NUCLEAR SCIENCE ABSTRACTS

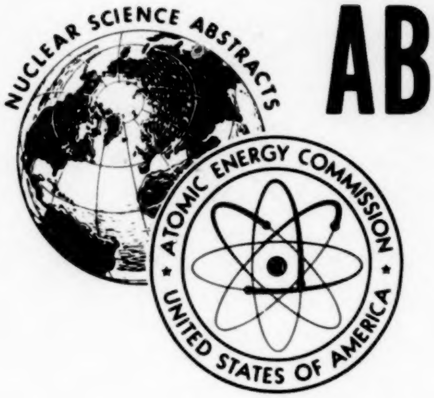

Volume 30 Number 11

Abstracts 28911-31460

December 15, 1974

UNITED STATES ATOMIC ENERGY COMMISSION

REPORT COLLECTIONS IN THE UNITED STATES

The libraries listed below purchase and maintain microfiche collections of USAEC and foreign reports that are abstracted in *NSA*. Their collections also include *NSA* and its indexes, AEC's Technical Progress Reviews, AEC-sponsored translations, conference proceedings published by AEC, and various bibliographic tools. Most of these libraries have microfiche reader-printers or other photocopy facilities with which to reproduce enlarged copies from microfiche. Charges for reproduction services vary.

Report collections of USAEC reports in countries other than the United States are listed on the inside back cover.

ALABAMA
Auburn, Auburn University
Tuskegee Institute, Tuskegee Institute

ALASKA
College, University of Alaska

ARIZONA
Tucson, University of Arizona

CALIFORNIA
Davis, University of California
Los Angeles, University of California
Santa Barbara, University of California

COLORADO
Boulder, University of Colorado

DISTRICT OF COLUMBIA
Washington, Library of Congress

FLORIDA
Gainesville, University of Florida

GEORGIA
Atlanta, Georgia Institute of Technology

HAWAII
Honolulu, University of Hawaii

IDAHO
Pocatello, Idaho State University

ILLINOIS
Urbana, University of Illinois

INDIANA
Lafayette, Purdue University

IOWA
Ames, Iowa State University

KANSAS
Manhattan, Kansas State University

KENTUCKY
Lexington, University of Kentucky

MARYLAND
Baltimore, Johns Hopkins University
College Park, University of Maryland

MASSACHUSETTS
Cambridge, Massachusetts Institute of Technology
Worcester, Worcester Polytechnic Institute

MICHIGAN
Ann Arbor, University of Michigan

MISSISSIPPI
State College, Mississippi State University

MISSOURI
Columbia, University of Missouri
Kansas City, Linda Hall Library

NEW JERSEY
Princeton, Princeton University

NEW MEXICO
Albuquerque, University of New Mexico

NEW YORK
Albany, New York State Library
Albany, State University at Albany
Ithaca, Cornell University
New York, Columbia University
Rochester, University of Rochester
Syracuse, Syracuse University
Troy, Rensselaer Polytechnic Institute

NORTH CAROLINA
Raleigh, North Carolina State University

OHIO
Cincinnati, University of Cincinnati
Cleveland, Cleveland Public Library

OHIO (Continued)
Columbus, Ohio State University
Toledo, University of Toledo

OKLAHOMA
Norman, University of Oklahoma

PENNSYLVANIA
Philadelphia, University of Pennsylvania
Pittsburgh, Carnegie Library
University Park, Pennsylvania State University

PUERTO RICO
San Juan, University of Puerto Rico

SOUTH CAROLINA
Columbia, University of South Carolina

TENNESSEE
Knoxville, University of Tennessee

TEXAS
Austin, University of Texas
College Station, Texas A & M University
Houston, Rice University

UTAH
Salt Lake City, University of Utah

VIRGINIA
Blacksburg, Virginia Polytechnic Institute
Charlottesville, University of Virginia

WASHINGTON
Pullman, Washington State University
Seattle, University of Washington

WEST VIRGINIA
Morgantown, West Virginia University

WISCONSIN
Madison, University of Wisconsin

USAEC reports so indicated in *Nuclear Science Abstracts* are offered for sale by National Technical Information Service, U. S. Department of Commerce, Springfield, Virginia 22151.

Volume 30, Number 11, December 15, 1974

NUCLEAR SCIENCE ABSTRACTS

A semimonthly publication of the USAEC Office of Information Services
Published by the USAEC Technical Information Center

Nuclear Science Abstracts provides the only comprehensive abstracting and indexing coverage of the international nuclear science literature. It covers scientific and technical reports of the U. S. Atomic Energy Commission and its contractors, other U. S. Government agencies, other governments, universities, and industrial and research organizations. In addition, books, conference proceedings, individual conference papers, patents, and journal literature on a worldwide basis are abstracted and indexed. Each issue of *Nuclear Science Abstracts* includes four indexes: subject, personal author, corporate author, and report number.

The following organizations scan and abstract the nuclear science literature in their respective countries for input to the International Nuclear Information System of the International Atomic Energy Agency. By special agreement, the input to INIS is simultaneously sent to the USAEC Technical Information Center to enhance the timeliness of coverage of that literature in *Nuclear Science Abstracts.*

- Atomic Energy of Canada Limited
- Australian Atomic Energy Commission
- Danish Atomic Energy Commission
- Finnish Atomic Energy Commission
- French Atomic Energy Commission
- Japan Atomic Energy Bureau–Atomic Energy Research Institute
- Commissie Nucleaire Informatieverzorging (Netherlands)
- Institutt for Atomenergi (Norway)
- Aktiebolaget Atomenergi (Sweden)
- United Kingdom Atomic Energy Authority
- Zentralstelle für Atomkernenergie-Dokumentation (West Germany)

Numerous organizations, societies, and publishers throughout the world provide *Nuclear Science Abstracts* with advance page-proof copy of their publications.

A list of the journals scanned regularly and the abbreviations used appears in the January 15 issue of *Nuclear Science Abstracts* and is supplemented in the July 15 issue. The January 15 issue also describes the scope and arrangement of the subject matter covered in *Nuclear Science Abstracts.* The subject matter covered is also described in TID-4552, *Subject Scope of Nuclear Science Abstracts,* available free from the USAEC Technical Information Center, P. O. Box 62, Oak Ridge, Tennessee 37830. An outline of the subject categories appears in the Contents of each issue.

HOW TO OBTAIN NUCLEAR SCIENCE ABSTRACTS

Nuclear Science Abstracts is available to the public on a subscription basis from the Superintendent of Documents, U. S. Government Printing Office, Washington, D. C. 20402.

NSA is issued in two volumes per calendar year, one beginning January 15, the other July 15. Each volume consists of twelve issues.

For the two 12-issue volumes, the annual subscription rate is $75.50 for domestic subscribers and $94.50 for foreign subscribers. A single issue costs $3.25 domestic rates or $4.07 foreign rates. Domestic rates apply to the United States, Canada, Mexico, and Central and South American countries except Argentina, Brazil, Guyana, French Guiana, Surinam, and British Honduras.

Indexes are cumulated for each volume, i.e., on a six-month volume basis. Each volume index is priced at $35.70 for domestic subscribers and $45.10 for foreign subscribers.

Previous *NSA* cumulative indexes are available:

From Johnson Reprint Corporation, 111 Fifth Avenue, New York, N. Y. 10003:

Vols. 1–4, Subjects and Authors (1948–1950), $30.00.

From Technical Information Center, P. O. Box 62, Oak Ridge, Tennessee 37830:

Vols. 5–10, Subjects and Authors (1951–1956), $5.25.

Vols. 11–15, Subjects (1957–1961), $19.00.
Vols. 11–15, Personal Authors (1957–1961), $14.25.
Vols. 11–15, Corporate Authors (1957–1961), $2.50.

From Superintendent of Documents, U. S. Government Printing Office, Washington, D. C. 20402:

Vols. 16–20, Subjects (1962–1966), $36.00.
Vols. 16–20, Personal Authors (1962–1966), $22.50.

Vols. 16–20, Corporate Authors (1962–1966), $3.75.

Vol. 26, Subjects and Authors (1972), $37.75.

Vol. 27, Subjects, Authors, and Report Numbers (Jan.–June 1973), $16.90.

Vol. 28, Subjects and Authors (July–Dec. 1973), $18.55.

Cumulative Report Number Index, Vols. 1–15 Revised, $4.00.
Cumulative Report Number Index, Vols. 16–20 Revised, $5.50.
Cumulative Report Number Index, Vols. 21–28, $9.35.

From Xerox University Microfilms, 300 North Zeeb Road, Ann Arbor, Michigan 48106:

Vols. 21–25, Subjects, Authors, and Corporate Authors (1967–1971), $195.00.

Nuclear Science Abstracts is available on an exchange basis to universities, research institutions, industrial firms, and publishers of scientific information. Government agencies may obtain *NSA* free of charge. Inquiries should be directed to the USAEC Technical Information Center, P. O. Box 62, Oak Ridge, Tennessee 37830.

Nuclear Science Abstracts is also available on 16-mm and 35-mm microfilm in reel or cartridge from Princeton Microfilm Corporation, Alexander Road, Princeton, New Jersey 08540. The cost of Vols. 1–26 (1948–1972) including *Abstracts of Declassified Documents* (1947–1948) is $730.00. The indexes for *Nuclear Science Abstracts* Vols. 1–26 (1948–1972) are also available for $385.00. The cost of each volume (six months) of *NSA* and its indexes is $45.

INDEXES TO NSA

Comprehensive indexes appear in each issue and are cumulated at the end of each volume. The report number indexes will be cumulated on both a volume and two-volume basis. Multivolume cumulations have been issued as indicated above.

All documents abstracted are indexed by subjects and personal authors. Report literature is indexed also by corporate author and report number. Each of these indexes in every issue is preceded by an introduction explaining in detail the organization of the index and the principles by which it is compiled. The reader is referred to these explanations for information not found in the brief summaries below.

Personal Authors

Each author's name is indexed in the form appearing on the document abstracted, with the exception that given names are reduced to initials:

SMITH, H., Planetary nebulae: two types, 29:13374
SMITH, H.R. Jr., Principles of electron beam technology, 29:13155
SMITH, J., See HOEGERMAN, S.F., 29:13035
See HOEGERMAN, S.F., 29:13037

Subjects

The subject index consisting of entries naming specific materials, objects, and processes is arranged alphabetically. Document titles, informative phrases, or both specific to these entries are arranged alphabetically under the entries.

Examples:

REACTOR LICENSING/SPAIN
Harmonization of the licensing conditions including environmental protection for the siting of nuclear power plants, 29:14745
REACTOR MATERIALS/STRESS ANALYSIS
Problems on nuclear reactor structure at elevated temperature, 29:14654
REACTOR PROTECTION SYSTEMS
HTGR gas turbine power plant control and safety studies. Quarterly progress report for the period July 1, 1973--September 30, 1973, 29:14846 (GULF-GA-A-12799)

Corporates

Technical report literature is indexed using the name of the organization or institution responsible for the issuance of the report.

14452 (WASH-1278) CTR ENGINEERING SYSTEMS STUDY REVIEW MEETING, GERMANTOWN, MARYLAND, SEPTEMBER 19 AND 20, 1973. Gough, W. C. **(USAEC Division of Controlled Thermonuclear Research, Washington, D. C.).** 1973. 258p. (CONF-730971-). Dep. NTIS $7.60.

is indexed as:

USAEC DIVISION OF CONTROLLED THERMONUCLEAR RESEARCH, WASHINGTON, D.C.
CTR engineering systems study review meeting, Germantown, Maryland, September 19 and 20, 1973, 29:14452 (WASH-1278)

Report Numbers

Technical report literature is also indexed using report numbers. This index includes information on where individual reports may be obtained. While not reports, patents and conference papers are indexed here as a matter of convenience.

WANL-M-FR-	(Non-AEC)	
72-5	29-13170	See N-73-31498
73-2	29-13070	See N-73-27584
WAPD-TM-	(Misc.)	
1126	29-14648	Dep. NTIS, $3.00
WARD-RB-		
3045-3	29-14647	AT
WARD-XS-		
3045-4	29-14784	AT
WASH-		
1208(12-73)	29-14582	Dep. NTIS, $3.00
1271	29-14451	Dep. NTIS, $7.60
1273	29-13005	NTIS, $4.00
1278	29-14452	Dep. NTIS, $7.60
1283	29-15003	Dep. NTIS, $7.50
WCAP-	(Misc.)	
7757	29-14785	
7758	29-14786	

AVAILABILITY OF PUBLICATIONS ABSTRACTED

Public availability of all U. S. Atomic Energy Commission reports is indicated in the report number indexes. The availability of other reports, when known, is also indicated. The availability of some unnumbered reports is given in the abstract.

Dissertations from *Dissertation Abstracts International, Part B* that are included in *Nuclear Science Abstracts* are available from University Microfilms, Inc., 315 N. First Street, Ann Arbor, Michigan 48103.

Information on the availability of the published literature and unpublished conference papers abstracted in *Nuclear Science Abstracts* can be obtained from the USAEC Technical Information Center, P. O. Box 62, Oak Ridge, Tennessee 37830.

TABLE OF CONTENTS

Volume 30, Number 11, December 15, 1974

Category *Page*

CHEMISTRY 2917
Analytical and Separations Chemistry 2917
Activation and Nuclear Reaction Procedures 2917
Chemical and Spectral Procedures 2920
Radiometric and Radiochemical Procedures 2922
Separation Procedures 2924
Inorganic, Organic, and Physical Chemistry 2925
Chemical and Physicochemical Properties 2925
Isotope Effects 2926
Isotope Exchange and Isotope Separation 2928
Radiation Chemistry 2929
Radiochemistry and Nuclear Chemistry 2934
Hot-Atom Chemistry 2934
Properties of Radioactive Materials 2934
Radioactive Waste Treatment 2939
Radioisotope Production 2939
Reactor Fuel Reprocessing 2940

CONTROLLED THERMONUCLEAR RESEARCH 2941
Confinement and Heating 2941
Diagnostics 2941
Kinetics (General) 2943
Kinetics (Experimental) 2943
Kinetics (Theoretical) 2943
Production 2945
Stability 2945
Thermonuclear Engineering and Equipment 2946
Wave Phenomena 2949

ENGINEERING 2950
Energy Conversion 2950
Facilities and Equipment 2953
Heat Transfer and Fluid Flow 2955
Materials Testing 2956
Nuclear Explosions 2957
Protective Structures and Equipment 2959

ENVIRONMENTAL AND EARTH SCIENCES 2960
Minerals and Ores 2960
Radioactive Effluents 2961
Radioactivity Monitoring and Transport 2961
Atmosphere 2963
Soil 2967
Water 2968
Ecosystems and Food Cycles 2969
Radiometric Techniques 2969
Site Surveys 2970
Thermal Effluents 2973
Chemical Effluents 2974

INSTRUMENTATION 2977
Radiation Detection Instruments 2977
General Detectors and Monitors 2977
Radiation Dosimeters 2981

Category *Page*

INSTRUMENTATION (Cont'd.)
Nuclear Spectroscopic Instrumentation 2983
High Energy Physics Instrumentation 2984
Radiometric Instruments 2986
Miscellaneous Instruments 2987

ISOTOPE AND RADIATION SOURCE TECHNOLOGY . 2990
Isotope Separation (Industrial) 2990
Isotopic Power Sources 2990
Radiation Sources 2990
Design and Fabrication 2990
Industrial Uses 2990

LIFE SCIENCES 2992
Radiation Effects on Biochemicals 2992
Radiation Effects on Cells 2993
Radiation Effects on Microorganisms 2995
Radiation Effects on Plants 2996
Radiation Effects on Animals 2998
Man 2998
Vertebrates 3001
Invertebrates 3005
Radionuclide Effects (Internal Source) 3005
Man 3005
Animals 3006
Microorganisms 3008
Nuclide Kinetics and Toxicology 3008
Man 3008
Animals 3009
Plants 3012
Microorganisms 3012
New Tracer Techniques 3012

MATERIALS 3019
Ceramics and Cermets 3019
Metals and Alloys 3024
Corrosion and Erosion 3024
Preparation and Fabrication 3025
Properties, Structure, and Phase Studies 3026
Radiation Effects 3035
Other Materials 3037

NUCLEAR MATERIALS AND WASTE MANAGEMENT . 3040
Accountability and Safeguards 3040
Disposal and Storage 3040
Handling Equipment and Procedures 3040
Transportation 3040

PARTICLE ACCELERATORS 3042
Design, Development, and Operation 3042
Auxiliaries and Components 3042
Ion Sources and Injection and Extraction Systems . . . 3043
Ion Optics and Field Calculations 3043
Storage Rings 3043
Experimental Facilities 3044

TABLE OF CONTENTS (continued)

Category — *Page*

- **PHYSICS (ASTROPHYSICS AND COSMOLOGY)** 3046
  - Cosmic Radiation . . . 3046
  - Stars . . . 3048
  - Quasi-Stellar, Radio, and X-Ray Sources . . . 3055
  - Solar Phenomena . . . 3057
  - Galaxies . . . 3062
  - Cosmology . . . 3066
  - Planetary Phenomena . . . 3067
- **PHYSICS (ATMOSPHERIC)** . . . 3069
  - Auroral and Ionospheric Phenomena . . . 3069
  - Effects of Nuclear Detonations . . . 3072
  - Magnetospheric Phenomena . . . 3072
- **PHYSICS (ATOMIC AND MOLECULAR)** . . . 3076
  - Beams and Their Reactions . . . 3076
  - Atomic and Molecular Properties . . . 3077
  - Positronium, Muonium, and Muonic and Mesic Atoms and Molecules . . . 3079
  - Collision Phenomena . . . 3079
  - Atomic Theory . . . 3084
- **PHYSICS (ELECTROFLUID AND MAGNETOFLUID)** . . 3085
- **PHYSICS (HIGH-ENERGY)** . . . 3086
  - Particle Interactions and Properties (Experimental) . . . 3086
    - *Electromagnetic* . . . 3086
    - *Weak* . . . 3087
    - *Strong (Baryon-induced)* . . . 3087
    - *Strong (Meson-induced)* . . . 3089
  - Particle Interactions and Properties (Theoretical) . . . 3090
    - *General* . . . 3090
    - *Electromagnetic* . . . 3092
    - *Weak* . . . 3094
    - *Strong (General)* . . . 3095
    - *Strong (Baryon No. = 0)* . . . 3097
    - *Strong (Baryon No. = 1)* . . . 3098
    - *Strong (Baryon No. ≥ 2)* . . . 3099
  - Particle Invariance Principles and Symmetries . . . 3100
    - *General* . . . 3100
    - *Applications (Electromagnetic and Weak)* . . . 3101
    - *Applications (Strong)* . . . 3101
  - Scattering Theory . . . 3102
- **PHYSICS (LOW-TEMPERATURE)** . . . 3103
  - Superfluidity . . . 3103
  - Superconductivity . . . 3103
  - Equipment and Devices . . . 3105
- **PHYSICS (NUCLEAR)** . . . 3108
  - Neutron Interactions with Matter . . . 3108
  - Nuclear Properties and Reactions, $A \leq 5$ . . . 3108
  - Nuclear Properties and Reactions, $6 \leq A \leq 19$ . . . 3110
  - Nuclear Properties and Reactions, $20 \leq A \leq 38$ . . . 3113
  - Nuclear Properties and Reactions, $39 \leq A \leq 58$ . . . 3114

Category — *Page*

PHYSICS (NUCLEAR) (Cont'd.)

  - Nuclear Properties and Reactions, $59 \leq A \leq 89$ . . . 3115
  - Nuclear Properties and Reactions, $90 \leq A \leq 149$ . . . 3117
  - Nuclear Properties and Reactions, $150 \leq A \leq 189$ . . . 3119
  - Nuclear Properties and Reactions, $190 \leq A \leq 219$ . . . 3121
  - Nuclear Properties and Reactions, $A \geq 220$ . . . 3121
  - Nuclear Theory . . . 3123
- **PHYSICS (RADIATION AND SHIELDING)** . . . 3130
  - Radiation Physics . . . 3130
  - Radiation Protection Standards . . . 3131
  - Radiation Source Calibration and Standardization . . . 3131
  - Shielding Calculations and Experiments . . . 3132
- **PHYSICS (THEORETICAL)** . . . 3133
  - General . . . 3133
  - Quantum Field Theories . . . 3133
  - Gravitation and General Relativity . . . 3136
- **REACTOR TECHNOLOGY AND REGULATION** 3138
  - Power Reactors, Non-Breeding, BWR-Type . . . 3138
  - Power Reactors, Non-Breeding, PWR-Type . . . 3138
  - Power Reactors, Non-Breeding, Graphite Moderated . . . 3140
  - Power Reactors, Non-Breeding, Otherwise Moderated . . . 3141
  - Power Reactors, Breeding . . . 3141
  - Research, Test, and Experimental Reactors . . . 3142
  - Production and Materials Testing and Processing Reactors . . . 3143
  - Propulsion and Package Reactors . . . 3144
  - Reactor Safety and Environmental Aspects . . . 3144
  - Reactor Theory and Calculation . . . 3147
  - Reactor Components and Accessories . . . 3148
  - Reactor Fuels . . . 3149
  - Reactor Control Systems . . . 3149
  - Nuclear Power Plant Economics . . . 3150
  - Reactor Fuel Cycle Economics . . . 3150
  - Reactor Licensing and Regulation . . . 3150
- **GENERAL** . . . 3152
  - Civilian Defense . . . 3152
  - Energy Utilization and Economics . . . 3152
  - Information Handling . . . 3152
  - Law . . . 3152
  - Management . . . 3153
  - Mathematics and Computers . . . 3153
  - Miscellaneous . . . 3155
    - *Chemistry* . . . 3155
    - *Life Sciences* . . . 3157
    - *Materials* . . . 3157
    - *Physics and Engineering* . . . 3161
- **CORPORATE INDEX** . . . INDEX-1
- **PERSONAL AUTHOR INDEX** . . . INDEX-11
- **SUBJECT INDEX** . . . INDEX-57
- **REPORT NUMBER INDEX** . . . INDEX-170

STAFF OF NUCLEAR SCIENCE ABSTRACTS

Editor and Production Manager
David E. Bost

Assistant Editor
Lee M. Thompson

Associate Editors
M. Catherine Grissom
Robert C. Kelly
Sidney F. Lanier
Henry D. Raleigh
Charles E. Stuber

Report Evaluators
John H. Mitchell
Mary H. Newman

Descriptive Cataloging Specialist
J. Paul Meredith

Subject Heading Specialist
Dora H. Moneyhun

Corporate Author Specialist
Clara L. Fox

Report Number Specialist
Helen W. White

Information Specialists
E. Ray Bedford
Jane G. Buchanan
D. Lamar Cason
David C. Cunningham
Theodore F. Davis
James R. Dulaney
Darrell O. Galde
Martha W. Gerrard
Everett J. Hoffman
Carolyn D. Houston
Lynda H. Kern
W. Hugh Kinser
Lisbeth C. Lieberman
William D. Matheny
Jean F. Peckham
Mona H. Raridon
Julia S. Redford
Stanley J. Rimshaw
Jesse W. Rushing
Robert W. Rutkowski
Francis S. Sachs
Lila B. Smith
Polly C. Summers
Helen L. Ward
Lawrence T. Whitehead
Milton O. Whitson
Martha C. Wilson

Publishing Coordinator
Charles R. Bruce

Computer Processing Coordinator
Noboru Kawakami

Communication concerning the editorial policy and content of *Nuclear Science Abstracts* should be addressed to the Editor, *Nuclear Science Abstracts*, USAEC Technical Information Center, P. O. Box 62, Oak Ridge, Tennessee 37830.

Use of funds for printing this publication approved by the Director of the Office of Management and Budget, June 19, 1972.

Volume 30, Number 11 December 15, 1974

NUCLEAR SCIENCE ABSTRACTS

CHEMISTRY

Analytical and Separations Chemistry

Refer also to abstracts 29359 and 31371.

28911 MODERN METHODS OF DETERMINATION OF ZIRCONIUM (SURVEY). Dolgorev, A. V.; Pal'nikova, T. I.; Podchainova, V. N. Ind. Lab. (USSR) (Engl. Transl.); 40: No. 2, 157-165(Feb 1974).

Translated from Zavod. Lab.; 40: No. 2, 129-136(Feb 1974).

A review is presented of gravimetric, titrimetric, photometric, extraction, and spectral methods reported in studies published up through 1972. 105 references. (JSR)

Activation and Nuclear Reaction Procedures

Refer also to abstracts 29510 and 29524.

28912 (AED-CONF-73-479-009) NONDESTRUCTIVE DETERMINATION OF BORON IN GLASSES USING A ^{241}Am–Be NEUTRON SOURCE. Ostermann, P.; Staerk, H.; Henkelmann, R. (Technische Univ. Muenchen, Garching (F. R. Germany). Inst. fuer Radiochemie). 1973. 4p. (In German). INIS.

From 4th seminar "activation analysis" of the Bundesanstalt fuer Materialpruefung; Berlin, F. R. Germany (11 Oct 1973).

The prompt gamma radiation with $E(\gamma) = 477$ keV generated in the $^{10}B(n,\alpha)^7Li$ nuclear reaction is the basis of the nondestructive and quantitative determination of boron in glass. The irradiation device is a 300-mCi ^{241}Am-Be neutron source fitted into a small lead cube, a paraffin block as neutron moderator, as well as a Pb-Bi alloy shield for the absorption of fast neutrons and gammas of the source. The prompt gamma radiation is measured in a multichannel analyzer with a 3 in. × 3 in. NaI(Tl)-scintillation crystal which is shielded against thermal neutrons by a ^{6}LiF cap. Several possibilities for moderation and shielding with the goal to obtain optimum flux conditions in the sample position and the background radiation of the detector are described, and the influence of detector dimensions as well as problems of the neutron source intensity are discussed. For the determination of B_7O_3-contents in glasses, several standard glass samples with known B_7O_3 concentrations have been used as calibration standards. The influences of tray dimensions, layer thickness and particle size of the samples and of the neutron self-absorption with higher boron contents have been studied. The method allows the determination of B_7O_3-concentrations above 0.1% with an accuracy of 2-4% within 10 minutes. (INIS)

28913 (IEA-316) APPLICATION OF NEUTRON ACTIVATION ANALYSIS TO THE DETERMINATION OF GOLD IN MINERALS. Garcia Agudo, E.; Seignemartin, C. L.; Duarte, U. (Instituto de Energia Atomica, Sao Paulo (Brazil)). Nov 1973. 20p. (In Portuguese). Dep. NTIS (US Sales Only) $4.00.

There is a general need for more sensitive techniques in gold analysis, not only in samples for gold prospection, but also for geochemical studies. In this work, the applicability of neutron activation analysis for gold assay in different kinds of samples, like quartzites, basic rocks with sulfides, sulfides (pyrite, chalcopyrite, etc.), and alluvium, was studied. Small samples, usually less than 1 g, are used in activation analysis, but as gold is not uniformly distributed, for gold prospection it is necessary to analyze bigger samples. For these cases, the irradiation time and neutron flux were adjusted for activating 100-g samples, assuring in this way the representativity of the analysis. A detection limit of about 10 ppB was obtained using this technique. For small samples (about 200 mg), the detection limit was of 0.1 ppM, varying with the sample composition. All the analyses were instrumental, not being necessary for the chemical separation of gold. The gamma spectra of the activated samples are included. (auth)

28914 (IEA-326) APPLICATION OF ACTIVATION ANALYSIS TO THE DETERMINATION OF POLLUTANTS IN THE ATMOSPHERE. Miyamaru, M.; Lima, F. W. (Instituto de Energia Atomica, Sao Paulo (Brazil)). Feb 1974. 15p. (In Portuguese). Dep. NTIS (US Sales Only) $4.00.

Thermal neutron activation is used to analyze the elements mercury, bromine, arsenic, antimony, and selenium, quantitatively, present in the atmosphere at the campus of the University of São Paulo. The elements are collected in "Millipore" filters by suctioning about 40 cubic meters of air through the filter. Chemical separation is achieved by distillation of bromine and bromides of the other four elements, which are, lately, retained individually in anion exchanger resins. Arsenic and selenium are collected in the same resin column. Zinc, sodium, scandium, iron, copper, samarium, lanthanum, potassium, tungsten, and chromium were qualitatively identified in the residue of the distillation. A Ge(Li) counter was used for the qualitative analysis of the elements in the residue and NaI(Tl) for the quantitative determination of arsenic, bromine, antimony, selenium, and mercury. All concentrations found are below maximum permissible levels for those five elements. Gold and uranium were also identified in the various samples analyzed. (auth)

28915 (N-74-20335) TRACE-ELEMENT ANALYSIS OF 1000 ENVIRONMENTAL SAMPLES PER YEAR USING INSTRUMENTAL NEUTRON ACTIVATION ANALYSIS. Sheibley, D. W. (National Aeronautics and Space Administration, Cleveland, Ohio (USA). Lewis Research Center). Mar 1974. 25p. (NASA-TM-X-71519; E-7724). NTIS $4.25.

The technology and methods developed at the Plum Brook Reactor to analyze 1000 samples per year and report data on as many as 56 elements are described. The manpower for the complete analysis of 20 to 24 samples per week required only 3 to 3.5 hours per sample. The solutions to problems encountered in sample preparation, irradiation, and counting are discussed. The automation of data reduction is described. Typical data on various sample matrices are presented. (auth)

28916 (N-74-20470) TRACE GEOCHEMISTRY OF LUNAR MATERIAL. Final Report. Morrison, G. H. (Cornell Univ., Ithaca, N. Y. (USA). Dept. of Chemistry). 31 Jan 1974. 12p. (NASA-CR-137386). NTIS $4.00.

The lunar samples from the Apollo 16 and 17 flights which were analyzed include soil, igneous rock, anorthositic gabbro, orange soil, subfloor basalt, and norite breccia. Up to 57 elements including majors, minors, rare earths and other trace elements were determined in the lunar samples. The analytical techniques used were spark source mass spectrometry and neutron activation analysis. The latter was done either instrumentally or with group radiochemical separations. The differences in abundances of the elements in lunar soils at the various sites are discussed. With regard to the major elements only Si is about the same at all the sites. A detailed analysis which was performed on a sample of the Allende meteorite is summarized. (auth)

28917 (NP-20122, pp 85-86) NONDESTRUCTIVE DETERMINATION OF THE NITROGEN (PROTEIN) CONTENT IN SINGLE KERNELS OF SEEDS. Sundqvist, B. (Tandem Accelerator Lab., Uppsala); Goenczi, L.; Bergman, R.; Lindh, U. Jan 1974.

28918 (NP-20122, pp 87) ANALYSIS OF THE NITROGEN AND CARBON CONTENT IN ORGANIC BULK MATTER BY FAST-NEUTRON INDUCED GAMMA RADIATION. Bergman, R. (Gustaf Werner Inst., Uppsala); Bergqvist, I.; Conde, H.; Stroemberg, L. G.; Lindholm, A.; Nilsson, L.; Nordborg, C. Jan 1974.

28919 (PAEC(A)-7332(Suppl.1)) ACTIVATION ANALYSIS: A LITERATURE SEARCH. (Philippine Atomic Energy Commission, Diliman, Quezon City). 4 Oct 1973. 233p. Dep. NTIS (US Sales Only) $14.75.

This bibliography contains 1,266 entries which were abstracted in NSA during the period December 1972 to January 1974. (LK)

28920 BETATRON ACTIVATION ANALYSIS OF CUPRIFEROUS FLOTATION PULP. Kaminski, R.; Matenko, J.; Mencel, J.; Janiczek, J.; Kielsznia, R. Nukleonika; 19: No. 6, 593-605(1974). (In Polish).

A method of copper determination in cupriferous flotation pulp by photo-activation analysis using betatron and another equipment intended for copper determination in dry samples is described. An activation was achieved with 14.9-MeV γ photons. The excitation activity was investigated by using two scintillation detectors and a fast coincidence circuit with resolution time τ = 80 ns. The precision of method was determined as ±4.25% in 0.95 confidence level for pulp with concentration 5% Cu and ±24% for 0.06% Cu. (auth)

28921 MULTIELEMENT DETERMINATION IN MARKET-GARDEN SOILS BY INSTRUMENTAL PHOTON ACTIVATION ANALYSIS. Chattopadhyay, A.; Jervis, R. E. (Univ. of Toronto). Anal. Chem.; 46: No. 12, 1630-1639(Oct 1974).

An instrumental method has been developed for simultaneous photon activation analysis of 30 elements in vegetable crop-growing organic soils using a 45-MeV electron linear accelerator. The method consists of a simultaneous irradiation of a multielement standard and the environmental soil samples at 15, 20, 22, 35, and 44 MeV maximum bremsstrahlung energies for 1 hour to determine concentrations of 27 elements by a high-resolution Ge(Li) detector. Three more elements can be determined by continuing the irradiation for 4 hours at 20 MeV. Guidelines for selecting appropriate activation products and their gamma-rays have been described. The concentrations of several of the elements determined have been independently checked through the use of alternative nuclides and gamma-rays. A comparison of the accuracy of this activation method with other standard analytical techniques, notably atomic absorption spectrophotometry, has been carried out by analyzing a few elements in soils by the latter technique. Agreement among the several analytical methods compared ranged between 2 and 10%. The accuracy of photon activation technique has also been evaluated by analyzing the Standard Reference Materials. The limits of detection for all 30 elements analyzed varied between 10 and 8000 nanograms depending on the nuclide measured. (auth)

28922 NONDESTRUCTIVE DETERMINATION OF SOME TRACE ELEMENTS IN TANTALUM BY PROTON ACTIVATION ANALYSIS. Krivan, V. (Max-Planck-Institut fuer Metallforschung, Schwaebisch Gmuend, Ger.); Swindle, D. L.; Schweikert, E. A. Anal. Chem.; 46: No. 12, 1626-1629(Oct 1974).

Trace concentrations of titanium, iron, zirconium, niobium, molybdenum, and tungsten have been determined nondestructively and simultaneously in high-purity tantalum. The determination is based on the analysis of the γ-ray spectra of the radionuclides produced by bombarding thick samples with a 15-MeV proton beam via the following principal reactions: ^{48}Ti(p,n)^{48}V, ^{56}Fe(p,n)^{56}Co, ^{90}Zr(p,n)^{90}Nb, ^{93}Nb(p,n)^{93m}Mo, and ^{182}W(p,2n)^{181}Re. The trace elements have been determined at levels comprised between 0.1 to 35 ppm, with a relative precision of 8.5 to 25%. The detection limits for a 5 μA-hr irradiation range from 0.005 ppm for zirconium to 0.5 ppm for tungsten. (auth)

28923 RADIOCHEMICAL SEPARATION OF FLUORINE BY ADSORPTION ON HAFNIUM DIOXIDE: APPLICATION TO THE DETERMINATION OF OXYGEN BY ACTIVATION ANALYSIS WITH CHARGED PARTICLES. Kohn, A.; Barrandon, J. N.; Debrun, J. L.; Valladon, M.; Vialatte, B. (CNRS, Orleans Cedex, France). Anal. Chem.; 46: No. 12, 1737-1741(Oct 1974).

Low concentrations of oxygen in metals and semiconductors are best determined by activation analysis with charged particles. The main problem, in most cases, is to perform a good radiochemical separation of ^{18}F, produced by nuclear reaction on oxygen. Adsorption of fluorine on hafnium dioxide, from nitric acid solutions, is studied here in detail as a possible method to perform this radiochemical separation. Applications in the case of the determination of oxygen in copper, cobalt, and silver are presented. (auth)

28924 COMPARISON OF ANALYTICAL TECHNIQUES FOR INORGANIC POLLUTANTS. Coleman, R. F. (Lab. of the Government Chemist, London). Anal. Chem.; 46: No. 12, 989A-990A; 992A; 994A-996A(Oct 1974).

Analytical methods which are applied to inorganic pollutants found in water, food, or collected on air filters from the atmosphere are discussed. The following methods are compared on the basis of sensitivity, accuracy, precision, multielement capability, and range of application: optical and electron microscopy, atomic absorption and fluorescence spectroscopy, mass spectrometry, atomic emission spectroscopy, neutron activation analysis, x-ray fluorescence spectrometry, and anodic stripping voltammetry. (LK)

28925 ELEMENTAL ANALYSIS OF PROTEIN-CONTAINING FOOD MATERIALS FROM VARIOUS SOURCES. Furr, A. K. (Virginia Polytechnic Inst., Blacksburg); Kosikowski, F. V.; Bache, C. A.; Lisk, D. J. J. Food Sci.; 39: No. 5, 887-891(1974).

Concentrations of elements in food materials were determined by neutron activation analysis. The following samples were analyzed: fish protein, dried seaweed, fermented sheep's milk, yeast protein, fermented rice, soybean protein, commercial dog food, and commercial sodium alginate. Results are tabulated and the significance of various elements is discussed. (HLW)

28926 ASSAY OF SILVER IN ORES BY NEUTRON ACTIVATION. Gorshkov, V. V.; Basargin, N. N.; Smakhtin, L. A.; Sinitsyna, T. S. Ind. Lab. (USSR) (Engl. Transl.); 40: No. 2, 226-228(Feb 1974).

Translated from Zavod. Lab.; 40: No. 2, 181-184(Feb 1974).

A method was developed for the neutron-activation determination of Ag in ores preceded by selected concentration of the Ag. The Ag is isolated by its coprecipitation as p-dimethylaminobenzylidene rhodaninate with 2,4-dinitroaniline as coprecipitant to provide more complete and rapid coprecipitation of the Ag complex. The completeness of the separation was determined in the presence of a number of elements. The results obtained on specimens and standards of ores of various compositions were compared with the results of spectral and atomic absorption analyses with satisfactory agreement. (JSR)

28927 USE OF NH_4-FORM CHELEX 100 CHELATING RESIN OF LOW INDUCED ACTIVITIES FOR NEUTRON ACTIVATION ANALYSIS OF MANGANESE IN SEAWATER. Hirose, A.; Kobori, K.; Ishii, D. (Nagoya Univ., Japan). Nippon Kagaku Kaishi; 1974: No. 5, 900-904(May 1974). (In Japanese).

A method has been developed for the determination of manganese in seawater by neutron activation using Chelex 100 chelating resin as a pre-irradiation concentration agent. Chelex 100 resin (0.5 ~ 1 g as wet basis) was packed into a column (0.65 cm ϕ × 10 cm) and purified by washing with 2N HNO_3 and 2N NH_4OH, and finally transformed into NH_4-form by washing with 0.1N NH_4OH until pH of effluent became above 6. Seawater (0.1 ~ 0.5 l), previously filtrated with a 0.45 μ pore-sized membrane filter, was passed through above column at a flow rate of within 1.5 ml/min to separate manganese from seawater. The resin was transferred into a polyethylene bag and dried in an electric oven at 75°C for 10 hours and heat-sealed off. The resin samples together with standards were irradiated with pneumatic tube system of JRR-2 reactor at a flux of 7×10^{13} n/cm^2/sec for 20 minutes. After cooling for about 3 hours, the irradiated resin was slurried with water and transferred into a column previously packed with 0.1 g of Dowex A-1 chelating resin, then treated with 50 ml/g/wet resin of 0.1N KNO_3 to elute out the interfering nuclides such as ^{24}Na and ^{82}Br. The γ-activities from ^{56}Mn in resin were counted with a Ge(Li) detector after cooling for about 5 ~ 6 hrs. At present, the chemical yield of manganese was over 98%. And, the blank was 0.003 μg/g/wet resin. The minimum determinable and detectable masses are thus presumed to be about 0.03 μg per 500 ml of seawater (10-fold of blank) and 0.006 μg per 500 ml of seawater (2-fold of blank), respectively. (auth)

28928 DETERMINATION OF ZINC IN THE PRESENCE OF SCANDIUM BY ACTIVATION ANALYSIS COMBINED WITH THIN-LAYER CHROMATOGRAPHIC SEPARATION. Maki, Y.; Nojiri, T. (Industrial Research Inst. of Kanagawa Prefecture, Yokohama, Japan). Jap. Anal.; 23: No. 6, 604-609(Jun 1974). (In Japanese).

The determination of zinc contained in the sample such as airborne by non-destructive neutron activation analysis by measuring a γ-ray spectrum is disturbed by scandium accompanied with zinc. It is difficult to distinguish the photo-peak with 1115 keV of ^{65}Zn (half life; 245 days) from that with 1120 keV of ^{46}Sc (half life; 83.9 days), even though a Ge(Li) detector is used. These radioactive nuclides are produced by the thermal neutron irradiation of target elements, ^{64}Zn and ^{45}Sc whose thermal neutron cross section and natural abundance are 0.64 barn and 48.9%, and 23 barn and 100%, respectively. In this report, after separation of neutron-irradiated zinc and scandium by thin-layer chromatography (TLC), zinc was identified by a NaI (Tl) scintillation detector which was not superior to Ge(Li) detector in the resolution of measuring of γ-ray spectrum, but excellent in the counting efficiency and the maintenance. The sample solutions were prepared as follows: after irradiation of scandium oxide or zinc metal by thermal neutron (flux: 1×10^{12} n/cm^2/sec) in a reactor for 6 hours, samples were dissolved with an acid. The solutions were developed on cellulose as an adsorbent, with a mixture of n-propanol and 3N HCl in a volume ratio (10 : 1) as a developer which is the most excellent one in several kinds of mixed solutions. The developed spot of zinc was overlapped on the acid front with sharp shape and the R_f values were 0.74 for zinc and 0.02 for scandium. The sample solutions including different ratios of scandium to zinc such as 50 μg : 0 μg, 50 μg : 1 μg, 50 μg : 5 μg, 50 μg : 50 μg, 50 μg : 500 μg were developed by using the TLC system. No trace of scandium could be detected in each of these zinc fractions on the thin-layer plates. Next, the determination limit of zinc was examined by measuring γ-ray photo-peak of ^{65}Zn and total γ-ray of ^{65}Zn. Zinc was separated by the TLC system above mentioned from the sample solution containing cobalt, scandium, iron and zinc of which R_f values were 0.02, 0.02, 0.45 and 0.74, respectively, in order to exclude the radio-activities of ^{60}Co, ^{46}Sc and ^{59}Fe which were produced by the irradiation of thermal neutron to target elements. These radioactive nuclides disturb the identification of the photo-peak of ^{65}Zn by a NaI(Tl) detector for their long half-lives and γ-ray energy more than 1 MeV. More than 5 μg of zinc can be determined by measuring the γ-ray spectrum and moreover the determination limit of zinc was found to be about 1 μg with an error of 20% by counting total γ-ray of ^{65}Zn in the zinc spot developed on the thin-layer plate. (auth)

28929 RADIOACTIVATION ANALYSIS IN THERMAL AND EPITHERMAL NEUTRONS OF THE IBR-30 REACTOR OF JINR. Byu, N. K.; Vyropaev, V. Ya.; Dien, F. K.; Zhuravleva, E. L.; Khien, F. Z. Sov. Radiochem. (Engl. Transl.); 15: No. 6, 861-864(1973).

Translated from Radiokhimiya; 15: No. 6, 853-858(1973).

Results of activation analysis of rocks in thermal and epithermal neutron channels of the IBR-30 reactor are reported. Physical parameters of these two channels for activation were measured and on this basis a comparison was made of the analysis sensitivity for some elements in these channels. (LK)

28930 TRACE ELEMENT BEHAVIOR IN SOIL OF SOME INDONESIAN SAWAH'S AND IN SLUDGE OF AN INDONESIAN RIVER. Routma, J. P. W. (Interuniversitair Reactor Instituut, Delft, Netherlands). Delft Progr. Rep., Ser. A-F; 1: No. 1, 5-16 (Sep 1973).

Soil and sludge samples were taken during the beginning of the rainy season from three sawah's at various height levels near Tjiparaj and from the Tji Tarum River near the inflow of six side rivers along a 200 km stretch. These samples were purified from particles bigger than 16 μm by a sedimentation procedure. They were analyzed by nondestructive neutron activation analysis (NAA) for 22 elements (Na, K, Cs, Cu, Au, Hg, Cr, Mn, Fe, Co, As, Sb, Br, Sc, La, Ce, Eu, Yb, Tb, Hf, Ta, Th) and by destructive NAA for Zn, Cu, and Hg. Indications were obtained regarding absolute concentrations in sawah soils and about mobilization and absorption phenomena in tropical river. Moreover, certain elements (i.e., mercury) in river sludge show strong variations at specific points along the river. This might indicate the presence of geographical areas. This should be further investigated. Finally some soil and fish samples from the near-shore part of the Java Sea were analyzed to measure the possible consequences of mercury discharge for the environment. (NL)

28931 SIMULTANEOUS ANALYSIS OF URANIUM AND THORIUM BY THE DELAYED FISSION NEUTRON COUNTING METHOD. Lee, C. (Atomic Energy Research Inst., Seoul); Kim, H. J.; Bak, H. I. J. Korean Nucl. Soc.; 6: No. 2, 80-88 (Jun 1974).

A small modification in the procedure of Amiel's delayed neutron counting method is attempted for the simultaneous determination of uranium and thorium in geological samples. This analytical procedure is found to hold good accuracy over the wide range of concentration ratio of two elements. Details of the development and evaluation of the method are described. The sensitivity obtained from the method is less than 0.1 μg for uranium and it is about 5 μg for thorium. (auth)

28932 OXYGEN CONTENT USING A 14-MeV NEUTRON ACTIVATION AND DIRECT-COUNTING TECHNIQUE. Philadelphia; American Society for Testing and Materials (1973). 6p. (ASTM-E-385-73).

This method covers the measurement of oxygen concentration in almost any matrix by using a 14-MeV neutron activation and direct-counting technique. Essentially the same system can be used to determine oxygen concentrations ranging from over 50% to about 10 ppM or less depending on the sample size and available 14-MeV neutron flux. The method can be used on either solid or liquid samples, provided that they can be made to conform in size, shape, and density during irradiation and counting to a standard sample of known oxygen content. (LK)

28933 MEASUREMENT OF ATOMIC CONCENTRATION PROFILES IN THIN FILMS USING NONRESONANT NUCLEAR REACTIONS. Wise, P. J.; Barnes, D. G.; Neild, D. J. (Univ. of Manchester, Eng.). J. Phys., D (London); 7: No. 11, 1475-1481(21 Jul 1974).

A general experimental technique and computational procedure is described for the quantitative determination of concentration profiles of atomic species in thin films. The theoretically expected charged-particle energy spectrum resulting from the bombardment of the sample by energetic charged particles is calculated and then compared with the experimentally observed spectrum to obtain the concentration profiles. This technique has been applied to the determination of diffusion coefficients, oxidation rates, and film thicknesses for a variety of samples. (auth)

28934 TRACE ELEMENTS IN PRECIPITATION AND CLOUD WATER IN THE AREA OF HEIDELBERG, MEASURED BY INSTRUMENTAL NEUTRON ACTIVATION ANALYSIS. Bogen, J. (Univ., Heidelberg). Atmos. Environ.; 8: No. 8, 835-844(Aug 1974).

The concentrations of the trace elements Cl, La, K, Co, In, Fe, Sc, Mn, Cs, Br, Ag, Sb, Cd, Cr, Hg, Ce, and Sm in rain water residues, collected in Heidelberg (April to June 1971) were determined by thermal neutron irradiation in a flux of 3×10^{11}n cm^{-2} s^{-1} and γ-ray spectrometry using Ge(Li)-detectors. Cloud water was collected aboard an airplane at different heights from stratiform clouds and treated like rain for comparison of the trace element concentrations in rain and cloud water. Considering the concentration of an element, i, relative to the concentration of the element sodium, three groups of elements were found, the main sources of which were presumed to be the ocean (Cl, Br), the earth's surface (La, Fe, Sc, Mn, Cr, Sm) and anthropogenous production (Ag, Sb, Co). A comparison of cloud and rain water concentrations shows constant values inside the cloud between 3500 and 2500 m, decreasing concentrations between 2500 and 2000 m, and constant or increasing values for all elements not originating in the ocean between the lowest cloud level and the earth's surface. The concentration of elements which are specific for an aerosol production on the surface of the ocean increased with height, due to the special meteorological situation. (auth)

28935 DETERMINATION OF RARE EARTHS AND THORIUM IN APATITES BY THERMAL AND EPITHERMAL NEUTRON-ACTIVATION ANALYSIS. Brunfelt, A. O.; Roelandsts, I. (Univ. of Oslo). Talanta; 21: No. 6, 513-521(Jun 1974).

A procedure is described for the non destructive determination of Na, Mn, La, Nd, Sm, Eu, Gd, Tb, Dy, Ho, Er, Yb, Lu, and Th in apatites by thermal and epithermal neutron-activation of independent portions of the material. The method was applied to three apatites with different contents. The precision obtained was better than ± 5% for La, Ce, Sm, Eu, Gd, Tb, and Dy and ± 20% for Yb, Nd, Ho, Er, and Lu for an apatite with a total rare earth oxide content of the order of 1%. Determination of Ce, Tb, and Yb could only be carried out with thermal neutron-activation analysis, while Gd, Ho and Er could only be determined after irradiation with epithermal neutrons. (auth)

28936 METHOD FOR DETERMINING SUGAR/STARCH CONTENTS IN AQUEOUS SOLUTIONS. Chatters, R. M.; Kimbrell, J. E.; Slater, S. D. (to United States Atomic Energy Commission). US Patent 3,826,617. 30 Jul 1974. Filed date 31 Oct 1972. 8p.

A method is reported for determining simple reducing sugar concentration in aqueous solutions. It consists of several steps, including rendering the solution strongly basic, adding a solution consisting of potassium iodide and ^{203}HgI$_2$ to the basic solution, heating the resulting solution to an elevated temperature near boiling for a period of time to reduce the radio-mercury to elemental mercury. The elemental mercury is sorbed on diatomaceous earth, separating the diatomaceous earth–mercury solids. Then the retained solids are analyzed for ^{203}Hg. In an alternative embodiment, nonradioactive mercury (as mercury iodide) may be used with neutron activation to form a radio-mercury isotope, such as ^{203}Hg, which can then be analyzed. Starch concentration may also be determined by first converting any starch present to a simple reducing sugar by enzymatic hydrolysis, the sugar concentration then being determined by this method. (Official Gazette)

Chemical and Spectral Procedures

Refer also to abstracts 29625, 31370, and 31373.

28937 (BNWL-1850(Pt.3), pp 1-3) POTENTIAL APPLICATION OF ATOMIC ABSORPTION AND ANODIC STRIPPING VOLTAMMETRY TO THE PRECIPITATION SCAVENGING PROGRAM. Lee, R. N. Apr 1974.

In Pacific Northwest Laboratory annual report for 1973 to the USAEC Division of Biomedical and Environmental Research. Part 3. Atmospheric sciences.

Rain samples from the April 16, 1971 in-cloud scavenging experiment have been analyzed by flameless atomic absorption and anodic stripping voltammetry. These techniques appear to be of potential value to the in-cloud scavenging program. However, more extensive work is required to evaluate the potential of anodic stripping voltammetry. (auth)

28938 (CNEA-363) APPLICATION OF A MASS SPECTROMETER TO THE METHOD OF DETERMINATION OF GASES IN METALS BY VACUUM FUSION. Andreone, C. A.; Simkin, Y. R.; Zuzek, E. (Comision Nacional de Energia Atomica, Buenos Aires (Argentina). Departamento de Metalurgia). 1973. 12p. (In Spanish). Dep. NTIS (US Sales Only) $4.00.

A method was developed for the determination of gases in metals applying the vacuum fusion technique and using a quadrupole mass spectrometer as analyzer. The fundamental principle of the method is given, the apparatus is described and the calibration of same, which permits the simultaneous identification of oxygen, nitrogen, and hydrogen, is discussed. (auth)

28939 (CNEA-366) CHRONOAMPEROMETRIC DETERMINATION OF IODINE IN URINE. Botbol, M.; Casabe, J.; Garcia, E. E. (Comision Nacional de Energia Atomica, Buenos Aires (Argentina). Departamento de Quimica). 1973. 12p. (In Spanish). Dep. NTIS (US Sales Only) $4.00.

A procedure is described for the determination of total iodine in urine, based on its measurement as iodate by means of linear potential scan voltametry. The iodine in the sample is converted to inorganic iodide by ignition in alkaline medium and then separated on an anionic ion-exchange resin. The iodide is eluted with a solution of sodium perchlorate and oxidized to iodate by means of bromine in slightly acid medium. The iodate is reduced on a hanging drop electrode by a chronoamperometric technique with a linear potential scan from −0.5 to −1.5 V vs SCE in a supporting electrolyte composed of 0.9 M sodium perchlorate -0.005 M borax at pH 8.5. As described, the procedure allows the determination of urinary iodine contents ranging from 0.035 to 0.65 ppM. (auth)

28940 (EUR-4859) ANALYSIS OF ECE DATA ON THE BASIS OF ISOTOPIC WEIGHT FRACTIONS. Kroeckel, H. (Commission of the European Communities, Brussels (Belgium)). 1972. 78p. INIS.

The uranium masses of batches of fuel elements of the ISPRA-I reactor are determined on the basis of isotopic weight fractions measured during the reprocessing campaigns. This calculation provides for information permitting the assessment of the validity of such analysis for accurate uranium mass determination and the investigation of the errors involved. (INIS)

28941 (JUL-1063-CT) LABORATORY AND HOT-CELL STUDIES CONCERNING THE IN-LINE POLAROGRAPHIC DETERMINATION OF URANIUM IN THE AQUEOUS WASTE STREAM OF THE KFA-TBP 23/25 PROCESS. Merz, I.; Kaiser, G. (Kernforschungsanlage Juelich G.m.b.H. (F.R. Germany). Inst. fuer Chemische Technologie). Apr 1974. 30p. (In German). INIS. 14 figs.; 3 tabs.; 11 refs. With abstract.

In flowsheet studies for the KFA-TBP 23/25 process, in-line polarography was applied in the laboratory as well as in the hot cells to control the uranium content of the IAW streams. While the detection limit was 3 mg/l in the laboratory, only uranium concentrations ≥15 mg/l in fission product-containing solutions could be determined. Disturbances due to fission or radiolysis products could only partly be suppressed by the addition of increased amounts of methanol and ascorbic acid; solutions practically free of uranium also always exhibited a horizontal stage at the depolarization voltage of uranium. However, it is not clear to what species this can be assigned. (GE)

28942 (N-74-18812) INTERLABORATORY COMPARISON OF CHEMICAL ANALYSIS OF URANIUM MONONITRIDE. Merkle, E. J.; Davis, W. F.; Halloran, J. T.; Graab, J. W. (National Aeronautics and Space Administration, Cleveland, Ohio (USA). Lewis Research Center). Mar 1974. 23p. (NASA-TN-D-7536; E-7674). NTIS $3.00.

Analytical methods were established in which the critical variables were controlled, with the result that acceptable interlaboratory agreement was demonstrated for the chemical analysis of uranium mononitride. This was accomplished by using equipment readily available to laboratories performing metallurgical analyses. Agreement among three laboratories was shown to be very good for uranium and nitrogen. Interlaboratory precision of ±0.04% was achieved for both of these elements. Oxygen was determined to ±15 ppM at the 170-ppM level. The carbon determination gave an interlaboratory precision of ±46 ppM at the 320-ppM level. (auth)

28943 (RISO-297) COMPILATION OF X-RAY INTERACTION DATA FOR X-RAY FLUORESCENCE ANALYSIS OF GEOLOGICAL SAMPLES. Gwozdz, R.; Kunzendorf, H.; Rose-Hansen, J. (Danish Atomic Energy Commission, Risoe. Research Establishment). Dec 1973. 61p. Dep. NTIS (US Sales Only) $6.25.

X-ray interaction data useful in x-ray fluorescence analysis of geological samples were compiled on a Univac 1110 computer by means of a Fortran IV program. Based on fit coefficients the tabulations include values for the photoelectric absorption coefficient, the coherent and incoherent scattering coefficients, the ratio of the total scattering coefficient to the total x-ray attenuation coefficient, the ratio of the coherent to the incoherent scattering coefficient, and the half-range of characteristic $K\alpha$ x rays for 14 oxides, international geochemical reference samples, selected minerals, and selected fluxing agents. A graphical representation of some of these data is also included. For the geological samples are also tabulated x-ray interaction data for the radiation of 9 radioisotopes commonly used in energy-dispersive x-ray fluorescence analysis. (auth)

28944 (UCID-15952) SPECTROGRAPHIC DETERMINATION OF TRACE IMPURITIES IN HIGH PURITY URANIUM OXIDE. Morris, W. F. (California Univ., Livermore (USA). Lawrence Livermore Lab.). 12 Nov 1971. 14p. Dep. NTIS $4.00.

A spectrographic method for the determination of Al, B, Ba, Be, Bi, Ca, Cd, Co, Cr, Cu, Fe, Ga, Ge, K, Mg, Mn, Mo, Na, Nb, Ni, Pb, Sb, Si, Sn, Sr, Ti, Tl, V, Zn, and Zr in high-purity U_3O_8 ($99.5^+\%$) is given. The method can be applied to the analysis of uranium metal or any uranium compound which can be converted to oxide either by direct ignition in a muffle furnace at 850°C or by acid dissolution followed by ignition. (LK)

28945 DETERMINATION OF SMALL AMOUNTS OF ZIRCONIUM IN WOOL. Inglis, A. S.; Nicholls, P. W. (CSIRO, Melbourne, Australia). J. Text. Inst.; 64: No. 7, 445-447(1973).

The atomic-absorption method of Grossman and Inglis (Anal. Abstr., 1972, 23: 486) for determining Zr in tanned hide was unsatisfactory for use with the levels of Zr (<1%) in flame-proofed and metal-treated wools. The procedure is modified by ashing the sample to decompose amino acids and convert sulfates into oxides; the ash is dissolved in 10% HF, and this solution is subjected to atomic-absorption analysis (loc. cit.). Precision was good for Zr contents down to 0.02%, and the results agreed with the spectrophotometric procedure of Savvin (Ibid., 1962, 9, 1352). However, the spectrophotometric method, although more sensitive, was less precise. (Anal. Abstr.)

28946 DETERMINATION OF RARE EARTHS IN PLUTONIUM BY X-RAY EMISSION ANALYSIS. Miller, A. G. (Atlantic Richfield Hanford Co., Richland, WA). Contract AT(45-1)-2130. Anal. Chem.; 46: No. 12, 1720-1724(Oct 1974).

A sensitive and accurate method for measuring trace rare earths in plutonium by x-ray emission analysis has been developed. Plutonium is separated from the rare earths by solvent extraction using tri-isooctylamine. The rare earths are then carrier-precipitated as fluorides and collected on a membrane filter in an "infinitely thin" layer. The rare earths on the filter are counted and ratioed to a terbium internal standard. This work has dealt with samarium, europium, gadolinium, dysprosium, and the elements that produce spectral interferences. However, the method is equally applicable to the other rare earths, assuming spectral interferences are avoided. Detection limits are on the order of 0.1 μg. The relative standard deviation for spike recoveries of the four rare earths at the 1-μg level is 8%. (auth)

28947 NEW DISCRETE ATOMIZATION CELL FOR ATOMIC FLUORESCENCE SPECTROMETRY. Molnar, C. J.; Winefordner, J. D. (Univ. of Florida, Gainesville). Anal. Chem.; 46: No. 12, 1807-1810(Oct 1974).

This system allows the use of both pulsed and continuous modes of sampling, which results in improved absolute limits of detection. No deleterious effects to the linear dynamic ranges result. (auth)

28948 SEPARATION OF TRACE METAL IMPURITIES FROM NUCLEAR GRADE URANIUM BY LONG-CHAIN AMINE EXTRACTION AND DIRECT DETERMINATION BY ATOMIC ABSORPTION

SPECTROPHOTOMETRY. de Moraes, S.; Abrao, A. (Instituto de Energia Atomica, Sao Pualo, Brazil). Anal. Chem.; 46: No. 12, 1812-1814(Oct 1974).

Solvent extraction separation of trace concentrations of Cd, Ag, Au, Hg, Pb, and Bi in uranium from HCl–KI media is investigated for analytical applications. Direct burning of the organic phase in an AA spectrophotometer provides enhanced absorbance, and precision in the range 2–12%. (auth)

28949 SPECTROCHEMICAL METHOD FOR DETERMINATION OF TELLURIUM IN GEOLOGICAL MATERIALS. Schoenfeld, I.; Berman, A. (Soreq Nuclear Research Centre, Yavne, Israel). Anal. Chem.; 46: No. 12, 1826-1827(Oct 1974).

This method consists of volatilization of tellurium and dc-arc excitation of the distillate. The precision is about 20%, the accuracy about 10%. (auth)

28950 BERYLLIUM CONTENT OF NBS STANDARD REFERENCE ORCHARD LEAVES. Florence, T. M.; Farrar, Y. J.; Dale, L. S.; Batley, G. E. (Australian Atomic Energy Commission Research Establishment, Lucas Heights). Anal. Chem.; 46: No. 12, 1874-1876(Oct 1974).

Results from an analysis of beryllium content of NBS Orchard Leaves by the Morin fluorimetric method, emission spectrography, and gas chromatography are reported. From fluorimetric and emission spectrographic studies it was concluded that NBS Standard Reference Orchard Leaves contains a total beryllium content (acid soluble + silicons residue) of 0.030 ± 0.004 ppm (dry basis) and that the sample contains no beryllium compounds which are volatile below 800°C. (LK)

28951 SPECTRAL ASSAY OF COMPONENTS IN ALLOYS (EXCHANGE OF EXPERIENCE). Miskar'yants, V. G. (State Research and Planning Inst. for the Rare-Metal Industry, Moscow). Ind. Lab. (USSR) (Engl. Transl.); 40: No. 2, 224-225(Feb 1974).

Translated from Zavod. Lab.; 40: No. 2, 179-180(Feb 1974).

A spectral method, based on powdering the sample and exciting the spectrum in a spark discharge, was developed for determining alloying components in alloys whose compositions vary within wide limits. Turnings from the alloy are dissolved in H_2SO_4 with the addition of $(NH_4)_2SO_4$. The solution is evaporated and the residue fired. The resulting powder is finely ground, mixed with vaseline grease, and excited with a spark discharge. The method was tested on an alloy of known composition for the determination of W, Mo, and Zr. The values obtained were compared with the results of chemical analysis and with the marker's values. The results are tabulated. (JSR)

28952 ABSORPTION X-RAY RADIOMETRIC ANALYSIS USING THE $K\alpha_2$ LINES OF THE CHARACTERISTIC RADIATION OF TARGETS. Kokhov, E. D.; Dines, V. L.; Voronov, B. F. Ind. Lab. (USSR) (Engl. Transl.); 40: No. 2, 200-202(Feb 1974).

Translated from Zavod. Lab.; 40: No. 2, 160-162(Feb 1974).

The absorption x-ray radiometric analysis method was applied to the determination of Sm using the $K\alpha_2$ lines of Ho and Er targets as the characteristic radiation of the two targets. Excitation sources of ^{170}Tm and ^{241}Am were used and gave approximately the same results. The analytical results were substantially affected by the position of the selective filters. The effect of additives can be minimized by the selection of the proper l_2/l_1 ration (with l_1 and l_2 being the thicknesses of the samples for radiation fluxes with different energies). Analysis results obtained with pure Sm solutions and with admixtures of La, Nd, No, Ce, and Eu were tabulated. These results show that Eu decreased and sensitivity of the method by causing high readings for Sm. Otherwise the method offers a sufficiently high selectivity with respect to admixtures and can be used in automated instrumentation for monitoring technological solutions. (JSR)

28953 EXTRACTION SPECTROPHOTOMETRIC DETERMINATION OF SCANDIUM WITH XYLENOL ORANGE AND ETHYLTRIDODECYLAMMONIUM BROMIDE. Shijo, Y. (Utsunomiya Univ., Japan). Nippon Kagaku Kaishi; 1974: No. 5, 889-893(May 1974). (In Japanese).

A spectrophotometric method of determination of scandium was studied by the solvent extraction of scandium-xylenol orange chelate into xylene solution of ethyltridodecylammonium bromide (ETDA). The scandium-XO-ETDA complex was extracted into aromatic hydrocarbons such as benzene, toluene, xylene, but not into polar solvents such as n-butanol, ethylacetate, methylisobutylketone, and nitrobenzene. The extracted complex had an absorption maximum at 520 nm. Its maximum extraction was obtained when the pH of the aqueous phase was adjusted to 6.0 ~ 6.7. The extraction rate of the complex was fast and equilibrium was attained by shaking for 10 sec. Beer's law was seen up to 7.0 μg scandium per 5.0 ml of xylene. The molar absorption coefficient of the complex was 2.7×10^4 $cm^{-1}/mol^{-1}/l$ at 520 nm. Composition of the complex was estimated to be Sc : XO : ETDA = 1 : 1 : 2 by the mole ratio, continuous variation and mobile equilibrium methods. Consequently it may be assumed that the ternary complex was an ion association system with $\{ScHR^{2-}\} \cdot \{(ETDA^+)_2\}$ structure. Triethylene-tetramine and o-phenanthroline can be used for the masking of many metal ions, but the presence of vanadium, aluminum, beryllium, thorium, zirconium, uranium, bismuth, lanthanum, nitrate, perchlorate, citrate, EDTA interfered with the determination seriously. (auth)

28954 ATOMIC ABSORPTION SPECTROMETRY OF IMPURITIES IN HIGH PURITY TANTALUM WITH HEATED GRAPHITE ATOMIZER. Ishibashi, W.; Sato, M.; Hashimoto, M. (Showa Denko K. K., Tokyo). Jap. Anal.; 23: No. 6, 597-603(Jun 1974). (In Japanese).

For the determination of impurities in high-purity tantalum powders, atomic absorption spectrometry using a heated graphite tube as an atomizer was studied. In comparison with another method, this method has no contamination risk from the pretreatment of the sample, and the operation is performed rapidly and easily. Some factors for the determination, (1) the effect of the carrier gas flow rate on the sensitivity, (2) the effect of a state of sample on the absorption peak, (3) the relation between the spectral intensity and the duration of absorption, and (4) the relation between the spectral intensity and the furnace temperature are examined. The more the carrier gas rate increases, the more the sensitivity decreases. The flow rate variation of 0.1 l/min. corresponds to the absorption spectral intensity variation of 5% or so. For this reason, the flow rate variation was fixed within 0.05 l/min in the determination. The relation between the spectral intensity and the duration of absorption shows that the element is vaporized more rapidly in an aqueous solution than the tantalum powder. Therefore, when the impurities at different states contained in a substance are measured, it is better to determine the elements by the use of the peak area method than the peak height method. The peak height increases with the atomizing temperature, but the peak area is a constant above a certain temperature. The resulting value does not depend on the amounts of sample, and the value from the peak area method has better accuracy than that from the peak height method. In case of copper in tantalum powders, standard relative deviation was 3.5%, and the detection limit was 5×10^{-11} g. The time for a determination was 5 minutes. Cr, Fe, Mn, Ni, and Si were determined similarly. (auth)

28955 DETERMINATION OF BERYLLIUM WITH NITRYLTRIMETHYLPHOSPHONIC ACID IN THE PRESENCE OF ALKALINE EARTH METALS. Morozova, S. S.; Nikitina, L. V.; Dyatlova, N. M.; Serebryakova, G. V. (All-Union Scientific-Research Inst. of Chemical Reagents and Special Purity Chemicals, Moscow). Zh. Anal. Khim.; 29: No. 7, 1323-1326(Jul 1974). (In Russian).

A gravimetric method is suggested of determining beryllium in acid media (pH 1.8–2.5) with nitryltrimethylphosphonic acid using various buffer solutions. Buffer solution components glycine, phthalic, and citric acid do not enter the complexes of beryllium with NTP. 100-Fold amounts of Mg, Ca, Ba, and Sr do not interfere. (auth)

28956 EXTRACTION–SPECTROPHOTOMETRIC METHODS OF DETERMINING 0.0–0.000n% ALUMINUM IN MATERIALS OF METALLURGICAL MANUFACTURE (EXCHANGE OF EXPERIENCE). Gorlova, M. N. (All-Union Inst. of Light Alloys, Moscow). Ind. Lab. (USSR) (Engl. Transl.); 40: No. 1, 36-37 (Jan 1974).

Translated from Zavod. Lab.; 40: No. 1, 27-28(Jan 1974).

Extraction-spectrophotometric methods of determining microgram amounts of aluminum in metallic W, Mo, Nb, Ti, Mg, Zn, Ni, and Fe. The extraction agent was a 1% solution of 8-hydroxyquinoline in chloroform. Unithiol, hydrogen peroxide, and potassium cyanide were the complexing agents. Relative standard deviation of the method is ≤15% for a concentration of $n \cdot 10^{-3}$%. (LK)

28957 SPECTROCHEMICAL ANALYSIS OF URANIUM OXIDE BY GALLIUM OXIDE CARRIER DC ARC TECHNIQUE. Philadelphia; American Society for Testing and Materials (1970). 6p. (ASTM-E-402-70).

This method covers the semi-quantitative spectrochemical analysis of high-purity U_3O_8 for Ag, Al, As, Au, B, Be, Bi, Ba, Cd, Co, Cr, Cs, Cu, Fe, Ge, In, Mg, Mn, Mo, K, Li, Na, Ni, P, Pb, Rb, Sb, Si, Sn, Tl, V, and Zn. The method can be applied to those samples of uranium and uranium compounds, or both, which can be converted to the black oxide from U_3O_8 and which are of approximately 99.5% purity or better. (LK)

28958 COMMENTS ON OXYGEN ANALYSIS OF SODIUM BY EQUILIBRATION WITH VANADIUM: AN ASSESSMENT. Smith, D. L. (Argonne National Lab., Ill. (USA)). J. Nucl. Mater.; 51: No. 2, 280-282(Jun 1974).

Hooper and Trevillion claim to have clearly demonstrated that the oxygen activity in liquid sodium cannot be determined by the vanadium-wire equilibration method. On the basis of their "theoretical" analysis, Hooper and Trevillion conclude that claims made in the literature for the range of application of the method are "unfounded", and that the method is not useful because of its non-equilibrium nature. Although Hooper and Trevillion are quick to reject the experimental data on which the method was based primarily because the results do not agree with their calculated values, they fail to consider the magnitude of the uncertainty in the calculated values that arises from reasonable variations in the fundamental thermodynamic data used in their calculations. The differences between the experimental and theoretical values are not unreasonable when one considers legitimate uncertainties in all the data. Hooper and Trevillion are also apparently unaware of the general acceptance and support that the vanadium equilibration method has received from investigators at other laboratories. (auth)

28959 CONDUCTIMETRIC AND HIGH-FREQUENCY TITRATION CONDITIONS FOR NIOBIUM BY AROMATIC AMINES IN AQUEOUS-ORGANIC MEDIUM. Manakova, L. I.; Bausova, N. V. (Inst. of Chemistry, Sverdlovsk, USSR). Tr. Inst. Khim., Ural. Nauch. Tsentr, Akad. Nauk SSSR; No. 25, 162-164(1973). (In Russian).

The possibility of the conductimetric and high-frequency titration of hydrofluoric acid solutions of Nb in aqueous-organic medium was studied. Solutions of the following aromatic amines were used as the titrating agent: benzidine, tolidine, and α-naphthylamine. The clearest deflection on the conductimetric and high-frequency titration curves was found during the titration of 1% solutions of benzidine in medium containing 80% methanol, ethanol, and acetone. A method for the simultaneous determination of Nb and Si in a medium of 95% acetone by the high-frequency titration method was proposed. (tr-auth)

28960 COLORIMETRIC DETERMINATION OF MOLYBDENUM IN ORGANIC-RICH SOIL. Stanton, R. E.; Mockler, M.; Newton, S. (Hunting Technical Services Ltd., Boreham Wood, Eng.). J. Geochem. Explor.; 2: No. 1, 37-40(1973).

Application of the Zn dithiol method of Stanton and Hardwick (Analyt. Abstr., 1968, 15: 5700), modified by carrying out the fusion with $K_2S_2O_7$ in a multiple-fusion rack (Marranzino and Wood, Analyt. Chem., 1956, 28: 273), to soils rich in organic material yields erroneously low results, especially in the range 0.2 to 10 ppM of Mo. Digestion of samples with HNO_3-HClO_4 overnight at room temperature, followed by evaporation of the mixture to dryness and leaching of the residue with 6M-HCl, gave more accurate results and better reproducibility for up to 110 ppM of Mo. (Anal. Abstr.)

28961 CHEMICAL ANALYSIS OF ZIRCONIUM AND ZIRCONIUM-BASE ALLOYS. Philadelphia; American Society for Testing and Materials (1968). 38p. (ASTM-E-146-68).

Procedures are presented for chemical analysis of Zr and Zr-base alloys having chemical compositions within specified limits. Fifteen analytical procedures are included. (JRD)

28962 PREPARATION, PROPERTIES, AND ANALYTICAL APPLICATION OF THORIUM N-PHENYL-O-NITROBENZOHYDROXAMATE. Agrawal, Y. K.; Rao, V.; Shashimohan, A. L. (Indian Inst. of Tech., Bombay). Talanta; 21: No. 6, 626-629 (Jun 1974).

A new complex of thorium(IV) with N-phenyl-o-nitrobenzohydroxamic acid (PNHA) was prepared by reacting an aqueous solution of thorium with an alcholic solution of PNHA at 60°C and adjusting the pH to 4 to 4.5. The infrared spectra and thermal analysis of the complex are discussed. The use of PNHA for gravimetric determination of thorium is described. (auth)

28963 DIRECT DETERMINATION ON NANOGRAM AMOUNTS OF IODINE BY ATOMIC-ABSORPTION SPECTROSCOPY USING A GRAPHITE-TUBE ATOMIZER. Adams, M. J.; Kirkbright, G. F.; West, T.S. (Imperial Coll. of Science and Tech., London). Talanta; 21: No. 6, 573-579(Jun 1974).

The direct determination of iodine by AAS at its 183.0 and 178.2 nm resonance lines by using a small graphite-tube atomizer, electrodeless discharge-lamp source, and vacuum monochromator is described. Optimum conditions for the determination of iodine have been established; similar sensitivity is obtained when iodide or iodate samples are examined. With 10 μl aqueous samples sensitivities (for 1% absorption) of 4×10^{-10}g and 2×10^{-10}g of I were obtained at 183.0 and 178.2 nm respectively; a detection limit of 2×10^{-9}g was observed at both lines. Non-specific molecular absorption from common inorganic salts causes interference with the determination; the iodine non-resonance line at 184.4 nm may be employed to correct for this interference when moderate amounts of common salts are present. (auth)

28964 EXTRACTIVE SEPARATION OF MOLYBDENUM AS Mo(V) XANTHATE FROM IRON, VANADIUM, TUNGSTEN, COPPER, URANIUM AND OTHER ELEMENTS. Yatirajam, V.; Ram, J. (Univ. of Kurukshetra, India). Talanta; 21: No. 6, 439-443(Jun 1974).

A simple and selective extraction of molybdenum is described. Tungsten is masked with tartaric acid and molybdenum(VI) is reduced in 2M hydrochloric acid by boiling with hydrazine sulphate. Iron, copper, and vanadium are then masked with ascorbic acid, thiourea and potassium hydrogen fluoride respectively. The molybdenum(V) is extracted as its xanthate complex into chloroform, from 1M hydrochloric acid that is 0.4M potassium ethyl xanthate. The complex is decomposed by excess of liquid bromine, and the molybdenum is stripped into alkaline hydrogen peroxide solution. The molybdenum is then determined by standard methods. Large amounts of Cu(II), Mn(II), Fe(III), Ti(IV), Zr, Ce(IV), V(V), Nb, Cr(VI), W(VI), U(VI), Re(VII), and Os(VIII) do not interfere. Several synthetic samples and ferromolybdenum have been rapidly and satisfactorily analysed by the method. (auth)

28965 DETERMINATION OF TRACES OF Mo IN SOILS AND GEOLOGICAL MATERIALS BY SOLVENT EXTRACTION OF THE MOLYBDENUM-THIOCYANATE COMPLEX AND ATOMIC ABSORPTION. Kim, C. H.; Owens, C. M.; Smythe, L.E. (New South Wales Univ., Kensington, Australia). Talanta; 21: No. 6, 445-454(Jun 1974).

Comprehensive studies of the extraction of the molybdenum thiocyanate complex with methyl isobutyl ketone resulted in an improved method for the determination of traces of molybdenum in soils and geological materials by atomic-absorption spectroscopy. The method is applicable in the range 1 to 500 ppM Mo, with 1-g samples, giving relative standard deviations not exceeding about 8% at a level of 1 ppM. The limit of detection is 0.1 ppM. There are few interferences, and large quantities of iron are without effect. (auth)

28966 3-NITROSO-4-HYDROXY-5, 6-BENZOCOUMARIN AS A SELECTIVE REAGENT FOR THE SPECTROPHOTOMETRIC DETERMINATION OF RUTHENIUM(III). Kohli, N.; Singh, R. P. (Univ. of Delhi). Talanta; 21: No. 6, 638-641(Jun 1974).

The pinkish-violet complex developed on interaction of ruthenium(III) with 3-nitroso-4-hydroxy-5, 6-benzocoumarin (NHBC) in the pH range 5.5 to 8.0 can be extracted into n-butanol. The complex has an absorption maximum at 520 nm. Maximum colour development takes place after heating for 20 min on a steam-bath and the extracted complex is stable for at least 92 hr. Beer's law is followed up to 7.4 ppM of ruthenium. The molar absorptivity is 1.04×10^4 1/mole^{-1}/cm^{-1}. The composition of the complex is 1:2 (ruthenium:NHBC). None of the other platinum metals was found to interfere in the determination of ruthenium, even though present in large excess. (auth)

28967 MICRO-SAMPLE ANALYSIS BY SPARK SOURCE MASS SPECTROMETRY. Bingham, R. A.; Vossen, P. G. T. (AEI Scientific Apparatus Ltd., Urmston, Manchester, UK). J. Mass Spectrom. Ion Phys.; 14: No. 3, 259-266(Jul 1974).

The abundances of the neodymium isotopes in a 1 microgram sample of neodymium oxide were determined using the AEI MS702R spark source mass spectrometer in order to evaluate the precision of analysis for small samples. Gold was used as the support material for the sample. Three different modes of analysis were evaluated, namely (1) simultaneous detection of all masses on the photographic plate, (2) magnetic scanning, with electrical detection of the individual and total ion currents and recording of the individual/total ion current ratio, and (3) electrical switching between masses, with electrical detection as in (2). It is shown that satisfactory results are obtained for all three modes of analysis. The time required for acquiring the data and subsequent evaluation is discussed for each mode. The neodymium isotope abundances are calculated and compared with published values for natural neodymium. (auth)

Radiometric and Radiochemical Procedures

Refer also to abstracts 29418, 29439, 29440, 29443, 29444, 29561, 29809, and 29817.

28968 (AED-CONF-74-084-007) EXTENSION OF QUANTITATIVE ELECTRON BEAM MICROANALYSIS TO SOLIDS CONTAINING LIGHT ELEMENTS. Weisweiler, W. (Karlsruhe Univ. (TH)

(F.R. Germany). Inst. fuer Chemische Technik). 1974. 11p. (In German). (CONF-740342-2). INIS.

From meeting of lecturers in chemistry; Stuttgart, F. R. Germany (31 Mar 1974).

17 figs.; 1 tab.; 18 refs.

With regard to the extension of microanalysis by electron beams to solids with elements of the 3rd and 2nd period, using spectra and data the following are dealt with: sample contamination, mass absorption coefficients, x-ray intensities of the standards, position of energy of the x-ray line, differential and integral measurement of intensity, microanalysis of porous as well as of electrical nonconducting samples. (GE)

28969 (DP-MS-73-77) DETERMINATION OF PROMETHIUM-147 IN AQUEOUS ENVIRONMENTAL SAMPLES. Milham, R. C. (Du Pont de Nemours (E. I.) and Co., Aiken, S. C. (USA). Savannah River Lab.). 1974. Contract AT(07-2)-1. 11p. (CONF-740702-8). Dep. NTIS $4.00.

From Health Physics Society annual meeting; Houston, Texas, USA (7 Jul 1974).

An improved method for isolating and beta counting ^{147}Pm in aqueous environmental samples at the Savannah River Laboratory is described. Interference from ^{141,144}Ce is eliminated by cation exchange with Dowex 1-X2. The liquid cation exchanger HDEHP is used to separate Pm from ^{103,106}Ru and ^{95}Zr-^{95}Nb by reversed phase partition chromatography. Decontamination of ^{147}Pm from interferences is greater than 10^3. Analyses of control spikes during the past three years show the method to have a sensitivity of 10 pCi/l, and a recovery of 90 ± 6% when using a 100-ml sample. (auth)

28970 (HASL-300(Suppl. 2)) HASL PROCEDURES MANUAL. Harley, J. H. (ed.). (USAEC Health and Safety Lab., New York). Aug 1974. 173p. Dep. NTIS $7.60.

Annual revision pages to the HASL procedure manual are presented. (LK)

28971 (NVO-AEIC-74-1, pp 107-118) DETERMINATION OF ^{239}Pu AND ^{241}Am IN LARGE NAEG VEGETATION SAMPLES. Major, W. J.; Lee, K. D.; Wessman, R. A.; Melgard, R. (LFE Environmental Analysis Labs. Div., Richmond, CA). Jul 1974.

In dynamics of plutonium in desert environments. Nevada Applied Ecology Group progress report as of January 1974.

Samples of vegetation collected from various locations at the Nevada Test Site were analyzed for ^{239}Pu and ^{241}Am. A method was developed for the radiometric analysis of ^{239}Pu and ^{241}Am in various types of woody vegetation in amounts ranging from 300 to 500 g dry weight. Methods of sample preparation are described. Radiochemical isotope dilution analysis was also performed for ^{239}Pu using ^{236}Pu tracer. Also, if ^{241}Am was too low for instrumental measurement or a confirmation of the instrumental measurement was required, isotope dilution analysis for ^{241}Am was performed using ^{243}Am tracer. Comparisons are made between radiochemical and instrumental analyses of ^{241}Am. (CH)

28972 (TRITA-KKE-7403) RESEARCH REPORT FOR 1972–1973. (Kungliga Tekniska Hoegskolan, Stockholm (Sweden). Institutionen foer Kaernkemi). 13 Mar 1974. 60p. (In Swedish). Dep. NTIS (US Sales Only) $6.00.

Two sections of this report were abstracted and indexed separately. (LK)

For abstracts of individual sections see: 28973 and 29603.

28973 (TRITA-KKE-7403, pp 23-24) X-RAY FLUORESCENCE ANALYSIS OF LEAD. Mar 1973. (In Swedish).

A gamma radiation source containing ^{57}Co has been constructed and tested for analysis of lead. The accuracy is 1,000 μg/g for routine analysis and 100 μg/g in extreme cases. The accuracy is planned to be improved with a new detector. (SW)

28974 RADIOMETRIC METHOD FOR THE ESTIMATION OF IODINE COMPLEXING DEGREE IN IODOPHOR PREPARATIONS. Lucka, B. (Instytut Badan Jadrowych, Swierk, Poland). Nukleonika; 19: No. 6, 505-510(1974). (In Polish).

The radiometric method for estimating the complexing degree of iodine in iodophor preparations was elaborated. The method consists in measurements of iodine-131 (or iodine-125) activities, distributed between the aqueous and organic phases. The elaborated radiometric method seems to be quicker and more universal than the spectrophotometric method. (auth)

28975 RADIOMETRIC ANALYSIS OF THORIUM AND URANIUM. Abraham, M.; Rai, M. S. (Birla Inst. of Tech. and Science, Pilani, India). Metals Miner. Rev.; 11: No. 11, 16-17 (1972).

Radiometric analysis is used to test the efficiency of some of the precipitation methods for thorium and uranium analysis, so that a comparative account of the efficiency of various precipitation processes for the estimation of thorium and uranium can be judged. (Indian Sci. Abstr.)

28976 NOVEL METHODS IN THE ANALYSIS OF CESIUM. Bende, E.; Szabo, A. (Megyei Elelmiszerellenorzo es Vegyvizsgalo Intezet, Gyor, Hungary). Izotoptechnika; 17: No. 8, 413-419(Aug 1974). (In Hungarian).

A literature survey was made on the methods for the analysis of radioactive cesium contamination of foodstuffs. (42 references) (auth)

28977 SIMULTANEOUS DETERMINATION OF ALPHA-EMITTING NUCLIDES OF RADIUM THROUGH CALIFORNIUM IN SOIL. Sill, C. W.; Puphal, K. W.; Hindman, F. D. (Atomic Energy Commission, Idaho Falls, ID). Anal. Chem.; 46: No. 12, 1725-1737(Oct 1974).

A procedure is described by which virtually all alpha-emitting nuclides can be determined in soil, either singly or in any combination on a single sample. The sample is decomposed completely by a combination of potassium fluoride and pyrosulfate fusions with simultaneous volatilization of hydrogen fluoride and silicon tetrafluoride. The cake is dissolved in dilute hydrochloric acid and all alpha emitters are precipitated with barium sulfate. An option is provided by which uranium can be obtained in a separate fraction to eliminate mutual interference with ^{237}Np. The barium sulfate is dissolved in acidic aluminum nitrate and the elements from thorium through plutonium are extracted into Aliquat-336. Acid-deficient aluminum nitrate is then added to the aqueous phase to reduce the acidity, and americium, curium, and californium are extracted into fresh Aliquat-336. Thorium is removed by scrubbing the first organic extract with 10M hydrochloric acid, and protactinium, uranium, neptunium, and plutonium are stripped with a mixture of perchloric and oxalic acids. Americium, curium, and californium are stripped from the second organic extract with 8M nitric acid. Each fraction is electrodeposited and analyzed by alpha spectrometry with few interferences. Overall recovery excluding electrodeposition ranges from 88% for protactinium to 99% for plutonium. (auth)

28978 SEQUENTIAL DETERMINATION OF RADIUM-226, RADIUM-228, ACTINIUM-227, AND THORIUM ISOTOPES IN ENVIRONMENTAL AND PROCESS WASTE SAMPLES. Percival, D. R.; Martin, D. B. (Atomic Energy Commission, Idaho Falls, ID). Anal. Chem.; 46: No. 12, 1742-1749(Oct 1974).

A procedure is described for the sequential determination of ^{226}Ra, ^{228}Ra, ^{227}Ac, thorium isotopes, and, in some cases, ^{231}Pa in environmental and process waste samples at 0.1 to 0.001 of the concentration guides specified by Federal regulations. The radionuclides are separated from gross sample constituents by coprecipitation with lead sulfate. Radium is separated on a small quantity of barium sulfate precipitated from a diethylenetriaminepentaacetate solution of the lead sulfate. Actinium-227 and thorium are then separated sequentially from the barium sulfate supernate by extraction into bis(2-ethylhexyl)phosphoric acid. Any one or more of the radionuclides may be excluded from the analysis by omitting certain independent steps. Over-all recoveries are 99% for radium and 95% for actinium and thorium. Accuracy, precision, and the effects of chemical and radiochemical interferences are discussed. (auth)

28979 DETERMINATION OF MOLYBDENUM IN PLUTONIA CERMETS BY X-RAY FLUORESCENCE SPECTROMETRY. Woltermann, H. A.; Strohm, W. W. (Mound Lab., Miamisburg, OH). Contract AT(33-1)-Gen-53. Anal. Chem.; 46: No. 12, 1822-1823(Oct 1974).

An x-ray fluorescence procedure is developed to determine the weight fraction of molybdenum in ^{238}PuO$_2$/molybdenum cermet fuel. This method has a relative standard deviation of approximately 1%. (auth)

28980 APPLICATION OF NUCLEAR PHYSICS METHODS FOR THE DETERMINATION OF THE DEPTH OF LITIUM IONS PENETRATION IN THE GLASSES WITH CRYSTALLIZED SURFACE. Pomorski, L. (Inst. of Nuclear Physics, Krakow); Madeja, M.; Jarzmik, B.; Bugajski, W. Szklo Ceram.; 24: 225-229(1974). (In Polish).

The thickness of a modified layer in glasses with crystallized surface determines the mechanical strength of the material. The surface concentration of litium ions was determined by the means of accelerated alpha particles and protons. (auth)

28981 UNKNOWN ALPHA-EMITTERS IN NATURE. Bogdanov, R. V.; Kuznetsov, R. A. Sov. Radiochem. (Engl. Transl.); 15: No. 6, 865-868(1973).

Translated from Radiokhimiya; 15: No. 6, 858-861(1973).

A study was made of a series of samples of igneous and sedimentary rocks to check on the hypothesis of the existence in nature of an unknown transuranium element, which volatilizes from aqueous solutions and is an alpha-emitter with an energy of 4.4 to 4.7 MeV. Chemical and alpha-spectrometric investigations showed that the samples studied contained no unknown alpha-emitters with the chemical properties of eka-osmium, eka-mercury, or eka-astatine down to a concentration limit of 10^{-10}–10^{-11} g/g (assuming a half-life of 10^9 yr). (auth)

28982 FRACTIONAL DETERMINATION OF ^{95}Zr AND ^{95}Nb IN A MIXTURE BY REVERSE PHASE CHROMATOGRAPHY. Chekmarev, A. M.; Chibrikin, V. V.; Yagodin, V. G.; Yagodin, G. A. Sov. Radiochem. (Engl. Transl.); 15: No. 6, 894-895 (1973).

Translated from Radiokhimiya; 15: No. 6, 881-882(1973).

^{95}Zr and ^{95}Nb were determined by reverse phase chromatography on paper and gamma counting. The method proposed makes it possible to use a mixture of isotopes without their preliminary separation and also makes it possible to study the intereffect of the elements. (LK)

28983 USE OF ETHYL ALCOHOL AND ACETIC ACID TO PREPARE SAMPLES OF SODIUM COOLANT FOR RADIOCHEMICAL ANALYSIS. Poznyak, G. I.; Rozhdestvenskaya, L. N. Sov. Radiochem. (Engl. Transl.); 15: No. 6, 915-916(1973).

Translated from Radiokhimiya; 15: No. 6, 897-898(1973).

Acetic acid and ethanol were used in the development of a method for radiochemical analysis of the sodium coolant of the BOR-60 reactor. Data from the study indicate that it is advantageous to use acetic acid as the solvent for sodium coolant and acetate solutions of sodium for radiochemical analysis. (LK)

28984 DETERMINATION OF RUTHENIUM-106 IN SEA WATER. Terada, K.; Nishimura, K.; Kiba, T. (Kanazawa Univ., Japan). J. Radiat. Res.; 15: No. 1, 7-13(Mar 1974).

A simple and effective method for determining ^{106}Ru in seawater is presented. After the seawater is heated with oxidants (potassium peroxodisulfate and potassium periodate) in potassium hydroxide solution, ruthenium tetraoxide is extracted into carbon tetrachloride from the aqueous solution adjusted to pH 4-6, and then back-extracted with a hydrochloric acid solution containing sodium hydrogen sulfite. Ruthenium metal is precipitated from the solution by adding magnesium powder, filtered, washed and dried under reduced pressure at room temperature. Chemical yield of ruthenium is measured by gravimetry, and the β-activity is measured by a low-background β-ray spectrometer, "Picobeta". The overall yield of ruthenium was 88-92% and the whole chemical procedure takes about 6 hours. The analytical results for ^{106}Ru in seawater samples collected from several locations and depths of the Japan Sea are presented. (auth)

28985 METHOD OF ^{3}H-DETERMINATION IN HAIR. Bilkiewicz, J. (Central Lab. for Radiological Protection, Warsaw). Postepy Fiz. Med.; 8: No. 1-2, 1-6(1973). (In Polish).

A method is described of determining the content of tritium in hair by performing combustion in a glass flask filled with oxygen and distilling of the water directly to a liquid scintillator. The activities of the samples were determined in the liquid scintillation, Packard Tri-Carb type, Model 3315 spectrometer. The mean recovery of tritium was 94.5 ± 5.4%, and the relative standard deviation for parallel determinations was 20.8%. The method was improved and simplified by modifying the combustion flask and by dissolving water in dioxane which was partly added to the liquid scintillator for activity measurements. The mean recovery of tritium was similar to that in the distillation method and it was equal to 93.0 ± 4.7%; the accuracy, however, was higher. The minimum detectable radioactivity in both methods was 86 pCi per sample. The method can also be used for tritium determinations in tissue samples. (auth)

28986 GAMMA-RAY ASSAY OF LOW-ENRICHED URANIUM WASTE. Walton, R. B.; Whitted, E. I.; Forster, R. A. (Univ. of California, Los Angeles). Nucl. Technol.; 24: No. 1, 81-92(Oct 1974).

A method based on the detection of 0.767- and 1.001-MeV gamma rays from ^{234m}Pa was developed for the assay of ^{238}U in large containers of uranium waste. Detailed calibration and assay procedures were obtained for 3½- × 4- × 4-ft plywood boxes of combustible waste. The gamma rays were detected with a large NaI crystal and a line-source "standard" box was used for calibration. The calibration was extended over a wide range of box weights using Monte Carlo calculations of gamma-ray attenuation. The error in the calibration is <6% (2σ); much larger assay errors can result from the heterogeneities in the waste and from the age dependence of the ^{238}U daughters. The detection limit for a 5-min count is about 30 g ^{238}U in a typical box of combustibles. Data generated for the box problem, together with additional Monte Carlo calculations, were used to devise a simple analytical model applicable for the assay of boxes and cylinders in a range of practical geometries. The essential feature of this model is a flux buildup factor which accounts for Compton-scattered photons. (15 fig) (auth)

28987 NO RADIOACTIVE SILVER DETECTABLE IN SILVER–URANIUM ORE. Merritt, W. F. (Atomic Energy of Canada Ltd., Chalk River, Ont.). Nature (London); 250: No. 5464, 351(26 Jul 1974).

Further observations are reported concerning the alleged finding of ^{108m}Ag and ^{110m}Ag in some Ag bars processed from uraniferous Ag ores of Eastern European origin (see Nature 240: 463(1972) and 243: 461(1973)). It had been suggested by some authors that the presence of these isotopes was due to mining with nuclear explosives, and by other authors that their presence was due to (α,n) reactions and spontaneous fission reactions of U in the Ag ores. A sample uraniferous Ag ore was assayed by the present author, using x-ray fluorescence spectroscopy, and found to contain 6.8% Ag and 0.97% U. No radioactive Ag γ peaks were detected, leading to the conclusion that the radioactive Ag found in the bullion was not of natural origin. (UK)

28988 SENSITIVITY IN TRACE-ELEMENT ANALYSIS BY p,α AND ^{16}O INDUCED X-RAYS. Folkmann, F.; Borggreen, J.; Kjeldgaard, A. (Niels Bohr Institutet, Copenhagen (Denmark)). Nucl. Instrum. Methods; 119: No. 1, 117-123(1 Jul 1974).

With direct application in mind the sensitivity of ion-induced x-ray trace-element analysis was investigated as a function of projectile atomic number. For 3 and 5 MeV/amu p, α and ^{16}O ions K and L x-ray yields were measured for six elements between Cu and Pb and background radiation from matrices consisting of C, Al, and V. The importance of nuclear processes and the Compton scattering of the associated γ rays is emphasized as a limiting factor for the sensitivity when the radiation is recorded in a solid-state detector. (auth)

Separation Procedures

Refer also to abstracts 29138 and 29149.

28989 (ANL-Trans-960) RECENT RESULTS IN THE APPLICATION OF COLUMN EXTRACTION CHROMATOGRAPHY IN INORGANIC ANALYSIS. Stronski, I. Translated from Isotopenpraxis; 9: 273-279(1973). 18p. Dep. NTIS $4.00.

The application of extraction chromatography in the separation of lanthanides, transplutonium elements, lanthanides from transplutonium elements, actinides, and uranium from its fission products is discussed. (LK)

28990 (ANL-Trans-961) CONTRIBUTION TO THE SEPARATION OF RARE EARTHS BY EXTRACTION CHROMATOGRAPHY WITH DI(2-ETHYLHEXYL) PHOSPHORIC ACID. II. Behavior of the Matrix and Its Influence on the Microcomponents. Herrmann, E.; Grosse-Ruyken, H.; Chalkin, W. Translated from J. Chromatogr.; 87: 351-363(1973). 16p. Dep. NTIS $4.00.

The use of extraction chromatography with undiluted di(2-ethylhexyl)phosphoric acid as the stationary phase for macro/micro separations of lanthanides has been studied. Macro amounts of a rare earth element are retained on the column bed from weakly acidic solutions in the form of tris(dialkyl phosphates). By elution with diluted mineral acids an asymmetrical peak with a sharp front and a long tail is observed. The position A of the front, normalized to the unity di(2-ethylhexyl)phosphoric acid volume on the column, depends on the loading B (expressed in %) of the column with rare earth ions and on the partition coefficient D for this element in tracer concentration. This dependence can be expressed by the following equation: $\log A = \log D - 0.036\ B - 0.15$. The influence of the macro amount of the given rare earth element on the behavior of the other lanthanides present in tracer concentration has also been investigated. When the micro element has a lower atomic number than the macro element and $A_{macro}/D_{micro} \geq 1.5$, it is possible to isolate the tracer with a yield of more than 80% and with an enrichment factor of about 10^6. But in this case the loading of the column should be no more than about 50% of the maximum column capacity. In the opposite case, when the tracer has the higher atomic number, the isolation process of micro elements is less sensitive to the macro amount. In some cases even the total column capacity could be used. But as a result of the tailing effects the enrichment factors are usually reduced to values of about 10^3 – 10^4. (auth)

28991 (BLG-487) SEPARATION OF ^{137}Cs AND ^{90}Sr FROM HIGHLY RADIOACTIVE FISSION PRODUCT SOLUTIONS. Baetslé, L.; Huys, D.; Speeckaert, Ph. (Centre d'Etude de l'Energie Nucleaire, Mol (Belgium)). Dec 1973. 36p. Dep. NTIS (US Sales Only) $5.00.

Separation of ^{137}Cs and ^{90}Sr from fission products in nitric acid solutions with inorganic ion exchangers has been studied at three different activity levels. At trace level a comparison was made between the uptake capacity of titanium phosphate (TiP) and hexacyanoferrate (FeMo) for Cs and the ability to reuse the ion exchange columns during several loading and regeneration cycles. Titanium phosphate is advantageous when Cs has to be separated and purified, but hexacyanoferrate (FeMo) is useful as storage material. The separation of ^{90}Sr from waste solutions in HNO_3 solution can be achieved with polyantimonic acid but the exchange kinetics are not very favorable. Confirmation tests with ^{137}Cs and ^{90}Sr at 5 Ci/l mixed fission products have shown that decontamination factors of 10^3 may easily be obtained. Hot cell tests with mixed fission product solutions at 100 Ci/l level in 2 to 7 M HNO_3 have indicated that titanium phosphate has to be preferred to hexacyanoferrate (FeMo) when ^{137}Cs is to be separated during tests with repeated loading and regeneration cycles. Strontium-90 adsorbed on polyantimonic acid is difficult to remove by elution with HNO_3 or $Pb(NO_3)_2$, therefore volatilization with hydrochloric acid gas at 250 to 300°C was investigated as a possible alternative. (auth)

28992 CRYOTECH '73: THE PRODUCTION AND USE OF INDUSTRIAL GASES. Proceedings of the British Cryogenics Council Conference, Brighton, England, November 13–15, 1973. Guildford, Eng.; IPC Business Press Ltd. (1974). 128p. (CONF-731145-). £7.00.

Nineteen papers were presented at the conference. Two papers were abstracted separately. (LK)

For abstracts of individual papers see: 28993 and 31206.

28993 RECOVERY OF RARE GASES IN AIR SEPARATION AND AMMONIA PLANTS. Streich, M.; Daimer, P. (Linde AG, Munich). pp 31-35 of Cryotech '73: the Production and Use of Industrial Gases. Guildford, Eng.; IPC Business Press Ltd. (1974).

From the production and use of industrial gases symposium; Brighton, UK (13 Nov 1973). See CONF-731145-.

This paper concentrates on two processes: first, the production of krypton and xenon from air; and, second, the recovery of helium from a helium-hydrogen-nitrogen mixture. (auth)

28994 SYNTHESIS OF REPRODUCIBLE TIN(IV) BASED ION EXCHANGERS: SEPARATION OF LANTHANUM(III) FROM YTTRIUM(III), EUROPIUM(III), AND LUTETIUM(III). Qureshi, M.; Kumar, R.; Sharma, V. (Aligarh Muslim Univ., India). Anal. Chem.; 46: No. 12, 1855-1858(Oct 1974).

Five reproducible, water-insoluble compounds of Sn(IV) are synthesized. The antimonate has highest chemical and thermal stability and the arsenate shows greatest ion-exchange capacity. Stannic selenite columns are used for separation studies. (auth)

28995 ATMOSPHERE PURIFICATION OF XENON, RADON, AND RADON DAUGHTER ELEMENTS. Stein, L. (to United States Atomic Energy Commission). US Patent 3,829,551. 13 Aug 1974. Filed date 27 Mar 1973. 6p.

A method is described for purifying an atmosphere of xenon, radon, and radon daughter elements by passing the atmosphere containing these elements through a reaction bed of dioxygenyl hexafluoroantimonate, which oxidizes the xenon, radon, and radon daughter elements to their respective fluorides which remain in the reaction bed and are thus removed from the atmosphere, and recirculating the purified atmosphere. The method is also useful for separating the before-named elements from krypton. (Official Gazette)

28996 ION EXCHANGE ADSORPTION OF Pu(IV) AT EXTREMELY LOW CONCENTRATIONS IN A CHELATING RESIN. Matsuzuru, H.; Wadachi, Y. (Japan Atomic Energy Research Inst., Tokai). Nippon Kagaku Kaishi; 1974: No. 4, 617-621(Apr 1974). (In Japanese).

The equilibrium and kinetics of ion exchange of adsorption of Pu(IV) (1.5×10^{-7} mol/l) have been studied with a chelating resin, Dowex A-1 (polystyrene-divinylbenzene copolymer containing iminodiacetic acid as a functional group). The distribution coefficient K_d of Pu(IV) increased with increasing pH of the solution until pH 3.5, beyond which the K_d increased. The ionic strength which was varied from 0.01 to 0.5 did not affect the K_d value in the pH range of 2 ~ 3.5, whereas above pH 4 the K_d value varied with ionic strength. The mass-action low holds for the adsorption of Pu(IV) at pH 3, but not for the adsorption at pH 5. These results may probably be due to the fact that Pu(IV) is adsorbed on this resin throughout the pH range of 2 ~ 3.5 by chelate formation mechanism between monomeric Pu(IV) ion and the iminodiacetic group of the resin, but Pu(IV) at above pH 4 exists predominantly as polymeric species which is adsorbed on the resin surface by the colloidal adsorption mechanism. The rate of the ion exchange adsorption of Pu(IV) was independent of the ionic strength and of the particle size of the resin, and was not explained by a kinetic equation with film or particle diffusion. These results support the view that rate determining step of the reaction is the chelate formation reaction between Pu(IV) and iminodiacetic group of the resin. The apparent activation energy obtained from the first-order rate constant was 18.4 kcal/mol at ionic strength of 0.1 and pH 3. (auth)

28997 CHROMATOGRAPHY ON FINELY DISPERSED IONITES ON INERT SUPPORTS. Moskvin, L. N.; Miroshnikov, V. S. Sov. Radiochem. (Engl. Transl.); 15: No. 6, 896-897(1973).

Translated from Radiokhimiya; 15: No. 6, 882-883(1973).

It was shown that a finely dispersed sorbent on an inert support (polytetrafluoroethylene) can be used for chromatographic concentration and separation of substances. Chromatography of carrier-free ^{89}Sr is reported. (LK)

28998 SORPTION METHOD OF ISOLATING URANIUM AND OTHER VALUABLE METALS FROM SEA WATER. Ryabinin, A. I.; Romanov, A. S.; Doroshenko, G. A.; Lazareva, E. A. Sov. Radiochem. (Engl. Transl.); 15: No. 6, 898-899(1973).

Translated from Radiokhimiya; 15: No. 6, 884-885(1973).

Results of testing a sorbent prepared from titanium hydroxide and anionite AN-2F are reported. The sorbent is designed for isolating uranium and accompanying microelements from ocean water. (LK)

28999 SORPTION OF TETRAVALENT ELEMENTS BY MORDENITE. II. Sorption of Pu(IV). Grebenshchikova, V. I.; Chernyavskaya, N. B.; Andreeva, N. R. Sov. Radiochem. (Engl. Transl.); 15: No. 6, 771-775(1973).

Translated from Radiokhimiya; Vol. 15, No. 6, 761-766(1973).

It was established that the absorption of $Pu^{(IV)}$ by H-mordenite in 0.5-0.1 N HNO_3 has an ion exchange mechanism. The capacity of H-mordenite for $Pu^{(IV)}$ was determined. It was shown that mordenite may be used as a sorbent for the separation of surge amounts of plutonium from Na, Ca, Ba, Eu, and Th in 0.1 N HNO_3. It was established that polymeric forms of $Pu^{(IV)}$ are hardly absorbed by mordenite and this may be used in the study of the state of $Pu^{(IV)}$ in solutions. (auth)

29000 EXTRACTION OF NIOBIUM IN PHOSPHORIC ACID SOLUTIONS BY ALKALI METALS AND AMMONIUM SALTS. Shtin, A. P. (Inst. of Chemistry, Sverdlovsk, USSR). Tr. Inst. Khim., Ural. Nauch. Tsentr, Akad. Nauk SSSR; No. 25, 149-151 (1973). (In Russian).

Niobium phosphates containing a monovalent cation were extracted by the effects of alkali metal phosphates and ammonia on phosphoric acid solutions of Nb. The conditions for the formation of this compound were established. (tr-auth)

29001 SELECTIVE ION-EXCHANGERS CONTAINING PHOSPHORUS IN THEIR FUNCTIONAL GROUPS. I. Sorption and Separation of Some Bivalent and Trivalent Ions. Marhol, M.; Beranova, H.; Cheng, K. L. (Nuclear Research Inst., Rez, Czech.). J. Radioanal. Chem.; 21: No. 1, 177-186(1974).

From 7th radiochemical conference; Marianske Lazne, Czechoslovakia (Apr 1973).

A series of selective ion-exchangers was synthetized, containing phosphinic or phosphonic acid functional groups. The selective sorption of Sc^{3+}, Fe^{3+}, Ga^{3+}, In^{3+}, Al^{3+}, Pb^{2+}, Co^{2+}, and Ca^{2+} ions in 0.1–4.0M HNO_3 medium was investigated using a batch experiment technique. The selectivity of these exchangers generally decreased in the order: Sc > Fe > In > Ga > Al > La > Pb > Cu > Co > Ca. The observed large differences in selectivity resulted in effective separation procedures of scandium from lanthanides, and gallium (or indium) from bivalent elements. The selective separation of these ions from their different mixtures is also possible. (auth)

Inorganic, Organic, and Physical Chemistry

Chemical and Physicochemical Properties

Refer also to abstracts 29122, 29658, 29970, 30022, and 30049.

29002 (ORNL-TM-760) SOLUBILITY AND STABILITY OF STRUCTURAL METAL DIFLUORIDES IN MOLTEN FLUORIDE MIXTURES. Blood, C. M. (Oak Ridge National Lab., Tenn. (USA)). 9 Jan 1964. Contract W-7405-eng-26. 54p. Dep. NTIS $5.75.

Studies of the corrosion of nickel alloys by molten fluorides of interest as nuclear reactor fuel-solvents led to the determination of equilibrium quotients for the reduction by hydrogen of dissolved impurities, NiF_2, FeF_2, and CrF_2, and also to the determination of the solubilities of NiF_2 and FeF_2 in the molten fluorides. This information is useful for practical purposes (the removal of Ni and

Fe impurities from molten fluorides) and also is a source of fundamental information regarding the solution behavior of the molten fluorides and the chemical properties of the impurities. Equilibrium quotients are reported for NiF_2 at 550 to 625°C in NaF–ZrF_4 melts having an NaF concentration of 53 and 60 mole %; for NiF_2 at 600°C in NaF–ZrF_4 having an NaF concentration of 43, 48, and 56 mole %; for NiF_2 at 500 to 600°C in LiF–BeF_2 (62 mole % LiF); for FeF_2 at 600 to 800°C in NaF–ZrF_4 (53 mole % NaF) and in LiF–BeF_2 (62 mole % LiF); and for CrF_2 at 750 to 850°C in NaF–ZrF_4 (53 mole % NaF) and in LiF–BeF_2 (62 mole % LiF). Solubilities are reported for NiF_2 at 550 to 625°C in NaF–ZrF_4 (53 mole % NaF); for NiF_2 at 600°C in NaF–ZrF_4 having an NaF concentration of 43, 48, 56, and 60 mole %; for NiF_2 at 475 to 600°C in LiF–BeF_2 (62 mole % LiF); and for FeF_2 at 500 and 550°C in LiF–BeF_2 (62 mole % LiF). In LiF–BeF_2 (62 mole % LiF) the saturating phases were crystalline NiF_2, FeF_2, and CrF_2. In the NaF–ZrF_4 solvents, the saturating phases were NaF · NiF_2 · $2ZrF_4$, NaF · FeF_2 · $2ZrF_4$ and NaF · CrF_2 · $2ZrF_4$, and the apparent solubility depended on the amount of solute added to the molten mixtures. For NiF_2 and FeF_2 in the LiF–BeF_2 solvent, a combination of the equilibrium quotients and solubilities will yield experimental equilibrium constants which suggest revisions of some thermochemical quantities and estimates. Better activity coefficients for NiF_2, FeF_2, and CrF_2 can be expected when the calculations have been completed. (auth)

29003 COMPETITIVE RADIOPROTECTION AND RADIOSENSITIZATION IN CHEMICAL SYSTEMS. Greenstock, C. L.; Chapman, J. D.; Raleigh, J. A.; Shierman, E.; Reuvers, A. P. (Atomic Energy of Canada Ltd., Pinawa, Manitoba). Radiat. Res.; 59: No. 3, 556-571(Sep 1974).

The kinetics of the action of radioprotective and radiosensitizing agents were studied in model chemical systems. Electron affinic sensitizers react with "target" free radicals either of DNA or of its mononucleotide components by redox processes involving radical oxidation or radical-sensitizer adduct formation. The effectiveness of both processes for a given class of radiosensitizers increases with the electron affinity of the radiosensitizers, with nitrofurans, benzoquinone, and oxygen being the most effective. A threshold for sensitization occurs at a sensitizer redox potential of approximately −0.3 V vs SCE required to oxidize the DNA radicals. The nitrofurans add to and oxidize DNA target radicals, whereas, for benzoquinone, radioinduced binding to target radicals predominates. Radioprotection may involve either OH-scavenging or H-donation. The action of H-donating species such as cysteamine was found to involve competition with sensitizers for the same target free radicals, presumably sugar radicals formed by OH attack. Steady-state radiolysis allows measurement of the ratios of rate constants for the competing reactions between target radicals and either protectors and sensitizers, or different sensitizers including oxygen. These rate constants have, where possible, been verified by direct experimental measurement using pulse radiolysis. The radiosensitizing effect of the cellular radiosensitizer Diamide is affected in chemical systems by added H-donating species. It appears to act by both an "electron affinic" mechanism and also by chemically inactivating the H-donating species which would otherwise repair potential target free radical damage. (auth)

29004 THERMAL ENHANCEMENT OF THE RADIOSENSITIVITY USING CULTURED NORMAL AND NEOPLASTIC CELLS. Kim, J. H.; Kim, S. H.; Hahn, E. (Memorial Sloan–Kettering Cancer Center, New York). Amer. J. Roentgenol., Radium Ther. Nucl. Med.; 121: No. 4, 860-864(Aug 1974).

From 74th annual meeting of the American Roentgen Ray Society, Montreal, Quebec (25 Sep 1973).

Cultures of normal tissue are relatively insensitive to heat, while malignant cells in culture are highly sensitive to thermal treatment. This differential thermal sensitivity is most pronounced when the cells of normal and neoplastic tissues are exposed to heat in their exponential growth phase. Dose survival curves of x irradiated HeLa and $_3T_3$ cells with and without postirradiation thermal treatment showed that the neoplastic HeLa line exhibited significant enhancement of radiosensitivity when the irradiated cells were exposed to elevated temperatures (42°C for 3 hours). Similar heat treatment of irradiated $_3T_3$ fibroblasts did not appreciably enhance the radiation response. The potential significance of these findings for clinical radiotherapy is discussed. (auth)

29005 *INTERRELATIONSHIP OF THERMODYNAMIC AND KINETIC PARAMETERS OF REDOX REACTIONS.* Kuznetsov, K. E.; Letnikov, F. A. (Inst. of the Earth's Crust, Irkutsk, USSR). *Russ. J. Phys. Chem. (Engl. Transl.)*; 47: No. 12, 1707-1709 (Dec 1973).

Translated from Zh. Fiz. Khim.; 47: No. 12, 3039-3042(Dec 1973).

Analysis of published data on uranium and neptunium reactions reveals a linear relation between the Gibbs functions of reaction and of activation for oxidation-reduction reactions occurring in perchloric acid solutions. The variation of the free energy of activation with the free energy of reaction is much greater with endothermic than with exothermic reactions. (auth)

29006 ON OXIDE FLUORIDES $A_{12}M(IV)M_3(VI)O_8F_{18}$ WITH URANIUM, MOLYBDENUM, AND TUNGSTEN. Fleckenstein, J.; Kemmler-Sack, S.; Ruedorff, W. (Tuebingen Univ. (F. R. Germany). Lab. fuer Anorganische und Analytische Chemie). Z. Naturforsch., b; 29: No. 1/2, 124-126(Jan 1974). (In German).

1 fig.; 4 tabs.; 3 refs.

Lattice constants and analysis data of compounds $A_{12}M(IV)(Mo,W)_3O_8F_{18}$ with A = Cs, Rb, K and M(IV) = U, Ce as well as of $A_{12}M(IV)U(VI)M(VI)O_8F_{18}$ with A = Cs, Rb, M = Ce, U, Mo, W, $1/\chi$-T diagrams of $Rb_{12}UW_3O_8F_{18}$ and $Rb_{12}Mo(IV)Mo_3(IV)O_8F_{18}$ as well as molecular susceptibilities of U(IV) with dependence on temperature are given. (GE)

Isotope Effects

Refer also to abstract 29068.

29007 (AED-CONF-74-084-004) ISOTOPE EFFECTS IN THE BOUNDARY LAYER OF INORGANIC SOLUTIONS. Heumann, K. G.; Hoffmann, R. (Technische Univ. Darmstadt (F.R. Germany). Fachbereich Anorganische Chemie und Kernchemie). 1974. 12p. (In German). (CONF-740342-3). INIS.

From meeting of lecturers in chemistry; Stuttgart, F.R. Germany (31 Mar 1974).

7 dias.

Calculated differences of the ion radii of some alkali and alkaline earth isotopes, dependence of the hydration number of some cations on the ion radius, the bubble spray formation procedure, a test equipment for the spray tests with Li and Ca salt solutions, the dependence of the calcium isotope effect with spray tests (0.375 m and 4.75 m $CaCl_2$ solution) on the temperature in the gas phase, as well as the lithium isotope effect (LiF and LiI solution) are described. (GE)

29008 (IAE-2309) ISOTOPIC ORDERING IN CeD_2H. Somenkov, V. A.; Ehntin, I. R.; Kost, M. E.; Shil'stein, S. Sh. (Gosudarstvennyj Komitet po Ispol'zovaniyu Atomnoj Ehnergii SSSR, Moscow. Inst. Atomnoj Ehnergii). 1973. 20p. (In Russian). INIS.

By a neutronographic method in temperature interval from 4.2 to 300°K a study was made on the distribution of hydrogen isotopes along the octa- and tetrahedral internodes in cerium trihydride having a mixed isotopic composition CeD_2H. It is shown that the H atoms fall into the octapores of the fcc-metal lattice with a greater probability (C_n^0 = 4.3 at T = 300°K) than with a chaotic distribution (C_n^0 = 0.33). With a decrease in temperature the value of C_n^0 increases (C_n^0 = 0.53 at T = 4.2 to 78°K). The physical reason for the redistribution of hydrogen isotopes along the matrix internodes is a decrease in the energy of the local oscillations of hydrogen on transfer of H into the octapores. On the basis of local, hydrogen oscillation frequencies in the trihydride CeH_3 as determined from inelastic neutron scattering experiments it was possible to calculate the temperature dependence for the probability that hydrogen will fall into the octapores. At room temperature the experimental and calculated probability values agree satisfactorily, while at low temperatures the experimentally measured probability C_n^0 is less than the calculated value. This behavior is most likely connected with a decrease in hydrogen mobility. (JSR)

29009 MÖSSBAUER EFFECT STUDY OF THE DEUTERATED AND HYDROGENATED HYDRATES OF FERROUS CHLORIDE. Brunot, B. (I. Physikalisches Institut der Universität zu Köln, Universitätsstrasse 14, 5 Köln 41, West Germany). J. Chem. Phys. 61: No. 6, 2360-2366 (15 Sept 1974).

A detailed study of isotope effects on Mössbauer hyperfine parameters is presented. Isomer shifts and quadrupole splittings for $FeCl_2 \cdot nH_2O$ and $FeCl_2 \cdot nD_2O$, where n = 1, 2, 4, and 6, were measured between 90 and 273°K. Identical isomer shifts δ were observed for the mono–, tetra–, and hexahydrates. Concerning the dihydrates, different δ were found with parallel temperature dependence. For the four studied hydrates, different quadrupole splittings ϵ were measured for the deuterated and the hydrogenated compounds. The temperature dependence of δ and ϵ were briefly analyzed with reference to structure and chemical bond considerations. A summary study of Debye–Waller factors suggested that a comparative investigation of lattice dynamics for the deuterated and hydrogenated hydrates is possible. (auth)

29010 *DO SN2 REACTIONS GO THROUGH ION PAIRS?* The Isotope Effect Criterion. Raaen, V. F.; Juhlke, T.; Brown, F. J.; Collins, C. J. (Oak Ridge National Lab., TN). J. Amer. Chem. Soc.; 96: No. 18, 5928-5930(4 Sep 1974).

Carbon-14 and α-deuterium isotope effects were determined during hydrolyses of benzyl chloride, p-methylbenzyl chloride, and 2-octyl brosylate in bicarbonate-buffered aqueous acetone. From the results it was concluded that the high k^{12}/k^{14} and low k_H/k_D values for benzyl and p-methylbenzyl chlorides signify classic SN2 transition states. *(LK)*

29011 KINETICS OF THE SELECTIVE HYDROGENATION OF DIMETHYLETHYNYLCARBINOL OVER PALLADIUM IN THE *VAPOR PHASE. II. Reaction Between Dimethylethynylcarbinol* and Deuterium and the Kinetic Isotopic Effect. Levin, D. Z.; Prokof'ev, E. P.; Gudkov, B. S.; Kiperman, S. L.; Besprozvannyi, M. A. *(Inst. of Organic Chemistry, Moscow).* Kinet. Catal. (USSR) (Engl. Transl.); 15: No. 1, 80-85(1974).

Translated from Kinet. Katal.; 15: No. 1, 98-103(1974).

A study was made of the reaction between dimethylethynylcarbinol and deuterium in the vapor phase over a palladium catalyst in a gradientless system at temperatures of 153 and 203°C. With the replacement of hydrogen by deuterium, the kinetic isotopic effects in the hydrogenation reaction of dimethylethynylcarbinol are equal to 1.8–1.9. A theoretical calculation of the kinetic isotopic effect on the basis of a reaction mechanism proposed in a previous communication leads to values close to the experimental. The methods of IR-(infrared) spectroscopy, PMR (paramagnetic resonance), and mass spectrometry were used to obtain data on the distribution of deuterium in the reaction products. (auth)

29012 HYDROGENATION AND DEUTERATION OF OLEFINS IN THE PRESENCE OF COBALT TRIETHYLALUMINUM-BIS (ACETYLACETONATE). Shmidt, F. K.; Krasnopol'skaya, S. M.; Lipovich, V. G.; Bazhenov, B. A. (Irkutsk Polytechnic Inst., USSR). Kinet. Catal. (USSR) (Engl. Transl.); 15: No. 1, 70-74 (1974).

Translated from Kinet. Katal.; 15: No. 1, 86-91(1974).

An investigation has been made of the hydrogenation and deuteration of 1-hexene and cyclohexene in the presence of a complex organometallic catalyst based on $Co(C_5H_7O_2)_2$. It has been shown that, in parallel with deuteration, there is exchange in the olefins and migration of the double bond. Measurements have been made of the kinetic isotope effects in hydrogenation of 1-hexene and cyclohexene, as well as the orders of the reactions with respect to olefin, hydrogen, and catalyst. The mechanism of the hydrogenation reaction on this catalyst is discussed. (auth)

29013 ISOTOPE EFFECT IN THE VAPOR PRESSURE OF CARBON TETRAFLUORIDE. Ustinov, V. I.; Petropavlov, M. V. Russ. J. Phys. Chem. (Engl. Transl.); 47: No. 12, 1697-1699 (Dec 1973).

Translated from Zh. Fiz. Khim.; 47: No. 12, 3021-3024(Dec 1973).

The isotope effect with respect to carbon in the vapor pressure of carbon tetrafluoride has been measured at 90°K, the p_h/p_l ratio being recorded by an accurate mass-spectrometric method for determining the $^{13}C/^{12}C$ ratio at the level of natural carbon-13 concentrations. The "positive" carbon isotope effect has been calculated theoretically for carbon tetrafluoride to give good agreement with experimental results. (auth)

29014 ^{67}Zn NMR ANOMALOUS SOLVENT ISOTOPE EFFECT IN AQUEOUS SOLUTIONS. Epperlein, B. W.; Krueger, H.; Lutz, O.; Schwenk, A. (Tuebingen Univ. (F. R. Germany). Physikalisches Inst.). Z. Naturforsch., a; 29: No. 4, 660-661(Apr 1974).

1 tab.; 12 refs.

For ^{67}Zn NMR lines of solutions of $ZnCl_2$, $ZnBr_2$, and ZnI_2 in H_2O and D_2O an anomalous solvent isotope effect is reported. In D_2O solutions the lines are shifted to higher frequencies. The difference between the shieldings in H_2O and D_2O is, e.g., $\Delta(H_2O) - \Delta(D_2O) = (13.1 \pm 0.7)$ ppM for a concentration of 0.02 moles zinc bromide per mole solvent. (auth)

29015 THE ISOTOPE EFFECT FOR DIFFUSION OF SILVER IN GOLD. Herzig, C.; Wolter, D. (Muenster Univ. (F. R. Germany). Inst. fuer Metallforschung). Z. Metallk.; 65: No. 4, 273-278(Apr 1974). (In German).

4 figs.; 3 tabs.; 41 refs.

The diffusion and the isotope effect of silver-105 and silver-110m were measured in gold single crystals at different temperatures. In addition, two experiments were performed to determine the isotope effect of silver in silver, which yield $f_0 \times \Delta K = 0.69$ as a mean value. The temperature dependence of the tracer diffusion coefficient is given by an Arrhenius-relation which agrees very well with data from literature. The temperature dependence of the isotope effect results of silver in gold indicates a divacancy contribution in the diffusion process. From the results estimations of values of f_2 and ΔK according to given theoretical models are discussed. (auth)

29016 EXCESS ENERGY DEPENDENCE OF RADIATIONLESS TRANSITIONS IN NAPHTHALENE VAPOR: COMPETITION BETWEEN INTERNAL CONVERSION AND INTERSYSTEM CROSSING. Fischer, S. F. (Northwestern Univ., Evanston, IL); Stanford, A. L.; Lim, E. C. J. Chem. Phys.; 61: No. 2, 582-593 (15 Jul 1974).

Experimental and theoretical evidence for effective internal conversion to the ground state from highly vibrationally excited states is presented for naphthalene-h_8 and -d_8. The evidence is based upon both the variation of the deuteron effect and strong exponential increase of the nonradiative decay rate as observed in the excess energy region between 10,000 and 18,000 cm^{-1}. The calculations are only consistent with the experiments if it is assumed that the excess energy does not redistribute completely according to the statistical weighting among the normal modes but rather stays in the class of strongly accepting modes. (auth)

29017 ACYLAL HYDROLYSIS. The Hydrolysis of 3-(p-Nitrophenoxy)phthalide, α-Acetoxybenzyl p-Nitrophenyl Ether, and 3-(Para-Substituted Thiophenyl)phthalides. Fife, T. H.; De, N. C. (Univ. of Southern California, Los Angeles). J. Amer. Chem. Soc.; 96: No. 19, 6158-6165(18 Sep 1974).

The rates of hydrolysis of the acylals 3-(p-nitrophenoxy)phthalide, α-acetoxybenzyl p-nitrophenyl ether, and 3-(para-substituted thiophenyl)phthalides have been measured at 30° in H_2O. In hydrolysis of these compounds hydronium ion and hydroxide ion catalysis takes place. There is also a pH-independent spontaneous reaction. The pH-independent hydrolysis of 3-(p-nitrophenoxy)phthalide is characterized by a ΔS^* of –47.1 eu, indicating solvent involvement in the reaction. In the hydronium ion catalyzed hydrolysis of α-acetoxybenzyl p-nitrophenyl ether ΔS^* is –17.6 eu. There is pronounced catalysis of the hydrolysis of these compounds by the base component of the buffer. In the case of the p-nitrophenoxy acylals there is both a first-order and a second-order dependence on base concentration, suggesting base catalysis of nucleophilic attack by a second molecule of base or a kinetic equivalent. With the 3-(para-substituted thiophenyl)phthalides there is strict first-order dependence on the concentration of the catalyzing base. From the D_2O solvent isotope effect for ethanolamine catalysis of the hydrolysis of 3-(p-nitrothiophenyl)phthalide ($k_B^H/k_B^D = 1.8$) it can be inferred that catalysis is by a general base mechanism involving proton transfer in the rate-determining step. The Hammett ρ value for ethanol-amine catalysis is 0.55 and that for hydroxide ion is 0.42. It is apparent that these acylals are hydrolyzing as esters not acetals. (auth)

29018 *ENTROPIC CONTROL OF PHOTOCHEMICAL REACTIVITY.* The Transition State for γ-Hydrogen Abstraction of Alkyl Phenyl Ketones. Lewis, F. D.; Johnson, R. W.; Kory, D. R. *(Northwestern Univ., Evanston, IL). J. Amer. Chem. Soc.; 96:* No. 19, 6100-6107(18 Sep 1974).

The photochemical reactivity of several alkyl phenyl ketones, having similar n,π^* triplet energies and γ C–H bond strengths but differing in conformational mobility, has been investigated. Measurements of Arrhenius activation parameters show that the rate enhancements in conformationally restricted molecules are entirely entropic in origin. Rate factors of 5 to 8 for each internal rotation which must be frozen in the transition state are observed. Primary and secondary kinetic deuterium isotope effects have been measured for photochemical γ-hydrogen abstraction. The results are consistent with an unsymmetrical transition state with less than 50% γ C–H bond breaking. The transition state model for γ-hydrogen abstraction is in accord with experimental results and recent theoretical predictions. (auth)

29019 VIBRATIONAL RELAXATION OF HF(v=1) AND DF(v=1) BY H_2 AND D_2. Bott, J.F. (The Aerospace Corporation, El Segundo, California 90009); J. Chem. Phys. 61: No. 7, 2530-2535 (1 Oct 1974).

The vibrational relaxation times of DF(v=1) in the presence of H_2 have been measured in a combined shock tube laser–induced fluorescence experiment at temperatures from 440 to 690°K and 295°K. The data fall along an extrapolation of previously obtained high temperature shock tube data. Data are presented also for the relaxation of HF(v=1) by H_2 and DF(v=1) by D_2. (auth)

29020 ISOTOPE EFFECTS ON PARTITION FUNCTIONS AND THERMODYNAMIC QUANTITIES OF THE STABLE DIATOMIC HYDRIDES. Bron, J.; Paul, S. O. (Natal Univ., Durham, South Africa). J. Chem. Soc., Faraday Trans., II; 70: No. 7, *1294-1300(1974).*

The logarithms of partition functions of diatomic hydrides (in the ideal gas phase) were calculated by a direct summation method at various temperatures in the range 200 to 800°K. The least squares method was used to fit a curve to the calculated values. Thermodynamic quantities are readily evaluated from the coefficients for the equations of the curves. These coefficients are listed for several isotopic species. The temperature dependence of equilibrium constants and related changes in thermodynamic quantities, as well as the effects of substituting different isotopes (including H, D and T) in similar exchange equilibria, have been determined and compared with earlier results. (auth)

29021 SECONDARY DEUTERIUM ISOTOPE EFFECT IN THE CYCLOADDITION OF DIMETHYLKETEN TO STYRENE. Isaacs, N. S.; Hatcher, B. G. (Univ. of Reading, Eng.). J. Chem. Soc., Chem. Commun.; No. 15, 593-594(7 Aug 1974).

The secondary deuterium isotope effect for the cycloaddition of dimethylketen to [α - ^{2}H]-styrene has been found to give $k_H/k_D = 0.8$ *and the mechanistic implications of this value are* discussed. (auth)

29022 DEUTERIUM ISOTOPE EFFECTS IN DEUTERATED STYRENES. Baird, M. C. (Queen's Univ., Kingston, Ont.). J. Magn. Resonance; 14: No. 2, 117-120(May 1974).

The catalytic decarbonylation of threo-PhCHDCHDCOCl by $RhCl(PPh_3)_3$ at 200°C yields all isomers of d_1- and d_2-styrene deuterated on the vinyl positions, permitting the calculation of the ^{1}H chemical shifts of all the compounds. The deuterium isotope shifts are 1.0 to 1.1 Hz (H gem to D), 0.3 to 0.4 Hz (H cis to D), and 0.7 to 0.8 Hz (H trans to D). In the cases of dideuterated compounds, the shifts are approximately additive. (auth)

29023 SECONDARY DEUTERIUM ISOTOPE EFFECTS IN PROTON TRANSFERS FROM 2-NITROPROPANE. Davies, M. H. (Univ. of Stirling, Eng.). J. Chem. Soc., Perkin Trans., II; No. 9, 1018-1025(1974).

Kinetic and equilibrium secondary isotope effects have been measured for the deprotonation of 2-nitropropane by hydroxide and acetate ions. Although the Bronsted coefficients deduced lie between 0 and 1, they cannot be regarded as 'degrees of proton transfer' within the formalism of the Marcus theory. The isotope effects are interpreted in terms of two contributions, one of which does not change monotonically along the reaction coordinate. A recently reported dependence of the primary isotope effect upon isotopic solvent composition is discussed in the context of the rule of the geometric mean. A revised value of the equilibrium constant for iodination of the 2-nitropropyl anion is reported. (auth)

Isotope Exchange and Isotope Separation

Refer also to abstract 29826.

29024 (LA-tr-74-18) ENRICHMENT OF CARBON AND NEON ISOTOPES BY GAS PHASE CHROMATOGRAPHY. Part 1. Blanc, C.; Huynh, C. T.; Espagno, L. Translated from J. Chromatogr.; 28: 177-193(1967). 23p. Dep. NTIS $4.25.

The chromatography of carbon monoxide and neon has enabled us to obtain a considerable enrichment of the isotopes carbon-12 and -13 and neon-20 and -22 without attaining a complete separation in one single stage. In order to determine the distribution of the isotopes in the chromatographic peak, a mass spectrometer is used in conjunction with the gas chromatograph. The spectrometer gives continuous information concerning the concentrations of the two isotopes. As a result of this information, a new quantity ρ, the enrichment factor, is defined. This factor ρ is the product of the resolving power, which characterizes the analytical efficiency of the column and the relative difference in adsorption constants of the two isotopes. (auth)

29025 (LA-tr-74-19) ENRICHMENT OF CARBON AND NEON ISOTOPES BY GAS PHASE CHROMATOGRAPHY. Part 2. Blanc, C.; Huynh, C. T.; Espagno, L. Translated from J. Chromatogr.; 28: 194-208(1967). 18p. Dep. NTIS $4.00.

In a preceding article, the apparatus used for following the separation of isotopes in a chromatographic peak was described, for the case where the chromatograph does not completely separate the isotopes. A new quantity, the enrichment factor ρ, is defined which characterizes an isotopic chromatographic experiment. According to the model proposed, this factor is the product of the resolving power, which characterizes the analytical efficacy of the column and the relative difference of the adsorption constants of the two isotopes. In the present paper, the results obtained by gas chromatography on solid stationary phases for the enrichment of carbon-12 and -13 isotopes and neon-20 and -22 are given. The temperature and length of the column have a considerable influence on the isotopic enrichment, while the sample volume, the rate of flow of the carrier gas and the cross section of the column are less important. In addition, the enrichment is independent of the initial isotopic concentrations in the sample. Finally, it is shown that the proposed model agrees well with the results. (auth)

29026 (MLM-2171(LD)) TRITIUM EFFLUENT CONTROL PROJECT. Progress Report: April–June 1974. Kershner, C. J. (Mound Lab., Miamisburg, Ohio (USA)). 12 Sep 1974. Contract AT-33-1-GEN-53. 20p. Dep. NTIS $4.00.

The fabricator of the helium purification system now being built for glovebox atmosphere decontamination suggested a substitution for the requested adsorber bed packing in the purifier. In order to evaluate this suggestion, a 77°K adsorption isotherm was measured for hydrogen on a sample of the suggested Grace 5A sieve at equilibrium cold pressures ranging from 0.0029 to 0.0284 torr. The results of these measurements indicate that the Grace 5A and a coconut charcoal previously tested have similar adsorption characteristics for hydrogen at equilibrium. Thus, the Linde 5A sieve previously found superior to the charcoal would also be more suitable than the Grace 5A as the purifier bed packing. Mound has reaffirmed the original specification of this adsorbent. In studies on cryogenic adsorbate separation, a three-bed, temperature-zoned, chromatographic separation technique is described. Performance data obtained with a prototype of the first bed in the series operating at −131°C with 5A molecular sieve adsorbent showed that the system was capable of selectively separating hydrogen/nitrogen and oxygen as required for processing the regeneration gas from the glovebox atmosphere detritiation system. For hydrogen isotope distillation a direct reading thermometer was developed for the temperature range from 20 to 30°K. The readout is nearly linear in this range and may be extended to 300°K with slight loss of linearity. In studies on tritiated liquid waste decontamination, four determinations of the separation factor were made with the GE regenerative cell operating in the fuel cell mode. An effort was made in these experiments to "equilibrate" the H–D gas in the chamber before the experiment was begun and to use a maximum throughput in order that errors in gas isotopic analysis be minimized. The separation factor observed for these experiments ranged from 1.30 to 1.49 with an average of 1.42. Screening tests were initiated for the 16 organic liquids initially chosen for extractive distillation studies. Out of the original 16 only seven were found that did not form low boiling azeotropes with water. In a test consisting of fractional distillation with tritiated water, three of these seven appeared to increase the vapor pressure of HTO relative to H_2O. In catalytic exchange detritiation studies, a project was initiated to develop a tritium separation and concentration process based on a H_2/H_2O catalytic exchange technique which can possibly be used to detritiate contaminated water from light water reactors, fuel reprocessing plants, and tritium handling laboratory facilities. (auth)

29027 ISOTOPE EXCHANGE OF CHLORINE-36 IN THE SYSTEMS: GASEOUS HYDROGEN CHLORIDE–γ-PICOLINE HYDROCHLORIDE AND GASEOUS HYDROGEN CHLORIDE–STOICHIOMETRIC SOLVATE OF HYDROGEN CHLORIDE WITH γ-PICOLINE HYDROCHLORIDE. Zielinski, M.; Torbicki, H.; Szpilowski, S. (Jagiellonian Univ., Krakow). Rocz. Chem.; 48: No. 6, 1107-1109(1974).

Results from a study on the physicochemical parameters determining the kinetics of isotope exchange of ^{36}Cl between gaseous hydrogen chloride and γ-picoline hydrochloride are reported. (LK)

29028 INVESTIGATION OF THE CATALYTIC PROPERTIES OF COMPOUNDS OF THE $LnMeO_3$ TYPE IN THE HOMOMOLECULAR EXCHANGE OF OXYGEN. Sazonov, L. A.; Moskvina, Z. V.; Artamonov, E. V. (Inst. of Catalysis, Novosibirsk, USSR). Kinet. Catal. (USSR) (Engl. Transl.); 15: No. 1, 100-105(1974).

Translated from Kinet. Katal.; 15: No. 1, 120-126(1974).

The homomolecular exchange of oxygen on compounds of the $LaMeO_3$ type, where Me represents Cr^{3+}, Mn^{3+}, Fe^{3+}, Co^{3+}, and Ni^{3+}, and $NdCoO_3$ and $SmCoO_3$ was investigated in a broad range of temperatures. The reaction rates and activation energies were determined. On the basis of the data obtained, a conclusion was drawn that the cation of the transition element plays the determining role in the high temperature region of exchange, and the cation of the rare earth element plays the determining role in the low temperature region of exchange. (auth)

29029 INVESTIGATION OF LOW-TEMPERATURE HOMOMOLECULAR ISOTOPIC OXYGEN EXCHANGE ON TITANIUM DIOXIDE. Griva, A. P.; Nikisha, V. V.; Shelimov, B. N.; Kazanskii, V. B. (Inst. of Organic Chemistry, Moscow). Kinet. Catal. (USSR) (Engl. Transl.); 15: No. 1, 86-89(1974).

Translated from Kinet. Katal.; 15: No. 1, 104-108(1974).

Study has been made of the kinetics of low-temperature homomolecular isotopic oxygen exchange on partially reduced titanium dioxide. It was found that exchange is accompanied by oxidation of the reduced oxide, and catalyzed by intermediate forms of oxygen resulting from the reoxidation. Correlation of the ESR spectra of the catalyst with the rate of isotopic exchange suggested that one such form might be the O^- anion-radical. (auth)

29030 INVESTIGATIONS ON THE STRUCTURE OF μ-OXO-CHLORORUTHENATE(IV) BY THE ISOTOPIC EXCHANGE METHOD. Wajda, S.; Hyla-Kryspin, I. (Univ., Warsaw). Nukleonika; 19: No. 6, 511-519(1974). (In Polish).

Kinetics of exchange of the radiochlorine in the $(Ru_2OCl_{10})^{4-}$–$^{36}Cl^-$ system were examined. The isotopic exchange reaction is close to second order with respect to Cl^- and to first order with respect to the complex. Kinetic measurements of exchange process in the discussed system confirm the D_{4h} symmetry of the complex and that C_{4v} each of metallic nuclei. On the basis of experimental data the mechanism of isotopic exchange is proposed. The character of induction time changes indicates that the exchange process is conditioned by formation of the transition complex. (auth)

29031 *ISOTOPE EXCHANGE REACTIONS. IX.* Calculation of the Partition Function Ratios of Isotopic Molecules with the Aid of the Increment in the Trace of the GF-Matrix. Denisov, D. A.; Knyazev, D. A.; Shafeeva, M. V. (Moscow Inst. of Chemical Engineering). Russ. J. Phys. Chem. (Engl. Transl.); 47: No. 12, 1672-1674(Dec 1973).

Translated from Zh. Fiz. Khim.; 47: No. 12, 2975-2979(Dec 1973).

A new version of computational relations defining the ratio of the partition functions of isotopic forms of molecules in terms of the increment in the trace of the GF-matrix is proposed. (auth)

29032 ISOTOPIC STUDY OF WATER GAS REACTION CATALYZED BY PLATINUM. Masuda, M.; Miyahara, K. (Hokkaido Univ., Sapporo). Bull. Chem. Soc. Jap.; 47: No. 5, 1058-1063 (May 1974).

By the use of ^{13}C- and ^{18}O-labelled carbon dioxide and D_2 gas, water gas reaction over an evaporated Pt film was studied at temperatures 380–450°C under constant elimination of water vapor with cold traps. The reaction of CO_2 and H_2 was as rapid as that of CO_2 and D_2, the mixture of H_2 and D_2 changing rapidly into an equilibrium mixture of H_2, HD, and D_2 in the course of the reaction with CO_2. The mixture of $C^{18}O_2$ and CO_2 was also rapidly equilibrated by the reaction with H_2. The exchange reactions of ^{18}O and ^{13}C between CO_2 and CO in the course of the water gas reaction were similarly observed. The theory of the stoichiometric number on the rate-determining step was applied to the results. From the results and the observed rate equation of the water gas reaction, $V = k[CO_2]^{0.6}[H_2]^{0.5}[CO]^{-0.5}$, the reaction was supposed to be caused by the sequence of steps, $CO_2 \rightleftharpoons CO_2(a)$, $H_2 \rightleftharpoons 2H(a)$, $CO_2(a) + H(a) \rightleftharpoons X(a)$, $X(a) \rightleftharpoons CO(a) + OH(a)$, $CO(a) \rightleftharpoons CO$, and $OH(a) + H(a) \rightleftharpoons H_2O$, and to be rate-controlled by the third and fourth steps, where (a) denotes the adsorbed state and X(a) is an intermediate to rule out the direct conversion of $CO_2(a) + H(a)$ into $CO(a) + OH(a)$. (auth)

29033 INVESTIGATIONS OF HYDROGEN–DEUTERIUM EXCHANGE IN α-CHYMOTRYPSIN. Kanta, L.; Siemton, I. Z. (Univ. of Wroclaw). Acta Biochim. Pol.; 20: 15-23(1973).

H-D exchange in α-chymotrypsin at pD 4.6, in the temperature range 9 to 40°C, was investigated. On this basis the activation energy and the values of enthalpy and entropy of activation were obtained. These data lead to the conclusion that local segmental conformational motions are responsible for the observed rate of exchange. Addition of salt ($CaCl_2$, $MgCl_2$, and NaCl) has only little influence on the rate of exchange. (auth)

29034 ISOTOPIC SEPARATION OF NITROGEN-15. III. Effect of the Degree of Oxidation of the Reflux Gases for the System NO, NO_2–HNO_3. Nielsen, J.; Guernier, G.; Enjalbert, M. (Institut de Genie Chimique, Toulouse). Chem. Eng. Sci.; 29: No. 8, 1673-1680(Aug 1974). (In French).

A spectrophotometer was built to measure NO_2 concentration in a mixture of nitrogen oxides. The coefficient of oxidation of these vapors, at fixed pressure and temperature is linear with the NO_2 concentration in the gas. In reduction of nitric acid with SO_2, a constant coefficient of oxidation of nitrogen oxides has been obtained using the spectrophotometer as the controller in the regulation loop. The influence of this parameter on the isotopic separation of nitrogen 15 is described; reflux gas with a coefficient of oxidation of 25% is recommended for the first stage of a separation process using a 57% weight nitric acid feed. (auth)

Radiation Chemistry

Refer also to abstracts 28941, 29003, 29131, 29142, 29649, and 29650.

29035 (TRG-Report-2434) INTERACTION OF THERMAL AND CATALYTIC PROCESSES IN THE GASIFICATION OF GRAPHITE IN CO_2 MIXTURES. Palmer, J. E. M.; Lind, R.; Linacre, J.; Keep, C. W. (UKAEA Reactor Group, Springfields). Jul 1974. 13p. Dep. NTIS (US Sales Only) $4.00.

A laboratory C-14-labelled analogue of a nuclear graphite was used to study the reactions of graphite with CO_2-based gas mixtures, under radiation, over the temperature range 350 to 750°C. Thermal blank experiments before and after irradiation covered the same temperature range. At the lower temperatures, radiolytic reactions provide the principal graphite gasification mechanism but, at the higher temperatures, thermal reactions predominate. Differences in reaction rate with gas composition are discussed. The low radiolytic reaction rate ($g \sim 0.1$) found in gas mixtures containing $CO/H_2O/CH_4$, at low temperatures, increase at high temperature as the protective effect of these additives is lost, and the rates approach the uninhibited value ($g \sim 3.0$) at about 800°C. In addition, during the experiments, the graphite became contaminated with nickel and iron and the effects of this on the reactions are considered. (auth)

29036 STRUCTURE DISARRANGEMENT CAUSED IN γ-IRRADIATED DNA IN VITRO. Fonarar'ov, A. B.; Shugalii, O. V.; Todorov, I. M.; Paskevich, I. F. (Inst. of Molecular Biology and Genetics, Kiev). Dopov. Akad. Nauk Ukr. RSR, Ser. B; No. 7, 641-645(Jul 1974). (In Ukrainian).

Gamma irradiation of DNA with doses of 1–5 kR is shown to cause the defects not in sucrose-phosphate skelets but in a double helix without disturbing the covalent bonds. The defects of this type are not at random distribution which is probably due to the cooperative effect of the event. (auth)

29037 RADIATION COPOLYMERIZATION OF ETHYLENE OXIDE WITH ACRYLONITRILE. Yakovleva, M. K.; Sheinker, A. P.; Abkin, A. D. (Scientific-Research Physical-Chemical Inst., Moscow). Vysokomol. Soedin., Ser. B; 16: No. 5, 382-384(May 1974). (In Russian).

The copolymer formed in the gamma (^{60}Co) irradiation of a triethylamine solution of ethylene oxide and acrylonitrile was enriched in the latter for all initial ratios of the monomers. Kinetic data at −78°C showed at least 30% conversion of the monomer occurring at a constant rate. Reaction at 25°C produced only acrylonitrile homopolymer. With increase in the ethylene oxide in the starting mixture, the copolymer yield decreased. (MG)

29038 KINETIC STUDY OF DOUBLE BONDS IN POLYETHYLENE IRRADIATED BY GAMMA RAYS. Hosoi, F. (Japan Atomic Energy Research Inst., Tokai); Mitsui, H.; Ushirokawa, M.; Kagiya, T. Kobunshi Ronbunshu; 31: No. 2, 94-99(Feb 1974). (In Japanese).

The effects of γ rays on the double bonds of polyethylene were investigated from a kinetic point of view. Various polyethylenes ranging in the number-average molecular weight ($\overline{M}_n$) from 1500 to 114,000 were used. When polyethylene was irradiated in vacuo at 30°C, the formations of hydrogen and trans-vinylene unsaturation (t-V) were observed, while terminal vinyl(Vi) and vinylidene(Vd) contents decreased. The rates of these reactions were given as follows: $R_H = d[H_2]/dt = 1.03 \times 10^{-6}\ \overline{M}_n{}^{0.10}I$; $R_{t-v} = d[t-V]/dt = 1.01 \times 10^{-7}\ \overline{M}_n{}^{0.28}I$; $R_{vi} = -d[Vi]/dt = 2.58 \times 10^{-3}\ \overline{M}_n{}^{0.33}I[Vi]$; $R_{vd} = -d[Vd]/dt = 6.57 \times 10^{-4}\ \overline{M}_n{}^{0.47}I[Vd]$; where R is the rate (mole/g-PE · hr), and I the dose rate (Mrad/hr). The methyl group content remained unaltered by the irradiation. The reaction mechanism was discussed for the formation of hydrogen and t–V, and the disappearance of Vi and Vd. The latter reaction was also examined on the basis of the estimated activation energies. (auth)

29039 ELECTRON SCAVENGING IN THE RADIOLYSIS OF SUPERCRITICAL ETHANE, ETHYLENE, n–BUTANE, AND ISOBUTANE. Nishikawa, M.; Yamaguchi, Y.; Fujita, K. (Department of Pure and Applied Sciences, University of Tokyo, 3–8–1 Komaba, Meguro–ku, Tokyo, Japan). J. Chem. Phys. 61: No. 6, 2356-2359 (15 Sept 1974).

Free ion yields in the radiolysis of supercritical ethane and ethylene at 50°C, and n–butane and isobutane at 170°C were estimated as a function of density from the nitrogen yields observed upon electron scavenging by N_2O with the use of the square root model, $G(N_2) = G(N_2)_{fi} + G(N_2)_{gi}(A[N_2O])^{1/2}$. The estimated G_{fi} in the hydrocarbon gases were in the decreasing order $C_2H_6 > i-C_4H_{10} > n-C_4H_{10} > C_2H_4$ for the density range 0.12–0.24 g/ml. The density–normalized range of electrons estimated from G_{fi} values decreased sharply with an increase in density for C_2 hydrocarbons, while it was practically constant for butanes over the entire range studied (0.12–0.42 g/ml). The variation of A values with density was discussed in terms of the concomitant change in the electron mobilities. (auth)

29040 EFFECTS OF IONIZING RADIATION ON TYROSINE. Box, H.C.; Budzinski, E.E.; Freund, H.G. (Biophysics Department, Roswell Park Memorial Institute, Buffalo, New York 14203). J. Chem. Phys. 61: No. 6, 2222-2226 (15 Sept 1974).

Two oxidation products and one reduction product were identified in single crystals of tyrosine HCl irradiated at 4.2°K. Both oxidation products are associated with the loss of an electron from the phenol ring of tyrosine. The reduction product is the result of electron addition to the carboxyl group. The identification of these species followed from an analysis of proton hyperfine couplings measured by the ENDOR technique. (auth)

29041 SOME PHYSICAL AND CHEMICAL PROPERTIES OF FRACTIONS SEPARATED FROM GAMMA-IRRADIATED CORN STARCH. Akulova, I. S.; Putilova, I. N.; Tregubov, N. N. Sb. Nauch. Tr., Mosk. Tekhnol. Inst. Pishch. Prom.; No. 20, 64-72(1971). (In Russian).

Fractionations were made of corn starch irradiated with doses of 50 and 100 Mrad by the method of fractional precipitation from an alcohol-water mixture. The fractionation products were characterized by the content of reducing material, the degree of polymerization, the capacity of binding iodine, the viscosity of the solution, and the size of the axial ratio of the molecule. The mean molecular weight of the fractions, calculated from the characteristic viscosity, varied in the limits from 13,240 to 1959. (tr-auth)

29042 ELECTRON RADIATION DAMAGE OF THIN FILMS OF GLYCINE, DIGLYCINE, AND AROMATIC AMINO ACIDS. Lin, S. D. (Univ. of Chicago). Radiat. Res.; 59: No. 3, 521-526(Sep 1974).

The radiation damage induced by 25 keV electrons to five amino acids and one peptide was studied by following various damage monitors accessible in a simple scanning electron microscope equipped with a spectrometer. It was found that change in crystalline structure, loss of mass, and damage to the aromatic parts of the amino acids constitute different stages of the damage process. From the measured characteristic doses necessary to induce various damages, the G values can be estimated. They are of the same order of magnitude as those determined from radiological studies. (auth)

29043 REACTIONS OF THE RADIOLYTICALLY GENERATED HYDROXYCYCLOHEXADIENYL RADICAL IN AQUEOUS BENZENE SYSTEMS. Bhatia, K. (Carnegie-Mellon Univ., Pittsburgh). Radiat. Res.; 59: No. 3, 537-555(Sep 1974).

The radiolysis of N_2O-saturated aqueous benzene solutions was investigated by aqueous liquid chromatographic methods. It is shown that phenol, biphenyl, and at least five unidentified nonvolatile phenol-like substances with absorption spectra in the region 210 to 290 nm similar to that of phenol were produced upon the γ radiolysis of the N_2O-saturated neutral aqueous benzene solution. Several of these products including phenol and biphenyl were primarily produced by postirradiation reactions since the yields of these products increased upon storing the irradiated solutions. It is concluded that hydroxycyclohexadienyl radical produced by the addition of the radiolytically generated hydroxyl radical to benzene was primarily converted to products other than phenol and/or biphenyl. Phenol formation in post irradiation reactions was and biphenyl formation was not acid catalyzed. Phenylphenols were identified among products of postirradiation reactions. The nature and composition of products formed in the pulse and the γ radiolysis conditions was, as expected, different. The analyses of the γ-irradiation solutions indicated that the number of products and their concentration ratios in the N_2O-saturated, aerated, and deaerated solutions was different. The product composition of aerated and deaerated systems was also significantly altered due to postirradiation reactions. (auth)

29044 REACTIONS OF SECONDARY FREE RADICALS IN THE IRRADIATED FROZEN AQUEOUS SOLUTIONS OF AMINO ACID AND PEPTIDES. Usatyi, A. F.; Panin, V. I. Biofizika; 18: No. 3, 439-446(1973). (In Russian).

Reactions of secondary free radicals in irradiated frozen aqueous solutions containing mixtures of amino acids (1 M) and peptides (0.1 M) were investigated by the ESR method. As a result of amino acid disamination, the radicals $R^{\cdot}_A$ appeared, which tear the hydrogen atom off the amino acid residue of neighboring peptide molecules. The transfer of free valency was followed by the corresponding ESR spectrum changes. The final radicals have the following configuration $\sim NH-\dot{C}H-CO\sim$, R = H, CH_3 etc. Two stages of the processes are revealed. Activation energy of the "rapid" stage depends on the reagent structure. The "slow" stage is a diffusive control process. Resonance patterns of nonradical fragments (R_A = H) are registered in the NMR-H^1 spectra of irradiated peptides solutions. (auth)

29045 STUDIES ON THE PREPARATION OF MORTAR–PLASTIC COMPOSITE. Pyun, H. C.; Lee, K. H. (Atomic Energy Research Inst., Seoul). J. Korean Nucl. Soc.; 6: No. 2, 73-79(Jun 1974).

Preparation of the mortar–plastic composites (MPC) was studied with styrene, methyl methacrylate, and vinyl acetate as monomers. Radiation, thermal-catalytic, and radiation-catalytic methods were used as curing methods. Almost all of the above monomers and methods were useable for preparing MPC. Although the thermal-catalytic method was excellent for obtaining MPC in a short time, the tensile strength of the product was less than those obtained by the radiation method. It was possible to prepare MPC which included up to about 10% plastics and strengthened about ten times based on acid resistances and tensile strength compared with the control. The improvement of the properties is much superior to concrete–plastic composites. (8 figures) (auth)

29046 TREATMENT OF EXHAUST GAS WITH ELECTRON BEAM IRRADIATION. I. Treatment of Exhaust Gas in Batch Type Apparatus. Kawamura, K.; Aoki, S. (Ebara Mfg. Co. Ltd., Tokyo). Ehara Jiho; No. 88, 9-14(Jun 1974). (In Japanese).

In order to examine the possibility of new method of processing exhaust gas with electron beam irradiation, change in the composition of gas due to the irradiation was measured on combustion gas of heavy oil containing about 1,000 ppM of sulfur dioxide by using a linear accelerator. The generation of white smoke-like aerosol was observed with the desulfurization of 80 to 90%, when an absorbed dose of about 3 megarads was given. Further, it was confirmed that the desulfurization rate depended on the energy of the electron beam, temperature of the reaction, and initial concentration of sulfur dioxide. In regard to the mechanism of the disappearance of sulfur dioxide, there are still many unclarified matters, but it can be concluded that the exhaust gas treatment with electron beam irradiation is effective at least in the laboratory test. (auth)

29047 REDUCTION OF METHYL ACETATE WITH SEVERAL HYDROSILANES UNDER GAMMA IRRADIATION. Nakao, R.; Fukumoto, T.; Tsurugi, J. (Radiation Center of Osaka Prefecture, Sakai, Japan). Bull. Chem. Soc. Jap.; 47: No. 4, 932-934(Apr 1974).

The reduction of methyl acetate with chlorinated hydrosilanes, $HSiCl_{3-n}R_n$(R = CH_3 or OCH_3, n = 0–2), and triethylsilane under γ-irradiation was studied. The hydrosilanes other than triethylsilane reduce the ester to ethyl methyl ether. The reaction rate is proportional to the hydrosilane concentration and is independent of the methyl acetate concentration. The results indicate that the rate-determining step in the reduction reaction is the hydrogen abstraction from the hydrosilanes. The reactivities of the chlorinated hydrosilanes in the reaction increase with the progressive chlorine substitution on the silicon atom and may be due to the susceptibility of each H–Si bond toward free radicals,

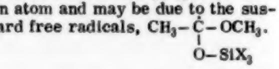

$CH_3-\underset{\underset{O-SiX_3}{|}}{\dot{C}}-OCH_3$.

(auth)

29048 CHEMICAL BEHAVIOR OF INTERMEDIATES PRODUCED IN SULFURIC ACID GLASS BY GAMMA IRRADIATION. I. Reactivities of Mobile Electrons with Inorganic Ions. Sasaki, T. (Japan Atomic Energy Research Inst., Tokai). Bull. Chem. Soc. Jap.; 47: No. 3, 529-533(Mar 1974).

The yield of the trapped hydrogen atom, H_t, produced in the 6 M sulfuric acid matrix at 77°K was decreased by the presence of an electron scavenger. Based on the competition reaction kinetics, the reactivities of mobile electrons, e^-_m, with metallic and oxygen-containing ions were determined from the decrease in the H_t yield. It was found that e^-_m is scavenged most efficiently with the TeO_4^{2-} ion. The relative reaction rates of e^-_m with oxyanions were generally larger than those of the corresponding e^-_{aq} reactions. On the other hand, a good accordance in the reaction rates for both forms of electrons was observed in the cases of the reactions with metallic ions. An interpretation was given to the discrepancy in the observed reaction rates that e^-_m in the epithermal energy region goes over the Coulomb barrier, which is too high for e^-_{aq} to pass through, and thus reacts more efficiently with anionic species than does e^-_{aq}. Some unstable intermediates produced at 77°K polymerized with the solute during the thermal annealing. The ESR and optical spectra of the polymerized cadmium and molybdenum are shown, together with those of the primarily produced species. (auth)

29049 RADIATION CHEMICAL STUDIES WITH CYCLOTRON BEAMS. III. Heavy-Ion Radiolysis of Liquid Aliphatic Ketones. Matsui, M.; Imamura, M. (Inst. of Physical and Chemical Research, Wako, Japan). Bull. Chem. Soc. Jap.; 47: No. 5, 1113-1116(May 1974).

The liquid-phase radiolysis of acetone, methyl ethyl ketone, and diethyl ketone with ^4He-, ^{12}C-, and ^{14}N-ions was carried out with the intention of discovering the specific reactions taking place in a very high LET region. The heavy ions were accelerated at various energies with an IPCR cyclotron, the LET of which was up to 80 eV/Å. The radiolytic yields of the main gaseous products, hydrogen and carbon monoxide, were found to increase appreciably with an increase in the LET and to reach the maximum values in the LET region between 50 and 70 eV/Å. The ratios of the two yields, $G(H_2)/G(CO)$, also increase substantially with an increase in the LET. These results, as well as the variations in the yields of saturated and unsaturated hydrocarbons, appear to indicate a thermal-spike effect which may bring about the thermal decomposition of free radicals, giving rise to the enhanced $G(H_2)$ and G(CO) values in the high LET region. (auth)

29050 ELECTRON SPIN RESONANCE STUDY ON FREE RADICALS IN THE CHEMICAL CARCINOGEN, 1,2-DIMETHYLHYDRAZINE INDUCED BY X-RAY IRRADIATION. Morita, N. (Kagoshima Univ., Japan); Hayashi, T.; Yunoki, K.; Kawano, I. Kagoshima Daigaku Igaku Zasshi; 25: No. 3, 249-252(Dec 1973). (In Japanese).

Prior to the examination of chemical reactivity of 1,2-dimethylhydrazine known as a chemical carcinogen, x-ray irradiation was performed for the examination of produced free radicals by means of electron spin resonance (ESR). X-ray irradiation was performed for 12 to 24 hours continually at room temperature using 30 KV, 10 mA, and a copper target for measurements with a JES-ME-3X type apparatus manufactured by Nihon Denshi. The conditions were the sweep range of the magnetic field of 3200 ± 100 G, 3000 ± 1000 G, and 3270 ± 100 G changed according to purpose, response 10 sec, gain 10 × 100, 10 × 10, and 6.3 × 10, and modulation width 4G and 10G and power 10 mW according to purpose. The ESR spectrum consists of about twelve lines spread over approximately 180 gauss. It is suggested that a radical of this type exhibits hyperfine splitting characteristic for a -N-N-fragment of 1,2-dimethylhydrazine. The free radicals obtained were stable for over several weeks. (JA)

29051 QUANTITATIVE STUDY OF THE RADIOLYSIS OF $FeSO_4 \cdot 7H_2O$ USING MOESSBAUER EFFECT. Kellershohn, C.; Soubirou, F.; Hubert, C. (Centre Hospitalier Universitaire Necker–Enfants–Malades, Paris). J. Phys. (Paris), Colloq.; No. 1, 73-75(1974). (In French).

From meeting on hyperfine interactions as detected by nuclear radiations; Liege, Belgium (11 Sep 1973).

The irradiation by x-rays of polycrystalline samples of $FeSO_4$ $7H_2O$ in a normal atmosphere and at room temperature leads to the formation of Fe^{3+}, probably in the form of ferric hydroxide as deduced from the isomeric shift and the quadrupole splitting. The 10-mg of samples of Fe/cm^2 are irradiated by means of an x-ray tube under constant voltage of 50 kV and the spectra taken at room temperature by a constant acceleration spectrometer equipped with a ^{57}Co–Pd source. The variation of the proportion of Fe^{3+} according to the dose of radiation is determined by comparison of the Moessbauer spectra of the irradiated samples with those of reference mixtures of $FeSO_4 \cdot 7H_2O$ and of an iron hydroxide having the same Moessbauer parameters as the Fe^{3+} ion resulting from the irradiation. The quantity of energy necessary for the production of an Fe^{3+} ion from a molecule of $FeSO_4 \cdot 7H_2O$ is deduced from the experimental data and compared with the energy necessary to obtain the same effect on ferrous sulfate in aqueous solution. Some implications of the results obtained are discussed. (FR)

29052 MOESSBAUER SPECTROSCOPIC STUDY OF THE EFFECT OF REACTOR RADIATION ON THE IRON(III) ACETYLACETONATE-TRIETHYLALUMINUM CATALYST. Sokol'skii, D. V.; Khlystov, A. S.; Dautov, L. M.; Marusich, N. I.; Noskova, N. F. (Inst. of Organic Catalysis and Electrochemistry, Alma-Ata, USSR). Russ. J. Phys. Chem. (Engl. Transl.); 47: No. 12, 1734-1737(Dec 1973).

Translated from Zh. Fiz. Khim.; 47: No. 12, 3088-3092(Dec 1973).

Mössbauer spectra of the $Fe(Acac)_3-Al(C_2H_5)_3$ system with irradiated iron(III), acetylacetonate were recorded and phenylacetylene was hydrogenated in the presence of this system. With increase of the integral flux of thermal neutrons from 10^6 to 10^{16} neutron cm^{-2}, the amount of Fe^{2+} and the number of quadrupole splittings are seen to increase. The rate of hydrogenation increases on the catalyst with irradiated iron(III) acetylacetonate until the attainment of a flux of 10^8 neutron cm^{-2} and then remains constant. (auth)

29053 EFFECT OF IRRADIATION OF METAL IONS ON ADSORPTION PROPERTIES OF SEMICONDUCTOR MATERIALS. I. Adsorption Properties of Oxidized Surface of Silicon. Sotnikov, V. S.; Beletskii, P. N.; Baru, V. G. Sov. Radiochem. (Engl. Transl.); 15: No. 6, 900-902(1973).

Translated from Radiokhimiya; 15: No. 6, 886-888(1973).

It was shown that a change in the radioactivity of the ions (Cu, Ag, Au, Hg, and P) by three orders does not have an appreciable effect on their adsorption. It was confirmed by radioactivation analysis that the amounts of adsorption of radioactive and nonradioactive metal ions on a silicon surface are the same. The experimental results agree with theoretical estimates of the effect of the reaction on the adsorption capacity of oxidized silicon. (auth)

29054 OXIDATIVE DEGRADATION PRODUCTS OF IRRADIATED POLYETHYLENE. Morisaki, S. (Research Inst. of Industrial Safety, Tokyo). Thermochim. Acta; 9: No. 2, 159-169(Jun 1974).

Oxidative thermal degradation products of polyethylenes at various temperatures crosslinked with electron beams were analyzed with gas chromatography and mass spectrometry techniques. Carbon monoxide and carbon dioxide were determined at a temperature range of 200 to 340°C, and the activation energies of the unirradiated and the irradiated polyethylene (at 100 Mrad) are 13.5 and 11.4 kcal/mole, respectively. C_1 to C_8 hydrocarbons produced in air and in nitrogen are determined at temperatures from 400 to 450°C for the polyethylenes. The irradiated polyethylene produces less hydrocarbons in air than the unirradiated polyethylene, contrary to the fact that the cross-linked polymer evolves more hydrocarbons than the unirradiated polymer in a nitrogen atmosphere. Aldehydes and ketones are observed in the volatile oxidative degradation products, and these carbonyl compounds increase quantitatively with increase of temperature up to about 460°C. It is concluded that irradiated polyethylene is thermally more unstable in the absence of oxygen and more easily oxidizable at low degradation temperatures in air than unirradiated polyethylene. Irradiated polyethylene, however, is more heat-stable than unirradiated polyethylene from the standpoint of the ignition process. (NL)

29055 RADIATION-INDUCED RADICALS IN THYMINE AND ITS DERIVATIVES IN LOW TEMPERATURE GLASSES. Kaalhus, O.; Johansen, S. A. (Norsk Hydro's Inst. for Cancer Research, Oslo). Ann. N. Y. Acad. Sci.; 222: 432-445(31 Dec 1973).

X-ray-induced radicals in frozen acid, neutral and alkaline glasses containing thymine or thymine derivatives were studied by ESR spectroscopy. Previous findings in a sulfuric acid glass indicate that radiation-induced electrons are converted into mobile hydrogen atoms, which eventually become trapped. This mobile hydrogen species produces a different thymine radical at 77°K than hydrogen atoms thermally released from traps at 103°K. Annealing at 153°K shows that the former radical, an ESR doublet with a h.f.s. of 16 gauss, is the precursor of the latter, the 5-thymyl octet radical. The thymine anion is observed in both an alkaline NaOH glass and a neutral glycol/water glass. This ESR doublet has a smaller splitting, 12 G, in agreement with theoretical predictions. On thermal annealing, the doublet abstracts a molecular fragment from the solvent. Conversely, it is protonated at C_6 by optical bleaching. (auth)

29056 IONIC FREE RADICALS INDUCED BY IONIZING RADIATION IN ORIENTED DNA. Graeslund, A.; Ehrenberg, A.; Rupprecht, A. (Univ. of Stockholm). Ann. N. Y. Acad. Sci.; 222: 374-386(31 Dec 1973).

The DNA samples containing either 6% LiCl or 1% NaCl of the dry sample weight were equilibrated in a humid atmosphere, or dried for one week and equilibrated in an atmosphere containing heavy water. This procedure gave a water content of approximately 30% of the total sample weight. The samples were γ-irradiated at 77°K with 450 krad from a ^{60}Co source, and were kept, handled and investigated at that temperature thereafter, unless otherwise stated. The ESR spectra were recorded on a Varian V-4502 spectrometer, equipped with 100 kHz modulation, a 12-inch magnet and a V-4531 multipurpose cavity or a V-4533 cylindrical cavity. A modified microwave bridge enabled work at low microwave power. (auth)

29057 RADIATION-CHEMICAL STUDIES ON THE GENERATION OF LEAD AND TIN RADICALS. Jungbluth, H.; Moeckel, H.; Wendenburg, J. (Hahn-Meitner-Institut fuer Kernforschung Berlin G.m.b.H. (F. R. Germany). Sektor Strahlenchemie). Z. Naturforsch., b; 29: No. 5/6, 379-384(May 1974). (In German).

5 figs.; 3 tabs.; 8 refs.

Triphenyltin chloride and acetate, the corresponding lead compounds, and tribenzyltin chloride are effective electron scavengers in γ-irradiated glasses of 2-methyltetrahydrofuran at 77°K. The reaction with the electrons leads to the formation of tin and lead radicals via dissociative electron capture. Only in the case of the benzyl compound is the molecular anion formed. Wavelength of absorption, extinction coefficients, and relative rate constants are reported. The formation of lead radicals is confirmed by observation of their ESR absorption. (auth)

29058 ACCELERATING EFFECT OF HALOGENATED METHANE ON THE RADIATION DEGRADATION OF POLYTETRAFLUOROETHYLENE. Hagiwara, M. (Japan Atomic Energy Research Inst., Takasaki); Tagawa, T.; Tsuchida, E.; Shinohara, I.; Kagiya, T. Kobunshi Ronbunshu; 31: No. 5, 336-340(May 1974). (In Japanese).

Polytetrafluoroethylene(I) was irradiated with γ rays in vacuo, in air atmosphere or in oxygen containing vapor of halogenated methane. Tensile strength and elongation at breaking point were reduced rapidly with dose. The reduction of the mechanical strength was accelerated by the irradiation in the presence of air, or by the application of heat after the irradiation. Further, the degradation was found to proceed effectively at elevated temperature, especially in the presence of gaseous mixture of oxygen and halogenated methane. Mass spectrometric analysis of the evolved gases showed that the degradation in air atmosphere proceeded with formation of CO_2 and CO. On the other hand, by gas chromatographic analysis CF_2Cl_2 and $CFCl_3$ were found to evolve when CCl_4 was added as a halogenated methane, and CF_2Cl_2, CHF_2Cl, $CFCl_3$, $CHFCl_2$, CH_2Cl_2, and CCl_4 were formed in the case of $CHCl_3$. Infrared absorption spectra of the irradiated samples were almost the same as that of the original I. From those experimental results a mechanism of acceleration of the degradation in the presence of halogenated methane was interpreted in terms of a radical chain reaction. (auth)

29059 MELTING BEHAVIOR OF NYLON 6. Todoki, M. (Toray Industries, Inc., Otsu, Japan); Kawaguchi, T. Kobunshi Ronbunshu; 31: No. 2, 106-111(Feb 1974). (In Japanese).

Melting of nylon 6 yarns has been studied by differential scanning calorimetry. γ-ray irradiation of the samples in gaseous acetylene provided an effective technique for suppressing reorganization during the heating process by introducing cross-links into the amorphous region. Acetylene molecules which diffused into the amorphous region serve as a cross-linking agent and also as a sensitizer. The optimum dose was determined empirically and it was small enough to minimize the damage of the crystal lattices. The melting curves thus obtained are considered to give melting points strictly inherent to the original crystallites in the nylon 6 yarns. Undrawn nylon 6 yarns exhibited very broad melting curves with a peak at about 155°C. By heat treatment the peak became sharp and shifted to a higher temperature. Drawn nylon 6 yarns exhibited sharp melting curves with a peak at temperatures higher than those of the undrawn yarns. (auth)

29060 PREVRASHCHENIE KOMPLEKSNYKH SOEDINENII POD DEISTVIEM SVETA, RADIATSII I TEMPERATURY. (Conversion of Complex Compounds Under the Action of Light, Radiation, and Temperature). Lazerko, G. A.; Neokladnovoi, L. N. (eds.). Minsk; Izdatel'stvo BGU im. V. I. Lenin (1973). 160p.

This collection of articles presents the results of studies on the photolysis and radiolysis of complex compounds of Pt, Rh, Co, and Cu containing various organic and inorganic ligands in solution and solid phase at temperatures of 77° and 300°K. New data were obtained on the mechanism of elementary processes, the effect of structure, and the composition of the outer and inner coordination spheres on the above processes. The following studies were carried out: photochemical conversion of complex Co(III) compounds with a mixed coordination sphere (chap. 1), photolysis of frozen cupric chloride solutions (chap. 2), photolysis of $K_3[Rh(C_2O_4)_3] \cdot 3H_2O$ (chap. 3), photochemistry of outer sphere, complexes of trivalent cobalt (chap. 4), new data on the photochemistry of Pt(IV) complexes (chap. 5), effect of uv and gamma radiation on aqueous solution of Cu(II) complexes with amino-acids (chap. 6), radiation-chemical conversions in solutions of Pt(II) and Pt(IV) complexes (chap. 7), study of the radiolysis of solid Co(III) compounds by EPR method (chap. 8), reaction of hydrogen atoms with Co(III) complexes (chap. 9), kinetics of the thermolysis of acido- and di acido aminocobaltichloride (chap. 10), reactivity of acido- and di acido aminocobaltichloride in an atmosphere of ammonia (chap. 11), kinetics for the formation of uranium tetrachloride ammoniates (chap. 12), the type of coordination of thiourea and pyridine metal complexes on a sulfo cation exchanger (chap. 13), the effect of complexing copper, cadmium and zinc ions with pyridine and ammonium in a cation exchanger on the adsorption of aniline and phenol (chap. 14), effect of solvent and electrolyte on the sensitivity of ion exchange methods in investigating complex formation (chap. 15), polar hydroxy complexes of hexavalent uranium (chap. 16), and a spectroscopic study of the photolysis of Rh(III) pyridinates. Five of the sections were abstracted separately for NSA. (SJR)

For abstracts of individual sections see: 29061–29063, 29124, and 29125.

29061 EFFECT OF ULTRAVIOLET LIGHT AND GAMMA RADIATION ON AQUEOUS SOLUTIONS OF Cu(II) COMPLEXES WITH AMINO ACIDS. Il'yukevich, L. A. pp 64-72 of Prevrashchenie Kompleksnykh Soedinenii Pod Deistviem Sveta, Radiatsii i Temperatury. Lazerko, G. A. (ed.). Minsk; Izdatel'stvo BGU im. V. I. Lenin (1973). (In Russian).

Results are presented of a study of photo- and radioinduced conversions of aerated aqueous solutions of Cu(II) complexes containing glycine, alpha-alanine, and serine. An analogy is found in the final decomposition products formed under the action of both types of radiation. Radiation-chemical yields and yields of reaction products at $\lambda = 253$ nm were determined. It was established that oxidation–reduction processes occur only on excitation of the complex in the electron-transition band. (SJR)

29062 RADIATION-CHEMICAL CONVERSIONS IN SOLUTIONS OF Pt(II) AND Pt(IV) COMPLEXES. Karaban, A. A.; Shagisultanova, G. A. pp 72-81 of Prevrashchenie Kompleksnykh Soedinenii Pod Deistviem Sveta, Radiatsii i Temperatury. Lazerko, G. A. (ed.). Minsk; Izdatel'stvo BGU im. V. I. Lenin (1973). (In Russian).

A study was carried out on the radiolysis of solutions of Pt(IV) complexes having different compositions: $(Pt\ en_3)Cl_4$, trans-$(Pt\ en_2\ Cl_2)Cl_2$ and $(Pt\ gly_3)Cl$, where en = $NH_2CH_2CH_2NH_2$ and gly = $NH_2CH_2COO^-$. On the basis of an analysis of the radiolysis products and the character of the effect of acceptors of oxidative radicals and of the hydrated electrons, conclusions were made on the mechanism of the radiation-chemical conversions of these complexes. By means of the EPR method it is proved that an intermediate Pt(III) complex is formed during radiolysis of frozen solutions. In addition studies were made on model reactions of a series of Pt(II) and Pt(IV) complexes with atomic hydrogen generated by a high-frequency, electrodeless discharge. (SJR)

29063 STUDIES OF RADIOLYSIS OF SOLID, Co(III) COMPOUNDS BY THE EPR METHOD. Neokladnova, L. N.; Pansevich, V. V.; Poznyak, A. L. pp 81-92 of Prevrashchenie Kompleksnykh Soedinenii Pod Deistviem Sveta, Radiatsii i Temperatury. Lazerko, G. A. (ed.). Minsk; Izdatel'stvo BGU im. V. I. Lenin (1973). (In Russian).

A study was made on the radiolysis of complexes containing various amino- and acido-ligands in the solid phase by the EPR method. Irradiation was carried out at 77 and 300°K. In the EPR spectra of complexes irradiated at 300°K, signals of parameter centers containing Co(II) were detected. Radiolysis at 77°K is accompanied by the formation of Cl_2^-, NO_2, and a number of other paramagnetic centers and radicals detected by EPR. The radiation-chemical yield of Co(II) was determined. (SJR)

29064 LONG-LIVED RADIATION-INDUCED FREE RADICALS IN ANOXIC WET DNA AS STUDIED BY ELECTRON SPIN RESONANCE SPECTROSCOPY. Jones, W. B. G.; Brustad, T. (Norsk Hydro's Inst. for Cancer Research, Oslo). Ann. N. Y. Acad. Sci.; 452-459(31 Dec 1973).

Previous studies by the authors show that some of the radiation-induced DNA transients are remarkably long-lived, persisting in aqueous solutions at room temperature for times in excess of 40 minutes. That these transients are likely to be free radicals which can readily react with the nitroxyls led them to investigate the long-lived radiation-induced free radicals in anoxic wet DNA, since the pulse radiolysis work and the binding studies taken together made it seem likely a specific component base (or bases) in DNA constituted the main target(s) for nitroxyl attack. If this were true, they hoped to be able to resolve the ESR spectra characteristic of this (these) specific target(s). Because of the limitations in sensitivity of the ESR spectrometer, it was not possible to use a true DNA solution so the authors devised a method for preparing a hydrated DNA which gave a good ESR signal with excellent reproducibility, in terms of both the ESR spectrum and the radical yield. (LK)

29065 EFFECTS OF MOLECULAR MOTION IN THE ESR SPECTRUM OF BrO_3^{2-} IONS IN $KBrO_3$ SINGLE CRYSTALS. Byberg, J. R.; Jensen, S. J. K.; Kirkegaard, B. S. (Univ. of Aarhus, Denmark). J. Chem. Phys.; 61: No. 1, 138-145(1 Jul 1974).

The ESR spectra at X band of BrO_3^{2-} defects in $KBrO_3$ crystals are investigated in the temperature interval 26–250°K. Spectra recorded below 115°K correspond to three distinct orientations of BrO_3^{2-} in the lattice. Above 115°K the three spectra merge into a single spectrum. The observed spectral changes are described in terms of the jump model, assuming that BrO_3^{2-} "jumps" between the three equivalent orientations. The model describes satisfactorily the temperature dependence of positions and shapes of all hyperfine lines between 80 and 160°K except for the static field B_0 directed along the trigonal axis of the crystal. Assumption of a moderate temperature dependence of the static spin Hamiltonian extends the range of agreement with experiment to 200°K for most orientations of B_0. (auth)

29066 FLASH PHOTOLYSIS STUDY OF THE GAS PHASE RECOMBINATION OF HYDROXYL RADICALS. Trainor, D. W.; von Rosenberg, C. W. Jr. (AVCO Everett Research Lab., Inc., MA). J. Chem. Phys.; 61: No. 3, 1010-1015(1 Aug 1974).

Rate constants are reported for the reactions $OH + OH \rightarrow H_2O + O$ (where k_1 is the rate constant) and $OH + OH + N_2 \rightarrow H_2O_2 + N_2$ (where k_5 is the rate constant) measured in a room temperature flash photolysis experiment. Hydroxyl radicals were produced by the photodecomposition of water vapor, and time resolved absorption spectroscopy was utilized to determine the absolute OH concentration. Specific rate constants obtained are $k_1 = 2.1 \pm 0.2 \times 10^{-12}$ cm^3/sec and $k_5 = 2.5 \pm 0.3 \times 10^{-31}$ cm^6/sec. (auth)

29067 ESR SPECTRA OF PF_2 AND SF_3 RADICALS. Colussi, A. J. (National Research Council of Canada, Ottawa); Morton, J. R.; Preston, K. F.; Fessenden, R. W. J. Chem. Phys.; 61: No. 3, 1247-1248(1 Aug 1974).

The radical PF_3 was prepared by irradiation of 5 mole % PF_3 in a C_2F_6 matrix with 2.8-MeV electrons and by UV photolysis of PF_2Cl in the liquid phase. The spectrum of SF_3 was observed in the liquid phase by photolyzing a solution of H_2S or D_2S and CF_3OF in Freon 13 at −110°C. (LK)

29068 TRAPPED ELECTRONS IN C_2H_5OD GLASSES γ-−IRRADIATED AT 4°K. Perkey, L.M.; Farhataziz; Hentz, R.R. (Department of Chemistry and the Radiation Laboratory, University of Notre Dame, Indiana 46556). J. Chem. Phys. 61: No. 7, 2979-2980 (1 Oct 1974).

Optical absorption spectra were determined for electrons in C_2H_5OH and C_2H_5OD glasses after γ irradiation and measurement at 4°K. Contrary to results reported in the literature, there is no significant difference between the spectra obtained with C_2H_5OH and C_2H_5OD. Both spectra correspond to the infrared spectrum (with absorption maximum at 1500 nm) attributed to trapped electrons, i.e., electrons in shallow unrelaxed traps, rather than to the spectrum (with $\gamma_{max} \simeq 500$ nm at 4°K) of solvated electrons, i.e., electrons in relaxed traps. Consequently, it is concluded that γ irradiation of C_2H_5OD at 4°K produces trapped electrons that are indistinguishable from those produced by γ irradiation of C_2H_5OH at 4°K. (AIP)

29069 ESR STUDY OF PARAMAGNETIC CENTERS IN IRRADIATED $Ba(ClO_3)_2 \cdot H_2O$ AND $Ba(ClO_3)_2 \cdot D_2O$ SINGLE CRYSTALS. Suryanarayana, D.; Sobhanadri, J. (Department of Physics, Indian Institute of Technology, Madras−600036 , India). J. Chem. Phys. 61: No. 7, 2827-2833 (1 Oct 1974).

ESR study of γ−irradiated $Ba(ClO_3)_2 \cdot H_2O$ revealed three main centers which are identified as O_3^-, ClO_2, and (ClO_2-H_2O) radicals, trapped at two distinct sites. The parameters of the spin Hamiltonian have been determined from single crystal and powdered samples. The principal values for O_3^- and ClO_2 centers agree with those reported in other systems. The chlorine center having "superhyperfine" interaction with the two protons of water of crystallization has been identified as a (ClO_2-H_2O) radical. The principal values of the g tensor are $g_{xx}=2.0023$, $g_{yy}=2.0065$, and $g_{zz}=2.0150$; those of the A tensor are $a_{xx}=102.11$, $a_{yy}=53.22$, and $a_{zz}=7.79$ G. The parameters of the hyperfine coupling of ^{35}Cl with the first proton are $a_{xx}=8.6$, $a_{yy}=5.0$, and $a_{zz}=5.0$ G, with $a_{iso}=6.2$ G, and those for the second proton are $a_{xx}=2.5$, $a_{yy}=1.2$, and $a_{zz}=1.2$ G. The (ClO_2-H_2O) center is found to be bleached at temperatures (above 120°C), where the crystal loses its water of hydration. On exposing the irradiated crystal to uv light, the two chlorine centers ClO_2 and (ClO_2-H_2O) are fully bleached, followed by an increase in the concentration of the O_3^- center. (auth)

29070 REDUCTION IN ELECTRON IRRADIATION DAMAGE TO ORGANIC COMPOUNDS BY CONDUCTING COATINGS. Salih, S. M.; Cosslett, V. E. (Cambridge Univ., Eng.). Phil. Mag.; 30: No. 1, 225-228(Jul 1974).

By coating crystals of anthracene or coronene with a thin evaporated layer of aluminum or gold their sensitivity to electron irradiation, as judged by fading of the diffraction pattern, is reduced by a factor of three to five. (auth)

29071 RADIATION CHEMISTRY OF DNA-MODEL COMPOUNDS. V. PHOSPHATE ELIMINATION FROM RIBOSE-5-PHOSPHATE AFTER OH RADICAL ATTACK AT C4. Stelter, L.; von Sonntag, C.; Schulte-Frohlinde, D. (Max-Planck-Institut fuer Kohlenforschung, Munich). Int. J. Radiat. Biol.; 25: No. 5, 515-519(May 1974).

The products of ^{60}Co γ radiolysis of ribose-5-phosphate in aqueous solution were reduced with $NaBD_4$, trimethylsilylated, and analyzed by combined gas-liquid chromatography and mass spectrometry, to give evidence for the formation of inorganic phosphate and 5-deoxy-D-erythropentos-4-ulose. A mechanism is proposed for the formation of these products, and the implications for strand-breakage in DNA by γ rays discussed. (UK)

29072 STUDIES ON IRRADIATION OF AGAR−AGAR IN THE SOLID STATE. On the Changes of Penetration of Agar−Agar Hydrogel Produced by Irradiation. Nisizawa, M. (Defense Academy, Yokosuka, Kanagawa, Japan). Radiat. Eff.; 21: No. 4, 221-224(1974).

The effects of radiation on the formation of the agar-agar hydrogel were studied by measuring the penetration changes at different radiation doses and concentrations of added substances (sugar and potato starch). The behavior of penetration against the radiation and the added substances was observed as follows. The experimental equations for the penetration changes were given by (A) $P = a(\log X)^2 + b(\log X) + c$; (B) $P = b - a \log t$; (C) $P = b - a \log S$, where P is the relative penetration of the agar-agar hydrogel, X is the radiation dose, t is the elapsed time after irradiation, S is the concentration of the added substances, and a, b and c are adjustable constants. (auth)

29073 UNSTABLE INTERMEDIATES. CXXXVII. α-Bromoalkyl Radicals in Irradiated Organic Bromides: An Electron Spin Resonance Study. Mishra, S. P.; Neilson, G. W.; Symons, M. C. R. (Univ. of Leicester, Eng.). J. Chem. Soc., Faraday Trans., II; 70: No. 7, 1165-1174(1974).

Exposure of a range of organic bromides to ^{60}Co γ-rays at 77°K, either pure or in perdeuteromethanol gave, among others. radicals having esr features thought to be characteristic of α-bromo radicals, $R_2\dot{C}Br$. Analyses of such spectra are given, including the use of selected single crystal spectra and measurements at different microwave frequencies. The effect of the large bromine quadrupole interaction is indicated. It is concluded that the unpaired electron is delocalized onto bromine to the extent of ~19%, this being relatively insensitive to the nature of the other substituents. Exposure of bromomaleic acid to hydrogen atoms gave an α-bromo radical exhibiting a large hyperfine coupling (38 G) to a single hydrogen, which was shown to be the added atom by use of deuterium in place of hydrogen. For the radical $H_2C=CH\dot{C}HBr$ structure $H_2\dot{C}-CH=CHBr$ makes only a minor contribution. Possible radiation mechanisms are discussed. (auth)

29074 ELECTRON SPIN RESONANCE ABSORPTION SPECTRUM OF HCO_3^{2-} MOLECULE-IONS IN IRRADIATED SINGLE-CRYSTAL CALCITE. Cass, J.; Kent, R. S.; Marshall, S. A.; Zager, S. A. (Argonne National Lab., IL). J. Magn. Resonance; 14: No. 2, 170-181(May 1974).

ESR and ENDOR spectra of γ-irradiated naturally occurring single-crystal calcite have revealed the existence of a stable and hitherto undetected molecule-ion defect associated with hydrogen. The ESR absorption spectrum consists of six hyperfine structure doublets arising from paramagnetic centers with effective spin S = 1/2 and I = 1/2 at two sets of three equivalent lattice sites. From the mean of the principal values of the orthorhombic g tensor as well as from the intensity and magnitude of ^{13}C self-hyperfine structure and superhyperfine structure, the center appears to be similar to the CO_3^{3-} molecule-ion. ENDOR data identify the associated nucleus to be ^1H. Analysis of the isotropic and anisotropic contributions to the orthorhombic ^1H hyperfine structure tensor indicates that about 2.5% of the unpaired electron spin density is localized on the proton. From this and other evidence obtained from temperature-dependent linewidth studies over the range 200 to 300°K, it is suggested that the proton is a constituent of the paramagnetic molecule-ion. It is proposed that the defect center is HCO_3^{2-} and that it arises from the ionization of bicarbonate ion impurities in calcite. (auth)

29075 RADIOLYSIS OF ALKALINE-EARTH FLUORIDES. Call, P. J. (Oxford Univ.); Hayes, W.; Scott, J. P.; Hughes, A. E. (Oxford Univ.). J. Phys., C (London); 7: No. 14, 2417-2428(21 Jul 1974).

Alkaline earth fluorides were irradiated at temperatures between 4 and 300°K using electrons of energy 70 keV, 300 keV, and 1 MeV. The coloration produced was investigated by both EPR and optical methods. At 77°K and lower temperatures, a rapid first-stage coloration occurs, which saturates and is followed by a slower second-stage coloration. The first stage is characterized by perturbed F centers and compensating V_K centres. It seems that the perturbed F centers are associated with nearby interstitial fluorine ions but impurities may also be directly involved. The second stage is characterized by the production of isolated F centers and compensating H centers and appears to be the result of intrinsic radiolysis. Thermally induced annealing of the first- and second-stage coloration is investigated. The first stage coloration of BaF_2 is described in some detail in an Appendix. (auth)

29076 UNSTABLE INTERMEDIATES. CXLVI. Electron Spin Resonance Spectra for Linear $BrCN^-$ and Br_2CN Radicals in Irradiated Cyanogen Bromide Crystals. Mishra, S. P.; Neilson, G. W.; Symons, M. C. R. (Univ. of Leicester, Eng.). J. Chem. Soc., Faraday Trans., II; 70: No. 7, 1280-1287(1974).

On exposure to ^{60}Co γ-rays at 77°K, two well defined paramagnetic centers are formed in crystalline cyanogen bromide. One, identified as $BrCN^-$ had ^{81}Br hyperfine and g-tensors parallel to the molecular axis and for this and other reasons is thought to be linear, with the unpaired electron in a σ^* orbital largely confined to bromine and carbon. This makes an interesting contrast with the isostructural radicals $F\dot{C}O$ and $Cl\dot{C}O$ which are reported to be strongly bent. The other well-defined radical, containing two equivalent bromine atoms, is identified as $Br_2\dot{C}N$. A third, poorly defined radical containing two strongly coupled bromine atoms and exhibiting a large positive g-shift is tentatively identified as the cation dimer, $(BrCN)_2^+$. A fourth radical, formed on exposure of solutions of cyanogen bromide in dilute solution in acetic acid to γ-rays at 77°K is tentatively identified as H(Br)$\dot{C}$N. The structures of these new species are discussed together with possible damage mechanisms. (auth)

29077 RADIATION EFFECTS IN POLYETHYLENE FILMS STUDIED BY PULSE RADIOLYSIS. Johnson, G. R. A.; Willson, A. (Newcastle Upon Tyne Univ., Eng.). J. Chem. Soc., Chem. Commun.; No. 15, 577-578(7 Aug 1974).

Pulse radiolysis of polyethylene film produces an optical absorption band attributed to the trapped electron and, with aromatic compounds as scavengers, results in the formation of ions and excited states from these additives; the technique is applicable to films of other translucent materials. (auth)

29078 MOESSBAUER SPECTROSCOPIC STUDIES OF THE EFFECT OF THE OXALATE ANION IN THE SECOND COORDINATION SPHERE ON THE OXIDATION STATE OF ^{57}Fe PRODUCED IN EC-DECAY. Sano, H.; Ohnuma, T. (Tokyo Metropolitan Univ. (Japan). Faculty of Science). Chem. Phys. Lett.; 26: No. 3, 348-349(1 Jun 1974).

^{57}Fe-Mössbauer emission spectra of ^{57}Co-labelled $Co(NH_3)_{6\,2}(C_2O_4)_3 \cdot 4H_2O$ and $[Co(en)_{3\,2}](C_2O_4)_3 \cdot 9H_2O$ show an increased yield of ^{57}Fe(II) species. The stabilization of ferrous ^{57}Fe species is attributed to the consequences of an autoradiolytic process involving oxalate anions in the second co-ordination sphere. (auth)

29079 TRANSIENT SPECTRUM FROM NANOSECOND PULSE RADIOLYSIS OF LIQUID AMMONIA. Belloni, J.; Cordier, P.; Delaire, J. (Paris-11 Univ., 91-Orsay (France). Lab. de Physico-Chimie des Rayonnements). Chem. Phys. Lett.; 27: No. 2, 241-244(15 Jul 1974).

In addition to the absorption of the ammoniated electron, the transient absorption spectrum of irradiated liquid ammonia contains two ultraviolet bands at 250 nm and 320 nm. The latter is shown to be due neither to the NH_2 ion nor to NH singlet. There is conflicting evidence concerning its possible assignment to NH triplet. The G value of the ammoniated electron was found to be 3.0 at −48°C. At −45°C, the ammoniated electron decays with concurrent first and second order kinetics and it reacts with Cu^{2+} with the rate constant 1.5×10^{11} l mole^{-1} sec^{-1}. (auth)

29080 CHROMIUM–CARBON BONDS IN AQUEOUS SOLUTIONS. A Pulse Radiolytic Study. Cohen, H.; Meyerstein, D. (Negev Nuclear Research Center, Beersheba, Israel). Inorg. Chem.; 13: No. 10, 2434-2443(Oct 1974).

The specific rates of reaction of 16 aliphatic radicals with $Cr(H_2O)_6^{2+}$ were determined. The absorption spectra due to the chromium–carbon bonds in the products of these reactions were measured. The specific rates of aquation of these complexes as a function of pH were determined. The effects of the structure of the aliphatic radicals on these spectra and specific rates of reactions are discussed in detail. It was found that chromium induces water elimination when a β-hydroxyl group is present. Pulsed electrons at 5 MeV and γ radiation were used for the experiments. (auth)

29081 REACTION OF THE HYDRATED ELECTRON WITH BENZENE STUDIED BY PULSE RADIOLYSIS. Marketos, D. G. (Demokritos Nuclear Research Center, Athens); Marketou-Mantaka, A.; Stein, G. J. Phys. Chem.; 78: No. 20, 1987-1992(26 Sep 1974).

The reaction of the hydrated electron with benzene was studied by electron pulse radiolysis. The rate constant of this reaction was found $(1.3 \pm 0.5) \times 10^7$ M^{-1} sec^{-1} by following the pseudo-first-order disappearance of e_{aq}^- at 600 nm, in Ar-saturated aqueous benzene solutions, at pH 11 and 13, in the presence of OH radical scavengers (tert-butyl and isobutyl alcohol). The bimolecular rate constants of the disappearance of $C_6H_7\cdot$ and $C_6H_6OH\cdot$ were also determined as $(1.25 \pm 0.22) \times 10^9$ and $(7.05 \pm 0.35) \times 10^8$ M^{-1} sec^{-1}, respectively. The absorption maxima of the transient species $C_6H_6^-$, $C_6H_7\cdot$, and $C_6H_6OH\cdot$ were found at 312, 311, and 313 nm, respectively, and their molar extinction coefficients were calculated as $\epsilon^{312}_{C_6H_6^-} = 2450$ (±13%), $\epsilon^{311}_{C_6H_7\cdot}$ 5350 (±10%), and $\epsilon^{313}_{C_6H_6OH\cdot}$ 4700 (±13%) M^{-1} cm^{-1}. The observed absorption at 312 nm, under conditions where mostly electrons are present (pH neutral to 13, Ar-saturated, tert-butyl alcohol present), is consistent with the assumption that this absorption is due to the formation of $C_6H_6^-$ (B^-), which, under the present experimental conditions, rapidly disappears by bimolecular radical reactions before protonation. (auth)

29082 METHOD FOR PREPARATION OF BIOCOMPATIBLE AND BIOFUNCTIONAL MATERIALS AND PRODUCT THEREOF. Hoffman, A. S.; Schmer, G. (to United States Atomic Energy Commission). US Patent 3,826,678. 30 Jul 1974. Filed date 6 Jun 1972. 14p.

A method for the preparation of biocompatible and biofunctional surfaces is reported. It involves radiation grafting of a reactable compound selected from the group consisting of polymers and copolymers onto an inert polymeric substrate and thereafter chemically bonding a biologically active molecule to the reactable compound. Specific embodiments include chemically bonding of human serum albumin, heparin, streptokinase, prostaglandin E-1 and mixtures thereof of hydrogels of varying compositions with or without an intermediate smaller molecule or chemical "arm," such as ϵ-amino caproic acid or 1,4 diamino butane, the hydrogels having been previously radiation-grafted to tough inert polymeric substrate. A highly synergistic effect is achieved for hydrogels containing high water contents, e.g., above about 55%, when the chemically bonding of the biologically active molecules is carried out via an intermediate smaller molecule or chemical arm. For thin film substrates having radiation-grafted thereto hydrogels with $-CO_2H$ pendant functional groups which are activated with a carbodiimide solution, a quick wash of the thin film with ice water is required to effect subsequent chemical bonding of the biologically active molecules to the activated surface. The same technique is also required where a chemical arm is employed which has $-CO_2H$ pendant functional groups. (Official Gazette)

Radiochemistry and Nuclear Chemistry

Refer also to abstracts 31333 and 31334.

Hot-Atom Chemistry

Refer also to abstract 29078.

29083 (AED-CONF-74-084-002) SEPARATION OF RADIONUCLIDES USING ALKYL RADICALS. Hoffmann, P. (Technische Univ. Darmstadt (F.R. Germany). Fachbereich Anorganische Chemie und Kernchemie). 1974. 5p. (In German). (CONF-740342-1). INIS.

From meeting of lecturers in chemistry; Stuttgart, F.R. Germany (31 Mar 1974).

7 figs.

In investigation of complex nuclear reaction mixtures in the gas phase, alkyl compounds of the elements, readily volatile, are used at fairly high temperatures for the 3rd–7th main group and the 2nd subgroup. Th-288 is a suitable source for the elements Pb, Bi, Tl, and Po, which form the alkyl compounds. To prepare the alkyl compounds, one starts with alkyl radicals, which are obtained from $Pb(alkyl)_4$. An apparatus for gas phase reactions and separations is described, the alkyl radicals react in it with the radioactive secondary products of Th-228. The thermal stability of the alkyls is used to separate them. The number of separated atoms of Pb-212, Bi-212, Tl-208 was determined as a function of heating temperature. The α spectra, which were obtained by transport with ethyl radicals of Bi-212, Rn-220, Po-216, Po-212 were recorded and discussed. (GE)

29084 IDENTIFICATION OF HIGH-BOILING TRITIUM-LABELED COMPOUNDS FORMED IN REACTIONS OF TRITIUM RECOIL ATOMS WITH BENZENE. Ivanov, Yu. A.; Kukin, P. P.; Filatov, E. S. Sov. Radiochem. (Engl. Transl.); 15: No. 6, 910-912(1973).

Translated from Radiokhimiya; 15: No. 6, 893-895(1973).

High-boiling tritium-labeled compounds were identified by thin-layer chromatography on adsorption plates with heptane, chloroform, and their mixtures as the mobile phase. (LK)

29085 TRAJECTORY STUDIES OF HOT ATOM REACTIONS. II. An Unrestricted Potential for CH_5. Valencich, T.; Bunker, D. L. (Univ. of California, Irvine). J. Chem. Phys.; 61: No. 1, 21-29(1 Jul 1974).

An approximate empirical potential energy hypersurface has been fitted to a combination of experimental results and molecular structural information, by means of a trajectory analysis, without the restrictions imposed in Part I. On the basis of this, predictions are made for the incident energy dependence of the reactive cross sections when the reactants are $T + CH_4$, $T + CD_4$, $D + CH_4$, $H + CD_4$, and $H + CH_4$. The scattering properties and some aspects of the energy disposal in these reactions are also examined, and the most characteristic molecular dynamic features of the reactions are described. (auth)

Properties of Radioactive Materials

Refer also to abstracts 28941, 28986, 29006, 29053, 29078, 29384, 29648, and 29809.

29086 (AEC-tr-7575) RUTHENIUM VOLATILITY DURING VITRIFICATION OF FISSION PRODUCTS. Part II. Fixation on a Steel Tube. Peroxide Decomposition. de Bettencourt, A. O.; Jouan, A. (CEA Centre d'Etudes Nucleaires de Fontenay-aux-Roses, 92 (France)). Jan 1969. Translation of CEA-R-3663(2). 28p. Dep. NTIS $4.50.

A study on the thermal decomposition of ruthenium peroxide, RuO_4, and its deposition on steel channels is reported. The published literature on the properties of this compound is reviewed, and then in the first part of the study, its deposition on a steel tube is reported. A gas containing RuO_4 labeled with ^{106}Ru was passed through a stainless steel tube in which there was a temperature gradient decreasing in the direction of passage of the gas. The temperature at which the RuO_4 is deposited or fixed on the tube was determined, and the effect of gas velocity on this deposition was studied. In the second part, both static and kinetic methods were used to study the decomposition of ruthenium peroxide to the dioxide, $RuO_4 \rightarrow RuO_2 + O_2$. RuO_4 gas was introduced into the receiver located inside an electric furnace. The reaction was followed by gamma counting. (auth)

29087 (UCID-15809) METHOD OF ESTIMATING THE TOTAL CURIES IN GAS SAMPLES. Morris, G. A. (California Univ., Livermore (USA). Lawrence Livermore Lab.). 3 Mar 1971. Contract W-7405-eng-48. 9p. Dep. NTIS $4.00.

A method of estimating the number of curies of radioactive material in gas samples from device tests was found and some correlation of such estimates with radiation-meter readings outside the shielded samples was derived. (auth)

29088 BINDING OF ^{63}Ni TO RABBIT SERUM α_1-MACROGLOBULIN IN VIVO AND IN VITRO. Decsy, M. I.; Sunderman, F. W. Jr. (Univ. of Connecticut, Farmington). Bioinorg. Chem.; 3: No. 2, 95-105(1974).

Nickeloplasmin, the nickel-containing α_1-macroglobulin in rabbit serum, was labelled with ^{63}Ni in vivo and in vitro. Serums were obtained from rabbits at 2 and 8 hours after an iv injection of $^{63}NiCl_2$. Isolation of serum ^{63}Ni-nickeloplasmin which was labelled in vivo was accomplished by successive fractionations by column chromatography on Sephadex G-200 and by preparative electrophoresis on acrylamide gel. Labelling of nickeloplasmin with ^{63}Ni in vitro was achieved by mixing (a) serum ultrafiltrates from rabbits which had received iv $^{63}NiCl_2$, with (b) concentrated proteins obtained by ultrafiltration of serums collected from the same rabbits prior to injection of $^{63}NiCl_2$. ^{63}Ni-nickeloplasmin preparations which were labelled in vivo or in vitro yielded a single protein band on analytical acrylamide gel electrophoresis and were identified as an α_1-macroglobulin by immunodiffusion and immunoelectrophoresis. Nickeloplasmin was not labelled in vitro after incubation of dialyzed serum proteins with $^{63}NiCl_2$ nor after incubation of crude serum macroglobulins with $^{63}NiCl_2$. These findings suggest that ^{63}Ni-nickeloplasmin might be a ternary complex of serum α_1-macroglobulin with an ultrafiltrable ^{63}Ni-constituent of serum. (auth)

29089 COMPOUNDS OF RARE GASES. Wilhelmova, L.; Cejnar, F.; Peka, I. (Praha a Ustav Jaderneho Vyzkumu, Rez, Czech.). Chem. Listy; 68: No. 8, 775-791(Aug 1974). (In Czech).

Compounds of rare gases are reviewed with special respect to their preparation, physico-chemical properties, and their possible practical utilization. (auth)

29090 PREPARATION AND CHARACTERIZATION OF A NEW THALLIUM(I) URANATE(VI), Tl_4UO_5. Giridharan, A. S.; Udupa, M. R.; Aravamudan, G. (Indian Inst. of Tech., Madras). Z. Anorg. Allg. Chem.; 407: No. 3, 345-349(Aug 1974).

A new thallium(I) uranate(VI) of composition Tl_4UO_5 was isolated and characterized by x-ray, IR and chemical analyses. The compound dissociated into thallium(I) oxide and Tl_2UO_4 on heating to 230°C and its subsequent thermal behavior depended on the volatilization and oxidation characteristics of the thallium(I) oxide released. (auth)

29091 GASEOUS HALIDE COMPLEXES AND THEIR STABILITY. Binnewies, M.; Schaefer, H. (Univ., Muenster, Ger.). Z. Anorg. Allg. Chem.; 407: No. 3, 327-344(Aug 1974). (In German).

The following new complex molecules were observed by mass spectroscopy: $TlCuCl_2$, $TlCuCl_3$, $TlInCl_4$, Tl_2InCl_5, $CuInCl_4$, Cu_2InCl_5, Cu_3InCl_6, $CuIn_2Cl_7$, $CuAlCl_4$, Cu_2AlCl_5, Cu_3AlCl_6, $CuAl_2Cl_7$, $Cu_2Al_2Cl_8$, $AgThCl_5$, and $CuTh_2Cl_9$. The heats of formation of a number of complex molecules from the binary gaseous chlorides were determined: $TlCdCl_3$, $TlPbCl_3$, $TlInCl_4$, $CuThCl_5$, $TlThCl_5$, $CuUCl_5$, $TlUCl_5$, $CdPbCl_4$, $BeInCl_5$, $ZnInCl_5$, $SnInCl_5$, $InUCl_8$, Tl_2InCl_5, Cu_2ThCl_6, $CuTh_2Cl_9$, Tl_2ThCl_6, Cu_2UCl_6, Tl_2UCl_6, TlU_2Cl_9, Be_2InCl_7, Be_3InCl_9, and $ThUCl_8$. Associative enthalpies for the formation of molecules Cu_4Cl_4, Cu_5Cl_5, Tl_2Cl_2, Sn_2Cl_4, In_2Cl_6, Th_2Cl_8, and U_2Cl_8 were determined. (LK)

29092 MECHANISM OF REDUCTION OF 1-METHYL-4-THIOCYANATOURACIL BY BISULFIDE. A Route to in Vitro Labeling of tRNAs with Sulfur-35. Pal, B. C.; Schmidt, D. G. (Oak Ridge National Lab., TN). J. Amer. Chem. Soc.; 96: No. 18, 5943-5944(4 Sep 1974).

The mechanism of the reaction of R SCN with SH^- was investigated and results indicated that 70% of the reaction proceeds with ring C-S bond fission. Attempts to label mixed E. coli · tRNAs in vitro with $^{35}SH^-$ were successful. It was demonstrated that the radioactivity was located in the 4-thiouridine moiety of the tRNA. (MCG)

29093 CHEMISTRY OF AMERICIUM. II. Behavior of Am(III), Am(V), and Am(VI) in Column Chromatography, With bis(2-ethylhexyl)Phosphoric Acid Used as the Extractant. Hara, M.; Suzuki, S. (Tohoku Univ., Sendai). Bull. Chem. Soc. Jap.; 47: No. 3, 635-638(Mar 1974).

The behavior of Am(III), Am(V), and Am(VI) in column chromatography with bis(2-ethylhexyl)phosphoric acid (HDEHP) used as the extractant were investigated in comparison with that of Np(IV), Np(V), and Np(VI). When the solution of Am(VI) was submitted to the column chromatography, it was found that Am(VI) was rapidly reduced to Am(V) and partially to Am(III) by HDEHP, irrespective of the conditions, such as the flow rate, the acidity, and the composition and temperature of the influent. The optimum conditions for the separation of Am(V) and Am(III) and for the preparation of the Am(V) solution were established by utilizing the difference in the adsorbability on the column bed between Am(III) and Am(V). When a freshly prepared Am(V) solution was submitted to column chromatography, it was found that Am(V) was also reduced to Am(III) as well as Am(VI) by HDEHP. The percentage of the Am(V) fraction eluted strongly depended on the conditions in the column chromatography, but it was found to be constant within the limits of experimental error under definite conditions as long as the same column was used. This fact was applied to the determination of the Am(V) content in the mixed solution of Am(III) and Am(V). The content of Am(V) decreased slowly in the nitrate, acetate, sulfate, and perchlorate solutions at lower temperatures, but it rapidly decreased in the chloride, iodide, sulfite, and hydrogen peroxide solutions even at 0°C. The content of Am(V) decreased more rapidly at higher temperatures, and the kinetic analysis showed that the reduction of Am(V) apparently followed the first-order kinetics in the acetate solutions. (auth)

29094 MAGNETIC SUSCEPTIBILITIES OF OCTACOORDINATED URANIUM(IV) COMPLEXES. Yoshimura, T.; Miyake, C.; Imoto, S. (Osaka Univ., Suita, Japan). Bull. Chem. Soc. Jap.; 47: No. 3, 515-518(Mar 1974).

Magnetic susceptibility measurements were carried out on octacoordinated uranium(IV) complexes, such as tetrakis(acetylacetonato)uranium(IV), tetrakis(trifluoroacetylacetonato)uranium(IV), tetrakis(benzoylacetonato)uranium(IV), tetrakis(dibenzoylmethanoto) uranium(IV), tetrakis(thenoyltrifluoroacetonato)uranium (IV), tetrakis(cupferronato)uranium (IV), and uranium(IV)tetrachloride, in the temperature range from room temperature to the temperature of liquid nitrogen or liquid helium. The Curie-Weiss law holds above the temperature of liquid nitrogen, with a magnetic moment of 3.5–2.92 BM. For the latter two complexes, a temperature-independent paramagnetism was observed in the low temperature range; the other complexes also seemed to show the same trend. We tried to interpret the magnetic behavior on the basis of the crystal-field model of the square antiprism structure or the dodecahedron structure of the complexes. (auth)

29095 FUSIBILITY DIAGRAM OF THE SYSTEM $LiCl-UCl_4-ThCl_4$. Desyatnik, V. N.; Vokhmyakov, A. N.; Kurbatov, N. N.; Raspopin, S. P. (Ural Polytechnic Inst., Sverdlovsk, USSR). Izv. Vyssh. Ucheb. Zaved., Tsvet. Met.; No. 3, 107-109(1974). (In Russian).

Fusibility diagrams of the $LiCl-UCl_4-ThCl_4$ system showed that the components of the system form a low-melting composition which may be used as an electrolyte in preparing, refining, or separating U and Th by an electrolytic method. (tr-auth)

29096 POST-EFFECTS OF ELECTRON CAPTURE IN ^{57}Co IN SYSTEMS CONTAINING COBALT NITRATE AND SULFATE. Bondarevskii, S. I.; Tarasov, V. A.; Shcherbakov, E. E. Sov Radiochem. (Engl. Transl.); 15: No. 6, 913-914(1973).

Translated from Radiokhimiya; 15: No. 6, 895-897(1973).

Post-effects of electron capture in ^{57}Co in frozen solutions were studied using carrier-free preparations of $^{57}CoSO_4$ and $^{57}Co(NO_3)$, samples of $CoSO_4$ and $Co(NO_3)_2 \cdot 6N_2O$ labeled with ^{57}Co, and their frozen solutions in CH_3OH, $(CN_3)_2CO$, H_2SO_4, and HNO_3. The results obtained agree with the results for converted isomeric transition in ^{119m}Sn in frozen alcohol, acetone, and acid solutions, are explained by the model proposed by Bondarevskii and Tarasov [Radiokhimiya 14(1), 162 (1972)], and indicate the analogy in the effect of the properties of the immediate environment of the decaying atoms on their form of stabilization in a converted isomeric transition in ^{119m}Sn and in an electron capture in ^{57}Co. (LK)

29097 POST-EFFECT OF ELECTRON CAPTURE IN ^{57}Co ATOMS SORBED ON CATION EXCHANGE RESINS WITH DIFFERENT DEGREES OF CROSS-LINKING. Ablesimov, N. E.; Bondarevskii, S. I. Sov. Radiochem. (Engl. Transl.); 15: No. 6, 908-909(1973).

Translated from Radiokhimiya; 15: No. 6, 892-893(1973).

The Moessbauer method was used to study the post-effect of EC in ^{57}Co atoms on cationites of the type KU-2 and KB-4 with different degrees of cross-linking. In samples of KU-2 the fraction of Fe(III) increases with a decrease in the DVB content of the copolymer; in KB-4 it is practically constant. This can be explained by a difference in the sorption mechanism for the two ionites; KU-2 resins have an ionic type of bond, while transition metal ions are sorbed in KB-4 resins through the formation of a coordination group. (LK)

29098 POST-EFFECT OF ELECTRON CAPTURE IN THE EUTECTIC ($NH_4NO_3-LiNO_3$):^{57}Co AT 77°K. Bondarevskii, S. I.; Izotov, V. I.; Ozernoi, A. N. Sov. Radiochem. (Engl. Transl.); 15: No. 6, 906-907(1973).

Translated from Radiokhimiya; 15: No. 6, 891-892(1973).

The effect of the concentration of $^{57}Co^{2+}$ and Cl^- on the yield of the valence forms of the daughter atoms ^{57m}Fe in quenched melts of the eutectic mixture $LiNO_3$ (27.5 mole %) + NH_4NO_3 (72.5 mole %) was studied. An increase in chloride ion concentration causes the formation of the associates $[CoCl_x(NO_3)_{4-x}]^{2-}$ up to the tetrachloro complex. The independence of the Fe(II)/Fe(III) ratio in the nuclear gamma resonance emission spectra of the chloride ion concentration up to m = 2.5 for samples with a cobalt content m = 0.5 is explained by the low ratio of the numbers of Cl and Co atoms. (LK)

29099 EFFECT OF PHYSICO-CHEMICAL PROPERTIES OF LOCAL ENVIRONMENT OF ^{57}Co MOESSBAUER ATOMS SORBED ON ION EXCHANGE MATERIALS ON THEIR STABILIZATION FORM AFTER ELECTRON CAPTURE. Ablesimov, N. E.; Bondarevskii, S. I. Sov. Radiochem. (Engl. Transl.); 15: No. 6, 903-905(1973).

Translated from Radiokhimiya; 15: No. 6, 889-891(1973).

The stabilization forms of ^{57}Co atoms sorbed on anionites (titanium hydroxide and the carbocationite KB-4P-2) after electron capture and the effect on the ratio of these forms of various organic and inorganic adsorbates in different aggregation states were studied. Results show that the occurrence of post-effects of nuclear conversions in atoms sorbed on ion exchange materials depends on the strength of the bond of the radioactive atom to the ionite matrix and on the electron acceptor properties of the immediate environment of the Moessbauer atoms. (LK)

29100 REACTION OF DI-2-ETHYLHEXYLPHOSPHORIC ACID AND ITS URANYL SALT WITH DILUENTS. IV. SOLUTIONS OF $(HR)_2$ AND $UO_2(HR_2)_2$ IN CARBON TETRACHLORIDE. Rozen, A. M.; Yurkin, V. G. Sov. Radiochem. (Engl. Transl.); 15: No. 6, 869-871(1973).

Translated from Radiokhimiya; 15: No. 6, 862-864(1973).

From the vapor pressures of CCl_4 the activity coefficients of D2EHPA $(HR)_2$ and its uranyl salt $UO_2(HR_2)_2$ in mixtures with CCl_4 at 10, 25, and 40°C were determined. The heats of mixing were also determined. The high negative nonideality of the solutions with an extremely small negative enthalpy of mixing is explained mainly by the athermal entropy effect due to dimerization of the D2EHPA, which leads to an increase in the size of the molecules and a decrease both in their polarity and their capacity for chemical interaction with CCl_4. The enthalpy of the weak chemical interaction of CCl_4 with $(HR)_2$ and $UO_2(HR_2)_2$ was estimated. (auth)

29101 REACTION OF DI-2-ETHYLHEXYLPHOSPHORIC ACID AND ITS URANYL SALT WITH DILUENTS. V. Solutions of $(HR)_2$ and $UO_2(HR_2)_2$ in Chloroform. Rozen, A. M.; Yurkin, V. G. Sov. Radiochem. (Engl. Transl.); 15: No. 6, 872-874(1973).

Translated from Radiokhimiya; 15: No. 6, 864-866(1973).

From the vapor pressure of $CHCl_3$ the activity coefficients of D2EHPA $(HR)_2$ and its uranyl salt $UO_2(HR_2)_2$ in mixtures with $CHCl_3$ at 10, 25, and 40°C were determined. The heats of mixing were also determined. The high negative nonideality of the solutions is explained by the athermal entropy effect and the chemical interaction of $(HR)_2$ and $UO_2(HR_2)_2$ with $CHCl_3$; the latter is somewhat weakened in comparison with analogous systems with TBP because of the dimerization of D2EHPA. The enthalpy of the chemical interaction of $CHCl_3$ with $(HR)_2$ and $UO_2(HR_2)_2$ was estimated. (auth)

29102 KINETICS OF URANIUM(IV)–NEPTUNIUM(VI) REACTION IN TRIBUTYL PHOSPHATE SOLUTIONS. Frolova, L. M.; Timofeev, G. A.; Rykov, A. G. Sov. Radiochem. (Engl. Transl.), 15: No. 6, 875-877(1973).

Translated from Radiokhimiya; 15: No. 6, 867-868(1973).

The results of studying the kinetics of the oxidation of uranium (IV) by neptunium (VI) ions are reported. The kinetics of the uranium (IV)–neptunium (VI) reaction were studied spectrophotometrically, and the reaction rate was determined from the change with time in the concentration of neptunium (V) accumulating. (LK)

29103 KINETICS OF OXIDATION OF URANIUM OXYSULFIDE. Dunaeva, K. M.; Dubrovin, A. V.; Koval'chuk, V. Yu.; Ippolitova, E. A. Sov. Radiochem. (Engl. Transl.); 15: No. 6, 878-880(1973).

Translated from Radiokhimiya; 15: No. 6, 869-870(1973).

Results from the study on the kinetics of oxidation of uranium oxysulfide to uranyl sulfate over the temperature range 400-500°C are reported. (LK)

29104 SOME CHARACTERISTICS OF THE REACTION OF AMERICIUM(VI) WITH REDUCING AGENTS IN AQUEOUS SOLUTIONS. Shilov, V. P.; Nikolaevskii, V. B.; Krot, N. N. Sov. Radiochem. (Engl. Transl.); 15: No. 6, 881-882(1973).

Translated from Radiokhimiya; 15: No. 6, 871-872(1973).

The reaction of americium (VI) with following complex forming agents was studied: oxalic acid, EDTA, tartaric acid, citric acid, hydrochloric acid, formic acid, formaldehyde, lithium sulfates, hydrogen peroxide, hydrazine, and hydroxylamine. (LK)

29105 OXIDATION–REDUCTION REACTIONS OF ACTINIDE ELEMENTS. XXIII. Kinetics of Neptunium(V)–Americium(V) Reaction in Perchlorate Solutions. Rykov, A. G.; Timofeev, G. A.; Chistyakov, V. M. Sov. Radiochem. (Engl. Transl.); 15: No. 6, 883-885(1973).

Translated from Radiokhimiya; 15: No. 6, 872-874(1973).

The kinetics of the neptunium(V)–americium(V) reaction were studied spectrophotometrically. The oxidation of neptunium(V) by americium(V) ions is an irreversible reaction of overall second order. (LK)

29106 OXIDATION–REDUCTION REACTIONS OF ACTINIDE ELEMENTS. XXIV. Kinetics of Uranium(IV)–Iron(III) Reaction in Water–Isopropanol Solutions. Rykov, A. G.; Frolava, L. M.; Timofeev, G. A. Sov. Radiochem. (Engl. Transl.); 15: No. 6, 886-887(1973).

Translated from Radiokhimiya; 15: No. 6, 875-876(1973).

Results from a study of the kinetics of the uranium(IV)–iron(III) reaction in water–isopropanol solutions are reported. The rate of the oxidation–reduction reaction is determined not by the properties of the components of the solvent, but primarily by its donor power as a whole. (LK)

29107 DEPOLYMERIZATION OF COLLOIDAL NEPTUNIUM IN NITRIC ACID SOLUTIONS. Ramazanov. L. M.; Goncharuk, L. V.; Sokhina, L. P. Sov. Radiochem. (Engl. Transl.); 15: No. 6, 888-891(1973).

Translated from Radiokhimiya; 15: No. 6, 876-879(1973).

A study was made of the depolymerization of colloidal neptunium by nitric acid solutions (4 and 6 M). Freshly prepared colloidal neptunium is broken down by nitric acid with a concentration ≥4 M. The rate of depolymerization increases with an increase in the acidity of the solution. The time for complete depolymerization equals ~17 h in 4 M nitric acid and 3 h in 6 M. Raising the temperature to 50°C reduces the time for complete depolymerization of colloidal neptunium in 4 M nitric acid to 40 min. It was established that with a nitric acid concentration less than 4 M there is coagulation and precipitation of a polymer and its breakdown is considerably retarded. (auth)

29108 COMPOUNDS OF TETRAVALENT URANIUM WITH COMPLEX CATIONS OF PLATINUM. Grinberg, A. A.; Petrzhak, G. I.; Lozhkina, G. S. Sov. Radiochem. (Engl. Transl.); 15: No. 6, 892-893(1973).

Translated from Radiokhimiya; 15: No. 6, 879-880(1973).

The following complex salts of uranium (IV) were synthesized for the first time: $[Pt(NH_3)_4]_2[U(C_4H_4O_6)_2(C_2O_4)_2]$–tetrammineplatinum (II) ditartratodioxalatouraneate and $[Pt(NH_3)_6][U(C_2O_4)_4] \cdot 3H_2O$–hexammineplatinum (IV) tetraoxalatouraneate. The derivative of uranooxalic acid with the quadruply charged cation of platinum (IV) is much less soluble in water than salts of uranooxalic acid with singly, triply, and quadruply charged complex cations. (auth)

29109 STABILIZATION OF DAUGHTER ^{99m}Tc AFTER β-DECAY OF ^{99}Mo IN THE HEXACARBONYL MOLYBDENUM MOLECULE. Nefedov, V. D.; Mikulai, V. Sov. Radiochem. (Engl. Transl.); 15: No. 6, 855-860(1973).

Translated from Radiokhimiya; 15: No. 6, 846-852(1973).

A method was developed for determining the chemical forms of stabilization of ^{99m}Tc after β-decay of ^{99}Mo in the molybdenum hexacarbonyl molecule. The main chemical forms in which the ^{99m}Tc is stabilized are as follows: the complex cation $[^{99m}Tc(CO)_6]^+$

(yield about 65%), so-called "volatile" ^{99m}Tc (not extracted into the aqueous phase, 30%), and pertechnate $^{99m}TcO_4^-$. The yield of the complex cation is mainly independent of the medium in which the decay occurs (carbonyl crystals) and the carbonyl in organic solvents). The chemical consequences of the β-decay of ^{99}Mo in the $Mo(CO)_6$ molecule may be used as a convenient method of obtaining the complex cation $[^{99m}Tc(CO)_6]^+$ in tracer amounts. (auth)

29110 REACTION OF URANIUM WITH A MIXTURE OF LITHIUM AND CALCIUM FLUORIDES. Kashcheev, I. N.; Zolotarev, A. B. Sov. Radiochem. (Engl. Transl.); 15: No. 6, 833-836(1973).

Translated from Radiokhimiya; 15: No. 6, 823-826(1973).

It was established that under nonequilibrium conditions uranium passes into a melt of alkali metal fluorides with the formation of an involatile uranium fluoride and the liberation of an alkali metal. When uranium passes into a melt of an $LiF-CaF_2$ mixture two salt layers are formed and of these the lower has a considerable uranium content, while the upper has a low concentration of this metal. An investigation of the change in the uranium content in these layers and their relative amount with time showed that the limiting stage of the process is diffusion of the reaction components to the interphase. (auth)

29111 ELECTROCHEMICAL INVESTIGATION OF AMALGAMS OF RARE EARTH METALS. I. Main Electrochemical Properties of Amalgams of Rare Earth Elements. Usenova, K. A.; Aigaraeva, M. M.; Osipova, G. V.; Enikeev, R. Sh. Sov. Radiochem. (Engl. Transl.); 15: No. 6, 837-841(1973).

Translated from Radiokhimiya; 15: No. 6, 826-831(1973).

Homogeneous amalgams of REM, which have no stable divalent state, decompose in aqueous solutions in accordance with a first-order reaction equation of their potentials are kept constant during the decomposition process; heterogeneous amalgams of these metals decompose at a constant rate under the given conditions. On the basis of the differences in the laws of decomposition of homogeneous and heterogeneous amalgams of REM in aqueous solutions it is possible to determine the solubility of these metals in mercury. (auth)

29112 REACTION BETWEEN PLUTONIUM(III) AND NITROUS ACID. II. Kinetics of Forward Reaction. Koltunov, V. S.; Marchenko, V. I. Sov. Radiochem. (Engl. Transl.); 15: No. 6, 787-790(1973).

Translated from Radiokhimiya; 15: No. 6, 777-781(1973).

A study was made of the kinetics of oxidation of Pu^{3+} ions by nitrous acid in HNO_3 solution with an ionic strength $\mu = 2$. It was found that the order of reaction relative to Pu(III)equals 1, relative to HNO_2 and H^+ ions 0.5, and relative to NO_3^- ions ~0.4. The rate constant of the reaction $k_1 = 1.55\ M^{-1.4} \cdot min^{-1}$ at 25°C with $\mu = 2$. The thermodynamic activation parameters were determined: $\Delta H_1^* = 13.9$ kcal/mole, $\Delta S_1^* = -19.1$ cal/mole · deg, and $\Delta F_1^* = 19.6$ kcal/mole. The mechanism of the reaction between Pu(III)and HNO_2 corresponding to the kinetic results obtained is discussed. The slow stage of the reaction is the reaction of Pu^{3+} ions with nitrogen peroxide. (auth)

29113 REACTION BETWEEN PLUTONIUM(III) AND NITROUS ACID. III. Kinetics of Reverse Reaction. Koltunov, V. S.; Marchenko, V. I. Sov. Radiochem. (Engl. Transl.); 15: No. 6, 791-795(1973).

Translated from Radiokhimiya; 15: No. 6, 781-786(1973).

A study was made of the kinetics of the reduction of Pu^{4+} ions by nitrous acid in nitric acid solution with an ionic strength $\mu = 2$. It was established that the reaction is first order with respect to Pu(IV)and HNO_2. The order of reaction with respect to H^+ ions equals 1. The rate constant of the reaction $k_2 = 1.22 \pm 0.22\ min^{-1}$ at 25°C with $\mu = 2$. The thermodynamic parameters of the activation of the reaction were determined: $\Delta H_2^* = 23.4$ kcal/mole, $\Delta S_2^* = 12.1$ kcal/mole · deg, and $\Delta F_2^* = 19.8$ kcal/mole. The mechanism of the reaction between Pu(IV)and HNO_2, which includes as the slow stage the reaction of Pu^{4+} and NO_2^- ions, was discussed. (auth)

29114 KINETICS OF REDUCTION OF PLUTONIUM(VI) BY OXALATE IONS. Zakharova, F. A.; Orlova, M. M.; Krot, N. N. Sov. Radiochem. (Engl. Transl.); 15: No. 6, 796-799(1973).

Translated from Radiokhimiya; 15: No. 6, 786-789(1973).

By a spectrophotometric method a study was made of the kinetics of reduction of plutonium(VI) by oxalate ions in relation to temperature, the concentration of oxalic acid, and the pH. It was shown that the reaction of Pu(VI) with oxalic acid proceeds by a complex mechanism, which includes a stepwise complex formation reaction. The rate of reduction of Pu(VI) by oxalic acid is strongly dependent on temperature. From the temperature dependence of the rate constant of the reduction we found the activation energy of the reaction in 0.02 M $H_2C_2O_4$ with an H^+ concentration of 1 M and $\mu = 1$, E = 27.86 kcal/mole. Great similarity was observed in the behavior of PuO_2^{2+} and NpO_2^{2+} ions in oxalate media. (auth)

29115 KINETICS OF REDUCTION OF NEPTUNIUM BY HYDRAZINE. III. Reduction of Np(V) To Np(IV) In Perchloric Acid. Koltunov, V. S.; Tikhonov, M. F. Soc. Radiochem. (Engl. Transl.); 15: No. 6, 800-804(1973).

Translated from Radiokhimiya; 15: No. 6, 789-794(1973).

The kinetics of the reduction of Np(V) to Np(IV) in $HClO_4$ solution with an ionic strength $\mu = 5$ over the ranges $[H^+] = 2-4.9$ M and $[N_2H_4] = 0.1-1$ M at temperatures of 61−92°C were investigated by a spectrophotometric method. It was shown that the reaction proceeds by two parallel routes, namely, through the disproportionation of Np(V) and through the direct reaction of Np(V) with hydrazine. The stoichiometry of both reactions is described by the equation $2NpO_2^+ + 2N_2H_4 + 8H^+ = 2Np^{4+} + 2NH_4^+ + N_2 + 4H_2O$. The rate of reduction of Np(V) by hydrazine without taking into account the disproportionation is given by $-d[Np(V)]/dt = k[Np(V)][N_2H_4][H^+]^3$, where $k = (5.80 \pm 0.36) \cdot 10^{-4}\ M^{-4} \cdot min^{-1}$ at 92°C with $\mu = 5$. The activation energy of the reaction is 24.5 ± 0.5 kcal/mole, the enthalpy of activation $\Delta H^* = 23.9$ kcal/mole, the entropy $\Delta S^* = 7$ entropy units, and the free energy of activation $\Delta F^* = 21.8$ kcal/mole (at 25°C). The mechanism of the reaction consists of the interaction of $NpO_2H_2^{3+}$ and $N_2H_6^{2+}$ ions in the slow stage, dimerization of the N_2H_3 radicals formed and decomposition of the tetrazine in subsequent fast stages. (auth)

29116 FORMATION OF COLLOIDAL NEPTUNIUM IN NITRIC ACID SOLUTIONS. Sokhina, L. P; Ramazanov, L. M.; Goncharuk, L. V. Sov. Radiochem. (Engl. Transl.); 15: No. 6, 805-810(1973).

Translated from Radiokhimiya; 15: No. 6, 794-801(1973).

By spectrophotometry and dialysis it was shown that neptunium(IV) in nitric acid solutions (≤0.3 M) may exist in a colloidal state. Conditions were found for obtaining colloidal neptunium(IV) by dissolving neptunium(IV) hydroxide in weak acid (≤0.3 M) at a temperature ≥50°C and also by diluting concentrated acid solutions of tetravalent neptunium with boiling water. The neptunium colloid formation process is more intensive the lower the acidity and the higher the temperature of weakly acid solutions. Depending on these conditions, up to 70% of the neptunium in a solution may be in a colloidal form. (auth)

29117 PREPARATION OF COMPLEX PERXENATES OF SOME ACTINIDE ELEMENTS. Gusev, Yu. K.; Mefod'eva.; M. P.; Kirin, I. S. Sov. Radiochem. (Engl. Transl.); 15: No. 6, 811-813(1973).

Translated from Radiokhimiya; 15: No. 6, 801-804(1973).

Some perxenates of Th(IV), U(VI), Np(VI), and Pu(VI) were isolated in a solid form. The complex nature of the compounds obtained was noted. (auth)

29118 COMPLEX FORMATION OF ACTINIDES AND LANTHANIDES WITH O-PHTHALIC, 3-NITROPHTHALIC, AND 4-NITROPHTHALIC ACIDS. I. Complex Formation of Uranium. Nikol'skii, B. P.; Krylov, L. I.; Zakhvataev, B. B.; Lyubtsev, R. I. Sov. Radiochem. (Engl. Transl.); 15: No. 6, 814-819(1973).

Translated from Radiokhimiya; No. 6, 804-809(1973).

By an ion exchange method we studied complex formation of uranium(VI) with o-phthalic, 3-nitrophthalic, and 4-nitrophthalic acids. In weakly acid solutions (pH = 3.2 to 3.6) complexes are formed with only anions of the second stage in the dissociation of the organic acids and the stability constants of complexes of uranyl with the anions of o-phthalic, 3-nitrophthalic, and 4-nitrophthalic acids with an ionic strength I = 1.0 ($NaNO_3$) are 1.3×10^4 for o-phthalic, 4×10^3 for 3-nitrophthalic, and 4×10^3 for 4-nitrophthalic acid. One ligand is present in the complex formed in the solution. It was shown that at pH = 3.2-3.6 no complexes are formed by uranium with anions of the first stage of dissociation of the organic acids studied. Thus, the introduction of a nitro group into the molecule of o-phthalic acid in positions 3 and 4 has the same, relatively weak effect on the stability of complexes of the corresponding anions with the uranyl ion in aqueous solution. (auth)

29119 COMPLEX FORMATION OF ACTINIDES AND LANTHANIDES WITH ORTHOPHTHALIC, 3-NITROPHTHALIC, AND 4-NITROPHTHALIC ACIDS. II. Complex Formation of Radioeuropium. Nikol'skii, B. P.; Krylov, L. I.; Zakhvataev, B. B. Sov. Radiochem. (Engl. Transl.); 15: No. 6, 820-822(1973).

Translated from Radiokhimiya; 15: No. 6, 810-813(1973).

Complex formation of europium with o-phthalic, 3-nitrophthalic, and 4-nitrophthalic acids was studied by ion exchange methods. It was shown that in weakly acid solutions (pH = 3.0-4.4) complexes are formed with anions of the second stage of dissociation of the organic acids. The stability constants of the complexes of europium with anions of orthophthalic, 3-nitrophthalic, and 4-nitrophthalic acids were calculated for a solution ionic strength I = 1.0 ($NaNO_3$) at T = 20°C: $K_{0-pht} = 0.6 \cdot 10^4$, $K_{3-npht} = 2.5 \cdot 10^2$, and $K_{4-npht} = 1.98 \cdot 10^2$. It was shown that at pH = 3-4.4 there is no complex formation between europium and anions of the first dissociation stage of the acids studied. (auth)

29120 INVESTIGATION OF COMPLEX FORMATION OF POLONIUM BY AN ION EXCHANGE METHOD. Ampelogova, N. I. Sov. Radiochem. (Engl. Transl.); 15: No. 6, 823-829(1973).
Translated from Radiokhimiya; 15: No. 6, 813-820(1973).

The concentration stability constants of the following complexes of polonium were determined by an ion exchange method: nitrates ($\beta_1 = 3.6 \pm 1$, $\beta_2 = 14 \pm 1.5$, $\beta_3 = 20 \pm 3$), sulfates ($\beta_1 = 29 \pm 7.5$, $\beta_2 = 2.4 \pm 0.9 \cdot 10^3$), acetates ($\beta_1 = 3.2 \pm 0.5 \cdot 10^2$, $\beta_2 = 7 \pm 1 \cdot 10^4$, $\beta_3 = 1.5 \cdot 10^7$), and oxalates ($\beta_1 = 1.7 \pm 0.2 \cdot 10^5$, $\beta_2 = 5.5 \pm 0.5 \cdot 10^9$). It was shown that the stability of polonium complexes decreases in the following sequence: $OH^- > Acac^- > TTA^- > HEDTA^{3-} > C_2O_4^{2-} > DBP^- > HCitr^{2-} \geq Tart^{2-} > HNTA^{2-} > Ac^- > Cl^- > SO_4^{2-} (\approx PO_4^{3-}) > NO_3^- \gg ClO_4^-$. (auth)

29121 HYDROLYSIS OF TRANSURANIUM ELEMENTS. II. Hydrolysis of Americium(III) in the Presence of Ions With Positive and Negative Hydration Energies. Korotkin, Yu. S. Sov. Radiochem. (Engl. Transl.); 15: No. 6, 776-781(1973).
Translated from Radiokhimiya; 15: No. 6, 766-772(1973).

The hydrolysis of americium(III) ions (10^{-6} M) was studied in HNO_3 and $HClO_4$ solutions with a constant ionic strength over the pH range of 1–11. It was shown that ions with positive and negative hydration energies have different effects on the hydrolysis process. It was shown that reliable data on hydrolysis processes may be obtained by means of distribution chromatography on paper. (auth)

29122 DERIVATOGRAPHIC INVESTIGATIONS ON THE THERMAL DEGRADATION OF PYRIDINE, ISOQUINOLINE, α,α-DIPYRIDYL AND O-PHENANTROLINE, RESP. BICHROMATE- OR CHROMATE-ION CONTAINING METAL COMPLEXES. II. Zinc (II)-, Cadmium(II)-, and Manganese(II)-Complexes. III. Mercury (I and II)-, Uranyl-, Thorium-, Lanthanum-, and Iron-Complexes. Lorant, B. (Hauptstadt, Budapest). Thermochim. Acta; 9: No. 1, 67-75(May 1974). (In German).

Complexes were prepared of zinc(II), cadmium(II), manganese(II), mercury(I and II), uranium, thorium(IV), lanthanum, and iron ions with pyridine, isoquinoline, α,α-dipydiyl, or o-phenantroline ligands and bichromate of chromate ions. As is the case with Cu(II), Ni(II) and Co(II) complexes, the initial decomposition temperatures increase from the pyridine complexes to the phenantroline complexes. The decompositions generally took place in two steps, but sometimes in one step only. Among the zinc complexes some were found in which base was present instead of water of hydration in the crystal lattice. The final products were the corresponding metal oxides, apart from chromium(III) oxide, or the corresponding chromates in the case of insufficient heating. With the mercury complexes the oxides were removed completely. Some complexes decomposed explosively. The formulas were checked. Several complexes contained water of hydration. The analytical usefulness is equal to that of the complexes dealt with in the first article of this series (Thermochim. Acta, vol. 6 (1973) p. 205). (NL)

29123 LABELLED COMPOUNDS. P. 18. Chlorine Exchange Between Antimony(III) Chloride-(^{36}Cl) and Hexachloropropene (1). Boberg, F.; Kresse, J. (Technische Univ. Clausthal, Clausthal-Zellerfeld (F. R. Germany). Organisch-Chemisches Inst.). Z. Naturforsch., b; 29: No. 3/4, 213-218(Apr 1974). (In German).

$SbCl_3$-(^{36}Cl) is prepared from $SbCl_3$ and NaCl-(^{36}Cl). In the homogeneous system $SbCl_3$-(^{36}Cl)/$CCl_3-CCl \rightarrow CCl_2$/$CH_2Cl_2$ and in the heterogeneous system $SbCl_3$-(^{36}Cl)/$CCl_3-CCl \rightarrow CCl_2$, with solid $SbCl_3$-(^{36}Cl), at 0 to 65°C $CCl_3-CCl \rightarrow CCl_2$ is only labelled at C-1 and C-3; at 150°C in the system $SbCl_3$-(^{36}Cl)/$CCl_3-CCl \rightarrow CCl_2$ C-2 is labelled too. Carbenium intermediates explain the chlorine exchange, in accordance with investigations with ^{14}C-labelled compounds too. The distribution of ^{36}Cl and ^{14}C in the molecule is proved by reactions to other labelled compounds. (auth)

29124 KINETICS OF FORMING AMMONIATES OF URANIUM TETRACHLORIDE. Torgoiskaya, T. I.; Ragotskaya, E. A. pp 115-122 of Prevrashchenie Kompleksnykh Soedinenii Pod Deistviem Sveta, Radiatsii i Temperatury. Lazerko, G. A. (ed.). Minsk; Izdatel'stvo BGU im. V. I. Lenin (1973). (In Russian).

By a gravimetric method a study was made on the effect of the temperature and pressure of ammonia on the rate of reaction of uranium tetrachloride with gaseous ammonia. It was found that at −20°C the reaction rate as a function of ammonia pressure is given by the following relation: $K = K_0 p_{NH_3}^{2.5}$. An increase in temperature decreases the reaction rate and content of ammonia in the products, and has no effect on the course of the kinetic curves. The limiting reaction step for the formation of uranium tetrachloride ammoniates over the interval of temperatures and pressures under study (with the exception of 0°C and a pressure of 200 mm Hg std) is the chemical process. At 0°C and an ammonia pressure of 200 mm Hg std the reaction rate is determined by a diffusion process. By a thermogravimetric method it was found that the decomposition of the $UCl_4 \cdot 7.6\ NH_3$ occurs in stages. The temperature intervals for a stable state of the intermediate compounds were determined. (SJR)

29125 CONDITIONS FOR FORMING POLYNUCLEAR HYDROXY COMPLEXES OF HEXAVALENT URANIUM. Davydov, Yu. P.; Efremenkov, V. M.; Skriptsova, A. B. pp 143-147 of Prevrashchenie Kompleksnykh Soedinenii Pod Deistviem Sveta, Radiatsii i Temperatury. Lazerko, G. A. (ed.). Minsk; Izdatel' stvo BGU im. V. I. Lenin (1973). (In Russian).

By the method of dialysis a study was made on conditions for forming polynuclear hydroxy complexes of U(VI). The degree of polymerization was investigated as a function of the concentration of uranium in solution and of the solution pH. At a pH of 6, particles of low molecular weight are formed in solution over the whole interval of uranium concentrations under study (10^{-6} to 10^{-4} molar); at a pH of 6.5 the degree of polymerization of hydrolyzed forms of uranium depends on the concentration of uranium in solution. In the region of low uranium concentrations the degree of polymerization is higher than in the region of higher uranium concentrations. At a pH of 7 and higher a visible precipitate of uranium hydroxide falls out. Analysis of the solution shows that polymeric hydrolyzed forms of uranium are present along with monomeric forms. (SJR)

29126 APPARATUS FOR OBTAINING WATER-FREE URANIUM COMPOUNDS FROM SUSPENSIONS. Pirk, H.; Ploeger, F.; Vietzke, H. (to Nukem Nuklear-Chemie und-Metallurgie GmbH). Canadian Patent 941,155. 5 Feb 1974.

Dry nuclear pure powdered uranium compounds are obtained from suspensions using an apparatus including a vertically disposed fluidized bed vessel of nuclear safe geometry having an inlet for fluidizing gas in the form of a sintered metal floor. The wall of the vessel is heated and moist powder in solid form is fed into the upper end of the vessel. Dry powder is withdrawn from the lower end of the vessel. A gas-permeable porous filter is disposed within the vessel near the upper end thereof, and a gas outlet conduit conveys fluidizing gas from the vessel. (CA)

29127 STABILIZED URANYL NITRATE COMPOSITIONS AND URANIUM IMPREGNATION METHOD. Elson, R. E.; Heminger, R. D.; Tully, G. R. Jr. (To United States Atomic Energy Commission). US Patent 3,826,753. 30 Jul 1974. Filed date 24 Oct 1958. 8p.

A method is described for the stabilization of uranyl nitrate dihydrate dissolved in tertiary butyl alcohol. The stabilizing agent is either lactic acid, acetic acid, chloroacetic acid, or acetic anhydride. The stabilized solution is then used for the impregnation of graphite in the production of fuel for nuclear reactors. (JSR)

29128 HEAT CAPACITY OF α-SODIUM URANATE (α-Na_2UO_4) FROM 5 TO 350 K. Standard Gibbs Energy of Formation at 298.15 K. Osborne, D. W.; Flotow, H. E.; Dallinger, R. P.; Hoekstra, H. R. (Argonne National Lab., IL). J. Chem. Thermodyn.; 6: No. 8, 751-756(Aug 1974).

The molar heat capacity of α-Na_2UO_4 was determined by adiabatic calorimetry from 5 to 350°K. No unusual thermally related phenomena were observed. The following thermodynamic results were calculated: heat capacity at constant pressure: C^0 (298.15 K) = (146.67 ± 0.29)J K^{-1} mol^{-1}; standard entropy: S^0(298.15 K) = (166.02 ± 0.33)J K^{-1} mol^{-1}; enthalpy increment: $\{H^0(298.15\ K) - H^0(0)\}$ = (26227 ± 52)J mol^{-1}; standard Gibbs energy divided by temperature $\{G^0(298.15\ K) - H^0(0)\}/298.15\ K$ = −(78.05 ± 0.16) J K^{-1} mol^{-1}. The enthalpy of formation of α-Na_2UO_4 reported by O'Hare and Hoekstra and the entropies of α-Na_2UO_4, Na, U, and O were used to calculate the standard Gibbs energy of formation ΔG_f^0(α-Na_2UO_4, c, 298.15 K) = −(1745.8 ± 3.6) kJ mol^{-1}. (auth)

29129 URANIUM TETRABROMIDE STRUCTURE. A New MX_4 Structure Type. Taylor, J. C.; Wilson, P. W. (Australian Atomic Energy Commission Research Establishment, Lucas Heights). J. Chem. Soc., Chem. Commun.; No. 15, 598-599 (7 Aug 1974).

UBr_4 is a new MX_4 structure type, the configuration around the uranium atom being the pentagonal bipyramid [UBr $Br_{6/2}$]. (auth)

29130 VAPOR PRESSURE OF PROTACTINIUM PENTABROMIDE. Weigel, F.; Hoffman, G.; Wishnevsky, V. (Univ., Munich). J. Chem. Soc., Dalton Trans.; No. 14, 1473-1476(1974).

The vapor pressure of protactinium pentabromide, measured using a silica-membrane gauge, is represented by equations (i) and (ii). ln P(atm) = (19.27 ± 0.8) − (12,399 ± 44)(1/T) (491 to 556 K) (i) ln P(atm) = (11.61 ± 0.02) − (8,136 ± 13)(1/T) (556 to 635 K) (ii) Interpretation of the experimental results yields the following thermodynamic parameters: ΔH_s = 103.1 ± 0.4 kJ mol^{-1}; ΔS_s = 160.2 ± 0.8 J K^{-1} mol^{-1}; ΔH_e = 67.6 ± 0.1 kJ mol^{-1}; ΔS_e = 96.6 ±

0.4 J K^{-1} mol^{-1}; $\Delta H_f = 35.40 \pm 0.4$ kJ mol^{-1}; and $\Delta S_f = 63.6 \pm 0.4$ J K^{-1} mol^{-1}. The extrapolated boiling point is 701°K. (auth)

29131 PHOTOCHEMISTRY OF THE URANYL ION. Burrows, H. D.; Kemp, T. J. (Univ. of Coimbra). Chem. Soc. Rev.; 3: No. 2, 139-165(1974).

The review falls under the following headings: structure and bonding; spectroscopy and photophysics (absorption spectrum, luminescence, energy transfer); solution photochemistry of UO_2^{2+} (excitation of complexes, intermolecular abstraction of a hydrogen atom by U^{VI*}, intermolecular electron transfer to excited uranyl ion, energy transfer); reactions of intermediate species; applications of the photochemistry of uranyl compounds; some comparisons with other metal ions. (UK)

29132 OXIDATION OF FREE AND COORDINATED THIOLS BY NEPTUNIUM(VI). Weschler, C. J. (Argonne National Lab., IL); Sullivan, J. C.; Deutsch, E. Inorg. Chem.; 13: No. 10, 2360-2366 (Oct 1974).

The Np(VI) oxidation of thioglycolic acid (tga) was quantitatively investigated under conditions where the reaction involves a 1-equiv oxidation at sulfur. This reaction follows the rate law $-d(\ln [Np(VI)])/dt = (a + b/[H^+])[tga]$; at 25° and $\mu = 1.00$ F ($LiClO_4$), $a = 3.5 \pm 0.7$ F^{-1} sec^{-1}, $b = 34.2 \pm 0.3$ sec^{-1}, and the corresponding activation parameters are $\Delta H_a^{*} = 6 \pm 3$ and $\Delta H_b^{\ddagger} = 14.2 \pm 0.2$ kcal/mol and $\Delta S_a^{*} = -37 \pm 11$ and $\Delta S_b^{\ddagger} = -3.7 \pm 0.5$ eu. The Np(VI) oxidation of methyl thioglycolate follows a similar rate law with values of a and b at 25° and $\mu = 1.00$ F ($LiClO_4$) of 58 ± 2 F^{-1} sec^{-1} and 2.7 ± 0.1 sec^{-1}, respectively. These results are interpreted as indicating that the net rate of oxidation of tga deprotonated at at the carboxyl group (b^{COO}) is 12 times greater than the net rate of oxidation of tga deprotonated at the sulfhydryl group (b^S); however, the specific rate of oxidation of the latter form ($k_2^S = b^S/K^S$) is 10^3 times greater than that of the former ($k_2^{COO} = b^{COO}/K^{COO}$) since the acid dissociation constant of the carboxyl group (K^{COO}) is about 10^4 times greater than that of the sulfhydryl group (K^S). Qualitative observations were also made on the Np(VI) oxidation of coordinated thiolato ligands in the complexes $[Cr(en)_2(SCH_2COO)]^+$, $[Co(en)_2(SCH_2COO)]^+$, $[Cr(en)_2(SCH_2CH_2NH_2)]^{2+}$, $[Co(en)_2(SCH_2CH_2NH_2)]^{2+}$, $[Cr(en)_2(SCH_2CH_2COO)]^+$, $[Cr(en)_2(SC_6H_4COO)]^+$, and $[Cr(en)_2(OH_2)(OOCCH_2SH)]^{2+}$. The last two complexes consume roughly 1 equiv of Np(VI)/mol of complex and can be considered to undergo the same type of oxidation as free thiols. The other complexes undergo multiequivalent, multistep oxidations often involving oxidation of the thiol carbon backbone. Chromium(III)-thiolato complexes are oxidized much more rapidly than analogous cobalt(III) complexes and coordinated tga is oxidized much more rapidly than coordinated cysteamine or coordinated thiopropionic acid. Rationalization to account for these observations are presented. (auth)

Radioactive Waste Treatment

Refer also to abstracts 29026 and 30108.

29133 (CEA-R-4550) STUDY OF DIFFUSION/LEACHING PHENOMENA WITH GLASSES. Application of Risk Evaluation to Long-Term Storage. Imbert, J. C.; Pacaud, F. (CEA Centre de Marcoule, 30 - Bagnols-sur-Ceze (France). Service des Ateliers Pilotes). Aug 1974. 88p. (In French). Dep. NTIS (US Sales Only) $7.50.

The leaching of glasses formed from highly radioactive wastes was studied. The following leaching agents were investigated: water for temperatures of less than 100°C; molten nitrates for temperatures in excess of 100°C; solutions having various different pH values or charged with sodium chloride or cesium; dry or wet air. The measurement of the various quantities of radioisotopes washed out can be used to determine the overall apparent coefficient of diffusion and long half-life fission products such as cerium, cesium, ruthenium, and strontium. The activation and diffusion energies can be determined. (auth)

29134 STUDIES ON THE SORPTION AND FIXATION OF CESIUM BY VERMICULITE. II. Lee, S. H. (Atomic Energy Research Inst., Seoul). J. Korean Nucl. Soc.; 6: No. 2, 97-111 (Jun 1974).

The adsorption mechnism of ^{137}Cs in low-level radioactive solution by vermiculite treated with Na ion is studied in order to investigate its use for radioactive effluent treatment. The beneficial role of Na-vermiculite is that Na ion can induce a wider c-axis spacing in which Cs ion can be sorbed in vermiculite. Cation exchange capacity and distribution coefficient of cesium seems to be influenced by the variation of c-axis spacing of vermiculite. Comparative identification and detection with the characteristic analyses of x-ray diffraction and electron diffraction patterns, differential thermal analysis, and electron microscopy of Na-, K-, and Cs-vermiculite are studied for the phenomena of Cs adsorption by vermiculite. The importance of the utilization in terms of adsorption and fixation of cesium involving vermiculite is discussed. It is found that Na-vermiculite would be a valuable outside charging material for high-level radioactive liquid waste underground storage tank to prevent pollution of underground water (13 fig, 4 tables) (auth)

29135 SORPTION OF IRIDIUM ON SILVER, MERCURY, LEAD, AND THALLIUM FORMS OF NATURAL ZEOLITE (CLINOPTILOLITE) AND VERMICULITE. Gradev, G. (Institut po Yaderna Fizika i Yaderna Energetika, Sofia (Bulgaria)). Radiochim. Acta; 19: No. 2, 66-69(1973). (In German).

5 figs.; 11 refs.

The sorption of iridium on natural zeolite (clinoptilolite) and vermiculite was investigated. Iridium(III) and iridium(IV) in the form of anion complexes are sorbed on a silver, mercury, thallium, and lead form of zeolite, due to the formation of sedimentary compounds. The sorption capacities of the above mentioned forms of zeolite at different pH were determined. The investigations were carried out with iridium-192 (by the method of radioactive indicators). These results are used for the processing of liquid radioactive wastes containing iridium-192, silver-110m, thallium-204, mercury-203. (auth)

29136 THE TREATMENT AND DISPOSAL OF RADIOACTIVE WASTES. Krause, H.; Starch, M. (Kernforschungszentrum Karlsruhe (F. R. Germany). Abt. Dekontaminationsbetriebe). VDI (Ver. Deut. Ing.) Z.; 116: No. 9, 715-719(Jun 1974). (In German).

54 refs.

The development of the treatment of radioactive wastes in the years 1972/73 and the methods applied during this period with respect to the processing and solidification as well as to storage and disposal are reviewed. The report contains a selected bibliography. (GE)

29137 CURRENT STORAGE POSSIBILITIES OF BLOCKS WITH SOLIDIFIED RADIOACTIVE WASTES AT THE INSTITUTE OF NUCLEAR RESEARCH. Dlouhy, Z. (Inst. of Nuclear Research, Rez, Czech.). Nukleon; No. 1, 19-22(1973). (In Czech).

A method is described of solidifying liquid radioactive wastes, proposed for the specific conditions of the Nuclear Research Institute at Řež, Czechoslovakia. The efficient method listed of solidification of wastes into bitumen is being elaborated for laboratory conditions with the aim of verifying the feasibility of solidifying substances of a specific activity of 100 Ci/l. The problem is also discussed of final disposal of the resulting products. The desired properties of solidified wastes and of the storage site are listed. (Nuclear Sci. Abstr. Czeck.)

Radioisotope Production

Refer also to abstract 30142.

29138 (GSI-tr-74/15) PREDICTION OF THE BEHAVIOR OF SUPERHEAVY ELEMENTS AND THEIR CHLORIDES DURING THERMOCHROMATOGRAPHIC SEPARATION. Eichler, B. May 1974. 12p. (In German). INIS.

8 figs.; 2 tabs.; 40 refs. With abstract. Translation of the Russian report JINR-P-12-7767.

By extrapolation of thermodynamic parameters, the most probable chemical properties of the superheavy elements during their evaporation in a stream of hydrogen or chlorine were determined. The standard heats of sublimation of these elements and their chlorides were estimated. The results are discussed with a view to the possibility of a thermochromatographic separation of nuclear reaction products. The main possibility of selective separation of the elements with Z = 112-117 in a hydrogen stream is shown. (GE)

29139 PROCESS FOR THE PRODUCTION OF TECHNETIUM-99m FROM NEUTRON IRRADIATED MOLYBDENUM TRIOXIDE. Robson, J. (to Australian Atomic Energy Commission). US Patent 3,833,469. 3 Sep 1974. Priority date 31 Aug 1971, Australia. 8p.

A process for producing solutions containing radioactive technetium-99m comprises irradiating molybdenum oxide in a nuclear reactor, heating the powdered product in a tube in a flowing gas stream at a temperature in the range 700 to 950°C, passing the vaporized ^{99m}Tc compound together with any vaporized molybdenum compound through a filter held at a temperature in the range 300 to 700°C, condensing the ^{99m}Tc compound in a condenser, taking-up the ^{99m}Tc compound in a liquid, and removing the liquid containing the ^{99m}Tc compound in a sterile container. (Official Gazette)

29140 RADIONUCLIDE GENERATOR PRODUCTION METHOD. Brown, J. L.; Harris, O. A. (to Mallinckrodt Chemical Works). US Patent 3,833,509. 3 Sep 1974. Filed date 2 Sep 1971. 10p.

Commercially important radionuclide generators utilize an alumina sorbent on which is adsorbed a parent radionuclide. The eluate from such generators contains significant quantities of aluminum ions in addition to the desired daughter radionuclide. Washing the alumina with an acetate fixing solution during the production of the generators substantially reduces the aluminum ion content of eluates obtained therefrom. A ^{99m}Tc generator is described. (Official Gazette)

29141 POSSIBILITY OF PREPARING ENRICHED AMERICIUM-242g BY ELUTION OF RECOIL ATOMS FROM ZEOLITE. Shafiev, A. I.; Vityutnev, V. M.; Ivanov, V. M.; Yakovlev, G. N. Sov. Radiochem. (Engl. Transl.); 15: No. 6, 830-832(1973).

Translated from Radiokhimiya; 15: No. 6, 820-823(1973).

On the example of the preparation of americium-242g it was shown that it is possible in principle to prepare enriched isotopes of actinides by elution of recoil atoms from zeolites. The enrichment factor depends on the conditions of treatment of the zeolite–americium-241 target before irradiation and the composition of the solution used for eluting the recoil atoms. The yield of recoil atoms depends both on the nature of the eluting solution and on the contact time of this solution with the material of the target. (auth)

29142 VOLATILITY OF MICROAMOUNTS OF THALLIUM FROM PbF_2 CRYSTALS IRRADIATED WITH HIGH-ENERGY PROTONS. Fast Gas Thermochromatographic Method of Obtaining Short-Lived Thallium Isotopes. Vandlik, Ya.; Vandlik, T.; Zaitseva, N. G.; Mate, Z.; Makhunka, I. Sov. Radiochem. (Engl. Transl.); 15: No. 6, 842-849(1973).

Translated from Radiokhimiya; 15: No. 6, 831-840(1973).

An investigation was made of some characteristics of the behavior of microamounts of thallium during sublimation, transfer, and deposition in relation to a series of parameters which affect the processes occurring during the sublimation of volatile compounds of heavy metals from a PbF_2 crystal powder irradiated with protons with $E_p = 660$ MeV. It was shown that efficient isolation of microamounts of thallium from irradiated PbF_2 is possible by gas thermochromatography. A rapid gas thermochromatographic method was developed for obtaining radiochemically pure, highly radioactive preparations of thallium in a form suitable for direct isotopic separation in order to obtain short-lived monoisotopic sources of thallium with $T \geq 1$ min for nuclear spectroscopic investigations. (auth)

29143 ISOLATION OF CARRIER-FREE RADIOACTIVE ISOTOPE COBALT-57 FROM NICKEL TARGET IRRADIATED ON CYCLOTRON. Sevast'yanov, Yu. G.; Bezmaternykh, A. S.; Volkova, L. S.; Ksenofontov, E. G. Sov. Radiochem. (Engl. Transl.); 15: No. 6, 850-854(1973).

Translated from Radiokhimiya; 15: No. 6, 841-846(1973).

Refinement of an ion exchange method for separating microamounts of cobalt and macroamounts of nickel in 9 M HCl is reported. Turnings of irradiated nickel were dissolved by heating in concentrated HCl with gradual addition of H_2O_2. After the dissolution the solution was adjusted to 2-2.5M $NiCl_2$ – 5-4M HCl and passed through a Dowex 1 × 8 column. The column was washed free from nickel with 9 M HCl and the ^{57}Co was eluted with 4 M HCl. The ^{55}Fe was eluted with 1 M HCl. For further purification of the ^{57}Co the solution was adjusted to 5M with respect to HCl and passed through another Dowex column at a rate of 0.2 ml/min with subsequent elution with 5M HCl solution. (LK)

29144 RADIONUCLIDE GENERATOR PRODUCTION METHOD. (to Mallinckrodt Chemical Works). Netherlands Patent 7,211,772. 29 Aug 1972. Priority Date 2 Sep 1971, USA. 22p. (In Dutch).

Commercially important radionuclide generators utilize an alumina sorbent on which is absorbed a parent radionuclide. The eluate from such generators contains significant quantities of aluminum ions in addition to the desired daughter radionuclide. Washing the alumina with an acetate fixing solution during the production of the generators substantially reduces the aluminum ion content of eluates obtained therefrom. (NL)

Reactor Fuel Reprocessing

Refer also to abstract 28940.

29145 (NP-20106) MIDWEST FUEL RECOVERY PLANT TECHNICAL STUDY REPORT. (General Electric Co., Morris, Ill. (USA). Midwest Fuel Recovery Plant). 5 Jul 1974. 52p.

Results of a study on the fundamental technical problems of the Aquafluor process and equipment and an assessment of the effect of these technical problems on the outlook for the operating capability of the plant are presented. (LK)

29146 APPARATUS AND METHOD FOR PROCESSING SPENT NUCLEAR FUEL ELEMENTS. Cherel, C. (to Saint-Gobain Techniques Nouvelles). Canadian Patent 941,145. 5 Feb 1974.

A method and apparatus for fragmenting spent nuclear fuel elements contained in bundles of metallic tubes which are secured together are described. The inert ends of the tubes are removed and then the tubes are advanced step by step through a shear so that the exposed piece is sheared off. The sheared fragments fall, under gravity, into a selected collector from which they pass into a solvent while later fragments fall into a second selected collector. (CA)

29147 THE DISPOSAL SYSTEM IN THE NUCLEAR FUEL CYCLE. Schmidt-Kuester, W. J. (Bundesministerium fuer Forschung und Technologie, Bonn (F. R. Germany)). Atomwirt., Atomtech.; 19: No. 7, 340-345(Jul 1974). (In German).

From reactor meeting; Berlin, F. R. Germany (2 Apr 1974). 4 figs.; 1 tab.

The German Ministry of Research and Technology (BMFT) has set up a disposal concept within the nuclear fuel cycle, where reprocessing, fuel recycling, waste treatment and waste disposal represent an integrated overall system. Bearing in mind the planned nuclear energy increase, this system has to be fully operable at least in 1985 in the Federal Republic of Germany. Medium and low-level radioactive wastes will be finally stored at the site of the reprocessing plant. This means that the choice of site depends on the deposit facility. High-level radioactive waste is intermediately stored as a solidified product. The final disposal of high-level radioactive wastes, which can be done in salt mines in Germany, will not be realized unless a careful testing of the ultimate disposal concepts has been done. The system applies to the LWR, HTR, and fast-breeder fuel cycle and must include the removal of dismantled nuclear plants. The concept is based on the assumption that reprocessing and waste treatment is mainly carried out by private enterprises. (auth)

29148 METHOD FOR THE SUPPRESSION OF HYDROGEN DURING THE DISSOLUTION OF ZIRCONIUM AND ZIRCONIUM ALLOYS. Carter, D. G. Jr. (To United States Atomic Energy Commission). US Patent 3,832,439. 27 Aug 1974. Filed Date 10 Jan 1973. 4p.

The evolution of hydrogen during dissolution of zirconium and zirconium alloys in an ammonium fluoride and ammonium nitrate solution (Zirflex Process) is suppressed by the presence of copper in the solution, while the rate at which the zirconium is dissolved is improved by the addition of sodium nitrite. (Official Gazette)

29149 DECONTAMINATING URANIUM BY REACTION WITH ClF_3 AND HF AND VOLATIZING THE UF_6 PRODUCT. Gustison, R. A.; Bernhardt, H. A.; Barber, E. J.; Benton, S. T. (To United States Atomic Energy Commission). US Patent 3,825,650. 23 Jul 1974. Filed Date 18 Jun 1954. 8p.

A fluorination process for the recovery and decontamination of U from Pu, fission products and other impurities is discussed. The method is based on the dissolution of the U in a liquid fluorination solution containing ClF_3 and HF at mole ratios which will prevent the formation of UF_6-containing axeotropes. The UF_6 is fractionally distilled. The process also provides for the recovery of the fluorination reagent for further dissolution of U. The recovery is achieved by reacting the monofluoride with fluorine over a catalyst of Cu, Ag, or Ni. The process is suitable for both the U metal and compounds, particularly oxides, fluorides, and oxyfluorides. The resulting UF_6 is of sufficient purity for introduction into a gaseous diffusion cascade. (JSR)

29150 PROCESS FOR SEPARATION OF PROTACTINIUM, THORIUM, AND URANIUM FROM NEUTRON-IRRADIATED THORIUM. Gresky, A. T.; Savolainen, J. E.; McDuffee, W. T. Jr.; Wischow, R. P. (to United States Atomic Energy Commission). US Patent 3,825,649. 23 Jul 1974. Filed date 7 Aug 1956. 22p.

Protectinium, uranium, and thorium are separated from an aqueous nitric acid solution of neutron-irradiated thorium containing these elements and fission products by contacting, under net nitrate deficient conditions, the acid solution with an organic solution of a trialkyl phosphate in an inert organic diluent, thereby preferentially extracting uranium and thorium into the organic phase while confining protactinium and fission products to the aqueous phase. After scrubbing the organic phase with an aqueous solution of an inorganic nitrate salt to remove small amounts of protactinium and fission products, the two phases are separated and thorium and uranium are separately recovered from the organic phase. (Official Gazette)

CONTROLLED THERMONUCLEAR RESEARCH

Confinement and Heating

Refer also to abstract 30655.

29151 (CLM-R-135) SUMMARY OF CONTAINMENT EXPERIMENTS ON THE PROTO-CLEO STELLARATOR. Lees, D. J. (UKAEA Research Group, Abingdon. Culham Lab.). May 1974. 17p. Dep. NTIS (US Sales Only) $4.00. UK 50 pence.

The importance of fluctuations on plasma containment is discussed and an attempt made to arrive at momentum balance for the ions and electrons. It is concluded that although plasma can be contained for periods as long as expected on the basis of loss solely by collisions, it cannot be conclusively demonstrated that this is the sole mechanism of plasma loss, since evidence for the existence of the diffusion driven current cannot be found. (auth)

29152 (COO-2277-4) HIGH BETA CAPTURE AND MIRROR CONFINEMENT OF LASER-PRODUCED PLASMAS. Semiannual Report, January 1, 1974 Through July 31, 1974. Haught, A. F.; Polk, D. H.; Woo, J. T.; Fader, W. J.; Tomlinson, R. G.; Jong, R. A.; Ard, W. B.; Mensing, A. E. (United Aircraft Corp., East Hartford, Conn. (USA). Research Labs.). 31 Jul 1974. Contract AT(11-1)-2277. 79p. Dep. NTIS $7.00.

The program to investigate the use of a dense, mirror confined, laser-produced plasma as the target for an energetic neutral injection beam with the goal of creating and sustaining a high temperature, high density, steady state, mirror confined fusion plasma is discussed. Earlier studies in this program have demonstrated that laser heating of a small solid particle in vacuum is an effective means for producing a dense, warm plasma which upon expansion can be captured and confined in a minimum-B mirror magnetic field. Calculations were carried out which show that the confined laser produced can provide collisional trapping of an injected neutral beam for a time sufficient to allow buildup to a steady state determined by the balance between collisional ionization of the injected neutrals and the plasma scattering losses. From the calculations, a 10 keV, 1.0 A equivalent neutral beam incident upon a laser produced target plasma confined in a 15 kG, mirror ratio and well depth = 2, 32 cm long minimum-B magnetic field will result in the formation of a 10^{12} cm^{-3}, 10 keV steady state plasma. The UARL Laser Initiated Target Experiment (LITE) is designed to achieve these parameters. In this report period, further investigations have been carried out to improve the reproducibility of high temperature laser plasma production with the larger (>50 μm dia) particles of interest for use as the target in the LITE program. Design features to reduce or eliminate the particle position-focal spot variation identified as the source of the problem have been incorporated in the LITE experimental system. Theoretical studies have included Fokker-Planck calculations of the evolution of a LITE target plasma to injection sustained steady state including the effects of charge exchange with the background neutrals, multispecies Fokker-Planck calculations of the decay of a confined LiH target plasma taking into account the presence of the lithium ions, and analysis of the Li III line radiation from the plasma for use as an electron density diagnostic during the target plasma decay. The development of the LITE facility which has comprised the major effort during this report period is described. The LITE experimental system consists of a coupled neutral beam source, experiment chamber, and beam termination tank and is being assembled in two parts: (1) the laser and experiment chamber mounted on the support base for plasma production experiments and confinement studies, and (2) the neutral beam source and dump tank progressively assembled and operated separately as a beam line test stand. The experiment chamber and laser with which the target production and confinement experiments will be carried out are discussed. The feedback particle suspension system which has not previously been described is presented in detail and the neutral beam line sub-assembly is treated. To acquire and reduce the data from the different plasma diagnostics, a computer based data handling system is being incorporated into the LITE facility. The configuration and development of the capabilities of this system are discussed. (auth)

29153 (LA-5639-MS) NEW TECHNIQUE FOR NONLINEAR OPTICAL PROBLEMS. Elliott, C. J.; Henderson, D. B. (Los Alamos Scientific Lab., N. Mex. (USA)). May 1974. Contract W-7405-eng-36. 11p. Dep. NTIS $4.00.

The propagation of high intensity or high power laser pulses presents a variety of nonlinear optical problems requiring self-consistent study. This method treats arbitrary three-dimensional problems with unlimited phase distortion and is similar to the particle-in-cell (PIC) methods of hydrodynamics and electromagnetic plasma simulation. The numerical algorithm is based on Maxwell's equations and is applied to laser-fusion reactor and laser amplifier problems. (auth)

29154 (NP-20140) ARC DISCHARGES IN A CURVED MAGNETIC FIELD. Schueller, F. C. (Stichting voor Fundamenteel Onderzoek der Materie, Jutphaas (Netherlands). Instituut voor Plasma-Physica). Jun 1974. 151p. Dep. NTIS (US Sales Only) $10.75.

Thesis.

An experiment on arc discharges in hydrogen in a curved magnetic field is described. During a few milliseconds the discharge current was flowing between two electrodes along the field lines of a toroidal magnetic field over an angle of 258°. The major radius of the discharge vessel was 0.45 m and the minor radius 0.075 m. The current was supplied by a delay line and could be made as large as 32 kA. The largest obtainable value of the magnetic field was 2 T: the filling pressure could be varied between 5×10^{-2} and 5 torr. At high filling pressure diamagnetic confinement caused such large pressure gradients that, together with the centrifugal force induced by the column rotation, Rayleigh-Taylor instabilities developed. At low filling pressure the discharges were stable notwithstanding the large plasma velocities (up to 9×10^3 m/sec, i.e., nearly the local sound velocity). Kink instabilities developed in regions where the local Kruskal limit was exceeded. (MOW)

29155 ANOMALOUS SCATTERING OF THE ENERGY OF A PLASMA JET INTERACTING WITH A GAS TARGET. Kartashev, K. B.; Pistunovich, V. I.; Platonov, V. V.; Ryutov, V. D.; Filimonova, E. A. JETP Lett. (USSR) (Engl. Transl.); 19: No. 8, 263-264(20 Apr 1974).

Translated from Zh. Eksp. Teor. Fiz., Pis'ma Red.; 19: No. 8, 493-496(20 Apr 1974).

Anomalous scattering of the energy of a plasma jet interacting with a gas target was observed. The observed phenomenon is manifest in the charge exchange of a plasma jet with current density $j \geq 10$ A/cm^2. (auth)

29156 RADIATION BALANCE AND ELECTRON TEMPERATURE IN A NEUTRALIZED MIGMA. Miller, R. A. (Fusion Energy Institute, Fusion Energy Corporation, Princeton, N. J. 08540, U. S. A.). Nucl. Instrum. Methods; 119: No. 2, 275-278 (15 Jul 1974).

The development of the concept of electrons in a migma is summarized. The equilibrium temperature of electrons in a neutralized migma is calculated by setting the energy gained by the electrons from the ions through Chandrasekhar's dynamical friction equal to the energy lost to radiation. Depending on the amount of reabsorption, for 2 MeV ions and local density $\eta_e = \eta_d = 10^{15}$ cm^{-3} the electron temperature will be between 30 and 80 keV; the cooling time constant for the ions will be from 1.7 to 7 s. It is found that synchrotron radiation dominates bremsstrahlung. (auth)

29157 INTENSE FAST ATOM-BEAM PRODUCTION WITH A GROUNDED LARGE-AREA ION SOURCE. Fumelli, M. (Association Euratom-CEA, Centre d'Etudes Nucleaires de Fontenay-aux-Roses, 92 (France). Groupe de Recherches sur la Fusion Controlee). Nucl. Instrum. Methods; 118: No. 2, 337-342(15 Jun 1974).

A neutral hydrogen atom beam of 1 A (equivalent), 18 keV energy, with small divergence angle (≈1°) has been obtained using a grounded ion source. This source, a prototype capable of delivering a total ion beam of 2 A, utilizes a large-area multi-aperture three-electrode extraction system. The neutralizer (a hydrogen gas cell adjacent to the extraction system where the accelerated ions are partially converted into fast atoms by charge exchange and dissociation) was biased at the negative potential corresponding to the desired beam energy. At the exit of the neutralizer, in this set-up there is a strong electric field which decelerates the energetic ions remaining in the beam. This field removes the unneutralized fraction from the beam; furthermore it is possible to provide for the energy recovery of this fraction. This is a very important point in view of the future needs of the thermo-nuclear fusion. This disposition also simplifies the ion-source power system and the control of the source parameters. (auth)

Diagnostics

Refer also to abstracts 29156, 29176, 29212, and 31241.

29158 (ORNL-TM-4672) SPECTROSCOPIC STUDY IN THE VACUUM ULTRAVIOLET OF A NEON PLASMA IN ELMO. Cobble, J. A. (Oak Ridge National Lab., Tenn. (USA)). Sep 1974. Contract W-7405-eng-26. 111p. Dep. NTIS $8.75.

Thesis. Submitted to Univ. of Tennessee, Knoxville.

ORNL's ELMO device contains an electron-cyclotron-heated plasma in a simple mirror trap. The relative intensities of line radiation in the vacuum ultraviolet for five charge states of neon in ELMO were measured with a calibrated, grazing incidence spectrometer. Theoretical models for the excitation and ionization of atomic systems in the plasma are based on an optically thin, corona approximation in which atom–electron collisions play the main part. The resulting population-balance equations for excited states in the excitation model are employed to measure the temperature of cold electrons which form the background plasma. Once this parameter is known, the density ratios of the various charge states present may be determined. Absolute densities of ions and electrons following from pressure measurements are next presented. Comparison of experimental results with the theoretical ionization model permits the estimation of a particle containment time and an ion temperature. Calculated plasma parameters are consistent with previous measurements of these variables when such measurements exist, and there is qualitative agreement with the estimates when no other assessment is available. (auth)

29159 (SAND-74-5262) NANOSECOND TIME RESOLVED X-RAY DIAGNOSTICS OF RELATIVISTIC ELECTRON BEAM INITIATED EVENTS. Kuswa, G. W.; Chang, J. (Sandia Labs., Albuquerque, N. Mex. (USA)). 1974. 11p. (CONF-740809-7). Dep. NTIS $4.00.

From 23rd annual conference on applications of x-ray analysis; Denver, Colorado, USA (7 Aug 1974).

The dynamic behavior of a test sample during and shortly after it has been irradiated by an intense relativistic electron beam (REB) is of great interest to the study of beam energy deposition. Since the sample densities are far beyond the cutoff in the optical region, flash x-radiography techniques have been developed to diagnose the evolution of the samples. The conventional approach of analyzing the dynamic behavior of solid densities utilizes one or more short x-ray bursts to record images on photographic emulsion. This technique is not useful in the presence of the intense x-rays from the REB interacting with the sample. Two techniques are reported for isolating the film package from the REB x-ray pulse. (auth)

29160 (UCID-15392) X-RAY MEASUREMENTS ON ELECTRON DISTRIBUTION IN ASTRON. Beal, J. W.; Lamb, W. A. S. (California Univ., Livermore (USA). Lawrence Livermore Lab.). 4 Oct 1968. Contract W-7405-eng-48. 12p. Dep. NTIS $4.00.

Measurements of the trapped electron layer in Astron using x-ray techniques are described. In these measurements calibrated scintillator, photomultiplier tube assemblies were arranged axially along the Astron vacuum tank. Observations were made of x-rays generated when the trapped electrons struck a tungsten wire probe. These probes were inserted radially into the trapping region. The lifetime of the trapped electron distribution against scattering on the fully inserted probe is the order of milliseconds. (MOW)

29161 (UCID-15625) FAST, HIGH SENSITIVITY 10.6 MICRON INTERFEROMETER. Condit, W. C. (California Univ., Livermore (USA). Lawrence Livermore Lab.). 4 Feb 1970. 16p. Dep. NTIS $4.00.

In response to a need to measure plasma densities of order $10^{13}/\mathrm{cm}^2$ over distances of order 1 cm, with spatial resolution of 1 mm or less and risetimes of 100 nsec or less, a Michelson interferometer was set up using a CO_2 laser as the radiation source and a Philco gold doped germanium detector for readout. The configuration is described. (MOW)

29162 (UCRL-75557) LLL COMPACT 10-PS STREAK CAMERA, 1974 UPDATE. Thomas, S. W.; Houghton, J. W.; Tripp, G. R.; Coleman, L. W. (California Univ., Livermore (USA). Lawrence Livermore Lab.). 20 Aug 1974. 8p. (CONF-740915-2). Dep. NTIS $4.00.

From 11th international congress on high speed photography; London, UK (15 Sep 1974).

A 10-ps streak camera was designed in order to simplify operation, reduce manufacturing costs, and improve appearance. The electronics were simplified, a film indexer added, and a contacted slit was evaluated. Data supports a 10-ps resolution. (auth)

29163 SPECTROSCOPIC METHODS FOR DIAGNOSTICS OF SUPERDENSE HOT PLASMA. Vinogradov, A.V.; Sobel'man, I.I.; Yukov, E.A. Sov. J. Quantum Electron. 4: No. 2, 149-154 (Aug 1974).

A review is given of the capabilities of spectroscopic methods for diagnostics of superdense plasma in a wide range of temperatures and densities. A detailed analysis is given of four methods based on: 1) broadening and shift of the x–ray lines of ions; 2) measurement of the relative intensities of intercombination and resonance lines; 3) appearance of plasma satellites; 4) Raman scattering of x rays (produced by an external source) on Langmuir plasma oscillations. It is shown that a combination of all four methods provides diagnostic means for investigating plasmas with electron densities of $10^{22}-10^{26}$ cm^{-3} and with temperatures in the range 0.1 – 10 keV. (auth)

29164 ELECTRON ENERGY DISTRIBUTION IN THE AFTERGLOW. I. Blagoev, A.B.; Kagan, Y.M.; Kolokolov, N.B.; Lyagushchenko, R.I. (A. A. Zhdanov Leningrad State University). Sov. Phys.–Tech. Phys. 19: No. 2, 211-214 (Aug 1974).

The electron energy distribution function in the afterglow is usually assumed to be a Maxwellian. However, one might expect a considerable departure from this distribution for fast electrons. In the present paper we describe a method for the experimental determination of the electron energy distribution and the densities of charged particles and metastable atoms in the afterglow. The results of measurements in helium carried out in a tube 2.7 in diameter at pressures of 1 and 2 torr and currents of 0.45 and 1.8 A are presented. The high–energy part of the distribution function exhibits effects due to metastables. (auth)

29165 ELECTRON ENERGY DISTRIBUTION IN THE AFTERGLOW. II. Blagoev, A.B.; Kagan, Y.M.; Kolokolov, N.B.; Lyagushchenko, R.I. (A. A. Zhdanov Leningrad State University). Sov. Phys.–Tech. Phys. 19: No. 2, 215-219 (Aug 1974).

The results of probe measurements on the distribution function in the afterglow of a helium plasma at pressures of 1 and 2 torr and currents of 0.45 and 1.8 A are presented. The distribution function in the energy range 4 – 20 eV has a complex nonmonotonic form. The number of electrons in this energy range is many orders of magnitude greater than in a Maxwellian distribution with the temperature of the slow electrons T_e. These characteristics are due to the production of fast electrons in reactions in which metastable atoms participate. The results of the experiment are compared with theoretical calculations of the distribution function in the afterglow. The agreement is satisfactory. Absolute measurements of the distribution function of the fast electrons and a comparison with theoretical calculation enable us to determine the constants and cross sections of the elementary processes. The following values are obtained: the cross section $\sigma_1 \simeq 0.6 \cdot 10^{-16}$ cm^2 for collisions of the second kind $\mathrm{He}\,(2^3{}_2\mathrm{S}_1)+e \rightarrow \mathrm{He}(1^1\mathrm{S}_0)+e$, the constant $\beta_2 \simeq 10^{-9}$ $\mathrm{cm}^3 \cdot \mathrm{sec}^{-1}$ for the reaction $\mathrm{He}(2^3\mathrm{S}_1)+\mathrm{He}(2^3{}_2\mathrm{S}_1) \rightarrow \mathrm{He}_2^+ + e$, and the constant $\beta_3 \simeq 2 \cdot 10^{-9}$ $\mathrm{cm}^3 \cdot \mathrm{sec}^{-1}$ for the reaction $\mathrm{He}(2^3\mathrm{S}_1)+\mathrm{He}(2^3\mathrm{S}_1) \rightarrow \mathrm{He}^+ + \mathrm{He} + e$. (auth)

29166 ELECTRON ENERGY DISTRIBUTION IN A HIGH–FREQEUNCY DISCHARGE IN AN AXIAL MAGNETIC FIELD. Vagner, S.D.; Virolainen, V.A.; Kagan, Y.M.; Kalmykova, T.A. (Karelian State Pedagogical Institute, Petrozavodsk). Sov. Phys.–Tech. Phys. 19: No. 2, 290-291 (Aug 1974).

The second–derivative method is used to measure the electron energy distribution functions in a high–frequency helium discharge. The functions are used to calculate the ionization rate. When an axial magnetic field is applied the ionization rate increases sharply from the axis of the tube towards the walls. This effect is due to a change in the radial electron distribution caused by the magnetic field. (auth)

29167 NEW METHOD FOR OBTAINING PROBE CHARACTERISTICS. Osipov, Y.I. (P. N. Lebedev Physics Institute, Academy of Sciences of the USSR, Moscow). Sov. Phys.–Tech. Phys. 19: No. 2, 296-298 (Aug 1974).

A new method is proposed for obtaining probe characteristics. This method avoids the difficulties which arise in studying plasmas with high particle densities and high energy densities. (auth)

29168 COLD–ELECTRON TEMPERATURE MEASUREMENTS IN ELMO BY EXCITATION RATE RATIOS OF VACUUM ULTRAVIOLET TRANSITIONS. Cobble, J.A. (Oak Ridge National Laboratory, Oak Ridge, Tennessee 37830). Appl. Opt. 13: No. 9, 2003-2005 (Sept 1974).

The cold–electron kinetic temperature (T_{ce}) in the ELMO plasma has been measured spectroscopically. (AIP) (auth)

29169 LIGHT SCATTERING FROM Ne, Ar, AND Xe ARCS. Vriens, L.; Adriaansz, M. (Philips Research Laboratories, Eindhoven, The Netherlands). J. Appl. Phys. 45: No. 10, 4422-4431 (Oct 1974).

A procedure is described whereby nonresonant polarized and depolarized Rayleigh, electronic Raman, and Thomson scattering are used as a diagnostic tool for high–pressure nonhomogeneous plasmas. The method is applied to 0.1 – 3 atm Ne, Ar, and Xe arcs, with currents not exceeding 3 A. Polarized Rayleigh scattering is dominant in these cases. Radial gas temperature and density distributions, an axis electron density, and upper limits of excited state and electron densities are obtained. The temperature range covered extends from about 350 K (near the wall) up to 4500 K (at the axis of a 2–A 3–atm Ne arc).

A comparison with spectroscopically obtained temperatures is shown to yield interesting information on the deviations from local thermodynamic equilibrium. (auth)

29170 PROPOSED METHOD OF MEASURING THE CURRENT DISTRIBUTION IN A TOKAMAK PLASMA. Bretz, N. (Plasma Physics Laboratory, Princeton University, Princeton, New Jersey 08540). Appl. Opt. 13: No. 5, 1134-1140 (May 1974).

It is shown that the current distribution in a typical Tokamak plasma can be measured by a light scattering technique. The direction of the total magnetic field is measured accurately enough that the magnitude of the small poloidal component can be found. The field direction is measured by observing the scattered frequency spectrum of CO_2 laser light. The usual Gaussian spectrum becomes modulated at the electron cyclotron frequency when the difference between the incident and scattered wave vectors is nearly perpendicular to the magnetic field. The harmonics can be superimposed with a Fabry–Perot interferometer and their collective width resolved as the scattering direction is changed. The SNR is high only when the detector is shielded against background radiation. (auth)

29171 DIAGNOSTICS OF DENSE LASER PLASMAS BASED ON THE SPECTRA OF HYDROGEN–LIKE AND HELIUM–LIKE MULTIPLY CHARGED IONS. Aglitskii, E.V.; Boiko, V.A.; Vinogradov, A.V.; Yukov, E.A. Sov. J. Quantum Electron. 4: No. 3, 322-328 (Sept 1974).

An investigation was made of the spectra of Mg XI, Mg XII, Al XII, and Al XIII ions generated by laser radiation focused on solid targets. The relative intensities of the allowed and forbidden lines and of the lines beginning from self–ionized levels yielded the electron density ($Ne_e \simeq 10^{20}$ cm^{-3}) and temperature ($kT_e \simeq 300$ eV) of the radiating region. The method employed was suitable for the diagnostics of plasmas with $N_e \simeq 10^{23}$ cm^{-3} provided the spectra of strongly ionized hydrogen–like and helium–like ions were observed. (auth)

29172 COLLECTOR PROBE MEASUREMENTS OF THE PARAMETERS OF A LASER PLASMA AT LONG DISTANCES. Antonov, A.V.; Zaritskii, A.R.; Zakharov, S.D. Sov. J. Quantum Electron. 4: No. 3, 342-344 (Sept 1974).

Investigations were made of the distributions of the electron and ion velocities using probe and transit–time collector methods. Experimental results were compared with a theoretical model of plasma expansion in a self–consistent electric field. It was found that at distances from the target exceeding the dimensions of the focusing region the electron and ion components interacted weakly with one another. (auth)

Kinetics (General)

29173 (IPP-3/12) ON THE ENERGY DISTRIBUTION OF ELECTRONS IN A PROTON-ELECTRON PLASMA WITH DENSITIES HIGHER THAN THE SOLID-STATE DENSITY. Wulff, H. (Max-Planck-Institut fuer Plasmaphysik, Garching/Muenchen (F.R. Germany)). May 1974. 18p. (In German). INIS.

With abstract in English.

This paper proves that Fermi electrons have to be bound, which has hitherto gone unnoticed. The distinction between bound and free electrons, valid for low-density plasmas, is extended to high densities and a new energy distribution function for the electrons is given. It is found that for plasmas in which a Bohr sphere defined by a_B^3 (a_B = Bohr radius) contains more than one electron the Pauli principle is incompatible with the virial theorem. (auth)

29174 (UCRL-75910) X-RAY ANALYSIS FOR ELECTRON BEAM ENHANCEMENT IN THE PLASMA FOCUS DEVICE. Gullickson, R. L.; Barlett, R. H. (California Univ., Livermore (USA). Lawrence Livermore Lab.). 2 Aug 1974. 15p. (CONF-740809-3). Dep. NTIS $4.00.

From 23rd annual conference on applications of x-ray analysis; Denver, Colorado, USA (7 Aug 1974).

The plasma focus device, a form of linear pinch discharge, produces an intense x-ray and neutron (D_2) burst from a magnetically heated dense plasma. Rapidly changing magnetic fields at pinch time generate large axial electric fields which accelerate electrons and ions. In the experiments reported here the x-ray production during the plasma pinch of a 96 kilojoule (at 20 kV) plasma focus device was measured. The purpose of these experiments was to evaluate the energy in accelerated electrons in the plasma focus device and to learn how to enhance these electron bursts. Well focused, megampere electron beams at a few hundred kilovolts, lasting less than 10 nanoseconds have applications in fusionable pellet heating experiments. (1) X-rays were monitored to evaluate these electron bursts using a defocusing bent crystal spectrometer, doubly diffused silicon (PIN) detectors, with Ross filters, thermoluminescent dosimeters (TLDs) with filters, and x-ray pinhole photography. Thermoluminescent dosimeters indicated maximum x-ray yields of 140 joules above 3 keV at 57.3 kilojoules stored energy (16 kV) for a conversion efficiency to x-rays of 0.2%. 40 joules are above 60 keV and 15 joules above 80 keV. The hard x-ray pulse typically rises in 3 ns and frequently has a pulse width less than 10 ns. The low energy x-ray spectrum consists almost entirely of lines from the high Z anode insert, and the high energy spectrum is characteristic of a nonthermal power law distribution with an exponent of 2.2 ± 0.8. Peak hard x-ray production is obtained at 1 torr deuterium in contrast to peak neutron production (3×10^{10}) at 5 torr. The addition of argon reduces total x-ray yield and increases the relative fraction of soft x-rays. These measurements suggest that the plasma focus produces 1200 joules of electrons with an average energy of 150 keV, in 10 nanoseconds with a stored energy of 57.3 kilojoules. This is a power of 1.2×10^{11} watts and power density of 1.5×10^{13} watts cm^{-2}. (auth)

29175 MODELIROVANIE I METODY RASCHETA FIZIKO-KHIMICHESKIKH PROTSESSOV V NIZKOTEMPERATURNOI PLAZME. (Simulation and Methods for Calculating Physical-Chemical Processes in Low-Temperature Plasmas). Polak, L. S. (ed.). Moscow; Izdatel'stvo Nauka (1974). 271p.

The physics and chemistry of processes, the principles of modeling gas discharges of different types, and methods for calculating stable and optimized generators for low-temperature plasmas (constant current, high and super-high frequencies) are considered. Methods for calculating stabilized electric arcs with consideration of transfer of the radiation, disturbance of the temperatures of components of the plasma, the effect of nonlinear properties of the plasma on the parameters of the arc post, a turbulent model of the arc of constant current, and problems of the generalization properties of an electric arc are considered. Special sections are devoted to the contracted induced discharge and the SVCh plasma generator. Some physicochemical processes in a low-temperature plasma and the effect of electron collisions and electron-activated states on disintegration of molecules, dissociation recombination of electrons and molecular ions, and chemical reactions under turbulent conditions are considered. The book is designed for physicists, chemists, and specialists in the field of low-temperature plasmas. 151 illustrations, 30 tables, 774 references. (tr-auth)

Kinetics (Experimental)

Refer also to abstract 30313.

29176 NUMERICAL ANALYSIS OF INTERFEROGRAMS OF ASYMMETRIC PLASMA OBJECTS. Gribkov, V.A.; Isakov, A.I.; Kalachev, N.V.; Krokhin, O.N.; Sklizkov, G.V. Sov. J. Quantum Electron. 4: No. 2, 203-205 (Aug 1974).

Interferometric studies of dense, rapidly expanding plasmas require the use of lasers emitting pulses of $\sim 10^{-10}-10^{-11}$ sec duration. Since the emission lines are wide, it is necessary to analyze interferograms by methods which ensure the maximum precision for a small number N of experimental points. Moreover, it is important to know the error resulting from such analysis and the optimal number N_{opt} of points to be analyzed. The present paper reports the results of numerical calculations, carried out on an M–220 computer, of the values of N_{opt} and of the error in the Van Voorhis method for three typical profiles of electron density in a plasma focus. The values of N_{opt} and of the errors in the parabola and Van Voorhis methods are refined for a plasma jet (these parameters have been estimated earlier analytically). A diagnostic method is suggested for asymmetric plasmas, and typical electron density profiles are calculated for Rayleigh–Taylor instability modes, which develop in pinches. (auth)

29177 SPATIAL STRUCTURE OF AN EXPANDING LASER PLASMA CONSISTING OF ALUMINUM IONS AND NUCLEI. Bykovskii, Y.A.; Kozyrev, Y.P.; Sil'nov, S.M.; Sharkov, B.Y. Sov. J. Quantum Electron. 4: No. 3, 405-406 (Sept 1974).

The angular structure characteristics of the expansion of multiply charged aluminum ions and nuclei were determined for the first time for a wide range of densities of radiation fluxes ($10^8-5 \cdot 10^{13}$ W/cm^2) reaching the target. The experimental results were generalized to a wide spectrum of masses and radiation flux densities and this made it possible to provide a description of the expansion of a laser plasma in vacuum. The phenomenon of "self–focusing" of beams of ions of maximum density, whose angle of expansion was 20–30° (symmetric about the normal to the target), was detected for the first time. This phenomenon and the results obtained should be useful in those cases where a sharp directionality of ion sources would be needed as, for example, in injection of ions into accelerators. (auth)

Kinetics (Theoretical)

Refer also to abstracts 30183 and 30196.

29178 (CEA-N-1711) CALCULATION OF THE NEUTRON SPECTRA FROM NUCLEAR REACTIONS IN FOCUS TYPE DEUTERIUM PLASMAS. I. General Presentation and Mathematical Analysis. Genta, P.; Millet, F.; Vezin, R. (CEA Centre d'Etudes de Limeil, 94 - Villeneuve-Saint-Georges (France)). 27 Feb 1974. 220p. (In French). Dep. NTIS (US Sales Only) $14.00.

The work undertaken over the last few years on the Focus discharge has established the existence of two operational regimes, i.e., a regime characterized by a relatively isotropic neutron emission and justified by a thermonuclear model; and a highly anisotropic regime (revealed by high resolution measurements of neutron spectra in the 0 to 90° region). A detailed beam-target model leads to calculations which clearly show these anisotropies. This model has been generalized for constant particle-target velocities v_T. The systematic use of the generalized cross section term (which turns out to be a very practical mathematical treatment) enables the S(E,Ω) integral to be used for calculating neutron spectra. An example is presented in which this calculation (which is intended for a uniquely deuteron population) is applied to a Maxwellian type distribution. In the case where two populations can be introduced, a detailed mathematical analysis of the integral enables it to be calculated on a computer using exact analytical formulas. (FR)

29179 (CLM-R-133) COMPUTATION OF MHD EQUILIBRIA IN TOKAMAK. Thomas, C. L.; Haas, F. A. (UKAEA Research Group, Abingdon. Culham Lab.). Jan 1974. 16p. Dep. NTIS (U. S. Sales Only) $4.00. UK 50 pence.

A code (TOPE) was written to study MHD equilibria in Tokamak. Four different models of the equilibrium and the numerical techniques appropriate to each are considered. Where possible, asymptotic analysis has been developed, and used (a) to elucidate the qualitative features of the models, and (b) to check the code. The results are presented as a series of examples. (auth)

29180 (UCID-15316) NUCLEAR CORRECTION FOR GENESIS. Warren, D. T. (California Univ., Livermore (USA). Lawrence Livermore Lab.). Mar 1968. 32p. Dep. NTIS $4.75.

The present Genesis code includes no allowance for the potential energy of the nuclei of the atoms in their interaction with each other. (Their interaction with the electrons is, of course, included in the Thomas–Fermi calculations.) A description of the calculation that is being added to the Genesis code to include this nuclear potential energy is presented. The equations are assembled in Appendix II. Where they are derivable, the derivation is given in Appendix I. The assumptions behind the derivations are outlined, and the quality of the fit obtained is indicated. (auth)

29181 (UCID-15487) RUNAWAY EFFECTS IN THE INDUCTIVELY EXCITED LEVITRON. Hartman, C. W. (California Univ., Livermore (USA). Lawrence Livermore Lab.). 13 May 1969. 6p. Dep. NTIS $4.00.

In the levitron, the inductive/resistive electric field along B nearly always exceeds the Dreicer value $E_{\|}$ $\lambda \approx T_e$ $\lambda = 1/n\sigma$. Thus, enhanced resistivity or runaways can be important. For typical gun or ohmically produced plasmas enhanced resistivity appears to prevent runaways while not adding appreciably to the pump-out rate. On the other hand, hot electron plasmas produced by microwave heating are under very strong runaway conditions (actually energetic electron production involves runaway of $v_\perp$ in the microwave heating field) if not mirror trapped. The objective of this note is to point out that collisional isotropization of an initially mirror trapped hot electron plasma is essentially precluded by runaway effects under typical levitron conditions. It should be emphasized that this effect is not considered to be the dominant one in preventing isotropization in present experiments where banana-super banana effects appear to be important, but rather serves to define experimental conditions appropriate to the observation of isotropization. (auth)

29182 (UCID-15513) CALCULATING ELECTRON SYNCHROTRON RADIATION LOSS FROM A FUSION PLASMA. Carlson, G. A. (California Univ., Livermore (USA). Lawrence Livermore Lab.). 6 Aug 1969. 16p. Dep. NTIS $4.00.

A practical method is described for the calculation of electron synchrotron radiation loss from a plasma slab. The loss is a function of plasma parameters and vacuum wall reflectivity. (auth)

29183 (UCID-15628) CONSIDERATION OF A "BRUTE-FORCE" APPROACH TO THE ACHIEVEMENT OF HIGHER DENSITY IN THE PRESENCE OF INSTABILITY. Futch, A. H.; Damm, C. C. (California Univ., Livermore (USA). Lawrence Livermore Lab.). 25 Mar 1970. 10p. Dep. NTIS $4.00.

The question of the stability of a high-density plasma in which the ion distribution is determined by coulomb collisions between the ions is central for the approach to a fusion-reaction regime in open-ended systems. An estimate is given for the technological requirements for achievement of a collision-dominated density regime in the ALICE Baseball plasma, in the presence of instability losses during the buildup. If such a "brute-force" or "punch-through" procedure could be made to work, one could avoid the tedious and difficult sequence of programming the plasma temperature and density up from a low level (~1 keV, 10^8 ions/cm^3), where a collisional regime can be achieved stably. In order to make this estimate, it is assumed that the trapping processes for the ions are direct Lorentz ionization and inverted cascade of the excited neutral atoms in the beam. The loss processes are assumed to be charge exchange instability losses, and collisional scattering into the mirror loss cone with the characteristic times τ_{cx}, τ_l, and τ_s, respectively. τ_{cx} and τ_l are assumed to be independent of density while $\tau_s(n^+)$ is inversely proportional to density. (MOW)

29184 (UCID-15647) CALCULATED ION-DENSITY SPATIAL DISTRIBUTION IN ALICE BASEBALL I. Foote, J. H. (California Univ., Livermore (USA). Lawrence Livermore Lab.). 11 May 1970. 29p. Dep. NTIS $4.50.

The spatial distribution of the ion density was calculated for the plasma of the Alice Baseball I controlled thermonuclear research experiment, using the single-particle-orbit computer code TIBRO and its auxiliary routines. Computed ion orbits representing 105 trapping positions are weighted and summed to obtain the density results. Possible collective particle effects are not included in these calculations. Data are obtained for the conditions where the trapped-ion loss rate on the streaming gas in the beam region is zero times and ten times the loss rate on the background gas in the same region. The resulting two density distributions are similar. In both cases the center of the plasma is surrounded by a region of higher density (25 to 60% higher) a few cm out from the center. The density then gradually decreases from this peak-density region out to the last closed magnetic-field contour inside the vacuum-chamber wall, where it becomes zero. The peak-density region around the center is less pronounced in the high-streaming case because the streaming removes a larger fraction of those particles near the center. (auth)

29185 (UCID-15712) THERMALLY AVERAGED GAUNT FACTORS IN NON-RELATIVISTIC ELECTRON-ION BREMSSTRAHLUNG. Shaw, W. M. (California Univ., Livermore (USA). Lawrence Livermore Lab.). Jul 1970. 33p. Dep. NTIS $4.75.

Thermally averaged Gaunt factors are defined for electron–ion bremsstrahlung in a nondegenerate plasma. For nonrelativistic bremsstrahlung in a pure Coulomb field two approximations are used to obtain thermally averaged Gaunt factors. These results are compared with the accurate results of Karzas and Latter, who used Sommerfeld's exact cross section to obtain their thermally averaged Gaunt factor. The comparisons reveal that the Born–Elwert approximation yields a useful numerical description of bremsstrahlung in a fully ionized plasma. Finally, an empirical fit to the Karzas and Latter Gaunt factor is presented. (auth)

29186 (UCID-15820) DECAY OF PLASMA CURRENTS AND CHARGE IN BEAM PLASMA EXPERIMENTS. Briggs, R. J. (California Univ., Livermore (USA). Lawrence Livermore Lab.). 1 Mar 1971. 13p. Dep. NTIS $4.00.

Using a relatively high plasma conductivity, the decay of plasma currents after the electron beam pulse is readily observable. The question as to whether charge neutralization can proceed by axial currents flowing in the highly conducting channel to the end of the tank and back through the tank wall was investigated. It is shown how a simple "transmission line" model can accurately describe the longest current and charge decay times in the experimental configuration. The model allows one to match up a variety of initial conditions and get numbers for the relative magnitudes of the current and charge as a function of time. (MOW)

29187 (UCID-16003(Rev. 1)) ANALYTICAL EXPRESSION FOR THE E-LAYER ELECTRON VELOCITY DISTRIBUTION. Christofilos, N. C.; Porter, G. D. (California Univ., Livermore (USA). Lawrence Livermore Lab.). 5 Mar 1972. 8p. Dep. NTIS $4.00.

Distribution functions which are a function of the constants of motion, namely the canonical angular momentum and the electron energy, are obtained from the Vlasov equation. It is assumed that the E layer is thin in the radial direction and that all the electrons have the same canonical angular momentum and energy. Analytical expressions are obtained for the velocity distribution of the E layers. (MOW)

29188 (UCID-16004) OBSERVATIONS ON THE CHANGE OF THE LENGTH OF THE E-LAYER DURING STACKING. Christofilos, N. C.; Hester, R. E.; Sherwood, W. A.; Stallard, B. W.; Porter, G. D.; Weiss, P. B. (California Univ., Livermore (USA).

Lawrence Livermore Lab.). 11 Mar 1972. 13p. Dep. NTIS $4.00.

The question of elongation or contraction of the E layer during pulse stacking was studied. It is shown that conditions exist resulting in contraction of the E-layer length during the stacking phase resulting in a value of $\alpha \approx 0.5$ or less in most of the E layers. Therefore, by proper choice of the ramp parameters, e.g., the region between the inflector and the trap, the transverse temperature T corresponding to the collective axial velocity of the E layer can be small in comparison to T_m of the E layer. As a result, the E-layer length either remains unchanged or it contracts. (MOW)

29189 (UCRL-51598) HYBRID-1, A TWO-DIMENSIONAL FOKKER-PLANCK CODE. Mirin, A. A. (California Univ., Livermore (USA). Lawrence Livermore Lab.). 28 Jun 1974. Contract W-7405-eng-48. 82p. Dep. NTIS $5.45.

The basic equations and methods used to solve the two-dimensional Fokker-Planck equation for ions and electrons are summarized. The ion equation is integrated using a second order, alternating direction, implicit difference scheme. An implicit algorithm is used to integrate the electron equation. A detailed description of the program and a listing are included. (auth)

29190 THE INFLUENCE OF EXCITED STATES ON THE REACTIVE THERMAL CONDUCTIVITY OF AN L. T. E. HYDROGEN PLASMA. Capitelli, M. (Bari Univ. (Italy). Dipartimento di Chimica). Z. Naturforsch., a; 29: No. 5/6, 953-954(Jun 1974). 2 tabs.; 5 refs.

The influence of excited states on the reactive thermal conductivity of an L. T. E. hydrogen plasma has been studied by making realistic assumptions on the cross sections of these species. (GE)

29191 HYPERNETTED CHAIN SOLUTIONS FOR THE CLASSICAL ONE-COMPONENT PLASMA UP TO $\Gamma = 7000$. Ng, K. (Department of Physics and Astronomy, University of Florida, Gainesville, Florida 32611). J. Chem. Phys. 61: No. 7, 2680-2689 (1 Oct 1974).

The hypernetted chain equation has been solved numerically for the classical one-component plasma in a uniform background up to $\Gamma = 7000$, where $\Gamma = (Ze)^2/kTa$ and a is the ion-sphere radius. Numerical results are presented. The distribution functions and thermodynamical quantities obtained are in good agreement with the Monte Carlo results in the fluid region. The average potential energy $\bar{U}/NkT$ is in error by less than 0.8% for $20 \leq \Gamma \leq 160$ and approaches -0.8995Γ as Γ approaches infinity. The pressure and the free energy calculated do not show any evidence of a phase transition. However, the distribution function g(r) for $\Gamma \gtrsim 1500$ has an unusual behavior between $2.5 < r < 4.0$, resembling somewhat that of a hcp crystal. If we assume the sum of the bridge diagram to be of the form $B(r) = -\lambda\Gamma/r$ where $\lambda = 0.6$ erf (0.024Γ), the distribution function calculated agrees to within about ± 0.02 with the Monte Carlo g(r) in the whole fluid region. (auth)

29192 BREAK OF THE CURRENT SHEATH IN A NONCYLINDRICAL Z PINCH. Vikhrev, V. V.; Korzhavin, M. (Inst. of Atomic Energy, Moscow). JETP Lett. (USSR) (Engl. Transl.); 19: No. 8, 279-280(20 Apr 1974).

Translated from Zh. Eksp. Teor. Fiz., Pis'ma Red.; 19: No. 8, 528-531(20 Apr 1974).

The motion of a turbulization wave is considered for the case when the magnetic field is determined by the discharge current. The motion of such a wave can explain the sharp increase of the velocity of convergence of the current layer in the "break" regime in a noncylindrical z pinch. (auth)

Production

Refer also to abstract 29159.

29193 • (SLA-74-5242) SPECTRAL ANALYSIS OF X RAYS FROM LASER-INDUCED PLASMAS. Cuderman, J. F.; Glibert, K. M. (Sandia Labs., Albuquerque, N. Mex. (USA)). [nd]. 10p. (CONF-740809-1). Dep. NTIS $4.00.

From 23rd annual conference on applications of x-ray analysis; Denver, Colorado, USA (7 Aug 1974).

Laser interaction experiments have been conducted on Sandia Laboratories' four-beam laser system. In these experiments, pulses of 1.06 μm light of up to 50 J each were focused in a tetrahedral geometry onto CD_2 microspheres. A 22-channel x-ray spectrometer which utilizes silicon diodes with appropriate K-edge prefilters was used for x-ray measurements. Typically, bremsstrahlung recombination spectra were observed in the photon regime below about 5 keV. The electron temperatures for this part of the spectrum ranged from a few hundred eV to 1 keV with up to 15 percent of the total laser energy converted to x rays. Less than one percent of the total energy emitted as x rays appeared in the energy regime above 5 keV. (auth)

29194 METHOD OF OBTAINING A MEDIUM HAVING A NEGATIVE ABSORPTION COEFFICIENT IN THE X-RAY AND ULTRAVIOLET SPECTRAL RANGE AND A LASER FOR PRACTICAL APPLICATION OF SAID METHOD. Jaegle, P.; Carillon, A.; Dhez, P.; Jamelot, G.; Sureau, A.; Cukier, M.; Dupeyrat, M.; Vogel, C. (to Agence National De Valorisation de la Recherche). US Patent 3,826,996. 30 Jul 1974. Priority Date 28 May 1971, France. 14p.

A plasma is formed from a material in which the ions possess discrete metastable energy states interacting with the energy states of the continuum which are populated by the free electrons of the plasma. Population inversion is achieved between a number of these metastable states and states of lower energy, negative absorption being then produced for the transition which couples the metastable states with the states of lower energy. In order to form the plasma, a giant-pulse laser beam is caused to interact in vacuum with a solid target and is focused within the target near the surface through which the beam passes, the beam power being such as to ensure sufficiently populated metastable states of the ions of the material. (Official Gazette)

Stability

Refer also to abstracts 29154 and 29176.

29195 (LA-5693-MS) THEORY OF DRIFT-CONE MODES OF COLLISIONLESS PLASMA IN CYLINDRICAL GEOMETRY. McCrory, R. L. Jr.; McCune, J. E. (Los Alamos Scientific Lab., N. Mex. (USA)). Jul 1974. Contract W-7405-eng-36. 13p. Dep. NTIS $4.00.

The problem of the collisionless electrostatic flute-like drift-cone instability of a hot, fully ionized plasma in a magnetic field in cylindrical geometry is considered. The cylindrical plasma model includes those sources of free energy available to drive the instability inherent in many mirror confinement devices, i.e., radially varying density gradients and velocity space "loss-cone" like distribution functions. The zeroth order density distribution is a Gaussian in the radial direction. In this theoretical treatment, a singular integral equation is derived for the Hankel transform for each azimuthal component of the perturbed electrostatic potential in the plasma. The treatment includes the finite Larmor radius corrections to all orders of a_i/R (a_i is the ion Larmor radius, R the plasma radius) for those cases where the quantity is less than unity. One finds the radial eigenmodes of the system without resorting to the "local approximation" and the results give the cylindrical geometry marginal stability boundaries for the nonlocal flute-like drift-cone modes which indicates that the critical values of R/a_i are substantially lower than have previously been reported. These cylindrical results were applied to the Livermore 2X machine. The results show that the frequency at threshold for the drift-cone modes is sensitive to the ion-electron temperature ratio but relatively insensitive to a_i/R. (auth)

29196 (TID-26639) INVESTIGATION OF UNIVERSAL PLASMA INSTABILITIES. Annual Progress Report No. 9. (Maryland Univ., College Park (USA). Inst. for Fluid Dynamics and Applied Mathematics). 1 Jun 1974. Contract AT(40-1)-3405. 11p. Dep. NTIS $4.00.

The investigation reports on turbulence in collisionless plasma, anomalous plasma resistivity, and catalytic plasma heating. Catalytic heating describes the enhancement of the ohmic heating in a tokamak device caused by increasing the ohmic resistance of the plasma by artificial means. Other research on plasma measurements and instrumentation is described. A program for measuring the conductivity of anisotropic plasma is discussed. Summaries are also given for the following research areas: (1) parametric excitation of ion-acoustic waves, (2) nonlinear pulling effects in beam-plasma interactions, and (3) nonlinear saturation of aperiodic plasma instabilities. (MOW)

29197 (UCID-15540) NEGATIVE MASS INSTABILITIES IN BEAM INJECTED PLASMAS. Horton, W. (California Univ., Livermore (USA). Lawrence Livermore Lab.). 14 Aug 1969. 17p. Dep. NTIS $4.00.

In building up a plasma by beam injection techniques it is necessary to remain with $\omega_{pi}^2/\Omega_i^2 < 4\,\Delta^2$ to be stable against the ion-cyclotron modes with negative mass effects under conditions where $\Delta^2 = T_{||}/T_\perp \lesssim 4a_i/L_m$ and $L_p/a_i < \sqrt{M/m}$. Typically, the two latter conditions are satisfied in neutral injection experiments in the Baseball devices. The mode is sensitive to the pitch angle spread of the distribution function and suggests that the injection be done to maximize the spread. Further work is needed to determine whether the modes are eliminated in a collisionally broadened distribution where the present calculations are inadequate. (auth)

29198 (UCID-15711) SOME COMMENTS ON THE TRANSVERSE RESISTIVE WALL INSTABILITY (OR, "LNS REVISITED"). Neil, V. K. (California Univ., Livermore (USA). Lawrence Livermore Lab.). 13 Aug 1970. 9p. Dep. NTIS $4.00.

The first order force used in the treatment of transverse motion of a particle beam is discussed. A simple model of a beam inside a conducting pipe is given. The equation of motion for a particle in the beam is given for both the unperturbed and perturbed states. Resistivity of the wall is considered. The instability is then examined by means of the Vlasov equation in a self-consistent manner. (MOW)

29199 (UCID-15996) REDUCTION OF HOSE GROWTH BY CURRENT TAILORING. Bevc, V.; Lee, E. P. (California Univ., Livermore (USA). Lawrence Livermore Lab.). 11 Feb 1972. Contract W-7405-eng-48. 14p. Dep. NTIS $4.00.

The resistive hose distortion of a short pulse of relativistic electrons is reduced by several orders of magnitude by programming its current to increase from head to tail. (auth)

29200 PARAMETRIC INSTABILITY OF AN ELECTRON BEAM IN A MAGNETIC FIELD. Pasynok, A.I.; Repalov, N.S. (Physicotechnical Institute, Academy of Sciences of the Ukrainian SSR, Khar'kov). Sov. Phys.—Tech. Phys. 19: No. 2, 177-180 (Aug 1974).

A linear theory is developed for the oscillations of an electron beam in a spatially periodic electrostatic field in a presence of a homogeneous magnetic field. In contrast to the case $H_0 \to \infty$, there are additional resonance regions due to the intersection of branches of the dispersion diagram. The conditions under which such resonances occur are studied; expressions are obtained for the maximum growth rates in these resonance regions; the dependence of the growth rate on the period of the modulating field and on the magnitude of the magnetic field are found. (auth)

29201 ATTACHMENT INSTABILITY IN AN EXTERNALLY IONIZED DISCHARGE. Douglas—Hamilton, D.H.; Mani, S.A. (Avco Everett Research Laboratory, Inc., Everett, Massachusetts 02149). J. Appl. Phys. 45: No. 10, 4406-4415 (Oct 1974).

A new type of plasma instability is described in an electron—beam ionized discharge. This instability occurs in the form of current oscillations in gas mixtures in which the dissociative attachment rate increases strongly with electric field. It has been observed experimentally in He : H_2O 74 : 2 and in He : CO_2 1 : 1 and 9 : 1 mixtures. A theoretical analysis which describes the onset of instability is presented, and a physical explanation is given. The region of instability in parameter space of ionization source function S and electric field E is presented for certain gas mixtures. The transient phenomena in this type of discharge appear to be controlled by electron attachment, and a theoretical explanation of the observed current overshoot has been provided. (auth)

29202 EXPLOSIVE AND HIGH-FREQUENCY INSTABILITY OF ELECTROMAGNETIC WAVES IN A TWO ELECTRON STREAM SYSTEM. Plotkin, E. E.; Fainshtein, S. M. (Gorky Polytechnical Inst., USSR). Izv. Vyssh. Ucheb. Zaved., Radiofiz.; 17: No. 3, 333-337(1974). (In Russian).

The explosive and hf-instability of electromagnetic waves in a system of two electron streams is investigated. The synchronization conditions for interacting waves are clarified. It is shown that a hf-electromagnetic wave may be effectively generated in the system. Estimations for the laboratory plasma are given. (auth)

Thermonuclear Engineering and Equipment

Refer also to abstract 29243.

29203 (BNL-19043) RECOIL ENERGY DISTRIBUTIONS IN CTR-RELATED NEUTRON SPECTRA. Parkin, D. M.; Goland, A. N. (Brookhaven National Lab., Upton, N. Y. (USA)). 1974. 7p. (CONF-741017-9). Dep. NTIS $4.00.

From meeting of the American Nuclear Society; Washington, District of Columbia, USA (27 Oct 1974).

The dependence of the primary recoil energy spectrum upon the incident neutron spectra from several CTR neutron sources is examined. The purpose of this investigation is to provide necessary guidelines for the selection of an intense neutron source for simulating fusion-reactor neutron spectra. The computer code evaluates the probability P(T), that a recoil of energy T is produced. It calculates the differential primary recoil energy spectrum rather than just the fraction of recoils with energies above T. (MOW)

29204 (CLM-R-132) BUNDLE DIVERTORS AND TOPOLOGY. Taylor, J. B. (UKAEA Research Group, Abingdon. Culham Lab.). Feb 1974. 5p. Dep. NTIS (U. S. Sales Only) $4.00. UK 50 pence.

It is pointed out that a perfect "bundle divertor", composed of magnetic surfaces, is topologically impossible. (auth)

29205 (GSI-tr-73/20) COMPLETE NUCLEAR FUSION REACTIONS. Kalinkin, B. N.; Permyakov, V. P. Nov 1973. 50p. (In German). INIS.

15 figs.; 57 refs. Translation of the Russian report JINR-P-4-7312.

Following a review of the models for the formation of a compound nucleus with processes of complete nuclear fusion, the influence of large angular momenta on the effective cross-section for compound-nucleus formation has been particularly examined. Then the process, competing with nuclear fusion of the fission of heavy nuclei by ions, is dealt with, and in particular the mechanism of inelastic collisions in the fission and the distribution of the fission products. Finally, the various possible effects of the dynamics of nuclear fusion with complex nuclei are discussed. (GE)

29206 (LA-5336) ENGINEERING DESIGN STUDY OF A REFERENCE THETA-PINCH REACTOR (RTPR). Krakowski, R. A.; Ribe, F. L.; Coultas, T. A.; Hatch, A. J. (eds.). (Los Alamos Scientific Lab., N. Mex. (USA); Argonne National Lab., Ill. (USA)). Mar 1974. Contract W-7405-eng-36. 144p. (ANL-8019). Dep. NTIS $7.60.

An engineering conceptual design study of a fusion reactor power plant based on the theta-pinch concept is described. A high-beta, deuterium—tritium (DT) plasma is produced by means of a programmed pulsed magnetic field in an approximately toroidal chamber having major and minor radii of 56 and 0.5 meters, respectively. The field produces a short, fast implosion stage followed by a longer adiabatic compression stage during which the DT fusion occurs. The DT burn stage has a duration of ~ 0.080 sec, and the cycle time is 10 sec. To protect the first wall after the burn, a gas blanket is used to cool the plasma in a slowly decreasing magnetic field. The fusion reactor power plant consists of 10 major systems as follows: implosion heating, plasma compression and confinement, magnetic energy transfer and storage, first wall, blanket, biological shield, fuel supply and removal, fuel-ash reprocessing, lithium processing, and energy conversion. Liquid lithium is the primary coolant. Other materials include alumina, provisionally chosen as the first-wall insulator, niobium as the first-wall and blanket structural material, beryllium as the neutron breeder, and graphite as a moderator. Two energy conversion schemes are considered: i) a conventional, low-temperature system which uses a Na-steam cycle, and ii) an advanced, high-temperature steam system which uses a potassium topping cycle. Special attention is given to plasma burn dynamics, overall energy balance, blanket neutronics and thermal response, radiation shielding, radiation effects on and corrosion of construction materials, thermal and irradiation response of the Al_2O_3-Nb first wall, and tritium recovery and containment. Unique features of the design include a novel superconducting magnetic energy transfer and storage system and a modular blanket structure which permits easy access for maintenance. The engineering design is detailed enough to provide the basis for an environmental impact study (Vol. II) and an assessment of future research and development (Vol. III). (auth)

29207 (LA-5699-MS) MAGNETICALLY PROTECTED FIRST WALL FOR A LASER-INDUCED THERMONUCLEAR REACTION. Devaney, J. J. (Los Alamos Scientific Lab., N. Mex. (USA)). Jul 1974. Contract W-7405-eng-36. 6p. Dep. NTIS $4.00.

A modest magnetic field (3-kG) is found to protect a cylindrical wall (240-cm radius) against both the alpha pulse and the DT debris plasma from a laser-induced thermonuclear microexplosion (100-MJ). The calculations indicate that the Debye lengths are sufficiently small compared to the minimum possible dimensions so that both the α particles and the debris behave collectively. The explosion compresses the magnetic field to as much as 21 kG against a negligible-resistance coil or cylindrical sleeve. Expansions from 102 to 222 cm are possible depending on the residual gas density. The expanding plasmas are demonstrated to be weakly stable over a large part of their expansion. The instabilities that do develop are slow, allowing time for adequate pressure relief at the ends. (auth)

29208 (ORNL-TM-4619) SHIELDING DESIGN CALCULATIONS FOR ORMAK-F/BX. Gabriel, T. A.; Santoro, R. T.; Engle, W. W. Jr. (Oak Ridge National Lab., Tenn. (USA)). Aug 1974. Contract W-7405-eng-26. 35p. Dep. NTIS $4.75.

Calculations are presented which are oriented toward the initial shielding design for the ORMAK-F/BX, the ORNL version of a first-generation injection-heated d–T ("Wetwood") burning TOKAMAK-type thermonuclear reactor. The calculations include heating rates in the reactor system with special interest on the heating in the superconducting magnet regions, radiation-damage studies in insulating and current-conducting material, shield and interior wall activation and personnel dosimetry, building and wall composition and thickness, and void-streaming problems associated with entry ports into the reactor plasma region. (auth)

29209 (ORNL-TM-4657) DUOPIGATRON II ION SOURCE. Davis, R. C.; Jernigan, T. C.; Morgan, O. B.; Stewart, L. D.; Stirling, W. L. (Oak Ridge National Lab., Tenn. (USA)). Aug 1974. Contract W-7405-eng-26. 28p. Dep. NTIS $4.50.

The DuoPIGatron ion source concept at Oak Ridge has proven itself capable to provide multiampere beams at tens of kilovolts. The DuoPIGatron II operates very reliably at 6 to 8 A total output current in the voltage range of 25 to 35 kV. Impurity level is easily maintained below 0.4% and the 0.2 sec pulses show no appreciable wear on the copper acceldecel electrode system after thousands of pulses with duty cycles up to 10%. The 7 cm diameter grids are 50% transparent and optimum curvature of the grids allows about 60 to 65% of the current to be incident on a 9 cm diameter target 100 cm from the source. Beam ion and neutral species fractions have been measured as a function of total source current. Studies of the ion source plasma show an m = 1 helical instability to be present. Probe measurements show a density variation of about 25 to 30% across the extraction grid. Instantaneous density variations from ±10% to ±40%, depending on radius, are observed to be driven by the instability at 250 to 400 kHz. A stabilizer has been developed which reduces the oscillation amplitude by about an order of magnitude. Studies at extraction voltages up to 10 kV show that the use of the stabilizer yields a less divergent beam and higher current output through a single aperture either on axis or 1.8 cm from the source axis. (auth)

29210 (ORNL-TM-4666) EQUILIBRIUM AND STABILITY OF ELLIPTICAL CROSS SECTION TOKAMAK. Harris, E. G. (Oak Ridge National Lab., Tenn. (USA)). Sep 1974. Contract W-7405-eng-26. 26p. Dep. NTIS $4.50.

If a cylindrical column of plasma in a uniform axial magnetic field carries a uniform current density parallel to the axis and is surrounded by a perfectly conducting cylindrical shell of elliptic cross section, then the magnetic surfaces are concentric similar elliptic cylinders. If this cylinder is now bent into a torus of large aspect ratio, then to first order in the inverse aspect ratio, the magnetic surfaces retain their shape but are shifted relative to one another. The amount of this shift is calculated. Localized flute instabilities of the Suydam type are stabilized by the toroidal curvature. The physical origin of this stabilization is the line tying of regions of bad curvature to regions of good curvature. A stability criterion is calculated. The effect of finite conductivity on this stabilization mechanism is evaluated and shown to be unimportant. (auth)

29211 (RL-74-077) METHOD FOR THE CALCULATION OF THE MAGNETOSTATIC FIELD FROM A WIDE CLASS OF CURRENT GEOMETRIES. Rosten, H. I. (Science Research Council, Chilton (UK). Rutherford Lab.). May 1974. 76p. Dep. NTIS (US Sales Only) $6.75.

Thesis. Submitted to Reading Univ. (England).

The filamentary approach to the calculation of the magnetic field due to current sources (iron free) is generalized. Important examples from high energy physics and fusion research are treated. It is also of general interest to magnet designers in the electrical engineering industry. (auth)

29212 (UCID-15434) PROPOSED 2X DATA SYSTEM. Coensgen, F. H.; Cummins, W. F.; Nexsen, W. E.; Vogtlin, G. (California Univ., Livermore (USA). Lawrence Livermore Lab.). 20 Dec 1968. Contract W-7405-eng-48. 9p. Dep. NTIS $4.00.

A primary function of any data system for 2X is the provision for on-line data reduction of those critical measurements which serve as monitors of the experiment. Among these are: (1) thermonuclear reaction rate on both linear and log plots, (2) plasma density on linear and log plots, (3) the ion energy distribution as a function of time (this measurement which is derived from the charge exchange flux through the use of a multichannel mass-energy analyzer may use as many as 10 to 20 channels), (4) correlation of multiple ion probe and/or electron probe data, (5) electron temperature as a function of time (derived by means of neutral beam techniques), and (6) end-loss patterns or radial density distributions. The diagnostics of this experiment are changed frequently as the need for different information arises, but the foregoing list is typical. The proposed on-line analysis consists mainly of simple arithmetic operations, calculation of standard functions, and, at most, simple integration and iteration schemes. (MOW)

29213 (UCID-15448) LEVITRONS AND THE SUPERCONDUCTING LEVITRON: A SUMMARY. Hartman, C. W. (California Univ., Livermore (USA). Lawrence Livermore Lab.). 3 Feb 1969. 14p. Dep. NTIS $4.00.

A brief summary is given of levitron experiments to date. The design considerations, experimental details, and experimental program for the superconducting levitron are also detailed. (auth)

29214 (UCID-15481) NOTE ON THE ASTRON GUN DESIGN. Beal, J. W. (California Univ., Livermore (USA). Lawrence Livermore Lab.). 7 May 1969. 11p. Dep. NTIS $4.00.

The accelerating potential distribution of the Astron gun and its effects on the beam envelop are discussed. In particular, two potential distributions are considered: (1) a theoretical potential distribution as derived, and (2) the potential distribution as it exists in the present high gradient gun. The results indicate that for present gun potential distribution, the beam is overfocussed and blows up rapidly thereafter. For the case of the theoretical potential distribution, the beam is not overfocussed. (MOW)

29215 (UCID-15511) MTSE II FIELD CALCULATION. Anderson, C. J. (California Univ., Livermore (USA). Lawrence Livermore Lab.). 4 Jun 1969. 19p. Dep. NTIS $4.00.

A summary of magnetic field calculations for the MTSE II experiment is given. The MTSE II machine is similar to the 2X II machine. The calculations presented are to aid in comparing the results of the two experiments, and to use the Mafco code on the Livermore CDC 3600 computer. Three classes of calculations are included: (1) mirror coils and Ioffe bars, (2) added mirror ends and reflector bars, and (3) added images of Ioffe and reflector bars. (MOW)

29216 (UCID-15624) PROCEDURE FOR DEUTERATING TITANIUM. Finlayson, V. A. (California Univ., Livermore (USA). Lawrence Livermore Lab.). 7 Mar 1970. 12p. Dep. NTIS $4.00.

A description and operation procedure for the facility used in deuterating titanium elements used in the 2X plasma guns are given. Basically the facility is a vacuum furnace in which titanium rings may first be purified by annealing and later presented with a known amount of deuterium for absorption. The ratio of the number of atoms of deuterium absorbed to the number of titanium atoms is approximately 0.90 : 1. When the ratio reaches 0.94 : 1, the titanium becomes mechanically weak and crumbles. (auth)

29217 (UCID-15650) PRELIMINARY REPORT OF DIRECT RECOVERY STUDY. (California Univ., Livermore (USA). Lawrence Livermore Lab.). 15 May 1970. 134p. Dep. NTIS $9.75.

A study group was set up at the Lawrence Radiation Laboratory to assess the problems associated with direct conversion of charged particle kinetic energy to electrical energy. The primary objective was to delineate a systematic approach to the development of a direct converter. The study group met weekly beginning in mid-December 1969, with an extensive set of minutes resulting therefrom. This report is a condensed and edited version of the minutes of those meetings as well as a view of what a direct conversion system might look like and a suggested program towards its realization. (auth)

29218 (UCID-15660) ALICE VACUUM SYSTEM: SEPT. 1969. Goodman, R. K.; Hunt, A. L. (California Univ., Livermore (USA). Lawrence Livermore Lab.). 8 Jun 1970. 18p. Dep. NTIS $4.00.

The ALICE vacuum system as of September 1969 is generally described. Typical operating conditions and procedures are given. (auth)

29219 (UCID-15695) SURFACE CURRENTS ON A TOROID THAT RESULT IN A UNIFORM, AXIAL MAGNETIC FIELD INSIDE THE TORUS. Cooper, R. K.; Neil, V. K. (California Univ., Livermore (USA). Lawrence Livermore Lab.). 24 Jul 1970. 21p. Dep. NTIS $4.25.

Toroidal coordinates were used in the study. For a uniform axial field B the vector potential is easily found in cylindrical coordinates r,ϕ,z. In the equation $A_\phi = Br/2 + \Phi/r$ the first term yields the proper field, and the second term yields no field. (Φ is an arbitrary constant.) All current on the toroidal surface is in the ψ-direction, which is the same as the ϕ-direction in cylindrical coordinates. The problem is broken into two parts; first one finds a distribution of surface current that yields $A_\psi (\equiv A_\phi) = Br/2$ inside the torus. This surface current is a particular solution to the problem at hand, but not necessarily the most desirable. Second one finds a distribution of surface current that yields $A_\psi = \Phi/r$ inside the torus. An arbitrary amount of this second solution may be added to the first solution without changing the field inside. The second solution controls to some degree the field outside the torus. (MOW)

29220 (UCID-15806) RADIATION AND HEAT DEPOSITION ANALYSIS OF THE PROPOSED MIRROR FUSION EXPERIMENT (MFX). Kearney, J. P. (California Univ., Livermore (USA). Lawrence Livermore Lab.). 19 Feb 1971. 17p. Dep. NTIS $4.00.

The Mirror Fusion Experiment (MFX) is intended to demonstrate electric power production by a fusion reactor using a D-^{3}He fuel cycle and direct conversion of the energy of the charged particles produced by this reaction. This large step in the LRL mirror program necessitates an extensive investigation into the quantities of radiation produced by sustained fusion reactions and the consequences of that radiation. The operating characteristics of the plasma are described from the standpoint of power production and the radiation and thermodynamic effects on the reactor surrounding the plasma. (auth)

29221 (UCID-15939) ENERGY RECOVERY OF A LITHIUM ION BEAM. Price, R. H. (California Univ., Livermore (USA). Lawrence Livermore Lab.). 1 Nov 1971. 36p. Dep. NTIS $5.00.

Experiments were done to demonstrate that by recovering the energy from an ion beam and feeding it back to the ion accelerator, beam power levels could be produced which were much larger (15 times larger) than the power input from the power supply. Various sources of power loss from the beam are discussed and energy recovery efficiencies as high as 92.3% are demonstrated with a 10 keV, one microampere lithium ion beam. (auth)

29222 (UCID-15953) ADEQUACY OF LITHIUM SUPPLIES AS A FUSION ENERGY SOURCE. Holdren, J. P. (California Univ., Livermore (USA). Lawrence Livermore Lab.). 8 Dec 1971. Contract W-7405-eng-48. 9p. Dep. NTIS $4.00.

Even the most conservative estimates of exploitable lithium supplies lead to the conclusion that D−T fusion reactors, breeding their tritium from natural lithium, could meet an electricity demand much larger than today's for centuries. (auth)

29223 (UCID-15956) WEAK INTERACTION OF A NEUTRALIZED E-LAYER WITH RESISTORS. Fessenden, T. J. (California Univ., Livermore (USA). Lawrence Livermore Lab.). 29 Nov 1971. 24p. Dep. NTIS $4.25.

A simplified theoretical description of the interaction of the moving E-layer fields with the Astron resistor structures is given. It is shown that, if the interaction is weak, the resistors slow the axial motion of the layer without affecting its axial rotation. Computer calculations are given which may be used to estimate the energy dissipated per unit length of the entire layer and of each electron for various situations. These curves are useful for adjusting the coupling of the layer to the resistor structures. (auth)

29224 (UCID-15977) BACK CURRENT IN AN E-LAYER. I. Berk, H. L.; Pearlstein, L. D. (California Univ., Livermore (USA). Lawrence Livermore Lab.). 20 Dec 1971. 9p. Dep. NTIS $4.00.

It is shown that an E-layer develops a back current which usually tends to cancel the current of newly injected current sources. (auth)

29225 (UCID-16057) RESISTOR BEAM BUGS: SCIENTIFIC EXPLANATION. Cooper, R. K.; Neil, V. K. (California Univ., Livermore (USA). Lawrence Livermore Lab.). 12 Jun 1972. Contract W-7405-eng-48. 17p. Dep. NTIS $4.00.

The so-called resistor beam bug has proven to be a very useful diagnostic tool for determining the amount of beam current flowing inside a conducting pipe. The bug is also useful for determining the transverse position of the beam centroid relative to the geometric center of the pipe. The bug consists of a gap in the pipe to interrupt the return currents in the wall. The gap is then bridged by a large number of resistors in parallel. An exact analytic treatment of the voltage across the gap as a function of azimuth and time seems impossible. Expressions are derived for the voltage using a transmission line model. (MOW)

29226 WAVE−WAVE COUPLING IN MULTIPLE-ION PLASMAS. Brice, N. (Cornell Univ., Ithaca, NY). J. Geophys. Res.; 79: No. 16, 2519-2520(1 Jun 1974).

It is pointed out that the presence of more than one ion in a plasma opens up several possibilities for wave−wave coupling that are not available in a single-ion plasma. This can be demonstrated by using the parallelogram construction on an $\omega-k$ diagram. Such a diagram for three ions (hydrogen, helium, and oxygen) appropriate to wave propagation in the upper ionosphere is given. (JFP)

29227 MEDUSA. A One-Dimensional Laser Fusion Code. Christiansen, J. P.; Ashby, D. E. T. F.; Roberts, K. V. (UKAEA Research Group, Abingdon. Culham Lab.). Comput. Phys. Commun.; 7: No. 5, 271-287(May 1974).

The feasibility of laser fusion as a method for generating controlled thermonuclear power has so far been mainly based on computer simulation. MEDUSA 1 has been written to investigate in one space dimension some of the hydrodynamic and plasma processes that take place in a small pellet which is irradiated by laser light. The plasma is described by 4 main dependent variables ρ, μ, T_i, T_e, which represent respectively the density, velocity and ion and electron temperatures. These are functions of the time t and of a single space variable r which can be chosen to correspond to slab, cylindrical or spherical geometry as required. Subsidiary variables represent the chemical composition of the plasma in terms of the fractions of the various ionic species that are present, the composition varying in space and time due to the thermonuclear reactions that occur. The Navier-Stokes equations are supplemented by separate heat conduction equations for the ion and electron temperatures and a variety of additional effects are included. A lagrangian difference mesh is employed, the integration scheme being explicit for the hydrodynamics and implicit for the heat conduction equations using the Crank-Nicholson scheme and the Gauss elimination method. Several iterations are performed at each time-step in order to take into account the non-linear dependence of the physical coefficients on the density and temperatures and to ensure convergence. (auth)

29228 PRELIMINARY APPRAISAL OF A FUSION/FISSION (HYBRID) REACTOR BASED ON THE LINEAR THETA PINCH. Bosler, G. E.; Dudziak, D. J.; Ellis, W. R. (Los Alamos Scientific Lab., NM). pp 710-718 of 9th Intersociety Energy Conversion Engineering Conference Proceedings. New York; American Society of Mechanical Engineers (1974).

From 9th Intersociety Energy Conversion Engineering Conference; San Francisco, California, USA (26 Aug 1974). See CONF-740805-.

In order to produce a useful output of energy, a D−T fusion reactor must exceed the Lawson "breakeven" criterion ($n\tau \approx 10^{20}$ m^{-3} s, where n is the ion number density and τ is the confinement time) by roughly an order of magnitude. One such device in which this might be accomplished is the linear theta pinch, in which a long cylinder of reacting plasma is contained (radially) in a straight uniform magnetic field. The maximum plasma density which can be contained at thermonuclear temperature (e.g., 10 keV) is approximately 2×10^{23} m^{-3}, set by strength of materials considerations ($B_{max} \approx 40$ tesla, corresponding to a magnetic pressure of 650 MPa on the coil). In order to achieve $n\tau$ values of 10^{21} m^{-3} s, therefore, the plasma must remain confined for ~5 ms. Assuming that plasma confinement is limited by particle flow out of the open ends at essentially the ion thermal velocity, the machine length required to achieve this is ~1.2 km. A significant reduction in the required reactor length can be made by using the 14-MeV neutrons from the plasma to create neutron multiplication and exoergic fission reactions in a surrounding blanket made of Uranium-238 or some other fissionable material. By this means the energy release per neutron can be increased from ~19 MeV [14 MeV birth energy plus ~5 MeV from the ^{6}Li(n,α)t tritium breeding reaction in the blanket] to approximately 200 MeV, with an attendant reduction in the effective Lawson criterion by a factor of ~10. Such an arrangement is sometimes called a fusion/fission hybrid, and in the case of the Linear Theta-Pinch Reactor (LTPR), offers the advantage of a greatly reduced circulating power fraction (by a factor of ~10, other things being equal), in addition to a greatly reduced length (~200−400 metres). We compare predicted reactor parameters and neutronics characteristics for several blanket variations. Structural and moderating materials are included in the neutronics analysis, and provision is made for coil cooling by flowing helium. Neutron and gamma-ray heating, and radiation damage effects are evaluated. Neutronic calculations are performed in one-dimensional cylindrical geometry, using the discrete ordinates transport code DTF-IV. Multigroup transport is calculated with an S_4 quadrature and 25-group, P_3 cross sections. All cross sections are derived from the Los Alamos Nuclear Data File. (auth)

29229 ECONOMIC AND ENVIRONMENTAL ASPECTS OF A FIRST-GENERATION FUSION POWER PLANT. Mills, R. G. (Princeton Univ., NJ). pp 726-730 of 9th Intersociety Energy Conversion Engineering Conference Proceedings. New York; American Society of Mechanical Engineers (1974).

From 9th Intersociety Energy Conversion Engineering Conference; San Francisco, California, USA (26 Aug 1974). See CONF-740805-.

The Reactor Studies Group at Princeton has recently completed a thorough, self-consistent conceptual design of a first generation fusion power plant. Selection of form, operating cycle, and materials has been made to avoid most known problems and to minimize the number of assumptions necessary due to lack of knowledge in plasma physics and materials damage. This plant has not been optimized in any sense, but is merely one reference design against which to test the effects of varying parameters or varying assumptions. Nevertheless it appears that even a first generation power plant will be attractive economically and environmentally acceptable. A brief description of the system is given together with cost estimates. (auth)

29230 CONCEPTUAL DESIGN OF A SERIES OF LASER-FUSION POWER PLANTS OF 100 TO 3000 MW(e). Fraas, A. P. (Oak Ridge National Lab., TN). pp 738-747 of 9th Intersociety Energy Conversion Engineering Conference Proceedings. New York; American Society of Mechanical Engineers (1974).

From 9th Intersociety Energy Conversion Engineering Conference; San Francisco, California, USA (26 Aug 1974). See CONF-740805-.

The many boundary conditions that must be met to give a commercially viable laser-fusion reactor are outlined. These provide the rationale for choosing the lithium vortex of the Blascon system as the basis for evolving a set of six conceptual designs of laser-fusion power plants. The choice of power conversion system and tritium recovery system largely condition the plant layout and the lithium through-put for the reactor. Analytical and experimental studies are correlated to establish the probable effects of the blast for a range of design conditions. These studies show that the vortex system can be proportioned so that, for a typical energy release of ~2 × 10^8 J per pulse, the stress induced in a 4 m diameter, 5 cm thick spherical pressure vessel with a 22 cm radius vortex cavity will be of the order of only 0.7 kg/mm^2 (1000 psi). Further, the shape of the vortex cavity will be only moderately disturbed by the blast, its original shape will be restored in a fraction of a second, and there should be essentially no blowback through the muffler arrangement of the injection port. The principal limitations on the pulse rate will be in the laser system and in the rate of heat dissipation by eddy diffusion in the vortex. The latter limitation for the design conditions chosen appears to be about 3 sec. The outstanding questions appear to be the feasibility of getting a suitable laser system and pellet geometry. In addition, there are important questions with respect to the validity of the scaling relations used in going from the model tests to actual units. (auth)

29231 HIGH POWER Nd:GLASS LASER FOR FUSION APPLICATIONS. Soures, J.; Kumpan, S.; Hoose, J. (Laboratory for Laser Energetics of the College of Engineering & Applied Science, University of Rochester, Rochester, New York 14627). Appl. Opt. 13: No. 9, 2081-2094 (Sept 1974).

Experiments on laser—induced thermonuclear fusion require high brightness lasers capable of producing subnanosecond pulses with total energy content of several kilojoules. Of existing laser media, Nd:glass appears to be the best choice for meeting these criteria. In this paper we discuss the problems of designing a high power Nd:glass laser system. A detailed description of an operating two—beam system producing subnanosecond pulses with a maximum energy of 350 J per beam is presented, along with an extensive description of beam diagnostic techniques. A four beam version of this system became operational on 3 April 1974 and is now producing energies in excess of a kilojoule in subnanosecond pulses. (auth)

29232 THERMONUCLEAR FUSION POWER. Roberts, K. V. (United Kingdom Atomic Energy Authority, Springfields, Eng.). Environ. Change; 2: No. 5, 329-338(Jan 1974).

A general account is given of thermonuclear fusion power. A brief introductory survey is made of other energy sources including nuclear fission. The nuclear fusion reactions of deuterium and tritium are described as well as the use of lithium as a raw material for producing tritium. The physical basis of the machines designed to produce hot plasma is outlined, and the need to confine the hot plasma until it has had time to react is explained. Confinement devices depending on magnetic fields are considered, and the effectiveness of various configurations of field discussed. The possibilities of inertial confinement, and the use of specially developed lasers to heat the plasma, are shown. The radiation hazards of fusion reactors are compared with hazards involved in the use of fission reactors. Possible designs of large scale thermonuclear reactors, and the international research programs directed towards the development of such reactors, are described. (UK)

Wave Phenomena

29233 (UCRL-51631(Pt.1)) INTERACTION OF INTENSE MICROWAVE RADIATION AND FULLY IONIZED HYDROGEN PLASMA. Part 1. High-Density System. Ensley, D. L. (California Univ., Livermore (USA). Lawrence Livermore Lab.). 26 Jul 1974. Contract W-7405-eng-48. 48p. Dep. NTIS $4.00.

The interaction of intense standing-wave radiation and a fully ionized plasma is investigated for $\omega/\omega_{pe} < 1$. The high-density case is treated here, for which $\nu_e/\omega \gtrsim 1$ at corona densities satisfying the confinement relation, but for which there is no average confinement. It is demonstrated that under certain realizable circumstances the energy-absorption time of the plasma is less than the inertial disassembly time, and that the radiation/plasma interface is stable for perturbations less than the external field radiation wavelength. (auth)

29234 EXCITATION OF ELECTROMAGNETIC ION CYCLOTRON WAVES BY FAST IONS. Kaladze, T.D.; Lominadze, D.G.; Stepanov, K.N. Sov. Phys.—Tech. Phys. 19: No. 2, 175-176 (Aug 1974).

The growth rate is computed for ion cyclotron waves that propagate across the magnetic field in a deuterium plasma. The waves are excited by a low—density beam of fast ions that result from fusion reactions. (auth)

29235 SCATTERING BY ION—ACOUSTIC WAVES IN A RECTANGULAR WAVEGUIDE. Troitskii, S.V. (A. M. Gor'kii Khar'kov State University). Sov. Phys.—Tech. Phys. 19: No. 2, 181-184 (Aug 1974).

An analytical expression is obtained for the scattering cross section for the fundamental mode in a rectangular waveguide containing a plasma in which there is a direct drift of the electrons with respect to the ions. Using linear theory, we study scattering conditions close to threshold, where the fluctuation level in the plasma is anomalously large. An experiment is described which involves scattering by ion—acoustic oscillations in a helium positive column located in a rectangular waveguide. (auth)

29236 MULTIMODE PARAMETRIC INTERACTIONS IN A PLASMA WITH LOW—FREQUENCY PUMPING. Sorokin, Y.M.; Stepanov, N.S. (N. I. Lobachevskii Gor'kii State University). Sov. Phys.—Tech. Phys. 19: No. 2, 185-189 (Aug 1974).

Multimode processes are analyzed in an isotropic, collisionless electron plasma whose density varies as a function of position and time under the influence of a low—frequency pumping wave. The spectrum of the high—frequency perturbation is assumed to be broad (on the scale of the pumping frequency) and smooth, so that the problem can be reduced to one of analyzing a single first—order partial differential equation for a complex amplitude. In this system, the perturbation spectrum can periodically shift upward or downward and undergo deformation, and the total wave energy can change. Synchronization of the pump with the high—frequency signal causes a monotonic shift of the spectrum upward (or downward), a simultaneous compression (or expansion) of the spectrum, and an increase (or decrease) in the total wave energy, depending on the particular phase relations. Both the boundary—value problem and the initial—value problem are solved. (auth)

29237 SCATTERING OF HIGH—FREQUENCY ELECTROMAGNETIC WAVES BY ION—ACOUSTIC OSCILLATIONS IN A BOUNDED PLASMA. Shaptala, V.G. (A. M. Gor'kii Khar'kov State University). Sov. Phys.—Tech. Phys. 19: No. 2, 193-196 (Aug 1974).

The scattering of high—frequency electromagnetic wave by regular ion—acoustic oscillations is studied in a plane homogeneous plasma with and without a fixed magnetic field parallel to the plasma boundary. The problem is treated in the hydrodynamic approximation and the nonlinearity is assumed to be weak. Expressions are found for the electromagnetic waves emitted into the vacuum at frequencies $\Omega_n = \Omega + n\omega$ (Ω is the frequency of the electromagnetic wave and ω is the frequency of the ion—acoustic wave, $n = \pm 1, \pm 2, \ldots$) for the case of total internal reflection and for transparency. It is shown that the amplitude of the scattered wave increases as the frequency of the probing signal approaches the plasma frequency. (auth)

29238 GENERATION OF BERNSTEIN MODES IN A BEAM—PLASMA SYSTEM. Fedorenko, V.N. (A. F. Ioffe Physicotechnical Institute, Academy of Sciences of the USSR, Leningrad). Sov. Phys.—Tech. Phys. 19: No. 2, 171-174 (Aug 1974).

The correlation of fluctuating electric fields associated with Bernstein modes in a beam—plasma system is analyzed. The criteria for the kinetic instability of Bernstein modes are analyzed. Certain experimental results are interpreted. (auth)

ENGINEERING

Energy Conversion

Refer also to abstracts 29217 and 31207–31209.

29239 (JUL-73) IMPLANTED ENERGY CONVERSION SYSTEM. Annual Report, 8 July 1972–8 July 1973. Johnston, R. P. (McDonnell Douglas Astronautics Co., Richland, Wash. (USA). Donald W. Douglas Labs.). Jul 1973. 104p. (MDC-G4418; PH-43-67-1408-6). NTIS $4.50.

Progress toward developing an implantable power source for an artificial heart based on the stirling cycle principle is described. During recent acute animal implant tests spanning up to 28 h, a completely implanted radioisotope-fueled power source achieved full ventricle relief without external power or control while assuming the full pumping load of the arterial side of the cardiovascular system. Bench tests show that the power source provides ventricle relief at blood flow to 10 liters/minute. The engine operated continuously at designed power for over seven months during an electrically heated laboratory life test. (GRA)

29240 DIRECT HEAT REJECTION PATH RADIOISOTOPIC THERMOELECTRIC GENERATOR. Snyder, D. L.; Himes, J. H.; Pravda, M. F. (to Isotopes, Inc.). US Patent 3,833,428. 3 Sep 1974. Filed date 25 Sep 1969. 10p.

Compression springs on the hot side, bias the thermoelectric elements of the radioisotopic-powered thermoelectric generator into contact with the casing wall. The bus straps, which electrically connect the cold ends of the thermoelectric elements, are bonded directly to the inner wall of the casing by a pressure sensitive epoxy adhesive which is preferably a dielectric but a good thermal conductor thereby eliminating the need for cold-end hardware. (Official Gazette)

29241 HIGH PERFORMANCE THERMAL INSULATION FOR AN IMPLANTABLE ARTIFICIAL HEART. Stoner, D. R. (Westinghouse Electric Corp., Trafford, PA); Svedberg, R. C.; Chi, J. W. H.; Vojnovich, T. pp 275-289 of Heat Transmission Measurements in Thermal Insulations. Tye, R. P. Philadelphia; American Society for Testing and Materials (1974).

From heat transmission measurements in thermal insulations conference; Philadelphia, Pennsylvania, USA (16 Apr 1973).

The practicability of an implantable artificial heart is strongly dependent on the availability of a high performance, compact, and lightweight thermal insulation system to contain the radioisotope energy source. The insulation system must limit losses to less than 0.024 W/cm^2 to maintain an acceptable thermal efficiency with the Stirling engine heat source at 870°C. On the basis of the overall system requirements, vacuum metal foil insulation is the only acceptable choice. Concentric nickel foil cups were utilized in place of the standard spiral-wrapped foil design with mitered corners, thereby eliminating a serious heat leak and the structural problems generally associated with the corners. Initial total system thermal performance tests have been very encouraging and predict that a system heat loss of 2 W can be met with about 35 to 40 foil cup layers. Since the implantable system is to be designed for a sealed ten-year lifetime under static vacuum, measurements are also being made to determine the long-time performance and outgassing characteristics of the nickel packages. (auth)

29242 HEAT TRANSMISSION MEASUREMENTS IN THERMAL INSULATIONS. Conference Held at Philadelphia, Pennsylvania, April 16–17, 1973. Tye, R. P. ASTM Special Technical Publication 544. Philadelphia; American Society for Testing and Materials (1974). 316p. (ASTM-STP-544; CONF-730479–). $30.75.

Nineteen papers were presented. A separate abstract was prepared for one paper. The remaining 18 papers on heat transfer measurements in thermal insulations were not in scope for NSA. (LCL)

29243 9TH INTERSOCIETY ENERGY CONVERSION ENGINEERING CONFERENCE PROCEEDINGS, SAN FRANCISCO, CALIFORNIA, AUGUST 26–30, 1974. New York; American Society of Mechanical Engineers (1974). 1356p. (CONF-740805-).

One hundred sixty-four papers were presented at the conference. A separate abstract was prepared for each of 26 papers. The remaining papers were not within the scope of NSA. (RCK)

For abstracts of individual papers see: 29228–29230, 29244–29263, 31210, 31238, and 31239.

29244 RTG TECHNOLOGY DEVELOPMENT: WHERE WE ARE/WHERE WE ARE GOING. Goldenberg, N. (Atomic Energy Commission, Washington, DC). pp 144-146 of 9th Intersociety Energy Conversion Engineering Conference Proceedings. New York; American Society of Mechanical Engineers (1974).

From 9th Intersociety Energy Conversion Engineering Conference; San Francisco, California, USA (26 Aug 1974). See CONF-740805-.

Recent advances in RTG technology show promise of doubling current efficiencies. Existing conversion technology is reviewed and compared with technologies currently in development. The status and projections of the selenide thermoelectric program is presented. The objective of the heat source technology program is discussed and the concept of "no identifiable failure mechanism" defined. The increased emphasis on noble metal technology is examined. (auth)

29245 MODULAR HEAT SOURCE FOR ^{244}Cm AND ^{238}Pu. Aller, P. F.; Miskuff, R. J. (Teledyne Isotopes, Timonium, MD). pp 147-151 of 9th Intersociety Energy Conversion Engineering Conference Proceedings. New York; American Society of Mechanical Engineers (1974).

From 9th Intersociety Energy Conversion Engineering Conference; San Francisco, California, USA (26 Aug 1974). See CONF-740805-.

A radioisotope heat source is presented to satisfy the following: (1) provide a significant improvement over state-of-the art heat source performance; (2) be optimally integrable with a thermoelectric converter; (3) contain either ^{244}curium or ^{238}plutonium fuel; (4) be adaptable to a large range of power levels with little or no modification; and (5) meet newly established safety criteria. The design approach consisted first of itemizing all known requirements or desirable characteristics and categorizing them. All existing heat source technologies were examined and evaluated in detail with respect to the parameters desired for this heat source. The design characteristics and safety attributes were then used to generate a number of heat source designs. The considerations examined included shapes, materials, capsule construction, insulation techniques, vents, number of heat sources, arrangement of heat sources, isolation from thermopile, and shielding. The following analyses were applied: (1) safety, the important parameters being probability of failure due to launch pad abort (blast, fire, and impact), probability of failure due to reentry melting of capsule or excessive thermal stresses in heat shield, probability of failure due to impact, burial, and post impact oxidation, recovery probability of capsules after reentry and impact, and overall hazards per individual unit; (2) reliability; (3) cost; (4) weight; and (5) integration, with important characteristics such as venting, interchangeability of fuel (^{244}curium or ^{238}plutonium), facility of fueling, and modularity (growth potential). The design approach followed and its utilization for optimum design selection is described. The final heat source design is described and its performance, both nominal and during probable abort conditions, is discussed. The heat source, as characterized, is compared with other state-of-the-art heat sources. (auth)

29246 FABRICATION AND TESTING OF A THERMOELECTRIC RING CONVERTER SEGMENT FOR SPACE APPLICATIONS. Elsner, N. B.; Bradshaw, G. B.; Shearer, C. H.; Morris, C. C. (General Atomic Co., San Diego, CA). pp 165-170 of 9th Intersociety Energy Conversion Engineering Conference Proceedings. New York; American Society of Mechanical Engineers (1974).

From 9th Intersociety Energy Conversion Engineering Conference; San Francisco, California, USA (26 Aug 1974). See CONF-740805-.

The RING converter is a second generation, lightweight modular generator that evolves from the TRANSIT thermoelectric converter technology. The TRANSIT has operated successfully in orbit since launch in September, 1972. This newer design is an upgrading with respect to: (1) lower fabrication costs; (2) ease of assembly; (3) higher tolerance for launch vibration conditions; (4) increased efficiency; (5) longer lifetime; (6) power output to 500 watts(e) and above; and (7) growth potential. In the past year, the first RING converter segment was fabricated and tested under simulated space conditions at JPL in Pasadena. The fabricating methods discussed include vacuum warm pressing the N type PbTe and P type segmented PbSnMnTe/BiSbTe thermoelectric elements, the laser welding of the elements to the radiator structure, assembly of the super insulation incorporating micapost hold-downs, and laser welding of the heat collectors to the thermoelectric elements. The test data obtained with the RING converter is presented and compared with laboratory and space data measured on the TRANSIT generator. (auth)

29247 SILICON GERMANIUM TECHNOLOGY PROGRAM AT JPL. Stapfer, G.; Truscello, V. C. (California Inst. of Tech., Pasadena). pp 171-176 of 9th Intersociety Energy Conversion Engineering Conference Proceedings. New York; American Society of Mechanical Engineers (1974).

From 9th Intersociety Energy Conversion Engineering Conference; San Francisco, California, USA (26 Aug 1974). See CONF-740805-.

The upcoming space exploration missions at JPL will utilize Radioisotope fueled Thermoelectric Generators (RTGs) to provide the necessary electrical spacecraft power. To support these missions, the Nuclear Power Sources Group at JPL has been conducting a comprehensive materials technology program. Under the auspices of the Atomic Energy Commission, the high temperature silicon germanium thermopile and associated thermal insulation system, being developed for the MHW program, has been evaluated. Some of the more recent results of this program are evaluated. The paper addresses itself primarily to the areas of material compatibilities and material degradation. Material compatibility areas which were studied and analyzed are the interaction phenomena which occur between the basic SiGe unicouple and its surrounding thermal insulation. The primary material degradation mechanisms which have been studied and analyzed are the thermal and electrical changes of the thermal insulation material; however, material degradation occurring within the thermoelectric material itself is also discussed. Also included are the results obtained from metallographic examinations of unicouples and insulation materials which have operated at various operating temperatures and conditions. (auth)

29248 PERFORMANCE TESTING OF THERMOELECTRIC GENERATORS AT JPL. Rouklove, P.; Truscello, V. (California Inst. of Tech., Pasadena). pp 177-184 of 9th Intersociety Energy Conversion Engineering Conference Proceedings. New York; American Society of Mechanical Engineers (1974).

From 9th Intersociety Energy Conversion Engineering Conference; San Francisco, California, USA (26 Aug 1974). See CONF-740805-.

One phase of the thermoelectric program at JPL is the performance evaluation of thermoelectric generators. At present 12 generators, ranging in output power from 800 μW to 170 W, are undergoing tests. The results of the tests of some of these generators are presented with emphasis on three generators of advanced concept: A Transit type generator, a "High Performance Generator" (HPG) and a Ring Converter generator. The behavior of other generators, representing Nimbus, Pioneer and Viking technology, is summarized. Results of the long term (50,000 to 60,000 h) life tests of some of these generators are presented. (auth)

29249 SNAP 19 VIKING RTG FLIGHT CONFIGURATION AND INTEGRATION TESTING. Brittain, W. M.; Christenbury, S. T. (Teledyne Isotopes, Timonium, MD). Contract AT(49-15)-3069. pp 185-192 of 9th Intersociety Energy Conversion Engineering Conference Proceedings. New York; American Society of Mechanical Engineers (1974).

From 9th Intersociety Energy Conversion Engineering Conference; San Francisco, California, USA (26 Aug 1974). See CONF-740805-.

Application of RTG's to the Viking-75 mission presents a significant challenge in the areas of thermal and electrical integration. The wide variation in thermal environments experienced during the mission phases directly influences the electrical power profile for the RTG's. Due to planetary quarantine requirements for microorganisms, fueled RTG's will be sterilized for the first time, along with the lander, while contained in a biocanister. During subsequent ground operations and launch, the RTG's/lander will remain in the biocanister. The Viking-75 mission environments and lander interface requirements which influence the design of the RTG, as well as RTG-related constraints are discussed. The baseline RTG design evolved from these considerations is presented with particular emphasis on the design features which make the Viking RTG unique. These features include a gas management system employing a separate gas reservoir to maintain the RTG hot junction and heat source temperatures within a desired range throughout the various mission phases, as well as a specially profiled housing/radiator assembly which facilitates both ground cooling of the RTG's prior to launch and thermal control of the lander after landing. Also presented is the expected RTG electrical performance when subjected to the various mission environments/requirements, such as "power-up" operations in Mars orbit just prior to the entry, and thermal cycling on the Martian surface after landing. (auth)

29250 OPERATIONAL TESTING OF THE HIGH PERFORMANCE THERMOELECTRIC GENERATOR (HPG-02). Russo, F. A. (Teledyne Isotopes, Timonium, MD). pp 193-196 of 9th Intersociety Energy Conversion Engineering Conference Proceedings. New York; American Society of Mechanical Engineers (1974).

From 9th Intersociety Energy Conversion Engineering Conference; San Francisco, California, USA (26 Aug 1974). See CONF-740805-.

The activities and observations leading to the successful development of the HPG-02, a thermoelectric generator of 165 W output and specific power of greater than 2 W per pound are described. Test results showing the temperature equalization effects of the heat pipes on the heat rejection surfaces and the attendant power performance characteristics are presented. In addition, experimental data on relevant long term heat pipe and thermoelectric tests are presented to support the predicted behavior of this generator. It is concluded that the HPG-02 provides an "off-the-shelf" state of the art power source capable of providing at least 130 W for 5 y. (auth)

29251 10% EFFICIENT ECONOMIC RTG DESIGN. Liberman, A. R.; Osmeyer, W. E. (Teledyne Isotopes, Timonium, MD). pp 197-203 of 9th Intersociety Energy Conversion Engineering Conference Proceedings. New York; American Society of Mechanical Engineers (1974).

From 9th Intersociety Energy Conversion Engineering Conference; San Francisco, California, USA (26 Aug 1974). See CONF-740805-.

A new RTG design study has resulted in a modular reference design for a nominal 400 W(e) end-of-mission (EOM) ^{244}Cm fueled Economic Radioisotope Thermoelectric Generator (ERTG). The ERTG exhibits beginning-of-life (BOL) specific power of over 11 W per kg and fits an envelope .20 × .92 × 1.53 meters. The modular construction of the ERTG allows convenient selection of unit power levels from 80 to 800 W, in 80 W increments, with only minor changes to the housing length and configuration. The ERTG reference design, its predicted performance, and key related information on the selenide thermoelectrics and the copper–water heat pipes are discussed. (auth)

29252 COST EFFECTIVE DESIGNING FOR THE ECONOMIC RTG. Schumann, F. A.; Barnett, W. J. (Teledyne Isotopes, Timonium, MD). pp 204-208 of 9th Intersociety Energy Conversion Engineering Conference Proceedings. New York; American Society of Mechanical Engineers (1974).

From 9th Intersociety Energy Conversion Engineering Conference; San Francisco, California, USA (26 Aug 1974). See CONF-740805-.

The Economic Radioisotope Thermoelectric generator to be fueled with ^{244}Cm or ^{238}Pu for generation of 400 W(e) after 5 y of unattended mission operation is being developed. The approach taken to optimize the cost is described. (TFD)

29253 LIGHT-WEIGHT RADIOISOTOPE THERMOELECTRIC GENERATOR DESIGN. Schock, A. (Fairchild Space and Electronics Co., Germantown, MD). Contract AT(49-15)-3063. pp 209-221 of 9th Intersociety Energy Conversion Engineering Conference Proceedings. New York; American Society of Mechanical Engineers (1974).

From 9th Intersociety Energy Conversion Engineering Conference; San Francisco, California, USA (26 Aug 1974). See CONF-740805-.

Design concepts to reduce RTG weights are described. These concepts are in the area of the isotope heat source, the thermoelectric converter, and the radiator. Their effectiveness is demonstrated by means of an illustrative design for a 360-W, plutonium-fueled generator with springloaded selenide elements. The generator, including necessary safety provisions for various abort modes, has an EOM specific power of 5 to 6 W/lb. (auth)

29254 FAULT TOLERANT SEQUENCING (FTS) SHUNT REGULATOR. Andrews, R. E.; Ebersole, T. J. (General Electric Co., Philadelphia). pp 242-250 of 9th Intersociety Energy Conversion Engineering Conference Proceedings. New York; American Society of Mechanical Engineers (1974).

From 9th Intersociety Energy Conversion Engineering Conference; San Francisco, California, USA (26 Aug 1974). See CONF-740805-.

Spacecraft electrical power subsystems are required to provide continuous control or regulation of the power bus which is used by all the spacecraft subsystems. Somewhat dependent on the type of power source available, there are various voltage regulation techniques that can be employed for a particular spacecraft power subsystem. The design description and test results of a shunt regulated power bus which is applicable to various primary power sources are presented. For the purpose of defining design parameters, the characteristics of the Multihundred Watt Radioisotope Thermoelectric Generator (MHW-RTG), which is to be used as the prime power source for a deep space mission, was used. Shunt regulation has been determined to be the best technique for the MHW-RTG as it maintains constant loading which provides continuous operation near the peak power point. The Failure Tolerant Sequencing (FTS) shunt regulator system is described with specific emphasis on the design approach which uses a majority voting of linear error amplifiers and series redundancy to enhance reliability. Failure modes are discussed to show that regulation is not affected and normal operation continues. An arrangement is employed to significantly reduce the power dissipation in the electronics by sequencing shunt elements as required to maintain voltage regulation. The principles which allow lower power dissipation as well as the simplicity of the sequencing circuitry is described. System requirements dictate the need for fast response to load changes and a low dynamic impedance presented to the regulated bus. The approach used to meet these needs is described, and breadboard test results verify compliance. During development, integration testing was performed with the FTS shunt regulator controlling the operation of an electrically heated RTG. The results of these successful tests show the similarity to tests performed with laboratory simulation of the power source. (auth)

29255 DEVELOPMENT OF A REFLUX CONDENSING HEAT PIPE FOR EMERGENCY COOLING OF LARGE COBALT-60 HEAT SOURCE. Chi, J. W. H.; Philips, E. C. (Westinghouse Electric Corp., Pittsburgh). pp 695-700 of 9th Intersociety Energy Conversion Engineering Conference Proceedings. New York; American Society of Mechanical Engineers (1974).

From 9th Intersociety Energy Conversion Engineering Conference; San Francisco, California, USA (26 Aug 1974). See CONF-740805-.

Inert gas controlled, reflux condensing type sodium heat pipes were proposed for the emergency cooling system of the large (30 kW) cobalt-60 heat source. The system is automatic and self-regulating. Prototype heat pipes were built and tested to verify the design, to study the operating characteristics, and to perform long duration and cyclic tests. The results showed that the heat pipes functioned successfully as designed. Moreover, potential sodium migration and hydrogen diffusion problems could not be detected after a total cumulative test time of 836 d. (auth)

29256 OPTIMIZATION OF THE BETA-VOLTAIC CELL. Wei, L. S. (Atomic Energy of Canada Ltd., Ottawa). pp 719-725 of 9th Intersociety Energy Conversion Engineering Conference Proceedings. New York; American Society of Mechanical Engineers (1974).

From 9th Intersociety Energy Conversion Engineering Conference; San Francisco, California, USA (26 Aug 1974). See CONF-740805-.

The beta-voltaic cell, which comprises one or two slabs of radioactive promethium oxide in contact with the surface of surfaces of a silicon n/p diode, has been extensively investigated in an effort to optimize its parameters for high short-circuit current and power conversion efficiency. The model used for the analysis has been verified by experimental data to ensure its validity. (auth)

29257 ADVANCED BETAVOLTAIC POWER SOURCES. Olsen, L. C. (Joint Center for Graduate Study, Richland, WA). pp 754-762 of 9th Intersociety Energy Conversion Engineering Conference Proceedings. New York; American Society of Mechanical Engineers (1974).

From 9th Intersociety Energy Conversion Engineering Conference; San Francisco, California, USA (26 Aug 1974). See CONF-740805-.

Betavoltaic batteries currently being manufactured utilize silicon junction devices coupled to ^{147}Pm beta sources. This technology can be characterized by a power density of approximately 1000 μW/cm^3, assuming no shielding. In order to achieve acceptable dose-rates, shielding must be added such that the power density is typically reduced to 50 μW/cm^3. Greater than 5 μW/cm^3 is provided for 7 to 9 y. A very significant improvement in the betavoltaic state-of-art will result if practical techniques for further reducing the concentration of ^{146}Pm can be developed. Other advances in betavoltaic energy conversion will result from choosing different semiconductor devices and/or beta emitting material. ^{147}Pm and ^{3}H appear to be the most useful isotopes. In both cases, it is desirable to utilize large band gap semiconductors. It appears that with advanced devices, ^{147}Pm and ^{3}H systems will be capable of providing > 5 μW/cm^3 for 20 y. (auth)

29258 IMPLANTABLE THERMAL CONVERTER AS POWER SOURCE FOR AN ARTIFICIAL HEART. Frank, G.; Keller, H.; Plitz, W.; Richter, C.; Schmid, P.; von Reth, R. D. (Messerschmitt-Boelkow-Blohm GmbH, Ger.). pp 775-781 of 9th Intersociety Energy Conversion Engineering Conference Proceedings. New York; American Society of Mechanical Engineers (1974).

From 9th Intersociety Energy Conversion Engineering Conference; San Francisco, California, USA (26 Aug 1974). See CONF-740805-.

Design considerations are discussed to use a miniature thermal engine with a gas cycle as a power source for an artificial heart. As heat source a radioisotope capsule is anticipated with a thermal storage unit serving as buffer for varying power demand. An enlarged thermal storage charged periodically transcutaneously can be used as a less controversial alternative to radioisotope fuel. At higher pressures engines with operating frequencies at the physiological heart beat rate or well above seem to be feasible. Comparison of pneumatic or hydraulic power transmission efficiency reveals by far the highest losses for a low pressure hydraulic coupling. The interaction between a high pressure blood pump with integrated actuator and the thermal engine as a system is considered. The resulting reference model for component evaluation is presented. Results of the component testing with emphasis on regenerator efficiency and energy balance are shown and compared with thermodynamic calculations. Initial test results with a pilot controlled solenoid valve with minimized electric power consumption, a high pressure blood-pump and a simple circulatory simulation loop are followed by a projection of the system applied as an assist or total replacement device. (auth)

29259 NUCLEAR ARTIFICIAL HEART BENCH MODEL. Pouchot, W. D. (Westinghouse Electric Corp., Large, PA); Daniels, A. Contract AT(11-1)-3043. pp 782-790 of 9th Intersociety Energy Conversion Engineering Conference Proceedings. New York; American Society of Mechanical Engineers (1974).

From 9th Intersociety Energy Conversion Engineering Conference; San Francisco, California, USA (26 Aug 1974). See CONF-740805-.

A bench model version of a nuclear-powered total artificial heart system has been constructed and tested. The construction and test of the bench model of the heart system was a part of a broader U. S. Atomic Energy Commission program. The objective of the AEC program was to assess the practicability of developing a fully implantable nuclear-powered total artificial heart system powered by the thermal energy of plutonium-238 and having a minimum weight and volume and a minimum life of ten years. The bench model was constructed to obtain experimental information on the potential capabilities of a Stirling-mechanical system to satisfy AEC practicability criteria. A Stirling-mechanical system was selected during prior analytical studies as being the most promising candidate for a nuclear-powered total artificial heart system. (auth)

29260 UNCONVENTIONAL STIRLING ENGINES FOR THE ARTIFICIAL HEART APPLICATION. Martini, W. R. (McDonnell Douglas Astronautics Co., Richland, WA); Emigh, S. G.; White, M. A.; Griffith, W. R.; Hinderman, J. D.; Johnston, R. P.; Perrone, R. E.; Feigenbutz, L. V. pp 791-798 of 9th Intersociety Energy Conversion Engineering Conference Proceedings. New York; American Society of Mechanical Engineers (1974).

From 9th Intersociety Energy Conversion Engineering Conference; San Francisco, California, USA (26 Aug 1974). See CONF-740805-.

The DWDL heart power source program combines the high efficiency of Stirling engines with the reliability, efficiency, and flexibility of hydraulic power transfer and control to ensure long system life and physiological effectiveness. Extended life testing has already been achieved with an engine module; animal in-vivo tests with an assist heart have consistently demonstrated required performance by biological synchronization and effective ventricle relief. The present System 5 can reliably meet near-term thousand-hour animal in-vivo test goals as far as the durability and efficacy of the power source are concerned. Carefully planned development of System 6 will produce major reductions in size and required input power. Research engine tests have provided the basis for achieving performance goals and the approach for further improvement is well established. The near term goal is 33 W heat input with 16 W input projected for normal physical activity. Another goal is reduction of engine module volume to 0.9 liter. Demonstrated reliability of 292 d for the engine and 35 d for the full system, as well as effectiveness of the artificial heart power source in short-term in-vivo tests indicate that life-limiting problems are blood pump reliability and the machine-animal interface; these were indicated by recent longer-term in-vivo testing. (auth)

29261 STATUS OF A THERMOCOMPRESSOR-POWERED IMPLANTABLE ARTIFICIAL HEART SYSTEM. Moise, J. C.; Faeser, R. J.; Rudnicki, M. I. (Aerojet Liquid Rocket Co., Sacramento, CA). pp 799-804 of 9th Intersociety Energy Conversion Engineering Conference Proceedings. New York; American Society of Mechanical Engineers (1974).

From 9th Intersociety Energy Conversion Engineering Conference; San Francisco, California, USA (26 Aug 1974). See CONF-740805-.

Development continued on fully implantable left ventricular assist and total heart replacement systems utilizing a radioisotope-powered Stirling cycle thermocompressor and pneumatic actuation and control system. The recent effort has concentrated on reducing size, improving the durability and exploring physiological compatibility through in vitro and longer duration in vivo testing. These efforts resulted in the design and fabrication of heart assist and total heart replacement systems of improved durability and with weight and volume believed to be low enough for initial clinical use. (auth)

29262 NUCLEAR-FUELED CIRCULATORY SUPPORT SYSTEMS. XIII. Augmented Performance of the Tidal Regenerator Engine. Hagen, K. G. (Thermo Electron Corp. Research and Development Center, Waltham, MA); Ruggles, A. E.; Huffman, F. N.; Daly, B. D. T.; Migliore, J. J.; Hughes, D. A.; Norman, J. C. pp 805-812 of 9th Intersociety Energy Conversion Engineering Conference Proceedings. New York; American Society of Mechanical Engineers (1974).

From 9th Intersociety Energy Conversion Engineering Conference; San Francisco, California, USA (26 Aug 1974). See CONF-740805-.

Continued development of a nuclear-powered implantable vapor cycle circulatory support system has emphasized improvement in engine efficiency and control. The engine efficiency has been increased from 6 to 10% by incorporating effective liquid regeneration. This improvement has yielded a 50% augmentation in system cardiac output. Control refinements have featured a passive boiler temperature controller and the development of an Si-Ge thermoelectric module with an output potential of 12 V. This high voltage output provides increased net electric power generation efficiency by eliminating the dc-dc converter required with the earlier Bi-Te module. A binary cycle version of the engine using a Dowtherm-A topping cycle on the basic steam cycle is under development. Results of initial breadboard testing have demonstrated engine efficiency as high as 13%. (auth)

29263 HIGH VOLTAGE MINIATURE RADIOISOTOPE THERMOELECTRIC GENERATORS. Raag, V. (Syncal Corp., Sunnyvale, CA). pp 824-825 of 9th Intersociety Energy Conversion Engineering Conference Proceedings. New York; American Society of Mechanical Engineers (1974).

From 9th Intersociety Energy Conversion Engineering Conference; San Francisco, California, USA (26 Aug 1974). See CONF-740805-.

A thermoelectric technology that enables the obtainment of high direct output voltages from thermoelectric power conversion devices at very low levels of power output is discussed. The technology is unique inasmuch as it enables the concurrent obtainment of high direct voltage and conversion efficiency from miniature thermoelectric generators; conventional thermoelectric technology enables only one of these parameters to be maximized. (auth)

Facilities and Equipment

Refer also to abstracts 29231, 30002, and 31111.

29264 (AED-CONF-73-600-001) SOLUTION OF THE PROBLEM OF DESIGNING LINERS FOR PRESTRESSED PRESSURE VESSELS. Albrecht, W. (Steinmueller (L.u.C.) G.m.b.H., Gummersbach (F. R. Germany)). 1973. 21p. (In German). INIS.

From experts meeting of the company L. and C. Steinmueller: examples of large scale plants in the generation of steam and building of equipment; Gummersbach, F. R. Germany (29 May 1973).

Following the explanation of the principle of prestressed-concrete vessel/liner, the basic problems of this type of construction are described from the viewpoint of a manufacturer using a few reactor examples. These problems are mainly strength problems and affect the bond between the liner and the concrete, buckling as a result of high pressure load, balancing of the liner forces between metal sheets of varying thicknesses, as well as the anchoring on penetrations. (INIS)

29265 (GA-A-12903) SECONDARY JAW CRUSHER DEVELOPMENT. Baxter, B. J.; Gasparovic, A.; Bond, A. H. (General Atomic Co., San Diego, Calif. (USA)). 26 Mar 1974. Contract AT(04-3)-167. 43p. Dep. NTIS $4.00.

The results are reported of experiments performed with conventional jaw crushers to evaluate the suitability of these machines to reduce standard fuel and control rod elements to less than $^3/_{16}$-in. ring-size particles with the further requirement that after crushing, the coated fuel particles should remain intact. Such fuel element reduction is required for HTGR head-end fuel reprocessing. The jaw crusher was found to be the most suitable device. (LCL)

29266 (LA-5683-MS) MODEL FOR THE CW POWER OUTPUT OF THE HF CHEMICAL LASER. Mjolsness, R. C. (Los Alamos Scientific Lab., N. Mex. (USA)). Jul 1974. Contract W-7405-eng-36. 12p. Dep. NTIS $4.00.

A radiation model is presented for inclusion in hydrodynamics codes calculating steady-state chemical lasing conditions. The model assumes that if sufficient gain exists for lasing to occur, then P-branch lasing occurs for $3 \rightarrow 2$, $2 \rightarrow 1$ and $1 \rightarrow 0$ transitions at the (local) J value corresponding to maximum zero power gain. For simplicity, all HF states with $v > 3$ are ignored. The theory yields the local and total power output, the local specific intensity of the radiation field and the local distribution of the HF population among the vibrational states. Very crude predictions could be obtained for the spectral distribution of the emitted radiation, although the theory is not well suited to that purpose. (auth)

29267 (RDT-E-1-19T(6-74)) CLASS 2 VALVES FOR LIQUID METAL SERVICE. (USAEC Division of Reactor Research and Development, Washington, D. C.). Jun 1974. 33p. RSO.

A standard is presented which establishes the requirements for the performance, design, fabrication, handling, marking, packaging, shipping, testing, inspection, and quality assurance of austenitic stainless steel valves for service in high-temperature systems using liquid metals or gases containing liquid metal vapor. (LCL)

29268 (UCID-15371) F-M DETECTION IN THE ARGON ION LASER. Stoll, H. M. (California Univ., Livermore (USA). Lawrence Livermore Lab.). 1 Oct 1968. 11p. Dep. NTIS $4.00.

Using a uniphase, cw, 10 mW He-Ne laser, it was demonstrated that frequency modulation on the order of one axial mode spacing may be discriminated by a Fabry-Perot interferometer with a cavity length equal to the axial mode spacing of the laser. However, an essential limitation in using a He-Ne laser in such applications is its low power output. Experimental results indicate that the desired high power output and fine detection resolution are obtainable from the properly controlled output of a cw, uniphase, multimode argon ion laser. (auth)

29269 (UCID-15833) BLADE-TYPE METAL-CUTTING TOOL FOR QUICK REMOVAL OF STOCK IN ROUGHING WORK. Gordon, C. M. (California Univ., Livermore (USA). Lawrence Livermore Lab.). Apr 1971. Contract W-7405-Eng-48. 10p. Dep. NTIS $4.00.

A cutting tool of an unusual blade-type design has been tested on a number of different metals at LRL and has been found to be quite effective in removing stock during roughing operations. This tool uses a unique approach to the cutting process and has several specific advantages over conventional cutting methods. These advantages derive from the tool's long life and its ability to remove large quantities of material quickly. (auth)

29270 (UCID-15860) ALIGNING A SPECTRA PHYSICS He-Ne LASER MODEL 125. Leavitt, G. (California Univ., Livermore (USA). Lawrence Livermore Lab.). 7 Dec 1970. 5p. Dep. NTIS $4.00.

A brief description of laser mirror alignment procedures is given. The technique uses another laser beam reflecting from the mirrors. (MOW)

29271 (UCID-16290) X-RAY LASERS: NECESSARY CONDITIONS AND SOME POSSIBLE APPROACHES. Slutz, S.; Zimmerman, G.; Lokke, W.; Chapline, G.; Wood, L. (California Univ., Livermore (USA). Lawrence Livermore Lab.). 25 May 1973. 40p. (CONF-730597-1). Dep. NTIS $5.00.

From USNRL x-ray laser symposium; Washington, District of Columbia, USA (29 May 1973).

After recalling the basic physics constraints on the most straightforward type of XRL operation, that involving creation of a population inversion between radiatively connected bound states of a highly stripped ion, these criteria were used in evaluation of the well-known XRL experiment of the University of Utah group. Some fundamental aspects of the transport of an XRL beam through a material medium, such as air, was then reviewed. The approach taken by the study group at Livermore to the design of XRL experiments is briefly reviewed, and highlights of current results are mentioned. It is noted that attainment of soft XRL action with use of extant lasers ($E \lesssim 10$ joules, $\tau \sim 10^{-12}$ sec) as pumping sources seems possible. (MOW)

29272 (UCRL-74898) SOME NECESSARY CONDITIONS ON X-RAY LASER ACTION. Slutz, S.; Zimmerman, G.; Lokke, W.; Chapline, G.; Wood, L. (California Univ., Livermore (USA).

Lawrence Livermore Lab.). 19 Jul 1973. 16p. (CONF-730705-27). Dep. NTIS $4.00.

From 6th European conference on controlled fusion and plasma physics; Moscow, USSR (30 Jul 1973).

The necessary conditions for XRL action are considered. These include the required dimensions of an XRL system; the necessary pumping power to overcome pumping losses and still possibly produce a population inversion great enough to overcome propagation losses, and the propagation losses themselves, most notably photoelectric opacity. The overwhelming difficulties in producing a free-bound XRL system and the somewhat more mild technical difficulties of a free-free system are discussed. The only sufficient condition which has been noted is that $\gtrsim 2$ (resonant) photons pass over each excited oscillator in the lifetime of the excitation. This condition points up the fact that an XRL is necessarily a rather spectacular device in operation, and that XRL action will be very unequivocally discerned when it occurs. (MOW)

29273 METHOD OF MEASURING THE MOBILITY, CONCENTRATION, AND ISOTOPE COMPOSITION OF RADIOACTIVE IONS. Matulyavichyus, V. P. Meas. Tech. (USSR) (Engl. Transl.); 17: No. 2, 257-258(Feb 1974).

Translated from Izmer. Tekh.; 17: No. 2, 60-61(Feb 1974).

An apparatus for collecting and measuring radioactive ions in the atmosphere is described. The aerosols are charged and collected on a thin wire electrode as they are pumped through a chamber. The wire is then counted using nuclear emulsions. (WHK)

29274 THEORY OF TRAVELING-WAVE ELECTRONIC RAMAN LASER: STOKES-ANTI-STOKES COUPLING IN THE STEADY STATE. Yuen, S. Y. (Massachusetts Inst. of Tech., Cambridge); Lax, B.; Wolff, P. A. Phys. Rev., A; 10: No. 1, 416-434(Jul 1974).

A detailed theory of traveling-wave electronic Raman lasers is constructed, which applies in particular to the spin-flip Raman lasers of Patel and others. Ten equations are set up describing explicitly the behavior of the Stokes field, the anti-Stokes field, the input laser field, and the electronic system. Solutions of these equations are obtained in the sinusoidal steady-state limit. Depletion of the input laser field is accounted for in an approximate but novel fashion in the form of photon-number conservation. We are able to express the steady-state output power in terms of the system parameters and the boundary pump excitation alone. Analytic formulas are given for the linear gain, the threshold pump power, and the Stokes as well as the anti-Stokes power output. They describe, among other things, the saturation and fluorescence behavior of the electronic Raman laser. Various intuitive interpretations are provided for the analytical results. Our detailed predictions are in good agreement with experiments. (auth)

29275 FLOW DISTRIBUTION FOR HEAT EXCHANGERS. Wolowodiuk, W.; Dawson, B. E.; Anelli, J. (to United States Atomic Energy Commission). US Patent 3,830,292. 20 Aug 1974. Filed date 1 May 1972. 4p.

A heat exchanger is described where one fluid is flowed over tubes carrying another fluid to place said fluid in indirect heat exchange in which problems of erosion, temperature gradient, and vibrations at the area where the tubes are joined to a tube sheet are eliminated. A fluid inlet spaced from the tube sheet feeds fluid into an annular flow chamber which encircles the tubes and has an annular perforated plate closer to the tubes than the inlet and perforated so that the resistance to flow of fluid through the plate at different locations on it is a function of the distance from the inlet. (3 claims, 2 drawing figures) (Official Gazette)

29276 FREEZING-UP SHAFT SEAL FOR MACHINES FOR THE TRANSPORT OF LIQUIDS AND GASES IN NUCLEAR POWER. Matal, O. Czech Patent 146,660. 15 Dec 1972. Filed Date 28 Feb 1972. 2p.

A freezing-up seal for machine shafts was proposed for use in machines transporting liquids and gases in nuclear power plants. The seal is especially suitable for the sealing of sliding bearings lubricated with a liquid metal. The seal consists of a liquid metal cooler placed inside the seal body. The cooler supports at least one spring pressing the sealing mass well against the seal body and the shaft. The liquid metal cooler prevents the liquid metal from the direct contact with the coolant, and also controls the coolant flow in the helical groove to avoid non-uniform cooling of the liquid metal, thus preventing any possible leakage through the freezing-up shaft seal. The pressure spring effects a permanent compression of the sealing mass during operation. (Nuclear Sci. Abstr. Czech.)

29277 INDUSTRIAL TECHNIQUE. (to Babcock and Wilcox Co.). Netherlands Patent 7,210,084. 21 Jul 1972. Priority Date 27 Aug 1971, USA. 20p. (In Dutch).

In accordance with an embodiment of the invention, an array of apertured flat plates support the tubes in a heat exchanger. Each aperture has at least three bights that provide individual fluid passageways when the associated tube is lodged in place. At least three inwardly protruding members that separate the bights restrain tube movement. Each of these members define arcs of a circle that has a diameter which is only slightly larger than the outside diameter of the respective tube. During heat exchanger assembly, this slightly larger diameter of the circle defined by the inwardly protruding members accommodates departures in the tubing from a perfectly straight condition. In operation, the individual tubes will tend to lay against one or two of the members in each aperture in almost line contact to prevent "crevice corrosion." The gap between the outer surface of the tube and the member or members with which it is not in contact, moreover, is so great that crevice corrosion in this region also is essentially overcome. (auth)

29278 ONCE-THROUGH VAPOR GENERATOR. (to Babcock and Wilcox Co.). Netherlands Patent 7,300,178. 5 Jan 1973. Priority Date 18 Jan 1965, USA. 15p. (In Dutch).

A method of vaporizing and superheating a fluid by circulating it through a heat exchanger in indirect heat transfer relationship with a heating fluid at mass flow rates below 400,000 lbs/hr/ft^2 is described. Prior to passing the vaporizable fluid through the heat exchanger it is mixed with a portion of vaporized fluid which has absorbed heat, in the course of its passage about the tubes, to thereby heat the feedfluid to substantially saturation temperature. Additionally, the invention comprises a vertically elongated heat exchanger having a bundle of heat exchanger tubes extending between a pair of spaced tube sheets. A cylindrically shaped shroud encloses the bundle of tubes for a substantial portion of its length, thereby providing a riser chamber about the tubes and an annular downcomer passage between the shroud and the heat exchanger shell. Openings are provided through the upper end of the shroud for admitting vapor, generated within the chamber, into the annular passageway wherein it mixes and heats the feedfluid by direct contact. The once-through vapor generators using low mass flows and in the nucleate boiling domain can be utilized in combination with nuclear reactors, particularly of the pressurized water type. (NL)

29279 TRANSVERSE MODE CONTROL IN A DISTRIBUTED FEEDBACK SEMICONDUCTOR LASER. Somekh, S. (California Inst. of Tech., Pasadena). Proc. IEEE (Inst. Elec. Electron. Eng.); 62: No. 2, 277-278(Feb 1974).

Transverse modes in a distributed feedback semiconductor laser are discussed. A scheme for discriminating between these modes is suggested. (auth)

29280 NEODYMIUM GLASS LASER HAVING ROOM TEMPERATURE OUTPUT AT WAVELENGTHS SHORTER THAN 1060 NM. Shaw, R. R.; Robinson, C. C. (to American Optical Corp.). US Patent 3,825,500. 23 Jul 1974. Filed date 31 Aug 1972. 10p.

Laserable material doped with a quantity of neodymium ions in a low concentration which results in the glass exhibiting a ratio of fluorescent intensity peaked at 920 nanometers over a fluorescent intensity peaked at approximately 1060 nanometers of at least 0.4 as measured by a Cary Model 14 spectrophotometer is discussed. The glasses enable the generation of laser light in a waveband with an optical center at about 920 nanometers at room temperature (approximately 20°C) when positioned in a laser cavity which is resonant at 920 nanometers. Four such laserable glasses are given. (Official Gazette)

29281 INTEGRAL CAPACITOR LATERAL DISCHARGE LASER. Otto, W. F.; Milton, R. D. (to Secretary of the Army). US Patent 3,828,277. 6 Aug 1974. Filed date 3 Jul 1973. 4p.

A high pressure gas laser is described in which uniform electrical field distribution is obtained for lateral discharge in the gas by employing a capacitor formed within the laser cavity. The laser may be a parallelepiped with capacitor plates forming two opposite rides of the parallelepiped. One of the plates is coated with a ceramic dielectric. Alternatively, the laser may be a conductive circular cylinder with a center electrode, and with a ceramic dielectric coating on the inside of the cylinder. A high voltage source is connected to the laser. Emission occurs when the capacitor charges to a high enough voltage to discharge through the gas. For better charge distribution, the coating may be covered by a resistive layer, or may have a mosaic of isolated conductors thereon. (Official Gazette)

29282 HIGH EFFICIENCY ACOUSTO-OPTICAL Q-SWITCH. Cohen, M. G. (to Quantronix Corp.). US Patent 3,828,276. 6 Aug 1974. Filed date 25 May 1973. 6p.

This invention relates to laser Q-switches, and, more particularly, to acousto-optical Q-switches for solid state laser media of the type which inherently produce unpolarized light. (Official Gazette)

29283 GAS LASER. Kindl, H.; Westermeier, H. (to Siemens Aktiengesellschaft). US Patent 3,826,998. 30 Jul 1974. Priority date 20 Feb 1970, F.R. Germany. 4p.

A gas laser assembly is described that includes an elongated tube having a mirror mount closing one end of the tube wherein a fitting on the tube end has a circumferentially weakened wall section and wherein the mirror is mounted on the fitting on the opposite side of the weakened wall section from the tube. The fitting preferably includes a closing window serving as a mounting for the mirror and secured to the fitting so that the adjustment of mirror angle can be effected externally of the device without permitting gas escape. The weakened wall section is in the form of a circumferential recess formed in the metal fitting or in the form of a circumferential stiffening corrugation. (Official Gazette)

29284 LASER PUMPED BY PHOTOIONIZATION GENERATED, ELECTRICALLY HEATED PLASMA. Javan, A.; Levine, J. S. (to Massachusetts Inst. of Tech.). US Patent 3,826,997. 30 Jul 1974. Filed date 30 Oct 1972. 6p.

A description is given of a laser with a photon energy spectrum lying below the ionization potential of the lasing constituent of the gas and heating of the plasma with an electric field at a voltage less than the avalanche breakdown voltage of the gas but high enough to effectively raise the lasing constituent to its lasing level. (Official Gazette)

29285 ON THE GAS TEMPERATURE IN COAXIAL ELECTRIC–DISCHARGE CO_2 FLOW LASERS. Shwartz, J.; Margalith, E. (Department of Aeronautical Engineering, Technion–Israel Institute of Technology, Haifa, Israel). J. Appl. Phys. 45: No. 10, 4469-4476 (Oct 1974).

An analytic and experimental investigation on the dependence of gas temperature on flow and discharge characteristics is presented. The entire range of slow– to fast–flowing coaxial CO_2 electric lasers is considered. As is known, at low flow rates the gas temperature is proportional to the electric power input per unit length, while at high flow rates the gas end temperature is proportional to the ratio of total electric power and gas mass flow rate. In addition, gas pressure and entrance Mach number were found to have a noticeable effect on gas temperature; the temperature tends to increase with increasing pressure and to decrease with increasing Mach number. The agreement between theory and experiment is fairly good, so that estimates of gas temperature at given flow and discharge conditions can be obtained. Also presented is an experimental correlation between laser power output (or efficiency) and gas temperature. Finally, scaling laws for temperature–limited coaxial flow CO_2 electric lasers are proposed. (auth)

29286 INTERACTION OF RADIATION WITH AN ACTIVE MEDIUM IN A MULTIMODE REGIME OF PULSE GENERATION. Lariontsev, E. G.; Skuybina, I. P. (Moscow State Univ.). Izv. Vyssh. Ucheb. Zaved., Radiofiz.; 17: No. 3, 354-359(1974). (In Russian).

The influence of the nonlinearity of solid-state laser active medium on the time radiation structure caused by the interference between generated longitudinal modes is considered. (auth)

29287 NATURAL WIDTH OF THE SPECTRUM OF TWO-FREQUENCY GASEOUS LASER MODES IN AUTONOMOUS REGIME AND SYNCHRONIZED BY A LIGHT SIGNAL. Poyzner, B. N.; Portnova, T. S.; Tsidulko, I. M. (Tomsk State Univ., USSR). Izv. Vyssh. Ucheb. Zaved., Radiofiz.; 17: No. 3, 350-353 (1974). (In Russian).

By passing from the Lamb equations to the system of equations for the mode amplitude and phase fluctuations caused by the delta-correlated noises acting independently at the mode frequencies, expressions are derived for the natural width of the spectrum of modes and the power of amplitude fluctuations. Based on the data for the helium-neon laser, the latter values are numerically estimated at symmetric and asymmetric mode tuning with respect to the radiation contour, as well as at the different lengths of the optical resonator. The conclusions are compared with the results obtained by the other authors. Similar expressions and numerical estimations are obtained for the regime of phase mode synchronization by a light signal with the frequency equal to the half-sum of the mode frequencies in which the natural width of the spectrum of modes and the level of amplitude fluctuations may decrease. (auth)

29288 DESIGN RELATIONSHIPS AND FAILURE THEORIES IN PROBABILISTIC FORM. Smith, C. O. (Detroit Univ., Mich. (USA)). Nucl. Eng. Des.; 27: No. 2, 286-292(May 1974).

The engineering profession has become increasingly concerned with the adequacy of design calculations. This concern indicates a need for critical evaluation of designs based on arbitrary multipliers, such as safety factors or worst-case treatment. Design has customarily been based on applied loading, geometry, and handbook property values to give a deterministic solution. This paper presents (1) the Soderberg, Goodman, Gerber, and elliptical design relationships; and (2) the maximum shear and distortion energy failure theories in probabilistic form. Inherent in these equations are the facts that (a) design variables are generally characterized by spectra of values, rather than unique values; and (b) a small, but finite, probability of failure must be recognized in any design. By coupling the mean static and mean alternating stresses (and their standard deviations) with the strengths available in a material (and their standard deviations) in one of the four design relationships using an appropriate theory of failure, the reliability of a given design can be calculated. Conversely, for a given reliability, the appropriate size can be determined. Illustrations are provided. The influence of range (different standard deviations) of variables on reliability is demonstrated. A comparison is made between safety factor and reliability. (auth)

29289 SPARE PARTS RESERVATION OF COMPONENTS SUBJECTED TO WEAR-OUT AND/OR FATIGUE ACCORDING TO A WEIBULL DISTRIBUTION. Birolini, A. (Eidgenoessische Technische Hochschule, Zurich (Switzerland)). Nucl. Eng. Des.; 27: No. 2, 293-298(May 1974).

This contribution discusses the determination of the number n of spare parts necessary to cover with probability $\geq W$ replacement requirements during the time interval (0,T) for the case where only a single part is used at a time. It is assumed that the lifespan of the parts is distributed according to a Weibull distribution with shape parameter $\beta \geq 1$. For small values of n, $1 \leq n \leq 10$, charts of $n = n$ (T/MTTF, W, β) are given for $W =$ 0.99, 0.95, 0.9, 0.75 and $\beta = 1$, 1.2, 1.5, 2, 3, 4 (MTTF is the mean of the lifespans). For large values of n, an asymptotic approximation is derived from the central limit theorem. An important result of this study is to show that the asymptotic formula obtained–which, irrespective of the exact form of the distribution function of the lifespan depends on the coefficient of variation σ/MTTF only–gives good approximations for relatively small values of n. In fact, for $n \geq 10$ and $\beta \geq 1$, the error is $< \pm 1$ spare part for $5\% \leq W \leq 95\%$ and $< \pm 2.2$ spare parts for $1\% \leq W \leq 99\%$. The widespread application of the Weibull distribution (for example to approximate the distribution of the lifespans of electronic and mechanical parts subjected to wear-out and/or fatigue) is then briefly discussed. (auth)

29290 A STATUS REPORT ON COMPUTATIONAL TECHNIQUES FOR FINITE ELEMENT ANALYSES. Melosh, R. J. (Virginia Polytechnic Inst. and State Univ., Blacksburg (USA)). Nucl. Eng. Des.; 27: No. 2, 274-285(May 1974).

Fifteen years of research, development, and application of the finite element concept, primarily to structural analysis, has yielded a host of techniques for computer implementation. The importance of using these techniques is shown by an estimated reduction in total computer costs by a factor of 20 over not using them. The techniques which play an important role in currently available computer software are described. Research work in the engineering literature is indicated which can be expected to stimulate development of new techniques in the next decade. It concludes that the thrust for better techniques will be provided by the expanding need for software in newer applications such as nuclear fusion, fracture mechanics, bioengineering simulations, and vehicle crashes. New techniques will yield computer software which more highly automates finite element use, will more efficiently solve large sets of equations, and which will be engineering discipline transportable. (auth)

Heat Transfer and Fluid Flow

Refer also to abstracts 29275, 29460, 29464, and 31280.

29291 TWO-PHASE FLOW AND HEAT TRANSFER AT THE BOUNDARY LAYER OF A THIN BODY OF REVOLUTION. Baikov, V. I. Inzh.-Fiz. Zh.; 26: No. 6, 991-994(Jun 1974). (In Russian).

The effect of transverse bends of the body and of injection on the flow and heat transfer in the two-phase boundary layer of a thin parabolic body of revolution was studied. The possibility of essential reduction of friction resistance and heat transfer in the two-phase boundary layer against a single-phase flow at comparatively low flow rates of the gas injected was found. It is shown that an increase in transverse bends of the body results in increasing friction resistance and heat transfer. (auth)

29292 DERIVATION OF TRANSFER FUNCTIONS IN BOILING LOOPS. Takahashi, R. (Tokyo Inst. of Tech.). Bull. Tokyo Inst. Technol. (Engl. Ed.); No. 121, 109-123(Mar 1974).

A transfer function model of boiling loops which were used to study flow instability is formulated. It is now possible to estimate steam void propagation velocity in the simple form, because the assumption of Bankoff's relation of slip ratio is made. Dependency of flow instability on changes in heat transfer is described explicitly in this model, because heat conduction of the heater and the boundary conduction at the heater wall appears to be the closest to phenomena. (auth)

29293 NEW APPROACH TO PREDICTING PRESSURE DROP IN TWO-PHASE FLOWS. Trela, M. Pr. Inst. Masz. Przeply.; No. 64, 41-57(1974).

A method of deriving analytical formulas for local values of friction factor and void fraction in two-phase flow is presented. Use was made of the experimental values of these coefficients, as given by Martinelli and Nelson for water flow. On the grounds of the theory of similitude a method was proposed for applying the derived formulas to the calculation of the pressure drop in two-phase flows of media other than water. (auth)

Materials Testing

Refer also to abstracts 29900, 29931, 29952, 30044, 30083, 30143, 30144, and 31200.

29294 (AD-776394) DETERMINATION OF THE FEASIBILITY OF USING BETA RADIATION BACKSCATTER FOR THE DETECTION OF SURFACE CONTAMINATION OF METAL PANELS. Gruber, H. T.; Bradbury, E. J.; Melton, C. W.; Rhoten, M. L. (Battelle Columbus Labs., Ohio (USA)). 15 Mar 1974. Contract DAAJ01-73-C-0858. 41p. (USAAVSCOM-TR-73-31). NTIS $3.25.

The beta backscatter technique was determined to be feasible for the measurement of contaminants and surface preparation coatings. Titanium and aluminum honeycomb panels with bonded and disbonded areas were examined to identify contaminants or surface preparation properties which result in disbonding and surface preparation coatings which result in acceptable bonds. The poor bonding of the titanium panels was between the metal skin and the primer coating. Electron microscopy showed that the surface of the titanium skin was too smooth to favor physical bonding. Further examination showed there were no bonded areas suitable for analysis. The skins of the aluminum panels showed the bonded areas exhibited a microetch pit structure which was not present in the poorly bonded areas. It was concluded that the lack of bond of the aluminum panels was not the result of surface contamination but rather a function of the pickling parameters and perhaps the annealing of the aluminum. (auth)

29295 (AD-776900) EXPERIMENTAL NEUTRON RADIOGRAPHY SYSTEM USING CALIFORNIUM-252. Final Report. Barnes, E. G.; Drucker, G.; Jentisch, A.; Helf, S. (Picatinny Arsenal, Dover, N. J. (USA)). Mar 1974. 28p. (PA-TR-4629). NTIS $3.25.

Neutron radiography was studied as a method for the nondestructive examination of loaded army munitions items. A 10 mg ^{252}Cf source was acquired and facilities for its use as a primary neutron source were developed. A versatile source-handling mechanism which accommodates a number of different experiments was devised by modifying a standard ^{60}Co source system, and was incorporated as an integral part of the storage/shipping container. Two moderator designs have been used thus far. Applications of neutron radiography using the Cf source have included 100% examination of a pilot production run of 1,300 explosive boosters, as well as a variety of other small munitions items. (auth)

29296 (UCID-15777) ACOUSTIC EMISSION MONITORING OF PROOF TESTS ON CANISTERS AND RELATED HARDWARE. Harris, D. O.; Roth, B. G.; Kuhn, B. A. (California Univ., Livermore (USA). Lawrence Livermore Lab.). 14 Jan 1971. 18p. Dep. NTIS $4.00.

Proof tests on canisters and related hardware for underground nuclear tests are conducted routinely at the Nevada Test Site pull test facility. The investigation was to determine the feasibility and desirability of acoustic monitoring of the proof tests, for it is believed that acoustic emission can provide valuable information on the integrity of structures. The results of five proof tests are presented and discussed herein. The test results indicate that the pull tester is sufficiently quiet to allow acquisition of meaningful acoustic emission data for assessment of the integrity of canisters and related hardware. In addition, preliminary results indicate that the acoustic emission source can be approximately located by comparing the activity on the various channels. However, all of the parts tested "good," and it remains to be determined whether or not acoustic emission can provide sufficient warning of impending failure to allow detection of an occasional "bad" part. Past experience indicates that this can be done. To definitely demonstrate failure detection, a part must be deliberately damaged or pulled to failure. Tentative plans for such a test are now underway. (auth)

29297 (UCID-15867) DESIGN OF A PASSIVE CRACK DETECTOR SYSTEM. Parker, R. (California Univ., Livermore (USA). Lawrence Livermore Lab.). 1 Jul 1971. Contract W-7405-Eng-48. 15p. Dep. NTIS $4.00.

An inexpensive, passive crack detector system was developed to determine how soon after exposure to radiation a mechanical component would crack. The system was designed so that switches were activated, initially from the radiation and later from the g loading associated with the experiment. This allowed current from cadmium batteries to flow through a conductive element on the surface of the test component. An interruption of the current by the formation of a crack was recorded on a passive current integrating device in series with the conductive element. Upon recovery, the records may be visually inspected to determine when, if any, cracks occurred. The entire package, including spring loaded contacts to the conductive element, occupies a few cubic inches of space, and operates reliably in severe thermal, shock, and radiation environments. Detailed calculations, drawings, redundancy, and testing procedures for the system elements are described. (auth)

29298 TECHNIQUE OF AUTORADIOGRAPHY. Second Revised and Enlarged Edition. Rogers A. W. Amsterdam; Elsevier (1973). 379p.

Theoretical and practical aspects of autoradiography are treated extensively. Special attention is paid to the concept of resolution, to quantitative evaluations of autoradiographs and to the possibilities and limitations of different nuclear emulsions. One chapter is devoted to electron microscope autoradiography. Each chapter contains a list of references. (NL)

29299 MULTICHANNEL PROCESSING OF DIGITAL RADIOMETRIC DATA IN SEQUENTIAL RECORDING OF A FINITE NUMBER OF COUNTS. Pokrovskii, A. V.; Selivanov, V. G. (Tomsk Polytechnical Inst., USSR). Sov. J. Nondestruct. Test. (Engl. Transl.); 9: No. 6, 637-642(Dec 1973).

Translated from Defektoskopiya; 9: No. 6, 7-13(1973).

A quasioptimal algorithm is considered for detecting the signal from a defect with two unknown parameters when the number of readings is finite. It is found that low efficiency results from algorithms for processing single observations when the signals are weak. A multichannel procedure is proposed for data processing that substantially increases the probability of observing the signal from a threshold defect. (auth)

29300 DIGITAL PROCESSORS FOR SERVOHYDRAULIC MATERIAL TESTING SYSTEMS. Mayr, P.; Schmalenbach, E. (Karlsruhe Univ. (TH) (F. R. Germany). Inst. fuer Werkstoffkunde 1); Neher, F. (Studiengesellschaft fuer Wissenschaftliche Datenverarbeitung G.m.b.H., Verlautenheide (F. R. Germany). Elektronische Rechenanlagen). Materialpruefung; 16: No. 7, 191-196 (Jul 1974). (In German).

5 figs.; 1 tab.; 2 refs.

Because of technical and commercial advantages, digital processors are being increasingly used in material testing systems for data acquisition, generation of command signals and digital control. The fundamental aspects of the hard- and software of a digital data processor subsystem are discussed. (auth)

29301 NUCLEAR RADIATION CONVERSION ENHANCEMENT WITH INHOMOGENEOUS CONVERTERS AND INTENSIFIERS. Harms, A. A.; Molson, L. D. (McMaster Univ., Hamilton, Ontario (Canada). Dept. of Engineering Physics). Nucl. Instrum. Methods; 119: No. 2, 389-393(15 Jul 1974).

Nuclear radiation conversion enhancement in converters and intensifying screens is investigated. It is found that independent variations in the isotopic and atomic concentrations can contribute significantly to an increase in radiation conversion and, as a consequence, can lead to a significant degree of image enhancement in nuclear particle radiography. (auth)

29302 ISOTOPIC CONVERSION IN GADOLINIUM-EXPOSURE NEUTRON IMAGING. Harms, A. A.; McCormack, G. (McMaster Univ., Hamilton, Ontario (Canada). Dept. of Physics). Nucl. Instrum. Methods; 118: No. 2, 583-587(15 Jun 1974).

The role of isotopic conversion in gadolinium as it relates to neutron imaging is investigated by both analytical and experimental means. Particular emphasis is placed on the internal-conversion electron spectra in ^{156}Gd and ^{158}Gd. It is found that gadolinium converters enriched in ^{157}Gd show a measure of optical-density enhancement which is a function of converter thickness. (auth)

Nuclear Explosions

Refer also to abstracts 29296, 29335, 29345, 29348, 29362, 29378, 29379, 29386, 29387, 29412, 29459, and 29619.

29303 (AD-776672) REGIONAL ATTENUATION OF SHORT-PERIOD P AND S WAVES IN THE UNITED STATES. Der, Z. A.; Masse, R. P.; Gurski, J. P. (Teledyne Geotech, Alexandria, Va. (USA)). 22 Jan 1974. Contract F08606-74-C-0006. 47p. (SDAC-TR-74-1). NTIS $3.25.

Regional distribution of anelastic attenuation beneath the United States was investigated using amplitudes and dominant periods of short period P and S waves originating from deep focus earthquakes in South America and the circumpacific seismic belt, recorded at LRSM (long range seismic measurement) stations. The observed regional distribution pattern shows high attenuation in the western United States, including California, and a less pronounced high attenuation region in the northeastern U. S. This distribution pattern is similar to that reported by Solomon and Toksoz (1970) for long period S waves, but differs from it sufficiently to indicate lateral variations in the frequency dependence of the average crust-upper mantle attenuation across the U. S. The relative changes of short period P and S wave amplitudes can be sufficiently explained by assuming a complex shear modulus; no losses in compression are indicated. (auth)

29304 (AD-776815) EXTENDED ARRAY EVALUATION PROGRAM. Special Report No. 5. Selection of Reference Waveforms for Matched Filter Processing of Long Period Signals from Seismic Events. Unger, R. (Texas Instruments, Inc., Dallas (USA)). 24 Oct 1973. Contract F33657-72-C-0725. 86p. NTIS $4.00.

In an attempt to find optimum reference waveforms for matched filtering long period signals, several reference waveforms varying in duration and signal contents were taken from Alaskan Long Period Array recordings of major events in the Sinkiang Province area. Each of these reference waveforms was used as a matched filter in processing a number of other events in the same area. The events differ in magnitude, location and depth. Analysis of the signal-to-noise ratio gains (relative to bandpass filtering) showed that optimum processing of all events required a large number of reference waveforms. This processing yielded up to 8 db improvement over to-date routine matched filter processing of Central Asia events. Several other aspects of reference waveform matched filtering also are discussed. (auth)

29305 (AD-777151) SEISMIC DISCRIMINATION. Semiannual Technical Summary Report, 1 July–31 December 1973. Chinnery, M. A. (Massachusetts Inst. of Tech., Lexington (USA). Lincoln Lab.). 31 Dec 1973. 100p. (ESD-TR-73-348). NTIS $4.00.

The analysis of the data for the international seismic month is nearing completion. The effects of crust and upper-mantle structure on the short-period signals received at LASA and NORSAR are described. Further work on interfering Rayleigh waves and on the phase PP is included, together with several studies in global seismology. Development of a seismic computer terminal system for the ARPA network is progressing satisfactorily. (auth)

29306 (AD-777315) EXTENDED ARRAY EVALUATION PROGRAM. Quarterly Report No. 6, 1 July–30 September 1973. Harley, T. W. (Texas Instruments, Inc., Dallas (USA)). 25 Oct 1973. Contract F33657-72-C-0725. 13p. NTIS $3.00.

The sixth quarterly report summarizes progress made under the extended evaluation of ALPA, NORSAR, and VLPE programs. Work to date in the following areas is summarized: NORSAR long period evaluation; NORSAR short period evaluation; VLPE evaluation; research; and seismic system study. (GRA)

29307 (AD-777580) BLAST WAVE BOUNDARY LAYER MEASUREMENT. Final Report, September 1971–August 1973. Carpenter, H. J.; Hove, D. T.; Batt, R. G.; Dillinger, B. L.; Crawford, D. R. (TRW Systems Group, Redondo Beach, Calif. (USA)). Mar 1974. 309p. (AFWL-TR-73-211). NTIS $7.25.

Blast wave boundary layer development at the ground surface was measured at approximately the 60 psi and 30 psi shock overpressure stations during Middle Gust Event IV 100-ton TNT surface-tangent sphere explosion, after an instrument checkout test at the 24 psi station on Middle Gust III. Static pressure, pitot pressure, surface shear, and flow temperature were measured to define the boundary layer over a clean hard surface. The dynamic measurements were made with rakes extending to 12 in. above the surface. In addition to defining the boundary layer, some of the data, specifically the inviscid flow (uppermost) measurements, are useful for comparison with two-dimensional computer code calculations of the airblast from 100-ton TNT surface-tangent explosions. One such comparison is made. (auth)

29308 (AD-777748) DIRECT INTERACTION EFFECTS IN EMP. Longmire, C. L. (Mission Research Corp., Santa Barbara, Calif. (USA)). 28 Jan 1974. Contract DASA01-69-C-0058. 26p. (DNA-3249T). NTIS $3.25.

For the electromagnetic pulse produced by nuclear explosions, a substantial amount of work has been applied to the calculation of that part of the EMP due to the interaction of the bomb gamma rays with the natural environment, e.g., the atmosphere or the ground surface. In EMP vulnerability studies of systems, the effect of the environmental EMP on the system is taken into account. When the system itself is exposed to the gamma rays, it may make its own contribution to the EMP to which it is subjected. This direct interaction EMP depends very much on the system. A few illustrative examples are discussed. (GRA)

29309 (AWRE-O-31/74) FOULNESS MULTI-TON AIR BLAST SIMULATOR. Part 1. Early Development: The Gun Driven Facility. Clare, P. M.; Rowe, R. D. (UKAEA Weapons Group, Aldermaston. Atomic Weapons Research Establishment). Jul 1974. 46p. Dep. NTIS (US Sales Only) $5.50.

The development and performance of a blast simulator for studying the vulnerability of military equipment to nuclear explosions are described. The blast simulator is an explosively driven shock tube that simulates weapons in the multi-ton range. (TFD)

29310 (LAMS-2610) COMPUTATIONS ON THE PARAMETER VALUES INSIDE OF THE E. M. SOURCE. Suydam, B. R. (Los Alamos Scientific Lab., N. Mex. (USA)). 6 Apr 1961. Contract W-7405-eng-36. 10p. Dep. NTIS $4.00.

Equations are developed for calculating the radial electric field and the azimuthal magnetic field inside the conducting sphere of an atomic explosion. (TFD)

29311 (PB-231011) PLOWSHARE TECHNOLOGY ASSESSMENT, PROSPECTIVES FOR NUCLEAR-STIMULATED GEOTHERMAL POWER IN THE WESTERN U. S. Sandquist, G. M. (Western Interstate Nuclear Board, Lakewood, Colo. (USA)). Feb 1973. 115p. (NSF/RA/G-73-014). NTIS $4.50.

The feasibility of using nuclear explosives to stimulate the output of geothermal sites is examined for the Western U. S. Actual explosive applications appear limited to marginal geothermal sites where explosive yield of 100 kt or less is adequate. (GRA)

29312 (PNE-RB-59) PROJECT RIO BLANCO: RESULTS FROM THE INITIAL ALLUVIAL WATER QUALITY PROGRAM. Knutson, C. F. (CER Geonuclear Corp., Las Vegas, Nev. (USA)). 1 Oct 1973. 39p.

An alluvial water quality evaluation program for the Rio Blanco Event was implemented and made part of the Water Pollution Control Permit for the detonation dated May 4, 1973. Weekly water samples were collected from wells during the period May 24, 1973 to Aug. 3, 1973. Analysis of these samples determined that there was no significant change in water quality nor was any radioactivity (other than background) detected. (auth)

29313 (PNE-RB-60) PROJECT RIO BLANCO: COMPARATIVE POSTDETONATION HYDROLOGIC TESTING. Knutson, C. F. (CER Geonuclear Corp., Las Vegas, Nev. (USA)). 31 Jan 1974. 53p.

Predetonation Project Rio Blanco hydrologic testing provided information on three aspects of the hydrologic regime in the emplacement well area: (1) transmissivity and water quality data from each of the three aquifers–alluvium, A aquifer (above the Mahogany Zone), and B aquifer (below the Mahogany Zone); (2) A and B aquifer continuity information resulting from tests of well pairs completed in the same aquifer; and (3) A to B aquifer interference testing to determine degree of communication across the Mahogany Zone. The predetonation testing sequence was replicated by a postdetonation hydrologic testing program. This report presents the results of the postdetonation testing program and compares these results with the information developed and reported predetonation. (auth)

29314 (SLA-74-0210) ARCHIVING GUIDE TO MICROBAROGRAPH RECORDS OF NUCLEAR AND CHEMICAL EXPLOSION TESTS. Reed, J. W. (Sandia Labs., Albuquerque, N. Mex. (USA)). Aug 1974. Contract AT(29-1)-789. 19p. Dep. NTIS $4.00.

Microbarograph records of airblast waves, made at distances of 20 km to over 500 km from various nuclear test explosions (1953 through 1973) and from certain chemical high-explosives tests, have been placed in permanent archives. These records, which contain detailed information on airblast propagation that has never been completely evaluated and reported, are not amenable to current microstorage techniques and cannot be reproduced by future experimenters. This report was prepared to guide future investigators to the archive storage boxes and filing system. Included are brief summaries of the test operations, projects, events, and purposes of microbarography, as well as a selected bibliography on Sandia microbarography and blast prediction operations. (auth)

29315 (UCID-15727) FIELD MEASUREMENT OF THE PERMEABILITY OF NTS ALLUVIUM. Pasternak, A.; McMullen, E. T. (California Univ., Livermore (USA). Lawrence Livermore Lab.). 28 Jul 1970. 11p. Dep. NTIS $4.00.

The permeability to gas flow of the medium surrounding an emplaced device is an important factor affecting containment criteria at the Nevada Test Site. Specifically, the permeability in part determines the proper depth of burial, particularly for small devices. For small devices, preventing the flow of radioactive cavity gas through the medium to the surface and its release to the atmosphere is likely to be the governing factor (rather than cratering effects) in determining depth of burial. An estimate of the permeability of Nevada Test Site alluvium has been obtained by carrying out air flow tests in a partially cased emplacement hole. Downhole pressures and air flow rates were measured in quasi-steady-state experiments. Measurements were also taken of transient pressure buildup and decay. The data for the steady-state experiments have been fitted to radial (cylindrical) flow and spherical flow models and the permeability of the medium calculated. It is estimated that the permeability of NTS alluvium is 9.5 darcies. The grout and casing of the emplacement hole were leak checked by placing a tracer gas (Freon-12) downhole and monitoring the area around surface ground zero with a halogen leak detector. No leaks were found. (auth)

29316 (UCID-15736) COMPRESSIBILITY AND STRENGTH BEHAVIOR OF DIAGONAL LINE ALLUVIUM. Heard, H. C.; Stephens, D. R. (California Univ., Livermore (USA). Lawrence Livermore Lab.). 14 Oct 1970. 8p. Dep. NTIS $4.00.

Present methods of calculating the physical effects resulting from an underground nuclear explosion require, as input, two types of deformational properties characterizing the nearby rock material. These are the pressure-volume and shear stress–mean pressure behavior of rocks as deduced from static tests simulating the peak pressures to be expected at cavity radii ranging from < 1 to > 10 radii. The principal reason for these material response calculations in the Diagonal Line Event is to predict whether the line-of-sight pipe will be closed by the passage of the shock wave or whether a ball valve will be required to contain the device debris. Diagonal Line is a DASA-sponsored event scheduled for hole UE-11c, near Area 5 in Area 11. The material is relatively dry alluvium, and the working point is at a depth of about 850 ft–several hundred feet above the local water table. The U. S. Geological Survey has furnished lithological, chemical composition and logging data. This report covers the P–V properties and shear stress–mean pressure response to 30 kbar and 7 kbar, respectively. (auth)

29317 (UCID-15771) SHOAL POSTSHOT ENVIRONMENT. Korver, J. A.; Boardman, C. R.; Rawson, D. E. (California Univ., Livermore (USA). Lawrence Livermore Lab.). 4 Feb 1964. 14p. Dep. NTIS $4.00.

The 12.5 kiloton device was detonated at a depth of 1205 ft in granite. The rock type ranges from a porphyritic granite to granodiorite. Though the formation is extensively faulted and jointed, the area around the shot point would be considered relatively massive, with a fracture frequency of ~1/ft. Major objectives of interest to the Plowshare program to be obtained in the postshot exploration of the Shoal Event were as follows: (1) test cavity radius and chimney height scaling equation for granite; (2) determine gamma radiation and temperature profiles in the chimney and cavity areas; (3) determine particle size distribution in the chimney and, possibly, the extent of fracturing beyond the chimney; and (4) investigate water table fluctuations caused by the explosion and the transport of radionuclides in the ground water. The results of these investigations are reported. (TFD)

29318 (UCID-15802(Rev. 1)) OPERATION CANNIKIN: ELECTRONIC AND ELECTRICAL SCIENTIFIC MEASUREMENTS AND SUPPORT PLAN. Pre-Operational Report. Hamm, T. Jr. (California Univ., Livermore (USA). Lawrence Livermore Lab.). 28 Feb 1971. Contract W-7405-eng-48. 131p. Dep. NTIS $9.75.

The electronics and electrical program for the Cannikin Event encompasses the instrumentation and power to obtain device performance and ground motion data. The equipment and experiments are defined as well as the methods used for recording these signals. Locations of the transducers and recording stations are described, along with time schedules of the events and readiness dates. (TFD)

29319 (UCID-15818) LAMINAR GAS FLOW THROUGH LOOSELY PACKED OVERTON SAND. Rozsa, R. B.; Skinner, D. F. (California Univ., Livermore (USA). Lawrence Livermore Lab.). 24 Mar 1971. Contract W-7405-Eng-48. 23p. Dep. NTIS $4.25.

The resistance to gas flow of stemming materials used to backfill emplaced devices is an important factor in evaluating containment of radioactive gases generated in nuclear test explosions. A simple laboratory experiment to measure the permeability of loosely packed Overton sand under steady state laminar gas flow conditions is described. The sand used in the experiments has a nominal particle size of about 2.5×10^{-2} cm. The porosity and permeability of the loose packed material was determined to be 0.35 and 13.2 darcies, respectively. Transient flow experiments are compared with numerically calculated predictions and good agreement is found. Recommendations are made to extend this work to other stemming materials and to investigate the turbulent flow regime. (auth)

29320 (UCID-15855) "SUPER" H. E. MACHINE CONCEPT. House, P. A. (California Univ., Livermore (USA). Lawrence Livermore Lab.). 8 Dec 1970. 11p. Dep. NTIS $4.00.

A unique new idea in high explosive (H. E.) pipe closures is presented. Special design features cause device induced gross overpressuration to enhance continued pipe closure. This design is an engineering attempt to prevent the usual early millisecond type failure, or bypass, of the first H. E. machine in a pipe string. Motivation for construction of the new machine is outlined, based on past experience and future design goals. The H. E. machine system and its method of operation is illustrated. Computer techniques used to predict response and thus aid in the physical design are described. (auth)

29321 (UCID-15865) FEASIBILITY OF TWO SCHEMES FOR DETECTING THE ENVELOPE OF A γ-RAY BURST UNDERGROUND. Bevensee, R. M. (California Univ., Livermore (USA). Lawrence Livermore Lab.). 28 Jun 1971. Contract W-7405-eng-48. 11p. Dep. NTIS $4.00.

Two schemes are discussed for measuring the envelope of a γ-ray burst from a nuclear explosion a mile or more underground and transmitting the information to the surface of the earth. In the first scheme, a beam of rays passes through an acidic aqueous solution, through which a laser beam (≈5000 Å) passes perpendicularly. The γ-rays create hydrated electrons which attenuate the laser beam accordingly. One can then generate an electromagnetic signal proportional to the laser beam intensity (by an electron multiplication scheme for example) either underground or on the earth's surface. In the latter case the laser beam can be transmitted through a light pipe to the surface. In the second scheme an electron current that is proportional to γ-ray intensity, the generation of which is not considered herein, excites (by loop coupling) a low-loss waveguide near cutoff. The electron current is modulated so as to have its spectrum centered at a frequency above the cutoff frequency. Stationary-phase analysis, assuming compensation of the frequency-dependent attenuation in the waveguide above cutoff, indicates that (a) frequency modulation of the electron current, such as would be employed in chirp radar, would be undesirable and (b) the waveguide output signal would unambiguously define the spectrum of the γ-ray intensity over the approximate range $-f_c$ to $+f_c$, f_c being the waveguide cutoff frequency. It is concluded that either scheme is a feasible means of detecting the envelope of an underground γ-ray burst, without being unduly costly. (auth)

29322 (UCID-15874) PRELIMINARY EQUATION-OF-STATE DATA FOR BANEBERRY ALTERED TUFF. Stephens, D. R.; Heard, H. C.; Schock, R. N. (California Univ., Livermore (USA). Lawrence Livermore Lab.). 13 Jul 1971. Contract W-7405-eng-48. 11p. Dep. NTIS $4.00.

An altered tuff from NTS location Ue8f, 1114-ft level, was examined as an aid in interpreting the Baneberry event. The rock, compared with other NTS rocks, was very weak and ductile. If the sample was representative of the working point medium, then, compared with other NTS events at comparable yield, the shock resulting from Baneberry would have been more intense, ground motions would have been larger, and seismic coupling should have been very efficient. In addition, pipe closure by the shock should have been very effective. These conclusions are consistent with the observed Baneberry phenomenology. (auth)

29323 (UCID-15919) FIELD MEASUREMENTS OF PERMEABILITY OF NTS ALLUVIUM IN AREA 10. Morris, G. A.; Snoeberger, D. F.; Morris, C. J.; DuVal, V. L. (California Univ., Livermore (USA). Lawrence Livermore Lab.). 11 Oct 1971. Contract W-7405-eng-48. 11p. Dep. NTIS $4.00.

A measurement of the permeability of NTS alluvium around hole U-10am-5 was completed. Tracer tests were also done using SF_6 to investigate the possible presence of cracks or highly permeable paths to the surface. This is the same hole used by Pasternak and McMullen for similar tests, but the region has since been subjected to shock from a nearby nuclear explosion. Transient tests were conducted at a number of flowrates and included buildup and decay of down-hole pressures for permeability calculations. No significant gas leaks or paths were found. The permeability calculated is in the range 8 to 16 darcies and does not show any large change from that reported by Pasternak and McMullen. (auth)

29324 (UCID-15981) NUMERICAL SIMULATION OF AIR-INJECTION EXPERIMENTS IN NTS ALLUVIUM. Rozsa, R. B.; Morris, G. A. (California Univ., Livermore (USA). Lawrence Livermore Lab.). 15 Jan 1972. Contract W-7405-eng-48. 13p. Dep. NTIS $4.00.

The gas flow properties of the medium surrounding an underground emplaced nuclear device are important in evaluating potential containment problems. The presence of faults or large cracks is significant in that, if early gas flow is turbulent enough, erosion will result and the flow path will widen. This, together with the high driving pressure available before chimney collapse, can result in the venting of large quantities of gas. Even when early-time dynamic venting is not a problem, late-time seepage can result if the permeability is high enough and the source pressure remains above ambient pressure for a long time. To study the flow of gas through Nevada Test Site alluvium, comprehensive air-injection experiments were conducted in July 1971 using a 454-ft-deep hole, U10am-5. Transient pressurization and decay runs were made with seven different flow rates. Numerical simulation calculations using a two-dimensional radial-flow model are described. It was found that the simple laminar Darcy flow relationship did not adequately describe the measured pressure histories, especially at the higher flow rates. The use of a more complicated expression including a turbulence factor resulted in good agreement for all flow rates. Within the limits of accuracy of the field data, the laminar permeability was calculated to be 8 ± 0.5 darcies and the porosity 0.4 ± 0.1. (TFD)

29325 (UCID-15983) GENERATION OF SEISMIC WAVES BY NUCLEAR EXPLOSIVES AND POSSIBILITIES FOR EVADING A TEST-BAN TREATY. Holzer, F. (California Univ., Livermore (USA). Lawrence Livermore Lab.). 31 Jan 1972. Contract W-7405-eng-48. 12p. Dep. NTIS $4.00.

Study of the seismic and geological data pertaining to underground nuclear explosions suggests several possibilities for conducting nuclear weapons tests clandestinely in an attempt to evade a test-ban treaty. Explosions with yields up to 10 kt in alluvium would give seismic signals less than Richter magnitude 4 and could be detonated without collapse craters if the alluvium were deep enough. Ignoring the subsidence or collapse-crater phenomenon, 15 to 20 kt could be detonated in alluvium without exceeding magnitude 4. Yields of 50 kt could be detonated either in a decoupling cavity without exceeding magnitude 4 or could be part of a series of explosions designed to simulate an earthquake. Finally, 100 kt or perhaps more could be detonated clandestinely by hiding its seismic signals in those of a large earthquake. (auth)

29326 (UCID-15985) INVESTIGATION OF TRITIUM DECONTAMINATION. Interim Research Report. Wethington, J. A. Jr. (California Univ., Livermore (USA). Lawrence Livermore Lab.). 18 Jan 1972. Contract AT(40-1)-4201. 14p. Dep. NTIS $4.00.

The use of nuclear explosions for releasing gas trapped in low permeability formations contaminates the well effluents with radioactivity. One of the most persistent of these activities, tritium, appears in the hydrocarbon fraction and in the water fraction which emerges from the chimney as steam mixed with the methane. Work on Gasbuggy suggested that tritium-containing hydrocarbons would be the major sources for injection of tritium into the environment, but studies at Rulison showed that HTO production might be the limiting factor in using such gas deposits. Decontamination of the HTO by isotopic exchange reactions with hydrocarbons and H-containing rocks is discussed. (TFD)

29327 (UCID-16107) ELAT-DEAD SEA CANAL. Nordyke, M. D. (California Univ., Livermore (USA). Lawrence Livermore Lab.). 11 Aug 1972. Contract W-7405-eng-48. 22p. Dep. NTIS $4.25.

The feasibility of using nuclear explosions to construct a canal from the vicinity of Elat on the Gulf of Aqaba to the Dead Sea to utilize the enormous depth below sea level and the high rate of evaporation of the Dead Sea to generate electric power is discussed. (TFD)

Protective Structures and Equipment

29328 (LA-UR-74-1132) VENTILATION DESIGN MODIFICATIONS AT LOS ALAMOS SCIENTIFIC LABORATORY MAJOR PLUTONIUM OPERATIONAL AREAS. Stafford, R. G.; Gallimore, J. C. Jr.; Mitchell, R. N.; Maraman, W. J.; McNeese, W. D. (Los Alamos Scientific Lab., N. Mex. (USA)). 1974. 20p. (CONF-740807-17). Dep. NTIS $4.00.

From 13th air cleaning conference; San Francisco, California, USA (12 Aug 1974).

Major ventilation design modifications in plutonium operational areas at Los Alamos have occurred during the past two years. An additional stage of HEPA filters has been added to DP West glovebox process exhaust resulting in significant effluent reductions. The additional stage of HEPA filters is unique in that each filter may be individually DOP tested. Radiological filter efficiencies of each process exhaust stage is presented. DP West room air ventilation systems have been modified to incorporate a single stage of HEPA filters in contrast to a previous American Air Filter PL-24 filtration system. Plutonium effluent reductions of 10^2 to 10^3 have resulted in these new systems. Modified DOP testing procedures for room air filtration systems are discussed. Major plutonium areas of the CMR Building utilizing Aerosolve 95 process exhaust filtration systems have been upgraded with two stages of HEPA filters. Significant reductions in effluent are evident. A unique method of DOP testing each bank of HEPA filters is discussed. Radiological efficiencies of both single and two-stage filters are discussed. (auth)

29329 (RFP-2215) VENTILATION DESIGN FOR NEW PLUTONIUM RECOVERY FACILITY. Oliver, A. J.; Amos, C. L. (Dow Chemical U. S. A., Golden, Colo. Rocky Flats Div.). [nd]. 18p. (CONF-740807-18). Dep. NTIS $4.00.

From 13th air cleaning conference; San Francisco, California, USA (12 Aug 1974).

The new Plutonium Recovery Facility at the Rocky Flats Plant will replace an existing facility of similar nature which was placed into operation in 1952. In 1968 it was determined that the old building would require extensive modification to meet the ever increasingly stringent objectives of a plutonium handling facility. Approval was given to proceed with a new replacement building incorporating the best and latest technology available. The methods by which the confinement of contamination and air treatment are being handled in this facility are reported. (TFD)

29330 (UCID-15941) LLL SPRAY DAMPER PROJECT. Gaskill, J. R.; Murrow, J. L. (California Univ., Livermore (USA). Lawrence Livermore Lab.). 12 Nov 1971. 4p. Dep. NTIS $4.00.

Experimental work is being carried out at Lawrence Livermore Laboratory on the use of water sprays to protect exhaust ventilation ductwork and downstream filters from the effects of fire gases. The experimental setup is described, and preliminary results are given. (auth)

ENVIRONMENTAL AND EARTH SCIENCES

29331 ENVIRONMENTAL ASSESSMENT OF RESOURCE DEVELOPMENT. Kerri, K. D. (Sacramento State Coll., CA). J. Sanit. Eng. Div., Amer. Soc. Civil Eng.; 98: No. SA2, 361-374 (Apr 1972).

Desired contents and expectations of environmental impact statements as required by the "National Environmental Policy Act" and the California "Environmental Quality Act" are discussed by representatives of the disciplines of biology, botany, soils, administration, engineering, fisheries, wildlife, zoology, and anthropology. Use of the matrices is outlined to provide a systematic approach to evaluate potential impacts, compare alternative solutions, identify critical actions, and indicate environmental conditions sensitive to the resource development project under consideration. Measurement and estimation of potential impact on water quality, aquatic organisms, wildlife, and the soil mantle are discussed. Annual plants and birds are proposed as possible indicator organisms to reveal the extent and magnitudes of resource development impacts on the environment. Anthropologists document the need to protect and scientifically evaluate the contents of archaeological sites. (auth)

Minerals and Ores

Refer also to abstract 28987.

29332 ZONAL'NOST' GIDROTERMAL'NYKH RUDNYKH MESTOROZHDENII. (Zonality of Hydrothermal Ore Deposits. Volume I. Zonality of Deposits of Tin, Tungsten, Molybdenum, and Some Groups of Less-Common Metals). Sokolov, G. A. (ed.). Moscow; Izdatel'stvo Nauka (1974). 298p.

Nine papers are included. A separate abstract was prepared for each of 2 papers. The remaining 7 papers were not within the scope of NSA. (LCL)

For abstracts of individual papers see: 29333 and 29334.

29333 ZONALITY OF THORIUM–NIOBIUM MINERALIZATION IN ALBITITES. Omel'yanenko, B. I. pp 276-283 of Zonal'-nost' Gidrotermal'nykh Rudnykh Mestorozhdenii. Vol I. Sokolov, G. A. (ed.). Moscow; Izdatel'stvo Nauka (1974). (In Russian).

Sodium metasomatites formed in precontact parts of the nepheline-syenite massives contain thorium-niobium and zirconium deposits. The minerals chlorite, pyrochlore, and zircon are localized in definite zones of the metasomatic bodies, pyrochlore and zircon in the inner and thorite in the intermediate and outer zones. In the localization of the thorite the lithological composition of the initial material is very significant. Thorium precipitation from solution is affected by quartz and calcite in the enclosing rock. Knowledge of the place of the ore minerals in the metasomatic zonality is important both for clarifying the conditions of transfer and deposition of the ore elements and for prospecting. (tr-auth)

29334 HYPOGENIC ZONALITY IN HYDROTHERMAL URANIUM DEPOSITS. Tishkin, A. I. pp 284-295 of Zonal'nost' Gidrotermal'nykh Rudnykh Mestorozhdenii. Vol. I. Sokolov, G. A. (ed.). Moscow; Izdatel'stvo Nauka (1974). (In Russian).

The nature of the chief types and formations of hydrothermal uranium deposits and a summary of the literature on studies of zonality in them are presented. For the industrially important deposits of pitchblende-sulfides and pitchblende-carbonates, data are given on the zonality of the ore fields, deposits, and separate ore bodies. Zonality in veins and precipitates and in oreoles of metasomatic changes in rocks and element dispersion are characterized. Practical recommendations are made based on zonality data. (tr-auth)

29335 GEOLOGY AND MINERAL RESOURCES OF THE GREATER GREEN RIVER BASIN. Symposium and Core Seminar, Casper, Wyoming, September 17–19, 1973. Schell, E. M.; McAuslan, E. R.; Renfro, A. R.; Walker, R. E. (eds.). Casper, WY; Wyoming Geological Association (1973). 247p. (CONF-7309115-).

Thirty-one papers are included. Two are abstracted individually for NSA. (JGB)

For abstracts of individual papers see: 29336 and 29459.

29336 URANIUM IN THE GREAT DIVIDE BASIN, WYOMING. McKeel, B. K. (Atomic Energy Committee, Salt Lake City). pp 131-138 of Geology and Mineral Resources of the Greater Green River Basin. Schell, E. M. (ed.). Casper, WY; Wyoming Geological Association (1973).

From symposium and core seminar on the geology and mineral resources of the greater Green River basin; Casper, Wyoming, USA (17 Sep 1973). See CONF-7309115-.

The Great Divide Basin might contain significant low-grade uranium deposits. An apparent lack of high-grade deposits might be due to the dispersal of uranium mineralization in the immense, unrestricted sand bodies, highly mobile frontal systems, and the apparent scarcity of carbon trash to aid in the precipitation of uranium. Uranium deposits of higher grades may occur at greater depths that have not been adequately explored. Potential uranium deposits of the Great Divide Basin are expected to occur largely as rolls resulting from solution-front activity. The potential host rocks are arkosic sands of the Battle Spring Formation of early and middle Eocene age and possibly the uppermost Fort Union Formation of Paleocene age. (auth)

29337 ORIGIN OF CARBONATITIC MAGMA IN THE LIGHT OF THE Pb-U-Th ISOTOPE SYSTEM. Lancelot, J. R.; Allegre, C. J. (Paris-6 Univ., 75 (France). Inst. de Physique du Globe). Earth Planet. Sci. Lett.; 22: No. 3, 233-238(Jun 1974).

The concentrations of U, Th, and Pb as well as the isotopic composition of lead have been determined in nine African carbonatites. The observed compositions show radiogenic isotope enrichments analogous to those of the alkali rocks from the Atlantic islands. The results as a whole reveal a mixing phenomenon that can receive two very different interpretations at the present time: (1) A component, originating from the mantle is contaminated by crustal lead inside the magmatic chamber situated in the continental crust (radiogenic lead from the embedding crustal rocks being preferentially extracted by the gaseous phase individualized in the magmatic chamber). (2) The mixing of a tholeiitic component with a radiogenic one from deep origin, corresponding to J. Morgan's "plumes" which would originate from the innermost part of the mantle, with high ^{238}U/^{204}Pb and ^{87}Rb/^{86}Sr ratios. (auth)

29338 ^{40}Ar/^{39}Ar DATING OF THE LONG RANGE DIKES, NEWFOUNDLAND. Stukas, V. (Dalhousie Univ., Halifax, Nova Scotia (Canada). Inst. of Oceanography); Reynolds, P. H. (Dalhousie Univ., Halifax, Nova Scotia (Canada). Dept. of Physics). Earth Planet. Sci. Lett.; 22: No. 3, 256-266(Jun 1974).

Stepwise outgassing experiments were performed on eleven whole rock samples from a sequence of diabase dikes from the Great Northern Peninsula. Gas released at high temperatures ($> \simeq 925-950$°C) was consistently characterized by anomalously high apparent ages. These are attributed to the release of excess radiogenic argon, gas which probably resides in the mineral augite. At temperatures below $\simeq 700$°C, a wide range in apparent age was observed. On the other hand, the medium temperature region ($\simeq 700-950$°C) is characterized by a relatively small range in apparent age. Data points corresponding to this region are rather well correlated in an isochron-type diagram; the slope of the best-fitting straight line corresponds to an age $t = 605 \pm 10$ m.y. It is suggested that the outgassing of unaltered plagioclase is dominating the age spectra in this temperature interval. Consequently, 605 ± 10 m.y. is taken as the time of emplacement of the Longe Range dike swarm. This event may have marked the opening of a proto-Atlantic Ocean. The Acadian Orogeny (perhaps the ocean-closing event $\simeq 380$ m.y. ago) appears to be recorded in the low–medium temperature regions in the cases of two rather extensively altered samples. (auth)

29339 Rb-Sr AND K-Ar AGE DETERMINATIONS, AND OXYGEN ISOTOPE DATA FOR THE GLEN CANNEL GRANOPHYRE, ISLE OF MULL, ARGYLLSHIRE, SCOTLAND. Beckinsale, R. D. (UKAEA Weapons Group, Aldermaston. Atomic Weapons Research Establishment). Earth Planet. Sci. Lett.; 22: No. 3, 267-274(Jun 1974).

A seven point Rb-Sr whole rock isochron for the Glen Cannel granophyre gives an age and initial ^{87}Sr/^{86}Sr ratio of 60.4 ± 1.9 m.y. and 0.7094 ± 0.0003 respectively (errors $1\sigma, \gamma\beta = 1.47 \times 10^{-11}$ yr^{-1}). K-Ar ages for two of the samples on the isochron average about 56 ± 1 m.y. Oxygen isotope data show that the granophyre is strongly depleted in ^{18}O with an average $\delta\,^{18}$O of about -2.3‰ (SMOW) as a result of massive interaction with meteoric ground water at approximate temperatures in the range 300–450°C. It is suggested that the Rb-Sr isochron reflects the point in time when the circulation of meteoric water ceased and that the K-Ar ages reflect continued radiogenic ^{40}Ar loss at lower temperatures after this. The initial ^{87}Sr/^{86}Sr ratio for the Glen

Cannel granophyre (0.7094 ± 0.0003) is significantly higher than that found that for a very fresh dolerite plug in northern Mull (0.7030 ± 0.0001). The high initial ratio and peralkaline chemistry of the granophyre are interpreted as effects of the rock/groundwater interaction in central Mull and do not exclude the possibility that the original acid magma was derived via fractional crystallization of a tholeiitic basalt liquid. The igneous activity in Mull appears to have been of quite short duration, probably not more than about 10 m.y. It was essentially confined to the Paleocene and ended in the Lower Eocene. (auth)

29340 DETERMINATION OF ^{87}Sr/^{86}Sr IN CENOZOIC ANDESITES AND THE RELATED ROCKS OF NORTHWEST SARDINIA (ITALY). Dupuy, C. (Univ., Montpellier, France); McNutt, R. H.; Coulon, C. Geochim. Cosmochim. Acta; 38: No. 8, 1287-1296(Aug 1974). (In French).

Initial isotopic ratios of strontium were determined in some calc-alkali rocks of Sardinia. The values of these ratios are from 0.7044 and 0.7047 in two basalts, and from 0.7063 to 0.7081 in five andesites. A dacite and a rhyolite have intermediate values of 0.7056 and 0.7058. It is suggested that increase of radiogenic strontium in andesite is most likely related to a contamination process involving water expelled from an underthrusting plate. This water also contributes to the increase in the potassium and related trace element contents in andesites. In spite of the ^{87}Sr/^{86}Sr difference between basalt and andesite, a cogenetic relationship between these two kinds of rocks cannot be precluded. (auth)

Radioactive Effluents

Refer also to abstracts 28995, 29369, 29468, and 30110.

29341 (DUN-8133) DOUGLAS UNITED NUCLEAR, INC. REACTOR AND FUEL PRODUCTION FACILITIES 1972 ENVIRONMENTAL RELEASE REPORT. Dabrowski, T. E. (Douglas United Nuclear, Inc., Richland, Wash. (USA)). 1 Mar 1973. 13p. Dep. NTIS $4.00.

During Calendar Year 1972, an estimated total of 4,000,000 pounds of waste materials, including approximately 1 gram of radionuclides, were discharged to the environs in liquid effluent streams emanating from Douglas United Nuclear, Inc. operated facilities. During the same period, approximately 2,000,000 pounds of reported waste materials, including a small fraction of a gram of reported radionuclides, were discharged to the atmosphere from Douglas United Nuclear Inc. operated facilities. (auth)

29342 (RISO-M-1726) COMPARISON OF MATHEMATICAL MODELS FOR CALCULATION OF EXTERNAL GAMMA DOSES ORIGINATING FROM RELEASES OF RADIOACTIVITY TO THE ATMOSPHERE. Hedemann Jensen, P. (Danish Atomic Energy Commission, Risoe. Research Establishment). Jul 1974. 176p. (In Danish). Dep. NTIS (US Sales Only) $12.00.

A brief description is given of different mathematical models for estimating external gamma doses from a continuous plume of radioactive gases (iodines and noble gases) released to the atmosphere from a nuclear plant, and the uncertainties of such estimates are discussed. Gamma doses from unit releases of fourteen noble gases and iodines were calculated from these models and compared with the doses calculated from the computer program GDOS, which is an implementation of a gamma dose model developed at Riso. Good agreement was found between GDOS and seven other models, one of which was experimentally verified within a downwind distance of a few kilometres. Estimated gamma doses from unit releases of fourteen noble gases and iodines for two weather categories (Pasquill types D and F), and with three different release heights (0, 24 and 100 metres) calculated with four of the models (including GDOS), are given tabularly and graphically for values of downwind distances from 0.1 to 50 kilometres. (auth)

29343 ATOMIC ENERGY. V. Parr, H.; Bryne, K. H.; Hofseth, P.; Riekeles, J. pp 86-117 of Report From the Norwegian Nature Conservancy Association, Prepared by the Association's Energy Group. Parr, H. (ed.). Oslo; Norges Naturvernforbund (1974). (In Norwegian)

The chapter is divided into three sections. In the first a brief survey of commercial nuclear power, followed by an outline of the nuclear fuel cycle, leads to a short general discussion of radioactivity and ionizing radiation. The principal radioactive materials resulting from power reactor operation are then presented and discussed. Thereafter the biological effects of radiation, acute, delayed and genetic, are described and finally the ICRP recommendations are given. The second section deals with the environmental aspects of nuclear power. The disposal of high active and low active waste is discussed at some length, and the toxic and safeguards aspects of plutonium more briefly. The consequences of reactor accidents are discussed on the basis of WASH-740 and WASH-1250. The release of radioactivity during normal operation and fast breeder reactors are finally treated briefly. The short third section presents as a conclusion that the hazards and uncertainties involved in nuclear energy are so serious that they outweigh its advantages. (NO)

29344 GORYACHIE AEROZOL'NYE CHASTITSY PRI TEKHNICHESKOM ISPOL'ZOVANII ATOMNOI ENERGII. (Hot Aerosol Particles During Commercial Use of Atomic Energy). Bykhovskii, A. V.; Zaraev, O. M. Moscow; Atomizdat (1974). 256p.

A broad range of problems encountered in ensuring radiation protection from the contamination of the atmosphere with highly active aerosol particles is considered. Modern concepts of the radiation hazard from aerosols and special features of its evaluation and control, related to the presence of hot aerosol particles in radioactive aerodispersed systems are discussed. The basic mechanisms of formation of hot aerosol particles in the commercial use of atomic energy, in particular, nuclear reactors and gamma sources, and in nuclear fuel production and reprocessing are also discussed. The specific activity and composition of the nonactive components of hot particles helps in identifying the sources of contamination of the air of industrial premises with radioactive aerosols. The book is designed for physicists, engineers, health physicists, and students engaged in studying the causes and prevention of aerosol contamination. (tr-auth)

Radioactivity Monitoring and Transport

Refer also to abstracts 29439, 29453, 29454, 29490, 29494, and 31204.

29345 (AD-629357) OFF-SITE SURVEILLANCE. Final Report. Report on Project Dribble, Salmon Event, Tatum Salt Dome, Mississippi, 22 October 1964. Carter, M. W.; Placak, O. R. (Southeastern Radiological Health Lab., Montgomery, Ala. (USA)). Feb 1966. 60p. (VUF-1021). NTIS $6.00.

The most significant knowledge gained during the salmon event was that large numbers of people can be successfully evacuated, and a comprehensive off-site radiological safety program can be successfully conducted in a populated area if the confidence of the people toward the operation is maintained. Considering the many occasions that the people were contacted relative to the surveys of the area and evacuation activities, extreme precautions were necessary to maintain the confidence of the people. In developing evacuation procedures, it was learned that each family had to be considered on an individual basis, and that questions relative to the operation had to be answered truthfully and as precisely as possible. The people in the area expressed considerable concern relative to when the shot would be detonated and what the effects might be on them and their surroundings. They expressed major concern over possible damage to their water wells due to structural or radiological effects. (auth)

29346 (GAT-781) PORTSMOUTH GASEOUS DIFFUSION PLANT ENVIRONMENTAL MONITORING REPORT, 1973. Kalmon, B.; Koehler, F. A. (Goodyear Atomic Corp., Piketon, Ohio (USA)). 3 May 1974. Contract AT(33-2)-1. 27p. Dep. NTIS $4.00.

At the Portsmouth Gaseous Diffusion Plant the ambient atmosphere and all effluent streams are sampled and analyzed regularly for conformance to applicable environmental standards. Additionally, because fluorides are used in the gaseous diffusion plant and because some states, not including Ohio, have established standards for fluorides in air, the concentrations of fluorides in the ambient atmosphere are measured routinely. Also, the concentrations of fluorides in vegetation are measured because fluoride ingestion can cause adverse effects in livestock. Atmospheric pollution resulting from a coal-fired steam plant is assessed periodically by measuring the concentrations of particulate matter and SO_2 in the steam plant stacks. With the exception of particulate matter from the steam plant and the possible exception of chromium in the cooling water discharge, none of the average annual concentrations of either radioactive or non-radioactive pollutants in the ambient atmosphere, in gaseous effluent streams, or in liquid effluent streams have exceeded applicable standards. However, higher average concentrations are reported this year than were reported in 1972 because the method of computation specified in AEC Manual Chapter 0513 has been changed. The average background radiation levels measured at the plant boundaries were no greater than those measured at a point approximately 4.5 miles southwest of the plant. There is no evidence that the operation of the plant has contributed to the background radiation. The calculated maximum radioactivity dose (lung burden) at the plant boundary, based on airborne emissions from the plant, was 6 mrem; at the same location the whole-body exposure resulting from continuous exposure to background radiation was 119 mr. (For comparison: estimates of diagnostic medical radiation vary, two estimates being 72 mrem per year and 165 mrem per year.) (auth)

29347 (NLCO-1109) FEED MATERIALS PRODUCTION CENTER ENVIRONMENTAL MONITORING ANNUAL REPORT FOR 1973. (National Lead Co. of Ohio, Cincinnati (USA)). 1 Apr 1974. Contract AT(30-1)-1156. 28p. Dep. NTIS $4.50.

Environmental monitoring data collected at the Feed Materials Production Center (FMPC) during 1973 are summarized. Data are presented for both radioactive and non-radioactive contaminants in environmental samples. These data show that the average offsite concentrations of radioactive contaminants from FMPC operations were no greater than 0.6% of the guide levels published in AEC Manual Chapter 0524. The resulting offsite radiation exposures would, therefore, be a small fraction of the standards for uncontrolled areas. (auth)

29348 (PNE-RB-51-9) RADIOLOGICAL MONITORING PROGRAM, PERIOD COVERING FEBRUARY 4, 1974–APRIL 30, 1974. (Eberline Instrument Corp., Santa Fe, N. Mex. (USA)). 1974. 20p.

For CER Geonuclear Corp., Las Vegas, NV.

Beta radioactivity in air particulate samples increased in March and April to a peak of 0.47 pCi/m^3 from a mid-winter low of 0.02 pCi/m^3. A seasonal increase is always noted in the spring, but this increase is more than usual and is attributable to injection of year old fission products from the upper atmosphere inventory due to spring mixing of the upper and lower atmosphere. The presence of a fission product mixture consistent with the time delay since the June 26, 1973 test by the Peoples Republic of China indicates that this test is responsible for most of the increase in the spring of 1974. The increase is not attributable to Rio Blanco because it was typical of levels measured throughout the US by Eberline and by the Environmental Protection Agency. For example, gamma isotopic analysis of composite filters from the southeastern US showed the presence of the same approximately year-old fission product mixture at similar concentrations as measured at Rio Blanco. Vegetation samples were collected on March 29, 1974. ^{89}Sr, tritium, and gamma emitters (other than natural ^{40}K) were not detected in any of the samples. The concentration of ^{90}Sr ranged from 0.04 to 0.18 pCi/g (dry weight) and is attributable to worldwide fallout. TLD data for this period indicated an average background dose rate of 3.0 mrem/week. This is higher than the dose rate measured during the winter (2.25 mrem/week) and is attributable to increased dose rate from terrestrial sources due to the melting of the winter snow cover. Water samples collected during March, 1974 did not indicate the presence of any unexpected radioactivity. Gross beta concentrations ranged up to a maximum of 8 ± 4 pCi/l. Tritium was measured in some of the samples by electrolytic enrichment and liquid scintillation counting. Concentrations of tritium ranged from 0.12 ± 0.08 to 0.25 ± 0.08 pCi/ml. This tritium is attributable to natural production in the atmosphere and worldwide fallout from weapons testing. This concentration is a small fraction of the peak in 1963 caused by weapons testing in the atmosphere. Gamma emitters, other than natural radioactivity were not detected in samples collected on March 29, 1974. ^{137}Cs was measured in soil samples collected on March 29, 1974 with concentrations ranging from less than 0.09 to 0.9 pCi/g (dry weight). Tritium and gamma emitters (except natural radioactivity) were not detected in any of the samples. None of the environmental samples from the Rio Blanco site indicate the presence of any radioactivity attributable to Project Rio Blanco. (auth)

29349 (SCPRI(RM)-2-1974) REPORT OF ACTIVITY, FEBRUARY 1974. (Service Central de Protection Contre les Rayonnements Ionisants, 78– Le Vesinet (France)). 1974. 15p. (In French). Dep. NTIS (US Sales Only) $4.00.

Data are presented on levels of radioactivity in the environment in France during February 1974. Samples monitored included atmospheric dusts (air at ground level, high altitude air), rainwater, surface water, underground water, irrigation water, drinking water, food chains (milk, plants, cattle, fish), sea water around nuclear plant (^{7}Be, ^{95}Zr and ^{95}Nb, ^{103}Ru, ^{131}I, ^{137}Cs, ^{140}Ba and ^{140}La, ^{90}Sr, ^{106}Ru and ^{106}Rh, ^{226}Ra, ^{54}Mn, U and T). (FR)

29350 (SCPRI(RM)-2-1974(Suppl.)) ANNEX TO MONTHLY REPORT, FEBRUARY 1974. Detail of Results of Measurement. (Service Central de Protection Contre les Rayonnements Ionisants, 78– Le Vesinet (France)). 1974. 23p. (In French). Dep. NTIS (US Sales Only) $4.25.

Tabulated data are presented on the radioactivity in environmental samples collected throughout France during February 1974. (CH)

29351 (UCC-ND-279) ENVIRONMENTAL MONITORING REPORT, CALENDAR YEAR 1973. (Paducah Gaseous Diffusion Plant, Ky. (USA)). 30 Apr 1974. Contract W-7405-eng-26. 28p. Dep. NTIS $4.50.

Air, water, soil, and grass in the vicinity of the Paducah Gaseous Diffusion Plant were continuously or periodically sampled during 1973. Analyses for materials known to be in plant effluents were made to provide effluent control information and to determine compliance with applicable air and water quality standards. The analyses showed all effluents to be in compliance with applicable state and federal standards (except Cr^{6+}). The steam plant and incinerator met applicable state and federal emissions standards. The air analyses for radioactivity indicate concentrations at all off-site sampling stations averaged less than 2.4% of the applicable Radioactivity Concentration Guide. The potential dose to the critical organ (lung) was also less than 2.4% of the allowable dose of 1.5 rem per year for off-site persons. The "fencepost dose" was calculated to be less than 0.036 rem per year. Air and grass off-site analyses for fluorides met the Kentucky air quality requirements. Soil samples collected to provide historical background data were analyzed for uranium. The results ranged from 1.6 to 2.1 ppM at the AEC property boundary. Background concentration is about 1.0 ppM. There are no comparable standards, but these values appear to be far below a level of environmental significance. There was no detectable change in chemical, physical, or radioactive characteristics of either the Ohio River or ground water attributable to Paducah Gaseous Diffusion Plant Operations. The results of water sample analyses of the Ohio River show the chromium and fluoride concentrations were in compliance with the requirements of the applicable Kentucky regulations. The concentrations of hexavalent chromium at the mouth of the combined Big and Little Bayous are slightly in excess of the Ohio River Valley Sanitation Commission (ORSANCO) discharge standard of 0.05 mg/liter. A chromate treatment facility is presently being designed and will insure compliance with existing standards. (auth)

29352 (UCC-ND-280) ENVIRONMENTAL MONITORING REPORT: UNITED STATES ATOMIC ENERGY COMMISSION, OAK RIDGE FACILITIES. Calendar Year 1973. (Union Carbide Corp., Oak Ridge, Tenn. (USA). Nuclear Div.). 2 May 1974. Contract W-7405-eng-26. 46p. Dep. NTIS $5.50.

The Environmental Monitoring Program for the Oak Ridge area includes sampling and analysis of air, water from surface streams, several food products, flora, and soil for both radioactive and nonradioactive materials. A summary of the results of the program for calendar year 1973 is presented. Surveillance of radioactivity in the Oak Ridge environs indicates the atmospheric concentrations of radioactivity were not significantly different from other areas in East Tennessee. Concentrations of radioactivity in the Clinch River and in fish collected from the river were less than one percent of the permissible concentration and intake guides for individuals in the off-site environment. While some radioactivity was released to the environment from plant operations, measurements in the Oak Ridge area show that environmental levels were well below established standards. The maximum potential exposure at the perimeter of the AEC-controlled area was calculated to be 0.48 mrem/year to the whole body and 17.8 mrem/year to the lung which are 0.09% and 1.2%, respectively, of the AEC Manual Chapter 0524 allowable standard. The maximum potential exposure to an Oak Ridge resident was calculated to be 0.17 mrem/year to the whole body and 4.8 mrem/year to the lung. These calculated exposures are 0.03% and 0.3%, respectively, of the allowable standard. The average exposure to an Oak Ridge resident was estimated to be 0.1 mrem/year as compared to approximately 100 mrem/year from natural background radiation. (auth)

29353 RADIATION IN MAN'S ENVIRONMENT. Titterton, E. W. (Australian National Univ., Canberra). Aust. J. Forensic Sci.; 6: No. 2, 96-100(Dec 1973).

From 21st plenary scientific session of the academy; Sydney, Australia (20 Sep 1973).

Fallout levels are compared with other radiation effects in everyday life as well as with other hazards which we all accept without question, but which are far more damaging than fallout. A number of legal, moral and ethical questions are then considered. (AT)

29354 ECOLOGICAL FACTORS IN THE SITING, DESIGN, AND OPERATION OF A NUCLEAR POWER STATION. Davy, D. R.; Giles, M. S.; Charash, E. Proc. Ecol. Soc. Aust.; 5: 153-168(1970).

It is shown that the safe disposal of radioactive waste arising from a nuclear power station will present no insoluble problem. The effects on the local ecology can be minimized by careful attention to design and operational procedures. Several ecological factors have been defined and discussed. The mechanisms of distribution of both gaseous and air-borne effluent are well understood. Discharges of liquid effluent involve the physical movement of large volumes of water, normal industrial wastes, transfer of heat and some release of radioactivity. An outline has been given of the factors to be taken into account in setting discharge limits for radioactivity. (auth)

29355 ENVIRONMENTAL RADIOACTIVITY AND RADIATION EXPOSURE. G-I-T (Glas- Instrum.-Tech.) Fachz. Lab.; 18: No. 6, 601(Jun 1974). (In German).

The German Federal Ministry of Internal Affairs published recently the 1972 annual report on environmental radioactivity and radiation exposure. A summarizing presentation is given and an evaluation of the results obtained from over 50 measuring stations during the year reported to the public within the framework of the official control of the environmental radioactivity and radiation exposure. (GE)

Atmosphere

Refer also to abstracts 28937, 29410, 29435, 29450, 29452, 29468, 29477, 29478, 29480, 29482, 29484–29486, 29610–29612, and 29719.

29356 (AED-CONF-74-157-005) HEALTH PHYSICS AND TECHNICAL CONSIDERATIONS CONCERNING THE CONTROL OF GASEOUS EFFLUENTS FROM NUCLEAR POWER PLANTS. Fitoussi, L. (Bayerisches Landesinstitut fuer Arbeitsmedizin, Muenchen (F.R. Germany)). 1974. 6p. (In French). (CONF-740556-7). INIS.

From seminar on the monitoring of radioactive effluents; Karlsruhe, F. R. Germany (14 May 1974).

4 figs.; 1 tab.; 9 refs. With abstract in English and French.

The nature and importance of the radioactive risks of the gaseous releases from a nuclear power plant are analyzed and attention is focused on the preponderant radioactive risk and the populations concerned. For the monitoring of the releases and the evaluation of their consequences, a simple measuring device is proposed. This device used with appropriate models allows the direct calculation of the ground level external irradiation. The generalization of this technique would make the comparison of the results easier if the correspondence factors $\text{rem} \cdot h^{-1}/\text{Ci} \cdot m^{-3}$ met with general agreement. (auth)

29357 (ARMS-71.6.5) AERIAL RADIOLOGICAL MEASURING SURVEY OF THE MAINE YANKEE ATOMIC POWER PLANT, SEPTEMBER 1971. (EG and G, Inc., Las Vegas, Nev. (USA)). Aug 1974. 19p. (EGG-1183-1605). Dep. NTIS $4.00.

The Aerial Radiological Measuring System (ARMS) was used to survey the area surrounding the Maine Yankee Atomic Power Plant during September 1971, prior to reactor start-up. The survey measured terrestrial gamma radiation. A high-sensitivity detection system collected gamma-ray spectral and gross-count data. The data were then computer processed into a map of a 530 square mile area showing isoexposure contours three feet above the ground. Exposure rates and isotopes identified are consistent with normal terrestrial background radiation. (auth)

29358 (ARMS-72.6.2) AERIAL RADIOLOGICAL MEASURING SURVEYS OF THE TURKEY POINT STATION, APRIL 1972. (EG and G, Inc., Las Vegas, Nev. (USA)). Jul 1974. 19p. (EGG-1183-1602). Dep. NTIS $4.00.

The Aerial Radiological Measuring System (ARMS) was used to survey the area surrounding the Turkey Point nuclear power station during April 1972, prior to reactor start-up. The survey measured terrestrial background gamma radiation. A high-sensitivity detection system collected gamma spectral and gross-count data. The data were then computer processed into a map of a 175 square mile area showing isoexposure contours three feet above the ground. Exposure rates and isotopes identified are consistent with normal terrestrial background radiation. (auth)

29359 (BNWL-1850(Pt.3), pp 4-16) QUILLAYUTE AIR REFERENCE STATION. Perkins, R. W.; Ludwick, J. D.; Thomas, C. W.; Petersen, M. R.; Cooper, J. A. Apr 1974.

In Pacific Northwest Laboratory annual report for 1973 to the USAEC Division of Biomedical and Environmental Research. Part 3. Atmospheric sciences.

The Quillayute Air Base has been selected for the air reference station necessary to sample and monitor air constituents. Installing of appropriate instrumentation there is near completion, and a large variety of air constituents is now under study using sampling and monitoring techniques. High-volume air filtration provides samples for measuring the concentration of a wide spectrum of radionuclides, while their physical size distribution is determined from high-volume impactor samples. Plans for gaseous radionuclide measurements are also being implemented. Monitoring is under way for the gaseous constituents ozone and nitrogen oxides while plans for carbon monoxide and oxides of sulfur are near completion. A constant monitor is kept on the particulate air levels as well as a rather detailed analysis of some 30 stable elements from sampling of these particulates. Size and elemental distributions are continually measured as well. The hemispheric concentrations of certain organic constituents are measured by coordinating the meteorological watch for fresh air masses with certain sampling techniques. (auth)

29360 (BNWL-1850(Pt.3), pp 16-17) PARTICLE SIZE DISTRIBUTIONS OF MANMADE AND NATURAL RADIONUCLIDES. Young, J. A. Apr 1974.

In Pacific Northwest Laboratory annual report for 1973 to the USAEC Division of Biomedical and Environmental Research. Part 3. Atmospheric sciences.

At Richland, Washington greater than 90% of the short-lived radon and thoron daughters and 88% of the cosmogenic ^{7}Be were present on particles too small (1.1 μm) to have appreciable settling velocities. The percentage of nuclear weapons radionuclides present on particles larger than 1.1 μm is fairly large soon after a nuclear test, but decreases fairly rapidly with time. (auth)

29361 (BNWL-1850(Pt.3), pp 20-23) ATMOSPHERIC NATURAL AEROSOLS AND FALLOUT PARTICULATES DURING 1973 AT RICHLAND, WASHINGTON AND POINT BARROW, ALASKA. Thomas, C. W. Apr 1974.

In Pacific Northwest Laboratory annual report for 1973 to the USAEC Division of Biomedical and Environmental Research. Part 3. Atmospheric sciences.

Radionuclide concentration at Richland decreased two- to tenfold during 1973, reflecting the lack of high-yield testing during 1971 and 1972. Time variations in the atmospheric concentrations of ^{238}Pu and ^{239}Pu at Richland and Point Barrow since 1964 have been typical of nuclear weapons-produced radionuclides except for the increase in the ^{238}Pu concentration from 1965 to 1968 resulting from the SNAP-9A burnup. (auth)

29362 (BNWL-1850(Pt.3), pp 23-25) BEHAVIOR AND CHARACTERISTICS OF RADIOACTIVE DEBRIS FROM THE CHINESE NUCLEAR WEAPONS TEST OF JUNE 26, 1973. Jenkins, C. E.; Perkins, R. W. Apr 1974.

In Pacific Northwest Laboratory annual report for 1973 to the USAEC Division of Biomedical and Environmental Research. Part 3. Atmospheric sciences.

Debris from the Chinese test of June 26, 1973 was first observed at Richland 8 days later. The maximum radioiodine dose from the grass-milk-child-thyroid chain was estimated to be only 1 mrem on the west coast and 12 mrem in Minnesota. (auth)

29363 (BNWL-1850(Pt.3), pp 114-117) MODEL FOR CUMULUS WASHOUT OF COSMOGENIC RADIONUCLIDES. Davis, W. E. Apr 1974.

In Pacific Northwest Laboratory annual report for 1973 to the USAEC Division of Biomedical and Environmental Research. Part 3. Atmospheric sciences.

A model is presented in an attempt to explain observed ^{24}Na measurements in rainwater from cumulus clouds. Results indicate that values measured on June 9, 1972 can be explained only when evaporation is included. Also values for rising with no mixing require ~97% evaporation of rainwater during fall to the ground as compared to ~70% evaporation for a 50% linear mixing rate with environmental air during rise. (auth)

29364 (BNWL-1850(Pt.3), pp 121-132) POSTULATED ESTIMATE OF WET VERSUS DRY DEPOSITION DOWNWIND OF A POINT SOURCE OF POLLUTION. Slinn, W. G. N. Apr 1974.

In Pacific Northwest Laboratory annual report for 1973 to the USAEC Division of Biomedical and Environmental Research. Part 3. Atmospheric sciences.

A simple postulate is advanced, which permits an estimate of the relative magnitudes of wet and dry deposition downwind of a point source of pollution. The postulate is an extension of Chamberlain's estimate of the dry deposition velocity. It is assumed that the deposition velocity for aerosol particles is the product of $u_*^2/\bar{u}$ by a particle-size-dependent collection efficiency. With this assumption and approximations for the washout coefficient, the ratio of wet to dry deposition is found to be independent of the characteristics of the pollution. Comparisons of the theoretical results are made with available experimental data, and although the theory permits a reasonable interpretation of the data, it is seen that more data is needed before unequivocal conclusions can be drawn. (auth)

29365 (BNWL-1850(Pt.3), pp 133-135) WET AND DRY ATMOSPHERIC RADIOACTIVE TRACERS. Nevissi, A.; Beck, J. N.; man, L. C.; Hales, J. M.; Mahalingam, R. Apr 1974.
In Pacific Northwest Laboratory annual report for 1973 to the USAEC Division of Biomedical and Environmental Research. Part 3. Atmospheric sciences.

A study is under way to evaluate the relative importance of all processes which remove radioiodine in all its forms from the atmosphere. The washout of gaseous iodine is shown to be dependent on the gas phase and liquid phase mass transfer resistance and on the changing partition coefficient as the concentration in the droplet changes. Application of the models developed to the very limited data available shows qualitative agreement. Washout rates are lower with realistic evaluation of the influence of liquid phase resistance. The more recently developed EPAEC model was applied to an initial case for various iodine release rates. Continued study is planned. (auth)

29366 (BNWL-1850(Pt.3), pp 136-137) DEVELOPMENT OF AN IDEAL SAMPLER FOR BELOW-CLOUD SCAVENGING STUDIES. Glover, D. W.; Hales, J. M. Apr 1974.
In Pacific Northwest Laboratory annual report for 1973 to the USAEC Division of Biomedical and Environmental Research. Part 3. Atmospheric sciences.

Attempts made to design and fabricate an "ideal" rain sampler, i.e., one that allows zero dry deposition or resuspension, are discussed briefly. Such samplers are necessary for obtaining uncontaminated samples for washout studies. The suggested designs have not been field tested. (LCL)

29367 (BNWL-1850(Pt.3), pp 148-149) EFFECTS OF RADIOACTIVITY ON ICE NUCLEATION. Rosinski, J. (National Center for Atmospheric Research, Boulder, CO); Langer, G.; Nagamoto, C. T.; Thomas, C. W.; Wogman, N. A.; Young, J. A. Apr 1974.
In Pacific Northwest Laboratory annual report for 1973 to the USAEC Division of Biomedical and Environmental Research. Part 3. Atmospheric sciences.

Supercooled drops containing dissolved radionuclides froze at warmer temperatures than drops containing no radionuclides. (auth)

29368 (BNWL-1850(Pt.3), pp 149-151) RADIONUCLIDE CONCENTRATION MINIMUMS FROM 6 TO 9 km. Young, J. A.; Davis, W. E.; Wogman, N. A. Apr 1974.
In Pacific Northwest Laboratory annual report for 1973 to the USAEC Division of Biomedical and Environmental Research. Part 3. Atmospheric sciences.

Radionuclide concentrations measured 1.5 km above a cirrus deck were an order of magnitude lower, and concentrations within the cirrus were an order of magnitude higher than would be expected on the basis of the measured concentrations in the rest of the vertical profile, indicating that cirrus scavenging could be responsible for the downward transport of radioactivity. (auth)

29369 (BNWL-1850(Pt.3), pp 163-168) DRY DISPOSITION PROCESSES ON VEGETATION CANOPIES. Droppo, J. G. Apr 1974.
In Pacific Northwest Laboratory annual report for 1973 to the USAEC Division of Biomedical and Environmental Research. Part 3. Atmospheric sciences.

A brief review of forestry and agricultural literature relating to processes of dry deposition on plant canopies is presented. The results are summarized in terms of development of a model for dry deposition processes in a vegetation canopy. Various aspects of the processes in both high and low vegetation are discussed. (auth)

29370 (BNWL-1850(Pt.3), pp 201-203) RESUSPENSION OF TRACER PARTICLES BY WIND. Sehmel, G. A.; Lloyd, F. D. Apr 1974.
In Pacific Northwest Laboratory annual report for 1973 to the USAEC Division of Biomedical and Environmental Research. Part 3. Atmospheric sciences.

A particle resuspension rate of 1.2×10^{-10} fraction/s removed by wind stresses was determined for a submicrometer inert molybdenum tracer deposited on a sandy soil surface. (auth)

29371 (BNWL-1850(Pt.3), pp 204-211) RESUSPENSION BY WIND AT ROCKY FLATS. Sehmel, G. A.; Lloyd, F. D. Apr 1974.
In Pacific Northwest Laboratory annual report for 1973 to the USAEC Division of Biomedical and Environmental Research. Part 3. Atmospheric sciences.

A field experiment at Rocky Flats was conducted to initially determine plutonium air concentration dependency on wind speed and sampling height and to determine the respirable particle size distribution and subsequently to determine plutonium resuspension rates from ground source samples concurrently collected by HASL. Radiochemical plutonium analyses for filter samples are awaited from DOW at Rocky Flats. Airborne soil size distributions indicate that airborne concentrations of respirable soil particles increase proportionately with the wind speed to the 4th to 6th power. (auth)

29372 (BNWL-1850(Pt.3), pp 212-214) RESUSPENSION SOURCE CHANGE AT ROCKY FLATS. Sehmel, G. A.; Orgill, M. M. Apr 1974.
In Pacific Northwest Laboratory annual report for 1973 to the USAEC Division of Biomedical and Environmental Research. Part 3. Atmospheric sciences.

The plutonium resuspension model developed for sampling station S-8 was used to predict resuspension for the time period following the model data base time period. Observed airborne plutonium concentrations being greater than predicted are attributed to changes in source characteristics caused by soil disturbance. (auth)

29373 (BNWL-1850(Pt.3), pp 214-219) REGIONAL WIND RESUSPENSION OF DUST. Orgill, M. M.; Sehmel, G. A.; Bander, T. J. Apr 1974.
In Pacific Northwest Laboratory annual report for 1973 to the USAEC Division of Biomedical and Environmental Research. Part 3. Atmospheric sciences.

Particle wind resuspension is important in planning and operation in the nuclear power industry. To obtain a better understanding of the frequency, duration and occurrence of wind resuspension (dusty) periods on a regional scale, the frequency of dusty periods throughout the country is being determined from hourly meteorological observations. Dust storm criteria are being initially defined and tested for this study using the hourly weather observations from the Hanford Area. (auth)

29374 (BNWL-1850(Pt.3), pp 219-222) INTERSTAGE PARTICLE LOSSES IN A HIGH-VOLUME CASCADE IMPACTOR. Sehmel, G. A. Apr 1974.
In Pacific Northwest Laboratory annual report for 1973 to the USAEC Division of Biomedical and Environmental Research. Part 3. Atmospheric sciences.

Commercially available 20-cfm cascade impactors were evaluated under field sampling conditions for particle sampling bias caused by interstage losses. Particles larger than respirable are being deposited throughout the cascade impactor. (auth)

29375 (BNWL-1850(Pt.3), pp 223-227) ASSESSMENT OF THE LONG-TERM EXPOSURE DUE TO RESUSPENSION. Horst, T. W.; Droppo, J. G.; Elderkin, C. E. Apr 1974.
In Pacific Northwest Laboratory annual report for 1973 to the USAEC Division of Biomedical and Environmental Research. Part 3. Atmospheric sciences.

A simple model of the interaction between an airborne pollutant and the underlying surface is postulated, which includes the processes of deposition, fixation by the soil, resuspension and redeposition. This model is used to calculate the ratio between the exposure to the resuspended material and the exposure to the primary material. Utilizing current estimates of model parameters, this ratio could range from 5 to 5×10^{-4}. In the case where resuspension is locally balanced by redeposition, however, this range is narrowed to from 0.5 to 0.05. Horizontal homogeneity is a sufficient condition for this balance to hold true. (auth)

29376 (BNWL-1850(Pt.3), pp 228-233) AIRBORNE RELEASE OF ^{137}Cs FROM A CONTAMINATED AREA DURING A RANGE FIRE. Mishima, J.; Schwendiman, L. C. Apr 1974.
In Pacific Northwest Laboratory annual report for 1973 to the USAEC Division of Biomedical and Environmental Research. Part 3. Atmospheric sciences.

To aid in evaluation of the potential airborne hazard during a range fire, the distribution and fractional airborne release of ^{137}Cs involved with various contaminated materials on the surface of prairie land were measured. The distribution was determined by collecting and measuring the ^{137}Cs content of all surface materials including soil to a depth of 1 cm in ten random 1-m^2 plots. Approximately 90%of the ^{137}Cs activity measured was found in the soil. Little of the ^{137}Cs involved in the soil was airborne during fires promoted by gasoline under static or flowing air conditions. Fractional airborne releases of 4×10^{-4} and 10^{-3} were obtained during fires where a combination of organic litter and animal droppings was involved at wind speeds of 2.5 and 20 mph respectively. Radioactive particles in the ashes were entrained to the extent of 6×10^{-3} at 2.5 mph and 4×10^{-2} at 20 mph, in a 24-h period immediately after the fire. (auth)

29377 (COM-74-10799) NUMERICAL PREDICTION OF THE MESOSCALE TRANSPORT OF ATMOSPHERIC EFFLUENTS: PHILOSOPHY AND MORPHOLOGY OF EXPERIMENTAL MODELS FOR PREDICTING THE WIND AND POTENTIAL RADIOLOGICAL FIELDS OVER THE NEVADA TEST SITE. Randerson, D.; Cornett, J. S. (National Oceanic and Atmospheric Administration, Las Vegas, Nev. (USA). Air Resources Lab.). May 1973. Contract NVO-SF-54-351. 63p. (NOAA-TM-ERL-ARL-37; ARLV-351-28). NTIS $6.25.

Two experimental numerical models are described and tentatively verified. One model predicts the mesoscale wind field over mountainous terrain and the other model forecasts the temporal and spatial changes in the airborne radioactivity field that might be associated with an accidental release of debris during nuclear testing on the Nevada Test Site. A mesoscale wind-prediction model is derived from the assumption of the conservation of vertical wind shear for a time period of at least 6 hr over an area 160 × 160 N MI. This assumption is closely analogous to the conservation of horizontal vorticity. Verification of the wind-prediction model is accomplished through two different modes. The radiological-prediction model is difficult to verify, but preliminary results look realistic. (auth)

29378 (NVO-410-24) OPERATION WHETSTONE: ON-SITE RADIOLOGICAL SAFETY REPORT, JULY 1964–JUNE 1965. Mullen, O. W. (comp.); Eubank, B. F. (ed.). (Reynolds Electrical and Engineering Co., Inc., Las Vegas, Nev. (USA)). Jan 1969. Contract AT(26-1)-410. 53p. Dep. NTIS $5.75.

WHETSTONE was the name assigned to the series of underground nuclear experiments conducted at the Nevada Test Site from July 1, 1964 through June 30, 1965. Remote radiation measurements were taken during and after each nuclear experiment by a telemetry system. Monitors with portable radiation detection instruments surveyed reentry routes into ground zeroes before other planned entries were made. Continuous surveillance was provided while persons were in radiation areas and appropriate precautions were taken to protect personnel from unnecessary exposure to radiation. Protective clothing and equipment was issued as needed. Complete radiological safety and industrial hygiene coverage was provided during drilling and mining operations. Telemetered and portable radiation detector measurements are recorded. Detection instrumentation used are described and specific operational procedures are defined. (auth)

29379 (NVO-410-25) OPERATION TOGGLE: ON-SITE RADIOLOGICAL SAFETY REPORT, JULY 1972–JUNE 1973. Mullen, O. W. (Comp.); Eubank, B. F. (ed.). (Reynolds Electrical and Engineering Co., Inc., Las Vegas, Nev. (USA)). May 1974. Contract AT(26-1)-410. 27p. Dep. NTIS $4.50.

TOGGLE was the name assigned to the series of underground nuclear experiments conducted at the Nevada Test Site from July 1, 1972 to June 30, 1973. The tests publicly announced by the U. S. Atomic Energy Commission are considered here. Remote radiation measurements were taken during and after each nuclear experiment by a telemetry system. Monitors with portable radiation detection instruments surveyed reentry routes into ground zeroes before other planned entries were made. Continuous surveillance was provided while personnel were in radiation areas and appropriate precautions were taken to protect persons from unnecessary exposure to radiation and toxic gases. Protective clothing and equipment were issued as needed. Complete radiological safety and industrial hygiene coverage was provided during drilling and mineback operations. Telemetered and portable radiation detector measurements are listed. Detection instrumentation used are described and specific operational procedures are defined. (auth)

29380 (ORNL-TM-4375) GROUND LEVEL AIR CONCENTRATIONS OF DUST PARTICLES DOWNWIND FROM A TAILINGS AREA DURING A TYPICAL WINDSTORM. Mills, M. T.; Dahlman, R. C.; Olson, J. S. (Oak Ridge National Lab., Tenn. (USA)). Sep 1974. Contract W-7405-eng-26. 65p. Dep. NTIS $5.00.

The atmospheric transport of contaminants is an important aspect of the environmental evaluation for a particular installation. An atmospheric transport model for suspension by wind of toxic particulates that have been deposited upon the ground surface is described. Dimensional arguments are given relating suspension and saltation rates. Sample calculations of ground level air concentrations are carried out for a square tailings area containing uranium mill dust. A list of the computer code and sample output from this code are included. (auth)

29381 (ORNL-TM-4674) PROGRAM FOR COMPUTING THE DISPERSION OF AIRBORNE CONTAMINANTS. Stephenson, R. L. (Oak Ridge National Lab., Tenn. (USA)). Sep 1974. Contract W-7405-eng-26. 50p. Dep. NTIS $5.50.

A FORTRAN program for computing the distribution of airborne pollutants has been written in two versions. One is for the IBM-360 machines and intended for calculations involving large numbers of sources. The other is a tutorial version, written for a PDP-10. The latter version provides the capability to visualize the effect of proposed sources and study the effect of changing the relevant parameters. In both versions, the output displays the calculated concentration of pollutants in the form of a rudimentary map. (auth)

29382 DATA. Section III. Air and Deposition. Radiat. Data Rep.; 15: No. 8, 506-517(Aug 1974).

March 1974 measurements of the gross β-activity in surface air and precipitation at 68 sampling stations in the US, 24 stations in Canada, and in surface air only at 12 South American Stations, and at 18 stations in California are reported. HASL data on the monthly deposition of ^{90}Sr at 35 sites in the US and at 29 sites in Central and South America during Jan through Dec 1972 are tabulated. (LCL)

29383 CALCULATIONS OF DOSES, POPULATION DOSES, AND POTENTIAL HEALTH EFFECTS DUE TO ATMOSPHERIC RELEASES OF RADIONUCLIDES FROM U. S. NUCLEAR POWER REACTORS IN 1972. Radiat. Data Rep.; 15: No. 8, 477-482(Aug 1974).

Atmospheric emissions of radionuclides during 1972 reported by operators of 14 boiling water nuclear power reactors and 2 pressurized water nuclear power reactors in the United States were analyzed to calculate resulting doses in the general offsite environment. A sector-averaged diffusion equation, using facility generated onsite annual average meteorology, was used to propagate the emissions from the release point to a radius of 80 km. In 1972, 4.88 megacuries of radioactivity were released to the atmosphere from 16 reactors on 13 sites. The resulting whole body population dose was calculated to be 1649 personrem to a population of 29.2 million people. The potential health effects induced by external radiation from nuclear power plant emissions in 1972 were less than those induced by natural background and occupational radiation exposures. (auth)

29384 STATE OF ^{90}Sr, ^{137}Cs, AND ^{144}Ce IN RADIOACTIVE FALLOUT. Pavlotskaya, F. I.; Surotkevichiene, R.; Levine, G. P. Tr., Inst. Eksp. Meteorol.; 21: No. 1, 112-118(1971). (In Russian).

Studies on worldwide fallout in 1958-1968 showed differences in distribution of the soluble and insoluble fractions of radionuclides. At all observation points, the water-soluble fractions were in the order ^{90}Sr > ^{137}Cs > ^{144}Ce, with average values of 78, 62, and 16%, respectively. The mobility of the radionuclides in the insoluble fraction differed. More than 90% of the water-insoluble ^{90}Sr and up to from 65 to 70% of the ^{137}Cs and ^{144}Ce dissolved in 1 N CH_3COOH and 1 N HCl. This indicates that the largest part of the water-insoluble fraction is in the exchangeable or mobile state and not in the form of difficultly soluble compounds (e.g., CeO_2). In the water-soluble state the radionuclides are cations, anions, or neutral. The ^{90}Sr distribution between the three forms is 90, 6, and 4.0%; the ^{137}Cs is 72, 16, and 12%; and ^{144}Ce is 55, 18, and 27%. There is some tendency to an increase in the relative fraction of the ^{90}Sr and ^{137}Cs in the anionic form and to a decrease in the neutral form in the winter compared to summer. The difference in mobility of the radionuclides in the insoluble fraction and in the cationic, anionic, and neutral states indicates the formation of different chemical compounds. (tr-auth)

29385 WASHOUT OF RADIOACTIVE IMPURITIES FROM THE ATMOSPHERE IN THE CENTRAL CAUCASUS MOUNTAINS. Avramenko, A. S.; Makhon'ko, K. P. Tr., Inst. Eksp. Meteorol.; 21: No. 1, 155-168(1971). (In Russian).

The coefficient of washout of radioactive dusts from the subcloud layer of the atmosphere was determined from measurements of impurities in the precipitates at two different heights in 1968-1969. Average values for nuclear explosion products were 3×10^{-5} per second for continuous rain, twice this for showers, and five times this for snow. Measurements during continuous rainfall above and below the slope of the mountain indicated an average rate of rise of air currents of about 0.6 m/sec. With an increase in the rate of precipitation, the washout coefficient at first decreased rapidly, reached a minimum at 1 mm/hr, and then increased. The role of vertical air currents was shown in the characteristic dependence observed. Measurements of short-lived radon decay products showed a strong coincidence of precipitation samples taken at two heights with a radiotelephone. Because of the short lives, the effect of fluctuation in concentration of natural radioactivity in the precipitates and in the air and of fluctuations in the precipitation rate was so large that the washout coefficient for these products could not be determined for rain; for snow the value was 9×10^{-5} per second with an error of 95%. A similar dependence of the specific radioactivity of the precipitation on time was not observed in 313 observations on background with large fluctuations in measured values. Despite the large scatter in the radioactivity of the precipitation, a decrease was noted in the radioactivity of the precipitation with increase in precipitation rate. A polar diagram of the radioactivity in the air and in the precipitation showed that the concentration of short-lived radon decay products near the earth's surface chiefly affects the exhalation in a radius of several kilometers and the concentration in the precipitation, in a radius of tens of kilometers. (tr-auth)

29386 CALCULATION OF FRACTIONATION EFFECTS FOLLOWING ATMOSPHERIC NUCLEAR EXPLOSIONS. Izraehl, Yu. A. Tr., Inst. Eksp. Meteorol.; 21: No. 1, 97-102(1971). (In Russian).

Fractionation coefficients for radioisotopes in aerosols formed in nuclear explosions were calculated, using Raoul's law and assuming thermodynamic equilibrium between liquid and gaseous fractions. The fraction of heavy radioisotopes condensed on aerosols was calculated as a function of time after an explosion. Fractionation coefficients for ^{132}Te, ^{90}Sr, ^{89}Sr, and ^{137}Cs were calculated as a function of the particle radii. Calculations were for the nearest traces of surface explosions and agreed well with isotope fractionation measured in the American low-yield explosion "small-boy". (tr-auth)

29387 RADIOACTIVE PARTICLE FORMATION AFTER NUCLEAR EXPLOSIONS IN THE TROPOSPHERE. Izraehl, Yu. A.; Ter-Saakov, A. A. Tr., Inst. Eksp. Meteorol.; 21: No. 1, 91-97(1971). (In Russian).

A theoretical scheme of aerosol radioactivity in the fireball of a nuclear explosion was examined. Formulas were derived for the radioactivity of the aerosol particles as a function of the particle radius. The Zr, La, Y, and other refractory element vapors condensed at temperatures above the boiling points of the soil substance particles (~2300°C), i.e., under conditions far from thermodynamic equilibrium. In some cases the radioisotopes condensed on the surface of the molten particles, i.e. at thermodynamic equilibrium (2300 to 1400°C), and in others, on the solid particle surfaces. Thus particles are activated by radioisotopes that have gaseous matrix precursors with half-lives from 10 sec to several minutes (^{89}Sr, ^{90}Sr, ^{137}Cs, ^{140}Ba). The effect of fallout of large particles from the cloud at the moment of activation is calculated. (tr-auth)

29388 CONCENTRATIONAL DISTRIBUTION OF FISSION PRODUCTS OVER TROPICAL ZONE OCEANS AND ITS RELATION TO ATMOSPHERIC PROCESSES. Dmitrieva, G. V.; Krasnopevtsev, Yu. V.; Malakhov, S. G. Tr., Inst. Eksp. Meteorol.; 21: No. 1, 20-33(1971). (In Russian).

Data (for 1967-68) are examined on the wide differences in fission product concentrations over the ocean in different tropical zones. In the air over the Indian and Western Pacific Oceans, the radioisotope distribution is not uniform. The nonuniformity is due to portions of the more radioactive air entering the tropical zone from the subtropical or from middle latitudes (winter hemisphere) where quasi-meridional cold fronts have passed. These invasions in some cases may lead to formation of separate regions of lines of conversions in the equatorial belt. Air moving from the extratropical latitudes to the equatorial belt sometimes flows, under definite meteorological conditions, through the equator and may be included in the circulation of the other hemisphere. Possibly transfer of air from the southern hemisphere to the northern may cause typhoons in the Pacific Ocean, which then may move to the cyclone latitudes. (tr-auth)

29389 VERTICAL DISTRIBUTION OF RADIOACTIVE AEROSOLS IN THE TROPOSPHERE ABOVE THE EUROPEAN PART OF THE USSR IN 1964–1967. Nazarov, L. E.; Volokitina, L. A.; Gaziev, Ya. I.; Kuzenko, A. F.; Malakhov, S. G.; Vasil'ev, A. S. Tr., Inst. Eksp. Meteorol.; 21: No. 1, 4-20(1971). (In Russian).

Data on the vertical distribution of radon decay products and nuclear explosion aerosols in the subject area are presented. An aerosynoptic analysis of cases of significant increase and decrease in fission product concentrations in the layer of air near the earth in the Sub-Moscow region, showed that the stratospheric aerosols are transferred to the upper troposphere through a break or funnel of the tropopuase on the cyclonic periphery of the stream. On the earth the radioactive spot appears most often under the anticyclonic periphery of the stream. From the simplest theoretical schemes of vertical distribution of fission product and short-lived radon decay products concentrations, the vertical coefficient of turbulent diffusion and rates of vertical regular movement were determined. (tr-auth)

29390 FORMATION OF SECONDARY AEROSOLS IN THE ATMOSPHERE AFTER VENTILATED UNDERGROUND NUCLEAR EXPLOSIONS. Petrov, V. N.; Ter-Saakov, A. A. Tr., Inst. Eksp. Meteorol.; 21: No. 1, 103-105(1971). (In Russian).

In underground nuclear explosions, as a result of destruction of the rocks in the explosion zone and formation of cracks in the surface of the earth, excess pressure or ventilation may cause release of radioactive products to the atmosphere. Direct release of non-gaseous radioactive products is unlikely because they are sorbed on the underground rocks, and probably the main products released will be weakly chemically active or inert gases such as isotopes of krypton and xenon. Nonvolatile radioisotopes in the atmosphere may be decay products of radioactive gases. Non-gaseous radioisotopes formed in the atmosphere precipitate on atmospheric dust particles and form the so-called "secondary" aerosols. A model for formation of gaseous radioisotope decay products in underground nuclear explosions is presented. (tr-auth)

29391 SCAVENGING OF RADIOACTIVE MATERIAL FROM THE ATMOSPHERE BY SURFACE CONDENSATION. Styro, B. I.; Dargene, N. P. Tr., Inst. Eksp. Meteorol.; 21: No. 1, 175-183(1971). (In Russian).

Simultaneous measurements were made of the radioactivity of the air and on dew from the upper and lower surfaces of polyethylene film spread on short-trimmed grass. The dew was collected in two ways: several single sheets of film were spread on the grass and samples were taken immediately after dew formed and each hour thereafter all night; and a single polyethylene film was changed every hour on the area selected and the radioactivity in the dew was determined. Dew samples collected by the first method were called "old dew," and by the second method, "new dew." The short-lived alpha activity was due to decay of ^{213}Po, ^{214}Pb, and ^{214}Bi. For old dew it varied from 0.1 to 24.5×10^{-11} Ci/ml, and for new, from 0.1 to 26×10^{-11} Ci/ml. The parameter of removal of radioactivity from the air was 0.02 to 1×10^{-4} sec^{-1} for old dew and 0.3 to 1×10^{-4} for new. The parabolic dependence of the radioactivity of new dew on the specific radioactivity of the air indicates an increase in fallout rate with increase of radioactivity in the air. Graphs of the dependence of the specific activity and coefficient of nonradioactive removal of radioactive substances by old dew on the amount of dew indicates that the atmosphere is purified by direct condensation of water vapor on radioactive aerosols and by electrical interaction of aerosol particles with dew drops. (tr-auth)

29392 SIZE-DISTRIBUTION RELATION OF HIGH-ACTIVITY PARTICLES IN THE TROPOSPHERE IN SEPTEMBER–DECEMBER 1967. Gaziev, Yu. I.; Malakhov, S. G.; Nazarov, L. E. Tr., Inst. Eksp. Meteorol.; 21: No. 1, 105-111(1971). (In Russian).

Under the subject conditions, high-activity particles of artificial radioactive aerosols "grew" for about 2 months. The particles studied were 0.9 μm or greater in dia. According to data obtained near the earth and in the upper troposphere, the integral and differential distributions of these particles by size were exponential. The average exponent for the troposphere was (1.4 ± 0.2)d μm^{-1}. The fractionation coefficients for ^{144}Ce, ^{141}Ce, and ^{103}Ru relative to ^{95}Zr among radioactive particles with a diameter from 2 to 6 μm were approximately the same as reported in the literature for micron-size particles of the air in nuclear explosions. The residence time in the stratosphere of particles of 2.5 to 6 μm diameter was about 4.5 months. The rate of self-purification of the lower troposphere from radioactive particles of 1 to 6 μm diameter was about 2 km/hr. (tr-auth)

29393 WASHOUT OF HYGROSCOPIC AND NONHYGROSCOPIC AEROSOLS WITH CLOUD DROPLETS. Burtseva, I. I.; Burtseva, L. V. Tr., Inst. Eksp. Meteorol.; 21: No. 1, 147-155 (1971). (In Russian).

The effect of hygroscopicity on washout of 0.1- to 0.5-μm aerosols by cloud droplets was studied by comparing the behavior of hygroscopic radioactive $^{32}P_2O_5$ aerosols with nonhygroscopic $^{89}SrCO_3$. The hygroscopic material take up by droplets was twice that of the nonhygroscopic. (tr-auth)

29394 SPECIFIC RADIOACTIVITY DISTRIBUTION IN RAIN DROPS. Styro, B. I.; Vebrene, B. K. Tr., Inst. Eksp. Meteorol.; 21: No. 1, 135-138(1971). (In Russian).

The droplet distribution curves for uniform dispersion and localized radioisotope concentrations in clouds. The location of the maximum on the curves depended on the amount of isotope. The specific radioactivity of the rain changed with time of its precipitation, the first maximum occurring several minutes after the isotope was introduced into the cloud and the second after 10 to 15 min. The very rapid appearance (3 to 4 min) of radioactive droplets on the ground indicates the speed of the descending currents. (tr-auth)

29395 RELATION BETWEEN WASHOUT OF RADIOACTIVITY AND NONRADIOACTIVE IONS IN THE ATMOSPHERE BY PRECIPITATION. Piskunov, L. I.; Tarasov, S. I. Tr., Inst. Eksp. Meteorol.; 21: No. 1, 184-188(1971). (In Russian).

A correlation between radioactive and nonradioactive impurities washed out from the atmosphere by precipitations is presented. Chloride and sulfate ions were selected to represent the nonradioactive impurities because, unlike the radioactive impurities, their background is constant in the continental regions studied. The ratio of radioactivity to chlorides and sulfates in atmospheric precipitation is seen from the identical expressions for their washout. The state of the radioactivity of the atmosphere can be evaluated approximately. For determining the equilibrium constants, precise observations are needed under conditions where concentrations of impurities are at background level. It is suggested that the absence of a correlation between radioactive components washed out by rain and background concentrations of nonradioactive ions may indicate anomalous phenomena. (tr-auth)

29396 USE OF NATURALLY RADIOACTIVE SUBSTANCES IN STUDYING TURBULENT EXCHANGE AND SELF-SCAVENGING OF THE ATMOSPHERE WITH SURFACE LAYER MEASUREMENTS. Bakulin, V. N.; Sen'ko, E. E.; Starikov, B. G.; Trufakin, V. A. Tr., Inst. Eksp. Meteorol.; 21: No. 1, 168-175(1971). (In Russian).

From day-long measurements of thoron diffusion and thoron and ^{212}Pb concentrations at 1 and 5 meters height, an average of 5 cm/sec was found for the rate of increase in the coefficient of turbulence with height in the summer anticyclone by day and 3 cm/sec at night. From the data the average coefficient of turbulence in the lower kilometer layer of the troposphere was determined from surface layer measurements. In the absence of thoron and ^{212}Pb, radon could not be calculated under quasistationary conditions, and nonstationary models of its behavior in the atmosphere had to be used. Around the earth a good indicator of the time course of turbulent exchange is the ratio between the decay products of radon. The maxima of the disturbance of equilibrium in the radon series are in the morning and evening in the periods of establishment and destruction of the night inversion. In the morning hours there are unusual distributions in height of radioactive substances due to mechanical destruction of the inversions. Data are given for the coefficients of washout of radioactive aerosols by precipitation, based on ^{212}Pb, radon, and ^{210}Pb measurements. (tr-auth)

29397 STOCHASTIC APPROACH TO STUDYING RADIOACTIVITY OF CLOUD AND RAIN DROPLETS. Avramenko, A. S. Tr., Inst. Eksp. Meteorol.; 21: No. 1, 138-147(1971). (In Russian).

Experiments were done on the use of the stochastic approach to problems of radioactivity of clouds and rain drops. A general system of equations is described which can be used to calculate the distribution function for cloud droplets from the activity for the radioactive series of natural decay products in the atomic state. For the case where the concentration of the radioactive elements can be neglected an equilibrium solution is given. Based on the distribution found, the dependence of the number of nonradioactive rain drops on their size is calculated. A comparison of theoretical dependences with experimental data found in the literature shows good agreement. (tr-auth)

29398 THEORIES OF RADIOACTIVITY TAKEUP BY RAIN DROPS. Avramenko, A. S.; Makhon'ko, K. P. Tr., Inst. Eksp. Meteorol.; 21: No. 1, 119-134(1971). (In Russian).

An approximate diagram of the takeup of radioactivity by rain drops during their formation and precipitation from clouds is presented. Processes occurring in the cloud with regular rising currents, which lead to the distribution on the ground of the specific radioactivity of rain drops according to amounts, are considered. Comparison of theoretical calculations of the concentration of nuclear fission products in rain drops of different sizes with experimental data of the authors and from the literature gave a coefficient of washout of radioactive aerosol particles by cloud droplets of 10^{-3} sec^{-1} and establishment of the existence of a reverse dependence between the concentration of nuclear fission products in cloud drops and their radii. For rain drops the dependence is close to the reverse. The distribution of specific radioactivity of rain drops according to size may lead to an increase in the specific radioactivity of rain water at the end of a short shower as a result of a decrease in the size of the rain drops. (tr-auth)

29399 RATE OF FALLOUT OF ^{137}Cs AND ^{90}Sr AEROSOLS FROM THE ATMOSPHERE. Zykova, A. S.; Telushkina, E. L.; Rublevskii, V. P.; Efremova, G. P.; Kuznetsova, G. A. Tr., Inst. Eksp. Meteorol.; 21: No. 1, 63-65(1971). (In Russian).

Data are presented on the density of fallout of ^{137}Cs and ^{90}Sr aerosols in Moscow from 1962 to 1968 and on the concentration of these isotopes in the air near the earth. The ratio of ^{137}Cs to ^{90}Sr in the radioactive precipitation was larger in all cases than that in the air. This suggests that the rate of fallout of aerosols carrying ^{137}Cs is somewhat greater than that of the aerosols carrying ^{90}Sr, but values averaged 1.7 ± 0.4 cm/sec for ^{137}Cs and 1.6 ± 0.4 cm/sec for ^{90}Sr. (tr-auth)

29400 LONG-LIVED RADON DAUGHTERS AS ATMOSPHERIC RADIOACTIVE TRACERS. Nevissi, A.; Beck, J. N.; Kuroda, P. K. (Univ. of Arkansas, Fayetteville). Health Phys.; 27: No. 2, 181-188(Aug 1974).

The activities of ^{210}Pb, ^{210}Bi and ^{210}Po were measured in a large number of rain and snow samples that fell at Fayetteville, Arkansas. It was found that in nearly 82% of the samples measured, the residence times calculated from the ^{210}Bi/^{210}Pb and ^{210}Po/^{210}Pb ratios were found to be either concordant or near concordant. The discordant residence times are shown to result from the mixing of two different air masses, which results in the failure of the assumption of steady state atmospheric condition. By assuming a residence time of 4 days for aerosols near the surface of the earth, an average residence of 35 days is calculated for tropospheric aerosols. (auth)

29401 NATURAL β-ACTIVITY OF THE AIR IN THE ATMOSPHERIC SURFACE LAYER. Barr, S. (Drexel Univ., Philadelphia). Atmos. Environ.; 8: No. 8, 867(Aug 1974).

Favourable comment is made on the paper of Israelsson et al. (Atmos. Environ. 7; 1127-1137(1973)). It is stated that their observations on vertical concentration gradients yield valuable insight into physical processes in the atmospheric boundary layer. It is hoped that the authors pursue the physical interpretation of their data in such a way as to identify the main sensitivities in the observations. It is important to account for time dependence in the transport processes as reported in the paper. In surveying the turbulent transfer processes, it is of central importance to note the strong interdependence between winds, temperatures and activity profiles. (UK)

Soil

Refer also to abstracts 29133, 29443, and 31254.

29402 RADIOACTIVE CONTAMINATION OF SOME ARABLE SOILS IN THE LOWER SILESIA IN 1972. Glowiak, B.; Malysowa, E.; Pacyna, J.; Borys, J. (Instytut Ochrony Srodowiska Politechniki, Wroclaw). Nukleonika; 19: No. 6, 587-592(1974). (In Polish).

The contents of ^{90}Sr and ^{137}Cs were determined in arable soil samples taken from eight spots in the Lower Silesia. The mean content of ^{90}Sr was 27.6 mCi/km^2, and that of ^{137}Cs was as high as 52.1 mCi/km^2. The level of contamination of Lower Silesian arable soils with ^{90}Sr found in 1972 was approximate to that of 1964, increasing in heavier and heavier soils. (auth)

29403 ^{90}Sr AND ^{137}Cs DISTRIBUTION IN DIFFERENT TYPES OF SOILS. Belova, E. I.; Antropova, Z. G. Tr., Inst. Eksp. Meteorol.; 21: No. 1, 77-80(1971). (In Russian).

The ^{90}Sr and ^{137}Cs profiles were determined in five types of virgin soil, 10 years after being contaminated. The studies were made under natural conditions on artificially contaminated areas of turf podzol, gray sand, leached chernozem, meadow solod, and salt marsh soils. The effect of forest litter on the migration rate and distribution of these nuclides along the soil profile in the 10-year period was observed. The ^{137}Cs content of the upper 0- to 4-cm layer was in the order: meadow solod < turf podzol < gray sand < salt marsh < leached chernozem, while the ^{90}Sr order was: meadow solod < turf podzol < salt marsh < gray sand < leached chernozem. (tr-auth)

29404 ^{90}Sr DISTRIBUTION AND MIGRATION IN SOILS. Gedeonov, L. I.; Rosyanov, S. P.; Vinogradov, V. K. Tr., Inst. Eksp. Meteorol.; 21: No. 1, 80-87(1971). (In Russian).

Results are presented of studies on the ^{90}Sr distribution in soil, from which the radioactivity load of the soil cover and the rate of ^{90}Sr migration to the deep soil can be estimated. The data may be used in studies on the mechanism of ^{90}Sr migration in soil. Radiochemical analyses for ^{90}Sr in soil samples taken at depths down to 30 cm showed that in 1964-1965 the ^{90}Sr was mainly in the first 15 cm of soil, but detectable amounts were found in the 15- to 20-cm layer. The ^{90}Sr distribution along the profile of loamy soil may, to a first approximation, be described as an exponential function. Calculations using this relation show that ^{90}Sr penetrates to depths of more than from 40 to 60 cm. Translocation of fission products in the soil cover is due to a combination of physico-chemical processes in the soil, particularly, ^{90}Sr diffusion and transfer of isotopes in solution. The coefficient of ^{90}Sr diffusion in chernozem and turf-podzol under average annual moisture conditions was 0.49 to 0.84×10^{-7} cm^2/sec. The vertical distribution of ^{90}Sr in soils was calculated from these coefficients as a function of diffusion only. Comparison of the calculated diffusion with that obtained from radiochemical data showed that, in loamy chernozem, ^{90}Sr migrates chiefly by diffusion. In sandy loam turf-podzol soils this process is comparable with others. (tr-auth)

29405 ^{137}Cs, ^{90}Sr, AND ^{210}Pb IN SOILS OF THE ARCTIC REGIONS. Troitskaya, M. N.; Ibatullin, M. S.; Litver, B. Ya.; Nizhnikov, A. N.; Ramzaev, P. V.; Teplykh, L. A. Tr., Inst. Eksp. Meteorol.; 21: No. 1, 72-76(1971). (In Russian).

The role of soil in contamination of subsequent links of the chain by natural and artificial radionuclides in the Far North regions is considered. It is shown that there are geographic variations in the level of artificially contaminated soil, but that the ^{137}Cr/^{90}Sr ratio in the soil in all regions is from 1.3 to 1.6. Experimental data on the mechanism of contamination of lichens, a basic food of northern deer, by natural and artificial nuclides are presented. Analytical data for museum samples (1900-1945) indicate the absence of any connection between high ^{210}Pb levels in the north and nuclear explosions. The ^{239}Pu level in plants of some regions of the Far North was determined. (tr-auth)

29406 BUILDUP OF ^{90}Sr IN SOILS. Tyuryukanova, E. B. Tr., Inst. Eksp. Meteorol.; 21: No. 1, 66-71(1971). (In Russian).

The ^{90}Sr distribution in the soils of the Russian plains was found to be very unequal. In sandy soils the ^{90}Sr content was lower than in loam and depended on the humus concentration of the soil and its qualitative make up. Accumulation of ^{90}Sr in soils was determined both by its physico-chemical composition and regional-geochemical conditions. The nature of the run-off had considerable effect. In most soils the ^{90}Sr was concentrated in the upper layer (0 to 5, 0 to 20 cm). (tr-auth)

29407 HORIZONTAL WATER MIGRATION OF ^{90}Sr. Vodovozova, I. G. Tr., Inst. Eksp. Meteorol.; 21: No. 1, 87-90 (1971). (In Russian).

In spring thaws, strontium fallout on the earth's surface migrates with the water formed. Data are given on the physicochemical state of the migrating strontium, showing that 73% is in the cationic form. Atmospheric precipitations falling on the soil and entering into the migration process leach out the soluble strontium from the soil, and essentially 100% of that in run-off and rivers is cationic. The cationic ^{90}Sr in flood waters is discharged to rivers. (tr-auth)

29408 DETERMINATION OF FALLOUT RADIOISOTOPES FROM THEIR CONTENT IN THE ANNUAL LAYERS OF HIGH-MOUNTAIN GLACIERS. Davydov, E. N.; Makhon'ko, K. P.; Tsevelev, M. A.; Shulepko, Z. S. Tr., Inst. Eksp. Meteorol.; 21: No. 1, 33-42(1971). (In Russian).

Results are presented of the determination of the ^{90}Sr, ^{137}Cs, ^{144}Ce, ^{54}Mn, ^{106}Ru, and ^{210}Pb in the annual layers of snow and ice of high-mountain glaciers in the Caucasus and Tyan'-Shan. Comparison of the annual fall-out values for ^{137}Cs, determined from the ^{137}Cs content in these layers in the period 1963-1967 showed agreement of the data. In 1956-1967, the ^{90}Sr fraction in these layers was 10% of its atmospheric fallout, which corresponds approximately to the fraction of Sr in nonsoluble form. About 90% of the ^{90}Sr and about 40% of the ^{210}Pb falling out on the glacier from the atmosphere migrated with the melting water, but the ^{137}Cs did not migrate. From changes in fall-out of different isotopes with time, determined from their contents in the annual layers, the half-life of fission products from the atmosphere was estimated to be 11 months and of ^{54}Mn, 28 months. (tr-auth)

29409 CONCENTRATION EFFECTS OF ^{137}Cs, ^{65}Zn, ^{60}Co, AND ^{106}Ru SORPTION BY MARINE SEDIMENTS WITH GEOCHEMICAL IMPLICATIONS. Duursma, E. K. (IAEA, Monaco). Neth. J. Sea Res.; 6: No. 1-2, 225-240(Apr 1973).

The reactions of ^{137}Cs, ^{65}Zn, ^{106}Ru, and ^{60}Co and several types of marine sediment were measured as functions of equilibration time, carrier and sediment concentrations, and salinity. Large values of the distribution coefficient found for each isotope at low sediment concentrations (<0.5 mg/ml) are attributed to enhancement of particle formation by aggregation or nucleation of the radioisotope with the sediment particles in suspension; this nucleation would be masked by adsorption at high sediment concentrations. Uptake of ^{137}Cs was proportional to the illite concentration of the sediments and probably involves an ion-exchange reaction with K, the others showed less specific adsorption. All radioisotope sediment reactions could be represented by the Freundlich isotherm model. The difficulty of predicting geochemical consequences of the experimental results is discussed. The role of sediments as adsorbents in the distribution of trace element and radioactive pollutants is suggested as the main regulating mechanism in areas with concentrated suspensions where nucleation is negligible, such as coastal waters. At very low suspension concentrations, nucleation may be a widespread mechanism in the control of trace element budgets in marine environments. (Pollut. Abstr.)

Water

29410 (BNWL-1850(Pt.3), pp 175-176) DETERMINATION OF AEROSOL DEPOSITION RATES ON A LAKE SURFACE USING RADON DAUGHTERS. Young, J. A. Apr 1974.

In Pacific Northwest Laboratory annual report for 1973 to the USAEC Division of Biomedical and Environmental Research. Part 3. Atmospheric sciences.

A deposition velocity of 1.5 cm sec^{-1} and a vertical eddy diffusion coefficient of 43 cm^2 sec^{-1} at a depth of 6 ft were calculated from the measured concentrations of the short-lived radon daughters ^{214}Pb and ^{214}Bi in Lake Crescent water. (auth)

29411 DATA. Section II. Water. Radiat. Data Rep.; 15: No. 8, 499-505(Aug 1974).

The following radiation monitoring data are reported: α and β activity of surface waters in Kansas monitored during Jan through June 1972; tritium content of drinking water sampled during Jan through March 1974 at 76 US stations; and tritium content in atmospheric precipitation sampled at 19 US stations during Jan through March 1974. (LOL)

29412 DATA. Section IV. Other Data. Radiat. Data Rep.; 15: No. 8, 518-547(Aug 1974).

Data from environmental monitoring during Jan through Dec 1972 at US nuclear facilities are presented. For the Argonne National Laboratory data are reported on the: α-, β-, and γ-radioactivity in surface air; Pu, Th, U, ^{41}Ar and ^{3}H in surface air; radioactivity in ANL area surface waters; ^{238}Pu and ^{239}Pu in area soils and benthic material; ^{239}Pu in grass; ^{137}Cs and ^{90}Sr in area milk; and dose rate to humans in areas near ANL. For the Bettis Atomic Power Laboratory, data are reported on: the total radioactivity of area surface waters; ^{137}Cs content in silts; and radiation dose to man. For the Paducah Plant data are reported on the: α- and β-activity in surface air; and U content in surface waters and soil. An underground nuclear test detonated on July 10, 1974 at the Nevada Test Site is reported. (LCL)

29413 RADIOACTIVITY IN BRAZILIAN MINERAL WATERS. Hainberger, P. L.; de Oliveira Paiva, I. R.; Salles Andrade, H. A.; Zundel, G.; Cullen, T. L. (Pontifica Universidade Catolica, Rio de Janeiro). Contract AT(11-1)-3437. Radiat. Data Rep.; 15: No. 8, 483-488(Aug 1974).

Samples of mineral waters from various parts of Brazil were analyzed for their radium content. ^{226}Ra activity ranged from nondetectable to 94.1 pCi/liter, and ^{228}Ra ranged from nondetectable to 152 pCi/liter. (auth)

29414 KINETICS OF THE SELF-PURIFICATION OF A BODY OF WATER CONTAINING STRONTIUM-90 AS A RESULT OF ABSORPTION OF THE RADIONUCLIDE BY THE BOTTOM DEPOSITS. Safronova, N. G. (Agrophysical-Scientific-Research Inst., Leningrad). Sov. J. Ecol. (Engl. Transl.); 4: No. 2, 101-105(Jan 1974).

Translated from Ekologiya; 4: No. 2, 12-18(1973).

A previously proposed diffusion model of the self-purification of natural water as a result of the absorption of ^{90}Sr by the bottom deposits agrees with the experimental data on the kinetics of the change in the concentration of ^{90}Sr in the water of an experimental lake. Together with the diffusion mechanism of self-purification, a factor of self-purification that can be considered within the framework of the model operates in the lake. Simple computational formulas for the dependence of the concentration of ^{90}Sr in the water on the time were obtained, permitting a long-range prognosis for the experimental lake. (Pollut. Abstr.)

Ecosystems and Food Cycles

Refer also to abstracts 28971, 29438, 29440, 29441, 29444, 29445, 29447–29449, 29455, and 29817.

29415 (CONF-740826-3) PLUTONIUM IN THE LAURENTIAN GREAT LAKES: FOOD-CHAIN RELATIONSHIPS. Marshall, J. S.; Waller, B. J.; Yaguchi, E. M. (Argonne National Lab., Ill. (USA)). 1974. Contract W-31-109-eng-38. 15p. Dep. NTIS $4.00.

From international association of limnology meeting; Winnipeg, Canada (22 Aug 1974).

Samples of water, plankton, benthus, and fish were collected from the Great Lakes in 1972 and 1973. The samples were analyzed for ^{239}Pu and ^{137}Cs and results are tabulated. It was concluded that the data are consistent with the hypothesis that sorption of plutonium by phytoplankton and the subsequent settling of phytodetritus or zooplankton fecal pellets is a major mechanism for removing plutonium from Great Lakes waters. The results indicate that although the concentration of plutonium in phytoplankton is several thousand times that in the water, it decreases by an order of magnitude in each successive link in the food chains leading to man. (HLW)

29416 (COO-3167-102) PROGRESS REPORT, JUNE 1, 1973–MAY 31, 1974. Comar, C. L.; Thompson, J. C. Jr.; Wentworth, R. A. (New York State Veterinary Coll., Ithaca (USA). Dept. of Physical Biology). 1974. Contract AT(11-1)-3167. 47p. Dep. NTIS $5.50.

Separate abstracts were prepared for two sections of this report. (CH)

For abstracts of individual sections see: 29417 and 29438.

29417 (COO-3167-102, pp 1-27) PHASE I. Radiation and Radioisotope Studies With Laboratory and Domestic Animals. 1974.

In progress report, June 1, 1973–May 31, 1974.

Data are summarized from studies conducted over a 10-yr time period on critical pathways in animal and human food chains for fallout ^{137}Cs, ^{131}I, and ^{90}Sr. Pathways leading to the contamination of milk, fruits, and vegetables and the relation of the consumption of these foods to the radiation dose to human populations are discussed. (CH)

29418 (NVO-AEIC-74-1, pp 43-49) GENERAL STATISTICAL CONSIDERATIONS IN ENVIRONMENTAL PLUTONIUM STUDIES. Eberhardt, L. L.; Gilbert, R. O. (Battelle Pacific Northwest Labs., Richland, WA). Jul 1974.

In dynamics of plutonium in desert environments. Nevada Applied Ecology Group progress report as of January 1974.

The high sampling variability encountered in environmental plutonium studies, along with high analytical costs, makes it very important that efficient sampling plans be used. However, efficient sampling depends on explicit and simple statements of the objectives of the study. When there are multiple objectives, as in the Nevada Applied Ecology Group (NAEG) study, it may be difficult to devise a wholly suitable sampling scheme. Sampling for long-term changes in plutonium concentration may also be complex and expensive. Further attention to problems associated with compositing samples is recommended, as is the consistent use of random sampling as a basic technique. (auth)

29419 (SRO-641-13) RADIOACTIVE TRACER STUDIES OF SOIL AND LITTER ARTHROPOD FOOD CHAINS. Progress Report, November 1, 1973–October 31, 1974. Crossley, D. A. Jr. (Georgia Univ., Athens (USA). Dept. of Entomology). 25 Jul 1974. Contract AT(38-1)-641. 36p. Dep. NTIS $5.00.

Studies of radionuclide turnover and mineral element movement based on experimental results and interpretations of field data are described. Models for assimilation and retention of radioactive materials were tested in a laboratory experiment using crickets (Acheta domesticus); models were found to yield equivalent predictions of equilibrium whole-body burdens of radioactivity. Experimental measurement of radionuclide turnover by mites and collembolans is described, using two different systems of detection. An electron microprobe technique for elemental analysis of individual microarthropods yielded preliminary results, and further applications of the technique are planned. Analysis of data on fallout ^{137}Cs concentrations in food chains of granitic outcrop systems in Georgia is presented. Those food chains contain ^{137}Cs concentrations 3 to 5 times higher than in surrounding areas. (auth)

29420 (ZAED-BIBL-02-12) BIBLIOGRAPHIES IN NUCLEAR SCIENCE AND TECHNOLOGY. Section 02: Contamination and Decontamination of Foods. Number 12. Fischer, E. (comp.). (Bundesforschungsanstalt fuer Lebensmittelfrischhaltung, Karlsruhe (F. R. Germany)). Jul 1974. 41p. Dep. NTIS (US Sales Only) $5.25.

Annotated references are presented to some 200 publications from the world literature from 1971 to 1973 on the contamination and decontamination of foods. English translations of all titles and author, subject, and corporate indexes are included. (CH)

29421 DATA. Section I. Milk and Food. Radiat. Data Rep.; 15: No. 8, 489-498(Aug 1974).

Data on the ^{137}Cs and ^{90}Sr content in milk at 63 sampling stations in the US, 16 in Canada, and 7 stations in Central and South America and Puerto Rico are reported for March 1974 and for the 12-month period from April 1973 through March 1974. (LCL)

29422 KHEMORADIOEKOLOGIYA PELAGIALI I BENTALI (METALLAKH I IKH RADIONUKLIDY V GIDROBIONTAKH I SREDE). (Chemoradioecology of the Pelagic Zone and the Benthos (Metals and Radionuclides in the Hydrobiont and Environment)). Polikarpov, G. G. (ed.). Kiev; Izdatel'stvo Naukova Dumka (1974). 271p.

The radioecology of the pelagic and benthos organisms is examined. Experimental data and materials from expeditionary research on the ecological aspects of the distribution, exchange mechanism, and accumulation of radioactive and stable metals in the hydrobiont are reported. (tr-auth)

29423 COMPARISON OF EXTERNAL IRRADIATION AND CONSUMPTION OF COWS' MILK AS CRITICAL PATHWAYS FOR ^{137}Cs, ^{54}Mn AND ^{144}Ce–^{144}Pr RELEASED TO THE ATMOSPHERE. Voilleque, P. G.; Pelletier, C. A. (Idaho Operations Offices, Idaho Falls). Health Phys.; 27: No. 2, 189-199(Aug 1974).

Models and data obtained from a 4 yr study of the behaviour of fallout radionuclides on and near a Michigan dairy farm are used to compare external irradiation and the consumption of cows' milk as critical pathways for the exposure of the population to ^{137}Cs, ^{54}Mn and ^{144}Ce-^{144}Pr released to the atmosphere. Direct radiation from radioactive material deposited on ground and plant surfaces is found to be the more limiting exposure route for ^{137}Cs and ^{54}Mn. Ingestion of contaminated milk is the more restrictive pathway for ^{144}Ce-^{144}Pr; the derived value is comparable to the limit based on the lung dose from direct inhalation by a standard man. The limiting continuous air concentrations that would produce, at equilibrium, either yearly dose equivalents of (a) 170 mrem to the gonads (population average), of (b) 500 mrem to the lower large intestine (LLI) of the critical group and less than 170 mrem to the LLI of the average member of the population are 6.8×10^{-13} μCi/cm^3, 1.7×10^{-11} μCi/cm^3 and 2.9×10^{-11} μCi/cm^3 for ^{137}Cs, ^{54}Mn and ^{144}Ce-^{144}Pr respectively. The models employed and details of the calculations made to derive these air concentrations are presented. (auth)

Radiometric Techniques

Refer also to abstracts 29370, 29388, 29389, 29393, 29394, 29396, 29410, 29475, 29476, 29481, and 29605.

29424 (BNWL-1850(Pt.3), pp 44-49) ESTIMATION OF MEAN CROSSWIND CONCENTRATION PROFILES FROM "INSTANTANEOUS" CROSSWIND TRAVERSES. Nickola, P. W.; Clark, G. H. Apr 1974.

In Pacific Northwest Laboratory annual report for 1973 to the USAEC Division of Biomedical and Environmental Research. Part 3. Atmospheric sciences.

Detailed real-time concentration histories available from use of the ^{85}Kr inert gas tracer system permit the simulation of aircraft crosswind traverses through a diffusing plume. The results of such simulations are presented for a tracer release in a thermally stable atmosphere. The standard error of estimate of the peak crosswind exposure was found to be in excess of 100% of the true value for a single traverse at either 800 or 1600 m from the source. This error is reduced to 25 to 30% if 6 traverses are presumed to have been flown. For crosswind integrated exposures standard errors are found to be about 40% and 15% for one and six traverses respectively. Standard errors for other numbers of traverses are presented graphically. (auth)

29425 (BNWL-1850(Pt.3), pp 49-60) MEASUREMENT OF PARTICULATE PLUME DEPLETION BY COMPARISON WITH INERT GAS PLUMES. Nickola, P. W.; Clark, G. H. Apr 1974.

In Pacific Northwest Laboratory annual report for 1973 to the USAEC Division of Biomedical and Environmental Research. Part 3. Atmospheric sciences.

The successes and shortcomings of the 1972–73 series of multitracer releases are reviewed. Tracers were dispersed to the atmosphere simultaneously from an elevation of 26 m. Although the particulate tracer, zinc sulfide, showed strong evidence of depletion in the near-ground layers, problems in calibration of the tracer assay technique complicate the specification of the magnitude of this depletion. Estimation of the zinc sulfide deposition was accomplished through comparison with the nondepositing, inert gas tracer, krypton-85. The krypton displayed strong evidence of "reflection" from the ground on one of the three experiments examined. The density of vertical samplers on the field measurement grid is currently not great enough to permit mass balance computation of high confidence. Following release into an unstable atmosphere, about 1% of the particulate zinc sulfide is estimated to have deposited before the plume reached 200 m. During one release into a stable atmosphere, 0 to 1% of the tracer deposited during movement to 812 m. During release into a somewhat less stable atmosphere, from 3 to 6% of the particulate zinc sulfide was deposited during traversal to 842 m. (auth)

29426 (BNWL-1850(Pt.3), pp 60-63) FITTING AN ANALYTICAL CURVE TO SOME EXPERIMENTAL DIFFUSION DATA. Clark, G. H.; Nickola, P. W. Apr 1974.

In Pacific Northwest Laboratory annual report for 1973 to the USAEC Division of Biomedical and Environmental Research. Part 3. Atmospheric sciences.

A technique has been developed for fitting a Gaussian curve to crosswind concentration distributions observed in atmospheric plumes. The effects of truncating observations to successively smaller portions of the crosswind distribution are presented. Comparison of statistics (σ_z and $\bar{z}$) generated from a truncated observed distribution and from the "complete" (observed plus extrapolated) crosswind integrated distribution reveals minor differences. (auth)

29427 (BNWL-1850(Pt.3), pp 152-155) FEASIBILITY STUDY OF THE USE OF INERT TRACERS IN THE NATIONAL HAIL RESEARCH EXPERIMENT. Young, J. A.; Wogman, N. A.; Thomas, C. W.; Tanner, T. M. Apr 1974.

In Pacific Northwest Laboratory annual report for 1973 to the USAEC Division of Biomedical and Environmental Research. Part 3. Atmospheric sciences.

Six tracers released sequentially into the updrafts of convective storms in northeast Colorado spread extensively through the storm system and were nearly completely scavenged. (auth)

29428 PECULIARITIES OF THE UPPER CLOUD LAYER AND SUGGESTIONS FOR USING RADIOACTIVE TRACER TECHNIQUES IN STUDYING MERIDIONAL CURRENTS. Romanov, N. N. Tr., Inst. Eksp. Meteorol.; 21: No. 1, 45-47(1971). (In Russian).

Based on an analysis of numerous accounts of pilots and observations of the authors in research flights in aeroplanes, a relation was established between the development of clouds in the upper strata and the direction of the wind with the largest meridional component. Regardless of the nature of the barometric field, clouds develop with south and southwest stable currents and are destroyed (or are absent) with north and northeast currents. This relation appears more clearly in the lower latitudes and is weak at higher latitudes. This pattern may be the result of stable vertical currents arising in the meridional currents in the turning of the earth. Direct measurements of the vertical movement with radioactive tracers are proposed, using appropriately selected synoptic arrangements. (tr-auth)

29429 NEUTRON LOGGING OF FORMATION POROSITY AND CHLORINITY. Bell, R. G. (to Schlumberger Technology Corp.). US Patent 3,833,809. 3 Sep 1974. Filed date 9 May 1973. 12p.

An embodiment of the invention shows a pulse neutron technique for measuring earth formation porosity. For example, the inelastic neutron scattering gamma radiation emitted from a formation in a broad energy range provides a measure of the porosity in a way that is free of formation fluid and matrix composition influences. Preferably, the inelastic scattering gamma rays characterizing this measurement are observed in a 10 microsecond interval that is initiated during an early part of each neutron pulse. The observed inelastic scattering gamma ray activity is normalized to compensate for variations in neutron source strength. The normalized data then is converted directly into a formation porosity output. (Official Gazette)

29430 IRREGULARITIES IN DENDROCHRONOLOGICAL CALIBRATION. Ottaway, B.; Ottaway, J. H. (Univ. of Edinburgh). Nature (London); 250: No. 5465, 407-408(2 Aug 1974).

A discussion is presented on the interpretation of irregularities or "wiggles" in the Suess curve used for calibrating radiocarbon dates in terms of dendrochronology. Most of these "wiggles" are likely to be artefacts, but in view of some changes expected to have occurred in the ^{14}C content of the atmosphere it is important to identify them by a method that does not depend on "intuition". Such a method is described. (UK)

Site Surveys

Refer also to abstracts 28971, 29354, 29377, 29462, and 29468.

29431 (BNWL-1850(Pt.3), pp 27-30) METHOD FOR DETERMINING MONIN-OBUKHOV L's FROM PROFILES OF SUBJECTIVELY ESTIMATED MEAN WIND SPEEDS AND TEMPERATURES. Powell, D. C. Apr 1974.

In Pacific Northwest Laboratory annual report for 1973 to the USAEC Division of Biomedical and Environmental Research. Part 3. Atmospheric sciences.

A method has been developed for calculating Monin-Obukhov L values using wind and temperature data from the four lowest levels of the Hanford 400-ft tower. The L values computed by this method are compared to L values computed from flux data from sonic anemometers. For one unstable case and for one stable case the agreement is quite good. For a slightly stable case, where the estimates of L differ by an order of magnitude, other logic favors the L as estimated from the 400-ft tower data. (auth)

29432 (BNWL-1850(Pt.3), pp 30-32) DEPENDENCE OF SITE EVALUATION OF ROUGHNESS LENGTH AND DISPLACEMENT LENGTH ON VALUE CHOSEN FOR VON KARMAN'S CONSTANT. Powell, D. C. Apr 1974.

In Pacific Northwest Laboratory annual report for 1973 to the USAEC Division of Biomedical and Environmental Research. Part 3. Atmospheric sciences.

By using sets of values of Von Karman's constant, roughness length, and displacement length, the gradient calculation method developed in the preceding paper may be extended to calculate values of the friction velocity. The criterion for validation is agreement of friction velocity values so calculated with those calculated from concurrent sonic anemometer data. When this is done using 0.35 or 0.40 for Von Karman's constant, the associated sets of values of roughness length and displacement length differ significantly. These results indicate that a new value of Von Karman's constant should not be adopted for profile analysis of data for a particular site unless the roughness length and displacement length values assumed for the site are reevaluated. This information will be used in diffusion-deposition models at Hanford. (auth)

29433 (BNWL-1850(Pt.3), pp 33-38) POWER SPECTRAL ANALYSIS OF TWO PERIODS OF TURBULENCE DATA FOR VERY STABLE CONDITIONS. Powell, D. C.; Horst, T. W. Apr 1974.

In Pacific Northwest Laboratory annual report for 1973 to the USAEC Division of Biomedical and Environmental Research. Part 3. Atmospheric sciences.

Sonic anemometer data from heights of 60, 15, and 7.5 m have been analyzed for two 55-min periods during which the critical Richardson number was attained at heights between 15 and 30 m. The best organization of the spectra was achieved by plotting dimensionless spectra, normalized by individual variances, as functions of dimensional frequency. For the less stable 55-min period the spectra from the 60-m level organize well with the spectra from the lower levels except at the lower frequencies which are not included in the normalizing variances. The frequencies of maximum spectral energy at 15 and 7.5 m for the three components average less than 60% of the values predicted by previous modeling. The parameterization of the data achieved by using the dimensionless frequency of maximum spectral energy f_m is found to be in no way inferior to that using the dimensionless frequency f_0 proposed by the A.F.C.R.L. investigators. (auth)

29434 (BNWL-1850(Pt.3), pp 38-44) COMPARISON OF DIFFUSION-DEPOSITION MODEL COMPONENTS WITH EXPERIMENTAL RESULTS. Elderkin, C. E.; Powell, D. C.; Clark, G. H.; Nickola, P. W. Apr 1974.

In Pacific Northwest Laboratory annual report for 1973 to the USAEC Division of Biomedical and Environmental Research. Part 3. Atmospheric sciences.

Estimations of crosswind integrated exposures (CIE) are made with the Hanford diffusion-deposition model using a measured vertical velocity spectrum and a Hay-Pasquill β value from analysis of concurrent turbulence data. The crosswind integrated exposures of both depositing and nondepositing tracers are modeled reasonably well by the measured spectrum and the experimentally indicated β value of 8, although both these components differ significantly from the model-derived values. The model for deposition velocity is extended, the application of which supports the parameterization given in previous reports. (auth)

29435 (BNWL-1850(Pt.3), pp 68–71) MESOSCALE TRANSPORT AND DIFFUSION STUDIES. Wendell, L. L.; Sandusky, W. F. Apr 1974.

In Pacific Northwest Laboratory annual report for 1973 to the USAEC Division of Biomedical and Environmental Research. Part 3. Atmospheric sciences.

In progress is an investigation of the validity of using the single-point wind in mesoscale radiological assessments on and around the Hanford site. Work at another AEC Site has shown the practice to be unreliable. Tower data are being analyzed and used to construct wind field trajectories for comparison with constant-volume balloon trajectories and trajectories constructed with a single-point wind. The appropriateness of the use of constant-volume balloon trajectories as an indication of mesoscale transport is being tested by aircraft sampling of an SF_6 plume in the vicinity of the balloons along their trajectories. (auth)

29436 (BNWL-1850(Pt.3), pp 72–73) MODEL TO COMPUTE LOW-LEVEL MONTGOMERY STREAM FUNCTIONS. Davis, W. E. Apr 1974.

In Pacific Northwest Laboratory annual report for 1973 to the USAEC Division of Biomedical and Environmental Research. Part 3. Atmospheric sciences.

The model to compute Montgomery stream functions was improved by incorporating water vapor. An error analysis was performed on the model comparing radiosondes taken at three sites in the grid. Results indicated errors in the Montgomery stream function with a standard deviation greater than $\pm 0.05 \times 10^7$ $cm^2\ sec^{-2}$ would be exceeded at ~100 mb less than the sfc pressure at all sites for November 1972 data. (auth)

29437 (BNWL-1850(Pt.3), pp 267–270) ALE RESERVE CLIMATOLOGY FOR 1973. Thorp, J. M. Apr 1974.

In Pacific Northwest Laboratory annual report for 1973 to the USAEC Division of Biomedical and Environmental Research. Part 3. Atmospheric sciences.

The Arid Lands Ecology Reserve microclimatological program will encompass 5 years of monthly maximum and minimum temperatures and monthly precipitation data at the end of calendar year 1973. An interim climatological summary of these data is planned for publication in 1974. Bioyear precipitation for 1973 was the least in the 5 years of record. A range fire burned over some 9000 acres of ALE land in August. (auth)

29438 (COO-3167-102, pp 28–45) AGRICULTURAL IMPACTS OF NUCLEAR POWER GENERATION IN NEW YORK STATE. 1974.

In progress report, June 1, 1973–May 31, 1974.

New York State will be used as a model for studies on the environmental effects of continued nuclear power plant expansion. New York State was chosen as a model inasmuch as this state has a contiguous electric power generating pool; numerous nuclear power generating reactors of various types and sizes are in operation, under construction, or in planning stages; a nuclear fuel reprocessing plant is located in the western part of the state; and the state is one of the major dairy, fruit, and vegetable growing areas of the country. Agricultural data are presented which have been assembled which conform to the major land form regions in New York State and which are located within or adjacent to existing or projected nuclear facilities. (CH)

29439 (NVO-AEIC-74-1) DYNAMICS OF PLUTONIUM IN DESERT ENVIRONMENTS. Nevada Applied Ecology Group Progress Report as of January 1974. Dunaway, P. B.; White, M. G. (Eds.). (USAEC Nevada Operations Office, Las Vegas). Jul 1974. 377p. (NVO-142). Dep. NTIS $10.60.

Separate abstracts were prepared for 24 sections of this report. (CH)

For abstracts of individual sections see: 28971, 29418, 29440–29455, 29494, 29616, 29617, and 29809–29811.

29440 (NVO-AEIC-74-1, pp 7–16) SOILS ELEMENT ACTIVITIES, OCTOBER 1972–SEPTEMBER 1973. Fowler, E. B.; Essington, E. H. (Los Alamos Scientific Lab., NM). Jul 1974.

In dynamics of plutonium in desert environments. Nevada Applied Ecology Group progress report as of January 1974.

A general review is presented of soil element activities at selected areas of the Nevada Test Site during the year October, 1972 to September, 1973. Areas declassified, areas sampled, and analytical results for ^{239}Pu, ^{240}Pu, and ^{241}Am are briefly discussed. Changes found in the ratio of $^{239-240}$Pu to ^{241}Am, as well as the implications of the changing ratio, are presented. It is suggested that the observed increasing ratio with depth of soil profile may be related to differential solubility of the two radionuclides, and that with passing time, ^{241}Am may become the radionuclide of prime concern in regard to uptake by plants and cycling in ecosystems. A modified analytical method for plutonium in soils is discussed. (CH)

29441 (NVO-AEIC-74-1, pp 17–19) REECo FIELD ACTIVITIES AND SAMPLE LOGISTICS IN SUPPORT OF THE NEVADA APPLIED ECOLOGY GROUP. Kayuha, H. J.; Aoki, I.; Wireman, D. L. (Reynolds Electrical and Engineering Co., Inc., Las Vegas, NV). Jul 1974.

In Dynamics of plutonium in desert environments. Nevada Applied Ecology Group progress report as of January 1974.

The field activities and sample logistics of Reynolds Electrical and Engineering Co., Inc. (REECo), in support of the Nevada Applied Ecology Group (NAEG) plutonium studies in the Test Range complex at the Nevada Test Site are discussed. Field instrument measurements, determination of sampling sites, and procedures used in preparation of samples are included. To date, the REECo preparation facility has processed 5758 soil samples and 400 vegetation samples. Also, there are 2528 samples stored in the sample library, in addition to 36 4- × 4- × 4-foot pallets of samples collected at and around NTS between the mid-50s–early 60s. Small animal samples are collected and prepared for chemical analysis and histo-pathological examination. (CH)

29442 (NVO-AEIC-74-1, pp 21–27) SOIL SURVEYS OF FIVE PLUTONIUM-CONTAMINATED AREAS ON THE TEST RANGE COMPLEX IN NEVADA. Leavitt, V. D. (National Environmental Research Center, Las Vegas, NV). Jul 1974.

In dynamics of plutonium in desert environments. Nevada Applied Ecology Group progress report as of January 1974.

Soil characteristics in five areas located on the Nevada Test Site were surveyed. Most of the surface soils in the areas have a gravelly texture and are typically classified as gravelly sandy loam. The majority of the surveyed land is either floodplain or alluvial fan with deep soils having well-developed profiles and platy structure. All of the soils are alkaline, ranging in pH from 7.0 to 9.0. Two general categories of vegetation are found in the study areas, low and high desert shrub. The low desert shrubs are predominantly creosotebush (Larrea divaricata) and white bursage (Franseria dumosa). The high desert shrubs are mostly fourwing saltbush (Atriplex canescens), winterfat (Eurotia lanata), and bud sagebrush (Artemisia spinescens). (CH)

29443 (NVO-AEIC-74-1, pp 29–42) DISTRIBUTION AND CHARACTERIZATION OF PLUTONIUM IN SOILS FROM NEVADA TEST SITE. Tamura, T. (Oak Ridge National Lab., TN). Jul 1974.

In dynamics of plutonium in desert environments. Nevada Applied Ecology Group progress report as of January 1974.

The distribution and characterization of Pu in three selected surface soil samples from two areas at Nevada Test Site were determined. Analytical methods are described for determination of total Pu content, Pu distribution in different particle size fractions, and short-time digestion leachability by HNO_3. Leaching with HNO_3 revealed that 65 to 91% of the Pu could be leached. The leaching results suggest the possibility of using the acid extraction as a means of predicting the availability of Pu in soils. Preliminary data suggest that Pu in the coarser size fractions is PuO_2, whereas plutonium associated with the finer size particles possibly is a hydrous PuO_2. (auth)

29444 (NVO-AEIC-74-1, pp 51–89) STATISTICAL ANALYSIS OF Pu IN SOIL AT THE NEVADA TEST SITE: SOME RESULTS. Gilbert, R. O.; Eberhardt, L. L. (Battelle Pacific Northwest Labs., Richland, WA). Jul 1974.

In dynamics of plutonium in desert environments. Nevada Applied Ecology Group progress report as of January 1974.

The statistical field sampling design being used to estimate surface soil inventory in Areas 13 and 5 of the Nevada Test Site (NTS) is described and discussed. We estimate that the total amount of $^{239-240}$Pu in the upper 5 cm of soil inside the outer fence region of Area 13 is 39 curies with a standard error of 5 curies. This estimate is obtained from soil samples collected at randomly chosen locations according to a stratified random sampling plan. Correlation and regression analyses are computed, which indicates that lab γ scans on soil samples for ^{241}Am can, in general, predict quite well the concentrations of $^{239-240}$Pu present in the soil in Area 13. This suggests the determination of $^{239-240}$Pu may not be required on all soil samples in this area. This also appears to be the case for Area 5, although the lab analyses are incomplete. Average Pu/Am ratios are obtained for Areas 13, 5, and the Tonopah Test Range (TTR). The average ratio for TTR appears to be considerably greater than those for Area 13 or 5. There is also some evidence to suggest that the Pu/Am ratio may not be constant over all levels of ^{241}Am for the lower count per minute (cpm) regions of Areas 13 and 5. (auth)

29445 (NVO-AEIC-74-1, pp 91-106) SOME ECOLOGICAL ATTRIBUTES AND PLUTONIUM CONTENTS OF PERENNIAL VEGETATION IN AREA 13 (NAEG VEGETATION STUDIES). Romney, E. M.; Wallace, A.; Gilbert, R. O.; Bamberg, S. A.; Childress, J. D.; Kinnear, J. E.; Ackerman, T. L. (Univ. of California, Los Angeles). Jul 1974.

In dynamics of plutonium in desert environments. Nevada Applied Ecology Group progress report as of January 1974.

Data are presented on the ecological attributes of vegetation in Area 13, Nevada Test Site (NTS), as well as data on the content of $^{239-240}$Pu and ^{241}Am in samples of vegetation collected in conjunction with the soil sampling program in Area 13. Prominent shrub and grass species in the fallout pattern of Area 13 include Artemisia spinescens, Atriplex canescens, Atriplex confertifolia, Eurotia lanata, Grayia spinosa, Kochia americana, Lycium andersonii, and Oryzopsis hymenoides. Individual or codominant species distinguished local association patterns of varied size within the fenced study area. Preliminary results showed rather uniform distributions of $^{239-240}$Pu and ^{241}Am among individual samples of the same plant species collected within an intensive study plot. However, there was considerable variation in the contamination levels between different species, presumably from superficial entrapment of resuspended particulate material. Concentrations in Eurotia lanata were three to five times higher than in other species sampled from the same study site. The $^{239-240}$Pu and ^{241}Am generally tended to decrease in samples of vegetation collected at increasing distances from ground zero, but there were poor correlations between vegetation and soil $^{239-240}$Pu concentrations in isopleth strata within the fenced grazing area. Results showed inconsistencies in the Pu/Am ratios for vegetation and soil. Lower ratios found in vegetation samples indicate that preferential uptake and concentration of ^{241}Am through plant roots might have occurred in the Project 57 area. (auth)

29446 (NVO-AEIC-74-1, pp 119-133) ANALYSIS OF VEGETATION COVER IN CERTAIN Pu-CONTAMINATED AREAS USING AERIAL PHOTOGRAPHY. Rhoads, W. A. (EG and G, Inc., Goleta, CA). Jul 1974.

In dynamics of plutonium in desert environments. Nevada Applied Ecology Group progress report as of January 1974.

Two methods of estimating vegetation cover were developed using aerial photographs; both are less expensive and do not contribute to disturbance of the areas compared to standard methods of measuring vegetation cover on the ground. Cover values for five Pu-contaminated areas at Nevada Test Site and Tonopah Test Range are presented. (auth)

29447 (NVO-AEIC-74-1, pp 135-141) ROLE OF SOIL MICROORGANISMS IN THE MOVEMENT OF PLUTONIUM. Au, F. H. F. (National Environmental Research Center, Las Vegas, NV). Jul 1974.

In dynamics of plutonium in desert environments. Nevada Applied Ecology Group progress report as of January 1974.

Microbial studies which are completed or in progress were designed to determine the ability of microorganisms to absorb plutonium, to quantify the uptake, and to determine the microbial population of soils of the Nevada Test Site (NTS). Results of the microbial inventory of Area 13 (NTS) showed that about 2% of the Aspergillus was near the surface of the hummock and increased with distance away from the plants. Penicillium, on the other hand, showed an inverse pattern in that its relative abundance decreased away from the plants. A method was developed for in vitro studies in which aerial fungal spores were collected to determine soluble plutonium uptake from agar medium. The concentration of plutonium in mature spores was approximately one-fourth of that in the growth medium. (auth)

29448 (NVO-AEIC-74-1, pp 151-161) GRAZING STUDIES ON SELECTED PLUTONIUM-CONTAMINATED AREAS IN NEVADA. Smith, D. D. (National Environmental Research Center, Las Vegas, NV). Jul 1974.

In dynamics of plutonium in desert environments. Nevada Applied Ecology Group progress report as of January 1974.

A grazing study in a Pu contaminated area of the Nevada Test Site was initiated in May of 1973 and is proceeding on schedule. This includes the monthly collection of ingesta samples from fistulated steers, the quarterly sacrifice and sampling of a goat, and the semiannual sacrifice and sampling of selected adult and young cattle. No data are yet available. Bone ash samples collected from the NTS beef herd for the years 1958 to 1967 have been obtained from the University of Nevada, Reno, and submitted for plutonium and americium analyses. During 1972, cattle from three different herds on and around the Nevada Test Site were sampled to determine the tissue burdens of plutonium and uranium. The uranium content of the tissues sampled was relatively consistent among the three herds; however, the ^{239}Pu was about 20 times higher in femurs from the Roller Coaster herd than in the Searchlight cattle. This ratio was lower in edible tissues. Using the maximum concentrations observed in beef tissue, the hypothetical maximum bone dose for a man ingesting 250 g/day for 50 years was calculated to be 9.7 mrem from beef muscle or 36.4 mrem for beef liver. (auth)

29449 (NVO-AEIC-74-1, pp 187-212) ECOLOGICAL STUDIES OF VERTEBRATES IN PLUTONIUM-CONTAMINATED AREAS OF THE NEVADA TEST SITE. Moor, K. S.; Bradley, W. G. (Univ. of Nevada, Las Vegas). Jul 1974.

In dynamics of plutonium in desert environments. Nevada Applied Ecology Group progress report as of January 1974.

Various standard census methods were employed during the period March 1972 to August 1973, to obtain a qualitative and quantitative inventory of the vertebrate biota in three plutonium-contaminated study areas of the Nevada Test Site (NTS). Data are presented on the vertebrate composition, relative abundance, and seasonal status in the study areas of snakes, lizards, birds, and rodents. Concentrations of ^{239}Pu and ^{241}Am were determined in the pelt, G.I. tract, and carcass of nine rodents (Dipodomys microps) resident of Area 13 for at least six months. Maximum ^{239}Pu values obtained in nCi/g ash were 2.44 × 10^{0}, 4.74 × 10^{0}, and 8.58 × 10^{-3} for the pelt, G.I. tract, and carcass, respectively. ^{241}Am values were 2.87 × 10^{-1}, 5.49 × 10^{-1}, and not detectable for the pelt, G.I. tract, and carcass, respectively. (auth)

29450 (NVO-AEIC-74-1, pp 221-233) RESUSPENSION ELEMENT STATUS REPORT. Phelps, P. L.; Anspaugh, L. R. (Univ. of California, Livermore). Jul 1974.

In dynamics of plutonium in desert environments. Nevada Applied Ecology Group progress report as of January 1974.

An intensive study on the resuspension of Pu at the Nevada Test Site has been initiated. The main thrust of the study is to develop a mathematical model for describing the concentrations of Pu in surface air as a function of the source and driving forces. It is intended that the model be a basis for assessing potential health hazards and developing cleanup recommendations. In addition, the study is providing an opportunity to develop a generalized resuspension model, applicable in general for establishing environmental and biological assessment of nuclear projects involving Pu. (auth)

29451 (NVO-AEIC-74-1, pp 235-239) MEASUREMENTS OF METEOROLOGICAL PARAMETERS. Kennedy, N. C.; Booth, H. G. (Air Resources Lab., Las Vegas, NV). Jul 1974.

In dynamics of plutonium in desert environments. Nevada Applied Ecology Group progress report as of January 1974.

Methods used for obtaining meteorological information at air sampling locations at the Nevada Test Site are described. Measurements of wind direction and speed, temperature, and precipitation were made and these data are being used in the analysis of Pu samples obtained for resuspension studies. (CH)

29452 (NVO-AEIC-74-1, pp 265-297) RESULTS AND DATA ANALYSIS: RESUSPENSION ELEMENT STATUS REPORT. Anspaugh, L. R.; Phelps, P. L. (Univ. of California, Livermore). Jul 1974.

In dynamics of plutonium in desert environments. Nevada Applied Ecology Group progress report as of January 1974.

The long-range goal of the Nevada Applied Ecology Group resuspension studies is to produce a set of equations which can be used to predict the time-dependent average concentration of resuspended material downwind from a source of any geometrical configuration and soil surface characteristics. Preliminary data are presented on the resuspension of ^{239}Pu, ^{240}Pu, and ^{241}Am at the Nevada Test Site as a function of particle size and meteorological parameters. Samples were collected using ultrahigh-volume air samplers. These preliminary results have already found practical application in another AEC program which has the goal of evaluating the potential hazards associated with the reoccupation of the Eniwetok Atoll. The use of the Nevada Test Site (NTS) data and expertise to predict the levels of resuspended air activity arising from the aged Eniwetok source is discussed. (CH)

29453 (NVO-AEIC-74-1, pp 311-319) DISTRIBUTION AND INVENTORY ELEMENT ACTIVITIES ON-NTS AND OFF-NTS. Church, B. W. (Atomic Energy Commission, Las Vegas, NV); Brady, D. N.; Aoki, I.; Bliss, W. A. Jul 1974.

In dynamics of plutonium in desert environments. Nevada Applied Ecology Group progress report as of January 1974.

Activities of the Nevada Applied Ecology Group during 1973 are summarized. Activities included investigations of all plutonium-contaminated areas on and near the Nevada Test Site (NTS). Data are included on the content of ^{239}Pu, ^{240}Pu, ^{241}Am, gross γ activity, and specific γ-emitting constituents of the gross γ spectra in soil samples collected at various locations. (CH)

29454 (NVO-AEIC-74-1, pp 321-327) INFORMATION SUPPORT FOR THE NEVADA APPLIED ECOLOGY GROUP. Oen, C. J. (Oak Ridge National Lab., TN). Jul 1974.

In dynamics of plutonium in desert environments. Nevada Applied Ecology Group progress report as of January 1974.

A computer file of 2,500 references on the environmental aspects of plutonium, uranium, and the Nevada Test Site (NTS) has been developed. Recent emphasis on the historic (pre-1962) literature on plutonium and uranium accounts for over 400 references. These early AEC-sponsored reports are primarily on exposure, radionuclide contamination, and radioactivity resulting from nuclear testing at the NTS or on the medical and biological aspects of plutonium and uranium. Services available include published bibliographies, customized bibliographies, and assistance in locating documents. A manual file of documents rounds out this information resource. (auth)

29455 (NVO-AEIC-74-1, pp 331-360) NAEG PLUTONIUM STUDY MODELING PROGRAM: PLUTONIUM TRANSPORT AND DOSE ESTIMATION MODEL. Martin, W. E.; Bloom, S. G.; Yorde, R. J. Jr. (Battelle Columbus Labs., Ohio). Jul 1974.

In dynamics of plutonium in desert environments. Nevada Applied Ecology Group progress report as of January 1974.

A computer program based on a matrix exponential method was used to solve a system of ordinary differential equations which simulate the behavior of ^{239}Pu in desert ecosystems such as those found at and near the Nevada Test Site. The model was used to estimate the rates of ^{239}Pu transport, via several environmental pathways, to Standard Man, who was assumed to live in a contaminated area. These estimates were then used to calculate radiation doses and dose commitments, as a function of time, to different organs (pulmonary lymph nodes, skeleton, lungs, kidney, liver, and G.I. tract). (auth)

29456 (ORNL-NSF-EP-73) ORRMIS: OAK RIDGE REGIONAL MODELING INFORMATION SYSTEM. Part I. Durfee, R. C. (Oak Ridge National Lab., Tenn. (USA)). Sep 1974. Contract W-7405-eng-26. 112p. Dep. NTIS $8.75.

A geographically oriented information system is being developed by the Regional Environmental Systems Analysis Program at Oak Ridge National Laboratory (ORNL). The system is being designed to operate either as a stand-alone inquiry-retrieval system or as a communications supervisor for use with simulation models. The primary purpose of ORRMIS is to provide the data management capability for analysis models which forecast the spatial distribution and ecological effects of activities within a geographical region. The geographic orientation of the system may, however, be replaced with a more general adjacency relationship thereby extending its use to non-geographic models. (auth)

29457 (RT/PROT-(74)13) 1973 METEOROLOGICAL YEARBOOK OF THE EUREX SITE AT SALUGGIA. (Comitato Nazionale per l'Energia Nucleare, Saluggia (Italy)). Apr 1974. 80p. (In Italian). Dep. NTIS (US Sales Only) $7.00.

The observed atmospheric phenomena and climatological methods applied, with emphasis of the salient feature of the meteorological year 1973, are described. (tr-auth)

29458 (UCID-15895) FIELD MEASUREMENT OF PERMEABILITIES IN NTS AREA 9. Snoeberger, D. F.; Morris, C. J.; Morris, G. A. (California Univ., Livermore (USA). Lawrence Livermore Lab.). 23 Aug 1971. Contract W-7405-eng-48. 14p. Dep. NTIS $4.00.

A measurement was completed of permeability to a depth of 1200 ft in an exploratory hole in Area 9 at NTS. The method consisted of successive air-injection tests on the empty hole and after each of four stages of backfilling with cement. The data include flow rate, temperature, and the buildup and decay of pressure in the hole. Preliminary calculations showed that the average permeability of the region for the full hole is about 4 darcies, assuming a radial cylindrical model and steady-state flow. Similarly, the permeabilities of the surface alluvium, the tuff layer underlying the alluvium, and the Grouse Canyon Ashfall are all in the 2-to-12-darcy range. Tracer gas, SF_6, added after bringing the top of the cement to 457 ft indicated flow paths to other holes and to the ground surface within 150 ft of the hole tested. (auth)

29459 ECOLOGICAL CONSIDERATIONS OF PROJECT WAGON WHEEL. Dolenc, M. R. (El Paso Natural Gas Co., TX). pp 215-223 of Geology and Mineral Resources of the Greater Green River Basin. Schell, E. M. (ed.). Casper, WY; Wyoming Geological Association (1973).

From symposium and core seminar on the geology and mineral resources of the greater Green River basin; Casper, Wyoming, USA (17 Sep 1973). See CONF-7309115-.

Project Wagon Wheel, a nuclear fracturing experiment designed for the northern portion of the Greater Green River Basin, is currently conceived to employ five 100 kiloton nuclear explosives, sequentially fired, and emplaced in a single well at depths between 9,220 to 11,570 feet. Studies conducted include the geology, hydrology, meteorology, seismicity, background radioactivity, culture and bioenvironmental aspects of the site under consideration. Some of the ecological considerations discussed include radioactivity, ground motion effects, structural effects, hydrologic effects, the effects on wildlife and fish habitats and the environmental effects of an influx of people on the land use of the area should this technique be successful in developing the gas resources of the Pinedale Unit. It is concluded that most of the above effects will be minimal and that nuclear fracturing can be safely employed as a completion technique on a portion of this unit. (auth)

Thermal Effluents

Refer also to abstracts 29417, 29468, 29488, 31252, 31255, 31257, and 31308.

29460 (BNWL-1850(Pt.3), pp 240-254) SIMPLE MODEL FOR BOUYANT PLUMES BASED ON THE CONSERVATION LAWS. Slinn, W. G. N. Apr 1974.

In Pacific Northwest Laboratory annual report for 1973 to the USAEC Division of Biomedical and Environmental Research. Part 3. Atmospheric sciences.

Equations for the steady-state rise of a buoyant plume are derived directly from the conservation laws for mass, momentum and energy. Top-hat profiles are used and it is assumed that there is no horizontal pressure gradient across the plume's boundary. In the resulting equations there are four unspecified quantities: the drag and heat transfer coefficients, the entrainment velocity and heat production. Results are shown for the (isentropic) case when all these quantities are zero as well as for cases with various combinations of these quantities different from zero and using simple relaxation models. In this way some insight is gained into their separate effects on the plume's properties. Results of a simple model to account for a mean wind are also demonstrated. The need for more field data is obvious. (auth)

29461 (BNWL-SA-5058) AQUATIC PHYSIOLOGY OF THERMAL AND CHEMICAL DISCHARGES. Schneider, M. J.; Becker, C. D.; Fickeisen, D. H.; Thatcher, T. O.; Wolf, E. G.; Hunt, E. L. (Battelle Pacific Northwest Labs., Richland, Wash. (USA)). Jun 1974. 32p. (CONF-740820-2). Dep. NTIS $4.75.

From symposium on the physical and biological effects on the environment of cooling systems and thermal discharges at nuclear power stations; Oslo, Norway (26 Aug 1974).

The United States Atomic Energy Commission has been operating the Hanford Works in Washington State, U.S.A., since the 1940's, and throughout this time, investigations of the ecological effects of reactor discharges have been conducted. Data are summarized from studies on the effects of fatigue on thermal tolerance in fish, the behavioral response of fish influenced by thermal plumes and the effect of thermal experience on fish sensory physiology, the effects of heat and gas supersaturation on fish, the effects of cold shock on fish, and the effects of heat and pollutant chemicals on fish. (CH)

29462 (CONF-740813-2) MIGRATORY BEHAVIOR OF FISH TAGGED AT A NUCLEAR POWER PLANT DISCHARGE INTO LAKE MICHIGAN. Romberg, G. P.; Spigarelli, S. A.; Prepejchal, W.; Thommes, M. M. (Argonne National Lab., Ill. (USA)). 1974. 31p. Dep. NTIS $4.75.

From 17th conference on Great Lakes research; Hamilton, Ontario, Canada (12 Aug 1974).

With the proliferation of nuclear power plants on Lake Michigan, much concern has been expressed over the effects of plume "residence" and abnormal temperature exposures on the physiology and migratory behavior of important fish species. A mark and recapture study was conducted at the Point Beach Nuclear Plant to describe the migratory behavior of fish at this thermal discharge. A total of 1781 fish (7 species) were captured, tagged and released during 1972 and 1973. As of August 1, 1974, 14% of the tagged fish have been recaptured, primarily by sport fishermen. Eighty four percent of the recaptures by fishermen occurred at locations other than Point Beach, and the number of recaptures generally decreased with distance. Rainbow trout tended to be the most migratory, but individuals of each species showed extensive movements. Experimental temperature sensitive fish tags indicated that the majority of fish recaptured at Point Beach spent less than 10% of their time at discharge temperature. Brown trout exhibited a stronger attraction to discharge waters than did rainbow trout or chinook salmon. High percentages of recapture for most species suggest negligible mortalities due to plume "residence" or the tagging procedure and imply that Lake Michigan sport fishermen are annually harvesting a substantial proportion of the fish stocks. (auth)

29463 (ORNL-tr-2781) SYMPOSIUM ON THE EFFECT OF HOT WATER OF THERMOELECTRIC PLANTS ON THE HYDROLOGY AND BIOLOGY OF RESERVOIRS (ABSTRACTS) MARCH 24–26, 1971, BOROK, USSR. Butorin, N. V.; Mordukhay-Boltovski, F. D.; Sinelnikov, V. E. (eds.). (Oak Ridge National Lab., Tenn. (USA)). 1971. Translated from Russian. (CONF-710360-(Absts.)). 87p. Dep. NTIS $7.50.

From symposium on the effect of hot water of thermoelectric plants on the hydrology and biology of reservoirs; Borok, USSR (24 Mar 1971).

Abstracts, in English, of 43 papers given at the conference are included. Each paper discusses the effects of thermal effluents from power plants on the thermal, hydraulic, or biological conditions in cooling reservoirs. (LCL)

29464 MATHEMATICAL AND PHYSICAL MODELS OF HEAT DISSIPATION. pp 33-54 of Thermal Discharges at Nuclear Power Stations. Vienna; International Atomic Energy Agency (1974).

See STI/DOC–10/155.

The basic principles and applications of mathematical modelling of heat dissipation from thermal effluents discharged into surface waters, e.g. rivers, open sea, bays, etc, and into the atmosphere are described. Hydraulic modeling and field studies of thermal plumes in surface waters and the use of atmospheric plume rise and diffusion models are discussed. (LCL)

29465 PHYSICAL–CHEMICAL EFFECTS OF COOLING SYSTEMS AND THERMAL DISCHARGES ON THE ENVIRONMENT. pp 55-68 of Thermal Discharges at Nuclear Power Stations. Vienna; International Atomic Energy Agency (1974).

See STI/DOC–10/155.

The possible physical and chemical effects on the environment of power plants thermal effluents discharged into surface waters or into the atmosphere via cooling towers are described. (LCL)

29466 BIOLOGICAL EFFECTS OF THERMAL DISCHARGES FROM NUCLEAR POWER PLANTS. pp 69-108 of Thermal Discharges at Nuclear Power Stations. Vienna; International Atomic Energy Agency (1974).

See STI/DOC–10/155.

Concern about the effects of thermal discharges on the biota are reviewed briefly to provide some understanding of current research on thermal effects and to indicate what future research is required. Ecosystem responses to thermal discharges in water bodies are described. (LCL)

29467 POSSIBLE EFFECTS OF THERMAL EFFLUENTS ON FISH: A REVIEW. Sylvester, J. R. Environ. Pollut. (London); 3: No. 3, 205-215(Jul 1972).

Literature on specific considerations of thermal effluents (metabolism, thermal shock, reproduction and development, acclimation and lethal limits, fluctuations and sensing, temperature preferences, and synergism) is reviewed. Thermal stress has general and specific effects on fish physiology. In general, over a species-specific temperature range, increasing temperatures increase metabolic rates and other activity. Deviations from optimal temperature could cause a cessation of spawning behavior or an increase of abnormal fry. The final level of temperature acclimation is a function of species, size, condition, and past environment. Most fish can acclimate faster to higher temperatures than to lower temperatures. Fluctuating temperatures increase thermal resistance in some species. Temperature preferences in fish are a function of acclimation temperature and of the species-specific optimum temperature. Slight increases in temperature can be lethal because of synergism. (Pollut. Abstr.)

Chemical Effluents

Refer also to abstracts 28930, 29351, 29366, 29425, 29435, 29461, 29612, and 29613.

29468 (BNWL-1850(Pt.3)) PACIFIC NORTHWEST LABORATORY ANNUAL REPORT FOR 1973 TO THE USAEC DIVISION OF BIOMEDICAL AND ENVIRONMENTAL RESEARCH. Part 3. Atmospheric Sciences. Simpson, C. L. (Battelle Pacific Northwest Labs., Richland, Wash. (USA)). Apr 1974. Contract AT(45-1)-1830. 292p. Dep. NTIS $7.60.

Fifty-seven sections are included. A separate abstract was prepared for each section. (LCL)

For abstracts of individual papers see: 28937, 29359–29376, 29410, 29424–29427, 29431–29437, 29460, 29469–29488, and 29609–29613.

29469 (BNWL-1850(Pt.3), pp 17-19) TRACE POLLUTANT EMISSIONS IN FOSSIL FUEL COMBUSTION. Rancitelli, L. A.; Abel, K. H.; Weimer, W. C. Apr 1974.

In Pacific Northwest Laboratory annual report for 1973 to the USAEC Division of Biomedical and Environmental Research. Part 3. Atmospheric sciences.

Measurements of trace elements in coal and flyash indicate that substantial amounts of the potentially toxic elements Se, Hg, and As are emitted into the atmosphere by the Centralia coal-fired electric plant. (auth)

29470 (BNWL-1850(Pt.3), pp 63-67) SURFACE FLUX MODEL FOR DIFFUSION, DEPOSITION, AND RESUSPENSION. Horst, T. W. Apr 1974.

In Pacific Northwest Laboratory annual report for 1973 to the USAEC Division of Biomedical and Environmental Research. Part 3. Atmospheric sciences.

A model of the diffusion-deposition-resuspension transport process is developed which accounts for the effect of deposition and resuspension on the airborne concentrations by representing the net vertical flux of material at the surface due to these processes as an areal source of material for further downwind diffusion. The diffusion process is modeled by the standard Gaussian plume. This model is used to show that the assumptions of the source depletion model of deposition overestimate surface air concentrations and, hence, the deposition flux by factors of 2 to 4 for moderately strong deposition, $V_d/\overline{u} = 10^{-2}$. These results can be used to define the limits within which the source depletion model may be used with acceptable accuracy. (auth)

29471 (BNWL-1850(Pt.3), pp 94-99) CHARACTERISTICS OF AEROSOLS FROM ST. LOUIS. Alkezweeny, A. J. Apr 1974.

In Pacific Northwest Laboratory annual report for 1973 to the USAEC Division of Biomedical and Environmental Research. Part 3. Atmospheric sciences.

Aerosol particle size distributions were measured over St. Louis. It was found that the concentrations of particles of all sizes generally decrease with an increase in altitude and that the size distributions in the same location show a considerable daily variation. The volume distribution measured with time peaked around 0600 for particles greater than 0.45 μm. At noon an increase in the particles less than 0.45 μm and in the Aitken nuclei concentrations was observed. Even though a decrease in the Aitken nuclei count was measured downwind of St. Louis, it was associated with an increase in the concentrations of larger particles. (auth)

29472 (BNWL-1850(Pt.3), pp 100-101) PRELIMINARY IN-PLUME MEASUREMENTS NEAR CENTRALIA. Alkezweeny, A. J. Apr 1974.

In Pacific Northwest Laboratory annual report for 1973 to the USAEC Division of Biomedical and Environmental Research. Part 3. Atmospheric sciences.

Preliminary in-plume measurements of trace gases and particulates were conducted near Centralia, Washington. A maximum of 0.28 ppM NO_x concentration was detected. The measurement suggested that aerosol particles leaving the stack undergo significant coagulation. (auth)

29473 (BNWL-1850(Pt.3), pp 102-105) CONCENTRATIONS AND RATES OF REMOVAL OF CONTAMINANTS FROM THE ATMOSPHERE IN AND DOWNWIND OF ST. LOUIS. Young, J. A.; Tanner, T. M.; Thomas, C. W.; Wogman, N. A.; Petersen, M. R. Apr 1974.

In Pacific Northwest Laboratory annual report for 1973 to the USAEC Division of Biomedical and Environmental Research. Part 3. Atmospheric sciences.

The atmospheric concentrations of trace elements, sulfates, SO_2, freons and CO were measured upwind, in, and downwind of St. Louis to determine the rates at which these contaminants are removed from the atmosphere by dry deposition and chemical reactions. (auth)

29474 (BNWL-1850(Pt.3), pp 105-107) VERTICAL PROFILES OF TRACE GASES IN ST. LOUIS. Alkezweeny, A. J. Apr 1974.
In Pacific Northwest Laboratory annual report for 1973 to the USAEC Division of Biomedical and Environmental Research. Part 3. Atmospheric sciences.

Airborne and ground measurements of NO_x and NO have shown their concentrations at 1,000 ft above the ground to be higher than those at the ground and to decrease with altitude above that elevation. (auth)

29475 (BNWL-1850(Pt.3), pp 109-111) PROGRESS REPORT ON IN-CLOUD SCAVENGING IN FRONTAL STORMS. Davis, W. E.; Young, J. A.; Thorp, J. M. Apr 1974.
In Pacific Northwest Laboratory annual report for 1973 to the USAEC Division of Biomedical and Environmental Research. Part 3. Atmospheric sciences.

The successful in-cloud release of tracers in a storm on December 5, 1973, near Quillayute, Washington is reported. Suggestions are made for work to be completed before the next test series. (auth)

29476 (BNWL-1850(Pt.3), pp 111-114) SUMMARY OF CURRENT FINDINGS FROM THE ANALYSIS OF 1972 QUILLAYUTE SCAVENGING EXPERIMENTS. Davis, W. E. Apr 1974.
In Pacific Northwest Laboratory annual report for 1973 to the USAEC Division of Biomedical and Environmental Research. Part 3. Atmospheric sciences.

The results of two in-cloud releases of tracers in two frontal storms at Quillayute, Washington are reported: on March 21, 1972, In and AgI were released with little or no deposition; on March 31, 1972 a rhodamine release showed values to 5x background detected in ground samples. (auth)

29477 (BNWL-1850(Pt.3), pp 117-120) COMPARISON OF THE WASHOUT COEFFICIENT FOR A POLYDISPERSE AEROSOL TO THAT FOR AN AEROSOL OF FIXED PARTICLE SIZE. Dana, M. T.; Hales, J. M. Apr 1974.
In Pacific Northwest Laboratory annual report for 1973 to the USAEC Division of Biomedical and Environmental Research. Part 3. Atmospheric sciences.

When a polydisperse aerosol is involved in a calculation of washout coefficient, considerable error can result from an attempt to characterize the distribution by a single "representative" particle size. If the differential washout coefficient is expressed as $\Lambda = cr^{\alpha}$ and aerosol removal is expressed in terms of mass, the error is not eliminated unless the chosen representative size is the $(\alpha/2 + 3)$th geometric mean particle radius. (auth)

29478 (BNWL-1850(Pt.3), pp 138-140) EXTENSION OF THE ANALYSIS OF PLUME WASHDOWN TO INCLUDE DIFFUSION. Slinn, W. G. N. Apr 1974.
In Pacific Northwest Laboratory annual report for 1973 to the USAEC Division of Biomedical and Environmental Research. Part 3. Atmospheric sciences.

An extension is presented of an analysis of plume washdown caused by reversible washout of gases. The extension is to include diffusion. The results show that in the mean the plume falls at the washdown velocity $H'J_0$ where J_0 is the rainfall rate and H' is the dimensionless Henry's law constant for the gas, and that diffusion is slightly enhanced. (auth)

29479 (BNWL-1850(Pt.3), pp 141-143) PRECIPITATION SCAVENGING OF INORGANIC POLLUTANTS FROM METROPOLITAN SOURCES: ST. LOUIS, JULY 1973. Dana, M. T.; Hales, J. M.; Hane, C. E.; Thorp, J. M. Apr 1974.
In Pacific Northwest Laboratory annual report for 1973 to the USAEC Division of Biomedical and Environmental Research. Part 3. Atmospheric sciences.

An additional series of rain scavenging experiments in St. Louis was conducted, this time using a large array of collectors. Some nine convective storms were sampled, and over 400 individual rain samples were analyzed for SO_2, SO_4^{2-}, NO_2^-, NO_3^-, NH_4^+, and H^+. (auth)

29480 (BNWL-1850(Pt.3), pp 143-146) CONVECTIVE STORM MODELING AND ITS POSSIBLE APPLICATION TO PRECIPITATION SCAVENGING PROBLEMS. Hane, C. E. Apr 1974.
In Pacific Northwest Laboratory annual report for 1973 to the USAEC Division of Biomedical and Environmental Research. Part 3. Atmospheric sciences.

The use of numerical convective cloud modeling in precipitation scavenging research is discussed. A particular two-dimensional time-dependent squall line model is described, which includes a parametrization scheme for the microphysics of cloud and rain. Possible initial steps for the use of this model in scavenging research are discussed. (auth)

29481 (BNWL-1850(Pt.3), pp 146-147) ENTRAINMENT OF TRACERS NEAR THE SIDES OF CONVECTIVE CLOUDS. Young, J. A.; Tanner, T. M.; Thomas, C. W.; Wogman, N. A. Apr 1974.
In Pacific Northwest Laboratory annual report for 1973 to the USAEC Division of Biomedical and Environmental Research. Part 3. Atmospheric sciences.

Tracers released sequentially at 10 to 13.5 thousand ft near the upwind sides of two convective towers near St. Louis spread between the towers and were almost completely scavenged by the precipitation. (auth)

29482 (BNWL-1850(Pt.3), pp 157-162) DRY DEPOSITION OF PARTICLES. Sehmel, G. A.; Hodgson, W. H.; Sutter, S. L. Apr 1974.
In Pacific Northwest Laboratory annual report for 1973 to the USAEC Division of Biomedical and Environmental Research. Part 3. Atmospheric sciences.

Deposition velocities for monodispersed particles were measured for deposition onto surfaces of both 1.6 and 3.8 cm dia crushed gravel. Deposition velocities are greater for the larger gravel. For the larger gravel about 20% of the deposited particles were found below the top layer of gravel, suggesting that particle deposition may be enhanced in thick, coarse beds. (auth)

29483 (BNWL-1850(Pt.3), pp 169-170) ELEMENTAL CONTENT OF TRACE ELEMENTS IN VEGETATION COLLECTED AT CENTRALIA, WASHINGTON. Rancitelli, L. A.; Abel, K. H.; Weimer, W. C. Apr 1974.
In Pacific Northwest Laboratory annual report for 1973 to the USAEC Division of Biomedical and Environmental Research. Part 3. Atmospheric sciences.

Samples of vegetation collected around the Centralia coal-fired electric plant contained concentrations of As, Hg, Sb, and Se that were up to an order of magnitude higher than the concentrations measured in Alaskan vegetation samples. (auth)

29484 (BNWL-1850(Pt.3), pp 171-174) PARTICLE DEPOSITION RATES ON A WATER SURFACE AS A FUNCTION OF PARTICLE DIAMETER AND AIR VELOCITY. Sehmel, G. A.; Sutter, S. L. Apr 1974.
In Pacific Northwest Laboratory annual report for 1973 to the USAEC Division of Biomedical and Environmental Research. Part 3. Atmospheric sciences.

Deposition rates of airborne monodispersed particles onto a water surface were determined in a wind tunnel. Average air velocities over water were 2.2, 7.2, 13.8 m/s, and particle diameters were from 0.3 to 28 μm. For particles greater than 1 μm, deposition rates increased with both particle diameter and wind speed. For particles less than 1 μm diam, phoretic forces are comparable to transport forces from eddy diffusion and Brownian diffusion. Minimum deposition velocities are approximately 1×10^{-2} cm/sec. Maximum deposition velocity was 37 cm/sec, the largest ever reported for any surface. (auth)

29485 (BNWL-1850(Pt.3), pp 179-187) ANALYTICAL INVESTIGATIONS OF INERTIAL DEPOSITION OF SMALL AEROSOL PARTICLES FROM LAMINAR FLOWS ONTO LARGE OBSTACLES. Part A. General Formulation. Slinn, W. G. N. Apr 1974.
In Pacific Northwest Laboratory annual report for 1973 to the USAEC Division of Biomedical and Environmental Research. Part 3. Atmospheric sciences.

Rather than follow the usual formulation of the inertial deposition problem, a continuum model is presented which replaces Newton's second law by a continuity equation and a pseudomomentum equation. Some features of the general solution are discerned and it is seen that regular perturbation methods fail both at large and small Stokes numbers. (auth)

29486 (BNWL-1850(Pt.3), pp 188-199) ANALYTICAL INVESTIGATIONS OF INERTIAL DEPOSITION OF SMALL AEROSOL PARTICLES FROM LAMINAR FLOWS ONTO LARGE OBSTACLES. Part B. Large Stokes Number Solution by the Method of Matched Asymptotic Expansion. Slinn, W. G. N. Apr 1974.
In Pacific Northwest Laboratory annual report for 1973 to the USAEC Division of Biomedical and Environmental Research. Part 3. Atmospheric Sciences.

The reason for the failure of the regular perturbation techniques used in Part A is identified. The method of matched asymptotic expansions is applied to obtain the first order correction to the collection efficiency at large Stokes numbers. Analytical continuation of the solution to a result valid for all Stokes numbers is discussed, and it is concluded that the most productive procedure would be to gain information about the small Stokes number limit. This will be described in Part C. (auth)

29487 (BNWL-1850(Pt.3), pp 235-239) MEASUREMENTS OF DRIFT FROM A MECHANICAL DRAFT COOLING TOWER. Alkezweeny, A. J.; Glover, D. W.; Lee, R. N.; Sloot, J. W.; Wolf, M. A. Apr 1974.

In Pacific Northwest Laboratory annual report for 1973 to the USAEC Division of Biomedical and Environmental Research. Part 3. Atmospheric sciences.

Measurements were made at the Oak Ridge Gaseous Diffusion Plant to determine the air concentrations and surface deposition rates of chromium in solution in drift droplets originating from a mechanical draft cooling tower. Observed deposition fluxes were about 1 mg/(m^2-h) within 50 m of the tower and approximately two orders of magnitude lower at 1 km. Air concentrations over that same distance were observed to decrease by less than an order of magnitude with values of approximately 40 ng m^{-3} observed to distances of about 100 m. Air concentration and deposition flux appear unrelated, the former probably due to downwash of fine droplets at the tower. The chromium circulation rate during these measurements, based on a chromate concentration of 15 ppM in the circulating water, was 76 kg/h. Work is continuing in the effort to utilize the experimental results for improvement of drift models. (auth)

29488 (BNWL-1850(Pt.3), pp 254-266) ANALYTICAL SEARCH FOR THE STOCHASTIC-DOMINATING PROCESS IN THE DRIFT-DEPOSITION PROBLEM. Slinn, W. G. N. Apr 1974.

In Pacific Northwest Laboratory annual report for 1973 to the USAEC Division of Biomedical and Environmental Research. Part 3. Atmospheric sciences.

The random processes in the drift-deposition problem are examined separately to see if any one of them dominates the statistical properties of the outcome. The three prime candidates are assumed to be the drop size distribution, the distribution of breakaway points, and turbulent diffusion. It is seen that the drop size distribution probably has dominant influence on the deposition of the large-size (drift or carry-over) drops. Turbulence has a comparable influence on the deposition of the small drops for downwind distances of the order of 10 tower heights and then dominates for large downwind distances, provided the atmosphere is not stable. Uncertainties in details of how the drops break free from the plume's updraft preclude an accurate evaluation of this effect and seriously limit the accuracy of any drift-deposition prediction. To remedy this, more field data is needed. (auth)

29489 (UCRL-75902(Rev.1)) HAS MAN, THROUGH INCREASING EMISSIONS OF PARTICULATES, CHANGED THE CLIMATE. Ellsaesser, H. W. (California Univ., Livermore (USA). Lawrence Livermore Lab.). 1 Aug 1974. 24p. (CONF-740921-2). Dep. NTIS $4.25.

From atmospheric-service exchange of particulates and gaseous pollutants symposium; Richland, Washington, USA (4 Sep 1974).

Diverse data relating to natural and anthropogenic particulate emissions and trends in atmospheric turbidity are reviewed. It is estimated that man now contributes 13.6% of the 3.5×10^9 tons of primary and secondary particulates presently emitted to the atmosphere annually. Values derived for the anthropogenic effect on the trend in total airborne particulates (if assumed monotonic) range from 0.06 to 0.4% increase per year. Since such an effect would be only marginally detectable in the available record, the much larger rates of increase published as proof of an upward trend must be due to local or temporary effects and cannot be representative of a global trend. On the other hand almost all urban areas plagued by dirty skies prior to the 1940's have shown in recent years measurable improvement in terms of visibility, dust fall, suspended particulates or the ratio of sunshine in the central city to that at an outlying station. This leads to the conclusion that while an anthropogenic upward trend in airborne particulates existed in the past, it was halted and may even have been reversed over the past few decades. (auth)

29490 (UCRL-76014(Rev. 1)) FAST RESPONSE LIGHT SCATTERING MEASUREMENTS OF THE CHARACTERISTICS OF WIND SUSPENDED AEROSOLS. Porch, W. M.; Shinn, J. H. (California Univ., Livermore (USA). Lawrence Livermore Lab.). Aug 1974. 22p. (CONF-740921-3). Dep. NTIS $4.25.

From atmospheric-service exchange of particulates and gaseous pollutants symposium; Richland, Washington, USA (4 Sep 1974).

An experiment was performed to study dust suspension by wind in Plains, Texas. A vertical pair of nephelometers at heights above ground of 35.5 and 166 cm and anemometers at various heights were used. The nephelometer measures the integrated light scattering coefficient due to aerosols and air, i.e., the amount of dust in air. From the experiments it was concluded that: nephelometer measurements of dust (biased toward the respirable fraction) show strong correlation with simultaneous wind measurements; the vertical gradient of the nephelometer signals which is a measure of the flux shows a very strong power law relation to the friction velocity; and the frequency response and spectral density comparisons of the wind and dust data has proven to be a valuable tool in understanding the physical properties of dust suspension by wind. (LCL)

INSTRUMENTATION

Radiation Detection Instruments

29491 DIGITAL PERIOD METER. Sheets, W. R. (Dow Chemical, Golden, CO). Nucl. Technol.; 24: No. 1, 99-101(Oct 1974).

A digital readout-type period meter was used to monitor period information during critical mass experiments. Its range of measurement extends from ½ to 1000 sec. It can be used to measure the slope of any linearly changing signal. By using a logarithmic amplifier in conjunction with the meter, it will measure an exponential slope. It provides a greater readout range and is less susceptible to noise than the conventional differentiating operational amplifier types. Noise frequency periods are much shorter than the periods measured during an experiment. The input stage has a cutoff frequency allowing typical experiment periods to be measured, but above the cutoff frequency response decreases at 20 db per decade. Contrary to this, the conventional differentiating operational amplifier-type period meter increases in response above its cutoff frequency. The error in period readings was found to be less than 5% probable error. (auth)

General Detectors and Monitors

Refer also to abstracts 29321, 29704, 30127, and 30843.

29492 (CEA-R-4543) STUDY OF THE DETECTION OF NUCLEAR PARTICLES IN LIQUID DIELECTRICS. Prunier, J. (CEA Centre d'Etudes Nucleaires de Grenoble, 38 (France)). Jul 1974. 127p. (In French). Dep. NTIS (U. S. Sales Only) $9.50.

Thesis. Submitted to Universite Scientifique et Medicale de Grenoble (France).

Gas-filled multidetectors are very much used in the fields of nuclear medicine and of high-energy physics as particle localization devices. However, their use is limited by their loss of detection efficiency for energetic x or γ rays (energy greater then 80 keV) or for weakly ionizing charged particles. The choice of more dense detection media suppresses this inconvenience. For this use, liquefied noble gases have very much interesting detection and electron transport properties. The work described concerns essentially liquid argon and xenon. Liquid krypton has been put aside because of its strong nuclear noise caused by the isotope ^{85}Kr. After a short recall about nuclear detection and certain characteristic properties of these liquids, the experimental preparation of the liquids (purification and analysis) and the cryogenics for liquefaction of the noble gases are described. In a third chapter, the pulse ionization chamber mode (parallel plate or cylindrical chamber) is studied with a particular attention devoted to electron transport properties. The next chapter concerns the study of the proportional mode and the amplification caused by electronic avalanches. In the fifth chapter are investigated the properties caused by the addition of molecular impurities. Then, in the last part, problems about particle localization in a liquid dielectric-filled multidetector prototype are examined. It is concluded that liquid argon and xenon are promising detection media but on the condition that they should be very pure. Liquid argon is the most interesting to use in pulse ionization chamber mode detectors while liquid xenon is advised when a high detection efficiency or a proportional mode operation is necessary. (auth)

29493 (LUIP-CR-74-3) IDENTIFICATION OF HEAVY IONS IN NUCLEAR EMULSIONS IN THE HUNDREDS OF MeV INTERVAL. Jensen, M. (Lund Univ. (Sweden). Fysiska Institutionen). Apr 1974. 40p. Dep. NTIS (US Sales Only) $5.25.

The method of charge identification in nuclear emulsions by measurement of mean track width (MTW) and the rate of change of MTW are described, and the expected charge resolution is calculated as a function of charge, energy and measured track length. Measurements have been made on tracks from heavy ions in the charge interval $4 \leq Z \leq 14$ which interact with emulsion nuclei. It is shown that if the energy of the collision can be approximately determined by an independent method, charge identification can be made using comparatively short tracks (3 cm). (auth)

29494 (NVO-AEIC-74-1, pp 241-246) ULTRA HIGH VOLUME AIR SAMPLER. Goluba, R. W. (Univ. of California, Livermore). Jul 1974.

In dynamics of plutonium in desert environments. Nevada Applied Ecology Group progress report as of January 1974.

An air sampler with a nominal volumetric flow rate of 1500 m^3/hr was developed in order that a measurable amount of ^{239}Pu could be collected in as short a time span as 2 hr. The design of the unit is patterned after an air sampler built by Asikainen and Blomqvist (1970) which had a flow rate of 1000 m^3/hr. The air flow through the sampler is maintained by a centrifugal blower thats inlet is attached to one side of a large plenum. The filter, which measures 0.6 × 1.7 m, is mounted horizontally on top of the plenum at a height of 1.3 m above ground level. The blower exhausts through a 0.3-m diameter of 3-m-long sheet metal duct, which is inclined at an angle of 10° with respect to the ground. The length of the duct precludes any interference of the exhaust flow stream with the air intake to the sampler. The duct is inclined so that the exhaust flow stream dissipates without directly striking the ground, which would artificially introduce aerosol into the air. The centrifugal blower is a 0.4-m-diameter wheel with radial blades and is driven by a 7.5-hp electric motor. (auth)

29495 (UCID-15372) IDENTIFICATION AND MEASUREMENT OF LOW-ENERGY ELECTRONS BY CLOUD CHAMBER TECHNIQUES: THE OXYGEN AND NEON AUGER-ELECTRON PROBLEM. Weston, W. F. (California Univ., Livermore (USA). Lawrence Livermore Lab.). 21 Aug 1968. 23p. Dep. NTIS $4.25.

A source of monoenergetic x-rays was used to produce photoelectrons in an expansion cloud chamber. The incident x-rays had energies in the 4.5 to 8.6 keV range. The positive and negative ions composing the photoelectron track were separated by an electric field and the tracks were photographed by two cameras, giving a stereoscopic view of the tracks. The individual droplets in the auger-electron blob or spheroid were counted. The auger spheroid at the high energy end of the photoelectron track was distinguished from the spheroid at the low energy end of the track by relative differences in the numerical density of droplets along the track and differences in size of the two spheroids. The data indicate that the small spheroid at the beginning of the track can confidently be identified as the track of an auger electron from either the oxygen or neon atoms. The respective measured energies are 513 ± 75 eV and 820 ± 54 eV. The expected energies are 514 eV and 822 eV. (auth)

29496 (UCID-15761) SINGLE PULSE AREA MEASUREMENT SYSTEM (SPAMS). Campbell, D. E. (California Univ., Livermore (USA). Lawrence Livermore Lab.). 20 Nov 1970. 14p. Dep. NTIS $4.00.

A measurement system under development will electronically integrate the area of a pulse generated by x-ray-sensitive detectors. An analog gate at the integrator input determines the period of integration. The gate width and gate position are adjustable, allowing extremely selective integration periods. The input impedance of this system is 10 kΩ permitting paralleling of several channels on a single-signal cable (0.5% of charge is removed for each channel used). A SPAMS package will consist of six channels in a standard Nuclear Instrumentation Module System (NIMS) bin. The output of each channel is an analog level proportional to the area of segment integrated. This level will be multiplexed and digitized by the Nevada Automated Diagnostic System (NADS) groups for transmission to the control point building. Provisions are being included in the design to make the system self-calibrating and computer-interactive. (auth)

29497 (UCID-15775) CONSTRUCTION OF AN ADJUSTABLE CARRYING HANDLE FOR THE FIDLER DETECTOR. Taylor, R. D. (California Univ., Livermore (USA). Lawrence Livermore Lab.). 17 Dec 1970. 7p. Dep. NTIS $4.00.

The FIDLER low energy x- and gamma-ray detector has been used extensively for plutonium contamination surveys under laboratory and field conditions. To maintain a fixed counting geometry for these measurements, the detector must be carried over the contaminated surface at a fixed height—normally about 12 inches. The design of an adjustable carrying handle that has been developed for this purpose is described. (WHK)

29498 DEVELOPMENT OF NEUTRON SENSITIVE PCP IONIZATION CHAMBER. Lee, H. Y.; Kim, J. K. (Atomic Energy Research Inst., Seoul). J. Korean Nucl. Soc.; 6: No. 1, 27-35(Mar 1974).

A neutron-sensitive ionization chamber was successfully developed by an improved technique for reactor instrumentation. This instrument is 50mm in diameter and 87cm in length, and can yield a current of 14μA when in a neutron flux of around 10^9 nv. The normally required voltage is +350V. The instrument may be removed from operating flux and disassembled immediately without special precautions from radiation. (auth)

29499 DIAGRAMS OF SENSITIVITY IN RESPECT TO THE ZENITH ANGLE FOR SCINTILLATION TELESCOPES OF ARBITRARY GEOMETRY. Blokh, Ya. L.; Dorman, L. I.; Libin, I. Ya. Kosm. Luchi; No. 14, 141-156(1974). (In Russian).

Calculations of the sensitivity diagrams with respect to the zenith angle θ were performed for telescopes of any geometry, the fringe effects and the path length l of the particle being taken into account. A general analytical expression for such sensitivity diagrams was obtained. The calculations of the sensitivity diagrams with respect to the zenith angle were carried out by different researchers. Detailed investigations of sensitivity diagrams for a vertical and an azimuthal telescopes are presented. (auth)

29500 NEUTRON SUPERMONITOR. Blokh, Ya. L.; Kapustin, I. N. Kosm. Luchi; No. 14, 136-140(1974). (In Russian).

The functional circuit of a neutron supermonitor is considered. A detailed analysis is given of factors affecting the data level stability of the instrument, and the degree to which these factors affect different types of cosmic ray variations was studied. An attempt was made to choose optimal parameters for the most significant elements for determining the stability of the data level. In addition to the ordinary recording the difference between data with a small dead time and data with a large dead time, it is suggested that use be made of these data because the data are nearly free from the counter radioactivity and the μ-meson component contributions. (auth)

29501 SEMI-AUTOMATIC PHOTOMETER FOR DETERMINING HEAVY NUCLEUS CHARGES OF COSMIC RAYS IN NUCLEAR PHOTOEMULSION. Kulikov, V. N.; Pyatigorskii, G. A.; Yakubovskii, E. A.; Gagarin, Yu. F.; Ivanova, N. S. Kosm. Luchi; No. 14, 170-173(1974). (In Russian).

In recent years the problem of charge identification has acquired a great importance. A semi-automatic photometer for cosmic ray nucleus charge determination is described. The constructive features of the instrument present certain advantages in regard to the charge determination. (auth)

29502 CONTENT OF RADIUM, URANIUM, RADIOTHORIUM, AND THORIUM IN SOME SCINTILLATORS. Severnyi, S. A. Kosm. Luchi; No. 14, 162-164(1974). (In Russian).

Experimenting on low intensity radiation recording imposes severe restrictions on the permissible contamination of the radiation detectors by radioactive elements. The necessity for contamination control is discussed. (auth)

29503 RADIATION DETECTION. Channon, H. E. S.; Crawley, J. C. W.; McWilliam, A. D. Netherlands Patent 7,211,897. 31 Aug 1972. Priority Date 1 Sep 1971, United Kingdom of Great Britain and Northern Ireland. 11p. (In Dutch).

An elongated scintillation crystal assembly was designed for use in the radioisotope scanning of living bodies and inanimate objects. The assembly is made up of a plurality of individual crystals lying face to face, with material at the interfaces between the crystals that establishes an optical coupling between them. The crystals are preferably identical and of square section, the thickness being considerably less than the square side dimension; the optically-coupling material is preferably a thixotropic grease. Also, the invention provides a method for constructing the elongated scintillation crystal assembly as well as a method for spreading the coupling material in paste or liquid form on at least one of the pairs of surfaces between the adjacent crystals in the assembly. The surfaces are preferably rubbed down with fine emery paper and then polished in alcohol. With this invention a high-speed scanning procedure for living organs is provided. (NL)

29504 SOLID STATE RADIATION SENSITIVE FIELD ELECTRON EMITTER AND METHODS OF FABRICATION THEREOF. (to Westinghouse Electric Corp.). Netherlands Patent 7,301,833. 9 Feb 1973. Priority Date 11 Feb 1972, USA. 31p. (In Dutch).

A solid state radiation sensitive field emitter cathode comprising a single crystal semiconductor member having a body portion with a uniform array of closely-spaced and very sharp electron emitting projections from one surface in the form of needles or whisker-like members is described. Electrons are emitted into vacuum when a planar-parallel positive anode is mounted in close proximity to the surface. The cathode is responsive to input radiation such as electrons or light directed onto the cathode in modifying the electron emission from the array of electron emitter projections. The method of manufacturing the cathode by providing a predetermined pattern of mosaic of islands of a material exhibiting a greater etch-resistant property than the semiconductor material on a wafer of a semiconductor material and then etching out between and beneath the islands to undercut to a point where the islands are supported by only a small whisker of the semiconductor material is described. Removal of the islands results in an electron emitter being exposed from beneath each island wherein carriers generated within the body portion and also carriers generated within the depletion regions of the tips diffuse to the electron emitter projections wherein establishment of a high electric field at the tips of the electron emitter projections results in electron emission primarily due to conduction band tunneling. The device provides about 10^6 emitting points of close proximity so as to effect photograph-like imaging. (NL)

29505 NUCLEAR IMAGING SYSTEMS. (to Raytheon Corp.). Netherlands Patent 7,214,774. 1 Nov 1972. Priority Date 1 Nov 1971, USA. 19p. (In Dutch).

A nuclear imaging system is described for mapping the source of high energy nuclear particles from a living organ which has selectively absorbed a radioactive compound by spatially coding the energy from the source in a Fresnel pattern on a detector and decoding the detector output to produce an image of the source. The coding is produced by a Fresnel zone plate interposed between the nuclear energy source and the detector whose position is adjustable with respect to the detector. By adjusting the zone plate to a plurality of positions, data from a plurality of cross-sectional slices are produced from which a three-dimensional image of the nuclear source may be obtained. (NL)

29506 NEW EXTRAPOLATION METHOD FOR THE DETERMINATION OF SATURATED IONIZATION CURRENTS. Klumpar, J.; Jirousek, P. (Tschechoslowakischen Akademie, Prague). Isotopenpraxis; 10: No. 6, 233-236(Jun 1974). (In German).

After a short account of the theoretical bases for the existing methods to determine saturated ionization currents, e.g., in pressure chambers, a new empirical mode of extrapolation with the independent variable U^{-x} is described. Introducing relative reciprocals of the current and voltages, integers, u, for the voltages relative to their maximum value and a table for the constant values $(10/u)^x$, the extrapolation by this mode will be more convenient. (auth)

29507 USE OF PARTICLE TRACK DETECTORS IN THE INVESTIGATION OF STATIC REACTOR PARAMETERS. Jozefowicz, K. Nukleonika; 19: No. 6, 557-563(1974). (In Russian).

The technique of particle track detectors, especially fission track detectors is described. Examples of application of these detectors for the determination of reaction rate distribution and fission rate ratio of fissionable isotopes are given. (auth)

29508 EFFICIENCY OF THE ANTICOINCIDENCE METHOD APPLIED TO THE G. M. WINDOW COUNTERS. Sirbu, M. (Institutul de Fizica Atomica, Bucharest). Stud. Cercet. Fiz.; 25: No. 2, 253-256(1973). (In Rumanian).

The anticoincidence installation is described, and the results obtained are presented. The results are given for the G. M. window counters made in Romania and the Philips 18.515 and 18.516 counters. Conclusions are presented. (auth)

29509 CONTINUOUS IN-LINE MONITOR FOR UF_6 ENRICHMENT. Reilly, T. D.; Martin, E. R.; Parker, J. L.; Speir, L. G.; Walton, R. B. (Los Alamos Scientific Lab., NM). Nucl. Technol.; 23: No. 3, 318-327(Sep 1974).

A system has been developed to measure continuously the ^{235}U and ^{234}U enrichment in the UF_6 product of a gaseous diffusion plant. The measurements are made on liquid UF_6 prior to withdrawal into product cylinders. The ^{235}U enrichment is measured to a relative accuracy of 0.5% at two sigma by counting the 185.7-keV gamma ray from ^{235}U with an NaI detector. The ^{234}U enrichment is measured with a neutron detector counting (α,n) neutrons from UF_6. The neutron system can measure either ^{234}U enrichment directly or ^{235}U enrichment indirectly (for low-enriched uranium, 2 to 5% ^{235}U, the two enrichments are nearly proportional). The accuracy of the neutron measurement is 2.5% at two sigma. The gamma and neutron measurements are independent and could be used singly if only one isotope were desired. Both are required to measure ^{235}U and ^{234}U enrichment. The system is presently installed at the Goodyear Atomic Corporation gaseous diffusion plant in Piketon, Ohio. (auth)

29510 A TELESCOPE COUNTER DETECTION SYSTEM APPLIED TO LOW-ENERGY ION-BEAM SURFACE ANALYSIS. Thomas, J-P.; Engerran, J. (Lyon-1 Univ., 69–Villeurbanne (France). Inst. de Physique Nucleaire); Cachard, A.; Tardy, J. (Lyon-1 Univ., 69–Villeurbanne (France)). Nucl. Instrum. Methods; 119: No. 2, 373-380(15 Jul 1974).

Coincidence detection (telescope counter) of charged particles emitted using low-energy backscattering and nuclear reactions is applied to surface analysis and thin film studies. Principles and characteristics of the electronic set-up are described. Performances dealing mainly with resolution and count rate are discussed and illustrated with typical experiments. For proton detection and light-element analysis, the system shows its usefulness as well for depth resolution improvement as for reliability in numerous applications. Comparisons are made between backscattering, (d,p), and (d,α) reactions, using classical single detection and telescope detection. (auth)

29511 A COMPARISON OF POLARIZATION VALUES FOR D–D NEUTRONS OBTAINED FROM MOTT-SCHWINGER AND ^{4}He SCATTERING. Maayouf, R. M. A.; Galloway, R. B. (Edinburgh Univ. (UK)). Nucl. Instrum. Methods; 118: No. 2, 343-347(15 Jun 1974).

Measurements of the polarization of neutrons emitted from the ^{2}H(d,n)^{3}He reaction for a mean deuteron energy of 330 keV are presented. The measurements were carried out for neutrons emitted from a 350 keV thick Ti–D target at 47° using Mott–Schwinger scattering from Pb and U and for neutrons emitted at 50° using scattering from helium. The value of polarization deduced from Mott–Schwinger scattering is $-(13.7 \pm 1.5)\%$ in good agreement with the value $-(13.7 \pm 0.7)\%$ obtained using scattering from helium. The agreement between these neutron polarization values obtained by quite different techniques serves to give confidence both in the polarization values themselves and in the usefulness of Mott–Schwinger scattering in this field. The values reported are consistent with others published recently, for both thin and thick Ti–D targets, in the deuteron energy range 200 to 800 keV. (auth)

29512 ELECTRONIC PROCESSES IN LIQUID XENON. Derenzo, S. E. (California Univ., Berkeley (USA). Lawrence Berkeley Lab.); Mast, T. S.; Zaklad, H.; Muller, R. A.; Prunier, J.; Allemand, R.; Laval, M.; Thomas, G. Nucl. Instrum. Methods; 118: No. 2, 611-614(15 Jun 1974).

An article recently published by Prunier et al. entitled "Some properties of xenon liquid-filled nuclear detectors" is commented on. The article describes an experiment to measure electronic phenomena in liquid xenon using single-wire cylindrical chambers. A criticism of their interpretation of their experimental observations is given. A rebuttal to the criticism is presented by Prunier et al. (WHK)

29513 AUTOMATIC CORRECTIONS FOR DEADTIME EFFECTS AND LINESHAPE CHANGES DUE TO SOURCE DECAY IN POSITRON-ANNIHILATION EXPERIMENTS. Tennant, D. C.; Martel, P.; Buyers, W. J. L.; Kim, S. M. (Atomic Energy of Canada Ltd., Chalk River, Ontario). Nucl. Instrum. Methods; 118: No. 2, 367-371(15 Jun 1974).

Correction systems are described for minimizing the changes in deadtime losses and in lineshape produced by the variation in count rate from intense, short-halflife sources. Application to the counting of ^{64}Cu annihilation radiation in positron experiments employing angular-correlation and Doppler techniques is described. Both techniques have been improved by decreasing, by an order of magnitude, their sensitivities to change of counting rate. (auth)

29514 THE NEEDLE CHAMBER: A NEW HIGHLY VERSATILE DETECTOR. Grunberg, C.; Le Devehat, J. (CEA Centre d'Etudes Nucleaires de Saclay, 91–Gif-sur-Yvette (France). Dept. de Physique Nucleaire). Nucl. Instrum. Methods; 118: No. 2, 457-463(15 Jun 1974).

The main features of a new X-Y detector are described. This counter, based on gaseous multiplication, is made of needle arrays, each needle behaving as a proportional counter. High counting rates (2×10^5/needle s), high amplification factor (up to 10^7), related with a high mechanical reliability make this counter of great interest in a large area. (auth)

29515 A NEUTRON MONITOR WITH A ROTATING RHODIUM DISK. Braumandl, F.; Schreckenbach, K.; von Egidy, T. (Technische Univ. Muenchen, Garching (F.R. Germany). Physik-Dept.). Nucl. Instrum. Methods; 118: No. 2, 381-382(15 Jun 1974).

A neutron monitor has been constructed which uses the activation of rhodium by thermal neutrons. A rhodium disk is rotating between the neutron beam and proportional counters. The gamma background is subtracted automatically. A neutron flux of 10^5 n/cm^{2}s can be measured with a relative precision of 10^{-3} in the presence of a gamma flux of about 10^7 γ/cm^{2}s. (auth)

29516 SHORT-LIVED RADIOACTIVITY INDUCED IN Ge(Li) GAMMA-RAY DETECTORS BY NEUTRONS. Bunting, R. L.; Kraushaar, J. J. (Colorado Univ., Boulder (USA). Nuclear Physics Lab.). Nucl. Instrum. Methods; 118: No. 2, 565-572 (15 Jun 1974).

A number of low-energy transitions have been observed when a Ge(Li) detector is irradiated with neutrons having a broad spectrum of energies. Some of the transitions are from isomers produced by the neutron reactions on the germanium isotopes. Peaks at 53.53 and 66.59 keV are from 0.53 s ^{73m}Ge, 139.88 keV from 46 s ^{75m}Ge, and at 22.7, 175.2, and 197.91 keV from 21.9 ms ^{71m}Ge. The presence of these delayed transitions and those from other reactions can lead to misidentification of gamma rays in certain reaction studies since they are not broadened as are the peaks from inelastic neutron excitation. The half-lives of ^{71m,73m,75m}Ge have been determined to be (21.5 ± 0.4) ms, (499 ± 11) ms, and (45.8 ± 3.1) s respectively. (auth)

29517 EFFICIENCIES AND RESPONSE FUNCTIONS OF NaI(Tl) CRYSTALS FOR GAMMA RAYS FROM THICK DISK SOURCES. Belluscio, M.; De Leo, R.; Pantaleo, A.; Vox, A. (Bari Univ. (Italy). Istituto di Fisica). Nucl. Instrum. Methods; 118: No. 2, 553-563(15 Jun 1974).

A Monte-Carlo program for the determination of the response functions and total and peak efficiencies of NaI detectors for gamma-rays from thick sources is described. With respect to previous calculations, the present one allows the determination of the efficiency curves for higher gamma-ray energies because the secondary electrons are followed in the source and in the detector. The influence on the efficiency curves of the source thickness and of the bremsstrahlung photon and electron leakages is evaluated. Some results obtained with the present program have been compared with other experimental or calculated data. (auth)

29518 MEASUREMENT OF THE GEOMETRY FACTORS OF Ge(Li) DETECTORS. Grosswendt, B.; Waibel, E. (Physikalisch-Technische Bundesanstalt, Braunschweig (F.R. Germany)). Nucl. Instrum. Methods; 118: No. 2, 547-552(15 Jun 1974). (In German).

For two different Ge(Li) detectors finite solid-angle correction factors Q_k ($k = 1, \ldots, 6$) have been measured using the collimated-beam method. For seven source-detector distances, values of Q_k are given using three different thresholds in the measured pulse-height spectra for the gamma-ray energies 0.661 MeV and 1.25 MeV. The comparison between the experimentally determined attenuation factors and those calculated by using photo-peak and total gamma-ray attenuation coefficients shows some discrepancies for low threshold values in the pulse-height spectra. (auth)

29519 SEMICONDUCTOR CONTACTS TO SILICON SURFACE-BARRIER DETECTORS. Andersson, L. P.; Hyder, A.; Misra, M. (Uppsala Univ. (Sweden). Fysiska Institutionen). Nucl. Instrum. Methods; 118: No. 2, 537-539(15 Jun 1974).

The rectifying properties of evaporated and sputtered contacts of germanium and silicon on the (1,1,1) surface of n-type silicon crystals are studied. It is found that the coated germanium or silicon forms a barrier with a barrier height between 0.65 and 0.70 eV and that the formation of the barrier is dependent upon the processing used. (auth)

29520 N-TYPE CADMIUM TELLURIDE SURFACE-BARRIER NUCLEAR RADIATION DETECTORS. Dabrowski, A. J.; Iwanczyk, J. (Institute of Nuclear Research, Warsaw (Poland)); Triboulet, R. (Centre National de la Recherche Scientifique, 92–Meudon-Bellevue (France). Lab. de Magnetisme et de Physique du Solide). Nucl. Instrum. Methods; 118: No. 2, 531-535(15 Jun 1974).

Low-resistivity (10^2 to 10^4 cm) n-type CdTe surface-barrier detectors have been produced and measured. The energy resolution at 300°K was found to be 32 keV (fwhm) for 6.050 MeV α-particles and 14 keV (fwhm) for 59.5 keV γ-rays. The average energy required to produce the free electron-hole pair in n-type CdTe single crystals at 300 K for α-particles was determined experimentally, and a value of $\epsilon_{\mathrm{CdTe},\alpha} = 4.43 \pm 0.03$ eV was obtained. (auth)

29521 EXPERIMENTAL FLIGHT OF A LARGE SPHERICAL GAS SCINTILLATOR. Fowler, P. H.; Walker, R. N. F.; Moses, R. T.; Worley, A. (Bristol Univ. (UK). H. H. Wills Physics Lab.). Nucl. Instrum. Methods; 119: No. 2, 381-387(15 Jul 1974).

A spherical argon-nitrogen gas scintillation detector of diameter 119 cm has been constructed and operated successfully during a six-hour high-altitude balloon flight. Primary cosmic-ray nuclei in the charge range $14 \leq Z \leq 26$ were detected. The number of iron-group nuclei detected was consistent with previous results. This large detector, with a geometrical factor of 7 m^{2}sr, was designed as a simple engineering test on which to base the construction of larger, more versatile instruments. (auth)

29522 LATENT FADING IN SOLID-STATE TRACK ETCHING DETECTORS. Piesch, E.; Sayed, A. M. (Karlsruhe Nuclear Research Center, Health Physics Division, Karlsruhe, Germany). Nucl. Instrum. Methods; 119: No. 2, 367-371(15 Jul 1974).

Results are given for the latent track stability of fission fragments as well as neutron-induced recoils and α-particles found in Makrofol E and cellulose acetate after a storage time of up to 28 d at a temperature of 0 to 50°C and at relative air humidities of 0 to 97%. (auth)

29523 WAVELENGTH SHIFTERS FOR XENON PROPORTIONAL SCINTILLATION COUNTERS. Alves, M. A. F.; Dos Santos, M. C. M.; Policarpo, A. J. P. L. (Coimbra Univ. (Portugal)). Nucl. Instrum. Methods; 119: No. 2, 405-406 (15 Jul 1974).

Recent work with a xenon proportional scintillation counter (Xe PS counter) has shown that it features a good energy resolution; for example, full widths at half maximum of 500 eV and 100 eV are obtained for 5.9 keV and 277 eV, respectively. Detector capacitance, electronic or photomultiplier noises do not give any significant contribution to its performance. From 277 eV to 25 keV there is no nonlinearity of practical importance; and no peak shift was detected till about 10^5 counts per second. For the particular counters used the photomultiplier contribution to the resolution is important, slightly larger than that arising from the intrinsic parameters, the Fano factor and the energy per ion pair. Then, to improve the energy resolution, a good light-collection system together with an efficient wavelength shifter should be used. Relative efficiencies of p-terphenyl, sodium salicylate and p-quaterphenyl, as wavelength shifters for xenon proportional scintillation counters, are reported. (auth)

29524 HIGH SENSITIVITY PHOTONEUTRON DETECTOR FOR "NON-DESTRUCTIVE" SUBMICROANALYSIS OF BERYLLIUM. Quandt, U.; Herr, W. (Koeln Univ. (F.R. Germany). Inst. fuer Kernchemie). Nucl. Instrum. Methods; 119: No. 2, 279-285 (15 Jul 1974). (In German).

Submicrogram quantities of Be are determined "non-destructively" by utilizing photon activation. A special neutron counting device was developed consisting of 8 high-pressure, ^{10}B-enriched BF_3-counters installed into 1 m^3 of reactor-grade graphite with an outside paraffin reflector. In order to overcome "γ-pulse pile-up" effects, each of the $^{10}BF_3$-counters has an individual high-voltage supply and its own amplifier discriminator circuit. A strong ^{124}Sb γ-source (2 to 3 Ci) shielded by 70 kg of pure Bi-metal—the latter having a lower σ_{th} than Pb—was used. Because of an effective neutron-γ pulse discrimination, obtained by appropriate electronics and MCA spectroscopy as well, the neutron yield has been raised considerably. An additional shield of concrete (10 t) together with paraffin and 3000 l borated water reduced the background due to cosmic rays by a factor of ~40. By means of these improvements a lower detection limit (2σ) of 10 ppb Be was achieved in a counting time of 100 min. The minimum sample weight needed (10 g) is 10 times less than commonly required. Interferences of certain elements by neutron and γ self-absorption were considered by taking the respective calibration curves. Be contents down to 11 ppb were determined in normal rocks and in selected material of geological interest thus proving that the formerly reached "limit of detection" was put down by more than 2 orders of magnitude. (auth)

29525 FURTHER MEASUREMENT OF THE TRACK LENGTHS OF HEAVY IONS IN MICA. Blok, H.; Hanappe, F.; Kiely, F. M.; Pate, B. D.; Peter, J. (Simon Fraser Univ., Burnaby, British Columbia (Canada). Dept. of Chemistry). Nucl. Instrum. Methods; 119: No. 2, 307-312(15 Jul 1974).

The track lengths in mica track detectors have been measured for Al, Ar, Ca, Cr, Ni, Se, Kr, and Ag ions, in the energy range 0 to 1.5 MeV/amu. The data from this study (which show departures from monotonic dependence of the range on projectile charge, mass and energy) and from a previous study have been compared with relevant theories for the stopping of heavy ions in matter. It is concluded that the Lindhard-Scharff-Schiott theory does not apply well to this range of ion masses and energies. A relationship between the track length and the energy, mass (charge) of the ion has been derived. (auth)

29526 SOME FEATURES IN THE DEPENDENCE OF THE PULSE-HEIGHT DEFECT IN SEMICONDUCTOR DETECTORS ON DETECTED PARTICLE ENERGY. Kassirov, S. A.; Kovshevny, G. G.; Kotov, A. A.; Resnik, V. R.; Solyakin, G. E.; Terent'ev, N. K. (AN SSSR, Leningrad. Inst. Yadernoj Fiziki). Nucl. Instrum. Methods; 119: No. 2, 301-305(15 Jul 1974).

The pulse-height defect (PHD) in surface-barrier silicon detectors has been measured for (8 to 17) MeV ^{19}F, (4 to 18) MeV ^{27}Al, (7 to 25) MeV ^{40}Ca and (6 to 38) MeV ^{58}Ni ions. Ions have been obtained by elastic scattering of ^{252}Cf spontaneous-fission fragments on the appropriate scatterers. Simultaneous measurement of the semiconductor detector response and the time of flight for a given ion make it possible to determine PHD for every event. The results are discussed under assumption that there is a very thin surface layer that can account for the origin of the main part of the PHD. (auth)

29527 EFFECT OF ELECTRONS AND X-RAYS ON ALPHA-PARTICLE REGISTRATION IN T-CELLIT DETECTOR. Varnagy, M.; Csikai, J.; Szegedi, S. (Kossuth Lajos Tudomanyegyetem, Debrecen (Hungary). Kiserleti Fizikai Intezet). Nucl. Instrum. Methods; 119: No. 2, 261-267(15 Jul 1974).

Alpha-irradiated cellulose acetate (T-Cellit) foils were exposed to 1.7 MeV electrons as well as to x-rays from a 60 kV Roentgen tube. These foils were then etched with solutions of various compositions and temperature. The electron and x-ray irradiation caused marked changes in the bulk etching rate of the polymer and in the diameter of the alpha-particle tracks. These changes depend on the composition and temperature of the etchant as well as on the electron and x-ray doses. The possible consequences of the results are discussed. (78 references) (auth)

29528 LUMINESCENCE RESPONSE OF THIN PLASTIC SCINTILLATOR DETECTORS TO FISSION FRAGMENTS FROM PROTON-INDUCED FISSION OF ^{232}Th, ^{235}U AND ^{238}U. Muga, L.; Clem, A.; Griffith, G. (Florida Univ., Gainesville (USA)); Plendl, H. S.; Eaker, R.; Holub, R. (Florida State Univ., Tallahassee (USA)). Nucl. Instrum. Methods; 119: No. 2, 255-260(15 Jul 1974).

The luminescence response of a thin-film detector to fragments from the fission of ^{232}Th, ^{235}U, and ^{238}U induced by 10 to 18 MeV protons was determined. Measurements were made in coincidence with signals from a surface-barrier solid state detector, and the detector responses were displayed for each energy as two-parameter plots. Detector responses to ^{252}Cf spontaneous-fission fragments were determined for comparison. Results are consistent with previous work at comparable energies. The possible significance of a previously observed change in symmetric-to-asymmetric fission ratio near 15 MeV bombarding energy, and the applicability of thin-film detectors to identification of unknown fissioning nuclides are discussed. (auth)

29529 DEAD-TIME CALIBRATOR. Zidek, V.; Plch, J. (Institute for Research, Production and Application of Radioisotopes, Prague, Czechoslovakia). Nucl. Instrum. Methods; 119: No. 2, 247-249(15 Jul 1974).

In many cases the accuracy of the counting rate determination is limited by an error of the dead-time correction. This problem is very serious in the field of absolute activity measurements. It can be solved if an optimal arrangement of the counting system is found which is characterized by a single dead time and if this dead time can be measured accurately. A method of dead-time measurement based on the time interval density measurement is proposed. (auth)

29530 A PERTURBATION METHOD FOR CALCULATING THE RATE OF CHARGE COLLECTION IN A SEMICONDUCTOR DETECTOR. El-Kharadly, L. A.; El-Ibiary, M. Y. (Cairo Univ. (Egypt). Faculty of Engineering). Nucl. Instrum. Methods; 119: No. 1, 113-116(1 Jul 1974).

A new method for calculating the rate of charge collection in a semiconductor detector is introduced in which the motion of a charge carrier is treated as a perturbation to the space charges and electric potentials created within the detector by the bias voltage. The method leads to a formula which is applicable to partially depleted, punch-through, and over-biased detectors of any shape. The analysis allows for the presence of fixed charges and for the discontinuity in the electric field and potential of mobile point charges. The results of the new approach confirm the contention that Ramo's theorem is always suitable for calculating the rate of charge collection in a semiconductor detector and that the power-balance approach cannot be used except in the case of a fully compensated detector. A discussion of the theoretical treatment and the experimental observations of Strokan et al. which were considered to support the power-balance approach, is given. (auth)

29531 SEMICONDUCTOR COUNTERS FOR NUCLEAR RADIATIONS PRODUCED BY ION IMPLANTATION. Peterstroem, S.; Holmen, G. (Chalmers Tekniska Hoegskola, Goeteborg (Sweden). Institutionen foer Fysik). Nucl. Instrum. Methods; 119: No. 1, 151-155(1 Jul 1974).

Junction counters for nuclear radiations without a metal layer on the sensitive surface have been produced by ion implantation in high-resistivity silicon at room temperature. The p-n junction was made by a boron implant, surrounded by a ring-shaped aluminium implant giving good electrical contact to the boron layer.

The energy resolution and the window thickness of the counters were measured after annealing at different temperatures. Two counter sizes were produced. Counters of 10 mm diameter, annealed at 275°C, had a best resolution of 17 keV measured at room temperature. Counters of 15 mm diameter, annealed at 275°C were tested at both room temperature and 77°K. The resolution was found to be 24 and 16 keV, respectively, which agrees with theoretical estimates. A window thickness of 0.1 μm was obtained for the best of the counters. Some of the counters have been used in medical applications and have proved to resist influence of the environment much better than surface barrier detectors. (auth)

29532 THE ETCHING OF CELLULOSE NITRATE PLASTIC. Gruhn, T. A.; Benton, E. V.; Andrus, C. H. (San Francisco Univ., Calif. (USA). Dept. of Physics). Nucl. Instrum. Methods; 119: No. 1, 131-133(1 Jul 1974).

The mechanism of etching of a cellulose nitrate track detector employing camphor as plasticizer has been studied. It was found that nitrocellulose itself is rapidly degraded by common hydroxide etchants to soluble, non-polymeric species. Camphor, on the other hand, is not attacked by the etchants nor is it soluble in them to any great extent. Thus, as etching proceeds a layer of camphor builds up at the surface. This layer is the principal factor governing the nature of the etching for a given set of conditions. Differences in reactivity of the alkali hydroxides are explained in terms of their differing solubilities in organic media. Studies of this type are aimed toward a more fundamental understanding of the bulk and track etch processes. (auth)

29533 SPHERICAL HARMONIC ANALYSIS OF SATELLITE ANISOTROPY MEASUREMENTS. Sanderson, T. R.; Page, D. E. (European Space Research and Technology Centre, Noordwijk (Netherlands)). Nucl. Instrum. Methods; 119: No. 1, 177-182 (1 Jul 1974).

A method is described whereby a particle distribution measured by a detector telescope mounted on a spinning satellite can be represented by an equivalent set of spherical harmonics. The response of the telescope is determined for each term of the harmonic expansion, and fitted to a set of satellite data, enabling the zero order, and first and second harmonics to be found. The effects of sectoring are introduced, and the limitations of both the sectoring and the finite telescope opening angle upon the angular resolution are evaluated. A method is outlined for including particle scattering in the calculations. (auth)

29534 PRELIMINARY RESULTS ON MERCURIC IODIDE NUCLEAR RADIATION DETECTORS. Ponpon, J. P.; Stuck, R.; Siffert, P. (Centre National de la Recherche Scientifique, 67—Strasbourg (France). Lab. de Physique des Rayonnements et d'Electronique Nucleaire); Schwab, C. (Strasbourg-1 Univ., 67 (France)). Nucl. Instrum. Methods; 119: No. 1, 197-198(1 Jul 1974).

Nuclear radiation detectors prepared on red mercuric iodide single crystals grown by a vapor-phase technique are investigated with regard to detection performance, energy requested per electron-hole pair and charge carrier mobility. Polarization phenomena are also considered. (auth)

29535 A FAST NEUTRON-GAMMA DISCRIMINATOR. Betz, P.; Braun, G.; Hammel, G.; Urban, J. (Freiburg Univ. (F.R. Germany). Fakultaet fuer Physik). Nucl. Instrum. Methods; 119: No. 1, 199-203(1 Jul 1974).

In the past many pulse-shape discrimination (PSD) circuits have been developed to distinguish between neutrons and gammas detected in organic scintillators. In most cases time-to-amplitude converters (TAC) are used to measure the time difference between the zero crossing points of the doubly clipped pulses corresponding to neutrons and gammas, respectively. Because of the long processing time involved using these systems (~5 μs) the PS information must always be added to the fast-timing information by a slow coincidence. The circuit described provides the PS information within 300 ns and allows to gate the fast-timing signal with the logic neutron or gamma information. (auth)

29536 THE PERFORMANCE OF SINGLE CHARGED-PARTICLE DETECTORS UNDER ISOTROPIC IRRADIATION. Kolchin, A. A.; Lebedev, V. V.; Skrebtsov, G. P. (AN SSSR, Leningrad. Fiziko-Tekhnicheskij Inst.). Nucl. Instrum. Methods; 119: No. 1, 93-96(1 Jul 1974).

The following characteristics are considered for a single detector under isotropic irradiation: (a) geometric factor with a non-zero energy threshold; (b) path-length distribution of particles passing through the detector; (c) energy-loss distribution of charged particles passing through the detector; (d) gamma-radiation detection efficiency. The concept of a detector-response function is introduced for the case of isotropic radiation flux. The relation between these characteristics and the ways of their derivation are shown. The first two of these characteristics are obtained for detectors with the sensitive volume in the form of a sphere, a parallelepiped, and a rectangular cylinder. (auth)

29537 THE EFFECT OF FRAGMENT ANISOTROPY ON FISSION-CHAMBER EFFICIENCY. Carlson, G. W. (California Univ., Livermore (USA). Lawrence Livermore Lab.). Nucl. Instrum. Methods; 119: No. 1, 97-100(1 Jul 1974).

A method is given for calculating the inefficiency of a fission chamber because of the loss of fragments in the foil. The method includes the effects of the anisotropy in the fragment angular distribution because of both angular and linear momentum given to the nucleus by the incident neutron. A numerical example for a ^{239}Pu chamber shows that the linear-momentum effect is larger than the angular-momentum effect, but less than 1% at neutron energies below 15 MeV. (auth)

Radiation Dosimeters

29538 (COO-1105-212) THERMOLUMINESCENT RESPONSE OF TLD-100 TO 1 TO 25 keV ELECTRONS. Progress Report, July 15, 1973—July 15, 1974. Laskey, J. B.; Moran, P. R. (Wisconsin Univ., Madison (USA)). [nd]. Contract AT(11-1)-1105. 6p. Dep. NTIS $4.00.

LiF (TLD-100) high sensitivity ribbons have been irradiated with monoenergetic electrons (1 to 25 keV). Irradiations necessarily occur in a specially constructed vacuum chamber since the electron ranges are short even in air. Ribbons exposed to 5 and 25 keV electrons have a much higher TL response near 100°C than when they are irradiated with ^{137}Cs gammas. Except for these shape differences, the TL response vs. dose is not unlike that for ^{137}Cs, but at 1 kV no supralinearity is observed. For a constant number of electrons striking the samples the TL response increases roughly as the cube of the electron energy. Implications are discussed. (auth)

29539 (DEMO-74/5) INTERNATIONAL INTERCOMPARISON OF CHEMICAL DOSIMETERS FOR IN-PILE USE. A Report of Measurements Made in the Greek Research Reactor-1 at Nuclear Research Center "Democritos", Athens, Greece, 3—8 July 1972 by Eight Reactor Calorimetry and Radiation Chemistry Groups from Eight Member States of the IAEA. Marketos, D. G.; Boyd, A. W. (eds.). *(Democritus Nuclear Research Center, Athens Greece)).* Apr 1974. 80p. Dep. NTIS (US Sales Only) $7.00.

Separate abstracts were prepared for the 12 papers presented. *(WHK)*

For abstracts of individual papers see: 29540—29550 and 31230.

29540 *(DEMO-74/5, pp 10-14) MEASUREMENTS WITH THE* SWIERK CALORIMETER. Panta, P. P. (Inst. of Nuclear Research, Warsaw). Feb 1973.

A description is presented of the Swierk calorimeter which is an isothermal or constant temperature type calorimeter. It contains a graphite sample and chromel-alumel thermocouple. Calibration measurements are described and the absorbed dose rates of mixed pile radiation are given. (INIS)

29541 (DEMO-74/5, pp 15-19) MEASUREMENTS WITH HUNGARIAN CALORIMETER. Bod, L. (Kozponti Fizikai Kutato Intezet, Budapest). Feb 1973.

A description is presented of the Hungarian calorimeter which is an isothermal or steady state temperature difference type calorimeter. It contains a graphite sample and copper-constantan thermocouple. Calibration measurements are described and the absorbed dose rates are given. (INIS)

29542 (DEMO-74/5, pp 20-22) MEASUREMENTS WITH THE CHALK RIVER CALORIMETER. Boyd, A. W. (Chalk River Nuclear Labs., Ont.). Feb 1973.

A description is presented of the Chalk River calorimeter which is designed to determine the absorbed dose rate in graphite. It is operated in the quasi-adiabatic mode. Calibration measurements are described and the absorbed dose rates tabulated. *(INIS)*

29543 (DEMO-74/5, pp 23-25) MEASUREMENTS BY ISOTOPE EXCHANGE BETWEEN ^{14}CO AND ^{12}CO$_2$. Wickham, A. J. *(Central Electricity Generating Board, Berkeley, Eng.). Feb* 1973.

A description is presented of a chemical dosemeter using isotopic *exchange between CO and CO$_2$ as a measure for absorbed* radiation dose. Silica ampoules were used and the CO labelled with ^{14}C. The progress of isotope exchange reactions is presented and absorbed dose rates given. (INIS)

29544 (DEMO-74/5, pp 26-30) MEASUREMENTS BY FLUOROCARBON DOSIMETRY. Proksch, E.; Gehringer, P. (Oesterreichische Studiengesellschaft fuer Atomenergie GmbH, Seibersdorf, Austria). Feb 1973.

A description of gamma dose rate measurements using radiolytic decomposition of fluorocarbons is presented. The method consists in measuring the production of F-cyclohexane (C_6) from irradiated F-methylcyclohexane (C_7) by gas chromatography. The preparation of the samples and the dose rates measured are discussed. (INIS)

29545 (DEMO-74/5, pp 31-34) MEASUREMENTS WITH THE HYDROGEN SULFIDE DOSIMETER. Boyd, A. M. (Chalk River Nuclear Labs., Ont.). Feb 1973.

A description of a hydrogen sulfide dosemeter is given. The hydrogen sulfide was contained in a quartz capsule and the absorbed dose rate values are tabulated. (INIS)

29546 (DEMO-74/5, pp 35-43) RADIOCHROMIC DOSIMETRY MEASUREMENTS. Humpherys, K. C. (EG and G, Inc., Santa Barbara, CA). Feb 1973.

A description is presented of two colorimetric dosemeters, a nylon solid solution of hexahydroxyethyl pararosaniline-cyanide and a polychlorostyrene solid solution of malachite green-methoxide. The experimental irradiation, and calibration is described and the absorbed dose rates tabulated. (INIS)

29547 (DEMO-74/5, pp 44-52) MEASUREMENTS WITH DICARBOXYLIC ACID DOSIMETERS. Gal, O.; Draganic, I. (Institut za Nuklearne Nauke Boris Kidric, Belgrade). Feb 1973.

A description is presented of radiation dose rate measurements using three systems of dicarboxylic acid dosemeters: aqueous oxalic acid, solid oxalic acid and solid succinic acid. The experimental procedure and the obtained values of dose rates are tabulated. (INIS)

29548 (DEMO-74/5, pp 53-60) MEASUREMENTS WITH AQUEOUS OXALIC ACID. Panta, P. P. (Inst. of Nuclear Research, Warsaw). Feb 1973.

A description is presented of radiation dose rate measurements using an aqueous oxalic acid dosemeter. The experimental procedure and the obtained values of dose rates are tabulated. (INIS)

29549 (DEMO-74/5, pp 61-63) MEASUREMENTS WITH CYCLOHEXANE DOSIMETERS. Boyd, A. W. (Chalk River Nuclear Labs., Ont.). Feb 1973.

A radiation dosemeter based on cyclohexane is described. The cyclohexane is enclosed in a quartz capsule. The absorbed dose rates are presented. (INIS)

29550 (DEMO-74/5, pp 64-68) GENERAL DISCUSSION AND SUMMARY. Boyd, A. W. (Chalk River Nuclear Labs., Ont.). Feb 1973.

This summary presents, for purposes of comparisons, all the results obtained for absorbed dose rate values by calorimetry and chemical dosimetry which are described in detail in each of the individual papers of the conference. (INIS)

29551 (LA-UR-74-1232) PASSIVE ENVIRONMENTAL NEUTRON DOSIMETER. Apt, K. E.; Schiager, K. J. (Los Alamos Scientific Lab., N. Mex. (USA)). 1974. Contract W-7405-eng-36. 8p. (CONF-740701-2). Dep. NTIS $4.00.

From 2nd international conference on nuclear methods in environmental research; Columbia, Missouri, USA (29 Jul 1974).

A passive environmental neutron dosimeter has been developed for use in the environs of the Clinton P. Anderson Meson Physics Facility. The dosimeter is a 0.25-m-diam spherical polyethylene moderator which incorporates 2 fission-fragment track registry assemblies. Enriched ^{235}U serves as the fission radiator, and 10-μm-thick polycarbonate foil is the fission-track registry material. Latent fission tracks are chemically etched with base and subsequently counted with an automatic digital spark counter system. The neutron dosimeter is insensitive to radiation other than neutrons, and an exposed registry foil becomes a permanent record of integrated neutron dose equivalent. The dosimeter response is approximately proportional to the incident neutron dose equivalent. Calibration and field exposures indicate that dose equivalent values as low as 0.1 mrem can be accurately measured. The environmental neutron dosimeter in conjunction with thermoluminescent dosimetry materials has been used to characterize environmental radiation levels resulting from nuclear accelerator operations. (auth)

29552 (UCID-15836) ELECTRONICS FOR THE LRL AUTOMATED PERSONNEL THERMOLUMINESCENCE DOSIMETRY SYSTEM. Shapiro, E. G.; Jones, D. E.; Petrock, K. F.; Samardzich, B. G. (California Univ., Livermore (USA). Lawrence Livermore Lab.). 17 May 1971. Contract W-7405-eng-48. 21p. Dep. NTIS $4.25.

The electronics associated with the LRL thermoluminescence dosimetry system have two separate functions: to encode the employee identification number on a TLD personnel badge and to decode and record the badge identification number with its associated TLD data. The data are recorded on a computer card, which is then used to update the individual employee's dosimetry file. A detailed description of both modes of operation is given. (WHK)

29553 OPTIMAL ANNEALING OF NATURAL BERYL FOR THERMOLUMINESCENT DOSIMETRY. Moon, P. S. (Atomic Energy Research Inst., Seoul). J. Korean Nucl. Soc.; 6: No. 1, 3-8(Mar 1974).

Annealing of natural beryl powder used for thermoluminescent dosimetry was investigated in order to eliminate the effects of previous exposure. Through analysis of the glow curve, the optimal annealing treatment was found to be one-hour annealing at 1450°C, but annealing for one hour at 550°C was sufficient for reuse of natural beryl powder. There are two distinguished glow peaks at 65°C and 200°C of heating temperature during readout process. The 65°C glow peak fades away rapidly, but the 200°C glow peak remains very stable. It is, therefore, quite feasible to use the 200°C glow peak for thermoluminescent dosimetry. (7 figures) (auth)

29554 DISCRIMINATION OF NEUTRON ENERGIES WITH THE AID OF THE NUCLEAR TRACK METHOD. Faengewisch, G. L.; Scharmann, A. (Giessen Univ. (F. R. Germany). 1. Physikalisches Inst.). Kerntechnik; 16: No. 5, 193-197(May 1974). (In German, English).

4 figs.; 13 refs. Part of a thesis by Faengewisch, G. L.

The nuclear track method is increasingly used in neutron dosimetry. Additional information on the energy of the impinging neutrons can be obtained by making use of neutron-induced threshold reactions. In principle, it is possible to use (n,f) and (n,α) reactions. As the use of fissionable materials presents certain disadvantages, the experiments described in this paper were based on the use of (n,α) converters. If dosimeter sandwiches, consisting of materials entering into (n,α) reactions and of nuclear track detectors sensitive to alpha particles, are irradiated with fast neutrons it is possible to clearly distinguish between, for example, 3.3 MeV neutrons, 14.9 MeV neutrons and fission neutrons. This is due to differences in the sensitivity of individual converter/detector combinations based on the energy dependence of the response of the detector to neutrons and of the cross-section of the (n,α) reaction induced in the converters. (auth)

29555 DOSIMETRY OF THE SIN BIOMEDICAL PION BEAM WITH TISSUE-EQUIVALENT IONIZATION CHAMBERS. Cabeza, L. (Zurich Univ. (Switzerland). Strahlenbiologisches Inst.). Fortschr. Geb. Roentgenstr. Nuklearmed.; 121: No. 1, 109-114(Jul 1974).

4 figs.; 2 tabs.; 26 refs.

Small, tissue-equivalent ionization chambers with high-pressure gas filling are described. Their calibration with a calorimeter is discussed, and the advantages of comparisons with Monte Carlo calculations of absorbed dose and with a biological dosimeter are examined. (auth)

29556 CALORIMETRIC AND IONIZATION MEASUREMENTS OF STOPPING POWER IN CARBON FOR 19.5 GeV ELECTRONS. Kase, K. R.; Domen, S. R. (Stanford Linear Accelerator Center, Calif. (USA)). Nucl. Instrum. Methods; 118: No. 2, 469-475 (15 Jun 1974).

A portable carbon calorimeter built at the National Bureau of Standards was used in a 19.5 GeV electron beam at the Stanford Linear Accelerator to measure the absorbed dose. The dose measurements were normalized to a given number of incident electrons by monitoring the electron intensity with a transmission ion chamber previously calibrated against a quantameter in the same beam. The simultaneous measurements of integrated electron intensity and absorbed dose allowed a direct determination of stopping power in carbon for 19.5 GeV electrons. The measured value of 1.80 MeV cm^2/g is within 6% of the calculated value. (auth)

29557 FAST-NEUTRON PERSONNEL DOSIMETRY WITH SOLID-STATE TRACK RECORDERS. Gold, R. (Joint Center for Graduate Study, Richland, Washington, USA); Armani, R. J.; Rusch, G. K.; Yule, T. J. (Argonne National Lab., Ill. (USA)). Nucl. Instrum. Methods; 118: No. 2, 383-399(15 Jun 1974).

Aluminum-covered and cadmium-covered Solid-State Track Recorders (SSTR) consisting of pre-etched mica and asymptotically thick ^{235}U foils have been used to monitor the fast-neutron dose received by personnel at the Zero-Power Reactor (ZPR) facilities (Argonne-East). Neutron spectra and absolute integral measurements were carried out at representative locations throughout the ZPR working environment. SSTR dosimeters were exposed at the same locations. Doses inferred from the SSTR data are compared to those derived from the measured neutron spectra or to doses determined with portable rem meters. On this basis, the applicability of the SSTR dosimetry method has been (conservatively) established. (auth)

Nuclear Spectroscopic Instrumentation

Refer also to abstracts 30159 and 31125.

29558 (IFA-FN-44-1974) RESOLUTION FUNCTION FOR THE ROTATING-CRYSTAL SPECTROMETER. Popa, N. C. (Institutul de Fizica Atomica, Bucharest (Romania)). 1974. 24p. Dep. NTIS (U. S. Sales Only) $4.25.

The resolution function in the $(\vec{Q},\omega)$ space for the rotating-crystal time-of-flight spectrometer is defined. All the instrumental components bringing a contribution to the uncertainties in the measured energy and momentum transfers are taken into account. A detailed analysis of the monochromator unit transmission, including the Doppler effect influence, is presented. An analytic expression is derived for the resolution function in the Gaussian approximation. (auth)

29559 (IFA-FN-45-1974) RESOLUTION OF SLOW NEUTRON SPECTROMETERS. I. General Method to Calculate the Resolution Function. II. Resolution Function for Time of Flight Diffractometry. Stoica, A. D. (Institutul de Fizica Atomica, Bucharest (Romania)). 1974. 27p. Dep. NTIS (U. S. Sales Only) $4.50.

Starting from a general definition of the resolution function one gets a rigorous method of calculating the shape of this function. In the computation the tensors of the probability moments of the parameters controlled in the measuring device are used. The application to TDF neutron spectrometry is discussed. (auth)

29560 (JUL-1050-FF) THEORY OF MULTI-VARIABLE CORRELATION TECHNIQUES FOR TIME-OF-FLIGHT EXPERIMENTS. Amadori, R. (Kernforschungsanlage Juelich G.m.b.H. (F. R. Germany). Inst. fuer Festkoerperforschung; Technische Hochschule Aachen (F.R. Germany)). Mar 1974. 149p. (In German). INIS.

17 figs.; 12 tabs.; 51 refs. With abstract.

The determination of the energy distribution of particles by means of time-of-flight spectrometry is equivalent to the problem of the identification of linear systems, in particular to the determination of the response function of linear systems. Following a presentation of the fundamentals of the correlation methods for the determination of the response function and a few general aspects of the system identification, specific higher correlation functions of binary pseudostatistic sequences are derived. The known results of the correlation method for uni-variable systems with Poisson statistics are compiled and optimization possibilities are dealt with in detail. By using the properties of non-correlated binary pseudostatic sequences, the correlation method is applied to two different time-of-flight experiments which correspond to specific multi-variable systems, and is derived assuming the Poisson statistics gain factors of these multi-variable correlation methods compared with the corresponding conventional methods. Finally, the extent to which a certain type of digital filtering of the response function can increase the gain factors for systems with Poisson statistics is investigated for the uni-variable correlation method as well as for the multivariable correlation methods considered. (auth)

29561 METHODS, APPARATUS, AND FLEXIBLE CONTAINERS FOR HANDLING LIQUID SAMPLES FOR SCINTILLATION SPECTROMETRY. (to Packard Instrument Co.). Netherlands Patent 7,214,381. 24 Oct 1972. Priority Date 26 Oct 1971, USA. 15p. (In Dutch).

A sample container for liquid scintillation spectrometry analysis is described. The container is in the form of a flexible bag made up of a layered, light-transmissive polyester film which is heat sealed. A centrally disposed flask-like portion is circular in the plane of the layers with a diameter approximating the diameters of the photomultiplier tubes. Thus an optimum counting geometry for the container structure is provided. The provision of the flexible containers in a continuous strip enables a simplified handling in the detection apparatus. The sample containers are squeezed in between the photomultiplier tubes. The close optical coupling between the tubes and the container minimizes lost light. (NL)

29562 GAMMA-RAY ATTENUATION IN APPLIED SCINTILLATION SPECTROMETRY. Polyakov, V. I.; Chechetkin, Yu. V. Sov. At. Energy (Engl. Transl.); 35: No. 4, 939-940 (Oct 1973).

Translated from At. Energ. (USSR); 35: No. 4, 274-275(Oct 1973).

The γ-ray attenuation coefficient was calculated for making corrections in γ spectra measurements. The energy dependence of the γ-ray attenuation coefficient is plotted. (WHK)

29563 A METHOD OF ON-LINE SPECTRA EVALUATION BY MEANS OF A SMALL COMPUTER EMPLOYING FOURIER TRANSFORMS. Blinowska, K. J.; Wessner, E. F. (Oesterreichische Studiengesellschaft fuer Atomenergie G.m.b.H., Seibersdorf. Forschungszentrum). Nucl. Instrum. Methods; 118: No. 2, 597-604(15 Jun 1974).

A method of on-line gamma-spectra evaluation by means of a small computer, employing Fourier transforms, is described. The program performs the acquisition and recording of data, then the Fourier transform properties are used to smooth the spectra. By employing appropriate apparatus functions in the transform domain an improvement of resolution is achieved which permits in cases of good statistics to resolve peaks spaced as close as 1/10 of fwhm. The program is written partly in PALF-Assembler, partly in FOCAL-12 and can be run on a PDP-12 computer with 8k memory. With slight changes it is also possible to run it on a PDP-8. (auth)

29564 A HIGH-RESOLUTION MASS-IDENTIFICATION SYSTEM FOR HEAVY IONS. Zeidman, B.; Henning, W.; Kovar, D. G. (Argonne National Lab., Ill. (USA)). Nucl. Instrum. Methods; 118: No. 2, 361-365(15 Jun 1974).

A ΔE-E surface-barrier detector time-of-flight telescope in heavy-ion reactions yields 150 keV energy resolution and 84 ps time resolution in routine operation. Fast analog circuitry, pile-up rejection, and direct computer-memory access allow high count rates that are desirable for the study of heavy-ion transfer reactions at extreme forward angles. (auth)

29565 A 1Ge(Li)-3NaI(Tl) DETECTOR SYSTEM FOR γ-γ ANGULAR CORRELATION MEASUREMENTS. Hayashi, T.; Uehara, S.; Seo, T. (Kyoto Univ., Kumatori, Osaka (Japan). Research Reactor Inst.). Nucl. Instrum. Methods; 118: No. 2, 541-545(15 Jun 1974).

A multi-detector system consisting of one Ge(Li) and three NaI(Tl) detectors has been constructed for measuring γ-γ angular correlations. In the present apparatus the angular positions of the three NaI(Tl) detectors are interchanged in cyclic repetition, so that different characteristics of the NaI(Tl) detectors and associated circuitries can be averaged. Whole operations including goniometer driving and data taking are performed automatically under the instruction of a programmed controller. The performance of the system has been tested by measuring the g-factor of the 100 keV level in ^{182}W. (auth)

29566 THE APOLLO GAMMA-RAY SPECTROMETER. Harrington, T. M.; Marshall, J. H. (MDH Industries, Inc., Pasadena, California, USA); Arnold, J. R.; Peterson, L. E. (California Univ., La Jolla, San Diego (USA)); Trombka, J. I. (National Aeronautics and Space Administration, Greenbelt, Md. (USA). Goddard Space Flight Center); Metzger, A. E. (California Inst. of Tech., Pasadena (USA)). Nucl. Instrum. Methods; 118: No. 2, 401-411(15 Jun 1974).

A γ-ray spectrometer has been flown on the Apollo 15 and 16 spacecrafts to determine the lunar-surface composition and measure the cosmic γ-ray flux. The instrument included a NaI(Tl) scintillation crystal coupled to a 7.6 cm photomultiplier tube, a plastic mantle for anti-coincidence rejection of charged particles, and 511 channels of analysis. Boom-mounted operation permitted a significant reduction in the background. The data were transmitted on an event-by-event basis. About 22% of the lunar surface was mapped and spectra of the cosmic γ-ray flux over an energy range of 0.065 to 27.5 MeV have been obtained. (auth)

29567 EXPERIMENTAL EQUIPMENT FOR SPECTROMETRY OF ELECTRONS AND PROTONS BETWEEN 0.4 AND 30 keV ABOARD THE AUREOLE SATELLITE. Guyader, J. C.; Bouyssou, J.; Crasnier, J.; Sauvaud, J. A. (Toulouse-3 Univ., 31 (France). Centre d'Etude Spatiale des Rayonnements). Nucl. Instrum. Methods; 118: No. 2, 497-503(15 Jun 1974). (In French).

The equipment for the ARCADE program aboard the AUREOLE satellite is described, more particularly the low-energy spectrometers for measuring protons and electrons between 0.4 and 30 keV. These spectrometers, consisting of an electrostatic analyzer and a measuring system operating at constant current with a windowless electron multiplier, are well adapted for detection of auroral particles. Examples of the results of the ARCADE experiment are given. (auth)

29568 8192-CHANNEL SQUARE-ROOT PULSE-HEIGHT ANALYZER. Binns, W. R.; Carpenter, H. C. (McDonnell Douglas Corp., St. Louis, Mo. (USA)). Nucl. Instrum. Methods; 119: No. 2, 355-360(15 Jul 1974).

A versatile, high-precision, 8192-channel, square-root pulse-height analyzer which possesses an unusually large dynamic range of 1000 is described. This instrument was developed for use in a balloon-borne cosmic-ray detector but can easily be adapted to other detector systems. (auth)

29569 ENERGY SPECTROMETRY OF PROTONS BY MEANS OF A DIELECTRIC TRACK DETECTOR. Lueck, H. B. (Zentralinstitut fuer Kernforschung, Rossendorf bei Dresden (German Democratic Republic)). Nucl. Instrum. Methods; 119: No. 2, 403-404(15 Jul 1974).

The energy resolution of a cellulose nitrate detector has been investigated in a range from 500 to 1600 keV. The full width at half-maximum (fwhm) has been found to improve from 50 to 25 keV with increasing energy. (auth)

29570 A SUMMING Ge(Li)-COMPTON SPECTROMETER. Ivanov, V. B.; Shipilov, V. I. (State Committee of Atomic Energy, Scientific Research Institute of Atomic Reactors, Dimitrovgrad, USSR). Nucl. Instrum. Methods; 119: No. 2, 313-320(15 Jul 1974).

The experimental results of the investigation of a summing Compton spectrometer based on two planar Ge(Li) detectors made in a single germanium ingot are presented. It is shown that the spectrometer beginning with a background-to-useful activities ratio equal to 4 has a better sensitivity than a single-crystal spectrometer in the energy range 0.5 to 2 MeV. Theoretical expressions have been given for the comparison between γ-spectrometers. (auth)

29571 SPECTROMETER FOR ON-LINE ANALYSIS OF RADIONUCLIDES (SOLAR). Stoffels, J. J. (Battelle Pacific Northwest Labs., Richland, Wash. (USA)). Nucl. Instrum. Methods; 119: No. 2, 251-254(15 Jul 1974).

A mass spectrometer has been built for on-line analysis of fission product nuclides. The spectrometer ion source is located inside the thermal column of a TRIGA reactor and consists of a high-temperature oven containing fissile target material. Fission product nuclides born in the target are thermally ionized and accelerated out of the reactor through a 2.3 m long flight tube. Outside the reactor the ion beam is deflected 90° by an electrostatic mirror. Mass analysis of the ions takes place in a 30.5 cm radius, 60° deflection magnetic field. The system is intended initially to measure relative independent and cumulative yields of Rb, Cs, Br, and I isotopes with half-lives as short as 0.1 s. Other applications include nuclear spectroscopy, delayed-neutron emission measurements, and measurements of nuclidic masses and nuclear moments of the separated isotopes produced by the system. (auth)

29572 THE RESOLUTION FUNCTION FOR THE ROTATING-CRYSTAL SPECTROMETER. Popa, N. C. (Institutul de Fizica Atomica, Bucharest (Romania)). Nucl. Instrum. Methods; 119: No. 2, 237-246(15 Jul 1974).

The resolution function in (Q,ω) space for the rotating-crystal time-of-flight spectrometer is defined. All the instrumental components giving contributions to the uncertainties in the measured energy- and momentum-transfers are taken into account. A detailed analysis of the monochromator-unit transmission, including the Doppler effect influence, is presented. An analytic expression is derived for the resolution function in the Gaussian approximation. (auth)

29573 PERFORMANCE OF A HEAVY-ION TIME-OF-FLIGHT SPECTROMETER. Cormier, T. M.; Galik, R. S.; Cosman, E. R.; Lazzarini, A. J. (Massachusetts Inst. of Tech., Cambridge (USA). Dept. of Physics). Nucl. Instrum. Methods; 119: No. 1, 145-150 (1 Jul 1974).

A heavy-ion time-of-flight spectrometer has been brought into operation at the Brookhaven National Laboratory (BNL) MP tandem-Van-de-Graff facility. The start detector consists of a very thin plastic scintillation detector and the stop detector is a commercial surface-barrier detector. The design and operation of the spectrometer are discussed. An overall time resolution of ~0.3 ns is found to be routinely attainable under realistic experimental conditions. Plans to include a magnetic quadrupole lens in the flight path as well as the ultimate application of the spectrometer are discussed. (auth)

29574 A SIMPLE METHOD OF ORIENTATING SINGLE CRYSTALS ON TIME-OF-FLIGHT NEUTRON SPECTROMETERS. Minor, W.; Rajca, A.; Giebultowicz, T. (Warsaw Univ. (Poland). Instytut Fizyki Doswiadczalnej). Nucl. Instrum. Methods; 119: No. 1, 141-144(1 Jul 1974).

A method is presented for orientating single crystals of any structure directly on a time-of-flight neutron spectrometer. In this method white radiation is used as in the Laue diffraction technique. While neutron Laue diffraction patterns are difficult to obtain, the information necessary for orientating the crystal can be obtained from the spectra of transmitted neutrons. The transmission patterns are easily measured by using an additional detector. The results of orientating a zinc single crystal are presented as an experimental test. (auth)

29575 A LARGE PLASTIC SCINTILLATOR AS ANTICOINCIDENCE SHIELD FOR BETA-RADIATION DETECTORS. Roedel, W.; Peter, H. (Heidelberg Univ. (F. R. Germany). 2. Physikalisches Inst.). Nucl. Instrum. Methods; 119: No. 1, 135-139 (1 Jul 1974).

The response of a NE 102A plastic scintillator, 600 mm in diameter and 600 mm long, to electrons and thus to cosmic-ray secondaries (especially to neutrons) has been investigated. The background of a beta-ray detector placed into a well of the scintillator has been studied. By anticoincidence operation the background of the beta-ray detector is reduced by a factor of 37, but no statistically significant correlation between the beta-detector background and the response of the scintillator to neutrons could be found. The minimum background rate of the beta detector (with 1.5″ window diameter) is 0.155 counts per minute. (auth)

High Energy Physics Instrumentation

Refer also to abstract 30574.

29576 REFRIGERATING SYSTEMS FOR THE BIG CERN BUBBLE CHAMBER. Giger, U.; Pagani, P.; Trepp, C. (Sulzer Bros. Ltd., Winterthur, Switzerland). Sulzer Tech. Rev.; 56: No. 2, 54-60(1974).

A combined helium-hydrogen refrigerator has been installed for cooling the new CERN bubble chamber at Geneva. The cool-down of the bubble chamber and magnet, as well as emergency operation and control of the refrigerator are described. Besides the choice of basic conception and circuit, the plant components are dealt with too. The function of the bubble chamber and the development of the CERN proton synchrotron are described in order to facilitate understanding of the relationship between the Sulzer cryogenic plant and the CERN bubble chamber. Installations and equipment not manufactured by Sulzer are also mentioned. (auth)

29577 INVESTIGATION OF A 90-CHANNEL Pb GLASS CHERENKOV HODOSCOPE. Astvatsaturov, R. G.; Ivanv, V. I.; Knapik, E.; Khachaturyan, M. N.; Khvastunov, M. S.; Kramarenko, V. A.; Kulakov, B. A.; Malakhov, A. I.; Melkumov, G. L. (Joint Inst. for Nuclear Research, Dubna, USSR). Nukleonika; 19: No. 6, 575-581(1974). (In Russian).

The properties of the 90-channel Pb glass Cherenkov hodoscope were investigated in the electron beam at 2.3 and 5 GeV. The average energy resolutions (full width at half maximum) are as follows: 2.0 GeV, 7.2%; 3.0 GeV, 6.0%; and 4.0 GeV, 5.3%. (auth)

29578 100-CHANNEL SCINTILLATION TELESCOPE. Alekseev, E. N.; Bakatanov, V. N.; Voevodskii, A. V.; Dadykin, V. Ya.; Kozerivskii, V. A.; Konovalov, Yu. N.; Maslov, V. N.; Mikheev, S. P.; Stepanov, V. I. Kosm. Luchi; No. 14, 187-189(1974). (In Russian).

A 100-channel scintillation telescope is described. It allows an uninterrupted registration of cosmic ray intensity to be accomplished. A liquid scintillator is used in this installation. The telescope consists of 4 layers, situated in 1.3 m distance one above another. The area of each layer is 12.25 m^2. It permits counting rates of 2, 3, and 4 layers coincidence to be registered. The statistical error for 4 layers coincidence is 0.07 per cent for one hour. Also it allows the registration of the intensity of the inclined component of cosmic rays with the maximum direction 53° to zenith in the East, West, North and South directions with the statistical accuracy 0.13 per cent for one hour. (auth)

29579 PRIMARY AUTOMATIC PROCESSING ALGORITHMS FOR DATA OBTAINED AT COSMIC RAY STATIONS. Blokh, Ya. L.; Inozemtseva, O. I.; Okulov, Yu. I. Kosm. Luchi; No. 14, 174-186(1974). (In Russian).

An account of the methods proposed for a primary reduction of cosmic ray station data in view of a subsequent computer processing is given. A detailed description of the data arriving at the station's output unit is given. A dispersion analysis of these data is presented; methods of exposing the malfunctions of the instrumentation are described, and the form of the function is found which approximates cosmic ray intensity so that it can be used for the reduction of the data to a zero level. (auth)

29580 METHODS OF SEARCH OF GAMMA-RADIATION POINT SOURCES BY TWO GROUPS OF DETECTORS. Pavlov, I. V.; Stepanyan, A. A. Kosm. Luchi; No. 14, 165-169(1974). (In Russian).

Different methods of searching for point sources of gamma radiation with the energy of 10^{13} eV using Cherenkov radiation recordings of extensive air showers were studied. Scanning by two detector groups is proposed; it permits the elimination, to a considerable degree, of the effect of the transparent variations in the analysis of the observational data. Preliminary experimental data are presented on the correlation of the transparence along different directions during the recording of the Cherenkov flashes of extensive air showers. (auth)

29581 TELESCOPE WITH PROPORTIONAL GAS-DISCHARGE COUNTERS FOR ANALYSIS OF HIGH-ENERGY COSMIC RAY VARIATIONS. Frantsuz, E. T. Kosm. Luchi; No. 14, 157-161 (1974). (In Russian).

A general-purpose fourfold coincidence meson telescope is described. The telescope has an effective registration area of 12 m^2 and measures high-energy particle fluxes coming from the vertical and sixteen azimuthal directions. The telescope has three independent registration channels for the vertical direction. The schemes are presented of the amplifier-discriminator and of the pulse duration gate for pulses entering the coincidence gates. The telescope is supposed to be used for recording the hard component of the cosmic rays at sea-level and underground at the depth to 100 m. w. e. The telescope is provided with SGM-14 gas-discharge proportional counters. (auth)

29582 ABOUT THE USE OF PROPORTIONAL COUNTERS FOR REGISTRATION OF COSMIC RAY MESON COMPONENT. Blokh, Ya. L.; Dmitriev, A. B.; Eroshenko, E. A.; Leonov, V. Kh.; Franpuz, E. T. Kosm. Luchi; No. 14, 128-131(1974). (In Russian).

The results are considered of the study of certain characteristics of large proportional counters SGM-14 produced by the home industry as well as of small proportional counters made out of the ordinary counters SM-5G through overfilling them with cyclohexane. Differential spectra and counting responses are presented which show that the length of plateau in the proportionality range of these counters is no less than 200 V and that the plateau slope does not exceed 2% for 100 V in case of small counters and 2 to 3% for 100 V in case of large counters. The efficiency, life-time, and the temperature coefficients of the counters in the most probable temperature range were studied. The results of the measurements of the delay of the pulse front relative to the moment when the ionizing particle traverses the counter are given. The characteristics (input resistance, gain, frequency properties, resolving time, and some others) are discussed and some recommendations are given concerning the use of electronic methods necessary for work with large and small proportional counters. (auth)

29583 INPUT CONTROL OF COUNTERS CU-51 FOR ASSEMBLING AZIMUTHAL AND CALIBRATION TELESCOPES T/SKL AND ET/SKL. Egorov, Yu. A.; Leonov, V. Kh.; Seregina, N. G. Kosm. Luchi; No. 14, 132-135(1974). (In Russian).

The scheme of an instrument for a comparatively fast recording of the SM-5G counters counting responses in the voltage range 1100 to 1600 V is described. The experience gained from recording the characteristics of more than 800 counters is analyzed, and some suggestions are made for modernization of the instrument with the aim of improving the accuracy of the estimation of the counting rate of the counter under test by means of automatic periodic comparison with the counting rate of a standard counter. The recorded characteristics are analyzed and recommendations are given for the altering of the number of ordered counters. (auth)

29584 APPLICATION OF MICROWAVE TECHNIQUES TO HIGH-ENERGY PHYSICS EXPERIMENTS AT ARGONNE NATIONAL LABORATORY. Chang, C. T. M.; Dawson, J. W.; Fuja, R. E.; Kustom, R. L.; Moretti, A. (Argonne National Lab., IL). Proc. IEEE (Inst. Elec. Electron. Eng.); 62: No. 1, 25-32(Jan 1974).

High-energy physics research as conducted at Argonne National Laboratory is characterized by transport of beams of highly relativistic charged particles, and detection and analysis of the interaction of these particles with one another. Microwave systems find application in both areas. In beam transport, rf separators are frequently used to physically separate particles of different quantum mass. Microwave discharge chambers are used for particle detection and polarized proton targets are used to analyze the scattering of particles. (auth)

29585 MULTI-STRIP SCINTILLATION COUNTERS (MSSC). Lee, L. Y.; Allred, J. C.; Goodman, C. (Houston Univ., Tex. (USA)). Nucl. Instrum. Methods; 119: No. 1, 29-33(1 Jul 1974).

Using binary-coded light-pipe systems, a single-layer, position-sensitive scintillation counter is demonstrated which can respond at a rate up to 10^8 Hz with a relatively small number of photomultiplier tubes. These devices may also be used as position-sensitive gamma-ray detectors. (auth)

29586 ENERGY-LOSS SPECTROMETER FOR LOW-ENERGY PION SCATTERING. Barbini, R.; Faini, S.; Guaraldo, C.; Schaerf, C.; Scrimaglio, R. (Comitato Nazionale per l'Energia Nucleare, Frascati (Italy). Laboratori Nazionali di Frascati). Nucl. Instrum. Methods; 119: No. 1, 35-42(1 Jul 1974).

The performance of an energy-loss spectrometer is reported together with a detailed discussion of the basic parameters of such a system and in particular the second-order aberrations. The system constructed consists of two uniform-field 70° bending sectors in a configuration symmetrical to first order, with an image point in the symmetry plane. The system has been tested with the LEALE-LNF low-energy positive and negative pion beams. The magnets were set at zero degrees facing each other. The contributions of the aberrations and of multiple Coulomb scattering in air, helium and thin windows to the momentum resolution of the two magnet systems have been evaluated and the total momentum resolution compared with the experiment at various energies for positive and negative pions. (auth)

29587 FURTHER RESULTS ON THE OPERATION OF HIGH-ACCURACY DRIFT CHAMBERS. Breskin, A.; Charpak, G.; Gabioud, B.; Sauli, F.; Trautner, N. (European Organization for Nuclear Research, Geneva (Switzerland)); Duinker, W. (Rijksuniversiteit Utrecht (Netherlands)); Schultz, G. (Strasbourg-1 Univ., 67 (France)). Nucl. Instrum. Methods; 119: No. 1, 9-28 (1 Jul 1974).

Optimization of the working parameters in the drift chambers with adjustable electric fields permits stable operation and high accuracies. Full saturation of the drift velocity leads to remarkable improvements, namely a very linear space-time correlation for perpendicular tracks, and simple geometrical distortion of linearity for inclined tracks. The same results can be obtained when properly tilting the electric field equipotentials in a wide range of external magnetic fields. This simple behavior should allow a practical use, even for large systems, of the intrinsic high accuracy of the drift chambers (100 to 200 μm). They appear then as a very promising high-resolution fast detector for high-energy particle physics. (auth)

29588 LOW-PRESSURE DRIFT CHAMBERS FOR HEAVILY IONIZING PARTICLES. Breskin, A.; Charpak, G.; Sauli, F. (European Organization for Nuclear Research, Geneva (Switzerland)). Nucl. Instrum. Methods; 119: No. 1, 7-8(1 Jul 1974).

Drift chambers have been operated at pressures of 20 mm, 43 mm and 87 mm Hg of methylal vapor. At the lowest pressure an accuracy of 1.5 mm (fwhm) is obtained with α-particles. (auth)

29589 TWO-DIMENSIONAL DRIFT CHAMBERS. Breskin, A.; Charpak, G.; Sauli, F.; Santiard, J. C. (European Organization for Nuclear Research, Geneva (Switzerland)). Nucl. Instrum. Methods; 119: No. 1, 1-5(1 Jul 1974).

By using simple thin delay lines, of a diameter smaller than 2 mm, and parallel to the sense wire of a drift chamber it is possible to measure the position of the avalanche along the sense wire. With a drift chamber of 150 cm length accuracies between 2 mm and 3 mm along the wire are obtained. The delay line can be placed in the cathode or can be used between two sense wires very closely spaced in order to solve the right-left ambiguity. (auth)

29590 STUDY OF A PION-STOPPING TELESCOPE BY TIME-OF-FLIGHT METHODS. Calligaris, F.; Ciuti, P.; Giacomich, R. (Trieste Univ. (Italy). Instituto di Fisica). Nucl. Instrum. Methods; 119: No. 2, 229-235(15 Jul 1974).

A pion-stopping telescope has been improved by the time-of-flight technique; some results of measurements are presented. The method gives a valid tool for rejecting spurious counts due to "apparent" stops in the target and supplies also useful information about the range of the pions stopped in the target. (auth)

29591 180° MAGNETIC SPECTROMETER WITH HELIUM-FILLED STREAMER CHAMBER. Balestra, F.; Busso, L.; Garfagnini, R.; Piragino, G. (Turin Univ. (Italy). Instituto di Fisica); Barbini, R.; Guaraldo, C.; Scrimaglio, R. (Comitato

Nazionale per l'Energia Nucleare, Frascati (Italy). Laboratori Nazionali di Frascati); Falomkin, I. V.; Kulyukin, M. M.; Shcherbakov, Yu. A. (Joint Inst. for Nuclear Research, Dubna (USSR)). Nucl. Instrum. Methods; 119: No. 2, 347-353(15 Jul 1974).

The experimental apparatus exposed to the LNF-LEALE pion beam to measure the large-angle pion-nucleus scattering is described. This 180° spectrometer consists of a streamer chamber filled with helium at atmospheric pressure placed in a magnetic field and used for identification of scattering events. The required degree of localization and brightness of the tracks is obtained without using a Blumlein system. Finally, the momentum resolution obtainable with this spectrometer has been evaluated by a Monte-Carlo technique. (auth)

29592 LOW-DEAD-TIME DELAY-LINE READ-OUT FOR POSITION-SENSITIVE PROPORTIONAL COUNTERS. Anderson, A. N. (Idaho Univ., Moscow (USA)); Barrett, R. J. (Case Western Reserve Univ., Cleveland, Ohio (USA)); Wadlinger, E. A. (Virginia Univ., Charlottesville (USA)). Nucl. Instrum. Methods; 119: No. 2, 365-366(15 Jul 1974).

A method is presented for circumventing the long dead times (25 μs) which usually accompany the read-out of helical proportional chambers and other position-sensitive detectors with delay-line read-out. (auth)

29593 MULTI-WIRE PROPORTIONAL CHAMBER WITH CHARGE DIVISION READING. Chaminade, R.; Durand, J. M.; Faivre, J. C.; Pain, J. (CEA Centre d'Etudes Nucleaires de Saclay, 91 - Gif-sur-Yvette (France). Dept. de Physique Nucleaire). Nucl. Instrum. Methods; 118: No. 2, 477-481(15 Jun 1974). (In French).

A new reading system for multiwire proportional chambers is described. It permits a good rapidity with a very simple electronic data acquisition system. The resolution can be better than 0.5 mm with a reading gap of 36 mm. (auth)

29594 HIGH-RESOLUTION CRYOGENIC SPARK CHAMBERS. Atac, M.; Taylor, W. E. (National Accelerator Lab., Batavia, Ill. (USA)). Nucl. Instrum. Methods; 118: No. 2, 413-417(15 Jun 1974).

A cluster of four narrow-gap (2.5 mm) spark chambers containing eight wires per millimeter has been built and operated at low temperatures (as low as 118 K). Results obtained from these chambers indicate that the width of the spark column is reduced at lower temperatures due to the increased gas density. Electron diffusion and deviation of the spark column from the true particle trajectory are greatly reduced at lower temperatures with narrow-gap spark chambers. Space resolutions less than $\sigma = 70$ μm(hwhm) have been achieved and even better resolutions are predicted from the observed temperature dependence. (auth)

29595 HIGH-RESOLUTION IONIZATION MEASUREMENTS IN THE REGION OF THE RELATIVISTIC RISE. Aderholz, M.; Lazeyras, P.; Lehraus, I.; Matthewson, R.; Tejessy, W. (European Organization for Nuclear Research, Geneva (Switzerland)). Nucl. Instrum. Methods; 118: No. 2, 419-430(15 Jun 1974).

Results of a 62-layer gas proportional counters test at 9 GeV/c are given. The achieved resolution in the ionization was 9.4% fwhm for 4 cm layer thickness and Ar + 5% CH_4 gas mixture. The ionization ratio of pions and protons was 1.21 ± 0.01 for argon at atmospheric pressure. Other gas mixtures were also tested. The results of the experiment were used for design improvements of a 128 layer ionization detector proposed for identification of fast secondaries emerging from the 3.7 m bubble chamber working at SPS energies. (auth)

29596 A CALORIMETER FOR 300 GeV NEUTRONS AND PROTONS. Jones, L. W.; Chanowski, J. P.; Gustafson, H. R.; Longo, M. J.; Skubic, P. L.; Stone, J. L. (Michigan Univ., Ann Arbor (USA)); Cork, B. (Argonne National Lab., Ill. (USA)). Nucl. Instrum. Methods; 118: No. 2, 431-434(15 Jun 1974).

A total-absorption calorimeter made of alternating layers of iron and plastic scintillators for determining the energies of hadrons has been built and tested in beams at the National Accelerator Laboratory. The calorimeter is being used in an experiment to measure neutron total cross sections. The design of the calorimeter is described and its performance is reported. The resolution of the calorimeter for 300 GeV protons is found to be 12.8% fwhm. (auth)

29597 A HIGH-RESOLUTION SCINTILLATION COUNTER WITH PARTICLE IDENTIFICATION FOR USE WITH PIONS. Axen, D.; Duesdieker, G.; Felawka, L.; Ingram, C. H. Q.; Jones, G.; Salomon, M.; Westlund, W. (British Columbia Univ., Vancouver (Canada). Dept. of Physics). Nucl. Instrum. Methods; 118: No. 2, 435-443(15 Jun 1974).

A plastic scintillation counter used to determine the energy of positive pions and protons is described. The measured energy resolution and efficiency for 50 MeV pions are 1 MeV and 87% respectively. Fast response permits high-count-rate operation and pion identification. This stopping counter is useful for positive pions of energies up to about 100 MeV. (auth)

29598 STUDY OF TOTAL-ABSORPTION COUNTERS FOR VERY-HIGH-ENERGY PARTICLES. Baroncelli, A. (Instituto Superiore di Sanita, Rome (Italy). Laboratori di Fisica). Nucl. Instrum. Methods; 118: No. 2, 445-451(15 Jun 1974).

The development of the nuclear-electromagnetic cascade initiated by a strongly interacting particle has been studied by means of the Monte Carlo method. The model used to simulate the cascade inside an indefinite homogeneous medium is described. The performance of a total-absorption counter of the sample type, consisting of a sandwich of absorbers and scintillator plates, is discussed. The resolution is studied as a function of the geometry and of the incident particle energy in the range 5 to 300 GeV. The results of the calculation show that at 300 GeV an energy resolution of about ±4% can be achieved. (auth)

29599 TRANSITION COUNTERS FOR πK DIFFERENTIATION ABOVE 400 GeV. Wang, C. L. (Brookhaven National Lab., Upton, N. Y. (USA)). Nucl. Instrum. Methods; 118: No. 2, 453-456(15 Jun 1974).

New data on a counter based on transition radiation from 0.4 to 2.8 GeV electrons indicate that πK differentiation above 400 GeV can be expected, and that to differentiate these particles in a beam of variable energy one simply has to adjust the discriminator level or the threshold of the counter - a procedure much simpler than changing the pressure of threshold gas Cherenkov counters. In addition, a useful application of majority coincidence logic for "magnetless" transition-radiation detectors of fast resolving time and good rejection radio is suggested. (auth)

29600 A LARGE FAST WATER CHERENKOV COUNTER. Carlson, P. J.; Johansson, E. (Stockholm Univ. (Sweden). Fysiska Institutionen). Nucl. Instrum. Methods; 118: No. 2, 465-468(15 Jun 1974).

A description is given of a large-volume Cherenkov counter with diffuse reflecting inside walls. Particular attention is given to the timing properties and it is shown that the chosen combination of the reflectivity of the walls and the number of photomultiplier tubes gives an output rise time of about 12 ns. The performance of the counter in two experiments is discussed. (auth)

29601 COMPUTATION OF POTENTIAL IN A MULTIWIRE PROPORTIONAL COUNTER OF ARBITRARY CROSS-SECTION. Symm, G. T. (National Physical Lab., Teddington (UK)). Nucl. Instrum. Methods; 118: No. 2, 605-607(15 Jun 1974).

A potential problem arising in connection with the design of multiwire proportional counters is here solved numerically by an integral equation method. Typical results are illustrated by computer-drawn contours and graphs. (auth)

Radiometric Instruments

29602 (BDX-613-1028(Rev.)) BETA BACKSCATTER MEASUREMENTS OF ALUMINUM COATINGS ON MYLAR SUBSTRATES. Heckman, R. V. (Bendix Corp., Kansas City, Mo. (USA)). Sep 1974. Contract AT(29-1)-613. 21p. Dep. NTIS $4.00.

A method was developed, using specialized beta backscatter equipment, to nondestructively measure the thickness of 0- to 450-microinch (0 to 0.0114 mm) aluminum foil on an aluminum-mylar-aluminum laminate. Measurement precision is greater than 3 percent. The sensitivity of various isotope sources is discussed, and promethium 147 is shown to be the best for the application. (auth)

29603 (TRITA-KKE-7403, pp 25-26) RADIOMETRIC METHOD FOR EGGSHELLS. Mar 1973. (In Swedish).

A radiometric method for measurement of the thickness of eggshells has been improved. The method has been adapted to hen eggs and is intended for use in hen breeding and egg laying control. The results have also been tested in control of marshhauler eggs. (SW)

29604 RADIOISOTOPE METHOD OF MEASURING THE MEAN FIBRE DIAMETER OF WOOL SAMPLES. Downes, A. M. (CSIRO, Prospect, Australia). Wool Technol. Sheep Breed.; 20: No. 2, 29-34(Dec 1973).

In order to measure mean fiber diameter by the radioisotope method, there are three stages - preparation of test specimens containing a known amount of carbon-14, measurement of radioactivity by means of a liquid scintillation spectrometer, and calculation of results from a previously determined calibration equation. The theoretical and practical aspects of the method are described. The method has been rigorously tested over a three year period. For standard tops the mean 95% confidence limits for a single measurement on one test specimen is about ± 0.36 microns. For core samples and for sheep mid-side samples the corresponding value is about ± 0.65 microns. These limits are well within those accepted for the air-flow method. The mean fiber diameters of standard tops, as measured by the radioisotope method agreed almost perfectly with the mean results obtained in about 80 other laboratories by the air-flow method. The radioisotope method is therefore an acceptable alternative to the air-flow method. (auth)

29605 APPROXIMATION FOR TIME RELATIONSHIPS IN PULSED GAMMA–GAMMA LOGGING. Dyad'kin, I. G.; Krasil'nikov, B. N.; Starikov, V. N. Sov. At. Energy (Engl. Transl.); 35: No. 4, 936-938(Oct 1973).

Translated from At. Energ. (USSR); 35: No. 4, 272-273(Oct 1973).

Pulsed $\gamma-\gamma$ logging (PGGL) is based on measurement of the time distribution of γ radiation from a pulsed source scattered by rock; it increases the reliability of determinations of rock density because it decreases the effect of neighboring zones considerably. Formulas for the determination of the time distribution of γ rays scattered in rock are presented for probes of various lengths, and good agreement with the results of Monte Carlo calculations are demonstrated. These experessions were obtained by transformation of the well-known time-dependent solutions for the neutron transport equation. (WHK)

29606 COMPARATIVE ANALYSIS OF THE ACCURACY OF ABSOLUTE AND RELATIVE METHODS OF THICKNESS MEASUREMENT USING SCATTERED RADIATION. Troitskii, I. N. Sov. J. Nondestruct. Test. (Engl. Transl.); 9: No. 6, 661-665 (Dec 1973).

Translated from Defektoskopiya; 9: No. 6, 36-41(1973).

The accuracy of absolute and relative methods of measuring the thickness of an irradiated object is investigated taking into account fluctuations in the scattered radiation. Relations are given which enable one to determine which of the methods of measurement is preferable, depending on the accuracy with which the recorded radiation power is known. (auth)

29607 CONTRIBUTION OF FLUCTUATIONS IN THE PARAMETERS OF THE OBJECT TO THE PROCESS TAKING PLACE AT THE OUTPUT OF A RADIOMETRIC DEVICE. Zav'yalkin, F. M.; Kvasnitsa, M. S. (Tomsk Polytechnic Inst., USSR). Sov. J. Nondestruct. Test. (Engl. Transl.); 9: No. 6, 647-650(Dec 1973).

Translated from Defektoskopiya; 9: No. 6, 19-23(1973).

The process taking place at the output of a radiometric apparatus is described for cases in which statistically specified fluctuations occur in the parameters of the object under test (thickness, linear attenuation coefficient of the flux of radiation). Exact and approximate expressions are derived for calculating the effect of fluctuations in the object parameters on the functional error of the instrument. (auth)

29608 GENERAL APPROACH TO THE DESIGN OF RADIATION GAUGES. Notea, A.; Segal, Y. (Technion-Israel Inst. of Tech., Haifa). Nucl. Technol.; 24: No. 1, 73-80(Oct 1974).

A procedure was developed for characterization and optimization of gages, based on nuclear or atomic radiation. It provides a logical and organized method to obtain the optimal design parameters of the gage, limits of detection, resolving power, etc. The dominant concept in the procedure is a characterization function which correlates the variables that have to be measured, the design parameters of the gage, its response and uncertainty. Gages with linear and exponential responses were analyzed to demonstrate the generality of the approach and the use of the concepts. (auth)

Miscellaneous Instruments

Refer also to abstracts 29254, 29297, 29300, 29374, 29490, 30572, and 31111.

29609 (BNWL-1850(Pt.3), pp 73-75) DEVELOPMENT OF A SONIC ANEMOMETER SYSTEM. Horst, T. W.; Bander, T. J. Apr 1974.

In Pacific Northwest Laboratory annual report for 1973 to the USAEC Division of Biomedical and Environmental Research. Part 3. Atmospheric sciences.

A three-dimensional sonic anemometer was designed for mounting on an aircraft, constructed and laboratory tested. A noseboom for mounting the anemometer was also constructed and flight-tested. Further testing of both elements of this system is required prior to operational use. (auth)

29610 (BNWL-1850(Pt.3), pp 75-79) EVALUATION OF AN AIRBORNE FLUORESCENT PARTICLE COUNTER FOR ATMOSPHERIC TRACER STUDIES. Orgill, M. M.; Nickola, P. W. Apr 1974.

In Pacific Northwest Laboratory annual report for 1973 to the USAEC Division of Biomedical and Environmental Research. Part 3. Atmospheric sciences.

A Model 110 automatic fluorescent particle counter is being evaluated in an aircraft for utilizing the instrument in field dispersion, transport and deposition studies. Results to date indicate that typical crosswind and downwind concentration profiles can be obtained, but tracking of plumes beyond 7 km has not been totally successful. (auth)

29611 (BNWL-1850(Pt.3), pp 80-83) REAL-TIME SYSTEM FOR DETECTION OF THE ATMOSPHERIC TRACER SULFUR HEXAFLUORIDE. Lee, R. N.; Miller, M. C. Apr 1974.

In Pacific Northwest Laboratory annual report for 1973 to the USAEC Division of Biomedical and Environmental Research. Part 3. Atmospheric sciences.

An SF_6 tracer gas detection system built for aircraft operation has undergone tests to determine its qualitative performance. The primary component of this system is a gas chromatograph equipped with an electron capture detector. During operation, continuous flow of an atmospheric sample through a column possessing an affinity for oxygen allows real-time description of an SF_6 plume before arrival of the oxygen frontal. The column, which is rejuvenated by an argon backflush, permits sampling for 1-min intervals during each 6 to 8 min of flight time. (auth)

29612 (BNWL-1850(Pt.3), pp 87-93) AIRBORNE LABORATORY FOR AIR POLLUTION STUDY. Alkezweeny, A. J. Apr 1974.

In Pacific Northwest Laboratory annual report for 1973 to the USAEC Division of Biomedical and Environmental Research. Part 3. Atmospheric sciences.

A description is given of air pollution and cloud physics instrumentation aboard a Cessna 411 aircraft. The aircraft is capable of continuously measuring and recording aerosol particle size distributions and concentrations of Aitken nuclei, cloud condensation nuclei, ice nuclei, and concentrations of trace gases, as well as meteorological and aircraft parameters. All the data are measured and recorded automatically on magnetic tape and/or strip-chart recorders. The aircraft is currently in use for characterization of aerosol and trace gases in polluted and unpolluted atmospheres. (auth)

29613 (BNWL-1850(Pt.3), pp 176-178) FLUX METER FOR DIRECT FIELD MEASUREMENT OF DEPOSITION AND RESUSPENSION RATES. Hales, J. M.; Horst, T. W. Apr 1974.

In Pacific Northwest Laboratory annual report for 1973 to the USAEC Division of Biomedical and Environmental Research. Part 3. Atmospheric sciences.

A conceptual design for a dry-deposition flux meter is described. A prototype of this design will be constructed and tested during the coming year. (auth)

29614 (IFA-CRD-57-1974) PROGRAMS FOR EXPERIMENTAL DATA PROCESSING ON PDP-8/I COMPUTER. Duma, M. (Institutal de Fizica Atomica, Bucharest (Romania)). 1974. 13p. Dep. NTIS (US Sales Only) $4.00.

The functions FADC and FDIS have been rewritten aiming to use the FOCAL'69 in connection with the Series 50/50 Nuclear Data Analyzer and 7004B X-Y Recorder. In the new versions these functions are dependent on two parameters and are used to read or write the information acquired by the 4096 channel analyzer of the ND-50/50 system and to utilize the space just below the extended functions. These functions have been used to write programs for off-line processing of experimental data acquired by the ND-50/50 system. (auth)

29615 (JPRS-61338, pp 1-3) INTERATOMINSTRUMENT TO COORDINATE EE NUCLEAR INSTRUMENTATION TECHNOLOGY. Kaspar, J. Translated from Zapisnik; No. 1, 30-31(Jan 1974).

The formation of the interatominstrument (IAI) organization, an international economic association for nuclear instrumentation technology, is announced. The intergovernmental agreement was signed by representatives of the Bulgarian, Hungarian, GDR, Polish, USSR, and Czechoslovak governments. (WHK)

29616 (NVO-AEIC-74-1, pp 247-254) SALTATION AND CREEP SAMPLER. Reichman, J. M. (Univ. of California, Livermore). Jul 1974.

In dynamics of plutonium in desert environments. Nevada Applied Ecology Group progress report as of January 1974.

Motion of windblown sand close to the ground can occur by two mechanisms. The first of these mechanisms is creep, which is the rolling motion of sand along the ground. The second mechanism occurs when wind speed increases and sand hops along the ground in short, arching paths; this is saltation. Measurement of these mechanisms of sand movement, together with the resuspended sand, is necessary for the understanding of the total flux of windborne soil. Various devices have been used to measure saltation and creep. In order to develop an efficient sampling unit, several of these devices were evaluated to determine the most efficient. Modifications then were made to further increase efficiency. Testing of the units was conducted under controlled conditions at Livermore in order that more reproducibility could be obtained than would be possible at the Nevada Test Site (NTS). (auth)

29617 (NVO-AEIC-74-1, pp 255-263) IN SITU OPTICAL PARTICLE SIZE ANALYSIS OF AMBIENT AEROSOL. Koval, J. S. (Univ. of California, Livermore). Jul 1974.

In dynamics of plutonium in desert environments. Nevada Applied Ecology Group progress report as of January 1974.

The efficiency of the Climet Particle Analyzer, a light-scattering instrument capable of sizing and counting aerosol particles in the range 0.5 to 10 μm in diameter, is discussed. (CH)

29618 (UCID-15828) NEW NADS: COMPATIBLE ALPHA MEASURING SYSTEM. Lindsey, J. S. (California Univ., Livermore (USA). Lawrence Livermore Lab.). 25 Jan 1971. 6p. Dep. NTIS $4.00.

The development of a deflecting photodiode tube with readout system for measuring and storing alpha information is described. (WHK)

29619 (UCID-16026) MAGREC FINAL REPORT. Wichner, R. (California Univ., Livermore (USA). Lawrence Livermore Lab.). 1 Feb 1972. Contract W-7405-eng-48. 20p. Dep. NTIS $4.00.

The development of an improved device to record fast transients created by nuclear events that uses a continuous magnetic thin film as the recording medium is described. The electrical signal is recorded in the form of a domain wall and it is read out electronically. The recorder has a risetime on the order of a nanosecond and a dynamic range of better than 30 db. Readout of the record is compatible with computer cycle times. (auth)

29620 SIMPLE DEVICE USING CAPACITANCE SWITCHES FOR DATA ENTRY IN MAN–MACHINE SYSTEMS. Danchak, M.; Moyer, W. R.; Tatarczuk, J. R.; Becker, M. (Rensselaer Polytechnic Inst., Troy, NY). Contract AT(11-1)3058. Nucl. Technol.; 23: No. 3, 337-39(Sep 1974).

A simple design for the priority input of 32 function switches in a man-machine system was developed. The use of no-bounce capacitance switches required additional logic circuitry to alleviate the problem of slow rise time inherent in this method of data entry. (auth)

29621 ALKALI METAL LEAK DETECTOR METHOD AND APPARATUS. (to Varian Associates). Netherlands Patent 7,217,247. 18 Dec 1972. Priority Date 16 Dec 1971, USA. 18p. (In Dutch).

A method and apparatus for detecting alkali metal leaks comprising a sputter-ion pump for creating vacuum and measuring hydrogen pressure in the vacuum are described. The sputter-ion pump is fitted with a probe that has a diaphragm permeable to hydrogen (e.g., palladium). Hydrogen gas passing through the diaphragm of the probe causes an increase in the pressure within the pump. The current drawn by the pump is proportional to the pressure within the pump over a wide pressure range. Thus, the presence of hydrogen within the pump can be observed by monitoring pressure within the pump directly or by monitoring the current drawn by the pump during its operation. The change in pressure will generate a signal which activates an alarm or recording device. Since the permeability of the diaphragm is affected by changes in temperature of the diaphragm, compensating means can be provided. In situations where regular (nonisotopic) hydrogen is normally present in the region external to the sodium containment structure a deuterium-containing hydrogen compound is disposed in the region proximate to the sodium containment structure, and the sputter-ion or other vacuum pump is coupled to a mass spectrometer. When deuterium is detected by the mass spectrometer, an alarm or recording device is thereupon activated. (NL)

29622 FLUID PRESSURE REGULATING AND CONTROL DEVICE. (to Westinghouse Electric Corp.). Netherlands Patent 7,214,024. 17 Oct 1972. Priority Date 27 Oct 1971, USA. 17p. (In Dutch).

A controlled leakage face-type device is provided to control the flow of a fluid from a high pressure region to a low pressure region. An annular barrier member or ring is movably mounted in a housing having a face therein confronting a face on the ring. A hydrostatic balancing system is utilized to control the leak rate through the interface passage between the confronting faces under various operating conditions. This permits a small stable leakage to be maintained in the "closed" position so that the use of injection water and/or cold loop concepts are feasible to control the temperature and particulate content of the effluent. The hydrostatic balancing system includes a variable seating force whose magnitude depends on the fluid conditions between the faces. Thus, the device is constructed to remain in balance over the large change in lifting forces that results when the fluid changes phase. In a typical reactor the nominal operating pressure can be raised from 2250 psi to 2425 psi. Thus, the reactor can operate at a higher temperature which greatly improves its efficiency. (NL)

29623 CHOOSING THE BASIC PARAMETERS OF A BUFFER MEMORY DEVICE IN THE HPD COMPUTER SYSTEM BY A METHOD OF STATISTICAL MODELING. Klarin, A. P.; Solov'ev, G. N. Sb. Statei, Mosk. Inzh.-Fiz. Inst.; No. 4, 155-162(1971). (In Russian).

From use of digital and analog computers in nuclear science and engineering; Moscow, USSR (1971).

This study investigates the relation between capacity and velocity parameters of a buffer memory device intended for the accumulation of information entering at a random moment of time from the coded circuits of a HPD computer, the smoothing out of this information with time, and its transmission to a digital computer for subsequent treatment according to definite algorithms. The study is carried out by using the method of statistical modeling. The results of the modeling are presented. (SJR)

29624 MONITOR FOR RADIATION-INDUCED HEATING. Wallin, W. R.; Lowery, V. W.; Smith, R. R. (to United States Atomic Energy Commission). US Patent 3,826,921. 30 Jul 1974. Filed Date 26 Apr 1973. 6p.

A susceptive material that is to be examined with respect to radiation-induced heating is sealed within a capsule composed of a material such as stainless steel. The remaining capsule volume is filled with a liquid metal that has a greater coefficient of thermal expansion than the capsule walls. The liquid expansion permanently deforms the capsule in an amount representative of its maximum temperature. The capsule is coaxially supported within an outer container, thus forming a gas-filled annulus having a known resistance to heat transfer. The heat generated by irradiation of the susceptive material is determined by the temperature difference required for its transfer across the annulus. (9 Claims, 2 Drawing Figures) (Official Gazette)

29625 A NEW MASS SPECTROMETER FOR ISOTOPIC ANALYSIS. Fenner, N. C.; Jackson, M. C.; Powell, R. E.; Roberts, J. W.; Young, W. A. P. (UKAEA Weapons Group, Aldermaston. Atomic Weapons Research Establishment). J. Mass Spectrom. Ion Phys.; 14: No. 3, 245-258(Jul 1974).

A single stage, 30 cm radius mass spectrometer with 90° magnetic deflection has been built for isotopic analysis of solid samples. The sample throughput is high and analyses are made with a precision approaching 0.1%. The source is a turret design that will accommodate six single or triple filament beads at one loading, and the source accelerating plates are in the Nier arrangement. The collector slit is adjustable between 0 and 1.5 mm and is rotatable through an angle of ±5° for alignment. The collector system consists of a scintillation detector with a Faraday bucket as an alternative. A retardation grid is mounted between the slit and the detector to reject ions that have lost energy due to gas scattering in the flight tube. This arrangement produces a flat top to the peak and an abundance sensitivity of less than 10^{-6} in the uranium region. The beam spread at the focus is 18 μm at the 10% beam intensity points. The magnet power unit can be varied to cover masses 2 to 300 at 8 kV EHT and peak scanning is by a double ramp. The stability of the current is $< 2 \times 10^{-5}$ in 30 minutes. The high tension unit can be varied between 0 and 10 kV and is stable to $< 5 \times 10^{-5}$ over one hour. The filament current supples will give currents up to 6 amps and the stability is $\sim 2 \times 10^{-5}$ for 30 minutes. (auth)

29626 INTERACTION EFFECT OF ENTRY VELOCITY AND POSITION ON QUADRUPOLE MASS FILTER RESOLUTION. Nagarajan, R.; Ghosh, P. K. (Indian Inst. of Tech., Kanpur.

Dept. of Chemistry). J. Mass Spectrom. Ion Phys.; 14: No. 3, 267-271 (Jul 1974).

From numerical calculations of ion trajectories in a quadrupole field, upper bounds on the initial displacement and radial velocity for zero initial phase have been obtained for 100% ion transmission in the resolution range $m/\Delta m = 100$ to 1000. An empirical expression relating the maximum possible resolution as a function of initial velocity and position involving a position-velocity interaction term has been obtained to fit the calculated results. (auth)

29627 TEST SYSTEM FOR CAMAC MODULES. Meyer, J. M.; Berst, J. D.; Metzger, G. (Centre National de la Recherche Scientifique, 67-Strasbourg (France). Lab. de Physique du Noyau et de Physique des Particules). Nucl. Instrum. Methods; 118: No. 2, 589-595(15 Jun 1974). (In French).

A software system is described which allows static and dynamic tests of CAMAC modules. For this purpose, a special application language, LA TAUC, where the vocabulary is specialized and a familiar syntax is used, is provided for non-programmers. (auth)

29628 REFERENCE PULSERS FOR CALIBRATION PURPOSES. Manfredi, P. F.; Maranesi, P.; Varoli, V. (Politecnico di Milano (Italy). Centro Studi Nucleari E. Fermi). Nucl. Instrum. Methods; 118: No. 2, 487-495(15 Jun 1974).

The pulse generators have been developed that are suitable for testing and calibrating high-accuracy analog signal processors as well as high-resolution analog-to-digital converters. One of them has 20 ppM integral non-linearity, 10 ppM/°C thermal drift and 100 ns risetime. The other unit, which features 100 ppM nonlinearity and 15 ppM/°C drift, has a risetime lower than 10 ns. It was exhaustively proved that both generators enable the designers and the users of pulse instruments to measure their linearity, stability and resolution in a very reliable way. (auth)

29629 A STUDY OF ION PATHS IN CURVED PARALLEL-PLATE ELECTRON MULTIPLIERS WITH PERPENDICULAR MAGNETIC FIELD. Janney, R. B.; Tove, P. A. (Uppsala Univ. (Sweden)). Nucl. Instrum. Methods; 118: No. 2, 509-513(15 Jun 1974).

A computer study of ion paths in curved parallel-plate electron multipliers with a perpendicular magnetic field is performed. The implications on the avoidance of ion feedback and on the possible construction of a mass detector are discussed. Ions may be introduced in these multipliers either directly or by ionization from the avalanching electrons. With given multiplier dimensions and magnetic field strength it is found that the structure is able to transport ions of only one mass. The influence of initial ion velocities which can be present is investigated. For low-energy ions it is found that a longitudinal velocity spread is unimportant while velocities perpendicular to the plates may influence the paths significantly. (auth)

29630 LOGARITHMIC DIGITAL-ANALOG CONVERSION FOR VARYING PARAMETERS IN CAMAC DEVICES. Andert, K.; Gabriel, F.; Shuravin, V. A. (Joint Inst. for Nuclear Research, Dubna (USSR)). Nucl. Instrum. Methods; 119: No. 2, 361-363(15 Jul 1974).

Some methods of digital-analog conversion, necessary for a series of devices in the Camac system with analog functions are discussed. A logarithmic method which allows to perform conversion in a very large range ($1:10^4$ and larger) with a high stability (about 10^{-4}/°C) is considered. (auth)

29631 RISE-TIME JITTER REDUCTION IN TIMING AND AMPLITUDE-DISCRIMINATION CIRCUITS. Abbattista, N.; Marangelli, B.; Marino, D.; Plantamura, V. L. (Bari Univ. (Italy). Instituto di Fisica). Nucl. Instrum. Methods; 119: No. 2, 407-409(15 Jul 1974).

When dealing with signals from nuclear devices, one generally has to analyze a single characteristic parameter, while the others must be held constant. Unfortunately, the other parameters are really variable, affecting the precision of analysis of the parameter of interest. For instance, amplitude discrimination and timing are affected by rise-time variation of the input signals. In order to improve the performances of the circuits that carry out these operations, it is shown in this work how, utilizing a signal whose amplitude is a function of rise time—which modifies the operating conditions of the circuits—a compensation is accomplished that reduces the rise-time jitter influence. (auth)

29632 A FOCUSSING LOW-ANGLE NEUTRON DIFFRACTOMETER. Nunes, A. C. (Brookhaven National Lab., Upton, N. Y. (USA)). Nucl. Instrum. Methods; 119: No. 2, 291-293 (15 Jul 1974).

Low-angle neutron scattering is yielding valuable information on the quaternary structure of macro-molecular aggregates in solution. To obtain the angular resolution necessary for these experiments (a few hundredths of a degree) such broad samples require either long neutron flight paths or systems of Soller slits. The former system, though it allows the use of position-sensitive or multiple-detector systems to increase one's data acquisition rate, unfortunately requires a great deal of space. The latter system, while small and relatively inexpensive, limits one to single-detector step scans over the scattering pattern of interest. A converging non-reflecting Soller slit providing a focussed neutron beam for neutron scattering experiments is described. (auth)

29633 PRECISE DETERMINATION OF INHOMOGENEOUS MAGNETIC FIELD COMPONENTS WITH A HALL PROBE. Kiselev, Yu. T.; Burgov, N. A.; Gerzon, S. A.; Terekhov, Yu. V.; Ushakov, V. I.; Chumakov, M. M. (Gosudarstvennyj Komitet po Ispol'zovaniyu Atomnoj Ehnergii SSSR, Moscow. Inst. Teoreticheskoj i Ehksperimental'noj Fiziki). Nucl. Instrum. Methods; 119: No. 2, 323-325(15 Jul 1974).

The possibility of precise determination of inhomogeneous magnetic field components with a Hall probe is shown. The adjustment technique, a set of necessary probe calibrations, and the method of mathematical treatment of the results of the measurements are described. (auth)

29634 DEVELOPMENT OF A CAMAC CRATE CONTROLLER FOR CONNECTION TO A COMPUTER CDC 1700. Moritz, J. (Karlsruhe Univ. (TH) (F. R. Germany). Inst. fuer Experimentelle Kernphysik); Sindt, H. (Deutsches Elektronen-Synchrotron (DESY), Hamburg (F. R. Germany)). Nucl. Instrum. Methods; 119: No. 1, 107-112(1 Jul 1974).

A CAMAC crate controller is described which directly connects a CAMAC crate to a 16-bit computer CDC 1700 without use of a branch highway and branch driver. With a few minor exceptions the controller complies fully with the CAMAC standard. (auth)

29635 A CORRELATION CHOPPER OR CHOPPER WITH CODING DISK. Graffstein, A. (Institute of Nuclear Research, Warsaw (Poland)). Nucl. Instrum. Methods; 119: No. 1, 101-105(1 Jul 1974).

The properties of various decoding methods of results obtained by a correlation chopper are analyzed. A new method of diminishing the background was demonstrated. Some conclusions leading to construction of new devices are presented. (auth)

ISOTOPE AND RADIATION SOURCE TECHNOLOGY

Isotope Separation (Industrial)

Refer also to abstract 29487.

29636 PROCESS FOR SEPARATING URANIUM ISOTOPES. (to Mobil Oil Corp.). Netherlands Patent 7,216,867. 12 Dec 1972. Priority Date 12 Jan 1972, USA. 13p. (In Dutch).

A process for separating uranium isotopes, i.e., $^{235}UF_6$ from $^{238}UF_6$ utilizing shock separation techniques is described. The gaseous uranium hexafluoride is introduced at supersonic velocity into a circular duct. Within the supersonic parallel flow stream a number of hollow probes are placed at different distances along the axis of flow. The hollow probes having critical dimensions relative to the mean free path of the flow stream in front of the probes so as to cause a detached stationary shock to form ahead of each of the leading edges of the probes. The process gives much better results than the process according to which all the probes are placed in the same transverse plane. (NL)

29637 STRONG FOCUSING ION SOURCES. Alexandru, G. (Institutul de Fizica Atomica, Bucharest). Stud. Cercet. Fiz.; 25: No. 2, 249-251(1973). (In Rumanian).

The advantages of strong focusing ion sources used for electromagnetic isotope separation and mass spectrometers are presented. (auth)

Isotopic Power Sources

Refer also to abstracts 29239 and 29242–29263.

Radiation Sources

Refer also to abstracts 29295 and 31125.

29638 PROCESSING OF THE RESPONSE FUNCTIONS OBTAINED BY RADIOTRACER MEASUREMENTS. II. Approximation of the Measured Relations and Smoothing of Variations by Means of Laguerre Functions. Thyn, J. (Inst. for Research, Production, and Use of Radioisotopes, Prague). Radioisotopy; 15: No. 3, 329-355(1974). (In Czech).

The feasibility of using Laguerre functions for the approximation of experimental curves obtained in radiotracer measurements by means of a count-rate meter, i.e., of step-like curves with statistical variations, was investigated. It was found that the first eleven Laguerre functions are sufficient for a good approximation of common unimodal relations. The advantages of the approximations are demonstrated on graphic correlations, indicating that under given precision requirements of the obtained information, substantially smaller amounts of activity are required for the experiment, if the Laguerre functions are used for the processing of experimental relations. (auth)

29639 EVALUATION OF RESPONSE FUNCTIONS WHICH ARE OBTAINED WHEN RADIOISOTOPES ARE USED AS A TRACER. I. Application of the Scaler. Thyn, J. (Inst. for Research, Production, and Use of Radioisotopes, Prague). Radioisotopy; 15: No. 3, 307-328(1974). (In Czech).

There were studied two kinds of errors in the measurement of the residence time distributions using radioactive tracers, when the scaler is used, i.e., (1) the error which originates from the stairstep registration of the continuous function; and (2) the error which originates from the statistical nature of the radioactive disintegration. Charts were prepared from which the optimal time step can be found. When the scaler works with this time step then only a minimum number of the dates is used and a minimum error is obtained. A chart is presented which can be utilized for estimation of activity which is needed for an experiment. (auth)

Design and Fabrication

29640 KRYPTON SOURCE. Fowler, R. J. (to Secretary of the Navy). US Patent 3,833,815. 3 Sep 1974. Filed date 18 Feb 1969. 4p.

A radiation source for use in an arming system for airborne weapons comprising a stainless steel sphere filled with krypton-85 (^{85}Kr) radioactive gas at high pressure and having gold plated internal surfaces to form Bremsstrahlung targets which continuously emit gamma radiation when subjected to the beta radiation from the ^{85}Kr is described. A depleted uranium or tungsten shield surrounds the steel sphere and means are provided for pivoting part of the shield away from the steel sphere to permit the gamma radiation to escape and irradiate part of the path followed by a released bomb. The ^{85}Kr may be harmlessly dissipated in the atmosphere, if desired, by activation of an explosive squib fixed to a fill tube on the sphere. (Official Gazette)

29641 RAPID PRODUCTION OF THIN Kr SOURCES. Houdayer, A. J.; Mark, S. K.; Moore, R. B. (McGill Univ., Montreal, Quebec (Canada). Foster Radiation Lab.). Nucl. Instrum. Methods; 118: No. 2, 615-616(15 Jun 1974).

In conventional nuclear beta and gamma spectroscopy, one often encounters the problems of fabricating a thin radioactive source with a relatively short half-life (few minutes), particularly when the source is a gas produced by the bombardment of a solid target with energetic projectiles. This communication describes a technique for the rapid production of thin Kr sources. It has been used in a series of investigations on the decay properties of the neutron-deficient Kr nuclides lying far from the beta stability line. (auth)

Industrial Uses

Refer also to abstract 29681.

29642 (AD-777550) PRESERVATION OF ENZYME INACTIVATED LAMB SLICES: EFFECTS OF FREEZE DESICCATION AND LOW DOSE IRRADIATION. Rao, B. Y. K.; Shults, G. W.; Wierbicki, E. (Army Natick Labs., Mass. (USA)). Feb 1974. 21p. (FL-180). NTIS $3.00.

The purpose of the present study was to develop a shelf stable product, having satisfactory texture and flavor characteristics, by combination treatments of heat, freeze-desiccation (partial dehydration), and low dose radiation. The following conclusions were drawn from the ambient temperature storage studies conducted over a period of ninety days on the enzyme inactivated, freeze-desiccated lamb slices, vacuum packed in flexible pouches and irradiated with 0.25, 0.5 and 1.0 mrad doses at 0 to 4°C: 0.25 mrad dose was not found to be adequate for the ambient temperature storage of flexible packed, enzyme inactivated, freeze-desiccated lamb samples; a dose of 0.5 and 1.0 mrad appears to be optimum for the ambient temperature storage of enzyme inactivated, partially dehydrated lamb slices and a dose of 1.0 mrad for the non-dehydrated, enzyme inactivated lamb slices; at an irradiation dose of 1.0 mrads, the non-dehydrated lamb slices scored slightly higher than the partially dehydrated lamb slices in technological panel evaluations for the sensory characteristics and preference. (auth)

29643 FIRST GAMMA-IRRADIATION PLANT FOR SEWAGE-SLUDGE HYGIENIZATION. Hernhut, H.; Bosshard, E. (Sulzer Bros. Ltd., Winterthur, Switzerland). Sulzer Tech. Rev.; 56: No. 2, 77-81(1974).

The purpose and mode of operation of the first gamma-irradiation plant for the hygienization of sewage-sludge are described. Radiation protection, safety precautions, and radiation-technological considerations are also discussed. (auth)

29644 INVESTIGATIONS ON MATERIAL TRANSPORT AND DUST FORMATION IN REVOLVING FURNACES FOR CLINKERING BY ISOTOPIC TRACING. Torok, I. (Szilikatipari Kutato es Tervezo Intezet, Budapest). Izotoptechnika; 17: No. 8, 400-405(Aug 1974). (In Hungarian).

The determination of material transport, dwelling time,place of dust formation and adhesion in dry and wet furnaces with $^{24}Na_2CO_3$ tracer is reported. (auth)

29645 SURFACE IRRADIATION OF SPHERICAL VEGETABLES AND FRUITS. Kalman, B.; Kiraly, Z. (Kozponti Elelmiszeripari Kutato Intezet, Budapest). Izotoptechnika; 17: No. 8, 388-395(Aug 1974). (In Hungarian).

A revolving facility for the homogeneous superficial irradiation of apricots, peaches, tomatoes, apples, etc. with fast electrons is described. (auth)

29646 VARIANCE IN THE EVALUATION OF DATA OBTAINED IN RADIOISOTOPIC TRACER INVESTIGATIONS. Rona, V. (MTA Izotop Intezete, Budapest). Izotoptechnika; 17: No. 8, 375-387(Aug 1974). (In Hungarian).

The effect and interaction of different aggressive media and their action time in qualifiying protective coatings are described. Tests of the acceptability of the systematic error found in a dilution process based on the "gasometer" principle is discussed. (auth)

29647 STERILIZATION METHOD AND PRODUCT. Stephenson, M.; Hartley, G. H. (to Ethicon, Inc.). Canadian Patent 944,691. 2 Apr 1974.

A method of sterilizing polyurethane adhesive forming components by exposure to high-energy radiation, e.g., a cobalt-60 source and the sterilized products produced are described. (CA)

LIFE SCIENCES

29648 SMALL QUANTITIES. Cook, L. M. (Texas State Dept. of Health, Austin). Health Phys.; 27: No. 2, 231(Aug 1974).

It is contended that such small quantities as that of 1.2×10^{-11865} μCi/ml of ^{58}Co which appeared in an article by Inoue and Morisawa (Health Phys.; 26: 53(1973)) are meaningless and that such numbers are actually zero. Such a concentration of radioactive material represents very much less than one atom in the entire universe. (UK)

Radiation Effects on Biochemicals

Refer also to abstracts 29036, 29071, and 31333.

29649 (JEN-284) RADIOMIMETICITY OF THE SYSTEM H_2O_2/Fe(II) ON NUCLEIC ACID COMPONENTS. Kinetic Study. Cirauqui, R.; Mingot, F.; Davila, C. A. (Junta de Energia Nuclear, Madrid (Spain)). 1974. 117p. (In Spanish). Dep. NTIS (US Sales Only) $9.00.

Results of a kinetic study of the action of a redox system on DNA monomers confirmed the radiomimetic character of this system. Assuming that in both cases, γ radiolysis of aerated aqueous solutions and action of H_2O_2/Fe(II) system in the same conditions, the reactive species is the OH radical, kinetic expressions are proposed that are confirmed by the experimental results reported. Some of the accepted G-values are corrected in view of the findings. Also these results give evidence mechanisms of molecular repair after radical attack. (auth)

29650 (JEN-286) STRUCTURAL STUDY OF DNA DISCONTINUITIES BY ENZYMATIC POLYMERIZATION. Delgado, M. D.; Mingot, F.; Davila, C. A. (Junta de Energia Nuclear, Madrid (Spain)). 1974. 269p. (In Spanish). Dep. NTIS (US Sales Only) $16.50.

The use of mechanistic knowledge of the in vitro DNA polymerization reaction in order to obtain information on local structure of radioinduced alterations in DNA irradiated in solution is described. By comparison of DNA samples, degraded by γ radiation, DNase treatment, and mechanical disruption, as they act as substrate for DNA polymerase, differences in local structure of the internucleotide discontinuities are demonstrated. The adequacy of the proposed expressions for the description of the polymerization are an indirect proof of the DNA degradation theory by haplotomic mechanism previously developed. The values obtained for some macromolecular parameters confirm previously supposed values. (auth)

29651 EFFECT OF γ IRRADIATION ON THE CHARGE AND SIZE PROPERTIES OF HORSERADISH PEROXIDASE: INDIVIDUAL ISOENZYMES. Delincee, H.; Radola, B. J. (Institut Fuer Strahlentechnologie, Karlsruhe, Ger.). Radiat. Res.; 59: No. 3, 572-584(Sep 1974).

Individual isoenzymes of horseradish peroxidase (EC 1.11.1.7) were irradiated in dilute aqueous solution with ^{60}Co γ rays. By thin-layer isoelectric focusing of the irradiated isoenzymes, it was found that their charge properties were extensively modified. After irradiation, enzyme activity was distributed as well defined zones with isoelectric points identical with those of isoenzymes present in the unirradiated complete isoenzyme system of horseradish peroxidase, and as a rather diffuse activity "smearing between and above the distinct zones. For the near-neutral and basic isoenzymes there was a dose-dependent shift of the enzymatically active components to lower isoelectric points, whereas for the acidic isoenzymes this shift was reversed. Enzymatically active aggregates were revealed by thin-layer gel chromatography. Aggregation depended strongly on enzyme concentration, in the most dilute solution only traces of aggregates, mainly dimers, being formed. The isoelectric pattern of the remaining monomer dominates the pattern of the unfractionated isoenzyme. Already at low degrees of inactivation the charge properties of the monomer were distinctly modified. The findings indicate that the radiation-induced changes of the composite enzyme of horseradish peroxidase are the sum of the alterations of the individual isoenzymes. (auth)

29652 UNIQUE FORMS OF FAST-SEDIMENTING BU LAMBDA DNA IN A SUPERINFECTED E. COLI LYSOGEN. Marburger, K.; Hewitt, R. (Univ. of Texas, Houston). Virology; 55: No. 2, 400-409(Oct 1973).

When a lysogenic (immune) culture of Escherichia coli C thy-321 is superinfected with lambda phage in which 5-bromouracil (BU) has been substituted for the normal DNA base thymine, a large percentage of the linear BU lambda DNA injected into the cells is converted into a covalently closed circular monomer while a smaller amount is converted into DNA forms which sediment faster than the covalently closed circular monomer in both neutral and alkaline sucrose gradients. These unique BU-DNA structures form independently of coinfecting thymine lambda DNA, which forms only the covalently closed circular monomer. It has been found that the formation of the unique forms of fast-sedimenting BU lambda DNA is dependent upon the multiplicity of infection, i.e., the percent of unique forms is greatly reduced in cells superinfected at a multiplicity of infection of less than 1.0. This suggests that there is some type of atypical, intracellular interaction between two or more BU λ DNA molecules. Other observations concerning certain physical characteristics of these unique forms, such as their sedimentation properties in alkaline and neutral sucrose gradients following exposure to ultraviolet (uv) light, indicate that they are structures which differ from each other in molecular weight rather than in superhelical density. (auth)

29653 EFFECT OF X RAYS ON THE PHOSPHORYLATION OF HISTONE f_1 IN THYMOCYTES. Danceva, K. I.; Nikolova, R. H. Suvrem. Med.; 24: No. 2, 15-19(1973).

X rays applied in vitro in a dose of 100 R inhibit phosphorylation of histone f_1 isolated after incubation of thymocyte suspension. This is established by the quantity of the phosphates in histone f_1 and by the incorporation of ^{32}P. In the first 10 minutes dithiotreitol increases phosphorylation of histone f_1 in intact thymocytes followed by a considerable inhibition. In the irradiated thymocytes dithiotreitol exerts a protective effect by phosphorylation of histone f_1. The protector increases the O_2 consumption which is possibly due to the effects of phosphorylation on respiration. (Abstr. Bulg. Sci. Med. Lit.)

29654 CHEMICAL STUDY OF THE MECHANISM OF THE RADIOPROTECTIVE EFFECT OF AET. Horvath, M. Honvedorvos; 26: No. 1, 37-52(1974). (In Hungarian).

In an aqueous solution of pH greater than 7, AET is converted to MEG (mercaptoethylguanidine), which contains a free SH-group, and under suitable conditions (physiological pH, room temperature, a few hours of incubation), it is bound in vitro with reactive SH-groups of proteins. By lengthening the reaction time, increasing the pH and using carbamide, "latent" SH-groups and disulphide bonds may also react. Irradiation with ^{60}Co does not split off the mixed disulphide bond of AET and protein. Paper electrophoresis shows a certain protective effect of the AET bond with albumin, and on binding with hemoglobin this effect is not seen. The formation of methemoglobin and denaturation appear between 1 to 5 Mrad with hemoglobin bound with AET. (tr-auth)

29655 CHANGES IN GENETIC CELL MATERIAL DURING THE ACTION OF IONIZING RADIATION. Benenyo, T. Honvedorvos; 26: No. 1, 53-66(1974). (In Hungarian).

At the level of microscopic studies radiation damage of nuclear cell material appears in the form of chromosomal aberrations whose behavior during cell division determines cell survivability. Changes in the exchange of certain elements of the chromatin which are caused by irradiation are considered in separate sections. Radiation DNA damage takes place by the same radiochemical mechanism in all living organisms, but recovery is different and namely in this respect is found the reason for the different radiation sensitivity of various types of living organisms. The study considers 3 main types of repair mechanisms known at present, and discusses the differences in repair of damage caused by ultraviolet and by x rays. On the basis of radiation-chemical changes in DNA and biophysical explanations of the DNA-Histone bond, and as a consequence of electron structure, different sensitivity of the components and migration properties of the energy absorbed in the nucleoprotein complex, attention is turned to the fact that the histones are damaged more strongly than the DNA and that the most threatened parts of the DNA molecule are the thymine zones. Delay in division and the occurrence of chromosomal aberrations as a result of irradiation may be closely connected with characteristic changes of the histone ϕ, ϕ, and ϕ. In spite of the fact that the spindle-shaped threads do not belong in a close sense to the chromatin substances, their participation in the occurrence of aberrations cannot be excluded in view of their biochemical properties. The possibilities of therapeutic intervention include a heightening of the natural recuperative power of the cell, and the authors discuss in detail the possibility of using cell proliferation, purine replacement and hormone therapy with the purpose of forestalling pathological states brought on by irradiation. (tr-auth)

29656 ESR STUDIES OF RADIATION DAMAGE IN NUCLEIC ACIDS, BASES, NUCLEOSIDES, AND NUCLEOTIDES. Wyard, S. J.; Elliott, J. P. (Guy's Hospital Medical School, London). Ann. N. Y. Acad. Sci.; 222: 628-639(31 Dec 1973).

Studies on the use of electron spin resonance spectroscopy to determine radiation damage in biological molecules are reviewed. The significance of these studies for increasing the differential radiosensitivity between cancer cells and normal cells is emphasized. Studies are reviewed under the following headings: single crystal studies at room temperature; single crystal studies at low temperature; studies in frozen solutions; studies in liquid solutions; and radical species in irradiated DNA. (HLW)

29657 SIGNIFICANCE OF FREE RADICALS FOR THE INACTIVATION OF TRYPSIN BY uv-IRRADIATION. Investigations by Means of ESR Spectroscopy. Nemec, H. W. Freiburg, Ger.; Freiburg Univ. (1973). 127p. (In German). INIS.

Thesis. 47 figs.; 13 tabs.; 119 refs. With abstract. Available from Freiburg Univ., F. R. Germany. Partly published in Biophysik, v. 6 (1970).

Trypsin was irradiated with uv light in different organic suspension media. The irradiation was carried out using light from the 254 nm mercury resonance line and from different regions of wavelength. It was shown that there is a direct radiation effect and that uv irradiation of oxygen-free suspensions gives similar results to an irradiation in vacuum. After irradiation at 278°K, it could be shown by means of ESR spectroscopy that in trypsin there are long-lived free radicals. Essentially, the unpaired electrons are localized at the C_α atoms of the polypeptide chain and at the sulphur atoms of the cystine radical. Besides the ESR measurement, the decrease of the enzymatic activity was investigated and the quanta yield for the radical formation, Φ_r, and for the inactivation, Φ_I, were determined. For trypsin, after irradiation with uv light at a wavelength 254 nm, it was found that $\Phi_r = 1.7 \times 10^{-3}$ and $\Phi_I = 2.4 \times 10^{-2}$. Thus a value of 0.07 radicals per inactivated molecule was obtained. The long-lived free radicals thus have no influence on the inactivation of the enzyme but are an expression of the damage already taken place. An analysis of these radicals, however, permits conclusions to be drawn on the effect of radiation as there is a greater yield of inactivation quanta with increasing sulphur radical yield. Both radiation effects are mainly attributed to the formation of primary sulphur radicals. For the formation of the secondary sulphur radicals of the type RS from the primary radicals, various transfer mechanisms are assumed. The size of the share of sulphur radicals in the total radical concentration, (RS), decreases with increasing dielectric constants epsilon of the suspension medium according to (RS) approximately $1/\epsilon$. It can be concluded from the present results that central importance must be attributed to the disulphide fracture for the inactivation. Besides the absorption by the cystine radicals, especially those quanta absorbed from the tryptophane radicals can lead to the disulphide fracture. Furthermore, it can be concluded that cross-linking reactions also contribute to the enzyme inactivation. (GE)

29658 PHOTOCHEMICAL ADDITION OF AMINO ACIDS TO THYMINE. Schott, H. N.; Shetlar, M. D. (Univ. of California, San Francisco). Biochem. Biophys. Res. Commun.; 59: No. 3, 1112-1116(5 Aug 1974).

The ultraviolet-light-induced photoreactivity of thymine with the twenty-two common amino acids was surveyed. Lysine, arginine, cysteine, and cystine have been found to be reactive in forming heteroadducts. The results suggest that lysine and arginine may be involved in the experimentally observed ultraviolet induced crosslinking of histones to DNA in DNA-histone complexes. (auth)

29659 KINETICS OF THE CHANGES OF MOUSE HEMOGLOBIN UNDER UV-IRRADIATION. Artyukhov, V. G.; Shmelev, V. P. (Voronezh State Univ., USSR). Biofizika; 18: No. 3, 497-501 (1973). (In Russian).

Spectral study of structural changes of mouse hemoglobin under uv irradiation was carried out. It is shown that photooxidation of its molecules proceeds with a relatively high yield, which equals 0.164. Kinetics of absorption change was studied at 576 mμ of oxyhemoglobin solutions uv-irradiated at 20 to 50°C. It is found that the temperature increase of the irradiated solutions up to 40 to 50°C is accompanied by a deep fall of oxyhemoglobin absorption at 576 mμ. Values of the constants of oxyhemoglobin photooxidation rates at these temperatures were determined. The temperature effect on irradiation of oxyhemoglobin solutions manifests itself in an increase of oxidation rate of its molecules. Different doses of uv irradiation are shown to affect the values of activation energy of oxyhemoglobin photooxidation. An increase of the doses brings about a significant decrease of the activation energy of this photoprocess. (auth)

29660 COMMENT ON "FURTHER DATA ON DNA STRAND BREAKAGE BY VARIOUS RADIATION QUALITIES". Baverstock, K. F.; Horgan, V. J. (Medical Research Council, Harwell, Eng.). Int. J. Radiat. Biol.; 25: No. 5, 513(May 1974).

A correction to the doses reported in a previous paper (Neary, G. J., Horgan, V. J., Bance, D. A., and Stretch, A., Int. J. Radiat. Biol., 1972, 22, 525) on strand-breakage of DNA by ^{60}Co γ rays, gave new values of 70.1 ± 3.3 breaks/Mrad for single-strand breaks, and 3.95 ± 0.16 breaks/Mrad for double-strand breaks, which have been confirmed by further experiments. The corrected results show that the strand breaks per Mrad for ^{60}Co are greater than those for protons by a factor of 1.51. The implications of the revised values are discussed. (UK)

29661 EFFECTS OF CERTAIN DENATURANTS ON THE ABSORPTION SPECTRA OF HEMOGLOBIN FROM CHICK EMBRYOS IRRADIATED WITH ULTRAVIOLET RADIATION DURING EARLY EMBRYOGENESIS. Lwin, K. (Boris Kidric Inst., Belgrade). Iugoslav. Physiol. Pharmacol. Acta; 7: No. 3, 367-374(1971).

Denaturation of hemoglobin with alkali, acid, urea, and/or heat followed by spectrophotometric measurements revealed that the difference spectra of hemoglobin from irradiated embryos were different from those of hemoglobin from the controls, the difference being more pronounced in the uv-than in the visible region. This suggests structural changes in the polypeptide chain and possibly in the general configuration of hemoglobin. (Bull. sci, Sect. A)

Radiation Effects on Cells

29662 (UCRL-75441) CELL CYCLE KINETICS AND RADIATION THERAPY. Mendelsohn, M. L. (California Univ., Livermore (USA). Lawrence Livermore Lab.). 23 Aug 1974. 46p. (CONF-740715-13). Dep. NTIS $5.50.

From 5th international radiation research congress meeting; Seattle, Washington, USA (14 Jul 1974).

The application of cell cycle kinetics to radiation therapy is one hope of significantly improving therapeutic results. Three classes of approach are available: the combined use of intracyclic differential sensitivity and cell synchronization; the application of cycle-linked radiation sensitizers and chemotherapeutic agents to affect cycling versus noncycling cells; and the selection of therapeutic intensity on the basis of repopulation rates of tumor and relevant normal tissue before and after perturbation. A survey of how each approach could be used and of the available kinetic data suggests that there is much to be learned about the kinetic properties of tumor and normal tissue before these approaches are likely to bear fruit. (auth)

29663 STUDIES ON RADIORESISTANCE WITH HeLa CELLS: RADIOSENSITIVITY AND CHROMOSOME CONSTITUTION. Koiwai, S.; Muta, N. (Sapporo Medical Coll.). Radiat. Res.; 59: No. 3, 717-723(Sep 1974).

The chromosome complements of cells of the radioresistant line, which had been derived from HeLa strain by repeated x-irradiation in our previous experiment, were compared with those of the unirradiated original strain of cells. The modal chromosome number of the radioresistant 5 kR line of HeLa cells was found to be 64, and that of the original HeLa strain to be 71. The 5 kR line of cells contained one or two abnormally long acrocentric chromosomes which were almost absent in the parent line. The radiosensitive line of cells from a clone that was obtained by a single cell culture of the original HeLa strain was also examined to confirm the correlation between chromosome constitution and radiosensitivity. From these results and several authors' reports, it was concluded, concerning tumor cells, that the differences in chromosome numbers and karyotypes are simply markers which are useful in distinguishing the resistant line from the original strain. (auth)

29664 RADIATION-INDUCED DNA SYNTHESIS IN NORMAL AND STIMULATED HUMAN LYMPHOCYTES. Darzynkiewicz, Z. (Boston Biomedical Research Inst.). Exp. Cell Res.; 69: 356-360(Dec 1971).

The rate of DNA repair, as measured by unscheduled incorporation of ^{3}H-thymidine following ultraviolet light irradiation, increases during stimulation of lymphocytes by phytohemagglutinin. This increase is parallel in time with a rise in DNA polymerase activity which occurs during stimulation, but is almost two orders of magnitude lower than the increase in enzyme activity. The rate of DNA repair in granulocytes is five times lower than in unstimulated lymphocytes. The possible involvement of DNA polymerase in DNA repair replication is discussed. (auth)

29665 SENSITIVITY TO RADIATION AND INSENSITIVITY TO VINBLASTINE OF THE INDUCER FUNCTION OF THYMUS-DERIVED CELLS. Ito, T.; Cudkowicz, G. (State Univ. of New York, Buffalo). Cell. Immunol.; 2: 595-601(Dec 1971).

Thymic antigen-reactive cells stimulated by sheep erythrocytes generate specific inducer cells facilitating differentiation and maturation of marrow precursors into immunocytes (direct and indirect plaque-forming cells). This function is abolished by in vitro exposure of inducer cells to 1000 rads of gamma rays, but not by their in vivo exposure to the drug vinblastine which is cytocidal for cells entering mitosis. Thus, the cooperative function of inducer cells in anti-sheep immune responses is radiosensitive even when the cells are not dividing. Other helper functions of thymus-derived cells are radioresistant, e.g., the function of carrier-specific cells and of cells reconstituting spleens of thymectomized mice. Differences in radiosensitivity of helper functions suggest that more than one cell type and/or mechanism may be utilized for triggering marrow-derived precursors of immunocytes. (auth)

29666 RADIATION-INDUCED DNA SYNTHESIS IN NUCLEI OF HEN ERYTHROCYTES REACTIVATED IN HETEROKARYONS. Darzynkiewicz, Z. (Boston Biomedical Research Inst.). Exp. Cell Res.; 69: 477-481(Dec 1971).

The effect of ultraviolet irradiation on ^{3}H-thymidine incorporation by erythrocyte nuclei before and after reactivation was investigated. The nuclei reactivated in heterokaryons responded to uv irradiation with an eight-to-fifteen-fold increased rate of ^{3}H-thymidine incorporation. Enlargement of the reactivated hen erythrocyte nuclei was due to the migration of proteins from the heterokaryon cytoplasm into the nuclei. Results indicated that among the macromolecules entering the reactivated nuclei were enzymes capable of repairing DNA. (HLW)

29667 MACROPHAGE – LYMPHOCYTE SYNERGY IN THE PRODUCTION OF OSTEOCLAST ACTIVATING FACTOR. Horton, J. E. (Walter Reed Army Medical Center, Washington, DC); Oppenheim, J. J.; Mergenhagen, S. E.; Raisz, L. G. J. Immunol.; 113: No. 4, 1278-1287(Oct 1974).

Supernatants from cultures of activated normal human peripheral blood leukocytes contain a factor which stimulates osteoclastic bone resorption in vitro. The present study indicates that osteoclast activating factor (OAF) is produced by phytohemagglutinin-activated mononuclear cells within 6 hr of activation, and that peak production is associated with increased amino acid incorporation into protein but precedes increased thymidine incorporation into DNA. Granulocytes, platelets, and red cells were not necessary for the production of OAF, since mononuclear cells purified on Ficoll-Hypaque gradients and devoid of these elements produced as much OAF as unseparated leukocytes. Granulocyte extracts did not show bone-resorbing activity. The production of OAF by mononuclear cells was impaired by irradiation, suggesting that it is made by radiosensitive lymphocytes rather than radioresistant macrophages. However, OAF was not produced by lymphocytes purified on glass-bead columns although these cells could respond to phytohemagglutinin with increased thymidine and amino acid incorporation. Purified macrophages also failed to produce substantial bone-resorbing activity. However, when a small number of irradiated but viable macrophages (5×10^4 cells/ml) was added to glass bead-purified lymphocytes (2×10^6 cells/ml), OAF production was as great as with unseparated mononuclear cell populations. These results suggest that OAF is produced by lymphocytes, but that its production is dependent on macrophage-lymphocyte interaction. OAF is a unique bone-resorbing factor which may play an important role in bone lesions associated with chronic inflammation and neoplasia. The cellular mechanisms for its production participate in the pathogenesis of these disorders. (auth)

29668 LACK OF RECOVERY FROM RADIATION DAMAGE ON COLONY FORMING ABILITY AND ON MEMBRANE CHARGE IN A BURKITT LYMPHOMA CELL LINE. Sato, C. (Aichi Cancer Center, Nagoya, Japan); Kojima, K.; Matsuzawa, T.; Sairenji, T.; Hinuma, Y. J. Radiat. Res.; 15: No. 1, 25-31 (Mar 1974).

A Burkitt lymphoma cultured cell line, P3HR-1, was found to be very radiosensitive ($n = 1$, $D_0 = 67$ R) and showed no substantial recovery by dose-fractionation. Measurement of electrophoretic mobility of whole cells and isolated nuclei after irradiation demonstrated that the loss of negative charge on the membrane was irreversible in this cell line. Analysis of frequency distribution pattern of electrophoretic mobility indicated a good correlation between the loss of colony forming ability and the irreversible loss of membrane charge. The surface saccharides responsible for electrokinetic behavior of the P3HR-1 cells mainly consisted of sialic acid and chondroitine sulfate, but not of hyaluronic acid. The mobility reduction by the removal of these saccharides was reversible and did not result in cell death. (auth)

29669 HISTONE F1 PHOSPHORUS CONTENT AND DNA SYNTHESIS IN SLOWLY-GROWING SUBLINES OF L5178Y-S CELLS. Szumiel, I.; Rosiek, O.; Beer, J. Z.; Budzicka, E.; Sablinski, J.; Kopec, M. (Inst. of Nuclear Research, Warsaw). Bull. Acad. Pol. Sci., Ser. Sci. Biol.; 21: 7-12(1973).

Slowly-growing sublines were isolated by cloning from x-irradiated cell populations of L5178Y-S cells. Phosphorus content of histone F1 and ^{3}H-thymidine incorporation into DNA were determined for 7 such sublines with various mean doubling times. It was found that both histone F1 phosphorylation and the ability to incorporate ^{3}H-thymidine into DNA are impaired in these sublines and that degree of the impairment correlates with the proliferation rate. (auth)

29670 EFFECT OF X IRRADIATION ON HYDROCARBON METABOLISM AND ON HYDROCARBON-INDUCED LETHALITY AND TRANSFORMATION IN CELLS DERIVED FROM MOUSE PROSTATE. Marquardt, H. (Sloan-Kettering Inst. for Cancer Research, New York). Z. Krebsforsch. Klin. Onkol.; 80: No. 3, 223-228(1973).

In M2 cells derived from C3H mouse prostate which are x-irradiated (250 R) 48 before treatment the lethality induced by 3-methylcholanthrene is significantly increased, whereas that induced by N-methyl-N′-nitro-N-nitrosoguanidine is not altered. The effect of prior x-irradiation on the rate of malignant transformation in vitro is as follows: that caused by 3-methylcholanthrene is markedly decreased, that caused by the K-region epoxide of 3-methylcholanthrene is significantly increased, while that caused by dimethylbenz(a)anthracene or by N-methyl-N′-nitro-N-nitrosoguanidine is not influenced. The data suggest that the effect of x rays on methylcholanthrene-induced transformation in vitro is due to altered methylcholanthrene metabolism. (GE)

29671 DISSOCIATION OF HISTONE AND DNA SYNTHESIS IN X-IRRADIATED HeLa CELLS. Bases, R.; Mendez, F. (Albert Einstein Coll. of Medicine, New York). Exp. Cell. Res.; 69: 289-294(Dec 1971).

Although histone synthesis and DNA synthesis are normally very well coordinated in HeLa cells, their histone synthesis proved relatively resistant to inhibition by ionizing radiation. During the first 24 h after 1000 R the rate of cellular DNA synthesis progressively fell to small fractions of control values while histone synthesis continued with much less relative reduction. Acrylamide gel electropherograms of the acid soluble nuclear histones synthesized by irradiated HeLa cells were qualitatively normal. (auth)

29672 RATE OF DNA REPAIR IN PROGERIC AND NORMAL HUMAN FIBROBLASTS. Epstein, J.; Williams, J. R.; Little, J. B. (Harvard Univ., Boston). Biochem. Biophys. Res. Commun.; 59: No. 3, 850-857(5 Aug 1974).

The rate of rejoining of γ-ray induced DNA strand breaks was measured in diploid skin fibroblasts from normal subjects at early and middle passage through their in vitro lifespan and compared to the rate of rejoining observed in cells from 4 patients with symptoms of the Hutchinson-Gilford Progeria syndrome of precocious aging. The rate of rejoining observed in middle passage diploid cells was less than that in cells in very early passage. The rate of rejoining in progeric cells varied markedly among cells from different patients but was significantly less than the rate in normal diploid cells. The reason for this decreased rate of DNA strand rejoining in progeric cells is not clear, but it may be related to accelerated in vitro senescence which is observed in some progeric cell strains. (auth)

29673 DNA REPAIR IN HUMAN PROGEROID CELLS. Regan, J. D.; Setlow, R. B. (Oak Ridge National Lab., TN). Biochem. Biophys. Res. Commun.; 59: No. 3, 858-864(5 Aug 1974).

Human diploid fibroblast cells derived from normal subjects and from patients with progeria or progeroid syndromes were examined for the extent of their ability to repair γ-induced single-strand breaks in their DNA. Cells irradiated and incubated as monolayers showed normal repair in all cell lines studied. Progeroid cells that were treated with trypsin, irradiated, and allowed to repair in suspension with shaking showed slightly less repair after long times than did normal cells. However, if the cells were not shaken, the progeroid cells remaining in suspension showed

DNA degradation and an inability to repair DNA strand breaks in contrast to normal cells. (auth)

29674 METRONIDAZOLE (FLAGYL). A Radiosensitizer of Hypoxic Cells. Asquith, J. C. (Mount Vernon Hospital, Northwood, Eng.); Foster, J. L.; Willson, R. L.; Ings, R.; McFadzean, J. A. Brit. J. Radiol.; 47: No. 560, 474-481(Aug 1974).

The radiosensitizing properties of metronidazole were studied using bacteria, bean roots, and mammalian cells in vitro as test systems. Metronidazole has been shown to sensitize only anoxic cells in a concentration-dependent manner, a maximum enhancement ratio of 1 · 9 being obtained at 8 mmol/1. metronidazole concentration for mammalian cells. The effect of added SH compounds on the sensitizing effect of metronidazole was studied in bacteria and bean roots. Metronidazole sensitized bacteria to the effects of neutron irradiation by a factor of only 1 · 4. The mechanism of sensitization by metronidazole is discussed in the light of pulse radiolysis and ESR data, and its action compared with that of oxygen. Pharmacological data presented suggest that in vivo testing of metronidazole should be possible and that any radiosensitizing effects shown may be related to measured serum concentrations. (auth)

29675 MECHANISMS OF INHIBITION OF THE POSTIRRADIATION RECOVERY IN CELLS. IV. The Effect of Caffeine and Acriflavine on Gamma and X-Ray Induced Unscheduled DNA Synthesis in HeLa Zh-63 Cells. Semenova, E. G.; Volkova, Z. M.; Zhestyanikov, V. D. (Inst. of Cytology, Leningrad). Tsitologiya; 16: No. 8, 1010-1015(Aug 1974). (In Russian).

The effect of caffeine and acriflavine on x-ray induced unscheduled DNA synthesis did not involve changes in the distribution of the x-ray cells (5 krad) in asynchronous culture. Caffeine (10^{-2} M) and acriflavine ($5 \cdot 10^{-6}$ M) inhibited the unscheduled DNA synthesis in the asynchronous and synchronized (G_1-phase) culture after gamma irradiation (100 krad), and in the synchronized culture (G_2-phase) after gamma irradiation of 5 and 100 krad. Caffeine (10^{-2} to $2 \cdot 10^{-3}$ M) reduces the survival of x-irradiated HeLa Zh-63 cells, while acriflavine ($5 \cdot 10^{-7}$ M) has no such effect. (auth)

Radiation Effects on Microorganisms

Refer also to abstract 29674.

29676 (SLA-74-0065) MEASUREMENT OF THE RADIATION INACTIVATION OF ATTENUATED POLIOVIRUS BY THE PLAQUE ASSAY TECHNIQUE. Trujillo, R. E. (Sandia Labs., Albuquerque, N. Mex. (USA)). Aug 1974. Contract AT(29-1)-789. 48p. Dep. NTIS $5.50.

The γ inactivation of attenuated polio virus at various dose rates is presented. This study of virus inactivation depended upon the application of the plaque assay technique in monitoring virus survival after exposure to ionizing radiation. This plaque assay technique is described in sufficient detail to allow those unfamiliar with the required tissue culture and virology techniques to engage in further studies on this virus. (auth)

29677 MALIGNANT TRANSFORMATION OF HAMSTER EMBRYO FIBROBLASTS FOLLOWING EXPOSURE TO ULTRAVIOLET-IRRADIATED HUMAN CYTOMEGALOVIRUS. Albrecht, T.; Rapp, F. (Pennsylvania State Univ., Hershey). Virology; 55: No. 1, 53-61(Sep 1973).

Following exposure to ultraviolet-irradiated cytomegalovirus, clones of noncontact inhibited hamster embryo fibroblasts were isolated. A continuous cell line (Cx-90-3B) was established from one of these clones, which proved oncogenic when inoculated into weanling golden Syrian hamsters. Cytomegalovirus antigens could be demonstrated in the cytoplasm and on the surface of Cx-90-3B cells using human convalescent sera. Furthermore, serum from tumor bearing animals was shown to contain antibody to cytomegalovirus specified antigens. These observations are similar to those previously reported for herpes simplex viruses and represent the first demonstration that human cytomegalovirus has transforming potential in mammalian cells. (auth)

29678 POSTIRRADIATION FATE OF BACTERIOPHAGE LAMBDA DNA IN THE HOST CELL. Trgovcevic, Z.; Petronovic, D.; Zgaga, V. (Ruder Boskovic Inst., Zegreb). Virology; 55: No. 1, 266-274(Sep 1973).

The postirradiation fate of lambda cI857 DNA in the host cell was investigated under conditions which prevent phage vegetative development. Like other episomes, lambda cI857 DNA can be present in the host either integrated in the host chromosome or located in the cytoplasm. It has been shown by the technique of DNA–DNA hybridization that, after gamma irradiation chromosomally integrated lambda cI857 DNA is degraded to about the same extent as the bacterial DNA. In contrast, extrachromosomally located lambda cI857 DNA is insensitive to radiation-induced degradation, as shown by infection with radioactively labeled lambda cI857 prior to irradiation; under the same set of experimental conditions, the host DNA is susceptible to degradation. The biological implications of these findings are discussed. (auth)

29679 PROTEINS INDUCED IN BACILLUS SUBTILIS INFECTED WITH BACTERIOPHAGE ϕ29. Carrascosa, J. L.; Vinuela, E.; Salas, M. (Inst. G. Maranon, Madrid). Virology; 56: No. 1, 291-299(Nov 1973).

Bacteriophage ϕ29 induces, in uv-irradiated B. subtilis, the synthesis of 12 nonstructural proteins as well as the 7 structural polypeptides which form the viral particle. The molecular weight of the nonstructural polypeptides amounts to 180,000 daltons; if all these proteins are phage-coded, this corresponds to about 30% of the information content of ϕ29 DNA. The phage-induced polypeptides can be classified as early and late proteins, according to the time of their appearance after infection. All the structural proteins as well as three nonstructural proteins are late proteins. The remaining nonstructural proteins appear early after infection. (auth)

29680 REPAIR OF γ-RAY-INDUCED DAMAGE IN BACTERIOPHAGE LAMBDA. Srivastava, B. S. (Univ., Brussels). Virology; 55: No. 2, 550-553(Oct 1973).

Bacteriophage λ was gamma-irradiated in nutrient broth and plated on radiosensitive and radioresistant strains of Escherichia Coli K12. The number of single-strand breaks induced in phage DNA by irradiation was essentially the same for all bacterial strains, but there was a difference in the ability of the phages and bacterial mutants to repair phage DNA during post-radiation incubation. Essentially all breaks were repaired in wild-type bacteria demonstrating that a wild-type phage-bacterial system possesses an efficient system to repair single-strand breaks. (HLW)

29681 TEKHNOLOGICHESKIYE OSNOVY RADIATSIONNOY OBRABOTKI PISHCHEVYKH PRODUKTOV. (Technological Foundations for Radiation Treatment of Food Products). Frumkin, M. L.; Koval'skaya, L. P.; Gel'fand, S. Yu. Moscow; Izdatel'stvo Pishchevaya Promyshlennost (1973). 408p.

The results of research conducted at the All-Union Scientific Research Institute of the Canning and Vegetable Drying Industry are summarized and literature data on irradiation of plant (fruit, berries, and vegetables) and animal (meat and meat products) raw materials are presented. Particular attention was accorded to the use of low doses of ionizing radiation (gamma rays and accelerated electrons) which do not have a negative influence on the quality of the products. Data are presented on investigations dealing with the development of technological approaches for irradiating fruits, berries, and vegetables, as well as intermediate meat products, and culinary and sausage products. Physiological and biochemical changes which arise in plant and animal tissues under the influence of ionizing radiation are described. Methods are presented for the inhibition of undesirable changes in quality during irradiation and on subsequent storage. (JPRS)

29682 CHEMICAL NATURE OF THE ENDS OF DNA SINGLE-STRAND BREAKS PRODUCED BY IONIZING γ RADIATION IN VIVO AND PATHWAYS OF THEIR REPARATION. Gaziev, A. I.; Sergeeva, S. A.; Zakrzhevskaya, D. T. (Inst. of Biophysics, Puscino, USSR). Stud. Biophys.; 42: No. 3, 203-218(1974). (In Russian).

Single-strand breaks with 5'OH, $5'PO_4$, and 3'OH ends indicated by phosphate, polynucleotidkinase, and DNA ligase reactions are registered in DNA from cell of E. coli of wild type and deficient in DNA polymerase I, isolated immediately after their γ-irradiation. The total quantity of single-strand breaks with 5' ends corresponds to those registered with the method of sedimentation in a gradient of alkaline sucrose. The yield of breaks with different ends does not equal the total yield of single-strand breaks in DNA in vivo and depends on the dose. The quantity of $5'PO_4$ groups is larger than that of 3'OH ones. Most (70–40% at doses of 10–30 krad) of the single-strand breaks with $5'PO_4$ and 3'OH ends are bound by ligase. During the short period of postradiation incubation the end groups of ligase-specific breaks in DNA of the cells deficient in DNA polymerase I changes to a form not capable of binding with ligase. This results from exonuclease attacks on ligase-specific substrate points to the DNA molecule. However, transformation of ligase into a ligase adenylate complex during irradiation contributes to the partial rapid reparation of single-strand breaks in E. coli DNA independently of DNA polymerase I. The rest of the breaks recover only after DNA-polymerase reassemblage of the polynucleotide chain. (auth)

29683 SPECIFICITY AND FREQUENCY OF ULTRAVIOLET-INDUCED REVERSION OF AN ISO-1-CYTOCHROME C OCHRE MUTANT IN RADIATION-SENSITIVE STRAINS OF YEAST. Lawrence, C. W.; Stewart, J. W.; Sherman, F.; Christensen, R. (Univ. of Rochester, NY). J. Mol. Biol.; 85: No. 1, 137-162 (5 May 1974).

The basis for the specific pattern of ultraviolet-induced reversion of cyc 1-9, an ochre allele of the structural gene for iso-1-cytochrome c, was examined in radiation-sensitive strains of yeast. Previous analysis, using RAD+ strains, showed that 21 out of 23 cyc 1-9 revertants induced by ultraviolet light arose by A.T to G · C transition at the first position in the UAA codon, the remaining two occurring by A.T to T.A transversion at the second position (Stewart et al. J. Mol. Biol.; 68: 83-96(1972), Sherman & Stewart. Genetics, in the press, (1974)). All possible base-pair substitutions could be obtained with the aid of other mutagens. It has now been shown that this specificity depends largely on the action of the RAD6 locus, since ultraviolet-induced revertants of cyc 1-9 arose by a variety of base-pair substitutions in a strain carrying the rad 6-1 allele. Induced reversion frequencies in strains carrying this allele are much lower than normal, though significantly higher than the spontaneous frequency, and the strains are more sensitive to the lethal effects of both ultraviolet and x radiation. The pheno-typically similar rad 18-2 mutation, which appears to block the same repair pathway as rad 6-1, also has some effect on the reversion specificity, but its action depends on the presence of other, unidentified, mutations. Specificity was, however, completely unaltered in an excision-defective strain carrying the rad 1-2 allele. Induced reversion frequency of cyc 1-9 was much higher than normal in this strain. Photoreactivation studies indicated that pyrimidine dimers were responsible for most of the revertants in RAD+, rad 1, and rad 6 strains. These experiments show that the RAD 6+ locus is intimately concerned with error-prone repair, and suggest that excision repair is substantially error-free. (auth)

29684 BASE-PAIR DELETION AT A FRAMESHIFT HOTSPOT IN SALMONELLA. Ino, I. (Johns Hopkins Univ., Baltimore); Yourno, J. J. Mol. Biol.; 85: No. 2, 301-307(15 May 1974).

A frameshift mutation induced by x rays in the histidinol dehydrogenase gene of Salmonella is shown to be a deletion of a G · C pair (−1) from a DNA repeat of three G · C pairs. This repeat is a hotspot for frameshifts induced by intercalating agents. Most of these are externally suppressible and test as an addition of a G · C pair (+1). There is no evidence for external suppression of the −1 frameshift. The results are consistent with previous suggestions that: (a) repeating DNA sequences are frameshift hotspots because these have an intrinsic tendency to mispair; and (b) frameshifts produced by radiation damage generally are deletions. The intercalating agents fail to revert the −1 frameshift to prototrophy; DNA repeats of at least three G · C pairs seem necessary for these intercalating agents to induce frameshifts by stabilizing mispairing. (auth)

Radiation Effects on Plants

Refer also to abstract 29674.

29685 ASCORBIC ACID CONTENT IN DIFFERENT STAGES OF RIPENESS OF FRUITS PEPPER UNDER THE EFFECT OF E1 AND IRRADIATION BY ^{60}Co. Zderkiewicz, T.; Dyduch, J. Acta Agrobot.; 25: 171-178(1972). (In Polish).

Investigations on the ascorbic acid content during subsequent stages of ripeness of pepper fruits submitted to the influence of E1 and irradiation by ^{60}Co are presented. Considerable variation was found in the ascorbic acid content in the pepper fruit, depending on the ripeness stage, the E1 concentration, and the dose of ^{60}Co. The highest content of this compound was found at the intermediate ripeness stage, the lowest at the technical ripeness stage. E1 caused vitamin C increase at the concentration of 0.03 and 0.125%, and ^{60}Co at the 5000 R dose. (auth)

29686 RECIPROCAL TRANSLOCATION AS A NEW APPROACH TO BREEDING SEEDLESS WATERMELON. I. Some Characters of F$_1$ Hybrids with Six Reciprocal Translocations. Watanabe, T. (Kyoto Univ. of Education). Bull. Kyoto Educ. Univ., Ser. B; No. 41, 19-39(Sep 1972). (In Japanese).

Dry seeds of watermelon varieties including strains, parents of the hybrid watermelon (A × B strains, Nagaoka kohai Kodama), were irradiated with 20, 25, 30 and 35 R doses of x-rays. The induced reciprocal translocation (RT's) heterozygotes were self-pollinated and then from their progeny the reciprocal translocation homozygotes were selected. The increases of RT's heterozygotes are made from their reirradiation of the seeds and also from successive crossings among the resultants. Before 1971 we made the F$_1$ hybrid with six reciprocal translocations. In spite of the vigorous growth of the main vines of the plant, they produce a small number of very poor male flowers. Female flowers are as successful as those of the control plants and fruits set well with normal pollination by the normal control pollen grains. Pollen fertility of the F$_1$ hybrid shows about 1 per cent level of good pollen grains. The theoretical pollen fertility in the F$_1$ hybrids was calculated by the formula $Y = Kd^t$ (Yamashita 1952), where Y = pollen fertility, K = constant (K is usually 1), d = disjunctional coefficient, t = number of RT-sets combined. The observed pollen fertility very well fitted the theoretical pollen fertility. The number of seeds per fruit (average weight of five fruits is about 2.1 kg) is significantly reduced to the level of 4.6 grains of seeds. This corresponds to the reduction of about 97 per cent against that of the control fruit seed number. The fruit is somewhat inclined to deformity in morphology due to the lesser number of seeds in the fruit. Some characters, namely, seed germination, vegetative growth and development, flowering of female flowers, pollination and fertilization, fruit-setting and early ripening of the fruits are the same as those of the control plants. (auth)

29687 VEGETATION CHARACTERISTICS OF LENS ESCULENTA (MOENCH) FOLLOWING IRRADIATION WITH THERMAL NEUTRONS. Uhlik, J. Sb. Vys. Sk. Zemed. Praze, Fak. Agron., Rada A; 5: No. 1, 127-143(1972). (In Czech).

Preliminary findings are presented on the effect of thermal neutrons on generation M$_1$ of lentil (Lens esculenta (Moench)). The study aimed at finding the range of efficient doses of thermal neutrons that had not so far been investigated in view of their biological effect. Also the variability was observed of various vegetation characteristics due to the conditions of the site during five seasons with extremely different climatic conditions. Doses between 8×10^{11} n/cm^{-2} and 5×10^{12} n/cm^{-2} did not considerably affect the number of germinated seeds related to controls. In a greenhouse, doses of about 10^{12} n/cm^{-2} to 3.3×10^{12} n/cm^{-2} resulted in a decrease in the number of sprouted plants, in dependence on the manner of cultivation. The growth of roots was inhibited by a dose of 6.5×10^{11} n/cm^{-2}. Thermal neutron irradiation was also found to affect the length of the plants. The greatest differences were observed on the 35th day after irradiation, the smallest on the 90th day. Climatic factors were observed to affect considerably the length of stems, the number of surviving plants, and the fertility of the plants. The range of practical and useful doses was limited by doses of 1.5×10^{12} n/cm^{-2} and 5×10^{12} n/cm^{-2} in dependence on the conditions of cultivation. Under less suitable cultivation conditions a dose of 5×10^{12} n/cm^{-2} was lethal, while under good conditions only a dose of 6×10^{12} n/cm^{-2} was observed to show the same effect. (INIS)

29688 RESISTANCE TO USTILAGO MYADIS OF WD LINEAGE PROGENY AFTER CHRONIC GAMMA IRRADIATION. Rousek, J. (Vysoka Skola Zemedelska, Prague). Sb. Vys. Sk. Zemed. Praze, Fak. Agron., Rada A; 5: No. 2, 105-111(1972). (In Czech).

The effect of chronic gamma irradiation on the sensitivity of maize to smut (Ustilago maydis) was studied. Progeny I$_4$ of the WD lineage maize were infested with smut. Part of the progeny were irradiated in a gamma field in generation I$_1$. The differences were statistically processed. The irradiation resulted in greater differences between the original offspring generation and generation M$_4$ than in the controls as far as the resistance to smut was concerned. Inbreeding did not affect the resistance. (auth)

29689 EFFECT OF CHRONIC AND ACUTE GAMMA IRRADIATION ON SPECIFIC RECOMBINATION CAPABILITY OF LINEAGE WD MAIZE. Cerny, J. (Vysoka Skola Zemedelska, Prague). Sb. Vys. Sk. Zemed. Praze, Fak. Agron., Rada A; 5: No. 2, 85-104(1972). (In Czech).

In maize of the WD lineage the effect of gamma radiation on the alteration of the specific recombination capability was studied. Plants were exposed to chronic irradiation in doses of 8734 to 88 R, while dry seeds were exposed to acute irradiation by a dose of 10,000 R. The chronic and acute irradiations were found to effect genetic changes of the specific recombination capability of said lineage which resulted in extending the genotype and phenotype variabilities of hybrids F$_1$ of generations M$_3$ and M$_4$ and the parental species W9. As against controls, gamma radiation was ascertained to reduce average values of the number of days before maize panicle flowering and of the height of the experimental plants. (auth)

29690 EFFECT OF GAMMA RADIATION ON GENERATION M$_2$ OF LENS ESCULENTA MOENCH. Uhlik, J. (Vysoka Skola

Zemedelska, Prague). Sb. Vys. Sk. Zemed. Praze, Fak. Agron., Rada A; 5: No. 2, 113-127(1972). (In Czech).

The effect was investigated of gamma radiation on lentil (Lens esculenta (Moench)). Irradiation at doses of 2 to 16 kR was not found to substantially affect the number of sprouted plants. The effect of irradiation increased with increasing number of days after planting. Characteristic of the irradiation was a rapid reduction of the relative number of plants following mean doses and a slight reduction of the relative number following lower as well as higher doses. Radiosensitivity was also affected by climatic conditions. Doses exceeding 16 kR were lethal for plants grown in suitable conditions. Doses of 12 to 13 kR were critical for plants grown in less suitable conditions. (auth)

29691 RADIOECOLOGY OF POGONATUM URNIGERUM (L.) PAL. BEAUV. Sarosiek, J.; Kola, W.; Orda, A. (Univ. of Wroclaw). Acta Soc. Bot. Pol.; 42: 241-252(1973).

Within the area of the radiation anomaly near Kowary (Sudetes), the moss Pogonatum urnigerum grows on sites with natural gamma radiation of the soil within the limits of 0.05 to 0.91 mR/h. By way of detailed ecological analysis, five stenotopic habitats of P. urnigerum were singled out, differing, however, in radiation level. On these microhabitats the intrapopulation variability, radioactivity and ecological properties of the P. urnigerum populations were investigated. It was demonstrated that radiation within the above mentioned range is an essential ecological factor conditioning the ecotype differences in Pogonatum urnigerum, and among them the developmental anomalies. (auth)

29692 STUDIES ON THE USE OF U-120 CYCLOTRON AND FAST NEUTRON GENERATOR IN NEUTRON IRRADIATION OF SEEDS FOR MUTATION. Huczkowski, J. (Inst. of Nuclear Physics, Krakow). Hodowla Rosl., Aklim. Nasien.; 17: 145-159(1973). (In Polish).

Fast neutrons produced in the U-120 cyclotron and fast neutron generator were used for the irradiation of seeds aiming at radiation induction of mutation. The neutrons of mean energy of 5.5 MeV were obtained from nuclear reactions of ^{9}Be(d,n)^{10}B and ^{9}Be(α,n)^{12}C in the cyclotron. The 14.1-MeV neutrons were produced from the reaction of ^{3}H(d,n)^{4}He in the fast neutron generator. Barley seed of Himalaya and Damazy varieties as well as wheat seed of Ciano 67 variety were irradiated. The irradiation effect was measured by the method of reduction of seedling height in a growth chamber, recommended by the international program of FAO/IAEA. The results obtained proved the U-120 cyclotron to be fit for neutron irradiation of seed for the needs of plant breeding and that the irradiation conditions were either similar or even better than that obtained in the nuclear reactors of the international program FAO/IAES. The mentioned installations are capable of treating seed with neutron doses of 1000 R for 24 minutes at a distance of 20 cm from the target. The gamma contamination was by 130 R lower than that obtained from the reactors adapted specially to irradiation of seed. Mean energy of neutron produced in the cyclotron was three times higher than that obtained from the nuclear reactor. The advantage of the cyclotron is a possibility of regulating the doses of irradiated objects, even a big one, by changing the distance of them from the beryl target. (auth)

29693 USE OF X-RAYS IN SUGAR BEET BREEDING. Szota, Z. (Plant Breeding and Acclimatization Inst., Bydgoszcz, Poland). Hodowla Rosl., Aklim. Nasien.; 17: 121-127(1973). (In Polish).

Dry seed, germinated seed, and young plants at the cotyledon stage were given x-ray treatment. The tolerant dose for dry seed was 30 to 40 kR, while that for germinated seed was 12 to 15 kR, and that for young plants was 8 kR respectively. The selection within the irradiated material did not result in obtaining of mutants that could be valuable both with regard to economic characters and the resistance to fungal diseases. It is likely that sugar beet breeders are in a position of improving sugar beet varieties without troublesome methods of mutation breeding as the mutability among the existing varieties is still great. (auth)

29694 INDUCED MUTATION IN PEAS. XXVI. Genetically Conditioned Differences in Radiation Sensitivity. IV. Blixt, S. Agri Hort. Genet.; 28: No. 9, 55-116(1970).

Four pea lines at three different levels of gamma sensitivity were crossed, and the sensitivity of the lines in the F_1 and F_2-generations were studied. The criteria of radiation effect used were the dose for fifty per cent germination inhibition, growth inhibition, survival of main shoot and of main and secondary shoot, and the dose producing spotting degree 2.5. The characteristics studied in relation to sensitivity have been the number of recessive genes, flowering time and the genes A, Cor, D, Di, F, Fs, Gri, I, Kp, Kpa, Le, Mifo, O, P1, R, U, and V. Of the four lines used, line 180 was the most radiation-resistant, the lines 1147 and 1241 the most radiation-sensitive, while line 1405 was intermediate. The F_1-generations showed that the different criteria used for measuring sensitivity probably reflected radiation effects on different mechanisms. Also, the different crosses differed with respect to sensitivity: crosses involving line 180 were generally more resistant than those not involving this line. The results indicate that the gene A is of the first importance in determining the sensitivity; recessivity for this gene results in a low level of resistance to gamma radiation. In genotypes dominant or heterozygous for A, the sensitivity is influenced by the number of double-recessive genes present in the genotype. The results from the analysis of the F_2-generations showed a clear effect of the gene R in chromosome VII, genotypes recessive for this gene being more sensitive. Chromosome I was also found to be connected with sensitivity. Radiation sensitivity in micro-organisms and the relation of these results to the results from Pisum are discussed. (auth)

29695 MECHANISMS OF THE INHIBITORS OF CELL POST-IRRADIATION RECOVERY. III. Increase in the Chromosomal Damage Rate by Caffeine Treatment of X Irradiated Buckwheat Cells. Erupnova, G. F.; Seitkhozhaev, A. I. (Inst. of Cytology, Leningrad). Tsitologiya; 16: No. 8, 1005-1009(Aug 1974). (In Russian).

Post-irradiation treatment with caffeine ($1 \cdot 10^{-4}$ M) of the root-tip cells of diploid and tetraploid buckwheat increased markedly the yield of chromosome aberrations. The delay of the cell cycle occurred (extended S and G). The chromosome aberrations rate increased more in the tetraploid buckwheat cells rather than in the diploid buckwheat cells. Caffeine is supposed to inhibit the restoration of the chromosome breaks, and the cells of tetraploid buckwheat are supposed to have a stronger reparation system. (auth)

29696 CHROMOSOMAL ABERRATIONS INDUCED BY GAMMA IRRADIATION OF CREPIS CAPILLARIS SEEDLINGS AT DIFFERENT PERIODS OF INTERPHASE. Luchnik, N. V.; Fesenko, E. V.; Ovchinnikova, V. G.; Morozov, K. N. (Research Inst. of Medical Radiology, Obninsk, USSR). Genetika; 10: No. 8, 47-57 (Aug 1974). (In Russian).

Seedlings of Crepis capillaris were irradiated with 200 and 400 rads of gamma rays (^{60}Co) and fixations were done at hourly intervals during the first postirradiation cell cycle. Types and frequencies of chromosomal aberrations as well as the number of labelled metaphases were studied. The significant heterogeneity between roots with respect to labelling index took place in spite of their random variation with respect to aberration frequency. An appreciable number of chromosome type aberrations including dicentrics and rings was observed at all fixation times, thus the type of aberration did not depend on the state of chromosome duplication. Peaks for relative frequencies of different discontinuities form the succession: gaps—chromatid breaks—double gaps—isolocus breaks. A higher radiation dose favored the formation of chromatid exchanges at the expense of chromosome ones, a similar interrelation was observed also for isochromatid and chromosome breaks. A classical interpretation of the observed pattern of aberrations in the cell cycle appear to be insufficient. The results obtained indicate a significant importance of the stages of intermolecular proofs in the development of a primary lesion. The mechanism of proofs is radiosensitive, if a damage affects the frequency and the type of aberrations. (auth)

29697 DOSE-RESPONSE FOR FREQUENCY OF CHROMATID ABERRATIONS INDUCED BY X RAYS AT G_2 AND S STAGES OF THE MITOTIC CYCLE IN CREPIS CAPILLARIS ROOT TIPS. Kaznadzei, V. V.; Protopopova, E. M. (Inst. of Developmental Biology, Moscow). Genetika; 10: No. 8, 58-70(Aug 1974). (In Russian).

A study was made of dose-response for chromatid aberration yield at G_2 and S stages of the mitotic cycle in x irradiated Crepis capillaris root tips. With respect to dose-response for the yield of exchange-type aberrations during the mitotic cycle, two-break component existed exclusively at the S stage. At the G_2 stage it was replaced with one-break component. The dose-response for frequency of terminal fragments reveals in general a linear kinetics, showing a certain two-break component. A detailed comparative analysis of dose-response curves for chromatid aberration yield during the mitotic cycle suggests that two alternative mechanisms of the aberration formation, i.g., according to principles of "break" and "exchange" exist simultaneously. (auth)

29698 STUDIES ON INTER-RELATIONSHIP OF QUANTITATIVE TRAITS IN M_3 AND M_4 GENERATIONS FOLLOWING MUTAGENIC TREATMENTS IN SORGHUM. Sreeramulu, K. (Tamilnadu Agricultural Univ., Coimbatore, India). Z. Pflanzenzuecht.; 68: No. 4, 287-293(1972).

The effects of physical (x and γ rays) and chemical (EMS) mutagens on few quantitative characters, namely height of plant, weight of ear and grain in cultivated Sorghum (Co. 18) for the induced polygenic variability were examined and the interrelationship of these characters in M_3 and M_4 generations were studied. The mean of the different quantitative traits showed an increase as well as decrease in the treated M_3 and M_4 populations when compared to the untreated control population. But, in general, the mean showed a tendency to approach the control following mutagen treatments. The variance differed in magnitude in the different quantitative traits following treatments with mutagens. In M_3, all treatments showed an increase in variance except 30 kR x rays in all the characters, whereas in M_4 there was an increase as well as decrease in variance in the treated population compared to the control. Intergeneration correlation for the components of variation in M_4 over M_3 was worked out for the 3 characters. The γ values were found to be not significant in treated as well as control population in respect of plant height, where as they were found to be significant in 20 and 40 kR x rays for weight of ear and in control for grain yield. The induced quantitative variation and the interrelationship appeared to depend not only on the type of treatment but also on the character chosen for study. (Indian Sci. Abstr.)

29699 RADIOSENSITIZATION OF HYPOXIC CELLS WITH METRONIDAZOLE. Hall, E. J. (Columbia Univ., New York); Chapman, J. D. Brit. J. Radiol.; 47: No. 560, 513-514(Aug 1974).

Drugs that act as hypoxic radiosensitizers to human tumor cells could constitute an eminently practical advance in radiotherapy, since they would be much more widely available to radiotherapists than high LET radiation, and at a fraction of the cost. Metronidazole, which is extremely non-toxic and can be maintained at a prolonged high concentration in human blood, has been studied as a hypoxic radiosensitizer, using the growth of Vicia faba seedlings as a test system, with (a) 210 kV x rays and (b) 15-MeV monoenergetic neutrons. Metronidazole (6 mM) reduced the oxygen enhancement ratio for x rays from 2.8 to 1.9, and for 15-MeV d → T neutrons from 1.67 to 1.36. The aerated cells were unaffected. Electron-affinic radiosensitizers could therefore prove beneficial in radiotherapy with neutrons, as well as with low LET radiation sources, since metronidazole, although not an outstanding sensitizer, enhanced the expression of radiation damage generated in hypoxia by radiations of different LETs. (U.K.)

Radiation Effects on Animals

Refer also to abstracts 29827 and 29828.

Man

Refer also to abstracts 29003, 29342, 29343, 29346, 29347, 29351–29353, 29362, 29378, 29379, 29383, 29412, 29452, 29662, and 29829.

29700 (AED-CONF-74-030-004) GENETIC RADIATION EFFECTS. Stephan, G. (Bundesgesundheitsamt, Neuherberg/Muenchen (F. R. Germany). Abt. fuer Strahlenhygiene). 1974. 9p. (In German). INIS.

From symposium on safety aspects of implanted cardiac pacemakers, with special regard to radionuclide batteries; Berlin, F. R. Germany (1 Mar 1974).

The conditions and processes involved in genetic damage due to ionizing radiation and the various types of mutations are reviewed. The genetic risk from radionuclide-powered cardiac pacemakers can only be evaluated when the dose rate of the radiation source, the type of emitted radiation and the distance between radiation source and irradiation object, in this case the gonads, are known. The radiation dose to the gonads of ^{147}Pm or ^{238}Pu-powered cardiac pacemakers, calculated for a period of ten years, varies between 5 and 10 mrem/h, depending on the distance between the implanted source and the gonads. These values are valid for the conditions in air, whereas the conditions in the human body are different as the radiation is attenuated by the tissues, the attenuation increasing with greater distance. Another important factor in the estimation of the radiogenetic risk is the age of patients who, in most of the cases (about 98%), have passed the age of reproductiveness at the time they have their first cardiac pacemaker implanted. For comparison, the ICRP standards for the maximum permissible occupational dose to workers and the maximum permissible dose to the population, as well as the dose resulting from the natural radiation exposure are given. (INIS)

29701 (AED-CONF-74-140-004) INDIRECT TECHNIQUE AND PROBLEMS OF RADIATION PROTECTION IN PEDIATRIC X-RAY DIAGNOSTICS. Heinrich, H.; Schuster, W.; Ullrich, H. 1974. 6p. (In German). (CONF-740465-2). INIS.

From x-ray congress meeting; Baden-Baden, F.R. Germany (25 Apr 1974).

The equivalence of direct and indirect x-ray pictures is demonstrated and the advantages of the indirect pictures such as e.g., the minute doses per picture and thus a lesser burden to the patient, are shown. The saving factor can be as much as 20. The experience gained with this method by the x-ray department of the University Clinic Erlangen are demonstrated using several examples. The geometric enlargements can be reduced to a little over 1. The skin and gonadal doses alone due to the small geometrical enlargements are reduced by a factor of 2.9. By means of constructive measures this factor can even be enlarged to 3.3. There is naturally a dose reduction for the investigating team. (GE)

29702 (AED-CONF-74-221-006) SPECIAL LABORATORY-CHEMICAL EXAMINATION TECHNIQUES. Thefeld, W.; Hoffmeister, H. (Bundesgesundheitsamt, Berlin (F.R. Germany). Inst. fuer Sozialmedizin und Epidemiologie). 1974. 13p. (In German). (CONF-740662-4). INIS.

From 15th annual meeting of the Vereinigung Deutscher Strahlenaerzte e.V. on the authorized physician within the meaning of the radiation protection laws; Karlsruhe, F.R. Germany (14 Jun 1974).

1 fig.; 1 tab.; 46 refs. Available from ZAED.

Although up to present, only little experience could be gained with laboratory chemical investigations on patients who had suffered a radiation accident, a lot can be said for including this method in diagnostics along with the haematological and cytological methods. The conditions that these investigations must fulfill are given. An attempt is made, by demonstrating the radiation-induced changes of individual metabolic systems (amino acids, especially tryptophane and its metabolites, nucleic acids and their decomposition products, enzymes, proteins, electrolytes, amongst others) to point out the biochemical parameters whose laboratory chemical determination in blood or urine promises to be successful in the diagnosis of radiation damage. (GE)

29703 (AED-CONF-74-221-007) MEDICAL EVALUATION OF MEASURED VALUES FOLLOWING RADIATION EXPOSURE. Oster, H. (Bayerisches Landesinstitut fuer Arbeitsmedizin, Muenchen (F.R. Germany)). 1974. 6p. (In German). (CONF-740662-2). INIS.

From 15th annual meeting of the Vereinigung Deutscher Strahlenaerzte e.V. on the authorized physician within the meaning of the radiation protection laws; Karlsruhe, F.R. Germany (14 Jun 1974).

Difficulties encountered in practical health physics when trying to fulfill the requirements laid down in paragraph 35 of the X-Ray Ordinance are discussed. The essential problem for the physician in this field is to find an answer to the question of how the excessive radiation doses verified by the physicist are to be purposefully utilized in his practical work. The basic considerations in this connection are: 1. How should the individual values measured in personnel dosimetry be evaluated and which facts and factors are to be taken into account by the authorized physician? 2) To what extent and in what way should other types of radiation exposure be taken into account? 3) What conclusions should be drawn by the authorized physician with respect to his examinations and what subsequent measures should be taken? Based on present-day knowledge in this field, this paper tries to give an answer to these questions. (GE)

29704 (KFK-1851) IN-VIVO MEASUREMENT OF THE GAMMA AND NEUTRON DOSE RATE ON PATIENTS WITH ^{238}Pu PACEMAKERS IMPLANTED. Piesch, E.; Burgkhardt, B.; Kollmeier, W. (Kernforschungszentrum Karlsruhe (F. R. Germany). Abt. Strahlenschutz und Sicherheit). Jun 1974. 31p. Dep. NTIS (U. S. Sales Only) $4.75.

In vivo measurements on Medtronic ^{238}Pu-powered heart pacemaker were performed with a proportional counter for the measurement of neutrons and with thermoluminescence dosimeters and a scintillation dose rate meter for gamma measurements. The paper discusses the technique of phantom calibration, the in-vivo measurement of the neutron emission rate and the estimation of dose equivalent. Results are presented for phantom and in-vivo measurement at different positions from the ^{238}Pu source. The dose equivalent rate from neutrons and gamma rays was measured on seven patients with ^{238}Pu-pacemakers implanted and was found to be 5.6 ± 0.1 mrem/h and 2.54 ± 0.5 mrem/h, respectively at the surface of the pacemaker in 1.25 cm distance from the center of the source. (auth)

29705 (RT/FI-(74)16) NEUTRON RADIOGRAPHY: BIOMEDICAL APPLICATIONS. Giannini, M. (Comitato Nazionale per l'Energia Nucleare, Rome (Italy)). Mar 1974. 18p. (In Italian). (CONF-731149-1). Dep. NTIS (US Sales Only) $4.00.

From conference on bioengineering; Milan, Italy (20 Nov 1973).

After a brief description of neutron radiography as a complementary technique to conventional x-ray radiography, the applications of this method to biomedical problems are examined. Living materials have such a high hydrogen content that scattering of thermal neutrons constitutes a serious problem. Two different approaches discussed include the use of fast neutrons, and the replacement of hydrogen with deuterium in various tissues. (auth)

29706 CHANGES IN THE NUMBER OF CIRCULATING LYMPHOCYTES WITH CHROMOSOMAL ABERRATIONS FOLLOWING A SINGLE EXPOSURE OF THE PELVIS TO X-IRRADIATION IN CANCER PATIENTS. Tamura, H.; Sugiyama, Y.; Sugahara, T. (Kyoto Univ.). Radiat. Res.; 59: No. 3, 653-657 (Sep 1974).

The percentage of lymphocytes with chromosomal aberrations in the peripheral blood of patients with cervical cancer increased to reach a peak 6 hr after a single ^{60}Co γ-irradiation of the pelvis, then decreased during the next 14 hours to the number recorded 20 min after irradiation. These findings may have important implications for the study of lymphocyte kinetics and for biological dosimetry. (auth)

29707 HUMAN LYMPHOCYTE AS A RADIOBIOLOGICAL DOSIMETER AFTER TOTAL BODY IRRADIATION. Silberstein, E. B.; Ewing, C. J.; Bahr, G. K.; Kereiakes, J. G. (Cincinnati General Hospital). Radiat. Res.; 59: No. 3, 658-664(Sep 1974).

Lymphocytes from seven patients receiving 100 or 200 rads of cobalt-60 total body irradiation for therapy of metastatic tumors have been cultured with phytohemagglutinin, harvested at 48 hr, and examined for the incidence of chromosome aberrations. The mean yield of dicentric plus ring forms per cell were found to be 0.043 at 100 rads and 0.098 at 200 rads. These were compared to the only other human data available for homogeneous total body irradiation, that of Buckton et al. who employed doses of 25–50 rads. By a one-way analysis of variance there is no significant difference between the dicentric plus ring yield per cell for the available data at 25, 50, 100, or 200 rads. Individual variation in response to a homogeneous dose of total body irradiation may diminish the value of lymphocyte chromosome aberrations as a radiation dosimeter. (auth)

29708 EFFECT OF GRADED DOSES OF IONIZING RADIATION ON THE HUMAN TESTIS. Rowley, M. J.; Leach, D. R.; Warner, G. A.; Heller, C. G. (Pacific Northwest Research Foundation, Seattle). Radiat. Res.; 59: No. 3, 665-678(Sep 1974).

A portable unit was developed to provide uniform irradiation of the human testes. The device had built-in radiological protection and provided a dosage independent of the subject geometry, uniform to within ±5%. Single doses, between 8 and 600 rad, were administered to the testes of human subjects. Observations were made both before and following irradiation. Parameters evaluated included sperm concentration, motility and morphology, seminal fluid volume, plasma and urinary gonadotropin and testosterone levels, urinary estrogens, and comparison of testicular biopsies taken before and after irradiation in the same subject. Dose-response relationships and recovery times were determined for each dose range studied. (auth)

29709 RADIATION CHARACTERISTICS AND CONTROLS. I. Crandell, C. E. (Univ. of North Carolina, Chapel Hill). Dent. As.; 42: 17-20; 21-23(Nov 1973).

Radiation protection of dental patients and personnel is reviewed under the following headings: somatic and gonadal damage to human tissues; fundamental principles of radiation; legal responsibilities of the professions in radiological health; safe levels of radiation; advisory groups on radiation protection; maximum permissible exposure of patients and personnel; reduction of radiation hazards; and radiation measurement. (HLW)

29710 CAUSE OF DEATH IN RADIOLOGICAL WORKERS. Analysis of Cause of Death in Japanese Radiological Technicians, 1966 to 1972. Kitabatake, T.; Watanabe, T. (Niigata Univ., Japan). Acta Med. Biol. (Niigata); 21: No. 2, 107-111(Sep 1973).

From 1966 to 1972, 134 deaths were reported among Japanese radiological technicians in the Japan Radiological Technicians Association. This observed value is extremely less than the expected; this finding is probably due to an omission of case findings. Of 134, 6 skin cancer deaths and 2 aplastic anemia deaths were found. Both of these are significantly frequent as compared with the expected number. Leukemia was seen in 5 cases, but there is no statistically significant difference between the observed and expected values. The observed average year of death is 52.7 years while the expected is 48.6 years. (auth)

29711 CODE OF PRACTICE AGAINST RADIATION HAZARDS. London; Imperial College of Science and Technology ([nd]). 78p.

The subject is introduced by a section setting out rules for the conduct of radiation work. The code of practice is divided into sections entitled: legislation, administrative organization, personnel supervision, hazards from ionizing radiation, X-ray equipment, particle accelerators, University of London Reactor Centre, classification of radionuclides and grading of radiochemical laboratories, methods of handling sealed and unsealed radioactive materials, source control, storage, transport, disposal of radioactive waste, monitoring, accidents and emergencies, training and instruction. Appendices contain specimen forms, identity cards and record cards for radioactive materials, signs and notices, and maximum permissible levels of surface contamination. (UK)

29712 PROBLEMS OF SPACE RADIOBIOLOGY AND RADIATION SAFETY IN SPACE MISSIONS. Tobais, K. A.; Grigor'ev, Yu. G. Kosm. Biol. Aviakosmicheskaya Med.; 8: 12-21(1974). (In Russian).

The main criteria of assaying radiation hazards of different space flights and qualitative characteristics of these criteria are presented. The results of space radiobiology investigations are given. Approaches to the establishment of allowable levels of an exposure of astronauts to irradiation are described. Purposes of advanced researches are determined. (auth)

29713 INFLUENCE OF FRACTIONATION ON ACUTE AND LATE REACTIONS IN VOCAL CORD CARCINOMA. Loeffler, R. K. (Radiation Center, Massilon, OH). Amer. J. Roentgenol., Radium Ther. Nucl. Med.; 121: No. 4, 748-753(Aug 1974).

From 55th annual meeting of the American Radium Society; Colorado Springs, CO (22 Apr 1973).

Four schedules for the x or γ treatment of localized vocal cord carcinoma were compared, to establish a relationship between daily and total dose, and acute and late normal tissue reactions. All patients were treated 5 days per week. All of those who received 200 R daily (6,000 R in 30 treatments) developed a confluent mucositis and minimal to moderate subsequent aryepiglottic edema. Patients who received 180 R daily (6,480 R in 36 treatments) developed a patchy mucositis. Those who received 170 R daily (7,140 R or 6,400 rads in 42 treatments) developed only a brisk erythema, with decreasing incidence and severity of edema. At 160 R daily (6,880 R in 43 treatments) only a mild erythema developed, with no visible edema at any time. Local recurrence rates of about 10 percent for T_1 lesions, and of about 25 per cent for T_2 and T_3 lesions, indicate that the decrease in reactions with longer fractionation has been achieved without loss of tumor control. Even minimal improvement in functional status following treatment for this highly curable malignancy well justifies the inconvenience of the increased number of treatments. (auth)

29714 CANCER MORTALITY FOLLOWING IRRADIATION IN INFANCY FOR HEMANGIOMA. Li, F. P.; Cassady, J. R.; Bernett, E. (National Cancer Inst., Boston). Radiology; 113: No. 1, 177-178(Oct 1974).

Three cancer deaths were found (versus 2.4 expected) in a record-linkage study of 4,746 patients irradiated in infancy for hemangioma of the skin. Only one tumor arose in proximity to the treatment field and may have been induced by radiation. The findings show no significant excess cancer deaths following low-level irradiation, but occurrence of non-lethal cancers of skin or other organs was not evaluated. (auth)

29715 FOLLOW-UP ON THE LONG-TERM EFFECTS OF THERAPEUTIC IRRADIATION ON BONE MARROW. Sykes, M. P.; Chu, F.; Gee, T. S.; McKenzie, S. (Memorial Sloan-Kettering Cancer Center, New York). Radiology; 113: No. 1, 179-180(Oct 1974).

Results are reported from a survey on patients who had received prophylactic chest-wall irradiation for breast cancer in 1964. Sternal and iliac crest marrows were obtained in five of these women. While all iliac crest marrows were normocellular, four of the five sternal marrow aspirates remained aplastic 13 to 16 years after irradiation. The fifth was moderately hypocellular. Results were similar in three autopsied patients. Since the regeneration of bone marrow following 4,500 rads is unlikely in a 14-year period, a diagnostic marrow study from such a site would be of no value. (auth)

29716 HISTOCHEMICAL CHANGES IN CANCER OF THE CORPUS UTERI AFTER EXPERIMENTAL IRRADIATION. Bagaturiya, G. D.; Kvesitadze, T. (Inst. of Oncology, Tbilisi, USSR). Tr. Nauch.-Issled. Inst. Onkol. Gruz. SSR; 7: 193-196 (1972). (In Russian).

Morphological and histochemical methods were used to study changes in tumor tissue (experimental cancer of the corpus uteri) after x-ray therapy (single dose 500 rads, total 500 to 6000 rads).

Structural changes directly related to the dose were discovered. Irradiation decreased the amount of ribonucleoprotein (RNP) in the tumor cells with a shift of their isoelectric point to the alkaline side. Nucleolar RNP frequently disappeared, an indication that RNP synthesis decreased or was absent in these cells. Irradiation also reduced the amount of deoxyribonucleoprotein (depending on the degree of cell differentiation in the tumor cells), increased the amount of acid mucopolysaccharides (in both the stroma and parenchymatous structures of the tumor), and sharply decreased the amount of glycogen. (Referativnyi Zh.)

29717 PROSTHESIS SET FOR RADIOPROTECTION OF THE EYE. Mitrov, G.; Dobrev, D. Onkologiya (Sofia); 9: No. 4, 186-190(1972).

Prostheses for radioprotection of the eye were manufactured to be used in case of percutaneous radiation treatment in this area. The prostheses were made of lead 2 mm thick and Superpont or Superacryl type of methyl metacrylate. Two plastic layers, an upper covering layer and a lower in contact with the conjunctive, were shaped and stratified over a lead folio folded and modeled in a desired form. Methyl metacrylate protects the eye from direct contact with the metal, i.e., it makes the prosthesis nontraumatic and at the same time functions as a filter by absorbing secondary electrons (originating from the lead). Prostheses are constructed according to the form of the eye in the sizes: large, medium, and small. Each pack contains one prosthesis for full protection of the eye, one for protection of the central part only and three with open edges for irradiation of various parts of the eye. Protection is adequate for irradiation with an energy not exceeding 220 kV. (Abstr. Bulg. Sci. Med. Lit.)

29718 GONAD DOSES OF IRRADIATION OF PATIENTS IN X-RAY STUDIES. Stavitskii, R. V. Med. Radiol.; 19: No. 8, 32-37(1974). (In Russian).

The experimental study on the gonad and surface exposure dose was made on a series of bone-parafin phantoms simulating people of 4 age groups: 0 to 2, 3 to 7, 8 to 14, and 15 years and older. The dependence of the gonad dose rate for males and females was determined as a function of the voltage of the x-ray tube. The gonad dose rate and the coefficients of transition from the surface to the gonad dose was calculated for males and females for various irradiated areas. (JSR)

29719 NUCLEAR TESTING. Baxter, P. Aust. J. Forensic Sci.; 6: No. 2, 89-95(Dec 1973).

From 21st plenary scientific session of the academy; Sydney, Australia (20 Sep 1973).

A discussion is given of the biological radiation effects arising from nuclear fallout. The five radioactive materials which are discussed include: iodine 131; strontium 90; cesium 137; carbon 14 and tritium. The effects of natural radiation arising from cosmic rays are also described, and it is concluded that there is no measurable effect on health. The concept of threshold dose is discussed and is compared with predictions obtained from extrapolated high dose experiments. (AT)

29720 REAL RISKS OF THE NUCLEAR TESTS. Fliegner, J. R. Aust. J. Forensic Sci.; 6: No. 2, 101-104(Dec 1973).

From 21st plenary scientific session of the academy; Sydney, Australia (20 Sep 1973).

An argument is presented against nuclear weapons testing. Radiation effects from fallout deposits such as ^{131}I, ^{137}Cs and ^{90}Sr are considered, as well as short-time radiation doses on children and adults. Estimates of increases in cancer caused by radioactive fallout are given. These estimates are based on the linear irradiation effect rather than a threshold effect. It is concluded that there is a great deal of uncertainty about the effects of nuclear atmospheric testing. (AT)

29721 EXPERIENCE OF USE OF REDUCED TYPE OF GLUTATHIONE TO PREVENT SIDE EFFECTS OF RADIOTHERAPY AND ANTINEOPLASTIC CHEMOTHERAPY. Shimizu, T.; Nomatsu, K.; Hiratsuka, H.; Ichinose, M. (Oita Red Cross Hospital, Japan). Rinsho To Kenkyu; 51: No. 5, 1431-1436(May 1974). (In Japanese).

The use of reduced type of glutathione (glutide) was examined for preventing side effects of radiotherapy and chemotherapy. Examinations were performed on 49 cases which received glutide, including 10 cases aged from 32 to 68 to which radiotherapy was given, and 30 cases aged from 33 to 76 to which antineoplastic drugs were given. In the radiotherapy group, daily dose of x irradiation was 200 R and the total dose ranged from 2,000 to 6,000 R. Concomitantly, 400 mg/day of glutide was given intravenously in total doses ranging from 400 mg × 5 to 400 mg × 50, every day or in combination every day and intermittently. The number of leukocytes was compared between groups in the concomitant use of glutide and the control groups without using glutide. Decrease of leukocytes was observed in 66.7% of the control group. In the groups with glutide including both radiotherapy group and antineoplastic chemotherapy group, decrease of leukocytes was less than in the control groups: decrease of leukocytes occurred in 10% of radiotherapy group and in antineoplastic chemotherapy group, it was in 20 to 33.3%. In these groups, decrease of thrombocytes occurred in only 14.3% of radiotherapy group and in 0 to 10% of chemotherapy group. These results accorded with the fact that the groups using glutide showed no significant biochemical changes before and after the radiotherapy and chemotherapy. (JA)

29722 EXPERIMENTAL USAGE OF CYSTEINE IN RADIATION THERAPY. Ohshima, T. (Tokyo Teishin Hospital); Tsukiyama, I.; Kinoshita, F.; Maekawa, A. Rinsho Hoshasen; 19: No. 5, 339-343(May 1974). (In Japanese).

In order to protect from side effects of radiation therapy, Hysthiol (C-G), a mixture of cysteine and glucose, was used as a radiation protective agent. Subjects were selected from the patients with cancer of the breast and with uterine cancer who had received ^{60}Co γ therapy. In addition, these patients were divided into two groups, 33 patients with C-G administration and 30 patients without C-G administration. The effect of C-G was compared using as criteria the number of leukocytes and erythrocytes, hemoglobin, hematocrit, blood platelets, the state of radiation sickness and pulmonary function before and after irradiation. C-G had the effect of preventing leukopenia and radiation sickness. There was a significant difference between before and after irradiation in the counts of leukocytes. In erythrocytes, hemoglobin, hematocrit, blood platelets and pulmonary function, there was a significant difference between the groups with and without C-G administration. (JA)

29723 STUDIES ON THE RADIATION PROTECTION PROPERTIES OF FENCHLORFOS AND ITS ROLE IN THE RADIOPROTECTION MECHANISM. Panke, R.; Wisniewski, K.; Sarosiek, W.; Daniluk, J.; Szymanski, A. (Medical Academy, Bialystok, Poland). Postepy Fiz. Med.; 8: 79-85(1973). (In Polish).

Radioprotection properties of fenchlorfos were investigated to estimate the survival following radiation toxemia and metabolic changes, which may effect the radioprotection mechanism. (auth)

29724 SYSTEMATICS OF IATROGENIC CARCINOGENESIS. Thomas, C. (Univ., Freiburg i. B.). Verh. Deut. Ges. Kreislaufforsch.; 56: 126-132(1972). (In German).

Iatrogenic cancers following the use of ionizing radiation for therapy or diagnosis are discussed. Carcinogenic properties of the following drugs are reviewed; arsenic, chlornaphazin, paraffin, and coal-tar containing skin creams. The importance of testing drugs in animals before administering to humans is emphasized. Carcinogenic properties of the following compounds are pointed out: urethane, isonicotinic hydrazide, griseofulvin, chloroform, tannic acid, thiouracil, plastics, and iron dextran. (HLW)

29725 DOSE-LIMITING TISSUES IN RELATION TO TYPES AND LOCATION OF TUMORS. Implications for Efforts to Improve Radiation Dose Distributions. Suit, H. D.; Goitein, M. (Massachusetts General Hospital, Boston). Eur. J. Cancer; 10: No. 4, 217-224(Apr 1974).

From 2nd meeting on fundamental and practical aspects of the application of fast neutrons in clinical radiotherapy; The Hague, Netherlands (3 Oct 1973).

The potential gains to be expected from improved dose distributions which can, for example, be obtained from large field, low LET, energy modulated proton beams are considered. Increases in tumor control probability, which resulted from improvements in dose distribution in the past are discussed. Limitations on the maximum dose that can be delivered and on possible ways in which normal tissue tolerance can be extended are considered. The impact of improved dose distributions on management of a number of diseases, particularly cancer of the urinary bladder, is discussed. It is concluded that, for sites in which conventional radiotherapy can deliver doses of the order of 7000 rad in 7 weeks, improvements in local control are unlikely and any improvements in results may be in the form of a reduction of morbidity. However, significantly higher frequency of local control may be achieved in those normal tissue-tumor situations in which doses are currently limited to about 5000 rad in 5 weeks but could be increased to levels >6000 rad in 6 weeks by use of improved dose distribution patterns obtainable with proton beams. (auth)

29726 RBE OF CYCLOTRON NEUTRONS FOR EFFECTS ON NORMAL TISSUES. Hornsey, S.; Field, S. B. (Hammersmith Hospital, London). Eur. J. Cancer; 10: No. 4, 231-234(Apr 1974).

From 2nd meeting on fundamental and practical aspects of the application of fast neutrons in clinical radiotherapy; The Hague, Netherlands (3 Oct 1973).

The RBE for damage to various normal tissues was shown to be dependent on the tissue at risk and on the dose per fraction used. At present there is no method of predicting the RBE for any tissue. (auth)

29727 INFLUENCE OF IONIZING RADIATION ON ALKALINE PHOSPHATASE ACTIVITY IN HUMAN PERIPHERAL BLOOD LEUKOCYTES AND BONE MARROW CELLS. Bartnikowa, W. Folia Haematol. (Leipzig); 100: 385-394(1973). (In German).

In men irradiation with x ray or gamma rays caused a momentary increase of activity of the alkaline phosphatase in the granulocytes of the bone marrow and the peripheral blood, the activity of the enzyme in the blood serum being not influenced. The radiation energy is not to be regarded as a specifically effective factor being able to cause fluctuations of activity of alkaline phosphatase in the hemopoietic system, since, for example, similar changes may also be caused by an operation stress. The dependence of the alkaline phosphatase activity on the body area being irradiated proves that in the granulocytes the adrenal glands play a part for the mechanism of alkaline phosphatase stimulation induced by irradiation. (auth)

29728 CHANGES OF THE BRONCHO-VASCULAR SYSTEM OF THE LUNG UNDER THE INFLUENCE OF LOCAL γ IRRADIATION. Kapanadze, B. B. (Scientific Research Inst. of Medical Radiology, Moscow). Med. Radiol.; 19: No. 9, 16-23(Sep 1974). (In Russian).

By studying the condition of the lung after the application of equivalent doses of γ therapy under the conditions of micro- and macro-fractionated irradiation, the transitory changes of the vessels of the lung with fractionation of the dose into micro fractions and their irreversible affection after fractionation of the dose into macro fractions were established. This made it possible to recommend macro-fractionated γ therapy only in such cases when the efficacy of micro-fractionated irradiation is dubious. (auth)

29729 CHANGES IN THE CARDIOVASCULAR SYSTEM IN RADIATION AND MEDICINAL TREATMENT OF LUNG CANCER. Shoikhet, Ya. N. Med. Radiol.; 19: No. 9, 23-27(Sep 1974). (In Russian).

Results of radiocardiographical and rheopulmonographic investigations conducted for the purpose of a thorough assessment of changes in the cardiovascular system in the process of radiation and medicinal treatment of lung cancer before treatment, upon its completion, and 6 to 8 weeks after it are presented. The investigations have displayed a rise in heart ejection by the end of the treatment course and its subsequent fall 6 to 8 weeks after it. By this time the blood volume in the lungs decreases drastically. The contractile capacity of the myocardium diminishes too. (auth)

29730 CONDITION OF THE NERVOUS AND VASCULAR SYSTEMS AFTER RADIATION TREATMENT OF LYMPHOGRANULOMATOSIS. Oliper, T. V.; Khmelevskaya, Z. I. (Scientific Research Inst. of Medical Radiology, Moscow). Med. Radiol.; 19: No. 9, 31-36(Sep 1974). (In Russian).

The article presents the results of neurological observation of 200 patients suffering from lymphogranulomatosis in the process of radiation therapy and after it. It was shown that early reaction to irradiation developed only in single cases (6 to 8.5%). In $\frac{1}{3}$ of the patients after radiation therapy light general or more often regional vascular disorders and focal changes of the nervous system developed, which, in cases of prolonged remission, were gradually smoothed over. Complications in later periods were revealed in 9 patients: in 4 patients they were expressed in the development of the Lermitt syndrome, in 5 patients development of dermatofibrosis in the irradiated zone (4000 to 5000 rad) with persistent compression of the vascular-nervous bundle in 3 of them. Irradiation of the spinal cord to a dose not higher than 3000 rad during 3 to 4 weeks in a 3-year observation period did not entail the development of myelitis. (auth)

29731 CHROMOSOME ABERRATIONS IN LYMPHOCYTES OF PERIPHERAL BLOOD AFTER RADIATION THERAPY. Guzeev, G. G.; Sevan'kaev, A. V.; Baisogolov, G. D. (Scientific Research Inst. of Medical Radiology, Moscow). Med. Radiol.; 19: No. 9, 36-39(Sep 1974). (In Russian).

Results are presented of the frequency of the cells with chromosome aberrations in patients with malignant neoformations of the urinary bladder before and after radiation therapy course. It was noted that during irradiation on the accelerators the level of aberrant cells was two times less than that during irradiation on cobalt units. (auth)

29732 PREVENTION OF THROMBO-EMBOLISM DURING RADIOTHERAPY OF CARCINOMA OF THE UTERINE CERVIX. Joswig, E. H.; Joswig-Priewe, H. (Univ., Goettingen, Ger.). Geburtsh. Frauenheilk.; 33: 988-993(1973). (In German).

At the University Hospital for Women in Göttingen the mortality from thrombo-embolism was 1.45%, the morbidity from embolism 2.63%, and the morbidity from thrombophlebitis 4.35% during radiotherapy for carcinoma of the cervix without routine preventive measures in 345 patients. Since 1968, routine prophylaxis of thrombosis is carried out during the radium insertions. Any patient with latent or overt cardiac failure is digitalized. Patients with varicose veins have tensor bandages applied to their legs. Immediately after the radium insertion a 24 intravenous drip with 20,000 units of heparin was administered. From 1968 to 1971, 263 patients received this prophylaxis during a total of 583 radium insertions. The mortality from embolism decreased to 76%, the morbidity from embolism to 1.1%, and the morbidity from thrombophlebitis to 1.90%. The incidence of superficial thrombophlebitis increased from 1.45% to 4.5%. The comparability of the two groups is discussed. The striking decrease of the incidence of early severe thrombo-embolic complications is attributed to the preventive measures. It can be expected that treatment with anticoagulants following the radium insertion during the complete course of radiotherapy could lower the complication from embolism even further and may improve the five year survival rate. Significant bleeding due to the prophylactic measures was not observed. Blood coagulation studies are not necessary. The presence of hypertension over 200 mm Hg or active gastric or intestinal ulcers is a contraindication to the prophylactic treatment. It was possible to give prophylactic treatment to 97.4% of all patients. (auth)

29733 TREATMENT OF ADVANCED TUMOURS OF HEAD AND NECK WITH FAST NEUTRONS. Catterall, M.; Vonberg, D. D. (Medical Research Council, London). Brit. Med. J.; 3: No. 5924, 137-143(20 Jul 1974).

The use of fast neutrons for the treatment of the first 100 cases of advanced tumors of the head and neck at the Hammersmith Hospital is described. Altogether 62 patients showed complete regression of the tumors, and only two recurred. Tumors of the buccal cavity and salivary glands responded particularly well and the relief of pain and ulceration was striking. Side effects were not serious and did not differ from those seen with supervoltage radiation, apart from the reaction of the skin. Follow-up was short, however, owing to deaths from metastases, and out of 76 patients treated more than one year previously only 30 survived. The results obtained so far indicate that it is now justifiable to use fast neutrons for the treatment of cases which have not metastasized, so that the effects on tumors and adjacent normal tissues can be observed for several years after treatment. (UK)

29734 ALKALINE PHOSPHATASE ACTIVITY OF GRANULOCYTES (FAG) IN WORKERS IN RADIOLOGICAL LABORATORIES. Holowiecki, J.; Kaweeka, J.; Katowicach, M. Acta Haematol. Pol.; 5: No. 1, 29-33(1974). (In Polish).

In 57 workers in four laboratories of radiology and in 54 healthy subjects, FAG activity was determined by the Gomori method in a modification repeating them two times at intervals of several weeks. The mean FAG activity in controls was 46 (±24 S.D.), in workers from radiological laboratories it was 33 (±26 S.D.) and in those working over 5 years it was 28 (±27 S.D.). These differences are statistically significant ($p < 0.01$). The correlation coefficient between the duration of employment and FAG activity was $r = 0.162$. The results are discussed in the light of reports on more frequent incidence of leukemias in radiologists. (auth)

Vertebrates

Refer also to abstracts 29661 and 29781.

29735 (CONF-731222-1) RESPONSE OF SPERMATOGONIA OF THE MOUSE TO HYCANTHONE, AND A COMPARISON WITH THE EFFECT OF γ RAYS. Oakberg, E. F. (Oak Ridge National Lab., Tenn. (USA)). 1973. 23p. Dep. NTIS $4.25.

From 13th international symposium on physiologica and genetic aspects of reproduction, Salvador, Brazil, December 2–7, 1973.

Studies on the response of mouse spermatogonia to hycanthone (an antischistosomal drug) and x or γ irradiation showed that certain aspects of the response of spermatogonia to hycanthone are similar to those of radiation. These include the high incidence of cell necrosis at 15 hrs, the high sensitivity of A_2-In spermatogonia, and the resistance of spermatocytes and spermatids. Important differences also occur, the most marked being the difference between the lethal dose and spermatogonial killing. For example, both 600 R of x rays and 150 mg/kg of hycanthone have similar animal toxicity, yet survival of type A spermatogonia after these doses is 34% for hycanthone and only $\sim$3% for x rays.

Data for γ ray exposures giving comparable survival showed a lower relative effectiveness for hycanthone at low doses, and a greater effectiveness at high doses. The difference in sensitivity between A_3-In and earlier (A_s-A_2) spermatogonia observed with γ rays is even greater with hycanthone. This results in a more rapid regeneration of the seminiferous epithelium after hycanthone. The data presented, and the comparison of hycanthone with γ rays, demonstrate some of the parameters which must be considered in a thorough evaluation of the effect of any noxious agent on sensitive tissues and cells. (CH)

29736 (RT/BIO-(74)10) OSMOTIC HAEMOLYSIS AS A MEANS OF STUDYING ERYTHROPOIETIC STRESSES: RESPONSE TO ACUTE ANAEMIA AND ACUTE IRRADIATION. Briganti, G.; Galloni, G. (Comitato Nazionale per l'Energia Nucleare, Rome (Italy)). Apr 1974. 29p. Dep. NTIS (US Sales Only) $4.50.

In the rat, young red blood cells are relatively resistant to osmotic lysis. For instance about 1% of red blood cells from normal animals do not lyse when exposed to 0.25% NaCl for 10 minutes at room temperature. By injecting ^{59}Fe labeled red blood cells in normal rats and then measuring the disappearance of activity from the resistant cells it has been shown that cells lose their resistance to lysis within twelve hours of entering the circulation for the conditions of lysis mentioned. The number of resistant cells is the product of the rate of red cells production and the time for which the cells remain resistant. Osmotic lysis therefore provides a simple method for estimating the rate of red cell production since the duration for which the cells are resistant can be determined by counting techniques. In response to bleeding determined and together with knowledge of the time for which the cells are resistant it is possible to determine the change in red cell production during the period of recovery. Similar experiments were done on irradiated rats, following the red cell production during the period of recovery after 200 rad whole-body x-irradiation. (auth)

29737 X-RADIATION-SENSITIVITY OF RAT LIVER TO INTERPHASE DEATH. Jackson, K. L.; Christensen, G. M.; Hebard, D. W.; Parker, R. G. (Univ. of Washington, Seattle). Radiat. Res.; 59: No. 3, 585-596(Sep 1974).

The response of the liver to local irradiation of the surgically exteriorized left anterior lobe during a period of 9 wk following exposures of 5−40 kR is described. Decrease in irradiated left lobe weight relative to shielded right lobe weight was dose-dependent and exhibited a maximum response by 20 days. Histological examination and DNA analysis indicate there was a radiation-dose-related loss of parenchymal cells. Incorporation of ^{3}H-labeled leucine relative to weight change indicated that metabolically dead cells were rapidly removed from the irradiated lobe. The findings do not clarify whether interphase death of parenchymal cells was a direct response to irradiation or resulted indirectly from radiation-induced vascular damage. The estimated curve for survival of hepatocytes from interphase death in vivo as a function of dose has an extrapolation number of 2.7 and a D_0 of 9.1 kR. (auth)

29738 EFFECT OF IRRADIATION ON GASTROINTESTINAL DRUG ABSORPTION IN MICE AND RATS. Hurwitz, S.; Doull, J. (Univ. of Kansas, Kansas City). Radiat. Res.; 59: No. 3, 606-613(Sep 1974).

X-irradiation inhibits gastrointestinal absorption of nutrients by damaging the intestinal mucosal cells, which actively transport these chemicals. The results of the present study demonstrate that sublethal doses of x-irradiation delay the passive gastrointestinal absorption of an acidic drug, sulfadiazine, and a basic drug, quinine, in mice. This effect is detectable 2 hr after radiation exposure and is most pronounced in the first 3 postirradiation days. Both the magnitude and the duration of the effect are related to the radiation dose (25 to 800 R in mice and 200 to 800 R in rats). The effect was not demonstrable when sulfadiazine was given by intraperitoneal or intraduodenal rather than by intragastric administration after which more of the drug was retained in the stomachs of rats irradiated 21 hr earlier. Head irradiation, which is known to delay gastric emptying, lowered blood levels of sulfadiazine after gastric administration, and shielding partially protected against this delayed drug absorption. This effect was most pronounced in whole-body-irradiated rats. Thus, delayed gastric emptying is the major cause of inhibited gastrointestinal drub absorption in the first 3 days after irradiation of mice and rats. (auth)

29739 HYDROLYSIS OF 2′,3′-CYCLIC ADENOSINE MONOPHOSPHATE AND 3′,5′-CYCLIC ADENOSINE MONOPHOSPHATE IN SUBCELLULAR FRACTIONS OF NORMAL AND NEOPLASTIC MOUSE SPLEEN. Konings, A. W. T.; Pierce, D. A. (State Univ. of Groningen, Netherlands). Life Sci.; 15: No. 3, 491-499(1 Aug 1974).

A comparison was made between the capacity to hydrolyse 2′,3′-cyclic adenosine monophosphate and 3′,5′-cyclic adenosine monophosphate in subcellular fractions of normal and neoplastic (lymphosarcoma) spleen of C_{57}BL mice. The effect of x-irradiation on these activities was tested. Subcellular fractionation of normal and lymphosarcoma spleen points to a different overall localization of the enzymes. The 2′,3′-cyclic nucleotide phosphodiesterase (2′,3′-cAMPase) has its highest specific activity in the particulate fractions of the cell, while the data on 3′,5′-cyclic nucleotide phosphodiesterase (3′,5′-cAMPase) show the highest activity in the soluble fraction. The 2′,3′-cAMPase activity is higher in the tumor as compared to the normal tissue, while the opposite holds for 3′,5′-cAMPase. Total body irradiation of normal mice with a dose of 600 rads of x-rays results in a clear drop in 2′,3′-cAMPase 48 hours after the exposure. The 3′,5′-cAMPase is hardly affected at this time. Neither imidazol nor Mg^{2+} has any influence on the 2′,3′-cAMPase. The pH optimum for 3′,5′-cAMPase and 2′,3′-cAMPase appears to be 7.7 and 6.2 respectively. This report suggests a no-identity of the two enzymes in mouse spleen, a situation different from that found in certain plants. (auth)

29740 AROMATIC AMINO ACID DECARBOXYLASE ACTIVITY OF RAT BRAIN AND ITS PARTS FOLLOWING EXPOSURE TO IONIZING RADIATION. Drsata, J.; Hais, I. M. (Charles Univ., Hradec Kralove, Czech.). Radiat. Res.; 59: No. 3, 724-726(Sep 1974).

Aromatic L-amino acid decarboxylase activity was estimated in whole rat brain or its main parts at various time intervals (1 to 5 days) following 500, 800, and 1000 R of whole-body x-irradiation and 3 days after 10,000 R of head-only γ-irradiation. The enzyme was relatively resistant. Changes observed in some of the groups following 800 R whole-body irradiation are sufficient to account for the changes in brain amine levels reported in the literature. (auth)

29741 X-RADIATION-INDUCED INTESTINAL LESIONS IN PROTEIN-DEFICIENT RATS. Deo, M. G.; Verma, K. (Inst. of Medical Sciences, New Delhi). Arch. Pathol.; 98: No. 4, 269-273(Sep 1974).

Morphologic alterations in the jejunum following a single dose of 200 rads whole-body or 650 rads focal x-radiation to the abdomen were studied in protein-deficient rats and pair-fed controls. A similar study was also made in animals fed a stock diet but having weights similar to those of the protein-deficient animals at the time of x-radiation. That group served as the weight control. The protein-deficient animals showed less cellular degeneration, necrosis, and inflammatory response when compared with the controls. On the other hand, recovery as judged by the rate of reappearance of mitoses was tardy in the deficient animals. The jejunal crypts of the deficient animals contained a higher number of megalocytes when compared with the number found in the controls, following focal x-radiation. Protein deficiency may increase susceptibility of the host to x-radiation by interfering with the rate of recovery and not by excessive tissue damage. (auth)

29742 KINETICS OF RECOVERY IN IRRADIATED COLONIC MUCOSA OF THE MOUSE. Withers, H. R.; Mason, K. A. (Univ. of Texas, Houston). Cancer; 34: No. 3, 896-903(Sep 1974).

From 2nd national conference on cancer of the colon and rectum; Bal Harbour, FL (27 Sep 1973).

There is an increasing interest in radiotherapy as a pre or postoperative adjuvant to surgery in the curative treatment of rectosigmoid cancer. This is a concept completely unrelated to palliative treatment, and therefore the response of incidentally irradiated intestine needs to be understood in order that maximally curative doses of radiotherapy may be used safely. There are two aspects of radiation injury: early mucosal injury and late fibrosis. The acute response of colonic mucosa of the mouse to single and multiple doses of gamma rays was studied. The radiosensitivity of colonic mucosal cells is similar to that of other cells of epithelial origin, both normal and neoplastic. Two factors predominate in the response of colonic mucosa to multifraction irradiation: (A) the ability of cells to repair non-lethal radiation damage between dose-fractions; and (B) the regenerative capacity of surviving cells. These two aspects of the response of colonic mucosa and other cell renewal systems are discussed. The capacity of colonic mucosa to repair nonlethal damage is similar to that of other epithelial cells. It is likely from available radiobiology studies that neoplastic cells and normal cells are equally capable of this repair. However, the normal mucosa possesses a great capacity for regeneration, and this is probably the mechanism that provides the radiotherapist with a margin of safety in the postoperative treatment of residual small deposits of rectosigmoid cancer. (auth)

29743 RADIATION AND HYPERTHERMAL RESPONSE OF NORMAL TISSUE IN SITU. Robinson, J. E.; Wizenberg, M. J.;

McCready, W. A. (Univ. of Maryland, Baltimore). Radiology; 113: No. 1, 195-198(Oct 1974).

From 59th scientific assembly and annual meeting of the Radiological Society of North America; Chicago, IL (25 Nov 1973).

Experiments were conducted to determine the effects of hyperthermal treatment on the radiation sensitivity of normal mouse skin. Hyperthermal treatment by itself produces no measurable response but enhances radiation sensitivity which increases with treatment temperature. Skin treated at 41°C was 1.18 times more sensitive than that treated at normal 37.5°C, and at 43°C the thermal enhancement ratio (TER) was 2.06. When compared with parallel studies using C3H mammary tumors, TER of 4.33 at 43°C, it appears that thermal sensitization of normal skin is appreciably less than for tumor. Hyperthermal treatment produces a favorable therapeutic ratio which increases with treatment temperature over the range studied. (auth)

29744 INCREASED CURES USING FRACTIONATED EXPOSURES OF X IRRADIATION AND HYPERTHERMIA IN THE LOCAL TREATMENT OF THE RIDGWAY OSTEOGENIC SARCOMA IN MICE. Hahn, E. W.; Alfieri, A. A.; Kim, J. H. (Sloan-Kettering Inst., New York). Radiology; 113: No. 1, 199-202(Oct 1974).

From 59th scientific assembly and annual meeting of the Radiological Society of North America; Chicago, IL (25 Nov 1973).

Experiments were carried out to determine the effect of heat and/or x rays on the Ridgway osteogenic sarcoma in mice. Tumors averaging 0.9 ± 0.2 cm in diameter were exposed to 200 rads and/or heat three times on alternate days. Tumor core temperatures of 42.5 ± 0.5°C were maintained for 15, 30, or 45 minutes immediately before or after x irradiation. Heat alone did not effect cures whereas radiation alone cured 8 of 18 animals (44%). In contrast, 71 of the 74 animals (96%) receiving the combined treatment were cured. Radiation was equally effective whether given immediately before or after tumor hyperthermia. There were no differences in cure rates in the 15-, 30-, or 45-minute heat radiation groups. (auth)

29745 INFLUENCE OF RADIATION ON THE LAYERS OF TUMORS IN THE EARLY FORMATION OF TUMORS. Pavicic, S. (Faculty of Medicine, Zagreb); Milas, I. (Faculty of Medicine, Zagreb). Libri Oncol.; 1: No. 4, 171-178(1972).

The tumors first appeared if the number of injected tumor cells were larger. Likewise, they first appeared in unirradiated legs if the number of injected cells were larger than 10^5. Extended latency of tumors in irradiated legs depended on the amount of dosage given during the treatment. Dosages of 100 roentgens did not lead to extended latency. Dosages of 500 roentgens extended latency two days, and 1,000, 3,000, and 6,000 roentgens extended latency to four days. (Bull. Sci. Sect. A)

29746 EFFECT OF A COMBINATION OF ANTIBIOTICS AND AET ON THE SURVIVAL OF IRRADIATED ANIMALS. Borhegyi, L.; Benko, G. Honvedorvos; 26: No. 1, 28-34(1974). (In Hungarian).

On the basis of an estimate of the survival of mice subjected to various doses of whole-body irradiation it is concluded that with the use of a combination of AET and antibiotics (mainly Tetranpyrrolidinomethyl-oxytetracyclin) it is possible to obtain beneficial results in the prophylaxis and therapy of the infection syndrome of radiation sickness, mainly in the minimum lethal irradiation dose. Antibiotics introduced under these conditions could potentiate an AET dose of 0.5 mM/kg. This result indicates the beneficial effect of AET on immunity of the organism and the effect of AET in decreasing tissue penetrability. The combined treatment can successfully supplement agents combating the early reactions of severe radiation sickness. (tr-auth)

29747 TIME COURSE OF THE RADIOPROTECTIVE EFFECT AND THE FORMATION OF ENDOGENOUS COLONIES OF HAEMOPOIETIC CELLS IN MOUSE SPLEEN FOLLOWING THE ADMINISTRATION OF SODIUM FLUOROACETATE. Novak, L.; Sikulova, J.; Kolacny, I.; Slotova, J. (Inst. of Biophysics, Brno). Folia Biol. (Prague); 20: No. 4, 277-282(1974).

The time course of changes in the degree of radioprotection by 5 mg/kg of sodium fluoroacetate (FAc) given at different time intervals before lethal x-irradiation was investigated in mice. Comparison of the data obtained on survival, respiratory exchange, ESC formation, mitotic index and accumulation of citrate in brain and liver tissues indicated that the number of ESC correlated with the radioprotective effect measured as survival only at the peak of the protection against lethal damage, i.e., 1 hr after FAc, while the inhibition of the rate of respiratory exchange and of the mitotic activity in femoral marrow followed a time course closely resembling that of the survival over the whole range. The increase in citrate content coincided in time with the onset of the respiratory exchange inhibition. A hypothesis is proposed in the discussion that the protective effect of FAc might be associated with an inhibition of metabolic processes, in particular, the total volume of macroergic bonds formed, which is reflected, among others, in the depression of mitotic activity of bone marrow. This action may obviously have a favorable effect upon survival even at those time intervals between FAc application and exposure where no equivalent protection of colony-forming stem cells is manifested. (auth)

29748 EFFECT OF TOTAL IRRADIATION ON THE DEVELOPMENT OF LEUKEMIA L_{1210} IN F_1-HYBRIDS. Malaise, E. Onkologiya (Sofia); 9: No. 4, 163-172(1972).

Results are reported of a study of the effect of irradiation with sublethal x-ray dose on the survival and the leukemic cell population reduplication time in mice F_1 ($DBA_2xC_{57}Bl$), which received by intraperitoneal injection different amounts of L_{1210} cells. Exposure to roentgen rays of mice F_1 was shown to inhibit the hybrid effect. The survival time and the leukemic cell population reduplication time were shortened. (Under similar experimental conditions the effect of roentgen irradiation on these same parameters in animals of line DBA_2 was negligible). (auth)

29749 INFLUENCE OF BLOOD OXYGENATION DURING IN VITRO IRRADIATION UPON THE YIELD OF DICENTRIC CHROMOSOMAL ABERRATIONS IN LYMPHOCYTES. Liniecki, J.; Bajerska, A.; Karniewicz, W. (Inst. of Occupational Medicine, Lodz, Poland). Bull. Acad. Pol. Sci., Ser. Sci. Biol.; 21: 69-76 (1973).

Freshly drawn venous blood, blood oxygenated by equilibration with expired air and whole-blood nonstimulated (PHA_) microcultures of lymphocytes (average partial oxygen tension of 30, 150 and 177 mm Hg, respectively) were irradiated with x-ray doses in the range from 50 to 450 rads, and dicentric aberrations scored in metaphasal figures of lymphocytes cultured for 51 h. Whereas the dose-effect relationship for irradiated PHA(_) cultures and the aerated blood were not significantly different from each other, that for the venous blood was displaced significantly toward lower values of the dependent variable. When the dose response curves were fitted to equation of the type $y_d = ax^\beta$, the values of the exponent β were significantly higher ($\beta = 1.5$) for all three series than that for PHA (+) cultures irradiated in previous studies ($\beta =$ 1.1 to 1.2). Additionally, the effect of temperature during irradiation of the venous blood upon aberration yield was studied and found much less pronounced than that operating for irradiated PHA (+) cultures. On basis of available data, it is postulated that in vitro irradiation of venous blood should yield an adequate reference system for in vitro vs in vivo dose-effect comparisons. (auth)

29750 DEVELOPMENT OF HUMORAL IMMUNITY IN LETHALLY IRRADIATED MICE RECONSTITUTED WITH FETAL LIVER. Sherwin, W. K.; Rowlands, D. T. Jr. (Univ. of Pennsylvania, Philadelphia). J. Immunol.; 113: No. 4, 1353-1360 (Oct 1974).

A model system of ontogeny was utilized to investigate the development of humoral immunity. Lethally irradiated adult C3H mice were reconstituted with syngeneic fetal liver. These mice were immunized at various times after reconstitution with a series of eight antigens: the bacteriophages F2 T4 and ϕX-174; the hapten carrier complexes 2,4 dinitrophenyl-bovine serum albumin and fluorescein bovine serum albumin; and the small proteins, hen egg lysozyme, sperm whale myoglobin, and bovine pancreatic ribonuclease. Subsequent antibody production to the bacteriophage was assayed using a bacteriophage neutralization technique. To detect antibody directed against the haptens or small proteins, the appropriate hapten or protein was first coupled to T4, and then a modified bacteriophage neutralization technique was employed. Individual mice responded to the various antigens in a sequential pattern which was basically the same for all mice within the strain. This hierarchy of responsiveness could not be explained on the basis of different immunogenicities of the antigens nor on different sensitivities of the antibody assays. Instead, we propose that the hierarchy results from the ordered maturation of lymphopoietic elements in the fetal liver inoculum. (auth)

29751 DESYNCHRONIZATION OF THE DIURNAL RHYTHM OF ACID PHOSPHATASE ACTIVITY IN MALE GONADS OF MICE UNDER THE INFLUENCE OF UV AND X-RAYS RADIATION. Barbacka, G.; Surowiak, J. (Jagiellonian Univ., Krakow). Acta Biol. Cracov., Ser. Zool.; 16: 71-85(1973).

By means of histochemical and biochemical methods, acid phosphatase activity was studied in the testes of male mice in the course of 24 hours in the spring and winter seasons and different geographical longitudes, and the influence of large doses of x radiation (50 kVp 20 mA, 2100 R) and uv (about 80,000 ergs/sec/cm^2)

on this rhythm was observed. The findings showed that the diurnal rhythm of this enzyme is somewhat different in interstitial tissue than in the epithelium of the convoluted tubules of the testes. Both types of radiation desynchronized this rhythm within several hours after exposure. Significant differences of diurnal rhythm of acid phosphatase activity were also observed in different seasons of the year and different geographical longitudes. (auth)

29752 GOMORI-POSITIVE GLIA IN UV-IRRADIATED MICE. Srebro, Z.; Lach, H. (Medical Academy, Krakow). Acta Biol. Cracov., Ser. Zool.; 16: 43-48(1973).

A single, massive dose of uv was applied to the skin of the back of adult, female albino mice. The irradiated animals were killed after 12 h, 24 h, and 48 h following the irradiation. The brains of the animals were examined histologically from preparations stained with Gomori's chrome haematoxylin method. A significant increase in number of periventricular glial cells showing Gomori-positive granulations was found in the hypothalamus of irradiated animals in comparison with unirradiated, control mice. A tendency to return towards normal level was observed 48 h post irradiation. (auth)

29753 EFFECTS OF CARBON PARTICLES ON PHAGOCYTIC ACTIVITY OF RETICULOENDOTHELIAL SYSTEM IN X-IRRADIATED MICE. Nakamura, S. (Osaka Public Health Inst.); Mori, K. J. J. Radiat. Res.; 15: No. 1, 14-18(Mar 1974).

The effects of carbon particles and x irradiation on phagocytic activity of reticuloendothelial system (RES) were studied. Administration of 1 mg of carbon particles per mouse did not decrease the phagocytic activity of RES, but slightly enhanced the activity. A functional blockade of RES was observed in the mice administered more than 5 mg of carbon particles. In the mice given 10 mg of carbon particles, the blockade continued for about a week after the treatment. The degree of blockade caused by the administration of carbon particles was not affected even by x irradiation with 500 R. (JA)

29754 EXPERIMENTAL OCULAR IRRADIATION WITH ACCELERATED PROTONS. Constable, I. J.; Koehler, A. M. (Retina Foundation, Boston). Invest. Ophthalmol.; 13: No. 4, 280-287(Apr 1974).

High-energy proton beams of 7 mm. diameter or less were used to irradiate monkey eyes. When the Bragg peak was positioned immediately in front of the retina, it was possible to apply an acute radiation burn to a discrete area of the retina and choroid while delivering much smaller doses to other ocular and orbital tissues. The minimal scatter, finite penetration, and advantageous dose-distribution curve for soft tissues make this mode of radiotherapy very attractive for the treatment of ocular and orbital tumors. (auth)

29755 AUTORADIOGRAPHIC STUDIES OF DNA-REPAIR IN THE RETINA OF RABBITS. Pichler, L.; Hofer, H.; Gumpel-Mayer, T. F. Invest. Ophthalmol.; 13: No. 4, 290-293(Apr 1973).

DNA repair in ^{60}Co-γ-irradiated (60,000 rad) rabbit retinae was investigated by autoradiography. A repair mechanism has been shown to exist at the same high degree in cells of the ganglion layer and inner nuclear layer, but, however, to a much lesser extent in the cells of the outer nuclear layer of these retinae. (auth)

29756 DIRECT RELATIONSHIP BETWEEN IMMUNE COMPETENCE AND THE SUBCUTANEOUS GROWTH RATE OF A MALIGNANT MURINE LUNG TUMOR. Yuhas, J. M.; Pazmino, N. H.; Proctor, J. O.; Toya, R. E. (Oak Ridge National Lab., TN). Cancer Res.; 34: 722-728(Apr 1974).

Studies were conducted on the transplantability and growth in syngeneic hosts of a malignant alveolar cell carcinoma of the BALB/c mouse lung. In untreated mice, the cancer can be established with fewer than 100 cells and grows with a volume doubling time of 3.1 days. Total-body irradiation of the host with 500 R 2 hr prior to s.c. inoculation with tumor cells does not affect the transplantability of the tumor but significantly suppresses its growth rate. This suppression of the growth rate is not associated with a generalized body weight loss and cannot be induced by localized irradiation. Injection of hydrocortisone acetate prior to tumor inoculation or use of immunologically crippled senescent hosts yields a similar suppression. Further, suppression of the growth rate of the cancer by total-body irradiation can be reversed by transplantation of syngeneic lymph node or spleen cells immediately after irradiation. It is unlikely that this reduced growth rate of s.c. tumors in immunosuppressed hosts results from inhibition of immunological reactions which stimulate growth or from a preferential loss of "blocking" factors, since metastasis proceeds more rapidly in immunosuppressed hosts and splenectomy does not slow the growth of the s.c. tumor. (auth)

29757 TYROSINE AMINOTRANSFERASE INDUCTION IN RAT LIVER AS A RESPONSE TO IRRADIATION OR FLASH BURN INJURIES. Henderson, T. R.; Jones, R. K. (Lovelace Foundation for Medical Education and Research, Albuquerque, NM). J. Trauma; 14: No. 4, 317-324(Apr 1974).

Tyrosine aminotransferase activity (TAT) was measured in rat liver to determine the extent to which thermal or irradiation injury, or both, resulted in induction of TAT synthesis, and to determine the relationship between the severity of injury and the extent of TAT induction. Flash burns elicited increased TAT activity in the liver, and the extent of induction was related to the severity of burn injury. Thermal injuries to the skin alone resulted in a detectable increase in TAT activity in about 30% of the animals, while deeper burns resulted in a uniform induction in all animals. The highest TAT activity occurred in the livers of animals just prior to death from thermal injuries. Irradiation alone did not lead to a detectable increase in TAT activity, but resulted in a superinduction effect in animals exposed to skin burns. The latter was considered to result from interference with repressor formation due to genetic damage, resulting in uncontrolled TAT synthesis. Thus it appears that one of the events associated with the exaggerated catabolism of proteins following severe burns is the induction of enzyme synthesis in the liver. The manner by which excessive synthesis of enzymes such as TAT in the liver can contribute towards a poor prognosis is discussed. (auth)

29758 RESPONSE OF JEJUNAL MUCOSA TO FRACTIONATED DOSES OF NEUTRONS OR γ-RAYS. Withers, H. R.; Chu, A. M.; Mason, K. A.; Reid, B. O.; Barkley, H. T.; Smathers, J. B. (Univ. of Texas, Houston). Eur. J. Cancer; 10: No. 4, 249-252(Apr 1974).

From 2nd meeting on fundamental and practical aspects of the application of fast neutrons in clinical radiotherapy; The Hague, Netherlands (3 Oct 1973).

The $\mathrm{RBE}_{n+\gamma/\gamma}$ of fast neutrons produced by the ^{9}Be(d,n)^{10}B reaction (E_d = 50 MeV) relative to ^{60}Co γ rays for killing of jejunal crypt stem cells has been measured over a wide range of doses beginning at 400 rad of γ-rays, and extending to doses as high as 1600 rad. Dose-equivalent values for recovery as a function of the size of the dose-per-fraction were measured. When γ doses up to about 400 rad were given, about 60% of the dose was "recovered." With neutron doses of 100 to 200 rad, the recovered dose amounted to only about 13% of the given dose. (auth)

29759 CELLULAR REPAIR AFTER X OR GAMMA IRRADIATION DETERMINED FOR SEVERAL GROSS CRITERIA ON ANIMALS AND PATIENTS. Wambersie, A. (Univ., Louvain, Belgium). Eur. J. Cancer; 10: No. 4, 235-239(Apr 1974).

From 2nd meeting on fundamental and practical aspects of the application of fast neutrons in clinical radiotherapy; The Hague, Netherlands (3 Oct 1973).

The shape of survival curves for several mammalian cell types was studied by assessing the "recovered dose" (early recovery) for different sizes of fractions. The following "gross" end-points were used: skin reactions and intestinal death in mice, tumor regression, gross skin and mucosal reactions in patients. The increase of dose necessary to attain the chosen biological effect was determined when a single irradiation dose D_s was split into two equal doses $2D_i$ or when N fractions ($N \times D_s$) were "split" into 2N equal "subfractions" ($N \times 2D_i$); i was the interval between the two "subfractions" D_i and the overall treatment time was kept constant. From the data obtained conclusions are drawn about the shape of cell survival curves in the low dose region and some implications for fast neutron therapy are discussed. (auth)

29760 DEVELOPMENT AND INVOLUTION OF MAMMARY GLAND EPITHELIAL TISSUE UNDER X IRRADIATION, CYCLOPHOSPHAMIDE, AND ANTILYMPHOCYTE SERUM TREATMENT. Krushchov, N. G.; Samoilov, V. I.; Kurovska, M.; Skurskaya, M. G.; Suetina, I. A. (Moscow State Univ.). Ontogenez; 4: No. 5, 481-487 (Jul 1973). (In Russian).

X irradiation and treatment with cyclophosphamide and antilymphocyte serum resulted in retardation of the gland tissue involution and a sharp, short-term increase in the secretory activity in experimentally induced development and involution of the mammary gland parenchyma in rats and mice. Since x irradiation in the doses used causes leukopenia, sharply inhibiting the migration of neutrophils and macrophages in the tissue, it is suggested that a deficiency in neutrophils and macrophages also leads to a retardation of involution (resorption) of epithelial structures of the mammary gland. A decrease in the threshold concentrations of hormones (prolactin) in the blood, which affects the epithelium, may explain the increase in tissue penetrability and the short-term increase in secretory activity. The action of cyclophosphamide was similar to that of radiation but less marked. (tr-INIS)

29761 CHANGES IN GLYCOGEN LOCALIZATION AND CONTENT AND ACTIVITY OF ENZYMES METABOLIZING GLYCOGEN IN RAT BRAIN DURING MATURATION UNDER NORMAL CONDITIONS AND AFTER GAMMA IRRADIATION. Oseenda, M.; Smialek, M.; Pronaszko, A.; Nowakowski, W. Neuropatol. Pol.; 8: No. 4, 375-387(1970). (In Polish).

In the maturating brains of rats an increase in glycogen content was found in the period of development. It was characterized by a twofold leap between the 5th and 8th, and the 10th and 14th day of life. The rise of the glycogen level did not occur in parallel to the cytological maturation of brain tissue. Phosphorylase activity appeared successively in various brain structures during development, in phylogenic order together with the appearance of glycogen. Glycogen does not exhibit a predilection for localization in the germinal zones. In rats subjected to whole-body irradiation on the 4th day of life with a 300 R dose of gamma rays, a short and reversible increase in glycogen content occurred in the early period after exposure (24 to 96 h). The dynamics of these changes did not differ from that observed in the brains of adult animals under similar experimental conditions. The localization of glycogen and phosphorylases remained unchanged after irradiation. Phosphorylase activity, between the 5th and 8th day of life greatly increased in the cortex and subcortical nuclei. In this period glycogen was mainly present in the white matter both in astro- and oligodendroglia. (auth)

29762 EFFECT OF IONIZING RADIATION ON ALKALINE PHOSPHATASE ACTIVITY IN HEMATOPOIETIC CELLS OF MOUSE AND RAT. Bartnikowa, W. Folia Haematol. (Leipzig); 100: No. 4, 377-384(1973). (In German).

Activity fluctuations of alkaline phosphatase can be observed in the spleen and bone marrow cells of mice and rats after a single total-body irradiation. This irradiation, however, is not able to produce an activity increase of alkaline phosphatase in those cells that previously had no enzyme activity. On the other hand various strong fluctuations of activity can be proved after irradiation in the same cell type, with the surroundings of the tissue where the cells are located apparently exercising a great influence. (auth)

29763 CHANGES IN OXYGENATION AND RADIOSENSITIVITY OF THE TUMOR AFTER IRRADIATION. Rampan, Yu. I.; Yarmonenko, S. P. (Inst. of Experimental and Clinical Oncology, Moscow). Med. Radiol.; 19: No. 9, 47-52(Sep 1974). (In Russian).

Experiments were made of 140 albino mongrel mice with a solid form of ascitic cancer ELD. The polarographic method established reoxygenation of anoxic tumor cells during the period from 24 to 72 hours following irradiation of the tumor in a dose of 1000 R. The antitumor effect of fractionated irradiation (1000 R × 2) became significantly intensified if the second irradiation was made during the period of the most marked oxygenation of the tumor. (auth)

29764 REVIEW OF RBE VALUES OF 15 MeV NEUTRONS FOR EFFECTS ON NORMAL TISSUES. Broerse, J. J. (Gezondheidsorganisatie TNO, Rijswijk, Netherlands). Eur. J. Cancer; 10: No. 4, 225-230(Apr 1974).

From 2nd meeting on fundamental and practical aspects of the application of fast neutrons in clinical radiotherapy; The Hague, Netherlands (3 Oct 1973).

Values of the relative biological effectiveness (RBE) of fast neutrons for effects on normal tissues depend not only on the neutron energy and the dose, but also on the type of tissue irradiated. Values of the RBE of 15 MeV neutrons are reviewed for rapidly proliferating rodent tissues, such as mouse bone marrow, mouse intestine, and rat skin treated with single and fractionated irradiations. In addition, RBE values were obtained for rodent tissues with relatively long cell life times, such as the vascular endothelium, the spinal cord and the lung. In general, the normal tissue data indicated that for doses between 50 and 250 rad the RBE values ranged up to values of about 2, but depend on the fractionation regimen. (auth)

29765 TOXICITY TO RABBIT RETINA OF EPITHERMAL NEUTRON BEAM. Kroyhn, D. L. (New York Eye and Ear Infirmary); Newton, J. C.; Barsa-Newton, M. C.; Jacobson, J. H.; Straub, R. F. Int. J. Nucl. Med. Biol.; 1: No. 4, 181-186 (Jun 1974).

A comparison was made between the 24-hr effects of fully thermalized and partially thermalized atomic pile radiation on four metabolic indicators in rabbit retina. The purpose was to estimate the retinal toxic effect of each quality of radiation relative to the thermal neutron fluence available in the posterior ocular segment for neutron–^{10}boron heavy particle radiation [^{10}B(n,α)^{7}Li]. Cadmium filtration was omitted. The indicators were rates of oxygen consumption, anaerobic glycolysis, and activities of cytochrome oxidase and succinic dehydrogenase. In all determinations, ‘‘epithermal’’ pile radiation was significantly more toxic than fully thermalized radiation relative to thermal neutron fluence in the target area. Toxicity varied directly with dose in both cases. Up to a dose of 5×10^{12} neutrons cm^{-2} sec^{-1}, little acute retinal metabolic damage occurred with fully thermalized pile radiation, which remains the choice in investigation of neutron-boron therapy in the posterior ocular segment. (auth)

Invertebrates

29766 (SAND-74-6017) EFFECT OF TEMPERATURE ON THE RADIATION SENSITIVITY OF ASCARIS EGGS. Dognon, A. Translated by Patricia Newman from Compt. Rend. Soc. Biol.; 94: 466-468(1926). 6p. Dep. NTIS $4.00.

The sensitivity of a cell (Ascaris egg) to x rays does not appear to be directly related to its activity. It continues to increase for temperatures much higher than the optimum for this activity. The over-all sensitivity no longer varies with temperature above 15 to 20°C. It can be separated into a constant element and an element that varies rapidly with temperature, where its nearly constant coefficient is about 4 at 10°C. This element can apparently be severely reduced by a reduction in gas exchanges. (auth)

29767 INSENSITIVITY OF SERIALLY TRANSFERRED TETRAHYMENA PYRIFORMIS W. TO IRRADIATED MEDIA. Srinivas, H.; Vakil, U. K.; Sreenivasan, A. (Bhabha Atomic Research Centre, Bombay). Radiat. Res.; 59: No. 3, 710-716(Sep 1974).

The sensitivity of Tetrahymena pyriformis to irradiated normal media has been examined during four successive transfers. Morphological, physiological as well as chemical characteristics of the cells with respect to growth, size, shape, response to heat-shock synchronization, oxidative metabolism, and the contents of certain cell constituents were not affected. Hydrogen peroxide formed in the medium due to radiolysis is decomposed rapidly by Tetrahymena. This may explain the resistance of cells to known toxic effects of irradiated media. (auth)

29768 CHROMOSOME LOSS FOLLOWING X-RAY IRRADIATION OF MATURE OOCYTES FROM DROSOPHILA MELANOGASTER. Luetolf, H. U. (Eidgenoessiche Technische Hochschule, Zurich). Arch. Genet.; 47: 99-120(1973). (In German).

The purpose of the present studies was to investigate on a quantitative level the contribution of chromosome loss to the over-all rate of x-ray induced dominant lethals in mature oocytes of Drosophila melanogaster. For these investigations, the dose response curves for x-ray induced loss of the chromosomes X, 2, and 3 in mature oocytes were determined. The frequency of X-chromosome loss was measured by the number of X*/O-males resulting from a cross of irradiated wildtype females (stock: Berlin wild) to untreated X*/Y*-males (X* = ywspl sn^3, Y* = y$^+$ YB^S). For the detection of loss of the autosomes 2 and 3, the above type of irradiated females were mated to males with the compound chromosomes C(2L)RM,b; C(2R)RM,cn; and C(3L)RM,st; C(3R)RM,p^p, respectively. The compound-2 and compound-3 test systems used allow for selective recovery of about ¼ of the flies which received via the maternal pronucleus, either no autosome (chromosome loss or nondisjunction) or two autosomes (nondisjunction). Also approximately ¼ of animals containing newly formed compound autosomes were recovered. With very few exceptions (e.g., triploids), other combinations of gametes lead to zygotes which, due to aneuploidy, die before reaching pupal or adult stages of development. The experimental results did not provide a simple correlation between the size of the individual chromosomes and the frequency at which they were lost after x irradiation. This result is possibly due to factors localized on the chromosomes of the stocks used, which may modify the radiation-induced rates of chromosome loss. The combined data suggest that, when wildtype females are irradiated and crossed to untreated wildtype males, about 50% of the dominant lethals result in breakage-fusion-bridge cycles and about 10% represent a loss of one of the chromosomes X, 2, or 3. (auth)

Radionuclide Effects (Internal Source)

Man

Refer also to abstracts 29343, 29452, 29700, 29702, 29719, 29720, and 29829.

29769 (AED-CONF-74-016-002) THOROTRAST-INDUCED NEOPLASMS. van Kaick, G.; Wimmer, B.; Lorenz, D. (Deutsches Krebsforschungszentrum, Heidelberg (F.R. Germany). Inst. fuer Nuklearmedizin). 1974. 7p. (In German). INIS.

From German cancer congress; Muenchen, F. R. Germany (14 Feb 1974).

The clinical findings and causes of death of 1850 thorotrast patients have been compared with the data of a corresponding control group. Although the investigations have not been completed, the following statements can be made at this stage: By far the greatest part of the thorotrast patients died from diseases which cannot be attributed to the thorotrastosis. There is a greater risk of patients with thorotrastosis of the RES of developing liver tumors, leukemia, liver cirrhosis or myelophthisis. There is no upper limit of latency periods of the chronic irradiation, the longest latency period determined so far for a liver tumor being 39 years. As regards the other thorotrast storing organs such as spleen, lymph nodes and bones not containing marrow, no increase in neoplastic diseases could be observed. Among the cases investigated, there was no indication of a malignant tumor within the range of a thorotrast paravasate, nor of an enhanced occurrence of lung tumors as a result of the exhaled radioactive thoron. These preliminary results of the follow-up study indicate that there is an increase in the incidence of liver tumors and leukemias with prolonged latency period, i.e. with increasing total dose. (GE)

29770 (AED-CONF-74-030-003) SPECIAL INDICATION AND CONTRAINDICATIONS FOR THE IMPLANTATION OF CARDIAC PACEMAKERS WITH RADIONUCLIDE BATTERIES. Seipel, L.; Buchta, I.; Loogen, F. (Duesseldorf Univ. (F.R. Germany). 1. Medizinische Klinik B). 1974. 9p. (In German). INIS.

From symposium on safety aspects of implanted cardiac pacemakers, with special regard to radionuclide batteries; Berlin, F. R. Germany (1 Mar 1974).

In principle, the same indications are true for long-lived pacemakers as for conventional aggregates. The indication is merely limited by the expectation of life of the patient for economical reasons. The ECGs of 30 patients who had isotope pacemakers implanted in them in 1972 and 1973 exhibited the same rhythmic disturbances as the cases with conventional pacemakers which are described in detail. From the medical point of view there are no contraindications for long-lived pacemakers. It only seems worthwhile from an economical viewpoint, to implant in those patients who have a corresponding expectation of life. Important for a prognosis is the cardial state of the patient as well as the etiology of the rhythmic disturbance. A few chosen criteria are shown regarding this aspect. Considering the criteria, the number of patients in question is relatively small. Whether the isotope pacemakers will be more widely used in the coming years or whether they will be replaced by other long-lived aggregates, remains to be seen in the future. (INIS)

29771 (CONF-740930-1) CELL MEDIATED IMMUNITY AS AN EARLY DIAGNOSTIC TEST FOR OSTEOSARCOMA IN HUMAN RADIUM CASES. Lloyd, E. L.; Menon, M.; Mitchen, J. L. (Argonne National Lab., Ill. (USA)). 1974. 16p. Dep. NTIS $4.00.

From 14th Hanford biology symposium on radiation and the lymphatic system; Richland, Washington, USA (30 Sep 1974).

Lymphocytes from patients carrying a body burden greater than 0.3 μCi ^{226}Ra have been tested for specific cytotoxicity to four different osteosarcoma cell lines as well as normal human fibroblasts. Cytotoxicity indices (defined as the ratio of the number of target cells remaining, after treatment with the patients lymphocytes, relative to the values obtained with normal control subjects) have been calculated. With one exception, no cytotoxicity was observed. This is in agreement with the fact that no fresh osteosarcomas were diagnosed. The patient, in which cytotoxicity was observed, was suffering from an inflammatory lesion involving bone due to a foreign body reaction at the time of the first test. When the test was repeated 10 months later no cytotoxicity was observed. No significant nonspecific cytotoxicity was observed using lymphocytes taken from normal control subjects with any of the target cell lines used. (auth)

29772 (LA-UR-74-1300) HUMAN EXPERIENCE. Richmond, C. R. (Los Alamos Scientific Lab., N. Mex. (USA)). 1974. Contract W-7405-eng-36. 38p. (CONF-740115-1). Dep. NTIS $5.00.

From Plutonium information meeting; Los Alamos, New Mexico, USA (4 Jan 1974).

Data are summarized on the biological effects of Pu on man, based on the results of periodic medical studies on several hundred personnel with known body burdens of ^{239}Pu or ^{238}Pu, including 25 exposed in 1944 and 1945 to ^{239}Pu at doses resulting in body burdens of 10 or more nanicuries. The role of the US Transuranium Registry in the collection of data on Pu uptake by man for an epidemiological study of pathological effects, if any, is discussed. It is pointed out that medical studies so far have shown no adverse effects attributable to Pu, even after 30 years. (CH)

29773 PLUTONIUM. I. Questions of Health in a New Industry. Gillette, R. Science; 185: No. 4156, 1027-1032 (20 Sep 1974).

Questions of plutonium exposure by personnel at the Nuclear Fuels Services West Valley Processing Plant are considered along with some other exposure incidents at various places. (MCG)

29774 RESULTS AND COMPLICATIONS OF THE TREATMENT OF BECHTEREW'S DISEASE WITH THORIUM X. Laschner, W. (Karl-Marx Univ., Leipzig). Z. Orthop. Ihre Grenzgeb.; 111: 743-748(Oct 1973). (In German).

Good subjective results of Thorium X treatment of Bechterew's disease were tested by clinical examination both before and after treatment. In 51 patients an increase in joint-range could be ascertained. Undesirable side-effects are also described. During radiotherapy 9 cases of iridocyclitis, 1 case of gastric ulcer, and another with normochromic anemia were observed. Tests of serum lability, normal before the start of treatment, became abnormal during or after it in a comparatively large number of cases. A further number of cases was submitted to chemical tests, where Thorium X therapy had been given more than 3 years previously. Here, too, chemical changes were found, but no actual damage could be proved. (auth)

29775 PLASMA TSH AND SERUM T-4 LEVELS IN LONGER-TERM FOLLOW-UP OF PATIENTS TREATED WITH ^{131}I FOR THYROTOXICOSIS. Toft, A. D. (Univ. of Edinburgh); Irvine, W. J.; Hunter, W. M.; Seth, J. Brit. Med. J.; 3: No. 5924, 152-153(20 Jul 1974).

The plasma TSH levels of patients euthyroid after iodine-131 therapy given for thyrotoxicosis are reported. The mean serum T-4 level in the euthyroid patients with a high plasma TSH was significantly lower, though still in the normal range, than that in the euthyroid patients with a normal plasma TSH level. Since no patient with a normal plasma TSH level after iodine-131 treatment 6 to 18 years earlier for thyrotoxicosis developed hypothyroidism over a two year period, the follow-up of such patients need not be so rigorous as that of similarly treated euthyroid patients with raised plasma TSH levels in whom hypothyroidism developed at the rate of 5% per year. (UK)

Animals

Refer also to abstract 29805.

29776 (BNWL-SA-4870) LONG-TERM EFFECTS OF INTRATRACHEALLY INSTILLED ^{253}EsCl$_3$ IN RATS. Ballou, J. E.; Dagle, G. E.; Morrow, W. G. (Battelle Pacific Northwest Labs., Richland, Wash. (USA)). 1974. Contract AT(45-1)-1830. 16p. (CONF-740702-7). Dep. NTIS $4.00.

From Health Physics Society annual meeting; Houston, Texas, USA (7 Jul 1974).

Einsteinium-253 ($T_{1/2}$ = 20.5 days; 6.6 MeV alpha) is a transuranic element formed by multiple neutron capture in the heavier actinide elements. The unique physical properties of ^{253}Es may be exploited in comparative biological effects studies with ^{239}Pu ($T_{1/2} \cong$ 24,000 years, 5.2 MeV alpha) in order to explore the effect of radiation dose rate and radiation dose distribution on the induction of latent effects such as lung and bone tumors. Results are reported of preliminary investigations in rats to determine the carcinogenicity of intratracheally instilled ^{253}EsCl$_3$. The intratracheal mode of administration was employed rather than the more natural inhalation route in order to conserve radionuclide and administer an accurately metered dose. Radiation doses of sufficient magnitude to severely damage the lung and markedly shorten the life span were notably non-carcinogenic. The low incidence of tumors is undoubtedly related to the fact that animals did not survive long enough for the long latency period of tumorigenesis to be expressed. (CH)

29777 (BNWL-SA-5065) CARCINOGENICITY OF IODINE-131 RELATIVE TO AGE AT EXPOSURE. Sikov, M. R.; Mahlum, D. D. (Battelle Pacific Northwest Labs., Richland, Wash. (USA)). [nd]. 10p. (CONF-740715-10). Dep. NTIS $4.00.

From 5th international radiation research congress meeting; Seattle, Washington, USA (14 Jul 1974).

Adult, prenatal, and newborn rats were given various doses of ^{131}I or ^{125}I orally and the thyroid and pituitary glands were examined histologically at death or until 30-mo of age for signs of carcinogenesis or other pathological changes in relation to the radiation dose at various ages. The results indicate that weanling rats were the most sensitive age group. (CH)

29778 (COO-119-249) RESEARCH IN RADIOBIOLOGY. Annual Report of Work in Progress in the Internal Irradiation Program. Jee, W. S. S. (Utah Univ., Salt Lake City (USA). Radiobiology Div.). 31 Mar 1974. Contract AT(11-1)-119. 340p. Dep. NTIS $20.00.

Data are included on the pathological findings at autopsy of beagles given single intravenous injections of various doses of ^{226}Ra, ^{228}Ra, ^{239}Pu, ^{228}Th, ^{90}Sr, ^{241}Am, ^{249}Cf, or ^{252}Cf. Most of the animals were euthanized when death appeared imminent, for some of which this was 10-yr post-injection. Data are included on the calculated average dose to the skeletion in rods and the incidence of osteosarcomas and other neoplasms. Separate abstracts were prepared for 14 sections of the report. (CH)

For abstracts of individual sections see: 29779, 29780, and 29796–29807.

29779 (COO-119-249, pp 268-280) EARLY HEMATOLOGIC EFFECTS OF CURIUM AND EINSTEINIUM IN BEAGLES. Dougherty, J. H. 31 Mar 1974.

In research in radiobiology. Annual report of work in progress in the internal irradiation program.

The hematologic changes following a single injection of curium (^{244}Cm + ^{243}Cm) at the 5-dose level, or einsteinium (^{253}Es) at the three and five dose levels into a small number of adult beagles have been summarized for the first 9 to 12 months following injection. These actinide elements are surface-seeking alpha emitters with the einsteinium having a very short half-life (20.5 days). The early hematologic effects follow the typical patterns of early granular leukocyte and erythrocyte depression as seen after injection of high dose levels of other transuranic elements. However, the rates and magnitude of recovery of the various cells are much more rapid in dogs injected with the short lived ^{253}Es. (auth)

29780 (COO-119-249, pp 311-321) CORTISOL METABOLISM IN SKIN OF BEAGLES BEARING ^{241}Am: A POSSIBLE PRE-NEOPLASTIC CHANGE IN STEROID METABOLISM. Nabors, C. J. Jr.; Hinckley, J. S. 31 Mar 1974.

In research and radiobiology. Annual report of work in progress in the internal irradiation program.

Skin from beagles bearing ^{241}Am with and without tumors and controls was studied. The metabolism of cortisol-4-^{14}C was significantly elevated over controls in both ^{241}Am groups. This metabolic alteration may indicate a pre-neoplastic change in ^{241}Am injected beagles. (auth)

29781 (COO-3268-5) EMBRYOTOXICITY OF ASTATINE-211. Borras, C.; Brent, R. L.; Gorson, R. O.; Lamb, J. F. (Thomas Jefferson Univ., Philadelphia, Pa. (USA). Stein Research Center; Medi-Physics, Inc., Emeryville, Calif. (USA)). [nd]. 5p. (CONF-740926-2). Dep. NTIS $4.00.

From 1st world congress of nuclear medicine and exhibition meeting; Tokyo, Japan (30 Sep 1974).

Pregnant rats were given ^{211}At by intravenous injection at doses ranging from 0.127 μCi to 0.893 μCi of ^{211}At/g/rat body mass, with the absorbed doses to the embryonic site ranging from 43 to 302 rads. The rats were examined at various time intervals for an increase in embryo lethality and a decrease in both fetal and placental mass. Progeny were examined for the incidence of congenital malformations. The pathological changes induced by internal irradiation from ^{211}At are compared with those induced by external exposure to x radiation of the same dose range. (CH)

29782 EFFECT OF INTERNALLY DEPOSITED PLUTONIUM-239 ON THE LYSOSOMES OF RAT LIVER. Danpure, C. J.; Taylor, D. M. (Inst. of Cancer Research, Sutton, Eng.). Radiat. Res.; 59: No. 3, 679-692(Sep 1974).

The effects of plutonium-239, an α-particle emitting radionuclide which deposits mainly in the lysosomes, on the activity of various lysosomal enzymes have been studied in rat liver. The effects observed were compared with those produced by the $\beta + \gamma$ radiation from colloidal gold-198. Following administration of 0.5 μCi polymeric ^{239}Pu the specific activities of acid deoxyribonuclease and aryl sulphatase were increased by 30 days and remained elevated at 1 yr. β-Glucuronidase, acid β-glycerophosphatase, and cathepsin D showed increased specific activity at time intervals longer than 6 mo after injection of ^{239}Pu. All the enzymes studied showed decreased sedimentability at 30 days but this returned to approximately normal limits at longer time intervals. In comparison the administration of 0.5 mCi ^{198}Au colloid also caused increased specific activity of deoxyribonuclease II, β-glucuronidase, and acid β-glycerophosphatase, but did not decrease the enzyme sedimentabilities. It is concluded that at least some of the pathological effects known to be produced by ^{239}Pu and ^{198}Au may be explained in terms of lysosomal changes. (auth)

29783 EFFECT OF ^{239}PuO$_2$ PARTICLE NUMBER AND SIZE ON THE FREQUENCY AND DISTRIBUTION OF CHROMOSOME ABERRATIONS IN THE LIVER OF THE CHINESE HAMSTER. Brooks, A. L.; Retherford, J. C.; McClellan, R. O. (Inhalation Toxicology Research Inst., Albuquerque, NM). Radiat. Res.; 59: No. 3, 603-709(Sep 1974).

Chinese hamsters were injected intravenously with ^{239}Pu citrate or ^{239}PuO$_2$ particles. There were four particle sizes injected: 0.17, 0.30, 0.44, and 0.84 μm, which would vary the local radiation dose and dose rate to the surrounding cells. Additional hamsters were injected with graded levels of activity from 6×10^{-5} to 6×10^{-3} μCi/g using 0.30 μm ^{239}PuO$_2$ particles. This changes the particle number and the average dose rate. An experiment was also conducted to determine the retention and distribution of the particles using ^{51}Cr to trace the ^{239}PuO$_2$ particles. The particles were concentrated in the reticuloendothelial system with 90% of the injected activity in the liver, 3% in the spleen, and the remainder in either the bone or bone marrow. Autoradiographic studies with ^{239}Pu showed that there was particle clumping causing high local doses to the liver cells in all particle sizes studied. The ^{239}Pu citrate produced a linear increase in the chromosome aberration frequency with a slope of 4.8×10^{-3} aberrations/cell/rad. The chromosome aberration frequency increased with increasing average dose following injection of the ^{239}PuO$_2$ particles. This increase in response plateaued at higher average doses. There was little evidence of an effect of particle size on the aberration frequency. When local dose was related to aberration frequency, the smaller the particles the greater the effectiveness in producing chromosome damage. Following injection of all particle sizes, the nonuniform distribution of dose was reflected in a nonuniform distribution of chromosome damage in the cell population with up to 13 aberrations in an individual cell. The number of cells at risk following particulate deposition is much less than from uniform distribution of the same total activity. This may indicate that long-term risks from ^{239}PuO$_2$ particles would be less than that from uniformly distributed ^{239}Pu citrate. (auth)

29784 PATHOLOGICAL CHANGES IN MICE FOLLOWING THE INTRAPERITONEAL ADMINISTRATION OF RADIONUCLIDES. Huvos, A. G.; Rogoff, E. E.; Hilaris, B. S.; Hahn, E. W. (Memorial Sloan–Kettering Cancer Center, New York). Radiology; 113: No. 1, 203-207(Oct 1974).

From 59th scientific assembly and annual meeting of the Radiological Society of North America; Chicago, IL (25 Nov 1973).

Various doses of either ^{32}P or ^{198}Au were given to mice and autopsies were performed 5, 8, 10, 15, and 90 days later. Control animals received intraperitoneal saline injections. If given in sufficient intraperitoneal doses to mice, both ^{32}P and ^{198}Au can cause morbidity and/or death. The death is related to pathological changes in the gastrointestinal tract including goblet-cell hypersecretion and blunting of the mucosal folds in both large and small intestines with increased numbers of mitotic figures seen at the base of the intestinal crypts, splitting and degeneration of the myofibers with focal necrosis, and increased mesothelial proliferation. (auth)

29785 MORPHOLOGY AND ENZYME HISTOCHEMISTRY OF ^{224}Ra-INDUCED OSTEOSARCOMAS OF THE MOUSE. Goessner, W.; Hindringer, B.; Luz, A.; Schwabe, M. (Gesellschaft fuer Strahlen- und Umweltfoschung mbH, Nuremberg). Z. Krebsforsch. Klin. Onkol.; 78: No. 3, 225-235(1972). (In German).

The induction of osteosarcomas by the short-living osteotropic alpha emitter ^{224}Ra was studied in a large long-term experiment. Within the framework of these experiments the different structure and the enzyme pattern of the induced tumors were investigated. Male and female mice, aged 3–4 weeks, had received ^{224}Ra in the form of chloride, the doses varying between 5 and 100 μCi/kg. Only freshly removed tumors of sacrificed animals were used for the present investigation. The osteoblastic sarcomas showed various types of differentiation dependent on their location in the skeleton. Generally, tumors of the head region did not show any special osteoblastic cells, whereas in tumors of other skeletal sites osteoblasts, osteoclasts and even blood-forming tissue were frequently observed. The histochemical demonstration of alkaline and acid phosphatase revealed different patterns of enzyme activity. (GE)

29786 FOLLICULAR DAMAGE TO BOVINE OVARY FROM RADIOIODINE. Reddi, O. S. (Osmania Univ., Hyderabad, India). Indian J. Anim. Sci.; 42: No. 9, 648-650(1972).

The effect of iodine-131 in zebu cows at a dose level of 5 mCi or 0.014 μCi per g body weight was investigated up to 28 days. Twenty zebu cows were injected subcutaneously with the said dose. A batch of 10 were used for uptake measurements and the other batch of 10 for gonadal cell mortality. Two cows each, from both the groups were sacrificed on 3rd, 7th, 14th, 21st, and 28th days. Oocyte damage and uptake of iodine-131 by ovaries were studied for that period. The oocyte mortality increased steadily reaching a peak by 28th day, whereas the iodine-131 present in ovaries decreased as a result of decay. The cell death on the 3rd day was due to the iodine-131 present until that time, whereas the effect observed on the 28th day may be due to the residual effect of radioiodine. The fact that 0.003% of injected activity on 3rd day would cause about 75% mortality by 28th day points out the possible hazards of radioiodine in medicine. (Indian Sci. Abstr.)

29787 SOMATIC MUTATION BY ENDOGENOUS RADIOCARBON. Tamers, M. A. (Nova Univ., Fort Lauderdale, FL). Int. J. Nucl. Med. Biol.; 1: No. 4, 227-228(Jun 1974).

The probability of a naturally occurring radiocarbon atom decaying in a strategic position, such as in a DNA base on a gene, during a human lifetime is shown to be high. Furthermore there is a high probability that the ^{14}N atom thus produced will remain in position in the DNA base molecule, in the site of the decayed ^{14}C atom. This endogenous radiocarbon mechanism is distinct from the radioinduced mutation mechanism, and the possible relevance of this chemical transmutation to the etiology of diseases such as cancer is discussed. The process of aging could also result from somatic mutations and therefore be related to the incidence of endogenous radiocarbon. The possibility of experimental assessment of this radiocarbon effect by observation of laboratory animals raised on a radiocarbon free diet is suggested. (UK)

Microorganisms

29788 COMPARATIVE INVESTIGATION OF MUTAGENIC EFFECTS OF INCORPORATED ISOTOPES OF THE MOST IMPORTANT ORGANOGENIC ELEMENTS. VI. Comparison of Lethal and Mutagenic Effects of the Decay of ^{32}P and ^{35}S Incorporated into Cells of Escherichia Coli WP-2S Try$^-$. Pluchennik, G. (Univ., Warsaw). Genetika; 10: No. 8, 129-136(Aug 1974). (In Russian).

Quantitative data are obtained on the induction of the lethal effect of the Try$^-$ → Try$^+$ reversion in Escherichia coli WP-2S Try$^-$ by the decay of incorporated ^{32}P and ^{35}S. The data obtained were compared to similar data obtained for E. coli WP-2 Try$^-$. The frequency of Try$^-$ → Try$^+$ reversions induced in E. coli WP-2S Try$^-$ by the decay, of ^{32}P was ten times that induced in E. coli WP-2 Try$^-$. A conclusion is drawn about the substantial effect of the state of the reparative mechanism on the probability of the transition of the primary lesion of DNA structure into hereditarily fixed mutation. (auth)

Nuclide Kinetics and Toxicology

Refer also to abstract 29439.

Man

Refer also to abstracts 29423, 29455, 29773, 29846, and 29857.

29789 DISTRIBUTION OF RADIOACTIVE AND STABLE CESIUM IN THE HUMAN BODY. Pietrzak-Flis, J. (Central Lab. for Radiological Protection, Warsaw). pp 335-339 of Health Physics Problems of Internal Contamination. Budapest; Akademiai Kiado (1973).

From proceedings of the IRPA second European congress on radiation protection; Budapest, Hungary (3 May 1972).

The concentration of stable and radioactive cesium and potassium was determined in the different tissues from eleven autopsies. The highest concentration of the above elements was in muscles and it was slightly lower in pancreas and spleen. The lowest concentration of ^{137}Cs was found in bones. Concentration of ^{137}Cs in brain was close to the average in all tissues. The average amount of stable cesium, estimated for the body of the standard man, was 0.92 ± 0.28 mg. (auth)

29790 PLUTONIUM(II): WATCHING AND WAITING FOR ADVERSE EFFECTS. Gillette, R. Science; 185: No. 4157, 1140-1143(27 Sep 1974).

The role of the US Transuranium Registry, established by the AEC in 1968, is the collection of medical data on Pu personnel to find correlations, if any, between the body burden of Pu or other radioactive elements and any changes in longevity or patterns of disease that develop. Medical data have been accumulated to date on some 6000 nuclear personnel, including autopsy findings on some 40 consenting individuals. The value of this epidemiological study in assessing the health hazards of Pu is pointed out. The AEC has made cooperation with the registry entirely voluntary on the part of private industry now engaged in the production of Pu fuels for nuclear power reactors. The value of participation in the registry to the Pu fuel industry is pointed out in the event of legal suits for compensation of employees for injuries attributed to Pu exposure. The value of the data accumulated by the registry to scientists is pointed out in the event changes are considered in the present standards for maximum permissible body burden of Pu, established in the late 1940's as 40 nanocuries. (CH)

29791 ABSORPTION OF ^{47}Ca FROM DIGESTIVE TRACT IN PATIENTS WITH UROLITHIASIS. Lorenz, J.; Hrynczuk, B.; Janukowicz-Lorenz, H. (Medical Academy, Wroclaw). Pol. Tyg. Lek.; 28: No. 23, 862-865(1973). (In Polish).

In 23 patients with urolithiasis and 13 controls absorption of calcium from the digestive tract was determined after oral administration of ^{47}Ca. The radioactivity was measured in the serum 30, 60, and 120 minutes after administration of the isotope expressing it in percent of administered dose per one litre of serum. Besides that the percentage of ^{47}Ca dose excreted with urine during 4 hours was determined. It was found that ^{47}Ca absorption from the digestive tract was increased and accelerated in case of urolithiasis. No significant difference was demonstrated between the groups with regard to the amount of isotope excreted with urine during 4 hours. There was also no parallelism between the degree of calcium absorption and the amount of this element excreted in 24-hour urine. (auth)

29792 PHARMACODYNAMICS OF ^{197}Au AND ^{195}Au LABELED AUROTHIOMALATE IN BLOOD. Correlation with Course of Rheumatoid Arthritis, Gold Toxicity, and Gold Excretion. Gottlieb, N. L.; Smith, P. M.; Smith, E. M. (Univ. of Miami, FL). Arthritis Rheum.; 17: No. 2, 171-183(1974).

The relationships between serum stable gold (^{197}Au) concentration and serum and whole blood radioactive gold (^{195}Au) disappearance curves to clinical course and gold excretion are analyzed in this prospective clinical-metabolic study of 18 patients with active rheumatoid arthritis (RA). Patients received a standard course of Myochrysine (^{197}Au aurothiomalate), were given ^{195}Au labeled aurothiomalate to monitor current dose dynamics, and clinically evaluated at regular intervals. Stable and radiogold concentrations in blood were measured serially on an outpatient basis and during periods of hospitalization using neutron activation analysis and standard radiometric techniques. Serum concentrations of both isotopes failed to correlate with clinical course and toxicity. Serum radiogold disappearance curves were similar in patients who received radioactive gold on two or more occasions, despite changes in clinical course. Whole blood radiogold disappearance curves however were significantly different in most and least improved patients. These findings, and others reported herein, suggest that (a) the probable interstitial or intracellular mechanism(s) of action of gold on the inflammatory process are not dependent upon serum gold concentrations and (b) they raise the possibility that whole blood radiogold disappearance curves would provide a means of selecting those patients who will derive maximum therapeutic benefit from chrysotherapy. (auth)

29793 ESTIMATION OF RADIATION DOSES FROM I. V. ADMINISTRATION OF SELENITE Na$_2$^{75}SeO$_3$. Textoris, R. (Safarik Univ., Kosice, Czech.); Pokorna, I. Cesk. Radiol.; 27: No. 5, 295-298(Sep 1973). (In Slovak).

The feasibility of applying ^{75}Se in the diagnostics of tumors was studied. The detectors were placed above the kidneys, the liver, the thyroid, and the thigh. Measurements were carried out in two patients i.v. administered ^{75}Se in selenite over 34 days after the radioisotope application. Also, the activity of blood samples was measured. The retention curves and the proportion of cumulated activity thus obtained served for calculation of the cumulated activity in the kidneys, the liver, and in the thyroid. The results show that the application of selenite Na$_2$^{75}SeO$_3$ is feasible in spite of the long half-life of ^{75}Se. The absorbed doses were found to be fairly low and absolutely acceptable. (Nucl. Sci. Abstr. Czeck.)

29794 TISSUE-BLOOD ^{131}I AND ^{133}Xe TRANSFER IN THE PRESENCE OF RAISED CAPILLARY FILTRATION. Roztocil, K.; Prerovsky, I.; Novak, P. (Inst. for Clinical and Experimental Medicine, Prague). Physiol. Bohemoslov.; 23: No. 4, 327-332 (1974).

The induction of venous occlusion of 60 torrs was followed by temporary arrest of isotope clearance. In the next phase, up to the release of venous occlusion, when fluid filters into the extravascular space, the rate of ^{131}I clearance was higher than before occlusion. The rate of ^{133}Xe clearance during the same period did not attain the level of the initial values. The findings are in agreement with the concept that transcapillary blood-tissue fluid shifts influence the transport of substances into the blood. The possible application of this relationship should be taken into account when using clearance methods for local blood flow evaluation. (auth)

Animals

Refer also to abstracts 29419, 29420, 29448, 29449, 29778, 29786, and 29859.

29795 (CEA-R-4591) METABOLISM OF TRITIUM-LABELLED SODIUM ACETATE, IN THE RAT. A Radiation Protection Approach. Jeanmaire, L.; Vernois, Y.; Bullier, D.; Gros, R. (CEA Centre d'Etudes Nucleaires de Fontenay-aux-Roses, 92 (France). Dept. de Protection). Aug 1974. 34p. (In French). Dep. NTIS (U. S. Sales Only) $4.75.

The tissue distribution of the tritium-labeled sodium acetate was followed in rats for 240 days. Absorption following oral and intraperitoneal administration, urinary and fecal excretion, and uptake by some twenty tissues was followed through time. Most of the acetate was quickly changed into water and a small percentage of the activity (about 1 percent) was incorporated into the organic matter. The longer excretion half-life was in the range of 70 days, but it seemed longer for some organs. The exposure of these organs due to the longer half-life should be considered as compared with that due to tritiated water. (auth)

29796 (COO-119-249, pp 120-124) EVALUATION OF LONG-TERM ZnDTPA THERAPY IN BEAGLES. Taylor, G. N.; Roberts, L.; Williams, J. L.; Shabestari, L. 31 Mar 1974.

In research and radiobiology. Annual report of work in progress in the internal irradiation program.

Administration of ZnNa$_3$DTPA subcutaneously to ^{241}Am-injected beagles, either daily or five times daily, in daily doses of up to about 0.36 m Moles/kg (10 times the recommended daily human dosage of DTPA) has not produced any serious symptoms during daily therapy 7 days per week extending over a period of eight months. The only detectable change observed, thus far, was an occasional, slight melena, which was detectable only by chemical procedures. Clinical illness was not produced. Increased toxicity was not observed when the daily dose was divided into five equally spaced injections. (auth)

29797 (COO-119-249, pp 125-148) DECORPORATION OF ^{241}Am IN BEAGLES BY DTPA. Lloyd, R. D.; McFarland, S. S.; Taylor, G. N.; Williams, J. L.; Mays, C. W. 31 Mar 1974.

In research and radiobiology. Annual report of work in progress in the internal irradiation program.

Chelation treatments using daily subcutaneous injections of ZnNa$_3$DTPA were begun two weeks after the intravenous administration of ^{241}Am-citrate to six beagles. Retention of americium in the liver and in non-liver tissue (mainly skeleton) was followed serially in the living dogs by a combination of total-body and partial-body counting. During the first seven months of DTPA therapy, roughly the same fraction of deposited ^{241}Am was removed from two dogs by one injection each day of 0.030 m moles of DTPA per kg body mass as from two other dogs by 0.036 m moles/kg body given in five injections per day. Increasing the daily amount by factors of 11 and 150 in the two remaining dogs only slightly increased the removal of ^{241}Am. By two months of chelation therapy, americium retention in non-liver tissue was about $\frac{1}{2}$ and in liver was less than $\frac{1}{10}$ of the respective pretreatment values, while liver ^{241}Am had correspondingly decreased to about $\frac{1}{100}$ of pretreatment retention by 5 months of DTPA administration. Non-liver retention at five months averaged about 40% of pretreatment values and had decreased to 34% by seven months of chelation therapy. (auth)

29798 (COO-119-249, pp 149-160) ALTERNATE METHODS FOR ADMINISTERING CHELATING AGENTS IN DECORPORATION THERAPY. Stevens, W.; Atherton, D. R.; Grube, B. J.; Bruenger, F. W. 31 Mar 1974.

In research and radiobiology. Annual report of work in progress in the internal irradiation program.

The effects of the molecular structure of chelating agents and the effect of mode of administration on the removal of ^{241}Am and other actinides from mammals were investigated in rats. Preliminary results are reported on the effectiveness of DTPA in comparison with various preparations of diethylenetriamine pentaacetic acid (DTPA), ethylenebis glycol (α-aminoethylether) tetraacetic acid (EGTA), ethylenediaminediacetic acid (EDDA), N-hydroxyl ethylenediaminetriacetic acid (HEDTA), and methanesulfonate of desferrioxamine B or desferal (DFOA). (CH)

29799 (COO-119-249, pp 161-169) DECORPORATION OF ^{241}Am FROM BONE USING DTPA AND OSTEOPOROTIC AGENTS. Fisher, D. R.; Taysum, D. H.; Mays, C. W.; Kimmel, D.; Brammer, D.; Brammer, T.; McFarland, S. S. 31 Mar 1974.

In research and radiobiology. Annual report of work in progress in the internal irradiation program.

Total-body retention of ^{241}Am was evaluated sequentially in thirty C57 black mice (male and female) each injected intraperitoneally with 0.08 μCi ^{241}Am in citrate solution at 132 days of age. The objective was to determine whether decorporation by the zinc trisodium chelate of diethylenetriaminepentaacetic acid (Zn-DTPA) could be enhanced by osteoporotic agents. In the first experiment, 3 to 24 days after ^{241}Am administration, the daily subcutaneous injections of heparin (1600 U. S. P. units/kg/day) plus ZnDTPA (0.036 m mole/kg/day) had no detectable effect on decorporation compared to the action of physiological saline plus ZnDTPA. In a second experiment continuing with mice previously treated with saline plus ZnDTPA in the first experiment, the daily subcutaneous injections of parathyroid extract (400 USP units/kg/day) plus ZnDTPA during 24 to 45 days after ^{241}Am administration removed about 11% more ^{241}Am than was removed by saline plus ZnDTPA during this period. (auth)

29800 (COO-119-249, pp 170-179) EFFECTS OF PHYTOHEMAGGLUTININ-P (PHA-P) ON BONE CELLS OF THE TIBIAL AND FEMORAL METAPHYSIS OF THE RATS. Wang, T. M.; Jee, W. S. S. 31 Mar 1974.

In research in radiobiology. Annual report of work in progress in the internal irradiation program.

In rats treated with PHA, past observations such as blast cell transformation and increased DNA synthesis have been confirmed. However, no work has been done concerning PHA effects on bone and bone cells. The current studies found the labeling index of osteoprogenitor cells was increased by higher doses (25 and 50 mg/kg/day) of PHA. In addition, the number of osteoblasts was decreased at all doses, and the number of osteoclasts was increased at all doses. PHA is of special interest because of the possibility that it may affect the bone and bone cells and provide insight into the development of new endpoints of radiation damage in the growing skeleton. (auth)

29801 (COO-119-249, pp 180-233) PLUTONIUM, DIPHOSPHONATES, AND BONE. Jee, W. S. S.; Kimmel, D. B.; Miller, S. C.; Yee, J. A.; Woodbury, L. A.; Dell, R. 31 Mar 1974.

In research and radiobiology. Annual report of work in progress in the internal irradiation program.

Ethane-1-hydroxy-1, 1-diphosphonate (EHDP) inhibited the uptake of ^{239}Pu at the bone surface, when it was given for as little as five days before injection of ^{239}Pu into rats. In evaluating its other effects, it was deduced that EHDP reduced the rate of bone resorption. It was also shown that dichloromethylene diphosphonate (Cl$_2$MDP) was five to ten times more effective in inhibiting bone resorption than EHDP. Administration of EHDP increased dramatically the rate of osteoclast nuclei production while also increasing somewhat the rate of osteoclast nuclei attrition. Studies on osteoblasts indicated that EHDP inhibited the differentiation of osteoblasts by inhibiting DNA synthesis in osteoprogenitor cells from which osteoblast nuclei are derived. (auth)

29802 (COO-119-249, pp 234-246) EINSTEINIUM STUDIES IN BEAGLES. Lloyd, R. D.; Dockum, J. G.; Atherton, D. R.; Mays, C. W.; Williams, J. L. 31 Mar 1974.

In research in radiobiology. Annual report of work in progress in the internal irradiation program.

The early excretion, retention, and tissue distribution of einsteinium was studied following the intravenous injection of ^{253}Es citrate into six young adult beagles. Although the first day's urinary excretion by two of these animals was about three and six times the average of the other four dogs, excretion of the ^{252}Cf contaminant in the injection solution by these same individuals was also much higher. The ratio of excreted Cf to excreted Es in the first day's urine averaged 0.68 for all six dogs and was 0.66 and 0.72 in the two animals which excreted an abnormally high fraction of their injected Es. We have never seen previously such anomalous excretion within any group of beagles injected with Cf, Cm, Am, or Pu. Of the other transuranium elements which we have studied, Es appears to most closely resemble Cf in its excretion, retention, and tissue distribution. The ^{253}Es concentration of exsanguinated tissues was about equal in skeleton and liver, the two tissues of highest concentration. Thyroid concentration was about $\frac{1}{4}$ to $\frac{1}{3}$ that of the skeleton. (auth)

29803 (COO-119-249, pp 247-254) EARLY RETENTION AND DISTRIBUTION OF ^{253}Es BY THE BEAGLE. Atherton, D. R.; Bruenger, F. W.; Stevens, W. 31 Mar 1974.

In research in radiobiology. Annual report of work in progress in the internal irradiation program.

Einsteinium-253 in 0.08 M citric acid-sodium citrate buffer at pH 3.5 was given by intravenous injection to 10 beagles. The concentration of the einsteinium in plasma for the first 48 hours following injection is adequately described by a three component exponential equation. The circulating nuclide diminishes to insignificance in less than six days. The major deposition sites are liver and skeleton. Less of the injected einsteinium is retained by the liver than has been observed for any of the actinides except ^{228}Th. Skeletal retention and urinary excretion are highly variable and appear to be at least somewhat related. (auth)

29804 (COO-119-249, pp 255-267) EARLY SUBCELLULAR DISTRIBUTION OF EINSTEINIUM IN CANINE LIVERS. Bruenger, F. W.; Grube, B. J.; Atherton, D. R.; Buster, D. S.; Stevens, W. 31 Mar 1974.

In research in radiobiology. Annual report of work in progress in the internal irradiation program.

Studies of the subcellular distribution of actinide elements were enlarged to include ^{253}Es. Beagles were injected with 3 μCi of the nuclide in 0.08 M citrate buffer of pH 3.5 per kg of body weight. Liver specimens were obtained either by serial surgical liver biopsies or at time of sacrifice of the animal. The nuclide was first associated with soluble liver proteins (mainly ferritin). With increasing time after injection, einsteinium became associated with subcellular liver organelles. The concentration of einsteinium in the crude mitochondrial fraction was usually higher than it was in the crude lysosomal fraction. In the mitochondrial fraction 41% was either membrane bound or associated with sedimentable granular material and 59% was present in soluble form at 7 days. A considerable but variable fraction of the nuclide remained bound to ferritin. Lysosomes and heavier organelles are involved in the binding. Less einsteinium deposits in the liver than do other actinides except ^{228}Th and biological variation is greater. (auth)

29805 (COO-119-249, pp 281-307) ^{210}Pb RETENTION, EXCRETION, AND DISTRIBUTION IN BEAGLES FOLLOWING INTRAVENOUS INJECTION. Lloyd, R. D.; Mays, C. W.; Atherton, D. R.; Bruenger, F. W. 31 Mar 1974.

In research in radiobiology. Annual report of work in progress in the internal irradiation program.

Carrier-free ^{210}Pb was administered intravenously to 10 young adult beagles in a sodium citrate citric acid solution at pH 3.5. Retention was determined by total-body counting of the 47 keV γ ray. Total excreta collections from 3 dogs for the first 3 weeks after injection were assayed intact for their ^{210}Pb content by γ counting. About $^3/_4$ of the excreted ^{210}Pb appeared in the feces. The fraction of the injected activity still in the circulating blood was 0.4 at 1 day, 0.14 at 1 week, and 0.03 at 1 month. By 1 hour following injection, red cells had more than 99% of the ^{210}Pb that was in blood. During the first 1600 days after administration the retention of injected Pb in the dogs could be described by an equation. One dog sacrificed 28 days after administration had about 63% of the retained ^{210}Pb in the skeleton, 20% in the liver, 8% in the blood, and 9% in other soft tissues. Assuming a skeletal mass equal to 7.5% of body weight at injection, the skeleton had the highest concentration of any tissue measured. Liver concentration was about 0.8 times that of the skeleton. Relative liver concentration was much lower in 2 dogs sacrificed 1100 and 1497 days after injection, 0.03 and 0.005 times that in the skeleton, which contained 97% and 99%, respectively, of the ^{210}Pb retained in the total-body at death. The effectiveness, rad for rad, of injected ^{210}Pb for osteosarcoma production in beagles appeared to be not greatly different from that of ^{226}Ra. At long times after injection, the ^{210}Po/^{210}Pb ratio in the skeleton was close to 1.0. (auth)

29806 (COO-119-249, pp 308-310) TRANSURANIUM ELEMENTS IN GONADAL TISSUE. Mays, C. W.; Lloyd, R. D.; Atherton, D. R. 31 Mar 1974.

In research in radiobiology. Annual report of work in progress in the internal irradiation program.

Young adult beagles were injected intravenously with transuranium elements in citrate solution. Data are presented on the gonadal retention of ^{239}Pu, ^{241}Am, ^{243}Cm, ^{244}Cm, ^{249}Cf, and ^{252}Cf from one to 2127 days after injection. (CH)

29807 (COO-119-249, pp 322-325) EFFECTS OF DTPA ON TISSUE CULTURED FIBROBLASTS. Nabors, C. J. Jr. 31 Mar 1974.

In research in radiobiology. Annual report of work in progress in the internal irradiation program.

An in vitro method for evaluating relative toxicities of various chelating agents was evaluated. Preliminary studies have shown that Ca-DTPA is toxic to L-929 fibroblasts in concentrations ranging from 2.3×10^{-3} to 2.3×10^{-5} M. In contrast, Zn-DTPA was not toxic below 2.2×10^{-5} M. This system may provide a rapid means of screening proposed decorporation agents for potential toxicity. (auth)

29808 (F-599) DAILY EXCRETION RATE OF IODINE CALCULATED FROM THE RELATIONSHIP IODINE PER GRAM CREATININE IN A SINGLE AFTERNOON URINE SAMPLE. Mathisen, Oe. (Forsvarets Forskningsinstitutt, Kjeller (Norway)). Feb 1974. 10p. (In Norwegian). Dep. NTIS (US Sales Only) $4.00.

A method is sometimes used, in which the daily renal iodine excretion of an individual is calculated on the basis of the iodine to creatinine ratio in a single afternoon urine sample. The present results based on measurements of urine samples from 57 healthy males may seem to question this practice. The variability in the individual 24 hour creatinine clearance appears to be too large to warrant its use as a reference substance. (auth)

29809 (NVO-AEIC-74-1, pp 143-150) IN VITRO PLUTONIUM STUDIES USING THE ARTIFICIAL RUMEN AND SIMULATED ABOMASAL AND INTESTINAL FLUIDS. Barth, J.; Mullen, A. A. (National Environmental Research Center, Las Vegas, NV). Jul 1974.

In dynamics of plutonium in desert environments. Nevada Applied Ecology Group progress report as of January 1974.

An artificial rumen, and simulated abomasal and intestinal fluids procedure were used to study in vitro the alimentary solubility and biological availability of various forms of plutonium in ruminants. Plutonium was added to viable rumen juice and incubated for 24 hr. This juice was converted to simulate the digestive stages of the abomasum, duodenum, jejunum, and lower small intestine by the addition of enzymes, bile, and adjustment of the pH. Samples were collected from these digestive stages for soluble plutonium analysis by liquid scintillation. (auth)

29810 (NVO-AEIC-74-1, pp 163-185) ABSORPTION, DISTRIBUTION, AND EXCRETION OF PLUTONIUM BY DAIRY CATTLE. Stanley, R. E.; Bretthauer, E. W.; Sutton, W. W. (National Environmental Research Center, Las Vegas, NV). Jul 1974.

In dynamics of plutonium in desert environments. Nevada Applied Ecology Group progress report as of January 1974.

In order to obtain information on the significance of the milk link in man's food chain as a source of plutonium exposure and to gain additional information on plutonium deposition patterns in ruminants, a series of metabolism studies with dairy cows was initiated. Two groups of Holstein dairy cows, four cows in each group, were studied to examine the physiological transport of ingested ^{238}Pu citrate and $^{238}PuO_2$. Approximately 3 mCi of Pu citrate per animal was administered in an acute treatment to the first group, while 1 mCi of Pu dioxide was given daily to each animal for 19 consecutive days in the second group. Samples of blood, milk, urine, and feces were taken during and after oral dosing, while tissue collections were made at necropsy 6 to 13 weeks after treatment. The major portion of plutonium activity was excreted in the feces. However, recovered activity in urine and milk following both the acute dose of Pu citrate and the multiple doses of Pu dioxide confirmed the physiological uptake and transport to milk was not great and, on a percent of oral dose basis, was observed to be 2×10^{-4} and 2×10^{-5} following the Pu citrate and Pu dioxide treatments, respectively. (auth)

29811 (NVO-AEC-74-1, pp 213-220) DISTRIBUTION OF INGESTED PLUTONIUM IN CHICKENS AND SUBSEQUENT TRANSPORT TO EGGS. Mullen, A. A. (National Environmental Research Center, Las Vegas, NV). Jul 1974.

In dynamics of plutonium in desert environments. Nevada Applied Ecology Group progress report as of January 1974.

Soluble ^{238}Pu citrate and relatively insoluble particulate $^{238}PuO_2$ were administered orally to two groups of laying hens daily for two weeks. The yolks, whites, and shells from the eggs were analyzed for their plutonium content. Yolks from the eggs of chickens fed Pu citrate appeared to be the only egg fractions in which Pu activity was observed. This activity reached a peak of 0.0155% of the administered dose nine days after the initial ingestion. The activity decreased with a biological half-life of 1.85 ± 0.48 days and an indication of a longer half-life of >25 days. Ten chickens from each group were sacrificed 12 days after the final administration of Pu. Tissue samples were collected to determine the amount of Pu present in the edible portions and feathers of the chickens. The remaining chickens were sacrificed 30 days after the final dose was administered. Preliminary results indicate little Pu remained in either the tissues or feathers obtained from either group of chickens at time of sacrifice. (auth)

29812 ELIMINATION OF INTRAVENOUSLY INJECTED ^{125}I-TOLUIDINE BLUE IN RABBITS. Normann, E. Acta Pharm. Toxicol.; 34: 254-259(1974).

The elimination of intravenously injected ^{125}I-toluidine blue was studied in rabbits. Within 5 minutes after the injection, approximately 80% of the dye had been metabolized, being present in the plasma and urine in a colorless state. As much as 99% of the label was recovered in the urine and feces within 3 days. It is therefore assumed that in future clinical parathyroid scintigraphy, the absorbed radiation dose with radioiodinated dye will be smaller than with ^{75}Se-selenomethionine, the currently used radiopharmaceutic compound for the parathyroids. (auth)

29813 DECORPORATION OF ^{239}Pu AND ^{241}Am IN THE RAT AND HAMSTER BY Zn–DTPA. Volf, V.; Seidel, A. (Kernforschungszentrum, Karlsruhe, Ger.). Radiat. Res.; 59: No. 3, 638-644(Sep 1974).

The influence of Zn–DTPA on the retention of ^{239}Pu and ^{241}Am injected intraperitoneally in the form of citrate into rats and Syrian hamsters was examined. In all untreated animals, ^{239}Pu was retained mainly by the skeleton and ^{241}Am mainly in the liver. In the hamster liver, however, the residence time of the radioactive deposit was considerably longer. Six doses of Zn–DTPA (10 or 100 μmole·kg^{-1}) given over the next month were more effective in rats than in hamsters; the liver burden was reduced more than the skeletal one and ^{241}Am was removed more effectively than ^{239}Pu. Difficulties in predicting the behavior of radionuclides and effectiveness of therapeutic removal in various mammalian species are discussed. (auth)

29814 EFFECT OF COPPER AND CADMIUM ON ^{65}Zn ABSORPTION IN ZINC-DEFICIENT AND ZINC-SUPPLEMENTED RATS. Evans, G. W.; Grace, C. I.; Hahn, C. (Agricultural Research Service, Grand Forks, ND). Bioinorg. Chem.; 3: No. 2, 115-120(1974).

The effect of oral copper and cadmium on ^{65}Zn transport to the carcass and ^{65}Zn uptake by the small intestine was examined in zinc-deficient and zinc-supplemented rats. Neither copper nor cadmium, when administered orally with ^{65}Zn–Zn in ratios of 1000:1, 100:1, or 10:1, affected ^{65}Zn transport to the carcass in zinc-deficient rats, but both elements inhibited ^{65}Zn transport to the carcass in zinc-supplemented rats. Copper had little or no effect on ^{65}Zn uptake by the intestine in either group, whereas cadmium markedly decreased intestinal ^{65}Zn uptake in both deficient and supplemented rats. The experimental results suggest that zinc absorption consists of two independent processes: zinc uptake by the intestinal epithelial cells and zinc transport from the lumen to the blood. (auth)

29815 COMPARISON OF ^{115m}Ca RETENTION IN RATS FOLLOWING DIFFERENT ROUTES OF ADMINISTRATION. Stara, J. F.; Crocker, W. C.; Malanchuk, M.; Iltis, R. (EPA, Cincinnati). Environ. Res.; 6: No. 4, 473-478(Dec 1973).

Cadmium-115m was administered by 4 routes: oral, inhalation, intraperitoneal and intravenous injection. The retention curve for each route of administration was divided into 2 components. The 1st component reflected the initial rapid clearance of ^{115m}Cd primarily by the gastrointestinal tract and the 2nd component indicated the absorption and turnover of ^{115m}Cd. Extrapolation of the 2nd component to the intercept gave initial absorption values of 93%, 91%, 41%, and 2.3% for i.p., i.v., inhalation, and oral routes, respectively. Immediately after inhalation exposure, 9.7% of the total inhaled Cd was present in the lungs. The route of administration did not significantly influence the rate of elimination and biological half-life of the 2nd component of the whole body retention curve. (Pollut. Abstr.)

29816 EFFECTS OF COPPER, MERCURY, AND ZINC ON THE UPTAKE AND DISTRIBUTION OF CADMIUM-115m IN THE ALBINO RAT. Shank, K. E.; Vetter, R. J. (Purdue Univ., Lafayette, IN). Environ. Lett.; 6: No. 1, 13-18(1974).

The effects of Cu, Hg, and Zn on the uptake and distribution of ^{115m}Cd in the albino rat were investigated. Different ratios of the metals and Cd were administered simultaneously. The animals were posed i.p. and were sacrificed 24 hr postinjection. The samples analyzed for ^{115m}Cd content included the liver, kidneys, and whole blood. The metals produced an increase in Cd uptake in the liver and a decrease in the kidneys but had no significant effect on Cd concentration in the blood. (Pollut. Abstr.)

29817 ^{210}Po RADIOACTIVITY IN ORGANS OF SELECTED TUNAS AND OTHER MARINE FISH. Hoffman, F. L.; Hodge, V. F.; Folsom, T. R. (Univ. of California, San Diego). J. Radiat. Res.; 15: No. 2, 103-106(Jun 1974).

Polonium-210 activity was measured in organs of 10 oceanic fish from three families. Various tissues from 10 species were analyzed (albacore, bluefin, yellowfin, skipjack, black skipjack, Pacific bonito, and Pacific mackerel), as well as three other species often caught off Southern California (jack mackerel, yellowtail and broomtail grouper). Samples of 0.5 to 1.0 gm were covered with HNO_3 and spiked with ^{208}Po. After digestion at reflux temperatures with the addition of small amounts of H_2O_2, when necessary, the polonium was autoplated onto silver disks. Samples were counted below 300 or 450 mm^2 silicon surface barrier detectors which were monitored by pulse-height analyzers. The highest polonium radioactivities were found either in tissues of the pyloric caecal masses or in the intestinal contents of these fish. The liver was found to have rather high polonium concentrations. Intense activities of ^{210}Po were also found in the spleen, kidney, and gall bladder of the albacore, gall bladder of the yellowfin, and kidney of the skipjack. In the grouper, polonium activities were high in the caecal mass and in the intestinal contents; little was found elsewhere. The high polonium concentrations associated with the digestive organs of these large marine fish are not significantly higher than those found in the same organs of the tiny fish that they often eat. Thus, it appears that there are mechanisms by which polonium is sequestered in the digestive tract and discharged as waste material back to the ocean in a concentrated form possibly available to lower organisms who feed upon detrital material. (JA)

29818 INFLUENCE OF IRRADIATION ON THE INCORPORATION OF RADIONUCLIDES. Jaworowski, Z.; Bilkiewicz, J.; Radwan, I. (Central Lab. for Radiological Protection, Warsaw). pp 303-306 of Health Physics Problems of Internal Contamination. Budapest; Akademiai Kiado (1973).

From proceedings of the IRPA second European congress on radiation protection; Budapest, Hungary (3 May 1972).

The influence of internal irradiation on the incorporation rate of ^{239}Pu, ^{226}Ra, ^{210}Pb, ^{144}Ce, and ^{3}H in hair and other tissues has been studied on rabbits and rats. In tritium experiments internal irradiation effects were compared with those caused by external x-ray exposure. (auth)

29819 COMPARATIVE STUDY OF THE INCORPORATION OF ^{32}P INTO THE PHOSPHOLIPIDS OF MEMBRANES FROM NOVIKOFF HEPATOMA ASCITES CELLS AND LIVER CELLS FROM NORMAL AND TUMOR BEARING ANIMALS. Anghileri, L. J. (GHS Klinik, Essen). Z. Krebsforsch.; 80: 301-306 (28 Dec 1973). (In German).

The incorporation of ^{32}P into the phospholipids of membranes and whole cells of the ascitic Novikoff hepatoma and the livers from normal and tumor bearing animals has been studied. The higher specific activity of the phospholipid from membranes of ascites cells and of liver cells from tumor bearing animals indicates a higher metabolic rate. The membranes of ascites cells show less phospholipid phosphorus than the membranes of liver cells. No drastic deviations were observed in the composition of the phospholipid of tumor-cell membranes when compared to the phospholipid of liver cell membranes. Phospholipid from membranes and whole cells shows a fairly similar composition. (auth)

29820 EFFECT OF DELAYED LYMPHADENECTOMY ON $^{239}PuO_2$ TRANSLOCATION IN DOGS. Gomez, L. S.; Bistline, R. W.; Dagle, G. E.; Lebel, J. L.; Watters, R. L. (Colorado State Univ., Fort Collins). Health Phys.; 27: No. 2, 213-215 (Aug 1974).

The translocation of high-fired $^{239}PuO_2$ via the lymphatic system from a simulated puncture wound in the left dorsal metacarpus of beagles was studied. Plutonium build-up in the first major lymph node draining the implant site was determined by in vivo counting of the 17-keV x-ray complex with a thin NaI(Tl) detector. Lymphadenectomy was performed on half of the dogs 14 days after plutonium implant. All dogs were killed 49 days after plutonium implant and the radioactivity in selected tissues was determined. Comparisons were made between lymphadenectomized and intact dogs. Higher levels of plutonium were found in the liver, spleen, and hepatic lymph nodes of lymphadenectomized dogs than in the intact dogs. These results are compared with results obtained from earlier studies in which lymphadenectomy occurred on the day of plutonium implant. The possible use of lymphadenectomy as a therapeutic procedure for workers contaminated with plutonium is discussed. (auth)

29821 INTERNAL DEPOSITION OF INGESTED CERIUM IN SUCKLING MICE. Naharin, A.; Feige, Y.; Lubin, E.; Sadeh, T. (Israel Atomic Energy Commission, Yavne). Health Phys.; 27: No. 2, 207-211(Aug 1974).

Post partum albino mice were injected intraperitoneally with ^{144}Ce-citrate at different times during the lactation period. Twenty-four hours and 4 weeks later, the suckling neonates were sacrificed and the ^{144}Ce content in their digestive tract, liver, and carcass determined by gamma counting. The fraction of ^{144}Ce absorbed from the gastrointestinal tract was calculated. It is one to two orders of magnitude above the currently accepted values for gastrointestinal absorption of lanthanides in adult mice. The discriminatory characteristics of the gastrointestinal tract in early life, as derived from these experiments, are discussed in the light of other relevant investigations. (auth)

29822 REMOVAL BY DTPA OF INTERNALLY DEPOSITED ^{241}Am. A Comparative Study on Rats and Syrian Hamsters. Seidel, A. (Kernforschungszentrum, Karlsruhe, Ger.). Int. J. Nucl. Med. Biol.; 1: No. 4, 197-200(Jun 1974).

^{241}Am(III)–citrate was injected intraperitoneally into rats and Syrian hamsters. Its metabolic behavior in both species showed some differences: a higher deposition of ^{241}Am in the skeleton and kidneys as well as a longer residence time in the liver of the hamster. Ca–DTPA was more effective in mobilizing ^{241}Am from the rat liver whereas the removal from the kidneys was more pronounced in the hamster. As to the skeletal burden, the chelate was equally effective in both species. The data are discussed from the theoretical point of view. (auth)

29823 DECONTAMINATION OF SWINE, SHEEP, AND CATTLE SURFACE-CONTAMINATED WITH FISSION PRODUCTS. II. Removal of Radionuclides of Zirconium, Niobium, Ruthenium, and Cerium. Havlicek, F.; Hrusovsky, J.; Mach, J. (Military Veterinary Research Inst., Prague). Voj. Zdravot. Listy; 42: No. 4, 177-179(Jul 1973). (In Czech).

The decontamination efficiency of water and various chelating agents, complex-forming agents and commercial detergents in swine, sheep, and cattle experimentally contaminated with ^{95}Zr–^{95}Nb, ^{106}Ru, and ^{144}Ce was studied. For the radionuclides investigated, a 1% solution of EDTA and Jar-extra (commercial detergent) in combination was found to show the optimum decontamination ability. The use of EDTA and Jar-extra solutions alone, or water alone showed lesser ability. The experiment followed up on a study into the decontamination of farmyard animals surface-contaminated with Cs, Sr, and I. (Nuclear Sci. Abstr. Czeck.)

29824 UNEXPECTED COMPLICATION IN THE USE OF ^{169}Yb–DTPA WITH RESPECT TO HOSPITAL HEALTH PHYSICS. Pauwels, E. K. J. (Rijksuniversiteit, Leiden); Van Damme, K. J. Int. J. Nucl. Med. Biol.; 1: No. 4, 228-229(Jun 1974).

The radiopharmaceutical ^{169}Yb–DTPA has some very favorable characteristics for the scintigraphic imaging of cerebrospinal fluid pathways. However, unexpected ^{169}Yb contamination was detected in whole body ^{40}K counting examinations of several infants after ^{169}Yb–DTPA had been used in the diagnosis of non-resorptive hydrocephalus in a 2-year old child. This contamination was traced to the cotton napkins of the babies, and further investigation showed that trace amounts of the ^{169}Yb complex were strongly absorbed onto the cotton material, with the cross contamination having occurred during the cleaning process in the hospital laundry. Prolonged cleaning did not result in appreciable decrease in the contamination level. In addition, an undesirable accumulation of the ^{169}Yb–DTPA in meningo-encephalitic structures has been reported elsewhere, and it is therefore recommended that ^{111}In–DTPA is used in place of ^{169}Yb–DTPA in cisternography and ventriculography. (UK)

Plants

29825 INFLUENCE OF SOIL PLUTONIUM CONCENTRATION OF PLUTONIUM UPTAKE AND DISTRIBUTION IN SHOOTS AND ROOTS OF BARLEY. Wildung, R. E.; Garland, T. R. (Battelle Pacific Northwest Lab., Richland, WA). J. Agr. Food Chem.; 22: No. 5, 836-838(1974).

A split-root (soil-nutrient solution) plant culture technique was employed to determine the effect of soil plutonium concentration on the uptake and distribution of Pu in the shoots and roots of barley. Although the absolute concentrations of Pu in plant tissues (micro-Curies of Pu/gram of plant tissue) decreased with decreased soil Pu concentration, the concentration factors (micro-Curies of Pu/gram of plant tissue per micro-Curies of Pu/gram of soil) were markedly higher below a soil Pu level of 10 μCi/g which was used previously to establish soil-plant concentration factors. This effect may have resulted from a concentration-dependent change in Pu availability to plants or from a toxic effect of Pu on the plants and subsequent inhibition of uptake. The concentration of Pu in roots exceeded the shoots by factors of 3 to 8 depending on soil Pu concentration, and Pu was shown to be translocated downward in the roots after uptake from the soil. The results indicate the advisability of further delineation of Pu uptake by plants at environmental levels of Pu with particular emphasis on root crops. Furthermore, studies should be undertaken to establish the role of roots in the transport of Pu in soil and the solubility, chemical form, and availability to plants of Pu released on decomposition of plant roots. (auth)

Microorganisms

Refer also to abstract 29447.

29826 FRACTIONATION OF SULFUR ISOTOPES BY THE YEAST SACCHAROMYCES CEREVISIAE. McCready, R. G. L. (Univ. of California, Los Angeles); Kaplan, I. R.; Din, G. A. Geochim. Cosmochim. Acta; 38: No. 8, 1239-1253(Aug 1974).

Growing and resting cell suspensions of Baker's yeast (Saccharomyces cerevisiae) were permitted to metabolize sulfite and sulfate under a variety of environmental conditions. Enrichment of S^{32} in the H_2S released during reduction of sulfate under growing conditions was consistently lower ($\delta S^{34} < -25‰$) than enrichment during reduction of sulfite under similar conditions ($\delta S^{34} \sim -30$ to $-50‰$). Yeast cells harvested from a sulfite medium released small quantities of H_2S when suspended in glucose-sulfate solution; cells from a sulfate growth medium did not. The enrichment of H_2S in S^{32} by sulfite-grown resting cells suspended in either SO_4^{2-} or SO_3^{2-} solutions was about 10‰ less than the maximum obtained during growth on sulfite. Isotopic fractionation was always significantly less in assimilated, than in dissimilated sulfur. (auth)

New Tracer Techniques

Refer also to abstracts 29088, 29092, 29794, 29812, and 29824.

29827 (AD-774860) RESEARCH IN BIOLOGICAL AND MEDICAL SCIENCES INCLUDING IN BIOCHEMISTRY, COMMUNICABLE DISEASE AND IMMUNOLOGY, INTERNAL MEDICINE, NUCLEAR MEDICINE, PHYSIOLOGY, PSYCHIATRY, SURGERY, AND VETERINARY MEDICINE. Volume I. Annual Progress Report, 1 July 1972–30 June 1973. (Walter Reed Army Inst. of Research, Washington, D. C. (USA)). 30 Jun 1973. 717p. NTIS $13.00.

29828 (AD-776967) RESEARCH IN BIOLOGICAL AND MEDICAL SCIENCES INCLUDING BIOCHEMISTRY, COMMUNICABLE DISEASE AND IMMUNOLOGY, INTERNAL MEDICINE, NUCLEAR MEDICINE, PHYSIOLOGY, PSYCHIATRY, SURGERY, AND VETERINARY MEDICINE. Volume II. Annual Progress Report, 1 July 1972–30 June 1973. (Walter Reed Army Inst. of Research, Washington, D. C. (USA)). 30 Jun 1973. 594p. NTIS $11.00.

29829 (AED-CONF-74-221-004) RESULTS OF THE MEDICAL EXAMINATIONS. Zimmer, R. (Bayerisches Landesinstitut fuer Arbeitsmedizin, Muenchen (F.R. Germany)). 1974. 10p. (In German). (CONF-740662-3). INIS.

From 15th annual meeting of the Vereinigung Deutscher Strahlenaerzte e.V. on the authorized physician within the meaning of the radiation protection laws; Karlsruhe, F.R. Germany (14 Jun 1974).

3 tabs.

The development and results of medical investigations carried out according to the regulations of the first Radiation Protection Ordinance and the old X-Ray Ordinance are given. The problem in question is how the human organism reacts to the summation of the smallest doses and what measures should be taken in order to avoid radiation damage from the start. In order to enable optimal health control of professionally radiation-exposed persons, it is essential to have a comprehensive cooperation between physicists, radiochemists, and the doctor. For all those coming into contact with open radioactive substances, the controlling of incorporation is an additional rigid part of the medical supervision. The control of those in contact with α emitters and some β emitters such as e.g., ^{3}H, ^{14}C and ^{32}P, is somewhat difficult. A direct "in vivo" measurement of this is not possible but the indirect excretion method can be used. Finally, two interesting examples of accidents with radioactive materials are presented. (GE)

29830 (CONF-740708-20) ADVANTAGES OF THEORETICAL MODELS IN INTERPRETING CEREBRAL TRANSIT CURVES. Itti, R.; Planiol, T.; Floyrac, R. (Tours Univ., 37 (France). Lab. de Biophysique). [nd]. 11p. (In French). (SM-185/86). Dep. NTIS (U. S. Sales Only) $4.00.

From symposium on dynamic studies with radioisotopes in clinical medicine and research; Knoxville, Tennessee, USA (15 Jul 1974).

Dynamic cerebral blood flow measurements made with a γ camera at 10 min and at three hours following the intravenous injection of ^{99m}Tc-pertechnetate were used for the evaluation of cerebral pathology. The advantages of using mathematical models of cerebral blood flow in interpreting the scan data are discussed. (CH)

29831 (CONF-740708-52) LIVER STUDIES WITH VARIOUS RADIOACTIVE TRACERS AND METHODS. Zita, G.; Uiberrak, H.; Csirik, J.; Schwarz, K.K. (Kaiserin-Elisabeth-Spital, Vienna (Austria). Ludwig Boltzmanninstitut fuer Nuklearmedizinische Gastroenterologie). 1974. 10p. (SM-185/6). Dep. NTIS (US Sales Only) $4.00.

From symposium on dynamic studies with radioisotopes in clinical medicine and research; Knoxville, Tennessee, USA (15 Jul 1974).

Investigations were carried out to recognize present problems and to find any useful method for diagnostic application of radioisotope scanning in the evaluation of liver diseases. Various studies with certain radioactive colloids and dyes showed some new findings. With colloids a new index LTI was calculated from time activity curves of the heart and liver. This parameter may give a value for the tracer's uptake in liver tissue. The new as well as the known parameters of halftime and fractional turnover rate give useless findings with colloids even in normal subjects. This fact seems to be caused by extrahepatical uptake and the spread of particle sizes. The results with colloids led to the conclusion that the function of the RES and the liver cells can not be differentiated by these investigations. (CH)

29832 (COO-2427-4) BIOLOGIC CONSIDERATIONS IN ANATOMIC IMAGING WITH RADIONUCLIDES. Progress Report, July 1973–June 1974. Potchen, E. J. (Johns Hopkins Univ., Baltimore, Md. (USA). School of Medicine). 1974. Contract AT(11-1)-2427. 14p. Dep. NTIS $4.00.

An experimental program is described that was designed with the objective of determining the diagnostic utility of brain, bone, and liver scans. The data for these scans was generated by a three-step process consisting of a prospective questionnaire, an outcome determination, and a follow-up questionnaire to determine the disposition of the patient. (CH)

29833 RADIOIMMUNOASSAY FOR MYOSIN IN CULTURED SKELETAL MUSCLE CELLS. Holberton, E. J.; Goldspink, G. (Univ. of Hull, Eng.). Exp. Cell Res.; 79: 471-174(Jun 1973).

Procedures are described for the preparation of myosin and labelling myosin with ^{3}H-iodoacetic acid. Cell cultures were prepared from dissociated muscle tissue derived from 11-day chick embryos. Assay curves for progressive dilutions of labeled and unlabeled myosin followed the same slope; equal reactivity in terms of standard and unknown myosins was also established. (HLW)

29834 MICROASSAY FOR PROTEOLYTIC ENZYMES USING A NEW RADIOACTIVE ANILIDE SUBSTRATE. Roffman, S.; Troll, W. (New York Univ., N. Y.). Anal. Biochem.; 61: No. 1, 1-5(Sep 1974).

The synthesis of benzoyl-DL-arginine [^{3}H]anilide hydrochloride is described and it is shown to be a sensitive substrate for papain and trypsin. The virtual stability of the radioactive anilide to spontaneous hydrolysis serves to assay submicrograms of both trypsin and papain. Rates as low as 16 pmoles of anilide hydrolyzed per minute can be measured when used in a continuous radioactive assay. (auth)

29835 MEASUREMENT OF SERUM FERRITIN BY A 2-SITE IMMUNORADIOMETRIC ASSAY. Miles, L. E. M.; Lipschitz, D. A.; Bieber, C. P.; Cook, J. D. (Stanford Univ., CA). Anal. Biochem.; 61: No. 1, 209-224(Sep 1974).

A 2-site immunoradiometric assay (2-site IRMA) for human serum ferritin is carried out by reaction of the ferritin solution with a solid-phase anti(human ferritin), followed by a second reaction in which the insoluble product is incubated with purified, radioactively labeled anti(human ferritin). Unreacted labeled antibodies remain in solution and are washed away. As the amount of ferritin increases, the radioactivity in the solid-phase increases. Factors affecting the assay were evaluated including concentration and stability of solid-phase antibody, variation in temperature, reaction times, and reagent concentrations, stability and storage of antibody coated tubes, effect of tube washing cycles, effect of serum proteins and anticoagulants, organ specificity of ferritin. A paradoxical fall in dose-response was seen at high dose. Statistical analysis, dose interpolation, and automatic data processing were carried out by a generalization of the logit/log method and computer programs used in conventional radioimmunoassay. The dependence of the variance on the position on the dose-response curve is different than that seen in radioimmunoassay systems and is reflected in a greater effective assay range. 2-Site IRMA may also have advantages in reagent stability, specificity, antigen protection, and suitability for automation. The properties of 2-site IRMA are closely related to the usual IRMA assay system, but 2-site IRMA is more economical in antigen, is unlikely to be subject to deleterious allosteric reactions, and has a lower zero dose-response (0.5–2% of the total radioactivity in the system). (auth)

29836 SOLID PHASE RADIOIMMUNOASSAY FOR PLANT VIRUSES. Ball, E. M. (Univ. of Nebraska, Lincoln). Virology; 55: No. 2, 516-520(Oct 1973).

In a radioimmunoassay procedure, adapted to the antigenic analysis of plant viruses, antibody was irreversibly attached to the walls of disposable polystyrene tubes. In the direct test, labeled antigen was effectively assayed in a range of 10 to 100 ng/ml. In the indirect test, unlabeled antigen from 0.5 to 5.0 μg/ml and a constant amount of labeled antigen were added sequentially to antibody-coated tubes. The latter procedure was applied effectively to serological differentiation of virus strains and of coat-protein and intact virus rods. (auth)

29837 MEASUREMENT OF CEREBRAL INFARCTION EDEMA WITH SODIUM-22. Brunson, B.; Robertson, J. T.; Morgan, H.; Friedman, B. I. (Univ. of Tennessee, Memphis). Stroke; 4: 461-464(1973).

Sodium 22 was used to determine quantitatively cerebral infarction edema in cats after occlusion of the middle cerebral artery. A comparison was made of the sodium 22 edema determination with the wet weight-dry weight method of edema determination. There was a high degree of correlation between the two methods. The sodium 22 method of measuring cerebral infarction edema was less time consuming and easier than the wet weight-dry weight method, and served as a reliable means of quantitatively comparing the edema content in the hemispheres of animals with stroke. (auth)

29838 PRINCIPLES AND METHODS FOR USING ELECTRONIC COMPUTERS IN CLINICAL RADIOISOTOPIC DIAGNOSIS. Sivoshinskii, D. S.; Narkevich, B. Ya.; Gurarii, K. N. (Inst. of Experimental and Clinical Oncology, Moscow). Vestn. Akad. Med. Nauk SSSR; 28: No. 5, 16-19(1973). (In Russian).

A brief review is given of the different uses of computers in radioisotopic clinical diagnosis. The development of a computer complex at the Institute of Experimental and Clinical Oncology is outlined and its basic characteristics are given. The need for cooperation between the physician and the computer specialists in order to obtain the optimum results and to expand the utility of the computer complex is indicated. (JSR)

29839 URINE ^{113m}In-EDTA TIME CONCENTRATION CURVE AND REDISTRIBUTION OF GLOMERULAR FILTRATION IN THE DOG. Ito, K.; Nakamura, T. (Research Inst. of Brain and Blood Vessels, Akita, Japan). Rinsho Seiri; 4: No. 3, 268-272 (May 1974). (In Japanese).

The urine time concentration curve represents the frequency distribution of the passage time from the glomerulus to the measured site. Therefore, a method was developed for evaluating the redistribution of intrarenal glomerular filtration from the urine ^{113m}In-EDTA time concentration curve in dogs. The method requires catheterization of one renal artery, a sudden injection of 2mC of ^{113m}In-EDTA, glomerular substance, into the renal artery, and recording of the concentration curve of ureter urine by a collimator (2 inch crystal) during the control period and hemorrhagic hypotension or saline infusion. During hemorrhagic hypotension, total glomerular filtration rate (GFR) decreased from 16.8 ml/min to 13.4 ml/min ($P < 0.05$), sodium excretion from 66.0 μEq/min to 14.9 μEq/min ($P < 0.05$), and fractional sodium excretion from 2.7% to 1.1% ($P < 0.05$). A ratio of build-up time to appearance time obtained from the ^{113m}In-EDTA curve decreased significantly ($P < 0.05$) during hemorrhagic hypotension. This transformation of the shape of the curve may show that the superficial (short) nephron GFR decreased more than did the juxtamedullary (long) nephron GFR. During acute saline loading, total GFR, sodium excretion, and fractional sodium excretion increased significantly. However, a characteristic of the shape of the ^{113m}In-EDTA curve observed by appearance time and build-up time was not changed significantly by saline loading. (auth)

29840 STUDY ON THE BLOOD-CEREBROSPINAL FLUID BARRIER. I. Permeability of RISA^{131}I at Twenty-Four Hours After Intravenous Administration. Miyazaki, M.; Kanao, K.; Fujita, M.; Gemba, H.; Shimazaki, K. (Sumito Hospital, Osaka). Rinsho Shinkeigaku; 14: No. 3, 281-285(Mar 1974). (In Japanese).

The blood-cerebrospinal fluid barrier was investigated by means of RISA^{131}I on subjects with various neurological diseases. Permeability was expressed by percentage of cerebrospinal fluid (CSF) and plasma RISA^{131}I net cpm ratio. This report deals with results only 24 hours after intravenous administration with concomitant sampling of blood and CSF. Control samples consisted of 25 patients with a variety of diseases in which increased permeability was not suspected. Permeability in this group was 0.30 ± 0.28%. Increased permeability was observed in various types of meningitis and Guillain-Barré syndrome. This increased permeability gradually decreased in parallel with clinical recovery. Increased permeability in these diseases was positively correlated to protein value in CSF but not to cell count. Increased protein content, however, was not correlated to permeability in cerebral tumor and in degenerative diseases when studied 24 hours after isotope administration but did correlate when sampled 72 to 96 hours after administration. This could be explained on the basis of plasma-CSF isotope equilibrium; namely, this equilibrium is reached 72 to 96 hours after isotope administration in non-inflammatory diseases, whereas in the inflammatory state the equilibrium is attained earlier than the above interval. No increased permeability was observed in acute and subacute stages of cerebrovascular accident. (auth)

29841 RETICULOENDOTHELIAL FUNCTION TEST IN RABBIT AND MAN. Experimental and Clinical Investigation on Artificial Fat Cream and ^{131}IAA. Matsumura, K. (Tokyo Medical and Dental Univ.). Nippon Monaikei Gakkai Kaishi; 13: No. 3, 119-132(Jan 1974). (In Japanese).

The Fatogen colorimetric method, triglyceride method, and ^{131}I aggregated albumin (^{131}IAA) method as reticuloendothelial function tests were examined. Fatogen was given in doses of 50, 100, or 150 mg/kg, and the latter dosage was suitable for Fatogen colorimetric method. There was a marked individual difference between the phagocytic index K of normal rabbits in Fatogen colorimetric method and the mean K value was 0.0508 (SD ± 0.0158). After the injection of 0.05 mg/kg of ^{131}IAA to rabbits, the radioactivity decreased almost along an exponential curve. There was a relatively small individual difference between the K value of normal rabbits in ^{131}IAA method and the mean K value was 0.0303 (SD ± 0.008). In ^{131}IAA method, ACTH, Solcoseryl, and Zymosan stimulated the reticuloendothelial system, and cortisone inhibited it. When Zymosan was given to splenectomized rabbits, acceleration of the function disappeared. Spleen extract obtained from the normal rabbits accelerated the reticuloendothelial function. Spleen extract obtained at the time of acceleration of reticuloendothelial function after the injection of Zymosan showed accelerating effects of the reticuloendothelial function, and the same effect was also found in the splenectomized rabbits. When 0.05 mg/kg or 0.025 mg/kg of ^{131}IAA was given to normal persons, the radioactivity decreased almost along the exponential curve in 2 to 12 minutes after the injection of ^{131}IAA. The mean K value was 0.0789 (SD ± 0.0141) in the injection of 0.025 mg/kg of ^{131}IAA. (JA)

29842 CLINCIAL EXPERIENCE WITH RADIOIMMUNOLOGICAL TSH DETERMINATION. Lauridsen, U. B.; Deckert, T.; Friis, T.; Kirkegaard, C.; Hansen, J. M.; Siersbaek-Nielsen, K. Ugeskr. Laeger; 136: No. 25, 1365-1368(1974). (In Danish).

By means of a radioimmunological method the serum TSH levels were measured in euthyroid patients and patients with thyroid disturbances both prior to treatment and during treatment. In 128 euthyroid patients the TSH concentrations were found to average 1.9 μU/ml with 95% limits 0–4.8 μU/ml and immeasurable values in 36%. In 97 hyperthyroid patients significantly lower values were encountered averaging 1.5 μU/ml with 95% limits 0–3.5 μU/ml while immeasurable values were encountered in 47%. In 40 hypothyroid patients greatly increased values were encountered averaging 116 μU/ml with 95% limits 36–290 μU/ml. Significant increase in serum TSH was encountered in euthyroid men aged over 60 years. No sex difference was found in the individual age groups. The group with atoxic goitre did not differ significantly from the control group. In hyperthyroid patients receiving antithyroid therapy raised TSH values were encountered in half of the patients with lowered serum thyroxine while all patients with normal serum thyroxine with a few exceptions had normal TSH values. Among hypothyroid patients receiving substitution therapy with l-thyroxine raised serum TSH values were encountered in all patients with low serum thyroxine values and in half of the patients with serum thyroxine levels corresponding to the lower half of the normal range. This indicates that the endogenic TSH stimulation in these patients is not eliminated until serum thyroxine values are high in the normal range. It is concluded that TSH determination is of value as well in the diagnosis of primary myxoedema as in follow-up control of patients receiving substitution therapy with l-thyroxine and in hyperthyroid patients receiving antithyroid therapy, whereas it has no clinical value in the diagnosis of hyperthyroidism. (auth)

29843 ^{99m}Tc PYROPHOSPHATE FOR DIAGNOSTIC BONE IMAGING. Weber, D. A.; Keyes, J. W. Jr; Benedetto, W. J.; Wilson, G. A. (Univ. of Rochester, NY). Radiology; 13: No. 1, 131-137(Oct 1974).

The kinetics and imaging characteristics of ^{99m}Tc-labeled stannous pyrophosphate were evaluated in 30 patients. Blood chemistries, urinalyses, serial blood activity measurements, and 24-hour fractionated urine activity assays were obtained in selected patient studies. Digital gamma camera images were recorded on magnetic disk and quantitatively analyzed. Total body rectilinear scans were also recorded. Results indicate that ^{99m}Tc pyrophosphate is useful for bone imaging. Preparations yielded reproducibly high binding efficiencies; soft tissue clearance was rapid; no pharmacologic effects were observed; and count levels and contrast between lesion-involved bone and normal bone were adequate. Image quality was acceptable between 1 and 6 hours after administration. Abnormal areas were detected at all imaging times; however, the best image quality was usually observed in the delayed views. (auth)

29844 COMBINED CONTRAST AND RADIONUCLIDE ANGIOGRAPHY OF THE LIVER. Waxman, A. D.; Finck, E. J.; Siemsen, J. K. (Univ. of Southern California Medical Center, Los Angeles). Radiology; 113: No. 1, 123-129(Oct 1974).

In 18 patients with known focal liver disease intra-arterial ^{99m}Tc sulfur colloid angiography and subsequent static scans were found to be superior to contrast angiography in evaluation of small avascular hepatic lesions. Radionuclide angiography was inferior to contrast angiography in evaluation of small hypervascular lesions. Large vascular or avascular lesions were detected equally well by both methods. Intravenous radionuclide perfusion distribution studies were equal or slightly inferior to the intra-arterial method in detecting hepatic lesions. The intravenous radionuclide study was superior in determining arterialization of the hepatic bed. Vascular lesions of the left lobe and inferior border of the liver were better detected by the intra-arterial injection of radiocolloid than by the intravenous route. The combined use of all three techniques was superior to any single modality in evaluation of hepatic lesions. (auth)

29845 GALLIUM–TECHNETIUM SUBTRACTION SCANNING FOR THE LOCALIZATION OF SUBPHRENIC ABSCESS. Damron, J. R.; Beihn, R. M.; Selby, J. B.; Rosenbaum, H. D. (Veterans Administration Hospital, Lexington, KY). Radiology; 113: No. 1, 117-122(Oct 1974).

Diagnosing subphrenic abscesses may still be difficult even with radioisotope scanning techniques using ^{67}Ga-citrate. To enhance the imaging of such abscesses, a gallium–technetium subtraction scan was produced simultaneously allowing image subtraction of liver, spleen, and even lungs. Since ^{99m}Tc localizes only in those organs, only those areas are erased, and the specific area of gallium localization is more clearly defined. Abscesses were unequivocally detected only by this technique in the four cases presented. (auth)

29846 CLINICAL EVALUATION OF TUMOR SCANNING WITH ^{57}Co-BLEOMYCIN. Suzuki, Y.; Hisada, K.; Hiraki, T.; Ando, A. (Kanazawa University Hospital, Japan). Radiology; 113: No. 1, 139-143(Oct 1974).

Tumor scanning with ^{57}Co-bleomycin was carried out in 46 patients with an overall accuracy of 66% in malignant tumors. There were no genuine false positive results in four benign lesions. Since ^{57}Co-bleomycin is excreted rapidly through the kidneys, a high tumor-to-blood ratio is obtained a short time after injection. Although its long physical half-life may restrict its routine use, ^{57}Co-bleomycin might provide a valuable adjunct in the work-up of malignant tumors when used in properly selected patients. (auth)

29847 DUAL CAMERA STUDIES OF PULMONARY FUNCTION WITH COMPUTER PROCESSING OF DATA. Loken, M. K.; Ponto, R. A.; Kronenberg, R. S.; Williams, L. E.; Goldberg, M. E. (Univ. of Minnesota Hospital, Minneapolis). Amer. J. Roentgenol., Radium Ther. Nucl. Med.; 121: No. 4, 761-771(Aug 1974).

Xenon-133 and two scintillation cameras arranged to view both anterior and posterior lung fields were used routinely for evaluation of pulmonary function. Scintiphotograms were obtained from both cameras throughout the course of both perfusion and ventilation portions of the study. In addition, data from both cameras were digitized and stored on line in a dedicated computer for further analysis. Computer processing of data permits quantitative information to be obtained on perfusion, ventilation, and clearance of the radioactive gas from selected regions of the anterior and posterior lung fields. Ventilation-perfusion ratios and washout times are likewise calculated by computer. (auth)

29848 DETECTION AND LOCALIZATION OF AN OCCULT VESICOENTERIC FISTULA. Prokop, E. K.; Buddemeyer, E. U.; Strauss, H. W.; Wagner, H. N. Jr. (Johns Hopkins Medical Institutions, Baltimore). Amer. J. Roentgenol., Radium Ther. Nucl. Med.; 121: No. 4, 811-818(Aug 1974).

Detection and localization of an enterovesicular fistula in a patient with chronic inflammatory bowel disease and recurrent urinary tract infection was accomplished by following a bolus of orally administered ^{198}Au colloid as it traversed the gastrointestinal tract with serial scintiphotos and simultaneously monitoring the activity in the urine. When significant tracer was found in the urine, multiple scans of the abdomen were obtained to determine the location of the tracer. To confirm the site of the fistula, the tracer was mixed with barium and administered per rectum. Radiographs were obtained when significant activity was found in the urine. (auth)

29849 PITFALLS IN ^{99m}Tc POLYPHOSPHATE SKELETAL IMAGING. Thrall, J. H.; Ghaed, N.; Geslien, G. E.; Pinsky, S. M.; Johnson, M. C. (Walter Reed Army Medical Center, Washington, DC). Amer. J. Roentgenol., Radium Ther. Nucl. Med.; 121: No. 4, 739-747(Aug 1974).

The quality of ^{99m}Tc polyphosphate scans was evaluated in 600 bone scans of patients with various bone lesions. In all age groups quality was adversely affected by free TcO_4^-. This should be suspected if excessive background is present or marked accumulation is noted in the thyroid gland. Other causes of error are discussed. (CH)

29850 VALUE OF ^{99m}Tc-DIPHOSPHONATE (HEDSPA) AS A SKELETAL SCANNING AGENT. Papadimitriou, J.; Vezeridis, M.; Constantinidis, M.; Chiotelis, E.; Constandinidis, C.; Tountas, C. (Athens Univ.). Amer. J. Roentgenol., Radium Ther. Nucl. Med.; 121: No. 4, 735-738(Aug 1974).

A new bone seeking agent, namely the organic compound diphosphate labeled with ^{99m}Tc was tried in 21 patients for skeletal scanning. In three cases, although the clinical and roentgenographic evidence of bone lesions was absent, bone metastases were found and these were confirmed histologically. The organic diphosphonate is more stable compared to the inorganic polyphosphates and the images obtained are excellent. (auth)

29851 USE OF MULTIPLE RADIONUCLIDE IMAGING TO DIFFERENTIATE THE FOCAL INTRAHEPATIC LESION. Muroff, L. R.; Johnson, P. M. (Columbia Univ., New York). Amer. J. Roentgenol., Radium Ther. Nucl. Med.; 121: No. 4, 728-734(Aug 1974).

From 74th annual meeting of the American Roentgen Ray Society; Montreal, Quebec (25 Sep 1973).

Thirty-five patients with various focal intrahepatic mass lesions were evaluated with scans using multiple radionuclides (^{99m}Tc-colloid, ^{113m}In, ^{75}Se, and ^{111}In). Comparison of the blood pool scans with angiography and histology demonstrated an excellent correlation of these studies. Diagnostic accuracy was improved by separating the blood pool scans into three categories. Each category suggested, at most, one further study to provide specific diagnostic information. Thus, by utilizing three radiopharmaceuticals, one can be more specific in preoperative diagnoses. (auth)

29852 DIAGNOSIS OF BARRETT'S ESOPHAGUS WITH RADIOISOTOPES. Gordon, F.; Ramirez-Degollado, J.; Munoz, R.; Cuaren, A.; Landa, L. (Hospital General del Centro Medico Nacional, Mexico City). Amer. J. Roentgenol., Radium Ther. Nucl. Med.; 121: No. 4, 716-719(Aug 1974).

The replacement of the normal stratified squamous lining of the lower esophagus by columnar epithelium similar to that of the stomach is known as Barrett's esophagus. Patients who have this disease develop in most cases esophagitis and ulceration. Diagnosis of Barrett's esophagus with ^{99m}Tc pertechnetate scanning is a fast, easy, reliable and innocuous method, that may be used as a complementary procedure in the study of patients suspected of having this disease. (auth)

29853 QUANTITATIVE THYROID SCANNING: A RELIABLE THYROID FUNCTION TEST. Arkles, L. B. (Repatriation General Hospital, Melbourne). Amer. J. Roentgenol., Radium Ther. Nucl. Med.; 121: No. 4, 705-713(Aug 1974).

Quantitative thyroid scanning using ^{99m}Tc-pertechnetate is a simple, reliable, and informative test of thyroid function and preferable in many ways to ^{131}I uptake studies in the diagnosis of thyrotoxicosis. The information provided is complementary to in vitro thyroid function tests and is likely to remain so, despite the recent advances in the latter field. Calculation of extrathyroidal neck radioactivity and percentage uptake would not appear to be an essential prerequisite for satisfactory intravenous $^{99m}TcO_4^-$ thyroid function studies. Quantitative thyroid scanning is not suitable as a routine screening test, but is a valuable examination in the diagnosis of thyrotoxicosis. (auth)

29854 CLINICAL EVALUATION OF PREOPERATIVE LIVER SCINTIGRAPHY IN GASTRIC CARCINOMA PATIENTS. Watanabe, K.; Kawahira, K.; Matsuura, K. (Kyushu Univ., Fukuoka). Amer. J. Roentgenol., Radium Ther. Nucl. Med.; 121: No. 4, 720-727 (Aug 1974).

The surgical and liver scintigraphic (^{198}Au colloid and ^{99m}Tc colloid) findings were compared for evaluation of preoperative diagnostic value in 150 cases of gastric carcinoma with extension to the muscularis and serosa. There was correlation in 90% of the cases, with a false negative rate of 16%, and a false positive rate of 6.6%. Liver metastases were detected in 89%, when the liver was palpable, compared to 75% in those with nonpalpable livers. Four of the 150 cases had small scintigraphically undetectable metastatic foci. Although search for liver metastases at laparotomy may be inconclusive in confirming the presence of metastases, the scintigraphic detection rate correlated closely with the surgical findings. Preoperative liver scintigraphy is therefore considered to be of great diagnostic value. (auth)

29855 ENHANCEMENT OF PANCREATIC CONCENTRATION OF ^{75}Se-SELENOMETHIONINE. Winston, M. A.; Guth, P.; Endow, J. S.; Blahd, W. H. (Veterans Administration Wadsworth Hospital, Los Angeles). J. Nucl. Med.; 15: No. 8, 662-666(Aug 1974).

In order to improve the reliability of pancreas scanning, particularly the elimination of falsely abnormal scans, we have tested the effects of various stimulatory regimens upon the uptake of ^{75}Se-selenomethionine by the rat pancreas. Urecholine proved to have a mild stimulatory effect while the parasympatholytic agent propantheline bromide had a reverse action. The combination of urecholine, followed by pancreazymin, caused a marked enhancement of tracer uptake. This combined regimen was further evaluated in human subjects with encouraging results. Falsely abnormal results have been largely eliminated, and side effects have been quite tolerable. It is proposed that parasympathetic stimulation is required for optimal pancreatic function. (auth)

29856 PRACTICAL APPLICATION OF A SIMPLIFIED VITAMIN B_{12} RADIOASSAY. Shafer, R. B.; Ripley, D.; McMahon, J.; Doscherholmen, A. (Veterans Administration Hospital, Minneapolis). J. Nucl. Med.; 15: No. 8, 688-692(Aug 1974).

A simplified radioassay for the measurement of serum vitamin B_{12} concentration was reassessed. Results of the radioassay were compared with results from the Euglena gracilis assay in 76 normal volunteers, 19 patients with Addisonian pernicious anemia, and 45 patients with gastric resection. Normal range of the radioassay was 200 to 900 pg/ml with a mean of 514 ± 156 pg/ml. Clear separation without overlap was possible by both methods between normal volunteers and vitamin B_{12}-deficient patients with pernicious anemia or gastric resection. The simplicity, economy, and reproducibility of the assay is stressed. Large numbers of sera can be assayed in a short period of time with very little expense and the test results made available within 24 hr. All equipment required can be found in the routine chemistry and nuclear medicine laboratories. The use of naturally occurring specific-binding substances with minimum preparation and cost seems an alternative answer to the rising expense of the prepackaged kits. (auth)

29857 TISSUE CLEARANCE OF ^{131}I FROM LOWER-LIMB BLOOD VESSELS IN DIABETICS. Poniecki, A.; Grabowski, R.; Franecki, G. (Medical Academy, Bialystok, Poland). Wiad. Lek.; 26: 1119-1123(1973). (In Polish).

Fifty subjects were studied including 20 healthy controls and 30 diabetics taking into account the age, sex, form and duration of the disease. Determinations of tissue clearance of ^{131}I from the blood vessels of lower limbs demonstrated a significantly delayed disappearance of radioactivity in diabetics which was in part correlated with the duration of diabetes and sex of the patient. The investigations suggest a frequent presence of occult changes in lower-limb capillary vessels in diabetes confirming the usefulness of the isotope method for their detection. (auth)

29858 COMPARATIVE STUDY OF PLACENTAL LOCATION BY USING ^{51}Cr AND THE DOPPLER EFFECT. Franck, C. (Chile Univ., Santiago). Rev. Chil. Obstet. Ginecol.; 37: No. 1, 18-23(1971). (In Spanish).

A placental location technique using erythrocytes labeled with ^{51}Cr is described. Some results were obtained in all the cases studied. A comparison with the ultrasonic results using the Doppler effect showed less satisfactory results. The diagnosis was correct in 65% of the cases with 34% false results in the cases of placenta previa studied. A comparative survey was made of the results obtained in different publications and some characteristics of the isotopes used in placental location were analyzed. (tr-auth)

29859 AFFINITY OF ^{111}In-BLEOMYCIN FOR MALIGNANT TUMORS. Akiba, H.; Kakehi, H.; Kawana, M. (Chiba Univ., Japan). Nippon Igaku Hoshasen Gakkai Zasshi; 34: No. 3, 162-168(Mar 1974). (In Japanese).

The affinity of ^{111}In-bleomycin for malignant tumors of the rat and those of human beings was investigated. The agent was injected intravenously to the rats that bore subcutaneous transplants of Yoshida sarcoma or ascites hepatoma of AH 109A. They were sacrificed 1, 2, 3, or 5 days after the injection. The radioactivity of the tumor, blood, muscle, liver, kidney, bone, and spleen was measured by a well-type scintillation counter. Tumor to muscle concentration ratio of Yoshida sarcoma was 5.8, and that of AH 109A was 7.1. Kidney to muscle ratio was 13 invariably. The ratios of liver or spleen to muscle were 6 to 7. That of blood to muscle was 0.4. The whole-body retention of the radionuclide at 24 hours of the injection was about $\frac{1}{3}$ the dose. Twenty-eight patients with neoplasms were investigated with ^{111}In-bleomycin, and the results were positive in 21 of them. In four cases its deposition was uncertain. Eight of the 28 were also examined with ^{67}Ca citrate and all the cases were positive. The results appear to indicate good results for tumor imaging with ^{111}In-bleomycin. (auth)

29860 STUDIES ON RADIOIMMUNOASSAY OF LUTEINIZING HORMONE OF RABBIT. Ichii, H.; Yamaji, K.; Fukada, N.; Tanizawa, O.; Kurachi, K. (Osaka Univ.). Nippon Sanka Fujinka Gakkai Zasshi; 26: No. 1, 67-68(Jan 1974). (In Japanese).

In order to measure rabbit luteinizing hormone (LH) in the blood, a new radioimmunoassay was established by the combination of the serum of a guinea pig with anti-sheep LH and ^{125}I labeled rat LH antigen. This method enabled the measurement of rabbit LH. The LH levels in the blood were measured at various times after the injection of LH-RH or $CuSO_4$ by this method, and the method was found to be sufficiently sensitive to LH dynamics in the blood. It is concluded that this method greatly contributes to make clear the mechanism of ovulation in rabbit as a model. (JA)

29861 DOUBLE ANTIBODY RADIOIMMUNOASSAY FOR HUMAN URINARY FOLLICLE STIMULATING HORMONE. Watanabe, N. (Chiba Univ., Japan). Nippon Naibumpi Gakkai Zasshi; 50: No. 4, 797-812(Apr 1974). (In Japanese).

Methods for the radioimmunoassay of follicle stimulating hormone (HUFSH) in the urine are described using FSH in the high purified human urine FSH (HUFSH) and FSH in the anti-human urine (anti-HUFSH) as well as the studies on the change of the excretion rate of FSH in the urine of a normal matured woman and of a pregnant woman. Purified urinary FSH, 920 IU (immunopotency)/mg, labeled with ^{125}I to specific activity of 100 to 120 μCi/μg was used. (JA)

29862 DETERMINATION OF PROLACTIN IN THE BLOOD BY RADIOIMMUNOASSAY. Onishi, T.; Miyai, K.; Kumahara, Y. (Osaka Univ.). Rinsho Kagaku; 15: No. 5, 595-599(May 1974). (In Japanese).

Human prolactin in the blood was labeled by ^{125}I, and radioimmunoassay was done. Prolactin in the blood was determined in healthy cases, in the cases with hypothyroidism and hyperthyroidism, in the cases with pituitary adenoma and galactorrhea, and in the healthy cases with the administration of TRH of chlorpromazine. The secretion of prolactin was distributed to high value in the cases with hypothyroidism. In cases with hyperthyroidism, these values were within normal limits. In the cases with pituitary adenoma and galactorrhea, it showed high value. When TRH and chlorpromazine were administered, its secretion was increased. From these results, the determination of the prolactin in the blood in various pathological states seemed to play as important a role as the clinical examination. (JA)

29863 RADIOIMMUNOASSAY FOR SEX STEROID HORMONE. VI. Radioimmunoassay for Δ^4-Androstenedione. Yoshida, T.; Tanemori, K.; Inatomi, K.; Ozaki, H.; Takagi, S. (Nihon Univ., Tokyo). Horumon To Rinsho; 22: No. 5, 671-676(May 1974). (In Japanese).

A method is described for the radioimmunoassay for Δ^4-A-dione in male and female adults in which tritium was used as the tracer. That is to say, Δ^4-A-dione was separated and purified from ether extracts in the plasma by Sephadex LH 20 column chromatography. These prepared substances were reacted to rabbit anti-serum. Radioimmunoassay was done after separation of antibody-bound type and free type was achieved by the ammonium sulfate analysis. The values of Δ^4-A-dione in the peripheral blood were 1.22 ± 0.33 ng/ml (N = 23) in the adult males and 1.12 ± 0.27 ng/ml (N = 41) in the adult females by this method. The purification and the reproducibility by this measurement method were satisfactory. Therefore, this method seemed to be one of the useful methods for the clinical diagnosis. (JA)

29864 DATA PROCESSING SYSTEM FOR NUCLEAR MEDICINE. Saito, K.; Fujiki, Y.; Oobayashi, I.; Asahina, K. (Tokyo Shibaura Electric Co. Ltd., Kawasaki, Japan). Toshiba Rebyu; 29: No. 6, 574-578(Jun 1974). (In Japanese).

Nuclear medicine, which performs diagnosis of cancer, measurement of blood flow and quantitative analysis of hormone, etc., by the use of radioisotopes as tracer, is making rapid progress of late. The reason the nuclear medicine took the lead of other medical fields in adopting the data processing system is that the system can utilize the processing techniques of radiation measurement and that it can accept the data that have digital character. The processing system of this sort makes high-speed on-line collection of γ-camera data and forms scintigrams on core memories. It can also perform various types of image processing, such as elimination of quantum noise inherent in scintigram data and correction of uniformity, or obtain histograms in time series from original data groups. Although it has made progress in company with the popularization of γ cameras, the data processing system is also making important contribution to labor saving in computation of regional cerebral blood flow, hormone quantity, etc. (auth)

29865 RADIOISOTOPE PLACENTOGRAPHY WITH ^{113m}In. Its Value in the Diagnosis and Treatment of Placenta Praevia. Bravo, A.; Benavides, I.; Claure, H.; Stevenson, C. (Univ., Chile, Santiago). Rev. Chil. Obstet. Ginecol.; 36: No. 5, 276-289(1971). (In Spanish).

The different methods for the diagnosis of placenta praevia are reviewed. Placentary scintigraphy with ^{113m}In at doses of 1 to 1.5 mci was carried out on 63 pregnant women with hemorrhage of the third month. The diagnostic precision of the placentary implantation with this technique was 96.8% compared with the Doltone technique with a certainty of 55.3%. The therapeutic plan used in placenta praevia at the Santiago Maternity Hospital consists in prolonged hospitalization under obstetric observation until childbirth, use of radioisotopic placentography, colpocytograms, use of uterine relaxants, elective Caesarian operation (90%) in the case of lower lateral, marginal, or central placenta praevia, and prompt pediatric care of the newborn. This therapeutic plan in placenta praevia reduces appreciably obstetric acute anemia from 57.4% to 1.8%, fetal hypoxia from 27% to 5.45%, prematurity from 39.6% to 16.36%, and prenatal mortality from 20.69% to 7.27%. (tr-auth)

29866 ASYNCHRONOUS TURNOVER OF THE THIN FILAMENT PROTEINS, ACTIN, TROPOMYOSIN, AND TROPONIN BY A CONTINUOUS DOUBLE ISOTOPE METHOD. Funabiki, R.; Cassens, R. G. (Univ. of Wisconsin, Madison). J. Nutr. Sci. Vitaminol.; 19: 361-368(Aug 1973).

The relative turnover rate of protein components of the thin filament was measured by a continuous double isotope method. Both ^{3}H-lysine and ^{14}C-lysine were administered continuously in the diet to male adult rabbits for 7 days. On the 7th day, the ^{14}C-lysine was discontinued while the ^{3}H-lysine was continued for 14 additional days. The relative turnover rate of the protein components was estimated from the ^{3}H/^{14}C ratios of the isolated protein of the same animal. From the different ratios of ^{3}H/^{14}C of each protein fraction, asynchronous turnover of the thin filament proteins (actin, tropomyosin and troponin) was concluded. The order of degree in relative turnover rate is as follows: troponin > tropomyosin > actin. (auth)

29867 USE OF A DOUBLE ISOTOPE METHOD IN THE DETERMINATION OF ANTIBODY AFFINITY. Gaze, S.; West, N. J.; Steward, M. W. (Kennedy Inst. of Rheumatology, London). J. Immunol. Methods; 3: 357-364(1973).

A double isotope method for the determination of antibody affinity using ammonium sulfate globulin precipitation is described and appraised. The incorporation of a ^{22}Na-volume marker in addition to the ^{125}I-labelled antigen eliminates the usual necessity to wash the globulin precipitates and enables larger numbers of samples to be assayed rapidly and reliably. Affinity values for anti-hapten and anti-protein antibodies determined by these two methods are compared and although higher values were obtained with the double isotope method the affinities of sera assayed by both methods are ordered similarly. (auth)

29868 IDENTIFICATION OF SPARGANUM GROWTH FACTOR BY A RADIORECEPTOR ASSAY FOR GROWTH HORMONE. Tsushima, T.; Friesen, H. G.; Chang, T. W.; Raben, M. S. (Univ. of Manitoba, Winnipeg). Biochem. Biophys. Res. Commun.; 59: No. 3, 1062-1068(5 Aug 1974).

The growth hormone-like substance of Spirometra mansonoides in the incubation medium of the worm as well as in serum from infested rats was studied with the radioreceptor assay (RRA) for growth hormone (GH). Sparganum growth factor (SGF) inhibited the binding of hGH tracer to the rabbit liver receptor in a parallel manner to human GH. Serum concentrations of SGF in normal rats increased to a level equivalent to 1 μg/ml hGH eight days after subcutaneous implantation of 50 worms. Upon gel filtration in G-100 Sephadex, SGF eluted in the fractions corresponding to a molecular weight of approximately 70,000. The Rf of SGF upon polyacrylamide disc gel electrophoresis was 0.32 and after gel isoelectrofocusing, the growth factor was detected in gel segment of pH 6.0. (auth)

29869 ADRENAL IMAGING WITH RADIOIODOCHOLESTEROL IN THE DIAGNOSIS OF ADRENAL DISORDERS. Anderson, B. G.; Beierwaltes, W. H. (Univ. of Michigan, Ann Arbor). Advan. Intern. Med.; 19: 327-343(1974).

Intravenous injections of ^{131}I-19-iodocholesterol were given to patients and a scintillation camera was used for imaging and determination of % uptake. Results for 100 patients are tabulated according to abnormal adrenal scans and adrenal disorders. Preliminary assessment of the utility of ^{131}I-19-iodocholesterol for adrenal scanning and prospective uses are discussed. (HLW)

29870 RADIOIMMUNOASSAY FOR PLASMA INSULIN USING ZIRCONYL PHOSPHATE GEL. Coffey, J. W.; Nagy, C. F.; Lenusky, R.; Hansen, H. J. (Hoffman–La Roche Inc., Nutley, NJ). Biochem. Med.; No. 9, 54-61(Jan 1974).

A procedure for the detection of immunoreactive insulin in human plasma is described. The procedure is a rapid radioimmunoassay (3 hr) which uses zirconyl phosphate gel (Z-gel) at a pH of 6.25 to adsorb antibody-bound insulin while leaving free insulin in solution. Thirty-two samples of human plasma which had been assayed for immunoreactive insulin using a commercially available assay (Pharmacia Fine Chemicals, Piscataway, NJ) were also assayed on a blind basis for immunoreactive insulin using the Z-gel technique. A statistical comparison of the data obtained by the two methods yielded a highly significant ($P < 0.01$) coefficient of correlation (0.998). A known amount of bovine insulin was added to each of these plasma samples, and the Z-gel assay repeated. The mean percentage recovery of added insulin was 100.4 ± 17.0 (SD). In addition, the insulin response of two healthy individuals to the ingestion of 100 g of glucose was determined using the Z-gel assay. The insulin response curves were similar to those described by other investigators. (auth)

29871 APPLICATION OF ^{133}Xe IN MEASURING PERIPHERAL BLOOD FLOW. Zadak, Z.; Hottmar, Z. (Military Medical Research and Postgraduate Inst., Hradec Kralove, Czech.). Sb. Ved. Pr. VLVDU Hradci Kralove; 62: 181-193(1972). (In Czech).

Xenon-133 in a solution was applied in the determination of peripheral blood flow. The method using ^{133}Xe, described elsewhere, was found very advantageous as against other indicators. It was found especially useful in measuring higher values of blood flow. It is not time consuming and does not strain the person examined. (Nuclear Sci. Abstr. Czeck.)

29872 EXPERIMENTAL APPLICATION OF ^{133}Xe IN MEASURING MINUTE VOLUME OF BLOOD. Zadak, Z.; Hottmar, Z. (Military Medical Research and Postgraduate Inst., Hradec Kralove, Czech.). Sb. Ved. Pr. VLVDU Hradci Kralove; 62: 157-179(1972). (In Czech).

A new method of measuring hemodynamic values using ^{133}Xe, described elsewhere, was applied in experiments aiming at determining the relations of hemodynamic constants during physical effort. The radionuclide was applied intravenously before and after the strain to which experimental persons were exposed on a bicycle ergometer. Investigated were also the effects of increased temperature on people at rest and of high doses of atropine on people at rest. The method yielded good results showing considerable changes in hemodynamic indicators. (Nuclear Sci. Abstr. Czeck.)

29873 APPLICATION OF ^{133}Xe IN MEASURING MINUTE VOLUME OF BLOOD. Zadak, Z.; Hottmar, Z. (Military Medical Research and Postgraduate Inst., Hradec Kralove, Czech.). Sb. Ved. Pr. VLVDU Hradci Kralove; 62: 125-155(1972). (In Czech).

A bloodless method is described elaborated for the measurement of hemodynamic values, mainly of cardiac output. The method makes it possible to determine the desired hemodynamic values in very short time intervals. The method also offers an advantage of a minimum load imposed on the person examined and of a possibility of measuring the values during physical effort. (Nuclear Sci. Abstr. Czeck.)

29874 RADIOIMMUNOLOGICAL DETERMINATION OF PROTEOHORMONES. Sedlak, J.; Antonic, B. (East-Slovakian Iron Works, Kosice-Saca, Czech.). Prakt. Lek.; 53: No. 14, 577-559 (20 Jul 1973). (In Slovak).

The procedure for determining the growth hormone is presented as the model for the radioimmunological determination of the proteohormone. A list is presented of complete sets for the determination of proteohormones as well as a list of apparatus available in Czechoslovakia for measuring the radioactivity of labelled samples. (Nuclear Sci. Abstr. Czeck.)

29875 CLINICAL STUDIES OF MYOCARDIAL SCINTIGRAPHY WITH ^{131}I-MAA. Konishi, H.; Abe, H.; Shirai, O.; Hayashi, M.; Muraoka, T. (Kyoto Univ.). Mayakkangaku; 14: No. 1, 45-50(Jan 1974). (In Japanese).

Myocardial scintigraphy with ^{131}I-MAA was carried out in 25 patients with coronary arterial diseases (22 with angina, 3 with infarct, and 1 with fistula) to prepare scintigrams by computer. Following the selective coronary arteriography, 100 to 200 μCi of ^{131}I-MAA diluted with about 5 mg of physiological sodium chloride solution was injected into the left coronary artery for a few minutes. Using Anger-type scinticamera, the image was taken by polaroid camera and recorded in magnetic tape within a few hours. The data was improved by smoothing and gradual approximation method, and the count was divided into 20 levels to express as iso-count curve. The scintigram was evaluated by paying attention to positional changes of the highest count point and morphological changes of iso-count curve. Coronary arteriograms, images by scintiscanner and scinticamera, computer scintigrams of 7 patients and so on were shown. All the patients, that showed more than 50% of narrowing in the findings of coronary arterial arteriography, showed abnormalities in scintigram. All the patients that had abnormal findings in electrocardiogram showed abnormalities in scintigram, but the site was not always the same. Seven patients that had no abnormal change in electrocardiogram showed abnormalities in scintigram. Electrocardiogram and arterial pressure of the patients revealed no abnormality after the injection of ^{131}I-MAA. (JA)

29876 RADIOIMMUNOASSAY OF ANGIOTENSIN. Fukuchi, S.; Takeuchi, T.; Nishizato, K.; Nakajima, K.; Ito, A. (Tohoku Univ., Sendai). Rinsho Seijinbyo; 4: No. 3, 275-278(Mar 1974). (In Japanese).

In order to determine plasma renin activity, the plasma with pH 5.5 was incubated for 3 hours at 37°C, and angiotensin I was obtained. This angiotensin I was determined by radioimmunoassay. In addition, the plasma angiotensin II was determined by similar incubation of the plasma as the determination of renin. Angiotensin I and II were labeled by ^{131}I, and were incubated for 18 hours at 5°C. Then, the radioactivity was measured. The determination of the plasma renin activity is an indispensable examination method for the diagnosis in the cases with each hypertension. (JA)

29877 MODIFICATION OF RADIOIMMUNOASSAY METHOD OF HUMAN GROWTH HORMONE ESTIMATION. Samuel, A. M.; Deshpande, U. R. Indian J. Med. Res.; 61: No. 1, 98-104(1973).

Radioimmunoassays are increasingly useful techniques in the detection of very minute concentrations of circulating substances especially hormones. Certain modifications in the technique were studied. Labelling procedure was simplified by a simple device of a polyethylene tubing. The time of incubation of the assay system has been reduced from 4 to 5 days to 26 hr by incubating the assay at 37°C instead of 4°C. There was no loss of sensitivity or reproducibility by changing the temperature of incubation. HGH-free serum for the normalization of the assay system was done by use of charcoal treated donor serum instead of hypopituitary or horse serum used by others. The absence of endogenous HGH in the charcoal treated serum has been tested by various criteria. Optimum amounts of charcoal dextran have been studied for the separation of the bound and free fractions at the end of the incubation of the assay. (Indian Sci. Abstr.)

29878 UPTAKE AND METABOLISM OF [4-^{14}C]TESTOSTERONE IN HUMAN BREAST CANCER GROWN IN ORGAN CULTURE. Geir, A. (Hebrew Univ., Jerusalem); Horn, H.; Lichtshtein, E.; Finkelstein, M.; Levij, I. S. Acta Endocrinol.; 75: 195-204(1974).

The uptake and metabolism of [4-^{14}C] testosterone was studied in 10 tissue samples of human female breast grown in organ culture. Four samples were from carcinomas, 4 were non-cancerous tissue from the uninvolved part of the cancer bearing breast, and two were from fibroadenomas. In all cases, testosterone was metabolized to androstenedione, androsterone, dihydrotestosterone, androstanedione, and androstanediol. The non-cancerous tissues showed greater retention, uptake and conversion of testosterone into metabolites than the cancerous tissues. The retention of testosterone in the fibroadenomas samples was lower than that in samples of either cancerous or non-cancerous tissue. The uptake and conversion of testosterone into metabolites in one case of fibroadenoma was similar to that seen in cancerous tissue samples but in the other case it was considerably higher. (auth)

29879 STUDY ON MECHANISMS OF NERVOUS SYSTEM DISTURBANCE BY RADIOACTIVELY LABELED CHINOFORM.

Takasu, T. (Tokyo Univ.). Rinsho Shinkeigaku; 14: No. 1, 232-237(Mar 1974). (In Japanese).

In order to demonstrate the pathogenesis of chinoform, ^{131}I- or ^{14}C-labeled chinoform, and ^{59}Fe- and ^{65}Zn-labeled metallic salt were administered to mice, rats, dogs, and monkeys, and were traced by autoradiography and scintillation counter. There were various differences by organs in the absorption and the distribution. Chinoform was extremely incorporated especially in the retina, the dorsal root ganglion, the nerve root and the peripheral nerves of the nervous systems. In addition, there were changes in the metabolism and the distribution of chinoform and metallic salt which were given to the animals in pre-treatment with a large amount of chinoform. From these results, in the mechanism of the nervous system disturbance by chinoform poisoning, neuron disturbance was assumed to be directly affected by chinoform. In addition, it was supposed that chinoform has strong affinity with metallic ion, and has the possibility to produce the poisoning in the nervous systems as a metallic chelate in the whole body. (JA)

29880 ECG CHANGES IN SELECTIVE CORONARY ANGIOGRAPHY AND MYOCARDIAL SCINTIGRAPHY. Aldor, E.; Heeger, H. (Hanusch-Krankenhauses, Vienna). Z. Kardiol.; 62: No. 12, 1078-1084(Dec 1973). (In German).

In 50 nonselected patients with coronary heart disease the ECG changes that occur during selective coronary angiography were analyzed. There is no connection between the degree of the changes and the anatomic substrate in the coronary arteries. It seems that hypoxia cannot be the cause of the ECG response because Ringer solution and ^{131}I-Albumin did not develop it. Iodine-131 Albumin, which is used by myocardial scintigraphy, shows other characteristics in the electrocardiogram caused by hypoxia. Changes at the myocardial membrane conductance are discussed for the origin of the ECG response on contrast medium. (auth)

29881 ^{125}I-LABELLING OF CANDIDA ALBICANS BY ELECTROLYSIS. Viken, K. E. (Trondheim Central Hospital, Norway). Acta Pathol. Microbiol. Scand., Sect. B; 82: 219-222(1974).

The aim of this investigation was to establish an easy method for radiolabelling of large quantities of heat-killed Candida albicans. The yeast particles were to be used in studies of phagocytosis in human monocytes cultured in vitro. The results show that it is possible to label quantities of 3–4 × 10^9 Candida particles in one single run by electrolysis of a Na ^{125}I solution. The surface antigens of the Candida were found to be intact after the electrolytic iodination process. (auth)

29882 UPTAKE AND RELEASE OF ^{3}H-MITOMYCIN C IN MOUSE P-388 CELL CULTURES. Oerstavik, J. (Univ. of Oslo). Acta Pathol. Microbiol. Scand., Sect. B; 82: 270-276 (1974).

Mouse P-388 cells were grown in suspension culture and exposed to ^{3}H-labelled mitomycin C for 1 hour. With concentrations from 0.5 to 50 μg of ^{3}H-mitomycin C per ml cell culture, about 0.01% of the radioactivity added was found in washed cells. Most of the intracellular antibiotic was present as cold acid soluble material, but significant amounts of tritium were found in the nucleic acid- and protein fractions. The ratio of ^{3}H per weight unit was of the same order of magnitude for DNA and RNA, but substantially lower for cell protein. Double labelling experiments using ^{14}C-thymidine and ^{3}H-mitomycin C were carried out to study the specific loss of antibiotic from the cells during post-treatment incubation. Cold TCA soluble ^{3}H-mitomycin C was rapidly released from the cells during the first hours after they had been transferred to non-radioactive growth medium. Loss of ^{3}H-radioactivity from the RNA- and protein fractions roughly paralleled the loss of ^{14}C radioactivity from the DNA fraction over a period of 3 days. The content of ^{3}H-radioactivity in the DNA-containing cell fraction increased during the first day of post-treatment incubation, followed by a substantial drop during the second day. This drop was far more extensive than the corresponding loss of ^{14}C radioactivity. During the third day after exposure to mitomycin C the drops in ^{3}H and ^{14}C in the DNA fraction were not significantly different. (auth)

29883 ^{67}Ga-SCINTIGRAPHY IN MALIGNANT LESIONS OF THE LUNG. Hjelms, E.; Dyrbye, M. (Gentofte Hospital, Copenhagen). Scand. J. Resp. Dis.; 55: 1-4(1974).

Gallium-67 scintigraphy was carried out in 107 patients with proven or suspected cancer of the lung. A pathological accumulation was found in 72 of the 92 patients with malignant lesions, and in 5 out of the 12 cases with benign lesions of the lung. It is therefore concluded that the examination is of very limited value in the diagnoses of malignant tumors of the lung because it affords no possibility for distinguishing the malignant lesions from the benign ones. (auth)

29884 TOTAL-BODY WATER DETERMINATION WITH A PRACTICAL INTERNAL STANDARD METHOD. Eberstadt, P. L. (Instituto Nacional de Energia Nuclear, Mexico City). Int. J. Nucl. Med. Biol.; 1: No. 4, 191-195(Jun 1974).

Knowing the total-body water content of their patients, physicians can reach important conclusions. So far, complex methodology has been an obstacle to the easy obtainment of precise data. The presented method with scintillation counting, using an internal standard, employed two identical vials with equal quenching. Both of the vials contained the same amount of sample, but only one of them a known amount of HTO. With the proposed mathematical handling of the readings the efficiency could be determined and with the concentration of HTO in the samples, the HTO diffusible space could be determined. To test the procedure, urine and serum samples taken 24 hr after oral HTO served to determine the total-body water. The results for men were: 64.9% of the body weight of 23.1/m^2 of the body surface; women: 56.6% of the body weight of 19.1/m^2 of body surface. The perfect reproducibility, accuracy and simplicity of the procedure offer an excellent and practical method to determine total body water. (auth)

29885 WEIGHT PARAMETERS OF ADULT HUMAN SKELETON. Borisov, B. K.; Marei, A. N. (Ministry of Health, Moscow). Health Phys.; 27: No. 2, 224-229(Aug 1974).

The aim of the study reported was to investigate weight proportions of individual bones in a total adult human skeleton. These data are necessary for calculation of the total skeletal content of oesteotropic elements (isotopes) from determinations performed on single bones. The fresh weight of individual bones in both the male and female skeleton, the mass proportions of both male and female skeletons % of total skeletal weight contributed by various bones, the ash weight/fresh weight ratios for various bones of adult human skeleton and the weight of the ash obtained from individual bones of human adults are tabulated. It is concluded that: (1) The weight of the skeleton in adult humans of typical body build amounts on the average to 14.2% of body weight. This relative value is sex-independent. (2) On the average, the weight of the skeleton of an adult male is 15% higher than that of a typical female. (3) The proportion of ash in the skeleton in the studied sample amounted to 22% of the fresh weight of the skeleton. (UK)

29886 LOCALIZATION OF INFECTIOUS PROCESSES WITH GALLIUM CITRATE (Ga-67). Blair, D. C.; Carroll, M.; Silva, J.; Fekety, F. R. Jr. (Univ. of Michigan, Ann Arbor). J. Amer. Med. Ass.; 230: No. 1, 82-85(7 Oct 1974).

Thirty patients received ^{67}Ga citrate for scintiscanning in a search for abscesses and other covert infections (25 intra-abdominal and 5 extra-abdominal). Abnormal areas of isotope uptake were found in 25 patients; of these, six had proven infections; 15 had clinically established infections (but confirmatory tissue diagnostic procedures were not performed); one scan was false-positive; and three abnormal scans revealed tumors. This noninvasive scanning procedure has proved useful in identifying sites of inflammation. (auth)

MATERIALS

29887 DAMPING AND ELASTIC CHARACTERISTICS OF PLASMA-SPRAYED COATINGS OF W, NICHROME, ZIRCONIA, AND Cr–Ni SPINELS. Zolotukhin, I. V.; Akinin, K. G.; Abramov, V. V.; Netusov, Yu. K.; Skorobogatov, V. S.; Svedomtsev, N. V. (Voronezh Pedagogical Inst., USSR). Strength Mater. (USSR) (Engl. Transl.); 5: No. 9, 1120-1123(Sep 1973).

Translated from Probl. Prochnosti; 5: No. 9, 86-89(Sep 1973).

The damping (absorption coefficient) and elastic modulus were measured in order to determine the effect of plasma spraying conditions. The low values of the elastic modulus are discussed; porosity does not affect its temperature dependence but only determines its absolute value. (DLC)

Ceramics and Cermets

Refer also to abstracts 28933, 29008, 30018, 30021, 31223, and 31231.

29888 (AD-903226) JFET HARDENING AND HIGH DOSE RATE STUDY. Long, D. M.; Swant, D. H.; Casey, R. H.; Palchefsky, J. W. (General Electric Co., Philadelphia, Pa. (USA)). Jun 1972. 126p. (AFCRL-72-0335). NTIS $9.50.

Results of a study to assess transient response hardening techniques for junction field effect transistors (JFETS) are presented. Their high dose rate behavior was also studied. The hardening analysis shows that by minimizing the device area, and using gold doping or a built-in E-field in the substrate, the JFET response can be made less than the response of typical transistor packages. The lowest response is achieved by JFETS on sapphire. The high dose rate analysis yielded models which establish upper and lower bounds on the photocurrent in the high injection region. Measurements of JFET photocurrent comply with the expected response. The channel response of JFETS is shown to be small at high dose rates, and sceptre predictions of secondary photocurrent at high dose rates agree well with experimental data. Pulse injection measurements on low voltage devices showed burnout levels comparable to diodes, while high voltage units were much more sensitive, apparently due to surface instability. (GRA)

29889 (MLM-2172(OP)) PULSE NMR STUDIES OF RADIATION DAMAGE IN METAL TRITIDES. Bowman, R. C. Jr.; Attalla, A. (Mound Lab., Miamisburg, Ohio (USA)). 1974. Contract AT-33-1-GEN-53. 15p. (CONF-740715-11). Dep. NTIS $4.00.

From fifth international radiation research congress meeting; Seattle, Washington, USA (14 Jul 1974).

The effects of triton decay in LiT and UT_3, which are regarded as representative ionic and actinide metal tritides, were investigated by pulse NMR techniques. Lithium metal, molecular tritium, and ^3He are observed in LiT; only ^3He is detected in UT_3. These radiation damage products were characterized with respect to their concentrations, nuclear spin–lattice relaxation times, and spin–spin relaxation times. The influences of temperature and irradiation dose on the formation and distribution of these species were also studied. (auth)

29890 (SAND-74-0193) J-INTEGRAL AS A FAILURE CRITERION FOR A BORSIC–Al COMPOSITE. Hoover, W. R.; Allred, R. E. (Sandia Labs., Albuquerque, N. Mex. (USA)). Aug 1974. Contract AT(29-1)-789. 32p. Dep. NTIS $4.75.

The fracture toughness behavior of a unidirectional Borsic–Al composite was examined in three-point bending at three different loading rates (3.3×10^{-4}, 20, and 130 in./s). The load-deflection traces indicated that crack "pop-in" occurred prior to maximum load at all three testing speeds. The load-deflection response was significantly nonlinear under the quasistatic conditions while being essentially linear to pop-in at the most rapid loading condition. This change in load–deflection response with loading rate was the result of a strain-rate sensitive matrix yield strength. The fracture toughness was observed to increase with increased loading rate. To determine if the apparent strain-rate sensitive fracture was due to the nonlinear behavior, Rice's J-integral was evaluated over a wide range of crack lengths under static loading conditions. The critical J values varied continuously with crack length; hence the J-integral was inappropriate as a failure criterion. However, a similar but theoretically different parameter, the critical potential energy release rate, L_c, was found to be constant over a wide range of crack lengths. In addition, L_c was found to be constant to within ±4% over the loading rate range tested. Thus the L_c approach may be an effective failure criterion for unidirectional Borsic–Al composites in three-point bending. (13 fig., 4 tables) (auth)

29891 (UCID-15859) YIELD SURFACES FOR BERYLLIUM BORIDE CERAMICS. Holt, A. C. (California Univ., Livermore (USA). Lawrence Livermore Lab.). Jun 1971. 7p. Dep. NTIS $4.00.

Estimates of yield surfaces of Be_2B, BeB_4, and BeB_6 are given. A mathematical form for these surfaces that is convenient for incorporation into the KO one-dimensional hydro code is proposed. It is noted that the results are approximate and are presented as a stop-gap until measurements can be made. (JRD)

29892 EFFECT OF ADDITIVES OF YTTRIUM AND ALUMINIUM OXIDES ON SINTERING AND PROPERTIES OF LANTHANUM HEXABORIDE. Shlyuko, V. Ya.; Morozov, V. V.; Besov, A. V.; Chernyak, L. V.; Guzenko, L. V. (Kiev Polytechnical Inst.). Porosh. Met., Akad. Nauk Ukr. SSR; No. 7, 29-33 (Jul 1974). (In Russian).

Yttrium oxide additives to 4 wt % are determined to activate the shrinkage process, the maximum compaction occurring at 2 wt % of Y_2O_3. Aluminium oxide additives into lanthanum hexaboride deactivate the sintering process. Yttrium oxide additives are shown to increase resistivity and resistance to ion bombardment and to decrease somewhat the work function at 0.5 wt %. (auth)

29893 PRODUCTION OF COMPLEX ZIRCONIUM–TUNGSTEN CARBIDE ON SEMI-INDUSTRIAL SCALE. Grebenkina, V. G.; Karasev, A. I.; Pedanov, L. G.; Shumilova, R. G. (Inst. of Problems in Materials Science, Kiev). Porosh. Met., Akad. Nauk Ukr. SSR; No. 7, 80-83(Jul 1974). (In Russian).

Conditions are studied for obtaining complex zirconium tungsten carbide on a semi-industrial scale. Hydrogen-shielded sintering of a mixture of zirconium carbide–tungsten and soot in the Tamman furnace at 2300°C for 2 h is shown to be the optimal condition and for obtaining a solid solution with the highest fixed carbon content. (auth)

29894 PREPARATION AND SOME MAGNETIC PROPERTIES OF URANIUM OXIDE DOPED YIG CRYSTALS. Krishnan, R. (CNRS, Bellevue, France). Phys. Status Solidi (a); 24: No. 2, K147-K149(16 Aug 1974).

$Y_3Fe_5O_{12}$ (YIG) crystals were grown by the molten flux method, using UO_2. Single crystals of 10 to 15 mm size were obtained. The magnetization (190 ± 2 G at 4°K) is identical to that of pure YIG. The anisotropy constants were determined to be $K_1 = -2.5 \times 10^4$ erg/cm^3 and K_2 = negligibly small. The U^{3+} $5f^3$ and U^{4+} $5f^2$ ions are similar to Nd^{3+} $4f^3$ and Pr^{3+} $4f^2$, respectively, which should result in high anisotropy. This discrepancy is unexplained. (DLC)

29895 COINCIDENCE TWIST BOUNDARIES IN MUSCOVITE, KAOLINITE, AND MoO_3. de Diego, N.; Serna, J.; Bru, L. (Univ. Complutense, Madrid). Phys. Status Solidi (a); 24: No. 2, 613-620(16 Aug 1974).

By means of electron microscopy and electron diffraction, configurations which take place during random sedimentation processes were studied in muscovite, kaolinite, and MoO_3. Twist boundaries about [001] axis in muscovite and kaolinite, and about [010] axis in MoO_3 were observed. Measurements of the rotation angles of these boundaries revealed the existence of preferred misorientation angles. A geometrical model was built up in order to explain the observed configurations in terms of the coincidence site model. This geometrical model does not consider the rotation of two lattices, but the rotation of two ion networks. Results support the validity of the model for the crystals studied. Furthermore it is allowed to assume that these preferred orientations correspond to low-energy configurations. (7 figures) (auth)

29896 ELECTRICAL CONDUCTIVITY IN METAL/OXIDE/ELECTROLYTE SYSTEMS. Odynets, L. L.; Chekmasova, S. S. (Petrozavod State Univ., USSR). Sov. Electrochem. (Engl. Transl.); 9: No. 8, 1113-1115(Aug 1973).

Translated from Elektrokhimiya; 9: No. 8, 1117-1180(Aug 1973).

The temperature dependence of the voltage–current characteristics was studied using the Ta/Ta_2O_5 (anodic)/electrolyte (1N H_3PO_4) system. The contributions to the conduction (defects, electronic, ionic) were separated. Results indicate that the ohmic part is determined by the conductivity along the through-defects of the oxide film filled with electrolyte, and that in the 0.5–0.85 U_F (anodic voltage) range, the main contribution is from the electron current which flows through a continuous oxide layer and obeys a Poole–Frenkel type dependence. (DLC)

29897 EFFECT OF PLASTIC DEFORMATION ON SOME PHYSICAL PROPERTIES OF NIOBIUM MONOCARBIDE IN THE HOMOGENEITY REGION. Bychkov, A. Kh.; Neshpor, V. S.; Ordan'yan, S. S. (Leningrad Technological Inst.). Porosh. Met., Akad. Nauk Ukr. SSR; No. 7, 51-57(Jul 1974). (In Russian).

Polycrystalline NbC samples manifest a noticeable effect of work hardening during plastic deformation above the viscous–brittle transition temperature. The hardening grows with an increase in the content of carbon vacancies in niobium monocarbide lattice. The carbide electric resistance also grows due to increase in concentration of the point defects. The deformation rates being equal, the absolute increase in electric resistance and thermal emf of niobium monocarbide samples is maximum at $x = 0.81 - 0.84$, which is conditioned by the greatest sensitivity of these compositions corresponding to the maximum statistical weight of the stable electronic configurations of $sp^3(s^2p^3)$-type to the Fermi surface charge made by plastic deformation. (auth)

29898 MICRO-X-RAY SPECTRUM ANALYSIS OF INTERPHASE INTERACTION IN THE SYSTEMS "REFRACTORY COMPOUND–LIQUID METAL". Samsonov, G. V.; Sharkin, O. P.; Panasyuk, A. D.; D'yakonova, L. V. (Inst. of Problems in Materials Science, Kiev). Porosh. Met., Akad. Nauk Ukr. SSR; No. 7, 63-68(Jul 1974). (In Russian).

Interaction of liquid Ni with ZrB_2 was studied by means of micro-x-ray spectrum analysis. Ni is dissolved in ZrB_2 (~0.6 wt %) and ZrB_2 is dissolved in the Ni drop. The effect of the oxide films on the ZrB_2 surface was studied as applied to Ni distribution in the boride phase. The Ni solubility increases due to formation of lower boride phases (ZrB). The effect of ZrO_2 film on the interaction and solubility of Ni in the boride phases was studied. Thick oxide films, being defective, are shown to accelerate Ni diffusion into the boride phase. (auth)

29899 ABRASIVE WEAR-RESISTANCE AND FAILURE CHARACTER OF TITANIUM AND ZIRCONIUM BORIDES SURFACE LAYERS. Dan'kin, A. A.; Svetlopolyanskaya, T. P.; Oreshkin, V. D.; Svetlopolyanskii, V. I. Porosh. Met., Akad. Nauk Ukr. SSR; 88-92(Jul 1974). (In Russian).

The intensity of abrasive erosion of titanium and zirconium borides is analyzed depending on the angle of attack at constant rate of the abrasive jet; the character of the surface layer failure in the samples is considered. The observed phenomena are interpreted on the basis of configuration model of the substance. Wear resistance of titanium and zirconium borides is compared with that of steel X18H10T. (auth)

29900 CALORIMETRIC DETERMINATION OF THE HEAT RESISTANCE OF RING-SHAPED SAMPLES OF BRITTLE ELECTRIC CONDUCTORS. Popov, V. P.; Lanin, A. G.; Manyukhin, V. P. Strength Mater. (USSR) (Engl. Transl.); 5: No. 10, 1260-1263(Oct 1973).

Translated from Probl. Prochnosti; 5: No. 10, 96-99(Oct 1973).

A method is proposed for testing the heat resistance of ring-shaped samples of brittle electric conductors by heating in the inductor of a high-frequency generator and cooling the internal surface of the samples by water (temperature interval 100-300°C). The heat current at fracture is determined from the flow and heating up of the cooling water. The error of the measurement does not exceed ±10%. Values of the second criterion of heat resistance were determined on samples of dimensions 50 × 3 × 10 mm for the carbides $ZrC_{0.93}$ and $NbC_{0.93}$; they amount to 23×10^2 and 19×10^2 W/m, respectively. (auth)

29901 MAGNETIZATION AND MOESSBAUER SPECTRA OF NONCRYSTALLINE $Y_3Fe_5O_{12}$. Popma, J. A.; van Diepen, A. M. (Philips Research Labs., Eindhoven, Netherlands). Mater. Res. Bull.; 9: No. 9, 1119-1128(Sep 1974).

Non-crystalline Y_3FeO_{12} is studied by x-ray, electron microscope, magnetic susceptibility, and Moessbauer effect techniques. The material appears to consist of x-ray amorphous platelets of several microns, which are agglomerations of particles of about 200 Å. Moessbauer spectra at room temperature show Fe in tetrahedral surrounding, while at liquid helium temperature hyperfine splitting for both octahedral and tetrahderal sites is observed. Magnetization measurements show that individual particles order magnetically at ~850°K, much higher than well-crystallized YIG (560°K). These differences are consistent with a high degree of crystallographic disorder and a small particle size. Crystallographic ordering and particle growth are induced by annealing. At 680°C crystalline YIG is formed. (auth)

29902 MAGNETIC PROPERTIES OF VANADIUM OXIDE V_3O_7. Bayard, M.; Grenier, J. C.; Pouchard, M.; Hagenmuller, P. (CNRS, Talance, France). Mater. Res. Bull.; 9: No. 9, 1137-1142(Sep 1974). (In French).

Magnetic susceptibility and magnetization measurements on V_3O_7 from 4.2 to 600°K characterize a paramagnetic behavior above 18°K; the samples follow a Curie-Weiss law with a Curie constant in good agreement with a spin only value $S = \frac{1}{2}$ per V^{4+}. At lower temperature the magnetic ordering may be attributed to a metamagnetic behavior resulting from the layer type structure. (auth)

29903 SYNTHESIS OF HIGH PRESSURE $Cd_2V_2O_7$ AND RELATED COMPOSITIONS. Sleight, A. W. (E. I. Du Pont de Nemours and Co., Wilmington, DE). Mater. Res. Bull.; 9: No. 9, 1185-1190(Sep 1974).

$Cd_2V_2O_7$-II has been prepared at about 80 kbars pressure. This new compound has a structure related to that of pyrochlore, but the symmetry is distorted from cubic to monoclinic. Solid solutions of the types $Cd_2V_{2-x}Nb_xO_7$ and $Cd_{2-x}A_xV_2O_7$ (A = In or Tl) were prepared at 58 kbars. Attempts to confirm previous reports of $A^{1+}A^{3+}V_2O_7$ pyrochlores were unsuccessful. (auth)

29904 ELECTRON MICROSCOPE STUDY OF SOME NON-STOICHIOMETRIC TUNGSTEN OXIDES. Sundberg, M.; Tilley, R. J. D. (Univ. of Bradford, Eng.). J. Solid State Chem.; 11: No. 2, 150-160(Oct 1974).

Large crystals of WO_3 have been reduced to a composition of approximately $WO_{2.91}$ at 3 different temperatures, 950, 1000, and 1070°C. After reduction the crystals were examined by optical microscopy and transmission electron microscopy. The crystals were faulted in a variety of ways and rarely perfectly ordered. Large crystals heated at 1070°C supported oxygen loss by formation of $\{103\}$ CS planes while crystals heated at 950°C contained $\{102\}$ CS planes. At 1000°C $\{102\}$ and $\{103\}$ CS planes coexisted. It was found that the way in which the WO_3 structure accommodated oxygen loss was a function of composition and of temperature. In all experiments, some vapor transport also took place, resulting in the growth of needle shaped crystals. These were always members of the W_nO_{3n-2} homologous series of oxides, and contained $\{103\}$ CS planes, irrespective of the formation temperature. (auth)

29905 THERMODYNAMIC PROPERTIES AND MUTUAL DIFFUSION IN THE SYSTEM UC–ZrC. Fedorov, G. B.; Gusev, V. N.; Zagryazkin, V. N.; Smirnov, E. A. Sov. At. Energy (Engl. Transl.); 35: No. 4, 928-931(Oct 1973).

Translated from At. Energ. (USSR); 35: No. 4, 267-269(Oct 1973).

Data on diffusion in three-component systems incorporating one interstitial element are used to calculate the coefficients of mutual diffusion in UC–ZrC. The activities of these monocarbides are calculated using statistical thermodynamics methods. Results are presented in tables and graphs are discussed. Results show that as ZrC is added the strength of the interatomic bonds in the solid solutions in the UC–ZrC system increase. (JRD)

29906 MNOGOKOMPONENTNYE DIFFUZIONNYE POKRYTIYA. (Multicomponent Diffusion Coatings). Lyakhovich, L. S. (ed.). Minsk; Izdatel'stvo Nauka i Tekhnika (1974). 288p.

Processes and results are discussed of simultaneous diffusion penetration of steels and alloys by two or more chemical elements, which in many cases cause the formation, on the surfaces of metals, of diffusion layers whose properties surpass the quality of the layers of multicomponent saturation. Information is presented on the processes of saturation of steels and alloys by a large number of elements simultaneously with B, Si, and Al and with combinations of three elements. Methods for obtaining multicomponent coatings and their structure and properties are studied. The prospects for using mathematical planning of experiments for studies on physical-chemical processing are shown. The book is designed for scientists working in the field of protective coatings on metals and is useful for industrial workers, graduate students, and beginning workers. (tr-auth)

29907 ESR SPECTRA AND IONIC STATES IN THE SYSTEM $V_2O_5-SnO_2$. Anufrienko, V. F.; Chupina, M. A.; Kurina, L. N.; Savel'eva, N. V. (Inst. of Catalysis, Novosibirsk, USSR). Inorg. Mater. (USSR) (Engl. Transl.); 10: No. 1, 69-72(Jan 1974).

Translated from Izv. Akad. Nauk SSSR, Neorg. Mater.; 10: No. 1, 87-90(Jan 1974).

A study of the ESR spectra of the system $V_2O_5-SnO_2$ suggests the formation of microregions of bronzes for V_2O_5 doped with tin, and the formation of a solid solution of substitution for vanadium doped with SnO_2. (auth)

29908 SYNTHESIS AND MAGNETIC PROPERTIES OF SAMARIUM AND EUROPIUM TITANONIOBATES. Krylov, E. I.; Borisov, A. E.; Makurin, Yu. N.; Kasimov, G. G. (Ural Polytechnic Inst., Sverdlovsk, USSR). Inorg. Mater. (USSR) (Engl. Transl.); 10: No. 1, 58-61(Jan 1974).

Translated from Izv. Akad. Nauk SSSR, Neorg. Mater.; 10: No. 1, 74-77(Jan 1974).

Synthesis conditions, chemical analysis results, lattice parameters, and temperature dependences of the magnetic susceptibilities are given for samarium and europium titanoniobates. The graph of the magnetic susceptibility obeys the Van Vleck law between 77 and 300°K. (auth)

29909 EFFECT OF COMPLEX ADMIXTURES OF RARE-EARTH OXIDES ON SINTERING OF CERIUM DIOXIDE. Leonov, A. I.; Trusova, E. M.; Sadikova, N. S. (Inst. of Silicate Chemistry, Moscow). Inorg. Mater. (USSR) (Engl. Transl.); 10: No. 1, 55-57(Jan 1974).

Translated from Izv. Akad. Nauk SSSR, Neorg. Mater.; 10: No. 1, 71-73(Jan 1974).

The effect of complex admixtures of rare-earth oxides on sintering of cerium dioxide is investigated. They establish the additive effect of ions with similar dimensions and the same valence. Lanthanum oxide forms with matrix defects (CeO_2) microphases with a higher energy than those formed by any other rare-earth oxide. (auth)

29910 SYNTHESIS, SINTERING, AND MICROSTRUCTURE OF THE SOLID SOLUTIONS $CaO-La_2O_3$. Popil'skii, R. Ya.; Baranova, T. F.; Pankratova, V. S.; Ievleva, Zh. I.; Belyanina, R. G.; Golovkina, N. E.; Shmatko, B. A. (Moscow Chemical-Technological Inst.). Inorg. Mater. (USSR) (Engl. Transl.); 10: No. 1, 50-54(Jan 1974).

Translated from Izv. Akad. Nauk SSSR, Neorg. Mater.; 10: No. 1, 65-70(Jan 1974).

Specimens were obtained of a ceramic consisting of solid solutions of CaO in La_2O_3. The preparation procedure is based on coprecipitation of carbonates or oxalates from a mixed solution of La and Ca nitrates. The effects on the sinterability by the amount of CaO incorporated, heat treatment, pressing, and roasting conditions were investigated. (auth)

29911 SURFACE STABILIZATION AND PROPERTIES OF ZrO_2-BASED SOLID SOLUTIONS. Leonov, A. I.; Sadikova, N. S.; Trusova, E. M. (Inst. of Silicate Chemistry, Moscow). Inorg. Mater. (USSR) (Engl. Transl.); 10: No. 1, 47-49(Jan 1974).

Translated from Izv. Akad. Nauk SSSR, Neorg. Mater.; 10: No. 1, 62-64(Jan 1974).

The phenomenon of surface stabilization of cubic solid solutions ZrO_2-CaO is due to the decrease in the specific surface and (presumably) to coherent linking of microcrystals and formation of surface submicrophases. (auth)

29912 PREPARATION AND PROPERTIES OF VANADIUM MONOCARBIDE IN THE REGION OF HOMOGENEITY. .Samsonov, G. V.; Naumenko, V. Ya.; Okhremchuk, L. N.; Rud, V. M.; Lemeshko, A. M. (Inst. of Problems in Materials Science, Kiev). Inorg. Mater. (USSR) (Engl. Transl.); 10: No. 1, 39-42(Jan 1974).

Translated from Izv. Akad. Nauk SSSR, Neorg. Mater.; 10: No. 1, 52-56(Jan 1974).

Vanadium carbide phases of relatively high purity in the region of homogeneity were obtained. The character of the concentration dependences of the electrophysical properties indicates that the electronic structure of vanadium carbide is similar to that of carbides of transition metals of group IV. (auth)

29913 PHASE CHANGES IN HIGH-ALUMINA CERAMIC UNDER THE INFLUENCE OF IONIZING RADIATION. Antonova, N. P.; Kotyukov, N. S.; Medvedovskaya, E. I.; Naidenova, G. A. Inorg. Mater. (USSR) (Engl. Transl.); 10: No. 1, 99-101(Jan 1974).

Translated from Izv. Akad. Nauk SSSR, Neorg. Mater.; 10: No. 1, 122-125(Jan 1974).

Investigations of the radiation stability of various high-alumina ceramic materials reveal that the most stable ones in fluxes of ionizing radiation are the high-alumina materials 22KhS and Mikrolit M-7, which consist of α-alumina with a little vitreous phase. The high-alumina material GB-7, containing boron in the vitreous phase, does not exhibit structural changes under irradiation by doses of up to 1×10^{20} neutrons/cm^2. A dose of 2×10^{20} neutrons/cm^2 leads to crystallization of the vitreous phase. The mullite–corundum materials MG-2 and Uralit, which have admixtures of other crystalline phases in addition to the main crystalline phase of α-alumina, undergo some structural changes even after irradiation with a dose of 2×10^{19} neutrons/cm^2. The material UF-46 begins to change after irradiation with a dose of 1×10^{20} neutrons/cm^2. (auth)

29914 CONDITIONS FOR THREE-DIMENSIONAL CORRESPONDENCE IN THE HETEROEPITAXIAL GROWTH OF ZrC. Gert, L. M.; Babad-Zakhryapin, A. A.; Makhinko, V. R.; Yushina, L. R. Inorg. Mater. (USSR) (Engl. Transl.); 10: No. 1, 128-130(Jan 1974).

Translated from Izv. Akad. Nauk SSSR, Neorg. Mater.; 10: No. 1, 155-156(Jan 1974).

Thick layers of ZrC were grown on a monocrystalline Mo substrate. The effect of layer growth rate on the intrinsic texture of ZrC was determined: for growth rates of 0.3 to 1.5μ/min and a substrate temperature of 1450°C, the intrinsic texture is [110] or [110] + [100], whereas rates > 1.5μ/min result only in the [100] texture. A block pattern is present in the microstructure, with a tendency toward natural faceting which is perfected when the layer growth rate is increased. Sharp inhomogeneity is produced when a substrate temperature of 1650°C is used. (DLC)

29915 INTRINSIC DEFECT CONDUCTIVITY OF VANADIUM PENTOXIDE. Volzhenskii, D. S.; Pashkovskii, M. V.; Prokopchuk, L. F. (Lvov State Univ.). Inorg. Mater. (USSR) (Engl. Transl.); 10: No. 1, 140-141(Jan 1974).

Translated from Izv. Akad. Nauk SSSR, Neorg. Mater.; 10: No. 1, 165-166(Jan 1974).

The integral photosensitivity of V_2O_5 single crystals, grown under excess oxygen pressure, was investigated in the infrared. The photosignal vs illumination time show a sum of two exponentials, whose relaxation times agree with that for the formation of a complex from a vacancy and an interstitial O atom with electron localization, and with that for the first stage of formation of a Frenkel defect. (DLC)

29916 TEMPERATURE DEPENDENCE OF THE ELASTIC CONSTANTS OF NONSTOICHIOMETRIC ZIRCONIUM CARBIDES. Baranov, V. M.; Knyazev, V. I.; Korostin, O. S. (Moscow Engineering-Physics Inst.). Strength Mater. (USSR) (Engl. Transl.); 5: No. 9, 1074-1077(Sep 1973).

Translated from Probl. Prochnosti; 5: No. 9, 45-47(Sep 1973).

A study was made of the composition dependence (C/Zr = 0.75 to 1) and the temperature dependence (0 to 2100°C) of the elastic characteristics of ZrC_x. Young's modulus E and the Poisson ratio were used; the bulk compression modulus and Debye temperature were derived. The composition dependence indicates that the interatomic bonds become stronger as the C content increases. For temperatures below 0.5 T_m, $E = E_a - BT \exp(-T_0/T)$. When $T > 0.5\ T_m$, there is a deviation from linearity: $E = E_a - BT\exp(-T_0/T) - C\exp(-H/RT)$. H is close to the heat of formation of ZrC. Similar results were obtained for VC. (DLC)

29917 FREQUENCY CHARACTERISTICS OF ANODIC OXIDE FILMS: EFFECTS OF ANODIZATION VOLTAGE. Lee, D. N. (Inst. of Science and Tech., Seoul); Yoon, Y. K. J. Korean Nucl. Soc.; 6: No. 1, 14-22(Mar 1974).

Effects of anodization voltage on frequency characteristics of anodic oxide films on tantalum were analyzed based on the following impedance equations: $1/C_f = [\ln \omega\tau_w + P\ln(\tau_w/\tau_0)]/[C_0(1+P)\ln(\tau_w/\tau_0)]$ and $\tan\delta_f = \omega C_f R_f = \{\omega\tau_w[(\pi/2) - \tan^{-1}\omega\tau_0] + P\ln(\tau_w/\tau_0)\}/\{\omega\tau_w[\ln \omega\tau_w + P\ln(\tau_w/\tau_0)]\}$. Here R_f, C_f, and $\tan\delta_f$ are equivalent series resistance in ohm, equivalent series capacitance in farad, and dielectric loss of anodic oxide films respectively. Parameters P, τ_0, τ_w, and C_0 are defined as follows: $P = (d-w)/w$, $\tau_0 = \kappa\rho_0$, $\tau_w = \kappa\rho_w$, and $C_0 = \kappa A/d$, where d is the thickness of oxide film, w is the diffusion layer thickness, ρ_0 is the resistivity of oxide film at the interface of metal and the oxide, ρ_w is the resistivity of oxide film at intrinsic region and A is the area of the film and $\kappa = 0.0885 + 10^{-12} \times$ dielectric constant (farad/cm). It was shown that dielectric loss and frequency dependence of equivalent series capacitance decrease as anodization voltage increases. This is a consequence of the fact that the thickness of diffusion layer increases a little with increasing anodization voltage whereas the total oxide thickness is proportional to the anodization voltage. The negative deviation of measured values from the relation, $\tan\delta_f = 0.682\ \Delta C_f$, was also discussed based on the impedance equations given above. Here ΔC_f is the change in capacitance between 0.1 and 1 kHz. (12 figures) (auth)

29918 SOLUBILITY OF HYDROGEN IN VANADIUM AND NIOBIUM AT HIGH TEMPERATURES. Mazaev, A. A.; Avarbe, R. G. Izv. Akad. Nauk SSSR, Metal.; No. 3, 91-94(1974). (In Russian).

The solubility was studied at 1273 to 2273°K and pressures up to 25 atm. The solubility in both metals decreased exponentially with increase in temperature and, to a first approximation, followed the Siberts law. Thermodynamic analysis was carried out of the equilibrium in the V–H, Nb–H, and Ta–H systems. From five models it was established that the solubility of hydrogen in the systems studied may be described by three constants: frequency of oscillation of the hydrogen atoms in the metal lattice, pair energy of the Me–H interaction, and pair energy of the H–H interaction. (tr-auth)

29919 NEW USES IN TECHNOLOGY BOOST DEMAND FOR RARE EARTHS. Ind. Miner. (London); No. 82, 9-31(Jul 1974).

29920 SOME PROPERTIES OF MATERIALS OF THE SYSTEMS $Si_3N_4-ZrO_2$. Finkel'shtein, I. M. (Inst. of Problems in Materials Science, Kiev). Porosh. Met., Akad. Nauk Ukr. SSR; No. 6, 96-99(Jun 1974). (In Russian).

Results are presented of studies in some properties of materials of the system $Si_3N_4-ZrO_2$ obtained by hot casting. The properties of the materials including ultimate bending strength, compressive strength as affected by thermocycling, and thermal and heat resistance are shown. The linear thermal expansion coefficient and modulus of normal elasticity are measured. (auth)

29921 NEW ASPECT OF GRAIN GROWTH OF SOL-GEL URANIA. Suzuki, H.; Hase, T.; Iseki, T. (Tokyo Inst. of Tech.). J. Nucl. Sci. Technol. (Tokyo); 11: No. 4, 146-152(Apr 1974).

Grain growth in sol-gel urania compacts was determined as a function of temperature by observing with scanning electron microscope the fractured surface of compacts heated up to predetermined temperatures at a constant rate of heating. Rapid grain growth, unexplainable by currently accepted square or cubic growth kinetics, was observed to occur in the sintered compact when the density reached 70 to 75% T. D., which was attained at about 1000°C in the case of heating rate of 5°C/min. It was considered that this rapid grain growth proceeded by plastic flow of which driving force was the surface tension of the grains, when a large number of primary grains were closely packed against each other, i.e., arranged in quite high coordination number. A rough estimation showed that the rate of coalescence of grains was dependent on the temperature and the grain size or the surface tension of the material, and that the multi-grain-coalescence model, which was previously reported for the case of sintering of BeO, could also be applied to sol-gel urania. (auth)

29922 INITIAL-STAGE SINTERING OF SOL-GEL URANIA. Suzuki, H. (Tokyo Inst. of Tech.); Hase, T.; Hattori, T.; Nakabayashi, M. J. Nucl. Sci. Technol. (Tokyo); 11: No. 5, 208-215(May 1974).

The initial-stage sintering mechanism of hyperstoichiometric urania prepared by sol-gel process was determined in relation to temperature during constant rate heating (CRH). The urania powder used in this experiment was prepared by crushing in Ar atmosphere the microspheric gel of UO_2 obtained by sol-gel process, and reducing the resulting powder by heating in H_2 for 1 h at 500°C. The results obtained from densification measurements indicated that the initial-stage sintering proceeded in two phases governed by different shrinkage mechanisms, as follows. The sintering up to 675°C is due to a mechanism such as rearrangement of grains and/or plastic flow. Sintering at 750 to 800°C is interpreted as being controlled by uranium volume diffusion. The estimated diffusion coefficient is $D = 1.42 \times 10^{-6} \exp(-52{,}500/RT)\ cm^2/s$. This value agreed in order of magnitude with the uranium diffusion coefficients measured by other workers for hyperstoichiometric urania. (auth).

29923 STRUCTURE DETERMINATION OF BORON NITRIDE TRANSFORMED BY SHOCK COMPRESSION. Sawaoka, A.; Soma, T.; Saito, S. (Tokyo Inst. of Tech.). Jap. J. Appl. Phys.; 13: No. 5, 891-892(May 1974).

29924 NEW PHASE TRANSITIONS IN NON-STOICHIOMETRIC U_3O_{8-x} AT HIGH TEMPERATURES. I. Thermogravimetric Study. Matsui, T.; Tsuji, T.; Naito, K. (Nagoya Univ., Japan). J. Nucl. Sci. Technol. (Tokyo); 11: No. 5, 216-222(May 1974).

The phase equilibrium of non-stoichiometric U_3O_{8-x} has been studied by thermogravimetry in the range $765 \leqq T \leqq 995$°C and $10^{-4} \leqq P_{O_2} \leqq 1$ atm. The results suggest the presence of six phases within the U_3O_{8-x} phase, separated by second (or higher) order transitions. The relative partial molar free energies, enthalpies, and entropies within each of the six phases, as well as the standard free energies, enthalpies and entropies for the phase changes are calculated and compared with previous works. (auth)

29925 FABRICATION OF HIGH-DENSITY UO_2 AND $(U_{0.75}Pu_{0.25})O_2$ BY HOT PRESSING. Hart, P. E. (Battelle Pacific Northwest Labs., Richland, Wash. (USA)). J. Nucl. Mater.; 51: No. 2, 199-202(Jun 1974).

The hot pressing behavior of hyperstoichiometric UO_2 and $(U,Pu)O_2$ powders has been evaluated. Specimens with densities in excess of 99% theoretical can be fabricated with this technique at temperatures of 1000°C or less. (auth)

29926 FABRICATION OF (Pu-U) OXIDE MICROSPHERES USING AN INTERNAL GELATION METHOD. Louwrier, K. P.; Schoenherr, H. (Commission of the European Communities, Karlsruhe (F. R. Germany). European Inst. for Transuranium Elements). J. Nucl. Mater.; 51: No. 2, 232-236(Jun 1974).

The application of an internal gelation sol-gel method for the preparation of $(U,Pu)O_2$ microspheres is described. A mixture of PuO_2 sol, a concentrated denitrated uranyl nitrate solution, urea and hexamethylenetetramine are injected into a glass column containing paraffin oil and tetrachloroethylene in an upward flow. The reaction conditions for the different Pu/U ratios are given as well as the optimum washing conditions. The drying and thermal treatment of the spheres are discussed and densities and chemical compositions of the spheres are given. Some sphere cross sections are presented. (auth)

29927 EPITAXIAL GROWTH OF UO_2 THIN FILMS EVAPORATED ON NaCl SUBSTRATES WITH COLLOIDAL CENTRES. Birjega, M. I.; Popescu-Pogrion, N.; Topa, V.; Vasiliu, F. (Institutul de Fizica Atomica, Bucharest (Romania)). J. Nucl. Mater.; 51: No. 2, 261-265(Jun 1974).

There is now an accumulation of experimental results which demonstrates that alkali halide substrate imperfections such as F-centers produced by electron bombardment or x-ray irradiation enhance epitaxial orientation and structural perfection of vacuum-evaporated thin films. Some experimental results are presented which give evidence of similar effects promoted by Pb, Ag, and Na colloids in the epitaxial growth of UO_2 thin films simultaneously evaporated on freshly air-cleaved (100) surfaces of three types of NaCl substrates; pure, doped with Pb or Ag, and electrolytically colored (in order to obtain Pb, Ag, or Na colloidal centers). (auth)

29928 THE STRUCTURE OF VACUUM-EVAPORATED UO_2 THIN FILMS. Popescu-Pogrion, N.; Vasiliu, F.; Birjega, M. I. (Institutul de Fizica Atomica, Bucharest (Romania)). J. Nucl. Mater.; 51: No. 2, 255-260(Jun 1974).

A brief review of the methods used for obtaining thin polycrystalline and monocrystalline UO_2 films, by evaporation or sputtering in vacuum on alkali halide substrates, is presented. The presence of weak subsidiary reflections in the diffraction patterns of nearly epitaxial UO_2 thin films is attributed to crystallites grown in two (110) orientations, rotated 90° relative to each other. Some similarities in the growth behavior of the thin UO_2 and CaF_2 films on the NaCl substrates are outlined. Finally the mean parameters are summarized which are necessary to ensure the epitaxial growth. These are the substrate temperature between 320 and 350°C, the existence of colloidal centers (Pb°, Ag°, Na°) in the NaCl substrate, the preheating treatment of the NaCl substrate at 400°C, and the deposition rate exceeding 5 Å/s. (auth)

29929 LATTICE DEFECTS AND ATOMIC RADII IN UO_2 AND PuO_2. Blank, H. (Commission of the European Communities, Karlsruhe (F. R. Germany). European Inst. for Transuranium Elements). J. Nucl. Mater.; 51: No. 2, 269-270(Jun 1974).

Attention is drawn to the fact that any ionic model for the actinide dioxides based on ionic radii does not fit into a coherent physical picture. For example there are strong differences (by roughly a factor of two) between the melting points and the elastic constants of truly ionic compounds like NaCl and CaF_2 and oxides like MgO, UO_2, ThO_2 and PuO_2. Also, the relatively good stability of C-type sesquioxides such as Pu_2O_3 is difficult to understand in the ionic picture because in these compounds $^1/_4$ of the oxygen atoms has been removed from the fluorite-type structure with only very slight lattice distortions. This lattice could not be stable if the frame of the structure really was constituted by the large, soft, doubly charged $0^{=}$ ions, as required by the ionic model. (auth)

29930 IRRADIATION DAMAGE IN REACTION-BONDED SILICON CARBIDE. Matthews, R. B. (Atomic Energy of Canada Ltd., Pinawa, Manitoba. Whiteshell Nuclear Research Establishment). J. Nucl. Mater.; 51: No. 2, 203-208(Jun 1974).

Reaction-bonded SiC loses nearly 50% of its fracture strength when exposed to neutron irradiation. Young's modulus also decreases rapidly. The damage occurs soon after exposure and levels out with continuing exposure up to $3 \times 10^{21}\ n/cm^2$. Both α and β-SiC undergo a nearly isotropic expansion that saturates with increasing irradiation. Silicon undergoes a very small expansion and mechanical property degradation. The strength reduction in SiC is explained in terms of differential lattice expansions between SiC and Si which result in misfit strains and subsequent crack growth and critical flaw size extension. (auth)

29931 A TECHNIQUE FOR MEASURING THE DENSITY OF SMALL FRAGMENTS OF HIGH-DENSITY MATERIALS BOTH BEFORE AND AFTER IRRADIATION. Rose, K. S. B.; Williams, J.; Potts, G. (UKAEA Research Group, Harwell. Atomic

Energy Research Establishment). J. Nucl. Mater.; 51: No. 2, 195-198(Jun 1974).

A method for determining the density of small fragments of unirradiated and irradiated UO_2 to an absolute accuracy of ±0.6% using a density gradient column is described. The specimens are suspended in PTFE "carriers" and the combined specimen plus "carrier" density measured. Changes in UO_2 density of 0.08% can be detected. The method is, in principle, applicable to any solid that does not react with the liquids in the density column. The main error comes from measuring the mass of the specimen. (auth)

29932 STABILIZATION UNDER HIGH PRESSURE OF CARBIDE PHASES IN THE MOLYBDENUM: CARBON SYSTEM. Shinyaev, A. Ya.; Fedorov, V. B.; Gorshkova, L. V.; Chernov, D. B. (Inst. of Metallurgy, Moscow). Sov. Phys. - Dokl. (Engl. Transl.); 18: No. 10, 673-674(Apr 1974).

Translated from Dokl. Akad. Nauk SSSR; 212: No. 6, 1336-1338 (Oct 1973).

A study was made of the phase composition of Mo–C alloys (36 to 43 at. % C) at 1500°C and 25 kbar. In all the alloys, hexagonal η-carbide is contained after the 1500°C, 25 kbar anneal; the cubic α phase was observed only when it was present initially. Thus, it is shown that high pressure stabilizes Mo monocarbides; 25 kbar lowers the dissociation temperature of the hexagonal η carbide from 1650 to 1380°C. (DLC)

29933 PRODUCTION OF OXYGEN VACANCIES BY ELASTIC COLLISIONS IN ALKALINE EARTH OXIDES. Hughes, A. E. (UKAEA Research Group, Harwell, Eng.). J. Phys. (Paris), Colloq.; No. 9, 515-518(1973).

From 1st international conference on lattice defects in ionic crystals; Marseilles, France (2 Jul 1973).

Production of oxygen vacancies in MgO and CaO by 400-keV and 3-MeV protons was measured at approximately 15, 77, and 300°K. The stable defect production rate is substantially lower than expected according to simple knock-on radiation damage theory, and is only about a factor of two higher at low temperatures than at room temperature. No annealing of vacancies occurs when the sample is warmed up to room temperature after low-temperature irradiation, even in the presence of irradiation. It is suggested that escape of the interstitial from a critical recombination region around its vacancy is the controlling step for stable damage, and that the escape probability is highest at low temperatures. (FR)

29934 FUELED MODERATOR COMPOSITION. Johnson, P. D. (to United States Atomic Energy Commission). US Patent 3,825,499. 23 Jul 1974. Filed date 7 Jul 1959. 8p.

A method of preparing homogeneous UO_2–BeO ceramic fuel compositions is described. A solution of Be and U salts is prepared and contacted by hydroxyl ions to coprecipitate Be and U hydrous oxides. The precipitate is separated from the aqueous solution and thermally decomposed to form the homogeneous UO_2–BeO composition. (JRD)

29935 EFFECT OF ALTERED VALENT CATIONS ON OXYGEN PRESSURE OVER URANIA. Winslow, G. H. (Argonne National Lab., IL). High Temp. Sci.; 6: No. 3, 237-245(Sep 1974).

The substitution of an overall charge balance and an equilibrium relation between concentrations of altered valent cations in place of two charge balances separately written for the hyper- and hypostoichiometric regions of urania makes it possible to use the anion vacancy–anion interstitial model of nonstoichiometry to describe the observed oxygen partial pressures for oxygen/uranium ratios from the lower phase boundary to 2.1 and up to 2700°K without arbitrary changes in parameters. It is concluded that an additional process such as a structural change must be included to describe the observed pressures for oxygen/uranium ratios from 2.1 to the upper phase boundary, and that the values of $p(O_2)$ presently predicted along the lower phase boundary for $T < \sim 1850°K$ are questionable. (auth)

29936 KNUDSEN EFFUSION AND MASS SPECTROMETRIC STUDIES OF THE VAPORIZATION OF $Y_2O_3(s)$. Dissociation Energy of YO(g). Liu, M. B. (Illinois Inst. of Tech., Chicago); Wahlbeck, P. G. High Temp. Sci.; 6: No. 3, 179-189(Sep 1974).

Results from vaporization experiments agreed with the conclusion of Ackermann, Rauh, and Thorn that $Y_2O_{3-x}(s)$ vaporizes congruently with $x = 0.004 \pm 0.001$. The vapor species in equilibrium with $Y_2O_{3-x}(s)$ were identified with a Bendix time-of-flight mass spectrometer; YO(g) was found to be dominant over the species Y(g). It was concluded that the principal vaporization reaction is $Y_2O_3(s) = 2\ YO(g) + O(g)$. Measurements of the effusion rate of vapor in equilibrium with yttria were performed using a vacuum balance. For the above chemical equilibrium in a Knudsen cell, the partial pressures of YO(g) at 2342 to 2614°K also were determined from mass spectrometer intensities, using a Ag calibration procedure. From these measurements and auxiliary thermodynamic data, $D_0^\circ[YO(g)]$ was calculated and compared to other available values of $D_0^\circ[YO(g)]$. A value of 170.3 kcal is recommended. (auth)

29937 ION–BACKSCATTERING STUDY OF LiOH–TO–Li_2O CONVERSION ON A LiH SUBSTRATE. Myers, S.M. (Sandia Laboratories, Albuquerque, New Mexico 87115). J. Appl. Phys. 45: No. 10, 4320-4329 (Oct 1974).

Elastic proton backscattering has been used to study the mechanism by which LiOH corrosion layers on LiH are converted to Li_2O. The concentration–vs–depth profile was measured during vacuum anneals in the temperature range 200–280 °C, over which the conversion rate varied by two orders of magnitude. Conversion was found to proceed via two reaction fronts, one advancing from the LiH–LiOH interface, the other from the surface. Both H_2 and H_2O were evolved during the reaction. The results are interpreted in terms of H_2O being formed at both reaction fronts, and then diffusing respectively to the LiH substrate and to the surface. Water reaching the LiH substrate then reacts to produce H_2, while H_2O at the surface is released. The conversion rate on the LiH substrate is related quantitatively to the static equilibrium pressure of H_2O over a mixture of bulk LiOH and Li_2O in the absence of LiH. Values for this thermodynamic quantity have been reported in the literature. From the analysis it is concluded that H_2O formation at the reaction fronts is the rate–determining step in the conversion. The activation energy for the conversion process is 31 kcal/mole. (auth)

29938 OXIDATION OF ZrB_2, TaB_2, NbB_2, AND W_2B_5 IN ATOMIC OXYGEN AND BY ANODIC POLARIZATION. Lavrenko, V. A.; Yagupolskaya, L. N.; Kuznetsova, L. I.; Doroshenko, L. K.; Lugovskaya, E. S. (Materials Research Inst., Kiev). Oxidation Metals; 8: No. 3, 131-137(Jun 1974).

The investigated materials, both in the gas medium and in the electrolyte, were highly resistant to corrosion. The composition of the surface compounds was examined during the oxidation. High resistance to oxidation is explained by the B_2O_3 oxide. Oxidation of borides in both atomic oxygen and in 1 N H_2SO_4 takes place at comparable rates, the corrosion resistance in the two media being similar. (auth)

29939 EVALUATION OF GLANCING ANGLE X-RAY DIFFRACTION AND MeV ^{4}He BACKSCATTERING ANALYSES OF SILICIDE FORMATION. Lau, S. S. (California Inst. of Tech., Pasadena); Chu, W. K.; Mayer, J. W.; Tu, K. N. Thin Solid Films; 23: No. 2, 205-213(Sep 1974).

Nickel and palladium silicide films have been used in an evaluation of MeV-range ^{4}He backscattering, as measured by the Read x-ray camera and the Seemann–Bohlin x-ray diffractometer. Identical samples of untextured, textured and epitaxial crystalline layers have been studied by all three techniques. Backscattering spectrometry techniques give concentration ratios and silicide layer thicknesses. Glancing angle x-ray diffraction is required for positive phase identification and structural analysis. The Seemann–Bohlin diffractometer is capable of quantitative structural analysis; however, the Read camera is adequate in phase identification of silicide formation. (auth)

29940 NONLINEAR HIGH-FIELD CONDUCTIVITY IN Nb_2O_5 THIN FILMS. Lalevic, B.; Fuschillo, N.; Annamalai, N. K. (Rutgers–The State Univ., New Brunswick, NJ). Thin Solid Films; 23: No. 2, 249-256(Sep 1974).

The conduction mechanism in thin amorphous films of Nb_2O_5 with Nb counterelectrodes has been investigated for undoped films and for films doped with Nb by a low energy implantation–diffusion process occurring during sputtering of the Nb counterelectrodes. For films with evaporated electrodes, the conductance G versus the applied voltage V showed three regions: (a) an ohmic region at low fields up to a field $E_1 = 1.33 \times 10^5$ V/cm; (b) a nonlinear dependence of the form $I \propto V^m$, where $m = 3.8$, at intermediate fields; and (c) for fields $E > 1.2 \times 10^6$ V/cm an exponential dependence of G on V corresponding to the Poole–Frenkel field-assisted emission mechanism. Films with sputtered Nb electrodes exhibited ohmic regions up to a field $E_1 = 4 \times 10^4$ V/cm (where E_1 decreases with increasing sputtering voltage), a relation $G \propto V^4$ at intermediate fields up to $E = 8.3 \times 10^4$ V/cm, and then an exponential dependence of G on V corresponding to the Poole-type emission mechanism. The conductance and capacitance increased in films with sputtered Nb electrodes and were found to increase, while the thermal activation energy decreased, with increasing sputtering voltage. The above results indicate an increase of coulombic donor sites in Nb_2O_5 films as a consequence of the Nb implantation–diffusion process. (auth)

29941 STRUCTURE OF THE DOUBLE OXIDE $UMo_{10}O_{32}$. Serezhkin, V.N.; Kovba, L.M.; Trunov, V.K. (M. V. Lomonosov Moscow State University). Sov. Phys.–Crystallogr. 19: No. 2, 231-233 (Sept 1974).

Results of an x-ray diffraction investigation of the crystal structure of the double oxide $UMo_{10}O_{32}$ are presented. Interatomic distances are tabulated and structural relationship to the $\beta-UMo_2O_8$ structure is confirmed. (AIP)

Metals and Alloys

Refer also to abstracts 29294 and 30093.

Corrosion and Erosion

Refer also to abstracts 29906, 31223, and 31250.

29942 (AD-777170) THERMAL AND MECHANICAL EFFECTS ON THE CORROSION BEHAVIOR OF Ti-6Al-4V. Report for January 1971-January 1972. Dull, D. L.; Raymond, L. (Aerospace Corp., El Segundo, Calif. (USA)). 31 Mar 1974. Contract F04701-73-C-0074. 32p. (SAMSO-TR-74-73). NTIS \$3.25.

Anodic and cathodic polarization behaviors of Ti-6Al-4V were determined by potentiostatic and galvanostatic techniques in deaerated 1, 5, and 10N sulfuric acid solutions. In the active region, metallurgical processing, which included cold rolling and thermal treatment, had no effect on the corrosion behavior. It is suggested that a titanium hydride film exists on the titanium alloy surface. In the passive region, plastic deformation resulting from cold rolling increased the passive current density, whereas crystallographic texturing had no effect. The introduction of an alpha prime phase, resulting from thermal treatment, produced an additional peak in the passive region. (auth)

29943 (CONF-730230-(Absts.)) CORROSION AND CORROSION RESISTANCE. IX. Tutzing Symposium of the DECHEMA, February 26-March 1, 1973, Tutzing Castle, Starnberger Lake. (DECHEMA Deutsche Gesellschaft fuer Chemisches Apparatewesen e.V., Frankfurt am Main (F. R. Germany)). Feb 1973. 116p. (In German).

Thirty-two papers and discussions are compiled: "Corrosion Research Program", corrosion of semiconductors and semiconducting coatings on metals, kinetics of anodic oxide layers on Ta, impedance and phase displacement on passive Zr electrodes in acid solution, kinetics of anodic dissolution of Mo in aqueous and nonaqueous electrolytes, kinetics of Fe corrosion in various aqueous media, morphological studies during dissolution and refining of Fe, theory of pitting corrosion on basis of very small pits, electrochemical studies on titanium hydride, effect of H_2 gas on steel at room temperature, effect of water content on corrosion in monocarboxylic acids, effects of two phases on corrosion of Zr alloys with Zr-V example reactions between solids and gases, high-temperature corrosion of Ni and Ni-Cr alloys in a Cl_2-O_2 atmosphere, nitration of Fe and Ti, scaling of Fe in sulfur- and oxygen-containing gases, high-temperature corrosion of SiC and Si_3N_4, hot corrosion in diesel motors, corrosion of metals in alkali sulfate and V_2O_5 melts, stress corrosion of $AlZnMg_3$, effect of cathodic polarization on stress corrosion of X5CrNi189 steel, by stress corrosion of austenitic Cr-Ni steel, strength behavior of Cr-Ni steels, erosion in rapidly flowing liquids, corrosion of Ni in HCl under oxygen partial pressure and different corrosion inhibitors, inhibitors in the corrosion of Fe in NaCl solutions in O_2, protective coatings on hot galvanized steel tubes, cold condensation of anodic oxide layers on Al, vapor deposited and galvanic deposited metallic coatings, cathodic corrosion protection of Zn and Al coatings, protective behavior and complex resistance of polymer surface coatings, and compatibility of cathodic corrosion protection with protective coatings and barnacle-protective coatings on ship's hulls. (JSR)

29944 (Y-1949) ELECTROCHEMISTRY OF AQUEOUS CORROSION: URANIUM AND ITS ALLOYS. Bullock, J. S.; Brown, A. D.; Dobbins, A. G. (Oak Ridge Y-12 Plant, Tenn. (USA)). 19 Sep 1974. Contract W-7405-eng-26. 70p. Dep. NTIS \$5.45.

A literature review revealed four main points concerning U and U alloys: (1) their electrochemistry is profoundly dependent on the pH of the environment, due to participation of H^+ in many of the corrosion reactions; (2) chloride (halide) ion lowers their metal/solution potential relative to other ions (operationally, the significance of this fact is that the anodic reaction rate must be increased); (3) hydrogen charging of their surfaces changes the oxide conductivity and lowers their corrosion resistance, while adding good hydrogen recombination catalysts increases their corrosion resistance; (4) the rate of the $H^+ \rightarrow H_2$ and $O_2 \rightarrow H_2O_2$ reduction processes is highly dependent on the state of the surface. Experimental studies of the alloys of U with Zr, Ti, and Nb have been conducted in a variety of environments. Correlating these studies with literature data allowed several conclusions to be drawn concerning the corrosion of U and its alloys, as well as concerning methods of studying the corrosion. (131 references, 22 fig.) (auth)

29945 CORROSION FATIGUE STRENGTH OF A TITANIUM ALLOY AT ELEVATED TEMPERATURE. Khutyz, A. M.; Shamanin, Yu. A. Tr. Leningrad. Korablestroitel'nogo Inst.; No. 75, 129-132(1971).

A study was made of a Ti alloy with an $\alpha + \beta$ structure, alloyed with Al and Zr and having the following mechanical characteristics: $\sigma_B = 830$ Mn/m², $\sigma_{0.2} =$ Mn/m², $\delta_5 = 9\%$, $\psi = 23\%$, $a_H = 70$ N_oM/cm^2. Tests were carried out on 7.5-mm round smooth specimens with a localized fracture point, and on round specimens with an annular V-profile notch, using bending and rotation on a machine with cantilever loading. For notched specimens, the theoretical concentration coefficient $\alpha_\sigma = 4$. Rotational direction change frequency was 2000 cycles/min and tests were carried out at 20° and 90-100° in air and corrosive media over 20×10^6 cycles. The media contained (g/l tap water) NaCl 26.5, $MgCl_2$ 0.87, $MgSO_4$, $7H_2O$ 0.68, CuCl 1.1, KCl 0.73, $NaHCO_3$ 0.2, and NaBr 0.08, simulating sea water. For smooth specimens, a corrosive environment and rise in temperature to 95-100° slightly reduce the durability and life of specimens, while for notched specimens a corrosive environment markedly reduces specimen life, but a rise in temperature of the environment completely eliminates its effect. (Corrosion Abstr.)

29946 SURFACE PROTECTION IN NUCLEAR POWER PLANT. Schliesing, H.; Herms, R. Werkst. Korros.; 24: No. 6, 507-513(Jun 1973).

Coatings used in nuclear power plants are necessarily high density abrasion-resistant types with the additional requirement of being capable of decontamination from radiation. The major usage is epoxy resin coatings but in the case of steel work for safety shields, an alkali silicate/zinc dust paint is generally used. It is also recommended that hot-dip galvanized steel with a chromate surface treatment be used for general steelwork because of the ease of further coating with the specialized epoxies. (Corrosion Abstr.)

29947 STUDY OF THE CORROSION RESISTANCE OF TITANIUM ALLOYS AND SOME STEELS DURING CONDENSATION OF ALKYLPHENOL WITH FORMALDEHYDE. Yusifov, V. G.; Allakhverdieev, G. A.; Kazimov, A. M.; Agalarova, A. F.; Agadzhanov, Kh. S. Azerb. Neft. Khoz.; No. 4, 40-41(1972). (In Russian).

The corrosion resistance was determined of steels 3, AT-3, and EI-943 and Ti alloys VTZ-1, VT-14, VT1-O, OT-4, VT5, Ti + 5% Ta, and Ti + 33% Mo during alkylphenol-formaldehyde condensation, and a study was made of the influence of formalin and HCl feed conditions on corrosion behavior. Under existing operating conditions, none of the materials showed satisfactory resistance (corrosion rate 0.4-4.0 g/m² · h). However, combined feed of formalin and HCl after raising the alkylphenol to the operating temperature markedly raised the resistance of Ti alloys, which permitted a considerable increase in equipment service life without substantial changes in design or technology. (Corrosion Abstr.)

29948 REACTIONS OF BORON AND SILICON CARBIDE WITH TUNGSTEN AND TITANIUM. Dzyadykevich, Yu. V. Inorg. Mater. (USSR) (Engl. Transl.); 10: No. 1, 32-34(Jan 1974).

Translated from Izv. Akad. Nauk SSSR, Neorg. Mater.; 10: No. 1, 44-46(Jan 1974).

A comparison of the pattern of interaction of boron and silicon carbide fibers with a Ti matrix reveals the higher resistance of SiC fibers with respect to both the matrix and the substrate. An SiC coating can be recommended as a diffusion barrier in the manufacture of boron fibers. Silicon carbide fibers are suitable for strengthening titanium-based compositions during prolonged residence below 1000°C, and for brief residence periods as far as a temperature of 1300°C. (auth)

29949 KINETICS OF MOLYBDENUM-RHENIUM ALLOY OXIDATION. Vasil'eva, A. G.; Vasilevskaya, I. I.; Bibikova, V. I.; Nisel'son, L. A. Izv. Akad. Nauk SSSR, Metal.; No. 3, 230-232(1974). (In Russian).

Alloy MR-47VP was oxidized in a current of oxygen in a series of exothermic reactions, self-accelerating at temperature above 700°C. Up to 710°C, the process took place in the kinetic zone and at temperatures around 700°C, in the diffusion zone. In the oxidative roasting, the optimum temperature interval is 750-770°C. (tr-auth)

29950 STUDY ON MASS TRANSFER PHENOMENA IN THE SODIUM LOOP OF STRUCTURAL MATERIALS OF THE LIQUID

METAL FAST-BREEDER REACTOR. Ishikawajima-Harima Giho; 14: No. 3, 258-265(May 1974). (In Japanese).

In programming research and development of the liquid metal fast-breeder reactor (LMFBR), the evaluation of sodium corrosion of the structural materials is inescapable. The clarification of carbon related mass-transfer phenomena is particularly indispensable in designing the secondary system of the LMFBR. The sodium loop, for a study of material corrosion problems, was installed in 1972, and the carburization and decarburization behaviors of the test materials, i.e. ferritic $2\frac{1}{4}$ Cr−1Mo and SUS 316 steels, intended for the LMFBR's steam generator were examined first. It was shown in the $2\frac{1}{4}$ Cr−1Mo steel that decarburization in annealed specimens was much larger than that in the specimens otherwise heat-treated, i.e. normalization-tempering or stress-relieving after annealing. This phenomenon was revealed by the noticeable differences in weight loss per surface area and was confirmed by carbon content analysis into the surface of the specimens, stripped of a thin layer, after retention in the loop at 550°C for 1000 h. The detailed specifications of the testing loop are presented, together with a part of the experimental results obtained by this facility. (auth)

29951 THE STABILITY OF VANADIUM AND OF THE ALLOY V-3Ti-15Nb IN LIQUID LITHIUM AT 700°C. Borgstedt, H. U. (Kernforschungszentrum Karlsruhe (F. R. Germany). Inst. fuer Material- und Festkoerperforschung). J. Nucl. Mater.; 51: No. 2, 221-226(Jun 1974). (In German).

Unalloyed vanadium was deoxidized at 700°C in liquid lithium; deep cavities were formed in a zone 100 μm wide around grain boundaries. The alloy V-3Ti-15Nb proved to be stable against deoxidation and there was no grain-boundary attack by lithium. Both vanadium and the vanadium alloy however became carbonized, when unstabilized stainless steel was also immersed in the lithium (as was the case in these experiments). The interior of the steel capsule was observed to have become decarbonized. Lithium scarcely attacks vanadium alloys at all at 700°C, provided the transport of oxygen and carbon is prevented. (auth)

29952 AQUEOUS CORROSION TESTING OF SAMPLES OF ZIRCONIUM AND ZIRCONIUM ALLOYS. Philadelphia; American Society for Testing and Materials (1968). 8p. (ASTM-G-2-67).

A standard prescribing requirements for aqueous corrosion testing of Zr and Zr alloys for nuclear and associated applications is presented. (JRD)

29953 OXIDATION MECHANISM OF Ni_3Al CONTAINING YTTRIUM. Kuenzly, J. D.; Douglass, D. L. (Univ. of California, Los Angeles). Oxidation Metals; 8: No. 3, 139-178(Jun 1974).

Oxidation of Ni_3Al (Ni−13.2 wt % Al) with and without additions of 0.5 wt % Y was studied at 900−1200°C in air. None of the commonly accepted rate laws were followed by the kinetics. Although the weight gains of samples containing Y were consistently 10 to 20% greater than those without yttrium, the steady-state scaling rates were identical. X-ray diffraction was used to determine the kinetics of growth of the protective alpha-alumina layer. The alumina growth followed the parabolic rate law under all conditions studied. The rate-controlling transport process in alumina was enhanced diffusion of oxygen down grain boundaries. The presence of Y as nickel-rich intermetallics promoted the formation of nickel aluminate (spinel). A marked increase in scale adherence was observed for short times. At longer times, however, the outer layer of spinel and unreacted nickel oxide spalled off along with some of the inner alumina layer. Loss of adherence was caused by a complex Y−aluminum oxide which formed by the reaction of yttria and alumina. The poor scale adherence on Ni_3Al was due to the formation of voids at the alloy−oxide interface. These voids concentrated the athermal stresses above the oxide-to-metal adherence strength. The voids were produced as a result of the selective oxidation of aluminum resulting from a "Kirkendall" effect in the substrate. During the selective oxidation process, a vacancy flux directed from the matrix to the metal oxide interface resulted in a supersaturation of vacancies. Equilibrium was maintained by the condensation of excess vacancies. The presence of Y as either nickel-rich intermetallics or internal oxide prevented the voids from forming. The Y-rich particles relieved the matrix of vacancy supersaturation by providing vacancy sinks. A necessary and sufficient condition for an effective vacancy sink appears to be the presence of an incoherent boundary between particle and matrix. (32 figures, 31 references) (auth)

29954 EFFECT OF OXYGEN ON THE CORROSION OF VANADIUM AND V−20% Ti BY LIQUID LITHIUM. DeVan, J. H.; Klueh, R. L. (Oak Ridge National Lab., TN). Nucl. Technol.; 24: No. 1, 64-72(Oct 1974).

The partitioning of oxygen between liquid lithium and alpha vanadium was investigated between 600 and 1000°C. At all test temperatures, the interstitial oxygen content of the vanadium was decreased by contact with lithium, even when the lithium contained excess Li_2O. Vanadium containing as much as 2200 ppM oxygen resisted lithium attack at 815°C. Additions of oxygen to the lithium did not enhance the dissolution of vanadium. The oxygen content of V−20% Ti also was decreased by exposure to lithium at 800 and 1000°C; however, the decrease at 800°C was apparently slowed by the diffusion kinetics of oxygen in the alloy. (auth)

29955 EFFECT OF LITHIUM VAPOR ON THE STRUCTURE OF MONOCRYSTALS OF REFRACTORY METALS AND ALLOYS. Larikov, L. N.; Cherepin, V. T.; Belkov, V. M.; Vasil'ev, M. A.; Ivashchenko, Yu. N.; Isaichev, V. I.; Maksimenko, E. A. (Inst. of Metal Physics, Kiev). Fiz.-Khim. Mekh. Mater.; 10: No. 4, 34-38(1974). (In Russian).

The effect of Li vapor on the crystal structure of monocrystals of Mo, W, and alloys based on these metals was studied as a function of the crystallographic orientation and the structural state of the samples. The concentration distribution of Li on the surface and inside the materials was studied. The mechanism for the diffusion of Li was explained. (tr-auth)

29956 CORROSION OF SHEET AND WELDED JOINT SPECIMENS OF INCOLOY 825-LOW CARBON ($C \leq 0.03\%$) IN HNO_3 (HUEY) AND HF SOLUTIONS. de Gregorio, G.; Bernabai, U. (Univ., Rome). Com. Naz. Energ. Nucl., Notiz.; 20: No. 6, 45-53(Jun 1974). (In Italian).

Results of corrosion tests carried out in HNO_3 65% boiling solutions (Huey) and HF solutions on Incoloy 825-low carbon ($C \leq 0.03\%$) sheet and welded joint specimens are discussed. Knife line corrosion (KLC) has been observed in both HNO_3 and HF solutions: the influence of heat treatments on KLC and the heat treatment procedures to eliminate KLC have been investigated. (auth)

29957 STRESS CORROSION CRACKING OF ZIRCONIUM IN METHANOL−HCl SOLUTIONS. De, P. K.; Elayaperumal, K.; Balchandra, J. (Bhabha Atomic Research Centre, Bombay). Trans. Soc. Advan. Electrochem. Sci. Technol.; 5: No. 1, 15-20 (Jan 1970).

Preliminary data on the stress corrosion of cracking behavior of Kroll zirconium in a mixture of methanol and hydrochloric acid have been obtained. The results indicated the following: (1) Cold worked zirconium is resistant to stress corrosion cracking in MeOH + HCl solution under all conditions tested. Annealed samples are susceptible under most of the conditions. (2) Susceptibility of annealed zirconium was found to increase with temperature of the medium. (3) Pure methanol is not corrosive but becomes so by addition of HCl. MeOH + 0.4% HCl mixture was the most corrosive, with further addition of HCl decreasing the corrosiveness. Complete passivity is achieved when HCl concentration is greater than 2%. Specimens were found to get embrittled by the treatment. Ductility tests showed that, after exposure to the MeOH−HCl solution, ductility was decreased in the cases of annealed zirconium, the effect being greater in boiling solution, whereas it remained unaffected in the case of cold worked specimens. The observations were explained on the basis of a hydrogen embrittlement mechanism. (auth)

Preparation and Fabrication

29958 (UCID-15926) PLUTONIUM FOUNDRY PRACTICES AT THE LAWRENCE LIVERMORE LABORATORY. Rose, R. L. (California Univ., Livermore (USA). Lawrence Livermore Lab.). 22 Oct 1971. Contract W-7405-eng-48. 15p. Dep. NTIS $4.00.

Plutonium and plutonium alloys are routinely cast in the LLL plutonium foundry. Various shapes such as rods, plates, and slabs, are cast to meet LLL R&D needs, as well as the needs of other facilities with joint programs. The foundry consists of two vacuum-induction casting units, one arc-casting unit, and work boxes to facilitate all foundry operations. (auth)

29959 NUCLEATION AND GROWTH OF W FILMS EVAPORATED ON NaCl. Asselin, G. P.; Wayman, C. M. (Univ. of Illinois, Urbana). Phys. Status Solidi (a); 24: No. 2, 675-690 (16 Aug 1974).

Evaporated tungsten films deposited on vacuum- and air-cleaved NaCl substrates at 350°C follow classical thin film nucleation and growth processes. At 250°C or lower, a very high density of initial nuclei leads to an apparent monolayer-like film growth process; however, such films reach a certain thickness and "break up", after which the growth of well-defined, isolated particles occurs. In most cases, the evaporated tungsten films exhibited a strong {100} texture. The degree of texturing and the particle morphology both depend on the substrate temperature and nature (vacuum- vs air-cleaved). In all of the films observed, two phases were found:

α (bcc) and β (A15); both of these appear to be substrate-nucleated. The β-structure was observed at all substrate temperatures and conditions employed. However, on vacuum-cleaved substrates at 350°C, both the α and β phases transformed to a new phase, γ (f.c.c.), at a film thickness near 72 Å. (28 references) (auth)

29960 EFFECT OF ELECTROLYSIS CONDITIONS ON THE CURRENT EFFICIENCY OF THE DEPOSITION AND COMPOSITION OF CHROMIUM–MOLYBDENUM ALLOY. Shluger, M. A.; Shirokova, N. V. Sb. Tr., Mosk. Vech. Met. Inst.; No. 12, 460-463(1972). (In Russian).

Results are reported from a study of the electrodeposition of a Cr–Mo alloy in relation to the electrolysis conditions. Bright and semibright light-grey deposits were obtained at 40 to 70°C with current densities of 60-100 A/dm^2. (Ref. Zh.)

29961 CHEMICAL VAPOR DEPOSITION OF URANIUM AND PLUTONIUM. Crisler, L. R.; Eggerman, W. G. (to United States Atomic Energy Commission). US Patent 3,832,222. 27 Aug 1974. Filed date 27 Dec 1972. 6p.

U or Pu is deposited upon a substrate by vaporizing triscyclopentadienyluranium (IV) chloride or plutonium(III) tricyclopentadienide, heating the substrate upon which the Pu or U is to be deposited to from about 600°C to about 900°C, and contacting the vaporized compound with the heated substrate to deposit a coating of U or Pu respectively. (Official Gazette)

29962 COLD-WELD TYPE CAPSULES FOR RADIOISOTOPE PRODUCTION. Yamabayashi, H.; Shikata, E.; Masaki, N.; Okane, S. (Japan Atomic Energy Research Inst., Tokai). Nippon Genshiryoku Gakkaishi; 16: No. 5, 276-281(May 1974). (In Japanese).

Three types of Al capsules, sealed hermetically by cold-welding, were manufactured for radioisotope production in nuclear reactors. The cold-welding was performed simply by drawing the capsules through a steel die or by pressing between steel dies, thus eliminating the demerits inherent in arc-welding, currently used. The capsules thus cold-welded were submitted to airtightness and burst tests in order to ascertain the practical acceptability of the resulting-welds. It was found that the airtightness of the capsules was reliably high up to 300°C, and tests with He leak detector showed that the leak rate was below 10^{-8} atm · cc/s in more than 95% of the capsules. The burst pressure of the capsules exceeded 25 kg/cm^2 at room temperature, but decreased with rising temperature, and at 300°C it was $\frac{1}{2} \sim \frac{1}{4}$ of the room temperature value. Most of the capsules subjected to burst test broke at the position of the cold-weld. The exceptions were some of the die-press welded capsules, which ruptured in the side wall. These tests confirmed that the present method of sealing by cold-welding should be a safe and easy means of preparing capsules for radioisotope production. (auth)

29963 POROSHKOVAYA METALLURGIYA ZHAROPROCHNYKH SPLAVOV I TUGOPLAVKIKH METALLOV. (Powder Metallurgy of Heat-Resistant Alloys and Refractory Metals). Rakovskii, V. S.; Silaev, A. F.; Khodkin, V. I.; Fatkullin, O. Kh. Moscow; Metallurgiya (1974). 184p.

The principles and physico-chemical bases of some new technological processes of powder metallurgy are examined. These include the production of powders by sputtering in plasma, sputtering of melts, and shaping by pulsed heaters. The powder metallurgy of Ti, W, Cr, and their alloys and nickel-base heat-resistant alloys is discussed. Methods for the production of the initial powders and processes for forming, sintering, and processing the products with pressure are examined. (146 references) (tr-auth)

29964 MOLYBDENUM AND MOLYBDENUM ALLOY FORGINGS. Philadelphia; American Society for Testing and Materials (1974). 3p. (ASTM-B-384-74).

Specifications for semifinished shapes of Mo and Mo alloy forgings are presented. Included are unalloyed arc-cast Mo, unalloyed powder metallurgy Mo, arc-cast Mo–0.5% Te alloy, and powder metallurgy TZM. (JRD)

29965 MACROETCHING METALS AND ALLOYS. Philadelphia; American Society for Testing and Materials (1968). 17p. (ASTM-E-340-68).

A standard method for macroetching metals and alloys to reveal their macrostructure is presented. (JRD)

29966 FABRICATION PROCEDURES FOR UNALLOYED MOLYBDENUM. Moorhead, A. J.; DiStefano, J. R.; McDonald, R. E. (Oak Ridge National Lab., TN). Nucl. Technol.; 24: No. 1, 50-63(Oct 1974).

Procedures were developed to fabricate molybdenum components for a complex chemical processing system. Closed-end $3\frac{1}{8}$-in.-OD containers up to 12 in. long were back extruded using ZrO_2-coated plungers and dies, and blank preheat temperatures of 1600 to 1700°C. It was found that ductile molybdenum tubing could be prepared by careful control of process variables and removal of contamination introduced during fabrication. By using either the gas tungsten-arc or the electron-beam process, complex components were fabricated by welding. Two important factors found to minimize weld hot cracking were stress relieving and preheating of components before welding. Radial compressive tests indicated glove-box welds were superior to field welds, but there was no correlation of weld properties with cleaning procedure or strain rate. (13 fig) (auth)

29967 PREPARATION OF NEW β–W PHASES BY FILM–DEPOSITION TECHNIQUES. Kammerdiner, L.; Luo, H.L. (Department of Applied Physics and Information Science, University of California, San Diego, La Jolla, California 92037). J. Appl. Phys. 45: No. 10, 4590-4593 (Oct 1974).

By sputtering and evaporation simultaneously, β–W phases Nb_3In, Nb_3Pb, and Nb_3Tl have been prepared. Lattice constants were measured for all samples and found to increase with decreasing substrate temperatures. These values were respectively: 5.303 ± 0.002 A, 5.333 ± 0.005 A, and 5.297 ± 0.005 A. The extended range in producing unstable phases by film–deposition techniques as opposed to conventional methods is considered. (auth)

29968 VAPOR–GROWN TUNGSTEN WHISKERS INDUCED BY VACUUM DISCHARGES. Okuyama, F. (Department of Fine Measurements, Nagoya Institute of Technology, Gokiso–cho, Syowa–ku, Nagoya, Japan). J. Appl. Phys. 45: No. 10, 4239-4241 (Oct 1974).

Characteristic vapor–grown tungsten whiskers on tungsten substrates were studied by means of a field emission and a transmission electron microscope. The whisker growth was found to be induced by high–field vacuum discharges caused by tungsten oxide vapors. By transmission electron microscopy of a typical specimen, evidence was obtained that the whisker growth can be accounted for by the screw–dislocation mechanism of crystal growth. (auth)

29969 NICKEL BRAZING BELOW 1025°C OF UNTREATED INCONEL 718. Use of a Getter Makes Nickel Brazing of Inconel 718 and X-750 Below 1025°C (1875°F) as easy as Nickel Brazing of Stainless Steels in Vacuum. Christensen, J.; Roerbo, K. (Danish Atomic Energy Commission, Roskilde, Denmark). Weld. J. (N. Y.); 53: No. 10, 460s-464s(Oct 1974).

Nickel brazing of untreated Ni–Cr–Fe high temperature alloys containing reactive metals such as Ta, Ti, and Nb normally requires brazing temperatures above 1075°C and a vacuum better than 10^{-5} mm Hg. Brazing of these alloys at lower temperatures and/or at higher pressures has previously involved a time consuming pretreatment in which the oxides formed by the reactive metals are eliminated. A method is described in which the dewetting effect of these oxides is eliminated during the brazing cycle by means of a getter material, e.g. zirconium. The new process applied to Inconel 718 and X-750 and with BNi6 and BNi7 as brazing filler metals results in perfect wetting and joint filling at 1025°C under a vacuum of only 10^{-2} mm Hg. The only pretreatment necessary for Inconel 718 and X-750 is degreasing. Corrosion tests on the brazed joints in water at 290°C have shown a corrosion rate of 0.3 to 2.3 μm/year; this may be compared with heat treated and unbrazed Inconel 718 which has shown a corrosion rate of less than 0.1 μm/year. (auth)

29970 MECHANISM OF NIOBIUM PENTOXIDE REDUCTION IN AN ALUMINO–THERMAL PROCESS. Lyakishev, N. P.; Demkin, Yu. L; Bogdanov, N. A. Izv. Akad. Nauk SSSR, Metal.; No. 3, 74-76(1974). (In Russian).

X-ray and metallographic analysis confirmed the existence in the slag system $Nb_2O_5–Al_2O_3$ of the compounds $9Nb_2O_5 \cdot Al_2O_3$, $NbAlO_4$, and α-Al_2O_3. A mechanism is suggested in which the compounds are formed with a gradually decreasing niobium content. (tr-auth)

29971 JOINT REDUCTION OF NIOBIUM, ALUMINIUM, AND GERMANIUM CHLORIDES BY HYDROGEN. Petrusevich, I. V.; Nisel'son, L. A.; Kozlov, F. N.; Bogdanov, V. P.; Abramov, V. V. Izv. Akad. Nauk SSSR, Metal.; No. 3, 77-79(1974). (In Russian).

The superconducting compounds obtained in the joint reduction by hydrogen of a mixture of $NbCl_5$, $GeCl_4$, and $AlCl_3$, in a study of the isothermic cuts $(3NbCl_5 + GeCl_4) + AlCl_3$, $(5NbCl_5 + AlCl_3) + GeCl_4$, $3NbCl_5 + xAlCl_3 + (1 - x)GeCl_4$, were shown to be germanides of Nb alloyed with small (1 – 3 at. %) amounts of Al and to have transition temperatures in the superconducting state around 20–20.5°K. (tr-auth)

Properties, Structure, and Phase Studies

Refer also to abstracts 28933, 29015, 31251, and 31279.

29972 (AD-765318) FATIGUE-CRACK GROWTH OF Ti−6Al−2Cb−1Ta−0.8 Mo ALLOY IN AIR AND NATURAL SEAWATER ENVIRONMENTS. Cares, W. R.; Cooker, T. W. Jul 1973. 15p. (NRL-MR-2617). NTIS.

Studies of low-cycle fatigue-crack propagation in air and natural seawater environments were conducted on a Ti−6Al−2Nb−1Ta−0.8 Mo alloy. The effects of cathodic polarization of the alloy in seawater were evaluated. The alloy was tested as single-edge-notched, side-grooved samples in zero-to tension loading, and results were analyzed in terms of crack-tip stress-intensity parameters. The alloy showed no evidence of fatigue sensitivity to either natural seawater or to applied cathodic potential. Results are in agreement with other studies on a similar Ti−6Al−2Nb−1Ta−0.8 Mo alloy and a Ti−6Al−4V alloy of similar yield strength and fracture toughness, but are in sharp contrast to the high degree of environmental sensitivity previously exhibited by a Ti−7Al−2Nb−1Ta alloy. (GRA) (Corros. Abstr.)

29973 (AD-774890) MECHANICAL PROPERTIES OF METAL MATRIX COMPOSITES SUBJECTED TO CYCLIC TEMPERATURE CHANGES. Annual Report, 1 July 1972−30 June 1973. Wright, M. A. (Tennessee Univ., Tullahoma (USA). Space Inst.). Aug 1973. Contract N00014-71-C-0121-0003. 105p. NTIS $4.50.

The mechanical properties of 6061 aluminum reinforced with fibers of stainless steel, 34 vol % SiC, 27 vol % boron, and 45 vol % boron cross-plied 0/90 degrees, were determined in the as-received condition and after thermal fatigue. The properties included longitudinal and transverse strength and modulus, major and minor Poisson's ratio, density, and fracture toughness. It was concluded that the nature of the damage produced by exposing these materials to cyclic temperature variations consisted of voids and cracks that were solely connected with the matrix or matrix-fiber bond. (GRA)

29974 (AD-775334) FATIGUE AND IMPACT RESISTANCE OF DUAL-MATRIX BORON−ALUMINUM COMPOSITES. Final Report. Hancock, J. R.; Shaw, G. G. (Midwest Research Inst., Kansas City, Mo. (USA)). Feb 1974. Contract N00014-70-C-0212. 14p. NTIS $3.00.

The effects of a soft, plastic interface zone and of heat treatments on the axial fatigue resistance and on the Charpy impact behavior of boron−6061 aluminum composites were determined. Interfacial-microstructures and composite fatigue resistance were compared with those previously determined for current, state-of-the-art boron−6061 aluminum composites. It was concluded that (a) matrix crack-tip stresses are relatively unimportant in determining the axial fatigue resistance of boron-aluminum composites, (b) a soft, plastic interface zone will only be effective in improving fatigue resistance in composites with a high-strength metal matrix having poor toughness, and (c) phase-boundary migration into boron filaments may occur during boron−aluminum interdiffusion instead of inert-marker movement into the aluminum matrix. (auth)

29975 (AD-775359) MECHANICAL BEHAVIOR OF METAL MATRIX COMPOSITES. Final Report, 1 April 1972−30 April 1973. Scheirer, S. T.; Toth, I. J. (TRW, Inc., Cleveland, Ohio (USA)). May 1973. Contract F33615-72-C-1601. 92p. (TRW-ER-7274-9; AFML-TR-73-178). NTIS $4.00.

A study of certain factors influencing tensile, fatigue, and creep behavior in B−Al and B/SiC−Ti composite materials was performed. The effects of controlled composite imperfections (including filament spacing defects, aligned filament breakage, and improper fiber-matrix bond condition) on tensile and fatigue behavior were investigated. Fatigue behavior of B/SiC−Ti was studied for a variety of loading conditions. (GRA)

29976 (AD-776621) STRESS−VELOCITY RELATIONS FOR DISLOCATIONS IN NIOBIUM. Walson, R. P.; Birnbaum, H. K. (Illinois Univ., Urbana (USA)). Feb 1974. Contract N00014-67-A-0305-0020. 20p. NTIS $3.00.

The stress-velocity relations for screw and mixed dislocations in high-purity niobium were studied at 298 and 196°K. ETCH-pitting methods were used to reveal the dislocation positions after stress pulses in tension and compression. Attention was particularly directed towards establishing any asymmetry in the motion of dislocations on the (112). No asymmetry was observed for either screw or mixed dislocations moving on the (112). The motion at 298°K at low stresses was limited by extrinsic barriers while that at 196°K and high stresses seemed limited by intrinsic dislocation drag. (auth)

29977 (COO-2172-7) GRAIN BOUNDARY SLIDING AND STRUCTURE. Progress Report, December 1, 1973−November 30, 1974. Li, C. Y. (Cornell Univ., Ithaca, N. Y. (USA). Dept. of Materials Science and Engineering). 1 Sep 1974. Contract AT(11-1)-2172. 15p. Dep. NTIS $4.00.

Research devoted to development of concepts and methods for characterization of polycrystalline solids is reported. Results of investigations are presented on work hardening, plastic equation of state, creep, and grain boundary sliding in 316 stainless steel. (JRD)

29978 (EURFNR-1163) CREEP-RUPTURE BEHAVIOR OF THE ALLOY INCONEL 625 IN THREE DIFFERENT PRETREATMENT STATES. Schirra, M. (Kernforschungszentrum Karlsruhe (F. R. Germany). Inst. fuer Material- und Festkoerperforschung). Feb 1974. Translation of KFK-1925. 28p. Dep. NTIS $4.50.

Work performed under United States−Euratom Fast Reactor Exchange Program.

The creep and time-to-rupture behavior of the matrix hardening nickel base alloy Inconel 625 was investigated in the temperature range 650-800°C. Three different thermo-mechanical pretreatments were employed. These were hot rolled finish, annealing at 870°C, and solution treatment. The temperature range of this study is for samples which have undergone treatments well above the temperatures normally employed. The results show an anomalous stress dependence of creep and time-to-rupture at around 750°C. The reason is to be found in the very complex precipitation processes occuring while the stress is applied. The results are explained according to newer findings about precipitation in this type of alloy. (auth)

29979 (N-74-19370) INTERNAL FRICTION MEASUREMENT IN HIGH PURITY TUNGSTEN SINGLE CRYSTAL. Rieu, G. E. (National Aeronautics and Space Administration, Cleveland, Ohio (USA). Lewis Research Center). Feb 1974. 18p. (NASA-TM-X-71506; E-7882). NTIS $4.00.

Internal friction peaks observed after small deformation in high purity tungsten single crystals between liquid helium temperature and 800°K in the frequency range 30 to 50 kHz are studied as a function of orientation. An orientation effect is observed in the internal friction spectra due to the creation of internal stresses. The elementary processes related to these peaks are discussed in terms of kink generation and geometric kink motion on screw and edge dislocations in an internal stress field. (STAR)

29980 (N-74-19371) INTERNAL FRICTION PEAKS OBSERVED IN EXPLOSIVELY DEFORMED POLYCRYSTALLINE Mo, Nb, AND Cu. Rieu, G. E.; Grimes, H. H.; Romain, J. F.; DeFouquet, J. (National Aeronautics and Space Administration, Cleveland, Ohio (USA). Lewis Research Center). Jan 1974. 11p. (NASA-TM-X-71507; E-7918). NTIS $4.00.

Explosive deformation (50 kbar range) induced, in Cu, Mo, and Nb, internal friction peaks identical to those observed after large normal deformation. The variation of the peaks with pressure for Mo and Nb leads to an explanation of these processes in terms of double kink generation in screw and edge dislocations. (STAR)

29981 (NRL-Report-7780) PREVENTION AND CONTROL OF SUBCRITICAL CRACK GROWTH IN HIGH-STRENGTH METALS. Judy, R. J. Jr.; Goode, R. J. (Naval Research Lab., Washington, D. C. (USA)). 2 Aug 1974. 15p.

The integrity of structures that must operate in hostile environments depends on both the resistance to the propagation of cracks and the resistance to fracture of the structural material. Design procedures established to assure structural integrity are intended to enable designers systematically to take account of applicable parameters and their relation to various structures. The three-part Ratio Analysis Diagram (RAD) system was developed to provide an analysis technique for ascertaining the significance of fracture, stress-corrosion cracking, and sustained-load cracking in terms of the relationships of critical stress level to flaw size. (auth)

29982 (SLA-73-1121) METALLURGICAL PROCESSING AND PULSED REACTOR FUEL PERFORMANCE. Hickerson, J. P. Jr. (Sandia Labs., Albuquerque, N. Mex. (USA)). Jul 1974. Contract AT(29-1)-789. 89p. Dep. NTIS $7.50.

Because of an intermittent fracture problem with Sandia Pulsed Reactor II fuels, a study was undertaken to develop metallurgical methods for improving fuel performance. It was concluded that fatigue failure was largely responsible for fuel fractures and that changes in fuel processing were the most practical means of achieving improvement. A hot forging step was chosen for investigation. Four prototype fuel plates of depleted U−10Mo alloy were produced under contract at National Lead Company of Ohio. Two plates were fabricated by conventional casting while two were fabricated by upset forging cast cylinders to final dimensions. Test specimens cut from these plates were examined metallographically, tensile tested, fatigue tested, and Charpy impact tested. It was found that after forging tensile strength and high temperature elongation increased, fatigue properties were more consistent, and Charpy toughness increased. Furthermore, casting porosity was found to be removed by the hot working step. Mechanical property improvements could be attributed to a grain size reduction and the dispersal of grain boundary carbide networks effected by the forging operation. (auth)

29983 (WAPD-TM-1157) HYDIZ: A 2-DIMENSIONAL COMPUTER PROGRAM FOR MIGRATION OF INTERSTITIAL SOLUTES OF FINITE SOLUBILITY IN A THERMAL GRADIENT (LWBR Development Program). Marino, G. P. (Bettis Atomic Power Lab., Pittsburgh, Pa. (USA)). Jun 1974. Contract AT(36-1)-GEN-14. 44p. Dep. NTIS $5.25.

A numerical method for the calculation of solute distribution in systems of finite solubility under general 2-dimensional thermal distributions is presented. Results are compared to available experimental data; agreement is quite good to date. The method of solution is a time-explicit finite differencing technique which allows for general solute ingress rates at the specimen boundaries, finite precipitation rates of any second phase (Zr_2H_3 in the H−Zr system), and the solution of the Onsager-type flux equations required for systems containing multiple driving forces (i.e., $\vec{\nabla}C$ and $\vec{\nabla}T$ in this case). Very few parameter adjustments on the diffusivity and solubility were needed to fit theory and experiment. A problem is solved which shows that this numerical method yields the known steady-state solution which is calculable in closed form for an artificial case in which no precipitation occurs. (auth)

29984 MECHANICAL PROPERTIES OF MULTICOMPONENT ALLOYS BASED ON Ti−Al−Sn (Zr) α-SOLID SOLUTION WITH β-STABILIZING ELEMENTS. Mikheev, V. S. (Inst. of Metallurgy, Moscow). Strength Mater. (USSR) (Engl. Transl.); 5: No. 10, 1253-1256(Oct 1973).

Translated from Probl. Prochnosti; 5: No. 10, 89-92(Oct 1973).

Optimum compositions were established for high-strength, ductile multicomponent titanium alloys containing 5.5 to 7% Al, 1.5 to 2.5% Sn, 2% Mo, 2% V, 0.3-0.5% Cr, 0.10-0.20% Fe, 0.3-0.5% Si, and 0.01% of B and for alloys containing 2.5-3% Zr (without Sn) and alloyed with a total of 11-13% of the same elements. Increase in the Al content to 8.9% or the Zr content to 15% leads to an increase in the hardness to 387 and 460 HB respectively, to an increase in the strength, and to a considerable decrease in the ductile characteristics. Heat treatment has a large effect on the mechanical properties of the multicomponent titanium alloys. In the alloy containing 8.9% Al (total alloying elements 15.76%), high-temperature annealing (t = 1000°C) with subsequent quenching in water and tempering at t = 500°C increases the strength to 170 kgf/mm^2; the elongation remains unchanged, and the reduction increases by 1.9−2.7 times. (auth)

29985 LEVEL OF THE EQUICOHESIVE TEMPERATURE OF THE Mo ALLOY VM-1A IN SHORT-TIME TESTS IN VACUO. Konoplenko, V. P.; Artyukhina, L. L.; Ovsepyan, E. S.; Vinogradova, V. S. (Moscow Engineering Physics Inst.). Strength Mater. (USSR) (Engl. Transl.); 5: No. 10, 1211-1215(Oct 1973).

Translated from Probl. Prochnosti; 5: No. 10, 51-55(Oct 1973).

Under high-temperature stress conditions in vacua of 5×10^{-4} and 5×10^{-5} mm Hg, the equicohesive temperature of the alloy VM-1A (Mo−0.009% C−0.21% Zr−0.15% Ti−0.01 to 0.04% Ta) is approximately 1250°C. The reduction in the residual oxygen by preliminary triple flushing out of the chamber with argon leads to a rise in the equicohesive temperature of the alloy to approximately 1450°C. As a result of protecting the surface of the specimens with a coating of $MoSi_2$, the equicohesive temperature of the alloy in a vacuum of 5×10^{-4} mm Hg increases to more than 1500°C. The character of the failure of the alloy VM-1A is determined by the rate of growth of the microcracks formed at the surface grain boundaries, which are saturated with residual oxygen during high-temperature testing in vacuo. (auth)

29986 ADAPTATION OF METALLIC MATERIALS TO THE CONDITIONS OF UTILIZATION. Vieillard-Baron, B. (Societe Creusot-Loire, Paris). Ann. Mines; No. 5, 55-66(May 1974). (In French).

Metallic materials are often used in new and requiring conditions of utilization. Examples from nuclear, petroleum, and chemical industries show how the problems were solved by metallurgists. Producers and users have to act in concert in order to find the best compromise between the specifications and the costs. (FR)

29987 EFFECT OF SMALL ADDITIONS OF BERYLLIUM ON SOME PROPERTIES OF ALUMINUM AND THE ALUMINUM ALLOY AL11. Mezhbezher, I. L.; Militsyn, K. N. Tr. Mosk. Inst. Radiotekh., Elektron. Avtomat.; 41: 249-254(1973). (In Russian).

Results are given from a study of the effects of small additions of Be (0.05-0.4%) on the engineering and mechanical properties of Al and the Al alloy AL11 (Zn 8.6-8.8, Si 7.4-7.8, Mg 0.55-0.6%) mainly in the form of pressure castings but with mould and sand castings for comparison. Additions to the pressure-cast alloy of small amounts of Be (0.05%) increase the ultimate tensile strength (UTS) by 10-30% and stabilize its value and increase the elongation by ≥100% at room temperature. Raising the Be to 0.3-0.4% increases the UTS to 27-31 kg/mm^2, and reduces the elongation by 2-3%. Increase in the mold temperature and in the superheating of the melt of Be-containing Al increases its fluidity but somewhat decreases the linear upsetting property. The fluidity of the alloy is little affected by Be, i.e., it is slightly raised with Be ≤ 0.05%, then slightly reduced with Be 0.05−0.1%, and then effectively constant with Be ≥ 0.1%. In general, Be additions improve the surface purity of the castings. (Ref. Zh.)

29988 NIMONIC ALLOYS AND OTHER NICKEL-BASE HIGH-TEMPERATURE ALLOYS. Betterodge, W.; Heslop, J. (eds.). London; Edward Arnold (1974). 512p.

Chapters by different authors are entitled: high-temperature alloys and the aircraft gas turbine, history of the alloys, range of alloys, constitution and strengthening mechanisms, metallography and structure, heat treatment, melting and ingot casting, hot working, cold working, physical properties, short-time mechanical properties, long-time mechanical properties, castings, powder products, corrosion properties, joining, machining, analysis, testing and inspection methods, applications. (UK)

29989 CRYSTAL AND MAGNETIC STRUCTURE OF INTERMETALLIC COMPOUNDS OF THE TYPE $Th(Co_xFe_{1-x})_5$. Elemans, J. B. A. A. (Kamerlingh Onnes Laboratorium, Leiden); Buschow, K. H. J. Phys. Status Solidi (a); 24: No. 2, 393-399 (16 Aug 1974).

The series $Th(Co_xFe_{1-x})_5$ was investigated by means of neutron diffraction. All compounds investigated (x = 0, 0.2, 0.4, 0.6, and 1.0) were found to crystallize in the hexagonal $CaCu_5$ type of structure. Their lattice constants were determined at 4.2°K as well as at room temperature. It is shown that only part of these compounds are true ferromagnets. For the compounds with x = 0 and x = 0.2, antiferromagnetic components are also present, leading to a doubling of the magnetic unit cell. For all compounds investigated, the magnetic structure is given in detail. (auth)

29990 SPECIFIC HEAT IN TbZn AND HoZn COMPOUNDS. Morin, P. (CNRS, Grenoble, France); Pierre, J.; Chaussy, J. Phys. Status Solidi (a); 24: No. 2, 425-432(16 Aug 1974).

The specific heat of the CsCl-type structure equiatomic compounds TbZn and HoZn was measured between 20 and 300°K. The lattice contribution is determined on the isomorphous compound YZn. The two alloys show in the ordering range a rotation of the moments at 63°K for TbZn and at 23°K for HoZn. The transition is a first order one. The magnetic properties are explained in terms of molecular field, and the crystalline field parameters are deduced. However, a spin wave model seems to account better for the magnetic excitations of these systems. (7 figures) (auth)

29991 INTERNAL FRICTION OF POLYCRYSTALLINE Re FOLLOWING TORSIONAL DEFORMATION AT LIQUID NITROGEN TEMPERATURE. Callens-Raadschelders, M. (Rijksuniversitair Centrum Antwerpen, Mol, Belgium); De Batist, R. Phys. Status Solidi (a); 24: No. 2, 467-472(16 Aug 1974).

Aging treatments at room temperature, following deformation at liquid nitrogen temperature on a polycrystalline hcp rhenium specimen result in a partial recovery of the damping and the modulus defect, together with the introduction of a relaxation peak. The experimental observations are interpreted in terms of dislocations moving, during aging, from a position nonparallel with a Peierls valley, into a position in a Peierls valley and hence changing their behavior from string-like to double-kink generation conditioned. (auth)

29992 SYSTEMATIC CONTROL OF DOPING CHARACTERISTICS OF n-InSb BY NUCLEAR REACTIONS. Kuchar, F. (Univ., Vienna); Fantner, E.; Bauer, G. Phys. Status Solidi (a); 24: No. 2, 513-518(16 Aug 1974).

Nuclear transmutations by thermal neutrons are used to control the doping characteristics of n-InSb in a systematic way. The concentration of the produced donors is determined by an analysis of Hall effect and mobility measurements in a temperature range where ionized impurity scattering dominates. This concentration agrees very well with the additional donor concentrations calculated from the total flux of the thermal neutrons. (auth)

29993 MAGNETIC PROPERTIES OF CeBi. Bartholin, H. (Laboratoire de Magnetisme et Service National des Champs

Intenses, Grenoble, France); Florence, D.; Tcheng-si, W.; Vogt, O. Phys. Status Solidi (a); 24: No. 2, 631-636(16 Aug 1974).

Magnetization measurements are made along different crystallographic directions of cerium bismuth single crystals as a function of a high static magnetic field up to 150 kOe and temperatures between 2 and 30°K. The existence of two antiferromagnetic phases in zero magnetic field is confirmed. With magnetic fields, multiple-step magnetization behavior is observed. In the magnetic phase diagram, some particular points are found where the transition lines seem to converge. At low temperatures, a small remanent magnetization is observed. (5 figures) (auth)

29994 CHARACTERISTICS OF MOS CAPACITORS FORMED ON p-TYPE InSb. Korwin-Pawlowski, M. L.; Heasell, E. L. (Univ. of Waterloo, Ont.). Phys. Status Solidi (a); 24: No. 2, 649-(16 Aug 1974).

MOS capacitors were fabricated on p-type InSb using anodized as well as evaporated silicon monoxide layers and their C – U plots studied. It was found possible to obtain carrier accumulation or depletion at the surface, depending upon the previous chemical treatment of InSb. Surface state densities between 5×10^{10} and 5×10^{12} cm^{-2} were measured in these structures at 77°K. (auth)

29995 PRECISION CASTING OF ALLOY Ti–6Al–4V. Koni, D. M.; Lasker, M. F. pp 33-38 of Vakuum. Metallurgiya. Moscow; Izd'vo Metallurgiya (1973).

The mechanical properties and structure of the titanium alloy Ti–6Al–4V, melted and cast in vacuum induction furnaces, were investigated. The cast alloy has a combination microstructure of acicular alpha- and alpha'-phases. Alloy samples, annealed at 705°C for two hours, have a microstructure similar to the cast structure. This heat treatment gives the alloy the best heat resistance and workability and has little effect on mechanical properties. Inasmuch as the microstructure in the cast and annealed states is very similar, the strength and ductility properties of length were approximately the same. However, time and temperature of quenching to the solid solution and conditions of aging significantly influence strength and ductility. It was shown that soaking for less than 10 seconds yields a lower strength indicator. Alloy composition strongly affects mechanical properties. For example, a change in oxygen content by 0.01% can reduce or increase tensile strength by 7.03-10.54 kg/mm^2. Mechanical properties of Ti–6Al–4V castings in the cast and annealed states were analogous, with the exception of crack nucleation energy where indicators for the cast alloy were 67% higher. (Ref. Zh.)

29996 STRESS RELAXATION AND STRAIN-AGE CRACKING IN RENE 41 WELDMENTS. Franklin, J. E. (International Nickel Co., Suffern, NY); Savage, W. F. Weld, J. (N.Y.); 53: No. 9, 380-s-387-s(Sep 1974).

From 55th AWS annual meeting; Houston, TX (6 May 1974).

Electron microscopy studies show that stress relaxation behavior is influenced by gamma prime precipitation during welding and postweld heat treatment. (12 figs.) (auth)

29997 SIGN REVERSAL OF THE 4f CONTRIBUTION TO THE HYPERFINE FIELD AT Sm IN PARAMAGNETIC SAMARIUM COMPOUNDS. Malik, S. K.; Vijayaraghavan, R. (Tata Inst. of Fundamental Research, Bombay). Phys. Rev., B; 10: No. 1, 283-286(1 Jul 1974).

In paramagnetic rare-earth compounds, in the presence of an applied magnetic field, the 4f electrons produce a field at the rare-earth nuclear site, which, for the free Sm^{3+} ion, is positive at all temperatures. It is shown that because of crystal-field effects, the 4f contribution to the hyperfine field at Sm reverses its sign at one or two temperatures, unlike in the free ion. Exchange interaction between Sm^{3+} ions, in the presence of crystal fields, may induce or suppress the sign reversals in the hyperfine field. (auth)

29998 DISPERSNOUPROCHNENNYE MATERIALY. (Dispersion-Hardened Materials). Portnoi, K. I.; Babich, B. N. Uspekhi Sovremennogo Metallovedeniya. Moscow; Metallurgiya (1974). 200p.

Theoretical problems of the hardening of metals and alloys by dispersed stable inclusions of particles of refractory compounds are considered. The effect of the hardening particles on the formed structure of the dispersion-hardened alloys in the processes of deformation and thermal processing and their role in increasing the heat resistance is shown. The criteria for selecting the hardening phase and methods for introducing the particles into the matrix are discussed. Processes for obtaining the initial powdered mixtures are described along with their conversion to semifabricates. Data on the preparation, physico-mechanical properties, and use of dispersion-hardened alloys of 20 industrially important metals are described. The book is designed for scientific workers, construction people, and engineers specializing in the field of metallurgy and behavior of metals. It may be used by undergraduate and graduate students in metallurgy institutes. (43 illustrations, 33 tables, 248 references) (tr-auth)

29999 BRAZING ALLOY. Bradburn, E. H.; Tidwell, J. T. (to United States Atomic Energy Commission). US Patent 3,829,313. 13 Aug 1974. Filed date 7 Mar 1973. 4p.

An aluminum base brazing alloy for aluminum is described which is resistant to a fluorine and fluoride atmosphere containing silicon and zinc; the silicon is present as a discontinuous phase. (Official Gazette)

30000 FIELD ION MICROSCOPE OBSERVATIONS OF THE THREE-FOLD SYMMETRIC DISSOCIATION OF $\frac{1}{2}a(111)$ SCREW DISLOCATIONS IN MOLYBDENUM. Seidman, D. N.; Burke, J. J. (Cornell Univ., Ithaca, NY). Acta Met.; 22: No. 10, 1301-1314 (Oct 1974).

A field ion microscope (FIM) study has been performed of the dislocation structure which exists in the $\{222\}$ planes and environs of molybdenum specimens. The dislocation structure always consisted of three-fold symmetric dissociated $\frac{1}{2}a\langle 111\rangle$ screw dislocations which emerged normal to the $\{222\}$ planes. Employing the pulsed field evaporation technique it was shown that the dissociated dislocation structure consisted of a $ka\langle 111\rangle$ type partial screw dislocation (where k is a constant) which emerged normal to the $\{222\}$ planes and three stacking faults on the $\{110\}$ planes that intersected one another along a $\langle 111\rangle$ type direction. The three stacking faults exhibited three-fold symmetry about the $\langle 111\rangle$ type vector. This represents the first experimental observation of a three-fold symmetric dissociated $\frac{1}{2}a\langle 111\rangle$ screw dislocation in any body-centered cubic metal. The dislocation structure was produced in situ in the FIM specimen at a specimen temperature of less than 50°K as a result of the molybdenum specimen yielding to electric field induced shear stresses. It is pointed out that the observations are so far typical to the FIM and that the exact role played by the electric field induced stresses, surface image effect and the small tip size on dislocation geometry remain to be determined. (auth)

30001 DIFFUSION IN THE Mo–Ni, Mo–Fe, AND Mo–Co SYSTEMS. Heijwegen, C. P.; Rieck, G. D. (Univ. of Tech., Eindhoven, Netherlands). Acta Met.; 22: No. 10, 1269-1281 (Oct 1974).

Interdiffusion phenomena at temperatures between 800 and 1300°C have been investigated in the Mo–Ni, Mo–Fe, and Mo–Co systems using the diffusion couple technique combined with the techniques of microscopy, microprobe analysis, x-ray diffraction, and microindentation hardness testing. The layer growth of the α-solid solutions obeys the parabolic law only above 1000°C. The layer growth of the intermetallic phases δ-(MoNi) and μ-(Fe_7Mo_6) is parabolic, that in the μ-(Co_7Mo_6) phase only in incremental couples. It is shown that the diffusion coefficients of the α-solid solutions of the three binary systems are independent of concentration. Arrhenius' relation applies in all cases, and a number of Q values have been calculated. Marker experiments show that only in the α-solid solutions with Ni and Fe, the Mo atoms diffuse fastest. (auth)

30002 APPARATUS FOR STUDYING THE KINETICS OF THE LIBERATION OF INERT GASES FROM MATERIALS DURING ISOTHERMAL ANNEALING. Skorov, D. M.; Dashkovskii, A. I.; Zaluzhnyi, A. G.; Storozhuk, O. M. Sov. At. Energy (Engl. Transl.); 35: No. 4, 932-933(Oct 1973).

Translated from At. Energ. (USSR); 35: No. 4, 269-271(Oct 1973).

A description is presented of an apparatus for use in studying the kinetics of the liberation of inert gases from materials during the process of isothermal annealing. The apparatus consists of a stainless steel high-vacuum chamber with a heater made of molybdenum or tungsten wire wound on an insulating tube in which the sample to be studied is placed. A getter-ion pump, operating in the sorption mode evacuates only the chemically active gases, so that inert gases evolved from the sample in the annealing process accumulate in an active volume which is measured. Sample annealing is carried out in a vacuum of about 10^{-7} mm Hq. (JRD)

30003 INTERACTION OF TUNGSTEN WITH LIQUID ALUMINUM. Eremenko, V. N ; Antonchenko, R. V.; Dybkov, V. I.; Natanzon, Ya. V. (Inst. of Problems in Materials Science, Kiev). Dopov. Akad. Nauk Ukr. SSR, Ser. B.; No. 7, 621-623(Jul 1974). (In Ukrainian).

The process of tungsten dissolution in liquid aluminum is controlled by the rate of tungsten atoms transition through the boundary diffusive layer. Data on solubility constants of the dissolution rate and coefficients of diffusion of tungsten in liquid aluminum are obtained by the method of rotated disk at 700 to

850°C. Intermetallic layer consisting of WAl_5 grows on the boundary of tungsten with aluminum at 750 to 850°C. It has a weak adherence with tungsten. (auth)

30004 RECRYSTALLIZATION GRAIN COARSENING IN THE TUNGSTEN–NICKEL SYSTEM. Geguzin, Ya. E.; Klinchuk, Yu. I. (Kharkov State Univ.). Fiz. Metal. Metalloved.; 37: No. 5, 1099-1101(May 1974). (In Russian).

In previous works an equation was derived describing the kinetics of recrystallization. Experimental studies were made on W wires with additions of Ni in order to verify this equation. The recrystallization was made in the temperature interval from 1100 to 1400°C and the dimensions of the grains were determined by metallography. The dependence of the average grain size on the duration of the annealing was determined. The test results showed that the recrystallization kinetics were controlled by diffusion mass transfer and not by processes at the grain boundaries. The temperature dependence of the diffusion coefficient was found. (JSR)

30005 VOLUME AND TEMPERATURE DEPENDENCE OF THE ELECTRONIC TRANSPORT PROPERTIES OF FLUID ALKALIS IN THE SEMICONDUCTING RANGE. Freyland, W.; Pfeifer, H P.; Hensel, F. (Univ., Marburg, Ger.). pp 1327-1330 of Amorphous and Liquid Semiconductors. Stuke, J. (ed.). London; Taylor and Francis Ltd. (1974).

From 5th international conference on amorphous and liquid semiconductors; Garmisch-Partenkirchen, Germany (3 Sep 1973).

New experimental data are presented on the electrical conductivity (σ) of fluid potassium and cesium and on the absolute thermoelectric power (S) of cesium. Special emphasis is given to the density range where the transition from metallic to nonmetallic behavior occurs. For densities larger than 1 g/cm^3 the temperature coefficient of cesium at constant volume $[(\partial \ln \sigma)/(\partial \ln T)]_V$ is negative; it is positive for densities smaller than 1 g/cm^3 and rises up to 50 at a density of about 0.5 g/cm^3. For conductivities smaller than about 300 Ω^{-1} cm^{-1} a plot of $\ln \sigma$ versus S of cesium gives a straight line with a slope of $1.7 \times 10^{4\circ}$/V. (auth)

30006 NONEQUILIBRIUM CRYSTALLIZATION OF ALUMINUM–MOLYBDENUM ALLOYS. Dobatkin, V. I.; Sizova, R. M. (All-Union Light-Alloy Inst., Moscow). Izv. Vyssh. Ucheb. Zaved., Tsvet. Met.; No. 3, 117-120(1974). (In Russian).

Data obtained on Al–Mo alloys agree with data on Al–Cr and Al–Zr alloys and confirm the theory of nonequilibrium crystallization of alloys of peritectic systems according to the type of solid solutions, in agreement with metastable phase diagrams. (tr-auth)

30007 CO-SOLUBILITY OF NEODYMIUM AND ZINC IN SOLID MAGNESIUM. Drits, M. E.; Padezhnova, E. M.; Miklina, N. V. Izv. Akad. Nauk SSSR, Metal.; No. 3, 225-229(1974). (In Russian).

Microstructure studies were used to determine the phase composition of Mg–Nd–Zn alloys containing up to 3 wt % Nd and up to 8 wt % Zn. In equilibrium with the solid solution based on magnesium, the phases Mg_9Nd, X, Y, Z, MgZn were found. Micro x-ray-spectral analysis showed the chemical composition of the ternary phase of the Mg–Nd–Zn system to be: $X = MgNd_4Zn_5$, $Y = Mg_6Nd_2Zn_7$, $Z = Mg_2Nd_2Zn_9$. (tr-auth)

30008 EFFECT OF CARBON ON THE PLASTICITY AND NATURE OF BREAKDOWN OF POLYCRYSTAL Mo. Movchan, B. A.; Statkevich, V. N.; Malashenko, I. S. Izv. Akad. Nauk SSSR, Metal.; No. 3, 199-206(1974). (In Russian).

Based on the authors' and literature data, the effect of carbon on the nature of the breakdown and plasticity of polycrystal molybdenum at room temperature was generalized. For removal of intercrystal grains of Mo, an equilibrium structural state must be formed at the boundaries and in the volume of the grains. This is done by an equilibrium distribution of the impurities by means of a thorough purification, thermal processing, alloying, or addition of elements to form the same two-phase structure along the grain boundaries and in the matrix. The second phase in Mo shows a hardening action in the temperature interval 70 to 1500°C, simultaneously ensuring stability at a sufficiently high level of plasticity and uniform distribution of the deformation throughout the volume of the metal. (39 references) (tr-auth)

30009 EFFECT OF COLD DEFORMATION ON PHASE TRANSITION IN Ti–Nb ALLOYS. Kadykova, G. N.; Gadzoeva, M. M.; Obkhodova, T. V. Izv. Akad. Nauk SSSR, Metal.; No. 3, 165-172(1974). (In Russian).

In the process of cold deformation of hardened alloys with 25-40% Nb containing α''-phase after hardening, a body-centered tetragonal phase is formed with c/a = 1.11 for the 30% Nb alloy. The c/a ratio decreases with increasing Nb content. The body-centered tetragonal phase disappears when the material is heated to 250°C. With aging, both the hardened and the cold-deformed alloys with 25 to 40% Nb begin to form an ω–phase and then an α–phase. Cold deformation decreases the temperature of the upper limit of existence of the ω–phase and of α–phase formation and increases the amount of α–phase formed with aging. In alloys with 45 to 65% Nb, the α–phase is formed in the aging regime studied only in samples after preliminary cold deformation. (tr-auth)

30010 PSEUDOASYMMETRY OF [110] SLIP IN TUNGSTEN SINGLE CRYSTALS. Chupyatova, L. P.; Kurdyumov, V. G.; Morozova, N. P.; Pikunov, M. V.; Shishkov, V. V. (Inst. of Metallography and Physics of Metals, Moscow). Sov. Phys.–Dokl. (Engl. Transl.); 18: No. 11, 741-743(May 1974).

Translated from Dokl. Akad. Nauk SSSR; 213: No. 2, 325-328 (Nov 1973).

Experimental studies were conducted on low-purity W crystals; critical shear stresses (CSS) were estimated for the various slip systems. Results show two types of $\{110\}$ slips which differ markedly in the level of CSS. The difference in the yield points for orientations close to $|001|$ and $|011|$ can be explained by asymmetry of slip in plane $\{112\}$, and an analogous effect can also be attained for $\{110\}$ slip. However, it is shown that asymmetry of shear is not characteristic of $\{110\}$ slip. (DLC)

30011 $(\alpha \rightarrow \omega)$ TRANSITION IN TITANIUM AND ZIRCONIUM IN SHOCK WAVES. Kutsar, A. R.; German, V. N.; Nosova, G. I. (Inst. of Metallography and Physics of Metals, Moscow). Sov. Phys.–Dokl. (Engl. Transl.); 18: No. 11, 733-734(May 1974).

Translated from Dokl. Akad. Nauk SSSR; 213: No. 1, 81-84 (Nov 1973).

The $\alpha \rightarrow \omega$ transition was established in Ti and Zr in shock waves. The formation of ω phase for a compression impulse of 5 μ sec and a temperature behind the front of 200 to 300°K indicates an athermic martensitic transition. Preservation of the ω phase shows that the transition is hysteretic. (DLC)

30012 METHOD OF DETERMINING THE RELATIVE ELONGATION OF LIGHT ALLOYS CLOSE TO THE SOLIDUS ON AN IMASh-5S-65 UNIT. Boldyrev, A. M.; Dorofeev, E. B.; Tolokonnikov, N. P. (Voronezh Polytechnic Inst., USSR). Ind. Lab. (USSR) (Engl. Transl.); 40: No. 2, 270-272(Feb 1974).

Translated from Zavod. Lab.; 40: No. 2, 219-221(Feb 1974).

A method is proposed by determining the relative elongation of light alloys by heating the test material to a temperature close to the solidus and then applying a load until failure. A typical tensile chart obtained with this method is given for a Mg–Zn–Ce system alloy. The temperature relations as determined by three different metals for the same system are shown graphically and indicate that the method of determining the high-temperature ductility of a metal provides high accuracy and reproducibility of results. (JSR)

30013 EFFECT OF STRESS CONCENTRATION ON THE MECHANICAL PROPERTIES OF Mo SPECIMENS WITH A PROTECTIVE COATING IN TESTS IN AN OXIDIZING ATMOSPHERE. Zelenyuk, E. E.; Shkolyar, V. S.; Sosnovskii, L. A.; Epik, A. P. (Inst. of Problems in Strength, Kiev). Strength Mater. (USSR) (Engl. Transl.); 5: No. 9, 1087-1090(Sep 1973).

Translated from Probl. Prochnosti; 5: No. 9, 56-59(Sep 1973).

The short-term strength of smooth specimens at 800-1500°C is lower than the strength of specimens with notches. The values of the ultimate strength obtained in tests on all types of specimen in air are somewhat lower than the corresponding values obtained in vacuo. The ductility of notched specimens in tests in an oxidizing atmosphere is two or three times lower than that of smooth specimens. The nature of the $\epsilon - \tau$ relationship for smooth specimens in vacuo is similar to that in air. The value of the plastic deformation at which cracks appear in the coating depends to a large extent on the rate of plastic deformation and the temperature. The extent of plastic deformation in creep and long-term strength tests on smooth specimens in air is twice as low as in tests in vacuo, whereas for notched specimens they are practically the same. The long-term strength of coated specimens in air is practically the same as that of the base in vacuo. The long-term strength of smooth specimens tested in an oxidizing atmosphere is practically the same as that of notched specimens. (auth)

30014 EFFECT OF MICROADDITIONS OF Ni ON THE MECHANICAL PROPERTIES OF Mo AND ITS ALLOYS WITH C. Malashenko, I. S.; Statkevich, V. N.; Shchukin, A. A. (Inst. of Electric Welding, Kiev). Strength Mater. (USSR) (Engl. Transl.); 5: No. 9, 1081-1086(Sep 1973).

Translated from Probl. Prochnosti; 5: No. 9, 51-55(Sep 1973).

The temperature dependence of the strength and plasticity of unalloyed Mo, Mo–Ni, and Mo–Ni–C alloys was studied in order to determine the effect of Ni at temperatures at which deformation aging sets in. A rise in the Ni and C content results in softening upon annealing, with the maximum effect occurring at 0.03 to 0.06% Ni. Ni either increases the content of interstitial impurities (C) or facilitates the migration of C atoms in Mo. (DLC)

30015 TERNARY SYSTEM Cd–Ga–Te. Derid, O. P.; Demina, T. V.; Markus, M. M. (Kishinev Polaytechnical Inst., USSR). Inorg. Mater. (USSR) (Engl. Transl.); 10: No. 1, 11-13 (Jan 1974).

Translated from Izv. Akad. Nauk SSSR, Neorg. Mater.; 10: No. 1, 18-20(Jan 1974).

Using thermal, x-ray phase, and metallographic analyses, together with microhardness measurements of cast and annealed alloys, it is shown that the system CdTe–Ga and CdTe–GaTe are quasibinary. It was found that the system CdTe–Ga contains a degenerate eutectic with a melting point of 28°C. Solubility of the components CdTe and Ga is not observed; the system CdTe–GaTe is of the eutectic type. The eutectic contains 25 mole % CdTe and has a melting point of 785°C. The solubility of GaTe in CdTe at 785°C is < 4 mole %. (auth)

30016 SYSTEM Ce–Ge. Rustamov, P. G.; Nasibov, I. O.; Alieva, M. M. (Azerbaidzhan State Pedagogic Inst., Baku). Inorg. Mater. (USSR) (Engl. Transl.); 10: No. 1, 7-10(Jan 1974).

Translated from Izv. Akad. Nauk SSSR, Neorg. Mater.; 10: No. 1, 13-17(Jan 1974).

The system Ce–Ge phase diagram was constructed from differential thermal, x-ray, and microstructural analyses and microhardness measurements. The system contains the compounds Ce_5Ge_3, CeGe, Ce_2Ge_3, and $CeGe_2$. The compound Ce_5Ge_3 is formed by a peritectic reaction. At 600°C, $CeGe_2$ is converted from the low-temperature to the high-temperature modification. (auth)

30017 MECHANICAL PROPERTIES OF SINTERED MAGNESIUM–BERYLLIUM ALLOYS. Zelenskii, V. F.; Savchenko, V. I.; Bovkunenko, A. S. (Physical-Technical Inst., Kharkov). Porosh. Met., Akad. Nauk Ukr. SSR; No. 6, 90-95(Jun 1974). (In Russian).

Production technique and results of studies in distillation magnesium–beryllium alloys prepared by combination of distillation method and that of powder metallurgy are reported. A considerable increase in heat resistance and plasticity of these alloys as compared with the alloys obtained by hot pressing of magnesium and beryllium powders was observed. (auth)

30018 X-RAY SPECTROSCOPY ANALYSIS OF THE URANIUM 5f DISTRIBUTION IN THE METAL AND IN UO_2. Bonnelle, C.; Lachere, G. (Univ., Paris). J. Phys. (Paris); 35: No. 3, 295-299(Mar 1974). (In French).

The M(IV) and M(V) emission spectra of uranium in the metal and in UO_2 were analyzed and compared with the absorption spectra. The lines corresponding to the 5f distributions were identified and their relative intensities are discussed as functions of the cross-section for interactions of the excitation-electrons with the target, the self-absorption, and the excited state localization. The $5f^n$ states of the uranium metal were observed about 2 eV below, and the $5f^{n+1}$ < 1 eV above the Fermi level. Shifts were seen between the metal and oxide spectra. (auth)

30019 STRUCTURE AND PHASE-BOUNDARY ENERGIES OF THE DIRECTIONALLY SOLIDIFIED InSb–MnSb–NiSb, InSb–FeSb, AND InSb–CrSb EUTECTIC ALLOYS. Umehara, Y.; Koda, S. (Tokai Univ., Tokyo). Metallography; 7: No. 4, 313-331(Aug 1974).

The eutectic alloys of InSb–MSb where M is a metal of Mn, Ni, Fe, and Cr, have been directionally solidified at various rates of solidification in order to investigate the structure change due to the solidification condition, and the boundary energy between InSb and MSb phases was determined from a dislocation model of interface boundary. (auth)

30020 SOLUBILITY AND DIFFUSION OF COBALT IN INDIUM. Albrecht, W. W.; Frohberg, G.; Wever, H. (Technische Univ. Berlin (F. R. Germany). Inst. fuer Metallforschung). Z. Metallk.; 65: No. 4, 279-284(Apr 1974). (In German).

9 figs.; 14 refs.

Indium has a solubility of some 10^{-6} at. % Co at the melting point with a heat of solution of 24 kcal/mol. The solubility depends on the dislocation density. During the diffusion penetration, profiles are formed which can be explained by none of the mathematical analyses known so far. It is assumed that the dislocations are mainly responsible for the diffusion. The unknown structure of the dislocation network thus has a decisive influence on the penetration profiles. This concept is confirmed by autoradiographic exposures. For a small depth of penetration, an activation energy of 6 kcal/mol and a D_0 of 1.2×10^{-5} cm^2/sec at a dislocation density of about $10^6/cm^2$ can be calculated. (auth)

30021 HIGH-MELTING METALS AND METALLIC COMPOUNDS. Haag, H. (Starck (Herrmann C.) Berlin, Goslar (F. R. Germany). Lab. fuer Hartstoffkunde). Metall; 28: No. 7, 725-730(Jul 1974). (In German).

2 figs.; 1 tab.; 3 refs.

High-melting metals such as W, Mo, Nb, Ta and high-melting carbides, nitrides, borides, and silicides are important materials in cemented-carbide metallurgy, industry of superalloys, electronics, and nuclear industry. A survey is given on production, special properties, and applications of high-melting materials. (GE)

30022 REACTIONS OCCURRING DURING ANNEALING OF VIa AND Va METALS IN OXYGEN, WATER VAPOR, AND AIR AT LOW PRESSURES. Jehn, H. (Max-Planck-Institut fuer Metallforschung, Stuttgart (F. R. Germany). Inst. fuer Werkstoffwissenschaften). Metall; 28: No. 7, 699-705(Jul 1974). (In German).

12 figs.; 1 tab.; 64 refs.

A survey is given on the reaction during annealing of W, Mo, Ta, Nb, and V in O_2, steam, N_2, air, H_2, and CH_4 at low pressures. The metal losses of W and Mo were particularly examined and compared to the respective results for Ta and Nb. The oxygen-pickup of Ta, Nb, and V in steam is described and compared to the behavior in an oxygen atmosphere. (auth)

30023 INTER-CRYSTALLITE INTERNAL ADSORPTION IN LOW-ALLOY MOLYBDENUM. Arkharov, V. I.; Drachinskii, A. S.; Pisarenko, V. A.; Samoilenko, Z. A.; Trefilov, V. I. (Donetsk Physico-Technological Inst., USSR). Fiz. Metal. Metalloved.; 37: No. 2, 335-338(Feb 1974). (In Russian).

The alloy Mo–0.5% Ti–0.05% Zr–0.012% C was investigated by electron-microscope fractography; quantitative x-ray spectroscope, x-ray structure, and scanning electron microscope studies of fractures; and displacement of the characteristic lines of the x-ray spectrum. As a result of annealing at 1400–2000°C, the enriching material of the solid solution is fixed in the inter-crystallite zones. Tempering after annealing leads to disintegration of this material. The observed phenomena are explained from the viewpoint of the theory of intercrystallite internal adsorption. (tr-auth)

30024 DIFFRACTION OF X RAYS ON STACKING FAULTS IN METALS WITH HCP LATTICES. Shishmakov, A. S.; Mirzaev, D. A.; Khmelinin, Yu. F.; Adamesku, R. A. (Ural Polytechnic Inst., Sverdlovsk, USSR). Fiz. Metal. Metalloved.; 37: No. 2, 313-321(Feb 1974). (In Russian).

The diffraction effects from stacking faults were examined on the {1010} and (0001) planes of crystals with hcp lattices. Calculation formulas were derived for the experimental determination of the probability of deformation stacking faults. The use of this method makes it possible to obtain data on the existence of defects of both types in some metals and alloys with hcp lattices. Experimental data are provided for Co, Ti, Zr, Be, Ti–Al, and Ti–Sn. (tr-auth)

30025 SPECIFIC HEAT AND SUPERCONDUCTING PROPERTIES OF Zr–Mo ALLOYS. Yasohama, K.; Ogasawara, T. (Nihon Univ., Tokyo). J. Phys. Soc. Jap.; 36: No. 5, 1349-1355(May 1974).

The low-temperature specific heat of bcc alloys of zirconium base Zr–Mo was measured in order to investigate their superconducting properties. It was observed that the small addition of Mo to Zr results in a steep rise of the electronic specific heat coefficient γ and a decrease of the Debye temperature Θ_D. From the knowledge of γ and Θ_D the variation of the superconducting transition temperature, T_c, of zirconium with molybdenum concentration was analyzed with the McMillan theory, and it is suggested that an enhancement of T_c due to the small addition of molybdenum may be ascribed to the sharp rise of the electronic density of states at the Fermi surface. (auth)

30026 FORMATION OF A NETWORK OF SPHERICAL MICROPORES AND THE RELATION OF THIS WITH THE GK PROPERTIES OF TUNGSRAM-MADE TUNGSTEN METAL PREPARED WITH OXIDE ADDITIVES CONTAINING K, Si, AND Al. Millner, T. Acta Tech. Acad. Sci. Hung.; 75: No. 1-4, 309-319 (1973).

It is known that sintered tungsten rods prepared from tungsten powder doped with K, Si, and Al consist of large crystals, and the recrystallized wires produced therefrom also consist of long crystals, due to the 10 to 50 ppM additive traces remaining in them. Several conditions are recognizable for this large-crystal (GK) effect of which the following are the most probable. (1) Secondary β-W must be formed during the wet hydrogen reduction of doped WO_3. (2) The additive traces must contain sufficient K for producing a network of micropores filled with K vapor in the metal. (3) This must give rise to a state of internal stress. (4) The additive traces must contain a sufficient number of foreign atoms to produce a network of microdimensional foreign-phase particles, preferably of mullite ($3\ Al_2O_3 \cdot 2\ SiO_2$) or leucite ($KAlSi_2O_6$) composition. (5) Sufficient quantities of Al-containing additive traces must remain for enabling the Al atoms to decrease the probability of nucleation inside the metal fibers at recrystallization. (Hung. Tech. Abstr.).

30027 STUDY OF SOME HIGH-TEMPERATURE STRENGTH PROPERTIES OF THE NIOBIUM ALLOYS 5VMTs, 5VMTsU, AND 5VTTs AT 1100°C. Tsvilyuk, I. S.; Pyl'nikov, V. I.; Men'shikh, V. A. (Inst. of Problems of Strength, Kiev). Strength Mater. (USSR) (Engl. Transl.); 5: No. 11, 1332-1335(Nov 1973).

Translated from Probl. Prochnosti; 5: No. 11, 39-42(Nov 1973).

A comparative study of the high-temperature strength properties of niobium alloys showed that alloys 5VMTs (5.3W−2.1Mo−0.72 Zr) and 5VMTsU (4.9W−2.0Mo−1.15Zr) are superior to alloy 5VTTs (4.5W−2Ta−3.45Zr). The equations $\epsilon = A\sigma^n$ and $\tau = B\sigma^{-\beta}$ cannot represent the test results over a wide range of stresses; this fact limits the assumption previously made that the equations can be used to extrapolate the high-temperature strength properties of niobium alloys. Use of the stress dependence of the minimum creep rates to determine the conventional creep limits may in many cases lead to substantial errors. (5 figs, 3 tables) (DLC)

30028 EFFECT OF CYCLIC DEFORMATION ON THE DISLOCATION STRUCTURE AND MECHANICAL PROPERTIES OF MOLYBDENUM, CHROMIUM, AND TUNGSTEN. Kovsh, S. V.; Kotko, V. A.; Polotskii, I. G.; Prokopenko, G. I.; Trefilov, V. I.; Firstov, S. A. (Inst. of Metal Physics, Kiev). Strength Mater. (USSR) (Engl. Transl.); 5: No. 11, 1306-1311(Nov 1973).

Translated from Probl. Prochnosti; 5: No. 11, 15-20(Nov 1973).

Under the effect of elastic vibrations in Mo, a mosaic structure arises with large angles of misorientation (3−5°). The mean subgrain size is about 2 μ. Formation of misoriented mosaic structure in Mo, Cr, and W takes place upon cyclic loading with amplitudes and exposure times at which cracks due to fatigue appear. It is shown that the application of intermediate anneals up to 800°C and electrolytic polishing in order to remove the surface layer can substantially decrease the number of microcracks observed in the surface layer. The hardening achieved in molybdenum by low-frequency cyclic loading is comparable to the hardening that can be achieved by 90% plastic deformation in rolling. The yield stress of cyclically loaded samples amounts to 110−120 kg/mm^2 as compared to 50−60 kg/mm^2 in the initial state. The transition temperature to cold brittleness is lowered by 20−30°C. Cyclic loading of molybdenum samples leads to a change of the character of brittle fracture. While in the initial recrystallized state the fracture is primarily intergranular, after cyclic loading transgranular fracture was observed. (6 figs) (auth)

30029 NUCLEAR GAMMA-RESONANCE ON NUCLEI OF ^{57}Fe IMPURITY IN TUNGSTEN−RHENIUM ALLOYS. Budagovskii, S. S.; Bykov, V. N.; Gavrilyuk, M. I.; Ivanyushkin, E. M.; Rudnev, I. I.; Solov'ev, V. A. Fiz. Metal. Metalloved.; 37: No. 1, 171-173(Jan 1974). (In Russian).

The nuclear gamma-resonance spectrum of ^{57}Fe in the sigma phase of the W−Re system consists of 3 lines, the appearance of which indicates a difference in the electronic structure of the atoms occupying nonequivalent nodes in the crystal lattice of the sigma phase. The ratio of the areas under the respective lines is $S^3 : S^1 : S^2 = 4.6 : 2.3 : 1$, characteristic of the relative number of nodes in the crystalline lattice of the sigma phase. Data indicate that the electronic structure of atoms forming the sigma phase is similar to that of tungsten in the solution W−Re, but that the electronic structure close to the nodes with coordination numbers 12 and 14 differs from that of pure W and Re. (MG)

30030 STACKING FAULTS IN REFRACTORY METALS AND ALLOYS. Noskova, N. I.; Pavlov, V. A. (Inst. of Physics of Metals, Moscow). Fiz. Metal. Metalloved.; 37: No. 1, 142-147 (Jan 1974). (In Russian).

X-ray methods were used to determine the diffraction maxima (110), (200), and (211) in the field of coherent dispersion−units in strongly deformed pure metals and solid solutions. Molybdenum, tantalum, niobium, and the solid solutions Mo + Ta with Ta contents of 16.6, 34.6, and 61.4 at. % and Mo + Nb with Nb contents of 49 and 74 at. % were studied. The measured dimensions of units in pure metals agreed with literature data. Anisotropy of the dimensions of units, explained by the use of different diffraction maxima, was absent in pure Mo and insignificant in Ta and Nb. In solid solutions, the anisotropy of the dimensions of the units was greater than in pure metals. The latter may indicate a change in the stacking defect energy in the alloying. (tr-auth)

30031 MAGNETIC PROPERTIES OF ALLOYS OF THE TbCu−YCu SYSTEM. Basha, A. F.; Chechernikov, V. I.; Lisitsyn, L. M. (Moscow State Univ.). Fiz. Metal. Metalloved.; 37: No. 1, 195-198(Jan 1974). (In Russian).

The magnetic properties of the compound TbCu were studied during the replacement of Tb with Y at 77 to 300°K. Solid solutions of the TbCu−YCu system containing 30, 40, 60, and 80 at. % YCu were used. The magnetic properties were studied in both the magneto-ordered state and in the paramagnetic region. The dependence of the Curie temperature, Neel temperature, and magnetic susceptibility on the composition of the system was determined. It was established that in the systems studied, antiferromagnetic ordering occurs which is weakened with the extent of dilution. The energy state of the Tb ions does not change during this phenomenon. (JSR)

30032 ANOMALY OF THERMAL EXPANSION OF DYSPROSIUM CLOSE TO THE FERROMAGNETIC TRANSITION POINT. Petrenko, N. S.; Popov, V. P.; Finkel, V. A.; Belovol, V. S. (Gorky State Univ., USSR). Fiz. Metal. Metalloved.; 37: No. 1, 186-189(Jan 1974). (In Russian).

A hysteresis effect observed in the thermal expansion of dysprosium at phase transition was suggested to be related to the orienting action of a magnetic field directed along the axis of the sample. Measurements on dysprosium samples of 99.6 and 99.8% purity at 80°K showed a 2.6-Oe magnetic field, which confirms the theory. (MG)

30033 TYPES OF CRACKS IN W MONOCRYSTALS DEFORMED BY COMPRESSION AT 77°K. Chupyatova, L. P.; Kurdyumov, V. G.; Morozova, N. P.; Prokhorova, O. N.; Shishkov, V. V. (Central Scientific Research Inst. of Ferrous Metallurgy, Moscow). Fiz. Metal. Metalloved.; 37: No. 1, 204-206 (Jan 1974). (In Russian).

Three types of cracks are discussed briefly: cracks due to interaction of twins of one system, those due to collisions of twins of two systems, and those formed inside twin layers. (MG)

30034 STRUCTURE OF ALLOYS OF COBALT WITH RARE EARTHS OF THE APPROXIMATE COMPOSITION RCo_5. Gorbunov, V. I.; Grunau, L. M.; Potapov, N. N. (Central Scientific Research Inst. of Ferrous Metallurgy, Moscow). Fiz. Metal. Metalloved.; 37: No. 1, 119-123(Jan 1974). (In Russian).

X-ray and microstructural methods were used in studying the structure of cast and annealed alloys of Co with Ce, Sm, Gd, Er, and Y in the composition area $R_2Co_7 - RCo_5 - R_2Co_{17}$. It was shown that the structure of these alloys depends not only on the processes taking place in crystallization but also by the conversion to the solid state. (tr-auth)

30035 VARIATION OF ACTIVATION VOLUME AND ENTHALPY DURING TENSILE STRAINING OF ALPHA-URANIUM AT ROOM TEMPERATURE. Carvalhinhos, H. J.; Loureiro, P. Metalurgia (Sao Paulo); 29: No. 187, 377-384(Jun 1973). (In Portuguese).

Tensile tests demonstrated for α−U the applicability of an equation for the rate of plastic deformation in shear in a study of the variation of activation enthalpy and activation volume during constant strain rate. The apparent activation volumes provided by tests involving sudden variations in strain rate were equal for the same applied stresses and the same strains and decreased from 1.5×10^{-21} to 0.5×10^{-21} cm^3 for applied stresses >35−40 kg/mm^2 and strains >2%. The apparent activation enthalpy obtained by varying the temperature ±20°C during the constant strain rate tests was 1.06−1.07 eV for stresses > ~30 kg/mm^2. Abrupt variations in temperature during the relaxation tests revealed that the apparent activation enthalpy determined by this method is practically constant above 35−40 kg/mm^2 and equal to 1.21 ± 0.09 eV. At lower stresses the apparent activation enthalpy assumes higher values. The values of the apparent activation volume and activation enthalpy obtained for stresses >35−40 appear to be compatible with the hypothesis that the Peierls−Nabarro mechanism controls the plastic deformation of α-U under the given test conditions. (Metals Abstr.)

30036 EFFECT OF THE VOLUME DISPARTIY BETWEEN THE PRECIPITATION PHASE AND THE MATRIX ON THE SCATTERING OF X RAYS BY AGING ALLOYS. Gitgarts, M. I.; Ivashin, V. V. Sov. Phys. - Dokl. (Engl. Transl.); 18: No. 11, 744-746 (May 1974).

Translated from Dokl. Akad. Nauk SSSR; 213: No. 3, 563-566 (Nov 1973).

X-ray scattering by an aging alloy with a negative ΔV/V was studied. The alloy was industrial-grade EP199, a Ni−Cr−W−Mo−Al−Ti alloy; aging regimes at 750 to 850°C were employed. The patterns have diffuse maxima on the side of smaller scattering angles relative to the regular reflections, in agreement with theory. (DLC)

30037 FIELD-ION MICROSCOPIC STUDY OF AGED MARTENSITE IN AN IRON–NICKEL–COBALT–MOLYBDENUM ALLOY. Edneral, A. F.; Kirienko, V. I.; Potapov, L. P. (Inst. of Metallography and Metal Physics, Moscow). Sov. Phys. - Dokl. (Engl. Transl.); 18: No. 11, 747-748(May 1974).

Translated from Dokl. Akad. Nauk SSSR; 213: No. 3, 567-568 (Nov 1973).

The structure of Fe–16%Ni–15%Co–5%Mo(N16K15M5 alloy) was studied after quenching from 1000°C and aging at 440° for 16 h. A field-ion microscope with hydrogen as imaging gas was used. Results indicate that during the aging process, Mo-rich precipitates are formed, with a size between 10 and 80 Å (average 30 Å). (DLC)

30038 EFFECT OF PLASTIC DEFORMATION ON QUADRUPOLE INTERACTION IN Al, Nb, AND Au ALLOYED WITH Hf. Klyucharev, V. A.; Bozhko, V. P. (Physico-Technological Inst., Kazan). Fiz. Metal. Metalloved.; 37: No. 2, 446-448(Feb 1974). (In Russian).

Measurements of the perturbation angle of correlation showed that plastic deformation of non-ordered solid solutions of Al(Hf), Nb(Hf), and Au(Hf) crystallized in the cubic system leads to an increase in the constant of the quadrupole bond, i.e., of the effective local gradient of the electric field on the nucleus. Similar experiments showed a basic connection between the quadrupole interaction and the different types of defects in the crystal structure. (MG)

30039 STRUCTURAL CHANGES IN Mo WORKED WITH ULTRASOUND. Kotko, V. A.; Prokopenko, G. I.; Firstov, S. A. (Inst. of Metal Physics, Moscow). Fiz. Metal. Metalloved.; 37: No. 2, 444-445(Feb 1974). (In Russian).

Electron microscope studies of samples of molybdenum (type TsM-6) treated with ultrasound for 5 at 300°C showed the most significant structural changes localized in a narrow pre-surface area less than 100 μm thick. Increasing the ultrasound-treatment time to 1 min did not increase the thickness of the changed layer. The microhardness of the samples was increased by the processing, the increase in strength being related to formation of a cellular structure. (MG)

30040 STRUCTURE OF ALLOYS OF THE Nb–Ti–Zr SYSTEM. Close Order of Displacement in Solid Solutions. Tyapkin, Yu. D.; Lyasotskii, I. V.; Malienko, E. I. (Inst. of Metal Science and Physics of Metals, Moscow). Fiz. Metal. Metalloved.; 37: No. 1, 107-118(Jan 1974). (In Russian).

Diffusion distribution in Nb–Ti–Zr alloys with 50 at. % Nb, described with a presentation of fluctuating displacement waves, is related to the presence of close-order displacements characteristic of coordination of atoms in the ω-phase. Models of structures corresponding to the determined close order, which qualitatively explain the peculiarities of the observed diffusion distribution, are examined. (tr-auth)

30041 ORIENTATION RELATION BETWEEN PHASES IN $SmCo_5$–BASE ALLOYS. Magat, L. M.; Makarova, G. M.; Korotkova, M. N.; Solina, L. V. (Inst. of Physics of Metals, Moscow). Fiz. Metal. Metalloved.; 37: No. 1, 221-224(Jan 1974). (In Russian).

Data show that in the cast alloy $SmCo_5$, besides the basic phase with this composition, there is an area of varying composition enriched in Co. There are also oriented precipitates of a rhombohedral phase, Sm_2Co_7, i.e., a phase with a lower Co content. Other compositions are also suggested. (MG)

30042 IZDANIYA ZA 1970–1972 GODY IZDATEL'STVA METALLURGIYA. Annotirovannyi Ukazatel'. (Publications from 1970–1972 of the Metallurgical Publishers. Annotated Index). Starobinskaya, N. G. Moscow; Metallurgiya (1974). 199p.

An annotated index is presented of books, periodical literature, pamphlets, and other materials published by the Metallurgy Publishers. Abstracts are given for each item cited. The topics considered are general questions of metallurgy, physicochemical principles of the metallurgical industry, technology of ferrous metallurgy, technology of non-ferrous metallurgy, pressure processing of ferrous and nonferrous metals, powder metallurgy, physics of metals and metallurgy, thermal, thermomechanical, and thermochemical processing of steels and alloys, corrosion and protection of metals, methods of study and quality control of metals and alloys, equipment and automation of ferrous and nonferrous mills, thermal techniques and energetics of ferrous and nonferrous metallurgy, economics and planning of metallurgical industries, processing of scrap metal, and health care and safety techniques. (786 references) (JSR)

30043 PARAPROCESS NEAR CURIE TEMPERATURE AND CRITERIA OF APPEARANCE OF TEMPERATURE OF MAGNETIC COMPENSATION IN COMPOUNDS OF RARE EARTHS WITH IRON. Nikitin, S. A.; Bisliev, A. M. (Moscow State Univ.). Fiz. Metal. Metalloved.; 37: No. 1, 81-87(Jan 1974). (In Russian).

Using the molecular field theory, the paraprocess compounds of the heavy rare earths with iron, of the type RFe_2 and RFe_3, was studied. From the theory an equation of the type $\alpha\mu + \beta\mu^3 = H$ was derived, where μ = the magnetism and α and β are coefficients expressing through the atomic constants the exchange integrals and the temperature. The equation was satisfied in the experiment, close to the Curie temperature. The dependence of α and β on the atomic number is largely determined by the parameter ξ, which is the absolute value of the ratio of the magnetic sublattices at the Curie point. It was established that the criterion of appearance of the magnet compensation temperature is $\xi < 1$. (tr-auth)

30044 STEEL CASTINGS UP TO 2 IN. IN THICKNESS. Philadelphia; American Society for Testing and Materials (1972). 3p. (ASTM-E-446-72).

Standard reference radiographs for steel castings are presented illustrating various types and degrees of discontinuities occurring in steel castings. Methods for radiograph preparation are outlined along with procedures for radiograph evaluation. (JRD)

30045 EXPERIMENTAL, VERY HIGH-TEMPERATURE, LIQUID–URANIUM EQUATION OF STATE. Gathers, G. R.; Shaner, J. W.; Young, D. A. (Univ. of California, Livermore). Phys. Rev. Lett.; 33: No. 2, 70-72(8 Jul 1974).

U wire samples under very high confining gas pressures are heated ohmically into the liquid phase. The sample diameter is measured after achievement of thermodynamic equilibrium. Enthalpy–volume isobars and resistivity–enthalpy curves are obtained. The data are fitted with a soft-sphere theory of liquids, and the critical point of U is estimated. (auth)

30046 COMPRESSION AND ANHARMONICITY OF RARE–EARTH METALS. Reynolds, C.L. Jr.; Barker, R.E. Jr. (Department of Materials Science, University of Virginia, Charlottesville, Virginia 22901). J. Chem. Phys. 61: No. 7, 2548-2549 (1 Oct 1974).

In a recent paper Gust and Royce have presented some equation of state data and given evidence of an electronic interaction during the compression of the rare–earth metals. We have shown that their data are in agreement with an anharmonicity postulate and the coefficients in the compression equation, $-\Delta V/V_0 = a_1p + a_2p^2 + a_1p^3$, have been calculated. The anharmonicity coefficient $C_2 \equiv a_2/a_1^2$, was found to be -1.58. (auth)

30047 EXPERIMENTAL VERIFICATION OF A MODEL FOR THE MAGNETIZATION REVERSAL IN RCo_5 PARTICLES. Searle, C.W. (Air Force Materials Laboratory, Wright–Patterson Air Force Base, Ohio 45433). J. Appl. Phys. 45: No. 10, 4581-4585 (Oct 1974).

A model relating the nucleation field for RCo_5 particles (R stands for any rare–earth element) to the domain–wall energy has been refined and it now predicts some interesting experimentally observable effects. The experimental verification of the predicted effects puts the model on a strong experimental foundation. The model explains the origin of the superior magnetic properties for $SmCo_5$ particles observed at the Air Force Materials Laboratory. (auth)

30048 SUPERCONDUCTIVITY OF Nb–Al–Zr ALLOYS. Pan, V. M.; Latysheva, V. I.; Sudovtsov, A. I. (Inst. of Metal Physics, Kiev). Metallofizika; No. 50, 83-86(1974). (In Russian).

By metallographic, x-ray, and hardness analyses, a study was made on Nb–Al–Zr alloys in the Nb-rich region. The phase boundaries at 750 and 1700°C were established. The maximum solubility of zirconium in Nb_3Al is about 4 at. %. It was established that the Nb_3Al phase does not penetrate deep into the ternary system more than by 10 at. % Zr. Superconducting transition temperatures were measured in a number of ternary alloys. It is shown that additions of zirconium above 1.5 at. % decrease the critical temperature of the Nb_3Al compound. (SJR)

30049 SOLUBILITY OF TIN AND GERMANIUM IN LIQUID SODIUM. The Sodium–Tin Partial Phase Diagram. Hubberstey, P.; Pulham, R. J. (Univ. of Nottingham, Eng.). J. Chem. Soc., Dalton Trans.; No. 14, 1541-1544(1974).

The solubility of tin (up to 6.9 atom %) and of germanium (up to 1.0 atom %) in liquid sodium was determined by thermal analysis and electrical-resistance methods. The compound NaGe precipitates from dilute solutions of germanium in sodium. Partial molar enthalpies and entropies of solution in sodium for tin (with respect to $Na_{15}Sn_4$) and germanium (with respect to NaGe) are 46.8 and 44.3 kJ mol^{-1} and 50.7 and 29.7 J K^{-1} mol^{-1} respectively. A simple thermochemical cycle is used to demonstrate that metallic tin and lead dissolve exothermically in liquid sodium but that carbon dissolves endothermically; the cycle is also used to derive solvation energies for the elements Pb, Sn, and C. The sodium-tin phase diagram is augmented over the range 0 to 6.9 atom % Sn. (auth)

30050 LATTICE DYNAMICAL STUDY OF THE RECOILLESS FRACTION OF ^{57}Fe IN Ni, Mo, W, α-Fe AND Cu. Sneh. (Meerut Univ., India). Indian J. Pure Appl. Phys.; 12: No. 3, 182-184(Mar 1974).

The recoilless fraction of 14.4 keV transition of ^{57}Fe in Ni, Mo, W, α-Fe, and Cu host lattices has been calculated at different temperatures using angular force models of lattice dynamics. At high temperatures, the anharmonic contribution also has been taken into account. (auth)

30051 NATURE OF THE DEFORMATION AND FLOW OF METALS AT AND NEAR THE INTERFACE DURING ABRASION, AND ITS RELATION TO THE FRICTION. Lin, D. S.; Wilman, H. (Imperial Coll. of Science and Tech., London). Faraday Spec. Discuss. Chem. Soc.; No. 2, 46-55(1972).

From solid/solid interfaces conference; Nottingham, England (18 Sep 1972).

The direction of flow of various metals (Pb, Al, Au, Ag, 62.1 at. % Au–Ag alloy, Cu, Ni, 25.7 at. % Ni–Cu, Mo, W, U, Ti, Mg, and Zn) past the faces of a ploughing Vickers diamond pyramid of dihedral angle 136° is shown in ploughing (a) parallel to the side of the initial square indentation, (b) parallel to the diagonal, (c) in an intermediate asymmetrical direction. In all these cases, with this obtuse indenter, the metal flow at the interface is close to the direction lying in a plane through the ploughing direction, normal to the surface of the specimen. Approximate theoretical expressions are derived for the friction coefficient π for such conditions. The form of the flow past an indenter is also indicated by observations on the ploughing of macroscopic metal pyramids and cones in Plasticene built from superposed layers of different colors. Observations are also made on the widths of grooves ploughed by the diamond on various metals, compared with the width of the static indentation. These are considered in relation to the theoretical expressions and the factors which may affect the groove development. (auth)

30052 RESISTIVITY AND TCR OF ERBIUM FILMS COMPARED WITH THE PREDICTIONS OF THE COLUMNAR MODEL. Singh, B.; Ling, C. C.; Surplice, A. (Univ. of Keele, Eng.). Thin Solid Films; 23: No. 2, S50-S52(Sep 1974).

Variations of Er film resistivity as function of film thickness are presented in a diagram in which experimental data can be compared with the best fit calculated by the method of least squares. Equations are given that provide a good fit to the resistivity data and a satisfactory fit to the temperature coefficient of resistance for Er films. (JRD)

30053 REVIEW OF CURRENT STATUS OF YIELDING FRACTURE MECHANICS. Turner, C. E. (Imperial Coll. of Science and Tech., London); Burdekin, F. M. At. Energy Rev.; 12: No. 3, 439-503(1974).

Fracture mechanics can be defined as the study of fracture of materials in terms of the general laws of applied mechanics and macro-scale properties of particular materials. It is essentially concerned with the behavior of cracks in a body under stress, and with characterizing local conditions at the tip of a crack in terms of external loading and geometry, whereby the onset of fracture can be described. Many structural components may contain fabrication defects, or cracks may arise during service from fatigue, corrosion, or damage. The fitness for purpose of a flawed component may thus have to be assessed in the context of design or service of nuclear plant. Fracture mechanics is seen as a theoretical tool whereby such an assessment can be quantified. For materials that fail with extremely limited ductility, the principle of linear elasticity can be used. Such analyses of fracture behavior are termed linear elastic fracture mechanics. For many materials, however, deviations from linearity and/or elasticity occur before fracture, to an extent that may be significant, thus falling outside the range of validity of linear elastic analyses. These problems come within the field known as yielding fracture mechanics. Recent developments and the current status of treatments developed for assessing the behavior of cracks in materials which undergo various degrees of yielding before fracture are reviewed. Particular attention is given to the crack opening displacement concept, and the crack tip J contour integral method. It is concluded that these are closely related attempts to elicit a one-parameter characterization of elastic plastic crack tip stress fields; that either is a useful yardstick of the major geometric and stress level features of differing fracture circumstances for a given degree of through thickness constraint; and that as presently formulated neither are completely convincing in taking account of variations of in-plane constraint. (auth)

30054 EFFECT OF RARE EARTH METALS ON ANTIMAGNETISM OF CHROMIUM. Butylenko, A. K.; Rakitskii, A. N.; Shofman, N. L. (Inst. of Metal Physics, Kiev). Metallofizika; No. 50, 77-83(1974). (In Russian).

A study was made of the effect of rare-earth, f-transition metals on the antiferromagnetism of Cr when introducing the rare earth into Cr in amounts up to solid solution saturation. It is shown that metals of the cerium subgroup preferentially refine the chromium, and do not have any noticeable effect on the Neel point of chromium. Metals of the yttrium subgroup, on being dissolved in chromium in large amounts, somewhat raise the Neel point, and change the character of the temperature dependence curves of the electrical resistance in the region of the Neel point, but not to such a degree as the d-transition metals. (SJR)

30055 STUDY OF THE SUBSTRUCTURE OF DEFORMED AND ANNEALED SINGLE CRYSTALS OF MOLYBDENUM. Levikov, E. A.; Levikova, L. V.; Fedorova, L. I. (Inst. of Technical Physics, Kazan). Metallofizika; No. 50, 70-77(1974). (In Russian).

A study was made of the substructure of single-crystal molybdenum deformed in the (001) plane and [110] rolling direction, and of annealed single-crystal Mo by electron-microscopic and x ray analysis, and also by measuring the microhardness. It is shown that for all degrees of reduction (13 to 64%) and annealing temperatures (600 to 1000°C), there is a chaotic distribution of dislocations. The dislocation density was determined. The main increase in dislocation density takes place up to a deformation of 20%, and increases insignificantly with a further increase in degree of reduction. The continuous character of the deformation in molybdenum up to $\epsilon \sim 50\%$ was established. Annealing the samples up to 1000°C did not change the character of the distribution of dislocations, although the dislocation density decreases. (SJR)

30056 EFFECT OF TEMPERATURE AND RHENIUM IMPURITY ON THE AMPLITUDE-DEPENDENT, INTERNAL FRICTION OF TUNGSTEN. Benieva, T. Ya.; Golub, T. V. (Inst. of Metal Physics, Kiev). Metallofizika; No. 50, 59-61(1974). (In Russian).

On single crystals of tungsten and W–0.1 wt % Re, a study was made on the amplitude-temperature dependence of the internal friction. The value of the critical micro-shear-tension τ_{cr} and its temperature dependence were found for both samples. The temperature dependence for the length of dislocation segments L_c was determined. It is proposed that the observed anomaly in parameters characterizing the mobility of dislocations in W–Re is associated with a change in the temperature dependence of the degree of dislocation fastening by the impurity atoms. (SJR)

30057 ELECTRON MICROSCOPIC AND X-RAY STUDY OF THE STRUCTURE OF DEFORMED POLYCRYSTALLINE MOLYBDENUM. Kaverina, S. N.; Kotko, V. A.; Perlovich, Yu. A.; Trefilov, V. I.; Firstov, S. A. (Inst. of Metal Physics, Kiev). Metallofizika; No. 50, 40-47(1974). (In Russian).

Structural and textural studies were carried out on molybdenum of the type MT and TsM-2A over a wide range of degrees of deformation (2 to 90%) in the temperature interval of 20 to 950°C. It was found that during rolling with large reductions in the sheet, a texture is formed with prevalence of the components (001) [110] and (111) [112]. A substantial difference is noted in dimensions and shape of the cells which have been deformed in the sections corresponding to the main texture components. Regions with a (111) rolling plane are work hardened more easily than the (001) type region. An anomalous change was found in the texture and mechanical properties of molybdenum deformed at 200°C, which possibly is connected with the development of a process of dynamic deformation aging. (20 references, 8 figs.) (SJR)

30058 EFFECT OF CARBIDE-FORMING ELEMENTS ON THE PROPERTIES OF CHROMIUM AND ITS ALLOYS WITH RARE EARTHS. Rakitskii, A. N.; Trefilov, V. I. (Inst. of Metal Physics, Kiev). Metallofizika; No. 50, 31-36(1974). (In Russian).

A study was made on the effect of small additions of Ti, Zr, Hf, Nb, and Ta on the plastic properties of Cr and its rare earth alloys. It is shown that additions of Ti, Nb, and Ta in amounts of 0.2 to 0.5% decrease the transition temperature (T_x) of Cr and its La alloys. It was established that additions of carbide-forming elements noticeably increase the deformation strengthening of Cr. Annealing of deformed samples at 1100°C did not result in a significant loss in strength, while unalloyed Cr becomes completely disordered even at 900°C. Cr–La alloys containing Nb and Ta possess a sufficient reserve of plasticity in the recrystallized state. (7 figs, 28 references) (SJR)

30059 ELECTRICAL RESISTANCE AS A FUNCTION OF TEMPERATURE IN PURE AND DOPED BETA-TANTALUM

FILMS. Kushnir, A. J.; Worobey, W. (Bell Telephone Labs., Allentown, PA). Thin Solid Films; 23: No. 2, 195-203(Sep 1974).

The electrical resistance as a function of temperature has been measured for both pure and nitrogen-doped β-Ta films over the temperature range 2 to 300°K. A calibrated Auger spectroscopy system was used to analyze the film samples quantitatively for dopant and impurity concentration. The undoped film samples were prepared under conditions expected to give a high degree of purity. These samples had resistance versus temperature curves characterized by a broad maximum occurring between 100 and 250°K and a small but well-defined resistance minimum at 15°K. A resistance minimum effect in tantalum has not been reported previously. Adding nitrogen to the films by reactive sputtering tended to reduce the temperature at which the maximum occurred (in films from a given system), but did not affect the temperature of the minimum. Detailed data on the resistance minimum showed that below 10°K the resistance had a logarithmic temperature dependence, indicating the possibility of magnetic scattering (the Kondo effect). Analysis of the films for potentially magnetic impurities revealed that Fe was present in an amount between 10 and 50 ppM. (auth)

Radiation Effects

Refer also to abstracts 29070, 30481, and 31231.

30060 (AD-777433) IRRADIATION EFFECTS ON REACTOR STRUCTURAL MATERIALS. Semiannual Progress Report, 1 August 1973–31 January 1974. Steele, L. E. (Naval Research Lab., Washington, D. C. (USA)). Mar 1974. 74p. (NRL-MR-2752). NTIS $4.00.

Information is presented on (1) effect of hold-time on fatigue crack propagation in thermally aged, annealed and 25% cold-worked 304 stainless steel; (2) notch ductility retention of A543 submerged arc and electroslag weld deposits after irradiation; (3) temperature and dose rate dependence of void nucleation and growth in heavy ion bombarded nickel; (4) studies of the mobility of helium in vanadium; (5) effect of cyclotron-implanted helium on the fatigue behavior of 316 stainless steel; and (6) notch toughness of irradiated 316 stainless steel weld. (GRA)

30061 (AD-777728) STUDY OF BASIC PROCESSES IN RADIATION DAMAGE. Final Report, 1 April 1971–30 November 1973. McDonald, R. E. (Lockheed Missiles and Space Co., Palo Alto, Calif. (USA). Lockheed Palo Alto Research Lab.). 15 Apr 1974. Contract N00014-71-C-0290. 49p. (LMSC-D-401278). NTIS $3.25.

Polarized radioactive nuclei are produced and implanted in metallic and semiconductor hosts. Resonance depolarization reveals the interaction between host and implant, giving information on radiation damage, implant site location, and motion via structure in the resonance line shape. (auth)

30062 (AED-CONF-74-044-009) RADIATION DAMAGE IN REACTOR STRUCTURAL MATERIALS—FORMATION OF PORES AND ITS SIMULATION. Giesecke, P.; Jahnke, B. (Technische Univ. Darmstadt (F.R. Germany). Inst. fuer Reaktortechnik). 1974. 7p. (In German). (CONF-740340-2). INIS.

From exhibition and experts meeting on nuclear technology; Frankfurt am Main, F.R. Germany (18 Mar 1974).

2 refs.

In order to assess the "equivalence" of information about the irradiation behavior of reactor structural materials obtained by neutron and ion irradiation experiments, this review theoretically analyzes the equivalence energy, equivalence dose, equivalence temperature, and the formation of pores in various experiments. As to the ion irradiation, the advantages of implantation of low-energy ions are: (a) the same equivalence energies, for those of fast neutrons of a reactor lie below 100 keV, and (b) the neutron equivalence dose can be achieved within a few minutes. Swelling has been found to be less frequent in precipitation-hardened alloys. (GE)

30063 (AED-CONF-74-089-006) INFLUENCE OF NEUTRON IRRADIATION ON CRITICAL DATA OF TYPE II SUPERCONDUCTORS. Bauer, H.; Saur, E. J.; Schweitzer, D. G. 1974. 4p. (CONF-740451-8). INIS.

From conference on solid state physics; Freudenstadt, F.R. Germany (1 Apr 1974).

3 figs.; 5 refs. Available from ZAED.

The experiment and the results concerning critical temperatures, critical currents, lattice constants, demonstrated by six quenching curves in transverse field for Nb_3Sn diffusion wires prior to and after irradiation with thermal neutrons are described. (GE)

30064 (AED-CONF-74-089-037) DIFFERENTIAL MAGNETIC ANALYSIS OF THE RADIATION-INDUCED DIFFUSION IN NICKEL–BERYLLIUM ALLOYS. Biswanger, H.; Sizmann, R. (Kraftwerk Union A.G., Erlangen (F.R. Germany)). 1974. 5p. (In German). (CONF-740451-9). INIS.

From conference on solid state physics; Freudenstadt, F.R. Germany (1 Apr 1974).

3 figs.

The radiation-induced precipitation of beryllium out of supersaturated nickel–beryllium alloys was examined. The concentration displacements (due to irradiation with 2.5 MeV electrons) of the dissolved beryllium were individually observed as a function of the irradiation dose, the flow density, and the irradiation temperature for each concentration value. The measurement of the temperature dependence of the magnetization was carried out by a mutual induction method in an alternating magnetic field. The differential method to analyze radiation-induced diffusion processes permits the investigation of various discharging diffusion processes in which one sample is next to another but spatially separated. (GE)

30065 (BNWL-1839) INVESTIGATIONS OF THE MICROSTRUCTURE OF HEAVY ION BOMBARDED NICKEL. Brimhall, J. L. (Battelle Pacific Northwest Labs., Richland, Wash. (USA)). Jul 1974. Contract AT(45-1)-1830. 29p. Dep. NTIS $4.00.

The microstructure of pure nickel bombarded with Ni ions in the temperature range 180 to 450°C has been studied. The defect structure consists of small dislocation loops and stacking fault tetrahedra (SFT) which are of vacancy type. Large dislocation loops and dislocation fragments comprise the interstitial type damage. The small loops and SFT formed a fcc defect lattice similar to the void lattice. The preference of the vacancies to form dislocation type defects rather than voids can be related to the high displacement rate during ion bombardment. Several explanations are given for the defect lattice although no one explanation is completely adequate. (auth)

30066 (UCID-16109) ION BOMBARDMENT SIMULATION OF 14 MeV NEUTRON DAMAGE IN THIN NIOBIUM FILMS. Mohr, P. (California Univ., Livermore (USA). Lawrence Livermore Lab.). 3 Nov 1972. Contract W-7405-eng-48. 20p. Dep. NTIS $4.00.

Thin (~1000 Å) vapor-deposited foils of niobium were bombarded with Nb^+ ions in the as-deposited and annealed conditions. Ion dose range was 10^{13} to 10^{17} ions/cm^2. Bombardment temperatures ranged from 25 to 850°C. Incident ion energy was 80 to 100 keV. Examination by transmission electron microscopy of foils bombarded at the lower temperatures revealed an extremely high density of very small (< 100 Å) features believed to be interstitial loops. The range of the induced features extended 700 to 800 Å from the incident face. The apparent density increases with dose. Foils bombarded at somewhat higher temperatures (e.g., 600°C) showed a greatly reduced density of larger (100 to 1000 Å) oriented features (also believed to be interstitial in character) that appear to lie in an orthogonal array. Considerable foil growth was observed with bombardment at all temperatures. Attempts to perform mechanical properties tests on the thin unsupported niobium foils were largely unsuccessful. Sheet specimens (0.5 mm thick) bombarded on one face showed no measurable or detectable surface strain differences attributable to bombardment when strained at room temperature to the point of maximum load. (auth)

30067 POINT DEFECT CLUSTERS IN NEUTRON-IRRADIATED Mo. I. Dose Dependence of the Number Density and the Mean Diameter of Radiation-Induced Dislocation Loops. Niebel, K. (Univ., Stuttgart); Wilkens, M. Phys. Status Solidi (a); 24: No. 2, 591-600(16 Aug 1974).

Molybdenum foils with a nominal purity of 99.95% were recrystallized and degassed at 2300°C and subsequently neutron-irradiated at 80°C with six different doses between 0.5×10^{18} and 24×10^{18} fast neutrons/cm^2. The radiation damage was studied by transmission electron microscopy. The number density, n_l, and the mean diameter, $\bar{d}$, of the small dislocation loops (mainly of interstitial type) were carefully investigated. It is found that n_l and $\bar{d}$ increase with irradiation time t proportional to t^x and t^y, respectively, with $x \approx 0.27$ and $y \approx 0.185$. A modification of the time exponents due to the finite resolution of the electron microscope is discussed. (auth)

30068 DETERMINATION OF THE VELOCITY AND LOCAL DENSITY OF MOBILE DISLOCATIONS WITHIN SLIP BANDS IN NEUTRON-IRRADIATED Cu BY HIGH SPEED CINEMATOGRAPHY. Neuhaeuser, H.; Rodloff, R. (Technische Univ., Brunswick). Phys. Status Solidi (a); 24: No. 2, 549-555(16 Aug 1974).

The relation between the growth rates of slip bands in depth (S) and in length (ν_L) as resolved by high-speed cinematography on the front surface of n-irradiated Cu crystals is used to determine the mean distance d (or local mobile density) of dislocations within the moving dislocation groups. Typical values are $\nu_L = 3$ mm/s, d = 0.35 μm. The observations suggest that ν_L approximates the velocity of screw dislocations emerging from source regions near the surface. The effective free activation enthalpy ΔG deduced directly from ν_L agrees closely with the value determined indirectly from measurements of the CRSS. (auth)

30069 EFFECT OF RADIOACTIVE IRRADIATION ON THE DEGREE OF CAVITATION EROSION OF ALUMINUM. Zhidenko, G. L. Tr. Nikolaev. Korablestroit. Inst.; No. 67, 107-112(1973). (In Russian).

Determinations were made of the effects of hard γ irradiation on the cavitation erosion of Al foil specimens. Results were treated statistically to yield general relationships. The radiation lowered the level of cavitation erosion. (Ref. Zh.)

30070 ENERGY TRANSFER TO A TUNGSTEN LATTICE BY ION BOMBARDMENT. Winters, H. F.; Horne, D. (IBM Research Lab., San Jose, CA). Phys. Rev., B; 10: No. 1, 55-63 (1 Jul 1974).

The energy transferred to a tungsten lattice under bombardment by noble-gas and nitrogen ions has been measured for energies between 25 and 600 eV. A linear relationship was found between the energy transferred and the initial kinetic energy over the entire range for Xe^+ and Kr^+ and between 150 and 600 eV for N_2^+ and 75 to 600 eV for He^+. A nonlinear relationship was found for Ne^+ and Ar^+ over most of the energy range. The fractional energy transferred was found to be between 0.4 and 0.6 for all gases measured. It is shown that the experimental data can be qualitatively explained on the basis of the binary-collision model. (auth)

30071 EFFECT OF ELECTRON-BEAM REMELTING ON THE HIGH-TEMPERATURE DUCTILITY OF STEEL 1Kh18N10T IRRADIATED WITH AN INTEGRATED FLUX OF $2.7 \cdot 10^{21}$ NEUTRONS/CM^2. Vorob'ev, A. N.; Bykov, V. N.; Belomyttsev, Yu. S.; Dmitriev, V. D.; Smelova, M. E. Sov. At. Energy (Engl. Transl.); 35: No. 4, 934-935(Oct 1973).

Translated from At. Energ. (USSR); 35: No. 4, 271-272(Oct 1973).

Results show that 1Kh18N10T steel may be obtained in a state in which it is not subject to high-temperature embrittlement on irradiation with an integrated neutron flux of 2.7×10^{21} neutrons/cm^2. The quantity of nuclear reaction products (helium, lithium, and hydrogen) formed in electron-beam melted 1Kh18N10T steel by irradiation with an integrated neutron flux of 2.7×10^{21} neutrons/cm^2 is insufficient to produce high-temperature embrittlement. (auth)

30072 EFFECT OF INTENSE REACTOR IRRADIATION ON THE SHEAR MODULUS AND VISCOSITY OF IRON. Grinik, E. U.; Efimov, A. I.; Karasev, V. S.; Landsman, V. S.; Paliokha, M. I. Sov. At. Energy (Engl. Transl.); 34: No. 5, 487-489(May 1973).

Translated from At. Energ. (USSR); 34: No. 5, 397-399(May 1973).

Reactor radiation effects on Fe during irradiation at $\sim 2.2 \times 10^{20}$ n/cm^2 were investigated. It was found that the grain-boundary maximum of iron's viscosity decreases when the integral neutron flux increases and when the flux is $\sim 0.5 \times 10^{20}$ n cm^{-2}, it degenerates into an inflection point. This phenomenon, as with the shear-modulus variation, is caused by the increased density of accumulations of radiation defects which decrease the grain-boundary slip. Further change in the viscosity near the grain-boundary relaxation temperatures is related to change of the high-temperature viscosity background (no peak arises for the grain-boundary relaxation). (auth)

30073 STRESS-RUPTURE PROPERTIES OF HELIUM-INJECTED ZIRCALOY-4. Furuta, T.; Kawasaki, S. (Japan Atomic Energy Research Inst., Tokai). J. Nucl. Sci. Technol. (Tokyo); 11: No. 6, 268-269(Jun 1974).

30074 EFFECTS OF LOW TEMPERATURE IRRADIATION WITH HEAVY IONS ON SUPERCONDUCTOR NIOBIUM. Klaumuenzer, S.; Ischenko, G.; Mueller, P. (Erlangen-Nuernberg Univ., Erlangen (F. R. Germany). Physikalisches Inst.). Z. Phys.; 268: No. 2, 189-196(Jun 1974).

7 figs.; 2 tabs.; 20 refs.

To study the effects of heavy ion irradiation at low temperature on the type II superconductor Nb, the transition temperature T_c, the normal state residual resistivity ρ_B, and the transition width ΔT_{ph} using oxygen ions of 25 MeV and subsequent thermal annealing were measured. The samples were held at temperatures <20°K during irradiation in a cryostat for in situ measurements. The maximum oxygen fluence was about 2×10^{15} cm^{-2} corresponding a relatively high defect concentration. The critical temperature decreases with increasing residual resistivity. The gap anisotropy parameter is $\langle a^2 \rangle = 0.008$, subsequent annealing shows a hysteresis of T_c versus ρ_B. The resistivity saturation value $\Delta\rho_{BS} = 2.55$ ηω cm was obtained and different recovery stages were found. Significant broadening of transition width during irradiation was observed. T_c and ΔT_{ph} anneal to 60% in the temperature interval of (60−90)°K. Oxygen induced effects as a simulation method of high neutron damage are compared with irradiation measurements using neutrons and deuterons. (auth)

30075 A MODEL FOR THE CALCULATION OF THE DEFECT PRODUCTION RATIO. Kaletta, D.; Ehrlich, K. (Kernforschungszentrum Karlsruhe (F. R. Germany). Inst. fuer Material- und Festkoerperforschung). J. Nucl. Mater.; 51: No. 2, 227-231(Jun 1974). (In German).

A simple procedure is proposed for calculating the number of defects produced in a damage cascade by a primary knock-on atom of known energy. The calculation is based on a real interatomic potential for the elastic Ni−Ni interaction. The proposed methods are compared with other models for estimating the cascade factor. (auth)

30076 SOME COMMENTS ON DAMAGE ALIGNMENT IN NEUTRON-IRRADIATED ZIRCONIUM ALLOYS. Northwood, D. O.; Gilbert, R. W. (Atomic Energy of Canada Ltd., Chalk River, Ontario. Chalk River Nuclear Labs.). J. Nucl. Mater.; 51: No. 2, 271-276(Jun 1974).

The observation of damage alignment in neutron-irradiated Zircaloy-2 is reported, and certain features of this damage are described. One example of defect alignment was in annealed Zircaloy-2 pressure tube material irradiated at 563°K to a fluence of 7.8×10^{25} nm^{-2} (E > 1 MeV). This fluence resulted in about 10 displacements per atom (dpa) which is the minimum dpa required to form aligned defects in ion-bombarded material. The alignment direction was parallel to the trace of the basal plane; however the damage alignment remained after post-irradiation annealing for one hour at 675°K. (auth)

30077 A POSSIBLE MECHANISM FOR THE FORMATION OF A FERROMAGNETIC PHASE IN STAINLESS STEEL Fe/Cr/Ni/Mo, 17/11/8/2 (TYPE 316L) IRRADIATED IN THE PILE. Baron, J. L.; Cadalbert, R.; Delaplace, J. (CEA Centre d'Etudes Nucleaires de Saclay, 91 - Gif-sur-Yvette (France). Dept. de Technologie). J. Nucl. Mater.; 51: No. 2, 266-268 (Jun 1974). (In French).

The results are summarized of experiments indicating that the occurrence of ferromagnetism in 316L steels is at least in part explained by the conversion of austenite to ferrite, induced by hydrogen resulting from nuclear reactions in the Rapsodie reactor. (INSPEC)

30078 CHANGES IN ELECTRICAL RESISTANCE, LENGTH, SEEBECK COEFFICIENT AND HALL EMF OF α-PLUTONIUM UNDER NEUTRON IRRADIATION IN LIQUID NITROGEN AND ISOCHRONAL ANNEALING. Raetsky, V. M. (Nauchno-Issledovatel'skij Inst. Atomnykh Reaktorov, Dimitrovgrad (USSR)). J. Nucl. Mater.; 51: No 2, 246-254(Jun 1974).

The results on radiation damage in α-plutonium under fission-fragment irradiation are presented. These changes are compared with those caused by self-irradiation in plutonium as well as to property changes in alpha-uranium, aluminium and copper under irradiation by fission fragments, α-particles + recoil nuclei, and electrons. The shape of the isochronal annealing curves for α-plutonium differs essentially from the Van Buren and Thompson schemes. A damage state simulation is proposed, suggesting fluctuations in bond type resulting from the destruction of long-range crystallographic order and describing with a single approach the changes in alpha, beta, and delta-plutonium volumes under low-temperature irradiation. It is assumed that the observed effects resulted from a strongly pronounced covalent interaction in α-plutonium. (auth)

30079 INTERCONNECTION BETWEEN IRRADIATION CREEP AND INTERSTITIAL LOOP FORMATION IN FCC METALS. Herschbach, K.; Schneider, W. (Kernforschungszentrum Karlsruhe (F. R. Germany). Inst. fuer Material- und Festkoerperforschung). J. Nucl. Mater.; 51: No. 2, 215-220(Jun 1974).

The creep strain resulting from stress-assisted, preferential loop nucleation was calculated for both the uniaxial and the biaxial stress state. Taking the texture into account the calculated creep is about one half as large as the observed creep. This small discrepancy can be reduced further by assuming that more than just three interstitials constitute a nucleus and/or by also taking into account the stress-assisted loop growth. A contribution to the creep strain may further arise from stress-assisted, anisotropic swelling. It is concluded that these processes might account for all or a larger part of irradiation-induced creep. (auth)

30080 X-RAY STUDY OF THE ORIENTATION DEPENDENCE OF RADIATION DEFECTS IN THE CRYSTALLINE LATTICE OF Mo IRRADIATED WITH HIGH-ENERGY PARTICLES. Kritskaya, V. K.; Il'ina, V. A.; Vasil'ev, A. A.; Kuznetsova, A. P.; Sharov, B. V. (Inst. of Metal Science and Physics of Metals, Moscow). Fiz. Metal. Metalloved.; 37: No. 2, 307-312(Feb 1974). (In Russian).

Fast electron and neutron irradiation of monocrystal samples of molybdenum with different orientations ([100], [110], [111], and [211]) was studied. Different x-ray effects related to the type of radiation were observed. An orientation dependence of the radiation damage was shown. (tr-auth)

30081 KINETICS OF ACCUMULATION OF RADIATION DEFECTS IN METALS AT TEMPERATURES OF STAGE II OF RECOVERY WITH CONSIDERATION OF TRANSITION PROCESSES. Pletnev, M. N.; Platov, Yu. M. (Inst. of Metallurgy, Moscow). Fiz. Metal. Metalloved.; 37: No. 2, 429-431(Feb 1974). (In Russian).

An equation is derived which indicates the effect of radiation on metals when transition processes are taken into consideration. From this equation were calculated, using experimental data from another source, the effective radii of capture of additive atoms. Data are tabulated for copper with the additives Ni, Mn, Au, Mg, and Sb, showing the effect of consideration of transition processes. (MG)

30082 CHANGES IN THE INTERNAL FRICTION SPECTRUM OF IRRADIATED OR DEFORMED PURE Al AND Al SOLID SOLUTIONS AT 77°K. Grynszpan, R.; Dimitrov, O. (CNRS, Vitry-sur-Seine, France). Mem. Sci. Rev. Met.; 71: No. 4, 251-257 (Apr 1974). (In French).

From autumn meeting on metallurgy; Chatenay-Malabry, France (2 Oct 1972).

The internal friction spectrum and shear modulus of pure Al and Al solid solutions containing between 0.005 and 0.020 at. % Mg, Ag, Cu, Ti, or Cr were studied after irradiation in a fast neutron beam or strain hardening at low temperature. No internal friction maximum was observed in irradiated Al. The internal friction peak spectra of the irradiated Al alloys present characteristics in relation with the alloying element. A temperature range exists in which the modulus of the irradiated alloys is lower than in the recovered condition at 400°K. (FR)

30083 EXAMINATION OF FUEL ELEMENT CLADDING INCLUDING THE DETERMINATION OF THE MECHANICAL PROPERTIES. Philadelphia; American Society for Testing and Materials (1972). 15p. (ASTM-E-453-72).

Procedures are presented for post-irradiation examination of nuclear fuel elements, selection of material and tests for radiation studies, determination of radiation conditions, conduction of tests for mechanical properties of cladding, and the reporting of data. Detailed guidelines are provided for post-irradiation examination of fuel cladding and for better correlation and interpretation of the data in the field of radiation effects. The procedures may be applied to metallic cladding from all types of fuel elements and the tests for determining mechanical properties of the fuel element cladding described could be used in planning radiation effect tests for evaluation of materials for cladding and other components in nuclear reactors. (JRD)

30084 PROPERTIES OF TZM AND NUCLEAR BEHAVIOR OF TZM BRAZEMENTS. Various Properties of TZM and Zr−5Be and Au−18Ni Brazing Filler Metals are Determined for Brazing TZM to Zr and to Steel. Semeniuk, A.; Brady, G. R. (Whiteshell Nuclear Research Establishment, Pinawa, Manitoba). Weld. J. (N.Y.); 53: No. 10, 454s-459s(Oct 1974).

On the basis of its low rate of hydrogen permeation, TZM (0.5Ti−0.08Zr-Mo) was considered for incorporation as a hydrogen barrier in transition joints between steel and zirconium alloys in 400°C organic-cooled nuclear reactors. To aid with the joint design an investigation was conducted to determine the following properties of TZM: (1) tensile and yield strength at 20 and 400°C, (2) impact strength from 20 to 500°C, (3) coefficient of thermal expansion, (4) corrosion behavior in organic coolants (HB-40) and CO_2 atmospheres, (5) hydrogen permeation rate. Since brazing was selected for joining TZM to either steel or zirconium alloys, tests were conducted to select suitable brazing filler metals. Initially, 16 filler metals were screened using wettability tests. Filler metals having sufficient wettability were then used to fabricate corrosion specimens for testing in organic coolant, and in wet and dry CO_2. Only two alloys, Zr−5Be for joining TZM to Zr, and Au−18Ni for joining TZM to steel, showed promise for further testing. Corrosion test results for Zr−5Be are presented graphically for various material and environment combinations. Corrosion of Au−18Ni was negligible in the organic coolant and in the CO_2 atmospheres. The tensile strength of butt-brazed specimens of TZM/Zr and TZM/steel were compared in the unirradiated and irradiated conditions at ambient temperature and at 400°C. Results show that Zr−5Be was not damaged by irradiation but Au−18Ni was severely damaged and would require shielding even in moderate irradiation fields. On the basis of the various small specimen tests it was concluded that TZM could be used as a hydrogen barrier in transition joints, however further research and development is necessary on prototype joints before they are accepted for nuclear applications. (auth)

30085 EMPIRICAL SWELLING EQUATIONS FOR SOLUTION-ANNEALED TYPE 304 STAINLESS STEEL. Foster, J. P. (Westinghouse Advanced Reactors Division, Madison, PA); Strain, R. V. Nucl. Technol.; 24: No. 1, 93-98(Oct 1974).

Bilinear and power law swelling equations were developed for solution-annealed Type 304 stainless steel from Treat Tubing heat 136272. All of the temperatures and fluences were calculated with the same thermal-hydraulic computer code. This procedure insured that all the data were evaluated on a consistent basis. The swelling equations were different from other empirical equations because of differences in the swelling data and the form of the swelling equation. The bilinear equation is recommended for the analysis of experimental data and will be used in the analysis of residual stress measurements made on the same lot of tubing. (10 fig) (auth)

30086 EFFECT OF TEMPERATURE AND ELECTROMAGNETIC RADIATION ON THE ELECTRICAL RESISTANCE OF DEFORMED MOLYBDENUM. Dekhtyar, I. Ya.; Danil'chenko, B. A.; Chirko, I. L.; Shalaev, A. M. (Inst. of Metal Physics, Kiev). Metallofizika; No. 50, 86-89(1974). (In Russian).

A study was made on the change in electrical resistance of molybdenum samples deformed by twisting (degree of deformation of 5, 10, and 25%) and given a ^{60}Co gamma ray dose of 10^9 R. The Mo samples were first subjected to low-temperature annealing at 100 to 140°C. A decrease in the electrical resistance was observed during the low-temperature annealing process. The curve for the change in electrical resistance during annealing of the irradiated samples shows a tendency to saturation. This behavior agrees with theoretical concepts in the theory of focusons. The observed changes are associated with the relaxation of internal stresses in the inhomogeneously deformed samples. (SJR)

30087 IONIC EMISSION YIELD FOR ALLOYS, DEPENDENCE ON THE NATURE OF THE SOLUTE. II. Interpretation. Blaise, G.; Slodzian, G. (Paris Univ., Orsay, France). J. Phys. (Paris); 35: No. 3, 243-261(Mar 1974). (In French).

The secondary ion emission of dilute alloys is explained by means of auto-ionizing processes. The probability with which auto-ionizing states are created on the outcoming atom determines the ion yield; this probability is computed according to the local electronic structure of solute atoms in the alloys. The model gives a fair account of the observed enhancement effects. (FR)

Other Materials

Refer also to abstracts 28933, 28980, 29070, 29367, 30145, 30151, and 31127.

30088 (AD-774654) ION IMPLANTATION OF SEMICONDUCTORS, METALS, AND ALLOYS. Interim Report No. 7, 1 September 1971−31 August 1973. Carter, G.; Grant, W. A. (Salford Univ. (UK)). 31 Aug 1973. 23p. (AFOSR-TR-74-104). NTIS $4.25.

The effect of heavy ion implantation in GaAs, GaP, CdS, and Al_2O_3 was investigated using electron microscopy and Rutherford backscattering based on channeling. The variation of damage with ion dose, the annealing behavior of implanted material, and the lattice location of the foreign implants were investigated. (auth)

30089 (AED-CONF-74-206-001) CHANGES OF DIMENSIONS, MODULUS OF ELASTICITY AND HEAT CONDUCTIVITY DURING REGRAPHITIZATION BY NEUTRON IRRADIATION. Delle, W. (Kernforschungsanlage Juelich G.m.b.H. (F.R. Germany)). 1974. 2p. (In German). (CONF-740466-1). INIS.

From meeting of the working group carbon of the Deutsche Keramische Gesellschaft; Karlsruhe, F.R. Germany (26 Apr 1974).

Available from ZAED.

In addition to the radiation damage, a radiation-induced graphitization (re-ordering of poorly ordered areas) occurs during neutron irradiation of graphite. The competing influence of both effects is discussed with a view to the changes of dimensions, of E-module, and of heat-conductivity. (GE)

30090 (IAE-2266) INVESTIGATION INTO RADIATION DEFECTS IN IRRADIATED PYROGRAPHITE. Platonov, P. A.; Chugunov, O. K.; Alekseev, S. I.; Vindryavskii, B. A.; Karpukhin, V. I.; Tumanov, Yu. P.; Chernyshev, A. A. (Gosudarstvennyj Komitet po Ispol'zovaniyu Atomnoj Ehnergii SSSR, Moscow. Inst. Atomnoj Ehnergii). 1973. 15p. (In Russian). INIS.

Defect formation in pyrolytic graphite with different degrees of ideal structure and irradiated with neutrons from 100 to 850°C at doses of 6×10^{20} n/cm^2 ($E < 0.18$ MeV) was studied. A quantitative evaluation was made of the concentration and form of the defects from x-ray structural analysis, electron microscopy, and cold neutron scattering (<5 Å). The data were compared with the results of theoretical calculations of the number of defects formed with consideration of annealing in displacement peak. (tr-auth)

30091 LUMINESCENCE OF POWDERED URANIUM GLASSES. Eubanks, A.G.; McGarrity, J.M.; Silverman, J. (Laboratory for Radiation and Polymer Science, University of Maryland, College Park, Maryland). J. Opt. Soc. Am. 64: No. 9, 1194-1199 (Sept 1974).

Cathodoluminescence and photoluminescence efficiencies of powdered uranium glasses were measured. Absolute radiant exitance spectra of the glasses were determined during excitation with 100–350 keV electrons and with 253.7 nm light. The spectra are the same for both excitation processes. The glasses luminesce over the wavelength range 470–630 nm. Maxima occur at 518, 534, and 563 nm. The most efficient glass in the series had the composition, by weight percent, 29.40 B_2O_3, 58.80 SiO_2, 9.80 Na_2O, and 2.00 UO_2. Powders of 8.6 and 4.6 μm particle sizes of the glass have cathodoluminescence efficiencies of (1.1 ± 0.1) % for electrons with 100–350 keV energies. The photoluminescence radiant efficiency is (12 ± 1) %. (auth)

30092 MOESSBAUER EFFECT METHODOLOGY. Volume VIII. Proceedings of the Eighth Symposium, New York City, New York, January 28, 1973. Gruverman, I. J.; Seidel, C. W. (eds.). New York; Plenum Publishing Corporation (1973). 291p. (CONF-730117-). $22.50.

From 8th symposium on Mössbauer effect methodology; New York, New York, USA (28 Jan 1973).

Information in the book is presented in sixteen papers. An abstract was prepared for one paper. Other papers were previously abstracted in NSA as 28: 01212 and 28: 04166. Papers for which no abstracts were prepared are concerned with spectroscopy and Moessbauer effect application. (JRD)

30093 MOESSBAUER SPECTROSCOPY OF FROZEN EUROPIUM AMMONIA SOLUTIONS. Brown, J. P.; Cohen, R. L.; West, K. W. (Bell Telephone Lab., Inc., Murray Hill, NJ). pp 3-10 of *Moessbauer Effect Methodology*. Vol. VIII. Gruverman, I. J. (ed.). New York; Plenum Publishing Corp. (1973).

From 8th symposium on Mössbauer effect methodology; New York, New York, USA (28 Jan 1973). See CONF-730117-.

Results of a Moessbauer study of Eu in frozen ammonia are presented. Experimental data show that europium is in the divalent state when in frozen ammonia solutions; that europium hexamine is indeed metallic; and that the OMS model, Oesterreicher, Mammano, and Sienko [Solid State Chem. 1: 10 (1969)], is not a satisfactory one for europium hexamine. Additional analysis of the europium hexamine data has recently been published, and a full paper describing this research is in preparation. (auth)

30094 FERROMAGNETISM OF EuO AND EuS. Lara, S.; Xavier, R. M. (Centro Brasileiro de Pesquisas Fisicas, Rio de Janeiro). Notas Fis., Cent. Brasil. Pesqui. Fis.; 21: No. 14, 277-288(1974).

The indirect magnetic interaction in semiconductors is used to evaluate the exchange parameters for EuO and EuS respectively. The exchange parameters $J_{eff}(EuO) \simeq (0.06 \pm 0.02)$eV and $J_{eff}(EuS) \simeq (0.08 \pm 0.04)$eV estimated by this method are in reasonable agreement with those found in the literature for rare-earth systems. (auth)

30095 ATOMIC DISPLACEMENT CROSS SECTIONS FOR CARBON FROM ENDF/B-III DATA. Morgan, W. C. (Battelle Pacific Northwest Labs., Richland, Wash. (USA)). J. Nucl. Mater.; 51: No. 2, 209-214(Jun 1974).

Atomic displacement cross sections were derived from the data in materials file 1165 (Carbon-12) of the third version of the Evaluated Nuclear Data File (ENDF/B-III), using the Lindhard theoretical treatment for the stopping cross sections of carbon ions in carbon. A comparison of the differences between previous estimates of the carbon atoms displacement functions and the results of these calculations indicate that the use of the atomic displacement cross sections presented herein should improve the correlations of damage production in different irradiation facilities. (auth)

30096 ELEMENTARY MODEL FOR RADIO-INDUCED DAMAGE IN IN-PILE GRAPHITE: CORRELATION BETWEEN TEMPERATURE AND FLUX. Genthon, J. P.; Micaud, G. (CEA Centre d'Etudes Nucleaires de Saclay, 91 - Gif-sur-Yvette (France). Service de Physico-Chimie des Materiaux). J. Nucl. Mater.; 51: No. 2, 237-245(Jun 1974). (In French).

A model based on displacement spikes is examined (and confirmed) for the primary defects induced by neutron bombardment. It is shown that, before any random annealing takes place, these spikes consist of about 4 stably displaced atoms, either isolated or grouped as interstitials or vacancies. There are no vacancy-type defects with activation energies less than 4 eV. The effects of irradiation temperature on dimensional changes in graphite (as published in the literature) are readily described in terms of this model. In particular, this model permits one to account for the effect of dose rate on the defect concentration. At low temperatures ($T \lesssim 300$°C), the theoretical treatment is equivalent to the currently accepted empirical treatment, and it extrapolates well to higher temperatures. A series of experiments is presented which helps to refine the model for high temperature and sets a lower limit of 4 eV for the vacancy activation energy in the displacement spike. $Q = 4$ eV is proposed for the purposes of temperature correction in the range 600 to 1400°C. More generally, as a first approximation, the model shows that a temperature rise of 7% (in degrees Kelvin) compensates for a 10-fold increase of flux, at constant fluence. (auth)

30097 THERMAL ACCOMMODATION COEFFICIENTS OF INERT GASES ON STAINLESS STEEL AND UO_2. Ullman, A.; Acharya, R.; Olander, D. R. (California Univ., Berkeley (USA). Lawrence Berkeley Lab.). J. Nucl. Mater.; 51: No. 2, 277-279 (Jun 1974).

One of the most uncertain aspects of the determination of the temperature distribution in oxide fuel pins is the conductance of the fuel-cladding gap. The gap conductance is generally taken to be the sum of heat transfer by conduction via contact points between the two rough solids and by conduction through the gaps in the remainder of the gap. The parameter α is the thermal accommodation coefficient, which reflects the completeness of energy exchange between the gas and the solid. In view of the absence of data on this parameter, α of helium and xenon on stainless steel and UO_2 has been measured. (auth)

30098 ANNEALING CHARACTERISTICS OF *ION–IMPLANTED p–CHANNEL MOS TRANSISTORS.* Nakamura, K.; Kamoshida, M. (L C Division, Nippon Electric Company, Limited, 1753 Shimonumabe, Kawasaki 211 Japan). J. Appl. Phys. 45: No. 10, 4262-4267 (Oct 1974).

The annealing characteristics of 50–keV $(2-3) \times 10^{11}/cm^2$ $^{11}B^+$–implanted p–channel MOS transistors were investigated from 300 to 900 °C. Below 500 °C, the number of activated atoms N_{II} decreased rapidly with decreasing anneal temperature and the C–V characteristics showed gradual distortions. This was presumably due to surface states induced by the ion implantation. Above 500 °C. N_{II} increased only slightly with increasing anneal temperature and the slope of the C–V characteristics in the transition region was larger than that of the unimplanted sample. Corresponding to the above features, the gain term increased near 500 °C to a value about 30% larger than that of the unimplanted sample, while the breakdown voltage decreased below 500 °C. Equivalent noise voltage decreased abruptly from 500 to 600 °C. However, at lower drain current levels, the generation–recombination noise spectrum did not disappear, even after a 900 °C anneal. In addition, reverse–annealing–like phenomena were observed in the equivalent noise voltage between 350 and 450 °C. The results of recombination velocity measurements wer consistent qualitatively with the results of equivalent noise–voltage measurements. Furthermore, device stability was confirmed by positive and negative bias–temperature treatments (250 °C, 1 h, $E_{ox} = \pm 6.7 \times 10^5$ V/cm) for devices annealed above 450 °C. (auth)

30099 REPLY TO "COMMENTS ON 'LUMINESCENCE FROM ELECTRON–IRRADIATED SILICON' ". Jones, C.E. (Department of Physics, Lehigh University, Bethlehem, Pennsylvania 18015); Streetman, B.G.; Noonan, J.R. J. Appl. Phys. 45: No. 10, 4655-4655 (Oct 1974).

Recent experimental and analytical results indicate that the 0.97–eV luminescence from irradiated Si is characterized by monoclinic symmetry. The assignment of symmetry class for other luminescence peaks in this material is incomplete. (auth)

30100 IMPLANT DOSE PROFILE DEPENDENCE OF ELECTRICAL CHARACTERISTICS OF ION–IMPLANTED MOS TRANSISTORS. Kudoh, O.; Nakamura, K.; Kamoshida, M. (IC

Division, Nippon Electric Co., Ltd. 1753 Shimonumabe, Kawasaki 211, Japan). J. Appl. Phys. 45: No. 10, 4514-4519 (Oct 1974).

Ion−implanted MOS transistors were fabricated and their electrical characteristics, such as threshold voltage, effective mobility, etc., were measured. In the $^{11}B^+$−implanted p−channel case, threshold voltage V_T can be shifted linearly with implant dose. These shifts ΔV_T were entirely determined by the net dose entering silicon. On the other hand, in the $^{11}B^+$−implanted n−channel case, threshold voltage shift ΔV_T varied sublinearly with dose and showed strong dose profile dependence. The profiles were varied with changing implantation energies and annealing times. These results can be interpreted in accordance with the rapid decrease of the maximum surface depletion layer X_{dmax} with the implant dose increase. Numerical calculations of threshold voltage shifts accounting for nonuniformly implanted profiles were compared with observed results. Good agreement was obtained. Effective mobilities μ_{eff} of $^{11}B^+$−implanted p− and n−channel MOS transistors also showed different dose dependences. In the low−dose region, effective mobilities of $^{11}B^+$−implanted p−channel MOSFET remained almost unchanged, but those of the n−channel case decreased monotonically with dose increase. Qualitative arguments, taking into account surface scattering and impurity scattering effects, and rough calculations are presented. (auth)

30101 COMMENTS ON "LUMINESCENCE FROM ELECTRON−IRRADIATED SILICON". Walker, J. (J. J. Thomson Physical Laboratory, University of Reading, Whiteknights, Reading RG6 2AF, England). J. Appl. Phys. 45: No. 10, 4653-4654 (Oct 1974).

Zero−phonon transitions at 0.79 and 0.97 eV observed in electron−irradiated silicon have been ascribed by previous workers to the K center and the divacancy, respectively, on the basis of their production and annealing behavior. This paper shows that, contrary to the original interpretation, the uniaxial stress results on these lines indicate monoclinic symmetry, which is consistent with the proposed models. The stress results on a third zero−phonon line at 1.045 eV are reinterpreted. (auth)

30102 OBSERVATION AND ANALYSIS OF THE PRIMARY ^{29}Si HYPERFINE STRUCTURE OF THE E′ CENTER IN NON-CRYSTALLINE SiO_2. Griscom, D. L.; Friebele, E. J.; Sigel, G. H. (Naval Research Lab., Washington, DC). Solid State Commun.; 15: No. 3, 479-483(1 Aug 1974).

Primary ^{29}Si hyperfine structure of E′ centers in γ-irradiated glassy silica has been observed and analyzed by computer line shape simulation methods. The data and analyses indicate that the E′ defect in non-crystalline SiO_2 is structurally identical to its well known analog in α-quartz, except for a statistical distribution in defect bond angles 0.7 deg in the glasses which is not manifest in the crystalline form. (auth)

30103 EFFECT OF OXYGEN ON UNENCAPSULATED CADMIUM SULFIDE SOLAR CELLS. Bryant, F. J.; Glew, R. W. (Univ. of Hull, Eng.). Thin Solid Films; 23: No. 2, S53-S56(Sep 1974).

The behavior of Cu_2S/CdS-junction solar cells under irradiation by electrons at 100 keV is reported. Results show that a physical model of CdS solar cells should incorporate the significant role played by oxygen in determining the open circuit voltage. A three-layer heterojunction structure should also be considered. (JRD)

NUCLEAR MATERIALS AND WASTE MANAGEMENT

Accountability and Safeguards

Refer also to abstracts 28940, 28986, and 29578.

30104 (FRNC-TH-50) SAFEGUARDING THE PEACEFUL USES OF NUCLEAR ENERGY BY STATES. Le Guelte, G. (Paris-2 Univ., 75 (France)). 1970. 427p. (In French). INIS. Thesis.

Eight agreements or series of agreements have come into force for the past 25 years. Each of them had different purposes, as well as different geographical and technical extent and different safeguards systems. All those treaties, except the N.P.T., apply only on limited areas, or on limited parts of the nuclear activity in the countries interested. Two main safeguards systems have been experienced: the one by I.A.E.A., can only control facilities or materials limitatively designated. On the other hand, the Euratom safeguards system ensures that one country does not use atomic energy for purposes prohibited by international regulations. The N.P.T., which is the only agreement able to limit the member of nuclear weapons countries, adopted the I.A.E.A. safeguards system. The efficiency of safeguards is limited from a technical point of view, and it does not permit the solving of a crisis if one country that openly violates international regulations. (INIS)

30105 (TID-26630) REPORT OF THE ADVISORY PANEL ON SAFEGUARDING SPECIAL NUCLEAR MATERIAL. (Ad Hoc Advisory Panel on Safeguarding Special Nuclear Materials (USA)). 10 Mar 1967. 125p. Dep. NTIS $9.25.

The establishment, workings, and recommendations of the Ad Hoc Advisory Panel on Safeguarding Special Nuclear Materials for maintaining and strengthening the safeguards program both nationally and internationally are reported. (TFD)

Disposal and Storage

Refer also to abstracts 29136, 29137, 29147, 29341, 29343, 29344, 29346, 29347, 29351, and 29369.

30106 (BNWL-B-223-11) ADVANCED WASTE MANAGEMENT STUDIES PROGRESS REPORT, APRIL–JUNE 1974. Schneider, K. J. (comp.). (Battelle Pacific Northwest Labs., Richland, Wash. (USA)). Jul 1974. Contract AT(45-1)-1830. 70p. Dep. NTIS $6.50.

This interim progress report describes Pacific Northwest Laboratory (PNL) activities in the Advanced Methods of Radioactive Waste Disposal Studies. PNL is studying and evaluating currently envisioned, potential long-term, radioactive waste management concepts. The purpose of the study is to identify feasible long-term waste management systems including variations in fuel cycles and their components, identify the research and development necessary for their establishment, and estimate the schedule and costs associated with selected systems. The study is being conducted so that alternative waste management systems can be evaluated on common bases and so that the future course of development for long-term management systems can be planned. Three basic types of waste management concepts are under study: (1) terrestrial disposal, (2) extraterrestrial disposal, and (3) transmutation processing. The terrestrial concepts involve disposal of waste in geologic formations, ice sheets, and seabeds. The extraterrestrial concept involves disposal of waste to various locations in space. Transmutation involves partial elimination of some offensive waste nuclides. There are several sub-concepts within each major concept (e.g., transmutation by accelerators, fission reactors, or fusion reactors). Each concept is being evaluated in terms of the total waste management system needed to support it. A significant part of the study is development of measures of safety/risk associated with the waste management schemes. (auth)

30107 (BNWL-B-334) RADIOACTIVE WASTE MANAGEMENT FOR NUCLEAR ENERGY CENTER. Winegardner, W. K.; Kaser, J. D. (Battelle Pacific Northwest Labs., Richland, Wash. (USA)). Jan 1974. Contract AT(45-1)-1830. 28p. Dep. NTIS $4.50.

Information developed during a brief study concerning the management of radioactive wastes within a Nuclear Energy Center (NEC) is presented. In addition to nuclear reactors for generating electrical power, the center includes an enrichment plant, fuel reprocessing plant, and fuel fabrication plant which also serve reactors outside the center. Facilities for treating and storing both high and low waste are described. Waste inventories are projected and estimated costs of the waste management facilities are presented. Benefits and problems are also briefly discussed. The information is generally applicable to NEC's at a variety of locations. Because of time limitations and the nature of the study, information was developed from preliminary data. There is no intent to imply that waste management schemes are optimum in relation to the center. (auth)

30108 (ICP-1045) EVALUATION OF QUINOL CLATHRATE FOR FISSION PRODUCT NOBLE GAS STORAGE. Staples, B. A.; Pence, D. T. (Allied Chemical Corp., Idaho Falls, Idaho (USA)). Jul 1974. Contract AT(10-1)-1375. 17p. Dep. NTIS $4.00.

The properties of quinol clathrate as they relate to the containment and storage of fission product noble gases are described. The most serious limitation of quinol clathrate for containment and storage of fission product noble gases is its thermal instability. Based on the reported thermal stability and some heat transfer calculations presented in this document, the maximum loading of quinol clathrate appears to be less than 5 cc of gas per gram of clathrate, about 7% of the theoretical capacity. Because of this limitation, quinol clathrate does not appear to be an economically suitable material for long-term containment of fission product noble gases. (auth)

30109 RADIOACTIVE WASTE STORAGE. Boldt, A. L. (to United States Atomic Energy Commission). US Patent 3,828,197. 6 Aug 1974. Filed date 17 Apr 1973. 4p.

High-level radioactive wastes are stored in a heavy walled metal cask which is stored in the open where natural convection of air over the cask removes the decay heat. If the waste is solely from plutonium-recycle pressurized-water reactors, the high neutron dose rate around the cask must be reduced by surrounding the cask in its storage position with crushed graphite or placing cooling fins on the cask and employing neutron shielding material such as polyethylene between the fins. (Official Gazette)

30110 NUCLEAR WASTE DISPOSAL IN THE OCEANS. Nielsen, S. O. (Symplexor Inc., Holte, Denmark). Science; 185: No. 4157, 1183(27 Sep 1974).

Several methods proposed for the disposal of nuclear wastes in the oceans are briefly reviewed from the standpoint of long-time safety. The safety aspects of the disposal of solidified wastes in glass containers at ocean depths of 5000m are compared with disposal in mausoleums. (CH)

Handling Equipment and Procedures

30111 NUCLEAR REACTOR FUEL ROD SPLITTER. Duncan, R.; Cellier, F. (to Westinghouse Electric Corp.). US Patent 3,831,248. 27 Aug 1974. Filed date 31 May 1972. 8p.

An apparatus for recovering fuel pellets from a fuel rod by cutting the rod lengthwise into two separate halves to allow fuel pellets therein to drop out of the rod cavity is described. A fuel rod is positioned in axial alignment with a stationary set of cutters on a table, and a winch on the other end of the table pulls the rod through the cutters, which cut grooves almost through the opposite sides of the rod. The rod is then caused to spread open, and fuel rod pellets fall into a receptacle for later disposition. The split halves of the fuel rod are then of a size and configuration convenient for efficient handling and disposal. (Official Gazette)

30112 SAFE HANDLING OF RADIATION SOURCES. Oberhofer, M. Thiemig-Taschenbuecher, Band 46. Munich; Verlag Karl Thiemig (1974). 250p. DM 28,-.

This book does not present regulations and explanations, but offers guidance in the practical procedures of radiation protection. It describes how man, who cannot perceive the danger of radiation with his natural senses, should conduct himself in a radiation field–how he should work with sealed and unsealed radiation sources. The book describes the appropriate equipment and discusses typical incidents and accidents. Ample use is made of sketches and photographs throughout the booklet. A subject index is included. (TFD)

Transportation

30113 (AD-777254) TANDEM TOWING TESTS OF THE MHU-12/M TRAILER. Final Report, October 1972–December 1973. Gray, G. W. (Air Force Special Weapons Center, Kirtland AFB, N. Mex. (USA)). Mar 1974. 30p. (AFSWC-TR-73-49). NTIS $3.25.

Two MHU-12/M trailers in tandem behind a 1½-ton truck were subjected to braking and road tests on roads of various surface conditions at speeds to 20 miles per hour. Three load conditions of the trailers were used in the tests, i.e., unloaded, a low center-of-gravity load at near rated capacity, and a high center-of-gravity load at near rated capacity. Speeds above 15 miles per hour were judged hazardous and are not recommended. Towing of a loaded trailer in tandem behind an unloaded trailer proved to be extremely unstable and resulted in breaking the tow bar of the aft trailer during a panic stop. No extremely hazardous behavior was noted towing two loaded trailers in tandem at speeds to 15 miles per hour. (auth)

30114 (ORNL-TM-3992) LMFBR-37-FUEL-ELEMENT SHIPPING CASK SIMULATION: TEST ASSEMBLY OPERATION AND DATA. Klima, B. B. (Oak Ridge National Lab., Tenn. (USA)). Aug 1974. Contract W-7405-eng-26. 195p. AT.

A test apparatus has been designed and fabricated to simulate a shipping cask for 37 LMFBR fuel elements arranged in a horizontal hexagonal array. The test equipment was fabricated in the ORNL shops, and installed and operated in Building 9201-3 at the Y-12 Plant. The data collected from the runs made using this equipment, with sodium, helium, argon, and vacuum as the heat transfer media are presented. (auth)

30115 (Y-DD-155) SAFETY ANALYSIS REPORT FOR PACKAGING (OAK RIDGE Y-12 PLANT MODEL VCD PACKAGE FOR ENRICHED URANIUM SOLUTION). Dyer, H. R. (Oak Ridge Y-12 Plant, Tenn. (USA)). Sep 1974. Contract W-7405-eng-26. 22p. Dep. NTIS $4.00.

An evaluation of the Y-12 Model VCD shipping container for enriched uranium solutions was made to demonstrate its compliance with federal regulations governing the interstate transport of fissile materials. Destructive testing and engineering evaluations were made to demonstrate the structural integrity and thermal resistance of the package in meeting the physical testing described in the AEC regulations. Reactor transport theory computer codes were used to analyze the criticality safety of the package containing enriched uranium solutions. Results of this evaluation show that the package complies with all applicable regulations. Analysis of the Y-12 Model VCD shipping container indicates that aqueous solutions containing any enrichment in the ^{235}U isotope meets the requirements for Fissile Class II shipments. Limitations on each package consist of a maximum volume of 13.5 liters of true solution and a contained ^{235}U mass not to exceed 7.86 kgs. (auth)

30116 (Y-DD-156) SAFETY ANALYSIS REPORT FOR PACKAGING (OAK RIDGE Y-12 PLANT FOAMGLAS SHIPPING PACKAGE FOR ENRICHED URANIUM). Mee, W. T. (Oak Ridge Y-12 Plant, Tenn. (USA)). Sep 1974. Contract W-7405-eng-26. 35p. Dep. NTIS $4.00.

A simple and relatively inexpensive package has been evaluated for use in shipping unirradiated dry enriched uranium materials. Physical test results and nuclear criticality safety analyses associated with the transportation of the packages have been compared with the criteria in regulations on transportation by the U. S. Atomic Energy Commission (AECM-0529). It is concluded that the Y-12 Foamglas Shipping Container meets the requirements for Fissile Class II shipments of any ^{235}U enriched dry uranium compounds and metal with a restriction of 19 kg ^{235}U contained in each package. It is further concluded that the Fissile Class I criteria are satisfied for enriched uranium dry compounds and metal if the mass per package is limited to 3.7 kilograms of ^{235}U. Restrictions on the size and shape of enriched uranium materials to be shipped are defined by the inner container dimensions of not greater than 6.19 in. in di. by 8.75 in. in height. (auth)

PARTICLE ACCELERATORS

Design, Development, and Operation

Refer also to abstracts 30855 and 30952.

30117 (GSI-tr-74/10) ON THE COLLECTIVE ACCELERATION OF HEAVY IONS—DEPARTMENT FOR NEW METHODS OF ACCELERATION OF THE JINR. Barabosch, L. S.; Beljajew, L. N.; Dolbilov, G. V.; Iwanov, I. N.; Inkin, V. D.; Kowalenko, A. D.; Nowikov, V. G.; Perelstein, E. A.; Sarenzew, V. P.; Swiridov, V. A.; Rochlov, I. M. Apr 1974. 35p. (In German). INIS. 15 figs.; 30 refs. Translation from Russian of the report JINR-P-9-7697.

After a brief introduction to the particularities of particle beams of a collective accelerator and evaluation of some parameters (energy gain per nucleon, accelerated ion number, instabilities), as well as enumeration of hitherto existing results and present projects of collective heavy-ion accelerators (Berkeley, Karlsruhe, Garching, Maryland), the collective electron-ring heavy-ion accelerator of the Department for New Methods of Acceleration of the JINR is closely dealt with: important parameters, the electron injector (pulsed linear accelerator), the accelerating inductor, the pulsed high-voltage generator, the electron source, beam focussing and feeder system for the magnetic field, the mechanical accelerator set-up, the ADGESATOR to form electron-rings (magnetic field, ring parameter, feeder system for pulsed coils, chamber, ion charging of the ring, ion acceleration), the control, beam diagnostics and measuring techniques. (auth)

30118 NUCLEAR STRUCTURE FACILITY 20/30 MV TANDEM ACCELERATOR. Tait, N. R. S.; Voss, G. P. (Daresbury Nuclear Physics Lab., Warrington, Eng.). Particle Accel.; 5: No. 4, 181-197(1973).

A large electrostatic accelerator has been designed to provide a nuclear structure facility in Britain. The machine is intended to operate initially at 20 MV with subsequent upgrading to 30 MV. The general features of the accelerator are described and the main dimensions are specified. The electrostatic design and beam optics of the machine are discussed and a description is given of the design and layout of the stack, intershield and center terminal. An extensive high voltage test program is under way using a variety of dc and pulsed sources, and surge phenomena in Van de Graaff accelerators are being studied both theoretically and experimentally using surge measurement devices that are under development at the laboratory. Details are also given of a high current inductive charging system and a number of other devices such as a fast data link employing a light diode and a color TV operating in conjunction with a small computer. The general layout of the facility is described and some details are given of the control and counting room, the experimental areas, and of shielding wall thicknesses. (auth)

30119 GEOMETRY AND OPTICS OF SYNCHROTRON RADIATION. Sabersky, A. P. (Stanford Linear Accelerator Center, CA). Particle Accel.; 5: No. 4, 199-206(1973).

The geometrical-optical properties of synchrotron radiation coming from a curving, relativistic electron beam do not fit into any usual category of light or radiation source. The center of the apparent source of radiation depends on the position of the observer with respect to the orbit, and the source has an axial extent which is a function of the sizes of the beam and the observation aperture. The beam image formed by focusing the synchrotron light is subject to distortions and depth of field errors. These errors are calculated, and, in some cases, methods of correction are given. The limits put on resolution by geometrical effects are given. Beam orbit changes cause errors in the angular acceptance of observation systems: these effects can also be corrected. The dimensions of the diffuse shadows cast by rays from the finite-sized source impinging on edges are calculated. (auth)

30120 SHORT ELECTRON LINAC OF SIDE-COUPLED STRUCTURE WITH LOW INJECTION VOLTAGE. Ono, K.; Takata, K.; Shigemura, N. (Tokyo Shibaura Electric Co., Ltd., Takatsu, Japan). Particle Accel.; 5: No. 4, 207-214(1973).

An electron linac with an overall length of 35 cm only has been constructed for medical use. The accelerating tube is a side-coupled structure with $Z_{eff}/Q = 6350\Omega/m$, where 2 bunching cells trap electrons well with the injection voltage as low as 5 kV. With an input power of 2 MW from a 3-GHz magnetron, 4-MeV, 100-mA beam pulses with 2 μs duration are obtained, where the beam diameter is 1 mm without any focusing magnet. The structure and the gun with an oxide cathode are sealed off together and evacuated by a 1 liter/s ion pump. (auth)

Auxiliaries and Components

30121 (LA-tr-74-30) HIGH-CURRENT ELECTRON ACCELERATOR WITH SUPPLY BY INDUCTIVE STORAGE. Dubovoi, L. V.; Roife, I. M.; Serendenko, E. V.; Stekol'nikov, B. A.; Shapiro, V. B. (Nauchno-Issledovatel'skij Inst. Ehlektrofizicheskoj Apparatury, Leningrad (USSR)). 1973. Translated by A. D. Cernicek from NIIEFA-T-0176. 11p. Dep. NTIS $4.00.

The high-voltage circuit of the high-current electron accelerator supply by an inductive storage-transformer is considered. The experimental model of the "Indus-1" accelerator with the extracted electron beam energy of ~1 kJ at pulse duration of ~5 msec is described. (auth)

30122 FLUX THEOREM FOR THE DESIGN OF MAGNET COIL ENDS. Mills, F. E.; Morgan, G. H. (Brookhaven National Lab., Upton, NY). Particle Accel.; 5: No. 4, 227-235 (1973).

Analytical expressions are developed for the Fourier expansion coefficients integrated along the axis of the field of iron-free multipole magnets, or magnets having an infinitely permeable concentric circular shield. The method makes use of the mutual inductance of the magnet and an idealized, infinitely-long cos $n\theta$ current sheet concentric with and interior to the magnet. The expressions obtained are used to verify a previously-known ideal end structure and also to compute the harmonics in a real magnet end on which measurements have been made. (auth)

30123 APPLICATION OF ELECTRICALLY CONDUCTIVE COATINGS TO INSULATING TUBES OF SWITCHING MAGNETS FOR PARTICLE ACCELERATORS. Tilles, E. B.; Nissen, R. F. (to United States Atomic Energy Commission). US Patent 3,822,146. 2 Jul 1974. Filed date 5 Jul 1972. 4p.

Indium is applied in controlled amounts to the interior of an insulating tube used in a switching magnet for a high-energy particle accelerator. The indium is then oxidized to form indium sesquioxide. Electrical resistance of the indium sesquioxide is controlled by varying the thickness of the coating. The invention is of especial utility in preventing the buildup of surface charges on such tubes. (Official Gazette)

30124 CHARGE MEASURING UNIT OF THE PULSED ELECTRON BEAM IN THE VAN de GRAAFF ACCELERATOR. Sawicki, A.; Orzechowski, T. (Instytut Badan Jadrowych, Swierk, Poland). Nukleonika; 19: No. 6, 583-586(1974).

The operating principles and circuit design of the current measuring unit are described, by means of which a measurement of charge of the pulsed electron beam in the Van de Graaff electron accelerator can be carried out without physical contact with the beam. The measuring head is composed of a ferroxcube torroid on which a number of turns of copper wire is wound forming a winding. The range of current in the beam is from 0.5 to 500 mA. (auth)

30125 AN AUTOMATIC RUNNING SYSTEM FOR A 500 kV VAN DE GRAAFF GENERATOR. Wene, C.-O.; Karlsson, E. (Tekniska Hoegskolan, Lund (Sweden). Institutionen foer Kaernfysik). Nucl. Instrum. Methods; 119: No. 2, 395-396(15 Jul 1974).

Small Van de Graaff generators with terminal voltages below 1 MV but capable of giving high beam currents are versatile tools with wide application in material analysis, solid-state, atomic and nuclear physics. A common feature for most applications is the need for a stable beam at a fixed energy and current during a long period. The inherent stability and simplicity of small single-stage Van de Graaff generators suggest that the role of the operator in these applications could be almost completely taken over by a comparatively simple integrated system for supervising the running of the accelerator and additional equipment. Besides a considerable reduction in running costs, this would enable users to run the generator single-handed over periods of several days. Such a system has been built and installed at a High Voltage AN-400 generator. This system will also automatically condition the generator up to a pre-set voltage. It has now been used for more than 2500 h and has increased the beam time available by a factor of 2 to 3 without demanding more personnel. In special applications, it has been able to run the generator for up to three days continuously without any human interference. (auth)

30126 HIGH-POWER STANDING-WAVE TRIPERIODIC STRUCTURE FOR POSITRON ACCELERATION. Bensussan, A.; Tran, D. T.; Tronc, D. (CGR-MeV, Domaine de Corbeville, Orsay, France). Nucl. Instrum. Methods; 118: No. 2, 349-355 (15 Jun 1974).

A high-power and high-gradient triperiodic structure has been built for positron acceleration. A mean power of 20 kW/m, i.e., 1 kW per accelerating cell, and a peak field of 15.3 MV/m, with a pulse duration of 13.6 μs, were obtained without any sparking. The structure has been tested in accelerating electrons. Positron acceleration is scheduled for early 1974. (auth)

30127 LOW-INTENSITY BEAM MONITORING WITH AN IMAGE-INTENSIFIED SCINTILLATOR DETECTOR. Kanstein, L. L.; Morgado, R. E.; Norgren, D. U.; Sorensen, R. W. (California Univ., Berkeley (USA). Lawrence Berkeley Lab.). Nucl. Instrum. Methods; 118: No. 2, 483-485(15 Jun 1974).

A compact, light-weight, image-intensified scintillator detector with video output developed for low-intensity ($<10^{10}$ particles/cm^{2}s) beam monitoring is described. (auth)

Ion Sources and Injection and Extraction Systems

30128 METAL VAPOR CONFINEMENT IN VACUUM. Bacal, M. (Ecole Polytechnique, Paris); Reichelt, W. Rev. Sci. Instrum.; 45: No. 6, 769-772(Jun 1974).

A new method for confining a metal vapor at a pressure of about 10^{-3} torr, with extremely low loss of metal into the vacuum chamber surrounding the metal cell, has been demonstrated; it consists in recycling the metal, condensed in the liquid state; its return to the high pressure region is ensured by capillarity. Two versions of the new cell, built for different applications, are described: a heat pipe heated lithium cell, characterized by a high uniformity of temperature, and a cesium cell, equipped with a surface ionization gauge for cesium pressure measurement, and a LiF window. Measurements carried out with the surface ionization gauge in the cesium cell led to a ratio 10^3 between the cesium atom flux at the center of the canal and at its port. The contribution of direct metal loss from the hot central region of the canal and that due to desorption from the canal ports is discussed. The study is directed toward charge exchange cell design for production of negative ion beams. (auth)

30129 SLOW BEAM EXTRACTION FROM THE JINR SYNCHROPHASOTRON. Issinskii, I. B.; Kalyonov, S. V.; Kulakova, E. M.; Novikov, S. A.; Omel'chenko, B. D.; Pavlov, N. I.; Sikolenko, V. F.; Vasilishin, B. V.; Volkov, V. I.; Zinoviev, L. P. (Joint Inst. for Nuclear Research, Dubna, USSR). Particle Accel.; 5: No. 4, 215-226(1973).

A slow extraction system designed at the Laboratory of High Energies operates on the $\nu_x = 2/3$ radial betatron resonance and permits extraction of more than 90 per cent of a circulating beam by means of two internal magnets. The high magnetic field operating region is large enough to permit a gain in amplitude at the septum-magnet entrance of about 17 cm per turn and to avoid influence of the field nonlinearity upon the beam emittance. Resonance conditions are created by means of two pole-face windings. The first of these builds up the second azimuthal harmonic of the sextupolar perturbation and the second one reduces the field index from the operating point ($n = 0.67$) to its resonance value ($n = 0.624$). The first internal lens placed downstream from the septum magnet focuses the beam in a horizontal plane to create an intermediate image located between the septum and extraction magnets. Under these conditions average values along each particle path in the accelerator fringing field are approximately equal and, consequently, the transverse phase volume distortions are small. As the average beam angle at the septum-magnet entrance changes during the extraction time, the septum-magnet field is modulated accordingly. The beam bending in the extraction magnet is large enough (about 100 mrad) to steer the beam outside the vacuum chamber and to avoid a significant influence of the fringing field in the next quadrant. The preliminary calculation of the extraction system was made by the analytical method and then on a computer taking into account the circulating beam characteristics, measured distribution n(x), accelerator structure and contribution of pole-face winding currents. Adjustment and experimental study of the system showed a good agreement with calculated results. The applications of real time feedback control loops into power supplies of the resonance winding and septum magnet allows us to improve significantly the extraction uniformity and to eliminate a slow drift of the beam entering the extraction magnet. The beam size on the first external target is 4×18 mm^2. The slow extracted beam efficiency has been determined in the reaction on carbon and by measuring the correlation of integrated particle fluxes around the accelerator proportional to the number of protons lost inside the accelerator chamber with the extracted system on and off. According to this method, the efficiency is 94 ± 0.5 per cent. (auth)

30130 BEAMS OF Be$^+$ FROM AN RF ION SOURCE. Norbeck, E.; York, R. C. (Iowa Univ., Iowa City (USA). Dept. of Physics and Astronomy). Nucl. Instrum. Methods; 118: No. 2, 327-328(15 Jun 1974).

A conventional radio-frequency ion source for a Van de Graaff accelerator was modified so that it produced beryllium ions when chlorine gas was used in the source. Analyzed Be$^+$-beam currents of 0.15 μA were produced. The modification had no effect on the operation of the source when hydrogen or helium were used. (auth)

Ion Optics and Field Calculations

30131 (UCID-16583) STATIC COMPRESSION OF RELATIVISTIC ELECTRON RINGS. Christofilos, N. C. (California Univ., Livermore (USA). Lawrence Livermore Lab.). 17 Sep 1968. Contract W-7405-eng-48. 12p. Dep. NTIS $4.00.

The process of formation and compression of electron rings for collective ion acceleration was studied. The parameters of the compression and the electron beam are given for compression at 4 MeV (at Astron Facility). (WHK)

30132 ELECTRON ORBITS IN THE ERA (ELECTRON RING ACCELERATOR) WITH AN ELECTROSTATIC-TYPE INFLECTOR SYSTEM. Toyama, H. (Nagoya Univ., Japan); Ishizuka, H. Particle Accel.; 5: No. 4, 237-240(1973).

Electron orbits in the ERA with an inflector system are calculated. The operational condition for effective capture of the electron beam is presented. (auth)

30133 METHOD AND MEANS FOR REDUCING THE POWER DENSITY OF AN INTERNAL CYCLOTRON BEAM. (to Cycotron Corp.). Netherlands Patent 7,301,442. 1 Feb 1973. Priority date 4 Feb 1972, USA. 9p. (In Dutch).

A method and apparatus are described for reducing the power density of the internal beam in an isochronous cyclotron at its extraction radius or an internal target wherein the internal beam in its orbits near and at the extraction or target radius is spread axially by applying to it a time-varying electrostatic field tuned to the natural axial oscillation frequency of the beam in such orbits. (auth)

30134 SYMMETRIZED DOUBLE-MONOCHROMATOR SYSTEMS. Hinterberger, F. (Bonn Univ. (F. R. Germany). Inst. fuer Strahlen- und Kernphysik). Nucl. Instrum. Methods; 119: No. 1, 43-49(1 Jul 1974).

A system of three triplet lenses is investigated with regard to the trajectory symmetrization in magnetic double-monochromator systems. Double-dispersive and non-dispersive telescopic modes can be realized for mirror-symmetric as well as anti-symmetric arrangements without changing the hardware geometry. Beside the symmetry fit certain asymmetry constraints can be adjusted in order to match special phase-space transformation properties. The resulting ion-optical structures are discussed with the aid of geometrical light optics as well as first-order matrix theory. (auth)

30135 RAPID MEASUREMENT OF THE EFFECTIVE FIELD BOUNDARY OF HOMOGENEOUS FIELD MAGNETS. Halbach, K. (California Univ., Berkeley (USA). Lawrence Berkeley Lab.). Nucl. Instrum. Methods; 119: No. 2, 329-331(15 Jul 1974).

It is often sufficient to express the beam optical properties of the fringe field of a magnet by describing its effective field boundary. It is shown how the effective field boundary can be measured very rapidly and accurately. (auth)

30136 A MAGNETIC FIELD CLAMP WITH BENEFICIAL SATURATION EFFECTS. Halbach, K. (California Univ., Berkeley (USA). Lawrence Berkeley Lab.). Nucl. Instrum. Methods; 119: No. 2, 327-328(15 Jul 1974).

It is shown that a certain amount of saturation is desirable in some magnetic field clamps. A specific field-clamp design is given that allows precise adjustment of the saturation effects in the field clamp. (auth)

Storage Rings

30137 (BNL-19192) RESONANCE EXCITATION BY DISTORTION OF THE β-FUNCTION COUPLED WITH A LONG RANGE SPACE CHARGE FORCE. Month, M. (Brookhaven National Lab., Upton, N. Y. (USA)). 12 Aug 1974. 19p. Dep. NTIS $4.00.

It is shown how a long range space charge force, such as that produced by image fields of a single beam, can combine with a lattice design having large β variations, such as occurs in machines with low β insertions, to induce characteristic resonance behavior. The significant aspect of the image force, distinguishing it from beam self forces or beam-beam forces, is its long range nature. This means that the force field does not diminish outside the beam, but extends, and increases, for amplitudes approaching the image boundary. Although the image force is highly nonlinear, it will, by itself, excite no resonances, since its azimuthal Fourier decomposition is essentially composed of 0th harmonic. It is pointed out that low periodicity, large β variations are harmonically rich and can provide the necessary azimuthal harmonics for resonance excitation. The resonance characteristics of this type of system are developed, emphasizing the influence of the two main parameters, the maximum β value and the image tune shift. The impact on storage ring design is discussed. (auth)

30138 (UCID-15685) PRELIMINARY ORBITS AND STRUCTURE OF A HIGH INTENSITY STORAGE RING. Beal, J. W. (California Univ., Livermore (USA). Lawrence Livermore Lab.). 13 Jul 1970. 10p. Dep. NTIS $4.00.

The computer program SYNCH was used for the variation of parameters for optimization of the design of the proposed High Intensity Storage Ring. The optimized storage ring structure is shown, and storage ring parameters are given. (WHK)

30139 (UCID-15686) NOTE ON THE INCOHERENT SPACE CHARGE LIMIT IN THE HIGH INTENSITY STORAGE RING. Beal, J. W. (California Univ., Livermore (USA). Lawrence Livermore Lab.). 13 Jul 1970. 7p. Dep. NTIS $4.00.

The transverse space-charge forces influence the frequency of betatron oscillations in such a way as to impose an upper limit on the number of particles that can be accommodated within a given storage ring design. The limit is such that the betatron frequency is shifted to the nearest machine resonance. In practice, a careful optimization of the machine design is necessary to achieve a balance between lattice design, aperture, and injection energy to achieve the desired intensity. Calculations for the High Intensity Storage Ring are given. (WHK)

30140 (UCID-15735) QUADRUPOLE FIELDS IN A TOROIDAL GEOMETRY FOR THE HIGH INTENSITY STORAGE RING. Beal, J. W. (California Univ., Livermore (USA). Lawrence Livermore Lab.). 2 Sep 1970. 14p. Dep. NTIS $4.00.

As envisioned for the High Intensity Storage Ring (HISR), the magnetic guide field will be a superposition of n = 0 dipole bending fields coupled with independent quadrupole focusing fields. Since the HISR is designed for low rigidity particles, approximately 5-MeV kinetic energy electrons, relatively weak field strengths are required. For this reason and also for increased flexibility, it was determined to produce these fields without ferrous materials and to use only the appropriate set of current-carrying conductors. Results of numerical calculations pertaining to the quadrupole field component produced by a set of finite conductors are described. (WHK)

Experimental Facilities

Refer also to abstracts 29584 and 29591.

30141 (BNL-19153) AGS SECONDARY BEAMS AND PARAMETERS, FY75. Berley, D.; Wang, C. L. (Brookhaven National Lab., Upton, N. Y. (USA)). 25 Jun 1974. 21p. Dep. NTIS $4.25.

A compilation is presented of the AGS secondary beam parameters and fluxes. (auth)

30142 (LA-UR-74-1263) RADIOISOTOPES FROM A MEDIUM-ENERGY ACCELERATOR: THE CLINTON P. ANDERSON MESON PHYSICS FACILITY RADIOISOTOPE PROGRAM. O'Brien, H. A. Jr.; Ogard, A. E.; Grant, P. M. (Los Alamos Scientific Lab., N. Mex. (USA)). 1974. 5p. (CONF-740926-3). Dep. NTIS $4.00.

From 1st world congress of nuclear medicine and exhibition meeting; Tokyo, Japan (30 Sep 1974).

The linac and the isotope production facility are briefly described, and the medical radioisotope research program is outlined. (WHK)

30143 RADIOGRAPHY OF STEEL COMPONENTS WITH A LINEAR ELECTRON ACCELERATOR. Angelov, B. P.; Levin, V. M.; Nikolaev, V. M.; Prudnikov, I. A.; Rumyantsev, V. V.; Tronov, B. N. Sov. J. Nondestruct. Test. (Engl. Transl.); 9: No. 6, 651-653(Dec 1973).

Translated from Defektoskopiya; 9: No. 6, 23-27(1973).

The detail sensitivity is considered for steel components up to 500 mm thick, the source being a linear accelerator providing up to 8 MeV. It is shown that the use of a plate standard with grooves (GOST-7512-69), this being placed on the source side, indicates that the limit of detection is not more than 0.5%, whereas the figure becomes 1.2–1.3% when a system with holes is employed. (auth)

30144 BETATRON ELECTRON INTERNAL-FLAW DETECTOR. Boiko, V. I.; Gorbunov, V. I.; Evstigneev, V. V.; Sviryakin, D. I. (Tomsk Polytechnical Inst., USSR). Sov. J. Nondestruct. Test. (Engl. Transl.); 9: No. 6, 643-646(Dec 1973).

Translated from Defektoskopiya 9: No. 6, 13-19(1973).

A scintillation system for flaw detection using fast monoenergetic electrons is described; the method employs evaluation of the contrast sensitivity and resolving power. The basic parameters of the apparatus have been measured. (auth)

30145 A NEW TECHNIQUE FOR THE PRODUCTION OF CARBON FOILS. Keeling, M. J. (Auckland Univ. (New Zealand). Dept. of Physics). Nucl. Instrum. Methods; 119: No. 2, 401 (15 Jul 1974).

A method is described using the evaporation of sucrose in vacuo with a high partial pressure of water vapor to provide a release agent. This system combines a number of advantageous features. These are: (1) As the release agent contains only carbon, hydrogen, and oxygen, foil contamination can be reduced. Methods using detergents, sodium chloride, cesium iodide, etc., have been shown to leave traces of the release agent in the foil. The absence of contaminants such as sodium, sulphur, phosphorus, is frequently advantageous when foils are used as target backings, i.e., for elemental analysis. (2) As the release agent is applied to the substrate in vacuo there is less chance of dust particles being entrained in the layer with consequent pinhole problems. (3) This system produces foils which are very easy to float, even down to the 1 $\mu g/cm^2$ range of thickness. (auth)

30146 NEUTRONS FROM THE 2 MeV DEUTERON BOMBARDMENT OF THICK ^{7}Li TARGETS. Jones, D. T. L.; Bartle, C. M. (Wisconsin Univ., Madison (USA). Dept. of Physics). Nucl. Instrum. Methods; 118: No. 2, 525-529(15 Jun 1974).

The spectra of neutrons produced in the ^{7}Li(d,n)^{8}Be reaction have been measured at a deuteron energy of 2 MeV using thick ^{7}Li targets in order to investigate the feasibility of using this source for radiotherapy. The time-of-flight technique was used and spectra were obtained at lab angles from 0° to 90° in 10° intervals. Total neutron yields and average neutron energies were determined from the data. Some measurements were also taken with the source viewed through various thicknesses of water and wax absorbers in order to harden the spectra. (auth)

30147 SUMMING OF HARMONIC FREQUENCIES BY A RESONANT CABLE FOR PULSE GENERATION ON A CAPACITIVE BEAM DEFLECTOR. Paulin, A. (Schweizerisches Inst. fuer Nuklearforschung, Villigen). Nucl. Instrum. Methods; 118: No. 2, 317-319(15 Jun 1974).

The feasibility of constructing a beam chopper by beam deflection using capacitive plates as a termination of a quarter wavelength cable has been demonstrated experimentally. The results agree well with theoretical predictions and indicate no technical obstacle to the use of beam choppers of this kind with various particle beams. (auth)

30148 WOBBLE TARGET HOLDER FOR THIN TARGETS IN INTENSE LIGHT- AND HEAVY-ION BEAMS. Hoffmann, D.; Sobotta, G.; Becker, K.; Genz, H.; Richter, A.; Schrieder, G. (Bochum Univ. (F. R. Germany). Inst. fuer Experimentalphysik). Nucl. Instrum. Methods; 118: No. 2, 321-326(15 Jun 1974).

A simple movable target holder for nuclear targets bombarded by intense light- and heavy-ion beams has been developed. It has been tested with proton and oxygen beams of the Dynamitron-Tandem accelerator on the low-melting-point targets selenium and bismuth. Significant improvements in maximum beam current with respect to breaking and evaporation of the targets were achieved. (auth)

30149 NMR CALIBRATION OF A POLARIZED NUCLEAR TARGET, PART OF WHICH IS RADIATION-DAMAGED. Wollan, D. S. (Virginia Polytechnic Inst., Blacksburg (USA). Dept. of Physics). Nucl. Instrum. Methods; 119: No. 2, 397-399(15 Jul 1974).

An NMR method is proposed for calibrating the decreased dynamic nuclear polarization in the radiation-damaged part of a nuclear target crystal when the beam area is smaller than the crystal. (auth)

30150 A HIGH-QUALITY MUON BEAM IN THE 10–15 GeV ENERGY RANGE. Flatte, S. M.; Heusch, C. A.; Seiden, A. (California Univ., Santa Cruz (USA)). Nucl. Instrum. Methods; 119: No. 2, 333-345(15 Jul 1974).

The design and performance of a muon beam built at the Stanford Linear Accelerator Center is described. The transport system delivers 14 GeV positive muons with a spot size of $\sigma \sim 4$ mm in each plane, divergence of $\sigma \sim 2$ mrad in each plane, momentum bite of ±1%, a total of 1.6% halo, with a π contamination of $(4 \pm 1.5) \times 10^{-5}$. With present incident beam power limitations due to primary target design, the flux is ~40000 muons/s. The full power of SLAC would yield 170000 muons/s. (auth)

30151 THE PREPARATION OF SELF-SUPPORTING ^{13}C-FOILS USING ENRICHED METHANE GAS. Keller, R.; Mueller, H. H. (Zurich Univ. (Switzerland)). Nucl. Instrum. Methods; 119: No. 2, 321-322(15 Jul 1974).

A method for the preparation of self-supporting carbon foils enriched with ^{13}C of thickness ranging between 10 and 50 μg/cm^2 is outlined. A gas discharge in highly enriched methane gas was used to deposit the carbon layer on a nickel foil. (auth)

30152 LINEAR ACCELERATOR NEUTRON SOURCE FOR NEUTRON SCATTERING. Harling, O. K. (Battelle Pacific Northwest Labs., Richland, Wash. (USA)). Nucl. Instrum. Methods; 119: No. 2, 217-227(15 Jul 1974).

Various aspects of the use of a pulsed linear electron accelerator as a source for neutron-scattering research are explored. Neutron production and moderation is discussed. Comparisons are made between the source strengths and neutron-scattering capability of steady-state reactors and some pulsed-accelerator sources. Design considerations of spectrometers for the pulsed-source application are discussed. A brief description is provided of a potential neutron-scattering facility based upon an electron linear-accelerator source. (auth)

30153 A SIMPLE FAST SWEEPING SYSTEM FOR EXTRACTED CYCLOTRON BEAMS. Hood, J. T.; Goldworm, R. A.; Macias, E. S.; Sarantites, D. G. (Washington Univ., St. Louis, Mo. (USA). Dept. of Chemistry). Nucl. Instrum. Methods; 119: No. 2, 213-215(15 Jul 1974).

A simple system for sweeping an extracted cyclotron beam on and off an adjustable aperture at various repetition rates and duty cycles is described. This system permits lifetime measurements of delayed γ-rays to be made over a range of 0.5 to 5000 μs. The application of this system for the study of the 3.29 and 159 μs isomeric states in ^{115}Sn populated by the (p,nγ) reaction at 8.0 MeV is described. (auth)

30154 A MECHANICAL BEAM CHOPPER SYSTEM FOR THE MEASUREMENT OF HALF-LIVES IN THE MILLISECOND REGION. Hashizume, A.; Kumagai, H.; Tendow, Y.; Katou, T. (Institute of Physical and Chemical Research, Wako, Saitama (Japan)). Nucl. Instrum. Methods; 119: No. 2, 209-212(15 Jul 1974).

A mechanical beam chopper system combined with a Ge(Li) γ-ray detector has been developed which enables to measure half-lives of isomeric states in the range from 1 to 900 ms. Values of (8.39 ± 0.11) ms for the half-life of the 2.757 MeV isomeric state in ^{132}Xe, (5.25 ± 0.24) ms for the 95.2 keV state in ^{171}Yb and (6.19 ± 0.08) ms for the 382 keV state in ^{90}Nb were obtained. (auth)

30155 POLARIZATION DECAY OF AN ETHYLENE GLYCOL POLARIZED PROTON TARGET IN AN INTENSE PROTON BEAM. Petri, H. R.; Abshire, G. W. (Indiana Univ., Bloomington (USA). Dept. of Physics). Nucl. Instrum. Methods; 119: No. 2, 205-207 (15 Jul 1974).

The first measurements of the decay of the polarization of an ethylene glycol target irradiated in an intense proton beam are examined as a function of the incident flux. Fits to the data using four functional forms are discussed. Using the form $P = P_0 \exp(-\phi/\phi_0)$, the characteristic flux ϕ_0 is determined to be $(2.00 \pm 0.18) \times 10^{14}$ protons/cm^2. Data on the decay of the relaxation time are also included. (auth)

30156 A HIGH-INTENSITY SUPERCONDUCTING MUON CHANNEL. Dibitonto, D.; Hitlin, D. (Stanford Univ., Calif. (USA). High-Energy Physics Lab.). Nucl. Instrum. Methods; 119: No. 1, 189-196(1 Jul 1974).

The design of a high-intensity muon channel with an acceptance of more than 2 sr is considered. The channel consists of two superconducting magnets; a toroid and a solenoid. Monte Carlo calculations are performed to optimize the channel's design parameters for maximum muon beam intensity. The channel can provide 1.4×10^9 muons/s when used in conjunction with a 1 mA, 400 MeV electron linac. (auth)

30157 A COOLING SYSTEM FOR THIN TRITIATED TITANIUM TARGETS. Morales, J. R.; Romero, J. L.; Brandan, M. E. (Chile Univ., Santiago. Departamento de Fisica). Nucl. Instrum. Methods; 119: No. 1, 91-92(1 Jul 1974).

A low-temperature device was built in order to avoid tritium evaporation from thin tritiated titanium foils under deuteron beam impact. A method to determine tritium loss is described. (auth)

30158 THE UNIVERSITY OF MICHIGAN CYCLOTRON FACILITY FOR RESEARCH IN NUCLEAR STRUCTURE. Parkinson, W. C.; Petersen, J. F.; Day, R. H.; DuPlantis, D. C.; Gray, W. S.; Bardwick, J. (Michigan Univ., Ann Arbor (USA). Cyclotron Lab.). Nucl. Instrum. Methods; 119: No. 1, 61-89(1 Jul 1974).

A number of improvements have been made in The University of Michigan 83″ sector focused cyclotron since its original construction. The reasons for the changes and the resulting improvement in the production of stable high-quality beams for nuclear research are described. A brief description of the total facility for research in nuclear structure is given. (auth)

30159 THE UNIVERSITY OF MICHIGAN NEUTRON TIME-OF-FLIGHT FACILITY. Parkinson, W. C.; Petersen, J. F.; Day, R. H.; Polichar, R. M.; Julien, P. F.; DuPlantis, D. C. (Michigan Univ., Ann Arbor (USA). Cyclotron Lab.). Nucl. Instrum. Methods; 119: No. 1, 51-60(1 Jul 1974).

The time-of-flight spectrometer now in use with The University of Michigan's 83″ cyclotron facility is an extension and modification of earlier versions the basis of which is the natural phase bunching of the circulating beam in the cyclotron. This paper describes the facility and indicates the type and quality of measurements that are being made. (auth)

PHYSICS (ASTROPHYSICS AND COSMOLOGY)

30160 (CONF-730693-) PARTICLES AND FIELDS IN SPACE. Proceedings of the Summer School, Balatonfured, 5-15 June 1973. Kiraly, P.; Sebestyen, A.; Somogyi, A. J. (eds.). (Kozponti Fizikai Kutato Intezet, Budapest (Hungary)). 1974. 284p. (In English and Russian).

The conference included 10 papers. Separate abstracts were prepared for each paper. (JFP)

For abstracts of individual papers see: 30182, 30183, 30296, 30297, 30341–30344, 30679, and 31019.

30161 PROBLEMY KOSMICHESKOI FIZIKI. (Problems of Cosmic Physics). Vsekhsvyatskii, S. K. (ed.). Kiev; Izdatel'stvo Kievskogo Universiteta (1973). 205p.

The book included 26 chapters. Separate abstracts were prepared for 14 chapters. Other chapters were outside the subject scope of NSA. (JFP)

For abstracts of individual chapters see: 30209–30213, 30308, 30309, 30354, 30395, 30396, 30415, and 30544–30546.

Cosmic Radiation

Refer also to abstracts 29499–29501, 29533, 29579–29583, 30297, 30432, 30579, 30585, and 30611.

30162 XENON ISOTOPE ANOMALIES IN THE CARBONACEOUS CHONDRITE MURRAY. Kuroda, P.K.; Beck, J.N.; Efurd, D.W.; Miller, D.K. (Department of Chemistry, University of Arkansas, Fayetteville, Arkansas 72701). J. Geophys. Res. 79: No. 26, 3981-3992 (10 Sept 1974).

Isotopic compositions have been measured mass spectrometrically for xenon fractions released from the carbonaceous chondrite Murray in stepwise heating experiments. The isotopic ratios varied quite considerably; for example, the ^{136}Xe/^{132}Xe ratio in the 1000°C fraction was almost identical to the atmospheric ratio (0.330), whereas the ratio in the 1300°C fraction agreed with that in Sucor (0.305). It appears that these variations can best be explained as being due to the fact that reservoirs of two isotopically distinct gases (solar and planetary) exist in the meteorite and that mixtures of these gases in various proportions are being released at different temperatures. The major difference in the isotopic compositions of solar and planetary xenon can be attributed to a mass–dependent fractionation process, which must have occurred during the early stages of the history of the solar system. The abundance ratios of the xenon isotopes are also altered by the cosmic ray irradiation and neutron capture processes. According to this interpretation, it is unnecessary to assume the existence of the so–called carbonaceous chondrite fission component. The decay products of extinct radionuclides ^{129}I and ^{244}Pu did not alter the xenon isotopic ratios significantly in the case of the carbonaceous chondrite Murray. The light isotopes ^{124}Xe and ^{126}Xe in the earth's atmosphere appear to be partially of cosmic ray origin. (auth)

30163 THE DISTRIBUTION OF COSMIC RAYS IN THE GALAXY AND THEIR DYNAMICS AS DEDUCED FROM RECENT γ-RAY OBSERVATIONS. Puget, J.L.; Stecker, F.W. (Theoretical Studies Group, NASA Goddard Space Flight Center, Greenbelt, Maryland). Astrophys. J. 191: No. 2, 323-329 (15 July 1974).

Recent data from SAS–2 on the galactic γ–ray line flux as a function of longitude reveal a broad maximum in the γ–ray intensity in the region $|l| \lesssim 30°$. These data, when unfolded, imply that the low–energy (1–10 GeV) galactic cosmic–ray flux varies with galactocentric distance and is about an order of magnitude higher than the local value in a toroidal region between 4 and 5 kpc from the galactic center. We further show that this enhancement can be plausibly accounted for by first–order Fermi acceleration, compression, and trapping of cosmic rays consistent with present ideas of galactic dynamics and galactic structure theory. Our calculations indicate that cosmic rays in the 4–5 kpc region are trapped and accelerated over a mean time of the order of a few million years or about 2–4 times the assumed trapping time in the solar region of the Galaxy. Cosmic–ray nucleons, cosmic–ray electrons, and ionized hydrogen gas are found to have a strikingly similar distribution in the Galaxy according to both the observational data and the theoretical model discussed here. (auth)

30164 CHARGE COMPOSITION AND ENERGY SPECTRA OF COSMIC–RAY NUCLEI AT ENERGIES ABOVE 20 GeV PER NUCLEON. Júliusson, E. (Enrico Fermi Institute and Department of Physics, Laboratory for Astrophysics and Space Research, University of Chicago). Astrophys. J. 191: No. 2, 331-348 (15 July 1974).

An instrument to measure the charge composition and energy spectra of cosmic–ray nuclei of charge $Z=3$ and above has been exposed for a net total of 7.6 m^2 sr hours in three balloon flights during 1971 and 1972. The instrument is a scintillation–Cerenkov counter telescope, including two gas Cerenkov counters for energy measurements above 20 GeV per nucleon, and up to about 100 GeV per nucleon. In this paper we present the charge composition and energy spectra that have been measured in that energy range. The nuclear composition has been found to change with energy. The flux of nuclei produced by spallation of source nuclei in the Galaxy has been found to decrease faster with increasing energy than the flux of source nuclei. The carbon to oxygen ratio measured above 20 GeV is significantly lower than measured at low energy. Iron exhibits a flatter energy spectrum than other nuclei. The results are interpreted as showing that the high–energy nuclei have traversed less material than the low–energy nuclei. (auth)

30165 CHARGE COMPOSITION OF COSMIC RAYS BETWEEN 4 AND 100 GV. Golden, R. L.; Adams, J. H.; Badhwar, G. D.; Deney, C. L.; Lindstrom, P. J.; Heckman, H. H. (Johnson Space Center, Houston, TX). Nature (London); 249: No. 5460, 814-816(28 Jun 1974).

Measurements of the ratios of L nuclei to M nuclei and of VH nuclei to M nuclei are reported as obtained using a magnetic spectrometer carried by balloon flights made from Texas in August 1969 and from Argentina in November 1970. A computer controlled microscope with a measuring accuracy of ±2.5 μm was used to measure trajectories. Rigidity spectra of nuclei with $Z \geq 3$ are shown. Analysis gave a spectral index of -2.6 ± 0.1. Charge measurement was carried out using a television microscope to measure track area, and the charge distribution is shown graphically; the charge composition is also shown as a function of rigidity. No evidence was found that the VH spectrum is steeper than the M spectrum. (UK)

30166 KOSMICHESKIE LUCHI V MEZHPLANETNOM PROSTRANSTVE. (Cosmic Rays in Interplanetary Space). Miroshnichenko, L. I. Moscow; Izdatel'stvo Nauka (1973). 160p.

This monograph reviews the methods and equipment used in cosmic ray measurements, the time-dependent variations of cosmic rays, and the history of cosmic ray detection and studies. Modern theories concerning sun-earth relations, the interplanetary magnetic field, the acceleration and propagation of cosmic particles and their penetration in the magnetosphere and atmosphere are set forth in the context of the practical aspects of radio communications, space navigation, and radiation safety of space flight. An updated classification of cosmic ray variations is given, covering seasonal, diurnal, 11-day, 27-day, solar-day, Forbush effect-related, and anomalous variations and their mechanisms and nature. The impact of cosmic rays on life on earth is also considered. (IAA)

30167 COSMIC RAY DIFFUSION AND ANISOTROPY. Skilling, J. (Cambridge Univ., Eng.); McIvor, I.; Holmes, J. A. Mon. Notic. Roy. Astron. Soc.; 167: No. 3, 87P-91P(Jun 1974).

The effects are investigated of a turbulent magnetic field on the "leaky box" model of galactic cosmic ray confinement. It is found that within the galactic disk cosmic rays diffuse in three dimensions with a mean free path of about 30 pc. If cosmic rays are produced by supernovae, rays are observed at earth from about 2000 separate sources. The local value of their anisotropy is determined by conditions local to those magnetic field lines which pass near the sun. (auth)

30168 EQUILIBRIUM STATISTICAL MECHANICS OF RELATIVISTIC PARTICLES WITH VARIABLE MASSES. I. Nonquantal Theory. Hakim, R. (Observatoire de Meudon, France). J. Math. Phys. (N. Y.); 15: No. 8, 1310-1319(Aug 1974).

The necessity for statistical mechanics of relativistic particles endowed with variable rest masses essentially arises from astrophysics (when dealing with clusters of stars or galaxies which do exhibit a mass spectrum) and from the statistical bootstrap model of Hagedorn and Frautschi for inclusive reactions of elementary particles. This series is begun with the simplest case of classical particles since this case demonstrates more clearly the main features of the theory. Moreover, this classical case is an excellent approximation for the statistical bootstrap near the "hadronic boiling point." First the one-particle distribution function is derived using the standard maximization procedure, in the implicit case of a uniform mass spectrum. It is shown that the actual mass spectrum possesses a part due to thermal agitation. An equation of states is derived. Other distributions are obtained (energy, 4-velocity). In the case of weak collisions, space-time correlations for the numerical and proper energy densities are derived and applied to the hadronic matter near the "hadronic boiling point." Finally, several extensions of these ideas are discussed. (auth)

30169 ORIGIN OF COSMIC RAYS. Pacheco, J. A. de F. (Univ., Sao Paulo, Brazil). Astrophys. Lett.; 15: No. 3, 155-158 (Nov 1973).

From the recent data on the L/M ratio, an energy-dependent diffusion coefficient was calculated. The implication of the results on the origin of cosmic rays is analyzed. (auth)

30170 THE UNIQUE COSMIC-RAY HISTORY OF THE MALAKAL CHONDRITE. Cressy, P. J. Jr. (National Aeronautics and Space Administration, Greenbelt, Md. (USA). Goddard Space Flight Center); Rancitelli, L. A. (Battelle Pacific Northwest Labs., Richland, Wash. (USA)). Earth Planet. Sci. Lett.; 22: No. 3, 275-283(Jun 1974).

Cosmogenic radionuclides, including ^{22}Na, ^{26}Al, and ^{54}Mn, were measured in a sample of the recently-fallen Malakal hypersthene chondrite. The high ^{26}Al activity, 79 ± 2 dpm/kg, greatly exceeds the levels expected from elemental production rates, shielding considerations, or comparisons with other ordinary chondrites, and can only be explained by exposure to a uniquely high cosmic-ray flux. Calculations including noble gas, ^{3}H, and ^{53}Mn data from other laboratories require a two-stage irradiation. Malakal's most probable history is: exposure in excess of 4 m.y. to an effective cosmic-ray flux approximately three times that experienced by other chondrites, an orbit change (very possibly caused by a collision), and a final period of about 2 m.y. during which it was exposed to a "normal" cosmic-ray flux. (auth)

30171 PION INCLUSIVE DISTRIBUTION AT COSMIC-RAY ENERGIES AND COMPARISON WITH ISR DATA. Rodrigues, W. A. Jr.; Turtelli, A. Jr. (Univ., Estadual, Campinas, Brazil). Nuovo Cim., 23A: No. 2, 227-236(21 Sep 1974).

The inclusive spectra for π^0-mesons constructed from the data obtained by Brasil-Japan emulsion chamber experiment with Câmara 15 (40 m^2), exposed at Mount Chacaltaya, Bolivia (5220 m, 550 g/cm^2), in 1969–70 covering the energy range 15 TeV < E_{lab} < 240 TeV are presented. A comparison with ISR data is presented, and it is pointed out that the available data on pion yield are compatible with a production mechanism occurring in two steps: first, uncorrelated clusters are produced (the unique link being, of course, energy-momentum conservation) and, then, they decay isotropically into pions. (auth)

30172 FOKKER–PLANCK COEFFICIENT FOR PITCH-ANGLE SCATTERING OF COSMIC RAYS. Fisk, L. A. (Goddard Space Flight Center, Greenbelt, MD); Goldstein, M. L.; Klimas, A. J.; Sandri, G. Astrophys. J.; 190: No. 2, 417-428(1 Jun 1974).

For the case of homogeneous, isotropic magnetic field fluctuations, it is shown that most theories which are based on the quasi-linear and adiabatic approximations yield the same integral for the Fokker–Planck coefficient for the pitch-angle scattering of cosmic rays. For example, despite apparent differences, the theories due to Jokipii and to Klimas and Sandri yield the same integral. It is also shown, however, that this integral in most cases has been evaluated incorrectly in the past. For small pitch angles, the errors in previous evaluations are fortuitously of minor importance. For large pitch angles, however, these errors become more significant; and for pitch angles of 90°, the actual Fokker-Planck coefficient contains a delta-function which has been overlooked in the past. The implications of these corrections on the ability to relate cosmic-ray diffusion coefficients to observed properties of the interplanetary magnetic field are discussed. (auth)

30173 THE POSSIBLE INFLUENCE OF JUPITER ON COSMIC RADIATION AT THE EARTH. Swinson, D.B. (The University of New Mexico, Department of Physics and Astronomy, Albuquerque, New Mexico 87131). J. Geophys. Res. 79: No. 25, 3695-3700 (1 Sept 1974).

Analysis of cosmic ray data in sidereal time from underground mu–meson telescopes at different depths in New Mexico and in Bolivia indicates the presence of a long–term modulation of the cosmic ray anisotropy in sidereal time. The period of this modulation is close to 11 or 12 years. These new data, along with data from the underground telescope at Hobart, are examined in relation to suggestions that such a long–term modulation in the cosmic ray anisotropy in sidereal time can be produced by a possible shielding of incoming galactic cosmic rays by Jupiter's magnetosphere. This model is reviewed in the light of the new cosmic ray data presented here and the data on Jupiter's magnetosphere obtained in the flyby by Pioneer 10. These data suggest that it is unlikely that Jupiter's magnetosphere is capable of causing the observed modulation. A correlation between the phase of the modulation and the cycle of solar activity is noted. (auth)

30174 A SEARCH FOR A COSMOLOGICAL COMPONENT OF THE SOFT X–RAY BACKGROUND IN THE DIRECTION OF M31. Margon, B. (Space Sciences Laboratory, University of California, Berkeley, CA 94720); Bowyer, S.; Cruddace, R.; Heiles, C.; Lampton, M.; Troland, T. Astrophys. J. Lett. 191: No. 3, L117-L119 (1 Aug 1974).

Results of an experiment to search for absorption of the soft ($E \leqslant 0.28$ keV) diffuse X–ray background by M31, the Andromeda Nebula, are presented. Both X–ray and 21–cm observations were obtained with high spatial resolution; the X–ray detector had a 2° field of view, and the 21–cm data were taken with 20′ resolution. The results establish that at least 48±5 percent of the soft X–ray flux has a local source, but that the remainder may be of distant origin and therefore of cosmological significance. (auth)

30175 FLUCTUATION STUDIES OF LARGE AIR SHOWERS: THE COMPOSITION OF PRIMARY COSMIC RAY PARTICLES OF ENERGY E_p APPROXIMATELY 10^{18} eV. Watson, A. A.; Wilson, J. G. (Univ. of Leeds, Eng.). J. Phys., B (London); 7: No. 10, 1199-1212(1 Jul 1974).

The time sequence of detection of Cherenkov light in the deep-water detectors used at Haverah Park is used to establish a shower parameter insensitive to the total energy of the primary particles but yielding a measure of fluctuations of development among showers. Values of departure of individual showers from the mean behavior now established are most readily understood if some of the primary particles of energy $E_p \sim 10^{18}$ eV are light, probably protons but perhaps α particles. (auth)

30176 ENERGY SPECTRUM OF PRIMARY COSMIC RAYS ABOVE 10^{12} eV. Kempa, J.; Wdowczyk, J.; Wolfendale, A. W. (Inst. of Nuclear Research, Warsaw). J. Phys., B (London); 7: No. 10, 1213-1221(1 Jul 1974).

Recent direct experimental measurements of the primary proton spectrum have given a power law with differential slope γ_d – 2.75 for energy less than about 10^{12} eV. Extrapolation of this spectrum gives intensities on the order of those derived from extensive air showers in the region of 10^{18} to 10^{19} eV. The data from a variety of experiments which had previously indicated intensities significantly above this spectrum, particularly in the range 10^{14} to 10^{16} eV, are re-examined critically. It is concluded that the intensities are indeed higher and that a single exponent is quite inadequate to describe the spectral range 10^{10} to 10^{20} eV. (auth)

30177 PRODUCTION SPECTRUM OF CHARGED COSMIC RAY PIONS AND THE PRIMARY COSMIC RAY NUCLEON SPECTRUM. Bhattacharyya, D. P. (Indian Association for Cultivation of Science, Calcutta). J. Phys., B (London); 7: No. 10, 1222-1226(1 Jul 1974).

The production spectrum of charged pions and the primary cosmic ray nucleon spectrum have been derived from the experimental muon spectrum determined near the geomagnetic equator at the zenith angles 45°W and 60°W. The derived pion spectrum follows the relation $P(E_\pi)dE_\pi = (0.22 \pm 0.03)E_\pi^{-(2.65 \pm 0.12)} dE_\pi$ and the primary spectrum agrees with the relation $N(E_p)dE_p = 2.9E_p^{-2.65}\,dE_p$. The results have been compared with the values expected from the vertical muon spectrum. (auth)

30178 COUPLING CONSTANTS FOR THE COSMIC RAY MUON COMPONENT. Singhal, K. P. (Physical Research Lab., Ahmedobad, India). J. Phys., B (London); 7: No. 10, 1227-1238(1 Jul 1974).

An apparatus employing twin telescopes to study the azimuthal variation of cosmic ray muon intensity was operated at Ahmedabad (geographic 23°N, 73°E; geomagnetic latitude 14°N). Fourteen directions were scanned for long time intervals to give a counting rate accuracy of about 0.4% for each direction. Experimental results are presented. Variation in the coupling constant values in the rigidity range 12 to 26 GV is rather flat. Some implications of this behavior are discussed. A theoretical method is described for the estimation of coupling constants applicable to muon telescopes. Correction for the fact that alpha particles and heavy particles have a cut-off (in terms of momentum per nucleon) at half the value for protons is incorporated in the calculation. The method is verified by comparing the theoretical results with experimental data on the latitude effect (namely, for zenith direction) and on the azimuth effect for fixed zenith angles. Theoretically estimated coupling constants for different zenith angles and different atmospheric depths are presented. (auth)

30179 VARIATIONS OF COSMIC RAY INTENSITY IN CONSEQUENCE OF THE SEMIDIURNAL ANISOTROPY. El Bedewi, F.; Goned, A.; Tolba, M. F. (Ain Shams Univ., Cairo). Planet. Space Sci.; 22: No. 8, 1185-1192(Aug 1974).

The different types of cosmic ray intensity variations arising from the semidiurnal anisotropy are evaluated for different stations taking into consideration the effect of the Earth's axis inclination. Appropriate values of the parameters of the anisotropy together with accurate values of coupling and normalization constants are used in the calculations. The results predict the appearance of semiannual and diurnal waves as a consequence of a semidiurnal anisotropy. The form of the generated waves is found to be dependent on the characteristics of the station's asymptotic cone of acceptance as well as the season of detection. The characteristics of these waves together with that of the semidiurnal variation are discussed in detail. (auth)

30180 RISING INELASTIC CROSS-SECTION AND THE ATTENUATION OF COSMIC RAY NUCLEONS IN THE ATMOSPHERE. Yekutieli, G. (Weizmann Inst. of Science, Rehovoth (Israel). Dept. of Physics). Phys. Lett., B; 51: No. 1, 93-95 (8 Jul 1974).

The intensity of C.R. nucleons in the atmosphere is calculated at high energies for energy-dependent inelastic cross-sections. It is found that the spectrum of C.R. nucleons becomes steeper with atmospheric depth (x g/cm^2) and behaves like $E^{-\gamma-xB/\Lambda}$. (auth)

30181 MONTE CARLO COMPUTATION FOR ISOTOPIC ANALYSIS OF COSMIC RAYS BY MEANS OF THE EARTH'S MAGNETIC FIELD. Hubert, P. (CEA Centre d'Etudes Nucleaires de Saclay, 91–Gif-sur-Yvette (France). Service d'Electronique Physique). Nucl. Instrum. Methods; 119: No. 1, 183-188 (1 Jul 1974).

A Monte Carlo computation has been performed to evaluate a method of cosmic-ray isotopic analysis by means of the earth's magnetic field. This procedure requires the numerical integration of a large number of randomly chosen trajectories. It takes into account the shape of the external spectrum, the geometrical conditions of the experiment and the properties of the detector. Numerical application is given in the case of a possible satellite experiment. (auth)

Stars

Refer also to abstracts 30380, 30913, and 31019.

30182 (CONF-730693-, pp 43-102) BLACK-HOLE PHYSICS: AN INTRODUCTION. Sexl, R. U. (CERN, Geneva). 1974.

From proceedings of the summer school on particles and fields in space; Balatonfured, Hungary (5 Jun 1973).

Lectures are given on an introduction to black-hole physics. They cover the elementary theory of stellar structure and relativistic effects, the theory of black holes, and the search for black holes. Many connections between elementary particle physics and astrophysics are shown. (JFP)

30183 (CONF-730693-, pp 161-181) INTRODUCTION TO THE PHYSICS OF INTERSTELLAR PLASMAS. Abonyi, I. (Roland Eoetvoes Univ., Budapest). 1974.

From proceedings of the summer school on particles and fields in space; Balatonfured, Hungary (5 Jun 1973).

The treatment covers continuum hydrodynamics particularly the motion of discontinuity surfaces. (JFP)

30184 THE PALOMAR RADIAL–VELOCITY SPECTROMETER. Griffin, R.F. (Cambridge Observatories); Gunn, J.E. Astrophys. J. 191: No. 2, 545-556 (15 July 1974).

A photoelectric radial–velocity spectrometer has been constructed for the 200–inch (5–m) telescope by modifying the existing coudé spectrograph; useful inovations have been made in both the design and the operation of the instrument. Internal evidence suggests that errors can be kept down to ~ 0.1 km s^{-1} on bright stars ($V \lesssim 10$). Observations of a set of very bright stars are more accurate than any velocities available for comparison; the rms discrepancy from Cambridge photoelectric observations is 0.48 km s^{-1}. (auth)

30185 THE T TAURI EMISSION NEBULA. Schwartz, R.D. (Department of Astronomy, University of Washington, Seattle, Washington 98195). Astrophys. J. 191: No. 2, 419-432 (15 July 1974).

Photoelectric and spectrographic data on the emission–line spectrum of T Tauri have been used to study the physical conditions in the circumstellar gas envelope which is estimated to extend to about 0.1 a.u. from the star, and the southward–extended emission nebula which extends to about 1500 a.u. from the star. Independent reddening analyses of the star and the extended nebula suggest the presence of a circumstellar dust envelope which is exterior to the circumstellar gas envelope but interior to the bulk of the nebula. The relative intensities of the emission lines of [O II], [O III], [N I], [N II], and [S II] suggest that $3 \times 10^3 \lesssim N_e \lesssim 10^4$ cm^{-3}, $7000°$ K $\lesssim T_e \lesssim 9000°$ K, in the resolved extended nebula. Forbidden lines arising from the "inner nebula" defined as that region exterior to the circumstellar gas envelope extending to about 400 a.u. from the star indicate $10^4 \lesssim N_e \lesssim 4 \times 10^4$ cm^{-3}, $9000°$ K $\lesssim T_e \lesssim 13{,}000°$ K. The larger intensity ratios of [O III]/[O II] and the blue/red [S II] lines in the inner nebula as compared with the extended nebula indicate the presence of higher excitation in the inner region nebula. The Balmer line flux from the from the circumstellar gas envelope is consistent with a region optically thin in the Balmer lines with an average density of $N_e \simeq 4 \times 10^9$ cm^{-3} and a volume of about 10^{37} cm^3. The photoelectric measurements indicate that the total energy emitted by the envelope–nebula gas system in emission lines, free–bound, and free–free radiation is of the order of 10^{33} ergs s^{-1}, about 1 percent of the luminosity of T Tau. It is estimated that about 90 percent of this energy is emitted by the circumstellar gas envelope, and the remainder by the inner and extended nebula. It is suggested that mechanical–energy input to the circumstellar gas envelope from the stellar convection zone can provide a significant fraction of the energy needed to maintain ionization of the envelope. Sufficient diffuse Lyman continuum radiation may emerge from the ionized envelope to produce the surrounding nebula. The relevance of this model for the interpretation of the emission–line spectra of other T Tauri stars and the Herbig–Haro objects is discussed. (auth)

30186 CHARGE AND PARTICLE CONSERVATION IN BLACK–HOLE DECAY. Carter, B. (Observatoire de Paris–Meudon, 92190 Meudon, France). Phys. Rev. Lett 33: No. 9, 558-561 (26 Aug 1974).

The qualitative consequences of Hawking's prediction of thermal emission from black holes are considered. Whereas mass and angular momentum loss proceeds on cosmologically long time scales, on the other hand electric discharge will take place extremely rapidly. Hypothetical mechanisms for baryon and lepton conservation are discussed. (auth)

30187 DISK–ACCRETION ONTO A BLACK HOLE. I. TIME–AVERAGED STRUCTURE OF ACCRETION DISK. Page, D.N.; Thorne, K.S. (California Institute of Technology, Pasadena, California). Astrophys. J. 191: No. 2, 499-506 (15 July 1974).

An analysis is given of the time–averaged structure of a disk of material accreting onto a black hole. The analysis is valid even if the disk is highly dynamical. It assumes only that the hole is stationary and axially symmetric (e.g., that it is a Kerr hole); that the disk lies in the equatorial plane of the hole, with its material moving in nearly geodesic circular orbits; that the disk is thin; and that radial heat transport is negligible compared with heat losses through the surface of the disk. The most important result of the analysis is an explicit, algebraic expression for the radial dependence of the time–averaged energy flux emitted from the disk's surface, F(r). (auth)

30188 DISK–ACCRETION ONTO A BLACK HOLE. II. EVOLUTION OF THE HOLE. Thorne, K.S. (California Institute of Technology, Pasadena, California). Astrophys. J. 191: No. 2, 507-519 (15 July 1974).

When a black hole swallows matter and radiation from an accretion disk, its mass M and angular momentum $J \equiv Ma$ change–i.e., the hole evolves. The details of that evolution are calculated. The accreting matter, by itself, would spin the hole up to $a = M$ ("extreme–Kerr hole") after a modest amount of accretion ($\Delta M/M_i \sim 1.5$). However, the radiation emitted by the disk and swallowed by the hole produces a counteracting torque, which prevents spin–up beyond a limiting state of $(a/M)_{\rm lim} \simeq 0.998$. This limiting state corresponds to a maximum efficiency of 30 percent for the hole's conversion of accreting mass into outgoing photon energy. In § IV it is argued that realistic phenomena ignored in this calculation (magnetic fields dragged down the hole by accreting matter; heating of outer parts of disk by X–rays from inner parts;...) might not change significantly the values $(a/M)_{\rm lim} \simeq 0.998$ and (maximum efficiency) $\simeq 0.30$. (auth)

30189 PERTURBATION OF A SLOWLY ROTATING BLACK HOLE BY A STATIONARY AXISYMMETRIC RING OF MATTER. I. EQUILIBRIUM CONFIGURATIONS. Will, C.M. (University of Chicago). Astrophys. J. 191: No. 2, 521-531 (15 July 1974).

We present and discuss the equations in general relativity that describe black holes surrounded by stationary axisymmetric rings or disks of matter, and develop a scheme for treating the effects of the matter and of a small amount of rotation of the hole as perturbations of vacuum Schwarzschild black hole. When specialized to a stationary axisymmetric ring of matter in orbit around a slowly rotating black hole, the equations lead to a sequence of configurations parametrized by the irreducible mass M_{ir} of the black hole (related to the area of its horizon), the angular velocity ω_H of the horizon, and the rest mass m and proper circumferential radius R of the ring. For any given M_{ir}, m, and R the total mass of a configuration is a minimum for a particular nonzero value of ω_H. Other properties of these configurations are discussed. (auth)

30190 A QUANTITATIVE STUDY OF SILICATE EXTINCTION. Day, K.L.; Steyer, T.R.; Huffman, D.R. (Department of Physics, University of Arizona). Astrophys. J. 191: No. 2, 415-418 (15 July 1974).

Quantitative measurements of silicate extinction, coupled with Mie theory indicate that previously used mass absorption coefficients for silicates are considerably too low. Information is presented leading to the conclusion that silicates have an almost negligible effect in producing extinction in the visible region of the general interstellar extinction curve. (auth)

30191 THE COMPOSITION OF RR LYRAE STARS. Rodgers, A.W. (Mount Stromlo and Siding Spring Observatory, Research School of Physical Sciences, Australian National University). Astrophys. J. 191: No. 2, 433-437 (15 July 1974).

A calibration of Preston's ΔS composition parameter in terms of [Ca/H] is presented and its implications for the range of composition exhibited by field and cluster RR Lyrae stars are discussed. Some stars with halo kinematics, or located in the halo, are as metal rich as those in the galactic disk. (auth)

30192 PULSATIONAL STABILITY OF STARS IN THERMAL IMBALANCE. III. ANALYSIS IN TERMS OF ABSOLUTE VARIATIONS. Cox, J.P. (Joint Institute for Laboratory Astrophysics, University of Colorado National Bureau of Standards; and Department of Physics and Astrophyics, Boulder, Colorado 80302); Davey, W.R.; Aizenman, M.L. Astrophys. J. 191: No. 2, 439-455 (15 July 1974).

A cubic equation has been derived for the eigenvalues, in terms of absolute variations, for stars in thermal imbalance; an analogous equation for relative variations is also presented, for completeness, in an appendix. No approximations (other than very general ones such as spherical symmetry, etc.) have been made in these equations regarding either the degree of adiabaticity in the pulsations or the motion of the unperturbed model. Solutions of these equations yield explicit integral expressions for the appropriate stability coefficients in the case where the pulsation period is small compared with the time scale for the secular motion of the unperturbed model. It is shown that the modified energy approach of Davey and Cox is fully equivalent to these integral expressions in the above case, for both absolute and relative variations, provided that the pulsations are assumed to be quasi—adiabatic. However, it is shown that, as far as the equivalence proofs are concerned, this assumption is normally sufficiently accurate for all real evolving stars except highly luminous, low—mass red supergiants. It is also shown in another appendix that the above integral expressions for the stability coefficient for absolute variations are equivalent to the energy approach of Axel and Perkins, at least in a certain class of cases. Computationally convenient forms of the integral expressions are presented, and it is shown that certain important simplifications are usually possible. Finally, it is pointed out by reference to work now in progress that all of the basic assumptions underlying the present integral expression approach have now been essentially confirmed. (auth)

30193 A DETERMINATION BY THE ZEEMAN EFFECT OF THE MAGNETIC FIELD STRENGTH IN THE WHITE DWARF G99—37. Angel, J.R.P. (Department of Astronomy, University of Texas at Austin, and Institute of Astronomy, Cambridge, England); Landstreet, J.D. Astrophys. J. 191: No. 2, 457-464 (15 July 1974).

The detailed wavelength dependence of circular polarization in G99—37 has been measured with the multi—channel spectrophotometer at the Hale telescope. A strong polarization feature is found associated with the G—band of CH, present in this white dwarf. The magnetic circular dichroism of this band is obtained by calculating the magnetic perturbation to first order of both energy eigenvalues and eigenfunctions of the CH molecule. From these results stellar profiles of absorption and polarization across the band are derived for different fields, taking into account the effect of radiative transfer. A good fit to the observations is obtained with an effective field $H = 3.6 \times 10^6$ gauss. An estimate of the strength and wavelength dependence of continuous circular polarization is made for this field strength, assuming He^- as the dominant opacity, and is in agreement with the observations. (auth)

30194 STRUCTURE OF SOLID IRON IN SUPERSTRONG NEUTRON—STAR MAGNETIC FIELDS. Chen, H. (School of Natural Science, Institute for Advanced Study, Princeton, New Jersey); Ruderman, M.A.; Sutherland, P.G. Astrophys. J. 191: No. 2, 473-477 (15 July 1974).

The structure of iron atoms, molecular chains, and condensed matter in superstrong magnetic fields ($1-5 \times 10^{12}$ gauss) is investigated. The binding energy for an iron atom is about $5-10 \times 10^4$ eV; the cohesive energy of an iron lattice is about $10-20 \times 10^3$ eV per atom. This binding may have important consequences for particle emission at the expected temperatures and electric fields on pulsar surfaces. (auth)

30195 RADIATIVE TRANSFER OF PARTIALLY POLARIZED LIGHT. Acquista, C.; Anderson, J.L. (Department of Physics, Stevens Institute of Technology, Hoboken, New Jersey 07030). Astrophys. J. 191: No. 2, 567-576 (15 July 1974).

The transfer of partially polarized radiation through an atmosphere composed of arbitrary scatterers is studied here. A transfer equation is derived for the case where the scatterers are at rest and then generalized to the case where the scatterers are in arbitrary state of motion. The terms in the transfer equation are then exhibited for the case of Compton scattering. (auth)

30196 A NEW NODAL EXPANSION FOR CLASSICAL PLASMAS. Buckholtz, T.J. (L—O, Lawrence Livermore Laboratory, Livermore, California 94550). Ann. Phys. (N.Y.) 86: No. 2, 197-232 (Aug 1974).

In calculating the equation of state for plasmas we find that diagrammatic expansions for the free energy become unwieldy at high density. At best, many terms must be retained in order to obtain meaningful results. We present a new expansion technique which can be applied to plasmas in the interiors of Jupiter and white dwarf stars. In such cases the older techniques are unsatisfactory because of the size of the ion coupling parameter. Our work yields expansions for which this parameter is supplanted by ion correlation functions, which can be supplied by external computations. In this paper we assume a two—species plasma of classical particles, thereby focusing on combinatorial techniques. The final result is a new nodal expansion in terms of ion correlation functions and an electron coupling parameter. (auth)

30197 DO PULSARS MAKE SUPERNOVAE? II. CALCULATIONS OF LIGHT CURVES FOR TYPE II EVENTS. Bodenheimer, P. (Lick Observatory, Board of Studies in Astronomy and Astrophysics, University of California, Santa Cruz); Ostriker, J.P. Astrophys. J. 191: No. 2, 465-471 (15 July 1974).

By performing numerical hydrodynamical calculations we examine the hypothesis that pulsars can produce supernova explosions—that the electromagnetic energy radiated by a newly formed rotating neutron star can drive off the remaining envelope of a red—giant star whose initial mass lies in the range 3—8 $M_\odot$. The initial configuration is taken to be a model of a red—giant envelope with mass M_{env} in which a neutron star with rotational energy E is embedded. The outward motion of the envelope is followed numerically, through a phase in which the material is confined to a relatively thin spherical shell, up to the point where the optical thickness of the shell becomes small. Radiative energy losses from the surface become important during the later stages of the calculation: the resulting light curves for a number of assumed values of M_{env} and E are compared with observations of supernovae. Reasonable agreement can be obtained with a number of different observed properties, but best agreement occurs for masses slightly less than 3 $M_\odot$. In all cases, the predicted time for the light to rise to maximum is somewhat too long to be consistent with observations. It is suggested that the calculated rise time will be significantly shortened if the presence of a dust—laden circumstellar envelope around the original red giant is taken into account. (auth)

30198 ISLAND SOLUTIONS IN LINEAR SERIES OF STATIC STELLAR MODELS WITH CORE HELIUM AND SHELL HYDROGEN BURNING FOR $M = 5,7$, AND 9 $M_\odot$. Lauterborn, D.; Siquig, R.A. (Joint Institute for Laboratory, Astrophysics, University of Colorado and National Bureau of Standards). Astrophys J. 191: No. 2, 589-592 (15 July 1974).

Linear series of static stellar models with core helium and shell hydrogen burning are presented for models with total mass $M = 4,5,7$, and 9 $M_\odot$, and for core masses $0.15 < M_c/M < 0.40$. Triple solutions are encountered over a certain range of core masses. Under certain conditions (large total mass, small value of l/H_p, and an adequately chosen chemical composition) parts of the linear series can become separated and form a disconnected branch of "island" solutions. Models along some of the linear series are tested for secular stability. The implications of the results for mass loss from Cepheids are discussed. (auth)

30199 IDENTIFICATION OF STARS IN THE DIRECTION OF THE LARGE MAGELLANIC CLOUD. Fehrenbach, C.; Duflot, M. (Observatory, Haute-Provence, France). Astron. Astrophys., Suppl. Ser.; 16: No. 3, 365-444(Sep 1974). (In French).

Stars of the Large Magellanic Cloud are identified on charts published by Hodge and Wright (1967). Galactic stars in the direction of the LMC were marked on the chart (listed in the catalog of Fehrenbach and Duflot 1970 — Fehrenbach and Duflot 1973). (auth)

30200 URCA PROCESSES IN CONVECTIVE STELLAR CORES. Paczynski, B. (Inst. of Astronomy, Warsaw). Astrophys. Lett.; 15: No. 3, 147-149(Nov 1973).

URCA processes lead to a local cooling if there is a local statistical equilibrium between electron capture and beta decay. Convection in cool and degenerate matter leads to the URCA processes with a global statistical equilibrium between the captures and decays within the whole convective region. Local statistical equilibrium is lost and this leads to a local heating by the URCA electrons. URCA processes are driven by the mechanical work performed by convective motions. About 25% of the mechanical energy is dissipated into heat and about 75% is lost with neutrinos. Therefore it is the mechanical energy of convective motions that is lost with the URCA neutrinos. In order to stabilize carbon burning the heat released by this burning must be efficiently transformed into the mechanical energy of convective motions. (auth)

30201 DIFFUSION AND ISOTOPE ANOMALIES IN PECULIAR A–B STARS. Michaud, G. (Univ., Montreal). Astrophys. Lett.; 15: No. 3, 143-146(Nov 1973).

The diffusion theory can explain the isotope anomaly of Hg in Mn–Hg stars. In spite of the relatively small mass difference among the isotopes, the mass difference is important because the radiation and gravitational forces tend to cancel in the configuration that time-dependent calculations tend to relax to. The lighter isotopes then leave the star more easily. (auth)

30202 STOKES FORMULATION OF NON-LTE RADIATIVE TRANSFER IN A MAGNETIC FIELD. House, L. L. (National Center for Atmospheric Research, Boulder, CO); Steinitz, R. Astrophys. Lett.; 15: No. 3, 129-133(Nov 1973).

The vector equation of radiative transfer and the associated equations of statistical equilibrium for the treatment of polarized radiation in a magnetic field are presented. The formulation is derived from quantum mechanics and allows for departures from local thermodynamic equilibrium. The radiation field is expressed in terms of the Stokes parameters. The equations reduce to Unno's when local thermodynamic equilibrium is imposed, and they reduce to the "standard" scalar problem when the magnetic field vanishes. This formulation allows a more general interpretation of the Stokes profiles as a function of frequency and thus can lead to better estimates of vector magnetic fields as derived from strong lines. (auth)

30203 WAVELENGTH DEPENDENCE OF CIRCULAR POLARIZATION IN GD 229. Landstreet, J. D. (Univ. of Western Ontario); Angel, J. R. P. Astrophys. J., Lett.; 190: No. 1, L25-L26(15 May 1974).

Circular polarization measurements of GD 229 in narrow wavelength bands show structure down to the instrumental resolution of 160 Å. The data do not indicate any significant variability on a night-to-night basis in any region of the spectrum. (auth)

30204 SPECTRUM OF THE POLARIZED WHITE DWARF GD 229. Greenstein, J. L.; Schmidt, M.; Searle, L. (California Inst. of Tech., Pasadena). Astrophys. J., Lett.; 190: No. 1, L27-L28(15 May 1974).

The spectrum of the polarized white dwarf GD 229 shows broad absorptions at λλ3890, 4150, 5300, 6410, and 7120. Variability of the absorption at λ4150 is suspected. Similarities and differences with the polarized white dwarf Gr +70°8247 are discussed. (auth)

30205 OPTICAL STUDIES OF UHURU SOURCES. VIII. Observations of 92 Possible Counterparts of X-Ray Sources. Jones, C. A.; Chetin, T.; Liller, W. (Havard Coll. Observatory, Cambridge, MA). Astrophys. J., Lett.; 190: No. 1, L1-L3(15 May 1974).

A total of 92 stars located at or near Uhuru x-ray source positions were observed photometrically from the Cerro Tololo Inter-American Observatory. Measurements are summarized in a (U – B, B – V)-diagram, and the data are tabulated for the more interesting stars. (auth)

30206 RELATIVISTIC STELLAR STABILITY: PREFERRED-FRAME EFFECTS. Ni, W. T. (California Inst. of Tech., Pasadena). Astrophys. J.; 190: No. 1, 131-136(15 May 1974).

The PPN (parametrized post-Newtonian) formalism was previously used to analyze relativistic influences on stellar stability in nearly all metric theories of gravity. That analysis omitted all "preferred-frame" terms. Possible preferred-frame effects on stellar stability are examined and no new instabilities are found. In particular, it is shown that: Although terms linear in the preferred-frame velocity w (time-odd terms, analogous to viscosity and energy generation) change the shapes of the normal modes, their symmetry properties prevent them from changing the characteristic frequencies. Thus, no new vibrational or secular instabilities can occur. Terms quadratic in w do not change either the shapes of the normal modes or the characteristic frequencies for radial pulsations (except for the effects due to the renormalization of the gravitation constant which does not affect stability). Thus, they have no influence on radial stability. Terms quadratic in w do change both the normal modes and the characteristic frequencies of nonradial pulsations; but in the limit of a neutral mode these changes vanish. Hence, there is not modification of the criterion for convective stability; i.e., the standard Schwarzschild criterion remains valid. (auth)

30207 HIGH-RESOLUTION FOURIER SPECTRA OF STARS AND PLANETS. Connes, P.; Michel, G. (CNRS, Orsay, France). Astrophys. J., Lett.; 190: No. 1, L29-L32(15 May 1974).

High resolution near infrared spectra (1-2.5 μ) were recorded with a fast-stepping large-maximum-path-difference interferometer coupled to the Palomar 500-cm telescope. Samples of stellar and planetary spectra are given. (auth)

30208 EFFECTIVE POTENTIALS NEAR A KERR–NEWMAN NAKED SINGULARITY. Bergamini, R. (Univ., Bologna); Denardo, G.; Treves, A. Lett. Nuovo Cim.; 11: No. 3, 183-186 (21 Sep 1974).

The effective potentials near a Kerr–Newman naked singularity endowed with charge and spin are considered. Effective potentials are useful to describe the motion of test particles in curved space-time- a technique extensively used in the case of black holes. (JFP)

30209 LIGHT-VARIATIONS INVESTIGATION OF VARIABLE STARS AND SATELLITES BY MEANS OF COMPUTER. Grigorevskii, M. V.; Vykhrestyuk, S. S.; Belotserkovskii, B. E.; Vatsura, V. V.; Vorob'eva, V. A.; Kurlanov, A. D.; Chernov, V. S. (Odessa State Univ.). pp 147-158 of Problemy Kosmicheskoi Fiziki. Vsekhsvyatskii, S. K. (ed.). Kiev; Izdatel'stvo Kievskogo Universiteta (1973). (In Russian).

The experience of the application of a digital computer in Odessa Observatory for variable stars observations processing is considered. The same programs are being successfully applied to photometric observations of artificial earth satellites too. (auth)

30210 SPECTROPHOTOMETRY OF ECLIPSING BINARY V 367 CYGNI. Karetnikov, V. G. (Odessa State Univ.); Perekresnyi, S. M. pp 159-167 of Problemy Kosmicheskoi Fiziki. Vsekhsvyatskii, S. K. (ed.). Kiev; Izdatel'stvo Kievskogo Universiteta (1973). (In Russian).

The investigation of energy distribution in the spectrum, spectrophotometric gradients for three spectral regions, monochromatic light curves, intensities of the emission line H_α and the equivalent widths of the hydrogen lines $H_8 - H_{14}$ and the electron densities by using 41 spectrograms of eclipsing binary V 367 Cygny with dispersion of 166 Å/mm at the line H_γ was carried out. The results were discussed. It was shown that in the system there is a powerful gas envelope observing both in the continuous and line spectrum. It surrounds the primary component of the system, besides, there are some features of the envelope around the secondary component as well as around all the system. (auth)

30211 PERIODS OF THREE RR LYRAE TYPE STARS. Gusev, P. P. (Odessa State Univ.). pp 168-173 of Problemy Kosmicheskoi Fiziki. Vsekhsvyatskii, S. K. (ed.). Kiev; Izdatel'stvo Kievskogo Universiteta (1973). (In Russian).

The behavior of the periods RV Cr B, XZ, Cyg, and AR Her was studied within the recent years. New elements are obtained. (auth)

30212 IONIZATION SHOCK WAVES IN STARS. Klimishin, I. A. (Lvov State Univ.). pp 174-181 of Problemy Kosmicheskoi Fiziki. Vsekhsvyatskii, S. K. (ed.). Kiev; Izdatel'stvo Kievskogo Universiteta (1973). (In Russian).

The approximative analysis of the question of ionization degree behind the shock wave front moving in the hydrogen stellar atmosphere is given. It is shown that by a density $Q \geq 10^{-10}$ g/cm^3 and shock wave velocity $D \geq 40$ km/sec with satisfactory exactness the Saha formula may be used. The expression for estimation of ionization degree before shock wave front connected with the absorption of Lyman continuum quantum is proposed. (auth)

30213 GENETIC CONNECTION BETWEEN STARS O–BO AND DIFFUSE NEBULAE. Gordeladze, Sh. G.; Belyi, A. G. (Kiev Polytechnic Inst.). pp 182-186 of Problemy Kosmicheskoi Fiziki. Vsekhsvyatskii, S. K. (ed.). Kiev; Izdatel'stvo Kievskogo Universiteta (1973). (In Russian).

The estimation of the lower limit of number of spectral classes O–BO stars which are not connected genetically with the diffuse nebulae is given. The distribution of these stars according to the spectral subclasses and depending on relative velocity of stars and nebulae is given. It was found that about 10% of total number of stars O are not connected genetically with the nebulae. There is reason to suppose that the number of such stars is actually much more. (auth)

30214 ON THE GENERALIZED ERGOSPHERE OF THE KERR-NEWMAN GEOMETRY. Denardo, G. (Trieste Univ. (Italy). Istituto di Fisica Teorica); Hively, L. (Western Electric Corp., Princeton, N. J. (USA)); Ruffini, R. (Princeton Univ., N. J. (USA). Joseph Henry Labs.). Phys. Lett., B; 50: No. 2, 270-272(27 May 1974).

The formula for the size at the generalized ergosphere given by Denardo and Ruffini for the Reissner-Nordstrom metric is shown to apply in complete generality to the case of any black hole. The structure of the ergosurface is discussed and analytic formulae are given for various asymptotic limits. (auth)

30215 MODELS FOR NUCLEI OF PLANETARY NEBULAE AND ULTRAVIOLET STARS. Katz, J. I.; Malone, R. C.; Salpeter, E. E. (Cornell Univ., Ithaca, NY). Astrophys. J.; 190: No. 2, 359-363(1 Jun 1974).

A series of stellar models was evolved, all with a total mass of 0.65 $M_{\odot}$, an initial carbon-oxygen core of mass 0.60 $M_{\odot}$, an intermediate helium mantle, and an outer hydrogen-rich envelope, with mass varying from case to case. Although the most hydrogen-rich cases resulted in red giants, cases with less than 0.01 $M_{\odot}$ in the hydrogen envelope evolved at high surface temperature. The early stages of development of these models are similar to observed central stars of planetary nebulae. The later stages (when the nebula should be very thin optically) still have a high luminosity; the relevance to "ultraviolet stars" will be discussed. (auth)

30216 POPULATION SYNTHESIS APPLIED TO EIGHT YOUNG MAGELLANIC CLOUD GLOBULAR CLUSTERS. Heckman, T.M. (Department of Astronomy, Harvard College Observatory, Cambridge, Massachusetts 02138). Astron. J. 79: No. 10, 1040-1046 (Oct 1974).

The technique of population synthesis is applied to reddening corrected 11 color data for eight young globular clusters in the Magellanic Clouds. A local luminosity function is used for all clusters. From the computed stellar populations, masses are determined for five of the clusters. These masses are found to be two to three times smaller than those for old Milky Way globulars. The synthesized populations are also compared to theoretical H—R diagrams. All seven clusters in the LMC are found to be redder in integrated light than the theoretical cluster of a corresponding age, with an opposite effect found in the only SMC cluster studied. These results are tentative since neither the photometric system nor the stellar synthesis groups available were optimal for young star clusters. (auth)

30217 INVESTIGATION OF A MILKY WAY REGION IN CANIS MAJOR. Clariá, J.J. (Observatorio Astronómico, Universidad Nacional, Córdoba, Argentina). Astron. J. 79: No. 10, 1022-1039 (Oct 1974).

Photoelectric measurements in the standard UBV system are presented for 247 stars, most of them of early—type, in a Milky Way field in Canis Major. The intensity of the H_{β} line was measured photoelectrically on 153 OB stars. In addition, spectral types on the MK system were determined from objective prism plates (dispersion 113 Å/mm at H_{γ}) for 172 program stars. Color excesses and distance moduli of all the program stars are assembled in a catalog. Space distribution of early—type stars in the region is nearly constant within different intervals of absolute magnitude. The population of high—luminosity B stars is smaller than that of lower luminosity B stars, which is in agreement with the known luminosity functions up to 600 pc from the Sun. High—luminosity stars with distances less than 900 pc generally present reddening smaller than 0.20. Beyond this distance, the reddening increases noticeably and shows great variations indicating the existence of irregularly distributed obscuring clouds. Low—luminosity B stars with distances from the Sun less than 1 kpc are uniformly reddened. The mean E (B—V) color excess obtained for these stars is 0.08±0.04. The investigation reveals the existence of a group of young OB stars together with excited gas and obscuring matter, which almost certainly belong to the association called Canis Major OB1 in the Catalogue of Star Clusters and Associations. In addition, this paper presents new distances of the H II regions of the zone and the main exciting stars. (auth)

30218 FURTHER OBSERVATIONS FOR CIRCULARLY POLARIZED RADIATION FROM WHITE DWARFS AND X-RAY SOURCES. Brown, D.N.; Rich, A.; Williams, W.L. (Department of Physics, University of Michigan, Ann Arbor). Astrophys. J. Lett. 191: No. 3, L111-L112 (1 Aug 1974).

We have searched for broad—band optical circular polarization in the radiation, from eight white dwarfs, four of which are of spectral type DC, with negative results. In addition, we have obtained negative results from observations of the optical components of Cen X—3 and SMC X—1, and for Sco X—1. (auth)

30219 NEAR—INFRARED MAGNITUDES AND (V—K) COLORS OF GLOBULAR CLUSTERS. Grasdalen, G.L. (Kitt Peak National Observatory, Tucson, Arizona 85726). Astron. J. 79: No. 10, 1047-1051 (Oct 1974).

Near—infrared (J,H,K) mag are reported for 13 globular clusters. Using available visual photometry, the mean intrinsic (V—K) color of globular clusters is found to be 2.19±0.08. This is in good agreement with predictions based on the stellar content of globular clusters. The (V—K) color does not appear to be strongly correlated with the cluster's integrated spectral type. The (V—K) color also places weak constraints on the main—sequence luminosity function of globular clusters. (auth)

30220 CLASSIFICATION OF UNIDENTIFIED SOURCES FROM A 2—μ SOUTHERN SKY SURVEY. Blanco, V.M.; Hansen, O.L. (Cerro Tololo Inter—American Observatory, La Serena, Chile). Astron. J. 79: No. 10, 1052-1053 (Oct 1974).

21 unidentified sources from a 2—μ southern sky survey by Price (1968) have been examined with objective prism plates, and most of them have been classified. Except for one carbon star and three sources that were too faint for classification, the sources were M stars with a preponderance of late types. (auth)

30221 BROAD—BAND 20—μ PHOTOMETRY OF 63 STARS. Simon, T. (Institute for Astronomy, University of Hawaii, Honolulu, Hawaii 96822). Astron. J. 79: No. 10, 1054-1055 (Oct 1974).

Broad—band 20—μ photometry is presented for 63 stars. The majority are late—type variables; 12 are early—type stars of spectral classes WR through G. Seven visual variables (all but one classified as Miras) vary in brightness at 20 μ. Eight nonvariable stars, potential photometric standards at long wavelengths, are also included in the survey. (auth)

30222 LUMINOSITIES AND TEMPERATURES OF M DWARF STARS FROM INFRARED PHOTOMETRY. Veeder, G.J. (Hale Observatories, California Institute of Technology, Carnegie Institution of Washington, Pasadena, California 91109). Astron. J. 79: No. 10, 1056-1072 (Oct 1974).

Broad—band infrared photometry at 1.65, 2.2, and 3.5 μ has yielded accurate bolometric magnitudes for a large number of M type dwarf stars. The intrinsic dispersion in these stars is found to be ~±0.4 mag in M_b vs V—K and M_b vs R—I magnitude—color diagrams. This dispersion in the lower main sequence may be the result of differential blanketing in the UBVRI filter bands and, thus, there may not be a unique main sequence for the intrinsically faint M dwarfs. Analysis shows that one parameter is sufficient to describe the blanketing in all of the UBVRI bands for all types of M dwarfs. In general, late M dwarfs seem to have lower effective temperatures than are predicted by theoretical models. M dwarfs that belong to the halo population on the basis of their large space motions tend to be subluminous in M_b vs V—K and M_b vs R—I magnitude—color diagrams although they have a large scatter. In these diagrams, stars with hydrogen emission lines average ~0.3 bolometric magnitude brighter than M dwarfs without any emission lines. The data for late dwarfs with known masses imply the empirical mass—luminosity relation: $L/L_{\odot} \propto (M/M_{\odot})^{2.2 \pm 0.2}$ for stars fainter than $M_b = 7.5$. (auth)

30223 ROTATIONAL VELOCITIES IN THE ORION ASSOCIATION. Sharpless, S. (C. E. Kenneth Mees Observatory, University of Rochester, Rochester, New York 14627). Astron. J. 79: No. 10, 1073-1075 (Oct 1974).

The effects of rotational velocity on narrow—band hydrogen line indices are discussed. A new comparison is made between the $<V \sin i>$ vs spectral type relationships for early—type stars in the Orion Belt and Orion Nebula Cluster regions. No gross difference in the rotational properties of stars in these two regions appears to exist. (auth)

30224 ANGULAR DIAMETER OF μ GEMINORUM. White, N.M. (Lowell Observatory, Flagstaff, Arizona 86001). Astron. J. 79: No. 10, 1076-1078 (Oct 1974).

Four highly consistent and independent lunar occultation observations have been made of the M3 III star, μ Geminorum. A diameter of 0.0121±0.0001 arcsec has been obtained on the assumption of a uniform disk. The total flux determined from the magnitude at 1.04 μ, I (104), and the observed diameter yielded a relatively high—effective temperature of 3880°K. The linear radius is found to be 81 ± 20 $R_{\odot}$. (auth)

30225 DIAMETER OF — GEMINORUM M3 III FROM LUNAR OCCULTATION. Ridgway, S.T.; Wells, D.C.; Carbon, D.F. (Kitt Peak National Observatory, Tucson, Arizona 85726). Astron. J. 79: No. 10, 1079-1081 (Oct 1974).

From a three—channel observation the angular diameter is found to be 0.0137±0.0010 arcsec. We deduce an effective temperature of 3680 ± 150°K, a radius of 90 ± 30 $R_{\odot}$, and a surface gravity log (g) =0.7±0.4. (auth)

30226 STUDY OF δ SCUTI VARIABLES. Elliott, J.E. (University of Texas, Austin, Texas 78712). Astron. J. 79: No. 10, 1082-1090 (Oct 1974).

UBV photoelectric observations have been made on 14 known or suspected δ Scuti stars with $m_v < 6.5$. Observing techniques were designed to detect brightness variations on the order of 0.015 and periods of from one to four hours. Of the four suspected ^{m} variables studied, one, HR 3889, was found definitely variable. It is of interest because of its fairly large Δm_1 index and because its close companion is a spectroscopic binary. New P—C—L and P—L relations are presented, and a case is made for a possible separation of variables on the basis of mass, period, and log g. (auth)

30227 BEAT PHENOMENON IN TAU PEG. Michael, J.L.; Seeds, M.A. (Joseph R. Grundy Observatory, Franklin and Marshall College, Lancaster, Pennsylvania 17604). Astron. J. 79: No. 10, 1091-1092 (Oct 1974).

Analysis of photoelectric observations made on seven nights provides a solution to the beat variation of the Delta Scuti star Tau Peg. The two periods 0.05433 and 0.04895 days produce a beat in the amplitude of the star's variation with a period of 0.4943 days. Similar results are obtained from two nights of data published by Fesen (1973). This solution fails to predict the lack of variation found on one night by Breger (1969). (auth)

30228 PHOTOMETRIC STUDY OF EE AQUARII. Williamon, R.M. (University of Florida, Gainesville, Florida 32601). Astron. J. 79: No. 10, 1093-1099 (Oct 1974).

Photoelectric observations of the eclipsing variable EE Aquarii were obtained in yellow, blue, and ultraviolet light during 1970 and 1971. The resulting light curves indicate rather severe interaction between the components. A determination of the elements of the system consistent among the three colors and based on the Russell method is presented. (auth)

30229 PROGRESS TOWARDS AN INTERPRETATION OF STELLAR SPECTRA. Mihalas, D. (High Altitude Observatory, National Center for Atmospheric Research, Boulder, Colorado 80302). Astron. J. 79: No. 10, 1111-1121 (Oct 1974).

A review is given of recent work on the interpretation of stellar spectra, with particular emphasis on the effects of departures from LTE, and extended and expanding envelopes. A prospectus for future work in potentially rewarding areas is offered. (auth)

30230 EVIDENCE FOR THE EXISTENCE OF A MASSIVE COMPANION TO X PERSEI (=2U 0352+30?). Hutchings, J.B.; Cowley, A.P.; Crampton, D.; Redman, R.O. (Dominion Astrophysical Observatory). Astrophys. J. Lett. 191: No. 3, L101-L104 (1 Aug 1974).

Radial−velocity measurements of X Persei of spectra obtained from 1920 to 1974 reveal a probable periodicity of about 584 days. The broad Balmer absorption lines and the emission move in antiphase and suggest the existence of a companion of mass at least 30 $M_\odot$. (auth)

30231 GRAVITIONAL RADIATION FROM STELLAR COLLAPSE. Thuan, T.X.; Ostriker, J.P. (Princeton University Observatory). Astrophys. J. Lett. 191: No. 3, L105-L107 (1 Aug 1974).

A uniform density, uniformly rotating, pressureless star of mass M and Schwarzschild radius $r_{Sch}\equiv 2GM/c^2$, collapsing from large radius to a pancake of radius r_{min}, can radiate up to 91.6 times more energy than two masses (totaling M) falling from infinity to final separation r_{min}. These calculations, valid for $(r_{Sch}/r_{min}) < 1$, when used to estimate the energy in a single pulse from a 1.4 $M_\odot$ collapsing white dwarf, indicate that current detectors will observe events occurring not more than $\sim 10^2$ lt−yr from us. (auth)

30232 INFLUENCE OF BINARIES ON RED DWARF DENSITY DISTRIBUTIONS. Weistrop, D. (Perkins Observatory, Ohio State University, Columbus, Ohio 43210). Astron. J. 79: No. 9, 954-958 (Sept 1974).

Density distributions and luminosity functions for red dwarfs are recalculated, assuming the presence of unresolved binaries in the data. Previous conclusions concerning the enhanced luminosity function of these stars, and their concentration to the galactic plane remain unchanged. Arguments in favor of the "missing mass" in the solar neighborhood being supplied by faint red dwarfs are strengthened. (auth)

30233 FAINT O−B3 STARS IN THE NORMA SECTION OF THE MILKY WAY. Muzzio, J.C. (Steward Observatory, University of Arizona, Tucson, Arizona 85721). Astron. J. 79: No. 9, 959-963 (Sept 1974).

Three fields in the galactic plane in Norma have been searched for faint OB stars by means of photographic UBV photometry. The magnitude limits of the search are $9.2 < V < 15.2$, $9.2 < V < 15.7$, and $8.8 < V < 14.7$, respectively, for the three fields Norma II, III, and IV. Nearly 100 stars have been found with spectral types of B3 or earlier as inferred from the colors. Many of these stars appear to be related to known optical H II regions; in some of these the total visual extinction exceeds five magnitudes. Our results support the existence of a total visual extinction of 2 to 3 mag within 2 kpc of the Sun in the directions of our fields. No firm conclusions regarding the spiral structure in the interval $326° < l < 333°$ can yet be drawn. (auth)

30234 PHOTOMETRY OF A PLEIADES CANDIDATE AND COMPOSITE WHITE DWARFS. Greenstein, J.L. (Hale Observatories, California Institute of Technology, Carnegie Institution of Washington, Pasadena, California 91109). Astron. J. 79: No. 9, 964-966 (Sept 1974).

The possible membership of LB 1497 (EG 25) in the Pleiades is examined; that it might have evolved without explosion from a parent star of more than 6 $M_\odot$ presents evolutionary difficulties. The suggestion that it might have a faint, close companion, and has therefore lost most of its mass, seems untenable; spectrophotometry shows no red or infrared excess. The companion would have to be fainter than $M = +15$, i.e., less than 0.1 $M_\odot$. The method does reveal other composite white dwarfs, one of which, GD 325 (DB+dM), is not yet resolved visually. GD 325 is an important astrometric object. (auth)

30235 ON THE DISTRIBUTION OF BINARY SYSTEM MASS RATIOS. Trimble, V. (Department of Physics and Astronomy, University of Maryland, College Park, Maryland 20742). Astron. J. 79: No. 9, 967-973 (Sept 1974).

Mass ratios have been calculated for all binary systems in the Sixth Catalogue of the Orbital Elements of Spectroscopic Binary Systems and the 1971 and 1973 supplements to it, and their distribution function is presented. The total sample is clearly bimodal, with peaks near mass ratios of 0.3 and 1.0, and the bimodality is preseved when only systems with known angles of orbital inclination are considered. It is also present in the subsample of unevolved systems, which suggests that there may be two populations of binaries formed in different ways. The distribution of mass ratios of the single−lined systems alone can be fitted satisfactorily with a hyperbola or parabola for analytic purposes. The power law fit adopted by previous workers is not satisfactory, and this analysis shows a greater preponderance of low−mass ratio systems than previously found. Between two and five percent of the single−line systems have mass ratios greater than one. Separating the binaries by spectral type does not reveal any striking differences, though the OB systems may be rather more strongly concentrated toward small mass ratios than the others, and systems with MK class I and II primaries may have a slight deficiency of low−mass ratios. (auth)

30236 PARALLAXES AND PROPER MOTIONS OF TWELVE NEARBY STARS DETERMINED WITH THE SPROUL 24−IN. REFRACTOR. Lippincott, S.L. (Sproul Observatory, Swarthmore College, Swarthmore, Pennsylvania 19081). Astron. J. 79: No. 9, 974-978 (Sept 1974).

Parallaxes and proper motions are determined from observations covering approximately three decades. The formal probable errors of the parallaxes range from ± 0.″003 to ± 0.″008. A revised weighted system adopted in 1973 is discussed. (auth)

30237 PROPER MOTIONS OF FAINT BLUE STARS NEAR THE GALACTIC ANTICENTER. I. Cudworth, K.M. (Lick Observatory, Board of Studies in Astronomy and Astrophysics, University of California, Santa Cruz, California 95064). Astron. J. 79: No. 9, 979-980 (Sept 1974).

Proper motions with a mean error to ± 1.″0/cent. have been measured for most of the faint blue stars found by Rubin and Losee (1971) in a field near the galactic anticenter. A few of these stars have detectable proper motions and are probably nearby white dwarfs, but most must be distant, and thus, of higher luminosity. (auth)

30238 ANALYSIS OF A ONE−PARAMETER FAMILY OF TRIPLE CLOSE APPROACHES OCCURRING IN STELLAR SYSTEMS. Szebehely, V. (University of Texas, Austin, Texas 78712). Astron. J. 79: No. 9, 981-983 (Sept 1974).

This paper is the first part of a trilogy dedicated to the role of triple encounters in the evolution of stellar systems. It shows how a symmetric triple collision may be perturbed to obtain a family of asymmetric triple close approaches with arbitrary high escape velocities and with the formation of binaries. The main result is that as the perturbation approaches zero, the product of the semimajor axis of the binary and the square of the escape velocity approach a value dependent only on the participating masses. The second part will describe results of the extensive numerical integrations, will offer detailed information on the one−parameter family of orbits generated, and will outline the intricate numerical techniques and controls used, without which no reliable numerical results may be obtained regarding the dynamic behavior of multicomponent stellar systems. The third and last part offers applications in stellar and galactic dynamics. In a parametric presentation it gives actual sizes of binaries formed and values of escape−velocities generated for triplets formed of Sun−like stars, of white dwarfs, of neutron stars, and of triple systems of galaxies. (auth)

30239 NGC 6193: AN EMISSION REGION WITH A HIGH RATIO OF TOTAL TO SELECTIVE EXTINCTION?. Herbst, W. (David Dunlap Observatory, University of Toronto, Richmond Hill, Ontario, Canada). Astron. J. 79: No. 9, 941-944 (Sept 1974).

Seven stars associated with emission and reflection nebulosities surrounding the galactic cluster NGC 6193 are used to determine the ratio of total to selective extinction in the region. An anomalously high value of $R=5.6\pm0.3$ is derived. The distance modulus and color−magnitude diagram for the cluster, which contains the peculiar Of star HD 148937, are obtained. (auth)

30240 OBSERVATIONS OF THE H 85α LINE FROM PLANETARY NEBULAE. Terzian, Y. (Department of Physics, University of Montreal, Montreal, Canada); Higgs, L.A.; MacLeod, J.M.; Doherty, L.H. Astron. J. 79: No. 10, 1018-1021 (Oct 1974).

Observations of the H 85α line from the planetary nebulae M1−78, NGC 6543, 7662, and 3242 have been made using the 46−m telescope at the Algonquin Radio Observatory. The line was definitely detected in the first three objects and may have been detected in NGC 3242. In all cases the line is wide, with a width comparable to that predicted from the known expansion velocities of the nebulae. The line strengths correspond to LTE electron temperatures in the expected region of 7000−13 000 K. (auth)

30241 STELLAR ATMOSPHERES: THE SOURCES OF INTERSTELLAR MOLECULES. Shimizu, M. (Tokyo Univ.). Int. Astron. Union Symp.; No. 52, 405-412(1973).

From conference on interstellar dust and related topics; Albany, NY (29 May 1972).

The analysis of the abundance of interstellar molecules in compact H II regions suggests that the molecules are formed in stellar atmospheres (possibly of protostars or of late type stars), transported to the location of the neutral clouds in the compact H II regions, and shielded from decomposition due to stellar radiation by the dust in the clouds. Cometary nuclei and interstellar dust are argued from the astrochemical point of view to be dirty ice of the second kind (or a sort of frozen interstellar molecules). The chemical structure of the primordial solar nebula is discussed under the assumption that long-period comets consist of the most primordial substances of the solar system. (auth)

30242 DUST, STAR, AND HYDROGEN DISTRIBUTIONS IN THE ORION ASSOCIATION. Isobe, S. (Tokyo Astronomical Observatory). Int. Astron. Union Symp.; No. 52, 433-444(1973).

From conference on interstellar dust and related topics; Albany, NY (29 May 1972).

From the star counts on the Palomar Sky Survey prints, dust and star distributions in the Orion Association are studied. The hydrogen distribution in the same region is obtained from an H alpha photograph. It is found that a considerable part of the interstellar absorption on the line of sight is due to the circumstellar dust grains in the Orion Association. (auth)

30243 HIGH VELOCITIES AND COCOON STARS. Dopita, M. A. (Univ. of Manchester, Eng.). Nature (London); 250: No. 5465, 397-398(2 Aug 1974).

It is stated that the existence of "cocoon" stars seems fairly well established from observations of infrared point sources (see Astrophys. J. 147: 799 (1967) and Mon. Not. R. Ast. Soc. 160: 1 (1972)), and these are frequently associated with compact H II regions and OH masers. The author suggests that break-up of the neutral gas and dust shell around such a star could conceivably produce the observed high velocities in large scale gas movements, giving rise to the split, asymmetric or broadened emission line profiles observed in many H II regions. (UK)

30244 DUST PARTICLES AND MOLECULES IN THE EXTENDED ATMOSPHERES OF CARBON STARS. Gilra, D. P. (Washburn Observatory, Madison, WI). Int. Astron. Union Symp.; No. 52, 517-528(1973).

From conference on interstellar dust and related topics; Albany, NY (29 May 1972).

It is shown that the absorption due to a circumstellar shell containing solid silicon carbide particles can very nicely explain the observed strong violet opacity in stars in which the carbon to oxygen ratio is greater than 1. It has been shown by Friedemann and Gilman that solid SiC particles can form in the cooler outer layers of such stars. Thermal re-emission from SiC particles is predicted to be in the 10-13 micron region, and recent infrared observations by Hackwell show an emission band in this region, thereby strongly supporting the SiC suggestion. It is also shown that the opacity due to C3 pseudocontinuum is not adequate to explain the observed violet opacity. It is suggested that the vibrational bands of C3 and SiC2 molecules should be among the major opacity sources in the infrared spectra of the late N-type carbon stars and some of the observed bands may be, at least in part, due to these molecules. (auth)

30245 RADIATIVE TRANSITIONS INVOLVING THE $(2p^2)$ $^3P^e$ METASTABLE AUTODETACHING STATE OF H^-. Jacobs, V.L.; Bhatia, A.K.; Temkin, A. (Theoretical Studies Group, Goddard Space Flight Center, National Aeronautics and Space Administration, Greenbelt, Maryland). Astrophys. J. 191: No. 3, 785-788 (1 Aug 1974).

The absorption coefficient for the free−bound transition $H(1s) + e^- + \hbar\omega \rightarrow H^-(2p^2, {}^3P^e)$ is calculated (together with the differential emission rate for the inverse process) using 1s−2s−2p close−coupling continuum wave functions and a Hylleraas bound−state wave function. A maximum in the absorption and emission spectra is found to occur at a photon wavelength of 1219.5 Å, which is 2 Å closer to the Lα line than predicted by the calculations of Drake and is in closer agreement with the stellar absorption feature identified by Heap and Stecher. The free−bound absorption process appears to be a significant source of continuous ultraviolet opacity. (auth)

30246 RATE COEFFICIENTS FOR ELECTRON EXCITATION OF THE FIRST RESONANCE TRANSITION IN H, Li, Na, Ca, Ca^+, AND Ba^+ CALCULATED FROM EXPERIMENTAL DATA. Crandall, D.H.; Dunn, G.H.; Gallagher, A.; Hummer, D.G.; Kunasz, C.V.; Leep, D.; Taylor, P.O. (Joint Institute for Laboratory Astrophysics, University of Colorado). Astrophys. J. 191: No. 3, 789-793 (1 Aug 1974).

By fitting cubic splines augmented with special functional forms for low and high energies to cross−section data determined experimentally at discrete values of the electron energy, we obtain an interpolation that can be visually inspected and adjusted to prevent the appearance of spurious features. The familiar integral expressing the rate coefficient in terms of the cross−sections can then be evaluated with no further approximation. This procedure is applied here to cross−section data for the first resonance transition of H, Li, Na, Ca, Ca^+, and Ba^+. The resulting collisional de−excitation rate coefficient, from which the excitation−rate coefficient can be determined by the detailed balance relation, is tabulated in each case for electron temperatures in the interval from 10^3 to 10^5°K and is expressed in terms of a Chebyshev expansion valid for this range of temperature. (auth)

30247 ON THE PASSAGE OF RADIATION THROUGH INHOMOGENEOUS, MOVING MEDIA. V. LINE ABSORPTION AND FREQUENCY VARIATIONS OF OPTICAL DEPTH. Lerche, I. (Enrico Fermi Institute and Department of Physics, University of Chicago). Astrophys. J. 191: No. 3, 753-757 (1 Aug 1974).

In a rapidly moving, rapidly shearing medium in which individual partially ionized atoms absorb radiation at a fixed frequency, ν_L, in their rest frames, we demonstrate that the optical distance an observer can "see" into the medium depends sensitively on both the angle of observation relative to the flow direction and the observing frequency. For instance, observations at perpendicular incidence using frequencies much lower than ν_L, and observations in the direction of motion at frequencies much higher than ν_L, both show strong absorption relative to the absorption taking place at high frequencies ($\nu > \nu_L$) (perpendicular incidence) and low frequencies ($\nu > \nu_L$) (parallel incidence), respectively. (auth)

30248 ON THE PASSAGE OF RADIATION THROUGH INHOMOGENEOUS, MOVING MEDIA. VI. DISPERSION EFFECTS ON PHASE AND RAY PATHS IN A PLANE, DIFFERENTIALLY SHEARING MEDIUM. Lerche, I. (Enrico Fermi Institute and Department of Physics, University of Chicago, Chicago, Illinois). Astrophys. J. 191: No. 3, 759-762 (1 Aug 1974).

Using the phase and ray−path equations given in the first paper of this series, we illustrate how dispersive effects change the behavior of waves propagating in a plane, differentially shearing medium from the behavior obtaining for constant refractive index. The major effect is, apparently, to cause an angular spreading of a slim pencil of rays normally incident on the slab. In other words, the dispersive effects do just that−they disperse a thin angular beam of radiation. This result is clearly of importance in the pulsar propagation problem, where a narrow angular spread is required to account for the small pulse width−relative to the pulse period. (auth)

30249 ON THE PASSAGE OF RADIATION THROUGH INHOMOGENEOUS, MOVING MEDIA. VII. CONCERNING THE VALIDITY OF THE GEOMETRICAL OPTICS APPROXIMATION. Lerche, I. (Enrico Fermi Institute and Department of Physics, University of Chicago, Chicago, Illinois). Astrophys. J. 191: No. 3, 763-769 (1 Aug 1974).

We give the two coupled second−order differential equations that must be solved in order to obtain exact solutions for electromagnetic wave propagation in a plane differentially shearing medium of constant refractive index, n, and of velocity $V = \hat{x}V(y)$. For the simple case of normal incidence we demonstrate that the time−averaged power flow is solely in the upstream direction at any point in the medium (for $n < 1$). The upgoing wave is balanced by a reflected wave from the critical height occurring at $V(y) = cn < c$. The upgoing ray path is shown to agree with the WKB (i.e., geometrical optics) ray path at high frequencies where the WKB analysis is expected to be valid. It is also pointed out that the instantaneous (not time averaged) power flow depends on the initial conditions and does not, in general, give rise to zero net power flow normal to the slab. (auth)

30250 ARE STELLAR SURFACE HEAVY−ELEMENT ABUNDANCES SYSTEMATICALLY ENHANCED? Joss, P.C. (Institute for Advanced Study, Princeton, New Jersey). Astrophys. J. 191: No. 3, 771-774 (1 Aug 1974).

Stellar surface heavy−element abundances may be substantially higher than interior abundances if there is appreciable accretion of chemically fractionated matter after Hayashi−phase convection has terminated. The plausibility of appreciable accretion is discussed, and some possible observational consequences of enhanced surface heavy–element abundances are investigated. These consequences include a reduced solar neutrino flux, systematic variations in surface abundance along the main sequence and along the giant branch, and relatively low heavy–element abundances among planetary nebulae and white dwarfs and in the interstellar medium. There is marginal observational evidence in support of the hypothesis of enhanced stellar surface heavy–element abundances. (auth)

30251 ULTRAVIOLET PHOTOMETRY FROM THE ORBITING ASTRONOMICAL OBSERVATORY. XVI. THE STELLAR LYMAN–ALPHA ABSORPTION LINE. Savage, B.D.; Panek, R.J. (Space Astronomy Laboratory, Washburn Observatory, University of Wisconsin–Madison). Astrophys. J. 191: No. 3, 659-674 (1 Aug 1974).

The Wisconsin far–ultraviolet spectrometer on OAO–2 has observed the stellar Lα line at 1216 Å in 29 lightly reddened stars ranging in spectral type from B2.5 to B9. For these stars, Lα equivalent widths have been derived by fitting synthetic profiles to the observed spectra. This procedure corrects for a small amount of blending between the stellar Lα line and a stellar Si III line at 1206.5 Å. The final equivalent widths, which include a small correction for interstellar Lα absorption, range from α15 Å at spectral type B2.5 to ~65 Å at spectral type B8. For the late–B stars the Lα line removes 2 to 3 percent of the total stellar flux. For our sample of stars (24 dwarfs, four giants, and one supergiant) the strength of Lα correlates quite well with measures of the Balmer discontinuity and Balmer line strengths. With the exception of the one supergiant, luminosity classification does not appear to strongly influence the Lα line strength. The observed Lα equivalent widths have been compared with the predictions of Mihalas's grid on non–LTE model atmospheres. With the possible exception of the stars of high luminosity, the calculations and observations are in basic agreement over their range of overlap ($T_e = 15{,}000° - 20{,}000°K$). We have shown that in a number of cases the stellar Lα line influences the interstellar column densities reported in the OAO–2 interstellar Lα survey. Because of this contamination the OAO–2 interstellar column densities toward lightly reddened B2 and B1.5 stars should be regarded as only upper limits. (auth)

30252 INFRARED OBSERVATIONS OF Be STARS FROM 2.3 TO 19.5 MICRONS. Gehrz, R.D.; Hackwell, J.A. (Department of Physics and Astronomy, University of Wyoming); Jones, T.W. Astrophys. J. 191: No. 3, 675-684 (1 Aug 1974).

Infrared observations of 33 "classical" Be stars and 26 early–type comparison objects are presented. Excess infrared radiation in the 2.3–19.5 μ spectral region was observed for 28 of the 33 Be stars. Circumstellar–dust emission models are ruled out. Free–free emission from a hot ($T_s \geq 10{,}000°K$) circumstellar plasma shell is found to be the most likely source of the excess infrared radiation. A typical Be star shell, assuming a shell radius to thickness ratio of 5, is shown to be characterized by an electron density of 3.7×10^{11} cm^{-3}, a radius of 2.5×10^{12} cm(~4R•), and a Thomson optical depth of 0.16. The infrared excess in Be stars tends to decrease as spectral type becomes late. A number of the survey stars were tested for infrared variability with negative results. (auth)

30253 SPECTROSCOPIC OBSERVATIONS OF INTERESTING SOUTHERN STARS NOTED ON SOUTHERN OBJECTIVE–PRISM PLATES. Stephenson, C.B. (Warner and Swasey Observatory, Case Western Reserve University). Astrophys. J. 191: No. 3, 685-689 (1 Aug 1974).

We report on slit spectrograms of eight southern stars, six of which are discussed here for the first time. These are culled from an objective–prism survey of the entire Milky Way, and include a new M dwarf which is an HD star, and a unique star similar to HR 7606. All are south of declination –33°. (auth)

30254 NEW HIGH–DISPERSION RADIAL VELOCITY CURVES OF W SAGITTARII. Jacobsen, T.S. (Department of Astronomy, Seattle, Washington). Astrophys. J. 191: No. 3, 691-697 (1 Aug 1974).

Radial–velocity curves of W Sgr for 1969 and 1973 have been constructed from the author's definitive measurements of 20 high–dispersion spectrograms taken by Wallerstein with the coudé spectrographs at Mount Wilson, Kitt Peak, and Cerro Tololo. The curves were compared with the author's high–dispersion curves constructed from his Mills three–prism spectrograms of 1923 and 1925. From an intercomparison of the various curves the following results emerge: (1) To a first approximation the systemic velocity varies in an estimated period of 80 years in a manner well described by Keplerian orbital elements. (2) The shape of the curve representing the short–period pulsation of 7.59+ days is definitely variable with time. There is definite evidence of a 51–year separation between two similar shapes. A comparison with curves of lower dispersion by Curtiss, Stibbs, and Evans suggest the possibility of a 17–year periodicity in the changing shapes. (3) The average spectroscopic pulsation period between 1923 and 1973 is derived. Comparison of this value with the four best–determined photometric periods reveals an increase in period between 1872 and about 1917 at the average rate of 1.364 s per year, and a linearly decreasing period at the rate of 0.134 s per year after about 1917. The apparent spectroscopic pulsation period for $\gamma = -27.58$ km s^{-1} should be given by $7.594875 - 0.00000155(t - 1938.6)$ mean solar days. (4) The spectra show interstellar D–lines of Na I at a constant velocity of –4.20 km s^{-1}. (auth)

30255 REACTION RATES OF INTEREST IN LATE STAGES OF STELLAR NUCLEOSYNTHESIS. Vlieks, A.E.; Morgan, J.F.; Blatt, S.L. (Department of Physics, Ohio State University). Astrophys. J. 191: No. 3, 699-704 (1 Aug 1974).

Stellar reaction rates have been calculated from experimental cross–sections for the ^{54}Fe(α,n), ^{46}Ti(α,n), ^{50}Cr(α,n), ^{51}V(α,n), ^{45}Sc(α,n), and ^{58}Ni(α,p) reactions in the temperature range $1 \leq T_9 \leq 5$. A comparison with some recent theoretical calculations indicates the actual rates to be somewhat smaller than those obtained from the statistical compound–nucleus model. To enhance their usefulness in nucleosynthesis calculations, the reaction rates have been fitted to an analytic function of temperature valid throughout the temperature domain considered. (auth)

30256 NUCLEOSYNTHESIS IN WHITE–DWARF ATMOSPHERES. Hoyle, F.; Clayton, D.D. (Department of Space Physics and Astronomy, Rice University, Houston). Astrophys. J. 191: No. 3, 705-710 (1 Aug 1974).

We propose events by which both s– and r–process nucleosynthesis may occur on the surfaces of white–dwarf stars. The main requirement is that the accreted hydrogen be mixed with comparable numbers of ^{12}C (or other alpha nuclei) before a runaway capture of protons takes place. Subsequent events offer many possibilities for nucleosynthesis and stars of peculiar composition. A new mechanism for a surface s–process due to few–MeV protons is also described. Concluding comments concern cosmic γ–ray bursts and the origin of anomalous low–energy galactic cosmic rays. (auth)

30257 A STUDY OF NUCLEOSYNTHESIS DURING EXPLOSIVE CARBON BURNING. Pardo, R.C.; Couch, R.G. (Center for Nuclear Studies, University of Texas, Austin); Arnett, W.D. Astrophys. J. 191: No. 3, 711-725 (1 Aug 1974).

Nucleosynthesis during explosive carbon burning is reexamined. Dominant reactions are determined and listed as an aid to experimental studies. Nucleosynthesis is examined at higher temperatures and higher neutron excess than considered previously. Simple approximations to the complete network of nuclear reactions are developed and presented. New implications of these results for stellar evolution and nucleosynthesis are discussed. Explosive carbon burning gives a signature which is quantitatively equivalent to that expected from the explosion of a massive ($8 \lesssim M/M_\odot \lesssim 80$) star. (auth)

30258 IRON PRODUCTION BY ^{12}C–DETONATION SUPERNOVAE. Arnett, W.D. (Department of Astronomy, University of Texas, Austin). Astrophys. J. 191: No. 3, 727-729 (1 Aug 1974).

A procedure which is relatively insensitive to the details of galactic evolutionary models is used to examine the production of iron–group nuclei to be expected from the carbon–detonation supernova model. The requirement that iron production be such as to reproduce the observed Fe/(C+O) abundance ratio places severe constraints on either (1) the frequency of such events or (2) the amount of iron–group elements ejected from such an event. (auth)

30259 ELECTRON–ION RELAXATION IN A DENSE PLASMA. Littleton, J.E.; Buchler, J. (Belfer Graduate School of Science, Yeshiva University, New York, New York). Astrophys. J. 191: No. 3, 731-737 (1 Aug 1974).

The electron–ion relaxation time is computed for a two–temperature plasma under the conditions of arbitrary relativity and strong degeneracy of the electrons. The results are applied to the shock–front structure in detonating stellar matter. Nuclear processes take place on a time scale much shorter than the thermal equilibration time, for which it is concluded that an examination of the microscopic structure of the shock front must treat the plasma as two fluids. (auth)

30260 LIMIT ON X–RAY EMISSION FROM A SUPERNOVA DURING MAXIMUM LIGHT. Sprott, G.F.; Bradt, H.V.; Clark, G.W.; Lewin, W.H.G.; Schnopper, H.W. (Department of Physics and Center for Space Research, Massachusetts Institute of Technology, Cambridge, Massachusetts); Pigatto, L.; Rosino, L. Astrophys. J. 191: No. 3, 739-742 (1 Aug 1974).

The MIT 1–60 keV X–ray detector on the OSO–7 satellite observed the supernova SN 1971s in NGC 493 during the period of its optical rise and maximum. The data were examined for steady and pulsed X–ray emission. Analysis of the light curve shows that the supernova was most likely of Type II. The upper limit (3 σ) to the continuous X–ray luminosity during the week of the optical rise and maximum is $\sim 5 \times 10^{43}$ ergs s^{-1} (1–5 keV), a factor of 40 less than previous upper limits for this portion of the light curve. The upper limit to the energy of an X–ray pulse of duration between 2 seconds and 3 minutes is $\sim 5\times10^{44}$ ergs (1–9 keV). The data examined for such a pulse covered 31 percent of the total observation time. (auth)

30261 CRITERIA FOR PION CONDENSATION THRESHOLDS IN NEUTRON STAR MATTER. Au, C. K.; Baym, G. (Illinois Univ., Chicago (USA). Dept. of Physics); Flowers, E. (New York Univ., N. Y. (USA). Dept. of Physics). Phys. Lett., B; 51: No. 1, 1-4(8 Jul 1974).

Sawyer [Phys. Rev. Lett., 31: 1556(1973)] has raised a serious objection to the criterion used by Migdal to predict the onset of the spontaneous appearance of negative pions (pion condensation) in neutron star matter. In this communication the detailed criteria are presented for the onset of pion condensation, by a second-order phase transition, in terms of the pion Green's function in matter, with the hope of resolving the apparently conflicting approaches to this problem. (NL)

30262 POSSIBLE EVIDENCE FOR CONTINUED EJECTION OF RR TELESCOPII. Friedjung, M. (Centre National de la Recherche Scientifique, 75–Paris (France). Inst. d'Astrophysique). Astrophys. Space Sci.; 29: No. 1, L5-L6(Jul 1974).

Fe II and Fe II intensity measures enable the size of the region containing singly ionized iron to be estimated. Calculations for a phase near maximum light support a continued ejection model. (auth)

30263 CALCULATIONS OF PROXIMITY EFFECTS IN CLOSE BINARY SYSTEMS. Budding, E. (Manchester Univ. (UK)). Astrophys. Space Sci.; 29: No. 1, 17-39(Jul 1974).

The proximity effects in the light curves of close binary systems are investigated with the aid of facilities provided by a high-speed, digital computer. The treatment follows, to a large extent, that summarized by Kopal (1959) and makes extensive use of the alpha-functions and related integrals provided by that author. The "ellipticity" and "reflection" effects are studied individually and different expressions are checked and compared. Test data are drawn continually from the well known system SZ Cam for which a "rectified" (in a more realistic sense) light curve is ultimately produced. (auth)

30264 ON THE SEMICONVECTIVE ZONE IN THE CORE-HELIUM-BURNING STARS. Saio, H. (Tohoku Univ., Sendai (Japan). Faculty of Science). Astrophys. Space Sci.; 29: No. 1, 41-49(Jul 1974).

The validity of current ideas to set up the semiconvective zone of the stellar models in core-helium-burning phase has been considered mainly from the viewpoint of timescales related to the mechanism. The time-scale of outward motion of the convective shell has been estimated as being longer than that of evolution. From this point of view, it might be said that the models constructed with semiconvective zone are not appropriate for the core-helium-burning stars. (auth)

Quasi-Stellar, Radio, and X-Ray Sources

Refer also to abstracts 30174, 30197, 30218, 30365, and 31183.

30265 OBSERVATIONS OF GALACTIC CARBON MONOXIDE EMISSION AT 2.6 MILLIMETERS. Wilson, W.J.; Schwartz, P.R.; Epstein, E.E.; Johnson, W.A.; Etcheverry, R.D.; Mori, T.T.; Berry, G.G.; Dyson, H.B. (Electronics Research Laboratory, The Aerospace Corporation, El Segundo, California). Astrophys. J. 191: No. 2, 357-374 (15 July 1974).

A wide variety of galactic sources have been observed at 2.6 mm (115,271.2 MHz) to determine the extent and strength of interstellar $^{12}C^{16}O$. Extended regions of CO emission were found in the direction of 32 H II regions and five supernova remnants. The CO emission was found to be larger in spatial extent than the 6–cm continuum H II emission, and CO emission maxima appear to be related to continuum emission peaks and infrared sources in several sources. Except near optically dark nebulae, little CO emission was detected away from the galactic plane. Radial velocities of the CO emission are within 10 km s^{-1} of the OH, H II (109α), and H_2CO velocities measured by other observers for the same sources. $^{13}C^{16}O$ was also measured in many of the stronger sources. The optical depths calculated for $^{12}C^{16}O$ range between 20 and 120, if the terrestrial value of 1/89 is assumed for the ratio of $^{13}C/^{12}C$. For excitation temperatures in the range of 10°– 50° K, the calculated projected densities range from 10^{18} to 2.5×10^{19} molecules cm^{-2}. (auth)

30266 THE INTERPRETATION OF BROAD EMISSION LINES IN HIGH–REDSHIFT QSOS. Stoner, R.E.; Ptak, R. (Department of Physics, Bowling Green State University, Bowling Green, Ohio); Ellis, D. Astrophys. J. 191: No. 2, 291-300 (15 July 1974).

Emission–line profiles for the most intense lines visible in high–redshift quasars (Lα λ1216, C IV λ1550, N V λ1240, Si IV λ1397, Si III] λ1888, and C III] λ1909) have been computed in a radially streaming, suprathermal ion model. Cross–sections for producing radiation in these lines by excitation during certain atomic collisions have been computed for this purpose. We report the results of these calculations and compare the profiles with those observed in the quasars 1331+170 and OQ 172. Interpretation of the observed profiles on the basis of the model requires slightly higher redshifts than previously assigned to these objects; systematic discrepancies among redshifts computed from the peaks in the different emission–line profiles are then explained naturally through atomic collision physics. Excellent fits to observed profiles are obtained with very few free parameters. We discuss the features of the model and ways in which they can be modified without destroying the basic agreement with observations. (auth)

30267 HIGH–FREQUENCY OBSERVATIONS OF POSSIBLE "HEAVY–ELEMENT" RECOMBINATION LINES. Chaisson, E.J. (Center for Astrophysics, Harvard College Observatory and Smithsonian Astrophysical Observatory). Astrophys. J. 191: No. 2, 411-414 (15 July 1974).

A possible heavy–element recombination line that arises in a predominantly neutral region toward three galactic nebulae is observed at 8.3 GHz. If our heavy–element interpretation is correct, the data suggest an abundance ratio [Mg+Si+S+Fe]/[C] that agrees reasonably well with the cosmic value. (auth)

30268 4.8–SECOND PULSED X–RAYS FROM CENTAURUS X–3 AT ENERGY GREATER THAN 7 keV. Ulmer, M.P.; Baity, W.A.; Wheaton, W.A.; Peterson, L.E. (University of California, San Diego). Astrophys. J. 191: No. 2, 593-595 (15 July 1974).

We searched the hard X–ray data, from the OSO–7 satellite, for the 4.8–second pulsations detected by Uhuru at lower energies. A pulse with a 4.841973±0.000009 s period was found in the ~7–11 keV range from 1971 December 18.0 to 21.4 observations, with a ratio of pulsed to total flux of 45±10 percent. In the 11–22 keV range, 2 σ upper limits were ~80 percent pulsed fraction assuming an 80 percent ON duty cycle. For two other intervals (1971 December 21.4–25.8 and 1972 January 22.9–26.0), we obtained only 2 σ upper limits of ~60–80 percent pulsed fraction over the entire ~7–22 keV range, again assuming an 80 percent ON duty cycle. (auth)

30269 A MODEL FOR THE TRANSIENT X–RAY SOURCES. Van Horn, H.M.; Hansen, C.J. (Joint Institute for Laboratory Astrophysics, University of Colorado and National Bureau of Standards, Boulder, Colorado). Astrophys. J. 191: No. 2, 479-481 (15 July 1974).

We suggest a model for the transient X–ray sources in which an accreted, hydrogen–rich envelope is heated by high–density electron captures to the point where a thermonuclear shell flash can occur. Some observational tests of the model are suggested. (auth)

30270 A SPECTROSCOPIC ANALYSIS OF HZ HERCULIS. Crampton, D.; Hutchings, J.B. (Dominion Astrophysical Observatory). Astrophys. J. 191: No. 2, 483-491 (15 July 1974).

Measurements from 49 spectra of HZ Her are presented. Emission lines of N III, He II, and N V are shown to be associated with the neutron star, together with a weak continuum. Velocities, spectrophotometry, and light curves of the primary suggest that it has an off–axis hot spot. Calculations of profile distortions for a simple model of this nature fit the spectroscopic observations. The spectroscopic results yield masses of ~ 2.0 $M_\odot$ and 1.0 $M_\odot$ for the primary and X–ray sources, respectively. (auth)

30271 COLOR VARIATIONS OF SCORPIUS X–1. Mook, D.E.; Messina, R.J. (Department of Physics and Astronomy, Dartmouth College, Hanover, New Hamshire); Pel, J.; Hiltner, W.A. Astrophys. J. 191: No. 2, 493-498 (15 July 1974).

Simultaneous five–color photometry of Sco X–1 is reported. Linear relations between pairs of the various magnitudes are obtained. As an illustration of how such data may be used to test models of the continuum emitting region, a simple, self–absorption bremsstrahlung model is compared with the observations; this type of comparison is shown to be independent of distance to the source, interstellar extinction, or absolute flux calibration of the photometric system. (auth)

30272 SPECTROMETRIC PROPERTIES OF CRYSTALS FOR X-RAY ASTRONOMY. I. Burek, A.J.; Barrus, D.M.; Blake, R.L. (The University of Chicago). Astrophys. J. 191: No. 2, 533-543 (15 July 1974).

Preliminary results are reported on measurements of X–ray reflection coefficients, rocking–curve width estimates, and factors that influence these for KAP, EDDT, and ADP crystals. The agreement between parameters measured in our laboratory and others over a period of some 10 years, and the uniformity among our samples, indicate that KAP as commercially supplied is amenable to a single theoretical description. This permits application of X–ray diffraction theory, which we outline and compare to measurements with good agreement. (auth)

30273 POSSIBLE NATURE OF SOME UNUSUAL OH SOURCES. Cohen, M.; Baudry, A. (Univ. of California, Berkeley). Astrophys. Lett.; 15: No. 3, 151-154(Nov 1973).

Possible optical identifications are suggested for four "star-like" OH sources, and pumping mechanisms are briefly discussed. (auth)

30274 ACCELERATION AND RADIATION OF COSMIC RAY ELECTRONS FROM PULSARS. Shen, C. S. (Purdue Univ., Lafayette, IN). Astrophys. Lett.; 15: No. 3, 135-138(Nov 1973).

The general property of radiation reaction in a large-scale field is discussed. The radiation spectrum and the maximum energy gain of a relativistic electron accelerated by the Gunn–Ostriker mechanism and under arbitrary radiation damping are derived. It is found that the radiation converted from the low-frequency wave should be cut off at a few 10^{10} eV for the Crab pulsar. (auth)

30275 RELATION BETWEEN THE RADIATED AND RECEIVED POWERS DUE TO GYRATING ELECTRONS IN AMBIENT PLASMA. Ko, H. C.; Chuang, C. W. (Ohio State Univ., Columbus). Astrophys. Lett.; 15: No. 3, 125-127(Nov 1973).

It is shown that the rate of energy radiated per unit of time, solid angle, and frequency interval by a gyrating electron in an ambient magnetoactive plasma is related to the rate of energy received per unit of time, solid angle, and frequency interval by a distant observer, by the factor $|1 - v \cos \psi\, \partial(k \cos \theta)/\partial\omega|$. Errors in the synchrotron emissivity formula in the current literature are discussed. (auth)

30276 IDENTIFICATION OF SOUTHERN QUASI-STELLAR OBJECTS. IV. Peterson, B. A. (Australian National Univ., Canberra); Bolton, J. G.; Shimmins, A. J. Astrophys. Lett.; 15: No. 3, 109-113(Nov 1973).

Forty new southern quasi-stellar objects were found from combined radio and optical observations. (auth)

30277 IDENTIFICATION OF SOME FAINT RADIO SOURCES THAT HAVE FLAT SPECTRA. Fanaroff, B. L.; Willson, M. A. G. (Cavendish Lab., Cambridge, Eng.). Astrophys. Lett.; 15: No. 3, 115-117(Nov 1973).

New identifications are presented for some faint radio sources that have flat radio spectra. A smaller fraction of faint sources with flat spectra in the sample are associated with quasars visible on the Palomar Sky Survey prints than was found in previous studies of samples of bright sources. (auth)

30278 NOTE ON LINEAR POLARIZATION IN THE EMISSION FRAME FOR RADIO GALAXIES AND QUASARS. Vallée, J.P. (Department of Astronomy and David Dunlap Observatory, University of Toronto, Toronto, Canada). Astron. J. 79: No. 10, 1015-1017 (Oct 1974).

There is empirical evidence that the percentage of integrated linear polarization at the emitted wavelength of 6 cm (PEO6) is a sensitive parameter to investigate the depolarization in extragalactic radio sources. PEO6 increases with increasing source linear size, but decreases with increasing redshift, radio luminosity, and brightness temperature in the emission frame. (auth)

30279 ON THE SHORT–TIMESCALE VARIABILITY OF OJ 287. Kiplinger, A.L. (Department of Astronomy, University of Texas at Austin). Astrophys. J. Lett. 191: No. 3, L109-L110 (1 Aug 1974).

Power spectra of two optical observational runs of OJ 287 do not confirm the existence of a 39–minute variation as indicated by Visvanathan and Elliot and Frolich. (auth)

30280 THE CRAB NEBULA AS A CALIBRATION SOURCE FOR X-RAY ASTRONOMY. Toor, A.; Seward, F.D. (Lawrence Livermore Laboratory, University of California, Livermore, California 94550). Astron. J. 79: No. 10, 995-999 (Oct 1974).

A new high–quality observation of the 2– to 60–keV spectrum of the Crab Nebula is presented. Previous x–ray spectral measurements are critically reviewed and compared with this new measurement. Within the accuracy of the observations, which span a period of eight years, the Crab can be considered a steady x–ray source, producing a constant spectrum suitable for checking the response of x–ray instruments. (auth)

30281 INTENSE RADIO SOURCES AT 1400 MHz. II. ADDITIONS TO THE BDFL SAMPLE. Bridle, A.H. (Astronomy Group, Department of Physics, Queen's University at Kingston, Ontario, Canada); Fomalont, E.B. Astron. J. 79: No. 10, 1000-1005 (Oct 1974).

Sixteen sources with 1.4–GHz integrated flux densities greater than 1.7 Jy and $|b| > 5°$ have been added to the 424 in the BDFL catalog (Paper I) between declinations $-5°$ and $+70°$, on the evidence of new 1.4–GHz observations at the NRAO 300–ft telescope. The BDFL "complete sample" of sources with $S_{1.4} > 2.00$ Jy in the region of sky between declinations $-5°$ and $70°$ at $|b| > 20°$ has consequently been slightly revised. Five new sources have been added and two sources deleted. The revised BDFL "complete" sample of 237 sources (Table V of this paper) is estimated to be $99 \pm 1\%$ complete. Data on the additional sources are given in Table II of this paper, which also presents new data on 14 sources from the BDFL catalog. All sources with 1.4–GHz flux densities greater than 1.5 Jy in the Ohio $40°-63°$ survey at $|b| > 5°$ have now been observed at the 300–ft telescope, and the flux–density accuracy of this survey is assessed. (auth)

30282 OPTICAL IDENTIFICATIONS FROM THE NRAO 5–GHz RADIO SURVEY. Johnson, K.H. (Steward Observatory, University of Arizona, Tucson, Arizona 85721). Astron. J. 79: No. 10, 1006-1014 (Oct 1974).

Optical identifications are given for sources comprising a portion of the NRAO 5–GHz radio survey, largely on the basis of accurate radio positions measured with the RRE interferometer and optical positions measured on the Palomar Sky Survey plates. More than 80% of the sources can be identified with objects visible on these plates; more than half of these are quasars or quasar–like objects. (auth)

30283 OPTICAL IDENTIFICATIONS AND RADIO SPECTRA OF SOURCES FOUND BY THE MICHIGAN 8–GHz SURVEY. Brandie, G.W. (Radio Astronomy Observatory, The University of Michigan, Ann Arbor, Michigan 48104); Bridle, A.H. Astron. J. 79: No. 9, 903-917 (Sept 1974).

Optical counterparts have been found or confirmed for over 80% of the 55 sources found by an 8–GHz survey of $\simeq 0.8$ steradian of sky between declinations $-4°$ and $+5°$. More than two–thirds of the identifications are with stellar objects. The 1.4– to 13.5–GHz spectra of the sources have been determined and classified using a radio analogue of the optical "two–color" diagram. The galaxies cluster in a region of the "two–color" diagram different from that occupied by the QSS. The sources have thus been divided into two main spectral classes —class "G", consisting entirely of nonvariable galaxies and empty fields, and class "Q", consisting of variable stellar objects with only a small proportion of "deviant" galaxies. Some of the stellar objects are neutral in color and may be quasars of very high redshift. (auth)

30284 SEARCH FOR CIRCULAR POLARIZATION IN COMPACT RADIO SOURCES AT A WAVELENGTH OF 2.2 CM. Seaquist, E.R. (David Dunlap Observatory, University of Toronto, Richmond Hill, Ontario, Canada); Gregory, P.C.; Clarke, T.R. Astron. J. 79: No. 9, 918-922 (Sept 1974).

A search has been made for circular polarization in ten compact radio sources at a wavelength of 2.2 cm. Marginal detections were obtained from two sources: 3C273 and 3C345. A new polarization feed which permitted simultaneous measurements of all four Stokes parameters is briefly described. The results are discussed with reference to the radiation mechanism. (auth)

30285 NGC 520 CHAIN OF QUASARS. Arp, H. (Hale Observatories, Carnegie Institution of Washington, California Institute of Technology, Pasadena, California 91109). Astron. J. 79: No. 9, 923-924 (Sept 1974).

In claiming that the line of QSR's originating from the exploding galaxy NGC 520 is not statistically significant, Barnothy has introduced quasars in the area that are fainter in radio strength and drawn from incomplete surveys. That author adopts a density of QSR's around NGC 520 which is roughly ten times the average density of QSR's over the sky. As indicated by Arp in the original paper, however, only the chain, which represents a density increase of about five over the average, represents the real density excess of QSR's in the NGC 520 area. The peculiar galaxies additional to NGC 520 claimed by Barnothy to be in the area are known to be smaller, fainter, and peculiar in only minor ways compared to the extremely disrupted NGC 520. (auth)

30286 FURTHER INTERFEROMETER OBSERVATIONS OF THE WATER VAPOR SOURCES IN W49. Knowles, S.H.; Johnston, K.J. (E. O. Hulburt Center for Space Research, Naval Research Laboratory, Washington, D.C. 20375); Moran, J.M.; Burke, B.F.; Lo, K.Y.; Papadopoulos, G.D. Astron. J. 79: No. 9, 925-932 (Sept 1974).

Interferometer maps have been made over an extended period of both low–velocity and high–velocity features in the water vapor source W49N; W49S has also been observed. The W49N source consists of six regions whose relative position remains stable with time, and whose geometric sizes are 10–20 times their apparent sizes. The negative high–velocity emission comes mainly from a nebular region of size 3000 astronomical units by 400 astonomical units, which also contains the strong and persistent -7 km/sec feature. No relation between radial velocity and spatial position is discernable in this nebula, nor among the six regions. (auth)

30287 FIRST CELESTIAL WATER VAPOR SOURCES OBSERVED AT ITAPETINGA RADIO OBSERVATORY, BRAZIL. Kaufmann, P.; Fogarty, W.G.; Scalise, E. Jr.; Schaal, R.E. (Centro de

Rádio Astronomia e Astrofisica, Universidade Mackenzie, São Paulo, Brazil). Astron. J. 79: No. 9, 933-937 (Sept 1974).

Stronger H_2O sources in the southern sky were confirmed, showing flux densities about four times larger than previously reported. VY Canis Majoris has shown a strong reduction in intensity by June 1973. The presence of H_2O emission found in H2−3 tends to confirm the nature of this source as a compact HII region rather than a planetary nebulae. H2−3 is also the first known source of H_2O emission that is associated with OH in absorption. (auth)

30288 SEARCH FOR OPTICAL PULSATIONS FROM CEN X-3. Lasker, B. M. (Cerro Tololo Inter-American Observatory, Casilla, Chile). Nature (London); 250: No. 5464, 308(26 Jul 1974).

It is stated that the optical system identified with the x-ray source Cen X-3 is very suitable for high frequency optical studies since it provides the possibility of observing optical effects related to the 4.842 sec. x-ray pulsations. Observations were made at the Cerro Tololo Inter-American Observatory in Chile using an S-20 photomultiplier, with no filter, and making 1 m sec. integrations onto magnetic tape. Average upper limits of the optical pulsations for three sets of data were 0.031, 0.11, and 0.14%. Detected optical pulsations for Her X-1 are of the same fractional order of magnitude as the observed upper limit for Cen X-3 reported, and comparisons are made between these two x-ray objects. (UK)

30289 ORIGIN OF QSO ABSORPTION LINES. Opher, R. (National Aeronautics and Space Administration, Moffett Field, CA). Nature (London); 250: No. 5464, 310-311(26 Jul 1974).

The origin of absorption lines in QSOs is stated to be a puzzle. It has been suggested that they result from matter lying along the line of sight of the QSO but not associated with it. It has also been suggested that the lines arise "locally" from matter expelled from the QSO core, with radiation pressure acting as the driving mechanism. Any model that attempts to explain the formation of QSO absorption lines must explain the highly multiple spectra that are sometimes seen, and the distribution of the multiplicities. What is termed the "plasmoid mechanism" is discussed in connection with QSO "clouds", the "plasmoids" consisting of relativistic particles in a magnetic field. A possible alternative to the "plasmoid mechanism" is also discussed and it is shown that some large relative bulk motions in QSO "clouds" can be dissipated without the presence of strong magnetic fields and without large adiabatic expansions. (UK)

30290 ABSORPTION OF GAMMA RAYS IN INTENSE X-RAY SOURCES. Herterich, K. (Max-Planck-Institut fuer Extraaterrestrische Physik, Munich). Nature (London); 250: No. 5464, 311-312(26 Jul 1974).

A suggestion that intense x-ray sources could act as γ-ray sources is examined, but it is stated that there is no experimental evidence to support this. This means either that no γ-rays are produced or that they are absorbed before they leave the source. It can be shown that γ-rays are strongly absorbed as a result of pair production with x-ray photons, and calculations are given describing the absorption of γ-rays in some intense x-ray sources, using recent data. The x-ray sources Her X-1, Cyg X-1 and the Crab pulsar are amongst the astrophysical sources considered. It is shown that γ-rays cannot be expected above 10 MeV, although if there are pulsed γ-rays from the Crab above 10 MeV, as claimed by some authors, this would not contradict the present arguments. (UK)

30291 H ALPHA EMISSION IN CYGNUS X−1. Hutchings, J.B.; Cowley, A.P.; Crampton, D. (Dominion Astrophysical Observatory); Fahlmann, G.; Glaspey, J.W.; Walker, G.A.H. Astrophys. J. 191: No. 3, 743-748 (1 Aug 1974).

Observations are presented of the Hα region of the spectrum of Cygnus X−1, from spectrograms and Image Isocon scans. The feature is a broad emission broken by one or more blended absorption features. It is argued that the emission arises in an accretion ring surrounding the X−ray source. The configuration of the ring and evidence for mass−loss from its outer layer are discussed and some model calculations presented. An inclination of the system of $i \sim 30°$ is suggested, and a mass−ratio M_p/M_x of less than 2. (auth)

30292 DAILY OBSERVATIONS OF CYGNUS X−3 AT 10.5 AT GHz DURING THE PERIOD 1973 JULY−OCTOBER. Hughes, V.A.; Woodsworth, A. (Astronomy Group, Queen's University of Kingston, Ontario); Gregory, P.C.; Sequist, E.R. Astrophys. J. 191: No. 3, 749-751 (1 Aug 1974).

The 46−meter telescope of the Algonquin Radio Observatory was used to obtain daily flux densities of Cygnus X−3 at 10.5 GHz. The activity of the source was sporadic, but no event was observed which had an amplitude greater than 20 percent that of the major outburst of 1973 September 2. The maxima of a number of previously unpublished outbursts are tabulated. (auth)

30293 ON THE TIME EVOLUTION OF QUASAR LUMINOSITY AND REDSHIFT DISTRIBUTION. Meiseles, R.; Kozlovsky, B.; Shaviv, G. (Tel Aviv Univ. (Israel). Dept. of Physics and Astronomy). Astrophys. Space Sci.; 29: No. 1, 221-231(Jul 1974).

The possibility to predict the redshift distribution on the basis of certain assumptions about the time-dependence of quasar luminosity is discussed. It is found that for a certain general class of models that resembles the spinar model for quasars only specific combinations of parameters give rise to acceptable results. Further consequences are discussed. (auth)

30294 SIMULTANEOUS HARD X-RAY AND OPTICAL OBSERVATIONS OF SCO X-1 AND A MODEL OF SEMI-OPAQUE X-RAY SOURCES. Kasahara, I. (Nagoya Univ. (Japan). Dept. of Physics). Astrophys. Space Sci.; 29: No. 1, 191-210(Jul 1974).

Simultaneous observations of hard x-ray and optical emission from Sco X-1 were carried out at Hyderabad, India, on April 16 and 19, 1972. During the first and the second observations Sco X-1 was on the average in a bright phase of B = 12.5 mag. and a slightly darker phase of B = 12.7 mag. respectively. During the first observation the x-ray intensity in the energy range 20 to 40 keV measured with balloon-borne scintillation counters showed an enhancement of a factor of about two in coincidence with an optical flare of $B \cong 0.2$ mag., whereas the apparent temperature derived from the x-ray spectrum observed in the energy range 20 to 35 keV showed no appreciable change. Both the x-ray intensity and the apparent temperature observed on April 19 are considerably lower than those observed on April 16. Taking into account the effect of radiative transfer in a hot plasma, the electron density and the optical depth for electron scattering of the plasma cloud are derived as $n_e \sim 3 \times 10^{16}$ cm^{-3} and $\tau_{es} \sim 10$ for the quiescent bright phase. The flare is explained by an increase of the plasma mass by about 30% and an increase of τ_{es} by $\tau_{es} \sim 1$ without appreciable change of the plasma temperature. The results on April 19 are interpreted as indicating that the quiescent dark phase may be characterized by a decrease of the plasma mass, its contraction and lower temperature. (auth)

30295 THE MASS-ANGULAR MOMENTUM-DIAGRAM AND THE BLACK HOLE LIMIT. Brosche, P. (Bonn Univ. (F. R. Germany). Astronomische Institute). Astrophys. Space Sci.; 29: No. 1, L7-L8(Jul 1974).

The ratio angular momentum/mass squared of a wide variety of astronomical objects lies about 10^3 times above the value $G/c = 2.2 \times 10^{-18}$ cm^2 g^{-1} s^{-1} for extremely fast rotating black holes. (auth)

Solar Phenomena

Refer also to abstracts 30400, 30401, 30413, 30418, and 31423.

30296 (CONF-730693-, pp 231-253) CONSIDERATIONS ON THE NEUTRAL COMPONENT RELATIVE TO THE AUGUST 4, 1972 SOLAR EVENT. Cortellessa, P.; Paizis, C. (Univ., Milan). 1974.

From proceedings of the summer school on particles and fields in space; Balatonfured, Hungary (5 Jun 1973).

The observation on board the OSO-7 satellite of the gamma-ray line at 2.2 MeV associated with the August 4, 1972 solar event suggests the production of neutrons in the flare region. From the observed gamma-ray intensities at 0.51, 2.2, 4.4, and 6.1 MeV, the neutron and high energy gamma-ray fluxes are estimated from π^0 decay that should have been expected at 1 A.U. A comparison is made of the estimated solar neutron flux with the best upper limits obtained experimentally up to now. (auth)

30297 (CONF-730693-, pp 255-277) PROPERTIES AND MODELS OF SOLAR FLARES AND COSMIC RADIATION. Krivsky, L. (Ondrejov Observatory, Czech.); Pinter, S. 1974. (In Russian).

From proceedings of the summer school on particles and fields in space; Balatonfured, Hungary (5 Jun 1973).

30298 ON THE NATURE OF THE ASYMPTOTICALLY ADIABATIC SOLUTION OF THE TWO−FLUID SOLAR WIND. Roxburgh, I.W. (High Altitude Observatory, Boulder, Colorado). Astrophys. J. 191: No. 2, 557-561 (15 July 1974).

It is shown that there are four degrees of freedom in the asymptotically adiabatic solutions of the solar−wind models. The electron and proton temperatures tend to equality at large distances like $T_0 r^{-4/3}$, T_0 being the same for both the electron and proton gases. For a given T_0 there exists another branch of solutions that converge on to this in an asymptotically irregular manner like $S_0 r^{(\beta/2-4/3)} \exp(-\beta r)$, where β is a constant, known in terms of T_0, and S_0 represents the extra degree of freedom required to specify arbitrarily the density and electron and proton temperature at the Sun. (auth)

30299 RISE TIME IN 20–32 keV IMPULSIVE X–RADIATION. Vorpahl, J.A. (University of California, San Diego); Takakura, T. Astrophys. J. 191: No. 2, 563-565 (15 July 1974).

A study was made of the hard X–ray component in the impulsive phase of solar flares. In 36 randomly chosen events the value for the slope in differential electron power spectrum, $E^{-\delta}$ electrons cm^{-2} s^{-1} keV^{-1}, was related to the 20–32 keV spike rise time (e–folding) as $t_{rise} = 0.56 \exp(0.88\delta)$ in the thin–target model and $t_{rise} = 0.10 \exp(0.88\delta)$ in the thick–target picture. In the thin–target model, the above empirical relation would imply that the acceleration of electrons can last longer when the acceleration rate is smaller. An alternative interpretation would be that an impulsive hard X–ray burst is a superposition of two components emitted from thin and thick targets; when the former predominates the duration is longer and the photon spectral index is larger, and vice versa. (auth)

30300 CORONAL INHOMOGENEITIES AND SOLAR RADIO EMISSIONS. Leblanc, Y. (Observatoire de Paris). pp 312-340 of Summer School on Plasma Physics and Solar Radioastronomy. Vol. 1. Mangeney, A. (ed.). Meudon, France; Observatoire de Paris-Meudon (1973).

From proceedings of the summer school on plasma physics and solar radioastronomy; Ile de Re, France (4 Sep 1972).

Coronal inhomogeneities can play an important part in solar radio emissions. It is shown how they influence many observations in the meter, decameter and kilometer wavelength ranges. Scattering mechanisms are reviewed and computation techniques are given. The theoretical results are compared with data. (auth)

30301 TYPE III RADIO BURSTS. Berthomieu, G. (Observatoire de Nice). pp 299-311 of Summer School on Plasma Physics and Solar Radioastronomy. Vol. 1. Mangeney, A. (ed.). Meudon, France; Observatoire de Paris-Meudon (1973).

From proceedings of the summer school on plasma physics and solar radioastronomy; Ile de Re, France (4 Sep 1972).

The results of observations of type III radio bursts are presented. These bursts are generally interpreted as being excited by the passage through the corona, of a stream of particles having velocities of the order of one third of the velocity of light. Two models are presented for these bursts: one is based on the stabilization on the stream, the other is based on a quasi-linear behavior of the stream. (auth)

30302 TYPE I SOLAR RADIO EMISSION. Bourgeret, J. L. (Observatoire de Paris). pp 341-361 of Summer School on Plasma Physics and Solar Radioastronomy. Mangeney, A. (ed.). Meudon, France; Observaroire de Paris-Meudon ([nd]).

From proceedings of the summer school on plasma physics and solar radioastronomy; Ile de Re, France (4 Sep 1972).

The main characteristics of type I solar radio emissions are recalled: microscopic features of storm bursts and of the background continuum, storm centers and polarization phenomena. The results of high resolution spectrometry and interferometry are presented; an interpretation is given. (auth)

30303 SOLAR ULTRAVIOLET FLUX BELOW 50 KILOMETERS. Ackerman, M. (Institut d'Aeronomie Spatiale de Belgique, Brussels). Can. J. Chem.; 52: No. 8, 1505-1509(15 Apr 1974).

The available values of the solar flux from 1700 A to 4000 Å are presented. The penetration of this radiation in the stratosphere is discussed and the role of scattering on direct and global radiation in the troposphere is emphasized. (auth)

30304 RESONANCE IN A SEMI-INFINITE ISOTHERMAL ATMOSPHERE. Zhugzhda, Yu. D. (Inst. of Terrestrial Magnetism, Ionosphere, and Radio-wave Propagation, Moscow). Astrophys. Lett.; 15: No. 3, 119-124(Nov 1973).

Worrall's resonance in the isothermal atmosphere is considered. This resonance is proven to be impossible in a semi-infinite atmosphere. Resonant excitation of Lamb's wave in a semi-infinite atmosphere is considered, and the possible mechanism of five-minute oscillation dissipation in the solar atmosphere is discussed. Lamb's wave in the magnetic field is considered and running penumbral wave is discussed. (auth)

30305 RADIO EMISSIONS ASSOCIATED WITH THE EMERGENCE OF NEW MAGNETIC FLUX FROM THE SOLAR PHOTOSPHERE. Sheridan, K. V.; McLean, D. J.; Smerd, S. F. (CSIRO, Sydney). Astrophys. Lett.; 15: No. 3, 139-142(Nov 1973).

The emergence of new magnetic flux was accompanied by explosive activity observed with the Culgoora radioheliograph at 80 and 160 MHz. The senses of polarization were opposite for the two widely separated sources corresponding to the forward and reverse strokes of several U-bursts. Opposite senses of polarization and different positions distinguished the Type I storms before and after the explosive activity. (auth)

30306 A 10.5 YEAR PERIOD FOR THE SLOWLY VARYING COMPONENT OF THE SOLAR RADIO FLUX. Covington, A. E. (National Research Council, Ottawa). J. Roy Astron. Soc. Can.; 68: 31-35(Feb 1974).

A basic period of 10.5 years has been found from the Ottawa 10.7 cm daily radio flux observations and is identical to that found in recent studies of the more extensive sunspot numbers. Assuming this period, it is predicted that the next radio minimum will occur in January 1975 with an error of plus or minus one solar rotation. (auth)

30307 SOME STUDIES ON SOLAR X-RAY FLARE-ASSOCIATED OPTICAL FLARES, MICROWAVE BURSTS, AND SUDDEN IONOSPHERIC DISTURBANCES. Dasgupta, M. K.; Sarkar, S. K. (Univ. of Calcutta). Indian J. Radio Space Phys.; 1: No. 4, 256-260(1972).

Different classes of solar optical flares, microwave bursts at 4995 MHz and sudden ionospheric disturbances have been examined in relation to 1575 solar x-ray flares (or bursts) recorded in the 0.5-3A band by SOLRAD-9 satellite during the period December 1968 to March 1970. X-ray flares have been found to be associated with all these events, the overall percentage association values being 46.5, 60.5 and 47.2 respectively. Bright Hα flares have been found to be more effective in producing x-ray flares. In relation to microwave bursts, x-ray flares show greater association with gradual rise and fall flares and also with impulsive type of bursts. Peak flux spectra of x-ray flare-associated bursts under both these types show three distinct types of distribution, viz. "inverted U" type showing one peak (I), "complex" or "zigzag" type having more than one peak (II) and peak flux increasing with frequency (III). 18 ref. (Indian Sci. Abstr.)

30308 ELECTRICAL CONDUCTIVITY OF THE MATTER IN THE SUBPHOTOSPHERIC LAYERS OF THE SUN. Krivodubskii, V. N. (Kiev State Univ.). pp 3-15 of Problemy Kosmicheskoi Fiziki. Vsekhsvyatskii, S. K. (ed.). Kiev; Izdatel'stvo Kievskogo Universiteta (1973). (In Russian).

The method of kinetic equation is applied to the research of inhomogeneous ionized gas in the magnetic field. Boltsman's equation is solved to the second approximation by the method of Enskog–Chapman. The formulas of the densities of electrical currents caused by the electric field strength, the pressure; concentration and temperature gradients in the presence of magnetic field and the formulae for calculating the longitudinal σ_0, transversal σ_1 and Hall's σ_2 conductivities are deduced. The values of the electrical conductivities of plasma of the convective zone of the sun are calculated. σ_0 changes from $2.88 \cdot 10^{12}$ CGSE at a depth of 400 km beneath the photosphere to $2.46 \cdot 10^{16}$ CGSE at a depth of 200,000 km beneath the photosphere, σ_1–from $1.56 \cdot 10^{12}$ CGSE to $2.46 \cdot 10^{16}$ CGSE, σ_2–from $7.47 \cdot 10^{10}$ CGSE to $3.08 \cdot 10^{12}$ CGSE. (auth)

30309 CONNECTION OF THE OPTICAL FLARES WITH THE SOLAR RADIO BURSTS. Nesmyanovich, A. T. (Kiev State Univ.); Sizonenko, Yu. V.; Chernomaz, V. P.; Podstrigach, T. S. pp 16-21 of Problemy Kosmicheskoi Fiziki. Vsekhsvyatskii, S. K. (ed.). Kiev; Izdatel'stvo Kievskogo Universiteta (1973). (In Russian).

It is compared 102 light curves of the flares with profiles of radio bursts observed on seven frequencies (100 to 9100 MHZ) in 1966 to 1970. (auth)

30310 IS THERE A REAL NEED FOR DOUBLING THE SOLAR EUV FLUXES? Prasad, S. S.; Furman, D. R. (Univ. of Florida, Gainesville). J. Geophys. Res.; 79: No. 16, 2463-2468(1 Jun 1974).

The need for doubling the solar EUV flux, which has recently been suggested in the literature is examined. Two independent approaches were used: comparison between electron production and loss using ion composition and density data and comparison between observed and calculated electron fluxes. The finding is that the reasonings so far advanced for doubling the solar EUV flux are not compelling. It is felt that the conclusive demonstration of the need should come from repeated careful measurements of the solar EUV flux and/or definitive analysis of a more comprehensive set of simultaneously measured ionospheric data. In the meantime, attention should also be devoted to a search for possible alternative ways out of the difficulties presently encountered with the lower values of the solar EUV fluxes. (auth)

30311 MASS SPECTROMETRIC ISOTOPE DILUTION ANALYSES OF TIN IN STONY METEORITES AND STANDARD ROCKS. de Laeter, J. R.; McCulloch, M. T.; Rosman, K. J. R. (West Australian Inst. of Technology, South Bentley). Earth Planet. Sci. Lett.; 22: No. 3, 226-232(Jun 1974).

The abundance of tin in 21 stony meteorites and 12 standard rocks has been determined by the stable isotope dilution technique. The measurements of the Cl chondrite Orgueil give a cosmic abundance for tin of 3.7 (with respect to Si = 10^6 atoms) and thus substantiate the peak in the cosmic abundance curve due to the closed proton shell for Z = 50. The low abundance of tin in ordinary chondrites allows tin to be reassigned to the strongly depleted group of elements in the context of the Larimer–Anders model. The values for the standard rocks are in reasonable agreement with the presently accepted abundances of tin, except for the diabase W-1 and tonalite T-1 for which significantly lower values were obtained. (auth)

30312 COMMENT ON "PROPAGATION ANISOTROPIES OF SOLAR FLARE PROTONS AND ELECTRONS AT LOW ENERGIES IN INTERPLANETARY SPACE" BY R. K. PYLE. Roelof, E. C. (Johns Hopkins Univ., Silver Spring, MD). J. Geophys. Res.; 79: No. 19, 2931-2935(1 Jul 1974).

It is shown that a significant bias was introduced in the method of analysis of the directional data from the University of Chicago Pioneer detector used by Pyle (1973) for the study of propagation anisotropies of solar flare protons and electrons at low energies in interplanetary space. (JFP)

30313 SOLAR-FLARE AND LABORATORY PLASMA PHENOMENA. Lee, T. N. (Naval Research Lab., Washington, DC). Astrophys. J.; 190: No. 2, 467-479(1 Jun 1974).

Systematic comparisons between solar flares and a laboratory discharge indicate that a number of similarities and interesting contrasts exist between the two in the following areas: the thermal and nonthermal (suprathermal) x-ray continuum spectra, the emission line spectra (>6 keV) of iron, the spectral and temporal behavior of microwave and x-radiations, and the plasma ejection. These together with consistent scaling factors of observed quantities which exist between the two cases suggest that some of the basic physical processes involved in both cases could be of similar origin. (auth)

30314 HYDRAULIC CONCENTRATION OF MAGNETIC FIELDS IN THE SOLAR PHOTOSPHERE. II. Bernoulli Effect. Parker, E. N. (Univ. of Chicago). Astrophys. J.; 190: No. 2, 429-436(1 Jun 1974).

The magnetic filaments in the solar photosphere are subject to vigorous kneading and massaging by the convective turbulence at, and beneath, the visible surface. It is shown that the Bernoulli effect of the consequent surging of fluid up and down along the filaments is a major factor in concentrating the magnetic pressure of the filament (the mean square field). The mean field is also increased if the phase velocity of the external massaging exceeds the Alfvén speed within the filament. The net observational magnetic result of the surging, then, depends upon the response of the observing instrument, and whether it essentially observes the mean field, the rms field, or whether there are saturation effects. The hydraulic effects responsible for the formation of the concentrated magnetic filaments are part of the dynamical picture of spicules, pointed out a decade ago. Hence it is suggested that the chromospheric mottles (spicules) seen in Hα are in fact the intense magnetic filaments that carry most of the magnetic flux across the photospheric boundary of the sun. (auth)

30315 DYNAMICS OF THE SOLAR MAGNETIC FIELD. I. Method of Examination of Force-Free Magnetic Fields. Nakagawa, Y. (High Altitude Observatory, Boulder, CO). Astrophys. J.; 190: No. 2, 437-440(1 Jun 1974).

In the solar atmosphere, prevailing physical conditions indicate that below the photospheric level the magnetic field is subject to passive change due to fluid motions, while above the photospheric level the magnetic field must satisfy closely the force-free conditions. On the basis of such understandings a practical method of studying the evolution of a general force-free magnetic field in the solar atmosphere utilizing magnetograph observations is described. It is assumed that at the level of magnetograph observations the magnetic field is subject to changes by purely horizontal fluid motions, and these changes are accompanied by adjustments in the distribution of the electric currents such that the magnetic field above the level of magnetograms remains force-free. Then it is shown that the fluid motions can be determined uniquely from the successive magnetograms and that the evolution of general force-free magnetic fields in the solar atmosphere in response to the changes in the magnetograms can be examined. The details of the formulations are presented, together with discussions of their physical significance. (auth)

30316 DYNAMICS OF THE SOLAR MAGNETIC FIELD. II. The Energy Spectrum of Large-Scale Solar Magnetic Fields. Nakagawa, Y.; Levine, R. H. (High Altitude Observatory, Boulder, CO). Astrophys. J.; 190: No. 2, 441-446(1 Jun 1974).

The energy spectrum of large-scale solar magnetic fields is obtained as a function of the circumferential wave number k along the heliographic latitudinal circle from the full-disk magnetograms of the Kitt Peak National Observatory covering one solar rotation. It is shown that the spectra in the higher latitudinal zones are different from those in the lower latitudinal zones. For the lower latitudinal zones between 35°N and 30°S, the energy spectrum is closely characterized by k^{-1} dependence, while for the higher latitudinal zones the spectrum follows approximately k^{-3} dependence. It is then shown that these dependences can be interpreted in terms of the theory of passive response of the magnetic field to turbulent fluid motions, and that the difference between the k^{-1} and k^{-3} dependences can be attributed to the difference in the balance between the magnetic energy supply and dissipation in the higher and lower latitudinal zones. (auth)

30317 ACCELERATION OF THERMAL PARTICLES IN COLLAPSING MAGNETIC REGIONS. Levine, R. H. (High Altitude Observatory, Boulder, CO). Astrophys. J.; 190: No. 2, 447-456 (1 Jun 1974).

The acceleration of thermal particles in the vicinity of a magnetic neutral sheet is discussed. This process is considered as the archetypal low intensity process at a newly formed neutral sheet. The collapse of the field toward the neutral sheet produces acceleration by secularly increasing the velocity component perpendicular to the sheet. The average energy increase for a thermal distribution of particles is calculated both with and without the inclusion of Coulomb losses by accelerated particles to particles in the accelerating region. Emphasis is placed on the conditions necessary for acceleration in the presence of Coulomb losses. The applicability of this approach to regions which collapse very fast is discussed. (auth)

30318 NEW THEORY OF CORONAL HEATING. Levine, R. H. (High Altitude Observatory, Boulder, CO). Astrophys. J.; 190: No. 2, 457-466(1 Jun 1974).

An alternative to the heating of the corona by shocks or waves is examined. It is argued that the corona is interspersed with magnetic neutral surfaces which collapse and accelerate particles to a few times their thermal velocity in the manner described previously. The accelerated particles travel through the corona and lose their increased energy through Coulomb collisions. It is shown that this mechanism can provide the energy balance needed by the corona and that such acceleration can account for regions of enhanced or decreased heating in the corona. (auth)

30319 OBSERVED DEPARTURES FROM LTE IN STELLAR Fe I LINES. I. The Sun. Smith, M. A. (Univ. of Toledo). Astrophys. J.; 190: No. 2, 481-486(1 Jun 1974).

The recent calculation of the excitation and ionization equilibrium of the Fe I atom in the sun by Athay and Lites has made possible a simple division of observed Fe I transitions into three groups, so that a convenient comparison of the predicted departures of each of these groups can be made with observed solar lines. The observed data, taken from the Michigan photoelectric solar atlas, consist of core depths and line strengths for lines measured at $\mu = 1$ and 0.3. The result of comparison of this non-LTE model with observations is that two of the three groups show identical departures from LTE, while the third (high-excitation) group shows only very little deviation from LTE. The actual departures for the former groups are only 50 to 60 percent of the Athay and Lites predictions. While the character of the observed departures is roughly that predicted, it is suggested that a few estimates of collisional-excitation cross sections be modified. Nonetheless their basic-model reference atom appears to provide a very good representation of the real behavior of Fe I atoms in the solar atmosphere. As only the central cores of strong lines are found to be affected, one can even amplify Holweger's assertion that non-LTE excitation of the Fe I atom has a negligible effect on the determination of the Fe abundance and of the microturbulent velocity parameter in the sun. (auth)

30320 CORONAL EXPANSION AND SOLAR WIND. Hundhausen, A. J. Physics and Chemistry in Space. Volume 5. New York; Springer-Verlag (1972). 247p.

An attempt is made to combine the solar wind observations from a decade of spacecraft exploration in interplanetary space with recent theories of the solar corona. After discussion of the dynamical and chemical processes basic to the coronal expansion, attention is focused on two characteristic forms of solar wind variability—long-lived localized streams and transient shock waves. Both of these are found to arise from the interaction between the coronal plasma and magnetic field. (LBS)

30321 INTERPLANETARY STREAM INTERFACES. Burlaga, L.F. (Laboratory for Extraterrestrial Physics, NASA Goddard Space Flight Center, Greenbelt, Maryland 20771). J. Geophys. Res. 79: No. 25, 3717-3725 (1 Sept 1974).

At 1 AU there is a distinct boundary (the stream interface) in the interaction region of a stream in the solar wind, characterized by an abrupt (approximately a factor of 2 change in $<10^6$ km) drop in density, a similar increase in temperature, and a small increase in speed. In some cases this is a tangential discontinuity, in others it is probably evolving into a tangential discontinuity. It is suggested that stream interfaces form in the interplanetary medium as a consequence of the nonlinear evolution of streams generated by an increase in temperature in the solar envelope. This evolution eventually leads to the formation of a reverse shock behind the interface and a forward shock ahead of it. Two instances in which both a stream interface and a reverse shock had developed at 1 AU are presented. Examples of flare—generated shocks that passed through a stream and were observed near a stream interface are also presented. It is shown that stream interfaces are definitely not the same structures that others have identified as piston boundaries. It is noted that slow shocks, like stream interfaces, always occur ahead of streams and may develop in the interplanetary medium. The importance of small—scale interplanetary dynamical processes, especially the development of discontinuities, is emphasized. (auth)

30322 PROPAGATION OF SUDDEN DISTURBANCES THROUGH A NONHOMOGENEOUS SOLAR WIND. Hirshberg, J.; Nakagawa, Y. (High Altitude Observatory, National Center for Atmospheric Research, Boulder, Colorado 80302); Wellck, R.E. J. Geophys. Res. 79: No. 25, 3726-3730 (1 Sept 1974).

In the earliest studies of the propagation of solar flare disturbances through the solar wind the problem was treated as being spherically symmetric. However, typically interplanetary conditions at 1 AU are dominated by a series of high—velocity streams, each preceded by a density peak. Earlier calculations have indicated that velocity and density inhomogeneities have important effects on transit times and strengths of propagating disturbances. Other workers have numerically investigated the effect of streams on the propagation of shocks confined to remain strong throughout the propagation to 1 AU. However, the constraint that the interplanetary shock remain strong throughout its propagation is unrealistic, since the shocks observed in space at 1 AU often have low or intermediate Mach numbers. We here report on a calculation in which a sudden spherically symmetric disturbance is introduced at 30 R_s and allowed to propagate through a solar wind containing a velocity stream. No restriction is made on the evolution of the strength of the disturbance as it propagates. It was found that at 1 AU the disturbance remained strong in the low—velocity part of the stream and that it propagated from the sun relatively slowly. In the high—velocity region the disturbance reached 1 AU more rapidly but was weaker. Near the density peak the form of the disturbance seen at 1 AU was highly distorted. In other words, it is shown that the calculated transit time, strength, and form of the disturbance at 1 AU depend markedly on the position within the stream at which it is observed. (auth)

30323 LATITUDINAL DISTRIBUTION OF SOLAR WIND VELOCITY AND ITS RELATION TO SOLAR EUV CORONA. Watanabe, T.; Shibasaki, K.; Kakinuma, T. (Research Institute of Atmospherics, Nagoya University, Toyokawa, Aichi, Japan). J. Geophys. Res. 79: No. 25, 3841-3844 (1 Sept 1974).

The solar wind velocity in high latitudes up to 64°N is derived from the interplanetary scintillation of 3C48 in 1972 and 1973, and the relation between latitudinal distribution of the solar wind velocity and of the brightness of solar EUV corona is examined. In May—June 1972 the solar wind velocity tended to increase with increasing heliographic latitude of the source of observed solar wind, while the intensity of the EUV corona weakened with increasing latitude. In May—June 1973 the solar wind velocity did not noticeably increase with latitude, and average brightness of the EUV corona in low and high latitudes was approximately the same. Hence it is suggested that the latitudinal distribution of the solar wind velocity is inversely related to the brightness distribution of the solar EUV corona. (auth)

30324 ON ELECTRON HEAT CONDUCTION IN THE SOLAR WIND. Hollweg, J.V. (High Altitude Observatory, National Center for Atmospheric Research, Boulder, Colorado 80303). J. Geophys. Res. 79: No. 25, 3845-3850 (1 Sept 1974).

First, it is pointed out that Perkins' work on the helioclassical electron conductivity in the solar wind is missing an important term. This term essentially removes Perkins' helioclassical reduction of the heat flux below the classical Spitzer—Härm value. Second, a speculative discussion of an alternative approach is presented. It is argued that heat current instabilities may be effective in substantially reducing the heat flux, and approximate formulas are presented for the heat flux when the instabilities are operating. However, these formulas must be regarded merely as speculations as to the end result of a difficult and as yet unsolved problem in nonlinear plasma physics. (auth)

30325 SWEET'S MECHANISM IN THE SOLAR WIND. Burlaga, L.F.; Scudder, J.D. (Laboratory for Extraterrestrial Physics, NASA/Goddard Space Flight Center, Greenbelt, Maryland 20771). Astrophys. J. Lett. 191: No. 3, L149-L152 (1 Aug 1974).

Direct evidence for Sweet's mechanism is presented. This process occurs in the solar wind, at D—sheets near 1 a.u. Conductivities on the order of 10^4 esu are obtained, which is on the order of the local plasma frequency, implying that the effective "collision" frequency is on the order of the plasma frequency. The lateral extent of D—sheets is approximately 0.01 to 0.001 a.u. Hundreds of such D—sheets are probably present between the orbits of Venus and Earth at any instant. (auth)

30326 ULTRAVIOLET FLUORESCENT PUMPING OF OH 18—CENTIMETER RADIATION IN COMETS. Mies, F.H. (National Bureau of Standards). Astrophys. J. Lett. 191: No. 3, L145-L148 (1 Aug 1974).

In the absence of collisions, optical pumping of cometary OH by solar ultraviolet radiation determines the relative population of OH molecules in the Λ—doubled levels of the $^2\Pi_{3/2}$ ground state. The distribution is extremely sensitive to the heliocentric radial velocity of the comet, and at appropriate velocites the level populations will be either inverted or anti—inverted. Thus the OH 18—cm spectrum of a comet, measured with respect to the 10°K galactic background at 1665 and 1667 MHz, may be observed either in emission or in absorption at different periods during the trajectory. Optical pumping also will produce an alignment of the magnetic sublevels along the axis of the incident solar radiation, and variable degrees of linear polarization are expected. (auth)

30327 SUN AND COSMIC RAYS. Pomerantz, M. A.; Duggal, S. P. (Franklin Inst., Swarthmore, PA). Rev. Geophys. Space Phys.; 12: No. 3, 343-361(Aug 1974).

Solar phenomena produce cosmic ray intensity variations over a wide range of time scales. The observed flux is modulated and rendered anisotropic as the particles propagate in the solar wind, and it is occasionally enhanced by the sporadic emission of solar cosmic rays. Both quasi-static phenomena (the long-term omnidirectional intensity variation and the steady state diurnal anisotropy) and transient fluctuations (disturbed daily variation and Forbush decrease) as well as the spatial distribution of solar flare particles are represented by a theoretical model that prescribes the role of the several solar-controlled parameters that characterize the electromagnetic properties of the interplanetary medium. Considerable information concerning the ambient conditions has been obtained with spacecraft. However, the in situ measurements are confined to a limited region near the ecliptic plane. Consequently, in some cases, theoretical predictions based upon them are not in accord with observations of cosmic ray intensity variations. Thus the modulations and anisotropies must be treated in a three-dimensional framework. It is therefore reasonable to attempt to deduce the properties of the relevant inaccessible regions of the heliosphere from observations of the sun itself. These properties can be determined by relating the various cosmic ray phenomena to changes during a solar cycle and from one cycle to another. To this end, data covering at least two solar cycles are studied to determine the solar cycle dependence of the following effects: long-term variations in the omnidirectional intensity, Forbush decreases, solar diurnal variations, and solar cosmic ray events (ground level enhancement and polar cap absorption). (auth)

30328 COMPARISON OF ACTIVITY IN SOLAR CYCLES 18, 19, AND 20. Dodson, H. W.; Hedeman, E. R.; Mohler, O. C. (Univ. of Michigan, Pontiac). Rev. Geophys. Space Phys.; 12: No. 3, 329-341(Aug 1974).

Although solar activity cycles are in general remarkably similar, cycles 18, 19, and 20, with maximums in 1947.5, 1958.2, and 1968.9, respectively, differed in the heights of their maximums, in the patterns of their development, and to a certain extent in the character of their manifestations of solar activity. Of the 20 solar cycles since 1755, the maximums in sunspot numbers for cycles 18, 19, and 20 rank as 3, 1, and 10, respectively. Cycle 18, with a maximum smoothed monthly sunspot number of 151.8, was the cycle of "giant" spots. Cycle 19, with the highest recorded maximum, 201.3, included many large spots but failed to produce spots with areas equal to those of cycle 18. The highest known daily 2800-MHz flux occurred in cycle 18, not in cycle 19. Cycle 20, with a sunspot maximum of only 110.6, appears to have been close to the average cycle of the last 220 years. An attempt is made to compare the general levels of flare production in the three cycles. Cycle 19 is estimated to have been more flare-rich than cycle 18 by a much smaller factor than the original data implied. In cycle 20, general flare production drops conspicuously. Two types of flare-rich centers of activity are recognized, viz., those with extraordinarily high numbers of flares of Hα importance ≥ 1 and those with unusually high frequency of flares with comprehensive indices of 11 or greater (great ionizing and radio frequency emission as well as Hα area). A list of the most flare-rich regions in cycles 18, 19, and 20 is presented. In addition, the times and locations of the ~100 greatest individual flares in the three cycles have been tabulated. North-south asymmetry of sunspots and the shapes of the mean sunspot curves were not the same for the three cycles. The minimums between the cycles differed in duration and residual activity. Solar magnetic measurements exhibit the 22-year period and make polarity patterns alike in cycles 18 and 20. Summarized coronal measurements from the Pic-du-Midi Observatory for 1944–1973 suggest that the relationships between coronal intensities and other measures of solar activity are complex. Emphasis on times of the greatest solar activity in cycles 18–20 leads to a certain sense of positive relationship between events on the sun and geophysical phenomena. Geophysical uncertainties abound, however, if consideration drops to just above average solar circumstances. Comments are made on certain problems in solar-terrestrial relationships. (auth)

30329 SPECTRAL CLASSIFICATIONS IN THE Fe XIX TO Fe XXIII ISOELECTRONIC SEQUENCES. Fawcett, B. C.; Galanti, M.; Peacock, N. J. (Science Research Council, Abingdon, Eng.). J. Phys., B (London); 7: No. 10, 1149-1153(11 Jul 1974).

Emission lines are classified belonging to $2s^22p^n$-$2s2p^{n+1}$ transition arrays in the ions Ti XVII, V XVII to XX, Mn XVIII, Mn XIX, Fe XIX and Fe XX. The source of these ions is the plasma produced at metallic surfaces irradiated with a neodymium laser beam with a focused power density in the range of 10^{12} to 10^{13} W cm^{-2} at the target surface. The data reported can be applied to the interpretation of solar flare spectra. (auth)

30330 RATIO OF THE TEMPERATURES OF THE QUIET SUN AND THE CENTRE OF THE MOON AT $\lambda = 1.3$ mm. Wrixon, G. T. (University Coll., Cork, Ireland); Schneider, M. V. Nature (London); 250: No. 5464, 314(26 Jul 1974).

It has been proposed to use the Moon as a radiometric calibration standard for observations of extended sources in the infrared millimetre, and microwave portions of the spectrum. In this connection measurements were made of the ratio of the quiet sun temperature to that of the center of the new Moon at 231 CHz ($\lambda = 1.3$ mm). The 36ft telescope at the National Radio Astronomy Observatory was used for measurements made on June 30th 1973. Assuming that the temperature of the quiet Sun was 5,800 K at $\lambda = 1.3$ mm the value 124.5 K was derived for the central lunar temperature at new Moon. (UK)

30331 LONG TERM PERIODICITIES IN THE SUNSPOT CYCLE. Cohen, T. J.; Lintz, P. R. (Teledyne Geotech, Alexandria, VA). Nature (London); 250: No. 5465, 398-399(2 Aug 1974).

It is stated that the existence of a long period (~179 yr.) periodicity in the solar cycle is suggested by the planetary theory of sunspots. The present authors consider that although such a periodicity probably exists it is not caused by primary long term excitation but is in the nature of a "beat" phenomenon. An analysis was made of sunspot data acquired back to 1750 by what is termed the "maximum entropy spectral analysis method", and from the results the existence of a long period (160 to 190) variation in sunspot activity appears certain. Sinusoids were obtained that interfered with one another to produce beat effects. The results were also used to predict future sunspot activity, using a value of 179 yr. for the periodicity. (UK)

30332 STRUCTURE AND EVOLUTIONARY HISTORY OF THE SOLAR SYSTEM. IV. Alfven, H.; Arrhenius, G. (California Univ., La Jolla, San Diego (USA)). Astrophys. Space Sci.; 29: No. 1, 63-159(Jul 1974).

The fourth part of an analysis of the solar system is presented. The chemical composition of the planets and satellites is studied: heavy elements are more abundant in the outermost and innermost regions of the systems. It is shown that observations of meteorites provide information on processes in jet streams and on early fractionation and condensation. The location of the different groups of secondary bodies is a result of a plasma phenomenon occurring at the critical velocity limit. The structure of the different groups of bodies is considered and it is shown that the mass distribution is a function of the spin of the central body. (auth)

30333 SOLAR FLARES AS SOURCES OF ENERGETIC PARTICLES. de Feiter, L. D. (Space Research Lab. of the Astronomical Institute at Utrecht, The Netherlands). Space Sci. Rev.; 16: No. 1-2, 3-43(Jun-Jul 1974).

A review is presented of the present status of knowledge of solar-flare phenomena with special emphasis on the production of suprathermal particles and their solar effects. Of these energetic particles electrons play an important role since they produce the x-ray and radio-bursts observed during many flares. Also, during their slowing down to thermal energies they contribute to the heating of localized regions in the solar atmosphere, through energy exchange with the ambient electrons. Observable radiations of energetic protons, and other nuclei, are produced through nuclear interactions leading to the emissions of gamma-ray lines. Detectable fluxes of these gamma-ray lines are produced only in the most powerful flares. Also the nuclei that enter into deeper layers of the solar atmosphere transfer most of their kinetic energy to the ambient plasma. (auth)

30334 TYPE III BURSTS. Solar Radio Group Utrecht (Astronomical Institute at Utrecht, The Netherlands). Space Sci. Rev.; 16: No. 1-2, 45-89(Jun-Jul 1974).

One of the purposes of this paper is to stress the fact that the solar type III radio burst is not the simple phenomenon it is sometimes suggested to be. Therefore its various properties derived from observations of the past 20 years are presented, and a few theories invoked to describe the basic features are reviewed. This may serve as an introduction to the subject. (auth)

30335 TYPE-III RADIO BURSTS AND THEIR INTERPRETATION. Smith, D. F. (High Altitude Observatory, Boulder, Colo. (USA)). Space Sci. Rev.; 16: No. 1-2, 91-144(Jun-Jul 1974).

The observations of Type-III solar radio bursts are briefly reviewed to set requirements on a model for their interpretation. The most important of these requirements is that the source must be an electron stream which is in a state of continuous quasilinear relaxation and which initially must have a nearly monotonically decreasing velocity distribution. The problem of constructing a model is broken into three parts: (1) The plasma wave source which depends on the interaction of the electron stream with electron plasma waves. (2) The radiation source which depends on the interaction of plasma waves and transverse electromagnetic waves or in a magnetized plasma the ordinary and extraordinary modes of magnetoionic theory. (3) The propagation of radiation between the source and the observer which depends on the transmission of radiation through a scattering refracting absorbing magnetized plasma. (auth)

30336 SATELLITE OBSERVATIONS OF TYPE III SOLAR RADIO BURSTS AT LOW FREQUENCIES. Fainberg, J.; Stone, R. G. (National Aeronautics and Space Administration, Greenbelt, Md. (USA). Goddard Space Flight Center). Space Sci. Rev.; 16: No. 1-2, 145-188(Jun-Jul 1974).

30337 NON-RELATIVISTIC SOLAR ELECTRONS. Lin, R. P. (California Univ., Berkeley (USA). Space Sciences Lab.). Space Sci. Rev.; 16: No. 1-2, 189-256(Jun-Jul 1974).

This review summarizes both the direct spacecraft observations of nonrelativistic solar electrons, and observations of the x-ray and radio emission generated by these particles at the Sun and in the interplanetary medium. These observations bear on three physical processes basic to energetic particle phenomena: (1) the acceleration of particles in tenuous plasmas; (2) the propagation of energetic charged particles in a disordered magnetic field, and (3) the interactions of energetic charged particles with tenuous plasmas to produce electromagnetic radiation. Because these electrons are frequently accelerated and emitted by the Sun, mostly in small and relatively simple flares, it is possible to define a detailed physical picture of these processes. In many small solar flares nonrelativistic electrons accelerated during flash phase constitute the bulk of the total flare energy. Thus the basic flare mechanism in these flares essentially converts the available flare energy into fast electrons. Nonrelativistic electrons exhibit a wide variety of propagation modes in the interplanetary medium, ranging from diffusive to essentially scatter-free. This variability in the propagation may be explained in terms of the distribution of interplanetary magnetic field fluctuations. Type III solar radio burst emission is generated by these electrons as they travel out to 1 AU and beyond. Recent in situ observations of these electrons at 1 AU, accompanied by simultaneous observations of the low-frequency radio emission generated by them at 1 AU provide quantitative information on the plasma processes involved in the generation of Type III bursts. (auth)

30338 RELATIVISTIC ELECTRON EVENTS IN INTERPLANETARY SPACE. Simnett, G. M. (California Univ., Riverside (USA). Dept. of Physics). Space Sci. Rev.; 16: No. 1-2, 257-323 (Jun-Jul 1974).

This review is concerned with relativistic electron events observed in interplanetary space. The different types of events are identified and illustrated. The relationships between solar x-ray and radio emissions and relativistic electrons are examined, and the relevance of the observations to solar flare acceleration models is discussed. A statistical analysis of electron spectra, the electron/proton ratio and propagation from the flare site to the Earth is presented. A model is outlined which can account for the release of electrons from the Sun in a manner consistent with observations of energetic solar particles and electromagnetic solar radiation. (auth)

30339 THE SOLAR TEMPERATURE REVERSAL AND CONVECTIVE MOTIONS. Skalafuris, A. J. (Naval Research Lab., Washington, D.C. (USA)). Astrophys. Space Sci.; 29: No. 1, L9-L17(Jul 1974).

Given an equation of state, the three equations of mass, momentum, and energy conservation determine the vortex-free flow fields in a star. The solar data processed by Athay (1966) is a measure of the dissipation of the fluid, while the use of an empirical temperature profile (BCA, 1968) permits values for the gradients in the equations of fluid flow rendering them algebraic, with solutions independent of boundary conditions. This approach serves as a consistency check on the methods with which data have been processed by inquiring to what degree the basic conservation laws have been satisfied, and by directly implying a velocity field can be scrutinized for its observational consequences. It is found that the most consistent interpretation to this data is that the temperature minimum should not be coincident with flux maximum as the BCD model photosphere is, and that the temperature profile must rise higher at the 1500 km region above optical depth one. Furthermore, more emissions must occur in the U−V metals at this region to support such a temperature increase, but at least an order of magnitude decrease in H$^-$ emission should also be expected, as well as some suppression of the Balmer. As a theoretical consequence horizontal stratification of the velocity field occurs, suggesting either cellular motions or differential rotation with surface velocities as high as 60 kms^{-1}, but on the average near 30 to 40 kms^{-1}, across the solar surface. (auth)

Galaxies

Refer also to abstracts 30167, 30174, 30213, 30216, 30217, 30241, 30242, 30267, and 30278.

30340 (COM-74-50233/7) GALACTIC COSMIC RAY MODULATION IN THE OUTER SOLAR SYSTEM: SOLAR WIND CONSEQUENCES. Suess, S. T.; Fisk, L. A.; Holzer, T. E. (National Oceanic and Atmospheric Administration, Boulder, Colo. (USA)). Nov 1973. 17p. (NOAA-TR-ERL-285; SEL-26; NOAA-74021906). GPO $0.55.

It has recently been suggested that "quiet-time electron increases" may be indicative of a galactic cosmic ray modulation region in the outer solar system that is quite distinct from the modulation region in the inner solar system. The effects of an outer modulation region on the solar wind expansion are considered. It was found that the effects are somewhat more important than those associated with only an inner modulation region, when the same constraints on galactic cosmic ray energy density are applied. It was also found that the existence of an outer modulation region will not lead to a shock-free solar wind transition to subsonic flow (or even to a weakly shocked transition) in the absence of an interstellar neutral gas, and that the cosmic ray effects are less important than those of the neutral gas in the presence of an interstellar atomic hydrogen gas of density 0.1/cc. (auth)

30341 (CONF-730693-, pp 103-131) ELECTRICALLY CHARGED GALAXY AND ITS INTERNAL AND COSMOLOGICAL CONSEQUENCES. Bagge, E. (Univ., Kiel). 1974.

From proceedings of the summer school on particles and fields in space; Balatonfured, Hungary (5 Jun 1973).

The treatment covers the galactic electrical charge, cosmological consequences of electrically charged galaxies, the stopping power of highly ionized gases for charged relativistic particles, and the origin of the large spaced magnetic field in the galaxy. (JFP)

30342 (CONF-730693-, pp 133-160) ANGULAR DISTRIBUTION OF HIGH ENERGY CHARGED PARTICLES IN THE GALAXY. Somogyi, A. J. (Central Research Inst. for Physics, Budapest). 1974.

From proceedings of the summer school on particles and fields in space; Balatonfured, Hungary (5 Jun 1973).

The discussion covers the difficulties of measuring galactic angular distribution, experimental results and their interpretation. (JFP)

30343 (CONF-730693-, pp 183-209) GALACTIC ELECTRONS AND ELECTROMAGNETIC RADIATION. Dilworth, C. (Univ., Milan). 1974.

From proceedings of the summer school on particles and fields in space; Balatonfured, Hungary (5 Jun 1973).

Lectures are given on the present state of knowledge of the electrons of the cosmic radiation acceleration in the galaxy and that of the astronomies, x- and γ-ray astronomy, from which one hopes to derive further information on both the sources and the propagation of cosmic rays. (JFP)

30344 (CONF-730693-, pp 211-230) MODULATION INDUCED ON YOUNG SUPERNOVAE UV AND IR LUMINOSITY BY DUST GRAINS. Aiello, S. (Univ., Florence). 1974.

From proceedings of the summer school on particles and fields in space; Balatonfured, Hungary (5 Jun 1973).

The discussion covers dust condensation in galactic explosions, condensation of cosmic dust in supernovae explosions, experimental evidence, the supernova dust envelope, and modulation of dust of ultraviolet and infrared luminosity. It is concluded that the Hoyle and Wickramasinghe model of dust envelope associated with the expanding shell of supernovae gives plausible results for the modulation of ultraviolet and infrared luminosities after the explosion. Present evidence from infrared and soft x ray observations in the Crab nebula and from visible observations also support the dust envelope model. (JFP)

30345 TURNOVER RADIO SPECTRA OF ELLIPTICAL GALAXIES. Noonan, T.W. (Brockport State College, Brockport, New York). Astrophys. J. 191: No. 2, 301-304 (15 July 1974).

The turnover (peaked) radio spectra of elliptical galaxies with known redshifts show a correlation between the power density at the peak and the frequency at the peak. (auth)

30346 NGC 1068: POSSIBLE 3−MILLIMETER RADIO VARIABILITY. Fogarty, W.G.; Epstein, E.E.; Mottmann, J. (Electronics Research Laboratory, The Aerospace Corporation, Los Angeles, California 90009). Astrophys. J. 191: No. 2, 305-308 (15 July 1974).

Recent measurements of the 3.3−mm flux density of the Seyfert galaxy NGC 1068 indicate a detection approximately 4 standard deviations above the value implied by an extrapolation of the longer−wavelength radio data. This result, plus our two previously reported detections, together with the fact that over 7 years most of our observations are consistent with the extrapolated flux value, imply that the 3−mm flux of NGC 1068 may be variable. A standard statistical test indicates approximately 0.1 percent significance for the hypothesis that the flux is constant. (auth)

30347 X−RAY IONIZATION AND THE HELIUM ABUNDANCE IN 3C 120. Shields, G.A. (Hale Observatories, California Institute of Technology, Carnegie Institution of Washington). Astrophys. J. 191: No. 2, 309-316 (15 July 1974).

Strong He I line emission can arise in a nebula photoionized by a soft X−ray continuum, because of preferential absorption of the higher−frequency photons by He^0 rather than H^0. Using this mechanism, we can account for the strong helium lines of the Seyfert galaxy 3C 120 with a helium abundance as small as N(He)/N(H) =0.09, rather than 0.23, the value that results from the conventional analysis. We present models for 3C 120 with ionization by an exponential continuum or by dilute blackbody radiation. The broad hydrogen and helium lines come from filaments with $N=10^9-10^{12}$ cm^{-3} located 0.3−10 pc from the continuum source, and the forbidden lines come from filaments with $N \lesssim 5 \times 10^5$ cm^{-3} located $\gtrsim$ 100 pc from the continuum source. The forbidden−line intensities imply a large abundance of neon. Predictions of the models include substantial steepening of the Balmer decrement by collisional excitation, strong ultraviolet emission lines of H I, C II, and Mg II, and a thermal infrared luminosity possibly exceeding 10^{46} ergs s^{-1}. (auth)

30348 GAS DENSITY AND THE RATE OF STAR FORMATION IN M33. Madore, B.F.; Van den Bergh, S. (David Dunlap Observatory, University of Toronto, Richmond Hill, Ontario, Canada); Rogstad, D.H. Astrophys. J. 191: No. 2, 317-321 (15 July 1974).

Star counts in M33 are compared with high−resolution radio observations of neutral hydrogen gas. These observations suggest that (1) the gas layer is thinner near the center of M33 than it is in the outer parts; (2) the rate of star formation depends more critically on surface gas density in the outer region of M33 than it does in the inner parts of this object; and (3) the relation between gas density and number of bright stars is similar to the relation between gas density and number density of H II regions. (auth)

30349 FORMATION AND DESTRUCTION RATES OF INTERSTELLAR H_2. Jura, M. (Princeton University Observatory). Astrophys. J. 191: No. 2, 375-379 (15 July 1974).

The interstellar ultraviolet field near 1000 Å is calculated at several locations within 200 pc of the Sun. We include the possibility that interstellar clouds are mutually self−shielding in the Lyman bands, and at the Sun the computed H_2 photodestruction rate is 2×10^{-11} s^{-1}. Also, a value of the H_2 formation rate, R, of 10^{17} cm^3 s^{-1} is consistent with observations toward stars in which n(H_2) is very low. Using these rates, we find that the total densities of hydrogen nuclei within observed clouds are $\sim20(10^{-17}/R)$ cm^{-3} and, therefore, "standard clouds" may be ~10 percent H_2. Our results also apply to HD; and by assuming a deuterium abundance, we can infer that $n(H^+) \lesssim 10^{-2}$ cm^{-3}. Consequently, the hydrogen ionization rate is probably not much higher than about 5×10^{-17} s^{-1}. (auth)

30350 STATISTICAL PROPERTIES OF INTERSTELLAR CLOUDS. Hobbs, L.M. (Yerkes Observatory, University of Chicago). Astrophys. J. 191: No. 2, 395-399 (15 July 1974).

Several statistical properties of 37 interstellar clouds toward 17 stars are considered. Primary among these are the differential distribution functions for the column densities and the line widths obtained directly from interferometric scans of the individual components of the k I λ7699 line. A comparison of the K I absorption with the corresponding H I absorption then determines other cloud properties. For the column–density range $N_H \gtrsim 1.7 \times 10^{20}$ cm^{-2}, various parameters of the resulting average cloud include $N_H = 7 \times 10^{20}$ cm^{-2}, b=1.5 km s^{-1}, v=4.6 kpc^{-1}. The distribution of hydrogen column densities obeys a power law, $\psi(N_H) \propto N_H^{-2}$. (auth)

30351 IONIZATION OF THE LOW–DENSITY INTERSTELLAR MEDIUM. Torres–Peimbert, S.; Lazcano–Araujo, A.; Peimbert, M. (Instituto de Astronomia, Universidad Nacionale Autónoma de México). Astrophys. J. 191: No. 2, 401-410 (15 July 1974).

The fraction of O and early B–type stars embedded in H II regions has been obtained for the solar neighborhood. It is found that a substantial fraction of the OB stars are outside the faintest H II regions detectable on the Palomar Sky Survey plates. This fraction increases from 44 percent for O5 stars to 83 percent for B5 stars, and is independent of reddening for the sample considered. The hydrogen ionizing radiation due to OB stars not embedded in H II regions in 1.3×10^{-14} photons cm^{-3} s^{-1} in the plane of the Galaxy. The integrated spectrum of this flux is similar to that of an 07 star. These results imply that a very important source of ionization of the "intercloud medium" is due to O and B stars not associated with normal H II regions. The z distribution of the stars inside and outside H II regions is presented. This study is based on 2883 OB stars. For M33, the ionization is also obtained for the interarm H II region and amounts to 2×10^{-13} s^{-1} and 7×10^{-14} s^{-1} at distances to the nucleus of $2'$ and $5'$, respectively. All the evidence available indicates that most of the ionization in the interarm H II region is due to late O stars and early B stars, so that cloud collisions, X–rays, and cosmic rays are ruled out as substantial sources of ionization. (auth)

30352 SPECTRAL SURVEY OF THE SOUTHERN MILKY WAY. I. General Description and Catalog I (l = 306–318°). Sundman, A.; Loden, L. O.; Nordstroem, B. (Stockholm Univ., Saltsjoebaden, Sweden). Astron. Astrophys., Suppl. Ser.; 16: No. 3, 445-510(Sep 1974).

As a result of a spectral survey in progress at the Stockholm Observatory, finding lists are being prepared for early and very late type stars in the southern Milky Way. In the present paper, which contains an introductory description of catalogs to be published, the observational material, the principles of the spectral classification, and the card catalogue and catalogue I are presented, which covers the region l = 306–308°, b = +3–−3°. (auth)

30353 DISTRIBUTION OF ORBITAL ECCENTRICITIES OF THE GLOBULAR CLUSTERS. Peterson, C. J. (Univ. of California, Berkeley). Astrophys. J., Lett.; 190: No. 1, L17-L20 (15 May 1974).

Under the assumption that the size of a globular cluster is limited by the tidal force field of the galaxy, the perigalacticon distances were computed for 41 clusters. These new data were combined with the observed radial velocities and positions in a simple model to estimate the distribution of orbital eccentricities. (auth)

30354 U. B. V. PHOTOMETRY OF THE IRREGULAR GALAXY NGC 4753. Shapovalova, A. I. (Kiev State Univ.). pp 187-194 of Problemy Kosmicheskoi Fiziki. Vsekhsvyatskii, S. K. (ed.). Kiev; Izdatel'stvo Kievskogo Universiteta (1973). (In Russian)

The results of detailed three-color photometry of the irregular galaxy NGC 4753 are presented. The integral magnitudes, U–B, B–V colors are found. The absolute magnitudes of galaxy and nucleus are obtained: $M_B = -20^m,23$ $M_B^N = -16^m,4$. The distribution of brightness and colors along the main axes and two dark bands is given. U–B, B–V diagram is constructed. The dependences of the relative intensities and the mean surface brightnesses from B–V color are investigated. The similarity of NGC 4753 with M 82 is noted. The brightness and U–V, B–V colors for every area of size $9'',8 \times 9'',8$ are presented. (auth)

30355 ION IMPLANTATION EFFECTS IN "COSMIC" DUST GRAINS. Bibring, J. P.; Langevin, Y.; Maurette, M.; Meunier, R. (Laboratoire Rene-Bernas, Orsay (France)); Jouffrey, B.; Jouret, C. (Centre National de la Recherche Scientifique, 31 - Toulouse (France). Lab. d'Optique Electronique). Earth Planet. Sci. Lett.; 22: No. 3, 205-214(Jun 1974).

Cosmic dust grains, whatever their origin may be, have probably suffered a complex sequence of events including exposure to high doses of low-energy nuclear particles and cycles of turbulent motions. High-voltage electron microscope observations of micron-sized grains either naturally exposed to space environmental parameters on the lunar surface or artificially subjected to space simulated conditions strongly suggest that such events could drastically modify the mineralogical composition of the grains and considerably ease their aggregation during collisions at low speeds. Furthermore, combined mass spectrometer and ionic analyzer studies show that small carbon compounds can be both synthesized during the implantation of a mixture of low-energy D, C, N ions in various solids and released in space by ion sputtering. The present results have implications concerning the origin of small molecules in interstellar or circumstellar clouds, the "aging" or cosmic dust grains in space, and the "sticking" process in the solar nebula. (auth)

30356 A NEW INFRARED COMPLEX AND MOLECULAR CLOUD IN ORION. Gatley, I. (California Institute of Technology, 1201 East California Blvd., Pasadena, CA 91109); Becklin, E.E.; Matthews, K.; Neugebauer, G.; Penston, M.V.; Scoville, N. Astrophys. J. Lett. 191: No. 3, L121-L125 (1 Aug 1974).

A new complex of infrared sources $\sim 1'$ across has been discovered in Orion. Associated with this cluster is an extended $\sim 6'$ molecular cloud producing intense CO emission. Its measured infrared luminosity is less than $\sim 500\ L_\odot$. The complex is hypothesized to be composed of pre–main–sequence sources. Several arguments suggest that these stars heat dust in the larger molecular cloud and thus cause the strong CO emission. The complex is not associated with a known visible or radio continuum feature, and searches over a $0^\circ.7 \times 0^\circ.7$ field show no other comparable unknown 2.2–μ sources. (auth)

30357 ON THE THEORY OF H_2 ROTATIONAL EXCITATION. Spitzer, L. Jr.; Gould Zweibel, E. (Princeton University Observatory). Astrophys. J. Lett. 191: No. 3, L127-L130 (1 Aug 1974).

The equilibrium populations of the H_2 rotational levels are calculated and compared with the excitation observed in interstellar clouds. The excitation processes considered include collisions with H atoms and electrons and downward radiative cascading following photon excitation or molecule formation. If the probability, β, of ultraviolet photon absorption is less than the mean value of 5×10^{-10} s^{-1}, the computed excitation temperature $T_{2,4}$, corresponding to the relative population of the levels J=2 and 4, is between 200° and 400°K, for a gas temperature of 80°K, and $n(H\ I) \leq 10^2$ cm^{-3}; this is the range of observed excitation temperatures for clouds with strong H_2 lines, for which β is reduced by shielding. To explain the excitation temperatures of about 1000°K observed in some weak–line clouds requires either that β is some 10 times its mean value, corresponding to a cloud position relatively close to an early–type star, or that the cloud is dense [$n(H\ I) > 10^2$] and possibly also hot ($T \simeq 10^3$). (auth)

30358 NEUTRAL POTASSIUM IN DUSTY CLOUDS. Lutz, B.L. (Department of Earth and Space Sciences, State University of New York at Stony Brook). Astrophys. J. Lett. 191: No. 3, L131-L134 (1 Aug 1974).

Observations of interstellar neutral potassium in the spectra of 26 early–type stars are reported along with upper limits for 13 additional stars. Correlation of the derived column densities is shown to be consistent with the "cosmic" potassium–to–hydrogen ratio and ultraviolet shielding if a normal gas–to–dust ratio is assumed. (auth)

30359 DETECTION OF INTERSTELLAR METHYLAMINE. Kaifu, N. (National Radio Astronomy Observatory, Green Bank, West Virginia); Morimoto, M.; Nagane, K.; Akabane, K.; Iguchi, T.; Takagi, K. Astrophys. J. Lett. 191: No. 3, L135-L137 (1 Aug 1974).

Interstellar methylamine, CH_3NH_2, has been discovered in its α, $5_{15}-5_{05}$(73.0 GHz) and s, $4_{14}-4_{04}$(86.1 GHz) transitions in Sgr B2 and Ori A, using the 6–m telescope at Mitaka and 11–m telescope at Kitt Peak. Column density of methylamine is consistently estimated from these observations to be 4×10^{15} cm^{-2} in Sgr B2. The 1–0 transition of $HC^{15}N$(86.1 GHz) and the 2,2–1,1 transition of SO(86.1 GHz) have also been detected during these observations. (auth)

30360 DETECTION OF INTERSTELLAR METHYLAMINE BY ITS $2_{02} \rightarrow 1_{10}$ A_a–STATE TRANSITION. Fourikis, N. (Division of Radiophysics, CSIRO, Sydney, Australia); Takagi, K.; Morimoto, M. Astrophys. J. Lett. 191: No. 3, L139-L141 (1 Aug 1974).

Interstellar methylamine has been detected by its $2_{02} \rightarrow 1_{10}$ A_a–state transition. This transition has been observed in emission in the direction of Sgr B2 and Ori A with the Parkes 64–m radio telescope. A four–component multiplet has been detected in the direction of Sgr B2, but only the main (F=3–2) line at 8777.38 MHz has been detected in the direction of Ori A. Relative to the recently detected millimeter lines, these lines are much more intense than would be expected in thermodynamic equilibrium. We discuss the excitation temperatures of the molecular clouds and their corresponding column densities, and outline the difficulties arising in such calculations. (auth)

30361 IS H^- A SOURCE OF DIFFUSE INTERSTELLAR LINES? Herbst, E.; Patterson, T.A.; Norcross, D.W. (Joint Institute for Laboratory Astrophysics, University of Colorado and National Bureau of Standards); Lineberger, W.C. Astrophys. J. Lett. 191: No. 3, L143-L144 (1 Aug 1974).

The photodetachment spectrum of H^- has been investigated under high resolution in the vicinity of 4430, 4890, and 6180 Å. No resonances have been found. These negative results prove conclusively that H^- autoionization is not the source of the diffuse interstellar lines at these wavelengths. Similarly, C^-, and O^- have been ruled out as candidates for the 4890 and 4430 Å interstellar absorption lines, respectively. (auth)

30362 AN OH SURVEY OF THE HOFFMANN 100−μ SOURCES. Dickinson, D.F.; Chaisson, E.J. (Center for Astrophysics, Harvard College Observatory and Smithsonian Astrophysical Observatory, Cambridge, Massachusetts 02138). Astron. J. 79: No. 9, 938-940 (Sept 1974).

The Hoffmann 100−μ sources were searched at all four lambda−doublet frequencies of the ground state of OH. This molecule is observed in the direction of most of these far−infrared objects. No general correlation with 1720−MHz maser emission was found (as had been suggested on theoretical grounds). (auth)

30363 vB 130: A NEBULOUS CLUSTER WITH AN ABNORMAL EXTINCTION LAW. Racine, R. (David Dunlap Observatory and Erindale College, University of Toronto, Richmond Hill, Ontario, Canada). Astron. J. 79: No. 9, 945-947 (Sept 1974).

Photometric and spectroscopic observations of fourteen stars in a small nebulous cluster in Cygnus are reported. A ratio $A_V/E(B-V) = 8.1 \pm 1.2$ m.e. is found for the absorbing material surrounding the cluster. It is suggested that such large values of R need not apply to all the interstellar material in the line of sight and may only be valid in the immediate vicinity of the cluster. (auth)

30364 MONTE CARLO CALCULATIONS OF THE SURFACE BRIGHTNESS PROFILES OF SPHERICAL DARK NEBULAE. Witt, A.N.; Stephens, T.C. (Ritter Astrophysical Research Center, University of Toledo, Toledo, Ohio 43606). Astron. J. 79: No. 9, 948-953 (Sept 1974).

Theoretical surface brightness profiles of spherical dark nebulae of both uniform density and a density $\propto r^{-2}$ are being discussed. The albedo and asymmetry factor of the dust grains and the optical radius measured from the cloud center were the variable parameters in this study, which further assumed an isotropically incident radiation field. The occurrence of dark cores in the surface brightness profiles is examined and their frequent existence in galactic dark nebulae is interpreted as resulting from a strongly forward scattering phase function and a high optical depth of the associated objects. The shape and depth of the profiles of the dark cores is closely related to the internal density distribution of the clouds and it is suggested that detailed observations of the surface brightness profiles of dark nebulae will reveal important information on the type of their internal density distribution and, thus, their evolutionary status. A determination of the dust albedo from the maximum surface brightness of dark clouds is found to be uncertain, at least at low−galactic latitudes, due to interference from line−of−sight diffuse galactic light. (auth)

30365 X−RAY OBSERVATIONS OF THE LARGE MAGELLANIC CLOUD BY THE COPERNICUS SATELLITE. Rapley, C.G.; Tuohy, I.R. (University College London, Mullard Space Science Laboratory, Department of Physics and Astronomy, Holmbury St. Mary, Dorking, Surrey, England). Astrophys. J. Lett. 191: No. 3, L113-L116 (1 Aug 1974).

The X−ray sources in the Large Magellanic Cloud have been observed using the Mullard Space Science Laboratory instrumentation on board the Copernicus satellite. We have located LMC X−1 to an accuracy of 2' and find that it is associated with part of the Henize H α nebulosity N159 and the intense radio object MC 77. The Be−type supergiant star R149 lies close to our minimum χ^2 position. LMC X−2 is situated in the upper half of the Uhuru error box, and the supergiant R96 is suggested as a possible optical candidate. We have located LMC X−3 to be better than 1'.0, and only two stars brighter than ~17 mag lie within the error circle. The intensities of LMC X−2 and LMC X−3 differ significantly form those previously published. A search for LMC X−4 has detected no flux. We discuss the possible nature of the three bright LMC X−ray sources, their relationship with optical and radio features, and the implications concerning their state of evolution. (auth)

30366 OBSERVATIONS OF INTERACTIONS BETWEEN INTERPLANETARY AND GEOMAGNETIC FIELDS. Burch, J. L. (Goddard Space Flight Center, Greenbelt, MD). Rev. Geophys. Space Phys.; 12: No. 3, 363-378(Aug 1974).

Magnetospheric effects associated with variations of the north-south component of the interplanetary magnetic field (IMF) are examined in light of recent experimental and theoretical results. Although the occurrence of magnetospheric substorms is statistically related to periods of southward IMF, the details of the interaction are not understood. In particular, attempts to separate effects resulting directly from the interaction between interplanetary and geomagnetic fields from those associated with substorms have produced conflicting results. One can, however, say with some assurance that the transfer of magnetic flux from the day side to the night side magnetosphere, as evidenced by equatorward motion of the polar cusp and increases of the magnetic energy density in the lobes of the geomagnetic tail, is a direct consequence of the southward IMF. On the other hand, the formation of a macroscopic X-type neutral line at tail distances less than 35 R_E appears to be a substorm phenomenon. Although other plasma and field phenomena in the outer magnetosphere and at low altitudes may be directly associated with the southward IMF, the evidence is less convincing. The quantitative results that have been obtained are compared with current theoretical models of the reconnection process. (auth)

30367 GAS AND DUST IN INTERSTELLAR CLOUDS. Davies, R. D. (Victoria Univ., Manchester, Eng.). Int. Astron. Union Symp.; No. 52, 251-255(1973).

From conference on interstellar dust and related topics; Albany, NY (29 May 1972).

Detailed measurements have been made of the H, OH and H_2CO lines formed in the L 1534 dense dust cloud; some H and H_2CO observations have been made of the dust cloud lying behind the Orion cluster. These indicate a similar distribution of the 3 species throughout the dust clouds. Studies of H, OH and H_2CO absorption features in clouds lying in front of bright radio sources provide estimates of the physical conditions in regions of molecule formation. (auth)

30368 INTERFEROMETRIC STUDIES OF OH SOURCES ASSOCIATED WITH H II REGIONS AND IR OBJECTS. Davies, R. D. (Victoria Univ., Manchester, Eng.). Int. Astron. Union Symp.; No. 52, 423-432(1973).

From conference on interstellar dust and related topics; Albany, NY (29 May 1972).

An interferometer with a 24 km baseline has been used to map components of OH sources to a precision of a few hundredths of a second of arc. The W3 OH source which is associated with an H II region appears to be rotating slowly. There is evidence for Zeeman splitting in the components of this source. The IR/OH sources NML Cygnus and VY CMa are found to be expanding objects with a large rate of mass outflow. Rotation is also evident in both these objects. (auth)

30369 MIXING OF NEUTRAL GAS AND DUST WITH THE IONIZED GAS OF H II REGIONS. Lortet-Zuckermann, M. C. (Meudon Observatoire, Hauts-de-Seine, France). Int. Astron. Union Symp.; No. 52, 477-481(1973).

From conference on interstellar dust and related topics; Albany, NY (29 May 1972).

30370 DUST IN THE LARGE MAGELLANIC CLOUD. Johnson, H. M. Int. Astron. Union Symp.; No. 52, 471-476(1973).

From conference on interstellar dust and related topics; Albany, NY (29 May 1972).

A brief review of extinction effects is followed by a discussion of new Cerro Tololo Schmidt plates. They were exposed on parts of the LMC with filters which reveal the presence or absence of a continuum, such as one scattered on dust, in H II regions. The results are presented in comparison with the Orion nebula which was observed in the same way. The continuum is always relatively weak in those LMC H II regions which are significantly larger than Orion, but the continuum averages strong in the Orion-class and point-image nebulae. (auth)

30371 VARIATIONS OF INTERSTELLAR ULTRA-VIOLET ABSORPTION. Isobe, S. (Tokyo Astronomical Observatory). Int. Astron. Union Symp.; No. 52, 11-19(1973).

From conference on interstellar dust and related topics; Albany, NY (29 May 1972).

Mixtures of graphite core-ice mantle grains of relatively large mean grain radius and graphite grains are shown to provide good fits to observed interstellar extinction curves. This finding and the rationalization of Greenberg's (1968) assumptions regarding the ultraviolet absorbency of ice are believed to warrant the conclusions that: (1) there are relatively large grains in interstellar clouds; (2) there are relatively small grains in intercloud regions; and (3) there are graphite grains, approximately 0.02 microns in size, present as kernels of the graphite core-ice mantle grains in all regions of interstellar space. (IAA)

30372 4830 MHz FORMALDEHYDE LINE OBSERVATIONS OF DARK CLOUDS IN IC 1795/W3/. Minn, Y. K. (Max-Planck-Institut fuer Radioastronomie, Bonn); Greenberg, J. M. Int. Astron. Union Symp.; No. 52, 269-275(1973).

From conference on interstellar dust and related topics; Albany, NY (29 May 1972).

30373 INTERSTELLAR DUST AND RELATED TOPICS. Proceedings of the Symposium, Albany, New York, May 29–June 2, 1972. Greenberg, J. M.; van de Hulst, H. O. (Eds.). IAU Symposium, No. 52. Dordrecht, Netherlands; D. Reidel Publishing Company (1973). 540p. $44.80.

Theoretical studies and observations of interstellar dust are described in papers dealing with the passive properties of dust grains, their physical and chemical activities in the interstellar medium, and their interactions in association with stars. The papers are grouped according to the principal topics of (1) extinction and polarization, (2) diffuse interstellar features, (3) dust around and in close association with stars, (4) reflection nebulae and other aspects of dust scattering properties, (5) alignment mechanisms, (6) distribution of molecules and processes of molecule formation, (7) radiation effects on dust, (8) physical and chemical interactions of dust with the ambient medium, and (9) gas and dust in H II regions. (IAA)

30374 CYANOACETYLENE: NEW LINES AND SOURCES IN THE GALAXY. Morris, M. (Chicago Univ.); Turner, B. E.; Zuckerman, B.; Palmer, P. Int. Astron. Union Symp.; No. 52, 381-385(1973).

From conference on interstellar dust and related topics; Albany, NY (29 May 1972).

It is suggested that in the case of optically obscured regions cyanoacetylene is particularly useful as a probe in the study of large molecular clouds because of its large abundance and large number of detectable rotational lines. Observations of four successive rotational lines of HC3N are reported. A limited map with points spaced by one arcminute intervals was made of the 72.8 GHz emission in Sgr B2. (IAA)

30375 NEW INFRARED SOURCES ASSOCIATED WITH H II REGIONS. Wynn-Williams, C. G.; Becklin, E. E.; Neugebauer, G. (California Inst. of Tech., Pasadena). Int. Astron. Union Symp.; No. 52, 459-463(1973).

From conference on interstellar dust and related topics; Albany, NY (29 May 1972).

The H II regions studied have generally been those which contain OH or H2O maser sources and which have been shown to contain compact condensations of ionized gas which may be connected with star formation processes. A brief account of two such sources, W3 and NGC 7538, is given. On the basis of the reported observations it is concluded that in general H II condensations are infrared sources in the range from 3 to 20 microns. The condensations are hidden optically by large quantities of obscuring matter. (IAA)

30376 OPTICAL AND CHEMICAL STUDIES ON SIMULATED INTERSTELLAR GRAIN MATERIALS. McCullough, J. D.; Floyd, G. R.; Prince, R. H.; Duley, W. W. (York Univ., Toronto). Int. Astron. Union Symp.; No. 52, 327-333(1973).

From conference on interstellar dust and related topics; Albany, NY (29 May 1972).

The possibility that many different diffuse interstellar absorption features may be produced by the same type of absorbing atom in different hydrocarbon matrices on interstellar grains has been examined experimentally. The present study shows that absorption bands due to Na atoms in various hydrocarbon matrices can occur within the wavelength range 5400 to 5800 A. A study of the molecules generated from the radiation-induced polymerization of C2H2 at 55 K is also reported. It is shown that C6H6 is an abundant product of this polymerization and may therefore be an important constituent of interstellar grains. (auth)

30377 STUDY OF THE INTERSTELLAR DIFFUSE ABSORPTION FEATURES. Wu, C. C. (Washburn Observatory, Madison, WI). Int. Astron. Union Symp.; No. 52, 91-95(1973).

From conference on interstellar dust and related topics; Albany, NY (29 May 1972).

Interstellar diffuse absorption features recently observed are discussed. They are shown to suggest that: (1) the diffuse 4430-A band absorption feature may be produced by preionization of H(-), and (2) the features at wavelengths 5780 A and 5797 A may be due to pure electronic transitions of impurity centers in solid grains. (IAA)

30378 REDSHIFT OF A GALAXY NEAR 4C11.50. Stockton, A. (Univ. of Hawaii, Honolulu). Nature (London); 250: No. 5464, 308(26 Jul 1974).

It is known that near the position of the radio source 4C 11.50 a pair of QSOs exists, separated by 4.8 arc sec. and having redshifts of 0.4359 and 1.901. The presence of a 19 mag. galaxy has also been noted, 10 arc sec. west of the brighter lower redshift QSO (4C 11.50a). Plates taken with a 244 cm telescope indicate that this "galaxy" is actually a close group of three galaxies. (UK)

30379 DYNAMIC EVIDENCE ON MASSIVE CORONAS OF GALAXIES. Einasto, J.; Kaasik, A.; Saar, E. (Astrophysical Observatory, Toravere, Estonia, USSR). Nature (London); 250: No. 5464, 309-310(26 Jul 1974).

It is stated that an unresolved problem in galactic astronomy is the mass discrepancy observed in clusters of galaxies. The virial mass of the cluster per galaxy and the mass-luminosity ratio is considerably larger than for individual galaxies. The discrepancy cannot be a result of expansion and cannot be due to recent origin of clusters, since such ideas would contradict present knowledge of the evolution and ages of galaxies. It is here suggested, as an alternative hypothesis, that clusters of galaxies are stabilized by hidden matter. Another way of resolving the mass discrepancy is to suppose that the masses of individual galaxies have been underestimated. An attempt is made to calculate more exact information on the distribution of mass in the outer regions of galaxies. It is suggested that galaxies contain a previously unrecognized "corona", the parameters of which are as far as possible deduced, but to determine total masses and dimensions of galactic "coronas" more distant test bodies are needed. For this purpose isolated pairs of galaxies may be used, with secondary galaxies serving as test bodies for determining the mass distribution of primary galaxies. Data were collected on 105 pairs of galaxies of known types, radial velocities, and estimated magnitudes and dimensions. There were enough pairs in the sample to allow estimation of the masses of "coronas" separately for primary elliptical galaxies and for bright and intermediate spiral galaxies. It is found that the presence of such massive "coronas" in galaxies considerably reduces and may even remove the virial mass discrepancy in clusters of galaxies. The mass-luminosity ratio rises to about 100 for spiral and 120 for elliptical galaxies. According to new estimates the total mass density of matter in galaxies is 20% of the critical cosmological density. (UK)

30380 RADIATIVE TRANSFER IN CIRCUMSTELLAR DUST CLOUDS. Code, A. D. (Washburn Observatory, Madison, WI). Int. Astron. Union Symp.; No. 52, 505-515(1973).

From conference on interstellar dust and related topics; Albany, NY (29 May 1972).

Radiation transfer is described for several simple models in which the distinction between interstellar extinction and interstellar absorption becomes important. It tries to indicate the manner in which the presence of nearby dust clouds can influence the observed flux from stars. For stars with significant infrared excesses neither the nature of the embedded star nor the optical depth of the dust cloud can be determined by the usual techniques employing color excesses and ratios of total to selective absorption. (IAA)

30381 THE DENSITY PROFILES OF RICH CLUSTERS OF GALAXIES. Yahil, A. (Princeton University Observatory, and Institute for Advanced Study, Princeton, New Jersey). Astrophys. J. 191: No. 3, 623-631 (1 Aug 1974).

The density profiles of rich clusters of galaxies are investigated through the analysis of published galaxy counts. The main feature of the (three–dimensional) spatial density is the proportionality law $\rho \propto r^{-2}$. The detectability of deviations from this singular density is scrutinized, and corollaries bearing on the determination of masses of clusters of galaxies and on the cosmological picture of the Universe are discussed. A realistic cutoff to the singular density profile at $5H_{100}{}^{-1}$ Mpc yields a lower limit $\Omega \geqslant 0.25$ to the density of the Universe, and an upper limit $z \leqslant 3$ to the redshift at the epoch of formation of clusters of galaxies, but the limits can be relaxed if the cutoff radius is smaller. (auth)

30382 RADIO EMISSION FROM MARKARIAN 6. Sramek, R.A. (National Radio Astronomy Observatory, Charlottesville, Virginia); Tovmassian, H.M. Astrophys. J. 191: No. 3, 633-637 (1 Aug 1974).

Interferometer synthesis maps of the Seyfert galaxy Markarian 6 at 11.1–cm and 3.7–cm wavelengths are given. The source is dominated by a bright radio core presumably associated with the optical nucleus. There is also a faint background component which is displaced ~2° from the nucleus. The spectral index of the core is very steep with $\alpha = -1.22$, while the spectral index of the background component is fairly flat. No variations in the core flux density between October 1970 and September 1973 are seen at either frequency despite an optical outburst which occurred in the nucleus between 1968 February and 1969 January. (auth)

30383 A STUDY OF THE H I ABSORPTION IN THE GALAXY M82 BY RADIO INTERFEROMETRY. Weliachew, L. (Owens Valley Radio Observatory, California Institute of Technology). Astrophys. J. 191: No. 3, 639-644 (1 Aug 1974).

The continuum source located in the Irr II galaxy M82 has been studied in H I absorption at 21–cm wavelength. Absorption by gas located in M82 has been detected and mapped with an east–west interferometer. The maximum baseline length was approximately 4500 λ. The velocity resolution was 21 km s^{-1}. The positions of 15 velocity centroids of the H I absorption have been determined to within 1"–3" accuracy relative one another. This allows direct comparison with Heckathorn's recent optical study. For the first time close agreement is found between the systemic velocities of M82 determined by optical and radio methods. While Heckathorn finds a velocity of 243 ± 3 km s^{-1}, the present study yields 240 ± 10 kms^{-1}. The variation of the H I radial velocity across the central region is much more consistent with optical emission lines than with optical absorption lines. Several features of the velocity field are then discussed particularly in the framework of the dustscattering models recently proposed by Sanders and Balamore for M82. (auth)

30384 TWO CHAINS OF INTERESTING SOUTHERN GALAXIES: NGC 7172–7173–7174–7176 AND NGC 7201–7203–7204. Rubin, V.C. (Department of Terrestrial Magnetism, Carnegie Institution of Washington, Washington, D.C.). Astrophys. J. 191: No. 3, 645-651 (1 Aug 1974).

Photographs in the blue and red spectral regions and spectra are presented for two southern chains of galaxies. The morphological types range from ellipticals to early–type spirals with much gas and dust. The velocity dispersion is very small among the galaxies, giving evidence that the two chains form a single group. (auth)

30385 ROTATIONAL EXCITATION OF HCN BY COLLISIONS. Green, S. (Department of Chemistry, Columbia University, New York, New York 10027); Thaddeus, P. Astrophys. J. 191: No. 3, 653-657 (1 Aug 1974).

Rate constants for rotational excitation of HCN by collisions with low–energy He atoms (kinetic temperatures below 100°K) have been computed from first principles. The accuracy of individual rates is conservatively estimated to be ±50 percent above 30°K and within a factor of 2 below 20°K. These rates are also believed to be representative of excitation by collisions with H_2. (auth)

30386 A GALACTIC MODEL WITH A PULSATING ACTIVE NUCLEUS. III. Evolution of Rare-Light Elements. Ohnishi, T. (Kyoto Univ., Uji (Japan). Inst. of Atomic Energy). Astrophys. Space Sci.; 29: No. 1, 3-16(Jul 1974).

The accumulation and distribution of rare-light elements in the Galaxy are investigated according to a model of the Galaxy in which there exists a pulsating active nucleus whose activity decreases with time. The abundances of rare-light elements rapidly decrease on approaching the galactic center whereas the most abundant region of these elements is the annular region at the radial distance of $r = 8 \sim 14$ kpc from the galactic center. In the inner region of $r \leq 8$ kpc the abundances of these elements have varied by two to three orders of magnitude from the early days of the galactic history till now, but in $r \gtrsim 8$ kpc they have been almost constant within a factor of 2. It has become clear that if the nuclides D, ^3He, ^7Li, ^{10}B, and ^{11}B have been produced mainly by the shock process taking place in the outer envelope of Type-II supernova, they must have been created by the mass fractions of the supernova of some 2.7×10^{-3}, 1.7×10^{-4}, 6.9×10^{-8}, 1.7×10^{-7}, and 7.9×10^{-7}, respectively, to account for the solar system abundances. (auth)

30387 EFFECTS OF AN AMBIENT MEDIUM ON THE EMISSION, ABSORPTION AND SCATTERING OF WAVES BY ATOMS AND MOLECULES. Melrose, D. B. (Australian National Univ., Canberra. Dept. of Theoretical Physics). Astrophys. Space Sci.; 29: No. 1, 211-219(Jul 1974).

A theory describing the interaction between atoms or molecules (or other systems with discrete energy eigenvalues) and waves in an arbitrary mode in an arbitrary ambient medium is developed. Rules for generalizing formulas describing processes for waves in vacuo to include the effects of a medium are stated and the illustrative examples of multipole radiation, the photo-electric effect and Rayleigh and Raman scattering are given. The following specific results are discussed: (1) In an isotropic medium with refractive index $n(\omega)$, the rate of transitions with frequency ω is $n(\omega)$, $n^3(\omega)$, ... times that in vacuo for electric dipole, magnetic dipole, or electric quadrupole, ..., transitions. (2) The conventional multipole expansion is inadequate when waves with a longitudinal component of polarization exist, but this does not affect the theory of electric and magnetic dipole transitions. A possible astrophysical application of resonant scattering by molecules of electron plasma waves is discussed briefly. (auth)

30388 DISSIPATION OF MAGNETIC FLUX AND MAGNETIC ENERGY IN PARTIALLY IONIZED GASES. Byrne, J. C.; Burman, R. R. (Western Australia Univ., Nedlands. Dept. of Physics). Astrophys. Space Sci.; 29: No. 1, 179-189(Jul 1974).

Macroscopic equations of motion are used to derive several forms of the generalized Ohm's law for partially ionized ternary gases in magnetic fields, and a conductivity σ is defined that is independent of the magnetic field. A flux theorem is derived using a velocity u_H that can be defined to be the velocity of magnetic field lines; u_H is only slightly different from the velocity of the electron component of the gas. It is shown that σ is the conductivity relevant to the decay of magnetic flux through any surface moving everywhere with velocity u_H. The rate of increase of the thermal energy density of the gas arising through collisions between particles of different species can be resolved into Joule heating at the rate j^2/σ, where j is the current density, and heating associated with ambipolar drift. The latter, contrary to what has been claimed by some authors, is not necessarily fully compensated by a decrease in the energy of the electromagnetic field. In many applications such compensation does occur, but it may not in interstellar clouds where large amounts of gravitational energy can be made available by collapse, and then both heating and an increase in electromagnetic field energy may occur. (auth)

30389 THE MASS OF M33. Lohmann, W. (Max-Planck-Institut fuer Astronomie, Heidelberg (F.R. Germany)). Astrophys. Space Sci.; 29: No. 1, 61-62(Jul 1974). (In German).

According to the Bottlinger law the mass of M33 is determined with $(1.29 \pm 0.23) \times 10^{10} M_\odot$ from measurements of the velocities of the neutral hydrogen by Warner et al. (1973). (auth)

30390 GRAVITATIONAL INSTABILITY OF A ROTATING PLASMA. Sharma, R. C. (Himachal Pradesh Univ., Calcutta (India)). Astrophys. Space Sci.; 29: No. 1, L1-L4(Jul 1974).

The gravitational instability of an infinite homogeneous self-gravitating rotating plasma in the presence of a uniform vertical magnetic field has been studied to include the FLR effects. It has been found that the Jeans' criterion of instability remains unaffected even if rotation and FLR effects are included. The effect of rotation is to decrease the Larmor radius by an amount depending upon the wave number of perturbation. The particular cases of the effect of FLR and rotation on the waves propagated along and perpendicular to the magnetic field have been discussed. (auth)

Cosmology

Refer also to abstract 30770.

30391 SCALAR WAVES IN THE MIXMASTER UNIVERSE. II. Particle Creation. Hu, B. L. (Inst. for Advanced Study, Princeton, NJ). Phys. Rev., D; 9: No. 12, 3263-3281(15 Jun 1974).

Solutions to the complete time-dependent scalar wave equation in the mixmaster universe are presented. Differential equations for the mode amplitudes are given corresponding to field expansions in terms of the asymmetric- and the symmetric-top wave functions and for both minimal and conformal couplings of the scalar field to gravity. The theory of quantized fields in the mixmaster space is summarized. Creation and annihilation operators in the Heisenberg picture develop in time under a general Bogolubov transformation which expresses mathematically the physical processes of particle creation and mode mixing. The problem of particle creation is discussed here in the light of the classical theory of wave propagation. In the adiabatic limit when the expansion of the universe is slow, little production takes place. Higher-order expressions for the production amount are derived by the method of successive WKB approximations. Finally, numerical solutions of the wave equation for the uncoupled modes are presented. The effects of geometric shape, level energy, and particle mass on production are studied for the characteristic "small oscillation" and "bounce" solutions of the mixmaster universe. The anisotropic dynamics of the background gives rise to strong directional effects in particle creation. Production of particles of higher mass or energy is less abundant and less sensitive to the shape or level. (auth)

30392 POSSIBLE EVIDENCE FOR A LARGE MAGNETIC FIELD IN THE ORION INFRARED NEBULA. Beichman, C. A. (Univ. of Hawaii, Manoa); Chaisson, E. J. Astrophys. J., Lett.; 190: No. 1, L21-L24(15 May 1974).

Two independent observational results suggest that a magnetic field of milligauss strength permeates the Orion infrared nebula/molecular cloud. First, the large degree of infrared polarization is best explained in terms of preferential absorption by elongated silicate grains aligned by a ~10-milligauss field. Second, the microwave OH emission features appear to show a classical Zeeman pattern, suggesting a longitudinal field strength of about 3 milligauss. (auth)

30393 STEPS TOWARD THE HUBBLE CONSTANT. II. THE BRIGHTEST STARS IN LATE−TYPE SPIRAL GALAXIES. Sandage, A.; Tammann, G.A. (Hale Observatories, Carnegie Institution of Washington, California Institute of Technology). Astrophys. J. 191: No. 3, 603-621 (1 Aug 1974).

Identification and photometry of the brightest blue and red supergiant stars are given for the highly resolved galaxies NGC 2366, NGC 4236, IC 2574, Ho I, and Ho II in the NGC 2403−M81 group. The data are based on plates taken with the Hale 5−meter telescope and on new photoelectric sequences, or on photographic transfers to other photoelectric sequences. Brightest stars in the Large Magellanic Cloud, the Small Magellanic Cloud, and the solar neighborhood have been selected by analysis of recent data in the literature. This material, together with less complete data for NGC 6822, IC 1613, and M33, gives a calibration of the absolute blue magnitude of the brightest stars in terms of either the luminosity of the parent galaxy or the luminosity class. The absolute magnitudes range from $M_B(1st) = -8.0$ for $M_B(gal) = -14.5$ to $M_B(1st) = -10.0$ for $M_B(gal) = -20.7$. The standard deviation of a single galaxy about the mean correlation line is σ $(M_B) \simeq 0.5$ mag. The correlation of M(star) and M(galaxy) is significant at the 2.5 σ level, and can be understood as a consequence of the normalization of a common luminosity function to the total luminosity of each parent galaxy. A test of the assumption that six galaxies of the NGC 2403 group are closely at the distance of the parent galaxy was made by determining the individual distances by the H II region calibration of Paper I and by the bright−star criterion here. The mean distance to the six galaxies is 3.09 ± 0.13 Mpc (the standard deviation of the single galaxy distance is ± 0.30 Mpc). There are no significant differences (larger than $\sim 1.5\sigma$) in our distances to any of the six members of the group. The brightest red supergiants [chosen such that $(B-V)_0 \gtrsim 2.0$] have a remarkably small dispersion in absolute magnitude, and the magnitudes do not depend on the luminosity of the parent galaxy. The calibration gives $M_v^0(max) = -7.9 \pm 0.1$ mag. Brighter stars are guillotined either by downward sloping evolutionary tracks from their brighter main−sequence progenitors, or by the sharp onset (at $M_v \simeq -8$) of some physical process that drastically shortens the life of a brighter red supergiant. Bright blue irregular variables are not so well defined in absolute luminosity. Although they are very luminous at maximum light $[\langle M_B \rangle \simeq -9.4 \pm \simeq 0.5]$, some members of the class, such as η Car, become so much brighter $(M_B \simeq -14)$ at certain times that the stars, as a class, are apparently unsuitable as accurate distance indicators. (auth)

Planetary Phenomena

Refer also to abstracts 30166, 30173, 30195, 30207, 30330, 30341, 30451, and 30544.

30394 ANOMALIES IN THE COMPOSITION OF INTERPLANETARY HEAVY IONS WITH $0.01 < E < 40$ MeV PER AMU. Chan, J. H.; Price, P. B. (Univ. of California, Berkeley). Astrophys. J., Lett.; 190: No. 1, L39-L41(15 May 1974).

Analysis of tracks in plastic detectors on Apollo 17 shows that at energies from ~2 to ~10 MeV per amu, the composition of interplanetary heavy ions is quite different from that of either solar particles or galactic cosmic rays. C + N, Mg + Si, and $Z \geq 20$ are depleted with respect to 0, and Li + Be + B are missing. The existence of a peculiar bump in the oxygen energy spectrum is confirmed. (auth)

30395 CONCERNING THE ORIGIN AND THE DYNAMICS OF INTERPLANETARY DUST. Koutchmy, S. L. (Paris Astrophysical Inst.). pp 28-33 of Problemy Kosmicheskoi Fiziki. Vsekhsvyatskii, S. K. (ed.). Kiev; Izdatel'stvo Kievskogo Universiteta (1973). (In Russian)

The classical hypotheses concerning the zodiacal light and the F-corona are mentioned. Then recent observations are reviewed which suggest that homogeneous models must be revised: infrared observations of the heliocentric dust cloud, photographical observations of the "diffuse external reinforcement" during the 1970−total solar eclipse and of structure superposed on that expected for the zodiacal light out of the plane of the ecliptic. Finally some suggestions are made for future observations. (auth)

30396 INVESTIGATION OF ULTRAVIOLET ABSORPTION IN THE CONTINUOUS SPECTRUM OF JUPITER. Gerasimenko, S. N. (Kiev State Univ.). pp 65-68 of Problemy Kosmicheskoi Fiziki. Vsekhsvyatskii, S. K. (ed.). Kiev; Izdatel'stvo Kievskogo Universiteta (1973). (In Russian)

The variations of ultraviolet absorption in the continuous spectrum of Jupiter as well as in course of time and on planetary disk are studied. It is concluded that the variations of UV-absorption on the disk are global. (auth)

30397 DAY AIRGLOW EMISSIONS OF 5577-A AND 6300 OI LINES IN MARTIAN ATMOSPHERE. Ghosh, S. N.; Jain, S. K. (Allahabad Univ., India). Indian J. Meteorol. Geophys.; 23: No. 1, 23-28(1972).

Emissions of 5577A and 6300A lines of OI in Martian atmosphere have been investigated. It has been found that for the 5577 A line there are 2 peaks at 90 and 120 km and its total intensity is about 3.5 kR. For 6300 A line, its emission profile is obtained for 2 values of quenching coefficients, namely, $1X10^{-13}cm^3Sec^{-1}$ and $1X10^{-12}cm^{-3}Sec^{-1}$. (20 ref.) (Indian Sci. Abstr.)

30398 LARGE-AMPLITUDE HYDROMAGNETIC WAVES. Barnes, A. (Max Planck Institut fuer Physik und Astrophysik, Munich); Hollweg, J. V. J. Geophys. Res.; 79: No. 16, 2302-2318 (1 Jun 1974).

Several aspects of the theory of large-amplitude hydromagnetic waves and their behavior in the interplanetary medium are examined. The characteristic modes of the full (i.e. nonlinearized) MHD equations and their modification by collisionless and finite-frequency effects are considered. Special attention is given to the transverse Alfvén mode, which is undamped and characterized by strictly constant pressure, density, and $|B|$; this seems to be the predominant propagating fluctuation at 1 AU. It is shown that its propagation in the small-wavelength (WKB) approximation is essentially identical to that of the small-amplitude Alfvén wave of linearized theory. It is also suggested that its presence at 1 AU may provide a natural explanation of the observed power anisotropy of the fluctuations. A second-order analysis is used to study fluctuations that are not characteristic modes. It is found that for a small range of propagation directions, and subject to third-order effects, a finite-amplitude wave can exist that is linearly polarized with δB perpendicular to both B_0 and k: such a wave can damp nonlinearly. But the situation is different for other directions of propagation, and the analysis suggests a possible explanation for the presence of the transverse Alfvén mode at 1 AU. The results are used to discuss several possible mechanisms by which hydromagnetic waves may heat the solar wind. (auth)

30399 DISCUSSION OF INTERPLANETARY POSTSHOCK FLOWS WITH TWO EXAMPLES. Ogilvie, K. W.; Burlaga, L. F. (Goddard Space Flight Center, Greenbelt, MD). J. Geophys. Res.; 79: No. 16, 2324-2330(1 Jun 1974).

Plasma and magnetometer observations of two types of flare-associated shock flows are described and compared with present models. One type represents a class of flows in which the shock is followed by a stream and separated from it by a region in which density, temperature, and speed decrease monotonically. Neither the blast wave model nor the two-stage model, in which the stream and the shock are attributed to the same flare, can quantitatively describe this class. The other type is characterized by a complex region between the shock and the following stream, which has many discontinuities and fluctuations but in which there is no increase in helium concentration. This class of event is not describable in terms of the conventional pictures presented, for example, by Hundhausen. These two types of flow can be distinguished by using ground magnetograms, since the first type shows no sudden impulses following the shock, whereas the second type shows many. It is suggested that the complexity of postshock flows is often due to the interaction of the shock with streams having different origins from that of the shock. A stream that is observed to follow a shock by ~1 day has either a source different from that of the shock or an acceleration not described by the accepted solar wind expansion models. (auth)

30400 RELIABILITY OF THE DAILY QUICK LOOK SOLAR WIND VELOCITIES AS INDICATORS OF INTERPLANETARY ACTIVITY. Intriligator, D. S. (Univ. of Southern California, Los Angeles). J. Geophys. Res.; 79: No. 16, 2491-2492(1 Jun 1974).

It is shown that the daily quick look solar wind velocities based on the Ames Research Center solar wind plasma data obtained on the Pioneer spacecraft are surprisingly reliable indicators of interplanetary activity. These velocities, which are published in the monthly Solar Geophysical Data by NOAA, can appropriately be used in correlation studies with an average accuracy of ±5%. This accuracy reflects the "jitter" in the solar wind velocity during quiescent intervals and across high speed streams. (auth)

30401 INTERACTION BETWEEN AN IMPACT-PRODUCED NEUTRAL GAS CLOUD AND THE SOLAR WIND AT THE LUNAR SURFACE. Lindeman, R. A. (Rice Univ., Houston, TX); Vondrak, R. R.; Freeman, J. W.; Snyder, C. W. J. Geophys. Res.; 79: No. 16, 2287-2296(1 Jun 1974).

On April 15, 1970, the Apollo 13 S-IVB stage impacted the nighttime lunar surface approximately 140 km west of the Apollo 12

Alsep site and 410 km west of the dawn terminator. Beginning 20 s after impact the suprathermal ion detector experiment and the solar wind spectrometer observed a large flux of positive ions (maximum flux $\sim 3 \times 10^8$ ions/cm^{2}s sr) and electrons. Two separate streams of ions were observed: a horizontal flux that appeared to be deflected solar wind ions and a smaller vertical flux of predominantly heavy ions (>10 amu), which probably were material vaporized from the S-IVB stage. An examination of the data shows that collisions between neutral molecules and hot electrons (50 eV) were probably an important ionization mechanism in the impact-produced neutral gas cloud. These electrons, which were detected by the solar wind spectrometer, are thought to have been energized in a shock front or some form of intense interaction region between the cloud and the solar wind. Thus strong ionization and acceleration are seen under conditions approaching a collisionless state. (auth)

30402 VOLATILE ELEMENT INFLUX ON VENUS FROM COMETARY IMPACTS. Lewis, J. S. (Massachusetts Inst. of Tech., Cambridge (USA). Dept. of Earth and Planetary Sciences). Earth Planet. Sci. Lett.; 22: No. 3, 239-244(Jun 1974).

Several different reasonably concordant methods of estimating the flux of carbonaceous chondrite and cometary material (both meteoric dust and comet nuclei) through the inner solar system are shown to imply that such sources may have a dominant effect on the present abundances of several important constituents of the atmosphere of Venus. In particular, the entire supply of hydrogen compounds on Venus may owe its origin to infall of such material. The escape rate of atomic hydrogen may be in approximate balance with the influx rate of hydrogen in the forms of bound meteoritic water and cometary ices. It is suggested that the atmospheric inventories of H, S, Cl, F and possibly N on Venus are provided by infall, and need not be endogenous to Venus. (auth)

30403 POWER SPECTRA OF THE INTERPLANETARY MAGNETIC FIELD, 0.7 TO 1.6 AU. Blake, D. H.; Belcher, J. W. (Massachusetts Inst. of Tech., Cambridge). J. Geophys. Res.; 79: No. 19, 2891-2893(1 Jul 1974).

Power spectra of the fluctuations in the interplanetary magnetic field were obtained from a number of spacecraft. Russell (1972) and Childers and Russell (1972) have recently reviewed published power spectra of the interplanetary field. The computation of power spectra in the frequency range from 1.16×10^{-5} Hz to 2.96×10^{-3} Hz corresponded to periods from 1 day to 5.86 min. The data used for these spectra were taken during the Mariner 4 and Mariner 5 missions and cover a radial distance from 0.7 to 1.6 AU. (auth)

30404 ABSORPTION OF TRAPPED PARTICLES BY JUPITER'S MOONS. Hess, W. N. (National Oceanic and Atmospheric Administration, Boulder, CO); Birmingham, T. J.; Mead, G. D. J. Geophys. Res.; 79: No. 19, 2877-2880(1 Jul 1974).

Absorption effects of the four innermost moons were included in the radial transport equations for electrons and protons in Jupiter's magnetosphere. It is found that the phase space density n at 2 R_j for electrons with equatorial pitch angles of <69° is reduced by a factor of 4.2×10^4 when lunar absorption is included in the calculation. For protons with equatorial pitch angles of <69° the corresponding reduction factor is 2.3×10^6. The effect of the satellites becomes progressively weaker for both electrons and protons as equatorial pitch angles of $\pi/2$ are approached because the likelihood of impacting a satellite becomes progressively smaller. The large density decreases that are found at the orbits of Io, Europa, and Ganymede result in corresponding particle flux decreases that should be observed by spacecraft making particle measurements in Jupiter's magnetosphere. The characteristic signature of satellite absorption should be a downward-pointing vertex in the flux versus radius curve at the L value corresponding to each satellite. (auth)

30405 BURSTS OF RELATIVISTIC ELECTRONS FROM JUPITER OBSERVED IN INTERPLANETARY SPACE WITH THE TIME VARIATION OF THE PLANETARY ROTATION PERIOD. Chenette, D.L.; Conlon, T.F.; Simpson, J.A. (Enrico Fermi Institute, University of Chicago, Chicago, Illinois 60637). J. Geophys. Res. 79: No. 25, 3551-3558 (1 Sept 1974).

Bursts of Jovian electrons in the energy range 3–30 MeV have been detected to distances of the order of 1 AU from the planet. The duration of each burst was about 2–3 days, and the maximum intensity increased with increasing distance from the sun. These events could not be correlated with known solar activity. The conclusion that these electrons originated at Jupiter and were accelerated within the Jovian magnetosphere is based on the following observations of three bursts. (1) The power spectrum of the temporal variations of the 6– to 30–MeV electron flux showed a persistent peak at Jupiter's rotation frequency, 2.8×10^{-5} Hz (corresponding to the 10–hour rotation period) out to distances $> 10^8$ km from the planet; (2) the slope, or spectral index, of the differential energy spectrum measured as a function of time displayed the 10–hour cyclic variation in the value of the index, which was earlier discovered by our group as being characteristic of the electrons within the Jovian magnetosphere; (3) the value of the spectral index was anticorrelated with the flux level of the 6– to 30–MeV electrons, an effect that was found inside the magnetosphere on the inbound pass; (4) the 10–hour variations of both the spectral index and the number density observed in the bursts analyzed so far are in phase with the corresponding variations inside the Jovian magnetosphere for $R \gtrsim 50\ R_j$; and (5) overall, the bursts were anisotropic, their direction of propagation being toward the sun along the average interplanetary magnetic field. We also note that the particles in the bursts propagated across the average interplanetary magnetic field to reach Pioneer 10, and we discuss some of the implications. The analysis of these events provides a new tool for the study of the propagation of particles in the interplanetary medium. (auth)

30406 MEASUREMENTS OF THE JOVIAN RADIATION BELTS. Fillius, R.W.; McIlwain, C.E. (Physics Department, University of California at San Diego, La Jolla, California 92037). J. Geophys. Res. 79: No. 25, 3589-3599 (1 Sept 1974).

The University of California at San Diego trapped radiation detector measured proton and electron fluxes, angular distributions, and energy spectra throughout the Pioneer 10 flyby of Jupiter last December. Here the instrumentation and calibrations are described, and good values for particle fluxes in the inner and outer regions are presented. The major features of the Jovian radiation belts are described, with preliminary discussions of their meanings. (auth)

30407 THE POSITION AND STOKES PARAMETERS OF THE INTEGRATED 21–CENTIMETER RADIO EMISSION OF JUPITER AND THEIR VARIATION WITH EPOCH AND CENTRAL MERIDIAN LONGITUDE. Berge, G.L. (Owens Valley Radio Observatory, and Division of Geological and Planetary Sciences, California Institute of Technology, Pasadena, California). Astrophys. J. 191: No. 3, 775-784 (1 Aug 1974).

Interferometer observations of Jupiter using short antenna spacings were made in 1968 and 1970 at 21.1 cm wavelength and in 1971 at 18.7 cm. The flux density, centroid position, and complete polarization state of the integrated emission were determined at many different central meridian longitudes. A small displacement of the emission centroid from the center of the planet may have been detected. Of greater importance, perhaps, is that a displacement larger than about 0.15 radii is rules out. The observations confirm the slow decrease in flux density over a period of years, and extend the time base to 11 years, during which there has been no start of a recovery from the decline. The variation of flux density and polarization with central meridian longitude changed character in several respects from earlier observations. Some, but not all, of these changes can be explained by the change in our aspect angle D_E since the earlier observations. (auth)

30408 THE EQUILIBRIUM OF A ROTATING BODY OF ARBITRARY DENSITY. Lanzano, P. (Naval Research Lab., Washington, D.C. (USA)). Astrophys. Space Sci.; 29: No. 1, 161-178(Jul 1974).

Clairaut's theory of rotational equilibrium is extended to third order terms in a small parameter. It has been feasible to obtain the Clairaut equation, which governs the deformation of the equipotential surfaces within a rapidly rotating mass in hydrostatic equilibrium, as an ordinary differential equation. This has been achieved by eliminating the two integral terms which appeared in the original formulation. It is expected that the numerical integration of this newly obtained equation will contribute toward a more precise solution of certain geophysical problems—e.g., the determination of the geoid to an accuracy of ±1m, and the correction to the travel-time of seismic waves; it should also assist in some planetary questions like the determination of the exterior shape for the rapidly rotating planets Jupiter and Saturn. (auth)

30409 DIRECT SIMULATION OF COLLISION PROCESSES. II. The Growth of Planetesimals. Dodd, R. J.; Napier, W. M. (Royal Observatory, Edinburgh (UK)). Astrophys. Space Sci.; 29: No. 1, 51-59(Jul 1974).

The mass distribution of protoplanets is studied by a Monte Carlo technique. It is assumed that the bodies coalesce on collision and that their self-gravitation is important. It is found that over most of the mass range a distribution of the form $n(m) \alpha m^{-q}$ develops, with q tending to ~1.8. However, there is an overabundance of large masses relative to the power law; in particular the simulations indicate the growth of a large nucleus which progressively dominates the growth process. It is also found that the axial inclinations of the planets are best explained if they grew out of a coagulating medium comprising planetesimals with random velocities ~5 km s^{-1} and masses up to 10^{-2} of the embryo masses. The inclinations of the giant planets are consistent with a fluccole-type origin of these bodies. (auth)

PHYSICS (ATMOSPHERIC)

Auroral and Ionospheric Phenomena

Refer also to abstract 29226.

30410 (AD-776969) ROUTINE OPERATION OF DIGISONDE AT MAYNARD, MASSACHUSETTS. Final Report, 1 September 1971–31 August 1972. Bibl, K.; Reinisch, B. W.; Smith, S.; Temple, R. K. (Lowell Technological Inst., Mass. (USA). Research Foundation). Jun 1973. Contract F19628-72-C-0061. 64p. (LTIRF-356/IP; AFCRL-TR-73-0348). NTIS $3.75.

Digital ionosonde DGS 128-3 was operated and maintained at Maynard, Massachusetts, during the period from 31 August 1971 to 31 August 1972. Continuous monitoring of the ionosphere by vertical pulse sounding produced twelve months of ionospheric data for E- and F-region studies. Digital data, obtained for more than 98 percent of the entire period, was recorded continuously on magnetic tape. Hourly ionograms were produced on-line by a printer using a special number font. Magnetic tape and hourly ionograms, collected daily, were reduced and scaled for seventeen URSI parameters and presented for publication in the AFCRL geophysics and space data bulletin. A unique calibration scheme was implemented which automatically recorded the system amplitude versus frequency response and system linearity. (auth)

30411 CHARACTERISTICS OF THE TURBULENT ATMOSPHERE ON THE BASIS OF RADIO SOURCE SCINTILLATION DATA. Stankevich, K. S. Izv. Vyssh. Ucheb. Zaved., Radiofiz.; 17: No. 5, 666-673(1974). (In Russian).

Based upon the theory of radio wave propagation in the turbulent atmosphere, an analysis is made of the data on radio source scintillations in the troposphere at large zenith angles. It is shown that the reasons for scintillations are the amplitude fluctuations of radio waves passing through the turbulent atmospheric layer. The characteristics of the turbulent atmosphere are obtained: C_n = (1 to 3) · 10^{-7} and the thickness of the atmospheric inhomogeneous layer H = (3 to 4) km. (tr-auth)

30412 INHERENT ELECTROMAGNETIC AND ELECTROSTATIC OSCILLATIONS OF A SPHERICAL CAVITY IN PLASMA. Kormilitsin, B. T.; Zush, Ya. Ya. (Rizhskii Plytechnical Inst., USSR). Izv. Vyssh. Ucheb. Zaved., Radiofiz.; 17: No. 5, 779-781(1974). (In Russian).

On the assumption of a plasma with constant electron concentration with a spherical cavity in it free of electrons, equations are derived describing the inherent electromagnetic oscillation of the cavity, using the known expressions for the dielectric constant of cold collisionless plasma and the equations of classical electrodynamics. The dependence of the normalized dimension of the resonance spherical cavity in the plasma on the ratio of the resonance and plasma frequencies is shown. Some mechanical values related to the electromagnetic field of the oscillation of the cavity in the plasma are studied. (JSR)

30413 SATELLITE MEASUREMENTS OF SOLAR X-RAY FLUX AND GROUND OBSERVATIONS OF SUDDEN IONOSPHERIC DISTURBANCES. Lastovicka, J.; Smilauer, J. (Geophysical Inst., Prague). Geofys. Sb.; 19: 305-316(1971).

Processes are reviewed controlling the ionospheric D-layer, especially those that are the cause of anomalous conditions of radiowave propagation (SID-events). Attention is paid to the effect of solar x-ray flux, the intensity of which was measured in several energy bands in the period of September through December 1969 using the data telemetered from the Solrad-9 satellite. The satellite equipment and the device for the reception and evaluation of the telemetry information are described. The events of enhanced intensity of solar x-rays confirm the dominating effect of x-rays upon the lower ionosphere only for x-ray fluxes exceeding a level of about 10^{-13} Wm^{-2} s^{-1} in the 1 to 8 Å band. (1 f, 4 t) (Nuclear Sci. Abstr. Czeck.)

30414 LOCAL CHANGES OF THE ATMOSPHERIC ELECTRIC FIELD BY EAS IONIZATION. Bonino, G.; Dardo, M. (CNR, Turin). Lett. Nuovo Cim.; 10: No. 17, 757-761(24 Aug 1974).

An investigation is made of the changes in the atmospheric electric field caused by the motion of the electrons and the molecular ions produced by extensive air showers of different primary energies, with particular attention given to the radial dependence of pulse amplitude and temporal variations. The calculations are focused primarily on the electron component of the EAS. (LBS)

30415 ELECTROMAGNETIC RADIATION INFLUENCE UPON THE PLASMA VARIATION SPECTRA. Bondarenko, V. I.; Yukhimuk, A. K.; Pavlenko, V. N. pp 22-27 of Problemy Kosmicheskoi Fiziki. Vsekhsvyatskii, S. K. (ed.). Kiev; Izdatel'stvo Kievskogo Universiteta (1973). (In Russian)

The coupling of the electromagnetic wave and plasma is considered on the kinematic theory base. The excitation conditions of the ionosound and magnetosound vibrations of the magnetized plasma are found when the ion distribution function is Maxwellian and anisotropic ($T_{\parallel i} \neq T_{\perp i}$). (auth)

30416 VARIATION OF F-REGION POSITIVE ION DENSITY WITH SOLAR ACTIVITY. Ghosh, S. N.; Gupta, S. K. (Alahabad Univ., India). Indian J. Radio Space Phys.; 1: No. 4, 249-255(1972).

Rates of production of positive ion N_2^+, N^+, O^+, O_2^+ and NO^+ by photoionization and other chemical reactions have been calculated in the altitude range 120-400 Km for three different levels of solar activity. These levels of solar activity are characterized by three representative values. Variations of the flux of the solar extreme ultraviolet radiation incident upon the atmosphere, neutral particle densities, electron density and temperature, with solar activity have been calculated using laboratory measured values of the rate coefficient of ion-neutral reactions. Computed ion density profiles have been compared with the observed data. (38 ref.) (Indian Sci. Abstr.)

30417 LATITUDE DISTRIBUTION OF THE REGULARITY IN F_2-REGION IRREGULARITIES. Chaudhary, C. P. (Bengal Engineering Coll., Howrah, India). J. Inst. Telecommun. Eng.; 19: No. 3, 157-162(1973).

The ratio V' of maximum electron number density existing at any time to the maximum electron density at the level of maximum electron production for solar zenith distance X = 0 has been computed for F_2-layer heights from observed data during the year 1963 for seven ionospheric observatories extending in the lattiude range 76.4°N-51.7°S. Residue V_r obtained after subtracting theoretically Chapman value V from V for a particular observatory in a definite season and for the particular phase of sunspot cycle, when plotted against local time Ψ, indicates that the V_r-Ψ profile is regular. This characteristic termed 'regularity in F_2 region irregularity' has definite cyclic components which vary regularly with latitude and show solar control other than the photoionization effect of the sun. If Menzel and Bailey interpretation of equatorial anomaly is true then so-called equatorial anomaly or winter anomaly is no longer an anomaly in the sense and findings of this paper and comes under a regular feature of the F_2-region caused by some other agent such as the solar corpuscular emission, Mitra's view of 'distillation' of charge particles from equator to subequatorial zone is also supported by the findings. (11 ref.) (Indian Sci. Abstr.)

30418 PROPAGATION OF VLF AND ELF WAVES SUDDEN IONOSPHERIC DISTURBANCES. Gupta, S. P.; Singh, A. K.; Tantry, B. A. P. (Banaras Hindu Univ., India). Indian J. Radio Space Phys.; 1: No. 4, 261-264(1972).

The attenuation factors are calculated from the usual mode theory considerations adopting explicitly determined exponential model for electron density profiles both during normal and disturbed conditions. The calculations show that while in the ELF range the attenuation decreases during any type of flare, in the VLF range both increase and decrease could occur depending on the frequency and the type of flare. All these theoretical results are qualitatively in agreement with the explicit results reported by other workers. The effect of geomagnetic field has also been considered on the propagation of VLF and ELF waves during solar flares and is found to introduce significant changes in the east-to-west asymmetric propagation. (22 ref.) (Indian Sci. Abstr.)

30419 IONOSPHERIC ABSORPTION ON 2.4 MHz AT WALTAIR. Madhusudhanarao, D. N.; Ramana, K. V. V. (Andhra Univ., Waltair, India). Indian J. Radio Space Phys.; 2: No. 1, 86-88(1973).

Results of a preliminary investigation on the 2.4 MHz radio wave absorption in ionosphere using the AL technique are presented. It has been found that the diurnal variation parameter n (cos X index) has a wide range of values from 0.3 to 1.5 with a mean of 0.62 ± 0.003 (P.e). The cos X index n is found to have significant positive correlation with sun-spot number. The seasonal variation of the monthly mean noon-time absorption indicates an increase in equinoctial months. (18 ref.) (Indian Sci. Abstr.)

30420 DEPENDENCE OF FADING FREQUENCY ON CHARACTERISTICS OF IONOSPHERIC IRREGULARITIES. Hanumathsastri, J.; Ramachandra Rao, B. (National Physical Lab., New Delhi). Indian J. Radio Space Phys.; 2: No. 1, 88-90 (1973).

A study has been made of the relationship between frequency and the parameters that describe the nature and movement of ionospheric irregularities responsible for fading. It is noticed that the fading frequency is directly correlated with true drift speed and random velocity, and inversely with the structure size. (Indian Sci. Abstr.)

30421 FREQUENCY OF OCCURRENCE OF POSITIVE GEOMAGNETIC BAYS AT TRIVANDRUM. Sastri, N. S.; Hingorani, J. U. (Indian Inst. of Geomagnetism, Colaba, India). Indian J. Radio Space Phys.; 1: No. 4, 144-145(1972).

Frequency of occurrence of positive bays recorded at Trivandrum during the period 1958-69 is examined. Monthly frequency appears to be modulated by a composite of annual and semi-annual waves. The maximum indiurnal frequency is around midnight. (Indian Sci. Abstr.)

30422 TOTAL ELECTRON CONTENT MEASUREMENTS OVER KURUKSHETRA. Sant Prakash, L. J. B. (Regional Coll. of Education, Bhopal, India). Indian J. Radio Space Phys.; 1: No. 4, 269-272(1972).

An analysis has been made of the results of total electron content of the ionosphere derived from Faraday rotation measurements of 40 MHz satellite (S-66) signals at Kurukshetra (lat. 29.9°N, long. 76.8°E, dip 45.6°) for the period June 1968–April 1969. Day to day variation, seasonal anomaly and semi-annual effect have been observed in the electron content at this station. During daytime the electron content has always been found to increase towards the south and decrease towards the north of Kurukshetra but during night-time the electron content has, at times, been found to increase towards north of Kurukshetra, although no unusual magnetic activity has been reported on such occasions. This may be due to larger influx of ionization on such occasions from the upper atmosphere. (23 ref.) (Indian Sci. Abstr.)

30423 OBSERVATIONS OF THE CONJUGATE SAR ARCS OF SEPTEMBER 28–30, 1967. Reed, E. I. (Goddard Space Flight Center, Greenbelt, MD); Blamont, J. E. J. Geophys. Res.; 79: No. 16, 2524-2525(1 Jun 1974).

A description is given of the September 28 to 30 stable subauroral red arcs. This phenomenon was noted to be worldwise in its extent and located on the same L shell in the northern and in the southern hemispheres. It appeared near L = 3, moved equatorward to L = 2.4 and later moved to, or reformed, near L = 2.9. Its intensities were variable over the nearly two days of observations and, apparently influenced by the composition of the lower thermosphere, averaged 60% greater in the northern hemisphere. (JFP)

30424 ESRO 4 GAS ANALYZER RESULTS. II. Direct Measurements of Changes in the Neutral Composition During an Ionospheric Storm. Proelss, G. W.; von Zhan, U. (Univ., Bonn). J. Geophys. Res.; 79: No. 16, 2535-2539(1 Jun 1974).

Direct measurements of the neutral composition at ionospheric heights with the gas analyzer aboard Esro 4 reveal large decreases in the atomic oxygen to molecular nitrogen ratio during the ionospheric storm in late February 1973. A comparison shows that these changes in the neutral composition correlate well with decreases in the F_2 layer critical frequency observed at different ionosonde stations. The data presented therefore strongly support previous theoretical studies that delineate neutral composition changes as the major cause for negative ionospheric storm effects. It is suggested that ionospheric and neutral upper atmospheric storm data could be used to supplement each other. (auth)

30425 OXYGEN RECOMBINATION IN THE TROPICAL NIGHTGLOW. Julienne, P. S. (Naval Research Lab., Washington, DC); Davis, J.; Oran, E. J. Geophys. Res.; 79: No. 16, 2540-2543 (1 Jun 1974).

In order to explain O I lines in the tropical nightglow, complete and reasonably accurate recombination and emission rate coefficients are used to construct a detailed radiative cascade model of a recombining oxygen plasma. Effective recombination coefficients are given for all low quantum number O I levels for the two limiting cases of zero and infinite optical depth of the resonance lines. The direct recombination coefficients for the S levels, and to a lesser extent the P levels, are significantly smaller than those previously quoted in the literature. The quantitative evaluation of radiative cascading in the optically thin limit predicts an order of magnitude lower intensity for the 1304-Å line than that predicted by a recently published optically thin model using an estimate of the cascade contributions to the intensity. However, the optically thick model, which is more realistic for the F_2 region than the thin model, predicts a 1304-Å intensity in good agreement with observations of the 1304-Å line. (auth)

30426 SATELLITE OBSERVATIONS OF THE EQUATORIAL Mg II DAYGLOW INTENSITY DISTRIBUTION. Gerard, J. C.; Monfils, A. (Univ., Liege). J. Geophys. Res.; 79: No. 16, 2544-2550(1 Jun 1974).

Continuous measurements of the Mg II (2796–2803 Å) doublet intensity in the equatorial dayglow were obtained at dusk during the period March 19 to May 23, 1972, by using the TD1 A UV astronomical satellite looking upward. These data confirm that the glow observed near the equator can be accounted for by resonance scattering of sunlight by Mg^+ ions present at altitudes exceeding 530 km. Isophote maps are presented showing the morphology and dynamics of the phenomena. It is clear that the emission zones are closely related to the position of the dip equator and present either a single or a double peak. Important latitudinal asymmetries are frequently observed: it is suggested that they reflect differences in the height distribution of the ion layer in the two hemispheres, in agreement with the results of ionospheric and satellite observations. A statistical analysis of longitude and planetary magnetic activity effects is made. A maximum occurrence frequency is reached in the Asian sector (60 to 150°W). Important day-to-day variations are observed on some occasions, but the average daily intensity is not affected by Kp. (auth)

30427 PRELIMINARY REPORT OF NUMERICAL SIMULATION OF TYPE 2 IRREGULARITIES IN THE EQUATORIAL ELECTROJET. McDonald, B. E.; Coffey, T. P.; Ossakow, S.; Sudan, R. N. (Naval Research Lab., Washington, DC). J. Geophys. Res.; 79: No. 16, 2551-2554(1 Jun 1974).

A two-dimensional numerical solution of the basic equations believed to describe the electrojet structure was performed to determine whether the basic mechanism that produces small-scale structure in type-two irregularities is one-dimensional steepening or two-dimensional turbulence. The computer simulation is briefly discussed, and the results of the simulation are compared with experiment. (JFP)

30428 INDICATIONS OF A LONGITUDINAL COMPONENT IN AURORAL PHENOMENA. Stenbaek-Nielsen, H. C. (Univ. of Alaska, Fairbanks). J. Geophys. Res.; 79: No. 16, 2521-2523 (1 Jun 1974).

A number of independent observations indicate the presence of a longitudinal component in auroral activity arising from asymmetries in the earth's internal magnetic field. The longitudinal component follows the difference in conjugate ionospheric magnetic field strengths, the higher activity being in the hemisphere with the lower field strength. Observations indicate maximums in auroral phenomena in the Alaskan–Siberian sector of the northern auroral zone and near Syowa, Antarctica, in the southern auroral zone. (auth)

30429 OBSERVATION OF A TWO-TEMPERATURE ION ENERGY DISTRIBUTION IN REGIONS OF POLAR WIND FLOW. Maier, E. J. (Goddard Space Flight Center, Greenbelt, MD); Hoffman, J. H. J. Geophys. Res.; 79: No. 16, 2444-2447(1 Jun 1974).

In many regions of the ionosphere the distribution functions of the particles are highly time dependent because of the variation in energy deposition and particle ionization rates. At present, it is recognized that the electrons, the ions, and the neutral gases exist at three generally distinct temperatures that approach one another at low altitudes, where the mutual collision frequencies are sufficiently high. In the high latitude region, and especially at higher altitudes, a greater deviation from equilibrium is expected as a consequence of the complex flow patterns of ionization, downward energy conduction, and mass flow. A study was made of deviations from thermal equilibrium among the ions by considering that the "light" ions H^+ and He^+ may be at a different temperature from the "heavy" ion O^+. Further, the case in which thermal protons are observed to be flowing relative to the assumed static ambient oxygen ions is studied in particular. The proton flow is assumed to be along the direction of the magnetic field. Of the cases tested, it is found that the measured proton temperature is from 1 to 10 times the measured oxygen ion temperature. Such temperature enhancements may be expected both because of the energy transfer associated with the ion flow and as a consequence of the preferential energy coupling from the light ion distribution in the exosphere. (auth)

30430 INTERRELATIONSHIP BETWEEN THE >130 keV ELECTRON TRAPPING BOUNDARY, THE VHF RADAR BACKSCATTER, AND THE VISUAL AURORA. Romick, G. J. (Univ. of Alaska, Fairbanks); Ecklund, W. L.; Greenwald, R. A.; Balsley, B. B.; Imhof, W. L. J. Geophys. Res.; 79: No. 16, 2439-2443 (1 Jun 1974).

A coordinated program between satellite, VHF radar, and optical auroral observations was carried out in Alaska during the spring of 1972. On 18 days in February, March, and April the positions of the >130-keV isotropic and cutoff trapping boundaries in the evening sector of the oval were determined on satellite 1971-89a. On 9 of these days, simultaneous VHF 50-MHz auroral radar backscatter echoes were observed to lie equatorward of the cutoff trapping boundary regardless of the phase of the auroral substorm. The analysis of these data with respect to substorm phase, Dst, and position of the aurora shows that the motion of the trapping boundary is a dynamic feature of the substorm that can be monitored and approximately located by the VHF radar echoes. (auth)

30431 GLOBAL DISTRIBUTION OF NATURAL AND MAN-MADE IONOSPHERIC ELECTRIC FIELDS AT 200 kHz AND 540 kHz AS OBSERVED BY OGO 6. Laaspere, T.; Semprebon, L. C. (Darmouth Coll., Hanover, NH). J. Geophys. Res.; 79: No. 16, 2393-2401(1 Jun 1974).

The experiment on the polar-orbiting Ogo 6 spacecraft (perigee 400 km, apogee 1100 km) yielded real time analog data in several broad band channels and essentially continuous tape-recorded data from two narrow band (200 Hz) receivers operating at 200 and 540 kHz. The results show that the worldwide distribution of signals at 200 and 540 kHz falls into a number of different categories: naturally generated broad band (auroral) hiss at polar latitudes with typical 200-kHz intensities of around $0.1\ \mu V\ m^{-1}\ Hz^{-1/2}$, maximum intensities of up to several $\mu V\ m^{-1}\ Hz^{-1/2}$, and generally lower intensities at 540 kHz; nighttime mid-latitude enhancements of a few microvolts per meter, which probably result either from a superposition of signals from a number of 200- and 540-kHz stations or from interference from intense signals of much higher frequencies; well defined signal peaks associated with individual ground stations operating at 200 kHz (these upward-propagating signals appear to be guided along the earth's magnetic field and may reach an intensity of several hundred microvolts per meter); striking signal enhancements in the conjugate region of a low latitude 200-kHz station (Achkhabad), suggesting propagation in the whistler mode to the opposite hemisphere; and occasional signal enhancements at the magnetic equator, which are at present unexplained. (auth)

30432 ANOMALOUS BEHAVIOR OF F-REGION DURING THE SOLAR ECLIPSE OF SEPTEMBER 22, 1968. Venkatachari, R.; Sharma, L. H.; Chakrabarty, D. K. (National Physical Lab., New Delhi). Indian J. Radio Space Phys.; 1: No. 4, 246-248(1972).

Effects observed on ionograms and in cosmic radio noise absorption at Delhi for the eclipse of 22 Sept. 1968 (max. obscuration 81% at ground) are presented. Both fOF_2 and cosmic noise absorption showed anomalous increase during the eclipse. The implications of these observations are discussed. Estimates of electron temperature in the F region from absorption measurements and the changes in it indicate a decrease near the maximum of the eclipse. (Indian Sci. Abstr.)

30433 ACTIVE EXPERIMENTS STIMULATING WAVES AND PARTICLE PRECIPITATION WITH SMALL IONOSPHERIC BARIUM RELEASES. Kelley, M. C. (Univ. of California, Berkeley); Pedersen, A.; Fahleson, U. V.; Jones, D.; Koehn, D. J. Geophys. Res.; 79: No. 19, 2859-2867(1 Jul 1974).

Explosions of small barium canisters in the ionosphere were observed to stimulate a number of changes in the ambient medium. These included perturbations of the electric field, emission of at least three distinct types of waves, an increase in the flux of energetic particles, and enhancements in plasma density and temperature. The dc field changes and lowest frequency wave mode were confined to a relatively small volume, probably centered at the point of explosion, and propagated up magnetic field lines to the observation point, which in each case was on a sounding rocket. The two higher frequency modes also were detected along magnetic field lines from the point of explosion but seemed to be observable in larger volumes of space, possibly because of either a generation or a propagation effect. Change in the flux of energetic particles (electrons of >15 keV) was delayed by a few hundred milliseconds from the first indications of the explosion, the suggestion being that the enhanced precipitation was stimulated by a wave propagating up into the upper ionosphere or magnetosphere. (auth)

30434 IONOSPHERIC ION FLOW VELOCITIES FROM MEASUREMENTS OF THE ION DISTRIBUTION FUNCTION TECHNIQUE. Green, D. W.; Whalen, B. A. (National Research Council of Canada, Ottawa). J. Geophys. Res.; 79: No. 19, 2829-2833(1 Jul 1974).

A technique for sampling the ionospheric ion distribution function using a cylindrical plate electrostatic energy analyzer for the expressed purpose of detecting electric field-induced motions is presented. It is shown that data derived from a typical sounding rocket flight of this instrument may be used to determine unambiguously the ion flow velocity and that this technique is virtually unaffected by perturbing effects due to wake and sheath, which sometimes interfere with other related convective electric field measurements (e.g., double probes). Ion densities and temperatures may also be extracted from the data, although with somewhat less precision. (auth)

30435 SELF-CONSISTENT ELECTROSTATIC FIELD MAPPING IN THE HIGH-LATITUDE IONOSPHERE. Chiu, Y. T. (Aerospace Corp., El Segundo, CA). J. Geophys. Res.; 79: No. 19, 2790-2802(1 Jul 1974).

In an attempt to study the possible connections between upper and lower atmospheric electricity, the restricted boundary value problem of self-consistent electrostatic field mapping in the collision-dominated lower ionosphere is solved. Although large scale size perpendicular fields can penetrate the ionosphere, the associated self-consistent parallel fields are much more sensitive to the parameters of the ionosphere and atmosphere. Above 150 km the parallel field is generally 10^{-3} to 10^{-4} times the magnitude of the perpendicular field; however, below 100 km the two fields become comparable in magnitude. It is found that the magnetospheric origin of perpendicular electric fields measured at low altitude and high latitude regions cannot be ascertained unless simultaneous subsidiary observations such as magnetic disturbances and perpendicular scale sizes are also considered. (auth)

30436 ION LAYER FORMATION BY UNIFORM NEUTRAL WINDS IN THE NIGHTTIME E REGION. Rowe, J. F. Jr.; Gieraltowski, G. F. (National Astronomy and Ionosphere Center, Arecibo, Puerto Rico). J. Geophys. Res.; 79: No. 19, 2917-2920(1 Jul 1974).

A simplified model of plasma motion in the low latitude nighttime E region is used to investigate the role of uniform horizontal neutral winds in the formation of sporadic E layers. Numerical results show that thick layers may be formed in the mid-E region by plasma compression at the altitude where ion-neutral collisions destroy the ability of horizontal winds to move ionization vertically. It is hypothesized that this mechanism accounts for the appearance of early morning sporadic E layers that are observed to form near 125 km at low latitudes following descents of the F layer. (auth)

30437 CONDUCTIVITY RATIO EFFECTS ON THE DRIFT AND DEFORMATION OF F-REGION BARIUM CLOUDS COUPLED TO THE E-REGION IONOSPHERE. Scannapieco, A. J. (Science Applications, Inc., McLean, VA); Ossakow, S. L.; Book, D. L.; McDonald, B. E.; Goldman, S. R. J. Geophys. Res.; 79: No. 19, 2913-2916(1 Jul 1974).

The nonlinear motion of an F region barium release electrostatically coupled to the E region ionosphere is studied by numerical simulation. The effect of varying the ratio of the height-integrated Pedersen conductivity at the barium cloud (Σ_p^b) to that of the background ionosphere (Σ_p^1) and the formation of striations are discussed. (auth)

30438 INDUCTIVE ELECTRIC FIELD OF A FIELD-ALIGNED CURRENT SYSTEM. Murphy, C. H.; Wang, C. S.; Kim, J. S. (State Univ. of New York, Albany). J. Geophys. Res.; 79: No. 19, 2901-2903(1 Jul 1974).

Some preliminary results of a calculation of the inductive electric field produced by a time-dependent field-aligned current system are presented. The current model consists of a partial ring current joined to an ionospheric electrojet by field-aligned currents to represent a possible substorm current configuration. When a time variation for the current that is characteristic of the magnetic sub-storm is used, it is found that inductive electric fields of as much as 0.38 mV/m can be produced parallel to the magnetic field. It is estimated that the possible energy change of a charged particle due to such an electric field can be of the order of several keV. (auth)

30439 FURTHER DISCUSSION OF THE CYCLOTRON INSTABILITY. Lin, C. S. (Univ. of Washington, Seattle); Parks, G. K. J. Geophys. Res.; 79: No. 19, 2894-2897(1 Jul 1974).

The cyclotron instability is examined for arbitrary ratios of hot- to cold-plasma densities, resonant velocities, and wave frequencies. It is found that the cyclotron linear growth rate has a maximum when the resonant velocity is near the thermal velocity of the plasma distribution. A criterion for increasing the growth rate by increasing the cold-plasma density is derived. (auth)

30440 ELECTROMAGNETIC EFFECTS ON INSTABILITIES IN THE EQUATORIAL ELECTROJET. Kaw, P.K.; Chaturvedi, P.K.; Ivanov, A.A. (Physical Research Laboratory, Ahmedabad, India). J. Geophys. Res. 79: No. 25, 3802-3806 (1 Sept 1974).

A generalized fluid treatment for the excitation of electrostatic-electromagnetic waves in a weakly ionized inhomogeneous plasma with magnetized electrons, collision—dominated ions, and a cross—field electron streaming is presented. The relevance of the results to observable phenomena in the electrojet region of the ionosphere is discussed. (auth)

30441 RELATION OF THE PLASMA SHEET TO THE NIGHTTIME AURORAL OVAL. Lassen, K. (Danish Meteorological Institute, Geophysical Section, Lyngbyvej, Copenhagen, Denmark). J. Geophys. Res. 79: No. 25, 3857-3858 (1 Sept 1974).

The projection along the magnetic lines of force of the outer boundary of the plasma sheet onto the ionosphere is shown to follow closely the poleward edge of a mass plot of auroral arcs in a corrected magnetic latitude—time diagram. Projections of single points of the inner edge of the plasma sheet are situated along the equatorward boundary of the auroral area. It is concluded that the plasma sheet maps down onto the ionosphere in the nighttime auroral precipitation area. (auth)

30442 VELOCITY DISTRIBUTION OF IONOSPHERIC LOW-ENERGY ELECTRONS. Ashihara, O.; Takayanagi, K. (Tokyo Univ.). Planet. Space Sci.; 22: No. 8, 1201-1217(Aug 1974).

The velocity distribution function of ionospheric electrons is calculated in the low-energy (<8.7 eV) region. This is the first realistic model calculation for studying the transition of the distribution function from the nonthermal to the thermal part without assuming the Maxwellian distribution for the latter. The calculation is made for four altitudes between 120 and 250 km. All the relevant atomic collision processes are taken into account. Contributions of each individual process to determining the distribution function are discussed. The calculation shows that the deviation of the thermal energy part of the distribution function from Maxwellian in the region around the mean kinetic energy is within several percent. A much larger deviation is found at other portions of the function (still within the thermal part) especially at lower altitudes. In the Appendix, some features of the distribution function at higher energy regions are discussed. (auth)

30443 TEMPERATURES IN THE POLAR WIND. Bailey, G. J.; Moffett, R. J. (Univ. of Sheffield, Eng.). Planet. Space Sci.; 22: No. 8, 1193-1199(Aug 1974).

The thermal structure of the plasma in the polar wind is examined. With $O^+ - H^+$ Joule heating as the mechanism for heating the plasma, it is found that O^+ and H^+ temperatures are significantly greater than the electron temperature. With the adopted input parameters the $O^+ - H^+$ temperature difference is relatively small. (auth)

30444 INCOHERENT SCATTER SOUNDING OF THE IONOSPHERE. Beynon, W. J. G. (University Coll. of Wales, Aberystwyth, Eng.). Contemp. Phys.; 15: No. 4, 329-352(Jul 1974).

The incoherent scatter technique for sounding the ionosphere, first introduced in 1958, is now recognized as being the most accurate and convenient means of measuring a number of basic physical parameters of the ionosphere. Theory indicates that the technique can provide direct data on electron density, electron temperature, ion temperature, ion composition, plasma drift velocity and flux of precipitating electrons. The knowledge of these data then enables information on a number of other parameters such as the strengths of electric fields, neutral air temperature and neutral wind speed to be deduced. Such measurements can be made continuously in time and over a wide range of altitudes—from just below 100 km to 1000 km and beyond. (auth)

30445 LONGITUDINAL, SEASONAL, AND SOLAR CYCLE EFFECTS ON IONOSPHERIC F-REGION DISTURBANCES. Rajaram, G.; Rastogi, R. G. (Physical Research Lab., Ahmedabad, India). Riv. Ital. Geofis.; 22: 391-404(1973).

The longitudinal, seasonal, and solar cycle differences in the behavior of the F-region during periods of geomagnetic disturbance are discussed. The degree of disturbance in f0F2 as a function of latitude is shown for stations closely separated in dip and ranging from 89 deg N dip to 83 deg S dip. Two longitude zones are considered: the west (American) zone with low equatorial geomagnetic field and the east (Australasian) zone with high equatorial geomagnetic field. Several parameters of F-region disturbance are plotted against latitude to bring out these differences. An important point is that in low sunspot years the major part of the earth's latitudes experience increased f0F2 during disturbances, both by day and by night. In high sunspot years the peak effect on f0F2 occurs in the winter mid-latitudes and is more by night than by day. (IAA)

30446 CALCULATION OF THE LUNAR DIURNAL ATMOSPHERIC TIDE. Geller, M. A.; Schoeberl, M. R. (Illinois Univ., Urbana). Riv. Ital. Geofis.; 22: 379-384(1973).

Classical tidal calculations are made for the atmospheric response to the lunar diurnal component of the moon's gravitational forcing (period equal to 25.82 mean solar hours). The calculated amplitudes for the lunar diurnal oscillation in surface pressure agree with the observations of Malin and Chapman (1970) except at Hong Kong where ocean tidal effects appear to be dominant. Calculations of the lunar diurnal wind oscillation at the ground and at 100 km are also made. The annual variation in the lunar diurnal oscillation in surface pressure as reported by Malin and Chapman appears to be unexplainable in terms of annually varying atmospheric temperature structure. (IAA)

30447 INVESTIGATION OF A FINE REGULAR STRUCTURE AND RANDOM IONOSPHERIC IRREGULARITIES BY THE METHOD OF INCOHERENT RADIO WAVE SCATTERING. Misyura, V. A.; Novozhilov, V. I.; Erokhin, Yu. G.; Bludov, V. Ya.; Novozhilov, V. I.; Erokhin, Yu. G.; Bludov, V. Ya.; Belyi, A. F.; Trukhan, M. G.; Rozumenko, V. T. (Kharkov State Univ.). Izv. Vyssh. Ucheb. Zaved., Radiofiz.; 17: No. 7, 950-958(1974). (In Russian).

The peculiarities, possibilities and difficulties of the incoherent scattering method in investigations of the fine structure of regular profiles of the ionospheric parameters, their gradients and nonstationarity, as well as the large scale irregularities are considered. The measurements of the electron density profiles in F_2-, F_1-, E-, $-E_s$-, D-regions, in interlayer hollows and plateau, as well as of large scale irregularities of the ionosphere and their motion are illustrated. A sufficient reliability of measurements for the height $z \gtrsim 90$ km and difficulties at $z < 90$ km are pointed out. (auth)

Effects of Nuclear Detonations

30448 ELECTROMAGNETIC PULSE FROM NUCLEAR DETONATIONS. Price, G. H. (Stanford Research Inst., Menlo Park, CA). Rev. Geophys. Space Phys.; 12: No. 3, 389-400 (Aug 1974).

Models of the processes whereby a nuclear detonation emits a coherent electromagnetic pulse fall into three classes: those involving Compton electron currents produced by interaction of prompt γ radiation from the detonation with the environment, those involving photoelectron currents produced by the similar interaction of primary x radiation from the detonation, and those involving perturbation of the ambient magnetic field by the expanding plasma surrounding the detonation point. For each model considered the cause of the asymmetry in the current system necessary for the radiation of a signal is discussed. These causes include the earth-atmosphere interface, the atmospheric density gradient, anisotropy of the environment by virtue of the presence of the earth's magnetic field, nonuniform emission of the energetic radiation (γ and x rays) by the detonation, and asymmetries of the delivery vehicle and device case. The available experimental data are then examined in the light of the models. These data suffice to establish the models as probably being correct in their identification of the principal processes whereby the nuclear electromagnetic pulse is generated, but they are inadequate for a quantitative assessment of the accuracy of the models. (auth)

Magnetospheric Phenomena

Refer also to abstract 30366.

30449 (AD-776660) THERMAL AND SUPRATHERMAL PLASMA DENSITIES IN THE OUTER MAGNETOSPHERE. Progress Report. Gurnett, D. A.; Frank, L. A. (Iowa Univ., Iowa City (USA). Dept. of Physics and Astronomy). Oct 1973. Contract N00014-68-A-0196. 31p. NTIS $1.75.

Using the low frequency cutoff of electromagnetic noise trapped in the magnetosphere at frequencies above the local plasma frequency it is now possible to make very accurate, plus or minus 1%, electron density measurements in the low density region between the magnetopause and plasmapause. This technique for measuring the total plasma density was used, together with measurements of the suprathermal proton intensities with the Lepedea instrumentation on the IMP-6 spacecraft, to determine the thermal proton densities in the region between the plasmapause and magnetopause. (GRA)

30450 (COM-74-50228/7) SOME ACTIVE MAGNETOSPHERE EXPERIMENTS TO BE PERFORMED BY THE PLASMA PHYSICS AND ENVIRONMENTAL PERTURBATION LABORATORY. Bernstein, W.; Evans, D. S. (National Oceanic and Atmospheric Administration, Boulder, Colo. (USA)). Jul 1973. 77p. (NOAA-TR-ERL-286; SEL-27; NOAA-74021907). GPO $1.15.

A number of general studies that have been proposed for PPEPL/shuttle program are considered in qualitative detail both from the theoretical and practical points of view. The selection of experimental programs was restricted to those which may be considered active as opposed to refinements of the passive observational programs done previously. It is concluded that while these new studies were scientifically worthwhile and could be performed in principle, in most cases insufficient attention had been paid to the practical details of the experiments. Several specific areas of study, stressing in particular the practical feasibility of the proposed experiments, are recommended. In addition, recommendations are made for further theoretical study, where appropriate. (auth)

30451 SYNCHROTRON LOSS RATES OF ENERGETIC MAGNETOSPHERIC ELECTRONS. Baker, J. C. (Calspan Corp., Buffalo). J. Geophys. Res.; 79: No. 16, 2503-2505(1 Jun 1974).

Loss rates due to synchrotron radiation were calculated for electrons in the earth's magnetosphere with energies in the range 2 to 10 MeV. These loss rates are compared with measured rates and are shown to be of little importance for the earth. For Jupiter's magnetosphere the effect is much more pronounced. (auth)

30452 EXACT SOLUTIONS FOR CERTAIN AXISYMMETRIC PROBLEMS OF INDUCTION IN THIN NONUNIFORM SHEETS. Ashour, A. A. (Cairo Univ.). J. Geophys. Res.; 79: No. 16, 2479-2486(1 Jun 1974).

A general relation between the axisymmetric induction problems for the infinite plane and the spherical sheets is obtained. By using this relation and starting with the uniform plane and spherical sheets and an axial inducing dipole, exact solutions are obtained for induction in these two sheets when they have special axisymmetric distributions of conductivity. These distributions are given by $\sigma = \sigma_0 a^2/\rho^2$, $\sigma = 2\sigma_0 a^2/(a^2 + \rho^2)$ in the case of the plane sheet, where ρ is the distance from a fixed point in the sheet, and $\sigma = \sigma_1/(1 + \epsilon \cos \theta)$, $0 \leq \epsilon \leq 1$ in the case of the spherical sheet, where θ is the colatitude (σ_0, σ_1, a, and ϵ are constants). The conductivity in each case decreases gradually as one goes away from a fixed point in the sheet. The sheets are thus suitable models for representing the ionosphere (neglecting the nonisotropic character of its conductivity) or a large ocean. The exact solutions obtained are particularly useful in testing the accuracy of the iteration techniques, which are applied in the numerical solutions of the equations to which induction problems are reduced. As an example, numerical results for induction in the spherical shell by a uniform inducing field are given in the two cases when the time variations of the field are either periodic or aperiodic. (auth)

30453 ELECTRON ECHO EXPERIMENT 1: COMPARISON OF OBSERVED AND THEORETICAL MOTION OF ARTIFICIALLY INJECTED ELECTRONS IN THE MAGNETOSPHERE. McEntire, R. W.; Hendrickson, R. A.; Winckeler, J. R. (Univ. of Minnesota, Minneapolis). J. Geophys. Res.; 79: No. 16, 2343-2354(1 Jun 1974).

On August 13, 1970, a sounding rocket launched from Wallops Island, Virginia, was used to successfully inject a controlled beam of energetic electrons into the trapping region of the earth's magnetosphere. The Aerobee 350 rocket carried a high voltage electron gun, electron detectors, receivers to measure the electric field of waves generated by the experiment, and other apparatus to a peak altitude of 350 km. During a 10-min flight, more than 3000 16-ms-long 70-mA pulses of 35- to 43-keV electrons were injected into the magnetosphere with pitch angles within 25° of the local 90° mirror angle. The electrons, trapped in the geomagnetic field, bounced between the mirror point near the rocket and the southern conjugate point (−66° latitude, −82° longitude) while they were drifting eastward across field lines on a drift shell of constant McIlwain L parameter (2.56) under the gradient and curvature forces. Since Wallops Island conjugate mirror altitudes are at least 300 km lower than the injection altitudes, all returning electrons were backscattered from the atmosphere in the southern hemisphere. The rocket was launched eastward in an attempt to intercept the returning electrons, and for a 90-s interval about L apogee, electrons were detected returning from one, two, and in one case, three complete bounces to the southern hemisphere. The analyzed electron data agree well with echo patterns predicted from theoretical particle motion in models of the geomagnetic field combined with Monte Carlo studies of energy loss and diffusion in the conjugate point atmosphere. Observed bounce times, drift displacements, and cross L diffusion were in substantial agreement with theory. However, the returning flux was lower than predicted, and discrepancies between theory and experiment were observed at large diffusion distances. This experiment, Electron Echo 1, verified the concept of using controlled particle beams as magnetospheric probes, showing that such beams are sufficiently stable to be intercepted after bounces to the conjugate point and back. (auth)

30454 THERMAL AND SUPRATHERMAL PLASMA DENSITIES IN THE OUTER MAGNETOSPHERE. Gurnett, D. A.; Frank, L. A. (Univ. of Iowa, Iowa City). J. Geophys. Res.; 79: No. 16, 2355-2361(1 Jun 1974).

By using the low frequency cutoff of electromagnetic noise trapped in the magnetosphere at frequencies above the local plasma frequency it is now possible to make very accurate, ±1%, electron density measurements in the low density region between the magnetopause and plasmapause. This technique for measuring the total plasma density was used, together with measurements of the suprathermal proton intensities with the Lepedea instrumentation on the Imp 6 spacecraft, to determine the thermal proton densities in the region between the plasmapause and magnetopause. Although the thermal protons usually account for a significant fraction, ~50%, of the total proton density in this region, in some cases, particularly at the larger radial distances, the density of the thermal protons sometimes drops to a very small fraction, <5%, of the total density, and nearly all of the plasma consists of suprathermal particles. Usually, the high energy tail of the thermal proton distribution is sufficiently intense to be detected at low energies within the Lepedea energy range. When the high energy tail of the thermal distribution can be detected, it is possible to determine the temperature of the thermal protons. The temperature in a typical case is found to be 80,000°K. This high temperature for the thermal protons, which are presumably of ionospheric origin, agrees with earlier Ogo 5 measurements reported by Serbu and Maier. (auth)

30455 NEAR-EARTH MAGNETIC DISTURBANCE IN TOTAL FIELD AT HIGH LATITUDES. I. Summary of Data from Ogo 2, 4, and 6. Langel, R. A. (Goddard Space Flight Center, Greenbelt, MD). J. Geophys. Res.; 79: No. 16, 2363-2371(1 Jun 1974).

Variations in the total (i.e., scalar) magnetic field data from the polar orbiting Ogo 2, 4, and 6 spacecraft (altitudes 400−1510 km) are summarized for invariant latitudes above 55°. Data from all degrees of magnetic disturbances are included. The data are presented in terms of the quantity ΔB (i.e., measured field magnitude minus the field magnitude from a spherical harmonic model of the quiet field). The total field variations at the satellite form two regions: a region of the positive ΔB between about 2200 and 1000 MLT with its maximum near 0300 and 72° and a region of negative ΔB between about 1000 and 2200 MLT with its maximum near 1500 and 75°. In the negative ΔB region, $|\Delta B|$ is greatest in summer and least in winter and shows a substantial decrease with increasing altitude. The $|\Delta B|$ in the positive ΔB region, on the other hand, shows no seasonal variation and only a small decrease with increasing altitude. The $|\Delta B|$ increases with the Ap index in both regions. (auth)

30456 NEW-EARTH MAGNETIC DISTURBANCE IN TOTAL FIELD AT HIGH LATITUDES. II. Interpretation of Data from Ogo 2, 4, and 6. Langel, R. A. Goddard Space Flight Center, Greenbelt, MD). J. Geophys. Res.; 79: No. 16, 2373-2392(1 Jun 1974).

Variations in the scalar magnetic field (ΔB) from the polar-orbiting Ogo 2, 4, and 6 spacecraft, with supporting vector magnetic field data from surface observatories, are analyzed at dipole latitudes above 55°. Data from all degrees of magnetic disturbance are included, the emphasis being on periods when Kp = 2− to 3+. Although individual satellite passes at low altitudes confirm the existence of electrojet currents, neither individual satellite passes nor contours of average ΔB are consistent with latitudinally narrow electrojet currents as the principal source of ΔB at the satellite. The total field variations at the satellite form a region of positive ΔB between about 2200 and 1000 MLT and a region of negative ΔB between about 1000 and 2200 MLT. Further characteristics are given by Langel (1974a). The ratio of ΔB magnitudes in these positive and negative regions is variable. The characteristics of the negative ΔB region indicate a latitudinally broad ionospheric source. Equivalent current systems were derived from satellite data in the negative ΔB region for summer, winter, and equinox seasons for Kp = 2− to 3+. Comparison of the surface magnetic disturbance caused by the equivalent current with the measured average surface disturbance shows good agreement except in localized details. Because ΔB decreases very slowly with altitude in the positive ΔB region, it is not possible to account for this disturbance in terms of ionospheric currents. The contribution to the satellite ΔB due to a model electrojet that reproduced the measured average surface horizontal disturbance was computed. When the contribution to ΔB from this model electrojet is removed from the measured satellite ΔB, the remaining ΔB is constant with altitude within experimental error. This nonelectrojet ΔB is estimated to be about 50−80, 20−30, and 7−15 γ for Kp ≥ 4−, 2− to 3+, and 1−to 1+, respectively. It is concluded that most, if not all, of the nonelectrojet positive ΔB is extraionospheric in origin. Some of this nonionospheric ΔB is caused by the equatorial current sheet (ring current), but some data cannot be accounted for in terms of this source. Definitive identification of all sources of positive ΔB is not possible at this time. (auth)

30457 ULF GEOMAGNETIC POWER NEAR L = 4. III. Statistical Study of Power Spectra in Conjugate Areas During December Solstice. Surkan, A. J. (Univ. of Nebraska, Lincoln);

Lanzerotti, L. J. J. Geophys. Res.; 79: No. 16, 2403-2412(1 Jun 1974).

Results are reported of statistical studies of 2-hour power spectra of nonoverlapping H component magnetic record segments. The records were obtained in January 1972 at an antarctic magnetometer station (Siple) near L = 4 and at three stations (L ~4.4, ~4.0, ~3.2) at approximately the same magnetic longitude in the northern conjugate area. The K index measured near the longitude of the stations was ≤5 during the interval studied. (The explicit dependence of magnetic power on geomagnetic activity is examined in part four of this series (Lanzerotti and Surkan, 1974).) It is found that during more disturbed periods, higher power levels are accompanied by steeper spectral slopes; this finding implies a concentration of energy at the lower frequencies at these times. Relatively higher power levels are observed during the local afternoon and late evening than during other periods of the day. On the basis of power levels and spectral slopes, Siple (L ~4) is more nearly conjugate to a northern station at L ~4.4 than to a station at L ~4 during the 1971–1972 December solstice period. This finding may arise from hemispherical differences in ionospheric conductivities and, as such, may be dependent upon season. (auth)

30458 ULF GEOMAGNETIC POWER NEAR L = 4. IV. Relationship to the Fredericksburg K Index. Lanzerotti, L. J. (Bell Telephone Labs., Murray Hill, NJ); Surkan, A. J. J. Geophys. Res.; 79: No. 16, 2413-2419(1 Jun 1974).

The total power and slope of 2-hour nonoverlapping H component geomagnetic power spectra obtained during a 12-day period in January 1972 are statistically related at corresponding times to the K indices determined at the longitude of the stations and the global Dst indices. Although the power level increases and the spectral slope steepens with more positive K and more negative Dst values, there is no one-to-one relation between the spectral parameters (power and best-fit slope) and the geomagnetic indices. Thus it is not readily possible to accurately predict the latitudinal distribution of geomagnetic power from a given value of the K index. It is proposed that the introduction of geophysical indices based upon geomagnetic power levels should eventually provide more physical insight into geomagnetic disturbance phenomena. (auth)

30459 HEATING OF THE HIGH-LATITUDE THERMOSPHERE DURING MAGNETICALLY QUIET PERIODS. Reber, C. A.; Hedin, A. E. (Goddard Space Flight Center, Greenbelt, MD). J. Geophys. Res.; 79: No. 16, 2457-2461(1 Jun 1974).

A persistent mid- to high-latitude heating phenomenon is observed in both hemispheres in data from the Ogo 6 quadrupole mass spectrometer. The phenomenon is evidenced by an increase in N_2 density (indicative of a thermospheric temperature rise) and a depletion in helium (indicating an upwelling of air). The composition changes maximize near 0900 and 2100 UT, appear to corotate with the local magnetic pole, and are larger near equinox than near the summer solstice. The variation in latitude of the peak in the winter helium density (as a function of UT) is a specific manifestation of this general heating phenomenon. (auth)

30460 ROLE OF SOLAR LOCAL TIME IN POLAR CAP MAGNETIC VARIATIONS. Langel, R. A. (Goddard Space Flight Center, Greenbelt, MD); Svalgaard, L. J. Geophys. Res.; 79: No. 16, 2493-2495(1 Jun 1974).

The role of the earth's main field in controlling the morphology of magnetic disturbance is usually accounted for by use of invariant latitude and MLT (magnetic local time) as a coordinate system. Magnetic disturbance from ionospheric currents is also controlled by ionospheric conductivity. At high latitudes, where SLT (solar local time) can be very different from MLT, the use of only MLT can give misleading results. In particular, those diurnal magnetic variations in the polar cap that change characteristics between interplanetary magnetic sectors have a tendency to peak near noon SLT rather than noon MLT at Alert, where noon MLT and noon SLT differ by more than 10 hours. Because of the sparsity of magnetic observatories it is not possible to completely separate SLT and MLT effects. (auth)

30461 DIURNAL VARIATION OF THE REGION WITH VECTOR MAGNETIC FIELD CHANGES ASSOCIATED WITH FIELD-ALIGNED CURRENTS. Zmuda, A. J.; Armstrong, J. C. (John Hopkins Univ., Silver Spring, MD). J. Geophys. Res.; 79: No. 16, 2501-2502(1 Jun 1974).

The diurnal variation of the region with the magnetic changes observed by Triad at 800-km altitude by using the results of 350 data passes obtained in real time at a ground station at College, Alaska, during the period January 19 through May 24, 1973. (JFP)

30462 VLF WAVE INJECTION INTO THE MAGNETOSPHERE FROM SIPLE STATION, ANTARCTICA. Helliwell, R. A.; Katsufrakis, J. P. (Stanford Univ., CA). J. Geophys. Res.; 79: No. 16, 2511-2518(1 Jun 1974).

Radio signals in the 1.5- to 16-kHz range transmitted from Siple Station, Antarctica (L = 4), are used to control wave-particle interactions in the magnetosphere. Observations at the conjugate point show signal growth and triggered emissions including risers, fallers, and hooks. Growth rates of the order of 100 dB/s and total gains up to 30 dB are observed. Triggered emissions may be cut off or have their frequency rate of change altered by Siple pulses. Similar effects occur in association with harmonics from the Canadian power system. The observed temporal growth is predicted by a recently proposed feedback model of cyclotron interaction. Plasma instability theories predicting only spatial growth are not in accord with these observations. Possible applications include study of nonlinear plasma instability phenomena, diagnostic measurements of energetic particles trapped in the magnetosphere, modification of the ionosphere through control of precipitation, and VLF communication through the magnetosphere. (auth)

30463 VARIABILITY OF MID-LATITUDE MAGNETIC PARAMETERS USED TO CHARACTERIZE MAGNETOSPHERIC SUBSTORMS. Clauer, C. R.; McPherron, R. L. (Univ. of California, Los Angeles). J. Geophys. Res.; 79: No. 19, 2898-2900 (1 Jul 1974).

It was previously shown how mid-latitude magnetograms could be used to derive quantitative parameters that describe a magnetospheric substorm (Clauer and McPherron, 1974). These parameters include the onset time of the magnetospheric substorm expansion, the meridian of first onset, the central meridian of the resulting expansion observed at mid-latitudes, and the extent of the event in local time. The results of determining these parameters for a group of 45 magnetospheric substorms are reported. Each event selected was isolated and well defined at mid-latitude and occurred during periods of auroral zone magnetic activity. It was found that the magnitude, central meridian, and extent of the magnetospheric substorm are highly variable. The results are interpreted in terms of a simple field-aligned diversion of the tail current through the auroral ionosphere. The results suggest that this field-aligned circuit can form at any local time in the night sector. Past controversy concerning the magnetospheric signature of magnetospheric substorms may, in part, be a consequence of neglecting this aspect of substorm behavior. For example, the finite extent of the disturbance at mid-latitudes suggests that a limited longitudinal sector of the tail is involved, and the variability of central meridians suggests that this sector may occur in different positions across the tail. (auth)

30464 DERIVATION OF MAGNETOSPHERIC ELECTRIC FIELDS FROM WHISTLER DATA IN A DYNAMIC GEOMAGNETIC FIELD. Block, L. P.; Carpenter, D. L. (Stanford Univ., CA). J. Geophys. Res.; 79: No. 19, 2783-2789(1 Jul 1974).

The whistler method of determining magnetospheric electric fields has until recently been applied on the assumption of a static dipole geomagnetic field. The effect on the whistler analysis of including both departures of the field from a dipole and temporal variations in the field are considered. Departures from a dipole field appear to have relatively small effects on the analysis or can be relatively easily taken into account when it is necessary. Temporal changes present a more serious problem. In the presence of a changing geomagnetic field the temporal change in equatorial gyrofrequency of a drifting whistler path will consist of two parts: the variation due to radial drift of the path in the presence of the inhomogeneous B field and the variation due to the changes in B with time. Given knowledge of the temporal variation of B, it is possible to infer the total (induced plus potential) electric field associated with the radial drift. A substorm event is analyzed in which cross-L inward drifts near L = 4 occurred as the night side B field (as reflected in the low latitude H component) exhibited a rapid increase. It was found that on a time scale of 15 min or greater the inferred total east–west electric field differed by ~20% from the field estimated on the assumption of a static magnetic field. It is possible that effects of B may be relatively more important on a shorter time scale or during disturbances much larger than those thus far investigated. Also, in one quiet period preceding a substorm it appeared that all or a major part of the inferred cross-L motions of the plasma could have been due to fluctuations in the magnetic field. It is stressed that both equatorial and ionospheric measurements of electric fields are needed, since certain types of distortions of the high altitude magnetosphere are not readily observed at ionospheric heights. (auth)

30465 ORIGIN OF THE PLASMA SHEET. Hill, T. W. (Rice Univ., Houston, TX). Rev. Geophys. Space Phys.; 12: No. 3, 379-388(Aug 1974).

The plasma sheet is a region of hot plasma (~10^7 °K) that surrounds the earth, filling the distant magnetosphere and separating the northern and southern lobes of the magnetospheric tail; its origin is one of the basic outstanding problems of magnetospheric physics. A critical review of the available observations indicates that the plasma sheet source must provide roughly $10^{25}-10^{26}$ particles/s to balance known loss mechanisms operating in the quiet time magnetosphere and that an adiabatic or quasiadiabatic ($\Delta E \propto E$) acceleration mechanism must provide most of the observed particle energy. These constraints together with auroral helium ion measurements indicate that the plasma sheet particles must originate in the solar wind rather than in the terrestrial ionosphere. The available hypotheses for a solar wind source are examined, and it is concluded that a two-step process of magnetopause diffusion plus electrostatic acceleration is the simplest source mechanism that is consistent with the available observations. (auth)

30466 PLASMA TAIL INTERPRETATIONS OF PRONOUNCED DETACHED PLASMA REGIONS MEASURED BY OGO 5. Chen, A.J.; Grebowsky, J.M. (Goddard Space Flight Center, Greenbelt, Maryland 20771). J. Geophys. Res. 79: No. 25, 3851-3856 (1 Sept 1974).

Measurements of the light ion thermal plasma distribution in the magnetosphere frequently show apparent isolated patches of enhanced plasma density in the trough region beyond the main plasmasphere. These patches of light ions viewed along a satellite orbit appear detached from the main plasmasphere. By using a simple time–dependent convection model to determine length of time a magnetic flux tube has been closed and in daylight (a rough indicator of the expected equatorial plasma density variation), the most prominent 'detached' regions measured by the mass spectrometer on Ogo 5 in the noon–dusk quadrant are seen on a global scale to be readily interpreted as filamentary extensions of the plasmasphere, called plasma tails. Hence on a global scale the pronounced detached regions may be attached to the main plasmasphere. (auth)

30467 PHASE RELATIONS IN THE MAGNETIC FIELD OF THE EQUATORIAL ELECTROJET. Park, D. (Williams College, Williamstown, Massachusetts 01267). J. Geophys. Res. 79: No. 25, 3874-3875 (1 Sept 1974).

It is shown by calculation that the phase relation between the vertical and horizontal components of the magnetic field produced by fluctuations of the equatorial electrojet can be established by means of a simple image construction in which the image current is situated at a complex distance below the ground level. (auth)

30468 A MODEL OF THE DISTRIBUTED MAGNETOSPHERIC CURRENTS. Olson, W.P. (McDonnell Douglas Astronautics Company, Huntington Beach, California 92647). J. Geophys. Res. 79: No. 25, 3731-3738 (1 Sept 1974).

A model of the quiet time ring current and the tail currents has been developed for quiet magnetic conditions and perpendicular incidence of the solar wind on the main (dipolar) field of the earth. Previous work of several authors has shown that these distributed currents flow throughout the magnetosphere and that they are produced by the drift of charged particles in the nonuniform magnetic field B and by plasma diamagnetism. The currents are modeled from a few thousand kilometers above the earth's surface to distances of over 200 R_e back in the tail of the magnetosphere. This procedure allows the computation of the magnetic field B_p, associated with these distributed currents to beyond lunar orbit. The currents are chosen so that B_p correctly models observed field features in the inner magnetosphere and the magnetotail. Although the tail currents can be formed continuously by the entry of magnetosheath particles into the equatorial flanks of the tail even during quiet times, the ring currents must be supplied at irregular (substorm or storm) intervals when dynamic processes are operative. These currents make significant contributions to the earth's surface field variations (e.g., in Sq and Dst). The formation of the tail currents implies that the magnetosphere is open (in the equatorial regions of the tail) to low–energy charged particles. This model work also suggests that when magnetospheric particles and fields are considered self–consistently, it is not possible to produce a magnetically closed magnetosphere. The static magnetic field associated with this distributed current model exhibits a neutral line beyond the orbit of the moon. The inclusion of the field associated with these distributed currents in a model of the total magnetic field should yield better agreement between observed magnetospheric particle and field phenomena and model calculations. (auth)

30469 DEPENDENCE OF FIELD–ALIGNED ELECTRON PRECIPITATION OCCURRENCE ON SEASON AND ALTITUDE. Berko, F.W.; Hoffman, R.A. (NASA Goddard Space Flight Center, Greenbelt, Maryland 20771). J. Geophys. Res. 79: No. 25, 3749-3754 (1 Sept 1974).

An examination of factors affecting the occurrence of field–aligned 2.3–keV electron precipitation has been performed by using data from more than 7500 orbits of the polar-orbiting satellite Ogo 4. Both season and altitude were found to be parameters that are directly related to the probability of occurrence. The highest probabilities occurred when the measurements were made at altitudes from 800 km to apogee (914 km), except during summer. In this altitude interval the electron precipitation was more likely to be field aligned during winter than during any other season. The analysis suggests the establishment by electrostatic charge layers of localized electric fields parallel to the magnetic field. The resulting potential distribution focuses the electron beam along the field lines in the region between the charge layers but destroys the focused beam below the lower layer, and thus an altitude dependence is created. (auth)

30470 LATITUDINAL CROSS SECTION OF THE AURORAL ELECTROJET AND ITS RELATION TO THE INTERPLANETARY MAGNETIC FIELD POLARITY. Kamide, Y.; Akasofu, S. (Geophysical Institute, University of Alaska, Fairbanks, Alaska 99701). J. Geophys. Res. 79: No. 25, 3755-3772 (1 Sept 1974).

The latitudinal dependence of the auroral electrojet profile across the Alaska meridian chain of observatories on the polarity of the interplanetary magnetic field (IMF) is semiquantitatively examined. It is found that for polar magnetic substorms associated with a northward IMF and a southward IMF of a small magnitude (1) the auroral electrojet is confined to a rather narrow area in higher latitudes (~ 70° in geomagnetic latitudes), (2) the total westward electrojet current intensity is smaller, and (3) the positive change in the low–latitude H component is smaller ($< 10\ \gamma$) than the corresponding quantities of substorms associated with the southward IMF of a large magnitude. The correlation between the total electrojet intensity and the low–latitude H change (ΔH) is higher than that between the AE index and ΔH. It is suggested that the total electrojet current intensity across the midnight meridian is a better measure for the intensity of magnetospheric substorms than the AE index. (auth)

30471 BEHAVIOR OF OUTER RADIATION BELT ELECTRONS (>1.5 MeV) DURING A GEOMAGNETICALLY DISTURBED TIME ON 8 MARCH 1970 AND ITS RELATIONSHIP TO MAGNETOSPHERIC PROCESSES. Haeusler, B.; Sckopke, N. (Max-Planck-Institut fuer Physik und Astrophysik, Garching, Ger.). Planet. Space Sci.; 22: No. 8, 1249-1264(Aug 1974).

Omnidirectional intensities of electrons with energies $E_e > 1.5$ MeV detected by a low orbiting polar satellite (GRS-A/AZUR) in the outer radiation belt are examined during disturbed times including the main phase of a very strong geomagnetic storm on 8 March 1970. The particle intensity features are discussed in relationship with proposed magnetospheric processes. It is found that a superposition of the two following effects can explain the particle behavior in the trapping region: (1) Radial diffusion. After the southward turning of the interplanetary field an inward motion of both the energetic electron belt and the plasmapause took place. This effect was observed at $L > 3\ R_E$ and it is attributed to enhanced magnetospheric electric field fluctuations. Later, a strong interplanetary shock impinged upon the magnetosphere which was related to the triggering of intense magnetospheric substorms; a further inward diffusion occurred at $L \lesssim 3\ R_E$, accompanied by an inward movement of the electron slot. A rough estimation of the diffusion coefficient leads to a power spectrum of the electric field fluctuations which seems to be consistent with experimentally determined power spectra (Mozer, J. Geophys. Res.; 76: 3651 (1971)). (2) Adiabatic response to ring current changes. Large energetic electron intensity decreases within the outer radiation belt are shown to be adiabatic changes due to ring current variations. The influence of the inflation of the magnetosphere due to the developing ring current is simultaneously observed by the decrease of the solar proton cutoff (1.7 to 2.5 MeV). (auth)

30472 PARTICLE SATURATION OF THE OUTER ZONE: A NONLINEAR MODEL. Schulz, M. (Aerospace Corp., El Segundo, Calif. (USA). Space Physics Lab.). Astrophys. Space Sci.; 29: No. 1, 233-242(Jul 1974).

Properties of the steady state and transient behavior of geomagnetically trapped radiation are analyzed by means of phenomenological equations that concisely summarize the operative dynamical processes. The equations provide for a realistic coupling between electromagnetic wave energy, particle intensity, and pitch-angle anisotropy of the context of the outer zone. Applications include magnetospheric enforcement of a limit on stably trapped particle flux, the smooth transition between weak pitch-angle diffusion and strong diffusion, parasitic particle precipitation by natural and man-made radio signals, natural and artificial injections of trapped radiation, and the consequences of magnetospheric cold-plasma injection. (auth)

PHYSICS (ATOMIC AND MOLECULAR)

Beams and Their Reactions

Refer also to abstracts 30511, 30526, 30549, and 30972.

30473 (AD-772833) ADVANCED ION SOURCE. Final Report, 21 March–21 June 1973 on Phase 1. King, H. J. (Hughes Research Labs., Malibu, Calif. (USA)). 21 Mar 1973. Contract F08606-73-C-0038. 58p. NTIS $3.75.

The analytic and experimental studies conducted during Phase 1 of the program indicate that it is possible to design both cesium and iodine sources to meet the specified brightness requirements of 200 and 100 A/cm squared sr respectively. No reasons were uncovered as to why these two types of sources cannot operate in the same vacuum environment in such a manner that the ion species available to the AMS can be rapidly changed. Prototype hardware will be developed in Phase 2 to demonstrate this ability. (auth)

30474 (AED-CONF-74-089-032) ENERGY AND CHARGE DISTRIBUTION OF BACKSCATTERED PARTICLES DURING BOMBARDMENT OF METAL SURFACES WITH PROTONS. Meischner, P.; Verbeek, H. (Max-Planck-Institut fuer Plasmaphysik, Garching/Muenchen (F. R. Germany)). 1974. 8p. (In German). (CONF-740451-12). INIS.

From conference on solid state physics; Freudenstadt, F. R. Germany (1 Apr 1974).

7 figs. Available from ZAED.

When bombarding a metal target with light ions, e.g., protons, at low primary energies (below 50 keV), firstly the Rutherford cross section is no longer valid, secondly, the multiple collisions largely contribute to backscattering; this makes the theoretical description more difficult. Below 20 keV, no surface barrier counters can be used as energy analyzers, the charged particles can merely be spectrometrically examined in an electromagnetic analyzer. As the number of neutral, backscattered hydrogen atoms increases rapidly with decreasing energy, experiments to directly determine the neutral backscattered particles were carried out by ionization in a gauged gas cell. The experimental set-up and mode of operation of the apparatus as well as the experiments with Ta as target in the range 0 to about 18 keV are described. (GE)

30475 (GSI-A1-74) THE PRODUCTION OF MULTICHARGED IONS WITH A DUOPLASMATRON ION SOURCE IN HIGH-CURRENT CONTINUOUS OPERATION. Krupp, H. (Gesellschaft fuer Schwerionenforschung m.b.H., Darmstadt (F.R. Germany)). Mar 1974. 86p. (In German). INIS.

41 figs.; 8 tabs.; 49 refs. With abstract.

The investigation of a duoplasmatron ion source, whose mode of operation and design is described in detail, with discharging currents up to over 20 A during continuous operation gave the following results: The joint action of the current emitted by the cathode, of the discharge current, the gas pressure at the cathode, the magnetic field configuration, and of the discharge length together with the discharge space geometry which has to be adapted to the gas used for operation, will reproducibly determine the yield of multicharged ions. By adjusting the cathode emission so that the potential of the cathode is equal to the floating potential of the dynode it is possible to considerably reduce the required discharge power, and thus to markedly increase the serviceable life of the ion source. Operation at high discharge current values offers the possibility of generating multi-charged ions with high intensities, requiring a very low discharge voltage and therefore a comparatively low discharge power. (auth)

30476 SEMICLASSICAL THEORY OF ATOM–SOLID-SURFACE COLLISIONS: APPLICATION TO He–LiF DIFFRACTION. Doll, J. D. (State Univ. of New York, Stony Brook). J. Chem. Phys.; 61: No. 3, 954-957(1 Aug 1974).

The semiclassical theory of gas–solid-surface collisions is applied to the diffractive He–LiF system. It is shown that uniform semiclassical results are in good agreement with high quality quantum-mechanical results. The present study suggests that classically forbidden contributions should not always be ignored when both classically allowed and forbidden contributions are present. The experimental results of O'Keefe et al. are examined. (auth)

30477 STRONG 4f RESONANCE EFFECTS IN RARE-EARTH APPEARANCE-POTENTIAL SPECTRA. Harte, W. E.; Szczepanek, P. S.; Leyendecker, A. J. (Lab. for Physical Sciences, College Park, MD). Phys. Rev. Lett.; 33: No. 2, 86-88(8 Jul 1974).

Soft-x-ray appearance-potential spectra of rare-earth elements are interpreted in terms of strong resonance interactions between the incident electrons and atomic 4f states. These interactions account for both the large intensity and the threshold shifts of the measured signal. This resonance persists in La, Ce, Pr, and Nd when present as only a few atomic percent in a NiCr alloy reflecting the local character of the interaction. (auth)

30478 SELF-DECOMPOSITION OF QUASI-NEUTRAL ION BEAM. Gabovich, M. D. (Inst. of Physics, Kiev). Ukr. Fiz. Zh. (Russ. Ed.); 19: No. 4, 692-694(Apr 1974). (In Russian)

Stationary state of a quasineutral ion beam passing through rarefied gas is not possible without a source of additional energy, and the ion beam itself is such a source. Coulomb collisions of ion beams with electrons neutralized by it and activation of Langmuir electron oscillations by an ion beam with subsequent conversion of the energy of the oscillations to electrons leads to the electrons obtaining additional energy and being ejected from the beam. The presentations of the mechanism of self-compensation of an ion beam permit evaluating the degree of compensation of the latter under different conditions. (tr-auth)

30479 THE INELASTIC SCATTERING OF He AND Ne FROM A (001) SURFACE OF SODIUM FLUORIDE. Mason, B.F.; Williams, B.R. (Electron Physics Section, Radio and Electrical Engineering Division, National Research Council, Ottawa, Canada K1A OR8). J. Chem. Phys. 61: No. 7, 2765-2778 (1 Oct 1974).

The inelastic scattering of He and Ne atoms from a cleaved (001) surface of NaF has been studied at different surface temperatures. The study was similar to that for the He–LiF system, in that the intensity of the inelastic streaks in the vicinity of diffraction peaks was explored as a function of detector location and crystal rotation. For diffraction peaks not too close to the normal, the phonon emission and absorption effects separated into regions on either side of the elastic peak, the latter events being on the side closest to the normal. At 140°K the phonon absorption events were less probable than phonon emission events, i.e., atoms tended to lose energy, while at higher surface temperature the probability of energy gain increased. The positions of the streaks moved predictably in space by varying the incident momentum of the beam, a parameter which also influenced the intensity of the streaks. Comparisons have been made to the He–LiF system using the elastic constants of the two materials. (auth)

30480 HELIUM SCATTERING FROM SOLID SURFACES. Weare, J.H. (Department of Chemistry, Revelle College, University of California, San Diego, La Jolla, California 92037). J. Chem. Phys. 61: No. 7, 2900-2910 (1 Oct 1974).

The quantum mechanical scattering of light atoms from well defined solid surfaces is studied via a simplified model of the gas surface system. The differential scattering cross section is calculated using a power series expansion with convergence properties similar to those of distorted wave perturbation theory. The cross section is averaged over the internal states of the system, and the temperature dependence of the one and two-phonon contributions is calculated. It is concluded that, at sufficiently low surface temperatures and beam energies, one-phonon contributions dominate. Comparison of these results with perturbation theory indicates that, for these experimental conditions, a first-order perturbation theory should be sufficient to interpret experiments. Arguments are given indicating that this first-order calculation may yield direct information about the local density of states of the system. This suggests that He scattering may be developed into an analytical tool, similar to bulk neutron scattering, giving direct information about surface chemical bonding. (auth)

30481 SPUTTERING EXPERIMENTS WITH SILVER SINGLE CRYSTALS AND THE CHANNELING PHENOMENA. Bhattacharya, R. S.; Basu, D.; Karmohapatro, S. B. (Saha Inst. of Nuclear Physics, Calcutta). Radiat. Eff.; 21: No. 4, 275-278(1974).

Sputtering yields of monocrystalline silver under irradiation with 7 to 30 keV Ar^+, Kr^+ and Xe^+ ions, not reported earlier, have been determined. The yield has been found to depend strongly on the orientation of the crystal and mass of the impinging ion. Onderdelinden's (Appl. Phys. Lett.; 8: 189 (1966)) model based on Lindhard's (Kgl. Danske. Vid. Selsk. Matt. Fys. Medd.; 34: No. 14 (1965)) theory of channeling is found to describe satisfactorily, the observed orientation and ion mass dependence of the yields for the ions of energy ~10 keV or above. The role of the barrier potential approximated in the model in predicting the experimental results is discussed. (auth)

30482 SPUTTERING YIELDS AND SPECIFIC ENERGY LOSSES OF Ar^+ IONS WITH ENERGIES FROM 5 TO 30 keV AT SiO_2. Bach, H.; Kitzmann, I.; Schroeder, H. (Jenaer Glaswerk Schott und Gen., Mainz). Radiat. Eff.; 21: No. 1, 31-36(1974).

Sputtering yields are determined from interference micrographs of the etched pits developing during ablation of discharged silica surfaces by a homogeneous Ar ion beam at normal incidence. The maximum of the sputtering yield was found to be 1.8 atoms per incident ion at about 20 keV. The bombardment of thin silica layers on a glass substrate results in photo-emission of sputtered target particles and ionoluminescence; specific energy losses are evaluated from the time-varying spectral and intensity distributions which can be observed during sputtering. Both these specific energy losses and those calculated from sputtering yields are compared with the results from the unified sputtering theory of Brandt and Laubert (Nucl. Instr. Meth.; 47: 201 (1967)) predicting proportionality of the sputtering yield and the specific energy losses. The experimentally determined energy losses show the same energy dependence among each other and are more energy dependent than the theoretical results. If the surface is not discharged during ablation, then the sputtering yields increase up to 75%; however, the energy losses evaluated from the distribution of luminescence and photo-emission do not increase by more than 25%, this indicates a change of the momentum distribution within the collision cascade due to an attractive force between negative-charged oxygen ions and the positive-charged surface of the target. (auth)

30483 ION BEAM SPUTTERING. The Effect of Incident Ion Energy on Atomic Mixing in Subsurface Layers. McHugh, J. A. (Knolls Atomic Power Lab., Schenectady, NY). Radiat. Eff.; 21: No. 4, 209-215(1974).

Secondary ion mass spectrometric methods were used to study the effect of incident ion energy on atomic mixing in subsurface layers. A Ta_2O_5 film containing a 50 Å ^{31}P-rich layer 230 Å below the surface was depth profiled for phosphorus using normal incidence ^{16}O primary particles of various energies (1.75 to 18.5 keV). A pronounced energy effect was observed in the widths of ^{31}P profiles generated by 4 keV ^{16}O. For 18.5 keV ^{16}O, the observed profile contained two distinct components—the ^{31}P-rich layer and the ^{31}P recoil distribution. This later condition prevails when the peak of the incident ion damage distribution occurs at a depth which equals or exceeds the distance from the surface to the ^{31}P-rich layer. The desirable primary ion beam energy for characterizing the true elemental distribution is dictated by the shape and location of the layer to be profiled. In most instances, a low energy beam is preferred. (auth)

30484 HYPERTHERMAL BEAMS SPUTTERED FROM ALKALIHALIDE SURFACES. Konnen, G. P.; Grosser, J.; Haring, A.; De Vries, A. E.; Kistemaker, J. (Stichting voor Fundamental Onderzoek der Materie, Amsterdam). Radiat. Eff.; 21: No. 3, 171-179(Mar 1974).

Velocity selected beams of atoms and molecules have been produced by sputtering from various alkalihalide surfaces under 6 keV Ar^+ ion bombardment. The mass spectrum and the velocity distribution of these particles have been analyzed in the range from 0 to 13000 m/s. In the low velocity part of the spectrum monatomic particles as well as polyatomic ones have been found. For velocities larger than 3000 m/s the number of sputtered molecules is very small compared to the number of atoms. In addition to typical sputtering velocity distributions, thermal distributions are also found, due to vaporization of the less effectively sputtered atoms from the crystals. Above a few eV the energy distribution of a given alkali or halogen atom is independent of the target from which it is sputtered. There are indications that some sputtered atoms and molecules are formed in long lived excited states. (auth)

30485 A CLOSE TO UNIVERSAL NEGATIVE ION SOURCE. Middleton, R.; Adams, C. T. (Pennsylvania Univ., Philadelphia (USA). Dept. of Physics). Nucl. Instrum. Methods; 118: No. 2, 329-336(15 Jun 1974).

A new type of negative ion source has been developed which utilizes a beam of cesium positive ions from a surface ionization source to sputter a hollow target cone. Among the many advantages of the source are high yield (e.g. >50 μA of C^-), negative ion species can be changed within minutes and the emittance is low. (auth)

30486 BACKSCATTERING MEASUREMENTS AND SURFACE ROUGHNESS. Schmid, K.; Ryssel, H. (Technische Univ., Muenchen (F.R. Germany)). Nucl. Instrum. Methods; 119: No. 2, 287-289(15 Jul 1974).

The backscattering spectra of He^+ particles in the MeV range measured on rough and polished silicon surfaces show different line-shapes. The surface edge of the spectrum of a rough sample (roughness about 3000 Å) was distinctly smoother than that of a polished sample. This behavior can be explained by a simple model. (auth)

Atomic and Molecular Properties

Refer also to abstracts 30102, 30329, 30527, and 30550.

30487 (AD-776343) ANALYSIS OF THE GROUND CONFIGURATION OF TRIVALENT THULIUM IN SINGLE-CRYSTAL YTTRIUM VANADATE. Wortman, D. E.; Leavitt, R. P.; Morrison, C. A. (Harry Diamond Labs., Washington, D. C. (USA)). Dec 1973. 19p. (HDL-TR-1653). NTIS $4.00.

An analysis was made of the optical spectrum of Tm^{3+} in YVO_4. The approach taken was to describe the Tm^{3+} free-ion energy levels as completely as possible and then to describe the effects of the crystal field on these levels. Results gave a new interpretation of the triplet H4 and triplet H5 multiplets and gave G factors in good agreement with the measurements. The effects of the hyperfine interaction and the spin-crystal-field interaction on the energy levels are discussed. (GRA)

30488 (AD-777042) MULTIPHOTON TRANSITIONS IN HELIUM BETWEEN 1S and 2S LEVELS. Jones, H. D. (Naval Ordnance Lab., White Oak, Md. (USA)). 27 Feb 1974. 20p. (NOLTR-74-4). NTIS $3.00.

An extension of the momentum-translation approximation to include many-electron systems is presented. The multiphoton 1S-2S transition amplitude for a helium atom in the presence of combined intense and weak electromagnetic fields is calculated. Nonperturbative behavior of the results is exhibited at high intensities. (auth)

30489 STEP–BY–STEP EXCITATION IN HELIUM. Gerasimov, G.N.; Startsev, G.P. Opt. Spectrosc. (USSR) 36: No. 5, 487-488 (May 1974).

The effective cross section for stepwise excitation of helium from the 2^3S_1 to the 2^1S_0 state by electron impact was measured experimentally. It was shown that with a change of the average electron energy from 0.2 to 1.0 eV the cross section changed within the limits of 1.5×10^{-16} to 8.0×10^{-16} cm^2. (auth)

30490 DETERMINATION OF THE SINGLET–TRIPLET SEPARATION OF H_2 BY A LEVEL-ANTICROSSING TECHNIQUE. Jost, R.; Lombardi, M. (Univ., Grenoble, France). Phys. Rev. Lett.; 33: No. 2, 53-56(8 Jul 1974).

It is shown that the singlet-triplet separation of H_2 must be lowered by 157.7 ± 0.2 cm^{-1} compared to the hitherto accepted value of Dieke. A new kind of "level anticrossing" method was used in which the anticrossing is due to the coupling of a singlet and a triplet state by spin-orbit or hyperfine Fermi contact interaction. (auth)

30491 CALCULATED PHOTOIONIZATION CROSS SECTIONS AND RELATIVE EXPERIMENTAL PHOTOIONIZATION INTENSITIES FOR A SELECTION OF SMALL MOLECULES. Rabalais, J. W.; Debies, T. P.; Berkosky, J. L.; Huang, J. T. J.; Ellison, F. O. (Univ. of Pittsburgh). J. Chem. Phys.; 61: No. 2, 516-528(15 Jul 1974).

The general equations for calculating photoionization cross sections of polyatomic molecules in the plane-wave and orthogonalized plane-wave approximations have been programmed for the electronic computer. Applications are described for the molecules H_2, CH_4, N_2, CO, H_2O, H_2S, and H_2CCH_2 for incident photon energies from threshold to 1500 eV. Relative photoionization band intensities for the above molecules are measured using NeI, HeI, and HeII resonance radiation. A simplified analysis of the intensities derived from electrostatic deflection analyzers is presented. The $^2P_{3/2}:^2P_{1/2}$ intensity ratios of the rare gases are determined with the three modes of excitation mentioned above. An analysis of the resolution capabilities of an electrostatic deflection spectrometer as a function of electron kinetic energy is presented. Relative experimental photoionization band intensities for the above molecules obtained by ionization with the three uv sources and MgK_α and AlK_α x-ray sources are compared with computed differential cross sections. Variations in computed cross sections as a function of the kinetic energy of the photoelectrons are discussed, and possible interpretations are proposed. (auth)

30492 FINE STRUCTURE OF THE METASTABLE $a^3\Sigma^+_u$ STATE OF THE HELIUM MOLECULE. Lichten, W.; McCusker, M.V.; Vierima, T.L. (Yale University, New Haven, Connecticut 06520). J. Chem. Phys. 61: No. 6, 2200-2212 (15 Sept 1974).

We have measured the spin–spin, electronic fine structure of the $a^3\Sigma^+_u$ metastable state of He_2 by means of a molecular beam, magnetic resonance apparatus, with the flowing afterglow of a pulsed, helium discharge as the source. The zero field separations in the $N=1$ and $N=3$ rotational levels, probably in the $v=0$ vibrational state, are (in MHz) $N=1$: $J=0 \leftrightarrow J=1$:2199.968 ± 0.01, $J=1 \leftrightarrow J=2$:873.668 ± 0.007; $N=3$: $J=2 \leftrightarrow J=3$:1323.911 ± 0.006, $J=3 \leftrightarrow J=4$:964.992 ± 0.006, where the errors quoted are three standard deviations of the mean. From these measurements and from a separate determination of the level order, the interaction constants for these states are the following (in MHz): spin–spin: λ: $-1098.773\pm0.005(N=1)$, $-1096.803\pm0.004(N=3)$, spin–rotation: γ: $-2.421\pm0.003(N=1)$, $-2.414\pm0.001(N=3)$, where the errors are 3σ. (auth)

30493 GROTRIAN CHARTS FOR ATOMS AND IONS OF RARE GASES. Yokozawa, M.; Matsuzaki, H.; Kamegaya, T.; Nakajima, M. (Technical Research Laboratories, NHK (Japan Broadcasting Corporation), 1–10–11, Kinuta, Setagaya–ku, Tokyo 157, Japan). J. Opt. Soc. Am. 64: No. 3, 396-397 (Mar 1974).

Grotrian charts for He I, He II; Ne I, Ne II; Ar I, Ar II; Kr I, Kr II; Xe I, Xe II in the vacuum ultraviolet region are reported. The data used in the present work came from Moore's Atomic Energy Levels and Kelly's Tabulation of Emission Lines in Vacuum ultraviolet. (AIP)

30494 LONG-RANGE $He_2(^3\Sigma^+_{g,u})$ POTENTIALS AND METASTABILITY EXCHANGE IN He*–He COLLISIONS. Hickman, A. P.; Lane, N. F. (Rice Univ., Houston, TX). Phys. Rev., A; 10: No. 1, 444-447(Jul 1974).

Previous semiempirical determinations by Fitzsimmons et al. of the asymptotic form of the potentials V_g and V_u for the helium molecular states $^3\Sigma^+_{g,u}$ are refined to include new experimental data. The resulting potentials yield cross sections for elastic scattering, diffusion, and metastability exchange in $He(2\ ^3S_1)$-$He(1\ ^1S_0)$ collisions in agreement with various experiments from 15 to 500°K. (auth)

30495 WIDTHS OF 4s AND 5s MULTIPLET COMPONENTS IN THE RARE EARTHS. McGuire, E. J. (Sandia Labs., Albuquerque, NM). Phys. Rev., A; 10: No. 1, 13-20(Jul 1974).

For multiplets formed by adding an s vacancy to an atom with a partially filled shell, it is shown that the Auger transition rate can be found from expressions that do not involve fractional-parentage coefficients of the partially filled shell. The proof requires a sum over final states and that the partially filled shell be in a state of maximum spin. Calculations are performed for the widths of the 4s and 5s multiplet components in the rare earths. The calculated 4s widths are considerably larger than the measured values, while the 5s widths are considerably smaller than the measured values. It is shown that these disagreements cannot be fully accounted for by the choice of Auger-electron energy. It is hypothesized that the cause of the disagreement is neglect of configuration interaction, and this is briefly discussed. (auth)

30496 QUANTUM-DEFECT THEORY OF EXCITED $^1\Pi^-_u$ LEVELS OF H_2. Atabek, O. (Paris Univ., Orsay, France); Dill, D.; Jungen, C. Phys. Rev. Lett.; 33: No. 3, 123-126 (15 Jul 1974).

Quantum-defect methods are used to calculate, by a single unified procedure, the full spectrum of $J = 1\ ^1\Pi^-_u$ Rydberg levels of H_2, extending from the lowest levels of the $2p\pi^-\ C^1\Pi^-_u$ state to the high members of the $np\pi^-$ series between the $H_2^+(v = 0)$ and $H_2^+(v = 1)$ ionization thresholds. Results for the C state are substantially improved over previous calculations based on direct integration of the vibrational Schroedinger equation, while results at higher energies reproduce with high accuracy the recently observed spectrum, including local perturbations. (auth)

30497 ENERGY DEPENDENCE IN INTERATOMIC POTENTIALS-He_2. Mittleman, M. H. (City Univ. of New York). Phys Rev., A; 10: No. 1, 442-443(Jul 1974).

The energy dependence in interatomic potentials is shown to be expressible as angular momentum dependence of the potential. This means that a potential determined by scattering for a given partial wave can also be used to analyze the question of the existence of a bound state in the same partial wave. This procedure is not available for the problem of the existence of He_2 because of the lack of experimental data. However, it is shown that scattering experiments of He + He were done at sufficiently low energy so that the extrapolation of the potential in energy necessitated by its energy dependence is too small to affect the existence of the bound state. (auth)

30498 PHOTOIONIZATION OF $He(n^{1,3}P)$ ATOMS EXCITED BY POLARIZED LIGHT. Jacobs, V. L. (Goddard Space Flight Center, Greenbelt, MD). Phys. Rev. Lett.; 32: No. 25, 1399-1402(24 Jun 1974).

The S and D partial-wave cross sections for photoionization from the 3^1P, 4^1P, 3^3P, and 4^3P states of helium are calculated for ejected-electron energies from 2.04 to 13.6 eV. It is shown that the S and D contributions may be combined to obtain the total cross section for arbitrary polarization states of the excited helium atoms and of the ionizing radiation. Good agreement is obtained with a recent experimental determination in which polarized $He(n^{1,3}P)$ atoms were excited and subsequently ionized by linearly polarized laser light. (auth)

30499 TEST OF THE PAULI EXCLUSION PRINCIPLE FOR ATOMIC ELECTRONS. Reines, F.; Sobel, H. W. (Univ. of California, Irvine). Phys. Rev. Lett.; 32: No. 17, 954(29 Apr 1974).

The Pauli exclusion principle was tested for atomic electrons giving a lifetime for such a violation, per iodine atom, of $>2 \times 10^{27}$ sec. This result is compared to a normal electromagnetic dipole transition, and a limit is set on a possible symmetric wave-function admixture to a K-shell electron wave function. (auth)

30500 ABSOLUTE CROSS SECTIONS FOR THE PHOTOIONIZATION OF $He(n^{1,3}P)$ ATOMS. Dunning, F. B.; Stebbings, R. F. (Rice Univ., Houston, TX). Phys. Rev. Lett.; 32: No. 23, 1286-1289(10 Jun 1974).

A molecular-beam apparatus is used in conjunction with a tunable laser to determine absolute cross sections for the photoionization of helium 3^1P, 4^1P, 5^1P, 3^3P, 4^3P, and 5^3P atoms excited optically from the $2^{1,3}S$ metastable levels. The photoionization cross section for each of these states is determined at the wavelength used for its excitation from the metastable state. The results are compared with those of recent unpublished calculations. (auth)

30501 INTENSITIES OF THE DIPOLE AND QUADRUPOLE ROTATION-VIBRATION SPECTRA OF HD. McKellar, A. R. W. (National Research Council of Canada, Ottawa). Can. J. Phys.; 52: No. 13, 1144-1151(1 Jul 1974).

The 1–0, 2–0, 3–0, and 4–0 rotation-vibration bands of HD were studied using a cooled multiple-traversal absorption cell and a grating spectrometer; intensities were measured for one electric quadrupole and 13 dipole transitions. There is particular interest in these intensities because HD has recently been detected on Jupiter by means of the 4–0 dipole band. Since the four bands were studied with the same gas samples and apparatus, possible errors in the measurement of their relative intensities were minimized. A rather large rotational dependence was found for the 1–0 band dipole transition moment. The present results are compared with theoretical intensity calculations, and it is concluded that there is good agreement for the quadrupole transition, but not for the dipole transitions. (auth)

30502 DIELECTRIC PROPERTIES OF HELIUM: QUANTUM STATISTICAL MECHANICS. Bruch, L.W. (Theoretical Chemistry Institute and Department of Physics, University of Wisconsin, Madison, Wisconsin 53706); Fortune, P.J.; Berman, D.H. J. Chem. Phys. 61: No. 7, 2626-2636 (1 Oct 1974).

Expressions for the second dielectric and Kerr virial coefficients and the first two moments of the associated spectral functions valid in quantum statistical mechanics are derived. Upper and lower bounds are derived for the second Kerr virial coefficient to enable an indirect evaluation when quantal effects are appreciable. Calculations of helium dielectric properties near 4 K are reported. The calculations incorporate approximations for the pair distribution function of gaseous helium and coupled Hartree–Fock results for the diatom polarizability. Structure factors calculated from the distribution functions and the calculated anisotropy moments are in good agreement with experiment. The calculated second dielectric virial coefficient at 4 K is in order–of–magnitude agreement with experiment and reflects an imprecise knowledge of the incremental mean polarizability of the helium diatom. (auth)

30503 WEAK HYPERFINE STRUCTURE MEASUREMENT USING THE MAGNETIC REPOLARIZATION EFFECT: APPLICATION TO N=1 v=1 $(1s\ 3d)^1\Sigma$ LEVEL OF H_2. Meliteres–Marechal, M.; Lombardi, M. (Laboratoire de Spectrométrie Physique, Université Scientifique et Médicale de Grenoble, B.P. 53, 38041 Grenoble–Cedex, France). J. Chem. Phys. 61: No. 7, 2600-2608 (1 Oct 1974).

The magnetic repolarization effect is studied in the case where the hyperfine structure (AIJ) of the considered excited atomic or molecular level is weaker than the natural width Γ. General expressions are given. It is shown that the amplitude of this effect varies as $(A/\Gamma)^2$ and that its value permits the determination of A when one compares the magnetic repolarization and depolarization effects. Such an effect is experimentally studied in the N=1, v=1 $(1s\ 3d)^1\Sigma$ level of H_2. A value of $A = (1 \pm 0.17)$ MHz is deduced, corresponding to $A/\Gamma = 0.15$.) (auth)

30504 DIELECTRIC PROPERTIES OF HELIUM: THE POLARIZABILITY OF DIATOMIC HELIUM. Fortune, P.J.; Certain, P.R. (Department of Chemistry and Theoretical Chemistry Institute, University of Wisconsin, Madison, Wisconsin 53706). J. Chem. Phys. 61: No. 7, 2620-2625 (1 Oct 1974).

Self–consistent field calculations of the dipole polarizability tensor of diatomic helium at four internuclear separations between $4a_0$ and $6a_0$ are reported. For larger separations, the calculations are shown to reduce to the point–dipole model of long–range polarizabilities. The computed polarizability is used in a companion paper to obtain estimates of the second dielectric constant virial coefficient, the Kerr constant virial, and the spectral moments for Raman scattering. (auth)

30505 THERMODYNAMICAL ACCOUNT OF THE PHOTOEMISSION SPECTRA OF THE RARE EARTHS. Johansson, B.

(Forskningsinstitutet foer Atomfysik, Stockholm). J. Phys., F (London); 4: No. 7, L169-L173(Jul 1974).

From the most reasonable assumption of a nonbonding property for the 4f electrons in the rare earths, thermodynamical principles can be utilized to account for their photoemission spectra. (auth)

30506 HELIUM DIATOM POLARIZABILITY AND THE DIELECTRIC PROPERTIES OF FLUID HELIUM. Fortune, P. J.; Certain, P. R.; Bruch, L. W. (Wisconsin Univ., Madison (USA). Theoretical Chemistry Inst.). Chem. Phys. Lett.; 27: No. 2, 233-236(15 Jul 1974).

A priori calculations of the helium diatom polarizability are combined with an evaluation of the pair distribution function of gaseous helium to yield the second dielectric virial coefficient at 4 and 322°K. Order of magnitude agreement with experimental data is found, but the isotopic dependence at 4°K is in conflict with experimental data. (auth)

30507 HYPERFINE STRUCTURE IN THE VISIBLE NO_2 SPECTRUM. Demtroeder, W.; Paech, F.; Schmiedl, R. (Fachbereich Physik, Universitaet Kaiserslautern, Kaiserslautern, Germany). Chem. Phys. Lett.; 26: No. 3, 381-386(1 Jun 1974).

The absorption spectrum of NO_2 has been recorded within the tuning range (7 GHz) of the single-mode argon laser line $\lambda = 5145$ Å. Using a well collimated NO_2 molecular beam it was possible to resolve the hfs splitting and to determine for several transitions the hfs splitting in the excited B_2 state. (auth)

30508 VIBRATIONAL RELAXATION OF D_2 IN THE RANGE 400−50°K. Lukasik, J.; Ducuing, J. (Paris-11 Univ., 91–Orsay (France)). Chem. Phys. Lett.; 27: No. 2, 203-205(15 Jul 1974).

The vibrational relaxation of n-D_2 by itself and by n-H_2 was studied in the interval 400−50°K. The results are compared to the recent n-H_2 studies in the similar temperature range and discussed in terms of various molecular parameters. (auth)

Positronium, Muonium, and Muonic and Mesic Atoms and Molecules

Refer also to abstracts 30620 and 30777.

30509 NEGATIVE MUON CAPTURE IN VERY LIGHT ATOMS. Haff, P.K., Tombrello, T.A. (California Institute of Technology, Pasadena, California 91109). Ann. Phys. (N.Y.) 86: No. 1, 178-192 (July 1974).

The transition rates for unbound muons to be captured into atomic bound states are calculated as functions of (1) incident muon center−of−mass energy, (2) muon principal quantum number n, and (3) muon (final) angular momentum l, for the hydrogen, helium, and lithium atoms. These rates reflect differences in electron binding energies. At muon energies of several hundred electron volts, lithium K−shell electrons are more likely to be ejected than the L−shell electron, while this behavior is reversed for energies —10 eV. However, in each case when the capture rate is folded with a muon stopping power function, the result is that more than half of the unbound muons are absorbed above 75 eV. Implications for experiments which look at muon transfer processes are noted. (auth)

30510 EFFICIENT POSITRONIUM FORMATION BY SLOW POSITRONS INCIDENT ON SOLID TARGETS. Canter, K. F.; Mills, A. P. Jr.; Berko, S. (Brandeis Univ., Waltham, MA). Phys. Rev. Lett.; 33: No. 1, 7-10(1 Jul 1974).

A beam of slow positrons in the few-eV region is directed at bakable solid targets in a vacuum of $(2-4) \times 10^{-8}$ torr. Measurements of the $2\gamma/3\gamma$ annihilation-yield ratio indicate the conversion of the incident positrons into positronium. The conversion efficiency depends on the target material and incident positron energy, varying from less than 25% at 300°K to 40 to 85% at 900°K. (auth)

30511 DIFFUSION OF SLOW POSITRONS FROM GOLD. Pendyala, S.; McGowan, J. W. (Univ. of Western Ontario, London). Can. J. Phys.; 52: No. 12, 1051-1056(15 Jun 1974).

An attempt was made to experimentally determine the diffusion length L_D of slow positrons (peak energy ~0.1 eV) in gold at room temperature by comparing the slow positron yield with phenomenological models for the yield. The diffusion of the slow positron is assumed to be similar to that of a thermal neutron diffusion in an absorbing and scattering medium. A collision mean free path of the slow positron in the electron gas under the Born approximation is estimated to be ~2 Å. This corresponds to a calculated value of the diffusion length $L_D \sim 250$ Å. The experimental value is ≤1000 Å. (auth)

30512 FINITE RANGE EFFECTS IN PIONIC ATOMS. Iachello, F.; Lande, A. (Rijksuniversiteit Groningen (Netherlands)). Phys. Lett., B; 50: No. 3, 313-315(10 Jun 1974).

Results of a phenomenological treatment of the effects of the finite range of the s-wave π-N interaction on level shifts in pionic atoms is presented. Final range effects are shown to be important in the derivation of the π-nucleus optical potential. (auth)

30513 POSITRON ANNIHILATION IN COLORED KCl. Smedskjaer, L.; Dannefaer, S. (Danmarks Tekniska Hoejskole, Lyngby). J. Phys., C (London); 7: No. 15, 2603-2613(7 Aug 1974).

Colouration in KCl has been investigated by means of optical absorption and positron annihilation measurements. In additively coloured KCl crystals, positronium is formed in the F centres having a pick-off lifetime close to 1 ns. Angular correlation data obtained by magnetic quenching of orthopositronium indicate that a positronium-like system is formed with a hyperfine splitting close to the value in vacuo. During the measurements a considerable amount of F centres and other defects are produced by the positron source. (auth)

30514 QUADRUPOLE MIXING IN HADRONIC ATOMS: AN ADDITIONAL PROBE OF THE HADRON−NUCLEUS INTERACTION. Leon, M. (Los Alamos Scientific Lab., N. Mex. (USA)). Phys. Lett., B; 50: No. 4, 425-428(24 Jun 1974).

The effect of the nuclear electric quadrupole moment on the yields of hadronic x-rays is calculated. For each negative hadron there are a few nuclei for which the effect is large and readily observable. Results are presented for kaonic atoms with distorted even−even nuclei. (auth)

30515 POPULATION OF MUONIC ^{3}He STATES FOLLOWING THE μ^- CATALYSED FUSION p μd → μ^3He. Holzwarth, G.; Kleber, M. (Technische Univ., Muenchen, Garching (F.R. Germany). Physik-Dept.). Phys. Lett., B; 51: No. 1, 17-18(8 Jul 1974).

Recoil due to emission of the 5.5 MeV γ-ray in the fusion reaction pμd → μ^3He and dynamical corrections to the Born−Oppenheimer approximation lead to excited muonic states in the final μ^3He atom. The branching ratios for the lowest excitations are calculated. (auth)

30516 POLARIZABILITY CONTRIBUTION TO THE ENERGY LEVELS OF THE MUONIC HELIUM $(\mu^4He)^+$. Bernabeu, J.; Jarskog, C. (European Organization for Nuclear Research, Geneva (Switzerland)). Nucl. Phys., B; 75: No. 1, 59-71(11 Jun 1974).

An experiment measuring the 2S−2P separation in the ion $(\mu^4He)^+$ is in progress at CERN. Comparison of the outcome of this experiment with the prediction of quantum electrodynamics requires the knowledge of the hadronic correction due to the two-photon exchange mechanism. Therefore, the correction to the energy levels of the ion $(\mu^4He)^+$ due to this mechanism has been calculated. The hadronic contribution to the 2S−2P separation is found to be ~16 Å which is about three times larger than the expected experimental uncertainty. (auth)

Collision Phenomena

Refer also to abstracts 30489, 30494, and 30508.

30517 (AEC-Conf-74-085-001) ION−X-RAY COINCIDENCE EXPERIMENTS IN SLOW Ne^+−Ne COLLISIONS. Sackmann, S.; Lutz, H. O.; Briggs, J. (Kernforschungsanlage Juelich G.m.b.H. (F. R. Germany); Koeln Univ. (F. R. Germany)). 1974. 10p. ZAED.

From conference on atomic physics, physics of transient phenomena, molecular physics and plasma physics; Stuttgart, Germany (4 Mar 1974).

Ne^+ ions of 235 and 263 primary energy are scattered from a dilute Ne gas target. Ne−K x-rays excited in these collisions are detected in coincidence with ions scattered through laboratory angles ranging from 3 to 36°. The impact parameter dependence of inner shell excitation thus derived matches well with the Briggs and Macek theory. (auth)

30518 (AEC-Conf-74-085-002) CROSS SECTION FOR THE Ar−L−X-RAY EMISSION IN COLLISIONS OF He^+, Ne^+, AND Ar^+ IONS WITH Ar ATOMS. Schartner, K. H.; Schaefer, H.; Hippler, R. (Giessen Univ. (F. R. Germany). 1. Physikalisches Inst.). 1974. 5p. INIS.

From conference on atomic physics, physics of transient phenomena, molecular physics and plasma physics; Stuttgart, Germany (4 Mar 1974).

Ar−L−x-ray production cross sections for collisions of He^+ Ne^+ and Ar^+ ions of energies between 100 keV and 1 MeV with Ar-atoms were measured. The results are in good agreement with comparable cross section data. (orig.)

30519 (AED-CONF-74-085-004) ANGULAR DISTRIBUTIONS FOR THE REACTIVE SCATTERING OF H AND D ATOMS BY POLYATOMIC MOLECULES. Schmidt, K. (Freiburg Univ. (F.R. Germany). Fakultaet fuer Physik). 1974. 3p. (In German). (CONF-740329-1). INIS.

From conference on atomic physics, physics of transient phenomena, molecular physics and plasma physics; Stuttgart, F.R. Germany (4 Mar 1974).

Several chemical elementary reactions have been studied in a molecular beam apparatus, and the results are discussed. (GE)

30520 (IAE-2269) CALCULATION OF INELASTIC TRANSITION CROSS SECTIONS ON BASIS OF SPECTRAL LINE BROADENING THEORY. Demura, A. V.; Leneva, A. E.; Lisitsa, V. S. (Gosudarstvennyj Komitet po Ispol'zovaniyu Atomnoj Ehnergii SSSR, Moscow. Inst. Atomnoj Ehnergii). 1973. 20p. (In Russian). INIS.

A connection is established for the inelastic transition cross section (in its dependence on velocity) with the whole contour form of broadened spectral line for the entire region of energies. In this transition between the Born and adiabatic limits in the problem of scattering there is inserted correspondingly a transition between the shock and static limits in the problem of line broadening. Cases are considered both of the absence and also the presence of an intersection point of terms that correspond respectively to a line contour form in the "negative" and "positive" regions. From these results it can be concluded that it is possible to use the results of the theory of line broadening in calculating inelastic transition cross sections with the region of intermediate energies of exciting particles being included. Concrete calculations were carried out in the case of a dipole interaction, for which there are exact solutions of the broadening problem. These solutions were used in calculating the transition cross section during a dipole interaction. The results are compared with the data of other authors. The possibilities of taking into account rotational effects are discussed. (tr-SJR)

30521 (IC-73-19) POLARIZATION OF THE RESONANCE LINES OF LITHIUM AND SODIUM ATOMS BY ELECTRON IMPACT. Tripathi, A. N.; Mathur, K. C.; Joshi, S. K. (International Centre for Theoretical Physics, Trieste (Italy)). 1973. 7p. INIS.

The polarization of the resonance lines of ^{6}Li, ^{7}Li and Na, excited by electron impact, are calculated using the Glauber approximation. The present results are in good agreement with experimental values and with other theoretical calculations in the energy range from 2 to 5 eV. (auth)

30522 SCATTERING FORM FACTORS OF ATOMS, MOLECULES, AND SOLIDS. Lam, L.; Ho, H. (City Univ. of New York). Lett. Nuovo Cim.; 11: No. 2, 159-160(14 Sep 1974).

A unified approach to the scattering form factors of atoms, molecules, and solids is presented based on the density-functional formalism of the inhomogeneous electron gas which takes both the inhomogeneity and the electron correlations into account. (JFP)

30523 EFFECTIVE CROSS SECTIONS AND PECULIARITIES OF ELECTRON EXCITATION OF THE CADMIUM ATOM. Sovter, V.V.; Zapesochnyi, I.P.; Shpenik, O.B. Opt. Spectrosc. (USSR) 36: No. 5, 482-486 (May 1974).

Investigations of the excitation functions of spectral lines of the cadmium atom (in the 2200–8200 Å spectral region) by electron impact were made from the threshold to 15 eV. Absolute excitation cross sections were determined. The excitation cross sections of lines in the ultraviolet and red spectral regions were determined. This enables evaluation of the rate of decrease in the cross sections of lines from high levels for most of the series. A group of maxima beyond the ionization threshold was found for the excitation functions of spectral lines. It is assumed that these maxima are determined by the autoionization states of cadmium. (auth)

30524 EXCITATION OF RESONANCE LINES OF K II IN ELECTRON–ATOM COLLISIONS. Vukstich, V.S.; Aleksakhin, I.S.; Zapesochnyi, I.P. Opt. Spectrosc. (USSR) 36: No. 5, 604-605 (May 1974).

The excitation and ionization of potassium atoms by electron impact is reported. Energy dependences of excitation of three K II transitions are also given. (AIP)

30525 INFRARED LASER ENHANCED REACTIONS: SPECTRAL DISTRIBUTION OF THE NO_2 CHEMILUMINESCENCE PRODUCED IN THE REACTION OF VIBRATIONALLY EXCITED O_3 WITH NO. Braun, W. (National Bureau of Standards, Washington, DC); Kurylo, M. J.; Kaldor, A.; Wayne, R. P. J. Chem. Phys.; 61: No. 2, 461-464(15 Jul 1974).

Vibrationally excited ozone, produced by CO_2 laser radiation, was found to react significantly faster with NO than does thermal O_3. The emission spectrum of the laser enhanced chemiluminescence from this reaction was measured from 520 to 810 nm. The lowest lying 1^2B_2 state was identified as the primary source of NO_2^* emission in the NO + O_3 reaction. One quantum of vibrational excitation in the reactant O_3 was found to introduce one quantum of vibrational energy in the product NO_2 (1^2B_2). The rate enhancement of the reaction channel producing $NO_2(1^2B_2)$ as a result of vibrational excitation of O_3 was 5.6 ± 1.0. Thus, only about 50% of the available vibrational energy is used to enhance this reaction. (auth)

30526 DESIGN OF A HIGH DENSITY ATOMIC HYDROGEN SOURCE AND DETERMINATION OF BALMER CROSS SECTIONS. Walker, J.D. Jr.; St. John, R.M. (Department of Physics and Astronomy, University of Oklahoma, Norman, Oklahoma 73069). J. Chem. Phys. 61: No. 6, 2394-2407 (15 Sept 1974).

A high density beam of atomic hydrogen was obtained from a Wood discharge and utilized in the measurement of electron–hydrogen atom collision cross sections. Balmer optical excitation cross sections were determined from observations of crossed electronic and atomic beams. In order to choose Wood discharge parameters to obtain a high degree of dissociation under conditions of a high gas throughput, the differential equations relating the production, loss, and flow of hydrogen atoms and molecules were formulated and solved. The solutions show that recombination of atoms on the metal electrodes greatly reduces the degree of dissociation in large diameter tubes. They further show that this effect can be nearly eliminated by placing short small diameter tubes, called constrictions, between the electrodes and the main tube. A Wood tube 2 cm in diameter and 2 m in length with these constrictions was constructed which produced an atomic to molecular density ratio of 11 at a throughput of 1000 mtorr-liter/sec. The atoms and molecules from the Wood tube were passed through a nozzle and formed into a beam which was crossed with a monoenergetic electron beam. In the crossed beam volume the atomic density was approximately 5.6×10^{12} cm^{-3} and the background molecular density was approximately 3.3×10^{13} cm^{-3}. Optical excitation data were obtained by observation at 90° to the crossed beams with a monochromator and photomultiplier detection system. The ratio of the atomic density with the Wood discharge on to the molecular density with the Wood discharge off in the crossed beam volume was determined from molecular light intensity measurements and a derived relation. Combining this ratio with Balmer optical excitation data with the Wood discharge on and off gave the ratio of the atomic and molecular Balmer cross sections. Absolute molecular Balmer cross sections were measured in a static gas apparatus for use in determining the absolute atomic Balmer cross sections. The atomic Balmer cross sections (in units of 10^{-20} cm^2) for H_α, H_β, H_γ, H_δ, and H_ϵ at 200 eV thus determined are 229.0, 72.4, 22.5, 12.9, and 6.5, respectively. All of these cross sections are within 23% of the theoretical optical cross sections determined under zero electric field conditions. (auth)

30527 INTEGRAL EQUATION APPROACH TO COLLINEAR REACTIVE SCATTERING: $A+BC\rightarrow AB+C$. Adams, J.T.; Smith, R.L.; Hayes, E.F. (Department of Chemistry, William Marsh Rice University, Houston, Texas 77001). J. Chem. Phys. 61: No. 6, 2193-2199 (15 Sept 1974).

An integral equation approach to collinear reactive scattering has been developed. The technique has been implemented on a computer for calculation of scattering matrices for the following reactions: $H+H_2\rightarrow H_2+H$; $D+H_2\rightarrow HD+H$; and $F+H_2\rightarrow HF+H$. The results of these calculations are found to be in good agreement with those obtained by earlier workers. The attractive features of this method are discussed. (auth)

30528 SCATTERING OF ALKALI HALIDES BY ELECTRONS. II. CsCl. Becker, W.G.; Fickes, M.G.; Slater, R.C.; Stern, R.C. (Department of Chemistry, Columbia University, New York, New York 10027). J. Chem. Phys. 61: No. 6, 2283-2289 (15 Sept 1974).

Scattering of CsCl by 0.47 to 15.7 eV electrons has been measured using the molecular beam recoil technique. Center of mass differential cross section models are adjusted to the scattering after transformation to apparatus space. Absolute total cross sections, approximately equal to the first Born approximation point dipole prediction at 15.7 eV, fall to 1/4 of the theory at 0.47 eV. Momentum transfer cross sections are dramatically smaller than the theory at low energies. (auth)

30529 IMPROVED MODIFIED WAVENUMBER APPROXIMATION APPLIED TO ELASTIC COLLISION. Nanbu, K. (Institute of High Speed Mechanics, Tohoku University, Sendai, Japan). J. Chem. Phys. 61: No. 6, 2189-2192 (15 Sept 1974).

A method to improve the usual modified wavenumber result is applied to an elastic collision problem. For an exponential repulsive potential, simple expressions for the phase shift are obtained. The partial cross sections obtained by this improved modified wavenumber approximation agree qualitatively with those of the exact numerical solutions. The total cross sections agree very well with the exact results. (auth)

30530 COMMENT ON THE SEMICLASSICAL SCATTERING OF RIGID SPHERES. Riley, M.E. (Sandia Laboratories, Albuquerque, New Mexico 87115); Siska, P.E. J. Chem. Phys. 61: No. 6, 2485-2485 (15 Sept 1974).

It is shown that the use of WKB phase shifts in certain semiclassical calculations of rigid sphere total cross sections gives more accurate values for the first−order expansion coefficient than the use of classical phase shifts. (AIP)

30531 KINETICS OF THE REACTION BETWEEN OXYGEN ATOMS AND CARBON DISULFIDE. Slagle, I. R.; Gilbert, J. R.; Gutman, D. (Illinois Inst. of Tech., Chicago). J. Chem. Phys.; 61: No. 2, 704-709(15 Jul 1974).

The open channels of the room temperature $O + CS_2$ reaction were identified by studying this reaction in high intensity undiscriminated crossed molecular beams using photoionization mass spectrometry to detect the products. Three open channels were identified: $O + CS_2 \rightarrow CS + SO$ (1); $O + CS_2 \rightarrow OCS + S$ (2); and $O + CS_2 \rightarrow CO + S_2$ (3). The overall rate constant (k) of the $O + CS_2$ reaction as well as the branching ratio (k_2/k) for channel (2) were measured at 302°K using a fast-flow reactor. They are $k = 4.0 \times 10^{-12}$ cm^3 p^{-1} sec^{-1}, and $k_2/k = 0.093$. Speculation on the branching ratios for channels (1) and (3) are offered based on the results of the crossed beam experiments. The possible roles of OCS production by channel (2) and CO production by channel (3) in the performance of the $O + CS_2$ chemical laser are mentioned. (auth)

30532 OBSERVATION OF ORBITING RESONANCES IN THE INTEGRAL CROSS SECTION OF H−Xe. Toennies, J.P.; Welz, W.; Wolf, G. (Max−Planck−Institut für Strömungsforschung, 34 Göttingen, Germany). J. Chem. Phys. 61: No. 6, 2461-2462 (15 Sept 1974).

Scattering theory predicts that the quasibound states of the effective atom−atom potential will lead to sharp resonances in the velocity dependence of the integral cross section at low energies. This phenomenon, called orbiting, is experimentally observed in a beam scattering experiment, using the H−Xe system. (AIP)

30533 ADIABATIC DISTORTED WAVE CALCULATION OF $H + H_2$ REACTIVE SCATTERING. Choi, B.H.; Tang, K.T. (Department of Physics, Pacific Lutheran University, Tacoma, Washington 98447). J. Chem. Phys. 61: No. 6, 2462-2464 (15 Sept 1974).

Previous theoretical studies of $H + H_2$ rearrangement scattering have been made for an adiabatic, distorted wave model and a close−coupling model. In this Communication a calculation is carried out of the $0 \rightarrow 1$ rotational transition cross sections using the adiabatic model, but without the linear assumption used in previous calculations. Comparison of the results indicates that further investigations would be useful. (AIP)

30534 QUANTUM RESONANCE EFFECTS IN ELECTRONIC−TO−VIBRATIONAL ENERGY TRANSFER IN MOLECULAR COLLISIONS. Zimmerman, I.H.; George, T.F. (Department of Chemistry, The University of Rochester, Rochester, New York 14627). J. Chem. Phys. 61: No. 6, 2468-2470 (15 Sept 1974).

Quantum mechanical calculations on halogen−H_2 collisions are carried out in order to investigate the possibility that resonant transfer of energy between vibrational and translational degrees of freedom may occur when the spacings of the relevant energy levels are sufficiently close to being the same. (AIP)

30535 DIFFERENTIAL CROSS SECTIONS FOR THE ELASTIC SCATTERING OF ELECTRONS FROM ATOMIC HYDROGEN. II. Medium Energies. Lloyd, C. R.; Teubner, P. J. O.; Weigold, E.; Lewis, B. R. (Flinders Univ. of South Australia, Bedford Park). Phys. Rev., A; 10: No. 1, 175-181(Jul 1974).

Differential cross sections for the elastic scattering of electrons from atomic and molecular hydrogen were measured at 30, 50, 100, and 200 eV. The results for atomic hydrogen are compared with various theoretical calculations based on both low energy and improved high energy approximations. The ratios of the total cross sections for elastic scattering of electrons from atomic and molecular hydrogen are also given for incident energies of 9.4, 12.0, 20, 30, 50, 100, and 200 eV. (auth)

30536 HIGH-ENERGY CALCULATION OF K-SHELL EJECTION CROSS SECTIONS AS A FUNCTION OF PROJECTILE CHARGE. Reading, J. F.; Fitchard, E. (Texas A and M Univ., College Station). Phys. Rev., A; 10: No. 1, 168-174(Jul 1974).

A high energy calculation of the K-shell ejection cross section $\sigma(Z_p)$ as a function of projectile charge Z_p is presented. Charge-transfer effects are not included. The wave function for the heavy projectile is written as $e^{i\vec{k}_e \cdot \vec{R}} F(-in, 1, ik_e|\vec{R}-\vec{r}| - i\vec{k}_e \cdot (\vec{R}-\vec{r}))\Gamma(1 + in)e^{-n\pi/2}$, as opposed to the Glauber approximation $e^{i\vec{k}_e \cdot \vec{R}} \exp(-in \int_{-\infty}^{Z} dZ|\vec{R}-\vec{r}|^{-1})$. These two approximations agree at large distances but differ as the electron and projectile approach closely to each other. A prediction is made that if T_m (the maximum classical energy an electron at rest may receive) is much greater than I_K then r_{12} will be less than unity. Here $r_{12} = \sigma(Z_1)Z_2^2/\sigma(Z_2)Z_1^2$, $Z_1 > Z_2$. Higher energy experiments are needed to confirm this theoretical result. (auth)

30537 L- AND M-SHELL IONIZATION OF VARIOUS ELEMENTS BY FAST-α-PARTICLE BOMBARDMENT. Thornton, S. T.; McKnight, R. H.; Karlowicz, R. R. (Univ. of Virginia, Charlottesville). Phys. Rev., A; 10: No. 1, 219-224(Jul 1974).

L-shell total ionization cross sections were measured for targets of Sn, Ag, Tb, Bi, and Au from bombardment of 1 to 5 MeV α particles. Similar M-shell x-ray cross sections were obtained for Tb, Bi, and Au. The L-shell cross sections were compared with theoretical calculations from the plane−wave Born approximation, the semiclassical approximation, and the binary-encounter approximation. The latter theory best reproduces the experimental data. A comparison of L-subshell transitions was also made between experiment and the three theories. (auth)

30538 INELASTIC COLLISIONS OF He^+ AND Ar. Isler, R. C. (Univ. of Florida, Gainesville). Phys. Rev., A; 10: No. 1, 117-125(Jul 1974).

Relative emission cross sections were measured for spectral lines in the vacuum ultraviolet region which are produced by collisions of He^+ with Ar over a range of energies from threshold to 10 keV. The lines investigated arise from the following excited states of Ar and Ar^+: for Ar, $3p^54s[^1P, ^3P]$; for Ar^+, $3s3p^6\,^2S$, $3d^2P$, $3d^2D$, $4s^2P$, and $4s'^2D$. Charge exchange at low collision energies is dominated by transfer into the $3s3p^6$ states. The cross section for exciting this configuration rises rapidly from threshold at 4.7 eV to a low energy maximum which occurs at 11.3 eV. By normalizing this data to the absolute emission cross section which has been determined by De Heer et al. at a collision energy of 2 keV, it is found that the cross section for exciting the $3s3p^6$ configuration is 5.4×10^{-17} cm^2 at the low energy maximum. Oscillations are observed in several of the emission cross sections which indicate interferences between the wave functions of one or more of the excited states of the quasimolecule. (auth)

30539 ELECTRON-LOSS CROSS SECTIONS FOR FAST, EXCITED He ATOMS IN H_2. Pedersen, E. H. (Univ. of Aarhus, Denmark). Phys. Rev., A; 10: No. 1, 110-116(Jul 1974).

By means of an optical detection technique, the electron-loss cross sections for He atoms in the excited states 3^3P, 4^3S, 4^1S, 5^3S, and 5^1S were measured in H_2 in the energy range 8 to 160 keV. These cross sections are compared to theoretical cross sections derived by means of the classical impulse approximation of Bates and Walker. In agreement with this theory, the present electron-loss cross sections are found to depend very little on the binding energy and the specific quantum state of the weakly bound electron being removed. Further, they are approximately equal to the total electron-scattering cross section taken at the same impact velocity, as also predicted by the mentioned theory. (auth)

30540 DIFFERENTIAL ELASTIC-SCATTERING MEASUREMENTS OF Xe^+ ON Xe AND Ar^+ ON Ar IN THE 20 TO 340-eV RANGE. Jones, P. R.; Conklin, G. M.; Lorents, D. C.; Olson, R. E. (Stanford Research Inst., Menlo Park, CA). Phys. Rev., A; 10: No. 1, 102-109(Jul 1974).

Relative measurements of the differential cross section for elastic scattering of Xe^+ on Xe and Ar^+ on Ar are reported in the energy range 20 to 340 eV and the angular range 1 to 15 deg (lab). The data are presented in terms of the reduced cross section $\rho(\theta) \equiv \theta \sin \theta\sigma(\theta)$ and the reduced angle $\tau \equiv E\theta$. The ρ-vs-τ plots for Xe^+ on Xe show complex oscillations which are attribute primarily to phase interference in scattering from three coherent pairs of gerade-ungerade potential curves. The six states involved are the electronic fine-structure states of Xe_2^+, four of which dissociate to $Xe + Xe^+(^2P_{3/2})$, and the other two to $Xe + Xe^+(^2P_{1/2})$. At larger values of τ the elastic scattering pattern is further complicated by potential-curve crossings and excitation to higher states, while at smaller τ potential wells give rise to two rainbow peaks. Two oscillatory patterns in the data were resolved from which two difference potentials were determined for Xe_2^+, $\Delta V_{JM}(R) \equiv |V_{JMg}(R) - V_{JMu}(R)|$: $\Delta V_{3/2,1/2} = 23e^{-1.23R}$, $3.5 \lesssim R \lesssim 5.5$; and $\Delta V_{1/2,1/2} = 2.0e^{-0.768R}$, $5 \lesssim R \lesssim 6.5$, in a.u. The Ar^+ on Ar data are in excellent agreement with scattering calculations based upon ab initio computations of the Π_u and Π_g potentials of Ar_2^+. (auth)

30541 ARGON L-SHELL IONIZATION BY 50- TO 600-keV H^+, D^+, H_2^+, AND He^+ IMPACT. Stolterfoht, N.; Schneider, D.; Ziem, P. (Hahn-Meitner-Institut fuer Kernforschung, Berlin). Phys. Rev., A; 10: No. 1, 81-91(Jul 1974).

Production of Auger electrons from the Ar L shell were studied in scattering experiments with 50- to 600-keV H^+, D^+, H_2^+, and He^+ impact on Ar. Electrons ejected at 150° with respect to the incident beam were measured using electrostatic parallel-plate spectrometers. Sets of electron spectra were acquired at different resolutions of 0.35-, 1.4-, and (1.7–2.4)-eV full width of half-maximum. Branching ratios for normal transitions from initial L_2 and L_3 vacancy states are compared with results of others. Satellite structures in the spectra are analyzed to determine probabilities for excitation of multiple-vacancy states $L_{23}M^1$. Intensities of Auger electrons from the L_1 and L_{23} shell are compared for an evaluation of the L_1-shell Coster-Kronig yield. Total cross sections for Ar L-shell ionization are obtained by integration of the Auger spectra and cross section ratios are studied for He$^+$ and D$^+$ impact. (auth)

30542 VARIATIONAL BOUNDS ON THE 1s-CHARGE-EXCHANGE AMPLITUDE IN PROTON–HYDROGEN-ATOM SCATTERING. Storm, D.; Rapp, D. (Univ. of Texas, Dallas). Phys. Rev. Lett.; 33: No. 3, 137-139(15 Jul 1974).

With a relatively simple trial wave function, nontrivial variational bounds are obtained on some transition amplitudes for the 1s-charge-exchange reaction in the impact-parameter model for H$^+$-H scattering. Preliminary results imply that the two-state traveling molecular expansion is superior to the two-state traveling atomic expansion below 25 keV, that the Euler-Lagrange variational method is not necessarily superior to the static method, and that neither is the "best variational method." (auth)

30543 LOW ENERGY ELECTRON COLLISIONS IN GASES: SWARM AND PLASMA METHODS APPLIED TO THEIR STUDY. Gilardini, A. Wiley Series in Plasma Physics. New York; John Wiley and Sons, Inc. (1972). 508p. $27.50.

The topics discussed are the general characteristics of fundamental electron collision processes, the electron distribution function and the transport parameters, experimental methods of measuring transport parameters, and experimental determinations of electron collision parameters. (JFP)

30544 EXCITATION OF SOME BANDS AND LINES IN COLLISIONS OF 0.4 TO 20 keV ELECTRONS WITH CO, CO$_2$, AND O$_2$ MOLECULES. Koval, A. G.; Koppe, V. T.; Danilevskii, N. P.; Popova, L. I. (Kharkov State Univ.). pp 69-80 of Problemy Kosmicheskoi Fiziki. Vsekhsvyatskii, S. K. (ed.). Kiev; Izdatel'stvo Kievskogo Universiteta (1973). (In Russian)

Emission cross sections of some bands of the CO$^+$ comet tail system, CO$^+$ Baldet–Johnson system, CO_2^+ Fox, Duffendack, Barker system, first negative system of O_2^+ and six multiplets of OI and OII excited by electron impact (E = 4kev) were measured. In some cases the relative values of these cross sections were compared with the values calculated with the help of the Frank–Condon factors. The dependence of the electron transition moment Re on internuclear distance r was calculated for the CO$^+$ comet tail system. The excitation functions for some molecular bands and multiplets OI and OII were measured at electrons energies between 0.4 and 20 kev. For analysis of measured excitation functions the Bethe–Born approximation was used. (auth)

30545 POPULATION OF THE ROTATIONAL AND VIBRATIONAL LEVELS OF EXCITED ELECTRONIC STATES OF NITROGEN MOLECULES PRODUCED IN COLLISIONS OF ELECTRONS WITH N$_2$ MOLECULES. Polyakova, G. N.; Erko, V. F.; Zats, A. V.; Fogel, Ya. M. (Kharkov Physical-Technical Inst.). pp 81-84 of Problemy Kosmicheskoi Fiziki. Vsekhsvyatskii, S. K. (ed.). Kiev; Izdatel'stvo Kievskogo Universiteta (1973). (In Russian)

It is shown that the rotational energy level distribution of N_2^+ ions produced in the process of ionization N$_2$ molecules by electrons with energies 30 to 300 eV does not deviate from the Bolzmann distribution. The rotational temperature of the N_2^+ ions is equal to the temperature of the nitrogen gas in the collision chamber. The populations of the vibrational levels v′ = 0 to 4 of the N_2^+ $(B\,\Sigma_u^+)$ ions are investigated in the energy range of electrons 30 to 300 eV. At the electron energies $E > 50$ eV the vibrational levels of N_2^+ ions are populated in accordance with the Franck–Condon principle. At electron energies $E < 50$ eV the abnormal populations of the investigated levels are observed. In collisions of electrons (energy 15 to 75 eV) with N$_2$ molecules the vibrational levels v′ = 0 to 3 of the C_π^3 state of N$_2$ molecule are populated in accordance with the Franck–Condon principle. (auth)

30546 EXPERIMENTAL INVESTIGATION OF THE EFFECTIVE CROSS SECTION OF EXCITATIONS OF BANDS OF SOME DECAY PRODUCTS OF WATER, AMMONIA, AND ACETONITRILE BY SLOW ELECTRONS. Sushanin, I. V. (Uzhgorod State Univ., USSR). pp 85-88 of Problemy Kosmicheskoi Fiziki. Vsekhsvyatskii, S. K. (ed.). Kiev; Izdatel'stvo Kievskogo Universiteta (1973). (In Russian)

The results of investigation of effective cross–sections of excitations of bands of radicals OH, NH, CH and CN by slow electrons are presented. (auth)

30547 CROSSED–MOLECULAR–BEAM STUDY OF THE KINEMATICS AND DYNAMICS OF CHARGE–TRANSFER COLLISIONS. Kaiser, E.W.; Crowe, A.; Falconer, W.E. (Bell Laboratories, Murray Hill, New Jersey 07974). J. Chem. Phys. 61: No. 7, 2720-2726 (1 Oct 1974).

Using a crossed–molecular–beam apparatus, the low energy product ions formed in a variety of resonant and near–resonant charge–transfer collisions at incident ion energies of 200 eV have been examined. Observation of the translational energy and angular distributions of these low energy product ions confirms that charge transfer takes place at large impact parameters with near–zero momentum transfer. (auth)

30548 NEGATIVE ION FORMATION FROM ENERGETIC COLLISIONS OF CESIUM WITH CO$_2$, CS$_2$, AND COS. Tang, S. Y.; Rothe, E.W. (Research Institute for Engineering Sciences and Department of Chemical Engineering, Wayne State University, Detroit Michigan 48202); Reck, G.P. J. Chem. Phys. 61: No. 7, 2592–2595 (1 Oct 1974).

An experiment is described in which cesium atoms, with kinetic energies in the range 10–350 eV, collide with CO$_2$, CS$_2$, and COS. The measured products are negative ions from charge exchange (NICE). The parent anions, CO$_2^-$, CS$_2^-$, and COS$^-$ are observed, as are other fragment ions. Intensity ratios for the various anions are measured as a function of cesium atom energy. The electron affinity of CO$_2$, determined from crude threshold measurements, lies in the range -2.1 to -1.1 eV, with a precision of about ± 0.25 eV. (auth)

30549 THE REACTION OF ATOMIC OXYGEN WITH SEVERAL ATMOSPHERIC IONS. Rutherford, J.A.; Vroom, D.A. (Intelcom Rad Tech, P. O. Box 80817, San Diego, California 92138). J. Chem. Phys. 61: No. 7, 2514-2519 (1 Oct 1974).

Cross sections for reactions of atomic oxygen with the ions H$^+$, O$^+$,N$^+$,N$^+{}_2$, O$^-$, and O$^-{}_2$ have been measured. The ion energies range from 1 to 500 eV. For all ions, the charge transfer processes have been considered. In addition, for N$^+{}_2$ the ion–molecule reaction leading to production of NO$^+$ has been studied. For the charge transfer reactions in which no accidentally resonant pathway exists, cross sections less than 10^{-17} cm^2 at 1 eV were measured. Where accidental resonance occurs, cross sections larger than 10^{-16} cm^2 at 1 eV were found. For N$^+$, both the ground and excited states of the ion were used in the measurements. The method used to form the atomic oxygen beam is discussed. (auth)

30550 EQUATIONS OF MOTION METHOD: INELASTIC ELECTRON SCATTERING FOR HELIUM AND CO$_2$ IN THE BORN APPROXIMATION. McCurdy, C.W. Jr.; McKoy, V. (Arthur Amos Noyes Laboratory of Chemical Physics, California Institute of Technology, Pasadena, California 91109). J. Chem. Phys. 61: No. 7, 2820-2826 (1 Oct 1974).

We have applied the equations of motion method to the computation of generalized oscillator strengths in helium and CO$_2$. The equations of motion approach yields excitation energies without the computation of separate ground and excited state wavefunctions, and is ideally suited for computing matrix elements of the operator used in the Born approximation. Our results for helium agree well with more extensive calculations [Y. Kim and M. Inokuti, Phys. Rev. 175, 176 (1968)]. We compare our generalized oscillator strengths for CO$_2$ with experiment, and discuss assignments including the peaks at 8.61 and 9.16 eV in the experimental energy loss spectrum. We also compute a valencelike $^1\Sigma^+{}_u$ state below the first ionization potential with a large oscillator strength ($f = 0.64$), which may be responsible for the proposed continuum absorption between 11–14 eV in CO$_2$. (auth)

30551 RAMAN PROCESS IN THE CASE OF MULTIPHOTON EXCITATION OF THE HYDROGEN MOLECULE IN AN INTENSE LASER BEAM. Devi, U.; Bhatnagar, S. (Univ. of Delhi). J. Phys., B (London); 7: No. 10, 1122–1130(11 Jul 1974).

The reduced transition amplitude for the multiphoton excitation with the emission of one Raman photon of the hydrogen molecule due to an intense EM field from the ground state $1s\sigma^1\Sigma_g^+$ to the excited state $B2p\sigma^1\Sigma_u^+$ has been calculated using a method due to Reiss (Phys. Rev. A.; 1: 803-18 (1970)). The intensity dependence of the transition probability has been numerically investigated. A major feature of the curve is the oscillatory behaviour for larger values of N where N is the number of photons absorbed in the process. (auth)

30552 TOTAL CROSS-SECTION CORRESPONDING TO THE DIFFERENTIAL CROSS-SECTION OF LINDHARD, NEILSEN, AND SCHARFF. Mueller, G. P. (Naval Research Labs., Washington, DC). Radiat. Eff.; 21: No. 4, 253-254(1974).

An exact expression is presented for the total cross-section associated with the Winterbon, Sigmund and Sanders (Mat. Fys. Medd. Dan. Vid. Selsk.; 37: No. 14 (1970)) version of the Lindhard, Nielsen and Scharff (Mat. Fys. Medd. Dan. vid. Selsk.; 36: No. 10 (1968)) differential cross-section for heavy ion-atom scattering. A series expansion form of the same quantity is also given. (auth)

30553 NEW TECHNIQUE FOR THRESHOLD EXCITATION SPECTROSCOPY. Cvejanovic, S.; Read, F. H. (Univ. of Manchester, Eng.). J. Phys., B (London); 7: No. 10, 1180-1193(11 Jul 1974).

A new technique has been developed for obtaining high resolution threshold excitation spectra in electron-atom and electron-molecule collisions. A very weak field penetrating into the target chamber produces a saddle point in the potential distribution which has the effect of focusing and enhancing the extraction efficiency of very low energy inelastically scattered electrons. Also the electron energy analyzer is used in a special mode which sharpens the pass band for low energy electrons. Examples of threshold excitation spectra of He, Ar, and N_2 are given, and the onsets of the 2^3S and 2^1S states of helium have been used to determine accurately the energy (19.361 ± 0.009 eV) of the 2^2S resonance in helium. (auth)

30554 ACCURATE TOTAL INELASTIC CROSS SECTION FOR H_2^+ COLLIDING WITH FAST CHARGED PARTICLES IN THE ADIABATIC APPROXIMATION. Liu, J. W. (Univ. of Indiana, Bloomington). Mol. Phys.; 28: No. 2, 343-351(Aug 1974).

A sum rule for the total inelastic cross section of H_2^+ colliding with fast charged particles is evaluated in the first Born approximation using the clamped nuclei [Born–Oppenheimer (B.O.)] wave function and the adiabatic wave function. The vibrational correction to this cross section is of almost the same magnitude for both wave functions, and its value is about 5 per cent of the total. The parameters for the sum rule which depend upon the internuclear distance R are evaluated from $R = 1.4\ a_0$ to $R = 2.6\ a_0$ for the B.O. wave function. These parameters are found to have better asymptotic behavior for small R than for large R. The experimental values of the total cross sections of proton production processes measured by the swarm technique are twice as large as the theoretical ones. Calculations for various internuclear distances (i.e., for various excited vibrational states of the ground electronic state) are also compared with experiment. It is found that the proton production cross section mainly results from electron impact on H_2^+ molecules in the vibrationally excited electronic ground state. Assuming that v = 2 is the most populous vibrational state, it is found that the B.O. or adiabatic approximations to the wave function underestimate the experimental value of the cross section, which seems to indicate that rotational and vibrational excitation dissociation processes may make a significant contribution. (auth)

30555 CARBON K-SHELL X-RAY PRODUCTION BY NEON ION IMPACT. Piacentini, R. D.; Salin, A. (Rosario Univ. Nacional, Argentina). J. Phys., B (London); 7: No. 10, L311-L313 (11 Jul 1974).

A one-electron two-centre model is proposed for calculations, in a molecular approximation, on vacancy production in the K-shell of atoms by heavy ion impact. Results are given and compared with available experimental measurements for Ne^+–C collisions. (auth)

30556 ATOMIC EXCITATION PROCESSES IN THE DISCHARGES OF RARE GAS ION ENGINES. Martin, A. R. (City Univ., London). J. Phys., B (London); 7: No. 10, 1161-1166 (11 Jul 1974).

The influence of metastable and short-lived excited states produced by electron-bombardment of atoms in the discharge plasma of ion engines using the rare gases has been considered. Theoretical Gryzinski cross sections (Phys. Rev.; 115: 374 (1959) and Phys. Rev.; 138: 336 (1965)) were used to investigate the effects of collisions on the excited states of the atoms. It was found that metastable atoms are rapidly excited to higher states from which ground-state transition is allowed, because of the large cross sections for this excitation, and that predicted electron energy losses due to atomic excitation collisions gave good agreement with experiment in the case of argon, krypton and xenon. Operation with neon, however, was anomalous. (auth)

30557 OUTER S-SHELL IONIZATION OF NEON, ARGON, AND KRYPTON BY PROTON IMPACT (125 keV-1200 keV). Hippler, R.; Schartner, K. H. (Univ., Giessen, Ger.). J. Phys., B (London); 7: No. 10, 1167-1173(11 Jul 1974).

The ionization of the neon 2s-, argon 3s-, and krypton 4s-shell has been studied by proton impact in the energy range 125 keV to 1200 keV. Total cross sections have been obtained by measuring light intensities resulting from the decay of the excited ions; the corresponding wavelengths lie in the vacuum ultraviolet region. The cross sections have been made absolute by comparing the signal rates resulting from 1 keV electron impact and 400 keV proton impact and using the known electron impact cross sections. The results are compared with electron impact data and with theoretical data. (auth)

30558 VIBRATIONAL ENERGY DISTRIBUTION IN CO_2^+ (A^2PI_u) IONS PRODUCED BY COLLISIONS OF H_2^+ AND He^+ IONS WITH CO_2. Bregman-Reisler, H.; Doering, J. P. (Johns Hopkins Univ., Baltimore, Md. (USA). Dept. of Chemistry). Chem. Phys. Lett.; 27: No. 2, 199-202(15 Jul 1974).

The relative populations of vibrational levels in the $A^2\Pi_u$ state of CO_2^+ were derived from measured band intensities of the CO_2^+ $A^2\Pi_u \rightarrow X^2\Pi_g$ emission system excited by charge transfer collisions of 100–5000 eV H_2^+ and He^+ ions with CO_2. At relative laboratory velocities above 4×10^7 cm/sec the vibrational energy distribution was independent of velocity, but differed from that obtained by photoelectron spectroscopy. At velocities below 4×10^7 cm/sec the relative populations of low vibrational states increased monotonically with decreasing projectile ion velocity. (auth)

30559 OPTICAL POTENTIAL CALCULATIONS FOR MOLECULAR COLLISIONS. Zimmerman, I. H.; George, T. F. (Rochester Univ., N. Y. (USA). Dept. of Chemistry). Chem. Phys. (Amsterdam); 4: No. 3, 315-336(Jun 1974).

The Feshbach optical formalism is applied to elastic nonreactive atom–diatom scattering on a single potential energy surface. The optical potential depends on G_Q, the resolvent of E–QHQ, where Q projects onto open as well as closed channels. A method for generating G_Q is developed which goes beyond the free-space approximation by partitioning the radial part of the intermolecular separation into a set of intervals, on each of which the projected interaction QVQ is represented by a constant diagonal form. The resulting G_Q is used in calculations on a model collinear system. The calculations are carried out with various approximations on the full nonlocal optical potential equation for $P\Psi$. Emphasis is placed on two of these, one of which is characterized by a local homogeneous equation for $P\Psi$, and the other by a local inhomogeneous equation for $P\Psi$. (auth)

30560 EQUIVALENCE AND CONSERVATION RULES FOR THE TOTAL INTEGRAL CROSS SECTION IN MOLECULAR COLLISIONS. McGuire, P. (Max-Planck-Institut fuer Stroemungsforschung, Goettingen (F.R. Germany)). Chem. Phys. (Amsterdam); 4: No. 3, 483-491(Jun 1974).

The rule of conservation of the total integral cross section $\sigma_T(j)$ is described in a general way using the opacity function. An equivalence rule which states that at the same initial kinetic energy, the total integral cross section from the initial state j is equal to that from the initial state j′, i.e., $\sigma_T(j) = \sigma_T(j)$ is also presented. Both rules are demonstrated with numerical examples in the He + H_2 collision system and counter-examples are also presented. Possible uses of the rules in the inversion of the intermolecular surface and as an experimental tool are also discussed. (auth)

30561 ENTROPY ANALYSIS OF PRODUCT ENERGY DISTRIBUTIONS IN NONREACTIVE INELASTIC COLLISIONS. Rubinson, M.; Steinfeld, J. I. (Massachusetts Inst. of Tech., Cambridge (USA). Dept. of Chemistry). Chem. Phys. (Amsterdam); 4: No. 3, 467-475(Jun 1974).

Final state distributions for inelastic collisions of I_2^* with rare gas atoms are analyzed with the recently introduced surprisal function. Both experimental data and classical trajectory results are compared. Both vibrational and rotational state distributions follow linear surprisal plots, with fairly large values of $\lambda = dI(\Delta E)/d(\Delta E)$, indicating relatively weak coupling between internal and translational degrees of freedom. The λ_v and λ_j values appear to be relatively independent of the initial state of the excited molecule and of the collision partner. (auth)

30562 DIMENSIONALITY CONTROL OF COUPLED SCATTERING EQUATIONS USING PARTITIONING TECHNIQUES. Englot, G.; Rabitz, H. (Princeton Univ., N. J. (USA). Dept. of Chemistry). Chem. Phys. (Amsterdam); 4: No. 3, 458-466(Jun 1974).

A method of variable reduction of the dimensionality of the coupled equations for inelastic scattering is presented, based upon a projection operator P with a restricted range of orbital angular momentum states. For rotational states in the range $0 \leq j \leq j^*$ and total angular momentum large, the coupled equations have dimensionality $(j^* + 1) \leq N \leq (j^* + 1)^2$, where the value of N is controlled by the choice of P. This is in contrast to conventional partitioning techniques which utilize further restrictions on the important molecular rotational states. The equations for the P subspace and its complementary Q subspace are decoupled by an approximation on the equation of motion of $Q\Psi_{scat}$. Information about scattering into the Q subspace is retained, within this degree of approximation, and is reintroduced at the end of the computation with little additional labor. The theory is developed in terms of atom–rigid-rotor scattering, although addition of vibrational modes would not in any way interfere with the basic techniques used. (auth)

30563 THE COLLINEAR COLLISION OF TWO DIATOMIC MOLECULES. An Application of the Adiabatic Approximation and the T- and K-Matrix Methods. Clarke, J. H.; Thiele, E. (Johns Hopkins Univ., Baltimore, Md. (USA). Dept. of Chemistry). Chem. Phys. (Amsterdam); 4: No. 3, 447-457(Jun 1974).

A "partial decoupling" scheme is presented by which the collinear collision of two diatomics is reduced to an atom–diatomic collinear collision with new definitions for the parameters E, m, and α. The pseudo atom–diatomic problem is studied using the adiabatic approximation of Thiele and Katz and the first order distorted wave T- and K-matrix methods. The results are compared with the numerical results of Riley and Kuppermann and it is concluded that their results are reliable only for the transitions 00 → 01 and 01 → 10. A set of "corrected" adiabatic transition probabilities is prepared and the approximate T- and K-matrix results are compared with this set. The accuracies of these approximate methods are then seen to be consistent with earlier conclusions concerning the application of the first order distorted wave approximation to atom–diatomic collinear collisions. (auth)

30564 FINITE-DIFFERENCE BOUNDARY-VALUE METHOD FOR DETERMINATION OF RESONANCE WIDTHS IN ATOMIC COLLISIONS. Truhlar, D. G. (Minnesota Univ., Minneapolis (USA). Dept. of Chemistry). Chem. Phys. Lett.; 26: No. 3, 377-380(1 Jun 1974).

A new quantum mechanical procedure, using the finite-difference boundary-value method and an equation derived by Hazi and Taylor for the stabilization method, is proposed for finding the widths or lifetimes of resonance states in atomic collisions. Numerical illustrations are presented. (auth)

Atomic Theory

Refer also to abstracts 30655 and 31459.

30565 (LA-5694-MS) THOMAS–FERMI CALCULATION OF POTENTIAL BETWEEN ATOMS. Lee, C. E.; Longmire, C. L.; Rosenbluth, M. N. (Los Alamos Scientific Lab., N. Mex. (USA)). Jul 1974. Contract W-7405-eng-36. 4p. Dep. NTIS $4.00.

A Thomas–Fermi model calculation of the potential energy for the collision of two neutral, identical atoms is developed. The classical scattering distribution for this potential is compared to Rutherford scattering. (auth)

30566 DEGENERATE PERTURBATION THEORY. Klein, D. J. (Univ. of Texas, Austin). J. Chem. Phys.; 61: No. 3, 786-798(1 Aug (1 Aug 1974).

A number of different perturbation formulations found in the literature are discussed. Although these formulations are derived in quite different ways, simple relations among these derivations are described and, in fact, some are shown to yield identical results. One of these degenerate perturbation theories resulting from different formulations due to Van Vleck, Kemble, and Primas, to des Cloizeaux, and to Buleavski is considered in greater detail. Its linked and cluster expansion properties and some other resummation techniques are briefly discussed. (auth)

30567 IMPROVED FIRST ORDER PERTURBATIVE CALCULATION OF THE GROUND STATE ENERGY OF ATOMS. Leal de Santos, M.; Santos, E. (Departamento de Optica, Universidad de Valladolid, Valladolid, Spain). J. Chem. Phys. 61: No. 6, 2471-2471 (15 Sept 1974).

It is shown that a fairly good approximation to the ground state energy of an atom or molecule is given by $E_0 \exp(E_1/E_0)$, where $E_0(E_1)$ is the zero (first) order perturbation calculation of the energy when the electron repulsion is taken as the perturbing term. (AIP)

30568 SELF-CONSISTENT TIME-DEPENDENT HARTREE–FOCK SCHEME. Joergensen, P. (Univ. of Aarhus, Denmark); Oddershede, J.; Ratner, M. (Univ. of Aarhus, Denmark). J. Chem. Phys.; 61: No. 2, 710-718(15 Jul 1974).

A self-consistent time-dependent Hartree–Fock scheme based on a Green's function approach was derived. The contour integral is performed analytically, which makes the computational effort per iteration comparable with a normal time-dependent Hartree–Fock calculation. The excitation energies are found as poles for the polarization propagator in the energy representation. The corresponding residues determine the transition moments. Comparison is made with other similar random-phase approximations. The scheme was applied to the π-electron systems of trans-butadiene, pyridine, and benzene. The triplet spectra of those molecules especially are considerably improved over normal time-dependent Hartree–Fock results. (auth)

30569 PLAUSIBLE ASSERTIONS FOR BUILDING-UP THE WAVE FUNCTIONS OF THE ATOMS WITH A SINGLE VALENCE ELECTRON. Ionescu-Pallas, N. J. (Institutul de Fizica Atomica, Bucharest). Stud. Cercet. Fiz.; 25: No. 2, 167-182(1973). (In Rumanian).

Analytic atomic wave functions having a structure similar to that arising in the hydrogen case were constructed. They account for many features of the atoms or ions with a single valence electron, such as the number of zeros and the asymptotic behavior of the functions (including the Slater limit for $r \to \infty$), the Ritz formula for the energy levels, the maintaining of the hydrogen-like spectral classification, etc. An approximate normalization of the wave functions was performed, by resorting to a semiclassical procedure corroborated with the trend of the functions in the vicinity of the nucleus. (auth)

PHYSICS (ELECTROFLUID AND MAGNETOFLUID)

30570 DEVELOPMENTS IN MECHANICS. Volume 7. Proceedings of the 13th Midwestern Mechanics Conference Held at Pittsburgh, Pennsylvania, August 13–15, 1973. Midwestern Mechanics Conference Publication. Pittsburgh; University of Pittsburgh (1973). 1055p. (CONF-730818-).

Seventy-one papers are included. A separate abstract was prepared for one. The remaining papers treated various topics in fluid mechanics and solid mechanics. (MHR)

For an abstract of an individual paper see: 30571.

30571 MHD FLOW IN VARIABLE-AREA CONDUCTING RECTANGULAR DUCTS. Walker, J. S. (Univ. of Illinois, Urbana); Ludford, G. S. S. pp 265-276 of Developments in Mechanics. Vol. 7. Pittsburgh; Univ. of Pittsburgh (1973).

From 13th midwestern mechanics conference; Pittsburgh, Pennsylvania, USA (13 Aug 1973). See CONF-730818-.

The flow of a liquid metal in a diverging or converging duct of rectangular cross section with perfectly conducting walls and an applied transverse magnetic field is studied. The field is assumed to be sufficiently strong for inertia to be neglected and for viscous effects to be confined to thin boundary layers. It is found that in the layers adjacent to the walls parallel to the magnetic field there is an overshoot in part of the velocity profile, which exactly cancels the deficiency in the rest of the profile. Consequently, the displacement thickness of each layer is zero and the inviscid core flow is not disturbed by the presence of these walls. Since three-dimensional MHD duct flows are normally quite different from their two-dimensional, fully developed counterparts, the present solution is remarkable in its close resemblance to the corresponding solution for a constant-area duct. (auth)

30572 METHOD AND DEVICE FOR MAGNETOHYDRODYNAMICALLY CONTROLLING THE FLOW RATE OF AN ELECTRICALLY CONDUCTIVE LIQUID. Gelfgat, J. M.; Lielausis, O. A.; Sunakslis, Y. M.; Shtern, A. G. (to Inst. of Physics, Academy of Sciences, Latvian, SSSR). British Patent 1,353,556. 22 May 1974. 9p.

Some disadvantages of conventional methods of controlling the flow rate of an electrically conducting liquid between the poles of a magnetic system are stated. In the method described regions are set up in this flow region having different conditions for current induction. This may be achieved by variations in the density of the magnetic field, by varying the flow velocity of the liquid, by varying the heat exchange of the liquid flow with the surrounding medium, or by varying the removal of electrical energy from the flow by the surrounding medium. Suitable devices are described. At least one pole of the magnetic system may have a number of alternating protrusions and recesses, or the pole may take the form of a set of plates with at least one plate mounted so as to be movable relative to the other plates. Alternatively the flow channel may have alternate widenings and contractions. It may also be provided with an external cooling jacket to vary the heat exchange, or it may have portions of different electrical conductivity. (UK)

30573 THE SKIN FRICTION ON ACCELERATED PLATES IN MAGNETOHYDRODYNAMICS. Wilks, G. (Strathclyde Univ., Glasgow (UK). Dept. of Mathematics). Appl. Sci. Res. (The Hague); 29: No. 2, 121-129(Apr 1974).

A uniform transverse magnetic field acts across an infinite flat plate immersed in a conducting fluid of arbitrary magnetic Prandtl number. The skin friction on the plate for the class of accelerated motions Ut^k is discussed for (a) a perfect conductor and (b) an insulator. Residual stresses are demonstrated in both instances. (auth)

PHYSICS (HIGH-ENERGY)

Particle Interactions and Properties (Experimental)

30574 (COO-1428-391) ANNUAL REPORT FOR PERIOD OCTOBER 1, 1973–SEPTEMBER 30, 1974. Fowler, E. C. (Purdue Univ., Lafayette, Ind. (USA)). 1974. Contract AT(11-1)-1428. 12p. Dep. NTIS $4.00.

Research is reported on various high energy physics experiments and on the feasibility of a muon monitor. (JFP)

30575 (TID-26638) HIGH ENERGY ACCELERATOR AND COLLIDING BEAM USER GROUP. Progress Report. (Maryland Univ., College Park (USA). Dept. of Physics and Astronomy). 1974. Contract AT(40-1)-2504. 30p. Dep. NTIS $4.50.

Research on experimental programs on strong, electromagnetic, and weak interactions is summarized. A list of publications is included. (JFP)

30576 (UCID-15787) CLOUD CHAMBER QUARK QUEST ONE YEAR REPORT. Clark, A. F.; Finn, H. F.; Hansen, N. E.; Smith, D. E.; Powell, W. M. (California Univ., Livermore (USA). Lawrence Livermore Lab.). Dec 1970. 39p. Dep. NTIS $5.00.

Experimental research on a search for quarks is reported. (JFP)

30577 PROCEEDINGS OF THE FIFTH HAWAII TOPICAL CONFERENCE IN PARTICLE PHYSICS, HONOLULU, HAWAII, AUGUST 8–21, 1973. Dobson, P. N. Jr.; Peterson, V. Z.; Tuan, S. F. (eds.). Honolulu, HI; University Press of Hawaii (1974). 718p. (CONF-730856-). $15.00.

Four papers are presented; a separate abstract is prepared for each paper. (LBS)

For abstracts of individual papers see: 30578, 30594, 30681, and 30691.

30578 EXPERIMENTAL REVIEW OF STRONG INTERACTIONS AT HIGH ENERGY. Morrison, D. R. O. (CERN, Geneva). pp 183-499 of Proceedings of the Fifth Hawaii Topical Conference in Particle Physics. Dobson, P. N. Jr. (ed.). Honolulu, HI; Univ. Press of Hawaii (1974).

From 5th topical conference in partial physics; Honolulu, Hawaii, USA (8 Aug 1973). See CONF-730856-.

Recent experimental results are reviewed. Brief comments are first given on resonances, quasi two-body reactions, and search for quarks. The following subjects are then discussed: total and inelastic cross sections; elastic scattering; concepts and models of reaction mechanisms; scaling–single particle distributions; multiplicity distributions; transverse momentum; charge distributions and quantum number exchange; correlations; diffraction dissociation; and phenomenological picture of high-energy reactions. (LBS)

30579 SEARCH FOR HEAVY PARTICLES IN COSMIC RAYS. Yock, P. C. M. (Auckland Univ. (New Zealand). Dept. of Physics). Nucl. Phys., B; 76: No. 1, 175-181(4 Jul 1974).

A search for heavy, long-lived particles has been made in the cosmic rays. The observations may possibly be explained in terms of known particles, but they appear to be more easily explained in terms of a flux $\geq 6.10^{-9}$ cm^{-2} sec^{-1} sr^{-1} of singly charged particles having mass $\gtrsim 6$ m_p. (auth)

Electromagnetic

Refer also to abstract 30874.

30580 (AD-773442) COHERENT SYNCHROTRON RADIATION FROM AN INTENSE RELATIVISTIC ELECTRON BEAM. Granatstein, V. L.; Herndon, M.; Parker, R. K.; Sprangle, P. (Naval Research Lab., Washington, D. C. (USA)). Jan 1974. 15p. NTIS $3.00.

When an intense relativistic electron beam was made to traverse a magnetic field of novel configuration, about 25 MW of microwave power was measured in a narrowband pulse $\delta\omega/\omega \leq 0.6\%$ centered near the relativistic electron cyclotron frequency. The emission angle was almost perpendicular to the applied magnetic field. The measured power is 10 to the 6th power larger than what can be accounted for on the basis of single particle synchrotron radiation. The process is thought to be similar to that previously reported in a low power (about 1 W) electron cyclotron maser. (auth)

30581 (RL-74-098) PHYSICS WITH AN ELECTRON–POSITRON STORAGE RING OF BEAM ENERGY E = 14 GeV. (Science Research Council, Chilton (UK). Rutherford Lab.). Jun 1974. 23p. Dep. NTIS (US Sales Only) $4.25.

It is stated that for the energy region under consideration, the electron–positron system can be used to study a wide range of fundamental physical interactions, which are considered under the following headings: hadron production in electron–positron annihilation; quantum electrodynamics (QED); weak interaction effects; nonannihilation production processes. (UK)

30582 OBSERVATION OF THE DECAY $K_L{}^0 \rightarrow \pi^+\pi^-\gamma$. Donaldson, G.; Hitlin, D.; Kennelly, R.; Kirkby, J.; Liu, J.; Rothenberg, A.; Wojcicki, S. (Physics Department and Stanford Linear Accelerator Center, Stanford University, Stanford, California 94305). Phys. Rev. Lett. 33: No. 9, 554-557 (26 Aug 1974).

We have measured the ratio Γ $(K_L{}^0 \rightarrow \pi^+\pi^-\gamma)/\Gamma$ $(K_L{}^0 \rightarrow \text{all})$ to be $(6.2 \pm 2.1) \times 10^{-5}$. The rate and Dalitz–plot distribution are consistent with CP conservation in this weak–electromagnetic decay. (auth)

30583 EXTRACTION OF $R = \sigma_L/\sigma_T$ FROM DEEP INELASTIC e–p AND e–d CROSS SECTIONS. Riordan, E.M.; Bodek, A.; Breidenbach, M.; Dubin, D.L.; Elias, J.E.; Friedman, J.I.; Kendall, H.W.; Poucher, J.S.; Sogard, M.R. (Physics Department and Laboratory for Nuclear Science, Massachusetts Institute of Technology, Cambridge, Massachusetts 02139); Coward, D.H. Phys. Rev. Lett. 33: No. 9, 561-564 (26 Aug 1974).

The quantity $R = \sigma_L/\sigma_T$ is extracted for the proton, deuteron, and neutron from deep inelastic e–p and e–d scattering cross sections measured in recent experiments at Stanford Linear Accelerator Center. For $\omega \leqslant 5$ the kinematic behavior of νR_p is consistent with scaling, indicative of spin–1/2 constituents in a parton model of the proton. We also find that, within large statistical errors, R_d and R_n are consistent with being equal to R_p. (auth)

30584 MUON–DEUTERON DEEP INELASTIC SCATTERING. Kim, I.J.; Entenberg, A.; Jöstlein, H.; Königsmann, K.; Kostoulas, I.; Melissinos, A.C.; Aslanides, E.; Lederman, L.; Limon, P.; May, M.; Rapp, P.; Gittleson, H.; Kirk, T.; Murtagh, M.; Tannenbaum, M.J.; Sculli, J.; White, T.; Yamanouchi, T. (Department of Physics and Astronomy, University of Rochester, Rochester, New York 14627). Phys. Rev. Lett. 33: No. 9, 551-554 (26 Aug 1974).

We have measured deep inelastic muon–deuteron scattering in the range $0.4 < Q^2 < 3.4$ and $1.6 < \nu < 5.6$ GeV. We have extracted the neutron structure function and find that $\nu W_2{}^n$ differs significantly from $\nu W_2{}^p$, as also found in e–d scattering. To compare μ–d and e–d scattering we form the ratio $r(Q^2) = (\nu W_2)_\mu{}^d/(\nu W_2)_e{}^d = N(1 + Q^2/\Lambda^2)^{-2}$, and find $N = 0.925 \pm 0.038$ and $1/\Lambda^2 = -0.019 \pm 0.016$. (auth)

30585 RADIO PULSES FROM EXTENSIVE AIR SHOWERS DURING THUNDERSTORMS: THE ATMOSPHERIC ELECTRIC FIELD AS A POSSIBLE CAUSE. Mandolesi, N.; Morigi, G.; Palumbo, G. G. C. (Consiglio Nazionale delle Ricerche, Bologna). J. Atmos. Terrest. Phys.; 36: No. 8, 1431-1435(Aug 1974).

Radio pulses from extensive air showers were observed during thunderstorms. The measured RF electric fields in the pulses observed at 46 to 65 and 110 MHz cannot be explained by the geomagnetic charge separation theory. Alternative causes are discussed; it is proposed that the thundercloud electric field is responsible for the observed pulses. (auth)

30586 PHOTOPRODUCTION OF π^- FROM DEUTERIUM AT LABORATORY ENERGIES 600 TO 1250 MeV. Scheffler, P. E.; Walden, P. L. (California Inst. of Tech., Pasadena (USA)). Nucl. Phys., B; 75: No. 1, 125-158(11 Jun 1974).

The differential cross section for the reaction $\gamma n \rightarrow \pi^- p$ was measured for laboratory photon energies between 600 and 1250 MeV, using a liquid deuterium target. The experiment used three different techniques to measure 900 independent cross section values. The measurements from the two most reliable techniques were then interpolated and averaged to produce a final sample of 343 cross section measurements covering 29 lab. photon energies. The data show that the amplitude to excite the $F_{15}(1688)$ resonance is small, in agreement with a quark model prediction. (auth)

30587 MEASUREMENTS OF INCLUSIVE PION ELECTROPRODUCTION. Bebek, C. J.; Brown, C. N.; Herzlinger, M.; Lichtenstein, C. A.; Pipkin, F. M.; Sisterson, L. K. (Harvard Univ., Cambridge, Mass. (USA). Cyclotron Lab.); Andrews, D.; Berkelman, K.; Cassel, D. G.; Hartill, D. L. (Cornell Univ., Ithaca, N. Y. (USA). Lab. of Nuclear Studies). Nucl. Phys., B; 75: No. 1, 20-46(11 Jun 1974).

Measurements of the inclusive pion electroproduction reaction $e^- + p \rightarrow e^- + \pi^\pm + X$ made at the Wilson Synchrotron Laboratory are reported. Data were taken at points with nominal (Q^2,W) values of (0.6, 2.67), (1.2, 2.67), (2.0, 2.67) and (1.2, 2.15) in (GeV^2, GeV). A more complete angular distribution was taken at (1.2, 2.67). The virtual photoproduction cross section for π^+ + missing mass is studied as a function of missing mass, Feynman scaling variables, Q^2 and W. The invariant cross section shows a simple behavior as a function of Q^2 and W. Its dependence on $P_\perp^2$, χ and ϕ is determined. (auth)

30588 π^0-ELECTROPRODUCTION ON HYDROGEN NEAR THRESHOLD AT FOUR-MOMENTUM TRANSFERS OF 0.2, 0.4 AND 0.6 GeV^2. Brauel, P.; Buesser, F. W.; Canzler, Th.; Cords, D.; Dix, W. R.; Felst, R.; Grindhammer, G.; Kollmann, W. D.; Krehbiel, H.; Meyer, J. (Deutsches Elektronen-Synchrotron (DESY), Hamburg (F.R. Germany)). Phys. Lett., B; 50: No. 4, 507-510(24 Jun 1974).

The reaction $e + p \rightarrow e + \pi^0 + p$ was measured near the one pion threshold by detecting the final electron and proton in coincidence for values of $q^2 = 0.2$, 0.4 and 0.6 GeV^2. The slope of the cross section at threshold is determined. The data are compared with those of the $e + p \rightarrow e + \pi^+ + n$ reaction, measured simultaneously, and with the results of pseudovector Born approximation and with dispersion theoretical calculations. (auth)

30589 π^0 ELECTROPRODUCTION AT THE $\Delta(1236)$ RESONANCE AT A FOUR-MOMENTUM TRANSFER OF $q^2 = 0.3$ (GeV/c)^2. Baetzner, K.; Beck, U.; Becks, K. H.; Drees, J.; Knop, G.; Kolanoski, H.; Leenen, M.; Moser, K.; Nietzel, Ch.; Schloesser, E.; Stier, H. E. (Bonn Univ. (F.R. Germany). Physikalisches Inst.). Nucl. Phys., B; 76: No. 1, 1-14(4 Jul 1974).

The reaction $e^- + p \rightarrow e^- + p + \pi^0$ has been studied in the region of the $\Delta(1236)$ resonance at a four-momentum transfer of the virtual photon of 0.3 (GeV/c)^2. Angles and momenta of the secondary electron and of the outgoing proton were measured in coincidence to obtain the angular dependence of the differential cross section. The angular distribution for s- and p-waves of the pion in the πN cm-system was fitted to the cross section for three W-bins around the maximum of the resonance. The contribution of the resonant multipoles M_{1+}, E_{1+} and S_{1+} to the cross section as well as the contribution of the background amplitudes M_{1-}, E_{0+} and S_{0+} are given. (auth)

30590 UPPER LIMIT ON THE $\rho^0 \rightarrow \eta\gamma$ BRANCHING RATIO. Nordberg, M. E. Jr. (Cornell Univ., Ithaca, N. Y. (USA). Lab. of Nuclear Studies); Abramson, J.; Andrews, D.; Harvey, J.; Lobkowicz, F.; May, E.; Nelson, C.; Singer, M.; Thorndike, E. H. (Rochester Univ., N. Y. (USA). Dept. of Physics and Astronomy). Phys. Lett., B; 51: No. 1, 106-108(3 Jul 1974).

An improved upper limit for the $\rho^0 \rightarrow \eta\gamma$ branching ratio is reported. Vector mesons are coherently photoproduced by a 7 to 9 GeV tagged photon beam incident on a copper target. Those undergoing radiative decays $V \rightarrow P\gamma$ and $P \rightarrow \gamma\gamma$ result in a final state of three gamma rays. The gamma rays pass through a magnetic field and three planes of anticoincidence counters and are then converted in 1½ radiation lengths of lead. Shower positions are measured in magnetostrictive-readout, strip spark chambers. Shower energies are measured in a 16-element, lead-perchlorate-filled Cherenkov shower counter. The branching ratio for $\rho^0 \rightarrow \eta\gamma$ is determined to be less than 0.1% at the 90% confidence level. (NL)

30591 ELECTROPRODUCTION OF η-MESONS AT THE $S_{11}(1535)$ RESONANCE. Beck, U.; Becks, K. H.; Burkert, V.; Drees, J.; Dresbach, B.; Gerhardt, B.; Knop, G.; Kolanoski, H.; Leenen, M.; Moser, K. (Bonn Univ. (F.R. Germany). Physikalisches Inst.). Phys. Lett., B; 51: No. 1, 103-105(8 Jul 1974).

The reaction $e^- + p \rightarrow e^- + p + \eta$ has been studied in the region of the $S_{11}(1535)$-resonance by detecting the recoil proton in coincidence with the scattered electron. The reaction has been observed at three four-momentum transfers of the virtual photon: $q^2 = 0.2$, 0.28 and 0.4 (GeV/c). First results of the differential cross section measurements are given and compared with quark model calculations. (auth)

Weak

Refer also to abstracts 30892 and 30902.

30592 (JINR-E2-7402) $K_L^0 \rightarrow K_S^0$ INCOHERENT REGENERATION ON ATOMIC ELECTRONS AT HIGH ENERGIES AND ELECTRIC RADIUS OF K^0 MESON. Lyuboshits, V. L. (Joint Inst. for Nuclear Research, Dubna (USSR). Lab. of High Energy). 1973. 7p. (In Russian). INIS.

The cross section for incoherent regeneration of K_S^0 mesons during interaction of K_L^0 mesons with atomic electrons was rapidly increased by increase of the energy of K_L^0 mesons. At very high energies (~100 GeV) the reaction $K_L^0 + e \rightarrow K_S^0$ can be used for the experimental determination of the mean square electric radius of K_L^0 mesons, characterizing the charge distribution. The energy spectrum of relativistic recoil electrons was examined and a numerical evaluation was made. (tr-auth)

30593 (PITHA-64(1972)) MEASUREMENT OF THE ENERGY DEPENDENCE OF THE DECAY MATRIX ELEMENT FOR $K_L^0 \rightarrow \pi^+\pi^-\pi^0$. Krenz, W. (Technische Hochschule Aachen (F.R. Germany). 3. Physikalisches Inst.). Feb 1972. 67p. (In German). INIS.

29 figs.; 13 tabs.; 56 refs. With abstract.

In the CERN-1.1 m^3 bubble chamber for heavy liquids, about 750,000 K_L^0 decays were photographed in order to measure the absolute decay rate of $K_L^0 \rightarrow 2\pi^0$. Thus the K_L^0 beam was conducted in a tube through the bubble chamber; the decay products could be observed in the chamber liquid (heavy freon). 190,000 pictures of this experiment amongst others were used to measure the energy dependence of the matrix element in the decay $K_L^0 \rightarrow \pi^+\pi^-\pi^0$. The pictures after complete $K_L^0 \rightarrow \pi^+\pi^-\pi^0$ decays were looked through in three European laboratories. In them both decay photons of the π^0 meson must have converted in the chamber and both traces of the charged pions have left the tube. For the final analysis 1,468 kinematically reconstructed decays were used. There was practically no background. The value found for the energy dependence of the matrix element is only compatible with a few earlier measurements. Isospin and current algebra predictions are in good agreement with the result. (auth)

30594 EXPERIMENTAL ASPECTS OF NEUTRINO INTERACTIONS. Perkins, D. H. (Oxford Univ.). pp 501-710 of Proceedings of the Fifth Hawaii Topical Conference in Particle Physics. Dobson, P. N. Jr. (ed.). Honolulu, HI; Univ. Press of Hawaii (1974).

From 5th topical conference in particle physics; Honolulu, Hawaii, USA (8 Aug 1973). See CONF-730856-.

Lectures are presented on the following topics: leptonic neutral weak currents; semilepton neutral weak currents; leptonic interactions; and inclusive neutrino–nucleon interactions. (LBS)

30595 THE $\Delta I = 1/2$ RULE IN NON-LEPTONIC WEAK DECAYS. Fayyazuddin (European Organization for Nuclear Research, Geneva (Switzerland)); Riazuddin (Islamabad Univ., Rawalpindi (Pakistan)). Nucl. Phys., B; 76: No. 1, 125-136(4 Jul 1974).

The $\Delta I = 1/2$ rule is investigated for non-leptonic decays in unified theories of weak and electromagnetic interactions. In such theories, weak interactions are mediated not only by gauge vector bosons, but also through the exchange of scalar Higgs bosons. Also in such theories, the electromagnetic and weak interaction parts of the Lagrangian and the mass term are completely specified. Hence the divergence of the weak current $\partial_\mu J_\mu$ is completely known. For a non-leptonic decay $\alpha(p) \rightarrow \beta(p' + k)$, one has $\langle\beta|i\partial_\mu J_\mu|\alpha\rangle = 0$ because of energy-momentum conservation for particles on the mass shell. The restrictions due to the above condition on non-leptonic decays are examined. In particular, it is discussed whether through such restrictions one can understand the suppression of $\Delta I = 3/2$ in non-leptonic decays. The conclusions are that for the eight-quark version of the Georgi–Glashow model, the $\Delta I = 1/2$ rule for parity-conserving decays is obtained only in the SU(3) limit. For the Salam–Weinberg model, it is found that parity-conserving non-leptonic decays arise in the first order of SU(3) symmetry breaking, while the parity-violating part can arise in the SU(3) limit. The violation of the $\Delta I = 1/2$ rule for parity-violating decays is of first order in SU(3) breaking, whereas it is of second order in SU(3) breaking for parity-conserving decays. (auth)

30596 MEASUREMENT OF THE SLOPE PARAMETER FOR THE NEUTRAL PION SPECTRUM IN $K_L^0 \rightarrow \pi^0\pi^+\pi^-$ DECAY. Bisi, V.; Ferrero, M. I. (Istituto Nazionale di Fisica Nucleare, Turin (Italy)). Phys. Lett., B; 50: No. 4, 504-506(24 Jun 1974).

The π^0 spectrum in the $K_L^0 \rightarrow 3\pi$ decay was measured using a wire chamber magnetic spectrometer. In the usual approximation, the matrix element can be expressed as $|M|^2 \sim 1 + 2a_0(M_K/M_\pi^2)(2T_\pi 0 - T_\pi 0_{max}) + a_1(M_K^2/M_\pi^4)(2T_\pi 0 - T_\pi 0_{max})^2$. $a_0 = -0.282 \pm 0.011$ and a_1 consistent with zero are obtained. (auth)

Strong (Baryon-induced)

Refer also to abstract 30663.

30597 (COO-1428-382) ANNUAL PROGRESS REPORT FOR THE PERIOD JUNE 1, 1973–MAY 31, 1974. Loeffler, F. J. (Purdue Univ., Lafayette, Ind. (USA)). 1974. Contract AT(11-1)-1428. 44p. Dep. NTIS $5.25.

Experimental research on strong interactions is summarized. A list of publications is included. (JFP)

30598 (IFVE-SPK-73-69) ANALYSIS OF DATA ON MULTIPARTICLE PRODUCTION IN PP-INTERACTIONS FROM 13 UP TO 300 GeV. Babintsev, V. V.; Vorob'ev, A. P.; Moiseev, A. M. (Gosudarstvennyj Komitet po Ispol'zovaniyu Atomnoj Ehnergii SSSR, Serpukhov. Inst. Fiziki Vysokikh Ehnergij). 1973. 24p. (In Russian). INIS.

Multiplicity distributions of secondary charged particles in pp interactions were studied from 13 to 300 GeV. The analysis of the existing models of multiple production showed that none of them describe all aspects of the experimental data. (tr-auth)

30599 (LA-UR-74-1333) MEASUREMENT OF PARITY VIOLATION IN PROTON–PROTON SCATTERING AT 15 MeV. Potter, J. M.; Bowman, J. D.; Hwang, C. F.; McKibben, J. L.; Mischke, R. E.; Nagle, D. E.; Debrunner, P. B.; Frauenfelder, H.; Sorenson, L. B. (Los Alamos Scientific Lab., N. Mex. (USA); Illinois Univ., Urbana (USA)). 1974. 7p. (CONF-740822-3). Dep. NTIS $4.00.

From conference on few body problems in nuclear and particle physics; Quebec, Canada (27 Aug 1974).

A recent measurement of the parity violation in proton–proton scattering at 15 MeV by measuring the helicity dependence of the total cross section is reported. The results showed a possible effect of $(1 \pm 4) \times 10^{-7}$ which is consistent with previous predictions. Since it is necessary that the methods by which these measurements were taken be extremely carefully scrutinized for any possible systematic errors, a discussion is given of the method of experimentation and systematic errors. (JFP)

30600 DIFFRACTIVE PROCESSES IN $\bar{p}p$ INTERACTIONS AT 5.1 GeV/c. Bastien, D. B.; Hodous, M. F.; Hulsizer, R. I.; Napier, A.; Pless, I. A.; Silverman, J. P.; Wolfson, J. (Massachusetts Inst. of Tech., Cambridge (USA). Lab. for Nuclear Science); Bastien, P. L.; Kirkpatrick, L. D.; Lubatti, H. J. (Washington Univ., Seattle (USA). Dept. of Physics). Phys. Lett., B; 50: No. 2, 290-294(27 May 1974).

The interaction $\bar{p}p \rightarrow \bar{p}p\,\pi^+\pi^-$ at 5.1 GeV/c has been investigated using the prism plot method. In addition to the $\Delta^{++}\bar{\Delta}^{--}$ final state, the three particle diffractive dissociation of the proton and antiproton into $(p\pi^+\pi^-)$ and $(\bar{p}\pi^+\pi^-)$ respectively was isolated. It is estimated that this process accounts for 30% of the final state. (auth)

30601 TWO BODY CORRELATIONS BETWEEN NEGATIVE PIONS IN pp INTERACTIONS AT 69 GeV/c. Derre, J.; Blumenfeld, H.; Jabiol, M. A.; Leveque, A.; Otwinowski, S.; Pauli, E. (CEA Centre d'Etudes Nucleaires de Saclay, 91 – Gif-sur-Yvette (France). Dept. de Physique des Particules Elementaires); Bumazshnov, V. H.; Ermolov, P. F.; Kistenev, E. P.; Nicolaencko, V. I. Phys. Lett., B; 50: No. 2, 287-289(27 May 1974).

Correlations between two π^- in pp interactions at 69 GeV/c are presented in terms of longitudinal and transversal variables. The dominant feature is the existence of a strong short range positive correlation between the two π^- in the central region. (auth)

30602 INFLUENCE OF THE KINEMATICAL CONSTRAINTS ON THE TRANSVERSE MOMENTUM CORRELATION FEATURES. Fridman, A. (McGill Univ., Montreal, Quebec (Canada). Dept. of Physics); Juillot, P. (Centre National de la Recherche Scientifique, 67 – Strasbourg (France). Centre de Recherches Nucleaires). Z. Phys.; 268: No. 3, 317-320(Jun 1974).

1 tab.; 6 refs.

The influence of the kinematical constraints on the transverse momentum correlation features in multiparticle processes is studied by means of the $dN/(dr_1dr_2)dN/dr_1dr_2$ distribution, r_1 and r_2 being the transverse momenta of the particles entering in each pair. Using a limited transverse momentum phase space we obtain for high energy reactions a simple analytical expression for $dN/(dr_1dr_2)$. This expression, similar to a phenomenological parametrization proposed for analyzing $\bar{p}$,p annihilation data, served to define a correlation parameter, the non vanishing value of which is due to the energy-momentum conservation constraints. (auth)

30603 NEGATIVE PION PRODUCTION IN PROTON-PROTON INTERACTIONS AT 69 GeV/c. Bumazshnov, V. A.; Ermolov, P. F.; Fenyuk, A. S.; Kistenev, E. P.; Moiseev, A. M.; Starchencko, E. A.; Vlasov, E. V. (Gosudarstvennyj Komitet po Ispol'zovaniyu Atomnoj Ehnergii SSSR, Serpukhov. Inst. Fiziki Vysokikh Ehnergij); Blumenfeld, H.; Derre, J.; Jabiol, M. A. Phys. Lett., B; 50: No. 2, 283-286(27 May 1974).

Inclusive spectra of π^- production for pp interactions are discussed at 69 GeV/c both in the central and in the fragmentation region and are compared to data at lower and higher energies. The p_T dependence of the invariant structure function is also analyzed. (auth)

30604 MULTIPLICITY IN PROTON-NUCLEUS INTERACTIONS AT 200 GeV/c. Gurtu, A.; Malhotra, P. K. (Tata Inst. of Fundamental Research, Bombay (India)); Mittra, I. S.; Sood, P. M. (Punjab Univ., Chandigarh (India). Dept. of Physics); Gupta, S. C.; Gupta, V. K.; Kaul, G. L.; Mangotra, L. K.; Prakash, Y.; Rao, N. K. Phys. Lett., B; 50: No. 3, 391-395(10 Jun 1974).

Experimental results on multiparticle production in proton-nucleus collisions based on an exposure of emulsion stack to 200 GeV/c proton beam at NAL are presented. It is found that the average charged particle multiplicity $\langle n_s \rangle = 13.0 \pm 0.4$, $D \equiv (\langle n_s^2 \rangle - \langle n_s \rangle^2)^{1/2} = 8.5 \pm 0.4$ and $\langle N_h \rangle = 7.3 \pm 0.2$. Energy dependence of $R_{em} = \langle n_s \rangle / \langle n_{ch} \rangle$, where $\langle n_{ch} \rangle$ is the charged particle multiplicity in pp collisions, is investigated in the range 7.1 – 8000 GeV/c. R_{em} attains a constant value of 1.71 ± 0.04 beyond 200 GeV/c and furthermore this value of R_{em} implies an A dependence $R_A = A^{0.13}$. It is found that even for p-nucleus collisions D increases linearly with $\langle n_s \rangle$ with about the same slope as for pp collisions. (auth)

30605 MEASUREMENT OF CHARGED PARTICLE MULTIPLICITIES ASSOCIATED WITH LARGE TRANSVERSE MOMENTUM PHOTONS IN PROTON-PROTON COLLISIONS. Finocchiaro, G.; Grannis, P.; Green, D.; Joestlein, H.; Kephart, R.; Thun, R. (State Univ. of New York, Stony Brook (USA)); Amendolia, S. R.; Bellettini, G.; Braccini, P. L.; Bradaschia, C. Phys. Lett., B; 50: No. 3, 396-402(10 Jun 1974).

The behavior of charged-particle multiplicities has been studied as a function of the transverse momentum of photons produced at 90° in proton-proton collisions. The data were obtained at the CERN Intersecting Storage Rings (ISR) at a centre-of-mass energy of 53 GeV and cover the transverse momentum range $0 < p_\perp < 4.5$ GeV/c. The total associated charge multiplicity increases with $p_\perp$ and most of the increase is found in a very wide cone opposite the detected photons. Partial multiplicities in the direction of the photons vary only slightly with $p_\perp$. However, multiplicities at small angles with respect to the beams decrease sharply with increasing $p_\perp$. (auth)

30606 CROSS-SECTIONS FOR RESONANCE PRODUCTION IN $\bar{p}n$ ANNIHILATIONS AROUND 2190 MeV CENTRE-OF-MASS ENERGY. Bertanza, L. (Univ., Pisa, Italy); Bigi, A.; Casali, R.; Lariccia, P.; Pazzi, R.; Bettini, A.; Mazzucato, M.; Sartori, G.; Sartori, S.; Zumerle, G.; Borreani, G.; Quassiati, B.; Rinaudo, G.; Vigone, M. Nuovo Cim., 23A: No. 2, 209-226(21 Sep 1974).

Resonance production cross sections in nonstrange annihilation channels were studied in the c.m. energy interval from 2.13 to 2.29 GeV where the first bump in the $\bar{N}N$ cross section for $I = 1$ had been observed. None of the resonance intermediate states analyzed shows a structure large enough to be mainly responsible for the enhancement. (auth)

30607 POSSIBLE EXISTENCE OF A DIPROTON RESONANCE. A Proposal of p–p Scattering Experiment at About 500 MeV. Furuichi, S. (Rikkyo Univ., Tokyo); Matsuda, M.; Watari, W. Nuovo Cim., 23A: No. 2, 375-389(21 Sep 1974).

The energy dependence of the $^1D_2$ phase shift of proton–proton scattering in the region between 500 MeV and 1000 MeV is discussed. The possible existence of a diproton resonance in this energy region is examined with available experimental data by means of the phase-shift analysis and the analysis of the Kantor amplitude. It is shown that solutions both with and without resonance are equally possible. For the purpose of removing this uncertainty, the usefulness of further experiments of proton–proton scattering at about 500 MeV is discussed. (auth)

30608 CHARGED PARTICLE MULTIPLICITY DISTRIBUTIONS FOR 32 GeV/c $K^\pm p$ AND $\bar{p}p$ INTERACTIONS FOR 50 GeV/c $\pi^\pm p$ INTERACTIONS. Akopdjanov, G. A.; Babincev, V. V.; Chliapnikov, P. V.; Ermolov, P. F.; Fenjuk, A. B.; Gerdyukov, L. N.; Gumenyuk, S. A.; Manyukov, B. A.; Moiseev, A. M.; Sulyaev, R. M. (Gosudarstvennyj Komitet po Ispol'zovaniyu Atomnoj Ehnergii SSSR, Serpukhov. Inst. Fiziki Vysokikh Ehnergij). Nucl. Phys., B; 75: No. 3, 401-412(25 Jun 1974).

Topological cross sections are presented for K^+p, K^-p and $\bar{p}p$ interactions at 32 GeV/c and for π^+p and π^-p interactions at 50 GeV/c observed in the 4.5 m Mirabelle hydrogen bubble chamber at Serpukhov. Parameters characterizing the behavior of the multiplicity distributions, namely $\langle n_c \rangle$, D and f_2 and the normalized moments are given. The dependence of these parameters on the energy and the nature of the beam particle is discussed. The multiplicity distributions obtained cannot be described by a single function in the KNO variables. (auth)

30609 EXPERIMENTAL RESULTS ON STRONG INTERACTIONS IN THE NAL HYDROGEN BUBBLE CHAMBER. Whitmore, J. (National Accelerator Lab., Batavia, Ill. (USA)). Phys. Rep.; 10: No. 5, 273-373(May 1974).

This report presents a review of the data obtained on high-energy hadronic interactions in the 30-in. hydrogen bubble chamber at the National Accelerator Laboratory. The emphasis is on a representation of the experimental results that have been acquired during the Laboratory's first year of operation. The five main topics discussed are (a) topological cross sections and multiplicity distributions, (b) studies of the diffraction process observed in some low multiplicity final states, (c) single particle inclusive spectra, (d) neutral particle production, and (e) multiparticle correlations. While most of the data come from pp collisions and may be compared to results from the ISR, some of the more recent results from πp interactions are included and are compared to πp data at lower energies as well as to the pp results. The comparison between the πp and pp data indicates the striking result that many of the properties of high energy collisions seem almost independent of the nature of the projectile and target particles and depend primarily on the available center-of-mass energy. (auth)

30610 STUDY OF DOUBLE DIFFRACTION DISSOCIATION IN THE REACTION $\pi^{\pm}p \rightarrow (3\pi)^{\pm}(N\pi)^{+}$ AT 16 GeV/c. Graessler, H.; Honecker, R.; Lauscher, P.; Otter, G. (Technische Hochschule Aachen (F. R. Germany). 3. Physikalisches Inst.); Roloff, H.; Spiering, Ch. (Deutsche Akademie der Wissenschaften zu Berlin (German Democratic Republic)); Boeckmann, K.; Bossen, G. J.; Kanazirsky, Ch.; Rost, M. (Bonn Univ. (F. R. Germany). Physikalisches Inst.). Nucl. Phys., B; 75: No. 1, 1-19(11 Jun 1974).

Evidence is examined for double diffraction dissociation in the reaction $\pi^{\pm}p \rightarrow (3\pi)^{\pm}(N\pi)^{+}$ with $(3\pi)^{\pm}$ masses between 1.0 and 1.2 GeV at 16 GeV/c incident beam momentum. The data considered are found to reveal: (a) isospin zero exchange, (b) the expected factorization properties, (c) a $d\sigma/dt'$ slope compatible with those deduced from single dissociation processes and elastic scattering, and (d) as shown by an analysis of D moments, $(3\pi)^{\pm}$ systems with the same typical spin parity composition as observed in the diffractive single dissociation reactions $\pi^{\pm}p \rightarrow (3\pi)^{\pm}p$. Comparison of the 16 GeV/c data with data of an 8 GeV/c experiment indicates an almost energy-independent cross section for the process investigated. (auth)

30611 ENERGY DEPENDENCE OF $\sigma_{p\text{-air}}$ UP TO 20 TeV. Gaisser, T. K. (Bartol Research Foundation, Swarthmore, Pa. (USA)); Yodh, G. B. (Maryland Univ., College Park (USA). Dept. of Physics). Nucl. Phys., B; 76: No. 1, 182-188(4 Jul 1974).

The observed neutral to charge ratio in unaccompanied atmospheric hadron fluxes is used to improve the cosmic ray lower bound on the p-air inelastic cross section between 0.5 and 20 TeV. The conclusion drawn about the magnitude of continued increase of σ_{pp} between 2 and 20 TeV depends on the model relation between σ_{pp} and σp-air. (auth)

30612 RAPIDITY-GAP SEPARATION AND STUDY OF SINGLE-DIFFRACTION DISSOCIATION IN pp COLLISIONS AT 12 AND 24 GeV/c. Benecke, J.; Breitenlohner, P.; Nissen-Meyer, S.; Schmitz, N.; Schrankel, W.; Schwarzschild, B.; van Hove, L. (Max-Planck-Institut fuer Physik und Astrophysik, Muenchen (F. R. Germany)); Blobel, V.; Fesefeldt, H.; Neumann, H. F. Nucl. Phys., B; 76: No. 1, 29-47(4 Jul 1974).

An event-by-event separation of the single-diffractive component in the inclusive reaction $p + p \rightarrow p + X$ is attempted with the 12 and 24 GeV/c bubble-chamber data, using a method involving largest rapidity gaps. The method yields a (non-strange) single-diffraction cross section of about 7 mb at both energies, dominated by two and four prongs. For the diffractive component the recoil mass distribution $d\sigma/dM_X^2$ shows a sharp peak near $M_X^2 = 2$ GeV^2 at both energies with a long tail that broadens significantly with increasing energy. This shape is reasonably well described by the diffractive terms of a triple-Regge fit to the full pp data. The slope parameter of the diffractive t distribution shows a precipitous drop with increasing M_X^2, levelling off abruptly at M_X^2 ~3 GeV^2. The mean charged multiplicity of the diffractive system appears to be linear in log M_X^2 and independent of s. (auth)

Strong (Meson-induced)

30613 (COO-1428-391(App.A-2)) STUDY OF PARTICLE SPECTRA AND CORRELATIONS IN THE REACTION $\pi^- + p \rightarrow$ n(forward) + (2π, 4π, 6π) AT 8.4 GeV/c. Alam, M. S.; Brabson, B. B.; Galloway, K. (Indiana Univ., Bloomington (USA)). 1974. 26p. (CONF-740713-25). Dep. NTIS $4.50.

From 17th international conference on high-energy physics; London, UK (1 Jul 1974).

Results are reported on particle spectra and invariant mass distributions from the reaction $\pi^+ + p \rightarrow$ n(forward) + (2π, 4π, 6π) at 8.4 GeV/c. The data were obtained with the SLAC 15-inch Rapid Cycling Bubble Chamber which was triggered by detecting fast forward neutrons interacting in downstream optical spark chambers. The main features of the data can be simulated by a Monte Carlo model which incorporates Lorentz-invariant phase space modified by exponential transverse momentum damping on each final state particle and, in addition, takes into account the geometrical constraints and triggering requirements of the system. Resonance production in some channels is seen to deviate from background distributions. (auth)

30614 ISOSPIN ANALYSIS OF THE DIFFRACTION DISSOCIATION PROCESSES IN K^+p INTERACTIONS AT 5 AND 8.2 GeV/c. Eskreys, A.; Figiel, J.; Malecki, P.; Zalewska, A. (Inst. of Nuclear Physics, Krakow). Acta Phys. Pol., B; 5: No. 4, 485-496(1974).

An analysis of the diffraction dissociation processes in K^+p interactions at 5 and 8.2 GeV/c K^+ incoming momentum is presented. An isospin analysis was performed for the single dissociation processes: $K^+ \rightarrow K^*(890)\pi$ and $p \rightarrow \Delta(1236)\pi$, observed in the reactions: $K^+p \rightarrow K^*(890)\pi N$ and $K^+p \rightarrow K\pi\Delta(1236)$. It confirmed the dominance of the $I = 1/2$ component in the Q bump and in the low mass $\Delta\pi$ enhancement. It is found that the interference term between the isospin $1/2$ and isospin $3/2$ amplitudes is small for Q region and is quite sizable for the low $\Delta\pi$ mass enhancement. (auth)

30615 STUDY OF π^+p INTERACTIONS WITH STRANGE PARTICLE PRODUCTION IN FIVE- AND SIX-BODY FINAL STATES AT 8 GeV/c. Sabau, M. N. (Institutul de Fizica Atomica, Bucharest). Stud. Cercet. Fiz.; 25: No. 2, 183-215(1973). (In Rumanian).

This paper is based on a doctoral dissertation. After a brief introduction, the technical procedures are described. The results are then presented and interpreted; these include the following: cross sections of the reactions studied, kinematical characteristics of the secondary particle, angular correlations between the meson pairs (Goldhaber effect), behavior of the transverse momentum in interactions with strange-particle production, behavior of the mean transverse momentum, and correlation between the transverse and longitudinal momenta in the center-of-mass system. Then resonance production is discussed, including resonance production in $\Lambda K\, m\pi$ reactions and resonance production in $NKK\, m\pi$ reactions. In the last section the author draws his conclusions. (21 figures, 8 tables) (RWR)

30616 INCLUSIVE π^- PRODUCTION IN π^+d INTERACTIONS AT 24 GeV/c. Sreedhar, V.; Chien, C. Y.; Feiock, D.; Zdanis, R. (Johns Hopkins Univ., Baltimore, Md. (USA)); Bromberg, C.; Ferbel, T.; Slattery, P. (Rochester Univ., N.Y. (USA)). Nucl. Phys., B; 75: No. 2, 285-301(18 Jun 1974).

Inclusive π^- production from π^+d interactions at 24 GeV/c has been studied using data obtained from the Brookhaven National Laboratory 80″ bubble chamber. Distributions of longitudinal momenta in the laboratory frame and the projectile frame, of χ (Feynman's scaling variable), and of rapidity in the center of mass frame are presented and compared with the corresponding distributions from the reaction $\pi^+p \rightarrow \pi^- +$ anything. The effect of Fermi momentum of the nucleons has been investigated and is found to be small. It is concluded that single particle inclusive π^- spectra from proton and from neutron targets are very different in this energy range. The two particle correlations among negative pions in the deuteron experiment have been investigated and the results are presented. (auth)

30617 HIGH STATISTICS STUDY OF THE REACTION $\pi^-p \rightarrow \pi^-\pi^+n$: APPARATUS, METHOD OF ANALYSIS, AND GENERAL FEATURES OF RESULTS AT 17 GeV/c. Grayer, G.; Hyams, B.; Jones, C.; Schlein, P.; Weilhammer, P. (European Organization for Nuclear Research, Geneva (Switzerland)); Blum, W.; Dietl, H.; Koch, W.; Lorenz, E.; Luetjens, G. Nucl. Phys., B; 75: No. 2, 189-245(18 Jun 1974).

A detailed account is given of a high statistics experiment measuring the reaction $\pi^-p \rightarrow \pi^-\pi^+n$ at 17.2 GeV/c. The spark chamber and counter triggering system are described. The methods of data analysis are described, in particular the determination of angular distributions from apparatus with limited acceptance. Experimental data and their interpretation are presented. (auth)

30618 THE REAL PART OF THE FORWARD SCATTERING AMPLITUDE IN $\pi^{\pm}p$ ELASTIC SCATTERING BELOW 2 GeV/c. Baillon, P.; Bricman, C.; Eberhard, Ph.; Ferro-Luzzi, M.; Perreau, J. M.; Tripp, R. D.; Ypsilantis, T. (European Organization for Nuclear Research, Geneva (Switzerland)); Declais, Y.; Seguinot, J. (Caen Univ., 14 (France)). Phys. Lett., B; 50: No. 3, 387-390(10 Jun 1974).

The differential cross section for $\pi^{\pm}p$ elastic scattering below 2 GeV/c has been measured at small forward pion angles by an electronics experiment. The interference effects observed between the Coulomb and the nuclear interaction have been used to determine the magnitude and sign of the real parts of the $\pi^{\pm}p$

forward scattering amplitude. The latter are compared to the values predicted by the dispersion relations. (auth)

30619 MEASUREMENT OF THE REAL PART OF THE FORWARD SCATTERING AMPLITUDE IN K^+p ELASTIC SCATTERING BETWEEN 0.9 AND 2.6 GeV/c. Baillon, P.; Bricman, C.; Ferro-Luzzi, M.; Perreau, J. M.; Tripp, R. D.; Ypsilantis, T. (European Organization for Nuclear Research, Geneva (Switzerland)); Declais, Y.; Seguinot, J. (Caen Univ., 14 (France)). Phys. Lett., B; 50: No. 3, 377-382(10 Jun 1974).

The differential cross section for K^+p elastic scattering has been measured in the forward meson direction ($0.0008 < t < 0.1$ GeV^2) in an electronics experiment at incident momenta between 0.9 and 2.6 GeV/c. The high statistics and absolute normalization of the data allow a good determination of the real part of the forward nuclear scattering amplitude by means of the Coulomb-nuclear interference effect. (auth)

30620 THE πd SCATTERING LENGTH FROM K_α X-RAYS. Bailey, J. (Science Research Council, Daresbury (UK). Daresbury Lab.); Bugg, D. V.; Jeremiah, D. R. (Queen Mary Coll., London (UK)); Gastaldi, U.; Polacco, E. (Pisa Univ. (Italy). Istituto di Fisica); Hattersley, P. (Birmingham Univ. (UK)); Klempt, E.; Neubecker, K. (Mainz Univ. (F. R. Germany)); Warren, J. (British Columbia Univ., Vancouver (Canada)). Phys. Lett., B; 50: No. 3, 403-406(10 Jun 1974).

X-rays from the K_α transition ($2P \rightarrow 1S$) of the π^-d mesic atom have been observed. Their energy, $2592.8^{+1.3}_{-2.0}$ eV, has been measured by the critical absorber technique, using the M_V absorption edge in bismuth. The strong interaction shift in the 1S state is −4.8 eV, corresponding to a scattering length $a(\pi d) = -(0.052^{+0.022}_{-0.017})$ m_π^{-1}, in agreement with recent calculations. The intensity ratio $K_\alpha/K_{total} = 0.548 \pm 0.015$. (auth)

30621 BACKWARD PRODUCTION OF ρ^0 AND f^0 MESONS IN π^+n INTERACTIONS AT 6 GeV/c. Dado, S.; Engler, A.; Kraemer, R. W.; Toaff, S.; Weisser, F. (Carnegie-Mellon Univ., Pittsburgh, Pa. (USA)); Diaz, J.; Dibianca, F.; Fickinger, W.; Robinson, D. K. (Case Western Reserve Univ., Cleveland, Ohio (USA)). Phys. Lett., B; 50: No. 2, 275-279(27 May 1974).

Backward production of ρ^0 and f^0 mesons in π^+n interactions at 6 GeV/c is presented. Total and differential cross sections are reported along with spin density matrix elements. (auth)

30622 A STUDY OF THE REACTIONS $\pi^-p \rightarrow K^*X$, $K^*\Sigma$ AND $K^*Y_1^*(1385)$ AT 3.93 GeV/c. Yaffe, D.; Abramovich, M.; Chaloupka, V.; Ferrando, A.; Korkea-Aho, M.; Losty, M. J.; Montanet, L.; Paul, E.; Zatz, J.; Zieminski, Z. (European Organization for Nuclear Research, Geneva (Switzerland)). Nucl. Phys., B; 75: No. 3, 365-387(25 Jun 1974).

The final states $K^{*0}(890)\Lambda$, $K^{*0}(890)\Sigma^0$ and $K^{*0}(890)$ $Y_1^*(1385)$ produced in π^-p interactions at 3.93 GeV/c have been investigated. The differential cross sections and spin density matrix elements are presented for the resonances as functions of momentum transfer, as well as the Λ and Σ^0 polarizations. The Σ^0 polarization is found to be positive and maximal. An amplitude analysis is performed for the $K^*\Lambda$ and $K^*\Sigma^0$ reactions, and it is found that one natural parity transversity amplitude is dominant for the latter. (auth)

30623 CROSS CHANNEL ISOSPIN AMPLITUDES FOR 3.9 GeV/c $\pi^+p \rightarrow \pi(N\pi)$ COMPARED WITH THE PREDICTIONS OF A DOUBLE EXCHANGE MODEL. Berlad, G.; Haber, B.; Hodous, M. F.; Hulsizer, R. I.; Kistiakowsky, V.; Levy, A.; Pless, I. A.; Singer, R. A.; Wolfson, J.; Yamamoto, R. K. (Massachusetts Inst. of Tech., Cambridge (USA)). Nucl. Phys., B; 75: No. 1, 93-111(11 Jun 1974).

A cross-channel isospin analysis has been carried out on a prism plot separated sample of 3.9 GeV/c $\pi^+p \rightarrow \pi(N\pi)$ events. An enhancement is observed in the low $(N\pi)$ invariant mass region for an $I = \frac{1}{2}$ state of the $N\pi$ system when the isospin for the cross channel is both $I_E = 0$ and 1. These results and those of similar analyses at 8 and 16 GeV/c are compared with the predictions of a double-exchange model and good agreement is obtained. Neither interpretation of this phenomenon as a resonance nor as a consequence of diffraction dissociation in the usual definition, nonresonating single pomeron exchange, explains all the features of the results. (auth)

30624 A MEASUREMENT OF $K^*(1420)$ DECAY BRANCHING RATIOS. Dehm, G.; Goebel, G.; Wittek, W.; Wolf, G. (Max-Planck-Institut fuer Physik und Astrophysik, Muenchen (F. R. Germany)); De-Jong, G.; Tavernier, S. (Brussels Univ. (Belgium)); Cornet, P.; Dufour, P.; Grard, F.; Henri, V. P. Nucl. Phys., B; 75: No. 1, 47-58(11 Jun 1974).

The decay branching ratios of $K^{*0}(1420)$ into $K^+\pi^-$, $K^0\pi^+\pi^-$ and $K^{*+}(892)\pi^-$ are measured in the charge exchange reaction $K^+d \rightarrow K^{*0}(1420)pp$, using data from a K^+d bubble chamber experiment at 4.6 GeV/c incident momentum. For the branching ratio $(K^*(1420) \rightarrow K^*(892)\pi)/K^*(1420) \rightarrow K\pi)$ a value of (0.54 ± 0.16) is obtained. The results are compared with previous measurements. (auth)

30625 LONGITUDINAL PHASE-SPACE ANALYSIS OF THE $K^+\pi^+\pi^-$ SYSTEM PRODUCED BY 10 GeV/c K^+ INCIDENT ON NUCLEI. Blind, R.; Engel, J. P.; Escoubes, B.; Guyonnet, J. L.; Paty, M.; Riester, J. L. (Strasbourg-1 Univ., 67 (France)). Nucl. Phys., B; 76: No. 1, 61-68(4 Jul 1974).

Interactions of 10 GeV/c K^+ incident on nuclei producing the $K^+\pi^+\pi^-$ system have been analyzed by the longitudinal phase-space technique, which improves the selection of coherent events and allows a suitable analysis of the $K^+\pi^+\pi^-$ mass spectrum. Taking into account the experimental resolution and form factor effects, and comparing the data with results on protons (hydrogen bubble chamber data), it appears that the low-mass region of the spectrum is favored by coherent production. Spin-parity analysis of the Q^+ confirms the 1^+ value. (auth)

Particle Interactions and Properties (Theoretical)

Refer also to abstract 30577.

General

30626 (COO-1428-389) ANNUAL PROGRESS REPORT, TASK B, FOR JUNE 1, 1973 - MAY 31, 1974. (Purdue Univ., Lafayette, Ind. (USA). Dept. of Physics). 1974. Contract AT(11-1)-1428. 22p. Dep. NTIS $4.25.

Theoretical high energy physics research activities are summarized. A list of publications is included. (JFP)

30627 (IAE-2286) MAGIC NUCLEI THEORY. Nosov, V. G.; Kamchatnov, A. M. (Gosudarstvennyj Komitet po Ispol'zovaniyu Atomnoj Ehnergii SSSR, Moscow. Inst. Atomnoj Ehnergii). 1973. 26p. (In Russian). INIS.

On the basis of Fermi-liquid concepts about the structure of the energy spectrum of nuclear material a coherent theory is developed for shell and magic oscillations of spherical nuclear masses. A "magic" relation is found between the dimensions of a system and the limiting momentum of a Fermi-distribution of quasiparticles: a whole number of DeBroglie half-wave lengths should fit on the diameter of the nucleus. An expression is obtained for a jump in nucleon binding energy in the vicinity of a magic nucleus. An analysis is carried out on the role of the residual interaction without which a spherical configuration of the system in general would not be in a state of stable equilibrium. It is shown that the zone width of the Fermi-boundary smearing by the residual interaction is proportional to the square of the orbital momentum vector of the quasiparticle. Values of the corresponding proportionality coefficient (of the binding constant between quasiparticles) were determined from experimental data involving 52 magic nuclei. A tendency for a fall in intensity of the residual interaction was demonstrated with an increase in dimensions of the nucleus. (tr-auth)

30628 (KFKI-74-49) D_2-TYPE REPRESENTATION OF THE CONFORMAL GROUP EXTENDED BY REFLECTIONS. Iwaki, A.; Szegoe, K. (Kozponti Fizikai Kutato Intezet, Budapest (Hungary)). 1974. 17p. (CONF-740653-2). Dep. NTIS (US Sales Only) $4.00.

From 9th symposium on particle physics; Balatonfured, Hungary (12 Jun 1974).

The d_2 type representation of the conformal group is examined. The explicit basis functions of the irreducible spaces are calculated, and there are invariant bilinear functional for them. The representation is extended to include reflections as well, and the representation of the extended group are examined. (auth)

30629 INVARIANTS OF BORN RECIPROCITY THEORY. Shamaly, A. (Univ. of Alberta, Edmonton). J. Math. Phys. (N. Y.); 15: No. 8, 1178-1180(Aug 1974).

In an attempt to use Born reciprocity theory as a possible scheme for explaining elementary particles all the invariants of this theory are calculated. It turned out that all the invariants are functions of the operator $(x^2 + p^2)$. Thus there is only one independent invariant which characterizes this theory. (auth)

30630 PARTON MODELS AND ASYMPTOTIC FREEDOM. Kogut, J. (Cornell Univ., Ithaca, NY); Susskind, L. Phys. Rev., D; 9: No. 12, 3391-3399(15 Jun 1974).

The scale-invariant parton model is generalized to describe fixed-point and asymptotically free gauge and nongauge theories. Q^2-dependent scaling laws for the moments of νW_2 are derived.

In fixed-point theories the moments scale as powers of Q^2, while in asymptotically free theories they scale as powers of $\ln Q^2$. The behaviors of the elastic form factors, the ratio σ_S/σ_T, and the mean-squared transverse momentum of hadron secondaries are discussed in the various theories. The experimental study of these quantities should distinguish clearly between the conventional parton-model and asymptotically free theories of strong interactions. (auth)

30631 DIRECT VARIATIONAL CALCULATION OF THE TWO-BODY DENSITY MATRIX. Rosina, M. (Univ., Ljubljana, Yugoslavia). pp 490-499 of Nuclear Many-Body Problem. Vol. 1. Calogero, F. (ed.). Bologna; Editrice Compositori (1973).

From symposium on present status and novel developments in the nuclear many-body problem; Rome, Italy (19 Sep 1972). See CONF-720933-P1.

30632 COUPLED DIFFUSION EQUATIONS OF THE HYPERSPHERICAL FORMALISM. Fabre de la Ripelle, M. (Paris Univ., Orsay, France). Compt. Rend., Ser. B; 278: No. 14, 627-629(1 Apr 1974). (In French).

A method for solving inelastic scattering problems with many-body final state channels is presented. A hyperspherical harmonic expansion method is used. (auth)

30633 PROCEEDINGS OF THE EIGHTH RECONTRE de MORIOND. Volume II. The Pomeron. Conference Held at Meribel-les-Allues, France, March 4–16, 1973. Tran Thanh Van, J. (ed.). Orsay, France; Centre National de la Recherche Scientifique (1973). 623p. (CONF-730334-P2).

The conference included 29 papers, which were abstracted previously in NSA. For abstracts of these papers refer to CONF-730334–P2 in a cumulative report number index. (JFP)

30634 SCALING DISTRIBUTION OF LARGE TRANSVERSE MOMENTA. Amati, D.; Caneschi, L. (European Organization for Nuclear Research, Geneva (Switzerland)). Phys. Lett., B; 50: No. 3, 373-376(10 Jun 1974).

The structure function of large k_T scaling law is computed in the framework of a multiperipheral or parton model. This function depends on two scaling variables. It is shown that recent NAL data are in perfect agreement with the same $1/k_T^8$ law observed at ISR. The observed apparent change of the scaling power is faked by the neglect of the dependence on one of the scaling variables. (auth)

30635 POSSIBLE REPRESENTATIONS OF LOCAL CURRENT ALGEBRA. Weyers, J. (European Organization for Nuclear Research, Geneva (Switzerland)). Phys. Lett., B; 50: No. 3, 349-351(10 Jun 1974).

Dashen and Gell-Mann (1966) derived equations, for the matrix elements of the vector and axial vector charge densities at $P_z = \infty$, which follow from the requirements of local current algebra and relativistic covariance. The problem of representation of local current algebra at infinite momentum is then whether one can find an infinite set of single particle hadronic states, including the known meson and baryon resonances, which obey these equations exactly. If such representations can be constructed, they provide an approximate description of the hadron spectrum (i.e., masses and spins of the mesons and baryons) as well as of all weak and electromagnetic transitions between any two levels of the spectrum. In this paper the problem is examined in the meson case and, for simplicity, discussion is restricted to vector currents only. (auth)

30636 INCLUSIVE PROCESSES AT LARGE TRANSVERSE MOMENTA. Teper, M. (Westfield Coll., London (UK)). Phys. Lett., B; 50: No. 2, 261-264(27 May 1974).

A general model for processes at large transverse momentum is constructed on the assumption that events with large transverse momentum particles possess short range correlations. It is shown that particle ratios and scaling properties are not sensitive to the detailed dynamics of large angle scattering, and also that the character of the inclusive spectrum can be understood in terms of (quasi-) elastic scattering. (auth)

30637 NULL-PLANE COMMUTATORS IN THE SPONTANEOUSLY BROKEN GAUGE THEORY OF VECTOR DOMINANCE. Banyai, L. (CNRS, Marseille). Nuovo Cim., 23A: No. 2, 348-356(21 Sep 1974).

Null-plane commutators of the currents in the spontaneously broken gauge theory of vector dominance are discussed, in comparison with those of the traditional field algebra model, using Dirac's canonical formalism. (auth)

30638 PROPERTIES OF THE FUNDAMENTAL INTERACTIONS. Volume 9, Part A. 1971 International School of Subnuclear Physics, Erice, Trapani, Sicily, July 8–26, 1971. Zichichi, A. (ed.). Bologna; Editrice Compositori (1973). 413p. (CONF-710744-(P9)(PA)).

There were nine lectures given. Separate abstracts were prepared for all lectures. (JFP)

For abstracts of individual lectures see: 30639–30644, 30686, 30702, and 30703.

30639 GENERALIZATION OF REGGE ASYMPTOTIC BEHAVIOR. Chew, G. F. (Univ. of California, Berkeley). pp 24-61 of Properties of the Fundamental Interactions. Vol. 9, Pt. A. Zichichi, A. (ed.). Bologna; Editrice Compositori (1973).

From Properties of the Fundamental Interaction NATO-MPI-MRST Advanced Study Institute meeting; Erice, Italy (8 Jul 1971). See CONF-710744-(P9)(PA).

A discussion is given of current conjectures about the extended significance of second-degree analyticity. These conjectures are those that relate general asymptotic power behavior to analytic structure in channel invariants and those that deal with special attributes of discrete powers (Regge poles). The topics include the Mueller formula relating inclusive cross sections to discontinuities, Regge poles, factorization, one Regge-pole model of single-particle inclusive cross sections, the triple Regge limit in single-particle inclusive distributions, and hints about the Regge spectrum from multiperipheral models. (JFP)

30640 OLD AND NEW IDEAS ABOUT CURRENTS AND THEIR COMMUTATORS. de Alfaro, V. (Univ., Turin). pp 62-101 of Properties of the Fundamental Interactions. Vol. 9, Pt. A. Zichichi, A. (ed.). Bologna; Editrice Compositori (1973).

From Properties of the Fundamental Interaction NATO-MPI-MRST Advanced Study Institute meeting; Erice, Italy (8 Jul 1971). See CONF-710744-(P9)(PA).

Lectures are given on the use of the infinite momentum limit which allows a brief review of some historically important features and the arrival at questions concerning the light cone. The discussion covers current algebra, representation of an ordered product, old fashioned perturbation theory: $p \to \infty$ limit and partons, p and q infinite: asymptotic sum rules, commutators of currents on the light cone, scaling and light cone commutators, light cone version of the asymptotic sum rules, the connection between the light cone and $p \to \infty$ limit of equal time commutator matrix element, and light cone commutators and sum rules. (JFP)

30641 HIGH ENERGY BEHAVIOR OF TOTAL AND ELASTIC CROSS SECTIONS. Martin, A. (CERN, Geneva). pp 220-241 of Properties of the Fundamental Interactions. Vol. 9, Pt. A. Zichichi, A. (ed.). Bologna; Editrice Compositori (1973).

From Properties of the Fundamental Interaction NATO-MPI-MRST Advanced Study Institute meeting; Erice, Italy (8 Jul 1971). See CONF-710744-(P9)(PA).

The Pomeranchuk theorem and elastic cross sections for particle–particle and particle–antiparticle collisions are considered in these lectures. Also considered are the equality of differential cross sections, fixed t dispersion relations and the phase problem, controlling the phase by positivity, the small t behavior. (JFP)

30642 DYNAMICAL MODELS BASED ON VECTOR-MESON DOMINANCE AND UNIVERSALITY. Sakurai, J. J. (Univ. of California, Los Angeles). pp 242-307 of Properties of the Fundamental Interactions. Vol. 9, Pt. A. Zichichi, A. (ed.). Bologna; Editrice Compositori (1973).

From Properties of the Fundamental Interaction NATO-MPI-MRST Advanced Study Institute meeting; Erice, Italy (8 Jul 1971). See CONF-710744-(P9)(PA).

The discussion covers a historical review of the basic ideas, vector-meson universality in purely hadronic processes, ρ-photon analogy; hadronic behavior of the photon, charged-pion photo- and electroduction and $\pi^- + p \to \rho^0 + n$, and inelastic electron–proton scattering. (JFP)

30643 PHYSICS OF THE LIGHT CONE. Preparata, G. (Univ., Rome). pp 308-357 of Properties of the Fundamental Interactions. Vol. 9, Pt. A. Zichichi, A. (ed.). Bologna; Editrice Compositori (1973).

From Properties of the Fundamental Interaction NATO-MPI-MRST Advanced Study Institute meeting; Erice, Italy (8 Jul 1971). See CONF-710744-(P9)(PA).

Progress in the physics of the light cone is reported covering the kinematical relevance of the light cone, products of operators near the light cone, how to work with the light cone expansions, measuring light cone singularities, the SLAC experiments, the BNL–Columbia massive μ-pairs production experiments, towards a theory of canonical dimensions, large mass behavior as described by the light cone, theory of dispersion relations, and some applications of light cone controlled mass dispersion relations. (JFP)

30644 DILATATIONS. Coleman, S. (Harvard Univ., Cambridge, MA). pp 358-399 of Properties of the Fundamental Interactions. Vol. 9, Pt. A. Zichichi, A. (ed.). Bologna; Editrice Compositori (1973).

From Properties of the Fundamental Interaction NATO-MPI-MRST Advanced Study Institute meeting; Erice, Italy (8 Jul 1971). See CONF-710744-(P9)(PA).

The progress of investigations of the theory of scale transformations or dilatations is reported. The formal theory of broken scale invariance, scale current and the conformal group, hidden scale invariance, the death of scale invariance, and the resurrection of scale invariance are covered. (JFP)

30645 RESEARCH FIELDS IN PHYSICS. Portland, OR; International Scholarly Book Services, Inc. (1974). 355p. $17.50.

Brief accounts are given of research in progress at the various institutions together with the names of the personnel involved given under the individual research fields of each department. Name and subject indexes are included. (JFP)

30646 PARTICLE KINEMATICS. Byckling, E.; Kajantie, K. New York; John Wiley and Sons, Inc. (1973). 325p. $21.95.

The topics discussed cover special relativity, phase space, two-particle final states, multiparticle production, inclusive reactions, kinematical reflections, and numerical methods of phase space integration. (JFP)

30647 DUAL STRINGS IN THE AMATA–TESTA QUARK IMPRISONMENT SCHEME. Olesen, P.; Tze, H. C. (Niels Bohr Institutet, Copenhagen (Denmark)). Phys. Lett., B; 50: No. 4, 482-486(24 Jun 1974).

Various schemes have been proposed with the purpose of imprisoning colored quarks and gluons. In the model by Amati and Testa strong interactions arise merely as boundary conditions on the more fundamental weak and electromagnetic interactions. While appealing, their work fails conspicuously to exhibit some kind of duality or, perhaps more desirable, the dual string structure to be expected from a hadrodynamics based on quark and gluon confinement. In this note, the theory of Amati and Testa is complemented by indicating that a dual string structure can in fact exist in the context of that scheme. (NL)

Electromagnetic

Refer also to abstract 31174.

30648 (IC-73-131) POSSIBILITY OF PRODUCING POLARIZED PHOTONS BY COMPTON SCATTERING OF POLARIZED RELATIVISTIC ELECTRONS. Amer, A. A.; Elshenawy, L. S. (International Centre for Theoretical Physics, Trieste (Italy)). Sep 1973. 8p. INIS.

Formulas for the differential cross section and the degrees of polarization of the scattered photon are obtained, assuming that the incident photons are unpolarized and the initial electron is arbitrarily polarized and possesses an arbitrary momentum. The cross section is independent of the initial polarization of the electron and so are the two degrees of linear polarization of the scattered photons. The degree of circular polarization of the scattered photon depends on the initial polarization of the electron and is zero if the initial electron is unpolarized. The formulas obtained suggest a method for obtaining a polarized beam of photons from an initially unpolarized beam by means of Compton scattering. (auth)

30649 (JINR-P2-7511) HIGH-ENERGY SCATTERING OF VECTOR PARTICLES BY EXTERNAL ELECTROMAGNETIC FIELD. Pervushin, V. N.; Temnikov, P. P. (Joint Inst. for Nuclear Research, Dubna (USSR). Lab. of Theoretical Physics). 1973. 15p. (In Russian). INIS.

An eikonal representation was obtained for the amplitude of the high energy scattering of particles with spin 1 and random abnormal magnetic moments in an external magnetic field. Corrections to the eikonal Weinberg representation, resulting from the presence of states with zero helicity in the scattered particles, were found. The scattering of particles for strong external fields was studied. (tr-auth)

30650 (NP-20072) MESON ELECTROMAGNETIC DECAYS FROM SU(4)$_W$ AND GENERALIZED VECTOR DOMINANCE. Gounaris, G. J. (Ioannina Univ. (Greece). Dept. of Physics). 10 Jun 1974. 12p. Dep. NTIS (US Sales Only) $4.00.

Using SU(4)$_W$ and generalized vector dominance (GVD) the electromagnetic meson decays are expressed in terms of the pion form factor. Ordinary VMD seems adequate for one-photon processes. Data indicate that U(3) is better in the constituent than in the current quark frame. (auth)

30651 (UCID-15808) COMPTON SCATTERING SUBROUTINE FOR MONTE CARLO CALCULATIONS. Winslow, A. M. (California Univ., Livermore (USA). Lawrence Livermore Lab.). Jul 1967. 29p. Dep. NTIS $4.50.

Since the compton scattering of radiation by electrons is an important aspect of radiation transport in astrophysics and other fields involving hot ionized gases. A relativistic Compton scattering subroutine was previously developed for transport calculations using the Monte Carlo method. A subroutine using the same approach is written and tested. The differences are explained as mostly due to a different method of averaging the results over the electron velocity distribution. (JFP)

30652 CONFORMAL SYMMETRY IN THE WEYL THEORY. Berger, S. B. (Massachusetts Inst. of Tech., Cambridge). Lett. Nuovo Cim.; 11: No. 2, 89-91(14 Sep 1974).

Weyl theory is investigated as the m = 0 conformal limit of Dirac theory. A finite-dimensional representation of the conformal and Poincare groups is obtained in terms of Dirac matrices. It is indicated that this representation may be of physical interest if a distinction is made between conformal generators and physical operators due to the noncompact nature of the conformal group. (JFP)

30653 ELECTROMAGNETIC-MASS FORMULA AND A MODEL OF BARYONS. Kitazoe, T.; Nakahara, K. (Kobe Univ., Japan). Lett. Nuovo Cim.; 11: No. 2, 95-98(14 Sep 1974).

A search is made for a simple law of the electromagnetic masses of baryons which may be expressed by a mass formula with a form more restricted than the ones already given previously. A model of baryons which realizes such a mass formula is considered. (JFP)

30654 DEEP INELASTIC ELECTROPRODUCTION IN RESONANCE REGION. Cross Section Ratio σ_n/σ_p. Kawabe, T. (Kyushu Univ., Fukuoka); Shiga, K. Lett. Nuovo Cim.; 11: No. 2, 125-128(14 Sep 1974).

The cross section ratio of neutron to proton target of deep inelastic electroproduction is studied by considering three dominating resonances P_{33}(1236), D_{13}(1520), and F_{15}(1690) with the assumption that the octet nucleon resonance scales but not the decuplet. (JFP)

30655 EFFECT OF INTENSE ELECTROMAGNETIC WAVE IN CHARGED-PARTICLE SCATTERING. Rahman, N. K. (CEN de Saclay, Gif-sur-Yvette, France). Phys. Rev., A; 10: No. 1, 440-441(Jul 1974).

The recent theoretical results of Kroll and Watson concerning charged-particle scattering in the presence of an intense electromagnetic wave are rederived by using the solution of the Schrödinger equation of a charged particle coupled to a plane-wave electromagnetic field in the dipole approximation and by utilizing the Born approximation. (auth)

30656 TIME-INDEPENDENT MULTICHANNEL SCATTERING THEORY FOR CHARGED PARTICLES. Gibson, A. G.; Chandler, C. (Univ. of New Mexico, Albuquerque). J. Math. Phys. (N. Y.); 15: No. 8, 1366-1377(Aug 1974).

Rigorous derivations are given of two time-independent formulas for the multichannel scattering operator for nonrelativistic charged particle systems. The derivations are based on Dollard's time-dependent theory and use techniques of spectral integration. The formulas involve a complex power of the resolvent operator, in contrast to short-range formulas. Bilateral Laplace transforms are used to derive a generalized multichannel resolvent equation and to prove existence and uniqueness of the solution. The formulas are applied to recover the well known two-body Coulomb scattering amplitude. (auth)

30657 IMPLICATIONS OF THE RECENT $e^+e^- \to$ HADRON + X DATA ON THE LEPTONIC WORLD. Nanopoulos, D. V.; Vlassopulos, S. D. P. (CERN, Geneva). Lett. Nuovo Cim.; 10: No. 17, 751-756(24 Aug 1974).

It is pointed out that the conventional parton model fails to explain recent CEA and SPEAR data concerning the e^+e^- annihilation into hadrons. A phenomenological analysis of the inclusive process is made, and it is suggested that a two-component picture in which diffraction dominates for small x, while the parton model takes up at large x, may be capable of explaining all of the e^+e^- data. An attempt is made to understand the consequences and implications of this analysis in other processes, and also its further implications in the world of leptons. (LBS)

30658 ELECTROMAGNETIC MASS DIFFERENCES IN A RELATIVISTIC QUARK MODEL. Escobar, C. O. (Instituto de Fisica Teorica, Sao Paulo, Brazil). Lett. Nuovo Cim.; 10: No. 17, 741-746(24 Aug 1974).

The electromagnetic-mass difference problem is investigated in a relativistic quark model in which the bound states are described by Bethe–Salpeter amplitudes. The π^+-π^0 and K^+-K^0 mass differences are explicitly calculated. (LBS)

30659 CLASSICAL-PARTICLE DESCRIPTION OF PHOTONS AND PHONONS. Joyce, W. B. (Bell Telephone Labs., Inc., Murray Hill, NJ). Phys. Rev., D; 9: No. 12, 3234-3256(15 Jun 1974).

An $\hbar$-free analogy-free synthesis of classical mechanics and geometrical optics (acoustics) is presented which embraces without distinction particles of both zero and finite rest energy. The point-particle Lagrangian and other classical-particle properties of a photon (corpuscle) in gallium phosphide are found explicitly. Further brief applications are given to Newtonian mechanics, relativistic particle dynamics, fluid-immersed-body dynamics, hole-electron recombination in semiconductors, electrostatic and magnetic lenses, standardization of particle-flux units, and the still-controversial question of optical and acoustical radiation pressure and momentum. (auth)

30660 CHARGE SYMMETRY AND NEUTRAL CURRENT IN A UNIFIED MODEL OF WEAK AND ELECTROMAGNETIC INTERACTIONS. Fayyazuddin (CERN, Geneva); Riazuddin. Nuovo Cim., A; 23A: No. 1, 33-50(1 Sep 1974).

It is pointed out that measurement of the ratio $\sigma^{\bar{\nu}N}/\sigma^{\nu N}$ and the V — A interference term for the high energy inclusive processes $\nu(\bar{\nu}) + N \to l^{\mp}$ + anything (N is the proton-neutron average) can give an estimate of the violation of charge symmetry in these processes. Then an expression is given for charge symmetry violation in terms of experimentally measured structure functions above the charm threshold for the above processes for the Salam-Weinberg model. In addition, predictions are given for the neutral current for the processes $\nu(\bar{\nu}) + N \to \nu(\bar{\nu})$ + anything, below and above the charm threshold for charged currents. It is pointed out that the predictions for the neutral current below the charm threshold are the same as those due to a phenomenological neutral current with SU_3 structure $\bar{\psi}\gamma_\mu(1 + \gamma_5)\,\frac{1}{2}\,(\lambda_3 + (1/\sqrt{3})\lambda_8 - \frac{1}{2}\sqrt{2/3}\lambda_0)\,\psi$, where $\psi = [P/N/\lambda]$. Light-cone algebra is used to obtain our results in the scaling region. (auth)

30661 J = 0 FIXED POLE IN THE VIRTUAL COMPTON AMPLITUDE OFF PROTON AND NEUTRON. Niegawa, A. (Osaka City Univ.); Sasaki, K. Lett. Nuovo Cim.; 11: No. 3, 221-227(21 Sep 1974).

In the consideration of the residue of the J = 0 fixed pole in the forward real and virtual Compton amplitude of protons and neutrons, it is found that the residues for the proton and neutron at an infinite mass squared of the virtual photon are positive definite, which excludes the assumption of a polynomial residue. The residue of the proton is larger than that of the neutron. Also the diffractive component to the residue is not small, roughly 60% or more. (JFP)

30662 QUARK MODEL PREDICTIONS FOR ELECTROPRODUCTION OF $\frac{3}{2}^+$ ISOBARS. Gorczyca, B. (DESY, Hamburg). Acta Phys. Pol., B; 5: No. 4, 569-577(1974).

The excited quark model and the additive quark model constraints on the angular decay distributions of B^* produced by virtual photons in the process $\gamma_{\text{virt}}\ B \to PB^*$ are obtained. Some of the quark model relations are compared with the experimental data to check the quark model, others are used to obtain for Δ^{++} the ratio of the cross sections for production by longitudinal and transverse photons on protons $R = \sigma_L/\sigma_T$. The agreement of the quark model predictions with experiment is found to be good. (auth)

30663 PROCEEDINGS OF THE EIGHTH RENCONTRE de MORIOND. Volume I. Electromagnetic and Weak Interactions. Conference Held at Meribel-les-Allues, France, March 4–16, 1973. Tran Thanh Van, J. (ed.). Orsay, France; Centre National de la Recherche Scientifique (1973). 398p. (CONF-730334-P1).

From eighth Rencontre de Moriond conference; Meribel-les-Allues, France (4 Mar 1973).

The conference included 16 papers that appeared previously in NSA as 30: 03404, 04529, 04530, 04584, 04604, 04605, 04606, 04607, 04608, 04609, 04610, 04611, 04650, 04651, 04652, 04722. (JFP)

30664 POLARIZATION IN ELECTRON POSITRON COLLIDING BEAMS AND THE WEAK INTERACTIONS. McDonald, A. (Oxford Univ. (UK). Dept. of Theoretical Physics). Nucl. Phys., B; 75: No. 2, 343-351(18 Jun 1974).

The differential cross sections for the processes $e^+e^- \to \mu^+\mu^-$ and $e^+e^- \to hX$ are evaluated for arbitrary states of electron and positron polarization. The magnitudes of the weak interaction effects manifested are estimated using models and are found to be large enough to be searched for by the next generation of e^+e^- machines. (auth)

30665 AN SU(3) ANALYSIS OF VECTOR MESON PHOTOPRODUCTION AND THE POMERON. Cocho, G.; Rotelli, P. (International Centre for Theoretical Physics, Trieste (Italy)). Nucl. Phys., B; 75: No. 2, 352-364(18 Jun 1974).

A study is made of the energy dependence and internal symmetry structure of vector-meson photoproduction data. It is found that the pomeron is neither an SU(3) singlet coupling in an SU(3) invariant manner, nor is it described by the simplest generalization of the f-f′ dominance model. (auth)

30666 MULTIPOLE (KINEMATIC) ANALYSIS OF THE REACTION $eN \to e\pi\Delta$. II. Scalar Amplitude Decomposition by Multipole Amplitudes. Zayats, A. A. (Physical-Technical Inst., Kharkov). Ukr. Fiz. Zh. (Russ. Ed.); 19: No. 4, 684-686(Apr 1974). (In Russian).

The breakdown of scalar amplitudes according to multipolar amplitudes was studied. A mathematical development of the problem gave multipolar breakdowns that may be used for analysis of different possible resonances of the mechanisms of the $eN \to e\pi\Delta$ processes. (MG)

30667 CONTRIBUTION OF HADRONS TO VACUUM POLARIZATION. Folomeshkin, V. N. Yadern. Fiz.; 19: No. 5, 1157 (May 1974). (In Russian).

New experimental data on the dependence of the cross section of the reaction $e^+e^- \to$ hadrons on the total energy in the nonresonance region were used to recalculate the contribution of hadrons to vacuum polarization. The total contribution of hadrons in $(g-2)/2$ is $a = (8.2, 8.4, 8.9) \times 10^{-8}$ at $s_{\max}$ to 25, 10^2, and 10^3 GeV, respectively. (JSR)

30668 SENILE SCALING IN ELECTRON–POSITRON ANNIHILATION. Gatto, R. (Rome Univ. (Italy). Istituto di Fisica); Preparata, G. (European Organization for Nuclear Research, Geneva (Switzerland)). Phys. Lett., B; 50: No. 4, 479–481(24 Jun 1974).

An important difference is pointed out between the approach to scaling behavior in deep inelastic scattering and annihilation. In the framework of the massive quark model a quantitative analysis of the breaking terms is carried out for the total and the one-particle inclusive cross sections. Good agreement with available data is found. (auth)

30669 PHASE SPACE AND MULTIHADRON PRODUCTION IN ANNIHILATION PROCESSES AT PRESENT ENERGIES. Lam, W. S.; Suhonen, E. (Bielefeld Univ. (F. R. Germany)). Phys. Lett., B; No. 4, 453–456(24 Jun 1974).

It is argued that at present energies phase space effects are dominant in e^+e^- and $\bar{p}p$ annihilation processes. The predictions of the invariant phase space model give a good agreement with $\bar{p}p$ annihilation data and with the main features observed in e^+e^- annihilation experiments. (auth)

30670 ABSORPTION CORRECTIONS IN A MUELLER REGGE ANALYSIS OF INCLUSIVE PHOTO- AND ELECTROPRODUCTION. Craigie, N. S.; Kramer, G. (Hamburg Univ. (F. R. Germany). 2. Inst. fuer Theoretische Physik). Nucl. Phys., B; 75: No. 3, 509-530(25 Jun 1974).

The photon fragmentation region of inclusive pion photo- and electroproduction is discussed in terms of a helicity-dependent Mueller–Regge model, in which cut contributions are taken into account. It is shown that the inadequacies of a pure Regge pole expansion can be corrected if certain types of Regge cut contributions are included. The transition from electroproduction to the photoproduction limit is shown to be non-smooth in the case of charged pions, and it is pointed out that normal triple-Regge mechanisms are unlikely to be important in the deep inelastic region. (auth)

30671 PION ELECTROPRODUCTION FROM NUCLEI NEAR THRESHOLD. Borie, E. (Michigan State Univ., East Lansing (USA). Dept. of Physics); Chandra, H.; Drechsel, D. (Mainz Univ. (F. R. Germany). Inst. fuer Kernphysik). Nucl. Phys., A; 226: No. 1, 58–70(24 Jun 1974).

The electroproduction of low-energy pions is calculated for experimental situations corresponding to the detection of only one of the outgoing particles. The final nuclear state is a superposition of particle–hole states, corresponding to the giant resonances. A comparison with the predictions of the Fermi gas model is made. The effect of final-state interactions was included by using a distorted-wave impulse approximation to describe electroproduction from nuclei. Distortion effects near threshold have a significant effect on the magnitude of the electroproduction cross section. (auth)

30672 ASYMPTOTIC NEAR FREEDOM. Bailin, D.; Love, A. (Sussex Univ., Brighton (UK). School of Mathematical and Physical Sciences). Nucl. Phys., B; 75: No. 1, 159-170(11 Jun 1974).

The possibility that the asymptotic behavior of the structure functions for electroproduction or neutrinoproduction is controlled by a renormalization group fixed point near the origin, but not at the origin, is discussed. (auth)

30673 CALCULATION OF ELECTROPRODUCTION OF MUON PAIRS IN THE LIGHT-CONE LIMIT. Evans, K. J. (Cambridge

Univ. (UK). Dept. of Applied Mathematics and Theoretical Physics). Nucl. Phys., B; 75: No. 1, 171-180(11 Jun 1974).

The covariant parton model is used to calculate the cross section for ep → $e\mu^+\mu^-$ + hadrons in the limit governed by the bilocal algebra on the light cone. Such an experiment may be feasible in the forseeable future, but the theoretically most interesting mechanisms would contribute only a small number of events. (auth)

30674 AN ANOMALOUS $\rho-\omega$ INTERFERENCE IN THE REACTION $e^+e^- \rightarrow 3\pi$. Achasov, N. N.; Kozhevnikov, A. A.; Shestakov, G. N. (AN SSSR, Novosibirsk. Inst. Matematiki). Phys. Lett., B; 50: No. 4, 448-452(24 Jun 1974).

It is shown that in the $\pi^+\pi^-$ meson mass spectrum in the reaction $e^+e^- \rightarrow \pi^+\pi^-\pi^0$ at $2E > 1$ GeV one should expect the anomalously large effect of the $\rho-\omega$ interference. It can be used as a tool for the elucidation of the details of the $e^+e^- \rightarrow V\pi$ reaction dynamics and also possibly for the determination of the electromagnetic $\rho-\omega$ mixing parameters. (auth)

30675 MUON-ELECTRON UNIVERSALITY AT HIGH ENERGIES AND HADRONIC CORRECTIONS TO $e^+e^- \rightarrow \mu^+\mu^-$. Karl, G. (European Organization for Nuclear Research, Geneva (Switzerland)). Nucl. Phys., B; 75: No. 1, 72-76(11 Jun 1974).

It is argued that unitarity and muon-electron universality are sufficient to determine the contribution of hadrons to the imaginary part of the forward amplitude for the process $e^+e^- \rightarrow \mu^+\mu^-$. With these assumptions Im $T_1^h(e^+e^- \rightarrow \mu^+\mu^-) = s\sigma(e^+e^- \rightarrow \text{hadrons})$ to all orders in α. Some consequences of this formula are discussed. (auth)

30676 DEEP INELASTIC STRUCTURE FUNCTIONS OF THE PHOTON. Worden, R. P. (Science Research Council, Chilton (UK). Rutherford Lab.). Phys. Lett., B; 51: No. 1, 57-62(8 Jul 1974).

Three independent structure functions of a real photon can be measured in photon–photon collisions in $e^\pm e^-$ storage rings. These are M_1 and M_L (related to the usual structure functions W_1 and νW_2, as defined for any target) and a third function M_3, which arises from the strong plane polarization of the colliding photons. It is shown, by using a dispersion relation in the photon mass, that M_3 and the longitudinal structure function M_L both scale and are independent of the vector-dominant hadronic structure of the real photon. Therefore, in a parton model, or in the quark light-cone algebra, they are given by the bare quark box diagrams, which also dominate when both photons have large q^2; this uniquely predicts the behavior $M_L = [(1/2\pi)\Sigma\, e_i^4]4x(1-x)$, $M_3 = [(1/2\pi)\Sigma\, e_i^4](-x^2)$ for the real photon structure functions in the Bjorken limit ($q_2^2 \rightarrow -\infty$, $q_1^2 = 0$, $x = q_2^2/2q_1 \cdot q_2$ = constant). (auth)

30677 SCALING IN e^+e^- ANNIHILATION INTO HADRONS. Di Giacomo, A.; Konishi, K. I. (Scuola Normale Superiore, Pisa (Italy)). Phys. Lett., B; 51: No. 1, 67-70(8 Jul 1974).

The possibility is discussed that the violation of scaling observed in e^+e^- annihilation is due to the opening of the baryon pair channels. One-particle distributions are assumed to scale apart from final-state interactions. The threshold effects are computed. (auth)

30678 THE PION FORM FACTOR AT A TIMELIKE MOMENTUM TRANSFER OF APPROXIMATELY 1 fm^{-1} FROM π^+ ELECTROPORDUCTION AT THRESHOLD. Del Guerra, A.; Giazotto, A.; Giorgi, M. A.; Stefanini, A. (Pisa Univ. (Italy). Istituto di Fisica); Kellett, B. H. (Glasgow Univ. (UK). Dept. of Natural Philosophy); Verzegnassi, C. (Trieste Univ. (Italy). Istituto di Fisica); Botterill, D. R.; Norton, P. R. (Science Research Council, Daresbury (UK). Daresbury Lab.). Phys. Lett., B; 50: No. 4, 487-490(24 Jun 1974).

From an extrapolation of threshold π^+ electroproduction data combined with a kinematical constraint at an unphysical point, the value of the pion form factor is derived at a time-like value of the momentum transfer $k_\pi^2 \simeq 1\ fm^{-2}$. The result is $F_\pi(k_\pi^2) = 1.19 \pm 0.1$. From this value, by using a twice-subtracted dispersion relation, $r_\pi \gtrsim 0.98 \pm 0.24$ fm is obtained. (auth)

Weak

30679 (CONF-730693-, pp 31-42) NEUTRINO MASS FROM ASTROPHYSICS. Marx, G.; Szalay, A. S. (Roland Eoetvoes Univ., Budapest). 1974.

From proceedings of the summer school on particles and fields in space; Balatonfured, Hungary (5 Jun 1973).

From the upper limit of the deceleration of extragalaxies and from the lower limit of the age of the universe one can put an upper limit on the mass density. Dividing mass density by particle number density one obtains information about the rest masses. Some upper limits and a possible mass of the neutrino are discussed. (JFP)

30680 GENERALIZED COVARIANCE PRINCIPLES AND NEUTRINO PHYSICS. Flato, M.; Piard, A. (Univ., Dijon, France). J. Math. Phys. (N. Y.); 15: No. 8, 1288-1294(Aug 1974).

The zero-mass Dirac equation admits a simple generalized covariance group which is an inhomogeneous Lorentz group G different from the Poincaré group. Its mathematical structure and unitary irreducible representations have been studied by Flato and Hillion [Phys. Rev. D 1, 1667(1970)]. Physical consequences concerning neutrino physics were then obtained by introduction of the Stokes parameters. The coverage includes presentation of the idea of generalized covariance, a summary of the main results obtained by Flato and Hillion, and introduction of the 14 dimensional unification group proper for the generalized covariance of the free neutrino equation. By the well known method of induced representations all the strongly continuous unitary irreducible representations of the 10-dimensional Dirac group G as well as of the 14-dimensional unification group G are studied. Particular zero-mass representations of G′ which are of interest at least for the study of the neutrino free-field theory are treated. These classes of unitary irreducible representations of G′ permit one to have two possible physical alternatives which are discussed. (auth)

30681 INTRODUCTION TO RENORMALIZABLE MODELS OF WEAK INTERACTIONS. Llewellyn Smith, C. H. (CERN, Geneva). pp 99-181 of Proceedings of the Fifth Hawaii Topical Conference in Particle Physics. Dobson, P. N. Jr. (ed.). Honolulu, HI; Univ. Press of Hawaii (1974).

From 5th topical conference in particle physics; Honolulu, Hawaii, USA (8 Aug 1973). See CONF-730856-.

The problem of constructing models of weak interactions which might describe the real world and to confront them with experiment is discussed. The relevance of renormalizability and the elements of renormalizable models are first discussed. Examples of various models and a recipe for model building are then discussed. (LBS)

30682 ELECTRON DECAY SPECTRUM IN MUON DECAY IN THE UNIFIED THEORY OF WEAK AND ELECTROMAGNETIC INTERACTIONS. Fukuda, R. (Kyoto Univ.); Sasaki, R. Lett. Nuovo Cim.; 10: No. 17, 765-770(24 Aug 1974).

Radiative corrections to the μ-e decay in the unified theory of weak and electromagnetic interactions are calculated in the one-loop order. Finite decay electron spectrum is obtained explicitly by using the dispersion method. (LBS)

30683 APPLICATION OF THE ON-MASS-SHELL CURRENT ALGEBRA TO THE K_{l3} FORM FACTOR. Golestaneh, A. A. (Univ. of Texas, Austin); Carlson, C. E. Nuovo Cim.; 23A: No. 1, 153-172(1 Sep 1974).

The K_{l3} decay amplitudes are evaluated with a current algebra formalism while keeping the pions on the mass shell. This calculation is done using a technique described previously, in which the axial vector currents are modified and the equal-time commutation relations of the new currents verified. As a result of using these new currents, and for not needing to extrapolate the pion mass, the reduction formula contains some terms which must be evaluated by summing over sets of the intermediate states. In this application it is noted that dominating intermediate states are the π, K^*, A_1, x mesons. and the two-particle systems (K^*K) and ($\varkappa K$). Using the known data for the π, K, K^* and A_1 mesons a surprising sensitivity of the ratio of the decay form factors, i.e., $\xi(0) \equiv f_-(0)/f_+(0)$, to the change of the $\varkappa$ mass, width and decay constant is found. Within the expected ranges of these parameters, values of $\xi(0)$ ranging from -0.1 to -0.85 can be obtained by the present treatment. (auth)

30684 CAN THE $\Delta I = 1/2$ SELECTION RULE IN THE $K \rightarrow 2\pi$ DECAY BE SATISFIED IN GAUGE THEORIES. Eliezer, S.; Ross, D. A. (Imperial Coll. of Science and Tech., London). Lett. Nuovo Cim.; 11: No. 3, 233-237(21 Sep 1974).

The ΔI selection rule in weak interactions is investigated by calculating the decay rates for $K^+ \rightarrow \pi^+\pi^0$ and $K_1^0 \rightarrow \pi^+\pi^-$ ($2\pi^0$). The calculations are performed by using the free-quark model to describe the kaon and pion states and the Salam–Weinberg model to describe the weak interaction. The calculation is made to first order in the weak interactions (tree-diagram approximation). Although the decay $K^+ \rightarrow \pi^+\pi^0$ should be suppressed relative to $K_1^0 \rightarrow 2\pi$, since the former is a pure ΔI process, it is found that the amplitudes are of the same order of magnitude, both being to first order in the SU(3)-breaking. (JFP)

30685 NEUTRON OPTICS AND WEAK CURRENTS. Stodolsky, L. (Max-Planck-Institut fuer Physik und Astrophysik, Muenchen (F. R. Germany)). Phys. Lett., B; 50: No. 3, 352-356(10 Jun 1974).

The weak interaction can produce two small but striking effects with low energy neutrons. With a transversely polarized neutron beam the polarization rotates in passing through matter; and with an unpolarized beam a longitudinal polarization develops. These effects are of first order in the weak coupling and can only be produced by parity violating forces. With the conventional weak interaction only the nucleons in the material contribute, with "neutral currents" electrons also interact weakly. Thus, if experiments on different materials are performed, "neutral currents" may be observed by detecting an electron contribution to the effect and furthermore the isotopic structure of the weak interaction between nucleons may be determined. (auth)

30686 QUARK PARTON MODEL FOR DEEP INELASTIC LEPTON SCATTERING. Gourdin, M. (CERN, Geneva). pp 102-137 of Properties of the Fundamental Interactions. Vol. 9, Pt. A. Zichichi, A. (ed.). Bologna; Editrice Compositori (1973).

From Properties of the Fundamental Interaction NATO-MPI-MRST Advanced Study Institute meeting; Erice, Italy (8 Jul 1971). See CONF-710744-(P9)(PA).

Lectures are given on an elementary understanding of the previous sophisticated languages for the quark parton model attempting to be quantitative and to use the available experimental data as much as possible. The topics discussed are kinematics, the parton model, the quark parton model, sum rules, positivity constraints, and symmetries. The total neutrino and antineutrino cross sections and polarization for inelastic electron scattering are considered. (JFP)

30687 DIMENSIONAL REGULARIZATION FOR WEAK INTERACTIONS. Delbourgo, R.; Prasad, V. B. (Imperial Coll. of Science and Tech., London). Nuovo Cim.; 23A: No. 2, 257-270 (21 Sep 1974).

In generalizing the current-current form of the weak Lagrangian to arbitrary dimensions two kinds of polar vector and two kinds of axial vector are encountered among the possible set of currents. One of these weak polar vector currents is not conserved except in four dimensions and undergoes a finite renormalization from quantum loops. (auth)

30688 CHARMED-PARTICLE PRODUCTION BY NEUTRINOS WITH THE WEINBERG SU(4) CURRENTS. Albright, C. H. (European Organization for Nuclear Research, Geneva (Switzerland)). Nucl. Phys., B; 75: No. 3, 539-545(25 Jun 1974).

Charmed-particle production by neutrinos is investigated with the quark parton model formalism. Emphasis is placed on the largest effects which can be tolerated by the present experimental data as well as those suggested by more conventional models. (auth)

30689 PION DISTRIBUTIONS IN INELASTIC NEUTRINO INTERACTIONS. Albright, C. H.; Cleymans, J. (European Organization for Nuclear Research, Geneva (Switzerland)). Nucl. Phys., B; 76: No. 1, 48-60(4 Jul 1974).

Using data on semi-inclusive pion electroproduction as input, the distribution of pions in the current fragmentation region is calculated in the framework of the quark parton model for inelastic neutrino interactions. Results for the π^+/π^- asymmetry are presented for both charged and neutral currents. These provide stringent tests of the parton fragmentation hypothesis and the Weinberg–Salam gauge model. (auth)

Strong (General)

Refer also to abstracts 30781 and 31147.

30690 NEW DESCRIPTION OF THE INITIAL STATES. Kupczynski, M. (Univ., Warsaw). Lett. Nuovo Cim.; 11: No. 2, 117-120(14 Sep 1974).

The idea that the initial ensemble E of two-particle states (one particle from the beam and one from the target) is a mixed ensemble with respect to some additional parameters is developed without introducing new parameters for the two-particle states. It is noted that this hypothesis is correct, it will require very serious changes in the strong-interaction elementary-particle physics. This hypothesis, if correct, would also explain the possibility of the violation of the optical theorem. (JFP)

30691 PARTONS. Feynman, R. P. (California Inst. of Tech., Pasadena). pp 1-97 of Proceedings of the Fifth Hawaii Topical Conference in Particle Physics. Dobson, P. N. Jr. (ed.). Honolulu, HI; Univ. Press of Hawaii (1974).

From 5th topical conference in particle physics; Honolulu, Hawaii, USA (8 Aug 1973). See CONF-730856-.

The general ideas of the parton concept are first described. It is then pointed out how the experiments on deep-inelastic scattering of electrons and neutrinos by nucleons give information about the nature and distribution of the partons. This is followed by a discussion of the applications of parton ideas to hadronic collisions. Diffraction dissociation and some theoretical problems are also discussed. (LBS)

30692 GEOMETRICAL INTERPRETATION OF PARAORDER 3 OF PARAQUARK MODEL. Morita, K. (Nagoya Univ., Japan). Lett. Nuovo Cim.; 10: No. 17, 779-783(24 Aug 1974).

It is shown that the paraorder 3 has a direct geometrical origin of being the dimensionality of the space and that the gauge group is V_3. (LBS)

30693 SEMICLASSICAL MODEL OF MULTIPARTICLE PRODUCTION. Rechenberg, H. R.; Robertson, D. C. (Max-Planck-Institut fuer Physik und Astrophysik, Munich). Acta Phys. Pol., B; 5: No. 4, 507-521(1974).

A model of multiparticle production in high energy hadron collisions developed by Heisenberg more than 20 years ago is reexamined and compared to recent data on multiplicities, dispersion of multiplicities and partial cross sections. It is found that, contrary to popular belief, the behavior of the multiplicity predicted by his strong coupling model is still consistent with the data. Predictions about the intimate connection between the so-called KNO-scaling, and the constancy of the inelastic cross section are discussed in the light of the present experimental results. (auth)

30694 GENERALIZATION OF REGGE-BEHAVED DAMA TO PRODUCTION PROCESSES. Jenkovszky, L. L. (Inst. of Theoretical Physics, Kiev); Timokhin, V. V. Acta Phys. Pol., B; 5: No. 4, 537-547(1974).

The properties of the generalization of a Regge-behaved dual amplitude with Mandelstam analyticity (DAMA) to production processes are studied. A procedure of analytic continuation of A_5 into the physical domain is suggested. The amplitude has necessary dual, asymptotic and resonance properties. (auth)

30695 EXTENDED HADRONS AND REGGE SLOPE. Lusanna, L. (National Inst. of Nuclear Physics, Florence). Lett. Nuovo Cim.; 11: No. 3, 213-217(21 Sep 1974).

A simple interpretation of the slope of the strongly interacting particles on Regge trajectories based upon the relativistic properties of hadrons, thought of as extended quasi-classical objects built of elementary constituents (quarks, partons, virtual hadrons) and endowed with an intrinsic angular momentum. (JFP)

30696 CHARGE DISTRIBUTIONS OF MANY PARTICLE FINAL STATES AND THE ENERGY DEPENDENCE OF FORWARD CHARGE EXCHANGE. Krzywicki, A.; Weingarten, D. (Paris-11 Univ., 91 – Orsay (France). Lab. de Physique Theorique et Particules Elementaires). Phys. Lett., B; 50: No. 2, 265-269(27 May 1974).

Possible dynamical origin of the energy dependence of charge exchange cross sections is described. The assumption is local compensation of charge in a certain class of many particle final states. (auth)

30697 A DUAL QUARK PRISON. Olesen, P. (Niels Bohr Institutet, Copenhagen (Denmark)). Phys. Lett., B; 50: No. 2, 255-257(27 May 1974).

Using semi-classical arguments it is pointed out that the closed dual string, which arises in the strong coupling limit of gauge field theories, has the possibility of imprisoning quarks. (auth)

30698 BINARY-COLLISION THEORY FOR MULTIHADRON PRODUCTION AMPLITUDES. Arnold, R. C. (Argonne National Lab., Ill. (USA)). Phys. Lett., B; 50: No. 3, 359-361(10 Jun 1974).

A model for hadron production amplitudes is proposed which includes dynamical correlations, determined from two-body reactions, between all pairs of particles. Qualitative results are obtained accounting for many of the characteristic features recently seen in high energy collisions, including: large transverse momentum inclusive cross-sections, broad multiplicity distributions, and strong clustering effects in rapidity. (auth)

30699 HEAVY PARTICLE PRODUCTION AND CLUSTER MODELS OF HIGH-ENERGY COLLISIONS. Bialas, A. (Max-Planck-Institut fuer Physik und Astrophysik, Muenchen (F. R. Germany)); Jacob, M. (European Organization for Nuclear Research, Geneva (Switzerland)); Pokorski, S. (Warsaw Univ. (Poland)). Nucl. Phys., B; 75: No. 2, 259-268(18 Jun 1974).

It is pointed out that the study of heavy particle production at high energies and the analysis of the associated pion multiplicity distribution may provide important indications concerning the origin of the clustering effects observed in very high energy collisions. (auth)

30700 TRANSVERSE MOMENTUM BOUNDS AND SCALING IN THE HYDRODYNAMICAL MODEL. Chaichian, M.; Satz, H. (European Organization for Nuclear Research, Geneva (Switzerland)); Suhonen, E. (Bielefeld Univ. (F. R. Germany)). Phys. Lett., B; 50: No. 3, 362-366(10 Jun 1974).

It is shown that the equation of state of an ideal relativistic gas, as applied in the hydrodynamical model, leads not only to deviations from scaling in longitudinal rapidity distributions, but also to an average transverse momentum increasing asymptotically as a power of the incident energy. To prevent such an increase, one must use the equation of state of an interacting gas, in which the velocity of sound becomes asymptotically equal to that of light. This then also restores scaling (up to logarithmic terms) in longitudinal rapidity. (auth)

30701 OVERLAP FUNCTION FROM THE MULTIPERIPHERAL MODEL. Jadach, S. (Uniwersytet Jagiellonski, Krakow (Poland)); Turnau, J. (Institute of Nuclear Physics, Krakow (Poland)). Phys. Lett., B; 50: No. 3, 369-372(10 Jun 1974).

Monte Carlo phase space calculations of the overlap function for Chan-Loskiewicz-Allison and Chew-Pignotti models were performed up to laboratory momentum 1500 GeV. Slope of the overlap function was found about four times smaller than the experimental value. Shrinkage of the elastic peak is close to that found in experiment. The qualitative explanation of these results is given, and the discrepancy with the recent estimates obtained by Hamer and Peierls, Hwa, and Henyey is explained. Finally, the analysis shows that the random walk picture of the multiperipheral models is not valid for realistic density of particles in rapidity scale. (auth)

30702 QUARK OR BOOTSTRAP: TRIUMPH OR FRUSTRATION FOR HADRON PHYSICS. Chew, G. F. (Univ. of California, Berkeley). pp 3-22 of Properties of the Fundamental Interactions. Vol. 9, Pt. A. Zichichi, A. (ed.). Bologna; Editrice Compositori (1973).

From Properties of the Fundamental Interaction NATO-MPI-MRST Advanced Study Institute meeting; Erice, Italy (8 Jul 1971). See CONF-710744-(P9)(PA).

The discussion covers electromagnetism as the bridge between real and quantum worlds, the hadron S matrix bootstrap, supplementary S matrix principles, and experimental implications from models. It is noted that particle physics is frequently likened to the peeling of successive layers from an onion to see what lies underneath. (JFP)

30703 STRONG INTERACTION DYNAMICS. Jacob, M. (CERN, Geneva). pp 138-219 of Properties of the Fundamental Interactions. Vol. 9, Pt. A. Zichichi, A. (ed.). Bologna; Editrice Compositori (1973).

From Properties of the Fundamental Interaction NATO-MPI-MRST Advanced Study Institute meeting; Erice, Italy (8 Jul 1971). See CONF-710744-(P9)(PA).

Lectures are presented illustrating with a few topical examples how present understanding of strong interaction dynamics in terms of Regge exchange can be put to a test. Inclusive interactions and Regge behavior are also considered. (JFP)

30704 GEOMETRO-DYNAMICAL SOLDERING OF THE INTERNAL AND EXTERNAL SPACES OF STRONGLY INTERACTING PARTICLES. Heskia, S. (London Univ.). Nuovo Cim.; 23A: No. 2, 321-330(21 Sep 1974).

The gravitational field of space-time is shown to "solder" the dynamical group $O_{4,1}$ of space-time to the internal symmetry group $S \supseteq O_{\text{int}3,1}$ describing the isospin. In an irreducible representation of the "soldered" group one can obtain the mass formula $m^2 = m_0^2 + \lambda^2[J(J+1) + I(I+1)]$ for the mesons. (auth)

30705 EFFECTIVE DEGREES OF FREEDOM IN STRONG INTERACTION PROCESSES. Fubini, S.; Rebbi, C. (CERN, Geneva). Nuovo Cim.; 23A: No. 2, 331-347(21 Sep 1974).

A scheme of approximation where strong-interaction processes with a purely longitudinal configuration of external momenta are described by fields which depend on longitudinal space-time variables only, but retain their full four-dimensional spin structure. The evolution of these fields is governed by an effective Lagrangian, which can be obtained from the four-dimensional Lagrangian using a variational method. The main features of the effective Lagrangians for one-dimensional and two-dimensional configurations of the external momentas are discussed briefly. (auth)

30706 MULTIPLE POMERON EXCHANGE AND FINAL STATE RESCATTERING. Schwimmer, A. (Weizmann Inst. of Science, Rehovoth (Israel). Dept. of Nuclear Physics). Nucl. Phys., B; 75: No. 3, 446-454(25 Jun 1974).

The influence of final state rescattering corrections on multiple pomeron exchange of a simple pole pomeron violates the Froissart bound even after the inclusion of these corrections. A self-consistent unitarity equation is set up and it is shown that its solution is an expanding black disk. The multiparticle properties of this solution are discussed. (auth)

30707 SPONTANEOUS SYMMETRY BREAKDOWN AND REGGE INTERCEPTS. Cahalan, R. F.; Frampton, P. H. (Syracuse Univ., N. Y. (USA). Dept. of Physics). Phys. Lett., B; 50: No. 4, 475-478 (24 Jun 1974).

By Regge slope methods a Nambu–Goldstone spontaneous symmetry breakdown and a Higgs mechanism inherent in a unit-intercept dual meson amplitude are exhibited. By introducing an Abelian gauge group corresponding to conservation of a pseudocharge, Regge intercept shifts are calculated; to lowest order, the leading Regge intercept of the Neveu–Schwarz model is lowered from $\alpha(0) = 1$ to $\alpha(0) = 1/3$. The method has the advantage over Bardakci's spurion method that massless scalar states are not required at any stage. (auth)

30708 GNOME MODEL AND DEEP-INELASTIC LEPTON-NUCLEON STRUCTURE FUNCTIONS. Tokuda, N. (Heidelberg Univ. (F. R. Germany). Inst. fuer Theoretische Physik und Mechanik). Nucl. Phys., B; 75: No. 1, 181-188(11 Jun 1974).

The gnome model for hadrons, a nonet scheme which has been proposed as an alternative to the quark model and which avoids certain well-known difficulties of the latter concerning fractional charge, spin and statistics is investigated. It is found that the gnome model gives the same results as the quark model for semileptonic decay and electromagnetic transition matrix elements. The bounds for deep-inelastic lepton-nucleon structure functions are not as restrictive as the ones from the quark model if only SU(2) invariance is imposed. SU(3) invariance together with duality gives more restrictive bounds. (auth)

30709 QUARK ADDITIVITY FOR MASS SPLITTINGS IN THE $p_z \to \infty$ FRAME. Cabibbo, N.; Testa, M. (European Organization for Nuclear Research, Geneva (Switzerland)). Phys. Lett., B; 51: No. 1, 96-98(8 Jul 1974).

It is found that the $p_z \to \infty$ constituent quark description of hadrons, which was successfully used to describe deep inelastic phenomena, also describes correctly the main features of SU(3)-breaking mass splittings. In particular, the observed D/F ratio in baryon mass splittings is explained in terms of the same configuration mixing introduced to interpret deep inelastic electroproduction. (NL)

30710 UNITARITY, PHENOMENOLOGY AND THE BARE POMERON. Bali, N. F. (Washington Univ., Seattle (USA). Dept. of Physics); Dash, J. W. (Argonne National Lab., Ill. (USA)). Phys. Lett., B; 51: No. 1, 99-102(8 Jul 1974).

The possibility of utilizing the multifireball expansion and a bare Pomeron at $\hat{\alpha}_0 = 0.85$ as an approximation to a solution of the s-channel unitarity equations explicitly connecting 2-body and inelastic phenomenology is discussed. A scale for Pomeron renormalization effects is inferred. (auth)

30711 LIKE PARTICLE CORRELATIONS AS A TOOL TO STUDY THE MULTIPLE PRODUCTION MECHANISM. Kopylov, G. I. (Joint Inst. for Nuclear Research, Dubna (USSR)). Phys. Lett., B; 50: No. 4, 472-474(24 Jun 1974).

The measurement of correlations between like pions in the inclusive processes $a + b \to \pi^{\pm} + \pi^{\pm} + X$ permits one to study the space–time mechanism of multiple production. Similar measurements for neutrons evaporated from highly excited nuclei give the shape of nuclei and their mean lives; for pions from the resonance decay, the mean resonance life. (auth)

30712 THE EFFECTS OF MOMENTUM CONSERVATION ON PIONIZATION. Shaw, K. R. (Cambridge Univ. (UK). Cavendish Lab.). Nucl. Phys., B; 76: No. 1, 116-124(4 Jul 1974).

The Mueller–Regge models of inclusive processes in the "pionization" region are constrained to obey momentum conservation. A separate representation in the fragmentation region is found to be necessary on both theoretical and phenomenological grounds. It is also argued that the Laplace transform technique of solving the constraint equations highlights the bad low-energy behavior of these models. (auth)

30713 STATISTICAL BOOTSTRAP MODEL WITHOUT EXOTIC FIREBALLS. Wambach, U. M. (Bielefeld Univ. (F. R. Germany)). Nucl. Phys., B; 76: No. 1, 109-115(4 Jul 1974).

The bootstrap model is generalized to include isospin quantum numbers under the restriction that no exotic fireballs participate in the bootstrap. The same definition of exoticity is applied as in the dual resonance and quark model. The explicit solution is derived and the singularity of the partition function which determines the highest temperature is investigated. Such a generalization of the statistical bootstrap model may be tested by comparing with charge distributions, correlations, and charge transfer measurements. (auth)

30714 OFF-MASS-SHELL DUAL AMPLITUDES. III. Schwarz, J. H. (California Inst. of Tech., Pasadena (USA)). Nucl. Phys., B; 76: No. 1, 93-108(4 Jul 1974).

The study of off-mass-shell amplitudes in the $\alpha(0) = 1$ Veneziano model is continued. A formula for the scalar analog of virtual Compton scattering is derived and the deep-inelastic and Regge limits are investigated. For suitable choice of a parameter, it is demonstrated that a scaling law (of the Bjorken type) holds, even though the hadrons of the model contain no point-like structures. Regge poles and fixed poles of the appropriate type are also found. All these desirable results emerge despite the fact that they have not been built into the construction in any obvious way. The few remaining problems—logarithmic divergences and conflicting constraints on the dimension of space-time—are quite plausibly attributable to deficiencies of the particular dual model rather than the approach to constructing currents. (auth)

30715 THE QUARK–PARTON PARADOX. Orzalesi, C. A. (Pavia Univ. (Italy). Istituto di Fisica). Phys. Lett., B; 51: No. 1, 63-66(8 Jul 1974).

The author heuristically discusses the paradox that quarks are seldom produced and show semiclassical parton features while at the same time they interact strongly and are deeply bound inside hadrons. Rising total cross sections are interpreted as partially due to the production of massive free quarks through "pionization" graphs. (auth)

30716 PION PHASE TRANSITION IN CHIRAL SYMMETRY BREAKING MODEL. Dashen, R. (Institute for Advanced Study, Princeton, N. J. (USA)); Manassah, J. T. (American Univ., Beirut (Lebanon)). Phys. Lett., B; 50: No. 4, 460–462(24 Jun 1974).

It is shown that, in the non-linear σ-model, one has a phase transition when the isospin chemical potential is equal to the meson mass. This result is shown to be generally true in the $SU(2) \times SU(2)$ symmetry breaking model. (auth)

30717 POSSIBILITY THAT THE POMERON–REGGEON CUT CONTAINS THE REGGE POLE. Desai, B. R. (California Univ., Riverside (USA). Dept. of Physics). Phys. Lett., B; 50: No. 4, 494–498(24 Jun 1974).

By using the triple Regge formalism for the sum over intermediate states, it is shown that the Reggeon–Pomeron cut inherits the Regge pole. This pole dominance of the cut is experimentally verified for non-Pomeron exchanges involving vector and tensor trajectories. Consequences of t-channel unitarity are discussed. (auth)

Strong (Baryon No. = 0)

Refer also to abstract 30791.

30718 (JINR-P2-7502) POSSIBLE DESCRIPTION OF THE ρ RESONANCE IN THE SIMPLEST MODEL OF THE $\pi\pi$-INTERACTION. Angelov, N.; Atanasov, A.; Garsevanishvili, V.; Matveenko, A. (Joint Inst. for Nuclear Research, Dubna (USSR). Lab. of Theoretical Physics). 1973. 10p. (In Russian). INIS.

The possibility of describing the ρ-resonance within the framework of the model with four-pion interactions was examined. The calculation was made with the local quasipotential equation. (tr-auth)

30719 KINEMATICAL ORIGIN OF THE CONFIGURATION MIXING IN THE CHIRAL ALGEBRA. Celeghini, E.; Sorace, E. (Univ., Florence). Lett. Nuovo Cim.; 11: No. 2, 166-168(14 Sep 1974).

It is shown that the configuration mixing of the chiral algebra can be obtained as a result of a well defined limit of particles are compound states belonging to irreducible representations of the classification group. The old suggestion of Gell-Mann that current quarks may be nothing else than a group substitute of the infinite boost on extended particles is therefore clearly demonstrated. Only mesons are considered. (JFP)

30720 RELATIVISTIC CORRECTION IN DOUBLE SCATTERING BY DEUTERONS. Ragusa, S.; Rosa, L. P.; Thome, Z. D. (International Centre for Theoretical Physics, Trieste, Italy). Nuovo Cim.; 23A: No. 1, 145-152(1 Sep 1974).

A relativistic correction to the double-scattering Glauber formula arising from the relativistic correction in the definition of the center-of-mass and relative coordinates is presented. An application is made to the rho photoproduction on deuterons. (auth)

30721 PROPERTIES OF THE NUCLEON–ANTINUCLEON FIREBALL. Vandermeulen, J. (Univ., Liege). Lett. Nuovo Cim.; 11: No. 3, 243-247(21 Sep 1974).

Results for $p\bar{p}$ annihilation at rest leading to pions in the final state, excluding the production of a $K\bar{K}$ pair, are compared with a simple version of the statistical bootstrap. The branching ratios, frequency distribution of pion multiplicities, average numbers of neutral and negative pions, and the charged pion momentum distribution are considered. (JFP)

30722 EXACT AND PERTURBATIVE SOLUTIONS OF THE VAN HOVE MODEL DESCRIBING NUCLEAR DIFFRACTION DISSOCIATION OF PIONS. Lukierski, J.; Turko, L. (Univ., Warsaw). Bull. Acad. Pol. Sci., Ser. Sci., Math., Astron. Phys.; 22: No. 6, (1974).

Solutions of the Van Hove model describing the dissociation of pions into continuum states from nuclei are discussed. An exact solution is given for the case of a separable continuum-continuum transition vertex. In the general case, when the off-diagonal elements of such a vertex are small, a perturbative solution is proposed. The formulas take into consideration the relativistic kinematics and the three-momentum loss to the nucleus. (auth)

30723 PHENOMENOLOGICAL UPPER AND LOWER BOUNDS ON THE $\pi\pi$ S-WAVE SCATTERING LENGTHS. Bonnier, B. (European Organization for Nuclear Research, Geneva (Switzerland)). Nucl. Phys., B; 75: No. 2, 333-342(18 Jun 1974).

Starting from a given phenomenological input (upper and lower bounds of the real and imaginary parts of the $\pi^0\pi^0$ and $\pi^+\pi^0$ amplitudes in the region $0.45\ \text{GeV} \leq E_{cm} \leq 1.9\ \text{GeV}$; $0 \leq t \leq 4\ \mu^2$) rigorous upper and lower bounds on the $\pi\pi$ S-wave scattering lengths are derived. (auth)

30724 SCALAR MULTIPLETS AND ASYMPTOTIC FREEDOM. Delbourgo, R. (Imperial Coll. of Science and Tech., London); Salam, A.; Strathdee, J. Nuovo Cim.; 23A: No. 2, 237-256(21 Sep 1974).

In a gauge theory of scalar mesons interacting with gauge vector particles, it is shown that scalar-meson four-point Green's functions are free of infinities, provided that the scalar mesons do not couple to any fermions in the model and there is no direct $\lambda\varphi^4$-term in the Lagrangian. The proof relies on a "gauge approximation" technique which systematically exploits the information provided by Ward-Takahashi identities. For non-Abelian gauge theories, the significance of this result is that a large class of scalar multiplets which can induce spontaneous symmetry breaking do not affect the issue of asymptotic freedom. In order to exploit the information of Ward-Takahashi identities the "axial gauge" is used in which there are no fictitious scalar particles and the identities assume their naive form, with $Z_1 = Z_2$ for all matter and gauge fields. (auth)

30725 A TWO-DIMENSIONAL MODEL FOR MESONS. 't Hooft, G. (European Organization for Nuclear Research, Geneva (Switzerland)). Nucl. Phys., B; 75: No. 3, 461–470 (25 Jun 1974).

A recently proposed gauge theory for strong interactions, in which the set of planar diagrams play a dominant role, is considered in one space and one time dimension. In this case, the planar diagrams can be reduced to self-energy and ladder diagrams, and they can be summed. The gauge field interactions resemble those of the quantized dual string, and the physical mass spectrum consists of a nearly straight "Regge trajectory." (auth)

30726 PION AND KAON FORM FACTORS AND HEAVY VECTOR MESONS. Zovko, N. (Karlsruhe Univ. (TH) (F. R. Germany). Inst. fuer Theoretische Kernphysik). Phys. Lett., B; 51: No. 1, 54-56(8 Jul 1974).

A zero parameter model of analytic pion and kaon form factors with supplementary dynamical constraints is presented. Contrary to the general belief, the predicted form factors have a t^{-2} behavior and fit the pion space-like data excellently. Some properties of heavy vector mesons are predicted and discussed. (auth)

30727 IS THE 0^+ NONET RESPECTABLE? Morgan, D. (Science Research Council, Chilton (UK). Rutherford Lab.). Phys. Lett., B; 51: No. 1, 71-78(8 Jul 1974).

A scheme of assignments for the 0^+ nonet is proposed with the S^* (1000) effect corresponding to resonance poles on both Sheet II and Sheet III, and with the ϵ located somewhere above 1100 MeV, e.g., at 1300 MeV. A tentative fit of the decay characteristics of these and the other nonet candidates, $\delta(970)$ and $\kappa(\sim 1200)$, is achieved with the mixing angle given by $\cos^2\theta_s \sim 0.13$ instead of the "ideal" value of $\frac{2}{3}$. (auth)

30728 THE $\eta-\eta'$ MIXING ANGLE FROM DUALITY AND AND QUARK MODEL. Bramon, A. (Universidad Autonoma de Barcelona (Spain)). Phys. Lett., B; 51: No. 1, 87-89(8 Jul 1974).

From simple quark model and duality arguments the $\eta-\eta'$ mixing angle is predicted to be $\theta = \arctan(-\frac{1}{2}\sqrt{2}) \approx -19.5°$. The available experimental data seem to support such a result. (auth)

30729 GENERALIZED VECTOR DOMINANCE AND THE PION FORM FACTOR. Boehm, M. (European Organization for Nuclear Research, Geneva (Switzerland)); Krammer, M. (Deutsches Elektronen-Synchrotron (DESY), Hamburg (F. R. Germany)). Phys. Lett., B; 50: No. 4, 457–459(24 Jun 1974).

The pion form factor has been calculated using the bound state

Bethe–Salpeter amplitudes and the quark form factor of a relativistic quark model. A generalized vector dominance structure and an asymptotic behavior in the space-like region $F_\pi(Q) \sim -0.33$ GeV^2/Q^2 is obtained. (auth)

Strong (Baryon No. = 1)

Refer also to abstracts 30512 and 31097.

30730 (ITEF-31) ANALYSIS OF $K_1^0K_1^0$ SYSTEM IN THE $\pi^- p \rightarrow nK^0 \bar{K}^0$ REACTION AT 40 GeV/c. Baloshin, O. N.; Blagorodov, A. M.; Bolonkin, B. V. (Gosudarstvennyj Komitet po Ispol'zovaniyu Atomnoj Ehnergii SSSR, Moscow. Inst. Teoreticheskoj i Ehksperimental'noj Fiziki). 1973. 14p. (In Russian). INIS.

An analysis is presented of ~500 events of the reaction $\pi^- p \rightarrow K_1^0K_1^0 n$ at a 40 GeV/c momentum. The mass spectrum of the $K_1^0K_1^0$ system has a significant excess of events in the region $1.0 < M_{KK} < 1.5$ GeV/c^2, and qualitatively agrees with distributions obtained at lower energies. Distributions were also obtained according to the cosine of the angle between the incident π^--meson and the K-meson in the center-of-inertia system of two K-mesons, and according to the square of the transmitted momentum from proton to neutron for various mass regions of the $K_1^0K_1^0$ system. From a comparison of the data with available data at lower energies in the region of small masses of the $K_1^0K_1^0$ system it is possible to obtain an effective Regge trajectory slope of $\alpha' = 1.2 \pm 0.2$ (GeV/c)$^{-2}$. (tr-SJR)

30731 OFF–SHELL πN AMPLITUDES VIA A MULTICHANNEL SEPARABLE POTENTIAL. Londergan, J.T. (Department of Physics, University of Wisconsin, Madison, Wisconsin 54706); McVoy, K.W.; Moniz, E.J. Ann. Phys. (N.Y.) 86: No. 1, 147-177 (July 1974).

The off–shell pion–nucleon transition matrix is a basic ingredient in theories of pion–nuclear interactions which, in the absence of fundamental theory of πN dynamics, must be obtained by a phenomenological extrapolation from the available on–shell data. As one means of performing such an extrapolation, we explore a multichannel separable potential model with the property that the off–shell elastic scattering amplitude is generated directly from the measured elastic–channel phase shifts. The off–shell πN partial–wave transition amplitudes determined by this procedure are compared with those calculated by Landau and Tabakin using a one–channel absorptive separable potential. We find that the absorptive separable potential approach provides a physically unreasonable off–shell extrapolation at energies where the on–shell amplitude is highly inelastic, and show that the difficulty is a direct consequence of the one–channel nature of that method. The multichannel extrapolation is free of these difficulties. (auth)

30732 PARAMETRIZATION OF LOW ENERGY πN PHASE SHIFTS. Pelosi, V.; Abram, M. (Univ., Milan). Lett. Nuovo Cim.; 11: No. 2, 111-116(14 Sep 1974).

Since recent determinations of πN phase shifts were shown to converge at least in the low energy region, not only qualitatively, but also numerically, an attempt is made to extract a corresponding dynamical content, as may be described, for instance, in the form of a potential, if any. As a first approximation in the energy region where inelastic processes are not yet at work, a spherical-well potential is considered, where the parameters are the depth and radius for each of the involved waves. (JFP)

30733 PRACTICAL EVALUATION OF THE ASYMPTOTIC REAL–PART BEHAVIOR AND THE SEARCH FOR A POSSIBLE SUBTRACTION CONSTANT IN THE CROSSING-ODD FORWARD PION–NUCLEON AMPLITUDE. Ferrari, E.; Lusignoli, M.; Violini, G. (Univ., Rome). Lett. Nuovo Cim.; 10: No. 17, 762-764(24 Aug 1974).

It is pointed out that the problem of calculation of the dispersive integral for evaluating the asymptotic real-part behavior of scattering amplitudes has been solved in a simple and straightforward way. The result is restated in a generalized form, covering also the crossing-odd case. The details and questions concerning the practical side of the problem are discussed. (LBS)

30734 ASYMPTOTIC CROSSING-EVEN PION–NUCLEON FORWARD SCATTERING AND DUALITY IN THE COMPLEX ENERGY PLANE. Ferrari, E.; Lusignoli, M. (Univ., Rome). Nuovo Cim., A; 23A: No. 1, 51-68(1 Sep 1974).

The problem of the asymptotic parametrization of the crossing-even forward pion-nucleon scattering amplitude is studied. A fit saturating the Froissart bound is obtained by satisfying complex-energy sum rules suggested by duality requirements in the complex energy plane in addition to the usual cross section and real-part fitting. A comparative discussion is made of various high energy fits of the same type obtained previously. Finally, the amplitude behavior in the complex energy plane is studied, and it is found that, for fits of this kind, the extreme asymptotic limit is experimentally unattainable. (auth)

30735 SU$_6$ QUARK MODEL, NUCLEON RESONANCE ELECTROPRODUCTION AND SPIN-DEPENDENT ELECTROPRODUCTION STRUCTURE FUNCTIONS. Osborn, H.; Woo, G. (Cambridge Univ., Eng.). Nuovo Cim., A; 23A: No. 1, 103-125(1 Sep 1974).

The electromagnetic resonance excitation form factors for proton and neutron initial states are calculated in the nonrelativistic symmetric quark model for resonances in the 56 (L = 0), 70 (L = 1) and 56 (L = 2). Initially the radial wave function for each supermultiplet is assumed arbitrary and the results are used to calculate the resonance part of both spin independent and dependent electroproduction structure functions. Following Close, Gilman and Karliner the scaling behavior of the structure functions is then discussed and relations with the naive quark-parton model made. Further a common radial wave function for all of the supermultiplets is assumed so there is then just a single undetermined form factor. Sum rules such as the Cabibbo–Radicati are considered and by demanding their saturation by the 56 and 70 additional dynamical constraints are derived. The observed helicity structure for excitation of the D_{13} and F_{15} is shown to arise naturally and change less dramatically with q^2 than for a harmonicoscillator model. (auth)

30736 ELASTIC-DIFFRACTION SLOPES OF π^+p AND K$^+$p SCATTERINGS. Yoshida, T. (Fukushima Univ., Japan). Lett. Nuovo Cim.; 11: No. 3, 228-232(21 Sep 1974).

The study of a previous relation between total cross sections of meson-baryon scattering with estimation of the contribution of various inelastic processes to shadow scattering is continued in the impact-parameter formalism instead of the partial waves, taking into consideration the impact-parameter dependence of the overlap functions. Since the experimental values of the diffraction parameter B for π^-p and K$^-$p are available at 25.2 and 40.1 GeV/c, B is calculated for π^+p and K$^+$p at these energies. (JFP)

30737 THE NΛK COUPLING CONSTANT. Baillon, P.; Bricman, C.; Ferro-Luzzi, M.; Perreau, J. M.; Tripp, R. D.; Ypsilantis, T. (European Organization for Nuclear Research, Geneva (Switzerland)); Declais, Y.; Seguinot, J. (Caen Univ., 14 (France)). Phys. Lett., B; 50: No. 3, 383-386(10 Jun 1974).

A dispersion relation analysis has been performed using the real parts of the K$^\pm$p forward scattering amplitudes measured over the incident momentum region from 1 to 3 GeV/c in an electronics experiment. Two possible values are found for the NΛK coupling constant. One of them is in very good agreement with the symmetry theory predictions. (auth)

30738 μ-PAIR PRODUCTION BY INELASTIC πp AND $\bar{p}$p COLLISIONS. Galfi, L. (Inst. for Theoretical Physics, Roland Eotvos Univ., Budapest, Hungary). Phys. Lett., B; 50: No. 3, 357-358(10 Jun 1974).

The massive μ-pair production in πp and in $\bar{p}$p scattering is investigated. The Drell-Yan parton-antiparton annihilation model of the process and the Kuti-Weisskopf relativistic quark model of hadrons are used. (auth)

30739 DETAILED PREDICTIONS FOR THE p–n STRUCTURE FUNCTIONS IN THEORIES WITH COMPUTABLE LARGE MOMENTA BEHAVIOR. Parisi, G. (Columbia Univ., New York (USA)). Phys. Lett., B; 50: No. 3, 367-368(10 Jun 1974).

If strong interactions are described by non Abelian gauge theories, detailed predictions are obtained for the q^2 dependence at fixed ω of the difference of the structure functions of the proton and neutron. (auth)

30740 SIMPLE Z_0^* MODEL. Johnson, R. C.; Vlassopulos, S. D. P. (European Organization for Nuclear Research, Geneva (Switzerland)). Phys. Lett., B; 50: No. 3, 343-348(10 Jun 1974).

A model for isoscalar KN scattering near the K*N threshold is constructed, and solved analytically in the approximation of retaining only pion exchange terms. Basic features of phenomenological phase shifts are reproduced, including a wide $J^P = \frac{1}{2}^+$ exotic resonance, Z_0^*(1800). (auth)

30741 COHERENT TRANSMISSION OF NEUTRAL KAONS IN MATTER AND FORWARD SCATTERING AMPLITUDES. Votruba, J. (Ceskoslovenska Akademie Ved, Prague. Fyzikalni Ustav). Phys. Lett., B; 50: No. 2, 273-274(27 May 1974).

A method is proposed which enables simultaneous measurement of total cross sections of K and $\bar{K}$ interactions with protons or nuclei and the difference of real parts of forward scattering amplitudes, in the transmission of neutral kaons through matter. (auth)

30742 ISOSPIN ANALYSIS OF THE REACTION $\pi^+p \rightarrow \pi(N\pi)$ AT 11.7 GeV/c. Evans, D. (Univ. of Durham, Eng.); Contri, R.; Cerrina Feroni, C.; Costa, G.; Pastore, F.; Lewin, C. Nuovo Cim.; 23A: No. 2, 291-303(21 Sep 1974).

The $\frac{1}{2}$- and $\frac{3}{2}$-isospin contributions of the $(N\pi)$ system produced in the $\pi^+p \rightarrow \pi(N\pi)$ reaction at 11.7 GeV/c were separated. The $I = \frac{1}{2}$ cross section, weakly dependent on the energy, is interpreted in terms of pomeron exchange. The dependence on LPS, the differential cross sections and $(N\pi)$ mass spectra of the $I = \frac{1}{2}, \frac{3}{2}$ contributions are investigated. The results support the conclusion that the $I = \frac{1}{2}$ amplitude is dominated by the diffractive dissociation of the proton; a simple factorization test of the amplitude is satisfactorily satisfied at 11.7 GeV/c. (auth)

30743 EXPERIMENTAL MANIFESTATIONS OF DUALITY IN KN INTERACTIONS AND IMPLICATIONS FOR THE BOOTSTRAP. York, M. J. (Univ. of Birmingham, Eng.). J. Phys., B (London); 7: No. 10, 1135-1140(1 Jul 1974).

It is suggested that various channel cross sections for K^-p interactions strongly exhibit their different duality properties in the resonance region as well as at high energies. In particular, it is argued that non-diffractive processes with no (u,t) dual amplitude are resonance dominated in the real part as well as the imaginary part. Thus, from a bootstrap point of view, the (u,t) amplitude should be considered the driving force behind the (s,t) and (s,u) amplitudes and reciprocally. (auth)

30744 N AND π EXCHANGE AMPLITUDES IN πN BACKWARD SCATTERING. Aye, T. M.; Islam, A. K. M. A. (Imperial Coll. of Science and Tech., London). J. Phys., B (London); 7: No. 10, 1141-1150(1 Jul 1974).

The dual absorptive model is applied to πN backward scattering in detail and through the fits to the available data, the $N(I_u = \frac{1}{2})$ and $\Delta(I_u = \frac{3}{2})$ exchange amplitudes are studied. The interaction radius R and the slope parameter B for the N amplitudes are found to be consistent with those of the forward scattering, while the slope parameter B for the Δ amplitude is found to be rather large. This inconsistency is attributed to the incorrect form of the ReΔ as given by the model. Possible mechanisms to produce the correct ReΔ are given. (auth)

30745 COMMENTS ON THE CALCULATION OF THE PION-NUCLEON COUPLING CONSTANT AND S-WAVE SCATTERING LENGTHS. Woolcock, W. S. (Cambridge Univ. (UK). Cavendish Lab.). Nucl. Phys., B; 75: No. 3, 455-460(25 Jun 1974).

It is pointed out that Coulomb barrier effects above 300 MeV may have a significant effect on the calculation of f^2 and $a_1 - a_3$ for pion–nucleon scattering. It is argued that Bugg et al. have overestimated the value of f^2. Uncertainties in their calculations, which cannot be included in the statistical error, are listed and discussed. (auth)

30746 MODELS FOR THE POMERON AND LOW ENERGY K^+p SCATTERING. Reid, A. W. (Max-Planck-Institut fuer Physik und Astrophysik, Muenchen (F. R. Germany)); Sutherland, D. G. (Glasgow Univ. (UK). Dept. of Natural Philosophy). Nucl. Phys., B; 75: No. 3, 426-445(25 Jun 1974).

Using a simple s-channel unitarity model for the pomeron, abstracted from a number of more ambitious schemes, the pomeron contribution is computed using low-energy data in K^+p scattering. The agreement with experiment obtained is qualitatively fair but in detail substantial discrepancies appear. Possible reasons for these discrepancies and suggestions for their future investigation are presented. (auth)

30747 THE STRUCTURE OF T-CHANNEL EXCHANGES IN KN SCATTERING. Elvekjaer, F. (European Organization for Nuclear Research, Geneva (Switzerland)); Martin, B. R. (University Coll., London (UK)). Nucl. Phys., B; 75: No. 3, 388-400(25 Jun 1974).

Recent phase-shift solutions are used to evaluate KN finite energy sum rule integrals in order to examine zeros and phases of the t-channel exchange amplitudes in the most model-independent way. The results suggest that the line reversal breaking in KN charge exchange observed for $p_L \lesssim 5.5$ GeV/c is due to a large exchange degeneracy breaking component in the A_2 exchange flip amplitude. The ρ exchange flip amplitude is well described by a Regge pole amplitude with NWSZ at $-t \sim 0.5$ (GeV/c)^2. The imaginary parts of ρ and ω exchange non-flip amplitudes are both peripheral. (auth)

30748 FINITE ENERGY BOUNDS FOR πN SCATTERING. Grassberger, P. (European Organization for Nuclear Research, Geneva (Switzerland)); Kuehnelt, H.; Schwela, D. (Vienna Univ. (Austria). Inst. fuer Theoretische Physik). Nucl. Phys., B; 75: No. 3, 493-508(25 Jun 1974).

Upper bounds on energy-averaged πN cross sections are given. By using low energy data and data from πN backward scattering and $N\bar{N} \rightarrow \pi\pi$ annihilation, typical results are $\sigma_{tot} \lesssim 80$ mb and $\sigma_{inel} \lesssim 30$ mb, for energies just above the phase-shift region. The bounds are based on assumptions similar to those underlying Froissart's bound and are equal to it asymptotically. However, at finite but large energies, they increase much more slowly than might have been anticipated on purely numerological grounds. Related problems in pp and Kp scattering are also discussed. (auth)

30749 A PARTIAL-WAVE ANALYSIS OF THREE BODY π^+ PROTON INTERACTIONS AT LOW ENERGY. Chavanon, P.; Dolbeau, J.; Smadja, G. (CEA Centre d'Etudes Nucleaires de Saclay, 91–Gif-sur-Yvette (France). Dept. de Physique des Particules Elementaires). Nucl. Phys., B; 76: No. 1, 157-168 (4 Jul 1974).

An independent partial-wave analysis of the reaction $\pi^+p \rightarrow \pi^+p\pi^0$ is presented for values of the center of mass energy between 1.58 and 1.97 GeV. In the frame of the generalized isobar model, ten waves are introduced for the $\pi\Delta$ channel and eight for the $N\rho$ channel. The results are compared with those of the analysis performed by the Berkeley-Stanford group. (auth)

30750 SUM RULES FOR FORWARD ELASTIC PION–NUCLEON SCATTERING. Maximon, L. C.; O'Connel, J. S. (National Bureau of Standards, Washington, D. C. (USA)). Phys. Lett., B; 51: No. 1, 31-34(8 Jul 1974).

A number of energy-weighted sum rules relating amplitudes and differential cross sections for forward elastic and charge-exchange scattering to the total pion–nucleon cross section are derived from dispersion relations. (auth)

Strong (Baryon No. ≥ 2)

Refer also to abstracts 30866, 31035, 31042, and 31062.

30751 (IC-73-6) BOSE DISTRIBUTION AND THE LORENTZ CONTRACTED GEOMETRIC MODEL. Wing-Yin, Yu. (International Centre for Theoretical Physics, Trieste (Italy)). 1973. 6p. INIS.

The Bose-type distribution employed by Hoang for the inclusive p-p reactions is shown to be simply related to Krisch's model of a Lorentz contracted interaction volume. Hoang's phenomenological scaling law, $1/p_{max}$, can be explained as the effect of a spherically symmetric interaction volume being squashed down in the beam direction. The formation of intermediate isobars is suggested. (auth)

30752 PARITY-NONCONSERVING EFFECTS IN THE REACTION $n + p \rightarrow d + \gamma$. Lassey, K. R.; McKellar, B. H. J. (Univ. of Melbourne). Lett. Nuovo Cim.; 11: No. 2, 161-165(14 Sep 1974).

The results of a series of calculations for different strong-interaction potentials and the standard parity-nonconserving potential for the reaction $n + d \rightarrow d + \gamma$ are reported. It is seen that variations in the parity-conserving potential produce significant variation in the photon circular polarization and variations in the potential are probably more significant than variations in the method of calculation in determining the calculated photon circular polarization, for which the observed value is shown. The calculations are based on the Danilov approximation. (JFP)

30753 RECENT DEVELOPMENTS IN MESON-THEORETICAL STUDIES OF THE NUCLEON–NUCLEON INTERACTION. Ueda, T. (Osaka Univ., Toyonaka, Japan). pp 3-50 of Nuclear Many-Body Problem. Vol. I. Calogero, F. (ed.). Bologna; Editrice Compositori (1973).

From symposium on present status and novel developments in the nuclear many-body problem; Rome, Italy (19 Sep 1972). See CONF-720933–P1.

30754 LONG RANGE CORRELATIONS IN THE PIONIZATION COMPONENT. Kajantie, K.; Ruuskanen, P. V. (Univ. of Helsinki). Lett. Nuovo Cim.; 11: No. 3, 207-212(21 Sep 1974).

Recent measurements of correlations between a pion in the plateau and a proton in the fragmentation region were carried out. A typical result is a correlation function which has a positive value at smaller x, a zero at about $x = 0.5$, a roughly constant negative value for $0.5 < x < 0.8$, and approaches a large negative value for x close to 1. This structure is quantitatively explained in terms of a model which essentially amounts to putting finite-energy corrections to a multiperipheral cluster model. The two-component pionization + diffraction picture for pp collisions is considered. (JFP)

30755 SOME ANALOGY OF THE NUCLEAR AND NUCLEON FRAGMENTATION PROCESSES. Zielinski, P. (Inst. of Nuclear Research, Warsaw). Acta Phys. Pol., B; 5: No. 4, 531-535(1974).

The results of several recent experiments suggest the existence of composite structure of the nucleon. Consequently some analogies in the properties of nucleons and nucei are arising. For example, the diffraction pattern of elastic proton-proton collision, emerging at high energies, is similar to that of the proton-nucleus collision. (auth)

30756 SEMI-INCLUSIVE RAPIDITY DISTRIBUTIONS IN A CLUSTER EMISSION MODEL FOR THE PIONIZATION COMPONENT. Sohlo, S. (Univ. of Helsinki). Lett. Nuovo Cim.; 11: No. 3, 201-206(21 Sep 1974).

It is shown that a multiperipheral model modified to take energy conservation for cluster emission into account results in observable effects on the semi-inclusive single-particle rapidity distributions. The simultaneous fitting of one- and two-particle densities to test models is emphasized. Pionization in the final state of proton-proton collisions is considered. (JFP)

30757 BOUND ON THE AVERAGE MULTIPLICITY OF PIONS IN P–P COLLISION AT SUPERHIGH ENERGY. Yokomi, H.; Yotsuyanagi, I. (Osaka Univ.). Lett. Nuovo Cim.; 11: No. 3, 195-200(21 Sep 1974).

It is found that the ISR data and the assumed scaling behavior predict that the dependence of the average multiplicity of pions on energy in superhigh-energy p + p collisions is overwhelmingly logarithmic in the energy region where the average multiplicity can be observed. (JFP)

30758 SCALING OF MULTIPLICITY DISTRIBUTION IN HADRON COLLISIONS AND DIFFRACTIVE-EXCITATION LIKE MODELS. Buras, A. J ; Dethlefsen, J. M.; Koba, Z. (Univ. of Copenhagen). Acta Phys. Pol., B; 5: No. 4, 473-483(1974).

Multiplicity distribution of secondary particles in inelastic hadron collision at high energy is studied in the semiclassical impact parameter representation. The scaling function is shown to consist of two factors: one geometrical and the other dynamical. A specific choice of these factors is proposed, which describe satisfactorily the elastic scattering, the ratio of elastic to total cross section and the simple scaling behaviour of multiplicity distribution in p-p collisions. Two versions of diffractive-excitation like models (global and local excitation) are presented as interpretation of our choice of dynamical factor. (auth)

30759 MULTIPLICITY DISTRIBUTIONS IN THE REACTION p + p → p + ANYTHING. Whitmore, J. (National Accelerator Lab., Batavia, Ill. (USA)); Derrick, M. (Argonne National Lab., Ill. (USA)). Phys. Lett., B; 50: No. 2, 280-282(27 May 1974).

It is shown that, for fixed mass of the system X, the charged particle multiplicity distribution in the reaction p + p → p + X is remarkably similar to the shape of the multiplicity distribution for the reaction p + p → anything observed at an equivalent fixed center of mass energy. (auth)

30760 THE POMERON-PARTICLE TOTAL CROSS SECTION AND DIFFRACTIVE PRODUCTION OF SHOWERS AT VERY HIGH ENERGIES. Kaidalov, A. B.; Ter-Martirosyan, K. A. (Institute of Theoretical and Experimental Physics, Moscow, USSR). Nucl. Phys., B; 75: No. 3, 471-482(25 Jun 1974).

The experimental data of ISR and NAL for the process pp → pX are used for the determination of the pomeron-particle total cross section and the triple-pomeron vertex. Estimates of the cross sections of the diffractive production of one and several showers of particles are given. It is shown that at $s \sim 10^3$ GeV^2 the cross section of all inelastic diffractive processes is ~6 mb and grows with energy. A theoretical estimate of the amplitude of pomeron–pomeron scattering is given. (auth)

30761 AN IMPACT PARAMETER DESCRIPTION OF SINGLE AND DOUBLE DIFFRACTION DISSOCIATION. Humble, S. (European Organization for Nuclear Research, Geneva (Switzerland)). Nucl. Phys., B; 76: No. 1, 137-156(4 Jul 1974).

An s-channel impact parameter model of inelastic diffraction dissociation is constructed which describes quantitatively the momentum transfer distributions of both pion and nucleon induced reactions. It is stressed that the impact parameter profile is peripheral and is approximately the same for all helicity amplitudes. From the fits to the data, the concept of a universal limiting strength (ULS) for each amplitude is deduced and its consequence for other diffractive processes, and the approximate TCHC hypothesis are discussed. Finally, detailed predictions are presented for the momentum transfer distributions in the double diffraction process NN → (Nπ) (Nπ), and compared with a simple t-channel picture of diffraction dissociation. (auth)

30762 POSSIBLE EFFECTS OF WEAKLY COUPLED NEUTRAL CURRENTS IN $pp \to l^+l^- + X$. Brown, R. W.; Mikaelian, K. O. (Case Western Reserve Univ., Cleveland, Ohio (USA)); Gaillard, M. K. (National Accelerator Lab., Batavia, Ill. (USA)). Nucl. Phys., B; 75: No. 1, 112-124(11 Jun 1974).

The possibility of observing weak neutral currents in the inclusive production of ordinary lepton pairs in high-energy proton-proton collisions is discussed. The signatures of interest are the charge asymmetry $\langle E_{l^+} - E_{l^-}\rangle$ and the polarization of the leptons. The weak interaction is considered to be mediated by a neutral vector boson and the calculations are done in the parton model. This model is also used to estimate the asymmetry background due to two-photon exchange. To obtain numerical results weak couplings suggested by the Weinberg theory are used. (auth)

30763 IS $\bar{p}$ PRODUCTION PERIPHERAL OR CENTRAL? Gaisser, T. K. (Bartol Research Foundation, Swarthmore, Pa. (USA)); Miettinen, H. I. (European Organization for Nuclear Research, Geneva (Switzerland)); Tan, C. I.; Tow, D. M. (Brown Univ., Providence, R. I. (USA). Dept. of Physics). Phys. Lett., B; 51: No. 1, 83-86(8 Jul 1974).

Experimental consequences of peripheral production of $N\bar{N}$ pairs are described and contrasted with an orthogonal set of predictions which follow if $N\bar{N}$ production occurs in central collisions. It is shown that current ISR experiments can easily distinguish between the two viewpoints, for example, by measuring the average multiplicity associated with $\bar{p}$ production. (auth)

30764 LARGE MOMENTUM TRANSFER REACTIONS, WITHOUT PARTONS. Fried, H. M. (Brown Univ., Providence, R. I. (USA). Dept. of Physics). Phys. Lett., B; 51: No. 1, 90-92 (8 Jul 1974).

Three recent experiments involving large 4-momentum transfer are compared to predictions of the hadronic bremsstrahlung model, without partons. The model is discussed in terms of associate multiplicity, inclusive cross sections and deep inelastic scattering. (auth)

30765 A RECURRENCE RELATION FOR THE POLARIZATION IN ELASTIC p–p SCATTERING IN THE FRAMEWORK OF A PARTON MODEL. Neal, H. A.; Nielsen, H. B. (Niels Bohr Institute, Copenhagen (Denmark)). Phys. Lett., B; 51: No. 1, 79-82(8 Jul 1974).

Recent studies have shown that it is possible to account for the general features of large angle elastic proton–proton differential cross sections in a model where each constituent of one proton scatters from at least one constituent of the other proton in such a way that all constituents remain near their mass shell. Each of the parton–parton scatters is assumed to occur at approximately the same angle, so that the outgoing partons can easily recombine to form the two final-state protons. In the present article it is shown that such a model, with additional assumptions regarding the scattering mechanisms at small $|t|$, leads to a nontrivial recurrence relation which is consistent with the structure recently reported in the high-energy p–p polarization and fixed-angle differential cross section. (auth)

Particle Invariance Principles and Symmetries

General

30766 PHYSICAL SIGNIFICANCE OF THE TOPOLOGY OF THE BONDI–METZNER–SACHS GROUP. Crampin, M. (Faculty of Mathematics, The Open University, Walton Hall, Walton, Bletchley, Buckshire, England); McCarthy, P.J. Phys. Rev. Lett. 33: No. 9, 547-550 (26 Aug 1974).

It has been proposed that the Bondi–Metzner–Sachs group affords a possible explanation for the discreteness of elementary–particle spins. This discreteness result depends on the topology given to the group. A careful analysis of representations in the "nuclear" topology indicates that discrete–spin representations (those subsumed by the original topology) describe bound gravitating systems ("elementary particles"), whereas the new continuous–spin representations, if physically realistic, describe scattering states of gravitating systems. (auth)

30767 GAUGE DEPENDENCE OF RENORMALIZATION GROUP PARAMETERS. Banyai, L. (Inst. of Physics, Bucharest); Marculescu, S.; Vescan, T. Lett. Nuovo Cim.; 11: No. 2, 151-155(14 Sep 1974).

Using 't Hooft's renormalization procedure in the version of Collins and Macfarlane, it is shown that the consistency relations including massive fermions are actually contained in the very definitions of the renormalization group parameters and their gauge independence in 't Hooft's renormalization is connected with the gauge independence of certain renormalization constants. (JFP)

30768 GEL'FAND-PATTERN TECHNIQUE APPLIED TO THE PHYSICALLY IMPORTANT SU(3) × SU(2) IS CONTAINED IN SU(6) DECOMPOSITION OF SU(6). Strand, A. E. (Univ. of Trondheim, Norway). J. Math. Phys. (N. Y.); 15: No. 8, 1197-1202(Aug 1974).

Explicit and easily computable formulas for the physical quantum numbers I_3, Y, and S_3, and also two additional quantum numbers for all states spanning an arbitrary irreducible representation of SU(6) are obtained by using Gel'fand-pattern technique. This result is accomplished by establishing a correspondence between the 3 diagonal $SU(3) \otimes SU(2)$ generators + 2 "quark-spin" generators, and the 5 "canonical" generators $H_1 - H_5$, the eigenvalues of which are given by the Gel'fand patterns of SU(6) in the ordinary way. The $SU(3) \otimes SU(2) \subset SU(6)$ content of the SU(6) representations taken as examples is displayed explicitly. The possibility of doing this suggests that Gel'fand patterns may be useful even in a non-maximal decomposition, although the patterns are intrinsically linked to the "canonical" chain of decomposition: $SU(n) \supset U_1(1) \otimes SU(n-1) \supset U_1(1) \otimes U_2(1) \otimes SU(n-2) \supset \ldots$ etc. The procedure developed in the case of SU(6) is generalized to the twofold non-maximal decomposition of $SU(mn) \supset SU(m) \otimes SU(n)$. (auth)

30769 GENERALIZED 6J-COEFFICIENTS AND THEIR SYMMETRIES. D'Adda, A. (Istituto Nazionale de Fisica Nucleare, Turin); D'Auria, R.; Ponzano, G. Nuovo Cim., A; 23A: No. 1, 69-102(1 Sep 1974).

A unifying treatment of SU_2 and $SU_{1,1}$ 6j-coefficients with discrete unitary representation is realized through a generalizing function Φ_{6j}. From the invariance properties of Φ_{6j}, as a by-product, the symmetry group of the $SU_{1,1}$ 6j-coefficient with discrete unitary representations is obtained. The asymptotic connection of Φ_{6j} with the generalized 3j-coefficients is pointed out. (auth)

30770 SPONTANEOUS CP-VIOLATION AND COSMOLOGY. Kobsarev, I. Yu.; Okun, L. B.; Zeldovich, Ya. B. (AN SSSR, Moscow. Inst. Fiziki Vysokikh Davlenij). Phys. Lett., B; 50: No. 3, 340-342(10 Jun 1974).

In the theories with spontaneous CP-symmetry breaking there must exist the domain structure of the vacuum. The cosmological implications of this structure are discussed. (auth)

30771 SCALING BEHAVIOR IN A CLASS OF MASSIVE NON-ABELIAN GAUGE THEORIES. Politzer, H. D. (Harvard Univ., Cambridge, Mass. (USA)); Ross, G. G. (Science Research Council, Chilton (UK). Rutherford Lab.). Nucl. Phys., B; 75: No. 2, 269-284(18 Jun 1974).

The ultraviolet behavior of a class of non-Abelian gauge theories with vector meson masses generated by the Higgs mechanism is examined. It is found that although these theories are not asymptotically free they may, over a considerable momentum range, behave as if they had an ultraviolet stable fixed point at the origin. Such quasi-stable theories could exhibit Bjorken scaling (up to powers of $\ln q^2$) over the experimentally observable domain. The possible types of quasi-stable theories and the effects of the Higgs scalars, which lead to the eventual total breakdown of scaling are discussed. (auth)

Applications (Electromagnetic and Weak)

30772 TEST OF THE SU_3 BREAKING IN INCLUSIVE ELECTROPRODUCTION OF HADRONS. Pal, B. K. (Imperial Coll. of Science and Tech., London). Lett. Nuovo Cim.; 11: No. 2, 103-106(14 Sep 1974).

The two-component duality idea is applied within the parton model to describe the deep inelastic reactions. The quark distribution within the nucleon is divided into two components such as three valence quarks plus a core of quark–antiquark pairs. The sea of core quarks is assumed to be composed of equal numbers of each type. This corresponds to the pomeron background part of the amplitudes. The electroproduction of π^+ and K^+ is considered. (JFP)

30773 SPONTANEOUS CP VIOLATION IN THE GENERALIZED GEORGI–GLASHOW MODEL. Szymacha, A.; Tatur, S. (Univ., Warsaw). Lett. Nuovo Cim.; 11: No. 2, 92-94(14 Sep 1974).

Previous calculations of CP violating effects were performed under the additional assumption that certain couplings in the original Lagrangian consistent with gauge invariance renormalizability and CP invariance are not important and may be disregarded for simplicity. It is proven that the smallness of the CP violation depends crucially on this additional assumption. It is shown that some of the disregarded terms do lead to the effects of the CP violation which are not suppressed automatically, and in order to make them small one is forced to introduce some parameters of order 10^{-3} into the theory. The couplings which are responsible for the effective CP violation are the Yukawa couplings between triplet of scalar CP-odd fields and fermion fields. (JFP)

30774 IS CHIRAL $SU_2 \times SU_2$ A HIDDEN SYMMETRY. Rest, J. (Argonne National Lab., IL). Lett. Nuovo Cim.; 11: No. 3, 177-178(21 Sep 1974).

Comments are made on chiral $SU(2) \times SU(2)$ symmetry of strong interactions in a previous model in which the physical-weak interaction charges satisfy the SU(2) algebra only in the symmetry limit, or when the three-momenta of all physical particles approach zero. The previous analysis of the K_{l3} form factors is repeated. (JFP)

30775 STRUCTURE AND EXPERIMENTAL CONSEQUENCES OF CHIRAL $SU_3 \times SU_3$ BREAKING. Ebrahim, A.; Serdaroglu, M. (Middle East Technical Univ., Ankara (Turkey)). Phys. Lett., B; 50: No. 2, 258-260(27 May 1974).

Chiral $SU_2 \times SU_2$ breaking, Cabibbo angle, non-electromagnetic isospin breaking, $\pi \to 3\pi$ decay rate, and pion and kaon mass differences are related to one another in a nonlinear Lagrangian model of broken chiral $SU_3 \times SU_3$ symmetry. The agreement with experiment is very good. (auth)

30776 DISTURBED NON-LINEAR CHIRAL $SU(3) \times SU(3)$ DYNAMICS AND CABIBBO'S ANGLE. Il'in, Yu. M.; Sabo, V. Ya. (Inst. of Theoretical Physics, Kiev). Ukr. Fiz. Zh. (Russ. Ed.); 19: No. 4, 682-684(Apr 1974). (In Russian).

A covariant deviation of symmetry was introduced into the chiral nonlinear $SU(3) \times SU(3)$ dynamics of 0^- mesons. The parameters of symmetry deviation were expressed through the observed mass spectra of pseudoscalar mesons, which makes possible the determination of Cabibbo's angle in terms of the mass of 0^- mesons. The value obtained for this angle agrees with the value obtained experimentally. (tr-auth)

30777 PARITY VIOLATIONS BY NEUTRAL CURRENTS IN MUONIC ATOMS. Bernabeu, J.; Ericson, T. E. O.; Jarlskog, C. (European Organization for Nuclear Research, Geneva (Switzerland)). Phys. Lett., B; 50: No. 4, 467-471(24 Jun 1974).

The 2S–1S transition in low Z muonic atoms is shown to be extremely sensitive to possible parity violation, such as may be introduced by neutral currents. The most striking effects of parity violation are found in the case of muonic Li and Be, where they are estimated to be of the order of 10% on the basis of current models. (auth)

Applications (Strong)

Refer also to abstracts 30707 and 30716.

30778 CONSISTENCY CONDITIONS IN THE THEORY OF SPONTANEOUS BREAKING OF CHIRAL SYMMETRY. Saliu, L.; Tataru, L. (Univ., Craiova, Romania). Stud. Cercet. Fiz.; 25: No. 2, 137-149(1973). (In Rumanian).

The most general form of the symmetry-breaking Hamiltonian belonging to a $(3,\bar{3}) + (\bar{3},3)$ representation of $SU_3 \otimes SU_3$ and fulfilling the consistency conditions of Dashen's theorems [Phys. Rev., D3, 1879(1971)] is determined. In the GMOR (Gell-Mann, Oakes, Renner) Model it is proved that there always exists an $SU_3 \otimes SU_3$ transformation generating an operator which satisfies the consistency conditions. These operators can have a CP-symmetry-breaking term, but do not have an electromagnetic-symmetry-breaking term. (auth)

30779 ELECTROMAGNETIC MASS BREAKING OF BARYONS IN BROKEN CHIRAL $SU(3) \times SU(3)$. Shern, C. S.; Shih, Y. M. (National Taiwan Normal Univ., Taipei). Chin. J. Phys. (Taiwan); 11: No. 2, 151-155(Oct 1973).

Assuming that the electromagnetic breaking term of $SU(3) \otimes SU(3)$ symmetry transforms like an element of $(1,8) \oplus (8,1)$ linear representation, one can calculate the mass difference of baryons among each SU(2) multiplet. With only one parameter which expresses the ratio of this breaking to that of G.O.R. term, one gets quite satisfactory results. (auth)

30780 NON-ZERO MASSES OF π, K, η AND κ MESONS AND ALGEBRAIC REALIZATION OF $SU(3) \times SU(3)$ CHIRAL SYMMETRY. Dubnickova, A. Z. (Joint Inst. for Nuclear Research, Dubna (USSR). Lab. of Theoretical Physics). Nucl. Phys., B; 76: No. 1, 169-174(4 Jul 1974).

An algebraic realization of $SU(3) \times SU(3)$ symmetry, with linearization on the SU(2) X Y subgroup taking into account masses of π, K, η mesons in virtual states is investigated. This is achieved by explicit breaking of the symmetry. The chosen form of the breaking term in the Lagrangian enables the parameter c appearing in the squared mass operator to be estimated. The obtained value of $c(c \sim -1.17)$ is very close to that predicted by Gell-Mann, Oakes and Renner. (auth)

30781 SU(3) SYMMETRY BREAKING AND SUPERFLUIDITY OF HADRONIC MATTER. Eliezer, S.; Weiner, R. (Imperial Coll. of Science and Technology, London (UK). Dept. of Physics). Phys. Lett., B; 50: No. 4, 463-466(24 Jun 1974).

SU(3) breaking of strong interactions is associated with superfluidity of hadronic matter. At high energies and large transverse momenta, a phase transition occurs and SU(3) becomes an exact symmetry. (auth)

Scattering Theory

Refer also to abstracts 30733, 31044, and 31141.

30782 (COO-3237-40) GENERAL DERIVATION OF BAECKLUND TRANSFORMATIONS FROM INVERSE SCATTERING PROBLEMS. Chen, H. H. (Institute for Advanced Study, Princeton, N. J. (USA)). Aug 1974. Contract AT(11-1)-3237. 10p. Dep. NTIS $4.00.

A general way to derive Baecklund transformations for nonlinear partial differential equations that are solvable by inverse scattering method in the scheme of Ablowitz, Kaup, Newell and Segur is demonstrated. (auth)

30783 TESTS FOR THE PURITY OF THE INITIAL ENSEMBLE OF STATES IN SCATTERING EXPERIMENTS. Kupczynski, M. (Univ., Warsaw). Lett. Nuovo Cim.; 11: No. 2, 121-124 (14 Sep 1974).

Systematic tests for the purity of the initial ensemble E are proposed and discussed. These tests are also applicable if the ensemble E is a mixture of a different type. The idea of the proposed tests is very simple. One must find the dependence of the estimated values of some physical quantities characterizing the scattering (weakly dependent on spin) on the geometry of the beam–target configuration. (JFP)

30784 ANALYTIC NONLOCAL POTENTIALS. II. Analyticity of the S Matrix, for Fixed L, its Representations, and a Dispersion Relation for Fixed T. Yao, T. H. (University Coll., London). J. Math. Phys. (N. Y.); 15: No. 8, 1211-1224(Aug 1974).

For a class of analytic short-ranged nonlocal potentials, the analyticity of the S matrix in the k plane, for fixed l is studied using the Fredholm method for the Lippman–Schwinger equation for the partial scattering solution, and contour deformation in the analytic continuation of the S matrix, thereby extending a representation of the S matrix in terms of Fredholm determinants. Also representation of the S matrix is obtained in terms of Jost functions, for $l = 0$. For a subclass of this class of potentials, one obtains a dispersion relation for the full scattering amplitude, for fixed t in the range $0 \geq t > -4\gamma^2$, where γ is some parameter of the potential, using summation of the partial amplitude expansion of the full amplitude. Analyticity properties of the partial scattering solution, for all l, and of the regular and Jost solutions, for $l = 0$, are also discussed. (auth)

30785 REPRESENTATIONS OF THE JOST SOLUTIONS AND THE S MATRIX FOR A CLASS OF ANALYTIC NONLOCAL POTENTIALS. Yao, T. H. (University Coll., London). J. Math. Phys. (N. Y.); 15: No. 8, 1232-1234(Aug 1974).

Representations of the Jost solutions, the Jost functions, and the S matrix are derived for analytic nonlocal potentials belonging to a double Laplace transform class, for the s-wave case, in terms of the spectral function for the potential. (auth)

30786 COMMENTS ON APPROXIMATIONS FOR THE OVERLAP EXPANSION. Nakazawa, K. (Wakayama Univ., Japan). Lett. Nuovo Cim.; 10: No. 17, 784-788(24 Aug 1974).

The complications introduced in the Glauber theory by overlapping isospin-dependent interactions are noted. The approximations concerning the overlap expansions of degrees zero and one are investigated for the square-well potential and for a potential with exponential tail. (LBS)

30787 DIPOLE GHOSTS AND UNITARITY. Karowski, M. (Max-Planck-Institut fuer Physik und Astrophysik, Munich). Nuovo Cim., A; 23A: No. 1, 126-136(1 Sep 1974).

An S-matrix defined by Feynman diagrams in a state space with indefinite norm is considered. The propagators may have, in addition to simple poles, also double poles in momentum space. A unitarization procedure is derived which projects the S-matrix on the physical subspace. (auth)

30788 CONNECTION BETWEEN FREDHOLM DETERMINANT AND JOST FUNCTION FOR NONLOCAL POTENTIALS. Ahmad, S. S. (Univ., Padua). Nuovo Cim.; 23A: No. 2, 362-374(21 Sep 1974).

The assertion that the Jost function of an s-wave nonlocal potential is equivalent to the ratio of the Fredholm determinants of the integral equations corresponding to the physical and regular solutions was analyzed in detail. The results were verified from first principles by taking into account a model (square well) separable potential. A numerical analysis reflects the influence of the results so obtained on the enhancement factor. (auth)

30789 EXPONENTIAL POTENTIAL AND THE KLEIN–GORDON EQUATION. Bawin, M. (Univ., Liege); Lavine, J. P. Nuovo Cim.; 23A: No. 2, 311-320(21 Sep 1974).

The s-wave radial Klein-Gordon equation was analytically solved with an exponential potential. The behavior of particle and antiparticle bound states and phase shifts was studied in detail as a function of the range and strength of the potential. Results were found to be qualitatively similar to those found for the square-well potential. As in the nonrelativistic case for the exponential potential, redundant poles appear in the S-matrix. Some difficulties connected with the interpretation of these results in the framework of a second-quantized theory are briefly considered. (auth)

30790 COULOMB T-MATRIX IN THE GLAUBER APPROXIMATION IN THE PRESENCE OF A LOW FREQUENCY ELECTROMAGNETIC FIELD. Choudhury, B. J.; Bhakar, B. S. (Univ. of Manitoba, Winnipeg). J. Phys., B (London); 7: No. 10, L314-L316(11 Jul 1974).

The recently proposed method of calculating the multiphoton bremsstrahlung cross section in the Glauber approximation has been applied to the Coulomb scattering problem. The low frequency limit of the cross section has been obtained by using the stationary phase approximation. (auth)

30791 A NEW PARAMETRIZATION FOR THE N/D METHOD. Dilley, J.; Gibson, L. R. (Ohio Univ., Athens (USA)). Nucl. Phys., B; 76: No. 1, 69-92(4 Jul 1974).

A new treatment of the left-hand cut for N/D problems is presented whereby, instead of poles, the cut is parametrized by a Legendre expansion which fixes the discontinuity. The method is tested through the use of analytic forms, and is found to work very well in a wide variety of circumstances. An extension is made to situations where there are errors in the input, and resulting problems are discussed. The method is applied to elastic pion-pion scattering. Both the rho and f_0 mesons are produced dynamically, but trouble is encountered for the s-waves. The relation of this trouble to ambiguities found in other s-wave calculations is discussed. (auth)

30792 A NEW METHOD IN THE THEORY OF MANY-BODY SCATTERING. Kouri, D. J. (Max-Planck-Institut fuer Stroemungsforschung, Goettingen (F. R. Germany)); Levin, F. S. (Brown Univ., Providence, R. I. (USA). Dept. of Physics). Phys. Lett., B; 50: No. 4, 421-424(24 Jun 1974).

New coupled equations for the transition (T) and reactance (K) operators for N-channel, many-body, rearrangement scattering are derived. The key to the new method is the channel coupling array, W, which links the various rearrangement channels together. By specializing W to the class of channel permuting arrays, it is shown that the (N−1)st iterate of the kernel of the coupled equations is connected. (auth)

PHYSICS (LOW-TEMPERATURE)

Superfluidity

30793 FORMULAE FOR KINETIC COEFFICIENTS IN THE CASE OF He II. Szprynger, A. (Instytut Niskich Temperatur i Badan Strukturalnych, Wroclaw). Bull. Acad. Pol. Sci., Ser. Sci., Math., Astron. Phys.; 22: No. 6, 625-629(1974).

Expressions are given for the kinetic coefficients in the case of superfluid helium. These expressions are certain limit values of suitable Green functions determined by the hydrodynamic approach. In particular, the introduction of the real part of the "sources of particles" enables one to obtain the formula for the thermal conductivity coefficient. (auth)

30794 SUPERFLUID PHASES OF LIQUID ^{3}He. Lounasmaa, O. V. (Helsinki Univ. of Tech.). Contemp. Phys.; 15: No. 4, 353-374(Jul 1974).

After introductory remarks the recent discovery of the superfluid phases of ^{3}He is described. This is followed by a discussion of the P, T-diagram below 3 mK. NMR and susceptibility measurements on liquid ^{3}He are then explained. Next, heat capacity and heat flow data are briefly mentioned and experiments involving the zero and fourth sound are described. The viscosity and the density of the normal component of liquid ^{3}He are then discussed. The paper is concluded by a theoretical section. (auth)

30795 FLUCTUATIONS AND SUPERFLUID FLOW. Gluck, P. (Bar-Ilan Univ., Ramat-Gan, Israel). Solid State Commun.; 15: No. 2, 375-376(15 Jul 1974).

The effects of fluctuations are considered on the properties of the oscillating superfluid flow in the analogue of the Josephson effect in superfluid helium. (auth)

30796 CONDENSATE DENSITY IN BOGOLYUBOV HYDRODYNAMICS. Szprynger, A. (Instytut Niskich Temperatur i Badan Strukturalnych, Wroclaw). Bull. Acad. Pol. Sci., Ser. Sci., Math., Astron. Phys.; 22: No. 6, 631-635(1974).

Starting from the Bogolyubov Hamiltonian for the superfluid Bose-system certain Green functions are determined in the hydrodynamic approximation. From their symmetry properties results a formula connecting the condensate density ρ_c with the entropy S and the particle density ρ. (auth)

30797 TEMPERATURE DEPENDENCE OF THE SECOND SOUND VELOCITY REDUCTION IN ROTATING LIQUID HELIUM. Lhuillier, D.; Vidal, F. (Ecole Normale Superieure, Paris). J. Phys., C (London); 7: No. 14, L254-L257(21 Jul 1974).

The second sound velocity decrease in rotating helium has been measured as a function of the temperature ($1.3 \leq T \leq 2.1$ K). The results are compared with two theories, both based on the Hall and Vinen (Proc.R.Soc.; A 238:204-14, 215-34 (1956)) moving vortex model. (auth)

30798 ULTRASONIC DISPERSION AND ATTENUATION NEAR THE LIQUID–GAS CRITICAL POINT OF ^{4}He. Roe, D. B.; Wallace, B. A.; Meyer, H. (Duke Univ., Durham, NC). J. Low Temp. Phys.; 16: No. 1/2, 51-72(Jul 1974).

Sound velocity and acoustic attenuation measurements are described at several frequencies between 0.5 and 5 MHz along the critical isochore of ^{4}He immediately above the critical point T_c. The dispersion is obtained with respect to the velocity measurements by Barmatz taken at 1.8 kHz along the critical isochore. The dispersion and attenuation results are analyzed following the theory of Kawasaki and using the more recent modifications resulting from the Fixman–Mistura approach as described by Garland and co-workers. The critical exponent for the correlation length divergence was determined to be $v = 0.66 \pm 0.04$ and found to have good internal consistency between certain constants appearing in the theoretical expressions for both sound dispersion and attenuation. These experimentally determined constants are compared with those calculated from other experiments. Deviations in the observed acoustic properties from the predicted ones are discussed. They are similar to those found in acoustic experiments and in light scattering experiments near the critical point of Xe. (auth)

30799 APPROACH TO A UNIFORM THEORY OF THE LIQUID AND SOLID PHASES OF ^{4}He AT ABSOLUTE ZERO. Feenberg, E. (Washington Univ., St. Louis). J. Low Temp. Phys.; 16: No. 1/2, 125-130(Jul 1974).

Theoretical studies of liquid ^{4}He have led to recognition of a plausible general form for the exact ground-state wave function. Arguments are presented supporting the view that the same form is adequate to describe the solid. The notion of a local density is used to adapt the form to the description of the two-phase density range. Van Hove's theorem holds for the ground state. (auth)

30800 TEMPERATURE, PRESSURE, AND CONCENTRATION DEPENDENCE OF THE THERMAL CONDUCTIVITY OF VERY DILUTE SOLUTIONS OF ^{3}He IN SUPERFLUID ^{4}He. Rosenbaum, R. L.; Landau, J.; Eckstein, Y. (Technion–Israel Inst. of Tech., Haifa). J. Low Temp. Phys.; 16: No. 1/2, 131-143(Jul 1974).

The thermal conductivity of ^{3}He–^{4}He solutions at saturated vapor pressure has been measured for the concentration range 0.011 to 1.3 mole % ^{3}He and the temperature range 84 to 650 mK. Measurements were made at 10 and 24 atm for several of the concentrations. The thermal conductivity of solutions at 24 atm does not differ greatly from the thermal conductivity of pure ^{4}He at this pressure. Qualitative agreement with the Baym and Ebner theory is achieved only if the boundary scattering of phonons is treated in a different manner than suggested by them. (auth)

30801 INTERACTION OF SURFACE ELECTRONS IN LIQUID HELIUM WITH OSCILLATIONS OF THE VAPOR–LIQUID INTERFACE. Shikin, V. B.; Monarkha, Yu. P. (Physico-Technical Inst. of Low Temperatures, Kharkov). J. Low Temp. Phys.; 16: No. 1/2, 193-208(Jul 1974).

A detailed analysis is presented of the interaction between surface electrons and thermal oscillations (ripplons) of the liquid helium surface. The results obtained enable us to check the validity of the many different approximate descriptions of the electron–ripplon interaction that have been given. The influence of the interaction upon the kinetics of surface electrons also has been studied, with a view to establishing the possibility of obtaining information on the capillary wave spectrum. (auth)

30802 THERMODYNAMIC FUNCTIONS OF IDEAL TWO- AND THREE-DIMENSIONAL FERMI GASES. Ebner, C.; Fu, H. H. (Ohio State Univ., Columbus). J. Low Temp. Phys.; 16: No. 1/2, 43-50(Jul 1974).

Several common thermodynamic functions of ideal two- and three-dimensional Fermi gases of spin $\frac{1}{2}$ have been tabulated as functions of $t = T/T_F$, where T is the temperature and T_F is the Fermi temperature. The tables, presented elsewhere, are discussed. The entries in the tables are given at intervals of $\delta t = 0.001$ for $0 \leq t \leq 5$. The functions which are tabulated are: (i) the reduced chemical potential $\zeta(t) \equiv \mu(t)/\mu(0)$, (ii) the reduced internal energy $u(t) = U(t)/U(0)$, (iii) the reduced entropy $s(t) = S(t)/Nk$, and (iv) the reduced magnetic susceptibility $\varphi(t) = \chi(t)/\chi(0)$. In these expressions, N is the number of particles in the gas and k is Boltzmann's constant. The first of these functions, $\zeta(t)$, is given to eight places beyond the decimal point, while the others are given to six places. (auth)

30803 EXPERIMENTS ON DYNAMIC PARALLEL MAGNETISM IN SUPERFLUID ^{3}He. Webb, R. A.; Kleinberg, R. L.; Wheatley, J. C. (Univ. of California, San Diego, La Jolla). Phys. Rev. Lett.; 33: No. 3, 145-148(15 Jul 1974).

Observations are reported on the ringing of parallel magnetization in superfluid ^{3}He when an incremental magnetic field parallel to a steady field is suddenly turned off. (auth)

30804 VELOCITY OF FOURTH SOUND. Revzen, M.; Shapiro, B.; Kuper, C. G.; Rudnick, J. (Technion-Israel Inst. of Tech., Haifa). Phys. Rev. Lett.; 33: No. 3, 143-145(15 Jul 1974).

The flow of a superfluid through the interstices of a porous medium is considered, taking account of the finite volume of the grains and the resulting hydrodynamic drag. A correction factor to the velocity of fourth sound is found, which reconciles a long-standing discrepancy between theory and experiment. (auth)

Superconductivity

Refer also to abstracts 29967, 29971, 30025, 30048, 30063, and 30074.

30805 (AED-CONF-74-089-005) PROXIMITY EFFECT ON THIN NbN-LAYERS. Reppel, G. W.; Saur, E. 1974. 5p. (In German). (CONF-740451-11). INIS.

From conference on solid state physics; Freudenstadt, F.R. Germany (1 Apr 1974).

3 dias.

For type 2 superconductors with high values of transition temperature and critical field, for which only small proximity effects are to be expected due to short coherence lengths, the reduction of T_c on thin niobium nitride layers which are coated with copper, silver and gold layers was measured. The NbN layers were prepared by the electron radiation evaporation of niobium onto sapphire bases and then underwent diffusion of nitrogen at 1,100°C. Each superconducting starting layer was treated several times with vapour with normal conductors of varying thickness or also with various metals; the layer thicknesses were determined by an interferometer. The transition curves of the NbN-metal double layers for Cu, Ag, the reduced transition temperatures (double layer, non-coated starting layer against metal layer thickness) were measured and compared with the calculations. (GE)

30806 NIOBIUM–GERMANIUM: BECOMING A PRACTICAL SUPERCONDUCTOR. Robinson, A. L. Science; 185: No. 4154, 846; 848(6 Sep 1974).

Past work on superconducting Nb_3Ge is reviewed along with information about commercial methods for fabricating Nb_3Ge with a high transition temperature. (MHR)

30807 PROGRAMS ON LARGE SCALE APPLICATIONS OF SUPERCONDUCTIVITY IN THE UNITED KINGDOM. Appleton, A. D. (International Research and Development Co. Ltd., Newcastle upon Tyne, Eng.). pp 639-649 of Superconducting Machines and Devices: Large Systems Applications. Foner, S. (ed.). New York; Plenum Publishing Corp. (1974).

From large scale applications of superconductivity and magnetism conference; Entreves, Italy (5 Sep 1973). See CONF-7309112-.

The activities on superconductivity in U.K. are summarized under the Science Research Council and research grants to universities and laboratories. Some other activities are mentioned briefly. (MHR)

30808 SPECIFIC HEAT OF 2H $NbSe_2$. Bevolo, A.J.; Shanks, H.R. (Ames Laboratory–USAEC and Department of Physics, Iowa State University, Ames, Iowa 50010). J. Appl. Phys. 45: No. 10, 4644-4648 (Oct 1974).

The specific heats of four samples of 2H $NbSe_2$ have been measured in the temperature range from 1 to 54 K. No anomalous behavior was found near 40 K where x–ray, NMR, and Hall–effect measurements have indicated the presence of a phase transition. An upper limit of 0.3 J/mole K has been placed on the magnitude of any anomaly in the heat capacity associated with this transition. Measurements of high–purity stoichiometric 2H $NbSe_2$ sample gave a superconducting transition temperature of 7.23 K, a specific heat jump (ΔC) in zero field of 240 mJ/mole K, and a Debye temperature of 204 K. A deviation from the usual T^3 behavior for the lattice contribution to the heat capacity was observed and assumed to be due to the two–dimensional layer structure of the compound. Our best estimate for the electronic coefficient of specific heat (γ) is about 10 ± 5 mJ/mole K^2. Based on the values for T_c and ΔC, the value for γ calculated from BCS theory is 23 mJ/mole K^2 for 2H $NbSe_2$ which is in disagreement with our estimated value for γ by a factor of 2. (auth)

30809 MULTIFILAMENT Nb_3Sn CONDUCTORS. Deis, D.W.; Gavaler, J.R.; Shaw, B.J. (Westinghouse Research Laboratories, Pittsburgh, Pennsylvania 15235). J. Appl. Phys. 45: No. 10, 4594-4597 (Oct 1974).

The superconducting and mechanical properties of multifilament Nb_3Sn wires prepared by the surface diffusion technique are described. Materials tested were 0.021– and 0.051–cm–diam wires with 392 filaments 6.6 or 16 μ in diameter. Electron microprobe and scanning electron microscope studies of Nb_3Sn layer thickness and matrix contamination have been carried out also. (auth)

30810 MAGNETIC AND SUPERCONDUCTING PROPERTIES OF NIOBIUM OXIDES. Khan, H. R. (Forschungsinstitut fuer Edelmetalle und Metallchemie, Schwabisch-Gmuend, Ger.); Raub, C. J.; Gardner, W. E.; Fertig, W. A.; Johnston, D. C.; Maple, M. B. Mater. Res. Bull.; 9: No. 9, 1129-1136(Sep 1974).

Low temperature magnetic susceptibilities of niobium oxides have been measured. A homogeneous sample of NbO prepared by arc melting and checked by using x-ray and metallographic techniques exhibits no ferromagnetism but becomes superconducting at 1.20°K. (auth)

30811 CRITICAL TEMPERATURE OF TRANSITION-METAL ALLOY SUPERCONDUCTORS. Lustfeld, H. (Univ., Hamburg). Solid State Commun.; 15: No. 2, 301-302(15 Jul 1974).

The critical temperature T_c of a superconducting transition-metal alloy is calculated using an approximation of Kerker and Bennemann (Solid State Commun.; 14:399 (1974)), but in contrast to that of Kerker and Bennemann the present approximation does not violate the time reversal and spin rotation symmetries. (auth)

30812 SPECIFIC HEAT OF SUPERCONDUCTING Pd–H ALLOYS. Mackliet, C. A.; Gillespie, D. J.; Schlinder, A. I. (Naval Research Lab., Washington, DC). Solid State Commun.; 15: No. 2, 207-210(15 Jul 1974).

The low temperature specific heat of a series of superconducting Pd–H alloys ($H/Pd \sim 0.83_5$ to 0.87_5) has been measured; broad yet very pronounced peaks whose widths are a function of hydrogen concentration are observed. An interesting scaling feature and a theoretical fitting of the data are discussed. A few results of some associated electrical resistance measurements are mentioned, and the possible role of Fe impurities in suppressing superconductivity in Pd–H alloys is considered. (auth)

30813 ISOTOPE EFFECT IN THE SUPERCONDUCTING PALLADIUM–HYDROGEN–DEUTERIUM SYSTEM. Skoskiewicz, T.; Szafranski, A. W.; Bujnowski, W.; Baranowski, B. (Polska Akademia Nauk, Warsaw). J. Phys., C (London); 7: No. 15, 2670-2676(7 Aug 1974).

The dependence of critical temperature on hydrogen (deuterium) content in palladium hydride (deuteride) was measured on samples hydrogenized under equilibrium conditions with H(D) at high pressure. The superconductivity transitions can be observed for atomic ratios of hydrogen (deuterium) to palladium H(D)/Pd above 0.83 (0.77). The critical temperatures of deuteride are about 2.5 K higher than those of hydride (at the same atomic ratios). The highest critical temperatures so far observed for the hydride and deuteride are 9.1 K and 10.7 K respectively. For both phases the effect of hydrostatic pressure is to decrease the critical temperature. The observed isotope effect does not support a metallic behavior of hydrogen in palladium but is in reasonable agreement with Ganguly's model for the superconductivity of palladium hydride or deuteride. (auth)

30814 SUPERCONDUCTING-NORMAL PHASE BOUNDARIES OF (La,Th)Ce SYSTEMS. Huber, J. G.; Fertig, W. A.; Maple, M. B. (Univ. of California, La Jolla, San Diego). Solid State Commun.; 15: No. 3, 453-457(1 Aug 1974).

The dependence of the superconducting transition temperature T_c on Ce impurity concentration n is reported for various (La,Th) Ce systems. These results document for the first time the evolution of the superconducting–normal phase boundary (T_c vs n curve) as an impurity undergoes a magnetic-nonmagnetic transition which for Ce impurities in (La,Th)Ce systems proceeds with increasing Th concentration. Observed for only the second time, re-entrant T_c vs n curves are reported for two La-rich La, Th host compositions. (auth)

30815 VORTEX LATTICE IN MAGNETIC SUPERCONDUCTORS. Krey, U. (Univ., Hamburg). Int. J. Magn.; 4: No. 2, 153-162(1973).

The vortex lattice of magnetic superconductors near H_{c2} is treated within a phenomenological approach, generalizing the energy functional of the Ginsburg–Landau theory by inclusion of the magnetic polarization J(r) of the nondilute spin system as an additional variable function besides the order parameter $\psi(r)$ of the pair condensate. For the validity of this approach, the thermal fluctuations of the quantity J must be smaller than the expectation value. This condition can even be fulfilled, if there is no spontaneous ferromagnetic spin order in the Meissner state, provided the magnetic fields near H_{c2} are strong enough to induce spin polarization within the mixed state. From the generalized functional, a system of coupled partial differential equations is derived, which is treated in a similar manner as for nonmagnetic superconductors near H_{c2}. The results are as follows: The critical external field H_{c2} differs from the value corresponding to nonmagnetic material, depending on the magnetic polarization and on the demagnetizing factor N, whereas the value of the internal induction B_{c2} is the same as for nonmagnetic superconductors. The condition $\kappa > 1/\sqrt{2}$, which is necessary and sufficient for the existence of a stable vortex lattice for nonmagnetic material, is replaced by several different conditions, which must be fulfilled at the same time, involving a variety of material parameters, a structure parameter depending on the lattice structure and on the magnetic correlation length, and the demagnetizing factor N. Moreover, the stable vortex lattice can be different from the well-known triangular one, especially, if the Ginzburg–Landau parameter κ is not much larger than $1/\sqrt{2}$. (auth)

30816 SUPERCONDUCTORS. Prakash, O. M. (Armam Technological Inst., Poona). Elec. India; 13: No. 2, 5-18(1973).

The phenomenon of superconductivity is explained and its effects are discussed. The types of superconductors and some of the theories of superconductivity are mentioned. The various applications of superconductivity in the fields of electrical engineering, electronics, defense, etc. are given. 47 ref. (Indian Sci. Abstr.)

30817 SELF-CONSISTENT PAIR POTENTIAL IN SUPERCONDUCTORS. I. The Superconductor–Insulator Boundary Near T_c. Bar-Sagi, J.; Kuper, C. G. (Technion–Israel Inst. of Tech., Haifa). J. Low Temp. Phys.; 16: No. 1/2, 73-85(Jul 1974).

A method valid at all temperatures below T_c is presented for the self-consistent solution of the Bogoliubov–de Gennes equations. Computation is reduced to manageable proportions by using an Ansatz for the pair potential, and determining the parameters in the Ansatz by requiring self-consistency. For the simple geometry of a semiinfinite slab of superconductor in contact with an insulator (or vacuum), the Ansatz $\Delta = \Delta_\infty \tanh \alpha z$ is found to be good close to the transition temperature and correctly recovers the Ginzburg–Landau theory as $T \rightarrow T_c$. (auth)

30818 KINETICS OF FLUX JUMPS IN TYPE-II SUPERCONDUCTING DISKS. Mukherjee, B. K.; Baird, D. C. (Royal Military Coll. of Canada, Kingston, Ont.). J. Low Temp. Phys.; 16: No. 1/2, 119-124(Jul 1974).

Experimental studies of the kinetics of flux jumps in type-II superconducting disks have shown that flux penetration into the specimen can be described by an exponential function of time. A phenomenological theory is presented which uses the concepts of flux pinning and flux flow viscosity to derive a function of the same form as that found experimentally. The function can be used to evaluate the average pinning force and the viscosity from experimental data on flux jumps. (auth)

30819 PHASE-SLIP CENTERS AND NONEQUILIBRIUM PROCESSES IN SUPERCONDUCTING TIN MICROBRIDGES. Skocpol, W. J.; Beasley, M. R.; Tinkham, M. (Harvard Univ., Cambridge, MA). J. Low Temp. Phys.; 16: No. 1/2, 145-167(Jul 1974).

It is shown experimentally that steps in the I–V curves of long, superconducting microbridges near T_c are due to spatially localized voltage units (interpreted as quantum phase-slip centers) which appear at local critical currents determined primarily by variations of T_c along the bridge. The ac Josephson effect associated with such centers was also observed. At low voltages each center carries a time-averaged supercurrent of $\sim\frac{1}{2} I_c$ and exhibits a temperature-independent differential resistance due to normal current flow governed by the quasiparticle diffusion length. Our phenomenological model of this behavior includes a simplified description of both the superfluid dynamics and the spatial healing of the resulting disequilibrium between superconducting pairs and quasiparticles. The data indicate that the relaxation time associated with the nonequilibrium is typical of inelastic scattering times for electrons near the Fermi surface of normal tin. (auth)

Equipment and Devices

30820 (LA-5684-PR) USAEC-DAT DC SUPERCONDUCTING POWER TRANSMISSION LINE PROJECT AT LASL. Progress Report, January 1–March 31, 1974. Keller, W. E.; Taylor, R. D. (comps.). (Los Alamos Scientific Lab., N. Mex. (USA)). Jul 1974. Contract W-7405-eng-36. 19p. Dep. NTIS $4.00.

A small tube covered by two layers of commercial Nb_3Sn tapes carried a current of about 39,000 A introduced by a dc transformer technique. Critical current tests in the range 13.8 to 17 K are reported for several Nb_3Sn tapes of varying width. At 13.8 K some tapes carried over 25% of their 4 K critical current. Operation of the 20-m test bed with a NbTi sample at 4 K and carrying 10,000 A is described. Superconducting materials developments include thick, chemical-vapor-deposition prepared Nb_3Ge coatings having at T_c of 16 K. (auth)

30821 COHERENT EFFECTS IN LARGE ARRAYS OF SUPERCONDUCTING BRIDGES. Palmer, D.W.; Mercereau, J.E. (California Institute of Technology, Pasadena, California 91109). Appl. Phys. Lett. 25: No. 8, 467-469 (15 Oct 1974).

Series arrays of nearly identical superconducting proximity effect bridges have been fabricated in Nb/Ta thin films. Arrays with up to 500 bridges respond cooperatively to incident radiation and produce voltage steps in response to incident 30–20000–MHz radiation at $V =$ (number of bridges in array) $\times$ $(h\nu/2e)$. (auth)

30822 UTILIZATION OF SUPERCONDUCTING DEVICES FOR THE GENERATION AND STORAGE OF ELECTRICAL ENERGY. Arch. Energiewirt.; 28: No. 10, 488-495(May 1974). (In German).

7 refs.

Concerning electrical machines, the increase in the performance of the turbosets, the possibilities given by the superconductor, materials, the application of superconductors for other electrical machines, the development work in different countries and the international cooperation, as well as possibilities of energy storage are considered. (GE)

30823 SUPERCONDUCTING MACHINES AND DEVICES: LARGE SYSTEMS APPLICATIONS. Conference Held at Entreves, Italy, September 5–14, 1973. Foner, S.; Schwartz, B. B. (eds.). NATO Advanced Study Institutes Series B. Physics. Volume 1. New York; Plenum Publishing Corporation (1974). 711p. . (CONF-7309112-). $39.50.

From large scale applications of superconductivity and magnetism conference; Entreves, Italy (5 Sep 1973).

Seventeen lectures are included. Separate abstracts were prepared for sixteen. The remaining lecture considered the use of hydrogen as an energy carrier. (MHR)

For abstracts of individual papers see: 30807 and 30824–30838.

30824 LARGE SCALE APPLICATIONS OF SUPERCONDUCTIVITY. Powell, J. (Brookhaven National Lab., Upton, NY). pp 1-85 of Superconducting Machines and Devices: Large Systems Applications. Foner, S. (ed.). New York; Plenum Publishing Corp. (1974).

From large scale applications of superconductivity and magnetism conference; Entreves, Italy (5 Sep 1973). See CONF-7309112-.

The following applications are discussed: energy generation–fusion, energy generation–MHD, energy storage–peaking power, energy modification–ac and dc generators and motors, energy transmission–ac and dc, magnetic levitation–high speed ground transportation, and industrial processing. (17 tables, 27 figures, 89 references)

30825 PRACTICAL SUPERCONDUCTING MATERIALS. Dew-Hughes, D. (Univ. of Lancaster, Eng.). pp 87-137 of Superconducting Machines and Devices: Large Systems Applications. Foner, S. (ed.). New York; Plenum Publishing Corp. (1974).

From large scale applications of superconductivity and magnetism conference; Entreves, Italy (5 Sep 1973). See CONF-7309112-.

The properties required of superconductors for commercial applications are briefly summarized. Each of these properties, i.e., critical temperature, critical field, critical current density, stability, alternating current losses, fabrication, and cost, are examined in turn. Methods for producing optimum values are discussed and reasonable estimates of upper limits which can be placed on these values are made. (4 tables, 8 figures, 125 references) (MHR)

30826 SUPERCONDUCTING MAGNETS. Brechna, H. (Federal Inst. of Tech., Zurich). pp 139-217 of Superconducting Machines and Devices: Large Systems Applications. Foner, S. (ed.). New York; Plenum Publishing Corp. (1974).

From large scale applications of superconductivity and magnetism conference; Entreves, Italy (5 Sep 1973). See CONF-7309112-.

The following topics are discussed: applications of superconducting magnets, examples of operating superconducting magnets, magnet systems, superconductor stabilization, inductive energy storage magnets, magnets for pulsed field applications, coil structure and pulsed magnet design, conductor configurations in pulsed magnets, and experience with pulsed magnets. (38 figures, 34 references) (MHR)

30827 SUPERCONDUCTING DC MACHINES. Appleton, A. D. (International Research and Development Co. Ltd., Newcastle upon Tyne, Eng.). pp 219-277 of Superconducting Machines and Devices: Large Systems Applications. Foner, S. (ed.). New York; Plenum Publishing Corp. (1974).

From large scale applications of superconductivity and magnetism conference; Entreves, Italy (5 Sep 1973). See CONF-7309112-.

The limitations of conventional dc motors are examined and how machine ratings could be increased by the use of superconductors with the homopolar type of geometry is indicated. Then the design of the superconducting machine is considered in more detail and the picture is built up towards the realization of practical hardware. Some of the more important design problems are considered. The Fawley motor is considered in detail and applications and further developments for superconducting dc machines are mentioned. (3 tables, 41 figures, 15 references) (MHR)

30828 APPLICATIONS OF SUPERCONDUCTIVITY TO AC ROTATING MACHINES. Smith, J. L. Jr.; Keim, T. A. (Massachusetts Inst. of Tech., Cambridge). pp 279-345 of Superconducting Machines and Devices: Large Systems Applications. Foner, S. (ed.). New York; Plenum Publishing Corp. (1974).

From large scale applications of superconductivity and magnetism conference; Entreves, Italy (5 Sep 1973). See CONF-7309112-.

The following topics are discussed: basic synchronous machine theory, experimental machines at MIT, thermal isolation and cryogenic refrigerator, and present problems, current developments, and future prospects. (46 figures, 38 references) (MHR)

30829 HIGH SPEED MAGNETICALLY LEVITATED AND PROPELLED MASS GROUND TRANSPORTATION. Iwasa, Y. (Massachusetts Inst. of Tech., Cambridge). pp 347-399 of Superconducting Machines and Devices: Large Systems Applications. Foner, S. (ed.). New York; Plenum Publishing Corp. (1974).

From large scale applications of superconductivity and magnetism conference; Entreves, Italy (5 Sep 1973). See CONF-7309112-.

The following topics are discussed: state of the art, principles of magnetic levitation, principles of linear motor propulsion, other important considerations for repulsive magnetic levitation system, cost estimates for a magneplane system, and current status of new transportation system research and development in various nations. (5 tables, 20 figures, 32 references) (MHR)

30830 TRANSMISSION OF ELECTRICAL ENERGY BY SUPERCONDUCTING CABLES. Bogner, G. (Siemens A. G., Erlangen, Ger.). pp 401-548 of Superconducting Machines and Devices: Large Systems Applications. Foner, S. (ed.). New York; Plenum Publishing Corp. (1974).

From large scale applications of superconductivity and magnetism conference; Entreves, Italy (5 Sep 1973). See CONF-7309112-.

The following topics are discussed: power transmission systems in existence and in process of development, a general comparison between superconducting dc and ac cables, superconducting cable concepts, cable conductors, electrical insulation, thermal insulation, cable cooling, cable joints, terminations, methods of laying various types of cables, operational reliability and monitoring, characteristic data of various cable types, economics of superconducting cables, and superconducting cable projects. (9 tables, 74 figures, 141 references) (MHR)

30831 TUNNEL JUNCTIONS FOR COMPUTER APPLICATIONS. Matisoo, J. (IBM Watson Research Center, Yorktown Heights, New York). pp 563-580 of Superconducting Machines and Devices: Large Systems Applications. Foner, S. (ed.). New York; Plenum Publishing Corp. (1974).

From large scale applications of superconductivity and magnetism conference; Entreves, Italy (5 Sep 1973). See CONF-7309112-.

The use of Josephson junctions as computer devices is described. A discussion of how the devices function, how they are made, what is known about them so far, and why they continue to look extremely interesting is presented. (MHR)

30832 HIGH GRADIENT MAGNETIC SEPARATION: AN INDUSTRIAL APPLICATION OF MAGNETISM. Kelland, D.; Kolm, H.; deLatour, C.; Maxwell, E.; Oberteuffer, J. (Massachusetts Inst. of Tech., Cambridge). pp 581-594 of Superconducting Machines and Devices: Large Systems Applications. Foner, S. (ed.). New York; Plenum Publishing Corp. (1974).

From large scale applications of superconductivity and magnetism conference; Entreves, Italy (5 Sep 1973). See CONF-7309112-.

The uses, principles, and characteristics of high gradient magnetic separations are discussed. The use of superconducting magnets in this application is mentioned briefly. (MHR)

30833 PROGRAMS ON LARGE SCALE APPLICATIONS OF SUPERCONDUCTIVITY IN FRANCE. Bronca, G. (Commissariat a l'Energie Atomique, Saclay, France). pp 595-600 of Superconducting Machines and Devices: Large Systems Applications. Foner, S. (ed.). New York; Plenum Publishing Corp. (1974).

From large scale applications of superconductivity and magnetism conference; Entreves, Italy (5 Sep 1973). See CONF-7309112-.

The most promising application for the future in France is the superconducting alternator. The program directions are: for the near future, magnets for applications in research especially high energy physics and for the far future generators for electric power systems. (MHR)

30834 PROGRAMS ON LARGE SCALE APPLICATIONS OF SUPERCONDUCTIVITY IN THE FEDERAL REPUBLIC OF GERMANY. Bogner, G. (Siemens AG, Erlangen, Ger.). pp 601-614 of Superconducting Machines and Devices: Large Systems Applications. Foner, S. (ed.). New York; Plenum Publishing Corp. (1974).

From large scale applications of superconductivity and magnetism conference; Entreves, Italy (5 Sep 1973). See CONF-7309112-.

The major applied programs in Germany are: superconducting materials, magnets for high energy physics and plasma physics, magnets for industrial or special applications, rotating electrical machinery, electric power transmission, land transportation systems, and high frequency cavities and Josephson elements. (MHR)

30835 PROGRAMS ON LARGE SCALE APPLICATIONS OF SUPERCONDUCTIVITY IN ITALY. Rizzuto, C. (Consiglio Nazionale delle Richerche, Genoa). pp 615-620 of Superconducting Machines and Devices: Large Systems Applications. Foner, S. (ed.). New York; Plenum Publishing Corp. (1974).

From large scale applications of superconductivity and magnetism conference; Entreves, Italy (5 Sep 1973). See CONF-7309112-.

The development of applied superconductivity in Italy is briefly outlined, including a few details on the research laboratories and low temperature facilities. (CES)

30836 PROGRAMS ON LARGE SCALE APPLICATIONS OF SUPERCONDUCTIVITY IN JAPAN. Yasukochi, K.; Ogasawara, T. (Nihon Univ., Tokyo). pp 621-634 of Superconducting Machines and Devices: Large Systems Applications. Foner, S. (ed.). New York; Plenum Publishing Corp. (1974).

From large scale applications of superconductivity and magnetism conference; Entreves, Italy (5 Sep 1973). See CONF-7309112-.

The history and current status of the large scale application of superconductivity in Japan are reviewed. The current programs are divided into five categories: MHD power generation systems, superconducting rotating machines, cryogenic power transmission systems, magnetically levitated transportation, and applications in high energy physics experiments. (MHR)

30837 PROGRAMS ON LARGE SCALE APPLICATIONS OF SUPERCONDUCTIVITY IN SWITZERLAND. Bratoljic, T. (Brown, Boveri and Co. Ltd., Baden, Switzerland); Meyer, G.; pp 635-637 of Superconducting Machines and Devices: Large Systems Applications. Foner, S. (ed.). New York; Plenum Publishing Corp. (1974).

From large scale applications of superconductivity and magnetism conference; Entreves, Italy (5 Sep 1973). See CONF-7309112-.

A short survey of the universities, institutions, and businesses involved and their essential activities is presented. (MHR)

30838 PROGRAMS ON LARGE SCALE APPLICATIONS OF SUPERCONDUCTIVITY IN THE UNITED STATES. Powell, R. L.; Fickett, F. R.; Birmingham, B. W. (National Bureau of Standards, Boulder, CO). pp 651-675 of Superconducting Machines and Devices: Large Systems Applications. Foner, S. (ed.). New York; Plenum Publishing Corp. (1974).

From large scale applications of superconductivity and magnetism conference; Entreves, Italy (5 Sep 1973). See CONF-7309112-.

In summary tables, an attempt was made to present, in a succinct manner, an overview of the large-scale applications of superconductivity in the U. S. A. For each project the following are listed: the institution or company actually doing the work; a person who was the main contact; a description of the magnet, device, or system; an indication of the type of program; the source and amount of funding at the present; the status of the project as of summer 1973; and any future plans and proposals. The projects covered are: generators for electric power systems; electric power transmission; machinery for propulsion systems and auxiliary power supplies; magnets for energy storage, MHD, and controlled thermonuclear reaction systems; magnets and cavities for high energy physics experiments; magnets for industrial and medical applications; and land transportation systems. (MHR)

30839 INDUCTANCE BRIDGE FOR CURRENT–QUANTUM–PHASE MEASUREMENTS IN SUPERCONDUCTORS AT ZERO FREQUENCY. Meservey, R.; Paraskevopoulos, D.; Gruenberg, L.W.; Tedrow, P.M. (Francis Bitter National Magnet Laboratory, Massachusetts Institute of Technology, Cambridge, Massachusetts 02139). J. Appl. Phys. 45: No. 10, 4601-4610 (Oct 1974).

A zero–frequency bridge has been developed for measuring the inductance and the current–vs–quantum–phase relation of superconductors. The current null detector is a SQUID magnetometer coupled to the bridge by a superconducting transformer. The bridge is balanced by adjusting precision resistors at room temperature. The theory of the bridge and analysis of the null–detector circuit for optimizing the sensitivity are given. For current–dependent inductors, a definition of inductance based on the quantum–phase difference is shown to be useful. Construction and operation of the bridge are described and measurements of inductance vs temperature for Al thin–film meander lines are presented. Zero–frequency measurements avoid the stray coupling to capacitances and normal metal inductances found in high–frequency measurements and the method could give high–precision absolute measurements. The sensitivity of the present instrument is such that an inductor of 4×10^{-7} H was measured to a relative precision of one part in 10^4 with a measuring current of 5×10^{-6} A. Considerable improvement is possible, especially for circuit elements of very small inductance such as Josephson junctions and weak–link superconductors. (auth)

30840 THE EFFECT OF CLADDING MATERIAL ON AC LOSSES OF COMMERCIAL Nb_3Sn TAPES. Bussière, J.F.; Garber, M.; Suenaga, M. (Power Transmission Project, Brookhaven National

Laboratory, Upton, New York 11973). J. Appl. Phys. 45: No. 10, 4611-4616 (Oct 1974).

ac losses of commercial Nb_3Sn tapes have been measured before and after removal of the normal metal cladding which is used to stabilize the superconductor. It is shown that materials which are frequently used to assist in bonding the normal metal to the Nb_3Sn surface give rise to hysteretic losses which are much larger than those of the Nb_3Sn itself in the low—field region of interest for power transmission, below 1000 Oe. Examples of such materials are superconductive Pb—Sn solders used in cladding tin—diffused tapes and ferromagnetic nickel flashes used in silver plating vapor—deposited tapes. These lossy materials are not essential and can be eliminated in tapes which are properly designed for power transmission. It is also shown that eddy curent losses are acceptably small for normal metal cladding thickness of the order of 25 μm ($\rho \sim 10^{-8}$ Ω cm). (auth)

30841 TECHNIQUE FOR FABRICATION OF SUPERCONDUCTING MICROBRIDGES AND SMALL JOSEPHSON TUNNEL JUNCTIONS. Yeh, J.T.C. (Department of Physics and Laboratory for Research on the Structure of Matter, University of Pennsylvania, Philadelphia, Pennsylvania 19174). J. Appl. Phys. 45: No. 10, 4617-4621 (Oct 1974).

A simple, versatile, and inexpensive technique for the fabrication of superconducting microbridges and small Josephson tunnel junctions is described. The technique is based on the use of fiber masks for the production of precisely controlled substrate channels and yields device dimensions of 1 μm or less. (auth)

30842 APPLICATION OF JOSEPHSON'S EFFECT IN SUPERCONDUCTORS FOR MEASUREMENTS OF VERY SMALL VOLTAGES. Jaszczuk, W.; Trojnar, E. Chlodnictwo; 7: No. 7, 10-11 (1972).

A practical potentiometer with a sensitivity about 10^{-11}V (source resistance $0.8 \cdot 10^{-6}$) for use at liquid helium temperatures is described. As a null detector a Josephson tunneling device consisting of a lead—tin solder bead encircling a 0.2 mm niobium wire has been used. The device has zero dc resistance and is useful in the detection of small voltages from sources having small internal resistances. (auth)

PHYSICS (NUCLEAR)

Neutron Interactions with Matter

Refer also to abstracts 31015, 31071, 31271, 31274, and 31275.

30843 (IAE-2271) NEUTRON SLOWING-DOWN IN ICE AND POLYETHYLENE AT LOW TEMPERATURES. Ishmaev, S. N.; Sadikov, I. P.; Chernyshov, A. A. (Gosudarstvennyj Komitet po Ispol'zovaniyu Atomnoj Ehnergii SSSR, Moscow. Inst. Atomnoj Ehnergii). 1973. 8p. (In Russian). INIS.

In connection with the problem of optimizing a pulsed source of slow neutrons on the IAE linear accelerator, a study was made of the effect of intense cooling of a hydrogen-containing moderator (H_2O and $(CH_2)_n$ polyethylene) at T = 300, 77, and 4.2°K on the pulse shape of moderated neutrons of various energies from 0.0018 to 0.090 eV. At low temperatures polyethylene turns out to be a better moderator than ice, which observation is explained by the high level density in the low-energy part of the normal oscillation spectrum. Cooling of polyethylene $(CH_2)_n$ to T = 4.2°K makes it possible to increase the amplitude of a 0.0018-eV neutron pulse by a factor of 7 and to increase the integral yield by a factor of 16 as compared with T = 300°K. For the energy region of 0.1 to 0.01 eV, by cooling the moderator it is possible to shorten the duration of the neutron pulse by a factor of 2 to 3 without a loss in intensity in flux maximum so that resolution conditions are substantially improved in time-of-flight spectroscopy for this energy range. (3 figures) (tr-auth)

30844 (IAE-2274) MEASUREMENT OF NEUTRON TEMPERATURE IN WATER BY DIFFERENTIAL AND INTEGRAL METHODS. Ermolaev, O. Ya.; Lomakin, S. S.; Lysov, V. V.; Panfilov, G. G.; Taraban'ko, V. A. (Gosudarstvennyj Komitet po Ispol'zovaniyu Atomnoj Ehnergii SSSR, Moscow. Inst. Atomnoj Ehnergii). 1973. 12p. (In Russian). INIS.

By means of a time-of-flight method and Westcott's method the spatial distribution of neutron temperature in water was measured. The system consisted of a graphite prism with dimensions 100 cm × 100 cm × 59.5 cm and, placed in the center of the prism, a cylindrical water tank 5.7 cm in radius. Measurements were carried out at points 0, 2, 4, 6, 8, 10, 12, 14, and 16 cm on the cylinder axis and at points 0, 0.52, 1.04, 1.56, 2.08, 2.60, 3.12, 3.64, 4.16, 4.68, and 5.20 cm along the cylinder radius. Neutron temperatures obtained by the Westcott method and by the time-of-flight method agreed well within the error limits. These results can serve as a basis for measuring neutron temperatures by Westcott's method under similar conditions in place of the complex, difficult time-of-flight method. (6 figures) (tr-auth)

30845 (IFA-DNBR-8-1974) STRUCTURE OF THE EVALUATED MICROSCOPIC NUCLEAR DATA LIBRARY "DANEM-I" FROM THE I.A.P. Badescu-Singureanu, Al. I.; Mateescu, S.; Gheorghe, D.; Deciu, N. (Institutul de Fizica Atomica, Bucharest (Romania)). 1974. 17p. (In Rumanian). Dep. NTIS (US Sales Only) $4.00.

The physical and logical structures of the DANEM-I library of evaluated microscopic nuclear data for reactors produced in the "Institute of Atomic Physics" are described in detail. (3 figures, 6 tables) (auth)

30846 (IFA-DNBR-9-1974) PHYSICAL QUANTITIES THE NUMERICAL VALUES OF WHICH WILL BE INCLUDED IN THE EVALUATED MICROSCOPIC NUCLEAR DATA LIBRARY "DANEM-I" FROM THE I.A.P. Badescu-Singureanu, A. I.; Mateescu, S.; Gheorghe, D.; Deciu, N. (Institutul de Fizica Atomica, Bucharest (Romania)). 1974. 31p. (In Rumanian). Dep. NTIS (US Sales Only) $4.75.

The main physical quantities the numerical values of which will be included in the "DANEM-I" library of evaluated microscopic nuclear data for reactors from the I.A.P., the relations between them, and the formats utilized to store these data in the library are described. (9 figures) (auth)

30847 (IRI-132-73-03) RKSPROG: A COMPUTER PROGRAM FOR INELASTIC COLD NEUTRON SCATTERING TIME-OF-FLIGHT MEASUREMENTS. de Mul, F. F. M.; Bregman, J. D. (Interuniversitair Reactor Instituut, Delft (Netherlands)). Jul 1973. 58p. INIS.

A computer program for the evaluation of time-of-flight spectra, resulting from inelastic cold neutron scattering experiments using a rotating-crystal spectrometer, is described. The program calculates double-differential scattering cross sections and intermediate scattering functions, both on an absolute scale and corrected for the experimental resolution, using the direct fast Fourier transformation method. (NL)

30848 (KFK-1959) MEASUREMENT AND CALCULATION OF NEUTRON SPECTRA AT A SODIUM–IRON INTERFACE. Kappler, F. (Kernforschungszentrum Karlsruhe (F.R. Germany). Inst. fuer Neutronenphysik und Reaktortechnik). Apr 1974. 90p. (In German). Dep. NTIS (US Sales Only) $7.50.

The problem of strong space-dependent neutron spectra at boundaries is studied at a sodium–iron interface. At a sodium–iron interface in slab geometry spatial neutron spectra from a 14-MeV neutron source were measured in the energy range from 100 eV to 4.5 MeV. For the energy E < 200 keV, the time-of-flight method was utilized, and for E > 200 keV, proton recoil detectors were used. In addition, calculations with the Karlsruhe transport codes DTK and SNOW were performed. The comparison of measured and calculated spectra, both a function of space and energy, showed that the spectrum around the sodium resonance is well described in 208 energy groups. To estimate the depth to which the flux depression at a resonance energy propagates into an adjacent material, a relation is given as a function of the resonance parameters and the properties of the material concerned. (24 figures, 8 tables) (auth)

30849 (NEANDC-97/U) LIST OF COMPUTER PROGRAMS FOR NEUTRON CROSS SECTION CALCULATIONS AND ANALYSIS. (Organization for Economic Co-Operation and Development, 75 - Paris (France)). Jan 1974. 27p. Dep. NTIS (US Sales Only) $4.00.

This list of computer codes is ordered alphabetically by country of origin and then by field of application; thermal scattering, resolved resonances, unresolved resonances, statistical model, optical model, and miscellany are the groupings used. It is felt that more than 80% of the codes in use today are included. (117 references) (RWR)

30850 (RT/FI-(74)10) POINT-DEPENDENT CALCULATIONS OF THE ANISOTROPIC DIFFUSION COEFFICIENT. Michelini, M.; Sallam, O. H. (Comitato Nazionale per l'Energia Nucleare, Rome (Italy)). Jan 1974. 98p. Dep. NTIS (US Sales Only) $8.00.

In the framework of the anisotropic diffusion method it has been suggested that more accurate flux distributions could be obtained if the coefficient D_k (K = X, Y, Z) were calculated mesh by mesh, for instance, by means of standard diffusion codes. This possibility is examined numerically in this report. (15 figures, 3 tables) (auth)

30851 (RT/FI-(74)19) MCDATA CODE. Cosimi, M. (Comitato Nazionale per l'Energia Nucleare, Rome (Italy)). Apr 1974. 21p. Dep. NTIS (US Sales Only) $4.25.

The MCDATA code provides the capability of handling in an automatic way cross section data sets generated by successive runs of the MC^2 code. Different retrieval options are provided, and the resulting libraries are organized in the formats required by many neutronics codes of general use in fast reactor design calculations. (auth)

30852 ABSOLUTE DETERMINATION OF THE FAST NEUTRON FLUXES BY USING THE FLOW-TYPE MANGANESE BATH METHOD. Wu, M. W.; Chou, J. C. (Inst. of Nuclear Energy Research, Taiwan). Chin. J. Phys. (Taiwan); 11: No. 2, 97-104(Oct 1973).

The absolute neutron flux produced in a Van de Graaff accelerator via the $^{7}Li(p,n)^{7}Be$-reaction was measured with the help of a circulated manganese bath. An elaborate process was developed for the absolute determination of the efficiency of the gamma detector adapting the circulating system. The absolute emission rate of an Am–Be neutron source was also determined with the bath method, which agrees well with the calculated value according to the given decay rate of ^{241}Am. (auth)

30853 ACOUSTIC EFFECT OF FAST NEUTRON BEAMS IN A SOLID BODY. Kalinichenko, A. I.; Lazurik-El'tsufin, V. T. (Kharkov State Univ.). Ukr. Fiz. Zh. (Russ. Ed.); 19: No. 3, 515-517(Mar 1974). (In Russian).

The contributions to the amplitude of the acoustic signal of dynamic and thermoelastic volume forces due to the interaction of a beam of fast neutrons in a thin plastic solid body were evaluated and compared. (tr-auth)

Nuclear Properties and Reactions, A ≤ 5

Refer also to abstracts 29511, 31098, and 31103.

30854 (AD-777030) CROSS SECTIONS OF PROTON–NUCLEUS INTERACTIONS AT HIGH ENERGIES. Silberberg, R.; Tsao, C. H. (Naval Research Lab., Washington, D.C. (USA)). 21 Dec 1973. 68p. (NRL-7593). NTIS $3.75.

The measured partial cross sections for high energy proton–nucleus interactions were compiled from more than 200 publications. The targets range from lithium to uranium; the products considered have mass number A > or = 6. A comparison of cross section induced by protons and ^{4}He is tabulated. Also a table of cross sections for (p,nx) reactions is given. These cross sections are useful for studies of interactions of cosmic rays and solar flare particles, as well as in radiation shielding and radiation therapy. These cross sections were used to develop semi-empirical equations for calculating partial cross sections that have not yet been measured. (auth) (GRA)

30855 (NP-20122, pp 29-33) d(p,2p)n REACTION. Johansson, A.; Sundqvist, B.; Amten, L.; Glantz, L.; Goenczi, L.; Koersner, I.; Ebenhoeh, W. (Tandem Accelerator Lab., Uppsala). Jan 1974.

30856 (UCID-16563) SELECTED ACTIVITIES IN PHOTONUCLEAR REACTIONS, 1973–1974. Berman, B. L. (comp.). (California Univ., Livermore (USA). Lawrence Livermore Lab.). 1974. Contract W-7405-eng-48. 11p. (CONF-740806-2). Dep. NTIS $4.00.

From Gordon conference; Tilton, New Hampshire, USA (Aug 1974).

Abstract-length summaries are given of the following topics: measurement of the ^{4}He(γ,p)-to-(γ,n) cross-section ratio; high-resolution photoneutron spectrum from ^{16}O; preliminary study of the ^{28}Si(γ,p) and ^{28}Si(γ,n) reactions; photofission and photoneutron cross-section measurements; and investigation of gamma-producing reaction mechanisms and gamma strength functions for 8- to 30-MeV photons by comparing (p,γ) and (d,γ) reactions. (4 figures) (RWR)

30857 ^{4}He NUCLEUS AND SOFT CORE POTENTIALS. Ulehla, I. (Rutherford High Energy Lab., Chilton, Eng.). pp 39-404 of Nuclear Many-Body Problem. Vol. I. Calogero, F. (ed.). Bologna; Editrice Compositori (1973).

From symposium on present status and novel developments in the nuclear many-body problem; Rome, Italy (19 Sep 1972). See CONF-720933–P1.

30858 NEW METHOD FOR EVALUATING THE DENSITY MATRIX AND ITS APPLICATION TO THE GROUND STATE FORM FACTOR. Fink, M. (Ruhr-Univ., Bochum, Ger.). pp 514-526 of Nuclear Many-Body Problem. Vol. I. Calogero, F. (ed.). Bologna; Editrice Compositori (1973).

From symposium on present status and novel developments in the nuclear many-body problem; Rome, Italy (19 Sep 1972). See CONF-720933–P1.

30859 CONVERGENCE OF THE HYPERSPHERICAL EXPANSION TREATMENT OF FEW-NUCLEON BOUND STATES. Ballot, J. L.; Beiner, M.; Fabre, M.; Fabre de la Ripelle, M. (Institut de Physique Nucleaire, Orsay, France). pp 565-588 of Nuclear Many-Body Problem. Vol. I. Calogero, F. (ed.). Bologna; Editrice Compositori (1973).

From symposium on present status and novel developments in the nuclear many-body problem; Rome, Italy (19 Sep 1972). See CONF-720933–P1.

30860 CENTRE OF MASS COORDINATE IN MANY-BODY THEORIES. Palumbo, F. (CNEN, Rome). pp 685-705 of Nuclear Many-Body Problem. Vol. I. Calogero, F. (ed.). Bologna; Editrice Compositori (1973).

From symposium on present status and novel developments in the nuclear many-body problem; Rome, Italy (19 Sep 1972). See CONF-720933–P1.

30861 VARIATIONAL CALCULATIONS OF REACTIONS INVOLVING LIGHT NUCLEI. Hackenbroich, H. H. (Univ., Cologne). pp 706-747 of Nuclear Many-Body Problem. Vol. I. Calogero, F. (ed.). Bologna; Editrice Compositori (1973).

From symposium on present status and novel developments in the nuclear many-body problem; Rome, Italy (19 Sep 1972). See CONF-720933–P1.

30862 TRITON BINDING ENERGY AND THE DEUTERON WAVE FUNCTION. de Groot, H.; Boersma, H. J. (Vrije Univ., Amsterdam). Lett. Nuovo Cim.; 11: No. 3, 238-242(21 Sep 1974).

The dependence of the triton binding energy on changes in the deuteron wave function is considered in the more realistic case when a tensor force is present and the deuteron properties are well reproduced. Separable tensor potentials are constructed having the same deuteron wave function as that of realistic tensor potentials taken from a phase-equivalent set given previously. (JFP)

30863 HARTREE-FOCK CALCULATIONS USING SUSSEX MATRIX ELEMENTS. Malta, C. P.; Sanderson, E. A. (Sussex Univ., Brighton (UK). School of Mathematical and Physical Sciences). Nucl. Phys., A; 225: No. 2, 189-204(10 Jun 1974).

Binding energies and single particle spectra for the spherical nuclei helium, oxygen and calcium are calculated in the Hartree-Fock approximation. Higher order corrections are also estimated and are of considerable significance. The interaction matrix elements used are those derived earlier from the two-nucleon phase shifts by Elliott et al. and a modified set which give better saturation properties. (auth)

30864 PRECISION LIFETIME MEASUREMENT WITH THE COINCIDENT HIGH-VELOCITY DSA METHOD. Hermans, J. A. J.; Engelbertink, G. A. P.; Bucurescu, D.; van Driel, M. A.; Eggenhuisen, H. H. (Rijksuniversiteit Utrecht (Netherlands). Fysisch Lab.). Phys. Lett., B; 50: No. 3, 337-339(10 Jun 1974).

The inverse reaction ^{2}H(^{32}S,pγ)^{33}S at E(^{32}S) = 38 MeV is used to measure the mean life of ^{33}S(1). Coincident Doppler broadened lineshapes measured for the slowing-down materials Mg, Al, Cu and Ag are analyzed with experimental stopping powers. The results for the different materials agree with each other and lead to a mean life of τ_m = 1.65 ± 0.04 ps. (auth)

30865 RENORMALIZATION OF THE AXIAL-VECTOR COUPLING CONSTANT IN NUCLEAR β-DECAY (III). Wilkinson, D. H. (Oxford Univ. (UK). Nuclear Physics Lab.). Nucl. Phys., A; 225: No. 3, 365-381(17 Jun 1974).

Axial-vector β-decay of nuclei of $A \leq 22$ is analyzed in the light of recent work on relativistic corrections to the axial matrix element and to the isoscalar magnetic moment. After allowance for relativity it appears that the average decay amplitude found in practice is (7.3 ± 3.8)% below that predicted by the best explicit wave-functions that are confined to the nominal major shell; this is about one half of the renormalization that has been predicted on the basis of the tensor component of the NN potential and about equal to that predicted from PCAC and empirical pion-nucleus properties. Analysis of the isoscalar magnetic moments suggests a "tensor force renormalization" of perhaps a little less than this and also that the renormalization of the effective axial coupling constant, additional to that due to the tensor force or to equivalent "pion-nucleus" effects, is small and possibly of the opposite sign, i.e. an enhancement of the decay rate. A form of the relativistic isoscalar magnetic moment associated with a potential that generates a realistic spin-orbit splitting is favored by the analysis of the isoscalar moments. Some qualitative discussion is given of possible relationships between the theoretical renormalization effects. (auth)

30866 UNITARITY CORRECTIONS TO PION-NUCLEUS SCATTERING LENGTHS. Myhrer, F.; Silbar, R. R. (Schweizerisches Inst. fuer Nuklearforschung, Villigen). Phys. Lett., B; 50: No. 3, 299-301(10 Jun 1974).

An important contribution to pion-nucleus scattering length calculations coming from off-shell unitarity in the pion-bound-nucleon amplitude is pointed out. How much this general result affects the pion-deuteron scattering length is shown explicitly by calculating the first term in the Faddeev multiple scattering series. (auth)

30867 ON PROTON-DEUTERON BACKWARD ELASTIC SCATTERING AT MEDIUM ENERGIES. Noble, J. V.; Weber, H. J. (Virginia Univ., Charlottesville (USA). Dept. of Physics). Phys. Lett., B; 50: No. 2, 233-236(27 May 1974).

Recent theoretical attempts at explaining pd backward elastic scattering at medium energies are examined. It is found that at present there is no convincing evidence for reaction mechanisms such as N*-isobar exchange or pion-nucleon exchange, besides the usual neutron transfer. (auth)

30868 ON THE DETERMINATION OF THE NUCLEON-NUCLEON SCATTERING PARAMETERS THROUGH FINAL STATE INTERACTIONS. Ligatto De Slobodrian, M. L. V. (Laval Univ., Quebec City (Canada)). Phys. Lett., B; 50: No. 2, 225-228(27 May 1974).

The systematic errors introduced in the determination of the nucleon-nucleon scattering length from final state interaction spectra, due to the omission of relevant processes in the ^{3}He (τ,α)2p reaction, are shown to be at least 0.2 fm. (auth)

30869 THE ^{3}He(γ,π^{+})^{3}H REACTION IN THE (3,3) RESONANCE REGION. Dover, C. B.; Yang, S. N. (Brookhaven National Lab., Upton, N. Y. (USA)). Phys. Lett., B; 50: No. 2, 217-221(27 May 1974).

Cross sections are calculated for ^{3}He(γ,π^{+})^{3}H in the impulse approximation, using realistic three-body wavefunctions obtained with the Reid potential. The discrepancies with experiment indicate the need for a proper estimate of the rescattering corrections as well as a better treatment of the nucleon momenta in the nucleus. (auth)

30870 APPROXIMATE D-STATES AND MESON EXCHANGE CURRENTS. Jackson, A. D.; Riska, D. O. (State Univ. of New York, Stony Brook (USA). Dept. of Physics). Phys. Lett., B; 50: No. 2, 207-210(27 May 1974).

A simple approximate form for the [21] D-state component of the 3-nucleon ground state wave function, which has correct asymptotic behavior is introduced and compared to a previously used form. The implications of approximate D-state wave functions in evaluation of meson exchange current effects are discussed. (auth)

30871 A MICROSCOPIC DESCRIPTION OF THE NEGATIVE PARITY RESONANCES IN THE MASS-4 SYSTEM BY THE COUPLED-CHANNEL METHOD. Ramavataram, S.; Rao, C. L.; Ramavataram, K. Laval Univ., Quebec City (Canada). Dept. de Physique). Nucl. Phys., A; 226: No. 1, 173-188(24 Jun 1974).

The negative parity resonances in the mass-4 system have been investigated in the 1p−1h approximation with the continuum treated by the coupled-channel method. The observed dipole photoreaction cross section of ^{4}He as well as the energy dependence of the phase shifts deduced from the p−^{3}He scattering are well reproduced by the theory. (auth)

30872 THE DEUTERON BREAKUP REACTION INDUCED BY PROTONS OF 65, 85 AND 100 MeV. Cheng, V. K. C.; Roos, P. G. (Maryland Univ., College Park (USA)). Nucl. Phys., A; 225: No. 3, 397-424(17 Jun 1974).

Coplanar energy sharing spectra for p + d breakup at 65, 85 and 100 MeV proton bombarding energies were measured using the University of Maryland sectored isochronous cyclotron by measuring the energies of either two protons or one proton and one neutron in coincidence. The detector angles were chosen to enhance either the p−p or p−n quasi-free scattering, or the p−n final-state interaction. The energy dependence of the peak cross section at equal symmetric quasi-free scattering angle pairs was extracted for the ^{2}H(p,2p)n and ^{2}H(p,pn)p reactions. Quasi-free angular distributions were obtained for the reaction ^{2}H(p,2p)n at 65 MeV and for the reaction ^{2}H(p,pn)p at 65, 85 and 100 MeV. The plane-wave impulse approximation theory can only qualitatively reproduce the shape of the quasi-free scattering peak in the energy sharing spectra and the shape of the p−p quasi-free angular distribution. The discrepancies observed between the plane-wave impulse approximation theory and the experimental data imply that the presence of the spectator particle (i.e., the multiple scattering effects) has a strong influence on the magnitude and the shape of the experimental results. Multiple scattering calculations were carried out in the three-body model of Aaron, Amado and Yam except that the S-wave separable two-body amplitudes were modified to fit two-nucleon elastic scattering data at higher energies. Comparisons of the results of these multiple scattering calculations to the experimental data show excellent quantitative agreement throughout the energy range and the angular region of this experiment, except for a few cases in which this model is inherently insufficient; namely, regions in which the Coulomb interaction is important, or regions for which a Hulthen wave function is inaccurate and the off-shell effects are not properly taken into account. (auth)

30873 NEUTRON-DEUTERON DIFFERENTIAL CROSS SECTION AT 26.5 MeV. Wang, J. C.; Brady, F. P.; King, N. S. P.; McNaughton, M. W. (California Univ., Davis (USA). Crocker Nuclear Lab.). Phys. Lett., B; 51: No. 1, 42-44(8 Jul 1974).

The angular distributions of 26.5 MeV neutrons scattered elastically by deuterons between 90° and 166° (c.m.) were measured by using charged-particle telescopes. The absolute n−d cross section (of ~5% precision) was obtained by normalizing to the precision n−p cross section. Within the errors the magnitude of the minimum cross section was found to be in agreement with that of the proton−deuteron cross section at the same energy and in disagreement with some recent results. (auth)

30874 AN EXPERIMENTAL INVESTIGATION OF π PHOTOPRODUCTION PROCESSES ON ^{3}He. Goggi, G.; Mantovani, G. C.; Piazzoli, A.; Scannicchio, D. (Pavia Univ. (Italy). Instituto di Fisica). Nucl. Phys., B; 75: No. 1, 77-92(11 Jun 1974).

Experimental results are reported on single and double π photoproduction on ^{3}He up to E_γ = 800 MeV. The cross sections per equivalent quantum, total cross sections as a function of the photon energy and angular distributions are given. In the double charged photoproduction channel the $P\pi^+$ and $P\pi^-$ invariant mass distributions are presented and compared with the predictions of an isobaric model assuming the impulse approximation. There is also evidence for $\pi^+\pi^+$ photoproduction in analogy with $\pi^+\pi^+$ and $\pi^-\pi^-$ production on ^{4}He seen in a previous experiment. The data seem generally consistent with the available theoretical predictions based on the impulse approximation. (auth)

Nuclear Properties and Reactions, 6 ≤ A ≤ 19

Refer also to abstracts 30146, 30611, 30671, 30854, 30856, 30860, 30863, 30865, 31023, 31066, 31077, 31085, 31092, and 31096–31098.

30875 (JINR-P1-7523) MULTIPLICITY AND CORRELATIONS OF SECONDARY PARTICLES PRODUCED IN π^--^{12}C COLLISIONS AT 40 GeV/c. Grishin, V. G.; Inogamova, T. Ya.; Inogamov, Sh. V. (Joint Inst. for Nuclear Research, Dubna (USSR). Lab. of High Energy). 1973. 18p. (In Russian). INIS.

An analysis of distributions according to multiplicity of secondary charged particles in π^--^{12}C-interactions at p = 40 GeV/c showed that the distributions are qualitatively described by the formulas of Poisson and Poi. The data on multiplicity for π^--^{12}C-interactions are described by the same universal curve as given by the results from π^-p- and the pp-interactions (scaling according to multiplicity). The growth in average multiplicity of charged particles with energy satisfies a log dependence for the π^--^{12}C and π^-p-interactions with the same slope parameters. The correlation in the generation of neutral and charged particles from π^--^{12}C-interactions has the form: $\langle n_{\pi^0} \rangle = (1.64 \pm 0.11) + (0.16 \pm 0.02)n_\pm$, and the coefficients coincide with analogous results for π^-p- and π^-n interactions at p = 40 GeV/c. Hence it can be concluded that secondary interactions in the carbon nucleus are not substantial for this phenomenon. (tr-auth)

30876 ^{12}C + α SCATTERING BY THE COUPLED CHANNEL RESONATING GROUP METHOD. Solution of the Redundancy and Non-Orthogonality Problem. Horiuchi, H. (Kyoto Univ.). Progr. Theor. Phys. (Kyoto); 51: No. 3, 745-759(Mar 1974).

A microscopic treatment of ^{12}C + α scattering is formulated in the framework of the coupled-channel resonating group method (CCRGM), using Feshbach's formulation for nucleon scattering. The ground rotational-band states of ^{12}C of spins L = 0, 2 and 4 are adopted in the channel coupling, and the wave functions of these three states are assumed to be described by the SU_3 model wave functions of (0.4) representation. Since in the interaction region three channels which are based on the three states L = 0, 2, 4 of ^{12}C are not orthogonal and even not independent of each other, we need to classify the states which are independent and orthogonal. The answer to this problem of the classification of the states is given systematically by solving the eigenvalue problem of the overlap kernel, whose eigenfunctions are classified entirely by the irreducible representation of the SU_3 group. In order to clarify the meaning of the CCRGM approach, we classify some important shell model states of a few-particle−hole excitation by means of our CCRGM scheme and give α spectroscopic factors of these states, by using the solutions of the eigenvalue problem of the overlap kernel. As an approximation of the CCRGM equation, the equation of the coupled-channel orthogonality condition model is formulated. (auth)

30877 PARTICLE CONFIGURATIONS OF GIANT E1 STATES IN THE ^{14}N(γ,p_2) AND ^{14}N(γ,p_0) PROCESSES. Baglin, J. E. E. (IBM Thomas J. Watson Research Center, Yorktown Heights, NY); Bentz, E. J.; Carr, R. W. Phys. Rev., C; 10: No. 1, 24-34(Jul 1974).

Angular distributions and absolute cross sections were measured for the ^{14}N(γ,p_2) and ^{14}N(γ,p_0) reactions, at giant resonance energies. The angular distributions are shown to be consistent with a model in which exclusively $(p_{1/2})^{-1}$ (2s 1d) giant dipole states populate the ^{13}C ground state by proton decay, and predominantly $(p_{3/2})^{-1}$ (2s 1d) giant dipole states feed the $3/2^-$ state of ^{13}C at 3.68 MeV. Branching calculations based on established spectroscopic factors further support this model. It is inferred that the ^{14}N dipole states of $(p_{3/2})^{-1}$ (2s 1d) character, which carry ~90% of the E1 strength and which dominate the (γ,p_2) process studied, do not contribute significantly to the (γ,p_0) process which has often previously been treated as representative of E1 absorption. (auth)

30878 SEARCH FOR THE LOWEST T = 2 STATE IN ^{14}C BY INELASTIC ELECTRON SCATTERING. Kline, F. J. (Catholic Univ. of America, Washington, DC); Crannell, H., Finn, J. M.; Hallowell, P. L.; O'Brien, J. T.; Werntz, C. W.; Fivozinsky, S. P.; Lightbody, J. W. Jr.; Penner, S. Nuovo Cim., A; 23A: No. 1, 137-144(1 Sep 1974).

A search for the lowest energy T = 2 state in ^{14}C was attempted employing inelastic electron scattering techniques. Spectra obtained at 61 and 81 MeV incident-electron energy and 145.7° scattering angle fail to reveal significant structure at the predicted resonance energy. The implications of this result are discussed in terms of the particle-hole model and the ground-state structure of the ^{14}B analog of this level. (auth)

30879 ELASTIC SCATTERING OF ^{12}C BY ^{12}C. Raman, S.; Fulmer, C. B.; Halbert, M. L.; Saltmarsh, M. J.; Snell, A. H.; Stelson, P. H. (Oak Ridge National Lab., TN). p 2 of Proceedings of the International Conference on Reactions Between Complex Nuclei. Vol. I and Suppl. Robinson, R. L. (ed.). New York; American Elsevier Publishing Co., Inc. (1974).

From international conference on reactions between complex nuclei; Nashville, Tennessee, USA (10 Jun 1974). See CONF-740637-(P1 and Suppl.).

30880 ENTRANCE CHANNEL EFFECTS IN THE ^{32}S SYSTEM: COMPARISON OF ^{12}C + ^{20}Ne AND ^{16}O + ^{16}O ELASTIC SCATTERING. Vandenbosch, R.; Webb, M. P.; Zisman, M. S. (Univ. of Washington, Seattle). p 9 of Proceedings of the International Conference on Reactions Between Complex Nuclei. Vol. I and Suppl. Robinson, R. L. (ed.). New York; American Elsevier Publishing Co., Inc. (1974).

From international conference on reactions between complex nuclei; Nashville, Tennessee, USA (10 Jun 1974). See CONF-740637-(P1 and Suppl.).

30881 THREE-ALPHA PARTICLE MODEL FOR ^{12}C GROUND STATE. Kawazoe, Y. (Tohoku Univ., Sendai); Tsukamoto, T.; Matsuzaki, H. Progr. Theor. Phys. (Kyoto); 51: No. 2, 428-437(Feb 1974).

The three-alpha model of ^{12}C is treated on the basis of the Eyges equation with separable potentials. The vertex functions are taken to assure the r^4 dependence of the alpha–alpha bound state wave function near the origin. The resulting three-alpha binding energy — after adding the Coulomb energy — does not reproduce the experimental value. However, the first minimum of the charge form factor coincides with the experimental one. (auth)

30882 QUASI-FREE CONTRIBUTIONS IN THE d + ^{6}Li REACTIONS AT LOW ENERGIES. Miljanic, D.; Hudomalj, J.; Mutchler, G. S.; Andrade, E.; Phillips, G. C. (Rice Univ., Houston, Tex. (USA). Bonner Nuclear Labs.). Phys. Lett., B; 50: No. 3, 330-332(10 Jun 1974).

The ^{6}Li(d,dd)α, ^{6}Li(d,dα)d and ^{6}Li(d,tp)α reactions were investigated at low bombarding energies with the purpose to determine the importance of quasi-free processes relative to sequential reactions. (auth)

30883 OPTICAL MODEL AND DWBA ANALYSIS OF THE ^{7}Li(d,d)- AND ^{7}Li(d,p$_0$)-REACTIONS IN THE ENERGY REGION 1.0 TO 2.6 MeV. Lombaard, J. M.; Friedland, E. (Pretoria Univ. (South Africa). Dept. of Physics). Z. Phys.; 268: No. 4, 413-417(Jul 1974).

4 figs.; 2 tabs.; 17 refs.

Absolute differential cross sections for the elastic scattering of deuterons by ^{7}Li have been determined in the energy range of 1.0 to 2.6 MeV. Two excitation curves measured at laboratory angles of 90° and 160° vary smoothly with energy. At higher energies an extremely strong enhancement of the cross section relative to the Rutherford value was observed at large angles. It was, however, possible to find realistic optical potentials that describe these distributions fairly well over the whole energy region. For two of these potentials good fits could be obtained with DWBA calculations on the ^{7}Li(d,p$_0$)-reaction, one of them yielding a spectroscopic factor in close agreement with shell model predictions. (auth)

30884 EFFECTIVE INTERACTION CALCULATIONS FOR NUCLEI OF MASS 6 TO 9. Kumar, N. (Australian National Univ., Canberra. Research School of Physical Sciences). Nucl. Phys., A; 225: No. 2, 221-252(10 Jun 1974).

Shell model calculations using the effective interaction approach of Talmi are reported for normal parity states in nuclei of mass number 6–9. To fit simultaneously the energies of levels in these nuclei, energy shifts of ground state rotational bands in ^{8}Be and ^{9}Be are introduced. These shifts have their origin in the deformations of nuclei. The obtained matrix elements fit the data better than those of earlier authors, and resemble the matrix elements obtained from realistic interactions such as the Hamada–Johnston potential. Theoretical predictions are compared with new experimental data. M1 radiative widths, log ft values, and spectroscopic factors for single- and two-nucleon transfers are given to help in the interpretation of new data. The need for carrying out more calculations for 1p shell nuclei with realistic forces is discussed. (auth)

30885 HIGH SPIN STATES IN THE $K^\pi = {1/2}^-$ BAND OF ^{19}F. Underwood, B. Y.; Wormald, M. N.; Anyas-Weiss, N.; Jelley, N. A.; Allen, K. W. (Oxford Univ. (UK). Nuclear Physics Lab.). Nucl. Phys., A; 225: No. 2, 253-266(10 Jun 1974).

Resonances in the ^{15}N(α,γ)^{19}F reaction at E_α = 5413 ± 5 keV and 6258 ± 5 keV, corresponding to levels in ^{19}F at E_x = 8288 ± 2 keV and 8957 ± 2 keV, have been studied. Angular distribution and $\omega\gamma$ measurements indicate that the level at 8288 keV has $J^\pi = {13/2}^-({9/2}^-)$, while that at 8957 keV has $J^\pi = {11/2}^+$. The values of $\omega\gamma$ are 0.53 ± 0.08 eV and 0.91 ± 0.17 eV, respectively. The 8288 keV level decays by a 22.4 ± 3.3 W.u. E2 transition to the ${9/2}^-$ state at 4032 keV and is suggested to be the ${13/2}^-$ member of the $K^\pi = {1/2}^-$ band. (auth)

30886 1p HOLE-STATES IN ^{16}O AND ^{16}N AND THE MASS DEPENDENCE OF THE 1p SPIN-ORBIT SPLITTING. Mairle, G.; Wagner, G. J. (Max-Planck-Institut fuer Kernphysik, Heidelberg (F. R. Germany)). Phys. Lett., B; 50: No. 2, 252-254 (27 May 1974).

The 1p hole strength distribution in mass 16 nuclei, measured in parallel ^{17}O(d,t)^{16}O and ^{17}O(d,τ)^{16}N experiments, exhibit differences of the effective $1d_{5/2}1p_{1/2}$ and $1d_{5/2}\,1p_{3/2}$ interactions which lead to a 1p spin-orbit splitting increasing strongly with the number of $1d_{5/2}$ nucleons. (auth)

30887 POSSIBLE RESONANCE ANOMALIES IN THE ^{16}O + ^{12}C. Branford, D.; Newton, J. O.; Robinson, J. M.; Nagorcka, B. N. (Australian National Univ., Canberra). J. Phys., B (London); 7: No. 10, 1193-1198(1 Jul 1974).

A strong correlation has been observed between the 0° and 180° excitation functions for the ^{12}C(^{16}O,α)^{24}Mg reaction leading to the 13.2 MeV 8$^+$ level. The possibility that this is due to exciting intermediate structure peaks at E_{cm} = 13.7, 14.7, 16.0, and 18.0 MeV, is considered. It is concluded that the reaction most probably excites a narrow resonance ($\Gamma \simeq$ 70 keV) with $J^\pi = 9^-$ or 10^+ at E_{cm} = 13.7 MeV. Weak evidence supporting the existence of anomalies at E_{cm} = 16.0 and 14.7 MeV is presented. The possibility that the reaction excites a band of quasi-molecular states is discussed. An alternative explanation of the strong correlation in the data, based on the assumption that the reaction proceeds preferentially through either even or odd angular momentum states, is also considered. (auth)

30888 DISTORTED WAVE BORN APPROXIMATION ANALYSIS FOR THE ^{16}O(^{3}He,α)^{15}O REACTION. El-Bedewi, F.; Shalaby, M. (Cairo Univ., El Mansura). J. Phys., B (London); 7: No. 10, 1183-1192(1 Jul 1974).

Angular distributions for the ^{16}O(^{3}He,α)^{15}O reaction induced by 15 MeV ^{3}He particles have been measured. Distributions characterized by single-nucleon pickup have been compared with the local zero range form of the DWBA. A normalization factor of 14.2 has been estimated and absolute spectroscopic factors have been extracted for excited states in ^{15}O up to 10 MeV. A discussion for the odd and even parity states has been given in the weak-coupling model. Neutron filling probabilities for the $1d_{5/2}$–$2s_{1/2}$ and $1d_{3/2}$ orbits have been calculated for the ^{16}O ground state. (auth)

30889 R-MATRIX AND PHASE-SHIFT ANALYSIS OF NEUTRON POLARIZATION MEASUREMENTS FROM n–^{16}O SCATTERING. Hickey, G. T.; Firk, F. W. K.; Holt, R. J.; Nath, R. (Yale Univ., New Haven, Conn. (USA). Electron Accelerator Lab.). Nucl. Phys., A; 225: No. 3, 470-480(17 Jun 1974).

The measured polarization of neutrons that have been elastically scattered from ^{16}O in the energy region from 1–4 MeV has been analyzed using a general, multi-level R-matrix reaction theory. A self-consistent set of resonance parameters and estimates of the effects of distant levels were found. These parameters were then used to predict the neutron differential and total cross sections from 0–4 MeV: the predictions are in good agreement with experimental results. In addition to the R-matrix analysis, a phase-shift analysis of the polarization measurements was also carried out. (auth)

30890 CONTINUUM SHELL-MODEL CALCULATION FOR NEUTRON SCATTERING FROM ^{11}B. Birkholz, J.; Heil, V. (Technische Univ. Darmstadt (F. R. Germany). Inst. fuer Kernphysik). Nucl. Phys., A; 225: No. 3, 429-442(17 Jun 1974).

The shell model, extended to continuum states, is applied to the calculation of cross sections for the elastic and inelastic scattering of neutrons from ^{11}B. The states of the target nucleus are described in the framework of the 1p shell intermediate coupling model of Kurath. The computed absolute cross sections, angular distributions and polarization of the scattered neutron are presented and compared with experimental data. (auth)

30891 PION-NUCLEUS TOTAL CROSS SECTIONS FROM 88 TO 860 MeV. Clough, A. S.; Turner, G. K. (Surrey Univ., Guildford (UK). Dept. of Physics); Allardyce, B. W.; Batty, C. J.;

Baugh, D. J.; McDonald, W. J.; Riddle, R. A. J.; Watson, L. H. (Science Research Council, Chilton (UK). Rutherford Lab.); Cage, M. E.; Pyle, G. J. Nucl. Phys., B; 76: No. 1, 15-28(4 Jul 1974).

Total cross sections for π^+ and π^- mesons on ^{6}Li, ^{7}Li, ^{9}Be and C have been measured in the energy range from 90 to 860 MeV, and for oxygen from 88 to 228 MeV. The results of calculations with Kisslinger and local optical model potentials, using different sets of parameters, are compared with the data for ^{6}Li, C and O. (auth)

30892 EXPERIMENTAL STUDY OF ^{19}Ne DECAY AND ITS SIGNIFICANCE TO THE STUDY OF NEUTRAL WEAK CURRENTS. Mann, F. M.; Kavanagh, R. W. (California Inst. of Tech., Pasadena (USA)). Phys. Lett., B; 51: No. 1, 49-50(8 Jul 1974).

An upper limit of 0.003% for the beta decay of ^{19}Ne to the 1.55 MeV level in ^{19}F has been determined. Its significance for a recently suggested experiment to study neutral weak currents is discussed. (auth)

30893 CLUSTER-MODEL CALCULATIONS OF THE ELECTRODISINTEGRATION OF LITHIUM. Gromadzki, Z.; Noble, J. V. (Virginia Univ., Charlottesville (USA). Dept. of Physics). Phys. Lett., B; 51: No. 1, 9-13(8 Jul 1974).

In an extension of previously derived cluster-model treatments of the lithium isotopes to continuum states, (longitudinal) electrodistintegration cross sections are calculated in the energy loss range 1.5 to 7.5 MeV, for momentum transfers $q^2 = 0$ to 1.5 fm^{-2}. (auth)

30894 LIFETIME MEASUREMENTS IN ^{17}N USING THE RECOIL-DISTANCE TECHNIQUE. Rogers, D. W. O.; Anyas-Weiss, N.; Becker, J. A.; Belote, T.A.; Dolan, S. P.; Randolph, W. L. (Oxford Univ. (UK). Nuclear Physics Lab.). Nucl. Phys., A; 226: No. 3, 445-453(8 Jul 1974).

Nuclear lifetimes in ^{17}N have been measured using the recoil-distance technique. Levels were populated with the ^{11}B(^{7}Li,p)^{17}N reaction at E ~ 6 MeV. By using multi-parameter data acquisition techniques, p–γ coincident pulse heights were collected with an annular particle detector placed near 180° and a Ge(Li) γ-ray detector at $\theta_\gamma = 0^0$. The resulting lifetimes were as follows [τ_m (E$_x$ MeV) = ps]: τ_m (1.85) = $41 \pm {}^{70}_{5}$, τ_m (1.91) = 11 ± 2, τ_m (2.53) = 33 ± 3, τ_m (3.63) = 12 ± 2. These results can be reasonably well explained either in terms of a weak-coupling model or by a shell model calculation which includes 2p–1h, 4p–3h, and 3p–2h configurations. (auth)

30895 THE ELECTROMAGNETIC DECAY OF ^{17}N. Rogers, D. W. O.; Becker, J. A.; Alexander, T. K.; Anyas-Weiss, N.; Belote, T. A.; Dolan, S. P.; Jelley, N. A.; Randolph, W. L. (Oxford Univ. (UK). Nuclear Physics Lab.). Nucl. Phys., A; 226: No. 3, 424-444(8 Jul 1974).

The radiative decay properties of the first 16 bound states in ^{17}N with E$_x$ < 5.8 MeV have been studied using the ^{11}B(^{7}Li,pγ)^{17}N reaction at E = 6 MeV. Proton-gamma coincidence data were taken with an annular particle detector located at 180° and a Ge(Li) detector placed at θ_γ = 3°, 45° and 90°. Angular distributions, branching ratios and Doppler shifts were measured. The resulting energies (keV), lifetimes (fs) and spin–parity assignments (those in brackets are probable assignments) were (1374, 93 ± 35, $3/2^-$), (1850, > 1 ps, $1/2^+$), (1907, > 1 ps, ($5/2^-$)), (2526, > 1 ps, ($5/2^+$)), 3129, 275 ± 80, ($7/2^-$)), (3203, < 30, ($3/2^-$)), (3629, > 1 ps, ($9/2^-$)), (3663, < 350), (3906, 52 ± 22, ($7/2^-$)), (4006, < 15, ($3/2^+$)), (4208, < 70), (4415, < 60), (5170, < 60), (5195, < 95), (5514, < 100, ($3/2^-$)), (5770, < 120). The properties of these levels are interpreted in terms of a weak coupling model in which a $p_{1/2}$ proton hole is coupled to levels in ^{18}O or two proton holes are coupled to the K = $1/2^+$ g.s. band in ^{19}F. A shell model calculation which includes 2p–1h negative-parity states and 3p–2h positive-parity states is also shown to provide a reasonable description of the bound states of ^{17}N. (auth)

30896 THE ^{6}Li(p,2p)^{5}He REACTION AT 100 MeV. Bhowmik, R. K.; Chang, C. C.; Roos, P. G.; Holmgren, H. D. (Maryland Univ., College Park (USA)). Nucl. Phys., A; 226: No. 3, 365-380(8 Jul 1974).

The ^{6}Li(p, 2p)^{5}He reaction has been studied at a proton bombarding energy of 100 MeV with good energy and angular resolution for proton separation energies up to 50 MeV. Data were taken for 17 coplanar symmetric angle pairs, yielding both energy sharing spectra and coplanar symmetric angular correlations for various regions of separation energy. The data for the ^{5}He ground state ($3/2^-$ resonance) does not show a significant minimum at zero recoil momentum— this result suggests a contribution from an s-state knockout leading to this continuum state. DWIA calculations are presented which reproduce most of the important features of the data. These calculations indicate the importance of both the distortion effects and the off-energy-shell effects at this energy. (auth)

30897 MOMENTUM-SPACE STUDY OF PION–NUCLEUS INELASTIC SCATTERING. Lee, T. S. H ; Tabakin, F. (Pittsburgh Univ., Pa. (USA). Dept. of Physics). Nucl. Phys., A; 226: No. 2, 253-281(1 Jul 1974).

The inelastic scattering of intermediate energy pions from ^{12}C is studied using a distorted-wave impulse approximation (DWIA). A flexible momentum space formulation is presented which permits examination of a wide variety of non-local pion–nucleus potentials. Inelastic differential cross sections for the 2^+(4.43 MeV) and 3^-(9.64 MeV) states of ^{12}C are generated from several phenomenological pion–nucleon collision matrices. Form factors for the inelastic transitions are obtained from the collective model and also from microscopic 1p–1h (Gillet–Vinh Mau) wave functions. The dramatic role of the (3,3) pion–nucleon resonance, along with an associated pion–nucleus absorption, is illustrated. The inelastic cross sections prove to be somewhat influenced by the off-shell pion–nucleon model, with the effect mostly confined to larger angles, and with changes that closely parallel those found earlier for elastic scattering. Back-angle inelastic cross sections are found to be large by a factor of about 10 compared to prior pion–^{12}C inelastic scattering calculations. This beneficial effect, relative to the available data, is attributed to a corresponding elastic scattering back-angle build-up, which arises mainly from transforming the pion–nucleon interaction to the pion–nucleus center-of-mass frame. The inelastic scattering diffraction patterns are found to depend on the location and tail of the form factor, but much less so on its internal form, which is indicative of a surface direct reaction. Normalization of the collective model form factor to known B(E2) and B(E3) values yields general agreement with the magnitude of the forward-angle inelastic 2^+ and 3^- cross sections. These simple features of calculated pion–^{12}C inelastic scattering encourage further application of the DWIA and of direct-reaction strong-absorption methods to pion scattering in the resonance region. (auth)

30898 MAGNETIC MOMENTS AND GT-TYPE β-DECAY MATRIX ELEMENTS IN NUCLEI WITH A LS DOUBLY CLOSED SHELL PLUS OR MINUS ONE NUCLEON. Shimizu, K.; Ichimura, M.; Arima, A. (State Univ. of New York, Stony Brook (USA). Dept. of Physics). Nucl. Phys., A; 226: No. 2, 282-318(1 Jul 1974).

The magnetic moments and GT-type β-decay matrix elements of nuclei with an ^{16}O core plus (minus) one nucleon and with a ^{40}Ca core plus (minus) one nucleon are studied from the point of view of configuration mixing in terms of second-order perturbation theory. It is found that the effect of the mixing of highly excited configurations through a tensor force is essential to explain the large reduction of the GT-type β-decay matrix elements. It is also found that modulus of the isovector parts of the gyromagnetic ratio, $g_{\tau s}$ and $g_{\tau l}$ are appreciably reduced by the configuration mixing. (auth)

30899 MEASUREMENT OF THE AVERAGE POLARIZATION OF ^{12}B PRODUCED BY POLARIZED MUONS IN THE $\mu^- + {}^{12}C \to \nu_\mu + {}^{12}B$ REACTION. Possoz, A.; Favart, D.; Grenacs, L.; Lehmann, J.; Macq, P.; Meda, D.; Palffy, L. (Louvain Univ. (Belgium)); Julien, J.; Samour, C. (CEA Centre d'Etudes Nucleaires de Saclay, 91–Gif-sur-Yvette (France)). Phys. Lett., B; 50: No. 4, 438-440(24 Jun 1974).

The average polarization of ^{12}B produced by the capture of polarized muons in ^{12}C has been measured by using recoil implantation techniques. From the result is deduced the average polarization of the ^{12}B ground state, ^{12}B(0), corresponding to the $^{12}C \to {}^{12}B(0)$ Gamow–Teller reaction: $J_\mu(0) = 0.43 \pm 0.10$. The sizeable deviation of this polarization from the value of $2/3$, characteristic of a "bare" $0^+ \to 1^+$ process, is fair evidence for induced axial-vector interaction(s) in muon capture. The ratio of the induced pseudoscalar and the axial-vector coupling constants is deduced to be $g_P^\mu/g_A^\mu = 12 \pm 5$. (auth)

30900 DWBA AND CCBA ANALYSIS OF SELECTED TRANSITIONS IN THE ^{12}C(d,τ)^{11}B REACTION AT E$_d$ = 80 MeV. Aspelund, O.; Ingham, D.; Djaloeis, A.; Kelleter, H.; Mayer-Boericke, C. (Kernforschungsanlage Juelich G.m.b.H. (F. R. Germany). Inst. fuer Kernphysik). Phys. Lett., B; 50: No. 4, 441-444(24 Jun 1974).

Angular distributions from the reaction ^{12}C(d,τ)^{11}B leading to the $3/2^-$ ground state and the 4.44 MeV excited ($5/2^-$) state in ^{11}B have been measured at E$_d$ = 80 MeV up to about 70° and 40°, respectively. The inclusion of second-order processes in the framework of CCBA calculations gives a good reproduction of the $3/2^-$ as well as of the DWBA-forbidden $5/2^-$ angular distribution. The strong dependence of the cross section on the sign of the deformation supports a positive β_2 value for ^{11}B. (auth)

Nuclear Properties and Reactions, $20 \leq A \leq 38$

Refer also to abstracts 30854, 30864, 30865, 30880, 30887, 30898, 30927, 30959, and 30960.

30901 (NP-20122, pp 35-38) NUCLEAR STRUCTURE STUDIES OF NUCLEI AROUND MASS NUMBER 23. Christiansson, J. E.; Dubois, J.; Jarneborn, L.; Odelius, H.; Roth, H. (Chalmers Univ. of Tech., Goteborg). Jan 1974.

30902 BETA ASYMMETRY OF ^{35}Ar AND THE DEDUCED VALUE OF THE VECTOR COUPLING CONSTANT. Mead, W. C. Princeton, NJ; Princeton Univ. (1974). 226p. University Microfilms Order No. 74-17,476.

Thesis (Ph.D.).

Two measurement techniques were employed to remeasure the beta asymmetry parameter. In the first measurement technique, the polarization of atoms in the detector cell was determined from studies of the atomic beam intensity profile. The result of the singles technique was A. = .33 ± .06. In the second technique, simultaneous observations of the ground-state decay asymmetry and the asymmetry of the Gamow–Teller transition to the 1.22-MeV $^1\!/_2+$ level of ^{35}Cl were made. The result of this method is .23 ± .05. In both techniques of measurement considerable attention is given to systematic errors which could influence the experimental results. The remeasured asymmetry value is discussed in terms of theoretical and experimental implications. The anomaly is considered unresolved. (RWR)

30903 PHENOMENOLOGICAL OCCUPATION PROBABILITIES, BINDING ENERGIES, AND THE NUCLEAR ONE-PARTICLE DENSITY MATRIX. Boffi, S.; Pacati, F. D. (Univ., Pavia, Italy). pp 500-513 of Nuclear Many-Body Problem. Vol. I. Calogero, F. (ed.). Bologna; Editrice Compositori (1973).

From symposium on present status and novel developments in the nuclear many-body problem; Rome, Italy (19 Sep 1972). See CONF-720933–P1.

30904 EVIDENCE FOR SIMPLE ALPHA-PARTICLE TRANSFER IN THE (^{20}Ne,^{16}O) REACTION. Menchaca-Rocha, A.; Cornell, J. C.; Fisher, P. S.; Paschopoulos, I.; Pilt, A. A.; Sinclair, D. (Nuclear Physics Lab., Oxford). Lett. Nuovo Cim.; 11: No. 3, 192-194(21 Sep 1974).

Results of the ^{12}C(^{20}Ne, ^{16}O)^{16}O reaction measured at incident energies of 108 and 147 MeV are presented. It is concluded that the rather large differential cross sections combined with a lack of population of the 11.1-MeV (4^+) level in oxygen-16 provide strong evidence that this reaction proceeds by rather pure alpha-particle transfer. (JFP)

30905 COULOMB NUCLEAR INTERFERENCE IN THE INELASTIC SCATTERING OF ^{16}O IONS FROM ^{24}Mg. Saladin, J. X.; Lee, I. Y.; Haight, R. C.; Vitoux, D. (Univ. of Pittsburg). p 15 of Proceedings of the International Conference on Reactions Between Complex Nuclei. Vol. I and Suppl. Robinson, R. L. (ed.). New York; American Elsevier Publishing Co., Inc. (1974).

From international conference on reactions between complex nuclei; Nashville, Tennessee, USA (10 Jun 1974). See CONF-740637-(P1 and Suppl.).

30906 INELASTIC TRANSFER IN THE SCATTERING OF ^{32}S ON ^{30}Si. Kohlmeyer, B.; Schneider, W. F. W.; Puehlhofer, F.; Bauer, G.; Bock, R. (Univ., Marburg, Ger.). p 17 of Proceedings of the International Conference on Reactions Between Complex Nuclei. Vol. I and Suppl. Robinson, R. L. (ed.). New York; American Elsevier Publishing Co., Inc. (1974).

From international conference on reactions between complex nuclei; Nashville, Tennessee, USA (10 Jun 1974). See CONF-740637-(P1 and Suppl.).

30907 THE COUPLED-CHANNEL BORN APPROXIMATION AND J-DEPENDENCE IN ^{30}Si(d,p)^{31}Si. Hoffmann, G. W.; Udagawa, T.; Coker, W. R.; McIntyre, J.; Mahlab, M. (Texas Univ., Austin (USA). Center for Nuclear Studies). Phys. Lett., B; 50: No. 2, 249-251(27 May 1974).

Statistically accurate angular distribution data have been obtained at extreme forward angles ($\theta = 2°-40°$) for ^{30}Si(d,p)^{31}Si leading to the 2.32 MeV ($^5\!/_2^+$) and 2.79 MeV ($^5\!/_2^+$) states, at E_d = 10 MeV. It is shown that the extreme difference in the angular distributions for these two states can be explained by coupled-channel Born approximation calculations taking into account contributions from inelastic scattering, essentially without adjustable parameters, and without inclusion of the deuteron d-state or other similar small corrections. (auth)

30908 THE DECAY OF THE GIANT DIPOLE RESONANCE IN ^{26}Mg TO T = $^3\!/_2$ STATES OF ^{25}Mg. Wolf, H.; Berg, U.; Wienhard, K. (Giessen Univ. (F. R. Germany). Inst. fuer Kernphysik). Phys. Lett., B; 50: No. 2, 244-246(27 May 1974).

The population of T = $^3\!/_2$ states in ^{25}Mg from the giant dipole resonance in ^{26}Mg was observed by the ^{26}Mg(γ,nγ′) reaction. The previously reported result, that neutron decay between 18.9 MeV and 23.0 MeV proceeds mainly to these states, could not be confirmed. Therefore the isospin splitting of the giant resonance of ^{26}Mg remains questionable. (auth)

30909 SPIN AND PARITY OF 4.98-MeV LEVEL OF ^{21}Na NUCLEUS. Mal'ko, A. I.; Soroka, V. I.; Stryuk, V. S. (Kiev Nuclear Research Inst.). Ukr. Fiz. Zh. (Russ. Ed.); 19: No. 3, 509-510(Mar 1974). (In Russian).

Experimental data on the polarization of protons elastically scattered on neon in the energy range 2.1 to 2.7 MeV showed the existence of a 4.98-MeV level of the compound ^{21}Na nucleus, whose spin and parity are $^1\!/_2^-$. The neon dispersion at a 90° angle can be used as an analyzer for proton polarization. The polarization reaches 70% and slowly changes with energy at a significant energy interval. (tr-auth)

30910 4.510 MeV LEVEL IN ^{27}Al. Price, H. G.; Twin, P. J.; James, A. N.; Sharpey–Schafer, J. F. (Univ. of Liverpool). J. Phys., B (London); 7: No. 10, 1151-1155(1 Jul 1974).

The 4.510 MeV level in ^{27}Al has been conclusively shown to have a j^π assignment of $^{11}\!/_2^+$. The branching ratio was measured to be 77 ± 2% to the 2.211 MeV $^7\!/_2^+$ state and 23 ± 2% to the 3.004 MeV $^9\!/_2^+$ state, the multipole mixing ratio for the latter transition being −1.16 ± 0.11. It is suggested that the 4.510 MeV $^{11}\!/_2^+$ and the 3.004 MeV $^9\!/_2^+$ levels are possibly members of $K^\pi = {}^{11}\!/_2^+$ and $K^\pi = {}^9\!/_2^+$ bands respectively obtained by coupling an $\Omega = {}^1\!/_2$ (Nilsson orbit 9) neutron to the 5^+ ground-state configuration of ^{26}Al. (auth)

30911 STATES IN ^{24}Mg POPULATED BY THE ^{10}B(^{16}O,d)^{24}Mg AND ^{12}C(^{16}O,α)^{24}Mg REACTIONS. Ford, J. L. C. Jr.; Gomez Del Campo, J.; Robinson, R. L.; Stelson, P. H. (Oak Ridge National Lab., Tenn. (USA)); Thornton, S. T. (Virginia Univ., Charlottesville (USA)). Nucl. Phys., A; 226: No. 2, 189-203(1 Jul 1974).

States in ^{24}Mg were populated by the ^{10}B(^{16}O,d) and ^{12}C(^{16}O,α) reactions. Excitation functions at 7° for many of the levels were measured for bombarding energies between 40 and 46 MeV for the ^{16}O + ^{12}C reaction, and from 44 to 46 MeV for the ^{16}O + ^{10}B reaction. The reactions appear to be predominantly due to compound nucleus formation, and general agreement was found in comparing the measured cross sections with Hauser–Feshbach calculations. The experimental cross sections for the members of the $K^\pi = 0^+$ and 2^+ rotational bands are particularly well reproduced by the calculations up through the 8^+ states. (auth)

30912 INVESTIGATION OF THE 3.46 MeV ISOMERIC LEVEL OF ^{38}K WITH THE ^{24}Mg(^{16}O,pnγ)^{38}K REACTION. van Driel, M. A.; Eggenhuisen, H. H.; Hermans, J. A. J.; Bucurescu, D.; van Rinsveldt, H. A.; Engelbertink, G. A. P. (Rijksuniversiteit Utrecht (Netherlands). Fysisch Lab.). Nucl. Phys., A; 226: No. 2, 326-346(1 Jul 1974).

The $\tau_{1/2}$ = 22 μs isomeric level of ^{38}K at an excitation energy of 3458.0 ± 0.2 keV is strongly populated in the ^{24}Mg(^{16}O,pnγ)^{38}K reaction. Delayed γ-rays are studied with Ge(Li), Si(Li), and NaI detectors. Accurate excitation energies, branching ratios and lifetimes of levels involved in the decay of the isomeric state are determined. The isomeric level predominantly decays by a dipole transition of 38.03 ± 0.03 keV with a total conversion coefficient of α_T = 0.42 ± 0.15. Mean lives of ^{38}K levels are measured with the recoil-distance method. The results are τ_m = 10.1 ± 0.9 ps, 1.41 ± 0.14 ns and 101 ± 15 ps for the levels at excitation energies of 0.46, 2.65 and 3.42 MeV, respectively. It is suggested that the $(1f_{7/2})^2$ structure of a low-lying $J^\pi = 7^+$ state in combination with the selection rules for γ-decay in a self-conjugate nucleus is responsible for the isomerism. (auth)

30913 CROSS SECTIONS OF THE ^{21}Ne(α,n)^{24}Mg AND ^{22}Ne(α,n)^{25}Mg REACTIONS AT LOW ENERGIES OF ASTROPHYSICAL INTEREST. Mak, H.-B.; Ashery, D.; Barnes, C. A. (California Inst. of Tech., Pasadena (USA)). Nucl. Phys., A; 226: No. 3, 493-505(8 Jul 1974).

The ^{21}Ne(α,n)^{24}Mg reaction has been studied over the energy range $E_{c.m.}$ = 1.4 to 2.57 MeV by neutron time-of-flight spectroscopy and by the detection of the subsequent γ-ray transitions in ^{24}Mg. The astrophysical cross-section factor S(0) was determined and reaction rates were calculated for temperatures up to 5 × 10^9K. In favorable circumstances, this reaction can provide a significant neutron flux for nucleosynthesis. The absolute normalization of the cross sections obtained in earlier work on the reaction ^{22}Ne(α,n)^{25}Mg has also been verified. (auth)

30914 ANTIPAIRING AND ANTISTRETCHING IN ^{22}Ne. Gruemmer, F.; Goeke, K.; Allaart, K.; Faessler, A. (Kernforschungsanlage Juelich G.m.b.H. (F. R. Germany). Inst. fuer Kernphysik). Nucl. Phys., A; 225: No. 3, 443-456(17 Jun 1974).

The ground state rotational band of ^{22}Ne has been investigated with the angular momentum- and particle number-projected Hartree–Bogoliubov theory. Variation before projections was performed in the framework of the constrained Hartree–Bogoliubov theory with the quadrupole moment and the degree of pairing as constraints. It is shown that there is a clear decrease of the pairing correlations (antipairing) and a decrease of the quadrupole deformation (antistretching) with increasing angular momentum. The antipairing effect appears to be essential to reproduce the experimentally known deviation of the spectrum from the $J(J + 1)$ rule. The antistretching indicated by the B(E2) values is much stronger than that indicated by the calculated static quadrupole moments. This amounts to a breakdown of the rotational picture which is possibly connected with the low band cut-off values in the sd shell. The antipairing effect decreases the antistretching only slightly. The interaction between the pairing and quadrupole degrees of freedom is found to be too weak to change the earlier conclusions concerning antipairing and antistretching in the whole sd shell. No inert core was assumed in the calculations. The effective G-matrix elements of the Hamada–Johnston potential were used as an interaction. (auth)

30915 TWO-PARTICLE INTRINSIC EXCITATIONS IN ^{22}Ne AND ^{26}Mg. Craig, G. (Technische Univ. Darmstadt (F. R. Germany). Inst. fuer Kernphysik). Nucl. Phys., A; 225: No. 3, 493-520(17 Jun 1974).

A basis of two-particle intrinsic states for ^{22}Ne and ^{26}Mg is defined in terms of the Hartree–Fock solutions for ^{20}Ne and ^{24}Mg. Mixing between the different intrinsic states is estimated from a deformed shell model. The model proceeds to describe the lowest 12 positive-parity states in ^{22}Ne and the lowest 15 in ^{26}Mg. Spin, parity and K-quantum number assignments are proposed. These results are also compared with the existing shell model and projection model interpretations of ^{22}Ne and ^{26}Mg. (auth)

Nuclear Properties and Reactions, $39 \leq A \leq 58$

Refer also to abstracts 30854, 30863, 30898, 30903, 30945, 30946, 30959, 30960, 31007, 31011, and 31096.

30916 (NP-20122, pp 41-45) NUCLEAR STRUCTURE OF ^{54}Mn. Alenius, G.; Arnell, S. E.; Selin, E.; Stankiewicz, O. (Chalmers Univ. of Tech., Goteborg). Jan 1974.

30917 SPIN AND PARITY OF THE FIRST EXCITED LEVEL IN ^{53}Fe. Sona, P.; Taccetti, N. (Univ., Florence). Lett. Nuovo Cim.; 10: No. 17, 776-778(24 Aug 1974).

Excited states in ^{53}Fe were populated via the ^{50}Cr(α,n)^{53}Fe reaction using a ^{4}He^{++} beam at 10 MeV. The total internal-conversion coefficient of the 741 keV γ ray was measured. A comparison with calculated values of the conversion coefficient for different assumptions on the spin and parity of the 741 keV level suggests that the $J = {}^{3}\!/_{2}^{-}$ assignment is strongly favored. (LBS)

30918 STUDY OF THE STRUCTURE OF THE ^{56}Ni DOUBLE MAGIC NUCLEUS. Gmitro, M. (Nuclear Research Inst., Rez, Czech.). pp 855-864 of Nuclear Many-Body Problem. Vol. I. Calogero, F. (ed.). Bologna; Editrice Compositori (1973).

From symposium on present status and novel developments in the nuclear many-body problem; Rome, Italy (19 Sep 1972). See CONF-720933–P1.

30919 ISOMERIC-YIELD RATIO OF ^{52}Mn^{g} AND ^{52}Mn^{m} PHOTOPRODUCTION FROM ^{55}Mn AT INTERMEDIATE ENERGIES. de Napoli, V.; Martins, J. B.; Persichelli, G.; Terranova, M. L. (Univ., Rome). Lett. Nuovo Cim.; 11: No. 3, 179-182(21 Sep 1974).

Yield measurements of the photoproduction of ^{52}Mn^{g} and ^{52}Mn^{m} from ^{55}Mn at bremsstrahlung energies from 0.3 to 1 GeV. Some previously published results are also discussed for the sake of completeness. The cross sections, spins, and half lives are also given for these isomers. (JFP)

30920 POLARIZATION IN HI INELASTIC SCATTERING IN THE COULOMB–NUCLEAR INTERFERENCE REGION AND COUPLED CHANNEL EFFECTS. Steadman, S. (Massachusetts Inst. of Tech., Cambridge); Belote, T.; Goldstein, R.; Grodzins, L.; Cline, D.; deVoigt, M. J. A.; Videbaek, F. p 20 of Proceedings of the International Conference on Reactions Between Complex Nuclei. Vol. I and Suppl. Robinson, R. L. (ed.). New York; American Elsevier Publishing Co., Inc. (1974).

From international conference on reactions between complex nuclei; Nashville, Tennessee, USA (10 Jun 1974). See CONF-740637-(P1 and Suppl.).

30921 DIFFICULTIES IN FITTING ANGULAR DISTRIBUTIONS IN THE ^{40}Ca(^{13}C,^{14}N)^{39}K (g.s.) REACTION. Bond, P. D.; Garrett, J. D.; Hansen, O.; Kahana, S.; LeVine, M. J.; Schwarzschild, A. Z. (Brookhaven National Lab., Upton, NY). p 55 of Proceedings of the International Conference on Reactions Between Complex Nuclei. Vol. I and Suppl. Robinson, R. L. (ed.). New York; American Elsevier Publishing Co., Inc. (1974).

From international conference on reactions between complex nuclei; Nashville, Tennessee, USA (10 Jun 1974). See CONF-740637-(P1 and Suppl.).

30922 EVIDENCE FOR QUASI-MOLECULAR K X-RAY EMISSION IN HEAVY ION COLLISIONS FROM THE OBSERVATION OF THE X-RAY DIRECTIONAL ANISOTROPY. Greenberg, J. S.; Davis, C. K.; Vincent, P. (Yale Univ., New Haven). p 135 of Proceedings of the International Conference on Reactions Between Complex Nuclei. Vol. I and Suppl. Robinson, R. L. (ed.). New York; Elsevier Publishing Co., Inc. (1974).

From international conference on reactions between complex nuclei; Nashville, Tennessee, USA (10 Jun 1974). See CONF-740637-(P1 and Suppl.).

30923 THE MAGNITUDE OF COMPOUND NUCLEUS EFFECTS IN Ca(d,p) REACTIONS. Brown, G.; Denning, A.; Haigh, J. G. B. (Bradford Univ. (UK)). Nucl. Phys., A; 225: No. 2, 267-299(10 Jun 1974).

The level structure of ^{41}Ca, ^{43}Ca, ^{45}Ca and ^{49}Ca has been studied by means of the (d,p) reaction at an incident energy of 10 MeV. Angular distributions have been obtained for all levels below an excitation energy of approximately 5.5 MeV, and spectroscopic factors are deduced for levels which have angular distributions typical of a stripping pattern. It is suggested that comparison of these results with those previously reported at $E_d = 7$ MeV reveals the presence of compound nucleus contributions for many levels of ^{41}Ca, and smaller contributions for some levels of ^{43}Ca. Hauser–Feshbach calculations are used to predict the magnitude of such contributions, and excellent agreement with experiment is obtained. (auth)

30924 CALCULATION OF THE 0^+ AND 2^+ GIANT RESONANCES IN Ni^{58}. Jakubassa, D. H. (Technische Univ. Muenchen, Garching (F. R. Germany). Physik-Department). Z. Phys.; 268: No. 4, 409-411(Jul 1974).

1 fig.; 4 tabs.; 6 refs.

Estimates of the excitation energy, width and sum rule fraction of the collective monopole and quadrupole vibrations indicate that the peak in the $62A^{-1/3}$ MeV region is a superposition of the 0^+ and 2^+ modes. (auth)

30925 ARE THERE LOW-LYING, INTRASHELL-EXCITED, HIGHLY DEFORMED STATES IN THE 1f-2p SHELL NUCLEI. Dhar, A. K.; Kulkarni, D. R.; Bhatt, K. H. (Physical Research Lab., Ahmedabad (India)). Phys. Lett., B; 50: No. 3, 323-326(10 Jun 1974).

It is shown that the improved effective interactions in the fp shell imply the existence of an excited band of states which is much more deformed than the ground state band for some fp shell nuclei. Such states are to a certain extent analogous to the fission isomers occurring in heavy nuclei. Their experimental identification would be interesting and might also help to further improve the effective interaction. (auth)

30926 DEUTERON BREAK-UP AND PROTON SCATTERING ON ^{58}Ni. Buta, A.; Lang, J.; Micek, S.; Mueller, R.; Unternaehrer, J.; Viatte, P. (Eidgenoessische Technische Hochschule, Zurich (Switzerland). Lab. fuer Kernphysik). Phys. Lett., B; 50: No. 3, 333-336(10 Jun 1974).

The break-up of deuterons on ^{58}Ni has been measured. Contrary to gold the energy-angle correlation shows a pronounced structure due to excitation of levels in the intermediate configuration ^{59}Cu. The proton spectra are confronted with the excitation curves for proton scattering on the same target. (auth)

30927 ^{40}Ca(n,α)^{37}Ar REACTION AT 14.1 MeV. Perng, C. C.; Lin, S. Y.; Chou, M. C.; Hsu, Y. C.; Hwang, J. L.; Hsu, Y. C. (National Taiwan Univ., Taipei). Chin. J. Phys. (Taiwan); 11: No. 2, 119-129(Oct 1973).

Alpha particles produced by the interaction of 14.1 MeV neutrons with ^{40}Ca were studied by using counter telescope technique. The well resolved groups of the alpha particles leading to ^{37}Ar* = 0, 1.41 to 1.61 and 2.22 to 3.52 MeV states were obtained. The strong forward peak in the angular distributions of these groups suggests a large contribution from direct reaction process, in contrast with the earlier investigations. The angular distribution of the ground state was analyzed with the incoherent combination of direct reaction process using DWBA method, and compound nucleus process by Hauser-Feshbach theory. The cross section of the ground state transition was found to be 1.7 ± 0.2 mb, in which the contribution due to compound nucleus process was less than 12%. For the unresolved groups of the alpha particles, corresponding to the highly excited states of ^{37}Ar the angular distribution is approximately symmetrical with respect to 90°, and is agreeable with the prediction of compound nucleus process. From the analysis of these groups, the level density parameter, nuclear temperature and spin cut-off parameter are evaluated. (auth)

30928 CONVERSION COEFFICIENT MEASUREMENTS IN ^{49}V. Fazzini, T.; Giannatiempo, A.; Maurenzig, P. R. (Univ., Florence). Nuovo Cim.; 23A: No. 2, 304-310(21 Sep 1974).

Conversion coefficient measurements were performed on several transitions in ^{49}V, from the ^{49}Ti(p,nγ)^{49}V reaction. Negative parity was established for the levels at 1022 keV ($^{11}/_{2}$, 1155 keV ($^{9}/_{2}$) and 2263 keV (probably $^{15}/_{2}$) and for the level at 2354 keV. The first few levels of a rotational band based on the $^{3}/_{2}^{+}$, 748 keV state were investigated. Positive parity was established for the 1140 keV $^{5}/_{2}$ state, for the 1602 keV state, whose spin was determined as $^{7}/_{2}$, and for the 2178 keV state for which a $^{9}/_{2}$ spin value is suggested. (auth)

30929 COMMENT ON ANOMALOUS (p,t) ANGULAR DISTRIBUTIONS DUE TO FORM FACTOR CANCELLATION. Ohnuma, H. (Tokyo Univ.). J. Phys. Soc. Jap.; 35: No. 6, 1786(Dec 1973).

The possibility is pointed out of obtaining angular distributions entirely different from normal pattern if two orbits with different N are involved in the transition. This is because of the difference in numbers of nodes of two-nucleon form factors. Calculations are performed for the ^{44}Ca(p,t) reaction at 52 MeV/c angular distributions and form factors are found. (JFP)

30930 LIFETIME MEASUREMENTS OF SOME STATES IN ^{53}Mn. Georgopulos, P. D. (Pennsylvania State Univ., University Park (USA). Dept. of Physics); Hoffman, E. J.; Patter, D. M. van (Bartol Research Foundation, Swarthmore, Pa. (USA)). Nucl. Phys., A; 226: No. 1, 1-8(24 Jun 1974).

The lifetimes of fourteen levels in ^{53}Mn have been extracted by use of the Doppler shift attenuation (DSA) method. The states were populated by the ^{50}Cr(α, pγ)^{53}Mn reaction at $E_{\alpha} = 8.9$ MeV. In order to reduce the uncertainty in the lifetimes of these states, an evaluation of the stopping-power in chromium for Mn ions was made by comparing the lifetime measurements extracted by the DSA method for the 1.53 MeV state in ^{55}Mn populated by the ^{52}Cr(α, pγ) reaction, with an independent measurement made by resonance fluorescence. (auth)

30931 THREE-BODY EFFECTIVE INTERACTIONS IN THE $F_{7/2}$ REGION. Yariv (Rajewski), Y. (Max-Planck-Institut fuer Kernphysik, Heidelberg (F. R. Germany)). Nucl. Phys., A; 225: No. 3, 382-396(17 Jun 1974).

The three-body effective forces in a pure $(0f_{7/2})^{n}$ model space are calculated to second order in perturbation theory. The full effect of the $(0f_{7/2}1p_{3/2})^{3}$ configuration on the effective interaction in the $(0f_{7/2})^{3}$ model space leading to three-body forces is calculated to all orders in G. The resulting three-body force matrix elements come out much weaker than demanded by phenomenological fits. Their main effect is to push the spectra as a whole up in energy, improving the fit of the calculated ground state binding energies to experiment. The biggest three-body-force contribution appears toward the end of the $f_{7/2}$ shell, where its main object is to compensate for Pauli violations arising from the two-body diagrams. (auth)

30932 SPIN-DEPENDENT EFFECTS IN INELASTIC SCATTERING. Amos, K.; Smith, R. (Melbourne Univ., Parkville (Australia). School of Physics). Nucl. Phys., A; 226: No. 3, 519-532(8 Jul 1974).

The differential cross sections for the inelastic scattering of 10 MeV, 19.6 MeV, 30.4 MeV, 40 MeV and 49.35 MeV protons to the 2^{+} state (1.409 MeV) in ^{54}Fe and of 19.6 MeV protons to the 2^{+} state (0.846 MeV) in ^{56}Fe are analyzed in conjunction with the available data on the asymmetries and spin-flip probability amplitudes. The scattering amplitudes for both one-step (valence plus core polarization) and two-step (intermediate resonance) processes are evaluated by using an antisymmetrized distorted wave approximation. Collective model representations for both the one-step (core polarization) and two-step (intermediate resonance) processes are used, and included are the effects of deforming the full Thomas spin-orbit potentials. The one-step processes are fixed by the analyses of the scattering of 30.4, 40 and 49.35 MeV protons, with the core polarization contributions being constrained by the B(E2) values for the γ-ray deexcitation of the 2^{+} states. The analyses of the 19.6 MeV data demonstrate the need for an extra (two-step) contribution to the reaction process, and are consistent with the virtual formation of an L = 3 giant resonance. The 10 MeV data most certainly demonstrate compound nucleus effects but could also have some strength due to the virtual formation of an intermediate L = 2 giant resonance. The resonance parameters are consistent with recent information concerning the mass variation of giant resonances. (auth)

30933 MAGNETIC ROTATION OF LEVELS OF ^{53}Mn AND ^{54}Mn FOLLOWING THE ^{53,54}Cr(p,n) AND ^{51}V(α,n) REACTIONS. Kerr, P. G.; Wender, S. A.; Cameron, J. A. (McMaster Univ., Hamilton, Ontario (Canada). Dept. of Physics). Nucl. Phys., A; 226: No. 3, 381-390(8 Jul 1974).

The low-lying levels of ^{53}Mn and ^{54}Mn have been studied using the ^{53,54}Cr(p,nγ) and ^{51}V(α,nγ) reactions. Angular distributions of γ-rays have been measured; and their integral rotations in iron alloy targets studied. The g-factor of the 377 keV, $^{5}/_{2}$-level of ^{53}Mn is $g = +1.15 \pm 0.17$. Products gτ have been found for the 55, 156, 368, 408 and 1072 keV levels of ^{54}Mn to be 124 ± 42, 360 ± 60, 75 ± 25, > 10 and 150 ± 80 ps, respectively. By using shell model estimates for the g-factors, the lifetimes of the levels have been deduced. An interpretation of the results in terms of shell model wave functions is given. (auth)

30934 STRUCTURE OF LOW-LYING 0^{+} STATES IN $f_{7/2}$ SHELL NUCLEI FROM INELASTIC ^{3}He SCATTERING. Morsch, H.-P. (Max-Planck-Institut fuer Kernphysik, Heidelberg (F. R. Germany)). Nucl. Phys., A; 226: No. 3, 506-518(8 Jul 1974).

Differential cross sections for inelastic ^{3}He scattering to the first 0^{+} excited states in ^{40}Ca, ^{44}Ca, ^{46}Ti and ^{48}Ti have been measured at 29 MeV. A consistent description of the experimental data has been obtained within a microscopic approach using $[(s_{1/2}d_{3/2})^{-2m}f_{7/2}^{n+2m}]$ and $[f_{7/2}^{n-2m}p_{3/2}^{2m}]$ particle-hole components. The calculated angular distributions are found to be extremely sensitive to the different particle-hole configurations. The best fits to the data are obtained for dominant contributions from $[d_{3/2}^{-2m}f_{7/2}^{n+2m}]$ components with $m \geqq 2$. Contributions from other components were found to be small, except for ^{40}Ca where evidence for a strong $(s_{1/2}^{-2m}f_{7/2}^{2m})$ component was found. The fact that such a strength is not obtained from the deformed shell model with prolate deformation may be evidence for oblate components in the ^{40}Ca wave function. A study of the effect of different forms of the effective interaction leads to a preference for a Gaussian shape. The results obtained here together with information from transfer reactions provide a consistent picture of ground and first excited 0^{+} states. (auth)

Nuclear Properties and Reactions, 59 ≤ A ≤ 89

Refer also to abstracts 30854, 30931, 30960, and 31092.

30935 (ORNL-4985) GAMMA-RAY PRODUCTION DUE TO NEUTRON INTERACTIONS WITH ^{68}Zn AND THE LEVEL STRUCTURE OF ^{68}Zn. Dickens, J. K. (Oak Ridge National Lab., Tenn. (USA)). Sep 1974. Contract W-7405-eng-26. 53p. Dep. NTIS $5.45.

Numerical values of differential cross sections for gamma rays produced by neutron interactions with ^{68}Zn were measured for an incident energy of 5.4 MeV and gamma-ray scattering angle of 55 deg. The dσ/dω data were obtained by using a 60-cm^{3} Ge(Li) detector. The data consist of cross section values for 164 gamma rays or gamma-ray groups having gamma-ray energies between 413 and 4998 keV. These data were analyzed to obtain information on the level structure of ^{68}Zn, and 131 transitions were assigned among 78 known or postulated new levels in ^{68}Zn. (22 figures, 1 table) (auth)

30936 SPALLATION OF COPPER BY HIGH-ENERGY ALPHA PARTICLES. Karol, P. J. (Carnegie-Mellon Univ., Pittsburgh). Phys. Rev., C; 10: No. 1, 150-155(Jul 1974).

There were 28 radionuclides produced by spallation of natural copper by 720 MeV α particles investigated by direct γ counting of irradiated targets. Although the isobaric yield distributions and mass yield curve are similar in many respects to those found in proton spallation, a suppression of yields of neutron deficient products is observed. Several interpretations of this latter phenomenon are critically discussed. (auth)

30937 NUCLEAR SPECTROSCOPY WITH THE ^{62}Ni(^{7}Li,^{6}He)^{63}Cu REACTION. White, R. L.; Kemper, K. W.; Charlton, L. A.; Gunn, G. D.; Norton, G. A.; Williams, M. E. (Florida State Univ., Tallahassee). p 65 of Proceedings of the International Conference on Reactions Between Complex Nuclei. Vol. I and Suppl. Robinson, R. L. (ed.). New York; American Elsevier Publishing Co., Inc. (1974).

From international conference on reactions between complex nuclei; Nashville, Tennessee, USA (10 Jun 1974). See CONF-740637-(P1 and Suppl.).

30938 MOESSBAUER INVESTIGATIONS ON ^{83}Kr. Kolk, B. Groningen, Netherlands; Rijksuniversiteit (1974). 138p.
Thesis.

Investigations on ^{83}Kr, using the Moessbauer effect of the 9.4-keV transition in ^{83}Kr, are described. The recoilless fraction f(T) of ^{83}Kr in solid krypton was studied because a large deviation existed between measured and theoretical f-values. The investigations, which led to the removal of this discrepancy, brought to light the following facts: first, an incorrect value of the maximum resonant-absorption cross section, based on a wrong value of the internal-conversion coefficient of the 9.4-keV γ-ray transition, had been used in the earlier evaluations of f(T). The conversion coefficient was remeasured and the new value was used in a re-analysis of the recoilless-fraction results; secondly, the recoilless fraction of the solid-krypton source turned out to be 40% lower than that of the solid-krypton absorber. This effect to lattice damage caused by after effects was attributed to arising from the highly converted decay preceding the resonant γ-ray transition. The ME effect of ^{83}Kr in β-hydroquinone sources and absorbers and in Rb halide sources was studied. From the ME spectra obtained with a Kr in β-hydroquinone absorber a new value of the quadrupole-moment ratio between the 9.4 keV and ground state of ^{83}Kr was derived. The ME effect of ^{83}Kr implanted in aluminum and iron are investigated. In aluminum an isomer shift was observed indicating an increase in the Kr contact density relative to that in solid krypton in agreement with conversion-electron results. This increase was attributed to overlap effects. The ME results obtained with ^{83m}KrFe sources indicate that at lowest implantation doses about 40% of the krypton atoms experience a large magnetic hyperfine field. With reservations due to poor statistics the authors conclude to a magnetic hyperfine field of about 1.4 mg for the highest-field fraction of krypton in iron. (NL)

30939 DESCRIPTION OF ODD-MASS COPPER NUCLEI WITH PARTICLE-CORE COUPLING MODELS. de Jager, J. L. Amsterdam; Vrije Univ. (1974). 110p.
Thesis.

The properties of odd-mass copper nuclei can be described by models in which an extra proton is coupled to the neighbouring nickel nuclei. In a first model, the particle-phonon model, the even-even nickel core nucleus is described as a quantized oscillating liquid drop. In a second model, the particle-core model, the core states are considered as eigenfunctions of a core Hamiltonian, for which no explicit form is assumed. In this model the interaction between particle and core is written as the sum of a dipole-dipole and a quadrupole-quadrupole interaction. With respect to the particle-phonon model, an advantage of this model is that the possible quadrupole moments of the core states are not necessarily zero. With a few assumptions, and introducing effective operators in the formula of the differential cross section for electron scattering in the Born approximation, the form factors are calculated in a rather simple way. In the case of ^{63}Cu, it becomes clear that measurements of the inelastic form factors can be a sharp test on these coupling models. Both models were studied by identical minimization procedures where the model parameters were varied to give the best possible reproduction of excitation energies, spectroscopic factors and electromagnetic properties. The particle-core model with two core states is applied to other odd-mass Cu isotopes. The systematics in the experimental and calculated properties (and in the values of the parameters) in the chain of nuclei, ^{59}Cu, ^{61}Cu, ^{63}Cu, ^{65}Cu and ^{67}Cu, are considered. It is investigated whether the inclusion of the next three core states in the particle-core model can reproduce properties of higher ^{63}Cu levels and improve the description of the few properties of the low-lying levels which were less well-reproduced with two core states. Finally, the electron scattering form factors for the six lowest states in ^{63}Cu are calculated with the method developed in chapter II, using the particle-phonon and particle-core wave functions obtained in chapter III. A comparison is made with the presently available experimental data. (NL)

30940 TARGET-SPIN EFFECTS ON ELASTIC SCATTERING CROSS SECTIONS. Satchler, G. R.; Fulmer, C. B. (Oak Ridge National Lab., Tenn. (USA)). Phys. Lett., B; 50: No. 3, 309-312 (10 Jun 1974).

It is shown, using a simple model and empirical results, that the odd-even differences in the scattering of He ions from ^{59}Co and ^{60}Ni can be explained as due to the scattering from the quadrupole moment which is allowed for the odd target nucleus but not the even. (auth)

30941 SPECTROSCOPY OF THE ^{69}Ga AND ^{71}Ga ISOTOPES WITH THE ^{69,71}Ga$(\alpha,\alpha'\gamma)^{69,71}$Ga AND ^{66,68}Zn$(\alpha,p\gamma)^{69,71}$Ga REACTIONS. Ivascu, M.; Bucurescu, D.; Popescu, D.; Avrigeanu, V.; Dragulescu, E. (Institutul de Fizica Atomica, Bucharest (Romania)); Semenescu, G.; Avrigeanu, M. (Comitetul de Stat pentru Energia Nucleara, Bucharest (Romania)). Nucl. Phys., A; 225: No. 2, 357-364(10 Jun 1974).

Excitation energies and mean lives of some low-lying levels in ^{69}Ga and ^{71}Ga have been measured by means of the ^{69,71}Ga $(\alpha,\alpha'\gamma)^{69,71}$Ga and ^{66,68}Zn $(\alpha,p\gamma)^{69,71}$Ga reactions. Gamma rays were detected at 90° in coincidence with the charged particles detected at $\theta_\alpha' = \pm 120°$ and $\theta_p = \pm 50°$. From DSA measurements, mean lives of $\tau_m = 2400 \pm 1000$, <160, 350 ± 100 and 480 ± 160 fs were determined for the ^{69}Ga levels at $E_x = 0.58$, 1.03, 1.11 and 1.34 MeV, respectively, and of $\tau_m = 2100 \pm 1000$, 350 ± 230, >1100, >300 and 1100 ± 700 fs for the ^{71}Ga levels at $E_x = 0.51$, 0.91, 0.97, 1.11 and 1.40 MeV, respectively. (auth)

30942 GAMMA-RAYS FROM THE DECAY OF ^{75}Ge. Venkataratnam, S.; Lakshminarayana, V. (Andhra Univ., Visakhapatnam, India). Nuovo Cim.; 23A: No. 2, 390-399(21 Sep 1974).

Gamma-ray spectra from the decay of 82.2 min ^{75}Ge were studied with a high resolution Ge(Li) detector by singles and coincidence methods. In addition to the already reported gamma transitions two new gamma-rays at energies 136 and 270 keV are observed. The transitions in the decay of ^{75}Ge are placed in a level scheme of ^{75}As consisting of levels at 199, 265, 401, 469, and 618 keV, the 401 keV level being introduced for the first time in the beta-decay, to account for a newly observed gamma-transition. The log ft values for the different beta-transitions are estimated. The level structure of ^{75}As is discussed. (auth)

30943 OPTICAL MODEL CALCULATIONS FOR THE SCATTERING OF RAPID NEUTRONS (8 to 15 MeV) BY Cr AND Fe. Bucurescu, D.; Ivascu, M.; Popescu, D.; Semenescu, G.; Titirici, M. (Inst. of Atomic Physics, Bucharest). Stud. Cercet. Fiz.; 24: No. 10, 1197-1200(1972). (In Rumanian).

Optical model calculations with two different average parameter sets were performed for the scattering of 8 to 15 MeV neutrons by the Cr and Fe nuclei. From a comparison with existing experimental data it is concluded that the set of Rosen et al. is the most indicated for data evaluations in this mass and energy range. (auth)

30944 LEVEL STRUCTURE OF ^{78}Kr. Sanderson, N. E.; Lisle, J. C.; Willmot, J. C. (Univ. of Manchester, Eng.). J. Phys., B (London); 7: No. 10, 1156-1166(1 Jul 1974).

States in ^{78}Kr have been excited by the decay of ^{78}Rb and by the reaction ^{68}Zn(^{12}C,2n) and a level scheme has been built up from the observed γ-ray spectra. The presence of a number of states, previously reported, has been confirmed and four new levels at 2572.5, 2900.2, 3160.7 and 3723.8 MeV are identified. Firm spin and parity assignments are made for states at 1016.9 MeV (0^+) and 1147.5 MeV (2^+) and tentative assignments for states at 1564.4 MeV (3^+) and 1872.5 MeV ($3,4^+$). (auth)

30945 GENERALIZED COLLECTIVE MODEL AND α-PARTICLE SCATTERING ON ^{56}Fe AND ^{48}Ti. Rebel, H.; Schweimer, G. W.; Habs, D.; Gils, H. J. (Kernforschungszentrum Karlsruhe (F. R. Germany). Zyklotronlaboratorium). Nucl. Phys., A; 225: No. 3, 457-469(17 Jun 1974).

The generalized collective model has been applied to the description of elastic and inelastic scattering of 104 MeV α-particles from ^{48}Ti and ^{56}Fe. The mass and stiffness parameters of the collective Hamiltonian have been determined phenomenologically by fitting the level spectra. From the solutions of the collective Hamiltonian the coupling matrix elements for coupled-channel calculations of the differential cross sections are calculated. The radial dependence of the nuclear density has been assumed to be a two-parameter Fermi distribution. The folding model has been used for describing the scattering mechanism. The procedure provides a unified description of observed level spectra, E2 properties, and α-particle scattering, and results in a general agreement. (auth)

30946 NUCLEAR STRUCTURE CALCULATION OF ^{50}Sc AND ANALYSIS OF THE ^{48}Ca(^{3}He,p)^{50}Sc REACTION. Engeland, T.; Osnes, E. (Oslo Univ. (Norway). Fysisk Institutt). Nucl. Phys., A; 226: No. 1, 45-57(24 Jun 1974).

The spectrum of ^{50}Sc has been calculated in the shell-model picture by including both the 2p1f and 3s2d1g single-particle orbitals and using the Kuo–Brown interaction. The wave functions were used to calculate the strength of the ^{48}Ca(^{3}He,p)^{50}Sc reaction to the 1^+ levels. The inclusion of the 3s2d1g shell leads to increased 1^+ cross sections, but the theoretical predictions are still below the experimental values. (auth)

30947 THE VARIATION OF THE LIFE-TIME OF ^{89}Zr IN $BaTiO_3$, $PbZrO_3$ AND ZrO_2. Auric, P.; Vargas, J. I. (CEA

Centre d'Etudes Nucleaires de Grenoble, 38 (France). Dept. de Recherche Fondamentale). Chem. Phys. Lett.; 27: No. 2, 229-232(15 Jul 1974).

The variation of the electron capture (EC) decay life-time of ^{89}Zr as a function of environment has been measured with respect to the antiferroelectric-paraelectric transition in $PbZrO_3$ and the results ($\Delta\lambda/\lambda \sim 0.1\%$) have been compared to similar observations in Ba Ti(^{89}Zr)O_3. In ZrO_2, the decay rate of ^{89}Zr is insensitive to the crystallographic change from the cubic to the monoclinic form. The ^{89}Zr EC decay rate shows a strong temperature dependence in the monoclinic phase. (auth)

30948 THE DETERMINATION OF THE DIFFERENTIAL ENERGY LOSS OF HEAVY IONS BACKSCATTERED FROM AN INFINITELY THICK SOLID TARGET. Schmidt-Boecking, H.; Ruehle, G.; Bethge, K. (Heidelberg Univ. (F. R. Germany). 2. Physikalisches Inst.). Nucl. Instrum. Methods; 118: No. 2, 357-360(15 Jun 1974).

A method is described to determine the differential energy loss of heavy ions from the spectrum of heavy ions elastically scattered from an infinitely thick target. Data over a fairly wide energy range can be obtained from a single measurement by a recursive and iterative calculation. The data obtained in this way for ^{16}O ions in Ni and Au targets are compared to those from other measurements. They differ by less than 5% over the whole energy range investigated (7-35 MeV). The same method also allows the calculation of the elastic or inelastic cross section from known energy loss applying the recurrence formula inversely. (auth)

30949 A STUDY OF ISOBARIC ANALOGUE RESONANCES IN ^{71}Ga. Ikossi, P. G.; Busch, C. E.; Clegg, T. B.; Ludwig, E. J.; Thompson, W. J. (North Carolina Univ., Chapel Hill (USA)). Nucl. Phys., A; 225: No. 3, 481-492(17 Jun 1974).

Differential cross-section and analyzing-power excitation functions were measured for elastic proton scattering from $E_p = 3.6$ to 6.4 MeV at $\theta_{c.m.} = 90°$, 115.8°, 129.8° and 155.3°. Differential cross-section angular distributions were measured at 3.56, 3.94, 5.78 and 8.98 MeV; and analyzing-power angular distributions, at 5.78 and 8.98 MeV. Optical-model parameters were deduced from these distributions. Resonance parameters were determined for eight analog resonances in ^{71}Ga, and neutron spectroscopic factors were calculated. These were compared with the results of previous (p,p) cross-section analyses and the results of (d,p) reactions leading to states in ^{71}Zn. (auth)

30950 LEVEL DENSITIES OF ^{63}Cu AND ^{65}Cu FROM THE ANALYSIS OF EVAPORATION SPECTRA. Pacer, J. C.; Wiley, J.; Lux, C. R.; Porile, N. T. (Purdue Univ., Lafayette, Ind. (USA). Dept. of Chemistry). Nucl. Phys., A; 226: No. 3, 413-423(8 Jul 1974).

The levels of ^{63}Cu and ^{65}Cu were populated in (p,p'), (p,α), (α,p) and (α,α') reactions induced by 12.5-16.0-MeV protons and 16.8-21.3-MeV α-particles. Energy spectra were measured between 30° and 150°, and the evaporation spectra were compared with the spin- and isospin-dependent statistical theory. The comparison permitted the determination of the level density parameter, a, and the pairing energy parameter, δ, in the Fermi gas model level density expression. It was found that, while a given set of parameters could give a good fit to the spectra obtained at a given energy, the energy dependence of some of the differential cross sections was not very well reproduced. The implications of this disagreement for the validity of the Fermi gas model level density are discussed. (auth)

Nuclear Properties and Reactions, $90 \leq A \leq 149$

Refer also to abstracts 30153, 30154, 30854, 30977, 31012, 31020, 31094, and 31104.

30951 (AD-773622) MOESSBAUER EFFECT AND RELATED PHENOMENA. Final Report, 1 November 1964-1 January 1972. Hanna, S. S. (Stanford Univ., Calif. (USA). Dept. of Physics). 10 Jan 1974. Contract DA-31-124-ARO(D)-294. 41p. (AROD-5378-16-P). NTIS $3.25.

The goals of the 7-year research project were as follows: measurement of magnetic moments of excited states of nuclei by the Mossbauer effect and angular correlation experiments; study of ferromagnetic phenomena by the Mossbauer effect and other techniques; study of rare earth and actinide elements; search for new Mossbauer nuclides; and study of new techniques for Mossbauer spectroscopy. Final progress in these various areas is described in the report. (Modified author abstract) (GRA)

30952 (NP-20122) ANNUAL REPORT, 1973. (Tandemacceleratorlaboratoriet, Uppsala (Sweden)). Jan 1974. 91p. Dep. NTIS (US Sales Only) $7.75.

The substantive sections of this report concern the tandem accelerator, the on-line computer, research instrumentation and methods, and, principally, research reports. Although the latter deal overwhelmingly with nuclear physics, work on atomic physics, solid-state physics, and physical biology is also reported. Sections on personnel, seminars, and publications and reports are included. Nine of the research reports, containing significant information, are title listed separately. (RWR)

For title listings of individual papers see: 28917, 28918, 30855, 30901, 30916, 30953-30955, and 30979.

30953 (NP-20122, pp 52-54) NUCLEAR SPECTROSCOPY OF ^{107}Cd. Nyman, B.; Dietrich, W.; Lannergard, C. O.; Baecklin, A.; Johansson, A. (Univ. of Uppsala). Jan 1974.

30954 (NP-20122, pp 57-58) SEARCH FOR LOW-SPIN POSITIVE PARITY STATES IN LIGHT ODD-MASS In NUCLEI. Dietrich, W.; Baecklin, A.; Lannergard, C. O.; Nyman, B.; Bergman, O. (Univ. of Uppsala). Jan 1974.

30955 (NP-20122, pp 67-70) STATIC ELECTRIC QUADRUPOLE MOMENT OF THE FIRST 2^+-STATE IN ^{110}Pd. Thun, J. E.; Falk, F.; Hasselgren, L.; Fahlander, C.; Ghumman, B. S. (Univ. of Uppsala). Jan 1974.

30956 (RT/FI-(74)17) LARA: A FORTRAN IV CODE FOR THE CALCULATION OF THE COMPOUND NUCLEUS CONTRIBUTION TO THE TOTAL RADIATIVE WIDTH IN MEDIUM AND HEAVY NUCLEI BASED ON THE BRINK-AXEL MODEL. Reffo, G.; Vaccari, M. (Comitato Nazionale per l'Energia Nucleare, Rome (Italy)). Mar 1974. 22p. Dep. NTIS (US Sales Only) $4.25.

Radiative widths of compound-nucleus levels are calculated on the basis of the Brink-Axel estimate by assuming electric dipole transitions only. When the level scheme is known, the transitions to the discrete levels are considered singularly. (auth)

30957 ANALYSIS OF ROTATIONAL AND QUASIROTATIONAL GROUND-STATE BANDS IN EVEN-EVEN NUCLEI. Varshni, Y. P. (Univ. of Ottawa). J. Phys. Soc. Jap.; 36: No. 2, 317-325(Feb 1974).

A detailed analysis of the applicability of two three-parameter expressions for the level energies has been carried out on the ground-state bands of 149 deformed even-even nuclei. It is shown that the expression $E_I = aI(I+1) + pI + qI^2(I+1)$ provides a satisfactory description of the experimental data, and gives better results amongst the two. A method of estimating I_c, the spin at which the "back-bending" effect is expected to take place, is also developed. (auth)

30958 GAMMA-GAMMA ANGULAR CORRELATION IN ^{147}Pm. Bhati, S. S.; Singh, N.; Mangal, P. C.; Trehan, P. N. (Punjab Univ., Chandigarh, India). J. Phys. Soc. Jap.; 36: No. 2, 326-330(Feb 1974).

Angular correlation studies have been carried out for seven cascades, viz. 275-410, 275-319, 596-91, 440-91, 398-91, 319-91 and 197-398 keV, in ^{147}Pm. Out of these, the 275-410 keV cascade was attempted for the first time. A spin assignment of $5/2^+$ was confirmed for the 490-keV level. The mixing ratios of 596, 440, 410, 398, 319 and 197 keV gamma rays were found to be M1 + (19$^{+[illegible]}_{-[illegible]}$)% E2, M1 + (25$^{+[illegible]}_{-[illegible]}$)% E2, E2 + 3.8% M3, M1 + (5 ± 1.5)% E2, M1 + (1.5$^{+[illegible]}_{-[illegible]}$)% E2 and M1 + (82 ± 4)% E2, respectively. The experimental transition probabilities for the 596, 440, 275, 197 and 91 keV gamma rays were calculated and compared with the single-particle estimates. (auth)

30959 SURVEY FOR ELEMENTS TO BE EXCITED BY GAMMA-RAYS FOLLOWING THERMAL NEUTRON CAPTURE IN VANADIUM. Kawarasaki, Y. (Japan Atomic Energy Research Inst., Tokai). J. Phys. Soc. Jap.; 36: No. 4, 907(Mar 1974).

Natural V was exposed to neutrons from a reactor. The capture gamma rays were scattered from targets of about 40 elements. A number of the elements investigated showed scattered peaks which should be strong enough to allow reduction of the level parameters. High-energy portions of the scattered gamma spectra from Ca, Ti, Nb, Sn, La, and Hg are shown as examples. (1 figure) (RWR)

30960 Q-VALUES AND EXCITATION FUNCTIONS OF NUCLEAR REACTIONS. Part c. Estimation of Unknown Excitation Functions and Thick Target Yields for p, d, ^3He, and α Reactions. Keller, K. A.; Lange, J.; Muenzel, H. Landolt-Boernstein Numerical Data and Functional Relationships in Science and Technology. Group I. Nuclear and Particle Physics. Volume 5.

Berlin; Springer-Verlag (1974). 262p. (In German and English). \$65.30.

A semiempirical procedure is described which permits the estimation of excitation functions and thick-target yields for reactions with p, d, ^{3}He, and α as projectiles and different outgoing channels. The accuracy is deemed sufficient for most practical purposes. (506 figures, 7 tables) (RWR)

30961 RATIO OF THE NUCLEAR MOMENTS OF ^{99}Ru AND ^{101}Ru FROM NMR STUDIES OF FERROMAGNETIC ALLOYS. Murphy, J. J. (Iona Coll., New Rochelle, NY); Burch, T. J.; Budnick, J. I. J. Phys. Soc. Jap.; 36: No. 3, 634-635(Mar 1974).

NMR investigations of Ru as an impurity in Fe, Co, and Ni hosts yield a resonance frequency ratio for the isotopes ^{99}Ru and ^{101}Ru, $\nu_{101}/\nu_{99} = 1.121 \pm 0.002$. Interpreting this as the ratio of nuclear moments and using the best available data for μ_{99} gives $\mu_{101} = 0.698 \pm 0.024\ \mu_N$. (auth)

30962 NUCLEAR ORIENTATION: FROM AN EXOTIC TO A MATURED METHOD IN NUCLEAR PHYSICS. Postma, H. (Rijksuniversiteit, Groningen, Netherlands). J. Phys. (Paris), Colloq.; No. 1, 29-34(1974).

From meeting on hyperfine interactions as detected by nuclear radiations; Liege, Belgium (11 Sep 1973).

Nuclear orientation has been applied in nuclear physics for over two decades. It started as a somewhat exotic demonstration in nuclear spectroscopy, but it has evolved to a useful technique in nuclear spectroscopy and some other fields of nuclear physics. The current possibilities and difficulties are considered in some detail. A few examples of nuclear orientation experiments are reviewed. Nuclear orientation can also be useful to obtain information on the nuclear hyperfine interaction in solids. (FR)

30963 LEVELS IN ^{130}Ba FED FROM ^{130}La DECAY. Droste, C.; Morek, T.; Nowicki, M.; Sayed, E.; Srebrny, J.; Starosta, W. (Univ., Warsaw). Acta Phys. Pol., B; 5: No. 4, 561-567(1974).

The level structure of ^{130}Ba was studied from the β^+-decay of ^{130}La. The gamma rays emitted in the decay were measured using a Ge(Li) detector. The ^{130}La isotope was produced in the ^{130}Ba(p,n) ^{130}La reaction at a proton energy of $E \simeq 9.5$ MeV. A ^{130}La → ^{130}Ba decay scheme is proposed. (auth)

30964 ISOMERIC STATES IN ^{97,98,99,100}Rh ISOTOPES. Sieniawski, J. (Inst. of Nuclear Physics, Krakow). Acta Phys. Pol., B; 5: No. 4, 549-560(1974).

Short-living isomeric states in neutron-deficient Rh isotopes were investigated with Ge(Li) detectors and a toroidal iron-free electron spectrometer. Decay schemes were proposed for ^{97m}Rh(44 *m*), ^{98m}Rh(3.5 *m*), and ^{110m}Rh(4.7 *m*). The properties of the isomeric transitions observed in Rh isotopes support the shell model interpretation of the low-lying excited states. (auth)

30965 IN-BEAM CONVERSION-ELECTRON SPECTRUM FOR THE ^{148}Sm(^{12}C,4n)^{156}Er REACTION. Gono, Y.; Zolnowski, D. R.; Haenni, D. R.; Sugihara, T. T. (Texas A and M Univ., College Station). p 157 of Proceedings of the International Conference on Reactions Between Complex Nuclei. Vol. I and Suppl. Robinson, R. L. (ed.). New York; Elsevier Publishing Co., Inc. (1974).

From international conference on reactions between complex nuclei; Nashville, Tennessee, USA (10 Jun 1974). See CONF-740637-(P1 and Suppl.).

30966 NUCLEAR DATA SHEETS FOR A = 143. Lemming, J. F. (Ohio Univ., Athens). Nucl. Data Sheets; 13: No. 2, 229-265(Oct 1974).

Level schemes and decay characteristics are presented for all nuclei with mass number 143. Experimental data, adopted values, comparisons with theory, and arguments for spin and parity assignments are given. The adopted level schemes and decay properties are based on data received before January 1, 1974. (auth)

30967 NUCLEAR DATA SHEETS FOR A = 136. Bunting, R. L.; Kraushaar, J. J. (Univ. of Colorado, Boulder). Nucl. Data Sheets; 13: No. 2, 191-228(Oct 1974).

The 1961 version of Nuclear Data Sheets for A = 136 was revised according to experimental data received before September 1, 1973. Selected experimental data, discussions for J^π assignments, and detailed level schemes are presented. Additional data now detail the decays of ^{136}Te, ^{136}Pm, and ^{136}Nd, and the level structure for ^{136}Xe, ^{136}Ba, ^{136}Ce, ^{136}Pr, and ^{136}Nd are improved significantly. The low-lying levels in ^{136}Ba are very well established. Additional information on the higher excitations in ^{136}Ba is needed, possibly through more definitive ^{135}Ba(n,γ)^{136}Ba experiments. The relative positions of the isomers in ^{136}I and the details of the level structure for ^{136}La and ^{136}Cs are still unknown. Areas of continuing experimental interest are the decays of ^{136m}I, ^{136}Nd, ^{136}Pm, and the quasi-rotational levels of ^{136}Ce and ^{136}Nd. The level structure of ^{136}Xe(^{136}Pr) will be subject to major additions (complete revision) in the near future. These new decay data were not included in this evaluation because of their preliminary nature. (auth)

30968 NUCLEAR DATA SHEETS FOR A = 130. Hiddleston, H. R.; Browne, C. P. (Univ. of Notre Dame, IN). Nucl. Data Sheets; 13: No. 2, 133-190(Oct 1974).

All information concerning nuclei with A = 130 received prior to January 1974 were evaluated and compiled. More than 250 papers were studied, and data from over 140 of these are used or cited in this work. This report supersedes the 1961 version of the Nuclear Data Sheets. The nuclei included range in Z from 49 to 60 and are In, Sn, Sb, Te, I, Xe, Cs, Ba, La, Ce, and Nd. No information on the Z = 59 nucleus, Pr, has yet been published for mass 130. The largest amount of information included concerns the (only) three stable even–even A = 130 nuclei, Te, Xe, and Ba. The least investigated are the levels of the odd–odd nuclei I, Cs, and La. The correspondence for levels of Te seen in decay work and those resulting from inelastic scattering is in need of further investigation. All level information for Xe is based on γ-ray investigations. Several reaction-gamma studies have been performed, but no other reaction data are available for Xe. Reaction studies for Ba are sparse, and reaction-gamma results account for most of the levels known. Possible discrepancies in the Ba data include the BE(2), Q_2 measurements for the first 2^+ state, and the half-life of the (11-ms) isomer. The β^+ decay from La (study in the preliminary stages) is also beginning to provide new level information for Ba. The In → Sn → Sb β^- decays have just recently begun to be established by use of mass-separated sources, and the Sb → Te decay is now well explored. The relative positions of the two Sb isomers and transitions between them have yet to be established. $\beta\gamma$-coincidence work is needed to verify Q^- measurements for this β^- chain, as well as to determine the relative positions of the various isomers. The Ce → La → Ba β^+-decay chain is of current interest, and Ce → La decay studies can be undertaken when the La → Ba results are more complete. The more neutron-deficient nuclei, La, Ce, and Nd, may be reached by (HI,xnγ) reactions. Levels for even–even Ce have been obtained from just such studies. The odd–odd nuclei I and Cs are not reached by decay, and level information for these nuclei is not yet available from reaction studies. (auth)

30969 BLOCKING WITH REALISTIC DECAY FUNCTIONS. Uguzzoni, A.; Verondini, E. (Univ., Bologna). Nuovo Cim.; 23A: No. 2, 200-208(21 Sep 1974).

The influence of a nonexponential decay on the determination of compound nuclear-reaction times by means of the blocking effect. In particular, with reference to the reaction ^{92}Mo(p,p′)^{92}Mo* (2^+, 1.5 MeV), the applicability of a cut-off model is shown. The difference between the reaction times deduced from experiments for exponential and nonexponential decay is calculated. (auth)

30970 CORRELATIONS BETWEEN (n,γ) AND (d,p) REACTIONS ON N = 82 NUCLEI. Gelletly, W. (Univ. of Manchester, Eng.). J. Phys., A (London); 7: No. 10, L128-L132(1 Jul 1974).

The measured strengths of excitation in the (n,γ) and (d,p) reactions on the N = 82 nuclei ^{138}Ba, ^{140}Ce, and ^{142}Nd are compared and it is found that they are strongly correlated for ^{138}Ba and ^{140}Ce but not for ^{142}Nd. The results for ^{138}Ba and ^{140}Ce may be explained in terms of the common unique parent assumption of Lane and Wilkinson (Phys. Rev.; 97: 1199 (1955)). This suggests the predominance of direct capture in the thermal neutron cross section for these nuclei, whereas the ^{142}Nd cross section is thought to be largely due to compound nucleus formation as is the general rule. (auth)

30971 PROBLEM OF PARTICLE-HOLE SYMMETRY IN EVEN–EVEN Cd AND Te NUCLEI. Scharff-Goldhaber, G. (Brookhaven National Lab., Upton, NY). J. Phys., B (London); 7: No. 10, L121-L124(1 Jul 1974).

A comparison of the pattern of level energies of the ground-state bands in even-even Cd and Te nuclei indicates that in Te nuclei for which proton and neutron orbits belong to the same major shell (50 → 82), pronounced neutron-proton interaction occurs. This explains the large $h_{11/2}$ admixture to the proton configuration of the neutron rich Te isotopes underlying the negative quadrupole moments commented on by Hall and Thomas (J. Phys. A.; Math. Nucl. Gen. 7: L8-10 (1974)). (auth)

30972 ATOMIC-BEAM MEASUREMENTS ON REFRACTORY ELEMENTS. Nuclear Spin Measurements of ^{99}Mo and ^{99m}Tc. Rubinsztein, H.; Lindgren, I.; Lindstroem, L.; Riedl, H.; Rosen, A. (Chalmers Tekniska Hoegskola, Goeteborg (Sweden). Institutionen foer Fysik). Nucl. Instrum. Methods; 119: No. 2, 269-274(15 Jul 1974).

A technique has been developed for making atomic-beam magnetic-resonance experiments on refractory elements. The atomic beam is produced by heating a small ball at the end of a wire by means of electron bombardment. The technique is primarily intended for radioactive work, and it is sensitive enough for investigations on neutron-deficient nuclei. In this work the spin values of two radioactive isotopes are reported, namely ^{99}Mo(67 h), $I = 1/2$, and ^{99m}Tc (6 h). $I = 1/2$. The measured spin values are compared with spectroscopic results and discussed in terms of the nuclear models. (auth)

30973 STUDY OF THE (p,np̃) REACTION ON THE ISOTOPES OF TIN. Whitten, C. A. Jr.; Chai, J.; Chirapatpimol, N.; Dunlop, W. H.; Igo; G. J. (California Univ., Los Angeles (USA). Dept. of Physics). Phys. Lett., B; 51: No. 1, 45-48(8 Jul 1974).

The cross sections for the (p,np̃) reaction, where the isobaric analogue state excited in the (p,n) charge-exchange reaction decays by proton (p̃) emission, have been measured for the ten stable isotopes of tin. These cross sections show effects due to the neutron decay channel, decay kinematics, and the nuclear structure of the target ground state. (auth)

30974 EXCITATION OF THE DEEPLY BOUND $g_{9/2}$ NEUTRON HOLE STATE IN ^{117}Sn BY A NEUTRON PICKUP REACTION WITH 81.7 MeV ^{3}He PARTICLES. Sakai, M.; Sekiguchi, M.; Soga, F.; Hirao, Y. (Tokyo Univ., Tanashi (Japan). Inst. for Nuclear Study); Yagi, K.; Aoki, Y. (Osaka Univ., Toyonaka (Japan)). Phys. Lett., B; 51: No. 1, 51-53(8 Jul 1974).

Neutron hole states have been investigated by neutron pickup reactions on ^{92}Mo, ^{118}Sn, ^{140}Ce and ^{208}Pb with 81.7 MeV ^{3}He particles. A strong effect of angular momentum mismatch has been observed to reduce the cross section for low-spin orbits. It causes the deeply bound $g_{9/2}$ orbit to appear in the spectrum of the α-particles from the ^{118}Sn(τ,α)^{117}Sn reaction as a strong broad peak. It may provide a nice tool for investigating the coupling mechanism between the deeply bound holes and the core. (auth)

30975 PROTON-HOLE STATES IN ^{115}In OBSERVED IN THE ^{116}Sn(d,^{3}He) REACTION. Hesselink, W. H. A.; Kooistra, B. R.; Put, L. W.; Siemssen, R. H.; van der Werf, S. Y. (Rijksuniversiteit Groningen (Netherlands). Kernphysisch Versneller Instituut). Nucl. Phys., A; 226: No. 2, 229-236(1 Jul 1974).

The ^{116}Sn(d, ^{3}He)^{115}In reaction has been investigated at E_d = 50 MeV. Thirteen transitions to states up to 3 MeV excitation energy were studied. The measured angular distributions were compared with DWBA calculations, and transferred angular momenta and spectroscopic factors were deduced. Levels at 1.04, 2.23 and 2.52 MeV were found to be excited most likely by $l = 3$ angular momentum transfer, in contrast to previous investigations at lower incident energies in which no $l = 3$ transitions have been observed. (auth)

30976 ATOMIC-BEAM INVESTIGATIONS OF SOME ANTIMONY NUCLIDES. Ekstroem, C.; Hogervorst, W.; Ingelman, S.; Wannberg, G. (Uppsala Univ. (Sweden). Fysiska Institutionen). Nucl. Phys., A; 226: No. 2, 219-228(1 Jul 1974).

The nuclear spins of some antimony isotopes and the hyperfine structure constants of ^{117}Sb have been measured by the atomic-beam magnetic resonance method. The results are as follows: for ^{116}Sb (16 min), $I = 3$; ^{116m}Sb (60.4 min), $I = 8$; ^{118m}Sb (5.0 h), $I = 8$; ^{120m}Sb (5.76 d), $I = 8$; ^{128}Sb (9.0 h), $I = 8$; and ^{117}Sb (2.8 h), $a = -305(5)$ MHz, $b = 3(21)$ MHz. The corresponding nuclear moments of ^{117}Sb, $\mu_I = 3.43(6)$ n.m. and $Q = 0.2(1.2)$ b, have been evaluated through a direct comparison with known values in the stable nucleus ^{121}Sb. The magnetic dipole moment, which deviates from an earlier measurement, is in good agreement with theoretical predictions. (auth)

Nuclear Properties and Reactions, $150 \leq A \leq 189$

Refer also to abstracts 30154, 30854, 30948, 30960, 30965, 31011, 31094, and 31125.

30977 (AEC-tr-7574) MASS-SPECTROMETRIC DETERMINATION OF NEUTRON CAPTURE CROSS-SECTIONS OF THE RARE EARTH ISOTOPES. Dobrozemsky, R.; Pichlmayer, F.; Viehboeck, F. P. Translated from J. Mass Spectrom. Ion Phys.; 6: 415-450(1971). 16p. Dep. NTIS $4.00.

For the determination of neutron capture cross sections of rare earth isotopes, the corresponding elements were electromagnetically separated and the highly enriched isotopes were irradiated with and without Cd shielding in the ASTRA reactor to an integrated neutron flux of about 10^{20}n cm^{-2}. Before and after irradiation, the isotopic abundances were measured by mass spectrometry. The pile capture cross section, the thermal capture cross section and the effective resonance integral for: ^{147}Sm, ^{148}Sm, ^{154}Gd, ^{156}Gd, ^{160}Dy, ^{161}Dy, ^{162}Dy, ^{163}Dy, ^{170}Yb, ^{171}Yb, ^{172}Yb, ^{173}Yb were obtained. (5 figures, 3 tables) (auth)

30978 (IAE-2289) INTENSITY FLUCTUATIONS OF γ-TRANSITIONS FROM THE ($\bar{n}$,γ) REACTION. Efimov, B. V. (Gosudarstvennyj Komitet po Ispol'zovaniyu Atomnoj Ehnergii SSSR., Moscow. Inst. Atomnoj Ehnergii). 1973. 20p. (In Russian). INIS.

Consideration is given to a technique of calculating the statistical distribution of intensities of typical gamma transitions from (n,γ) reactions on the assumption that fluctuations of reduced neutron widths Γ_n and of partial radiation widths $\Gamma_{\gamma ij}$ obey a Porter-Thomas distribution. As an example the case of the ^{155}Gd (n,γ) reaction is calculated. Consideration is given to methods of decreasing fluctuations of the average intensities of the gamma transitions by taking into account the self-indicator filter and the neutron spectrometry technique. Estimates are given of effects which can be obtained in finding the correlation between Γ_n^0 and $\Gamma_{\gamma ij}$ by means of the self-indicator filter. (tr-auth)

30979 (NP-20122, pp 63-65) INVESTIGATIONS OF THE LEVEL STRUCTURE AND LIFETIMES OF ODD Tm ISOTOPES. Lindskog, J.; Svensson, L. G.; Solhed, H.; Jonsson, N. G.; Darwish, S. (Univ. of Uppsala). Jan 1974.

30980 LOW-LYING STATES OF ^{181}Os. Kawakami, H.; Yoshikawa, N.; Kusakari, H.; Ishihara, M.; Ishii, K. (Tokyo Univ., Tanashi, Japan). J. Phys. Soc. Jap.; 36: No. 3, 623-628(Mar 1974).

Nuclear structure of ^{181}Os was investigated by in-beam gamma ray spectroscopy through the excitation function and beam-gamma timing measurements. The low-lying level scheme of ^{181}Os was proposed, and the half-life of the first excited state was obtained as 316 ± 18 ns. The dependence of the intensity ratio of the crossover to cascade transitions on the Nilsson orbit is discussed by taking into account the g-factor cancellation. The hindrance factor of the E1 transition between the first excited state ($9/2^+$ [624]) and the ground state ($7/2^-$ [514]) was estimated to be 3.7×10^3 in terms of the Nilsson estimate. (auth)

30981 FORWARD SCATTERING OF 2-MeV NEUTRONS FROM ORIENTED ^{165}Ho. Fasoli, U.; Galeazzi, G.; Toniolo, D.; Zago, G.; Zannoni, R. (Univ., Padua). Lett. Nuovo Cim.; 11: No. 3, 169-172(21 Sep 1974).

The first experimental evidence regarding the influence of the polarization of the target on the differential scattering cross sections for neutrons is reported. This effect was found through a measurement of the difference between the scattering cross section of 2-MeV neutrons by a holmium-165 target polarized normally to the scattering plane and that of another identical but unpolarized target. The effects of nuclear deformation and multiple scattering are noted. (JFP)

30982 PROCEEDINGS OF THE INTERNATIONAL CONFERENCE ON REACTIONS BETWEEN COMPLEX NUCLEI, NASHVILLE, TENNESSEE, JUNE 10-14, 1974. Volume I and Supplement. Robinson, R. L.; McGowan, F. K.; Ball, J. B.; Hamilton, J. H. (eds.). New York; American Elsevier Publishing Company, Inc. (1974). vp. (CONF-740637-(P1 and Suppl.)).

From international conference on reactions between complex nuclei; Nashville, Tennessee, USA (10 Jun 1974).

Volume 1 of the Proceedings of the International Conference on Reactions between Complex Nuclei (with its supplement) contains one-page contributions to the meeting, which were available to the participants. Twenty of the 221 contributions were selected for oral presentation in full. The papers fell into the categories of elastic and inelastic scattering, nuclear reactions, fission and fusion, spectroscopy, and instrumentation and other topics. The papers presented orally are separately title listed. (RWR)

For title listings of individual papers see: 30879, 30880, 30905, 30906, 30920-30922, 30937, 30965, 30983-30987, 30996, 30997, and 31063-31066.

30983 γ-RAY MULTIPLICITY AFTER (HI,xn) REACTION. Hagemann, G. B.; Broda, R.; Herskind, B.; Ishihara, M.; Ryde, H. (Univ. of Copenhagen). p 110 of Proceedings of the International Conference on Reactions Between Complex Nuclei. Vol. I and Suppl. Robinson, R. L. (ed.). New York; Elsevier Publishing Co., Inc. (1974).

From international conference on reactions between complex nuclei; Nashville, Tennessee, USA (10 Jun 1974). See CONF-740637-(P1 and Suppl.).

30984 QUASI-FISSION: A NEW TYPE OF REACTION OBSERVED IN BOMBARDING HEAVY NUCLEI BY ^{84}Kr AND ^{63}Cu IONS. Hanappe, F.; Ngo, C.; Peter, J.; Tamain, B. (Institut Physique Nucleaire, Orsay, France). p 116 of Proceedings of the International Conference on Reactions Between Complex Nuclei. Vol. I and Suppl. Robinson, R. L. (ed.). New York; Elsevier Publishing Co., Inc. (1974).

From international conference on reactions between complex nuclei; Nashville, Tennessee, USA (10 Jun 1974). See CONF-740637-(P1 and Suppl.).

30985 DECOUPLED ROTATIONAL BANDS IN ^{163,165}Yb. Riedinger, L. L. (Oak Ridge National Lab., TN); Stelson, P. H.; Eichler, E.; Hensley, D. C.; Johnson, N. R.; Robinson, R. L.; Sayer, R. O.; Smith, G. J.; Hagemann, G. B. p 175 of Proceedings of the International Conference on Reactions Between Complex Nuclei. Vol. I and Suppl. Robinson, R. L. (ed.). New York; Elsevier Publishing Co., Inc. (1974).

From international conference on reactions between complex nuclei; Nashville, Tennessee, USA (10 Jun 1974). See CONF-740637-(P1 and Suppl.).

30986 SEARCH FOR NEW ISOTOPES ^{186,187}Tl. Schmidt-Ott, W. D. (UNISOR, Oak Ridge, TN); Carter, H. K.; Spejewski, E. H. p 177 of Proceedings of the International Conference on Reactions Between Complex Nuclei. Vol. I and Suppl. Robinson, R. L. (ed.). New York; Elsevier Publishing Co., Inc. (1974).

From international conference on reactions between complex nuclei; Nashville, Tennessee, USA (10 Jun 1974). See CONF-740637-(P1 and Suppl.).

30987 SPHERICAL AND DEFORMED SHAPES IN ^{188}Hg. Hamilton, J. H. (Vanderbilt Univ., Nashville); Ramayya, A. V.; Bosworth, E. p 178 of Proceedings of the International Conference on Reactions Between Complex Nuclei. Vol. I and Suppl. Robinson, R. L. (ed.). New York; Elsevier Publishing Co., Inc. (1974).

From international conference on reactions between complex nuclei; Nashville, Tennessee, USA (10 Jun 1974). See CONF-740637-(P1 and Suppl.).

30988 NUCLEAR DATA SHEETS FOR A = 186. Schmorak, M. R. (Oak Ridge National Lab., TN). Nucl. Data Sheets; 13: No. 2, 267-303(Oct 1974).

The available experimental data pertaining to the nuclear structure of nuclei with A = 186 are compiled; the results from various decay and reaction measurements are compared and evaluated. Inconsistencies and discrepancies in the level schemes are discussed. Level properties and gamma-ray properties are presented. Level schemes for each of the A = 186 nuclei are presented first. Then, for each nucleus, are presented summaries of level properties and compilers' comments, followed by the experimental data and a reference list. Data received before March 1974 were included. (auth)

30989 DECAY PROPERTIES OF THREE ^{166}Lu ISOMERS AND THE DECAY OF ^{166}Hf. de Boer, F. W. N.; Goudsmit, P. F. A.; Koldewijn, P.; Meyer, B. J. (Instituut voor Kernphysisch Onderzoek, Amsterdam (Netherlands)). Nucl. Phys., A; 225: No. 2, 317-351(10 Jun 1974).

Two new isomers have been identified in ^{166}Lu with half-lives of 2.12 and 1.41 min in addition to the 2.65 min ground state. Decay properties of the ^{166}Lu isomers and of 6.77 min ^{166}Hf have been studied with high resolution Ge(Li) detectors, a Ge(Li)−NaI(Tl) Compton-suppression device and a Si(Li) detector, mounted in an electron transport solenoid. The isotope ^{166}Hf decays mainly to a $\{p[523]\uparrow - n[523]\downarrow\}_{1+}$ level in ^{166}Lu. The decay of this level feeds all three isomers. The 2.65, 1.41 and 2.12 min isomers are identified as $\{p[404]\downarrow + n[523]\downarrow\}_{6-}$, $\{p[411]\downarrow + n[523]\downarrow\}_{3-}$ and $\{p[402]\uparrow - n[523]\downarrow\}_{0-}$ configurations. All three show allowed unhindered β-decay to excited levels in ^{166}Yb. The 2^+ up to 8^+ members of the ground state band, the 2^+ up to 8^+ members of the γ-vibrational band, several octupole levels and 20 other states are excited. The values $Z_\gamma(2) = 0.053 \pm 0.004$ and $Z_\gamma(0) = 0.089 \pm 0.004$ are found for the mixing of the γ-vibrational and the ground state bands. This indicates that the intrinsic quadrupole moment of the γ-band is a factor of 0.6 smaller than that of the ground state band. A considerable mixing with higher vibrational states is probably present. The level sequence and energy spacings of 6 odd-parity levels could be explained from a Coriolis mixing calculation of the four $p[514]\uparrow \pm p[411]\downarrow$ and $p[523]\uparrow \pm p[411]\downarrow$ bands. The 6^+ and 7^+ members of the $p[404]\downarrow + p[402]\uparrow$ band were identified. Positron−γ coincidence measurements yield a Q-value of 5480 ± 160 keV for the ^{166}Lu ground state decay. (auth)

30990 ELECTROMAGNETIC TRANSITIONS IN SOME ODD-NEUTRON DEFORMED NUCLEI. Andrejtscheff, W.; Manfrass, P.; Schilling, K. D.; Seidel, W. (Zentralinstitut fuer Kernforschung, Rossendorf bei Dresden (German Democratic Republic)). Nucl. Phys., A; 225: No. 2, 300-316(10 Jun 1974).

By using the reactions ^{155,157}Gd(α,2n), ^{178}Hf(n,γ), and ^{177}Hf(α,2n), the following half-lives of excited nuclear states have been measured: $T_{1/2}$(188.1 keV in ^{157}Dy) = 1.00 ± 0.15 ns, $T_{1/2}$(161.9 KeV in ^{157}Dy) = 1.3 ± 0.2 μs, $T_{1/2}$(177.6 keV in ^{159}Dy) = 9.0 ± 0.5 ns, $T_{1/2}$(614.3 keV in ^{179}Hf) = 0.50 ± 0.15 ns, $T_{1/2}$(720.7 keV in ^{179}Hf) $\leq$ 0.3 ns, $T_{1/2}$(516.4 keV in ^{179}Hf) < 0.2 ns, and $T_{1/2}$(309.0 keV in ^{179}W) = 1.53 ± 0.10 ns. A Ge(Li) timing system was employed. Electromagnetic transition probabilities are calculated in the Nilsson model including pairing and band-mixing effects. Comparisons between theoretical and experimental results are performed. (auth)

30991 ON THE BACK-BENDING IN THE ROTATIONAL MOTION. Broglia, R. A. (State Univ. of New York, Stony Brook (USA). Dept. of Physics); Molinari, A.; Pollarolo, G. (Turin Univ. (Italy). Istituto di Fisica); Regge, T. (Institute for Advanced Study, Princeton, N. J. (USA)). Phys. Lett., B; 50: No. 3, 295-298(10 Jun 1974).

The anomalous behaviour of the moment of inertia, as a function of the angular momentum, for the ground and first excited rotational bands of ^{154}Gd is accounted for by the mechanism of bands hybridization. (auth)

30992 MIXING OF NILSSON CONFIGURATIONS IN ^{159}Tb. Winter, G.; Funke, L.; Kemnitz, P.; Sodan, H.; Will, E. (Zentralinstitut fuer Kernforschung, Rossendorf bei, Dresden). J. Phys., B (London); 7: No. 10, L125-L127(1 Jul 1974).

The excited states of ^{159}Tb have been studied in the reaction ^{160}Gd(p,2nγ)^{159}Tb using in-beam gamma ray spectroscopy. New levels of two strongly mixed negative-parity bands and of the known $K^\pi = \frac{1}{2}^+$ band have been identified. From an analysis of the E1 transitions de-exciting the $\frac{7}{2}^+$ [404] level to the coupled $\frac{7}{2}^-$ states, the mixing between them was evaluated to be 17%. In order to explain the experimental value of the decoupling parameter for the $\frac{1}{2}^+$ band, an influence of the $\frac{1}{2}^+$ [660] configuration is suggested. (auth)

30993 TRANSITION PROBABILITIES IN THE DOUBLY ODD NUCLEI ^{176}Lu AND ^{182}Ta. Andrejtscheff, W.; Manfrass, P.; Seidel, W. (Zentralinstitut fuer Kernforschung, Rossendorf bei Dresden (German Democratic Republic)). Nucl. Phys., A; 226: No. 1, 142-156(24 Jun 1974).

The depopulation of isomeric states in ^{176}Lu and ^{182}Ta was studied in the (n,γ) reaction by means of delayed $\gamma-\gamma$ coincidence measurements with NaI(Tl) and Ge(Li) detectors. The following half-lives, unknown so far, have been obtained for ^{176}Lu: $T_{1/2}$(198.0 keV) = 35.0 ± 1.0 ns, $T_{1/2}$(638.8 keV) = 8.0 ± 1.0 ns and $T_{1/2}$(662.1 keV) = 6.3 ± 0.5 ns; and for ^{182}Ta: $T_{1/2}$(270.4 keV) = 1.2 ± 0.2 ns, $T_{1/2}$(402.6 keV) = 1.00 ± 0.05 ns and $T_{1/2}$(443.6 keV) = 2.2 ± 0.2 ns. The existence of the isomeric level at 443.6 keV in ^{182}Ta was confirmed. Weisskopf hindrance factors have been deduced for the K- and Ω-forbidden transitions. The K-allowed transitions are considered in terms of the Nilsson model, with pairing correlations taken into account. The experimental results for the transitions de-exciting the 270.4-keV level in ^{182}Ta agree with earlier model predictions including band mixing effects. The influence of the pairing effect on K-allowed E1 transitions in doubly odd nuclei is demonstrated. (auth)

30994 LEVELS IN ^{179}Ta AND γ-RAY TRANSITION PROBABILITIES IN ^{179}Ta AND ^{183}Re. Manfrass, P.; Andrejtscheff, W.; Kemnitz, P.; Will, E.; Winter, G. (Zentralinstitut fuer Kernforschung, Rossendorf bei Dresden (German Democratic Republic)). Nucl. Phys., A; 226: No. 1, 157-172(24 Jun 1974).

The level scheme of the deformed odd-proton nucleus ^{179}Ta has been investigated by in-beam spectroscopic methods. Singles γ-ray spectra as well as prompt and delayed $\gamma-\gamma$ coincidences were measured in the reactions ^{179}Hf(d,2n) and ^{179}Hf(p,n). The proposed level scheme of ^{179}Ta contains, in addition to the ground state band $\frac{7}{2}^+$[404], the rotational bands built on the intrinsic states $\frac{9}{2}^-$[514], $\frac{5}{2}^+$[402], $\frac{1}{2}^+$[411] and $\frac{1}{2}^-$[541]. By nanosecond lifetime measurements with Ge(Li) detectors the following half-lives have been obtained for ^{179}Ta levels: $T_{1/2}$(238.6 keV) = 95 ± 5 ns, $T_{1/2}$(520.3 keV) = 350 ± 20 ns, $T_{1/2}$(628.1 keV) = 80 ± 10 ns. A three-quasiparticle state of $T_{1/2}$ = 8.6 ± 1 ms with spin and parity tentatively assigned as $I^\pi = (\frac{19}{2}, \frac{21}{2})^-$ has been identified at an excitation energy of 1253.3 keV. For the $\frac{9}{2}$, $\frac{1}{2}^-$[541] level in ^{183}Re, excited in the reaction ^{181}Ta(α,2n), a lifetime of $T_{1/2}$ = 2.0 ± 0.1 ns was measured. (auth)

30995 ONE-NUCLEON TRANSFER REACTIONS IN DEFORMED NUCLEI. Ascuitto, R. J.; King, C. H.; McVay, L. J. (Yale Univ., New Haven, Conn. (USA). Nuclear Structure Lab.); Soerensen, B. (Niels Bohr Institutet, Copenhagen (Denmark)). Nucl. Phys., A; 226: No. 3, 454-492(8 Jul 1974).

The one-nucleon transfer reaction on deformed nuclei has been computed with the inclusion of indirect inelastic transitions that go through intermediate rotational states. The specific examples considered are ^{171}Yb(d,p), ^{172}Yb(p,d) and ^{186}W(p,d). Anomalies in the shapes of experimental angular distributions with respect to predictions of the distorted-wave Born approximation are shown to be reproduced when these higher-order inelastic processes are taken into account. Consideration is also given to the deuteron optical potential needed for these studies. (auth)

Nuclear Properties and Reactions, $190 \leq A \leq 219$

Refer also to abstracts 30854, 30959, 30960, 30974, 30984, 31078, and 31094.

30996 REACTIONS PRODUCED BY ^{7}Li ON ^{197}Au. Quebert, J. L. (CENBG, Gradignan, France); Frois, B.; Sousbie, G.; Marquez, L.; Ost, R.; Bethge, K.; Gruber, G. p 80 on Proceedings of the International Conference on Reactions Between Complex Nuclei. Vol. I and Suppl. Robinson, R. L. (ed.). New York; American Elsevier Publishing Co., Inc. (1974).

From international conference on reactions between complex nuclei; Nashville, Tennessee, USA (10 Jun 1974). See CONF-740637-(P1 and Suppl.).

30997 MASSIVE TRANSFER REACTION ^{208}Pb(^{20}Ne,α)^{224}Th. Maguire, C. F.; Harvey, B. G.; Hendrie, D. L.; Scott, D. K.; Kraus, L.; Mahoney, J. A.; Terrien, Y.; Yagi, K.; von Oertzen, W. (Univ. of California, Berkeley). p 84 of Proceedings of the International Conference on Reactions Between Complex Nuclei. Vol. I and Suppl. Robinson, R. L. (ed.). New York; American Elsevier Publishing Co., Inc. (1974).

From international conference on reactions between complex nuclei; Nashville, Tennessee, USA (10 Jun 1974). See CONF-740637-(P1 and Suppl.).

30998 HIGHLY INELASTIC SCATTERING OF α-PARTICLES FROM ^{208}Pb. Ho, H. W.; Henley, E. M. (Washington Univ., Seattle (USA). Dept. of Physics). Nucl. Phys., A; 225: No. 2, 205-220(10 Jun 1974).

Excitation of single particle (neutron)-hole states in the continuum is investigated as a possible explanation of an enhancement in the cross section observed in inelastic α-particle scattering. Both quasi-bound states of the excited neutron with the nucleus and with the scattered α-particle, i.e. ^{5}He formation, are taken into account. It is found that the large energy loss part of the observed broad plateau in the inelastic α-spectrum can be accounted for by ^{5}He formation. However, it appears difficult to explain the lower energy peak by a pseudo-bound state of the neutron and nucleus. (auth)

30999 ISOSPIN EFFECTS UPON THE DECAY OF HIGHLY EXCITED NUCLEAR STATES. Woods, T. J. (Minnesota Univ., Minneapolis (USA)). Phys. Lett., B; 50: No. 3, 302-304(10 Jun 1974).

It is proposed that $T_<$ states which strongly mix with analog states to give states of mixed isospin results in the enhancement of the probability of proton decay from highly excited nuclear states. Such considerations are shown to explain the anomalies observed in the (p,n$\bar{p}$) reactions.

31000 STRENGTH OF THE MULTIPOLE PAIRING COUPLING CONSTANT. Broglia, R. A.; Nilsson, B. S. (Niels Bohr Institutet, Copenhagen (Denmark)); Bes, D. R. (Comision Nacional de Energia Atomica, Buenos Aires (Argentina)). Phys. Lett., B; 50: No. 2, 213-216(27 May 1974).

The wavefunctions obtained by diagonalizing the multipole pairing residual interaction proposed earlier by the authors are shown to account for the energies, inelastic scattering and one- and two-particle transfer cross sections of the nuclei ^{206}Pb and ^{210}Pb. From the analysis of these data, detailed information on the different multipole pairing matrix elements is obtained. It is found that the strength of all the different multipolarities of the pairing residual interaction is approximately the same and equal in average to $G_\lambda = 27/A$ MeV ($\lambda = 0$, 2, 4 and 6). (auth)

31001 L SHELL IONIZATION IN THE α DECAY OF ^{210}Po. Scott, R. D. (Scottish Research Reactor Centre, East Kilbride, Eng.). J. Phys., B (London); 7: No. 10, 1171-1182(1 Jul 1974).

The number of L x-rays of lead emitted per α disintegration of ^{210}Po has been measured, in terms of the known emission of neptunium L x-rays by ^{241}Am, using a thin Ge(Li) x-ray detector, a low geometry α particle counter and a weak (~4 μCi) source of ^{210}Po. The result, $(1.41 \pm 0.12) \times 10^{-4}$ L x-rays per α, is substantially lower than the results of previous measurements but is still in marked disagreement with the predictions of calculations based on the theoretical approach of Migdal (J. Phys. USSR.; 4: 449-53 (1941)). The result is in fair agreement with a recent calculation, using a special formulation of the binary encounter approximation, by Hansen (Phys. Rev.; A9: 40-3 (1974)). Previous theoretical and experimental work is reviewed and the results of a simple calculation of the L shell ionization probability, using the sudden approximation, are given. (auth)

31002 PHOTOFISSION IN GOLD AT INTERMEDIATE ENERGY. Areskoug, M.; Schroeder, B.; Lindgren, K.; Andersson, G.; Forkman, B. (Lund Univ. (Sweden). Fysiska Institutionen). Nucl. Phys., A; 226: No. 1, 93-108(24 Jun 1974).

By using the thick-target thick-catcher technique, the yields of 29 fission products from photofission in ^{197}Au induced by 600-MeV bremsstrahlung have been measured. From these values, mass and charge distributions have been determined. The experimental results are compared with cascade-evaporation calculations in combination with calculations based on the liquid drop model. (auth)

31003 CORE POLARIZATION IN INELASTIC PROTON SCATTERING FROM ^{209}Bi AT 61 MeV. Scott, A.; Owais, M. (Georgia Univ., Athens (USA)); Petrovich, F. (California Univ., Berkeley (USA). Lawrence Berkeley Lab.). Nucl. Phys., A; 226: No. 1, 109-130(24 Jun 1974).

The differential cross sections for the excitation of the 0.90 MeV ($2f_{7/2}$) and 1.61 MeV ($1i_{13/2}$) single proton levels and the multiplet of states at 2.62 MeV in ^{209}Bi have been measured with 61.2 MeV protons. The results of collective model calculations and microscopic model calculations with core polarization are compared with the data. It is found that L = 4,6, and 8 core admixtures are important in the 0.90 MeV transition. The shape of the differential cross section for the 1.61 MeV excitation very clearly indicates that L = 3 transfer is dominant in this transition. An 8% admixture of the $13/2^+$ member of the 2.62 MeV multiplet in the $1i_{13/2}$ single proton state is needed to explain the 1.61 MeV cross section. The cross section for the 2.62 MeV multiplet is consistent with the weak coupling model. (auth)

31004 THE l-FORBIDDEN $3p_{3/2} \rightarrow 2f_{5/2}$ M1 TRANSITION IN ^{207}Pb. Haeusser, O.; Fossan, D. B.; Olin, A.; Ward, D.; Witthuhn, W. (Atomic Energy of Canada Ltd., Chalk River, Ontario. Chalk River Nuclear Labs.); Warner, R. E. (Oberlin Coll., Ohio (USA)). Nucl. Phys., A; 225: No. 3, 425-428(17 Jun 1974).

The branching ratio for the transition from the 0.90 MeV second excited to the 0.57 MeV first excited state in ^{207}Pb has been measured to be (0.59 ± 0.09)%. The corresponding B(M1) exceeds recent theoretical predictions. (auth)

31005 MODEL INDEPENDENT EVALUATION OF THE INELASTIC e^- SCATTERING CROSS SECTIONS FROM THE 3^- (2.615 MeV) LEVEL IN ^{208}Pb. Rothhaas, H.; Friedrich, J.; Merle, K.; Dreher, B. (Mainz Univ. (F. R. Germany). Inst. fuer Kernphysik). Phys. Lett., B; 51: No. 1, 23-25(8 Jul 1974).

The radial transition charge density and the reduced transition probability of the 3^- level in ^{208}Pb are determined model-independently from inelastic e^- scattering cross sections. The results are compared with (α,α') experiments and theoretical calculations. (auth)

31006 DECOUPLED BANDS IN ODD-MASS MERCURY ISOTOPES. Proetel, D.; Benson, D. Jr.; Gizon, A.; Gizon, J.; Maier, M. R.; Diamond, R. M.; Stephens, F. S. (California Univ., Berkeley (USA). Lawrence Berkeley Lab.). Nucl. Phys., A; 226: No. 2, 237-252(1 Jul 1974).

The schemes of the low-lying high-spin states in mercury isotopes with A = 195, 197, and 199 have been studied by γ-ray spectroscopy following (α,xn) reactions on separated platinum targets. Two bands have been excited in each Hg nucleus, one with positive parity based on the isomeric $i_{13/2}$ state and one, probably with negative parity, starting at spin $21/2$. The positive-parity states are interpreted with the rotation-aligned coupling scheme as decoupled bands; this interpretation implies oblate deformation in these three Hg isotopes. The negative-parity states are discussed as a decoupled $i_{13/2}$ neutron state coupled to the 5^-, 7^-, 9^-, . . . states, recently discovered in doubly even mercury isotopes. (auth)

31007 HIGH ENERGY PROTON SCATTERING BY MEDIUM AND HEAVY NUCLEI. Boridy, E.; Feshbach, H. (Massachusetts Inst. of Tech., Cambridge (USA). Lab. for Nuclear Science). Phys. Lett., B; 50: No. 4, 433-437(24 Jun 1974).

The recent data on both elastic and inelastic scattering of 1 GeV protons by ^{40}Ca and ^{208}Pb are analyzed by means of the first term of the multiple scattering series for the optical potential and the DWIA. Theory and experiment agree quite well. Coulomb effects are taken into account. Neutron and proton ground state densities given by Hartree–Fock calculations employing a density-dependent Hamiltonian and which provide a good fit to elastic electron scattering are used. The Tassie form factors, normalized by comparison with inelastic electron scattering, are employed in the DWIA. (auth)

Nuclear Properties and Reactions, $A \geq 220$

Refer also to abstracts 30856, 31026, and 31333.

31008 (AERE-R-7680) ASSESSMENT OF KNOWN INDEPENDENT YIELDS AND THE CALCULATION OF THOSE UNKNOWN IN THE FISSION OF ^{232}Th, ^{233}U, ^{235}U, ^{238}U, ^{239}Pu, ^{240}Pu, AND ^{241}Pu. Crouch, E. A. C. (UKAEA Research Group, Harwell. Atomic Energy Research Establishment). May 1974. 42p. Dep. NTIS (US Sales Only) $5.25.

Known fractional independent and fractional cumulative yields were used to calculate the parameters of Gaussian distributions modified to take account of odd/even atomic number effects. These distributions were used to estimate unknown fractional independent yields. (13 tables, 744 data references) (auth)

31009 (EURFNR-1162) CONTRIBUTION TO THE MUTUAL RESONANCE SHIELDING OF ^{238}U AND ^{239}Pu. Broeders-Siep, I. (Kernforschungszentrum Karlsruhe (F. R. Germany). Inst. fuer Neutronenphysik und Reaktortechnik). Feb 1974. Translation of KFK-1890. 17p. Dep. NTIS $4.00.

Work performed under United States–Euratom Fast Reactor Exchange Program.

The material compositions of a typical sodium-cooled Fast Reactor are used to investigate the influence which the kind of description of the cross section of ^{238}U as a background material has on the effective (n,γ) and fission cross sections of ^{239}Pu, their temperature derivatives and the Doppler coefficient in the energy range between 10 and 465 eV. On one hand, the narrow-resonance (NR) approximation is used with an energy-averaged background cross section, σ_0, in which the contribution of ^{238}U is described in three different ways. In a fourth type of calculation, the full energy and temperature dependence of the ^{238}U total cross section is taken into account in the NR Approximation. The results are compared and discussed. (7 tables) (auth)

31010 (ORO-4282-14) INVESTIGATION OF THE REPORTED MASS DISTRIBUTION CURVES IN THE FISSION OF ^{233}U WITH 14.8 MeV NEUTRONS. James, W. D.; Adams, D. E.; Beck, J. N.; Kuroda, P. K. (Arkansas Univ., Fayetteville (USA). Dept. of Chemistry). 1974. Contract AT(40-1)-4282. 9p. Dep. NTIS $4.00.

The mass yield distribution of fission products in the fission of ^{233}U with 14.8-MeV neutrons was measured for eight mass chains in the symmetric region. This investigation was initiated to resolve existing discrepancies in published data with respect to the fission yields in the valley region and the peak-to-valley ratio. The absolute activities of the nuclides measured were determined from gross beta counting, and total yields were measured relative to ^{132}Te or ^{99}Mo. The standard yields were chosen due to the close agreement of previous data for those mass chains. The peak-to-valley ratio calculated was about 3.5. The fission yields measured in this work were compared to known existing values for 14.8-MeV neutron-induced fission of ^{233}U. (1 figure, 1 table) (auth)

31011 (UCID-15639) STATUS REPORT TO NCSAC. Bowman, C. D. (California Univ., Livermore (USA). Lawrence Livermore Lab.). 4 May 1970. 24p. Dep. NTIS $4.25.

This report begins by discussing progress on the 100-MeV Livermore Electron Accelerator Facility (as of early 1970) and the detection of transition radiation or visible bremsstrahlung. A number of projects in neutron physics are then presented: a doorway state in ^{53}Cr for gamma rays; theory for direct (γ,n) processes in ^{208}Pb; capture cross-section measurements on ^{165}Ho, ^{151}Eu, and natural Eu; measurements of α for ^{235}U from 50 eV to 28 keV; thermal-neutron cross sections of the Ca isotopes; calculation of (n,γ) cross sections; and evaluation of effective interactions. Work in fission physics included an attempt to assign resonance spins of ^{235}U and the keV fission cross section of ^{235}U. (9 figures, 3 tables) (RWR)

31012 MEASUREMENT OF INTERNAL CONVERSION CASCADING IN ^{235}U FISSION FRAGMENTS. Withee, C. J. Urbana, IL; Univ. of Illinois (1973). 143p. University Microfilms Order No. 74-12,254.

Thesis (Ph.D.).

Internal conversion cascading in fragments from thermal-neutron fission of ^{235}U was studied through a measurement of the x rays emitted by the fragments. Two high-resolution Si(Li) semiconductor detectors were used to measure the x rays. The yield of x rays was obtained for the events when two or more x rays were emitted from the same element for the cases of fission and not-fission coincidences and the events when both complementary fission fragments emitted an x ray in coincidence with fission. The yield of x rays from the different elements produced in fission was also measured for single x-ray fission coincidences. It was found that the odd-Z elements of the heavy-fragment region had a higher portion of their x rays emitted in multiple emission events than did the even-Z elements. In the light fragments, a strong restriction of multiple x-ray emission was seen around Z = 38. A dramatic increase in the single x-ray yield per fragment above Z = 57 was seen for the even-Z elements 58 and 60. This rise was not present in the multiple x-ray yields, and hence was attributed to the possible enhancement of single low-energy transitions in the even–even nuclei of these two elements. It was seen that, when a fission fragment emits an x ray, the probability of x-ray emission from the complementary fragment is very low. This result suggests an unequal sharing of the available angular momentum between the two fission fragments. (RWR)

31013 RESONANCE INTEGRALS OF URANIUM-235/URANIUM-238 MIXTURES. Underhill, G. K. Stanford, CA; Stanford University (1974). 249p. University Microfilms Order No. 74-13,698.

Thesis (Ph.D.).

A series of experiments was conducted to measure the shielding effects appearing in the resonance integrals for uranium-235 fission and uranium-238 capture, which originate from the presence of both uranium-238 and uranium-235 in uranium mixtures. This "mutual shielding" effect was investigated by mixing 0.22%- and 93.2%-enriched uranium dioxide powders with lead monoxide powder to obtain uranium dioxide/lead monoxide samples of various dilutions and enrichments. The infinite-dilution resonance integrals obtained were $I^{\infty}_{f,235} = 277.3 \pm 5.4$ barns and $I^{\infty}_{cap,238} = 269.4 \pm 5.2$ barns, based upon $I^{\infty}_{Au} = 1580.6$ barns. The ratio of the single-absorber effective resonance integral to the infinite-dilution resonance integral was measured for uranium-235 fission and uranium-238 capture as a function of the effective scattering cross section per absorber atom. These results are compared with values calculated using a discrete ordinates solution of the integral transport equation. For 15.1%-enriched uranium the fractional decrease of the uranium-235 resonance integral due to shielding of ^{238}U capture resonances was found to be in inverse proportion to the ratio of the effective resonance integral for uranium-238 capture. (RWR)

31014 ENERGY MEASUREMENTS OF DELAYED NEUTRON GROUPS FROM ^{235}U. Naeem, A. Blacksburg, VA; Virginia Polytechnic Inst. and State Univ. (1971). 165p. University Microfilms Order No. 74-16,725.

Thesis (Ph.D.).

The energy spectra of the delayed neutron groups from thermal fission of uranium-235 were measured with a helium-3 fast-neutron spectrometer. The neutron beam from the research reactor was mechanically chopped. The delayed neutrons were detected by a ^{3}He detector (4-inch active length, 10 atmosphere filling pressure). The mechanical chopper and a multichannel analyzer were synchronized such that the data were collected only when the neutron beam from the reactor was in an "off" state. Four chopper speeds were used to measure the delayed neutrons. A computer program was written to analyze the data. Average energies of the various groups were determined. (Diss. Abstr. Int., B)

31015 THERMAL NEUTRON CROSS SECTIONS OF FISSIONABLE ELEMENTS IN THE MULTILEVEL–MULTICHANNEL FORMALISM. Mihailescu, I. M. (Institutul de Fizica Atomica, Bucharest). Stud. Cercet. Fiz.; 25: No. 2, 231-248(1973). (In Rumanian).

After a brief introduction, formulas for neutron cross sections of elements in the multilevel–multichannel formalism are examined; the total, reaction, and scattering cross sections are included. Then the determination of the complex orthogonal transformation matrix and of the poles of the collision matrix is taken up; this is followed by determination of the R-matrix parameters. In the last sections the author gives his conclusions and references. (RWR)

31016 FINE STRUCTURES IN THE MASS YIELD OF ^{252}Cf FISSION FRAGMENTS FROM A DOUBLE-ENERGY MEASUREMENT. Bertin, A.; Bruno, M.; Massa, I.; Vannini, G.; Vitale, A. (Univ., Bologna). Nuovo Cim.; 23A: No. 2, 185-199(21 Sep 1974).

The results of a measurement of the kinetic energies of the complementary fragments released in the spontaneous fission of ^{252}Cf are reported. The pre-neutron emission values of the fragment masses are reconstructed starting from the energies measured. For low excitation energies of the fragments, six fine structures in the mass distribution are observed. These results are discussed referring to previous experimental data, and correlated with preferred even-even charge division in the fission process. (auth)

31017 PERTURBED ALPHA–GAMMA ANGULAR CORRELATION STUDIES OF RADON RECOILS INTO ALUMINIUM. Orre, B.; Norlin, L. O.; Falk, F.; Johansson, K.; Noreland, T.; Arnesen, A. (Uppsala Univ. (Sweden). Fysiska Institutionen). Phys. Lett., B; 51: No. 1, 39-41(8 Jul 1974).

The quadrupole interaction of ^{222}Rn and ^{220}Rn implanted by α-particle decay in Al metal and Al oxide has been investigated.

The experimental results indicate an electrical interaction in cubic Al metal not in agreement with earlier measurements using isotope implanted sources. (auth)

31018 TERNARY FISSION INDUCED BY 540 MeV Fe IONS ON URANIUM. Becker, H. J.; Vater, P.; Brandt, R.; Boos, A. H. (Marburg Univ. (F. R. Germany). Inst. fuer Kernchemie); Diehl, H. (Frankfurt Univ. (F. R. Germany). Inst. fuer Theoretische Physik). Phys. Lett., B; 50: No. 4, 445-447(24 Jun 1974).

The ratio of ternary to binary fission for uranium irradiated with 540 MeV Fe ions was found to be (4.3 ± 0.7)%, when fission fragments in the forward hemisphere of the laboratory system are investigated. The detector was mica, heated after irradiation for 1 hour at 500°C, so as to reveal only fission fragments as tracks. The relatively high yield of ternary fission is interpreted qualitatively on the basis of potential-energy curves for binary fission and prolate ternary fission. The two curves appear to be fairly similar for the two decay modes. (auth)

Nuclear Theory

Refer also to abstracts 30261, 30566, 30753, 30755, 30860, 30865, 30898, 30931, 31037, 31038, and 31141.

31019 (CONF-730693-, pp 1-30) NUCLEOSYNTHESIS OF THE LIGHT ELEMENTS AND THE INTERSTELLAR MEDIUM. Reeves, H. (CNRS, Paris). 1974.

From proceedings of the summer school on particles and fields in space; Balatonfured, Hungary (5 Jun 1973).

The discussion of light element nucleosynthesis covers the build-up of an evolutionary abundance curve, big-bang nucleosynthesis, pregalactic and galactic nucleosynthesis, the effect of stellar evolution, summary of the observations, and the rainy galaxy. (JFP)

31020 (IFA-FT-107-1974) ZEROS OF TRIPLE SCATTERING PARAMETERS AND SPIN–PARITY DETERMINATION OF A RESONANCE. Ion, D. B.; Topor, V. (Institutul de Fizica Atomica, Bucharest (Romania)). 1974. 21p. Dep. NTIS (U. S. Sales Only) $4.25.

A new method for spin–parity determination of a resonance is presented. This method is based on the triple-scattering experiments in the resonance energy region. It is shown that, if one of the triple scattering parameters $a(\theta) = \mathrm{Im}(gh^*)/\sigma_0$, $A(\theta)$, or $\beta(\theta)$ is measured for $0° \leq \theta \leq 180°$, then the spin and parity of the resonance are unambiguously determined by the zeros number and the sign of these parameters in the different angular intervals. (5 figures, 5 tables) (auth)

31021 (IFA-FT-108-1974) ONE- AND TWO-NUCLEON TRANSFER REACTIONS ON DEFORMED NUCLEI. Dumitrescu, O. (Institutul de Fizica Atomica, Bucharest (Romania)). 1974. 50p. Dep. NTIS (U. S. Sales Only) $5.25.

One- and two-nucleon-transfer reactions are analyzed first formally by applying the projection procedure in the sense of Feshbach and Weidenmüller. The generalized optical-model potentials for both elastic and inelastic channels are obtained in terms of renormalized interactions. A comparison with the empirical optical-model potential is made. By some numerical examples, some approximations and techniques for the scattering state vector, such as DWBA, coupled-channels theory, and adiabatic theory, are discussed. (10 figures, 3 tables) (auth)

31022 NEW DESCRIPTION OF NUCLEAR SCATTERING AT INTERMEDIATE ENERGIES AND PERMISSIBILITY OF GLAUBER EXPRESSION TO LARGE-ANGLE ELASTIC SCATTERING. Kohmura, T.; Negishi, T. (Tokyo Univ. of Education). Progr. Theor. Phys. (Kyoto); 51: No. 2, 518-527(Feb 1974).

Using the accumulative method for phase shifts, we show that the phase shifts for potential scattering are equal to the phase shifts in the Born approximation to first order in $\mu V/k^2$ with the reduced mass μ, the potential V and the momentum k. The phase shift δ_l at energies above several hundred MeV, being additive and smooth with l, is closely related to the phase function $\chi(b)$ in the eikonal expression. The phase shifts for scattering from a bound target particle are linear combinations (redistribution) of those for scattering in free space. The Glauber expression is shown to be valid for elastic scattering at angles up to $\theta_c \sim 40°$, and gives an order estimate of the differential cross section at angles $\theta > \theta_c$. A high-energy approximation leads to a new description of the scattering amplitude, valid also at angles $\theta < \theta_c$. With only a few terms, the expression in terms of Bessel functions reproduces the universal features of angular distributions for nuclear elastic scattering. (auth)

31023 NEW ANALYTICAL DERIVATION OF KERNELS IN THE RESONATING GROUP METHOD FOR COMPOSITE-PARTICLE SCATTERING AND MOLECULE-LIKE STRUCTURES. Derivation from Kernels in the Generator Coordinate Method and Application to $^{16}O + \alpha$. Kamimura, M.; Matsuse, T. (Kyushu Univ., Fukuoka). Progr. Theor. Phys. (Kyoto); 51: No. 2, 438-466(Feb 1974).

Exchange kernels in the resonating group method are derived analytically from those in the generator coordinate method without any use of inverse operators of Gauss transformation. The whole kernels of the $^{16}O + \alpha$ system with Coulomb interaction are given, divided into various exchange mechanisms. Derivation in the cases where two interacting nuclei have different oscillator parameters and where other channels are included is also presented. (auth)

31024 SELF–CONSISTENT CALCULATION OF THE OPTICAL POTENTIAL AND GROUND–STATE PROPERTIES OF NUCLEAR MATTER. Ho–Kim, Q. (Department of Physics, Laval University, Quebec, Canada G1K 7P4); Khanna, F.C. Ann. Phys. (N.Y.) 86: No. 2, 233-261 (Aug 1974).

On the basis of the Green–function formalism, we performed a self–consistent calculation of the self–energy Σ (k, ω) of a particle interacting with the infinite nuclear medium. The function Σ (k, ω) was mapped out in the energy–momentum plane, and the single–particle energy ω (k), momentum distribution ρ (k) and the "on–shell" part of the self–energy, Σ (k, ω (k)), were defined, from which all physical properties followed. In particular we investigated the ground–state properties of nuclear matter in two Λ–approximations of the T–matrix. In one, the intermediate two–particle propagator, Λ_{00}, represented free–particle propagation; in the other, called Λ_{11}, intermediate states included both interacting particles and holes. Pauli principle effects were included in both approximations. The second approximation was expected to be conserving because it included a large part of the rearrangement effects, which, we found, contributed ~6 MeV per particle to the average energy and ~28 MeV to the single–particle energy at zero momentum. The Hugenholtz–van Hove theorem was nearly satisfied, with only 1 MeV separating the chemical potential from the average energy. We also studied, in the Λ_{00}–approximation, the optical potential for the scattering of a particle by a large nucleus; it was directly related to the "on–shell" part of the self–energy. It was found that, below 100 MeV, the real part varied as (−90+0.584E) [MeV], and the imaginary part as (2.4+0.009 E) [MeV]. (auth)

31025 THE ENERGY DENSITY FORMALISM AND THE SHELL STRUCTURE EFFECTS. Beiner, M.; Lombard, R.J. (Institute de Physique Nucléaire, Division de Physique Théorique, 91406—Orsay—France). Ann. Phys. (N.Y.) 86: No. 2, 262-305 (Aug 1974).

The Brueckner formulation of the energy density formalism has been extended in order to take into account shell structure effects in the description of nuclear bulk properties. The energy density is calculated by using a density-dependent effective interaction of the type $V_{eff}=g(\rho)\ \delta\ (r_1-r_2)+\bar{V}_l(r_1-r_2)$. The function $g(\rho)$ can be determined from nuclear matter calculations. The second term of the interaction is a long-range part in the Moszkowski–Scott sense, which is supposed to contribute only in the surface of finite system and for which use is made of the gradient expansion. A phenomenological l·s term is also included. The nuclear ground states are described by products of neutron and proton B.C.S. wavefunctions. The pairing matrix elements are derived from a realistic two–body interaction. The ground state properties are obtained by minimizing the total energy with respect to effective single-particle orbitals and their corresponding occupation numbers. The variational principle leads to Hartree–Fock–BCS equations which can be solved by iterations. The calculations have been performed for a very large number of nuclei distributed throughout the periodic table. The method is shown to reproduce the bulk nuclear properties accurately: binding energies and radii are in good agreement with experiments. The calculated charge distributions yield good fits to experimental elastic electron scattering data. Finally, the single-particle levels close to the Fermi surface are also consistent with experimental spectroscopic data. (auth)

31026 SUPERHEAVY ELEMENTS AND THE STRUTINSKY PRESCRIPTION. Chasman, R.R. (Chemistry Division, Argonne National Laboratory, Argonne, Illinois 60439). Phys. Rev. Lett. 33: No. 9, 544-547 (26 Aug 1974).

Cases are found in which the Strutinsky prescription for single–particle corrections to the liquid–drop model fails. Estimates of the spontaneous–fission lifetimes of superheavy elements are found to be overly sensitive to small changes in the assumed single–particle level spectrum. (auth)

31027 INFLUENCE OF CORE EXCITATIONS ON THE DEUTERON STRIPPING REACTION WITH THE METHOD OF MANY–BODY GREEN FUNCTIONS. Ethofer, S. (Hahn–Meitner–Institut für Kernforschung Berlin, Sektor Kernphysik, Berlin–West, Germany); Schuck, P. Ann. Phys. (N.Y.) 86: No. 2, 306-330 (Aug 1974).

Within the scope of many–body Green functions we derive a formally exact expression for the (d,p) –stripping amplitude, which resembles the DWBA for this reaction. However, the distorted wavefunctions in the entrance and exit channel are defined with respect to the most general expressions for the optical potentials, as they are given by the mass operators of corresponding Dyson equations for correlation functions. In the same way the transition operator is a complicated many–body quantity which explicitly depends on the deuteron energy and contains for example contributions coming from the core excitations of the target nucleus. In this paper we are mainly interested in the latter effect and a numerical estimation of a crude model for the many–body effects of the transition operator reveals no pronounced (sharply resonant) energy dependence. The essential difference of our paper to other publications on the same subject is that we are dealing with the "Dyson equation" approach developed recently for higher Green functions. (auth)

31028 DETERMINATION OF REACTION AMPLITUDES FROM EXPERIMENTAL OBSERVABLES. Goldstein, G. R. (Tufts Univ., Medford, MA); Moravcsik, M. J.; Bregman, D. Lett. Nuovo Cim.; 11: No. 2, 137-141(14 Sep 1974).

A completely general prescription is given for necessary and sufficient conditions for reactions containing particles with arbitrary spins. The problem is treated in the context of a question common to all relevant situations: given a set of experimental observables, are the amplitudes uniquely determined? (JFP)

31029 BOUNDARY VALUE PROBLEM FOR INTEGRO-DIFFERENTIAL EQUATIONS. Huss, R.; Kalaba, R.; Vasudevan, R. (Univ. of California, Los Angeles). J. Math. Phys. (N. Y.); 15: No. 8, 1285-1287(Aug 1974).

A boundary value problem of a linear differential-integral equation is converted to a Cauchy system by means of parameter imbedding. Numerical results are shown for an equation from nuclear physics. (auth)

31030 FOUR-BODY CORRELATIONS IN NUCLEI. Yokoi, T. (Nagoya Univ., Japan). Progr. Theor. Phys. (Kyoto); 51: No. 3, 760-778(Mar 1974).

Dynamical aspects of four-body correlations are investigated. The dependence of four-quasi-particle energy spectra on the effective quasi-four-body interaction strength is qualitatively discussed. Conditions of the validity of quasi-particle approximations in the treatment of four-body correlations are given, and a schematic calculation of an imaginary solution is made. (auth)

31031 NUCLEAR MANY-BODY PROBLEM. Volume I. Proceedings of the International Symposium, Rome, Italy, September 19–23, 1972. Calogero, F.; Ciofi Degli Atti, C. (eds.). Bologna; Editrice Compositori (1973). 910p. (CONF-720933–P1).

Thirty-nine papers are included; the title of each paper is listed. (LBS)

For titles of individual papers see: 30631, 30753, 30857–30861, 30903, 30918, and 31032–31061.

31032 RIGOROUS CONSTRAINTS THAT NUCLEAR FORCES MUST SATISFY TO BE CONSISTENT WITH THE SATURATION PROPERTY OF NUCLEAR BINDING ENERGIES. Calogero, F. (Univ., Rome); Simonov, Yu. A. pp 51-126 of Nuclear Many-Body Problem. Vol. I. Calogero, F. (ed.). Bologna; Editrice Compositori (1973).

From symposium on present status and novel developments in the nuclear many-body problem; Rome, Italy (19 Sep 1972). See CONF-720933–P1.

31033 RELATIVISTIC ONE-BOSON-EXCHANGE POTENTIAL, TWO-NUCLEON DATA, NUCLEAR MATTER, AND NEUTRON MATTER PROPERTIES. Alzetta, R.; Erkelenz, K.; Holinde, K. (Institut fuer Theoretische Kernphysik, Bonn). pp 127-144 of Nuclear Many-Body Problem. Vol. I. Calogero, F. (ed.). Bologna; Editrice Compositori (1973).

From symposium on present status and novel developments in the nuclear many-body problem; Rome, Italy (19 Sep 1972). See CONF-720933–P1.

31034 REALISTIC TWO-NUCLEON PHENOMENOLOGICAL POTENTIAL. Ulehla, I. (Rutherford High Energy Lab., Chilton, Eng.). pp 145-160 of Nuclear Many-Body Problem. Vol. I. Calogero, F. (ed.). Bologna; Editrice Compositori (1973).

From symposium on present status and novel developments in the nuclear many-body problem; Rome, Italy (19 Sep 1972). See CONF-720933–P1.

31035 REALISTIC SUPER-SOFT-CORE POTENTIAL MODEL OF THE N–N INTERACTION. Sprung, D. W. L.; de Tourreil, R. (McMaster Univ., Hamilton, Ont.). pp 161-175 of Nuclear Many-Body Problem. Vol. I. Calogero, F. (ed.). Bologna; Editrice Compositori (1973).

From symposium on present status and novel developments in the nuclear many-body problem; Rome, Italy (19 Sep 1972). See CONF-720933–P1.

31036 NEW DETERMINATION OF MONGAN'S NON-LOCAL SEPARABLE POTENTIALS FOR NUCLEAR STRUCTURE CALCULATIONS. Meyer, J.; Nahabetian, R.; Pigeon, J.; Fayard, C.; Lamot, G. H.; El Baz, E. (Univ. Claude Bernard, Lyon). pp 176-182 of Nuclear Many-Body Problem. Vol. I. Calogero, F. (ed.). Bologna; Editrice Compositori (1973).

From symposium on present status and novel developments in the nuclear many-body problem; Rome, Italy (19 Sep 1972). See CONF-720933–P1.

31037 NEUTRON–NEUTRON EFFECTIVE RANGE PARAMETERS FROM FEW-NUCLEON EXPERIMENTS. Breunlich, W. H. (Univ. of California, Los Angeles). pp 183-195 of Nuclear Many-Body Problem. Vol. I Calogero, F. (ed.). Bologna; Editrice Compositori (1973).

From symposium on present status and novel developments in the nuclear many-body problem; Rome, Italy (19 Sep 1972). See CONF-720933–P1.

31038 NUCLEON–NUCLEON INTERACTION AND LOW-ENERGY PROPERTIES OF THREE-NUCLEON SYSTEMS. van Wageningen, R. (Univ., Amsterdam). pp 196-214 of Nuclear Many-Body Problem. Vol. I. Calogero, F. (ed.). Bologna; Editrice Compositori (1973).

From symposium on present status and novel developments in the nuclear many-body problem; Rome, Italy (19 Sep 1972). See CONF-720933–P1.

31039 GROUND-STATE PROPERTIES OF THREE-NUCLEON SYSTEMS: A REVIEW. Nunberg, P. (CNEN, Rome); Prosperi, D.; Pace, E. pp 215-289 of Nuclear Many-Body Problem. Vol. I. Calogero, F. (ed.). Bologna; Editrice Compositori (1973).

From symposium on present status and novel developments in the nuclear many-body problem; Rome, Italy (19 Sep 1972). See CONF-720933–P1.

31040 THREE-NUCLEON REACTIONS AND OFF-SHELL BEHAVIOR OF THE NUCLEON–NUCLEON INTERACTION. Lovas, I. (Central Research Inst. for Physics, Budapest). pp 290-314 of Nuclear Many-Body Problem. Vol. I. Calogero, F. (ed.). Bologna; Editrice Compositori (1973).

From symposium on present status and novel developments in the nuclear many-body problem; Rome, Italy (19 Sep 1972). See CONF-720933–P1.

31041 PRESENT STATUS AND OPEN PROBLEMS IN FEW-NUCLEON SYSTEMS. Slaus, I. (Rudjer Boskovic Inst., Zagreb). pp 315-333 of Nuclear Many-Body Problem. Vol. I. Calogero, F. (ed.). Bologna; Editrice Compositori (1973).

From symposium on present status and novel developments in the nuclear many-body problem; Rome, Italy (19 Sep 1972). See CONF-720933–P1.

31042 OFF-SHELL EFFECTS OF THE NUCLEON–NUCLEON FORCE IN NUCLEON–NUCLEON BREMSSTRAHLUNG. Drechsel, D. (Univ., Mainz). pp 334-348 of Nuclear Many-Body Problem. Vol. I. Calogero, F. (ed.). Bologna; Editrice Compositori (1973).

From symposium on present status and novel developments in the nuclear many-body problem; Rome, Italy (19 Sep 1972). See CONF-720933–P1.

31043 CALCULATIONS ON FEW-NUCLEON SYSTEMS WITH CORRELATED WAVE FUNCTIONS. Rosati, S. (Univ., Pisa, Italy); Fantoni, S. pp 345-375 of Nuclear Many-Body Problem. Vol. I. Calogero, F. (ed.). Bologna; Editrice Compositori (1973).

From symposium on present status and novel developments in the nuclear many-body problem; Rome, Italy (19 Sep 1972). See CONF-720933–P1.

31044 USE OF LIPPMANN–SCHWINGER EQUATIONS IN THE THREE-BODY PROBLEM. Gloeckle, W. (Univ., Heidelberg). pp 349-353 of Nuclear Many-Body Problem. Vol. I. Calogero, F. (ed.). Bologna; Editrice Compositori (1973).

From symposium on present status and novel developments in the nuclear many-body problem; Rome, Italy (19 Sep 1972). See CONF-720933–P1.

31045 CORRELATION EFFECTS ON THE GROUND-STATE ENERGY AND FORM FACTOR OF FEW-BODY SYSTEMS. Ciofi Degli Atti, C. (Istituto Superiore di Sanita, Rome). pp 376-396 of Nuclear Many-Body Problem. Vol. I. Calogero, F. (ed.). Bologna; Editrice Compositori (1973).

From symposium on present status and novel developments in the nuclear many-body problem; Rome, Italy (19 Sep 1972. See CONF-720933-P1.

31046 APPLICATION OF TROTTER'S FORMULA TO A FEW-NUCLEON PROBLEM. Fano, G. (Univ., Bologna). pp

405-410 of Nuclear Many-Body Problem. Vol. I. Calogero, F. (ed.). Bologna; Editrice Compositori (1973).
From symposium on present status and novel developments in the nuclear many-body problem; Rome, Italy (19 Sep 1972). See CONF-720933-P1.

31047 TWO-BODY T-MATRIX FACTORIZATION AND THREE-NUCLEON PROBLEM. Efimov, V. N. (Joint Inst. for Nuclear Research, Dubna, USSR); Fenin, Yu. I.; Tkachenko, E. G. pp 411-412 of Nuclear Many-Body Problem. Vol. I. Calogero, F. (ed.). Bologna; Editrice Compositori (1973).
From symposium on present status and novel developments in the nuclear many-body problem; Rome, Italy (19 Sep 1972). See CONF-720933-P1.

31048 MESON FIELD THEORY OF NUCLEI AND THE N-N INTERACTION. Green, A. E. S. (Univ. of Florida, Gainesville); Riewe, F.; Nack, M. L.; Miller, L. D. pp 415-474 of Nuclear Many-Body Problem. Vol. I. Calogero, F. (ed.). Bologna; Editrice Compositori (1973).
From symposium on present status and novel developments in the nuclear many-body problem; Rome, Italy (19 Sep 1972). See CONF-720933-P1.

31049 ENERGY DENSITY FORMALISM AND THE SHELL STRUCTURE OF NUCLEI. Lombard, R. J. (Institut de Physique Nucleaire, Orsay, France). pp 475-489 of Nuclear Many-Body Problem. Vol. I. Calogero, F. (ed.). Bologna; Editrice Compositori (1973).
From symposium on present status and novel developments in the nuclear many-body problem; Rome, Italy (19 Sep 1972). See CONF-720933-P1.

31050 HYPERSPHERICAL-EXPANSION APPROACH TO NUCLEAR BOUND STATES. Simonov, Yu. A. (Univ., Rome). pp 528-564 of Nuclear Many-Body Problem. Vol. I. Calogero, F. (ed.). Bologna; Editrice Compositori (1973).
From symposium on present status and novel developments in the nuclear many-body problem; Rome, Italy (19 Sep 1972). See CONF-720933-P1.

31051 HYPERSPHERICAL EXPANSION APPROACH FOR NUCLEAR REACTIONS. Raynal, J. (CEN, Saclay, France). pp 589-604 of Nuclear Many-Body Problem. Vol. I. Calogero, F. (ed.). Bologna; Editrice Compositori (1973).
From symposium on present status and novel developments in the nuclear many-body problem; Rome, Italy (19 Sep 1972). See CONF-720933-P1.

31052 APPLICATION OF THE GENERATOR COORDINATE METHOD TO NUCLEAR BOUND STATES AND TO SCATTERING. Mihailovic, M. V. (Univ., Ljubljana, Yugoslavia). pp 605-626 of Nuclear Many-Body Problem. Vol. I. Calogero, F. (ed.). Bologna; Editrice Compositori (1973).
From symposium on present status and novel developments in the nuclear many-body problem; Rome, Italy (19 Sep 1972). See CONF-720933-P1.

31053 GENERALIZED EULERIAN ANGLES AND THE COLLECTIVE MOTION OF MANY-PARTICLE SYSTEM. Filippov, G. F.; Ovcharenko, V. I.; Steshenko, A. I. (Inst. of Theoretical Physics, Kiev). pp 627-668 of Nuclear Many-Body Problem. Vol. I. Calogero, F. (ed.). Bologna; Editrice Compositori (1973).
From symposium on present status and novel developments in the nuclear many-body problem; Rome, Italy (19 Sep 1972). See CONF-720933-P1.

31054 LINEAR AND ANGULAR LOCALIZATION EFFECTS IN NUCLEAR STRUCTURE CALCULATIONS. Hilton, R. R. (Univ., Hacettepe, Ankara, Turkey). pp 669-684 of Nuclear Many-Body Problem. Vol. I. Calogero, F. (ed.). Bologna; Editrice Compositori (1973).
From symposium on present status and novel developments in the nuclear many-body problem; Rome, Italy (19 Sep 1972). See CONF-720933-P1.

31055 MICROSCOPIC APPROACHES TO THE OPTICAL-MODEL POTENTIAL. Jeukenne, J. P.; Lejeune, A.; Mahaux, C. (Univ., Liege). pp 748-771 of Nuclear Many-Body Problem. Vol. I. Calogero, F. (ed.). Bologna; Editrice Compositori (1973).
From symposium on present status and novel developments in the nuclear many-body problem; Rome, Italy (19 Sep 1972). See CONF-720933-P1.

31056 SCATTERING FROM CORRELATED SYSTEMS. Shakin, C. M.; Thaler, R. M. (Case Western Reserve Univ., Cleveland). pp 772-783 of Nuclear Many-Body Problem. Vol. I. Calogero, F. (ed.). Bologna; Editrice Compositori (1973).
From symposium on present status and novel developments in the nuclear many-body problem; Rome, Italy (19 Sep 1972). See CONF-720933-P1.

31057 DYNAMICAL IMPLICATIONS OF CORRELATIONS. Agodi, A. (Univ., Catania, Italy). pp 784-804 of Nuclear Many-Body Problem. Vol. I. Calogero, F. (ed.). Bologna; Editrice Compositori (1973).
From symposium on present status and novel developments in the nuclear many-body problem; Rome, Italy (19 Sep 1972). See CONF-720933-P1.

31058 EXACT METHODS FOR TREATING NONLINEAR PROBLEMS IN MANY-BODY THEORY. Schiffrer, G. (Univ., Catania, Italy). pp 805-827 of Nuclear Many-Body Problem. Vol. I. Calogero, F. (ed.). Bologna; Editrice Compositori (1973).
From symposium on present status and novel developments in the nuclear many-body problem; Rome, Italy (19 Sep 1972). See CONF-720933-P1.

31059 EFFECTIVE TWO-BODY INTERACTION FOR EQUIVALENT PARTICLES. Johnson, M. B. (Cornell Univ., Ithaca, NY); Molinari, A.; Bethe, H. A. pp 828-854 of Nuclear Many-Body Problem. Vol. I. Calogero, F. (ed.). Bologna; Editrice Compositori (1973).
From symposium on present status and novel developments in the nuclear many-body problem; Rome, Italy (19 Sep 1972). See CONF-720933-P1.

31060 RENORMALIZED EFFECTIVE NUCLEAR INTERACTION BY EXPLICIT TRUNCATION AND USE OF THE RESULTS OF A LARGE CONFIGURATION SPACE. Gupta, R. K. (Panjab Univ., India). pp 865-871 of Nuclear Many-Body Problem. Vol. I. Calogero, F. (ed.). Bologna; Editrice Compositori (1973).
From symposium on present status and novel developments in the nuclear many-body problem; Rome, Italy (19 Sep 1972). See CONF-720933-P1.

31061 STATUS OF POTENTIAL MODELS. de Tourreil, R. (Univ. Paris-Sud, Orsay, France). pp 872-887 of Nuclear Many-Body Problem. Vol. I. Calogero, F. (ed.). Bologna; Editrice Compositori (1973).
From symposium on present status and novel developments in the nuclear many-body problem; Rome, Italy (19 Sep 1972). See CONF-720933-P1.

31062 DIFFRACTIVE PRODUCTION OFF NUCLEI: SHADOW OF HADRONIC BREMSSTRAHLUNG. Bialas, A.; Czyz, W. (Max-Planck-Institut fuer Physik und Astrophysik, Munich). Acta Phys. Pol., B; 5: No. 4, 523-530(1974).
Diffractive production on nuclei is calculated using as an input a specific model for diffractive production on nucleons. In this model diffractive production is described as a shadow of non-diffractive multiple production of particles. The mechanism for non-diffractive production is taken to be hadronic bremsstrahlung of independently produced clusters. It is shown that such a model naturally explains the strikingly simple pattern of absorption observed in coherent production on nuclei. Possible generalizations of these results are indicated. (auth)

31063 IMPORTANCE OF COULOMB INTERACTION POTENTIALS IN HEAVY ION DWBA CALCULATIONS. DeVries, R. M. (Univ. of Rochester, NY); Satchler, G. R.; Cramer, J. G. p 61 of Proceedings of the International Conference on Reactions Between Complex Nuclei. Vol. I and Suppl. Robinson, R. L. (ed.). New York; American Elsevier Publishing Co., Inc. (1974).
From international conference on reactions between complex nuclei; Nashville, Tennessee, USA (10 Jun 1974). See CONF-740637-(P1 and Suppl.).

31064 FUSION OF HEAVY NUCLEI IN A CLASSICAL MODEL. Bass, R. (Univ., Frankfurt am Main). p 117 of Proceedings of the International Conference on Reactions Between Complex Nuclei. Vol. I and Suppl. Robinson, R. L. (ed.). New York; Elsevier Publishing Co., Inc. (1974).
From international conference on reactions between complex nuclei; Nashville, Tennessee, USA (10 Jun 1974). See CONF-740637-(P1 and Suppl.).

31065 MECHANISM OF HEAVY ION COLLISIONS LEADING TO A COMPOUND SYSTEM AND TO DEEP INELASTIC DIRECT REACTIONS. Gross, D. H. E.; Kalinowski, H. (Hahn-Meitner-Institut, Berlin). p 118 of Proceedings of the International Conference on Reactions Between Complex Nuclei. Vol. I and Suppl. Robinson, R. L. (ed.). New York; Elsevier Publishing Co., Inc. (1974).

From international conference on reactions between complex nuclei; Nashville, Tennessee, USA (10 Jun 1974). See CONF-740637-(P1 and Suppl.).

31066 MICROSCOPIC TREATMENT OF VISCOSITY IN HEAVY ION REACTIONS. Glas, D.; Mosel, U. (Univ., Giessen, Ger.). p 121 of Proceedings of the International Conference on Reactions Between Complex Nuclei. Vol. I and Suppl. Robinson, R. L. (ed.). New York; Elsevier Publishing Co., Inc. (1974).

From international conference on reactions between complex nuclei; Nashville, Tennessee, USA (10 Jun 1974). See CONF-740637-(P1 and Suppl.).

31067 CALCULATION METHOD FOR A HIGH MOMENT OF ENERGY SPECTRA. The Case When Intrinsic Spin is Fixed. Nomura, M. (Tokyo Univ.). Progr. Theor. Phys. (Kyoto); 51: No. 2, 489-505(Feb 1974).

A calculation method is developed which enables algebraic treatment of the isospin-fixed (or seniority-fixed or S-fixed) high moment of energy spectra in a many-body configuration. It is essential to get a recursion relation for the average energy of a many-body interaction and to solve it as a boundary condition problem. Shell model techniques and the branching diagram are well used. As a simple application of the result, the first three moments with isospin being fixed are evaluated for the case of the $(0g_{9/2})^n$ configuration. (auth)

31068 THEORY OF COLLECTIVE EXCITATIONS IN SPHERICAL ODD-MASS NUCLEI. III. Electromagnetic Properties of the Anomalous Coupling States. Kuriyama, A. (Kyushu Univ., Fukuoka); Marumori, T.; Matsuyanagi, K. Progr. Theor. Phys. (Kyoto); 51: No. 3, 779-810(Mar 1974).

Various electromagnetic properties of the anomalous coupling states with spin (j−1) are shown to be well explained by the new viewpoint of the dressed n-quasi-particle modes proposed in a previous paper. In this point of view, the anomalous coupling collective states with spin (j−1) are considered as the dressed three-quasi-particle modes, which are regarded as a kind of elementary excitation mode in odd-mass nuclei. The effects of couplings between dressed three-quasi-particle modes and one-quasi-particle modes are also discussed in this connection, including those with spin j, (j−1) and (j−2). (auth)

31069 A SIMPLE DESCRIPTION OF DIFFERENTIAL CROSS SECTIONS FOR HEAVY ION INDUCED REACTIONS. Kahana, S.; Bond, P. D.; Chasman, C. (Brookhaven National Lab., Upton, N. Y. (USA)). Phys. Lett., B; 50: No. 2, 199-203(27 May 1974).

A semi-quantitative picture of heavy-ion induced transfer reactions is presented for non-vanishing angular momentum transfer L. The distinctive physics of the heavy-ion reactions, as reflected in the phase and magnitudes of the radial integrals, plays a crucial role in the derivation. The result is a simplified and inclusive description of the angular shapes and magnetic-state (M) dependence of the partial cross sections σ_M^L. (auth)

31070 ON THE DETERMINATION OF THE EFFECTIVE BARRIER IN HEAVY ION COLLISIONS. Da Silveira, R. (Paris-11 Univ., 91-Orsay (France). Inst. de Physique Nucleaire). Phys. Lett., B; 50: No. 2, 237-240(27 May 1974).

A simple method is given to obtain the effective barrier V_e between two colliding heavy nuclei based on the fact that, for a given incident energy E, the rainbow angle is determined mainly by the ratio E/V_e and only to a small extent by the potential shape and parameters. (auth)

31071 THE ABSENCE OF EXCITED TARGET CONTRIBUTIONS TO E1 PARTIAL WIDTHS OF NEUTRON RESONANCES: AN EXPLANATION FROM THRESHOLD EFFECTS. Lane, A. M. (UKAEA Research Group, Harwell. Atomic Energy Research Establishment). Phys. Lett., B; 50: No. 2, 204-206(27 May 1974).

The success of the "valence model" of resonance neutron capture in certain nuclei shows that E1 partial widths can be dominated by target ground state contributions, i.e. excited states contribute very little. This cannot be understood solely in terms of the composition of the final states, which often have strong excited target components. An explanation is found in terms of threshold effects on the initial (resonance) state composition. (auth)

31072 THE DIFFRACTION DISSOCIATION OF DEUTERONS ON THE DIFFUSED EDGE NUCLEI. Sitenko, A. G.; Polozov, A. D.; Evlanov, M. V. (AN Ukrainskoj SSR, Kiev. Inst. Teoreticheskoj Fiziki). Phys. Lett., B; 50: No. 2, 229-232(27 May 1974).

The dependence of the cross sections of various diffraction processes on the diffuseness of the nuclear edge is calculated in the interaction of high-energy deuterons with nuclei. The dependence of the deuteron dissociation cross section on the mass number, conditioned by the influence of the nuclear edge diffuseness, is shown. (auth)

31073 NUCLEAR MUON CAPTURE: A SIMPLE MODEL. Kozlowski, T.; Zglinski, A. (Institute of Nuclear Research, Warsaw (Poland)). Phys. Lett., B; 50: No. 2, 222-224(27 May 1974).

A simple model of the nuclear muon capture, based on the giant resonance supermultiplet states excitation, is presented. A unified description of the total capture rate and the emitted particle spectra has been obtained. (auth)

31074 FRAGMENTATION OF HIGHLY EXCITED HEAVY IONS. Bhaduri, R. K. (McMaster Univ., Hamilton, Ontario (Canada). Dept. of Physics). Phys. Lett., B; 50: No. 2, 211-212(27 May 1974).

The observed universal momentum distribution of the fragments of a heavy ion resulting from high energy impact with a target is explained on the basis of a simple statistical model. (auth)

31075 QUANTIZED FRICTION AND THE CORRESPONDENCE PRINCIPLE: SINGLE PARTICLE WITH FRICTION. Kan, K.-K.; Griffin, J. J. (Maryland Univ., College Park (USA). Dept. of Physics and Astronomy). Phys. Lett., B; 50: No. 2, 241-243(27 May 1974).

A non-linear time-dependent Schrodinger equation is derived by means of physical arguments and the correspondence principle to describe a quantal system acted upon by a frictional force. It involves non-linear terms of the same type as those already derived by Kostin for the Schrodinger-Langevin problem. Exact solutions are exhibited in closed form for the case of an harmonic oscillator. They exhibit reasonable properties and support the belief that the equation proposed provides an appropriate physical description. (auth)

31076 K-ELECTRON CAPTURE TO POSITRON EMISSION RATIOS AND THE SECOND CLASS CURRENTS PROBLEM. Ledingham, K. W. D.; Gourlay, J. Y.; Campbell, M.; Fitzpatrick, M. L.; Baillie, A. D. (Glasgow Univ. (UK). Dept. of Natural Philosophy). Phys. Lett., B; 50: No. 2, 247-248(27 May 1974).

A recent review has shown that experimental K-electron capture to positron emission ratios disagree with theory. This disagreement may be removed by using a correction factor introduced when mesonic second class currents are considered. (auth)

31077 TREATMENT OF CONTINUA IN THE SHELL-MODEL THEORY OF NUCLEAR REACTIONS. Zaidi, S. A. A.; Tyan, Y. L. (Texas Univ., Austin (USA). Center for Nuclear Studies). Phys. Lett., B; 50: No. 3, 305-308(10 Jun 1974).

It is shown that by a suitable choice of the bound- and continuum-state functions used to perform shell-model calculations, the continuum-continuum interaction may be minimized. Approximate expressions for the scattering matrix elements are derived that are easily evaluated by simple extensions of the conventional shell-model calculations for bound states. Numerical calculations are performed for neutron scattering from ^{12}C within the framework of the deformed rotor model and compared with exact coupled-channel calculations. (auth)

31078 HOW GOOD IS THE COLLECTIVE MODEL. Bertsch, G.; Tsai, S. F. (Michigan State Univ., East Lansing (USA). Dept. of Physics). Phys. Lett., B; 50: No. 3, 319-322(10 Jun 1974).

Hartree-Fock RPA theories of ^{208}Pb are used as a testing ground for collective models of the inelastic scattering transition densities. For isoscalar transitions, the standard collective model and the Tassie model both provide excellent descriptions of the transition density to the strongest states. For the isovector dipole mode, two states are found. The lower state has a transition density resembling the Steinwedel-Jensen model, while the upper state has a transition density resembling the Goldhaber-Teller model. The energetics of the collective states, as summarized in heuristicly derived sum rules, are quite close to the results of the RPA calculations. (auth)

31079 NEW SOURCE OF DECOUPLING OF E1 STRENGTH FROM THE GDR: BOUNDARY CONDITION MIXING FOR s- AND p-WAVE NEUTRON STATES NEAR THRESHOLD. Gyarmati, B. (Inst. of Nuclear Research, Hungarian Academy of Sciences, Debrecen, Hungary); Lane, A. M. (UKAEA Research Group, Harwell. Atomic Energy Research Establishment); Zimanyi, J. (Central Research Institute, Budapest, Hungary). Phys. Lett., B; 50: No. 3, 316-318(10 Jun 1974).

Non-statistical effects in neutron capture reveal that E1 strength of neutron orbits of low l-value is partially decoupled from the GDR. Particle-hole diagonalisations with realistic forces do not show this effect. It is shown that it can arise from a new source, boundary condition mixing, which operates when fine-structure states are introduced. This may also explain the "pygmy dip" in E1 strength reported for masses ~195. (auth)

31080 STATIC VISCOSITY OF NUCLEAR MATTER. Wegmann, G. (Muenchen Univ. (F. R. Germany). Sektion Physik). Phys. Lett., B; 50: No. 3, 327-329(10 Jun 1974).

The static shear viscosity η_0 of symmetric nuclear matter is estimated. It is found that for reasonable nuclear temperatures the mean free path connected with η_0 is considerably larger than the nuclear radii. It is therefore concluded that the concept of viscosity cannot be applied to nuclear fission and heavy ion collisions without taking into account the nuclear surface. (auth)

31081 CENTRE OF MASS MOTION AND SINGLE PARTICLE SEPARATION ENERGIES IN HARTREE–FOCK THEORY. Khadkikar, S. B.; Kamble, V. B. (Physical Research Lab., Ahmedabad (India)). Nucl. Phys., A; 225: No. 2, 352-356(10 Jun 1974).

An expression for single particle separation energies taking into account centre of mass motion is derived. It is shown that the separation energy and the variational determinantal state of a nucleus are independent of the form of the Hamiltonian used. (auth)

31082 THEORY OF FRAGMENTATION DYNAMICS IN NUCLEUS-NUCLEUS COLLISIONS. Fink, H. J.; Maruhn, J.; Scheid, W.; Greiner, W. (Frankfurt Univ. (F. R. Germany). Inst. fuer Theoretische Physik). Z. Phys.; 268: No. 3, 321-331(Jun 1974).

5 figs.; 24 refs.

The fragmentation of a nuclear system is described by a dynamical coordinate, the fragmentation coordinate $\gamma = (A_1 - A_2)/(A_1 + A_2)$. The total Hamiltonian describing a binary heavy ion encounter includes a term which describes the fragmentation and its coupling to other degrees of freedom. It is a collective Hamiltonian which is calculated from the microscopic Asymmetric Two-Center Shell Model (ATCSM). The properties of this Hamiltonian are extensively discussed and methods for its solution are described. Formulae for cross sections of specific nuclear fragmentations including fusion are derived. (auth)

31083 THE TREATMENT OF TWO PARTICLES IN THE CONTINUUM IN A GREEN'S FUNCTION THEORY OF THE (d,p)-REACTION. Froebrich, P. (Hahn-Meitner-Institut fuer Kernforschung Berlin G. m. b. H. (F. R. Germany)). Z. Phys.; 268: No. 3, 307-311(Jun 1974).

1 fig.; 1 tab.; 7 refs.

It is shown that a numerical treatment of two particles in the continuum is possible in applying the Green's function method to the (d,p)-reaction. A basis set for shell model states including the continuum in an approximate way is established and applied to the expansion of the incoming deuteron wave function into these basis states. As a test for the convergence of this expansion the sum of the squares of the expansion coefficients is calculated and found to be 0.965 instead of 1. The main contribution comes from the bound-bound and the bound-continuum configurations. The continuum-continuum contributions can be practically neglected. (auth)

31084 EXPERIMENTAL PHOTONUCLEAR CROSS SECTION CALCULATION. Deberth, C.; Cirstoiu, B. (Inst. of Atomic Physics, Bucharest). Stud. Cercet. Fiz.; 24: No. 10, 1201-1210 (1972). (In Rumanian).

The method used to solve the experimental photonuclear cross section equation is discussed and formulated in terms of the unfolding distribution theory. The boundary conditions, needed to solve the photonuclear problem, are justified. The photonuclear problem to be solved is formulated in a matrix form and an algorithm is given. On the basis of this algorithm a BASIC FORTRAN IV program was written for an IBM 360/40 computer. (auth)

31085 INNER BREMSSTRAHLUNG IN ELECTROMAGNETIC ZERO–ZERO TRANSITIONS IN NUCLEI. Burkhardt, H.; Zia, R. K. P.; Owen, D. R. (Univ. of Birmingham, Eng.). J. Phys., B (London); 7: No. 10, 1167-1170(1 Jul 1974).

The general form of the final state distribution is given for inner bremsstrahlung by the electron pair produced in 0–0 nuclear transitions with no parity change. The expression for the resultant photon energy spectrum is given and evaluated numerically for the transition in ^{16}O. (auth)

31086 ON THE EFFECTIVE TWO BODY MAGNETIC DIPOLE OPERATOR. Shimizu, K.; Arima, A. (State Univ. of New York, Stony Brook (USA). Dept. of Physics). Phys. Lett., B; 50: No. 4, 417-420(24 Jun 1974).

Second-order corrections of magnetic moments are decomposed into one-body and two-body effects. The two-body effect is estimated for nuclei with two holes or two particles beyond an LS closed shell. The result shows that the effect is negligibly small. (auth)

31087 A NOTE ON DIFFRACTION PHENOMENA IN THE INELASTIC SCATTERING OF COMPLEX NUCLEI. Landowne, S.; Takigawa, N. (Hahn-Meitner-Institut fuer Kernforschung Berlin G.m.b.H. (F. R. Germany). Bereich Kern- und Strahlenphysik). Phys. Lett., B; 50: No. 4, 414-416(24 Jun 1974).

It is illustrated how oscillations in angular distributions for inelastic scattering of heavy ions can be produced by diffraction effects arising from the variation of the excitation amplitudes. (auth)

31088 π-CONDENSATION IN A FINITE SYSTEM AND PROPERTIES OF NUCLEI. Migdal, A. B.; Kirichenko, N. A.; Sorokin, G. A. (L. D. Landau Inst. for Theoretical Physics, Moscow, USSR). Phys. Lett., B; 50: No. 4, 411-413(24 Jun 1974).

π-condensation in a finite system and its influence on the shape of a nucleus and the moment of inertia are considered. Electron scattering on nuclei is discussed. (auth)

31089 QUALITATIVE FEATURES OF PAULI BREAK-UP FROM THE CONFIGURATION SPACE VIEWPOINT. Gambhir, B. L. (Rochester Univ., N. Y. (USA). Dept. of Physics and Astronomy); Griffin, J. J. (Maryland Univ., College Park (USA). Dept. of Physics and Astronomy). Phys. Lett., B; 50: No. 4, 407-410(24 Jun 1974).

A dimensionless measure of the effect of Pauli exclusion upon the neutron–proton interaction in a projectile deuteron is calculated in the zero-range approximation for a Hulthen deuteron. One learns thereby that the Pauli breakup matrix element is distributed differently in space from that for nuclear break-up and that the effect increases rapidly with decreasing energy to a large value at the lowest deuteron energies. (auth)

31090 A WEAK COUPLING MODEL FOR HIGH-SPIN STATES. Wiebicke, H. J.; Muenchow, L. (Zentralinstitut fuer Kernforschung, Rossendorf bei Dresden (German Democratic Republic)). Phys. Lett., B; 50: No. 4, 429-432(24 Jun 1974).

Weak coupling of a rotating core and an odd particle is used to explain the appearance of pure rotational bands, as well as decoupled aligned state bands, by simple geometrical properties. (auth)

31091 SELF-SCREENING OF THE PARTICLE–HOLE INTERACTION AND CORE POLARIZATION OF THE EFFECTIVE TWO-PARTICLE INTERACTION. Kuo, T. T. S. (State Univ. of New York, Stony Brook (USA). Dept. of Physics); Osnes, E. (Oslo Univ. (Norway). Fysisk Institutt). Nucl. Phys., A; 226: No. 2, 204-218(1 Jul 1974).

The diagrams of the Tamm–Dancoff and random-phase approximations (TDA and RPA) have been summed to calculate the core polarization of the effective interaction between two nucleons in the 1s0d and 1p0f shells. The large core-polarization corrections obtained in the TDA and particularly the RPA are strongly reduced when the self-screening corrections to the particle–hole and ground-state correlation vertices are included. The screening corrections serve to suppress the collectivity of the core phonons and, in particular, to stabilize the isoscalar monopole phonon in ^{40}Ca against collapse. When screening is included, the TDA and RPA give core-polarization corrections which are similar in magnitude and in many cases lead to good agreement with experiment. Because of neglected effects and other uncertainties, the qualitative rather than the quantitative features of the results are stressed. (auth)

31092 ON THE NUCLEAR I·L POTENTIAL. Love, W. G. (Georgia Univ., Athens (USA)). Nucl. Phys., A; 226: No. 2, 319-325(1 Jul 1974).

Formulas are given for calculating the I·L (target spin) potential arising from single nucleon exchange effects and the nucleon–projectile two-body spin–orbit force. An estimate of the strength of this potential is made for the scattering of ^{4}He from ^{9}Be and ^{59}Co. While the effects arising from single nucleon exchange are found to be much more important than those arising from the two-body spin–orbit force, neither mechanism is sufficiently important to explain the experimental data. (auth)

31093 INTERMEDIATE-STATE TRANSITION RATES IN THE EXCITON MODEL. Oblozinsky, P.; Ribansky, I.; Betak, E. (Slovenska Akademia Vied, Bratislava (Czechoslovakia). Fyzikalny Ustav). Nucl. Phys., A; 226: No. 2, 347-364(1 Jul 1974).

A new method is described for deriving the intermediate-state transition rates in the exciton model of nuclear reactions. Transition rates are derived for particle–hole state densities of the equidistant-spacing model both including and neglecting the Pauli exclusion principle. Ericson's and Williams' state-density formulas were used in calculations. The obtained relations for the Pauli-principle-corrected transition rates are compared with exact results of direct calculations. It is shown that these relations are sufficiently accurate, especially in the region where Williams' state density also works well. (auth)

31094 SHELL EFFECTS ON STATE DENSITIES WITH GIVEN NUMBER OF EXCITED PROTONS AND NEUTRONS. Berger, J. F. (CEA Centre d'Etudes de Bruyeres-le-Chatel, 92 – Montrouge (France)); Martinot, M. (CEA Centre d'Etudes Nucleaires de Saclay, 91 – Gif-sur-Yvette (France). Dept. de Physique Nucleaire). Nucl. Phys., A; 226: No. 3, 391-412(8 Jul 1974).

A new method is introduced to calculate particle – hole state densities which takes into account the complete structure in both the proton and neutron shells. The results are given for three nuclei: ^{208}Pb, ^{172}Yb and ^{117}Sn. They are compared with previous formulas and with two other expressions derived in the present paper. Strong shell effects are displayed and discussed. (auth)

31095 THE VALIDITY OF THE FACTORIZATION HYPOTHESIS FOR NUCLEUS-NUCLEUS CROSS SECTIONS AT HIGH ENERGIES. Barshay, S. (State Univ. of New York, Stony Brook (USA)); Dover, C. B.; Vary, J. P. (Brookhaven National Lab., Upton, N. Y. (USA)). Phys. Lett., B; 51: No. 1, 5-8(8 Jul 1974).

Nucleus – nucleus cross sections are calculated for a variety of projectile and target nuclei and a wide range of energy. Total, reaction and elastic cross sections, as well as the slopes of the elastic diffraction peak, exhibit an approximate factorization property when the nuclei differ by less than 50% in r.m.s. radii. A simple geometrical interpretation is provided for the failure of factorization which occurs when target and projectile differ greatly in size. (auth)

31096 TRANSPARENCY TO VECTOR POLARIZATION TRANSFER IN DEUTERON STRIPPING REACTIONS. Santos, F. D. (Junta de Energia Nuclear, Sacavem (Portugal). Lab. de Fisica e Engenharia Nucleares). Phys. Lett., B; 51: No. 1, 14-16(8 Jul 1974).

For certain deuteron polarizations, when the spin transfer is pure $s = {}^{1}\!/_{2}$, it is shown that deuteron stripping reactions are transparent to vector polarization transfer and the outgoing nucleon polarization is independent of scattering angle and deuteron energy. With $s = {}^{3}\!/_{2}$ contributions there is still considerable transparency at the stripping main peak in DWBA calculations. (auth)

31097 SENSITIVITY OF INELASTIC PION SCATTERING TO NON-LOCAL INTERACTIONS. Koltun, D. S.; Nalcioglu, O. (Rochester Univ., N. Y. (USA). Dept. of Physics and Astronomy). Phys. Lett., B; 51: No. 1, 19-22(8 Jul 1974).

It is shown that the excitation of nuclear electric dipole states by small-angle inelastic scattering of pions can be used to detect the degree of non-locality of the pion – nucleus scattering matrix. (auth)

31098 SELF-CONSISTENT WAVE FUNCTIONS, CENTER-OF-MASS MOTION AND HIGH-ENERGY PARTICLE – NUCLEUS SCATTERING. Ciofi degli Atti, C. (Istituto Superiore di Sanita, Rome (Italy). Laboratori di Fisica); Guardiola, R. (Barcelona Univ. (Spain). Departamento de Fisica Teorica). Phys. Lett., B; 51: No. 1, 26-30(8 Jul 1974).

Elastic electron and hadron scattering by ^{4}He and ^{16}O is calculated; for the latter nucleus Brueckner – Hartree – Fock (BHF) wave functions obtained in the harmonic oscillator representation are used. The effects of the center-of-mass motion spuriosity are estimated. (auth)

31099 STATISTICAL PROPERTIES OF A PAIRED NUCLEUS WITH FIXED QUASIPARTICLE NUMBER. Moretto, L. G. (California Univ., Berkeley (USA). Dept. of Chemistry). Phys. Lett., B; 51: No. 1, 35-38(8 Jul 1974).

The pairing Hamiltonian, diagonal in the quasiparticle space, has been used to determine the statistical and thermodynamical properties of a system with a fixed number of quasiparticles. The formalism can describe the phase transition occurring at fixed energy as the system relaxes from the initial to the equilibrium quasiparticle number. (auth)

31100 DOPPLER SHAPE OF A γ-LINE IN COULOMB EXCITATION. Erokhina, K. I.; Lemberg, I. Kh.; Pasternack, A. A. (AN SSSR, Leningrad. Fiziko-Tekhnicheskij Inst.). Nucl. Instrum. Methods; 118: No. 2, 373-380(15 Jun 1974).

Calculations of the Doppler-shifted γ-line shape in the case of Coulomb excitation and using a thick target are made. The energy loss as a result of elastic ion-atomic collisions is taken into account through approximating an exact expression of the Lindhard's theory. Taking into account multiple scattering of recoil nuclei is effected by using a specially introduced distribution function which makes it possible to calculate the first two moments. It is shown that the method in which only the first moment of a distribution is calculated to take into account multiple scattering may result in biased estimates of the life-time values obtained. The estimates of the errors inherent in the method under consideration are based on the calculations made. The expression for the γ-line shape is obtained in a form allowing a generalization in case of any kinematics of a nuclear reaction. (auth)

31101 INFLUENCE OF PAIRING AND OF THE SPIN PROJECTION DISTRIBUTION ON THE "CLASSICAL" ISOTHERMAL ROTATIONS OF A NUCLEUS. Moretto, L. G. (California Univ., Berkeley (USA). Dept. of Chemistry). Nucl. Phys., A; 226: No. 1, 9-30(24 Jun 1974).

The properties of spherical, paired nuclei with finite angular momentum are discussed in terms of "classical" rotations. Rotational quantities like the angular velocity and the moment of inertia are calculated both for the yrast line ($T = 0$) and for higher temperatures. Particular attention is paid to the superfluid features associated with the pairing correlation. Three different models are considered. The first model is characterized by a constant spacing in the single-particle levels and by a constant spin projection, and it is treated analytically in the zero-temperature limit. It is shown that this model leads to a very strong back-bending. Calculations accounting for the pairing fluctuations are shown. The second model differs from the first one in the spin projection distribution which, in analogy with a spherical shell model nucleus, is taken to be rectangular. Analytical calculations show that, while strong superfluid properties remain, the back-bending seen in the previous model disappears. The third model used is the shell model. Numerical calculations of the angular velocities and of the moments of inertia are compared with the results obtained from the previous two models. A remarkable agreement is observed between the second model and the shell model. (auth)

31102 FINITE SIZE α-PARTICLE CALCULATIONS OF ABSOLUTE α-DECAY FOR SPHERICAL NUCLEI. Furman, V. I.; Holan, S.; Kadmensky, S. G.; Stratan, G. (Joint Inst. for Nuclear Research, Dubna (USSR)). Nucl. Phys., A; 226: No. 1, 131-141(24 Jun 1974).

Recently, some important results have been obtained in calculating absolute α-decay widths, the calculations having been performed in the zero-range α-particle approximation. In this paper the effects of the finite size of the α-particle are considered. Two important effects have been found: (i) for the finite-size calculation, the absolute α-decay widths decrease by 2 to 3 orders of magnitude, and (ii) the finite-size effects are strongly dependent on the shell model configuration of the initial nucleus. In the framework of the superfluid model the absolute probabilities of finite-size α-particle emission have been calculated for the favored α transitions of more than 200 spherical nuclei. The theoretical α widths turn out to be smaller than the experimental ones by a factor of 10, which is approximately constant for all the nuclei studied. (auth)

31103 SOLUTIONS OF THE INTEGRAL EQUATIONS FOR FOUR IDENTICAL PARTICLES. Kharchenko, V. F. (AN Ukrainskoj SSR, Kiev. Inst. Teoreticheskoj Fiziki); Kuzmichev, V. E.; Shadchin, S. A. (AN Ukrainskoj SSR, Kiev. Inst. Yadernykh Issledovanij). Nucl. Phys., A; 226: No. 1, 71-92 (24 Jun 1974).

By using the separable representation of the scattering amplitudes for the subsystems $3 + 1$ and $2 + 2$, the integral equations for four identical particles with a separable two-particle interaction are reduced to a set of single-variable integral equations. By solving the equations obtained, the binding energies and wave functions of the low-lying 0^{+} states of the system of four identical bosons, as well as the scattering length of a particle scattered by three bound particles, are calculated. The solution of the set of integral equations describing the bound state of four nucleons is found by approximating the space wave function by a symmetric one, and the binding energy and wave function of the ^{4}He nucleus are calculated. (auth)

31104 A THREE PARAMETER NUCLEON – NUCLEUS OPTICAL MODEL ON THE ENERGY SHELL. Sinha, B.; Duggan, F. (King's Coll., London (UK). Wheatstone Physics Lab.). Nucl. Phys., A; 226: No. 1, 31-44(24 Jun 1974).

An optical model has been developed in which the imaginary potential has been calculated theoretically under the assumption that it arises entirely from the forward scattering amplitude of nucleon – nucleon scattering. The two-body effective interaction used to calculate the imaginary potential has a finite range, in contradistinction to a zero-range interaction used by previous authors. The real central part has also been generated theoret-

ically by folding in a two-body effective interaction with the target nucleon density. A simple local approximation has been used to calculate the exchange term. The spin–orbit potential is generated using the Blin-Stoyle prescription. This model, which consists of three depth parameters, predicts the elastic scattering and polarization data as well as the standard ten-parameter phenomenological model. The present model is a general one, which can be used for optical model analysis. (auth)

PHYSICS (RADIATION AND SHIELDING)

Radiation Physics

Refer also to abstracts 29556, 29562, 29718, 30482, and 30948.

31105 (UCID-15784) FINE STRUCTURE GENERALIZATION OF THE COMPTON FOKKER–PLANCK EQUATION. Cooper, G. (California Univ., Livermore (USA). Lawrence Livermore Lab.). Oct 1970. 31p. Dep. NTIS $4.75.

Some preliminary results are given on the differential model for multigroup calculations of radiation transport through a fully ionized medium. (JFP)

31106 RADIATION LEVELS OF MACRORADIOGRAPHY. Takahashi, S.; Sakuma, S; Ayakawa, Y.; Maekoshi, H.; Ohara, K. (Nagoya Univ., Japan). Radiology; 112: No. 3, 709-713(Sep 1974).

Macroradiography via 4 to 6 times magnification of a test chart in water phantoms of various thicknesses, using an x-ray tube with 50 μ focal spot, is described. Its MTF improves when water depth is reduced. Long exposure of a moving organ in a thick water phantom reduces its image quality. For macroradiography of the human body, the skin dose can be limited to less than 1 rad. Appropriate beam limitation as well as shortening of the focus-film distance, use of the fastest film-screen combination and high-voltage technique are recommended. Clinical macroradiography is described in detail. (auth)

31107 SIMPLIFIED METHOD FOR CALCULATING DOSE-RATE DISTRIBUTIONS FROM EXTENDED VOLUMES CONTAINING GAMMA EMITTERS. Kushelevsky, A. P.; Valley, J. F.; Lerch, P. (Ecole Polytechnique Federale, Lausanne, Switzerland). Brit. J. Radiol.; 47: No. 560, 471-473(Aug 1974).

A generalized practical method to calculate dose-rate distributions from extended homogeneous radioactive sources in an infinite aqueous medium, taking into account build-up and attenuation factors, is presented. The method is based on data given by Berger (MIRD pamphlet No. 2, Journal of Nuclear Medicine, 1968, 9, Supplement No. 1, p. 15). The case of a homogeneous spherical radioactive source is treated for purposes of illustration. (auth)

31108 BACK-SCATTERING FROM METALS IN SUPERFICIAL THERAPY WITH HIGH ENERGY ELECTRONS. Saunders, J. E.; Peters, V. G. (Ontario Cancer Treatment and Research Foundation, Hamilton). Brit. J. Radiol.; 47: No. 560, 467-470(Aug 1974).

In the treatment of ear, eyelid, nose and lip lesions with 3 to 8 MeV electrons, lead shields are often used to protect underlying tissue. The characteristics of electron back-scatter from lead and metals of different atomic number, Z, were investigated for electron beams in the above energy range using monocrystalline layers of LiF powder to measure dose. The dose from electron back-scatter increased approximately in proportion to $Z^{1/2}$ but decreased slightly with increasing primary electron energy. The energy of the back-scattered electrons was sufficient to penetrate several millimetres of polystyrene and increased with Z and primary energy. The overdosage produced by back-scatter from eye-shields in the total skin treatment of patients with 3.1 MeV electrons may be reduced from 80 per cent to 35 per cent by using 2.2 mm of stainless steel instead of lead. In the treatment of localized lesions at 6.4 MeV, the overdosage may be reduced from 73 per cent to 15 per cent by covering the lead with 2 mm of aluminium. (auth)

31109 SPECTRAL CHARACTERISTICS OF γ RADIATION ^{60}Co SCATTERED IN THIN RADIATORS. Kheteev, M. V.; Stavitskii, R. V. (All-Union Scientific-Research Inst. of Radiation Tech. and Dept. of Sanitation, Moscow). Med. Radiol.; 19: No. 7, 66-72(Jul 1974). (In Russian).

Results are presented of investigation conducted with the help of a spectrometer of complete absorption of spectral characteristics of ^{60}Co γ-radiation scattered in thin cylindric radiators. The influence of thickness and atomic number of the radiator on the quantitative composition of radiation is also considered. The results were given in the charts of contribution of different energy components to the general dose from scattered radiation; the dependence of the factors of accumulation upon the thickness and atomic number of the radiator was also shown. As an example, the spectra of the absorbed doses in bone tissue was considered. It was shown that the contribution of a low-energy part of the spectrum to the dose absorbed in bone tissue may be considerable. (auth)

31110 DOSE FIELDS IN CONVERGENT IRRADIATION BY A NARROW BEAM OF PROTONS. Blokhin, S. I.; Breev, V. M.; Kleinbok, Ya. L.; Lomanov, M. F.; Narinskii, V. M. Med. Radiol.; 19: No. 7, 50-56(Jul 1974). (In Russian).

A narrow beam of protons with energy of 200 MeV was obtained on the protonic synchrotron ITEP (Moscow) for convergent irradiation of the hypophysis. The system of forming and the technique of measuring dose fields are described. To measure dose distributions the authors used a hard radiodefect detector which records fragments of a heavy nucleus fission. Phantom measurements were made and isodose charts for round (diameter 5–7 mm) and oval (with axes of 6 and 8 mm) cross-sections were obtained. The obtained dose fields have high gradients on the margin: decrease from 75 down to 25 per cent of the dose was achieved as a distance of 5 mm along the temporal line and by 1.5 mm perpendicular to this line. The authors measured the dose equivalent in different regions of the patient's head which comprised 0.1 ÷ 1 per cent from the local dose at distances more than 10 mm from the margin of the beam. This makes it possible to apply a single dose to the hypophysis which is necessary for suppression of its function with insignificant radiation loading on the head and body of the patient. (auth)

31111 ASSESSMENT OF DIAGNOSTIC X-RAY EQUIPMENT. Airth, G. R. (Southmead Hospital, Westbury-on-Tryme, Bristol, Eng.). Brit. J. Radiol.; 47: No. 560, 512(Aug 1974).

Following a recent announcement that the DHSS has set up a Radiology Advisory Committee to assess and report on the value of new diagnostic x-ray equipment, the author points out that the British Institute of Radiology inaugurated a similar sub-committee 21 years ago, but this ceased to function in 1957. It is hoped by the author that the new Radiology Advisory Committee of the DHSS will be more successful in ensuring that its recommendations are followed up. (UK)

31112 INTRODUCTION TO THE DISCUSSION ON CHARACTERISTICS OF INSTALLATIONS FOR RADIOTHERAPY WITH FAST NEUTRONS AND OTHER TYPES OF HIGH-LET RADIATION. Bewley, D. K. (Hammersmith Hospital, London). Eur. J. Cancer; 10: No. 4, 201-202(Apr 1974).

From 2nd meeting on fundamental and practical aspects of the application of fast neutrons in clinical radiotherapy; The Hague, Netherlands (3 Oct 1973).

The clinical requirements for the potential use of high-LET radiations such as fast neutrons, heavy ions and negative pi-mesons in radiotherapy are briefly surveyed, and related to the projected and available facilities for the production of fast neutrons and negative pi-mesons described in eighteen of the papers presented at the Conference. (UK)

31113 ENERGY LOSS AND PROJECTED RANGE OF ALPHA PARTICLES IN ZINC TELLURIDE. Bontemps, A.; Ligeon, E.; Fontenille, J. (CEN, Grenoble, France). Radiat. Eff.; 21: No. 3, 181-184(Mar 1974).

The helium stopping cross section in zinc telluride was measured for energies varying from 300 keV to 2 MeV. Up to an energy $E\alpha \simeq 600$ keV, dE/dx is not far from $kE^{1/2}$ (Lindhard, Scharff and Schiott theory). Values given by the Bethe theory were reached only for $E\alpha > 1.6$ MeV. By a "bursting" method the projected range was also measured and the values are in accordance with those computed from the experimental data of dE/dx. (auth)

31114 HELIUM ION STOPPING CROSS SECTIONS IN BISMUTH, LEAD, AND TUNGSTEN. Borders, J. A. (Sandia Labs., Albuquerque, NM). Radiat. Eff.; 21: No. 3, 165-169(Mar 1974).

The stopping cross sections of He ions in bismuth, lead and tungsten have been measured at incident energies from 0.4 MeV to 1.9 MeV. The energy losses of helium ions in vacuum evaporated films of bismuth and lead and sputtered films of tungsten were determined using a backscattering technique. Atomic areal densities were measured by a microbalance technique for the bismuth and lead films. The thicknesses of the tungsten films were determined by multiple-beam interferometry and a density of 0.93× atomic density was assumed in order to evaluate the areal density. Brice's (Phys. Rev.; A6: 1791 (1972)) three parameter formula has been fit to the data. Comparison of the results has also been made with the semi-empirical calculations and the experimental results of Chu, et al. (Appl. Phys. Letters; 22: 437 (1973)) and those of Lin, et al. (Phys. Rev.; to be published). (auth)

31115 ELECTRONIC STOPPING POWER OF CHANNELLED IONS IN A MODEL INCORPORATING THE PAULI PRINCIPLE. Ali, S. P.; Gallagher, D. F. (Univ. of Western Ontario, London). J. Phys., C (London); 7: No. 14, 2434-2446(21 Jul 1974).

Electronic energy-loss calculations have been performed for incident ions with charges ranging from $Z_1 = 1$ to $Z_1 = 50$ channelling in Si, Ge, Al, Cu, Au and W crystals. The calculations are carried out within a model due to Cheshire which itself is an extension of a model employed by Briggs and Pathak. Energy-loss S_e against Z_1 curves have been constructed with an electron-ion interaction potential of Thomas–Fermi form. The dependence of this S_e against Z_1 relation for a given target (fixed Z_2) on the incident-ion speed v_1 has also been found as well as the S_e against Z_2 dependence for fixed Z_1 and v_1. Predictions of the model for the S_e against Z_1 dependence (fixed Z_2) are in fairly good general agreement with experiment, the experimental oscillatory structure of the curves being confirmed in the calculations. Although the model produces oscillatory structure in the S_e against Z_2 (fixed Z_1) curves as has been seen experimentally by Whitton, the theoretical oscillations are considerably out of phase with the experimental ones. Suggestions are made for refinements of the model to attempt to improve the agreement with experiment in both Z_1 and Z_2. (auth)

31116 NEGATIVE PIONS IN RADIOTHERAPY. A Brief Review. Raju, M. R. (Los Alamos Scientific Lab., NM). Eur. J. Cancer; 10: No. 4, 211-215(Apr 1974).

From 2nd meeting on fundamental and practical aspects of the application of fast neutrons in clinical radiotherapy; The Hague, Netherlands (3 Oct 1973).

The frequency and energy distribution of fast-neutron interaction products such as protons, alpha particles, and heavy recoils and those arising from negative pion absorption processes are similar. Because of these similarities in radiation quality of negative pions and fast neutrons in the treatment volume, the therapeutic experience of fast neutrons is relevant for negative pions as well. However, in the case of negative pions, dose deposited in the treatment volume extends to much lower LET values than for fast neutrons because a significant fraction of the dose is deposited by energy losses of negative pions. The biological effectiveness for nearly monoenergetic negative pions at the peak of the depth-dose distribution was found to be significantly higher than at the entrance. For pion beams of larger momentum spread that are therapeutically relevant, the differences in biological effectiveness are reduced considerably; however, a significant reduction in OER still can be expected. Considerable changes in biological effectiveness within the peak region have been found. These changes will be reduced when opposed fields of negative pions are used. Although the current knowledge on biological effects sheds some light regarding what to expect when negative pion beams are used in therapy, more work needs to be done with intense negative pion beams before its possible therapeutic use. (auth)

31117 RADIOBIOLOGY WITH HEAVY CHARGED PARTICLES DIRECTED AT RADIOTHERAPY. Todd, P. (Pennsylvania State Univ., University Park). Eur. J. Cancer; 10: No. 4, 207-210 (Apr 1974).

From 2nd meeting on fundamental and practical aspects of the application of fast neutrons in clinical radiotherapy; The Hague, Netherlands (3 Oct 1973).

Work is beginning in the United States directed at the treatment of tumours other than those of pituitary and brain using range-modulated heavy charged particles. The biological effectiveness and the oxygen dependence of the mixed radiations in the treatment zone are being evaluated by studying the inactivation of human cells in three-dimensional cultures. Experimental depth-survival profiles are presented for range-modulated protons, helium ions, and oxygen ions. In the cases of oxygen and helium ions a decreased O_2 dependence and increased effectiveness were observed. The use of a flat dose profile in the treatment zone did not necessarily lead to a flat survival profile. (auth)

31118 TRANSMISSION AND REFLECTION OF ELECTRONS BY FOILS. Seltzer, S. M.; Berger, M. J. (National Bureau of Standards, Washington, D. C. (USA)). Nucl. Instrum. Methods; 119: No. 1, 157-179(1 Jul 1974).

Monte Carlo calculations pertaining to the penetration of electron beams through foils are described. The method of calculation is validated by comparisons with experimental transport data at energies between 50 keV and 1 MeV. New data are presented on the transmission and reflection of electrons through beryllium, mylar, aluminum, and titanium foils, for incident beam energies between 100 and 400 keV. The results given include transmission and reflection coefficients and the energy spectra and angular distributions of transmitted electron beams. (auth)

31119 CALCULATIONS ON TISSUE EQUIVALENCE FOR STOPPING π^- MESONS. Armstrong, T. W.; Chandler, K. C. (Oak Ridge National Lab., Tenn. (USA)). Nucl. Instrum. Methods; 119: No. 1, 125-129(1 Jul 1974).

Calculations have been made of the energy deposition in tissue-equivalent plastic (Shonka type A-150) and tissue when both are placed in the stopping region of a negatively charged pion beam. The configuration considered is that of relatively small pieces of tissue-equivalent plastic (thicknesses of 50 and 3000 μm) placed in a large π^- capture region. The multiplicities and energies of the π^- capture products were determined using an intranuclear cascade-evaporation model, and the energy deposition was obtained using computed stopping powers and ranges. (auth)

31120 CALCULATED PARTICLE-PRODUCTION SPECTRA FROM π^- CAPTURES IN TISSUE, TISSUE-EQUIVALENT PLASTIC, SILICON, AND GERMANIUM. Armstrong, T. W.; Chandler, K. C (Oak Ridge National Lab., Tenn. (USA)). Nucl. Instrum. Methods; 118: No. 2, 515-524(15 Jun 1974).

An intranuclear-cascade-evaporation model has been applied to predict the energy spectra of the products (neutrons, protons, deuterons, tritons, ^{3}He's, alpha particles, and residual nuclei) from π^- capture in several materials (tissue, tissue-equivalent plastic, silicon, and germanium) of interest in pion dosimetry. Also, the energy spectra of the products from 90 MeV π^- interactions in tissue are computed. (auth)

31121 CHARGE-STATE AND ENERGY DISTRIBUTIONS OF XENON IONS IN CARBON. Loew, R. (Technion-Israel Inst. of Tech., Haifa. Dept. of Physics). Nucl. Instrum. Methods; 118: No. 2, 505-508(15 Jul 1974).

Equilibrium charge-state fractions and stopping power of Xe ions passing through a thin carbon foil were measured in the energy interval between 300–700 keV. (auth)

31122 ENERGY DISPERSION OF DEUTERONS DURING THEIR PASSAGE THROUGH MATTER. Influence of the State of the Surface. Weber, G.; Quaglia, L. (Liege Univ. (Belgium). Inst. de Physique Nucleaire). Nucl. Instrum. Methods; 118: No. 2, 573-581(15 Jun 1974). (In French).

In order to explain the large differences existing between the experimental and theoretical values of the energy dispersion of charged particles after passing through metallic absorbers, the surface effect of the absorber has been investigated. The superficial irregularities seem to be the main cause of the differences mentioned above. Furthermore, a very simple calculation allows the determination of an equivalent mean irregular depth from the dispersion measurements. (auth)

Radiation Protection Standards

Refer also to abstract 29790.

Radiation Source Calibration and Standardization

31123 (UCID-15938) GEOMETRIC SOLUTION OF FINITE X-RAY SOURCE IRRADIATING TWO CONCENTRIC CYLINDERS CONTAINING X-RAY ABSORBING MATERIAL. Robertson, T. V. (California Univ., Livermore (USA). Lawrence Livermore Lab.). 9 Nov 1971. 14p. Dep. NTIS $4.00.

A solution is presented for the following problem: a finite x-ray source at z = DT in a plane parallel to the xy plane irradiates a target of two concentric cylinders whose axis is the line z = DTF in the yz plane. The problem is approximated in two dimensions by a slit source of length SPS irradiating a cross section of the cylinders. The target material is described by four absorption coefficients α_i, $i = 1, 2, 3, 4$; such that a ray traveling a length l through material i will be attenuated by a factor of $e^{-l\alpha_i}$. The x-ray intensity at any x on the film is to be found. (MHR)

31124 CHARACTERISTICS OF ^{252}Cf NEUTRON SOURCES USED FOR RADIOTHERAPY. Anderson, L. L. (Sloan-Kettering Inst. for Cancer Research, New York). Eur. J. Cancer; 10: No. 4, 203-205(Apr 1974).

From 2nd meeting on fundamental and practical aspects of the application of fast neutrons in clinical radiotherapy; The Hague, Netherlands (3 Oct 1973).

Medical neutron sources using ^{252}Cf are currently available for both intracavitary and interstitial radiotherapy. Neutron absorbed dose distributions have been measured primarily with applicator tube sources but were little affected by variations in source encapsulation. Agreement among various laboratories was poorer for neutrons than for gamma rays, which typically contributed only about one third of the total absorbed dose near the source. Recommended neutron dosimetry data, corrected for geometrical attenuation, showed a slowly varying exponential decrease with distance from the source, with a value at 1 cm of about 2.4 rad $cm^2\ \mu g^{-1}\ hr^{-1}$. Measured average LETs ranged from 30 to 45 keV μ^{-1}, depending on the contribution of gamma rays to the dose. A new, small afterloading cell for interstitial brachytherapy will incorporate only enough beta ray filtration to reduce the beta-gamma dose rate at 0.5 cm to approximately the neutron dose rate level. (auth)

31125 INTENSITIES OF γ-RAYS IN THE DECAY OF ^{166m}Ho. Lingeman, E. W. A.; de Boer, F. W. N.; Meijer, B. J. (Instituut voor Kernphysisch Onderzoek, Amsterdam (Netherlands)). Nucl. Instrum. Methods; 118: No. 2, 609(15 Jun 1974).

A quite good relative intensity calibration of a semi-conductor γ-ray detector, as well as an energy calibration in the 80–1000 keV can be performed by using only ^{166m}Ho as a source. New values are given for relative γ-ray intensities in the decay of ^{166m}Ho, that can be used for intensity calibration. (auth)

Shielding Calculations and Experiments

Refer also to abstract 31271.

31126 (ORNL-RSIC-25(Suppl.2)) SHIELDING BENCHMARK PROBLEMS. Simmons, G. L. (Ed.). (Oak Ridge National Lab., Tenn. (USA)). Jul 1974. Contract W-7405-eng-26. 71p. Dep. NTIS $5.45.

The Benchmark Problems Group of the American Nuclear Society Shielding Standards Subcommittee (ANS-6) has selected several "benchmark" problems for testing computational methods of radiation transport. Problems are described and solution data are presented. It is anticipated that publication of these problems will serve to focus attention so that careful work will produce solutions which are representative of the state-of-the-art. The problems will also serve to specify standard configurations so that meaningful comparisons can be made between different calculational methods and between experimental and calculational results. Supplement 2 provides a calculational problem (polyethylene slab) which can be treated in one or two dimensions, and an experimental problem (deep neutron penetration in sodium) with calculational solutions. (auth)

31127 RADIATION ABSORBING SHIELD FOR PERSONNEL AND MATERIALS AND METHOD OF MAKING SAME. (to Dow Chemical Co.). Netherlands Patent 7,217,655. 27 Dec 1972. Priority Date 30 Dec 1971, USA. 17p. (In Dutch).

A radiation absorbing shield is constructed by providing within confining walls a continuous or particulate gelled aqueous solution containing suitable soluble and/or insoluble radiation absorbing metal salts, or metal particles uniformly dispersed throughout the gelled solution. Monomers, e.g. acrylamide, can be polymerized in the aqueous solution containing the radiation absorbing material, in situ, or they can be polymerized, dried and pulverized and mixed with the aqueous solution to form a particulate mass of gel utilizable as a shield against radiation. (NL)

31128 BARITES FROM BOGUSZOW AS AGGREGATE FOR ANTI-RADIATION CONCRETE SHIELDS. Pininska, J.; Wysokinski, L. (Univ. of Warsaw). Tech. Poszukiwan; 11: No. 41, 50-53(1973). (In Polish).

Barite is discussed from the viewpoint of the possibility of using it to produce concrete shields. Based on the Soviet Union, USA and French data parameters required for the mineral raw materials, in this case for barite, are given. Moreover, they describe research work carried out to determine the usefulness of the barite from Boguszów in production of concrete shields, and draw a conclusion that the barite under consideration corresponds to the world's standard. (auth) (Nucl. Sci. Abstr. Pol.)

31129 BUILDUP OF SCATTERED RADIATION BEHIND A SHADOW SHIELD. Generozov, V. L.; Sakovich, V. A.; Sakharov, V. M. Sov. At. Energy (Engl. Transl.); 35: No. 4, 926-927 (Oct 1973).

Translated from At. Energ. (USSR); 35: No. 4, 266-267(Oct 1973). This is a summary of paper No. 696/7156 with full copy held at TIC.

The Monte Carlo method has been used to calculate doses of scattered radiation at various distance from the surface of a shield of finite transverse dimensions for monodirectional and cosine disk sources neutrons and γ-rays. (MHR)

PHYSICS (THEORETICAL)

General

Refer also to abstracts 31075 and 31362.

31130 (AD-776408) GENERALIZED APPROXIMATIVE PROCEDURES IN THE MANY BODY PROBLEM. Final Technical Report. Kelson, I. (Tel Aviv Univ. (Israel)). Nov 1973. Contract DAJA37-72-C-4532. 39p. NTIS $5.00.

Properties of multiparticle spaces are investigated, which are common to diverse physical systems. Special emphasis is placed on the concept of independent particle motion and the mathematical tools relevant to its use. The concept of determinantal measure is introduced and discussed, and a procedure for calculating its space average is followed in some simple cases. Approximate methods for evaluating it in general are developed, studying combinational structural aspects of the single particle description. Generalized variational principles are briefly considered, and technical aspects of their application are qualitatively analyzed. (auth)

31131 (AD-776985) DISCRETE SPECTRUM OF SOLUTIONS OF THE WAVE EQUATION WITH STRONG CUBIC NONLINEARITY. Bisshopp, F. E. (Brown Univ., Providence, R. I. (USA). Div. of Applied Mathematics). May 1973. Contract NONR-562(42). 49p. NTIS $5.50.

The nonlinear wave equation, $\phi_{TT} - \Delta\phi + \phi^3 = 0$, has many solutions that are periodic in time and localized in space, all with infinite energies. The search for spherically symmetric solutions that are well represented by the simple approximation, $\phi(r,t) \cong A(r) \sin \omega t$, leads to a discrete spectrum of solutions $\phi_n(r,t;\omega)$. These solutions are discussed. (GRA)

31132 (JINR-P-4-7225) SELFCONSISTENT CALCULATION OF THE GREEN'S FUNCTIONS IN THE HUBBARD MODEL. Kuzemskii, A. L. (Joint Inst. for Nuclear Research, Dubna (USSR). Lab. of Theoretical Physics). 1973. 15p. (In Russian). INIS.

The Dyson equation for one-particle two-time temperature Green function was obtained in the problem on the correlation of electrons in narrow energy zones described by the Hubbard Hamiltonian. The method used is based on the introduction of irreducible Green functions. The precise representation obtained for the mass operator of the one-particle Green function was calculated in the limits of low density. (tr-auth)

31133 (JINR-P5-7344) SOME RELATIONS BETWEEN THE TYPES OF THE GENERATING SYSTEMS OF ABELIAN GROUPS AND THEIR DIRECT SUMMANDS. Lebedenko, V. M. (Joint Inst. for Nuclear Research, Dubna (USSR). Lab. of Theoretical Physics). 1973. 36p. (In Russian). INIS.

Some satisfactory conditions during which the Abelian groups possess or do not possess by heredity strongly reducible systems of the generatrix were obtained. The embedding theorems for classes of Abelian groups, characterized by combinations of types of generatrix systems (in the Dlab systematics) were shown. (tr-auth)

31134 QUANTUM MECHANICS. Volume I. Cohen-Tannoudji, C.; Diu, B.; Laloe, F. Paris; Hermann (1973). 890p. (In French).

This lecture on quantum mechanics covers waves and particles, introduction to the fundamental ideas of quantum mechanics; the postulates of quantum mechanics; application of these postulates to simple cases: spin ½ and two-level systems; one-dimensional harmonic oscillator; general properties of kinetic moments in quantum mechanics; particle in a central potential, the hydrogen atom. (auth)

31135 QUANTUM MECHANICS. Volume II. Cohen-Tannoudji, C.; Diu, B.; Laloe, F. Paris; Hermann (1973). 613p. (In French).

This lecture on quantum mechanics includes the quantum theory of scattering by a potential; the spin of electrons; kinetic moments; theory of stationary perturbations: fine and hyperfine structure of the hydrogen atom; time-dependent perturbations; systems of identical particles. (auth)

31136 QUANTUM PHYSICS. Berkeley Physics Course. Volume 4. Wichmann, E. H. Paris; Librairie Armand Colin (1974). 423p. (In French).

This course covers magnitudes of physical quantities in microphysics; energy levels; the wave and particle properties of photons; the wave nature of all material particles; the uncertainty principle and the theory of measurements; the wave mechanics of Schroedinger; theory of stationary states; the elementary particles and their interactions. (auth)

31137 SPECIAL THEORY OF RELATIVITY. pp 509-550 of Principles of Physics. II. Klimes, B.; Kracik, J.; Zenisek, A.; Slavik, J. B. (eds.). Prague; Academia (1972). (In Czech)

The foundations of the special relativity theory are presented in a brief and comprehensible form. (Nuclear Sci. Abstr. Czech.)

31138 SOME FORGOTTEN TERMS OF THE DIRAC-BREIT-PAULI EQUATION. Fraga, S.; Karwoski, J. (Univ. of Alberta, Edmonton). Can. J. Phys.; 52: No. 11, 1045(1 Jan 1974).

Two terms of the Dirac-Breit-Pauli equation, never considered before, are discussed. Their contribution to the total energy is of the same order of magnitude as the hyperfine structure interactions. (auth)

31139 SOLUTION OF THE SCHROEDINGER EQUATION USING PADE APPROXIMANTS TO SUM ASYMPTOTIC SERIES. McGuire, J. H.; Golden, J. E.; Nuttall, J. (Kansas State Univ., Manhattan). Rocky Mt. J. Math.; 4: No. 2, 375-376(Spr 1974).

The Pade approximant is used to sum the asymptotic series in 1/r to a form which at large r might be used as the basis for a variational trial wave function. For small r it is suggested using other wave functions and looking for a region of overlap where the two pieces of the wave function match. The radial Schroedinger equation is considered. (JFP)

31140 CONVERGENCE OF CERTAIN PADE APPROXIMANTS. Nuttall, J. (Univ. of Western Ontario, London). Rocky Mt. J. Math.; 4: No. 2, 269-272(Spr 1974).

A convergence theorem is found that did not use in its proof any information about the location of the poles of the Pade approximants. (JFP)

31141 EIGENSTATE EXPANSIONS IN A SOLUBLE MODEL OF IDENTICAL PARTICLE SCATTERING. Kouri, D. J. (Max-Planck-Institut fuer Stroemungsforschung, Goettingen (F. R. Germany)); Levin, F. S. (Brown Univ., Providence, R. I. (USA). Dept. of Physics). Nucl. Phys., A; 225: No. 3, 521-532(17 Jun 1974).

Solutions to the Schrödinger equation and the inhomogeneous equation for the case of two identical particles interacting with a center of force are studied. Eigenstate expansions for solving each equation are explicitly introduced; and their properties discussed. The case when the interparticle interaction v_{12} is zero is then examined; this is a completely soluble problem. The eigenstate expansion solutions for the Schrödinger and inhomogeneous equations are used to explore the means by which the correct solution is obtained. Finally, approximate solutions, obtained by truncating the eigenfunction expansions, are introduced. It is seen that both methods lead to the correct amplitude when $v_{12} = 0$, even though the approximate solution to the inhomogeneous equation does not lead, in the end, to an antisymmetric solution. (auth)

Quantum Field Theories

Refer also to abstracts 30771 and 31184.

31142 (IAE-2306) APPLICATION OF A CONFORMAL TRANSFORMATION GROUP FOR RELATIVISTIC THEORIES. Kotel'nikov, G. A. (Gosudarstvennyj Komitet po Ispol'zovaniyu Atomnoj Ehnergii SSSR, Moscow. Inst. Atomnoj Ehnergii). 1973. 8p. (In Russian). INIS.

Consideration is given to a generalization of the special relativity theory by a space-time, conformal transformation group with an invariant quadratic form. The theorem of velocity summation is presented. An expression for an invariant action integral is composed by means of which the invariance of the known equations of motion and of the Maxwell equations with respect to the conformal transformation group is demonstrated. Transformation properties are pointed out for the Planck constant ($c'\hbar' = c\hbar$), the eigen mass value, particular values of length and time, and of a series of other quantities. It is established that by the use of the conformal transformation group it is possible to construct a coherent relativistic theory. (SJR).

31143 (INIS-mf-1357) CLASSICAL AND RELATIVISTIC DOPPLER EFFECTS. Buonomano, V.; Moore, J. E. (Universidade Estadual de Campinas (Brazil). Instituto de Fisica). 1973. 11p. INIS.

A proof is given that the relativistic Doppler formula is completely derivable from any type theory of special relativity which assumes the existence of a "preferred" reference frame, "real" time dilations, "real" length contractions, and uses the classical distinction between the velocity of the source and the observer. (auth)

31144 (JINR-P2-7432) CONSTRUCTION OF NONLOCAL QUANTUM ELECTRODYNAMICS OF BOSONS WITH SPIN 0 AND 1. Efimov, G. V.; Namsrai, Kh. (Joint Inst. for Nuclear Research, Dubna (USSR). Lab. of Theoretical Physics). 1973. 26p. (In Russian). INIS.

The nonlocal quantum electrodynamics of particles with spin 0 and 1, satisfying the conditions of unitarity, macrocausality, relativity, and gradient-gauge invariance and finiteness, were constructed. (tr-auth)

31145 (KFKI-74-46) FIELD THEORIES WITHOUT WARD-IDENTITIES? Szegoe, K. (Kozponti Fizikai Kutato Intezet, Budapest (Hungary)). 1974. 24p. (CONF-740653-3). Dep. NTIS (US Sales Only) $4.25.

From 9th symposium on particle physics; Balatonfured, Hungary (12 Jun 1974).

A new technique is proposed in constructing field theories. Its essence is that instead of the common discreet spin variables a continuous complex variable is used which can be considered as the generalized Fourier-transformed of the common spin variables. Exploiting the transformation properties of the new object under Poincaré transformations, fields are constructed without superfluous components; interaction is introduced by their invariant coupling, as well as Lagrangian can be formed. As an example, quantum electrodynamics is treated in this formalism. Since in this formulation neither Ward-identities, nor gauge transformation of second kind, nor indefinite metric appear, it is hoped that a better insight could be obtained into the machinary of field theory. (auth)

31146 A THEORY OF ELEMENTARY COUPLINGS III. Wellner, M. (Physics Department, Syracuse University, Syracuse, New York 13210). Ann. Phys. (N.Y.) 86: No. 2, 331-351 (Aug 1974).

We further develop a recent method, based on compensation between Feynman diagrams, for obtaining a priori information on the spectrum and interactions (weak and strong) of the elementary particles. The theory is based on hadron octets or nonets of spin zero and one half, together with vector bosons including photons. It has the necessary ingredients of a realistic broken—symmetry gauge theory, the compensation method giving the rules for breaking the symmetry. In this article, the scope of the compensation principle is greatly enlarged, thanks to the inclusion of scalar mesons. The main point of this paper is to show in detail how the strong (Yukawa) couplings may be completely determined by the compensation relations. The numerical results are worked out in the limit of exact SU(3) for the weak couplings. The eta and charged kaon lifetimes can now be computed, and come out in fair agreement with the data. The strong $\Sigma\Lambda\pi$ coupling is no longer zero, as in parts I and II, but is still smaller than the current experimental estimates. The accurate mass formula $N^{-1}+\Xi^{-1}+\Sigma^{-1}=6(N+\Xi)^{-1}$ is rederived in a new framework, and appears to be connected with a simple SU(3) —breaking weak or superweak interaction. (auth)

31147 SCALING AND ASYMPTOTICALLY FREE MASSIVE YANG—MILLS FIELD. Hsu, J. P. (Univ. of Texas, Austin). Lett. Nuovo Cim.; 11: No. 2, 129-133(14 Sep 1974).

It is shown that one can make the Yang—Mills quanta massive without destroying the asymptotically free property. Thus, based on the massless Yang—Mills theory one can construct models of various interactions which could exhibit Bjorken scaling. A new way of constructing strong interaction models is suggested. (JFP)

31148 EQUIVALENCE OF YANG—FELDMAN AND ACTION PRINCIPLE QUANTIZATION. Nagpal, A. K. (Univ. of Delhi). Lett. Nuovo Cim.; 11: No. 2, 107-110(14 Sep 1974).

Although it is reasonable to suppose that the equivalence of the commutation relations obtained from the Yang—Feldman and action principle method for quantization holds in higher orders, it is interesting to know the origin of this equivalence, i.e., the cause of the invariance of the Johnson—Sudarshan anticommutator under this transformation of Gupta and Repko type. (JFP)

31149 INFRA-RED-FINITE CALCULATIONS IN QUANTUM ELECTRODYNAMICS. Zwanziger, D. (New York Univ., New York). Lett. Nuovo Cim.; 11: No. 2, 145-150(14 Sep 1974).

A detailed analysis of the infrared problem in quantum electrodynamics has resulted in a new type of cross section formula. In it, radiation-damping effects are accounted for nonperturbatively, and the remaining physics is contained in reduced S-matrix elements. Although the asymptotic in and out state spaces of the local quantum field theory involve coherent states of infinite numbers of photons, each reduced S-matrix element refers to a finite number of electrons and photons. It is obtained as the on-mass-shell value of a single Green function, calculated according to Feynman rules and multiplied by an appropriate power of p^2-m^2. (JFP)

31150 ASYMPTOTIC SOLUTION OF THE SET OF EQUATIONS FOR GREEN'S FUNCTIONS IN THE YANG—MILLS FIELD THEORY. Fradkin, E. S.; Kalashnikov, O. K. (Lebedev Inst. of Physics, Moscow). Lett. Nuovo Cim.; 10: No. 17, 771-775(24 Aug 1974).

The asymptotic solution of the exact set of equations for the Green's functions is obtained in the region of large values of the momenta. The absence of the "zero charge" difficulty follows from the explicit form of the solution thus obtained. (LBS)

31151 DERIVATION OF UNIFIED GAUGE THEORY FROM A GENERALIZED MINIMAL PRINCIPLE. Mainland, G. B.; O'Raifeartaigh, L. (Dublin Inst. for Advanced Studies). Lett. Nuovo Cim.; 10: No. 17, 733-736(24 Aug 1974).

It is pointed out that the two steps used in the derivation of conventional unified gauge theory can be reduced to a single step, which is a natural generalization of the Yang—Mills minimal principle and which starts from the free-fermion Lagrangian. The generalized minimal principle is then used to derive the Lagrangian for unified gauge theory in exact analogy with the ordinary Yang—Mills procedure. (LBS)

31152 UNITARY FOLDY—WOUTHUYSEN TRANSFORMATIONS FOR PARTICLES OF ARBITRARY SPIN. Tekumalla, A. R.; Santhanam, T. S. (MATSCIENCE, Madras). Lett. Nuovo Cim.; 10: No. 17, 737-740(24 Aug 1974).

The existence of a unitary Foldy—Wouthuysen transformation for arbitrary spin is established. An explicit form for the unitary FW transformation is calculated and applied to spin $^1/_2$, spin 1, and spin $^3/_2$ cases. (LBS)

31153 NOTE ON AN INFINITE-MASS LIMIT OF THE HIGGS MODEL. Tamura, S. (Hokkaido Univ., Sapporo). Progr. Theor. Phys. (Kyoto); 51: No. 2, 628-630(Feb 1974).

It is shown that the nontrivial massive vector meson model with self-coupling can be obtained in the Abelian model. (LBS)

31154 MATHEMATICS OF CONTEMPORARY PHYSICS. Proceedings of a Conference Held at London, England, August 23—September 11, 1971. Streater, R. F. (ed.). New York; Academic Press Inc. (1972). 281p. (CONF-710860-). $17.50.

The topics discussed are quantum field theory, functional analysis, boson quantum field models, states and representations in statistical mechanics, quantum scattering systems, linear fields, the free boson gas, self-adjointness of the locally correct generator of Lorentz transformations for $P(\phi)_2$, and algebras with quasi-local structure and factorizable representations. (JFP)

31155 CONFORMAL INVARIANT SPINOR THEORY WITH THIRD-ORDER DERIVATIVES. Duerr, H. P.; van der Merwe, P. duT. (Max-Planck-Institut fuer Physik und Astrophysik, Munich). Nuovo Cim.; 23A: No. 1, 1-32(1 Sep 1974).

It is demonstrated that a free Weyl spinor theory with third-order derivatives, which serve as an imbedding Lagrange theory for noncanonical spinor theories of the Heisenberg type, is not only scale invariant but invariant under the full 15-parameter conformal group. The spinor field transforms according to an irreducible representation for mass dimension $^1/_2$. In a canonical formulation of this theory, in which the spin-projected first and second derivatives of the field are considered as independent dynamical variables, the new fields are found to transform according to nondecomposable representations for mass dimension $^3/_2$ and $^5/_2$, which produces nonconventional features. The special conformal currents are explicitly constructed in the third-order and canonical formalism and their conservation is demonstrated. Proposals for a conform invariant theory with interaction are made. It is shown to support a number of aspects of gauge-invariant spinor theories studied earlier. Conformal invariance leads to several new features in the case of interacting theories and, in connection with the occurrence of nondecomposable representations, brings to light the limitations of gauge replacement procedures for introducing interacting theories. The theory can be immediately generalized to Dirac-type spinor theories and theories with internal degrees of freedom. (auth)

31156 VACUUM POLARIZATION TENSOR AND CURRENT OPERATOR IN QUANTUM ELECTRODYNAMICS WITH COMPENSATING CURRENT. Bechler, A. (Univ., Warsaw). Acta Phys. Pol., B; 5: No. 4, 453-472(1974).

The photon propagator in the compensating current dependent quantum electrodynamics, formulated previously, is investigated. In particular, it is shown that the vacuum polarization tensor can be defined in the same way as in conventional quantum electrodynamics. Since the theory is fully gauge-invariant, this tensor is a transverse quantity before renormalization and therefore there is no trouble with the quadratically divergent term in $\Pi^{\mu\nu}$ The problem of a proper definition of the current operator is also considered. It is shown that the definitions proposed by Heisenberg and Euler, Schwinger and Brandt can be generalized to the case of an arbitrary compensating current, described previously. The definition of the current gives a certain prescription of the regularization, which ensures transversity of the vacuum polarization tensor at every step of calculations. The difference between this method of regularization and other methods is also discussed. A perturbation expansion of the current operator is calculated up to the third order and it is shown that it is independent of the compensating current. (auth)

31157 MODIFICATION OF THE QUANTUM-MECHANICAL EQUATIONS FOR THE SYSTEM OF CHARGED DIRAC PARTICLES BY INCLUDING ADDITIONAL TENSOR TERMS OF THE PAULI TYPE. I. Janyszek, H. (Copernicus Univ., Turin). Acta Phys. Pol., B; 5: No. 4, 447-452(1974).

A new modified quasirelativistic equation (different from that of Breit) for N charged Dirac particles in the external stationary electromagnetic field is proposed. This equation is an amplified quantum-mechanical Bethe-Salpeter equation obtained by adding (in a semi-phenomenological manner) terms which take into account radiative corrections. The application of this approximate equation is limited to third order terms in the fine structure constant α. (auth)

31158 MULTIPLICATION LAW IN QUANTUM PHYSICS. I. The Non-Relativistic Quantum Mechanics. Kapuscik, E. (Inst. of Nuclear Physics, Krakow). Acta Phys. Pol., B; 5: No. 4, 497-505(1974).

A generalization of the Heisenberg quantum theoretical multiplication law is proposed. What kind of modification this introduces to the usual results of quantum mechanics is shown. The large domain of applicability of the generalized product is indicated. (auth)

31159 FIELD QUANTIZATION ON THE SURFACE X^2 = CONSTANT. Gromes, D.; Rothe, H. J.; Stech, B. (Heidelberg Univ. (F. R. Germany). Inst. fuer Theoretische Physik und Mechanik). Nucl. Phys., B; 75: No. 2, 313-332(18 Jun 1974).

In analogy to non-relativistic quantum field theory where the Galilei invariant plane t = const. is used for a description of bound (and scattering) states the hyperboloid x^2 = const. which is invariant under homogeneous Lorentz transformations is taken. The appropriate complete set of basis functions is given for the expansion of any scalar and spin $^1/_2$ field on the hyperboloid. The free Klein Gordon and Dirac fields are discussed in detail. In this formulation a multiparticle system can be described by a Lorentz covariant wave function. (auth)

31160 THE CALLAN-SYMANZIK EQUATION AND DIMENSIONAL REGULARIZATION. Holwerda, M. J.; van Neerven, W. L.; van Royen, R. P. (Katholieke Universiteit Nijmegen (Netherlands)). Nucl. Phys., B; 75: No. 2, 302-312(18 Jun 1974).

A study is made of the Callan-Symanzik equation using the dimensional regularization method. The final equation is far more general than in the usual derivation in that the effect of mass terms is explicitly included; moreover the momenta need not be restricted to the deep-Euclidean region when considering asymptotic limits. (auth)

31161 ANOMALOUS CURRENTS IN GAUGE FIELD THEORIES. Bardeen, W. A. (Stanford Univ., Calif. (USA). Dept. of Physics). Nucl. Phys., B; 75: No. 2, 246-258(18 Jun 1974).

Properties of symmetry currents are examined within the context of renormalizable gauge field theories. The existence of triangle anomalies requires that some of the symmetry currents must have well-defined gauge transformation properties. Exact low-energy theorems for certain matrix elements of the divergences of the currents are established to all orders in perturbation theory. (auth)

31162 VELOCITY OF LIGHT IS DIRECTION DEPENDENT. Marinov. S. Czech. J. Phys.; 24: No. 9, 965-970(1974).

Performing the so-called "coupled-mirrors" experiment, it is established that velocity of light measured along a given track on the earth's surface is different during the different hours of the day. (auth)

31163 WIDE ANGLE SCATTERING IN SOFTENED FIELD THEORY. Ezawa, Z. F. (Cambridge Univ., Eng.). Nuovo Cim.; 23A: No. 2, 271-290(21 Sep 1974).

The picture of Brodsky and Farrar for scattering processes at large transverse momentum is formulated in softened field theory. A modest softening of the quark-quark-gluon vertex is introduced to suppress unwanted logarithms in the formalism. It is shown that the electromagnetic form factors of the proton and the pion yield asymptotically behaviors which agree with the result of simple dimensional counting. The threshold behaviors of the deep inelastic structure functions are calculated for the proton and the pion to give $\sim(1 - \omega)^3$ and $\sim(1 - \omega)^2$, respectively. Thus the Drell-Yan-West relation holds in the case of the proton target but is violated in the case of the pion target. It is also proved that the asymptotic behaviors of wide-angle elastic $\pi\pi$ and pp scattering naively predicted by dimensional counting and conjectured by Brodsky and Farrar on the basis of simple Born diagrams are actually the next-to-leading-order terms. The highest-order terms come from a certain set of diagrams that Landshoff studied. (auth)

31164 CAUSALITY IN INDEFINITE METRIC THEORIES. Stapp, H. P. (Univ. of California, Berkeley). Nuovo Cim.; 23A: No. 2, 357-361(21 Sep 1974).

It has recently been claimed by Rechenberg and Sudarshan that theories with shadow states are consistent with macroscopic causality, even though they lack the normal physical-region analytic structure. This claim is based on a number of incorrect statements, which are pointed out. These errors invalidate the claim. (auth)

31165 SOME APPLICATIONS OF PADE APPROXIMANTS TO QUANTUM FIELD THEORY MODELS. Masson, D. (Univ. of Toronto). Rocky Mt. J. Math.; 4: No. 2, 261-267(Spr 1974).

The close connection between Pade approximants applied to a series of Stieltjes and the theory of positive symmetric operators in a Hilbert space is reviewed. This permits the establishment of useful criteria for the self-adjointness of a symmetric operator in terms of the determinateness of a Hamburger moment problem and the obtaining of a method of approximating such operators related to the [n/n + 1] Pade approximant. It is indicated how these results may be applied to a quantum field theory model to give a simple proof of the self-adjointness of the Hamiltonian and a method of solving the Hamiltonian eigenvalue problem using the [n/n + 1] Pade approximant. (JFP)

31166 STIELTJES TYPE CONTINUED FRACTIONS IN QUANTUM ELECTRODYNAMICS. Graffi, S.; Grecchi, V. (Instituto Nazionale di Fisica Nucleare, Bologna). Rocky Mt. J. Math.; 4: No. 2, 363-366(Spr 1974).

The exactly solvable vacuum polarization by an external constant electromagnetic field is examined. It is proven that the Stieltjes type continued fraction corresponding to the divergent perturbation expansion in the general case does not converge to the exact solution, the convergence taking place only for the vacuum polarization for a pure electric or a pure magnetic field. The summability of the perturbation expansion to the exact solution under the Borel method is also proven. (auth)

31167 CONSTRAINTS, CAUSALITY, AND LORENTZ INVARIANCE. Jenkins, J. D. (Univ. of Durham, Eng.). J. Phys., B (London); 7: No. 10, 1129-1134(1 Jul 1974).

Simple theories of interacting classical relativistic massive spin-1 and spin-$^3/_2$ fields are studied. In these examples, it is found that if a theory is acausal in the sense of Velo and Zwanziger (Phys. Rev.; 186: 1337-41, Phys. Rev.; 188: 2218-22 (1969)), it is also not Lorentz covariant. The breakdown of Lorentz covariance is seen to manifest itself in the constraints, which must be satisfied by the interacting fields, not determining all the dependent fields components simultaneously in all inertial frames of reference. Some remarks on the present state of massive spin-$^3/_2$ theories are made. (auth)

31168 TWO-LOOP DIAGRAMS IN YANG–MILLS THEORY. Jones, D. R. T. (Oxford Univ. (UK). Dept. of Theoretical Physics). Nucl. Phys., B; 75: No. 3, 531-538(25 Jun 1974).

A calculation of the renormalization constants of the Yang–Mills field to $O(g^4)$ is presented. The function $\beta(g)$ is hence evaluated to $O(g^5)$, and possible implications for gauge theories of the strong interactions are discussed. (auth)

31169 WEAK LSZ LIMITS AND REDUCTION FORMULA FOR THE NON-RELATIVISTIC COULOMBIC INTERACTION. Papanicolaou, N. (New York Univ., N. Y. (USA). Dept. of Physics). Nucl. Phys., B; 75: No. 3, 483-492(25 Jun 1974).

The asymptotic condition is stated in the case of a non-relativistic Coulombic potential (long-range interaction), and the corresponding LSZ reduction formula is established for the S-matrix elements of the theory. Since the Coulombic Green function is known in closed (non-perturbative) form, it can be rigorously proved that the resulting S-matrix is free of infinite Coulombic phases and coincides with Dollard's S-matrix. A brief discussion of the forward-scattering amplitude is also given. (auth)

31170 GENERAL FEATURES OF THE REGGEON CALCULUS WITH $\alpha > 1$. Cardy, J. L. (Science Research Council, Daresbury (UK). Daresbury Lab.). Nucl. Phys., B; 75: No. 3, 413-425(25 Jun 1974).

Some general properties of the reggeon calculus with input intercept greater than one are discussed, in an attempt to formulate a model yielding indefinitely rising cross sections which is consistent with t-channel unitarity. In general the leading behavior of the amplitude always factorizes. If interactions between reggeons are ignored the scattering is equivalent to that from a grey absorbing disk of radius 0 (ln s). Diagrams involving such interactions are subject to large-scale cancellations. These enable the model to give sensible results for inclusive cross sections. In quantum number exchange reactions, factorization of the Regge pole residues is weakly broken in the model. (auth)

31171 BROKEN CONFORMAL WARD IDENTITIES IN NON-ABELIAN GAUGE THEORIES. Sarkar, S. (European Organization for Nuclear Research, Geneva (Switzerland)). Phys. Lett., B; 50: No. 4, 499-503(24 Jun 1974).

Integrated broken conformal Ward identities for non-abelian gauge theories are derived. There exist anomalous terms linked to the ones in the Callan–Symanzik equations. Also, there are a gauge-dependent term that can be predicted classically and a new term involving Faddeev–Popov ghosts. These two terms cannot be neglected asymptotically relative to the other terms for gauge-variant Green's functions. (auth)

Gravitation and General Relativity

Refer also to abstract 30704.

31172 PRINCIPLE OF MATERIAL INDIFFERENCE IN RELATIVITY. Bressan, A. (Univ., Padua). Lett. Nuovo Cim.; 11: No. 2, 134-136(14 Sep 1974).

A serious material error written in describing the contents of a previous work on the principle of material (frame) indifference or the objectivity principle. Also various questions concerning relativistic versions of material indifference and involving also other papers are discussed. (JFP)

31173 QUANTIZATION AND THE SOURCE OF THE GRAVITATIONAL FIELD. Riegert, R. J. Lett. Nuovo Cim.; 11: No. 2, 99-102(14 Sep 1974).

A previous procedure, equivalent in conclusions in the case of electromagnetism to that of another work and in addition to possessing covariance it does not require the use of the equations of motion of the field sources, is investigated as applied to the gravitational field. To this end the Dirac equation for a spinor field in curved space is considered. (JFP)

31174 F-GRAVITY AND THE PROTON–ELECTRON MASS RATIO. Lord, E. A.; Sivaram, C.; Sinha, K. P. (Indian Inst. of Science, Bangalore). Lett. Nuovo Cim.; 11: No. 2, 142-144 (14 Sep 1974).

An attempt is made to explain the mass anomaly as arising from the different mechanisms of the gravitational interactions for hadrons and leptons (i.e., the ability of the proton to take part in strong gravitational interactions also) just as the anomalous electromagnetic properties of the nucleons can be traced to the different nature of their electromagnetic interactions. (JFP)

31175 CAUSAL BOUNDARIES FOR GENERAL RELATIVISTIC SPACE–TIMES. Budic, R.; Sachs, R. K. (Univ. of California, Berkeley). J. Math. Phys. (N. Y.); 15: No. 8, 1302-1309(Aug 1974).

Let M be a causally continuous space–time. Using indecomposable past and future sets in a symmetric way one constructs a causal completion N for M. N is a causal space; the chronology of M in N is the chronology of M. The extended Alexandrov topology for N makes N Hausdorff and M a densely imbedded subspace. M is globally hyperbolic if either the chronological future or the chronological past of each point in N–M is empty, causally simple if the causality of M in N is the causality of M. The standard examples of causal completions are special cases. (auth)

31176 APPROXIMATE INTERIOR SOLUTION IN BRANS–DICKE THEORY. Mahanta, M. N.; Reddy, D. R. K. (Indian Inst. of Tech., New Delhi). J. Math. Phys. (N. Y.); 15: No. 8, 1235-1237(Aug 1974).

An approximate interior solution of the field equations of Brans–Dicke theory is obtained for a static spherically symmetric metric which can be considered to be an analog of Schwarzschild's interior solution in Einstein's theory. (auth)

31177 GRAVITATIONAL FIELD IN FINSLER SPACES. Takano, Y. (Yokohama National Univ., Japan). Lett. Nuovo Cim.; 10: No. 17, 747-750(24 Aug 1974).

The equations of the gravitational field in Finsler spaces are proposed. The equations determining the metric tensor $g_{\mu\nu}$ as a function of x are shown to be reasonably and consistently assumed. Some preliminary discussions on these equations are also presented. (LBS)

31178 MODEL FOR THE INTERACTION BETWEEN A GRAVITATIONAL WAVE AND A CIRCULAR CURRENT. Grossiord, J. L.; Tourrenc, P. (Univ., Paris). Compt. Rend., Ser. B; 278: No. 13, 563-565(25 Mar 1974). (In French).

The variation in the angular velocity of a charge executing a spiral motion consecutive to the passage of a Gaussian gravitational pulse is studied. (auth)

31179 NONRENORMALIZABILITY OF QUANTIZED FERMION–GRAVITATION INTERACTIONS. Deser, S.; van Nieuwenhuizen, P. (Brandeis Univ., Waltham, MA). Lett. Nuovo Cim.; 11: No. 3, 218-220(21 Sep 1974).

It is reported that the coupling to spin-$\frac{1}{2}$ fermions, the remaining fundamental matter fields, is also one-loop nonrenormalizable. This is established by exhibiting a one-loop counter term proportional to the fourth power of the fermion axial current. This term does not vanish on shell, cannot be cancelled by other counter terms, and is absent in the original (Dirac–Einstein) action; therefore its presence is sufficient to prove nonrenormalizability. (JFP)

31180 SOLUTIONS OF THE EINSTEIN FIELD EQUATIONS FOR A ROTATING PERFECT FLUID. Krasinski, A. (Univ., Warsaw). Acta Phys. Pol., B; 5: No. 4, 411-436(1974).

The equations of isentropic rotational motion of a perfect fluid are investigated with use of the Darboux theorem. It is shown that, together with the equation of continuity, they ensure the existence of four scalar functions which constitute a dynamically distinguished set of coordinates. If in this system of coordinates the metric tensor is constant along the lines tangent to velocity and vorticity fields, then the field equations with $T_{ij} = (\epsilon + p)u_i u_j - pg_{ij}$ can be completely integrated. The resulting metrics divide into 3 families, first of which contains 6 types of new solutions with non-zero pressure. All of them are given explicitly in terms of hypergeometric or confluent hypergeometric functions, type IV being the only one containing entirely elementary functions. The second family contains only the solution of Gödel, and the third one—only the solution of Lanczos. (auth)

31181 QUANTIZATION IN STATIC GRAVITATIONAL FIELDS. Kramer, D.; Lotze, K. H. (Friedrich–Schiller Univ., Jena, Ger.). Acta Phys. Pol., B; 5: No. 4, 437-446(1974). (In German).

After some remarks dealing with the generators of unitary transformations the canonical quantization of free fields in a static space-time is considered: expansion of the field operators, complete and orthonormal systems of classical solutions, definition of creation and annihilation operators, occupation number representation of the Hamiltonian. (auth)

31182 TRACE ANOMALIES IN DIMENSIONAL REGULARIZATION. Capper, D. M. (Imperial Coll. of Science and Tech., London); Duff, M. J. Nuovo Cim., 23A: No. 1, 173-183(1 Sep 1974).

An unusual perturbation theory anomaly is pointed out. If there exists a trace identity valid in an arbitrary number of dimensions, then employing dimensional regularization can result in an amplitude satisfying the identity in an arbitrary number of dimensions, but the finite part of the amplitude violating it in four dimensions. An example given is the one-loop neutrino contribution to the graviton propagator. Anomalous behavior, of a different origin, also occurs in the one-loop photon contribution. Both kinds of anomaly can be removed at the expense of introducing n-dimensional, rather than 4-dimensional, counterterms. (auth)

31183 CAN EINSTEIN'S THEORY OF GRAVITATION BE TESTED BEYOND THE GEOMETRICAL OPTICS LIMIT? Mashhoon, B. (Princeton Univ., NJ). Nature (London); 250: No. 5464, 316-317(26 Jul 1974).

It is stated that the separation of quasar images into right and left circularly polarised radiation, such as that passing the Sun from 3C 273, permits measurement of the effect of gravitation on polarised radiation, and that such an experiment would appear to be the first in which Einstein's theory of gravitation can be tested beyond the geometric optics limit. The differential gravitational deflection of polarised radiation is estimated, and it is pointed out that although with present techniques it is too small to be measurable for the Sun, it is potentially observable for gravitationally collapsed objects, and may provide a means of measuring the angular momentum of the object. (UK)

31184 NONRENORMALIZABILITY OF EINSTEIN–YANG–MILLS INTERACTIONS AT THE ONE-LOOP LEVEL. Deser, S.; Tsao, H. S.; van Nieuwenhuizen, P. (Brandeis Univ., Waltham, Mass. (USA). Dept. of Physics). Phys. Lett., B; 50: No. 4, 491-493(24 Jun 1974).

The interactions between the quantized Einstein and quantized Yang–Mills fields are one-loop nonrenormalizable. The reason is that the free coupling constant of this system is not the dimensionless Yang–Mills coupling constant f but rather f divided by the fixed dimensional gravitational coupling constant κ, so that $f' = f/\kappa$ cannot occur in the coefficient of $R^2_{\mu\nu}$ on dimensional grounds. Likewise, increasing the number of gauge fields by increasing the dimension of the group increases the coefficient of $R^2_{\mu\nu}$ even further from its already positive Maxwell value. (NL)

REACTOR TECHNOLOGY AND REGULATION

31185 (JPRS-61338, pp 9-13) PROGRESS ON CZECHOSLOVAK NUCLEAR POWER PLANTS. Kaspar, J. Translated from Zapisnik; No. 26, 18-20(22 Dec 1973).

The development of nuclear power in Czechoslovakia is summarized. Plants completed, under construction, or planned are described. Safety and environmental concerns are discussed briefly. (JWR)

31186 EFFECTS OF SITING AND LOAD VARIATION FOR A 650 MW NUCLEAR STATION WITH AIR CONDENSERS. Potter, J. H. (Stevens Inst. of Tech., Hoboken, N. J. (USA)). Arch. Energiewirt.; 28: No. 10, 463-469(May 1974). (In German). 7 figs.; 4 tabs.; 5 refs.

The advantages of the air-cooled steam condenser are twofold, as it saves cooling water and avoids the steam plumes inevitably associated with wet cooling. A 650 MW(e) nuclear power plant is discussed considering the effects of site selection and load changes with respect to both air cooling and cooling by conventional methods. (GE)

Power Reactors, Non-Breeding, BWR-Type

Refer also to abstracts 31250, 31251, 31260, 31265, 31311–31313, 31317, and 31318.

31187 (BNWL-B-371) NEUTRONIC CALCULATIONS FOR EXPERIMENTS WITH LIGHT WATER REACTOR FUEL IN PBF. Jenquin, U. P.; Thomsen, D. H.; Heeb, C. M. (Battelle Pacific Northwest Labs., Richland, Wash. (USA)). Aug 1974. Contract AT(45-1)-1830. 39p. Dep. NTIS $5.00.

Experiments are to be performed in the PBF with fuel rods representative of light water reactor fuel. Neutronic calculations have been performed to specify the rod enrichment required to give desired powers. In one set of experiments there will be four identical test rods placed symmetrically in the center of PBF. In addition, a 16-rod experiment will be performed with varying enrichments in the rods in order to flatten the power distribution. The 4-rod experiments will utilize fuel representative of BWR, large PWR, and small PWR pins. BWR and large PWR 4-rod experiments will also be performed utilizing plutonium in the fuel. The 16-rod experiment will utilize large PWR pins enriched with U-235. It is desired that these rods produce a maximum power of 21 to 25 kW/ft. Linear power densities as a function of enrichment were determined for test pins enriched with either uranium-235 or plutonium. In addition, a calculation was made for a MAPI rod as a check of the methods versus ANC methods. Results of calculations for the test rods of interest are plotted. The results are presented as peak axial power versus enrichment assuming a PBF core power of 30 MW. To obtain 25 kW/ft in the 4-rod experiments, the BWR pins must be enriched to 8% ^{235}U, the large PWR pins must be enriched to 12% ^{235}U, and the small PWR pins must be enriched to 16% ^{235}U. For mixed oxide fuel, the BWR pins must be enriched to 6% Pu and the large PWR pins must be enriched to 9% Pu for the plutonium isotopic composition assumed. The radial and azimuthal power distributions within the test pins were also determined. The 16-rod bundle of large PWR pins is not capable of producing 25 kW/ft. With an average enrichment of 60%, the power (peak axial, average radial) is 16.6 kW/ft. (auth)

31188 STEAM POWER PLANT FOR NUCLEAR POWER STATIONS WITH BOILING WATER REACTORS. Heitmann, H. G. (to Kraftwerk Union A. G., Muelheim an der Ruhr (F. R. Germany)). German Patent 2136352. 1 Feb 1973. 6p. (In German). 2 figs.

A plant is described in which the condensed steam is able to undergo a cleaning process prior to being re-fed into the working fluid circuit. The condensates are led in a feedwater container through the intermediary of at least one cleaning device containing electromagnetic filters. Water from a water separator may also be fed into the cleaning equipment. (GE)

31189 NUCLEAR POWER AVAILABILITY. Holmin, N. ERA (Foeren. Elek. Ration. Anvaendning); 46: No. 5, 95-97(1973). (In Swedish).

The availability of nuclear power plant is an important factor in the planning of Sweden's future nuclear power program. Operating statistics for a world list of pressurized water reactors (PWR) and boiling water reactors (BWR) are presented and discussed. Experience with the larger light water reactors (LWR) is, as yet, limited. Availability has varied widely but the average figure is quite good. (SW)

31190 COMPARISON OF TWO- AND THREE-DIMENSIONAL CALCULATIONS OF SUPER PROMPT CRITICAL EXCURSIONS. Birkhofer, A.; Schmidt, A.; Werner, W. (Technische Univ., Munich). Nucl. Technol.; 24: No. 1, 7-12(Oct 1974).

Calculations of super prompt critical excursions induced by ramp variation of absorption cross sections are performed in various geometries (r, xy, rz, xyz). The time behavior of neutron flux and fuel temperature is analyzed, especially with regard to their dependence on geometry and rod velocity. The evaluations establish the need for genuine three-dimensional calculations to correctly predict peak flux and temperature distributions for situations where space-dependent feedback effects are essential. (auth)

31191 PROBLEMS OF EMERGENCY CORE COOLING SYSTEM. Suzuki, T. (Rissho Univ., Tokyo); Fujimoto, Y. Kagaku (Tokyo); 43: No. 1, 33-41(Jan 1973). (In Japanese).

First, general introduction to the problem of ECCS is given. The outline of experiments at National Reactor Testing Station in U. S. A. and the significance of ECCS for LWRs are briefly explained with reference to the accident at Windscale. The assumed release rate of radioactive iodine in case of assumed grave accident, from 6 LWRs operating or under construction in Japan is presented by a table. The authors stress that it is not unrealistic to assume that the abnormal conditions of reactor container, spray system and filter can occur at the same time with the rupture of primary coolant piping. In the second part, various movements among U. S. AEC, JCAE, plant makers, etc. are historically followed since May 1971. The outline of the LOFT project is also explained on the basis of Ergen Report and ORNL report (ORNL NSIC-24). Thirdly, the relation between the scale-up of power plants and semi-scale experiment (LOFT) is discussed. The lack of philosophy in applying or extrapolating the results of experiments to the safety evaluation of large power plants is pointed out. (JA)

31192 TRENDS IN STRUCTURAL MECHANICS. A UK Review of the 2nd International Conference on Structural Mechanics in Reactor Technology. I. Pressure Vessels and Containments. Burrow, R. E. D. (Taylor Woodrow Construction Ltd., Southall, Eng.). J. Brit. Nucl. Energy Soc.; 13: No. 3, 278-284(Jul 1974).

The main types of prestressed concrete pressure vessels and containment which were discussed at the 2nd International Conference on Structural Mechanics in Reactor Technology, Berlin, 1973, are reviewed and attention is drawn to those features which may have future significance. The multi-cavity vessel with wire-wound circumferential prestressing appears as the basis for a large proportion of future schemes. A few comments are offered concerning the treatment of ultimate load calculations and the significance of impact loading conditions, which are being specified for containment of LWRs. (UK)

31193 DEVELOPMENT OF NUCLEAR REACTOR INCORE INSTRUMENTS. Yokota, M.; Honma, T.; Yamada, M. (Japan Atomic Energy Research Inst., Tokai). Keisoku To Seigyo; 12: No. 12, 985-992(Dec 1973). (In Japanese).

The development of in-core instruments in JPDR is described. The main instruments developed are the flow meters at coolant inlet and outlet, void gauge, thermocouples and neutron detectors. These instruments offer useful data for analyzing the thermodynamic and hydrodynamic characteristics of reactors. (JA)

Power Reactors, Non-Breeding, PWR-Type

Refer also to abstracts 29357, 29358, 31187, 31189–31192, 31250, 31251, 31260, 31302, 31310, 31314–31316, and 31319–31322.

31194 (BAW-10096) B AND W QUALITY ASSURANCE PROGRAM FOR NUCLEAR EQUIPMENT. (Babcock and Wilcox Co., Lynchburg, Va. (USA). Nuclear Power Generation Div.). Aug 1974. 93p. Dep. NTIS $7.75.

B&W's Quality Assurance Program (QAP) is described. The report is divided into 18 sections conforming in format to the 18 requirements listed in Appendix B of 10 CFR 50. The program is implemented through the Nuclear Power Generation Division

(NPGD). The position and relationships of the NPGD within the Company's Corporate structure are described. An overview is presented of the QAP describing its implementation, its operation, the controls imposed on all suppliers (both corporate and vendor) and site consulting activities. Format guidance and criteria requirements for the preparation of information included in each section of this report were obtained from the AEC document, "Guidance for Submittal of Quality Assurance Program Description," dated October 3, 1973, as amended through discussions and meetings with the Regulatory Staff. Each of the criteria listed in this document and applicable to the Company's scope of supply was addressed. (auth)

31195 (BAW-10097) MARK C (17 × 17) FUEL ASSEMBLY. Research and Development. Stoudt, R. H.; Kern, R. C.; Walton, L. A. (Babcock and Wilcox Co., Lynchburg, Va. (USA). Nuclear Power Generation Div.). Aug 1974. 40p.

The research and development programs related to the B&W Mark C (17 × 17) fuel assembly are described. The programs provide data for analytical models, confirm predictions, and verify the adequacy of the design. A general description of the Mark C assembly is presented along with comparisons to the Mark B (15 × 15) fuel assembly. The report is organized in three main test areas: mechanical and hydraulic; critical heat flux; and rod swelling and burst. The test program scopes and objectives are discussed along with the test methods. (auth)

31196 APPARATUS FOR IN-CORE INSTRUMENTATION OF PRESSURIZED WATER REACTORS. Gruener, W.; Schabert, H. P.; Schubert, F. (to Siemens Aktiengesellschaft). US Patent 3,827,935. 6 Aug 1974. Priority date 24 Oct 1969, F. R. Germany. 8p.

A nuclear reactor of the pressured water type is equipped with an in-core instrumentation apparatus which has vertically displaceable instrumentation shafts passing from above through the head cover of the reactor pressure vessel. Yoke structures extend horizontally from each instrumentation shaft in the space between the cover and the core assembly. Finger-like groups of rigid instrument guide tubes for respective measuring probes extend from each yoke downward into the core assembly. (Official Gazette)

31197 HEAD CLOSURE SYSTEM. (to Westinghouse Electric Corp.). Netherlands Patent 7,211,400. 21 Aug 1972. Priority Date 13 Sep 1971, USA. 21p. (In Dutch).

In order to reduce the time required for refueling a nuclear reactor, the studs utilized for securing the head of the reactor pressure vessel are provided with modified breechblock threads at their lower ends, and also at their upper ends. After being detensioned, the studs are rotated 60° for disengagement from corresponding threads in a flange at the top of the pressure vessel and are lifted out of the stud holes when the head is removed. The studs are tensioned and detensioned by a plurality of portable hydraulic stud tensioning devices or tensioners which are attached to the upper ends of the studs by the modified breechblock threads at the upper ends of the studs. The tensioners are carried by a separate hoist system mounted on the closure head of the vessel. (NL)

31198 HEAD CLOSURE MECHANISM. (to Westinghouse Electric Corp.). Netherlands Patent 7,211,133. 15 Aug 1972. Priority Date 13 Sep 1971, USA. 16p. (In Dutch).

For the purpose of reducing the time required for removal and replacement of a reactor pressure vessel closure head, each stud utilized for securing the head on the pressure vessel is provided with modified breechblock threads at its lower end. After being unloaded, the studs are rotated 60° for disengagement from corresponding threads in a flange at the top of the pressure vessel and can be lifted out of the stud holes in the vessel flange along with the head when it is removed from the vessel. Each stud is provided with an individual hydraulic tensioning device, mounted on top of the head flange. (NL)

31199 SYSTEM FOR CONCENTRATING A MODERATING SOLUTION UTILIZED IN A PRESSURIZED WATER NUCLEAR POWER PLANT. (to Westinghouse Electric Corp.). Netherlands Patent 7,215,216. 10 Nov 1972. Priority Date 30 Nov 1971, USA. 13p. (In Dutch).

A system for concentrating a boric acid solution to a predetermined concentration and stripping the radioactive gases from the solution is described. The system is generally operable so that there is a continuous feed of weak boric acid solution and a continuous discharge of pure water from the system during the concentrating portion of the cycle and the system is operable so that when the boric acid solution reaches a predetermined concentration, the weak acid feed and pure water discharge are shut off, the pure water is recirculated through the system until the boric acid of predetermined concentration is removed to storage tanks. The system has sequentially-operated controls which minimize the thermodynamic shock as the system is switched from the recycle portion of the cycle to the distillate discharge portion of the cycle. (NL)

31200 REACTOR VESSEL IN-SERVICE INSPECTION ASSEMBLY. (to Westinghouse Electric Corp.). Netherlands Patent 7,215,811. 22 Nov 1972. Priority Date 22 Nov 1971, USA. 20p. (In Dutch).

A nuclear reactor vessel in-service inspection apparatus is described for inspection of weld areas which permits remote control, accurate positioning of a tool within the reactor vessel and comprises a positioning and support assembly comprising a central body portion from which a plurality of radially directed support arms extend. The extending ends of the support arms are adapted to seat on a predetermined portion of the reactor vessel to define a positional frame of reference for the inspection assembly relative to the reactor vessel. The repositioning and support assemblies include integral adjustment means whereby the radial extent of the support arms is simultaneously varied to permit the assembly to fit reactor vessels of varying diameter. A central column is connected to the positioning and support assembly which central column extends along the longitudinal axis thereof. One or more movable inspection assemblies are connected to the central column which inspection assemblies include drive means and position indicating means. Three specific inspection subassemblies are provided including a flange scanner, a nozzle scanner, and a vessel scanner. Each of these scanner assemblies employ multiprobe transmitter-receiver ultrasonic transducers to permit more accurate volumetric plotting of the state of the wall of the vessel. (NL)

31201 TRANSIENT CRITICAL HEAT FLUX AND SPACER GRID STUDIES. Zielke, L. A. (Babcock and Wilcox Research Center, Alliance, OH); Wilson, R. H. Nucl. Technol.; 24: No. 1, 13-19(Oct 1974).

Experimental studies of pressurized-water-reactor flow and power transients are performed on a 6-ft-long electrically heated 9-rod bundle in a square array. Flow transients are patterned after decay rates typical of reactor coolant pump coast-downs. Power transients are approximately 5% ramp increases. For the transient conditions tested, there is no premature occurrence of critical heat flux. Steady-state critical heat flux data for axial spacer grid separations of 10, 15, and 21 in. indicated there is no grid-spacing effect on critical heat flux by the Babcock & Wilcox Mark B2-style spacer grid at normal reactor flow rates. (auth)

31202 CONSTRUCTION AND OPERATION EXPERIENCE IN PWR POWER PLANTS. Fujii, G. (Kansai Electric Power Co. Inc., Osaka). Karyoku Hatsuden; 24: No. 1, 39-44(Jan 1973). (In Japanese).

Based on Kansai Electric Power Company's experiences in constructing and operating 7 PWR plants, some reflections are made on each stage of construction, test operation and commercial operation. The construction of Mihama No. 1 and No. 2 atomic power plants took longer period (by the factor of about 1.5) than the fossil fuel-fired plants of the same scale. For the plant operation, the operation record of Mihama No. 1 plant is presented. Within 29 months of operation, there were 19 shutdowns, of which about half were for preventive maintenance. Only a few troubles of reactor systems were experienced, whereas many troubles occurred in conventional machinery such as pumps, turbine, valves and pipings. The significance of radioactivity for repairing works is emphasized as compared with those for fossil fuel plant. It is also recommended that seawater should not be used within reactor containers because of its intensive corrosion effect. (JA)

31203 THEORY OF PUMP-INDUCED PULSATING COOLANT PRESSURE IN PRESSURIZED WATER REACTORS. Penzes, L. E. (Combustion Engineering, Inc., Windsor, Conn. (USA). Nuclear Power Dept.). Nucl. Eng. Des.; 27: No. 2, 176-188(May 1974).

The theory of pump-induced pulsating pressure distributions in a PWR coolant annulus is developed. The calculated pressure distribution can then be applied to predict the dynamic responses of the reactor internals. The mathematical analysis is formulated in accordance with the linearized Navier-Stokes equations by assuming a compressible, inviscid liquid. These equations are combined to form a single equation in terms of the unknown pressure distribution. The boundary conditions are two concentric rigid walls in the radial direction and any combination of closed, open, and piston-spring supported end conditions in the axial direction. The pulsating pump pressure which induces the pressure fluctuation in the annulus is prescribed at a small opening of the outer cylindrical wall (pump inlet of the reactor). An approximate solution is obtained by introducing the concept of time-dependent body force in the governing differential equations. With this conceptual substitution for the actual loading, the time-dependent, mixed boundary value problem can be represented as a forced vibration problem with homogeneous boundary conditions. This problem can then be solved by the method of normal modes. Numerical examples are provided which give the pressure distribution in the axial and circumferential directions of the annulus for various configurations of one and/or several pumps. (auth)

Power Reactors, Non-Breeding, Graphite Moderated

Refer also to abstract 31192.

31204 (AED-CONF-74-157-007) EXPERIENCE IN COMPLYING WITH AUTHORIZATION CONDITIONS FOR THE DISCHARGE OF LIQUID AND GASEOUS RADIOACTIVE EFFLUENTS FROM CEGB NUCLEAR STATIONS. Pepper, R. B. (Bayerisches Landesinstitut fuer Arbeitsmedizin, Muenchen (F.R. Germany)). 1974. 10p. (CONF-740556-6). INIS.

From seminar on the monitoring of radioactive effluents; Karlsruhe, F.R. Germany (14 May 1974).

6 tabs. With abstract.

For each of its 8 operational twin-reactor Magnox sites, the Central Electricity Generating Board has been granted separate authorizations for liquid and gaseous radioactive discharges. The conditions attached to the authorizations differ only in detail from station-to-station. An outline is given of the manner in which the Board complies with those conditions relating to the monitoring of effluents. Reference is made to problems in monitoring and evaluation which have arisen because of changes in plant operating conditions and in reactor and plant design. As a result of the regular re-assessment of techniques in use, the Board is satisfied that it has continued to comply with the authorization conditions. (auth)

31205 UTILIZATION OF METALLIC URANIUM IN POWER CHANNEL URANIUM-GRAPHITE REACTORS. Zhirnov, A. D.; Sirotkin, A. P.; Bryunin, S. V.; Pushkarev, V. I.; Runin, V. I. Sov. At. Energy (Engl. Transl.); 34: No. 6, 584-586(Jun 1973).

Translated from At. Energ. (USSR); 34: No. 6, 479-481(Jun 1973).

Investigations, carried out for the purpose of attaining large burnups in metallic uranium, indicate that difficulties connected with the swelling of metallic uranium during irradiation can be overcome. One of the methods allowing one to reduce to a minimum the effect of swelling on the efficiency of the fuel elements is the creation of a central hole in the fuel element and the application of external guards. It was experimentally established that in a fuel element with a 5% empty, internal space, a burnup in the 15,000-20,000 MW · day/ton U range is attainable. The allowable burnup rises with an increase in the empty space. (auth)

31206 INDUSTRIAL GASES FOR NUCLEAR POWER PLANT. Williams, A. G. (Central Electricity Generating Boark, Romney Marsh, Eng.). pp 112-119 of Cryotech '73: the Production and Use of Industrial Gases. Guildford, Eng.; IPC Business Press Ltd. (1974).

From the production and use of industrial gases symposium; Brighton, UK (13 Nov 1973). See CONF-731145-.

In addition to the gases used at conventional power stations, nuclear plants use large quantities of reactor coolant. The selection of a suitable coolant gas and the effect of impurities are discussed. The need to use helium instead of carbon dioxide at future stations is considered. Reactor coolant plays an essential role in nuclear plant safety. Large reserves must always be available. Requirements are a small continuous make-up with infrequent heavy demand for reactor filling, and the ability to inject at very high rate in emergency. The effects on the design of storage plant and on the supply contract are discussed. The coolant will undergo changes in service due to normal operation or fault conditions and undesirable impurities may result. At AGR stations certain levels of additives in the coolant are necessary. Coolant analysis and management to give an acceptable composition are discussed. Some impurities can be removed in filters or driers, some by treatment in catalyst beds. Some additives break down in the reactor itself. Typical plant is discussed. Other gases will be required as additives or treatment and the merits of purchase or on-site manufacture are considered. (auth)

31207 ENGINEERING ASPECTS OF MAGNETOHYDRODYNAMICS. Thirteenth Symposium Held at Stanford, California, March 26-28, 1973. University, MI; University of Mississippi (1973). 359p. (CONF-730311-). $15.00.

Sixty papers were presented. A separate abstract was prepared for each of 2 papers. The remaining 58 papers on nonequilibrium generators, combustion generators, liquid metal generators, facilities and materials, design studies, plasma flows and instabilities, and pollution and combustion plasma properties were not within the scope of NSA. (LCL)

For abstracts of individual papers see: 31208 and 31209.

31208 FEASIBILITY PROBLEMS ON UHTR FOR CLOSED CYCLE MHD-POWER PLANTS. Bohn, T.; Komarek, P.; Naoumidis, A.; Nickel, H.; Teuchert, E. (Kernforschungsanlage, Juelich, Ger.). pp I.8.1-I.8.11 of Engineering Aspects of Magnetohydrodynamics. University, MI; Univ. of Mississippi (1973).

From 13th symposium on engineering aspects of magnetohydrodynamics; Stanford, California, USA (26 Mar 1973). See CONF-730311-.

The present state of art and the foreseeable progress in ultra high temperature reactor (UHTR) technology with respect to MHD-application are reviewed. The requirements imposed from MHD-energy conversion on the reactor are summarized. Concerning the working gas, the disadvantage of argon due to its high reactivity coefficient is pointed out. Discussing the dependence of plant efficiency on the gas conditions for different power plant concepts, it is shown that the advantage of high efficiencies for nuclear MHD-power plants can only be proved if temperatures of from 1800 to 2000°K can be delivered by the reactor. A new operation modus for the pebble bed-HTR has been developed which permits increasing the average gas outlet temperature up to 100°C below the maximum permissible coated particle temperature. The conventional proven limit of coated particles is 1250°C so that the reactor presently permits providing heated helium at 1150°C. But there exists no general limit for that concept at even much higher temperatures if the material technology could be developed. Increasing the temperature of present coated particles above 1400°C for a long time causes failure of the particle due to chemical reactions between the kernel and the coating ("amoeba effect"). Theoretical and experimental considerations are presented, showing that the chemical interaction can be manipulated by additives in the kernel. Out-of-pile tests have been successful from 1750 to 2000°C. Also promising were investigations improving the fission product retention at high temperatures by doping the kernel with special refractory oxides. The fission product release of the kernel could be reduced by a factor up to 100. Finally the question of compatibility of cesium released into the gas with the graphite in the reactor is discussed. It has been proved experimentally that the Cs-partial pressure in the main gas flow must be kept below a certain critical threshold vapor pressure which depends on the lowest process temperature. According to these results an extremely high degree of Cs-separation must be provided which has not yet been proven. (auth)

31209 EXPLORATORY STUDY OF SEVERAL ADVANCED NUCLEAR-MHD POWER PLANT SYSTEMS. Williams, J. R.; Rosa, R. J.; Yang, Y. Y.; Clement, J. D. (Georgia Inst. of Tech., Atlanta). pp V.10.1-V.10.7 of Engineering Aspects of Magnetohydrodynamics. University, MI; Univ. of Mississippi (1973).

From 13th symposium on engineering aspects of magnetohydrodynamics; Stanford, California, USA (26 Mar 1973). See CONF-730311-.

In order for efficient multi-megawatt closed cycle nuclear-MHD systems to become practical, long-life gas cooled reactors with exit temperatures of about 2500°K or higher must be developed. Four types of nuclear reactors which have the potential of achieving this goal are the NERVA-type solid core reactor, the colloid core (rotating fluidized bed) reactor, the "light bulb" gas core reactor, and the "coaxial flow" gas core reactor. Research programs aimed at developing these reactors have progressed rapidly in recent years so that prototype power reactors could be operating by 1980. Three types of power plant systems which use these reactors have been analyzed to determine the operating characteristics, critical parameters and performance of these power plants. Overall thermal efficiencies as high as 80% are projected using an MHD turbine-compressor cycle with steam bottoming, and slightly lower efficiencies are projected for an MHD motor-compressor cycle. Nuclear analyses of several reactor configurations have shown that these reactors are capable of breeding, that is, they can produce more fissile fuel than is used. Applications of these plants include terrestrial power generation, space power in the multimegawatt range, and power for proposed satellite nuclear power stations. (auth)

31210 ROLE OF HELIUM-COOLED REACTORS IN MEETING THE ENERGY CRISIS AND CONSERVING RESOURCES. Meleso-d'Hospital, G. (General Atomic Co., San Diego, CA). pp 731-

737 of 9th Intersociety Energy Conversion Engineering Conference Proceedings. New York; American Society of Mechanical Engineers (1974).

From 9th Intersociety Energy Conversion Engineering Conference; San Francisco, California, USA (26 Aug 1974). See CONF-740805-.

Helium cooling is now being used in High Temperature Gas Cooled Reactors (HTGR) which operate on the uranium-233–thorium cycle with a high thermodynamic efficiency. Present HTGR power plants raise conventional steam conditions with wet cooling towers, but gas turbine HTGRs with dry cooling are under active development in order to improve siting capabilities of nuclear plants. Hot helium out of HTGRs could be used for various industrial processes, such as coal gasification or hydrogen production. Gas Cooled Fast Breeder Reactors would use much of the HTGR technology and should have a very good breeding ratio. GCFRs look like attractive fuel factories to produce U-233 which is the preferred fuel for HTGRs, thus greatly reducing the need for enrichment facilities and significantly improving the utilization of existing fissile resources. Finally, next century, fusion reactors could also perhaps be cooled by helium which would thus appear to be a very attractive coolant for nuclear power plants for a long time to come. 25 references. (auth)

31211 CALCULATION OF THE CORROSION RATE OF AN HTR CORE UNDER FAULT CONDITIONS. Hawtin, P.; Huber, R. A.; Wilmore, D.; Perring, J. K. (United Kingdom Atomic Energy Authority, Harwell, Eng.). J. Brit. Nucl. Energy Soc.; 13: No. 3, 261-269(Jul 1974).

A burst heat exchanger tube in an HTR can lead to very rapid ingress of water. It is possible that during the initial phases of such an incident, very high rates of corrosion will occur in the graphite core. Under these conditions the steady state models used for calculating the core corrosion rate under normal operating conditions may not be adequate, and a transient model will then become essential. A suitable transient model is therefore developed. The model assumes cylindrical symmetry, and that diffusion is the sole mechanism of transport into and out of the graphite pores. A computer program LIGHTER is described, which implements the transient model for a whole reactor situation. This implementation shows that the mathematical procedures represent a practicable method for assessing the course of an incident involving gross in-leakage of water into an HTR core. (auth)

31212 NEW METHODS OF MEASURING ^{238}U CAPTURE RATE AND FAST FLUXES IN A ZERO ENERGY HTR LATTICE. Beynon, A. J. (Central Electricity Generating Board, Berkeley, Eng.); Lewis, T. A.; Nauman, S. J. Brit. Nucl. Energy Soc.; 13: No. 3, 241-250(Jul 1974).

The reactor physics of HTGR lattices is studied in a zero energy assembly to verify power reactor design calculation methods. Among new techniques developed are those for measurement of relative conversion ratio (RCR) and for fast neutron flux distribution. For both techniques, the target accuracy has been estimated as $\pm 2\%$ (1σ). (UK)

31213 TRENDS IN STRUCTURAL MECHANICS. A UK Review of the 2nd International Conference on Structural Mechanics in Reactor Technology. VIII. Reactor Core. Gittus, J. H. (United Kingdom Atomic Energy Authority, Harwell, Eng.). J. Brit. Nucl. Energy Soc.; 13: No. 3, 305-321(Jul 1974).

A review is presented which discusses material from 25 of the papers presented at the 2nd International Conference on Structural Mechanics in Reactor Technology, Berlin, 1973, which is relevant to structural problems in the core of nuclear reactors. The areas of interest which are considered are: the effect of normal operation on the deformation and fracture of fuel particles for HTR and fast reactor fuels; transient effects in fast reactors; finite element computer models of fuels; finite element analysis of cladding deformation and effects of irradiation creep; mechanism of axial rachetting; analysis of behaviour of metal clad fuel during start-up; bowing of fuel pins; fast reactor fuel element modelling; effect of fuel pin vibrations, and analysis of behaviour of graphite components in HTRs. (UK)

31214 IMPROVEMENTS IN OR RELATING TO NUCLEAR REACTORS. Hough, W. R.; Quick, M. V. (to Nuclear Power Group Ltd.). British Patent 1,353,733. 22 May 1974. 4p.

A moderator core construction is described comprising an assembly of moderator blocks arranged in vertical columns with an upper layer of spacer blocks the sides of which abut the spacer blocks of adjacent columns so as to maintain a substantially constant pitch between the columns. The blocks beneath the spacer blocks in each column are spigotted together but spaced from the blocks of adjacent columns. The spacer blocks have recesses in their sides adapted to take a grab for removal purposes. The arrangement avoids keying of the blocks and the provision of retractable members in the spacer blocks. (UK)

Power Reactors, Non-Breeding, Otherwise Moderated

31215 NOT SUCH A BAD REACTOR. Rippon, S. New Sci.; 63: No. 910, 398-401(15 Aug 1974).

The progress of the design and construction of the 100 MW(e) prototype SGHWR at Winfrith UK is outlined. The plant went into operation in 1967 since when operating performance has been good and has completely confirmed the validity of the design. However there has been difficulty, until recently, in getting the SGHWR into the commercial nuclear power program. Now a 660 MW(e) version has been chosen for the next round of nuclear power plant ordering. Various aspects of the original Winfrith and the new commercial designs of the SGHWR are discussed. (UK)

31216 CANADIAN NUCLEAR POWER PROGRAMME. Gray, J. L. (Atomic Energy of Canada Ltd., Ottawa). J. Brit. Nucl. Energy Soc.; 13: No. 3, 227-238(Jul 1974).

An outline is given of the development of nuclear power reactors in Canada. The expected programme for nuclear plants to the end of 1996 is illustrated. Operating statistics for Pickering show the high satisfactory performance of the plant. Continuous refuelling assists in the high availability of the nuclear steam supply system, together with maximum burnup of all the fuel. Another significant achievement is the very low loss and low upkeep rate of the heavy water. Other desirable features of the Candu system which are discussed are its inherent safety, the low cost fuel-cycle, and the flexibility of the pressure tube system. The economics of choosing between enrichment of uranium or production of heavy water for use with natural uranium, and Canada's achievement in heavy water production are briefly discussed. Generating costs for Pickering are fully competitive with comparative coal-fired plants. (UK)

Power Reactors, Breeding

Refer also to abstracts 29621, 31210, 31249, 31253, 31258, 31263, 31264, and 31323.

31217 (CENC-1194(Vol.1)(Suppl.1)) LMFBR DEMONSTRATION PLANT STEAM GENERATING SYSTEM. (Combustion Engineering, Inc., Chattanooga, Tenn. (USA)). 23 Feb 1973. Contract AT(11-1)-3031. 250p. Dep. NTIS $15.50.

Following the selection of a reference concept design for a sodium heated steam generator to be used in the LMFBR Demonstration Plant, additional analyses were performed in a follow-on program to further develop the steam generators. A report of the work accomplished to date in the follow-on program is presented. Included are structural analyses of certain critical areas of the steam generator, sodium–water reaction analyses, steam generator transient analyses, and shell side flow distribution analyses. Revised drawings of the evaporator and superheater modules indicate a modification of the heat transfer surface. Specifications and drawings of the steam/water recirculating system are also included. (DG)

31218 (CENC-1194(Vol.2)(Suppl.1)) LMFBR DEMONSTRATION PLANT STEAM GENERATING SYSTEM. (Combustion Engineering, Inc., Chattanooga, Tenn. (USA)). Feb 1973. Contract AT(11-1)-3031. 206p. Dep. NTIS $13.50.

Supplementary information is presented on the following topics: (1) preliminary structural analysis of tube-to-tubesheet weld, (2) preliminary structural analysis at the sodium–argon interface, (3) sodium–water reaction structural analysis, (4) specifications for demonstration plant steam generators, (5) insulator tube test—effects on steam generator thermal sizing, (6) effect of steam pressure on steam generator design, and (7) shell side distribution and pressure loss calculations. (DG)

31219 (CENC-1197(Vol.1)) LMFBR SODIUM HEATED STEAM GENERATOR: TEST MODEL. (Combustion Engineering, Inc., Chattanooga, Tenn. (USA)). 23 Feb 1973. Contract AT(11-1)-3031. 248p. Dep. NTIS $15.50.

The reference concept design for the LMFBR sodium heated steam generator was selected to be a forced circulation, separate shell, modular, bayonet tube type. The preliminary design program provided for the detail design, fabrication, and test of a 30 MW(t) model of the steam generator concept. Work to characterize the test model evaporator and superheater modules, the steam/water recirculating system, and the manufacturing and test planning efforts is described. (HDR)

31220 (CENC-1197(Vol.3)) LMFBR SODIUM HEATED STEAM GENERATOR: TEST MODEL. (Combustion Engineering, Inc., Chattanooga, Tenn. (USA)). Feb 1973. Contract AT(11-1)-3031. 238p. Dep. NTIS $15.00.

The water/steam isolation and dump system design for the 30 MW(t) Steam Generator Test Model is described, and the design analysis of the evaporator and superheater blowdown system and of the dump tank and venting system are presented. The preliminary structural analysis of the steam generator piping system is included, and tabulations of stresses, forces, or moments due to pressure, expansion, weight, and static equivalent seismic loading effects are provided. (DG)

31221 (CENC-1197(Vol.4)) LMFBR SODIUM HEATED STEAM GENERATOR: TEST MODEL. (Combustion Engineering, Inc., Chattanooga, Tenn. (USA)). Feb 1973. Contract AT (11-1)-3031. 138p. Dep. NTIS $10.00.

Structural steel analyses for the LMFBR 30 MW(t) test model are presented. (DG)

31222 (CONF-740341-1) DESIGN PROGRESS ON THE LMFBR DEMONSTRATION PLANT. Subject No. 20. Kenney, J. (Westinghouse Electric Corp., Madison, Pa. (USA). Advanced Reactors Div.). 1974. 22p. Dep. NTIS $4.25.

From electric utility engineering conference; Pittsburgh, Pennsylvania, USA (3 Mar 1974).

The Clinch River Breeder Reactor development program is reviewed. Design specifications and physics characteristics of the reactor are included. (DCC)

31223 (GEAP-12511) THERMODYNAMIC DATA PROGRAM INVOLVING PLUTONIA AND URANIA AT HIGH TEMPERATURES. Quarterly Report No. 27, February 1, 1974—April 30, 1974. Adamson, M. G.; Aitken, E. A. (General Electric Co., Pleasanton, Calif. (USA). Vallecitos Nuclear Center). May 1974. Contract AT(04-3)-893. 26p. Dep. NTIS $4.00.

Progress is reported on the continuing scope of work related to fission product-cladding chemical interaction, sodium-fuel interaction, and oxygen and plutonium-uranium redistribution in temperature gradients. 3 references. (auth)

31224 (JAPFNR-154) DEVELOPMENT OF SODIUM FLOWMETER BY REAL TIME CORRELATION TECHNIQUE. II. Measurement of Flow Velocity in Mockup Fuel Assembly. Hasegawa, K.; Nishino, O.; Kawaguchi, T. (Tokyo Univ. (Japan)). Jan 1974. 16p. (PNC-N-251-73-06). Dep. NTIS (US Sales Only) $4.00.

For Power Reactor and Nuclear Fuel Development Corp., Tokyo.

A measuring system of flow velocity by cross correlation techniques has been constructed and tested by use of a liquid sodium test loop. In the test loop a model fuel assembly was prepared for study of temperature fluctuations in flow. There is also a rectifier at outlet of the fuel assembly. Two sheathed thermocouples are placed on the central axis of the rectifier assembly and used to detect the temperature fluctuations in turbulent flow. Velocity and temperature of flow through a central fuel element in the assembly are so adjustable that a mixed stream of flows with different temperatures is obtained at the outlet of the assembly. Such a stream has large temperature fluctuations at high frequency region above several Hz. Therefore, correlation functions can be calculated by a real-time correlator, and flow velocities at various flow rates are measured. On the central axis of the rectifier, the flow velocity depends on the flow rate in the central fuel element and has a good linearity with it. (auth)

31225 (KFK-1990) CALCULATION OF THE EFFECTS OF FISSION GAS IN A LMFBR, FOR THE ANALYSIS OF AN UNPROTECTED OVERPOWER TRANSIENT. Bogensberger, H. G.; Ronchi, C. (Kernforschungszentrum Karlsruhe (F. R. Germany). Inst. fuer Angewandte Systemtechnik und Reaktorphysik). Jun 1974. 36p. (EUR-4975). Dep. NTIS (U. S. Sales Only) $5.00.

A distribution model for the noble gases, created by fission, is applied in a computer program. The subroutine LANGZEIT calculates the "long time" behavior of the fission gas in a pin during "steady state" operation. The results of this calculation are used as the initial conditions for the subroutine KURZZEIT. This code permits the calculation of migration phenomena and pin swelling during an overpower transient. The results for 2 examples are shown and discussed. (10 references) (auth)

31226 (RCN-212) FAST REACTOR PROGRAMME. First Quarter 1974 Progress Report. Hoekstra, E. K. (comp.). (Stichting Reactor Centrum Nederland, Petten). Jun 1974. 80p. INIS.

Data on the spectra of the flux and adjoint flux of the STEK cores 4000, 3000, 2000, 1000 and 500 are given; the code FISPRO-RCN for routine calculations in capture cross sections is discussed. Post-irradiation examination results are given of fuel pin R54-F29, which failed after a 101-hour in-pile burst test, and of fuel pin R63-L09, used in the in-pile loss-of-cooling experiments. Progress on the lattice parameter, thermodynamic and vapor pressure measurements on U(C,N) is reported. It is shown that the formation of $Cs_2U_4O_{12}$ from oxide fuel causes a change in volume which may lead to swelling of the fuel and even fuel pin failure. The strain rate dependence of the tensile properties of steel DIN 1.4948 at room temperature, obtained with high speed tensile tests, is shown graphically. The influence of supersaturation on the decay of the particle number concentration of gold aerosols is shown. Progress is reported on the single-phase and two-phase sodium heat transfer experiments in electrically heated bundles and on the testing of the heaters used in such bundles; in the field of heat transfer in air data on the thermal entrance effect for various roughened rods are presented. (NL)

31227 APPARATUS FOR REFINING SODIUM. Shimoyashiki, S.; Makita, K.; Aoki, N. (to Hitachi Ltd.). US Patent 3,831,912. 27 Aug 1974. Priority Date 28 Sep 1971, Japan. 6p.

Refining or the removal of impurities from sodium traveling within a closed circuit for heat exchange of a fast breeder nuclear reactor or the like is obtained by means of a sodium refining chamber as a part of the circuit having netlike members disposed against the sodium flow and a heat exchanger for selectively heating and cooling the sodium as it flows around the netlike members for the precipitation of the impurities during cooling and for the remelting of the impurities during heating. The remelted impurities during heating are discharged through a discharge pipe in the lower portions of the sodium flow adjacent the netlike members. The netlike members are constructed of large mesh, knitted wire material having the wire strands constructed of a plurality of fine wires, with the adjacent layers of net having spaces between their faces. The net layers are preferably corrugated, with the direction of corrugation being inclined with respect to the direction of knitting and further being inclined with respect to the corrugations of an adjacent layer. The travel of the sodium through the netlike members is such that it will be in counter flow heat exchange relationship, with the interposition of a heat conductive flow separator, with the flowing liquid sodium that has just passed through the netlike members. (Official Gazette)

31228 FISSION GAS BEHAVIOR IN FAST REACTOR FUEL UNDER TRANSIENT POWER CONDITIONS. Dias, J. W.; Okrent, D.; Erdmann, R. C. (Univ. of California, Los Angeles). Nucl. Technol.; 24: No. 1, 20-32(Oct 1974).

An explanation was sought to explain the existence of the relatively large (~2000 Å) fission gas bubbles found in the unrestructured region of an EBR-II-irradiated mixed-oxide pin following a TREAT transient in which peak temperatures stayed below melting. Using a code like GRASS, it was found difficult to explain their existence by employing the bubble mobility values fit to experimental measurements in the region of 1500°C. A rather good fit was obtained if the greater bubble mobility that theory gives for the surface-diffusion mechanism was assumed to be applicable at higher temperatures; e.g., above 1800°C. Sensitivity studies showed that swelling is very sensitive to peak temperatures and the duration of the transient and to hydrostatic pressures in the fuel. If the surface-diffusion mechanism is applicable, considerable fuel swelling can occur due to bubble growth and coalescence. In addition, bubble drift due to temperature gradient is found to equal or exceed the effects of Brownian motion. 37 references. (auth)

31229 STUDY OF LOCAL BLOCKAGES IN FAST REACTOR SUB-ASSEMBLIES. Gregory, C. V.; Lord, D. J. (United Kingdom Atomic Energy Authority, Dounreay, Eng.). J. Brit. Nucl. Energy Soc.; 13: No. 3, 251-260(Jul 1974).

The consequences of a localized blockage in a fast reactor subassembly is examined. Past and current work is reviewed and results from recent theoretical work at the Dounreay Experimental Reactor Establishment using the code WAKE are reported. The code allows prediction of the behaviour of the recirculating "wake" region immediately downstream of either permeable or impermeable blockages. The implications of these results for the safety of power fast reactors are discussed; in particular it is shown that relatively large blockages, of the order of 100 sub-channels, have to form before significant local boiling can occur. (auth)

Research, Test, and Experimental Reactors

Refer also to abstracts 31270 and 31295.

31230 (DEMO-74/5, pp 3-9) DESCRIPTION OF THE GREEK RESEARCH REACTOR-1. Marketos, D. G.; Mitsonias, C. A. (Democritus Nuclear Research Center, Athens). Feb 1973.

The "Democritos" Greek Research Reactor-1 (GRR-1) is described. The reactor is a 5 MW, swimming pool-type, light water moderated, cooled and reflected, heterogeneous reactor. Details are given of core dimensions, fuel, cooling system, experimental holes and neutron flux intensities. (INIS)

31231 (HEDL-TME-74-37) FABRICATION, IRRADIATION, AND POSTIRRADIATION EXAMINATION OF MIXED OXIDE FUEL PIN PNL-3-8. Chastain, S. A.; Arey, T. T.; Henderson, R. G. (comps.). (Hanford Engineering Development Lab., Richland, Wash. (USA)). Jul 1974. Contract AT(45-1)2170. 61p. AT.

PNL 3-8 was an unencapsulated fuel pin of a 37-pin subassembly (PNL-3) which was irradiated in the EBR-II. This document presents a compilation of design, specification and fabrication data, along with a detailed description of the irradiation and the results of the post-irradiation examination of pin PNL 3-8. The 13.5-in. fuel column consisted of 75 wt% UO_2-25 wt% PuO_2 pellets with a smeared density of 88% TD. The 304 SS cladding had an outside diameter of 0.250 in. and was 0.016 in. thick. The fuel pins were wire wrapped with 304 SS. Total pin length was 60-51/64 in. PNL 3-8 was one of four pins removed from the subassembly for both nondestructive and destructive examination after an exposure of 326.04 equivalent full power days (at 50 MW). The pin operated at a peak linear power of 4.82 kW/ft and the peak cladding temperature was 820°F. Examination of the pin revealed no significant damage or deterioration. (auth)

31232 (IKE-6-79d) CALCULATION OF CORRECTION FACTORS FOR PULSED NEUTRON MEASUREMENTS IN THE ITR CRITICAL EXPERIMENT. Woerner, D. (Stuttgart Univ. (TH) (F.R. Germany). Inst. fuer Kernenergetik). Dec 1973. 68p. (In German). INIS.

With figs. and tabs.; 14 refs. With abstract. Available from the library of Stuttgart Univ.

The reactivities measured by means of the pulsed neutron techniques according to the methods of Sjoestrand, Gozani and Garelis and Russell exhibit a marked spatial dependence according to each system. It can be theoretically shown that the kinetic distortion and the occurrence of higher modes are responsible for this. According to the system, there is a partial or complete compensation for these two effects. Using the example of the measurements on core III of the ITR critical experiment, it could be shown that the strong spatial dependence of the measured results can be compensated for to a certain extent by correction by prompt and delayed spectra. It was shown that more extensive methods (Preskitt) are in general not justifiable with regard to the efforts for programming. (GE)

31233 (KURRI-TR-110, pp 4-8) SOME TECHNICAL PROBLEMS ON THE DYNAMIC STUDIES OF THE HIGH FLUX RESEARCH REACTOR. Wakabayashi, J. (Kyoto Univ.). 1972. (In Japanese).

The University Union in Japan is planning to build a two-separated core type High Flux Research Reactor. In the dynamic studies of this reactor, it is necessary to treat it as a coupled reactor. The flux dependency of the coupling parameters is one of the important problems in the power excursion calculation, and the burn-up dependency of the coupling parameters must be taken into consideration. In order to determine the coupling parameters of the reactor, both analytical and experimental studies using a critical assembly are considered necessary. Control of the neutron flux level at the beam holes is one of the important problems for the experimental users. Effective control using a computer would be performed by creating a numerical model of the reactor which could calculate the deviation of neutron flux at the beam holes due to the fine change of control rods. (auth)

31234 (KURRI-TR-110, pp 29-30) STUDY OF NUCLEAR PHYSICS USING A HIGH-FLUX REACTOR. Shikazono, N. (Japan Atomic Energy Research Inst., Tokai). 1972. (In Japanese).

The use of a high-flux reactor as a γ-ray source is described. Thermal neutron capture γ-rays produced inside the reactor are the most useful monochromatic γ-rays available. Examples of photoreaction studies which can be carried out with the capture γ-rays are presented. Experimental facilities which should be installed at the reactor are discussed. (JA)

31235 (KURRI-TR-110, pp 61-67) HIGH FLUX RESEARCH REACTOR AND RESEARCH ON REACTOR PHYSICS AND REACTOR ENGINEERING. Sumita, K. (Osaka Univ.). 1972. (In Japanese).

The necessity of a high flux research reactor in Japan is described. Reactor physics and reactor engineering problems to be solved in developing a new type of high flux reactor are discussed. Reactor physics and reactor engineering studies employing a high flux reactor as an intense neutron source are described in accordance with the classification of neutron beam experiments and radiation experiments. A list of about one hundred possible themes is presented. (auth)

31236 (UCID-15817) H. E. FIRING CHAMBERS FOR USE IN SUPER KUKLA REACTOR. (California Univ., Livermore (USA). Lawrence Livermore Lab.). 7 May 1971. 9p. Dep. NTIS $4.00.

31237 OPTIMIZATION OF THE CYCLICITY OF OPERATION OF A RESEARCH REACTOR. Konoplev, K. A.; Semenov, Yu. P. Sov. At. Energy (Engl. Transl.); 35: No. 4, 923-924 (Oct 1973).

Translated from At. Energ. (USSR); 35: No. 4, 263-266(Oct 1973). This is a summary of paper No. 693/7007 with full copy held at TIC.

The question of the most economical operation of research reactors is considered. An attempt is made to optimize the cyclicity of reactor operation (without solving the questions of the refinement of the physical parameters and reprocessing of fuel) and the parameters of the cycle for which the cost per unit thermal energy developed is a minimum are determined. Cores that permit cassette reloading are considered. (DG)

31238 LOFT INTEGRAL TEST FACILITY AND PROGRAM. Coplen, H. L. (Aerojet Nuclear Co., Idaho Falls, ID); Barber, R. W.; Ybarrondo, L. J.; Swanson, R. E. pp 701-709 of 9th Intersociety Energy Conversion Engineering Conference Proceedings. New York; American Society of Mechanical Engineers (1974).

From 9th Intersociety Energy Conversion Engineering Conference; San Francisco, California, USA (26 Aug 1974). See CONF-740805-.

LOFT (Loss-of-Fluid Test) is an "integral" nuclear reactor test facility which has been designed to simulate, as nearly as possible, all of the important effects that are anticipated to occur during a loss-of-coolant accident (LOCA) in a large pressurized water reactor (LPWR) type nuclear steam supply system. During the period of July 1969 to December 1970, a critical reassessment of the original LOFT-U design and program (LOFT-U was to study core meltdown and fission products transport without the use of ECCS) was conducted. The reassessment was initiated with a study of current industrial pressurized water reactor (PWR) plant safety analysis reports with particular attention to ECCS and reactor system design parameters. The objectives of the new design are to (a) assure the credibility and applicability of the experimental data to be acquired to the verification of the predictive analysis codes used for LPWRs currently being built and (b) maximize the experimental system's basic test capability. A minimum of 19 loss-of-coolant experiments (LOCEs) are planned in LOFT with various simulated line break locations and sizes, including some initial isothermal tests using a core simulator rather than the actual fuel assemblies. (auth)

Production and Materials Testing and Processing Reactors

31239 NUCLEAR ENERGY REQUIREMENTS FOR HYDROGEN PRODUCTION FROM WATER. Pangborn, J. B.; Gregory, D. P. (Inst. of Gas Tech., Chicago). pp 400-404 of 9th Intersociety Energy Conversion Engineering Conference Proceedings. New York; American Society of Mechanical Engineers (1974).

From 9th Intersociety Energy Conversion Engineering Conference; San Francisco, California, USA (26 Aug 1974). See CONF-740805-.

The Institute of Gas Technology (IGT), under the sponsorship of the American Gas Association (A.G.A.), is conducting a research program, now in its third year, to derive, evaluate, and experimentally test closed-cycle chemical reaction sequences for splitting water into hydrogen and oxygen. One of our conclusions is that for nuclear water-splitting, heat at high temperatures (from HTGR's) will be required to make thermochemical hydrogen production more attractive than electrolysis. Future-technology electricity generation could achieve high efficiencies, and this allows electrolysis to be an optional route of reasonable overall energy efficiency. Future nuclear energy supply is a serious consideration, and, therefore, efficient energy conversion is of paramount importance. 15 references. (auth)

Propulsion and Package Reactors

31240 (GKSS-74/E/15) NS OTTO HAHN. Research Report No. 4. The Oscillational Behaviour of the Second Core Support System. Witte, G. (Gesellschaft fuer Kernenergieverwertung in Schiffbau und Schiffahrt m.b.H., Geesthacht-Tesperhude (F.R. Germany)). 1974. 31p. (In German). INIS.
19 figs. With abstract.

The dynamic behaviour of the second core support system of the NS Otto Hahn was investigated. The eigenfrequencies were calculated and compared with the exciting frequencies, where an oscillation excitation through the flowing primary water was also not to be excluded. Oscillation measurements were then carried out with running primary pumps and tests to experimentally confirm the calculated eigenfrequencies, as required by the experts. The calculated eigenfrequencies could not be experimentally verified due to the heavy damping by the primary water and the little excitation energy available for technical reasons. However, after measuring the vibrations on the containment support system, an excitation due to propeller excited oscillations could safely be considered as out of the question. No oscillation excitation of the support system worth mentioning was observed with working primary pumps. (GE)

31241 (N-74-23299) DIAGNOSTICS OF SEEDED RF PLASMAS: AN EXPERIMENTAL STUDY RELATED TO THE GASEOUS CORE NUCLEAR REACTOR. Final Report, 1 September 1971–31 July 1973. Thompson, S. D.; Clement, J. D.; Williams, J. R. (Georgia Inst. of Tech., Atlanta (USA). School of Nuclear Engineering). 31 Jul 1973. 137p. (NASA-CR-138240). NTIS $10.00.

Measurements of the temperature profiles in an RF argon plasma were made over magnetic field intensities ranging from 20 amp turns/cm to 80 amp turns/cm. The results were compared with a one-dimensional numerical treatment of the governing equations and with an approximate closed form analytical solution that neglected radiation losses. The average measured temperatures in the plasma compared well with the numerical treatment, though the experimental profile showed less of an off center temperature peak than predicted by theory. This may be a result of the complex turbulent flow pattern present in the experimental torch and not modeled in the numerical treatment. The radiation term cannot be neglected for argon at the power levels investigated. The closed form analytical approximation that neglected radiation led to temperature predictions on the order of 1000 to 2000°K higher than measured or predicted by the numerical treatment which considered radiation losses. (auth)

31242 FUEL ELEMENT FOR A COMPACT POWER REACTOR. Wetch, J. R.; Dieckamp, H. M.; Wilson, L. A. (to United States Atomic Energy Commission). US Patent 3,822,185. 2 Jul 1974. Filed date 28 Mar 1961. 8p.

A fuel element design for a compact reactor capable of withstanding high temperatures and mechanical vibrations is presented. The moderator is incorporated in the fuel rod by hydriding an alloy of ^{235}U and Zr. The reactor uses a NaK eutectic coolant. (DG)

31243 DIE DEUTSCHE SEESCHIFFAHRT: STRUKTURWANDEL UND KUENFTIGE AUSSICHTEN. Vortrag Gehalten am 12. Dezember 1973 vor der Mitgliederversammlung (Jahreshauptversammlung) der Kernenergie-Studiengesellschaft, Hamburg. (German Marine Shipping: Changes in Structure and Future Development. General Meeting of the Nuclear Energy Research Society, Hamburg, Germany, December 12, 1973). Hellwig, F. Munich; Verlag Karl Thiemig AG (1974). Hellwig, F. Munich; Verlag Karl Thiemig AG (1974). 24p. (CONF-731220-1). $4.50.

A quantitative evaluation is made of the future development of nuclear marine shipping based on the total economic growth of the amount and cost of energy production. An attempt was made to indicate general trends with which the German shipping industry is faced and to predict their future course. (JSR)

Reactor Safety and Environmental Aspects

Refer also to abstracts 29343, 29356–29358, 29369, 29383, 29438, 29461, 29462, 31296, and 31323.

31244 (AEC-tr-7569) PRESENT RESEARCH OF ATOMIC ENERGY SAFETY. (Japan Atomic Energy Research Inst., Tokyo). 1973. Translation of Japanese Report. 135p. Dep. NTIS $9.75.

Information on the reactor safety research programs is presented concerning safety research on fuel materials, research on reactor pressure boundary, engineered safety test research on LOCA, experimental research on excursion accident, development and adjustment of reactor safety analysis code, research on evaluation of environmental radiation, research on radioactive waste disposal and treatment. (DCC)

31245 (AED-CONF-73-686-000) ANNUAL COLLOQUIUM 1973 OF THE PROJECT NUCLEAR SAFETY. (Kernforschungszentrum Karlsruhe (F.R. Germany). Projekt Nukleare Sicherheit). 1973. vp. (In German). (CONF-731224-). INIS.
From project nuclear safety conference; Karlsruhe, F. R. Germany (11 Dec 1973).
With figs., tabs., and refs. Available from ZAED.

A report is given on the state of the work of the "Project Nuclear Safety" (PNS) which mainly deals with the topics: emergency core cooling, core meltdown, dynamic stress of safety devices, filter and off-gas systems, radiological and ecological impact in the environment by nuclear power plants, decontamination processes, radiation protection, risk analysis, safety problems in the fuel cycle, waste heat problems, and the reactor safety information system. (RESI). (GE)

31246 (IRS-A-4) IRS LITERATURE 1965-1973. Schulz, W. Dec 1973. 34p. (In German). INIS.

The report summarizes and lists the activities and publications (papers, reports, information series, proceedings and status reports, etc.) of the Institute for Reactor Safety from 1965 to 1973. (GE)

31247 (JAERI-M-5560) PRELUDE-2: SEISMIC RESPONSE ANALYSIS CODE FOR BLOCK-TYPE FUEL CORE. Ikushima, T. (Japan Atomic Energy Research Inst., Tokyo). Feb 1974. 70p. (In Japanese). NTIS (U. S. Sales Only).

Computer code PRELUDE-2 has been prepared for analyzing the seismic response of cores with block-type fuel. The code was developed from PRELUDE-1, and the features are as follows: (1) the model is treated as a discontinuous multi-mass points system. (2) Any seismic wave can be taken as the input. (3) Each mass point has two degrees of freedom, such as (x,θ_x), (x,y), (x,z). (4) The time intervals for calculation, graphic representation of the results, and printout of the results can be chosen arbitrarily so that computer time is commensurate with the purpose of the calculation, and the accuracy desired. (5) Subroutines for CALCOMP plotting are available in the code. The code is written in FORTRAN IV and can be used with FACOM 230-60. (auth)

31248 (KFK-1908) SECOND BIANNUAL REPORT 1973. (Kernforschungszentrum Karlsruhe (F.R. Germany). Projekt Nukleare Sicherheit). Apr 1974. 251p. (In German). INIS.
With figs., tabs. and refs. With abstract in German and English.

The activities of the Nuclear Safety Project in the 2nd half of 1973 are outlined. The following items are mentioned in particular: Environmental impact of nuclear power plants and reprocessing stations; systematic behavior of nuclear facilities under accident conditions; distribution and reaction of fission products in connection with major accidents; mitigation and removal of the consequences of accidents; and safety assessment of nuclear facilities. (GE)

31249 (KFK-1935) TRANSPORT OF CORE MATERIALS DURING ACCIDENTS IN LMFBRs (SLUMPING). Angerer, G. (Kernforschungszentrum Karlsruhe (F.R. Germany). Inst. fuer Neutronenphysik und Reaktortechnik). Jun 1974. 54p. (In German). Dep. NTIS (US Sales Only) $5.75. .

During a pump-coast-down accident in a LMFBR with simultaneous failure of the whole reactor protection system fuel pins may melt. The relocation of the materials as a result of gravity, gas and vapor forces leads to feedbacks on the reactivity and therefore the reactor power, which influence the course of the accident considerably. The computer program SLB is a first attempt to describe the material transport during the accident theoretically. For this the reactor-core is subdivided into coolant channels radially, and into nodes axially. The material transport between the nodes of one and the same coolant channel is computed and the altered material distribution is given to a neutron kinetics program afterwards. As an example the course of pump-coast-down accidents with various values of a material movement parameter is computed. (auth)

31250 (ORNL-TM-4655(Vol.1)) QUARTERLY PROGRESS REPORT ON REACTOR SAFETY PROGRAMS SPONSORED BY THE DIVISION OF REACTOR SAFETY RESEARCH FOR APRIL–JUNE 1974. I. Light-water-reactor Safety. (Oak Ridge National Lab., Tenn. (USA)). Aug 1974. Contract W-7405-eng-26. 86p. Dep. NTIS $5.45.

Information on reactor safety programs for water-cooled reactors is presented concerning blowdown heat transfer studies, Nuclear Safety Information Center Operations, β and γ energy release from fission product decay in fuel materials, and zirconium metal–water oxidation kinetics. (DCC)

31251 (ORNL-TM-4655(Vol.2)) QUARTERLY PROGRESS REPORT ON REACTOR SAFETY PROGRAMS SPONSORED BY THE DIVISION OF REACTOR SAFETY RESEARCH FOR APRIL–JUNE 1974. Whitman, G. D. (Oak Ridge National Lab., Tenn. (USA)). Aug 1974. Contract W-7405-eng-26. 111p. Dep. NTIS $5.45.

Information on the heavy-section steel technology program for water cooled reactor pressure vessels is presented concerning fracture mechanics analyses and investigations, effect of high-temperature primary reactor water on the subcritical crack growth of reactor vessel steel, investigations of irradiated materials, pressure vessel investigations, and thermal shock investigations. (DCC)

31252 (STI/DOC-10/155) THERMAL DISCHARGES AT NUCLEAR POWER STATIONS. Their Management and Environmental Impacts. A Report Prepared by a Group of Experts as the Result of a Panel Meeting Held in Vienna, 23–27 October 1972. (International Atomic Energy Agency, Vienna (Austria)). May 1974. 164p. IAEA $8.00.

Separate abstracts were prepared for each of the 7 chapters included. (JWR)

For abstracts of individual papers see: 29464–29466, 31255–31257, and 31308.

31253 (UCLA-ENG-7343) POST-ACCIDENT CORE RETENTION FOR LMFBR'S. 2. Technical Report. Final Report for the Period 1 July 1972–30 June 1973. Catton, I.; Erdmann, R. C. (California Univ., Los Angeles (USA). School of Engineering and Applied Science). Jul 1973. Contract AT(04-3)-34. 226p. (UCLA-34P203-1B). Dep. NTIS $14.50.

Efforts during fiscal year 1973 are summarized for the following areas: design review and analysis of proposed post-accident core retention systems; review of experiments and preparation of data file; examination of retention phenomena and application to core retention design; secondary criticality. Post-accident heat removal concepts were analyzed. (66 figures, 11 tables, 130 references) (DLC)

31254 (UCRL-51494) DIFFUSION OF RADIOACTIVE FLUID THROUGH SOIL SURROUNDING A LARGE POWER-REACTOR STATION AFTER A CORE MELTDOWN ACCIDENT. Pitts, J. H.; Bowman, B. R.; Martin, R. W.; McKay, J. P. (California Univ., Livermore (USA). Lawrence Livermore Lab.). 21 Dec 1973. Contract W-7405-eng-48. 23p. Dep. NTIS $4.00.

The flow of fluids through the soil surrounding a large power-reactor station after a core meltdown accident was analyzed. Fracture of, or penetration through, a portion of the containment floor was assumed so that radioactive gases would be driven through the soil by pressure within the containment shell. Results for both one-dimensional ideal gas and multiphase flow were obtained using dimensionless variables so that results are applicable for all soil conditions. Two-dimensional results are included for a specific case where permeability of the soil varies spatially. These calculations show that the time required for radioactive gases to permeate to the ground surface are years for silty-type clays and about 10 h for sand-type soil. Heat transfer calculations that estimate the amount of steam generated should the core melt penetrate the containment floor and contact wet soil show that cooling systems must be in operation within four or five days in order to prevent overpressurization of the containment shell. Fluid motion existing in the region immediately around the containment shell and also caused by fissure propagation is mentioned. (auth)

31255 MAGNITUDE OF THERMAL DISCHARGES FROM A DEVELOPING NUCLEAR ECONOMY. pp 3-8 of Thermal Discharges at Nuclear Power Stations. Vienna; International Atomic Energy Agency (1974).

See STI/DOC-10/155.

The magnitude of thermal discharges from nuclear power reactors is examined with particular emphasis on the growth of nuclear power and on the thermal efficiency of the various reactor types. The cooling options available to nuclear power plants are also discussed. (JWR)

31256 ENGINEERING TECHNIQUES FOR NUCLEAR PLANT COOLING. pp 9-31 of Thermal Discharges at Nuclear Power Stations. Vienna; International Atomic Energy Agency (1974).

See STI/DOC-10/155.

Methods for the rejection of waste heat from nuclear power plants are examined. Heat rejection to surface water includes the following: rivers, streams, and canals; ponds, reservoirs, and lakes; and estuaries and coastal sites. Heat rejection to air includes cooling towers and spray ponds. Mixed systems are also briefly discussed. (JWR)

31257 THERMAL DISCHARGES AND THE SITING OF NUCLEAR POWER PLANTS. pp 129-149 of Thermal Discharges at Nuclear Power Stations. Vienna; International Atomic Energy Agency (1974).

See STI/DOC-10/155.

The need for careful selection of nuclear power plant sites to mitigate the environmental impact of waste heat disposal is discussed. Criteria for site selection are given and the relevant factors for the assessment of the thermal receptivity of a given environment are presented. (JWR)

31258 STUDY ON THE TEST OF SODIUM BOILING. I. Loss-of-Flow Test by a Single Pin. Kikuchi, Y. (Power Reactor and Nuclear Fuel Development Corp., Oarai, Japan). Doryokuro Giho; No. 9, 50-62(Dec 1973). (In Japanese).

A test of sodium boiling has been performed to analyze accidents of a fast breeder reactor. A description is presented of a simulated reactor loss-of-flow accident. Test equipment was constructed to simulate the fast reactor. Preheated sodium is fed into a test section using a pump. The sodium boils at the test section, joins with that from a by-pass, condenses, is stored in a head tank, and goes back to the pump. The test section simulates a single fuel pin and its surroundings. Various measuring instruments such as thermocouples, void taps, pressure transducers, electromagnetic flow meters, an accelerometer, and a microphone are included in the test section. The pump stop method and valve closure method were used for simulating the loss of flow. The results showed that the superheat of wall at initial boiling was affected by temperature rise rate. The higher the wall superheat, the higher the initially generated pressure at the beginning of boiling. The generated pressure when vapor disappeared was higher as re-entering liquid velocity was faster, and the obtained pressure is in agreement with the calculated value of sodium hammer phenomenon. A single bubble slug model is dominant for void pattern, and the observed results are in agreement with the calculated results by NAIS-P2 code. (JA)

31259 INDUSTRIAL TECHNIQUE. (to Babcock and Wilcox Co.). Netherlands Patent 7,211,781. 30 Aug 1972. Priority Date 1 Sep 1971, USA. 16p. (In Dutch).

Approximately 0.1% by weight of sodium silicate is added to an aqueous radioiodine absorbing decontamination spray mixture for discharge within a nuclear reactor containment building. The radioactive decontamination fluid preferably includes 1% by weight of sodium thiosulfate, 1.22% by weight of boric acid and 0.528% by weight of sodium hydroxide in a water solution. The added sodium silicate allows less expensive aluminum components to be used within the containment building because it inhibits a corrosive chemical reaction between the aluminum and the sodium hydroxide. Without the inhibitor, the aluminum-hydroxide reaction would lead to a potentially explosive mixture of hydrogen and oxygen within the containment building. (NL)

31260 MAXIMUM CREDIBLE ACCIDENT (MCA) OF LIGHT WATER REACTOR. Uchida, H. (Tokyo Univ.). Genshiryoku Kogyo; 20: No. 3, 13-16(Mar 1974). (In Japanese).

Of the two types of reactor plant accidents, i.e., in normal operation and maximum credible, the latter in light water plants is described on concept, safety countermeasures, and world trend. The maximum credible accident is equivalent to design basis accident (DBA). It is centered on loss-of-coolant accident. Worldly, the incidence of DBA is now commonly taken at less than 10^{-6}/reactor year. This rate, which is probability expression, however, affords fair amount of margin, being essentially desirable target value. Moreover, it is augmented by safety devices etc. incorporated in nuclear power plants. In viewing the nuclear safety of light-water power plants, therefore, it is necessary to grasp the conservative aspect of DBA. (JA)

31261 TRENDS IN STRUCTURAL MECHANICS. A UK Review of the 2nd International Conference on Structural Mechanics in Reactor Technology. V. Fast Reactor Containment. Leigh, K. M. (United Kingdom Atomic Energy Authority, Risley, Eng.). J. Brit. Nucl. Energy Soc.; 13: No. 3, 293-296(Jul 1974).

Comments are presented on some of the work described at the 2nd International Conference on Structural Mechanics in Reactor Technology, Berlin, 1973. They relate to certain aspects of fast reactor containment design. Two fault situations are of particular interest, i.e., accidents involving the whole core which have developed into super-prompt critical power excursions, and accidents in fuel sub-assemblies which result in the fuel becoming molten. Both these situations give rise to a number of structural mechanics problems involving the determination of the response of various reactor components to dynamic loadings. The studies on primary containment and on sub-assembly fault propagation described at the conference which apply to these problems are discussed. (UK)

31262 NUCLEAR ENERGY AND THE ENVIRONMENT. Clementel, E. Com. Naz. Energ. Nucl., Notiz.; 20: No. 7, 25-29 (Jul 1974). (In Italian).

The energy situation that has been developing in the last few years and its relations with society are analyzed. (auth)

31263 DESIGN OF THE PRIMARY CONTAINMENT FOR POOL AND LOOP ARRANGEMENTS OF LMFBRs. Huebel, H.; Koehler, M.; Lange, L. (Internationale Atomreaktorbau G.m.b.H. (INTERATOM), Bensberg; Koeln (F. R. Germany)); Cobb, E. C.; Leigh, K. M. (Nuclear Power Group Ltd., Risley (UK)). Nucl. Eng. Des.; 27: No. 2, 139-154(May 1974).

LMFBR prototypes use different technical concepts for the primary system: France and the UK are constructing pool-type reactors, the US and DEBENELUX have selected loop-type reactors. Obviously, the relationship between the technical concept and the possibilities of limiting the consequences of a hypothetical whole-core accident is a widely discussed question. Three modes of loading phenomena are considered: (1) the transient pressures due to expansion of a vaporized fuel; (2) the transient pressures given by a coherent sodium-fuel interaction; and (3) the "equilibrium" pressure given by transferring the excess heat in the fuel to an amount of sodium which produces the highest possible quasi steady-state pressure in the system. The structural response of the pool and loop systems are studied with respect to salient modes (2) and (3). Axial forces during the accident have to be transferred via the plug the core support to the reactor vessel support. The technical solutions depend on the primary system concept. The given structures can be supplemented by special devices to protect the cover and the vessel against excessive loads. To a first approximation, such safeguards are independent of the technical concept. Post-accident heat removal is accomplished for commercial plants preferably by in-vessel solutions. The expenditure for in-vessel solutions depends more on the singularities of a given design than on the particular design concept. The intermediate (primary/secondary sodium) heat exchanger is a critical component of the containment system. The coupling between the source of the accident and the intermediate heat exchanger is different in both systems. Pool and loop systems are both adequate in limiting the consequences of an unprevented nuclear excursion of a reasonable size. Advantages are well-balanced for both systems. (auth)

31264 ANALYSIS OF THE PRIMARY CONTAINMENT RESPONSE USING A HYDRODYNAMIC-ELASTIC-PLASTIC COMPUTER CODE. Chang, Y. W.; Gvildys, J.; Fistedis, S. H. (Argonne National Lab., Ill. (USA)). Nucl. Eng. Des.; 27: No. 2, 155-175(May 1974).

The dynamic response of the primary reactor containment system to a hypothetical core disruptive accident (HCDA) is determined from the basic equations of mass, momentum, and energy, together with the equations of state of the medium. These equations are first expressed in material coordinates, then set into finite difference form and solved numerically by computer using a hydrodynamic-elastic-plastic computer code, REXCO-HEP, developed at ANL. Propagation of pressure waves, loads imposed on different parts of the reactor components, and the resulting deformations are determined at every time step throughout the sequence of the calculation. As a sample calculation, the code was applied to analyze the response of the FFTF reactor to a 150 MWsec HCDA. The mathematical model is described in detail, particularly in the areas of modeling reactor internals and extending the time range to cover the entire excursion phenomenon. The results obtained from the computer analysis are discussed in detail. (auth)

31265 COMPARATIVE FORCED VIBRATION TEST OF TWO BWR-TYPE REACTOR BUILDINGS. Muto, K. (Muto Inst. of Structural Mechanics, Inc., Tokyo (Japan)); Hayashi, T. (Chugoku Electric Power Co. Inc., Hiroshima (Japan)); Omatsuzawa, K. (Tokyo Electric Power Co., Inc., Okuma, Fukushima (Japan). Fukushima Atomic Power Station); Ohta, T.; Uchida, K.; Kasai, Y. (Kajima Corporation, Minato-Ku, Tokyo, Japan). Nucl. Eng. Des.; 27: No. 2, 220-227(May 1974).

Comparative forced vibration testing of two GE 460 MW(e) BWR-type reactor buildings is discussed. The tested nuclear power plants are the Fukushima Nuclear Power Plant Unit No. 1 of the Tokyo Electric Power Company (hereinafter referred to as Fukushima) and the Shimane Nuclear Power Plant of the Chugoku Electric Power Company (Shimane). They are almost the same in both structure and function, but are built on rock of quite different rigidity. The shear wave velocity of Shimane is about three times that of Fukushima. The forced vibration tests were performed immediately after completion of each reactor building using a vibrator with a maximum exciting force of 3t. The computer simulation analyses were carried out using vibration models possessing different internal viscous damping factors for each structural element. Both the resonance periods and damping factors of Fukushima were found to be larger than those of Shimane. Thus, site selection of nuclear power plants must be reviewed as a matter of utmost importance from the viewpoint of seismic design. (auth)

31266 ELASTIC-PLASTIC DEFORMATION OF CYLINDRICAL PRESSURE VESSELS UNDER CYCLIC LOADING. Chang, T. Y. (Akron Univ., Ohio (USA). Dept. of Civil Engineering); Chu, S. C. (Army Weapons Command, Rock Island, Ill. (USA). Research and Engineering Div.). Nucl. Eng. Des.; 27: No. 2, 228-237(May 1974).

A numerical procedure based on the finite element method and incremental solution approach is presented for analyzing cylindrical pressure vessels deformed in the state of generalized plane strain. The structures considered are subjected to internal pressure, thermal gradients and axial forces, which are cyclic in nature. The materials are assumed to obey the von Mises yield criterion with kinematic strain hardening in which, during the process of plastic deformation, the yield surface is permitted to translate in the stress space and may change its size as a function of temperature. Based on Drucker's postulates for stable materials in the incremental theory of plasticity, a nonisothermal flow rule is deduced in the cylindrical coordinates. By use of the virtual work principle, the finite element equations with displacement formulations are derived. The numerical solution is then carried out by a step-by-step approach for small loading increments and an iteration scheme is employed for each loading step. Furthermore, the analysis method is extended to the determination of limit load and shakedown load of a vessel. Several problem cases are presented. (auth)

31267 GENERATION AND PROPAGATION OF PRESSURE WAVES DUE TO UNCONFINED CHEMICAL EXPLOSIONS AND THEIR IMPACT ON NUCLEAR POWER PLANT STRUCTURES. Geiger, W. (Battelle-Institut e.V., Frankfurt am Main (F. R. Germany)). Nucl. Eng. Des.; 27: No. 2, 189-198(May 1974).

In the field of external reactor safety, possible violent incidents outside the reactor building need to be assessed with regard to their potential for doing damage to nuclear power plants. The generation and propagation of pressure waves due to unconfined chemical explosions and their impact on nuclear power plant structures are discussed. A survey is made of the procedures by which the effects of gas explosions on nuclear power plant structures can be assessed. (auth)

31268 DYNAMIC TESTING OF FULL-SCALE NUCLEAR POWER PLANT STRUCTURES AND EQUIPMENT. Smith, C. B. (Applied Nucleonics Company, Inc., Village Station, Los Angeles, California, USA). Nucl. Eng. Des.; 27: No. 2, 199-208(May 1974).

Three steps are required in the design of reliable nuclear power plants to be located in seismic areas. In addition to development of realistic analytical models, it is necessary to perform dynamic tests to verify the models and acquire the information needed to establish the dynamic parameters for modeling. The third and final step is to perform high level proof tests to validate analysis and test results. An overview of dynamic testing methods is presented. Testing can be performed in the laboratory or in the field. Laboratory tests are useful because a wide range of effects can be studied, and test parameters are more easily controlled. Care must be exercised to insure that the laboratory situation faithfully reproduces the actual structure in such details as supports, appurtenances, appendages, and mounting methods. In general, laboratory methods permit high level excitation of structures weighing up to a few metric tons (a few facilities in the world have capabilities up to 100 t). Since actual structures of interest to nuclear power plant designers often weigh up to 10,000 t, field testing is also important. Test procedures have been developed, using portable structural vibrators, for testing structures as large as nuclear power plant containment buildings. High level tests can be performed using explosives buried in the soil to excite structures. Recent work performed by the author demonstrates that explosive tests which produce a predetermined, specified response spectrum can be conducted. (auth)

31269 METHODS FOR THE IDENTIFICATION OF DYNAMIC PARAMETERS OF MATHEMATICAL STRUCTURAL MODELS

FROM EXPERIMENTAL DATA. Ibanez, P. (Applied Nucleonics Company, Inc., Village Station, Los Angeles, California, USA). Nucl. Eng. Des.; 27: No. 2, 209-219(May 1974).

The dynamic analysis of complex and critical structures, such as nuclear power plants, must employ both theoretical and experimental analysis and must also combine these two approaches to provide a unified description of the structure. A theoretical a priori model is useful in planning a vibration test, while the data obtained from such testing can be used to modify the a priori model so that it reproduces the experimental data. Several mathematical methods are illustrated which are useful in planning the placement of excitors and accelerometers; in analyzing data to identify resonant frequencies, modal damping and mode shapes; in modifying the mass and stiffness properties of the a priori model (consequently indicating improved methods of modeling in future studies); and in identifying unknown forces acting on the structure, once a good model has been obtained. Central to these methods is the use of a generalization of the inverse of a matrix (the pseudo-inverse) and the availability of efficient computer software for its computation. The properties of the pseudo-inverse allow it to calculate weighted least-mean-square and weighted minimum-norm solutions to ill-conditioned linear systems. It is consequently a versatile tool in the analysis of vibrating systems where the number of measurement and forcing points are often different and the confidence in different measurements and models varies. (auth)

Reactor Theory and Calculation

Refer also to abstracts 31009 and 31232.

31270 (EURFNR-1189) EXPERIMENTS IN PURE URANIUM LATTICES WITH UNIT $_\infty$. Assemblies SNEAK-8/8Z; UK 1 and UK 5 in ERMINE and HARMONIE. Chaudat, J. P.; Darrouzet, M.; Fischer, E. A. (comps.). (Kernforschungszentrum Karlsruhe (F.R. Germany). Inst. fuer Angewandte Systemtechnik und Reaktorphysik; CEA Centre d'Etudes Nucleaires de Cadarache, 13-Saint-Paul-les-Durance (France); CEA Centre d'Etudes Nucleaires de Fontenay-aux-Roses, 92 (France). Div. d'Etude et de Developpement des Reacteurs). 1973. 146p. (KFK-1865; CEA-R-4552). Dep. NTIS (US Sales Only) $5.45.

Work performed under United States-Euratom Fast Reactor Exchange Program.

Physics measurements in pure uranium lattices with k_∞ (production/absorption) close to unity were carried out in the critical facility SNEAK at KARLSRUHE (cores 8 and 8Z), the fast thermal coupled facility ERMINE at FONTENAY-AUX-ROSES (cores UK 1 and UK 5) and the exponential experiment HARMONIE at CADARACHE (core UK 5). k_∞ was experimentally determined from the central cell worth (SNEAK and ERMINE) or from the material buckling (HARMONIE). The reaction rate ratios were measured using the techniques developed at the different laboratories. In addition, the differential neutron spectrum was measured in some assemblies. All the experimental results were analyzed using the GfK and CEA methods, thus providing an extensive intercomparison of experimental techniques on one side, and of cross section data on the other side. The experimental results were then combined, and extrapolated to obtain best estimates for the parameters of a pure homogeneous uranium medium of exactly unit k_∞. This medium is proposed as a standard for nuclear data testing. 19 references. (auth)

31271 (IKE-6-75d) INVESTIGATIONS ON THE SHIELDING OF POWER REACTORS. Rexer, G. (Stuttgart Univ. (TH) (F.R. Germany). Inst. fuer Kernenergetik). Sep 1973. 45p. (In German). INIS.

14 figs.; 11 tabs.; 25 refs. With abstract. Available from the library of Stuttgart Univ.

A review is given on frequently applied standard calculation methods for the treatment of radiation transport problems. Attention is focussed on the methods of the discrete ordinates for one and two-dimensional geometries. The advantages and disadvantages of this process are compared with the removal-diffusion methods and the Monte Carlo method. The calculation of a reactor shield using the standard methods described is illustrated. The results of the calculations with a one-dimensional S_N-code are compared with measurements. (GE)

31272 (JAERI-M-5590) CONVERGENCE ACCELERATION ALGORITHMS OF THE ITERATIVE METHODS USED IN NUCLEAR REACTOR ANALYSIS CODES. Nakahara, Y.; Fujimura, T. (Japan Atomic Energy Research Inst., Tokyo). Mar 1974. 48p. (In Japanese). NTIS (U. S. Sales Only).

A systematic review has been made of the convergence acceleration algorithms for iterative methods to solve finite difference equations in commonly used neutron transport and diffusion codes. Also included are the recent studies on new acceleration algorithms not yet tested for the nuclear codes. The acceleration algorithms were evaluated through the available results of numerical experiments. It was found that the most promising are the coarse mesh rebalancing, the CCP, the line overrelaxation, the Chebyschev acceleration, and the modified Wielandt methods. It is possible to make an extensive improvement in the convergence rates of codes by revising them, using a suitable combination of the methods mentioned. (auth)

31273 (RT/FI-(74)26) POISSON-ALGEBRAIC DISTRIBUTIONS: ANOTHER FAMILY OF GENERALIZED POISSON PROFILES IN NUCLEAR-REACTOR NOISE-ANALYSIS. Zingoni, E.; Pacilio, N.; Jorio, V. M. (Comitato Nazionale per l'Energia Nucleare, Rome (Italy)). May 1974. 11p. Dep. NTIS (US Sales Only) $4.00.

A new family of Poisson generalized distributions is presented. The initiative offers a progressive contribution for seeking compact generating functions that might approximate the generating function of the Pal-Mogilner-Zolotukhin-Bell-Babala distribution. (auth)

31274 (RT/FI-(74)30) FLUXES AND EFFECTIVE MULTIPLICATION FACTOR EVALUATION BY ESCAPE PROBABILITIES. Bitelli, G.; Torelli, L. (Comitato Nazionale per l'Energia Nucleare, Rome (Italy)). Jun 1974. 12p. Dep. NTIS (US Sales Only) $4.00.

A collision method in finite one dimensional geometry is presented to calculate fluxes and effective multiplication factor of multiplying systems. This method makes use of escape probabilities instead of collision probabilities; by this choice numerical difficulties are overcome. A numerical example is compared with the results obtained by the transport method and calculation times are given. (auth)

31275 TRANSMISSION METHOD TO MEASURE CAPTURE RATES IN FAST REACTORS. Kuhn, D. (Gesellschaft fuer Kernforschung mbH, Karlsruhe, Ger.). Ann. Nucl. Sci. Eng.; 1: No. 5, 323-328(May 1974).

A method is described to measure neutron capture rates of materials in a cavity in the center of a fast reactor. The method is based on neutron transmission through a probe of the material to be investigated and can be used also in zero power facilities. Some measurements were done for ^{235}U and for ^{238}U. On account of the special detector used, it is limited, however, to sufficiently hard neutron energy spectra. (auth)

31276 NUCLEAR DATA ACCURACY CONSIDERATIONS IN REACTOR DESIGN. Ghani, A.; Ikramulhaq, M.; Chohan, A. S. (Federal Public Service Commission, Karachi, Pakistan). J. Natur. Sci. Math.; 12: No. 2, 221-237(Oct 1972).

Nuclear data requirements for various reactor calculations are summarized. Certain suggestions are also advanced for the purpose of developing self-sufficiency and confidence in writing the basic computer codes required in reactor design work. The different errors that are introduced in the multi-group diffusion approach are also briefly discussed. (auth)

31277 USE OF SUPERPOSITION IN CALCULATING THE TEMPERATURE OF A REACTOR CORE COOLED BY A LIQUID METAL. Sholokhov, A. A.; Minashin, V. E. Sov. At. Energy (Engl. Transl.); 35: No. 4, 925-926(Oct 1973).

Translated from At. Energ. (USSR); 35: No. 4, 264-265(Oct 1973). This is a summary of paper No. 695/7141 with full copy held at TIC.

A method is presented in which Green's functions are employed in the calculation of the time-dependent temperature distribution in a liquid metal cooled reactor core. (DG)

31278 KINETIC EXPERIMENTS IN REACTOR PHYSICS. Yamamuro, N. (Tokyo Inst. of Tech.); Kaneko, Y.; Nakamura, T.; Furuhashi, A.; Nishina, K. Nippon Genshiryoku Gakkaishi; 16: No. 3, 111-127(Mar 1974). (In Japanese).

A number of workers in Japan have undertaken neutronic kinetic experiments in reactor physics during the past decade, and the theoretical background for these experiments has been established. Many of the important reports related to these studies have appeared in the Journal of Nuclear Science & Technology. The present survey briefly reviews the work covered by outstanding papers published in this Journal, as well as some particularly noteworthy reports that have appeared in foreign journals in the same period. Pulsed neutron experiments in multiplying and non-multiplying systems are discussed separately for thermal reactor physics and fast reactor physics. Statistical correlation methods are covered in such forms as Rossi-α, Feynman-α, zero-count probability, polarity correlation and reactivity determination problems. Progress in neutron wave propagation studies is reviewed in respect to both theoretical and experimental aspects. (auth)

Reactor Components and Accessories

Refer also to abstracts 29264, 29267, 29276, 29622, 29937, 29950, 31256, and 31261.

31279 (RT/MET-(73)1) CHARACTERIZATIONS OF FUEL ELEMENT CLADDING TUBES. Fizzotti, C.; Sala, L.; Traversi, G. (Comitato Nazionale per l'Energia Nucleare, Rome (Italy)). 23 Apr 1973. 47p. (In Italian). Dep. NTIS (US Sales Only) $5.50.

Destructive and non-destructive methods developed at the Laboratory of Material Technology to test cladding tubes for fuel elements are described and discussed. The employed methods include dimensional, non-destructive, mechanical, structural and corrosion controls; they have been successfully applied to zirconium alloy and stainless steel cladding tubes. (auth)

31280 (WAPD-TM-1085) SAFR4: A PROGRAM TO EVALUATE THE STABILITY OF A RIGID BLADE IN PARALLEL FLUID FLOW. Zanoni, E. A. (Bettis Atomic Power Lab., Pittsburgh, Pa. (USA)). Apr 1974. Contract AT(36-1)-GEN-14. 38p. Dep. NTIS $5.00.

SAFR4 is a computer program based on an analysis for the prediction of flow-induced instability of a rigid flat blade in parallel fluid flow submerged in a stepped rectangular flow duct. The blade is suspended from its downstream end and may have two rigid body degrees of freedom. The fluid conservation equations are linearized by assuming small perturbations about the steady-state-centered blade conditions. A semi-empirical formulation of the cross flow is also included in SAFR4. The theory required to understand the basis for SAFR4 is presented as well as a sample problem to illustrate the program's use. (auth)

31281 CHEMICAL IMMOBILIZATION OF FISSION PRODUCTS REACTIVE WITH NUCLEAR REACTOR COMPONENTS. Grossman, L. N.; Kaznoff, A. I.; Clukey, H. V. (to General Electric Co.). US Patent 3,826,754. 30 Jul 1974. Filed Date 16 Jun 1971. 10p.

A method of immobilizing deleterious fission products produced in nuclear fuel materials during nuclear fission chain reactions through the use of additives is described. The additives are disposed with the nuclear fuel materials in controlled quantities to form new compositions preventing attack of reactor components, especially nuclear fuel clad, by the deleterious fission products. (Official Gazette)

31282 PROCESS FOR CONVERTING HEAT PRODUCED BY A NUCLEAR REACTOR TO ELECTRICAL ENERGY. Stahl, W. F. (to Westinghouse Electric Corp.). US Patent 3,826,091. 30 Jul 1974. Filed Date 24 May 1971. 6p.

A thermodynamic process for converting heat produced by a nuclear reactor to electrical energy by utilizing a liquid metal as a primary fluid and sulfur dioxide as a secondary fluid is described. The sulfur dioxide is expanded in a turbo-generator set, condensed and recycled through a closed secondary fluid loop. (Official Gazette)

31283 SYSTEM AND METHOD FOR OPERATING A STEAM TURBINE WITH INDEPENDENT OVERSPEED PROTECTION ESPECIALLY ADAPTED FOR A NUCLEAR REACTOR POWERED STEAM TURBINE. Conrad, J. D. Jr.; Gangloff, W. C. Jr.; Luongo, M. C. (to Westinghouse Electric Corp.). US Patent 3,826,094. 30 Jul 1974. Filed Date 14 Oct 1971. 16p.

In a steam turbine an overspeed protection system and method is provided which operates completely independently of the conventional steam valve controller or governor. Existing hydraulically actuated valves such as stop valves, governor valves, interceptor valves, etc., are deactivated by draining hydraulic control fluid through specially provided dump valves. A pair of dump valves is provided for each of the steam flow valves. Three turbine speed sensing transducers operating independently provide signals which are translated through three corresponding check circuits into related overspeed check signals. The three resulting check signals relating to overspeed are translated through majority switching logic into two dump valve trip signals. Each set of such trip signals operates one of the pair of dump valves on each steam control valve. (Official Gazette)

31284 SPRING CLAMPING DEVICE IN NUCLEAR REACTORS. Knoedler, D.; Steinke, A.; Kroepf, H. (to Siemens A. G., Berlin (F. R. Germany); Siemens A. G., Muenchen (F. R. Germany)). German Patent 2140170. 22 Feb 1973. 17p. (In German). 9 figs.

The object of the invention is a space-saving and simple support for a non-vibrational fuel element seating in the flow of the cooling medium. A spring clamping device is arranged between each fuel element (containing a large number of fuel rods) and one of the two grid plates supporting them, the device being in contact with the grid plate and fuel element. Fitting pins ensure a torsion-resistant support. The clamping device is so constructed as to influence the entry of the cooling medium in the fuel element in the manner desired (throttling, direction). (GE)

31285 NOZZLE FOR THE COVER OF A NUCLEAR REACTOR PRESSURE VESSEL. Bazant, E.; Cerjak, H.; Scholz, M. Czech Patent 146,221. 15 Nov 1972. Filed Date 7 Dec 1971. 3p.

An assembly is proposed of the nozzle and the cover of a nuclear reactor pressure vessel. With the attachment proposed, the nozzle consists of a combined tube equipped, in the region of its passage through the cover, with an austenitic lining tube. This leads through the cover, down to approximately the lower wall of the cover where it is welded to the inner cladding of the cover. Two methods of attaching the combined tube and the inner cladding of the cover are described. (Nuclear Sci. Abstr. Czech.)

31286 PRESSURE VESSEL PENETRATION TECHNIQUES. (to Combustion Engineering Inc.). Netherlands Patent 7,217,555. 22 Dec 1972. Priority Date 23 Dec 1971, USA. 32p. (In Dutch).

A manner of penetrating a reactor pressure vessel with hydraulic control lines is described. The control lines, in the form of a bundle of tubes, penetrate the side of the reactor vessel at a point below the junction of the main vessel portion and head. The penetration location is out of the main coolant flow path. Internally in the pressure vessel the control lines are positioned in the annulus between the reactor core barrel and the pressure vessel internal wall as they are directed upward into the area encompassed by the vessel head. Disconnecting means is provided in a location which is accessible with the head removed whereby the control lines may be readily separated when the core barrel is removed. So there is no control line penetration of the vessel head thus providing a "clean" head which may be readily removed after unbolting. Accordingly, the penetration is located in a comparatively protected area whereby damage is less likely to occur. (NL)

31287 PRESSURE VESSEL PENETRATION TECHNIQUE. (to Combustion Engineering Inc.). Netherlands Patent 7,217,571. 22 Dec 1972. Priority Date 23 Dec 1971, USA. 31p. (In Dutch).

The removable head of a pressure vessel enclosure for a nuclear reactor is penetrated by a bundle of hydraulic control lines. The vessel top head is provided with a single aperture and a connector assembly is installed in the aperture; the connector assembly providing leak proof coupling of external control lines to corresponding internal control lines of the bundle. (NL)

31288 INDUSTRIAL TECHNIQUE. (to Babcock and Wilcox Co.). Netherlands Patent 7,215,142. 3 Nov 1972. Priority Date 13 Dec 1971, USA. 13p. (In Dutch).

Aid in positioning fuel elements in a nuclear reactor core is discussed. The corner edges of the peripheral band that binds the fuel element grid structure together, as well as the ends of the individual grid plates that protrude beyond the last marginal rows of fuel rods in each of the fuel elements are chamfered or bevelled. Thus, when fuel elements are being inserted, relocated or withdrawn from a reactor core the sloping edges of the grid structures in adjacent elements slide past without locking together or otherwise undesirably engaging each other. (NL)

31289 TRENDS IN STRUCTURAL MECHANICS. A UK Review of the 2nd International Conference on Structural Mechanics in Reactor Technology. VII. Reliability Analysis. Salmons, B. H. (British Nuclear Design and Construction Ltd., Whetstone, Eng.). J. Brit. Nucl. Energy Soc.; 13: No. 3, 302-304(Jul 1974).

Some impressions gained at the 2nd International Conference on Structural Mechanics in Reactor Technology, Berlin, 1973, from the sessions on reliability analysis, are described. Principles and implications are considered but the mechanics of the mathematics involved are not described. The components considered are mainly pressure vessels and ducts but some statistics on failure rates due to creep rupture of fast reactor fuel rods are also examined. (UK)

31290 TRENDS IN STRUCTURAL MECHANICS. A UK Review of the 2nd International Conference on Structural Mechanics in

Reactor Technology. VI. Inelastic Structural Analysis. Head, J. L. (Imperial Coll. of Science and Tech., London). J. Brit. Nucl. Energy Soc.; 13: No. 3, 296-301(Jul 1974).

A selective review is presented from papers given at the 2nd International Conference on Structural Mechanics in Reactor Technology, Berlin, 1973. Attention is focused on two aspects of the general problem of inelastic structural analysis of reactor components, i.e., advances in the formulation and verification of the constitutive equations of materials in a reactor environment, and on advances in computational methods. Some specific analyses of special interest are also briefly discussed. (UK)

31291 LARGE USER-ORIENTATED SYSTEMS OF PROGRAMS FOR STRUCTURAL ANALYSIS AND DESIGN. Jezernik, A.; Miller, M. C. (Central Electricity Generating Board, London (UK). Computing Dept.). Nucl. Eng. Des.; 27: No. 2, 238-273(May 1974).

The trend in the use of structural analysis programs is towards larger, more highly integrated user-orientated systems. The main aim of organizing structural analysis program systems appears to be to provide users with more versatile tools to reduce the required man-days and computing costs and to increase the scope and potential of the programs. A large modular system is described constituting the most widely used structural analysis packages developed by the CEGB. The principal motivation in developing the system is to rationalize and simplify the considerable diversification of applications and techniques currently available. The applications encompass elastic, thermal, dynamic, creep, and plastic analyses of arbitrary two-dimensional and three-dimensional structures. The system uses a standardized form of input for all applications and provides user-aids such as mesh generation, error facilities, output facilities (online and graphical) as integrated system modules. Calculational packages integrated at present into the system comprise FLHE-BERSAFE (thermal and elastic, two and three dimensions), TESS (creep and plasticity, two dimensions), STAG21 (visco-elastic, two dimensions). Various element types and a comprehensive selection of different solution techniques based mainly on the finite element displacement model can be used in the analyses. All data presented to the system are in the form of files (data-lists) stored on 3330 magnetic disks. A comprehensive permanent disk library containing thermal and mechanical properties of the most commonly used materials is available to all users. The system is designed to be "open-ended" in the sense that new subsystems can be augmented easily. It is envisaged that these additions will include structural analysis applications which are strictly outside the area of finite element analysis, e.g., frameworks. The internal structure and mode of operation of the system are described in detail. Several diverse examples of nuclear design problems which have been studied are given. Examinations of and comparison with other large structural analysis systems currently available are given, and a discussion of possible future developments in this field is presented. (auth)

Reactor Fuels

Refer also to abstracts 28940, 29145–29147, 29926, 29934, 29982, 30083, 30097, and 30111.

31292 FUEL ASSEMBLY FOR A NUCLEAR REACTOR. Jabsen, F. S. (to Babcock and Wilcox Co.). US Patent 3,828,868. 13 Aug 1974. Filed Date 12 Jan 1973. 4p.

A nuclear reactor fuel assembly in which both fuel rods and control rod guide tubes are held in a predetermined parallel spacing relation by a pair of spaced end grids is described. The guide tubes are secured to the end grids by releaseable connection means that allow the tubes to be installed and individually replaced with the fuel rods already installed in the assembly. (Official Gazette)

31293 FUEL ROD FABRICATION. Silk, E. J.; Moore, C. A. (to Babcock and Wilcox Co.). US Patent 3,828,518. 13 Aug 1974. Filed Date 12 Jan 1971. 4p.

A process of sealing the external junction between an endclosure and a long fuel rod of a slender nature in a controlled gaseous environment by a rotating electrode passing through a predetermined path around the periphery of the junction is described. (Official Gazette)

31294 HYDROGEN DIFFUSION SEAL FOR NUCLEAR REACTOR FUEL RODS. Ploeger, M.; Gregorius, K.; Peehs, M. (to Siemens A. G., Berlin (F. R. Germany); Siemens A. G., Muenchen (F. R. Germany)). German Patent 2146346. 22 Mar 1973. 9p. (In German).
2 figs.

The hydrogen diffusion seal is intended for fuel rods which contain a mixture of nuclear fuel as well as a metal hydride moderator inside a stainless steel cladding tube and preferably are cooled by a liquid metal. Between the nuclear fuel and the cladding tube, there is a coat of aluminum or aluminum alloy on both parts. The composition and application of this coat are described. (GE)

Reactor Control Systems

31295 (KURRI-TR-110, pp 9-14) KUR ON-LINE COMPUTER SYSTEM. Hayashi, M.; Fujine, S. (Kyoto Univ.). 1972. (In Japanese).

The following aspects of the on-line computer system used in the KUR control system are described: (1) the composition of the KUR on-line computer system, (2) problems in interfacing the computer system with the existing KUR instruments, (3) the developing software. The possibility of the application of the Parallel Processing Multi-Minicomputer system at the high flux research reactor is discussed. (auth)

31296 (NP-20130) 10 YEARS: LABORATORY FOR REACTOR CONTROL AND PLANT SAFETY. (Technische Univ. Muenchen (F.R. Germany)). Jan 1974. 112p. (In German). Dep. NTIS (US Sales Only) $8.75.

The work done on reactor control and safety in the period from 1963 to 1973 is briefly summarized. This includes studies on reactor statics and dynamics, operating techniques and thermohydraulics, system analysis and process monitoring, and process data processing. A tabulation of the publications during this 10-year period is appended. (tr-auth)

31297 TEMPERATURE CONTROL AND EMERGENCY PROTECTION AGAINST PERILOUS TEMPERATURES IN NUCLEAR REACTOR. Strnad, M.; Sourek, J.; Voles, J. Czech Patent 146,450. 15 Dec 1972. Filed Date 7 Dec 1971. 2p.

A temperature control and emergency protection system against excessive temperatures in a nuclear reactor is proposed. The system is based on the use of temperature sensing probes operating on the principle of phase transformation of substances. The sensors are located at the inlets of the control and protection system loop. The system eliminates the disadvantages of currently used thermocouples and resistance thermometers such as rapid aging, the need of frequent calibration, and of complex and expensive compensating circuits, as well as of stabilized sources of reference voltage and temperature. (Nuclear Sci. Abstr. Czech.)

31298 TOP ACTUATED REACTOR CONTROL SYSTEM. (to Combustion Engineering Inc.). Netherlands Patent 7,217,556. 22 Dec 1972. Priority Date 23 Dec 1971, USA. 32p. (In Dutch).

A nuclear reactor control system employing a plurality of low worth absorber elements which can be individually moved between two positions respectively commensurate with full insertion and full retraction is described. Each absorber element actuator assembly is a top actuated device located entirely within the reactor pressure vessel and utilizing hydraulic pressure to control and monitor absorber element position. (NL)

31299 CONTROL LINE DISCONNECT ASSEMBLY. (to Combustion Engineering Inc.). Netherlands Patent 7,217,568. 22 Dec 1972. Priority Date 23 Dec 1971, USA. 31p. (In Dutch).

A multiple seal, single bolt connector for coupling a plurality of first conduits to a like plurality of second conduits is described. The apparatus is characterized by upper and lower flange devices which are respectively joined to the first and second conduits, a multiple apertured seal plate disposed between the flange devices and means for aligning and holding the connector in the assembled position. (NL)

31300 ELECTRIC POWER PLANT SYSTEM AND METHOD FOR OPERATING A STEAM TURBINE ESPECIALLY OF THE NUCLEAR TYPE WITH ELECTRONIC REHEAT CONTROL OF A CYCLE STEAM REHEATER. (to Westinghouse Electric Corp.). Netherlands Patent 7,301,065. 25 Jan 1973. Priority Date 27 Jan 1972, USA. 45p. (In Dutch).

An electronic system is provided for operating a nuclear electric power plant with electronic steam reheating control applied to the nuclear turbine system in response to low-pressure turbine temperatures and the control is adapted to operate in plurality of different automatic control modes to control reheating steam flow and other steam conditions, each of such modes of control permitting turbine temperature variations within predetermined constraints and according to predetermined functions of time. (NL)

31301 METHODS FOR MEASURING THE REACTIVITY AND EIGENVALUE OF NUCLEAR REACTORS. Albrecht, R. W.; Hess, G. M. (to USAEC, Washington, D. C.). German Patent 2335516. 24 Jan 1974. 23p. (In German).
3 figs.

A method for automatic reactivity measurement of a nuclear reactor in on-line-operation is described, which also allows the determination of the prompt eigenvalues. The method is based on the evaluation of two noise signals produced by measuring the neutron flux fluctuation at different positions within the core. (GE)

31302 BLOCK CONTROL OF A PWR TYPE REACTOR. Lempert, J.; Loehr, U.; Stevens, H. H.; Stuermer, W. (Babcock-Brown Boveri Reaktor G. m. b. H., Mannheim (F. R. Germany)). Brennst.-Waerme-Kraft; 26: No. 7, 308-313(1974). (In German).
12 figs.; 2 tabs.

The behavior of the control systems of two PWR type reactors, of which one is in operation and the other in the planning stage is described. The control of the reactor, of the steam generator, and of the turbine is dealt with individually. The control behavior of the plant in operation is described and illustrated by diagrams. Finally, the simulated control behavior of the plant still in planning is presented. (GE)

31303 A SIMPLE TIME OPTIMAL DIGITAL CONTROL FOR NUCLEAR REACTORS. D'Attellis, C. E.; Lorenzetti, J. R.; Reyes, C. H. (Comision Nacional de Energia Atomica, Buenos Aires (Argentina)). Nucl. Instrum. Methods; 119: No. 2, 295-299(15 Jul 1974).

A time optimal control between two stationary power states of a nuclear reactor has been obtained with a digital computer using a simple algorithm, which provides a smooth approximation to the final state without overshoot. The results obtained by means of a digital simulation are given. (auth)

Nuclear Power Plant Economics

Refer also to abstract 29243.

31304 (DEU-74-2) THE IMPACT OF NUCLEAR POWER PLANTS ON THE ECONOMIC STRUCTURE. Schmitt, D.; Schulz, W. (Koeln Univ. (F.R. Germany). Energiewirtschaftliches Inst.). 1974. 75p. (In German). INIS.
1 fig.; 4 tabs.

Following an introduction into the setup and methodics of the investigation, the concepts of economic structure and regional structural improvement are explained. The indirect effects of a nuclear power plant on the regional economic structure have been individually examined (site selection and the effect of energy costs; electricity consumption, power consumption, and siting of the most important current-consuming products; load volume and siting of large process-heat consumers, nuclear energy generation plants and regional energy supply). Furthermore, the immediate effects of a nuclear power plant on the regional economical structure are examined from the standpoints of employment, income, and taxes. (GE)

31305 (JUL-1077) NUCLEAR DISTRICT-HEATING AND NUCLEAR LONG-DISTANCE ENERGY. Bohn, T.; Dietrich, G.; Kugeler, K.; Kugeler, M.; Niessen, H. F.; Schlenker, H. V. (Kernforschungsanlage Juelich G.m.b.H. (F.R. Germany). Inst. fuer Reaktorentwicklung). Jun 1974. 68p. (In German). Dep. NTIS (US Sales Only) $6.50.

A first survey is given about the possibilities of nuclear energy for heating of residential and industrial buildings. The costs and quantities are only a first rough estimate. Nevertheless the results permit the conclusion, that nuclear energy will have economical advantages in comparison with conventional systems for district-heating. "Nuclear District-Heating" is a contribution to relieve the environment of pollution by using waste heat of electricity producing processes as is "Nuclear Long-Distance Energy" with it decentralized electricity production. (auth)

31306 (WASH-1334) PROJECTIONS OF LABOR REQUIREMENTS FOR ELECTRICAL POWER PLANT CONSTRUCTION 1974-2000. (USAEC Oak Ridge Operations Office, Tenn.; USAEC Division of Reactor Research and Development, Washington, D. C.). Aug 1974. 137p. Dep. NTIS $5.45.

Estimates of the labor force required for the construction of central station electrical power plants during the period 1974 through 2000 are presented. Projections for nuclear and fossil fuel plant construction and for the various trades involved are given. (JWR)

31307 ENERGY CRISIS AND NUCLEAR ENERGY. Energy Consumption and Expected Growth. Oeye, O. G. W. (Institut for Atomenergie, Kjeller, Norway). Fra Fys. Verden; 36: No. 2, 31-38(1974). (In Norwegian).

The growing realization of the necessity of restricting the rate of consumption of non-renewable resources is coupled with the need for continued growth in energy consumption in order to meet future requirements. The conclusion is that, due to resource and pollution limitation in the use of fossil fuel, nuclear power must be exploited. The objections to this, based on risk of accidents and limited fuel resources, are mentioned and discussion in the light of Farmer's criteria and the effectiveness of fast breeder and gas-cooled and heavy-water reactors, respectively. Loss of coolant accidents are discussed and the results in the WASH-740 report evaluated. Finally safety factors connected with reprocessing and radioactive waste disposal are considered. It is concluded that nuclear power is a feasible and necessary alternative. (NO)

31308 BENEFICIAL USES OF WASTE HEAT. pp 109-127 of Thermal Discharges at Nuclear Power Stations. Vienna; International Atomic Energy Agency (1974).
See STO/DOC-10/155.

Possibilities for the use of waste heat from nuclear power plants are discussed. Physical applications of low-grade heat include space heating and sewage and water treatment. Process heat applications include district heating, desalination, and sewage and water treatment. Biological applications include fresh and salt water aquaculture. (JWR)

31309 LONG TERM INVESTMENT CONSIDERATIONS OF CONJUNCTIVE DESALTING SYSTEMS. Morley English, J.; Young, N. A. (Univ. of California, Los Angeles). Desalination; 13: No. 3, 359-371(1973).

From 4th international symposium on fresh water from the sea; Heidelberg, Germany (9 Sep 1973).

Previous research, which dealt with the desirability of considering water projects in a long-range context, the measurements and costs of technological progress, and the value of preserving flexibility in future decision making, was combined and applied to the evaluation of the proposed prototype 40-mgd Diablo Canyon desalination plant. An alternative to the desalination plant is very large-scale aqueduct. The two projects are evaluated together as complementary components of a long-range project against the alternative of earlier construction of the aqueduct. The analysis concerns the interest rate, growth rate, demand elasticity, planning horizon, number of planning periods, and area growth rate in parametric form. A simplified numerical example is given. (NL)

Reactor Fuel Cycle Economics

31310 EQUILIBRIUM APPROACH TO OPTIMAL IN-CORE FUEL MANAGEMENT FOR PRESSURIZED WATER REACTORS. Chitkara, K.; Weisman, J. (Univ. of Cincinnati). Nucl. Technol.; 24: No. 1, 33-49(Oct 1974).

As an equilibrium core configuration is reached after only a few refueling cycles, equilibrium core energy costs dominate plant economics. Optimization of these costs can therefore lead to nearly optimum energy costs over plant life. A simple reactor state model has been developed that can predict equilibrium core conditions without reference to previous cycles. By coupling this model to an assignment and direct search algorithm, the refueling procedure and core power at equilibrium are determined so that energy costs are minimized. The equilibrium core parameters are then used to establish pre-equilibrium core conditions. 26 references. (auth)

Reactor Licensing and Regulation

31311 (DOCKET-50010-305) DRESDEN NUCLEAR POWER STATION, UNITS 1, 2, AND 3. Semiannual Report, January–June 1974. (Commonwealth Edison Co., Chicago, Ill. (USA)). 21 Aug 1974. 290p. (DOCKET-50237-598; DOCKET-50249-486). Dep. NTIS $17.50.

Dresden operations are summarized including changes in design, chronological history, fuel performance, procedure changes, surveillance, results of periodic containment leak rate testing, experiments, personnel changes, power generation, shutdowns, and maintenance. (FS)

31312 (DOCKET-50133-195) HUMBOLDT BAY POWER PLANT, UNIT 3. Semiannual Operations Report, January–June

1974. (Pacific Gas and Electric Co., San Francisco, Calif. (USA)). 29 Aug 1974. 71p. Dep. NTIS $6.75.

Information is presented concerning operation, changes in facility design, performance characteristics, surveillance testing, results of periodic containment leak rate tests, experiments, power generation, shutdowns, maintenance, radioactive effluent releases, solid radioactive wastes, environmental monitoring, and occupational personnel radiation exposure. (FS)

31313 (DOCKET-50220-315) NINE MILE POINT NUCLEAR STATION, UNIT 1. Semiannual Report of Operation, January–June 1974. (Niagara Mohawk Power Corp., Syracuse, N. Y. (USA)). 1974. 72p. Dep. NTIS $6.75.

Net electric generation totaled 1,165,735 MWh with the unit on load 48.6% of the period. Electric production was 46.8% of the 610 MW net electric capacity which is equivalent to 90.46 registered capacity for the period the unit was on line. The unit was shutdown for annual overhaul and refueling March 30, 1974. Cumulative net electrical power generated to the end of the period totaled 12,760,288 MWh. Summaries are presented concerning maintenance, instrumentation and control, inspections, primary containment testable penetrations and isolation valves, radiation protection, radiochemistry, and personnel changes. (FS)

31314 (DOCKET-50250-283) TURKEY POINT PLANT, UNITS 3 AND 4. Semiannual Operating Report No. 4, January–June 1974. (Florida Power and Light Co. (USA)). 27 Aug 1974. 130p. (DOCKET-50251-263). Dep. NTIS $9.50.

Turkey Point-3 reactor reached rated power of 2200 MW(t) on March 9th. Main steam line vibration problems caused Unit 4 to be limited to 80% rated power. Modifications to the unit allowed the unit to escalate to 100% rated power (2200 MW(t)) on March 11, 1974. On November 1, 1973 all company bargaining unit employees including licensed and unlicensed operators and maintenance personnel below the supervisor level went on strike. Operation of both units continued during the strike, using supervisors and technicians in all capacities. The strike ended February 2. Information is presented on power generation, maintenance, shutdowns, changes, tests, experiments, radioactive effluent releases, environmental monitoring, and personnel monitoring. (FS)

31315 (DOCKET-50269-284) OCONEE NUCLEAR STATION, UNITS 1 AND 2. Semiannual Operating Report, January–June 1974. (Duke Power Co., Charlotte, N.C. (USA)). 30 Jun 1974. 373p. (DOCKET-50270-230). Dep. NTIS $21.75.

Information is presented concerning operations, maintenance, changes, tests, experiments, and staff changes. The non radiological environmental surveillance report and appendices on tabulated water quality data, southwest reservoir investigations, plume mapping, and operational environmental radioactivity monitoring data are included. (FS)

31316 (DOCKET-50285-249) FORT CALHOUN STATION, UNIT 1. Semiannual Report, January–June 1974. (Omaha Public Power District, Nebr. (USA)). 28 Aug 1974. 205p. Dep. NTIS $13.25.

The power ascension testing program at the attainment of full power is discussed. The plant was administratively limited in power pending investigation and resolution of vibration in the main steam lines and the main steam isolation valves. Completion of power range testing at 100% is delayed until the vibration problem is corrected. Information is presented concerning shutdowns, maintenance, changes, tests, experiments, radioactive gaseous releases, radioactive liquid effluents, radioactive solid wastes, environmental monitoring, and occupational personnel radiation exposures. (FS)

31317 (DOCKET-50298-233) COOPER NUCLEAR STATION. Semiannual Operating Report, January–June 1974. (Nebraska Public Power District, Columbus (USA)). 1974. 135p. Dep. NTIS $9.75.

Information is presented concerning reactor operation, power generation, shutdowns, tests, facility changes, specification changes, procedure changes, personnel changes, maintenance, effluent and waste disposal, and personnel radiation exposure. (FS)

31318 (DOCKET-50331-277) DUANE ARNOLD ENERGY CENTER. Semiannual Operating Report, February 22–June 30, 1974. (Iowa Electric Light and Power Co., Cedar Rapids (USA)). 29 Aug 1974. 104p. Dep. NTIS $8.25.

Significant activities from the date of obtaining the operating license to the end of the reporting period are presented. The major plant activity involved the implementation of an improved simultaneous preoperational and start-up test program. Information is presented concerning power generation, shutdowns, maintenance, tests, changes, experiments, primary coolant chemistry, occupational personnel radiation exposure, FSAR changes, and radioactive effluents. (FS)

31319 (DOCKET-50510-1) BLUE HILLS STATION, UNITS 1 AND 2. License Application. (Gulf States Utilities Co., Beaumont, Tex. (USA)). 22 Aug 1974. 184p. (DOCKET-50511-1). Dep. NTIS $12.25.

An application is presented to construct and operate two nuclear electric generating units to be located in Newton County, Texas two miles southwest of Toledo Bend Reservoir, 17 miles east of Sam Rayburn Reservoir, 25 miles east-northeast of Jasper and 10 miles north of Wiergate and Burkeville. Two PWR type reactors with an evaluated power of 2966 MW(t) are to be employed. The units are to be completed in 1981. (FS)

31320 (DOCKET-STN-50516-1) JAMESPORT NUCLEAR POWER STATION, UNITS 1 AND 2. License Application. (Long Island Lighting Co., Hicksville, N. Y. (USA)). 28 Aug 1974. 78p. (DOCKET-STN-50517-1). Dep. NTIS $7.00.

An application is presented for the construction and operation of two similar nuclear power reactors which will be located approximately 65 miles east of New York City on the north shore of Long Island Sound northeast of Riverhead and approximately three miles west of Mattituck Creek Inlet. The two units are replicas of Waterford-3 Reactor. The PWR type cores are designed for a warranted power output of 3,411 MW(t) with a reactor coolant pump heat output of 14 MW(t) with a warranted NSSS output of 3,425 MW(t). A 5% increase in steam flow results in a maximum NSSS output of 3,565 MW(t). The facility has the capability to generate approximately 1153 MW(e) per unit. (FS)

31321 (FIND-50335) FIND: ST. LUCIE PLANT, UNIT 1. Williams, W. H. (ed.). (USAEC Technical Information Center, Oak Ridge, Tenn.). Jul 1974. 26p. Dep. NTIS $4.00.

An index is presented for the docket report material submitted in conjunction with the application for a nuclear power plant construction permit and operating license. The index citations are to the beginnings of major headings, sections, responses, etc., and refer to grid coordinates on microfiche sheets prepared for each docket report. (DCC)

31322 (FIND-50389) FIND: ST. LUCIE PLANT, UNIT 2. Carter, E. P. (ed.). (USAEC Technical Information Center, Oak Ridge, Tenn.). Aug 1974. 26p. Dep. NTIS $4.00.

An index is presented for the docket report material submitted in conjunction with the application for a nuclear power plant construction permit and operating license. The index citations are to the beginnings of major headings, sections, responses, etc., and refer to grid coordinates on microfiche sheets prepared for each docket report. (DCC)

31323 (TID-26631) PREAPPLICATION SAFETY EVALUATION OF THE GAS COOLED FAST BREEDER REACTOR, GENERAL ATOMIC COMPANY. Project No. 456. (USAEC Directorate of Licensing, Washington, D.C.). 1 Aug 1974. 308p. Dep. NTIS $18.50.

Safety considerations for the GCFR Reactor are presented under the following headings: site characteristics; design of structures, systems, and components; reactor; reactor coolant systems; engineered safety features; instrumentation and controls; electric power; auxiliary systems; steam and power conversion system; radioactive waste system; radiation protection; conduct of operations; initial tests and operation; and accident analysis. (DCC)

GENERAL

Civilian Defense

Refer also to abstract 31332.

Energy Utilization and Economics

31324 (LA-UR-74-741) ENERGY AND CRYOENGINEERING. Hammel, E. F. (Los Alamos Scientific Lab., N. Mex. (USA)). [nd]. 20p. (CONF-740509-8). Dep. NTIS $4.00.

From 5th international cryogenic engineering conference; Kyoto, Japan (7 May 1974).

Cryoengineering technologies relating to energy sources include instrumentation, handling of LNG, and fusion reactions. Cryogenic magnetometers utilizing SQUIDS are now available, sensitive gravimeters are being developed, and bolometers may be deployed in satellites for detecting geothermal anomalies. Two major approaches are discussed in which a plasma is confined magnetically and the recent technology of inertial confinement. Superconducting technology applicable in the mid-term energy requirement is superconducting magnetic separators, large air separation plants for coal gasification, cryopumping for stack gas cleanup, and cryoresistive power transmission. (MCW)

31325 (LA-UR-74-1085) CONTROL SYSTEM DESIGN AND SIMULATION FOR SOLAR HEATED STRUCTURES. Murray, H. S.; Hafer, J. F.; Shipley, J. P.; Springer, T. E.; Balcomb, J. D.; Hedstrom, J. C. (Los Alamos Scientific Lab., N. Mex. (USA)). 1974. Contract W-7405-eng-36. 29p. (CONF-740811-4). Dep. NTIS $4.50.

From meeting of the international Solar Energy Society; Fort Collins, Colorado, USA (19 Aug 1974).

Results are given for some methods of control of building environment using solar energy systems. The control problem differs from that of conventional heating and cooling systems in two major respects: (1) the temperature of the energy source of the system is constantly fluctuating, (2) the system performance criteria must include consideration of minimizing the energy requirements of the auxiliary heat source. The model includes a description of the dynamics of a single-glazed flat plate solar collector, energy storage system, auxiliary heating system, and the structure. A hybrid computer implementation is chosen for the model. One year of operation is simulated in 8.76 minutes. This allows an economical evaluation of an entire year of operation using various control modes and parameters. Actual hourly data for insolation, ambient temperature, and wind velocity are used to force the model. These data are stochastically reconstructed to introduce inputs with fluctuations occurring as fast as 15 seconds. Several different control schemes are investigated, including one that is near-optimal for a portion of the system and, for comparison, one that is similar to classical controllers. Results of simulation of a year's operation with each of the control schemes are presented, and it is shown that a suboptimal controller works quite well. Implications of each controller are discussed. (auth)

31326 (LA-UR-74-1093) DESIGN AND TESTING OF A STRUCTURALLY INTEGRATED STEEL SOLAR COLLECTOR UNIT BASED ON EXPANDED FLAT METAL PLATES. Moore, S. W.; Balcomb, J. D.; Hedstrom, J. C. (Los Alamos Scientific Lab., N. Mex. (USA)). 1974. Contract W-7405-eng-36. 35p. (CONF-740811-3). Dep. NTIS $4.75.

From meeting of the international Solar Energy Society; Fort Collins, Colorado, USA (19 Aug 1974).

The LASL flat plate collector design is based on combining the solar collector into a structural unit so that the collector doubles as the building roof. It is weather tight and insulated. It is easily installed and maintained by building craftsmen. Two mild steel plates are welded and pressure expanded to form a heat transfer panel. Extensions of the plates provide a structural C-beam support on the bottom and a glazing trough on the top. Glass is added on the top and insulation on the bottom to complete the unit. The collectors are two feet wide by ten feet or longer. Factor-assembled cost predictions are $2.50 to $3.00 per square foot, based on large scale mass production. Test data taken over several months confirming the performance of the collectors are presented. Preliminary test data on electro-deposited selective surfaces are given. Materials selection, design, manufacturing, and coolant fluid selection considerations are discussed. The effect of various heat leakage paths is discussed. The selection of materials and design for the glass support is discussed. (auth)

31327 (UCRL-75353) MATERIALS SCREENING PROGRAM FOR THE LLL GEOTHERMAL PROJECT. Lorensen, L. E. (California Univ., Livermore (USA). Lawrence Livermore Lab.). 9 Jan 1974. 11p. (CONF-740222-2). Dep. NTIS $4.00.

From symposium on engineering for the materials/energy challenge; Albuquerque, New Mexico, USA (28 Feb 1974).

In order to assist in the development of the Lawrence Livermore Laboratory's "Total Flow Concept" for the utilization of hot geothermal brine, a materials selection and screening program has been started. Polymers and composites resistant to the high temperatures, hot brine, and erosive conditions present in a flowing well are being sought. Ultimately fabrication into pipes, turbine nozzles, and turbine blades will be required. Test specimens and test equipment are being obtained. The program outline is presented and a few limited test results reported. (auth)

Information Handling

Refer also to abstract 29456.

Law

31328 AEC OMNIBUS LEGISLATION, 1974. Report by the Joint Committee on Atomic Energy, Ninety-Third Congress, Second Session, Senate. Washington, DC; Joint Committee on Atomic Energy (1974). 19p. GPO.

The Joint Committee on Atomic Energy, having considered S.3669, to amend the Atomic Energy Act of 1954, as amended, and the Atomic Weapons Rewards Act of 1955, reported recommendations that the bill pass with the one amendment. The changes in the Acts are published. The committee recommended enactment of H.R.15416 and S.3669. Comments concerning the rationale for individual sections of the bill are stated. (MCW)

31329 AEC OMNIBUS LEGISLATION, 1974. Report by the Joint Committee on Atomic Energy, Ninety-Third Congress, Second Session, House of Representatives. Washington, DC; Joint Committee on Atomic Energy (1974). 19p. GPO.

The Joint Committee on Atomic Energy, having considered H.R.15416, to amend the Atomic Energy Act of 1954, as amended, and the Atomic Weapons Rewards Act of 1955, report favorably, with one amendment, and recommend that the bill pass. The committee recommends enactment of H.R.15416 and S.3669. Comments concerning the rationale for individual sections of the bill are stated. (MCW)

31330 REVISING AND AMENDING THE PRICE-ANDERSON INDEMNITY PROVISIONS OF THE ATOMIC ENERGY ACT OF 1954, AS AMENDED. Report by the Joint Committee on Atomic Energy, Ninety-Third Congress, Second Session, Senate. Washington, DC; Joint Committee on Atomic Energy (1974). 36p. GPO.

A report is presented on the public hearings on the possible modification or extension of the Price-Anderson Act that were held on January 31, March 27 and 28, 1974 and hearings on H.R.14408, S.3254, and S.3452 that were held on May 9, 10, 14, 15, 16, 1974. An informal planning committee consisting of personnel from the Joint Committee staff, the AEC, the legal profession, the commercial power and insurance industries, and public citizen groups were in attendance. The Act, designed to protect the public and the emerging nuclear industry by assuring the availability of funds for the payment of claims in the unlikely event of a catastropic nuclear incident, is scheduled to expire on Aug. 1, 1977. The changes in the existing law are presented and in a statement, Dr. N. C. Rasmussen recommends phasing out the governmental responsibility for nuclear insurance and shifting the responsibility to insurance companies and the nuclear industry. (MCW)

31331 PUBLIC WORKS FOR WATER AND POWER DEVELOPMENT AND ATOMIC ENERGY COMMISSION APPROPRIATION BILL, 1975, NINETY-THIRD CONGRESS, SECOND SESSION, HOUSE OF REPRESENTATIVES. Washington, DC; Committee on Appropriations (1974). 76p. GPO.

The Committee on Appropriations submits the report in explanation of the Public Works bill for 1975. The Committee has recommended funds to provide for the full planning and construction capability for hydroelectric power projects for the Corpe of Engineers and the Bureau of Reclamation. A total of 29 new planning starts and 27 new construction starts are announced in developing needed electric power, more adequate water supply, flood control, additional and improved waterways for navigation, recreation and other services. Funds for other agencies include the AEC, the Water Resources Council, TVA, the Federal Power Commission and several Federal Power Administrations, including Bonneville Power Administration, Southeast Power Administration, Southwest Power Administration, and Alaska Power Administration, the River Basin Commissions, and programs of the Appalachian Regional Development Commission. (MCW)

Management

Refer also to abstract 30110.

31332 (BNL-19097(Rev.)) ANNUAL REPORT OF THE BROOKHAVEN DCPA CONTRACT GROUP. Greenhouse, N. A. (Brookhaven National Lab., Upton, N. Y. (USA)). Jul 1974. 25p. Dep. NTIS $4.25.

The DCPA Contract Group at Brookhaven National Laboratory was organized in May, 1973, in response to the needs of the Defense Civil Preparedness Agency. Its primary objective has been the development of a dual-use RADEF capability through programs designed to effectively utilize Civil Defense instrument and manpower resources in response to peacetime radiation accidents. During the past year, the contract group has focused on reactor accident response and the assessment of radioactive effluents in the environment which directly affect public health. Additional efforts were directed at modification of C-D instruments for improved characteristics or to perform special functions, evaluation of RADEF resources in transportation accident response, and the evaluation of DCPA and state RADEF training courses for peacetime application. (auth)

31333 (CEA-N-1688) DEPARTMENT OF FUNDAMENTAL RESEARCH, GRENOBLE, SEMIANNUAL BULLETIN NO. 4. (CEA Centre d'Etudes Nucleaires de Grenoble, 38 (France)). 1973. 179p. (In French and English). Dep. NTIS (US Sales Only) $12.00.

Research carried out during the second half of 1973 is presented. In the field of nuclear physics, this research concerned fission and fission products. The following aspects of solid state physics were investigated: defects and other effects produced by irradiation; magnetic properties of transition elements, rare earth compounds and alloys, and actinides (together with studies of the relevant hyperfine parameters); structure of transition element compounds, alloys, and complexes, and of semiconductors and insulators. Research in the fields of chemistry, physics, and biophysics concerned principally: free stable radicals; biological radical spin labeling; stereochemistry and conformation (NMR) studies; hyperfine deviations due to ^{13}C. Biological research was conducted on the structure and function of proteins, the structure and function of biological membranes, the effects of ionizing radiations on nucleic acids, the mineral nutrition of plants, the cellular differentiation of hematopoietic strain cells, and the structure and function of amino acids. The time-of-flight neutron spectrometer used in conjunction with Melusine is described as well as the Fourier transform system of the NMR XL 100 spectrometer, and nuclear and ion microanalysis applications in botanical physiology. (FR)

31334 HAHN-MEITNER-INSTITUT FUER KERNFORSCHUNG JAHRESBERICHT 1973. (Hahn-Meitner-Institut fuer Kernforschung Annual Report 1973). Maass, K. E. (ed.). Berlin, F. R. Germany; HMI (1974). 80p. (In German). (HMI-146).

9 figs.; 1 tab.

This annual report 1973 reviews the general development of the Hahn-Meitner-Institute for Nuclear Research and the scientific results of the research and development programs; it further describes the scientific-technical laboratories and facilities and the relationships of the HMI with other institutions and lists of the scientific publications and lectures given by members of the Institute as well as lectures read by other scientists. (GE)

Mathematics and Computers

31335 (CNEA-365) DOUBLE OPTIMIZATION IN LINEAR DISCRETE SYSTEMS. D'Attellis, C. E. (Comision Nacional de Energia Atomica, Buenos Aires (Argentina)). 1973. 12p. (In Spanish). Dep. NTIS (U. S. Sales Only) $4.00.

An algorithm is described which realizes a double optimization in single-input, linear, time-invariant, sampled-data systems: minimal time and minimal energy consumed. (auth)

31336 (COO-3077-44) CONNECTION BETWEEN SINGULAR PERTURBATIONS AND SINGULAR ARCS. Part 2. A Theory for the Linear Regulator. Jameson, A. (New York Univ., N. Y. (USA). AEC Computing and Applied Mathematics Center). 1973. Contract AT(11-1)-3077. 8p. Dep. NTIS $4.00.

Singular perturbation theory is applied to obtain the asymptotic solution for nearly singular optimal control of a constant linear system in a finite time interval. In the limit as the control cost is reduced to zero, the initial control is found to have an impulse-like behavior, while the outer solution yields a singular arc. (auth)

31337 (EDFB-IBP-74-4) SAFT: STRUCTURAL ANALYSIS OF FOREST TREES. West, D.; Kelsey, C. T.; Stephenson, R. L.; Goff, F. G. (Oak Ridge National Lab., Tenn. (USA)). Aug 1974. Contract W-7405-eng-26. 35p. Dep. NTIS $4.00.

A Fortran program, SAFT, was developed that summarizes the density distribution of forest trees by species and size class and calculates stand density characteristics by plot. The program was written specifically to be used with the IBP Standard Format-Forest Service Plot Tapes. The program listing and sample output listing generated from actual data are also presented. (auth)

31338 (HMI-B-149) USE OF THE CAMAC SYSTEM FOR ON-LINE DATA PROCESSING IN MEDICINE. Kolibach, D.; Metzler, H. G.; Pangritz, H.; Schmidt, V.; Uhlmann, B. (Hahn-Meitner-Institut fuer Kernforschung Berlin G.m.b.H. (F. R. Germany). Bereich Datenverarbeitung und Elektronik). Aug 1974. 96p. (In German). Dep. NTIS (U. S. Sales Only) $8.00.

For on-line data acquisition and data handling in the medical field the use of autonomous minisystems is proposed because of safety considerations and uncomplicated implementation. Such minisystems generally will be coupled to larger computing systems providing extensive computing power and data base management. Autonomous minisystems can be implemented with great advantage by using the internationally standardized CAMAC instrumentation system. Automation of the clinical laboratory is discussed. (tr-auth)

31339 (IS-3444) PROGRAM CORRECTNESS IN A MULTIPROGRAMMED MULTIPROCESSOR ENVIRONMENT. Moon, L. C. (Ames Lab., Iowa (USA)). Aug 1974. Contract W-7405-eng-82. 24p. Dep. NTIS $4.25.

Levitt's method for proving correctness of a program in a multiprogramming multiprocessor environment is described. Simple examples are supplied to illustrate the strong and weak points of the method. (auth)

31340 (IS-M-18) PL/I BASED MULTI-TASKING OPERATING SYSTEM. Campbell, J. H.; Covert, G. F. (Ames Lab., Iowa (USA); Iowa State Univ. of Science and Technology, Ames (USA). Computation Center). 1973. 5p. (CONF-731204-3). Dep. NTIS $4.00.

From Digital Equipment Computers Users' Society symposium; San Francisco, California, USA (27 Dec 1973).

A PL/I based programming language and its attendant operating system is described. The programming language contains multi-tasking, external interrupt handling, and experimental communication facilities that allow the users to operate in a real-time multi-programmed environment. (auth)

31341 (LBL-3072) MAPEDIT SYSTEM FOR AUTOMATIC MAP DIGITIZATION. Holmes, H. H.; Austin, D. M.; Benson, W. H. (California Univ., Berkeley (USA). Lawrence Berkeley Lab.). 6 Aug 1974. Contract W-7405-eng-48. 21p. Dep. NTIS $4.00.

A system for the automatic digitization of polygon boundaries is described. Digitized map files are created from a driver tape containing identification codes and approximate centroids of polygonal boundaries (e.g., census tracts), and a film image of the map. The digitizer scans on the film plane in an automatic line-following mode, producing the first stage of the map file for the editing system. The MAPEDIT system, which can be used either interactively or in batch mode, reads maps in several standard formats and provides for combining and selecting maps by census (or other) geocodes or by longitude and latitude. This system provides several stages of data compression, analysis, and verification, including algorithms for detecting straight lines, finding corners, fitting insets of maps together and matching boundaries common to a pair of polygons. Auxiliary programs (1) provide a very high resolution (1 part in 25,000) C.R.T. plot of the map, (2) allow a detailed examination and editing of the map, and (3) supply missing geocodes using auxiliary tapes such as the Medlist tapes. (auth)

31342 (MC-19-1974) SOFTWARE EXTENDED FLOATING-POINT FEATURE. Zamfirescu, I.; Constantinescu, S. (Institutul de Fizica Atomica, Bucharest (Romania)). 1974. 25p. Dep. NTIS (US Sales Only) $4.25,

A software extended floating-point feature operates with numbers whose length varies from 8 through 160, decimal digits. Operands length can be modified in increments of 8 decimal digits, even during the computation. A floating point number consists of a signed fraction. The quantity expressed by this number is the product of the fraction and the number 100,000,000 raised to the power of the exponent. The fraction is expressed as a number in 100,000,000 radix, having a radix point to the left of the high order digit. A set of 7 operators designed for this feature are "assembler" written programs, that can be used as "function" subprograms in "FORTRAN" language. Operators structure allows the usage of "FORTRAN" I/O statements as I/O statements for this extended floating-point feature as well as the writing of a string of extended floating point operations as a single "FORTRAN" statement. The chosen number representation, as an integer unidimensional array, allowed the utilization of fixed-point machine instructions, which lead to the minimum execution time per operation. (auth)

31343 (NOAA-TM-ERL-ARL-43) PROGRAM DESCRIPTIONS: SUPPLEMENT TO MESOSCALE WIND FIELDS AND TRANSPORT ESTIMATES DETERMINED FROM A NETWORK OF WIND TOWERS. Wendell, L. L. (National Oceanic and Atmospheric Administration, Idaho Falls, Idaho (USA). Air Resources Lab.). May 1974. 53p.

A computer program was developed to analyze objectively two-dimensional wind data from a mesoscale network of stations. The result is a graphic display of the network wind field at any particular time and a plot of computed air trajectories as a function of time and point of origin. A brief description, a list of input variables, and program listings for the computer program are provided. (auth)

31344 (ORNL-TM-4588) SUBROUTINE CAUCHY: COMPLEX ROOTS OF A FUNCTION USING A CAUCHY INTEGRAL TECHNIQUE. Beasley, C. O. Jr.; Meier, H. K. (Oak Ridge National Lab., Tenn. (USA)). Aug 1974. Contract W-7405-eng-26. 24p. Dep. NTIS $4.25.

A description of the subroutine CAUCHY, the program for finding zeros of an analytic function $f(z)$ within a contour in the z-plane, is given. Examples of types of functions for which this program is most advantageous as well as types of functions that show its weaknesses are given. (auth)

31345 (SAND-74-5236) STIFFNESS AND NON-STIFF DIFFERENTIAL EQUATION SOLVERS. Shampine, L. F. (Sandia Labs., Albuquerque, N. Mex. (USA)). 1974. 15p. (CONF-740665-1). Dep. NTIS $4.00.

From meeting of Mathematical Research Institute; Oberwolfach, F. R. Germany (9 Jun 1974).

The effects of stiffness are investigated for production codes for solving non-stiff ordinary differential equations. First, a practical view of stiffness as related to methods for non-stiff problems is described. Second, the interaction of local error estimators, automatic step size adjustment, and stiffness is studied and shown normally to prevent instability. Third, a practical test for stiffness in variable order Adams codes is developed. Numerical results for working codes are presented for each topic. (auth)

31346 (SLA-73-0409) FAULT TREE DRAWING PROGRAM USERS INSTRUCTIONS. Oliver, D. A. (Sandia Labs., Albuquerque, N. Mex. (USA)). Apr 1973. 31p. Dep. NTIS $4.75.

Procedures are outlined for the preparation of input data for the Fault Tree Drawing Program and for the computer processing requirements on the CDC-6600 computer and Calcomp plotters. (auth)

31347 (UCID-15388) SECOND-ORDER DIFFERENCE EQUATIONS FOR A NON-UNIFORM TRIANGLE MESH. Winslow, A. M. (California Univ., Livermore (USA). Lawrence Livermore Lab.). Sep 1968. Contract W-7405-eng-48. 14p. Dep. NTIS $4.00.

The difference equations are derived for the simplest type of second-order scheme, in which the additional nodes are put at the mid-points of the triangle sides. This scheme is compared in accuracy and computational effort with first-order schemes having the same number of nodes (and correspondingly more triangles). (MCW)

31348 (UCID-15478) NUMERICAL SOLUTIONS OF POISSON'S EQUATION BY FOURIER TRANSFORM METHODS. Crowley, W. P. (California Univ., Livermore (USA). Lawrence Livermore Lab.). Apr 1969. 13p. Dep. NTIS $4.00.

The solution of Poisson's equation was considered in a rectangular domain as a numerical boundary value problem and ways of solving it by techniques involving linear transformations were listed. The most accurate method is probably that in which a double transformation is used to reduce the differential equation to an algebraic equation and involves $\sim K^2L^2$ multiplications. The other two methods (Hockney's and Veronis') involve the use of a single transformation to reduce Poisson's equation to a system of ordinary difference equations. One-dimensional considerations indicate that of the two, Hockney's method is the more accurate. For simplicity, functions were assigned zero on the boundary. In general, if cosine as well as sine functions are used as basis vectors this restriction may be changed so that all smooth periodic functions are acceptable. Although the single transform methods are appealing because they are faster than the double transform methods they have additional advantages; consider functions that are periodic in one dimension but not periodic in the other. The function may be expanded in the dimension in which it is periodic, and the difference equations solved in the other dimension. Consider also the solution of Poisson's equation in polar geometry. It is quite natural then to expand in the angular dimension (assuming the function to be periodic in that dimension) and to solve the difference equations in the radial dimension. The use of Fast Fourier Transform Techniques enhances the value of the methods outlined here. It is possible that these techniques make feasible the double transform method. (MCW)

31349 (UCID-15743) NUMERICAL DECONVOLUTION. Blair, J. (California Univ., Livermore (USA). Lawrence Livermore Lab.). 6 Sep 1968. 39p. Dep. NTIS $5.00.

Some methods for numerically solving the problem of determining the input to a linear, time invariant physical system from knowledge of the output of the system are developed and interpreted. (MCW)

31350 (UCID-15753) CODE DESCRIPTION: FOFT. Ryder, H. A. (California Univ., Livermore (USA). Lawrence Livermore Lab.). 26 Feb 1968. 14p. Dep. NTIS $4.00.

A computer code in FORTRAN is described to calculate the flux measured by each channel as a function of the black-body temperature of the source. The flux is determined by folding a normalized black-body spectrum with the response function and dividing the signal for the channel by the integral product. (auth)

31351 (UCID-15765) SOLUTION OF LARGE COUPLED SETS OF KINETIC EQUATIONS. Gelinas, R. J. (California Univ., Livermore (USA). Lawrence Livermore Lab.). Sep. 1970. 18p. Dep. NTIS $4.00.

The solution is needed of large coupled sets of kinetic equations that are time-constant-limited, or stiff, sets of ordinary nonlinear differential equations required to calculate the temporal evolution of nonequilibrium radiating systems such as those in astrophysics, in regard to the kinetics of simple chemical laser systems, and in models of the photochemistry of the atmosphere relevant to air pollution. An attempt is made to qualitatively make clear the nature of stiffness, its causes, its effects, and requirements of numerical methods that are expected to adequately deal with these problems. A subroutine that represents the current state of the art is recommended on a basis dealing with the nonequilibrium radiation systems. (MCW)

31352 (UCID-15840) POLAROID VECTOGRAPH PROCESS AND APPLICATION AS APPLIED TO STEREO LASER AND COMPUTER-GENERATED 3-DIMENSIONAL FORMS. Rogers, A. M. (California Univ., Livermore (USA). Lawrence Livermore Lab.). 21 May 1971. Contract W-7405-Eng-48. 12p. Dep. NTIS $4.00.

The need for greater depth perception of photographic images generated by computers and holograms onto film was solved by applying the Polaroid Vectograph process to this problem. Vectographs made from these computer-generated films are quite impressive as they display complex shapes and forms viewed in three-dimension form. (auth)

31353 (UCID-15945) SPACE WAVE FIELDS OF SUBSURFACE ELECTROMAGNETIC SOURCES IN PLANAR LAYERED MEDIA. Lytle, R. J. (California Univ., Livermore (USA). Lawrence Livermore Lab.). 15 Dec 1971. Contract W-7405-eng-48. 13p. Dep. NTIS $4.00.

Equations are developed for the space wave fields generated by a subsurface electromagnetic source operated in an $(N + 1)$ layered medium composed of $N-1$ finite-thickness layers. (auth)

31354 (UCID-15947) ENERGY MINIMIZATION METHOD FOR COMPUTER DECONVOLUTION. Gathers, G. R. (California Univ., Livermore (USA). Lawrence Livermore Lab.). 29 Oct 1971. Contract W-7405-eng-48. 14p. Dep. NTIS $4.00.

An energy minimization scheme to reduce noise in recorded data before submitting it to computer deconvolution is described. By adding one more constraint—with Lagrangian multipliers—to those used in the usual energy minimization schemes, this technique avoids the necessity for using arbitrary adjustable parameters. The theory of the method is described and a simple example of its use is worked out in detail. (auth)

31355 (UCID-15992) INTRODUCTION TO EXTRAPOLATION METHODS FOR THE NUMERICAL SOLUTION OF DIFFERENTIAL EQUATIONS. Chang, J. S. (California Univ., Livermore (USA). Lawrence Livermore Lab.). Feb 1972. Contract W-7405-eng-48. 36p. Dep. NTIS $5.00.

Richardson's original rationale for the name "deferred approach to the limit" is described. Other names for this class of methods are also known as Richardson extrapolation, extrapolation to the limit, extrapolation methods, and Romberg integration and have been applied to numerical differentiation, numerical integration, numerical solution of ordinary and partial differential equations, numerical solution of integral equations, numerical solution of functional equations, and other discrete approximation processes. The existing theory of the extrapolation methods is discussed. (MCW)

31356 (UCRL-75662) DIGITAL IMAGE PROCESSING WITH PSEUDO-COLOR. Radewan, C. H. (California Univ., Livermore (USA). Lawrence Livermore Lab.). 5 Aug 1974. 9p. (CONF-740823-5). Dep. NTIS $4.00.

From 18th annual meeting of the Society of Photo-Optical Instrumentation Engineers; San Diego, California, USA (19 Aug 1974).

Pseudo-color processing is a technique that maps each of the grey levels of a black and white image into an assigned color. This colored image, when displayed, can make the identification of certain features easier for the observer. The mappings are computationally simple and fast. This makes pseudo-color an attractive technique for use on digital image processing systems that are designed to be used in the interactive mode. The application of several pseudo-color mapping schemes is discussed. Various color maps can give contrast enhancement effects, contouring effects, or grey level mapping (depicting areas of a given grey level). Pseudo-color schemes can also be designed to preserve or remove intensity information. Since the nature of the original black and white image can determine the success or failure of a particular color scheme, it is necessary to find a rational approach to the design and selection of the color maps. Some methods of designing color schemes that use ideas from the fields of colorimetry and visual perception are described. (auth)

Miscellaneous

31357 (ANL/ES-30) ENVIRONMENTAL IMPACT HANDBOOK FOR HIGHWAY SYSTEMS. Wolsko, T. D.; Nelson, K. E.; Habegger, L. J. (Argonne National Lab., Ill. (USA)). Jun 1974. Contract W-31-109-eng-38. 139p. Dep. NTIS $10.00.

A general background for transportation planners on the considerations that should be given to the environmental impact analysis of proposed highways is provided. It contains a description of the major environmental effects and describes the considerations that should be given to impact analysis and statement preparation. The primary emphasis of the report is to describe quantitative analysis techniques for assessing the air and noise impacts of highways. Noncomputerized techniques are presented, along with procedures for analysis and example calculations. These models, having application to a limited number of highway designs, are simplified versions of more complex computerized models, and their capacity is intended to provide air and noise quantitative analysis capability for the inexperienced highway planner. (auth)

31358 (ORNL-tr-2801) MICRO- AND MACROTURBULENCE. Hofmann, A. Translated by R. Gregg Mansfield from Promet - Meteorol. Fortbild.; No. 1/2, 1-40(1971). 86p. Dep. NTIS $7.50.

Thirteen chapters on turbulence follow a test consisting of thirty-six questions. The chapters are: Turbulence: the necessary chaos in the atmosphere; What is microturbulence; How is turbulence measured today; What is macroturbulence actually; The scales as a first principle of order for all atmospheric turbulence phenomenons; What is a turbulence spectrum; What does the turbulence spectrum in the atmosphere look like; What is the real purpose of turbulence theories; Between production and dissipation of turbulence energy; The social function of turbulence; Asocial behavior of macroturbulence; What is clear-air turbulence, where does it occur, and results of flight measurements; and Turbulence and building construction. (MCW)

31359 (PTB-L-2) SCIENTIFIC PUBLICATIONS, REPORTS AND EXTERNAL LECTURES IN 1973 COMPILED BY REFERAT SCHRIFTTUM. (Physikalisch-Technische Bundesanstalt, Braunschweig (F.R. Germany)). Apr 1974. 40p. (In German). INIS.

The compilation of literature contains: (1) scientific publications, PBT-reports and external lectures for 1973 arranged by the special departments of the PTB (from the Annual Report 1973 of the PTB); (2) scientific publications in special periodicals for 1973 alphabetized by authors; (3) PTB-reports in 1973 alphabetized by authors; and (4) external lectures for 1973 alphabetized by authors. (auth)

31360 (SCR-610) HUMAN ERROR QUANTIFICATION. Swain, A. D.; Altman, J. W.; Rook, L. W. Jr. (Sandia Labs., Albuquerque, N. Mex. (USA)). Apr 1963. 21p. (CONF-621106-1). Dep. NTIS $4.25.

From 6th annual meeting of the Human Factors Society; New York, New York, USA (28 Nov 1962).

Quantitative estimates of human performance can help the systems engineer balance human factors against other aspects of system design. Although methods for quantifying human factors evaluation certainly have not been perfected, starts toward such quantification have been made. Some quantifying techniques used at the American Institute for Research are discussed. (auth)

31361 (UCID-15722) DETERMINATION OF GEOGRAPHIC POSITION FROM RECTANGULAR COORDINATES. Progress Report, March-June 1970. Beers, F. T. III. (California Univ., Livermore (USA). Lawrence Livermore Lab.). 19 Mar 1970. 67p. Dep. NTIS $6.50.

Three memos are presented and are entitled: location of position references used by the GPL-A; accuracy of position standards used for GPL-A testing; and reduction of California coordinates to geographic position. The California coordinate system is a rectangular or Cartesian coordinate system used to represent a small portion of the Earth's surface. Within this system, a surveyor may work in a rectangular set of coordinates, obviating the tedious spherical trigonometry that could otherwise be involved. The coordinate system is based on Lambert conformal conic projections for different zones within the state. The conical projection is limited in its ability to represent the Earth's surface without introducing abnormal distortion. A code CALCOORD is presented for reducing California coordinate positions to latitude and longitude positions. A derivation of the formulae used in converting California coordinates to geographic position and vice versa is included. (MCW)

31362 (UCID-16014) PROGRAM IONS: TWO-DIMENSIONAL FOKKER-PLANCK EQUATION FOR IONS AND ELECTRONS. Mirin, A. A. (California Univ., Livermore (USA). Lawrence Livermore Lab.). 13 Mar 1972. Contract W-7405-eng-48. 34p. Dep. NTIS $4.75.

Program IONS solves the two-dimensional Fokker-Planck equation for ions and electrons, with the assumption that the electron distribution is Maxwellian. The ion equation is advanced using a second-order, alternating direction implicit (A.D.I.) difference scheme. A second-order Runge-Kutta method is used to advance the electron equation. (auth)

31363 (UCRL-51537) DEVELOPMENT OF AN AIR POLLUTION MODEL FOR THE SAN FRANCISCO BAY AREA. Second Semiannual Report to the National Science Foundation. (California Univ., Livermore (USA). Lawrence Livermore Lab.). 27 Feb 1974. Contract W-7405-eng-48. 123p. Dep. NTIS $5.45.

The operational planning group has completed the choice of instrumentation; coordinating and gathering data from various sources; planning where, when, and how these measurements are to be taken; planning and managing flight operations; developing a usable data storage system to achieve the data; and making the data available for model verification studies. Eighty-one fixed sites were selected to provide wind speed and direction data. Fixed vertical soundings providing wind, temperature, and humidity are available at three locations, and fixed vertical wind observations are available from two additional sites. Observations of pollutant concentrations are available from twenty-three fixed sites. Portable and mobile site observation points are designated. Flight plans have been filed. The air pollution model for the San Francisco Bay area consists of a suite of submodels that are coupled into the Livermore Regional Air Quality model. The meteorological data that have been gathered, analyzed, and entered into the data bank are available as input to MACAW, a mass consistent windfield model. The topography model is essentially complete, but modifications are needed on the source emission model. (MCW)

Chemistry

31364 (AED-CONF-74-072-002) MEASUREMENTS OF PERSISTENCE LENGTH AND TEMPERATURE DEPENDENCE OF THE RADIUS OF GYRATION IN BULK ATACTIC POLYSTYRENE. Wignall, G. D.; Ballard, D. G. H.; Schelten, J. (Technische Univ. Darmstadt (F.R. Germany). Inst. fuer Reaktortechnik). 1974. 6p. (CONF-740343-1). INIS.

From meeting on deformation and yield in high-polymer solutions, melts and solids; Wuerzburg, F. R. Germany (18 Mar 1974).

6 figs.; 2 tabs.; 16 refs. With abstract.

Measurements of radius of gyration, $\langle S^2\rangle^{1/2}$, and persistence length of polymer molecules in bulk atactic polystyrene have been made by means of low angle neutron scattering. The measured values of $\langle S^2\rangle^{1/2}$ lie close to those measured in Theta solvents and have a molecular weight dependence of $M^{\frac{1}{2}+\epsilon}$ where $\epsilon = 0.04 \pm 0.04$. The molecular configuration agrees closely with that of a random coil with a persistence length approximately 10 A. These measurements support the model of an unperturbed Gaussian coil for this polymer. Measurements of $\langle S^2\rangle^{\frac{1}{2}}$ throughout the glass transition region indicate that the overall conformation of the polymer chain does not change on heating through this region. (orig.)

31365 (AED-CONF-74-089-024) TEMPERATURE DEPENDENCE OF THE LATTICE DISTORTION IN THE ONE-DIMENSIONAL CONDUCTOR $K_2Pt[CN]_4Br_3 \times 3D_2O$. Renker, K.; Pintschovius, L. (Kernforschungszentrum Karlsruhe (F.R. Germany). Inst. fuer Angewandte Kernphysik). 1974. 7p. (In German). (CONF-740451-7). INIS.

From conference on solid state physics; Freudenstadt, F.R. Germany (1 Apr 1974).

8 figs.; 1 tab.; 3 refs. With abstract.

Based upon neutron measurements, a theoretical analysis of crystal models and a quantitative treatment with discussion of spectra of $K_2Pt[CN_4]Br_2 \times 2D_2O$ are presented. (GE)

31366 (BDX-613-1064) ELECTRODEPOSITING PLATINUM AND PLATINUM–IRIDIUM ALLOYS FROM MOLTEN CYANIDES: CHEMICAL PROCESS STUDIES. Harding, W. B. (Bendix Corp., Kansas City, Mo. (USA)). Sep 1974. Contract AT(29-1)-613. 35p. Dep. NTIS $4.00.

Studies were made of iridium and platinum plating baths produced by adding the metals to molten sodium cyanide both electrolytically and as cyanide salts. The electrode reactions were studied using efficiency measurements, voltammetry, cyclic voltammentry, and chronopotentiometry. Electrode efficiencies in the iridium process were low (about 20 percent) because of competing electrode reactions. The competing reactions were not identified, but the data suggested they involve a cyclic process of oxidation and reduction of iridium compounds, although the possibility that the reactions involved impurities was not ruled out. The electrode efficiencies in the platinum process are about 80 percent but the anode efficiency is somewhat uncertain because of decrepitation. The platinum electrolyte tends to decompose. (auth)

31367 (BDX-613-1099(Rev.)) SOLUBILITY PARAMETERS AND EVAPORATION RATE ANALYSIS IN ORGANIC RESIDUE CHARACTERIZATION. Jackson, L. C. (Bendix Corp., Kansas City, Mo. (USA)). Sep 1974. Contract AT(29-1)-613. 15p. Dep. NTIS $4.00.

Solubility parameter and evaporative rate analysis technologies were combined to establish a fundamental relationship between the two on the basis of known surface contamination by organic molecules. Surface tension measurements confirmed the relationship. Statistical analysis of the data showed high correlation confidence levels which gave significance to the use of the Meseran Surface Analyzer. Formulas useful in converting radioactive count measurements to solubility parameter values are presented. The latter characterizes a molecule as to its functional groups and, therefore, its activity. (auth)

31368 (SLA-73-7063) INSTRUMENTAL LIMITATION TO THE RATE OF KINETIC PROCESSES MEASURABLE BY TIME-RESOLVED MASS SPECTROMETRY. Rice, J. K.; Truby, F. K. (Sandia Labs., Albuquerque, N. Mex. (USA)). [nd]. 2p. (CONF-740554-1). Dep. NTIS $4.00.

From 22nd annual conference on mass spectrometry and allied topics; Philadelphia, Pennsylvania, USA (19 May 1974).

The technique of time-resolved mass spectrometry was applied to measurement of fast chemical reaction rates. Chemical reactions in a reaction cell are initiated by a flash lamp. The products effuse through an orifice in the cell and drift to the ionization region. If ionized, these species are accelerated, filtered according to their respective charge-to-mass ratios, and detected. The rate of a particular reaction can often be determined by monitoring the time dependence of a suitable product or reactant. An effect that limits the maximum rate that can be measured is described. This effect is based on the fact that particles effusing from a reaction cell have a range of velocities. Particles leaving the cell at one time in the reaction can arrive at the ionizer in conjunction with particles that left the cell at a different time. If the interference produced by this effect is severe enough, information concerning the underlying chemical reaction rates can be completely lost. The severity of this effect depends on the size of the ionizer and its distance from the cell, the velocity spread, and the reaction frequency of interest. (MCW)

31369 (UCID-15623) ANALYSIS OF PLASTIC-BONDED EXPLOSIVES CONTAINING HMX, AMMONIUM PERCHLORATE, ALUMINUM, AND VITON. Selig, W.; Crossman, G. L. (California Univ., Livermore (USA). Lawrence Livermore Lab.). 2 Apr 1970. 8p. Dep. NTIS $4.00.

Methods for the analysis of plastic-bonded explosives containing (1) HMX, ammonium perchlorate, and Viton or (2) HMX, ammonium perchlorate, aluminum, and Viton are presented. Viton is determined gravimetrically by extraction of the other constituents with concentrated nitric acid. If aluminum is present, it is analyzed titrimetrically in an aliquot of the nitric acid solution with EDTA. Ammonium perchlorate is analyzed by combustion in an oxygen bomb, and subsequent potentiometric titration of the resulting chloride with mercuric nitrate. HMX is calculated by difference. (auth)

31370 (UCID-15671) GAS CHROMATOGRAPHIC ANALYSIS OF BIS(2-FLUORO-2,2-DINITROETHYL) FORMAL (FEFO). Clarkson, J. E.; DuVal, V. L. (California Univ., Livermore (USA). Lawrence Livermore Lab.). 22 Jul 1970. 7p. Dep. NTIS $4.00.

A method for the quantitative analysis of bis(2-fluoro-2,2-dinitroethyl) formal (FEFO) is described. The FEFO is analyzed by a gas-chromatographic method, using on OV-3 column, temperature programming, and flame-ionization detectors. The standard deviation is 0.1% for a set of determinations run at the same time and 0.2 to 0.4% over several months. (MCW)

31371 (UCID-15872) SOURCE IDENTIFICATION BY MULTI-ELEMENT ANALYSIS OF DIURNAL SAMPLES. Wesolowski, J. J.; John, W.; Kaifer, R. (California Univ., Livermore (USA). Lawrence Livermore Lab.). 12 Jul 1971. 19p. Dep. NTIS $4.00.

Evidence for the existence of a non-automotive source of lead, probably N-NW of Elliot Cove, California was obtained by measuring the concentrations of Pb and Br in particulates collected from ambient air for two-hour time intervals and correlating this information with wind data. For one of the episodes, a two-hour Pb average as high as 11 $\mu g/m^3$ was recorded with a corresponding Br/Pb ratio of less than 0.037. A multi-element analysis of the samples using neutron activation analysis will be undertaken to determine more precisely the nature of the source. (auth)

31372 (UCID-15910) PROPERTIES OF THE HIGH EXPLOSIVE LX-09-0. Dobratz, B. M. (Comp.). (California Univ., Livermore (USA). Lawrence Livermore Lab.). 17 Sep 1971. Contract W-7405-eng-48. 29p. Dep. NTIS $4.50.

LX-09-0 is an explosive composition having slightly higher energy and greater thermal stability than PBX-9404-03. Measurement and determination of thermal, physical, compatibility, and sensitivity properties are described and compared with those of PBX-9404-03. (auth)

31373 (UCID-15972) ANALYSIS OF EXPLOSIVE SIMULANT 90503. Selig, W.; Crossman, G. L.; Estes, Z. E.; Boyles, L. (California Univ., Livermore (USA). Lawrence Livermore Lab.). 3 Jan 1972. Contract W-7405-eng-48. 5p. Dep. NTIS $4.00.

A method for the analysis of explosive simulant 90503, containing cyanuric acid, melamine, nitrocellulose (NC), and tris-β-chloroethylphosphate (CEF) is presented. CEF is extracted with methylene chloride. The remainder is digested with hot water, which converts an amount of cyanuric acid equivalent to the melamine present to the melamine cyanurate complex. The excess of cyanuric acid is removed by filtration. Finally, NC is extracted with acetone, leaving a residue of melamine cyanurate. (auth)

31374 (UCRL-51629) LX-10-1: A HIGH-ENERGY PLASTIC-BONDED EXPLOSIVE. Humphrey, J. R. (California Univ., Livermore (USA). Lawrence Livermore Lab.). 18 Jul 1974. Contract W-7405-Eng-48. 17p. Dep. NTIS $4.00.

The properties of LX-10-1, a special high-energy plastic-bonded explosive are described. LX-10-1 has greater energy, has better thermal stability and creep properties, is easier to prepare, and has fewer compatibility problems than either PBX-9404 or LX-09-1. (auth)

31375 (UCRL-51636) INVESTIGATION OF POLYION-SMALL ION ELECTROSTATIC INTERACTION EFFECTS IN POLYELECTROLYTE SOLUTIONS. Ermak, D. L. (California Univ., Livermore (USA). Lawrence Livermore Lab.). 6 Sep 1974. Contract W-7405-eng-48. 190p. Dep. NTIS $12.50.

Thesis.

A theoretical and computational study has been made on the effects of the polyion-small ion electrostatic interaction upon the dynamic and equilibrium properties of the ions in polyelectrolyte solutions at thermodynamic equilibrium. In these solutions each ion experiences a fluctuating electrostatic force due to equilibrium fluctuations in the distribution of the other ions. Of main interest were the effect of these interactions upon the polyion diffusion coefficient, the average electrostatic energy of each ion species, and the degree to which the small ions electrically shield the polyions. Treating the polyions as charged Brownian particles, the polyion motion is described using the Langevin equation which is modified to include the electrostatic force due to the small ions. Assuming that this force is random and independent of the polyion motion, the polyion diffusion coefficient is shown to be increased. This increase is expressed in terms of the mean square value and the correlation time of the electrostatic force on the polyions. The equilibrium properties of the polyions are described using the Debye-Hückel theory. In order to study quantitatively the effects of this interaction, a computer technique was developed for simulating the motion of the ions through the solution. Each ion undergoes a diffusive motion which is perturbed by the electrostatic force of the other ions. The model system studied consists of spherically symmetric ions in a uniform dielectric solvent. Computer experiments were conducted on systems containing polyions from 20 Å to 90 Å in diameter with the majority of the calculations being carried out with 45 Å diameter polyions. The polyion–small ion electrostatic interaction was found to increase the diffusion coefficient of the model polyions. For the systems studied, the increase was generally less than 10% and was strongly dependent upon the polyion charge and size, and the small ion charge and mobility, while only slightly affected by changes in the polyion concentration. For a given system, the increase was largest when there were only enough small ions to balance the charge of the polyions. Increasing the number of neutral small ion pairs per polyion decreased the polyion diffusion coefficient toward its uncharged value. The computer results were markedly different from those predicted by the self-consistent field theory of Stephen and a comparison of the two is presented. The average electrostatic energy of each ion species and the small ion distribution function relative to a central polyion was also calculated in each computer run. These results were compared with those of the Debye-Hückel theory for polyions at zero concentration. As the small ion shielding length becomes shorter than $\frac{1}{2}$ the mean distance between polyions, the computer and Debye-Hückel results for the polyion electrostatic energy are in fairly good agreement. The computer simulation technique developed in this work was extended so that the shielded polyion–polyion electrostatic interaction can also be studied. A series of computer calculations was conducted in which the small ion distribution was taken to be uniform and therefore the electrostatic shielding of the polyions was minimal. In contrast to the polyion-small ion interaction, the polyion–polyion interaction was found to decrease the polyion diffusion coefficient. (auth)

Life Sciences

31376 (CONF-740663-1) RECENT CHANGES OF THE FORAMINIFERAL ASSEMBLAGES OF JOBOS BAY AND SURROUNDINGS, PUERTO RICO. Seiglie, G. A. (Puerto Rico Univ., Mayaguez; Puerto Rico Nuclear Center, Mayaguez). 1973. Contract AT(40-1)-1833. 16p. Dep. NTIS $4.00.

From 7th Caribbean geological conference; Guadeloupe, France (30 Jun 1974).

A core 41.5 cm long was taken in Mar Negro Lagoon at a water depth of 4 m. The most important biogenic grains in the sand fraction of the core were Halimeda, molluscs, and foraminifers. Halimeda is the most abundant constituent of the sand from 41.5 to 22 cm in the core. It indicates a skeletal sand flat slowly increasing its mud content. The number of Halimeda fragments decreases from 26 to 0 cm. Molluscs are well preserved and maintain their shell color from 41.5 to 22 cm in the core. Shells show several degrees of preservation from 22 cm to 16 cm, and from 16 cm to the top of the core, shells are thin and fragmentary. Foraminifers constitute the dominant group of the sand size grains from 19 cm to the top of the core. Miliolids are the dominant group of foraminifers from 41.5 cm to 25 cm in the core, while specimens of Ammonia are scarce. The number of miliolids decrease dramatically from 26 cm to 20 cm probably because of dissolution of the tests. They are rare in the present living faunas. Ammonia is the dominant foraminifer from 25 cm to the top of the core. This core may be taken as a model for the evolution from a skeletal sand flat to a coastal lagoon with depths from 2.5 m to 4.5 m. Samples were taken in Mar Negro Bay at a water depth of 2.7 m to be compared with the core of Mar Negro Lagoon. The bay is in an evolutionary stage equivalent to that at depths of 6 cm to 22 cm in the core from the lagoon. Tests of dead miliods (living ones are present) are dissolved, and Ammonia is the dominant foraminifer, indicating the probable onset of stress conditions. A core 35 cm long was taken at a water depth of 2 m in the northwestern part of Jobos Bay, south of the Aguirre plant. This was the dumping area of Central Aguirre until December 1971. An Elphididae assemblage is dominant from 35 cm to 15 cm of depth in the core, where Ammonia is rare or absent. Ammonia is dominant from 15 cm to the top of the core. Its dominance indicates the onset of stress conditions in the area. Decrease of specific diversity and extreme deformation of individuals of Ammonia are related to pollution. (auth)

31377 (COO-1332-103) VERTEBRATE BEHAVIOR AND ECOLOGY. Progress Report, July 1, 1973–June 30, 1974. Tester, J. R.; Siniff, D. B. (Minnesota Univ., St. Paul (USA). Dept. of Ecology and Behavioral Biology). Jul 1974. Contract AT(11-1)-1332. 87p. Dep. NTIS $7.50.

A system was designed to use a small computer to record and partially process telemetry and environmental data at Cedar Creek Laboratory. Ten new portable tracking receivers using a frequency synthesizer as the tuning oscillator were built and are currently being tested and used in the field. Preliminary designs for heart rate transmitters were field tested and some improvements were made in the design of conventional transmitters. Lithium batteries have been functioning in 30 transmitters for nine months in the field in a pilot study to test this power source. The radio signal coming from the tracking antennas made it possible to record data directly onto magnetic tape. Efforts continued in investigations on habitat selection and vegetation analysis and a computer program was developed to visually display the vegetation pattern on a cathode ray scope to allow an operator to verify or correct line segments. Gray (Sciurus carolinensis), fox (S. niger), and red squirrels (Tamiasciurus hudsonicus) are being studied in three oak stands at Cedar Creek. Radios were placed on 48 squirrels and 146 additional squirrels were ear-tagged. Observations to detect effects of the radio collar on behavior are being made at an artificial feeding station and on squirrels held in a large outdoor pen. Analysis of data collected on gray squirrels last year indicated home ranges varied from 9.7 to 69.0 acres. Overlap of home ranges suggests that this species may not be territorial. Circadian activity patterns revealed a very consistent relationship between time of activity and sunrise and sunset. Analysis of data is continuing for all three species and an evaluation is planned of interspecific relations. (auth)

31378 (NYO-3406-18) PIEZOELECTRIC MECHANICAL-MICROPIPETTE STIMULATOR. Technical Report No. 10. Reynolds, G. T. (Princeton Univ., N. J. (USA)). 12 Feb 1970. Contract AT(30-1)-3406. 13p. Dep. NTIS $4.00.

A simple mechanical stimulating technique capable of controlled displacements and providing a time reference for the precise initiation of the stimulation of light-emitting organisms is described. Its effectiveness when applied to a number of different dinoflagellates (Noctiluca, Pyrocystis, Gonyaulax, Ctenophore) is compared with electrical and chemical techniques. A thin-walled piezoelectric cylinder is an integral part of the suction micropipette that holds the specimen. A schematic of the stimulator is shown. (MCW)

31379 (RFP-2151) DIRECT DETERMINATION OF BERYLLIUM IN URINE BY FLAMELESS ATOMIC ABSORPTION SPECTROMETRY. Hurlbut, J. A. (Dow Chemical U. S. A., Golden, Colo. Rocky Flats Div.). 20 Aug 1974. Contract AT(29-1)-1106. 8p. Dep. NTIS $4.00.

A direct, flameless, atomic absorption method for the determination of beryllium in urine is described. A heated graphite atomizer is used, and the method is simple, rapid, and utilizes aqueous standards. Ten picograms of beryllium can be detected, and the sensitivity is 0.2 micrograms per liter. Ashing does not alter the recovery of beryllium and is not necessary. (auth)

31380 (RT/BIO-(74)7) APPLICATION OF SEQUENTIAL ESTIMATION METHODS TO COUNTS OF PHYTOPLANKTON. Moeller, F.; Zattera, A. (Comitato Nazionale per l'Energia Nucleare, Rome (Italy)). Feb 1974. 74p. Dep. NTIS (U. S. Sales Only) $6.75.

The methods of sequential estimation applicable to the counting method of algae developed by Utermöhl are described. The Stein's method seems the most convenient applicable to the type Utermöhl sedimentation cells. With such method can be realized a high economy of time that often can be 30 times less than that necessary for counting all the algae on the whole sedimentation surface. (auth)

Materials

31381 (AED-CONF-74-089-025) HIGHLY RESOLVED ELECTRON ENERGY LOSS SPECTROSCOPY OF AMORPHOUS GERMANIUM AND SILICON LAYERS. Schroeder, B. 1974. 7p. (In German). (CONF-740451-13). INIS.

From conference on solid state physics; Freudenstadt, F. R. Germany (1 Apr 1974).

New results and knowledge acquired on highly resolved energy loss measurements on amorphous Ge and Si layers are reported. Energy losses in the region of the energy gap and the fundamental absorption (band edge) are discussed. (GE)

31382 (AED-CONF-74-089-027) SHORT-RANGE ORDER IN LIQUID LITHIUM-LEAD ALLOYS. Ruppersberg, H.; Speicher, W. (Universitaet des Saarlandes, Saarbruecken (F.R. Germany). Fachbereich Angewandte Physik). 1974. 5p. (In German). (CONF-740451-10). INIS.

From conference on solid state physics; Freudenstadt, F.R. Germany (1 Apr 1974).

8 figs.; 9 refs.

The x-ray diffraction, neutron diffraction, density and compressibility of various liquid alloys in the Li–Pb system were measured. Lead atoms have a preference for being surrounded by lithium atoms, the intermetallic compounds LiPb exhibit an extremely negative excess volume. The molecular volume of the alloys was determined being the method of the maximum bubble pressure, and for various mixtures of Li–Pb, the (partial) structure factors $i_{SS}(s)$ or $a_{ij}(o)$ as well as the so-called short-range order parameters were also determined. (GE)

31383 (AED-CONF-74-254-001) USE OF FINE-GRAINED ELECTROGRAPHITE IN METAL WORKING. Wiemer, H.; Persicke, H.; Huetsch, W. (Ringsdorff-Werke G.m.b.H., Bonn-Bad Godesberg (F.R. Germany)). 1974. 8p. (In German). (CONF-740664-2). INIS.

From general meeting of the Deutsche Gesellschaft fuer Metallkunde e.V.; Bonn, F.R. Germany (4 Jun 1974).

16 figs.

A survey is given of the manufacturing processes, properties and fields of application of the materials group artificial coal. (GE)

31384 (BDX-613-1036(Rev.)) STATIC COMPRESSIVE TESTING OF RIGID POLYURETHANE FOAM. Neet, T. E.; DeGisi, S. L. (Bendix Corp., Kansas City, Mo. (USA)). Oct 1974. Contract AT(29-1)-613. 49p. Dep. NTIS $4.00.

The relationships between the compressive strength and modulus and the test temperature and density of 11 foam systems are presented. The results of the study are graphically illustrated. (auth)

31385 (BDX-613-1082(Rev.)) PROCESS EVALUATION OF NEW CELLULAR SILICONE MATERIAL. Edman, G. W. IV. (Bendix Corp., Kansas City, Mo. (USA)). Sep 1974. Contract AT(29-1)-613. 25p. Dep. NTIS $4.00.

The processing characteristics of some new cellular silicone formulations were studied and evaluated. The major difference between these experimental materials and currently used cellular silicones is the manufacturing process of the base gum, with an expected benefit of improved processability of the filled raw material. To determine the relative processability of the experimental materials, sample parts were molded at various molding pressures. The wall thickness variation of the resultant finished parts was compared to that obtained for standard material counterparts processed under the same conditions. Additional tests of physical and chemical properties were performed to determine if there was an equivalency between the two materials as forecasted. Results of the wall thickness evaluation and observations made during sample fabrication indicate that the experimental materials do indeed process more readily than standard formulations, but the projected equivalency of finished part properties was not met. The two formulations are, however, sufficiently similar to warrant consideration of the new cellular silicone as an adequate replacement for current-use materials in future applications. (auth)

31386 (BDX-613-1133(Rev.)) TEMPERATURE DEPENDENT PROPERTIES OF POTTING MATERIALS. Walker, J. M. (Bendix Corp., Kansas City, Mo. (USA)). Sep 1974. Contract AT(29-1)-613. 30p. Dep. NTIS $4.00.

The mechanical, electrical, and thermal properties of a general purpose epoxy potting compound, filled with either glass microspheres or aluminum oxide and catalyzed with either diethanolamine or Epon Z are discussed. Twelve formulation-cure cycle combinations were chosen for evaluation. The temperature properties from −65 to 400°F of four of the combinations are given. Modulus versus temperature polynomials were calculated for the diethanolamine catalyzed material. (auth)

31387 (BDX-613-1155(Rev.)) MASS ANODIZATION OF TANTALUM–NITRIDE RESISTORS. Peltier, A. J. (Bendix Corp., Kansas City, Mo. (USA)). Sep 1974. Contract AT(29-1)-613. 24p. Dep. NTIS $4.00.

Mass anodization of tantalum-nitride films with sheet resistivities not exceeding 200 ohms per square to meet ±10% tolerance requirements on resistors above 100 ohms has been shown feasible. The anodization system that was developed for this study is capable of producing yields of approximately 80% under those conditions. Although anodization trimming on films with sheet resistivities as high as 600 ohms per square is now feasible, further work is necessary to successfully anodize films above 600 ohms per square and resistors below 100 ohms. The work was done to establish a method of anodizing tantalum nitride resistor films on microcircuit substrates. (auth)

31388 (BNL-19161) POLYMER-CONCRETE FOR USE IN THE REPAIR OF DETERIORATED BRIDGE DECKS. Kukacka, L. E.; Fontana, J.; Steinberg, M. (Brookhaven National Lab., Upton, N. Y. (USA)). 1974. 30p. Dep. NTIS $4.50.

One of the most severe problems facing the highway industry is the rapid deterioration of highway-type structures. As part of a concerted effort to solve this problem, research is being performed to determine if concrete-polymer materials can be used for the repair of deteriorated and delaminated bridge decks. Polymer-concrete (PC) consists of an aggregate mixed with a monomer which is subsequently polymerized in place. It is mixed and placed using techniques similar to those used for portland cement concrete and after curing produces a high-strength, durable material. Process variables studied include monomer-type, aggregate size distribution, and polymerization method. Field testing of PC has been progress for ~3 y and to date deterioration has not been observed. One test on a major arterial highway in New York City has been in progress for 7 months. Based on the success obtained in this experiment and in concurrent laboratory evaluations, further work on the same highway is scheduled for September 1974. These data are summarized. (auth)

31389 (CONF-740644-1) ROCK MAGNETITES WITH POSITIVE ANISOTROPY CONSTANTS AT 300°K. Griscom, D. L.; O'Horo, M. P.; Weeks, R. A. (Naval Research Lab., Washington, D. C. (USA); Xerox Corp., Webster, N. Y. (USA). Webster Research Center; Oak Ridge National Lab., Tenn. (USA)). 1974. 9p. Dep. NTIS $4.00.

From Takesi Nagata conference; Pittsburgh, Pennsylvania, USA (3 Jun 1974).

The use of ferromagnetic resonance as an easy and reliable method of measuring both the sign and magnitude of the anisotropy field of fine-grained ferromagnetic minerals is discussed with emphasis on submicroscopic magnetites. The FMR discussion involves studying the resonant absorption of microwaves by a sample as a function of a laboratory applied magnetic field. Computer-simulated powder spectra for cubic anisotropy for an X-band spectrometer frequency (9.5 GHz) and room-temperature X-band FMR spectra of ferric ion spinel precipitates in a DSDP basalt and two synthetic glasses are shown. The best characterized sample investigated to show the positive anisotropy constants at 300°K is a calcium alumino-boro-silicate glass melted to contain ferric and ferrous ions in a 2 : 1 ratio and precipitated at 600°C. The FMR spectra of a separate of green glass balls from Apollo 15 lunar sample 15426 believed to contain magnetite-like phases were analyzed. (MCW)

31390 (COO-1436-41) TRANSPORT AND THERMODYNAMIC PROPERTIES OF SOLIDS. Progress Report, September 1, 1973–August 31, 1974. Grace, R. E.; Dayananda, M. A. (Purdue Univ., Lafayette, Ind. (USA). School of Materials Engineering). 1974. Contract AT(11-1)-1436. 19p. Dep. NTIS $4.00.

Research on ternary diffusion in solid solution alloys was reported. Specific research projects deal with diffusion in the Cu–Zn–Ni, Ni–Fe–Al, and Ni–Al systems. The report is a general summary of projects either recently completed or in progress. Two separate research reports were completed during the year and are included as an appendix. These concern diffusion studies in Ni–Al alloys, and atomic mobilities and vacancy wind effects for diffusion in ternary Ag–Zn–Cd solid solutions. (MCW)

31391 (COPPE-TP-8/72) CORROSION STUDY OF THE SUPERPLASTIC ALLOYS 70/30 AND 80/20 ZINC ALUMINUM IN A HUMID ATMOSPHERE. de Ferran, E. M. (Rio de Janeiro Univ. (Brazil). Coordenacao dos Programmas de Pos-Graduacao de Engenharia). Jun 1972. 18p. (In Portuguese). INIS.

The corrosion resistance in a humid atmosphere was examined for the alloys 70/30% Zn-Al and 80/20% Zn-Al (by weight), and for various 70/30 and 80/20 Zn-Al alloys with small additions of Cu or Mg. The corrosion evaluation was made using the quick assay steam test and measuring after the test the thickness of the corrosion layer and the loss of mechanical properties in a tensile test. It was verified that the simple alloys 70/30 and 80/20 Zn-Al corrode considerably and that small additions of Mg and principally 0.5% of Cu improve appreciably the corrosion resistance. (INIS)

31392 (JINR-P14-7974) HEMATITE PHASE DIAGRAM IN A MAGNETIC FIELD. I. Low-Temperature Modification. Balanda, M.; Nitts, V. V. (Joint Inst. for Nuclear Research, Dubna (USSR). Lab. of Neutron Physics). 1974. 20p. (In Russian). Dep. NTIS (U. S. Sales Only) $4.00.

Thermodynamic consideration is made of the hematite crystal behavior in the external magnetic field at the temperature below the Morin point. On the basis of experimental data analysis it is shown that in the phase diagram there is a line of tricritical and that of critical points. (auth)

31393 (KFK-1978) DETERMINATION OF MINERAL-OIL IN THE HELIUM-CIRCUIT OF A REFRIGERATION-PLANT. Niekusch, E.; Schweer, K. H. (Kernforschungszentrum Karlsruhe (F. R. Germany). Inst. fuer Radiochemie). May 1974. 13p. (In German). Dep. NTIS (US Sales Only) $4.00.

A method for determining small amounts of mineral oil in the helium-circuit of a low-temperature apparatus is described. The gas was washed with an organic solvent (in this case carbon tetrachloride) and the solution was eventually enriched by a careful distillation. A content of mineral oil in the solution was examined by measuring the infrared absorption band at 3.4 μ. On the basis of a calibration curve, which is linear up to 0.3 mg mineral oil/ml solvent, the content of mineral oil can be quickly determined. The interpretation of the entire IR spectrum gives a qualitative insight in the composition of the sample. Different parts of the low-temperature apparatus were checked in this way, and the content of mineral oil in helium ranged from 0.45 to 1.36 wt ppM. (auth)

31394 (KHFTI-73-25, pp 19-23) CRYOVACUUM HYDROGEN ADSORPTION BY SMALL-SIZED, ACTIVATED MINERAL COAL WITHOUT A BINDER. Breslavets, K. G.; Kogan, V. S.; Mishchenko, B. A.; Koz'min, G. V.; Loskutov, A. I.; Tsai, M. I. 1973. (In Russian).

On the basis of comparing data on characteristic pore volumes obtained from experiments on the adsorption of benzene at 20°C, hydrogen at 20.4°K, and hydrogen at a temperature drift from 50 to 20.4°K, reasons are proposed for the character of the distribution in adsorption volumes according to micropore size in the ultramicropore region ($d < 5.8$ Å). It is shown that as a result of a 20% burnoff of the mineral coal a large volume of ultramicropores still remain in the coal. As a result the adsorption volumes according to benzene are 50% less than the volumes according to hydrogen, and hydrogen adsorption at 20.4°K has an activated character. According to its adsorption capacity for hydrogen at 20.4°K the active coal with a 20% burnoff without binder is a factor of 2 to 2.5 less effective than a composite active coal with the same burnoff, but the active coal without binder is more effective by approximately the same amount than the BAU coal. In order to increase the parameters of the active coal without binder as an adsorbent for cryovacuum equipment, apparently, it is necessary to obtain greater activation that would possibly increase the total volume of micropores, shift the maximum from the region of ultramicropores towards greater pore sizes, and improve the kinetic characteristics of the adsorbent. The study has added to knowledge on how microporous structure originates and develops in carbon adsorbents during the production process, and notes directions for further experiments on adsorbent treatments that are optimal for cryovacuum technique. (tr-SJR)

31395 (LA-5637-T) ELECTRONIC STRUCTURE AND OPTICAL PROPERTIES OF SOME FIRST ROW TRANSITION METAL OXYHALIDES. Jasinski, J. P. (Los Alamos Scientific Lab., N. Mex. (USA)). Jun 1974. Contract W-7405-eng-36. 205p. Dep. NTIS $10.60.

Thesis. Submitted to Univ. of Virginia, Charlottesville.

A molecular orbital calculation has been performed on two closed shell, d^0, molecules in C_{2v} symmetry (CrO_2F_2 and CrO_2Cl_2) and two closed shell, d^0, molecules in C_{3v} symmetry (MnO_3F and MnO_3Cl) using the SCF-Xα-SW method. The theoretical results are related to the parent tetrahedral ions (CrO_4^{2-} and MnO_4^-) and to the gas phase optical absorption spectrum of each of the molecules of interest. It has been found in the molecules C_{3v} symmetry that the ordering of ground state electronic energy levels can be grouped into a tetrahedral format nearly identical to that for the parent MnO_4^- ion. Electronic orbital transitions and excited state assignments have been made with the aid of vibrational data for the absorption bands in the visible and near ultraviolet regions. Descent in symmetry results in only a minor perturbation of the electronic absorption spectrum of MnO_4^-. The effects of the halide charge transfer first became significant with the second electronic orbital transition from the highest filled bonding P orbitals to the central metal d orbitals. A similar grouping of ground state electronic energy levels occurs with the two molecules of C_{2v} symmetry. Assignment of orbital transitions and excited states have also been made with the aid of the optical spectrum of each molecule in the visible and near ultraviolet regions. While the orbital electronic transitions parallel those in the parent ion, CrO_4^{2-}, a tremendous amount of overlap of excited states occurs. With this observation, many anomalies in the excited state optical spectrum for each molecule have been explained. In each molecule the lowest energy orbital transition is assigned to a charge transfer transition from the non-bonding highest filled group of p orbitals to the first unoccupied group of d metal orbitals. The charge density on these filled nonbonding orbitals in the dichloro substituted species is located primarily on the chloride ligands. In CrO_2F_2 the charge density on these orbitals is located primarily on the oxide ligands much like the parent molecule. In CrO_2Cl_2 a large splitting of excited states occurs while in CrO_2F_2 only a small separation of states has been found. The optical spectra of the two systems in C_{2v} symmetry show a greater deviation from the parent ions than do the two systems in C_{3v} symmetry. However, the ground state electronic structure and assigned orbital transitions in each of the four molecules exhibit a marked similarity to the parent ions. (auth)

31396 (SAND-74-0135) DIELECTRIC STRENGTH OF X-CUT QUARTZ AFTER THERMALLY INDUCED STRESS CYCLING: APPLICATION TO UNDERSTANDING THE SANDIA QUARTZ GAUGE. Seager, C. H. (Sandia Labs., Albuquerque, N. Mex. (USA)). Aug 1974. Contract AT(29-1)-789. 12p. Dep. NTIS $4.00.

The possible origins of the so-called ''-X anomaly'' in the Sandia Quartz gage are discussed. Recently, experiments were performed to determine the dielectric strength of SiO_2 under conditions simulating some aspects of gage operation. These data as well as the work of Korzo suggest that quartz that has been severely thermally or mechanically strained may break down at electric fields considerably below those characterizing unstrained single crystal quartz. It is concluded that these facts enhance the possibility that the ''-X anomally'' is a breakdown phenomenon despite the low fields characterizing its occurrence. (auth)

31397 (SLA-73-1073) RF HYBRID MICROCIRCUIT SOLDERING TECHNIQUES. Olson, H. C.; Knauss, G. L. (Sandia Labs., Albuquerque, N. Mex. (USA)). Aug 1974. Contract AT(29-1)-789. 44p. Dep. NTIS $5.25.

Progress on the development of hybrid microcircuit technology is described. To minimize the inductance caused by "flying wires" it was desirable to attach most applique parts to the hybrid circuits using a solder alloy. The hybrid circuits have 60 kÅ of gold as the metallization to which the applique parts are attached. The solder development activities, equipment, and assembly techniques using a 50%, by weight, lead-indium solder alloy are described. (auth)

31398 (UCID-15369) ELASTIC CONSTANTS OF FRACTURED HARDHAT GRANODIORITE. Stephens, D. R. (California Univ., Livermore (USA). Lawrence Livermore Lab.). 24 Oct 1968. 13p. Dep. NTIS $4.00.

The rigidity modulus (G) of fractured Hardhat granodiorite was measured to pressures of 1 kbar by a one-dimensional stress-strain experiment. The results show that above 0.5 kbar the data agree within experimental error with predictions from a fracture model due to Walsh. To predict the rigidity modulus from the fracture model, the bulk modulus as a function of pressure is needed; this is now known for several rock types. The assumption inherent in the model is that the rock contains a small number of noninteracting cracks; this is the basis for prediction of a nonzero G at zero pressure. As pressure increases, cracks close; and at 0.5 kbar the requirements of the model are apparently satisfied and G can be predicted within the experimental error of 10 to 20%. More accurate experiments on other rock types are needed to find whether the fracture model can be used to predict G at pressures above 0.5 kbar. If this can be done, the experimental work necessary to describe the elastic constants of fractured rock can be greatly simplified. (auth)

31399 (UCID-15454) LOW PRESSURE PHASE TRANSITION IN NaCl. Royce, E. B. (California Univ., Livermore (USA). Lawrence Livermore Lab.). Jan 1969. 17p. Dep. NTIS $4.00.

The NaCl → CsCl structure transition in NaCl most probably takes place between 220 and 270 kbar on the Hugoniot. A well-separated two-wave structure reported in porous samples near 30 kbar in shock compressed NaCl is shown to have arisen from the impedance-mismatch shock attenuation system and is not an indication of a phase transition. The phase transition observed in shock-compressed (100) crystals of NaCl at 29 kbar appears to have been real, though the volume change is quite small. (auth)

31400 (UCID-15586) GENERALIZED SHOCK HUGONIOTS. McMaster, W. H.; Schroeder, R. C. (California Univ., Livermore (USA). Lawrence Livermore Lab.). 8 Dec 1969. 36p. Dep. NTIS $5.00.

Results of studies on compression measurements and shock data are presented. The proper form is shown for the generalized and reference equation of state for a given temperature along with an explanation of how data for all solids, liquids, and gases scale to the reference curve. This scaling, then determines the appropriate value of S and a new modulus $M = \rho_0 C^2$ in a manner more accurate than previous scaling methods. Thus the generalized Hugoniot becomes a two parameter equation of state for all materials. Many of the parameter values can be obtained from static measurements. The modulus M correlates with the molar volume (or atomic radii) to indicate the electron shell responsible for the compressibility. Two types of phase changes can be handled by the parameters S and ρ_0C^2, and it is shown how changes in S may be related to electronic transitions. (auth)

31401 (UCID-15662) NOTES ON APPLICATION OF SOLID ELECTROLYTE TANTALUM CAPACITORS IN COUPLING AND BYPASS SERVICE. Graham, H. (California Univ., Livermore (USA). Lawrence Livermore Lab.). 5 Aug 1968. 6p. Dep. NITS $4.00.

The performance of the solid electrolyte tantalum capacitor is evaluated. It has eliminated the capacitance-temperature problem, reduced to a negligibly small value the series inductance, practically eliminated the capacitance-frequency trouble, and eliminated dissociation and thermal effects from drying out the electrolyte. (MCW)

31402 (UCID-15669) THERMAL IGNITION OF AN EXPLOSIVE BY SURFACE FRICTION. Edwards, A. L. (California Univ., Livermore (USA). Lawrence Livermore Lab.). 20 Jan 1964. 13p. Dep. NTIS $4.00.

A simplified model for thermal ignition of an explosive by surface friction was analyzed with the help of the HARC heat conduction and chemical reaction code. The calculations showed that LX-04-0 when subjected to a constant heating rate such as might occur in a shear zone resulting from friction, ignited when the rate of heat release from exothermic decomposition was equal to the initial heating rate. For ignition times between 0.6 and 1.2 milliseconds, approximately the times involved in the drop test, this equality of heating rates occurs at 385 to 395°C. It is concluded that for LX-04-0, any heating rate resulting in a temperature of about 390°C in a time of about one millisecond will cause an ignition. (MCW)

31403 (UCID-15739) TENSILE AND COMPRESSION TEST METHODS FOR RIGID PLASTIC FOAMS. Rinde, J. A. (California Univ., Livermore (USA). Lawrence Livermore Lab.). 22 Oct 1970. 8p. Dep. NTIS $4.00.

Test methods are described for use in testing rigid plastic foams such as polystyrene bead foams and polyurethane foams having densities less than 0.25 g/cm^3. Information is included on apparatus, test specimens, and procedure. (JRD)

31404 (UCID-15815) CHEMICAL COMPOSITIONS OF VARIOUS PLASTIC MATERIALS. Rinde, J. A. (California Univ., Livermore (USA). Lawrence Livermore Lab.). 14 Sep 1970. 41p. Dep. NTIS $5.25.

Data on composition of plastic materials are given in tables. Selected trade names, empirical formulas, density values, and maximum continuous temperature use data are included. (JRD)

31405 (UCID-15845) RESIDUAL STRESSES AND BIREFRINGENCE IN POLYCARBONATE PLASTIC. Kirkwood, W. F.; Rothstein, R. J. (California Univ., Livermore (USA). Lawrence Livermore Lab.). 1 Jun 1971. Contract W-7405-Eng-48. 10p. Dep. NTIS $4.00.

Samples of polycarbonate plate stock and injection-molded shells were examined after being subjected to environments similar to those expected in the manufacturing process. The resulting state of stress in the parts was determined by photoelastic stress analysis and strain gage techniques. Birefringent effects caused by thermal gradients and stress freezing were segregated, and the effects of these states on the material were evaluated. (auth)

31406 (UCID-15846) CONSISTENT VAPOR EQUATION OF STATE FOR SOLIDS. McCauley, E.; Osborn, J. (California Univ., Livermore (USA). Lawrence Livermore Lab.). 1 Jun 1971. Contract W-7405-eng-48. 44p. Dep. NTIS $5.25.

Results of investigations concerned with derivation and implementation of new equations of state for solids are presented. Information is included on existing equation of state, equation of state for the vapor region, and virial equation of state for the vapor region. (JRD)

31407 (UCID-15901) EVALUATION OF LOAD-DEFLECTION TESTS OF 0.060-IN.-THICK Y-3333 CELLULAR SILICONE. Murray, R. C. (California Univ., Livermore (USA). Lawrence Livermore Lab.). 1 Sep 1971. Contract W-7405-eng-48. 33p. Dep. NTIS $4.75.

The mechanical response of Y-3333 cellular silicone is important because of the material's function as a cushioning material. The cushioning behavior is strongly dependent on the exercising conditions the material is subjected to before it is tested, as well as on other test parameters. An investigation was made of the effects of various load-deflection test conditions, and it makes recommendations for improving material acceptance testing on 0.060-in.-thick Y-3333 cellular silicone. (auth)

31408 (UCID-15962) KINETICS OF ENERGY RELEASE OF HETEROGENEOUS HIGH EXPLOSIVES. Cheung, H. (California Univ., Livermore (USA). Lawrence Livermore Lab.). 15 Dec 1971. Contract W-7405-eng-48. 6p. Dep. NTIS $4.00.

The rate of energy release during detonation of a heterogeneous explosive may be considered as proceeding in at least two consecutive steps: (1) A fast step during which part of the chemical energy is released within a fraction of a microsecond. (2) Subsequently, the remaining energy is released slowly over a period of 10^{-3} sec or longer. In many such explosives, the rate of the second step is determined by diffusion of reactants. In this report the effects of chemical reaction rates and diffusion rates on the rate of energy release during the second (slow) step are compared. It is shown that diffusional processes are probably at least two orders of magnitude slower than chemical processes under detonation conditions. (auth)

31409 (UCID-16023) MECHANICAL PROPERTIES OF A SHALE FROM SITE U-2. Abey, A. E.; Bonner, B. P.; Heard, H. C.; Schock, R. N. (California Univ., Livermore (USA). Lawrence Livermore Lab.). 21 Apr 1972. Contract W-7405-eng-48. 21p. Dep. NTIS $4.25.

The mechanical properties of shale from Site U-2 were tested under pressure in the range to 30 kbar. Tests included hydrostatic and quasihydrostatic pressure-volume determinations, uniaxial strength tests as a function of confining pressure, and three-dimensional stress-strain measurements up to failure. The results indicate, in general, that the shale is a weak relatively incompressible rock, although some of the material near the surface is more compressible. (auth)

31410 (UCID-16076) ACOUSTIC EMISSION MONITORING OF RING-CRACKING IN GLASS AND ALUMINA. Kuhn, B. A. (California Univ., Livermore (USA). Lawrence Livermore Lab.). 7 Jul 1972. Contract W-7405-eng-48. 11p. Dep. NTIS $4.00.

Experiments were conducted to determine whether acoustic emission monitoring of ring cracking in glass and alumina is feasible. Pyrex 7740 was selected for the preliminary investigation to allow a visual correlation to be made, along with the acoustic emission data. The test results on the glass showed an excellent correlation between the visual ring crack propagation and the rapid increase in the acoustic emission rate. Tests were also conducted on alumina. The acoustic emission data from the alumina provided the same type of rapid increase in acoustic emission activity, at the onset of ring cracking, that was observed in the glass. A microscopic inspection of the fracture surface on the alumina showed that a ring crack did form, providing sufficient evidence that acoustic emission could be used to detect ring cracking in an opaque material. (auth)

31411 (UCRL-51626) EFFECT OF FLUID CONTENT ON THE MECHANICAL PROPERTIES OF WESTERLY GRANITE. Duba, A. G.; Heard, H. C.; Santor, M. L. (California Univ., Livermore (USA). Lawrence Livermore Lab.). 30 Jul 1974. Contract W-7405-eng-48. 20p. Dep. NTIS $4.00.

Jacketed samples of Westerly granite with water concentrations ranging from 0 to 20% total volume were loaded to failure under conditions of uniaxial stress up to 600 MPa confining pressure. Unjacketed samples, exposed directly to the pressure medium, were tested similarly. The volume and viscosity of fluid available to the intergranular porosity in the granite during uniaxial stress loading significantly influenced the compressive strength. Dry and saturated specimens (0.8% water) were loaded to 700 MPa confining pressure under conditions of uniaxial strain. Large differences in loading paths were observed between the saturated and dry granite. The pressure-volume curves determined to 300 MPa indicate only slightly less compression for the saturated granite (0.8% water) than for the dry material. Under axial load, the saturated material exhibited less volume decrease than the dry. This difference in compression during axial loading is attributed to water redistribution in the cracks of the rock. (auth)

31412 (UCRL-75499(Rev.1)) MAGNETIC ORDER IN CERTAIN ALKALI AMPHIBOLES, A MOESSBAUER INVESTIGATION. Borg, R. J.; Borg, I. Y. (California Univ., Livermore (USA). Lawrence Livermore Lab.). 21 Aug 1974. 14p. (CONF-740905-2). Dep. NTIS $4.00.

From international conference on the applications of the Mossbauer effect; Bendor, France (2 Sep 1974).

The appearance of magnetic hyperfine splitting (mhfs) was used to determine the magnetic ordering temperature for a few selected alkali amphiboles. This class of minerals has the monoclinic crystal structure and the general formula $(Na,Ca)_{2-3}$ $(Fe^{+2}, Fe^{+3}, Mg, Al)_5$ $Si_8O_{22}(OH, F)_2$. The iron can occupy three distinct crystallographic sites, yet the mhfs collapses with increasing temperature in the manner of less complex magnetic substances. In spite of the overall complexity, the much greater mhfs of Fe^{+3} easily separates lines 1 and 6 from all resonant absorption due to Fe^{+2}. Thus, relevant Moessbauer and magnetic parameters can be determined. The temperature dependence of the mhfs departs substantially from the usual Brillouin-like function. Magnetic susceptibility data on a single specimen indicate the ordering to be antiferromagnetic. The stacking sequence formed by the three sites is a one-dimensional chain parallel to the c axis. Each chain is separated from adjacent chains by linked SiO_4 tetrahedra. Thus, direct exchange can only occur within the chain, and a type of super-exchange must exist between chains. (auth)

31413 (Y-1955) THERMAL CONDUCTIVITY OF CARBON FOAM. Lore, J. D.; Richards, H. L.; Ward, M. E. (Oak Ridge Y-12 Plant, Tenn. (USA)). Sep. 1974. Contract W-7405-eng-26. 31p. Dep. NTIS $4.00.

Carbon foam materials, carbonized to 1273 K and graphitized to 3273 K prior to testing, were evaluated for thermal conductivity by three steady-state techniques: guarded hot plate, comparative apparatus, and radial flow. Tests were conducted over the temperature interval from 300 to 2800 K. Analyses were made of the material fabrication parameters, pertinent physical properties, and employed test techniques. Interpretation of data and a comparison with the findings of other laboratories were accomplished. (auth)

Physics and Engineering

31414 (AERE-R-7776) MEASUREMENTS OF THREE VELOCITY COMPONENTS AND THEIR CORRELATIONS IN A MODEL FURNACE WITH AND WITHOUT COMBUSTION. Baker, R. J.; Hutchinson, P.; Khalil, E. E.; Whitelaw, J. H. (UKAEA Research Group, Harwell. Atomic Energy Research Establishment). Jul 1974. 16p. Dep. NTIS (US Sales Only) $4.00.

Measured values of three components of mean velocity and the corresponding normal stresses are reported in the flow within an enclosure which is representative of a small-scale furnace with an axi-symmetric, swirling flow configuration. The measurements were obtained in isothermal air flow and in a combusting mixture of air and natural gas: exit swirl numbers of zero and 0.52 were investigated for both the isothermal and combusting cases. The flow configuration was that of a cylindrical chamber, 900 mm long by 300 mm in diameter. At one end, the chamber was closed except for a co-axial burner nozzle with annulus and jet dimensions of 55 mm outside diameter, 27 mm inside diameter and 12 mm jet diameter. At the other end, the chamber was closed except for a central hole of 90 mm diameter through which the air or combustion products flowed to exhaust. For all measurements, air emerged from the nozzle annulus with an average axial velocity of 5 m/s. For the isothermal measurements, air also emerged from the jet nozzle with an average axial velocity of 0 or 2.2 m/s for the non-swirling and swirling flows respectively. The jet air was replaced by natural gas, with a velocity of 5 m/s for the combustion measurements; this corresponds to an equivalence ratio of unity. A laser anemometer was used to obtain the measurements and comprised an argon-ion laser, a rotating diffraction grating as beam splitter and frequency shifter, transmission and collection optical components, a photomultiplier and a filter-bank signal processor. The grating provided a frequency shift of ±0.54 MHz and allowed measurements in regions of high turbulence intensity and negative mean velocity. The filter bank consisted of 50 filters spanning the range from 0.6 to 6 MHz, which with the frequency shift indicated above and the optical arrangement employed, corresponded to a measurable velocity range of −2 m/s to 23 m/s. (auth)

31415 (ANL-8111) PROTECTION CIRCUIT FOR A LIQUID-NITROGEN TRAP FILLER. Scott, R. G. (Argonne National Lab., Ill. (USA)). Jul 1974. Contract W-31-109-eng-38. 4p. Dep. NTIS $4.00.

A simple circuit is described that substitutes a timed fill for a demand fill in the event of sensor or fill-tube failure thereby avoiding damage and unnecessary shutdown of the system. (auth)

31416 (BDX-613-1115(Rev.)) DEVELOPMENT OF PROCESSES FOR HYBRID MICROCIRCUITS CONTAINING BEAM-LEAD DEVICES. Blazek, R. J.; Blakely, J. N. (Bendix Corp., Kansas City, Mo. (USA)). Aug 1974. Contract AT(29-1)-613. 157p. Dep. NTIS $7.60.

The process-development and prove-in work of this program established a complete technology for manufacturing hybrid microcircuits containing beam-lead devices. Previous microcircuits contained chip-and-wire semiconductors. The principal contributions of this work to the existing microcircuit technology were a thermocompression bonding process to bond the gold beam leads and lead frames to the microcircuit substrate and the precision process controls necessary to ensure adequate pull strength on bonds that cannot be nondestructively tested. Other pertinent processes also were refined as needed to provide high microcircuit reliability. These processes and techniques have been released for use in manufacturing seven types of microcircuits for a coded electronic switch. (auth)

31417 (BDX-613-1134(Rev.)) AUTOMATIC RADAR-SENSITIVITY MEASUREMENT. Final Report. Hardinger, K. E. (Bendix Corp., Kansas City, Mo. (USA)). Sep 1974. Contract AT(29-1)-613. 31p. Dep. NTIS $4.00.

Work is described that resulted in development of the necessary techniques to automatically measure radar receiver and system sensitivity. Both measurement speed and repeatability are improved over that possible by manual methods. Combined logic and analog techniques were used to derive a system suitable for both in-process and final-assembly tests on radar systems and rf subassemblies. (auth)

31418 (BDX-613-1135(Rev.)) USE OF EN-7 TO ENCAPSULATE ANALYZER ASSEMBLIES. Final Report. Elmore, R. D. (Bendix Corp., Kansas City, Mo. (USA)). Sep 1974. Contract AT(29-1)-613. 14p. Dep. NTIS $4.00.

The feasibility of using EN-7 as a substitute for Adiprene L100 curing agent for analyzer encapsulation was investigated. Since many analyzer assemblies cannot tolerate the usual EN-7 cure temperatures, this investigation was limited to a maximum cure temperature of 71°C. The results of these tests indicate that a 20-hour cure at 49°C is adequate to provide sufficient hardness if followed by additional room-temperature cure. (auth)

31419 (BDX-613-1144(Rev.)) DETECTION AND SUPPRESSION OF TRANSISTOR OSCILLATION DURING POWER BURN-IN. Schmitt, R. W. (Bendix.Corp., Kansas City, Mo. (USA)). Sep. 1974. Contract AT(29-1)-613. 35p. Dep. NTIS $4.00.

A method was developed for suppressing parasitic oscillation of transistors operating under test conditions through the use of ferrite cores and capacitors. The Hewlett-Packard Model 8554L spectrum analyzer is recommended for detecting unknown rf noise. (auth)

31420 (COPPE-TP-6/72) SPECTROSCOPY OF AUGER ELECTRONS AND ITS USE IN METALLURGY. Losch, W. H. P. (Rio de Janeiro Univ. (Brazil). Coordenacao dos Programmas de Pos-graduacao de Engenharia). Jun 1972. 21p. (In Portuguese). INIS.

The theoretical and experimental basis of the spectroscopy of Auger electrons and some applications in physical metallurgy are described. This method permits, under conditions of ultra-high vacuum, a chemical analysis of the surface planes up to a depth of only 2 to 3 atom layers. (INIS)

31421 (IFA-FT-109-1974) LANDAU DIAMAGNETISM. Angelescu, N.; Nenciu, G.; Bundaru, M. (Institutul de Fizica Atomica, Bucharest (Romania)). 1974. 36p. Dep. NTIS (US Sales Only) $5.00.

The grand-canonical partition function of an assembly of free spinless electrons in a magnetic field enclosed in a box Λ (Dirichlet boundary conditions) is shown to be an entire function of the fugacity Z and the magnetic field H, by proving the tracenorm convergence of the perturbation series in powers of H for the statistical semigroup. (SFL)

31422 (IKE-5-175) HEAT PIPE WORK IN EUROPE. Groll, M. (Institut fuer Reaktorsicherheit der Technischen Ueberwachungs-Vereine e.V., Koeln (F.R. Germany)). Mar 1974. 28p. INIS.

With abstract. Available from ZAED.

A comprehensive survey of heat pipe work in Europe is given. The contents of this report is based to a large extent on papers presented at the 1st International Heat Pipe Conference 1973 in Stuttgart. (auth)

31423 (LA-UR-74-1167) INTEGRATING ECLIPSE OPTICS INTO THE AEC AIR FORCE FLYING LABORATORY. Brixner, B. (Los Alamos Scientific Lab., N. Mex. (USA)). 1973. Contract W-7405-eng-36. 16p. (CONF-740823-3). Dep. NTIS $4.00.

From 18th annual meeting of the Society of Photo-Optical Instrumentation Engineers; San Diego, California, USA (19 Aug 1974). 1974).

Airborne expeditions in 1965, 1966, 1970, 1972, and 1973 resulted in measuring the temperature, density, structure, motions, and composition of the sun's corona during total solar eclipses. It was necessary to fit the eclipse optics into the already-completed flying laboratory. Five aspects of the problem involved obtaining optical elements that meet the optical specification; providing stabilized instrument platforms to reduce image-motion blur; getting instruments small enough to fit into the cramped space available; getting the fuselage modified for special windows and the mounting of instruments; and getting to the right place at the right time to follow the shadow. The data will be available for a study of the sun's behavior throughout its eleven-year cycle (MCW)

31424 (LBL-2574) MICROSECOND PULSE TECHNIQUE FOR HEAT CAPACITY MEASUREMENT. Chen, T. H. (California Univ., Berkeley (USA). Lawrence Berkeley Lab.). May

1974. Contract W-7405-eng-48. 82p. Dep. NTIS $7.25.

Thesis.

A refined thermal pulsing technique for measuring heat capacity of metals at high pressure is described. The technique originally involved measurements of the rate of temperature rise in the sample when a constant current power input was added for a constant current power input was added for a short period of time. When the technique was applied to a highly conducting sample, the results were found to be poor because the heat leak from the sample to the surrounding medium was appreciable. Efforts were therefore directed towards improving measuring techniques and refining mathematical equations to account for the heat leakage. The technique was improved to render an essentially constant heat capacity of aluminum with pressure at room temperature. The major limitation at present still lies in the lack of quality measuring devices. Heat capacity of iron in vacuum between room temperature and 1100°K was measured with the thermal pulsing technique to demonstrate its versatility. Differences in heat capacity between an annealed sample and a cold-worked sample were noted. The drastic change in heat capacity of iron in the vicinity of the magnetic phase transition was measured with an error less than 2%. (auth)

31425 (LBL-2781) EXCITON ENHANCED RAMAN SCATTERING OF LO PHONONS IN TRIGONAL Se. Amer, N.; Petroff, Y.; Shen, Y. R.; Yu, P. Y. (California Univ., Berkeley (USA). Lawrence Berkeley Lab.). Jun 1974. Contract W-7405-eng-48. 5p. (CONF-740722-1). Dep. NTIS $4.00.

From 12th international conference on the physics of semiconductors; Stuttgart, F. R. Germany (15 Jul 1974).

Resonance enhancements in the Raman cross-section of longitudinal optical (LO) phonons in trigonal Se were measured around its excitonic absorption edge at low temperatures. Results are explained in terms of resonant scattering of LO phonons via the Fröhlich interaction. (auth)

31426 (MLM-2098) IMPROVED PETN PARTICLE SIZE ANALYSES. Bonekowski, N. R. (Mound Lab., Miamisburg, Ohio (USA)). 15 Aug 1974. Contract AT-33-1-GEN-53. 15p. Dep. NTIS $4.00.

A significant improvement in obtaining more precise and accurate particle size distribution data for explosive powder evaluation studies has been realized. The improved capability of the Model T Coulter Counter over its predecessor, the Model A is evaluated. A Digital Equipment Corporation PDP-12A laboratory computer was used to statistically evaluate data collected using both models on National Bureau of Standards glass beads and three samples of pentaerythritol tetranitrate (PETN) high explosive with various surface areas; scanning electron photomicrographs of the samples are included. Also, computer printouts of particle size data and graphic comparisons of the performance of both Coulter Counter models are included. The Model T proved to be faster than the Model A, easier to calibrate, able to cover a greater range of particle sizes, and capable of analyzing a wide variety of sample geometries. (auth)

31427 (RISO-M-1714) ADDITIVE STRENGTH CONTRIBUTIONS. Andreasen, V. (Danish Atomic Energy Commission, Risoe. Research Establishment). Apr 1974. 95p. (In Danish). Dep. NTIS (U. S. Sales Only) $7.75.

A literary review of theories and models proposed for dispersion hardening, solid solution hardening, grain boundary hardening, and workhardening of dispersion hardening alloys is given. The movement of a dislocation line through an array of different kinds of obstacles was examined in order to investigate the interaction between different hardening mechanisms. Experimentally the plastic deformation at room temperature of Cu, Cu–Ag, Cu–Al_2O_3, and Cu–Ag–Al_2O_3 alloys was examined as a function of composition and volume fraction. The alloys were in the form of polycrystals and single crystals, and the single crystals were deformed in the [112]-direction. The solid solution hardening is shown to be additive to the other strengthening mechanisms. The workhardening from the dispersed particles was determined and found to be in agreement with the theories proposed by Ashby and Hart. In polycrystals an interaction between grain boundary hardening and dispersion hardening was found and this interaction can be determined by computer simulation. The Hall-Petch relation is not obeyed in this case. (auth)

31428 (SAND-74-0149) ALARM COMMUNICATIONS AND DISPLAY SEGMENT (ACADS). Technical Order Publications Plan (CDRL Item 20). Sandia Labs., Albuquerque, N. Mex. (USA)). Aug 1974. Contract AT(29-1)-789. 8p. Dep. NTIS $4.00.

31429 (SAND-74-0153) RANGE-SCAN RADAR IMAGES AND THEIR APPLICATION TO MAP-MATCHING ESTIMATION OF LOCATION. James, L. T.; Aronson, E. A. (Sandia Labs., Albuquerque, N. Mex. (USA)). Sep 1974. Contract AT(29-1)-789. 17p. Dep. NTIS $4.00.

The results are reported of experiments that demonstrate that a pulse radar sensor with a nondirectional antenna pattern produces images containing enough character to serve as signatures of the sensor's location when operating over the types of scenes considered. This property is a necessary condition if this type of sensor is to be employed in the design of a map-matching location-estimation system for use in improving the navigation accuracy of airborne inertial navigation systems. (auth)

31430 (SLA-74-0347) TEST OF A MAGNETIC BEARING FOR OPTICAL SCANNER APPLICATIONS. Abbink, R. E. (Sandia Labs., Albuquerque, N. Mex. (USA)). Sep 1974. Contract AT(29-1)-789. 14p. Dep. NTIS $4.00.

An electro-optical measurement technique is described for the determination of angular stability of a rotating shaft. Demonstrated measurement resolution is on the order of 0.1 arc second. This technique is applied to the performance evaluation of a development model, radially passive, magnetic bearing system. Results are discussed in terms of using this type of bearing system in a high resolution optical scanner. (auth)

31431 (SLA-74-5239) PERFORMANCE CHARACTERISTICS OF SANDIA LABORATORIES 5.8-METRE-DIAMETER EXPLOSIVELY DRIVEN BLAST SIMULATOR. Vigil, M. G. (Sandia Labs., Albuquerque, N. Mex. (USA)). 1973. 15p. (CONF-740931-1). Dep. NTIS $4.00.

From 4th international symposium military applications of blast simulators; Berkshire, UK (9 Sep 1974).

Simulator performance as established from twenty-one tests are discussed. The simulator has a 1.8 m-dia driver. Blast waves are expanded through a conical section to a 5.8 m-dia test section. Data on explosive charge weights, charge lengths, static overpressure ratios, and shock Mach numbers are tabulated. (JRD)

31432 (UCID-15203) EVALUATION OF DOWNHOLE ALIGNMENT BY MEANS OF AN ALTERNATING MAGNETIC DIPOLE FIELD. Hurdlow, W. R. (California Univ., Livermore (USA). Lawrence Livermore Lab.). Sep 1967. 13p. Dep. NTIS $4.00.

A theoretical and experimental study of an electromagnetic system to align subsurface instrumentation is described. The conclusions are that the design goal of ±2° ($\pm 3.5 \times 10^{-2}$ rad) orientation using a magnetic dipole antenna array was theoretically and practically attainable 1000 meters in Earth. (MCW)

31433 (UCID-15373) APPLICATION OF A COMPUTER-SIMULATED PERCEPTRON TO A COMPLEX PHOTOGRAPHIC SCENE. Leary, R. H. (California Univ., Livermore (USA). Lawrence Livermore Lab.). Sep 1968. 11p. Dep. NTIS $4.00.

PERC is a digital computer simulation of a Perceptron designed to be used in conjunction with Gales' OBJLOC, a program for the location of objects in a complex photographic scene. OBJLOC operates on digitized photographs, attempting the location of a desired object through a subroutine that generates truth values from questions about the local density pattern around individual points in the photograph. (MCW)

31434 (UCID-15383) PHOTOELASTOMETRIC RECORDING OF STRESS WAVES. Cunningham, D. M.; Brown, G. W.; Griffith, J. C. (California Univ., Livermore (USA). Lawrence Livermore Lab.). 15 Oct 1968. Contract W-7405-eng-48. 15p. Dep. NTIS $4.00.

A very sensitive fast-responding photomultiplier tube and laser light source were used to record stress-optic data associated with a moving stress wave. By using a grey-field (which is halfway between a dark and light field) polariscope, optical-electrical recordings were obtained that were linearly proportional to strain. A discriminatory record results that exhibits a higher signal-to-noise ratio than semiconductor strain gages. Gage length can be varied from 0.005 in. upwards. (auth)

31435 (UCID-15496) 36 INCH MITER VALVE DESIGN. Holl, P. M.; Kopytoff, V. (California Univ., Livermore (USA). Lawrence Livermore Lab.). 16 Jun 1969. 35p. Dep. NTIS $4.75.

The design and fabrication of a unique gas valve is described. The very special installation and operational requirements are met with an innovative design executed to advantage by employing arc welded steel fabrications for major static and dynamic components. (auth)

31436 (UCID-15597) OUTLINE OF DEVELOPMENTS IN MAGNETIC CIRCUIT THEORY. Buntenbach, R. (California Univ., Livermore (USA). Lawrence Livermore Lab.). 16 Dec 1969. 34p. Dep. NTIS $4.75.

An analytical approach to the design of magnetic components and systems is presented. Information and discussions are included on the coexistence of electric and magnetic phenomena, errors and corrective measures, dimensional equivalence and magnetic impedance, the permeance–capacitance analogy, the reactance of a permeance, analogous quantities, analogous circuit laws, tellegen gyrators, transfer equations, impedence relations, inductors on conducting cores, and response of conducting cores. (JRD)

31437 (UCID-15611) TWO NUMERICAL EXAMPLES OF RAYLEIGH–TAYLOR INSTABILITY FOR A SYSTEM OF FIVE DIFFERENT DENSITIES. Crowley, W. P. (California Univ., Livermore (USA). Lawrence Livermore Lab.). 15 Feb 1970. 14p. Dep. NTIS $4.00.

The amplitude of a small perturbation on the interface separating two fluids, a light fluid accelerating a heavy fluid, will at first grow exponentially in time. For two semi-infinite fluids, the growth rate of this Rayleigh–Taylor instability is $\sigma^2 = gk\alpha$, where g is the acceleration, k is the wave-number of the perturbation and α is the Atwood number, $\alpha = (p - p')/(p + p')$. The theory is limited to incompressible, irrotational, inviscid flows where the product of the wave-number and the amplitude is small, $k\eta \ll 1$. Calculations are presented for decreasing the growth rate by inserting three new materials between the two original materials. In one problem, the new densities were chosen on the basis of a linear density gradient, and in the second problem, the densities were chosen so that the Atwood number is a constant for all interfaces. The experiments were also carried out on a one-dimensional compressible Lagrangian code (ODL) in which the STABIL equations were included so as to simulate the two-dimensional aspects of the perturbation. (MCW)

31438 (UCID-15618) SOME NUMERICAL EXPERIMENTS WITH LOW ATWOOD NUMBER INCOMPRESSIBLE RAYLEIGH–TAYLOR INSTABILITIES. Crowley, W. P. (California Univ., Livermore (USA). Lawrence Livermore Lab.). 10 Apr 1970. 27p. Dep. NTIS $4.50.

Some numerical calculations for two-fluid Rayleigh–Taylor instabilities, were reported using the MAC technique with inviscid calculations spanning a range of Atwood numbers between 0.05 and 0.8. It was found that for low Atwood numbers the growth rates were substantially less than those predicted by linear theory, attributable to a fluid resistance proportional to the square of the velocity. Perturbations were large enough to place the solutions in the nonlinear regime for the duration of the calculation. With the strong dependence on Atwood number, it was thought that the problem might show some anomalous results for low Atwood numbers. The Viecelli version of the MAC code was used, and no anomalous behavior was found for the linear (small amplitude) case. It appears that the crossover from linear to nonlinear regions occur at $\eta = 0.1$. A simple analytic expression for the perturbation amplitude in the transition between the exponential and the spike and bubble regions based on results presented here is proposed. Three cases are considered with a fluid of density ρ underlying a fluid of density ρ' in a gravitational field. The cases involve deep fluids with large initial perturbation; deep fluids with small initial perturbation; and a shallow fluid with small initial perturbation. (MCW)

31439 (UCID-15649) STEADY-STATE, AC-TEMPERATURE TECHNIQUE FOR MEASURING THE SPECIFIC HEAT OF ELECTRICAL CONDUCTORS. Finnila, R. M. (California Univ., Livermore (USA). Lawrence Livermore Lab.). 1 Dec 1967. 9p. Dep. NTIS $4.00.

A theoretical discussion of a steady-state technique for measuring the high temperature specific heat of an electrical conductor is presented. If the conductor is heated by an alternating current of frequency ν to an average temperature $\bar{T}$, then it is shown that the specific heat can often be measured by using the following formula: $c_p(T) \approx \bar{P}/(2\pi\nu m\Delta T_a)$, where $\bar{P}$ = average electrical power per unit length, m = mass per unit length, and ΔT_a = the amplitude of the ac component of the temperature. (auth)

31440 (UCID-15682) DYNAMIC INTERFEROMETRIC HOLOGRAPHY. Morehouse, J. H. (California Univ., Livermore (USA). Lawrence Livermore Lab.). 10 Jul 1970. 25p. Dep. NTIS $4.25.

Dynamic interferometric holography is the technique in which holography is used to photographically record transient or steady-state surface strains. In developing the technique, the mechanics of the holographic process were thoroughly studied. The response of the laser cavity and the influence of the holographic setup on the resulting holograms were optimized for the existing equipment. A high degree of repeatability was reached in producing clear, bright, double-pulsed holograms. The system was then used to record dynamic strains due to impact loading. The limitations and applicability of the method to other surface-deformation problems are discussed. (MCW)

31441 (UCID-15723) THERMAL CONDUCTIVITY OF A HARD SPHERE SOLID. Gass, D. M.; Alder, E. J.; Wainwright, T. E. (California Univ., Livermore (USA). Lawrence Livermore Lab.). Aug 1970. 10p. Dep. NTIS $4.00.

The thermal conductivity of an fcc hard sphere solid was evaluated by molecular dynamics computation. From near close-packing to melting, the results are in virtual agreement with the Enskog theory. The dominant potential contribution yields nearly the Enskog value, while the kinetic and cross terms deviate less than 20%, in opposite directions, from the predicted values. The deviations of the heat-flux autocorrelation function from an exponential are discussed. (auth)

31442 (UCID-15769) ELECTRO-OPTIC METHOD OF TRACKING AN ELECTRON-BEAM WELD. Leavitt, G. A. (California Univ., Livermore (USA). Lawrence Livermore Lab.). 1 Dec 1970. 13p. Dep. NTIS $4.00.

Recommendations were made that for post-weld inspection specification they be made in terms of Joules delivered at the weld per inch of weld for a given spot size. Specifying welds in this manner requires a new instrumentation system for measuring the weld parameters. The system consists of a calorimeter, a magnetic pickup coil to measure the actual beam current, a flying wire scanner to measure spot size, and an optical scanner to monitor the precision with which the weld spot tracks the seam in a workpiece. The design and performance of the optical scanner are described. The scanner can reliably detect both seams and weld spots. (MCW)

31443 (UCID-15773) TEST METHODS FOR HIGH PACKING DENSITY DIGITAL MAGNETIC TAPE RECORDERS. Nugent, T. J. (California Univ., Livermore (USA). Lawrence Livermore Lab.). 18 Nov 1970. 9p. Dep. NTIS $4.00.

Test procedures are recommended to supplement IRIG 106-69 for testing magnetic recorders. Tests for 1) signal-to-noise ratio, 2) error rate (dropout), 3) flutter, and 4) inter-channel time displacement error (skew) are described. (WHK)

31444 (UCID-15803) MATHEMATICAL REVIEW OF INTRODUCTORY WAVE MECHANICS. Habberstad, J. L. (California Univ., Livermore (USA). Lawrence Livermore Lab.). 12 Feb 1971. 119p. Dep. NTIS $9.00.

The review includes fundamental mathematics definitions, fundamental concepts of mechanics of waves, fundamentals of shock mechanics, and equations of state. (It does not concern quantum mechanics, as the title might imply.) (JRD)

31445 (UCID-15811) PRESSURE, FORCE, AND MASS CALIBRATION LABORATORY. Field, J. (California Univ., Livermore (USA). Lawrence Livermore Lab.). 26 May 1970. 17p. Dep. NTIS $4.00.

The calibration of pressure and force transducers at LRL and the interrelationship of other LRL standards facilities are discussed. A description of static and dynamic calibration services with accuracies and ranges is included. Some precautions with respect to manufacturer specifications versus user understanding are also considered. (auth)

31446 (UCID-15816) CAIN SYSTEM FIELD TEST. Robertson, R. D. (California Univ., Livermore (USA). Lawrence Livermore Lab.). 1 Feb 1971. Contract W-7405-eng-48. 47p. Dep. NTIS $5.25.

An automatic access control system utilizing a computer as a central controller and individually coded badges for employee identification, was field tested under controlled conditions. System performance was made fail-safe. Authorized accesses were granted in most cases with no perceptible delay. The system logs all valid and invalid access attempts. Central control operators are automatically notified of the nature and location of any unauthorized entry attempts. The badge used for such an attempt is identified to the operator at the time of the alarm. Badges contain no information that reveal to unauthorized persons what accesses are possible. (auth)

31447 (UCID-15829) BREMSSTRAHLUNG POLARIZATION FROM COMMERCIAL X-RAY TUBES. Slivinsky, V. W. (California Univ., Livermore (USA). Lawrence Livermore Lab.). 15 May 1970. 13p. Dep. NTIS $4.00.

Measurements made to determine the variation of polarization with x-ray energy from commonly used x-ray tubes at voltages which are commonly used for operating these tubes are presented and discussed. The polarization effect on x-ray scattering is also examined. (WHK)

31448 (UCID-15866) SOME THOUGHTS ON NEGATIVE RESISTANCE AS IT APPLIES TO HIGH FREQUENCY IMPEDANCE MEASUREMENTS. Bostwick, W. E. (California Univ., Livermore (USA). Lawrence Livermore Lab.). 25 Jun 1971. 5p. Dep. NTIS $4.00.

31449 (UCID-15890) RADIATION FROM BURIED ANTENNAS Miller, E. K.; Burke, G. J. (California Univ., Livermore (USA).

Lawrence Livermore Lab.). 12 Aug 1971. 35p. Dep. NTIS $4.75.

An integral equation technique previously developed for the analysis of wire antennas located in free space over a conducting half space is here extended to the treatment of antennas immersed in the conducting medium. As before two methods are considered for this purpose, one an essentially rigorous technique based upon the Sommerfeld integrals and the other an approximate approach which uses a modified plane-wave transmission coefficient. The latter is found to agree as expected with the asymptotic far-field hemispherical expansion of Baños. (auth)

31450 (UCID-15898) STATE RELATIONSHIPS FOR MAXIMAL-LENGTH SEQUENCE GENERATORS. Latorre, V. R. (California Univ., Livermore (USA). Lawrence Livermore Lab.). 6 Oct 1971. Contract W-7405-eng-48. 4p. Dep. NTIS $4.00.

A method of devising switching circuitry to perform operations on Galois-field elements was previously outlined. A summary is made on pertinent parts of the method with regard to computing the state of a maximal-length shift register after a fixed number of shifts, given an arbitrary initial state. Steps are outlined that are required to build a logic circuit that calculates successors of arbitrary states of the register. (MCW)

31451 (UCID-15907) TORSION PENDULUM FOR LASER ENERGY MEASUREMENT. Bostwick, W. E. (California Univ., Livermore (USA). Lawrence Livermore Lab.). 7 Sep 1971. 16p. Dep. NTIS $4.00.

Two devices were combined for a possible laser energy measurement experiment. The first device was a simulated blackbody absorber using platinum as a resistance element in a conventional bridge to sense the temperature rise. The second device is described as a torsion pendulum, using light pressure to measure pulse laser output. Its sensitivity can be accurately calculated. In an original experiment with the torsion pendulum, the mirrors would disintegrate due to the laser beam energy. In the new measuring device, the mirrors took the form of a high-temperature material with a high polish, becoming elements of a resistance bridge directly. Equation development and calculations are followed for the new device and it is believed that the torsion pendulum has possibilities as a pulsed laser energy measuring device. (MCW)

31452 (UCID-15955) COMMUNICATION SYSTEM DESIGN. Latorre, V. R. (California Univ., Livermore (USA). Lawrence Livermore Lab.). 27 Dec 1971. Contract W-7405-eng-48. 19p. Dep. NTIS $4.00.

Equations necessary to permit the design engineer to determine the transmitter power required to provide a specified type and grade of service for a communication system are developed. Factors such as antenna gains, noise figures, bandwidths, and path losses are considered in detail, and their role in the overall expression for required power is developed. Various parameters that enter into the analysis are defined and final expressions for the required transmitter power are derived. The Friis transmission formula is developed and then the effects of external and receiver noise are included. The equation for the effective noise figure at the input to a loss-free antenna is derived. (auth)

31453 (UCID-15998) SOME NOTES ON COAXIAL TERMINATIONS, SHORT-CIRCUITS, AND OPEN-CIRCUITS. Bostwick, W. E. (California Univ., Livermore (USA). Lawrence Livermore Lab.). 15 Feb 1972. Contract W-7405-eng-48. 6p. Dep. NTIS $4.00.

31454 (UCID-16032) EVALUATION OF GOLD-DOPED PERMALLOY FILMS USING FERROMAGNETIC RESONANCE TECHNIQUES. Hsieh, E. J.; Rogers, B.; Soohoo, R.; Tsai, C. (California Univ., Livermore (USA). Lawrence Livermore Lab.). 17 May 1972. Contract W-7405-eng-48. 11p. Dep. NTIS $4.00.

Permalloy films, with gold added up to 30% by weight, were evaluated using both microwave and UHF resonance measurements. Gold was found to be truly alloyed with Permalloy with the result that magnetic moment to volume ratio ($4\pi M$) was decreased with increases in the percentage of gold. The determination that gold improved the uniformity of the Permalloy films could not be affirmed. (auth)

31455 (UCID-16034) LORENTZ MICROSCOPIC OBSERVATION OF HEAD-ON DOMAIN WALLS IN MAGNETIC THIN FILMS. Hsieh, E. J.; Kelly, M.; Soohoo, R. (California Univ., Livermore (USA). Lawrence Livermore Lab.). 19 Apr 1972. Contract W-7405-eng-48. 11p. Dep. NTIS $4.00.

For the first time, head-on domain walls were formed on thin magnetic films in situ of an electron microscope and then manipulated on a microscopic scale. It was found that the microscopic head-on walls thus formed were the same type as the macroscopic walls formed in recordings of the MAGREC program. The correlation suggests that the present recording resolution of the MAGREC has not reached a limit and further improvement is possible. (auth)

31456 (UCID-16051) INSTRUMENTING THE LAPQ-1 AIRBORNE CLOUD-MAPPING RADAR FOR SHIPBOARD USE IN OPERATION DIAL TRAIN. Mortensen, W. K.; Border, E. D. (California Univ., Livermore (USA). Lawrence Livermore Lab.). 7 Jun 1972. Contract W-7405-eng-48. 31p. Dep. NTIS $4.75.

Two LAPQ-1 airborne K_a-band cloud-mapping radars were used on shipboard in Operation Dial Train during the summer of 1971 to collect radar cross-section data on various radar targets. The special instrumentation and recording equipment required, the modifications to the radar, and the problems encountered in preparing to operate the radar on board a ship at sea are described. Data obtained with the radar are not included. (auth)

31457 (UCID-16064) NEW PRECISION, HIGH-CONTRAST PHOTOGRAPHIC RESOLUTION TARGET. Herrmann, W. C. (California Univ., Livermore (USA). Lawrence Livermore Lab.). 23 Jun 1972. Contract W-7405-eng-48. 11p. Dep. NTIS $4.00.

A new precision, high-contrast photographic resolution test target has been constructed that can be used throughout the laboratory for determining the resolution of optical systems or total systems. It is designed to read in line pairs per millimeter. The overall dynamic range is 10 through 120 line pairs per millimeter in equal steps of 10 millimeters. This new Tech Photo Group Target 1 can be supplied in a range of sizes and in any one of a variety of supporting backgrounds. Directions are given for determining the maximum resolving power of a lens system. The test can be performed either visually or photographically. (auth)

31458 (UCID-16108) MEASUREMENT SYSTEM FOR THE PEAK TIME AND AMPLITUDE OF A PULSE. Rufer, R. P. (California Univ., Livermore (USA). Lawrence Livermore Lab.). 24 Mar 1972. Contract W-7405-eng-48. 34p. Dep. NTIS $4.75.

The specific measurement must be made of the peak amplitude of the pulse and the time at which the peak occurs. The system required will provide, in computer compatible format, time and amplitude information about a pulse, or series of pulses. These pulses will be of varying amplitude and time spacing, requiring wide dynamic range performance in the system. Methods and systems are described for the determinations. A practical system meeting the requirements of a wide variety of nanosecond pulse measurements is constructed. (MCW)

31459 (UCRL-13599) ANGULAR MOMENTUM COUPLING, POTENTIAL CURVES AND RADIATIVE SELECTION RULES FOR HEAVY DIATOMIC MOLECULES, WITH PARTICULAR REFERENCE TO Kr_2 AND Kr_2^+. Barr, T. L.; Dee, D.; Gilmore, F. R. (R and D Associates, Santa Monica, Calif. (USA)). Jun 1974. 32p. Dep. NTIS $4.75.

For Univ. of California. Lawrence Livermore Lab.

The coupling of electronic orbital angular momentum, spin, and molecular rotation of diatomic molecules is summarized, with emphasis on heavy molecules where the spin-orbital interaction is not small. The symmetry properties of diatomic wave functions are discussed and tabulated. The building up of molecular electronic states from states of the separated atoms, from states of the united atom, and from molecular orbitals is also explained. These principles and other data are applied to the construction of potential energy curves for Kr_2 and Kr_2^+, following the example of Mulliken for Xe_2 and Xe_2^+. Finally, the electric dipole selection rules for radiative transitions between electronic states are summarized and applied to Kr_2.

31460 (UCRL-75994) AUTOMATED INSPECTION OF IC PHOTOMASKS. Ciarlo, D. R.; Schultz, P. A.; Novotny, D. B. (California Univ., Livermore (USA). Lawrence Livermore Lab.). 19 Aug 1974. 8p. (CONF-740823-4). Dep. NTIS $4.00.

From 18th annual meeting of the Society of Photo-Optical Instrumentation Engineers; San Diego, California, USA (19 Aug 1974).

The results of a nationwide review of automated IC photomask inspection methods are presented. Major photomask inspection problems of detection of visual defects and registration errors, and the determination of critical dimensions and photoplate quality are discussed. This review indicates that for high-volume, large-scale integrated circuits, the greatest concern is for the detection of visual defects. Next in order of importance are the detection of registration errors, and then the accurate determination of critical dimensions. Automated inspection systems and technologies currently available for this are discussed including:

microdensitometer-digital computer systems, laser beam scanning systems, spatial filtering systems, and microscope-television-digital computer systems. Suggested criteria for an ideal photomask inspection system are the simultaneous inspection for 2-μm visual defects, the determination of registration tolerances to within ±0.5 μm, and the determination of the accuracy of the critical dimensions to tolerances of ±0.5 μm on a single photomask in ten minutes. (auth)

CORPORATE INDEX

In the Corporate Index, technical report literature is indexed using the name of the organization or institution responsible for issuing the report. Headings are provided for all report literature and for published literature for which a corporate approach is especially desirable, e.g., symposium and conference proceedings.

Each entry under a corporate heading gives the publication title and the *NSA* volume and abstract numbers. Report numbers, where applicable, are given in parentheses at the end of the entry.

INIS: Authority List for Corporate Entries and Report Number Prefixes (IAEA-INIS-6) is used in the standardization of corporate entries. IAEA-INIS-6 is available from INIS Section, International Atomic Energy Agency, P. O. Box 590, A-1011, Vienna, Austria and from the U. S. Atomic Energy Commission, Technical Information Center, P. O. Box 62, Oak Ridge, TN 37830.

A

AD HOC ADVISORY PANEL ON SAFEGUARDING SPECIAL NUCLEAR MATERIALS (USA)
- Report of the advisory panel on safeguarding special nuclear material, 30:30105 (TID-26630)

AEROSPACE CORP., EL SEGUNDO, CALIF. (USA)
- Thermal and mechanical effects on the corrosion behavior of Ti--6Al--4V. Report for January 1971--January 1972, 30:29942 (AD-777170)

AIR FORCE SPECIAL WEAPONS CENTER, KIRTLAND AFB, N.MEX. (USA)
- Tandem towing tests of the MHU-12/M trailer. Final report, October 1972--December 1973, 30:30113 (AD-777254)

ALLIED CHEMICAL CORP., IDAHO FALLS, IDAHO (USA)
- Evaluation of quinol clathrate for fission product noble gas storage, 30:30108 (ICP-1045)

AMERICAN SOCIETY FOR TESTING AND MATERIALS, PHILADELPHIA, PA.
- Heat transmission measurements in thermal insulations. Conference held at Philadelphia, Pennsylvania, April 16--17, 1973, 30:29242

AMES LAB., IOWA (USA)
- PL/I based multi-tasking operating system, 30:31340 (IS-M-18)
- Program correctness in a multiprogrammed multiprocessor environment, 30:31339 (IS-3444)

ARGONNE NATIONAL LAB., ILL. (USA)
- Cell mediated immunity as an early diagnostic test for osteosarcoma in human radium cases, 30:29771 (CONF-740930-1)
- Contribution to the separation of rare earths by extraction chromatography with di(2-ethylhexyl) phosphoric acid. II. Behavior of the matrix and its influence on the microcomponents, 30:28990 (ANL-Trans-961)
- Engineering design study of a Reference Theta-Pinch Reactor (RTPR), 30:29206 (LA-5336)
- Environmental impact handbook for highway systems, 30:31357 (ANL/ES-30)
- Migratory behavior of fish tagged at a nuclear power plant discharge into Lake Michigan, 30:29462 (CONF-740813-2)
- Plutonium in the Laurentian Great Lakes: food-chain relationships, 30:29415 (CONF-740826-3)
- Protection circuit for a liquid-nitrogen trap filler, 30:31415 (ANL-8111)
- Recent results in the application of column extraction chromatography in inorganic analysis, 30:28989 (ANL-Trans-960)

ARKANSAS UNIV., FAYETTEVILLE (USA). DEPT. OF CHEMISTRY
- Investigation of the reported mass distribution curves in the fission of ^{233}U with 14.8 MeV neutrons, 30:31010 (ORO-4282-14)

ARMY NATICK LABS., MASS. (USA)
- Preservation of enzyme inactivated lamb slices: effects of freeze desiccation and low dose irradiation, 30:29642 (AD-777550)

B

BABCOCK AND WILCOX CO., LYNCHBURG, VA. (USA). NUCLEAR POWER GENERATION DIV.
- B and W quality assurance program for nuclear equipment, 30:31194 (BAW-10096)
- Mark C (17 x 17) fuel assembly. Research and development, 30:31195 (BAW-10097)

BATTELLE COLUMBUS LABS., OHIO (USA)
- Determination of the feasibility of using beta radiation backscatter for the detection of surface contamination of metal panels, 30:29294 (AD-776394)

BATTELLE PACIFIC NORTHWEST LABS., RICHLAND, WASH. (USA)
- Advanced waste management studies progress report, April--June 1974, 30:30106 (BNWL-B-223-11)
- Airborne laboratory for air pollution study, 30:29612 (BNWL-1850(Pt.3))
- Airborne release of ^{137}Cs from a contaminated area during a range fire, 30:29376 (BNWL-1850(Pt.3))
- ALE reserve climatology for 1973, 30:29437 (BNWL-1850(Pt.3))
- Analytical investigations of inertial deposition of small aerosol particles from laminar flows onto large obstacles. Part A. General formulation, 30:29485 (BNWL-1850(Pt.3))
- Analytical search for the stochastic-dominating process in the drift-deposition problem, 30:29488 (BNWL-1850(Pt.3))
- Analytical investigations of inertial deposition of small aerosol particles from laminar flows onto large obstacles. Part B. Large stokes number solution by the method of matched asymptotic expansion, 30:29486 (BNWL-1850(Pt.3))
- Aquatic physiology of thermal and chemical discharges, 30:29461 (BNWL-SA-5058)
- Assessment of the long-term exposure due to resuspension, 30:29375 (BNWL-1850(Pt.3))
- Atmospheric natural aerosols and fallout particulates during 1973 at Richland, Washington and Point Barrow, Alaska, 30:29361 (BNWL-1850(Pt.3))
- Behavior and characteristics of radioactive debris from the Chinese nuclear weapons test of June 26, 1973, 30:29362 (BNWL-1850(Pt.3))
- Carcinogenicity of iodine-131 relative to age at exposure, 30:29777 (BNWL-SA-5065)
- Characteristics of aerosols from St. Louis, 30:29471 (BNWL-1850(Pt.3))
- Comparison of diffusion-deposition model components with experimental results, 30:29434 (BNWL-1850(Pt.3))
- Comparison of the washout coefficient for a polydisperse aerosol to that for an aerosol of fixed particle size, 30:29477 (BNWL-1850(Pt.3))
- Concentrations and rates of removal of contaminants from the atmosphere in an downwind of St. Louis, 30:29473 (BNWL-1850(Pt.3))
- Convective storm modeling and its possible application to precipitation scavenging problems, 30:29480 (BNWL-1850(Pt.3))
- Dependence of site evaluation of roughness length and displacement length on value chosen for Von Karman's constant, 30:29432 (BNWL-1850(Pt.3))
- Determination of aerosol deposition rates on a lake surface using radon daughters, 30:29410 (BNWL-1850(Pt.3))
- Development an an ideal sampler for below-cloud scavenging studies, 30:29366 (BNWL-1850(Pt.3))
- Development of a sonic anemometer system, 30:29609 (BNWL-1850(Pt.3))
- Dry deposition of particles, 30:29482 (BNWL-1850(Pt.3))
- Dry disposition processes on vegetation canopies, 30:29369 (BNWL-1850(Pt.3))
- Effects of radioactivity on ice nucleation, 30:29367 (BNWL-1850(Pt.3))
- Elemental content of trace elements in vegetation collected at Centralia, Washington, 30:29483 (BNWL-1850(Pt.3))
- Entrainment of tracers near the sides of convective clouds, 30:29481 (BNWL-1850(Pt.3))
- Estimation of mean crosswind concentration profiles from ''instantaneous'' crosswind traverses, 30:29424 (BNWL-1850(Pt.3))

  Evaluation of an airborne fluorescent particle counter for atmospheric tracer studies, 30:29610 (BNWL-1850(Pt.3))
  Extension of the anaysis of plume washdown to include diffusion, 30:29478 (BNWL-1850(Pt.3))
  Feasibility study of the use of inert tracers in the national hail research experiment, 30:29427 (BNWL-1850(Pt.3))
  Fitting an analytical curve to some experimental diffusion data, 30:29426 (BNWL-1850(Pt.3))
  Flux meter for direct field measurement of deposition and resuspension rates, 30:29613 (BNWL-1850(Pt.3))
  Interstage particle losses in a high-volume cascade impactor, 30:29374 (BNWL-1850(Pt.3))
  Investigations of the microstructure of heavy ion bombarded nickel, 30:30065 (BNWL-1639)
  Long-term effects of intratracheally instilled ^{253}EsCl$_3$ in rats, 30:29776 (BNWL-SA-4870)
  Measurement of particulate plume depletion by comparison with inert gas plumes, 30:29425 (BNWL-1850(Pt.3))
  Measurements of drift from a mechanical draft cooling tower, 30:29487 (BNWL-1850(Pt.3))
  Mesoscale transport and diffusion studies, 30:29435 (BNWL-1850(Pt.3))
  Method for determining Monin--Obukhov L's from profiles of subjectively estimated mean wind speeds and temperatures, 30:29431 (BNWL-1850(Pt.3))
  Model for cumulus washout of cosmogenic radionuclides, 30:29363 (BNWL-1850(Pt.3))
  Model to compute low-level Montgomery stream functions, 30:29436 (BNWL-1850(Pt.3))
  Neutronic calculations for experiments with light water reactor fuel in PBF, 30:31187 (BNWL-B-371)
  Pacific Northwest Laboratory annual report for 1973 to the USAEC Division of Biomedical and Environmental Research. Part 3. Atmospheric sciences, 30:29468 (BNWL-1850(Pt.3))
  Particle deposition rates on a water surface as a function of particle diameter and air velocity, 30:29484 (BNWL-1850(Pt.3))
  Particle size distributions of manmade and natural radionuclides, 30:29360 (BNWL-1850(Pt.3))
  Postulated estimate of wet versus dry deposition downwind of a point source of pollution, 30:29364 (BNWL-1850(Pt.3))
  Potential application of atomic absorption and anodic stripping voltammetry to the precipitation scavenging program, 30:28937 (BNWL-1850(Pt.3))
  Power spectral analysis of two periods of turbulence data for very stable conditions, 30:29433 (BNWL-1850(Pt.3))
  Precipitation scavenging of inorganic pollutants from metropolitan sources: St. Louis, July 1973, 30:29479 (BNWL-1850(Pt.3))
  Preliminary in-plume measurements near Centralia, 30:29472 (BNWL-1850(Pt.3))
  Progress report on in-cloud scavenging in frontal storms, 30:29475 (BNWL-1850(Pt.3))
  Quillayute air reference station, 30:29359 (BNWL-1850(Pt.3))
  Radioactive waste management for nuclear energy center, 30:30107 (BNWL-B-334)
  Radionuclide concentration minimums from 6 to 9 km, 30:29368 (BNWL-1850(Pt.3))
  Real-time system for detection of the atmospheric tracer sulfur hexafluoride, 30:29611 (BNWL-1850(Pt.3))
  Regional wind resuspension of dust, 30:29373 (BNWL-1850(Pt.3))
  Resuspension by wind at Rocky Flats, 30:29371 (BNWL-1850(Pt.3))
  Resuspension of tracer particles by wind, 30:29370 (BNWL-1850(Pt.3))
  Resuspension source change at Rocky Flats, 30:29372 (BNWL-1850(Pt.3))
  Simple model for bouyant plumes based on the conservation laws, 30:29460 (BNWL-1850(Pt.3))
  Summary of current findings from the analysis of 1972 Quillayute scavenging experiments, 30:29476 (BNWL-1850(Pt.3))
  Surface flux model for diffusion, deposition, and resuspension, 30:29470 (BNWL-1850(Pt.3))
  Trace pollutant emissions in fossil fuel combustion, 30:29469 (BNWL-1850(Pt.3))
  Vertical profiles of trace gases in St. Louis, 30:29474 (BNWL-1850(Pt.3))
  Wet and dry atmospheric removal processes for radioiodine, 30:29365 (BNWL-1850(Pt.3))

BAYERISCHES LANDESINSTITUT FUER ARBEITSMEDIZIN, MUENCHEN (F.R. GERMANY)
  Experience in complying with authorisation conditions for the discharge of liquid and gaseous radioactive effluents from CEGB nuclear stations, 30:31204 (AED-CONF-74-157-007)
  Health physics and technical considerations concerning the control of gaseous effluents from nuclear power plants, 30:29356 (AED-CONF-74-157-005)
  Medical evaluation of measured values following radiation exposure, 30:29703 (AED-CONF-74-221-007)
  Results of the medical examinations, 30:29829 (AED-CONF-74-221-004)

BENDIX CORP., KANSAS CITY, MO. (USA)
  Automatic radar-sensitivity measurement. Final report, 30:31417 (BDX-613-1134(Rev.))
  Beta backscatter measurements of aluminum coatings on mylar substrates, 30:29602 (BDX-613-1028(Rev.))
  Detection and suppression of transistor oscillation during power burn-in, 30:31419 (BDX-613-1144(Rev.))
  Development of processes for hybrid microcircuits containing beam-lead devices, 30:31416 (BDX-613-1115(Rev.))
  Electrodepositing platinum and platinum--iridium alloys from molten cyanides: chemical process studies, 30:31366 (BDX-613-1064(Rev.))
  Mass anodization of tantalum-nitride resistors, 30:31387 (BDX-613-1155(Rev.))
  Process evaluation of new cellular silicone material, 30:31385 (BDX-613-1082(Rev.))
  Solubility parameters and evaporation rate analysis in organic residue characterization, 30:31367 (BDX-613-1099(Rev.))
  Static compressive testing of rigid polyurethane foam, 30:31384 (BDX-613-1036(Rev.))
  Temperature dependent properties of potting materials, 30:31386 (BDX-613-1133(Rev.))
  Use of EN-7 to encapsulate analyzer assemblies. Final report, 30:31418 (BDX-613-1135(Rev.))

BETTIS ATOMIC POWER LAB., PITTSBURGH, PA. (USA)
  HYDIZ: a 2-dimensional computer progam for migration of interstitial solutes of finite solubility in a thermal gradient (LWBR Development Program), 30:29983 (WAPD-TM-1157)
  SAFR4: a program to evaluate the stability of a rigid blade in parallel fluid flow, 30:31280 (WAPD-TM-1085)

BROOKHAVEN NATIONAL LAB., UPTON, N.Y. (USA)
  AGS secondary beams and parameters, FY75, 30:30141 (BNL-19153)
  Annual report of the Brookhaven DCPA Contract Group, 30:31332 (BNL-19097(Rev.))
  Polymer-concrete for use in the repair of deteriorated bridge decks, 30:31388 (BNL-19161)
  Recoil energy distributions in CTR-related neutron spectra, 30:29203 (BNL-19043)
  Resonance excitation by distortion of the β-function coupled with a long range space charge force, 30:30137 (BNL-19192)

BROWN UNIV., PROVIDENCE, R.I. (USA). DIV. OF APPLIED MATHEMATICS
  Discrete spectrum of solutions of the wave equation with strong cubic nonlinearity, 30:31131 (AD-776985)

BUNDESFORSCHUNGSANSTALT FUER LEBENSMITTELFRISCHHALTUNG, KARLSRUHE (F.R. GERMANY)
  Bibliographies in nuclear science and technology. Section 02: contamination and decontamination of foods. Number 12, 30:29420 (ZAED-BIBL.-02-12)

BUNDESGESUNDHEITSAMT, BERLIN (F.R. GERMANY). INST. FUER SOZIALMEDIZIN UND EPIDEMIOLOGIE
  Special laboratory-chemical examination techniques, 30:29702 (AED-CONF-74-221-006)

BUNDESGESUNDHEITSAMT, NEUHERBERG
  Genetic radiation effects, 30:29700 (AED-CONF-74-030-004)

C

CALIFORNIA UNIV., BERKELEY (USA). LAWRENCE BERKELEY LAB.
  Exciton enhanced Raman scattering of LO phonons in trigonal Se, 30:31425 (LBL-2781)
  MAPEDIT system for automatic map digitization, 30:31341 (LBL-3072)
  Microsecond pulse technique for heat capacity measurement, 30:31424 (LBL-2574)

CALIFORNIA UNIV., LIVERMORE (USA). LAWRENCE LIVERMORE LAB.
  36 inch miter valve design, 30:31435 (UCID-15496)
  Acoustic emission monitoring of ring-cracking in glass and alumina, 30:31410 (UCID-16076)
  Acoustic emission monitoring of proof tests on canisters and related hardware, 30:29296 (UCID-15777)
  Adequacy of lithium supplies as a fusion energy source, 30:29222 (UCID-15953)
  Alice vacuum system: Sept. 1969, 30:29218 (UCID-15660)
  Aligning a spectra physics He--Ne laser Model 125, 30:29270 (UCID-15860)
  Analysis of plastic-bonded explosives containing HMX, ammonium perchlorate, aluminum, and Viton, 30:31369 (UCID-15623)
  Analysis of explosive simulant 90503, 30:31373 (UCID-15972)
  Analytical expression for the E-layer electron velocity distribution, 30:29187 (UCID-16003(Rev.1))
  Application of a computer-simulated Perceptron to a complex photographic scene, 30:31433 (UCID-15373)
  Automated inspection of IC photomasks, 30:31460 (UCRL-75994)
  Back current in an E-layer. I, 30:29224 (UCID-15977)
  Blade-type metal-cutting tool for quick removal of stock in roughing work, 30:29269 (UCID-15833)
  Bremsstrahlung polarization from commercial x-ray tubes, 30:31447 (UCID-15829)
  CAIN system field test, 30:31446 (UCID-15816)
  Calculated ion-density spatial distribution in Alice Baseball I, 30:29184 (UCID-15647)
  Calculating electron synchrotron radiation loss from a fusion plasma, 30:29182 (UCID-15513)

Cell cycle kinetics and radiation therapy, 30:29662 (UCRL-75441)
Chemical compositions of various plastic materials, 30:31404 (UCID-15815)
Cloud chamber quark quest one year report, 30:30576 (UCID-15787)
Code description: FOFT, 30:31350 (UCID-15753)
Communication system design, 30:31452 (UCID-15955)
Compressibility and strength behavior of Diagonal Line alluvium, 30:29316 (UCID-15736)
Compton scattering subroutine for Monte Carlo calculations, 30:30651 (UCID-15808)
Consideration of a ''brute-force'' approach to the achievement of higher density in the presence of instability, 30:29183 (UCID-15628)
Consistent vapor equation of state for solids, 30:31406 (UCID-15846)
Construction of an adjustable carrying handle for the FIDLER detector, 30:29497 (UCID-15775)
Decay of plasma currents and charge in beam plasma experiments, 30:29186 (UCID-15820)
Design of a passive crack detector system, 30:29297 (UCID-15867)
Determination of geographic position from rectangular coordinates. Progress report, March--June 1970, 30:31361 (UCID-15722)
Development of an air pollution model for the San Francisco Bay Area. Second semiannual report to the National Science Foundation, 30:31363 (UCRL-51537)
Diffusion of radioactive fluid through soil surrounding a large power-reactor station after a core meltdown accident, 30:31254 (UCRL-51494)
Digital image processing with pseudo-color, 30:31356 (UCRL-75662)
Dynamic interferometric holography, 30:31440 (UCID-15682)
Effect of fluid content on the mechanical properties of Westerly granite, 30:31411 (UCRL-51626)
Elastic constants of fractured Hardhat granodiorite, 30:31398 (UCID-15369)
Elat-Dead Sea canal, 30:29327 (UCID-16107)
Electro-optic method of tracking an electron-beam weld, 30:31442 (UCID-15759)
Electronics for the LRL automated personnel thermoluminescence dosimetry system, 30:29552 (UCID-15836)
Energy minimization method for computer deconvolution, 30:31354 (UCID-15947)
Energy recovery of a lithium ion beam, 30:29221 (UCID-15939)
Evaluation of gold-doped permalloy films using ferromagnetic resonance techniques, 30:31454 (UCID-16032)
Evaluation of downhole alignment by means of an alternating magnetic dipole field, 30:31432 (UCID-15203)
Evaluation of load-deflection tests of 0.060-in.-thick Y-3333 cellular silicone, 30:31407 (UCID-15901)
F-M detection in the argon ion laser, 30:29268 (UCID-15371)
Fast response light scattering measurements of the characteristics of wind suspended aerosols, 30:29490 (UCRL-76014(Rev.1))
Fast, high sensitivity 10.6 micron interferometer, 30:29161 (UCID-15625)
Feasibility of two schemes for detecting the envelope of a γ-ray burst underground, 30:29321 (UCID-15865)
Field measurements of permeability of NTS alluvium in Area 10, 30:29323 (UCID-15919)
Field measurement of the permeability of NTS alluvium, 30:29315 (UCID-15727)
Field measurement of permeabilities in NTS Area 9, 30:29458 (UCID-15895)
Fine structure generalization of the Compton Fokker--Planck equation, 30:31105 (UCID-15784)
Gas chromatographic analysis of bis(2-fluoro-2,2-dinitroethyl) formal (FEFO), 30:31370 (UCID-15671)
Generalized shock Hugoniots, 30:31400 (UCID-15586)
Generation of seismic waves by nuclear explosives and possibilities for evading a test-ban treaty, 30:29325 (UCID-15983)
Geometric solution of finite x-ray source irradiating two concentric cylinders containing x-ray absorbing material, 30:31123 (UCID-15938)
H.E. firing chambers for use in Super Kukla Reactor, 30:31236 (UCID-15817)
Has man, through increasing emissions of particulates, changed the climate, 30:29489 (UCRL-75902(Rev.1))
HYBRID-1, a two-dimensional Fokker--Planck code, 30:29189 (UCRL-51598)
Identification and measurement of low-energy electrons by cloud chamber techniques: the oxygen and neon auger-electron problem, 30:29495 (UCID-15372)
Instrumenting the LAPQ-1 airborne cloud-mapping radar for shipboard use in Operation Dial Train, 30:31456 (UCID-16051)
Interaction of intense microwave radiation and fully ionized hydrogen plasma. Part 1. High-density system, 30:29233 (UCRL-51631(Pt.1))
Introduction to extrapolation methods for the numerical solution of differential equations, 30:31355 (UCID-15992)
Investigation of polyion-small ion electrostatic interaction effects in polyelectrolyte solutions, 30:31375 (UCRL-51636)
Investigation of tritium decontamination. Interim research report, 30:29326 (UCID-15985)
Ion bombardment simulation of 14 MeV neutron damage in thin niobium films, 30:30066 (UCID-16109)
Kinetics of energy release of heterogeneous high explosives, 30:31408 (UCID-15962)
Laminar gas flow through loosely packed Overton sand, 30:29319 (UCID-15818)
Levitrons and the superconducting levitron: a summary, 30:29213 (UCID-15448)
LLL compact 10-ps streak camera, 1974 update, 30:29162 (UCRL-75557)
LLL spray damper project, 30:29330 (UCID-15941)
Lorentz microscopic observation of head-on domain walls in magnetic thin films, 30:31455 (UCID-16034)
Low pressure phase transition in NaCl, 30:31399 (UCID-15454)
LX-10-1: a high-energy plastic-bonded explosive, 30:31374 (UCRL-51629)
Magnetic order in certain alkali amphiboles, a Moessbauer investigation, 30:31412 (UCRL-75499(Rev.1))
MAGREC final report, 30:29619 (UCID-16026)
Materials screening program for the LLL geothermal project, 30:31327 (UCRL-75353)
Mathematical review of introductory wave mechanics, 30:31444 (UCID-15803)
Measurement system for the peak time and amplitude of a pulse, 30:31458 (UCID-16108)
Mechanical properties of a shale from Site U-2, 30:31409 (UCID-16023)
Method of estimating the total curies in gas samples, 30:29087 (UCID-15809)
MTSE II field calculation, 30:29215 (UCID-15511)
Negative mass instabilities in beam injected plasmas, 30:29197 (UCID-15540)
New NADS: compatible alpha measuring system, 30:29618 (UCID-15828)
New precision, high-contrast photographic resolution target, 30:31457 (UCID-16064)
Note on the Astron gun design, 30:29214 (UCID-15481)
Note on the incoherent space charge limit in the High Intensity Storage Ring, 30:30139 (UCID-15686)
Notes on application of solid electrolyte tantalum capacitors in coupling and bypass service, 30:31401 (UCID-15662)
Nuclear correction for Genesis, 30:29180 (UCID-15316)
Numerical deconvolution, 30:31349 (UCID-15743)
Numerical solutions of Poisson's equation by Fourier transform methods, 30:31348 (UCID-15478)
Numerical simulation of air-injection experiments in NTS alluvium, 30:29324 (UCID-15981)
Observations on the change of the length of the E-layer during stacking, 30:29188 (UCID-16004)
Operation Cannikin: electronic and electrical scientific measurements and support plan. Pre-operational report, 30:29318 (UCID-15802(Rev.1))
Outline of developments in magnetic circuit theory, 30:31436 (UCID-15597)
Photoelastometric recording of stress waves, 30:31434 (UCID-15383)
Plutonium foundry practices at the Lawrence Livermore Laboratory, 30:29958 (UCID-15926)
Polaroid vectograph process and application as applied to stereo laser and computer-generated 3-dimensional forms, 30:31352 (UCID-15840)
Preliminary equation-of-state data for Baneberry altered tuff, 30:29322 (UCID-15874)
Preliminary report of direct recovery study, 30:29217 (UCID-15650)
Preliminary orbits and structure of a high intensity storage ring, 30:30138 (UCID-15685)
Pressure, Force, and Mass Calibration Laboratory, 30:31445 (UCID-15811)
Procedure for deuterating titanium, 30:29216 (UCID-15624)
Program IONS: two-dimensional Fokker--Planck equation for ions and electrons, 30:31362 (UCID-16014)
Properties of the high explosive LX-69-0, 30:31372 (UCID-15910)
Proposed 2X data system, 30:29212 (UCID-15434)
Quadrupole fields in a toroidal geometry for the High Intensity Storage Ring, 30:30140 (UCID-15735)
Radiation and heat deposition analysis of the proposed Mirror Fusion Experiment (MFX), 30:29220 (UCID-15806)
Radiation from buried antennas, 30:31449 (UCID-15890)
Reduction of hose growth by current tailoring, 30:29199 (UCID-15996)
Residual stresses and birefringence in polycarbonate plastic, 30:31405 (UCID-15845)
Resistor beam bugs: scientific explanation, 30:29225 (UCID-16057)
Runaway effects in the inductively excited levitron, 30:29181 (UCID-15487)
Second-order difference equations for a non-uniform triangle mesh, 30:31347 (UCID-15388)
Selected activities in photonuclear reactions, 1973--1974, 30:30856 (UCID-16563)
Shoal postshot environment, 30:29317 (UCID-15771)
Single pulse area measurement system (SPAMS), 30:29496 (UCID-15761)

  - Solution of large coupled sets of kinetic equations, 30:31351 (UCID-15765)
  - Some comments on the transverse resistive wall instability (or, ''LNS revisited''), 30:29198 (UCID-15711)
  - Some necessary conditions on x-ray laser action, 30:29272 (UCRL-74898)
  - Some notes on coaxial terminations, short-circuits, and open-circuits, 30:31453 (UCID-15998)
  - Some numerical experiments with low atwood number incompressible Rayleigh--Taylor instabilities, 30:31438 (UCID-15618)
  - Some thoughts on negative resistance as it applies to high frequency impedance measurements, 30:31448 (UCID-15866)
  - Source identification by multi-element analysis of diurnal samples, 30:31371 (UCID-15872)
  - Space wave fields of subsurface electromagnetic sources in planar layered media, 30:31353 (UCID-15945)
  - Spectrographic determination of trace impurities in high purity uranium oxide, 30:28944 (UCID-15952)
  - State relationships for maximal-length sequence generators, 30:31450 (UCID-15898)
  - Static compression of relativistic electron rings, 30:30131 (UCID-16583)
  - Status report to NCSAC, 30:31011 (UCID-15639)
  - Steady-state, ac-temperature technique for measuring the specific heat of electrical conductors, 30:31439 (UCID-15649)
  - ''Super'' H.E. machine concept, 30:29320 (UCID-15855)
  - Surface currents on a toroid that result in a uniform, axial magnetic field inside the torus, 30:29219 (UCID-15695)
  - Tensile and compression test methods for rigid plastic foams, 30:31403 (UCID-15739)
  - Test methods for high packing density digital magnetic tape recorders, 30:31443 (UCID-15773)
  - Thermal conductivity of a hard sphere solid, 30:31441 (UCID-15723)
  - Thermal ignition of an explosive by surface friction, 30:31402 (UCID-15669)
  - Thermally averaged Gaunt factors in non-relativistic electron-ion bremsstrahlung, 30:29185 (UCID-15712)
  - Torsion pendulum for laser energy measurement, 30:31451 (UCID-15907)
  - Two numerical examples of Rayleigh--Taylor instability for a system of five different densities, 30:31437 (UCID-15611)
  - Weak interaction of a neutralized E-layer with resistors, 30:29223 (UCID-15956)
  - X-ray analysis for electron beam enhancement in the plasma focus device, 30:29174 (UCRL-75910)
  - X-ray lasers: necessary conditions and some possible approaches, 30:29271 (UCID-16290)
  - X-ray measurements on electron distribution in Astron, 30:29160 (UCID-15392)
  - Yield surfaces for beryllium boride ceramics, 30:29891 (UCID-15859)
- CALIFORNIA UNIV., LOS ANGELES (USA). SCHOOL OF ENGINEERING AND APPLIED SCIENCE
  - Post-accident core retention for LMFBR's. 2. Technical report. Final report for the period 1 July 1972--30 June 1973, 30:31253 (UCLA-ENG-7343)
- CEA CENTRE D'ETUDES DE LIMEIL, 94 - VILLENEUVE-SAINT-GEORGES (FRANCE)
  - Calculation of the neutron spectra from nuclear reactions in Focus type deuterium plasmas. I. General presentation and mathematical analysis, 30:29178 (CEA-N-1711)
- CEA CENTRE D'ETUDES NUCLEAIRES DE CADARACHE, 13 - SAINT-PAUL-LES-DURANCE (FRANCE)
  - Experiments in pure uranium lattices with unit /sub infinity/. Assemblies SNEAK-8/8Z; UK 1 and UK 5 in ERMINE and HARMONIE, 30:31270 (EURFNR-1189)
- CEA CENTRE D'ETUDES NUCLEAIRES DE FONTENAY-AUX-ROSES, 92 (FRANCE)
  - Ruthenium volatility during vitrification of fission products. Part II. Fixation on a steel tube. Peroxide decomposition, 30:29086 (AEC-tr-7575)
- CEA CENTRE D'ETUDES NUCLEAIRES DE FONTENAY-AUX-ROSES, 92 (FRANCE). DEPT. DE PROTECTION
  - Metabolism of tritium-labelled sodium acetate, in the rat. A radiation protection approach, 30:29795 (CEA-R-4591)
- CEA CENTRE D'ETUDES NUCLEAIRES DE FONTENAY-AUX-ROSES, 92 (FRANCE). DIV. D'ETUDE ET DE DEVELOPPEMENT DES REACTEURS
  - Experiments in pure uranium lattices with unit /sub infinity/. Assemblies SNEAK-8/8Z; UK 1 and UK 5 in ERMINE and HARMONIE, 30:31270 (EURFNR-1189)
- CEA CENTRE D'ETUDES NUCLEAIRES DE GRENOBLE, 38 (FRANCE)
  - Department of Fundamental Research, Grenoble, semiannual bulletin No. 4, 30:31333 (CEA-N-1688)
  - Study of the detection of nuclear particles in liquid dielectrics, 30:29492 (CEA-R-4543)
- CEA CENTRE DE MARCOULE, 30 - BAGNOLS-SUR-CEZE (FRANCE). SERVICE DES ATELIERS PILOTES
  - Study of diffusion/leaching phenomena with glasses. Application of risk evaluation to long-term storage, 30:29133 (CEA-R-4550)
- CENTRE D'ETUDE DE L'ENERGIE NUCLEAIRE, MOL (BELGIUM)
  - Separation of ^{137}Cs and ^{90}Sr from highly radioactive fission product solutions, 30:28991 (BLG-487)
- CER GEONUCLEAR CORP., LAS VEGAS, NEV. (USA)
  - Project Rio Blanco: comparative postdetonation hydrologic testing, 30:29313 (PNE-RB-60)
  - Project Rio Blanco: results from the initial alluvial water quality program, 30:29312 (PNE-RB-59)
- COMBUSTION ENGINEERING, INC., CHATTANOOGA, TENN. (USA)
  - LMFBR demonstration plant steam generating system, 30:31217 (CENC-1194(Vol.1)(Suppl.1))
  - LMFBR demonstration plant steam generating system, 30:31218 (CENC-1194(Vol.2)(Suppl.1))
  - LMFBR sodium heated steam generator: test model, 30:31221 (CENC-1197(Vol.4))
  - LMFBR sodium heated steam generator: test model, 30:31219 (CENC-1197(Vol.1))
  - LMFBR sodium heated steam generator: test model, 30:31220 (CENC-1197(Vol.3))
- COMISION NACIONAL DE ENERGIA ATOMICA, BUENOS AIRES (ARGENTINA)
  - Double optimization in linear discrete systems, 30:31335 (CNEA-365)
- COMISION NACIONAL DE ENERGIA ATOMICA, BUENOS AIRES (ARGENTINA). DEPARTAMENTO DE METALURGIA
  - Application of a mass spectrometer to the method of determination of gases in metals by vacuum fusion, 30:28938 (CNEA-363)
- COMISION NACIONAL DE ENERGIA ATOMICA, BUENOS AIRES (ARGENTINA). DEPARTAMENTO DE QUIMICA
  - Chronoamperometric determination of iodine in urine, 30:28939 (CNEA-366)
- COMITATO NAZIONALE PER L'ENERGIA NUCLEARE, ROME (ITALY)
  - Application of sequential estimation methods to counts of phytoplankton, 30:31380 (RT/BIO-(74)7)
  - Characterizations of fuel element cladding tubes, 30:31279 (RT/MET-(73)1)
  - Fluxes and effective multiplication factor evaluation by escape probabilities, 30:31274 (RT/FI-(74)30)
  - LARA: a FORTRAN IV code for the calculation of the compound nucleus contribution to the total radiative width in medium and heavy nuclei based on the Brink--Axel model, 30:30956 (RT/FI-(74)17)
  - MCDATA code, 30:30851 (RT/FI-(74)19)
  - Neutron radiography: biomedical applications, 30:29705 (RT/FI-(74)16)
  - Osmotic haemolysis as a means of studying erythropoietic stresses: response to acute anaemia and acute irradiation, 30:29736 (RT/BIO-(74)10)
  - Point-dependent calculations of the anisotropic diffusion coefficient, 30:30850 (RT/FI-(74)10)
  - Poisson-Algebraic distributions: another family of generalized Poisson profiles in nuclear-reactor noise-analysis, 30:31273 (RT/FI-(74)26)
- COMITATO NAZIONALE PER L'ENERGIA NUCLEARE, SALUGGIA (ITALY)
  - 1973 meteorological yearbook of the EUREX site at Saluggia, 30:29457 (RT/PROT-(74)13)
- COMMISSION OF THE EUROPEAN COMMUNITIES, BRUSSELS (BELGIUM)
  - Analysis of ECE data on the basis of isotopic weight fractions, 30:28940 (EUR-4859)
- COMMITTEE ON APPROPRIATIONS (U.S. SENATE), WASHINGTON, D.C.
  - Public works for water and power development and Atomic Energy Commission appropriation bill, 1975, Ninety-Third Congress, Second Session, House of Representatives, 30:31331
- COMMITTEE ON COMMERCE (U.S. SENATE), WASHINGTON, D.C.
  - Radiation control for health and safety. Hearings before the Committee on Commerce, United States Senate, Ninety-Third Congress, First Session, on Public Law 90-602, March 8, 9, and 12, 1973, 30:30445
- COMMONWEALTH EDISON CO., CHICAGO, ILL. (USA)
  - Dresden Nuclear Power Station, Units 1, 2, and 3. Semiannual report, January--June 1974, 30:31311 (DOCKET-50010-305)
- CORNELL UNIV., ITHACA, N.Y. (USA). DEPT. OF CHEMISTRY
  - Trace geochemistry of lunar material. Final report, 30:28916 (N-74-20470)
- CORNELL UNIV., ITHACA, N.Y. (USA). DEPT. OF MATERIALS SCIENCE AND ENGINEERING
  - Grain boundery sliding and structure. Progress report, December 1, 1973--November 30, 1974, 30:29977 (COO-2172-7)

D

- DANISH ATOMIC ENERGY COMMISSION, RISOE. RESEARCH ESTABLISHMENT
  - Additive strength contributions, 30:31427 (RISO-M-1714)
  - Comparison of mathematical models for calculation of external gamma doses originating from releases of radioactivity to the atmosphere, 30:29342 (RISO-M-1726)
  - Compilation of x-ray interaction data for x-ray fluorescence analysis of geological samples, 30:28943 (RISO-297)
- DECHEMA DEUTSCHE GESELLSCHAFT FUER CHEMISCHES APPARATEWESEN E.V., FRANKFURT AM MAIN (F.R. GERMANY)
  - Corrosion and corrosion resistance. IX. Tutzing symposium of the DECHEMA, February 26--March 1, 1973, Tutzing Castle, Starnberger Lake, 30:29943 (CONF-730230-(Absts.))

DEMOCRITUS NUCLEAR RESEARCH CENTER, ATHENS (GREECE)
International intercomparison of chemical dosimeters for in-pile use. A report of measurements made in the Greek Research Reactor-1 at Nuclear Research Center ''Democritos'', Athens, Greece, 3--8 July 1972 by eight reactor calorimetry and radiation chemistry groups from eight member states of the IAEA, 30:29539 (DEMO-74/5)
DEUTSCHES KREBSFORSCHUNGSZENTRUM, HEIDELBERG (F.R. GERMANY). INST. FUER NUKLEARMEDIZIN
Thorotrast-induced neoplasms, 30:29769 (AED-CONF-74-016-002)
DOUGLAS UNITED NUCLEAR, INC., RICHLAND, WASH. (USA)
Douglas United Nuclear, Inc. reactor and fuel production facilities 1972 environmental release report, 30:29341 (DUN-8133)
DOW CHEMICAL U.S.A., GOLDEN, COLO. ROCKY FLATS DIV.
Direct determination of beryllium in urine by flameless atomic absorption spectrometry, 30:31379 (RFP-2151)
Ventilation design for new Plutonium Recovery Facility, 30:29329 (RFP-2215)
DU PONT DE NEMOURS (E.I.) AND CO., AIKEN, S.C. (USA). SAVANNAH RIVER LAB.
Determination of promethium-147 in aqueous environmental samples, 30:28969 (DP-MS-73-77)
DUESSELDORF UNIV. (F.R. GERMANY). 1. MEDIZINISCHE KLINIK B
Special indication and contraindications for the implantation of cardiac pacemakers with radionuclide batteries, 30:29770 (AED-CONF-74-030-003)
DUKE POWER CO., CHARLOTTE, N.C. (USA)
Oconee Nuclear Station, Units 1 and 2. Semiannual operating report, January--June 1974, 30:31315 (DOCKET-50269-284)

E

EBERLINE INSTRUMENT CORP., SANTA FE, N.MEX. (USA)
Radiological monitoring program, period covering February 4, 1974--April 30, 1974, 30:29348 (PNE-RB-51-9)
EG AND G, INC., LAS VEGAS, NEV. (USA)
Aerial radiological measuring survey of the Maine Yankee Atomic Power Plant, September 1971, 30:29357 (ARMS-71.6.5)
Aerial radiological measuring surveys of the Turkey Point Station, April 1972, 30:29358 (ARMS-72.6.2)
ERLANGEN-NUERNBERG UNIV., ERLANGEN (F.R. GERMANY). KINDERKLINIK MIT POLIKLINIK
Indirect technique and problems of radiation protection in pediatric X-ray diagnostics, 30:29701 (AED-CONF-74-140-004)

F

FLORIDA POWER AND LIGHT CO. (USA)
Turkey Point Plant, Units 3 and 4. Semiannual operating report No. 4, January--June 1974, 30:31314 (DOCKET-50250-283)
FORSVARETS FORSKNINGSINSTITUTT, KJELLER (NORWAY)
Daily excretion rate of iodine calculated from the relationship iodine per gram creatinine in a single afternoon urine sample, 30:29808 (F-559)
FREIBURG UNIV. (F.R. GERMANY). FAKULTAET FUER PHYSIK
Angular distributions for the reactive scattering of H and D atoms by polyatomic molecules, 30:30519 (AED-CONF-74-085-004)

G

GENERAL ATOMIC CO., SAN DIEGO, CALIF. (USA)
Secondary jaw crusher development, 30:29265 (GA-A-12903)
GENERAL ELECTRIC CO., MORRIS, ILL. (USA). MIDWEST FUEL RECOVERY PLANT
Midwest Fuel Recovery Plant technical study report, 30:29145 (NP-20106)
GENERAL ELECTRIC CO., PHILADELPHIA, PA. (USA)
JFET hardening and high dose rate study, 30:29888 (AD-903226)
GENERAL ELECTRIC CO., PLEASANTON, CALIF. (USA). VALLECITOS NUCLEAR CENTER
Thermodynamic data program involving plutonia and urania at high temperatures. Quarterly report No. 27, February 1, 1974--April 30, 1974, 30:31223 (GEAP-12511)
GEORGIA INST. OF TECH., ATLANTA (USA). SCHOOL OF NUCLEAR ENGINEERING
Diagnostics of seeded rf plasmas: an experimental study related to the gaseous core nuclear reactor. Final report, 1 September 1971--31 July 1973, 30:31241 (N-74-23299)
GEORGIA UNIV., ATHENS (USA). DEPT. OF ENTOMOLOGY
Radioactive tracer studies of soil and litter arthropod food chains. Progress report, November 1, 1973--October 31, 1974, 30:29419 (SRO-641-13)
GESELLSCHAFT FUER KERNENERGIEVERWERTUNG IN SCHIFFBAU UND SCHIFFAHRT M.B.H., GEESTHACHT-TESPERHUDE (F.R. GERMANY)
NS Otto Hahn. Research Report No. 4. The oscillational behaviour of the second core support system, 30:31240 (GKSS-74/E/15)
GESELLSCHAFT FUER SCHWERIONENFORSCHUNG M.B.H., DARMSTADT (F.R. GERMANY)
The production of multicharged ions with a duoplasmatron ion source in high-current continuous operation, 30:30475 (GSI-A1-74)
GIESSEN UNIV. (F.R. GERMANY). 1. PHYSIKALISCHES INST.
Cross section for the Ar--L--x-ray emission in collisions of He^{+}-, Ne^{+}-, and Ar^{+}- ions with Ar atoms, 30:30518 (AED-CONF-74-085-002)
GIESSEN UNIV. (F.R. GERMANY). INST. FUER ANGEWANDTE PHYSIK
Influence of neutron irradiation on critical data of type II superconductors, 30:30063 (AED-CONF-74-089-006)
Proximity effect on thin NbN-layers, 30:30805 (AED-CONF-74-089-005)
GOODYEAR ATOMIC CORP., PIKETON, OHIO (USA)
Portsmouth Gaseous Diffusion Plant environmental monitoring report, 1973, 30:29346 (GAT-781)
GOSUDARSTVENNYJ KOMITET PO ISPOL'ZOVANIYU ATOMNOJ EHNERGII SSSR, MOSCOW. INST. ATOMNOJ EHNERGII
Application of a conformal transformation group for relativistic theories, 30:31142 (IAE-2306)
Calculation of inelastic transition cross sections on basis of spectral line broadening theory, 30:30520 (IAE-2269)
Intensity fluctuations of γ-transitions from the (anti n,γ) reaction, 30:30978 (IAE-2289)
Investigation into radiation defects in irradiated pyrographite, 30:30090 (IAE-2266)
Isotopic ordering in CeD_2H, 30:29008 (IAE-2309)
Magic nuclei theory, 30:30627 (IAE-2286)
Measurement of neutron temperature in water by differential and integral methods, 30:30844 (IAE-2274)
Neutron slowing-down in ice and polyethylene at low temperatures, 30:30843 (IAE-2271)
GOSUDARSTVENNYJ KOMITET PO ISPOL'ZOVANIYU ATOMNOJ EHNERGII SSSR, MOSCOW. INST. TEORETICHESKOJ I EHKSPERIMENTAL'NOJ FIZIKI
Analysis of $K_1^0K_1^0$ system in the $\pi^-p \to nK^0$ anti K^0 reaction at 40 GeV/c, 30:30730 (ITEF-31)
GOSUDARSTVENNYJ KOMITET PO ISPOL'ZOVANIYU ATOMNOJ EHNERGII SSSR, SERPUKHOV. INST. FIZIKI VYSOKIKH EHNERGIJ
Analysis of data on multiparticle production in pp-interactions from 13 up to 300 GeV, 30:30598 (IFVE-SPK-73-69)
GULF STATES UTILITIES CO., BEAUMONT, TEX. (USA)
Blue Hills Station, Units 1 and 2. License application, 30:31319 (DOCKET-50510-1)

H

HAHN-MEITNER-INSTITUT FUER KERNFORSCHUNG BERLIN G.M.B.H. (F.R. GERMANY). BEREICH DATENVERARBEITUNG UND ELEKTRONIK
Use of the CAMAC system for on-line data processing in medicine, 30:31338 (HMI-B-149)
HANFORD ENGINEERING DEVELOPMENT LAB., RICHLAND, WASH. (USA)
Fabrication, irradiation, and postirradiation examination of mixed oxide fuel pin PNL-3-8, 30:31231 (HEDL-TME-74-37)
HARRY DIAMOND LABS., WASHINGTON, D.C. (USA)
Analysis of the ground configuration of trivalent thulium in single-crystal yttrium vanadate, 30:30487 (AD-776343)
HUGHES RESEARCH LABS., MALIBU, CALIF. (USA)
Advanced ion source. Final report, 21 March--21 June 1973 on Phase 1, 30:30473 (AD-772833)

I

ILLINOIS UNIV., URBANA (USA)
Measurement of parity violation in proton--proton scattering at 15 MeV, 30:30599 (LA-UR-74-1333)
Measurement of internal conversion cascading in ${}^{235}U$ fission fragments, 30:31012
Stress--velocity relations for dislocations in niobium, 30:29976 (AD-776621)
INDIANA UNIV., BLOOMINGTON (USA)
Study of particle spectra and correlations in the reaction $\pi^+ + p \to n(forward) + (2\pi,4\pi,6\pi)$ at 8.4 GeV/c, 30:30613 (COO-1428-391(App.A-2))
INSTITUT FUER REAKTORSICHERHEIT DER TECHNISCHEN UEBERWACHUNGS-VEREINE E.V., KOELN (F.R. GERMANY)
Heat pipe work in Europe, 30:31422 (IKE-5-175)
INSTITUTE FOR ADVANCED STUDY, PRINCETON, N.J. (USA)
General derivation of Baecklund transformations from inverse scattering problems, 30:30782 (COO-3237-40)
INSTITUTO DE ENERGIA ATOMICA, SAO PAULO (BRAZIL)
Application of activation analysis to the determination of pollutants in the atmosphere, 30:28914 (IEA-326)
Application of neutron activation analysis to the determination of gold in minerals, 30:28913 (IEA-316)
INSTITUTUL DE FIZICA ATOMICA, BUCHAREST (ROMANIA)
Landau diamagnetism, 30:31421 (IFA-FT-109-1974)
One- and two-nucleon transfer reactions on deformed nuclei, 30:31021 (IFA-FT-108-1974)
Physical quantities the numerical values of which will be included in the evaluated microscopic nuclear data library ''DANEM-I'' from the I.A.P., 30:30846 (IFA-DNDR-9-1974)

  - Programs for experimental data processing on PDP-8/I computer, 30:29614 (IFA-CRD-57-1974)
  - Resolution function for the rotating-crystal spectrometer, 30:29558 (IFA-FN-44-1974)
  - Resolution of slow neutron spectrometers. I. General method to calculate the resolution function. II. Resolution function for time of flight diffractometry, 30:29559 (IFA-FN-45-1974)
  - Software extended floating-point feature, 30:31342 (MC-19-1974)
  - Structure of the evaluated microscopic nuclear data library ''DANEM-I'' from the I.A.P., 30:30845 (IFA-DNBR-8-1974)
  - Zeros of triple scattering parameters and spin--parity determination of a resonance, 30:31020 (IFA-FT-107-1974)
- INTERNATIONAL ATOMIC ENERGY AGENCY, VIENNA (AUSTRIA)
  - Thermal discharges at nuclear power stations. Their management and environmental impacts. A report prepared by a group of experts as the result of a panel meeting held in Vienna, 23--27 October 1972, 30:31252 (STI/DOC-10/155)
- INTERNATIONAL CENTRE FOR THEORETICAL PHYSICS, TRIESTE (ITALY)
  - Bose distribution and the Lorentz contracted geometric model, 30:30751 (IC-73-6)
  - Polarization of the resonance lines of lithium and sodium atoms by electron impact, 30:30521 (IC-73-19)
  - Possibility of producing polarized photons by Compton scattering of polarized relativistic electrons, 30:30648 (IC-73-131)
- INTERUNIVERSITAIR REACTOR INSTITUUT, DELFT (NETHERLANDS)
  - RKSPROG: a computer program for inelastic cold neutron scattering time-of-flight measurements, 30:30847 (IRI-132-73-03)
- IOANNINA UNIV. (GREECE). DEPT. OF PHYSICS
  - Meson electromagnetic decays from SU(4)/sub w/ and generalized vector dominance, 30:30650 (NP-20072)
- IOWA ELECTRIC LIGHT AND POWER CO., CEDAR RAPIDS (USA)
  - Duane Arnold Energy Center. Semiannual operating report, February 22--June 30, 1974, 30:31318 (DOCKET-50331-277)
- IOWA STATE UNIV. OF SCIENCE AND TECHNOLOGY, AMES (USA). COMPUTATION CENTER
  - PL/I based multi-tasking operating system, 30:31340 (IS-M-18)
- IOWA UNIV., IOWA CITY (USA). DEPT. OF PHYSICS AND ASTRONOMY
  - Thermal and suprathermal plasma densities in the outer magnetosphere. Progress report, 30:30449 (AD-776660)

J

- JAPAN ATOMIC ENERGY RESEARCH INST., TOKYO
  - Convergence acceleration algorithms of the iterative methods used in nuclear reactor analysis codes, 30:31272 (JAERI-M-5590)
  - PRELUDE-2: seismic response analysis code for block-type fuel core, 30:31247 (JAERI-M-5560)
  - Present research of atomic energy safety, 30:31244 (AEC-tr-7569)
- JOHNS HOPKINS UNIV., BALTIMORE, MD. (USA). SCHOOL OF MEDICINE
  - Biologic considerations in anatomic imaging with radionuclides. Progress report, July 1973--June 1974, 30:29832 (COO-2427-4)
- JOINT COMMITTEE ON ATOMIC ENERGY (U.S. CONGRESS), WASHINGTON, D.C.
  - AEC omnibus legislation, 1974. Report by the Joint Committee on Atomic Energy, Ninety-Third Congress, Second Session, Senate, 30:31328
  - AEC omnibus legislation, 1974. Report by the Joint Committee on Atomic Energy, Ninety-Third Congress, Second Session, House of Representatives, 30:31329
  - Revising and amending the Price--Anderson Indemnity Provisions of the Atomic Energy Act of 1954, as amended. Report by the Joint Committee on Atomic Energy, Ninety-Third Congress, Second Session, Senate, 30:31330
- JOINT INST. FOR NUCLEAR RESEARCH, DUBNA (USSR). LAB. OF HIGH ENERGY
  - K/sub L/^{0} + K/sub S/^{0} incoherent regeneration on atomic electrons at high energies and electric radius of K^0 meson, 30:30592 (JINR-E2-7402)
  - Multiplicity and correlations of secondary particles produced in π^---^{12}C collisions at 40 GeV/c, 30:30675 (JINR-P1-7523)
- JOINT INST. FOR NUCLEAR RESEARCH, DUBNA (USSR). LAB. OF NEUTRON PHYSICS
  - Hematite phase diagram in a magnetic field. I. Low-temperature modification, 30:31392 (JINR-P14-7974)
- JOINT INST. FOR NUCLEAR RESEARCH, DUBNA (USSR). LAB. OF THEORETICAL PHYSICS
  - Construction of nonlocal quantum electrodynamics of bosons with spin 0 and 1, 30:31144 (JINR-P2-7432)
  - High-energy scattering of vector particles by external electromagnetic field, 30:30649 (JINR-P2-7511)
  - Possible description of the rho resonance in the simplest model of the $\pi\pi$-interaction, 30:30718 (JINR-P2-7502)
  - Selfconsistent calculation of the Green's functions in the Hubbard model, 30:31132 (JINR-P4-7225)
  - Some relations between the types of the generating systems of Abelian groups and their direct summands, 30:31133 (JINR-P5-7344)
- JUNTA DE ENERGIA NUCLEAR, MADRID (SPAIN)
  - Radiomimeticity of the system H_2O_2/Fe(II) on nucleic acid components. Kinetic study, 30:29649 (JEN-284)
  - Structural study of DNA discontinuities by enzymatic polymerization, 30:29650 (JEN-286)

K

- KAISERIN-ELISABETH-SPITAL, VIENNA (AUSTRIA). LUDWIG BOLTZMANNINSTITUT FUER NUKLEARMEDIZINISCHE GASTROENTEROLOGIE
  - Liver studies with various radioactive tracers and methods, 30:29831 (CONF-740708-52)
- KARLSRUHE UNIV. (TH) (F.R. GERMANY). INST. FUER CHEMISCHE TECHNIK
  - Extension of quantitative electron beam microanalysis to solids containing light elements, 30:28968 (AED-CONF-74-084-007)
- KERNFORSCHUNGSANLAGE JUELICH G.M.B.H. (F.R. GERMANY)
  - Changes of dimensions, modulus of elasticity and heat conductivity during re-graphitization by neutron irradiation, 30:30089 (AED-CONF-74-206-001)
  - Ion--x-ray coincidence experiments in slow Ne$^+$--Ne collisions, 30:30517 (AED-CONF-74-085-001)
- KERNFORSCHUNGSANLAGE JUELICH G.M.B.H. (F.R. GERMANY). INST. FUER CHEMISCHE TECHNOLOGIE
  - Laboratory and hot-cell studies concerning the in-line polarographic determination of uranium in the aqueous waste stream of the KFA-TBP 23/25 process, 30:28941 (JUL-1063-CT)
- KERNFORSCHUNGSANLAGE JUELICH G.M.B.H. (F.R. GERMANY). INST. FUER FESTKOERPERFORSCHUNG
  - Theory of multi-variable correlation techniques for time-of-flight experiments, 30:29560 (JUL-1050-FF)
- KERNFORSCHUNGSANLAGE JUELICH G.M.B.H. (F.R. GERMANY). INST. FUER REAKTORENTWICKLUNG
  - Nuclear district-heating and nuclear long-distance energy, 30:31305 (JUL-1077)
- KERNFORSCHUNGSZENTRUM KARLSRUHE (F.R. GERMANY). ABT. STRAHLENSCHUTZ UND SICHERHEIT
  - In-vivo measurement of the gamma and neutron dose rate on patients with ^{238}Pu pacemakers implanted, 30:29704 (KFK-1851)
- KERNFORSCHUNGSZENTRUM KARLSRUHE (F.R. GERMANY). INST. FUER ANGEWANDTE KERNPHYSIK
  - Temperature dependence of the lattice distortion in the one-dimensional conductor $K_2Pt[CN]_4Br_3$ x $3D_2O$, 30:31365 (AED-CONF-74-089-024)
- KERNFORSCHUNGSZENTRUM KARLSRUHE (F.R. GERMANY). INST. FUER ANGEWANDTE SYSTEMTECHNIK UND REAKTORPHYSIK
  - Calculation of the effects of fission gas in a LMFBR, for the analysis of an unprotected overpower transient, 30:31225 (KFK-1990)
  - Experiments in pure uranium lattices with unit /sub infinity/. Assemblies SNEAK-8/8Z; UK 1 and UK 5 in ERMINE and HARMONIE, 30:31270 (EURFNR-1189)
- KERNFORSCHUNGSZENTRUM KARLSRUHE (F.R. GERMANY). INST. FUER MATERIAL- UND FESTKOERPERFORSCHUNG
  - Creep-rupture behavior of the alloy Inconel 625 in three different pretreatment states, 30:29978 (EURFNR-1163)
- KERNFORSCHUNGSZENTRUM KARLSRUHE (F.R. GERMANY). INST. FUER NEUTRONENPHYSIK UND REAKTORTECHNIK
  - Contribution to the mutual resonance shielding of ^{238}U and ^{239}Pu, 30:31009 (EURFNR-1162)
  - Measurement and calculation of neutron spectra at a sodium--iron interface, 30:30848 (KFK-1959)
  - Transport of core materials during accidents in LMFBRs (slumping), 30:31249 (KFK-1935)
- KERNFORSCHUNGSZENTRUM KARLSRUHE (F.R. GERMANY). INST. FUER RADIOCHEMIE
  - Determination of mineral-oil in the helium-circuit of a refrigeration-plant, 30:31393 (KFK-1978)
- KERNFORSCHUNGSZENTRUM KARLSRUHE (F.R. GERMANY). PROJEKT NUKLEARE SICHERHEIT
  - Annual colloquium 1973 of the Project Nuclear Safety, 30:31245 (AED-CONF-73-686-000)
  - Second biannual report 1973, 30:31248 (KFK-1908)
- KOELN UNIV. (F.R. GERMANY)
  - Ion--x-ray coincidence experiments in slow Ne$^+$--Ne collisions, 30:30517 (AED-CONF-74-085-001)
- KOELN UNIV. (F.R. GERMANY). ENERGIEWIRTSCHAFTLICHES INST.
  - The impact of nuclear power plants on the economic structure, 30:31304 (DEU-74-2)
- KOZPONTI FIZIKAI KUTATO INTEZET, BUDAPEST (HUNGARY)
  - D_2-type representation of the conformal group extended by reflections, 30:30628 (KFKI-74-49)
  - Field theories without Ward-identities, 30:31145 (KFKI-74-46)
  - Particles and fields in space. Proceedings of the summer school, Balatonfured, 5--15 June 1973, 30:30160 (CONF-730693-)
- KRAFTWERK UNION A.G., ERLANGEN (F.R. GERMANY)
  - Differential magnetic analysis of the radiation-induced diffusion in nickel-beryllium alloys, 30:30064 (AED-CONF-74-089-037)
- KUNGLIGA TEKNISKA HOEGSKOLAN, STOCKHOLM (SWEDEN). INSTITUTIONEN FOER KAERNKEMI
  - Research report for 1972--1973, 30:28972 (TRITA-KKE-7403)

L

- LOCKHEED MISSILES AND SPACE CO., PALO ALTO, CALIF. (USA). LOCKHEED PALO ALTO RESEARCH LAB.
  - Study of basic processes in radiation damage. Final report, 1 April 1971--30 November 1973, 30:30061 (AD-777728)
- LONG ISLAND LIGHTING CO., HICKSVILLE, N.Y. (USA)
  - Jamesport Nuclear Power Station, Units 1 and 2. License application, 30:31320 (DOCKET-STN-50516-1)
- LOS ALAMOS SCIENTIFIC LAB., N.MEX. (USA)
  - Computations on the parameter values inside of the E.M. source, 30:29310 (LAMS-2610)
  - Control system design and simulation for solar heated structures, 30:31325 (LA-UR-74-1085)
  - Design and testing of a structurally integrated steel solar collector unit based on expanded flat metal plates, 30:31326 (LA-UR-74-1093)
  - Electronic structure and optical properties of some first row transition metal oxyhalides, 30:31395 (LA-5637-T)
  - Energy and cryoengineering, 30:31324 (LA-UR-74-741)
  - Engineering design study of a Reference Theta-Pinch Reactor (RTPR), 30:29206 (LA-5336)
  - Human experience, 30:29772 (LA-UR-74-1300)
  - Integrating eclipse optics into the AEC Air Force flying laboratory, 30:31423 (LA-UR-74-1167)
  - Magnetically protected first wall for a laser-induced thermonuclear reaction, 30:29207 (LA-5699-MS)
  - Measurement of parity violation in proton--proton scattering at 15 MeV, 30:30599 (LA-UR-74-1333)
  - Model for the CW power output of the HF chemical laser, 30:29266 (LA-5683-MS)
  - New technique for nonlinear optical problems, 30:29153 (LA-5639-MS)
  - Passive environmental neutron dosimeter, 30:29551 (LA-UR-74-1232)
  - Radioisotopes from a medium-energy accelerator: the Clinton P. Anderson Meson Physics Facility radioisotope program, 30:30142 (LA-UR-74-1263)
  - Theory of drift-cone modes of collisionless plasma in cylindrical geometry, 30:29195 (LA-5693-MS)
  - Thomas--Fermi calculation of potential between atoms, 30:30565 (LA-5694-MS)
  - USAEC-DAT dc superconducting power transmission line project at LASL. Progress report, January 1--March 31, 1974, 30:30820 (LA-5684-PR)
  - Ventilation design modifications at Los Alamos Scientific Laboratory major plutonium operational areas, 30:29328 (LA-UR-74-1132)
- LOWELL TECHNOLOGICAL INST., MASS. (USA). RESEARCH FOUNDATION
  - Routine operation of Digisonde at Maynard, Massachusetts. Final report, 1 September 1971--31 August 1972, 30:30410 (AD-776969)
- LUND UNIV. (SWEDEN). FYSISKA INSTITUTIONEN
  - Identification of heavy ions in nuclear emulsions in the hundreds of MeV interval, 30:29493 (LUIP-CR-74-3)

M

- MARYLAND UNIV., COLLEGE PARK (USA). DEPT. OF PHYSICS AND ASTRONOMY
  - High Energy Accelerator and Colliding Beam User Group. Progress report, 30:30575 (TID-26638)
- MARYLAND UNIV., COLLEGE PARK (USA). INST. FOR FLUID DYNAMICS AND APPLIED MATHEMATICS
  - Investigation of universal plasma instabilities. Annual progress report No. 9, 30:29196 (TID-26639)
- MASSACHUSETTS INST. OF TECH., LEXINGTON (USA). LINCOLN LAB.
  - Seismic discrimination. Semiannual technical summary report, 1 July--31 December 1973, 30:29305 (AD-777151)
- MAX-PLANCK-INSTITUT FUER PLASMAPHYSIK, GARCHING
  - Energy and charge distribution of backscattered particles during bombardment of metal surfaces with protons, 30:30474 (AED-CONF-74-089-032)
  - On the energy distribution of electrons in a proton-electron plasma with densities higher than the solid-state density, 30:29173 (IPP-3/12)
- MCDONNELL DOUGLAS ASTRONAUTICS CO., RICHLAND, WASH. (USA). DONALD W. DOUGLAS LABS.
  - Implanted energy conversion system. Annual report, 8 July 1972--8 July 1973, 30:29239 (JUL-73)
- MEDI-PHYSICS, INC., EMERYVILLE, CALIF. (USA)
  - Embryotoxicity of astatine-211, 30:29781 (COO-3268-5)
- MIDWEST RESEARCH INST., KANSAS CITY, MO. (USA)
  - Fatigue and impact resistance of dual-matrix boron--aluminum composites. Final report, 30:29974 (AD-775334)
- MINNESOTA UNIV., ST. PAUL (USA). DEPT. OF ECOLOGY AND BEHAVIORAL BIOLOGY
  - Vertebrate behavior and ecology. Progress report, July 1, 1973--June 30, 1974, 30:31377 (COO-1332-103)
- MISSION RESEARCH CORP., SANTA BARBARA, CALIF. (USA)
  - Direct interaction effects in EMP, 30:29308 (AD-777748)
- MOUND LAB., MIAMISBURG, OHIO (USA)
  - Improved PETN particle size analyses, 30:31426 (MLM-2098)
  - Pulse NMR studies of radiation damage in metal tritides, 30:29689 (MLM-2172(OP))
  - Tritium Effluent Control Project. Progress Report: April--June 1974, 30:29026 (MLM-2171(LD))
- MUENCHEN (F.R. GERMANY)
  - Energy and charge distribution of backscattered particles during bombardment of metal surfaces with protons, 30:30474 (AED-CONF-74-089-032)
  - On the energy distribution of electrons in a proton-electron plasma with densities higher than the solid-state density, 30:29173 (IPP-3/12)
- MUENCHEN (F.R. GERMANY). ABT. FUER STRAHLENHYGIENE
  - Genetic radiation effects, 30:29700 (AED-CONF-74-030-004)

N

- NATIONAL AERONAUTICS AND SPACE ADMINISTRATION, CLEVELAND, OHIO (USA). LEWIS RESEARCH CENTER
  - Interlaboratory comparison of chemical analysis of uranium mononitride, 30:28942 (N-74-18812)
  - Internal friction peaks observed in explosively deformed polycrystalline Mo, Nb, and Cu, 30:29980 (N-74-19371)
  - Internal friction measurement in high purity tungsten single crystal, 30:29979 (N-74-19370)
  - Trace-element analysis of 1000 environmental samples per year using instrumental neutron activation analysis, 30:28915 (N-74-20335)
- NATIONAL LEAD CO. OF OHIO, CINCINNATI (USA)
  - Feed Materials Production Center environmental monitoring annual report for 1973, 30:29347 (NLCO-1109)
- NATIONAL OCEANIC AND ATMOSPHERIC ADMINISTRATION, BOULDER, COLO. (USA)
  - Galactic cosmic ray modulation in the outer solar system: solar wind consequences, 30:30340 (COM-74-50233)
  - Some active magnetosphere experiments to be performed by the Plasma Physics and Environmental Perturbation Laboratory, 30:30450 (COM-74-50228)
- NATIONAL OCEANIC AND ATMOSPHERIC ADMINISTRATION, IDAHO FALLS, IDAHO (USA). AIR RESOURCES LAB.
  - Program descriptions: supplement to mesoscale wind fields and transport estimates determined from a network of wind towers, 30:31343 (NOAA-TM-ERL-ARL-43)
- NATIONAL OCEANIC AND ATMOSPHERIC ADMINISTRATION, LAS VEGAS, NEV. (USA). AIR RESOURCES LAB.
  - Numerical prediction of the mesoscale transport of atmospheric effluents: philosophy and morphology of experimental models for predicting the wind and potential radiological fields over the Nevada Test Site, 30:29377 (COM-74-10799)
- NAUCHNO-ISSLEDOVATEL'SKIJ INST. EHLEKTROFIZICHESKOJ APPARATURY, LENINGRAD (USSR)
  - High-current electron accelerator with supply by inductive storage, 30:30121 (LA-tr-74-30)
- NAVAL ORDNANCE LAB., WHITE OAK, MD. (USA)
  - Multiphoton transitions in helium between 1S and 2S levels, 30:30488 (AD-777042)
- NAVAL RESEARCH LAB., WASHINGTON, D.C. (USA)
  - Coherent synchrotron radiation from an intense relativistic electron beam, 30:30580 (AD-773442)
  - Cross sections of proton--nucleus interactions at high energies, 30:30854 (AD-777030)
  - Irradiation effects on reactor structural materials. Semiannual progress report, 1 August 1973--31 January 1974, 30:30060 (AD-777433)
  - Prevention and control of subcritical crack growth in high-strength metals, 30:29981 (NRL-Report-7780)
  - Rock magnetites with positive anisotropy constants at 300°K, 30:31389 (CONF-740644-1)
- NEBRASKA PUBLIC POWER DISTRICT, COLUMBUS (USA)
  - Cooper Nuclear Station. Semiannual operating report, January--June 1974, 30:31317 (DOCKET-50298-233)
- NEW YORK STATE VETERINARY COLL., ITHACA (USA). DEPT. OF PHYSICAL BIOLOGY
  - Agricultural impacts of nuclear power generation in New York State, 30:29438 (COO-3167-102)
  - Phase I. Radiation and radioisotope studies with laboratory and domestic animals, 30:29417 (COO-3167-102)
  - Progress report, June 1, 1973--May 31, 1974, 30:29416 (COO-3167-102)
- NEW YORK UNIV., N.Y. (USA). AEC COMPUTING AND APPLIED MATHEMATICS CENTER
  - Connection between singular perturbations and singular arcs. Part 2. A theory for the linear regulator, 30:31336 (COO-3077-44)
- NIAGARA MOHAWK POWER CORP., SYRACUSE, N.Y. (USA)
  - Nine Mile Point Nuclear Station, Unit 1. Semiannual report of operation, January--June 1974, 30:31313 (DOCKET-50220-315)

O

- OAK RIDGE NATIONAL LAB., TENN. (USA)
  - DuoPIGatron II ion source, 30:29209 (ORNL-TM-4657)
  - Equilibrium and stability of elliptical cross section tokamak, 30:29210 (ORNL-TM-4666)
  - Gamma-ray production due to neutron interactions with **Zn and the level structure of **Zn, 30:30935 (ORNL-4985)
  - Ground level air concentrations of dust particles downwind from a tailings area during a typical windstorm, 30:29380 (ORNL-TM-4375)

- LMFBR-37-fuel-element shipping cask simulation: test assembly operation and data, 30:30114 (ORNL-TM-3992)
- ORRMIS: Oak Ridge Regional Modeling Information System. Part I, 30:29456 (ORNL-NSF-EP-73)
- Program for computing the dispersion of airborne contaminants, 30:29381 (ORNL-TM-4674)
- Quarterly progress report on reactor safety programs sponsored by the Division of Reactor Safety Research for April--June 1974, 30:31251 (ORNL-TM-4655(Vol.2))
- Quarterly progress report on reactor safety programs sponsored by the Division of Reactor Safety Research for April--June 1974. I. Light-water-reactor safety, 30:31250 (ORNL-TM-4655(Vol.1))
- Response of spermatogonia of the mouse to hycanthone, and a comparison with the effect of γ rays, 30:29735 (CONF-731222-1)
- Rock magnetites with positive anisotropy constants at 300°K, 30:31389 (CONF-740644-1)
- SAFT: structural analysis of forest trees, 30:31337 (EDFB-IBP-74-4)
- Shielding design calculations for ORMAK--F/BX, 30:29208 (ORNL-TM-4619)
- Shielding benchmark problems, 30:31126 (ORNL-RSIC-25(Suppl.2))
- Solubility and stability of structural metal difluorides in molten fluoride mixtures, 30:29002 (ORNL-TM-760)
- Spectroscopic study in the vacuum ultraviolet of a neon plasma in ELMO, 30:29158 (ORNL-TM-4672)
- Subroutine CAUCHY: complex roots of a function using a CAUCHY integral technique, 30:31344 (ORNL-TM-4588)
- Symposium on the effect of hot water of thermoelectric plants on the hydrology and biology of reservoirs (abstracts) March 24--26, 1971, Borok, USSR, 30:29463 (ORNL-tr-2781)

- OAK RIDGE Y-12 PLANT, TENN. (USA)
  - Electrochemistry of aqueous corrosion: uranium and its alloys, 30:29944 (Y-1949)
  - Safety analysis report for packaging (Oak Ridge Y-12 Plant Model VCD package for enriched uranium solution), 30:30115 (Y-DD-155)
  - Safety analysis report for packaging (Oak Ridge Y-12 Plant foamglas shipping package for enriched uranium), 30:30116 (Y-DD-156)
  - Thermal conductivity of carbon foam, 30:31413 (Y-1955)
- OESTERREICHISCHE STUDIENGESELLSCHAFT FUER ATOMENERGIE G.M.B.H., SEIBERSDORF. FORSCHUNGSZENTRUM
  - Mass-spectrometric determination of neutron capture cross-sections of the rare earth isotopes, 30:30977 (AEC-tr-7574)
- OMAHA PUBLIC POWER DISTRICT, NEBR. (USA)
  - Fort Calhoun Station, Unit 1. Semiannual report, January--June 1974, 30:31316 (DOCKET-50285-249)
- ORGANIZATION FOR ECONOMIC CO-OPERATION AND DEVELOPMENT, 75 - PARIS (FRANCE)
  - List of computer programs for neutron cross section calculations and analysis, 30:30849 (NEANDC-97/U)

P

- PACIFIC GAS AND ELECTRIC CO., SAN FRANCISCO, CALIF. (USA)
  - Humboldt Bay Power Plant, Unit 3. Semiannual operations report, January--June 1974, 30:31312 (DOCKET-50133-195)
- PADUCAH GASEOUS DIFFUSION PLANT, KY. (USA)
  - Environmental monitoring report, calendar year 1973, 30:29351 (UCC-ND-279)
- PARIS-2 UNIV., 75 (FRANCE)
  - Safeguarding the peaceful uses of nuclear energy by states, 30:30104 (FRNC-TH-50)
- PHILIPPINE ATOMIC ENERGY COMMISSION, DILIMAN, QUEZON CITY
  - Activation analysis: a literature search, 30:28919 (PAEC(A)-7332(Suppl.1))
- PHYSIKALISCH-TECHNISCHE BUNDESANSTALT, BRAUNSCHWEIG (F.R. GERMANY)
  - Scientific publications, reports and external lectures in 1973 compiled by Referat Schrifttum, 30:31359 (PTB-L-2)
- PICATINNY ARSENAL, DOVER, N.J. (USA)
  - Experimental neutron radiography system using californium-252. Final report, 30:29295 (AD-776900)
- PRINCETON UNIV., N.J. (USA)
  - Beta asymmetry of ^{35}Ar and the deduced value of the vector coupling constant, 30:30902
  - Piezoelectric mechanical-micropipette stimulator. Technical report No. 10, 30:31378 (NYO-3406-18)
- PUERTO RICO NUCLEAR CENTER, MAYAGUEZ
  - Recent changes of the foraminiferal assemblages of Jobos Bay and surroundings, Puerto Rico, 30:31376 (CONF-740663-1)
- PUERTO RICO UNIV., MAYAGUEZ
  - Recent changes of the foraminiferal assemblages of Jobos Bay and surroundings, Puerto Rico, 30:31376 (CONF-740663-1)
- PURDUE UNIV., LAFAYETTE, IND. (USA)
  - Annual progress report for the period June 1, 1973--May 31, 1974, 30:30597 (COO-1428-382)
  - Annual report for period October 1, 1973--September 30, 1974, 30:30574 (COO-1428-391)
- PURDUE UNIV., LAFAYETTE, IND. (USA). DEPT. OF PHYSICS
  - Annual progress report, task B, for June 1, 1973--May 31, 1974, 30:30626 (COO-1428-389)
- PURDUE UNIV., LAFAYETTE, IND. (USA). SCHOOL OF MATERIALS ENGINEERING
  - Transport and thermodynamic properties of solids. Progress report, September 1, 1973--August 31, 1974, 30:31390 (COO-1436-41)

R

- R AND D ASSOCIATES, SANTA MONICA, CALIF. (USA)
  - Angular momentum coupling, potential curves and radiative selection rules for heavy diatomic molecules, with particular reference to Kr_2 and Kr_2^+, 30:31459 (UCRL-13599)
- REYNOLDS ELECTRICAL AND ENGINEERING CO., INC., LAS VEGAS, NEV. (USA)
  - Operation TOGGLE: on-site radiological safety report, July 1972--June 1973, 30:29379 (NVO-410-25)
  - Operation WHETSTONE: on-site radiological safety report, July 1964--June 1965, 30:29378 (NVO-410-24)
- RINGSDORFF-WERKE G.M.B.H., BONN-BAD GODESBERG (F.R. GERMANY)
  - Use of fine-grained electrographite in metal working, 30:31383 (AED-CONF-74-254-001)
- RIO DE JANEIRO UNIV. (BRAZIL). COORDENACAO DOS PROGRAMMAS DE POS-GRADUACAO DE ENGENHARIA
  - Corrosion study of the superplastic alloys 70/30 and 80/20 zinc aluminum in a humid atmosphere, 30:31391 (COPPE-TP-8/72)
  - Spectroscopy of Auger electrons and its use in metallurgy, 30:31420 (COPPE-TP-6/72)

S

- SALFORD UNIV. (UK)
  - Ion implantation of semiconductors, metals, and alloys. Interim report No. 7, 1 September 1971--31 August 1973, 30:30088 (AD-774654)
- SANDIA LABS., ALBUQUERQUE, N.MEX. (USA)
  - Alarm communications and display segment (ACADS). Technical order publications plan (CDRL item 20), 30:31428 (SAND-74-0149)
  - Archiving guide to microbarograph records of nuclear and chemical explosion tests, 30:29314 (SLA-74-0210)
  - Dielectric strength of x-cut quartz after thermally induced stress cycling: application to understanding the Sandia Quartz gauge, 30:31396 (SAND-74-0135)
  - Fault Tree Drawing Program users instructions, 30:31346 (SLA-73-0409)
  - Human error quantification, 30:31360 (SCR-610)
  - Instrumental limitation to the rate of kinetic processes measurable by time-resolved mass spectrometry, 30:31368 (SLA-73-7063)
  - J-integral as a failure criterion for a Borsic--Al composite, 30:29690 (SAND-74-0193)
  - Measurement of the radiation inactivation of attenuated poliovirus by the plaque assay technique, 30:29676 (SLA-74-0065)
  - Metallurgical processing and pulsed reactor fuel performance, 30:29982 (SLA-73-1121)
  - Nanosecond time resolved x-ray diagnostics of relativistic electron beam initiated events, 30:29159 (SAND-74-5262)
  - Performance characteristics of Sandia Laboratories 5.8-metre-diameter explosively driven blast simulator, 30:31431 (SLA-74-5239)
  - Range-scan radar images and their application to map-matching estimation of location, 30:31429 (SAND-74-0153)
  - Rf hybrid microcircuit soldering techniques, 30:31397 (SLA-73-1073)
  - Spectral analysis of x rays from laser-induced plasmas, 30:29193 (SLA-74-5242)
  - Stiffness and non-stiff differential equation solvers, 30:31345 (SAND-74-5236)
  - Test of a magnetic bearing for optical scanner applications, 30:31430 (SLA-74-0347)
- SCIENCE RESEARCH COUNCIL, CHILTON (UK). RUTHERFORD LAB.
  - Method for the calculation of the magnetostatic field from a wide class of current geometries, 30:29211 (RL-74-077)
  - Physics with an electron--positron storage ring of beam energy E = 14 GeV, 30:30581 (RL-74-098)
- SERVICE CENTRAL DE PROTECTION CONTRE LES RAYONNEMENTS IONISANTS, 78 - LE VESINET (FRANCE)
  - Annex to monthly report, February 1974. Detail of results of measurement, 30:29350 (SCPRI(RM)-2-1974(Suppl.))
  - Report of activity, February 1974, 30:29349 (SCPRI(RM)-2-1974)
- SOUTHEASTERN RADIOLOGICAL HEALTH LAB., MONTGOMERY, ALA. (USA)
  - Off-site surveillance. Final report. Report on Project Dribble, Salmon Event, Tatum Salt Dome, Mississippi, 22 October 1964, 30:29345 (AD-629357)
- STANFORD UNIV., CALIF. (USA)
  - Resonance integrals of uranium-235/uranium-238 mixtures, 30:31013
- STANFORD UNIV., CALIF. (USA). DEPT. OF PHYSICS
  - Moessbauer effect and related phenomena. Final report, 1 November 1964--1 January 1972, 30:30951 (AD-773622)

STEINMUELLER (L.U.C.) G.M.B.H., GUMMERSBACH (F.R. GERMANY)
- Solution of the problem of designing liners for prestressed pressure vessels, 30:29264 (AED-CONF-73-600-001)

STICHTING REACTOR CENTRUM NEDERLAND, PETTEN
- Fast reactor programme. First quarter 1974 progress report, 30:31226 (RCN-212)

STICHTING VOOR FUNDAMENTEEL ONDERZOEK DER MATERIE, JUTPHAAS (NETHERLANDS). INSTITUUT VOOR PLASMA-FYSICA
- Arc discharges in a curved magnetic field, 30:29154 (NP-20140)

STUTTGART UNIV. (TH) (F.R. GERMANY). INST. FUER KERNENERGETIK
- Calculation of correction factors for pulsed neutron measurements in the ITR critical experiment, 30:31232 (IKE-6-79d)
- Investigations on the shielding of power reactors, 30:31271 (IKE-6-75d)

T

TANDEMACCELERATORLABORATORIET, UPPSALA (SWEDEN)
- Annual report, 1973, 30:30952 (NP-20122)

TECHNISCHE HOCHSCHULE AACHEN (F.R. GERMANY)
- Theory of multi-variable correlation techniques for time-of-flight experiments, 30:29560 (JUL-1050-FF)

TECHNISCHE HOCHSCHULE AACHEN (F.R. GERMANY). 3. PHYSIKALISCHES INST.
- Measurement of the energy dependence of the decay matrix element for K^0sub(L) $\rightarrow \pi^+ \pi^- \pi^0$, 30:30593 (PITHA-64(1972))

TECHNISCHE UNIV. DARMSTADT (F.R. GERMANY). FACHBEREICH ANORGANISCHE CHEMIE UND KERNCHEMIE
- Isotope effects in the boundary layer of inorganic solutions, 30:29007 (AED-CONF-74-084-004)
- Separation of radionuclides using alkyl radicals, 30:29083 (AED-CONF-74-084-002)

TECHNISCHE UNIV. DARMSTADT (F.R. GERMANY). INST. FUER REAKTORTECHNIK
- Measurements of persistence length and temperature dependence of the radius of gyration in bulk atactic polystyrene, 30:31364 (AED-CONF-74-072-002)
- Radiation damage in reactor structural materials - Formation of pores and its simulation, 30:30062 (AED-CONF-74-044-009)

TECHNISCHE UNIV. MUENCHEN (F.R. GERMANY)
- 10 years: Laboratory for Reactor Control and Plant Safety, 30:31296 (NP-20130)

TECHNISCHE UNIV. MUENCHEN, GARCHING (F.R. GERMANY). INST. FUER RADIOCHEMIE
- Nondestructive determination of boron in glasses using a ^{241}Am--Be neutron source, 30:28912 (AED-CONF-73-479-009)

TEL AVIV UNIV. (ISRAEL)
- Generalized approximative procedures in the many body problem. Final technical report, 30:31130 (AD-776408)

TELEDYNE GEOTECH, ALEXANDRIA, VA. (USA)
- Regional attenuation of short-period P and S waves in the United States, 30:29303 (AD-776672)

TENNESSEE UNIV., TULLAHOMA (USA). SPACE INST.
- Mechanical properties of metal matrix composites subjected to cyclic temperature changes. Annual report, 1 July 1972--30 June 1973, 30:29973 (AD-774890)

TEXAS INSTRUMENTS, INC., DALLAS (USA)
- Extended array evaluation program. Special report No. 5. Selection of reference waveforms for matched filter processing of long period signals from seismic events, 30:29304 (AD-776815)
- Extended array evaluation program. Quarterly report No. 6, 1 July--30 September 1973, 30:29306 (AD-777315)

THOMAS JEFFERSON UNIV., PHILADELPHIA, PA. (USA). STEIN RESEARCH CENTER
- Embryotoxicity of astatine-211, 30:29781 (COO-3268-5)

TOKYO UNIV. (JAPAN)
- Development of sodium flowmeter by real time correlation technique. II. Measurement of flow velocity in mockup fuel assembly, 30:31224 (JAPFNR-154)

TOURS UNIV., 37 (FRANCE). LAB. DE BIOPHYSIQUE
- Advantages of theoretical models in interpreting cerebral transit curves, 30:29830 (CONF-740708-20)

TRIER-KAISERSLAUTERN UNIV., KAISERSLAUTERN (F.R. GERMANY). FACHBEREICH PHYSIK
- Highly resolved electron energy loss spectroscopy of amorphous germanium and silicon layers, 30:31381 (AED-CONF-74-089-025)

TRW SYSTEMS GROUP, REDONDO BEACH, CALIF. (USA)
- Blast wave boundary layer measurements. Final report, September 1971--August 1973, 30:29307 (AD-777580)

TRW, INC., CLEVELAND, OHIO (USA)
- Mechanical behavior of metal matrix composites. Final report, 1 April 1972--30 April 1973, 30:29975 (AD-775359)

U

UKAEA REACTOR GROUP, SPRINGFIELDS
- Interaction of thermal and catalytic processes in the gasification of graphite in CO_2 mixtures, 30:29035 (TRG-Report-2434)

UKAEA RESEARCH GROUP, ABINGDON. CULHAM LAB.
- Bundle divertors and topology, 30:29204 (CLM-R-132)
- Computation of MHD equilibria in Tokamak, 30:29179 (CLM-R-133)
- Summary of containment experiments on the PROTO--CLEO stellarator, 30:29151 (CLM-R-135)

UKAEA RESEARCH GROUP, HARWELL. ATOMIC ENERGY RESEARCH ESTABLISHMENT
- Assessment of known independent yields and the calculation of those unknown in the fission of ^{232}Th, ^{233}U, ^{235}U, ^{238}U, ^{239}Pu, ^{240}Pu, and ^{241}Pu, 30:31008 (AERE-R-7680)
- Measurements of three velocity components and their correlations in a model furnace with and without combustion, 30:31414 (AERE-R-7776)

UKAEA WEAPONS GROUP, ALDERMASTON. ATOMIC WEAPONS RESEARCH ESTABLISHMENT
- Foulness multi-ton air blast simulator. Part 1. Early development: the gun driven facility, 30:29309 (AWRE-O-31/74)

UNION CARBIDE CORP., OAK RIDGE, TENN. (USA). NUCLEAR DIV.
- Environmental monitoring report: United States Atomic Energy Commission, Oak Ridge facilities. Calendar year 1973, 30:29352 (UCC-ND-280)

UNITED AIRCRAFT CORP., EAST HARTFORD, CONN. (USA). RESEARCH LABS.
- High beta capture and mirror confinement of laser-produced plasmas. Semiannual report, January 1, 1974 through July 31, 1974, 30:29152 (COO-2277-4)

UNIVERSIDADE ESTADUAL DE CAMPINAS (BRAZIL). INSTITUTO DE FISICA
- Classical and relativistic Doppler effects, 30:31143 (INIS-mf-1357)

UNIVERSITAET DES SAARLANDES, SAARBRUECKEN (F.R. GERMANY). FACHBEREICH ANGEWANDTE PHYSIK
- Short-range order in liquid lithium-lead alloys, 30:31382 (AED-CONF-74-089-027)

USAEC DIRECTORATE OF LICENSING, WASHINGTON, D.C.
- Preapplication safety evaluation of the gas cooled fast breeder reactor, General Atomic Company. Project No. 456, 30:31323 (TID-26631)

USAEC DIVISION OF REACTOR RESEARCH AND DEVELOPMENT, WASHINGTON, D.C.
- Class 2 valves for liquid metal service, 30:29267 (RDT-E-1-19T(6-74))
- Projections of labor requirements for electrical power plant construction 1974--2000, 30:31306 (WASH-1334)

USAEC HEALTH AND SAFETY LAB., NEW YORK
- HASL procedures manual, 30:28970 (HASL-300(Suppl.2))

USAEC NEVADA OPERATIONS OFFICE, LAS VEGAS
- Absorption, distribution, and excretion of plutonium by dairy cattle, 30:29810 (NVO-AEIC-74-1)
- Analysis of vegetation cover in certain Pu-contaminated areas using aerial photography, 30:29446 (NVO-AEIC-74-1)
- Determination of ^{239}Pu and ^{241}Am in large NAEG vegetation samples, 30:28971 (NVO-AEIC-74-1)
- Distribution and characterization of plutonium in soils from Nevada Test Site, 30:29443 (NVO-AEIC-74-1)
- Distribution and inventory element activities on-NTS and off-NTS, 30:29453 (NVO-AEIC-74-1)
- Distribution of ingested plutonium in chickens and subsequent transport to eggs, 30:29811 (NVO-AEIC-74-1)
- Dynamics of plutonium in desert environments. Nevada Applied Ecology Group progress report as of January 1974, 30:29439 (NVO-AEIC-74-1)
- Ecological studies of vertebrates in plutonium-contaminated areas of the Nevada Test Site, 30:29449 (NVO-AEIC-74-1)
- General statistical considerations in environmental plutonium studies, 30:29418 (NVO-AEIC-74-1)
- Grazing studies on selected plutonium-contaminated areas in Nevada, 30:29448 (NVO-AEIC-74-1)
- In situ optical particle size analysis of ambient aerosol, 30:29617 (NVO-AEIC-74-1)
- In vitro plutonium studies using the artificial rumen and simulated abomasal and intestinal fluids, 30:29809 (NVO-AEIC-74-1)
- Information support for the Nevada Applied Ecology Group, 30:29454 (NVO-AEIC-74-1)
- Measurements of meteorological parameters, 30:29451 (NVO-AEIC-74-1)
- NAEG plutonium study modeling program: plutonium transport and dose estimation model, 30:29455 (NVO-AEIC-74-1)
- REECo field activities and sample logistics in support of the Nevada Applied Ecology Group, 30:29441 (NVO-AEIC-74-1)
- Results and data analysis: resuspension element status report, 30:29452 (NVO-AEIC-74-1)
- Resuspension element status report, 30:29450 (NVO-AEIC-74-1)
- Role of soil microorganisms in the movement of plutonium, 30:29447 (NVO-AEIC-74-1)
- Saltation and creep sampler, 30:29616 (NVO-AEIC-74-1)
- Soil surveys of five plutonium-contaminated areas on the Test Range Complex in Nevada, 30:29442 (NVO-AEIC-74-1)
- Soils element activities, October 1972--September 1973, 30:29440 (NVO-AEIC-74-1)
- Some ecological attributes and plutonium contents of perennial vegetation in Area 13 (NAEG vegetation studies), 30:29445 (NVO-AEIC-74-1)

Statistical analysis of Pu in soil at the Nevada Test Site: some results, 30:29444 (NVO-AEIC-74-1)
Ultra high volume air sampler, 30:29494 (NVO-AEIC-74-1)
USAEC OAK RIDGE OPERATIONS OFFICE, TENN.
Projections of labor requirements for electrical power plant construction 1974--2000, 30:31306 (WASH-1334)
USAEC TECHNICAL INFORMATION CENTER, OAK RIDGE, TENN.
FIND: St. Lucie Plant, Unit 1, 30:31321 (FIND-50335)
FIND: St. Lucie Plant, Unit 2, 30:31322 (FIND-50389)
UTAH UNIV., SALT LAKE CITY (USA). RADIOBIOLOGY DIV.
Alternate methods for administering chelating agents in decorporation therapy, 30:29798 (COO-119-249)
Cortisol metabolism in skin of beagles bearing ^{241}Am: a possible pre-neoplastic change in steroid metabolism, 30:29780 (COO-119-249)
Decorporation of ^{241}Am from bone using DTPA and osteoporotic agents, 30:29799 (COO-119-249)
Decorporation of ^{241}Am in beagles by DTPA, 30:29797 (COO-119-249)
Early hematologic effects of curium and einsteinium in beagles, 30:29779 (COO-119-249)
Early retention and distribution of ^{253}Es by the beagle, 30:29803 (COO-119-249)
Early subcellular distribution of einsteinium in canine livers, 30:29804 (COO-119-249)
Effects of DTPA on tissue cultured fibroblasts, 30:29807 (COO-119-249)
Effects of Phytohemaglutinin-P (PHA-P) on bone cells of the tibial and femoral metaphysis of the rats, 30:29800 (COO-119-249)
Einsteinium studies in beagles, 30:29802 (COO-119-249)
Evaluation of long-term ZnDTPA therapy in beagles, 30:29796 (COO-119-249)
^{210}Pb retention, excretion, and distribution in beagles following intravenous injection, 30:29805 (COO-119-249)
Plutonium, diphosphonates, and bone, 30:29801 (COO-119-249)
Research in radiobiology. Annual report of work in progress in the internal irradiation program, 30:29778 (COO-119-249)
Transuranium elements in gonadal tissue, 30:29806 (COO-119-249)

V

VIRGINIA POLYTECHNIC INST. AND STATE UNIV., BLACKSBURG (USA)
Energy measurements of delayed neutron groups from ^{235}U, 30:31014

W

WALTER REED ARMY INST. OF RESEARCH, WASHINGTON, D.C. (USA)
Research in biological and medical sciences including biochemistry, communicable disease and immunology, internal medicine, nuclear medicine, physiology, psychiatry, surgery, and veterinary medicine. Volume II. Annual progress report, 1 July 1972--30 June 1973, 30:29828 (AD-776967)
Research in biological and medical sciences including in biochemistry, communicable disease and immunology, internal medicine, nuclear medicine, physiology, psychiatry, surgery, and veterinary medicine. Volume I. Annual progress report, 1 July 1972--30 June 1973, 30:29827 (AD-774860)
WESTERN INTERSTATE NUCLEAR BOARD, LAKEWOOD, COLO. (USA)
Plowshare technology assessment, prospectives for nuclear-stimulated geothermal power in the western U.S., 30:29311 (PB-231011)
WESTINGHOUSE ELECTRIC CORP., MADISON, PA. (USA). ADVANCED REACTORS DIV.
Design progress on the LMFBR demonstration plant. Subject No. 20, 30:31222 (CONF-740341-1)
WISCONSIN UNIV., MADISON (USA)
Thermoluminescent response of TLD-100 to 1 to 25 keV electrons. Progress report, July 15, 1973--July 15, 1974, 30:29538 (COO-1105-212)

X

XEROX CORP., WEBSTER, N.Y. (USA). WEBSTER RESEARCH CENTER
Rock magnetites with positive anisotropy constants at 300°K, 30:31389 (CONF-740644-1)

PERSONAL AUTHOR INDEX

Authors' surnames are indexed in the form appearing in the abstracted publication; given names are reduced to initials. Each author entry gives the publication title and the *NSA* volume and abstract numbers. Report numbers, where applicable, are given in parentheses at the end of the entry. For publications with multiple authors, an author entry is provided for each. Entries for the second and succeeding authors give a reference to the first author and the *NSA* volume and abstract number.

Because of problems involved in the mechanical preparation of this index, all accent marks are omitted. The following changes in spelling have been introduced to reduce some of the confusion which might result from omitting the accents:

Germanic	ä appears as	ae
Germanic	ö	oe
Germanic	ü	ue
Scandinavian	ø	oe

Also included are entries for multinational and multiorganizational collaborating groups.

A

ABBATTISTA, N., Rise-time jitter reduction in timing and amplitude-discrimination circuits, 30:29631
ABBINK, R.E., Test of a magnetic bearing for optical scanner applications, 30:31430 (SLA-74-0347)
ABE, H., See KONISHI, H., 30:29875
ABEL, K.H., See RANCITELLI, L.A., 30:29469
  See RANCITELLI, L.A., 30:29483
ABEY, A.E., Mechanical properties of a shale from Site U-2, 30:31409 (UCID-16023)
ABKIN, A.D., See YAKOVLEVA, M.K., 30:29037
ABLESIMOV, N.E., Effect of physico-chemical properties of local environment of ^{57}Co Moessbauer atoms sorbed on ion exchange materials on their stabilization form after electron capture, 30:29099
  Post-effect of electron capture in ^{57}Co atoms sorbed on cation exchange resins with different degrees of cross-linking, 30:29097
ABONYI, I., Introduction to the physics of interstellar plasmas, 30:30183 (CONF-730693-)
ABRAHAM, M., Radiometric analysis of thorium and uranium, 30:28975
ABRAM, M., See PELOSI, V., 30:30732
ABRAMOV, V.V., See PETRUSEVICH, I.V., 30:29971
  See ZOLOTUKHIN, I.V., 30:29887
ABRAMOVICH, M., See YAFFE, D., 30:30622
ABRAMSON, J., See NORDBERG, M.E. Jr., 30:30590
ABRAO, A., See DE MORAES, S., 30:28948
ABSHIRE, G.W., See PETRI, H.R., 30:30155
ACHARYA, R., See ULLMAN, A., 30:30097
ACHASOV, N.N., An anomalous rho-ω interference in the reaction $e^+e^- \to 3\pi$, 30:30674
ACKERMAN, M., Solar ultraviolet flux below 50 kilometers, 30:30303
ACKERMAN, T.L., See ROMNEY, E.M., 30:29445
ACQUISTA, C., Radiative transfer of partially polarized light, 30:30195
ADAMESKU, R.A., See SHISHMAKOV, A.S, 30:30024
ADAMS, C.T., See MIDDLETON, R., 30:30485
ADAMS, D.E., See JAMES, W.D., 30:31010
ADAMS, J.H., See GOLDEN, R.L., 30:30165
ADAMS, J.T., Integral equation approach to collinear reactive scattering: $A+BC \to AB+C$, 30:30527
ADAMS, M.J., Direct determination on nanogram amounts of iodine by atomic-absorption spectroscopy using a graphite-tube atomizer, 30:28963
ADAMSON, M.G., Thermodynamic data program involving plutonia and urania at hign temperatures. Quarterly report No. 27, February 1, 1974—April 30, 1974, 30:31223 (GEAP-12511)
ADERHOLZ, M., High-resolution ionization measurements in the region of the relativistic rise, 30:29595
ADRIAANSZ, M., See VRIENS, L., 30:29169
AGADZHANOV, Kh.S., See YUSIFOV, V.G., 30:29947
AGALAROVA, A.F., See YUSIFOV, V.G., 30:29947
AGLITSKII, E.V., Diagnostics of dense laser plasmas based on the spectra of hydrogen-like and helium-like multiply charged ions, 30:29171
AGODI, A., Dynamical implications of correlations, 30:31057
AGRAWAL, Y.K., Preparation, properties, and analytical application of thorium n-phenyl-o-nitrobenzohydroxamate, 30:28962
AHMAD, S.S., Connection between Fredholm determinant and Jost function for nonlocal potentials, 30:30788
AIELLO, S., Modulation induced on young supernovae uv and ir luminosity by dust grains, 30:30344 (CONF-730693-)
AIGARAEVA, M.M., See USENOVA, K.A., 30:29111
AIRTH, G.R., Assessment of diagnostic x-ray equipment, 30:31111
AITKEN, E.A., See ADAMSON, M.G., 30:31223
AIZENMAN, M.L., See COX, J.P., 30:30192
AKABANE, K., See KAIFU, N., 30:30359
AKASOFU, S., See KAMIDE, Y., 30:30470
AKIBA, H., Affinity of ^{111}In-bleomycin for malignant tumors, 30:29859
AKININ, K.G., See ZOLOTUKHIN, I.V., 30:29887
AKOPDJANOV, G.A., Charged particle multiplicity distributions for 32 GeV/c $K^{+-}p$ and anti pp interactions and for 50 GeV/c $\pi^{+-}p$ interactions, 30:30608
AKULOVA, I.S., Some physical and chemical properties of fractions separated from gamma-irradiated corn starch, 30:29041
ALAM, M.S., Study of particle spectra and correlations in the reaction $\pi^+ + p \to n(\text{forward}) + (2\pi,4\pi,6\pi)$ at 8.4 GeV/c, 30:30613 (COO-1428-391(App.A-2))
ALBRECHT, R.W., Methods for measuring the reactivity and eigenvalue of nuclear reactors, 30:31301
ALBRECHT, T., Malignant transformation of hamster embryo fibroblasts following exposure to ultraviolet-irradiated human cytomegalovirus, 30:29677
ALBRECHT, W., Solution of the problem of designing liners for prestressed pressure vessels, 30:29264 (ALD-CONF-73-600-001)
ALBRECHT, W.W., Solubility and diffusion of cobalt in indium, 30:30020
ALBRIGHT, C.H., Charmed-particle production by neutrinos with the Weinberg SU(4) currents, 30:30688
  Pion distributions in inelastic neutrino interactions, 30:30689
ALDER, B.J., See GASS, D.M., 30:31441
ALDOR, E., ECG changes in selective coronary angiography and myocardial scintigraphy, 30:29880
ALEKSAKHIN, I.S., See VUKSTICH, V.S., 30:30524
ALEKSEEV, E.N., 100-channel scintillation telescope, 30:29578
ALEKSEEV, S.I., See PLATONOV, P.A., 30:30090
ALENIUS, G., Nuclear structure of ^{54}Mn, 30:30916 (NP-20122)
ALEXANDER, T.K., See ROGERS, D.W.O., 30:30895
ALEXANDRU, G., Strong focusing ion sources, 30:29637
ALFIERI, A.A., See HAHN, E.W., 30:29744
ALFVEN, H., Structure and evolutionary history of the solar system. IV, 30:30332
ALI, S.P., Electronic stopping power of channelled ions in a model incorporating the Pauli principle, 30:31115
ALIEVA, M.M., See RUSTAMOV, P.G., 30:30016
ALKEZWEENY, A.J., Airborne laboratory for air pollution study, 30:29612 (BNWL-1850(Pt.3))
  Characteristics of aerosols from St. Louis, 30:29471 (BNWL-1850(Pt.3))
  Measurements of drift from a mechanical draft cooling tower, 30:29487 (BNWL-1850(Pt.3))
  Preliminary in-plume measurements near Centralia, 30:29472 (BNWL-1850(Pt.3))
  Vertical profiles of trace gases in St. Louis, 30:29474 (BNWL-1850(Pt.3))
ALLAART, K., See GRUEMMER, F., 30:30914
ALLAKHVERDIEEV, G.A., See YUSIFOV, V.G., 30:29947
ALLARDYCE, B.W., See CLOUGH, A.S., 30:30891
ALLEGRE, C.J., See LANCELOT, J.R., 30:29337
ALLEN, K.W., See UNDERWOOD, B.Y., 30:30885
ALLER, P.F., Modular heat source for ^{244}Cm and ^{238}Pu, 30:29245
ALLRED, J.C., See LEE, L.Y., 30:29585
ALLRED, R.E., See HOOVER, W.R., 30:29890
ALTMAN, J.W., See SWAIN, A.D., 30:31360

ALVES, M.A.F., Wavelength shifters for xenon proportional scintillation counters, 30:29523
ALZETTA, R., Relativistic one-boson-exchange potential, two-nucleon data, nuclear matter, and neutron matter properties, 30:31033
AMADORI, R., Theory of multi-variable correlation techniques for time-of-flight experiments, 30:29560 (JUL-1050-FF)
AMATI, D., Scaling distribution of large transverse momenta, 30:30634
AMENDOLIA, S.R., See FINOCCHIARO, G., 30:30605
AMER, A.A., Possibility of producing polarized photons by Compton scattering of polarized relativistic electrons, 30:30648 (IC-73-131)
AMER, N., Exciton enhanced Raman scattering of LO phonons in trigonal Se, 30:31425 (LBL-2781)
AMOS, C.L., See OLIVER, A.J., 30:29329
AMOS, K., Spin-dependent effects in inelastic scattering, 30:30932
AMPELOGOVA, N.I., Investigation of complex formation of polonium by an ion exchange method, 30:29120
AMTEN, L., See JOHANSSON, A., 30:30855
ANDERSON, A.N., Low-dead-time delay-line read-out for position-sensitive proportional counters, 30:29592
ANDERSON, B.G., Adrenal imaging with radioiodocholesterol in the diagnosis of adrenal disorders, 30:29869
ANDERSON, C.J., MTSE II field calculation, 30:29215 (UCID-15511)
ANDERSON, J.L., See ACQUISTA, C., 30:30195
ANDERSON, L.L., Characteristics of ^{252}Cf neutron sources used for radiotherapy, 30:31124
ANDERSSON, G., See ARESKOUG, M., 30:31002
ANDERSSON, L.P., Semiconductor contacts to silicon surface-barrier detectors, 30:29519
ANDERT, K., Logarithmic digital-analog conversion for varying parameters in Camac devices, 30:29630
ANDO, A., See SUZUKI, Y., 30:29846
ANDRADE, E., See MILJANIC, D., 30:30882
ANDREASEN, V., Additive strength contributions, 30:31427 (RISO-M-1714)
ANDREEVA, N.R., See GREBENSHCHIKOVA, V.I., 30:28999
ANDREJTSCHEFF, W., Electromagnetic transitions in some odd-neutron deformed nuclei, 30:30990
  Transition probabilities in the doubly odd nuclei ^{174}Lu and ^{182}Ta, 30:30993
  See MANFRASS, P., 30:30994
ANDREONE, C.A., Application of a mass spectrometer to the method of determination of gases in metals by vacuum fusion, 30:28938 (CNEA-363)
ANDREWS, D., See BEBEK, C.J., 30:30587
  See NORDBERG, M.E. Jr., 30:30590
ANDREWS, R.E., Fault tolerant sequencing (FTS) shunt regulator, 30:29254
ANDRUS, C.H., See GRUHN, T.A., 30:29532
ANELLI, J., See WOLOWODIUK, W., 30:29275
ANGEL, J.R.P., A determination by the Zeeman effect of the magnetic field strength in the white dwarf G99-37, 30:30193
  See LANDSTREET, J.D., 30:30203
ANGELESCU, N., Landau diamagnetism, 30:31421 (IFA-FT-109-1974)
ANGELOV, B.P., Radiography of steel components with a linear electron accelerator, 30:30143
ANGELOV, N., Possible description of the rho resonance in the simplest model of the $\pi\pi$-interaction, 30:30718 (JINR-P2-7502)
ANGERER, G., Transport of core materials during accidents in LMFBRs (slumping), 30:31249 (KFK-1935)
ANGHILERI, L.J., Comparative study of the incorporation of ^{32}P into the phospholipids of membranes from Novikoff hepatoma ascites cells and liver cells from normal and tumor bearing animals, 30:29819
ANNAMALAI, N.K., See LALEVIC, B., 30:29940
ANSPAUGH, L.R., Results and data analysis: resuspension element status report, 30:29452 (NVO-AEIC-74-1)
  See PHELPS, P.L., 30:29450
ANTONCHENKO, R.V., See EREMENKO, V.N., 30:30003
ANTONIC, B., See SEDLAK, J., 30:29874
ANTONOV, A.V., Collector probe measurements of the parameters of a laser plasma at long distances, 30:29172
ANTONOVA, N.P., Phase changes in high-alumina ceramic under the influence of ionizing radiation, 30:29913
ANTROPOVA, Z.G., See BELOVA, E.I., 30:29403
ANUFRIENKO, V.F., ESR spectra and ionic states in the system V_2O_5--SnO_2, 30:29907
ANYAS-WEISS, N., See ROGERS, D.W.O., 30:30894
  See ROGERS, D.W.O., 30:30895
  See UNDERWOOD, B.Y., 30:30885
AOKI, I., See CHURCH, B.W., 30:29453
  See KAYUHA, H.J., 30:29441
AOKI, N., See SHIMOYASHIKI, S., 30:31227
AOKI, S., See KAWAMURA, K., 30:29046
AOKI, Y., See SAKAI, M., 30:30974
APPLETON, A.D., Programs on large scale applications of superconductivity in the United Kingdom, 30:30807
  Superconducting dc machines, 30:30827
APT, K.E., Passive environmental neutron dosimeter, 30:29551 (LA-UR-74-1232)
ARAVAMUDAN, G., See GIRIDHARAN, A.S., 30:29090
ARD, W.B., See HAUGHT, A.F., 30:29152
ARESKOUG, M., Photofission in gold at intermediate energy, 30:31002
AREY, T.T., See CHASTAIN, S.A., 30:31231
ARIMA, A., See SHIMIZU, K., 30:30898
  See SHIMIZU, K., 30:31086
ARKHAROV, V.I., Inter-crystallite internal adsorption in low-alloy molybdenum, 30:30023
ARKLES, L.B., Quantitative thyroid scanning: a reliable thyroid function test, 30:29853
ARMANI, R.J., See GOLD, R., 30:29557
ARMSTRONG, J.C., See ZMUDA, A.J., 30:30461
ARMSTRONG, T.W., Calculated particle-production spectra from π^- captures in tissue, tissue-equivalent plastic, silicon, and germanium, 30:31120
  Calculations on tissue equivalence for stopping π^- mesons, 30:31119
ARNELL, S.E., See ALENIUS, G., 30:30916
ARNESEN, A., See ORRE, B., 30:31017
ARNETT, W.D., Iron production by ^{12}C-detonation supernovae, 30:30258
  See PARDO, R.C., 30:30257
ARNOLD, J.R., See HARRINGTON, T.M., 30:29566
ARNOLD, R.C., Binary-collision theory for multihadron production amplitudes, 30:30698
ARONSON, E.A., See JAMES, L.T., 30:31429
ARP, H., NGC 520 chain of quasars, 30:30285
ARRHENIUS, G., See ALFVEN, H., 30:30332
ARTAMONOV, E.V., See SAZONOV, L.A., 30:29028
ARTYUKHINA, L.L., See KONOPLENKO, V.P., 30:29985
ARTYUKHOV, V.G., Kinetics of the changes of mouse hemoglobin under uv-irradiation, 30:29659
ASAHINA, K., See SAITO, K., 30:29864
ASCUITTO, R.J., One-nucleon transfer reactions in deformed nuclei, 30:30995
ASHBY, D.E.T.F., See CHRISTIANSEN, J.P., 30:29227
ASHERY, D., See MAK, H.-B., 30:30913
ASHIHARA, O., Velocity distribution of ionospheric low-energy electrons, 30:30442
ASHOUR, A.A., Exact solutions for certain axisymmetric problems of induction in thin nonuniform sheets, 30:30452
ASLANIDES, E., See KIM, I.J., 30:30584
ASPELUND, O., DWBA and CCBA analysis of selected transitions in the ^{12}C(d,tau)^{11}B reaction at Esub(d) = 80MeV, 30:30900
ASQUITH, J.C., Metronidazole (Flagyl). A radiosensitizer of hypoxic cells, 30:29674
ASSELIN, G.P., Nucleation and growth of W films evaporated on NaCl, 30:29959
ASTVATSATUROV, R.G., Investigation of a 90-channel Pb glass Cherenkov hodoscope, 30:29577
ATABEK, O., Quantum-defect theory of excited ^{1}PI/sub u/$^-$ levels of H_2, 30:30496
ATAC, M., High-resolution cryogenic spark chambers, 30:29594
ATANASOV, A., See ANGELOV, N., 30:30718
ATHERTON, D.R., Early retention and distribution of ^{253}Es by the beagle, 30:29803 (COO-119-249)
  See BRUENGER, F.W., 30:29804
  See LLOYD, R.D., 30:29805
  See LLOYD, R.D., 30:29802
  See MAYS, C.W., 30:29806
  See STEVENS, W., 30:29798
ATTALLA, A., See BOWMAN, R.C. Jr., 30:29889
AU, C.K., Criteria for pion condensation thresholds in neutron star matter, 30:30261
AU, F.H.F., Role of soil microorganisms in the movement of plutonium, 30:29447 (NVO-AEIC-74-1)
AURIC, P., The variation of the lifetime of ^{89}Zr in $BaTiO_3$, $PbZrO_3$ and ZrO_2, 30:30947
AUSTIN, D.M., See HOLMES, H.H., 30:31341
AVARBE, R.G., See MAZAEV, A.A., 30:29918
AVRAMENKO, A.S., Stochastic approach to studying radioactivity of cloud and rain droplets, 30:29397
  Theories of radioactivity takeup by rain drops, 30:29398
  Washout of radioactive impurities from the atmosphere in the Central Caucasus mountains, 30:29385
AVRIGEANU, M., See IVASCU, M., 30:30941
AVRIGEANU, V., See IVASCU, M., 30:30941
AXEN, D., A high-resolution scintillation counter with particle identification for use with pions, 30:29597
AYAKAWA, Y., See TAKAHASHI, S., 30:31106
AYE, T.M., N and π exchange amplitudes in πN backward scattering, 30:30744

B

BABAD-ZAKHRYAPIN, A.A., See GERT, L.M., 30:29914
BABICH, B.N., See PORTNOI, K.I., 30:29998
BABINCEV, V.V., See AKOPDJANOV, G.A., 30:30608
BABINTSEV, V.V., Analysis of data on multiparticle production in pp-interactions from 13 up to 300 GeV, 30:30598 (IFVE-SPK-73-69)
BACAL, M., Metal vapor confinement in vacuum, 30:30128
BACH, H., Sputtering yields and specific energy losses of Ar^+ ions with energies from 5 to 30 keV at SiO_2, 30:30482
BACHE, C.A., See FURR, A.K., 30:28925
BADESCU-SINGUREANU, A.I., Physical quantities the numerical values of which will be included in the evaluated microscopic nuclear data library ''DANEM-I'' from the I.A.P., 30:30846 (IFA-DNBR-9-1974)
  Structure of the evaluated microscopic nuclear data library ''DANEM-I'' from the I.A.P., 30:30845 (IFA-DNBR-8-1974)
BADHWAR, G.D., See GOLDEN, R.L., 30:30165
BAECKLIN, A., See DIETRICH, W., 30:30954

See NYMAN, B., 30:30953
BAETSLE, L., Separation of ^{137}Cs and ^{90}Sr from highly radioactive fission product solutions, 30:28991 (BLG-487)
BAETZNER, K., π^0 electroproduction at the $\Delta(1236)$ resonance at a four-momentum transfer of $q^2=0.3(\mathrm{GeV}/c)^2$, 30:30589
BAGATURIYA, G.D., Histochemical changes in cancer of the corpus uteri after experimental irradiation, 30:29716
BAGGE, E., Electrically charged galaxy and its internal and cosmological consequences, 30:30341 (CONF-730693-)
BAGLIN, J.E.E., Particle configurations of giant El states in the $^{14}N(\gamma,p_2)$ and $^{14}N(\gamma,p_0)$ processes, 30:30877
BAHR, G.K., See SILBERSTEIN, E.B., 30:29707
BAIKOV, V.I., Two-phase flow and heat transfer at the boundary layer of a thin body of revolution, 30:29291
BAILEY, G.J., Temperatures in the polar wind, 30:30443
BAILEY, J., The πd scattering length from Ksub(α) X-rays, 30:30620
BAILIN, D., Asymptotic near freedom, 30:30672
BAILLIE, A.D., See LEDINGHAM, K.W.D., 30:31076
BAILLON, P., Measurement of the real part of the forward scattering amplitude in $K^{\pm}p$ elastic scattering between 0.9 and 2.6 GeV/c, 30:30619
  The NAK coupling constant, 30:30737
  The real part of the forward scattering amplitude in $\pi^{\pm}p$ elastic scattering below 2 GeV/c, 30:30618
BAIRD, D.C., See MUKHERJEE, B.K., 30:30818
BAIRD, M.C., Deuterium isotope effects in deuterated styrenes, 30:29022
BAISOGOLOV, G.D., See GUZEEV, G.G., 30:29731
BAITY, W.A., See ULMER, M.P., 30:30268
BAJERSKA, A., See LINIECKI, J., 30:29749
BAK, H.I., See LEE, C., 30:28931
BAKATANOV, V.N., See ALEKSEEV, E.N., 30:29578
BAKER, J.C., Synchrotron loss rates of energetic magnetospheric electrons, 30:30451
BAKER, R.J., Measurements of three velocity components and their correlations in a model furnace with and without combustion, 30:31414 (AERE-R-7776)
BAKULIN, V.N., Use of naturally radioactive substances in studying turbulent exchange and self-scavenging of the atmosphere with surface layer measurements, 30:29396
BALANDA, M., Hematite phase diagram in a magnetic field: I. Low-temperature modification, 30:31392 (JINR-P14-7974)
BALCHANDRA, J., See DE, P.K., 30:29957
BALCOMB, J.D., See MOORE, S.W., 30:31326
  See MURRAY, H.S., 30:31325
BALESTRA, F., 180° magnetic spectrometer with helium-filled streamer chamber, 30:29591
BALI, N.F., Unitarity, phenomenology and the bare pomeron, 30:30710
BALL, E.M., Solid phase radioimmunoassay for plant viruses, 30:29836
BALL, J.B., See ROBINSON, R.L., 30:30982
BALLARD, D.G.H., See WIGNALL, G.D., 30:31364
BALLOT, J.L., Convergence of the hyperspherical expansion treatment of few-nucleon bound states, 30:30859
BALLOU, J.E., Long-term effects of intratracheally instilled ^{253}EsCl$_3$ in rats, 30:29776 (BNWL-SA-4870)
BALOSHIN, O.N., Analysis of $K_1^0K_1^0$ system in the $\pi^-p \to nK^0$ anti K^0 reaction at 40 GeV/c, 30:30730 (ITEF-31)
BALSLEY, B.B., See ROMICK, G.J., 30:30430
BAMBERG, S.A., See ROMNEY, E.M., 30:29445
BANDER, T.J., See HORST, T.W., 30:29609
  See ORGILL, M.M., 30:29373
BANYAI, L., Gauge dependence of renormalization group parameters, 30:30767
  Null-plane commutators in the spontaneously broken gauge theory of vector dominance, 30:30637
BARABOSCH, L.S., On the collective acceleration of heavy ions - Department for new methods of acceleration of the JINR, 30:30117 (GSI-tr-74/10)
BARANOV, V.M., Temperature dependence of the elastic constants of nonstoichiometric zirconium carbides, 30:29916
BARANOVA, T.F., See POPIL'SKII, R.Ya., 30:29910
BARANOWSKI, B., See SKOSKIEWICZ, T., 30:30813
BARBACKA, G., Desynchronization of the diurnal rhythm of acid phosphatase activity in male gonads of mice under the influence of uv and x-rays radiation, 30:29751
BARBER, E.J., See GUSTISON, R.A., 30:29149
BARBER, R.W., See CUPLEN, H.L., 30:31238
BARBINI, R., Energy-loss spectrometer for low-energy pion scattering, 30:29586
  See BALESTRA, F., 30:29591
BARDEEN, W.A., Anomalous currents in gauge field theories, 30:31161
BARDWICK, J., See PARKINSON, W.C., 30:30158
BARKER, R.E. Jr., See REYNOLDS, C.L. Jr., 30:30046
BARKLEY, H.T., See WITHERS, H.R., 30:29758
BARLETT, R.H., See GULLICKSON, R.L., 30:29174
BARNES, A., Large-amplitude hydromagnetic waves, 30:30398
BARNES, C.A., See MAK, H.-B., 30:30913
BARNES, D.G., See WISE, P.J., 30:28933
BARNES, E.G., Experimental neutron radiography system using californium-252. Final report, 30:29295 (AD-776900)
BARNETT, W.J., See SCHUMANN, F.A., 30:29252
BARON, J.L., A possible mechanism for the formation of a ferromagnetic phase in stainless steel Fe/Cr/Ni/Mo, 17/11/8/2 (type 316L) irradiated in the pile, 30:30077
BARONCELLI, A., Study of total-absorption counters for very-high-energy particles, 30:29598
BARR, S., Natural β-activity of the air in the atmospheric surface layer, 30:29401
BARR, T.L., Angular momentum coupling, potential curves and radiative selection rules for heavy diatomic molecules, with particular reference to Kr$_2$ and Kr$_2^+$, 30:31459 (UCRL-13599)
BARRANDON, J.N., See KOHN, A., 30:28923
BARRETT, R.J., See ANDERSON, A.M., 30:29592
BARRUS, D.M., See BUREK, A.J., 30:30272
BAR-SAGI, J., Self-consistent pair potential in superconductors. I. The superconductor--insulator boundary near T/sub c/, 30:30817
BARSA-NEWTON, M.C., See KROYHN, D.L., 30:29765
BARSHAY, S., The validity of the factorization hypothesis for nucleus-nucleus cross sections at high energies, 30:31095
BARTH, J., In vitro plutonium studies using the artificial rumen and simulated abomasal and intestinal fluids, 30:29809 (NVO-AEIC-74-1)
BARTHOLIN, H., Magnetic properties of CeBi, 30:29993
BARTLE, C.M., See JONES, D.T.L., 30:30146
BARTNIKOWA, W., Effect of ionizing radiation on alkaline phosphatase activity in hematopoietic cells of mouse and rat, 30:29762
  Influence of ionizing radiation on alkaline phosphatase activity in human peripheral blood leukocytes and bone marrow cells, 30:29727
BARU, V.G., See SOTNIKOV, V.S., 30:29053
BASARGIN, N.N., See GORSHKOV, V.V., 30:28926
BASES, R., Dissociation of histone and DNA synthesis in x-irradiated HeLa cells, 30:29671
  Dissociation of histone and DNA synthesis in x-irradiated HeLa cells, 30:29666
BASHA, A.F., Magnetic properties of alloys of the TbCu--YCu system, 30:30031
BASS, R., Fusion of heavy nuclei in a classical model, 30:31064
BASTIEN, D.B., Diffractive processes in anti pp interactions at 5.1 GeV/c, 30:30600
BASTIEN, P.L., See BASTIEN, D.B., 30:30600
BASU, D., See BHATTACHARYA, R.S., 30:30481
BATLEY, G.E., See FLORENCE, T.M., 30:28950
BATT, R.G., See CARPENTER, H.J., 30:29307
BATTY, C.J., See CLOUGH, A.S., 30:30891
BAUDRY, A., See COHEN, M., 30:30273
BAUER, G., See KOHLMEYER, B., 30:30906
  See KUCHAR, F., 30:29992
BAUER, H., Influence of neutron irradiation on critical data of type II superconductors, 30:30063 (AED-CONF-74-089-006)
BAUGH, D.J., See CLOUGH, A.S., 30:30891
BAUSOVA, N.V., See MANAKOVA, L.I., 30:28959
BAVERSTOCK, K.F., Comment on ''further data on DNA strand breakage by various radiation qualities'', 30:29660
BAWIN, M., Exponential potential and the Klein--Gordon equation, 30:30789
BAXTER, B.J., Secondary jaw crusher development, 30:29265 (GA-A-12903)
BAXTER, P., Nuclear testing, 30:29719
BAYARD, M., Magnetic properties of vanadium oxide V$_3$O$_7$, 30:29902
BAYM, G., See AU, C.K., 30:30261
BAZANT, E., Nozzle for the cover of a nuclear reactor pressure vessel, 30:31285
BAZHENOV, B.A., See SHMIDT, F.K., 30:29012
BEAL, J.W., Note on the Astron gun design, 30:29214 (UCID-15481)
  Note on the incoherent space charge limit in the High Intensity Storage Ring, 30:30139 (UCID-15686)
  Preliminary orbits and structure of a high intensity storage ring, 30:30138 (UCID-15685)
  Quadrupole fields in a toroidal geometry for the High Intensity Storage Ring, 30:30140 (UCID-15735)
  X-ray measurements on electron distribution in Astron, 30:29160 (UCID-15392)
BEASLEY, C.O. Jr., Subroutine CAUCHY: complex roots of a function using a CAUCHY integral technique, 30:31344 (ORNL-TM-4588)
BEASLEY, M.R., See SKOCPOL, W.J., 30:30819
BEBEK, C.J., Measurements of inclusive pion electroproduction, 30:30587
BECHLER, A., Vacuum polarization tensor and current operator in quantum electrodynamics with compensating current, 30:31156
BECK, J.N., See JAMES, W.D., 30:31010
  See KURODA, P.K., 30:30162
  See NEVISSI, A., 30:29400
BECK, U., Electroproduction of eta-mesons at the S$_{11}$ (1535) resonance, 30:30591
  See BAETZNER, K., 30:30589
BECKER, C.D., See SCHNEIDER, M.J., 30:29461
BECKER, H.J., Ternary fission induced by 540 MeV Fe ions on uranium, 30:31018
BECKER, J.A., See ROGERS, D.W.O., 30:30895
  See ROGERS, D.W.O., 30:30894
BECKER, K., See HOFFMANN, D., 30:30148
BECKER, M., See DANCHAK, M., 30:29620

BECKER, W.G., Scattering of alkali halides by electrons. II. CsCl, 30:30528
BECKINSALE, R.D., Rb-Sr and K-Ar age determinations, and oxygen isotope data for the Glen Cannel granophyre, Isle of Mull, Argyllshire, Scotland, 30:29339
BECKLIN, E.E., See GATLEY, I., 30:30356
See WYNN-WILLIAMS, C.G., 30:30375
BECKS, K.H., See BAETZNER, K., 30:30589
See BECK, U., 30:30591
BEER, J.Z., See SZUMIEL, I., 30:29669
BEERS, F.T. III., Determination of geographic position from rectangular coordinates. Progress report, March—June 1970, 30:31361 (UCID-15722)
BEICHMAN, C.A., Possible evidence for a large magnetic field in the Orion infrared nebula, 30:30392
BEIERWALTES, W.H., See ANDERSON, B.G., 30:29869
BEIHN, R.M., See DAMRON, J.R., 30:29845
BEIL, R.G., Neutron logging of formation porosity and chlorinity, 30:29429
BEINER, M., The energy density formalism and the shell structure effects, 30:31025
See BALLOT, J.L., 30:30859
BELCHER, J.W., See BLAKE, D.H., 30:30403
BELETSKII, P.N., See SOTNIKOV, V.S., 30:29053
BELJAJEW, L.N., See BARABOSCH, L.S., 30:30117
BELKOV, V.M., See LARIKOV, L.N, 30:29955
BELLETTINI, G., See FINOCCHIARO, G., 30:30605
BELLONI, J., Transient spectrum from nanosecond pulse radiolysis of liquid ammonia, 30:29079
BELLUSCIO, M., Efficiencies and response functions of NaI(Tl) crystals for gamma rays from thick disk sources, 30:29517
BELOMYTTSEV, Yu.S., See VOROB'EV, A.N., 30:30071
BELOTE, T., See STEADMAN, S., 30:30920
BELOTE, T.A., See ROGERS, D.W.O., 30:30894
See ROGERS, D.W.O., 30:30895
BELOTSERKOVSKII, B.E., See GRIGOREVSKII, M.V., 30:30209
BELOVA, E.I., ^{90}Sr and ^{137}Cs distribution in different types of soils, 30:29403
BELOVOL, V.S., See PETRENKO, N.S., 30:30032
BELYANINA, R.G., See POPIL'SKII, R.Ya., 30:29910
BELYI, A.F., See MISYURA, V.A., 30:30447
BELYI, A.G., See GORDELADZE, Sh.G., 30:30213
BENAVIDES, I., See BRAVO, A., 30:29865
BENDE, E., Novel methods in the analysis of cesium, 30:28976
BENECKE, J., Rapidity-gap separation and study of single-diffraction dissociation in pp collisions at 12 and 24 GeV/c, 30:30612
BENEDETTO, W.J., See WEBER, D.A., 30:29843
BENENYO, T., Changes in genetic cell material during the action of ionizing radiation, 30:29655
BENIEVA, T.Ya., Effect of temperature and rhenium impurity on the amplitude-dependent, internal friction of tungsten, 30:30056
BENKO, G., See BORHEGYI, L., 30:29746
BENSON, D. Jr., See PROETEL, D., 30:31006
BENSON, W.H., See HOLMES, H.H., 30:31341
BENSUSSAN, A., High-power standing-wave triperiodic structure for positron acceleration, 30:30126
BENTON, E.V., See GRUHN, T.A., 30:29532
BENTON, S.T., See GUSTISON, R.A., 30:29149
BENTZ, E.J., See BAGLIN, J.E.E., 30:30877
BERANOVA, H., See MARHOL, M., 30:29001
BERG, U., See WOLF, H., 30:30908
BERGAMINI, R., Effective potentials near a Kerr--Newman naked singularity, 30:30208
BERGE, G.L., The position and Stokes parameters of the integrated 21-centimeter radio emission of Jupiter and their variation with Epoch and central meridan longitude, 30:30407
BERGER, J.F., Shell effects on state densities with given number of excited protons and neutrons, 30:31094
BERGER, M.J., See SELTZER, S.M., 30:31118
BERGER, S.B., Conformal symmetry in the Weyl theory, 30:30652
BERGMAN, O., See DIETRICH, W., 30:30954
BERGMAN, R., Analysis of the nitrogen and carbon content in organic bulk matter by fast-neutron induced gamma radiation, 30:28918 (NP-20122)
See SUNDQVIST, B., 30:28917
BERGQVIST, I., See BERGMAN, R., 30:28918
BERK, H.L., Back current in an E-layer. I, 30:29224 (UCID-15977)
BERKELMAN, K., See BEBEK, C.J., 30:30587
BERKO, F.W., Dependence of field-aligned electron precipitation occurrence on season and altitude, 30:30469
BERKO, S., See CANTER, K.F., 30:30510
BERKOSKY, J.L., See RABALAIS, J.W., 30:30491
BERLAD, G., Cross channel isospin amplitudes for 3.9 GeV/c $\pi^{+-}p \to \pi(N\pi)$ compared with the predictions of a double exchange model, 30:30623
BERLEY, D., AGS secondary beams and parameters, FY75, 30:30141 (BNL-19153)
BERMAN, A., See SCHOENFELD, I., 30:28949
BERMAN, B.L., Selected activities in photonuclear reactions, 1973--1974, 30:30856 (UCID-16563)
BERMAN, D.H., See BRUCH, L.W., 30:30502
BERNABAI, U., See DE GREGORIO, G., 30:29956
BERNABEU, J., Parity violations by neutral currents in muonic atoms, 30:30777
Polarizability contribution to the energy levels of the muonic helium $(\mu^{4}He)^{+}$, 30:30516
BERNETT, E., See LI, F.P., 30:29714
BERNHARDT, H.A., See GUSTISON, R.A., 30:29149
BERNSTEIN, W., Some active magnetosphere experiments to be performed by the Plasma Physics and Environmental Perturbation Laboratory, 30:30450 (COM-74-50228)
BERRY, G.G., See WILSON, W.J., 30:30265
BERST, J.D., See MEYER, J.M., 30:29627
BERTANZA, L., Cross-sections for resonance production in anti pn annihilations around 2190 MeV centre-of-mass energy, 30:30606
BERTHOMIEU, G., Type III radio bursts, 30:30301
BERTIN, A., Fine structures in the mass yield of ^{252}Cf fission fragments from a double-energy measurement, 30:31016
BERTSCH, G., How good is the collective model, 30:31078
BES, D.R., See BROGLIA, R.A., 30:31000
BESOV, A.V., See SHLYUKO, V.Ya., 30:29892
BESPROZVANNYI, M.A., See LEVIN, D.Z., 30:29011
BETAK, E., See OBLOZINSKY, P., 30:31093
BETHE, H.A., See JOHNSON, M.B., 30:31059
BETHGE, K., See QUEBERT, J.L., 30:30996
See SCHMIDT-BOECKING, H., 30:30948
BETTERODGE, W., Nimonic alloys and other nickel-base high-temperature alloys, 30:29988
BETTINI, A., See BERTANZA, L., 30:30606
BETZ, P., A fast neutron-gamma discriminator, 30:29535
BEVC, V., Reduction of hose growth by current tailoring, 30:29199 (UCID-15996)
BEVENSEE, R.M., Feasibility of two schemes for detecting the envelope of a γ-ray burst underground, 30:29321 (UCID-15865)
BEVOLO, A.J., Specific heat of 2H NbSe$_2$, 30:30808
BEWLEY, D.K., Introduction to the discussion on characteristics of installations for radiotherapy with fast neutrons and other types of high-LET radiation, 30:31112
BEYNON, A.J., New methods of measuring ^{238}U capture rate and fast fluxes in a zero energy HTR lattice, 30:31212
BEYNON, W.J.G., Incoherent scatter sounding of the ionosphere, 30:30444
BEZMATERNYKH, A.S., See SEVAST'YANOV, Yu.G., 30:29143
BHADURI, R.K., Fragmentation of highly excited heavy ions, 30:31074
BHAKAR, B.S., See CHOUDHURY, B.J., 30:30790
BHATI, S.S., Gamma--gamma angular correlation in ^{147}Pm, 30:30958
BHATIA, A.K., See JACOBS, V.L., 30:30245
BHATIA, K., Reactions of the radiolytically generated hydroxycyclohexadienyl radical in aqueous benzene systems, 30:29043
BHATNAGAR, S., See DEVI, U., 30:30551
BHATT, K.H., See DHAR, A.K., 30:30925
BHATTACHARYA, R.S., Sputtering experiments with silver single crystals and the channeling phenomena, 30:30481
BHATTACHARYYA, D.P., Production spectrum of charged cosmic ray pions and the primary cosmic ray nucleon spectrum, 30:30177
BHOWMIK, R.K., The ^{6}Li(p,2p)^{5}He reaction at 100 meV, 30:30896
BIALAS, A., Diffractive production off nuclei: shadow of hadronic bremsstrahlung, 30:31062
Heavy particle production and cluster models of high-energy collisions, 30:30699
BIBIKOVA, V.I., See VASIL'EVA, A.G., 30:29949
BIBL, K., Routine operation of Digisonde at Maynard, Massachusetts. Final report, 1 September 1971--31 August 1972, 30:30410 (AD-776969)
BIBRING, J.P., Ion implantation effects in 'cosmic' dust grains, 30:30355
BIEBER, C.P., See MILES, L.E.M., 30:29835
BIGI, A., See BERTANZA, L., 30:30606
BILKIEWICZ, J., Method of ^{3}H-determination in hair, 30:28985
See JAWOROWSKI, Z., 30:29818
BINGHAM, R.A., Micro-sample analysis by spark source mass spectrometry, 30:28967
BINNEWIES, M., Gaseous halide complexes and their stability, 30:29091
BINNS, W.R., 8192-channel square-root pulse-height analyzer, 30:29568
BIRJEGA, M.I., Epitaxial growth of UO$_2$ thin films evaporated on NaCl substrates with colloidal centres, 30:29927
See POPESCU-POGRION, N., 30:29928
BIRKHOFER, A., Comparison of two- and three-dimensional calculations of super prompt critical excursions, 30:31190
BIRKHOLZ, J., Continuum shell-model calculation for neutron scattering from ^{11}B, 30:30890
BIRMINGHAM, B.W., See POWELL, R.L., 30:30838
BIRMINGHAM, T.J., See HESS, W.N., 30:30404
BIRNBAUM, H.K., See WALSON, R.P., 30:29976
BIROLINI, A., Spare parts reservation of components subjected to wear-out and/or fatigue according to a Weibull distribution, 30:29289
BISI, V., Measurement of the slope parameter for the neutral pion spectrum in K^0sub(L) $\to \pi^0\pi^+\pi^-$ decay, 30:30596
BISLIEV, A.N., See NIKITIN, S.A., 30:30043

BISSHOPP, F.E., Discrete spectrum of solutions of the wave equation with strong cubic nonlinearity, 30:31131 (AD-776985)
BISSWANGER, H., Differential magnetic analysis of the radiation-induced diffusion in nickel-beryllium alloys, 30:30064 (AED-CONF-74-089-037)
BISTLINE, R.W., See GOMEZ, L.S., 30:29820
BITELLI, G., Fluxes and effective multiplication factor evaluation by escape probabilities, 30:31274 (RT/FI-(74)30)
BLAGOEV, A.B., Electron energy distribution in the afterglow. II, 30:29165
  Electron energy distribution in the afterglow. I, 30:29164
BLAGORODOV, A.M., See BALOSHIN, O.N., 30:30730
BLAHD, W.H., See WINSTON, M.A., 30:29855
BLAIR, D.C., Localization of infectious processes with gallium citrate (Ga-67), 30:29886
BLAIR, J., Numerical deconvolution, 30:31349 (UCID-15743)
BLAISE, G., Ionic emission yield for alloys, dependence on the nature of the solute. II. Interpretation, 30:30087
BLAKE, D.H., Power spectra of the interplanetary magnetic field, 0.7 to 1.6 AU, 30:30403
BLAKE, R.L., See BUREK, A.J., 30:30272
BLAKELY, J.N., See BLAZEK, R.J., 30:31416
BLAMONT, J.E., See REED, E.I., 30:30423
BLANC, C., Enrichment of carbon and neon isotopes by gas phase chromatography. Part 1, 30:29024 (LA-tr-74-18)
  Enrichment of carbon and neon isotopes by gas phase chromatography. Part 2, 30:29025 (LA-tr-74-19)
BLANCO, V.M., Classification of unidentified sources from a 2-μ southern sky survey, 30:30220
BLANK, H., Lattice defects and atomic radii in UO$_2$ and PuO$_2$, 30:29929
BLATT, S.L., See VLIEKS, A.E., 30:30255
BLAZEK, R.J., Development of processes for hybrid microcircuits containing beam-lead devices, 30:31416 (BDX-613-1115(Rev.))
BLIND, R., Longitudinal phase-space analysis of the $K^+\pi^+\pi^-$ system produced by 10 GeV/c K^+ incident on nuclei, 30:30625
BLINOWSKA, K.J., A method of on-line spectra evaluation by means of a small computer employing Fourier transforms, 30:29563
BLISS, W.A., See CHURCH, B.W., 30:29453
BLIXT, S., Induced mutation in peas. XXVI. Genetically conditioned differences in radiation sensitivity. IV, 30:29694
BLOBEL, V., See BENECKE, J., 30:30612
BLOCK, L.P., Derivation of magnetospheric electric fields from whistler data in a dynamic geomagnetic field, 30:30464
BLOK, H., Further measurement of the track lengths of heavy ions in mica, 30:29525
BLOKH, Ya.L., About the use of proportional counters for registration of cosmic ray meson component, 30:29582
  Diagrams of sensitivity in respect to the zenith angle for scintillation telescopes of arbitrary geometry, 30:29499
  Neutron supermonitor, 30:29500
  Primary automatic processing algorithms for data obtained at cosmic ray stations, 30:29579
BLOKHIN, S.I., Dose fields in convergent irradiation by a narrow beam of protons, 30:31110
BLOOD, C.M., Solubility and stability of structural metal difluorides in molten fluoride mixtures, 30:29002 (ORNL-TM-760)
BLOOM, S.G., See MARTIN, W.E., 30:29455
BLUDOV, V.Ya., See MISYURA, V.A., 30:30447
BLUM, W., See GRAYER, G., 30:30617
BLUMENFELD, H., See BUMAZSHNOV, V.A., 30:30603
  See DERRE, J., 30:30601
BOARDMAN, C.R., See KORVER, J.A., 30:29317
BOBERG, F., Labelled compounds. P. 18. Chlorine exchange between antimony(III) chloride-(^{36}Cl) and hexachloropropene (1), 30:29123
BOCK, R., See KOHLMEYER, B., 30:30906
BOD, L., Measurements with Hungarian calorimeter, 30:29541 (DEMO-74/5)
BODEK, A., See RIORDAN, E.M., 30:30583
BODENHEIMER, P., Do pulsars make supernovae. II. Calculations of light curves for type II events, 30:30197
BOECKMANN, K., See GRAESSLER, H., 30:30610
BOEHM, M., Generalized vector dominance and the pion form factor, 30:30729
BOERSMA, H.J., See DE GROOT, H., 30:30862
BOFFI, S., Phenomenological occupation probabilities, binding energies, and the nuclear one-particle density matrix, 30:30903
BOGDANOV, N.A., See LYAKISHEV, N.P., 30:29970
BOGDANOV, R.V., Unknown alpha-emitters in nature, 30:28981
BOGDANOV, V.P., See PETRUSEVICH, I.V., 30:29971
BOGEN, J., Trace elements in precipitation and cloud water in the area of Heidelberg, measured by instrumental neutron activation analysis, 30:28934
BOGENSBERGER, H.G., Calculation of the effects of fission gas in a LMFBR, for the analysis of an unprotected overpower transient, 30:31225 (KFK-1990)
BOGNER, G., Programs on large scale applications of superconductivity in the Federal Republic of Germany, 30:30834
  Transmission of electrical energy by superconducting cables, 30:30830
BOHN, T., Feasibility problems on UHTR for closed cycle MHD-power plants, 30:31208
  Nuclear district-heating and nuclear long-distance energy, 30:31305 (JUL-1077)
BOIKA, V.A., See AGLITSKII, E.V., 30:29171
BOIKO, V.I., Betatron electron internal-flaw detector, 30:30144
BOLDT, A.L., Radioactive waste storage, 30:30109
BOLDYREV, A.M., Method of determining the relative elongation of light alloys close to the solidus on an IMASh-5S-65 unit, 30:30012
BOLONKIN, B.V., See BALOSHIN, O.N., 30:30730
BOLTON, J.G., See PETERSON, B.A., 30:30276
BOND, A.H., See BAXTER, B.J., 30:29265
BOND, P.D., Difficulties in fitting angular distributions in the ^{40}Ca(^{13}C,^{14}N)^{39}K (g.s.) reaction, 30:30921
  See KAHANA, S., 30:31069
BONDARENKO, V.I., Electromagnetic radiation influence upon the plasma variation spectra, 30:30415
BONDAREVSKII, S.I., Post-effects of electron capture in ^{57}Co in systems containing cobalt nitrate and sulfate, 30:29096
  Post-effect of electron capture in the eutectic (NH$_4$NO$_3$--LiNO$_3$):^{57}Co at 77°K, 30:29098
  See ABLESIMOV, N.E., 30:29099
  See ABLESIMOV, N.E., 30:29097
BONEKOWSKI, N.R., Improved PETN particle size analyses, 30:31426 (MLM-2098)
BONINO, G., Local changes of the atmospheric electric field by EAS ionization, 30:30414
BONNELLE, C., X-ray spectroscopy analysis of the uranium 5f distribution in the metal and in UO$_2$, 30:30018
BONNER, B.P., See ABEY, A.E., 30:31409
BONNIER, B., Phenomenological upper and lower bounds on the $\pi\pi$ S-wave scattering lengths, 30:30723
BONTEMPS, A., Energy loss and projected range of alpha particles in zinc telluride, 30:31113
BOOK, D.L., See SCANNAPIECO, A.J., 30:30437
BOOS, A.H., See BECKER, H.J., 30:31018
BOOTH, H.G., See KENNEDY, N.C., 30:29451
BORDER, E.D., See MORTENSEN, W.K., 30:31456
BORDERS, J.A., Helium ion stopping cross sections in bismuth, lead, and tungsten, 30:31114
BORG, I.Y., See BORG, R.J., 30:31412
BORG, R.J., Magnetic order in certain alkali amphiboles, a Moessbauer investigation, 30:31412 (UCRL-75499(Rev.1))
BORGGREEN, J., See FOLKMANN, F., 30:28988
BORGSTEDT, H.U., The stability of vanadium and of the alloy V-3Ti-15Nb in liquid lithium at 700°C, 30:29951
BORHEGYI, L., Effect of a combination of antibiotics and AET on the survival of irradiated animals, 30:29746
BORIDY, E., High energy proton scattering by medium and heavy nuclei, 30:31007
BORIE, E., Pion electroproduction from nuclei near threshold, 30:30671
BORISOV, A.E., See KRYLOV, E.I., 30:29908
BORISOV, B.K., Weight parameters of adult human skeleton, 30:29885
BORRAS, C., Embryotoxicity of astatine-211, 30:29781 (COO-3268-5)
BORREANI, G., See BERTANZA, L., 30:30606
BORYS, J., See GLOWIAK, B., 30:29402
BOSLER, G.E., Preliminary appraisal of a fusion/fission (hybrid) reactor based on the linear theta pinch, 30:29228
BOSSEN, G.J., See GRAESSLER, H., 30:30610
BOSSHARD, E., See HERNHUT, H., 30:29643
BOSTWICK, W.E., Some notes on coaxial terminations, short-circuits, and open-circuits, 30:31453 (UCID-15998)
  Some thoughts on negative resistance as it applies to high frequency impedance measurements, 30:31448 (UCID-15866)
  Torsion pendulum for laser energy measurement, 30:31451 (UCID-15907)
BOSWORTH, E., See HAMILTON, J.H., 30:30987
BOTBOL, M., Chronoamperometric determination of iodine in urine, 30:28939 (CNEA-366)
BOTT, J.F., Vibrational relaxation of HF(v=1) and DF(v=1) by H$_2$ and D$_2$, 30:29019
BOTTERILL, D.R., See DEL GUERRA, A., 30:30678
BOURGERET, J.L., Type I solar radio emission, 30:30302
BOUYSSOU, J., See GUYADER, J.C., 30:29567
BOVKUNENKO, A.S., See ZELENSKII, V.F., 30:30017
BOWMAN, B.R., See PITTS, J.H., 30:31254
BOWMAN, C.D., Status report to NCSAC, 30:31011 (UCID-15639)
BOWMAN, J.D., See POTTER, J.M., 30:30599
BOWMAN, R.C. Jr., Pulse NMR studies of radiation damage in metal tritides, 30:29889 (MLM-2172(OP))
BOWYER, S., See MARGON, B., 30:30174
BOX, H.C., Effects of ionizing radiation on tyrosine, 30:29040
BOYD, A.M., Measurements with the hydrogen sulfide dosimeter, 30:29545 (DEMO-74/5)
BOYD, A.W., General discussion and summary, 30:29550 (DEMO-74/5)
  Measurements with cyclohexane dosimeters, 30:29549 (DEMO-74/5)
  Measurements with the Chalk River calorimeter, 30:29542 (DEMO-74/5)
  See MARKETOS, D.G., 30:29539
BOYLES, L., See SELIG, W., 30:31373
BOZHKO, V.P., See KLYUCHAREV, V.A., 30:30038
BRABSON, B.B., See ALAM, M.S., 30:30613

BRACCINI, P.L., See FINOCCHIARO, G., 30:30605
BRADASCHIA, C., See FINOCCHIARO, G., 30:30605
BRADBURN, E.H., Brazing alloy, 30:29999
BRADBURY, E.J., See GRUBER, H.T., 30:29294
BRADLEY, W.G., See MOOR, K.S., 30:29449
BRADSHAW, G.B., See ELSNER, N.B., 30:29246
BRADT, H.V., See SPROTT, G.F., 30:30260
BRADY, D.N., See CHURCH, B.W., 30:29453
BRADY, F.P., See WANG, J.C., 30:30873
BRADY, G.R., See SEMENIUK, A., 30:30084
BRAMMER, D., See FISHER, D.R., 30:29799
BRAMMER, T., See FISHER, D.R., 30:29799
BRAMON, A., The eta-eta' mixing angle from duality and quark model, 30:30728
BRANDAN, M.E., See MORALES, J.R., 30:30157
BRANDIE, G.W., Optical identifications and radio spectra of sources found by the Michigan 8-GHz survey, 30:30283
BRANDT, R., See BECKER, H.J., 30:31018
BRAWFORD, D., Possible resonance anomalies in the ^{16}O + ^{12}C, 30:30887
BRATOLJIC, T., Programs on large scale applications of superconductivity in Switzerland, 30:30837
BRAUEL, P., π^0-electroproduction on hydrogen near threshold at four-momentum transfers of 0.2, 0.4 and 0.6 GeV^2, 30:30588
BRAUMANDL, F., A neutron monitor with a rotating rhodium disk, 30:29515
BRAUN, G., See BETZ, P., 30:29535
BRAUN, W., Infrared laser enhanced reactions: spectral distribution of the NO_2 chemiluminescence produced in the reaction of vibrationally excited O_3 with NO, 30:30525
BRAVO, A., Radioisotope placentography with /sup 113m/In. Its value in the diagnosis and treatment of placenta praevia, 30:29865
BRECHNA, H., Superconducting magnets, 30:30826
BREEV, V.M., See BLOKHIN, S.I., 30:31110
BREGMAN, D., See GOLDSTEIN, G.R., 30:31028
BREGMAN, J.D., See DE MUL, F.F.M., 30:30847
BREGMAN-REISLER, H., Vibrational energy distribution in CO_2^+ (A^{2}PIsub(u)) ions produced by collisions of H_2^+ and He^+ ions with CO_2, 30:30558
BREIDENBACH, M., See RIORDAN, E.M., 30:30583
BREITENLOHNER, P., See BENECKE, J., 30:30612
BRENT, R.L., See BORRAS, C., 30:29781
BRESKIN, A., Further results on the operation of high-accuracy drift chambers, 30:29587
  Low-pressure drift chambers for heavily ionizing particles, 30:29588
  Two-dimensional drift chambers, 30:29589
BRESLAVETS, K.G., Cryovacuum hydrogen adsorption by small-sized, activated mineral coal with a binder, 30:31394 (KHFTI-73-25)
BRESSAN, A., Principle of material indifference in relativity, 30:31172
BRETTHAUER, E.W., See STANLEY, R.E., 30:29810
BRETZ, N., Proposed method of measuring the current distribution in a tokamak plasma, 30:29170
BREUHLICH, W.H., Neutron--neutron effective range parameters from few-nucleon experiments, 30:31037
BRICE, N., Wave--wave coupling in multiple-ion plasmas, 30:29226
BRICMAN, C., See BAILLON, P., 30:30618
  See BAILLON, P., 30:30619
  See BAILLON, P., 30:30737
BRIDLE, A.H., Intense radio sources at 1400 MHz. II. Additions to the BDFL sample, 30:30281
  See BRANDIE, G.W., 30:30283
BRIGANTI, G., Osmotic haemolysis as a means of studying erythropoietic stresses: response to acute anaemia and acute irradiation, 30:29736 (RT/BIO-(74)10)
BRIGGS, J., See SACKMANN, S., 30:30517
BRIGGS, R.J., Decay of plasma currents and charge in beam plasma experiments, 30:29186 (UCID-15820)
BRIMHALL, J.L., Investigations of the microstructure of heavy ion bombarded nickel, 30:30065 (BNWL-1839)
BRITTAIN, W.M., SNAP 19 Viking RTG flight configuration and integration testing, 30:29249
BRIXNER, B., Integrating eclipse optics into the AEC Air Force flying laboratory, 30:31423 (LA-UR-74-1167)
BRODA, R., See HAGEMANN, G.B., 30:30983
BROEDERS-SIEP, I., Contribution to the mutual resonance shielding of ^{238}U and ^{239}Pu, 30:31009 (EURFNR-1162)
BROERSE, J.J., Review of RBE values of 15 MeV neutrons for effects on normal tissues, 30:29764
BROGLIA, R.A., On the back-bending in the rotational motion, 30:30991
  Strength of the multipole pairing coupling constant, 30:31000
BROMBERG, C., See SREEDHAR, V., 30:30616
BRON, J., Isotope effects on partition functions and thermodynamic quantities of the stable diatomic hydrides, 30:29020
BRONCA, G., Programs on large scale applications of superconductivity in France, 30:30833
BROOKS, A.L., Effect of $^{239}PuO_2$ particle number and size on the frequency and distribution of chromosome aberrations in the liver of the Chinese hamster, 30:29783
BROSCHE, P., The mass-angular momentum-diagram and the black hole limit, 30:30295
BROWN, A.D., See BULLOCK, J.S., 30:29944
BROWN, C.N., See BEBEK, C.J., 30:30587
BROWN, D.N., Further observations for circularly polarized radiation from white dwarfs and x-ray sources, 30:30218
BROWN, F.J., See RAAEN, V.F., 30:29010
BROWN, G., The magnitude of compound nucleus effects in Ca(d,p) reactions, 30:30923
BROWN, G.W., See CUNNINGHAM, D.M., 30:31434
BROWN, J.L., Radionuclide generator production method, 30:29140
BROWN, J.P., Moessbauer spectroscopy of frozen europium ammonia solutions, 30:30093
BROWN, R.W., Possible effects of weakly coupled neutral currents in $pp \to l^+l^- + X$, 30:30762
BROWNE, C.P., See HIDDLESTON, H.R., 30:30968
BRU, L., See DE DIEGO, N., 30:29895
BRUCH, L.W., Dielectric properties of helium: Quantum statistical mechanics, 30:30502
  See FORTUNE, P.J., 30:30506
BRUENGER, F.W., Early subcellular distribution of einsteinium in canine livers, 30:29804 (COO-119-249)
  See ATHERTON, D.R., 30:29803
  See LLOYD, R.D., 30:29805
  See STEVENS, W., 30:29798
BRUNFELT, A.O., Determination of rare earths and thorium in apatites by thermal and epithermal neutron-activation analysis, 30:28935
BRUNO, M., See BERTIN, A., 30:31016
BRUNOT, B., Moessbauer effect study of the deuterated and hydrogenated hydrates of ferrous chloride, 30:29009
BRUNSON, B., Measurement of cerebral infarction edema with sodium-22, 30:29837
BRUSTAD, T., See JONES, W.B.G., 30:29064
BRYANT, F.J., Effect of oxygen on unencapsulated cadmium sulfide solar cells, 30:30103
BRYNE, K.H., See PARR, H., 30:29343
BRYUNIN, S.V., See ZHIRNOV, A.D., 30:31205
BUCHLER, J., See LITTLETON, J.E., 30:30259
BUCHTA, I., See SEIPEL, L., 30:29770
BUCKHOLTZ, T.J., New nodal expansion for classical plasmas, 30:30196
BUCURESCU, D., Optical model calculations for the scattering of rapid neutrons (8 to 15 MeV) by Cr and Fe, 30:30943
  See HERMANS, J.A.J., 30:30864
  See IVASCU, M., 30:30941
  See VAN DRIEL, M.A., 30:30912
BUDAGOVSKII, S.S., Nuclear gamma-resonance on nuclei of ^{57}Fe impurity in tungsten--rhenium alloys, 30:30029
BUDDEMEYER, E.U., See PROKOP, E.K., 30:29848
BUDDING, E., Calculations of proximity effects in close binary systems, 30:30263
BUDIC, R., Causal boundaries for general relativistic space--times, 30:31175
BUDNICK, J.I., See MURPHY, J.J., 30:30961
BUDZICKA, E., See SZUMIEL, I., 30:29669
BUDZINSKI, E.E., See BOX, H.C., 30:29040
BUESSER, F.W., See BRAUEL, P., 30:30588
BUGAJSKI, W., See POMORSKI, L., 30:28980
BUGG, D.V., See BAILEY, J., 30:30620
BUJNOWSKI, W., See SKOSKIEWICZ, T., 30:30813
BULLIER, D., See JEANMAIRE, L., 30:29795
BULLOCK, J.S., Electrochemistry of aqueous corrosion: uranium and its alloys, 30:29944 (Y-1949)
BUMAZSHNOV, V.A., Negative pion production in proton-proton interactions at 69 GeV/c, 30:30603
BUMAZSHNOV, V.H., See DERRE, J., 30:30601
BUMPEL-MAYER, T.F., See PICHLER, L., 30:29755
BUNDARU, M., See ANGELESCU, N., 30:31421
BUNKER, D.L., See VALENCICH, T., 30:29085
BUNTENBACH, R., Outline of developments in magnetic circuit theory, 30:31436 (UCID-15597)
BUNTING, R.L., Nuclear Data Sheets for A = 136, 30:30967
  Short-lived radioactivity induced in Ge(Li) gamma-ray detectors by neutrons, 30:29516
BUONOMANO, V., Classical and relativistic Doppler effects, 30:31143 (INIS-mf-1357)
BURAS, A.J., Scaling of multiplicity distribution in hadron collisions and diffractive-excitation like models, 30:30758
BURCH, J.L., Observations of interactions between interplanetary and geomagnetic fields, 30:30366
BURCH, T.J., See MURPHY, J.J., 30:30961
BURDEKIN, F.M., See TURNER, C.E., 30:30053
BUREK, A.J., Spectrometric properties of crystals for x-ray astronomy. I., 30:30272
BURGKHARDT, B., See PIESCH, E., 30:29704
BURGOV, N.A., See KISELEV, Yu.T., 30:29633
BURKE, B.F., See KNOWLES, S.H., 30:30286
BURKE, G.J., See MILLER, E.K., 30:31449
BURKE, J.J., See SEIDMAN, D.N., 30:30000
BURKERT, V., See BECK, U., 30:30591
BURKHARDT, H., Inner bremsstrahlung in electromagnetic zero--zero transitions in nuclei, 30:31085
BURLAGA, L.F., Interplanetary stream interfaces, 30:30321
  Sweet's mechanism in the solar wind, 30:30325
  See OGILVIE, K.W., 30:30399
BURMAN, R.R., See BYRNE, J.C., 30:30388
BURROW, R.E.D., Trends in structural mechanics. A UK review of the 2nd international conference on structural mechanics in reactor technology. I. Pressure vessels and containments, 30:31192

BURROWS, H.D., Photochemistry of the uranyl ion, 30:29131
BURTSEVA, I.I., Washout of hygroscopic and nonhygroscopic aerosols with cloud droplets, 30:29393
BURTSEVA, L.V., See BURTSEVA, I.I., 30:29393
BUSCH, C.E., See IKOSSI, P.G., 30:30949
BUSCHOW, K.H.J., See ELEMANS, J.B.A.A., 30:29989
BUSSIERE, J.F., The effect of cladding material on ac losses of commercial Nb_3Sn tapes, 30:30840
BUSSO, L., See BALESTRA, F., 30:29591
BUSTER, D.S., See BRUENGER, F.W., 30:29804
BUTA, A., Deuteron break-up and proton scattering on ^{58}Ni, 30:30926
BUTORIN, N.V., Symposium on the effect of hot water of thermoelectric plants on the hydrology and biology of reservoirs (abstracts) March 24--26, 1971, Borok, USSR, 30:29463 (ORNL-tr-2781)
BUTYLENKO, A.K., Effect of rare earth metals on antimagnetism of chromium, 30:30054
BUYERS, W.J.L., See TENNANT, D.C., 30:29513
BYBERG, J.R., Effects of molecular motion in the ESR spectrum of BrO_3^{2-} ions in $KBrO_3$ single crystals, 30:29065
BYCHKOV, A.Kh., Effect of plastic deformation on some physical properties of niobium monocarbide in the homogeneity region, 30:29897
BYCKLING, E., Particle kinematics, 30:30646
BYKHOVSKII, A.V., Hot aerosol particles during commercial use of atomic energy, 30:29344
BYKOV, V.N., See BUDAGOVSKII, S.S., 30:30029
  See VOROB'EV, A.N., 30:30071
BYKOVSKII, Y.A., Spatial structure of an expanding laser plasma consisting of aluminum ions and nuclei, 30:29177
BYRNE, J.C., Dissipation of magnetic flux and magnetic energy in partially ionized gases, 30:30388
BYU, N.K., Radioactivation analysis in thermal and epithermal neutrons of the IBR-30 reactor of JINR, 30:28929

C

CABEZA, L., Dosimetry of the SIN biomedical pion beam with tissue-equivalent ionization chambers, 30:29555
CABIBBO, N., Quark additivity for mass splittings in the psub(z) + infinity frame, 30:30709
CACHARD, A., See THOMAS, J.-P., 30:29510
CADALBERT, R., See BARON, J.L., 30:30077
CAGE, M.E., See CLOUGH, A.S., 30:30891
CAHALAN, R.F., Spontaneous symmetry breakdown and Regge intercepts, 30:30707
CALL, P.J., Radiolysis of alkaline-earth fluorides, 30:29075
CALLENS-RAADSCHELDERS, M., Internal friction of polycrystalline Re following torsional deformation at liquid nitrogen temperature, 30:29991
CALLIGARIS, F., Study of a pion-stopping telescope by time-of-flight methods, 30:29590
CALOGERO, F., Nuclear many-body problem. Volume I. Proceedings of the international symposium, Rome, Italy, September 19--23, 1972, 30:31031
  Rigorous constraints that nuclear forces must satisfy to be consistent with the saturation property of nuclear binding energies, 30:31032
CAMERON, J.A., See KERR, P.G., 30:30933
CAMPBELL, D.E., Single pulse area measurement system (SPAMS), 30:29496 (UCID-16761)
CAMPBELL, J.H., PL/I based multi-tasking operating system, 30:31340 (IS-M-18)
CAMPBELL, M., See LEDINGHAM, K.W.D., 30:31076
CANESCHI, L., See AMATI, D., 30:30634
CANTER, K.F., Efficient positronium formation by slow positrons incident on solid targets, 30:30510
CANZLER, Th., See BRAUEL, P., 30:30588
CAPITELLI, M., The influence of excited states on the reactive thermal conductivity of an L.T.E. hydrogen plasma, 30:29190
CAPPER, D.M., Trace anomalies in dimensional regularization, 30:31182
CARBON, D.F., See RIDGWAY, S.T., 30:30225
CARDY, J.L., General features of the reggeon calculus with $\alpha>1$, 30:31170
CARES, W.R., Fatigue-crack growth of Ti--6Al--2Cb-1Ta--0.8Mo alloy in air and natural sea water environments, 30:29972 (AD-765318)
CARILLON, A., See JAEGLE, P., 30:29194
CARLSON, C.E., See GOLESTANEH, A.A., 30:30683
CARLSON, G.A., Calculating electron synchrotron radiation loss from a fusion plasma, 30:29182 (UCID-15513)
CARLSON, G.W., The effect of fragment anisotropy on fission-chamber efficiency, 30:29537
CARLSON, P.J., A large fast water Cherenkov counter, 30:29600
CARPENTER, D.L., See BLOCK, L.P., 30:30464
CARPENTER, H.C., See BINNS, W.R., 30:29568
CARPENTER, H.J., Blast wave boundary layer measurements. Final report, September 1971--August 1973, 30:29307 (AD-777580)
CARR, R.W., See BAGLIN, J.E.E., 30:30877
CARRASCOSA, J.L., Proteins induced in Bacillus subtilis infected with bacteriophage phi29, 30:29679
CARROLL, M., See BLAIR, D.C., 30:29886
CARTER, B., Charge and particle conservation in black-hole decay, 30:30186
CARTER, D.G. Jr., Method for the suppression of hydrogen during the dissolution of zirconium and zirconium alloys, 30:29148
CARTER, E.P., FIND: St. Lucie Plant, Unit 2, 30:31322 (FIND-50389)
CARTER, G., Ion implantation of semiconductors, metals, and alloys. Interim report No. 7, 1 September 1971--31 August 1973, 30:30088 (AD-774654)
CARTER, H.K., See SCHMIDT-OTT, W.D., 30:30986
CARTER, M.W., Off-site surveillance. Final report. Report on Project Dribble, Salmon Event, Tatum Salt Dome, Mississippi, 22 October 1964, 30:29345 (AD-629357)
CARVALHINHOS, H.J., Variation of activation volume and enthalpy during tensile straining of alpha-uranium at room temperature, 30:30035
CASABE, J., See BOTBOL, M., 30:28939
CASALI, R., See BERTANZA, L., 30:30606
CASEY, R.H., See LONG, D.M., 30:29888
CASS, J., Electron spin resonance absorption spectrum of HCO_2^{2-} molecule-ions in irradiated single-crystal calcite, 30:29074
CASSADY, J.R., See LI, F.P., 30:29714
CASSEL, D.G., See BEBEK, C.J., 30:30587
CASSENS, R.G., See FUNABIKI, R., 30:29866
CATTERALL, M., Treatment of advanced tumours of head and neck with fast neutrons, 30:29733
CATTON, I., Post-accident core retention for LMFBR's. 2. Technical report. Final report for the period 1 July 1972--30 June 1973, 30:31253 (UCLA-ENG-7343)
CEJNAR, F., See WILHELMOVA, L., 30:29089
CELEGHINI, E., Kinematical origin of the configuration mixing in the chiral algebra, 30:30719
CELLIER, F., See DUNCAN, R., 30:30111
CERJAK, H., See BAZANT, E., 30:31285
CERNY, J., Effect of chronic and acute gamma irradiation on specific recombination capability of lineage WD maize, 30:29689
CERRINA FERONI, C., See EVANS, D., 30:30742
CERTAIN, P.R., See FORTUNE, P.J., 30:30506
  See FORTUNE, P.J., 30:30504
CHAI, J., See WHITTEN, C.A. Jr., 30:30973
CHAICHIAN, M., Transverse momentum bounds and scaling in the hydrodynamical model, 30:30700
CHAISSON, E.J., High-frequency observations of possible ''heavy-element'' recombination lines, 30:30267
  See BEICHMAN, C.A., 30:30392
  See DICKINSON, D.F., 30:30362
CHAKRABARTY, D.K., See VENKATACHARI, R., 30:30432
CHALKIN, W., See HERRMANN, E., 30:28990
CHALOUPKA, V., See YAFFE, D., 30:30622
CHAMINADE, R., Multi-wire proportional chamber with charge division reading, 30:29593
CHAN, J.H., Anomalies in the composition of interplanetary heavy ions with $0.01 < E < 40$ MeV per amu, 30:30394
CHANDLER, C., See GIBSON, A.G., 30:30656
CHANDLER, K.C., See ARMSTRONG, T.W., 30:31119
  See ARMSTRONG, T.W., 30:31120
CHANDRA, H., See BORIE, E., 30:30671
CHANG, C.C., See BHOWMIK, R.K., 30:30896
CHANG, C.T.M., Application of microwave techniques to high-energy physics experiments at Argonne National Laboratory, 30:29584
CHANG, J., See KUSWA, G.W., 30:29159
CHANG, J.S., Introduction to extrapolation methods for the numerical solution of differential equations, 30:31355 (UCID-15992)
CHANG, T.W., See TSUSHIMA, T., 30:29868
CHANG, T.Y., Elastic-plastic deformation of cylindrical pressure vessels under cyclic loading, 30:31266
CHANG, Y.W., Analysis of the primary containment response using a hydrodynamic-elastic-plastic computer code, 30:31264
CHANNON, H.E.S., Radiation detection, 30:29503
CHANOWSKI, J.P., See JONES, L.W., 30:29596
CHAPLINE, G., See SLUTZ, S., 30:29271
  See SLUTZ, S., 30:29272
CHAPMAN, J.D, See GREENSTOCK, C.L., 30:29003
  See HALL, E.J., 30:29699
CHARASH, E., See DAVY, D.R., 30:29354
CHARLTON, L.A., See WHITE, R.L., 30:30937
CHARPAK, G., See BRESKIN, A., 30:29588
  See BRESKIN, A., 30:29587
  See BRESKIN, A., 30:29589
CHASMAN, C., See KAHANA, S., 30:31069
CHASMAN, R.R., Superheavy elements and the Strutinsky prescription, 30:31026
CHASTAIN, S.A., Fabrication, irradiation, and postirradiation examination of mixed oxide fuel pin PNL-3-8, 30:31231 (HEDL-TME-74-37)
CHATTERS, R.M., Method for determining sugar/starch contents in aqueous solutions, 30:28936
CHATTOPADHYAY, A., Multielement determination in market-garden soils by instrumental photon activation analysis, 30:28921
CHATURVEDI, P.K., See KAW, P.K., 30:30440
CHAUDAT, J.P., Experiments in pure uranium lattices with unit /sub infinity/. Assemblies SNEAK-8/8Z; UK 1 and UK 5 in ERMINE and HARMONIE, 30:31270 (EURFNR-1189)
CHAUDHARY, C.P., Latitude distribution of the regularity in F_2-region irregularities, 30:30417
CHAUSSY, J., See MORIN, P., 30:29990

CHAVANON, P., A partial-wave analysis of three body π^+ proton interactions at low energy, 30:30749
CHECHERNIKOV, V.I., See BASHA, A.F., 30:30031
CHECHETKIN, Yu.V., See POLYAKOV, V.I., 30:29562
CHEKMAREV, A.M., Fractional determination of ^{95}Zr and ^{95}Nb in a mixture by reverse phase chromatography, 30:28982
CHEKMASOVA, S.S., See ODYNETS, L.L., 30:29896
CHEN, A.J., Plasma tail interpretations of pronounced detached plasma regions measured by Ogo 5, 30:30466
CHEN, H., Structure of solid iron in superstrong neutron-star magnetic fields, 30:30194
CHEN, H.H., General derivation of Baecklund transformations from inverse scattering problems, 30:30782 (COO-3237-40)
CHEN, T.H., Microsecond pulse technique for heat capacity measurement, 30:31424 (LBL-2574)
CHENETTE, D.L., Bursts of relativistic electrons from Jupiter observed in interplanetary space with the time variation of the planetary rotation period, 30:30405
CHENG, K.L., See MARHOL, M., 30:29001
CHENG, V.K.C., The deuteron breakup reaction induced by protons of 65, 85 and 100 MeV, 30:30872
CHEREL, C., Apparatus and method for processing spent nuclear fuel elements, 30:29146
CHEREPIN, V.T., See LARIKOV, L.N, 30:29955
CHERNOMAZ, V.P., See NESMYANOVICH, A.T., 30:30309
CHERNOV, D.B., See SHINYAEV, A.Ya., 30:29932
CHERNOV, V.S., See GRIGOREVSKII, M.V., 30:30209
CHERNYAK, L.V., See SHLYUKO, V.Ya., 30:29892
CHERNYAVSKAYA, N.B., See GREBENSHCHIKOVA, V.I., 30:28999
CHERNYSHEV, A.A., See PLATONOV, P.A., 30:30090
CHERNYSHOV, A.A., See ISHMAEV, S.N., 30:30843
CHETIN, T., See JONES, C.A., 30:30205
CHEUNG, H., Kinetics of energy release of heterogeneous high explosives, 30:31408 (UCID-15962)
CHEW, G.F., Generalization of Regge asymptotic behavior, 30:30639
  Quark or bootstrap: triumph or frustration for hadron physics, 30:30702
CHI, J.W.H., Development of a reflux condensing heat pipe for emergency cooling of large cobalt-60 heat source, 30:29255
  See STONER, D.R., 30:29241
CHIBRIKIN, V.V., See CHEKMAREV, A.M., 30:28982
CHIEN, C.Y., See SREEDHAR, V., 30:30616
CHILDRESS, J.D., See ROMNEY, E.M., 30:29445
CHINNERY, M.A., Seismic discrimination. Semiannual technical summary report, 1 July--31 December 1973, 30:29305 (AD-777151)
CHIOTELIS, E., See PAPADIMITRIOU, J., 30:29850
CHIRAPATPIMOL, N., See WHITTEN, C.A. Jr., 30:30973
CHIRKO, I.L., See DEKHTYAR, I.Ya., 30:30086
CHISTYAKOV, V.M., See RYKOV, A.G., 30:29105
CHITKARA, K., Equilibrium approach to optimal in-core fuel management for pressurized water reactors, 30:31310
CHIU, Y.T., Self-consistent electrostatic field mapping in the high-latitude ionosphere, 30:30435
CHLIAPNIKOV, P.V., See AKOPDJANOV, G.A., 30:30608
CHOHAN, A.S., See GHANI, A., 30:31276
CHOI, B.H., Adiabatic distorted wave calculation of $H+H_2$ reactive scattering, 30:30533
CHOU, J.C., See WU, M.W., 30:30852
CHOU, M.C., See PERNG, C.C., 30:30927
CHOUDHURY, B.J., Coulomb T-matrix in the Glauber approximation in the presence of a low frequency electromagnetic field, 30:30790
CHRISTENBURY, S.T., See BRITTAIN, W.M., 30:29249
CHRISTENSEN, G.M., See JACKSON, K.L., 30:29737
CHRISTENSEN, J., Nickel brazing below 1025 C of untreated Inconel 718. Use of a getter makes nickel brazing of Inconel 718 and X-750 below 1025 C (1875 F) as easy as nickel brazing of stainless steels in vacuum, 30:29969
CHRISTENSEN, R., See LAWRENCE, C.W., 30:29683
CHRISTIANSEN, J.P., MEDUSA. A one-dimensional laser fusion code, 30:29227
CHRISTIANSSON, J.E., Nuclear structure studies of nuclei around mass number 23, 30:30901 (NP-20122)
CHRISTOFILOS, N.C., Analytical expression for the E-layer electron velocity distribution, 30:29187 (UCID-16003(Rev.1))
  Observations on the change of the length of the E-layer during stacking, 30:29188 (UCID-16004)
  Static compression of relativistic electron rings, 30:30131 (UCID-16583)
CHU, A.M., See WITHERS, H.R., 30:29758
CHU, F., See SYKES, M.P., 30:29715
CHU, S.C., See CHANG, T.Y., 30:31266
CHU, W.K., See LAU, S.S., 30:29939
CHUANG, C.W., See KO, H.C., 30:30275
CHUGUNOV, O.K., See PLATONOV, P.A., 30:30090
CHUMAKOV, M.M., See KISELEV, Yu.T., 30:29633
CHUPINA, M.A., See ANUFRIENKO, V.F., 30:29907
CHUPYATOVA, L.P., Pseudoasymmetry of [110] slip in tungsten single crystals, 30:30010
  Types of cracks in W monocrystals deformed by compression at 77°K, 30:30033
CHURCH, B.W., Distribution and inventory element activities on-NTS and off-NTS, 30:29453 (NVO-AEIC-74-1)
CIARLO, D.R., Automated inspection of IC photomasks, 30:31460 (UCRL-75994)
CIOFI DEGLI ATTI, C., Correlation effects on the ground-state energy and form factor of few-body systems, 30:31045
  Self-consistent wave functions, center-of-mass motion and high-energy particle-nucleus scattering, 30:31098
  See CALOGERO, F., 30:31031
CIRAUQUI, R., Radiomimeticity of the system H_2O_2/Fe(II) on nucleic acid components. Kinetic study, 30:29649 (JEN-284)
CIRSTOIU, B., See DEBERTH, C., 30:31084
CIUTI, P., See CALLIGARIS, F., 30:29590
CLARE, P.M., Foulness multi-ton air blast simulator. Part 1. Early development: the gun driven facility, 30:29309 (AWRE-O-31/74)
CLARIA, J.J., Investigation of a Milky Way region in Canis Major, 30:30217
CLARK, A.F., Cloud chamber quark quest one year report, 30:30576 (UCID-15787)
CLARK, G.H., Fitting an analytical curve to some experimental diffusion data, 30:29426 (BNWL-1850(Pt.3))
  See ELDERKIN, C.E., 30:29434
  See NICKOLA, P.W., 30:29424
  See NICKOLA, P.W., 30:29425
CLARK, G.W., See SPROTT, G.F., 30:30260
CLARKE, J.H., The collinear collision of two diatomic molecules. An application of the adiabatic approximation and the T- and K-matrix methods, 30:30563
CLARKE, T.R., See SEAQUIST, E.R., 30:30284
CLARKSON, J.E., Gas chromatographic analysis of bis(2-fluoro-2,2-dinitroethyl) formal (FEFO), 30:31370 (UCID-15671)
CLAUER, C.R., Variability of mid-latitude magnetic parameters used to characterize magnetospheric substorms, 30:30463
CLAURE, H., See BRAVO, A., 30:29865
CLAYTON, D.D., See HOYLE, F., 30:30256
CLEGG, T.B., See IKOSSI, P.G., 30:30949
CLEM, A., See MUGA, L., 30:29528
CLEMENT, J.D., See THOMPSON, S.D., 30:31241
  See WILLIAMS, J.R., 30:31209
CLEMENTEL, E., Nuclear energy and the environment, 30:31262
CLEYMANS, J., See ALBRIGHT, C.H., 30:30689
CLINE, D., See STEADMAN, S., 30:30920
CLOUGH, A.S., Pion-nucleus total cross sections from 88 to 860 MeV, 30:30891
CLUKEY, H.V., See GROSSMAN, L.N., 30:31281
COBB, E.C., See HUEBEL, H., 30:31263
COBBLE, J.A., Cold-electron temperature measurements in ELMO by excitation rate ratios of vacuum ultraviolet transitions, 30:29168
  Spectroscopic study in the vacuum ultraviolet of a neon plasma in ELMO, 30:29158 (ORNL-TM-4672)
COCHO, G., An SU(3) analysis of vector meson photoproduction and the pomeron, 30:30665
CODE, A.D., Radiative transfer in circumstellar dust clouds, 30:30380
COENSGEN, F.H., Proposed 2X data system, 30:29212 (UCID-15434)
COFFEY, J.W., Radioimmunoassay for plasma insulin using zirconyl phosphate gel, 30:29870
COFFEY, T.P., See MCDONALD, B.E., 30:30427
COHEN, H., Chromium--carbon bonds in aqueous solutions. A pulse radiolytic study, 30:29080
COHEN, M., Possible nature of some unusual OH sources, 30:30273
COHEN, M.G., High efficiency acousto-optical Q-switch, 30:29282
COHEN, R.L., See BROWN, J.P., 30:30093
COHEN, T.J., Long term periodicities in the sunspot cycle, 30:30331
COHEN-TRANNOUDJI, C., Quantum mechanics. Volume II, 30:31135
  Quantum mechanics. Volume I, 30:31134
COKER, W.R., See HOFFMANN, G.W., 30:30907
COLEMAN, L.W., See THOMAS, S.W., 30:29162
COLEMAN, R.F., Comparison of analytical techniques for inorganic pollutants, 30:28924
COLEMAN, S., Dilatations, 30:30644
COLLINS, C.J., See RAAEN, V.F., 30:29010
COLUSSI, A.J., ESR spectra of PF_2 and SF_3 radicals, 30:29067
COMAR, C.L., Progress report, June 1, 1973--May 31, 1974, 30:29416 (COO-3167-102)
CONDE, H., See BERGMAN, R., 30:28918
CONDIT, W.C., Fast, high sensitivity 10.6 micron interferometer, 30:29161 (UCID-15625)
CONKLIN, G.M., See JONES, P.R., 30:30540
CONLON, T.F., See CHENETTE, D.L., 30:30405
CONNES, P., High-resolution Fourier spectra of stars and planets, 30:30207
CONRAD, J.D. Jr., System and method for operating a steam turbine with independent overspeed protection especially adapted for a nuclear reactor powered steam turbine, 30:31283
CONSTABLE, I.J., Experimental ocular irradiation with accelerated protons, 30:29754
CONSTANDINIDIS, C., See PAPADIMITRIOU, J., 30:29850
CONSTANTINESCU, S., See ZAMFIRESCU, I., 30:31342
CONSTANTINIDIS, M., See PAPADIMITRIOU, J., 30:29850
CONTRI, R., See EVANS, D., 30:30742
COOK, J.D., See MILES, L.E.M., 30:29835

COOK, L.M., Small quantities, 30:29648
COOKER, T.W., See CARES, W.R., 30:29972
COOPER, G., Fine structure generalization of the Compton Fokker--Planck equation, 30:31105 (UCID-15784)
COOPER, J.A., See PERKINS, R.W., 30:29359
COOPER, R.K., Resistor beam bugs: scientific explanation, 30:29225 (UCID-16057)
  Surface currents on a toroid that result in a uniform, axial magnetic field inside the torus, 30:29219 (UCID-15695)
COPLEN, H.L., LOFT integral test facility and program, 30:31238
CORDIER, P., See BELLONI, J., 30:29079
CORDS, D., See BRAUEL, P., 30:30588
CORK, B., See JONES, L.W., 30:29596
CORMIER, T.M., Performance of a heavy-ion time-of-flight spectrometer, 30:29573
CORNELL, J.C., See MENCHACA-ROCHA, A., 30:30904
CORNET, P., See DEHM, G., 30:30624
CORNETT, J.S., See RANDERSON, D., 30:29377
CORTELLESSA, P., Considerations on the neutral component relative to the August 4, 1972 solar event, 30:30296 (CONF-730693-)
COSIMI, M., MCDATA code, 30:30851 (RT/FI-(74)19)
COSMAN, E.R., See CORMIER, T.M., 30:29573
COSSLETT, V.E., See SALIH, S.M., 30:29070
COSTA, G., See EVANS, D., 30:30742
COUCH, R.G., See PARDO, R.C., 30:30257
COULON, C., See DUPUY, C., 30:29340
COULTAS, T.A., See KRAKOWSKI, R.A., 30:29206
COVERT, G.F., See CAMPBELL, J.H., 30:31340
COVINGTON, A.E., 10.5 year period for the slowly varying component of the solar radio flux, 30:30306
COWARD, D.H., See RIORDAN, E.M., 30:30583
COWLEY, A.P., See HUTCHINGS, J.B., 30:30230
  See HUTCHINGS, J.B., 30:30291
COX, J.P., Pulsational stability of stars in thermal imbalance. III. Analysis in terms of absolute variations, 30:30192
CRAIG, G., Two particle intrinsic excitations in ^{22}Ne and ^{26}Mg, 30:30915
CRAIGIE, N.S., Absorption corrections in a Mueller Regge analysis of inclusive photo- and electroproduction, 30:30670
CRAMER, J.G., See DEVRIES, R.M., 30:31063
CRAMPIN, M., Physical significance of the topology of the Bondi--Metzner--Sachs group, 30:30766
CRAMPTON, D., Spectroscopic analysis of HZ Herculis, 30:30270
  See HUTCHINGS, J.B., 30:30291
  See HUTCHINGS, J.B., 30:30230
CRANDALL, D.H., Rate coefficients for electron excitation of the first resonance transition in H, Li, Na, Ca, Ca^+, and Ba^+ calculated from experimental data, 30:30246
CRANDELL, C.E., Radiation characteristics and controls. I, 30:29709
CRANNELL, H., See KLINE, F.J., 30:30678
CRASNIER, J., See GUYADER, J.C., 30:29567
CRAWFORD, D.R., See CARPENTER, H.J., 30:29307
CRAWLEY, J.C.W., See CHANNON, H.E.S., 30:29503
CRESSY, P.J. Jr., The unique cosmic-ray history of the Malakal chondrite, 30:30170
CRISLER, L.R., Chemical vapor deposition of uranium and plutonium, 30:29961
CROCKER, W.C., See STARA, J.F., 30:29815
CROSSLEY, D.A. Jr., Radioactive tracer studies of soil and litter arthropod food chains. Progress report, November 1, 1973--October 31, 1974, 30:29419 (SRO-641-13)
CROSSMAN, G.L., See SELIG, W., 30:31369
  See SELIG, W., 30:31373
CROUCH, E.A.C., Assessment of known independent yields and the calculation of those unknown in the fission of ^{232}Th, ^{233}U, ^{235}U, ^{238}U, ^{239}Pu, ^{240}Pu, and ^{241}Pu, 30:31008 (AERE-R-7680)
CROWE, A., See KAISER, E.W., 30:30547
CROWLEY, W.P., Numerical solutions of Poisson's equation by Fourier transform methods, 30:31348 (UCID-15478)
  Some numerical experiments with low atwood number incompressible Rayleigh--Taylor instabilities, 30:31438 (UCID-15618)
  Two numerical examples of Rayleigh--Taylor instability for a system of five different densities, 30:31437 (UCID-15611)
CRUDDACE, R., See MARGON, B., 30:30174
CSIKAI, J., See VARNAGY, M., 30:29527
CSIRIK, J., See ZITA, G., 30:29831
CUAREN, A., See GORDON, F., 30:29852
CUDERMAN, J.F., Spectral analysis of x rays from laser-induced plasmas, 30:29193 (SLA-74-5242)
CUDKOWICZ, G., See ITO, T., 30:29665
CUDWORTH, K.M., Proper motions of faint blue stars near the galactic anticenter. I, 30:30237
CUKIER, M., See JAEGLE, P., 30:29194
CULLEN, T.L., See HAINBERGER, P.L., 30:29413
CUMMINS, W.F., See COENSGEN, F.H., 30:29212
CUNNINGHAM, D.M., Photoelastometric recording of stress waves, 30:31434 (UCID-15383)
CVEJANOVIC, S., New technique for threshold excitation spectroscopy, 30:30553
CZYZ, W., See BIALAS, A., 30:31062

D

DABROWSKI, A.J., N-type cadmium telluride surface-barrier nuclear radiation detectors, 30:29520
DABROWSKI, T.E., Douglas United Nuclear, Inc. reactor and fuel production facilities 1972 environmental release report, 30:29341 (DUN-8133)
D'ADDA, A., Generalized 6j-coefficients and their symmetries, 30:30769
DADO, S., Backward production of rho^0 and f^0 mesons in π^+n interactions at 6 GeV/c, 30:30621
DADYKIN, V.Ya., See ALEKSEEV, E.N., 30:29578
DAGLE, G.E., See BALLOU, J.E., 30:29776
  See GOMEZ, L.S., 30:29820
DAHLMAN, R.C., See MILLS, M.T., 30:29380
DAIMER, P., See STREICH, M., 30:28993
DALE, L.S., See FLORENCE, T.M., 30:28950
DALLINGER, R.P., See OSBORNE, D.W., 30:29128
DALY, B.D.T., See HAGEN, K.G., 30:29262
DAMM, C.C., See FUTCH, A.H., 30:29183
DAMRON, J.R., Gallium--technetium subtraction scanning for the localization of subphrenic abscess, 30:29845
DANA, M.T., Comparison of the washout coefficient for a polydisperse aerosol to that for an aerosol of fixed particle size, 30:29477 (BNWL-1850(Pt.3))
  Precipitation scavenging of inorganic pollutants from metropolitan sources: St. Louis, July 1973, 30:29479 (BNWL-1850(Pt.3))
DANCEVA, K.I., Effect of x rays on the phosphorylation of histon f_1 in thymocytes, 30:29653
DANCHAK, M., Simple device using capacitance switches for data entry in man--machine systems, 30:29620
DANIELS, A., See POUCHOT, W.D., 30:29259
DANIL'CHENKO, B.A., See DEKHTYAR, I.Ya., 30:30086
DANILEVSKII, N.P., See AOVAL, A.G., 30:30544
DANILUK, J., See PANKE, R., 30:29723
DAN'KIN, A.A., Abrasive wear-resistance and failure character of titanium and zirconium borides surface layers, 30:29899
DANNEFAER, S., See SMEDSKJAER, L., 30:30513
DANPURE, C.J., Effect of internally deposited plutonium-239 on the lysosomes of rat liver, 30:29782
DARDO, M., See BONINO, G., 30:30414
DARGENE, N.P., See STYRO, B.I., 30:29391
DARROUZET, M., See CHAUDAT, J.P., 30:31270
DARWISH, S., See LINDSKOG, J., 30:30979
DARZYNKIEWICZ, Z., Radiation-induced DNA synthesis in normal and stimulated human lymphocytes, 30:29664
DASGUPTA, M.K., Some studies on solar x-ray flare-associated optical flares, microwave bursts, and sudden ionospheric disturbances, 30:30307
DASH, J.W., See BALI, N.F., 30:30710
DASHEN, R., Pion phase transition in chiral symmetry breaking model, 30:30716
DASHKOVSKII, A.I., See SKOROV, D.M., 30:30002
DA SILVEIRA, R., On the determination of the effective barrier in heavy ion collisions, 30:31070
D'ATTELLIS, C.E., A simple time optimal digital control for nuclear reactors, 30:31303
  Double optimization in linear discrete systems, 30:31335 (CNEA-365)
D'AURIA, R., See D'ADDA, A., 30:30769
DAUTOV, L.M., See SOKOL'SKII, D.V., 30:29052
DAVEY, W.R., See COX, J.P., 30:30192
DAVIES, M.H., Secondary deuterium isotope effects in proton transfers from 2-nitropropane, 30:29023
DAVIES, R.D., Gas and dust in interstellar clouds, 30:30367
  Interferometric studies of OH sources associated with H II regions and ir objects, 30:30368
DAVILA, C.A., See CIRAUQUI, R., 30:29649
  See DELGADO, M.D., 30:29650
DAVIS, C.K., See GREENBERG, J.S., 30:30922
DAVIS, J., See JULIENNE, P.S., 30:30425
DAVIS, R.C., DuoPIGatron II ion source, 30:29209 (ORNL-TM-4657)
DAVIS, W.E., Model for cumulus washout of cosmogenic radionuclides, 30:29363 (BNWL-1850(Pt.3))
  Model to compute low-level Montgomery stream functions, 30:29436 (BNWL-1850(Pt.3))
  Progress report on in-cloud scavenging in frontal storms, 30:29475 (BNWL-1850(Pt.3))
  Summary of current findings from the analysis of 1972 Quillayute scavenging experiments, 30:29476 (BNWL-1850(Pt.3))
  See YOUNG, J.A., 30:29368
DAVIS, W.F., See MERKLE, E.J., 30:28942
DAVY, D.R., Ecological factors in the siting, design, and operation of a nuclear power station, 30:29354
DAVYDOV, E.N., Determination of fallout radioisotopes from their content in the annual layers of high-mountain glaciers, 30:29408
DAVYDOV, Yu.P., Conditions for forming polynuclear hydroxy complexes of hexavalent uranium, 30:29125
DAWSON, B.E., See WOLOWODIUK, W., 30:29275
DAWSON, J.W., See CHANG, C.T.M., 30:29584
DAY, K.L., A quantitative study of silicate extinction, 30:30190
DAY, R.H., See PARKINSON, W.C., 30:30158
  See PARKINSON, W.C., 30:30159
DAYANANDA, M.A., See GRACE, R.E., 30:31390
DE, N.C., See FIFE, T.H., 30:29017
DE, P.K., Stress corrosion cracking of zirconium in methanol--HCl solutions, 30:29957

DE ALFARO, V., Old and new ideas about currents and their commutators, 30:30640
DE BATIST, R., See CALLENS-RAADSCHELDERS, M., 30:29991
DEBERTH, C., Experimental photonuclear cross section calculation, 30:31084
DE BETTENCOURT, A.O., Ruthenium volatility during vitrification of fission products. Part II. Fixation on a steel tube. Peroxide decomposition, 30:29086 (AEC-tr-7575)
DEBIES, T.P., See RABALAIS, J.W., 30:30491
DE BOER, F.W.N., Decay properties of three ^{166}Lu isomers and the decay of ^{166}Hf, 30:30989
  See LINGEMAN, E.W.A., 30:31125
DEBRUN, J.L., See KOHN, A., 30:28923
DEBRUNNER, P.B., See POTTER, J.M., 30:30599
DECIU, N., See BADESCU-SINGUREANU, A.I., 30:30846
  See BADESCU-SINGUREANU, A.I., 30:30845
DECKERT, T., See LAURIDSEN, U.B., 30:29842
DECLAIS, Y., See BAILLON, P., 30:30737
  See BAILLON, P., 30:30618
  See BAILLON, P., 30:30619
DECSY, M.I., Binding of ^{63}Ni to rabbit serum α_1-macroglobulin in vivo and in vitro, 30:29088
DE DIEGO, N., Coincidence twist boundaries in muscovite, kaolinite, and MoO_3, 30:29895
DEE, D., See BARR, T.L., 30:31459
DE FEITER, L.D., Solar flares as sources of energetic particles, 30:30333
DE FERRAN, E.M., Corrosion study of the superplastic alloys 70/30 and 80/20 zinc aluminum in a humid atmosphere, 30:31391 (COPPE-TP-8/72)
DEFOUQUET, J., See RIEU, G.E., 30:29980
DEGISI, S.L., See NEET, T.E., 30:31384
DE GREGORIO, G., Corrosion of sheet and welded joint specimens of Incoloy 825-low carbon (C less than or equal to 0.03%) in HNO_3 (Huey) and HF solutions, 30:29956
DE GROOT, H., Triton binding energy and the deuteron wave function, 30:30862
DEHM, G., A measurement of K*(1420) decay branching ratios, 30:30624
DEIS, D.W., Multifilament Nb_3Sn conductors, 30:30809
DE JAGER, J.L., Description of odd-mass copper nuclei with particle-core coupling models, 30:30939
DE-JONG, G., See DEHM, G., 30:30624
DEKHTYAR, I.Ya., Effect of temperature and electromagnetic radiation on the electrical resistance of deformed molybdenum, 30:30086
DE LAETER, J.R., Mass spectrometric isotope dilution analyses of tin in stony meteorites and standard rocks, 30:30311
DELAIRE, J., See BELLONI, J., 30:29079
DELAPLACE, J., See BARON, J.L., 30:30077
DELATOUR, C., See KELLAND, D., 30:30832
DELBOURGO, R., Dimensional regularization for weak interactions, 30:30687
  Scalar multiplets and asymptotic freedom, 30:30724
DE LEO, R., See BELLUSCIO, M., 30:29517
DELGADO, M.D., Structural study of DNA discontinuities by enzymatic polymerization, 30:29650 (JEN-286)
DEL GUERRA, A., The pion form factor at a timelike momentum transfer of approximately 1 fm^{-1} from π^+ electroproduction at threshold, 30:30678
DELINCEE, H., Effect of γ irradiation on the charge and size properties of horseradish peroxidase: individual isoenzymes, 30:29651
DELL, R., See JEE, W.S.S., 30:29801
DELLE, W., Changes of dimensions, modulus of elasticity and heat conductivity during regraphitization by neutron irradiation, 30:30089 (AED-CONF-74-206-001)
DEMINA, T.V., See DERID, O.P., 30:30015
DEMKIN, Yu.I., See LYAKISHEV, N.P., 30:29970
DE MORAES, S., Separation of trace metal impurities from nuclear grade uranium by long-chain amine extraction and direct determination by atomic absorption spectrophotometry, 30:28948
DEMTROEDER, W., Hyperfine structure in the visible NO_2 spectrum, 30:30507
DE MUL, F.F.M., RKSPROG: a computer program for inelastic cold neutron scattering time-of-flight measurements, 30:30847 (IRI-132-73-03)
DEMURA, A.V., Calculation of inelastic transition cross sections on basis of spectral line broadening theory, 30:30520 (IAE-2269)
DENARDO, G., On the generalized ergosphere of the Kerr-Newman geometry, 30:30214
  See BERGAMINI, R., 30:30208
DENEY, C.L., See GOLDEN, R.L., 30:30165
DENISOV, D.A., Isotope exchange reactions. IX. Calculation of the partition function ratios of isotopic molecules with the aid of the increment in the trace of the GF-matrix, 30:29031
DENNING, A., See BROWN, G., 30:30923
DEO, M.G., X-radiation-induced intestinal lesions in protein-deficient rats, 30:29741
DE OLIVEIRA PAIVA, I.R., See HAINBERGER, P.L., 30:29413
DER, Z.A., Regional attenuation of short-period P and S waves in the United States, 30:29303 (AD-776672)
DERENZO, S.E., Electronic processes in liquid xenon, 30:29512
DERID, O.P., Ternary system Cd--Ga--Te, 30:30015
DERRE, J., Two body correlations between negative pions in pp interactions at 69 GeV/c, 30:30601
  See BUMAZSHNOV, V.A., 30:30603
DERRICK, M., See WHITMORE, J., 30:30759
DESAI, B.R., Possibility that the Pomeron-Reggeon cut contains the Regge pole, 30:30717
DESER, S., Nonrenormalizability of Einstein-Yang-Mills interactions at the one-loop level, 30:31184
  Nonrenormalizability of quantized fermion--gravitation interactions, 30:31179
DESHPANDE, U.R., See SAMUEL, A.M., 30:29877
DESYATNIK, V.N., Fusibility diagram of the system $LiCl$--UCl_4--$ThCl_4$, 30:29095
DETHLEFSEN, J.M., See BURAS, A.J., 30:30758
DE TOURREIL, R., Status of potential models, 30:31061
  See SPRUNG, D.W.L., 30:31035
DEUTSCH, E., See WESCHLER, C.J., 30:29132
DEVAN, J.H., Effect of oxygen on the corrosion of vanadium and V--20% Ti by liquid lithium, 30:29954
DEVANEY, J.J., Magnetically protected first wall for a laser-induced thermonuclear reaction, 30:29207 (LA-5699-MS)
DEVI, U., Raman process in the case of multiphoton excitation of the hydrogen molecule in an intense laser beam, 30:30551
DEVOIGT, M.J.A., See STEADMAN, S., 30:30920
DE VRIES, A.E., See KONNEN, G.P., 30:30484
DEVRIES, R.M., Importance of Coulomb interaction potentials in heavy ion DWBA calculations, 30:31063
DEW-HUGHES, D., Practical superconducting materials, 30:30825
DHAR, A.K., Are there low-lying, intrashell-excited, highly deformed states in the 1f-2p shell nuclei, 30:30925
DHEZ, P., See JAEGLE, P., 30:29194
DIAMOND, R.M., See PROETEL, D., 30:31006
DIAS, J.W., Fission gas behavior in fast reactor fuel under transient power conditions, 30:31228
DIAZ, J., See DADO, S., 30:30621
DIBIANCA, F., See DADO, S., 30:30621
DIBITONTO, D., A high-intensity superconducting muon channel, 30:30156
DICKENS, J.K., Gamma-ray production due to neutron interactions with ^{64}Zn and the level structure of ^{64}Zn, 30:30936 (ORNL-4985)
DICKINSON, D.F., An OH survey of the Hoffmann 100-μ sources, 30:30362
DIECKAMP, H.M., See WETCH, J.R., 30:31242
DIEHL, H., See BECKER, H.J., 30:31018
DIEN, F.K., See BYU, N.K., 30:28929
DIETL, H., See GRAYER, G., 30:30617
DIETRICH, G., See BOHN, T., 30:31305
DIETRICH, W., Search for low-spin positive parity states in light odd-mass In nuclei, 30:30954 (NP-20122)
  See NYMAN, B., 30:30953
DI GIACOMO, A., Scaling in e^+e^- annihilation into hadrons, 30:30677
DILL, D., See ATABEK, O., 30:30496
DILLEY, J., A new parametrization for the N/D method, 30:30791
DILLINGER, B.L., See CARPENTER, H.J., 30:29307
DILWORTH, C., Galactic electrons and electromagnetic radiation, 30:30343 (CONF-730693-)
DIMITROV, O., See GRYNSZPAN, R., 30:30082
DIN, G.A., See MCCREADY, R.G.L., 30:29826
DI NAPOLI, V., Isomeric-yield ratio of ^{52}Mn/sup g/ and ^{52}Mn/sup m/ photoproduction from ^{55}Mn at intermediate energies, 30:30919
DINES, V.L., See KOKHOV, E.D., 30:28952
DISTEFANO, J.R., See MOORHEAD, A.J., 30:29966
DIU, B., See COHEN-TRANNOUDJI, C., 30:31134
  See COHEN-TRANNOUDJI, C., 30:31135
DIX, W.R., See BRAUEL, P., 30:30588
DJALOEIS, A., See ASPELUND, O., 30:30900
DLOUHY, Z., Current storage possibilities of blocks with solidified radioactive wastes at the Institute of Nuclear Research, 30:29137
DMITRIEV, A.B., See BLOKH, Ya.L., 30:29582
DMITRIEV, V.D., See VOROB'EV, A.N., 30:30071
DMITRIEVA, G.V., Concentrational distribution of fission products over tropical zone oceans and its relation to atmospheric processes, 30:29388
DOBATKIN, V.I., Nonequilibrium crystallization of aluminum--molybdenum alloys, 30:30006
DOBBINS, A.G., See BULLUCK, J.S., 30:29944
DOBRATZ, B.M., Properties of the high explosive LX-09-0, 30:31372 (UCID-15910)
DOBREV, D., See MITROV, G., 30:29717
DOBROZEMSKY, R., Mass-spectrometric determination of neutron capture cross-sections of the rare earth isotopes, 30:30977 (AEC-tr-7574)
DOBSON, P.N. Jr., Proceedings of the fifth Hawaii topical conference in particle physics, Honolulu, Hawaii, August 8--21, 1973, 30:30577
DOCKUM, J.G., See LLOYD, R.D., 30:29802
DODD, R.J., Direct simulation of collision processes. II. The growth of planetesimals, 30:30409
DODSON, H.W., Comparison of activity in solar cycles 18, 19, and 20, 30:30328
DOERING, J.P., See BREGMAN-REISLER, H., 30:30558
DOGNON, A., Effect of temperature on the radiation sensitivity of Ascaris eggs, 30:29766 (SAND-74-6017)
DOHERTY, L.H., See TERZIAN, Y., 30:30240
DOLAN, S.P., See ROGERS, D.W.O., 30:30895
  See ROGERS, D.W.O., 30:30894
DOLBEAU, J., See CHAVANON, P., 30:30749

DOLBILOV, G.V., See BARABOSCH, L.S., 30:30117
DOLENC, M.R., Ecological considerations of Project Wagon Wheel, 30:29459
DOLGOREV, A.V., Modern methods of determination of zirconium (survey), 30:28911
DOLL, J.D., Semiclassical theory of atom--solid-surface collisions: application to He--LiF diffraction, 30:30476
DOMEN, S.R., See KASE, K.R., 30:29556
DONALDSON, G., Observation of the decay K/subL/^{0} + $\pi^+\pi^-\gamma$, 30:30582
DOPITA, M.A., High velocities and cocoon stars, 30:30243
DORMAN, L.I., See BLOKH, Ya.L., 30:29499
DOROFEEV, E.B., See BOLDYREV, A.M., 30:30012
DOROSHENKO, G.A., See RYABININ, A.I., 30:28996
DOROSHENKO, L.K., See LAVRENKO, V.A., 30:29938
DOSCHERHOLMEN, A., See SHAFER, R.B., 30:29856
DOS SANTOS, M.C.M., See ALVES, M.A.F., 30:29523
DOUGHERTY, J.H., Early nematologic effects of curium and einsteinium in beagles, 30:29779 (COO-119-249)
DOUGLAS-HAMILTON, D.H., Attachment instability in an externally ionized discharge, 30:29201
DOUGLASS, D.L., See KUENZLY, J.D., 30:29953
DOULL, J., See HURWITZ, S., 30:29738
DOVER, C.B., The ^{3}He(γ,π^+)^{3}H reaction in the (3,3) resonance region, 30:30869
  See BARSHAY, S., 30:31095
DOWNES, A.M., Radioisotope method of measuring the mean fibre diameter of wool samples, 30:29604
DRACHINSKII, A.S., See ARKHAROV, V.I., 30:30023
DRAGANIC, I., See GAL, O., 30:29547
DRAGULESCU, E., See IVASCU, M., 30:30941
DRECHSEL, D., Off-shell effects of the nucleon--nucleon force in nucleon--nucleon bremsstrahlung, 30:31042
  See BORIE, E., 30:30671
DREES, J., See BAETZNER, K., 30:30589
  See BECK, U., 30:30591
DREHER, B., See ROTHHAAS, H., 30:31005
DRESBACH, B., See BECK, U., 30:30591
DRITS, M.E., Co-solubility of neodymium and zinc in solid magnesium, 30:30007
DROPPO, J.G., Dry disposition processes on vegetation canopies, 30:29369 (BNWL-1850(Pt.3))
  See HORST, T.W., 30:29375
DROSTE, C., Levels in ^{130}Ba fed from ^{130}La decay, 30:30963
DRSATA, J., Aromatic amino acid decarboxylase activity of rat brain and its parts following exposure to ionizing radiation, 30:29740
DRUCKER, G., See BARNES, E.G., 30:29295
DUARTE, U., See GARCIA AGUDO, E., 30:28913
DUBA, A.G., Effect of fluid content on the mechanical properties of Westerly granite, 30:31411 (UCRL-51626)
DUBIN, D.L., See RIORDAN, E.M., 30:30583
DUBNICKOVA, A.Z., Non-zero masses of π,K, eta and kappa mesons and algebraic realization of SU(3) x SU(3) chiral symmetry, 30:30780
DUBOIS, J., See CHRISTIANSSON, J.E., 30:30901
DUBOVOI, L.V., High-current electron accelerator with supply by inductive storage, 30:30121 (LA-tr-74-30)
DUBROVIN, A.V., See DUNAEVA, K.M., 30:29103
DUCUING, J., See LUKASIK, J., 30:30508
DUDZIAK, D.J., See BOSLER, G.E., 30:29228
DUERR, H.P., Conformal invariant spinor theory with third-order derivatives, 30:31155
DUESDIEKER, G., See AXEN, D., 30:29597
DUFF, M.J., See CAPPER, D.M., 30:31182
DUFLOT, M., See FEHRENBACH, C., 30:30199
DUFOUR, P., See DEHM, G., 30:30624
DUGGAL, S.P., See POMERANTZ, M.A., 30:30327
DUGGAN, F., See SINHA, B., 30:31104
DUINKER, W., See BRESKIN, A., 30:29587
DULEY, W.W., See MCCULLOUGH, J.D., 30:30376
DULL, D.L., Thermal and mechanical effects on the corrosion behavior of Ti--6Al--4V. Report for January 1971--January 1972, 30:29942 (AD-777170)
DUMA, M., Programs for experimental data processing on PDP-8/I computer, 30:29614 (IFA-CRD-57-1974)
DUMITRESCU, O., One- and two-nucleon transfer reactions on deformed nuclei, 30:31021 (IFA-FT-108-1974)
DUNAEVA, K.M., Kinetics of oxidation of uranium oxysulfide, 30:29103
DUNAWAY, P.B., Dynamics of plutonium in desert environments. Nevada Applied Ecology Group progress report as of January 1974, 30:29439 (NVO-AEIC-74-1)
DUNCAN, R., Nuclear reactor fuel rod splitter, 30:30111
DUNLOP, W.H., See WHITTEN, C.A. Jr., 30:30973
DUNN, G.H., See CRANDALL, D.H., 30:30246
DUNNING, F.B., Absolute cross sections for the photoionization of He(n^3 ^{3}P) atoms, 30:30500
DUPEYRAT, M., See JAEGLE, P., 30:29194
DUPLANTIS, D.C., See PARKINSON, W.C., 30:30159
  See PARKINSON, W.C., 30:30158
DUPUY, C., Determination of ^{87}Sr/^{86}Sr in cenozoic andesites and the related rocks of northwest Sardinia (Italy), 30:29340
DURAND, J.M., See CHAMINADE, R., 30:29593
DURFEE, R.C., ORRMIS: Oak Ridge Regional Modeling Information System. Part I, 30:29456 (ORNL-NSF-EP-73)
DUURSMA, E.K., Concentration effects of ^{137}Cs, ^{65}Zn, ^{60}Co, and ^{106}Ru sorption by marine sediments with geochemical implications, 30:29409
DUVAL, V.L., See CLARKSON, J.E., 30:31370
  See MORRIS, G.A., 30:29323
DYAD'KIN, I.G., Approximation for time relationships in pulsed gamma--gamma logging, 30:29605
D'YAKONOVA, L.V., See SAMSONOV, G.V., 30:29898
D'YAKOV, V.A., Optical coherent radiation, 30:30112
DYATLOVA, N.M., See MOROZOVA, S.S., 30:28955
DYBKOV, V.I., See EREMENKO, V.N., 30:30003
DYDUCH, J., See ZDERKIEWICZ, T., 30:29685
DYER, H.R., Safety analysis report for packaging (Oak Ridge Y-12 Plant Model VCD package for enriched uranium solution), 30:30115 (Y-DD-155)
DYRBYE, M., See HJELMS, E., 30:29883
DYSON, H.B., See WILSON, W.J., 30:30265
DZYADYKEVICH, Yu.V., Reactions of boron and silicon carbide with tungsten and titanium, 30:29948

E

EAKER, R., See HUGA, L., 30:29528
EBENHOEH, W., See JOHANSSON, A., 30:30855
EBERHARD, Ph., See BAILLON, P., 30:30618
EBERHARDT, L.L., General statistical considerations in environmental plutonium studies, 30:29418 (NVO-AEIC-74-1)
  See GILBERT, R.O., 30:29444
EBERSOLE, T.J., See ANDREWS, R.E., 30:29254
EBERSTADT, P.L., Total-body water determination with a practical internal standard method, 30:29884
EBNER, C., Thermodynamic functions of ideal two- and three-dimensional Fermi gases, 30:30802
EBRAHIM, A., Structure and experimental consequences of chiral SU$_3$ x SU$_3$ breaking, 30:30775
ECKLUND, W.L., See ROMICK, G.J., 30:30430
ECKSTEIN, Y., See ROSENBAUM, R.L., 30:30800
EDMAN, G.W. IV, Process evaluation of new cellular silicone material, 30:31385 (BDX-613-1082(Rev.))
EDNERAL, A.F., Field-ion microscopic study of aged martensite in an iron--nickel--cobalt--molybdenum alloy, 30:30037
EDWARDS, A.L., Thermal ignition of an explosive by surface friction, 30:31402 (UCID-15669)
EFIMOV, A.I., See GRINIK, E.U., 30:30072
EFIMOV, B.V., Intensity fluctuations of γ-transitions from the (anti n,γ) reaction, 30:30978 (IAE-2289)
EFIMOV, G.V., Construction of nonlocal quantum electrodynamics of bosons with spin 0 and 1, 30:31144 (JINR-P2-7432)
EFIMOV, V.N., Two-body T-matrix factorization and three-nucleon problem, 30:31047
EFREMENKOV, V.M., See DAVYDOV, Yu.P., 30:29125
EFREMOVA, G.P., See ZYKOVA, A.S., 30:29399
EFURD, D.W., See KURODA, P.K., 30:30162
EGGENHUISEN, H.H., See HERMANS, J.A.J., 30:30864
  See VAN DRIEL, M.A., 30:30912
EGGERMAN, W.G., See CRISLER, L.R., 30:29961
EGOROV, Yu.A., Input control of counters CU-51 for assembling azimuthal and calibration telescopes T/SKL and ET/SKL, 30:29583
EHNTIN, I.R., See SOMENKOV, V.A., 30:29008
EHRLICH, K., See KALETTA, D., 30:30075
EICHLER, B., Prediction of the behaviour of superheavy elements and their chlorides during thermatochromatographic separation, 30:29138 (GSI-tr-74/15)
EICHLER, E., See RIEDINGER, L.L., 30:30985
EINASTO, J., Dynamic evidence on massive coronas of galaxies, 30:30379
EKSTROEM, C., Atomic-beam investigations of some antimony nuclides, 30:30976
ELAYAPERUMAL, K., See DE, P.K., 30:29957
EL BAZ, E., See MEYER, J., 30:31036
EL-BEDEWI, F., Distorted wave Born approximation analysis for the ^{16}O(^{3}He,α)^{15}O reaction, 30:30888
  Variations of cosmic ray intensity in consequence of the semidiurnal anisotropy, 30:30179
ELDERKIN, C.E., Comparison of diffusion-deposition model components with experimental results, 30:29434 (BNWL-1850(Pt.3))
  See HORST, T.W., 30:29375
ELEMANS, J.B.A.A., Crystal and magnetic structure of intermetallic compounds of the type Th(Co/sub x/Fe/sub 1-x/)$_5$, 30:29989
ELIAS, J.E., See RIORDAN, E.M., 30:30583
EL-IBIARY, M.Y., See EL-KHARADLY, L.A., 30:29530
ELIEZER, S., Can the ΔI = 1/2 selection rule in the K + 2π decay be satisfied in gauge theories, 30:30684
  SU(3) symmetry breaking and superfluidity of hadronic matter, 30:30781
EL-KHARADLY, L.A., A perturbation method for calculating the rate of charge collection in a semiconductor detector, 30:29530
ELLIOTT, C.J., New technique for nonlinear optical problems, 30:29153 (LA-5639-MS)
ELLIOTT, J.E., Study of delta Scuti variables, 30:30226

- ELLIOTT, J.P., See WYARD, S.J., 30:29656
- ELLIS, D., See STONER, R.E., 30:30266
- ELLIS, W.R., See BOSLER, G.E., 30:29228
- ELLISON, F.O., See RABALAIS, J.W., 30:30491
- ELLSAESSER, H.W., Has man, through increasing emissions of particulates, changed the climate, 30:29489 (UCRL-75902(Rev.1))
- ELMORE, R.D., Use of EN-7 to encapsulate analyzer assemblies. Final report, 30:31418 (BDX-613-1135(Rev.))
- ELSHENAWY, L.S., See AMER, A.A., 30:30648
- ELSNER, N.B., Fabrication and testing of a thermoelectric RING converter segment for space applications, 30:29246
- ELSON, R.E., Stablized uranyl nitrate compositions and uranium impregnation method, 30:29127
- ELVEKJAER, F., The structure of t-channel exchanges in KN scattering, 30:30747
- EMIGH, S.G., See MARTINI, W.R., 30:29260
- ENDOW, J.S., See WINSTON, M.A., 30:29855
- ENGEL, J.P., See BLIND, R., 30:30625
- ENGELAND, T., Nuclear structure calculation of ^{50}Sc and analysis of the ^{48}Ca(^{3}He,p)^{50}Sc reaction, 30:30946
- ENGELBERTINK, G.A.P., See HERMANS, J.A.J., 30:30864
  - See VAN DRIEL, M.A., 30:30912
- ENGERRAN, J., See THOMAS, J.-P., 30:29510
- ENGLE, W.W. Jr., See GABRIEL, T.A., 30:29208
- ENGLER, A., See DADO, S., 30:30621
- ENGLOT, G., Dimensionality control of coupled scattering equations using partitioning techniques, 30:30562
- ENIKEEV, R.Sh., See USENOVA, K.A., 30:29111
- ENJALBERT, M., See NIELSEN, J., 30:29034
- ENSLEY, D.L., Interaction of intense microwave radiation and fully ionized hydrogen plasma. Part 1. High-density system, 30:29233 (UCRL-51631(Pt.1))
- ENTENBERG, A., See KIM, I.J., 30:30584
- EPIK, A.P., See ZELENYUK, E.E., 30:30013
- EPPERLEIN, B.W., ^{67}Zn NMR anomalous solvent isotope effect in aqueous solutions, 30:29014
- EPSTEIN, E.E., See FOGARTY, W.G., 30:30346
  - See WILSON, W.J., 30:30265
- EPSTEIN, J., Rate of DNA repair in progeric and normal human fibroblasts, 30:29672
- ERDMANN, R.C., See CATTON, I., 30:31253
  - See DIAS, J.W., 30:31228
- EREMENKO, V.N., Interaction of tungsten with liquid aluminum, 30:30003
- ERICSON, T.E.O., See BERNABEU, J., 30:30777
- ERKELENZ, K., See ALZETTA, R., 30:31033
- ERKO, V.F., See POLYAKOVA, G.N., 30:30545
- ERMAK, D.L., Investigation of polyion-small ion electrostatic interaction effects in polyelectrolyte solutions, 30:31375 (UCRL-51636)
- ERMOLAEV, O.Ya., Measurement of neutron temperature in water by differential and integral methods, 30:30844 (IAE-2274)
- ERMOLOV, P.F., See AKOPDJANOV, G.A., 30:30608
  - See BUMAZSHNOV, V.A., 30:30603
  - See DERRE, J., 30:30601
- EROKHIN, Yu.G., See MISYURA, V.A., 30:30447
- EROKHINA, K.I., Doppler shape of a γ-line in Coulomb excitation, 30:31100
- EROSHENKO, E.A., See BLOKH, Ya.L., 30:29582
- ERUPNOVA, G.F., Mechanisms of the inhibitors of cell post-irradiation recovery. III. Increase in the chromosomal damage rate by caffeine treatment of x irradiated buckwheat cells, 30:29695
- ESCOBAR, C.O., Electromagnetic mass differences in a relativistic quark model, 30:30658
- ESCOUBES, B., See BLIND, R., 30:30625
- ESKREYS, A., Isospin analysis of the diffraction dissociation processes in $K^{+}p$ interactions at 5 and 8.2 GeV/c, 30:30614
- ESPAGNO, L., See BLANC, C., 30:29024
  - See BLANC, C., 30:29025
- ESSINGTON, E.H., See FOWLER, E.B., 30:29440
- ESTES, Z.E., See SELIG, W., 30:31373
- ETCHEVERRY, R.D., See WILSON, W.J., 30:30265
- ETHOFER, S., Influence of core excitations on the deuteron stripping reaction with the method of many-body Green functions, 30:31027
- EUBANK, B.F., See MULLEN, O.W., 30:29379
  - See MULLEN, O.W., 30:29378
- EUBANKS, A.G., Luminescence of powdered uranium glasses, 30:30091
- EVANS, D., Isospin analysis of the reaction $\pi^{+}p \to \pi(N\pi)$ at 11.7 GeV/c, 30:30742
- EVANS, D.S., See BERNSTEIN, W., 30:30450
- EVANS, G.W., Effect of copper and cadmium on ^{65}Zn absorption in zinc-deficient and zinc-supplemented rats, 30:29814
- EVANS, K.J., Calculation of electroproduction of muon pairs in the light-cone limit, 30:30673
- EVLANOV, M.V., See SITENKO, A.G., 30:31072
- EVSTIGNEEV, V.V., See BOIKO, V.I., 30:30144
- EWING, C.J., See SILBERSTEIN, E.B., 30:29707
- EZAWA, Z.F., Wide angle scattering in softened field theory, 30:31163

F

- FABRE, M., See BALLOT, J.L., 30:30859
- FABRE DE LA RIPELLE, M., Coupled diffusion equations of the hyperspherical formalism, 30:30632
  - See BALLOT, J.L., 30:30859
- FADER, W.J., See HAUGHT, A.F., 30:29152
- FAENGEWISCH, G.L., Discrimination of neutron energies with the aid of the nuclear track method, 30:29554
- FAESER, R.J., See MOISE, J.C., 30:29261
- FAESSLER, A., See GRUEMMER, F., 30:30914
- FAHLANDER, C., See THUN, J.E., 30:30955
- FAHLESON, U.V., See KELLEY, M.C., 30:30433
- FAINBERG, J., Satellite observations of type III solar radio bursts at low frequencies, 30:30336
- FAINI, S., See BARBINI, R., 30:29586
- FAINSHTEIN, S.M., See PLOTKIN, E.E., 30:29202
- FAIVRE, J.C., See CHAMINADE, R., 30:29593
- FALCONER, W.E., See KAISER, E.W., 30:30547
- FALK, F., See ORRE, B., 30:31017
  - See THUN, J.E., 30:30955
- FALOMKIN, I.V., See BALESTRA, F., 30:29591
- FANAROFF, B.L., Identification of some faint radio sources that have flat spectra, 30:30277
- FANO, G., Application of Trotter's formula to a few-nucleon problem, 30:31046
- FANTNER, E., See KUCHAR, F., 30:29992
- FANTONI, S., See ROSATI, S., 30:31043
- FARHATAZIZ, See PERKEY, L.M., 30:29068
- FARRAR, Y.J., See FLORENCE, T.M., 30:28950
- FASOLI, U., Forward scattering of 2-MeV neutrons from oriented ^{165}Ho, 30:30981
- FATKULLIN, O.Kh., See RAKOVSKII, V.S., 30:29963
- FAVART, D., See POSSOZ, A., 30:30899
- FAWCETT, B.C., Spectral classifications in the Fe XIX to Fe XXIII isoelectronic sequences, 30:30329
- FAYARD, C., See MEYER, J., 30:31036
- FAYYAZUDDIN, Charge symmetry and neutral current in a unified model of weak and electromagnetic interactions, 30:30660
  - The $\Delta I=1/2$ rule in non-leptonic weak decays, 30:30595
- FAZZINI, T., Conversion coefficient measurements in ^{49}V, 30:30928
- FEDORENKO, V.N., Generation of Bernstein modes in a beam-plasma system, 30:29238
- FEDOROV, G.B., Thermodynamic properties and mutual diffusion in the system UC--ZrC, 30:29905
- FEDOROV, V.B., See SHINYAEV, A.Ya., 30:29932
- FEDOROVA, L.I., See LEVIKOV, E.A., 30:30055
- FEENBERG, E., Approach to a uniform theory of the liquid and solid phases of ^{4}He at absolute zero, 30:30799
- FEHRENBACH, C., Identification of stars in the direction of the Large Magellanic Cloud, 30:30199
- FEIGE, Y., See NAHARIN, A., 30:29821
- FEIGENBUTZ, L.V., See MARTINI, W.R., 30:29260
- FEIOCK, D., See SREEDHAR, V., 30:30616
- FEKETY, F.R. Jr., See BLAIR, D.C., 30:29886
- FELAWKA, L., See AXEN, D., 30:29597
- FELST, R., See BRAUEL, P., 30:30588
- FENIN, Yu.I., See EFIMOV, V.N., 30:31047
- FENJUK, A.B., See AKOPDJANOV, G.A., 30:30608
- FENNER, N.C., A new mass spectrometer for isotopic analysis, 30:29625
- FENYUK, A.S., See BUMAZSHNOV, V.A., 30:30603
- FERBEL, T., See SREEDHAR, V., 30:30616
- FERRANDO, A., See YAFFE, D., 30:30622
- FERRARI, E., Asymptotic crossing-even pion--nucleon forward scattering and duality in the complex energy plane, 30:30734
  - Practical evaluation of the asymptotic real-part behavior and the search for a possible subtraction constant in the crossing-odd forward pion--nucleon amplitude, 30:30733
- FERRERO, M.I., See BISI, V., 30:30596
- FERRO-LUZZI, M., See BAILLON, P., 30:30737
  - See BAILLON, P., 30:30618
  - See BAILLON, P., 30:30619
- FERTIG, W.A., See HUBER, J.G., 30:30814
  - See KHAN, H.R., 30:30810
- FESEFELDT, H., See BENECKE, J., 30:30612
- FESENKO, E.V., See LUCHNIK, N.V., 30:29696
- FESHBACH, H., See BORIDY, E., 30:31007
- FESSENDEN, R.W., See COLUSSI, A.J., 30:29067
- FESSENDEN, T.J., Weak interaction of a neutralized E-layer with resistors, 30:29223 (UCID-15956)
- FEYNMAN, R.P., Partons, 30:30691
- FICKEISEN, D.H., See SCHNEIDER, M.J., 30:29461
- FICKES, M.G., See BECKER, W.G., 30:30528
- FICKETT, F.R., See POWELL, R.L., 30:30838
- FICKINGER, W., See DADO, S., 30:30621
- FIELD, J., Pressure, Force, and Mass Calibration Laboratory, 30:31445 (UCID-15811)
- FIELD, S.B., See HORNSEY, S., 30:29726
- FIFE, T.H., Acylal hydrolysis. The hydrolysis of 3-(p-nitrophenoxy)phthalide, α-acetoxybenzyl p-nitrophenyl ether, and 3-(para-substituted thiophenyl)phthalides, 30:29017
- FIGIEL, J., See ESKREYS, A., 30:30614
- FILATOV, E.S., See IVANOV, Yu.A., 30:29084
- FILIMONOVA, E.A., See KARTASHEV, K.B., 30:29155
- FILIPPOV, G.F., Generalized Eulerian angles and the collective motion of many-particle system, 30:31053
- FILLIUS, R.W., Measurements of the Jovian radiation belts, 30:30406

FINCK, E.J., See WAXMAN, A.D., 30:29844
FINK, H.J., Theory of fragmentation dynamics in nucleus-nucleus collisions, 30:31082
FINK, M., New method for evaluating the density matrix and its application to the ground state form factor, 30:30858
FINKEL, V.A., See PETRENKO, N.S., 30:30032
FINKEL'SHTEIN, I.M., Some properties of materials of the systems Si_3N_4--ZrO_2, 30:29920
FINKELSTEIN, M., See GEIR, A., 30:29878
FINLAYSON, V.A., Procedure for deuterating titanium, 30:29216 (UCID-15624)
FINN, H.F., See CLARK, A.F., 30:30576
FINN, J.M., See KLINE, F.J., 30:30878
FINNILA, R.M., Steady-state, ac-temperature technique for measuring the specific heat of electrical conductors, 30:31439 (UCID-15649)
FINOCCHIARO, G., Measurement of charged particle multiplicities associated with large transverse momentum photons in proton-proton collisions, 30:30605
FIRK, F.W.K., See HICKEY, G.T., 30:30889
FIRSTOV, S.A., See KAVERINA, S.N., 30:30057
  See KOTKO, V.A., 30:30039
  See KOVSH, S.V., 30:30028
FISCHER, E., Bibliographies in nuclear science and technology. Section 02: contamination and decontamination of foods. Number 12, 30:29420 (ZAED-BIBL.-02-12)
FISCHER, E.A., See CHAUDAT, J.P., 30:31270
FISCHER, S.F., Excess energy dependence of radiationless transitions in naphthalene vapor: competition between internal conversion and intersystem crossing, 30:29016
FISHER, D.R., Decorporation of ^{241}Am from bone using DTPA and osteoporotic agents, 30:29799 (COO-119-249)
FISHER, P.S., See MENCHACA-ROCHA, A., 30:30904
FISK, L.A., Fokker--Planck coefficient for pitch-angle scattering of cosmic rays, 30:30172
  See SUESS, S.T., 30:30340
FISTEDIS, S.H., See CHANG, Y.W., 30:31264
FITCHARD, E., See READING, J.F., 30:30536
FITOUSSI, L., Health physics and technical considerations concerning the control of gaseous effluents from nuclear power plants, 30:29356 (AED-CONF-74-157-005)
FITZPATRICK, M.L., See LEDINGHAM, K.W.D., 30:31076
FIVOZINSKY, S.P., See KLINE, F.J., 30:30878
FIZZOTTI, C., Characterizations of fuel element cladding tubes, 30:31279 (RT/MET-(73)1)
FLATO, M., Generalized covariance principles and neutrino physics, 30:30680
FLATTE, S.M., A high-quality muon beam in the 10-15 GeV energy range, 30:30150
FLECKENSTEIN, J., On oxifluorides $A_{12}M(IV)M_3(VI)O_8F_{18}$ with uranium, molybdenum, and tungsten, 30:29006
FLIEGNER, J.R., Real risks of the nuclear tests, 30:29720
FLORENCE, D., See BARTHOLIN, H., 30:29993
FLORENCE, T.M., Beryllium content of NBS standard reference orchard leaves, 30:28950
FLOTOW, H.E., See OSBORNE, D.W., 30:29128
FLOWERS, E., See AU, C.K., 30:30261
FLOYD, G.R., See MCCULLOUGH, J.D., 30:30376
FLOYRAC, R., See ITTI, R., 30:29830
FOGARTY, W.G., NGC 1068: possible 3-millimeter radio variability, 30:30346
  See KAUFMANN, P., 30:30287
FOGEL, Ya.M., See POLYAKOVA, G.N., 30:30545
FOLKMANN, F., Sensitivity in trace-element analysis by p,α and ^{16}O induced X-rays, 30:28988
FOLSOM, T.R., See HOFFMAN, F.L., 30:29817
FOMALONT, E.B., See BRIDLE, A.H., 30:30281
FOMARAR'OV, A.B., Structure disarrangement caused in γ-irradiated DNA in vitro, 30:29036
FONER, S., Superconducting machines and devices: large systems applications. Conference held at Entreves, Italy, September 5--14, 1973, 30:30823
FONTANA, J., See KUKACKA, L.E., 30:31388
FONTENILLE, J., See BONTEMPS, A., 30:31113
FOOTE, J.H., Calculated ion-density spatial distribution in Alice Baseball I, 30:29184 (UCID-15647)
FORD, J.L.C. Jr., States in ^{24}Mg populated by the $^{10}B(^{16}O,d)^{24}Mg$ and $^{12}C(^{16}O,\alpha)^{24}Mg$ reactions, 30:30911
FORKMAN, B., See ARESKOUG, M., 30:31002
FORSTER, R.A., See WALTON, R.B., 30:28986
FORTUNE, P.J., Dielectric properties of helium: The polarizability of diatomic helium, 30:30504
  Helium diatom polarizability and the dielectric properties of fluid helium, 30:30506
  See BRUCH, L.W., 30:30502
FOSSAN, D.B., See HAEUSSER, O., 30:31004
FOSTER, J.L., See ASQUITH, J.C., 30:29674
FOSTER, J.P., Empirical swelling equations for solution-annealed Type 304 stainless steel, 30:30085
FOURIKIS, N., Detection of interstellar methylamine by its 2_{02}-1_{10} A/sub a/-state transition, 30:30360
FOWLER, E.B., Soils element activities, October 1972--September 1973, 30:29440 (NVO-AEIC-74-1)
FOWLER, E.C., Annual report for period October 1, 1973--September 30, 1974, 30:30574 (COO-1428-391)
FOWLER, P.H., Experimental flight of a large spherical gas scintillator, 30:29521
FOWLER, R.J., Krypton source, 30:29640
FRAAS, A.P., Conceptual design of a series of laser-fusion power plants of 100 to 3000 MW(e), 30:29230
FRADKIN, E.S., Asymptotic solution of the set of equations for Green's functions in the Yang--Mills field theory, 30:31150
FRAGA, S., Some forgotten terms of the Dirac--Breit--Pauli equation, 30:31138
FRAMPTON, P.H., See CAHALAN, R.F., 30:30707
FRANCK, C., Comparative study of placental location by using ^{51}Cr and the Doppler effect, 30:29858
FRANECKI, G., See PONIECKI, A., 30:29857
FRANK, G., Implantable thermal converter as power source for an artificial heart, 30:29258
FRANK, L.A., See GURNETT, D.A., 30:30449
  See GURNETT, D.A., 30:30454
FRANKLIN, J.E., Stress relaxation and strain-age cracking in Rene 41 weldments, 30:29996
FRANPUZ, E.T., See BLOKH, Ya.L., 30:29582
FRANTSUZ, E.T., Telescope with proportional gas-discharge counters for analysis of high-energy cosmic ray variations, 30:29581
FRAUENFELDER, H., See PUTTER, J.N., 30:30599
FREEMAN, J.W., See LINDEMAN, R.A., 30:30401
FREUND, H.G., See BOX, H.C., 30:29040
FREYLAND, W., Volume and temperature dependence of the electronic transport properties of fluid alkalis in the semiconducting range, 30:30005
FRIDMAN, A., Influence of the kinematical constraints on the transverse momentum correlation features, 30:30602
FRIEBELE, E.J., See GRISCOM, D.L., 30:30102
FRIED, H.M., Large momentum transfer reactions, without partons, 30:30764
FRIEDJUNG, M., Possible evidence for continued ejection of RR Telescopii, 30:30262
FRIEDLAND, E., See LOMBAARD, J.M., 30:30883
FRIEDMAN, B.I., See BRUNSON, B., 30:29837
FRIEDMAN, J.I., See RIORDAN, E.M., 30:30583
FRIEDRICH, J., See ROTHHAAS, H., 30:31005
FRIESEN, H.G., See TSUSHIMA, T., 30:29868
FRIIS, T., See LAURIDSEN, U.B., 30:29842
FROEBRICH, P., The treatment of two particles in the continuum in a Green's function theory of the (d,p)-reaction, 30:31083
FROHBERG, G., See ALBRECHT, W.W., 30:30020
FROIS, B., See QUEBERT, J.L., 30:30996
FROLOVA, L.M., Kinetics of uranium(IV)--neptunium(VI) reaction in tributyl phosphate solutions, 30:29102
  See RYKOV, A.G., 30:29106
FRUMKIN, M.L., Technological foundations for radiation treatment of food products, 30:29681
FU, H.H., See EBNER, C., 30:30802
FUBINI, S., Effective degrees of freedom in strong interaction processes, 30:30705
FUJA, R.E., See CHANG, C.T.M., 30:29584
FUJII, G., Construction and operation experience in PWR power plants, 30:31202
FUJIKI, Y., See SAITO, K., 30:29864
FUJIMOTO, Y., See SUZUKI, T., 30:31191
FUJIMURA, T., See NAKAHARA, Y., 30:31272
FUJINE, S., See HAYASHI, M., 30:31295
FUJITA, K., See NISHIKAWA, M., 30:29039
FUJITA, M., See MIYAZAKI, M., 30:29840
FUKADA, N., See ICHII, H., 30:29860
FUKUCHI, S., Radioimmunoassay of angiotensin, 30:29876
FUKUDA, R., Electron decay spectrum in muon decay in the unified theory of weak and electromagnetic interactions, 30:30682
FUKUMOTO, T., See NAKAO, R., 30:29047
FULMER, C.B., See RAMAN, S., 30:30879
  See SATCHLER, G.R., 30:30940
FUMELLI, M., Intense fast atom-beam production with a grounded large-area ion source, 30:29157
FUNABIKI, R., Asynchronous turnover of the thin filament proteins, actin, tropomyosin, and troponin by a continuous double isotope method, 30:29866
FUNKE, L., See WINTER, G., 30:30992
FURMAN, D.R., See PRASAD, S.S., 30:30310
FURMAN, V.I., Finite size α-particle calculations of absolute α-decay for spherical nuclei, 30:31102
FURR, A.K., Elemental analysis of protein-containing food materials from various sources, 30:28925
FURUICHI, S., Possible existence of a diproton resonance. A proposal of p--p scattering experiment at about 500 MeV, 30:30607
FURUSHASHI, A., See YAMAMURO, N., 30:31278
FURUTA, T., Stress-rupture properties of helium-injected Zircaloy-4, 30:30073
FUSCHILLO, N., See LALEVIC, B., 30:29940
FUTCH, A.H., Consideration of a ''brute-force'' approach to the achievement of higher density in the presence of instability, 30:29183 (UCID-15628)

G

GABIOUD, B., See BRESKIN, A., 30:29587
GABOVICH, M.D., Self-decomposition of quasi-neutral ion beam, 30:30478
GABRIEL, F., See ANDERT, K., 30:29630
GABRIEL, T.A., Shielding design calculations for ORMAK--F/BX, 30:29208 (ORNL-TM-4619)
GADZOEVA, M.M., See KADYKOVA, G.N., 30:30009
GAGARIN, Yu.F., See KULIKOV, V.N., 30:29501
GAILLARD, M.K., See BROWN, R.W., 30:30762
GAISSER, T.K., Energy dependence of sigma sub(p-air) up to 20TeV, 30:30611
  Is anti p production peripheral or central, 30:30763
GAL, O., Measurements with dicarboxylic acid dosimeters, 30:29547 (DEMO-74/5)
GALANTI, M., See FAWCETT, B.C., 30:30329
GALEAZZI, G., See FASOLI, U., 30:30981
GALFI, L., μ-pair production by inelastic πp and anti pp collisions, 30:30738
GALIK, R.S., See CORMIER, T.M., 30:29573
GALLAGHER, A., See CRANDALL, D.H., 30:30246
GALLAGHER, D.F., See ALI, S.P., 30:31115
GALLIMORE, J.C. Jr., See STAFFORD, R.G., 30:29328
GALLONI, G., See BRIGANTI, G., 30:29736
GALLOWAY, K., See ALAM, M.S., 30:30613
GALLOWAY, R.B., See MAAYOUF, R.M.A., 30:29511
GAMBHIR, B.L., Qualitative features of Pauli break-up from the configuration space viewpoint, 30:31089
GANGLOFF, W.C. Jr., See CONRAD, J.D. Jr., 30:31283
GARBER, M., See BUSSIERE, J.F., 30:30840
GARCIA, E.E., See BOTBOL, M., 30:28939
GARCIA AGUDO, E., Application of neutron activation analysis to the determination of gold in minerals, 30:28913 (IEA-316)
GARDNER, W.E., See KHAN, H.R., 30:30810
GARFAGNINI, R., See BALESTRA, F., 30:29591
GARLAND, T.R., See WILDUNG, R.E., 30:29825
GARRETT, J.D., See BOND, P.D., 30:30921
GARSEVANISHVILI, V., See ANGELOV, N., 30:30718
GASKILL, J.R., LLL spray damper project, 30:29330 (UCID-15941)
GASPAROVIC, A., See BAXTER, B.J., 30:29265
GASS, D.M., Thermal conductivity of a hard sphere solid, 30:31441 (UCID-15723)
GASTALDI, U., See BAILEY, J., 30:30620
GATHERS, G.R., Energy minimization method for computer deconvolution, 30:31354 (UCID-15947)
  Experimental, very high-temperature, liquid--uranium equation of state, 30:30045
GATLEY, I., A new infrared complex and molecular cloud in Orion, 30:30356
GATTO, R., Senile scaling in electron-positron annihilation, 30:30668
GAVALER, J.R., See DEIS, D.W., 30:30809
GAVRILYUK, M.I., See BUDAGOVSKII, S.S., 30:30029
GAZE, S., Use of a double isotope method in the determination of antibody affinity, 30:29867
GAZIEV, A.I., Chemical nature of the ends of DNA single-strand breaks produced by ionizing γ radiation in vivo and pathways of their reparation, 30:29682
GAZIEV, Ya.I., See NAZAROV, L.E., 30:29389
GAZIEV, Yu.I., Size-distribution relation of high-activity particles in the troposphere in September--December 1967, 30:29392
GEDEONOV, L.I., ^{90}Sr distribution and migration in soils, 30:29404
GEE, T.S., See SYKES, M.P., 30:29715
GEGUZIN, Ya.E., Recrystallization grain coarsening in the tungsten--nickel system, 30:30004
GEHRINGER, P., See PROKSCH, E., 30:29544
GEHRZ, R.D., Infrared observations of Be stars from 2.3 to 19.5 microns, 30:30252
GEIGER, W., Generation and propagation of pressure waves due to unconfined chemical explosions and their impact on nuclear power plant structures, 30:31267
GEIR, A., Uptake and metabolism of [4-^{14}C]testosterone in human breast cancer grown in organ culture, 30:29878
GEL'FAND, S.Yu., See FRUMKIN, M.L., 30:29681
GELFGAT, J.M., Method and device for magnetohydrodynamically controlling the flow rate of an electrically conductive liquid, 30:30572
GELINAS, R.J., Solution of large coupled sets of kinetic equations, 30:31351 (UCID-15765)
GELLER, M.A., Calculation of the lunar diurnal atmospheric tide, 30:30446
GELLETLY, W., Correlations between (n,γ) and (d,p) reactions on N = 82 nuclei, 30:30970
GEMBA, H., See MIYAZAKI, M., 30:29840
GENEROZOV, V.L., Buildup of scattered radiation behind a shadow shield, 30:31129
GENTA, P., Calculation of the neutron spectra from nuclear reactions in Focus type deuterium plasmas. I. General presentation and mathematical analysis, 30:29178 (CEA-N-1711)
GENTHON, J.P., Elementary model for radio-induced damage in in-pile graphite: correlation between temperature and flux, 30:30096
GENZ, H., See HOFFMANN, D., 30:30148
GEORGE, T.F., See ZIMMERMAN, I.H., 30:30534
  See ZIMMERMAN, I.H., 30:30559
GEORGOPULOS, P.D., Lifetime measurements of some states in ^{53}Mn, 30:30930
GERARD, J.C., Satellite observations of the equatorial Mg II dayglow intensity distribution, 30:30426
GERASIMENKO, S.N., Investigation of ultraviolet absorption in the continuous spectrum of Jupiter, 30:30396
GERASIMOV, G.N., Step-by-step excitation in helium, 30:30489
GERDYUKOV, L.N., See AKOPDJANOV, G.A., 30:30608
GERHARDT, B., See BECK, U., 30:30591
GERMAN, V.N., See KUTSAR, A.R., 30:30011
GERT, L.M., Conditions for three-dimensional correspondence in the heteroepitaxial growth of ZrC, 30:29914
GERZON, S.A., See KISELEV, Yu.T., 30:29633
GESLIEN, G.E., See THRALL, J.H., 30:29849
GHAED, N., See THRALL, J.H., 30:29849
GHANI, A., Nuclear data accuracy considerations in reactor design, 30:31276
GHEORGHE, D., See BADESCU-SINGUREANU, A.I., 30:30846
  See BADESCU-SINGUREANU, A.I., 30:30845
GHOSH, P.K., See NAGARAJAN, R., 30:29626
GHOSH, S.N., Day airglow emissions of 5577-A and 6300 OI lines in Martian atmosphere, 30:30397
  Variation of F-region positive ion density with solar activity, 30:30416
GHUMMAN, B.S., See THUN, J.E., 30:30955
GIACOMICH, R., See CALLIGARIS, F., 30:29590
GIANNATIEMPO, A., See FAZZINI, T., 30:30928
GIANNINI, M., Neutron radiography: biomedical applications, 30:29705 (RT/FI-(74)16)
GIAZOTTO, A., See DEL GUERRA, A., 30:30678
GIBSON, A.G., Time-independent multichannel scattering theory for charged particles, 30:30656
GIBSON, L.R., See DILLEY, J., 30:30791
GIEBULTOWICZ, T., See MINOR, W., 30:29574
GIERALTOWSKI, G.F., See ROWE, J.F. Jr., 30:30436
GIESECKE, P., Radiation damage in reactor structural materials - Formation of pores and its simulation, 30:30062 (AED-CONF-74-044-009)
GIGER, U., Refrigerating systems for the big CERN bubble chamber, 30:29576
GILARDINI, A., Low energy electron collisions in gases: swarm and plasma methods applied to their study, 30:30543
GILBERT, J.R., See SLAGLE, I.R., 30:30531
GILBERT, R.O., Statistical analysis of Pu in soil at the Nevada Test Site: some results, 30:29444 (NVO-AEIC-74-1)
  See EBERHARDT, L.L., 30:29418
  See ROMNEY, E.M., 30:29445
GILBERT, R.W., See NORTHWOOD, D.O., 30:30076
GILES, M.S., See DAVY, D.R., 30:29354
GILLESPIE, D.J., See MACKLIET, C.A., 30:30812
GILLETTE, R., Plutonium. I. Questions of health in a new industry, 30:29773
  Plutonium(II): watching and waiting for adverse effects, 30:29790
GILMORE, F.R., See BARR, T.L., 30:31459
GILRA, D.P., Dust particles and molecules in the extended atmospheres of carbon stars, 30:30244
GILS, H.J., See REBEL, H., 30:30945
GIORGI, M.A., See DEL GUERRA, A., 30:30678
GIRIDHARAN, A.S., Preparation and characterization of a new thallium(I) uranate(VI), Tl_4UO_5, 30:29090
GITGARTS, M.I., Effect of the volume disparity between the precipitation phase and the matrix on the scattering of x rays by aging alloys, 30:30036
GITTLESON, H., See KIM, I.J., 30:30584
GITTUS, J.H., Trends in structural mechanics. A UK review of the 2nd international conference on structural mechanics in reactor technology. VIII. Reactor core, 30:31213
GIZON, A., See PROETEL, D., 30:31006
GIZON, J., See PROETEL, D., 30:31006
GLANTZ, L., See JOHANSSON, A., 30:30855
GLAS, D., Microscopic treatment of viscosity in heavy ion reactions, 30:31066
GLEW, R.W., See BRYANT, F.J., 30:30103
GLIBERT, K.M., See CUDERMAN, J.F., 30:29193
GLOECKLE, W., Use of Lippmann--Schwinger equations in the three-body problem, 30:31044
GLOVER, D.W., Development an an ideal sampler for below-cloud scavenging studies, 30:29366 (BNWL-1850(Pt.3))
  See ALKEZWEENY, A.J., 30:29487
GLOWIAK, B., Radioactive contamination of some arable soils in the Lower Silesia in 1972, 30:29402
GLUCK, P., Fluctuations and superfluid flow, 30:30795
GMITRO, M., Study of the structure of the ^{56}Ni double magic nucleus, 30:30918
GOEBEL, G., See DEHM, G., 30:30624
GOEKE, K., See GRUEMMER, F., 30:30914
GOENCZI, L., See JOHANSSON, A., 30:30855
  See SUNDQVIST, B., 30:28917
GOESSNER, W., Morphology and enzyme histochemistry of ^{224}Ra-induced osteosarcomas of the mouse, 30:29785
GOFF, F.G., See WEST, D., 30:31337
GOGGI, G., An experimental investigation of π photoproduction processes on ^{3}He, 30:30874
GOITEIN, M., See SUIT, H.D., 30:29725
GOLAND, A.N., See PARKIN, D.M., 30:29203

GOLD, R., Fast-neutron personnel dosimetry with solid-state track recorders, 30:29557
GOLDBERG, M.E., See LOKEN, M.K., 30:29847
GOLDEN, J.E., See MCGUIRE, J.H, 30:31139
GOLDEN, R.L., Charge composition of cosmic rays between 4 and 100 GV, 30:30165
GOLDENBERG, N., RTG technology development: where we are/where we are going, 30:29244
GOLDMAN, S.R., See SCANNAPIECO, A.J., 30:30437
GOLDSPINK, G., See HOLBERTON, E.J., 30:29833
GOLDSTEIN, G.R., Determination of reaction amplitudes from experimental observables, 30:31028
GOLDSTEIN, M.L., See FISK, L.A., 30:30172
GOLDSTEIN, R., See STEADMAN, S., 30:30920
GOLDWORM, R.A., See HOOD, J.T., 30:30153
GOLESTANEH, A.A., Application of the on-mass-shell current algebra to the K/sub 13/ form factor, 30:30683
GOLOVKINA, N.E., See POPIL'SKII, R.Ya., 30:29910
GOLUB, T.V., See BENIEVA, T.Ya., 30:30056
GOLUBA, R.W., Ultra high volume air sampler, 30:29494 (NVO-AEIC-74-1)
GOMEZ, L.S., Effect of delayed lymphadenectomy on $^{239}PuO_2$ translocation in dogs, 30:29820
GOMEZ DEL CAMPO, J., See FORD, J.L.C. Jr., 30:30911
GONCHARUK, L.V., See RAMAZANOV, L.M., 30:29107
  See SOKHINA, L.P., 30:29116
GONED, A., See EL BEDEWI, F., 30:30179
GONO, Y., In-beam conversion-electron spectrum for the $^{148}Sm(^{12}C,4n)^{156}Er$ reaction, 30:30965
GOODE, R.J., See JUDY, R.J. Jr., 30:29981
GOODMAN, C., See LEE, L.Y., 30:29585
GOODMAN, R.K., Alice vacuum system: Sept. 1969, 30:29218 (UCID-15660)
GORBUNOV, V.I., Structure of alloys of cobalt with rare earths of the approximate composition RCo_5, 30:30034
  See BOIKO, V.I., 30:30144
GORCZYCA, B., Quark model predictions for electroproduction of $3/2^+$ isobars, 30:30662
GORDELADZE, Sh.G., Genetic connection between stars O--B0 and diffuse nebulae, 30:30213
GORDON, C.M., Blade-type metal-cutting tool for quick removal of stock in roughing work, 30:29269 (UCID-15833)
GORDON, F., Diagnosis of Barrett's esophagus with radioisotopes, 30:29852
GORLOVA, N.N., Extraction--spectrophotometric methods of determining 0.0--n0.000n% aluminum in materials of metallurgical manufacture (exchange of experience), 30:28956
GORSHKOV, V.V., Assay of silver in ores by neutron activation, 30:28926
GORSHKOVA, L.V., See SHINYAEV, A.Ya., 30:29932
GORSON, R.O., See BORRAS, C., 30:29781
GOTTLIEB, N.L., Pharmacodynamics of ^{197}Au and ^{198}Au labeled aurothiomalate in blood. Correlation with course of rheumatoid arthritis, gold toxicity, and gold excretion, 30:29792
GOUDSMIT, P.F.A., See DE BOER, F.W.N., 30:30989
GOULD ZWEIBEL, E., See SPITZER, L. Jr., 30:30357
GOUNARIS, G.J., Meson electromagnetic decays from SU(4)/sub w/ and generalized vector dominance, 30:30650 (NP-20072)
GOURDIN, M., Quark parton model for deep inelastic lepton scattering, 30:30686
GOURLAY, J.Y., See LEDINGHAM, K.W.D., 30:31076
GRAAB, J.W., See MERKLE, E.J., 30:28942
GRABOWSKI, R., See PONIECKI, A., 30:29857
GRACE, C.I., See EVANS, G.W., 30:29814
GRACE, R.E., Transport and thermodynamic properties of solids. Progress report, September 1, 1973--August 31, 1974, 30:31390 (COO-1436-41)
GRADEV, G., Sorption of iridium on silver, mercury, lead, and thallium forms of natural zeolite (clinoptilolite) and vermiculite, 30:29135
GRAESSLER, H., Study of double diffraction dissociation in the reaction $\pi^{+-}p \to (3\pi)^{+-}(N\pi)^+$ at 16 GeV/c, 30:30610
GRAFFI, S., Stieltjes type continued fractions in quantum electrodynamics, 30:31166
GRAFFSTEIN, A., A correlation chopper or chopper with coding disk, 30:29635
GRAHAM, H., Notes on application of solid electrolyte tantalum capacitors in coupling and bypass service, 30:31401 (UCID-15662)
GRANATSTEIN, V.L., Coherent synchrotron radiation from an intense relativistic electron beam, 30:30580 (AD-773442)
GRANNIS, P., See FINOCCHIARO, G., 30:30605
GRANT, P.M., See O'BRIEN, H.A. Jr., 30:30142
GRANT, W.A., See CARTER, G., 30:30088
GRARD, F., See DEHM, G., 30:30624
GRASDALEN, G.L., Near-infrared magnitudes and (V-K) colors of globular clusters, 30:30219
GRASSBERGER, P., Finite energy bounds for πN scattering, 30:30748
GRAY, G.W., Tandem towing tests of the MHU-12/M trailer. Final report, October 1972--December 1973, 30:30113 (AD-777254)
GRAY, J.L., Canadian nuclear power programme, 30:31216
GRAY, W.S., See PARKINSON, W.C., 30:30158
GRAYER, G., High statistics study of the reaction $\pi^- p \to \pi^-\pi^+ n$: apparatus, method of analysis, and general features of results at 17 GeV/c, 30:30617
GREBENKINA, V.G., Production of complex zirconium--tungsten carbide on semi-industrial scale, 30:29893
GREBENSHCHIKOVA, V.I., Sorption of tetravalent elements by mordenite. II. Sorption of Pu(IV), 30:28999
GREBOWSKY, J.M., See CHEN, A.J., 30:30466
GRECCHI, V., See GRAFFI, S., 30:31166
GREEN, A.E.S., Meson field theory of nuclei and the N--N interaction, 30:31048
GREEN, D., See FINOCCHIARO, G., 30:30605
GREEN, D.W., Ionospheric ion flow velocities from measurements of the ion distribution function technique, 30:30434
GREEN, S., Rotational excitation of HCN by collisions, 30:30385
GREENBERG, J.M., Interstellar dust and related topics. Proceedings of the symposium, Albany, New York, May 29--June 2, 1972, 30:30373
  See MINH, Y.K., 30:30372
GREENBERG, J.S., Evidence for quasi-molecular K x-ray emission in heavy ion collisions from the observation of the x-ray directional anisotropy, 30:30922
GREENHOUSE, N.A., Annual report of the Brookhaven DCPA Contract Group, 30:31332 (BNL-19097(Rev.))
GREENSTEIN, J.L., Photometry of a Pleiades candidate and composite white dwarfs, 30:30234
  Spectrum of the polarized white dwarf GD 229, 30:30204
GREENSTOCK, C.L., Competitive radioprotection and radiosensitization in chemical systems, 30:29003
GREENWALD, R.A., See ROMICK, G.J., 30:30430
GREGORIUS, K., See PLOEGER, M., 30:31294
GREGORY, C.V., Study of local blockages in fast reactor sub-assemblies, 30:31229
GREGORY, D.P., See PANGBORN, J.B., 30:31239
GREGORY, P.C., See HUGHES, V.A., 30:30292
  See SEAQUIST, E.R., 30:30284
GREINER, W., See FINK, H.J., 30:31082
GRENACS, L., See POSSOZ, A., 30:30899
GRENIER, J.C., See BAYARD, M., 30:29902
GRESKY, A.T., Process for separation of protactinium, thorium, and uranium from neutron-irradiated thorium, 30:29150
GRIBKOV, V.A., Numerical analysis of interferrograms of asymmetric plasma objects, 30:29176
GRIFFIN, J.J., See GAMBHIR, B.L., 30:31089
  See KAN, K.-K., 30:31075
GRIFFIN, R.F., The Palomar radial-velocity spectrometer, 30:30184
GRIFFITH, G., See MUGA, L., 30:29528
GRIFFITH, J.C., See CUNNINGHAM, D.M., 30:31434
GRIFFITH, W.R., See MARTINI, W.R., 30:29260
GRIGOR'EV, Yu.G., See TOBAIS, K.A., 30:29712
GRIGOREVSKII, M.V., Light-variations investigation of variable stars and satellites by means of computer, 30:30209
GRIMES, H.H., See RIEU, G.E., 30:29980
GRINBERG, A.A., Compounds of tetravalent uranium with complex cations of platinum, 30:29108
GRINDHAMMER, G., See BRAUEL, P., 30:30588
GRINIK, E.U., Effect of intense reactor irradiation on the shear modulus and viscosity of iron, 30:30072
GRISCOM, D.L., Observation and analysis of the primary ^{29}Si hyperfine structure of the E' center in non-crystalline SiO_2, 30:30102
  Rock magnetites with positive anisotropy constants at 300°K, 30:31389 (CONF-740644-1)
GRISHIN, V.G., Multiplicity and correlations of secondary particles produced in $\pi^- - {}^{12}C$ collisions at 40 GeV/c, 30:30875 (JINR-P1-7523)
GRIVA, A.P., Investigation of low-temperature homomolecular isotopic oxygen exchange on titanium dioxide, 30:29029
GRODZINS, L., See STEADMAN, S., 30:30920
GROLL, M., Heat pipe work in Europe, 30:31422 (IKE-5-175)
GROMADZKI, Z., Cluster-model calculations of the electrodisintegration of lithium, 30:30893
GROMES, D., Field quantization on the surface x^2=constant, 30:31159
GROS, R., See JEANMAIRE, L., 30:29795
GROSS, D.H.E., Mechanism of heavy ion collisions leading to a compound system and to deep inelastic direct reactions, 30:31065
GROSSER, J., See KONNEN, G.P., 30:30484
GROSSE-RUYKEN, H., See HERRMANN, E., 30:28990
GROSSIORD, J.L., Model for the interaction between a gravitational wave and a circular current, 30:31178
GROSSMAN, L.N., Chemical immobilization of fission products reactive with nuclear reactor components, 30:31281
GROSSWENDT, B., Measurement of the geometry factors of Ge(Li) detectors, 30:29518
GRUBE, B.J., See BRUENGER, F.W., 30:29804
  See STEVENS, W., 30:29798
GRUBER, G., See QUEBERT, J.L., 30:30996
GRUBER, H.T., Determination of the feasibility of using beta radiation backscatter for the detection of surface contamination of metal panels, 30:29294 (AD-776394)

GRUEMMER, F., Antipairing and antistretching in ^{22}Ne, 30:30914
GRUENBERG, L.W., See MESERVEY, R., 30:30839
GRUENER, W., Apparatus for in-core instrumentation of pressurized water reactors, 30:31196
GRUHN, T.A., The etching of cellulose nitrate plastic, 30:29532
GRUNAU, L.M., See GORBUNOV, V.I., 30:30034
GRUNBERG, C., The needle chamber: a new highly versatile detector, 30:29514
GRUVERMAN, I.J., Moessbauer effect methodology. Volume VIII. Proceedings of the eighth symposium, New York City, New York, January 28, 1973, 30:30092
GRYNSZPAN, R., Changes in the internal friction spectrum of irradiated or deformed pure Al and Al solid solutions at 77°K, 30:30082
GUARALDO, C., See BALESTRA, F., 30:29591
  See BARBINI, R., 30:29586
GUARDIOLA, R., See CIOFI DEGLI ATTI, C., 30:31098
GUDKOV, B.S., See LEVIN, D.Z., 30:29011
GUERNIER, G., See NIELSEN, J., 30:29034
GULLICKSON, R.L., X-ray analysis for electron beam enhancement in the plasma focus device, 30:29174 (JCRL-75910)
GUMENYUK, S.A., See AKOPDJANOV, G.A., 30:30608
GUNN, G.D., See WHITE, R.L., 30:30937
GUNN, J.E., See GRIFFIN, R.F., 30:30184
GUPTA, R.K., Renormalized effective nuclear interaction by explicit truncation and use of the results of a large configuation space, 30:31060
GUPTA, S.C., See GURTU, A., 30:30604
GUPTA, S.K., See GHOSH, S.N., 30:30416
GUPTA, S.P., Propagation of VLF and ELF waves during sudden ionospheric disturbances, 30:30418
GUPTA, V.K., See GURTU, A., 30:30604
GURARII, K.N., See SIVOSHINSKII, D.S., 30:29838
GURNETT, D.A., Thermal and suprathermal plasma densities in the outer magnetosphere. Progress report, 30:30449 (AD-776660)
  Thermal and suprathermal plasma densities in the outer magnetosphere, 30:30454
GURSKI, J.P., See DER, Z.A., 30:29303
GURTU, A., Multiplicity in proton-nucleus interactions at 200 GeV/c, 30:30604
GUSEV, P.P., Periods of three RR Lyrae type stars, 30:30211
GUSEV, V.N., See FEDOROV, G.B., 30:29905
GUSEV, Yu.K., Preparation of complex perxenates of some actinide elements, 30:29117
GUSTAFSON, H.R., See JONES, L.W., 30:29596
GUSTISON, R.A., Decontaminating uranium by reaction with ClF_3 and HF and volatizing the UF_6 product, 30:29149
GUTH, P., See WINSTON, M.A., 30:29855
GUTMAN, D., See SLAGLE, I.R., 30:30531
GUYADER, J.C., Experimental equipment for spectrometry of electrons and protons between 0.4 and 30keV aboard the AUREOLE satellite, 30:29567
GUYONNET, J.L., See BLIND, R., 30:30625
GUZEEV, G.G., Chromosome aberrations in lymphocytes of peripheral blood after radiation therapy, 30:29731
GUZENKO, L.V., See SHLYUKO, V.Ya., 30:29892
GVILDYS, J., See CHANG, Y.W., 30:31264
GWOZDZ, R., Compilation of x-ray interaction data for x-ray fluorescence analysis of geological samples, 30:28943 (RISO-297)
GYARMATI, B., New source of decoupling of E1 strength from the GDR: boundary condition mixing for s- and p-wave neutron states near threshold, 30:31079

H

HAAG, H., High-melting metals and metallic compounds, 30:30021
HAAS, F.A., See THOMAS, C.L., 30:29179
HABBERSTAD, J.L., Mathematical review of introductory wave mechanics, 30:31444 (UCID-15803)
HABEGGER, L.J., See WOLSKO, T.D., 30:31357
HABER, B., See BERLAD, G., 30:30623
HABS, D., See REBEL, H., 30:30945
HACKENBROICH, H.H., Variational calculations of reactions involving light nuclei, 30:30851
HACKWELL, J.A., See GEHRZ, R.D., 30:30252
HAENNI, D.R., See GONO, Y., 30:30965
HAEUSLER, B., Behavior of outer radiation belt electrons (> 1.5 MeV) during a geomagnetically disturbed time on 8 March 1970 and its relationship to magnetospheric processes, 30:30471
HAEUSSER, O., The 1-forbidden 3psub(3/2) + 2fsub(5/2) M1 transition in ^{207}Pb, 30:31004
HAFER, J.F., See MURRAY, H.S., 30:31325
HAFF, P.K., Negative muon capture in very light atoms, 30:30509
HAGEMANN, G.B., γ-ray multiplicity after (HI,xn) reaction, 30:30983
  See RIEDINGER, L.L., 30:30985
HAGEN, K.G., Nuclear-fueled circulatory support systems. XIII. Augmented performance of the tidal regenerator engine, 30:29262
HAGENMULLER, P., See BAYARD, M., 30:29902
HAGIWARA, M., Accelerating effect of halogenated methane on the radiation degradation of polytetrafluoroethylene, 30:29058
HAHN, C., See EVANS, G.W., 30:29814
HAHN, E., See KIM, J.H., 30:29004
HAHN, E.W., Increased cures using fractionated exposures of x irradiation and hyperthermia in the local treatment of the Ridgeway osteogenic sarcoma in mice, 30:29744
  See HUVOS, A.G., 30:29784
HAIGH, J.G.B., See BROWN, G., 30:30923
HAIGHT, R.C., See SALADIN, J.X., 30:30905
HAINBERGER, P.L., Radioactivity in Brazilian mineral waters, 30:29413
HAIS, I.M., See DRSATA, J., 30:29740
HAKIM, R., Equilibrium statistical mechanics of relativistic particles with variable masses. I. Nonquantal theory, 30:30158
HALBACH, K., A magnetic field clamp with beneficial saturation effects, 30:30136
  Rapid measurement of the effective field boundary of homogeneous field magnets, 30:30135
HALBERT, M.L., See RAMAN, S., 30:30879
HALES, J.M., Flux meter for direct field measurement of deposition and resuspension rates, 30:29613 (BNWL-1850(Pt.3))
  See DANA, M.T., 30:29479
  See DANA, M.T., 30:29477
  See GLOVER, D.W., 30:29366
  See SCHWENDIMAN, L.C., 30:29365
HALL, E.J., Radiosensitization of hypoxic cells with metronidazole, 30:29699
HALLORAN, J.T., See MERKLE, E.J., 30:28942
HALLOWELL, P.L., See KLINE, F.J., 30:30878
HAMILTON, J.H., Spherical and deformed shapes in ^{188}Hg, 30:30987
  See ROBINSON, R.L., 30:30982
HAMM, T. Jr., Operation Cannikin: electronic and electrical scientific measurements and support plan. Pre-operational report, 30:29318 (UCID-15802(Rev.1))
HAMMEL, E.F., Energy and cryoengineering, 30:31324 (LA-UR-74-741)
HAMMEL, G., See BETZ, P., 30:29535
HANAPPE, F., Quasi-fission: a new type of reaction observed in bombarding heavy nuclei by ^{84}Kr and ^{63}Cu ions, 30:30984
  See BLOK, H., 30:29525
HANCOCK, J.R., Fatigue and impact resistance of dual-matrix boron--aluminum composites. Final report, 30:29974 (AD-775334)
HANE, C.E., Convective storm modeling and its possible application to precipitation scavenging problems, 30:29480 (BNWL-1850(Pt.3))
  See DANA, M.T., 30:29479
HANNA, S.S., Moessbauer effect and related phenomena. Final report, 1 November 1964--1 January 1972, 30:30951 (AD-773622)
HANSEN, C.J., See VAN HORN, H.M., 30:30269
HANSEN, H.J., See COFFEY, J.W., 30:29870
HANSEN, J.M., See LAURIDSEN, U.B., 30:29842
HANSEN, N.E., See CLARK, A.F., 30:30576
HANSEN, O., See BOND, P.D., 30:30921
HANSEN, O.L., See BLANCO, V.M., 30:30220
HANUMATHSASTRI, J., Dependence of fading frequency on characteristics of ionospheric irregularities, 30:30420
HARA, M., Chemistry of americium. II. Behavior of Am(III), Am(V), and Am(VI) in column chromatography, with bis(2-ethylhexyl)phosphoric acid used as the extractant, 30:29093
HARDING, W.B., Electrodepositing platinum and platinum--iridium alloys from molten cyanides: chemical process studies, 30:31366 (BDX-613-1064(Rev.))
HARDINGER, K.E., Automatic radar-sensitivity measurement. Final report, 30:31417 (BDX-613-1134(Rev.))
HARING, A., See KONNEN, G.P., 30:30484
HARLEY, J.H., HASL procedures manual, 30:28970 (HASL-300(Suppl.2))
HARLEY, T.W., Extended array evaluation program. Quarterly report No. 6, 1 July--30 September 1973, 30:29306 (AD-777315)
HARLING, O.K., Linear accelerator neutron source for neutron scattering, 30:30152
HARMS, A.A., Isotopic conversion in gadolinium-exposure neutron imaging, 30:29302
  Nuclear radiation conversion enhancement with inhomogeneous converters and intensifiers, 30:29301
HARRINGTON, T.M., The Apollo gamma-ray spectrometer, 30:29566
HARRIS, D.O., Acoustic emission monitoring of proof tests on canisters and related hardware, 30:29296 (UCID-15777)
HARRIS, E.G., Equilibrium and stability of elliptical cross section tokamak, 30:29210 (ORNL-TM-4666)
HARRIS, O.A., See BROWN, J.L., 30:29140
HART, P.E., Fabrication of high-density UO_2 and (Usub(0.75)Pusub(0.25))O_2 by hot pressing, 30:29925
HARTE, W.E., Strong 4f resonance effects in rare-earth appearance-potential spectra, 30:30477
HARTILL, D.L., See BEBEK, C.J., 30:30587
HARTLEY, G.H., See STEPHENSON, M., 30:29647
HARTMAN, C.W., Levitrons and the superconducting levitron: a summary, 30:29213 (UCID-15448)
  Runaway effects in the inductively excited levitron, 30:29181 (UCID-15487)
HARVEY, B.G., See MAGUIRE, C.F., 30:30997
HARVEY, J., See NORDBERG, M.E. Jr., 30:30590
HASE, T., See SUZUKI, H., 30:29921
  See SUZUKI, H., 30:29922
HASEGAWA, K., Development of sodium flowmeter by real time correlation technique. II. Measurement of flow velocity in mockup fuel assembly, 30:31224 (JAPFNR-154)

- **HASHIMOTO, M.**, See ISHIBASHI, W., 30:28954
- **HASHIZUME, A.**, A mechanical beam chopper system for the measurement of half-lives in the millisecond region, 30:30154
- **HASSELGREN, L.**, See THUN, J.E., 30:30955
- **HATCH, A.J.**, See KRAKOWSKI, R.A., 30:29206
- **HATCHER, B.G.**, See ISAACS, N.S., 30:29021
- **HATTERSLEY, P.**, See BAILEY, J., 30:30620
- **HATTORI, T.**, See SUZUKI, H., 30:29922
- **HAUGHT, A.F.**, High beta capture and mirror confinement of laser-produced plasmas. Semiannual report, January 1, 1974 through July 31, 1974, 30:29152 (COO-2277-4)
- **HAVLICEK, F.**, Decontamination of swine, sheep, and cattle surface-contaminated with fission products. II. Removal of radionuclides of zirconium, niobium, ruthenium, and cerium, 30:29823
- **HAWTIN, P.**, Calculation of the corrosion rate of an HTR core under fault conditions, 30:31211
- **HAYASHI, M.**, KUR on-line computer system, 30:31295 (KURRI-TR-110)
  - See KONISHI, H., 30:29875
- **HAYASHI, T.**, A 1Ge(Li)-3NaI(Tl) detector system for γ-γ angular correlation measurements, 30:29565
  - See MORITA, N., 30:29050
  - See MUTO, K., 30:31265
- **HAYES, E.F.**, See ADAMS, J.T., 30:30527
- **HAYES, W.**, See CALL, P.J., 30:29075
- **HEAD, J.L.**, Trends in structural mechanics. A UK review of the 2nd international conference on structural mechanics in reactor technology. VI. Inelastic structural analysis, 30:31290
- **HEARD, H.C.**, Compressibility and strength behavior of Diagonal Line alluvium, 30:29316 (UCID-15736)
  - See ABEY, A.E., 30:31409
  - See DUBA, A.G., 30:31411
  - See STEPHENS, D.R., 30:29322
- **HEASELL, E.L.**, See KORWIN-PAWLOWSKI, M.L., 30:29994
- **HEBARD, D.W.**, See JACKSUN, K.L., 30:29737
- **HECKMAN, H.H.**, See GOLDEN, R.L., 30:30165
- **HECKMAK, R.V.**, Beta backscatter measurements of aluminum coatings on mylar substrates, 30:29602 (BDX-613-1028(Rev.))
- **HECKMAN, T.M.**, Population synthesis applied to eight young Magellanic Cloud globular clusters, 30:30216
- **HEDEMAN, E.R.**, See DODSON, H.W., 30:30328
- **HEDEMANN JENSEN, P.**, Comparison of mathematical models for calculation of external gamma doses originating from releases of radioactivity to the atmosphere, 30:29342 (RISO-M-1726)
- **HEDIN, A.E.**, See REBER, C.A., 30:30459
- **HEDSTROM, J.C.**, See MOORE, S.W., 30:31326
  - See MURRAY, H.S., 30:31325
- **HEEB, C.M.**, See JENQUIN, U.P., 30:31187
- **HEEGER, H.**, See ALDOR, E., 30:29880
- **HEIJWEGEN, C.P.**, Diffusion in the Mo--Ni, Mo--Fe, and Mo--Co systems, 30:30001
- **HEIL, V.**, See BIRKHOLZ, J., 30:30890
- **HEILES, C.**, See MARGON, B., 30:30174
- **HEINRICH, H.**, Indirect technique and problems of radiation protection in pediatric X-ray diagnostics, 30:29701 (AED-CONF-74-140-004)
- **HEITMANN, H.G.**, Steam power plant for nuclear power stations with boiling water reactors, 30:31188
- **HELF, S.**, See BARNES, E.G., 30:29295
- **HELLER, C.G.**, See ROWLEY, M.J., 30:29708
- **HELLIWELL, R.A.**, VLF wave injection into the magnetosphere from Siple Station, Antarctica, 30:30462
- **HELLWIG, F.**, German marine shipping: changes in structure and future development. General meeting of the Nuclear Energy Research Society, Hamburg, Germany, December 12, 1973, 30:31243
- **HEMINGER, R.D.**, See ELSON, R.E., 30:29127
- **HENDERSON, D.B.**, See ELLIOTT, C.J., 30:29153
- **HENDERSON, R.G.**, See CHASTAIN, S.A., 30:31231
- **HENDERSON, T.R.**, Tyrosine aminotransferase induction in rat liver as a response to irradiation or flash burn injuries, 30:29757
- **HENDRICKSON, R.A.**, See MCENTIRE, R.W., 30:30453
- **HENDRIE, D.L.**, See MAGUIRE, C.F., 30:30997
- **HENKELMANN, R.**, See USTERMANN, P., 30:28912
- **HENLEY, E.M.**, See HO, H.W., 30:30998
- **HENNING, W.**, See ZEIDMAN, B., 30:29564
- **HENRI, V.P.**, See DEHM, G., 30:30624
- **HENSEL, F.**, See FREYLAND, W., 30:30005
- **HENSLEY, D.C.**, See RIEDINGER, L.L., 30:30985
- **HENTZ, R.R.**, See PERKEY, L.M., 30:29068
- **HERBST, E.**, Is H$^-$ a source of diffuse interstellar lines., 30:30361
- **HERBST, W.**, NGC 6193: an emission region with a high ratio of total to selective extinction, 30:30239
- **HERMANS, J.A.J.**, Precision lifetime measurement with the coincident high-velocity DSA method, 30:30864
  - See VAN DRIEL, M.A., 30:30912
- **HERMS, R.**, See SCHLIESING, H., 30:29946
- **HERNDON, M.**, See GRANATSTEIN, V.L., 30:30580
- **HERNHUT, H.**, First gamma-irradiation plant for sewage-sludge hygienization, 30:29643
- **HERR, W.**, See QUANDT, U., 30:29524
- **HERRMANN, E.**, Contribution to the separation of rare earths by extraction chromatography with di(2-ethylhexyl) phosphoric acid. II. Behavior of the matrix and its influence on the microcomponents, 30:28990 (ANL-Trans-961)
- **HERRMANN, W.C.**, New precision, high-contrast photographic resolution target, 30:31457 (UCID-15064)
- **HERSCHBACH, K.**, Interconnection between irradiation creep and interstitial loop formation in fcc metals, 30:30079
- **HERSKIND, B.**, See HAGEMANN, G.B., 30:30983
- **HERTERICH, K.**, Absorption of gamma rays in intense x-ray sources, 30:30290
- **HERZIG, C.**, The isotope effect for diffusion of silver in gold, 30:29015
- **HERZLINGER, M.**, See BEBEK, C.J., 30:30587
- **HESKIA, S.**, Geometro-dynamical soldering of the internal and external spaces of strongly interacting particles, 30:30704
- **HESLOP, J.**, See BETTERODGE, W., 30:29988
- **HESS, G.M.**, See ALBRECHT, R.W., 30:31301
- **HESS, W.N.**, Absorption of trapped particles by Jupiter's moons, 30:30404
- **HESSELINK, W.H.A.**, Proton-hole states in ^{115}In observed in the ^{116}Sn(d,^{3}He) reaction, 30:30975
- **HESTER, R.E.**, See CHRISTOFILOS, N.C., 30:29168
- **HEUMANN, K.G.**, Isotope effects in the boundary layer of inorganic solutions, 30:29007 (AED-CONF-74-084-004)
- **HEUSCH, C.A.**, See FLATTE, S.M., 30:30150
- **HEWITT, R.**, See MARBURGER, K., 30:29652
- **HICKERSON, J.P. Jr.**, Metallurgical processing and pulsed reactor fuel performance, 30:29982 (SLA-73-1121)
- **HICKEY, G.T.**, R-matrix and phase-shift analysis of neutron polarization measurements from n--^{16}O scattering, 30:30889
- **HICKMAN, A.P.**, Long-range He$_2$($^3\Sigma$/sub g.u/$^+$) potentials and metastability exchange in He*--He collisions, 30:30494
- **HIDDLESTON, H.R.**, Nuclear Data Sheets for A = 130, 30:30968
- **HIGGS, L.A.**, See TERZIAN, Y., 30:30240
- **HILARIS, B.S.**, See HUVOS, A.G., 30:29784
- **HILL, T.W.**, Origin of the plasma sheet, 30:30465
- **HILTNER, W.A.**, See MOOK, D.E., 30:30271
- **HILTON, R.R.**, Linear and angular localization effects in nuclear structure calculations, 30:31054
- **HIMES, J.H.**, See SNYDER, D.L., 30:29240
- **HINCKLEY, J.S.**, See NABORS, C.J. Jr., 30:29780
- **HINDERMAN, J.D.**, See MARTINI, W.R., 30:29260
- **HINDMAN, F.D.**, See SILL, C.W., 30:28977
- **HINDRINGER, B.**, See GOESSNER, W., 30:29785
- **HINGORANI, J.U.**, See SASTRI, N.S., 30:30421
- **HINTERBERGER, F.**, Symmetrized double-monochromator systems, 30:30134
- **HINUMA, Y.**, See SATO, C., 30:29668
- **HIPPLER, R.**, Outer s-shell ionization of neon, argon, and krypton by proton impact (125 keV-1200 keV), 30:30557
  - See SCHARTNER, K.H., 30:30518
- **HIRAKI, T.**, See SUZUKI, Y., 30:29846
- **HIRAO, Y.**, See SAKAI, M., 30:30974
- **HIRATSUKA, H.**, See SHIMIZU, T., 30:29721
- **HIROSE, A.**, Use of NH$_4$-form Chelex 100 chelating resin of low induced activities for neutron activation analysis of manganese in seawater, 30:28927
- **HIRSHBERG, J.**, Propagation of sudden disturbances through a nonhomogeneous solar wind, 30:30322
- **HISADA, K.**, See SUZUKI, Y., 30:29846
- **HITLIN, D.**, See DIBITONTO, D., 30:30156
  - See DONALDSON, G., 30:30582
- **HIVELY, L.**, See DENARDO, G., 30:30214
- **HJELMS, E.**, ^{67}Ga-scintigraphy in malignant lesions of the lung, 30:29883
- **HO, H.**, See LAM, L., 30:30522
- **HO, H.W.**, Highly inelastic scattering of α-particles fron ^{208}Pb, 30:30998
- **HOBBS, L.M.**, Statistical properties of interstellar clouds, 30:30350
- **HODGE, V.F.**, See HOFFMAN, F.L., 30:29817
- **HODGSON, W.H.**, See SEHMEL, G.A., 30:29482
- **HODOUS, M.F.**, See BASTIEN, D.B., 30:30600
  - See BERLAD, G., 30:30623
- **HOEKSTRA, E.K.**, Fast reactor programme. First quarter 1974 progress report, 30:31226 (RCN-212)
- **HOEKSTRA, H.R.**, See OSBORNE, D.W., 30:29128
- **HOFER, H.**, See PICHLER, L., 30:29755
- **HOFFMAN, A.S.**, Method for preparation of biocompatible and biofunctional materials and product thereof, 30:29082
- **HOFFMAN, E.J.**, See GEORGOPULOS, P.D., 30:30930
- **HOFFMAN, F.L.**, ^{210}Po radioactivity in organs of selected tunas and other marine fish, 30:29817
- **HOFFMAN, G.**, See WEIGEL, F., 30:29130
- **HOFFMAN, J.H.**, See MAIER, E.J., 30:30429
- **HOFFMAN, R.A.**, See BERKO, F.W., 30:30469
- **HOFFMANN, D.**, Wobble target holder for thin targets in intense light- and heavy-ion beams, 30:30148
- **HOFFMANN, G.W.**, The coupled-channel Born approximation and J-dependence in ^{30}Si(d,p)^{31}Si, 30:30907
- **HOFFMANN, P.**, Separation of radionucilides using alkyl radicals, 30:29083 (AED-CONF-74-084-002)
- **HOFFMANN, R.**, See HEUMANN, K.G., 30:29007
- **HOFFMEISTER, H.**, See THEFELD, W., 30:29702

HOFMANN, A., Micro- and macroturbulence, 30:31358 (ORNL-tr-2801)
HOFSETH, P., See PARR, H., 30:29343
HOGERVORST, W., See EKSTROEM, C., 30:30976
HO-KIM, Q., Self-consistent calculation of the optical potential and ground-state properties of nuclear matter, 30:31024
HOLAN, S., See FURMAN, V.I., 30:31102
HOLBERTON, E.J., Radioimmunoassay for myosin in cultured skeletal muscle cells, 30:29833
HOLDREN, J.P., Adequacy of lithium supplies as a fusion energy source, 30:29222 (UCID-15953)
HOLINDE, K., See ALZETTA, R., 30:31033
HOLL, P.M., 36 inch miter valve design, 30:31435 (UCID-15496)
HOLLWEG, J.V., On electron heat conduction in the solar wind, 30:30324
  See BARNES, A., 30:30398
HOLMEN, G., See PETERSTROEM, S., 30:29531
HOLMES, H.H., MAPEDIT system for automatic map digitization, 30:31341 (LBL-3072)
HOLMES, J.A., See SKILLING, J., 30:30167
HOLMGREN, H.D., See BHOWMIK, R.K., 30:30896
HOLMIN, N., Nuclear power availability, 30:31189
HOLOWIECKI, J., Alkaline phosphatase activity of granulocytes (FAG) in workers in radiological laboratories, 30:29734
HOLT, A.C., Yield surfaces for beryllium boride ceramics, 30:29891 (UCID-15859)
HOLT, R.J., See HICKEY, G.T., 30:30889
HOLUB, R., See MUGA, L., 30:29528
HOLWERDA, M.J., The Callan-Symanzik equation and dimensional regularization, 30:31160
HOLZER, F., Generation of seismic waves by nuclear explosives and possibilities for evading a test-ban treaty, 30:29325 (UCID-15983)
HOLZER, T.E., See SUESS, S.T., 30:30340
HOLZWARTH, G., Population of muonic ^{3}He states following the μ-catalysed fusion $p\mu d \to \mu {}^{3}\mathrm{He}$, 30:30515
HONECKER, R., See GRAESSLER, H., 30:30510
HONMA, T., See YOKOTA, M., 30:31193
HOOD, J.T., A simple fast sweeping system for extracted cyclotron beams, 30:30153
HOOSE, J., See SOURES, J., 30:29231
HOOVER, W.R., J-integral as a failure criterion for a Borsic--Al composite, 30:29890 (SAND-74-0193)
HORGAN, V.J., See BAVERSTOCK, K.F., 30:29660
HORIUCHI, H., ^{12}C + α scattering by the coupled channel resonating group method. Solution of the redundancy and non-orthogonality problem, 30:30876
HORN, H., See GEIR, A., 30:29878
HORNE, D., See WINTERS, H.F., 30:30070
HORNSEY, S., RBE of cyclotron neutrons for effects on normal tissues, 30:29726
HORST, T.W., Assessment of the long-term exposure due to resuspension, 30:29375 (BNWL-1850(Pt.3))
  Development of a sonic anemometer system, 30:29609 (BNWL-1850(Pt.3))
  Surface flux model for diffusion, deposition, and resuspension, 30:29470 (BNWL-1850(Pt.3))
  See HALES, J.M., 30:29613
  See POWELL, D.C., 30:29433
HORTON, J.E., Macrophage--lymphocyte synergy in the production of osteoclast activating factor, 30:29667
HORTON, W., Negative mass instabilities in beam injected plasmas, 30:29197 (UCID-15540)
HORVATH, M., Chemical study of the mechanism of the radioprotective effect of AET, 30:29654
HOSOI, F., Kinetic study of double bonds in polyethylene irradiated by gamma rays, 30:29038
HOTTMAR, Z., See ZADAK, Z., 30:29873
  See ZADAK, Z., 30:29871
  See ZADAK, Z., 30:29872
HOUDAYER, A.J., Rapid production of thin Kr sources, 30:29641
HOUGH, W.R., Improvements in or relating to nuclear reactors, 30:31214
HOUGHTON, J.W., See THOMAS, S.W., 30:29162
HOUSE, L.L., Stokes formulation of non-LTE radiative transfer in a magnetic field, 30:30202
HOUSE, P.A., ''Super'' H.E. machine concept, 30:29320 (UCID-15855)
HOVE, D.T., See CARPENTER, H.J., 30:29307
HOYLE, F., Nucleosynthesis in white-dwarf atmospheres, 30:30256
HRUSOVSKY, J., See HAVLICEK, F., 30:29823
HRYNCZUK, B., See LORENZ, J., 30:29791
HSIEH, E.J., Evaluation of gold-doped permalloy films using ferromagnetic resonance techniques, 30:31454 (UCID-16032)
  Lorentz microscopic observation of head-on domain walls in magnetic thin films, 30:31455 (UCID-16034)
HSU, J.P., Scaling and asymptotically free massive Yang--Mills field, 30:31147
HSU, Y.C., See PERNG, C.C., 30:30927
  See PERNG, C.C., 30:30927
HU, B.L., Scalar waves in the mixmaster universe. II. Particle creation, 30:30391
HUANG, J.T.J., See RABALAIS, J.W., 30:30491
HUBBERSTEY, P., Solubility of tin and germanium in liquid sodium. The sodium--tin partial phase diagram, 30:30049
HUBER, J.G., Superconducting-normal phase boundaries of (La,Th)Ce systems, 30:30814
HUBER, R.A., See HAWTIN, P., 30:31211
HUBERT, C., See KELLERSHOHN, C., 30:29051
HUBERT, P., Monte Carlo computation for isotopic analysis of cosmic rays by means of the Earth's magnetic field, 30:30181
HUCZKOWSKI, J., Studies on the use of U-120 cyclotron and fast neutron generator in neutron irradiation of seeds for mutation, 30:29692
HUDOMALJ, J., See MILJANIC, D., 30:30882
HUEBEL, H., Design of the primary containment for pool and loop arrangements of LMFBRs, 30:31263
HUETSCH, W., See WIEMER, H., 30:31383
HUFFMAN, D.R., See DAY, K.L., 30:30190
HUFFMAN, F.N., See HAGEN, K.G., 30:29262
HUGHES, A.E., Production of oxygen vacancies by elastic collisions in alkaline earth oxides, 30:29933
  See CALL, P.J., 30:29075
HUGHES, D.A., See HAGEN, K.G., 30:29262
HUGHES, V.A., Daily observations of Cygnus X-3 at 10.5 at GHz during the period 1973 July-October, 30:30292
HULSIZER, R.I., See BASTIEN, D.B., 30:30600
  See BERLAD, G., 30:30623
HUMBLE, S., An impact parameter description of single and double diffraction dissociation, 30:30761
HUMMER, D.G., See CRANDALL, D.H., 30:30246
HUMPHERYS, K.C., Radiochromic dosimetry measurements, 30:29546 (DEMO-74/5)
HUMPHREY, J.R., LX-10-1: a high-energy plastic-bonded explosive, 30:31374 (UCRL-51629)
HUNDHAUSEN, A.J., Coronal expansion and solar wind, 30:30320
HUNT, A.L., See GOODMAN, R.K., 30:29218
HUNT, E.L., See SCHNEIDER, M.J., 30:29461
HUNTER, W.M., See TUFT, A.D., 30:29775
HURDLOW, W.R., Evaluation of downhole alignment by means of an alternating magnetic dipole field, 30:31432 (UCID-15203)
HURLBUT, J.A., Direct determination of beryllium in urine by flameless atomic absorption spectrometry, 30:31379 (RFP-2151)
HURWITZ, S., Effect of irradiation on gastrointestinal drug absorption in mice and rats, 30:29738
HUSS, R., Boundary value problem for integro-differential equations, 30:31029
HUTCHINGS, J.B., Evidence for the existence of a massive companion to X Persei (=2U 0352+30.), 30:30230
  H alpha emission in Cygnus X-1, 30:30291
  See CRAMPTON, D., 30:30270
HUTCHINSON, P., See BAKER, R.J., 30:31414
HUVOS, A.G., Pathological changes in mice following the intraperitoneal administration of radionuclides, 30:29784
HUYNH, C.T., See BLANC, C., 30:29025
  See BLANC, C., 30:29024
HUYS, D., See BAETSLE, L., 30:28991
HWANG, C.F., See POTTER, J.M., 30:30599
HWANG, J.L., See PERNG, C.C., 30:30927
HYAMS, B., See GRAYER, G., 30:30617
HYDER, A., See ANDERSSON, L.P., 30:29519
HYLA-KRYSPIN, I., See WAJDA, S., 30:29030

I

IACHELLO, F., Finite range effects in pionic atoms, 30:30512
IBANEZ, P., Methods for the identification of dynamic parameters of mathematical structural models from experimental data, 30:31269
IBATULLIN, M.S., See TROITSKAYA, M.N., 30:29405
ICHII, H., Studies on radioimmunoassay of leteinizing hormone of rabbit, 30:29860
ICHIMURA, M., See SHIMIZU, K., 30:30898
ICHINOSE, M., See SHIMIZU, T., 30:29721
IEVLEVA, Zh.I., See POPIL'SKII, R.Ya., 30:29910
IGO, G.J., See WHITTEN, C.A. Jr., 30:30973
IGUCHI, T., See KAIFU, N., 30:30359
IKOSSI, P.G., A study of isobaric analogue resonances in ^{71}Ga, 30:30949
IKRAMULHAQ, M., See GHANI, A., 30:31276
IKUSHIMA, T., PRELUDE-2: seismic response analysis code for block-type fuel core, 30:31247 (JAERI-M-5560)
IL'IN, Yu.M., Disturbed non-linear chiral SU(3) x SU(3) dynamics and Cabibbo's angle, 30:30776
IL'INA, V.A., See KRITSKAYA, V.K., 30:30080
ILTIS, R., See STARA, J.F., 30:29815
IL'YUKEVICH, L.A., Effect of ultraviolet light and gamma radiation on aqueous solutions of Cu(II) complexes with amino acids, 30:29061
IMAMURA, M., See MATSUI, M., 30:29049
IMBERT, J.C., Study of diffusion/leaching phenomena with glasses. Application of risk evaluation to long-term storage, 30:29133 (CEA-R-4550)
IMHOF, W.L., See ROMICK, G.J., 30:30430
IMOTO, S., See YOSHIMURA, T., 30:29094
INATOMI, K., See YOSHIDA, T., 30:29863
INGELMAN, S., See EKSTROEM, C., 30:30976
INGHAM, D., See ASPELUND, O., 30:30900
INGLIS, A.S., Determination of small amounts of zirconium in wool, 30:28945
INGRAM, C.H.Q., See AXEN, D., 30:29597
INGS, R., See ASQUITH, J.C., 30:29674
INKIN, V.D., See BARABOSCH, L.S., 30:30117
INO, I., Base-pair deletion at a frameshift hotspot in Salmonella, 30:29684
INOGAMOV, Sh.V., See GRISHIN, V.G., 30:30875
INOGAMOVA, T.Ya., See GRISHIN, V.G., 30:30875
INOZEMTSEVA, O.I., See BLOKH, Ya.L., 30:29579

INTRILIGATOR, D.S., Reliability of the daily quick look solar wind velocities as indicators of interplanetary activity, 30:30400
ION, D.B., Zeros of triple scattering parameters and spin--parity determination of a resonance, 30:31020 (IFA-FT-107-1974)
IONESCU-PALLAS, N.J., Plausible assertions for building-up the wave functions of the atoms with a single valence electron, 30:30569
IPPOLITOVA, E.A., See DUNAEVA, K.M., 30:29103
IRVINE, W.J., See TOFT, A.D., 30:29775
ISAACS, N.S., Secondary deuterium isotope effect in the cycloaddition of dimethylketen to styrene, 30:29021
ISAICHEV, V.I., See LARIKOV, L.N, 30:29955
ISAKOV, A.I., See GRISKOV, V.A., 30:29176
ISCHENKO, G., See KLAUMUENZER, S., 30:30074
ISEKI, T., See SUZUKI, H., 30:29921
ISHIBASHI, W., Atomic absorption spectrometry of impurities in hign purity tantalum with heated graphite atomizer, 30:28954
ISHIHARA, M., See HAGEMANN, G.B., 30:30983
  See KAWAKAMI, H., 30:30980
ISHII, D., See HIROSE, A., 30:28927
ISHII, K., See KAWAKAMI, H., 30:30980
ISHIZUKA, H., See TOYAMA, H., 30:30132
ISHMAEV, S.N., Neutron slowing-down in ice and polyethylene at low temperatures, 30:30843 (IAE-2271)
ISLAM, A.K.M.A., See AYE, T.M., 30:30744
ISLER, R.C., Inelastic collisions of He^+ and Ar, 30:30538
ISOBE, S., Dust, star, and hydrogen distributions in the Orion association, 30:30242
  Variations of interstellar ultraviolet absorption, 30:30371
ISSINSKII, I.B., Slow beam extraction from the JINR synchrophasotron, 30:30129
ITO, A., See FUKUCHI, S., 30:29876
ITO, K., Urine /sup 131m/In-EDTA time concentration curve and redistribution of glomerular filtration in the dog, 30:29839
ITO, T., Sensitivity to radiation and insensitivity to vinblastine of the inducer function of thymus-derived cells, 30:29665
ITTI, R., Advantages of theoretical models in interpreting cerebral transit curves, 30:29830 (CONF-740708-20)
IVANOV, A.A., See KAW, P.K., 30:30440
IVANOV, V.B., A summing Ge(Li)-Compton spectrometer, 30:29570
IVANOV, V.M., See SHAFIEV, A.I., 30:29141
IVANOV, Yu.A., Identification of high-boiling tritium-labeled compounds formed in reactions of tritium recoil atoms with benzene, 30:29084
IVANOVA, N.S., See KULIKOV, V.N., 30:29501
IVANV, V.I., See ASTVATSATUROV, R.G., 30:29577
IVANYUSHKIN, E.M., See BUDAGOVSKII, S.S., 30:30029
IVASCU, M., Spectroscopy of the ^{69}Ga and ^{71}Ga isotopes with the ^{69} $^{71}Ga(\alpha,\alpha'\gamma)^{69}$ ^{71}Ga and ^{66} $^{68}Zn(\alpha,p\gamma)^{69}$ ^{71}Ga reactions, 30:30941
  See BUCURESCU, D., 30:30943
IVASHCHENKO, Yu.N., See LARIKOV, L.N, 30:29955
IVASHIN, V.V., See GITGARTS, M.I., 30:30036
IWAKI, A., D_2-type representation of the conformal group extended by reflections, 30:30628 (KFKI-74-49)
IWANCZYK, J., See DABROWSKI, A.J., 30:29520
IWANOV, I.N., See BARABOSCH, L.S., 30:30117
IWASA, Y., High speed magnetically levitated and propelled mass ground transportation, 30:30829
IZOTOV, V.I., See BONDAREVSKII, S.I., 30:29098
IZRAEHL, Yu.A., Calculation of fractionation effects following atmospheric nuclear explosions, 30:29386
  Radioactive particle formation after nuclear explosions in the troposphere, 30:29387

J

JABIOL, M.A., See BUMAZSHNOV, V.A., 30:30603
  See DERRE, J., 30:30601
JABSEN, F.S., Fuel assembly for a nuclear reactor, 30:31292
JACKSON, A.D., Approximate D-states and meson exchange currents, 30:30870
JACKSON, K.L., X-radiation-sensitivity of rat liver to interphase death, 30:29737
JACKSON, L.C., Solubility parameters and evaporation rate analysis in organic residue characterization, 30:31367 (BDX-613-1099(Rev.))
JACKSON. M.C., See FENNER, N.C., 30:29625
JACOB, M., Strong interaction dynamics, 30:30703
  See BIALAS, A., 30:30699
JACOBS, V.L., Photoionization of $He(n^1\ ^3P)$ atoms excited by polarized light, 30:30498
  Radiative transitions involving the $(2p^2)\ ^3P$/sup e/ metastable autodetaching state of H^-, 30:30245
JACOBSEN, T.S., New high-dispersion radial velocity curves of W sagittarii, 30:30254
JACOBSON, J.H., See KROYHN, D.L., 30:29765
JADACH, S., Overlap function from the multiperipheral model, 30:30701
JAEGLE, P., Method of obtaining a medium having a negative absorption coefficient in the x-ray and ultraviolet spectral range and a laser for practical application of said metnod, 30:29194
JAHNKE, B., See GIESECKE, P., 30:30062
JAIN, S.K., See GHOSH, S.N., 30:30397
JAKUBASSA, D.H., Calculation of the 0^+ and 2^+ giant resonances in Ni^{58}, 30:30924
JAMELOT, G., See JAEGLE, P., 30:29194
JAMES, A.N., See PRICE, H.G., 30:30910
JAMES, L.T., Range-scan radar images and their application to map-matching estimation of location, 30:31429 (SAND-74-0153)
JAMES, W.D., Investigation of the reported mass distribution curves in the fission of ^{233}U with 14.8 MeV neutrons, 30:31010 (ORO-4282-14)
JAMESON, A., Connection between singular perturbations and singular arcs. Part 2. A theory for the linear regulator, 30:31336 (COO-3077-44)
JANICZEK, J., See KAMINSKI, R., 30:28920
JANNEY, R.B., A study of ion paths in curved parallel-plate electron multipliers with perpendicular magnetic field, 30:29629
JANUKOWICZ-LORENZ, H., See LORENZ, J., 30:29791
JANYSZEK, H., Modification of the quantum-mechanical equations for the system of charged Dirac particles by including additional tensor terms of the Pauli type. I, 30:31157
JARLSKOG, C., See BERNABEU, J., 30:30777
JARNEBORN, L., See CHRISTIANSSON, J.E., 30:30901
JARSKOG, C., See BERNABEU, J., 30:30516
JARZMIK, B., See POMORSKI, L., 30:28980
JASINSKI, J.P., Electronic structure and optical properties of some first row transition metal oxyhalides, 30:31395 (LA-5637-T)
JASZCZUK, W., Application of Josephson's effect in superconductors for measurements of very small voltages, 30:30842
JAVAN, A., Laser pumped by photoionization generated, electrically heated plasma, 30:29284
JAWOROWSKI, Z., Influence of irradiation on the incorporation of radionuclides, 30:29818
JEANMAIRE, L., Metabolism of tritium-labelled sodium acetate, in the rat. A radiation protection approach, 30:29795 (CEA-R-4591)
JEE, W.S.S., Plutonium, diphosphonates, and bone, 30:29801 (COO-119-249)
  Research in radiobiology. Annual report of work in progress in the internal irradiation program, 30:29778 (COO-119-249)
  See WANG, T.M., 30:29800
JEHN, H., Reactions occurring during annealing of VIa and Va metals in oxygen, water vapor, and air at low pressures, 30:30022
JELLEY, N.A., See ROGERS, D.W.O., 30:30895
  See UNDERWOOD, B.Y., 30:30885
JENKINS, C.E., Behavior and characteristics of radioactive debris from the Chinese nuclear weapons test of June 26, 1973, 30:29362 (BNWL-1850(Pt.3))
JENKINS, J.D., Constraints, causality, and Lorentz invariance, 30:31167
JENKOVSZKY, L.L., Generalization of Regge-behaved DAMA to production processes, 30:30694
JENQUIN, U.P., Neutronic calculations for experiments with light water reactor fuel in PBF, 30:31187 (BNWL-B-371)
JENSEN, M., Identification of heavy ions in nuclear emulsions in the hundreds of MeV interval, 30:29493 (LUIP-CR-74-3)
JENSEN, S.J.K., See BYBERG, J.R., 30:29065
JENTISCH, A., See BARNES, E.G., 30:29295
JEREMIAH, D.R., See BAILEY, J., 30:30620
JERNIGAN, T.C., See DAVIS, R.C., 30:29209
JERVIS, R.E., See CHATTOPADHYAY, A., 30:28921
JEUKENNE, J.P., Microscopic approaches to the optical-model potential, 30:31055
JEZERNIK, A., Large user-orientated systems of programs for structural analysis and design, 30:31291
JIROUSEK, P., See KLUMPAR, J., 30:29506
JOERGENSEN, P., Self-consistent time-dependent Hartree--Fock scheme, 30:30565
JOESTLEIN, H., See FINOCCHIARO, G., 30:30505
  See KIM, I.J., 30:30584
JOHANSEN, S.A., See KAALHUS, O., 30:29055
JOHANSSON, A., D(p,2p)n reaction, 30:30855 (NP-20122)
  See NYMAN, B., 30:30953
JOHANSSON, B., Thermodynamical account of the photoemission spectra of the rare earths, 30:30505
JOHANSSON, E., See CARLSON, P.J., 30:29600
JOHANSSON, K., See ORRE, B., 30:31017
JOHN, W., See WESOLOWSKI, J.J., 30:31371
JOHNSON, G.R.A., Radiation effects in polyethylene films studied by pulse radiolysis, 30:29077
JOHNSON, H.M., Dust in the Large Magellanic Cloud, 30:30370
JOHNSON, K.H., Optical identifications from the NRAO 5-GHz radio survey, 30:30282
JOHNSON, M.B., Effective two-body interaction for equivalent particles, 30:31059
JOHNSON, M.C., See THRALL, J.H., 30:29549
JOHNSON, N.R., See RIEDINGER, L.L., 30:30985
JOHNSON, P.D., Fueled moderator composition, 30:29934
JOHNSON, P.M., See MUROFF, L.R., 30:29851

JOHNSON, R.C., Simple Z_0* model, 30:30740
JOHNSON, R.W., See LEWIS, F.D., 30:29018
JOHNSON, W.A., See WILSON, W.J., 30:30265
JOHNSTON, D.C., See KHAN, H.R., 30:30810
JOHNSTON, K.J., See KNOWLES, S.H., 30:30286
JOHNSTON, R.P., Implanted energy conversion system. Annual report, 8 July 1972--8 July 1973, 30:29239 (JUL-73)
  See MARTINI, W.R., 30:29260
JONES, C., See GRAYER, G., 30:30617
JONES, C.A., Optical studies of Uhuru sources. VIII. Observations of 92 possible counterparts of x-ray sources, 30:30205
JONES, C.E., Reply to ''Comments on 'Luminescence from electron-irradiated silicon' '', 30:30099
JONES, D., See KELLEY, M.C., 30:30433
JONES, D.E., See SHAPIRO, E.G., 30:29552
JONES, D.R.T., Two-loop diagrams in Yang-Mills theory, 30:31168
JONES, D.T.L., Neutrons from the 2MeV deuteron bombardment of thick ^{7}Li targets, 30:30146
JONES, G., See AXEN, D., 30:29597
JONES, H.D., Multiphoton transitions in helium between 1S and 2S levels, 30:30488 (AD-777042)
JONES, L.W., A calorimeter for 300GeV neutrons and protons, 30:29596
JONES, P.R., Differential elastic-scattering measurements of Xe$^+$ on Xe and Ar$^+$ on Ar in the 20 to 340-eV range, 30:30540
JONES, R.K., See HENDERSON, T.R., 30:29757
JONES, T.W., See GEHRZ, R.D., 30:30252
JONES, W.B.G., Long-lived radiation-induced free radicals in anoxic wet DNA as studied by electron spin resonance spectroscopy, 30:29064
JONG, R.A., See HAUGHT, A.F., 30:29152
JONSSON, N.G., See LINDSKOG, J., 30:30979
JORIO, V.M., See ZINGONI, E., 30:31273
JOSHI, S.K., See TRIPATHI, A.N., 30:30521
JOSS, P.C., Are stellar surface heavy-element abundances systematically enhanced., 30:30250
JOST, R., Determination of the singlet--triplet separation of H_2 by a level-anticrossing technique, 30:30490
JOSWIG, E.H., Prevention of thromboembolism during radiotherapy of carcinoma of the uterine cervix, 30:29732
JOSWIG-PRIEWE, H., See JOSWIG, E.H., 30:29732
JOUAN, A., See DE BETTENCOURT, A.O., 30:29085
JOUFFREY, B., See BIBRING, J.P., 30:30355
JOURET, C., See BIBRING, J.P., 30:30355
JOYCE, W.B., Classical-particle description of photons and phonons, 30:30659
JOZEFOWICZ, K., Use of particle track detectors in the investigation of static reactor parameters, 30:29507
JUDY, R.J. Jr., Prevention and control of subcritical crack growth in high-strength metals, 30:29981 (NRL-Report-7780)
JUHLKE, T., See RAAEN, V.F., 30:29010
JUILLOT, P., See FRIDMAN, A., 30:30602
JULIEN, J., See POSSOZ, A., 30:30899
JULIEN, P.F., See PARKINSON, W.C., 30:30159
JULIENNE, P.S., Oxygen recombination in the tropical nightglow, 30:30425
JULIUSSON, E., Charge composition and energy spectra of cosmic-ray nuclei at energies above 20 GeV per nucleon, 30:30164
JUNGBLUTH, H., Radiation-chemical studies on the generation of lead and tin radicals, 30:29057
JUNGEN, C., See ATABEK, O., 30:30496
JURA, M., Formation and destruction rates of interstellar H_2, 30:30349

K

KAALHUS, O., Radiation-induced radicals in thymine and its derivatives in low temperature glasses, 30:29055
KAASIK, A., See EINASTO, J., 30:30379
KADMENSKY, S.G., See FURMAN, V.I., 30:31102
KADYKOVA, G.N., Effect of cold deformation on phase transition in Ti--Nb alloys, 30:30009
KAGAN, Y.M., See BLAGOEV, A.B., 30:29165
  See BLAGOEV, A.B., 30:29164
  See VAGNER, S.D., 30:29166
KAGIYA, T., See HAGIWARA, M., 30:29058
  See HOSOI, F., 30:29038
KAHANA, S., A simple description of differential cross sections for heavy ion induced reactions, 30:31069
  See BUND, P.D., 30:30921
KAIDALOV, A.B., The pomeron-particle total cross section and diffractive production of showers at very high energies, 30:30760
KAIFER, R., See WESOLOWSKI, J.J., 30:31371
KAIFU, N., Detection of interstellar methylamine, 30:30359
KAISER, E.W., Crossed-molecular-beam study of the kinematics and dynamics of charge-transfer collisions, 30:30547
KAISER, G., See MERZ, I., 30:28941
KAJANTIE, K., Long range correlations in the pionization component, 30:30754
  See BYCKLING, E., 30:30646
KAKEHI, H., See AKIBA, H., 30:29859
KAKINUMA, T., See WATANABE, T., 30:30323
KALABA, R., See HUSS, R., 30:31029
KALACHEV, N.V., See GRIBKOV, V.A., 30:29176
KALADZE, T.D., Excitation of electromagnetic ion cyclotron waves by fast ions, 30:29234
KALASHNIKOV, O.K., See FRADKIN, E.S., 30:31150
KALDOR, A., See BRAUN, W., 30:30525
KALETTA, D., A model for the calculation of the defect production ratio, 30:30075
KALINICHENKO, A.I., Acoustic effect of fast neutron beams in a solid body, 30:30853
KALINKIN, B.N., Complete nuclear fusion reactions, 30:29205 (GSI-tr-73/20)
KALINOWSKI, H., See GROSS, D.H.E., 30:31065
KALMAN, B., Surface irradiation of spherical vegetables and fruits, 30:29645
KALMON, B., Portsmouth Gaseous Diffusion Plant environmental monitoring report, 1973, 30:29345 (GAT-781)
KALMYKOVA, T.A., See VAGNER, S.D., 30:29166
KALYONOV, S.V., See ISSINSKII, I.B., 30:30129
KAMBLE, V.B., See KHADKIKAR, S.B., 30:31081
KAMCHATNOV, A.M., See NOSOV, V.G., 30:30627
KAMEGAYA, T., See YOKOZAWA, M., 30:30493
KAMIDE, Y., Latitudinal cross section of the auroral electrojet and its relation to the interplanetary magnetic field polarity, 30:30470
KAMIMURA, M., New analytical derivation of kernels in the resonating group method for composite-particle scattering and molecule-like structures. Derivation from kernels in the generator coordinate method and application to $^{16}O + \alpha$, 30:31023
KAMINSKI, R., Betatron activation analysis of cupriferrous flotation pulp, 30:28920
KAMMERDINER, L., Preparation of new β-W phases by film-deposition techniques, 30:29967
KAMOSHIDA, M., See KUDOH, O., 30:30100
  See NAKAMURA, K., 30:30098
KAN, K.-K., Quantized friction and the correspondence principle: single particle with friction, 30:31075
KANAO, K., See MIYAZAKI, M., 30:29840
KANAZIRSKY, Ch., See GRAESSLER, H., 30:30610
KANEKO, Y., See YAMAMURO, N., 30:31278
KANSTEIN, L.L., Low-intensity beam monitoring with an image-intensified scintillator detector, 30:30127
KANTA, L., Investigations of hydrogen--deuterium exchange in α-chymotrypsin, 30:29033
KAPANADZE, B.B., Changes of the broncho-vascular system of the lung under the influence of local γ irradiation, 30:29728
KAPLAN, I.R., See MCCREADY, R.G.L., 30:29826
KAPPLER, F., Measurement and calculation of neutron spectra at a sodium--iron interface, 30:30848 (KFK-1959)
KAPUSCIK, E., Multiplication law in quantum physics. I. The non-relativistic quantum mechanics, 30:31158
KAPUSTIN, I.N., See BLOKH, Ya.L., 30:29500
KARABAN, A.A., Radiation-chemical conversions in solutions of Pt(II) and Pt(IV) complexes, 30:29062
KARASEV, A.I., See GREBENKINA, V.G., 30:29893
KARASEV, V.S., See GRINIK, E.U., 30:30072
KARETNIKOV, V.G., Spectrophotometry of eclipsing binary V 367 Cygni, 30:30210
KARL, G., Muon-electron universality at high energies and hadronic corrections to $e^+e^- \to \mu^+\mu^-$, 30:30675
KARLOWICZ, R.R., See THORNTON, S.T., 30:30537
KARLSSON, E., See WENE, C.-O., 30:30125
KARMOHAPATRO, S.B., See BHATTACHARYA, R.S., 30:30481
KARNIEWICZ, W., See LINIECKI, J., 30:29749
KAROL, P.J., Spallation of copper by high-energy alpha particles, 30:30935
KAROWSKI, M., Dipole ghosts and unitarity, 30:30787
KARPUKHIN, V.I., See PLATONOV, P.A., 30:30090
KARTASHEV, K.B., Anomalous scattering of the energy of a plasma jet interacting with a gas target, 30:29155
KARWOSKI, J., See FRAGA, S., 30:31138
KASAHARA, I., Simultaneous hard X-ray and optical observations of Sco X-1 and a model of semi-opaque X-ray sources, 30:30294
KASAI, Y., See MUTO, K., 30:31265
KASE, K.R., Calorimetric and ionization measurements of stopping power in carbon for 19.5 GeV electrons, 30:29556
KASER, J.D., See WINEGARDNER, W.K., 30:30107
KASHCHEEV, I.N., Reaction of uranium with a mixture of lithium and calcium fluorides, 30:29110
KASIMOV, G.G., See KRYLOV, E.I., 30:29908
KASPAR, J., Interatominstrument to coordinate EE nuclear instrumentation technology, 30:29615 (JPRS-61338)
  Progress on Czechoslovak Nuclear Power Plants, 30:31185 (JPRS-61338)
KASSIROV, S.A., Some features in the dependence of the pulse-height defect in semiconductor detectors on detected particle energy, 30:29526
KATOU, T., See HASHIZUME, A., 30:30154
KATOWICACH M., See HOLOWIECKI, J., 30:29734
KATSUFRAKIS, J.P., See HELLIWELL, R.A., 30:30462
KATZ, J.I., Models for nuclei of planetary nebulae and ultraviolet stars, 30:30215
KAUFMANN, P., First celestial water vapor sources observed at Itapetinga Radio Observatory, Brazil, 30:30287
KAUL, G.L., See GURTU, A., 30:30604

KAVANAGH, R.W., See MANN, F.M., 30:30692
KAVERINA, S.N., Electron microscopic and x-ray study of the structure of deformed polycrystalline molybdenum, 30:30057
KAW, P.K., Electromagnetic effects on instabilities in the equatorial electrojet, 30:30440
KAWABE, T., Deep inelastic electroproduction in resonance region. Cross section ratio sigma/sub n//sigma/sub p/, 30:30654
KAWAGUCHI, T., See HASEGAWA, K., 30:31224
  See TODUKI, M., 30:29059
KAWAHIRA, K., See WATANABE, K., 30:29654
KAWAKAMI, H., Low-lying states of ^{181}Os, 30:30980
KAWAMURA, K., Treatment of exhaust gas with electron beam irradiation. I. Treatment of exhaust gas in batch type apparatus, 30:29046
KAWANA, M., See AKIBA, H., 30:29859
KAWANO, I., See MORITA, N., 30:29050
KAWARASAKI, Y., Survey for elements to be excited by gamma-rays following thermal neutron capture in vanadium, 30:30959
KAWASAKI, S., See FURUTA, T., 30:30073
KAWAZOE, Y., Three-alpha particle model for ^{12}C ground state, 30:30881
KAWEEKA, J., See HOLOWIECKI, J., 30:29734
KAYUHA, H.J., REECo field activities and sample logistics in support of the Nevada Applied Ecology Group, 30:29441 (NVO-AEIC-74-1)
KAZANSKII, V.B., See GRIVA, A.P., 30:29029
KAZNADZEI, V.V., Dose-response for frequency of chromatid aberrations induced by x rays at G$_2$ and S stages of the mitotic cycle in Crepis capillaris root tips, 30:29697
KAZNOFF, A.I., See GROSSMAN, L.N., 30:31281
KEARNEY, J.P., Radiation and heat deposition analysis of the proposed Mirror Fusion Experiment (MFX), 30:29220 (UCID-15806)
KEELING, M.J., A new technique for the production of carbon foils, 30:30145
KEEP, C.W., See PALMER, J.E.M., 30:29035
KEIM, T.A., See SMITH, J.L. Jr., 30:30828
KELLAND, D., High gradient magnetic spearation: an industrial application of magnetism, 30:30832
KELLER, H., See FRANK, G., 30:29258
KELLER, K.A., Q-values and excitation functions of nuclear reactions. Part C. Estimation of unknown excitation functions and thick target yields for p, d, ^{3}He, and α reactions, 30:30960
KELLER, R., The preparation of self-supporting ^{13}C-foils using enriched methane gas, 30:30151
KELLER, W.E., USAEC-DAT dc superconducting power transmission line project at LASL. Progress report, January 1--March 31, 1974, 30:30820 (LA-5684-PR)
KELLERSHOHN, C., Quantitative study of the radiolysis of FeSO$_4$.7H$_2$O using Moessbauer effect, 30:29051
KELLETER, H., See ASPELUND, O., 30:30900
KELLETT, B.H., See DEL GUERRA, A., 30:30578
KELLEY, M.C., Active experiments stimulating waves and particle precipitation with small ionospheric barium releases, 30:30433
KELLY, M., See HSIEH, E.J., 30:31455
KELSEY, C.T., See WEST, D., 30:31337
KELSON, I., Generalized approximative procedures in the many body problem. Final technical report, 30:31130 (AD-776408)
KEMMLER-SACK, S., See FLECKENSTEIN, J., 30:29006
KEMMITZ, P., See MANFRASS, P., 30:30994
  See WINTER, G., 30:30992
KEMP, T.J., See BURROWS, H.D., 30:29131
KEMPA, J., Energy spectrum of primary cosmic rays above 10^{12} eV, 30:30176
KEMPER, K.W., See WHITE, R.L., 30:30937
KENDALL, H.W., See RIORDAN, E.M., 30:30583
KENNEDY, N.C., Measurements of meteorological parameters, 30:29451 (NVO-AEIC-74-1)
KENNELLY, R., See DONALDSON, G., 30:30582
KENNEY, J., Design progress on the LMFBR demonstration plant. Subject No. 20, 30:31222 (CONF-740341-1)
KENT, R.S., See CASS, J., 30:29074
KEPHART, R., See FINUCCHIARO, G., 30:30605
KEREIAKES, J.G., See SILBERSTEIN, E.B., 30:29707
KERN, R.C., See STOUDT, R.H., 30:31195
KERR, P.G., Magnetic rotation of levels of ^{53}Mn and ^{54}Mn following the ^{53} ^{54}Cr(p,n) and ^{51}V(α,n) reactions, 30:30933
KERRI, K.D., Environmental assessment of resource development, 30:29331
KERSHNER, C.J., Tritium Effluent Control Project. Progress Report: April--June 1974, 30:29026 (MLM-2171(LD))
KEYES, J.W. Jr., See WEBER, D.A., 30:29843
KHACHATURYAN, M.N., See ASTVATSATUROV, R.G., 30:29577
KHADKIKAR, S.B., Centre of mass motion and single particle separation energies in Hartree-Fock theory, 30:31081
KHALIL, E.E., See BAKER, R.J., 30:31414
KHAN, H.R., Magnetic and superconducting properties of niobium oxides, 30:30810
KHANNA, F.C., See HO-KIM, Q., 30:31024
KHARCHENKO, V.F., Solutions of the integral equations for four identical particles, 30:31103
KHETEEV, M.V., Spectral characteristics of γ radiation ^{60}Co scattered in thin radiators, 30:31109
KHIEN, F.Z., See BYU, N.K., 30:28929
KHLYSTOV, A.S., See SOKOL'SKII, D.V., 30:29052
KHMELEVSKAYA, Z.I., See OLIPER, T.V., 30:29730
KHMELININ, Yu.F., See SHISHMAKOV, A.S, 30:30024
KHODKIN, V.I., See RAKOVSKII, V.S., 30:29963
KHUTYZ, A.M., Corrosion fatigue strength of a titanium alloy at elevated temperature, 30:29945
KHVASTUNOV, M.S., See ASTVATSATUROV, R.G., 30:29577
KIBA, T., See TERADA, K., 30:28984
KIELSZNIA, R., See KAMINSKI, R., 30:28920
KIELY, F.M., See BLUK, H., 30:29525
KIKUCHI, Y., Study on the test of sodium boiling. I. Loss-of-flow test by a single pin, 30:31258
KIM, C.H., Determination of traces of Mo in soils and geological materials by solvent extraction of the molybdenum-thiocyanate complex and atomic absorption, 30:28965
KIM, H.J., See LEE, C., 30:28931
KIM, I.J., Muon-deuteron deep inelastic scattering, 30:30584
KIM, J.H., Thermal enhancement of the radiosensitivity using cultured normal and neoplastic cells, 30:29004
  See HAHN, E.W., 30:29744
KIM, J.K., See LEE, H.Y., 30:29498
KIM, J.S., See MURPHY, C.H., 30:30438
KIM, S.H., See KIM, J.H., 30:29004
KIM, S.M., See TENNANT, D.C., 30:29513
KIMBRELL, J.E., See CHATTERS, R.M., 30:28936
KIMMEL, D., See FISHER, D.R., 30:29799
KIMMEL, D.B., See JEE, W.S.S., 30:29801
KINDL, H., Gas laser, 30:29283
KING, C.H., See ASCUITTO, R.J., 30:30995
KING, H.J., Advanced ion source. Final report, 21 March--21 June 1973 on Phase 1, 30:30473 (AD-772833)
KING, N.S.P., See WANG, J.C., 30:30873
KINNEAR, J.E., See ROMNEY, E.M., 30:29445
KINOSHITA, F., See OHSHIMA, T., 30:29722
KIPERMAN, S.L., See LEVIN, D.Z., 30:29011
KIPLINGER, A.L., On the short-timescale variability of OJ 287, 30:30279
KIRALY, P., Particles and fields in space. Proceedings of the summer school, Balatonfured, 5--15 June 1973, 30:30160 (CONF-730693-)
KIRALY, Z., See KALMAN, B., 30:29645
KIRICHENKO, N.A., See MIGDAL, A.B., 30:31088
KIRIENKO, V.I., See EDNERAL, A.F., 30:30037
KIRIN, I.S., See GUSEV, Yu.K., 30:29117
KIRK, T., See KIM, I.J., 30:30584
KIRKBRIGHT, G.F., See ADAMS, M.J., 30:28963
KIRKBY, J., See DONALDSON, G., 30:30582
KIRKEGAARD, B.S., See BYBERG, J.R., 30:29065
KIRKEGAARD, C., See LAURIDSEN, U.B., 30:29842
KIRKPATRICK, L.D., See BASTIEN, D.B., 30:30600
KIRKWOOD, W.F., Residual stresses and birefringence in polycarbonate plastic, 30:31405 (UCID-15845)
KISELEV, Yu.T., Precise determination of inhomogeneous magnetic field components with a Hall probe, 30:29633
KISTEMAKER, J., See KONNEN, G.P., 30:30484
KISTENEV, E.P., See BUMAZSHNOV, V.A., 30:30603
  See DERRE, J., 30:30601
KISTIAKOWSKY, V., See BERLAD, G., 30:30623
KITABATAKE, T., Cause of death in radiological workers. Analysis of cause of death in Japanese radiological technicians, 1966 to 1972, 30:29710
KITAZOE, T., Electromagnetic-mass formula and a model of baryons, 30:30653
KITZMANN, I., See BACH, H., 30:30482
KJELDGAARD, A., See FOLKMANN, F., 30:28988
KLARIN, A.P., Choosing the basic parameters of a buffer memory device in the HPD computer system by a method of statistical modeling, 30:29623
KLAUMUENZER, S., Effects of low temperature irradiation with heavy ions on superconductor niobium, 30:30074
KLEBER, M., See HOLZWARTH, G., 30:30515
KLEIN, D.J., Degenerate perturbation theory, 30:30566
KLEINBERG, R.L., See WEBB, R.A., 30:30803
KLEINBOK, Ya. L., See BLOKHIN, S.I., 30:31110
KLEMPT, E., See BAILEY, J., 30:30620
KLIMA, B.B., LMFBR-37-fuel-element shipping cask simulation: test assembly operation and data, 30:30114 (ORNL-TM-3992)
KLIMAS, A.J., See FISK, L.A., 30:30172
KLIMES, B., Special theory of relativity, 30:31137
KLIMISHIN, I.A., Ionization shock waves in stars, 30:30212
KLINCHUK, Yu.I., See GEGUZIN, Ya.E., 30:30004
KLINE, F.J., Search for the lowest T = 2 state in ^{14}C by inelastic electron scattering, 30:30878
KLUEH, R.L., See DEVAN, J.H., 30:29954
KLUMPAR, J., New extrapolation method for the determination of saturated ionization currents, 30:29506
KLYUCHAREV, V.A., Effect of plastic deformation on quadrupole interaction in Al, Nb, and Au alloyed with Hf, 30:30038
KNAPIK, E., See ASTVATSATUROV, R.G., 30:29577
KNAUSS, G.L., See OLSON, H.C., 30:31397
KNOEDLER, D., Spring clamping device in nuclear reactors, 30:31284
KNOP, G., See BAETZNER, K., 30:30589
  See BECK, U., 30:30591

KNOWLES, S.H., Further interferometer observations of the water vapor sources in W49, 30:30286
KNUTSON, C.F., Project Rio Blanco: results from the initial alluvial water quality program, 30:29312 (PNE-RB-59)
  Project Rio Blanco: comparative postdetonation hydrologic testing, 30:29313 (PNE-RB-60)
KNYAZEV, D.A., See DENISOV, D.A., 30:29031
KNYAZEV, V.I., See BARANOV, V.M., 30:29916
KO, H.C., Relation between the radiated and received powers due to gyrating electrons in ambient plasma, 30:30275
KOBA, Z., See BURAS, A.J., 30:30758
KOBORI, K., See HIROSE, A., 30:28927
KOBSAREV, I.Yu., Spontaneous CP-violation and cosmology, 30:30770
KOCH, W., See GRAYER, G., 30:30617
KODA, S., See UMEHARA, Y., 30:30019
KOEHLER, A.M., See CONSTABLE, I.J., 30:29754
KOEHLER, F.A., See KALMON, B., 30:29346
KOEHLER, M., See HUEBEL, H., 30:31263
KOEHN, D., See KELLEY, M.C., 30:30433
KOELN, See HUEBEL, H., 30:31263
KOENIGSMANN, K., See KIM, I.J., 30:30584
KOERSNER, I., See JOHANSSON, A., 30:30855
KOGAN, V.S., See BRESLAVETS, K.G., 30:31394
KOGUT, J., Parton models and asymptotic freedom, 30:30630
KOHLI, N., 3-nitroso-4-hydroxy-5,6-benzocoumarin as a selective reagent for the spectrophotometric determination of ruthenium(III), 30:28966
KOHLMEYER, B., Inelastic transfer in the scattering of ^{32}S on ^{30}Si, 30:30906
KOHMURA, T., New description of nuclear scattering at intermediate energies and permissibility of Glauber expression to large-angle elastic scattering, 30:31022
KOHN, A., Radiochemical separation of fluorine by adsorption on hafnium dioxide: application to the determination of oxygen by activation analysis with charged particles, 30:28923
KOIWAI, S., Studies on radioresistance with HeLa cells: radiosensitivity and chromosome constitution, 30:29663
KOJIMA, K., See SATO, C., 30:29668
KOKHOV, E.D., Absorption x-ray radiometric analysis using the Kα_2 lines of the characteristic radiation of targets, 30:28952
KOLA, W., See SAROSIEK, J., 30:29691
KOLACNY, I., See NOVAK, L., 30:29747
KOLANOSKI, H., See BAETZNER, K., 30:30589
  See BECK, U., 30:30591
KOLCHIN, A.A., The performance of single charged-particle detectors under isotropic irradiation, 30:29536
KOLDEWIJN, P., See DE BOER, F.W.N., 30:30989
KOLK, B., Moessbauer investigations on ^{83}Kr, 30:30938
KOLLBACH, D., Use of the CAMAC system for on-line data processing in medicine, 30:31338 (HMI-B-149)
KOLLMANN, W.D., See BRAUEL, P., 30:30588
KOLLMEIER, W., See PIESCH, E., 30:29704
KOLM, H., See KELLAND, D., 30:30832
KOLOKOLOV, N.B., See BLAGOEV, A.B., 30:29165
  See BLAGOEV, A.B., 30:29164
KOLTUN, D.S., Sensitivity of inelastic pion scattering to non-local interactions, 30:31097
KOLTUNOV, V.S., Kinetics of reduction of neptunium by hydrazine. III. Reduction of Np(V) to Np(IV) in perchloric acid, 30:29115
  Reaction between plutonium(III) and nitrous acid. II. Kinetics of forward reaction, 30:29112
  Reaction between plutonium(III) and nitrous acid. III. Kinetics of reverse reaction, 30:29113
KOMAREK, P., See BOHN, T., 30:31208
KONI, D.M., Precision casting of alloy Ti--6Al--4V, 30:29995
KONINGS, A.W.T., Hydrolysis of 2',3'-cyclic adenosine monophosphate and 3',5'-cyclic adenosine monophosphate in subcellular fractions of normal and neoplastic mouse spleen, 30:29739
KONISHI, H., Clinical studies of myocardial scintigraphy with ^{131}I-MAA, 30:29875
KONISHI, K.I., See DI GIACOMO, A., 30:30677
KONNEN, G.P., Hyperthermal beams sputtered from alkali halide surfaces, 30:30484
KONOPLENKO, V.P., Level of the equicohesive temperature of the Mo alloy VM-1A in short-time tests in vacuo, 30:29985
KONOPLEV, K.A., Optimization of the cyclicity of operation of a research reactor, 30:31237
KONOVALOV, Yu.N., See ALEKSEEV, E.N., 30:29578
KOOISTRA, B.R., See HESSELINK, W.H.A., 30:30975
KOPEC, M., See SZUMIEL, I., 30:29669
KOPPE, V.T., See KOVAL, A.G., 30:30544
KOPYLOV, G.I., Like particle correlations as a tool to study the multiple production mechanism, 30:30711
KOPYTOFF, V., See HOLL, P.M., 30:31435
KORKEA-AHO, M., See YAFFE, D., 30:30622
KORMILITSIN, B.T., Inherent electromagnetic and electrostatic oscillations of a spherical cavity in plasma, 30:30412
KOROSTIN, O.S., See BARANOV, V.M., 30:29916
KOROTKIN, Yu.S., Hydrolysis of transuranium elements. II. Hydrolysis of americium(III) in the presence of ions with positive and negative hydration energies, 30:29121
KOROTKOVA, N.N., See MAGAT, L.M., 30:30041
KORVER, J.A., Shoal postshot environment, 30:29317 (UCID-15771)
KORWIN-PAWLOWSKI, M.L., Characteristics of MOS capacitors formed on p-type InSb, 30:29994
KORY, D.R., See LEWIS, F.D., 30:29018
KORZHAVIN, M., See VIKHREV, V.V., 30:29192
KOSIKOWSKI, F.V., See FURR, A.K., 30:28925
KOST, M.E., See SOMENKOV, V.A., 30:29008
KOSTOULAS, I., See KIM, I.J., 30:30584
KOTEL'NIKOV, G.A., Application of a conformal transformation group for relativistic theories, 30:31142 (IAE-2306)
KOTKO, V.A., Structural changes in Mo worked with ultrasound, 30:30039
  See KAVERINA, S.N., 30:30057
  See KOVSH, S.V., 30:30028
KOTOV, A.A., See KASSIROV, S.A., 30:29526
KOTYUKOV, N.S., See ANTONOVA, N.P., 30:29913
KOURI, D.J., A new method in the theory of many-body scattering, 30:30792
  Eigenstate expansions in a soluble model of identical particle scattering, 30:31141
KOUTCHMY, S.L., Concerning the origin and the dynamics of interplanetary dust, 30:30396
KOVAL, A.G., Excitation of some bands and lines in collisions of 0.4 to 20 keV electrons with Co, CO_2, and O_2 molecules, 30:30544
KOVAL, J.S., In situ optical particle size analysis of ambient aerosol, 30:29617 (NVO-AEIC-74-1)
KOVAL'CHUK, V.Yu., See DUNAEVA, K.M., 30:29103
KOVAL'SKAYA, L.P., See FRUMKIN, M.L., 30:29681
KOVAR, D.G., See ZEIDMAN, B., 30:29564
KOVBA, L.M., See SEREZHKIN, V.N., 30:29941
KOVSH, S.V., Effect of cyclic deformation on the dislocation structure and mechanical properties of molybdenum, chromium, and tungsten, 30:30028
KOVSHEVNY, G.G., See KASSIROV, S.A., 30:29526
KOWALENKO, A.D., See BARABOSCH, L.S., 30:30117
KOZERIVSKII, V.A., See ALEKSEEV, E.N., 30:29578
KOZHEVNIKOV, A.A., See ACHASOV, N.N., 30:30674
KOZLOV, F.N., See PETRUSEVICH, I.V., 30:29971
KOZLOVSKY, B., See MEISELES, R., 30:30293
KOZLOWSKI, T., Nuclear muon capture: a simple model, 30:31073
KOZ'MIN, G.V., See BRESLAVETS, K.G., 30:31394
KOZYREV, Y.P., See BYKOVSKII, Y.A., 30:29177
KRAEMER, R.W., See DADO, S., 30:30621
KRAKOWSKI, R.A., Engineering design study of a Reference Theta-Pinch Reactor (RTPR), 30:29206 (LA-5336)
KRAMARENKO, V.A., See ASTVATSATUROV, R.G., 30:29577
KRAMER, D., Quantization in static gravitational fields, 30:31181
KRAMER, G., See CRAIGIE, N.S., 30:30670
KRAMMER, M., See BOEHM, M., 30:30729
KRASIL'NIKOV, B.N., See DYAD'KIN, I.G., 30:29605
KRASINSKI, A., Solutions of the Einstein field equations for a rotating perfect fluid, 30:31180
KRASNOPEVTSEV, Yu.V., See DMITRIEVA, G.V., 30:29388
KRASNOPOL'SKAYA, S.M., See SHMIDT, F.K., 30:29012
KRAUS, L., See MAGUIRE, C.F., 30:30997
KRAUSE, H., The treatment and disposal of radioactive wastes, 30:29136
KRAUSHAAR, J.J., See BUNTING, R.L., 30:30967
  See BUNTING, R.L., 30:29516
KREHBIEL, H., See BRAUEL, P., 30:30588
KRENZ, W., Measurement of the energy dependence of the decay matrix element for K^0sub(L) + $\pi^+ \pi^- \pi^0$, 30:30593 (PITHA-64(1972))
KRESSE, J., See BOBERG, F., 30:29123
KREY, U., Vortex lattice in magnetic superconductors, 30:30815
KRISHNAN, R., Preparation and some magnetic properties of uranium oxide doped YIG crystals, 30:29894
KRITSKAYA, V.K., X-ray study of the orientation dependence of radiation defects in the crystalline lattice of Mo irradiated with high-energy particles, 30:30080
KRIVAN, V., Nondestructive determination of some trace elements in tantalum by proton activation analysis, 30:28922
KRIVODUBSKII, V.N., Electrical conductivity of the matter in the subphotospheric layers of the Sun, 30:30308
KRIVSKY, L., Properties and models of solar flares and cosmic radiation, 30:30297 (CONF-730693-)
KROECKEL, H., Analysis of ECE data on the basis of isotopic weight fractions, 30:28940 (EUR-4859)
KROEPF, H., See KNOEDLER, D., 30:31284
KROKHIN, O.N., See GRIBKOV, V.A., 30:29176
KRONENBERG, R.S., See LOKEN, M.K., 30:29847
KROT, N.N., See SHILOV, V.P., 30:29104
  See ZAKHAROVA, F.A., 30:29114
KROYHN, D.L., Toxicity to rabbit retina of epithermal neutron beam, 30:29765
KRUEGER, H., See EPPERLEIN, B.W., 30:29014
KRUPP, H., The production of multicharged ions with a duoplasmatron ion source in high-current continuous operation, 30:30475 (GSI-A1-74)
KRUSHCHOV, N.G., Development and involution of mammary gland epithelial tissue under x irradiation, cyclophosphamide, and antilymphocyte serum treatment, 30:29760

KRYLOV, E.I., Synthesis and magnetic properties of samarium and europium titanoniobates, 30:29908
KRYLOV, L.I., See NIKOL'SKII, B.P., 30:29118
See NIKOL'SKII, B.P., 30:29119
KRZYWICKI, A., Charge distributions of many particle final states and the energy dependence of forward charge exchange, 30:30696
KSENOFONTOV, E.G., See SEVAST'YANOV, Yu.G., 30:29143
KTAZIMOV, A.M., See YUSIFOV, V.G., 30:29947
KUCHAR, F., Systematic control of doping characteristics of n-InSb by nuclear reactions, 30:29992
KUDOH, O., Implant dose profile dependence of electrical characteristics of ion-implanted MOS transistors, 30:30100
KUEHNELT, H., See GRASSBERGER, P., 30:30748
KUENZLY, J.D., Oxidation mechanism of Ni$_3$Al containing yttrium, 30:29953
KUGELER, K., See BOHN, T., 30:31305
KUGELER, M., See BOHN, T., 30:31305
KUHN, B.A., Acoustic emission monitoring of ring-cracking in glass and alumina, 30:31410 (UCID-16076)
See HARRIS, D.O., 30:29296
KUHN, D., Transmission method to measure capture rates in fast reactors, 30:31275
KUKACKA, L.E., Polymer-concrete for use in the repair of deteriorated bridge decks, 30:31388 (BNL-19161)
KUKIN, P.P., See IVANOV, Yu.A., 30:29084
KULAKOV, B.A., See ASTVATSATUROV, R.G., 30:29577
KULAKOVA, E.M., See ISSINSKII, I.B., 30:30129
KULIKOV, V.N., Semi-automatic photometer for determining heavy nucleus charges of cosmic rays in nuclear photoemulsion, 30:29501
KULKARNI, D.R., See DHAR, A.K., 30:30925
KULYUKIN, M.M., See BALESTRA, F., 30:29591
KUMAGAI, H., See HASHIZUME, A., 30:30154
KUMAHARA, Y., See ONISHI, T., 30:29862
KUMAR, N., Effective interaction calculations for nuclei of mass 6 to 9, 30:30884
KUMAR, R., See QURESHI, M., 30:28994
KUMPAN, S., See SOURES, J., 30:29231
KUNASZ, C.V., See CRANDALL, D.H., 30:30246
KUNZENDORF, H., See GWOZDZ, R., 30:28943
KUO, T.T.S., Self-screening of the particle-hole interaction and core polarization of the effective two-particle interaction, 30:31091
KUPCZYNSKI, M., New description of the initial states, 30:30690
Tests for the purity of the initial ensemble of states in scattering experiments, 30:30763
KUPER, C.G., See BAR-SAGI, J., 30:30817
See REVZEN, M., 30:30804
KURACHI, K., See ICHII, H., 30:29860
KURBATOV, N.N., See DESYATNIK, V.N., 30:29095
KURDYUMOV, V.G., See CHUPYATOVA, L.P., 30:30010
See CHUPYATOVA, L.P., 30:30033
KURINA, L.N., See ANUFRIENKO, V.F., 30:29907
KURIYAMA, A., Theory of collective excitations in spherical odd--mass nuclei. III. Electromagnetic properties of the anomalous coupling states, 30:31068
KURLANOV, A.D., See GRIGOREVSKII, N.V., 30:30209
KURODA, P.K., Xenon isotope anomalies in the carbonaceous chondrite Murray, 30:30162
See JAMES, W.D., 30:31010
See NEVISSI, A., 30:29400
KUROVSKA, M., See KRUSHCHOV, N.G., 30:29750
KURYLO, M.J., See BRAUN, W., 30:30525
KUSAKARI, H., See KAWAKAMI, H., 30:30980
KUSHELEVSKY, A.P., Simplified method for calculating dose-rate distributions from extended volumes containing gamma emitters, 30:31107
KUSHNIR, A.J., Electrical resistance as a function of temperature in pure and doped beta-tantalum films, 30:30059
KUSTOM, R.L., See CHANG, C.T.M., 30:29584
KUSWA, G.W., Nanosecond time resolved x-ray diagnostics of relativistic electron beam initiated events, 30:29159 (SAND-74-5262)
KUTSAR, A.R., ($\alpha \to \omega$) transition in titanium and zirconium in shock waves, 30:30011
KUZEMSKII, A.L., Selfconsistent calculation of the Green's functions in the Hubbard model, 30:31132 (JINR-P4-7225)
KUZENKO, A.F., See NAZAROV, L.E., 30:29389
KUZMICHEV, V.E., See KHARCHENKO, V.F., 30:31103
KUZNETSOV, K.E., Interrelationship of thermodynamic and kinetic parameters of redox reactions, 30:29005
KUZNETSOV, R.A., See BOGDANOV, R.V., 30:28981
KUZNETSOVA, A.P., See KRITSKAYA, V.K., 30:30080
KUZNETSOVA, G.A., See ZYKOVA, A.S., 30:29399
KUZNETSOVA, L.I., See LAVRENKO, V.A., 30:29938
KVASNITSA, M.S., See ZAV'YALKIN, F.M., 30:29607
KVESITADZE, T., See BAGATURIYA, G.D., 30:29716

L

LAASPERE, T., Global distribution of natural and man-made ionospheric electric fields at 200 kHz and 540 kHz as observed by Ogo 6, 30:30431
LACH, H., See SREBRO, Z., 30:29752
LACHERE, G., See BONNELLE, C., 30:30018
LAKSHMINARAYANA, V., See VENKATARATNAM, S., 30:30942
LALEVIC, B., Nonlinear high-field conductivity in Nb$_2$O$_5$ thin films, 30:29940
LALOE, F., See COHEN-TRANNOUDJI, C., 30:31134
See COHEN-TRANNOUDJI, C., 30:31135
LAM, L., Scattering form factors of atoms, molecules, and solids, 30:30522
LAM, W.S., Phase space and multihadron production in annihilation processes at present energies, 30:30669
LAMB, J.F., See BORRAS, C., 30:29781
LAMB, W.A.S., See BEAL, J.W., 30:29160
LAMOT, G.H., See MEYER, J., 30:31036
LAMPTON, M., See MARGON, B., 30:30174
LANCELOT, J.R., Origin of carbonatitic magma in the light of the Pb-U-Th isotope system, 30:29337
LANDA, L., See GORDON, F., 30:29852
LANDAU, J., See ROSENBAUM, R.L., 30:30800
LANDE, A., See IACHELLO, F., 30:30512
LANDOWNE, S., A note on diffraction phenomena in the inelastic scattering of complex nuclei, 30:31087
LANDSMAN, V.S., See GRINIK, E.U., 30:30072
LANDSTREET, J.D., Wavelength dependence of circular polarization in GD 229, 30:30203
See ANGEL, J.R.P., 30:30193
LANE, A.M., The absence of excited target contributions to E1 partial widths of neutron resonances: an explanation from threshold effects, 30:31071
See GYARMATI, B., 30:31079
LANE, N.F., See HICKMAN, A.P., 30:30494
LANG, J., See BUTA, A., 30:30926
LANGE, J., See KELLER, K.A., 30:30960
LANGE, L., See HUEBEL, H., 30:31263
LANGEL, R.A., Near-earth magnetic disturbance in total field at high latitudes. I. Summary of data from Ogo 2, 4, and 6, 30:30455
New-earth magnetic disturbance in total field at high latitudes. II. Interpretation of data from Ogo 2, 4, and 6, 30:30456
Role of solar local time in polar a cap magnetic variations, 30:30460
LANGER, G., See RUSINSKI, J., 30:29367
LANGEVIN, Y., See BIBRING, J.P., 30:30355
LANIN, A.G., See POPOV, V.P., 30:29900
LANNERGARD, C.O., See DIETRICH, W., 30:30954
See NYMAN, B., 30:30953
LANZANO, P., The equilibrium of a rotating body of arbitrary density, 30:30408
LANZEROTTI, L.J., ULF geomagnetic power near L = 4. IV. Relationship to the Fredericksburg K index, 30:30458
See SURKAN, A.J., 30:30457
LARA, S., Ferromagnetism of EuO and EuS, 30:30094
LARICCIA, P., See BERTANZA, L., 30:30606
LARIKOV, L.N, Effect of lithium vapor on the structure of monocrystals of refractory metals and alloys, 30:29955
LARIONTSEV, E.G., Interaction of radiation with an active medium in a multimode regime of pulse generation, 30:29286
LASCHNER, W., Results and complications of the treatment of Bechterew's disease with thorium X, 30:29774
LASKER, B.M., Search for optical pulsations from Cen X--3, 30:30288
LASKER, M.F., See KONI, D.M., 30:29995
LASKEY, J.B., Thermoluminescent response of TLD-100 to 1 to 25 keV electrons. Progress report, July 15, 1973--July 15, 1974, 30:29538 (COO-1105-212)
LASSEN, K., Relation of the plasma sheet to the nighttime auroral oval, 30:30441
LASSEY, K.R., Parity-nonconserving effects in the reaction $n + p \to d + \gamma$, 30:30752
LASTOVICKA, J., Satellite measurements of solar x-ray flux and ground observations of sudden ionospheric disturbances, 30:30413
LATORRE, V.R., Communication system design, 30:31452 (UCID-15955)
State relationships for maximal-length sequence generators, 30:31450 (UCID-15898)
LATYSHEVA, V.I., See PAN, V.M., 30:30045
LAU, S.S., Evaluation of glancing angle x-ray diffraction and MeV ^{4}He backscattering analyses of silicide formation, 30:29939
LAURIDSEN, U.B., Clinical experience with radioimmunological TSH determination, 30:29842
LAUSCHER, P., See GRAESSLER, H., 30:30610
LAUTERBORN, D., Island solutions in linear series of static stellar models with core helium and shell hydrogen burning for M=5,7, and 9 M/subsun/, 30:30198
LAVINE, J.P., See BAWIN, M., 30:30789
LAVRENKO, V.A., Oxidation of ZrB$_2$, TaB$_2$, NbB$_2$, and W$_2$B$_5$ in atomic oxygen and by anodic polarization, 30:29938
LAWRENCE, C.W., Specificity and frequency of ultraviolet-induced reversion of an iso-1-cytochrome c ochre mutant in radiation-sensitive strains of yeast, 30:29683
LAX, B., See YUEN, S.Y., 30:29274
LAZAREVA, E.A., See RYABININ, A.I., 30:28996
LAZCANO-ARAUJO, A., See TORRES-PEIMBERT, S., 30:30351
LAZERKO, G.A., Conversion of complex compounds under the action of light, radiation, and temperature, 30:29060
LAZEYRAS, P., See ADERHOLZ, M., 30:29595
LAZURIK-EL'TSUFIN, V.T., See KALINICHENKO, A.I., 30:30853

LAZZARINI, A.J., See CORMIER, T.M., 30:29573
LEACH, D.R., See ROWLEY, M.J., 30:29708
LEAL DE SANTOS, M., Improved first order perturbative calculation of the ground state energy of atoms, 30:30567
LEARY, R.H., Application of a computer-simulated Perceptron to a complex photographic scene, 30:31433 (UCID-15373)
LEAVITT, G., Aligning a spectra physics He--Ne laser Model 125, 30:29270 (UCID-15860)
LEAVITT, G.A., Electro-optic method of tracking an electron-beam weld, 30:31442 (UCID-15769)
LEAVITT, R.P., See WORTMAN, D.E., 30:30487
LEAVITT, V.D., Soil surveys of five plutonium-contaminated areas on the Test Range Complex in Nevada, 30:29442 (NVO-AEIC-74-1)
LEBEDENKO, V.M., Some relations between the types of the generating systems of Abelian groups and their direct summands, 30:31133 (JINR-P5-7344)
LEBEDEV, V.V., See KOLCHIN, A.A., 30:29536
LEBEL, J.L., See GOMEZ, L.S., 30:29820
LEBLANC, Y., Coronal innomogeneities and solar radio emissions, 30:30300
LEDERMAN, L., See KIM, I.J., 30:30584
LE DEVEHAT, J., See GRUNBERG, C., 30:29514
LEDINGHAM, K.W.D., K-electron capture to positron emission ratios and the second class currents problem, 30:31076
LEE, C., Simultaneous analysis of uranium and thorium by the delayed fission neutron counting method, 30:28931
LEE, C.E., Thomas--Fermi calculation of potential between atoms, 30:30565 (LA-5694-MS)
LEE, D.N., Frequency characteristics of anodic oxide films: effects of anodization voltage, 30:29917
LEE, E.P., See BEVC, V., 30:29199
LEE, H.Y., Development of neutron sensitive PCP ionization chamber, 30:29498
LEE, I.Y., See SALADIN, J.X., 30:30905
LEE, K.D., See MAJOR, W.J., 30:28971
LEE, K.H., See PYUN, H.C., 30:29045
LEE, L.Y., Multi-strip scintillation counters (MSSC), 30:29585
LEE, R.N., Potential application of atomic absorption and anodic stripping voltammetry to the precipitation scavenging program, 30:28937 (BNWL-1850(Pt.3))
  Real-time system for detection of the atmospheric tracer sulfur hexafluoride, 30:29611 (BNWL-1850(Pt.3))
  See ALKEZWEENY, A.J., 30:29487
LEE, S.H., Studies on the sorption and fixation of cesium by vermiculite. II, 30:29134
LEE, T.N., Solar-flare and laboratory plasma phenomena, 30:30313
LEE, T.S.H., Momentum-space study of pion-nucleus inelastic scattering, 30:30897
LEENEN, M., See BAETZNER, K., 30:30589
  See BECK, U., 30:30591
LEEP, D., See CRANDALL, D.H., 30:30246
LEES, D.J., Summary of containment experiments on the PROTO--CLEO stellarator, 30:29151 (CLM-R-135)
LE GUELTE, G., Safeguarding the peaceful uses of nuclear energy by states, 30:30104 (FRNC-TH-50)
LEHMANN, J., See POSSOZ, A., 30:30899
LEHRAUS, I., See ADERHOLZ, M., 30:29595
LEIGH, K.M., Trends in structural mechanics. A UK review of the 2nd international conference on structural mechanics in reactor technology. V. Fast reactor containment, 30:31261
  See HUEBEL, H., 30:31263
LEJEUNE, A., See JEUKENNE, J.P., 30:31055
LEMBERG, I.Kh., See EROKHINA, K.I., 30:31100
LEMESHKO, A.M., See SAMSONOV, G.V., 30:29912
LEMMING, J.F., Nuclear Data Sheets for A = 143, 30:30966
LEMPERT, J., Block control of a PWR type reactor, 30:31302
LENEVA, A.E., See DEMURA, A.V., 30:30520
LENUSKY, R., See COFFEY, J.W., 30:29870
LEON, M., Quadrupole mixing in hadronic atoms: an additional probe of the hadron-nucleus interaction, 30:30514
LEONOV, A.I., Effect of complex admixtures of rare-earth oxides on sintering of cerium dioxide, 30:29909
  Surface stabilization and properties of ZrO_2-based solid solutions, 30:29911
LEONOV, V.Kh., See BLOKH, Ya.L., 30:29582
  See EGOROV, Yu.A., 30:29583
LERCH, P., See KUSHELEVSKY, A.P., 30:31107
LERCHE, I., On the passage of radiation through inhomogeneous moving media. V. Line absorption and frequency variations of optical depth, 30:30247
  On the passage of radiation through inhomogeneous, moving media. VI. Dispersion effects on phase and ray paths in a plane, differentially shearing medium, 30:30248
  On the passage of radiation through inhomogeneous, moving media. VII. Concerning the validity of the geometrical optics approximation, 30:30249
LETNIKOV, F.A., See KUZNETSOV, K.E., 30:29005
LEVEQUE, A., See DERRE, J., 30:30601
LEVIJ, I.S., See GEIR, A., 30:29878
LEVIKOV, E.A., Study of the substructure of deformed and annealed single crystals of molybdenum, 30:30055
LEVIKOVA, L.V., See LEVIKOV, E.A., 30:30055
LEVIN, D.Z., Kinetics of the selective hydrogenation of dimethylethynylcarbinol over palladium in the vapor phase. II. Reaction between dimethylethynylcarbinol and deuterium and the kinetic isotopic effect, 30:29011
LEVIN, F.S., See KOURI, D.J., 30:30792
  See KOURI, D.J., 30:31141
LEVIN, V.M., See ANGELOV, B.P., 30:30143
LEVINE, G.P., See PAVLOTSKAYA, F.I., 30:29384
LEVINE, J.S., See JAVAN, A., 30:29284
LEVINE, M.J., See BOND, P.D., 30:30921
LEVINE, R.H., Acceleration of thermal particles in collapsing magnetic regions, 30:30317
  New theory of coronal heating, 30:30318
  See NAKAGAWA, Y., 30:30316
LEVY, A., See BERLAD, G., 30:30623
LEWIN, C., See EVANS, D., 30:30742
LEWIN, W.H.G., See SPROTT, G.F., 30:30260
LEWIS, B.R., See LLOYD, C.R., 30:30535
LEWIS, F.D., Entropic control of photochemical reactivity. The transition state for γ-hydrogen abstraction of alkyl phenyl ketones, 30:29018
LEWIS, J.S., Volatile element influx on Venus from cometary impacts, 30:30402
LEWIS, T.A., See BEYNON, A.J., 30:31212
LEYENDECKER, A.J., See HARTE, W.E., 30:30477
LHUILLIER, D., Temperature dependence of the second sound velocity reduction in rotating liquid helium, 30:30797
LI, C.Y., Grain boundary sliding and structure. Progress report, December 1, 1973--November 30, 1974, 30:29977 (COO-2172-7)
LI, F.P., Cancer mortality following irradiation in infancy for hemangioma, 30:29714
LIBERMAN, A.R., 10% efficient economic RTG design, 30:29251
LIBIN, I.Ya., See BLOKH, Ya.L., 30:29499
LICHTEN, W., Fine structure of the metastable a$^3\Sigma^+$/subu/ state of the helium molecule, 30:30492
LICHTENSTEIN, C.A., See BEBEK, C.J., 30:30587
LICHTSHTEIN, E., See GEIR, A., 30:29878
LIELAUSIS, O.A., See GELFGAT, J.M., 30:30572
LIGATTO DE SLOBODRIAN, M.L.V., On the determination of the nucleon-nucleon scattering parameters through final state interactions, 30:30868
LIGEON, E., See BONTEMPS, A., 30:31113
LIGHTBODY, J.W. Jr., See KLINE, F.J., 30:30878
LILLER, W., See JONES, C.A., 30:30205
LIM, E.C., See FISCHER, S.F., 30:29016
LIMA, F.W., See MIYAMARU, M., 30:28914
LIMON, P., See KIM, I.J., 30:30584
LIN, C.S., Further discussion of the cyclotron instability, 30:30439
LIN, D.S., Nature of the deformation and flow of metals at and near the interface during abrasion, and its relation to the friction, 30:30051
LIN, R.P., Non-relativistic solar electrons, 30:30337
LIN, S.D., Electron radiation damage of thin films of glycine, diglycine, and aromatic amino acids, 30:29042
LIN, S.Y., See PERNG, C.C., 30:30927
LINACRE, J., See PALMER, J.E.M., 30:29035
LIND, R., See PALMER, J.E.M., 30:29035
LINDEMAN, R.A., Interaction between an impact-produced neutral gas cloud and the solar wind at the lunar surface, 30:30401
LINDGREN, I., See RUBINSZTEIN, H., 30:30972
LINDGREN, K., See ARESKOUG, M., 30:31002
LINDH, U., See SUNDQVIST, B., 30:28917
LINDHOLM, A., See BERGMAN, R., 30:28918
LINDSEY, J.S., New NADS: compatible alpha measuring system, 30:29618 (UCID-15828)
LINDSKOG, J., Investigations of the level structure and lifetimes of odd Tm isotopes, 30:30979 (NP-20122)
LINDSTROEM, L., See RUBINSZTEIN, H., 30:30972
LINDSTROM, P.J., See GOLDEN, R.L., 30:30165
LINEBERGER, W.C., See HERBST, E., 30:30361
LING, C.C., See SINGH, B., 30:30052
LINGEMAN, E.W.A., Intensities of γ-rays in the decay of sup(166m)Ho, 30:31125
LINIECKI, J., Influence of blood oxygenation during in vitro irradiation upon the yield of dicentric chromosomal aberrations in lymphocytes, 30:29749
LINTZ, P.R., See COHEN, T.J., 30:30331
LIPOVICH, V.G., See SHMIDT, F.K., 30:29012
LIPPINCOTT, S.L., Parallaxes and proper motions of twelve nearby stars determined with the Sproul 24-in. refractor, 30:30236
LIPSCHITZ, D.A., See MILES, L.E.M., 30:29835
LISITSA, V.S., See DEMURA, A.V., 30:30520
LISITSYN, L.M., See BASHA, A.F., 30:30031
LISK, D.J., See FURR, A.K., 30:28925
LISLE, J.C., See SANDERSON, N.E., 30:30944
LITTLE, J.B., See EPSTEIN, J., 30:29672
LITTLETON, J.E., Electron-ion relaxation in a dense plasma, 30:30259
LITVER, B.Ya., See TROITSKAYA, M.N., 30:29405
LIU, J., See DONALDSON, G., 30:30582
LIU, J.W., Accurate total inelastic cross section for H_2^+ colliding with fast charged particles in the adiabatic approximation, 30:30554
LIU, M.B., Knudsen effusion and mass spectrometric studies of the vaporization of Y_2O_3(s). Dissociation energy of YO(g), 30:29936

- LLEWELLYN SMITH, C.H., Introduction to renormalizable models of weak interactions, 30:30681
- LLOYD, C.R., Differential cross sections for the elastic scattering of electrons from atomic hydrogen. II. Medium energies, 30:30535
- LLOYD, E.L., Cell mediated immunity as an early diagnostic test for osteosarcoma in human radium cases, 30:29771 (CONF-740930-1)
- LLOYD, F.D., See SEHMEL, G.A., 30:29371
  - See SEHMEL, G.A., 30:29370
- LLOYD, R.D., Decorporation of ^{241}Am in beagles by DTPA, 30:29797 (COO-119-249)
  - Einsteinium studies in beagles, 30:29802 (COO-119-249)
  - ^{210}Pb retention, excretion, and distribution in beagles following intravenous injection, 30:29805 (COO-119-249)
  - See MAYS, C.W., 30:29806
- LO, K.Y., See KNOWLES, S.H., 30:30286
- LOBKOWICZ, F., See NORDBERG, M.E. Jr., 30:30590
- LODEN, L.O., See SUNDMAN, A., 30:30352
- LOEFFLER, F.J., Annual progress report for the period June 1, 1973--May 31, 1974, 30:30597 (COO-1428-382)
- LOEFFLER, R.K., Influence of fractionation on acute and late reactions in vocal cord carcinoma, 30:29713
- LOEHR, U., See LEMPERT, J., 30:31302
- LOEW, R., Charge-state and energy distributions of xenon ions in carbon, 30:31121
- LOHMANN, W., The mass of M33, 30:30389
- LOKEN, M.K., Dual camera studies of pulmonary function with computer processing of data, 30:29847
- LOKKE, W., See SLUTZ, S., 30:29272
  - See SLUTZ, S., 30:29271
- LOMAKIN, S.S., See ERMOLAEV, O.Ya., 30:30844
- LOMANOV, M.F., See BLOKHIN, S.I., 30:31110
- LOMBAARD, J.M., Optical model and DWBA analysis of the ^{7}Li(d,d)- and ^{7}Li(d,p$_0$)-reactions in the energy region 1.0 to 2.6 MeV, 30:30883
- LOMBARD, R.J., Energy density formalism and the shell structure of nuclei, 30:31049
  - See BEINER, M., 30:31025
- LOMBARDI, M., See JOST, R., 30:30490
  - See MELITERES-MARECHAL, M., 30:30503
- LOMINADZE, D.G., See KALADZE, T.D., 30:29234
- LONDERGAN, J.T., Off-shell πN amplitudes via a multichannel separable potential, 30:30731
- LONG, D.M., JFET hardening and high dose rate study, 30:29888 (AD-903226)
- LONGMIRE, C.L., Direct interaction effects in EMP, 30:29308 (AD-777748)
  - See LEE, C.E., 30:30565
- LONGO, M.J., See JONES, L.W., 30:29596
- LOOGEN, F., See SEIPEL, L., 30:29770
- LORANT, B., Derivatographic investigations on the thermal degradation of pyridine, isoquinoline, α,α-dipyridyl and o-phenantroline, resp. bichromate- or chromate-ion containing metal complexes. II. Zinc(II)-, cadmium(II)-, and manganese(II)-complexes. III. Mercury(I and II)-, uranyl-, thorium-, lanthanum-, and iron-complexes, 30:29122
- LORD, D.J., See GREGORY, C.V., 30:31229
- LORD, E.A., F-gravity and the proton--electron mass ratio, 30:31174
- LORE, J.D., Thermal conductivity of carbon foam, 30:31413 (Y-1955)
- LORENSEN, L.E., Materials screening program for the LLL geothermal project, 30:31327 (UCRL-75353)
- LORENTS, D.C., See JONES, P.R., 30:30540
- LORENZ, D., See VAN KAICK, G., 30:29769
- LORENZ, E., See GRAYER, G., 30:30617
- LORENZ, J., Absorption of ^{47}Ca from digestive tract in patients with urolithiasis, 30:29791
- LORENZETTI, J.R., See D'ATTELLIS, C.E., 30:31303
- LORTET-ZUCKERMANN, M.C., Mixing of neutral gas and dust with the ionized gas of H II regions, 30:30369
- LOSCH, W.H.P., Spectroscopy of Auger electrons and its use in metallurgy, 30:31420 (COPPE-TP-6/72)
- LOSKUTOV, A.I., See BRESLAVETS, K.G., 30:31394
- LOSTY, M.J., See YAFFE, D., 30:30622
- LOTZE, K.H., See KRAMER, D., 30:31181
- LOUNASMAA, O.V., Superfluid phases of liquid ^{3}He, 30:30794
- LOUREIRO, P., See CARVALHINHOS, H.J., 30:30035
- LOUWRIER, K.P., Fabrication of (Pu-U) oxide microspheres using an internal gelation method, 30:29925
- LOVAS, I., Three-nucleon reactions and off-shell behavior of the nucleon--nucleon interaction, 30:31040
- LOVE, A., See BAILIN, D., 30:30672
- LOVE, W.G., On the nuclear I.L potential, 30:31092
- LOWERY, V.W., See WALLIN, W.R., 30:29624
- LOZHKINA, G.S., See GRINBERG, A.A., 30:29108
- LUBATTI, H.J., See BASTIEN, D.B., 30:30600
- LUBIN, E., See NAHARIN, A., 30:29821
- LUCHNIK, N.V., Chromosomal aberrations induced by gamma irradiation of Crepis capillaris seedlings at different periods of interphase, 30:29696
- LUCKA, B., Radiometric method for the estimation of iodine complexing degree in iodophor preparations, 30:28974
- LUDFORD, G.S.S., See WALKER, J.S., 30:30571
- LUDWICK, J.D., See PERKINS, R.W., 30:29359
- LUDWIG, E.J., See IKOSSI, P.G., 30:30949
- LUECK, H.B., Energy spectrometry of protons by means of a dielectric track detector, 30:29569
- LUETJENS, G., See GRAYER, G., 30:30617
- LUETOLF, H.U., Chromosome loss following x-ray irradiation of mature oocytes from Drosophila melanogaster, 30:29768
- LUGOVSKAYA, E.S., See LAVRENKO, V.A., 30:29938
- LUKASIK, J., Vibrational relaxation of D$_2$ in the range 400-50°K, 30:30508
- LUKIERSKI, J., Exact and perturbative solutions of the Van Hove model describing nuclear diffraction dissociation of pions, 30:30722
- LUO, H.L., See KAMMERDINER, L., 30:29967
- LUONGO, M.C., See CONRAD, J.D. Jr., 30:31283
- LUSANNA, L., Extended hadrons and Regge slope, 30:30695
- LUSIGNOLI, M., See FERRARI, E., 30:30734
  - See FERRARI, E., 30:30733
- LUSTFELD, H., Critical temperature of transition-metal alloy superconductors, 30:30811
- LUTZ, B.L., Neutral potassium in dusty clouds, 30:30358
- LUTZ, H.O., See SACKMANN, S., 30:30517
- LUTZ, O., See EPPERLEIN, B.W., 30:29014
- LUX, C.R., See PACER, J.C., 30:30950
- LUZ, A., See GOESSNER, W., 30:29785
- LWIN, K., Effects of certain denaturants on the absorption spectra of hemoglobin from chick embryos irradiated with ultraviolet radiation during early embryogenesis, 30:29661
- LYAGUSHCHENKO, R.I., See BLAGOEV, A.B., 30:29165
  - See BLAGOEV, A.B., 30:29164
- LYAKHOVICH, L.S, Multicomponent diffusion coatings, 30:29906
- LYAKISHEV, N.P., Mechanism of niobium pentoxide reduction in an alumino--thermal process, 30:29970
- LYASOTSKII, I.V., See TYAPKIN, Yu.D., 30:30040
- LYSOV, V.V., See ERMOLAEV, O.Ya., 30:30844
- LYTLE, R.J., Space wave fields of subsurface electromagnetic sources in planar layered media, 30:31353 (UCID-15945)
- LYUBOSHITS, V.L., K/sub L/^{0} + K/sub S/^{0} incoherent regeneration on atomic electrons at high energies and electric radius of K^0 meson, 30:30592 (JINR-E2-7402)
- LYUBTSEV, R.I., See NIKOL'SKII, B.P., 30:29118

M

- MAASS, K.E., Hahn-Meitner-Institut fuer Kernforschung annual report 1973, 30:31334
- MAAYOUF, R.M.A., A comparison of polarization values for D-D neutrons obtained from Mott-Schwinger and ^{4}He scattering, 30:29511
- MACH, J., See HAVLICEK, F., 30:29823
- MACIAS, E.S., See HOOD, J.T., 30:30153
- MACKLIET, C.A., Specific heat of superconducting Pd--H alloys, 30:30812
- MACLEOD, J.M., See TERZIAN, Y., 30:30240
- MACQ, P., See POSSOZ, A., 30:30899
- MADEJA, M., See POMORSKI, L., 30:28980
- MADHUSUDHANARAO, D.N., Ionospheric absorption on 2.4 MHz at Waltair, 30:30419
- MADORE, B.F., Gas density and the rate of star formation in M33, 30:30348
- MAEKAWA, A., See OHSHIMA, T., 30:29722
- MAEKOSHI, H., See TAKAHASHI, S., 30:31106
- MAGAT, L.M., Orientation relation between phases in SmCo$_5$--base alloys, 30:30041
- MAGUIRE, C.F., Massive transfer reaction ^{208}Pb(^{20}Ne,α)^{224}Th, 30:30997
- MAHALINGAM, R., See SCHWENDIMAN, L.C., 30:29365
- MAHANTA, M.N., Approximate interior solution in Brans--Dicke theory, 30:31176
- MAHAUX, C., See JEUKENNE, J.P., 30:31055
- MAHLAB, M., See HOFFMANN, G.W., 30:30907
- MAHLUM, D.D., See SIKOV, M.R., 30:29777
- MAHONEY, J.A., See MAGUIRE, C.F., 30:30997
- MAIER, E.J., Observation of a two-temperature ion energy distribution in regions of polar wind flow, 30:30429
- MAIER, M.R., See PROETEL, D., 30:31006
- MAINLAND, G.B., Derivation of unified gauge theory from a generalized minimal principle, 30:31151
- MAIRLE, G., 1p hole-states in ^{16}O and ^{14}N and the mass dependence of the 1p spin-orbit splitting, 30:30886
- MAJOR, W.J., Determination of ^{239}Pu and ^{241}Am in large NAEG vegetation samples, 30:28971 (NVO-AEIC-74-1)
- MAK, H.-B., Cross sections of the ^{21}Ne(α,n)^{24}Mg and ^{22}Ne(α,n)^{25}Mg reactions at low energies of astrophysical interest, 30:30913
- MAKAROVA, G.M., See MAGAT, L.M., 30:30041
- MAKHINKO, V.R., See GERT, L.M., 30:29914
- MAKHON'KO, K.P., See AVRAMENKO, A.S., 30:29385
  - See AVRAMENKO, A.S., 30:29398
  - See DAVYDOV, E.N., 30:29408
- MAKHUNKA, I., See VANDLIK, Ya., 30:29142
- MAKI, Y., Determination of zinc in the presence of scandium by activation analysis combined with thin-layer chromatographic separation, 30:28928
- MAKITA, K., See SHIMOYASHIKI, S., 30:31227
- MAKSIMENKO, E.A., See LARIKOV, L.N, 30:29955
- MAKURIN, Yu.N., See KRYLOV, E.I., 30:29908
- MALAISE, E., Effect of total irradiation on the development of leukemia L$_{1210}$ in F$_1$-hybrids, 30:29748
- MALAKHOV, A.I., See ASTVATSATUROV, R.G., 30:29577

MALAKHOV, S.G., See DMITRIEVA, G.V., 30:29388
See GAZIEV, Yu.I., 30:29392
See NAZAROV, L.E., 30:29389
MALANCHUK, M., See STARA, J.F., 30:29815
MALASHENKO, I.S., Effect of microadditions of Ni on the mechanical properties of Mo and its alloys with C, 30:30014
See MOVCHAN, B.A., 30:30008
MALECKI, P., See ESKREYS, A., 30:30614
MALHOTRA, P.K., See GURTU, A., 30:30604
MALIENKO, E.I., See TYAPKIN, Yu.D., 30:30040
MALIK, S.K., Sign reversal of the 4f contribution to the hyperfine field at Sm in paramagnetic samarium compounds, 30:29997
MAL'KO, A.I., Spin and parity of 4.98-MeV level of ^{21}Na nucleus, 30:30909
MALONE, R.C., See KATZ, J.I., 30:30215
MALTA, C.P., Hartree-Fock calculations using Sussex matrix elements, 30:30863
MALYSOWA, E., See GLOWIAK, B., 30:29402
MANAKOVA, L.I., Conductimetric and high-frequency titration conditions for niobium by aromatic amines in aqueous-organic medium, 30:28959
MANASSAH, J.T., See DASHEN, R., 30:30716
MANDOLESI, N., Radio pulses from extensive air showers during thunderstorms: the atmospheric electric field as a possible cause, 30:30585
MANFRASS, P., Levels in ^{179}Ta and γ-ray transition probabilities in ^{179}Ta and ^{183}Re, 30:30994
See ANDREJTSCHEFF, W., 30:30993
See ANDREJTSCHEFF, W., 30:30990
MANFREDI, P.F., Reference pulsers for calibration purposes, 30:29628
MANGAL, P.C., See BHATI, S.S., 30:30958
MANGOTRA, L.K., See GURTU, A., 30:30604
MANI, S.A., See DOUGLAS-HAMILTON, D.H., 30:29201
MANN, F.M., Experimental study of ^{19}Ne decay and its significance to the study of neutral weak currents, 30:30892
MANTOVANI, G.C., See GOGGI, G., 30:30874
MANYUKHIN, V.P., See POPOV, V.P., 30:29900
MANYUKOV, B.A., See AKOPDJANOV, G.A., 30:30509
MAPLE, M.B., See HUBER, J.G., 30:30814
See KHAN, H.R., 30:30810
MARAMAN, W.J., See STAFFORD, R.G., 30:29328
MARANESI, P., See MANFREDI, P.F., 30:29628
MARANGELLI, B., See ABBATTISTA, N., 30:29631
MARBURGER, K., Unique forms of fast-sedimenting BU lambda DNA in a superinfected E. coli lysogen, 30:29652
MARCHENKO, V.I., See KOLTUNOV, V.S., 30:29112
See KOLTUNOV, V.S., 30:29113
MARCULESCU, S., See BANYAI, L., 30:30767
MAREI, A.N., See BORISOV, B.K., 30:29885
MARGALITH, E., See SHWARTZ, J., 30:29285
MARGON, B., A search for a cosmological component of the soft X-ray background in the direction of M31, 30:30174
MARHOL, M., Selective ion-exchangers containing phosphorus in their functional groups. I. Sorption and separation of some bivalent and trivalent ions, 30:29001
MARINO, D., See ABBATTISTA, N., 30:29631
MARINO, G.P., HYDIZ: a 2-dimensional computer progam for migration of interstitial solutes of finite solubility in a thermal gradient (LWBR Development Program), 30:29983 (WAPD-TM-1157)
MARINOV, S., Velocity of light is direction dependent, 30:31162
MARK, S.K., See HOUDAYER, A.J., 30:29641
MARKETOS, D.G., Description of the Greek Research Reactor-1, 30:31230 (DEMO-74/5)
International intercomparison of chemical dosimeters for in-pile use. A report of measurements made in the Greek Research Reactor-1 at Nuclear Research Center ''Democritos'', Athens, Greece, 3--6 July 1972 by eight reactor calorimetry and radiation chemistry groups from eight member states of the IAEA, 30:29539 (DEMO-74/5)
Reaction of the hydrated electron with benzene studied by pulse radiolysis, 30:29081
MARKETOU-MANTAKA, A., See MARKETOS, D.G., 30:29081
MARKUS, M.M., See DEMID, D.P., 30:30015
MARQUARDT, H., Effect of x irradiation on hydrocarbon metabolism and on hydrocarbon-induced lethality and transformation in cells derived from mouse prostate, 30:29670
MARQUEZ, L., See QUEBERT, J.L., 30:30996
MARSHALL, J.H., See HARRINGTON, T.M., 30:29566
MARSHALL, J.S., Plutonium in the Laurentian Great Lakes: food-chain relationships, 30:29415 (CONF-740826-3)
MARSHALL, S.A., See CASS, J., 30:29074
MARTEL, P., See TENNANT, D.C., 30:29513
MARTIN, A., High energy behavior of total and elastic cross sections, 30:30641
MARTIN, A.R., Atomic excitation processes in the discharges of rare gas ion engines, 30:30556
MARTIN, B.R., See ELVEKJAER, F., 30:30747
MARTIN, D.B., See PERCIVAL, D.R., 30:28978
MARTIN, E.R., See REILLY, T.D., 30:29509
MARTIN, R.W., See PITTS, J.H., 30:31254
MARTIN, W.E., NAEG plutonium study modeling program: plutonium transport and dose estimation model, 30:29455 (NVO-AEIC-74-1)
MARTINI, W.R., Unconventional Stirling engines for the artificial heart application, 30:29260
MARTINOT, M., See BERGER, J.F., 30:31094
MARTINS, J.B., See DI NAPOLI, V., 30:30919
MARUHN, J., See FINK, H.J., 30:31082
MARUMORI, T., See KURIYAMA, A., 30:31068
MARUSICH, N.I., See SOKOL'SKII, D.V., 30:29052
MARX, G., Neutrino mass from astrophysics, 30:30579 (CONF-730593-)
MASAKI, N., See YAMABAYASHI, H., 30:29962
MASHHOON, B., Can Einstein's theory of gravitation be tested beyond the geometrical optics limit, 30:31183
MASLOV, V.N., See ALEKSEEV, E.N., 30:29578
MASON, B.F., The inelastic scattering of He and Ne from a (001) surface of sodium fluoride, 30:30479
MASON, K.A., See WITHERS, H.R., 30:29758
See WITHERS, H.R., 30:29742
MASSA, I., See BERTIN, A., 30:31016
MASSE, R.P., See DER, Z.A., 30:29303
MASSON, D., Some applications of Pade approximants to quantum field theory models, 30:31165
MAST, T.S., See DERENZO, S.E., 30:29512
MASUDA, M., Isotopic study of water gas reaction catalyzed by platinum, 30:29032
MATAL, O., Freezing-up shaft seal of machines for the transport of liquids and gases in nuclear power, 30:29276
MATE, Z., See VANDLIK, Ya., 30:29142
MATEESCU, S., See BADESCU-SINGUREANU, A.I., 30:30846
See BADESCU-SINGUREANU, A.I., 30:30845
MATENKO, J., See KAMINSKI, R., 30:28920
MATHISEN, Oe., Daily excretion rate of iodine calculated from the relationship iodine per gram creatinine in a single afternoon urine sample, 30:29808 (F-599)
MATHUR, K.C., See TRIPATHI, A.N., 30:30521
MATISOO, J., Tunnel junctions for computer applications, 30:30831
MATSUDA, M., See FURUICHI, S., 30:30607
MATSUI, M., Radiation chemical studies with cyclotron beams. III. Heavy-ion radiolysis of liquid aliphatic ketones, 30:29049
MATSUI, T., New phase transitions in non-stoichiometric U_3O/sub 8-x/ at high temperatures. I. Thermogravimetric study, 30:29924
MATSUMURA, K., Reticuloendothelial function test in rabbit and man. Experimental and clinical investigation on artificial fat cream and ^{131}IAA, 30:29841
MATSUSE, T., See KAMIMURA, M., 30:31023
MATSUURA, K., See WATANABE, K., 30:29854
MATSUYANAGI, K., See KURIYAMA, A., 30:31068
MATSUZAKI, H., See KAWAZOE, Y., 30:30881
See YOKOZAWA, M., 30:30493
MATSUZAWA, T., See SATO, C., 30:29668
MATSUZURU, H., Ion exchange adsorption of Pu(IV) at extremely low concentrations in a chelating resin, 30:28996
MATTHEWS, K., See GATLEY, I., 30:30356
MATTHEWS, R.B., Irradiation damage in reaction-bonded silicon carbide, 30:29930
MATTHEWSON, R., See ADERHOLZ, M., 30:29595
MATULYAVICHYUS, V.P., Method of measuring the mobility, concentration, and isotope composition of radioactive ions, 30:29273
MATVEENKO, A., See ANGELOV, N., 30:30718
MAURENZIG, P.R., See FAZZINI, T., 30:30928
MAURETTE, M., See BIBRING, J.P., 30:30355
MAXIMON, L.C., Sum rules for forward elastic pion-nucleon scattering, 30:30750
MAXWELL, E., See KELLAND, D., 30:30832
MAY, E., See NORDBERG, M.E. Jr., 30:30590
MAY, M., See KIM, I.J., 30:30584
MAYER, J.W., See LAU, S.S., 30:29939
MAYER-BOERICKE, C., See ASPELUND, O., 30:30900
MAYR, P., Digital processors for servohydraulic material testing systems, 30:29300
MAYS, C.W., Transuranium elements in gonadal tissue, 30:29806 (COO-119-249)
See FISHER, D.R., 30:29799
See LLOYD, R.D., 30:29797
See LLOYD, R.D., 30:29805
See LLOYD, R.D., 30:29802
MAZAEV, A.A., Solubility of hydrogen in vanadium and niobium at high temperatures, 30:29918
MAZZUCATO, M., See BERTANZA, L., 30:30506
MCAUSLAN, E.R., See SCHELL, E.M., 30:29335
MCCARTHY, P.J., See CRAMPIN, M., 30:30765
MCCAULEY, E., Consistent vapor equation of state for solids, 30:31406 (UCID-15846)
MCCLELLAN, R.O., See BROOKS, A.L., 30:29763
MCCORMACK, G., See HARMS, A.A., 30:29302
MCCREADY, R.G.L., Fractionation of sulfur isotopes by the yeast Saccharomyces cerevisiae, 30:29826
MCCREADY, W.A., See ROBINSON, J.E., 30:29743
MCCRORY, R.L. Jr., Theory of drift-cone modes of collisionless plasma in cylindrical geometry, 30:29195 (LA-5693-MS)
MCCULLOCH, M.T., See DE LAETER, J.R., 30:30311
MCCULLOUGH, J.D., Optical and chemical studies on simulated interstellar grain materials, 30:30376

MCCUNE, J.E., See MCCRORY, R.L. Jr., 30:29195
MCCURDY, C.W. Jr., Equations of motion method: Inelastic electron scattering for helium and CO$_2$ in the Born approximation, 30:30550
MCCUSKER, M.V., See LICHTEN, W., 30:30492
MCDONALD, A., Polarization in electron positron colliding beams and the weak interactions, 30:30664
MCDONALD, B.E., Preliminary report of numerical simulation of Type 2 irregularities in the equatorial electrojet, 30:30427
  See SCANNAPIECO, A.J., 30:30437
MCDONALD, R.E., Study of basic processes in radiation damage. Final report, 1 April 1971—30 November 1973, 30:30061 (AD-777728)
  See MOORHEAD, A.J., 30:29966
MCDONALD, W.J., See CLOUGH, A.S., 30:30891
MCDUFFEE, W.T. Jr., See GRESKY, A.T., 30:29150
MCENTIRE, R.W., Electron Echo experiment 1: Comparison of observed and theoretical motion of artificially injected electrons in the magnetosphere, 30:30453
MCFADZEAN, J.A., See ASQUITH, J.C., 30:29674
MCFARLAND, S.S., See FISHER, D.R., 30:29799
  See LLOYD, R.D., 30:29797
MCGARRITY, J.M., See EUBANKS, A.G., 30:30091
MCGOWAN, F.K., See ROBINSON, R.L., 30:30982
MCGOWAN, J.W., See PENDYALA, S., 30:30511
MCGUIRE, E.J., Widths of 4s and 5s multiplet components in the rare earths, 30:30495
MCGUIRE, J.H, Solution of the Schroedinger equation using Pade approximants to sum asymptotic series, 30:31139
MCGUIRE, P., Equivalence and conservation rules for the total integral cross section in molecular collisions, 30:30560
MCHUGH, J.A., Ion beam sputtering. The effect of incident ion energy on atomic mixing in subsurface layers, 30:30483
MCILWAIN, C.E., See FILLIUS, R.W., 30:30406
MCINTYRE, J., See HOFFMANN, G.W., 30:30907
MCIVOR, I., See SKILLING, J., 30:30167
MCKAY, J.P., See PITTS, J.H., 30:31254
MCKEEL, B.K., Uranium in the Great Divide Basin, Wyoming, 30:29336
MCKELLAR, A.R.W., Intensities of the dipole and quadrupole rotation-vibration spectra of HD, 30:30501
MCKELLAR, B.H.J., See LASSEY, K.R., 30:30752
MCKENZIE, S., See SYKES, M.P., 30:29715
MCKIBBEN, J.L., See POTTER, J.M., 30:30599
MCKNIGHT, R.H., See THORNTON, S.T., 30:30537
MCKOY, V., See MCCURDY, C.W. Jr., 30:30550
MCLEAN, D.J., See SHERIDAN, K.V., 30:30305
MCMAHON, J., See SHAFER, R.B., 30:29856
MCMASTER, W.H., Generalized shock Hugoniots, 30:31400 (UCID-15586)
MCMULLEN, E.T., See PASTERNAK, A., 30:29315
MCNAUGHTON, M.W., See WANG, J.C., 30:30873
MCNEESE, W.D., See STAFFORD, R.G., 30:29328
MCNUTT, R.H., See DUPUY, C., 30:29340
MCPHERRON, R.L., See CLAUER, C.R., 30:30463
MCVAY, L.J., See ASCUITTO, R.J., 30:30995
MCVOY, K.W., See LONDERGAN, J.T., 30:30731
MCWILLIAM, A.D., See CHANNON, H.E.S., 30:29503
MEAD, G.D., See HESS, W.N., 30:30404
MEAD, W.C., Beta asymmetry of ^{35}Ar and the deduced value of the vector coupling constant, 30:30902
MEDA, D., See POSSOZ, A., 30:30899
MEDVEDOVSKAYA, E.I., See ANTONOVA, N.P., 30:29913
MEE, W.T., Safety analysis report for packaging (Oak Ridge Y-12 Plant foamglas shipping package for enriched uranium), 30:30116 (Y-DD-156)
MEFOD'EVA, M.P., See GUSEV, Yu.K., 30:29117
MEIER, H.K., See BEASLEY, C.O. Jr., 30:31344
MEIJER, B.J., See LINGEMAN, E.W.A., 30:31125
MEISCHNER, P., Energy and charge distribution of backscattered particles during bombardment of metal surfaces with protons, 30:30474 (AED-CONF-74-089-032)
MEISELES, R., On the time evolution of quasar luminosity and redshift distribution, 30:30293
MELESE-D'HOSPITAL, G., Role of helium-cooled reactors in meeting the energy crisis and conserving resources, 30:31210
MELGARD, R., See MAJOR, W.J., 30:28971
MELISSINOS, A.C., See KIM, I.J., 30:30584
MELITERES-MARECHAL, M., Weak hyperfine structure measurement using the magnetic repolarization effect: Application to N=1 v=1 (1s 3d)$^1\Sigma$ level of H$_2$, 30:30503
MELKUNOV, G.L., See ASTVATSATUROV, R.G., 30:29577
MELOSH, R.J., A status report on computational techniques for finite element analyses, 30:29290
MELROSE, D.B., Effects of an ambient medium on the emission, absorption and scattering of waves by atoms and molecules, 30:30387
MELTON, C.W., See GRUBER, H.T., 30:29294
MENCEL, J., See KAMINSKI, R., 30:28920
MENCHACA-ROCHA, A., Evidence for simple alpha-particle transfer in the (^{20}Ne,^{16}O) reaction, 30:30904
MENDELSOHN, M.L., Cell cycle kinetics and radiation therapy, 30:29662 (UCRL-75441)
MENDEZ, F., See BASES, R., 30:29671
  See BASES, R., 30:29666
MENON, M., See LLOYD, E.L., 30:29771
MEN'SHIKH, V.A., See TSVILYUK, I.S., 30:30027
MENSING, A.E., See HAUGHT, A.F., 30:29152
MERCEREAU, J.E., See PALMER, D.W., 30:30821
MERGENHAGEN, S.E., See HORTON, J.E., 30:29567
MERKLE, E.J., Interlaboratory comparison of chemical analysis of uranium mononitride, 30:28942 (N-74-18812)
MERLE, K., See ROTHHAAS, H., 30:31005
MERRITT, W.F., No radioactive silver detectable in silver—uranium ore, 30:28987
MERZ, I., Laboratory and hot-cell studies concerning the in-line polarographic determination of uranium in the aqueous waste stream of the KFA-TBP 23/25 process, 30:28941 (JUL-1063-CT)
MESERVEY, R., Inductance bridge for current-quantum phase measurements in superconductors at zero frequency, 30:30839
MESSINA, R.J., See MOOK, D.E., 30:30271
METZGER, A.E., See HARRINGTON, T.M., 30:29566
METZGER, G., See MEYER, J.M., 30:29627
METZLER, H.G., See KOLLBACH, D., 30:31338
MEUNIER, R., See BIBRING, J.P., 30:30355
MEYER, B.J., See DE BOER, F.W.N., 30:30989
MEYER, G., See BRATOLJIC, T., 30:30837
MEYER, H., See ROE, D.B., 30:30798
MEYER, J., New determination of Mongan's non-local separable potentials for nuclear structure calculations, 30:31035
  See BRAUEL, P., 30:30588
MEYER, J.M., Test system for CAMAC modules, 30:29627
MEYERSTEIN, D., See COHEN, H., 30:29080
MEZHBEZHER, I.L., Effect of small additions of beryllium on some properties of aluminum and the aluminum alloy AL11, 30:29987
MICAUD, G., See GENTHON, J.P., 30:30098
MICEK, S., See BUTA, A., 30:30926
MICHAEL, J.L., Beat phenomenon in Tau Peg, 30:30227
MICHAUD, G., Diffusion and isotope anomalies in peculiar A--B stars, 30:30201
MICHEL, G., See CONNES, P., 30:30207
MICHELINI, M., Point-dependent calculations of the anisotropic diffusion coefficient, 30:30850 (RT/FI-(74)10)
MIDDLETON, R., A close to universal negative ion source, 30:30485
MIES, F.H., Ultraviolet fluorescent pumping of OH 18-centimeter radiation in comets, 30:30326
MIETTINEN, H.I., See GAISSER, T.K., 30:30763
MIGDAL, A.B., π-condensation in a finite system and properties of nuclei, 30:31088
MIGLIORE, J.J., See HAGEN, K.G., 30:29262
MIHAILESCU, I.M., Thermal neutron cross sections of fissionable elements in the multilevel-multichannel formalism, 30:31015
MIHAILOVIC, M.V., Application of the generator coordinate method to nuclear bound states and to scattering, 30:31052
MIHALAS, D., Progress towards an interpretation of stellar spectra, 30:30229
MIKAELIAN, K.O., See BROWN, R.W., 30:30752
MIKHEEV, S.P., See ALEKSEEV, E.N., 30:29578
MIKHEEV, V.S., Mechanical properties of multicomponent alloys based on Ti--Al--Sn (Zr) α-solid solution with β-stabilizing elements, 30:29984
MIKLINA, N.V., See DRITS, M.E., 30:30007
MIKULAI, V., See NEFEDOV, V.D., 30:29109
MILAS, I., See PAVICIC, S., 30:29745
MILES, L.E.M., Measurement of serum ferritin by a 2-site immunoradiometric assay, 30:29835
MILHAM, R.C., Determination of promethium-147 in aqueous environmental samples, 30:28969 (DP-MS-73-77)
MILITSYN, K.N., See MEZHBEZHER, I.L., 30:29987
MILJANIC, D., Quasi-free contributions in the d+^{6}Li reactions at low energies, 30:30882
MILLER, A.G., Determination of rare earths in plutonium by x-ray emission analysis, 30:28946
MILLER, D.K., See KURODA, P.K., 30:30162
MILLER, E.K., Radiation from buried antennas, 30:31449 (UCID-16890)
MILLER, L.D., See GREEN, A.E.S., 30:31048
MILLER, M.C., See JEZERNIK, A., 30:31291
  See LEE, R.N., 30:29611
MILLER, R.A., Radiation balance and electron temperature in a neutralized sigma, 30:29156
MILLER, S.C., See JEE, W.S.S., 30:29801
MILLET, F., See GENTA, P., 30:29178
MILLNER, T., Formation of a network of spherical micropores and the relation of this with the GK properties of TUNGSRAM-made tungsten metal prepared with oxide additives containing K, Si, and Al, 30:30026
MILLS, A.P. Jr., See CANTER, K.F., 30:30510
MILLS, F.E., Flux theorem for the design of magnet coil ends, 30:30122
MILLS, M.T., Ground level air concentrations of dust particles downwind from a tailings area during a typical windstorm, 30:29380 (ORNL-TM-4375)
MILLS, R.G., Economic and environmental aspects of a first-generation fusion power plant, 30:29229
MILTON, R.D., See OTTO, W.F., 30:29281

MINASHIN, V.E., See SHOLOKHOV, A.A., 30:31277
MINGOT, F., See CIRAUQUI, R., 30:29649
  See DELGADO, M.D., 30:29650
MINN, Y.K., 4830 MHz formaldehyde line observations of dark clouds in IC 1795/#3/, 30:30372
MINOR, W., A simple method of orientating single crystals on time-of-flight neutron spectrometers, 30:29574
MIRIN, A.A., HYBRID-1, a two-dimensional Fokker--Planck code, 30:29189 (UCRL-51598)
  Program IONS: two-dimensional Fokker--Planck equation for ions and electrons, 30:31362 (UCID-16014)
MIROSHNICHENKO, L.I., Cosmic rays in interplanetary space, 30:30166
MIROSHNIKOV, V.S., See MOSKVIN, L.N., 30:28997
MIRZAEV, D.A., See SHISHMAKOV, A.S, 30:30024
MISCHKE, R.E., See POTTER, J.M., 30:30599
MISHCHENKO, B.A., See BRESLAVETS, K.G., 30:31394
MISHIMA, J., Airborne release of ^{137}Cs from a contaminated area during a range fire, 30:29376 (BNWL-1850(Pt.3))
MISHRA, S.P., Unstable intermediates. CXLVI. Electron spin resonance spectra for linear $BrCN^-$ and Br_2CN radicals in irradiated cyanogen bromide crystals, 30:29076
  Unstable intermediates. CXXXVII. α-bromoalkyl radicals in irradiated organic bromides: an electron spin resonance study, 30:29073
MISKAR'YANTS, V.G., Spectral assay of components in alloys (exchange of experience), 30:28951
MISKUFF, R.J., See ALLER, P.F., 30:29245
MISRA, M., See ANDERSSON, L.P., 30:29519
MISYURA, V.A., Investigation of a fine regular structure and random ionospheric irregularities by the method of incoherent radio wave scattering, 30:30447
MITCHELL, R.N., See STAFFORD, R.G., 30:29328
MITCHEN, J.L., See LLOYD, E.L., 30:29771
MITROV, G., Prostnesis set for radioprotection of the eye, 30:29717
MITSONIAS, C.A., See MARKETOS, D.G., 30:31230
MITSUI, H., See HOSOI, F., 30:29036
MITTLEMAN, M.H., Energy dependence in interatomic potentials-He_2, 30:30497
MITTRA, I.S., See GURTU, A., 30:30604
MIYAHARA, K., See MASUDA, M., 30:29032
MIYAI, K., See ONISHI, T., 30:29862
MIYAKE, C., See YOSHIMURA, T., 30:29094
MIYAMARU, M., Application of activation analysis to the determination of pollutants in the atmosphere, 30:28914 (IEA-326)
MIYAZAKI, M., Study on the blood-cerebrospinal fluid barrier. I. Permeability of RISA^{131}I at twenty-four hours after intravenous administration, 30:29840
MJOLSNESS, R.C., Model for the CW power output of tne HF chemical laser, 30:29266 (LA-5683-MS)
MOCKLER, M., See STANTON, R.E., 30:28960
MOECKEL, H., See JUNGBLUTH, H., 30:29057
MOELLER, F., Application of sequential estimation methods to counts of phytoplankton, 30:31380 (RT/BIO-(74)7)
MOFFETT, R.J., See BAILEY, G.J., 30:30443
MOHLER, D.C., See DODSON, H.W., 30:30328
MOHR, P., Ion bombardment simulation of 14 MeV neutron damage in thin niobium films, 30:30066 (UCID-16109)
MOISE, J.C., Status of a thermocompressor-powered implantable artificial heart system, 30:29261
MOISEEV, A.M., See AKOPDJANOV, G.A., 30:30608
  See BABINTSEV, V.V., 30:30598
  See BUMAZSHNOV, V.A., 30:30603
MOLINARI, A., See BROGLIA, R.A., 30:30991
  See JOHNSON, M.B., 30:31059
MOLNAR, C.J., New discrete atomization cell for atomic fluorescence spectrometry, 30:28947
MOLSON, L.D., See HARMS, A.A., 30:29301
MONARKHA, Yu.P., See SHIKIN, V.B., 30:30801
MONFILS, A., See GERARD, J.C., 30:30426
MONIZ, E.J., See LONDERGAN, J.T., 30:30731
MONTANET, L., See YAFFE, D., 30:30622
MONTH, M., Resonance excitation by distortion of tne β-function coupled with a long range space charge force, 30:30137 (BNL-19192)
MOOK, D.E., Color variations of Scorpius X-1, 30:30271
MOON, L.C., Program correctness in a multiprogrammed multiprocessor environment, 30:31339 (IS-3444)
MOON, P.S., Optimal annealing of natural beryl for thermoluminescent dosimetry, 30:29553
MOOR, K.S., Ecological studies of vertebrates in plutonium-contaminated areas of the Nevada Test Site, 30:29449 (NVO-AEIC-74-1)
MOORE, C.A., See SILK, E.J., 30:31293
MOORE, J.E., See BUONOMANO, V., 30:31143
MOORE, R.B., See HOUDAYER, A.J., 30:29641
MOORE, S.W., Design and testing of a structurally integrated steel solar collector unit based on expanded flat metal plates, 30:31326 (LA-UR-74-1093)
MOORHEAD, A.J., Fabrication procedures for unalloyed molybdenum, 30:29965
MORALES, J.R., A cooling system for thin tritiated titanium targets, 30:30157
MORAN, J.M., See KNOWLES, S.H., 30:30286
MORAN, P.R., See LASKEY, J.B., 30:29538
MORAVCSIK, M.J., See GOLDSTEIN, G.R., 30:31028
MORDUKHAY-BOLTOVSKI, F.D., See BUTORIN, N.V., 30:29463
MOREHOUSE, J.H., Dynamic interferometric holography, 30:31440 (UCID-15682)
MOREK, T., See DROSTE, C., 30:30963
MORETTI, A., See CHANG, C.T.M., 30:29584
MORETTO, L.G., Influence of pairing and of the spin projection distribution on the 'classical' isothermal rotations of a nucleus, 30:31101
  Statistical properties of a paired nucleus with fixed quasiparticle number, 30:31099
MORGADO, R.E., See KANSTEIN, L.L., 30:30127
MORGAN, D., Is the 0^+ nonet respectable, 30:30727
MORGAN, G.H., See MILLS, F.E., 30:30122
MORGAN, H., See BRUNSON, B., 30:29837
MORGAN, J.F., See VLIEKS, A.E., 30:30255
MORGAN, O.B., See DAVIS, R.C., 30:29209
MORGAN, W.C., Atomic displacement cross sections for carbon from ENDF/B-III data, 30:30095
MORI, K.J., See NAKAMURA, S., 30:29753
MORI, T.T., See WILSON, W.J., 30:30265
MORIGI, G., See MANDOLESI, N., 30:30585
MORIMOTO, M., See FOURIKIS, N., 30:30360
  See KAIFU, N., 30:30359
MORIN, P., Specific heat in TbZn and HoZn compounds, 30:29990
MORISAKI, S., Oxidative degradation products of irradiated polyethylene, 30:29054
MORITA, K., Geometrical interpretation of paraorder 3 of paraquark model, 30:30692
MORITA, N., Electron spin resonance study on free radicals in tne chemical carcinogen, 1,2-dimethylhydrazine induced by x-ray irradiation, 30:29050
MORITZ, J., Development of a CAMAC crate controller for connection to a computer CDC 1700, 30:29634
MORLEY ENGLISH, J., Long term investment considerations of conjunctive desalting systems, 30:31309
MOROZOV, K.N., See LUCHNIK, N.V., 30:29696
MOROZOV, V.V., See SHLYUKO, V.Ya., 30:29892
MOROZOVA, N.P., See CHUPYATOVA, L.P., 30:30033
  See CHUPYATOVA, L.P., 30:30010
MOROZOVA, S.S., Determination of beryllium with nitryltrimethylphosphonic acid in the presence of alkaline earth metals, 30:28955
MORRIS, C.C., See ELSNER, N.B., 30:29246
MORRIS, C.J., See MORRIS, G.A., 30:29323
  See SNOEBERGER, D.F., 30:29458
MORRIS, G.A., Field measurements of permeability of NTS alluvium in Area 10, 30:29323 (UCID-15919)
  Method of estimating the total curies in gas samples, 30:29087 (UCID-15809)
  See ROZSA, R.B., 30:29324
  See SNOEBERGER, D.F., 30:29458
MORRIS, M., Cyanoacetylene: new lines and sources in the galaxy, 30:30374
MORRIS, W.F., Spectrographic determination of trace impurities in high purity uranium oxide, 30:28944 (UCID-15952)
MORRISON, C.A., See WORTMAN, D.E., 30:30487
MORRISON, D.R.O., Experimental review of strong interactions at high energy, 30:30578
MORRISON, G.H., Trace geochemistry of lunar material. Final report, 30:28916 (N-74-20470)
MORROW, W.G., See BALLOU, J.E., 30:29776
MORSCH, H.-P., Structure of low-lying 0^+ states in fsub(7/2) shell nuclei from inelastic ^{3}He scattering, 30:30934
MORTENSEN, W.K., Instrumenting the LAPQ-1 airborne cloud-mapping radar for shipboard use in Operation Dial Train, 30:31456 (UCID-16051)
MORTON, J.R., See COLUSSI, A.J., 30:29067
MOSEL, U., See GLAS, D., 30:31066
MOSER, K., See BAETZNER, K., 30:30589
  See BECK, U., 30:30591
MOSES, R.T., See FOWLER, P.H., 30:29521
MOSKVIN, L.N., Chromatography on finely dispersed ionites on inert supports, 30:28997
MOSKVINA, Z.V., See SAZONOV, L.A., 30:29028
MOTTMANN, J., See FOGARTY, W.G., 30:30346
MOVCHAN, B.A., Effect of carbon on the plasticity and nature of breakdown of polycrystal Mo, 30:30008
MOYER, W.R., See DANCHAK, M., 30:29620
MUELLER, G.P., Total cross-section corresponding to the differential cross-section of Lindhard, Neilsen, and Scharff, 30:30552
MUELLER, H.H., See KELLER, R., 30:30151
MUELLER, P., See KLAUMUENZER, S., 30:30074
MUELLER, R., See BUTA, A., 30:30926
MUENCHOW, L., See WIEBICKE, H.J., 30:31090
MUENZEL, H., See KELLER, K.A., 30:30960
MUGA, L., Luminescence response of thin plastic scintillator detectors to fission fragments from proton-induced fission of ^{232}Th, ^{235}U and ^{238}U, 30:29528
MUKHERJEE, B.K., Kinetics of flux jumps in Type-II superconducting disks, 30:30818
MULLEN, A.A., Distribution of ingested plutonium in chickens and subsequent transport to eggs, 30:29811 (NVO-AEIC-74-1)
  See BARTH, J., 30:29809

MULLEN, D.W., Operation TOGGLE: on-site radiological safety report, July 1972--June 1973, 30:29379 (NVO-410-25)
Operation WHETSTONE: on-site radiological safety report, July 1964--June 1965, 30:29378 (NVO-410-24)
MULLER, R.A., See DERENZO, S.E., 30:29512
MUNOZ, R., See GORDON, F., 30:29852
MURAOKA, T., See KONISHI, H., 30:29875
MUROFF, L.R., Use of multiple radionuclide imaging to differentiate the focal intrahepatic lesion, 30:29851
MURPHY, C.H., Inductive electric field of a field-aligned current system, 30:30438
MURPHY, J.J., Ratio of the nuclear moments of ^{99}Ru and ^{101}Ru from NMR studies of ferromagnetic alloys, 30:30961
MURRAY, H.S., Control system design and simulation for solar heated structures, 30:31325 (LA-UR-74-1085)
MURRAY, R.C., Evaluation of load-deflection tests of 0.060-in.-thick Y-3333 cellular silicone, 30:31407 (UCID-15901)
MURROW, J.L., See GASKILL, J.R., 30:29330
MURTAGH, M., See KIM, I.J., 30:30584
MUTA, N., See KOIWAI, S., 30:29663
MUTCHLER, G.S., See MILJANIC, D., 30:30882
MUTO, K., Comparative forced vibration test of two BWR-type reactor buildings, 30:31265
MUZZIO, J.C., Faint O-B3 stars in the Norma section of the Milky Way, 30:30233
MYERS, S.M., Ion-backscattering study of LiOH-to-Li$_2$O conversion on a LiH substrate, 30:29937
MYHRER, F., Unitarity corrections to pion-nucleus scattering lengths, 30:30866

N

NABORS, C.J. Jr., Cortisol metabolism in skin of beagles bearing ^{241}Am: a possible pre-neoplastic change in steroid metabolism, 30:29780 (COO-119-249)
Effects of DTPA on tissue cultured fibroblasts, 30:29807 (COO-119-249)
NACK, M.L., See GREEN, A.E.S., 30:31048
NAEEM, A., Energy measurements of delayed neutron groups from ^{235}U, 30:31014
NAGAMOTO, C.T., See ROSINSKI, J., 30:29357
NAGANE, K., See KAIFU, N., 30:30359
NAGARAJAN, R., Interaction effect of entry velocity and position on quadrupole mass filter resolution, 30:29525
NAGLE, D.E., See POTTER, J.M., 30:30599
NAGORCKA, B.N., See BRANFORD, D., 30:30887
NAGPAL, A.K., Equivalence of Yang--Feldman and action principle quantization, 30:31148
NAGY, C.F., See COFFEY, J.W., 30:29870
NAHABETIAN, R., See MEYER, J., 30:31036
NAHARIN, A., Internal deposition of ingested cerium in suckling mice, 30:29821
NAIDENOVA, G.A., See ANTONOVA, N.P., 30:29913
NAITO, K., See MATSUI, T., 30:29924
NAKABAYASHI, M., See SUZUKI, H., 30:29922
NAKAGAWA, Y., Dynamics of the solar magnetic field. I. Method of examination of force-free magnetic fields, 30:30315
Dynamics of the solar magnetic field. II. The energy spectrum of large-scale solar magnetic fields, 30:30316
See HIRSHBERG, J., 30:30322
NAKAHARA, K., See KITAZOE, T., 30:30653
NAKAHARA, Y., Convergence acceleration algorithms of the iterative methods used in nuclear reactor analysis codes, 30:31272 (JAERI-M-5590)
NAKAJIMA, K., See FUKUCHI, S., 30:29876
NAKAJIMA, M., See YOKOZAWA, M., 30:30493
NAKAMURA, K., Annealing characteristics of ion-implanted p-channel MOS transistors, 30:30098
See KUDOH, O., 30:30100
NAKAMURA, S., Effects of carbon particles on phagocytic activity of reticuloendothelial system in x-irradiated mice, 30:29753
NAKAMURA, T., See ITO, K., 30:29839
See YAMAMURO, N., 30:31278
NAKAO, R., Reduction of methyl acetate with several hydrosilanes under gamma irradiation, 30:29047
NAKAZAWA, K., Comments on approximations for the overlap expansion, 30:30786
NALCIOGLU, O., See KOLTUN, D.S., 30:31097
NAMSRAI, Kh., See EFIMOV, G.V., 30:31144
NANBU, K., Improved modified wavenumber approximation applied to elastic collision, 30:30529
NANOPOULOS, D.V., Implications of the recent $e^+e^- \to$ hadron + X data on the leptonic world, 30:30657
NAOUMIDIS, A., See BOHN, T., 30:31208
NAPIER, A., See BASTIEN, D.B., 30:30600
NAPIER, W.M., See DODD, R.J., 30:30409
NARINSKII, V.M., See BLOKHIN, S.I., 30:31110
NARKEVICH, B.Ya., See SIVOSHINSKII, D.S., 30:29838
NASIBOV, I.O., See RUSTAMOV, P.G., 30:30016
NATANZON, Ya.V., See EREMENKO, V.N., 30:30003
NATH, R., See HICKEY, G.T., 30:30889
NAUMAN, S., See BEYNON, A.J., 30:31212
NAUMENKO, V.Ya., See SAMSONOV, G.V., 30:29912
NAZAROV, L.E., Vertical distribution of radioactive aerosols in the troposphere above the European part of the USSR in 1964--1967, 30:29389
See GAZIEV, Yu.I., 30:29392
NEAL, H.A., A recurrence relation for the polarization in elastic p--p scattering in the framework of a parton model, 30:30755
NEET, T.E., Static compressive testing of rigid polyurethane foam, 30:31384 (BDX-613-1035(Rev.))
NEFEDOV, V.D., Stabilization of daughter /sup 99m/Tc after β-decay of ^{99}Mo in the hexacarbonyl molybdenum molecule, 30:29109
NEGISHI, T., See KOHMURA, T., 30:31022
NEHER, P., See MAYR, P., 30:29300
NEIL, V.K., Some comments on the transverse resistive wall instability (or, ''LNS revisited''), 30:29198 (UCID-15711)
See COOPER, R.K., 30:29225
See COOPER, R.K., 30:29219
NEILD, D.J., See WISE, P.J., 30:28933
NEILSON, G.W., See MISHRA, S.P., 30:29073
See MISHRA, S.P., 30:29075
NELSON, C., See NORDBERG, M.E. Jr., 30:30590
NELSON, K.E., See WOLSKO, T.D., 30:31357
NEMEC, H.W., Significance of free radicals for the inactivation of trypsin by uv irradiation. Investigations by means of ESR spectroscopy, 30:29657
NENCIU, G., See ANGELESCU, N., 30:31421
NEOKLADNOVA, L.N., Studies of radiolysis of solid, Co(III) compounds by the EPR method, 30:29063
NEOKLADNOVOI, L.N., See LAZERKO, G.A., 30:29060
NESHPOR, V.S., See BYCHKOV, A.Kh., 30:29897
NESMYANOVICH, A.T., Connection of the optical flares with the solar radio bursts, 30:30309
NETUSOV, Yu.K., See ZOLOTUKHIN, I.V., 30:29887
NEUBECKER, K., See BAILEY, J., 30:30620
NEUGEBAUER, G., See GATLEY, I., 30:30356
See WYNN-WILLIAMS, C.G., 30:30375
NEUHAEUSER, H., Determination of the velocity and local density of mobile dislocations within slip bands in neutron-irradiated Cu by high speed cinematography, 30:30068
NEUMANN, H.F., See BENECKE, J., 30:30612
NEVISSI, A., Long-lived radon daughters as atmospheric radioactive tracers, 30:29400
NEWTON, J.C., See KROYHN, D.L., 30:29765
NEWTON, S., See STANTON, R.E., 30:28960
NEWTON J.D., See BRANFORD, D., 30:30887
NEXSEN, W.E., See COENSGEN, F.H., 30:29212
NG, K., Hypernetted chain solutions for the classical one-component plasma up to GAMMA=7000, 30:29191
NGO, C., See HANAPPE, F., 30:30984
NI, W.T., Relativistic stellar stability: preferred-frame effects, 30:30206
NICHOLLS, P.W., See INGLIS, A.S., 30:28945
NICKEL, H., See BUHN, T., 30:31208
NICKOLA, P.W., Estimation of mean crosswind concentration profiles from ''instantaneous'' crosswind traverses, 30:29424 (BNWL-1850(Pt.3))
Measurement of particulate plume depletion by comparison with inert gas plumes, 30:29425 (BNWL-1850(Pt.3))
See CLARK, G.H., 30:29426
See ELDERKIN, C.E., 30:29434
See ORGILL, M.M., 30:29610
NICOLAENCKO, V.I., See DERRE, J., 30:30601
NIEBEL, K., Point defect clusters in neutron-irradiated Mo. I. Dose dependence of the number density and the mean diameter of radiation-induced dislocation loops, 30:30067
NIEGAWA, A., J = 0 fixed pole in the virtual Compton amplitude off proton and neutron, 30:30561
NIEKUSCH, E., Determination of mineral-oil in the helium-circuit of a refrigeration-plant, 30:31393 (KFK-1976)
NIELSEN, H.B., See NEAL, H.A., 30:30765
NIELSEN, J., Isotopic separation of nitrogen-15. III. Effect of the degree of oxidation of the reflux gases for the system NO, NO$_2$--HNO$_3$, 30:29034
NIELSEN, S.O., Nuclear waste disposal in the oceans, 30:30110
NIESSEN, H.F., See BOHN, T., 30:31305
NIETZEL, Ch., See BAETZNER, K., 30:30589
NIKISHA, V.V., See GRIVA, A.P., 30:29029
NIKITIN, S.A., Paraprocess near Curie temperature and criteria of appearance of temperature of magnetic compensation in compounds of rare earths with iron, 30:30043
NIKITINA, L.V., See MOROZOVA, S.S., 30:28955
NIKOLAEV, V.M., See ANGELOV, B.P., 30:30143
NIKOLAEVSKII, V.B., See SHILOV, V.P., 30:29104
NIKOLOVA, R.H., See DANCEVA, K.I., 30:29653
NIKOL'SKII, B.P., Complex formation of actinides and lanthanides with orthophthalic, 3-nitrophthalic, and 4-nitrophthalic acids. II. Complex formation of radioeuropium, 30:29119
Complex formation of actinides and lanthanides with o-phthalic, 3-nitrophthalic, and 4-nitrophthalic acids. I. Complex formation of uranium, 30:29118
NILSSON, B.S., See BROGLIA, R.A., 30:31000
NILSSON, L., See BERGMAN, R., 30:28918
NISEL'SON, L.A., See PETRUSEVICH, I.V., 30:29971
See VASIL'EVA, A.G., 30:29949
NISHIKAWA, M., Electron scavenging in the radiolysis of supercritical ethane, ethylene, n-butane, and isobutane, 30:29039
NISHIMURA, K., See TERADA, K., 30:28984

NISHINA, K., See YAMAMURO, N., 30:31278
NISHINO, O., See HASEGAWA, K., 30:31244
NISHIZATO, K., See FUKUCHI, S., 30:29675
NISIZAWA, M., Studies on irradiation of agar--agar in the solid state. On the changes of penetration of agar--agar hydrogel produced by irradiation, 30:23072
NISSEN, R.F., See TILLES, E.B., 30:30123
NISSEN-MEYER, S., See BENECKE, J., 30:30512
NITTS, V.V., See BALANDA, M., 30:31392
NIZHNIKOV, A.N., See TROITSKAYA, M.N., 30:29405
NOBLE, J.V., On proton-deuteron backward elastic scattering at medium energies, 30:30857
  See GRONADZKI, Z., 30:30893
NOJIRI, T., See MAKI, Y., 30:28928
NOMATSU, K., See SHIMIZU, T., 30:29721
NOMURA, M., Calculation method for a high moment of energy spectra. The case when intrinsic spin is fixed, 30:31057
NOONAN, J.R., See JONES, C.E., 30:30099
NOONAN, T.W., Turnover radio spectra of elliptical galaxies, 30:30345
NORBECK, E., Beams of Be$^+$ from an rf ion source, 30:30130
NORCROSS, D.W., See HERBST, E., 30:30351
NORDBERG, M.E. Jr., Upper limit on the rho^0 → etaγ branching ratio, 30:30590
NORDBORG, C., See BERGMAN, R., 30:28918
NORDSTROEM, B., See SUNDMAN, A., 30:30352
NORDYKE, M.D., Elat-Dead Sea canal, 30:29327 (UCID-16107)
NORELAND, T., See ORRE, B., 30:31017
NORGREN, D.J., See KAVSTEIN, L.L., 30:30127
NORLIN, L.O., See ORRE, B., 30:31017
NORMAN, J.C., See HAGEN, K.G., 30:29262
NORMANN, E., Elimination of intravenously injected ^{125}I-toluidine blue in rabbits, 30:29812
NORTHWOOD, D.O., Some comments on damage alignment in neutron-irradiated zirconium alloys, 30:30075
NORTON, G.A., See WHITE, R.L., 30:30937
NORTON, P.R., See DEL GUERRA, A., 30:30578
NOSKOVA, N.F., See SOKOL'SKII, D.V., 30:29052
NOSKOVA, N.I., Stacking faults in refractory metals and alloys, 30:30030
NOSOV, V.G., Magic nuclei theory, 30:30527 (IAE-2285)
NOSOVA, G.I., See KUTSAR, A.R., 30:30011
NOTEA, A., General approach to the design of radiation gauges, 30:29508
NOVAK, L., Time course of the radioprotective effect and the formation of endogenous colonies of haemopoietic cells in mouse spleen following the administration of sodium fluoroacetate, 30:29747
NOVAK, P., See ROZTOCIL, K., 30:29794
NOVIKOV, S.A., See ISSINSKII, I.B., 30:30129
NOVOTNY, D.B., See CIARLO, D.R., 30:31460
NOVOZHILOV, V.I., See MISYURA, V.A., 30:30447
NOWAKOWSKI, W., See OSEENDA, M., 30:29761
NOWICKI, M., See DROSTE, C., 30:30963
NOWIKOV, V.G., See BARABOSCH, L.S., 30:30117
NUGENT, T.J., Test methods for high packing density digital magnetic tape recorders, 30:31443 (UCID-15773)
NUNBERG, P., Ground-state properties of three-nucleon systems: a review, 30:31039
NUNES, A.C., A focussing low-angle neutron diffractometer, 30:29632
NUTTALL, J., Convergence of certain Pade approximants, 30:31140
  See MCGUIRE, J.H, 30:31139
NYMAN, B., Nuclear spectroscopy of ^{107}Cd, 30:30953 (NP-20122)
  See DIETRICH, W., 30:30954

O

OAKBERG, E.F., Response of spermatogonia of the mouse to hycanthone, and a comparison with the effect of γ rays, 30:29735 (CONF-731222-1)
OBAYASHI, I., See SAITO, K., 30:29854
OBERTEUFFER, J., See KELLAND, D., 30:30832
OBKHODOVA, T.V., See KADYKOVA, G.N., 30:30009
OBLOZINSKY, P., Intermediate-state transition rates in the exciton model, 30:31093
O'BRIEN, H.A. Jr., Radioisotopes from a medium-energy accelerator: the Clinton P. Anderson Meson Physics Facility radioisotope program, 30:30142 (LA-UR-74-1253)
O'BRIEN, J.T., See KLINE, F.J., 30:30878
O'CONNEL, J.S., See MAXIMON, L.C., 30:30750
ODDERSHEDE, J., See JUERGENSEN, P., 30:30568
ODELIUS, H., See CHRISTIANSSON, J.E., 30:30901
ODYNETS, L.L., Electrical conductivity in metal/oxide/electrolyte systems, 30:29896
OEN, C.J., Information support for the Nevada Applied Ecology Group, 30:29454 (NVO-AEIC-74-1)
OERSTAVIK, J., Uptake and release of ^{3}H-mitomycin C in mouse P-388 cell cultures, 30:29862
OEYE, O.G.W., Energy crisis and nuclear energy. Energy consumption and expected growth, 30:31307
OGARD, A.E., See O'BRIEN, H.A. Jr., 30:30142
OGASAWARA, T., See YASOHAMA, K., 30:30025
  See YASUKOCHI, K., 30:30836
OGILVIE, K.W., Discussion of interplanetary postshock flows with two examples, 30:30399
OHARA, K., See TAKAHASHI, S., 30:31105
OHNISHI, T., A galactic model with a pulsating active nucleus. III. Evolution of rare-light elements, 30:30386
OHNUMA, H., Comment on anomalous (p,t) angular distributions due to form factor cancellation, 30:30929
OHNUMA, T., See SANO, H., 30:29078
O'HORO, M.P., See GRISCOM, D.L., 30:31389
OHSHIMA, T., Experimental usage of cysteine in radiation therapy, 30:29722
OHTA, T., See MUTO, K., 30:31265
OKANE, S., See YAMABAYASHI, H., 30:29962
OKHREMCHUK, L.N., See SAMSONOV, G.V., 30:29912
OKRENT, D., See DIAS, J.W., 30:31228
OKULOV, Yu.I., See BLUKH, Ya.L., 30:29579
OKUN, L.B., See KOBSAREV, I.Yu., 30:30770
OKUYAMA, F., Vapor-grown tungsten whiskers induced by vacuum discharges, 30:29968
OLANDER, D.R., See ULLMAN, A., 30:30097
OLESEN, P., A dual quark prison, 30:30697
  Dual strings in the Amata-Testa quark imprisonment scheme, 30:30647
OLIN, A., See HAEUSSER, O., 30:31004
OLIPER, T.V., Condition of the nervous and vascular systems after radiation treatment of lymphogranulomatosis, 30:29730
OLIVER, A.J., Ventilation design for new Plutonium Recovery Facility, 30:29329 (RFP-2215)
OLIVER, D.A., Fault Tree Drawing Program users instructions, 30:31346 (SLA-73-0409)
OLSEN, L.C., Advanced betavoltaic power sources, 30:29257
OLSON, H.C., Rf hybrid microcircuit soldering techniques, 30:31397 (SLA-73-1073)
OLSON, J.S., See MILLS, M.T., 30:29380
OLSON, R.E., See JONES, P.R., 30:30540
OLSON, W.P., A model of the distributed magnetospheric currents, 30:30468
OMATSUZAWA, K., See MUTO, K., 30:31265
OMEL'CHENKO, B.D., See ISSINSKII, I.B., 30:30129
OMEL'YANENKO, B.I., Zonality of thorium--niobium mineralization in albitites, 30:29333
ONISHI, T., Determination of prolactin in the blood by radioimmunoassay, 30:29862
ONO, K., Short electron linac of side-coupled structure with low injection voltage, 30:30120
OPHER, R., Origin of QSO absorption lines, 30:30289
OPPENHEIM, J.J., See HORTON, J.E., 30:29667
O'RAIFEARTAIGH, L., See MAINLAND, G.B., 30:31151
ORAN, E., See JULIENNE, P.S., 30:30425
ORDA, A., See SAROSIEK, J., 30:29691
ORDAN'YAN, S.S., See BYCHKOV, A.Kh., 30:29897
ORESHKIN, V.D., See DAN'KIN, A.A., 30:29899
ORGILL, M.M., Evaluation of an airborne fluorescent particle counter for atmospheric tracer studies, 30:29610 (BNWL-1850(Pt.3))
  Regional wind resuspension of dust, 30:29373 (BNWL-1850(Pt.3))
  See SEHMEL, G.A., 30:29372
ORLOVA, M.M., See ZAKHAROVA, F.A., 30:29114
ORRE, B., Perturbed alpha-gamma angular correlation studies of radon recoils into aluminium, 30:31017
ORZALESI, C.A., The quark-parton paradox, 30:30715
ORZECHOWSKI, T., See SAWICKI, A., 30:30124
OSBORN, H., SU$_6$ quark model, nucleon resonance electroproduction and spin-dependent electroproduction structure functions, 30:30735
OSBORN, J., See MCCAULEY, E., 30:31406
OSBORNE, D.W., Heat capacity of α-sodium uranate (α-Na$_2$UO$_4$) from 5 to 350 K. Standard Gibbs energy of formation at 298.15 K, 30:29128
OSEENDA, M., Changes in glycogen localization and content and activity of enzymes metabolizing glycogen in rat brain during maturation under normal conditions and after gamma irradiation, 30:29761
OSIPOV, Y.I., New method for obtaining probe characteristics, 30:29167
OSIPOVA, G.V., See USENOVA, K.A., 30:29111
OSMEYER, W.E., See LIBERMAN, A.R., 30:29251
OSNES, E., See ENGELAND, T., 30:30946
  See KUO, T.T.S., 30:31091
OSSAKOW, S., See MCDONALD, B.E., 30:30427
OSSAKOW, S.L., See SCANNAPIECO, A.J., 30:30437
OST, R., See QUEBERT, J.L., 30:30996
OSTER, H., Medical evaluation of measured values following radiation exposure, 30:29703 (AED-CONF-74-221-007)
OSTERMANN, P., Nondestructive determination of boron in glasses using a ^{241}Am--Be neutron source, 30:28912 (AED-CONF-73-479-009)
OSTRIKER, J.P., See BODENHEIMER, P., 30:30197
  See THUAN, T.X., 30:30231
OTTAWAY, B., Irregularities in dendrochronological calibration, 30:29430
OTTAWAY, J.H., See OTTAWAY, B., 30:29430
OTTER, G., See GRAESSLER, H., 30:30610
OTTO, W.F., Integral capacitor lateral discharge laser, 30:29281
OTWINOWSKI, S., See DERRE, J., 30:30601
OVCHARENKO, V.I., See FILIPPOV, G.F., 30:31053
OVCHINNIKOVA, V.G., See LUCHNIK, N.V., 30:29696
OVSEPYAN, E.S., See KONOPLENKO, V.P., 30:29985
OWAIS, M., See SCOTT, A., 30:31003
OWEN, D.R., See BURKHARDT, H., 30:31085
OWENS, C.H., See KIM, C.H., 30:28965

OZAKI, H., See YOSHIDA, T., 30:29863
OZERNOI, A.N., See BONDAREVSKII, S.I., 30:29098

P

PACATI, F.D., See BOFFI, S., 30:30903
PACAUD, F., See IMBERT, J.C., 30:29133
PACE, E., See NUNBERG, P., 30:31039
PACER, J.C., Level densities of ^{63}Cu and ^{65}Cu from the analysis of evaporation spectra, 30:30950
PACHECO, J.A.deF., Origin of cosmic rays, 30:30169
PACILIO, N., See ZINGONI, E., 30:31273
PACYNA, J., See GLOWIAK, B., 30:29402
PACZYNSKI, B., URCA processes in convective stellar cores, 30:30200
PADEZHNOVA, E.M., See DRITS, M.E., 30:30007
PAECH, F., See DEMTROEDER, W., 30:30507
PAGANI, P., See GIGER, U., 30:29576
PAGE, D.E., See SANDERSON, T.R., 30:29533
PAGE, D.N., Disk-accretion onto a black hole. I. Time-averaged structure of accretion disk, 30:30187
PAIN, J., See CHAMINADE, R., 30:29593
PAIZIS, C., See CORTELLESSA, P., 30:30295
PAL, B.C., Mechanism of reduction of 1-methyl-4-thiocyanatouracil by bisulfide. A route to in vitro labeling of tRNAs with sulfur-35, 30:29092
PAL, B.K., Test of the SU_3 breaking in inclusive electroproduction of hadrons, 30:30772
PALCHEFSKY, J.W., See LONG, D.M., 30:29888
PALFFY, L., See POSSOZ, A., 30:30899
PALIOKHA, M.I., See GRINIK, E.U., 30:30072
PALMER, D.W., Coherent effects in large arrays of superconducting bridges, 30:30821
PALMER, J.E.M., Interaction of thermal and catalytic processes in the gasification of graphite in CO_2 mixtures, 30:29035 (TRG-Report-2434)
PALMER, P., See MORRIS, M., 30:30374
PAL'NIKOVA, T.I., See DOLGOREV, A.V., 30:28911
PALUMBO, F., Centre of mass coordinate in many-body theories, 30:30860
PALUMBO, G.G.C., See MANDOLESI, N., 30:30585
PAN, V.M., Superconductivity of Nb--Al--Zr alloys, 30:30048
PANASYUK, A.D., See SAMSONOV, G.V., 30:29898
PANEK, R.J., See SAVAGE, B.D., 30:30251
PANFILOV, G.G., See ERMOLAEV, O.Ya., 30:30844
PANGBORN, J.B., Nuclear energy requirements for hydrogen production from water, 30:31239
PANGRITZ, H., See KOLLBACH, D., 30:31338
PANIN, V.I., See USATYI, A.F., 30:29044
PANKE, R., Studies on the radiation protection properties of fenchlorfos and its role in the radioprotection mechanism, 30:29723
PANKRATOVA, V.S., See POPIL'SKII, R.Ya., 30:29910
PANSEVICH, V.V., See NEOKLADNOVA, L.N., 30:29063
PANTA, P.P., Measurements with aqueous oxalic acid, 30:29548 (DEMO-74/5)
  Measurements with the Swierk calorimeter, 30:29540 (DEMO-74/5)
PANTALEO, A., See BELLUSCIO, M., 30:29517
PAPADIMITRIOU, J., Value of /sup 99m/Tc-diphosphonate (HEDSPA) as a skeletal scanning agent, 30:29850
PAPADOPOULOS, G.D., See KNOWLES, S.H., 30:30286
PAPANICOLAOU, N., Weak LSZ limits and reduction formula for the non-relativistic Coulombic interaction, 30:31169
PARASKEVOPOULOS, D., See MESERVEY, R., 30:30839
PARDO, R.C., A study of nucleosynthesis during explosive carbon burning, 30:30257
PARISI, G., Detailed predictions for the p-n structure functions in theories with computable large moments behaviour, 30:30739
PARK, D., Phase relations in the magnetic field of the equatorial electrojet, 30:30467
PARKER, E.N., Hydraulic concentration of magnetic fields in the solar photosphere. II. Bernoulli effect, 30:30314
PARKER, J.L., See REILLY, T.D., 30:29509
PARKER, R., Design of a passive crack detector system, 30:29297 (UCID-15867)
PARKER, R.G., See JACKSON, K.L., 30:29737
PARKER, R.K., See GRANATSTEIN, V.L., 30:30580
PARKIN, D.M., Recoil energy distributions in CTR-related neutron spectra, 30:29203 (BNL-19043)
PARKINSON, W.C., The University of Michigan cyclotron facility for research in nuclear structure, 30:30158
  The University of Michigan neutron time-of-flight facility, 30:30159
PARKS, G.K., See LIN, C.S., 30:30439
PARR, H., Atomic energy. V, 30:29343
PASCHOPOULOS, I., See MENCHACA-ROCHA, A., 30:30904
PASHKOVSKII, M.V., See VOLZHENSKII, D.S., 30:29915
PASKEVICH, I.F., See FONARAR'OV, A.B., 30:29036
PASTERNACK, A.A., See EROKHINA, K.I., 30:31100
PASTERNAK, A., Field measurement of the permeability of NTS alluvium, 30:29315 (UCID-15727)
PASTORE, F., See EVANS, D., 30:30742
PASYNOK, A.I., Parametric instability of an electron beam in a magnetic field, 30:29200
PATE, B.D., See BLOK, H., 30:29525
PATTERSON, T.A., See HERBST, E., 30:30361
PATY, M., See BLIND, R., 30:30625
PAUL, E., See YAFFE, D., 30:30622
PAUL, S.O., See BRON, J., 30:29020
PAULI, E., See DERRE, J., 30:30601
PAULIN, A., Summing of harmonic frequencies by a resonant cable for pulse generation on a capacitive beam deflector, 30:30147
PAUWELS, E.K.J., Unexpected complication in the use of ^{169}Yb--DTPA with respect to hospital health physics, 30:29824
PAVICIC, S., Influence of radiation on the layers of tumors in the early formation of tumors, 30:29745
PAVLENKO, V.N., See BONDARENKO, V.I., 30:30415
PAVLOTSKAYA, F.I., State of ^{90}Sr, ^{137}Cs, and ^{144}Ce in radioactive fallout, 30:29384
PAVLOV, I.V., Methods of search of gamma-radiation point sources by two groups of detectors, 30:29580
PAVLOV, N.I., See ISSINSKII, I.B., 30:30129
PAVLOV, V.A., See NOSKOVA, N.I., 30:30030
PAZMINO, N.H., See YUHAS, J.M., 30:29756
PAZZI, R., See BERTANZA, L., 30:30606
PEACOCK, N.J., See FAWCETT, B.C., 30:30329
PEARLSTEIN, L.D., See BERK, H.L., 30:29224
PEDANOV, L.G., See GREBENKINA, V.G., 30:29893
PEDERSEN, A., See KELLEY, M.C., 30:30433
PEDERSEN, E.H., Electron-loss cross sections for fast, excited He atoms in H_2, 30:30539
PEEHS, M., See PLOEGER, M., 30:31294
PEIMBERT, M., See TORRES-PEIMBERT, S., 30:30351
PEKA, I., See WILHELMOVA, L., 30:29069
PEL, J., See MOOK, D.E., 30:30271
PELLETIER, C.A., See VOILLEQUE, P.G., 30:29423
PELOSI, V., Parametrization of low energy πN phase shifts, 30:30732
PELTIER, A.J., Mass anodization of tantalum-nitride resistors, 30:31387 (BDX-613-1155(Rev.))
PENCE, D.T., See STAPLES, B.A., 30:30108
PENDYALA, S., Diffusion of slow positrons from gold, 30:30511
PENNER, S., See KLINE, F.J., 30:30878
PENSTON, M.V., See GATLEY, I., 30:30356
PENZES, L.E., Theory of pump-induced pulsating coolant pressure in pressurized water reactors, 30:31203
PEPPER, R.B., Experience in complying with authorisation conditions for the discharge of liquid and gaseous radioactive effluents from CEGB nuclear stations, 30:31204 (AED-CONF-74-157-007)
PERCIVAL, D.R., Sequential determination of radium-226, radium-228, actinium-227, and thorium isotopes in environmental and process waste samples, 30:28978
PEREKRESNYI, S.M., See KARETNIKOV, V.G., 30:30210
PERELSTEIN, E.A., See BARABOSCH, L.S., 30:30117
PERKEY, L.M., Trapped electrons in C_2H_5OD glasses γ-irradiated at 4°K, 30:29068
PERKINS, D.H., Experimental aspects of neutrino interactions, 30:30594
PERKINS, R.W., Quillayute air reference station, 30:29359 (BNWL-1850(Pt.3))
  See JENKINS, C.E., 30:29362
PERLOVICH, Yu.A., See KAVERINA, S.N., 30:30057
PERMYAKOV, V.P., See KALINKIN, B.N., 30:29205
PERNG, C.C., ^{40}Ca(n,α)^{37}Ar reaction at 14.1 MeV, 30:30927
PERREAU, J.M., See BAILLON, P., 30:30619
  See BAILLON, P., 30:30618
  See BAILLON, P., 30:30737
PERRING, J.K., See HAWTIN, P., 30:31211
PERRONE, R.E., See MARTINI, W.R., 30:29260
PERSICHELLI, G., See DI NAPOLI, V., 30:30919
PERSICKE, H., See WIEMER, H., 30:31383
PERVUSHIN, V.N., High-energy scattering of vector particles by external electromagnetic field, 30:30649 (JINR-P2-7511)
PETER, H., See ROEDEL, W., 30:29575
PETER, J., See BLOK, H., 30:29525
  See HANAPPE, F., 30:30984
PETERS, V.G., See SAUNDERS, J.E., 30:31108
PETERSEN, J.F., See PARKINSON, W.C., 30:30158
  See PARKINSON, W.C., 30:30159
PETERSEN, M.R., See PERKINS, R.W., 30:29359
  See YOUNG, J.A., 30:29473
PETERSON, B.A., Identification of southern quasi-stellar objects. IV, 30:30276
PETERSON, C.J., Distribution of orbital eccentricities of the globular clusters, 30:30353
PETERSON, L.E., See HARRINGTON, T.M., 30:29566
  See ULMER, M.P., 30:30268
PETERSON, V.Z., See DOBSON, P.N. Jr., 30:30577
PETERSTROEM, S., Semiconductor counters for nuclear radiations produced by ion implantation, 30:29531
PETRENKO, N.S., Anomaly of thermal expansion of dysprosium close to the ferromagnetic transition point, 30:30032
PETRI, H.R., Polarization decay of an ethylene glycol polarized proton target in an intense proton beam, 30:30155
PETROCK, K.F., See SHAPIRO, E.G., 30:29552
PETROFF, Y., See AMER, N., 30:31425
PETRONOVIC, D., See TRGOVCEVIC, Z., 30:29678
PETROPAVLOV, N.V., See USTINOV, V.I., 30:29013
PETROV, V.N., Formation of secondary aerosols in the atmosphere after ventilated underground nuclear explosions, 30:29390
PETROVICH, F., See SCOTT, A., 30:31003

PETRUSEVICH, I.V., Joint reduction of niobium, aluminum, and germanium chlorides by hydrogen, 30:29971
PETRZHAK, G.I., See GRINBERG, A.A., 30:29108
PFEIFER, H.P., See FREYLAND, W., 30:30005
PHELPS, P.L., Resuspension element status report, 30:29450 (NVO-AEIC-74-1)
  See ANSPAUGH, L.R., 30:29452
PHILIPS, E.C., See CHI, J.W.H., 30:29255
PHILLIPS, G.C., See MILJANIC, D., 30:30882
PIACENTINI, R.D., Carbon K-shell x-ray production by neon ion impact, 30:30555
PIARD, A., See FLATO, M., 30:30680
PIAZZOLI, A., See GOGGI, G., 30:30874
PICHLER, L., Autoradiographic studies of DNA-repair in the retina of rabbits, 30:29755
PICHLMAYER, F., See DOBROZEMSKY, R., 30:30977
PIERCE, D.A., See KONINGS, A.W.T., 30:29739
PIERRE, J., See MORIN, P., 30:29990
PIESCH, E., In-vivo measurement of the gamma and neutron dose rate on patients with ^{238}Pu pacemakers implanted, 30:29704 (KFK-1851)
  Latent fading in solid-state track etching detectors, 30:29522
PIETRZAK-FLIS, J., Distribution of radioactive and stable cesium in the human body, 30:29789
PIGATTO, L., See SPROTT, G.F., 30:30260
PIGEON, J., See MEYER, J., 30:31036
PIKUNOV, M.V., See CHUPYATOVA, L.P., 30:30010
PILT, A.A., See MENCHACA-ROCHA, A., 30:30904
PININSKA, J., Barites from Boguszow as aggregate for anti-radiation concrete shields, 30:31128
PINSKY, S.M., See THRALL, J.H., 30:29849
PINTER, S., See KRIVSKY, L., 30:30297
PINTSCHOVIUS, L., See RENKER, K., 30:31365
PIPKIN, F.M., See BEBEK, C.J., 30:30587
PIRAGINO, G., See BALESTRA, F., 30:29591
PIRK, H., Apparatus for obtaining water-free uranium compounds from suspensions, 30:29126
PISARENKO, V.A., See ARKHAROV, V.I., 30:30023
PISKUNOV, L.I., Relation between washout of radioactivity and nonradioactive ions in the atmosphere by precipitation, 30:29395
PISTUNOVICH, V.I., See KARTASHEV, K.B., 30:29155
PITTS, J.H., Diffusion of radioactive fluid through soil surrounding a large power-reactor station after a core meltdown accident, 30:31254 (UCRL-51494)
PLACAK, O.R., See CARTER, M.W., 30:29345
PLANIOL, T., See ITTI, R., 30:29830
PLANTAMURA, V.L., See ABBATTISTA, N., 30:29631
PLATONOV, P.A., Investigation into radiation defects in irradiated pyrographite, 30:30090 (IAE-2266)
PLATONOV, V.V., See KARTASHEV, K.B., 30:29155
PLATOV, Yu.M., See PLETNEV, M.N., 30:30081
PLCH, J., See ZIDEK, V., 30:29529
PLENDL, H.S., See MUGA, L., 30:29528
PLESS, I.A., See BASTIEN, D.B., 30:30600
  See BERLAD, G., 30:30623
PLETNEV, M.N., Kinetics of accumulation of radiation defects in metals at temperatures of stage II of recovery with consideration of transition processes, 30:30081
PLITZ, W., See FRANK, G., 30:29258
PLOEGER, F., See PIRK, H., 30:29126
PLOEGER, M., Hydrogen diffusion seal for nuclear reactor fuel rods, 30:31294
PLOTKIN, E.E., Explosive and high-frequency instability of electromagnetic waves in a two electron stream system, 30:29202
PLUCHENNIK, G., Comparative investigation of mutagenic effects of incorporated isotopes of the most important organogenic elements. VI. Comparison of lethal and mutagenic effects of the decay of ^{32}P and ^{35}S incorporated into cells of Escherichia coli WP-2S Try$^-$, 30:29788
PODCHAINOVA, V.N., See DOLGOREV, A.V., 30:28911
PODSTRIGACH, T.S., See NESMYANOVICH, A.T., 30:30309
POKORNA, I., See TEXTORIS, R., 30:29793
POKORSKI, S., See BIALAS, A., 30:30699
POKROVSKII, A.V., Multichannel processing of digital radiometric data in sequential recording of a finite numer of counts, 30:29299
POLACCO, E., See BAILEY, J., 30:30620
POLAK, L.S., Simulation and methods for calculating physical-chemical processes in low-temperature plasmas, 30:29175
POLICARPO, A.J.P.L., See ALVES, M.A.F., 30:29523
POLICHAR, R.M., See PARKINSON, W.C., 30:30159
POLIKARPOV, G.G., Chemoradioecology of the pelagic zone and the benthos (metals and radionuclides in the hydrobiont and environment), 30:29422
POLITZER, H.D., Scaling behaviour in a class of massive non-Abelian gauge theories, 30:30771
POLK, D.H., See HAUGHT, A.F., 30:29152
POLLAROLO, G., See BRUGLIA, R.A., 30:30991
POLOMESHKIN, V.N., Contribution of hadrons to vacuum polarization, 30:30667
POLOTSKII, I.G., See KOVSH, S.V., 30:30028
POLOZOV, A.D., See SITENKO, A.G., 30:31072
POLYAKOV, V.I., Gamma-ray attenuation in applied scintillation spectrometry, 30:29562
POLYAKOVA, G.N., Population of the rotational and vibrational levels of excited electronic states of nitrogen molecules produced in collisions of electrons with N_2 molecules, 30:30545
POMERANTZ, M.A., Sun and cosmic rays, 30:30327
POMORSKI, L., Application of nuclear physics methods for the determination of the depth of lithium ions penetration in the glasses with crystallized surface, 30:28980
PONIECKI, A., Tissue clearance of ^{131}I from lower-limb blood vessels in diabetics, 30:29857
PONPON, J.P., Preliminary results on mercuric iodide nuclear radiation detectors, 30:29534
PONTO, R.A., See LOKEN, M.K., 30:29847
PONZANO, G., See D'ADDA, A., 30:30769
POPA, N.C., Resolution function for the rotating-crystal spectrometer, 30:29558 (IFA-FN-44-1974)
  The resolution function for the rotating-crystal spectrometer, 30:29572
POPESCU, D., See BUCURESCU, D., 30:30943
  See IVASCU, M., 30:30941
POPESCU-POGRION, N., The structure of vacuum-evaporated UO_2 thin films, 30:29928
  See BIRJEGA, M.I., 30:29927
POPIL'SKII, R.Ya., Synthesis, sintering, and microstructure of the solid solutions CaO--La_2O_3, 30:29910
POPMA, J.A., Magnetization and Moessbauer spectra of non-crystalline $Y_3Fe_5O_{12}$, 30:29901
POPOV, V.P., Calorimetric determination of the heat resistance of ring-shaped samples of brittle electric conductors, 30:29900
  See PETRENKO, N.S., 30:30032
POPOVA, L.I., See KOVAL, A.G., 30:30544
PORCH, W.M., Fast response light scattering measurements of the characteristics of wind suspended aerosols, 30:29490 (UCRL-76014(Rev.1))
PORILE, N.T., See PACER, J.C., 30:30950
PORTER, G.D., See CHRISTOFILOS, N.C., 30:29187
  See CHRISTOFILOS, N.C., 30:29188
PORTNOI, K.I., Dispersion-hardened materials, 30:29998
PORTNOVA, T.S., See POYZNER, B.N., 30:29287
POSSOZ, A., Measurement of the average polarization of ^{12}B produced by polarized muons in the μ^- + ^{12}C + νsub(μ) + ^{12}B reaction, 30:30899
POSTMA, H., Nuclear orientation: from an exotic to a matured method in nuclear physics, 30:30962
POTAPOV, L.P., See EDNERAL, A.F., 30:30037
POTAPOV, N.N., See GORBUNOV, V.I., 30:30034
POTCHEN, E.J., Biologic considerations in anatomic imaging with radionuclides. Progress report, July 1973--June 1974, 30:29832 (COO-2427-4)
POTTER, J.H., Effects of siting and load variation for a 650 MW nuclear station with air condensers, 30:31186
POTTER, J.M., Measurement of parity violation in proton--proton scattering at 15 MeV, 30:30599 (LA-UR-74-1333)
POTTS, G., See ROSE, K.S.B., 30:29931
POUCHARD, M., See BAYARD, M., 30:29902
POUCHER, J.S., See RIORDAN, E.M., 30:30583
POUCHOT, W.D., Nuclear artificial heart bench model, 30:29259
POWELL, D.C., Dependence of site evaluation of roughness length and displacement length on value chosen for Von Karman's constant, 30:29432 (BNWL-1850(Pt.3))
  Method for determining Monin--Obukhov L's from profiles of subjectively estimated mean wind speeds and temperatures, 30:29431 (BNWL-1850(Pt.3))
  Power spectral analysis of two periods of turbulence data for very stable conditions, 30:29433 (BNWL-1850(Pt.3))
  See ELDERKIN, C.E., 30:29434
POWELL, J., Large scale applications of superconductivity, 30:30824
POWELL, R.E., See FENNER, N.C., 30:29625
POWELL, R.L., Programs on large scale applications of superconductivity in the United States, 30:30838
POWELL, W.M., See CLARK, A.F., 30:30576
POYZNER, B.N., Natural width of the spectrum of two-frequency gaseous laser modes in autonomous regime and synchronized by a light signal, 30:29287
POZNYAK, A.L., See NEOKLADNOVA, L.N., 30:29063
POZNYAK, G.I., Use of ethyl alcohol and acetic acid to prepare samples of sodium coolant for radiochemical analysis, 30:28983
PRAKASH, O.M., Superconductors, 30:30816
PRAKASH, Y., See GURTU, A., 30:30604
PRASAD, S.S., Is there a real need for doubling the solar EUV fluxes, 30:30310
PRASAD, V.B., See DELBOURGO, R., 30:30687
PRAVDA, M.F., See SNYDER, D.L., 30:29240
PREPARATA, G., Physics of the light cone, 30:30643
  See GATTO, R., 30:30668
PREPEJCHAL, W., See ROMBERG, G.P., 30:29462
PREROVSKY, I., See ROZTOCIL, K., 30:29794
PRESTON, K.F., See COLUSSI, A.J., 30:29067
PRICE, G.H., Electromagnetic pulse from nuclear detonations, 30:30448
PRICE, H.G., 4.510 MeV level in ^{27}Al, 30:30910
PRICE, P.B., See CHAN, J.H., 30:30394

PRICE, R.H., Energy recovery of a lithium ion beam, 30:29221 (UCID-15939)
PRINCE, R.H., See MCCULLOUGH, J.D., 30:30376
PROCTOR, J.D., See YUHAS, J.M., 30:29756
PROELSS, G.W., Esro 4 gas analyzer results. II. Direct measurements of changes in the neutral composition during an ionospheric storm, 30:30424
PROETEL, D., Decoupled bands in odd-mass mercury isotopes, 30:31006
PROKHOROVA, D.N., See CHUPYATOVA, L.P., 30:30033
PROKOF'EV, E.P., See LEVIN, D.Z., 30:29011
PROKOP, E.K., Detection and localization of an occult vesicoenteric fistula, 30:29848
PROKOPCHUK, L.F., See VOLZHENSKII, D.S., 30:29915
PROKOPENKO, G.I., See KOTKO, V.A., 30:30039
  See KOVSH, S.V., 30:30028
PROKSCH, E., Measurements by fluorocarbon dosimetry, 30:29544 (DEMO-74/5)
PRONASZKO, A., See OSEENDA, M., 30:29761
PROSPERI, D., See NUNBERG, P., 30:31039
PROTOPOPOVA, E.M., See KAZNADZEI, V.V., 30:29697
PRUDNIKOV, I.A., See ANGELOV, B.P., 30:30143
PRUNIER, J., Study of the detection of nuclear particles in liquid dielectrics, 30:29492 (CEA-R-4543)
PTAK, R., See STONER, R.E., 30:30266
PUEHLHOFER, F., See KOHLMEYER, B., 30:30906
PUGET, J.L., The distribution of cosmic rays in the galaxy and their dynamics as deduced from recent γ-ray observations, 30:30163
PULHAM, R.J., See HUBBERSTEY, P., 30:30049
PUPHAL, K.W., See SILL, C.W., 30:28977
PUSHKAREV, V.I., See ZHIRNOV, A.D., 30:31205
PUT, L.W., See HESSELINK, W.H.A., 30:30975
PUTILOVA, I.N, See AKULOVA, I.S., 30:29041
PYATIGORSKII, G.A., See KULIKOV, V.N., 30:29501
PYLE, G.J., See CLOUGH, A.S., 30:30891
PYL'NIKOV, V.I., See TSVILYUK, I.S., 30:30027
PYUN, H.C., Studies on the preparation of mortar--plastic composite, 30:29045

Q

QUAGLIA, L., See WEBER, G., 30:31122
QUANDT, U., High sensitivity photoneutron detector for 'non-destructive' submicroanalysis of beryllium, 30:29524
QUASSIATI, B., See BERTANZA, L., 30:30606
QUEBERT, J.L., Reactions produced by ^{7}Li on ^{197}Au, 30:30996
QUICK, M.V., See HOUGH, W.R., 30:31214
QURESHI, M., Synthesis of reproducible tin(IV) based ion exchangers: separation of lanthanum(III) from yttrium(III), europium(III), and lutetium(III), 30:28994

R

RAAEN, V.F., Do SN2 reactions go through ion pairs. The isotope effect criterion, 30:29010
RAAG, V., High voltage miniature radioisotope thermoelectric generators, 30:29263
RABALAIS, J.W., Calculated photoionization cross sections and relative experimental photoionization intensities for a selection of small molecules, 30:30491
RABEN, M.S., See TSUSHIMA, T., 30:29868
RABITZ, H., See ENGLOI, G., 30:30562
RACINE, R., VB 130: A nebulous cluster with an abnormal extinction law, 30:30363
RADEWAN, C.H., Digital image processing with pseudo-color, 30:31356 (UCRL-75662)
RADOLA, B.J., See DELINCEE, H., 30:29651
RADWAN, I., See JAWOROWSKI, Z., 30:29818
RAETSKY, V.M., Changes in electrical resistance, length, Seebeck coefficient and Hall emf of alpha-plutonium under neutron irradiation in liquid nitrogen and isochronal annealing, 30:30078
RAGOTSKAYA, E.A., See TORGOISKAYA, T.I., 30:29124
RAGUSA, S., Relativistic correction in double scattering by deuterons, 30:30720
RAHMAN, N.K., Effect of intense electromagnetic wave in charged-particle scattering, 30:30655
RAI, M.S., See ABRAHAM, M., 30:28975
RAISZ, L.G., See HORTON, J.E., 30:29667
RAJCA, A., See MINOR, W., 30:29574
RAJU, M.R., Negative pions in radiotherapy. A brief review, 30:31116
RAKITSKII, A.N., Effect of carbide-forming elements on the properties of chromium and its alloys with rare earths, 30:30058
  See BUTYLENKO, A.K., 30:30054
RAKOVSKII, V.S., Powder metallurgy of heat-resistant alloys and refractory metals, 30:29963
RALEIGH, J.A., See GREENSTOCK, C.L., 30:29003
RAM, J., See YATIRAJAM, V., 30:28964
RAMACHANDRA RAO, B., See HANUMATHSASTRI, J., 30:30420
RAMAN, S., Elastic scattering of ^{12}C by ^{12}C, 30:30879
RAMANA, K.V.V., See MADHUSUDHANARAO, D.N., 30:30419
RAMAVATARAM, K., See RAMAVATARAM, S., 30:30871
RAMAVATARAM, S., A microscopic description of the negative parity resonances in the mass-4 system by the coupled-channel method, 30:30871
RAMAYYA, A.V., See HAMILTON, J.H., 30:30987
RAMAZANOV, L.M., Depolymerization of colloidal neptunium in nitric acid solutions, 30:29107
  See SOKHINA, L.P., 30:29116
RAMIREZ-DEGOLLADO, J., See GORDON, F., 30:29852
RAMPAN, Yu.I., Changes in oxygenation and radiosensitivity of the tumor after irradiation, 30:29763
RAMZAEV, P.V., See TROITSKAYA, M.N., 30:29405
RANCITELLI, L.A., Elemental content of trace elements in vegetation collected at Centralia, Washington, 30:29483 (BNWL-1850(Pt.3))
  Trace pollutant emissions in fossil fuel combustion, 30:29469 (BNWL-1850(Pt.3))
  See CRESSY, P.J. Jr., 30:30170
RANDERSON, D., Numerical prediction of the mesoscale transport of atmospheric effluents: philosophy and morphology of experimental models for predicting the wind and potential radiological fields over the Nevada Test Site, 30:29377 (COM-74-10799)
RANDOLPH, W.L., See ROGERS, D.W.O., 30:30894
  See ROGERS, D.W.O., 30:30895
RAO, B.Y.K., Preservation of enzyme inactivated lamb slices: effects of freeze desiccation and low dose irradiation, 30:29642 (AD-777550)
RAO, C.L., See RAMAVATARAM, S., 30:30871
RAO, N.K., See GURTU, A., 30:30604
RAO, V., See AGRAWAL, Y.K., 30:28962
RAPLEY, C.G., X-ray observations of the large magellanic cloud by the Copernicus satellite, 30:30365
RAPP, D., See STORM, D., 30:30542
RAPP, F., See ALBRECHT, T., 30:29677
RAPP, P., See KIM, I.J., 30:30584
RASPOPIN, S.P., See DESYATNIK, V.N., 30:29095
RATNER, M., See JOERGENSEN, P., 30:30568
RAUB, C.J., See KHAN, H.R., 30:30810
RAWSON, D.E., See KORVER, J.A., 30:29317
RAYMOND, L., See DULL, D.L., 30:29942
RAYNAL, J., Hyperspherical expansion approach for nuclear reactions, 30:31051
READ, F.H., See CVEJANOVIC, S., 30:30553
READING, J.F., High-energy calculation of K-shell ejection cross sections as a function of projectile charge, 30:30536
REBBI, C., See FUBINI, S., 30:30705
REBEL, H., Generalized collective model and α-particle scattering on ^{56}Fe and ^{48}Ti, 30:30945
REBER, C.A., Heating of the high-latitude thermosphere during magnetically quiet periods, 30:30459
RECHENBERG, H.R., Semiclassical model of multiparticle production, 30:30693
RECK, G.P., See TANG, S.Y., 30:30548
REDDI, O.S., Follicular damage to bovine ovary from radioiodine, 30:29786
REDDY, D.R.K., See MAHANTA, M.N., 30:31176
REDMAN, R.O., See HUTCHINGS, J.B., 30:30230
REED, E.I., Observations of the conjugate SAR arcs of September 28-30, 1967, 30:30423
REED, J.W., Archiving guide to microbarograph records of nuclear and chemical explosion tests, 30:29314 (SLA-74-0210)
REEVES, H., Nucleosynthesis of the light elements and the interstellar medium, 30:31019 (CONF-730693-)
REFFO, G., LARA: a FORTRAN IV code for the calculation of the compound nucleus contribution to the total radiative width in medium and heavy nuclei based on the Brink--Axel model, 30:30956 (RT/FI-(74)17)
REGAN, J.D., DNA repair in human progeroid cells, 30:29673
REGGE, T., See BROGLIA, R.A., 30:30991
REICHELT, W., See BACAL, M., 30:30128
REICHMAN, J.M., Saltation and creep sampler, 30:29616 (NVO-AEIC-74-1)
REID, A.W., Models for the pomeron and low energy $K^{+}p$ scattering, 30:30746
REID, B.O., See WITHERS, H.R., 30:29758
REILLY, T.D., Continuous in-line monitor for UF_6 enrichment, 30:29509
REINES, F., Test of the Pauli exclusion principle for atomic electrons, 30:30499
REINISCH, B.W., See BIBL, K., 30:30410
RENFRO, A.R., See SCHELL, E.M., 30:29335
RENKER, K., Temperature dependence of the lattice distortion in the one-dimensional conductor $K_2Pt[CN]_4Br_3$ x $3D_2O$, 30:31365 (AED-CONF-74-089-024)
REPALOV, N.S., See PASYNOK, A.I., 30:29200
REPPEL, G.W., Proximity effect on thin NbN-layers, 30:30805 (AED-CONF-74-089-005)
RESNIK, V.R., See KASSIROV, S.A., 30:29526
REST, J., Is chiral SU_2 x SU_2 a hidden symmetry, 30:30774
RETHERFORD, J.C., See BROOKS, A.L., 30:29783
REUVERS, A.P., See GREENSTOCK, C.L., 30:29003
REVZEN, M., Velocity of fourth sound, 30:30804
REXER, G., Investigations on the shielding of power reactors, 30:31271 (IKE-6-75d)
REYES, C.H., See D'ATTELLIS, C.E., 30:31303
REYNOLDS, C.L. Jr., Compression and anharmonicity of rare-earth metals, 30:30046
REYNOLDS, G.T., Piezoelectric mechanical-micropipette stimulator. Technical report No. 10, 30:31378 (NYO-3406-18)

REYNOLDS, P.H., See STUKAS, V., 30:29338

RHOADS, W.A., Analysis of vegetation cover in certain Pu-contaminated areas using aerial photography, 30:29446 (NVO-AEIC-74-1)

RHOTEN, M.L., See GRUBER, H.T., 30:29294

RIAZUDDIN, See FAYYAZUDDIN, 30:30595

See FAYYAZUDDIN, 30:30660

RIBANSKY, I., See OBLOZINSKY, P., 30:31093

RIBE, F.L., See KRAKOWSKI, R.A., 30:29206

RICE, J.K., Instrumental limitation to the rate of kinetic processes measurable by time-resolved mass spectrometry, 30:31368 (SLA-73-7063)

RICH, A., See BROWN, D.N., 30:30218

RICHARDS, H.L., See LORE, J.D., 30:31413

RICHMOND, C.R., Human experience, 30:29772 (LA-UR-74-1300)

RICHTER, A., See HOFFMANN, D., 30:30148

RICHTER, C., See FRANK, G., 30:29256

RIDDLE, R.A.J., See CLOUGH, A.S., 30:30891

RIDGWAY, S.T., Diameter of μ Geminorum M3 III from lunar occultation, 30:30225

RIECK, G.D., See HEIJWEGEN, C.P., 30:30001

RIEDINGER, L.L., Decoupled rotational bands in ^{163} ^{165}Yb, 30:30985

RIEDL, H., See RUBINSZTEIN, H., 30:30972

RIEGERT, R.J., Quantization and the source of the gravitational field, 30:31173

RIEKELES, J., See PARR, H., 30:29343

RIESTER, J.L., See BLIND, R., 30:30625

RIEU, G.E., Internal friction measurement in high purity tungsten single crystal, 30:29979 (N-74-19370)

Internal friction peaks observed in explosively deformed polycrystalline Mo, Nb, and Cu, 30:29980 (N-74-19371)

RIEWE, F., See GREEN, A.E.S., 30:31048

RILEY, M.E., Comment on the semiclassical scattering of rigid spheres, 30:30530

RINAUDO, G., See BERTANZA, L., 30:30606

RINDE, J.A., Chemical compositions of various plastic materials, 30:31404 (UCID-15815)

Tensile and compression test methods for rigid plastic foams, 30:31403 (UCID-15739)

RIORDAN, E.M., Extraction of R=sigma/subL//sigma/subT/ from deep inelastic e-p and e-d cross sections, 30:30583

RIPLEY, D., See SHAFER, R.B., 30:29856

RIPPON, S., Not such a bad reactor, 30:31215

RISKA, D.O., See JACKSON, A.D., 30:30870

RIZZUTO, C., Programs on large scale applications of superconductivity in Italy, 30:30835

ROBERTS, J.W., See FENNER, N.C., 30:29625

ROBERTS, K.V., Thermonuclear fusion power, 30:29232

See CHRISTIANSEN, J.P., 30:29227

ROBERTS, L., See TAYLOR, G.N., 30:29796

ROBERTSON, D.C., See RECHENBERG, H.R., 30:30693

ROBERTSON, J.T., See BRUNSON, B., 30:29837

ROBERTSON, R.D., CAIN system field test, 30:31446 (UCID-15816)

ROBERTSON, T.V., Geometric solution of finite x-ray source irradiating two concentric cylinders containing x-ray absorbing material, 30:31123 (UCID-15938)

ROBINSON, A.L., Niobium--germanium: becoming a practical , superconductor, 30:30806

ROBINSON, C.C., See SHAW, R.R., 30:29280

ROBINSON, D.K., See DADO, S., 30:30621

ROBINSON, J.E., Radiation and hyperthermal response of normal tissue in situ, 30:29743

ROBINSON, J.M., See BRANFORD, D., 30:30887

ROBINSON, R.L., Proceedings of the international conference on reactions between complex nuclei, Nashville, Tennessee, June 10--14, 1974. Volume 1 and Supplement, 30:30982

See FORD, J.L.C. Jr., 30:30911

See RIEDINGER, L.L., 30:30985

ROBSON, J., Process for the production of technetium-99m from neutron irradiated molybdenum trioxide, 30:29139

ROCHLOV, I.M., See BARABOSCH, L.S., 30:30117

RODGERS, A.W., The composition of RR Lyrae stars, 30:30191

RODLOFF, R., See NEUHAEUSER, H., 30:30068

RODRIGUES, W.A. Jr., Pion inclusive distribution at cosmic-ray energies and comparison witn ISR data, 30:30171

ROE, D.B., Ultrasonic dispersion and attenuation near the liquid--gas critical point of ^{4}He, 30:30798

ROEDEL, W., A large plastic scintillator as anticoincidence shield for beta-radiation detectors, 30:29575

ROELANDSTS, I., See BRUNFELT, A.O., 30:28935

ROELOF, E.C., Comment on ''Propagation anisotropies of solar flare protons and electrons at low energies in interplanetary space'' by R. K. Pyle, 30:30312

ROERBO, K., See CHRISTENSEN, J., 30:29969

ROFFMAN, S., Microassay for proteolytic enzymes using a new radioactive anilide substrate, 30:29834

ROGERS, A.M., Polaroid vectograph process and application as applied to stereo laser and computer-generated 3-dimensional forms, 30:31352 (UCID-15840)

ROGERS, B., See HSIEH, E.J., 30:31454

ROGERS, D.W.O., Lifetime measurements in ^{17}N using tne recoil-distance technique, 30:30894

The electromagnetic decay of ^{17}N, 30:30895

ROGERS A.W., Technique of autoradiography. Second revised and enlarged edition, 30:29298

ROGOFF, E.E., See HUVOS, A.G., 30:29784

ROGSTAD, D.H., See MADORE, B.F., 30:30348

ROIFE, I.M., See DUBOVOI, L.V., 30:30121

ROLOFF, H., See GRAESSLER, H., 30:30610

ROMAIN, J.F., See RIEU, G.E., 30:29980

ROMANOV, A.S., See RYABININ, A.I., 30:28998

ROMANOV, N.N., Peculiarities of the upper cloud layer and suggestions for using radioactive tracer techniques in studying meridional currents, 30:29428

ROMBERG, G.P., Migratory behavior of fish tagged at a nuclear power plant discharge into Lake Michigan, 30:29462 (CONF-740813-2)

ROMERO, J.L., See MORALES, J.R., 30:30157

ROMICK, G.J., Interrelationship between the > 130 keV electron trapping boundary, the VHF radar backscatter, and the visual aurora, 30:30430

ROMNEY, E.M., Some ecological attributes and plutonium contents of perennial vegetation in Area 13 (NAEG vegetation studies), 30:29445 (NVO-AEIC-74-1)

RONA, V., Variance in the evaluation of data obtained in radioisotopic tracer investigations, 30:29646

RONCHI, C., See BOGENSBERGER, H.G., 30:31225

ROOK, L.W. Jr., See SWAIN, A.D., 30:31360

ROOS, P.G., See BHOWMIK, R.K., 30:30896

See CHENG, V.K.C., 30:30872

ROSA, L.P., See RAGUSA, S., 30:30720

ROSA, R.J., See WILLIAMS, J.R., 30:31209

ROSATI, S., Calculations on few-nucleon systems with correlated wave functions, 30:31043

ROSE, K.S.B., A technique for measuring the density of small fragments of high-density materials botn before and after irradiation, 30:29931

ROSE, R.L., Plutonium foundry practices at the Lawrence Livermore Laboratory, 30:29958 (UCID-15926)

ROSE-HANSEN, J., See GWOZDZ, R., 30:28943

ROSEN, A., See RUBINSZTEIN, H., 30:30972

ROSENBAUM, H.D., See DAMRON, J.R., 30:29845

ROSENBAUM, R.L., Temperature, pressure, and concentration dependence of the thermal conductivity of very dilute solutions of ^{3}He in superfluid ^{4}He, 30:30800

ROSENBLUTH, M.N., See LEE, C.E., 30:30565

ROSIEK, O., See SZUNIEL, I., 30:29669

ROSINA, M., Direct variational calculation of the two-body density matrix, 30:30631

ROSINO, L., See SPROTT, G.F., 30:30260

ROSINSKI, J., Effects of radioactivity on ice nucleation, 30:29367 (BNWL-1850(Pt.3))

ROSMAN, K.J.R., See DE LAETER, J.R., 30:30311

ROSS, D.A., See ELIEZER, S., 30:30684

ROSS, G.G., See POLITZER, H.D., 30:30771

ROST, M., See GRAESSLER, H., 30:30610

ROSTEN, H.I., Method for the calculation of the magnetostatic field from a wide class of current geometries, 30:29211 (RL-74-077)

ROSYANOV, S.P., See GEDEONOV, L.I., 30:29404

ROTELLI, P., See COCHO, G., 30:30665

ROTH, B.G., See HARRIS, D.O., 30:29296

ROTH, H., See CHRISTIANSSON, J.E., 30:30901

ROTHE, E.W., See TANG, S.Y., 30:30548

ROTHE, H.J., See GROMES, D., 30:31159

ROTHENBERG, A., See DONALDSON, G., 30:30582

ROTHHAAS, H., Model independent evaluation of the inelastic e^- scattering cross sections from the 3^- (2.615 MeV) level in ^{208}Pb, 30:31005

ROTHSTEIN, R.J., See KIRKWOOD, W.F., 30:31405

ROUKLOVE, P., Performance testing of thermoelectric generators at JPL, 30:29248

ROUSEK, J., Resistance to Ustilago myadis of WD lineage progeny after chronic gamma irradiation, 30:29688

ROUTMA, J.P.W., Trace element behavior in soil of some Indonesian sawah's and in sludge of an Indonesian river, 30:28930

ROWE, J.F. Jr., Ion layer formation by uniform neutral winds in the nignttime E region, 30:30436

ROWE, R.D., See CLARE, P.M., 30:29309

ROWLANDS, D.T. Jr., See SHERWIN, W.K., 30:29750

ROWLEY, M.J., Effect of graded doses of ionizing radiation on the human testis, 30:29708

ROXBURGH, I.W., On the nature of the asymptotically adiabatic solution of the two-fluid solar wind, 30:30298

ROYCE, E.B., Low pressure phase transition in NaCl, 30:31399 (UCID-15454)

ROZEN, A.M., Reaction of di-2-ethylhexylphosphoric acid and its uranyl salt with diluents. V. Solutions of $(HR)_2$ and $UO_2(HR_2)_2$ in chloroform, 30:29101

Reaction of di-2-ethylhexylphosphoric acid and its uranyl salt with diluents. IV. Solutions of $(HR)_2$ and $UO_2(HR_2)_2$ in carbon tetrachloride, 30:29100

ROZHDESTVENSKAYA, L.N., See POZNYAK, G.I., 30:28983

ROZSA, R.B., Laminar gas flow through loosely packed Overton sand, 30:29319 (UCID-15818)

Numerical simulation of air-injection experiments in NTS alluvium, 30:29324 (UCID-15981)

ROZTOCIL, K., Tissue-blood ^{131}I and ^{133}Xe transfer in the presence of raised capillary filtration, 30:29794
ROZUMENKO, V.T., See MISYURA, V.A., 30:30447
RUBIN, V.C., Two chains of interesting southern galaxies: NGC 7172-7173-7174-7176 and NGC 7201-7203-7204, 30:30384
RUBINSON, M., Entropy analysis of product energy distributions in nonreactive inelastic collisions, 30:30561
RUBINSZTEIN, H., Atomic-beam measurements on refractory elements. . Nuclear spin measurements of ^{99}Mo and sup(99m)Tc, 30:30972
RUBLEVSKII, V.P., See ZYKOVA, A.S., 30:29399
RUD, V.M., See SAMSONOV, G.V., 30:29912
RUDERMAN, M.A., See CHEN, H., 30:30194
RUDNEV, I.I., See BUDAGOVSKII, S.S., 30:30029
RUDNICK, J., See REVZEN, M., 30:30804
RUDNICKI, M.I., See MOISE, J.C., 30:29261
RUEDORFF, W., See FLECKENSTEIN, J., 30:29006
RUEHLE, G., See SCHMIDT-BOECKING, H., 30:30948
RUFER, R.P., Measurement system for the peak time and amplitude of a pulse, 30:31458 (UCID-16108)
RUFFINI, R., See DENARDO, G., 30:30214
RUGGLES, A.E., See HAGEN, K.G., 30:29262
RUMYANTSEV, V.V., See ANGELOV, B.P., 30:30143
RUNIN, V.I., See ZHIR[illegible]OV, A.D., 30:31205
RUPPERSBERG, H., Short-range order in liquid lithium-lead alloys, 30:31382 (AED-CONF-74-089-027)
RUSCH, G.K., See GOLD, R., 30:29557
RUSSO, F.A., Operational testing of the high performance thermoelectric generator (HPG-02), 30:29250
RUSTAMOV, P.G., System Ce--Ge, 30:30016
RUTHERFORD, J.A., The reaction of atomic oxygen with several atmospheric ions, 30:30549
RUUSKANEN, P.V., See KAJANTIE, K., 30:30754
RYABININ, A.I., Sorption method of isolating uranium and other valuable metals from sea water, 30:28998
RYDE, H., See HAGEMANN, G.B., 30:30983
RYDER, H.A., Code description: FOFT, 30:31350 (UCID-15753)
RYKOV, A.G., Oxidation--reduction reactions of actinide elements. XXIII. Kinetics of neptunium(V)--americium(V) reaction in perchlorate solutions, 30:29105
  Oxidation--reduction reactions of actinide elements. XXIV. Kinetics of uranium(IV)--iron(III) reaction in water--isopropanol solutions, 30:29106
  See FROLOVA, L.M., 30:29102
RYSSEL, H., See SCHMID, K., 30:30486
RYUTOV, V.D., See KARTASHEV, K.B., 30:29155

S

SAAR, E., See EINASTO, J., 30:30379
SABAU, M.N., Study of $\pi^{+}p$ interactions with strange particle production in five- and six-body final states at 8 GeV/c, 30:30615
SABERSKY, A.P., Geometry and optics of synchrotron radiation, 30:30119
SABLINSKI, J., See SZUMIEL, I., 30:29669
SABO, V.Ya., See IL'IN, Yu.M., 30:30776
SACHS, R.K., See BUDIC, R., 30:31175
SACKMANN, S., Ion--x-ray coincidence experiments in slow Ne^{+}--Ne collisions, 30:30517 (AED-CONF-74-085-001)
SADEH, T., See NAHARIN, A., 30:29821
SADIKOV, I.P., See ISHMAEV, S.N., 30:30843
SADIKOVA, N.S., See LEONOV, A.I., 30:29911
  See LEONOV, A.I., 30:29909
SAFRONOVA, N.G., Kinetics of the self-purification of a body of water containing strontium-90 as a result of absorption of the radionuclide by the bottom deposits, 30:29414
SAIO, H., On the semiconvective zone in the core-helium-burning stars, 30:30264
SAIRENJI, T., See SATO, C., 30:29658
SAITO, K., Data processing system for nuclear medicine, 30:29864
SAITO, S., See SAWAOKA, A., 30:29923
SAKAI, M., Excitation of the deeply bound gsub(9/2) neutron hole state in ^{117}Sn by a neutron pickup reaction with 81.7 MeV ^{3}He particles, 30:30974
SAKHAROV, V.M., See GENEROZOV, V.L., 30:31129
SAKOVICH, V.A., See GENEROZOV, V.L., 30:31129
SAKUMA, S, See TAKAHASHI, S., 30:31106
SAKURAI, J.J., Dynamical models based on vector-meson dominance and universality, 30:30642
SALA, L., See FIZZUTTI, C., 30:31279
SALADIN, J.X., Coulomb nuclear interference in the inelastic scattering of ^{16}U ions from ^{24}Mg, 30:30905
SALAM, A., See DELBOURGO, R., 30:30724
SALAS, M., See CARRASCOSA, J.L., 30:29679
SALIH, S.M., Reduction in electron irradiation damage to organic compounds by conducting coatings, 30:29070
SALIN, A., See PIACENTINI, R.D., 30:30555
SALIU, L., Consistency conditions in the theory of spontaneous breaking of chiral symmetry, 30:30778
SALLAM, O.H., See MICHELINI, M., 30:30850
SALLES ANDRADE, H.A., See HAINBERGER, P.L., 30:29413
SALMONS, B.H., Trends in structural mechanics. A UK review of the 2nd international conference on structural mechanics in reactor technology. VII. Reliability analysis, 30:31289
SALOMON, M., See AXEN, D., 30:29597
SALPETER, E.E., See KATZ, J.I., 30:30215
SALTMARSH, M.J., See RAMAN, S., 30:30879
SAMARDZICH, B.G., See SHAPIRO, E.G., 30:29552
SAMOILENKO, Z.A., See ARKHAROV, V.I., 30:30023
SAMOILOV, V.I., See KRUSHCHOV, N.G., 30:29760
SAMOUR, C., See POSSOZ, A., 30:30899
SAMSONOV, G.V., Micro-x-ray spectrum analysis of interphase interaction in the systems ''refractory compound--liquid metal'', 30:29898
  Preparation and properties of vanadium monocarbide in the region of homogeneity, 30:29912
SAMUEL, A.M., Modification of radioimmunoassay method of human growth hormone estimation, 30:29877
SANDAGE, A., Steps toward the Hubble constant. II. The brightest stars in late-type spiral galaxies, 30:30393
SANDERSON, E.A., See MALTA, C.P., 30:30863
SANDERSON, N.E., Level structure of ^{78}Kr, 30:30944
SANDERSON, T.R., Spherical harmonic analysis of satellite anisotropy measurements, 30:29533
SANDQUIST, G.M., Plowshare technology assessment, prospectives for nuclear-stimulated geothermal power in the western U.S., 30:29311 (PB-231011)
SANDRI, G., See FISK, L.A., 30:30172
SANDUSKY, W.F., See WENDELL, L.L., 30:29435
SANO, H., Moessbauer spectroscopic studies of the effect of the oxalate anion in the second coordination sphere on the oxidation state of ^{57}Fe produced in EC-decay, 30:29078
SANTHANAM, T.S., See TEKUMALLA, A.R., 30:31152
SANTIARD, J.C., See BRESKIN, A., 30:29589
SANTOR, M.L., See DUBA, A.G., 30:31411
SANTORO, R.T., See GABRIEL, T.A., 30:29206
SANTOS, E., See LEAL DE SANTOS, M., 30:30567
SANTOS, F.D., Transparency to vector polarization transfer in deuteron stripping reactions, 30:31096
SANT PRAKASH, L.J.B., Total electron content measurements over Kurukshetra, 30:30422
SARANTITES, D.G., See HOOD, J.T., 30:30153
SARANZEW, V.P., See BARABOSCH, L.S., 30:30117
SARKAR, S., Broken conformal Ward identities in non-abelian gauge theories, 30:31171
SARKAR, S.K., See DASGUPTA, M.K., 30:30307
SAROSIEK, J., Radioecology of Pogonatum urnigerum (L.) pal. beauv, 30:29691
SAROSIEK, W., See PANKE, R., 30:29723
SARTORI, G., See BERTANZA, L., 30:30606
SARTORI, S., See BERTANZA, L., 30:30606
SASAKI, K., See NIEGAWA, A., 30:30661
SASAKI, R., See FUKUDA, R., 30:30682
SASAKI, T., Chemical behavior of intermediates produced in sulfuric acid glass by gamma irradiation. I. Reactivities of mobile electrons with inorganic ions, 30:29048
SASTRI, N.S., Frequency of occurrence of positive geomagnetic bays at Trivandrum, 30:30421
SATCHLER, G.R., Target-spin effects on elastic scattering cross sections, 30:30940
  See DEVRIES, R.M., 30:31063
SATO, C., Lack of recovery from radiation damage on colony forming ability and on membrane charge in a Burkitt lymphoma cell line, 30:29668
SATO, M., See ISHIBASHI, W., 30:28954
SATZ, H., See CHAICHIAN, M., 30:30700
SAULI, F., See BRESKIN, A., 30:29588
  See BRESKIN, A., 30:29587
  See BRESKIN, A., 30:29589
SAUNDERS, J.E., Back-scattering from metals in superficial therapy with high energy electrons, 30:31108
SAUR, E., See REPPEL, G.W., 30:30805
SAUR, E.J., See BAUER, H., 30:30063
SAUVAUD, J.A., See GUYADER, J.C., 30:29567
SAVAGE, B.D., Ultraviolet photometry from the orbiting astronomical observatory. XVI. The stellar Lyman-Alpha absorption line, 30:30251
SAVAGE, W.F., See FRANKLIN, J.E., 30:29996
SAVCHENKO, V.I., See ZELENSKII, V.F., 30:30017
SAVEL'EVA, N.V., See ANUFRIENKO, V.F., 30:29907
SAVOLAINEN, J.E., See GRESKY, A.T., 30:29150
SAWAOKA, A., Structure determination of boron nitride transformed by shock compression, 30:29923
SAWICKI, A., Charge measuring unit of the pulsed electron beam in the Van de Graeff accelerator, 30:30124
SAYED, A.M., See PIESCH, E., 30:29522
SAYED, E., See DROSTE, C., 30:30963
SAYER, R.O., See RIEDINGER, L.L., 30:30985
SAZONOV, L.A., Investigation of the catalytic properties of compounds of the LnMeO$_3$ type in the homomolecular exchange of oxygen, 30:29028
SCALISE, E. Jr., See KAUFMANN, P., 30:30287
SCANNAPIECO, A.J., Conductivity ratio effects on the drift and deformation of F-region barium clouds coupled to the E-region ionosphere, 30:30437
SCANNICCHIO, D., See GOGGI, G., 30:30874
SCHAAL, R.E., See KAUFMANN, P., 30:30287

SCHABERT, H.P., See GRUENER, W., 30:31196
SCHAEFER, H., See BINNEWIES, M., 30:29091
  See SCHARTNER, K.H., 30:30518
SCHAERF, C., See BARBINI, R., 30:29586
SCHARFF-GOLDHABER, G., Problem of particle-hole symmetry in even--even Cd and Te nuclei, 30:30971
SCHARMANN, A., See FAENGEWISCH, G.L., 30:29554
SCHARTNER, K.H., Cross section for the Ar--L--x-ray emission in collisions of He^{+}-, Ne^{+}-, and Ar^{+}-ions with Ar atoms, 30:30518 (AED-CONF-74-085-002)
  See HIPPLER, R., 30:30557
SCHEFFLER, P.E., Photoproduction of π^- from deuterium at laboratory energies 600 to 1250 MeV, 30:30586
SCHEID, W., See FINK, H.J., 30:31082
SCHEIRER, S.T., Mechanical behavior of metal matrix composites. Final report, 1 April 1972--30 April 1973, 30:29975 (AD-775359)
SCHELL, E.M., Geology and mineral resources of the Greater Green River Basin. Symposium and core seminar, Casper, Wyoming, September 17--19, 1973, 30:29335
SCHELTEN, J., See WIGNALL, G.D., 30:31364
SCHIAGER, K.J., See APT, K.E., 30:29551
SCHIFFRER, G., Exact methods for treating nonlinear problems in many-body theory, 30:31058
SCHILLING, K.D., See ANDREJTSCHEFF, W., 30:30990
SCHIRRA, M., Creep-rupture behavior of the alloy Inconel 625 in three different pretreatment states, 30:29978 (EURFNR-1163)
SCHLEIN, P., See GRAYER, G., 30:30617
SCHLENKER, H.V., See BOHN, T., 30:31305
SCHLIESING, H., Surface protection in nuclear power plant, 30:29946
SCHLINDER, A.I., See MACKLIET, C.A., 30:30812
SCHLOESSER, E., See BAETZNER, K., 30:30589
SCHMALENBACH, E., See MAYR, P., 30:29300
SCHMER, G., See HOFFMAN, A.S., 30:29082
SCHMID, K., Backscattering measurements and surface roughness, 30:30486
SCHMID, P., See FRANK, G., 30:29258
SCHMIDT, A., See BIRKHOFER, A., 30:31190
SCHMIDT, D.G., See PAL, B.C., 30:29092
SCHMIDT, K., Angular distributions for the reactive scattering of H and D atoms by polyatomic molecules, 30:30519 (AED-CONF-74-085-004)
SCHMIDT, M., See GREENSTEIN, J.L., 30:30204
SCHMIDT, V., See KOLLBACH, D., 30:31338
SCHMIDT-BOECKING, H., The determination of the differential energy loss of heavy ions backscattered from an infinitely thick solid target, 30:30948
SCHMIDT-KUESTER, W.J., The disposal system in the nuclear fuel cycle, 30:29147
SCHMIDT-OTT, W.D., Search for new isotopes ^{186} ^{187}Tl, 30:30986
SCHMIEDL, R., See DEMTROEDER, W., 30:30507
SCHMITT, D., The impact of nuclear power plants on the economic structure, 30:31304 (DEU-74-2)
SCHMITT, R.W., Detection and suppression of transistor oscillation during power burn-in, 30:31419 (BDX-613-1144(Rev.))
SCHMITZ, N., See BENECKE, J., 30:30612
SCHMORAK, M.R., Nuclear Data Sheets for A = 186, 30:30988
SCHNEIDER, D., See STOLTERFOHT, N., 30:30541
SCHNEIDER, K.J., Advanced waste management studies progress report, April--June 1974, 30:30106 (BNWL-B-223-11)
SCHNEIDER, M.J., Aquatic physiology of thermal and chemical discharges, 30:29461 (BNWL-SA-5058)
SCHNEIDER, M.V., See WRIXON, G.T., 30:30330
SCHNEIDER, W., See HERSCHBACH, K., 30:30079
SCHNEIDER, W.F.W., See KUHLMEYER, B., 30:30906
SCHNOPPER, H.W., See SPROTT, G.F., 30:30260
SCHOCK, A., Light-weight radiosotope thermoelectric generator design, 30:29253
SCHOCK, R.N., See ABEY, A.E., 30:31409
  See STEPHENS, D.R., 30:29322
SCHOEBERL, M.R., See GELLER, M.A., 30:30446
SCHOENFELD, I., Spectrochemical method for determination of tellurium in geological materials, 30:28949
SCHOENHERR, H., See LUUWRIER, K.P., 30:29926
SCHOLZ, M., See BAZANT, E., 30:31285
SCHOTT, H.N., Photochemical addition of amino acids to thymine, 30:29658
SCHRANKEL, W., See BENECKE, J., 30:30612
SCHRECKENBACH, K., See BRAUMANDL, F., 30:29515
SCHRIEDER, G., See HOFFMANN, D., 30:30148
SCHROEDER, B., Highly resolved electron energy loss spectroscopy of amorphous germanium and silicon layers, 30:31381 (AED-CONF-74-089-025)
  See ARESKOUG, M., 30:31002
SCHROEDER, H., See BACH, H., 30:30482
SCHROEDER, R.C., See MCMASTER, W.H., 30:31400
SCHUBERT, F., See GRUENER, W., 30:31196
SCHUCK, P., See ETHOFER, S., 30:31027
SCHUELLER, F.C., Arc discharges in a curved magnetic field, 30:29154 (NP-20140)
SCHULTE-FROHLINDE, D., See STELTER, L., 30:29071
SCHULTZ, G., See BRESKIN, A., 30:29587
SCHULTZ, P.A., See CIARLO, D.R., 30:31460
SCHULZ, M., Particle saturation of the outer zone: a nonlinear model, 30:30472
SCHULZ, W., IRS literature 1965-1973, 30:31246 (IRS-A-4)
  See SCHMITT, D., 30:31304
SCHUMANN, F.A., Cost effective designing for the economic RTG, 30:29252
SCHUSTER, W., See HEINRICH, H., 30:29701
SCHWAB, C., See PONPON, J.P., 30:29534
SCHWABE, M., See GOESSNER, W., 30:29785
SCHWARTZ, B.B., See FONER, S., 30:30823
SCHWARTZ, P.R., See WILSON, W.J., 30:30265
SCHWARTZ, R.D., The T Tauri emission nebula, 30:30185
SCHWARZ, J.H., Off-mass-shell dual amplitudes. III, 30:30714
SCHWARZ, K.K., See ZITA, G., 30:29831
SCHWARZSCHILD, A.Z., See BOND, P.D., 30:30921
SCHWARZSCHILD, B., See BENECKE, J., 30:30612
SCHWEER, K.H., See NIEKUSCH, E., 30:31393
SCHWEIKERT, E.A, See KRIVAN, V., 30:28922
SCHWEIMER, G.W., See REBEL, H., 30:30945
SCHWEITZER, D.G., See BAUER, H., 30:30063
SCHWELA, D., See GRASSBERGER, P., 30:30748
SCHWENDIMAN, L.C., Wet and dry atmospheric removal processes for radioiodine, 30:29365 (BNWL-1850(Pt.3))
  See MISHIMA, J., 30:29376
SCHWENK, A., See EPPERLEIN, B.W., 30:29014
SCHWIMMER, A., Multiple pomeron exchange and final state rescattering, 30:30706
SCKOPKE, N., See HAEUSLER, B., 30:30471
SCOTT, A., Core polarization in inelastic proton scattering from ^{209}Bi at 61 MeV, 30:31003
SCOTT, D.K., See MAGUIRE, C.F., 30:30997
SCOTT, J.P., See CALL, P.J., 30:29075
SCOTT, R.D., L shell ionization in the α decay of ^{210}Po, 30:31001
SCOTT, R.G., Protection circuit for a liquid-nitrogen trap filler, 30:31415 (ANL-8111)
SCOVILLE, N., See GATLEY, I., 30:30356
SCRIMAGLIO, R., See BALESTRA, F., 30:29591
  See BARBINI, R., 30:29586
SCUDDER, J.D., See BURLAGA, L.F., 30:30325
SCULLI, J., See KIM, I.J., 30:30584
SEAGER, C.H., Dielectric strength of x-cut quartz after thermally induced stress cycling: application to understanding the Sandia Quartz gauge, 30:31396 (SAND-74-0135)
SEAQUIST, E.R., Search for circular polarization in compact radio sources at a wavelength of 2.2 cm, 30:30284
SEARLE, C.W., Experimental verification of a model for the magnetization reversal in RCo$_5$ particles, 30:30047
SEARLE, L., See GREENSTEIN, J.L., 30:30204
SEBESTYEN, A., See KIRALY, P., 30:30160
SEDLAK, J., Radioimmunological determination of proteohormones, 30:29874
SEEDS, M.A., See MICHAEL, J.L., 30:30227
SEGAL, Y., See NOTEA, A., 30:29608
SEGUINOT, J., See BAILLON, P., 30:30618
  See BAILLON, P., 30:30619
  See BAILLON, P., 30:30737
SEHMEL, G.A., Dry deposition of particles, 30:29482 (BNWL-1850(Pt.3))
  Interstage particle losses in a high-volume cascade impactor, 30:29374 (BNWL-1850(Pt.3))
  Particle deposition rates on a water surface as a function of particle diameter and air velocity, 30:29484 (BNWL-1850(Pt.3))
  Resuspension of tracer particles by wind, 30:29370 (BNWL-1850(Pt.3))
  Resuspension source change at Rocky Flats, 30:29372 (BNWL-1850(Pt.3))
  Resuspension by wind at Rocky Flats, 30:29371 (BNWL-1850(Pt.3))
  See ORGILL, M.M., 30:29373
SEIDEL, A., Removal by DTPA of internally deposited ^{241}Am. A comparative study on rats and Syrian hamsters, 30:29822
  See VOLF, V., 30:29813
SEIDEL, C.W., See GRUVERMAN, I.J., 30:30092
SEIDEL, W., See ANDREJTSCHEFF, W., 30:30993
  See ANDREJTSCHEFF, W., 30:30990
SEIDEN, A., See FLATTE, S.M., 30:30150
SEIDMAN, D.N., Field ion microscope observations of the three-fold symmetric dissociation of 1/2a(111) screw dislocations in molybdenum, 30:30000
SEIGLIE, G.A., Recent changes of the foraminiferal assemblages of Jobos Bay and surroundings, Puerto Rico, 30:31376 (CONF-740663-1)
SEIGNEMARTIN, C.L., See GARCIA AGUDO, E., 30:28913
SEIPEL, L., Special indication and contraindications for the implantation of cardiac pacemakers with radionuclide batteries, 30:29770 (AED-CONF-74-030-003)
SEITKHOZHAEV, A.I., See ERUPNOVA, G.F., 30:29695
SEKIGUCHI, M., See SAKAI, M., 30:30974
SELBY, J.B., See DAMRON, J.R., 30:29845
SELIG, W., Analysis of explosive simulant 90503, 30:31373 (UCID-15972)
  Analysis of plastic-bonded explosives containing HMX, ammonium perchlorate, aluminum, and Viton, 30:31369 (UCID-15623)
SELIN, E., See ALENIUS, G., 30:30916
SELIVANOV, V.G., See POKROVSKII, A.V., 30:29299
SELTZER, S.M., Transmission and reflection of electrons by foils, 30:31118
SEMENESCU, G., See BUCURESCU, D., 30:30943
  See IVASCU, M., 30:30941
SEMENIUK, A., Properties of TZM and nuclear behavior of TZM brazements. Various properties of TZM and Zr--5Be and Au--18Ni brazing filler metals are determined for brazing TZM to Zr and to steel, 30:30084

SEMENOV, Yu.P., See KONOPLEV, K.A., 30:31237
SEMENOVA, E.G., Mechanisms of inhibition of the postirradiation recovery in cells. IV. The effect of caffeine and acriflavine on gamma and x-ray induced unscheduled DNA synthesis in HeLa Zn-63 cells, 30:29675
SEMPREBON, L.C., See LAASPERE, T., 30:30431
SEN'KO, E.E., See BAKULIN, V.N., 30:29396
SEO, T., See HAYASHI, T., 30:29565
SEQUIST, E.R., See HUGHES, V.A., 30:30292
SERDAROGLU, M., See EBRAHIM, A., 30:30775
SEREBRYAKOVA, G.V., See MOROZOVA, S.S., 30:28955
SEREGINA, N.G., See EGOROV, Yu.A., 30:29563
SERENDENKO, E.V., See DUBOVOI, L.V., 30:30121
SEREZHKIN, V.N., Structure of the double oxide UMo$_{10}$O$_{32}$, 30:29941
SERGEEVA, S.A., See GAZIEV, A.I., 30:29682
SERNA, J., See DE DIEGO, N., 30:29895
SETH, J., See TOFT, A.D., 30:29775
SETLOW, R.B., See REGAN, J.D., 30:29673
SEVAN'KAEV, A.V., See GUZEEV, G.G., 30:29731
SEVAST'YANOV, Yu.G., Isolation of carrier-free radioactive isotope cobalt-57 from nickel target irradiated on cyclotron, 30:29143
SEVERNYI, S.A., Content of radium, uranium, radiothorium, and thorium in some scintillators, 30:29502
SEWARD, F.D., See TOOR, A., 30:30280
SEXL, R.U., Black-hole physics: an introduction, 30:30182 (CONF-730693-)
SHABESTARI, L., See TAYLOR, G.N., 30:29796
SHADCHIN, S.A., See KHARCHENKO, V.F., 30:31103
SHAFEEVA, M.V., See DENISOV, D.A., 30:29031
SHAFER, R.B., Practical application of a simplified vitamin B$_{12}$ radioassay, 30:29856
SHAFIEV, A.I., Possibility of preparing enriched americium-242g by elution of recoil atoms from zeolite, 30:29141
SHAGISULTANOVA, G.A., See KARABAN, A.A., 30:29062
SHAKIN, C.M., Scattering from correlated systems, 30:31056
SHALABY, M., See EL-BEDEWI, F., 30:30888
SHALAEV, A.M., See DEKHTYAR, I.Ya., 30:30086
SHAMALY, A., Invariants of Born reciprocity theory, 30:30629
SHAMANIN, Yu.A., See KHUTYZ, A.M., 30:29945
SHAMPINE, L.F., Stiffness and non-stiff differential equation solvers, 30:31345 (SAND-74-5236)
SHANER, J.W., See GATHERS, G.R., 30:30045
SHANK, K.E., Effects of copper, mercury, and zinc on the uptake and distribution of cadmium-115m in the albino rat, 30:29816
SHANKS, H.R., See BEVOLO, A.J., 30:30808
SHAPIRO, B., See REVZEN, M., 30:30804
SHAPIRO, E.G., Electronics for the LRL automated personnel thermoluminescence dosimetry system, 30:29552 (UCID-15836)
SHAPIRO, V.B., See DUBOVOI, L.V., 30:30121
SHAPOVALOVA, A.I., U.B.V. photometry of the irregular galaxy NGC 4753, 30:30354
SHAPTALA, V.G., Scattering of high-frequency electromagnetic waves by ion-acoustic oscillations in a bounded plasma, 30:29237
SHARKIN, O.P., See SAMSONOV, G.V., 30:29898
SHARKOV, B.Y., See BYKOVSKII, Y.A., 30:29177
SHARMA, L.H., See VENKATACHARI, R., 30:30432
SHARMA, R.C., Gravitational instability of a rotating plasma, 30:30390
SHARMA, V., See QURESHI, M., 30:28994
SHAROV, B.V., See KRITSKAYA, V.K., 30:30080
SHARPEY-SCHAFER, J.F., See PRICE, H.G., 30:30910
SHARPLESS, S., Rotational velocities in the Orion association, 30:30223
SHASHIMOHAN, A.L., See AGRAWAL, Y.K., 30:28962
SHAVIV, G., See MEISELES, R., 30:30293
SHAW, B.J., See DEIS, D.W., 30:30809
SHAW, G.G., See HANCOCK, J.R., 30:29974
SHAW, K.R., The effects of momentum conservation on pionization, 30:30712
SHAW, R.R., Neodymium glass laser having room temperature output at wavelengths shorter than 1060 Nm, 30:29280
SHAW, W.M., Thermally averaged Gaunt factors in non-relativistic electron-ion bremsstranlung, 30:29185 (UCID-15712)
SHCHERBAKOV, E.E., See BONDAREVSKII, S.I., 30:29096
SHCHERBAKOV, Yu.A., See BALESTRA, F., 30:29591
SHCHUKIN, A.A., See MALASHENKO, I.S., 30:30014
SHEARER, C.H., See ELSNER, N.B., 30:29246
SHEETS, W.R., Digital period meter, 30:29491
SHEIBLEY, D.W., Trace-element analysis of 1000 environmental samples per year using instrumental neutron activation analysis, 30:28915 (N-74-20335)
SHEINKER, A.P., See YAKOVLEVA, M.K., 30:29037
SHELIMOV, B.N., See GRIVA, A.P., 30:29029
SHEN, C.S., Acceleration and radiation of cosmic ray electrons from pulsars, 30:30274
SHEN, Y.R., See AMER, N., 30:31425
SHERIDAN, K.V., Radio emissions associated with the emergence of new magnetic flux from the solar photosphere, 30:30305
SHERMAN, F., See LAWRENCE, C.W., 30:29683
SHERN, C.S., Electromagnetic mass breaking of baryons in broken chiral SU(3) x SU(3), 30:30779
SHERWIN, W.K., Development of humoral immunity in lethally irradiated mice reconstituted with fetal liver, 30:29750
SHERWOOD, W.A., See CHRISTOFILOS, N.C., 30:29188
SHESTAKOV, G.N., See ACHASOV, N.N., 30:30674
SHETLAR, M.D., See SCHOTT, H.N., 30:29658
SHIBASAKI, K., See WATANABE, T., 30:30323
SHIELDS, G.A., X-ray ionization and the helium abundance in 3C 120, 30:30347
SHIERMAN, E., See GREENSTOCK, C.L., 30:29003
SHIGA, K., See KAWABE, T., 30:30654
SHIGEMURA, N., See ONO, K., 30:30120
SHIH, Y.M., See SHERN, C.S., 30:30779
SHIJO, Y., Extraction spectrophotometric determination of scandium with xylenol orange and ethyltridodecylammonium bromide, 30:28953
SHIKATA, E., See YAMABAYASHI, H., 30:29962
SHIKAZONO, N., Study of nuclear physics using a high-flux reactor, 30:31234 (KURRI-TR-110)
SHIKIN, V.B., Interaction of surface electrons in liquid helium with oscillations of the vapor--liquid interface, 30:30801
SHILOV, V.P., Some characteristics of the reaction of americium(VI) with reducing agents in aqueous solutions, 30:29104
SHIL'STEIN, S.Sh., See SOMENKOV, V.A., 30:29608
SHIMAZAKI, K., See MIYAZAKI, M., 30:29840
SHIMIZU, K., Magnetic moments and GT-type β-decay matrix elements in nuclei with a LS doubly closed shell plus or minus one nucleon, 30:30898
On the effective two body magnetic dipole operator, 30:31086
SHIMIZU, M., Stellar atmospheres: the sources of interstellar molecules, 30:30241
SHIMIZU, T., Experience of use of reduced type of glutathione to prevent side effects of radiotherapy and antineoplastic chemotherapy, 30:29721
SHIMMINS, A.J., See PETERSON, B.A., 30:30276
SHIMOYASHIKI, S., Apparatus for refining sodium, 30:31227
SHINN, J.H., See PORCH, W.M., 30:29490
SHINOHARA, I., See HAGIWARA, M., 30:29058
SHINYAEV, A.Ya., Stabilization under high pressure of carbide phases in the molybdenum: carbon system, 30:29932
SHIPILOV, V.I., See IVANOV, V.B., 30:29570
SHIPLEY, J.P., See MURRAY, H.S., 30:31325
SHIRAI, O., See KONISHI, H., 30:29875
SHIROKOVA, N.V., See SHLUGER, M.A., 30:29960
SHISHKOV, V.V., See CHUPYATOVA, L.P., 30:30033
See CHUPYATOVA, L.P., 30:30010
SHISHMAKOV, A.S, Diffraction of x rays on stacking faults in metals with hcp lattices, 30:30024
SHKOLYAR, V.S., See ZELENYUK, E.E., 30:30013
SHLUGER, M.A., Effect of electrolysis conditions on the current efficiency of the deposition and composition of chromium--molybdenum alloy, 30:29960
SHLYUKO, V.Ya., Effect of additivies of yttrium and aluminum oxides on sintering and properties of lanthanum hexaboride, 30:29892
SHMATKO, B.A., See POPIL'SKII, R.Ya., 30:29910
SHMELEV, V.P., See ARTYUKHOV, V.G., 30:29659
SHMIDT, F.K., Hydrogenation and deuteration of olefins in the presence of cobalt triethylaluminum-bis(acetylacetonate), 30:29012
SHOFMAN, N.L., See BUTYLENKO, A.K., 30:30054
SHOIKHET, Ya.N., Changes in the cardiovascular system in radiation and medicinal treatment of lung cancer, 30:29729
SHOLOKHOV, A.A., Use of superposition in calculating the temperature of a reactor core cooled by a liquid metal, 30:31277
SHPENIK, O.B., See SOVTER, V.V., 30:30523
SHTERN, A.G., See GELFGAT, J.M., 30:30572
SHTIN, A.P., Extraction of niobium in phosphoric acid solutions by alkali metals and ammonium salts, 30:29000
SHUGALII, O.V., See FONARAR'OV, A.B., 30:29036
SHULEPKO, Z.S., See DAVYDOV, E.N., 30:29408
SHULTS, G.W., See RAO, B.Y.K., 30:29642
SHUMILOVA, R.G., See GREBENKINA, V.G., 30:29893
SHURAVIN, V.A., See ANDERT, K., 30:29630
SHWARTZ, J., On the gas temperature in coaxial electric-discharge CO$_2$ flow lasers, 30:29285
SIEMSEN, J.K., See WAXMAN, A.D., 30:29844
SIEMSSEN, R.H., See HESSELINK, W.H.A., 30:30975
SIEMTON, I.Z., See KANTA, L., 30:29033
SIENIAWSKI, J., Isomeric states in ^{97} ^{98} ^{99} ^{100}Rh isotopes, 30:30964
SIERSBAEK-NIELSEN, K., See LAURIDSEN, U.B., 30:29842
SIFFERT, P., See PONPON, J.P., 30:29534
SIGEL, G.H., See GRISCOM, D.L., 30:30102
SIKOLENKO, V.F., See ISSINSKII, I.B., 30:30129

SIKOV, M.R., Carcinogenicity of iodine-131 relative to age at exposure, 30:29777 (BNWL-SA-5065)
SIKULOVA, J., See NOVAK, L., 30:29747
SILAEV, A.F., See RAKOVSKII, V.S., 30:29963
SILBAR, R.R., See MYHRER, F., 30:30866
SILBERBERG, R., Cross sections of proton--nucleus interactions at high energies, 30:30854 (AD-777030)
SILBERSTEIN, E.B., Human lymphocyte as a radiobiological dosimeter after total body irradiation, 30:29707
SILK, E.J., Fuel rod fabrication, 30:31293
SILL, C.W., Simultaneous determination of alpha-emitting nuclides of radium through californium in soil, 30:28977
SIL'NOV, S.M., See BYKOVSKII, Y.A., 30:29177
SILVA, J., See BLAIR, D.C., 30:29886
SILVERMAN, J., See EUBANKS, A.G., 30:30091
SILVERMAN, J.P., See BASTIEN, D.B., 30:30600
SIMKIN, Y.R., See ANDREONE, C.A., 30:28938
SIMMONS, G.L., Shielding benchmark problems, 30:31126 (ORNL-RSIC-25(Suppl.2))
SIMNETT, G.M., Relativistic electron events in interplanetary space, 30:30338
SIMON, T., Broad-band 20-μ photometry of 63 stars, 30:30221
SIMONOV, Yu.A., Hyperspherical-expansion approach to nuclear bound states, 30:31050
See CALOGERO, F., 30:31032
SIMPSON, C.L., Pacific Northwest Laboratory annual report for 1973 to the USAEC Division of Biomedical and Environmental Research. Part 3. Atmospheric sciences, 30:29468 (BNWL-1850(Pt.3))
SIMPSON, J.A., See CHENETTE, D.L., 30:30405
SINCLAIR, D., See MENCHACA-ROCHA, A., 30:30904
SINDT, H., See MORITZ, J., 30:29634
SINELNIKOV, V.E., See BUTORIN, N.V., 30:29463
SINGER, M., See NORDBERG, M.E. Jr., 30:30590
SINGER, R.A., See BERLAD, G., 30:30623
SINGH, A.K., See GUPTA, S.P., 30:30418
SINGH, B., Resistivity and TCR of erbium films compared with the predictions of the columnar model, 30:30052
SINGH, N., See BHATI, S.S., 30:30958
SINGH, R.P., See KOHLI, N., 30:28966
SINGHAL, K.P., Coupling constants for the cosmic ray muon component, 30:30178
SINHA, B., A three parameter nucleon-nucleus optical model on the energy shell, 30:31104
SINHA, K.P., See LORD, E.A., 30:31174
SINIFF, D.B., See TESTER, J.R., 30:31377
SINITSYNA, T.S., See GORSHKOV, V.V., 30:28926
SIQUIG, R.A., See LAUTERBORN, D., 30:30198
SIRBU, M., Efficiency of the anticoincidence method applied to the G. M. window counters, 30:29508
SIROTKIN, A.P., See ZHIRNOV, A.D., 30:31205
SISKA, P.E., See RILEY, M.E., 30:30530
SISTERSON, L.K., See BEBEK, C.J., 30:30587
SITENKO, A.G., The diffraction dissociation of deuterons on the diffused edge nuclei, 30:31072
SIVARAM, C., See LORD, E.A., 30:31174
SIVOSHINSKII, D.S., Principles and methods for using electronic computers in clinical , radioisotopic diagnosis, 30:29838
SIZMANN, R., See BISSWANGER, H., 30:30064
SIZONENKO, Yu.V., See NESMYANOVICH, A.T., 30:30309
SIZOVA, R.N., See DUBATKIN, V.I., 30:30006
SKALAFURIS, A.J., The solar temperature reversal and convective motions, 30:30339
SKILLING, J., Cosmic ray diffusion and anisotropy, 30:30167
SKINNER, D.F., See ROZSA, R.B., 30:29319
SKLIZKOV, G.V., See GRIBKOV, V.A., 30:29176
SKOCPOL, W.J., Phase-slip centers and nonequilibrium processes in superconducting tin microbridges, 30:30819
SKOROBOGATOV, V.S., See ZOLOTUKHIN, I.V., 30:29887
SKOROV, D.M., Apparatus for studying the kinetics of the liberation of inert gases from materials during isothermal annealing, 30:30002
SKOSKIEWICZ, T., Isotope effect in the superconducting palladium--hydrogen--deuterium system, 30:30813
SKREBTSOV, G.P., See KOLCHIN, A.A., 30:29536
SKRIPTSOVA, A.B., See DAVYDOV, Yu.P., 30:29125
SKUBIC, P.L., See JONES, L.W., 30:29596
SKURSKAYA, M.G., See KRUSHCHOV, N.G., 30:29760
SKUYBINA, I.P., See LARIONTSEV, E.G., 30:29286
SLAGLE, I.R., Kinetics of the reaction between oxygen atoms and carbon disulfide, 30:30531
SLATER, R.C., See BECKER, W.G., 30:30528
SLATER, S.D., See CHATTERS, R.M., 30:28936
SLATTERY, P., See SREEDHAR, V., 30:30616
SLAUS, I., Present status and open problems in few-nucleon systems, 30:31041
SLEIGHT, A.W., Synthesis of high pressure $Cd_2V_2O_7$ and related compositions, 30:29903
SLINN, W.G.N., Analytical investigations of inertial deposition of small aerosol particles from laminar flows onto large obstacles. Part B. Large stokes number solution by the method of matched asymptotic expansion, 30:29486 (BNWL-1850(Pt.3))
Analytical search for the stochastic-dominating process in the drift-deposition problem, 30:29488 (BNWL-1850(Pt.3))
Analytical investigations of inertial deposition of small aerosol particles from laminar flows onto large obstacles. Part A. General formulation, 30:29485 (BNWL-1850(Pt.3))
Extension of the anaysis of plume washdown to include diffusion, 30:29478 (BNWL-1850(Pt.3))
Postulated estimate of wet versus dry deposition downwind of a point source of pollution, 30:29364 (BNWL-1850(Pt.3))
Simple model for bouyant plumes based on the conservation laws, 30:29460 (BNWL-1850(Pt.3))
SLIVINSKY, V.W., Bremsstrahlung polarization from commercial x-ray tubes, 30:31447 (UCID-15829)
SLODZIAN, G., See BLAISE, G., 30:30087
SLOOT, J.W., See ALKEZWEENY, A.J., 30:29487
SLOTOVA, J., See NOVAK, L., 30:29747
SLUTZ, S., Some necessary conditions on x-ray laser action, 30:29272 (UCRL-74898)
X-ray lasers: necessary conditions and some possible approaches, 30:29271 (UCID-16290)
SMADJA, G., See CHAVANON, P., 30:30749
SMAKHTIN, L.A., See GORSHKOV, V.V., 30:28926
SMATHERS, J.B., See WITHERS, H.R., 30:29758
SMEDSKJAER, L., Positron annihilation in colored KCl, 30:30513
SMELOVA, M.E., See VOROB'EV, A.N., 30:30071
SMERD, S.F., See SHERIDAN, K.V., 30:30305
SMIALEK, M., See OSEENDA, M., 30:29761
SMILAUER, J., See LASTOVICKA, J., 30:30413
SMIRNOV, E.A., See FEDOROV, G.B., 30:29905
SMITH, C.B., Dynamic testing of full-scale nuclear power plant structures and equipment, 30:31268
SMITH, C.D., Design relationships and failure theories in probabilistic form, 30:29288
SMITH, D.D., Grazing studies on selected plutonium-contaminated areas in Nevada, 30:29448 (NVO-AEIC-74-1)
SMITH, D.E., See CLARK, A.F., 30:30576
SMITH, D.F., Type-III radio bursts and their interpretation, 30:30335
SMITH, D.L., Comments on oxygen analysis of sodium by equilibration with vanadium: an assessment, 30:28958
SMITH, E.M., See GOTTLIEB, N.L., 30:29792
SMITH, G.J., See RIEDINGER, L.L., 30:30985
SMITH, J.L. Jr., Applications of superconductivity to ac rotating machines, 30:30828
SMITH, M.A., Observed departures from LTE in stellar Fe I lines. I. The Sun, 30:30319
SMITH, P.M., See GOTTLIEB, N.L., 30:29792
SMITH, R., See AMOS, K., 30:30932
SMITH, R.L., See ADAMS, J.T., 30:30527
SMITH, R.R., See WALLIN, W.R., 30:29624
SMITH, S., See BIBL, K., 30:30410
SMYTHE, L.E., See KIM, C.H., 30:28965
SNEH, Lattice dynamical study of the recoilless fraction of ^{57}Fe in Ni, Mo, W, α-Fe and Cu, 30:30050
SNELL, A.H., See RAMAN, S., 30:30879
SNOEBERGER, D.F., Field measurement of permeabilities in NTS Area 9, 30:29458 (UCID-15895)
See MORRIS, G.A., 30:29323
SNYDER, C.W., See LINDEMAN, R.A., 30:30401
SNYDER, D.L., Direct heat rejection path radioisotopic thermoelectric generator, 30:29240
SOBEL, H.W., See REINES, F., 30:30499
SOBEL'MAN, I.I., See VINOGRADOV, A.V., 30:29163
SOBHANADRI, J., See SURYANARAYANA, D., 30:29069
SOBOTTA, G., See HOFFMANN, D., 30:30148
SODAN, H., See WINTER, G., 30:30992
SOERENSEN, B., See ASCUITTO, R.J., 30:30995
SOGA, F., See SAKAI, M., 30:30974
SOGARD, M.R., See RIORDAN, E.M., 30:30583
SOHLO, S., Semi-inclusive rapidity distributions in a cluster emission model for the pionization component, 30:30756
SOKHINA, L.P., Formation of colloidal neptunium in nitric acid solutions, 30:29116
See RAMAZANOV, L.M., 30:29107
SOKOLOV, G.A., Zonality of hydrothermal ore deposits. Volume I. Zonality of deposits of tin, tungsten, molybdenum, and some groups of less-common metals, 30:29332
SOKOL'SKII, D.V., Moessbauer spectroscopic study of the effect of reactor radiation on the iron(III) acetylacetonate-triethylaluminum catalyst, 30:29052
SOLAR RADIO GROUP UTRECHT, Type III bursts, 30:30334
SOLHED, H., See LINDSKOG, J., 30:30979
SOLINA, L.V., See MAGAT, L.M., 30:30041
SOLOV'EV, G.N., See KLARIN, A.P., 30:29623
SOLOV'EV, V.A., See BUDAGOVSKII, S.S., 30:30029
SOLYAKIN, G.E., See KASSIROV, S.A., 30:29526
SOMA, T., See SAWAOKA, A., 30:29923
SOMEKH, S., Transverse mode control in a distributed feedback semiconducor laser, 30:29279
SOMENKOV, V.A., Isotopic ordering in CeD_2H, 30:29008 (IAE-2309)
SOMOGYI, A.J., Angular distribution of high energy charged particles in the galaxy, 30:30342 (CONF-730693-)
See KIRALY, P., 30:30160
SONA, P., Spin and parity of the first excited level in ^{53}Fe, 30:30917
SODD, P.M., See GURTU, A., 30:30604

SOOHOO, R., See HSIEH, E.J., 30:31454
See HSIEH, E.J., 30:31455
SORACE, E., See CELEGHINI, E., 30:30719
SORENSEN, R.W., See KANSTEIN, L.L., 30:30127
SORENSON, L.B., See PUTTER, J.M., 30:30599
SOROKA, V.I., See MAL'KU, A.I., 30:30909
SOROKIN, G.A., See MIGDAL, A.B., 30:31088
SOROKIN, Y.M., Multimode parametric interactions in a plasma with low-frequency pumping, 30:29236
SOSNOVSKII, L.A., See ZELENYUK, E.E., 30:30013
SOTNIKOV, V.S., Effect of irradiation of metal ions on adsorption properties of semiconductor materials. I. Adsorption properties of oxidized surface of silicon, 30:29053
SOUBIROU, F., See KELLERSHOHN, C., 30:29051
SOUREK, J., See STRNAD, M., 30:31297
SOURES, J., High power Nd:glass laser for fusion applications, 30:29231
SOUSBIE, G., See QUEBERT, J.L., 30:30996
SOVTER, V.V., Effective cross sections and peculiarities of electron excitation of the cadmium atom, 30:30523
SPEECKAERT, Ph., See BAETSLE, L., 30:28991
SPEICHER, W., See RUPPERSBERG, H., 30:31382
SPEIR, L.G., See REILLY, T.D., 30:29509
SPEJEWSKI, E.H., See SCHMIDT-OTT, W.D., 30:30986
SPIERING, Ch., See GRAESSLER, H., 30:30610
SPIGARELLI, S.A., See ROMBERG, G.P., 30:29462
SPITZER, L. Jr., On the theory of H_2 rotational excitation, 30:30357
SPRANGLE, P., See GRANATSTEIN, V.L., 30:30580
SPRINGER, T.E., See MURRAY, H.S., 30:31325
SPROTT, G.F., Limit on X-ray emission from a supernova during maximum light, 30:30260
SPRUNG, D.W.L., Realistic super-soft-core potential model of the N--N interaction, 30:31035
SRAMEK, R.A., Radio emission from Markarian 6, 30:30382
SREBRNY, J., See DRUSTE, C., 30:30963
SREBRO, Z., Gomori-positive glia in uv-irradiated mice, 30:29752
SREEDHAR, V., Inclusive π^- production in π^+d interactions at 24 GeV/c, 30:30616
SREENIVASAN, A., See SRINIVAS, H., 30:29767
SREERAMULU, K., Studies on interrelationship of quantitative traits in M_3 and M_4 generations following mutagenic treatments in sorghum, 30:29698
SRINIVAS, H., Insensitivity of serially transferred Tetrahymena pyriformis W. to irradiated media, 30:29767
SRIVASTAVA, B.S., Repair of γ-ray-induced damage in bacteriophage lambda, 30:29680
STAERK, H., See OSTERMANN, P., 30:28912
STAFFORD, R.G., Ventilation design modifications at Los Alamos Scientific Laboratory major plutonium operational areas, 30:29328 (LA-UR-74-1132)
STAHL, W.F., Process for converting heat produced by a nuclear reactor to electrical energy, 30:31282
STALLARD, B.W., See CHRISTOFILOS, N.C., 30:29188
STANFORD, A.L., See FISCHER, S.F., 30:29015
STANKEVICH, K.S., Characteristics of the turbulent atmosphere on the basis of radio source scintillation data, 30:30411
STANKIEWICZ, O., See ALENIUS, G., 30:30916
STANLEY, R.E., Absorption, distribution, and excretion of plutonium by dairy cattle, 30:29810 (NVO-AEIC-74-1)
STANTON, R.E., Colorimetric determination of molybdenum in oganic-rich soil, 30:28960
STAPFER, G., Silicon germanium technology program at JPL, 30:29247
STAPLES, B.A., Evaluation of quinol clathrate for fission product noble gas storage, 30:30108 (ICP-1045)
STAPP, H.P., Causality in indefinite metric theories, 30:31164
STARA, J.F., Comparison of /sup 115m/Ca retention in rats following different routes of administration, 30:29815
STARCH, M., See KRAUSE, H., 30:29136
STARCHENCKO, E.A., See BUMAZSHNOV, V.A., 30:30603
STARIKOV, B.G., See BAKULIN, V.N., 30:29396
STARIKOV, V.N., See DYAD'KIN, I.G., 30:29605
STAROBINSKAYA, N.G., Publications from 1970--1972 of the Metallurgical Publishers. Annotated index, 30:30042
STAROSTA, W., See DROSTE, C., 30:30963
STARTSEV, G.P., See GERASIMOV, G.N., 30:30489
STATKEVICH, V.N., See MALASHENKO, I.S., 30:30014
See MOVCHAN, B.A., 30:30008
STAVITSKII, R.V., Gonad doses of irradiation of patients in x-ray studies, 30:29718
See KHETEEV, M.V., 30:31109
STEADMAN, S., Polarization in HI inelastic scattering in the Coulomb--nuclear interference region and coupled channel effects, 30:30920
STEBBINGS, R.F., See DUNNING, F.B., 30:30500
STECH, B., See GROMES, D., 30:31159
STECKER, F.W., See PUGET, J.L., 30:30163
STEELE, L.E., Irradiation effects on reactor structural materials. Semiannual progress report, 1 August 1973--31 January 1974, 30:30060 (AD-777433)
STEFANINI, A., See DEL GUERRA, A., 30:30578
STEIN, G., See MARKETOS, D.G., 30:29081
STEIN, L., Atmosphere purification of xenon, radon, and radon daughter elements, 30:28995
STEINBERG, M., See KUKACKA, L.E., 30:31388
STEINFELD, J.I., See RUBINSON, M., 30:30561
STEINITZ, R., See HOUSE, L.L., 30:30202
STEINKE, A., See KNOEDLER, D., 30:31284
STEKOL'NIKOV, B.A., See DUBOVOI, L.V., 30:30121
STELSON, P.H., See FORD, J.L.C. Jr., 30:30911
See RAMAN, S., 30:30879
See RIEDINGER, L.L., 30:30985
STELTER, L., Radiation chemistry of DNA-model compounds. V. Phosphate elimination from ribose-5-phosphate after OH radical attack at C4, 30:29071
STENBAEK-NIELSEN, H.C., Indications of a longitudinal component in auroral phenomena, 30:30428
STEPANOV, K.N., See KALADZE, T.D., 30:29234
STEPANOV, N.S., See SOROKIN, Y.M., 30:29236
STEPANOV, V.I., See ALEKSEEV, E.N., 30:29578
STEPANYAN, A.A., See PAVLOV, I.V., 30:29580
STEPHAN, G., Genetic radiation effects, 30:29700 (AED-CONF-74-030-004)
STEPHENS, D.R., Elastic constants of fractured Hardhat granodiorite, 30:31398 (UCID-16369)
Preliminary equation-of-state data for Baneberry altered tuff, 30:29322 (UCID-15074)
See HEARD, H.C., 30:29316
STEPHENS, F.S., See PROETEL, D., 30:31006
STEPHENS, T.C., See WITT, A.N., 30:30364
STEPHENSON, C.B., Spectroscopic observations of interesting Southern stars noted on southern objective-prism plates, 30:30253
STEPHENSON, M., Sterilization method and product, 30:29647
STEPHENSON, R.L., Program for computing the dispersion of airborne contaminants, 30:29381 (ORNL-TM-4674)
See WEST, D., 30:31337
STERN, R.C., See BECKER, W.G., 30:30528
STESHENKO, A.I., See FILIPPOV, G.F., 30:31053
STEVENS, H.H., See LEMPERT, J., 30:31302
STEVENS, W., Alternate methods for administering chelating agents in decorporation therapy, 30:29798 (COO-119-249)
See ATHERTON, D.R., 30:29803
See BRUENGER, F.W., 30:29804
STEVENSON, C., See BRAVO, A., 30:29865
STEWARD, M.W., See GAZE, S., 30:29867
STEWART, J.W., See LAWRENCE, C.W., 30:29683
STEWART, L.D., See DAVIS, R.C., 30:29209
STEYER, T.R., See DAY, K.L., 30:30190
STIER, H.E., See BAETZNER, K., 30:30589
STIRLING, W.L., See DAVIS, R.C., 30:29209
ST. JOHN, R.M., See WALKER, J.D. Jr., 30:30526
STOCKTON, A., Redshift of a galaxy near 4C11.50, 30:30378
STODOLSKY, L., Neutron optics and weak currents, 30:30685
STOFFELS, J.J., Spectrometer for on-line analysis of radionuclides (SOLAR), 30:29571
STOICA, A.D., Resolution of slow neutron spectrometers. I. General method to calculate the resolution function. II. Resolution function for time of flight diffractometry, 30:29559 (IFA-FN-45-1974)
STOLL, H.M., F-M detection in the argon ion laser, 30:29268 (UCID-15371)
STOLTERFOHT, N., Argon L-shell ionization by 50- to 600-keV H^+, D^+, H_2^+, and He^+ impact, 30:30541
STONE, J.L., See JONES, L.W., 30:29595
STONE, R.G., See FAINBERG, J., 30:30336
STONER, D.R., High performance thermal insulation for an implantable artificial heart, 30:29241
STONER, R.E., The interpretation of broad emission lines in high-redshift QSOS, 30:30266
STORM, D., Variational bounds on the 1s-charge-exchange amplitude in proton--hydrogen-atom scattering, 30:30542
STOROZHUK, O.M., See SKOROV, D.M., 30:30002
STOUDT, R.H., Mark C (17 x 17) fuel assembly. Research and development, 30:31195 (BAW-10097)
STRAIN, R.V., See FOSTER, J.P., 30:30085
STRAND, A.E., Gel'fand-pattern technique applied to the physically important SU(3) x SU(2) is contained in SU(6) decomposition of SU(6), 30:30768
STRATAN, G., See FURMAN, V.I., 30:31102
STRATHDEE, J., See DELBOURGO, R., 30:30724
STRAUB, R.F., See KROYHN, D.L., 30:29765
STRAUSS, M.W., See PROKOP, E.K., 30:29648
STREATER, R.F., Mathematics of contemporary physics. Proceedings of a conference held at London, England, August 23--September 11, 1971, 30:31164
STREETMAN, B.G., See JONES, C.E., 30:30099
STREICH, M., Recovery of rare gases in air separation and ammonia plants, 30:28993
STRNAD, M., Temperature control and emergency protection against perilous temperatures in nuclear reactor, 30:31297
STROEMBERG, L.G., See BERGMAN, R., 30:28918
STROHM, W.W., See WOLTERMANN, H.A., 30:28979

STRONSKI, I., Recent results in the application of column extraction chromatography in inorganic analysis, 30:28989 (ANL-Trans-960)
STRYUK, V.S., See MAL'KO, A.I., 30:30909
STUCK, R., See PONPON, J.P., 30:29534
STUERMER, W., See LEMPERT, J., 30:31302
STUKAS, V., ^{40}Ar/^{39}Ar dating of the long range dikes, Newfoundland, 30:29338
STYRO, B.I., Scavenging of radioactive material from the atmosphere by surface condensation, 30:29391
  Specific radioactivity distribution in rain drops, 30:29394
SUDAN, R.N., See MCDONALD, B.E., 30:30427
SUDOVTSOV, A.I., See PAN, V.M., 30:30048
SUENAGA, M., See BUSSIERE, J.F., 30:30840
SUESS, S.T., Galactic cosmic ray modulation in the outer solar system: solar wind consequences, 30:30340 (COM-74-50233)
SUETINA, I.A., See KRUSHCHOV, N.G., 30:29760
SUGAHARA, T., See TAMURA, H., 30:29706
SUGIHARA, T.T., See GONO, Y., 30:30965
SUGIYAMA, Y., See TAMURA, H., 30:29706
SUHONEN, E., See CHAICHIAN, M., 30:30700
  See LAM, W.S., 30:30669
SUIT, H.D., Dose-limiting tissues in relation to types and location of tumors. Implications for efforts to improve radiation dose distributions, 30:29725
SULLIVAN, J.C., See WESCHLER, C.J., 30:29132
SULYAEV, R.M., See AKOPDJANOV, G.A., 30:30608
SUMITA, K., High flux research reactor and research on reactor physics and reactor engineering, 30:31235 (KURRI-TR-110)
SUNAKSLIS, Y.M., See GELFGAT, J.M., 30:30572
SUNDBERG, M., Electron microscope study of some nonstoichiometric tungsten oxides, 30:29904
SUNDERMAN, F.W. Jr., See DECSY, M.I., 30:29088
SUNDMAN, A., Spectral survey of the southern Milky Way. I. General description and catalog I (l = 306--318°), 30:30352
SUNDQVIST, B., Nondestructive determination of the nitrogen (protein) content in single kernels of seeds, 30:28917 (NP-20122)
  See JOHANSSON, A., 30:30855
SUREAU, A., See JAEGLE, P., 30:29194
SURKAN, A.J., ULF geomagnetic power near L = 4. III. Statistical study of power spectra in conjugate areas during December solstice, 30:30457
  See LANZEROTTI, L.J., 30:30458
SUROTKEVICHIENE, R., See PAVLOTSKAYA, F.I., 30:29384
SUROWIAK, J., See BARBACKA, G., 30:29751
SURPLICE, A., See SINGH, B., 30:30052
SURYANARAYANA, D., ESR study of paramagnetic centers in irradiated $Ba(ClO_3)_2 \cdot H_2O$ and $Ba(ClO_3)_2 \cdot D_2O$ single crystals, 30:29069
SUSHANIN, I.V., Experimental investigation of the effective cross section of excitations of bands of some decay products of water, ammonia, and acetonitrile by slow electrons, 30:30546
SUSSKIND, L., See KOGUT, J., 30:30630
SUTHERLAND, D.G., See REID, A.W., 30:30746
SUTHERLAND, P.G., See CHEN, H., 30:30194
SUTTER, S.L., See SEHMEL, G.A., 30:29484
  See SEHMEL, G.A., 30:29482
SUTTON, W.W., See STANLEY, R.E., 30:29810
SUYDAM, B.R., Computations on the parameter values inside of the E.M. source, 30:29310 (LAMS-2610)
SUZUKI, H., Initial-stage sintering of sol-gel urania, 30:29922
  New aspect of grain growth of sol-gel urania, 30:29921
SUZUKI, S., See HARA, M., 30:29093
SUZUKI, T., Problems of emergency core cooling system, 30:31191
SUZUKI, Y., Clinical evaluation of tumor scanning with ^{57}Co-bleomycin, 30:29846
SVALGAARD, L., See LANGEL, R.A., 30:30460
SVEDBERG, R.C., See STONER, D.R., 30:29241
SVEDOMTSEV, N.V., See ZOLOTUKHIN, I.V., 30:29887
SVENSSON, L.G., See LINDSKOG, J., 30:30979
SVETLOPOLYANSKAYA, T.P., See DAN'KIN, A.A., 30:29899
SVETLOPOLYANSKII, V.I., See DAN'KIN, A.A., 30:29899
SVIRYAKIN, D.I., See BOIKO, V.I., 30:30144
SWAIN, A.D., Human error quantification, 30:31360 (SCR-610)
SWANSON, R.E., See COPLEN, H.L., 30:31238
SWANT, D.H., See LONG, D.M., 30:29888
SWINDLE, D.L., See KRIVAN, V., 30:28922
SWINSON, D.B., The possible influence of Jupiter on cosmic radiation at the earth, 30:30173
SWIRIDOV, V.A., See BARABOSCH, L.S., 30:30117
SYKES, M.P., Follow-up on the long-term effects of therapeutic irradiation on bone marrow, 30:29715
SYLVESTER, J.R., Possible effects of thermal effluents on fish: a review, 30:29467
SYMM, G.T., Computation of potential in a multiwire proportional counter of arbitrary cross-section, 30:29601
SYMONS, M.C.R., See MISHRA, S.P., 30:29073
  See MISHRA, S.P., 30:29076
SZABO, A., See BENDE, E., 30:28976
SZAFRANSKI, A.W., See SKOSKIEWICZ, T., 30:30813
SZALAY, A.S., See MARX, G., 30:30679
SZCZEPANEK, P.S., See HARTE, W.E., 30:30477
SZEBEHELY, V., Analysis of a one-parameter family of triple close approaches occurring in stellar systems, 30:30238
SZEGEDI, S., See VARNAGY, M., 30:29527
SZEGOE, K., Field theories without Ward-identities, 30:31145 (KFKI-74-46)
  See IWAKI, A., 30:30628
SZOTA, Z., Use of x-rays in sugar beet breeding, 30:29693
SZPILOWSKI, S., See ZIELINSKI, M., 30:29027
SZPRYNGER, A., Condensate density in Bogolyubov hydrodynamics, 30:30796
  Formulae for kinetic coefficients in the case of He II, 30:30793
SZUMIEL, I., Histone F1 phosphorus content and DNA synthesis in slowly-growing sublines of L5178Y-S cells, 30:29669
SZYMACHA, A., Spontaneous CP violation in the generalized Georgi--Glashow model, 30:30773
SZYMANSKI, A., See PANKE, R., 30:29723

T

TABAKIN, F., See LEE, T.S.H., 30:30897
TACCETTI, N., See SONA, P., 30:30917
TAGAWA, T., See HAGIWARA, M., 30:29058
TAIT, N.R.S., Nuclear structure facility 20/30 mV tandem accelerator, 30:30118
TAKAGI, K., See FOURIKIS, N., 30:30360
  See KAIFU, N., 30:30359
TAKAGI, S., See YOSHIDA, T., 30:29863
TAKAHASHI, R., Derivation of transfer functions in boiling loops, 30:29292
TAKAHASHI, S., Radiation levels of macroradiography, 30:31106
TAKAKURA, T., See VORPAHL, J.A., 30:30299
TAKANO, Y., Gravitational field in Finsler spaces, 30:31177
TAKASU, T., Study on mechanisms of nervous system disturbance by radioactively labeled chinoform, 30:29879
TAKATA, K., See ONO, K., 30:30120
TAKAYANAGI, K., See ASHIHARA, O., 30:30442
TAKEUCHI, T., See FUKUCHI, S., 30:29876
TAKIGAWA, N., See LANDOWNE, S., 30:31087
TAMAIN, B., See HANAPPE, F., 30:30984
TAMERS, M.A., Somatic mutation by endogenous radiocarbon, 30:29787
TAMMANN, G.A., See SANDAGE, A., 30:30393
TAMURA, H., Changes in the number of circulating lymphocytes with chromosomal aberrations following a single exposure of the pelvis to x-irradiation in cancer patients, 30:29706
TAMURA, S., Note on an infinite-mass limit of the Higgs model, 30:31153
TAMURA, T., Distribution and characterization of plutonium in soils from Nevada Test Site, 30:29443 (NVO-AEIC-74-1)
TAN, C.I., See GAISSER, T.K., 30:30763
TANEMORI, K., See YOSHIDA, T., 30:29863
TANG, K.T., See CHOI, B.H., 30:30533
TANG, S.Y., Negative ion formation from energetic collisions of cesium with CO_2, CS_2, and COS, 30:30548
TANIZAWA, O., See ICHII, H., 30:29860
TANNENBAUM, M.J., See KIM, I.J., 30:30584
TANNER, T.M., See YOUNG, J.A., 30:29481
  See YOUNG, J.A., 30:29473
  See YOUNG, J.A., 30:29427
TANTRY, B.A.P., See GUPTA, S.P., 30:30418
TARABAN'KO, V.A., See ERMOLAEV, O.Ya., 30:30844
TARASOV, L.V., See D'YAKOV, V.A., 30:30112
TARASOV, S.I., See PISKUNOV, L.I., 30:29395
TARASOV, V.A., See BONDAREVSKII, S.I., 30:29096
TARDY, J., See THOMAS, J.-P., 30:29510
TATARCZUK, J.R., See DANCHAK, M., 30:29620
TATARU, L., See SALIU, L., 30:30778
TATUR, S., See SZYMACHA, A., 30:30773
TAVERNIER, S., See DEHM, G., 30:30624
TAYLOR, D.M., See DANPURE, C.J., 30:29782
TAYLOR, G.N., Evaluation of long-term ZnDTPA therapy in beagles, 30:29796 (COO-119-249)
  See LLOYD, R.D., 30:29797
TAYLOR, J.B., Bundle divertors and topology, 30:29204 (CLM-R-132)
TAYLOR, J.C., Uranium tetrabromide structure. A new MX_4 structure type, 30:29129
TAYLOR, P.O., See CRANDALL, D.H., 30:30246
TAYLOR, R.D., Construction of an adjustable carrying handle for the FIDLER detector, 30:29497 (UCID-15775)
  See KELLER, W.E., 30:30820
TAYLOR, W.E., See ATAC, M., 30:29594
TAYSUM, D.H., See FISHER, D.R., 30:29799
TCHENG-SI, W., See BARTHOLIN, H., 30:29993
TEDROW, P.M., See MESERVEY, R., 30:30839
TEJESSY, W., See ADERHOLZ, M., 30:29595
TEKUMALLA, A.R., Unitary Foldy--Wouthuysen transformations for particles of arbitrary spin, 30:31152
TELUSHKINA, E.L., See ZYKOVA, A.S., 30:29399
TEMKIN, A., See JACOBS, V.L., 30:30245
TEMNIKOV, P.P., See PERVUSHIN, V.N., 30:30649
TEMPLE, R.K., See BIBL, K., 30:30410
TENDOW, Y., See HASHIZUME, A., 30:30154
TENNANT, D.C., Automatic corrections for deadtime effects and lineshape changes due to source decay in positron-annihilation experiments, 30:29513
TEPER, M., Inclusive processes at large transverse momenta, 30:30636
TEPLYKH, L.A., See TROITSKAYA, M.N., 30:29405

TERADA, K., Determination of ruthenium-106 in sea water, 30:28984
TEREKHOV, Yu.V., See KISELEV, Yu.T., 30:29633
TERENT'EV, N.K., See KASSIROV, S.A., 30:29526
TER-MARTIROSYAN, K.A., See KAIDALOV, A.B., 30:30760
TERRANOVA, M.L., See DI NAPOLI, V., 30:30919
TERRIEN, Y., See MAGUIRE, C.F., 30:30997
TER-SAAKOV, A.A., See IZRAEHL, Yu.A., 30:29387
  See PETROV, V.N., 30:29390
TERZIAN, Y., Observations of the H 85α line from planetary nebulae, 30:30240
TESTA, M., See CABIBBO, N., 30:30709
TESTER, J.R., Vertebrate behavior and ecology. Progress report, July 1, 1973--June 30, 1974, 30:31377 (COO-1332-103)
TEUBNER, P.J.O., See LLOYD, C.R., 30:30535
TEUCHERT, E., See BOHN, T., 30:31208
TEXTORIS, R., Estimation of radiation doses from i. v. administration of selenite $Na_2{}^{75}SeO_3$, 30:29793
THADDEUS, P., See GREEN, S., 30:30385
THALER, R.M., See SHAKIN, C.M., 30:31056
THATCHER, T.O., See SCHNEIDER, M.J., 30:29461
THEFELD, W., Special laboratory-chemical examination techniques, 30:29702 (AED-CONF-74-221-006)
THIELE, E., See CLARKE, J.H., 30:30563
THOMAS, C., Systematics of iatrogenic carcinogenesis, 30:29724
THOMAS, C.L., Computation of MHD equilibria in Tokamak, 30:29179 (CLM-R-133)
THOMAS, C.W., Atmospheric natural aerosols and fallout particulates during 1973 at Richland, Washington and Point Barrow, Alaska, 30:29361 (BNWL-1850(Pt.3))
  See PERKINS, R.W., 30:29359
  See ROSINSKI, J., 30:29367
  See YOUNG, J.A., 30:29427
  See YOUNG, J.A., 30:29473
  See YOUNG, J.A., 30:29481
THOMAS, J.-P., A telescope counter detection system applied to low-energy ion-beam surface analysis, 30:29510
THOMAS, S.W., LLL compact 10-ps streak camera, 1974 update, 30:29162 (UCRL-75557)
THOME, Z.D., See RAGUSA, S., 30:30720
THOMMES, M.M., See ROMBERG, G.P., 30:29462
THOMPSON, J.C. Jr., See COMAR, C.L., 30:29416
THOMPSON, S.D., Diagnostics of seeded rf plasmas: an experimental study related to the gaseous core nuclear reactor. Final report, 1 September 1971--31 July 1973, 30:31241 (N-74-23299)
THOMPSON, W.J., See IKOSSI, P.G., 30:30949
THOMSEN, D.H., See JENQUIN, U.P., 30:31187
'T HOOFT, G., A two-dimensional model for mesons, 30:30725
THORNDIKE, E.H., See NORDBERG, M.E. Jr., 30:30590
THORNE, K.S., Disk-accretion onto a black hole. II. Evolution of the hole, 30:30188
  See PAGE, D.N., 30:30187
THORNTON, S.T., L- and M-shell ionization of various elements by fast-α-particle bombardment, 30:30537
  See FORD, J.L.C. Jr., 30:30911
THORP, J.M., ALE reserve climatology for 1973, 30:29437 (BNWL-1850(Pt.3))
  See DANA, M.T., 30:29479
  See DAVIS, W.E., 30:29475
THRALL, J.H., Pitfalls in /sup 99m/Tc polyphosphate skeletal imaging, 30:29849
THUAN, T.X., Gravitional radiation from stellar collapse, 30:30231
THUN, J.E., Static electric quadrupole moment of the first 2^+-state in ^{110}Pd, 30:30955 (HP-20122)
THUN, R., See FINOCCHIARO, G., 30:30605
THYN, J., Evaluation of response functions which are obtained when radioisotopes are used as a tracer. I. Application of the scaler, 30:29639
  Processing of the response functions obtained by radiotracer measurements. II. Approximation of the measured relations and smoothing of variations by means of Laguerre functions, 30:29638
TIDWELL, J.T., See BRADBURN, E.H., 30:29999
TIKHONOV, M.F., See KULTUNOV, V.S., 30:29115
TILLES, E.B., Application of electrically conductive coatings to insulating tubes of switching magnets for particle accelerators, 30:30123
TILLEY, R.J.D., See SUNDBERG, M., 30:29904
TIMOFEEV, G.A., See FROLOVA, L.M., 30:29102
  See RYKOV, A.G., 30:29106
  See RYKOV, A.G., 30:29105
TIMOKHIN, V.V., See JENKOVSZKY, L.L., 30:30694
TINKHAM, M., See SKOCPOL, W.J., 30:30819
TISHKIN, A.I., Hypogenic zonality in hydrothermal uranium deposits, 30:29334
TITIRICI, M., See BUCURESCU, D., 30:30943
TITTERTON, E.W., Radiation in man's environment, 30:29353
TKACHENKO, E.G., See EFIMOV, V.N., 30:31047
TOAFF, S., See DADU, S., 30:30621
TOBAIS, K.A., Problems of space radiobiology and radiation safety in space missions, 30:29712
TODD, P., Radiobiology with heavy charged particles directed at radiotherapy, 30:31117
TODOKI, M., Melting behavior of Nylon 6, 30:29059
TODOROV, I.M., See FUNARAR'OV, A.B., 30:29036
TOENNIES, J.P., Observation of orbiting resonances in the integral cross section of H--Xe, 30:30532
TOFT, A.D., Plasma TSH and serum T-4 levels in longer-term follow-up of patients treated with ^{131}I for thyrotoxicosis, 30:29775
TOKUDA, N., Gnome model and deep-inelastic lepton-nucleon structure functions, 30:30708
TOLBA, M.F., See EL BEDEWI, F., 30:30179
TOLOKONNIKOV, N.P., See BOLDYREV, A.M., 30:30012
TOMBRELLO, T.A., See HAFF, P.K., 30:30509
TOMLINSON, R.G., See HAUGHT, A.F., 30:29152
TONIOLO, D., See FASOLI, U., 30:30981
TOOR, A., The Crab Nebula as a calibration source for x-ray astronomy, 30:30280
TOPA, V., See BIRJEGA, M.I., 30:29927
TOPOR, V., See ION, D.B., 30:31020
TORBICKI, H., See ZIELINSKI, M., 30:29027
TORELLI, L., See BITELLI, G., 30:31274
TORGOISKAYA, T.I., Kinetics of forming ammoniates of uranium tetrachloride, 30:29124
TOROK, I., Investigations on material transport and dust formation in revolving furnaces for Clinkering by isotopic tracing, 30:29644
TORRES-PEIMBERT, S., Ionization of the low-density interstellar medium, 30:30351
TOTH, I.J., See SCHEIRER, S.T., 30:29975
TOUNTAS, C., See PAPADIMITRIOU, J., 30:29850
TOURRENC, P., See GROSSIORD, J.L., 30:31178
TOVE, P.A., See JANNEY, R.B., 30:29629
TOVMASSIAN, H.M., See SRAMEK, R.A., 30:30382
TOW, D.M., See GAISSER, T.K., 30:30763
TOYA, R.E., See YUHAS, J.M., 30:29756
TOYAMA, H., Electron orbits in the ERA (electron ring accelerator) with an electrostatic-type inflector system, 30:30132
TRAINOR, D.W., Flash photolysis study of the gas phase recombination of hydroxyl radicals, 30:29066
TRAN, D.T., See BENSUSSAN, A., 30:30126
TRAN THANH VAN, J., Proceedings of the eighth Rencontre de Moriond. Volume II. The pomeron. Conference held at Meribel-les-Allues, France, March 4--16, 1973, 30:30633
  Proceedings of the eighth Rencontre de Moriond. Volume I. Electromagnetic and weak interactions. Conference held at Meribel-les-Allues, France, March 4--16, 1973, 30:30663
TRAUTNER, N., See BRESKIN, A., 30:29587
TRAVERSI, G., See FIZZOTTI, C., 30:31279
TREFILOV, V.I., See ARKHAROV, V.I., 30:30023
  See KAVERINA, S.N., 30:30057
  See KOVSH, S.V., 30:30028
  See RAKITSKII, A.N., 30:30058
TREGUBOV, N.N., See AKULOVA, I.S., 30:29041
TREHAN, P.N., See BHATI, S.S., 30:30958
TRELA, M., New approach to predicting pressure drop in two-phase flows, 30:29293
TREPP, C., See GIGER, U., 30:29576
TREVES, A., See BERGAMINI, R., 30:30208
TRGOVCEVIC, Z., Postirradiation fate of bacteriophage lambda DNA in the host cell, 30:29678
TRIBOULET, R., See DABROWSKI, A.J., 30:29520
TRIMBLE, V., On the distribution of binary system mass ratios, 30:30235
TRIPATHI, A.N., Polarization of the resonance lines of lithium and sodium atoms by electron impact, 30:30521 (IC-73-19)
TRIPP, G.R., See THOMAS, S.W., 30:29162
TRIPP, R.D., See BAILLON, P., 30:30619
  See BAILLON, P., 30:30618
  See BAILLON, P., 30:30737
TROITSKAYA, M.N., ^{137}Cs, ^{90}Sr, and ^{210}Pb in soils of the Arctic regions, 30:29405
TROITSKII, I.N., Comparative analysis of the accuracy of absolute and relative methods of thickness measurement using scattered radiation, 30:29606
TROITSKII, S.V., Scattering by ion-acoustic waves in a rectangular waveguide, 30:29235
TROJNAR, E., See JASZCZUK, W., 30:30842
TROLAND, T., See MARGON, B., 30:30174
TROLL, W., See ROFFMAN, S., 30:29834
TROMBKA, J.I., See HARRINGTON, T.M., 30:29566
TRONC, D., See BENSUSSAN, A., 30:30126
TRONOV, B.N., See ANGELOV, B.P., 30:30143
TRUBY, F.K., See RICE, J.K., 30:31368
TRUFAKIN, V.A., See BAKULIN, V.N., 30:29396
TRUHLAR, D.G., Finite-difference boundary-value method for determination of resonance widths in atomic collisions, 30:30564
TRUJILLO, R.E., Measurement of the radiation inactivation of attenuated poliovirus by the plaque assay technique, 30:29676 (SLA-74-0065)
TRUKHAN, M.G., See MISYURA, V.A., 30:30447
TRUNOV, V.K., See SEREZHKIN, V.N., 30:29941
TRUSCELLO, V., See ROUKLOVE, P., 30:29248
TRUSCELLO, V.C., See STAPFER, G., 30:29247
TRUSOVA, E.M., See LEONOV, A.I., 30:29911
  See LEONOV, A.I., 30:29909
TSAI, C., See HSIEH, E.J., 30:31454
TSAI, M.I., See BRESLAVETS, K.G., 30:31394
TSAI, S.F., See BERTSCH, G., 30:31078
TSAO, C.H., See SILBERBERG, R., 30:30854
TSAO, H.S., See DESER, S., 30:31184
TSEVELEV, M.A., See DAVYDOV, E.N., 30:29408
TSIDULKO, I.M., See POYZNER, B.N., 30:29287

TSUCHIDA, E., See HAGIWARA, M., 30:29058
TSUJI, T., See MATSUI, T., 30:29924
TSUKAMOTO, T., See KAWAZOE, Y., 30:30881
TSUKIYAMA, I., See OHSHIMA, T., 30:29722
TSURUGI, J., See NAKAO, R., 30:29047
TSUSHIMA, T., Identification of sparganum growth factor by a radioreceptor assay for growth hormone, 30:29868
TSVILYUK, I.S., Study of some high-temperature strength properties of the niobium alloys 5VMTs, 5VMTsU, and 5VTTs at 1100°C, 30:30027
TU, K.N., See LAU, S.S., 30:29939
TUAN, S.F., See DOBSON, P.N. Jr., 30:30577
TULLY, G.R. Jr., See ELSON, R.E., 30:29127
TUMANOV, Yu.P., See PLATONOV, P.A., 30:30090
TUOHY, I.R., See RAPLEY, C.G., 30:30365
TURKO, L., See LUKIERSKI, J., 30:30722
TURNAU, J., See JADACH, S., 30:30701
TURNER, B.E., See MORRIS, M., 30:30374
TURNER, C.E., Review of current status of yielding fracture mechanics, 30:30053
TURNER, G.K., See CLOUGH, A.S., 30:30891
TURTELLI, A. Jr., See RODRIGUES, W.A. Jr., 30:30171
TWIN, P.J., See PRICE, H.G., 30:30910
TYAN, Y.L., See ZAIDI, S.A.A., 30:31077
TYAPKIN, Yu.D., Structure of alloys of the Nb--Ti--Zr system. Close order of displacement in solid solutions, 30:30040
TYE, R.P., Heat transmission measurements in thermal insulations. Conference held at Philadelphia, Pennsylvania, April 16--17, 1973, 30:29242
TYURYUKANOVA, E.B., Buildup of ^{90}Sr in soils, 30:29406
TZE, H.C., See OLESEN, P., 30:30647

U

UCHIDA, H., Maximum credible accident (MCA) of light water reactor, 30:31260
UCHIDA, K., See MUTO, K., 30:31265
UDAGAWA, T., See HOFFMANN, G.W., 30:30907
UDUPA, M.R., See GIRIDHARAN, A.S., 30:29090
UEDA, T., Recent developments in meson-theoretical studies of the nucleon--nucleon interaction, 30:30753
UEHARA, S., See HAYASHI, T., 30:29565
UGUZZONI, A., Blocking with realistic decay functions, 30:30969
UHLIK, J., Effect of gamma radiation on generation M_2 of Lens esculenta Moench, 30:29690
  Vegetation characteristics of Lens esculenta (Moench) following irradiation with thermal neutrons, 30:29687
UHLMANN, B., See KOLLBACH, D., 30:31338
UIBERRAK, H., See ZITA, G., 30:29831
ULEHLA, I., ^{4}He nucleus and soft core potentials, 30:30857
  Realistic two-nucleon phenomenological potential, 30:31034
ULLMAN, A., Thermal accommodation coefficients of inert gases on stainless steel and UO_2, 30:30097
ULLRICH, H., See HEINRICH, H., 30:29701
ULMER, M.P., 4.8-second pulsed x-rays from Centaurus X-3 at energy greater than 7 keV, 30:30268
UMEHARA, Y., Structure and phase-boundary energies of the directionally solidified InSb--MnSb--NiSb, InSb--FeSb, and InSb--CrSb eutectic alloys, 30:30019
UNDERHILL, G.K., Resonance integrals of uranium-235/uranium-238 mixtures, 30:31013
UNDERWOOD, B.Y., High spin states in the Ksup(π)=1/2^{-} band of ^{19}F, 30:30885
UNGER, R., Extended array evaluation program. Special report No. 5. Selection of reference waveforms for matched filter processing of long period signals from seismic events, 30:29304 (AD-776815)
UNTERNAEHRER, J., See BUTA, A., 30:30926
URBAN, J., See BETZ, P., 30:29535
USATYI, A.F., Reactions of secondary free radicals in the irradiated frozen aqueous solutions of amino acid and peptides, 30:29044
USENOVA, K.A., Electrochemical investigation of amalgams of rare earth metals. I. Main electrochemical properties of amalgams of rare earth elements, 30:29111
USHAKOV, V.I., See KISELEV, Yu.T., 30:29633
USHIROKAWA, M., See HOSOI, F., 30:29038
USTINOV, V.I., Isotope effect in the vapor pressure of carbon tetrafluoride, 30:29013

V

VACCARI, M., See REFFO, G., 30:30956
VAGNER, S.D., Electron energy distribution in a high-freqeuncy discharge in an axial magnetic field, 30:29166
VAKIL, U.K., See SRINIVAS, H., 30:29767
VALENCICH, T., Trajectory studies of hot atom reactions. II. An unrestricted potential for CH_5, 30:29085
VALLADON, M., See KOHN, A., 30:28923
VALLEE, J.P., Note on linear polarization in the emission frame for radio galaxies and quasars, 30:30278
VALLEY, J.F., See KUSHELEVSKY, A.P., 30:31107
VAN DAMME, K.J., See PAUWELS, E.K.J., 30:29824
VAN DE HULST, H.O., See GREENBERG, J.M., 30:30373
VAN DEN BERGH, S., See MADORE, B.F., 30:30348
VANDENBOSCH, R., Entrance channel effects in the ^{32}S system: comparison of ^{12}C + ^{20}Ne and ^{16}O + ^{16}O elastic scattering, 30:30880
VAN DER MERWE, P.duT., See DUERR, H.P., 30:31155
VANDERMEULEN, J., Properties of the nucleon--antinucleon fireball, 30:30721
VAN DER WERF, S.Y., See HESSELINK, W.H.A., 30:30975
VAN DIEPEN, A.M., See POPMA, J.A., 30:29901
VANDLIK, T., See VANDLIK, Ya., 30:29142
VANDLIK, Ya., Volatility of microamounts of thallium from PbF_2 crystals irradiated with high-energy protons. Fast gas thermochromatographic method of obtaining short-lived thallium isotopes, 30:29142
VAN DRIEL, M.A., Investigation of the 3.46 MeV isomeric level of ^{38}K with the ^{24}Mg(^{16}O,pnγ)^{38}K reaction, 30:30912
  See HERMANS, J.A.J., 30:30864
VAN HORN, H.M., A model for the transient x-ray sources, 30:30269
VAN HOVE, L., See BENECKE, J., 30:30612
VAN KAICK, G., Thorotrast-induced neoplasms, 30:29769 (AED-CONF-74-016-002)
VAN NEERVEN, W.L., See HOLWERDA, M.J., 30:31160
VAN NIEUWENHUIZEN, P., See DESER, S., 30:31184
  See DESER, S., 30:31179
VANNINI, G., See BERTIN, A., 30:31016
VAN PATTER, D.M., See GEORGOPULOS, P.D., 30:30930
VAN RINSVELDT, H.A., See VAN DRIEL, M.A., 30:30912
VAN ROYEN, R.P., See HOLWERDA, M.J., 30:31160
VAN WAGENINGEN, R., Nucleon--nucleon interaction and low-energy properties of three-nucleon systems, 30:31038
VARGAS, J.I., See AURIC, P., 30:30947
VARNAGY, M., Effect of electrons and X-rays on alpha-particle registration in T-Cellit detector, 30:29527
VAROLI, V., See MANFREDI, P.F., 30:29628
VARSHNI, Y.P., Analysis of rotational and quasirotational ground-state bands in even--even nuclei, 30:30957
VARY, J.P., See BARSHAY, S., 30:31095
VASIL'EV, A.A., See KRITSKAYA, V.K., 30:30080
VASIL'EV, A.S., See NAZAROV, L.E., 30:29389
VASIL'EV, M.A., See LARIKOV, L.N, 30:29955
VASIL'EVA, A.G., Kinetics of molybdenum--rhenium alloy oxidation, 30:29949
VASILEVSKAYA, I.I., See VASIL'EVA, A.G., 30:29949
VASILISHIN, B.V., See ISSINSKII, I.B., 30:30129
VASILIU, F., See BIRJEGA, M.I., 30:29927
  See POPESCU-POGRION, N., 30:29928
VASUDEVAN, R., See HUSS, R., 30:31029
VATER, P., See BECKER, H.J., 30:31018
VATSURA, V.V., See GRIGOREVSKII, M.V., 30:30209
VEDRENE, B.K., See STYRO, B.I., 30:29394
VEEDER, G.J., Luminosities and temperatures of M dwarf stars from infrared photometry, 30:30222
VENKATACHARI, R., Anomalous behavior of F-region during the solar eclipse of September 22, 1968, 30:30432
VENKATARATNAM, S., Gamma-rays from the decay of ^{75}Ge, 30:30942
VERBEEK, H., See MEISCHNER, P., 30:30474
VERMA, K., See DEO, M.G., 30:29741
VERNOIS, Y., See JEANMAIRE, L., 30:29795
VERONDINI, E., See UGUZZONI, A., 30:30969
VERZEGNASSI, C., See DEL GUERRA, A., 30:30678
VESCAN, T., See BANYAI, L., 30:30767
VETTER, R.J., See SHANK, K.E., 30:29816
VEZERIDIS, M., See PAPADIMITRIOU, J., 30:29850
VEZIN, R., See GENTA, P., 30:29178
VIALATTE, B., See KOHN, A., 30:28923
VIATTE, P., See BUTA, A., 30:30926
VIDAL, F., See LHUILLIER, D., 30:30797
VIDEBAEK, F., See STEADMAN, S., 30:30920
VIEHBOECK, F.P., See DOBROZEMSKY, R., 30:30977
VIEILLARD-BARON, B., Adaptation of metallic materials to the conditions of utilization, 30:29986
VIERIMA, T.L., See LICHTEN, W., 30:30492
VIETZKE, H., See PIRK, H., 30:29126
VIGIL, M.G., Performance characteristics of Sandia Laboratories 5.8-metre-diameter explosively driven blast simulator, 30:31431 (SLA-74-5239)
VIGONE, M., See BERTANZA, L., 30:30606
VIJAYARAGHAVAN, R., See MALIK, S.K., 30:29997
VIKEN, K.E., ^{125}I-labelling of Candida albicans by electrolysis, 30:29881
VIKHREV, V.V., Break of the current sheath in a noncylindrical Z pinch, 30:29192
VINCENT, P., See GREENBERG, J.S., 30:30922
VINDRYAVSKII, B.A., See PLATONOV, P.A., 30:30090
VINOGRADOV, A.V., Spectroscopic methods for diagnostics of superdense hot plasma, 30:29163
  See AGLITSKII, E.V., 30:29171
VINOGRADOV, V.K., See GEDEONOV, L.I., 30:29404
VINOGRADOVA, V.S., See KONOPLENKO, V.P., 30:29985
VINUELA, E., See CARRASCOSA, J.L., 30:29679
VIOLINI, G., See FERRARI, E., 30:30733
VIROLAINEN, V.A., See VAGNER, S.D., 30:29166
VITALE, A., See BERTIN, A., 30:31016
VITOUX, D., See SALADIN, J.X., 30:30905
VITYUTNEV, V.M., See SHAFIEV, A.I., 30:29141

VLASOV, E.V., See BUMAZSHNOV, V.A., 30:30603
VLASSOPULOS, S.D.P., See JOHNSON, R.C., 30:30740
  See NANOPOULOS, D.V., 30:30657
VLIEKS, A.E., Reaction rates of interest in late stages of stellar nycleosynthesis, 30:30255
VODOVOZOVA, I.G., Horizontal water migration of ^{90}Sr, 30:29407
VOEVODSKII, A.V., See ALEKSEEV, E.N., 30:29578
VOGEL, C., See JAEGLE, P., 30:29194
VOGT, D., See BARTHOLIN, H., 30:29993
VOGTLIN, G., See COENSGEN, F.H., 30:29212
VOILLEQUE, P.G., Comparison of external irradiation and consumption of cows' milk as critical pathways for ^{137}Cs, ^{54}Mn and ^{144}Ce--^{144}Pr released to the atmosphere, 30:29423
VOJNOVICH, T., See STONER, D.R., 30:29241
VOKHMYAKOV, A.N., See DESYATNIK, V.N., 30:29095
VOLES, J., See STRNAD, M., 30:31297
VOLF, V., Decorporation of ^{239}Pu and ^{241}Am in the rat and namster by Zn--DTPA, 30:29813
VOLKOV, V.I., See ISSINSKII, I.B., 30:30129
VOLKOVA, L.S., See SEVAST'YANOV, Yu.G., 30:29143
VOLKOVA, Z.M., See SEMENOVA, E.G., 30:29675
VOLOKITINA, L.A., See NAZAROV, L.E., 30:29389
VOLZHENSKII, D.S., Intrinsic defect conductvity of vanadium pentoxide, 30:29915
VONBERG, D.D., See CATTERALL, M., 30:29733
VONDRAK, R.R., See LINDEMAN, R.A., 30:30401
VON EGIDY, T., See BRAUMANDL, F., 30:29515
VON OERTZEN, W., See MAGUIRE, C.F., 30:30997
VON RETH, R.D., See FRANK, G., 30:29258
VON ROSENBERG, C.W. Jr., See TRAINOR, D.W., 30:29066
VON SONNTAG, C., See STELTER, L., 30:29071
VON ZHAN, U., See PROELSS, G.W., 30:30424
VOROB'EV, A.N., Effect of electron-beam remelting on the high-temperature ductility of steel IKh18N10T irradiated with an integrated flux of $2.7 \cdot 10^{21}$ neutrons/cm^2, 30:30071
VOROB'EV, A.P., See BABINTSEV, V.V., 30:30598
VOROB'EVA, V.A., See GRIGOREVSKII, M.V., 30:30209
VORONOV, B.F., See KOKHOV, E.D., 30:26952
VORPAHL, J.A., Rise time in 20 to 32 keV impulsive x-radiation, 30:30299
VOSS, G.P., See TAIT, N.R.S., 30:30118
VOSSEN, P.G.T., See BINGHAM, R.A., 30:28967
VOTRUBA, J., Coherent transmission of neutral kaons in matter and forward scattering amplitudes, 30:30741
VOX, A., See BELLUSCIO, M., 30:29517
VRIENS, L., Light scattering from Ne, Ar, and Xe arcs, 30:29169
VROOM, D.A., See RUTHERFORD, J.A., 30:30549
VSEKHSVYATSKII, S.K., Problems of cosmic physics, 30:30161
VUKSTICH, V.S., Excitation of resonance lines of K II in electron-atom collisions, 30:30524
VYKHRESTYUK, S.S., See GRIGOREVSKII, M.V., 30:30209
VYROPAEV, V.Ya., See BYU, N.K., 30:28929

W

WADACHI, Y., See MATSUZURU, H., 30:28996
WADLINGER, E.A., See ANDERSON, A.N., 30:29592
WAGNER, G.J., See MAIRLE, G., 30:30886
WAGNER, H.N. Jr., See PROKOP, E.K., 30:29848
WAHLBECK, P.G., See LIU, M.B., 30:29936
WAIBEL, E., See GROSSWENDT, B., 30:29518
WAINWRIGHT, T.E., See GASS, D.M., 30:31441
WAJDA, S., Investigations on the structure of µ-oxochlororuthenate(IV) by the isotopic exchange method, 30:29030
WAKABAYASHI, J., Some technical problems on the dynamic studies of the high flux research reactor, 30:31233 (KURRI-TR-110)
WALDEN, P.L., See SCHEFFLER, P.E., 30:30586
WALKER, J., Comments on ''Luminescence from electron-irradiated silicon'', 30:30101
WALKER, J.D. Jr., Design of a high density atomic hydrogen source and determination of Balmer cross sections, 30:30526
WALKER, J.M., Temperature dependent properties of potting materials, 30:31386 (BDX-613-1133(Rev.))
WALKER, J.S., MhD flow in variable-area conducting rectangular ducts, 30:30571
WALKER, R.E., See SCHELL, E.M., 30:29335
WALKER, R.N.F., See FOWLER, P.H., 30:29521
WALLACE, A., See ROMNEY, E.M., 30:29445
WALLACE, B.A., See ROE, D.B., 30:30798
WALLER, B.J., See MARSHALL, J.S., 30:29415
WALLIN, W.R., Monitor for radiation-induced heating, 30:29624
WALSON, R.P., Stress--velocity relations for dislocations in niobium, 30:29976 (AD-776621)
WALTON, L.A., See STOUDT, R.H., 30:31195
WALTON, R.B., Gamma-ray assay of low-enriched uranium waste, 30:28986
  See REILLY, T.D., 30:29509
WAMBACH, U.M., Statistical bootstrap model without exotic fireballs, 30:30713
WAMBERSIE, A., Cellular repair after x or gamma irradiation determined for several gross criteria on animals and patients, 30:29759
WANG, C.L., Transition counters for πK differentiation above 400 GeV, 30:29599
  See BERLEY, D., 30:30141
WANG, C.S., See MURPHY, C.H., 30:30438
WANG, J.C., Neutron-deuteron differential cross section at 26.5 MeV, 30:30873
WANG, T.M., Effects of Phytohemaglutinin-P (PHA-P) on bone cells of the tibial and femoral metaphysis of the rats, 30:29800 (COO-119-249)
WANNBERG, G., See EASTROEM, C., 30:30976
WARD, D., See HAEUSSER, O., 30:31004
WARD, M.E., See LORE, J.D., 30:31413
WARNER, G.A., See ROWLEY, M.J., 30:29708
WARNER, R.E., See HAEUSSER, O., 30:31004
WARREN, D.T., Nuclear correction for Genesis, 30:29180 (UCID-15316)
WARREN, J., See BAILEY, J., 30:30620
WATANABE, K., Clinical evaluation of preoperative liver scintigraphy in gastric carcinoma patients, 30:29854
WATANABE, N., Double antibody radioimmunoassay for human urinary follicle stimulating hormone, 30:29861
WATANABE, T., Latitudinal distribution of solar wind velocity and its relation to solar EUV corona, 30:30323
  Reciprocal translocation as a new approach to breeding seedless watermelon. I. Some characters of F_1 hybrids with six reciprocal translocations, 30:29686
  See KITABATAKE, T., 30:29710
WATARI, W., See FURUICHI, S., 30:30607
WATSON, A.A., Fluctuation studies of large air showers: the composition of primary cosmic ray particles of energy E/sub p/ approximately 10^{18} eV, 30:30175
WATSON, L.M., See CLOUGH, A.S., 30:30891
WATTERS, R.L., See GOMEZ, L.S., 30:29820
WAXMAN, A.D., Combined contrast and radionuclide angiography of the liver, 30:29844
WAYMAN, C.M., See ASSELIN, G.P., 30:29959
WAYNE, R.P., See BRAUN, W., 30:30525
WDOWCZYK, J., See KEMPA, J., 30:30176
WEARE, J.H., Helium scattering from solid surfaces, 30:30480
WEBB, M.P., See VANDENBOSCH, R., 30:30880
WEBB, R.A., Experiments on dynamic parallel magnetism in superfluid ^{3}He, 30:30803
WEBER, D.A., /sup 99m/Tc pyrophosphate for diagnostic bone imaging, 30:29843
WEBER, G., Energy dispersion of deuterons during their passage through matter. Influence of the state of the surface, 30:31122
WEBER, H.J., See NOBLE, J.V., 30:30867
WEEKS, R.A., See GRISCOM, D.L., 30:31389
WEGMANN, G., Static viscosity of nuclear matter, 30:31080
WEI, L.S., Optimization of the beta-voltaic cell, 30:29256
WEIGEL, F., Vapor pressure of protactinium pentabromide, 30:29130
WEIGDLD, E., See LLOYD, C.R., 30:30535
WEILHAMMER, P., See GRAYER, G., 30:30617
WEIMER, W.C., See RANCITELLI, L.A., 30:29483
  See RANCITELLI, L.A., 30:29469
WEINER, R., See ELIEZER, S., 30:30781
WEINGARTEN, D., See KRZYWICKI, A., 30:30696
WEISMAN, J., See CHITKARA, K., 30:31310
WEISS, P.B., See CHRISTOFILOS, N.C., 30:29188
WEISSER, F., See DADO, S., 30:30621
WEISTROP, D., Influence of binaries on red dwarf density distributions, 30:30232
WEISWEILER, W., Extension of quantitative electron beam microanalysis to solids containing light elements, 30:28968 (AED-CONF-74-084-007)
WELIACHEW, L., A study of the H I absorption in the galaxy M82 by radio interferometry, 30:30383
WELLCK, R.E., See HIRSHBERG, J., 30:30322
WELLNER, M., A theory of elementary couplings. III, 30:31146
WELLS, D.C., See RIDGWAY, S.T., 30:30225
WELZ, W., See TOENNIES, J.P., 30:30532
WENDELL, L.L., Mesoscale transport and diffusion studies, 30:29435 (BNWL-1850(Pt.3))
  Program descriptions: supplement to mesoscale wind fields and transport estimates determined from a network of wind towers, 30:31343 (NOAA-TM-ERL-ARL-43)
WENDENBURG, J., See JUNGBLUTH, H., 30:29057
WENDER, S.A., See KERR, P.G., 30:30933
WENE, C.-O., An automatic running system for a 500kV Van de Graaff generator, 30:30125
WENTWORTH, R.A., See COMAR, C.L., 30:29416
WERNER, W., See BIRKHOFER, A., 30:31190
WERNTZ, C.W., See KLINE, F.J., 30:30878
WESCHLER, C.J., Oxidation of free and coordinated thiols by neptunium(VI), 30:29132
WESOLOWSKI, J.J., Source identification by multi-element analysis of diurnal samples, 30:31371 (UCID-15872)
WESSMAN, R.A., See MAJOR, W.J., 30:28971
WESSNER, E.F., See BLINOWSKA, K.J., 30:29563
WEST, D., SAFT: structural analysis of forest trees, 30:31337 (EDFB-IBP-74-4)
WEST, K.W., See BROWN, J.P., 30:30093
WEST, N.J., See GAZE, S., 30:29867
WEST, T.S., See ADAMS, M.J., 30:28963
WESTERMEIER, H., See KINDL, H., 30:29283

WESTLUND, W., See AXEN, D., 30:29597
WESTON, W.F., Identification and measurement of low-energy electrons by cloud chamber techniques: the oxygen and neon auger-electron problem, 30:29495 (UCID-15372)
WETCH, J.R., Fuel element for a compact power reactor, 30:31242
WETHINGTON, J.A. Jr., Investigation of tritium decontamination. Interim research report, 30:29326 (UCID-15985)
WEVER, H., See ALBRECHT, W.W., 30:30020
WEYERS, J., Possible representations of local current algebra, 30:30635
WHALEN, B.A., See GREEN, D.W., 30:30434
WHEATLEY, J.C., See WEBB, R.A., 30:30803
WHEATON, W.A., See ULMER, M.P., 30:30268
WHITE, M.A., See MARTINI, W.R., 30:29260
WHITE, M.G., See DUNAWAY, P.B., 30:29439
WHITE, N.M., Angular diameter of μ Geminorum, 30:30224
WHITE, R.L., Nuclear spectroscopy with the ^{62}Ni(^{7}Li,^{6}He)^{63}Cu reaction, 30:30937
WHITE, T., See KIM, I.J., 30:30584
WHITELAW, J.H., See BAKER, R.J., 30:31414
WHITMAN, G.D., Quarterly progress report on reactor safety programs sponsored by the Division of Reactor Safety Research for April--June 1974, 30:31251 (ORNL-TM-4655(Vol.2))
WHITMORE, J., Experimental results on strong interactions in the NAL hydrogen bubble chamber, 30:30609
  Multiplicity distributions in the reaction p + p → p + anything, 30:30759
WHITTED, E.I., See WALTON, R.B., 30:28986
WHITTEN, C.A. Jr., Study of the (p,np) reaction on the isotopes of tin, 30:30973
WICHMANN, E.H., Quantum physics. Berkeley physics course. Volume 4, 30:31136
WICHNER, R., MAGREC final report, 30:29619 (UCID-16026)
WICKHAM, A.J., Measurements by isotope exchange between ^{14}Co and ^{12}CO$_2$, 30:29543 (DEMO-74/5)
WIEBICKE, H.J., A weak coupling model for high-spin states, 30:31090
WIEMER, H., Use of fine-grained electrographite in metal working, 30:31383 (AED-CONF-74-254-001)
WIENHARD, K., See WOLF, H., 30:30908
WIERBICKI, E., See RAO, B.Y.K., 30:29642
WIGNALL, G.D., Measurements of persistence length and temperature dependence of the radius of gyration in bulk atactic polystyrene, 30:31364 (AED-CONF-74-072-002)
WILDUNG, R.E., Influence of soil plutonium concentration of plutonium uptake and distribution in shoots and roots of barley, 30:29825
WILEY, J., See PACER, J.C., 30:30950
WILHELMOVA, L., Compounds of rare gases, 30:29089
WILKENS, M., See NIEBEL, K., 30:30067
WILKINSON, D.H., Renormalization of the axial-vector coupling constant in nuclear β-decay (III), 30:30865
WILKS, G., The skin friction on accelerated plates in magnetohydrodynamcis, 30:30573
WILL, C.M., Perturbation of a slowly rotating black hole by a stationary axisymmetric ring of matter. I. Equilibrium configurations, 30:30189
WILL, E., See MANFRASS, P., 30:30994
  See WINTER, G., 30:30992
WILLIAMON, R.M., Photometric study of EE Aquarii, 30:30228
WILLIAMS, A.G., Industrial gases for nuclear power plant, 30:31206
WILLIAMS, B.R., See MASON, B.F., 30:30479
WILLIAMS, J., See ROSE, K.S.B., 30:29931
WILLIAMS, J.L., See LLOYD, R.D., 30:29797
  See LLOYD, R.D., 30:29802
  See TAYLOR, G.N., 30:29796
WILLIAMS, J.R., Exploratory study of several advanced nuclear-MHD power plant systems, 30:31209
  See EPSTEIN, J., 30:29672
  See THOMPSON, S.D., 30:31241
WILLIAMS, L.E., See LUKEN, M.K., 30:29847
WILLIAMS, M.E., See WHITE, R.L., 30:30937
WILLIAMS, W.H., FIND: St. Lucie Plant, Unit 1, 30:31321 (FIND-50335)
WILLIAMS, W.L., See BROWN, D.N., 30:30218
WILLMOT, J.C., See SANDERSON, N.E., 30:30944
WILLSON, A., See JOHNSON, G.R.A., 30:29077
WILLSON, M.A.G., See FANAROFF, B.L., 30:30277
WILLSON, R.L., See ASQUITH, J.C., 30:29674
WILMAN, H., See LIN, D.S., 30:30051
WILMORE, D., See HAWTIN, P., 30:31211
WILSON, G.A., See WEBER, D.A., 30:29843
WILSON, J.G., See WATSON, A.A., 30:30175
WILSON, L.A., See WETCH, J.R., 30:31242
WILSON, P.W., See TAYLOR, J.C., 30:29129
WILSON, R.H., See ZIELKE, L.A., 30:31201
WILSON, W.J., Observations of galactic carbon monoxide emission at 2.6 millimeters, 30:30265
WIMMER, B., See VAN KAICK, G., 30:29769
WINCKELER, J.R., See MCENTIRE, R.W., 30:30453
WINEFORDNER, J.D., See MOLNAR, C.J., 30:28947
WINEGARDNER, W.K., Radioactive waste management for nuclear energy center, 30:30107 (BNWL-B-334)
WING-YIN, Y., Bose distribution and the Lorentz contracted geometric model, 30:30751 (IC-73-6)
WINSLOW, A.M., Compton scattering subroutine for Monte Carlo calculations, 30:30651 (UCID-15808)
  Second-order difference equations for a non-uniform triangle mesh, 30:31347 (UCID-15388)
WINSLOW, G.H., Effect of altered valent cations on oxygen pressure over urania, 30:29935
WINSTON, M.A., Enhancement of pancreatic concentration of ^{75}Se-selenomethionine, 30:29855
WINTER, G., Mixing of Nilsson configurations in ^{159}Tb, 30:30992
  See MANFRASS, P., 30:30994
WINTERS, H.F., Energy transfer to a tungsten lattice by ion bombardment, 30:30070
WIREMAN, D.L., See KAYUHA, H.J., 30:29441
WISCHOW, R.P., See GRESKY, A.T., 30:29150
WISE, P.J., Measurement of atomic concentration profiles in thin films using nonresonant nuclear reactions, 30:28933
WISHNEVSKY, V., See WEIGEL, F., 30:29130
WISNIEWSKI, K., See PANKE, R., 30:29723
WITHEE, C.J., Measurement of internal conversion cascading in ^{235}U fission fragments, 30:31012
WITHERS, H.R., Kinetics of recovery in irradiated colonic mucosa of the mouse, 30:29742
  Response of jejunal mucosa to fractionated doses of neutrons or γ-rays, 30:29758
WITT, A.N., Monte Carlo calculations of the surface brightness profiles of spherical dark nebulae, 30:30364
WITTE, G., NS Otto Hahn. Research Report No. 4. The oscillational behaviour of the second core support system, 30:31240 (GKSS-74/E/15)
WITTEK, W., See DEHM, G., 30:30624
WITTHUHN, W., See HAEUSSER, O., 30:31004
WIZENBERG, M.J., See ROBINSON, J.E., 30:29743
WOERNER, D., Calculation of correction factors for pulsed neutron measurements in the ITR critical experiment, 30:31232 (IKE-6-79d)
WOGMAN, N.A., See ROSINSKI, J., 30:29367
  See YOUNG, J.A., 30:29368
  See YOUNG, J.A., 30:29473
  See YOUNG, J.A., 30:29427
  See YOUNG, J.A., 30:29481
WOJCICKI, S., See DONALDSON, G., 30:30582
WOLF, E.G., See SCHNEIDER, M.J., 30:29461
WOLF, G., See DEHM, G., 30:30624
  See TUENNIES, J.P., 30:30532
WOLF, H., The decay of the giant dipole resonance in ^{26}Mg to T=3/2 states of ^{25}Mg, 30:30908
WOLF, M.A., See ALKEZWEENY, A.J., 30:29487
WOLFENDALE, A.W., See KEMPA, J., 30:30176
WOLFF, P.A., See YUEN, S.Y., 30:29274
WOLFSON, J., See BASTIEN, D.B., 30:30600
  See BERLAD, G., 30:30623
WOLLAN, D.S., NMR calibration of a polarized nuclear target, part of which is radiation-damaged, 30:30149
WOLOWODIUK, W., Flow distribution for heat exchangers, 30:29275
WOLSKO, T.D., Environmental impact handbook for highway systems, 30:31357 (ANL/ES-30)
WOLTER, D., See HERZIG, C., 30:29015
WOLTERMANN, H.A., Determination of molybdenum in plutonia cermets by x-ray fluorescence spectrometry, 30:28979
WOO, G., See OSBORN, H., 30:30735
WOO, J.T., See HAUGHT, A.F., 30:29152
WOOD, L., See SLUTZ, S., 30:29271
  See SLUTZ, S., 30:29272
WOODBURY, L.A., See JEE, W.S.S., 30:29801
WOODS, T.J., Isospin effects upon the decay of highly excited nuclear states, 30:30999
WOODSWORTH, A., See HUGHES, V.A., 30:30292
WOOLCOCK, W.S., Comments on the calculation of the pion-nucleon coupling constant and s-wave scattering lengths, 30:30745
WORDEN, R.P., Deep inelastic structure functions of the photon, 30:30676
WORLEY, A., See FOWLER, P.H., 30:29521
WORMALD, M.R., See UNDERWOOD, B.Y., 30:30885
WOROBEY, W., See KUSHNIR, A.J., 30:30059
WORTMAN, D.E., Analysis of the ground configuration of trivalent thulium in single-crystal yttrium vanadate, 30:30487 (AD-776343)
WRIGHT, M.A., Mechanical properties of metal matrix composites subjected to cyclic temperature changes. Annual report, 1 July 1972--30 June 1973, 30:29973 (AD-774890)
WRIXON, G.T., Ratio of the temperatures of the quiet sun and the centre of the moon at lambda = 1.3 mm, 30:30330
WU, C.C., Study of the interstellar diffuse absorption features, 30:30377
WU, M.W., Absolute determination of the fast neutron fluxes by using the flow-type manganese bath method, 30:30852
WULFF, H., On the energy distribution of electrons in a proton-electron plasma with densities higher than the solid-state density, 30:29173 (IPP-3/12)
WYARD, S.J., ESR studies of radiation damage in nucleic acids, bases, nucleosides, and nucleotides, 30:29656
WYNN-WILLIAMS, C.G., New infrared sources associated with H II regions, 30:30375
WYSOKINSKI, L., See PININSKA, J., 30:31128

X

XAVIER, R.M., See LARA, S., 30:30094

Y

YAFFE, D., A study of the reactions $\pi^- p \to K^* X$, $K^* \Sigma$ and $K^* Y_1^*(1385)$ at 3.93 GeV/c, 30:30622
YAGI, K., See MAGUIRE, C.F., 30:30997
  See SAKAI, M., 30:30974
YAGODIN, G.A., See CHEKMAREV, A.M., 30:28982
YAGODIN, V.G., See CHEKMAREV, A.M., 30:28982
YAGUCHI, E.M., See MARSHALL, J.S., 30:29415
YAGUPOLSKAYA, L.N., See LAVRENKO, V.A., 30:29938
YAHIL, A., The density profiles of rich clusters of galaxies, 30:30381
YAKOVLEV, G.N., See SHAFIEV, A.I., 30:29141
YAKOVLEVA, M.K., Radiation copolymerization of ethylene oxide with acrylonitrile, 30:29037
YAKUBOVSKII, E.A., See KULIKOV, V.N., 30:29501
YAMABAYASHI, H., Cold-weld type capsules for radioisotope production, 30:29962
YAMADA, M., See YOKOTA, M., 30:31193
YAMAGUCHI, Y., See NISHIKAWA, M., 30:29039
YAMAJI, K., See ICHII, H., 30:29860
YAMAMOTO, R.K., See BERLAD, G., 30:30623
YAMAMURO, N., Kinetic experiments in reactor physics, 30:31278
YAMANOUCHI, T., See KIM, I.J., 30:30584
YANG, S.N., See DOVER, C.B., 30:30869
YANG, Y.Y., See WILLIAMS, J.R., 30:31209
YAO, T.H., Analytic nonlocal potentials. II. Analyticity of the S matrix, for fixed l, its representations, and a dispersion relation for fixed t, 30:30784
  Representations of the Jost solutions and the S matrix for a class of analytic nonlocal potentials, 30:30785
YARIV [RAJEWSKI], Y., Three-body effective interactions in the fsub(7/2) region, 30:30931
YARMONENKO, S.P., See RAMPAN, Yu.I., 30:29763
YASOHAMA, K., Specific heat and superconducting properties of Zr--Mo alloys, 30:30025
YASUKOCHI, K., Programs on large scale applications of superconductivity in Japan, 30:30836
YATIRAJAM, V., Extractive separation of molybdenum as Mo(V) xanthate from iron, vanadium, tungsten, copper, uranium and other elements, 30:28964
YBARRONDO, L.J., See COPLEN, H.L., 30:31238
YEE, J.A., See JEE, W.S.S., 30:29801
YEH, J.T.C., Technique for fabrication of superconducting microbridges and small Josepnson tunnel junctions, 30:30841
YEKUTIELI, G., Rising inelastic cross-section and the attenuation of cosmic rays nucleons in the atmosphere, 30:30180
YOCK, P.C.M., Search for heavy particles in cosmic rays, 30:30579
YODH, G.B., See GAISSER, T.K., 30:30611
YOKOI, T., Four-body correlations in nuclei, 30:31030
YOKOMI, H., Bound on the average multiplicity of pions in p--p collision at superhigh energy, 30:30757
YOKOTA, M., Development of nuclear reactor incore instruments, 30:31193
YOKOZAWA, M., Grotrian charts for atoms and ions of rare gases, 30:30493
YOON, Y.K., See LEE, D.N., 30:29917
YORDE, R.J. Jr., See MARTIN, W.E., 30:29455
YORK, M.J., Experimental manifestations of duality in KN interactions and implications for the bootstrap, 30:30743
YORK, R.C., See NORBECK, E., 30:30130
YOSHIDA, T., Elastic-diffraction slopes of $\pi^+ p$ and $K^+ p$ scatterings, 30:30736
  Radioimmunoassay for sex steroid hormone. VI. Radioimmunoassay for Δ^4-androstenedione, 30:29863
YOSHIKAWA, N., See KAWAKAMI, H., 30:30980
YOSHIMURA, T., Magnetic susceptibilities of octacoordinated uranium(IV) complexes, 30:29094
YOTSUYANAGI, I., See YOKOMI, H., 30:30757
YOUNG, D.A., See GATHERS, G.R., 30:30045
YOUNG, J.A., Concentrations and rates of removal of contaminants from the atmosphere in an downwind of St. Louis, 30:29473 (BNWL-1850(Pt.3))
  Determination of aerosol deposition rates on a lake surface using radon daughters, 30:29410 (BNWL-1850(Pt.3))
  Entrainment of tracers near the sides of convective clouds, 30:29481 (BNWL-1850(Pt.3))
  Feasibility study of the use of inert tracers in the national hail research experiment, 30:29427 (BNWL-1850(Pt.3))
  Particle size distributions of manmade and natural radionuclides, 30:29360 (BNWL-1850(Pt.3))
  Radionuclide concentration minimums from 6 to 9 km, 30:29368 (BNWL-1850(Pt.3))
  See DAVIS, W.E., 30:29475
  See ROSINSKI, J., 30:29367
YOUNG, N.A., See MORLEY ENGLISH, J., 30:31309
YOUNG, W.A.P., See FENNER, N.C., 30:29625
YOURNO, J., See INO, I., 30:29684
YPSILANTIS, T., See BAILLON, P., 30:30619
  See BAILLON, P., 30:30618
  See BAILLON, P., 30:30737
YU, P.Y., See AMER, N., 30:31425
YUEN, S.Y., Theory of traveling-wave electronic Raman laser: Stokes-anti-Stokes coupling in the steady state, 30:29274
YUHAS, J.M., Direct relationship between immune competence and the subcutaneous growth rate of a malignant murine lung tumor, 30:29756
YUKHIMUK, A.K., See BONDARENKO, V.I., 30:30415
YUKOV, E.A., See AGLITSKII, E.V., 30:29171
  See VINOGRADOV, A.V., 30:29163
YULE, T.J., See GOLD, R., 30:29557
YUNOKI, K., See MORITA, N., 30:29050
YURKIN, V.G., See ROZEN, A.M., 30:29101
  See ROZEN, A.M., 30:29100
YUSHINA, L.R., See GERT, L.M., 30:29914
YUSIFOV, V.G., Study of the corrosion resistance of titanium alloys and some steels during condensation of alkylphenol witn formaldehyde, 30:29947

Z

ZADAK, Z., Application of ^{133}Xe in measuring peripheral blood flow, 30:29871
  Application of ^{133}Xe in measuring minute volume of blood, 30:29873
  Experimental application of ^{133}Xe in measuring minute volume of blood, 30:29872
ZAGER, S.A., See CASS, J., 30:29074
ZAGO, G., See FASOLI, U., 30:30981
ZAGRYAZKIN, V.N., See FEDOROV, G.B., 30:29905
ZAIDI, S.A.A., Treatment of continua in the snell-model theory of nuclear reactions, 30:31077
ZAITSEVA, N.G., See VANDLIK, Ya., 30:29142
ZAKHAROV, S.D., See ANTONOV, A.V., 30:29172
ZAKHAROVA, F.A., Kinetics of reduction of plutonium(VI) by oxalate ions, 30:29114
ZAKHVATAEV, B.B., See NIKOL'SKII, B.P., 30:29118
  See NIKOL'SKII, B.P., 30:29119
ZAKLAD, H., See DERENZO, S.E., 30:29512
ZAKRZHEVSKAYA, D.T., See GAZIEV, A.I., 30:29682
ZALEWSKA, A., See ESKREYS, A., 30:30614
ZALUZHNYI, A.G., See SKOROV, D.M., 30:30002
ZAMFIRESCU, I., Software extended floating-point feature, 30:31342 (MC-19-1974)
ZANNONI, R., See FASOLI, U., 30:30981
ZANONI, E.A., SAFR4: a program to evaluate the stability of a rigid blade in parallel fluid flow, 30:31280 (WAPD-TM-1085)
ZAPESOCHNYI, I.P., See SOVTER, V.V., 30:30523
  See VUKSTICH, V.S., 30:30524
ZARAEV, O.M., See BYKHOVSKII, A.V., 30:29344
ZARITSKII, A.R., See ANTONOV, A.V., 30:29172
ZATS, A.V., See POLYAKOVA, G.N., 30:30545
ZATTERA, A., See MOELLER, F., 30:31380
ZATZ, J., See YAFFE, D., 30:30622
ZAV'YALKIN, F.M., Contribution of fluctuations in the parameters of the object to the process taking place at the output of a radiometric device, 30:29607
ZAYATS, A.A., Multipole (kinematic) analysis of the reaction $eN \to e\pi\Delta$. II. Scalar amplitude decomposition by multipole amplitudes, 30:30666
ZDANIS, R., See SHEEDHAR, V., 30:30616
ZDERKIEWICZ, T., Ascorbic acid content in different stages of ripeness of fruits pepper under the effect of El and irradiation by ^{60}Co, 30:29685
ZEIDMAN, B., A high-resolution mass-identification system for heavy ions, 30:29564
ZELDOVICH, Ya.B., See KOBSAREV, I.Yu., 30:30770
ZELENSKII, V.F., Mechanical properties of sintered magnesium--beryllium alloys, 30:30017
ZELENYUK, E.E., Effect of stress concentration on the mechanical properties of Mo specimens with a protective coating in tests in an oxidizing atmosphere, 30:30013
ZGAGA, V., See TRGOVCEVIC, Z., 30:29678
ZGLINSKI, A., See KOZLOWSKI, T., 30:31073
ZHESTYANIKOV, V.D., See SEMENOVA, E.G., 30:29675
ZHIDENKO, G.L., Effect of radioactive irradiation on the degree of cavitation erosion of aluminum, 30:30069
ZHIRNOV, A.D., Utilization of metallic uranium in power channel uranium-graphite reactors, 30:31205
ZHUGZHDA, Yu.D., Resonance in a semi-infinite isothermal atmosphere, 30:30304
ZHURAVLEVA, E.L., See BYU, N.K., 30:28929
ZIA, R.K.P., See BURKHARDT, H., 30:31085
ZICHICHI, A., Properties of the fundamental interactions. Volume 9, Part A. 1971 International School of Subnuclear Physics, Erice, Trapani, Sicily, July 8--26, 1971, 30:30638
ZIDEK, V., Dead-time calibrator, 30:29529
ZIELINSKI, M., Isotope exchange of chlorine-36 in the systems: gaseous hydrogen chloride--γ-picoline hydrochloride and gaseous hydrogen chloride--stoichiometric solvate of hydrogen chloride with γ-picoline hydrochloride, 30:29027
ZIELINSKI, P., Some analogy of the nuclear and nucleon fragmentation processes, 30:30755
ZIELKE, L.A., Transient critical heat flux and spacer grid studies, 30:31201
ZIEM, P., See STOLTERFOHT, N., 30:30541
ZIEMINSKI, Z., See YAFFE, D., 30:30622
ZIMANYI, J., See GYARMATI, B., 30:31079
ZIMMER, R., Results of the medical examinations, 30:29829 (AED-CONF-74-221-004)
ZIMMERMAN, G., See SLUTZ, S., 30:29272
  See SLUTZ, S., 30:29271

ZIMMERMAN, I.H., Optical potential calculations for molecular collisions, 30:30569
  Quantum resonance effects in electronic-to-vibrational energy transfer in molecular collisions, 30:30534
ZINGONI, E., Poisson-Algebraic distributions: another family of generalized Poisson profiles in nuclear-reactor noise-analysis, 30:31273 (RT/FI-(74)26)
ZINOVIEV, L.P., See ISSINSKII, I.B., 30:30129
ZISMAN, M.S., See VANDENBOSCH, R., 30:30880
ZITA, G., Liver studies with various radioactive tracers and methods, 30:29831 (CONF-740708-52)
ZMUDA, A.J., Diurnal variation of the region with vector magnetic field changes associated with field-aligned currents, 30:30461
ZOLNOWSKI, D.R., See GONO, Y., 30:30965
ZOLOTAREV, A.B., See KASHCHEEV, I.N., 30:29110
ZOLOTUKHIN, I.V., Damping and elastic characteristics of plasma-sprayed coatings of W, nichrome, zirconia, and Cr--Ni spinels, 30:29887
ZOVKO, N., Pion and kaon form factors and heavy vector mesons, 30:30726
ZUCKERMAN, B., See MORRIS, M., 30:30374
ZUMERLE, G., See BERTANZA, L., 30:30606
ZUNDEL, G., See HAINBERGER, P.L., 30:29413
ZUSH, Ya.Ya., See KORMILITSIN, B.T., 30:30412
ZUZEK, E., See ANDREONE, C.A., 30:28938
ZWANZIGER, D., Infra-red-finite calculations in quantum electrodynamics, 30:31149
ZYKOVA, A.S., Rate of fallout of ^{137}Cs and ^{90}Sr aerosols from the atmosphere, 30:29399

SUBJECT INDEX

The subject indexing of literature announced in *Nuclear Science Abstracts* is based on the use of descriptors* selected from a controlled thesaurus of terms. Subject descriptors and qualifiers (subheadings) are selected and presented in the following format:

SUBJECT DESCRIPTOR/QUALIFIER
Title (supplementary information), volume number:abstract number

For example:

```
REACTOR LICENSING/SPAIN
  Harmonization of the licensing conditions including
    environmental protection for the siting of nuclear
    power plants, 29:14745
REACTOR MATERIALS/STRESS ANALYSIS
  Problems on nuclear reactor structure at elevated
    temperature, 29:14654
REACTOR PROTECTION SYSTEMS
  HTGR gas turbine power plant control and safety studies.
    Quarterly progress report for the period July 1, 1973--
    September 30, 1973, 29:14846 (GULF-GA-A-12799)
```

The title may be supplemented with additional words, or a phrase, if it appears additional information would be helpful. Such title augmentation is routinely used to denote the presence of numerical data tabulations or new values of constants. In cases for which the title contains little or no information related to the subject entry, it may be replaced entirely by the supplementary information. A qualifier is not always required, and in such cases the title will follow the unqualified subject descriptor.

All index entries cite *NSA* volume and abstract numbers; the volume number precedes the colon and the abstract number follows it. Report numbers, where applicable, are included in parentheses after the abstract number. Published literature (journal article or book) can be identified by the absence of a report number.

The descriptors selected for use as subject terms are generally the names of specific materials, things, and processes. To the extent possible, a qualifier is selected to describe the properties of, or processes applied to, the subject term.

Index entries are selected to indicate the important ideas and concepts presented in the original literature, rather than words that may appear in the article. Within the available thesaurus terms, indexers select what seems the most probable or logical place to look for typical information. However, users of the index should consider synonymous or closely related terms.

Information is indexed for the greatest use to the greatest number of users. This requires that a topic be indexed using subject entries that most specifically describe it and not ordinarily its ultimate use. Only the most specific subject entries are made for a given topic. For example, information on the Yankee-Rowe nuclear power plant is indexed using the subject descriptor ROWE YANKEE REACTOR but not NUCLEAR POWER PLANTS, POWER REACTORS, or PWR TYPE REACTORS. To aid the user, narrower term (NT1) relationships are shown in the subject index as "See also" references. For complete broader term and narrower term relationships of descriptors, refer to IAEA-INIS-13. "See" references are incorporated when abbreviated or synonymous terms have been used.

Specific and general examples can be given as guidance, but for complete understanding, a study should be made of subject entry patterns used to index specific information.

The standard indexing patterns used for some specific subject areas follow.

Machine intervention is used to add collections of related entries to the cumulative indexes because of their unique, e.g., BIBLIOGRAPHIES, MEETINGS, and STANDARDS, or special, e.g., BIOLOGICAL RADIATION EFFECTS, CHEMICAL RADIATION EFFECTS, and PHYSICAL RADIATION EFFECTS, nature.

REACTOR TECHNOLOGY

Subject terms for reactors are of three types: (1) specific reactor names, e.g., BEPO REACTOR, INDIAN POINT-1 REACTOR; (2) reactors having a common physics or engineering characteristic, e.g., FBR TYPE REACTORS, SODIUM COOLED REACTORS; and (3) reactors having a common purpose, as POWER REACTORS, RESEARCH REACTORS.

Information on a specific reactor is indexed using the subject descriptor for that reactor name. Information on classes or types of reactors is indexed using subject descriptors for all applicable reactor types. For example, an article on a sodium-cooled fast breeder power reactor, without a specific name, is indexed using FBR TYPE REACTORS, SODIUM COOLED REACTORS, and POWER REACTORS. Where applicable, subject descriptors that name reactor components may be used, e.g., FUEL ELEMENTS, even though the term is also used as a qualifier of a general reactor term. Indexing is provided for materials used in reactor components when the information is peculiar to the material. For example, if the article deals with corrosion of stainless steel in a sodium cooled reactor, STAINLESS STEELS would be chosen as a pertinent subject descriptor.

In general, qualifiers of reactor subject descriptors are of two types. One type expresses reactor characteristics, e.g., REACTIVITY, and the other indicates components, e.g., CONTROL ELEMENTS.

---

*The descriptors used for indexing are selected from the thesaurus of the IAEA International Nuclear Information System (INIS). TIC is a major contributor to thesaurus concepts and maintenance. The thesaurus, IAEA-INIS-13, is available from the USAEC Technical Information Center, P. O. Box 62, Oak Ridge, TN 37830.

PARTICLE INTERACTIONS OF HIGH ENERGY PHYSICS

Information on particle-particle events is indexed using subject descriptors that name the particles involved. These subject descriptors have the form PION-NUCLEON INTERACTIONS, MESON-BARYON INTERACTIONS, etc. Such terms are constructed so that the lighter particle appears first in the combination.

A citation on cross sections of pion-neutron interactions would be found by referring to the entry PION-NEUTRON INTERACTIONS/CROSS SECTIONS. This is a dual entry of descriptors corresponding to the main heading-subheading combination of a more conventional index. Each citation under this entry will consist of the title of the article or the title with additional informative words.

Subject terms are also provided for specific models and theories. For example, OCTET MODEL, STRONG-COUPLING MODEL, SYMMETRY GROUPS, etc.

CHEMISTRY

Subject descriptors in chemistry are generally names of elements, isotopes, and compounds. Qualifiers designate properties, processes, and reactions as specifically as possible.

Compounds on which there are significant quantities of information in the literature of nuclear science and technology are indexed by using specific descriptors following the nomenclature of the literature, e.g., METHYL IODIDE, TBP, 2-METHYLPROPANE, URANIUM DIOXIDE, etc.

Compounds occurring less frequently are indexed using more general terms or combinations of terms. In such cases all of the descriptors used to describe the compounds may be selected as subject terms or only the ones of main importance. In these cases the complete compound is indicated in either the title or title augmentation. For example, ethyl bromide is indexed using the subject descriptor BROMINATED ALIPHATIC HYDROCARBONS, uranyl acetates is included as URANYL COMPOUNDS, and lithium fluoroberyllates appears as LITHIUM FLUORIDES and BERYLLIUM FLUORIDES.

Terms for chemical reactions, processes, and properties are not used as subject descriptors in indexing information on specific materials. Such terms are included for publications such as books, reviews, or general treatment of the subject.

LIFE SCIENCES

Information in this area is indexed using subject descriptors for specific animals, plants, microorganisms, biochemicals, biological systems and processes, cells, organs, radiation effects, and substances modifying radiation effects. DNA, BARLEY, HELA CELLS, BEAGLES, PATIENTS, BACILLUS SUBTILIS, LACTATE DEHYDROGENASE, and CHROMOSOMAL ABERRATIONS are examples of specific subject descriptors. While most descriptors are common names, genus and species names are sometimes used, e.g., DROSOPHILA. If the specific name of an organism or biochemical is not used, the name of a higher category is used instead. For example, clams are indexed using the subject descriptor MOLLUSCS, Anopheles pharoensis using MOSQUITOS, and glutamine oxalacetic acid transaminase using TRANSFERASES. Title augmentation is used to more completely identify the organisms or substances.

Subject descriptors naming incident radiation are used only if dose, RBE, or other radiation quality studies are made.

INSTRUMENTATION

Information in the field of instrumentation technology is indexed using the most specific subject descriptors available for the instrument, instrument component, or instrument application, e.g., SOLID SCINTILLATION DETECTORS, GAMMA SPECTROMETERS, INTEGRATED CIRCUITS, GAMMA DETECTION, etc. Qualifiers of subject descriptors are selected to indicate the attribute, characteristic, component, or application studied. In those cases where the application is indexed, a qualifier is selected to indicate the instrument used in the study, e.g., GAMMA DETECTION/LI-DRIFTED GE DETECTORS and NEUTRON DOSIMETRY/THERMOLUMINESCENT DOSEMETERS.

A

ABDOMEN/SCINTISCANNING
Gallium--technetium subtraction scanning for the localization of subphrenic abscess (Double tracer using /sup 99m/Tc for liver, spleen and lung scans), 30:29845
Localization of infectious processes with gallium citrate (Ga-67), 30:29886
ABSCESSES/DIAGNOSIS
Gallium--technetium subtraction scanning for the localization of subphrenic abscess (Double tracer using /sup 99m/Tc for liver, spleen and lung scans), 30:29845
Localization of infectious processes with gallium citrate (Ga-67), 30:29886
ABSOLUTE COUNTING/CALIBRATION
Dead-time calibrator, 30:29529
ABSORPTION SPECTROSCOPY/COMPARATIVE EVALUATIONS
Comparison of analytical techniques for inorganic pollutants, 30:28924
ACCELERATORS
See also BETATRONS
BEVATRON
BROOKHAVEN AGS
COLLECTIVE ACCELERATORS
ELECTRON-RING ACCELERATORS
ELECTROSTATIC ACCELERATORS
FRASCATI SYNCHROTRON
ISOCHRONOUS CYCLOTRONS
JINR SYNCHROTRON
LAMPF LINAC
LINEAR ACCELERATORS
MSU CYCLOTRONS
SACLAY LINAC
STANFORD 20-GEV LINAC
STORAGE RINGS
VAN DE GRAAFF ACCELERATORS
ACCELERATORS/ELECTROMAGNETS
Application of electrically conductive coatings to insulating tubes of switching magnets for particle accelerators (Patent), 30:30123
Flux theorem for the design of magnet coil ends, 30:30122
ACCELERATORS/POWER SUPPLIES
High-current electron accelerator with supply by inductive storage, 30:30121 (LA-tr-74-30)
ACCELERATORS/SYNCHROTRON RADIATION
Geometry and optics of synchrotron radiation, 30:30119
ACES
See QUARKS
ACETIC ACID ESTERS/CHEMICAL RADIATION EFFECTS
Reduction of methyl acetate with several hydrosilanes under gamma irradiation, 30:29047
ACETONE/RADIOLYSIS
Radiation chemical studies with cyclotron beams. III. Heavy-ion radiolysis of liquid aliphatic ketones, 30:29049
ACETYLENES
See ALKYNES
ACID PHOSPHATASE/DAILY VARIATIONS
Desynchronization of the diurnal rhythm of acid phosphatase activity in male gonads of mice under the influence of uv and x-rays radiation, 30:29751
ACID PHOSPHATASE/METABOLISM
Morphology and enzyme histochemistry of ^{224}Ra-induced osteosarcomas of the mouse, 30:29785
ACOUSTIC EMISSION TESTING/CONTAINERS
Acoustic emission monitoring of proof tests on canisters and related hardware, 30:29296 (UCID-15777)
ACRIFLAVINE/RADIOSENSITIVITY EFFECTS
Mechanisms of inhibition of the postirradiation recovery in cells. IV. The effect of caffeine and acriflavine on gamma and x-ray induced unscheduled DNA synthesis in HeLa Zh-63 cells, 30:29675
ACRYLONITRILE/CHEMICAL RADIATION EFFECTS
Radiation copolymerization of ethylene oxide with acrylonitrile (Gamma radiation), 30:29037
ACTIN/METABOLISM
Asynchronous turnover of the thin filament proteins, actin, tropomyosin, and troponin by a continuous double isotope method (^{14}C and tritium tracer techniques), 30:29865
ACTINIDES/EXTRACTION CHROMATOGRAPHY
Recent results in the application of column extraction chromatography in inorganic analysis, 30:28989 (ANL-Trans-960)
ACTINIDES/REMOVAL
Alternate methods for administering chelating agents in decorporation therapy (Removal of actinides from mammals), 30:29798 (COO-119-249)
ACTINIDES/RESEARCH PROGRAMS
Department of Fundamental Research, Grenoble, semiannual bulletin No. 4, 30:31333 (CEA-N-1688)
ACTINIUM 227/RADIOCHEMICAL ANALYSIS
Sequential determination of radium-226, radium-228, actinium-227, and thorium isotopes in environmental and process waste samples, 30:28978
ACTIVATED CARBON/SORPTIVE PROPERTIES
Cryovacuum hydrogen adsorption by small-sized, activated mineral coal with a binder (Adsorption of benzene at 20°C and hydrogen from 20.4 to 50°K), 30:31394 (KHFTI-73-25)
ACTIVATION ANALYSIS
Radioactivation analysis in thermal and epithermal neutrons of the IBR-30 reactor of JINR, 30:28929
ACTIVATION ANALYSIS/BIBLIOGRAPHIES
Activation analysis: a literature search, 30:28919 (PAEC(A)-7332(Suppl.1))
ACTIVATION ANALYSIS/COMPARATIVE EVALUATIONS
Comparison of analytical techniques for inorganic pollutants, 30:28924
ACTIVATION DETECTORS/PERFORMANCE
A neutron monitor with a rotating rhodium disk, 30:29515
ADENOCARCINOMAS
See CARCINOMAS
ADENOSINE MONOPHOSPHATE
See AMP
ADGEZATOR
See ELECTRON-RING ACCELERATORS
ADRENAL GLANDS/SCINTISCANNING
Adrenal imaging with radioiodocholesterol in the diagnosis of adrenal disorders (^{131}I tracer technique), 30:29869
ADVANCED GAS COOLED GRAPHITE REACTOR
See AGR TYPE REACTORS
AERODYNAMICS
Dependence of site evaluation of roughness length and displacement length on value chosen for Von Karman's constant, 30:29432 (BNWL-1850(Pt.3))
AEROSOL WASTES/SEDIMENTATION
Analytical search for the stochastic-dominating process in the drift-deposition problem, 30:29488 (BNWL-1850(Pt.3))
AEROSOLS
See also RADIOACTIVE AEROSOLS
AEROSOLS/LAMINAR FLOW
Analytical investigations of inertial deposition of small aerosol particles from laminar flows onto large obstacles. Part A. General formulation, 30:29485 (BNWL-1850(Pt.3))
Analytical investigations of inertial deposition of small aerosol particles from laminar flows onto large obstacles. Part B. Large stokes number solution by the method of matched asymptotic expansion, 30:29486 (BNWL-1850(Pt.3))
AEROSOLS/PARTICLE SIZE
In situ optical particle size analysis of ambient aerosol (Performance of particle analyzer for sizing and counting particles in range of 0.5 to 10 μm in diameter), 30:29617 (NVO-AEIC-74-1)
AEROSOLS/VAPOR CONDENSATION
Fast reactor programme. First quarter 1974 progress report, 30:31226 (RCN-212)
AEROSOLS/WASHOUT
Comparison of the washout coefficient for a polydisperse aerosol to that for an aerosol of fixed particle size, 30:29477 (BNWL-1850(Pt.3))
Precipitation scavenging of inorganic pollutants from metropolitan sources: St. Louis, July 1973, 30:29479 (BNWL-1850(Pt.3))
AET
(Aminoethylisothiuronium bromide.)
AET/CHEMICAL RADIATION EFFECTS
Chemical study of the mechanism of the radioprotective effect of AET (Gamma radiation; AET; MEG), 30:29654
AET/RADIOSENSITIVITY EFFECTS
Chemical study of the mechanism of the radioprotective effect of AET (Gamma radiation; AET; MEG), 30:29654
Effect of a combination of antibiotics and AET on the survival of irradiated animals (Tetron-pyrrolidinomettryl-oxytetracycline), 30:29746
AFTERGLOW/DISTRIBUTION FUNCTIONS
Electron energy distribution in the afterglow. II (Nonmonotonic form, constants and cross sections), 30:29165
AFTERGLOW/ENERGY SPECTRA
Electron energy distribution in the afterglow. I (Effects due to metastables, pressures of 1 and 2 torr, currents of 0.45 and 1.8 A), 30:29164
AGAR/CHEMICAL RADIATION EFFECTS
Studies on irradiation of agar--agar in the solid state. On the changes of penetration of agar--agar hydrogel produced by irradiation (Gamma radiation), 30:29072
AGR TYPE REACTORS/COOLANTS
Industrial gases for nuclear power plant, 30:31206
AIR
See also EARTH ATMOSPHERE
SURFACE AIR
AIR/ACTIVATION ANALYSIS
Comparison of analytical techniques for inorganic pollutants, 30:28924
AIR/CHEMICAL ANALYSIS
Application of activation analysis to the determination of pollutants in the atmosphere (Thermal neutrons), 30:28914 (IEA-326)
Comparison of analytical techniques for inorganic pollutants, 30:28924
AIR/DECONTAMINATION
Atmosphere purification of xenon, radon, and radon daughter elements, 30:28995

AIR/MIXING
Long-lived radon daughters as atmospheric radioactive tracers (^{210}Pb, ^{210}Bi, ^{210}Po), 30:29400
AIR FILTERS/PERFORMANCE TESTING
Ventilation design modifications at Los Alamos Scientific Laboratory major plutonium operational areas, 30:29328 (LA-UR-74-1132)
AIR POLLUTION
Environmental monitoring report: United States Atomic Energy Commission, Oak Ridge facilities. Calendar year 1973 (Monitoring), 30:29352 (UCC-ND-280)
Has man, through increasing emissions of particulates, changed the climate, 30:29489 (UCRL-75902(Rev.1))
Quillayute air reference station (Air sampling and monitoring in Washington State), 30:29359 (BNWL-1850(Pt.3))
Source identification by multi-element analysis of diurnal samples, 30:31371 (UCID-15672)
Surface flux model for diffusion, deposition, and resuspension, 30:29470 (BNWL-1850(Pt.3))
AIR POLLUTION/AEROSOL MONITORING
Concentrations and rates of removal of contaminants from the atmosphere in an downwind of St. Louis, 30:29473 (BNWL-1850(Pt.3))
Vertical profiles of trace gases in St. Louis (Nitrogen oxide measurements from ground level to 5500 ft), 30:29474 (BNWL-1850(Pt.3))
AIR POLLUTION/DIFFUSION
Program for computing the dispersion of airborne contaminants, 30:29381 (ORNL-TM-4674)
AIR POLLUTION/MEASURING INSTRUMENTS
Airborne laboratory for air pollution study, 30:29612 (BNWL-1850(Pt.3))
Flux meter for direct field measurement of deposition and resuspension rates, 30:29613 (BNWL-1850(Pt.3))
AIR POLLUTION/NUMERICAL SOLUTION
Postulated estimate of wet versus dry deposition downwind of a point source of pollution, 30:29364 (BNWL-1850(Pt.3))
AIR POLLUTION/PARTICLE SIZE
Characteristics of aerosols from St. Louis (Aircraft measurements of particle size distribution), 30:29471 (BNWL-1850(Pt.3))
AIR POLLUTION/RESEARCH PROGRAMS
Pacific Northwest Laboratory annual report for 1973 to the USAEC Division of Biomedical and Environmental Research. Part 3. Atmospheric sciences, 30:29468 (BNWL-1850(Pt.3))
AIR POLLUTION/SEDIMENTATION
Determination of aerosol deposition rates on a lake surface using radon daughters (^{214}Bi and ^{214}Pb tracer studies), 30:29410 (BNWL-1850(Pt.3))
Dry deposition of particles (Velocity of deposition on large and small crushed gravel), 30:29482 (BNWL-1850(Pt.3))
Particle deposition rates on a water surface as a function of particle diameter and air velocity, 30:29484 (BNWL-1850(Pt.3))
Postulated estimate of wet versus dry deposition downwind of a point source of pollution, 30:29364 (BNWL-1850(Pt.3))
AIR POLLUTION/SIMULATION
Development of an air pollution model for the San Francisco Bay Area. Second semiannual report to the National Science Foundation, 30:31363 (UCRL-51537)
AIR POLLUTION/TRACER TECHNIQUES
Measurement of particulate plume depletion by comparison with inert gas plumes (^{85}Kr tracer studies), 30:29425 (BNWL-1850(Pt.3))
AIR POLLUTION/WASHOUT
Precipitation scavenging of inorganic pollutants from metropolitan sources: St. Louis, July 1973, 30:29479 (BNWL-1850(Pt.3))
AIR SAMPLERS
See also CASCADE IMPACTORS
AIR SAMPLERS/DESIGN
Flux meter for direct field measurement of deposition and resuspension rates, 30:29613 (BNWL-1850(Pt.3))
Ultra high volume air sampler (Design specifications), 30:29494 (NVO-AEIC-74-1)
AIR SAMPLERS/OPERATION
Airborne laboratory for air pollution study, 30:29612 (BNWL-1850(Pt.3))
AIR SAMPLERS/PERFORMANCE
Real-time system for detection of the atmospheric tracer sulfur hexafluoride, 30:29611 (BNWL-1850(Pt.3))
AIR SAMPLERS/PERFORMANCE TESTING
Evaluation of an airborne fluorescent particle counter for atmospheric tracer studies, 30:29610 (BNWL-1850(Pt.3))
AIRGLOW/PHOTOMETRY
Satellite observations of the equatorial Mg II dayglow intensity distribution, 30:30426
AIRGLOW/RECOMBINATION
Oxygen recombination in the tropical nightglow, 30:30425
ALARM SYSTEMS
Alarm communications and display segment (ACADS). Technical order publications plan (CDRL item 20), 30:31428 (SAND-74-0149)
ALASKA/FALLOUT
Atmospheric natural aerosols and fallout particulates during 1973 at Richland, Washington and Point Barrow, Alaska, 30:29361 (BNWL-1850(Pt.3))
ALASKA/POLLUTION
Elemental content of trace elements in vegetation collected at Centralia, Washington (Comparison with Alaskan vegetation), 30:29483 (BNWL-1850(Pt.3))
ALBUMINS/CHEMICAL RADIATION EFFECTS
Method for preparation of biocompatible and biofunctional materials and product thereof (Graft polymerization using high-energy electrons, x or γ radiation, patent), 30:29082
ALDEHYDES
See also FORMALDEHYDE
RIBOSE
ALDEHYDES/GAS CHROMATOGRAPHY
Gas chromatographic analysis of bis(2-fluoro-2,2-dinitroethyl) formal (FEFO), 30:31370 (UCID-15671)
ALDEHYDES/NITRO COMPOUNDS
Gas chromatographic analysis of bis(2-fluoro-2,2-dinitroethyl) formal (FEFO), 30:31370 (UCID-15671)
ALDEHYDES/ORGANIC FLUORINE COMPOUNDS
Gas chromatographic analysis of bis(2-fluoro-2,2-dinitroethyl) formal (FEFO), 30:31370 (UCID-15671)
ALICE/ION DENSITY
Calculated ion-density spatial distribution in Alice Baseball I, 30:29184 (UCID-15647)
ALICE/PLASMA DENSITY
Consideration of a ''brute-force'' approach to the achievement of higher density in the presence of instability, 30:29183 (UCID-15628)
ALICE/VACUUM SYSTEMS
Alice vacuum system: Sept. 1969, 30:29218 (UCID-15660)
ALKALI METAL COMPOUNDS/SPUTTERING
Hyperthermal beams sputtered from alkali halide surfaces (6-keV Ar$^+$), 30:30484
ALKALINE EARTH METAL COMPOUNDS/RADIOLYSIS
Radiolysis of alkaline-earth fluorides (Electron beams), 30:29075
ALKALINE PHOSPHATASE/BIOLOGICAL RADIATION EFFECTS
Alkaline phosphatase activity of granulocytes (FAG) in workers in radiological laboratories, 30:29734
Effect of ionizing radiation on alkaline phosphatase activity in hematopoietic cells of mouse and rat (X rays), 30:29762
Influence of ionizing radiation on alkaline phosphatase activity in human peripheral blood leukocytes and bone marrow cells (X rays; γ rays), 30:29727
ALKALINE PHOSPHATASE/METABOLISM
Morphology and enzyme histochemistry of ^{224}Ra-induced osteosarcomas of the mouse, 30:29785
ALKANES
See also BUTANE
CYCLOALKANES
ETHANE
METHANE
ALKANES/CHEMICAL REACTION KINETICS
Chromium--carbon bonds in aqueous solutions. A pulse radiolytic study (Reaction of 16 aliphatic radicals with Cr $(H_2O)_6{}^{2+}$), 30:29080
ALKENES
See also ETHYLENE
ALKENES/CHEMICAL REACTION KINETICS
Chromium--carbon bonds in aqueous solutions. A pulse radiolytic study (Reaction of 16 aliphatic radicals with Cr $(H_2O)_6{}^{2+}$), 30:29080
ALKYNES/CHEMICAL REACTION KINETICS
Chromium--carbon bonds in aqueous solutions. A pulse radiolytic study (Reaction of 16 aliphatic radicals with Cr $(H_2O)_6{}^{2+}$), 30:29080
ALLOY-TZM/CORROSION
Properties of TZM and nuclear behavior of TZM brazements. Various properties of TZM and Zr--5Be and Au--18Ni brazing filler metals are determined for brazing TZM to Zr and to steel, 30:30084
ALLOY-TZM/MECHANICAL PROPERTIES
Properties of TZM and nuclear behavior of TZM brazements. Various properties of TZM and Zr--5Be and Au--18Ni brazing filler metals are determined for brazing TZM to Zr and to steel, 30:30084
ALLOY-TZM/STANDARDS
Molybdenum and molybdenum alloy forgings, 30:29964
ALLOY-TZM/WELDING
Properties of TZM and nuclear behavior of TZM brazements. Various properties of TZM and Zr--5Be and Au--18Ni brazing filler metals are determined for brazing TZM to Zr and to steel, 30:30084
ALLOYS
See also BRAZING ALLOYS
ALLOYS/CHEMICAL ANALYSIS
Spectral assay of components in alloys (exchange of experience), 30:28951
ALLOYS/CORROSION
Corrosion and corrosion resistance. IX. Tutzing symposium of the DECHEMA, February 26--March 1, 1973, Tutzing Castle, Starnberger Lake, 30:29943 (CONF-730230-(Absts.))
ALLOYS/CRACKS
Prevention and control of subcritical crack growth in high-strength metals (Ratio analysis diagram), 30:29981 (NRL-Report-7780)

ALLOYS/DISPERSION HARDENING
  Dispersion-hardened materials (Book), 30:29998
ALLOYS/DUCTILITY
  Method of determining the relative elongation of light alloys close to the solidus on an IMASh-53-65 unit, 30:30012
ALLOYS/ETCHING
  Macroetching metals and alloys, 30:29965
ALLOYS/METALLURGY
  Publications from 1970--1972 of the Metallurgical Publishers. Annotated index (Metallurgy; ferrous and nonferrous metals; processing of steels and alloys; corrosion), 30:30042
ALLOYS/USES
  Adaptation of metallic materials to the conditions of utilization (Nuclear, petroleum, and chemical industries), 30:29966
ALLUVIAL DEPOSITS/COMPRESSIBILITY
  Compressibility and strength behavior of Diagonal Line alluvium, 30:29316 (UCID-15736)
ALLUVIAL DEPOSITS/PERMEABILITY
  Field measurement of the permeability of NTS alluvium (Nuclear explosion containment), 30:29315 (UCID-15727)
  Field measurements of permeability of NTS alluvium in Area 10, 30:29323 (UCID-15919)
  Numerical simulation of air-injection experiments in NTS alluvium (Nuclear explosion containment), 30:29324 (UCID-15981)
ALLUVIAL DEPOSITS/SHEAR PROPERTIES
  Compressibility and strength behavior of Diagonal Line alluvium, 30:29316 (UCID-15736)
ALPHA DECAY
  Finite size α-particle calculations of absolute α-decay for spherical nuclei, 30:31102
ALPHA DETECTION/DIELECTRIC TRACK DETECTORS
  Effect of electrons and X-rays on alpha-particle registration in T-Cellit detector, 30:29527
ALPHA PARTICLES/ENERGY LOSSES
  Energy loss and projected range of alpha particles in zinc telluride, 30:31113
ALPHA PARTICLES/STOPPING POWER
  Energy loss and projected range of alpha particles in zinc telluride, 30:31113
ALPHA REACTIONS/CAPTURE
  High spin states in the Ksup(π)=1/2^{-} band of ^{19}F (From angular distribution and ωγ measurements at 5413 and 6258 MeV), 30:30865
ALPHA REACTIONS/COMPOUND-NUCLEUS REACTIONS
  Cross sections of the ^{21}Ne(α,n)^{24}Mg and ^{22}Ne(α,n)^{25}Mg reactions at low energies of astrophysical interest (Below 3 MeV), 30:30913
  Gamma spectra from ^{179}Hf (d,2n), ^{179}Hf (p,n), and ^{181}Ta (α,2n) reactions, 30:30994
  Level densities of ^{63}Cu and ^{65}Cu from the analysis of evaporation spectra (12.5- to 16.0-MeV protons, 16.8- to 21.3-MeV α), 30:30950
  Pt (α,xn), 34-50 MeV: γ spectra, 30:31006
  Reaction rates of interest in late stages of stellar nycleosynthesis (Estimate of reliability), 30:30255
  Spectroscopy of the ^{69}Ga and ^{71}Ga isotopes with the ^{69} ^{71}Ga(α,α'γ)^{69} ^{71}Ga and ^{66} ^{68}Zn(α,pγ)^{69} ^{71}Ga reactions, 30:30941
  Yield functions for ^{51}V(α,rγ) reaction at 7 to 15 MeV, 30:30916 (NP-20122)
ALPHA REACTIONS/ELASTIC SCATTERING
  Generalized collective model and α-particle scattering on ^{54}Fe and ^{48}Ti (104 MeV: angular distributions), 30:30945
  On the nuclear l.L potential, 30:31092
  Target-spin effects on elastic scattering cross sections, 30:30940
ALPHA REACTIONS/EXCITATION FUNCTIONS
  Q-values and excitation functions of nuclear reactions. Part C. Estimation of unknown excitation functions and thick target yields for p, d, ^{3}He, and α reactions (Up to 25 or 35 MeV), 30:30960
ALPHA REACTIONS/INELASTIC SCATTERING
  Generalized collective model and α-particle scattering on ^{54}Fe and ^{48}Ti (104 MeV: angular distributions), 30:30945
  Highly inelastic scattering of α-particles from ^{208}Pb (Mechanism for cross section enhancement), 30:30998
  Level densities of ^{63}Cu and ^{65}Cu from the analysis of evaporation spectra (12.5- to 16.0-MeV protons, 16.8- to 21.3-MeV α), 30:30950
  Spectroscopy of the ^{69}Ga and ^{71}Ga isotopes with the ^{69} ^{71}Ga(α,α'γ)^{69} ^{71}Ga and ^{66} ^{68}Zn(α,pγ)^{69} ^{71}Ga reactions, 30:30941
  The l-forbidden 3psub(3/2) + 2fsub(5/2) M1 transition in ^{207}Pb (Branching ratio from Coulomb excitation), 30:31004
ALPHA REACTIONS/SCATTERING
  ^{12}C + α scattering by the coupled channel resonating group method. Solution of the redundancy and non-orthogonality problem, 30:30876
  New analytical derivation of kernels in the resonating group method for composite-particle scattering and molecule-like structures. Derivation from kernels in the generator coordinate method and application to ^{16}O + α, 30:31023
ALPHA REACTIONS/SPALLATION
  Spallation of copper by high-energy alpha particles (720 MeV), 30:30936
ALPHA REACTIONS/THREE-NUCLEON TRANSFER REACTIONS
  Magnetic rotation of levels of ^{53}Mn and ^{54}Mn following the ^{53} ^{54}Cr(p,n) and ^{51}V(α,n) reactions (2.5- and 3.0-MeV protons, 7.5-MeV alphas; branching ratios, g, lifetimes), 30:30933
ALPHA REACTIONS/TOTAL CROSS SECTIONS
  The validity of the factorization hypothesis for nucleus-nucleus cross sections at high energies (2.1 GeV/nucleon; various combinations from ^{3}He + α to ^{120}Sn + ^{208}Pb), 30:31095
ALPHA SOURCES/RADIATION MONITORING
  Data. Section II. Water, 30:29411
  Data. Section IV. Other data, 30:29412
  Environmental monitoring report, calendar year 1973, 30:29351 (UCC-ND-279)
  Environmental monitoring report: United States Atomic Energy Commission, Oak Ridge facilities. Calendar year 1973, 30:29352 (UCC-ND-280)
  Feed Materials Production Center environmental monitoring annual report for 1973, 30:29347 (NLCO-1109)
  Operation WHETSTONE: on-site radiological safety report, July 1964--June 1965, 30:29378 (NVO-410-24)
  Operation TOGGLE: on-site radiological safety report, July 1972--June 1973, 30:29379 (NVO-410-25)
  Portsmouth Gaseous Diffusion Plant environmental monitoring report, 1973, 30:29346 (GAT-781)
  Radiological monitoring program, period covering February 4, 1974--April 30, 1974 (Rio Blanco site), 30:29348 (PNE-RB-51-9)
ALUMINIUM/BONDING
  Determination of the feasibility of using beta radiation backscatter for the detection of surface contamination of metal panels, 30:29294 (AD-776394)
ALUMINIUM/BRAZING
  Brazing alloy (Patent), 30:29999
ALUMINIUM/CHARGED-PARTICLE TRANSPORT
  Energy dispersion of deuterons during their passage through matter. Influence of the state of the surface, 30:31122
  Transmission and reflection of electrons by foils, 30:31118
ALUMINIUM/CHEMICAL REACTIONS
  Mechanism of niobium pentoxide reduction in an alumino--thermal process, 30:29970
ALUMINIUM/DEPOSITION
  Multicomponent diffusion coatings (Book), 30:29906
ALUMINIUM/ELECTRON COLLISIONS
  Transmission and reflection of electrons by foils, 30:31118
ALUMINIUM/EMISSION SPECTROSCOPY
  Spectrochemical analysis of uranium oxide by gallium oxide carrier dc arc technique (ASTM Standard E402), 30:28957
  Spectrographic determination of trace impurities in high purity uranium oxide, 30:28944 (UCID-15952)
ALUMINIUM/FABRICATION
  Cold-weld type capsules for radioisotope production, 30:29962
ALUMINIUM/ION CHANNELING
  Electronic stopping power of channelled ions in a model incorporating the Pauli principle (Incident ions Z = 1 to 50), 30:31115
ALUMINIUM/ION EXCHANGE
  Selective ion-exchangers containing phosphorus in their functional groups. I. Sorption and separation of some bivalent and trivalent ions, 30:29001
ALUMINIUM/METALLURGY
  Effect of small additions of beryllium on some properties of aluminum and the aluminum alloy AL11 (AL11 = Zn 8.7percent, Si 7.6percent, Mg 0.57percent; effects on tensile properties and casting), 30:29987
ALUMINIUM/PHYSICAL RADIATION EFFECTS
  Changes in the internal friction spectrum of irradiated or deformed pure Al and Al solid solutions at 77°K (Fast neutrons; additions of 0.005 to 0.02 at. percent of Mg, Ag, Cu, Ti, or Cr), 30:30082
ALUMINIUM/RADIATION EFFECTS
  Effect of radioactive irradiation on the degree of cavitation erosion of aluminum (Hard γ rays), 30:30069
ALUMINIUM/SOLVENT PROPERTIES
  Interaction of tungsten with liquid aluminum, 30:30003
ALUMINIUM/SPECTROPHOTOMETRY
  Extraction--spectrophotometric methods of determining 0.0--n0.000n% aluminum in materials of metallurgical manufacture (exchange of experience), 30:28956
ALUMINIUM/THICKNESS
  Beta backscatter measurements of aluminum coatings on mylar substrates, 30:29602 (BDX-613-1028(Rev.))
ALUMINIUM 26/COSMOCHEMISTRY
  The unique cosmic-ray history of the Malakal chondrite, 30:30170
ALUMINIUM 27/ENERGY LEVELS
  4.510 MeV level in ^{27}Al (J, π), 30:30910
ALUMINIUM ALLOYS
    See also ALUMINIUM BASE ALLOYS
             RENE 41
             ZIRCALOY

ALUMINIUM ALLOYS/AGING
Effect of the volume disparity between the precipitation phase and the matrix on the scattering of x rays by aging alloys (EP 199 (Ni--Cr--W--Mo--Al--Ti)), 30:30036
ALUMINIUM ALLOYS/CHEMICAL PREPARATION
Joint reduction of niobium, aluminum, and germanium chlorides by hydrogen (Transition temperature of Nb germanides alloyed with 1 to 3 at. percent al = 20 to 20.5°K), 30:29971
ALUMINIUM ALLOYS/CORROSION
Corrosion fatigue strength of a titanium alloy at elevated temperature (Ti--Al--Zr; simulated seawater), 30:29945
Thermal and mechanical effects on the corrosion behavior of Ti--6Al--4V. Report for January 1971--January 1972, 30:29942 (AD-777170)
ALUMINIUM ALLOYS/CORROSION RESISTANCE
Corrosion study of the superplastic alloys 70/30 and 80/20 zinc aluminum in a humid atmosphere, 30:31391 (COPPE-TP-8/72)
ALUMINIUM ALLOYS/CRYSTALLIZATION
Nonequilibrium crystallization of aluminum--molybdenum alloys, 30:30006
ALUMINIUM ALLOYS/DIFFUSION
Transport and thermodynamic properties of solids. Progress report, September 1, 1973--August 31, 1974, 30:31390 (COO-1436-41)
ALUMINIUM ALLOYS/FATIGUE
Fatigue-crack growth of Ti--6Al--2Cb-1Ta--0.8Mo alloy in air and natural sea water environments, 30:29972 (AD-765318)
ALUMINIUM ALLOYS/FRACTURE PROPERTIES
J-integral as a failure criterion for a Borsic--Al composite, 30:29890 (SAND-74-0193)
ALUMINIUM ALLOYS/MECHANICAL PROPERTIES
Fatigue and impact resistance of dual-matrix boron--aluminum composites. Final report (B--6061 Al), 30:29974 (AD-775334)
Mechanical behavior of metal matrix composites. Final report, 1 April 1972--30 April 1973 (B--Al;B/SiC--Ti;tensile, fatigue, and creep behavior;effects of defects), 30:29975 (AD-775359)
Mechanical properties of multicomponent alloys based on Ti--Al--Sn (Zr) α-solid solution with β-stabilizing elements (Additions of Mo, V, Cr, Fe, Si, B;properties at up to 950°C), 30:29984
Precision casting of alloy Ti--6Al--4V (Effects of heat treatments on mechanical properties), 30:29995
ALUMINIUM ALLOYS/OXIDATION
Oxidation mechanism of Ni_3Al containing yttrium (with and without 0.5 wt percent Y; 900 to 1200°C in air), 30:29953
ALUMINIUM ALLOYS/QUADRUPOLES
Effect of plastic deformation on quadrupole interaction in Al, Nb, and Au alloyed with Hf, 30:30038
ALUMINIUM ALLOYS/STACKING FAULTS
Diffraction of x rays on stacking faults in metals with hcp lattices (Ti--Al; Ti--Sn), 30:30024
ALUMINIUM ALLOYS/SUPERCONDUCTIVITY
Joint reduction of niobium, aluminum, and germanium chlorides by hydrogen (Transition temperature of Nb germanides alloyed with 1 to 3 at. percent al = 20 to 20.5°K), 30:29971
Superconductivity of Nb--Al--Zr alloys (Phase boundaries;solubility of Zr in Nb_3Al), 30:30048
ALUMINIUM ALLOYS/THERMAL FATIGUE
Mechanical properties of metal matrix composites subjected to cyclic temperature changes. Annual report, 1 July 1972--30 June 1973 (6064 Al reinforced with fibers of stainless steel, 34 vol % SiC, 27 vol % B, and 45 vol % B), 30:29973 (AD-774890)
ALUMINIUM BASE ALLOYS/METALLURGY
Effect of small additions of beryllium on some properties of aluminum and the aluminum alloy AL11 (AL11 = Zn 8.7percent, Si 7.6percent, Mg 0.57percent; effects on tensile properties and casting), 30:29987
ALUMINIUM IONS/X-RAY SPECTRA
Diagnostics of dense laser plasmas based on the spectra of hydrogen-like and helium-like multiply charged ions, 30:29171
ALUMINIUM OXIDES/CRACKS
Acoustic emission monitoring of ring-cracking in glass and alumina, 30:31410 (UCID-16076)
ALUMINIUM OXIDES/ION IMPLANTATION
Ion implantation of semiconductors, metals, and alloys. Interim report No. 7, 1 September 1971--31 August 1973, 30:30088 (AD-774654)
ALUMINIUM OXIDES/METALLURGICAL EFFECTS
Effect of additivies of yttrium and aluminum oxides on sintering and properties of lanthanum hexaboride, 30:29892
ALUMINIUM OXIDES/PHYSICAL RADIATION EFFECTS
Phase changes in high-alumina ceramic under the influence of ionizing radiation (Neutrons; γ rays), 30:29913
ALUMINIUM OXIDES/X-RAY FLUORESCENCE ANALYSIS
Compilation of x-ray interaction data for x-ray fluorescence analysis of geological samples, 30:28943 (RISO-297)
AMALGAMS
See MERCURY ALLOYS
AMERICIUM/EXTRACTION CHROMATOGRAPHY
Chemistry of americium. II. Behavior of Am(III), Am(V), and Am(VI) in column chromatography, with bis(2-ethylhexyl)phosphoric acid used as the extractant, 30:29093
AMERICIUM/HYDROLYSIS
Hydrolysis of transuranium elements. II. Hydrolysis of americium(III) in the presence of ions with positive and negative hydration energies, 30:29121
AMERICIUM/REDUCTION
Oxidation--reduction reactions of actinide elements. XXIII. Kinetics of neptunium(V)--americium(V) reaction in perchlorate solutions, 30:29105
Some characteristics of the reaction of americium(VI) with reducing agents in aqueous solutions, 30:29104
AMERICIUM 241/ALPHA SPECTROSCOPY
Simultaneous determination of alpha-emitting nuclides of radium through californium in soil, 30:28977
AMERICIUM 241/BIOLOGICAL RADIATION EFFECTS
Cortisol metabolism in skin of beagles bearing ^{241}Am: a possible pre-neoplastic change in steroid metabolism, 30:29780 (COO-119-249)
Research in radiobiology. Annual report of work in progress in the internal irradiation program (Pathological effects of bone-seeking radionuclides in beagles), 30:29778 (COO-119-249)
AMERICIUM 241/CLEARANCE
Removal by DTPA of internally deposited ^{241}Am. A comparative study on rats and Syrian hamsters, 30:29822
AMERICIUM 241/DIFFUSION
Resuspension of ^{239}Pu, ^{240}Pu, and ^{241}Am particles at Nevada Test Site; prediction of air concentrations of Pu due to resuspension at Eniwetok Atoll, 30:29452 (NVO-AEIC-74-1)
AMERICIUM 241/RADIATION MONITORING
Distribution and inventory element activities on-NTS and off-NTS (^{239}Pu, ^{240}Pu, and ^{241}Am content of soil samples from Nevada Test Site and environs), 30:29453 (NVO-AEIC-74-1)
Soils element activities, October 1972--September 1973 (^{214}Am, ^{239}Pu, and ^{240}Pu in soil at Nevada Test Site), 30:29440 (NVO-AEIC-74-1)
Some ecological attributes and plutonium contents of perennial vegetation in Area 13 (NAEG vegetation studies) (Botany of Nevada Test Site), 30:29445 (NVO-AEIC-74-1)
Statistical analysis of Pu in soil at the Nevada Test Site: some results (Statistical sampling design), 30:29444 (NVO-AEIC-74-1)
AMERICIUM 241/RADIOCHEMICAL ANALYSIS
Determination of ^{239}Pu and ^{241}Am in large NAEG vegetation samples (Nevada Test Site), 30:28971 (NVO-AEIC-74-1)
AMERICIUM 241/REMOVAL
Alternate methods for administering chelating agents in decorporation therapy (Removal of actinides from mammals), 30:29798 (COO-119-249)
Decorporation of ^{241}Am in beagles by DTPA, 30:29797 (COO-119-249)
Decorporation of ^{241}Am from bone using DTPA and osteoporotic agents (Additive effects of parathyroid extract), 30:29799 (COO-119-249)
Evaluation of long-term ZnDTPA therapy in beagles (Toxicity of ZnDTPA during prolonged chelation treatment for removal of ^{241}Am), 30:29796 (COO-119-249)
AMERICIUM 241/RETENTION
Decorporation of ^{239}Pu and ^{241}Am in the rat and hamster by Zn--DTPA, 30:29813
AMERICIUM 241/ROOT ABSORPTION
Influence of soil plutonium concentration of plutonium uptake and distribution in shoots and roots of barley (^{239}Pu, ^{240}Pu, ^{238}Pu, ^{241}Am), 30:29825
AMERICIUM 241/TISSUE DISTRIBUTION
Decorporation of ^{241}Am in beagles by DTPA, 30:29797 (COO-119-249)
Ecological studies of vertebrates in plutonium-contaminated areas of the Nevada Test Site (^{239}Pu and ^{241}Am content of GI tract, carcass, and pelt of rodents), 30:29449 (NVO-AEIC-74-1)
Transuranium elements in gonadal tissue (^{239}Pu, ^{241}Am, ^{243}Cm, ^{244}Cm, ^{249}Cf, and ^{252}Cf), 30:29806 (COO-119-249)
AMERICIUM 242/HOT ATOM CHEMISTRY
Possibility of preparing enriched americium-242g by elution of recoil atoms from zeolite, 30:29141
AMERICIUM 242/ISOTOPE PRODUCTION
Possibility of preparing enriched americium-242g by elution of recoil atoms from zeolite, 30:29141
AMERICIUM COMPLEXES/HOT ATOM CHEMISTRY
Possibility of preparing enriched americium-242g by elution of recoil atoms from zeolite, 30:29141
AMERICIUM NITRATES/REDUCTION
Chemistry of americium. II. Behavior of Am(III), Am(V), and Am(VI) in column chromatography, with bis(2-ethylhexyl)phosphoric acid used as the extractant, 30:29093
AMINES
See also AET
CYTOSINE
AMINES/COSMOCHEMISTRY
Detection of interstellar methylamine (Column density), 30:30359

Detection of interstellar methylamine by its $2_{02}+1_{10}$ A/sub a/-state transition (Thermodynamic equilibrium), 30:30360
AMINO ACIDS
See also DTPA
GLYCINE
TYROSINE
AMINO ACIDS/CHEMICAL RADIATION EFFECTS
Electron radiation damage of thin films of glycine, diglycine, and aromatic amino acids, 30:29042
AMINO ACIDS/PHOTOCHEMISTRY
Photochemical addition of amino acids to thymine (UV radiation), 30:29658
AMINO ACIDS/PHOTOLYSIS
Effect of ultraviolet light and gamma radiation on aqueous solutions of Cu(II) complexes with amino acids, 30:29061
AMINO ACIDS/RADIOLYSIS
Effect of ultraviolet light and gamma radiation on aqueous solutions of Cu(II) complexes with amino acids, 30:29061
Reactions of secondary free radicals in the irradiated frozen aqueous solutions of amino acid and peptides, 30:29044
AMINOACETIC ACID
See GLYCINE
AMINOETHYLISOTHIURONIUM BROMIDE
See AET
AMINOETHYLTHIOPSEUDOUREA
See AET
AMINOGLYCIDES
See AMINES
AMINOTRANSFERASES/METABOLISM
Tyrosine aminotransferase induction in rat liver as a response to irradiation or flash burn injuries (Gamma radiation), 30:29757
AMMONIA/CHEMICAL REACTION KINETICS
Kinetics of forming ammoniates of uranium tetrachloride, 30:29124
AMMONIA/MOESSBAUER EFFECT
Moessbauer spectroscopy of frozen europium ammonia solutions, 30:30093
AMMONIA/RADIOLYSIS
Transient spectrum from nanosecond pulse radiolysis of liquid ammonia, 30:29079
AMMONIA/WASHOUT
Precipitation scavenging of inorganic pollutants from metropolitan sources: St. Louis, July 1973, 30:29479 (BNWL-1850(Pt.3))
AMP
(Adenosine monophosphate.)
AMP/HYDROLYSIS
Hydrolysis of 2',3'-cyclic adenosine monophosphate and 3',5'-cyclic adenosine monophosphate in subcellular fractions of normal and neoplastic mouse spleen (X radiation), 30:29739
AMPHIBOLE/MAGNETIC PROPERTIES
Magnetic order in certain alkali ampniboles, a Moessbauer investigation, 30:31412 (UCRL-75499(Rev.1))
AMYLUM
See STARCH
ANALOG RESONANCES
See ISOBARIC ANALOGS
ANALOG STATES
See ISOBARIC ANALOGS
ANALOG-TO-DIGITAL CONVERTERS/CALIBRATION
Reference pulsers for calibration purposes, 30:29628
ANDROSTENEDIONE/RADIOIMMUNOASSAY
Radioimmunoassay for sex steroid hormone. VI. Radioimmunoassay for Δ^{4}-androstenedione (Tritium label), 30:29863
ANEMOMETERS/DESIGN
Development of a sonic anemometer system, 30:29609 (BNWL-1850(Pt.3))
ANGIOGRAPHY
See BIOMEDICAL RADIOGRAPHY
BLOOD VESSELS
ANGIOMAS/RADIOTHERAPY
Cancer mortality following irradiation in infancy for hemangioma, 30:29714
ANGIOTENSIN/RADIOIMMUNOASSAY
Radioimmunoassay of angiotensin (^{125}I), 30:29876
ANIMAL CELLS
See also SOMATIC CELLS
SPLEEN CELLS
THYMUS CELLS
TUMOR CELLS
ANIMAL CELLS/BIOLOGICAL RADIATION EFFECTS
Changes in genetic cell material during the action of ionizing radiation (Effects of uv and x radiation on DNA and nucleoproteins), 30:29655
Effect of x irradiation on hydrocarbon metabolism and on hydrocarbon-induced lethality and transformation in cells derived from mouse prostate (3-Methylcholanthrene, 7,12-dimethylbenz(a)anthracene, N-methyl-N'-nitro-N-nitrosoquanidine), 30:29670
Effect of total irradiation on the development of leukemia L_{1210} in F_1-hybrids (X Radiation; mice), 30:29748
Metronidazole (Flagyl). A radiosensitizer of hypoxic cells, 30:29674
ANIMAL CELLS/BIOLOGICAL REPAIR
Cellular repair after x or gamma irradiation determined for several gross criteria on animals and patients, 30:29759
ANIMAL CELLS/MORPHOLOGICAL CHANGES
Gomori-positive glia in uv-irradiated mice, 30:29752
ANIMAL CELLS/SURVIVAL CURVES
Cellular repair after x or gamma irradiation determined for several gross criteria on animals and patients, 30:29759
ANIMALS
(See specific animal names.)
See also VERTEBRATES
WILD ANIMALS
ANIMALS/SAMPLING
General statistical considerations in environmental plutonium studies (Sample selection), 30:29416 (NVO-AEIC-74-1)
REECo field activities and sample logistics in support of the Nevada Applied Ecology Group (Nevada Test Site ecological sample collection and preparation for Pu analysis), 30:29441 (NVO-AEIC-74-1)
ANL
(Argonne National Laboratory.)
ANL/RADIOACTIVITY
Data. Section IV. Other data (Monitoring), 30:29412
ANTENNAS/DESIGN
Communication system design, 30:31452 (UCID-15955)
ANTENNAS/ELECTROMAGNETIC RADIATION
Radiation from buried antennas, 30:31449 (UCID-15890)
ANTENNAS/PERFORMANCE
Automatic radar-sensitivity measurement. Final report, 30:31417 (BDX-613-1134(Rev.))
ANTHRACENE/CHEMICAL RADIATION EFFECTS
Reduction in electron irradiation damage to organic compounds by conducting coatings (Electron beams, Al or Au coatings), 30:29070
ANTIBIOTICS
See also MITOMYCIN
ANTIBIOTICS/RADIOSENSITIVITY EFFECTS
Effect of a combination of antibiotics and AET on the survival of irradiated animals (Tetron-pyrrolidinomettryl-oxytetracycline), 30:29746
ANTIBODIES/AFFINITY
Use of a double isotope method in the determination of antibody affinity (^{22}Na and ^{125}I tracer technique), 30:29867
ANTICORROSION
See CORROSION PROTECTION
ANTIKAONS NEUTRAL/TRANSMISSION
Coherent transmission of neutral kaons in matter and forward scattering amplitudes, 30:30741
ANTIMONY/ACTIVATION ANALYSIS
Application of activation analysis to the determination of pollutants in the atmosphere (Thermal neutrons), 30:28914 (IEA-326)
Multielement determination in market-garden soils by instrumental photon activation analysis, 30:28921
Trace element behavior in soil of some Indonesian sawah's and in sludge of an Indonesian river, 30:28930
Trace elements in precipitation and cloud water in the area of Heidelberg, measured by instrumental neutron activation analysis, 30:28934
ANTIMONY/EMISSION SPECTROSCOPY
Spectrochemical analysis of uranium oxide by gallium oxide carrier dc arc technique (ASTM Standard E402), 30:28957
Spectrographic determination of trace impurities in high purity uranium oxide, 30:28944 (UCID-15952)
ANTIMONY/FLUORESCENCE SPECTROSCOPY
New discrete atomization cell for atomic fluorescence spectrometry, 30:28947
ANTIMONY/UPTAKE
Elemental content of trace elements in vegetation collected at Centralia, Washington (Comparison with Alaskan vegetation), 30:29483 (BNWL-1850(Pt.3))
ANTIMONY 116/SPIN
Atomic-beam investigations of some antimony nuclides, 30:30976
ANTIMONY 117/HYPERFINE STRUCTURE
Atomic-beam investigations of some antimony nuclides, 30:30976
ANTIMONY 117/MAGNETIC DIPOLE MOMENTS
Atomic-beam investigations of some antimony nuclides, 30:30976
ANTIMONY 117/QUADRUPOLE MOMENTS
Atomic-beam investigations of some antimony nuclides, 30:30976
ANTIMONY 118/SPIN
Atomic-beam investigations of some antimony nuclides, 30:30976
ANTIMONY 120/SPIN
Atomic-beam investigations of some antimony nuclides, 30:30976
ANTIMONY 125/RADIATION MONITORING
Data. Section IV. Other data, 30:29412
ANTIMONY 128/SPIN
Atomic-beam investigations of some antimony nuclides, 30:30976

ANTIMONY 130/ENERGY LEVELS
  Nuclear Data Sheets for A = 130, 30:30968
ANTIMONY 130/NUCLEAR PROPERTIES
  Nuclear Data Sheets for A = 130, 30:30968
ANTIMONY ALLOYS/CRYSTAL DOPING
  Systematic control of doping characteristics of n-InSb by nuclear reactions (Thermal neutrons), 30:29992
ANTIMONY ALLOYS/ELECTRICAL PROPERTIES
  Characteristics of MOS capacitors formed on p-type InSb, 30:29994
ANTIMONY ALLOYS/MICROSTRUCTURE
  Structure and phase-boundary energies of the directionally solidified InSb--MnSb--NiSb, InSb--FeSb, and InSb--CrSb eutectic alloys, 30:30019
ANTIMONY CHLORIDES/ION EXCHANGE
  Labelled compounds. P. 18. Chlorine excnange between antimony(III) chloride-(^{36}Cl) and hexachloropropene (1), 30:29123
ANTIMONY CHLORIDES/LABELLING
  Labelled compounds. P. 18. Chlorine exchange between antimony(III) chloride-(^{36}Cl) and hexachloropropene (1), 30:29123
ANTIMUONS
  See MUONS PLUS
ANTIPROTON-NEUTRON INTERACTIONS/ANNIHILATION
  Cross-sections for resonance production in anti pn annihilations around 2190 MeV centre-of-mass energy, 30:30606
ANTIPROTONS/PARTICLE PRODUCTION
  Is anti p production peripheral or central, 30:30763
APATITES/ACTIVATION ANALYSIS
  Determination of rare earths and thorium in apatites by thermal and epithermal neutron-activation analysis, 30:28935
AQUATIC ECOSYSTEMS/RADIONUCLIDE MIGRATION
  Chemoradioecology of the pelagic zone and the benthos (metals and radionuclides in the nydrobiont and environment) (Book in Russian), 30:29422
  Concentration effects of ^{137}Cs, ^{65}Zn, ^{60}Co, and ^{106}Ru sorption by marine sediments with geocnemical implications, 30:29409
ARCTIC REGIONS/FALLOUT
  ^{137}Cs, ^{90}Sr, and ^{210}Pb in soils of the Arctic regions (Monitoring), 30:29405
ARCTIC REGIONS/NATURAL RADIOACTIVITY
  ^{137}Cs, ^{90}Sr, and ^{210}Pb in soils of the Arctic regions (Monitoring), 30:29405
ARGON/ELECTRON-ATOM COLLISIONS
  Atomic excitation processes in the discnarges of rare gas ion engines, 30:30556
  New technique for threshold excitation spectroscopy, 30:30553
ARGON/ION-ATOM COLLISIONS
  Argon L-shell ionization by 50- to 600-keV H$^+$, D$^+$, H$_2^+$, and He$^+$ impact (Branching ratios, excitation, multiple-vacancy states, total cross sections, ionization), 30:30541
  Cross section for the Ar--L--x-ray emission in collisions of He^{+-}, Ne^{+-}, and Ar^{+-} ions with Ar atoms (100 keV to 1 MeV), 30:30518 (AED-CONF-74-085-002)
  Crossed-molecular-beam study of tne kinematics and dynamics of cnarge-transfer collisions (200 eV), 30:30547
  Differential elastic-scattering measurements of Xe$^+$ on Xe and Ar$^+$ on Ar in the 20 to 340-eV range (Oscillations, interference, excitation, potential-curve crossings), 30:30540
  Inelastic collisions of He$^+$ and Ar (Cross sections, threshold to 10 keV), 30:30538
  Outer s-shell ionization of neon, argon, and krypton by proton impact (125 keV-1200 keV), 30:30557
ARGON/IONIZATION
  Outer s-shell ionization of neon, argon, and krypton by proton impact (125 keV-1200 keV), 30:30557
ARGON 35/BETA-PLUS DECAY
  Beta asymmetry of ^{35}Ar and the deduced value of the vector coupling constant, 30:30902
ARGON 37/ENERGY LEVELS
  ^{40}Ca(n,α)^{37}Ar reaction at 14.1 MeV, 30:30927
ARGON 38/ENERGY LEVELS
  Investigation of the 3.46 MeV isomeric level of ^{38}K with the ^{24}Mg(^{16}O,pnγ)^{38}K reaction (38 MeV: γ spectra; lifetimes of levels in ^{38}K, ^{38}Ar, ^{38}Cl), 30:30912
ARGON 41/RADIATION MONITORING
  Data. Section IV. Other data, 30:29412
ARGON IONS/CHANNELING
  Sputtering experiments with silver single crystals and the channeling phenomena, 30:30481
ARGON IONS/COLLISIONS
  Hyperthermal beams sputtered from alkali halide surfaces (6-keV Ar$^+$), 30:30484
  Sputtering experiments with silver single crystals and the channeling phenomena, 30:30481
  Sputtering yields and specific energy losses of Ar$^+$ ions with energies from 5 to 30 keV at SiO$_2$, 30:30482
ARGON IONS/ENERGY LOSSES
  Sputtering yields and specific energy losses of Ar$^+$ ions with energies from 5 to 30 keV at SiO$_2$, 30:30482
ARGON IONS/ION-ATOM COLLISIONS
  Cross section for the Ar--L--x-ray emission in collisions of He^{+-}, Ne^{+-}, and Ar^{+-} ions with Ar atoms (100 keV to 1 MeV), 30:30518 (AED-CONF-74-085-002)
  Crossed-molecular-beam study of the kinematics and dynamics of charge-transfer collisions (200 eV), 30:30547
  Differential elastic-scattering measurements of Xe$^+$ on Xe and Ar$^+$ on Ar in the 20 to 340-eV range (Oscillations, interference, excitation, potential-curve crossings), 30:30540
ARGON IONS/ION-MOLECULE COLLISIONS
  Crossed-molecular-beam study of the kinematics and dynamics of charge-transfer collisions (200 eV), 30:30547
ARGONNE NATIONAL LABORATORY
  See ANL
ARSENIC/ACTIVATION ANALYSIS
  Application of activation analysis to the determination of pollutants in the atmosphere (Thermal neutrons), 30:28914 (IEA-326)
  Multielement determination in market-garden soils by instrumental photon activation analysis, 30:28921
  Trace element behavior in soil of some Indonesian sawah's and in sludge of an Indonesian river, 30:28930
ARSENIC/EMISSION SPECTROSCOPY
  Spectrochemical analysis of uranium oxide by gallium oxide carrier dc arc technique (ASTM Standard E402), 30:28957
ARSENIC/STACK DISPOSAL
  Trace pollutant emissions in fossil fuel combustion, 30:29469 (BNWL-1850(Pt.3))
ARSENIC 75/ENERGY LEVELS
  Gamma-rays from the decay of ^{75}Ge, 30:30942
ARTHROPODS/RADIONUCLIDE KINETICS
  Radioactive tracer studies of soil and litter arthropod food chains. Progress report, November 1, 1973--October 31, 1974 (Fallout ^{137}Cs tracer), 30:29419 (SRO-641-13)
ASCARIS/RADIOSENSITIVITY
  Effect of temperature on the radiation sensitivity of Ascaris eggs (X radiation), 30:29766 (SAND-74-6017)
ASCORBIC ACID/BIOLOGICAL RADIATION EFFECTS
  Ascorbic acid content in different stages of ripeness of fruits pepper under the effect of El and irradiation by ^{60}Co, 30:29685
ASTATINE 211/TOXICITY
  Embryotoxicity of astatine-211 (Comparison of effects of internal ^{211}At with external x irradiation), 30:29781 (COO-3268-5)
ASTROCYTOMAS
  See NEOPLASMS
ASTRON/ELECTRON BEAMS
  Analytical expression for the E-layer electron velocity distribution, 30:29187 (UCID-16003(Rev.1))
  Back current in an E-layer. I, 30:29224 (UCID-15977)
  Observations on the change of the length of the E-layer during stacking, 30:29188 (UCID-16004)
  Weak interaction of a neutralized E-layer with resistors, 30:29223 (UCID-15956)
ASTRON/ELECTRON SOURCES
  Note on the Astron gun design, 30:29214 (UCID-15481)
ASTRON/PLASMA DIAGNOSTICS
  X-ray measurements on electron distribution in Astron, 30:29160 (UCID-15392)
ASTRON/RESISTORS
  Resistor beam bugs: scientific explanation, 30:29225 (UCID-16057)
ASTRON/TRAPPED ELECTRONS
  X-ray measurements on electron distribution in Astron, 30:29160 (UCID-15392)
ASTRONAUTS/MAXIMUM PERMISSIBLE EXPOSURE
  Problems of space radiobiology and radiation safety in space missions, 30:29712
ASTRONOMY/RESEARCH PROGRAMS
  Research fields in physics (Research topics listing), 30:30645
ASTROPHYSICS
  Problems of cosmic physics (Book), 30:30161
ASTROPHYSICS/MEETINGS
  Particles and fields in space. Proceedings of the summer school, Balatonfured, 5--15 June 1973, 30:30160 (CONF-730693-)
ASTROPHYSICS/TRANSPORT THEORY
  Compton scattering subroutine for Monte Carlo calculations, 30:30651 (UCID-15808)
ATMOSPHERIC PRECIPITATIONS
  See also RAIN
ATMOSPHERIC PRECIPITATIONS/RADIATION MONITORING
  Data. Section III. Air and deposition, 30:29382
  Data. Section II. Water, 30:29411
  Rate of fallout of ^{137}Cs and ^{90}Sr aerosols from the atmosphere, 30:29399
  Use of naturally radioactive substances in studying turbulent exchange and self-scavenging of the atmosphere with surface layer measurements, 30:29396
ATOM COLLISIONS
  See also ATOM-ATOM COLLISIONS
    ATOM-MOLECULE COLLISIONS
    ELECTRON-ATOM COLLISIONS
    ION-ATOM COLLISIONS

ATOM COLLISIONS/SCATTERING
Scattering form factors of atoms, molecules, and solids (Density-functional formalism, electron gas), 30:30522
ATOM-ATOM COLLISIONS
A model for the calculation of the defect production ratio, 30:30075
ATOM-ATOM COLLISIONS/INTERATOMIC FORCES
Thomas--Fermi calculation of potential between atoms, 30:30565 (LA-5694-MS)
ATOM-ATOM COLLISIONS/RESONANCE
Finite-difference boundary-value method for determination of resonance widths in atomic collisions, 30:30564
ATOM-MOLECULE COLLISIONS/ELASTIC SCATTERING
Improved modified wavenumber approximation applied to elastic collision, 30:30529
ATOM-MOLECULE COLLISIONS/INELASTIC SCATTERING
Dimensionality control of coupled scattering equations using partitioning techniques, 30:30562
Entropy analysis of product energy distributions in nonreactive inelastic collisions, 30:30561
ATOM-MOLECULE COLLISIONS/OPTICAL MODELS
Optical potential calculations for molecular collisions (Feshback formalism), 30:30559
ATOM-MOLECULE COLLISIONS/SCATTERING
Integral equation approach to collinear reactive scattering: A+BC+AB+C, 30:30527
ATOM-MOLECULE COLLISIONS/TOTAL CROSS SECTIONS
Equivalence and conservation rules for the total integral cross section in molecular collisions (Opacity function), 30:30560
ATOMIC ABSORPTION SPECTROSCOPY
See ABSORPTION SPECTROSCOPY
ATOMIC BOMBS
See NUCLEAR WEAPONS
ATOMIC CLOUDS
See RADIOACTIVE CLOUDS
ATOMIC ENERGY AGREEMENTS
Safeguarding the peaceful uses of nuclear energy by states, 30:30104 (FRNC-TH-50)
ATOMIC ENERGY CONTROL/INTERNATIONAL AGREEMENTS
Safeguarding the peaceful uses of nuclear energy by states, 30:30104 (FRNC-TH-50)
ATOMIC ENERGY LAWS
AEC omnibus legislation, 1974. Report by the Joint Committee on Atomic Energy, Ninety-Third Congress, Second Session, Senate, 30:31328
AEC omnibus legislation, 1974. Report by the Joint Committee on Atomic Energy, Ninety-Third Congress, Second Session, House of Representatives, 30:31329
ATOMIC EXPLOSIONS
See NUCLEAR EXPLOSIONS
ATOMIC WEAPONS
See NUCLEAR WEAPONS
ATOMS
See also MUONIC ATOMS
ATOMS/ELECTRONIC STRUCTURE
Degenerate perturbation theory, 30:30566
ATOMS/GROUND STATES
Improved first order perturbative calculation of the ground state energy of atoms, 30:30567
ATOMS/IONIZATION
Effect of intense electromagnetic wave in charged-particle scattering (Born and dipole approximations, Schroedinger equation), 30:30655
ATOMS/WAVE FUNCTIONS
Plausible assertions for building-up the wave functions of the atoms with a single valence electron, 30:30569
AURORAE/ASYMMETRY
Indications of a longitudinal component in auroral phenomena, 30:30426
AURORAE/ELECTROJETS
Latitudinal cross section of the auroral electrojet and its relation to the interplanetary magnetic field polarity, 30:30470
AURORAE/ELECTRON DENSITY
Interrelationship between the > 130 keV electron trapping boundary, the VHF radar backscatter, and the visual aurora, 30:30430
AURORAE/PHOTOMETRY
Observations of the conjugate SAR arcs of September 28-30, 1967, 30:30423
AURORAL ELECTROJETS
See ELECTROJETS
AURORAL OVAL/PLASMA SHEET
Relation of the plasma sheet to the nighttime auroral oval, 30:30441
AURORAL SUBSTORMS
See MAGNETIC BAYS
AUSTRALIA/RADIATION HAZARDS
Radiation in man's environment (Hazards from fallout as compared with other radiation sources in Australia), 30:29353
AUTORADIOGRAPHS
See IMAGES
AUTORADIOGRAPHY/REVIEWS
Technique of autoradiography. Second revised and enlarged edition (Book), 30:29298

B

BACILLUS SUBTILIS/BIOLOGICAL RADIATION EFFECTS
Proteins induced in Bacillus subtilis infected with bacteriophage phi29 (Ultraviolet radiation), 30:29679
BACTERIOPHAGES/BIOLOGICAL EFFECTS
Proteins induced in Bacillus subtilis infected with bacteriophage phi29 (Ultraviolet radiation), 30:29679
BACTERIOPHAGES/BIOLOGICAL RADIATION EFFECTS
Postirradiation fate of bacteriophage lambda DNA in the host cell (Escherichia coli), 30:29678
Repair of γ-ray-induced damage in bacteriophage lambda (Escherichia coli), 30:29680
BARIUM/ACTIVATION ANALYSIS
Multielement determination in market-garden soils by instrumental photon activation analysis, 30:28921
BARIUM/EMISSION SPECTROSCOPY
Spectrochemical analysis of uranium oxide by gallium oxide carrier dc arc technique (ASTM Standard E402), 30:28957
Spectrographic determination of trace impurities in high purity uranium oxide, 30:28944 (UCID-15952)
BARIUM/ION EXCHANGE
Sorption of tetravalent elements by mordenite. II. Sorption of Pu(IV), 30:28999
BARIUM 130/ENERGY LEVELS
Levels in ^{130}Ba fed from ^{130}La decay, 30:30963
Nuclear Data Sheets for A = 130, 30:30968
BARIUM 130/NUCLEAR PROPERTIES
Nuclear Data Sheets for A = 130, 30:30968
BARIUM 136/ENERGY LEVELS
Nuclear Data Sheets for A = 136, 30:30967
BARIUM 136/NUCLEAR PROPERTIES
Nuclear Data Sheets for A = 136, 30:30967
BARIUM 138/DEUTERON REACTIONS
Correlations between (n,γ) and (d,p) reactions on N = 82 nuclei (Excitation strengths), 30:30970
BARIUM 138/NEUTRON REACTIONS
Correlations between (n,γ) and (d,p) reactions on N = 82 nuclei (Excitation strengths), 30:30970
BARIUM 140/RADIATION MONITORING
Data. Section IV. Other data, 30:29412
Environmental monitoring report: United States Atomic Energy Commission, Oak Ridge facilities. Calendar year 1973, 30:29352 (UCC-ND-280)
Report of activity, February 1974 (Radioactivity of environmental samples collected throughout France during February 1974), 30:29349 (SCPRI(RM)-2-1974)
BARIUM 143/NUCLEAR PROPERTIES
Nuclear Data Sheets for A = 143, 30:30966
BARIUM COMPOUNDS/RADIATION CHEMISTRY
ESR study of paramagnetic centers in irradiated $Ba(ClO_3)_2 \cdot H_2O$ and $Ba(ClO_3)_2 \cdot D_2O$ single crystals (γ radiation), 30:29069
BARIUM IONS/EXCITATION
Rate coefficients for electron excitation of the first resonance transition in H, Li, Na, Ca, Ca^+, and Ba^+ calculated from experimental data (Transition probabilities), 30:30246
BARIUM SULFATES/X-RAY FLUORESCENCE ANALYSIS
Compilation of x-ray interaction data for x-ray fluorescence analysis of geological samples, 30:28943 (RISO-297)
BARLEY/MUTATIONS
Studies on the use of U-120 cyclotron and fast neutron generator in neutron irradiation of seeds for mutation (Barley; wheat), 30:29692
BARLEY/RADIONUCLIDE KINETICS
Influence of soil plutonium concentration of plutonium uptake and distribution in shoots and roots of barley (^{239}Pu, ^{240}Pu, ^{238}Pu, ^{241}Am), 30:29825
BARYONS
See also NUCLEONS
BARYONS/MASS DIFFERENCE
Electromagnetic mass breaking of baryons in broken chiral SU(3) x SU(3), 30:30779
BARYONS/MASS FORMULAE
Electromagnetic-mass formula and a model of baryons, 30:30653
BARYONS/MASS SPECTRA
Quark additivity for mass splittings in the psub(z) + infinity frame, 30:30709
BASALT/CHEMICAL COMPOSITION
Origin of carbonatitic magma in the light of the Pb-U-Th isotope system, 30:29337
BASALT/MAGNETIC PROPERTIES
Rock magnetites with positive anisotropy constants at 300°K, 30:31389 (CONF-740644-1)
BASALT/X-RAY FLUORESCENCE ANALYSIS
Compilation of x-ray interaction data for x-ray fluorescence analysis of geological samples, 30:28943 (RISO-297)
BASEBALL DEVICES/NEGATIVE MASS INSTABILITY
Negative mass instabilities in beam injected plasmas, 30:29197 (UCID-15540)
BASEDOW'S DISEASE
See HYPERTHYROIDISM

BEAGLES/BIOLOGICAL RADIATION EFFECTS
Early hematologic effects of curium and einsteinium in beagles (^{244}Cm, ^{243}Cm, and ^{253}Es), 30:29779 (COO-119-249)
Research in radiobiology. Annual report of work in progress in the internal irradiation program (Pathological effects of bone-seeking radionuclides in beagles), 30:29778 (COO-119-249)
BEAGLES/CHRONIC IRRADIATION
Research in radiobiology. Annual report of work in progress in the internal irradiation program (Pathological effects of bone-seeking radionuclides in beagles), 30:29778 (COO-119-249)
BEAGLES/RADIONUCLIDE KINETICS
Decorporation of ^{241}Am in beagles by DTPA, 30:29797 (COO-119-249)
Early retention and distribution of ^{253}Es by the beagle, 30:29803 (COO-119-249)
Early subcellular distribution of einsteinium in canine livers (^{253}Es), 30:29804 (COO-119-249)
Effect of delayed lymphadenectomy on ^{239}PuO$_2$ translocation in dogs, 30:29820
Einsteinium studies in beagles (^{253}Es tissue distribution), 30:29802 (COO-119-249)
Evaluation of long-term ZnDTPA therapy in beagles (Toxicity of ZnDTPA during prolonged chelation treatment for removal of ^{241}Am), 30:29796 (COO-119-249)
^{210}Pb retention, excretion, and distribution in beagles following intravenous injection, 30:29805 (COO-119-249)
Transuranium elements in gonadal tissue (^{239}Pu, ^{241}Am, ^{243}Cm, ^{244}Cm, ^{249}Cf, and ^{252}Cf), 30:29806 (COO-119-249)
BEAM BENDING MAGNETS
A magnetic field clamp with beneficial saturation effects, 30:30136
BEAM BENDING MAGNETS/MAGNETIC FIELDS
Rapid measurement of the effective field boundary of homogeneous field magnets, 30:30135
BEAM MONITORS/ELECTRONIC CIRCUITS
Charge measuring unit of the pulsed electron beam in the Van de Graaff accelerator (Torroidal winding pickup), 30:30124
BEAM MONITORS/PLASTIC SCINTILLATION DETECTORS
Low-intensity beam monitoring with an image-intensified scintillator detector, 30:30127
BEAM PULSERS
A simple fast sweeping system for extracted cyclotron beams, 30:30153
BEAM PULSERS/DESIGN
A mechanical beam chopper system for the measurement of half-lives in the millisecond region, 30:30154
BEAM SEPARATORS
(For velocity separation of secondary beams.)
BEAM SEPARATORS/RF SYSTEMS
Application of microwave techniques to high-energy physics experiments at Argonne National Laboratory, 30:29584
BEAM TRANSPORT/MONOCHROMATORS
Symmetrized double-monochromator systems, 30:30134
BEAM-PLASMA SYSTEMS/BEAM CURRENTS
Decay of plasma currents and charge in beam plasma experiments, 30:29186 (UCID-15820)
BEAM-PLASMA SYSTEMS/BERNSTEIN MODE
Generation of Bernstein modes in a beam-plasma system (Test-charge density, experimental results), 30:29238
BEAM-PLASMA SYSTEMS/HOSE INSTABILITY
Reduction of hose growth by current tailoring, 30:29199 (UCID-15996)
BEETS/MUTATIONS
Use of x-rays in sugar beet breeding, 30:29693
BENZANTHRACENE/BIOLOGICAL EFFECTS
Effect of x irradiation on hydrocarbon metabolism and on hydrocarbon-induced lethality and transformation in cells derived from mouse prostate (3-Methylcholanthrene, 7,12-dimethylbenz(a)anthracene, N-methyl-N'-nitro-N-nitrosoquanidine), 30:29670
BENZENE/ADSORPTION
Cryovacuum hydrogen adsorption by small-sized, activated mineral coal with a binder (Adsorption of benzene at 20°C and hydrogen from 20.4 to 50°K), 30:31394 (KHFTI-73-25)
BENZENE/CHEMICAL REACTION KINETICS
Reaction of the hydrated electron with benzene studied by pulse radiolysis (5-MeV electron pulses), 30:29081
BENZENE/HOT ATOM CHEMISTRY
Identification of high-boiling tritium-labeled compounds formed in reactions of tritium recoil atoms with benzene, 30:29084
BENZENE/RADIOLYSIS
Reactions of the radiolytically generated hydroxycyclohexadienyl radical in aqueous benzene systems (γ Radiation), 30:29043
BERYLLIUM/ABSORPTION SPECTROSCOPY
Direct determination of beryllium in urine by flameless atomic absorption spectrometry, 30:31379 (RFP-2151)
BERYLLIUM/CHARGED-PARTICLE TRANSPORT
Transmission and reflection of electrons by foils, 30:31118
BERYLLIUM/ELECTRON COLLISIONS
Transmission and reflection of electrons by foils, 30:31118
BERYLLIUM/EMISSION SPECTROSCOPY
Beryllium content of NBS standard reference orchard leaves, 30:28950
Spectrochemical analysis of uranium oxide by gallium oxide carrier dc arc technique (ASTM Standard E402), 30:28957
Spectrographic determination of trace impurities in high purity uranium oxide, 30:28944 (UCID-15952)
BERYLLIUM/FLUORESCENCE SPECTROSCOPY
Beryllium content of NBS standard reference orchard leaves, 30:28950
BERYLLIUM/GAS CHROMATOGRAPHY
Beryllium content of NBS standard reference orchard leaves, 30:28950
BERYLLIUM/GRAVIMETRIC ANALYSIS
Determination of beryllium with nitryltrimethylphosphonic acid in the presence of alkaline earth metals, 30:28955
BERYLLIUM/NUCLEAR REACTION ANALYSIS
High sensitivity photoneutron detector for 'non-destructive' submicroanalysis of beryllium, 30:29524
BERYLLIUM/STACKING FAULTS
Diffraction of x rays on stacking faults in metals with hcp lattices, 30:30024
BERYLLIUM 7/RADIATION MONITORING
Data. Section IV. Other data, 30:29412
Quillayute air reference station (Air sampling and monitoring in Washington State), 30:29359 (BNWL-1850(Pt.3))
Report of activity, February 1974 (Radioactivity of environmental samples collected throughout France during February 1974), 30:29349 (SCPRI(RM)-2-1974)
BERYLLIUM 9/ALPHA REACTIONS
On the nuclear I.L potential, 30:31092
BERYLLIUM 9/COSMOCHEMISTRY
A galactic model with a pulsating active nucleus. III. Evolution of rare-light elements, 30:30386
BERYLLIUM 9/PION REACTIONS
Pion-nucleus total cross sections from 88 to 860 MeV, 30:30891
BERYLLIUM ALLOYS/DIFFUSION
Differential magnetic analysis of the radiation-induced diffusion in nickel-beryllium alloys, 30:30064 (AED-CONF-74-089-037)
BERYLLIUM ALLOYS/FILLER METALS
Properties of TZM and nuclear behavior of TZM brazements. Various properties of TZM and Zr--5Be and Au--18Ni brazing filler metals are determined for brazing TZM to Zr and to steel, 30:30084
BERYLLIUM ALLOYS/MECHANICAL PROPERTIES
Mechanical properties of sintered magnesium--beryllium alloys, 30:30017
BERYLLIUM ALLOYS/PHYSICAL RADIATION EFFECTS
Differential magnetic analysis of the radiation-induced diffusion in nickel-beryllium alloys, 30:30064 (AED-CONF-74-089-037)
BERYLLIUM BORIDES/YIELD STRENGTH
Yield surfaces for beryllium boride ceramics, 30:29891 (UCID-15859)
BERYLLIUM CHLORIDES/FORMATION HEAT
Gaseous halide complexes and their stability, 30:29091
BERYLLIUM FLUORIDES/SOLVENT PROPERTIES
Solubility and stability of structural metal difluorides in molten fluoride mixtures, 30:29002 (ORNL-TM-760)
BERYLLIUM IONS/ION SOURCES
Beams of Be^+ from an rf ion source, 30:30130
BERYLLIUM MODERATORS
See BERYLLIUM
BERYLLIUM OXIDES/CHEMICAL PREPARATION
Fueled moderator composition (Patent), 30:29934
BESSEL DIFFERENTIAL EQUATION
See FOKKER-PLANCK EQUATION
BETA BACKSCATTERING GAGES
See RADIOMETRIC GAGES
BETA DECAY
See also BETA-PLUS DECAY
BETA DECAY/AXIAL-VECTOR CURRENTS
Renormalization of the axial-vector coupling constant in nuclear β-decay (III) (A123), 30:30865
BETA DECAY/CONFIGURATION MIXING
Magnetic moments and GT-type β-decay matrix elements in nuclei with a LS doubly closed shell plus or minus one nucleon, 30:30898
BETA SOURCES/FABRICATION
Rapid production of thin Kr sources, 30:29641
BETA SOURCES/RADIATION MONITORING
Data. Section III. Air and deposition, 30:29382
Data. Section II. Water, 30:29411
Data. Section IV. Other data, 30:29412
Environmental monitoring report, calendar year 1973, 30:29351 (UCC-ND-279)
Environmental monitoring report: United States Atomic Energy Commission, Oak Ridge facilities. Calendar year 1973, 30:29352 (UCC-ND-280)
Feed Materials Production Center environmental monitoring annual report for 1973, 30:29347 (NLCO-1109)
Operation WHETSTONE: on-site radiological safety report, July 1964--June 1965, 30:29378 (NVO-410-24)
Operation TOGGLE: on-site radiological safety report, July 1972--June 1973, 30:29379 (NVO-410-25)

Portsmouth Gaseous Diffusion Plant environmental monitoring report, 1973, 30:29346 (GAT-781)
Radiological monitoring program, period covering February 4, 1974--April 30, 1974 (Rio Blanco site), 30:29348 (PNE-RB-51-9)
BETA SPECTROMETERS/ANTICOINCIDENCE
A large plastic scintillator as anticoincidence shield for beta-radiation detectors, 30:29575
BETA-PLUS DECAY/SECOND-CLASS CURRENTS
K-electron capture to positron emission ratios and the second class currents problem, 30:31076
BETATRONS/ACCELERATOR FACILITIES
Betatron electron internal-flaw detector, 30:30144
BETAVOLTAIC CELLS/EFFICIENCY
Advanced betavoltaic power sources, 30:29257
BETAVOLTAIC CELLS/OPTIMIZATION
Optimization of the beta-voltaic cell, 30:29256
BETTIS/RADIOACTIVITY
Data. Section IV. Other data (Monitoring), 30:29412
BEVATRON
(6.2-GeV proton synchrotron at LBL.)
BEVATRON/BEAM MONITORING
Low-intensity beam monitoring with an image-intensified scintillator detector, 30:30127
BF3 COUNTERS/DESIGN
High sensitivity photoneutron detector for 'non-destructive' submicroanalysis of beryllium, 30:29524
BINARY STARS/BALMER LINES
Evidence for the existence of a massive companion to X Persei (=2U 0352+30.) (Massive stars, Balmer absorption lines), 30:30230
BINARY STARS/COSMIC X-RAY SOURCES
Spectroscopic analysis of HZ Herculis (Weak continuum), 30:30270
BINARY STARS/MASS
On the distribution of binary system mass ratios (Analytic purposes), 30:30235
BINARY STARS/ORBITS
Analysis of a one-parameter family of triple close approaches occurring in stellar systems (Participating masses), 30:30238
BINARY STARS/PROXIMITY EFFECT
Calculations of proximity effects in close binary systems, 30:30263
BINARY STARS/RED DWARF STARS
Influence of binaries on red dwarf density distributions (Galactic plane), 30:30232
BINARY STARS/SPECTROPHOTOMETRY
Spectrophotometry of eclipsing binary V 367 Cygni, 30:30210
BIOGEOCENOSES
See ECOSYSTEMS
BIOLOGICAL DOSEMETERS/BIOCHEMICAL REACTION KINETICS
Special laboratory-chemical examination techniques (Diagnosis of radiation injuries), 30:29702 (AED-CONF-74-221-006)
BIOLOGICAL DOSEMETERS/CHROMOSOMAL ABERRATIONS
Human lymphocyte as a radiobiological dosimeter after total body irradiation (Gamma radiation), 30:29707
BIOLOGICAL RADIATION EFFECTS
See also GENETIC RADIATION EFFECTS
RADIATION INJURIES
BIOLOGICAL RADIATION EFFECTS/DIAGNOSIS
Special laboratory-chemical examination techniques (Diagnosis of radiation injuries), 30:29702 (AED-CONF-74-221-006)
BIOLOGICAL RADIATION EFFECTS/DOSE-RESPONSE RELATIONSHIPS
Cellular repair after x or gamma irradiation determined for several gross criteria on animals and patients, 30:29759
Effect of graded doses of ionizing radiation on the human testis, 30:29708
Review of RBE values of 15 MeV neutrons for effects on normal tissues, 30:29764
BIOLOGICAL RADIATION EFFECTS/RESEARCH PROGRAMS
Department of Fundamental Research, Grenoble, semiannual bulletin No. 4, 30:31333 (CEA-N-1688)
BIOLOGY/RESEARCH PROGRAMS
Research fields in physics (Research topics listing), 30:30645
Research in biological and medical sciences including biochemistry, communicable disease and immunology, internal medicine, nuclear medicine, physiology, psychiatry, surgery, and veterinary medicine. Volume I. Annual progress report, 1 July 1972--30 June 1973, 30:29827 (AD-774860)
Research in biological and medical sciences including biochemistry, communicable disease and immunology, internal medicine, nuclear medicine, physiology, psychiatry, surgery, and veterinary medicine. Volume II. Annual progress report, 1 July 1972--30 June 1973, 30:29828 (AD-776967)
BIOMEDICAL RADIOGRAPHY/IMAGES
Radiation levels of macroradiography, 30:31106
BIOMEDICAL RADIOGRAPHY/NEUTRON SOURCES
Neutron radiography: biomedical applications, 30:29705 (RT/FI-(74)16)
BIOMEDICAL RADIOGRAPHY/RADIATION DOSES
Indirect technique and problems of radiation protection in pediatric X-ray diagnostics, 30:29701 (AED-CONF-74-140-004)
Medical evaluation of measured values following radiation exposure, 30:29703 (AED-CONF-74-221-007)
Radiation levels of macroradiography, 30:31106
BIOMEDICAL RADIOGRAPHY/RADIATION HAZARDS
Neutron radiography: biomedical applications, 30:29705 (RT/FI-(74)16)
BIOTITE/X-RAY FLUORESCENCE ANALYSIS
Compilation of x-ray interaction data for x-ray fluorescence analysis of geological samples, 30:28943 (RISO-297)
BISMUTH/ABSORPTION SPECTROSCOPY
Separation of trace metal impurities from nuclear grade uranium by long-chain amine extraction and direct determination by atomic absorption spectrophotometry, 30:28948
BISMUTH/ACTIVATION ANALYSIS
Multielement determination in market-garden soils by instrumental photon activation analysis, 30:28921
BISMUTH/CHARGED-PARTICLE TRANSPORT
Helium ion stopping cross sections in bismuth, lead, and tungsten, 30:31114
BISMUTH/EMISSION SPECTROSCOPY
Spectrochemical analysis of uranium oxide by gallium oxide carrier dc arc technique (ASTM Standard E402), 30:28957
Spectrographic determination of trace impurities in high purity uranium oxide, 30:28944 (UCID-15952)
BISMUTH/FLUORESCENCE SPECTROSCOPY
New discrete atomization cell for atomic fluorescence spectrometry, 30:28947
BISMUTH/ION COLLISIONS
L- and M-shell ionization of various elements by fast-α-particle bombardment (Cross sections, 1 to 5 MeV), 30:30537
BISMUTH/SEPARATION PROCESSES
Atmosphere purification of xenon, radon, and radon daughter elements (Patent, fluorination and adsorption), 30:28995
BISMUTH 209/EXCITATION
Core polarization in inelastic proton scattering from ^{209}Bi at 61 MeV, 30:31003
BISMUTH 209/KRYPTON 84 REACTIONS
Quasi-fission: a new type of reaction observed in bombarding heavy nuclei by ^{84}Kr and ^{63}Cu ions, 30:30984
BISMUTH 209/PROTON REACTIONS
Core polarization in inelastic proton scattering from ^{209}Bi at 61 MeV, 30:31003
Isospin effects upon the decay of highly excited nuclear states, 30:30999
BISMUTH 210/RADIATION MONITORING
Long-lived radon daughters as atmospheric radioactive tracers, 30:29400
BISMUTH 212/ALPHA SPECTRA
Separation of radionuclides using alkyl radicals, 30:29083 (AED-CONF-74-084-002)
BISMUTH 212/SEPARATION PROCESSES
Separation of radionuclides using alkyl radicals, 30:29083 (AED-CONF-74-084-002)
BISMUTH 214/RADIATION MONITORING
Determination of aerosol deposition rates on a lake surface using radon daughters (^{214}Bi and ^{214}Pb tracer studies), 30:29410 (BNWL-1850(Pt.3))
Scavenging of radioactive material from the atmosphere by surface condensation, 30:29391
BISMUTH ALLOYS/MAGNETIC PROPERTIES
Magnetic properties of CeBi (Orientation; 3 to 30°K), 30:29993
BLACK HOLES
Black-hole physics: an introduction, 30:30182 (CONF-730693-)
BLACK HOLES/ANGULAR MOMENTUM
The mass-angular momentum-diagram and the black hole limit, 30:30295
BLACK HOLES/DECAY
Charge and particle conservation in black-hole decay, 30:30186
BLACK HOLES/EQUILIBRIUM
Perturbation of a slowly rotating black hole by a stationary axisymmetric ring of matter. I. Equilibrium configurations (Equatorial plane, surrounding environment), 30:30189
BLACK HOLES/KERR FIELD
On the generalized ergosphere of the Kerr-Newman geometry, 30:30214
BLACK HOLES/MASS
The mass-angular momentum-diagram and the black hole limit, 30:30295
BLACK HOLES/ROTATION
Perturbation of a slowly rotating black hole by a stationary axisymmetric ring of matter. I. Equilibrium configurations (Equatorial plane, surrounding environment), 30:30189
BLACK HOLES/SINGULARITY
Effective potentials near a Kerr--Newman naked singularity (Test particle kinetics), 30:30208
BLACK HOLES/STAR ACCRETION
Disk-accretion onto a black hole. I. Time-averaged structure of accretion disk (Accreting material), 30:30187
Disk-accretion onto a black hole. II. Evolution of the hole (Maximum efficiency), 30:30188

BLACKBODY RADIATION/RADIATION FLUX
  Code description: FOFT (Calculates black-body radiation flux), 30:31350 (UCID-15753)
BLANKETS (BREEDING)
  See BREEDING BLANKETS
BLASTS
  See EXPLOSIONS
BLOOD
  See also BLOOD CELLS
BLOOD/DIFFUSION
  Study on the blood-cerebrospinal fluid barrier. I. Permeability of RISA^{131}I at twenty-four hours after intravenous administration, 30:29840
BLOOD/MEASURING METHODS
  Application of ^{133}Xe in measuring peripheral blood flow, 30:29871
  Experimental application of ^{133}Xe in measuring minute volume of blood, 30:29872
BLOOD/RADIONUCLIDE KINETICS
  Pharmacodynamics of ^{197}Au and ^{198}Au labeled aurothiomalate in blood. Correlation with course of rheumatoid arthritis, gold toxicity, and gold excretion, 30:29792
BLOOD CELLS
  See also ERYTHROCYTES
BLOOD CELLS/BIOLOGICAL RADIATION EFFECTS
  Chromosome aberrations in lymphocytes of peripheral blood after radiation therapy (γ ray; betatron), 30:29731
BLOOD CIRCULATION/BIOLOGICAL RADIATION EFFECTS
  Prevention of thrombo-embolism during radiotherapy of carcinoma of the uterine cervix (Radium inserts), 30:29732
BLOOD CIRCULATION/MEASURING METHODS
  Application of ^{133}Xe in measuring peripheral blood flow, 30:29871
  Application of ^{133}Xe in measuring minute volume of blood, 30:29873
BLOOD FLOW/MEASURING METHODS
  Application of ^{133}Xe in measuring minute volume of blood, 30:29873
BLOOD FLOW/TRACER TECHNIQUES
  Tissue-blood ^{131}I and ^{133}Xe transfer in the presence of raised capillary filtration, 30:29794
BLOOD FORMATION/BIOLOGICAL RADIATION EFFECTS
  Early hematologic effects of curium and einsteinium in beagles (^{244}Cm, ^{243}Cm, and ^{253}Es), 30:29779 (COO-119-249)
BLOOD VESSELS
  See also CAPILLARIES
BLOOD VESSELS/BIOLOGICAL RADIATION EFFECTS
  Changes of the broncho-vascular system of the lung under the influence of local γ irradiation (Following micro- or macro-fractionated therapy), 30:29728
  Condition of the nervous and vascular systems after radiation treatment of lymphogranulomatosis (Hodgkins disease), 30:29730
BLUE HILLS-1 REACTOR
  License application; annual reports; financial data, 30:31319 (DOCKET-50510-1)
BLUE HILLS-2 REACTOR
  License application; annual reports; financial data, 30:31319 (DOCKET-50510-1)
BODY FLUIDS
  See also CEREBROSPINAL FLUID
    MILK
    URINE
  Total-body water determination with a practical internal standard method (HTO scintillation counting), 30:29884
BODY FLUIDS/SOLVENT PROPERTIES
  In vitro plutonium studies using the artificial rumen and simulated abomasal and intestinal fluids (Uptake by ruminants), 30:29809 (NVO-AEIC-74-1)
BOILING WATER REACTORS
  See BWR TYPE REACTORS
BONE CELLS
  Effects of Phytohemaglutinin-P (PHA-P) on bone cells of the tibial and femoral metaphysis of the rats (Uptake of radioisotopes), 30:29800 (COO-119-249)
BONE DISEASES
  See SKELETAL DISEASES
BONE MARROW CELLS/BIOCHEMICAL REACTION KINETICS
  Effect of ionizing radiation on alkaline phosphatase activity in hematopoietic cells of mouse and rat (X rays), 30:29762
BONE MARROW CELLS/DELAYED RADIATION EFFECTS
  Follow-up on the long-term effects of therapeutic irradiation on bone marrow, 30:29715
BONE TISSUES/GAMMA DOSIMETRY
  Spectral characteristics of γ radiation ^{60}Co scattered in thin radiators, 30:31109
BONE TISSUES/RADIONUCLIDE KINETICS
  Plutonium, diphosphonates, and bone (Effects of EHDP on ^{239}Pu uptake by bone tissues), 30:29801 (COO-119-249)
BONE TISSUES/SCINTISCANNING
  /sup 99m/Tc pyrophosphate for diagnostic bone imaging, 30:29843
  Pitfalls in /sup 99m/Tc polyphosphate skeletal imaging, 30:29849
  Value of /sup 99m/Tc-diphosphonate (HEDSPA) as a skeletal scanning agent, 30:29850
BONES
  See SKELETON
BOOTSTRAP MODEL/HADRONS
  Quark or bootstrap: triumph or frustration for hadron physics (S matrix), 30:30702
BOOTSTRAP MODEL/ISOSPIN
  Statistical bootstrap model without exotic fireballs, 30:30713
BORIDES/DEPOSITION
  Multicomponent diffusion coatings (Book), 30:29906
BORIDES/PRODUCTION
  High-melting metals and metallic compounds, 30:30021
BORIDES/USES
  High-melting metals and metallic compounds, 30:30021
BORN APPROXIMATION
  See also COUPLED CHANNEL BORN APPROXIMATION
    DWBA
  Invariants of Born reciprocity theory, 30:30629
BORN CROSS SECTIONS
  See BORN APPROXIMATION
BORON/CHEMICAL REACTIONS
  Reactions of boron and silicon carbide with tungsten and titanium, 30:29948
BORON/EMISSION SPECTROSCOPY
  Spectrochemical analysis of uranium oxide by gallium oxide carrier dc arc technique (ASTM Standard E402), 30:28957
  Spectrographic determination of trace impurities in high purity uranium oxide, 30:28944 (UCID-15952)
BORON/NUCLEAR REACTION ANALYSIS
  Nondestructive determination of boron in glasses using a ^{241}Am--Be neutron source, 30:28912 (AED-CONF-73-479-009)
BORON/PHYSICAL RADIATION EFFECTS
  Study of basic processes in radiation damage. Final report, 1 April 1971--30 November 1973 (Implantation of polarized radioisotopes in metals and semiconductors), 30:30061 (AD-777728)
BORON/PRODUCTION
  High-melting metals and metallic compounds, 30:30021
BORON/USES
  High-melting metals and metallic compounds, 30:30021
BORON 10/COSMOCHEMISTRY
  A galactic model with a pulsating active nucleus. III. Evolution of rare-light elements, 30:30386
BORON 10/OXYGEN 16 REACTIONS
  States in ^{24}Mg populated by the ^{10}B(^{16}O,d)^{24}Mg and ^{12}C(^{16}O,α)^{24}Mg reactions (40 to 46 MeV: excitation functions), 30:30911
BORON 11/COSMOCHEMISTRY
  A galactic model with a pulsating active nucleus. III. Evolution of rare-light elements, 30:30386
BORON 11/LITHIUM 7 REACTIONS
  J, π, lifetimes from spectra from ^{11}B(^{7}Li, pγ) at 6.0 MeV, 30:30895
  Spectra from ^{11}B(^{7}Li, pγ) reaction at 6 MeV, 30:30894
BORON 11/NEUTRON REACTIONS
  Continuum shell-model calculation for neutron scattering from ^{11}B (0 to 10 MeV: cross sections, polarization), 30:30890
BORON 11/NUCLEAR DEFORMATION
  DWBA and CCBA analysis of selected transitions in the ^{12}C(d,tau)^{11}B reaction at Esub(d) = 60MeV, 30:30900
BORON 12/POLARIZED PRODUCTS
  Measurement of the average polarization of ^{12}B produced by polarized muons in the $\mu^- + {}^{12}C + \nu$sub(μ) + ^{12}B reaction, 30:30899
BORON 14/ENERGY LEVELS
  Search for the lowest T = 2 state in ^{14}C by inelastic electron scattering, 30:30878
BORON ADDITIONS
  Mechanical properties of multicomponent alloys based on Ti--Al--Sn (Zr) α-solid solution with β-stabilizing elements (Additions of Mo, V, Cr, Fe, Si, B;properties at up to 950°C), 30:29984
BORON ALLOYS/FRACTURE PROPERTIES
  J-integral as a failure criterion for a Borsic--Al composite, 30:29890 (SAND-74-0193)
BORON ALLOYS/MECHANICAL PROPERTIES
  Fatigue and impact resistance of dual-matrix boron--aluminum composites. Final report (B--6061 Al), 30:29974 (AD-775334)
  Mechanical behavior of metal matrix composites. Final report, 1 April 1972--30 April 1973 (B--Al;B/SiC--Ti;tensile, fatigue, and creep behavior;effects of defects), 30:29975 (AD-775359)
BORON ALLOYS/THERMAL FATIGUE
  Mechanical properties of metal matrix composites subjected to cyclic temperature changes. Annual report, 1 July 1972--30 June 1973 (6064 Al reinforced with fibers of stainless steel, 34 vol % SiC, 27 vol % B, and 45 vol % B), 30:29973 (AD-774890)
BORON NITRIDES/CRYSTAL STRUCTURE
  Structure determination of boron nitride transformed by shock compression, 30:29923
BOSONS
  See also MESONS
BOSONS/QUANTUM ELECTRODYNAMICS
  Construction of nonlocal quantum electrodynamics of bosons with spin 0 and 1 (Unitarity, macrocausality, relativity, gauge, invariance, finiteness), 30:31144 (JINR-P2-7432)

BOUNDARIES (GRAIN)
See GRAIN BOUNDARIES
BOVINE
See CATTLE
BRAIN/BIOLOGICAL RADIATION EFFECTS
Aromatic amino acid decarboxylase activity of rat brain and its parts following exposure to ionizing radiation (X radiation), 30:29740
Changes in glycogen localization and content and activity of enzymes metabolizing glycogen in rat brain during maturation under normal conditions and after gamma irradiation, 30:29761
Gomori-positive glia in uv-irradiated mice, 30:29752
BRAIN/BLOOD FLOW
Advantages of theoretical models in interpreting cerebral transit curves (/sup 99m/Tc-pertechnetate tracer), 30:29830 (CONF-740708-20)
BRAIN/EDEMA
Measurement of cerebral infarction edema with sodium-22 (Cats), 30:29837
BRAIN/SCINTISCANNING
Advantages of theoretical models in interpreting cerebral transit curves (/sup 99m/Tc-pertechnetate tracer), 30:29830 (CONF-740708-20)
BRAKING RADIATION
See BREMSSTRAHLUNG
BRAZIL/NATURAL RADIOACTIVITY
Radioactivity in Brazilian mineral waters (monitoring), 30:29413
BRAZING ALLOYS
Brazing alloy (Patent), 30:29999
BREAKUP REACTIONS/PAULI PRINCIPLE
Qualitative features of Pauli break-up from the configuration space viewpoint, 30:31089
BREASTS
See MAMMARY GLANDS
BREEDING BLANKETS/FISSION
Preliminary appraisal of a fusion/fission (hybrid) reactor based on the linear theta pinch, 30:29228
BREEDING BLANKETS/THERMAL INSULATION
Engineering design study of a Reference Theta-Pinch Reactor (RTPR), 30:29206 (LA-5336)
BREMSSTRAHLUNG
See also INTERNAL BREMSSTRAHLUNG
Thermally averaged Gaunt factors in non-relativistic electron-ion bremsstrahlung, 30:29185 (UCID-15712)
BREMSSTRAHLUNG/POLARIZATION
Bremsstrahlung polarization from commercial x-ray tubes, 30:31447 (UCID-15829)
BREMSSTRAHLUNG (MAGNETIC)
See SYNCHROTRON RADIATION
BRIDGES (ELECTRIC)
See ELECTRIC BRIDGES
BROMATES/CHEMICAL RADIATION EFFECTS
Effects of molecular motion in the ESR spectrum of BrO_3^{2-} ions in $KBrO_3$ single crystals (X radiation), 30:29065
BROMINE/ACTIVATION ANALYSIS
Application of activation analysis to the determination of pollutants in the atmosphere (Thermal neutrons), 30:28914 (IEA-326)
Trace element behavior in soil of some Indonesian sawah's and in sludge of an Indonesian river, 30:28930
Trace elements in precipitation and cloud water in the area of Heidelberg, measured by instrumental neutron activation analysis, 30:28934
BROMINE/CHEMICAL ANALYSIS
Source identification by multi-element analysis of diurnal samples, 30:31371 (UCID-15872)
BROOKHAVEN AGS
(Alternating-Gradient Synchrotron.)
BROOKHAVEN AGS/SECONDARY BEAMS
AGS secondary beams and parameters, FY75, 30:30141 (BNL-19153)
BRUECKNER MODEL
The energy density formalism and the shell structure effects, 30:31025
BUCKWHEAT/BIOLOGICAL RADIATION EFFECTS
Mechanisms of the inhibitors of cell post-irradiation recovery. III. Increase in the chromosomal damage rate by caffeine treatment of x irradiated buckwheat cells, 30:29695
BUILDING MATERIALS
See also CONCRETES
BUILDING MATERIALS/COMPARATIVE EVALUATIONS
Polymer-concrete for use in the repair of deteriorated bridge decks, 30:31388 (BNL-19161)
BUILDINGS
See also HOSPITALS
BUILDINGS/STRESS ANALYSIS
Large user-orientated systems of programs for structural analysis and design, 30:31291
BUILDINGS (CONTAINMENT)
See CONTAINMENT BUILDINGS
BUTANE/RADIOLYSIS
Electron scavenging in the radiolysis of supercritical ethane, ethylene, n-butane, and isobutane (Gamma radiation), 30:29039
BUTANOLS/SOLVENT PROPERTIES
Stablized uranyl nitrate compositions and uranium impregnation method (Patent), 30:29127
BUTYL ALCOHOLS
See BUTANOLS
BUTYRIC ALCOHOLS
See BUTANOLS
BWR TYPE REACTORS
See also COOPER REACTOR
DRESDEN-1 REACTOR
DRESDEN-2 REACTOR
DRESDEN-3 REACTOR
DUANE ARNOLD-1 REACTOR
FUKUSHIMA-1 REACTOR
HANFORD-2 REACTOR
HUMBOLDT BAY REACTOR
JPDR REACTOR
NEWBOLD ISLAND-1 REACTOR
NEWBOLD ISLAND-2 REACTOR
NINE MILE POINT-1 REACTOR
SHIMANE-1 REACTOR
BWR TYPE REACTORS/AVAILABILITY
Nuclear power availability, 30:31189
BWR TYPE REACTORS/CONDENSATES
Steam power plant for nuclear power stations with boiling water reactors (Patent), 30:31188
BWR TYPE REACTORS/ECCS
Problems of emergency core cooling system, 30:31191
BWR TYPE REACTORS/EXCURSIONS
Comparison of two- and three-dimensional calculations of super prompt critical excursions, 30:31190
BWR TYPE REACTORS/FUEL ELEMENTS
Neutronic calculations for experiments with light water reactor fuel in PBF, 30:31187 (BNWL-B-371)
BWR TYPE REACTORS/MAXIMUM CREDIBLE ACCIDENT
Maximum credible accident (MCA) of light water reactor, 30:31260
BWR TYPE REACTORS/PERFORMANCE
Nuclear power availability, 30:31189
BWR TYPE REACTORS/PRESSURE VESSELS
Quarterly progress report on reactor safety programs sponsored by the Division of Reactor Safety Research for April--June 1974, 30:31251 (ORNL-TM-4655(Vol.2))
Trends in structural mechanics. A UK review of the 2nd international conference on structural mechanics in reactor technology. I. Pressure vessels and containments, 30:31192
BWR TYPE REACTORS/REACTOR SAFETY
Quarterly progress report on reactor safety programs sponsored by the Division of Reactor Safety Research for April--June 1974. I. Light-water-reactor safety, 30:31250 (ORNL-TM-4655(Vol.1))
Quarterly progress report on reactor safety programs sponsored by the Division of Reactor Safety Research for April--June 1974, 30:31251 (ORNL-TM-4655(Vol.2))

C

C-REACTIVE PROTEIN
See GLOBULINS
CABIBBO ANGLE/PSEUDOSCALAR MESONS
Disturbed non-linear chiral SU(3) x SU(3) dynamics and Cabibbo's angle, 30:30776
CADMIUM/ABSORPTION SPECTROSCOPY
Separation of trace metal impurities from nuclear grade uranium by long-chain amine extraction and direct determination by atomic absorption spectrophotometry, 30:28948
CADMIUM/ACTIVATION ANALYSIS
Multielement determination in market-garden soils by instrumental photon activation analysis, 30:28921
Trace elements in precipitation and cloud water in the area of Heidelberg, measured by instrumental neutron activation analysis, 30:28934
CADMIUM/ELECTRON-ATOM COLLISIONS
Effective cross sections and peculiarities of electron excitation of the cadmium atom, 36:30523
CADMIUM/EMISSION SPECTROSCOPY
Spectrochemical analysis of uranium oxide by gallium oxide carrier dc arc technique (ASTM Standard E402), 30:28957
Spectrographic determination of trace impurities in high purity uranium oxide, 30:28944 (UCID-15952)
CADMIUM/FLUORESCENCE SPECTROSCOPY
New discrete atomization cell for atomic fluorescence spectrometry, 30:28947
CADMIUM 107/ENERGY LEVELS
Nuclear spectroscopy of ^{107}Cd, 30:30953 (NP-20122)
CADMIUM 115/RETENTION
Comparison of /sup 115m/Ca retention in rats following different routes of administration, 30:29815
CADMIUM 115/TISSUE DISTRIBUTION
Effects of copper, mercury, and zinc on the uptake and distribution of cadmium-115m in the albino rat, 30:29816
CADMIUM ALLOYS/DIFFUSION
Transport and thermodynamic properties of solids. Progress report, September 1, 1973--August 31, 1974, 30:31390 (COO-1436-41)
CADMIUM CHLORIDES/FORMATION HEAT
Gaseous halide complexes and their stability, 30:29091

CADMIUM COMPLEXES/PYROLYSIS
Derivatographic investigations on the thermal degradation of pyridine, isoquinoline, α,α-dipyridyl and o-phenantroline, resp. bichromate- or chromate-ion containing metal complexes. II. Zinc(II)-, cadmium(II)-, and manganese(II)-complexes. III. Mercury(I and II)-, uranyl-, thorium-, lanthanum-, and iron-complexes, 30:29122
CADMIUM COMPOUNDS/CHEMICAL PREPARATION
Synthesis of high pressure $Cd_2V_2O_7$ and related compositions, 30:29903
CADMIUM ISOTOPES/ENERGY LEVELS
Problem of particle-hole symmetry in even--even Cd and Te nuclei, 30:30971
CADMIUM SULFIDES/ION IMPLANTATION
Ion implantation of semiconductors, metals, and alloys. Interim report No. 7, 1 September 1971--31 August 1973, 30:30088 (AD-774654)
CADMIUM SULFIDES/PHYSICAL RADIATION EFFECTS
Effect of oxygen on unencapsulated cadmium sulfide solar cells, 30:30103
CADMIUM TELLURIDES/PHASE STUDIES
Ternary system Cd--Ga--Te, 30:30015
CAFFEINE/RADIOSENSITIVITY EFFECTS
Mechanisms of inhibition of the postirradiation recovery in cells. IV. The effect of caffeine and acriflavine on gamma and x-ray induced unscheduled DNA synthesis in HeLa Zn-63 cells, 30:29675
Mechanisms of the inhibitors of cell post-irradiation recovery. III. Increase in the chromosomal damage rate by caffeine treatment of x irradiated buckwheat cells, 30:29695
CALCITE/PHYSICAL RADIATION EFFECTS
Electron spin resonance absorption spectrum of HCO_3^{2-}-molecule-ions in irradiated single-crystal calcite (Gamma radiation), 30:29074
CALCIUM/ACTIVATION ANALYSIS
Multielement determination in market-garden soils by instrumental photon activation analysis, 30:28921
CALCIUM/EMISSION SPECTROSCOPY
Spectrographic determination of trace impurities in high purity uranium oxide, 30:28944 (UCID-15952)
CALCIUM/EXCITATION
Rate coefficients for electron excitation of the first resonance transition in H, Li, Na, Ca, Ca^+, and Ba^+ calculated from experimental data (Transition probabilities), 30:30246
CALCIUM/ION EXCHANGE
Selective ion-exchangers containing phosphorus in their functional groups. I. Sorption and separation of some bivalent and trivalent ions, 30:29001
Sorption of tetravalent elements by mordenite. II. Sorption of Pu(IV), 30:28999
CALCIUM 40/BINDING ENERGY
Hartree-Fock calculations using Sussex matrix elements (Single particle spectra), 30:30863
CALCIUM 40/CARBON 13 REACTIONS
Difficulties in fitting angular distributions in the $^{40}Ca(^{13}C,^{14}N)^{39}K$ (g.s.) reaction (As contrasted with $^{40}Ca(^{13}C,^{12}C)^{41}Ca$(g.s.) reaction at 60 and 68 MeV), 30:30921
CALCIUM 40/DENSITY MATRIX
Phenomenological occupation probabilities, binding energies, and the nuclear one-particle density matrix, 30:30903
CALCIUM 40/DEUTERON REACTIONS
The magnitude of compound nucleus effects in Ca(d,p) reactions (1w MeV: angular distributions, reaction mechanisms; spectroscopic factors), 30:30923
Transparency to vector polarization transfer in deuteron stripping reactions, 30:31096
CALCIUM 40/ENERGY LEVELS
Hartree-Fock calculations using Sussex matrix elements (Single particle spectra), 30:30863
Structure of low-lying 0^+ states in fsub(7/2) shell nuclei from inelastic ^3He scattering (29 MeV: differential cross sections, DWBA), 30:30934
CALCIUM 40/HELIUM 3 REACTIONS
Structure of low-lying 0^+ states in fsub(7/2) shell nuclei from inelastic ^3He scattering (29 MeV: differential cross sections, DWBA), 30:30934
CALCIUM 40/NEUTRON REACTIONS
$^{40}Ca(n,\alpha)^{37}Ar$ reaction at 14.1 MeV, 30:30927
CALCIUM 40/PROTON REACTIONS
High energy proton scattering by medium and heavy nuclei (1 GeV: differential cross sections, DWIA with Coulomb effects), 30:31007
CALCIUM 41/ENERGY LEVELS
The magnitude of compound nucleus effects in Ca(d,p) reactions (1w MeV: angular distributions, reaction mechanisms; spectroscopic factors), 30:30923
CALCIUM 42/DEUTERON REACTIONS
The magnitude of compound nucleus effects in Ca(d,p) reactions (1w MeV: angular distributions, reaction mechanisms; spectroscopic factors), 30:30923
CALCIUM 43/ENERGY LEVELS
The magnitude of compound nucleus effects in Ca(d,p) reactions (1w MeV: angular distributions, reaction mechanisms; spectroscopic factors), 30:30923
CALCIUM 44/DEUTERON REACTIONS
The magnitude of compound nucleus effects in Ca(d,p) reactions (1w MeV: angular distributions, reaction mechanisms; spectroscopic factors), 30:30923
CALCIUM 44/ENERGY LEVELS
Structure of low-lying 0^+ states in fsub(7/2) shell nuclei from inelastic ^3He scattering (29 MeV: differential cross sections, DWBA), 30:30934
CALCIUM 44/HELIUM 3 REACTIONS
Structure of low-lying 0^+ states in fsub(7/2) shell nuclei from inelastic ^3He scattering (29 MeV: differential cross sections, DWBA), 30:30934
CALCIUM 44/PROTON REACTIONS
Comment on anomalous (p,t) angular distributions due to form factor cancellation, 30:30929
CALCIUM 45/ENERGY LEVELS
The magnitude of compound nucleus effects in Ca(d,p) reactions (1w MeV: angular distributions, reaction mechanisms; spectroscopic factors), 30:30923
CALCIUM 47/INTESTINAL ABSORPTION
Absorption of ^{47}Ca from digestive tract in patients with urolithiasis, 30:29791
CALCIUM 48/DEUTERON REACTIONS
The magnitude of compound nucleus effects in Ca(d,p) reactions (1w MeV: angular distributions, reaction mechanisms; spectroscopic factors), 30:30923
CALCIUM 48/HELIUM 3 REACTIONS
Nuclear structure calculation of ^{50}Sc and analysis of the $^{48}Ca(^3He,p)^{50}Sc$ reaction, 30:30946
CALCIUM 49/ENERGY LEVELS
The magnitude of compound nucleus effects in Ca(d,p) reactions (1w MeV: angular distributions, reaction mechanisms; spectroscopic factors), 30:30923
CALCIUM CARBONATES
See also CALCITE
CALCIUM CARBONATES/X-RAY FLUORESCENCE ANALYSIS
Compilation of x-ray interaction data for x-ray fluorescence analysis of geological samples, 30:28943 (RISO-297)
CALCIUM FLUORIDES/CHEMICAL REACTIONS
Reaction of uranium with a mixture of lithium and calcium fluorides, 30:29110
CALCIUM IONS/EXCITATION
Rate coefficients for electron excitation of the first resonance transition in H, Li, Na, Ca, Ca^+, and Ba^+ calculated from experimental data (Transition probabilities), 30:30246
CALCIUM ISOTOPES/NEUTRON REACTIONS
Status report to NCSAC, 30:31011 (UCID-15639)
CALCIUM OXIDES/CRYSTAL STRUCTURE
Surface stabilization and properties of ZrO_2-based solid solutions, 30:29911
CALCIUM OXIDES/PHYSICAL RADIATION EFFECTS
Production of oxygen vacancies by elastic collisions in alkaline earth oxides (400-keV and 3-MeV protons; 15, 77, and 300°K), 30:29933
CALCIUM OXIDES/SINTERING
Synthesis, sintering, and microstructure of the solid solutions CaO--La_2O_3, 30:29910
CALCIUM OXIDES/X-RAY FLUORESCENCE ANALYSIS
Compilation of x-ray interaction data for x-ray fluorescence analysis of geological samples, 30:28943 (RISO-297)
CALCIUM SULFATES/X-RAY FLUORESCENCE ANALYSIS
Compilation of x-ray interaction data for x-ray fluorescence analysis of geological samples, 30:28943 (RISO-297)
CALHOUN-1 REACTOR/REACTOR OPERATION
Semiannual report, January--June 1974, 30:31316 (DOCKET-50285-249)
CALIFORNIA/FALLOUT
Data. Section III. Air and deposition (Monitoring), 30:29382
CALIFORNIUM 249/BIOLOGICAL RADIATION EFFECTS
Research in radiobiology. Annual report of work in progress in the internal irradiation program (Pathological effects of bone-seeking radionuclides in beagles), 30:29778 (COO-119-249)
CALIFORNIUM 249/TISSUE DISTRIBUTION
Transuranium elements in gonadal tissue (^{239}Pu, ^{241}Am, ^{243}Cm, ^{244}Cm, ^{249}Cf, and ^{252}Cf), 30:29806 (COO-119-249)
CALIFORNIUM 252/ALPHA SPECTROSCOPY
Simultaneous determination of alpha-emitting nuclides of radium through californium in soil, 30:28977
CALIFORNIUM 252/BIOLOGICAL RADIATION EFFECTS
Research in radiobiology. Annual report of work in progress in the internal irradiation program (Pathological effects of bone-seeking radionuclides in beagles), 30:29778 (COO-119-249)
CALIFORNIUM 252/NEUTRON DOSIMETRY
Characteristics of ^{252}Cf neutron sources used for radiotherapy, 30:31124
CALIFORNIUM 252/NEUTRON SOURCES
Experimental neutron radiography system using californium-252. Final report, 30:29295 (AD-776900)
CALIFORNIUM 252/SPONTANEOUS FISSION
Fine structures in the mass yield of ^{252}Cf fission fragments from a double-energy measurement, 30:31016
CALIFORNIUM 252/TISSUE DISTRIBUTION
Transuranium elements in gonadal tissue (^{239}Pu, ^{241}Am, ^{243}Cm, ^{244}Cm, ^{249}Cf, and ^{252}Cf), 30:29806 (COO-119-249)

CALORIMETRIC DOSEMETERS/CALIBRATION
Measurements with the Swierk calorimeter, 30:29540 (DEMO-74/5)
Measurements with Hungarian calorimeter, 30:29541 (DEMO-74/5)
Measurements with the Chalk River calorimeter, 30:29542 (DEMO-74/5)
CALORIMETRIC DOSEMETERS/COMPARATIVE EVALUATIONS
Comparison of in-core chemical and calorimetric dosemeter measurements, 30:29550 (DEMO-74/5)
CALORIMETRIC DOSEMETERS/PERFORMANCE
Calorimetric and ionization measurements of stopping power in carbon for 19.5 GeV electrons, 30:29556
CAMAC SYSTEM
(Computer Application to Measurement And Control.)
Development of a CAMAC crate controller for connection to a computer CDC 1700, 30:29634
CAMAC SYSTEM/DIGITAL-TO-ANALOG CONVERTERS
Logarithmic digital-analog conversion for varying parameters in Camac devices, 30:29630
CAMAC SYSTEM/PERFORMANCE TESTING
Test system for CAMAC modules, 30:29627
CAMAC SYSTEM/USES
Use of the CAMAC system for on-line data processing in medicine, 30:31338 (HMI-B-149)
CAMERAS
See also GAMMA CAMERAS
CAMERAS/DESIGN
LLL compact 10-ps streak camera, 1974 update, 30:29162 (UCRL-75557)
CAMP
See AMP
CANADA/FALLOUT
Data. Section III. Air and deposition (Monitoring), 30:29382
Data. Section I. Milk and food (monitoring), 30:29421
CANADA/NUCLEAR INDUSTRY
Canadian nuclear power programme, 30:31216
CANADA/NUCLEAR POWER PLANTS
Canadian nuclear power programme, 30:31216
CANALS (WATERWAYS)
See INLAND WATERWAYS
CANCER
See NEOPLASMS
CANDIDA/LABELLING
^{125}I-labelling of Candida albicans by electrolysis, 30:29881
CANNIKIN EVENT
Operation Cannikin: electronic and electrical scientific measurements and support plan. Pre-operational report, 30:29318 (UCID-15802(Rev.1))
CANONICAL EQUATIONS
See DIFFERENTIAL EQUATIONS
CAPACITORS/FABRICATION
Characteristics of MOS capacitors formed on p-type InSb, 30:29994
CAPACITORS/PERFORMANCE
Notes on application of solid electrolyte tantalum capacitors in coupling and bypass service, 30:31401 (UCID-15662)
CAPILLARIES/PERMEABILITY
Study on the blood-cerebrospinal fluid barrier. I. Permeability of RISA^{131}I at twenty-four hours after intravenous administration, 30:29840
CAPILLARIES/RADIONUCLIDE KINETICS
Tissue clearance of ^{131}I from lower-limb blood vessels in diabetics, 30:29857
CARBIDES/PRODUCTION
High-melting metals and metallic compounds, 30:30021
CARBIDES/USES
High-melting metals and metallic compounds, 30:30021
CARBINOL
See METHANOL
CARBON
See also ACTIVATED CARBON
GRAPHITE
CARBON/BIOLOGICAL EFFECTS
Effects of carbon particles on phagocytic activity of reticuloendothelial system in x-irradiated mice, 30:29753
CARBON/CHARGED-PARTICLE TRANSPORT
Calorimetric and ionization measurements of stopping power in carbon for 19.5 GeV electrons, 30:29556
Charge-state and energy distributions of xenon ions in carbon, 30:31121
CARBON/CHEMICAL ANALYSIS
Interlaboratory comparison of chemical analysis of uranium mononitride, 30:28942 (N-74-16812)
CARBON/CHEMICAL VAPOR DEPOSITION
A new technique for the production of carbon foils, 30:30145
CARBON/ION-ATOM COLLISIONS
Carbon K-shell x-ray production by neon ion impact, 30:30555
High-energy calculation of K-shell ejection cross sections as a function of projectile charge (Born approximation), 30:30536
CARBON/NUCLEAR REACTION ANALYSIS
Analysis of the nitrogen and carbon content in organic bulk matter by fast-neutron induced gamma radiation, 30:28918 (NP-20122)
CARBON/PHYSICAL RADIATION EFFECTS
Atomic displacement cross sections for carbon from ENDF/B-III data, 30:30095
CARBON/PION REACTIONS
Pion-nucleus total cross sections from 88 to 860 MeV, 30:30891
CARBON/SOLUBILITY
Solubility of tin and germanium in liquid sodium. The sodium--tin partial phase diagram, 30:30049
CARBON/THERMAL CONDUCTIVITY
Thermal conductivity of carbon foam, 30:31413 (Y-1955)
CARBON/THERMONUCLEAR REACTIONS
A study of nucleosynthesis during explosive carbon burning (Solar-system material), 30:30257
URCA processes in convective stellar cores, 30:30200
CARBON 12/ALPHA REACTIONS
^{12}C + α scattering by the coupled channel resonating group method. Solution of the redundancy and non-orthogonality problem, 30:30876
CARBON 12/BINDING ENERGY
Three-alpha particle model for ^{12}C ground state, 30:30881
CARBON 12/CARBON 12 REACTIONS
Elastic scattering of ^{12}C by ^{12}C (36 to 61 MeV (c.m.): 90^0 excitation function), 30:30879
CARBON 12/DEUTERON REACTIONS
DWBA and CCBA analysis of selected transitions in the ^{12}C(d,tau)^{11}B reaction at Esub(d) = 80MeV (Angular distribution), 30:30900
Transparency to vector polarization transfer in deuteron stripping reactions, 30:31096
CARBON 12/FORM FACTORS
Three-alpha particle model for ^{12}C ground state, 30:30881
CARBON 12/GROUND STATES
Three-alpha particle model for ^{12}C ground state, 30:30881
CARBON 12/ISOTOPE SEPARATION
Enrichment of carbon and neon isotopes by gas phase chromatography. Part 1, 30:29024 (LA-tr-74-18)
Enrichment of carbon and neon isotopes by gas phase chromatography. Part 2, 30:29025 (LA-tr-74-19)
CARBON 12/MUON REACTIONS
Measurement of the average polarization of ^{12}B produced by polarized muons in the μ^- + ^{12}C + νsub(μ) + ^{12}B reaction, 30:30899
CARBON 12/NEON 20 REACTIONS
Evidence for simple alpha-particle transfer in the (^{20}Ne,^{16}O) reaction (108 and 147 MeV, differential cross sections), 30:30904
CARBON 12/NEUTRON REACTIONS
Treatment of continua in the shell-model theory of nuclear reactions, 30:31077
CARBON 12/OXYGEN 16 REACTIONS
Possible resonance anomalies in the ^{16}O + ^{12}C, 30:30887
States in ^{24}Mg populated by the ^{10}B(^{16}O,d)^{24}Mg and ^{12}C(^{16}O,α)^{24}Mg reactions (40 to 46 MeV: excitation functions), 30:30911
CARBON 12/PION REACTIONS
Momentum-space study of pion-nucleus inelastic scattering (120 to 280 MeV: differential cross sections, form factors DWIA), 30:30897
Multiplicity and correlations of secondary particles produced in π^--^{12}C collisions at 40 GeV/c, 30:30875 (JINR-P1-7523)
Sensitivity of inelastic pion scattering to non-local interactions (75 to 120 MeV: differential cross sections), 30:31097
CARBON 12/THERMONUCLEAR REACTIONS
Iron production by ^{12}C-detonation supernovae (Severe constraints), 30:30258
CARBON 12 REACTIONS/COMPOUND-NUCLEUS REACTIONS
In-beam conversion-electron spectrum for the ^{148}Sm(^{12}C,4n)^{156}Er reaction (75 MeV), 30:30965
CARBON 12 REACTIONS/ELASTIC SCATTERING
Elastic scattering of ^{12}C by ^{12}C (36 to 61 MeV (c.m.): 90^0 excitation function), 30:30879
Entrance channel effects in the ^{32}S system: comparison of ^{12}C + ^{20}Ne and ^{16}O + ^{16}O elastic scattering (23.3 MeV (c.m.): angular distributions), 30:30880
CARBON 13/ENERGY LEVELS
Particle configurations of giant E1 states in the ^{14}N(γ,p_2) and ^{14}N(γ,p_0) processes, 30:30877
CARBON 13/FABRICATION
The preparation of self-supporting ^{13}C-foils using enriched methane gas, 30:30151
CARBON 13/ISOTOPE EFFECTS
Isotope effect in the vapor pressure of carbon tetrafluoride, 30:29013
CARBON 13/ISOTOPE SEPARATION
Enrichment of carbon and neon isotopes by gas phase chromatography. Part 1, 30:29024 (LA-tr-74-18)
Enrichment of carbon and neon isotopes by gas phase chromatography. Part 2, 30:29025 (LA-tr-74-19)
CARBON 13/ISOTOPIC EXCHANGE
Isotopic study of water gas reaction catalyzed by platinum, 30:29032
CARBON 13/TARGETS
The preparation of self-supporting ^{13}C-foils using enriched methane gas, 30:30151

CARBON 13 REACTIONS/ONE-NUCLEON TRANSFER REACTIONS
Difficulties in fitting angular distributions in the ^{40}Ca(^{13}C,^{14}N)^{39}K (g.s.) reaction (As contrasted with ^{40}Ca(^{13}C,^{12}C)^{41}Ca(g.s.) reaction at 60 and 68 MeV), 30:30921
CARBON 14/BIOLOGICAL RADIATION EFFECTS
Nuclear testing (^{131}I; ^{90}Sr; ^{137}Cs; ^{14}C; Tritium), 30:29719
CARBON 14/ELECTRON REACTIONS
Search for the lowest T = 2 state in ^{14}C by inelastic electron scattering (61 and 81 MeV), 30:30878
CARBON 14/ENERGY LEVELS
Search for the lowest T = 2 state in ^{14}C by inelastic electron scattering (61 and 81 MeV), 30:30878
CARBON 14/ISOTOPE EFFECTS
Do SN2 reactions go through ion pairs. The isotope effect criterion, 30:29010
CARBON 14/MUTAGENESIS
Somatic mutation by endogenous radiocarbon, 30:29787
CARBON DIOXIDE/ELECTRON-MOLECULE COLLISIONS
Equations of motion method: Inelastic electron scattering for helium and CO$_2$ in the Born approximation, 30:30550
Excitation of some bands and lines in collisions of 0.4 to 20 keV electrons with Co, CO$_2$, and O$_2$ molecules (Emission, cross sections, Bette-Born approximation), 30:30544
CARBON DIOXIDE/ION-MOLECULE COLLISIONS
Crossed-molecular-beam study of the kinematics and dynamics of charge-transfer collisions (200 eV), 30:30547
Vibrational energy distribution in CO$_2^+$ (A^{2}PIsub(u)) ions produced by collisions of H$_2^+$ and He$^+$ ions with CO$_2$, 30:30558
CARBON DIOXIDE/OSCILLATOR STRENGTHS
Equations of motion method: Inelastic electron scattering for helium and CO$_2$ in the Born approximation, 30:30550
CARBON DIOXIDE LASERS/GAS FLOW
On the gas temperature in coaxial electric-discharge CO$_2$ flow lasers (Gas composition of He:N$_2$:CO$_2$=80:15:5 by volume, laser efficiency), 30:29285
CARBON MONOXIDE/ATOM-MOLECULE COLLISIONS
Negative ion formation from energetic collisions of cesium with CO$_2$, CS$_2$, and COS, 30:30548
CARBON MONOXIDE/ELECTRON-MOLECULE COLLISIONS
Excitation of some bands and lines in collisions of 0.4 to 20 keV electrons with Co, CO$_2$, and O$_2$ molecules (Emission, cross sections, Bette-Born approximation), 30:30544
CARBON MONOXIDE/PHOTOIONIZATION
Calculated photoionization cross sections and relative experimental photoionization intensities for a selection of small molecules, 30:30491
CARBON MONOXIDE/RADIOWAVE RADIATION
Observations of galactic carbon monoxide emission at 2.6 millimeters (Visual extinction, excitation temperatures), 30:30265
CARBON SULFIDES/ATOM-MOLECULE COLLISIONS
Kinetics of the reaction between oxygen atoms and carbon disulfide (Rate constant, branching ratio), 30:30531
Negative ion formation from energetic collisions of cesium with CO$_2$, CS$_2$, and COS, 30:30548
CARBONIC ACID DERIVATIVES/BIOLOGICAL EFFECTS
Effect of x irradiation on hydrocarbon metabolism and on hydrocarbon-induced lethality and transformation in cells derived from mouse prostate (3-Methylcholanthrene, 7,12-dimethylbenz(a)anthracene, N-methyl-N'-nitro-N-nitrosoguanidine), 30:29670
CARBOXYLIC ACID SALTS/RADIOSENSITIVITY EFFECTS
Time course of the radioprotective effect and the formation of endogenous colonies of haemopoietic cells in mouse spleen following the administration of sodium fluoroacetate (X Radiation; mice), 30:29747
CARCINOGENESIS/REVIEWS
Systematics of iatrogenic carcinogenesis, 30:29724
CARCINOMAS/RADIOTHERAPY
Influence of fractionation on acute and late reactions in vocal cord carcinoma (Radiotherapny planning), 30:29713
CARDIAC OUTPUT
See BLOOD CIRCULATION
CARDIAC PACEMAKERS
Special indication and contraindications for the implantation of cardiac pacemakers with radionuclide batteries, 30:29770 (AED-CONF-74-030-003)
CARDIAC PACEMAKERS/GENETIC RADIATION EFFECTS
Genetic radiation effects (^{147}Pm and ^{238}Pu powered cardiac pacemakers), 30:29700 (AED-CONF-74-030-004)
CARDIAC PACEMAKERS/RADIATION DOSE DISTRIBUTIONS
In-vivo measurement of the gamma and neutron dose rate on patients with ^{238}Pu pacemakers implanted, 30:29704 (KFK-1851)
CARDIOVASCULAR DISEASES/DIAGNOSIS
Dual camera studies of pulmonary function with computer processing of data (^{133}Xe tracer), 30:29847
CARDIOVASCULAR SYSTEM
See also BLOOD VESSELS
CARDIOVASCULAR SYSTEM/BIOLOGICAL RADIATION EFFECTS
Changes in the cardiovascular system in radiation and medicinal treatment of lung cancer, 30:29729
CASCADE IMPACTORS/PERFORMANCE
Interstage particle losses in a high-volume cascade impactor, 30:29374 (BNWL-1850(Pt.3))
CASKS/DESIGN
Radioactive waste storage (Patent), 30:30109
CASKS/SAFETY
Safety analysis report for packaging (Oak Ridge Y-12 Plant model VCD package for enriched uranium solution), 30:30115 (Y-DD-155)
Safety analysis report for packaging (Oak Ridge Y-12 Plant foamglas shipping package for enriched uranium), 30:30116 (Y-DD-156)
CASKS/SIMULATION
LMFBR-37-fuel-element shipping cask simulation: test assembly operation and data, 30:30114 (ORNL-TM-3992)
CATHEPSINS/BIOCHEMICAL REACTION KINETICS
Effect of internally deposited plutonium-239 on the lysosomes of rat liver (Compared with effects from ^{198}Au), 30:29782
CATTLE
See also COWS
CATTLE/DECONTAMINATION
Decontamination of swine, sheep, and cattle surface-contaminated with fission products. II. Removal of radionuclides of zirconium, niobium, ruthenium, and cerium (^{95}Zr; ^{95}Nb; ^{106}Ru; ^{144}Ce), 30:29823
CATTLE/RADIONUCLIDE KINETICS
Grazing studies on selected plutonium-contaminated areas in Nevada (U and Pu uptake by cattle), 30:29448 (NVO-AEIC-74-1)
CAUSALITY
Causal boundaries for general relativistic space--times, 30:31175
Constraints, causality, and Lorentz invariance, 30:31167
CDC COMPUTERS/EQUIPMENT INTERFACES
Development of a CAMAC crate controller for connection to a computer CDC 1700, 30:29634
CDTE SEMICONDUCTOR DETECTORS/PERFORMANCE
N-type cadmium telluride surface-barrier nuclear radiation detectors, 30:29520
CEA GRENOBLE/RESEARCH PROGRAMS
Department of Fundamental Research, Grenoble, semiannual bulletin No. 4, 30:31333 (CEA-N-1688)
CELL KILLING/RADIOINDUCTION
X-radiation-sensitivity of rat liver to interphase death, 30:29737
CELL MEMBRANES/RADIONUCLIDE KINETICS
Comparative study of the incorporation of ^{32}P into the phospholipids of membranes from Novikoff hepatoma ascites cells and liver cells from normal and tumor bearing animals (Rats), 30:29819
CELL NUCLEI/BIOLOGICAL RADIATION EFFECTS
Dissociation of histone and DNA synthesis in x-irradiated HeLa cells (Ultraviolet radiation), 30:29666
CELLS (ANIMAL)
See ANIMAL CELLS
CENTRAL AMERICA/FALLOUT
Data. Section III. Air and deposition (Monitoring), 30:29382
Data. Section I. Milk and food (Monitoring), 30:29421
CEPHEIDS/MASS TRANSFER
Island solutions in linear series of static stellar models with core helium and shell hydrogen burning for M=5,7, and 9 M/subsun/ (Mass loss, secular stability), 30:30198
CEPHEIDS/RADIAL VELOCITY
New high-dispersion radial velocity curves of W sagittarii (Lower dispersion), 30:30254
CEREBROSPINAL FLUID/DIFFUSION
Study on the blood-cerebrospinal fluid barrier. I. Permeability of RISA^{131}I at twenty-four hours after intravenous administration, 30:29840
CERIUM/ACTIVATION ANALYSIS
Determination of rare earths and thorium in apatites by thermal and epithermal neutron-activation analysis, 30:28935
Radioactivation analysis in thermal and epithermal neutrons of the IBR-30 reactor of JINR, 30:28929
Trace element behavior in soil of some Indonesian sawah's and in sludge of an Indonesian river, 30:28930
Trace elements in precipitation and cloud water in the area of Heidelberg, measured by instrumental neutron activation analysis, 30:28934
CERIUM/DIFFUSION
Study of diffusion/leaching phenomena with glasses. Application of risk evaluation to long-term storage, 30:29133 (CEA-R-4550)
CERIUM/ELECTRON COLLISIONS
Strong 4f resonance effects in rare-earth appearance-potential spectra, 30:30477
CERIUM/SOLUBILITY
Electrochemical investigation of amalgams of rare earth metals. I. Main electrochemical properties of amalgams of rare earth elements (^{144}Ce tracer), 30:29111
CERIUM 130/ENERGY LEVELS
Nuclear Data Sheets for A = 130, 30:30968
CERIUM 130/NUCLEAR PROPERTIES
Nuclear Data Sheets for A = 130, 30:30968
CERIUM 136/ENERGY LEVELS
Nuclear Data Sheets for A = 136, 30:30967
CERIUM 136/NUCLEAR PROPERTIES
Nuclear Data Sheets for A = 136, 30:30967

CERIUM 140/DEUTERON REACTIONS
  Correlations between (n,γ) and (d,p) reactions on N = 82 nuclei (Excitation strengths), 30:30970
CERIUM 140/NEUTRON REACTIONS
  Correlations between (n,γ) and (d,p) reactions on N = 82 nuclei (Excitation strengths), 30:30970
CERIUM 141/RADIATION MONITORING
  Data. Section IV. Other data, 30:29412
  Quillayute air reference station (Air sampling and monitoring in Washington State), 30:29359 (BNWL-1850(Pt.3))
CERIUM 143/ENERGY LEVELS
  Nuclear Data Sheets for A = 143, 30:30966
CERIUM 143/NUCLEAR PROPERTIES
  Nuclear Data Sheets for A = 143, 30:30966
CERIUM 144/BIOLOGICAL RADIATION EFFECTS
  Comparison of external irradiation and consumption of cows' milk as critical pathways for ^{137}Cs, ^{54}Mn and ^{144}Ce--^{144}Pr released to the atmosphere, 30:29423
CERIUM 144/CHEMICAL STATE
  State of ^{90}Sr, ^{137}Cs, and ^{144}Ce in radioactive fallout, 30:29384
CERIUM 144/INTESTINAL ABSORPTION
  Internal deposition of ingested cerium in suckling mice, 30:29821
CERIUM 144/RADIATION MONITORING
  Data. Section IV. Other data, 30:29412
  Determination of fallout radioisotopes from their content in the annual layers of high-mountain glaciers, 30:29408
  Environmental monitoring report: United States Atomic Energy Commission, Oak Ridge facilities. Calendar year 1973, 30:29352 (UCC-ND-280)
CERIUM 144/RADIOECOLOGICAL CONCENTRATION
  Comparison of external irradiation and consumption of cows' milk as critical pathways for ^{137}Cs, ^{54}Mn and ^{144}Ce--^{144}Pr released to the atmosphere, 30:29423
CERIUM 144/REMOVAL
  Decontamination of swine, sheep, and cattle surface-contaminated with fission products. II. Removal of radionuclides of zirconium, niobium, ruthenium, and cerium, 30:29823
CERIUM 144/TISSUE DISTRIBUTION
  Influence of irradiation on the incorporation of radionuclides (^{239}Pu; ^{226}Ra; ^{210}Pb; ^{144}Ce; tritium), 30:29818
CERIUM ALLOYS/CRYSTAL STRUCTURE
  Structure of alloys of cobalt with rare earths of the approximate composition RCo$_5$, 30:30034
CERIUM ALLOYS/ELONGATION
  Method of determining the relative elongation of light alloys close to the solidus on an IMASh-5S-65 unit, 30:30012
CERIUM ALLOYS/MAGNETIC PROPERTIES
  Magnetic properties of CeBi (Orientation; 3 to 30°K), 30:29993
CERIUM ALLOYS/PHASE DIAGRAMS
  System Ce--Ge, 30:30016
CERIUM ALLOYS/SUPERCONDUCTIVITY
  Superconducting-normal phase boundaries of (La,Th)Ce systems, 30:30814
CERIUM COMPOUNDS/LATTICE PARAMETERS
  On oxifluorides A$_{12}$M(IV)M$_3$(VI)O$_8$F$_{18}$ with uranium, molybdenum, and tungsten (A = Cs, Rb, K and M(IV) = U, Ce, MoW), 30:29006
CERIUM COMPOUNDS/MAGNETIC SUSCEPTIBILITY
  On oxifluorides A$_{12}$M(IV)M$_3$(VI)O$_8$F$_{18}$ with uranium, molybdenum, and tungsten (A = Cs, Rb, K and M(IV) = U, Ce, MoW), 30:29006
CERIUM HYDRIDES
  Isotopic ordering in CeD$_2$H, 30:29008 (IAE-2309)
CERIUM OXIDES/SINTERING
  Effect of complex admixtures of rare-earth oxides on sintering of cerium dioxide (Sm$_2$O$_3$; Gd$_2$O$_3$; Y$_2$O$_3$; La$_2$O$_3$), 30:29909
CESIUM
  Metal vapor confinement in vacuum (Charge exchange cells for negative ion beam production), 30:30128
CESIUM/ACTIVATION ANALYSIS
  Multielement determination in market-garden soils by instrumental photon activation analysis, 30:28921
  Trace element behavior in soil of some Indonesian sawah's and in sludge of an Indonesian river, 30:28930
  Trace elements in precipitation and cloud water in the area of Heidelberg, measured by instrumental neutron activation analysis, 30:28934
CESIUM/ATOM-MOLECULE COLLISIONS
  Negative ion formation from energetic collisions of cesium with CO$_2$, CS$_2$, and COS, 30:30548
CESIUM/CHEMICAL ANALYSIS
  Novel methods in the analysis of cesium, 30:28976
CESIUM/DIFFUSION
  Study of diffusion/leaching phenomena with glasses. Application of risk evaluation to long-term storage, 30:29133 (CEA-R-4550)
CESIUM/ELECTRIC CONDUCTIVITY
  Volume and temperature dependence of the electronic transport properties of fluid alkalis in the semiconducting range (K and Cs), 30:30005
CESIUM/EMISSION SPECTROSCOPY
  Spectrochemical analysis of uranium oxide by gallium oxide carrier dc arc technique (ASTM Standard E402), 30:28957
CESIUM/THERMOELECTRIC PROPERTIES
  Volume and temperature dependence of the electronic transport properties of fluid alkalis in the semiconducting range (K and Cs), 30:30005
CESIUM/TISSUE DISTRIBUTION
  Distribution of radioactive and stable cesium in the human body (^{137}Cs; K), 30:29789
CESIUM 130/NUCLEAR PROPERTIES
  Nuclear Data Sheets for A = 130, 30:30968
CESIUM 136/NUCLEAR PROPERTIES
  Nuclear Data Sheets for A = 136, 30:30967
CESIUM 137/ABUNDANCE
  Calculation of fractionation effects following atmospheric nuclear explosions, 30:29386
CESIUM 137/ADSORPTION
  Studies on the sorption and fixation of cesium by vermiculite. II, 30:29134
CESIUM 137/BIOLOGICAL RADIATION EFFECTS
  Comparison of external irradiation and consumption of cows' milk as critical pathways for ^{137}Cs, ^{54}Mn and ^{144}Ce--^{144}Pr released to the atmosphere, 30:29423
  Nuclear testing (^{131}I; ^{90}Sr; ^{137}Cs; ^{14}C; Tritium), 30:29719
  Real risks of the nuclear tests (^{131}I; ^{137}Cs; ^{90}Sr), 30:29720
CESIUM 137/CHEMICAL STATE
  State of ^{90}Sr, ^{137}Cs, and ^{144}Ce in radioactive fallout, 30:29384
CESIUM 137/DIFFUSION
  Concentration effects of ^{137}Cs, ^{65}Zn, ^{60}Co, and ^{106}Ru sorption by marine sediments with geochemical implications, 30:29409
  ^{90}Sr and ^{137}Cs distribution in different types of soils, 30:29403
CESIUM 137/ION EXCHANGE
  Separation of ^{137}Cs and ^{90}Sr from highly radioactive fission product solutions, 30:28991 (BLG-487)
CESIUM 137/RADIATION MONITORING
  Airborne release of ^{137}Cs from a contaminated area during a range fire, 30:29376 (BNWL-1850(Pt.3))
  ^{137}Cs, ^{90}Sr, and ^{210}Pb in soils of the Arctic regions, 30:29405
  Data. Section IV. Other data, 30:29412
  Data. Section I. Milk and food, 30:29421
  Determination of fallout radioisotopes from their content in the annual layers of high-mountain glaciers, 30:29408
  Phase I. Radiation and radioisotope studies with laboratory and domestic animals (Fallout ^{137}Cs, ^{131}I, and ^{90}Sr in food chains), 30:29417 (COO-3167-102)
  Quillayute air reference station (Air sampling and monitoring in Washington State), 30:29359 (BNWL-1850(Pt.3))
  Radioactive contamination of some arable soils in the Lower Silesia in 1972, 30:29402
  Radiological monitoring program, period covering February 4, 1974--April 30, 1974 (Rio Blanco site), 30:29348 (PNE-RB-51-9)
  Rate of fallout of ^{137}Cs and ^{90}Sr aerosols from the atmosphere, 30:29399
  Report of activity, February 1974 (Radioactivity of environmental samples collected throughout France during February 1974), 30:29349 (SCPRI(RM)-2-1974)
CESIUM 137/RADIOECOLOGICAL CONCENTRATION
  Comparison of external irradiation and consumption of cows' milk as critical pathways for ^{137}Cs, ^{54}Mn and ^{144}Ce--^{144}Pr released to the atmosphere, 30:29423
  Environmental monitoring report: United States Atomic Energy Commission, Oak Ridge facilities. Calendar year 1973, 30:29352 (UCC-ND-280)
  Plutonium in the Laurentian Great Lakes: food-chain relationships (^{239}Pu; ^{137}Cs), 30:29415 (CONF-740826-3)
  Radioactive tracer studies of soil and litter arthropod food chains. Progress report, November 1, 1973--October 31, 1974 (Fallout ^{137}Cs tracer), 30:29419 (SRO-641-13)
CESIUM 137/TISSUE DISTRIBUTION
  Distribution of radioactive and stable cesium in the human body (^{137}Cs; K), 30:29789
CESIUM 143/NUCLEAR PROPERTIES
  Nuclear Data Sheets for A = 143, 30:30966
CESIUM CHLORIDES/ELECTRON-MOLECULE COLLISIONS
  Scattering of alkali halides by electrons. II. CsCl (0.47- to 15.7-eV electrons: cross sections), 30:30528
CESIUM COMPOUNDS/LATTICE PARAMETERS
  On oxifluorides A$_{12}$M(IV)M$_3$(VI)O$_8$F$_{18}$ with uranium, molybdenum, and tungsten (A = Cs, Rb, K and M(IV) = U, Ce, MoW), 30:29006
CESIUM COMPOUNDS/MAGNETIC SUSCEPTIBILITY
  On oxifluorides A$_{12}$M(IV)M$_3$(VI)O$_8$F$_{18}$ with uranium, molybdenum, and tungsten (A = Cs, Rb, K and M(IV) = U, Ce, MoW), 30:29006
CESTODES/HORMONES
  Identification of sparganum growth factor by a radioreceptor assay for growth hormone (^{125}I tracer technique), 30:29868
CHARGE-EXCHANGE INTERACTIONS/DIFFERENTIAL CROSS SECTIONS
  Charge distributions of many particle final states and the energy dependence of forward charge exchange, 30:30696

CHARGED PARTICLES
- See also ALPHA PARTICLES
  - DEUTERONS
  - IONS
  - TRITONS

CHARGED PARTICLES/DIRAC EQUATION
- Modification of the quantum-mechanical equations for the system of charged Dirac particles by including additional tensor terms of the Pauli type. I, 30:31157

CHARGED PARTICLES/ELECTRODYNAMICS
- Effect of intense electromagnetic wave in charged-particle scattering (Born and dipole approximations, Schroedinger equation), 30:30655

CHARGED-PARTICLE TRANSPORT THEORY/COMPUTER CODES
- Program IONS: two-dimensional Fokker--Planck equation for ions and electrons, 30:31362 (UCID-16014)

CHARM PARTICLES/PARTICLE PRODUCTION
- Charmed-particle production by neutrinos with the Weinberg SU(4) currents (0 to 180 GeV), 30:30688

CHEMICAL ANALYSIS
- See also ABSORPTION SPECTROSCOPY
  - ACTIVATION ANALYSIS
  - FLUORESCENCE SPECTROSCOPY
  - NUCLEAR REACTION ANALYSIS
  - X-RAY FLUORESCENCE ANALYSIS
- Sensitivity in trace-element analysis by p,α and ^{16}O induced X-rays, 30:28988

CHEMICAL ANALYSIS/MANUALS
- HASL procedures manual, 30:28970 (HASL-300(Suppl.2))

CHEMICAL ANALYSIS/STANDARDS
- Chemical analysis of zirconium and zirconium-base alloys (Book), 30:28961

CHEMICAL DOSEMETERS/COMPARATIVE EVALUATIONS
- Comparison of in-core chemical and calorimetric dosemeter measurements, 30:29550 (DEMO-74/5)
- International intercomparison of chemical dosimeters for in-pile use. A report of measurements made in the Greek Research Reactor-1 at Nuclear Research Center ''Democritos'', Athens, Greece, 3--8 July 1972 by eight reactor calorimetry and radiation chemistry groups from eight member states of the IAEA, 30:29539 (DEMO-74/5)

CHEMICAL DOSEMETERS/OPERATION
- Measurements by isotope exchange between ^{14}Co and $^{12}CO_2$, 30:29543 (DEMO-74/5)
- Measurements with the hydrogen sulfide dosimeter, 30:29545 (DEMO-74/5)

CHEMICAL DOSEMETERS/PERFORMANCE
- Measurements by fluorocarbon dosimetry, 30:29544 (DEMO-74/5)
- Measurements with dicarboxylic acid dosimeters, 30:29547 (DEMO-74/5)
- Measurements with aqueous oxalic acid, 30:29548 (DEMO-74/5)
- Measurements with cyclohexane dosimeters, 30:29549 (DEMO-74/5)

CHEMICAL EXPLOSIONS/SHOCK WAVES
- Archiving guide to microbarograph records of nuclear and chemical explosion tests, 30:29314 (SLA-74-0210)
- Blast wave boundary layer measurements. Final report, September 1971--August 1973, 30:29307 (AD-777580)

CHEMICAL EXPLOSIVES
- See also PETN
- Thermal ignition of an explosive by surface friction, 30:31402 (UCID-15669)

CHEMICAL EXPLOSIVES/CHEMICAL ANALYSIS
- Analysis of plastic-bonded explosives containing HMX, ammonium perchlorate, aluminum, and Viton, 30:31369 (UCID-15623)
- Analysis of explosive simulant 90503, 30:31373 (UCID-15972)

CHEMICAL EXPLOSIVES/CHEMICAL REACTION KINETICS
- Kinetics of energy release of heterogeneous high explosives, 30:31408 (UCID-15962)

CHEMICAL EXPLOSIVES/GAS CHROMATOGRAPHY
- Gas chromatographic analysis of bis(2-fluoro-2,2-dinitroethyl) formal (FEFO), 30:31370 (UCID-15671)

CHEMICAL EXPLOSIVES/NEUTRON RADIOGRAPHY
- Experimental neutron radiography system using californium-252. Final report, 30:29295 (AD-776900)

CHEMICAL EXPLOSIVES/PHYSICAL PROPERTIES
- LX-10-1: a high-energy plastic-bonded explosive, 30:31374 (UCRL-51629)
- Properties of the high explosive LX-09-0, 30:31372 (UCID-15910)

CHEMICAL REACTION KINETICS
- Instrumental limitation to the rate of kinetic processes measurable by time-resolved mass spectrometry, 30:31368 (SLA-73-7063)

CHEMICAL REACTION KINETICS/THERMODYNAMICS
- Interrelationship of thermodynamic and kinetic parameters of redox reactions, 30;29005

CHEMISTRY
- See also NUCLEAR CHEMISTRY
  - PHOTOCHEMISTRY
  - RADIATION CHEMISTRY
  - RADIOCHEMISTRY

CHEMISTRY/RESEARCH PROGRAMS
- Research fields in physics (Research topics listing), 30:30645

CHERENKOV COUNTERS
- Methods of search of gamma-radiation point sources by two groups of detectors (Cosmic gamma sources), 30:29580

CHERENKOV COUNTERS/ENERGY RESOLUTION
- Investigation of a 90-channel Pb glass Cherenkov hodoscope, 30:29577

CHERENKOV COUNTERS/PERFORMANCE
- A large fast water Cherenkov counter, 30:29600

CHEST/SCINTISCANNING
- Gallium--technetium subtraction scanning for the localization of subphrenic abscess (Double tracer using /sup 99m/Tc for liver, spleen and lung scans), 30:29845

CHICKENS/RADIONUCLIDE KINETICS
- Distribution of ingested plutonium in chickens and subsequent transport to eggs (^{238}Pu tracer), 30:29811 (NVO-AEIC-74-1)

CHINA/NUCLEAR EXPLOSIONS
- Behavior and characteristics of radioactive debris from the Chinese nuclear weapons test of June 26, 1973, 30:29362 (BNWL-1850(Pt.3))

CHINA CLAY
- See KAOLIN

CHINESE HAMSTER
- See HAMSTERS

CHIRAL SYMMETRY
- Structure and experimental consequences of chiral SU_3 x SU_3 breaking, 30:30775

CHIRAL SYMMETRY/SYMMETRY BREAKING
- Consistency conditions in the theory of spontaneous breaking of chiral symmetry, 30:30778
- Pion phase transition in chiral symmetry breaking model, 30:30716

CHLORATES/RADIATION CHEMISTRY
- ESR study of paramagnetic centers in irradiated $Ba(ClO_3)_2 \cdot H_2O$ and $Ba(ClO_3)_2 \cdot D_2O$ single crystals (γ radiation), 30:29069

CHLORIDES/PRECIPITATION SCAVENGING
- Relation between washout of radioactivity and nonradioactive ions in the atmosphere by precipitation, 30:29395

CHLORIDES/WASHOUT
- Relation between washout of radioactivity and nonradioactive ions in the atmosphere by precipitation, 30:29395

CHLORINE/ACTIVATION ANALYSIS
- Multielement determination in market-garden soils by instrumental photon activation analysis, 30:28921
- Trace elements in precipitation and cloud water in the area of Heidelberg, measured by instrumental neutron activation analysis, 30:28934

CHLORINE/BIOLOGICAL EFFECTS
- Aquatic physiology of thermal and chemical discharges, 30:29461 (BNWL-SA-5058)

CHLORINE 35/ENERGY LEVELS
- Investigation of the 3.46 MeV isomeric level of ^{38}K with the ^{24}Mg(^{16}O,pnγ)^{38}K reaction (38 MeV: γ spectra; lifetimes of levels in ^{38}K, ^{38}Ar, ^{35}Cl), 30:30912

CHLORINE 36/ISOTOPIC EXCHANGE
- Investigations on the structure of μ-oxochlororuthenate(IV) by the isotopic exchange method, 30:29030
- Isotope exchange of chlorine-36 in the systems: gaseous hydrogen chloride--γ-picoline hydrochloride and gaseous hydrogen chloride--stoichiometric solvate of hydrogen chloride with γ-picoline hydrochloride, 30:29027
- Labelled compounds. P. 18. Chlorine exchange between antimony(III) chloride-(^{36}Cl) and hexachloropropene (1), 30:29123

CHOLANTHRENE/BIOLOGICAL EFFECTS
- Effect of x irradiation on hydrocarbon metabolism and on hydrocarbon-induced lethality and transformation in cells derived from mouse prostate (3-Methylcholanthrene, 7,12-dimethylbenz(a)anthracene, N-methyl-N'-nitro-N-nitrosoquanidine), 30:29670

CHONDRITES/CHEMICAL COMPOSITION
- Mass spectrometric isotope dilution analyses of tin in stony meteorites and standard rocks, 30:30311
- The unique cosmic-ray history of the Malakal chondrite, 30:30170

CHONDRITES/ISOTOPE RATIO
- Xenon isotope anomalies in the carbonaceous chondrite Murrey, 30:30162

CHONDROSARCOMAS
- See SKELETAL DISEASES

CHOPPERS (NEUTRON)
- See NEUTRON CHOPPERS

CHROMATID DELETIONS
- See CHROMOSOMAL ABERRATIONS

CHROMIUM/ABSORPTION SPECTROSCOPY
- Atomic absorption spectrometry of impurities in high purity tantalum with heated graphite atomizer, 30:28954

CHROMIUM/ACTIVATION ANALYSIS
- Multielement determination in market-garden soils by instrumental photon activation analysis, 30:28921
- Trace element behavior in soil of some Indonesian sawah's and in sludge of an Indonesian river, 30:28930
- Trace elements in precipitation and cloud water in the area of Heidelberg, measured by instrumental neutron activation analysis, 30:28934

- CHROMIUM/DIFFUSION
  - Measurements of drift from a mechanical draft cooling tower (Air concentrations and surface deposition of Cr from gaseous diffusion plant cooling tower), 30:29487 (BNWL-1850(Pt.3))
- CHROMIUM/EMISSION SPECTROSCOPY
  - Spectrochemical analysis of uranium oxide by gallium oxide carrier dc arc technique (ASTM Standard E402), 30:28957
  - Spectrographic determination of trace impurities in high purity uranium oxide, 30:28944 (UCID-15952)
- CHROMIUM/MECHANICAL PROPERTIES
  - Effect of cyclic deformation on the dislocation structure and mechanical properties of molybdenum, chromium, and tungsten, 30:30028
- CHROMIUM/MONITORING
  - Environmental monitoring report, calendar year 1973, 30:29351 (UCC-ND-279)
  - Portsmouth Gaseous Diffusion Plant environmental monitoring report, 1973, 30:29346 (GAT-781)
- CHROMIUM/NEUTRON REACTIONS
  - Optical model calculations for the scattering of rapid neutrons (8 to 15 MeV) by Cr and Fe, 30:30943
- CHROMIUM/POWDER METALLURGY
  - Powder metallurgy of heat-resistant alloys and refractory metals (Book), 30:29963
- CHROMIUM/QUALITATIVE CHEMICAL ANALYSIS
  - Application of activation analysis to the determination of pollutants in the atmosphere, 30:28914 (IEA-326)
- CHROMIUM 50/ALPHA REACTIONS
  - Reaction rates of interest in late stages of stellar nycleosynthesis (Estimate of reliability), 30:30255
- CHROMIUM 52/NEUTRON REACTIONS
  - Status report to NCSAC, 30:31011 (UCID-15639)
- CHROMIUM 53/PHOTONUCLEAR REACTIONS
  - Status report to NCSAC, 30:31011 (UCID-15639)
- CHROMIUM 53/PROTON REACTIONS
  - Magnetic rotation of levels of ^{53}Mn and ^{54}Mn following the ^{53} ^{54}Cr(p,n) and ^{51}V(α,n) reactions (2.5- and 3.0-MeV protons, 7.5-MeV alphas; branching ratios, g, lifetimes), 30:30933
- CHROMIUM 54/PROTON REACTIONS
  - Magnetic rotation of levels of ^{53}Mn and ^{54}Mn following the ^{53} ^{54}Cr(p,n) and ^{51}V(α,n) reactions (2.5- and 3.0-MeV protons, 7.5-MeV alphas; branching ratios, g, lifetimes), 30:30933
- CHROMIUM ALLOYS
  - See also CHROMIUM BASE ALLOYS
    - INCULOY ALLOYS
    - NICHROME
    - NIMONIC
    - RENE 41
    - STAINLESS STEELS
- CHROMIUM ALLOYS/AGING
  - Effect of the volume disparity between the precipitation phase and the matrix on the scattering of x rays by aging alloys (EP 199 (Ni--Cr--W--Mo--Al--Ti)), 30:30036
- CHROMIUM ALLOYS/BRAZING ALLOYS
  - Nickel brazing below 1025 C of untreated Inconel 718. Use of a getter makes nickel brazing of Inconel 718 and X-750 below 1025 C (1875 F) as easy as nickel brazing of stainless steels in vacuum, 30:29969
- CHROMIUM ALLOYS/ELECTRODEPOSITION
  - Effect of electrolysis conditions on the current efficiency of the deposition and composition of chromium--molybdenum alloy, 30:29960
- CHROMIUM ALLOYS/ION EMISSION
  - Ionic emission yield for alloys, dependence on the nature of the solute. II. Interpretation, 30:30087
- CHROMIUM ALLOYS/MICROSTRUCTURE
  - Structure and phase-boundary energies of the directionally solidified InSb--MnSb--NiSb, InSb--FeSb, and InSb--CrSb eutectic alloys, 30:30019
- CHROMIUM ALLOYS/PLASTICITY
  - Effect of carbide-forming elements on the properties of chromium and its alloys with rare earths (Additions of Ti, Zr, Hf, Nb, Ta), 30:30058
- CHROMIUM ALLOYS/POWDER METALLURGY
  - Powder metallurgy of heat-resistant alloys and refractory metals (Book), 30:29963
- CHROMIUM BASE ALLOYS/NEEL TEMPERATURE
  - Effect of rare earth metals on antimagnetism of chromium, 30:30054
- CHROMIUM COMPOUNDS/CHEMICAL REACTION KINETICS
  - Chromium--carbon bonds in aqueous solutions. A pulse radiolytic study (Reaction of 16 aliphatic radicals with Cr $(H_2O)_6^{2+}$), 30:29080
- CHROMIUM COMPOUNDS/ELECTRONIC STRUCTURE
  - Electronic structure and optical properties of some first row transition metal oxyhalides, 30:31395 (LA-5637-T)
- CHROMIUM COMPOUNDS/OPTICAL PROPERTIES
  - Electronic structure and optical properties of some first row transition metal oxyhalides, 30:31395 (LA-5637-T)
- CHROMIUM FLUORIDES/SOLUBILITY
  - Solubility and stability of structural metal difluorides in molten fluoride mixtures, 30:29002 (ORNL-TM-760)
- CHROMIUM OXIDES/PLASMA ARC SPRAYING
  - Damping and elastic characteristics of plasma-sprayed coatings of W, nichrome, zirconia, and Cr--Ni spinels (Cr--Ni spinel), 30:29887
- CHROMIUM OXIDES/X-RAY FLUORESCENCE ANALYSIS
  - Compilation of x-ray interaction data for x-ray fluorescence analysis of geological samples, 30:28943 (RISO-297)
- CHROMIUM-MOLYBDENUM STEELS/MASS TRANSFER
  - Study on mass transfer phenomena in the sodium loop of structural materials of the liquid metal fast-breeder reactor, 30:29950
- CHROMOSOMAL ABERRATIONS/RADIOINDUCTION
  - Changes in genetic cell material during the action of ionizing radiation (Effects of uv and x radiation on DNA and nucleoproteins), 30:29655
  - Changes in the number of circulating lymphocytes with chromosomal aberrations following a single exposure of the pelvis to x-irradiation in cancer patients, 30:29706
  - Chromosomal aberrations induced by gamma irradiation of Crepis capillaris seedlings at different periods of interphase, 30:29696
  - Chromosome aberrations in lymphocytes of peripheral blood after radiation therapy (γ ray; betatron), 30:29731
  - Dose-response for frequency of chromatid aberrations induced by x rays at G_2 and S stages of the mitotic cycle in Crepis capillaris root tips, 30:29697
  - Effect of $^{239}PuO_2$ particle number and size on the frequency and distribution of chromosome aberrations in the liver of the Chinese hamster, 30:29783
  - Human lymphocyte as a radiobiological dosimeter after total body irradiation (Gamma radiation), 30:29707
  - Influence of blood oxygenation during in vitro irradiation upon the yield of dicentric chromosomal aberrations in lymphocytes (X Radiation), 30:29749
  - Mechanisms of the inhibitors of cell post-irradiation recovery. III. Increase in the chromosomal damage rate by caffeine treatment of x irradiated buckwheat cells, 30:29695
  - Reciprocal translocation as a new approach to breeding seedless watermelon. I. Some characters of F_1 hybrids with six reciprocal translocations (X radiation), 30:29686
- CHROMOSOMES/BIOLOGICAL RADIATION EFFECTS
  - Chromosome loss following x-ray irradiation of mature oocytes from Drosophila melanogaster, 30:29768
- CHROMOSOMES/KARYOTYPE
  - Studies on radioresistance with HeLa cells: radiosensitivity and chromosome constitution, 30:29663
- CHROMOSOMES/RESEARCH PROGRAMS
  - Department of Fundamental Research, Grenoble, semiannual bulletin No. 4, 30:31333 (CEA-N-1688)
- CHUGOKU ELECTRIC POWER COMPANY REACTOR
  - See SHIMANE-1 REACTOR
- CHUGOKU-1 REACTOR
  - See SHIMANE-1 REACTOR
- CLATHRATES
  - Evaluation of quinol clathrate for fission product noble gas storage, 30:30108 (ICP-1045)
- CLIMATES
  - Has man, through increasing emissions of particulates, changed the climate, 30:29489 (UCRL-75902(Rev.1))
- CLINCH RIVER/RADIATION MONITORING
  - Environmental monitoring report: United States Atomic Energy Commission, Oak Ridge facilities. Calendar year 1973, 30:29352 (UCC-ND-280)
- CLINCH RIVER BREEDER REACTOR/DESIGN
  - Design progress on the LMFBR demonstration plant. Subject No. 20, 30:31222 (CONF-740341-1)
- CLINCH RIVER BREEDER REACTOR/PLANNING
  - Design progress on the LMFBR demonstration plant. Subject No. 20, 30:31222 (CONF-740341-1)
- CLOSED-CYCLE MHD GENERATORS
  - Exploratory study of several advanced nuclear-MHD power plant systems, 30:31209
  - Feasibility problems on UHTR for closed cycle MHD-power plants, 30:31208
- CLOUDS
  - (Limited to clouds in the earth atmosphere; for interstellar clouds see COSMIC DUST or COSMIC GASES.)
  - See also RADIOACTIVE CLOUDS
- CLOUDS/DIFFUSION
  - Peculiarities of the upper cloud layer and suggestions for using radioactive tracer techniques in studying meridional currents, 30:29428
- CLOUDS/PRECIPITATION SCAVENGING
  - Convective storm modeling and its possible application to precipitation scavenging problems, 30:29480 (BNWL-1850(Pt.3))
  - Entrainment of tracers near the sides of convective clouds (Tantalum, iridium, gold, rhenium, and indium tracer measurements), 30:29481 (BNWL-1850(Pt.3))
  - Feasibility study of the use of inert tracers in the national hail research experiment (Inert gold, rhenium, and indium and ^{38}Cl and ^{39}Cl tracer measurements), 30:29427 (BNWL-1850(Pt.3))
  - Model for cumulus washout of cosmogenic radionuclides, 30:29363 (BNWL-1850(Pt.3))
  - Progress report on in-cloud scavenging in frontal storms, 30:29475 (BNWL-1850(Pt.3))
  - Radionuclide concentration minimums from 6 to 9 km, 30:29368 (BNWL-1850(Pt.3))

Summary of current findings from the analysis of 1972 Quillayute scavenging experiments, 30:29476 (BNWL-1850(Pt.3))
CLOUDS/RADIOACTIVITY
Stochastic approach to studying radioactivity of cloud and rain droplets, 30:29397
CLUSTERS (STAR)
See STAR CLUSTERS
COAL/SORPTIVE PROPERTIES
Cryovacuum hydrogen adsorption by small-sized, activated mineral coal with a binder (Adsorption of benzene at 20°C and hydrogen from 20.4 to 50°K), 30:31394 (KHFTI-73-25)
COASTAL WATERS/WATER POLLUTION
Recent changes of the foraminiferal assemblages of Jobos Bay and surroundings, Puerto Rico, 30:31376 (CONF-740663-1)
COATED FUEL PARTICLES/DEFORMATION
Trends in structural mechanics. A UK review of the 2nd international conference on structural mechanics in reactor technology. VIII. Reactor core (HTGR), 30:31213
COATED FUEL PARTICLES/FRACTURE PROPERTIES
Trends in structural mechanics. A UK review of the 2nd international conference on structural mechanics in reactor technology. VIII. Reactor core (HTGR), 30:31213
COBALT/ACTIVATION ANALYSIS
Multielement determination in market-garden soils by instrumental photon activation analysis, 30:28921
Radiochemical separation of fluorine by adsorption on hafnium dioxide: application to the determination of oxygen by activation analysis with charged particles (^{3}He and ^{4}He particles), 30:28923
Trace element behavior in soil of some Indonesian sawah's and in sludge of an Indonesian river, 30:28930
Trace elements in precipitation and cloud water in the area of Heidelberg, measured by instrumental neutron activation analysis, 30:28934
COBALT/EMISSION SPECTROSCOPY
Spectrochemical analysis of uranium oxide by gallium oxide carrier dc arc technique (ASTM Standard E402), 30:28957
Spectrographic determination of trace impurities in high purity uranium oxide, 30:28944 (UCID-15952)
COBALT/FLUORESCENCE SPECTROSCOPY
New discrete atomization cell for atomic fluorescence spectrometry, 30:28947
COBALT/ION EXCHANGE
Selective ion-exchangers containing phosphorus in their functional groups. I. Sorption and separation of some bivalent and trivalent ions, 30:29001
COBALT/STACKING FAULTS
Diffraction of x rays on stacking faults in metals with hcp lattices, 30:30024
COBALT 57/ELECTRON CAPTURE DECAY
Effect of physico-chemical properties of local environment of ^{57}Co Moessbauer atoms sorbed on ion exchange materials on their stabilization form after electron capture, 30:29099
Moessbauer spectroscopic studies of the effect of the oxalate anion in the second coordination sphere on the oxidation state of ^{57}Fe produced in EC-decay, 30:29078
Post-effects of electron capture in ^{57}Co in systems containing cobalt nitrate and sulfate, 30:29096
Post-effect of electron capture in ^{57}Co atoms sorbed on cation exchange resins with different degrees of cross-linking, 30:29097
Post-effect of electron capture in the eutectic (NH$_4$NO$_3$--LiNO$_3$):^{57}Co at 77°K, 30:29098
COBALT 57/ION EXCHANGE
Isolation of carrier-free radioactive isotope cobalt-57 from nickel target irradiated on cyclotron, 30:29143
COBALT 58/RADIATION HAZARDS
Small quantities (Radioactive materials concentrations), 30:29648
COBALT 59/ALPHA REACTIONS
On the nuclear I.L potential, 30:31092
COBALT 59/HELIUM 3 REACTIONS
Target-spin effects on elastic scattering cross sections, 30:30940
COBALT 60/COSMOCHEMISTRY
The unique cosmic-ray history of the Malakal chondrite, 30:30170
COBALT 60/DIFFUSION
Concentration effects of ^{137}Cs, ^{65}Zn, ^{60}Co, and ^{106}Ru sorption by marine sediments with geochemical implications, 30:29409
Solubility and diffusion of cobalt in indium, 30:30020
COBALT 60/RADIATION MONITORING
Data. Section IV. Other data, 30:29412
Environmental monitoring report: United States Atomic Energy Commission, Oak Ridge facilities. Calendar year 1973, 30:29352 (UCC-ND-280)
COBALT 60/RADIOISOTOPE HEAT SOURCES
Development of a reflux condensing heat pipe for emergency cooling of large cobalt-60 heat source, 30:29255
COBALT 60/SOLUBILITY
Solubility and diffusion of cobalt in indium, 30:30020
COBALT ALLOYS
See also COBALT BASE ALLOYS
RENE 41
COBALT ALLOYS/AGING
Field-ion microscopic study of aged martensite in an iron--nickel--cobalt--molybdenum alloy (Fe--16 percent Ni--15 percent Co--5 percent Mo; precipitation of Mo), 30:30037
COBALT ALLOYS/ION EMISSION
Ionic emission yield for alloys, dependence on the nature of the solute. II. Interpretation, 30:30087
COBALT ALLOYS/MAGNETIC PROPERTIES
Crystal and magnetic structure of intermetallic compounds of the type Th(Co/sub x/Fe/sub 1-x/)$_5$, 30:29989
COBALT ALLOYS/THERMAL DIFFUSION
Diffusion in the Mo--Ni, Mo--Fe, and Mo--Co systems, 30:30001
COBALT BASE ALLOYS/CRYSTAL STRUCTURE
Structure of alloys of cobalt with rare earths of the approximate composition RCo$_5$ (R = Ce, Sm, Gd, Er, Y), 30:30034
COBALT BASE ALLOYS/DOMAIN STRUCTURE
Experimental verification of a model for the magnetization reversal in RCo$_5$ particles (Sm/sub x/Nd/sub 1+-x/Co$_5$), 30:30047
COBALT BASE ALLOYS/PHASE STUDIES
Orientation relation between phases in SmCo$_5$--base alloys, 30:30041
COBALT COMPLEXES/AUTORADIOLYSIS
Moessbauer spectroscopic studies of the effect of the oxalate anion in the second coordination sphere on the oxidation state of ^{57}Fe produced in EC-decay (^{57}Co), 30:29078
COBALT COMPLEXES/RADIOLYSIS
Studies of radiolysis of solid, Co(III) compounds by the EPR method, 30:29063
COBALT NITRATES/RADIOCHEMISTRY
Post-effects of electron capture in ^{57}Co in systems containing cobalt nitrate and sulfate, 30:29096
COBALT SULFATES/RADIOCHEMISTRY
Post-effects of electron capture in ^{57}Co in systems containing cobalt nitrate and sulfate, 30:29096
COHERENT RADIATION
Coherent synchrotron radiation from an intense relativistic electron beam, 30:30580 (AD-773442)
COLD PLASMA/PHYSICAL PROPERTIES
Simulation and methods for calculating physical-chemical processes in low-temperature plasmas, 30:29175
COLD TRAPS/EQUIPMENT PROTECTION DEVICES
Protection circuit for a liquid-nitrogen trap filler, 30:31415 (ANL-8111)
COLLECTIVE ACCELERATORS
See also ELECTRON-RING ACCELERATORS
COLLECTIVE ACCELERATORS/MAGNETIC COMPRESSION
Static compression of relativistic electron rings, 30:30131 (UCID-16583)
COLLECTIVE MODEL/INELASTIC SCATTERING
How good is the collective model, 30:31078
COLLECTIVE MODEL/MANY-BODY PROBLEM
Generalized Eulerian angles and the collective motion of many-particle system, 30:31053
COLLISION MATRIX
See S MATRIX
COLLISIONLESS PLASMA/DRIFT INSTABILITY
Theory of drift-cone modes of collisionless plasma in cylindrical geometry, 30:29195 (LA-5693-MS)
COLLISIONLESS PLASMA/RESEARCH PROGRAMS
Investigation of universal plasma instabilities. Annual progress report No. 9, 30:29196 (TID-26639)
COLLISIONS
See also ATOM-ATOM COLLISIONS
ATOM-MOLECULE COLLISIONS
ELECTRON-ATOM COLLISIONS
ELECTRON-ION COLLISIONS
ELECTRON-MOLECULE COLLISIONS
ION-ATOM COLLISIONS
ION-MOLECULE COLLISIONS
MOLECULE-MOLECULE COLLISIONS
POSITRON COLLISIONS
COLLISIONS/INELASTIC SCATTERING
Calculation of inelastic transition cross sections on basis of spectral line broadening theory (Dipole interaction, rotational effects), 30:30520 (IAE-2269)
COLON
See LARGE INTESTINE
COLORADO/RADIOACTIVITY
Radiological monitoring program, period covering February 4, 1974--April 30, 1974 (Rio Blanco site), 30:29348 (PNE-RB-51-9)
COLORIMETRIC DOSEMETERS/CALIBRATION
Radiochromic dosimetry measurements, 30:29546 (DEMO-74/5)
COLORIMETRY
See ABSORPTION SPECTROSCOPY
COLUMBIUM
See NIOBIUM
COMETS/RADIOWAVE RADIATION
Ultraviolet fluorescent pumping of OH 18-centimeter radiation in comets (Magnetic sublevels), 30:30326
COMMUNICATIONS
Communication system design, 30:31452 (UCID-15955)

COMMUNITIES (ECOLOGICAL)
  See ECOSYSTEMS
COMPOSITE MODELS
  See also BOOTSTRAP MODEL
    PARTON MODEL
COMPOSITE MODELS/HADRONS
  Gnome model and deep-inelastic lepton-nucleon structure functions, 30:30708
COMPOSITE MODELS/U-3 GROUPS
  Geometrical interpretation of paraorder 3 of paraquark model, 30:30692
COMPOUND NUCLEI/ENERGY LEVELS
  LARA: a FORTRAN IV code for the calculation of the compound nucleus contribution to the total radiative width in medium and heavy nuclei based on the Brink--Axel model, 30:30956 (RT/FI-(74)17)
COMPOUND-NUCLEUS REACTIONS/NUCLEAR REACTION KINETICS
  Statistical properties of a paired nucleus with fixed quasiparticle number, 30:31099
COMPOUNDS (ORGANIC)
  See ORGANIC COMPOUNDS
COMPRESSION/MEASURING METHODS
  Generalized shock Hugoniots, 30:31400 (UCID-15586)
COMPTON EFFECT/VIRTUAL PARTICLES
  J = 0 fixed pole in the virtual Compton amplitude off proton and neutron, 30:30661
COMPTON SCATTERING
  See COMPTON EFFECT
COMPTON SPECTROMETERS/LI-DRIFTED GE DETECTORS
  A summing Ge(Li)-Compton spectrometer, 30:29570
COMPUTER CODES
  Compton scattering subroutine for Monte Carlo calculations, 30:30651 (UCID-15808)
  Ground level air concentrations of dust particles downwind from a tailings area during a typical windstorm (Mathematical model), 30:29380 (ORNL-TM-4375)
  List of computer programs for neutron cross section calculations and analysis, 30:30849 (NEANDC-97/U)
  Programs for experimental data processing on PDP-8/I computer, 30:29614 (IFA-CRD-57-1974)
  Software extended floating-point feature, 30:31342 (MC-19-1974)
COMPUTER CODES/C CODES
  Determination of geographic position from rectangular coordinates. Progress report, March--June 1970, 30:31361 (UCID-15722)
  Subroutine CAUCHY: complex roots of a function using a CAUCHY integral technique, 30:31344 (ORNL-TM-4588)
COMPUTER CODES/F CODES
  Code description: FOFT (Calculates black-body radiation flux), 30:31350 (UCID-15753)
COMPUTER CODES/G CODES
  Nuclear correction for Genesis, 30:29180 (UCID-15316)
COMPUTER CODES/H CODES
  HYBRID-1, a two-dimensional Fokker--Planck code, 30:29189 (UCRL-51598)
COMPUTER CODES/I CODES
  Program IONS: two-dimensional Fokker--Planck equation for ions and electrons, 30:31362 (UCID-16014)
COMPUTER CODES/L CODES
  LARA: a FORTRAN IV code for the calculation of the compound nucleus contribution to the total radiative width in medium and heavy nuclei based on the Brink--Axel model, 30:30956 (RT/FI-(74)17)
COMPUTER CODES/M CODES
  MCDATA code (For automatic handling of cross section data sets generated by successive runs of MC^2), 30:30851 (RT/FI-(74)19)
  MEDUSA. A one-dimensional laser fusion code, 30:29227
COMPUTER CODES/P CODES
  PRELUDE-2: seismic response analysis code for block-type fuel core, 30:31247 (JAERI-M-5560)
COMPUTER CODES/R CODES
  RKSPROG: a computer program for inelastic cold neutron scattering time-of-flight measurements, 30:30847 (IRI-132-73-03)
COMPUTER CODES/RELIABILITY
  Program correctness in a multiprogrammed multiprocessor environment, 30:31339 (IS-3444)
COMPUTER CODES/S CODES
  SAFR4: a program to evaluate the stability of a rigid blade in parallel fluid flow, 30:31260 (WAPD-TM-1085)
  SAFT: structural analysis of forest trees, 30:31337 (EDFB-IBP-74-4)
COMPUTER CODES/T CODES
  Computation of MHD equilibria in Tokamak (TOPE Code), 30:29179 (CLM-R-133)
COMPUTER GRAPHICS
  Program descriptions: supplement to mesoscale wind fields and transport estimates determined from a network of wind towers, 30:31343 (NOAA-TM-ERL-ARL-43)
COMPUTERS
  See also CDC COMPUTERS
    PDP COMPUTERS
  Principles and methods for using electronic computers in clinical radioisotopic diagnosis, 30:29838
COMPUTERS/JOSEPHSON JUNCTIONS
  Tunnel junctions for computer applications, 30:30831
COMPUTERS/MEMORY DEVICES
  Choosing the basic parameters of a buffer memory device in the HPD computer system by a method of statistical modeling, 30:29623
COMPUTERS/PROGRAMMING
  Software extended floating-point feature, 30:31342 (MC-19-1974)
CONCRETES/RADIATION TRANSPORT
  Barites from Boguszow as aggregate for anti-radiation concrete shields, 30:31128
CONCRETES/USES
  Polymer-concrete for use in the repair of deteriorated bridge decks, 30:31388 (BNL-19161)
CONDENSED AROMATICS
  See also ANTHRACENE
    BENZANTHRACENE
    CHOLANTHRENE
CONDENSED AROMATICS/CHEMICAL RADIATION EFFECTS
  Reduction in electron irradiation damage to organic compounds by conducting coatings (Electron beams, Al or Au coatings), 30:29070
CONDUCTORS (ELECTRIC)
  See ELECTRIC CONDUCTORS
CONFORMAL GROUPS
  Application of a conformal transformation group for relativistic theories, 30:31142 (IAE-2306)
  D_2-type representation of the conformal group extended by reflections, 30:30628 (KFKI-74-49)
CONGENITAL MALFORMATIONS/RADIOINDUCTION
  Embryotoxicity of astatine-211 (Comparison of effects of internal ^{211}At with external x irradiation), 30:29781 (COO-3268-5)
CONTAINERS
  See also CASKS
    PRESSURE VESSELS
CONTAINERS/ACOUSTIC EMISSION TESTING
  Acoustic emission monitoring of proof tests on canisters and related hardware, 30:29296 (UCID-15777)
CONTAINMENT
  (Means and methods for preventing the escape of fission products to the atmosphere, particularly in the case of reactor accidents.)
  See also CONTAINMENT BUILDINGS
    CONTAINMENT SYSTEMS
CONTAINMENT/DESIGN
  Design of the primary containment for pool and loop arrangements of LMFBRs, 30:31263
CONTAINMENT BUILDINGS/SPECIFICATIONS
  Trends in structural mechanics. A UK review of the 2nd international conference on structural mechanics in reactor technology. I. Pressure vessels and containments, 30:31192
CONTAINMENT SPRAY SYSTEMS/CORROSION INHIBITORS
  Industrial technique (Patent), 30:31259
CONTAINMENT SYSTEMS
  See also CONTAINMENT SPRAY SYSTEMS
CONTAINMENT SYSTEMS/PERFORMANCE
  Analysis of the primary containment response using a hydrodynamic-elastic-plastic computer code (Rexco-hep code; LMFBR), 30:31264
CONTROL SYSTEMS
  (For automated processes including feedback.)
  See also ON-LINE CONTROL SYSTEMS
    REACTOR CONTROL SYSTEMS
  Connection between singular perturbations and singular arcs. Part 2. A theory for the linear regulator, 30:31336 (COO-3077-44)
CONTROL THEORY (REACTOR)
  See REACTOR KINETICS
CONVERTERS (ANALOG-DIGITAL)
  See ANALOG-TO-DIGITAL CONVERTERS
CONVERTERS (IMAGE)
  See IMAGE CONVERTERS
COOLANT LOOPS
  See also REACTOR COOLING SYSTEMS
COOLANT LOOPS/FLOW MODELS
  Derivation of transfer functions in boiling loops, 30:29292
COOLERS
  See HEAT EXCHANGERS
COOLING SYSTEM (REACTOR)
  See REACTOR COOLING SYSTEMS
COOLING TOWERS
  Effects of siting and load variation for a 650 MW nuclear station with air condensers, 30:31186
COOLING TOWERS/GASEOUS WASTES
  Measurements of drift from a mechanical draft cooling tower (Air concentrations and surface deposition of Cr from gaseous diffusion plant cooling tower), 30:29487 (BNWL-1850(Pt.3))
COOLING TOWERS/PLUMES
  Analytical search for the stochastic-dominating process in the drift-deposition problem, 30:29488 (BNWL-1850(Pt.3))
COOPER REACTOR/REACTOR OPERATION
  Semiannual operating report, January--June 1974, 30:31317 (DOCKET-50298-233)
COORDINATES
  Determination of geographic position from rectangular coordinates. Progress report, March--June 1970, 30:31361 (UCID-15722)

COPPER/ABSORPTION SPECTROSCOPY
Atomic absorption spectrometry of impurities in high purity tantalum with heated graphite atomizer, 30:28954
COPPER/ACTIVATION ANALYSIS
Betatron activation analysis of cupriferrous flotation pulp (14.9-MeV photons), 30:28920
Radiochemical separation of fluorine by adsorption on hafnium dioxide: application to the determination of oxygen by activation analysis with charged particles (^{3}He and ^{4}He particles), 30:28923
Trace element behavior in soil of some Indonesian sawah's and in sludge of an Indonesian river, 30:28930
COPPER/ADSORPTION
Effect of irradiation of metal ions on adsorption properties of semiconductor materials. I. Adsorption properties of oxidized surface of silicon (Effect of radioactivity of adsorbed ions), 30:29053
COPPER/ALPHA REACTIONS
Spallation of copper by high-energy alpha particles (720 MeV), 30:30936
COPPER/DEBYE-WALLER FACTOR
Lattice dynamical study of the recoilless fraction of ^{57}Fe in Ni, Mo, W, α-Fe and Cu, 30:30050
COPPER/EMISSION SPECTROSCOPY
Spectrochemical analysis of uranium oxide by gallium oxide carrier dc arc technique (ASTM Standard E402), 30:28957
Spectrographic determination of trace impurities in high purity uranium oxide, 30:28944 (UCID-15952)
COPPER/HARDENING
Additive strength contributions, 30:31427 (RISO-M-1714)
COPPER/INTERNAL FRICTION
Internal friction peaks observed in explosively deformed polycrystalline Mo, Nb, and Cu, 30:29980 (N-74-19371)
COPPER/ION CHANNELING
Electronic stopping power of channelled ions in a model incorporating the Pauli principle (Incident ions Z = 1 to 50), 30:31115
COPPER/ION EXCHANGE
Sorption method of isolating uranium and other valuable metals from sea water, 30:28998
COPPER/ION-ATOM COLLISIONS
High-energy calculation of K-shell ejection cross sections as a function of projectile charge (Born approximation), 30:30536
COPPER/PHYSICAL RADIATION EFFECTS
Determination of the velocity and local density of mobile dislocations within slip bands in neutron-irradiated Cu by high speed cinematography, 30:30066
COPPER/QUALITATIVE CHEMICAL ANALYSIS
Application of activation analysis to the determination of pollutants in the atmosphere, 30:28914 (IEA-326)
COPPER 59/ENERGY LEVELS
Description of odd-mass copper nuclei with particle-core coupling models, 30:30939
COPPER 61/ENERGY LEVELS
Description of odd-mass copper nuclei with particle-core coupling models, 30:30939
COPPER 63/ALPHA REACTIONS
Level densities of ^{63}Cu and ^{65}Cu from the analysis of evaporation spectra, 30:30950
COPPER 63/ENERGY LEVELS
Description of odd-mass copper nuclei with particle-core coupling models, 30:30939
Level densities of ^{63}Cu and ^{65}Cu from the analysis of evaporation spectra, 30:30950
Nuclear spectroscopy with the ^{62}Ni(^{7}Li,^{6}He)^{63}Cu reaction, 30:30937
COPPER 63/PROTON REACTIONS
Level densities of ^{63}Cu and ^{65}Cu from the analysis of evaporation spectra, 30:30950
COPPER 65/ALPHA REACTIONS
Level densities of ^{63}Cu and ^{65}Cu from the analysis of evaporation spectra, 30:30950
COPPER 65/ENERGY LEVELS
Description of odd-mass copper nuclei with particle-core coupling models, 30:30939
Level densities of ^{63}Cu and ^{65}Cu from the analysis of evaporation spectra, 30:30950
COPPER 65/PROTON REACTIONS
Level densities of ^{63}Cu and ^{65}Cu from the analysis of evaporation spectra, 30:30950
COPPER 67/ENERGY LEVELS
Description of odd-mass copper nuclei with particle-core coupling models, 30:30939
COPPER ALLOYS
See also COPPER BASE ALLOYS
COPPER ALLOYS/DIFFUSION
Transport and thermodynamic properties of solids. Progress report, September 1, 1973--August 31, 1974, 30:31390 (COO-1436-41)
COPPER ALLOYS/HARDENING
Additive strength contributions, 30:31427 (RISO-M-1714)
COPPER ALLOYS/ION EMISSION
Ionic emission yield for alloys, dependence on the nature of the solute. II. Interpretation, 30:30087
COPPER ALLOYS/MAGNETIC PROPERTIES
Magnetic properties of alloys of the TbCu--YCu system (77 to 300°K; Curie point; Neel temperature; susceptibility), 30:30031
COPPER BASE ALLOYS/PHYSICAL RADIATION EFFECTS
Kinetics of accumulation of radiation defects in metals at temperatures of stage II of recovery with consideration of transition processes (Ni, Mn, Au, Mg, Sb additions), 30:30081
COPPER CHLORIDES/ENTHALPY
Gaseous halide complexes and their stability, 30:29091
COPPER CHLORIDES/FORMATION HEAT
Gaseous halide complexes and their stability, 30:29091
COPPER COMPLEXES/PHOTOLYSIS
Effect of ultraviolet light and gamma radiation on aqueous solutions of Cu(II) complexes with amino acids, 30:29061
COPPER COMPLEXES/RADIOLYSIS
Effect of ultraviolet light and gamma radiation on aqueous solutions of Cu(II) complexes with amino acids, 30:29061
COPPER SULFATES/X-RAY FLUORESCENCE ANALYSIS
Compilation of x-ray interaction data for x-ray fluorescence analysis of geological samples, 30:28943 (RISO-297)
COPPER SULFIDES/PHYSICAL RADIATION EFFECTS
Effect of oxygen on unencapsulated cadmium sulfide solar cells, 30:30103
CORE CATCHERS/DESIGN
Post-accident core retention for LMFBR's. 2. Technical report. Final report for the period 1 July 1972--30 June 1973, 30:31253 (UCLA-ENG-7343)
CORONA (SOLAR)
See SOLAR CORONA
CORROSION
See also ELECTROCHEMICAL CORROSION
CORROSION/MEETINGS
Corrosion and corrosion resistance. IX. Tutzing symposium of the DECHEMA, February 26--March 1, 1973, Tutzing Castle, Starnberger Lake, 30:29943 (CONF-730230-(Absts.))
CORROSION PROTECTION/MEETINGS
Corrosion and corrosion resistance. IX. Tutzing symposium of the DECHEMA, February 26--March 1, 1973, Tutzing Castle, Starnberger Lake, 30:29943 (CONF-730230-(Absts.))
CORTEX (ADRENAL)
See ADRENAL GLANDS
CORTISOL
See HYDROCORTISONE
CORUNDUM/PHYSICAL RADIATION EFFECTS
Phase changes in high-alumina ceramic under the influence of ionizing radiation (Neutrons; γ rays), 30:29913
COSMIC DUST/ABSORPTION
A quantitative study of silicate extinction (Circumstellar shells, Mie theory), 30:30190
COSMIC DUST/CHEMICAL COMPOSITION
Gas and dust in interstellar clouds, 30:30367
COSMIC DUST/DISTRIBUTION
Dust, star, and hydrogen distributions in the Orion association, 30:30242
COSMIC DUST/ION IMPLANTATION
Ion implantation effects in 'cosmic' dust grains, 30:30355
COSMIC DUST/MECHANICS
Concerning the origin and the dynamics of interplanetary dust, 30:30395
COSMIC DUST/MEETINGS
Interstellar dust and related topics. Proceedings of the symposium, Albany, New York, May 29--June 2, 1972, 30:30373
COSMIC DUST/MIXING
Mixing of neutral gas and dust with the ionized gas of H II regions, 30:30369
COSMIC DUST/ORIGIN
Concerning the origin and the dynamics of interplanetary dust, 30:30395
COSMIC DUST/RADIATION TRANSPORT
Radiative transfer in circumstellar dust clouds, 30:30380
COSMIC GAMMA BURSTS/ORIGIN
Nucleosynthesis in white-dwarf atmospheres (Infalling material, gamma ray bursts), 30:30256
COSMIC GAMMA SOURCES
See also COSMIC GAMMA BURSTS
COSMIC GAMMA SOURCES/ABSORPTION
Absorption of gamma rays in intense x-ray sources, 30:30290
COSMIC GAMMA SOURCES/RADIATION DETECTION
Methods of search of gamma-radiation point sources by two groups of detectors, 30:29580
COSMIC GASES/CHEMICAL COMPOSITION
4830 MHz formaldehyde line observations of dark clouds in IC 1795/W3/, 30:30372
Gas and dust in interstellar clouds, 30:30367
COSMIC GASES/DENSITY
Statistical properties of interstellar clouds (Power law), 30:30350
COSMIC GASES/EXCITATION
Investigation of a Milky Way region in Canis Major (Obscuring matter), 30:30217
COSMIC GASES/IONIZATION
Ionization of the low-density interstellar medium, 30:30351

COSMIC GASES/MIXING
Mixing of neutral gas and dust with the ionized gas of H II regions, 30:30369
COSMIC GASES/ULTRAVIOLET RADIATION
Formation and destruction rates of interstellar H_2, 30:30349
COSMIC PARTICLES
See COSMIC RADIATION
COSMIC RADIATION
See also COSMIC GAMMA BURSTS
PRIMARY COSMIC RADIATION
SECONDARY COSMIC RADIATION
Properties and models of solar flares and cosmic radiation, 30:30297 (CONF-730693-)
COSMIC RADIATION/ABSORPTION
Rising inelastic cross-section and the attenuation of cosmic rays nucleons in the atmosphere, 30:30180
COSMIC RADIATION/ANGULAR DISTRIBUTION
Angular distribution of high energy charged particles in the galaxy, 30:30342 (CONF-730693-)
COSMIC RADIATION/ANISOTROPY
Spherical harmonic analysis of satellite anisotropy measurements, 30:29533
COSMIC RADIATION/ATOMIC NUMBER
Charge composition of cosmic rays between 4 and 100 GV (Rigidity spectra), 30:30165
COSMIC RADIATION/ENERGY SPECTRA
Pion inclusive distribution at cosmic-ray energies and comparison with ISR data (15 to 240 TeV, production mechanism), 30:30171
Rising inelastic cross-section and the attenuation of cosmic rays nucleons in the atmosphere, 30:30180
COSMIC RADIATION/MODULATION
Galactic cosmic ray modulation in the outer solar system: solar wind consequences, 30:30340 (COM-74-50233)
COSMIC RADIATION/TRANSPORT THEORY
Fokker--Planck coefficient for pitch-angle scattering of cosmic rays (Magnetic field fluctuations), 30:30172
COSMIC RADIO SOURCES
See also H2 REGIONS
PULSARS
QUASARS
RADIO GALAXIES
SUPERNOVA REMNANTS
COSMIC RADIO SOURCES/CARBON MONOXIDE
Observations of galactic carbon monoxide emission at 2.6 millimeters (Visual extinction, excitation temperatures), 30:30265
COSMIC RADIO SOURCES/CHEMICAL COMPOSITION
Detection of interstellar methylamine (Column density), 30:30359
Detection of interstellar methylamine by its $2_{02}+1_{10}$ A/sub a/-state transition (Thermodynamic equilibrium), 30:30360
COSMIC RADIO SOURCES/COORDINATES
Optical identifications from the NRAO 5-GHz radio survey (Quasar-like objects), 30:30282
Optical identifications and radio spectra of sources found by the Michigan 8-GHz survey (Radio analogue), 30:30283
COSMIC RADIO SOURCES/INFRARED RADIATION
An OH survey of the Hoffmann 100-μ sources (Lambda-doublet frequencies), 30:30362
COSMIC RADIO SOURCES/LUMINOSITY
Intense radio sources at 1400 MHz. II. Additions to the BDFL sample (300-foot telescope), 30:30281
COSMIC RADIO SOURCES/OPTICAL PROPERTIES
Possible nature of some unusual OH sources, 30:30273
COSMIC RADIO SOURCES/SPECTRA
High-frequency observations of possible ''heavy-element'' recombination lines (Cosmic value), 30:30267
Identification of some faint radio sources that have flat spectra, 30:30277
COSMIC RADIO SOURCES/VARIATIONS
On the short-timescale variability of OJ 287 (Observational runs, power spectra), 30:30279
COSMIC RADIO SOURCES/WATER VAPOR
First celestial water vapor sources observed at Itapetinga Radio Observatory, Brazil (Reduction in intensity), 30:30287
Further interferometer observations of the water vapor sources in W49 (Geometric sizes), 30:30286
COSMIC RAY DETECTION/DATA PROCESSING
Primary automatic processing algorithms for data obtained at cosmic ray stations, 30:29579
COSMIC RAY DETECTION/GAS SCINTILLATION DETECTORS
Experimental flight of a large spherical gas scintillator, 30:29521
COSMIC RAY DETECTION/IONIZATION CHAMBERS
Neutron supermonitor (Cosmic ray neutron detection), 30:29500
COSMIC RAY DETECTION/NUCLEAR EMULSIONS
Semi-automatic photometer for determining heavy nucleus charges of cosmic rays in nuclear photoemulsion, 30:29501
COSMIC RAY DETECTION/PROPORTIONAL COUNTERS
About the use of proportional counters for registration of cosmic ray meson component, 30:29582
COSMIC RAY DETECTION/TELESCOPE COUNTERS
100-channel scintillation telescope, 30:29578
Diagrams of sensitivity in respect to the zenith angle for scintillation telescopes of arbitrary geometry, 30:29499
Input control of counters CU-51 for assembling azimuthal and calibration telescopes T/SKL and ET/SKL, 30:29583
Spherical harmonic analysis of satellite anisotropy measurements, 30:29533
Telescope with proportional gas-discharge counters for analysis of high-energy cosmic ray variations, 30:29581
COSMIC RAY PROPAGATION
Angular distribution of high energy charged particles in the galaxy, 30:30342 (CONF-730693-)
Cosmic ray diffusion and anisotropy, 30:30167
Galactic electrons and electromagnetic radiation, 30:30343 (CONF-730693-)
COSMIC RAY SPECTROMETERS/DESIGN
The Apollo gamma-ray spectrometer (For mapping lunar surface and measuring cosmic γ spectra), 30:29566
COSMIC X-RAY SOURCES/COORDINATES
X-ray observations of the large magellanic cloud by the Copernicus satellite (Error circle), 30:30365
COSMIC X-RAY SOURCES/EMISSION SPECTRA
Spectroscopic analysis of HZ Herculis (Weak continuum), 30:30270
COSMIC X-RAY SOURCES/GAMMA RADIATION
Absorption of gamma rays in intense x-ray sources, 30:30290
COSMIC X-RAY SOURCES/HARD X RADIATION
Simultaneous hard X-ray and optical observations of Sco X-1 and a model of semi-opaque X-ray sources, 30:30294
COSMIC X-RAY SOURCES/LUMINOSITY
A model for the transient x-ray sources (Shell flash, thermonuclear shell flash), 30:30269
COSMIC X-RAY SOURCES/PHOTOMETRY
Color variations of Scorpius X-1 (Absolute flux calibration), 30:30271
Optical studies of Uhuru sources. VIII. Observations of 92 possible counterparts of x-ray sources, 30:30205
COSMIC X-RAY SOURCES/POLARIZATION
Further observations for circularly polarized radiation from white dwarfs and x-ray sources (Negative results), 30:30218
COSMIC X-RAY SOURCES/PULSES
4.8-second pulsed x-rays from Centaurus X-3 at energy greater than 7 keV (Duty cycle, OSO-7 satellite), 30:30268
COSMIC X-RAY SOURCES/RADIOWAVE RADIATION
Daily observations of Cygnus X-3 at 10.5 at GHz during the period 1973 July-October (Major outburst), 30:30292
COSMIC X-RAY SOURCES/SPATIAL DISTRIBUTION
A search for a cosmological component of the soft X-ray background in the direction of M31 (Alternative interpretations, intergalactic medium), 30:30174
COSMIC X-RAY SOURCES/SPECTRA
H alpha emission in Cygnus X-1 (Optical primary, mass-loss), 30:30291
COSMIC X-RAY SOURCES/SUPERNOVAE
Limit on X-ray emission from a supernova during maximum light (Optical rise, observation time), 30:30260
COSMIC X-RAY SOURCES/VARIATIONS
Color variations of Scorpius X-1 (Absolute flux calibration), 30:30271
COSMIC X-RAY SOURCES/VISIBLE RADIATION
Search for optical pulsations from Cen X--3, 30:30288
COSMOLOGY
Scalar waves in the mixmaster universe. II. Particle creation (Heisenberg picture, Bogolyubov transformation), 30:30391
COSMOLOGY/CP INVARIANCE
Spontaneous CP-violation and cosmology, 30:30770
COSMOLOGY/GALAXIES
Electrically charged galaxy and its internal and cosmological consequences, 30:30341 (CONF-730693-)
COSMOLOGY/GALAXY CLUSTERS
The density profiles of rich clusters of galaxies (Cutoff radius), 30:30381
COSMOS
See UNIVERSE
COULOMB EXCITATION/GAMMA SPECTRA
Doppler shape of a γ-line in Coulomb excitation, 30:31100
COULOMB SCATTERING/S MATRIX
Coulomb T-matrix in the Glauber approximation in the presence of a low frequency electromagnetic field, 30:30790
COULOMB SCATTERING/SCATTERING AMPLITUDES
Time-independent multichannel scattering theory for charged particles, 30:30656
COULOMETRY
See VOLTAMETRY
COUNTERS (RADIATION)
See RADIATION DETECTORS
COUNTING CIRCUITS/DEAD TIME
Dead-time calibrator, 30:29529
COUPLED CHANNEL BORN APPROXIMATION/DEUTERON REACTIONS
The coupled-channel Born approximation and J-dependence in ^{30}Si(d,p)^{31}Si (Angular distributions), 30:30907
COW-MILKERS
See RADIOISOTOPE GENERATORS
COWS/RADIONUCLIDE KINETICS
Absorption, distribution, and excretion of plutonium by dairy cattle (^{238}Pu tracer), 30:29810 (NVO-AEIC-74-1)

CP INVARIANCE/COSMOLOGY
Spontaneous CP-violation and cosmology, 30:30770
CP INVARIANCE/KAONS NEUTRAL LONG-LIVED
Observation of the decay K/subL/^{0} → $\pi^+\pi^-\gamma$, 30:30582
CP INVARIANCE/SYMMETRY BREAKING
Spontaneous CP violation in the generalized Georgi--Glashow model (Coupling, lagrangian function), 30:30773
CRAB NEBULA/X-RAY SPECTRA
The Crab Nebula as a calibration source for x-ray astronomy (Diffuse component), 30:30280
CRACKS/MEASURING METHODS
Design of a passive crack detector system (Measurement of neutron-induced cracks), 30:29297 (UCID-15867)
CRBR REACTOR
See CLINCH RIVER BREEDER REACTOR
CREPIS/BIOLOGICAL RADIATION EFFECTS
Chromosomal aberrations induced by gamma irradiation of Crepis capillaris seedlings at different periods of interphase, 30:29696
Dose-response for frequency of chromatid aberrations induced by x rays at G_2 and S stages of the mitotic cycle in Crepis capillaris root tips, 30:29697
CRICETULUS
See HAMSTERS
CRITICALITY ACCIDENTS
See RADIATION ACCIDENTS
CRYOGENIC BUBBLE CHAMBERS/COOLING
Refrigerating systems for the big CERN bubble chamber, 30:29576
CRYOGENICS
Energy and cryoengineering, 30:31324 (LA-UR-74-741)
CRYOGENICS/MEETINGS
Cryotech '73: the production and use of industrial gases. Proceedings of the British Cryogenics Council conference, Brighton, England, November 13--15, 1973, 30:28992
CULTURE MEDIA/CHEMICAL RADIATION EFFECTS
Insensitivity of serially transferred Tetrahymena pyriformis W. to irradiated media, 30:29767
CURIUM 243/BIOLOGICAL RADIATION EFFECTS
Early hematologic effects of curium and einsteinium in beagles, 30:29779 (COO-119-249)
CURIUM 243/TISSUE DISTRIBUTION
Transuranium elements in gonadal tissue (^{239}Pu, ^{241}Am, ^{243}Cm, ^{244}Cm, ^{249}Cf, and ^{252}Cf), 30:29806 (COO-119-249)
CURIUM 244/ALPHA SPECTROSCOPY
Simultaneous determination of alpha-emitting nuclides of radium through californium in soil, 30:28977
CURIUM 244/BIOLOGICAL RADIATION EFFECTS
Early hematologic effects of curium and einsteinium in beagles, 30:29779 (COO-119-249)
CURIUM 244/RADIOISOTOPE HEAT SOURCES
10% efficient economic RTG design, 30:29251
Cost effective designing for the economic RTG, 30:29252
Modular heat source for ^{244}Cm and ^{238}Pu, 30:29245
CURIUM 244/TISSUE DISTRIBUTION
Transuranium elements in gonadal tissue (^{239}Pu, ^{241}Am, ^{243}Cm, ^{244}Cm, ^{249}Cf, and ^{252}Cf), 30:29806 (COO-119-249)
CURRENT ALGEBRA
See also NEUTRAL CURRENTS
SYMMETRY GROUPS
Old and new ideas about currents and their commutators (Lectures), 30:30640
CURRENT ALGEBRA/CONFIGURATION MIXING
Kinematical origin of the configuration mixing in the chiral algebra, 30:30719
CURRENT ALGEBRA/VECTOR CURRENTS
Possible representations of local current algebra, 30:30635
CURRENT COMMUTATORS
(For operators in current algebra; for electric circuitry see SWITCHES.)
Old and new ideas about currents and their commutators (Lectures), 30:30640
CUTTING TOOLS/DESIGN
Blade-type metal-cutting tool for quick removal of stock in roughing work, 30:29269 (UCID-15833)
CYANIDES/ELECTRON-ION COLLISIONS
Experimental investigation of the effective cross section of excitations of bands of some decay products of water, ammonia, and acetonitrile by slow electrons, 30:30546
CYANOCOBALAMIN
See VITAMIN B-12
CYCLES (THERMODYNAMIC)
See THERMODYNAMIC CYCLES
CYCLIC ADENOSINE MONOPHOSPHATE
See AMP
CYCLOALKANES
See also CYCLOHEXANE
CYCLOALKANES/RADIOLYSIS
Measurements by fluorocarbon dosimetry, 30:29544 (DEMO-74/5)
CYCLOHEXANE/RADIOLYSIS
Measurements with cyclohexane dosimeters, 30:29549 (DEMO-74/5)
CYTOCHROMES
Specificity and frequency of ultraviolet-induced reversion of an iso-1-cytochrome c ochre mutant in radiation-sensitive strains of yeast, 30:29683
CYTOSINE/RADIOSENSITIVITY EFFECTS
Experimental usage of cysteine in radiation therapy (Radioprotective effects), 30:29722
CZECHOSLOVAKIA/NUCLEAR POWER PLANTS
Progress on Czechoslovak Nuclear Power Plants, 30:31185 (JPRS-61338)
CZECHOSLOVAKIA/RADIOACTIVE WASTE STORAGE
Current storage possibilities of blocks with solidified radioactive wastes at the Institute of Nuclear Research, 30:29137

D

D REGION/SUDDEN IONOSPHERIC DISTURBANCE
Satellite measurements of solar x-ray flux and ground observations of sudden ionospheric disturbances, 30:30413
DATA ACQUISITION SYSTEMS
See also CAMAC SYSTEM
Simple device using capacitance switches for data entry in man--machine systems, 30:29620
DATA PROCESSING
Application of a computer-simulated Perceptron to a complex photographic scene, 30:31433 (UCID-15373)
Energy minimization method for computer deconvolution, 30:31354 (UCID-15947)
DATA PROCESSING/COMPUTER CODES
Programs for experimental data processing on PDP-8/I computer, 30:29614 (IFA-CRD-57-1974)
DATA STORAGE DEVICES
See MEMORY DEVICES
DAYGLOW
See AIRGLOW
DECALSO
See ION EXCHANGE MATERIALS
DECARBOXYLASE/BIOCHEMICAL REACTION KINETICS
Aromatic amino acid decarboxylase activity of rat brain and its parts following exposure to ionizing radiation (X radiation), 30:29740
DEFORMED NUCLEI/DEUTERON REACTIONS
One- and two-nucleon transfer reactions on deformed nuclei (Generalized optical model; DWBA, coupled-channels and adiabatic theory), 30:31021 (IFA-FT-108-1974)
DEFORMED NUCLEI/EXCITED STATES
Are there low-lying, intrashell-excited, highly deformed states in the 1f-2p shell nuclei, 30:30925
DEFORMED NUCLEI/PROTON REACTIONS
One- and two-nucleon transfer reactions on deformed nuclei (Generalized optical model; DWBA, coupled-channels and adiabatic theory), 30:31021 (IFA-FT-108-1974)
DEFORMED NUCLEI/ROTATIONAL STATES
Analysis of rotational and quasirotational ground-state bands in even--even nuclei, 30:30957
DELAYED NEUTRONS/ENERGY SPECTRA
Energy measurements of delayed neutron groups from ^{235}U, 30:31014
DEMOCRITUS REACTOR/DESIGN
Description of the Greek Research Reactor-1, 30:31230 (DEMO-74/5)
DENSIMETERS/DATA PROCESSING
Approximation for time relationships in pulsed gamma--gamma logging, 30:29605
DENTISTRY/RADIATION DOSES
Radiation characteristics and controls. I (Radiation protection of dental patients and personnel), 30:29709
DEOXYPENTOSE NUCLEIC ACID
See DNA
DEOXYRIBONUCLEIC ACID
See DNA
DEPLETED URANIUM
Metallurgical processing and pulsed reactor fuel performance, 30:29982 (SLA-73-1121)
DESALINATION/ECONOMICS
Long term investment considerations of conjunctive desalting systems, 30:31309
DESALINATION/SEAWATER
Long term investment considerations of conjunctive desalting systems, 30:31309
DESALINATION REACTORS/ECONOMICS
Long term investment considerations of conjunctive desalting systems, 30:31309
DESALINATION REACTORS/SEAWATER
Long term investment considerations of conjunctive desalting systems, 30:31309
DESOXYRIBONUCLEIC ACID
See DNA
DETECTORS (RADIATION)
See RADIATION DETECTORS
DETONATION WAVES
See SHOCK WAVES
DETONATIONS
Kinetics of energy release of heterogeneous high explosives, 30:31408 (UCID-15962)

DEUTERIUM/ATOM-MOLECULE COLLISIONS
Angular distributions for the reactive scattering of H and D atoms by polyatomic molecules, 30:30519 (AED-CONF-74-085-004)
Integral equation approach to collinear reactive scattering: A+BC→AB+C (Reaction of H, D, and F with H_2), 30:30527
DEUTERIUM/COSMOCHEMISTRY
A galactic model with a pulsating active nucleus. III. Evolution of rare-light elements, 30:30386
DEUTERIUM/HOT ATOM CHEMISTRY
Trajectory studies of hot atom reactions. II. An unrestricted potential for CH_4, 30:29085
DEUTERIUM/ISOTOPE EFFECTS
Acylal hydrolysis. The hydrolysis of 3-(p-nitrophenoxy)phthalide, α-acetoxybenzyl p-nitrophenyl ether, and 3-(para-substituted thiophenyl)phthalides, 30:29017
Deuterium isotope effects in deuterated styrenes, 30:29022
Do SN2 reactions go through ion pairs. The isotope effect criterion, 30:29010
Entropic control of photochemical reactivity. The transition state for γ-hydrogen abstraction of alkyl phenyl ketones, 30:29018
Excess energy dependence of radiationless transitions in naphthalene vapor: competition between internal conversion and intersystem crossing, 30:29016
Hydrogenation and deuteration of olefins in the presence of cobalt triethylaluminum-bis(acetylacetonate), 30:29012
Isotope effects on partition functions and thermodynamic quantities of the stable diatomic hydrides, 30:29020
Isotope effect in the superconducting palladium--hydrogen--deuterium system, 30:30813
Kinetics of the selective hydrogenation of dimethylethynylcarbinol over palladium in the vapor phase. II. Reaction between dimethylethynylcarbinol and deuterium and the kinetic isotopic effect, 30:29011
Moessbauer effect study of the deuterated and hydrogenated hydrates of ferrous chloride, 30:29009
Secondary deuterium isotope effect in the cycloaddition of dimethylketen to styrene, 30:29021
Secondary deuterium isotope effects in proton transfers from 2-nitropropane, 30:29023
Trapped electrons in C_2H_5OD glasses γ-irradiated at 4°K, 30:29068
Vibrational relaxation of HF(v=1) and DF(v=1) by H_2 and D_2, 30:29019
^{67}Zn NMR anomalous solvent isotope effect in aqueous solutions (Heavy water or water), 30:29014
DEUTERIUM/ISOTOPIC EXCHANGE
Investigations of hydrogen--deuterium exchange in α-chymotrypsin, 30:29033
Isotopic study of water gas reaction catalyzed by platinum, 30:29032
DEUTERIUM/KAON REACTIONS
A measurement of K*(1420) decay branching ratios, 30:30624
DEUTERIUM/MOLECULE-MOLECULE COLLISIONS
Vibrational relaxation of D_2 in the range 400-50°K, 30:30508
DEUTERIUM/NEUTRON REACTIONS
Neutron-deuteron differential cross section at 26.5 MeV, 30:30873
DEUTERIUM/PION REACTIONS
The πd scattering length from Ksub(α) X-rays, 30:30620
DEUTERIUM/PROTON REACTIONS
D(p,2p)n reaction (6 to 11.6 MeV: cross sections, spectra, separable-potential model with Yamaguchi form factors), 30:30855 (NP-20122)
On proton-deuteron backward elastic scattering at medium energies (Cross sections), 30:30867
Population of muonic ^{3}He states following the μ-catalysed fusion pμd→μ^{3}He, 30:30515
The deuteron breakup reaction induced by protons of 65, 85 and 100 MeV (Spectra, angular distributions), 30:30872
DEUTERIUM/SULFUR 32 REACTIONS
Precision lifetime measurement with the coincident high-velocity DSA method, 30:30864
DEUTERIUM/WAVE FUNCTIONS
Approximate D-states and meson exchange currents, 30:30870
DEUTERIUM COMPOUNDS/EMISSION SPECTRA
Intensities of the dipole and quadrupole rotation-vibration spectra of HD, 30:30501
DEUTERIUM IONS/ION-ATOM COLLISIONS
Argon L-shell ionization by 50- to 600-keV H^+, D^+, H_2^+, and He^+ impact (Branching ratios, excitation, multiple-vacancy states, total cross sections, ionization), 30:30541
High-energy calculation of K-shell ejection cross sections as a function of projectile charge (Born approximation), 30:30536
DEUTERON REACTIONS/BREAKUP REACTIONS
Deuteron break-up and proton scattering on ^{58}Ni, 30:30926
Qualitative features of Pauli break-up from the configuration space viewpoint, 30:31089
Quasi-free contributions in the d+^{6}Li reactions at low energies, 30:30882
DEUTERON REACTIONS/COMPOUND-NUCLEUS REACTIONS
Gamma spectra from ^{179}Hf (d,2n), ^{179}Hf (p,n), and ^{181}Ta (α,2n) reactions, 30:30994
The magnitude of compound nucleus effects in Ca(d,p) reactions (1ν MeV: angular distributions, reaction mechanisms; spectroscopic factors), 30:30923
DEUTERON REACTIONS/DIFFRACTION MODELS
The diffraction dissociation of deuterons on the diffused edge nuclei (Cross sections), 30:31072
DEUTERON REACTIONS/ELASTIC SCATTERING
Optical model and DWBA analysis of the ^{7}Li(d,d)- and ^{7}Li(d,p_0)-reactions in the energy region 1.0 to 2.6 MeV, 30:30883
DEUTERON REACTIONS/EXCITATION FUNCTIONS
Q-values and excitation functions of nuclear reactions. Part C. Estimation of unknown excitation functions and thick target yields for p, d, ^{3}He, and α reactions (Up to 25 or 35 MeV), 30:30960
DEUTERON REACTIONS/ONE-NUCLEON TRANSFER REACTIONS
One- and two-nucleon transfer reactions on deformed nuclei (Generalized optical model; DWBA, coupled-channels and adiabatic theory), 30:31021 (IFA-FT-108-1974)
One-nucleon transfer reactions in deformed nuclei (Indirect inelastic transitions through intermediate rotational states included), 30:30995
DEUTERON REACTIONS/PICKUP REACTIONS
1p hole-states in ^{15}O and ^{15}N and the mass dependence of the 1p spin-orbit splitting (Spectroscopic factors), 30:30886
DWBA and CCBA analysis of selected transitions in the ^{12}C(d,tau)^{11}B reaction at Esub(d) = 80MeV (Angular distribution), 30:30900
Proton-hole states in ^{115}In observed in the ^{116}Sn(d,^{3}He) reaction (50 MeV: angular distributions, DWBA; S), 30:30975
DEUTERON REACTIONS/STRIPPING
Correlations between (n,γ) and (d,p) reactions on N = 82 nuclei (Excitation strengths), 30:30970
Influence of core excitations on the deuteron stripping reaction with the method of many-body Green functions, 30:31027
Neutrons from the 2MeV deuteron bombardment of thick ^{7}Li targets, 30:30146
Optical model and DWBA analysis of the ^{7}Li(d,d)- and ^{7}Li(d,p_0)-reactions in the energy region 1.0 to 2.6 MeV, 30:30883
The coupled-channel Born approximation and J-dependence in ^{30}Si(d,p)^{31}Si (Angular distributions), 30:30907
The magnitude of compound nucleus effects in Ca(d,p) reactions (1ν MeV: angular distributions, reaction mechanisms; spectroscopic factors), 30:30923
The treatment of two particles in the continuum in a Green's function theory of the (d,p)-reaction, 30:31083
Transparency to vector polarization transfer in deuteron stripping reactions, 30:31096
DEUTERONS/BINDING ENERGY
New determination of Mongan's non-local separable potentials for nuclear structure calculations, 30:31036
DEUTERONS/ENERGY LOSSES
Energy dispersion of deuterons during their passage through matter. Influence of the state of the surface, 30:31122
DEUTERONS/STRUCTURE FUNCTIONS
Muon-deuteron deep inelastic scattering, 30:30584
DEUTERONS/WAVE FUNCTIONS
Triton binding energy and the deuteron wave function, 30:30862
DIAMAGNETISM
Landau diamagnetism, 30:31421 (IFA-FT-109-1974)
DIELECTRIC TRACK DETECTORS
Effect of electrons and λ-rays on alpha-particle registration in T-Cellit detector, 30:29527
Use of particle track detectors in the investigation of static reactor parameters, 30:29507
DIELECTRIC TRACK DETECTORS/ENERGY RESOLUTION
Energy spectrometry of protons by means of a dielectric track detector, 30:29569
DIELECTRIC TRACK DETECTORS/ETCHING
The etching of cellulose nitrate plastic, 30:29532
DIELECTRIC TRACK DETECTORS/LATENT IMAGES
Latent fading in solid-state track etching detectors, 30:29522
DIELECTRIC TRACK DETECTORS/PARTICLE TRACKS
Further measurement of the track lengths of heavy ions in mica, 30:29525
DIELECTRIC TRACK DETECTORS/PERFORMANCE
Discrimination of neutron energies with the aid of the nuclear track method (Using (n,α) converters), 30:29554
Fast-neutron personnel dosimetry with solid-state track recorders, 30:29557
Passive environmental neutron dosimeter (Polyethylene-moderated fission foil--dielectric track detector system), 30:29551 (LA-UR-74-1232)
DIETHYLENETRIAMINEPENTAACETIC ACID
See DTPA
DIFFERENTIAL EQUATIONS
See also DIRAC EQUATION
FOKKER-PLANCK EQUATION
KLEIN-GORDON EQUATION
POISSON EQUATION
SCHROEDINGER EQUATION

DIFFERENTIAL EQUATIONS/NUMERICAL SOLUTION
Introduction to extrapolation methods for the numerical solution of differential equations, 30:31355 (UCID-15992)
Second-order difference equations for a non-uniform triangle mesh, 30:31347 (UCID-15388)
Stiffness and non-stiff differential equation solvers, 30:31345 (SAND-74-5236)
DIFFRACTION MODELS/HADRON REACTIONS
Diffractive production off nuclei: shadow of hadronic bremsstranlung, 30:31062
DIFFRACTION MODELS/IMPACT PARAMETER
An impact parameter description of single and double diffraction dissociation, 30:30761
DIFFRACTION MODELS/PROTON REACTIONS
Some analogy of the nuclear and nucleon fragmentation processes, 30:30755
DIFFRACTION MODELS/PROTON-PROTON INTERACTIONS
Scaling of multiplicity distribution in hadron collisions and diffractive-excitation like models, 30:30758
Some analogy of the nuclear and nucleon fragmentation processes, 30:30755
DIGITAL-TO-ANALOG CONVERTERS/CAMAC SYSTEM
Logarithmic digital-analog conversion for varying parameters in Camac devices, 30:29630
DIGITIZERS
MAPEDIT system for automatic map digitization, 30:31341 (LBL-3072)
DIMERCAPTOETHANE
See DITHIOLS
DIMETHYLKETONE
See ACETONE
DIRAC EQUATION/ENERGY
Some forgotten terms of the Dirac--Breit--Pauli equation, 30:31138
DIRECT ENERGY CONVERTERS
See also BETAVOLTAIC CELLS
SOLAR CELLS
THERMOELECTRIC GENERATORS
DIRECT ENERGY CONVERTERS/MAGNETIC MIRRORS
Preliminary report of direct recovery study, 30:29217 (UCID-15650)
DIRECT REACTIONS/NUCLEAR REACTIONS
Mechanism of neavy ion collisions leading to a compound system and to deep inelastic direct reactions, 30:31065
DISTORTED WAVE BORN APPROXIMATION
See DWBA
DISTRICT HEATING
Nuclear district-heating and nuclear long-distance energy, 30:31305 (JUL-1077)
DISTURBANCES/ASYMPTOTIC SOLUTIONS
Connection between singular perturbations and singular arcs. Part 2. A theory for the linear regulator, 30:31336 (COO-3077-44)
DITHIOLS/RADIOSENSITIVITY EFFECTS
Effect of x rays on the phosphorylation of histon f_1 in thymocytes, 30:29653
DIVERTORS/MATHEMATICAL MODELS
Bundle divertors and topology, 30:29204 (CLM-R-132)
DNA
(Deoxyribonucleic acid.)
DNA/BIOLOGICAL RADIATION EFFECTS
Postirradiation fate of bacteriophage lambda DNA in the host cell (Escherichia coli), 30:29678
Unique forms of fast-sedimenting BU lambda DNA in a superinfected E. coli lysogen (Ultraviolet radiation), 30:29652
DNA/BIOLOGICAL REPAIR
Autoradiographic studies of DNA-repair in the retina of rabbits (Gamma radiation), 30:29755
Changes in genetic cell material during the action of ionizing radiation (Effects of uv and x radiation on DNA and nucleoproteins), 30:29655
Radiation-induced DNA synthesis in normal and stimulated human lymphocytes (Ultraviolet radiation), 30:29664
DNA/BIOSYNTHESIS
Dissociation of histone and DNA synthesis in x-irradiated HeLa cells (Ultraviolet radiation), 30:29666
Dissociation of histone and DNA synthesis in x-irradiated HeLa cells, 30:29671
Histone F1 phosphorus content and DNA synthesis in slowly-growing sublines of L5178Y-S cells, 30:29669
DNA/CHEMICAL RADIATION EFFECTS
Structural study of DNA discontinuities by enzymatic polymerization (γ radiation), 30:29650 (JEN-286)
Structure disarrangement caused in γ-irradiated DNA in vitro, 30:29036
DNA/RADIATION INJURIES
Base-pair deletion at a frameshift notspot in Salmonella (X rays), 30:29684
ESR studies of radiation damage in nucleic acids, bases, nucleosides, and nucleotides (Review), 30:29656
DNA/RADIOLYSIS
Applying statistics to analysis of corrosion data (Gamma radiation), 30:29056
Long-lived radiation-induced free radicals in anoxic wet DNA as studied by electron spin resonance spectroscopy, 30:29064
Radiation chemistry of DNA-model compounds. V. Phosphate elimination from ribose-5-phosphate after OH radical attack at C4 (γ radiation), 30:29071
Radiomimeticity of the system H_2O_2/Fe(II) on nucleic acid components. Kinetic study, 30:29649 (JEN-284)
DNA/STRAND BREAKS
Chemical nature of the ends of DNA single-strand breaks produced by ionizing γ radiation in vivo and pathways of their reparation (Escherichia coli), 30:29682
Comment on ''further data on DNA strand breakage by various radiation qualities'' (γ radiation. protons), 30:29660
DNA repair in human progeroid cells (Gamma radiation), 30:29673
Rate of DNA repair in progeric and normal human fibroblasts (Gamma radiation, Hutchinson--Gilford syndrome), 30:29672
Repair of γ-ray-induced damage in bacteriophage lambda (Escherichia coli), 30:29680
DNA REPLICATION/BIOLOGICAL RADIATION EFFECTS
Mechanisms of inhibition of the postirradiation recovery in cells. IV. The effect of caffeine and acriflavine on gamma and x-ray induced unscheduled DNA synthesis in HeLa Zh-63 cells, 30:29675
DOPPLER EFFECT/RELATIVITY THEORY
Classical and relativistic Doppler effects, 30:31143 (INIS-mf-1357)
DOSE FRACTIONATION
See FRACTIONATED IRRADIATION
DRESDEN-1 REACTOR/REACTOR OPERATION
Semiannual report, January--June 1974, 30:31311 (DOCKET-50010-305)
DRESDEN-2 REACTOR/REACTOR OPERATION
Semiannual report, January--June 1974, 30:31311 (DOCKET-50010-305)
DRESDEN-3 REACTOR/REACTOR OPERATION
Semiannual report, January--June 1974, 30:31311 (DOCKET-50010-305)
DRINKING WATER/RADIATION MONITORING
Data. Section II. Water, 30:29411
DROPLETS/FREEZING
Effects of radioactivity on ice nucleation, 30:29367 (BNWL-1850(Pt.3))
DRUGS
See also ANTIBIOTICS
CAFFEINE
RADIOPHARMACEUTICALS
RADIOPROTECTIVE SUBSTANCES
RADIOSENSITIZERS
DRUGS/CARCINOGENESIS
Systematics of iatrogenic carcinogenesis, 30:29724
DTPA/TOXICITY
Effects of DTPA on tissue cultured fibroblasts (Toxicity of Ca-DTPA and Zn-DTP), 30:29807 (COO-119-249)
Evaluation of long-term ZnDTPA therapy in beagles (Toxicity of ZnDTPA during prolonged chelation treatment for removal of ^{241}Am), 30:29796 (COO-119-249)
DUAL ABSORPTION MODEL/PION-NUCLEON INTERACTIONS
N and π exchange amplitudes in πN backward scattering, 30:30744
DUAL RESONANCE MODEL/MANDELSTAM REPRESENTATION
Generalization of Regge-behaved DAMA to production processes, 30:30694
DUAL RESONANCE MODEL/SYMMETRY BREAKING
Spontaneous symmetry breakdown and Regge intercepts (Higgs mechanism), 30:30707
DUANE ARNOLD-1 REACTOR/REACTOR OPERATION
Semiannual operating report, February 22--June 30, 1974, 30:31318 (DOCKET-50331-277)
DUODENUM
See SMALL INTESTINE
DUOPLASMATRONS/OPTIMIZATION
The production of multicharged ions with a duoplasmatron ion source in high-current continuous operation, 30:30475 (GSI-A1-74)
DUOPLASMATRONS/PERFORMANCE
The production of multicharged ions with a duoplasmatron ion source in high-current continuous operation, 30:30475 (GSI-A1-74)
DUOPLASMATRONS/SPECIFICATIONS
The production of multicharged ions with a duoplasmatron ion source in high-current continuous operation, 30:30475 (GSI-A1-74)
DUSTS
See also COSMIC DUST
DUSTS/DIFFUSION
Fast response light scattering measurements of the characteristics of wind suspended aerosols (Dust suspension by winds), 30:29490 (UCRL-76014(Rev.1))
Ground level air concentrations of dust particles downwind from a tailings area during a typical windstorm (Mathematical model), 30:29380 (ORNL-TM-4375)
Regional wind resuspension of dust, 30:29373 (BNWL-1850(Pt.3))
DWARF STARS
See also RED DWARF STARS
WHITE DWARF STARS
DWARF STARS/CHEMICAL COMPOSITION
The composition of RR Lyrae stars (Metal rich), 30:30191
DWARF STARS/LUMINOSITY
Luminosities and temperatures of M dwarf stars from infrared photometry (Intrinsically faint), 30:30222

DWARF STARS/PHOTOMETRY
  Ultraviolet photometry from the orbiting astronomical observatory. XVI. The stellar Lyman-Alpha absorption line (Upper limits), 30:30251
DWARF STARS/SPECTRA
  Spectroscopic observations of interesting Southern stars noted on southern objective-prism plates (R coronae borealis stars), 30:30253
DWBA
  (Distorted wave born approximation.)
  Importance of Coulomb interaction potentials in heavy ion DWBA calculations, 30:31063
DYNAMICS
  See MECHANICS
DYSON REPRESENTATION/GREEN FUNCTION
  Selfconsistent calculation of the Green's functions in the Hubbard model, 30:31132 (JINR-P4-7225)
DYSPROSIUM/ACTIVATION ANALYSIS
  Determination of rare earths and thorium in apatites by thermal and epithermal neutron-activation analysis, 30:28935
DYSPROSIUM/EXTRACTION CHROMATOGRAPHY
  Contribution to the separation of rare earths by extraction chromatography with di(2-ethylhexyl) phosphoric acid. II. Behavior of the matrix and its influence on the microcomponents, 30:28990 (ANL-Trans-961)
DYSPROSIUM/THERMAL EXPANSION
  Anomaly of thermal expansion of dysprosium close to the ferromagnetic transition point (Hysteresis; 80°K), 30:30032
DYSPROSIUM/X-RAY SPECTROSCOPY
  Determination of rare earths in plutonium by x-ray emission analysis, 30:28946
DYSPROSIUM 157/ENERGY-LEVEL TRANSITIONS
  Electromagnetic transitions in some odd-neutron deformed nuclei (Lifetimes, transition probabilities in Nilsson model with pairing and band mixing), 30:30990
DYSPROSIUM 159/ENERGY-LEVEL TRANSITIONS
  Electromagnetic transitions in some odd-neutron deformed nuclei (Lifetimes, transition probabilities in Nilsson model with pairing and band mixing), 30:30990
DYSPROSIUM 160/NEUTRON REACTIONS
  Mass-spectrometric determination of neutron capture cross-sections of the rare earth isotopes (Pile and thermal cross sections), 30:30977 (AEC-tr-7574)
DYSPROSIUM 161/NEUTRON REACTIONS
  Mass-spectrometric determination of neutron capture cross-sections of the rare earth isotopes (Pile and thermal cross sections), 30:30977 (AEC-tr-7574)
DYSPROSIUM 162/NEUTRON REACTIONS
  Mass-spectrometric determination of neutron capture cross-sections of the rare earth isotopes (Pile and thermal cross sections), 30:30977 (AEC-tr-7574)
DYSPROSIUM 163/NEUTRON REACTIONS
  Mass-spectrometric determination of neutron capture cross-sections of the rare earth isotopes (Pile and thermal cross sections), 30:30977 (AEC-tr-7574)

E

E LAYER
  See E REGION
E REGION/ELECTRON DENSITY
  Routine operation of Digisonde at Maynard, Massachusetts. Final report, 1 September 1971--31 August 1972, 30:30410 (AD-776969)
E REGION/LAYERS
  Ion layer formation by uniform neutral winds in the nighttime E region, 30:30436
EARTH ATMOSPHERE
  See also AIR
    IONOSPHERE
    MAGNETOSPHERE
    SURFACE AIR
    THERMOSPHERE
    TROPOSPHERE
  Development of an air pollution model for the San Francisco Bay Area. Second semiannual report to the National Science Foundation, 30:31363 (UCRL-51537)
  Relation between washout of radioactivity and nonradioactive ions in the atmosphere by precipitation, 30:29395
EARTH ATMOSPHERE/AIR POLLUTION
  Douglas United Nuclear, Inc. reactor and fuel production facilities 1972 environmental release report, 30:29341 (DUN-8133)
  Trace pollutant emissions in fossil fuel combustion, 30:29469 (BNWL-1850(Pt.3))
EARTH ATMOSPHERE/CONTAMINATION
  Douglas United Nuclear, Inc. reactor and fuel production facilities 1972 environmental release report, 30:29341 (DUN-8133)
  Formation of secondary aerosols in the atmosphere after ventilated underground nuclear explosions, 30:29390
  Hot aerosol particles during commercial use of atomic energy (Book in Russian), 30:29344
  Mesoscale transport and diffusion studies, 30:29435 (BNWL-1850(Pt.3))
  Numerical prediction of the mesoscale transport of atmospheric effluents: philosophy and morphology of experimental models for predicting the wind and potential radiological fields over the Nevada Test Site, 30:29377 (COM-74-10799)
  Regional wind resuspension of dust, 30:29373 (BNWL-1850(Pt.3))
EARTH ATMOSPHERE/DIFFUSION
  Comparison of diffusion-deposition model components with experimental results, 30:29434 (BNWL-1850(Pt.3))
  Dependence of site evaluation of roughness length and displacement length on value chosen for Von Karman's constant, 30:29432 (BNWL-1850(Pt.3))
  Evaluation of an airborne fluorescent particle counter for atmospheric tracer studies, 30:29610 (BNWL-1850(Pt.3))
  Fitting an analytical curve to some experimental diffusion data, 30:29426 (BNWL-1850(Pt.3))
  Real-time system for detection of the atmospheric tracer sulfur hexafluoride, 30:29611 (BNWL-1850(Pt.3))
  Surface flux model for diffusion, deposition, and resuspension, 30:29470 (BNWL-1850(Pt.3))
EARTH ATMOSPHERE/ELECTRIC FIELDS
  Local changes of the atmospheric electric field by EAS ionization, 30:30414
EARTH ATMOSPHERE/FALLOUT
  Radionuclide concentration minimums from 6 to 9 km, 30:29368 (BNWL-1850(Pt.3))
EARTH ATMOSPHERE/GRAVITATION
  Calculation of the lunar diurnal atmospheric tide, 30:30446
EARTH ATMOSPHERE/IONIZATION
  Local changes of the atmospheric electric field by EAS ionization, 30:30414
EARTH ATMOSPHERE/PRECIPITATION SCAVENGING
  Potential application of atomic absorption and anodic stripping voltammetry to the precipitation scavenging program, 30:28937 (BNWL-1850(Pt.3))
EARTH ATMOSPHERE/RADIATION MONITORING
  Long-lived radon daughters as atmospheric radioactive tracers, 30:29400
EARTH ATMOSPHERE/RADIOACTIVE AEROSOLS
  Particle size distributions of manmade and natural radionuclides, 30:29360 (BNWL-1850(Pt.3))
  Washout of radioactive impurities from the atmosphere in the Central Caucasus mountains, 30:29385
  Wet and dry atmospheric removal processes for radioiodine, 30:29365 (BNWL-1850(Pt.3))
EARTH ATMOSPHERE/TEMPERATURE DISTRIBUTION
  Method for determining Monin--Obukhov L's from profiles of subjectively estimated mean wind speeds and temperatures, 30:29431 (BNWL-1850(Pt.3))
EARTH ATMOSPHERE/THERMAL POLLUTION
  Physical--chemical effects of cooling systems and thermal discharges on the environment, 30:29465
EARTH ATMOSPHERE/TURBULENCE
  Micro- and macroturbulence, 30:31358 (ORNL-tr-2801)
  Power spectral analysis of two periods of turbulence data for very stable conditions, 30:29433 (BNWL-1850(Pt.3))
EARTH ATMOSPHERE/WIND
  Estimation of mean crosswind concentration profiles from ''instantaneous'' crosswind traverses (^{85}Kr tracer studies), 30:29424 (BNWL-1850(Pt.3))
  Method for determining Monin--Obukhov L's from profiles of subjectively estimated mean wind speeds and temperatures, 30:29431 (BNWL-1850(Pt.3))
EARTH PLANET/EQUILIBRIUM
  The equilibrium of a rotating body of arbitrary density, 30:30408
EARTHQUAKES/SEISMIC DETECTION
  Extended array evaluation program. Special report No. 5. Selection of reference waveforms for matched filter processing of long period signals from seismic events, 30:29304 (AD-776815)
  Extended array evaluation program. Quarterly report No. 6, 1 July--30 September 1973, 30:29306 (AD-777315)
  Regional attenuation of short-period P and S waves in the United States, 30:29303 (AD-776672)
  Seismic discrimination. Semiannual technical summary report, 1 July--31 December 1973, 30:29305 (AD-777151)
ECCS
  (Emergency core cooling system.)
ECCS/PERFORMANCE
  Problems of emergency core cooling system (PWR and BWR), 30:31191
ECOLOGICAL COMMUNITIES
  See ECOSYSTEMS
ECOSYSTEMS
  See also AQUATIC ECOSYSTEMS
    TERRESTRIAL ECOSYSTEMS
  Environmental assessment of resource development (Contents and expectations of environmental impact statements), 30:29331
ECOSYSTEMS/THERMAL POLLUTION
  Biological effects of thermal discharges from nuclear power plants, 30:29466
EDEMA/DIAGNOSIS
  Measurement of cerebral infarction edema with sodium-22 (Cats), 30:29837

EGGS/RADIOACTIVITY
Distribution of ingested plutonium in chickens and subsequent transport to eggs (^{238}Pu tracer), 30:29811 (NVO-AEIC-74-1)
EGGS/RADIOSENSITIVITY
Effect of temperature on the radiation sensitivity of Ascaris eggs (X radiation), 30:29766 (SAND-74-6017)
EGGS/X-RAY RADIOGRAPHY
Radiometric method for eggshells, 30:29603 (TRITA-KKE-7403)
EINSTEIN FIELD EQUATIONS/FLUIDS
Solutions of the Einstein field equations for a rotating perfect fluid, 30:31180
EINSTEIN GRAVITATION THEORY
See GENERAL RELATIVITY THEORY
EINSTEINIUM 253/BIOLOGICAL RADIATION EFFECTS
Early hematologic effects of curium and einsteinium in beagles, 30:29779 (COO-119-249)
Long-term effects of intratracheally instilled ^{253}EsCl$_3$ in rats, 30:29776 (BNWL-SA-4870)
EINSTEINIUM 253/TISSUE DISTRIBUTION
Early retention and distribution of ^{253}Es by the beagle, 30:29803 (COO-119-249)
Early subcellular distribution of einsteinium in canine livers, 30:29804 (COO-119-249)
Einsteinium studies in beagles (^{253}Es tissue distribution), 30:29802 (COO-119-249)
ELASTIC SCATTERING
See also COMPTON EFFECT
COULOMB SCATTERING
POTENTIAL SCATTERING
New description of nuclear scattering at intermediate energies and permissibility of Glauber expression to large-angle elastic scattering, 30:31022
ELASTIC SCATTERING/NUCLEAR REACTION KINETICS
Self-consistent wave functions, center-of-mass motion and high-energy particle-nucleus scattering, 30:31098
ELECTRIC BRIDGES/FABRICATION
Technique for fabrication of superconducting microbridges and small Josephson tunnel junctions, 30:30841
ELECTRIC BRIDGES/SUPERCONDUCTORS
Coherent effects in large arrays of superconducting bridges, 30:30821
Inductance bridge for current-quantum phase measurements in superconductors at zero frequency (Al thin-film meander lines, inductance vs temperature, SQUID magnetometer detector), 30:30839
Technique for fabrication of superconducting microbridges and small Josephson tunnel junctions, 30:30841
ELECTRIC CONDENSERS
See CAPACITORS
ELECTRIC CONDUCTORS/SPECIFIC HEAT
Steady-state, ac-temperature technique for measuring the specific heat of electrical conductors, 30:31439 (UCID-15649)
ELECTRIC DISCHARGES/DISTRIBUTION FUNCTIONS
Electron energy distribution in a high-freqeuncy discharge in an axial magnetic field (Second-derivative method), 30:29166
ELECTRIC DISCHARGES/PLASMA INSTABILITY
Arc discharges in a curved magnetic field, 30:29154 (NP-20140)
Attachment instability in an externally ionized discharge (High-pressure electron beam-sustainer discharge, 74:2 He:H$_2$O and 1:1 and 9:1 He:CO$_2$ mixtures), 30:29201
ELECTRIC FIELDS
Space wave fields of subsurface electromagnetic sources in planar layered media, 30:31353 (UCID-15945)
ELECTRIC GENERATORS
(Rotating generators only; excludes DIRECT ENERGY CONVERTERS.)
ELECTRIC GENERATORS/SUPERCONDUCTORS
Applications of superconductivity to ac rotating machines, 30:30828
Superconducting dc machines, 30:30827
ELECTRIC MOTORS
See MOTORS
ELECTRIC PULSES
See PULSES
ELECTROCHEMICAL CORROSION
Electrochemistry of aqueous corrosion: uranium and its alloys (Review), 30:29544 (Y-1949)
ELECTROJETS/INSTABILITY
Electromagnetic effects on instabilities in the equatorial electrojet, 30:30440
ELECTROJETS/MAGNETIC FIELDS
Phase relations in the magnetic field of the equatorial electrojet, 30:30467
ELECTROJETS/SIMULATION
Preliminary report of numerical simulation of Type 2 irregularities in the equatorial electrojet, 30:30427
ELECTROLYTES/CHEMICAL REACTIONS
Investigation of polyion-small ion electrostatic interaction effects in polyelectrolyte solutions, 30:31375 (UCRL-51636)
ELECTROMAGNETIC INTERACTIONS
See also COMPTON EFFECT
COULOMB SCATTERING
ELECTROPRODUCTION
PHOTON-PHOTON INTERACTIONS
PHOTOPRODUCTION
ELECTROMAGNETIC INTERACTIONS/MEETINGS
Proceedings of the eighth Rencontre de Moriond. Volume I. Electromagnetic and weak interactions. Conference held at Meribel-les-Allues, France, March 4--16, 1973, 30:30663
ELECTROMAGNETIC INTERACTIONS/RESEARCH PROGRAMS
High Energy Accelerator and Colliding Beam User Group. Progress report (Summaries of research activities at University of Maryland), 30:30575 (TID-26638)
ELECTROMAGNETIC ISOTOPE SEPARATION/SUPERCONDUCTING MAGNETS
High gradient magnetic spearation: an industrial application of magnetism, 30:30832
ELECTROMAGNETIC ISOTOPE SEPARATORS/ION SOURCES
Strong focusing ion sources, 30:29637
ELECTROMAGNETIC PULSES
Computations on the parameter values inside of the E.M. source, 30:29310 (LAMS-2610)
Direct interaction effects in EMP, 30:29308 (AD-777748)
ELECTROMAGNETIC RADIATION
See also BLACKBODY RADIATION
BREMSSTRAHLUNG
COHERENT RADIATION
GAMMA RADIATION
LASER RADIATION
SYNCHROTRON RADIATION
ELECTROMAGNETIC RADIATION/SCATTERING
Scattering of high-frequency electromagnetic waves by ion-acoustic oscillations in a bounded plasma (Probing signal), 30:29237
ELECTROMAGNETIC RADIATION/VELOCITY
Velocity of light is direction dependent, 30:31162
ELECTROMAGNETS
See also SUPERCONDUCTING MAGNETS
A magnetic field clamp with beneficial saturation effects, 30:30136
ELECTROMAGNETS/MAGNETIC FIELDS
Rapid measurement of the effective field boundary of homogeneous field magnets, 30:30135
ELECTROMAGNETS/SURFACE COATING
Application of electrically conductive coatings to insulating tubes of switching magnets for particle accelerators (Patent), 30:30123
ELECTRON BEAMS/MAGNETIC FIELDS
Parametric instability of an electron beam in a magnetic field (Effective exchange of energy), 30:29200
ELECTRON BEAMS/REFLECTION
Transmission and reflection of electrons by foils, 30:31118
ELECTRON BEAMS/SYNCHROTRON RADIATION
Coherent synchrotron radiation from an intense relativistic electron beam, 30:30580 (AD-773442)
Geometry and optics of synchrotron radiation, 30:30119
ELECTRON BEAMS/TRANSMISSION
Transmission and reflection of electrons by foils, 30:31118
ELECTRON COLLISIONS
See also ELECTRON-ATOM COLLISIONS
ELECTRON-ION COLLISIONS
ELECTRON-MOLECULE COLLISIONS
Low energy electron collisions in gases: swarm and plasma methods applied to their study (Book), 30:30543
ELECTRON COLLISIONS/POTENTIAL SCATTERING
Strong 4f resonance effects in rare-earth appearance-potential spectra, 30:30477
ELECTRON DETECTION/CHERENKOV COUNTERS
Investigation of a 90-channel Pb glass Cherenkov hodoscope, 30:29577
ELECTRON DETECTION/EXPANSION CHAMBERS
Identification and measurement of low-energy electrons by cloud chamber techniques: the oxygen and neon auger-electron problem, 30:29495 (UCID-15372)
ELECTRON DOSIMETRY/BACKSCATTERING
Back-scattering from metals in superficial therapy with high energy electrons, 30:31108
ELECTRON DOSIMETRY/CALORIMETRIC DOSEMETERS
Calorimetric and ionization measurements of stopping power in carbon for 19.5 GeV electrons, 30:29556
ELECTRON DOSIMETRY/THERMOLUMINESCENT DOSEMETERS
Thermoluminescent response of TLD-100 to 1 to 25 keV electrons. Progress report, July 15, 1973--July 15, 1974, 30:29538 (COO-1105-212)
ELECTRON MICROSCOPY
Electron radiation damage of thin films of glycine, diglycine, and aromatic amino acids, 30:29042
ELECTRON MICROSCOPY/COMPARATIVE EVALUATIONS
Comparison of analytical techniques for inorganic pollutants, 30:28924
ELECTRON MULTIPLIERS
A study of ion paths in curved parallel-plate electron multipliers with perpendicular magnetic field, 30:29629
ELECTRON PLASMA WAVES/AMBIPLASMA
Effects of an ambient medium on the emission, absorption and scattering of waves by atoms and molecules, 30:30387
ELECTRON PLASMA WAVES/WAVE PROPAGATION
Effects of an ambient medium on the emission, absorption and scattering of waves by atoms and molecules, 30:30387
ELECTRON PRECIPITATION/SEASONAL VARIATIONS
Dependence of field-aligned electron precipitation occurrence on season and altitude, 30:30469

ELECTRON REACTIONS/BREAKUP REACTIONS
  Cluster-model calculations of the electrodisintegration of lithium (Differential form factors), 30:30893
ELECTRON REACTIONS/ELASTIC SCATTERING
  Self-consistent wave functions, center-of-mass motion and high-energy particle-nucleus scattering, 30:31098
  The energy density formalism and the shell structure effects, 30:31025
ELECTRON REACTIONS/ELECTROPRODUCTION
  Pion electroproduction from nuclei near threshold (280 MeV), 30:30671
ELECTRON REACTIONS/INELASTIC SCATTERING
  Model independent evaluation of the inelastic e^- scattering cross sections from the 3^- (2.615 MeV) level in ^{208}Pb, 30:31005
  Search for the lowest T = 2 state in ^{14}C by inelastic electron scattering (61 and 81 MeV), 30:30878
ELECTRON SOURCES/DESIGN
  Note on the Astron gun design, 30:29214 (UCID-15481)
ELECTRON SPECTROMETERS
  Experimental equipment for spectrometry of electrons and protons between 0.4 and 30keV aboard the AUREOLE satellite, 30:29567
ELECTRON SPECTROSCOPY
  Spectroscopy of Auger electrons and its use in metallurgy, 30:31420 (COPPE-TP-6/72)
ELECTRON-ATOM COLLISIONS/ELASTIC SCATTERING
  Differential cross sections for the elastic scattering of electrons from atomic hydrogen. II. Medium energies (Total cross sections), 30:30535
ELECTRON-ATOM COLLISIONS/EXCITATION
  Atomic excitation processes in the discharges of rare gas ion engines, 30:30556
  Design of a high density atomic hydrogen source and determination of Balmer cross sections (20 to 440 eV), 30:30526
  Effective cross sections and peculiarities of electron excitation of the cadmium atom, 30:30523
  Excitation of resonance lines of K II in electron-atom collisions (20 to 200 eV), 30:30524
  New technique for threshold excitation spectroscopy, 30:30553
  Step-by-step excitation in helium (0.2 to 1.0 eV: cross sections), 30:30489
ELECTRON-ATOM COLLISIONS/INELASTIC SCATTERING
  Equations of motion method: Inelastic electron scattering for helium and CO_2 in the Born approximation, 30:30550
ELECTRON-ATOM COLLISIONS/IONIZATION
  Excitation of resonance lines of K II in electron-atom collisions (20 to 200 eV), 30:30524
ELECTRON-ATOM COLLISIONS/POLARIZATION
  Polarization of the resonance lines of lithium and sodium atoms by electron impact (Glauber theory), 30:30521 (IC-73-19)
ELECTRON-DEUTERON INTERACTIONS/DIFFERENTIAL CROSS SECTIONS
  Extraction of R=sigma/subL//sigma/subT/ from deep inelastic e-p and e-d cross sections, 30:30583
ELECTRON-ION COLLISIONS/EXCITATION
  Experimental investigation of the effective cross section of excitations of bands of some decay products of water, ammonia, and acetonitrile by slow electrons, 30:30546
ELECTRON-ION COLLISIONS/INELASTIC SCATTERING
  Accurate total inelastic cross section for H_2^+ colliding with fast charged particles in the adiabatic approximation, 30:30554
ELECTRON-MOLECULE COLLISIONS/ELASTIC SCATTERING
  Differential cross sections for the elastic scattering of electrons from atomic hydrogen. II. Medium energies (Total cross sections), 30:30535
ELECTRON-MOLECULE COLLISIONS/EXCITATION
  New technique for threshold excitation spectroscopy, 30:30553
  Population of the rotational and vibrational levels of excited electronic states of nitrogen molecules produced in collisions of electrons with N_2 molecules (30 to 300 eV, Franck-Condon principle), 30:30545
ELECTRON-MOLECULE COLLISIONS/INELASTIC SCATTERING
  Equations of motion method: Inelastic electron scattering for helium and CO_2 in the Born approximation, 30:30550
ELECTRON-MOLECULE COLLISIONS/SCATTERING
  Scattering of alkali halides by electrons. II. CsCl (0.47- to 15.7-eV electrons: cross sections), 30:30528
ELECTRON-MUON UNIVERSALITY/ELECTRON-POSITRON INTERACTIONS
  Muon-electron universality at high energies and hadronic corrections to $e^+e^- \to \mu^+\mu^-$, 30:30675
ELECTRON-NEUTRON INTERACTIONS/DIFFERENTIAL CROSS SECTIONS
  Extraction of R=sigma/subL//sigma/subT/ from deep inelastic e-p and e-d cross sections, 30:30583
ELECTRON-NUCLEON INTERACTIONS
    See also ELECTRON-NEUTRON INTERACTIONS
        ELECTRON-PROTON INTERACTIONS
ELECTRON-NUCLEON INTERACTIONS/PARTON MODEL
  Quark parton model for deep inelastic lepton scattering (Cross sections, lectures), 30:30686
ELECTRON-NUCLEON INTERACTIONS/QUARK MODEL
  Quark parton model for deep inelastic lepton scattering (Cross sections, lectures), 30:30686
ELECTRON-NUCLEON INTERACTIONS/SCATTERING AMPLITUDES
  Multipole (kinematic) analysis of the reaction $eN \to e\pi\Delta$. II. Scalar amplitude decomposition by multipole amplitudes, 30:30666
ELECTRON-POSITRON INTERACTIONS/ANNIHILATION
  An anomalous rho-ω interference in the reaction $e^+e^- \to 3\pi$ (2E > 1 GeV), 30:30674
  Implications of the recent $e^+e^- \to$ hadron + X data on the leptonic world, 30:30657
  Muon-electron universality at high energies and hadronic corrections to $e^+e^- \to \mu^+\mu^-$, 30:30675
  Phase space and multihadron production in annihilation processes at present energies, 30:30669
  Physics with an electron--positron storage ring of beam energy E = 14 GeV, 30:30581 (RL-74-098)
  Scaling in e^+e^- annihilation into hadrons, 30:30677
  Senile scaling in electron-positron annihilation, 30:30668
ELECTRON-POSITRON INTERACTIONS/CROSS SECTIONS
  Contribution of hadrons to vacuum polarization, 30:30667
ELECTRON-POSITRON INTERACTIONS/POLARIZATION
  Polarization in electron positron colliding beams and the weak interactions (Differential cross sections), 30:30664
ELECTRON-POSITRON INTERACTIONS/SCALING LAWS
  Scaling behaviour in a class of massive non-Abelian gauge theories, 30:30771
ELECTRON-PROTON INTERACTIONS/CROSS SECTIONS
  Calculation of electroproduction of muon pairs in the light-cone limit (Covariant parton model), 30:30673
ELECTRON-PROTON INTERACTIONS/DIFFERENTIAL CROSS SECTIONS
  Electroproduction of eta-mesons at the S_{11} (1535) resonance, 30:30591
  Extraction of R=sigma/subL//sigma/subT/ from deep inelastic e-p and e-d cross sections, 30:30583
  π^0 electroproduction at the $\Delta(1236)$ resonance at a four-momentum transfer of $q^2=0.3(GeV/c)^2$ (Angular distribution of s- and p-waves, cross sections), 30:30589
ELECTRON-PROTON INTERACTIONS/INCLUSIVE INTERACTIONS
  Measurements of inclusive pion electroproduction (Cross sections, angular distributions), 30:30587
ELECTRON-PROTON INTERACTIONS/PARTICLE PRODUCTION
  π^0-electroproduction on hydrogen near threshold at four-momentum transfers of 0.2, 0.4 and 0.6 GeV^2, 30:30588
ELECTRON-RING ACCELERATORS/BEAM DYNAMICS
  Electron orbits in the ERA (electron ring accelerator) with an electrostatic-type inflector system, 30:30132
ELECTRON-RING ACCELERATORS/RESEARCH PROGRAMS
  On the collective acceleration of heavy ions - Department for new methods of acceleration of the JINR, 30:30117 (GSI-tr-74/10)
ELECTRONIC CIRCUITS
    See also COUNTING CIRCUITS
        INTEGRATED CIRCUITS
        MICROELECTRONIC CIRCUITS
        PRINTED CIRCUITS
        SWITCHING CIRCUITS
        TIMING CIRCUITS
  Some notes on coaxial terminations, short-circuits, and open-circuits, 30:31453 (UCID-15998)
ELECTRONIC DATA PROCESSING
    See DATA PROCESSING
ELECTRONIC EQUIPMENT
    See also ANALOG-TO-DIGITAL CONVERTERS
        DIGITAL-TO-ANALOG CONVERTERS
        PULSE GENERATORS
        PULSE INTEGRATORS
  Interatominstrument to coordinate EE nuclear instrumentation technology, 30:29615 (JPRS-61338)
ELECTRONIC EQUIPMENT/MEASURING METHODS
  Automatic radar-sensitivity measurement. Final report, 30:31417 (BDX-613-1134(Rev.))
ELECTRONIC EQUIPMENT/SENSITIVITY
  Automatic radar-sensitivity measurement. Final report, 30:31417 (BDX-613-1134(Rev.))
ELECTRONIC EQUIPMENT/WEAR
  Spare parts reservation of components subjected to wear-out and/or fatigue according to a Weibull distribution, 30:29289
ELECTRONS
    See also SOLVATED ELECTRONS
        TRAPPED ELECTRONS
ELECTRONS/COSMIC RADIATION
  Acceleration and radiation of cosmic ray electrons from pulsars, 30:30274
  Galactic electrons and electromagnetic radiation, 30:30343 (CONF-730693-)
ELECTRONS/DIRAC OPERATORS
  Conformal symmetry in the Weyl theory, 30:30652
ELECTRONS/ENERGETIC SOLAR PARTICLES
  Solar flares as sources of energetic particles, 30:30333
ELECTRONS/GRAVITATION
  F-gravity and the proton--electron mass ratio, 30:31174
ELECTRONS/MASS
  F-gravity and the proton--electron mass ratio, 30:31174
ELECTRONS/RELAXATION
  Electron-ion relaxation in a dense plasma (Microscopic structure), 30:30259
ELECTRONS/SCAVENGING
  Electron scavenging in the radiolysis of supercritical ethane, ethylene, n-butane, and isobutane (Gamma radiation), 30:29039

Radiation-chemical studies on the generation of lead and tin radicals (By electron scavenging in γ-irradiated 2-MTHF glass at 77°K), 30:29057

ELECTRONS/SOLAR PARTICLES
Non-relativistic solar electrons, 30:30337
Relativistic electron events in interplanetary space, 30:30338

ELECTROPRODUCTION/CROSS SECTIONS
Deep inelastic electroproduction in resonance region. Cross section ratio sigma/sub n//sigma/sub p/, 30:30654

ELECTROPRODUCTION/INCLUSIVE INTERACTIONS
Absorption corrections in a Mueller Regge analysis of inclusive photo- and electroproduction, 30:30670

ELECTROPRODUCTION/STRUCTURE FUNCTIONS
Asymptotic near freedom, 30:30672

ELECTROSTATIC ACCELERATORS
See also VAN DE GRAAFF ACCELERATORS

ELECTROSTATIC ACCELERATORS/SPECIFICATIONS
Nuclear structure facility 20/30 MV tandem accelerator, 30:30118

ELECTROSTATIC PRECIPITATORS/DESIGN
Method of measuring the mobility, concentration, and isotope composition of radioactive ions, 30:29273

ELEMENT 108/ALPHA SPECTROSCOPY
Unknown alpha-emitters in nature, 30:28981

ELEMENT 112/ALPHA SPECTROSCOPY
Unknown alpha-emitters in nature, 30:28981

ELEMENT 117/ALPHA SPECTROSCOPY
Unknown alpha-emitters in nature, 30:28981

ELEMENTARY PARTICLES
See also HADRONS
LEPTONS
PHOTONS
POSTULATED PARTICLES
STRANGE PARTICLES
VIRTUAL PARTICLES

ELEMENTARY PARTICLES/BORN APPROXIMATION
Invariants of Born reciprocity theory, 30:30629

ELEMENTARY PARTICLES/COUPLING
A theory of elementary couplings. III (Compensation between Feynman diagrams), 30:31146

ELEMENTARY PARTICLES/MECHANICS
Particle kinematics (Book), 30:30646

ELEMENTARY PARTICLES/SPIN
Physical significance of the topology of the Bondi--Metzner--Sachs group, 30:30766

ELEMENTARY PARTICLES/SU GROUPS
Gel'fand-pattern technique applied to the physically important SU(3) x SU(2) is contained in SU(6) decomposition of SU(6), 30:30768

ELEMENTS
See also METALS

ELEMENTS/ACTIVATION ANALYSIS
Trace-element analysis of 1000 environmental samples per year using instrumental neutron activation analysis, 30:28915 (N-74-20335)

ELMO DEVICES/ELECTRON TEMPERATURE
Cold-electron temperature measurements in ELMO by excitation rate ratios of vacuum ultraviolet transitions, 30:29168

ELMO DEVICES/PLASMA DIAGNOSTICS
Cold-electron temperature measurements in ELMO by excitation rate ratios of vacuum ultraviolet transitions, 30:29168
Spectroscopic study in the vacuum ultraviolet of a neon plasma in ELMO, 30:29158 (ORNL-TM-4672)

EMBOLI/RADIOINDUCTION
Prevention of thrombo-embolism during radiotherapy of carcinoma of the uterine cervix (Radium inserts), 30:29732

EMBRYOS/BIOLOGICAL RADIATION EFFECTS
Embryotoxicity of astatine-211 (Comparison of effects of internal ^{211}At with external x irradiation), 30:29781 (COO-3268-5)

EMERGENCY CORE COOLING SYSTEM
See ECCS

EMISSION SPECTROSCOPY
See also FLUORESCENCE SPECTROSCOPY

EMISSION SPECTROSCOPY/COMPARATIVE EVALUATIONS
Comparison of analytical techniques for inorganic pollutants, 30:28924

EMISSION SPECTROSCOPY/PLASMA DIAGNOSTICS
Spectroscopic methods for diagnostics of superdense hot plasma, 30:29163

EMP
See ELECTROMAGNETIC PULSES

ENDOCRINE DISEASES
See also HYPERTHYROIDISM

ENDOCRINE DISEASES/DIAGNOSIS
Adrenal imaging with radioiodocholesterol in the diagnosis of adrenal disorders (^{131}I tracer technique), 30:29869

ENERGETIC SOLAR PARTICLES
See also SOLAR PARTICLES

ENERGETIC SOLAR PARTICLES/ORIGIN
Solar flares as sources of energetic particles, 30:30333

ENERGY CONVERSION/MEETINGS
9th intersociety energy conversion engineering conference proceedings, San Francisco, California, August 26--30, 1974, 30:29243

ENERGY SOURCES/PLANNING
Energy and cryoengineering, 30:31324 (LA-UR-74-741)

ENGINES
See MOTORS

ENIWETOK/RADIATION MONITORING
Resuspension of ^{239}Pu, ^{240}Pu, and ^{241}Am particles at Nevada Test Site; prediction of air concentrations of Pu due to resuspension at Eniwetok Atoll, 30:29452 (NVO-AEIC-74-1)

ENRICHED URANIUM/CRITICALITY
Safety analysis report for packaging (Oak Ridge Y-12 Plant Model VCD package for enriched uranium solution), 30:30115 (Y-DD-155)
Safety analysis report for packaging (Oak Ridge Y-12 Plant foamglas shipping package for enriched uranium), 30:30116 (Y-DD-156)

ENRICHED URANIUM/TRANSPORT
Safety analysis report for packaging (Oak Ridge Y-12 Plant Model VCD package for enriched uranium solution), 30:30115 (Y-DD-155)
Safety analysis report for packaging (Oak Ridge Y-12 Plant foamglas shipping package for enriched uranium), 30:30116 (Y-DD-156)

ENVIRONMENT
Environmental assessment of resource development (Contents and expectations of environmental impact statements), 30:29331

ENVIRONMENT/CONTAMINATION
Airborne release of ^{137}Cs from a contaminated area during a range fire, 30:29376 (BNWL-1850(Pt.3))
Ecological factors in the siting, design, and operation of a nuclear power station, 30:29354

ENVIRONMENT/INFORMATION SYSTEMS
ORRMIS: Oak Ridge Regional Modeling Information System. Part I, 30:29456 (ORNL-NSF-EP-73)

ENVIRONMENT/POLLUTION
Measurements of drift from a mechanical draft cooling tower (Air concentrations and surface deposition of Cr from gaseous diffusion plant cooling tower), 30:29487 (BNWL-1850(Pt.3))

ENVIRONMENT/RADIATION HAZARDS
Atomic energy. V (Norwegin Nature Conservancy Association), 30:29343

ENVIRONMENT/THERMAL POLLUTION
Ecological factors in the siting, design, and operation of a nuclear power station, 30:29354
Physical--chemical effects of cooling systems and thermal discharges on the environment, 30:29465

EPIPHYSIS (BONES)
See BONE TISSUES

EPOXIDES/ELECTRICAL PROPERTIES
Temperature dependent properties of potting materials, 30:31386 (BDX-613-1133(Rev.))

EPOXIDES/MECHANICAL PROPERTIES
Temperature dependent properties of potting materials, 30:31386 (BDX-613-1133(Rev.))

EPOXIDES/THERMODYNAMIC PROPERTIES
Temperature dependent properties of potting materials, 30:31386 (BDX-613-1133(Rev.))

EPOXY COMPOUNDS
See EPOXIDES

EQUATIONS (DIFFERENTIAL)
See DIFFERENTIAL EQUATIONS

EQUATORIAL ELECTROJETS
See ELECTROJETS

EQUILIBRIUM PLASMA/MATHEMATICAL MODELS
Computation of MHD equilibria in Tokamak, 30:29179 (CLM-R-133)

ERBIUM/ACTIVATION ANALYSIS
Determination of rare earths and thorium in apatites by thermal and epithermal neutron-activation analysis, 30:28935

ERBIUM/ELECTRIC CONDUCTIVITY
Resistivity and TCR of erbium films compared with the predictions of the columnar model, 30:30052

ERBIUM/EXTRACTION CHROMATOGRAPHY
Contribution to the separation of rare earths by extraction chromatography with di(2-ethylhexyl) phosphoric acid. II. Behavior of the matrix and its influence on the microcomponents, 30:28990 (ANL-Trans-961)

ERBIUM/FILMS
Resistivity and TCR of erbium films compared with the predictions of the columnar model, 30:30052

ERBIUM 156/HIGH SPIN STATES
In-beam conversion-electron spectrum for the ^{148}Sm(^{12}C,4n)^{156}Er reaction, 30:30965

ERBIUM 156/VIBRATIONAL STATES
In-beam conversion-electron spectrum for the ^{148}Sm(^{12}C,4n)^{156}Er reaction, 30:30965

ERBIUM 166/NEUTRON REACTIONS
Mass-spectrometric determination of neutron capture cross-sections of the rare earth isotopes (Pile and thermal cross sections), 30:30977 (AEC-tr-7574)

ERBIUM 167/NEUTRON REACTIONS
Mass-spectrometric determination of neutron capture cross-sections of the rare earth isotopes (Pile and thermal cross sections), 30:30977 (AEC-tr-7574)

ERBIUM ALLOYS/CRYSTAL STRUCTURE
  Structure of alloys of cobalt with rare earths of the approximate composition RCo_5, 30:30034
ERBIUM ISOTOPES/ENERGY-LEVEL TRANSITIONS
  γ-ray multiplicity after (HI,xn) reaction, 30:30983
ERYTHROBLASTS
  See BONE MARROW CELLS
ERYTHROCYTES/BIOLOGICAL RADIATION EFFECTS
  Osmotic haemolysis as a means of studying erythropoietic stresses: response to acute anaemia and acute irradiation (^{59}Fe tracer), 30:29736 (RT/BIO-(74)10)
ESCHERICHIA COLI/BIOLOGICAL RADIATION EFFECTS
  Comparative investigation of mutagenic effects of incorporated isotopes of the most important organogenic elements. VI. Comparison of lethal and mutagenic effects of the decay of ^{32}P and ^{35}S incorporated into cells of Escherichia coli WP-2S Try$^-$, 30:29788
ESCHERICHIA COLI/GENETIC RADIATION EFFECTS
  Comparative investigation of mutagenic effects of incorporated isotopes of the most important organogenic elements. VI. Comparison of lethal and mutagenic effects of the decay of ^{32}P and ^{35}S incorporated into cells of Escherichia coli WP-2S Try$^-$, 30:29788
ESOPHAGUS/SCINTISCANNING
  Diagnosis of Barrett's esophagus with radioisotopes (Scanning with /sup 99m/Tc tracer), 30:29852
ESTUARINE ECOSYSTEMS
  See AQUATIC ECOSYSTEMS
ETA MESONS/ELECTROPRODUCTION
  Electroproduction of eta-mesons at the S_{11} (1535) resonance, 30:30591
ETA MESONS/INTERFERENCE
  The eta-eta' mixing angle from duality and quark model, 30:30728
ETA MESONS/LIFETIME
  A theory of elementary couplings. III, 30:31146
ETA MESONS/MASS
  Non-zero masses of π,K, eta and kappa mesons and algebraic realization of SU(3) x SU(3) chiral symmetry, 30:30780
ETA-549
  See ETA MESONS
ETA-958 RESONANCES/INTERFERENCE
  The eta-eta' mixing angle from duality and quark model, 30:30728
ETCHING/STANDARDS
  Macroetching metals and alloys, 30:29965
ETHANE/ION-MOLECULE COLLISIONS
  Crossed-molecular-beam study of the kinematics and dynamics of charge-transfer collisions (200 eV), 30:30547
ETHANE/RADIOLYSIS
  Electron scavenging in the radiolysis of supercritical ethane, ethylene, n-butane, and isobutane (Gamma radiation), 30:29039
1,2-ETHANEDITHIOL
  See DITHIOLS
ETHANOL/CHEMICAL RADIATION EFFECTS
  Trapped electrons in C_2H_5OD glasses γ-irradiated at 4°K, 30:29068
ETHERS/CHEMICAL RADIATION EFFECTS
  Radiation copolymerization of ethylene oxide with acrylonitrile (Gamma radiation), 30:29037
ETHYLENE/RADIOLYSIS
  Electron scavenging in the radiolysis of supercritical ethane, ethylene, n-butane, and isobutane (Gamma radiation), 30:29039
ETHYLENE POLYMERS
  See POLYETHYLENES
EUFLAVINE
  See ACRIFLAVINE
EUROPIUM/ACTIVATION ANALYSIS
  Determination of rare earths and thorium in apatites by thermal and epithermal neutron-activation analysis, 30:28935
  Radioactivation analysis in thermal and epithermal neutrons of the IBR-30 reactor of JINR, 30:28929
  Trace element behavior in soil of some Indonesian sawah's and in sludge of an Indonesian river, 30:28930
EUROPIUM/EXTRACTION CHROMATOGRAPHY
  Contribution to the separation of rare earths by extraction chromatography with di(2-ethylhexyl) phosphoric acid. II. Behavior of the matrix and its influence on the microcomponents, 30:28990 (ANL-Trans-961)
EUROPIUM/ION EXCHANGE
  Sorption of tetravalent elements by mordenite. II. Sorption of Pu(IV), 30:28999
  Synthesis of reproducible tin(IV) based ion exchangers: separation of lanthanum(III) from yttrium(III), europium(III), and lutetium(III), 30:28994
EUROPIUM/NEUTRON REACTIONS
  Status report to NCSAC, 30:31011 (UCID-15639)
EUROPIUM/X-RAY SPECTROSCOPY
  Determination of rare earths in plutonium by x-ray emission analysis, 30:28946
EUROPIUM 143/NUCLEAR PROPERTIES
  Nuclear Data Sheets for A = 143, 30:30966
EUROPIUM COMPLEXES/CHEMICAL PREPARATION
  Complex formation of actinides and lanthanides with orthophthalic, 3-nitrophthalic, and 4-nitrophthalic acids. II. Complex formation of radioeuropium (^{152}Eu tracer), 30:29119
EUROPIUM COMPLEXES/MOESSBAUER EFFECT
  Moessbauer spectroscopy of frozen europium ammonia solutions, 30:30093
EUROPIUM COMPOUNDS/MAGNETIC SUSCEPTIBILITY
  Synthesis and magnetic properties of samarium and europium titanoniobates ($SmTiNbO_6$; $EuTiNbO6$), 30:29908
EUROPIUM OXIDES/FERROMAGNETISM
  Ferromagnetism of EuO and EuS, 30:30094
EUROPIUM SULFIDES/FERROMAGNETISM
  Ferromagnetism of EuO and EuS, 30:30094
EVEN-EVEN NUCLEI/ROTATIONAL STATES
  Analysis of rotational and quasirotational ground-state bands in even--even nuclei, 30:30957
EVEN-ODD NUCLEI/EXCITATION
  Theory of collective excitations in spherical odd--mass nuclei. III. Electromagnetic properties of the anomalous coupling states (N-quasi-particle modes), 30:31068
EXCHANGE INTERACTIONS/NUCLEAR POTENTIAL
  On the nuclear L.L potential, 30:31092
EXCITED STATES/DECAY
  Isospin effects upon the decay of highly excited nuclear states, 30:30999
EXCURSIONS/NEUTRON FLUX
  Comparison of two- and three-dimensional calculations of super prompt critical excursions (PWR and BWR), 30:31190
EXCURSIONS/TEMPERATURE DISTRIBUTION
  Comparison of two- and three-dimensional calculations of super prompt critical excursions (PWR and BWR), 30:31190
EXPANSION CHAMBERS/PARTICLE IDENTIFICATION
  Identification and measurement of low-energy electrons by cloud chamber techniques: the oxygen and neon auger-electron problem, 30:29495 (UCID-15372)
EXPERIMENTAL NEOPLASMS/BIOLOGICAL RADIATION EFFECTS
  Direct relationship between immune competence and the subcutaneous growth rate of a malignant murine lung tumor (X radiation), 30:29756
EXPLOSIONS
  See also CHEMICAL EXPLOSIONS
  NUCLEAR EXPLOSIONS
EXPLOSIONS/SIMULATORS
  Performance characteristics of Sandia Laboratories 5.8-metre-diameter explosively driven blast simulator, 30:31431 (SLA-74-5239)
EXTENSIVE AIR SHOWERS/IONIZATION
  Local changes of the atmospheric electric field by EAS ionization, 30:30414
EXTENSIVE AIR SHOWERS/RADIATION DETECTION
  Methods of search of gamma-radiation point sources by two groups of detectors, 30:29580
EXTENSIVE AIR SHOWERS/RADIOWAVE RADIATION
  Radio pulses from extensive air showers during thunderstorms: the atmospheric electric field as a possible cause, 30:30585
EXTENSIVE AIR SHOWERS/VARIATIONS
  Fluctuation studies of large air showers: the composition of primary cosmic ray particles of energy E/sub p/ approximately 10^{18} eV, 30:30175
EYES
  See also RETINA
EYES/BIOLOGICAL RADIATION EFFECTS
  Experimental ocular irradiation with accelerated protons (Monkeys), 30:29754
EYES/RADIATION PROTECTION
  Prosthesis set for radioprotection of the eye (Methyl methacrylate), 30:29717

F

F REGION/DISTURBANCES
  Radiation control for health and safety. Hearings before the Committee on Commerce, United States Senate, Ninety-Third Congress, First Session, on Public Law 90-602, March 8, 9, and 12, 1973, 30:30445
F REGION/ECLIPSE
  Anomalous behavior of F-region during the solar eclipse of September 22, 1968, 30:30432
F REGION/ELECTRIC CONDUCTIVITY
  Conductivity ratio effects on the drift and deformation of F-region barium clouds coupled to the E-region ionosphere, 30:30437
F REGION/ELECTRON DENSITY
  Latitude distribution of the regularity in F_2-region irregularities, 30:30417
  Routine operation of Digisonde at Maynard, Massachusetts. Final report, 1 September 1971--31 August 1972, 30:30410 (AD-776969)
F REGION/ION DENSITY
  Variation of F-region positive ion density with solar activity, 30:30416
F REGION/RADIO NOISE
  Anomalous behavior of F-region during the solar eclipse of September 22, 1968, 30:30432
F-1260 RESONANCES
  F-gravity and the proton--electron mass ratio, 30:31174
F-1260 RESONANCES/PARTICLE PRODUCTION
  Backward production of rho^0 and f^0 mesons in π^+n interactions at 6 GeV/c (Cross sections), 30:30621

FAILURES/PROBABILITY
  Design relationships and failure theories in probabilistic form, 30:29288
FALLOUT
  (For radioactive fallout only.)
  See also GLOBAL FALLOUT
    WASHOUT
FALLOUT/BIOLOGICAL RADIATION EFFECTS
  Nuclear testing (^{131}I; ^{90}Sr; ^{137}Cs; ^{14}C; Tritium), 30:29719
FALLOUT/DIFFUSION
  Numerical prediction of the mesoscale transport of atmospheric effluents: philosophy and morphology of experimental models for predicting the wind and potential radiological fields over the Nevada Test Site, 30:29377 (COM-74-10799)
  Vertical distribution of radioactive aerosols in the troposphere above the European part of the USSR in 1964--1967, 30:29389
FALLOUT/PRECIPITATION SCAVENGING
  Radionuclide concentration minimums from 6 to 9 km, 30:29368 (BNWL-1850(Pt.3))
FALLOUT/RADIATION HAZARDS
  Radiation in man's environment (Hazards from fallout as compared with other radiation sources in Australia), 30:29353
FALLOUT/RADIATION MONITORING
  Determination of fallout radioisotopes from their content in the annual layers of high-mountain glaciers, 30:29408
  Rate of fallout of ^{137}Cs and ^{90}Sr aerosols from the atmosphere, 30:29399
  Vertical distribution of radioactive aerosols in the troposphere above the European part of the USSR in 1964--1967, 30:29389
FAST FLUX TEST FACILITY REACTOR
  See FFTF REACTOR
FAST NEUTRONS/RBE
  Response of jejunal mucosa to fractionated doses of neutrons or γ-rays, 30:29758
  Review of RBE values of 15 MeV neutrons for effects on normal tissues, 30:29764
FAST NEUTRONS/TRANSMISSION
  Transmission method to measure capture rates in fast reactors, 30:31276
FAST REACTORS
  See also FFTF REACTOR
    GCFR TYPE REACTORS
    LMFBR TYPE REACTORS
FAST REACTORS/COATED FUEL PARTICLES
  Trends in structural mechanics. A UK review of the 2nd international conference on structural mechanics in reactor technology. VIII. Reactor core, 30:31213
FAST REACTORS/CONTAINMENT
  Trends in structural mechanics. A UK review of the 2nd international conference on structural mechanics in reactor technology. V. Fast reactor containment, 30:31261
FAST REACTORS/DOPPLER COEFFICIENT
  Contribution to the mutual resonance shielding of ^{238}U and ^{239}Pu, 30:31009 (EURFNR-1162)
FAST REACTORS/FUEL PINS
  Trends in structural mechanics. A UK review of the 2nd international conference on structural mechanics in reactor technology. VIII. Reactor core, 30:31213
FATS/METABOLISM
  Reticuloendothelial function test in rabbit and man. Experimental and clinical investigation on artificial fat cream and ^{131}IAA, 30:29841
FAULT TREE ANALYSIS
  Fault Tree Drawing Program users instructions, 30:31346 (SLA-73-0409)
FAULT TREE SYSTEMS
  See FAULT TREE ANALYSIS
FDR
  See OTTO HAHN REACTOR
FDR REACTOR
  See OTTO HAHN REACTOR
FECES/RADIATION MONITORING
  Absorption, distribution, and excretion of plutonium by dairy cattle (^{238}Pu tracer), 30:29810 (NVO-AEIC-74-1)
FEDERAL REPUBLIC OF GERMANY
  See GERMAN FEDERAL REPUBLIC
FEED MATERIALS PRODUCTION CENTER/ENVIRONMENT
  Feed Materials Production Center environmental monitoring annual report for 1973, 30:29347 (NLCO-1109)
FEED MATERIALS PRODUCTION CENTER/RADIATION MONITORING
  Feed Materials Production Center environmental monitoring annual report for 1973, 30:29347 (NLCO-1109)
FERMI GAS/THERMODYNAMICS
  Thermodynamic functions of ideal two- and three-dimensional Fermi gases, 30:30802
FERMIONS
  See also BARYONS
    LEPTONS
FERMIONS/PARTICLE INTERACTIONS
  Nonrenormalizability of quantized fermion--gravitation interactions, 30:31179
FERRATES
  See IRON OXIDES
FERRITE GARNETS/MAGNETIC PROPERTIES
  Preparation and some magnetic properties of uranium oxide doped YIG crystals ($Y_3Fe_5O_{12}$), 30:29894
FERRITIN/RADIOIMMUNOASSAY
  Measurement of serum ferritin by a 2-site immunoradiometric assay (^{125}I tracer technique), 30:29835
FESHBACH-PORTER-WEISSKOPF MODEL
  See OPTICAL MODELS
FFTF REACTOR/FUEL PINS
  Fabrication, irradiation, and postirradiation examination of mixed oxide fuel pin PNL-3-8, 30:31231 (HEDL-TME-74-37)
FIBROBLASTS
  Effects of DTPA on tissue cultured fibroblasts (Toxicity of Ca-DTPA and Zn-DTP), 30:29807 (COO-119-249)
  Malignant transformation of hamster embryo fibroblasts following exposure to ultraviolet-irradiated human cytomegalovirus, 30:29677
FIBROBLASTS/BIOLOGICAL RADIATION EFFECTS
  DNA repair in human progeroid cells (Gamma radiation), 30:29675
  Rate of DNA repair in progeric and normal human fibroblasts (Gamma radiation, Hutchinson--Gilford syndrome), 30:29672
FIBROBLASTS/RADIOSENSITIVITY
  Thermal enhancement of the radiosensitivity using cultured normal and neoplastic cells (Potential significance for radiotherapy), 30:29004
FIELD THEORIES
  See also QUANTUM FIELD THEORY
  Field theories without Ward-identities (Lagrangian formalism, Poincare group), 30:31145 (KFKI-74-46)
FIELD THEORIES/CAUSALITY
  Constraints, causality, and Lorentz invariance, 30:31167
FIELD THEORIES/LORENTZ INVARIANCE
  Constraints, causality, and Lorentz invariance, 30:31167
FILMS
  (Not for PHOTOGRAPHIC FILMS or NUCLEAR EMULSIONS.)
FILMS/CHEMICAL RADIATION EFFECTS
  Radiation effects in polyethylene films studied by pulse radiolysis (Electron beams), 30:29077
FILMS/NUCLEAR REACTION ANALYSIS
  Measurement of atomic concentration profiles in thin films using nonresonant nuclear reactions, 30:28933
FINITE ELEMENT METHOD/NUCLEAR ENGINEERING
  A status report on computational techniques for finite element analyses, 30:29290
FIRE EXTINGUISHERS/SPRAYS
  LLL spray damper project (Fire protection of ventilation systems), 30:29330 (UCID-15941)
FIREBALL MODEL/POMERANCHUK PARTICLES
  Unitarity, phenomenology and the bare pomeron, 30:30710
FIREBALL MODEL/PROTON-ANTIPROTON INTERACTIONS
  Properties of the nucleon--antinucleon fireball (Statistical bootstrap), 30:30721
FIRES/RADIATION HAZARDS
  Airborne release of ^{137}Cs from a contaminated area during a range fire, 30:29376 (BNWL-1850(Pt.3))
FISHES/BEHAVIOR
  Migratory behavior of fish tagged at a nuclear power plant discharge into Lake Michigan, 30:29462 (CONF-740813-2)
FISHES/PHYSIOLOGY
  Aquatic physiology of thermal and chemical discharges (Effects of chlorine), 30:29461 (BNWL-SA-5058)
FISHES/RADIONUCLIDE KINETICS
  Environmental monitoring report: United States Atomic Energy Commission, Oak Ridge facilities. Calendar year 1973 (Monitoring), 30:29352 (UCC-ND-280)
  Plutonium in the Laurentian Great Lakes: food-chain relationships (^{239}Pu; ^{137}Cs), 30:29415 (CONF-740826-3)
  ^{210}Po radioactivity in organs of selected tunas and other marine fish (Radioecological concentration in Pacific Ocean fishes), 30:29817
FISHES/THERMAL STRESSES
  Possible effects of thermal effluents on fish: a review, 30:29467
FISSILE MATERIALS
  (Materials containing nuclides capable of undergoing fission by interaction with slow neutrons.)
FISSILE MATERIALS/SAFEGUARDS
  Report of the advisory panel on safeguarding special nuclear material, 30:30105 (TID-26630)
FISSION CHAMBERS/EFFICIENCY
  The effect of fragment anisotropy on fission-chamber efficiency, 30:29537
FISSION FRAGMENT DETECTION/PLASTIC SCINTILLATION DETECTORS
  Luminescence response of thin plastic scintillator detectors to fission fragments from proton-induced fission of ^{232}Th, ^{235}U and ^{238}U, 30:29528
FISSION FRAGMENT SPECTROMETERS/OPERATION
  Spectrometer for on-line analysis of radionuclides (SOLAR), 30:29571
FISSION FRAGMENTS/ANGULAR DISTRIBUTION
  Ternary fission induced by 540 MeV Fe ions on uranium, 30:31018
FISSION FRAGMENTS/INTERNAL CONVERSION
  Measurement of internal conversion cascading in ^{235}U fission fragments, 30:31012

FISSION PRODUCTS/DIFFUSION
Concentrational distribution of fission products over tropical zone oceans and its relation to atmospheric processes, 30:29388
FISSION PRODUCTS/EXTRACTION CHROMATOGRAPHY
Recent results in the application of column extraction chromatography in inorganic analysis, 30:28989 (ANL-Trans-960)
FISSION PRODUCTS/FISSION YIELD
Assessment of known independent yields and the calculation of those unknown in the fission of ^{232}Th, ^{233}U, ^{235}U, ^{238}U, ^{239}Pu, ^{240}Pu, and ^{241}Pu (Odd--even Z effects), 30:31008 (AERE-R-7680)
Photofission in gold at intermediate energy, 30:31002
FISSION PRODUCTS/MASS NUMBER
Investigation of the reported mass distribution curves in the fission of ^{233}U with 14.8 MeV neutrons, 30:31010 (ORO-4282-14)
Photofission in gold at intermediate energy, 30:31002
FISSION PRODUCTS/PASSIVATION
Chemical immobilization of fission products reactive with nuclear reactor components (Patent), 30:31281
FISSION PRODUCTS/RADIATION MONITORING
Concentrational distribution of fission products over tropical zone oceans and its relation to atmospheric processes, 30:29388
FISSION PRODUCTS/RADIOACTIVITY
Theories of radioactivity takeup by rain drops, 30:29398
FISSION PRODUCTS/RESEARCH PROGRAMS
Department of Fundamental Research, Grenoble, semiannual bulletin No. 4, 30:31333 (CEA-N-1688)
FISSION PRODUCTS/SEPARATION PROCESSES
Decontaminating uranium by reaction with ClF_3 and HF and volatizing the UF_6 product (Patent), 30:29149
FISSION PRODUCTS/WASHOUT
Theories of radioactivity takeup by rain drops, 30:29398
FISSIONABLE MATERIALS
(materials containing nuclides capable of undergoing fission by any process.)
See also FISSILE MATERIALS
FISSIONABLE MATERIALS/NEUTRON REACTIONS
Thermal neutron cross sections of fissionable elements in the multilevel-multichannel formalism, 30:31015
FISSIONABLE MATERIALS MANAGEMENT
See NUCLEAR MATERIALS MANAGEMENT
FISSIONING PLASMA/TEMPERATURE DISTRIBUTION
Diagnostics of seeded rf plasmas: an experimental study related to the gaseous core nuclear reactor. Final report, 1 September 1971--31 July 1973 (Argon), 30:31241 (N-74-23299)
FLASKS
See CASKS
FLAT PLATE COLLECTORS/COMPUTER CALCULATIONS
Control system design and simulation for solar heated structures, 30:31325 (LA-UR-74-1085)
FLAT PLATE COLLECTORS/DESIGN
Design and testing of a structurally integrated steel solar collector unit based on expanded flat metal plates, 30:31326 (LA-UR-74-1093)
FLAT PLATE COLLECTORS/PERFORMANCE TESTING
Design and testing of a structurally integrated steel solar collector unit based on expanded flat metal plates, 30:31326 (LA-UR-74-1093)
FLORIDA/RADIOACTIVITY
Aerial radiological measuring surveys of the Turkey Point Station, April 1972, 30:29358 (ARMS-72.6.2)
FLOW (FLUID)
See FLUID FLOW
FLOW REGULATORS
See also VALVES
FLOW REGULATORS/LIQUID METALS
Method and device for magnetohydrodynamically controlling the flow rate of an electrically conductive liquid (Patent), 30:30572
FLOWMETERS/PERFORMANCE
Development of sodium flowmeter by real time correlation technique. II. Measurement of flow velocity in mockup fuel assembly (LMFBR), 30:31224 (JAPFNR-154)
FLUID FLOW
See also TWO-PHASE FLOW
SAFR4: a program to evaluate the stability of a rigid blade in parallel fluid flow, 30:31280 (WAPD-TM-1085)
FLUORESCENCE SPECTROSCOPY/COMPARATIVE EVALUATIONS
Comparison of analytical techniques for inorganic pollutants, 30:28924
FLUORIDES/MONITORING
Environmental monitoring report, calendar year 1973, 30:29351 (UCC-ND-279)
Portsmouth Gaseous Diffusion Plant environmental monitoring report, 1973, 30:29346 (GAT-781)
FLUORIDES/RADIOLYSIS
Radiolysis of alkaline-earth fluorides (Electron beams), 30:29075
FLUORINE/ATOM-MOLECULE COLLISIONS
Integral equation approach to collinear reactive scattering: $A+BC \rightarrow AB+C$ (Reaction of H, D, and F with H_2), 30:30527
FLUORINE 19/HIGH SPIN STATES
High spin states in the Kaup(π)=1/2$^-$ band of ^{19}F, 30:30885
FOAMS/COMPRESSIBILITY
Static compressive testing of rigid polyurethane foam, 30:31384 (BDX-613-1036(Rev.))
FOCK METHOD
See HARTREE-FOCK METHOD
FOKKER-PLANCK EQUATION/COMPTON EFFECT
Fine structure generalization of the Compton Fokker--Planck equation (Differential model), 30:31105 (UCID-15784)
FOKKER-PLANCK EQUATION/TWO-DIMENSIONAL CALCULATIONS
HYBRID-1, a two-dimensional Fokker--Planck code, 30:29189 (UCRL-51598)
Program IONS: two-dimensional Fokker--Planck equation for ions and electrons, 30:31362 (UCID-16014)
FOLDY-WOUTHUYSEN TRANSFORM/UNITARITY
Unitary Foldy--Wouthuysen transformations for particles of arbitrary spin, 30:31152
FOLIAGE
See LEAVES
FOLLICLE STIMULATING HORMONE
See FSH
FOOD
See also FRUITS
MEAT
MILK
VEGETABLES
FOOD/ACTIVATION ANALYSIS
Comparison of analytical techniques for inorganic pollutants, 30:28924
Elemental analysis of protein-containing food materials from various sources (Neutron activation analysis), 30:28925
FOOD/CHEMICAL ANALYSIS
Comparison of analytical techniques for inorganic pollutants, 30:28924
Novel methods in the analysis of cesium, 30:28976
FOOD/CONTAMINATION
Bibliographies in nuclear science and technology. Section 02: contamination and decontamination of foods. Number 12, 30:29420 (ZAED-BIBL.-02-12)
Phase I. Radiation and radioisotope studies with laboratory and domestic animals (Fallout ^{137}Cs, ^{131}I, and ^{90}Sr in food chains), 30:29417 (COO-3167-102)
FOOD CHAINS/RADIONUCLIDE KINETICS
Plutonium in the Laurentian Great Lakes: food-chain relationships (^{239}Pu; ^{137}Cs), 30:29415 (CONF-740826-3)
Progress report, June 1, 1973--May 31, 1974 (Radioactive effluents and radioisotope migration through food chains), 30:29416 (COO-3167-102)
Radioactive tracer studies of soil and litter arthropod food chains. Progress report, November 1, 1973--October 31, 1974 (Fallout ^{137}Cs tracer), 30:29419 (SRO-641-13)
FORESTS/DENSITY
SAFT: structural analysis of forest trees, 30:31337 (EDFB-IBP-74-4)
FORMALDEHYDE/COSMOCHEMISTRY
4830 MHz formaldehyde line observations of dark clouds in IC 1795/W3/, 30:30372
FORMIC ALDEHYDE
See FORMALDEHYDE
FOSSIL-FUEL POWER PLANTS/AEROSOL WASTES
Preliminary in-plume measurements near Centralia (Trace gases and particulates, power plant), 30:29472 (BNWL-1850(Pt.3))
Trace pollutant emissions in fossil fuel combustion, 30:29469 (BNWL-1850(Pt.3))
FOSSIL-FUEL POWER PLANTS/CONSTRUCTION
Projections of labor requirements for electrical power plant construction 1974--2000, 30:31306 (WASH-1334)
FOSSIL-FUEL POWER PLANTS/NONRADIOACTIVE WASTES
Elemental content of trace elements in vegetation collected at Centralia, Washington (Comparison with Alaskan vegetation), 30:29483 (BNWL-1850(Pt.3))
FOUR-BODY PROBLEM/BINDING ENERGY
Solutions of the integral equations for four identical particles, 30:31103
FOUR-BODY PROBLEM/CORRELATIONS
Correlation effects on the ground-state energy and form factor of few-body systems, 30:31045
FOUR-BODY PROBLEM/GIANT RESONANCE
A microscopic description of the negative parity resonances in the mass-4 system by the coupled-channel method, 30:30871
FOUR-BODY PROBLEM/INTEGRAL EQUATIONS
Solutions of the integral equations for four identical particles, 30:31103
FOUR-BODY PROBLEM/NUCLEONS
Calculations on few-nucleon systems with correlated wave functions (Binding energy, Coulomb energy), 30:31043
FOUR-BODY PROBLEM/SCATTERING AMPLITUDES
Solutions of the integral equations for four identical particles, 30:31103
FOUR-BODY PROBLEM/WAVE FUNCTIONS
Solutions of the integral equations for four identical particles, 30:31103
FRACTIONATED IRRADIATION/RBE
Cellular repair after x or gamma irradiation determined for several gross criteria on animals and patients, 30:29759

FRACTURE PROPERTIES/REVIEWS
Review of current status of yielding fracture mechanics, 30:30053
FRANCE/RADIATION MONITORING
Annex to monthly report, February 1974. Detail of results of measurement (Tabulated data on radioactivity in environmental samples collected throughout France during February 1974), 30:29350 (SCPRI(RM)-2-1974(Suppl.))
Report of activity, February 1974 (Radioactivity of environmental samples collected throughout France during February 1974), 30:29349 (SCPRI(RM)-2-1974)
FRASCATI SYNCHROTRON/ACCELERATOR FACILITIES
180° magnetic spectrometer with helium-filled streamer chamber, 30:29591
FREDHOLM EQUATION/POTENTIAL SCATTERING
Connection between Fredholm determinant and Jost function for nonlocal potentials, 30:30788
FREE RADICALS
See RADICALS
FRESH WATER ECOSYSTEMS
See AQUATIC ECOSYSTEMS
FRICKE DOSEMETERS
See CHEMICAL DOSEMETERS
FRUITS
(Edible parts of plants only.)
FRUITS/RADIOPRESERVATION
Surface irradiation of spherical vegetables and fruits, 30:29645
Technological foundations for radiation treatment of food products (Gamma radiation; electrons; book in Russian), 30:29661
FSH
(Follicle stimulating hormone.)
FSH/RADIOIMMUNOASSAY
Double antibody radioimmunoassay for human urinary follicle stimulating hormone (^{125}I tracer), 30:29861
FT. CALHOUN-1
See CALHOUN-1 REACTOR
FUEL ASSEMBLIES
See also FUEL ELEMENT CLUSTERS
FUEL ASSEMBLIES/CRITICAL HEAT FLUX
Transient critical heat flux and spacer grid studies (PWR), 30:31201
FUEL ASSEMBLIES/DESIGN
Mark C (17 x 17) fuel assembly. Research and development (PWR), 30:31195 (BAW-10097)
FUEL ASSEMBLIES/FLOW BLOCKAGE
Study of local blockages in fast reactor sub-assemblies, 30:31229
FUEL ASSEMBLIES/MOCKUP
Development of sodium flowmeter by real time correlation technique. II. Measurement of flow velocity in mockup fuel assembly (LMFBR), 30:31224 (JAPFNR-154)
FUEL ASSEMBLIES/PERFORMANCE TESTING
Mark C (17 x 17) fuel assembly. Research and development (PWR), 30:31195 (BAW-10097)
FUEL ASSEMBLIES/SPACERS
Fuel assembly for a nuclear reactor (Patent), 30:31292
FUEL BUNDLES
See FUEL ELEMENT CLUSTERS
FUEL CANS/DESTRUCTIVE TESTING
Characterizations of fuel element cladding tubes, 30:31279 (RT/MET-(73)1)
FUEL CANS/FAILURES
Fast reactor programme. First quarter 1974 progress report, 30:31226 (RCN-212)
FUEL CANS/FUEL-CLADDING INTERACTIONS
Chemical immobilization of fission products reactive with nuclear reactor components (Patent), 30:31281
FUEL CANS/INSPECTION
Examination of fuel element cladding including the determination of the mechanical properties, 30:30083
FUEL CANS/NONDESTRUCTIVE TESTING
Characterizations of fuel element cladding tubes, 30:31279 (RT/MET-(73)1)
FUEL CANS/RESEARCH PROGRAMS
Thermodynamic data program involving plutonia and urania at high temperatures. Quarterly report No. 27, February 1, 1974--April 30, 1974 (LMFBR), 30:31223 (GEAP-12511)
FUEL ELEMENT CLUSTERS/HEAT TRANSFER
Fast reactor programme. First quarter 1974 progress report, 30:31226 (RCN-212)
FUEL ELEMENT CLUSTERS/SPACERS
Industrial technique (Patent), 30:31288
FUEL ELEMENTS
See also FUEL ASSEMBLIES
FUEL CANS
FUEL PINS
FUEL PLATES
FUEL RODS
SPENT FUEL ELEMENTS
FUEL ELEMENTS/POWER DENSITY
Neutronic calculations for experiments with light water reactor fuel in PBF, 30:31187 (BNWL-B-371)
FUEL ELEMENTS/SUPPORTS
Spring clamping device in nuclear reactors (Patent), 30:31284
FUEL FABRICATION PLANTS/NONRADIOACTIVE WASTES
Douglas United Nuclear, Inc. reactor and fuel production facilities 1972 environmental release report, 30:29341 (DUN-8133)
FUEL FABRICATION PLANTS/RADIOACTIVE WASTES
Douglas United Nuclear, Inc. reactor and fuel production facilities 1972 environmental release report, 30:29341 (DUN-8133)
FUEL MANAGEMENT/OPTIMIZATION
Equilibrium approach to optimal in-core fuel management for pressurized water reactors, 30:31310
FUEL PINS/FISSION PRODUCTS
Calculation of the effects of fission gas in a LMFBR, for the analysis of an unprotected overpower transient, 30:31225 (KFK-1990)
Fission gas behavior in fast reactor fuel under transient power conditions, 30:31228
FUEL PINS/RESEARCH PROGRAMS
Thermodynamic data program involving plutonia and urania at high temperatures. Quarterly report No. 27, February 1, 1974--April 30, 1974 (LMFBR), 30:31223 (GEAP-12511)
FUEL PINS/STRESS ANALYSIS
Trends in structural mechanics. A UK review of the 2nd international conference on structural mechanics in reactor technology. VIII. Reactor core (HTGR), 30:31213
FUEL PINS/THERMAL CONDUCTION
Thermal accommodation coefficients of inert gases on stainless steel and UO_2, 30:30097
FUEL PLATES/FABRICATION
Metallurgical processing and pulsed reactor fuel performance (U--10 Mo alloy), 30:29982 (SLA-73-1121)
FUEL REPROCESSING PLANTS/ON-LINE MEASUREMENT SYSTEMS
Laboratory and hot-cell studies concerning the in-line polarographic determination of uranium in the aqueous waste stream of the KFA-TBP 23/25 process, 30:28941 (JUL-1063-CT)
FUEL REPROCESSING PLANTS/RADIOACTIVE WASTE DISPOSAL
Agricultural impacts of nuclear power generation in New York State (Preliminary survey agricultural data), 30:29438 (COO-3167-102)
FUEL RODS/SEALS
Hydrogen diffusion seal for nuclear reactor fuel rods (Patent), 30:31294
FUEL RODS/SEAM WELDING
Fuel rod fabrication (Patent), 30:31293
FUEL-CLADDING INTERACTIONS
Chemical immobilization of fission products reactive with nuclear reactor components (Patent), 30:31281
FUKUSHIMA-1 REACTOR/SEISMIC EFFECTS
Comparative forced vibration test of two BWR-type reactor buildings, 30:31265
FUMES
See AEROSOLS
FUNDAMENTAL PARTICLES
See ELEMENTARY PARTICLES
FURNACES
See also VACUUM FURNACES
FURNACES/GAS FLOW
Measurements of three velocity components and their correlations in a model furnace with and without combustion, 30:31414 (AERE-R-7776)
FURNACES/OPERATION
Investigations on material transport and dust formation in revolving furnaces for Clinkering by isotopic tracing, 30:29644
FUSION REACTIONS
(Heavy-ion reactions in which most or all of participating nucleons form single nucleus.)
FUSION REACTIONS/NUCLEAR REACTION KINETICS
Fusion of heavy nuclei in a classical model, 30:31064
FUSION REACTIONS/NUCLEAR REACTIONS
Mechanism of heavy ion collisions leading to a compound system and to deep inelastic direct reactions, 30:31065
FUSION REACTORS
See THERMONUCLEAR REACTORS

G

GADOLINIUM/ACTIVATION ANALYSIS
Determination of rare earths and thorium in apatites by thermal and epithermal neutron-activation analysis, 30:28935
GADOLINIUM/EXTRACTION CHROMATOGRAPHY
Contribution to the separation of rare earths by extraction chromatography with di(2-ethylhexyl) phosphoric acid. II. Behavior of the matrix and its influence on the microcomponents, 30:28990 (ANL-Trans-961)
GADOLINIUM/X-RAY SPECTROSCOPY
Determination of rare earths in plutonium by x-ray emission analysis, 30:28946
GADOLINIUM 143/NUCLEAR PROPERTIES
Nuclear Data Sheets for A = 143, 30:30966
GADOLINIUM 154/NEUTRON REACTIONS
Mass-spectrometric determination of neutron capture cross-sections of the rare earth isotopes (Pile and thermal cross sections), 30:30977 (AEC-tr-7574)
GADOLINIUM 154/ROTATIONAL STATES
On the back-bending in the rotational motion, 30:30991

GADOLINIUM 155/NEUTRON REACTIONS
Intensity fluctuations of γ-transitions from the (anti n,γ) reaction (Reduced-neutron and partial radiation widths), 30:30978 (IAE-2289)
GADOLINIUM 156/NEUTRON REACTIONS
Mass-spectrometric determination of neutron capture cross-sections of the rare earth isotopes (Pile and thermal cross sections), 30:30977 (AEC-tr-7574)
GADOLINIUM ALLOYS/CRYSTAL STRUCTURE
Structure of alloys of cobalt with rare earths of the approximate composition RCo_5, 30:30034
GADOLINIUM OXIDES
Effect of complex admixtures of rare-earth oxides on sintering of cerium dioxide, 30:29909
GALACTIC EVOLUTION/NUCLEOSYNTHESIS
A galactic model with a pulsating active nucleus. III. Evolution of rare-light elements, 30:30386
GALAXIES
See also GALAXY CLUSTERS
MAGELLANIC CLOUDS
MILKY WAY
RADIO GALAXIES
SEYFERT GALAXIES
GALAXIES/CHARGED PARTICLES
Angular distribution of high energy charged particles in the galaxy, 30:30342 (CONF-730693-)
GALAXIES/COSMIC GASES
Gas density and the rate of star formation in M33 (Initial collapse), 30:30348
Two chains of interesting southern galaxies: NGC 7172-7173-7174-7176 and NGC 7201-7203-7204 (Single group), 30:30384
GALAXIES/DOPPLER EFFECT
Redshift of a galaxy near 4C11.50, 30:30378
GALAXIES/ELECTRIC CHARGES
Electrically charged galaxy and its internal and cosmological consequences, 30:30341 (CONF-730693-)
GALAXIES/ELECTROMAGNETIC RADIATION
Galactic electrons and electromagnetic radiation, 30:30343 (CONF-730693-)
GALAXIES/ELECTRONS
Galactic electrons and electromagnetic radiation, 30:30343 (CONF-730693-)
GALAXIES/H2 REGIONS
Gas density and the rate of star formation in M33 (Initial collapse), 30:30348
GALAXIES/INTERFEROMETRY
A study of the H I absorption in the galaxy M82 by radio interferometry (Several features, velocity resolution), 30:30383
GALAXIES/MASS
Dynamic evidence on massive coronas of galaxies, 30:30379
The mass of M33, 30:30389
GALAXIES/PHOTOMETRY
Steps toward the Hubble constant. II. The brightest stars in late-type spiral galaxies (Mean correlation line), 30:30393
U.B.V. photometry of the irregular galaxy NGC 4753, 30:30354
GALAXIES/QUASARS
NGC 520 chain of quasars (Peculiar galaxies), 30:30285
GALAXIES/SPECTRA
Two chains of interesting southern galaxies: NGC 7172-7173-7174-7176 and NGC 7201-7203-7204 (Single group), 30:30384
GALAXIES/STATISTICAL MECHANICS
Equilibrium statistical mechanics of relativistic particles with variable masses. I. Nonquantal theory, 30:30168
GALAXY CLUSTERS/MASS
The density profiles of rich clusters of galaxies (Cutoff radius), 30:30381
GALAXY CLUSTERS/SPATIAL DISTRIBUTION
The density profiles of rich clusters of galaxies (Cutoff radius), 30:30381
GALLIUM/EMISSION SPECTROSCOPY
Spectrographic determination of trace impurities in high purity uranium oxide, 30:28944 (UCID-15952)
GALLIUM/ION EXCHANGE
Selective ion-exchangers containing phosphorus in their functional groups. I. Sorption and separation of some bivalent and trivalent ions, 30:29001
GALLIUM 69/ALPHA REACTIONS
Spectroscopy of the ^{69}Ga and ^{71}Ga isotopes with the ^{69} ^{71}Ga(α,α'γ)^{69} ^{71}Ga and ^{66} ^{68}Zn(α,pγ)^{69} ^{71}Ga reactions (Lifetimes, branching and mixing ratios), 30:30941
GALLIUM 69/ENERGY LEVELS
Spectroscopy of the ^{69}Ga and ^{71}Ga isotopes with the ^{69} ^{71}Ga(α,α'γ)^{69} ^{71}Ga and ^{66} ^{68}Zn(α,pγ)^{69} ^{71}Ga reactions (Lifetimes, branching and mixing ratios), 30:30941
GALLIUM 71/ALPHA REACTIONS
Spectroscopy of the ^{69}Ga and ^{71}Ga isotopes with the ^{69} ^{71}Ga(α,α'γ)^{69} ^{71}Ga and ^{66} ^{68}Zn(α,pγ)^{69} ^{71}Ga reactions (Lifetimes, branching and mixing ratios), 30:30941
GALLIUM 71/ENERGY LEVELS
Spectroscopy of the ^{69}Ga and ^{71}Ga isotopes with the ^{69} ^{71}Ga(α,α'γ)^{69} ^{71}Ga and ^{66} ^{68}Zn(α,pγ)^{69} ^{71}Ga reactions (Lifetimes, branching and mixing ratios), 30:30941
GALLIUM 71/ISOBARIC ANALOGS
A study of isobaric analogue resonances in ^{71}Ga, 30:30949
GALLIUM ARSENIDES/ION IMPLANTATION
Ion implantation of semiconductors, metals, and alloys. Interim report No. 7, 1 September 1971--31 August 1973, 30:30088 (AD-774654)
GALLIUM COMPOUNDS/PHOTONS
Classical-particle description of photons and phonons, 30:30659
GALLIUM PHOSPHIDES/ION IMPLANTATION
Ion implantation of semiconductors, metals, and alloys. Interim report No. 7, 1 September 1971--31 August 1973, 30:30088 (AD-774654)
GALLIUM TELLURIDES/PHASE STUDIES
Ternary system Cd--Ga--Te, 30:30015
GAMMA CAMERAS/DATA PROCESSING
Data processing system for nuclear medicine, 30:29864
GAMMA DETECTION
Feasibility of two schemes for detecting the envelope of a γ-ray burst underground, 30:29321 (UCID-15865)
GAMMA DETECTION/PARTICLE DISCRIMINATION
A fast neutron-gamma discriminator, 30:29535
GAMMA DETECTION/SOLID SCINTILLATION DETECTORS
Efficiencies and response functions of NaI(Tl) crystals for gamma rays from thick disk sources, 30:29517
GAMMA DOSIMETRY
Spectral characteristics of γ radiation ^{60}Co scattered in thin radiators, 30:31109
GAMMA DOSIMETRY/DOSE RATES
Simplified method for calculating dose-rate distributions from extended volumes containing gamma emitters, 30:31107
GAMMA DOSIMETRY/RADIATION DOSE DISTRIBUTIONS
Buildup of scattered radiation behind a shadow shield, 30:31129
GAMMA DOSIMETRY/SCINTILLATION COUNTERS
In-vivo measurement of the gamma and neutron dose rate on patients with ^{238}Pu pacemakers implanted, 30:29704 (KFK-1851)
GAMMA DOSIMETRY/SPATIAL DOSE DISTRIBUTIONS
Simplified method for calculating dose-rate distributions from extended volumes containing gamma emitters, 30:31107
GAMMA DOSIMETRY/THERMOLUMINESCENT DOSEMETERS
In-vivo measurement of the gamma and neutron dose rate on patients with ^{238}Pu pacemakers implanted, 30:29704 (KFK-1851)
GAMMA RADIATION/ABSORPTION SPECTRA
Spectral characteristics of γ radiation ^{60}Co scattered in thin radiators, 30:31109
GAMMA RADIATION/ANGULAR CORRELATION
A 1Ge(Li)-3NaI(Tl) detector system for γ-γ angular correlation measurements, 30:29565
GAMMA RADIATION/ATTENUATION
Gamma-ray attenuation in applied scintillation spectrometry, 30:29562
GAMMA RADIATION/COSMIC RAY FLUX
The distribution of cosmic rays in the galaxy and their dynamics as deduced from recent γ-ray observations (Trapping time), 30:30163
GAMMA RADIATION/RBE
Comment on ''further data on DNA strand breakage by various radiation qualities'' (γ radiation. protons), 30:29660
GAMMA RADIATION/SOLAR RADIATION
Considerations on the neutral component relative to the August 4, 1972 solar event, 30:30296 (CONF-730693-)
GAMMA RADIOGRAPHY
Radiography of steel components with a linear electron accelerator, 30:30143
GAMMA RADIOGRAPHY/DATA PROCESSING
Multichannel processing of digital radiometric data in sequential recording of a finite numer of counts, 30:29299
GAMMA SOURCES
(See also specific radioisotopes.)
See also COSMIC GAMMA SOURCES
GAMMA SOURCES/AERIAL MONITORING
Aerial radiological measuring survey of the Maine Yankee Atomic Power Plant, September 1971, 30:29357 (ARMS-71.6.5)
Aerial radiological measuring surveys of the Turkey Point Station, April 1972, 30:29358 (ARMS-72.6.2)
GAMMA SOURCES/CALIBRATION STANDARDS
Intensities of γ-rays in the decay of sup(166a)Ho, 30:31125
GAMMA SOURCES/DESIGN
Krypton source for arming airborne weapons; patent, 30:29540
GAMMA SOURCES/DOSE RATES
Simplified method for calculating dose-rate distributions from extended volumes containing gamma emitters, 30:31107
GAMMA SOURCES/RADIATION MONITORING
Distribution and inventory element activities on-NTS and off-NTS (^{239}Pu, ^{240}Pu, and ^{241}Am content of soil samples from Nevada Test Site and environs), 30:29453 (NVO-AEIC-74-1)
Operation WHETSTONE: on-site radiological safety report, July 1964--June 1965, 30:29378 (NVO-410-24)

Operation TOGGLE: on-site radiological safety report, July 1972--June 1973, 30:29379 (NVO-410-25)
Portsmouth Gaseous Diffusion Plant environmental monitoring report, 1973, 30:29346 (GAT-781)
Radiological monitoring program, period covering February 4, 1974--April 30, 1974 (Rio Blanco site), 30:29348 (PNE-RB-51-9)
GAMMA SPECTRA/DATA PROCESSING
A method of on-line spectra evaluation by means of a small computer employing Fourier transforms, 30:29563
GAMMA SPECTRA/DOPPLER EFFECT
Doppler shape of a γ-line in Coulomb excitation, 30:31100
GAMMA SPECTROMETERS
See also COMPTON SPECTROMETERS
GAMMA SPECTROMETERS/CALIBRATION
Intensities of γ-rays in the decay of sup(166m)Ho, 30:31125
GAMMA SPECTROMETERS/DESIGN
The Apollo gamma-ray spectrometer (For mapping lunar surface and measuring cosmic γ spectra), 30:29566
GAMMA SPECTROMETERS/PERFORMANCE
A 1Ge(Li)-3NaI(Tl) detector system for γ-γ angular correlation measurements, 30:29565
GAMMA SPECTROSCOPY/CORRECTIONS
Gamma-ray attenuation in applied scintillation spectrometry, 30:29562
GAS COOLANTS
See GASES
GAS COOLED FAST BREEDER REACTOR
See GCFR REACTOR
GAS COOLED FAST BREEDER REACTORS
See GCFR TYPE REACTORS
GAS COOLED REACTORS
See also AGR TYPE REACTORS
GCFR REACTOR
GCFR TYPE REACTORS
HTGR TYPE REACTORS
GAS COOLED REACTORS/CONTAINMENT BUILDINGS
Trends in structural mechanics. A UK review of the 2nd international conference on structural mechanics in reactor technology. I. Pressure vessels and containments, 30:31192
GAS COOLED REACTORS/COOLANTS
Industrial gases for nuclear power plant, 30:31206
GAS FUELED REACTORS/FISSIONING PLASMA
Diagnostics of seeded rf plasmas: an experimental study related to the gaseous core nuclear reactor. Final report, 1 September 1971--31 July 1973 (Argon), 30:31241 (N-74-23299)
GAS SCINTILLATION DETECTORS
Wavelength shifters for xenon proportional scintillation counters, 30:29523
GAS SCINTILLATION DETECTORS/PERFORMANCE
Experimental flight of a large spherical gas scintillator, 30:29521
GASEOUS DIFFUSION PLANTS/ENVIRONMENT
Portsmouth Gaseous Diffusion Plant environmental monitoring report, 1973, 30:29346 (GAT-781)
GASEOUS DIFFUSION PLANTS/GASEOUS WASTES
Measurements of drift from a mechanical draft cooling tower (Air concentrations and surface deposition of Cr from gaseous diffusion plant cooling tower), 30:29487 (BNWL-1850(Pt.3))
GASEOUS DIFFUSION PLANTS/ON-LINE MEASUREMENT SYSTEMS
Continuous in-line monitor for UF_6 enrichment, 30:29509
GASEOUS DIFFUSION PLANTS/RADIATION MONITORING
Portsmouth Gaseous Diffusion Plant environmental monitoring report, 1973, 30:29346 (GAT-781)
GASEOUS WASTES/CHEMICAL RADIATION EFFECTS
Treatment of exhaust gas with electron beam irradiation. I. Treatment of exhaust gas in batch type apparatus, 30:29046
GASES
See also AIR
COSMIC GASES
NATURAL GAS
GASES/MEETINGS
Cryotech '73: the production and use of industrial gases. Proceedings of the British Cryogenics Council conference, Brighton, England, November 13--15, 1973, 30:28992
GASES/RADIOACTIVITY
Method of estimating the total curies in gas samples, 30:29087 (UCID-15809)
GASES/WASHOUT
Extension of the anaysis of plume washdown to include diffusion, 30:29478 (BNWL-1850(Pt.3))
GASTROINTESTINAL TRACT/BIOLOGICAL RADIATION EFFECTS
Effect of irradiation on gastrointestinal drug absorption in mice and rats (Sulfadiazine;quinine;x radiation), 30:29738
Pathological changes in mice following the intraperitoneal administration of radionuclides (^{198}Au and ^{32}P), 30:29784
GASTROINTESTINAL TRACT/RADIONUCLIDE KINETICS
Absorption of ^{47}Ca from digestive tract in patients with urolithiasis, 30:29791
Internal deposition of ingested cerium in suckling mice, 30:29821
GAUGE INVARIANCE/AXIAL-VECTOR CURRENTS
Anomalous currents in gauge field theories, 30:31161
GCFR REACTOR/REACTOR SAFETY
Preapplication safety evaluation of the gas cooled fast breeder reactor, General Atomic Company. Project No. 456, 30:31323 (TID-26631)
GCFR TYPE REACTORS/PLANNING
Role of helium-cooled reactors in meeting the energy crisis and conserving resources, 30:31210
GCFR TYPE REACTORS/SPECIFICATIONS
Role of helium-cooled reactors in meeting the energy crisis and conserving resources, 30:31210
GE(LI) DETECTORS
See LI-DRIFTED GE DETECTORS
GEIGER-MUELLER COUNTERS/COINCIDENCE METHODS
Efficiency of the anticoincidence method applied to the G. M. window counters, 30:29508
GELS/CHEMICAL RADIATION EFFECTS
Method for preparation of biocompatible and biofunctional materials and product thereof (Graft polymerization using high-energy electrons, x or γ radiation, patent), 30:29082
GENE RECOMBINATION/RADIATION EFFECTS
Effect of chronic and acute gamma irradiation on specific recombination capability of lineage WD maize, 30:29689
GENERAL RELATIVITY THEORY
Principle of material indifference in relativity, 30:31172
GENERAL RELATIVITY THEORY/CAUSALITY
Causal boundaries for general relativistic space--times, 30:31175
GENERAL RELATIVITY THEORY/GRAVITATIONAL INTERACTIONS
Can Einstein's theory of gravitation be tested beyond the geometrical optics limit, 30:31183
GENERATORS (ELECTRIC)
See ELECTRIC GENERATORS
GENERATORS (PULSE)
See PULSE GENERATORS
GENERATORS (RADIOISOTOPE)
See RADIOISOTOPE GENERATORS
GENERATORS (STEAM)
See STEAM GENERATORS
GENETIC RADIATION EFFECTS
Genetic radiation effects (^{147}Pm and ^{238}Pu powered cardiac pacemakers), 30:29700 (AED-CONF-74-030-004)
GEOLOGIC DEPOSITS
See also URANIUM DEPOSITS
Zonality of hydrothermal ore deposits. Volume I. Zonality of deposits of tin, tungsten, molybdenum, and some groups of less-common metals (Book in Russian), 30:29332
GEOLOGIC DEPOSITS/POROSITY
Neutron logging of formation porosity and chlorinity, 30:29429
GEOMAGNETIC FIELD/DAILY VARIATIONS
Diurnal variation of the region with vector magnetic field changes associated with field-aligned currents, 30:30461
Role of solar local time in polar a cap magnetic variations, 30:30460
GEOMAGNETIC FIELD/DISTURBANCES
Near-earth magnetic disturbance in total field at high latitudes. I. Summary of data from Ogo 2, 4, and 6, 30:30455
Near-earth magnetic disturbance in total field at high latitudes. II. Interpretation of data from Ogo 2, 4, and 6, 30:30456
GEOMAGNETIC FIELD/INTERACTIONS
Observations of interactions between interplanetary and geomagnetic fields, 30:30366
GEOMAGNETIC FIELD/RADIOWAVE RADIATION
ULF geomagnetic power near L = 4. III. Statistical study of power spectra in conjugate areas during December solstice, 30:30457
ULF geomagnetic power near L = 4. IV. Relationship to the Fredericksburg K index, 30:30458
GEOMAGNETIC FIELD/TRAPPING
Particle saturation of the outer zone: a nonlinear model, 30:30472
GEOTHERMAL ENERGY/RECOVERY
Plowshare technology assessment, prospectives for nuclear-stimulated geothermal power in the western U.S., 30:29311 (PB-231011)
GEOTHERMAL RESOURCES/BRINES
Materials screening program for the LLL geothermal project, 30:31327 (UCRL-75353)
GERMAN FEDERAL REPUBLIC/NUCLEAR POWER PLANTS
The impact of nuclear power plants on the economic structure, 30:31304 (DEU-74-2)
GERMAN FEDERAL REPUBLIC/RADIATION MONITORING
Environmental radioactivity and radiation exposure (German Federal Republic), 30:29355
GERMAN FEDERAL REPUBLIC/RADIOACTIVE WASTE MANAGEMENT
The disposal system in the nuclear fuel cycle, 30:29147
GERMAN FEDERAL REPUBLIC/SHIP PROPULSION REACTORS
German marine shipping: changes in structure and future development. General meeting of the Nuclear Energy Research Society, Hamburg, Germany, December 12, 1973, 30:31243
GERMAN FR ORGANIZATIONS/RESEARCH PROGRAMS
Hahn-Meitner-Institut fuer Kernforschung annual report 1973, 30:31334

GERMANIUM
  Highly resolved electron energy loss spectroscopy of amorphous germanium and silicon layers, 30:31381 (AED-CONF-74-089-025)
GERMANIUM/EMISSION SPECTROSCOPY
  Spectrochemical analysis of uranium oxide by gallium oxide carrier dc arc technique (ASTM Standard E402), 30:28957
  Spectrographic determination of trace impurities in high purity uranium oxide, 30:28944 (UCID-15952)
GERMANIUM/ION CHANNELING
  Electronic stopping power of channelled ions in a model incorporating the Pauli principle (Incident ions Z = 1 to 50), 30:31115
GERMANIUM/PION REACTIONS
  Calculated particle-production spectra from π^- captures in tissue, tissue-equivalent plastic, silicon, and germanium, 30:31120
GERMANIUM/SOLUBILITY
  Solubility of tin and germanium in liquid sodium. The sodium--tin partial phase diagram, 30:30049
GERMANIUM 75/BETA-MINUS DECAY
  Gamma-rays from the decay of ^{75}Ge (Log ft value), 30:30942
GERMANIUM ALLOYS/CHEMICAL PREPARATION
  Joint reduction of niobium, aluminum, and germanium chlorides by hydrogen (Transition temperature of Nb germanides alloyed with 1 to 3 at. percent al = 20 to 20.5°K), 30:29971
GERMANIUM ALLOYS/PHASE DIAGRAMS
  System Ce--Ge, 30:30016
GERMANIUM ALLOYS/SUPERCONDUCTIVITY
  Joint reduction of niobium, aluminum, and germanium chlorides by hydrogen (Transition temperature of Nb germanides alloyed with 1 to 3 at. percent al = 20 to 20.5°K), 30:29971
  Niobium--germanium: becoming a practical superconductor (Nb_3Ge), 30:30806
GERMANY (FEDERAL REPUBLIC)
  See GERMAN FEDERAL REPUBLIC
GIANT CELLS
  See TUMOR CELLS
GIANT RESONANCE/ELECTRIC DIPOLE MOMENTS
  New source of decoupling of E1 strength from the GDR: boundary condition mixing for s- and p-wave neutron states near threshold, 30:31079
GIANT RESONANCE MODEL/MUON REACTIONS
  Nuclear muon capture: a simple model (Giant resonance supermultiplet states excitation), 30:31073
GIANT STARS
  See also RED GIANT STARS
  SUPERGIANT STARS
GIANT STARS/PHOTOMETRY
  Ultraviolet photometry from the orbiting astronomical observatory. XVI. The stellar Lyman-Alpha absorption line (Upper limits), 30:30251
GLACIERS/RADIONUCLIDE MIGRATION
  Determination of fallout radioisotopes from their content in the annual layers of high-mountain glaciers, 30:29408
GLASS/CATHODOLUMINESCENCE
  Luminescence of powdered uranium glasses, 30:30091
GLASS/CRACKS
  Acoustic emission monitoring of ring-cracking in glass and alumina, 30:31410 (UCID-16076)
GLASS/MAGNETIC PROPERTIES
  Rock magnetites with positive anisotropy constants at 300°K, 30:31389 (CONF-740644-1)
GLASS/NUCLEAR REACTION ANALYSIS
  Application of nuclear physics methods for the determination of the depth of lithium ions penetration in the glasses with crystallized surface, 30:28980
  Nondestructive determination of boron in glasses using a ^{241}Am--Be neutron source, 30:28912 (AED-CONF-73-479-009)
GLASS/PARTICLE SIZE
  Improved PETN particle size analyses, 30:31426 (MLM-2098)
GLASS/PHOTOLUMINESCENCE
  Luminescence of powdered uranium glasses, 30:30091
GLAUBER THEORY
  New description of nuclear scattering at intermediate energies and permissibility of Glauber expression to large-angle elastic scattering, 30:31022
GLAUBER THEORY/S MATRIX
  Coulomb T-matrix in the Glauber approximation in the presence of a low frequency electromagnetic field, 30:30790
GLIOBLASTOMAS
  See NEOPLASMS
GLOBAL FALLOUT/CHEMICAL STATE
  State of ^{90}Sr, ^{137}Cs, and ^{144}Ce in radioactive fallout, 30:29384
GLOBAL FALLOUT/DIFFUSION
  Concentrational distribution of fission products over tropical zone oceans and its relation to atmospheric processes, 30:29368
GLOBAL FALLOUT/RADIATION MONITORING
  Radiological monitoring program, period covering February 4, 1974--April 30, 1974 (Rio Blanco site), 30:29348 (PNE-RB-51-9)
GLOBULINS
  See also ANGIOTENSIN
  MYOSIN
GLOBULINS/LABELLING
  Binding of ^{63}Ni to rabbit serum α_1-macroglobulin in vivo and in vitro, 30:29088

GLOMERULI
  Urine /sup 131m/In-EDTA time concentration curve and redistribution of glomerular filtration in the dog, 30:29839
GLUCURONIDASE/BIOCHEMICAL REACTION KINETICS
  Effect of internally deposited plutonium-239 on the lysosomes of rat liver (Compared with effects from ^{198}Au), 30:29782
GLUTATHIONE/BIOLOGICAL EFFECTS
  Experience of use of reduced type of glutathione to prevent side effects of radiotherapy and antineoplastic chemotherapy, 30:29721
GLUTATHIONE/RADIOSENSITIVITY EFFECTS
  Experience of use of reduced type of glutathione to prevent side effects of radiotherapy and antineoplastic chemotherapy, 30:29721
GLYCINE/CHEMICAL RADIATION EFFECTS
  Electron radiation damage of thin films of glycine, diglycine, and aromatic amino acids, 30:29042
GLYCOCOLL
  See GLYCINE
GLYCOGEN/BIOLOGICAL RADIATION EFFECTS
  Changes in glycogen localization and content and activity of enzymes metabolizing glycogen in rat brain during maturation under normal conditions and after gamma irradiation, 30:29761
GOLD/ABSORPTION SPECTROSCOPY
  Separation of trace metal impurities from nuclear grade uranium by long-chain amine extraction and direct determination by atomic absorption spectrophotometry, 30:28948
GOLD/ACTIVATION ANALYSIS
  Application of neutron activation analysis to the determination of gold in minerals, 30:28913 (IEA-316)
  Radioactivation analysis in thermal and epithermal neutrons of the IBR-30 reactor of JINR, 30:28929
  Trace element behavior in soil of some Indonesian sawah's and in sludge of an Indonesian river, 30:28930
GOLD/ADSORPTION
  Effect of irradiation of metal ions on adsorption properties of semiconductor materials. I. Adsorption properties of oxidized surface of silicon (Effect of radioactivity of adsorbed ions), 30:29053
GOLD/EMISSION SPECTROSCOPY
  Spectrochemical analysis of uranium oxide by gallium oxide carrier dc arc technique (ASTM Standard E402), 30:28957
GOLD/ION CHANNELING
  Electronic stopping power of channelled ions in a model incorporating the Pauli principle (Incident ions Z = 1 to 50), 30:31115
GOLD/ION COLLISIONS
  L- and M-shell ionization of various elements by fast-α-particle bombardment (Cross sections, 1 to 5 MeV), 30:30537
GOLD/OXYGEN 16 REACTIONS
  The determination of the differential energy loss of heavy ions backscattered from an infinitely thick solid target (7-35 MeV), 30:30948
GOLD/POSITRON COLLISIONS
  Diffusion of slow positrons from gold (Scattering lengths, Born approximation), 30:30511
GOLD/QUALITATIVE CHEMICAL ANALYSIS
  Application of activation analysis to the determination of pollutants in the atmosphere, 30:28914 (IEA-326)
GOLD 186/NUCLEAR PROPERTIES
  Nuclear Data Sheets for A = 186, 30:30988
GOLD 195/EXCRETION
  Pharmacodynamics of ^{197}Au and ^{195}Au labeled aurothiomalate in blood. Correlation with course of rheumatoid arthritis, gold toxicity, and gold excretion, 30:29792
GOLD 195/TOXICITY
  Pharmacodynamics of ^{197}Au and ^{195}Au labeled aurothiomalate in blood. Correlation with course of rheumatoid arthritis, gold toxicity, and gold excretion, 30:29792
GOLD 197/EXCRETION
  Pharmacodynamics of ^{197}Au and ^{195}Au labeled aurothiomalate in blood. Correlation with course of rheumatoid arthritis, gold toxicity, and gold excretion, 30:29792
GOLD 197/LITHIUM 7 REACTIONS
  Reactions produced by ^{7}Li on ^{197}Au (32 MeV cross sections, reaction mechanisms), 30:30996
GOLD 197/PHOTONUCLEAR REACTIONS
  Photofission in gold at intermediate energy (600 MeV), 30:31002
GOLD 197/TOXICITY
  Pharmacodynamics of ^{197}Au and ^{195}Au labeled aurothiomalate in blood. Correlation with course of rheumatoid arthritis, gold toxicity, and gold excretion, 30:29792
GOLD 198/BIOLOGICAL RADIATION EFFECTS
  Effect of internally deposited plutonium-239 on the lysosomes of rat liver (Compared with effects from ^{198}Au), 30:29782

Pathological changes in mice following the intraperitoneal administration of radionuclides (^{198}Au and ^{32}P), 30:29784
GOLD ALLOYS
See also GOLD BASE ALLOYS
GOLD ALLOYS/QUADRUPOLES
Effect of plastic deformation on quadrupole interaction in Al, Nb, and Au alloyed with Hf, 30:30038
GOLD BASE ALLOYS/FILLER METALS
Properties of TZM and nuclear behavior of TZM brazements. Various properties of TZM and Zr--5Be and Au--18Ni brazing filler metals are determined for brazing TZM to Zr and to steel, 30:30084
GOLDHABER-TELLER MODEL
See GIANT RESONANCE MODEL
GONADS
See also OVARIES
TESTES
GONADS/RADIATION DOSES
Comparison of external irradiation and consumption of cows' milk as critical pathways for ^{137}Cs, ^{54}Mn and ^{144}Ce--^{144}Pr released to the atmosphere, 30:29423
Gonad doses of irradiation of patients in x-ray studies, 30:29718
GONADS/RADIONUCLIDE KINETICS
Transuranium elements in gonadal tissue (^{239}Pu, ^{241}Am, ^{243}Cm, ^{244}Cm, ^{249}Cf, and ^{252}Cf), 30:29806 (COO-119-249)
GRAIN BOUNDARIES/RESEARCH PROGRAMS
Grain boundary sliding and structure. Progress report, December 1, 1973--November 30, 1974, 30:29977 (COO-2172-7)
GRANITES/MECHANICAL PROPERTIES
Effect of fluid content on the mechanical properties of Westerly granite, 30:31411 (UCRL-51626)
GRANITES/X-RAY FLUORESCENCE ANALYSIS
Compilation of x-ray interaction data for x-ray fluorescence analysis of geological samples, 30:28943 (RISO-297)
GRANODIORITES/ELASTICITY
Elastic constants of fractured Hardhat granodiorite, 30:31398 (UCID-15369)
GRANODIORITES/X-RAY FLUORESCENCE ANALYSIS
Compilation of x-ray interaction data for x-ray fluorescence analysis of geological samples, 30:28943 (RISO-297)
GRAPHITE
See also PYROLYTIC GRAPHITE
GRAPHITE/CHEMICAL RADIATION EFFECTS
Interaction of thermal and catalytic processes in the gasification of graphite in CO_2 mixtures (Reactor irradiation), 30:29035 (TRG-Report-2434)
GRAPHITE/CORROSION
Calculation of the corrosion rate of an HTR core under fault conditions, 30:31211
GRAPHITE/IMPREGNATION
Stablized uranyl nitrate compositions and uranium impregnation method (Patent), 30:29127
GRAPHITE/PHYSICAL RADIATION EFFECTS
Changes of dimensions, modulus of elasticity and heat conductivity during re-graphitization by neutron irradiation, 30:30089 (AED-CONF-74-206-001)
Elementary model for radio-induced damage in in-pile graphite: correlation between temperature and flux, 30:30096
GRAPHITE/PRODUCTION
Use of fine-grained electrographite in metal working, 30:31383 (AED-CONF-74-254-001)
GRAPHITE/THERMAL CONDUCTIVITY
Thermal conductivity of carbon foam, 30:31413 (Y-1955)
GRAPHITE/USES
Use of fine-grained electrographite in metal working, 30:31383 (AED-CONF-74-254-001)
GRAPHITE MODERATED REACTORS
See also AGR TYPE REACTORS
HTGR TYPE REACTORS
LWGR TYPE REACTORS
GRAPHITE MODERATED REACTORS/MODERATORS
Improvements in or relating to nuclear reactors (Patent), 30:31214
GRAPHITE MODERATED REACTORS/SPACERS
Improvements in or relating to nuclear reactors (Patent), 30:31214
GRASS/RADIATION MONITORING
Environmental monitoring report, calendar year 1973, 30:29351 (UCC-ND-279)
GRASS/RADIONUCLIDE KINETICS
Data. Section IV. Other data, 30:29412
GRAVITATION
Can Einstein's theory of gravitation be tested beyond the geometrical optics limit, 30:31183
GRAVITATION/CONFORMAL GROUPS
D_2-type representation of the conformal group extended by reflections, 30:30628 (KFKI-74-49)
GRAVITATION/FIELD EQUATIONS
Approximate interior solution in Brans--Dicke theory, 30:31176
GRAVITATIONAL COLLAPSE/MAGNETIC FLUX
Dissipation of magnetic flux and magnetic energy in partially ionized gases, 30:30388
GRAVITATIONAL FIELDS/DIRAC EQUATION
Quantization and the source of the gravitational field (Spinor field, curved space, covariance), 30:31173
GRAVITATIONAL FIELDS/FIELD EQUATIONS
Gravitational field in Finsler spaces, 30:31177
GRAVITATIONAL FIELDS/PLASMA INSTABILITY
Gravitational instability of a rotating plasma, 30:30390
GRAVITATIONAL FIELDS/QUANTUM MECHANICS
Quantization in static gravitational fields, 30:31181
GRAVITATIONAL INTERACTIONS
F-gravity and the proton--electron mass ratio, 30:31174
GRAVITATIONAL INTERACTIONS/RENORMALIZATION
Nonrenormalizability of quantized fermion--gravitation interactions, 30:31179
Nonrenormalizability of Einstein-Yang-Mills interactions at the one-loop level, 30:31184
GRAVITATIONAL RADIATION
See also GRAVITONS
GRAVITATIONAL RADIATION/WHITE DWARF STARS
Gravitional radiation from stellar collapse (Point masses, Schwarzschild radius), 30:30231
GRAVITATIONAL WAVES/INTERACTIONS
Model for the interaction between a gravitational wave and a circular current, 30:31178
GRAVITONS/PARTICLE INTERACTIONS
Nonrenormalizability of quantized fermion--gravitation interactions, 30:31179
GRAVITONS/PROPAGATOR
Trace anomalies in dimensional regularization, 30:31182
GREAT LAKES
See also LAKE MICHIGAN
GREAT LAKES/RADIONUCLIDE MIGRATION
Plutonium in the Laurentian Great Lakes: food-chain relationships (^{239}Pu; ^{137}Cs), 30:29415 (CONF-740826-3)
GREEK RESEARCH REACTOR
See DEMOCRITUS REACTOR
GREEN FUNCTION/ASYMPTOTIC SOLUTIONS
Asymptotic solution of the set of equations for Green's functions in the Yang--Mills field theory, 30:31150
GREEN FUNCTION/DEUTERON REACTIONS
The treatment of two particles in the continuum in a Green's function theory of the (d,p)-reaction, 30:31083
GREEN FUNCTION/SELF-CONSISTENT FIELD
Selfconsistent calculation of the Green's functions in the Hubbard model, 30:31132 (JINR-P4-7225)
GREEN RIVER FORMATION/GEOLOGY
Geology and mineral resources of the Greater Green River Basin. Symposium and core seminar, Casper, Wyoming, September 17--19, 1973 (Leading abstract), 30:29335
GRIDS (COORDINATES)
See COORDINATES
GROUND WATER/RADIATION MONITORING
Environmental monitoring report, calendar year 1973, 30:29351 (UCC-ND-279)
GROUP THEORY
Some relations between the types of the generating systems of Abelian groups and their direct summands, 30:31133 (JINR-P5-7344)
GROUP THEORY/RENORMALIZATION
Gauge dependence of renormalization group parameters, 30:30767
GROWTH HORMONE
See STH
GRR REACTOR
See DEMOCRITUS REACTOR
GULF GENERAL ATOMIC FAST BREEDER REACTOR
See GCFR REACTOR

H

H2 REGIONS/CARBON MONOXIDE
Observations of galactic carbon monoxide emission at 2.6 millimeters (Visual extinction, excitation temperatures), 30:30265
H2 REGIONS/DISTANCE
Investigation of a Milky Way region in Canis Major (Obscuring matter), 30:30217
H2 REGIONS/INFRARED RADIATION
Interferometric studies of OH sources associated with H II regions and ir objects, 30:30368
New infrared sources associated with H II regions, 30:30375
H2 REGIONS/INTERSTELLAR GRAINS
Stellar atmospheres: the sources of interstellar molecules, 30:30241
H2 REGIONS/MIXING
Mixing of neutral gas and dust with the ionized gas of H II regions, 30:30369
H2 REGIONS/RADIATION SOURCES
New infrared sources associated with H II regions, 30:30375
H2 REGIONS/WATER VAPOR
First celestial water vapor sources observed at Itapetinga Radio Observatory, Brazil (Reduction in intensity), 30:30287
HADRON REACTIONS/MULTIPLE PRODUCTION
Diffractive production off nuclei: shadow of hadronic bremsstrahlung, 30:31062
HADRON-HADRON INTERACTIONS
See also MESON-MESON INTERACTIONS
NUCLEON-NUCLEON INTERACTIONS

HADRON-HADRON INTERACTIONS/PARTICLE MODELS
Scaling and asymptotically free massive Yang--Mills field, 30:31147
HADRON-HADRON INTERACTIONS/RESEARCH PROGRAMS
Annual progress report for the period June 1, 1973--May 31, 1974 (Summaries of research activities at Purdue University), 30:30597 (COO-1428-382)
HADRON-HADRON INTERACTIONS/TOTAL CROSS SECTIONS
The quark-parton paradox, 30:30715
HADRONS
See also BARYONS
MESONS
RESONANCE PARTICLES
HADRONS/BOOTSTRAP MODEL
Quark or bootstrap: triumph or frustration for hadron physics (S matrix), 30:30702
HADRONS/MESON NONETS
Gnome model and deep-inelastic lepton-nucleon structure functions, 30:30708
HADRONS/MULTIPLE PRODUCTION
Binary-collision theory for multihadron production amplitudes, 30:30698
HADRONS/QUARK MODEL
Quark or bootstrap: triumph or frustration for hadron physics (S matrix), 30:30702
HADRONS/REGGE TRAJECTORIES
Extended hadrons and Regge slope, 30:30695
HADRONS/SUPERFLUIDITY
SU(3) symmetry breaking and superfluidity of hadronic matter, 30:30781
HADRONS/VACUUM POLARIZATION
Contribution of hadrons to vacuum polarization, 30:30667
HAFNIUM/ACTIVATION ANALYSIS
Trace element behavior in soil of some Indonesian sawah's and in sludge of an Indonesian river, 30:28930
HAFNIUM 166/ELECTRON CAPTURE DECAY
Decay properties of three ^{166}Lu isomers and the decay of ^{166}Hf (Spectra, log ft, Q, branching ratios, K, J, π, L), 30:30989
HAFNIUM 179/DEUTERON REACTIONS
Gamma spectra from ^{179}Hf (d,2n), ^{179}Hf (p,n), and ^{181}Ta (α,2n) reactions, 30:30994
HAFNIUM 179/ENERGY-LEVEL TRANSITIONS
Electromagnetic transitions in some odd-neutron deformed nuclei (Lifetimes, transition probabilities in Nilsson model with pairing and band mixing), 30:30990
HAFNIUM 179/PROTON REACTIONS
Gamma spectra from ^{179}Hf (d,2n), ^{179}Hf (p,n), and ^{181}Ta (α,2n) reactions, 30:30994
HAFNIUM ALLOYS/PERTURBED ANGULAR CORRELATION
Effect of plastic deformation on quadrupole interaction in Al, Nb, and Au alloyed with Hf, 30:30038
HAIR/CHEMICAL ANALYSIS
Method of ^{3}H-determination in hair, 30:28985
HAIR/RADIONUCLIDE KINETICS
Influence of irradiation on the incorporation of radionuclides (^{239}Pu; ^{226}Ra; ^{210}Pb; ^{144}Ce; tritium), 30:29818
HALIDES
See also CHLORIDES
FLUORIDES
HALIDES/SPUTTERING
Hyperthermal beams sputtered from alkali halide surfaces (6-keV Ar^{+}), 30:30484
HALOGENS/ATOM-MOLECULE COLLISIONS
Quantum resonance effects in electronic-to-vibrational energy transfer in molecular collisions (H_2--halogen atom collisions), 30:30534
HAMSTERS/RADIONUCLIDE KINETICS
Removal by DTPA of internally deposited ^{241}Am. A comparative study on rats and Syrian hamsters, 30:29822
HARDENING/MATHEMATICAL MODELS
Additive strength contributions, 30:31427 (RISO-M-1714)
HARTREE-FOCK METHOD/BINDING ENERGY
Centre of mass motion and single particle separation energies in Hartree-Fock theory, 30:31081
HARTREE-FOCK METHOD/CENTER-OF-MASS SYSTEM
Centre of mass motion and single particle separation energies in Hartree-Fock theory, 30:31081
HARTREE-FOCK METHOD/TIME DEPENDENCE
Self-consistent time-dependent Hartree--Fock scheme (Green function), 30:30568
HE-3 COUNTERS/PERFORMANCE
Continuous in-line monitor for UF$_6$ enrichment, 30:29509
HEALTH PHYSICS
See RADIATION PROTECTION
HEAT CAPACITY
See SPECIFIC HEAT
HEAT EXCHANGERS/DESIGN
Flow distribution for heat exchangers (Patent), 30:29275
Industrial technique (patent), 30:29277
HEAT PIPES/DESIGN
Development of a reflux condensing heat pipe for emergency cooling of large cobalt-60 heat source, 30:29255
HEAT PIPES/PERFORMANCE TESTING
Development of a reflux condensing heat pipe for emergency cooling of large cobalt-60 heat source, 30:29255
HEAT PIPES/RESEARCH PROGRAMS
Heat pipe work in Europe, 30:31422 (IKE-5-175)
HEAT RESISTING ALLOYS/POWDER METALLURGY
Powder metallurgy of heat-resistant alloys and refractory metals (Book), 30:29963
HEAT RESISTING ALLOYS/REVIEWS
Nimonic alloys and other nickel-base high-temperature alloys (Book; aircraft gas turbine;strengthening;fabrication;heat treatment;physical and mechanical properties;forms), 30:29988
HEAT TRANSFER/BOUNDARY LAYERS
Two-phase flow and heat transfer at the boundary layer of a thin body of revolution, 30:29291
HEAT TRANSMISSION
See HEAT TRANSFER
HEATERS/TESTING
Fast reactor programme. First quarter 1974 progress report, 30:31226 (RCN-212)
HEAVY ION REACTIONS
See also CARBON 12 REACTIONS
CARBON 13 REACTIONS
KRYPTON 84 REACTIONS
LITHIUM 7 REACTIONS
NEON 20 REACTIONS
OXYGEN 16 REACTIONS
Quasi-fission: a new type of reaction observed in bombarding heavy nuclei by ^{84}Kr and ^{63}Cu ions, 30:30984
HEAVY ION REACTIONS/BREAKUP REACTIONS
Fragmentation of highly excited heavy ions, 30:31074
HEAVY ION REACTIONS/COMPOUND-NUCLEUS REACTIONS
Evidence for quasi-molecular K x-ray emission in heavy ion collisions from the observation of the x-ray directional anisotropy (^{58}Ni + ^{58}Ni, 70 MeV), 30:30922
Mechanism of heavy ion collisions leading to a compound system and to deep inelastic direct reactions, 30:31065
HEAVY ION REACTIONS/DIRECT REACTIONS
Mechanism of heavy ion collisions leading to a compound system and to deep inelastic direct reactions, 30:31065
HEAVY ION REACTIONS/ELASTIC SCATTERING
Microscopic treatment of viscosity in heavy ion reactions, 30:31066
HEAVY ION REACTIONS/FUSION REACTIONS
Fusion of heavy nuclei in a classical model, 30:31064
Mechanism of heavy ion collisions leading to a compound system and to deep inelastic direct reactions, 30:31065
Microscopic treatment of viscosity in heavy ion reactions, 30:31066
Theory of fragmentation dynamics in nucleus-nucleus collisions, 30:31082
HEAVY ION REACTIONS/INELASTIC SCATTERING
A note on diffraction phenomena in the inelastic scattering of complex nuclei, 30:31087
HEAVY ION REACTIONS/MEETINGS
Proceedings of the international conference on reactions between complex nuclei, Nashville, Tennessee, June 10--14, 1974. Volume 1 and Supplement, 30:30982
HEAVY ION REACTIONS/NUCLEAR REACTION KINETICS
Microscopic treatment of viscosity in heavy ion reactions, 30:31066
HEAVY ION REACTIONS/NUCLEAR REACTIONS
Mechanism of heavy ion collisions leading to a compound system and to deep inelastic direct reactions, 30:31065
HEAVY ION REACTIONS/ONE-NUCLEON TRANSFER REACTIONS
Importance of Coulomb interaction potentials in heavy ion DWBA calculations, 30:31063
HEAVY ION REACTIONS/POTENTIAL ENERGY
On the determination of the effective barrier in heavy ion collisions, 30:31070
HEAVY ION REACTIONS/SCATTERING
New analytical derivation of kernels in the resonating group method for composite-particle scattering and molecule-like structures. Derivation from kernels in the generator coordinate method and application to ^{16}O + α, 30:31023
HEAVY ION REACTIONS/SPALLATION
Theory of fragmentation dynamics in nucleus-nucleus collisions, 30:31082
HEAVY ION REACTIONS/THERMONUCLEAR REACTIONS
Complete nuclear fusion reactions (Angular momentum effects), 30:29205 (GSI-tr-73/20)
HEAVY ION REACTIONS/TOTAL CROSS SECTIONS
The validity of the factorization hypothesis for nucleus-nucleus cross sections at high energies (2.1 GeV/nucleon; various combinations from ^{3}He + α to ^{120}Sn + ^{208}Pb), 30:31095
HEAVY ION REACTIONS/TRANSFER REACTIONS
A simple description of differential cross sections for heavy ion induced reactions, 30:31069
HEAVY ION SPECTROMETERS/PERFORMANCE
Performance of a heavy-ion time-of-flight spectrometer, 30:29573
HEAVY ION SPECTROMETERS/TELESCOPE COUNTERS
A high-resolution mass-identification system for heavy ions, 30:29564
HEAVY NUCLEI/CORRELATIONS
Scattering from correlated systems, 30:31056
HEAVY NUCLEI/HEAVY ION REACTIONS
Importance of Coulomb interaction potentials in heavy ion DWBA calculations, 30:31063

On the determination of the effective barrier in heavy ion collisions, 30:31070
HEAVY NUCLEI/NEUTRON REACTIONS
  LARA: a FORTRAN IV code for the calculation of the compound nucleus contribution to the total radiative width in medium and heavy nuclei based on the Brink--Axel model, 30:30956 (RT/FI-(74)17)
HELA CELLS/BIOLOGICAL RADIATION EFFECTS
  Dissociation of histone and DNA synthesis in x-irradiated HeLa cells, 30:29671
  Mechanisms of inhibition of the postirradiation recovery in cells. IV. The effect of caffeine and acriflavine on gamma and x-ray induced unscheduled DNA synthesis in HeLa Zh-63 cells, 30:29675
HELA CELLS/CHROMOSOMAL ABERRATIONS
  Studies on radioresistance with HeLa cells: radiosensitivity and chromosome constitution, 30:29663
HELA CELLS/RADIOSENSITIVITY
  Studies on radioresistance with HeLa cells: radiosensitivity and chromosome constitution, 30:29663
  Thermal enhancement of the radiosensitivity using cultured normal and neoplastic cells (Potential significance for radiotherapy), 30:29004
HELIUM/ATOM-ATOM COLLISIONS
  Long-range He$_2$($^3\Sigma$/sub g,u/$^+$) potentials and metastability exchange in He*--He collisions (Cross sections, elastic scattering, excitation), 30:30494
HELIUM/ATOM-MOLECULE COLLISIONS
  Electron-loss cross sections for fast, excited He atoms in H$_2$ (8 to 160 keV), 30:30539
  Improved modified wavenumber approximation applied to elastic collision (Application to He--H$_2$), 30:30529
HELIUM/CHEMICAL ANALYSIS
  Determination of mineral-oil in the helium-circuit of a refrigeration-plant, 30:31393 (KFK-1978)
HELIUM/COLLISIONS
  Helium scattering from solid surfaces, 30:30480
  Semiclassical theory of atom--solid-surface collisions: application to He--LiF diffraction, 30:30476
  The inelastic scattering of He and Ne from a (001) surface of sodium fluoride, 30:30479
HELIUM/COSMOCHEMISTRY
  Island solutions in linear series of static stellar models with core helium and shell hydrogen burning for M=5,7, and 9 M/subsun/ (Mass loss, secular stability), 30:30198
  On the semiconvective zone in the core-helium-burning stars, 30:30264
  X-ray ionization and the helium abundance in 3C 120 (Time scale, forbidden-line intensities), 30:30347
HELIUM/DIELECTRIC PROPERTIES
  Dielectric properties of helium: Quantum statistical mechanics, 30:30502
HELIUM/DIFFUSION
  Irradiation effects on reactor structural materials. Semiannual progress report, 1 August 1973--31 January 1974, 30:30060 (AD-777433)
HELIUM/ELECTRON-ATOM COLLISIONS
  Equations of motion method: Inelastic electron scattering for helium and CO$_2$ in the Born approximation, 30:30550
  New technique for threshold excitation spectroscopy, 30:30553
  Step-by-step excitation in helium (0.2 to 1.0 eV: cross sections), 30:30489
HELIUM/ENERGY-LEVEL TRANSITIONS
  Multiphoton transitions in helium between 1S and 2S levels (Momentum-translation approximation), 30:30488 (AD-777042)
HELIUM/EXCITATION
  Step-by-step excitation in helium (0.2 to 1.0 eV: cross sections), 30:30489
HELIUM/INTERATOMIC FORCES
  Energy dependence in interatomic potentials-He$_2$ (Angular momentum), 30:30497
  Long-range He$_2$($^3\Sigma$/sub g,u/$^+$) potentials and metastability exchange in He*--He collisions (Cross sections, elastic scattering, excitation), 30:30494
HELIUM/METASTABLE STATES
  Fine structure of the metastable a$^3\Sigma^+$/subu/ state of the helium molecule, 30:30492
HELIUM/MUON REACTIONS
  Negative muon capture in very light atoms, 30:30509
HELIUM/MUONIC ATOMS
  Population of muonic ^{3}He states following the μ-catalysed fusion pμd$\to\mu^3$He, 30:30515
HELIUM/OSCILLATOR STRENGTHS
  Equations of motion method: Inelastic electron scattering for helium and CO$_2$ in the Born approximation, 30:30550
HELIUM/PHOTOIONIZATION
  Absolute cross sections for the photoionization of He(n^1 ^{3}P) atoms, 30:30500
  Photoionization of He(n^1 ^{3}P) atoms excited by polarized light, 30:30498
HELIUM/POLARIZABILITY
  Dielectric properties of helium: The polarizability of diatomic helium, 30:30504
  Helium diatom polarizability and the dielectric properties of fluid helium, 30:30506
HELIUM/SURFACE PROPERTIES
  Interaction of surface electrons in liquid helium with oscillations of the vapor--liquid interface, 30:30801
HELIUM/THERMAL CONDUCTION
  Thermal accommodation coefficients of inert gases on stainless steel and UO$_2$, 30:30097
HELIUM 3/COSMOCHEMISTRY
  A galactic model with a pulsating active nucleus. III. Evolution of rare-light elements, 30:30386
HELIUM 3/ELECTROMAGNETIC FORM FACTORS
  Convergence of the hyperspherical expansion treatment of few-nucleon bound states, 30:30859
HELIUM 3/FORM FACTORS
  Correlation effects on the ground-state energy and form factor of few-body systems, 30:31045
HELIUM 3/GROUND STATES
  Correlation effects on the ground-state energy and form factor of few-body systems, 30:31045
HELIUM 3/HELIUM 3 REACTIONS
  On the determination of the nucleon-nucleon scattering parameters through final state interactions, 30:30868
HELIUM 3/NEUTRON REACTIONS
  Variational calculations of reactions involving light nuclei, 30:30861
HELIUM 3/PHOTONUCLEAR REACTIONS
  An experimental investigation of π photoproduction processes on ^{3}He (Cross sections, angular distributions), 30:30874
  The ^{3}He(γ,π^+)^{3}H reaction in the (3,3) resonance region (Cross sections), 30:30869
HELIUM 3/PROTON REACTIONS
  A microscopic description of the negative parity resonances in the mass-4 system by the coupled-channel method, 30:30871
  Variational calculations of reactions involving light nuclei, 30:30861
HELIUM 3/SUPERFLUIDITY
  Experiments on dynamic parallel magnetism in superfluid ^{3}He, 30:30803
  Superfluid phases of liquid ^{3}He, 30:30794
HELIUM 3/THERMAL CONDUCTIVITY
  Temperature, pressure, and concentration dependence of the thermal conductivity of very dilute solutions of ^{3}He in superfluid ^{4}He, 30:30800
HELIUM 3/THREE-BODY PROBLEM
  Ground-state properties of three-nucleon systems: a review (Binding energy, charge form factor, magnetic moment), 30:31039
HELIUM 3/WAVE FUNCTIONS
  Approximate D-states and meson exchange currents, 30:30870
HELIUM 3 REACTIONS/ELASTIC SCATTERING
  Target-spin effects on elastic scattering cross sections, 30:30940
HELIUM 3 REACTIONS/EXCITATION FUNCTIONS
  Q-values and excitation functions of nuclear reactions. Part C. Estimation of unknown excitation functions and thick target yields for p, d, ^{3}He, and α reactions (Up to 25 or 35 MeV), 30:30960
HELIUM 3 REACTIONS/INELASTIC SCATTERING
  Structure of low-lying 0$^+$ states in fsub(7/2) shell nuclei from inelastic ^{3}He scattering (29 MeV: differential cross sections, DWBA), 30:30934
HELIUM 3 REACTIONS/PICKUP REACTIONS
  Distorted wave Born approximation analysis for the ^{16}O(^{3}He,α)^{15}O reaction (15 MeV; spectroscopic factors), 30:30888
  Excitation of the deeply bound gsub(9/2) neutron hole state in ^{117}Sn by a neutron pickup reaction with 81.7 MeV ^{3}He particles (Alpha spectra from reactions with ^{117}Sn and ^{208}Pb), 30:30974
  On the determination of the nucleon-nucleon scattering parameters through final state interactions, 30:30868
HELIUM 3 REACTIONS/STRIPPING
  Nuclear structure calculation of ^{50}Sc and analysis of the ^{48}Ca(^{3}He,p)^{50}Sc reaction, 30:30946
HELIUM 3 REACTIONS/TOTAL CROSS SECTIONS
  The validity of the factorization hypothesis for nucleus-nucleus cross sections at high energies (2.1 GeV/nucleon; various combinations from ^{3}He + α to ^{120}Sn + ^{208}Pb), 30:31095
HELIUM 4
    See also HELIUM II
  Approach to a uniform theory of the liquid and solid phases of ^{4}He at absolute zero, 30:30799
HELIUM 4/BACKSCATTERING
  Evaluation of glancing angle x-ray diffraction and MeV ^{4}He backscattering analyses of silicide formation, 30:29939
HELIUM 4/BINDING ENERGY
  Centre of mass coordinate in many-body theories, 30:30860
  Convergence of the hyperspherical expansion treatment of few-nucleon bound states, 30:30859
  Hartree-Fock calculations using Sussex matrix elements (Single particle spectra), 30:30863
  Solutions of the integral equations for four identical particles, 30:31103
HELIUM 4/ELECTROMAGNETIC FORM FACTORS
  Centre of mass coordinate in many-body theories, 30:30860
HELIUM 4/ENERGY LEVELS
  A microscopic description of the negative parity resonances in the mass-4 system by the coupled-channel method, 30:30871

Hartree-Fock calculations using Sussex matrix elements (Single particle spectra), 30:30863
HELIUM 4/FORM FACTORS
Correlation effects on the ground-state energy and form factor of few-body systems, 30:31045
New method for evaluating the density matrix and its application to the ground state form factor, 30:30858
HELIUM 4/GROUND STATES
Correlation effects on the ground-state energy and form factor of few-body systems, 30:31045
HELIUM 4/MUONIC ATOMS
Polarizability contribution to the energy levels of the muonic helium $(\mu^4\mathrm{He})^+$, 30:30516
HELIUM 4/NUCLEAR POTENTIAL
^{4}He nucleus and soft core potentials (Binding energy, nucleon density, form factor), 30:30857
HELIUM 4/PHOTONUCLEAR REACTIONS
A microscopic description of the negative parity resonances in the mass-4 system by the coupled-channel method, 30:30871
HELIUM 4/PROTON REACTIONS
Self-consistent wave functions, center-of-mass motion and high-energy particle-nucleus scattering, 30:31098
HELIUM 4/WAVE FUNCTIONS
Solutions of the integral equations for four identical particles, 30:31103
HELIUM 4/WAVE PROPAGATION
Ultrasonic dispersion and attenuation near the liquid--gas critical point of ^{4}He, 30:30798
HELIUM II/FOURTH SOUND
Velocity of fourth sound, 30:30804
HELIUM II/KINETICS
Formulae for kinetic coefficients in the case of He II (Green functions, hydrodynamics, thermal conductivity), 30:30793
HELIUM II/SECOND SOUND
Temperature dependence of the second sound velocity reduction in rotating liquid helium (1.3 to 2.1 K), 30:30797
HELIUM II/THERMAL CONDUCTIVITY
Temperature, pressure, and concentration dependence of the thermal conductivity of very dilute solutions of ^{3}He in superfluid ^{4}He, 30:30800
HELIUM IONS/BACKSCATTERING
Backscattering measurements and surface roughness, 30:30486
HELIUM IONS/COLLISIONS
L- and M-shell ionization of various elements by fast-α-particle bombardment (Cross sections, 1 to 5 MeV), 30:30537
HELIUM IONS/ENERGY LOSSES
Helium ion stopping cross sections in bismuth, lead, and tungsten, 30:31114
HELIUM IONS/ION-ATOM COLLISIONS
Argon L-shell ionization by 50- to 600-keV H^+, D^+, H_2^+, and He^+ impact (Branching ratios, excitation, multiple-vacancy states, total cross sections, ionization), 30:30541
Cross section for the Ar--L--x-ray emission in collisions of He^{+-}, Ne^{+-}, and Ar^{+-} ions with Ar atoms (100 keV to 1 MeV), 30:30518 (AED-CONF-74-085-002)
High-energy calculation of K-shell ejection cross sections as a function of projectile charge (Born approximation), 30:30536
Inelastic collisions of He^+ and Ar (Cross sections, threshold to 10 keV), 30:30538
HELIUM IONS/ION-MOLECULE COLLISIONS
Vibrational energy distribution in CO_2^+ (A^{2}PIsub(u)) ions produced by collisions of H_2^+ and He^+ ions with CO_2, 30:30558
HELIUM IONS/RADIOTHERAPY
Radiobiology with heavy charged particles directed at radiotherapy, 30:31117
HELIUM IONS/STOPPING POWER
Helium ion stopping cross sections in bismuth, lead, and tungsten, 30:31114
HELIUM METHOD
See ISOTOPE DATING
HEMANGIOMAS
See ANGIOMAS
HEMATITE/PHASE DIAGRAMS
Hematite phase diagram in a magnetic field. I. Low-temperature modification, 30:31392 (JINR-P14-7974)
HEMATOPOIESIS
See BLOOD FORMATION
HEMATOPOIETIC SYSTEM/BIOLOGICAL RADIATION EFFECTS
Time course of the radioprotective effect and the formation of endogenous colonies of haemopoietic cells in mouse spleen following the administration of sodium fluoroacetate (X Radiation; mice), 30:29747
HEMOGLOBIN/BIOLOGICAL RADIATION EFFECTS
Effects of certain denaturants on the absorption spectra of hemoglobin from chick embryos irradiated with ultraviolet radiation during early embryogenesis, 30:29661
Kinetics of the changes of mouse hemoglobin under uv-irradiation, 30:29659
HEMOLYSIS/RADIOINDUCTION
Osmotic haemolysis as a means of studying erythropoietic stresses: response to acute anaemia and acute irradiation (^{59}Fe tracer), 30:29736 (RT/BIO-(74)10)
HEMOPOIESIS
See BLOOD FORMATION
HENS
See CHICKENS
HEPARIN/CHEMICAL RADIATION EFFECTS
Method for preparation of biocompatible and biofunctional materials and product thereof (Graft polymerization using high-energy electrons, x or γ radiation, patent), 30:29082
HETEROZYGOTES
See HYBRIDIZATION
HIGH ENERGY PHYSICS/RESEARCH PROGRAMS
Annual progress report, task B, for June 1, 1973--May 31, 1974 (Summaries of theoretical research activities at Purdue University), 30:30626 (COO-1428-389)
Annual report for period October 1, 1973--September 30, 1974 (Summaries of research activities at Purdue University), 30:30574 (COO-1428-391)
Research fields in physics (Research topics listing), 30:30645
HIGH ENERGY PHYSICS/REVIEWS
Proceedings of the fifth Hawaii topical conference in particle physics, Honolulu, Hawaii, August 8--21, 1973, 30:30577
HIGH EXPLOSIVES
See CHEMICAL EXPLOSIVES
HIGH-BETA PLASMA/RESEARCH PROGRAMS
High beta capture and mirror confinement of laser-produced plasmas. Semiannual report, January 1, 1974 through July 31, 1974, 30:29152 (COO-2277-4)
HIGH-TEMPERATURE GAS-COOLED REACTOR
See HTGR TYPE REACTORS
HISTONES/BIOSYNTHESIS
Dissociation of histone and DNA synthesis in x-irradiated HeLa cells, 30:29671
HISTONES/CHEMICAL RADIATION EFFECTS
Changes in genetic cell material during the action of ionizing radiation (Effects of uv and x radiation on DNA and nucleoproteins), 30:29655
HISTONES/PHOSPHORYLATION
Effect of x rays on the phosphorylation of histon f_1 in thymocytes, 30:29653
Histone F1 phosphorus content and DNA synthesis in slowly-growing sublines of L5178Y-S cells, 30:29669
HODOSCOPES/SOLID SCINTILLATION DETECTORS
Multi-strip scintillation counters (MSSC), 30:29585
HOLMIUM/ACTIVATION ANALYSIS
Determination of rare earths and thorium in apatites by thermal and epithermal neutron-activation analysis, 30:28935
HOLMIUM 165/NEUTRON REACTIONS
Forward scattering of 2-MeV neutrons from oriented ^{165}Ho (Polarization, differential cross sections), 30:30981
Status report to NCSAC, 30:31011 (UCID-15639)
HOLMIUM 166/ENERGY-LEVEL TRANSITIONS
Intensities of γ-rays in the decay of sup(166m)Ho, 30:31125
HOLMIUM ALLOYS/SPECIFIC HEAT
Specific heat in TbZn and HoZn compounds (20 to 300°K; YZn; magnetic properties), 30:29990
HOLOGRAPHY
Polaroid vectograph process and application as applied to stereo laser and computer-generated 3-dimensional forms, 30:31352 (UCID-15840)
HOLOGRAPHY/USES
Dynamic interferometric holography, 30:31440 (UCID-15682)
HOMOGENEOUS PLASMA/ROTATION
Gravitational instability of a rotating plasma, 30:30390
HOMOZYGOTES
See HYBRIDIZATION
HORDEUM
See BARLEY
HORMONES
See also INSULIN
HORMONES/RADIOASSAY
Identification of sparganum growth factor by a radioreceptor assay for growth hormone (^{125}I tracer technique), 30:29868
HOSPITALS/CONTAMINATION
Unexpected complication in the use of ^{169}Yb--DTPA with respect to hospital health physics, 30:29824
HOT CELLS/VENTILATION
Ventilation design modifications at Los Alamos Scientific Laboratory major plutonium operational areas, 30:29328 (LA-UR-74-1132)
Ventilation design for new Plutonium Recovery Facility, 30:29329 (RFP-2215)
HOT LABS/VENTILATION
LLL spray damper project (Fire protection of ventilation systems), 30:29330 (UCID-15941)
HOT PLASMA
See also LASER-PRODUCED PLASMA
HOT PLASMA/LASER-RADIATION HEATING
Collector probe measurements of the parameters of a laser plasma at long distances, 30:29172
HOT PLASMA/PLASMA DIAGNOSTICS
Collector probe measurements of the parameters of a laser plasma at long distances, 30:29172
Numerical analysis of interferrograms of asymmetric plasma objects, 30:29176

  Spectroscopic methods for diagnostics of superdense hot plasma, 30:29163
HOT PLASMA/PLASMA EXPANSION
  Numerical analysis of interferrograms of asymmetric plasma objects, 30:29176
HTGR TYPE REACTORS
  Exploratory study of several advanced nuclear-MHD power plant systems, 30:31209
  Feasibility problems on UHTR for closed cycle MHD-power plants, 30:31208
HTGR TYPE REACTORS/COATED FUEL PARTICLES
  Trends in structural mechanics. A UK review of the 2nd international conference on structural mechanics in reactor technology. VIII. Reactor core, 30:31213
HTGR TYPE REACTORS/FUEL PINS
  Trends in structural mechanics. A UK review of the 2nd international conference on structural mechanics in reactor technology. VIII. Reactor core, 30:31213
HTGR TYPE REACTORS/MODERATORS
  Calculation of the corrosion rate of an HTR core under fault conditions, 30:31211
HTGR TYPE REACTORS/NEUTRON FLUX
  New methods of measuring ^{238}U capture rate and fast fluxes in a zero energy HTR lattice, 30:31212
HTGR TYPE REACTORS/PERFORMANCE
  Role of helium-cooled reactors in meeting the energy crisis and conserving resources, 30:31210
HTGR TYPE REACTORS/REACTOR KINETICS
  New methods of measuring ^{238}U capture rate and fast fluxes in a zero energy HTR lattice, 30:31212
HTGR TYPE REACTORS/SPECIFICATIONS
  Role of helium-cooled reactors in meeting the energy crisis and conserving resources, 30:31210
HUBBLE EFFECT
  Steps toward the Hubble constant. II. The brightest stars in late-type spiral galaxies (Mean correlation line), 30:30393
HUBBLE-HUMASON SHIFT
  See HUBBLE EFFECT
HUMAN CELLS
  See ANIMAL CELLS
HUMAN POPULATIONS/RADIATION DOSES
  Behavior and characteristics of radioactive debris from the Chinese nuclear weapons test of June 26, 1973, 30:29362 (BNWL-1850(Pt.3))
  Calculations of doses, population doses, and potential health effects due to atmospheric releases of radionuclides from U.S. nuclear power reactors in 1972, 30:29383
  Comparison of mathematical models for calculation of external gamma doses originating from releases of radioactivity to the atmosphere, 30:29342 (RISO-M-1726)
  Data. Section IV. Other data, 30:29412
  Environmental monitoring report, calendar year 1973, 30:29351 (UCC-ND-279)
  Environmental monitoring report: United States Atomic Energy Commission, Oak Ridge facilities. Calendar year 1973 (Monitoring), 30:29352 (UCC-ND-280)
  Feed Materials Production Center environmental monitoring annual report for 1973, 30:29347 (NLCO-1109)
  Grazing studies on selected plutonium-contaminated areas in Nevada (U and Pu uptake by cattle), 30:29448 (NVO-AEIC-74-1)
  Phase I. Radiation and radioisotope studies with laboratory and domestic animals (Fallout ^{137}Cs, ^{131}I, and ^{90}Sr in food chains), 30:29417 (COO-3167-102)
  Portsmouth Gaseous Diffusion Plant environmental monitoring report, 1973, 30:29346 (GAT-781)
  Radiation in man's environment (Hazards from fallout as compared with other radiation sources in Australia), 30:29353
HUMAN POPULATIONS/RADIATION HAZARDS
  Health physics and technical considerations concerning the control of gaseous effluents from nuclear power plants, 30:29356 (AED-CONF-74-157-005)
HUMAN POPULATIONS/RADIATION PROTECTION
  Environmental radioactivity and radiation exposure (German Federal Republic), 30:29355
  Off-site surveillance. Final report. Report on Project Dribble, Salmon Event, Tatum Salt Dome, Mississippi, 22 October 1964, 30:29345 (AD-629357)
HUMBOLDT BAY REACTOR/REACTOR OPERATION
  Semiannual operations report, January--June 1974, 30:31312 (DOCKET-50133-195)
HUTCHINSON ISLAND-1 REACTOR
  See LUCIE-1 REACTOR
HUTCHINSON ISLAND-2 REACTOR
  See LUCIE-2 REACTOR
HYBRIDIZATION
  Reciprocal translocation as a new approach to breeding seedless watermelon. I. Some characters of F$_1$ hybrids with six reciprocal translocations (X radiation), 30:29686
HYBRIDS
  See HYBRIDIZATION
HYDRATED ELECTRONS
  See SOLVATED ELECTRONS
HYDRIDE MODERATORS/CORROSION
  Ion-backscattering study of LiOH-to-Li$_2$O conversion on a LiH substrate (Surface hydrolysis reactions), 30:29937
HYDROCHLORIC ACID/CORROSIVE EFFECTS
  Stress corrosion cracking of zirconium in methanol--HCl solutions, 30:29957
HYDROCORTISONE/BIOLOGICAL EFFECTS
  Direct relationship between immune competence and the subcutaneous growth rate of a malignant murine lung tumor (X radiation), 30:29756
HYDROCORTISONE/METABOLISM
  Cortisol metabolism in skin of beagles bearing ^{241}Am: a possible pre-neoplastic change in steroid metabolism, 30:29780 (COO-119-249)
HYDROCYANIC ACID/EXCITATION
  Rotational excitation of HCN by collisions (Transition probabilities), 30:30385
HYDRODYNAMICS MODEL/MULTIPLE PRODUCTION
  Transverse momentum bounds and scaling in the hydrodynamical model, 30:30700
HYDRODYNAMICS MODEL/SCALING LAWS
  Transverse momentum bounds and scaling in the hydrodynamical model, 30:30700
HYDRODYNAMICS MODEL/TRANSVERSE MOMENTUM
  Transverse momentum bounds and scaling in the hydrodynamical model, 30:30700
HYDROFLUORIC ACID/CORROSIVE EFFECTS
  Corrosion of sheet and welded joint specimens of Incoloy 825-low carbon (C less than or equal to 0.03%) in HNO$_3$ (Huey) and HF solutions, 30:29956
HYDROGEN/ADSORPTION
  Cryovacuum hydrogen adsorption by small-sized, activated mineral coal with a binder (Adsorption of benzene at 20°C and hydrogen from 20.4 to 50°K), 30:31394 (KHFTI-73-25)
  Tritium Effluent Control Project. Progress Report: April--June 1974, 30:29026 (MLM-2171(LD))
HYDROGEN/ATOM-ATOM COLLISIONS
  Observation of orbiting resonances in the integral cross section of H--Xe (1.0 to 30 MeV (cm)), 30:30532
HYDROGEN/ATOM-MOLECULE COLLISIONS
  Adiabatic distorted wave calculation of H+H$_2$ reactive scattering (0.5 eV (cm)), 30:30533
  Angular distributions for the reactive scattering of H and D atoms by polyatomic molecules, 30:30519 (AED-CONF-74-085-004)
  Electron-loss cross sections for fast, excited He atoms in H$_2$ (8 to 160 keV), 30:30539
  Improved modified wavenumber approximation applied to elastic collision (Application to He--H$_2$), 30:30529
  Integral equation approach to collinear reactive scattering: A+BC+AB+C (Reaction of H, D, and F with H$_2$), 30:30527
  Quantum resonance effects in electronic-to-vibrational energy transfer in molecular collisions (H$_2$--halogen atom collisions), 30:30534
HYDROGEN/ATOMIC BEAMS
  Design of a high density atomic hydrogen source and determination of Balmer cross sections (20 to 440 eV), 30:30526
HYDROGEN/COSMOCHEMISTRY
  Dust, star, and hydrogen distributions in the Orion association, 30:30242
  Formation and destruction rates of interstellar H$_2$ (Absolute magnitude, total densities), 30:30349
  Island solutions in linear series of static stellar models with core helium and shell hydrogen burning for M=5,7, and 9 M/subsun/ (Mass loss, secular stability), 30:30198
HYDROGEN/DIFFUSION
  HYDIZ: a 2-dimensional computer progam for migration of interstitial solutes of finite solubility in a thermal gradient (LWBR Development Program), 30:29983 (WAPD-TM-1157)
HYDROGEN/ELECTRON-ATOM COLLISIONS
  Design of a high density atomic hydrogen source and determination of Balmer cross sections (20 to 440 eV), 30:30526
  Differential cross sections for the elastic scattering of electrons from atomic hydrogen. II. Medium energies (Total cross sections), 30:30535
HYDROGEN/ELECTRON-MOLECULE COLLISIONS
  Differential cross sections for the elastic scattering of electrons from atomic hydrogen. II. Medium energies (Total cross sections), 30:30535
HYDROGEN/ENERGY LEVELS
  Quantum-defect theory of excited ^{1}PI/sub u/$^{-}$ levels of H$_2$ (Rydberg levels, J), 30:30496
HYDROGEN/EXCITATION
  On the theory of H$_2$ rotational excitation (Mean value, gas temperature), 30:30357
  Rate coefficients for electron excitation of the first resonance transition in H, Li, Na, Ca, Ca^{+}, and Ba^{+} calculated from experimental data (Transition probabilities), 30:30246
HYDROGEN/G VALUE
  Chemical behavior of intermediates produced in sulfuric acid glass by gamma irradiation. I. Reactivities of mobile electrons with inorganic ions, 30:29048
HYDROGEN/HYPERFINE STRUCTURE
  Weak hyperfine structure measurement using the magnetic repolarization effect: Application to N=1 v=1 (1s 3d)^{1}I level of H$_2$, 30:30503

HYDROGEN/INTERSTELLAR SPACE
Is H^- a source of diffuse interstellar lines. (Negative results), 30:30361
HYDROGEN/ION-ATOM COLLISIONS
Variational bounds on the 1s-charge-exchange amplitude in proton--hydrogen-atom scattering, 30:30542
HYDROGEN/MASS SPECTROSCOPY
Application of a mass spectrometer to the method of determination of gases in metals by vacuum fusion, 30:28938 (CNEA-363)
HYDROGEN/MOLECULAR STRUCTURE
Determination of the singlet--triplet separation of H_2 by a level-anticrossing technique, 30:30490
HYDROGEN/MUON REACTIONS
Negative muon capture in very light atoms, 30:30509
HYDROGEN/PHOTOIONIZATION
Calculated photoionization cross sections and relative experimental photoionization intensities for a selection of small molecules, 30:30491
HYDROGEN/PHOTON-MOLECULE COLLISIONS
Raman process in the case of multiphoton excitation of the hydrogen molecule in an intense laser beam, 30:30551
HYDROGEN/PRODUCTION
Nuclear energy requirements for hydrogen production from water, 30:31239
HYDROGEN/SEPARATION PROCESSES
Tritium Effluent Control Project. Progress Report: April--June 1974, 30:29026 (MLM-2171(LD))
HYDROGEN/SOLUBILITY
Solubility of hydrogen in vanadium and niobium at high temperatures (1273 to 2273°K; up to 25 atm; V--H; Nb--H; Ta--H), 30:29918
HYDROGEN/ULTRAVIOLET RADIATION
Radiative transitions involving the $(2p^2)$ ^3P/sup e/ metastable autodetaching state of H^- (Transition probabilities, Hylleraas bound-state wave function), 30:30245
HYDROGEN/WASHOUT
Precipitation scavenging of inorganic pollutants from metropolitan sources: St. Louis, July 1973, 30:29479 (BNWL-1850(Pt.3))
HYDROGEN 2
See DEUTERIUM
HYDROGEN 3
See TRITIUM
HYDROGEN CHLORIDES
See HYDROCHLORIC ACID
HYDROGEN COMPOUNDS/EMISSION SPECTRA
Intensities of the dipole and quadrupole rotation-vibration spectra of HD, 30:30501
HYDROGEN FLUORIDES
See HYDROFLUORIC ACID
HYDROGEN IONS
See also HYDROGEN IONS 1 PLUS
HYDROGEN IONS 2 PLUS
HYDROGEN IONS/COSMOCHEMISTRY
Statistical properties of interstellar clouds (Power law), 30:30350
HYDROGEN IONS 1 PLUS/BACKSCATTERING
Energy and charge distribution of backscattered particles during bombardment of metal surfaces with protons (Less than 50 keV), 30:30474 (AED-CONF-74-089-032)
HYDROGEN IONS 1 PLUS/ION-ATOM COLLISIONS
Argon L-shell ionization by 50- to 600-keV H^+, D^+, H_2^+, and He^+ impact (Branching ratios, excitation, multiple-vacancy states, total cross sections, ionization), 30:30541
Outer s-shell ionization of neon, argon, and krypton by proton impact (125 keV-1200 keV), 30:30557
The reaction of atomic oxygen with several atmospheric ions (H^+, O^+, N^+, N^+_2, O^-, O^-_2, 1 to 500 eV), 30:30549
Variational bounds on the 1s-charge-exchange amplitude in proton--hydrogen-atom scattering, 30:30542
HYDROGEN IONS 2 PLUS/CHARGE EXCHANGE
Vibrational energy distribution in CO_2^+ (A^2PIsub(u)) ions produced by collisions of H_2^+ and He^+ ions with CO_2, 30:30558
HYDROGEN IONS 2 PLUS/ELECTRON-ION COLLISIONS
Accurate total inelastic cross section for H_2^+ colliding with fast charged particles in the adiabatic approximation, 30:30554
HYDROGEN IONS 2 PLUS/ION-ATOM COLLISIONS
Argon L-shell ionization by 50- to 600-keV H^+, D^+, H_2^+, and He^+ impact (Branching ratios, excitation, multiple-vacancy states, total cross sections, ionization), 30:30541
HYDROGEN IONS 2 PLUS/ION-MOLECULE COLLISIONS
Vibrational energy distribution in CO_2^+ (A^2PIsub(u)) ions produced by collisions of H_2^+ and He^+ ions with CO_2, 30:30558
HYDROGEN ISOTOPES
Isotopic ordering in CeD_2H, 30:29008 (IAE-2309)
HYDROGEN NITRATES
See NITRIC ACID
HYDROGEN PEROXIDE
Radiomimeticity of the system H_2O_2/Fe(II) on nucleic acid components. Kinetic study, 30:29649 (JEN-284)
HYDROGEN SULFATES
See SULFURIC ACID
HYDROGEN SULFIDES/PHOTOIONIZATION
Calculated photoionization cross sections and relative experimental photoionization intensities for a selection of small molecules, 30:30491
HYDROGEN SULFIDES/PHOTOLYSIS
ESR spectra of PF_2 and SF_3 radicals, 30:29067
HYDROGEN SULFIDES/RADIOLYSIS
Measurements with the hydrogen sulfide dosimeter, 30:29545 (DEMO-74/5)
HYDROXYL RADICALS/BIOCHEMICAL REACTION KINETICS
Radiomimeticity of the system H_2O_2/Fe(II) on nucleic acid components. Kinetic study, 30:29649 (JEN-284)
HYDROXYL RADICALS/COMETS
Ultraviolet fluorescent pumping of OH 18-centimeter radiation in comets (Magnetic sublevels), 30:30326
HYDROXYL RADICALS/COSMIC RADIO SOURCES
Possible nature of some unusual OH sources, 30:30273
HYDROXYL RADICALS/COSMOCHEMISTRY
Interferometric studies of OH sources associated with H II regions and ir objects, 30:30368
HYDROXYL RADICALS/ELECTRON-ION COLLISIONS
Experimental investigation of the effective cross section of excitations of bands of some decay products of water, ammonia, and acetonitrile by slow electrons, 30:30546
HYDROXYL RADICALS/INFRARED RADIATION
An OH survey of the Hoffmann 100-μ sources (Lambda-doublet frequencies), 30:30362
HYDROXYL RADICALS/RECOMBINATION
Flash photolysis study of the gas phase recombination of hydroxyl radicals, 30:29066
HYPERTHYROIDISM/DIAGNOSIS
Quantitative thyroid scanning: a reliable thyroid function test (99m-Tc tracer), 30:29853
HYPERTHYROIDISM/RADIOTHERAPY
Plasma TSH and serum T-4 levels in longer-term follow-up of patients treated with ^{131}I for thyrotoxicosis, 30:29775
HYPOPHYSIS
See PITUITARY GLAND

I

IAEA SAFEGUARDS
Safeguarding the peaceful uses of nuclear energy by states, 30:30104 (FRNC-TH-50)
ICE/NEUTRON TRANSPORT
Neutron slowing-down in ice and polyethylene at low temperatures (Moderator at 4.2, 77, and 300°K, 0.0018 to 0.090 eV), 30:30843 (IAE-2271)
ICE/NUCLEATION
Effects of radioactivity on ice nucleation, 30:29367 (BNWL-1850(Pt.3))
ICE/RADIOACTIVITY
Effects of radioactivity on ice nucleation, 30:29367 (BNWL-1850(Pt.3))
IGNEOUS ROCKS
See also BASALT
GRANITES
GRANODIORITES
TUFF
Determination of ^{87}Sr/^{86}Sr in cenozoic andesites and the related rocks of northwest Sardinia (Italy), 30:29340
IGNEOUS ROCKS/AGE ESTIMATION
Rb-Sr and K-Ar age determinations, and oxygen isotope data for the Glen Cannel granophyre, Isle of Mull, Argyllshire, Scotland, 30:29339
ILEUM
See SMALL INTESTINE
IMAGE CONVERTERS
Nuclear radiation conversion enhancement with inhomogeneous converters and intensifiers, 30:29301
IMAGE INTENSIFIERS
Nuclear radiation conversion enhancement with inhomogeneous converters and intensifiers, 30:29301
IMAGE SCANNERS
Test of a magnetic bearing for optical scanner applications, 30:31430 (SLA-74-0347)
IMAGE SCANNERS/DESIGN
Electro-optic method of tracking an electron-beam weld, 30:31442 (UCID-15769)
IMAGES/DATA PROCESSING
Digital image processing with pseudo-color, 30:31356 (UCRL-75662)
IMIDAZOLES/BIOLOGICAL EFFECTS
Hydrolysis of 2',3'-cyclic adenosine monophosphate and 3',5'-cyclic adenosine monophosphate in subcellular fractions of normal and neoplastic mouse spleen (X radiation), 30:29739
IMIDAZOLES/RADIOSENSITIVITY EFFECTS
Metronidazole (Flagyl). A radiosensitizer of hypoxic cells, 30:29674
Radiosensitization of hypoxic cells with metronidazole (Flagyl), 30:29699
IMMUNE REACTIONS
Direct relationship between immune competence and the subcutaneous growth rate of a malignant murine lung tumor (X radiation), 30:29756
IMMUNE REACTIONS/BIOLOGICAL RADIATION EFFECTS
Development of humoral immunity in lethally irradiated mice reconstituted with fetal liver (Gamma radiation), 30:29750

Macrophage--lymphocyte synergy in tne production of osteoclast activating factor (X Radiation), 30:29667
IMPEDANCE/MEASURING METHODS
  Some thoughts on negative resistance as it applies to high frequency impedance measurements, 30:31448 (UCID-15666)
IMPULSE
  See PULSES
IN CORE INSTRUMENTS
  (See also specific instruments.)
  Apparatus for in-core instrumentation of pressurized water reactors (Patent), 30:31196
  Monitor for radiation-induced heating (Patent), 30:29624
IN-CORE FUEL MANAGEMENT
  See FUEL MANAGEMENT
INCLUSION COMPLEXES
  See CLATHRATES
INCLUSIVE DISTRIBUTION
  See INCLUSIVE INTERACTIONS
INCLUSIVE INTERACTIONS
  (The group of all interactions of two particles producing a specific final state.)
  Strong interaction dynamics (Lectures, Regge exchange), 30:30703
INCLUSIVE INTERACTIONS/ELECTROPRODUCTION
  Test of the SU_3 breaking in inclusive electroproduction of hadrons (Duality, parton model, quarks, pomeron, scattering amplitudes, structure functions), 30:30772
INCLUSIVE INTERACTIONS/MULTIPLE PRODUCTION
  Like particle correlations as a tool to study the multiple production mechanism ($A + b \to \pi^+ + \pi^+ + X$), 30:30711
INCLUSIVE INTERACTIONS/PARTICLE MODELS
  Inclusive processes at large transverse momenta, 30:30636
INCLUSIVE INTERACTIONS/PIONIZATION
  The effects of momentum conservation on pionization, 30:30712
INCLUSIVE INTERACTIONS/STATISTICAL MECHANICS
  Equilibrium statistical mechanics of relativistic particles with variable masses. I. Nonquantal theory, 30:30168
INCOLOY ALLOYS/CORROSION
  Corrosion of sheet and welded joint specimens of Incoloy 825-low carbon (C less tnan or equal to 0.03%) in HNO_3 (Huey) and HF solutions, 30:29956
INCONEL 625/CREEP
  Creep-rupture behavior of the alloy Inconel 625 in three different pretreatment states, 30:29978 (EURFNR-1163)
INCONEL 625/RUPTURES
  Creep-rupture behavior of tne alloy Inconel 625 in three different pretreatment states, 30:29978 (EURFNR-1163)
INCONEL 718/BRAZING
  Nickel brazing below 1025 C of untreated Inconel 718. Use of a getter makes nickel brazing of Inconel 718 and X-750 below 1025 C (1875 F) as easy as nickel brazing of stainless steels in vacuum, 30:29969
INCONEL X750/BRAZING
  Nickel brazing below 1025 C of untreated Inconel 718. Use of a getter makes nickel brazing of Inconel 718 and X-750 below 1025 C (1875 F) as easy as nickel brazing of stainless steels in vacuum, 30:29969
INDEPENDENT-PARTICLE MODEL
  See SINGLE-PARTICLE MODEL
INDIUM/ACTIVATION ANALYSIS
  Multielement determination in market-garden soils by instrumental photon activation analysis, 30:28921
  Trace elements in precipitation and cloud water in the area of Heidelberg, measured by instrumental neutron activation analysis, 30:28934
INDIUM/EMISSION SPECTROSCOPY
  Spectrochemical analysis of uranium oxide by gallium oxide carrier dc arc technique (ASTM Standard E402), 30:28957
INDIUM/ION EXCHANGE
  Selective ion-exchangers containing phosphorus in their functional groups. I. Sorption and separation of some bivalent and trivalent ions, 30:29001
INDIUM/SOLVENT PROPERTIES
  Solubility and diffusion of cobalt in indium, 30:30020
INDIUM 111/TISSUE DISTRIBUTION
  Affinity of ^{111}In-bleomycin for malignant tumors (In patients and experimental rat tumors), 30:29859
INDIUM 115/ENERGY LEVELS
  Proton-hole states in ^{115}In observed in the ^{116}Sn(d,^{3}He) reaction (50 MeV: angular distributions, DWBA; S), 30:30975
INDIUM 115/NEUTRON REACTIONS
  Status report to NCSAC, 30:31011 (UCID-15639)
INDIUM 130/NUCLEAR PROPERTIES
  Nuclear Data Sheets for A = 130, 30:30968
INDIUM ALLOYS/CRYSTAL DOPING
  Systematic control of doping characteristics of n-InSb by nuclear reactions (Thermal neutrons), 30:29992
INDIUM ALLOYS/ELECTRICAL PROPERTIES
  Characteristics of MOS capacitors formed on p-type InSb, 30:29994
INDIUM ALLOYS/LATTICE PARAMETERS
  Preparation of new β-W phases by film-deposition techniques (Nb_3In, Nb_3Pb, and Nb_3Tl films, unstable phase range), 30:29967
INDIUM ALLOYS/SUPERCONDUCTIVITY
  Preparation of new β-W phases by film-deposition techniques (Nb_3In, Nb_3Pb, and Nb_3Tl films, unstable phase range), 30:29967
INDIUM ALLOYS/USES
  Rf hybrid microcircuit soldering techniques, 30:31397 (SLA-73-1073)
INDIUM CHLORIDES/ENTHALPY
  Gaseous halide complexes and their stability, 30:29091
INDIUM CHLORIDES/FORMATION HEAT
  Gaseous halide complexes and their stability, 30:29091
INDIUM COMPOUNDS/CHEMICAL PREPARATION
  Synthesis of high pressure $Cd_2V_2O_7$ and related compositions, 30:29903
INDIUM ISOTOPES/ENERGY-LEVEL TRANSITIONS
  Search for low-spin positive parity states in light odd-mass In nuclei, 30:30954 (NP-20122)
INDIUM ISOTOPES/ROTATIONAL STATES
  Search for low-spin positive parity states in light odd-mass In nuclei, 30:30954 (NP-20122)
INDUSTRIAL RADIOGRAPHY
  See also GAMMA RADIOGRAPHY
    NEUTRON RADIOGRAPHY
    X-RAY RADIOGRAPHY
  Betatron electron internal-flaw detector, 30:30144
INDUSTRIAL RADIOGRAPHY/STANDARDS
  Steel castings up to 2 in. in thickness, 30:30044
INFANTS/DELAYED RADIATION EFFECTS
  Cancer mortality following irradiation in infancy for hemangioma, 30:29714
INFANTS/RADIONUCLIDE KINETICS
  Unexpected complication in the use of ^{169}Yb--DTPA with respect to hospital health physics, 30:29824
INFECTIOUS DISEASES/DIAGNOSIS
  Enhancement of pancreatic concentration of ^{75}Se-selenomethionine (Stimulatory effect of urecholine followed by pancreazymin), 30:29855
  Localization of infectious processes with gallium citrate (Ga-67), 30:29886
INHOMOGENEOUS PLASMA/PLASMA DIAGNOSTICS
  Numerical analysis of interferrograms of asymmetric plasma objects, 30:29176
INLAND WATERWAYS/NUCLEAR EXCAVATION
  Elat-Dead Sea canal (Hydroelectric power generation), 30:29327 (UCID-16107)
INNER BREMSSTRAHLUNG
  See INTERNAL BREMSSTRAHLUNG
INSPECTION/STANDARDS
  Examination of fuel element cladding including the determination of the mechanical properties, 30:30083
INSTRUMENTS (MEASURING)
  See MEASURING INSTRUMENTS
INSULATION (THERMAL)
  See THERMAL INSULATION
INSULIN/RADIOIMMUNOASSAY
  Radioimmunoassay for plasma insulin using zirconyl phosphate gel (^{125}I tracer technique), 30:29870
INTEGRATED CIRCUITS/INSPECTION
  Automated inspection of IC photomasks, 30:31460 (UCRL-75994)
INTEGRATORS (PULSE)
  See PULSE INTEGRATORS
INTENSIFIERS (IMAGE)
  See IMAGE INTENSIFIERS
INTERFEROMETERS/PLASMA DENSITY
  Fast, high sensitivity 10.6 micron interferometer (Plasma diagnostics using Michelson interf$rometer), 30:29161 (UCID-15625)
INTERMEDIATE MASS NUCLEI/BINDING ENERGY
  Three-body effective interactions in the fsub(7/2) region, 30:30931
INTERMEDIATE MASS NUCLEI/ENERGY LEVELS
  Three-body effective interactions in the fsub(7/2) region, 30:30931
INTERMEDIATE MASS NUCLEI/EXCITATION
  Theory of collective excitations in spherical odd--mass nuclei. III. Electromagnetic properties of the anomalous coupling states (N-quasi-particle modes), 30:31068
INTERMEDIATE MASS NUCLEI/HEAVY ION REACTIONS
  Importance of Coulomb interaction potentials in heavy ion DWBA calculations, 30:31063
INTERMEDIATE MASS NUCLEI/NEUTRON REACTIONS
  LARA: a FORTRAN IV code for the calculation of the compound nucleus contribution to the total radiative width in medium and heavy nuclei based on the Brink--Axel model, 30:30956 (RT/FI-(74)17)
INTERMEDIATE MASS NUCLEI/NUCLEAR FORCES
  Three-body effective interactions in the fsub(7/2) region, 30:30931
INTERNAL BREMSSTRAHLUNG/ENERGY SPECTRA
  Inner bremsstrahlung in electromagnetic zero--zero transitions in nuclei, 30:31085
INTERNATIONAL ORGANIZATIONS
  Interatominstrument to coordinate EE nuclear instrumentation technology, 30:29615 (JPRS-61338)
INTERPLANETARY MAGNETIC FIELD/INTERACTIONS
  Observations of interactions between interplanetary and geomagnetic fields, 30:30366

INTERPLANETARY MAGNETIC FIELD/POLARIZATION
Latitudinal cross section of the auroral electrojet and its relation to the interplanetary magnetic field polarity, 30:30470
INTERPLANETARY SPACE/CHEMICAL COMPOSITION
Anomalies in the composition of interplanetary heavy ions with 0.01 < E < 40 MeV per amu, 30:30394
INTERPLANETARY SPACE/COSMIC DUST
Concerning the origin and the dynamics of interplanetary dust, 30:30395
INTERPLANETARY SPACE/COSMIC RADIATION
Cosmic rays in interplanetary space, 30:30166
INTERPLANETARY SPACE/ELECTRONS
Relativistic electron events in interplanetary space, 30:30338
INTERPLANETARY SPACE/HYDROMAGNETIC WAVES
Large-amplitude hydromagnetic waves, 30:30398
INTERPLANETARY SPACE/MAGNETIC FIELDS
Power spectra of the interplanetary magnetic field, 0.7 to 1.6 AU, 30:30403
INTERPLANETARY SPACE/SHOCK WAVES
Discussion of interplanetary postshock flows with two examples, 30:30399
INTERPLANETARY SPACE/SOLAR FLARES
Comment on ''Propagation anisotropies of solar flare protons and electrons at low energies in interplanetary space'' by R. K. Pyle, 30:30312
INTERSTELLAR GRAINS/ABSORPTION SPECTRA
Optical and chemical studies on simulated interstellar grain materials, 30:30376
Study of the interstellar diffuse absorption features, 30:30377
Variations of interstellar ultra-violet absorption, 30:30371
INTERSTELLAR GRAINS/CHEMICAL COMPOSITION
Optical and chemical studies on simulated interstellar grain materials, 30:30376
Stellar atmospheres: the sources of interstellar molecules, 30:30241
INTERSTELLAR GRAINS/GRAIN SIZE
Variations of interstellar ultra-violet absorption, 30:30371
INTERSTELLAR GRAINS/ION IMPLANTATION
Ion implantation effects in 'cosmic' dust grains, 30:30355
INTERSTELLAR GRAINS/MEETINGS
Interstellar dust and related topics. Proceedings of the symposium, Albany, New York, May 29--June 2, 1972, 30:30373
INTERSTELLAR MAGNETIC FIELDS/COSMIC RAY PROPAGATION
Cosmic ray diffusion and anisotropy, 30:30167
INTERSTELLAR SPACE/MOLECULES
Rotational excitation of HCN by collisions (Transition probabilities), 30:30385
INTERSTELLAR SPACE/NUCLEOSYNTHESIS
Nucleosynthesis of the light elements and the interstellar medium, 30:31019 (CONF-730693-)
INTERSTELLAR SPACE/PARTIAL IONIZATION
Dissipation of magnetic flux and magnetic energy in partially ionized gases, 30:30388
INTERSTELLAR SPACE/PLASMA
Introduction to the physics of interstellar plasmas, 30:30183 (CONF-730693-)
INTERSTELLAR SPACE/SCATTERING
Is H- a source of diffuse interstellar lines. (Negative results), 30:30361
INTERSTELLAR SPACE/SPECTRA
Is H- a source of diffuse interstellar lines. (Negative results), 30:30361
INTERSTITIAL CELL STIM HORMONE
See LH
INTERSTITIALS/DIFFUSION
HYDIZ: a 2-dimensional computer progam for migration of interstitial solutes of finite solubility in a thermal gradient (LWBR Development Program), 30:29583 (WAPD-TM-1157)
INVERSE SCATTERING PROBLEM
(Problem of determining scattering potential from phase shifts.)
General derivation of Baecklund transformations from inverse scattering problems, 30:30782 (COO-3237-40)
IODINE/ABSORPTION SPECTROSCOPY
Direct determination on nanogram amounts of iodine by atomic-absorption spectroscopy using a graphite-tube atomizer, 30:28963
IODINE/PAULI PRINCIPLE
Test of the Pauli exclusion principle for atomic electrons, 30:30499
IODINE/RENAL CLEARANCE
Daily excretion rate of iodine calculated from the relationship iodine per gram creatinine in a single afternoon urine sample, 30:29808 (F-599)
IODINE/VOLTAMETRY
Chronoamperometric determination of iodine in urine, 30:28939 (CNEA-366)
IODINE 125/CARCINOGENESIS
Carcinogenicity of iodine-131 relative to age at exposure (^{131}I and ^{125}I uptake by thyroid and pituitary glands), 30:29777 (BNWL-SA-5065)
IODINE 125/METABOLISM
Elimination of intravenously injected ^{125}I-toluidine blue in rabbits (Effectiveness for parathyroid scanning), 30:29812
IODINE 125/RADIOCHEMISTRY
^{125}I-labelling of Candida albicans by electrolysis, 30:29881
IODINE 125/RADIOMETRIC ANALYSIS
Radiometric method for the estimation of iodine complexing degree in iodophor preparations, 30:28974
IODINE 130/NUCLEAR PROPERTIES
Nuclear Data Sheets for A = 130, 30:30968
IODINE 131/BIOLOGICAL RADIATION EFFECTS
Nuclear testing (^{131}I; ^{90}Sr; ^{137}Cs; ^{14}C; Tritium), 30:29719
Real risks of the nuclear tests (^{131}I; ^{137}Cs; ^{90}Sr), 30:29720
IODINE 131/CAPILLARY FLOW
Tissue-blood ^{131}I and ^{133}Xe transfer in the presence of raised capillary filtration, 30:29794
IODINE 131/CARCINOGENESIS
Carcinogenicity of iodine-131 relative to age at exposure (^{131}I and ^{125}I uptake by thyroid and pituitary glands), 30:29777 (BNWL-SA-5065)
IODINE 131/CLEARANCE
Tissue clearance of ^{131}I from lower-limb blood vessels in diabetics, 30:29857
IODINE 131/DELAYED RADIATION EFFECTS
Plasma TSH and serum T-4 levels in longer-term follow-up of patients treated with ^{131}I for thyrotoxicosis, 30:29775
IODINE 131/RADIATION MONITORING
Behavior and characteristics of radioactive debris from the Chinese nuclear weapons test of June 26, 1973, 30:29362 (BNWL-1850(Pt.3))
Data. Section IV. Other data, 30:29412
Environmental monitoring report: United States Atomic Energy Commission, Oak Ridge facilities. Calendar year 1973, 30:29352 (UCC-ND-280)
Phase I. Radiation and radioisotope studies with laboratory and domestic animals (Fallout ^{137}Cs, ^{131}I, and ^{90}Sr in food chains), 30:29417 (COO-3167-102)
Report of activity, February 1974 (Radioactivity of environmental samples collected throughout France during February 1974), 30:29349 (SCPRI(RM)-2-1974)
IODINE 131/RADIOMETRIC ANALYSIS
Radiometric method for the estimation of iodine complexing degree in iodophor preparations, 30:28974
IODINE 131/RETENTION
Follicular damage to bovine ovary from radioiodine, 30:29786
IODINE 136/NUCLEAR PROPERTIES
Nuclear Data Sheets for A = 136, 30:30967
IODINE ISOTOPES/SEDIMENTATION
Wet and dry atmospheric removal processes for radioiodine, 30:29365 (BNWL-1850(Pt.3))
IODINE ISOTOPES/WASHOUT
Wet and dry atmospheric removal processes for radioiodine, 30:29365 (BNWL-1850(Pt.3))
ION ACOUSTIC WAVES/SCATTERING
Scattering by ion-acoustic waves in a rectangular waveguide (Boundary effects, analytical expression), 30:29235
Scattering of high-frequency electromagnetic waves by ion-acoustic oscillations in a bounded plasma (Probing signal), 30:29237
ION BEAMS/ENERGY TRANSFER
Energy transfer to a tungsten lattice by ion bombardment, 30:30070
ION BEAMS/KINETICS
Self-decomposition of quasi-neutral ion beam, 30:30478
ION BEAMS/RADIOTHERAPY
Introduction to the discussion on characteristics of installations for radiotherapy with fast neutrons and other types of high-LET radiation, 30:31112
ION BLOCKING
See ION CHANNELING
ION CHANNELING/ENERGY LOSSES
Electronic stopping power of channelled ions in a model incorporating the Pauli principle (Incident ions Z = 1 to 50), 30:31115
ION CHANNELING/STOPPING POWER
Electronic stopping power of channelled ions in a model incorporating the Pauli principle (Incident ions Z = 1 to 50), 30:31115
ION DETECTION/DIELECTRIC TRACK DETECTORS
Further measurement of the track lengths of heavy ions in mica, 30:29525
ION DETECTION/NUCLEAR EMULSIONS
Identification of heavy ions in nuclear emulsions in the hundreds of MeV interval, 30:29493 (LUIP-CR-74-3)
ION DETECTION/SI SEMICONDUCTOR DETECTORS
Some features in the dependence of the pulse-height defect in semiconductor detectors on detected particle energy, 30:29526
ION DOSIMETRY/DEPTH DOSE DISTRIBUTIONS
Radiobiology with heavy charged particles directed at radiotherapy, 30:31117
ION EXCHANGE
Selective ion-exchangers containing phosphorus in their functional groups. I. Sorption and separation of some bivalent and trivalent ions, 30:29001

ION EXCHANGE CHROMATOGRAPHY
  Chromatography on finely dispersed ionites on inert supports, 30:28997
ION EXCHANGE MATERIALS
  Post-effect of electron capture in ^{57}Co atoms sorbed on cation exchange resins with different degrees of cross-linking, 30:29097
ION SOURCES
  See also ALPHA SOURCES
    DUOPLASMATRONS
  Strong focusing ion sources, 30:29637
ION SOURCES/ATOMIC BEAMS
  Intense fast atom-beam production with a grounded large-area ion source, 30:29157
ION SOURCES/CHARGE EXCHANGE
  Metal vapor confinement in vacuum (Charge exchange cells for negative ion beam production), 30:30128
ION SOURCES/DESIGN
  Advanced ion source. Final report, 21 March--21 June 1973 on Phase 1, 30:30473 (AD-772833)
  DuoPIGatron II ion source, 30:29209 (ORNL-TM-4657)
ION SOURCES/ENERGY LOSSES
  Energy recovery of a lithium ion beam (Magnetic mirror geometry), 30:29221 (UCID-15939)
ION SOURCES/OPERATION
  Beams of Be$^+$ from an rf ion source, 30:30130
ION SOURCES/PERFORMANCE
  A close to universal negative ion source, 30:30485
ION WAVES/DISPERSION RELATIONS
  Excitation of electromagnetic ion cyclotron waves by fast ions (Refractive index, low-density beam), 30:29234
ION-ATOM COLLISIONS/CHARGE EXCHANGE
  Crossed-molecular-beam study of the kinematics and dynamics of charge-transfer collisions, 30:30547
ION-ATOM COLLISIONS/TOTAL CROSS SECTIONS
  Total cross-section corresponding to the differential cross-section of Lindhard, Neilsen, and Scharff, 30:30552
ION-DRAG ACCELERATORS
  See ELECTRON-RING ACCELERATORS
ION-MOLECULE COLLISIONS/CHARGE EXCHANGE
  Crossed-molecular-beam study of the kinematics and dynamics of charge-transfer collisions, 30:30547
IONIZATION CHAMBERS
  See also FISSION CHAMBERS
    LIQUID IONIZATION CHAMBERS
  Neutron supermonitor (Cosmic ray neutron detection), 30:29500
  New extrapolation method for the determination of saturated ionization currents, 30:29506
IONIZATION CHAMBERS/FABRICATION
  Development of neutron sensitive PCP ionization chamber, 30:29498
IONIZATION CHAMBERS/MULTI-CHANNEL ANALYZERS
  8192-channel square-root pulse-height analyzer, 30:29568
IONIZATION CHAMBERS/PARTICLE IDENTIFICATION
  High-resolution ionization measurements in the region of the relativistic rise, 30:29595
IONIZATION CHAMBERS/PERFORMANCE
  Development of neutron sensitive PCP ionization chamber, 30:29498
IONOSPHERE
  See also D REGION
    E REGION
    F REGION
IONOSPHERE/CHEMICAL COMPOSITION
  Esro 4 gas analyzer results. II. Direct measurements of changes in the neutral composition during an ionospheric storm, 30:30424
IONOSPHERE/CYCLOTRON INSTABILITY
  Further discussion of the cyclotron instability, 30:30439
IONOSPHERE/DATA ACQUISITION
  Routine operation of Digisonde at Maynard, Massachusetts. Final report, 1 September 1971--31 August 1972, 30:30410 (AD-776969)
IONOSPHERE/ELECTRIC CONDUCTIVITY
  Exact solutions for certain axisymmetric problems of induction in thin nonuniform sheets, 30:30452
IONOSPHERE/ELECTRIC FIELDS
  Global distribution of natural and man-made ionospheric electric fields at 200 kHz and 540 kHz as observed by Ogo 6, 30:30431
  Inductive electric field of a field-aligned current system, 30:30438
  Self-consistent electrostatic field mapping in the high-latitude ionosphere, 30:30435
IONOSPHERE/ELECTROMAGNETIC RADIATION
  Electromagnetic radiation influence upon the plasma variation spectra, 30:30415
IONOSPHERE/ELECTRON DENSITY
  Investigation of a fine regular structure and random ionospheric irregularities by the method of incoherent radio wave scattering, 30:30447
  Total electron content measurements over Kurukshetra, 30:30422
IONOSPHERE/ELECTRON PRECIPITATION
  Active experiments stimulating waves and particle precipitation with small ionospheric barium releases, 30:30433
IONOSPHERE/ELECTRON TEMPERATURE
  Temperatures in the polar wind, 30:30443
  Velocity distribution of ionospheric low-energy electrons, 30:30442
IONOSPHERE/ION DENSITY
  Ionospheric ion flow velocities from measurements of the ion distribution function technique, 30:30434
  Observation of a two-temperature ion energy distribution in regions of polar wind flow, 30:30429
IONOSPHERE/ION TEMPERATURE
  Temperatures in the polar wind, 30:30443
IONOSPHERE/MEASURING METHODS
  Incoherent scatter sounding of the ionosphere, 30:30444
IONOSPHERE/PLASMA DRIFT
  Ionospheric ion flow velocities from measurements of the ion distribution function technique, 30:30434
IONOSPHERE/PLASMA WAVES
  Electromagnetic effects on instabilities in the equatorial electrojet, 30:30440
  Inherent electromagnetic and electrostatic oscillations of a spherical cavity in plasma, 30:30412
  Wave--wave coupling in multiple-ion plasmas, 30:29226
IONOSPHERE/RADIOWAVE RADIATION
  Ionospheric absorption on 2.4 MHz at Waltair, 30:30419
IONOSPHERE/VARIATIONS
  Dependence of fading frequency on characteristics of ionospheric irregularities, 30:30420
IONOSPHERE/VERY HIGH TEMPERATURE
  Temperatures in the polar wind, 30:30443
IONOSPHERE/WAVE PROPAGATION
  Active experiments stimulating waves and particle precipitation with small ionospheric barium releases, 30:30433
  Wave--wave coupling in multiple-ion plasmas, 30:29226
IONS/RELAXATION
  Electron-ion relaxation in a dense plasma (Microscopic structure), 30:30259
IRIDIUM 186/ENERGY LEVELS
  Nuclear Data Sheets for A = 186, 30:30988
IRIDIUM 186/NUCLEAR PROPERTIES
  Nuclear Data Sheets for A = 186, 30:30988
IRIDIUM 192/CHEMISORPTION
  Sorption of iridium on silver, mercury, lead, and thallium forms of natural zeolite (clinoptilolite) and vermiculite, 30:29135
IRIDIUM ALLOYS/ELECTRODEPOSITION
  Electrodepositing platinum and platinum--iridium alloys from molten cyanides: chemical process studies, 30:31366 (BDX-613-1064(Rev.))
IRON
  See also IRON-ALPHA
IRON/ABSORPTION SPECTROSCOPY
  Atomic absorption spectrometry of impurities in high purity tantalum with heated graphite atomizer, 30:28954
IRON/ACTIVATION ANALYSIS
  Multielement determination in market-garden soils by instrumental photon activation analysis, 30:28921
  Nondestructive determination of some trace elements in tantalum by proton activation analysis, 30:28922
  Trace element behavior in soil of some Indonesian sawah's and in sludge of an Indonesian river, 30:28930
  Trace elements in precipitation and cloud water in the area of Heidelberg, measured by instrumental neutron activation analysis, 30:28934
IRON/CHEMICAL ANALYSIS
  Extraction--spectrophotometric methods of determining 0.0--n0.000n% aluminum in materials of metallurgical manufacture (exchange of experience), 30:28956
IRON/COSMOCHEMISTRY
  High-frequency observations of possible ''heavy-element'' recombination lines (Cosmic value), 30:30267
IRON/EMISSION SPECTROSCOPY
  Spectrochemical analysis of uranium oxide by gallium oxide carrier dc arc technique (ASTM Standard E402), 30:28957
  Spectrographic determination of trace impurities in high purity uranium oxide, 30:28944 (UCID-15952)
IRON/ION EXCHANGE
  Selective ion-exchangers containing phosphorus in their functional groups. I. Sorption and separation of some bivalent and trivalent ions, 30:29001
IRON/NEUTRON REACTIONS
  Optical model calculations for the scattering of rapid neutrons (8 to 15 MeV) by Cr and Fe, 30:30943
IRON/NEUTRON STARS
  Structure of solid iron in superstrong neutron-star magnetic fields (Quantized radii, binding energy), 30:30194
IRON/NEUTRON TRANSPORT
  Measurement and calculation of neutron spectra at a sodium--iron interface (14-MeV source), 30:30848 (KFK-1959)
IRON/NUCLEOSYNTHESIS
  Iron production by ^{12}C-detonation supernovae (Severe constraints), 30:30258
IRON/PHYSICAL RADIATION EFFECTS
  Effect of intense reactor irradiation on the shear modulus and viscosity of iron, 30:30072
IRON/QUALITATIVE CHEMICAL ANALYSIS
  Application of activation analysis to the determination of pollutants in the atmosphere, 30:28914 (IEA-326)

IRON/REDUCTION
  Oxidation--reduction reactions of actinide elements. XXIV. Kinetics of uranium(IV)--iron(III) reaction in water--isopropanol solutions, 30:29106
IRON/SPECIFIC HEAT
  Microsecond pulse technique for heat capacity measurement (1100°K), 30:31424 (LBL-2574)
IRON 52/EXCITED STATES
  Are there low-lying, intrashell-excited, highly deformed states in the 1f-2p shell nuclei, 30:30925
IRON 53/ENERGY LEVELS
  Spin and parity of the first excited level in ^{53}Fe, 30:30917
IRON 54/ALPHA REACTIONS
  Reaction rates of interest in late stages of stellar nycleosynthesis (Estimate of reliability), 30:30255
IRON 54/PROTON REACTIONS
  Spin-dependent effects in inelastic scattering (^{54}Fe, ^{56}Fe(p,p'), 10 to 49.35 MeV, 19.6 MeV: differential cross sections), 30:30932
IRON 56/ALPHA REACTIONS
  Generalized collective model and α-particle scattering on ^{56}Fe and ^{48}Ti (104 MeV: angular distributions), 30:30945
IRON 56/OXYGEN 16 REACTIONS
  Polarization in HI inelastic scattering in the Coulomb--nuclear interference region and coupled channel effects (^{56}Fe(^{16}O,^{16}O'), 43 MeV), 30:30920
IRON 56/PROTON REACTIONS
  Spin-dependent effects in inelastic scattering (^{54}Fe, ^{56}Fe(p,p'), 10 to 49.35 MeV, 19.6 MeV: differential cross sections), 30:30932
IRON 56 REACTIONS/FISSION
  Ternary fission induced by 540 MeV Fe ions on uranium (Branching ratio, potential energy surfaces), 30:31018
IRON 56 REACTIONS/TERNARY FISSION
  Ternary fission induced by 540 MeV Fe ions on uranium (Branching ratio, potential energy surfaces), 30:31018
IRON 57/CHEMICAL STATE
  Moessbauer spectroscopic studies of the effect of the oxalate anion in the second coordination sphere on the oxidation state of ^{57}Fe produced in EC-decay (^{57}Co), 30:29078
  Post-effect of electron capture in the eutectic (NH_4NO_3--$LiNO_3$):^{57}Co at 77°K, 30:29098
IRON 57/MOESSBAUER EFFECT
  Nuclear gamma-resonance on nuclei of ^{57}Fe impurity in tungsten--rhenium alloys, 30:30029
IRON ALLOYS
    See also INCONEL X750
             IRON BASE ALLOYS
             PERMALLOY
             RENE 41
             STEELS
IRON ALLOYS/DIFFUSION
  Transport and thermodynamic properties of solids. Progress report, September 1, 1973--August 31, 1974, 30:31390 (COO-1436-41)
IRON ALLOYS/ION EMISSION
  Ionic emission yield for alloys, dependence on the nature of the solute. II. Interpretation, 30:30087
IRON ALLOYS/MAGNETIC PROPERTIES
  Crystal and magnetic structure of intermetallic compounds of the type Th(Co/sub x/Fe/sub 1-x/)$_5$, 30:29989
IRON ALLOYS/MAGNETISM
  Paraprocess near Curie temperature and criteria of appearance of temperature of magnetic compensation in compounds of rare earths with iron, 30:30043
IRON ALLOYS/THERMAL DIFFUSION
  Diffusion in the Mo--Ni, Mo--Fe, and Mo--Co systems, 30:30001
IRON BASE ALLOYS
    See also INCOLOY ALLOYS
IRON BASE ALLOYS/AGING
  Field-ion microscopic study of aged martensite in an iron--nickel--cobalt--molybdenum alloy (Fe--16 percent Ni--15 percent Co--5 percent Mo; precipitation of Mo), 30:30037
IRON COMPLEXES
    See also FERRITIN
IRON COMPLEXES/PYROLYSIS
  Derivatographic investigations on the thermal degradation of pyridine, isoquinoline, α,α-dipyridyl and o-phenantroline, resp. bichromate- or chromate-ion containing metal complexes. II. Zinc(II)-, cadmium(II)-, and manganese(II)-complexes. III. Mercury(I and II)-, uranyl-, thorium-, lanthanum-, and iron-complexes, 30:29122
IRON COMPOUNDS
  Radiomimeticity of the system H_2O_2/Fe(II) on nucleic acid components. Kinetic study, 30:29649 (JEN-284)
IRON FLUORIDES/SOLUBILITY
  Solubility and stability of structural metal difluorides in molten fluoride mixtures, 30:29002 (ORNL-TM-760)
IRON IONS/EMISSION SPECTRA
  Spectral classifications in the Fe XIX to Fe XXIII isoelectronic sequences, 30:30329
IRON OXIDES
    See also HEMATITE
IRON OXIDES/MAGNETIC SUSCEPTIBILITY
  Magnetization and Moessbauer spectra of non-crystalline $Y_3Fe_5O_{12}$, 30:29901
IRON OXIDES/MOESSBAUER EFFECT
  Magnetization and Moessbauer spectra of non-crystalline $Y_3Fe_5O_{12}$, 30:29901
IRON OXIDES/X-RAY FLUORESCENCE ANALYSIS
  Compilation of x-ray interaction data for x-ray fluorescence analysis of geological samples, 30:28943 (RISO-297)
IRON SULFATES/RADIOLYSIS
  Quantitative study of the radiolysis of $FeSO_4.7H_2O$ using Moessbauer effect (X radiation), 30:29051
IRON SULFIDES/X-RAY FLUORESCENCE ANALYSIS
  Compilation of x-ray interaction data for x-ray fluorescence analysis of geological samples, 30:28943 (RISO-297)
IRON-ALPHA/DEBYE-WALLER FACTOR
  Lattice dynamical study of the recoilless fraction of ^{57}Fe in Ni, Mo, W, α-Fe and Cu, 30:30050
IRRADIATION CAPSULES/FABRICATION
  Cold-weld type capsules for radioisotope production, 30:29962
IRRADIATION PLANTS/DESIGN
  Surface irradiation of spherical vegetables and fruits, 30:29645
IRRADIATION PLANTS/OPERATION
  First gamma-irradiation plant for sewage-sludge hygienization, 30:29643
IRRADIATION RIGS
    See IRRADIATION CAPSULES
ISOBARIC ANALOGS/DECAY
  Isospin effects upon the decay of highly excited nuclear states, 30:30999
ISOBARIC SPIN
    See ISOSPIN
ISOBARS (NUCLEON)
    See N*RESONANCES
ISOCHRONOUS CYCLOTRONS
    See also MSU CYCLOTRONS
ISOCHRONOUS CYCLOTRONS/BEAM OPTICS
  Method and means for reducing the power density of an internal cyclotron beam, 30:30133
ISOENZYMES/BIOLOGICAL RADIATION EFFECTS
  Effect of γ irradiation on the charge and size properties of horseradish peroxidase: individual isoenzymes, 30:29651
ISOSPIN/SYMMETRY BREAKING
  Structure and experimental consequences of chiral SU_3 x SU_3 breaking, 30:30775
ISOTOPE DATING/ARGON 39
  ^{40}Ar/^{39}Ar dating of the long range dikes, Newfoundland, 30:29338
ISOTOPE DATING/ARGON 40
  ^{40}Ar/^{39}Ar dating of the long range dikes, Newfoundland, 30:29338
ISOTOPE DATING/ERRORS
  Irregularities in dendrochronological calibration (^{14}C), 30:29430
ISOTOPE EFFECTS
  Isotope effects in the boundary layer of inorganic solutions (Alkali and alkaline earth isotopes), 30:29007 (AED-CONF-74-084-004)
ISOTOPIC EXCHANGE/PARTITION FUNCTIONS
  Isotope exchange reactions. IX. Calculation of the partition function ratios of isotopic molecules with the aid of the increment in the trace of the GF-matrix, 30:29031
ISOTOPIC SPIN
    See ISOSPIN
ISPRA-1 REACTOR/FUEL ELEMENTS
  Analysis of ECE data on the basis of isotopic weight fractions, 30:28940 (EUR-4859)
ITALY/METEOROLOGY
  1973 meteorological yearbook of the EUREX site at Saluggia, 30:29457 (RT/PROT-(74)13)
ITR REACTOR/REACTIVITY
  Calculation of correction factors for pulsed neutron measurements in the ITR critical experiment, 30:31232 (IKE-6-79d)

J

JAMESPORT-1 REACTOR
  License application and annual report of applicant, 30:31320 (DOCKET-STN-50516-1)
JAMESPORT-2 REACTOR
  License application and annual report of applicant, 30:31320 (DOCKET-STN-50516-1)
JAPAN POWER DEMONSTRATION REACTOR
    See JPDR REACTOR
JEJUNUM
    See SMALL INTESTINE
JENSEN SARCOMA
    See EXPERIMENTAL NEOPLASMS
JINR SYNCHROTRON/BEAM EXTRACTION
  Slow beam extraction from the JINR synchrophasotron, 30:30129
JOSEPHSON JUNCTIONS/FABRICATION
  Technique for fabrication of superconducting microbridges and small Josephson tunnel junctions, 30:30841

JOSEPHSON JUNCTIONS/USES
  Application of Josephson's effect in superconductors for measurements of very small voltages, 30:30842
  Tunnel junctions for computer applications, 30:30831
JOST FUNCTION/POTENTIAL SCATTERING
  Connection between Fredholm determinant and Jost function for nonlocal potentials, 30:30788
JPDR REACTOR/IN CORE INSTRUMENTS
  Development of nuclear reactor incore instruments, 30:31193
JUNCTION DETECTORS/ION IMPLANTATION
  Semiconductor counters for nuclear radiations produced by ion implantation, 30:29531
JUNCTION DETECTORS/PERFORMANCE
  Semiconductor counters for nuclear radiations produced by ion implantation, 30:29531
JUNCTION TRANSISTORS/PHYSICAL RADIATION EFFECTS
  JFET hardening and high dose rate study, 30:29888 (AD-903226)
JUPITER PLANET/ABSORPTION SPECTRA
  Investigation of ultraviolet absorption in the continuous spectrum of Jupiter, 30:30396
JUPITER PLANET/COSMIC RAY FLUX
  The possible influence of Jupiter on cosmic radiation at the earth, 30:30173
JUPITER PLANET/EQUILIBRIUM
  The equilibrium of a rotating body of arbitrary density, 30:30408
JUPITER PLANET/MAGNETOSPHERE
  Synchrotron loss rates of energetic magnetospheric electrons, 30:30451
JUPITER PLANET/PLASMA
  New nodal expansion for classical plasmas, 30:30196
JUPITER PLANET/RADIATION BELTS
  Bursts of relativistic electrons from Jupiter observed in interplanetary space with the time variation of the planetary rotation period, 30:30405
  Measurements of the Jovian radiation belts, 30:30406
JUPITER PLANET/RADIOWAVE RADIATION
  The position and Stokes parameters of the integrated 21-centimeter radio emission of Jupiter and their variation with Epoch and central meridan longitude (Aspect angle, earlier observations), 30:30407
JUPITER PLANET/SATELLITES
  Absorption of trapped particles by Jupiter's moons, 30:30404
JUPITER PLANET/STOKES PARAMETERS
  The position and Stokes parameters of the integrated 21-centimeter radio emission of Jupiter and their variation with Epocn and central meridan longitude (Aspect angle, earlier observations), 30:30407

K

K CAPTURE/SECOND-CLASS CURRENTS
  K-electron capture to positron emission ratios and the second class currents problem, 30:31076
K-1240 RESONANCES/PARITY
  Longitudinal phase-space analysis of the $K^+\pi^+\pi^-$ system produced by 10 GeV/c K^+ incident on nuclei, 30:30625
K-1240 RESONANCES/SPIN
  Longitudinal phase-space analysis of the $K^+\pi^+\pi^-$ system produced by 10 GeV/c K^+ incident on nuclei, 30:30625
K-1420 RESONANCES/DECAY
  A measurement of $K^*(1420)$ decay branching ratios, 30:30624
K-892 RESONANCES/PARTICLE PRODUCTION
  A study of the reactions $\pi^- p \to K^*X$, $K^*\Sigma$ and $K^*Y_1^*(1385)$ at 3.93 GeV/c (Differential cross sections), 30:30622
K01
    See KAONS NEUTRAL SHORT-LIVED
K02
    See KAONS NEUTRAL LONG-LIVED
KANSAI-1 REACTOR
    See MIHAMA-1 REACTOR
KANSAI-2 REACTOR
    See MIHAMA-2 REACTOR
KANSAS/FALLOUT
  Data. Section II. Water (Monitoring), 30:29411
KAOLIN/GRAIN ORIENTATION
  Coincidence twist boundaries in muscovite, kaolinite, and MoO_3, 30:29895
KAON DETECTION/TRANSITION RADIATION DETECTORS
  Transition counters for πK differentiation above 400 GeV, 30:29599
KAON REACTIONS
  Longitudinal phase-space analysis of the $K^+\pi^+\pi^-$ system produced by 10 GeV/c K^+ incident on nuclei, 30:30625
KAON-DEUTERON INTERACTIONS/CHARGE-EXCHANGE INTERACTIONS
  A measurement of $K^*(1420)$ decay branching ratios, 30:30624
KAON-NUCLEON INTERACTIONS
    See also KAON-PROTON INTERACTIONS
KAON-NUCLEON INTERACTIONS/CHARGE-EXCHANGE INTERACTIONS
  The structure of t-channel exchanges in KN scattering, 30:30747
KAON-NUCLEON INTERACTIONS/MASS SPECTRA
  Longitudinal phase-space analysis of the $K^+\pi^+\pi^-$ system produced by 10 GeV/c K^+ incident on nuclei, 30:30625
KAON-NUCLEON INTERACTIONS/PHASE SPACE
  Longitudinal phase-space analysis of the $K^+\pi^+\pi^-$ system produced by 10 GeV/c K^+ incident on nuclei, 30:30625
KAON-NUCLEON INTERACTIONS/Z*RESONANCES
  Simple Z_0^* model, 30:30740
KAON-PROTON INTERACTIONS/BOOTSTRAP MODEL
  Experimental manifestations of duality in KN interactions and implications for the bootstrap, 30:30743
KAON-PROTON INTERACTIONS/CROSS SECTIONS
  Models for the pomeron and low energy K^+p scattering (S-channel unitarity model), 30:30746
KAON-PROTON INTERACTIONS/DIFFRACTION MODELS
  Elastic-diffraction slopes of π^+p and K^+p scatterings (25.2 and 40.1 GeV/c total cross sections, impact parameters), 30:30736
  Isospin analysis of the diffraction dissociation processes in K^+p interactions at 5 and 8.2 GeV/c, 30:30614
KAON-PROTON INTERACTIONS/DUALITY
  Experimental manifestations of duality in KN interactions and implications for the bootstrap, 30:30743
KAON-PROTON INTERACTIONS/MULTIPLICITY
  Charged particle multiplicity distributions for 32 GeV/c $K^{+-}p$ and anti pp interactions and for 50 GeV/c $\pi^{+-}p$ interactions (Topological cross sections), 30:30608
KAON-PROTON INTERACTIONS/SCATTERING AMPLITUDES
  Measurement of the real part of the forward scattering amplitude in $K^{+-}p$ elastic scattering between 0.9 and 2.6 GeV/c, 30:30619
  The NAK coupling constant, 30:30737
KAON-PROTON INTERACTIONS/TOTAL CROSS SECTIONS
  Coherent transmission of neutral kaons in matter and forward scattering amplitudes, 30:30741
  Finite energy bounds for πN scattering (Related problems in pp and Kp scattering), 30:30748
  Unitarity, phenomenology and the bare pomeron, 30:30710
KAONIC ATOMS/CONFIGURATION MIXING
  Quadrupole mixing in hadronic atoms: an additional probe of the hadron-nucleus interaction, 30:30514
KAONIC ATOMS/X-RAY SPECTRA
  Quadrupole mixing in hadronic atoms: an additional probe of the hadron-nucleus interaction, 30:30514
KAONS
    See also ANTIKAONS NEUTRAL
             KAONS NEUTRAL
             KAONS PLUS
KAONS/ELECTROMAGNETIC FORM FACTORS
  Pion and kaon form factors and heavy vector mesons, 30:30726
KAONS/LEPTONIC DECAY
  Application of the on-mass-shell current algebra to the K/sub l3/ form factor (Decay amplitudes, axial-vector currents,equal-time commutation relations), 30:30683
  Is chiral $SU_2 \times SU_2$ a hidden symmetry (Form factors), 30:30774
KAONS/LIFETIME
  A theory of elementary couplings. III, 30:31146
KAONS/MASS
  Non-zero masses of π,K, eta and kappa mesons and algebraic realization of SU(3) x SU(3) chiral symmetry, 30:30780
KAONS/MASS DIFFERENCE
  Structure and experimental consequences of chiral $SU_3 \times SU_3$ breaking, 30:30775
KAONS/PARTICLE RADII
  Pion and kaon form factors and heavy vector mesons, 30:30726
KAONS NEUTRAL
    See also KAONS NEUTRAL LONG-LIVED
             KAONS NEUTRAL SHORT-LIVED
KAONS NEUTRAL/MASS DIFFERENCE
  Electromagnetic mass differences in a relativistic quark model, 30:30658
KAONS NEUTRAL/PARTICLE RADII
  K/sub L/^{0} $\to$ K/sub S/^{0} incoherent regeneration on atomic electrons at high energies and electric radius of K^0 meson (Cross sections, 100 GeV), 30:30592 (JINR-E2-7402)
KAONS NEUTRAL/TRANSMISSION
  Coherent transmission of neutral kaons in matter and forward scattering amplitudes, 30:30741
KAONS NEUTRAL LONG-LIVED/DECAY
  Measurement of the energy dependence of the decay matrix element for K^0sub(L) $\to \pi^+ \pi^- \pi^0$, 30:30593 (PITHA-64(1972))
  Measurement of the slope parameter for the neutral pion spectrum in K^0sub(L) $\to \pi^0\pi^+\pi^-$ decay, 30:30596
  Observation of the decay K/subL/^{0} $\to \pi^+\pi^-\gamma$ (Branching ratio, Dalitz plot), 30:30582
KAONS NEUTRAL SHORT-LIVED/DECAY
  Can the $\Delta I = 1/2$ selection rule in the $K \to 2\pi$ decay be satisfied in gauge theories (Free-quark model, Salam-Weinberg model, decay amplitudes), 30:30684
KAONS NEUTRAL SHORT-LIVED/INCOHERENT SCATTERING
  K/sub L/^{0} $\to$ K/sub S/^{0} incoherent regeneration on atomic electrons at high energies and electric radius of K^0 meson (Cross sections, 100 GeV), 30:30592 (JINR-E2-7402)
KAONS NEUTRAL SHORT-LIVED/PION-PROTON INTERACTIONS
  Analysis of $K_1^0K_1^0$ system in the $\pi^-p \to nK^0$ anti K^0 reaction at 40 GeV/c (Regge trajectories), 30:30730 (ITEF-31)

KAONS PLUS/DECAY
Can the $\Delta I = 1/2$ selection rule in the $K \to 2\pi$ decay be satisfied in gauge theories (Free-quark model, Salam-Weinberg model, decay amplitudes), 30:30684
KAONS PLUS/ELECTROPRODUCTION
Test of the SU_3 breaking in inclusive electroproduction of hadrons (Duality, parton model, quarks, pomeron, scattering amplitudes, structure functions), 30:30772
KAONS PLUS/MASS DIFFERENCE
Electromagnetic mass differences in a relativistic quark model, 30:30658
KAPPA-725 RESONANCES/MASS
Non-zero masses of π,K, eta and kappa mesons and algebraic realization of SU(3) x SU(3) chiral symmetry, 30:30780
KASHIMA-1 REACTOR
See SHIMANE-1 REACTOR
KENTUCKY/AIR POLLUTION
Environmental monitoring report, calendar year 1973, 30:29351 (UCC-ND-279)
KENTUCKY/RADIOACTIVITY
Environmental monitoring report, calendar year 1973, 30:29351 (UCC-ND-279)
KENTUCKY/WATER POLLUTION
Environmental monitoring report, calendar year 1973, 30:29351 (UCC-ND-279)
KETONES
See also ACETONE
ANDROSTENEDIONE
TESTOSTERONE
KETONES/RADIOLYSIS
Radiation chemical studies with cyclotron beams. III. Heavy-ion radiolysis of liquid aliphatic ketones, 30:29049
KIDNEYS
See also GLOMERULI
KIDNEYS/METABOLISM
Urine /sup 131m/In-EDTA time concentration curve and redistribution of glomerular filtration in the dog, 30:29839
KINASES (PHOSPHOTRANSFERASES)
See PHOSPHOTRANSFERASES
KINETIC EQUATIONS
(Not for REACTOR KINETICS.)
KINETIC EQUATIONS/NUMERICAL SOLUTION
Solution of large coupled sets of kinetic equations, 30:31351 (UCID-15765)
KLEIN-GORDON EQUATION/POTENTIAL SCATTERING
Exponential potential and the Klein--Gordon equation (Bound states, phase shifts), 30:30789
KNOCK-ON ELECTRONS
See ELECTRONS
KRITO CRITICAL ASSEMBLY
See STEK REACTOR
KRYPTON/ELECTRON-ATOM COLLISIONS
Atomic excitation processes in the discharges of rare gas ion engines, 30:30556
KRYPTON/FABRICATION
Rapid production of thin Kr sources, 30:29641
KRYPTON/ION-ATOM COLLISIONS
Crossed-molecular-beam study of the kinematics and dynamics of charge-transfer collisions (200 eV), 30:30547
Outer s-shell ionization of neon, argon, and krypton by proton impact (125 keV-1200 keV), 30:30557
KRYPTON/IONIZATION
Outer s-shell ionization of neon, argon, and krypton by proton impact (125 keV-1200 keV), 30:30557
KRYPTON/MOLECULAR STRUCTURE
Angular momentum coupling, potential curves and radiative selection rules for heavy diatomic molecules, with particular reference to Kr_2 and Kr_2^+, 30:31459 (UCRL-13599)
KRYPTON/SEPARATION PROCESSES
Atmosphere purification of xenon, radon, and radon daughter elements (Patent, fluorination and adsorption), 30:28995
Recovery of rare gases in air separation and ammonia plants, 30:28993
KRYPTON 78/ENERGY LEVELS
Level structure of ^{78}Kr (J, π), 30:30944
KRYPTON 83/MOESSBAUER EFFECT
Moessbauer investigations on ^{83}Kr (Conversion coefficient of 9.4 keV transition), 30:30938
KRYPTON 84 REACTIONS
Quasi-fission: a new type of reaction observed in bombarding heavy nuclei by ^{84}Kr and ^{63}Cu ions, 30:30984
KRYPTON 85/GAMMA SOURCES
Krypton source for arming airborne weapons; patent, 30:29640
KRYPTON 85/RADIATION MONITORING
Environmental monitoring report: United States Atomic Energy Commission, Oak Ridge facilities. Calendar year 1973, 30:29352 (UCC-ND-280)
KRYPTON 85/STORAGE
Evaluation of quinol clathrate for fission product noble gas storage, 30:30108 (ICP-1045)
KRYPTON FLUORIDES/CHEMICAL PREPARATION
Compounds of rare gases, 30:29069
KRYPTON IONS/CHANNELING
Sputtering experiments with silver single crystals and the channeling phenomena, 30:30481
KRYPTON IONS/COLLISIONS
Sputtering experiments with silver single crystals and the channeling phenomena, 30:30481
KRYPTON IONS/ION-ATOM COLLISIONS
Crossed-molecular-beam study of the kinematics and dynamics of charge-transfer collisions (200 eV), 30:30547
KRYPTON IONS/ION-MOLECULE COLLISIONS
Crossed-molecular-beam study of the kinematics and dynamics of charge-transfer collisions (200 eV), 30:30547
KRYPTON IONS/MOLECULAR STRUCTURE
Angular momentum coupling, potential curves and radiative selection rules for heavy diatomic molecules, with particular reference to Kr_2 and Kr_2^+, 30:31459 (UCRL-13599)
KUPFFER CELLS
See RETICULOENDOTHELIAL SYSTEM
KUR REACTOR/ON-LINE CONTROL SYSTEMS
KUR on-line computer system, 30:31296 (KURRI-TR-110)
KYOTO UNIVERSITY REACTOR
See KUR REACTOR

L

L CELLS/CELL PROLIFERATION
Histone F1 phosphorus content and DNA synthesis in slowly-growing sublines of L5178Y-S cells (X radiation), 30:29669
L-S COUPLING/NUCLEAR POTENTIAL
On the nuclear I.L potential, 30:31092
LABORATORY EQUIPMENT
See also HOT CELLS
Piezoelectric mechanical-micropipette stimulator. Technical report No. 10, 30:31378 (NYO-3406-18)
LAKE MICHIGAN/THERMAL POLLUTION
Migratory behavior of fish tagged at a nuclear power plant discharge into Lake Michigan, 30:29462 (CONF-740813-2)
LAKES
See also GREAT LAKES
LAKE MICHIGAN
LAKES/CONTAMINATION
Determination of aerosol deposition rates on a lake surface using radon daughters (^{214}Bi and ^{214}Pb tracer studies), 30:29410 (BNWL-1850(Pt.3))
LAKES/RADIONUCLIDE MIGRATION
Kinetics of the self-purification of a body of water containing strontium-90 as a result of absorption of the radionuclide by the bottom deposits, 30:29414
LAMBS
See SHEEP
LAMPF LINAC/ISOTOPE PRODUCTION
Radioisotopes from a medium-energy accelerator: the Clinton P. Anderson Meson Physics Facility radioisotope program, 30:30142 (LA-UR-74-1263)
LAMPF LINAC/RADIATION MONITORS
Passive environmental neutron dosimeter (Polyethylene-moderated fission foil--dielectric track detector system), 30:29551 (LA-UR-74-1232)
LANTHANIDES
See RARE EARTHS
LANTHANUM/ACTIVATION ANALYSIS
Determination of rare earths and thorium in apatites by thermal and epithermal neutron-activation analysis, 30:28935
Radioactivation analysis in thermal and epithermal neutrons of the IBR-30 reactor of JINR, 30:28929
Trace element behavior in soil of some Indonesian sawah's and in sludge of an Indonesian river, 30:28930
Trace elements in precipitation and cloud water in the area of Heidelberg, measured by instrumental neutron activation analysis, 30:28934
LANTHANUM/ELECTRON COLLISIONS
Strong 4f resonance effects in rare-earth appearance-potential spectra, 30:30477
LANTHANUM/EXTRACTION CHROMATOGRAPHY
Contribution to the separation of rare earths by extraction chromatography with di(2-ethylhexyl) phosphoric acid. II. Behavior of the matrix and its influênce on the microcomponents, 30:28990 (ANL-Trans-961)
LANTHANUM/ION EXCHANGE
Selective ion-exchangers containing phosphorus in their functional groups. I. Sorption and separation of some bivalent and trivalent ions, 30:29001
Synthesis of reproducible tin(IV) based ion exchangers: separation of lanthanum(III) from yttrium(III), europium(III), and lutetium(III), 30:28994
LANTHANUM/QUALITATIVE CHEMICAL ANALYSIS
Application of activation analysis to the determination of pollutants in the atmosphere, 30:28914 (IEA-326)
LANTHANUM 130/BETA-PLUS DECAY
Levels in ^{130}Ba fed from ^{130}La decay, 30:30963
LANTHANUM 130/NUCLEAR PROPERTIES
Nuclear Data Sheets for A = 130, 30:30968
LANTHANUM 136/NUCLEAR PROPERTIES
Nuclear Data Sheets for A = 136, 30:30967

LANTHANUM 140/RADIATION MONITORING
  Data. Section IV. Other data, 30:29412
  Report of activity, February 1974 (Radioactivity of environmental samples collected throughout France during February 1974), 30:29349 (SCPRI(RM)-2-1974)
LANTHANUM 143/NUCLEAR PROPERTIES
  Nuclear Data Sheets for A = 143, 30:30966
LANTHANUM ALLOYS/PLASTICITY
  Effect of carbide-forming elements on the properties of chromium and its alloys with rare earths (Additions of Ti, Zr, Hf, Nb, Ta), 30:30058
LANTHANUM ALLOYS/SUPERCONDUCTIVITY
  Superconducting-normal phase boundaries of (La,Th)Ce systems, 30:30814
LANTHANUM BORIDES/SINTERING
  Effect of additivies of yttrium and aluminum oxides on sintering and properties of lanthanum hexaboride, 30:29892
LANTHANUM COMPLEXES/PYROLYSIS
  Derivatographic investigations on the thermal degradation of pyridine, isoquinoline, α,α-dipyridyl and o-phenantroline, resp. bichromate- or chromate-ion containing metal complexes. II. Zinc(II)-, cadmium(II)-, and manganese(II)-complexes. III. Mercury(I and II)-, uranyl-, thorium-, lanthanum-, and iron-complexes, 30:29122
LANTHANUM OXIDES
  Effect of complex admixtures of rare-earth oxides on sintering of cerium dioxide, 30:29909
LANTHANUM OXIDES/SINTERING
  Synthesis, sintering, and microstructure of the solid solutions CaO--La_2O_3, 30:29910
LAPLACE TRANSFORMATION
  Numerical deconvolution, 30:31349 (UCID-15743)
LARGE INTESTINE/RADIATION DOSES
  Comparison of external irradiation and consumption of cows' milk as critical pathways for ^{137}Cs, ^{54}Mn and ^{144}Ce--^{144}Pr released to the atmosphere, 30:29423
LARGE INTESTINE/RADIATION INJURIES
  Kinetics of recovery in irradiated colonic mucosa of the mouse (Gamma radiation, response of incidentially irradiated intestine), 30:29742
LARGE INTESTINE/SCINTISCANNING
  Detection and localization of an occult vesicoenteric fistula (^{198}Au colloid tracer), 30:29848
LASER MIRRORS/ALIGNMENT
  Aligning a spectra physics He--Ne laser model 125, 30:29270 (UCID-15860)
LASER RADIATION/MEASURING METHODS
  Torsion pendulum for laser energy measurement, 30:31451 (UCID-15907)
LASER RADIATION/WAVE PROPAGATION
  New technique for nonlinear optical problems, 30:29153 (LA-5639-MS)
LASER-PRODUCED PLASMA/METASTABLE STATES
  Method of obtaining a medium having a negative absorption coefficient in the x-ray and ultraviolet spectral range and a laser for practical application of said method (Patent), 30:29194
LASER-PRODUCED PLASMA/RESEARCH PROGRAMS
  High beta capture and mirror confinement of laser-produced plasmas. Semiannual report, January 1, 1974 through July 31, 1974, 30:29152 (COO-2277-4)
LASER-PRODUCED PLASMA/THERMONUCLEAR REACTIONS
  MEDUSA. A one-dimensional laser fusion code, 30:29227
LASER-PRODUCED PLASMA/X-RAY SPECTRA
  Spectral analysis of x rays from laser-induced plasmas, 30:29193 (SLA-74-5242)
LASER-RADIATION HEATING/NONLINEAR PROBLEMS
  New technique for nonlinear optical problems, 30:29153 (LA-5639-MS)
LASER-RADIATION HEATING/PLASMA EXPANSION
  Spatial structure of an expanding laser plasma consisting of aluminum ions and nuclei, 30:29177
LASERS
    See also CARBON DIOXIDE LASERS
             NEODYMIUM LASERS
  Interaction of radiation with an active medium in a multimode regime of pulse generation, 30:29286
  Natural width of the spectrum of two-frequency gaseous laser modes in autonomous regime and synchronized by a light signal, 30:29287
  Transverse mode control in a distributed feedback semiconducor laser, 30:29279
LASERS/CHEMICAL REACTIONS
  Model for the CW power output of the HF chemical laser, 30:29266 (LA-5683-MS)
LASERS/MODULATION
  F-M detection in the argon ion laser, 30:29268 (UCID-15371)
LASERS/POWER SUPPLIES
  Integral capacitor lateral discharge laser (Patent), 30:29281
LASERS/Q-SWITCHING
  High efficiency acousto-optical Q-switch (Patent), 30:29282
LASERS/RAMAN EFFECT
  Theory of traveling-wave electronic Raman laser: Stokes-anti-Stokes coupling in the steady state, 30:29274
LASERS/SPECIFICATIONS
  Gas laser (Patent), 30:29283
  Laser pumped by photoionization generated, electrically heated plasma (Patent), 30:29284
LASERS/X-RAY SOURCES
  Some necessary conditions on x-ray laser action, 30:29272 (UCRL-74898)
  X-ray lasers: necessary conditions and some possible approaches, 30:29271 (UCID-16290)
LATTICES (REACTOR)
    See REACTOR LATTICES
LEAD/ABSORPTION SPECTROSCOPY
  Separation of trace metal impurities from nuclear grade uranium by long-chain amine extraction and direct determination by atomic absorption spectrophotometry, 30:28948
LEAD/ABUNDANCE
  Origin of carbonatitic magma in the light of the Pb-U-Th isotope system, 30:29337
LEAD/ACTIVATION ANALYSIS
  Multielement determination in market-garden soils by instrumental photon activation analysis, 30:28921
LEAD/CHARGED-PARTICLE TRANSPORT
  Helium ion stopping cross sections in bismuth, lead, and tungsten, 30:31114
LEAD/CHEMICAL ANALYSIS
  Source identification by multi-element analysis of diurnal samples, 30:31371 (UCID-15872)
LEAD/DEFORMATION
  Nature of the deformation and flow of metals at and near the interface during abrasion, and its relation to the friction, 30:30051
LEAD/EMISSION SPECTROSCOPY
  Spectrochemical analysis of uranium oxide by gallium oxide carrier dc arc technique (ASTM Standard E402), 30:28957
  Spectrographic determination of trace impurities in high purity uranium oxide, 30:28944 (UCID-15952)
LEAD/FLUORESCENCE SPECTROSCOPY
  New discrete atomization cell for atomic fluorescence spectrometry, 30:28947
LEAD/ION EXCHANGE
  Selective ion-exchangers containing phosphorus in their functional groups. I. Sorption and separation of some bivalent and trivalent ions, 30:29001
  Sorption method of isolating uranium and other valuable metals from sea water, 30:28998
LEAD/MONITORING
  Quillayute air reference station (Air sampling and monitoring in Washington State), 30:29359 (BNWL-1850(Pt.3))
LEAD/SEPARATION PROCESSES
  Atmosphere purification of xenon, radon, and radon daughter elements (Patent, fluorination and adsorption), 30:28995
LEAD/SLIDING FRICTION
  Nature of the deformation and flow of metals at and near the interface during abrasion, and its relation to the friction, 30:30051
LEAD/SOLUBILITY
  Solubility of tin and germanium in liquid sodium. The sodium--tin partial phase diagram, 30:30049
LEAD/X-RAY FLUORESCENCE ANALYSIS
  X-ray fluorescence analysis of lead, 30:28973 (TRITA-KKE-7403)
LEAD 186/NUCLEAR PROPERTIES
  Nuclear Data Sheets for A = 186, 30:30988
LEAD 206/PAIRING INTERACTIONS
  Strength of the multipole pairing coupling constant, 30:31000
LEAD 206/X-RAY SPECTRA
  L shell ionization in the α decay of ^{210}Po, 30:31001
LEAD 207/ALPHA REACTIONS
  The l-forbidden 3psub(3/2) + 2fsub(5/2) M1 transition in ^{207}Pb (Branching ratio from Coulomb excitation), 30:31004
LEAD 207/ENERGY-LEVEL TRANSITIONS
  The l-forbidden 3psub(3/2) + 2fsub(5/2) M1 transition in ^{207}Pb (Branching ratio from Coulomb excitation), 30:31004
LEAD 208/ALPHA REACTIONS
  Highly inelastic scattering of α-particles from ^{208}Pb (Mechanism for cross section enhancement), 30:30998
LEAD 208/ELECTRON REACTIONS
  Model independent evaluation of the inelastic e^- scattering cross sections from the 3^- (2.615 MeV) level in ^{208}Pb, 30:31005
LEAD 208/ENERGY LEVELS
  Shell effects on state densities with given number of excited protons and neutrons, 30:31094
LEAD 208/ENERGY-LEVEL TRANSITIONS
  How good is the collective model, 30:31078
  Model independent evaluation of the inelastic e^- scattering cross sections from the 3^- (2.615 MeV) level in ^{208}Pb, 30:31005
LEAD 208/HELIUM 3 REACTIONS
  Excitation of the deeply bound gsub(9/2) neutron hole state in ^{117}Sn by a neutron pickup reaction with 81.7 MeV ^{3}He particles (Alpha spectra from reactions with ^{117}Sn and ^{208}Pb), 30:30974
LEAD 208/NEON 20 REACTIONS
  Massive transfer reaction ^{208}Pb(^{20}Ne,α)^{224}Th (99 MeV), 30:30997

LEAD 208/PROTON REACTIONS
  High energy proton scattering by medium and heavy nuclei (1 GeV: differential cross sections, DWIA with Coulomb effects), 30:31007
LEAD 210/PAIRING INTERACTIONS
  Strength of the multipole pairing coupling constant, 30:31000
LEAD 210/RADIATION MONITORING
  ^{137}Cs, ^{90}Sr, and ^{210}Pb in soils of the Arctic regions, 30:29405
  Determination of fallout radioisotopes from their content in the annual layers of high-mountain glaciers, 30:29408
  Long-lived radon daughters as atmospheric radioactive tracers, 30:29400
LEAD 210/TISSUE DISTRIBUTION
  Influence of irradiation on the incorporation of radionuclides (^{239}Pu; ^{226}Ra; ^{210}Pb; ^{144}Ce; tritium), 30:29818
  ^{210}Pb retention, excretion, and distribution in beagles following intravenous injection, 30:29805 (COO-119-249)
LEAD 212/RADIATION MONITORING
  Use of naturally radioactive substances in studying turbulent exchange and self-scavenging of the atmosphere with surface layer measurements, 30:29396
LEAD 212/SEPARATION PROCESSES
  Separation of radionuclides using alkyl radicals, 30:29083 (AED-CONF-74-084-002)
LEAD 214/RADIATION MONITORING
  Determination of aerosol deposition rates on a lake surface using radon daughters (^{214}Bi and ^{214}Pb tracer studies), 30:29410 (BNWL-1850(Pt.3))
  Scavenging of radioactive material from the atmosphere by surface condensation, 30:29391
LEAD ALLOYS/LATTICE PARAMETERS
  Preparation of new β-W phases by film-deposition techniques (Nb_3In, Nb_3Pb, and Nb_3Tl films, unstable phase range), 30:29967
LEAD ALLOYS/NEUTRON DIFFRACTION
  Short-range order in liquid lithium-lead alloys, 30:31382 (AED-CONF-74-089-027)
LEAD ALLOYS/PHASE DIAGRAMS
  Short-range order in liquid lithium-lead alloys, 30:31382 (AED-CONF-74-089-027)
LEAD ALLOYS/SUPERCONDUCTIVITY
  Preparation of new β-W phases by film-deposition techniques (Nb_3In, Nb_3Pb, and Nb_3Tl films, unstable phase range), 30:29967
LEAD ALLOYS/USES
  Rf hybrid microcircuit soldering techniques, 30:31397 (SLA-73-1073)
LEAD CHLORIDES/FORMATION HEAT
  Gaseous halide complexes and their stability, 30:29091
LEAD COMPOUNDS/CHEMICAL REACTIONS
  Radiation-chemical studies on the generation of lead and tin radicals (By electron scavenging in γ-irradiated 2-MTHF glass at 77°K), 30:29057
LEAD METHOD
  See ISOTOPE DATING
LEAD SULFIDES/X-RAY FLUORESCENCE ANALYSIS
  Compilation of x-ray interaction data for x-ray fluorescence analysis of geological samples, 30:28943 (RISO-297)
LEAK DETECTORS/DESIGN
  Alkali metal leak detector method and apparatus (Patent), 30:29621
LEAVES/CHEMICAL ANALYSIS
  Beryllium content of NBS standard reference orchard leaves, 30:28950
LEGUMINOSAE
  See also PISUM
  VICIA
LEGUMINOSAE/BIOLOGICAL RADIATION EFFECTS
  Effect of gamma radiation on generation M_2 of Lens esculenta Moench (Lentils), 30:29690
  Vegetation characteristics of Lens esculenta (Moench) following irradiation with thermal neutrons (Lentil), 30:29687
LEHMANN-SYMANZIK-ZIMMERMANN METHOD
  See LSZ THEORY
LEPTON-NUCLEON INTERACTIONS
  See also ELECTRON-NUCLEON INTERACTIONS
  NEUTRINO-NUCLEON INTERACTIONS
LEPTON-NUCLEON INTERACTIONS/STRUCTURE FUNCTIONS
  Gnome model and deep-inelastic lepton-nucleon structure functions, 30:30708
LEPTONS
  See also ELECTRONS
  MUONS
  NEUTRINOS
LEPTONS/PARTICLE PRODUCTION
  Possible effects of weakly coupled neutral currents in $pp\to l^+l^-+X$, 30:30762
LETHAL MUTATIONS/RADIOINDUCTION
  Chromosome loss following x-ray irradiation of mature oocytes from Drosophila melanogaster, 30:29768
LEUKEMIA
  Effect of total irradiation on the development of leukemia L_{1210} in F_1-hybrids (X Radiation; mice), 30:29748
LEVITRON DEVICES/REVIEWS
  Levitrons and the superconducting levitron: a summary, 30:29213 (UCID-15448)
LEVITRON DEVICES/RUNAWAY ELECTRONS
  Runaway effects in the inductively excited levitron, 30:29181 (UCID-15487)
LH
  (Luteinizing hormone.)
LH/RADIOIMMUNOASSAY
  Studies on radioimmunoassay of leteinizing hormone of rabbit (^{125}I tracer), 30:29860
LI-DRIFTED GE DETECTORS/CORRECTIONS
  Measurement of the geometry factors of Ge(Li) detectors, 30:29518
LI-DRIFTED GE DETECTORS/RADIOACTIVATION
  Short-lived radioactivity induced in Ge(Li) gamma-ray detectors by neutrons, 30:29516
LICHENS/RADIONUCLIDE KINETICS
  ^{137}Cs, ^{90}Sr, and ^{210}Pb in soils of the Arctic regions, 30:29405
LIGHT CONE/CURRENT COMMUTATORS
  Old and new ideas about currents and their commutators (Lectures), 30:30640
LIGHT CONE/REVIEWS
  Physics of the light cone, 30:30643
LIGHT NUCLEI/BETA DECAY
  Magnetic moments and GT-type β-decay matrix elements in nuclei with a LS doubly closed shell plus or minus one nucleon, 30:30898
  Renormalization of the axial-vector coupling constant in nuclear β-decay (III) (A123), 30:30865
LIGHT NUCLEI/ENERGY LEVELS
  Effective interaction calculations for nuclei of mass 6 to 9 (Shell-model calculations with Talmi effective interaction approach), 30:30884
LIGHT NUCLEI/NUCLEAR MAGNETIC MOMENTS
  Magnetic moments and GT-type β-decay matrix elements in nuclei with a LS doubly closed shell plus or minus one nucleon, 30:30898
LIGHT NUCLEI/NUCLEOSYNTHESIS
  Nucleosynthesis of the light elements and the interstellar medium, 30:31019 (CONF-730693-)
LIMESTONE/X-RAY FLUORESCENCE ANALYSIS
  Compilation of x-ray interaction data for x-ray fluorescence analysis of geological samples, 30:28943 (RISO-297)
LINACS
  See LINEAR ACCELERATORS
LINEAR ACCELERATORS
  See also LAMPF LINAC
  SACLAY LINAC
  STANFORD 20-GEV LINAC
LINEAR ACCELERATORS/ACCELERATOR FACILITIES
  A high-intensity superconducting muon channel (1 mA, 400 MeV electron linac facility), 30:30156
  Linear accelerator neutron source for neutron scattering, 30:30152
  Radiography of steel components with a linear electron accelerator, 30:30143
LINEAR ACCELERATORS/CONSTRUCTION
  Short electron linac of side-coupled structure with low injection voltage (4-MeV, 100 mA pulses), 30:30120
LINEAR THETA PINCH DEVICES/FISSION
  Preliminary appraisal of a fusion/fission (hybrid) reactor based on the linear theta pinch, 30:29228
LIPPMANN-SCHWINGER EQUATION/THREE-BODY PROBLEM
  Use of Lippmann--Schwinger equations in the three-body problem, 30:31044
LIQUID DROP MODEL/CORRECTIONS
  Superheavy elements and the Strutinsky prescription (Single-particle corrections to liquid-drop model), 30:31026
LIQUID IONIZATION CHAMBERS
  See also LIQUID PROPORTIONAL COUNTERS
LIQUID IONIZATION CHAMBERS/OPERATION
  Study of the detection of nuclear particles in liquid dielectrics, 30:29492 (CEA-R-4543)
LIQUID METAL COOLED REACTORS/REACTOR CORES
  Use of superposition in calculating the temperature of a reactor core cooled by a liquid metal, 30:31277
LIQUID METAL COOLED REACTORS/SECONDARY COOLANT CIRCUITS
  Process for converting heat produced by a nuclear reactor to electrical energy (Patent), 30:31282
LIQUID METAL FAST BREEDER REACTORS
  See LMFBR TYPE REACTORS
LIQUID PROPORTIONAL COUNTERS
  See also LIQUID IONIZATION CHAMBERS
  Electronic processes in liquid xenon (Comments on previous paper), 30:29512
LIQUID PROPORTIONAL COUNTERS/OPERATION
  Study of the detection of nuclear particles in liquid dielectrics, 30:29492 (CEA-R-4543)
LIQUID SCINTILLATION DETECTORS
  Methods, apparatus, and flexible containers for handling liquid samples for scintillation spectrometry (Patent), 30:29561
LIQUID WASTES/RADIOSTERILIZATION
  First gamma-irradiation plant for sewage-sludge hygienization, 30:29643
LITHIUM
  Metal vapor confinement in vacuum (Charge exchange cells for negative ion beam production), 30:30128

LITHIUM/CORROSIVE EFFECTS
  Effect of oxygen on the corrosion of vanadium and V--20% Ti by liquid lithium (600 to 1000°C), 30:29954
  The stability of vanadium and of the alloy V-3Ti-15Nb in liquid lithium at 700°C, 30:29951
LITHIUM/ELECTRON-ATOM COLLISIONS
  Polarization of the resonance lines of lithium and sodium atoms by electron impact (Glauber theory), 30:30521 (IC-73-19)
LITHIUM/EMISSION SPECTROSCOPY
  Spectrochemical analysis of uranium oxide by gallium oxide carrier dc arc technique (ASTM Standard E402), 30:28957
LITHIUM/EXCITATION
  Rate coefficients for electron excitation of the first resonance transition in H, Li, Na, Ca, Ca^+, and Ba^+ calculated from experimental data (Transition probabilities), 30:30246
LITHIUM/METALLURGICAL EFFECTS
  Effect of lithium vapor on the structure of monocrystals of refractory metals and alloys, 30:29955
LITHIUM/MUON REACTIONS
  Negative muon capture in very light atoms, 30:30509
LITHIUM/NUCLEAR REACTION ANALYSIS
  Application of nuclear physics methods for the determination of the depth of lithium ions penetration in the glasses with crystallized surface, 30:28980
LITHIUM 6/ABUNDANCE
  Adequacy of lithium supplies as a fusion energy source, 30:29222 (UCID-15953)
LITHIUM 6/COSMOCHEMISTRY
  A galactic model with a pulsating active nucleus. III. Evolution of rare-light elements, 30:30386
LITHIUM 6/DEUTERON REACTIONS
  Quasi-free contributions in the $d+{}^{6}Li$ reactions at low energies, 30:30882
LITHIUM 6/ELECTRON REACTIONS
  Cluster-model calculations of the electrodisintegration of lithium (Differential form factors), 30:30893
LITHIUM 6/PION REACTIONS
  Pion-nucleus total cross sections from 88 to 860 MeV, 30:30891
LITHIUM 6/PROTON REACTIONS
  The ${}^{6}Li(p,2p){}^{5}He$ reaction at 100 MeV (Angular correlations and distributions, energy and momentum distributions), 30:30896
LITHIUM 7/ABUNDANCE
  Adequacy of lithium supplies as a fusion energy source, 30:29222 (UCID-15953)
LITHIUM 7/COSMOCHEMISTRY
  A galactic model with a pulsating active nucleus. III. Evolution of rare-light elements, 30:30386
LITHIUM 7/DEUTERON REACTIONS
  Neutrons from the 2MeV deuteron bombardment of thick ${}^{7}Li$ targets, 30:30146
  Optical model and DWBA analysis of the ${}^{7}Li(d,d)$- and ${}^{7}Li(d,p_0)$-reactions in the energy region 1.0 to 2.6 MeV, 30:30883
LITHIUM 7/ELECTRON REACTIONS
  Cluster-model calculations of the electrodisintegration of lithium (Differential form factors), 30:30893
LITHIUM 7/PION REACTIONS
  Pion-nucleus total cross sections from 88 to 860 MeV, 30:30891
LITHIUM 7 REACTIONS/COMPOUND-NUCLEUS REACTIONS
  J, π, lifetimes from spectra from ${}^{11}B({}^{7}Li, p\gamma)$ at 6.0 MeV, 30:30895
  Spectra from ${}^{11}B({}^{7}Li, p\gamma)$ reaction at 6 MeV, 30:30894
LITHIUM 7 REACTIONS/ONE-NUCLEON TRANSFER REACTIONS
  Nuclear spectroscopy with the ${}^{62}Ni({}^{7}Li,{}^{6}He){}^{63}Cu$ reaction (34 MeV), 30:30937
LITHIUM 7 REACTIONS/STRIPPING
  Reactions produced by ${}^{7}Li$ on ${}^{197}Au$ (32 MeV cross sections, reaction mechanisms), 30:30396
LITHIUM ALLOYS/NEUTRON DIFFRACTION
  Short-range order in liquid lithium-lead alloys, 30:31382 (AED-CONF-74-089-027)
LITHIUM ALLOYS/PHASE DIAGRAMS
  Short-range order in liquid lithium-lead alloys, 30:31382 (AED-CONF-74-089-027)
LITHIUM CHLORIDES/MELTING POINTS
  Fusibility diagram of the system $LiCl$--UCl_4--$ThCl_4$, 30:29095
LITHIUM FLUORIDES/ATOM COLLISIONS
  Semiclassical theory of atom--solid-surface collisions: application to He--LiF diffraction, 30:30476
LITHIUM FLUORIDES/CHEMICAL REACTIONS
  Reaction of uranium with a mixture of lithium and calcium fluorides, 30:29110
LITHIUM FLUORIDES/SOLVENT PROPERTIES
  Solubility and stability of structural metal difluorides in molten fluoride mixtures, 30:29002 (ORNL-TM-760)
LITHIUM HYDRIDES/CORROSION
  Ion-backscattering study of LiOH-to-Li_2O conversion on a LiH substrate (Surface hydrolysis reactions), 30:29937
LITHIUM HYDRIDES/RADIATION EFFECTS
  Pulse NMR studies of radiation damage in metal tritides (Triton decay in LiT and UT_3), 30:29889 (MLM-2172(OP))
LIVER/CHROMOSOMAL ABERRATIONS
  Effect of ${}^{239}PuO_2$ particle number and size on the frequency and distribution of chromosome aberrations in the liver of the Chinese hamster, 30:29783
LIVER/METASTASES
  Clinical evaluation of preoperative liver scintigraphy in gastric carcinoma patients (${}^{198}Au$ colloid and /sup 99m/Tc colloid tracer), 30:29854
LIVER/RADIONUCLIDE KINETICS
  Early subcellular distribution of einsteinium in canine livers (${}^{253}Es$), 30:29804 (COO-119-249)
  Effect of delayed lymphadenectomy on ${}^{239}PuO_2$ translocation in dogs, 30:29820
  Internal deposition of ingested cerium in suckling mice, 30:29821
LIVER/RADIOSENSITIVITY
  X-radiation-sensitivity of rat liver to interphase death, 30:29737
LIVER/SCINTISCANNING
  Combined contrast and radionuclide angiography of the liver (/sup 99m/Tc-sulfur colloid tracer), 30:29844
  Liver studies with various radioactive tracers and methods (Critical evaluation of diagnostic value), 30:29831 (CONF-740708-52)
  Use of multiple radionuclide imaging to differentiate the focal intrahepatic lesion (/sup 99m/Tc, /sup 113m/In, ${}^{75}Se$, and ${}^{111}In$ tracer), 30:29851
LIVER CIRRHOSIS/DIAGNOSIS
  Combined contrast and radionuclide angiography of the liver (/sup 99m/Tc-sulfur colloid tracer), 30:29844
LMFBR TYPE REACTORS
  See also CLINCH RIVER BREEDER REACTOR
  FFTF REACTOR
  Apparatus for refining sodium (Patent), 30:31227
LMFBR TYPE REACTORS/CONTAINMENT
  Design of the primary containment for pool and loop arrangements of LMFBRs, 30:31263
LMFBR TYPE REACTORS/CORE CATCHERS
  Post-accident core retention for LMFBR's. 2. Technical report. Final report for the period 1 July 1972--30 June 1973, 30:31253 (UCLA-ENG-7343)
LMFBR TYPE REACTORS/FLOWMETERS
  Development of sodium flowmeter by real time correlation technique. II. Measurement of flow velocity in mockup fuel assembly, 30:31224 (JAPFNR-154)
LMFBR TYPE REACTORS/FUEL ASSEMBLIES
  Development of sodium flowmeter by real time correlation technique. II. Measurement of flow velocity in mockup fuel assembly, 30:31224 (JAPFNR-154)
  Study of local blockages in fast reactor sub-assemblies, 30:31229
LMFBR TYPE REACTORS/FUEL CANS
  Thermodynamic data program involving plutonia and urania at high temperatures. Quarterly report No. 27, February 1, 1974--April 30, 1974, 30:31223 (GEAP-12511)
LMFBR TYPE REACTORS/FUEL PINS
  Calculation of the effects of fission gas in a LMFBR, for the analysis of an unprotected overpower transient, 30:31225 (KFK-1990)
  Fission gas behavior in fast reactor fuel under transient power conditions, 30:31228
  Thermodynamic data program involving plutonia and urania at high temperatures. Quarterly report No. 27, February 1, 1974--April 30, 1974, 30:31223 (GEAP-12511)
LMFBR TYPE REACTORS/LOSS OF FLOW
  Study on the test of sodium boiling. I. Loss-of-flow test by a single pin, 30:31258
LMFBR TYPE REACTORS/MELTDOWN
  Post-accident core retention for LMFBR's. 2. Technical report. Final report for the period 1 July 1972--30 June 1973, 30:31253 (UCLA-ENG-7343)
  Transport of core materials during accidents in LMFBRs (slumping), 30:31249 (KFK-1935)
LMFBR TYPE REACTORS/REACTOR CORE DISRUPTION
  Analysis of the primary containment response using a hydrodynamic-elastic-plastic computer code (Rexco-hep code; LMFBR), 30:31264
  Post-accident core retention for LMFBR's. 2. Technical report. Final report for the period 1 July 1972--30 June 1973, 30:31253 (UCLA-ENG-7343)
LMFBR TYPE REACTORS/RESEARCH PROGRAMS
  Fast reactor programme. First quarter 1974 progress report (Reactor physics; fuel pin testing; cladding irradiation effects; aerosol behavior; heat transfer), 30:31226 (RCN-212)
LMFBR TYPE REACTORS/SPENT FUEL ELEMENTS
  LMFBR-37-fuel-element shipping cask simulation: test assembly operation and data, 30:30114 (ORNL-TM-3992)
LMFBR TYPE REACTORS/STEAM GENERATORS
  LMFBR demonstration plant steam generating system, 30:31217 (CENC-1194(Vol.1)(Suppl.1))
  LMFBR demonstration plant steam generating system, 30:31218 (CENC-1194(Vol.2)(Suppl.1))
  LMFBR sodium heated steam generator: test model, 30:31219 (CENC-1197(Vol.1))
  LMFBR sodium heated steam generator: test model, 30:31220 (CENC-1197(Vol.3))
  LMFBR sodium heated steam generator: test model (Structural steel analysis), 30:31221 (CENC-1197(Vol.4))
LOCAL GALAXY
  See MILKY WAY
LOCAL GROUP
  See GALAXIES

LOFT REACTOR/REACTOR EXPERIMENTAL FACILITIES
  LOFT integral test facility and program, 30:31238
LOFT REACTOR/RESEARCH PROGRAMS
  LOFT integral test facility and program, 30:31238
LORENTZ INVARIANCE
  Constraints, causality, and Lorentz invariance, 30:31167
LOS ALAMOS MESON PHYSICS FACILITY
  See LAMPF LINAC
LOSS OF FLOW/SIMULATION
  Study on the test of sodium boiling. I. Loss-of-flow test by a single pin (lmfbr), 30:31258
LOSS OF FLUID TEST REACTOR
  See LOFT REACTOR
LOW LEVEL COUNTERS/DESIGN
  A large plastic scintillator as anticoincidence shield for beta-radiation detectors, 30:29575
LSZ THEORY/COULOMB FIELD
  Weak LSZ limits and reduction formula for the non-relativistic Coulombic interaction, 30:31169
LSZ THEORY/S MATRIX
  Weak LSZ limits and reduction formula for the non-relativistic Coulombic interaction, 30:31169
LTH
  (Luteotropic hormone.)
LTH/RADIOIMMUNOASSAY
  Determination of prolactin in the blood by radioimmunoassay (^{125}I tracer), 30:29662
LUBRICATION/CHEMICAL ANALYSIS
  Determination of mineral-oil in the helium-circuit of a refrigeration-plant, 30:31393 (KFK-1978)
LUCIE-1 REACTOR/REACTOR LICENSING
  FIND: St. Lucie Plant, Unit 1, 30:31321 (FIND-50335)
LUCIE-2 REACTOR/REACTOR LICENSING
  FIND: St. Lucie Plant, Unit 2, 30:31322 (FIND-50389)
LUNAR MATERIALS/ACTIVATION ANALYSIS
  Trace geochemistry of lunar material. Final report, 30:28916 (N-74-20470)
LUNAR MATERIALS/MAGNETIC PROPERTIES
  Rock magnetites with positive anisotropy constants at 300°K, 30:31389 (CONF-740644-1)
LUNAR MATERIALS/MASS SPECTROSCOPY
  Trace geochemistry of lunar material. Final report, 30:28916 (N-74-20470)
LUNGS/BIOLOGICAL RADIATION EFFECTS
  Changes of the broncho-vascular system of the lung under the influence of local γ irradiation (Following micro- or macro-fractionated therapy), 30:29728
  Long-term effects of intratracheally instilled ^{253}EsCl$_3$ in rats, 30:29776 (BNWL-SA-4870)
LUNGS/EXPERIMENTAL NEOPLASMS
  Direct relationship between immune competence and the subcutaneous growth rate of a malignant murine lung tumor (X radiation), 30:29756
LUNGS/SCINTISCANNING
  Dual camera studies of pulmonary function with computer processing of data (^{133}Xe tracer), 30:29847
  ^{67}Ga-scintigraphy in malignant lesions of the lung, 30:29883
LUTEINIZING HORMONE
  See LH
LUTEOTROPIC HORMONE
  See LTH
LUTETIUM/ACTIVATION ANALYSIS
  Determination of rare earths and thorium in apatites by thermal and epithermal neutron-activation analysis, 30:28935
  Radioactivation analysis in thermal and epithermal neutrons of the IBR-30 reactor of JINR, 30:28929
LUTETIUM/ION EXCHANGE
  Synthesis of reproducible tin(IV) based ion exchangers: separation of lanthanum(III) from yttrium(III), europium(III), and lutetium(III), 30:28994
LUTETIUM 166/BETA-PLUS DECAY
  Decay properties of three ^{166}Lu isomers and the decay of ^{166}Hf (Spectra, log ft, Q, branching ratios, K, J, π, L), 30:30989
LUTETIUM 166/ELECTRON CAPTURE DECAY
  Decay properties of three ^{166}Lu isomers and the decay of ^{166}Hf (Spectra, log ft, Q, branching ratios, K, J, π, L), 30:30989
LUTETIUM 166/ENERGY LEVELS
  Decay properties of three ^{166}Lu isomers and the decay of ^{166}Hf (Spectra, log ft, Q, branching ratios, K, J, π, L), 30:30989
LUTETIUM 175/NEUTRON REACTIONS
  Coincidence spectra from ^{175}Lu (n,γ) and ^{181}Ta (n,γ) reactions with thermal neutrons, 30:30993
  Status report to NCSAC, 30:31011 (UCID-15639)
LUTETIUM 176/ENERGY-LEVEL TRANSITIONS
  Transition probabilities in the doubly odd nuclei ^{176}Lu and ^{182}Ta, 30:30993
LWGR TYPE REACTORS/NUCLEAR FUELS
  Utilization of metallic uranium in power channel uranium-graphite reactors, 30:31205
LYMPH NODES/RADIONUCLIDE KINETICS
  Effect of delayed lymphadenectomy on ^{239}PuO$_2$ translocation in dogs, 30:29820
LYMPHOCYTES/BIOLOGICAL RADIATION EFFECTS
  Radiation-induced DNA synthesis in normal and stimulated human lymphocytes (Ultraviolet radiation), 30:29664
LYMPHOCYTES/CHROMOSOMAL ABERRATIONS
  Changes in the number of circulating lymphocytes with chromosomal aberrations following a single exposure of the pelvis to x-irradiation in cancer patients, 30:29706
  Human lymphocyte as a radiobiological dosimeter after total body irradiation (Gamma radiation), 30:29707
  Influence of blood oxygenation during in vitro irradiation upon the yield of dicentric chromosomal aberrations in lymphocytes (X Radiation), 30:29749
LYMPHOID CELLS
  See LYMPHOCYTES
LYSOSOMES/BIOLOGICAL RADIATION EFFECTS
  Effect of internally deposited plutonium-239 on the lysosomes of rat liver (Compared with effects from ^{198}Au), 30:29782

M

MACHINE TOOLS/PERFORMANCE TESTING
  Secondary jaw crusher development, 30:29265 (GA-A-12903)
MACROPHAGES/BIOLOGICAL RADIATION EFFECTS
  Macrophage--lymphocyte synergy in the production of osteoclast activating factor (X Radiation), 30:29667
MAGELLANIC CLOUDS/COSMIC DUST
  Dust in the Large Magellanic Cloud, 30:30370
MAGELLANIC CLOUDS/COSMIC X-RAY SOURCES
  X-ray observations of the large magellanic cloud by the Copernicus satellite (Error circle), 30:30365
MAGELLANIC CLOUDS/LUMINOSITY
  Steps toward the Hubble constant. II. The brightest stars in late-type spiral galaxies (Mean correlation line), 30:30393
MAGELLANIC CLOUDS/STAR CLUSTERS
  Population synthesis applied to eight young Magellanic Cloud globular clusters (Corresponding age), 30:30216
MAGIC NUCLEI/ENERGY SPECTRA
  Magic nuclei theory, 30:30627 (IAE-2286)
MAGIC NUMBERS
  See MAGIC NUCLEI
MAGNESIUM/ACTIVATION ANALYSIS
  Multielement determination in market-garden soils by instrumental photon activation analysis, 30:28921
MAGNESIUM/CHEMICAL ANALYSIS
  Extraction--spectrophotometric methods of determining 0.0--n0.000n% aluminum in materials of metallurgical manufacture (exchange of experience), 30:28956
MAGNESIUM/COSMOCHEMISTRY
  High-frequency observations of possible ''heavy-element'' recombination lines (Cosmic value), 30:30267
MAGNESIUM/EMISSION SPECTROSCOPY
  Spectrochemical analysis of uranium oxide by gallium oxide carrier dc arc technique (ASTM Standard E402), 30:28957
  Spectrographic determination of trace impurities in high purity uranium oxide, 30:28944 (UCID-15952)
MAGNESIUM/FLUORESCENCE SPECTROSCOPY
  New discrete atomization cell for atomic fluorescence spectrometry, 30:28947
MAGNESIUM/OXYGEN 16 REACTIONS
  Investigation of the 3.46 MeV isomeric level of ^{38}K with the ^{24}Mg(^{16}O,pnγ)^{38}K reaction (38 MeV: γ spectra; lifetimes of levels in ^{38}K, ^{38}Ar, ^{38}Cl), 30:30912
MAGNESIUM 24/COSMOCHEMISTRY
  Cross sections of the ^{21}Ne(α,n)^{24}Mg and ^{22}Ne(α,n)^{25}Mg reactions at low energies of astrophysical interest, 30:30913
MAGNESIUM 24/OXYGEN 16 REACTIONS
  Coulomb nuclear interference in the inelastic scattering of ^{16}O ions from ^{24}Mg (20 to 30 MeV), 30:30905
MAGNESIUM 24/ROTATIONAL STATES
  States in ^{24}Mg populated by the ^{10}B(^{16}O,d)^{24}Mg and ^{12}C(^{16}O,α)^{24}Mg reactions, 30:30911
MAGNESIUM 25/COSMOCHEMISTRY
  Cross sections of the ^{21}Ne(α,n)^{24}Mg and ^{22}Ne(α,n)^{25}Mg reactions at low energies of astrophysical interest, 30:30913
MAGNESIUM 25/ENERGY LEVELS
  The decay of the giant dipole resonance in ^{26}Mg to T=3/2 states of ^{25}Mg, 30:30908
MAGNESIUM 26/ENERGY LEVELS
  Two particle intrinsic excitations in ^{22}Ne and ^{26}Mg, 30:30915
MAGNESIUM 26/PHOTONUCLEAR REACTIONS
  The decay of the giant dipole resonance in ^{26}Mg to T=3/2 states of ^{25}Mg, 30:30908
MAGNESIUM ALLOYS
  See also MAGNESIUM BASE ALLOYS
MAGNESIUM ALLOYS/ELONGATION
  Method of determining the relative elongation of light alloys close to the solidus on an IMASh-5S-65 unit, 30:30012
MAGNESIUM ALLOYS/MECHANICAL PROPERTIES
  Mechanical properties of sintered magnesium--beryllium alloys, 30:30017
MAGNESIUM BASE ALLOYS/PHASE STUDIES
  Co-solubility of neodymium and zinc in solid magnesium (Mg--Nd--Zn alloys containing up to 3 percent Nd and 8 percent Zn), 30:30007

MAGNESIUM CARBONATES/X-RAY FLUORESCENCE ANALYSIS
Compilation of x-ray interaction data for x-ray fluorescence analysis of geological samples, 30:28943 (RISO-297)
MAGNESIUM COMPOUNDS/BIOLOGICAL EFFECTS
Hydrolysis of 2',3'-cyclic adenosine monophosphate and 3',5'-cyclic adenosine monophosphate in subcellular fractions of normal and neoplastic mouse spleen (X radiation), 30:29739
MAGNESIUM IONS/X-RAY SPECTRA
Diagnostics of dense laser plasmas based on the spectra of hydrogen-like and helium-like multiply charged ions, 30:29171
MAGNESIUM OXIDES/PHYSICAL RADIATION EFFECTS
Production of oxygen vacancies by elastic collisions in alkaline earth oxides (400-keV and 3-meV protons; 15, 77, and 300°K), 30:29933
MAGNESIUM OXIDES/X-RAY FLUORESCENCE ANALYSIS
Compilation of x-ray interaction data for x-ray fluorescence analysis of geological samples, 30:28943 (RISO-297)
MAGNET COILS/DESIGN
Flux theorem for the design of magnet coil ends, 30:30122
MAGNET COILS/MAGNETIC FIELDS
Method for the calculation of the magnetostatic field from a wide class of current geometries, 30:29211 (RL-74-077)
Surface currents on a toroid that result in a uniform, axial magnetic field inside the torus, 30:29219 (UCID-15695)
MAGNETIC ANALYZERS
Energy-loss spectrometer for low-energy pion scattering, 30:29586
MAGNETIC BAYS
Latitudinal cross section of the auroral electrojet and its relation to the interplanetary magnetic field polarity, 30:30470
MAGNETIC BAYS/VARIATIONS
Frequency of occurrence of positive geomagnetic bays at Trivandrum, 30:30421
MAGNETIC BEARINGS/PERFORMANCE
Test of a magnetic bearing for optical scanner applications, 30:31430 (SLA-74-0347)
MAGNETIC BREMSSTRAHLUNG
See SYNCHROTRON RADIATION
MAGNETIC CIRCUITS/DESIGN
Outline of developments in magnetic circuit theory, 30:31436 (UCID-15597)
MAGNETIC COILS
See MAGNET COILS
MAGNETIC FIELDS
See also GEOMAGNETIC FIELD
Space wave fields of subsurface electromagnetic sources in planar layered media, 30:31353 (UCID-15945)
MAGNETIC FIELDS/KINETICS
Dynamics of the solar magnetic field. II. The energy spectrum of large-scale solar magnetic fields, 30:30316
MAGNETIC MATERIALS/DOMAIN STRUCTURE
Lorentz microscopic observation of head-on domain walls in magnetic thin films, 30:31455 (UCID-16034)
MAGNETIC MIRRORS
See also ELMO DEVICES
2X DEVICES
MAGNETIC MIRRORS/DIRECT ENERGY CONVERTERS
Preliminary report of direct recovery study, 30:29217 (UCID-15650)
MAGNETIC MIRRORS/MAGNETIC FIELDS
MTSE II field calculation, 30:29215 (UCID-15511)
MAGNETIC MIRRORS/NEUTRAL ATOM BEAM INJECTION
Energy recovery of a lithium ion beam, 30:29221 (UCID-15939)
MAGNETIC MIRRORS/OPERATION
Radiation and heat deposition analysis of the proposed Mirror Fusion Experiment (MFX), 30:29220 (UCID-15806)
MAGNETIC SPECTROMETERS/STREAMER SPARK CHAMBERS
180° magnetic spectrometer with helium-filled streamer chamber, 30:29591
MAGNETIC STARS/CHEMICAL COMPOSITION
Diffusion and isotope anomalies in peculiar A--B stars, 30:30201
MAGNETIC STARS/DIFFUSION
Diffusion and isotope anomalies in peculiar A--B stars, 30:30201
MAGNETITE/MAGNETIC PROPERTIES
Rock magnetites with positive anisotropy constants at 300°K, 30:31389 (CONF-740644-1)
MAGNETOHYDRODYNAMIC CHANNELS
See MHD CHANNELS
MAGNETOHYDRODYNAMICS
MHD flow in variable-area conducting rectangular ducts, 30:30571
MAGNETOHYDRODYNAMICS/FRICTION
The skin friction on accelerated plates in magnetohydrodynamcis, 30:30573
MAGNETOHYDRODYNAMICS/MEETINGS
Developments in mechanics. Volume 7. Proceedings of the 13th Midwestern Mechanics Conference held at Pittsburgh, Pennsylvania, August 13--15, 1973, 30:30570
Engineering aspects of magnetohydrodynamics. Thirteenth symposium held at Stanford, California, March 26--28, 1973, 30:31207
MAGNETOMETERS/OPERATION
Precise determination of inhomogeneous magnetic field components with a Hall probe, 30:29633
MAGNETOSPHERE/ELECTRIC FIELDS
Derivation of magnetospheric electric fields from whistler data in a dynamic geomagnetic field, 30:30464
MAGNETOSPHERE/ELECTRON BEAMS
Electron Echo experiment 1: Comparison of observed and theoretical motion of artificially injected electrons in the magnetosphere, 30:30453
MAGNETOSPHERE/ELECTRON DENSITY
Interrelationship between the > 130 keV electron trapping boundary, the VHF radar backscatter, and the visual aurora, 30:30430
MAGNETOSPHERE/MAGNETIC STORMS
Variability of mid-latitude magnetic parameters used to characterize magnetospheric substorms, 30:30463
MAGNETOSPHERE/PARAMETRIC INSTABILITIES
Particle saturation of the outer zone: a nonlinear model, 30:30472
MAGNETOSPHERE/PLASMA DENSITY
Thermal and suprathermal plasma densities in the outer magnetosphere. Progress report, 30:30449 (AD-776660)
Thermal and suprathermal plasma densities in the outer magnetosphere, 30:30454
MAGNETOSPHERE/RADIOWAVE RADIATION
VLF wave injection into the magnetosphere from Siple Station, Antarctica, 30:30462
MAGNETOSPHERE/RESEARCH PROGRAMS
Some active magnetosphere experiments to be performed by the Plasma Physics and Environmental Perturbation Laboratory, 30:30450 (COM-74-50228)
MAGNETOSPHERE/RING CURRENTS
A model of the distributed magnetospheric currents, 30:30468
MAGNETOSPHERE/SYNCHROTRON RADIATION
Synchrotron loss rates of energetic magnetospheric electrons, 30:30451
MAGNETOTAIL/PLASMA DENSITY
Plasma tail interpretations of pronounced detached plasma regions measured by Ogo 5, 30:30466
MAGNOX TYPE REACTORS/RADIOACTIVE WASTES
Experience in complying with authorisation conditions for the discharge of liquid and gaseous radioactive effluents from CEGB nuclear stations, 30:31204 (AED-CONF-74-157-007)
MAIN SEQUENCE STARS/CONVECTION
On the semiconvective zone in the core-helium-burning stars, 30:30264
MAINE/RADIOACTIVITY
Aerial radiological measuring survey of the Maine Yankee Atomic Power Plant, September 1971, 30:29357 (ARMS-71.6.5)
MAINE YANKEE REACTOR/AERIAL MONITORING
Aerial radiological measuring survey of the Maine Yankee Atomic Power Plant, September 1971, 30:29357 (ARMS-71.6.5)
MAIZE/DISEASE RESISTANCE
Resistance to Ustilago myadis of WD lineage progeny after chronic gamma irradiation (Maize), 30:29688
MAIZE/RADIATION EFFECTS
Effect of chronic and acute gamma irradiation on specific recombination capability of lineage WD maize, 30:29689
MAMMARY GLANDS/BIOLOGICAL RADIATION EFFECTS
Development and involution of mammary gland epithelial tissue under x irradiation, cyclophosphamide, and antilymphocyte serum treatment, 30:29760
MAN
See also INFANTS
PATIENTS
PERSONNEL
MAN/RADIATION DOSES
Comparison of external irradiation and consumption of cows' milk as critical pathways for ^{137}Cs, ^{54}Mn and ^{144}Ce--^{144}Pr released to the atmosphere, 30:29423
Medical evaluation of measured values following radiation exposure, 30:29703 (AED-CONF-74-221-007)
NAEG plutonium study modeling program: plutonium transport and dose estimation model (Computer model for evaluation of health hazards to man due to environmental ^{239}Pu, applied to Nevada Test Site), 30:29455 (NVO-AEIC-74-1)
MAN/RADIATION HAZARDS
Resuspension of ^{239}Pu, ^{240}Pu, and ^{241}Am particles at Nevada Test Site; prediction of air concentrations of Pu due to resuspension at Eniwetok Atoll, 30:29452 (NVO-AEIC-74-1)
MAN/RADIONUCLIDE KINETICS
Distribution of radioactive and stable cesium in the human body (^{137}Cs; K), 30:29789
NAEG plutonium study modeling program: plutonium transport and dose estimation model (Computer model for evaluation of health hazards to man due to environmental ^{239}Pu, applied to Nevada Test Site), 30:29455 (NVO-AEIC-74-1)
Tissue-blood ^{131}I and ^{133}Xe transfer in the presence of raised capillary filtration, 30:29794
MANGANESE/ABSORPTION SPECTROSCOPY
Atomic absorption spectrometry of impurities in high purity tantalum with heated graphite atomizer, 30:28954

MANGANESE/ACTIVATION ANALYSIS
  Determination of rare earths and thorium in apatites by thermal and epithermal neutron-activation analysis, 30:28935
  Multielement determination in market-garden soils by instrumental photon activation analysis, 30:28921
  Trace element behavior in soil of some Indonesian sawah's and in sludge of an Indonesian river, 30:28930
  Trace elements in precipitation and cloud water in the area of Heidelberg, measured by instrumental neutron activation analysis, 30:28934
  Use of NH_4-form Chelex 100 chelating resin of low induced activities for neutron activation analysis of manganese in seawater, 30:28927
MANGANESE/COSMOCHEMISTRY
  Diffusion and isotope anomalies in peculiar A--B stars, 30:30201
MANGANESE/EMISSION SPECTROSCOPY
  Spectrochemical analysis of uranium oxide by gallium oxide carrier dc arc technique (ASTM Standard E402), 30:28957
  Spectrographic determination of trace impurities in high purity uranium oxide, 30:28944 (UCID-15952)
MANGANESE/ION EXCHANGE
  Sorption method of isolating uranium and other valuable metals from sea water, 30:28998
MANGANESE 52/ISOMERIC TRANSITIONS
  Isomeric-yield ratio of ^{52}Mn/sup g/ and ^{52}Mn/sup m/ photoproduction from ^{55}Mn at intermediate energies (Lifetimes, 0.3 to 1 GeV), 30:30919
MANGANESE 52/NUCLEAR REACTION YIELD
  Isomeric-yield ratio of ^{52}Mn/sup g/ and ^{52}Mn/sup m/ photoproduction from ^{55}Mn at intermediate energies (Lifetimes, 0.3 to 1 GeV), 30:30919
MANGANESE 52/SPIN
  Isomeric-yield ratio of ^{52}Mn/sup g/ and ^{52}Mn/sup m/ photoproduction from ^{55}Mn at intermediate energies (Lifetimes, 0.3 to 1 GeV), 30:30919
MANGANESE 53/COSMOCHEMISTRY
  The unique cosmic-ray history of the Malakal chondrite, 30:30170
MANGANESE 53/ENERGY LEVELS
  Lifetime measurements of some states in ^{53}Mn (Doppler shift-attenuation method), 30:30930
  Magnetic rotation of levels of ^{53}Mn and ^{54}Mn following the ^{53} ^{54}Cr(p,n) and ^{51}V(α,n) reactions (2.5- and 3.0-MeV protons, 7.5-MeV alphas; branching ratios, g, lifetimes), 30:30933
MANGANESE 54/BIOLOGICAL RADIATION EFFECTS
  Comparison of external irradiation and consumption of cows' milk as critical pathways for ^{137}Cs, ^{54}Mn and ^{144}Ce--^{144}Pr released to the atmosphere, 30:29423
MANGANESE 54/COSMOCHEMISTRY
  The unique cosmic-ray history of the Malakal chondrite, 30:30170
MANGANESE 54/ENERGY LEVELS
  Magnetic rotation of levels of ^{53}Mn and ^{54}Mn following the ^{53} ^{54}Cr(p,n) and ^{51}V(α,n) reactions (2.5- and 3.0-MeV protons, 7.5-MeV alphas; branching ratios, g, lifetimes), 30:30933
MANGANESE 54/HIGH SPIN STATES
  Nuclear structure of ^{54}Mn, 30:30916 (NP-20122)
MANGANESE 54/RADIATION MONITORING
  Data. Section IV. Other data, 30:29412
  Determination of fallout radioisotopes from their content in the annual layers of high-mountain glaciers, 30:29408
  Report of activity, February 1974 (Radioactivity of environmental samples collected throughout France during February 1974), 30:29349 (SCPRI(RM)-2-1974)
MANGANESE 54/RADIOECOLOGICAL CONCENTRATION
  Comparison of external irradiation and consumption of cows' milk as critical pathways for ^{137}Cs, ^{54}Mn and ^{144}Ce--^{144}Pr released to the atmosphere, 30:29423
MANGANESE 55/PHOTONUCLEAR REACTIONS
  Isomeric-yield ratio of ^{52}Mn/sup g/ and ^{52}Mn/sup m/ photoproduction from ^{55}Mn at intermediate energies (Lifetimes, 0.3 to 1 GeV), 30:30919
MANGANESE ALLOYS/ION EMISSION
  Ionic emission yield for alloys, dependence on the nature of the solute. II. Interpretation, 30:30087
MANGANESE ALLOYS/MICROSTRUCTURE
  Structure and phase-boundary energies of the directionally solidified InSb--MnSb--NiSb, InSb--FeSb, and InSb--CrSb eutectic alloys, 30:30019
MANGANESE COMPLEXES/PYROLYSIS
  Derivatographic investigations on the thermal degradation of pyridine, isoquinoline, α,α-dipyridyl and o-phenantroline, resp. bichromate- or chromate-ion containing metal complexes. II. Zinc(II)-, cadmium(II)-, and manganese(II)-complexes. III. Mercury(I and II)-, uranyl-, thorium-, lanthanum-, and iron-complexes, 30:29122
MANGANESE COMPOUNDS/ELECTRONIC STRUCTURE
  Electronic structure and optical properties of some first row transition metal oxyhalides, 30:31395 (LA-5637-T)
MANGANESE COMPOUNDS/OPTICAL PROPERTIES
  Electronic structure and optical properties of some first row transition metal oxyhalides, 30:31395 (LA-5637-T)
MANGANESE IONS/EMISSION SPECTRA
  Spectral classifications in the Fe XIX to Fe XXIII isoelectronic sequences, 30:30329
MANGANESE OXIDES/X-RAY FLUORESCENCE ANALYSIS
  Compilation of x-ray interaction data for x-ray fluorescence analysis of geological samples, 30:28943 (RISO-297)
MANY-BODY PROBLEM
  See also FOUR-BODY PROBLEM
    THREE-BODY PROBLEM
    TWO-BODY PROBLEM
MANY-BODY PROBLEM/CENTER-OF-MASS SYSTEM
  Centre of mass coordinate in many-body theories, 30:30860
MANY-BODY PROBLEM/ENERGY SPECTRA
  Calculation method for a high moment of energy spectra. The case when intrinsic spin is fixed, 30:31067
MANY-BODY PROBLEM/MATHEMATICAL SPACE
  Generalized approximative procedures in the many body problem. Final technical report (Particle motion, variational principles), 30:31130 (AD-776408)
MANY-BODY PROBLEM/MEETINGS
  Nuclear many-body problem. Volume I. Proceedings of the international symposium, Rome, Italy, September 19--23, 1972, 30:31031
MANY-BODY PROBLEM/NONLINEAR PROBLEMS
  Exact methods for treating nonlinear problems in many-body theory, 30:31056
MANY-BODY PROBLEM/NUCLEI
  Dynamical implications of correlations, 30:31057
MANY-BODY PROBLEM/QUANTUM OPERATORS
  A new method in the theory of many-body scattering (Channel coupling), 30:30792
MANY-BODY PROBLEM/SCATTERING
  A new method in the theory of many-body scattering (Channel coupling), 30:30792
MANY-BODY PROBLEM/SPHERICAL HARMONICS
  Convergence of the hyperspherical expansion treatment of few-nucleon bound states, 30:30859
  Hyperspherical-expansion approach to nuclear bound states, 30:31050
MAPS
  MAPEDIT system for automatic map digitization, 30:31341 (LBL-3072)
MARINE ECOSYSTEMS
  See AQUATIC ECOSYSTEMS
MARS PLANET/PLANETARY ATMOSPHERES
  Day airglow emissions of 5577-A and 6300 OI lines in Martian atmosphere, 30:30397
MASS SPECTROMETERS/ION SOURCES
  Strong focusing ion sources, 30:29637
MASS SPECTROMETERS/MASS RESOLUTION
  Interaction effect of entry velocity and position on quadrupole mass filter resolution, 30:29626
MASS SPECTROMETERS/SPECIFICATIONS
  A new mass spectrometer for isotopic analysis, 30:29625
MASS SPECTROSCOPY/COMPARATIVE EVALUATIONS
  Comparison of analytical techniques for inorganic pollutants, 30:28924
MATERIALS TESTING
  Materials screening program for the LLL geothermal project, 30:31327 (UCRL-75353)
  Tensile and compression test methods for rigid plastic foams, 30:31403 (UCID-15739)
MATERIALS TESTING/ON-LINE CONTROL SYSTEMS
  Digital processors for servohydraulic material testing systems, 30:29300
MATERIALS TESTING/STANDARDS
  Aqueous corrosion testing of samples of zirconium and zirconium alloys, 30:29952
MATHEMATICS
  See also GROUP THEORY
  Double optimization in linear discrete systems, 30:31335 (CNEA-365)
  Numerical deconvolution, 30:31349 (UCID-15743)
  Subroutine CAUCHY: complex roots of a function using a CAUCHY integral technique, 30:31344 (ORNL-TM-4588)
MATHEMATICS/MEETINGS
  Mathematics of contemporary physics. Proceedings of a conference held at London, England, August 23--September 11, 1971, 30:31154
MAXIMUM CREDIBLE ACCIDENT/PROBABILITY
  Maximum credible accident (MCA) of light water reactor, 30:31260
MCA
  See MAXIMUM CREDIBLE ACCIDENT
MEASURING INSTRUMENTS
  See also ANEMOMETERS
    DENSIMETERS
    FLOWMETERS
    INTERFEROMETERS
    MAGNETOMETERS
    RADIATION DETECTORS
    RADIOMETRIC GAGES
    SPECTROMETERS
    THERMOCOUPLES
    THICKNESS GAGES
MEASURING INSTRUMENTS/ALIGNMENT
  Evaluation of downhole alignment by means of an alternating magnetic dipole field (1000 meters in the Earth), 30:31432 (UCID-15203)

MEAT/RADIOPRESERVATION
Preservation of enzyme inactivated lamb slices: effects of freeze desiccation and low dose irradiation, 30:29642 (AD-777550)
Technological foundations for radiation treatment of food products (Gamma radiation; electrons; book in Russian), 30:29681
MECHANICAL HEART/DESIGN
Nuclear artificial heart bench model (^{238}Pu heat source and Stirling cycle), 30:29259
MECHANICAL HEART/PERFORMANCE TESTING
Nuclear-fueled circulatory support systems. XIII. Augmented performance of the tidal regenerator engine, 30:29262
MECHANICAL HEART/POWER SUPPLIES
Implantable thermal converter as power source for an artificial heart, 30:29258
Unconventional Stirling engines for the artificial heart application, 30:29260
MECHANICAL HEART/RESEARCH PROGRAMS
Status of a thermocompressor-powered implantable artificial heart system (Radioisotope-powered Stirling cycle), 30:29261
MECHANICAL HEART/STIRLING ENGINES
Implanted energy conversion system. Annual report, 8 July 1972--8 July 1973, 30:29239 (JUL-73)
MECHANICAL HEART/THERMAL INSULATION
High performance thermal insulation for an implantable artificial heart (Radioisotope fueled), 30:29241
MECHANICAL STRUCTURES/DESIGN
Design relationships and failure theories in probabilistic form, 30:29288
MECHANICAL STRUCTURES/STRESS ANALYSIS
A status report on computational techniques for finite element analyses, 30:29290
Large user-orientated systems of programs for structural analysis and design, 30:31291
MECHANICAL STRUCTURES/WEAR
Spare parts reservation of components subjected to wear-out and/or fatigue according to a Weibull distribution, 30:29289
MECHANICS
See also QUANTUM MECHANICS
STATISTICAL MECHANICS
Particle kinematics (Book), 30:30646
MECHANICS/MEETINGS
Developments in mechanics. Volume 7. Proceedings of the 13th Midwestern Mechanics Conference held at Pittsburgh, Pennsylvania, August 13--15, 1973, 30:30570
MECHANICS/REVIEWS
Mathematical review of introductory wave mechanics (Classical mechanics of elastic and shock waves in solids and fluids), 30:31444 (UCID-15803)
MEDICAL PERSONNEL/DEATH
Cause of death in radiological workers. Analysis of cause of death in Japanese radiological technicians, 1966 to 1972, 30:29710
MEDICAL PERSONNEL/RADIATION PROTECTION
Radiation characteristics and controls. I (Radiation protection of dental patients and personnel), 30:29709
MEDICINE
See also BIOMEDICAL RADIOGRAPHY
DENTISTRY
NUCLEAR MEDICINE
PATIENTS
RADIOTHERAPY
Use of the CAMAC system for on-line data processing in medicine, 30:31338 (HMI-B-149)
MEDICINE/RESEARCH PROGRAMS
Research in biological and medical sciences including in biochemistry, communicable disease and immunology, internal medicine, nuclear medicine, physiology, psychiatry, surgery, and veterinary medicine. Volume I. Annual progress report, 1 July 1972--30 June 1973, 30:29827 (AD-774860)
Research in biological and medical sciences including biochemistry, communicable disease and immunology, internal medicine, nuclear medicine, physiology, psychiatry, surgery, and veterinary medicine. Volume II. Annual progress report, 1 July 1972--30 June 1973, 30:29828 (AD-776967)
MEDICINES
See DRUGS
MEGAKARYOCYTES
See BONE MARROW CELLS
MELANOCYTES
See ANIMAL CELLS
MELTDOWN
See also CORE CATCHERS
Diffusion of radioactive fluid through soil surrounding a large power-reactor station after a core meltdown accident, 30:31254 (UCRL-51494)
Post-accident core retention for LMFBR's. 2. Technical report. Final report for the period 1 July 1972--30 June 1973, 30:31253 (UCLA-ENG-7343)
Transport of core materials during accidents in LMFBRs (slumping), 30:31249 (KFK-1935)
MEMORY DEVICES/STATISTICAL MODELS
Choosing the basic parameters of a buffer memory device in the HPD computer system by a method of statistical modeling, 30:29623
MERCAPTANS
See THIOLS
MERCURY/ABSORPTION SPECTROSCOPY
Separation of trace metal impurities from nuclear grade uranium by long-chain amine extraction and direct determination by atomic absorption spectrophotometry, 30:28948
MERCURY/ACTIVATION ANALYSIS
Application of activation analysis to the determination of pollutants in the atmosphere (Thermal neutrons), 30:28914 (IEA-326)
Multielement determination in market-garden soils by instrumental photon activation analysis, 30:28921
Trace element behavior in soil of some Indonesian sawah's and in sludge of an Indonesian river, 30:28930
Trace elements in precipitation and cloud water in the area of Heidelberg, measured by instrumental neutron activation analysis, 30:28934
MERCURY/ADSORPTION
Effect of irradiation of metal ions on adsorption properties of semiconductor materials. I. Adsorption properties of oxidized surface of silicon (Effect of radioactivity of adsorbed ions), 30:29053
MERCURY/COSMOCHEMISTRY
Diffusion and isotope anomalies in peculiar A--B stars, 30:30201
MERCURY/SOLVENT PROPERTIES
Electrochemical investigation of amalgams of rare earth metals. I. Main electrochemical properties of amalgams of rare earth elements, 30:29111
MERCURY/STACK DISPOSAL
Trace pollutant emissions in fossil fuel combustion, 30:29469 (BNWL-1850(Pt.3))
MERCURY/UPTAKE
Elemental content of trace elements in vegetation collected at Centralia, Washington (Comparison with Alaskan vegetation), 30:29483 (BNWL-1850(Pt.3))
MERCURY 186/ENERGY LEVELS
Nuclear Data Sheets for A = 186, 30:30988
MERCURY 186/NUCLEAR PROPERTIES
Nuclear Data Sheets for A = 186, 30:30988
MERCURY 188/ENERGY LEVELS
Spherical and deformed shapes in ^{188}Hg, 30:30987
MERCURY 195/HIGH SPIN STATES
Decoupled bands in odd-mass mercury isotopes, 30:31006
MERCURY 197/HIGH SPIN STATES
Decoupled bands in odd-mass mercury isotopes, 30:31006
MERCURY 199/HIGH SPIN STATES
Decoupled bands in odd-mass mercury isotopes, 30:31006
MERCURY ALLOYS/ELECTROCHEMISTRY
Electrochemical investigation of amalgams of rare earth metals. I. Main electrochemical properties of amalgams of rare earth elements, 30:29111
MERCURY COMPLEXES/PYROLYSIS
Derivatographic investigations on the thermal degradation of pyridine, isoquinoline, α,α-dipyridyl and o-phenantroline, resp. bichromate- or chromate-ion containing metal complexes. II. Zinc(II)-, cadmium(II)-, and manganese(II)-complexes. III. Mercury(I and II)-, uranyl-, thorium-, lanthanum-, and iron-complexes, 30:29122
MESOCRICETUS
See HAMSTERS
MESON NONETS
Is the 0^+ nonet respectable, 30:30727
MESON RESONANCES
See also ETA-958 RESONANCES
F-1260 RESONANCES
KAPPA-725 RESONANCES
RHO-765 RESONANCES
VECTOR MESONS
MESON RESONANCES/PARTICLE PRODUCTION
Cross-sections for resonance production in anti pn annihilations around 2190 MeV centre-of-mass energy, 30:30606
MESON-MESON INTERACTIONS
See also PION-PION INTERACTIONS
MESON-MESON INTERACTIONS/GAUGE INVARIANCE
Scalar multiplets and asymptotic freedom (Green functions, Lagrangian functions, gauge approximation, word identities), 30:30724
MESONS
See also MESON RESONANCES
POMERANCHUK PARTICLES
PSEUDOSCALAR MESONS
Kinematical origin of the configuration mixing in the chiral algebra, 30:30719
MESONS/DECAY
Meson electromagnetic decays from SU(4)/sub w/ and generalized vector dominence (Pion form factor), 30:30650 (NP-20072)
MESONS/GAUGE INVARIANCE
A two-dimensional model for mesons, 30:30725
MESONS/MASS FORMULAE
Geometro-dynamical soldering of the internal and external spaces of strongly interacting particles, 30:30704
MESONS/MASS SPECTRA
Quark additivity for mass splittings in the psub(z) → infinity frame, 30:30709

METAGALAXY
See UNIVERSE
METALLURGY
(Use of a more specific term is recommended; see also EXTRACTIVE METALLURGY or FABRICATION.)
METALLURGY/BIBLIOGRAPHIES
Publications from 1970--1972 of the Metallurgical Publishers. Annotated index (Metallurgy; ferrous and nonferrous metals; processing of steels and alloys; corrosion), 30:30042
METALS
See also ACTINIDES
RARE EARTHS
TRANSITION ELEMENTS
METALS/CHEMICAL ANALYSIS
Application of a mass spectrometer to the method of determination of gases in metals by vacuum fusion, 30:28938 (CNEA-363)
METALS/CORROSION
Corrosion and corrosion resistance. IX. Tutzing symposium of the DECHEMA, February 26--March 1, 1973, Tutzing Castle, Starnberger Lake, 30:29943 (CONF-730230-(Absts.))
METALS/COSMOCHEMISTRY
The composition of RR Lyrae stars (Metal rich), 30:30191
METALS/CRACKS
Prevention and control of subcritical crack growth in high-strength metals (Ratio analysis diagram), 30:29981 (NRL-Report-7780)
METALS/CREEP
Interconnection between irradiation creep and interstitial loop formation in fcc metals, 30:30079
METALS/ETCHING
Macroetching metals and alloys, 30:29965
METALS/HARDENING
Additive strength contributions, 30:31427 (RISO-M-1714)
METALS/MACHINING
Blade-type metal-cutting tool for quick removal of stock in rougning work, 30:29269 (UCID-15833)
METALS/NONDESTRUCTIVE TESTING
Determination of the feasibility of using beta radiation backscatter for the detection of surface contamination of metal panels, 30:29294 (AD-776394)
METALS/PHYSICAL RADIATION EFFECTS
Interconnection between irradiation creep and interstitial loop formation in fcc metals, 30:30079
Study of basic processes in radiation damage. Final report, 1 April 1971--30 November 1973 (Implantation of polarized radioisotopes in metals and semiconductors), 30:30061 (AD-777728)
METALS/SPECIFIC HEAT
Microsecond pulse technique for heat capacity measurement, 30:31424 (LBL-2574)
METALS/SURFACE PROPERTIES
Determination of the feasibility of using beta radiation backscatter for the detection of surface contamination of metal panels, 30:29294 (AD-776394)
METALS/USES
Adaptation of metallic materials to the conditions of utilization (Nuclear, petroleum, and chemical industries), 30:29986
METASTASES/DIAGNOSIS
/sup 99m/Tc pyrophosphate for diagnostic bone imaging, 30:29843
Clinical evaluation of preoperative liver scintigraphy in gastric carcinoma patients (^{198}Au colloid and /sup 99m/Tc colloid tracer), 30:29854
METEOROLOGY
Method for determining Monin--Obukhov L's from profiles of subjectively estimated mean wind speeds and temperatures, 30:29431 (BNWL-1850(Pt.3))
METEOROLOGY/MANUALS
1973 meteorological yearbook of the EUREX site at Saluggia, 30:29457 (RT/PROT-(74)13)
METEOROLOGY/TRACER TECHNIQUES
Estimation of mean crosswind concentration profiles from ''instantaneous'' crosswind traverses (^{85}Kr tracer studies), 30:29424 (BNWL-1850(Pt.3))
Peculiarities of the upper cloud layer and suggestions for using radioactive tracer techniques in studying meridional currents, 30:29428
Use of naturally radioactive substances in studying turbulent exchange and self-scavenging of the atmosphere with surface layer measurements, 30:29396
METHACRYLIC ACID ESTERS
See also METHYL METHACRYLATE
METHACRYLIC ACID ESTERS/CHEMICAL RADIATION EFFECTS
Studies on the preparation of mortar--plastic composite (Radiation, thermal-catalytic, and radiation-catalytic methods; γ radiation), 30:29045
METHANE/HOT ATOM CHEMISTRY
Trajectory studies of hot atom reactions. II. An unrestricted potential for CH_4, 30:29085
METHANE/PHOTOIONIZATION
Calculated photoionization cross sections and relative experimental photoionization intensities for a selection of small molecules, 30:30491
METHANOL/CORROSIVE EFFECTS
Stress corrosion cracking of zirconium in methanol--HCl solutions, 30:29957
METHYL METHACRYLATE/BIOLOGICAL SHIELDING
Prosthesis set for radioprotection of the eye (Methyl methacrylate), 30:29717
5-METHYL URACIL
See THYMINE
METHYLTETRAHYDROFURAN
See MTHF
MHD CHANNELS/FLOW REGULATORS
Method and device for magnetohydrodynamically controlling the flow rate of an electrically conductive liquid (Patent), 30:30572
MICA
See also BIOTITE
MUSCOVITE
MICA/PARTICLE TRACKS
Further measurement of the track lengths of heavy ions in mica, 30:29525
MICE/BIOLOGICAL RADIATION EFFECTS
Pathological changes in mice following the intraperitoneal administration of radionuclides (^{198}Au and ^{32}P), 30:29784
MICE/RADIONUCLIDE KINETICS
Decorporation of ^{241}Am from bone using DTPA and osteoporotic agents (Additive effects of parathyroid extract), 30:29799 (COO-119-249)
Internal deposition of ingested cerium in suckling mice, 30:29821
MICHIGAN STATE UNIV CYCLOTRONS
See MSU CYCLOTRONS
MICROBIAL FLORA
See MICROORGANISMS
MICROELECTRONIC CIRCUITS/FABRICATION
Development of processes for hybrid microcircuits containing beam-lead devices, 30:31416 (BDX-613-1115(Rev.))
Mass anodization of tantalum-nitride resistors, 30:31387 (BDX-613-1155(Rev.))
MICROELECTRONIC CIRCUITS/SOLDERING
Rf hybrid microcircuit soldering techniques, 30:31397 (SLA-73-1073)
MICROELECTRONICS/SUPERCONDUCTORS
Technique for fabrication of superconducting microbridges and small Josephson tunnel junctions, 30:30841
MICROFLORA
See MICROORGANISMS
MICROORGANISMS
See also PROTOZOA
UNICELLULAR ALGAE
VIRUSES
YEASTS
MICROORGANISMS/RADIONUCLIDE KINETICS
Role of soil microorganisms in the movement of plutonium (Nevada Test Site studies), 30:29447 (NVO-AEIC-74-1)
MIDWEST FUEL RECOVERY PLANT
Midwest Fuel Recovery Plant technical study report, 30:29145 (NP-20106)
MIGMA DEVICES/ELECTRON TEMPERATURE
Radiation balance and electron temperature in a neutralized migma, 30:29156
MIGMA DEVICES/SYNCHROTRON RADIATION
Radiation balance and electrón temperature in a neutralized migma, 30:29156
MIHAMA-1 REACTOR/CONSTRUCTION
Construction and operation experience in PWR power plants, 30:31202
MIHAMA-1 REACTOR/REACTOR OPERATION
Construction and operation experience in PWR power plants, 30:31202
MIHAMA-2 REACTOR/CONSTRUCTION
Construction and operation experience in PWR power plants, 30:31202
MILITARY EQUIPMENT/BLAST EFFECTS
Foulness multi-ton air blast simulator. Part 1. Early development: the gun driven facility, 30:29309 (AWRE-O-31/74)
MILK/CONTAMINATION
Comparison of external irradiation and consumption of cows' milk as critical pathways for ^{137}Cs, ^{54}Mn and ^{144}Ce--^{144}Pr released to the atmosphere, 30:29423
MILK/RADIATION MONITORING
Absorption, distribution, and excretion of plutonium by dairy cattle (^{238}Pu tracer), 30:29810 (NVO-AEIC-74-1)
Data. Section IV. Other data, 30:29412
Data. Section I. Milk and food, 30:29421
Environmental monitoring report: United States Atomic Energy Commission, Oak Ridge facilities. Calendar year 1973, 30:29352 (UCC-ND-280)
Radiological monitoring program, period covering February 4, 1974--April 30, 1974 (Rio Blanco site), 30:29348 (PNE-RB-51-9)
MILKY WAY/CHEMICAL COMPOSITION
A galactic model with a pulsating active nucleus. III. Evolution of rare-light elements, 30:30386
MILKY WAY/PHOTOMETRY
Faint O-B3 stars in the Norma section of the Milky Way, 30:30233
MILKY WAY/PRIMARY COSMIC RADIATION
The distribution of cosmic rays in the galaxy and their dynamics as deduced from recent γ-ray observations (Trapping time), 30:30163

MILKY WAY/PULSATIONS
A galactic model with a pulsating active nucleus. III. Evolution of rare-light elements, 30:30386
MINERALS
See also AMPHIBOLE
APATITES
CORUNDUM
HEMATITE
MICA
MULLITE
VERMICULITE
Geology and mineral resources of the Greater Green River Basin. Symposium and core seminar, Casper, Wyoming, September 17--19, 1973 (Leading abstract), 30:29335
Zonality of hydrothermal ore deposits. Volume I. Zonality of deposits of tin, tungsten, molybdenum, and some groups of less-common metals (Book in Russian), 30:29332
MINERALS/ACTIVATION ANALYSIS
Application of neutron activation analysis to the determination of gold in minerals, 30:28913 (IEA-316)
MINERALS/X-RAY FLUORESCENCE ANALYSIS
Compilation of x-ray interaction data for x-ray fluorescence analysis of geological samples, 30:28943 (RISO-297)
MIRRORS (MAGNETIC)
See MAGNETIC MIRRORS
MISSISSIPPI/RADIATION MONITORING
Off-site surveillance. Final report. Report on Project Dribble, Salmon Event, Tatum Salt Dome, Mississippi, 22 October 1964, 30:29345 (AD-629357)
MISSOURI/AIR POLLUTION
Characteristics of aerosols from St. Louis (Aircraft measurements of particle size distribution), 30:29471 (BNWL-1850(Pt.3))
Concentrations and rates of removal of contaminants from the atmosphere in an downwind of St. Louis, 30:29473 (BNWL-1850(Pt.3))
Precipitation scavenging of inorganic pollutants from metropolitan sources: St. Louis, July 1973, 30:29479 (BNWL-1850(Pt.3))
Vertical profiles of trace gases in St. Louis (Nitrogen oxide measurements from ground level to 5500 ft), 30:29474 (BNWL-1850(Pt.3))
MITOMYCIN/UPTAKE
Uptake and release of ^{3}H-mitomycin C in mouse P-388 cell cultures, 30:29882
MODELS (NUCLEAR)
See NUCLEAR MODELS
MODELS (OPTICAL)
See OPTICAL MODELS
MODELS (PARTICLE)
See PARTICLE MODELS
MODELS (SHELL)
See SHELL MODELS
MODELS (STRUCTURAL)
See STRUCTURAL MODELS
MODERATING DETECTORS/PERFORMANCE
Passive environmental neutron dosimeter (Polyethylene-moderated fission foil--dielectric track detector system), 30:29551 (LA-UR-74-1232)
MODERATORS
(See also descriptors for specific moderator materials.)
See also HYDRIDE MODERATORS
MODERATORS/CORROSION
Calculation of the corrosion rate of an HTR core under fault conditions, 30:31211
MOESSBAUER EFFECT/MEETINGS
Moessbauer effect methodology. Volume VIII. Proceedings of the eighth symposium, New York City, New York, January 28, 1973 (Book), 30:30092
MOESSBAUER EFFECT/RESEARCH PROGRAMS
Moessbauer effect and related phenomena. Final report, 1 November 1964--1 January 1972 (Summaries of research at Stanford Univ.), 30:30951 (AD-773622)
MOLECULAR FLUORESCENCE SPECTROSCOPY
See FLUORESCENCE SPECTROSCOPY
MOLECULAR ORBITAL MODEL
See MOLECULES
MOLECULAR SIEVES/COMPARATIVE EVALUATIONS
Tritium Effluent Control Project. Progress Report: April--June 1974, 30:29026 (MLM-2171(LD))
MOLECULAR STRUCTURE/RESEARCH PROGRAMS
Department of Fundamental Research, Grenoble, semiannual bulletin No. 4, 30:31333 (CEA-N-1668)
MOLECULE COLLISIONS
See also ION-MOLECULE COLLISIONS
MOLECULE-MOLECULE COLLISIONS
PHOTON-MOLECULE COLLISIONS
MOLECULE COLLISIONS/SCATTERING
Scattering form factors of atoms, molecules, and solids (Density-functional formalism, electron gas), 30:30522
MOLECULE-MOLECULE COLLISIONS/ADIABATIC APPROXIMATION
The collinear collision of two diatomic molecules. An application of the adiabatic approximation and the T- and K-matrix methods, 30:30563
MOLECULE-MOLECULE COLLISIONS/K MATRIX
The collinear collision of two diatomic molecules. An application of the adiabatic approximation and the T- and K-matrix methods, 30:30563
MOLECULE-MOLECULE COLLISIONS/S MATRIX
The collinear collision of two diatomic molecules. An application of the adiabatic approximation and the T- and K-matrix methods, 30:30563
MOLECULES
See also MUONIC MOLECULES
MOLECULES/ORBITAL ANGULAR MOMENTUM
Angular momentum coupling, potential curves and radiative selection rules for heavy diatomic molecules, with particular reference to Kr_2 and Kr_2^+, 30:31459 (UCRL-13599)
MOLECULES/PERTURBATION THEORY
Degenerate perturbation theory, 30:30566
MOLYBDENUM/ABSORPTION SPECTROSCOPY
Colorimetric determination of molybdenum in oganic-rich soil, 30:28960
Determination of traces of Mo in soils and geological materials by solvent extraction of the molybdenum-thiocyanate complex and atomic absorption (Methyl isobutyl ketone solvent), 30:28965
MOLYBDENUM/ACTIVATION ANALYSIS
Multielement determination in market-garden soils by instrumental photon activation analysis, 30:28921
Nondestructive determination of some trace elements in tantalum by proton activation analysis, 30:28922
MOLYBDENUM/ANNEALING
Reactions occurring during annealing of VIa and Va metals in oxygen, water vapor, and air at low pressures, 30:30022
MOLYBDENUM/CHEMICAL ANALYSIS
Extraction--spectrophotometric methods of determining 0.0--n0.000n% aluminum in materials of metallurgical manufacture (exchange of experience), 30:28956
MOLYBDENUM/CRYSTAL STRUCTURE
Effect of lithium vapor on the structure of monocrystals of refractory metals and alloys, 30:29955
Structural changes in Mo worked with ultrasound, 30:30039
MOLYBDENUM/DEBYE-WALLER FACTOR
Lattice dynamical study of the recoilless fraction of ^{57}Fe in Ni, Mo, W, α-Fe and Cu, 30:30050
MOLYBDENUM/DEFORMATION
Nature of the deformation and flow of metals at and near the interface during abrasion, and its relation to the friction, 30:30051
MOLYBDENUM/DISLOCATIONS
Study of the substructure of deformed and annealed single crystals of molybdenum, 30:30055
MOLYBDENUM/EMISSION SPECTROSCOPY
Spectral assay of components in alloys (exchange of experience), 30:28951
Spectrochemical analysis of uranium oxide by gallium oxide carrier dc arc technique (ASTM Standard E402), 30:28957
Spectrographic determination of trace impurities in high purity uranium oxide, 30:28944 (UCID-15952)
MOLYBDENUM/FABRICATION
Fabrication procedures for unalloyed molytdenum (Extrusion; welding; vessels; tubes), 30:29966
MOLYBDENUM/INTERNAL FRICTION
Internal friction peaks observed in explosively deformed polycrystalline Mo, Nb, and Cu, 30:29980 (N-74-19371)
MOLYBDENUM/ION EXCHANGE
Sorption method of isolating uranium and other valuable metals from sea water, 30:28998
MOLYBDENUM/MECHANICAL PROPERTIES
Effect of stress concentration on the mechanical properties of Mo specimens with a protective coating in tests in an oxidizing atmosphere (Borosilicide coating; up to 1500°C), 30:30013
Effect of cyclic deformation on the dislocation structure and mechanical properties of molybdenum, chromium, and tungsten, 30:30028
MOLYBDENUM/PHYSICAL RADIATION EFFECTS
Effect of temperature and electromagnetic radiation on the electrical resistance of deformed molybdenum (^{60}Co γ rays), 30:30086
Point defect clusters in neutron-irradiated Mo. I. Dose dependence of the number density and the mean diameter of radiation-induced dislocation loops, 30:30067
X-ray study of the orientation dependence of radiation defects in the crystalline lattice of Mo irradiated with high-energy particles (Fast electrons and neutrons), 30:30080
MOLYBDENUM/PLASTICITY
Effect of carbon on the plasticity and nature of breakdown of polycrystal Mo, 30:30008
MOLYBDENUM/PRODUCTION
High-melting metals and metallic compounds, 30:30021
MOLYBDENUM/QUANTITATIVE CHEMICAL ANALYSIS
Extractive separation of molybdenum as Mo(V) xanthate from iron, vanadium, tungsten, copper, uranium and other elements, 30:28964
MOLYBDENUM/SCREW DISLOCATIONS
Field ion microscope observations of the three-fold symmetric dissociation of 1/2a(111) screw dislocations in molybdenum, 30:30000

MOLYBDENUM/SLIDING FRICTION
  Nature of the deformation and flow of metals at and near the interface during abrasion, and its relation to the friction, 30:30051
MOLYBDENUM/SOLVENT EXTRACTION
  Determination of traces of Mo in soils and geological materials by solvent extraction of the molybdenum-thiocyanate complex and atomic absorption (Methyl isobutyl ketone solvent), 30:28965
  Extractive separation of molybdenum as Mo(V) xanthate from iron, vanadium, tungsten, copper, uranium and other elements, 30:28964
MOLYBDENUM/STACKING FAULTS
  Stacking faults in refractory metals and alloys, 30:30030
MOLYBDENUM/STANDARDS
  Molybdenum and molybdenum alloy forgings, 30:29964
MOLYBDENUM/TEXTURE
  Electron microscopic and x-ray study of the structure of deformed polycrystalline molybdenum (MT and TsM-2A Mo), 30:30057
MOLYBDENUM/USES
  High-melting metals and metallic compounds, 30:30021
MOLYBDENUM/X-RAY FLUORESCENCE ANALYSIS
  Determination of molybdenum in plutonia cermets by x-ray fluorèscence spectrometry, 30:28979
MOLYBDENUM 92/PROTON REACTIONS
  Blocking with realistic decay functions (Compound-nuclear reaction times), 30:30969
MOLYBDENUM 99/SPIN
  Atomic-beam measurements on refractory elements. . Nuclear spin measurements of ^{99}Mo and sup(99m)Tc, 30:30972
MOLYBDENUM ADDITIONS
  Fatigue-crack growth of Ti--6Al--2Cb-1Ta--0.8Mo alloy in air and natural sea water environments, 30:29972 (AD-765318)
MOLYBDENUM ALLOYS
  See also INCONEL 718
    MOLYBDENUM BASE ALLOYS
    RENE 41
    STAINLESS STEEL-316
MOLYBDENUM ALLOYS/AGING
  Effect of the volume disparity between the precipitation phase and the matrix on the scattering of x rays by aging alloys (EP 199 (Ni--Cr--W--Mo--Al--Ti)), 30:30036
  Field-ion microscopic study of aged martensite in an iron--nickel--cobalt--molybdenum alloy (Fe--16 percent Ni--15 percent Co--5 percent Mo; precipitation of Mo), 30:30037
MOLYBDENUM ALLOYS/CORROSION RESISTANCE
  Study of the corrosion resistance of titanium alloys and some steels during condensation of alkylphenol with formaldehyde (Steels 3, AT-3, EI-943; Ti alloys VT2-1, VT-14; VT1-0, OT-4, VT5, Ti--5 percent Ta, Ti--33 percent Mo), 30:29947
MOLYBDENUM ALLOYS/CRYSTAL STRUCTURE
  Effect of lithium vapor on the structure of monocrystals of refractory metals and alloys (W--2 at. percent Rh; W--10 percent Mo; Mo--10 percent Re; Mo--27 percent Re), 30:29955
MOLYBDENUM ALLOYS/CRYSTALLIZATION
  Nonequilibrium crystallization of aluminum--molybdenum alloys, 30:30006
MOLYBDENUM ALLOYS/ELECTRODEPOSITION
  Effect of electrolysis conditions on the current efficiency of the deposition and composition of chromium--molybdenum alloy, 30:29960
MOLYBDENUM ALLOYS/ELECTRONIC STRUCTURE
  Specific heat and superconducting properties of Zr--Mo alloys, 30:30025
MOLYBDENUM ALLOYS/MECHANICAL PROPERTIES
  Mechanical properties of multicomponent alloys based on Ti--Al--Sn (Zr) α-solid solution with β-stabilizing elements (Additions of Mo, V, Cr, Fe, Si, B;properties at up to 950°C), 30:29984
  Study of some high-temperature strength properties of the niobium alloys 5VMTs, 5VMTsU, and 5VTTs at 1100°C (5VMTs = Nb--5.3W--2.1Mo--0.72Zr; 5VMTsU = Nb--4.9W--2.0Mo--1.15Zr; 5VTTs = 4.5W--2Ta--3.45Zr), 30:30027
MOLYBDENUM ALLOYS/METALLURGY
  Metallurgical processing and pulsed reactor fuel performance (U--10 Mo alloy), 30:29982 (SLA-73-1121)
MOLYBDENUM ALLOYS/OXIDATION
  Kinetics of molybdenum--rhenium alloy oxidation (MR-47VP), 30:29949
MOLYBDENUM ALLOYS/STACKING FAULTS
  Stacking faults in refractory metals and alloys (Mo--16.6, 34.6, and 61.4 at. percent Ta; Mo--49 and 74 at. percent Nb), 30:30030
MOLYBDENUM ALLOYS/THERMAL DIFFUSION
  Diffusion in the Mo--Ni, Mo--Fe, and Mo--Co systems, 30:30001
MOLYBDENUM BASE ALLOYS
  See also ALLOY-TZM
MOLYBDENUM BASE ALLOYS/CRYSTAL STRUCTURE
  Inter-crystallite internal adsorption in low-alloy molybdenum (Mo--0.5 percent Ti--0.05 percent Zr--0.012 percent C), 30:30023
MOLYBDENUM BASE ALLOYS/MECHANICAL PROPERTIES
  Effect of microadditions of Ni on the mechanical properties of Mo and its alloys with C, 30:30014
  Level of the equicohesive temperature of the Mo alloy VM-1A in short-time tests in vacuo (Mo--0,009 percent C--0.21 percent Zr--0.15 percent Ti--0.01 to 0.04 percent Te; MoSi$_2$ coatings), 30:29985
MOLYBDENUM BASE ALLOYS/STANDARDS
  Molybdenum and molybdenum alloy forgings, 30:29964
MOLYBDENUM CARBIDES/PHASE STUDIES
  Stabilization under high pressure of carbide phases in the molybdenum: carbon system (36 to 43 at. /percent/C; 1500°C; 25 kbar), 30:29932
MOLYBDENUM COMPOUNDS/LATTICE PARAMETERS
  On oxifluorides $A_{12}M(IV)M_3(VI)O_8F_{18}$ with uranium, molybdenum, and tungsten (A = Cs, Rb, K and M(IV) = U, Ce, MoW), 30:29006
MOLYBDENUM COMPOUNDS/MAGNETIC SUSCEPTIBILITY
  On oxifluorides $A_{12}M(IV)M_3(VI)O_8F_{18}$ with uranium, molybdenum, and tungsten (A = Cs, Rb, K and M(IV) = U, Ce, MoW), 30:29006
MOLYBDENUM OXIDES/CRYSTAL STRUCTURE
  Structure of the double oxide UMo$_{10}$O$_{32}$, 30:29941
MOLYBDENUM OXIDES/GRAIN ORIENTATION
  Coincidence twist boundaries in muscovite, kaolinite, and MoO$_3$, 30:29895
MONILIA
  See CANDIDA
MONITORS (REACTOR)
  See REACTOR CONTROL SYSTEMS
MONOCHROMATORS/BEAM OPTICS
  Symmetrized double-monochromator systems, 30:30134
MOON/GRAVITATION
  Calculation of the lunar diurnal atmospheric tide, 30:30446
MOON/SOLAR WIND
  Interaction between an inpact-produced neutral gas cloud and the solar wind at the lunar surface, 30:30401
MOON/TEMPERATURE MEASUREMENT
  Ratio of the temperatures of the quiet sun and the centre of the moon at lambda = 1.3 mm, 30:30330
MORTARS/CHEMICAL PREPARATION
  Studies on the preparation of mortar--plastic composite (Radiation, thermal-catalytic, and radiation-catalytic methods; γ radiation), 30:29045
MOS TRANSISTORS
  See also MOSFET
MOS TRANSISTORS/FABRICATION
  Characteristics of MOS capacitors formed on p-type InSb, 30:29994
MOS TRANSISTORS/PHYSICAL RADIATION EFFECTS
  Annealing characteristics of ion-implanted p-channel MOS transistors, 30:30098
  Implant dose profile dependence of electrical characteristics of ion-implanted MOS transistors, 30:30100
MOSFET/PHYSICAL RADIATION EFFECTS
  Implant dose profile dependence of electrical characteristics of ion-implanted MOS transistors, 30:30100
MOSSES
  See PLANTS
MOTORS
  See also ELECTRIC MOTORS
MOTORS/SUPERCONDUCTORS
  Applications of superconductivity to ac rotating machines, 30:30828
  Superconducting dc machines, 30:30827
MSU CYCLOTRONS/ACCELERATOR FACILITIES
  The University of Michigan cyclotron facility for research in nuclear structure, 30:30158
  The University of Michigan neutron time-of-flight facility, 30:30159
MSU CYCLOTRONS/BEAM PULSERS
  A simple fast sweeping system for extracted cyclotron beams, 30:30153
MSU CYCLOTRONS/TIME-OF-FLIGHT SPECTROMETERS
  The University of Michigan neutron time-of-flight facility, 30:30159
MTHF
  (Methyltetrahydrofuran.)
MTHF/RADIATION CHEMISTRY
  Radiation-chemical studies on the generation of lead and tin radicals (By electron scavenging in γ-irradiated 2-MTHF glass at 77°K), 30:29057
MUCOSA
  See MUCOUS MEMBRANES
MUCOUS MEMBRANES/BIOLOGICAL RADIATION EFFECTS
  Kinetics of recovery in irradiated colonic mucosa of the mouse (Gamma radiation, response of incidentially irradiated intestine), 30:29742
MULLITE/PHYSICAL RADIATION EFFECTS
  Phase changes in high-alumina ceramic under the influence of ionizing radiation (Neutrons; γ rays), 30:29913
MULTI-CHANNEL ANALYZERS/ELECTRONIC CIRCUITS
  8192-channel square-root pulse-height analyzer, 30:29568
MULTIPERIPHERAL MODEL/INCLUSIVE INTERACTIONS
  Semi-inclusive rapidity distributions in a cluster emission model for the pionization component, 30:30756
MULTIPERIPHERAL MODEL/MONTE CARLO METHOD
  Overlap function from the multiperipheral model, 30:30701

MULTIPERIPHERAL MODEL/PIONIZATION
Long range correlations in the pionization component (Multiperipheral cluster model), 30:30754
MULTIPERIPHERAL MODEL/POMERANCHUK POLES
Multiple pomeron exchange and final state rescattering, 30:30706
MULTIPLE PRODUCTION
Charge distributions of many particle final states and the energy dependence of forward charge exchange, 30:30696
Transverse momentum bounds and scaling in the hydrodynamical model, 30:30700
MULTIPLE PRODUCTION/PARTICLE MODELS
Binary-collision theory for multihadron production amplitudes, 30:30608
MULTIPLE PRODUCTION/REACTION KINETICS
Like particle correlations as a tool to study the multiple production mechanism ($A + b \to \pi^+ + \pi^+ + X$), 30:30711
MULTIPLE PRODUCTION/STRONG-COUPLING MODEL
Semiclassical model of multiparticle production, 30:30693
MULTIPLE PRODUCTION/TRANSVERSE MOMENTUM
Influence of the kinematical constraints on the transverse momentum correlation features, 30:30602
MULTIPLIER TUBES
See ELECTRON MULTIPLIERS
MULTIWIRE PROPORTIONAL CHAMBERS/ELECTRIC POTENTIAL
Computation of potential in a multiwire proportional counter of arbitrary cross-section, 30:29601
MULTIWIRE PROPORTIONAL CHAMBERS/OPERATION
Further results on the operation of high-accuracy drift chambers, 30:29587
Two-dimensional drift chambers, 30:29589
MULTIWIRE PROPORTIONAL CHAMBERS/PERFORMANCE
Low-pressure drift chambers for heavily ionizing particles, 30:29588
MULTIWIRE PROPORTIONAL CHAMBERS/READOUT SYSTEMS
Low-dead-time delay-line read-out for position-sensitive proportional counters, 30:29592
Multi-wire proportional chamber with charge division reading, 30:29593
MUON BEAMS/BEAM PRODUCTION
A high-quality muon beam in the 10-15 GeV energy range, 30:30150
MUON BEAMS/BEAM TRANSPORT
A high-intensity superconducting muon channel, 30:30156
MUON DETECTION
Annual report for period October 1, 1973--September 30, 1974 (Summaries of research activities at Purdue University), 30:30574 (COO-1428-391)
MUON REACTIONS/CAPTURE
Measurement of the average polarization of ^{12}B produced by polarized muons in the $\mu^- + {}^{12}C \to \nu sub(\mu) + {}^{12}B$ reaction, 30:30899
Negative muon capture in very light atoms, 30:30509
Nuclear muon capture: a simple model (Giant resonance supermultiplet states excitation), 30:31073
MUON-DEUTERON INTERACTIONS/INELASTIC SCATTERING
Muon-deuteron deep inelastic scattering, 30:30584
MUON-PROTON INTERACTIONS/INELASTIC SCATTERING
Muon-deuteron deep inelastic scattering, 30:30584
MUONIC ATOMS/AUGER EFFECT
Negative muon capture in very light atoms, 30:30509
MUONIC ATOMS/ENERGY LEVELS
Polarizability contribution to the energy levels of the muonic helium $(\mu^4He)^+$, 30:30516
MUONIC ATOMS/EXCITED STATES
Population of muonic ^3He states following the μ-catalysed fusion $p\mu d \to \mu^3He$, 30:30515
MUONIC ATOMS/P INVARIANCE
Parity violations by neutral currents in muonic atoms, 30:30777
MUONIC ATOMS/POLARIZABILITY
Polarizability contribution to the energy levels of the muonic helium $(\mu^4He)^+$, 30:30516
MUONIC MOLECULES
Population of muonic ^3He states following the μ-catalysed fusion $p\mu d \to \mu^3He$, 30:30515
MUONS
See also MUONS MINUS
MUONS PLUS
MUONS/DECAY
Electron decay spectrum in muon decay in the unified theory of weak and electromagnetic interactions, 30:30682
MUONS/PRIMARY COSMIC RADIATION
Production spectrum of charged cosmic ray pions and the primary cosmic ray nucleon spectrum, 30:30177
MUONS/SECONDARY COSMIC RADIATION
Coupling constants for the cosmic ray muon component, 30:30178
MUONS MINUS/ELECTROPRODUCTION
Calculation of electroproduction of muon pairs in the light-cone limit (Covariant parton model), 30:30673
MUONS MINUS/PAIR PRODUCTION
μ-pair production by inelastic πp and anti pp collisions, 30:30738
MUONS PLUS/ELECTROPRODUCTION
Calculation of electroproduction of muon pairs in the light-cone limit (Covariant parton model), 30:30673
MUONS PLUS/PAIR PRODUCTION
μ-pair production by inelastic πp and anti pp collisions, 30:30738
MUSCOVITE/GRAIN ORIENTATION
Coincidence twist boundaries in muscovite, kaolinite, and MoO_3, 30:29895
MUTATIONS
See also CHROMOSOMAL ABERRATIONS
LETHAL MUTATIONS
Somatic mutation by endogenous radiocarbon, 30:29787
MUTATIONS/RADIOINDUCTION
Base-pair deletion at a frameshift hotspot in Salmonella (X rays), 30:29684
Comparative investigation of mutagenic effects of incorporated isotopes of the most important organogenic elements. VI. Comparison of lethal and mutagenic effects of the decay of ^{32}P and ^{35}S incorporated into cells of Escherichia coli WP-2S Try⁻, 30:29788
Induced mutation in peas. XXVI. Genetically conditioned differences in radiation sensitivity. IV, 30:29694
Specificity and frequency of ultraviolet-induced reversion of an iso-1-cytochrome c ochre mutant in radiation-sensitive strains of yeast, 30:29683
Studies on the use of U-120 cyclotron and fast neutron generator in neutron irradiation of seeds for mutation (Barley; wheat), 30:29692
Studies on inter-relationship of quantitative traits in M_3 and M_4 generations following mutagenic treatments in sorghum (γ Rays; x rays; EMS), 30:29698
Use of x-rays in sugar beet breeding, 30:29693
MYLAR/CHARGED-PARTICLE TRANSPORT
Transmission and reflection of electrons by foils, 30:31118
MYLAR/ELECTRON COLLISIONS
Transmission and reflection of electrons by foils, 30:31118
MYOCARDIUM/SCINTISCANNING
Clinical studies of myocardial scintigraphy with ^{131}I-MAA, 30:29875
ECG changes in selective coronary angiography and myocardial scintigraphy (^{131}I), 30:29880
MYOSIN/RADIOIMMUNOASSAY
Radioimmunoassay for myosin in cultured skeletal muscle cells (Tritium tracer technique), 30:29833

N

N*RESONANCES/ELECTROPRODUCTION
Quark model predictions for electroproduction of $3/2^+$ isobars, 30:30662
SU_6 quark model, nucleon resonance electroproduction and spin-dependent electroproduction structure functions (Excitation form factors, sum rules), 30:30735
N*RESONANCES/PARTICLE PRODUCTION
Possible existence of a diproton resonance. A proposal of p--p scattering experiment at about 500 MeV, 30:30607
N-D METHOD/LEGENDRE POLYNOMIALS
A new parametrization for the N/D method, 30:30791
NASOPHARYNX
See PHARYNX
NATURAL GAS/DECONTAMINATION
Investigation of tritium decontamination. Interim research report, 30:29326 (UCID-15985)
NATURAL RADIOACTIVITY
(For unspecified naturally occuring radioisotopes only; not for BACKGROUND RADIATION.)
NATURAL RADIOACTIVITY/RADIATION MONITORING
Natural β-activity of the air in the atmospheric surface layer, 30:29401
NAVIGATIONAL INSTRUMENTS
Range-scan radar images and their application to map-matching estimation of location, 30:31429 (SAND-74-0153)
NEBULAE
See also CRAB NEBULA
PLANETARY NEBULAE
Genetic connection between stars O--B0 and diffuse nebulae, 30:30213
NEBULAE/BRIGHTNESS
Monte Carlo calculations of the surface brightness profiles of spherical dark nebulae (Evolutionary status), 30:30364
NEBULAE/EMISSION
The T Tauri emission nebula (Circumstellar shells), 30:30185
NEBULAE/HYDROGEN
On the theory of H_2 rotational excitation (Mean value, gas temperature), 30:30357
NEBULAE/INFRARED RADIATION
A new infrared complex and molecular cloud in Orion (Continuum feature), 30:30356
NEBULAE/MAGNETIC FIELDS
Possible evidence for a large magnetic field in the Orion infrared nebula, 30:30392
NEBULAE/SPECTRA
High-frequency observations of possible ''heavy-element'' recombination lines (Cosmic value), 30:30267

NEBULAE/SPECTROSCOPY
- VB 130: A nebulous cluster with an abnormal extinction law (Absorbing material), 30:30363

NEODYMIUM/ACTIVATION ANALYSIS
- Determination of rare earths and thorium in apatites by thermal and epithermal neutron-activation analysis, 30:28935

NEODYMIUM/ELECTRON COLLISIONS
- Strong 4f resonance effects in rare-earth appearance-potential spectra, 30:30477

NEODYMIUM/EXTRACTION CHROMATOGRAPHY
- Contribution to the separation of rare earths by extraction chromatography with di(2-ethylhexyl) phosphoric acid. II. Behavior of the matrix and its influence on the microcomponents, 30:28990 (ANL-Trans-961)

NEODYMIUM 130/NUCLEAR PROPERTIES
- Nuclear Data Sheets for A = 130, 30:30968

NEODYMIUM 136/ENERGY LEVELS
- Nuclear Data Sheets for A = 136, 30:30967

NEODYMIUM 136/NUCLEAR PROPERTIES
- Nuclear Data Sheets for A = 136, 30:30967

NEODYMIUM 142/DEUTERON REACTIONS
- Correlations between (n,γ) and (d,p) reactions on N = 82 nuclei (Excitation strengths), 30:30970

NEODYMIUM 142/NEUTRON REACTIONS
- Correlations between (n,γ) and (d,p) reactions on N = 82 nuclei (Excitation strengths), 30:30970

NEODYMIUM 143/ENERGY LEVELS
- Nuclear Data Sheets for A = 143, 30:30966

NEODYMIUM 143/NUCLEAR PROPERTIES
- Nuclear Data Sheets for A = 143, 30:30966

NEODYMIUM 150/OXYGEN 16 REACTIONS
- γ-ray multiplicity after (HI,xn) reaction (65 to 85 MeV), 30:30963

NEODYMIUM ALLOYS/DOMAIN STRUCTURE
- Experimental verification of a model for the magnetization reversal in RCo_5 particles (Sm/sub x/Nd/sub 1+-x/Co_5), 30:30047

NEODYMIUM ALLOYS/PHASE STUDIES
- Co-solubility of neodymium and zinc in solid magnesium (Mg--Nd--Zn alloys containing up to 3 percent Nd and 8 percent Zn), 30:30007

NEODYMIUM ISOTOPES/MASS SPECTROSCOPY
- Micro-sample analysis by spark source mass spectrometry (Nd isotopes in Nd_2O_3), 30:28967

NEODYMIUM LASERS/SPECIFICATIONS
- high power Nd:glass laser for fusion applications (Energy in excess of a kilojoule in subnanosecond pulses), 30:29231
- Neodymium glass laser having room temperature output at wavelengths shorter than 1060 Nm (Patent), 30:29280

NEODYMIUM OXIDES
- Effect of complex admixtures of rare-earth oxides on sintering of cerium dioxide, 30:29909

NEODYMIUM OXIDES/MICROANALYSIS
- Micro-sample analysis by spark source mass spectrometry (Nd isotopes in Nd_2O_3), 30:28967

NEOMYCIN
- See ANTIBIOTICS

NEON/AUGER EFFECT
- Identification and measurement of low-energy electrons by cloud chamber techniques: the oxygen and neon auger-electron problem, 30:29495 (UCID-15372)

NEON/COLLISIONS
- The inelastic scattering of He and Ne from a (001) surface of sodium fluoride, 30:30479

NEON/ELECTRON-ATOM COLLISIONS
- Atomic excitation processes in the discharges of rare gas ion engines, 30:30556

NEON/ION-ATOM COLLISIONS
- Ion--x-ray coincidence experiments in slow Ne^+--Ne collisions, 30:30517 (AED-CONF-74-085-001)
- Outer s-shell ionization of neon, argon, and krypton by proton impact (125 keV-1200 keV), 30:30557

NEON/IONIZATION
- Outer s-shell ionization of neon, argon, and krypton by proton impact (125 keV-1200 keV), 30:30557

NEON 19/BETA-PLUS DECAY
- Experimental study of ^{19}Ne decay and its significance to the study of neutral weak currents, 30:30892

NEON 20/CARBON 12 REACTIONS
- Entrance channel effects in the ^{32}S system: comparison of $^{12}C + ^{20}Ne$ and $^{16}O + ^{16}O$ elastic scattering (23.3 MeV (c.m.): angular distributions), 30:30880

NEON 20/ISOTOPE SEPARATION
- Enrichment of carbon and neon isotopes by gas phase chromatography. Part 1, 30:29024 (LA-tr-74-18)
- Enrichment of carbon and neon isotopes by gas phase chromatography. Part 2, 30:29025 (LA-tr-74-19)

NEON 20 REACTIONS/MANY-NUCLEON TRANSFER REACTIONS
- Massive transfer reaction $^{208}Pb(^{20}Ne,\alpha)^{224}Th$ (99 MeV), 30:30997

NEON 20 REACTIONS/STRIPPING
- Evidence for simple alpha-particle transfer in the $(^{20}Ne,^{16}O)$ reaction (108 and 147 MeV, differential cross sections), 30:30904

NEON 21/ALPHA REACTIONS
- Cross sections of the $^{21}Ne(\alpha,n)^{24}Mg$ and $^{22}Ne(\alpha,n)^{25}Mg$ reactions at low energies of astrophysical interest (Below 3 MeV), 30:30913

NEON 22/ALPHA REACTIONS
- Cross sections of the $^{21}Ne(\alpha,n)^{24}Mg$ and $^{22}Ne(\alpha,n)^{25}Mg$ reactions at low energies of astrophysical interest (Below 3 MeV), 30:30913

NEON 22/ENERGY LEVELS
- Two particle intrinsic excitations in ^{22}Ne and ^{24}Mg, 30:30915

NEON 22/ISOTOPE SEPARATION
- Enrichment of carbon and neon isotopes by gas phase chromatography. Part 1, 30:29024 (LA-tr-74-18)
- Enrichment of carbon and neon isotopes by gas phase chromatography. Part 2, 30:29025 (LA-tr-74-19)

NEON 22/NUCLEAR DEFORMATION
- Antipairing and antistretching in ^{22}Ne (Hartree--Bogolyubov theory), 30:30914

NEON 22/ROTATIONAL STATES
- Antipairing and antistretching in ^{22}Ne (Hartree--Bogolyubov theory), 30:30914

NEON 23/ENERGY LEVELS
- Nuclear structure studies of nuclei around mass number 23 (I, π, branching ratios), 30:30901 (NP-20122)

NEON IONS/ION-ATOM COLLISIONS
- Carbon K-shell x-ray production by neon ion impact, 30:30555
- Cross section for the Ar--L--x-ray emission in collisions of He^{+-}, Ne^{+-}, and Ar^{+-} ions with Ar atoms (100 keV to 1 MeV), 30:30518 (AED-CONF-74-085-002)
- Ion--x-ray coincidence experiments in slow Ne^+--Ne collisions, 30:30517 (AED-CONF-74-085-001)

NEOPLASMS
- See also ANGIOMAS
  - CARCINOMAS
  - EXPERIMENTAL NEOPLASMS
  - LEUKEMIA

NEOPLASMS/BIOLOGICAL RADIATION EFFECTS
- Influence of radiation on the layers of tumors in the early formation of tumors, 30:29745

NEOPLASMS/CHEMOTHERAPY
- Experience of use of reduced type of glutathione to prevent side effects of radiotherapy and antineoplastic chemotherapy, 30:29721

NEOPLASMS/DIAGNOSIS
- /sup 99m/Tc pyrophosphate for diagnostic bone imaging, 30:29843
- Affinity of ^{111}In-bleomycin for malignant tumors (In patients and experimental rat tumors), 30:29859
- Clinical evaluation of tumor scanning with ^{57}Co-bleomycin, 30:29846
- Combined contrast and radionuclide angiography of the liver (/sup 99m/Tc-sulfur colloid tracer), 30:29844
- Enhancement of pancreatic concentration of ^{75}Se-selenomethionine (Stimulatory effect of urecholine followed by pancreazymin), 30:29855
- Estimation of radiation doses from i. v. administration of selenite $Na_2{}^{75}SeO_3$, 30:29793
- ^{67}Ga-scintigraphy in malignant lesions of the lung, 30:29883
- Use of multiple radionuclide imaging to differentiate the focal intrahepatic lesion (/sup 99m/Tc, /sup 113m/In, ^{75}Se, and ^{111}In tracer), 30:29851

NEOPLASMS/RADIOINDUCTION
- Cancer mortality following irradiation in infancy for hemangioma, 30:29714
- Carcinogenicity of iodine-131 relative to age at exposure (^{131}I and ^{125}I uptake by thyroid and pituitary glands), 30:29777 (BNWL-SA-5065)
- Thorotrast-induced neoplasms, 30:29769 (AED-CONF-74-016-002)

NEOPLASMS/RADIOSENSITIVITY
- Radiation and hyperthermal response of normal tissue in situ (Comparison with mammary tumors in mice), 30:29743

NEOPLASMS/RADIOTHERAPY
- Dose-limiting tissues in relation to types and location of tumors. Implications for efforts to improve radiation dose distributions (Proton beams), 30:29725
- Experience of use of reduced type of glutathione to prevent side effects of radiotherapy and antineoplastic chemotherapy, 30:29721
- Histochemical changes in cancer of the corpus uteri after experimental irradiation (X Radiation), 30:29716
- Treatment of advanced tumours of head and neck with fast neutrons, 30:29733

NEPTUNIUM/ACTIVATION ANALYSIS
- Radioactivation analysis in thermal and epithermal neutrons of the 1BR-30 reactor of JINR, 30:28929

NEPTUNIUM/CHEMICAL PREPARATION
- Formation of colloidal neptunium in nitric acid solutions, 30:29116

NEPTUNIUM/CHEMICAL REACTION KINETICS
- Interrelationship of thermodynamic and kinetic parameters of redox reactions, 30:29005

NEPTUNIUM/CHEMICAL REACTIONS
- Oxidation of free and coordinated thiols by neptunium(VI) (Thioglycolic acid, methyl thioglycolate, and thiolato ligands in Cr and Co complexes), 30:29132

NEPTUNIUM/DEPOLYMERIZATION
- Depolymerization of colloidal neptunium in nitric acid solutions, 30:29107

NEPTUNIUM/OXIDATION
Oxidation--reduction reactions of actinide elements. XXIII. Kinetics of neptunium(V)--americium(V) reaction in perchlorate solutions, 30:29105
NEPTUNIUM/REDUCTION
Kinetics of uranium(IV)--neptunium(VI) reaction in tributyl phosphate solutions, 30:29102
Kinetics of reduction of neptunium by hydrazine. III. Reduction of Np(V) to Np(IV) in perchloric acid, 30:29115
NEPTUNIUM 237/ALPHA SPECTROSCOPY
Simultaneous determination of alpha-emitting nuclides of radium through californium in soil, 30:28977
NEPTUNIUM 237/RADIATION MONITORING
Data. Section IV. Other data, 30:29412
NEPTUNIUM 239/RADIATION MONITORING
Behavior and characteristics of radioactive debris from the Chinese nuclear weapons test of June 26, 1973, 30:29362 (BNWL-1850(Pt.3))
NEPTUNIUM COMPLEXES/CHEMICAL PREPARATION
Preparation of complex perxenates of some actinide elements, 30:29117
NERVOUS SYSTEM
Study on mechanisms of nervous system disturbance by radioactively labeled chinoform (^{131}I or ^{14}C and ^{59}Ta or ^{65}Zn labelling of salt), 30:29879
NERVOUS SYSTEM/BIOLOGICAL RADIATION EFFECTS
Condition of the nervous and vascular systems after radiation treatment of lymphogranulomatosis (Hodgkins disease), 30:29730
NEUTRAL CURRENTS
(Neutral currents occur in a process where a lepton scatters off another particle, does not change its charge, and a heavy neutral particle is exchanged between the lepton and the particle from which it scatters.)
NEUTRAL CURRENTS/WEAK INTERACTIONS
Experimental aspects of neutrino interactions, 30:30594
Neutron optics and weak currents, 30:30685
NEUTRINO REACTIONS/REVIEWS
Experimental aspects of neutrino interactions, 30:30594
NEUTRINO-ELECTRON INTERACTIONS/REVIEWS
Experimental aspects of neutrino interactions, 30:30594
NEUTRINO-NUCLEON INTERACTIONS/CROSS SECTIONS
Charmed-particle production by neutrinos with the Weinberg SU(4) currents (0 to 180 GeV), 30:30688
NEUTRINO-NUCLEON INTERACTIONS/INCLUSIVE INTERACTIONS
Charge symmetry and neutral current in a unified model of weak and electromagnetic interactions (Light-core algebra, cross sections,V-A interference structure functions), 30:30660
Pion distributions in inelastic neutrino interactions (Quark parton model), 30:30689
NEUTRINO-NUCLEON INTERACTIONS/PARTON MODEL
Quark parton model for deep inelastic lepton scattering (Cross sections, lectures), 30:30686
NEUTRINO-NUCLEON INTERACTIONS/QUARK MODEL
Quark parton model for deep inelastic lepton scattering (Cross sections, lectures), 30:30686
NEUTRINO-NUCLEON INTERACTIONS/REVIEWS
Experimental aspects of neutrino interactions, 30:30594
NEUTRINOS/DIRAC EQUATION
Generalized covariance principles and neutrino physics (Irreducible representations), 30:30680
NEUTRINOS/MASS
Neutrino mass from astrophysics, 30:30679 (CONF-730693-)
NEUTRINOS/STAR EVOLUTION
URCA processes in convective stellar cores, 30:30200
NEUTRINOS/STRUCTURE FUNCTIONS
Asymptotic near freedom (Neutrino production), 30:30672
NEUTRON BEAMS/BEAM OPTICS
Neutron optics and weak currents, 30:30685
NEUTRON BEAMS/MEV RANGE 10-100
Introduction to the discussion on characteristics of installations for radiotherapy with fast neutrons and other types of high-LET radiation, 30:31112
NEUTRON BEAMS/POLARIZATION
A comparison of polarization values for D-D neutrons obtained from Mott-Schwinger and ^{4}He scattering, 30:29511
NEUTRON BEAMS/RADIOTHERAPY
Introduction to the discussion on characteristics of installations for radiotherapy with fast neutrons and other types of high-LET radiation, 30:31112
NEUTRON CAPTURE
See NEUTRON BEAMS
NEUTRON CHOPPERS/CORRELATIONS
A correlation chopper or chopper with coding disk, 30:29635
NEUTRON DETECTION/ACTIVATION DETECTORS
A neutron monitor with a rotating rhodium disk, 30:29515
NEUTRON DETECTION/IONIZATION CHAMBERS
Development of neutron sensitive PCP ionization chamber, 30:29498
Neutron supermonitor (Cosmic ray neutron detection), 30:29500
NEUTRON DETECTION/PARTICLE DISCRIMINATION
A fast neutron-gamma discriminator, 30:29535
NEUTRON DIFFRACTOMETERS/GONIOMETERS
A simple method of orientating single crystals on time-of-flight neutron spectrometers, 30:29574
NEUTRON DIFFRACTOMETERS/OPERATION
A focussing low-angle neutron diffractometer, 30:29632
NEUTRON DOSIMETRY/DIELECTRIC TRACK DETECTORS
Discrimination of neutron energies with the aid of the nuclear track method (Using (n,α) converters), 30:29554
Fast-neutron personnel dosimetry with solid-state track recorders, 30:29557
NEUTRON DOSIMETRY/MODERATING DETECTORS
Passive environmental neutron dosimeter (Polyethylene-moderated fission foil--dielectric track detector system), 30:29551 (LA-UR-74-1232)
NEUTRON DOSIMETRY/PROPORTIONAL COUNTERS
In-vivo measurement of the gamma and neutron dose rate on patients with ^{238}Pu pacemakers implanted, 30:29704 (KFK-1851)
NEUTRON DOSIMETRY/RADIATION DOSE DISTRIBUTIONS
Buildup of scattered radiation behind a shadow shield, 30:31129
NEUTRON FLUX/COMPUTER CALCULATIONS
Point-dependent calculations of the anisotropic diffusion coefficient, 30:30850 (RT/FI-(74)10)
NEUTRON RADIOGRAPHY
Isotopic conversion in gadolinium-exposure neutron imaging, 30:29302
NEUTRON RADIOGRAPHY/CHEMICAL EXPLOSIVES
Experimental neutron radiography system using californium-252. Final report, 30:29295 (AD-776900)
NEUTRON RADIOGRAPHY/IMAGE CONVERTERS
Nuclear radiation conversion enhancement with inhomogeneous converters and intensifiers, 30:29301
NEUTRON REACTIONS
Gamma-ray production due to neutron interactions with ^{68}Zn and the level structure of ^{68}Zn (5.4 MeV: spectra, branching ratios, J, π), 30:30935 (ORNL-4985)
Physical quantities the numerical values of which will be included in the evaluated microscopic nuclear data library ''DANEM-I'' from the I.A.P., 30:30846 (IFA-DNBR-9-1974)
Thermal neutron cross sections of fissionable elements in the multilevel-multichannel formalism, 30:31015
NEUTRON REACTIONS/CAPTURE
Coincidence spectra from ^{175}Lu (n,γ) and ^{181}Ta (n,γ) reactions with thermal neutrons, 30:30993
Contribution to the mutual resonance shielding of ^{238}U and ^{239}Pu, 30:31009 (EURFNR-1162)
Correlations between (n,γ) and (d,p) reactions on N = 82 nuclei (Excitation strengths), 30:30970
Intensity fluctuations of γ-transitions from the (anti n,γ) reaction (Reduced-neutron and partial radiation widths), 30:30978 (IAE-2289)
Mass-spectrometric determination of neutron capture cross-sections of the rare earth isotopes (Pile and thermal cross sections), 30:30977 (AEC-tr-7574)
New source of decoupling of E1 strength from the GDR: boundary condition mixing for s- and p-wave neutron states near threshold, 30:31079
Resonance integrals of uranium-235/uranium-238 mixtures, 30:31013
Status report to NCSAC (Lawrence Livermore Lab.), 30:31011 (UCID-15639)
Transmission method to measure capture rates in fast reactors, 30:31275
NEUTRON REACTIONS/CAPTURE-TO-FISSION RATIO
Status report to NCSAC (Lawrence Livermore Lab.), 30:31011 (UCID-15639)
NEUTRON REACTIONS/COMPOUND-NUCLEUS REACTIONS
LARA: a FORTRAN IV code for the calculation of the compound nucleus contribution to the total radiative width in medium and heavy nuclei based on the Brink--Axel model, 30:30956 (RT/FI-(74)17)
NEUTRON REACTIONS/COMPUTER CODES
List of computer programs for neutron cross section calculations and analysis, 30:30849 (NEANDC-97/U)
Recoil energy distributions in CTR-related neutron spectra, 30:29203 (BNL-19043)
NEUTRON REACTIONS/DEUTERON REACTIONS
Correlations between (n,γ) and (d,p) reactions on N = 82 nuclei (Excitation strengths), 30:30970
NEUTRON REACTIONS/ELASTIC SCATTERING
Continuum shell-model calculation for neutron scattering from ^{11}B (0 to 10 MeV: cross sections, polarization), 30:30890
Neutron-deuteron differential cross section at 26.5 MeV, 30:30873
R-matrix and phase-shift analysis of neutron polarization measurements from n--^{16}O scattering (1 to 4 MeV: multilevel analysis), 30:30889
Variational calculations of reactions involving light nuclei, 30:30861
NEUTRON REACTIONS/FAST FISSION
Assessment of known independent yields and the calculation of those unknown in the fission of ^{232}Th, ^{233}U, ^{235}U, ^{238}U, ^{239}Pu, ^{240}Pu, and ^{241}Pu (Odd--even Z effects), 30:31008 (AERE-R-7680)
Contribution to the mutual resonance shielding of ^{238}U and ^{239}Pu, 30:31009 (EURFNR-1162)
Investigation of the reported mass distribution curves in the fission of ^{233}U with 14.8 MeV neutrons, 30:31010 (ORO-4282-14)

NEUTRON REACTIONS/FISSION
  Resonance integrals of uranium-235/uranium-238 mixtures, 30:31013
  Status report to NCSAC (Lawrence Livermore Lab.), 30:31011 (UCID-15639)
NEUTRON REACTIONS/INELASTIC SCATTERING
  Continuum shell-model calculation for neutron scattering from ^{11}B (0 to 10 MeV: cross sections, polarization), 30:30890
  RKSPROG: a computer program for inelastic cold neutron scattering time-of-flight measurements, 30:30847 (IRI-132-73-03)
NEUTRON REACTIONS/PICKUP REACTIONS
  ^{40}Ca(n,α)^{37}Ar reaction at 14.1 MeV, 30:30927
NEUTRON REACTIONS/RESEARCH PROGRAMS
  Status report to NCSAC (Lawrence Livermore Lab.), 30:31011 (UCID-15639)
NEUTRON REACTIONS/RESONANCE ABSORPTION
  The absence of excited target contributions to E1 partial widths of neutron resonances: an explanation from threshold effects, 30:31071
NEUTRON REACTIONS/RESONANCE INTEGRALS
  Mass-spectrometric determination of neutron capture cross-sections of the rare earth isotopes (Pile and thermal cross sections), 30:30977 (AEC-tr-7574)
  Resonance integrals of uranium-235/uranium-238 mixtures, 30:31013
NEUTRON REACTIONS/SCATTERING
  Forward scattering of 2-MeV neutrons from oriented ^{165}Ho (Polarization, differential cross sections), 30:30981
  Optical model calculations for the scattering of rapid neutrons (8 to 15 MeV) by Cr and Fe, 30:30943
  Treatment of continua in the shell-model theory of nuclear reactions, 30:31077
NEUTRON REACTIONS/THERMAL FISSION
  Assessment of known independent yields and the calculation of those unknown in the fission of ^{232}Th, ^{233}U, ^{235}U, ^{238}U, ^{239}Pu, ^{240}Pu, and ^{241}Pu (Odd--even Z effects), 30:31008 (AERE-R-7680)
  Energy measurements of delayed neutron groups from ^{235}U, 30:31014
  Measurement of internal conversion cascading in ^{235}U fission fragments, 30:31012
NEUTRON SOURCES
  (Excludes reactors even when used as neutron sources.)
NEUTRON SOURCES/DOSE RATES
  Characteristics of ^{252}Cf neutron sources used for radiotherapy, 30:31124
NEUTRON SOURCES/NEUTRON FLUX
  Absolute determination of the fast neutron fluxes by using the flow-type manganese bath method, 30:30852
NEUTRON SOURCES/NEUTRON SPECTRA
  Neutrons from the 2MeV deuteron bombardment of thick ^{7}Li targets, 30:30146
NEUTRON SOURCES/PERFORMANCE
  Linear accelerator neutron source for neutron scattering, 30:30152
NEUTRON SOURCES/PULSED NEUTRON TECHNIQUES
  Neutron slowing-down in ice and polyethylene at low temperatures (Moderator at 4.2, 77, and 300°K, 0.0018 to 0.090 eV), 30:30843 (IAE-2271)
NEUTRON SOURCES/RADIOTHERAPY
  Characteristics of ^{252}Cf neutron sources used for radiotherapy, 30:31124
NEUTRON SOURCES/TARGETS
  A cooling system for thin tritiated titanium targets, 30:30157
NEUTRON SPECTROMETERS/ENERGY RESOLUTION
  Resolution function for the rotating-crystal spectrometer, 30:29558 (IFA-FN-44-1974)
  The resolution function for the rotating-crystal spectrometer, 30:29572
NEUTRON SPECTROMETERS/GONIOMETERS
  A simple method of orientating single crystals on time-of-flight neutron spectrometers, 30:29574
NEUTRON SPECTROMETERS/RESOLUTION FUNCTIONS
  Resolution of slow neutron spectrometers. I. General method to calculate the resolution function. II. Resolution function for time of flight diffractometry, 30:29559 (IFA-FN-45-1974)
NEUTRON SPECTROMETERS/SHOWER COUNTERS
  A calorimeter for 300GeV neutrons and protons (Layered iron plates and plastic scintillators), 30:29596
NEUTRON SPECTROSCOPY/COMPUTER CODES
  RKSPROG: a computer program for inelastic cold neutron scattering time-of-flight measurements, 30:30847 (IRI-132-73-03)
NEUTRON STARS/MAGNETIC FIELDS
  Structure of solid iron in superstrong neutron-star magnetic fields (Quantized radii, binding energy), 30:30194
NEUTRON STARS/OBE MODEL
  Relativistic one-boson-exchange potential, two-nucleon data, nuclear matter, and neutron matter properties, 30:31033
NEUTRON STARS/ORBITS
  Analysis of a one-parameter family of triple close approaches occurring in stellar systems (Participating masses), 30:30238
NEUTRON STARS/PIONS MINUS
  Criteria for pion condensation thresholds in neutron star matter, 30:30261
NEUTRON STARS/STAR ACCRETION
  A model for the transient x-ray sources (Shell flash, thermonuclear shell flash), 30:30269
NEUTRON STARS/STAR EVOLUTION
  Do pulsars make supernovae. II. Calculations of light curves for type II events, 30:30197
NEUTRON TEMPERATURE/MEASURING METHODS
  Measurement of neutron temperature in water by differential and integral methods, 30:30844 (IAE-2274)
NEUTRON TRANSPORT THEORY
  Acoustic effect of fast neutron beams in a solid body, 30:30853
NEUTRON TRANSPORT THEORY/ALGORITHMS
  Convergence acceleration algorithms of the iterative methods used in nuclear reactor analysis codes, 30:31272 (JAERI-m-5590)
NEUTRON TRANSPORT THEORY/COMPUTER CALCULATIONS
  Point-dependent calculations of the anisotropic diffusion coefficient, 30:30850 (RT/FI-(74)10)
NEUTRON-NEUTRON INTERACTIONS/EFFECTIVE RANGE THEORY
  Neutron--neutron effective range parameters from few-nucleon experiments (D(π/sup minus/,2nγ), D(n,2np) reactions), 30:31037
NEUTRON-NEUTRON INTERACTIONS/SCATTERING LENGTHS
  Neutron--neutron effective range parameters from few-nucleon experiments (D(π/sup minus/,2nγ), D(n,2np) reactions), 30:31037
NEUTRONS
    See also FAST NEUTRONS
             SLOW NEUTRONS
NEUTRONS/ENERGY SPECTRA
  Measurement and calculation of neutron spectra at a sodium--iron interface (14-MeV source), 30:30848 (KFK-1959)
NEUTRONS/PRIMARY COSMIC RADIATION
  Production spectrum of charged cosmic ray pions and the primary cosmic ray nucleon spectrum, 30:30177
NEUTRONS/RBE
  RBE of cyclotron neutrons for effects on normal tissues, 30:29726
NEUTRONS/SOLAR PARTICLES
  Considerations on the neutral component relative to the August 4, 1972 solar event, 30:30296 (CONF-730693-)
NEUTRONS/STRUCTURE FUNCTIONS
  Detailed predictions for the p-n structure functions in theories with computable large momenta behaviour, 30:30739
  Muon-deuteron deep inelastic scattering, 30:30684
NEVADA TEST SITE
  Information support for the Nevada Applied Ecology Group (Computer file of references on environmental aspects of Pu, U, and Nevada Test Site), 30:29454 (NVO-AEIC-74-1)
NEVADA TEST SITE/AIR POLLUTION
  Operation WHETSTONE: on-site radiological safety report, July 1964--June 1965 (Monitoring), 30:29378 (NVO-410-24)
NEVADA TEST SITE/ECOLOGY
  Dynamics of plutonium in desert environments. Nevada Applied Ecology Group progress report as of January 1974, 30:29439 (NVO-AEIC-74-1)
  NAEG plutonium study modeling program: plutonium transport and dose estimation model (Computer model for evaluation of health hazards to man due to environmental ^{239}Pu, applied to Nevada Test Site), 30:29455 (NVO-AEIC-74-1)
NEVADA TEST SITE/METEOROLOGY
  Measurements of meteorological parameters, 30:29451 (NVO-AEIC-74-1)
  Numerical prediction of the mesoscale transport of atmospheric effluents: philosophy and morphology of experimental models for predicting the wind and potential radiological fields over the Nevada Test Site, 30:29377 (COM-74-10799)
NEVADA TEST SITE/PLANTS
  Analysis of vegetation cover in certain Pu-contaminated areas using aerial photography (Nevada Test Site), 30:29446 (NVO-AEIC-74-1)
  Some ecological attributes and plutonium contents of perennial vegetation in Area 13 (NAEG vegetation studies) (Botany of Nevada Test Site), 30:29445 (NVO-AEIC-74-1)
NEVADA TEST SITE/RADIATION MONITORING
  Determination of ^{239}Pu and ^{241}Am in large NAEG vegetation samples (Nevada Test Site), 30:28971 (NVO-AEIC-74-1)
  Distribution and inventory element activities on-NTS and off-NTS (^{239}Pu, ^{240}Pu, and ^{241}Am content of soil samples from Nevada Test Site and environs), 30:29453 (NVO-AEIC-74-1)
  Ecological studies of vertebrates in plutonium-contaminated areas of the Nevada Test Site (^{239}Pu and ^{241}Am content of GI tract, carcass, and pelt of rodents), 30:29449 (NVO-AEIC-74-1)
  Grazing studies on selected plutonium-contaminated areas in Nevada (U and Pu uptake by cattle), 30:29448 (NVO-AEIC-74-1)
  REECo field activities and sample logistics in support of the Nevada Applied Ecology Group (Nevada Test Site ecological sample collection and preparation for Pu analysis), 30:29441 (NVO-AEIC-74-1)

Resuspension of ^{239}Pu, ^{240}Pu, and ^{241}Am particles at Nevada Test Site; prediction of air concentrations of Pu due to resuspension at Eniwetok Atoll, 30:29452 (NVO-AEIC-74-1)
Role of soil microorganisms in the movement of plutonium, 30:29447 (NVO-AEIC-74-1)
Soils element activities, October 1972--September 1973 (^{214}Am, ^{239}Pu, and ^{240}Pu in soil at Nevada Test Site), 30:29440 (NVO-AEIC-74-1)
Statistical analysis of Pu in soil at tne Nevada Test Site: some results (Statistical sampling design), 30:29444 (NVO-AEIC-74-1)
NEVADA TEST SITE/RADIOACTIVITY
Operation WHETSTONE: on-site radiological safety report, July 1964--June 1965 (Monitoring), 30:29378 (NVO-410-24)
Operation TOGGLE: on-site radiological safety report, July 1972--June 1973 (Monitoring), 30:29379 (NVO-410-25)
NEVADA TEST SITE/SHRUBS
Soil surveys of five plutonium-contaminated areas on the Test Range Complex in Nevada (Geological and botany of Nevada Test Site), 30:29442 (NVO-AEIC-74-1)
NEVADA TEST SITE/SOILS
Distribution and characterization of plutonium in soils from Nevada Test Site, 30:29443 (NVO-AEIC-74-1)
Field measurement of permeabilities in NTS Area 9 (Soils in 2- to 12-darcy range), 30:29458 (UCID-15895)
Soil surveys of five plutonium-contaminated areas on the Test Range Complex in Nevada (Geological and botany of Nevada Test Site), 30:29442 (NVO-AEIC-74-1)
NEVADA TEST SITE/SURFACE CONTAMINATION
Resuspension element status report (Pu, Nevada Test Site), 30:29450 (NVO-AEIC-74-1)
NEVADA TEST SITE/VERTEBRATES
Ecological studies of vertebrates in plutonium-contaminated areas of the Nevada Test Site (^{239}Pu and ^{241}Am content of GI tract, carcass, and plet of rodents), 30:29449 (NVO-AEIC-74-1)
NEW YORK/ECOLOGY
Agricultural impacts of nuclear power generation in New York State (Preliminary survey agricultural data), 30:29438 (COO-3167-102)
NEWBORNS
See INFANTS
NICHROME/PLASMA ARC SPRAYING
Damping and elastic characteristics of plasma-sprayed coatings of W, nichrome, zirconia, and Cr--Ni spinels, 30:29887
NICKEL/ABSORPTION SPECTROSCOPY
Atomic absorption spectrometry of impurities in high purity tantalum with heated graphite atomizer, 30:28954
NICKEL/ACTIVATION ANALYSIS
Multielement determination in market-garden soils by instrumental photon activation analysis, 30:28921
NICKEL/CHEMICAL ANALYSIS
Extraction--spectrophotometric methods of determining 0.0--n0.000n% aluminum in materials of metallurgical manufacture (exchange of experience), 30:28956
NICKEL/DEBYE-WALLER FACTOR
Lattice dynamical study of the recoilless fraction of ^{57}Fe in Ni, Mo, W, α-Fe and Cu, 30:30050
NICKEL/EMISSION SPECTROSCOPY
Spectrochemical analysis of uranium oxide by gallium oxide carrier dc arc technique (ASTM Standard E402), 30:28957
Spectrograpnic determination of trace impurities in hign purity uranium oxide, 30:28944 (UCID-15952)
NICKEL/ION EXCHANGE
Sorption method of isolating uranium and other valuable metals from sea water, 30:28998
NICKEL/OXYGEN 16 REACTIONS
The determination of the differential energy loss of heavy ions backscattered from an infinitely thick solid target (7-35 MeV), 30:30948
NICKEL/PHYSICAL RADIATION EFFECTS
A model for the calculation of the defect production ratio, 30:30075
Investigations of the microstructure of heavy ion bombarded nickel, 30:30065 (BNWL-1839)
Irradiation effects on reactor structural materials. Semiannual progress report, 1 August 1973--31 January 1974, 30:30060 (AD-777433)
NICKEL/SOLUBILITY
Micro-x-ray spectrum analysis of interphase interaction in the systems ''refractory compound--liquid metal'' (Interaction of liquid Ni with ZrB_2), 30:29898
NICKEL 56/NUCLEAR STRUCTURE
Study of the structure of the ^{56}Ni double magic nucleus (Shell model), 30:30918
NICKEL 58/ALPHA REACTIONS
Reaction rates of interest in late stages of stellar nycleosynthesis (Estimate of reliability), 30:30255
NICKEL 58/DEUTERON REACTIONS
Deuteron break-up and proton scattering on ^{58}Ni, 30:30926
NICKEL 58/GIANT RESONANCE
Calculation of the 0^+ and 2^+ giant resonances in Ni^{58}, 30:30924
NICKEL 58/HEAVY ION REACTIONS
Evidence for quasi-molecular K x-ray emission in heavy ion collisions from the observation of the x-ray directional anisotropy (^{58}Ni + ^{58}Ni, 70 MeV), 30:30922
NICKEL 58/PROTON REACTIONS
Deuteron break-up and proton scattering on ^{58}Ni, 30:30926
NICKEL 60/ALPHA REACTIONS
Level densities of ^{63}Cu and ^{65}Cu from the analysis of evaporation spectra (12.5- to 16.0-MeV protons, 16.8- to 21.3-MeV α), 30:30950
Target-spin effects on elastic scattering cross sections, 30:30940
NICKEL 60/HELIUM 3 REACTIONS
Target-spin effects on elastic scattering cross sections, 30:30940
NICKEL 62/ALPHA REACTIONS
Level densities of ^{63}Cu and ^{65}Cu from the analysis of evaporation spectra (12.5- to 16.0-MeV protons, 16.8- to 21.3-MeV α), 30:30950
NICKEL 62/LITHIUM 7 REACTIONS
Nuclear spectroscopy with the ^{62}Ni(^{7}Li,^{6}He)^{63}Cu reaction (34 MeV), 30:30937
NICKEL 63/RADIOCHEMISTRY
Binding of ^{63}Ni to rabbit serum α_1-macroglobulin in vivo and in vitro, 30:29088
NICKEL ADDITIONS
Effect of microadditions of Ni on tne mechanical properties of Mo and its alloys with C, 30:30014
NICKEL ALLOYS
See also INCOLOY ALLOYS
NICKEL BASE ALLOYS
PERMALLOY
NICKEL ALLOYS/AGING
Field-ion microscopic study of aged martensite in an iron--nickel--cobalt--molybdenum alloy (Fe--16 percent Ni--15 percent Co--5 percent Mo; precipitation of Mo), 30:30037
NICKEL ALLOYS/BRAZING ALLOYS
Nickel brazing below 1025 C of untreated Inconel 718. Use of a getter makes nickel brazing of Inconel 718 and X-750 below 1025 C (1875 F) as easy as nickel brazing of stainless steels in vacuum, 30:29969
NICKEL ALLOYS/DIFFUSION
Transport and thermodynamic properties of solids. Progress report, September 1, 1973--August 31, 1974, 30:31390 (COO-1436-41)
NICKEL ALLOYS/FILLER METALS
Properties of TZM and nuclear behavior of TZM brazements. Various properties of TZM and Zr--5Be and Au--18Ni brazing filler metals are determined for brazing TZM to Zr and to steel, 30:30084
NICKEL ALLOYS/GRAIN GROWTH
Recrystallization grain coarsening in the tungsten--nickel system, 30:30004
NICKEL ALLOYS/ION EMISSION
Ionic emission yield for alloys, dependence on tne nature of the solute. II. Interpretation, 30:30087
NICKEL ALLOYS/MICROSTRUCTURE
Structure and phase-boundary energies of the directionally solidified InSb--MnSb--NiSb, InSb--FeSb, and InSb--CrSb eutectic alloys, 30:30019
NICKEL ALLOYS/THERMAL DIFFUSION
Diffusion in the Mo--Ni, Mo--Fe, and Mo--Co systems, 30:30001
NICKEL BASE ALLOYS
See also NICHROME
NIMONIC
RENE 41
NICKEL BASE ALLOYS/AGING
Effect of the volume disparity between the precipitation phase and the matrix on the scattering of x rays by aging alloys (EP 199 (Ni--Cr--W--Mo--Al--Ti)), 30:30036
NICKEL BASE ALLOYS/DIFFUSION
Differential magnetic analysis of the radiation-induced diffusion in nickel-beryllium alloys, 30:30064 (AED-CONF-74-089-037)
NICKEL BASE ALLOYS/OXIDATION
Oxidation mechanism of Ni_3Al containing yttrium (With and without 0.5 wt percent Y; 900 to 1200°C in air), 30:29953
NICKEL BASE ALLOYS/PHYSICAL RADIATION EFFECTS
Differential magnetic analysis of the radiation-induced diffusion in nickel-beryllium alloys, 30:30064 (AED-CONF-74-089-037)
NICKEL BASE ALLOYS/POWDER METALLURGY
Powder metallurgy of heat-resistant alloys and refractory metals (Book), 30:29963
NICKEL BASE ALLOYS/REVIEWS
Nimonic alloys and other nickel-base high-temperature alloys (Book; aircraft gas turbine;strengthening;fabrication;heat treatment;physical and mechanical properties;forms), 30:29988
NICKEL COMPOUNDS/MICROSTRUCTURE
Evaluation of glancing angle x-ray diffraction and MeV ^{4}He backscattering analyses of silicide formation, 30:29939
NICKEL FLUORIDES/SOLUBILITY
Solubility and stability of structural metal difluorides in molten fluoride mixtures, 30:29002 (ORNL-TM-760)

NICKEL OXIDES/PLASMA ARC SPRAYING
  Damping and elastic characteristics of plasma-sprayed coatings of W, nichrome, zirconia, and Cr--Ni spinels (Cr--Ni spinel), 30:29887
NIGHTGLOW
  See AIRGLOW
NIMONIC/REVIEWS
  Nimonic alloys and other nickel-base high-temperature alloys (Book; aircraft gas turbine;strengthening;fabrication;heat treatment;physical and mechanical properties;forms), 30:29988
NINE MILE POINT-1 REACTOR/REACTOR OPERATION
  Semiannual report of operation, January--June 1974, 30:31313 (DOCKET-50220-315)
NIOBATES/MAGNETIC SUSCEPTIBILITY
  Synthesis and magnetic properties of samarium and europium titanoniobates ($SmTiNbO_6$; EuTiNbO6), 30:29908
NIOBIUM/ACTIVATION ANALYSIS
  Nondestructive determination of some trace elements in tantalum by proton activation analysis, 30:28922
NIOBIUM/ANNEALING
  Reactions occurring during annealing of VIa and Va metals in oxygen, water vapor, and air at low pressures, 30:30022
NIOBIUM/CHEMICAL ANALYSIS
  Extraction--spectrophotometric methods of determining 0.0--n0.000n% aluminum in materials of metallurgical manufacture (exchange of experience), 30:28956
NIOBIUM/CHEMICAL PREPARATION
  Mechanism of niobium pentoxide reduction in an alumino--thermal process, 30:29970
NIOBIUM/CRYSTAL DEFECTS
  Effects of low temperature irradiation with heavy ions on superconductor niobium, 30:30074
NIOBIUM/DISLOCATIONS
  Stress--velocity relations for dislocations in niobium (298 and 196°K), 30:29976 (AD-776621)
NIOBIUM/EMISSION SPECTROSCOPY
  Spectrographic determination of trace impurities in high purity uranium oxide, 30:28944 (UCID-15952)
NIOBIUM/INTERNAL FRICTION
  Internal friction peaks observed in explosively deformed polycrystalline Mo, Nb, and Cu, 30:29980 (N-74-19371)
NIOBIUM/PHYSICAL RADIATION EFFECTS
  Effects of low temperature irradiation with heavy ions on superconductor niobium, 30:30074
  Ion bombardment simulation of 14 MeV neutron damage in thin niobium films, 30:30066 (UCID-16109)
NIOBIUM/PRODUCTION
  High-melting metals and metallic compounds, 30:30021
NIOBIUM/SOLVENT EXTRACTION
  Extraction of niobium in phosphoric acid solutions by alkali metals and ammonium salts, 30:29000
NIOBIUM/SOLVENT PROPERTIES
  Solubility of hydrogen in vanadium and niobium at high temperatures (1273 to 2273°K; up to 25 atm; V--H; Nb--H; Ta--H), 30:29918
NIOBIUM/STACKING FAULTS
  Stacking faults in refractory metals and alloys, 30:30030
NIOBIUM/TITRATION
  Conductimetric and high-frequency titration conditions for niobium by aromatic amines in aqueous-organic medium, 30:28959
NIOBIUM/USES
  High-melting metals and metallic compounds, 30:30021
NIOBIUM 90/ENERGY LEVELS
  A mechanical beam chopper system for the measurement of half-lives in the millisecond region, 30:30154
NIOBIUM 95/RADIATION MONITORING
  Data. Section IV. Other data, 30:29412
  Quillayute air reference station (Air sampling and monitoring in Washington State), 30:29359 (BNWL-1850(Pt.3))
  Report of activity, February 1974 (Radioactivity of environmental samples collected throughout France during February 1974), 30:29349 (SCPRI(RM)-2-1974)
NIOBIUM 95/RADIOCHEMICAL ANALYSIS
  Fractional determination of ^{95}Zr and ^{95}Nb in a mixture by reverse phase chromatography, 30:28982
NIOBIUM 95/REMOVAL
  Decontamination of swine, sheep, and cattle surface-contaminated with fission products. II. Removal of radionuclides of zirconium, niobium, ruthenium, and cerium, 30:29823
NIOBIUM ALLOYS
  See also INCONEL 718
    NIOBIUM BASE ALLOYS
NIOBIUM ALLOYS/CHEMICAL PREPARATION
  Joint reduction of niobium, aluminus, and germanium chlorides by hydrogen (Transition temperature of Nb germanides alloyed with 1 to 3 at. percent al = 20 to 20.5°K), 30:29971
NIOBIUM ALLOYS/CORROSION RESISTANCE
  Electrochemistry of aqueous corrosion: uranium and its alloys (Review), 30:29944 (Y-1949)
NIOBIUM ALLOYS/FATIGUE
  Fatigue-crack growth of Ti--6Al--2Cb-1Ta--0.8Mo alloy in air and natural sea water environments, 30:29972 (AD-765318)
NIOBIUM ALLOYS/PHASE TRANSFORMATIONS
  Effect of cold deformation on phase transition in Ti--Nb alloys, 30:30009
NIOBIUM ALLOYS/PHYSICAL RADIATION EFFECTS
  Influence of neutron irradiation on critical data of type II superconductors (Nb--Sn), 30:30063 (AED-CONF-74-089-006)
NIOBIUM ALLOYS/QUADRUPOLES
  Effect of plastic deformation on quadrupole interaction in Al, Nb, and Au alloyed with Hf, 30:30038
NIOBIUM ALLOYS/STACKING FAULTS
  Stacking faults in refractory metals and alloys (Mo--16.6, 34.6, and 61.4 at. percent Ta; Mo--49 and 74 at. percent Nb), 30:30030
NIOBIUM ALLOYS/SUPERCONDUCTIVITY
  Coherent effects in large arrays of superconducting bridges, 30:30821
  Joint reduction of niobium, aluminum, and germanium chlorides by hydrogen (Transition temperature of Nb germanides alloyed with 1 to 3 at. percent al = 20 to 20.5°K), 30:29971
NIOBIUM BASE ALLOYS/CRYSTAL STRUCTURE
  Structure of alloys of the Nb--Ti--Zr system. Close order of displacement in solid solutions (50 at./percent/Nb; diffusion distribution), 30:30040
NIOBIUM BASE ALLOYS/LATTICE PARAMETERS
  Preparation of new β-W phases by film-deposition techniques (Nb_3In, Nb_3Pb, and Nb_3Tl films, unstable phase range), 30:29967
NIOBIUM BASE ALLOYS/MECHANICAL PROPERTIES
  Study of some high-temperature strength properties of the niobium alloys 5VMTs, 5VMTsU, and 5VTTs at 1100°C (5VMTs = Nb--5.3W--2.1Mo--0.72Zr; 5VNTsU = Nb--4.9W--2.0Mo--1.15Zr; 5VTTs = 4.5W--2Ta--3.45Zr), 30:30027
NIOBIUM BASE ALLOYS/SUPERCONDUCTIVITY
  Multifilament Nb_3Sn conductors (Nb_3Sn surface layers on Nb-Cu composite), 30:30809
  Niobium--germanium: becoming a practical superconductor (Nb_3Ge), 30:30806
  Preparation of new β-W phases by film-deposition techniques (Nb_3In, Nb_3Pb, and Nb_3Tl films, unstable phase range), 30:29967
  Superconductivity of Nb--Al--Zr alloys (Phase boundaries;solubility of Zr in Nb_3Al), 30:30048
  The effect of cladding material on ac losses of commercial Nb_3Sn tapes (Pb-Sn and Ag-Sn solders, ferromagnetic nickel flashes, commercial superconducting Cu and Ag clad tapes), 30:30840
NIOBIUM BORIDES/OXIDATION
  Oxidation of ZrB_2, TaB_2, NbB_2, and W_2B_5 in atomic oxygen and by anodic polarization, 30:29938
NIOBIUM CARBIDES/DEFORMATION
  Effect of plastic deformation on some physical properties of niobium monocarbide in the homogeneity region (Work hardening; electric resistance; thermal emf; Fermi surface charge), 30:29897
NIOBIUM CARBIDES/THERMAL SHOCK
  Calorimetric determination of the heat resistance of ring-shaped samples of brittle electric conductors ($ZrC_{0.93}$; $NbC_{0.93}$), 30:29900
NIOBIUM HYDRIDES/PHASE STUDIES
  Solubility of hydrogen in vanadium and niobium at high temperatures (1273 to 2273°K; up to 25 atm; V--H; Nb--H; Ta--H), 30:29918
NIOBIUM NITRIDES/PROXIMITY EFFECT
  Proximity effect on thin NbN-layers, 30:30805 (AED-CONF-74-089-005)
NIOBIUM OXIDES/ELECTRIC CONDUCTIVITY
  Nonlinear high-field conductivity in Nb_2O_5 thin films, 30:29940
NIOBIUM OXIDES/MAGNETIC SUSCEPTIBILITY
  Magnetic and superconducting properties of niobium oxides, 30:30810
NIOBIUM OXIDES/REDUCTION
  Mechanism of niobium pentoxide reduction in an alumino--thermal process, 30:29970
NIOBIUM OXIDES/SUPERCONDUCTIVITY
  Magnetic and superconducting properties of niobium oxides, 30:30810
NIOBIUM SELENIDES/SPECIFIC HEAT
  Specific heat of 2H $NbSe_2$, 30:30808
NIOBIUM SELENIDES/SUPERCONDUCTIVITY
  Specific heat of 2H $NbSe_2$, 30:30808
NITRATES/MONITORING
  Environmental monitoring report, calendar year 1973, 30:29351 (UCC-ND-279)
NITRIC ACID/CORROSIVE EFFECTS
  Corrosion of sheet and welded joint specimens of Incoloy 825-low carbon (C less than or equal to 0.03%) in HNO_3 (Huey) and HF solutions, 30:29956
NITRIDES/PRODUCTION
  High-melting metals and metallic compounds, 30:30021
NITRIDES/USES
  High-melting metals and metallic compounds, 30:30021
NITRILES
  See also ACRYLONITRILE
NITRILES/COSMOCHEMISTRY
  Cyanoacetylene: new lines and sources in the galaxy, 30:30374

NITRILES/RADIOLYSIS
Unstable intermediates. CXLVI. Electron spin resonance spectra for linear BrCN- and Br_2CN radicals in irradiated cyanogen bromide crystals (Gamma radiation), 30:29076
NITROGEN/CHEMICAL ANALYSIS
Interlaboratory comparison of chemical analysis of uranium mononitride, 30:28942 (N-74-18812)
NITROGEN/ELECTRON-MOLECULE COLLISIONS
New technique for threshold excitation spectroscopy, 30:30553
Population of the rotational and vibrational levels of excited electronic states of nitrogen molecules produced in collisions of electrons with N_2 molecules (30 to 300 eV, Franck-Condon principle), 30:30545
NITROGEN/ION-MOLECULE COLLISIONS
Crossed-molecular-beam study of the kinematics and dynamics of charge-transfer collisions (200 eV), 30:30547
NITROGEN/MASS SPECTROSCOPY
Application of a mass spectrometer to the method of determination of gases in metals by vacuum fusion, 30:28938 (CNEA-363)
NITROGEN/NUCLEAR REACTION ANALYSIS
Analysis of the nitrogen and carbon content in organic bulk matter by fast-neutron induced gamma radiation, 30:28918 (NP-20122)
Nondestructive determination of the nitrogen (protein) content in single kernels of seeds (6-MeV deuterons), 30:28917 (NP-20122)
NITROGEN/PHOTOIONIZATION
Calculated photoionization cross sections and relative experimental photoionization intensities for a selection of small molecules, 30:30491
NITROGEN/ROTATIONAL STATES
Population of the rotational and vibrational levels of excited electronic states of nitrogen molecules produced in collisions of electrons with N_2 molecules (30 to 300 eV, Franck-Condon principle), 30:30545
NITROGEN/SEPARATION PROCESSES
Tritium Effluent Control Project. Progress Report: April--June 1974, 30:29026 (MLM-2171(LD))
NITROGEN/VIBRATIONAL STATES
Population of the rotational and vibrational levels of excited electronic states of nitrogen molecules produced in collisions of electrons with N_2 molecules (30 to 300 eV, Franck-Condon principle), 30:30545
NITROGEN 14/PHOTONUCLEAR REACTIONS
Particle configurations of giant E1 states in the ${}^{14}N(\gamma,p_2)$ and ${}^{14}N(\gamma,p_0)$ processes (Angular distribution, cross sections, spectroscopic factors), 30:30877
NITROGEN 15/ALPHA REACTIONS
High spin states in the Ksup(π)=$1/2^-$ band of ${}^{19}F$ (From angular distribution and ωγ measurements at 5413 and 6258 MeV), 30:30865
NITROGEN 15/ISOTOPE SEPARATION
Isotopic separation of nitrogen-15. III. Effect of the degree of oxidation of the reflux gases for the system NO, NO_2--HNO_3, 30:29034
NITROGEN 16/ENERGY LEVELS
1p hole-states in ${}^{16}O$ and ${}^{16}N$ and the mass dependence of the 1p spin-orbit splitting (Spectroscopic factors), 30:30886
NITROGEN 17/ENERGY LEVELS
Lifetime measurements in ${}^{17}N$ using the recoil-distance technique, 30:30894
The electromagnetic decay of ${}^{17}N$ (J, π, lifetimes from spectra from ${}^{11}B({}^{7}Li, p\gamma)$ at 6.0 MeV), 30:30895
NITROGEN IONS/ION-ATOM COLLISIONS
Crossed-molecular-beam study of the kinematics and dynamics of charge-transfer collisions (200 eV), 30:30547
The reaction of atomic oxygen with several atmospheric ions (H^+, O^+, N^+, N^+_2, O^-, O^-_2, 1 to 500 eV), 30:30549
NITROGEN IONS/ION-MOLECULE COLLISIONS
Crossed-molecular-beam study of the kinematics and dynamics of charge-transfer collisions (200 eV), 30:30547
NITROGEN OXIDES/AEROSOL MONITORING
Vertical profiles of trace gases in St. Louis (Nitrogen oxide measurements from ground level to 5500 ft), 30:29474 (BNWL-1850(Pt.3))
NITROGEN OXIDES/ATOM-MOLECULE COLLISIONS
Infrared laser enhanced reactions: spectral distribution of the NO_2 chemiluminescence produced in the reaction of vibrationally excited O_3 with NO, 30:30525
NITROGEN OXIDES/HYPERFINE STRUCTURE
Hyperfine structure in the visible NO_2 spectrum, 30:30507
NITROGEN OXIDES/MONITORING
Quillayute air reference station (Air sampling and monitoring in Washington State), 30:29359 (BNWL-1850(Pt.3))
NITROGEN OXIDES/WASHOUT
Precipitation scavenging of inorganic pollutants from metropolitan sources: St. Louis, July 1973, 30:29479 (BNWL-1850(Pt.3))
NITROSO COMPOUNDS/BIOLOGICAL EFFECTS
Effect of x irradiation on hydrocarbon metabolism and on hydrocarbon-induced lethality and transformation in cells derived from mouse prostate (3-Methylcholanthrene, 7,12-dimethylbenz(a)anthracene, N-methyl-N'-nitro-N-nitrosoquanidine), 30:29670
NOBLE GASES
See RARE GASES
NON-PROLIFERATION TREATY
Generation of seismic waves by nuclear explosives and possibilities for evading a test-ban treaty, 30:29325 (UCID-15983)
Safeguarding the peaceful uses of nuclear energy by states, 30:30104 (FRNC-TH-50)
NONAXIAL NUCLEI
See DEFORMED NUCLEI
NOVAE/EMISSION SPECTRA
Possible evidence for continued ejection of RR Telescopii, 30:30262
NOZZLES/WELDED JOINTS
Nozzle for the cover of a nuclear reactor pressure vessel (Patent), 30:31285
NUCLEAR CHEMISTRY/RESEARCH PROGRAMS
Research report for 1972--1973, 30:28972 (TRITA-KKE-7403)
NUCLEAR DATA COLLECTIONS
Physical quantities the numerical values of which will be included in the evaluated microscopic nuclear data library ''DANEM-I'' from the I.A.P., 30:30846 (IFA-DNBR-9-1974)
Structure of the evaluated microscopic nuclear data library ''DANEM-I'' from the I.A.P., 30:30845 (IFA-DNBR-8-1974)
NUCLEAR DATA COLLECTIONS/DATA PROCESSING
MCDATA code (For automatic handling of cross section data sets generated by successive runs of MC^2), 30:30851 (RT/FI-(74)19)
NUCLEAR EMULSIONS/PARTICLE IDENTIFICATION
Identification of heavy ions in nuclear emulsions in the hundreds of MeV interval, 30:29493 (LUIP-CR-74-3)
NUCLEAR EMULSIONS/PROTON REACTIONS
Multiplicity in proton-nucleus interactions at 200 GeV/c, 30:30604
NUCLEAR EMULSIONS/READOUT SYSTEMS
Semi-automatic photometer for determining heavy nucleus charges of cosmic rays in nuclear photoemulsion, 30:29501
NUCLEAR ENGINEERING
High flux research reactor and research on reactor physics and reactor engineering, 30:31235 (KURRI-TR-110)
NUCLEAR EXPLOSION DETECTION/SEISMIC WAVES
Extended array evaluation program. Special report No. 5. Selection of reference waveforms for matched filter processing of long period signals from seismic events, 30:29304 (AD-776815)
Extended array evaluation program. Quarterly report No. 6, 1 July--30 September 1973, 30:29306 (AD-777315)
Generation of seismic waves by nuclear explosives and possibilities for evading a test-ban treaty, 30:29325 (UCID-15983)
Seismic discrimination. Semiannual technical summary report, 1 July--31 December 1973, 30:29305 (AD-777151)
NUCLEAR EXPLOSIONS
See also CANNIKIN EVENT
RIO BLANCO EVENT
WAGON WHEEL EVENT
MAGREC final report (Magnetic film recorder for fast transients from nuclear events), 30:29619 (UCID-16026)
Preliminary equation-of-state data for Baneberry altered tuff, 30:29322 (UCID-15874)
NUCLEAR EXPLOSIONS/CONTAINMENT
Compressibility and strength behavior of Diagonal Line alluvium, 30:29316 (UCID-15736)
Field measurement of the permeability of NTS alluvium (Nuclear explosion containment), 30:29315 (UCID-15727)
Field measurements of permeability of NTS alluvium in Area 10, 30:29323 (UCID-15919)
Laminar gas flow through loosely packed Overton sand, 30:29319 (UCID-15818)
Numerical simulation of air-injection experiments in NTS alluvium (Nuclear explosion containment), 30:29324 (UCID-15981)
''Super'' H.E. machine concept, 30:29320 (UCID-15855)
NUCLEAR EXPLOSIONS/ELECTROMAGNETIC PULSES
Computations on the parameter values inside of the E.M. source, 30:29310 (LAMS-2610)
Direct interaction effects in EMP, 30:29308 (AD-777748)
Electromagnetic pulse from nuclear detonations, 30:30448
NUCLEAR EXPLOSIONS/FALLOUT
Behavior and characteristics of radioactive debris from the Chinese nuclear weapons test of June 26, 1973, 30:29362 (BNWL-1850(Pt.3))
NUCLEAR EXPLOSIONS/GAMMA DETECTION
Feasibility of two schemes for detecting the envelope of a γ-ray burst underground, 30:29321 (UCID-15865)
NUCLEAR EXPLOSIONS/RADIATION HAZARDS
Nuclear testing (${}^{131}I$; ${}^{90}Sr$; ${}^{137}Cs$; ${}^{14}C$; Tritium), 30:29719
Operation WHETSTONE: on-site radiological safety report, July 1964--June 1965 (Monitoring), 30:29378 (NVO-410-24)
Operation TOGGLE: on-site radiological safety report, July 1972--June 1973 (Monitoring), 30:29379 (NVO-410-25)
Real risks of the nuclear tests (${}^{131}I$; ${}^{137}Cs$; ${}^{90}Sr$), 30:29720

NUCLEAR EXPLOSIONS/RADIOACTIVE AEROSOLS
  Calculation of fractionation effects following atmospheric nuclear explosions, 30:29386
NUCLEAR EXPLOSIONS/RADIOACTIVE CLOUDS
  Radioactive particle formation after nuclear explosions in the troposphere, 30:29387
NUCLEAR EXPLOSIONS/RADIOACTIVITY
  Formation of secondary aerosols in the atmosphere after ventilated underground nuclear explosions, 30:29390
NUCLEAR EXPLOSIONS/SHOCK WAVES
  Archiving guide to microbarograph records of nuclear and chemical explosion tests, 30:29314 (SLA-74-0210)
NUCLEAR EXPLOSIONS/SIMULATION
  Blast wave boundary layer measurements. Final report, September 1971--August 1973, 30:29307 (AD-777580)
  Foulness multi-ton air blast simulator. Part 1. Early development: the gun driven facility, 30:29309 (AWRE-O-31/74)
NUCLEAR EXPLOSIONS/USES
  Elat-Dead Sea canal (Hydroelectric power generation), 30:29327 (UCID-16107)
  Investigation of tritium decontamination. Interim research report (Natural gas decont amination), 30:29326 (UCID-15985)
  Plowshare technology assessment, prospectives for nuclear-stimulated geothermal power in the western U.S., 30:29311 (PB-231011)
NUCLEAR EXPLOSIVES
  Acoustic emission monitoring of proof tests on canisters and related hardware, 30:29296 (UCID-15777)
NUCLEAR FORCES/BOSON-EXCHANGE MODELS
  Recent developments in meson-theoretical studies of the nucleon--nucleon interaction, 30:30753
NUCLEAR FORCES/BOUNDARY CONDITIONS
  Rigorous constraints that nuclear forces must satisfy to be consistent with the saturation property of nuclear binding energies, 30:31032
NUCLEAR FORCES/NUCLEON-NUCLEON INTERACTIONS
  Off-shell effects of the nucleon--nucleon force in nucleon--nucleon bremsstrahlung, 30:31042
NUCLEAR INDUSTRY/METALS
  Adaptation of metallic materials to the conditions of utilization, 30:29986
NUCLEAR INDUSTRY/RADIOACTIVE AEROSOLS
  Hot aerosol particles during commercial use of atomic energy (Book in Russian), 30:29344
NUCLEAR INSURANCE/LEGISLATION
  Revising and amending the Price--Anderson Indemnity Provisions of the Atomic Energy Act of 1954, as amended. Report by the Joint Committee on Atomic Energy, Ninety-Third Congress, Second Session, Senate, 30:31330
NUCLEAR MAGNETIC MOMENTS/CORRECTIONS
  On the effective two body magnetic dipole operator, 30:31086
NUCLEAR MAGNETIC MOMENTS/QUANTUM OPERATORS
  On the effective two body magnetic dipole operator, 30:31086
NUCLEAR MATERIALS MANAGEMENT
  AEC omnibus legislation, 1974. Report by the Joint Committee on Atomic Energy, Ninety-Third Congress, Second Session, Senate, 30:31328
  AEC omnibus legislation, 1974. Report by the Joint Committee on Atomic Energy, Ninety-Third Congress, Second Session, House of Representatives, 30:31329
NUCLEAR MATTER/BINDING ENERGY
  Status of potential models, 30:31061
NUCLEAR MATTER/GROUND STATES
  Self-consistent calculation of the optical potential and ground-state properties of nuclear matter, 30:31024
NUCLEAR MATTER/OBE MODEL
  Relativistic one-boson-exchange potential, two-nucleon data, nuclear matter, and neutron matter properties, 30:31033
NUCLEAR MATTER/PHASE TRANSFORMATIONS
  Criteria for pion condensation thresholds in neutron star matter, 30:30261
NUCLEAR MATTER/VISCOSITY
  Static viscosity of nuclear matter, 30:31080
NUCLEAR MEDICINE
  See also BIOMEDICAL RADIOGRAPHY
    RADIOPHARMACEUTICALS
    RADIOTHERAPY
    SCINTISCANNING
  Principles and methods for using electronic computers in clinical radioisotopic diagnosis, 30:29838
NUCLEAR MEDICINE/DATA PROCESSING
  Data processing system for nuclear medicine, 30:29864
NUCLEAR MODELS
  See also BRUECKNER MODEL
    COLLECTIVE MODEL
    LIQUID DROP MODEL
    PARTICLE-HOLE MODEL
    SHELL MODELS
NUCLEAR MODELS/EXCITONS
  Intermediate-state transition rates in the exciton model, 30:31093
NUCLEAR PHYSICS/RESEARCH PROGRAMS
  Annual report, 1973 (Tandem Accelerator Laboratory, Uppsala, Sweden), 30:30952 (NP-20122)
  Department of Fundamental Research, Grenoble, semiannual bulletin No. 4, 30:31333 (CEA-N-1688)
  Hahn-Meitner-Institut fuer Kernforschung annual report 1973, 30:31334
  Research fields in physics (Research topics listing), 30:30645
NUCLEAR POTENTIAL
  On the nuclear I.L potential, 30:31092
NUCLEAR POTENTIAL/NUCLEAR MATTER
  Status of potential models, 30:31061
NUCLEAR POTENTIAL/NUCLEI
  Status of potential models, 30:31061
NUCLEAR POTENTIAL/NUCLEON-NUCLEON INTERACTIONS
  Status of potential models, 30:31061
NUCLEAR POTENTIAL/OPTICAL MODELS
  Microscopic approaches to the optical-model potential, 30:31055
NUCLEAR POWER
  Energy crisis and nuclear energy. Energy consumption and expected growth, 30:31307
NUCLEAR POWER/RADIATION HAZARDS
  Atomic energy. V (Norwegin Nature Conservancy Association), 30:29343
NUCLEAR POWER PLANTS
  Nuclear district-heating and nuclear long-distance energy, 30:31305 (JUL-1077)
  Progress on Czechoslovak Nuclear Power Plants, 30:31185 (JPRS-61338)
NUCLEAR POWER PLANTS/CHEMICAL EXPLOSIONS
  Generation and propagation of pressure waves due to unconfined chemical explosions and their impact on nuclear power plant structures, 30:31267
NUCLEAR POWER PLANTS/CLOSED-CYCLE MHD GENERATORS
  Exploratory study of several advanced nuclear-MHD power plant systems, 30:31209
  Feasibility problems on UHTR for closed cycle MHD-power plants, 30:31208
NUCLEAR POWER PLANTS/CONSTRUCTION
  Projections of labor requirements for electrical power plant construction 1974--2000, 30:31306 (WASH-1334)
NUCLEAR POWER PLANTS/COOLING
  Engineering techniques for nuclear plant cooling, 30:31256
NUCLEAR POWER PLANTS/COOLING TOWERS
  Effects of siting and load variation for a 650 MW nuclear station with air condensers, 30:31186
NUCLEAR POWER PLANTS/COST
  Canadian nuclear power programme, 30:31216
NUCLEAR POWER PLANTS/ECONOMICS
  The impact of nuclear power plants on the economic structure, 30:31304 (DEU-74-2)
NUCLEAR POWER PLANTS/ENVIRONMENT
  Nuclear energy and the environment, 30:31262
NUCLEAR POWER PLANTS/MECHANICAL VIBRATIONS
  Methods for the identification of dynamic parameters of mathematical structural models from experimental data, 30:31269
NUCLEAR POWER PLANTS/PLANNING
  Canadian nuclear power programme, 30:31216
NUCLEAR POWER PLANTS/PROTECTIVE COATINGS
  Surface protection in nuclear power plant (Epoxy resin; coating of steel), 30:29946
NUCLEAR POWER PLANTS/PUMPS
  Freezing-up shaft seal of machines for the transport of liquids and gases in nuclear power (Patent), 30:29276
NUCLEAR POWER PLANTS/RADIOACTIVE WASTE DISPOSAL
  Agricultural impacts of nuclear power generation in New York State (Preliminary survey agricultural data), 30:29438 (COO-3167-102)
  Calculations of doses, population doses, and potential health effects due to atmospheric releases of radionuclides from U.S. nuclear power reactors in 1972, 30:29383
  Health physics and technical considerations concerning the control of gaseous effluents from nuclear power plants, 30:29356 (AED-CONF-74-157-005)
NUCLEAR POWER PLANTS/RADIOACTIVE WASTES
  Comparison of mathematical models for calculation of external gamma doses originating from releases of radioactivity to the atmosphere, 30:29342 (RISO-M-1726)
  Ecological factors in the siting, design, and operation of a nuclear power station, 30:29354
  Regional wind resuspension of dust, 30:29373 (BNWL-1850(Pt.3))
NUCLEAR POWER PLANTS/REACTOR SAFETY
  Second biannual report 1973, 30:31248 (KFK-1908)
NUCLEAR POWER PLANTS/SEISMIC EFFECTS
  Dynamic testing of full-scale nuclear power plant structures and equipment, 30:31268
NUCLEAR POWER PLANTS/SITE SELECTION
  Ecological factors in the siting, design, and operation of a nuclear power station, 30:29354
  Thermal discharges and the siting of nuclear power plants, 30:31257
NUCLEAR POWER PLANTS/STEAM TURBINES
  Electric power plant system and method for operating a steam turbine especially of the nuclear type with electronic reheat control of a cycle steam reheater (Patent), 30:31300

- System and method for operating a steam turbine with independent overspeed protection especially adapted for a nuclear reactor powered steam turbine (Patent), 30:31283
- NUCLEAR POWER PLANTS/STRUCTURAL MODELS
  - Large user-orientated systems of programs for structural analysis and design, 30:31291
  - Methods for the identification of dynamic parameters of mathematical structural models from experimental data, 30:31269
- NUCLEAR POWER PLANTS/THERMAL EFFLUENTS
  - Biological effects of thermal discharges from nuclear power plants, 30:29466
  - Ecological factors in the siting, design, and operation of a nuclear power station, 30:29354
  - Magnitude of thermal discharges from a developing nuclear economy, 30:31255
  - Thermal discharges at nuclear power stations. Their management and environmental impacts. A report prepared by a group of experts as the result of a panel meeting held in Vienna, 23--27 October 1972, 30:31252 (STI/DOC-10/155)
- NUCLEAR POWER PLANTS/WASTE HEAT
  - Beneficial uses of waste heat, 30:31308
- NUCLEAR REACTION ANALYSIS
  - (Chemical analysis based on detection and analysis of prompt nuclear reaction products, e.g., gamma rays, neutrons, or charged particles.)
  - Measurement of atomic concentration profiles in thin films using nonresonant nuclear reactions, 30:28933
- NUCLEAR REACTION ANALYSIS/RESEARCH PROGRAMS
  - Annual report, 1973 (Tandem Accelerator Laboratory, Uppsala, Sweden), 30:30952 (NP-20122)
- NUCLEAR REACTIONS
  - See also ALPHA REACTIONS
    - BREAKUP REACTIONS
    - CARBON 12 REACTIONS
    - CARBON 13 REACTIONS
    - COMPOUND-NUCLEUS REACTIONS
    - DEUTERON REACTIONS
    - DIRECT REACTIONS
    - ELECTRON REACTIONS
    - FUSION REACTIONS
    - HADRON REACTIONS
    - HEAVY ION REACTIONS
    - HELIUM 3 REACTIONS
    - KAON REACTIONS
    - KRYPTON 84 REACTIONS
    - LITHIUM 7 REACTIONS
    - MUON REACTIONS
    - NEON 20 REACTIONS
    - NEUTRINO REACTIONS
    - NEUTRON REACTIONS
    - NUCLEON REACTIONS
    - ONE-NUCLEON TRANSFER REACTIONS
    - OXYGEN 16 REACTIONS
    - PHOTONUCLEAR REACTIONS
    - PION REACTIONS
    - PRECOMPOUND-NUCLEUS EMISSION
    - PROTON REACTIONS
    - THERMONUCLEAR REACTIONS
    - TWO-NUCLEON TRANSFER REACTIONS
- NUCLEAR REACTIONS/COULOMB EXCITATION
  - Doppler shape of a γ-line in Coulomb excitation, 30:31100
- NUCLEAR REACTIONS/ELASTIC SCATTERING
  - Boundary value problem for integro-differential equations, 30:31029
- NUCLEAR REACTIONS/GENERATOR-COORDINATE METHOD
  - Application of the generator coordinate method to nuclear bound states and to scattering, 30:31052
- NUCLEAR REACTIONS/SCATTERING AMPLITUDES
  - Determination of reaction amplitudes from experimental observables, 30:31028
- NUCLEAR REACTIONS/SHELL MODELS
  - Treatment of continua in the shell-model theory of nuclear reactions, 30:31077
- NUCLEAR REACTIONS/SPHERICAL HARMONICS
  - Hyperspherical expansion approach for nuclear reactions, 30:31051
- NUCLEAR REACTIONS/VARIATIONAL METHODS
  - Variational calculations of reactions involving light nuclei, 30:30861
- NUCLEAR REACTORS
  - See REACTORS
- NUCLEAR STRUCTURE
  - Quantized friction and the correspondence principle: single particle with friction (Nonlinear time-dependent Schroedinger equation), 30:31075
- NUCLEAR STRUCTURE/CORRELATIONS
  - Four-body correlations in nuclei, 30:31030
- NUCLEAR STRUCTURE/ENERGY LEVELS
  - Shell effects on state densities with given number of excited protons and neutrons, 30:31094
- NUCLEAR STRUCTURE/MEETINGS
  - Nuclear many-body problem. Volume I. Proceedings of the international symposium, Rome, Italy, September 19--23, 1972, 30:31031
- NUCLEAR STRUCTURE/NONLOCAL POTENTIAL
  - New determination of Mongan's non-local separable potentials for nuclear structure calculations, 30:31036
- NUCLEAR STRUCTURE/PIONS
  - π-condensation in a finite system and properties of nuclei, 30:31088
- NUCLEAR STRUCTURE/SHELL MODELS
  - Linear and angular localization effects in nuclear structure calculations, 30:31054
- NUCLEAR WEAPON TESTS
  - See NUCLEAR EXPLOSIONS
- NUCLEAR WEAPONS/TRANSPORT
  - Tandem towing tests of the MHU-12/M trailer. Final report, October 1972--December 1973, 30:30113 (AD-777254)
- NUCLEASES/BIOCHEMICAL REACTION KINETICS
  - Effect of internally deposited plutonium-239 on the lysosomes of rat liver (Compared with effects from ^{198}Au), 30:29782
- NUCLEI
  - See also DEFORMED NUCLEI
    - EVEN-EVEN NUCLEI
    - EVEN-ODD NUCLEI
    - HEAVY NUCLEI
    - INTERMEDIATE MASS NUCLEI
    - LIGHT NUCLEI
    - MAGIC NUCLEI
    - ODD-EVEN NUCLEI
    - POLARIZED NUCLEI
- NUCLEI/BINDING ENERGY
  - Status of potential models, 30:31061
  - The energy density formalism and the shell structure effects, 30:31025
- NUCLEI/BOUND STATE
  - Application of the generator coordinate method to nuclear bound states and to scattering, 30:31052
  - Hyperspherical-expansion approach to nuclear bound states, 30:31050
- NUCLEI/COMPOSITE MODELS
  - Some analogy of the nuclear and nucleon fragmentation processes, 30:30755
- NUCLEI/CORRELATIONS
  - Dynamical implications of correlations, 30:31057
- NUCLEI/DENSITY MATRIX
  - Direct variational calculation of the two-body density matrix, 30:30631
  - New method for evaluating the density matrix and its application to the ground state form factor, 30:30856
- NUCLEI/ENERGY LEVELS
  - A mechanical beam chopper system for the measurement of half-lives in the millisecond region, 30:30154
  - Proceedings of the international conference on reactions between complex nuclei, Nashville, Tennessee, June 10--14, 1974. Volume 1 and Supplement, 30:30982
  - The energy density formalism and the shell structure effects, 30:31025
  - Zeros of triple scattering parameters and spin--parity determination of a resonance, 30:31020 (IFA-FT-107-1974)
- NUCLEI/ENERGY-LEVEL TRANSITIONS
  - Inner bremsstrahlung in electromagnetic zero--zero transitions in nuclei, 30:31085
- NUCLEI/HADRON REACTIONS
  - Diffractive production off nuclei: shadow of hadronic bremsstrahlung, 30:31062
- NUCLEI/HIGH SPIN STATES
  - A weak coupling model for high-spin states (Explained by simple geometrical arguments), 30:31090
- NUCLEI/LIFETIME
  - A simple fast sweeping system for extracted cyclotron beams, 30:30153
- NUCLEI/MANY-BODY PROBLEM
  - Generalized Eulerian angles and the collective motion of many-particle system, 30:31053
- NUCLEI/MOMENT OF INERTIA
  - π-condensation in a finite system and properties of nuclei, 30:31088
- NUCLEI/NUCLEAR RADII
  - The energy density formalism and the shell structure effects, 30:31025
- NUCLEI/PHASE TRANSFORMATIONS
  - π-condensation in a finite system and properties of nuclei, 30:31088
- NUCLEI/PRIMARY COSMIC RADIATION
  - Charge composition and energy spectra of cosmic-ray nuclei at energies above 20 GeV per nucleon (Source nuclei, spallation of source nuclei), 30:30164
- NUCLEI/ROTATION
  - Influence of pairing and of the spin projection distribution on the 'classical' isothermal rotations of a nucleus, 30:31101
- NUCLEI/ROTATIONAL STATES
  - A weak coupling model for high-spin states (Explained by simple geometrical arguments), 30:31090
- NUCLEI/SHAPE
  - π-condensation in a finite system and properties of nuclei, 30:31088
- NUCLEI/WAVE FUNCTIONS
  - Hyperspherical-expansion approach to nuclear bound states, 30:31050
- NUCLEI (CELLS)
  - See CELL NUCLEI

NUCLEIC ACIDS
See also DNA
RNA
NUCLEIC ACIDS/RADIATION INJURIES
ESR studies of radiation damage in nucleic acids, bases, nucleosides, and nucleotides (Review), 30:29656
NUCLEOGENESIS
See NUCLEOSYNTHESIS
NUCLEON ISOBARS
See N*RESONANCES
NUCLEON REACTIONS/ELASTIC SCATTERING
Zeros of triple scattering parameters and spin--parity determination of a resonance, 30:31020 (IFA-FT-107-1974)
NUCLEON-DEUTERON INTERACTIONS
Ground-state properties of three-nucleon systems: a review (Binding energy, charge form factor, magnetic moment), 30:31039
NUCLEON-DEUTERON INTERACTIONS/FADDEEV EQUATIONS
Three-nucleon reactions and off-shell behavior of the nucleon--nucleon interaction, 30:31040
NUCLEON-DEUTERON INTERACTIONS/NUCLEON-NUCLEON POTENTIAL
Three-nucleon reactions and off-shell behavior of the nucleon--nucleon interaction, 30:31040
NUCLEON-NUCLEON INTERACTIONS
See also NEUTRON-NEUTRON INTERACTIONS
PROTON-NEUTRON INTERACTIONS
PROTON-PROTON INTERACTIONS
NUCLEON-NUCLEON INTERACTIONS/BREMSSTRAHLUNG
Off-shell effects of the nucleon--nucleon force in nucleon--nucleon bremsstrahlung, 30:31042
NUCLEON-NUCLEON INTERACTIONS/DIFFRACTION MODELS
An impact parameter description of single and double diffraction dissociation, 30:30761
NUCLEON-NUCLEON INTERACTIONS/NUCLEAR FORCES
Off-shell effects of the nucleon--nucleon force in nucleon--nucleon bremsstrahlung, 30:31042
NUCLEON-NUCLEON INTERACTIONS/OBE MODEL
Recent developments in meson-theoretical studies of the nucleon--nucleon interaction, 30:30753
NUCLEON-NUCLEON INTERACTIONS/PHASE SHIFT
Realistic super-soft-core potential model of the N--N interaction, 30:31035
Status of potential models, 30:31061
NUCLEON-NUCLEON INTERACTIONS/SCATTERING LENGTHS
On the determination of the nucleon-nucleon scattering parameters through final state interactions ($^{3}He(^{3}He,\alpha)2p$), 30:30868
NUCLEON-NUCLEON INTERACTIONS/THREE-BODY PROBLEM
Nucleon--nucleon interaction and low-energy properties of three-nucleon systems, 30:31038
NUCLEON-NUCLEON INTERACTIONS/YUKAWA NONLOCAL THEORY
Meson field theory of nuclei and the N--N interaction, 30:31048
NUCLEON-NUCLEON POTENTIAL
Realistic two-nucleon phenomenological potential (Phase shift analysis), 30:31034
NUCLEON-NUCLEON POTENTIAL/CORRECTIONS
Self-screening of the particle-hole interaction and core polarization of the effective two-particle interaction (TDA and RPA), 30:31091
NUCLEON-NUCLEON POTENTIAL/OBE MODEL
Realistic super-soft-core potential model of the N--N interaction, 30:31035
Relativistic one-boson-exchange potential, two-nucleon data, nuclear matter, and neutron matter properties, 30:31033
NUCLEONS
See also NEUTRONS
PROTONS
NUCLEONS/COMPOSITE MODELS
Some analogy of the nuclear and nucleon fragmentation processes, 30:30755
NUCLEOPROTEINS/BIOSYNTHESIS
Histochemical changes in cancer of the corpus uteri after experimental irradiation (X Radiation), 30:29716
NUCLEOPROTEINS/CHEMICAL RADIATION EFFECTS
Changes in genetic cell material during the action of ionizing radiation (Effects of uv and x radiation on DNA and nucleoproteins), 30:29655
NUCLEOSIDES/RADIATION INJURIES
ESR studies of radiation damage in nucleic acids, bases, nucleosides, and nucleotides (Review), 30:29656
NUCLEOSYNTHESIS
See also THERMONUCLEAR REACTIONS
Iron production by ^{12}C-detonation supernovae (Severe constraints), 30:30258
Nucleosynthesis of the light elements and the interstellar medium, 30:31019 (CONF-730693-)
NUCLEOSYNTHESIS/CROSS SECTIONS
Reaction rates of interest in late stages of stellar nycleosynthesis (Estimate of reliability), 30:30255
NUCLEOSYNTHESIS/NEUTRON FLUX
Cross sections of the $^{21}Ne(\alpha,n)^{24}Mg$ and $^{22}Ne(\alpha,n)^{25}Mg$ reactions at low energies of astrophysical interest, 30:30913
NUCLEOSYNTHESIS/TEMPERATURE DEPENDENCE
A study of nucleosynthesis during explosive carbon burning (Solar-system material), 30:30257
NUCLEOTIDES
See also AMP
NUCLEOSIDES
NUCLEOTIDES/RADIATION INJURIES
ESR studies of radiation damage in nucleic acids, bases, nucleosides, and nucleotides (Review), 30:29656
NYLON/PHYSICAL RADIATION EFFECTS
Melting behavior of Nylon 6 (Gamma radiation), 30:29059

O

OCCLUSION COMPLEXES
See CLATHRATES
OCONEE-1 REACTOR/REACTOR CONTROL SYSTEMS
Block control of a PWR type reactor, 30:31302
OCONEE-1 REACTOR/REACTOR OPERATION
Semiannual operating report, January--June 1974, 30:31315 (DOCKET-50269-284)
OCONEE-2 REACTOR/REACTOR OPERATION
Semiannual operating report, January--June 1974, 30:31315 (DOCKET-50269-284)
ODD-EVEN NUCLEI/EXCITATION
Theory of collective excitations in spherical odd--mass nuclei. III. Electromagnetic properties of the anomalous coupling states (N-quasi-particle modes), 30:31068
OHIO/AIR POLLUTION
Feed Materials Production Center environmental monitoring annual report for 1973, 30:29347 (NLCO-1109)
Portsmouth Gaseous Diffusion Plant environmental monitoring report, 1973, 30:29346 (GAT-781)
OHIO/RADIOACTIVITY
Feed Materials Production Center environmental monitoring annual report for 1973, 30:29347 (NLCO-1109)
Portsmouth Gaseous Diffusion Plant environmental monitoring report, 1973, 30:29346 (GAT-781)
OHIO/WATER POLLUTION
Feed Materials Production Center environmental monitoring annual report for 1973, 30:29347 (NLCO-1109)
Portsmouth Gaseous Diffusion Plant environmental monitoring report, 1973, 30:29346 (GAT-781)
OILS/CHEMICAL ANALYSIS
Determination of mineral-oil in the helium-circuit of a refrigeration-plant, 30:31393 (KFK-1978)
OLEFINS
See ALKENES
OLIGONUCLEOTIDES
See NUCLEOTIDES
ON-LINE CONTROL SYSTEMS/MATERIALS TESTING
Digital processors for servohydraulic material testing systems, 30:29300
ON-LINE MEASUREMENT SYSTEMS
Methods for measuring the reactivity and eigenvalue of nuclear reactors (Patent), 30:31301
ONE-NUCLEON TRANSFER REACTIONS
One- and two-nucleon transfer reactions on deformed nuclei (Generalized optical model; DWBA, coupled-channels and adiabatic theory), 30:31021 (IFA-FT-108-1974)
OOCYTES/BIOLOGICAL RADIATION EFFECTS
Chromosome loss following x-ray irradiation of mature oocytes from Drosophila melanogaster, 30:29768
Follicular damage to bovine ovary from radioiodine (^{131}I), 30:29786
OPE POTENTIAL/D STATES
Approximate D-states and meson exchange currents, 30:30870
OPTICAL MICROSCOPY/COMPARATIVE EVALUATIONS
Comparison of analytical techniques for inorganic pollutants, 30:28924
OPTICAL MODELS/NUCLEAR POTENTIAL
A three parameter nucleon-nucleus optical model on the energy shell, 30:31104
Self-consistent calculation of the optical potential and ground-state properties of nuclear matter, 30:31024
OPTICAL SYSTEMS
Integrating eclipse optics into the AEC Air Force flying laboratory, 30:31423 (LA-UR-74-1167)
OPTICAL SYSTEMS/TESTING
New precision, high-contrast photographic resolution target, 30:31457 (UCID-16064)
OPTICAL THEOREM
New description of the initial states, 30:30690
OREGON/METEOROLOGY
Model to compute low-level Montgomery stream functions, 30:29436 (BNWL-1850(Pt.3))
ORES
See also SILVER ORES
THORIUM ORES
URANIUM ORES
ORES/CHEMICAL ANALYSIS
Assay of silver in ores by neutron activation, 30:28926
Spectrochemical method for determination of tellurium in geological materials, 30:28949
ORES/NUCLEAR REACTION ANALYSIS
Simultaneous analysis of uranium and thorium by the delayed fission neutron counting method, 30:28931
ORGANIC BROMINE COMPOUNDS
See also AET

ORGANIC BROMINE COMPOUNDS/RADIOLYSIS
Unstable intermediates. CXXXVII. α-bromoalkyl radicals in irradiated organic bromides: an electron spin resonance study (Gamma radiation), 30:29073
Unstable intermediates. CXLVI. Electron spin resonance spectra for linear $BrCN^-$ and Br_2CN radicals in irradiated cyanogen bromide crystals (Gamma radiation), 30:29076
ORGANIC CHLORINE COMPOUNDS/CHEMICAL RADIATION EFFECTS
Reduction of methyl acetate with several hydrosilanes under gamma irradiation, 30:29047
ORGANIC COMPOUNDS
See also ALDEHYDES
AMINES
CARBONIC ACID DERIVATIVES
KETONES
NUCLEIC ACIDS
NUCLEOTIDES
ORGANIC NITROGEN COMPOUNDS
ORGANIC POLYMERS
ORGANOMETALLIC COMPOUNDS
PROTEINS
ORGANIC COMPOUNDS/EVAPORATION
Solubility parameters and evaporation rate analysis in organic residue characterization (^{14}C tracer studies), 30:31367 (BDX-613-1099(Rev.))
ORGANIC COMPOUNDS/RADIOLYSIS
Radiation-induced radicals in thymine and its derivatives in low temperature glasses (X radiation), 30:29055
ORGANIC COMPOUNDS/SOLUBILITY
Solubility parameters and evaporation rate analysis in organic residue characterization (^{14}C tracer studies), 30:31367 (BDX-613-1099(Rev.))
ORGANIC FLUORINE COMPOUNDS/PHOTOLYSIS
ESR spectra of PF_2 and SF_3 radicals, 30:29067
ORGANIC FLUORINE COMPOUNDS/RADIOSENSITIVITY EFFECTS
Time course of the radioprotective effect and the formation of endogenous colonies of haemopoietic cells in mouse spleen following the administration of sodium fluoroacetate (X Radiation; mice), 30:29747
ORGANIC NITROGEN COMPOUNDS
See also ACRIFLAVINE
ACRYLONITRILE
AMINES
AMINO ACIDS
CAFFEINE
CYTOSINE
HEMOGLOBIN
IMIDAZOLES
NITRILES
NITROSO COMPOUNDS
NUCLEIC ACIDS
NUCLEOTIDES
PEROXIDASES
PROTEINS
QUINOLINES
THYMINE
VINBLASTINE
ORGANIC NITROGEN COMPOUNDS/RADIOLYSIS
Electron spin resonance study on free radicals in the chemical carcinogen, 1,2-dimethylhydrazine induced by x-ray irradiation, 30:29050
ORGANIC POLYMERS/CHEMICAL COMPOSITION
Chemical compositions of various plastic materials, 30:31404 (UCID-15615)
ORGANIC POLYMERS/MECHANICAL PROPERTIES
Tensile and compression test methods for rigid plastic foams, 30:31403 (UCID-15739)
ORGANIC POLYMERS/USES
Polymer-concrete for use in the repair of deteriorated bridge decks, 30:31388 (BNL-19161)
ORGANOMETALLIC COMPOUNDS/CHEMICAL RADIATION EFFECTS
Moessbauer spectroscopic study of the effect of reactor radiation on the iron(III) acetylacetonate-triethylaluminum catalyst, 30:29052
ORMAK DEVICES/SHIELDING
Shielding design calculations for ORMAK--F/BX, 30:29208 (ORNL-TM-4619)
OSMIUM 181/ENERGY LEVELS
Low-lying states of ^{181}Os, 30:30960
OSMIUM 186/ENERGY LEVELS
Nuclear Data Sheets for A = 186, 30:30988
OSMIUM 186/NUCLEAR PROPERTIES
Nuclear Data Sheets for A = 186, 30:30988
OSTEOSARCOMAS/DIAGNOSIS
Cell mediated immunity as an early diagnostic test for osteosarcoma in human radium cases (Negative results of cytotoxicity tests), 30:29771 (CONF-740930-1)
OSTEOSARCOMAS/RADIOINDUCTION
Morphology and enzyme histochemistry of ^{226}Ra-induced osteosarcomas of the mouse, 30:29785
^{210}Pb retention, excretion, and distribution in beagles following intravenous injection, 30:29805 (COO-119-249)
OSTEOSARCOMAS/RADIOTHERAPY
Increased cures using fractionated exposures of x irradiation and hyperthermia in the local treatment of the Ridgeway osteogenic sarcoma in mice, 30:29744
OTTO HAHN REACTOR/MECHANICAL VIBRATIONS
NS Otto Hahn. Research Report No. 4. The oscillational behaviour of the second core support system, 30:31240 (GKSS-74/E/15)
OVARIES/RADIONUCLIDE KINETICS
Follicular damage to bovine ovary from radioiodine (^{131}I), 30:29786
OXIRANS
See EPOXIDES
OXYCHLORIDES/ELECTRONIC STRUCTURE
Electronic structure and optical properties of some first row transition metal oxyhalides, 30:31395 (LA-5637-T)
OXYCHLORIDES/OPTICAL PROPERTIES
Electronic structure and optical properties of some first row transition metal oxyhalides, 30:31395 (LA-5637-T)
OXYFLUORIDES/ELECTRONIC STRUCTURE
Electronic structure and optical properties of some first row transition metal oxyhalides, 30:31395 (LA-5637-T)
OXYFLUORIDES/OPTICAL PROPERTIES
Electronic structure and optical properties of some first row transition metal oxyhalides, 30:31395 (LA-5637-T)
OXYFLUORIDES/SEPARATION PROCESSES
Decontaminating uranium by reaction with ClF_3 and HF and volatizing the UF_6 product (Patent), 30:29149
OXYGEN/ACTIVATION ANALYSIS
Oxygen content using a 14-MeV neutron activation and direct-counting technique (ASTM Standard E385), 30:28932
Radiochemical separation of fluorine by adsorption on hafnium dioxide: application to the determination of oxygen by activation analysis with charged particles (^{3}He and ^{4}He particles), 30:28923
OXYGEN/ATOM-MOLECULE COLLISIONS
Kinetics of the reaction between oxygen atoms and carbon disulfide (Rate constant, branching ratio), 30:30531
OXYGEN/AUGER EFFECT
Identification and measurement of low-energy electrons by cloud chamber techniques: the oxygen and neon auger-electron problem, 30:29495 (UCID-15372)
OXYGEN/BEAM PRODUCTION
The reaction of atomic oxygen with several atmospheric ions (H^+, O^+, N^+, N^+_2, O^-, O^-_2, 1 to 500 eV), 30:30549
OXYGEN/CHEMICAL ANALYSIS
Comments on oxygen analysis of sodium by equilibration with vanadium: an assessment, 30:28958
Interlaboratory comparison of chemical analysis of uranium mononitride, 30:28942 (N-74-18812)
OXYGEN/ELECTRON-MOLECULE COLLISIONS
Excitation of some bands and lines in collisions of 0.4 to 20 keV electrons with Co, CO_2, and O_2 molecules (Emission, cross sections, Bette-Born approximation), 30:30544
OXYGEN/ION-ATOM COLLISIONS
The reaction of atomic oxygen with several atmospheric ions (H^+, O^+, N^+, N^+_2, O^-, O^-_2, 1 to 500 eV), 30:30549
OXYGEN/MASS SPECTROSCOPY
Application of a mass spectrometer to the method of determination of gases in metals by vacuum fusion, 30:28938 (CNEA-363)
OXYGEN/PION REACTIONS
Pion-nucleus total cross sections from 88 to 860 MeV, 30:30891
OXYGEN/RADIOSENSITIVITY EFFECTS
Changes in oxygenation and radiosensitivity of the tumor after irradiation, 30:29763
Influence of blood oxygenation during in vitro irradiation upon the yield of dicentric chromosomal aberrations in lymphocytes (X Radiation), 30:29749
Metronidazole (Flagyl). A radiosensitizer of hypoxic cells, 30:29674
Radiosensitization of hypoxic cells with metronidazole (Flagyl), 30:29699
OXYGEN/SEPARATION PROCESSES
Tritium Effluent Control Project. Progress Report: April--June 1974, 30:29026 (MLM-2171(LD))
OXYGEN 15/ENERGY LEVELS
Distorted wave Born approximation analysis for the $^{16}O(^{3}He,\alpha)^{15}O$ reaction (15 MeV; spectroscopic factors), 30:30888
OXYGEN 16/ALPHA REACTIONS
New analytical derivation of kernels in the resonating group method for composite-particle scattering and molecule-like structures. Derivation from kernels in the generator coordinate method and application to $^{16}O + \alpha$, 30:31023
OXYGEN 16/BINDING ENERGY
Hartree-Fock calculations using Sussex matrix elements (Single particle spectra), 30:30863
OXYGEN 16/DENSITY MATRIX
Phenomenological occupation probabilities, binding energies, and the nuclear one-particle density matrix, 30:30903
OXYGEN 16/ELECTROMAGNETIC FORM FACTORS
Centre of mass coordinate in many-body theories, 30:30860
OXYGEN 16/ELECTRON REACTIONS
Pion electroproduction from nuclei near threshold (280 MeV), 30:30671
Self-consistent wave functions, center-of-mass motion and high-energy particle-nucleus scattering, 30:31098
OXYGEN 16/ENERGY LEVELS
1p hole-states in ^{16}O and ^{16}N and the mass dependence of the 1p spin-orbit splitting (Spectroscopic factors), 30:30886

Hartree-Fock calculations using Sussex matrix elements (Single particle spectra), 30:30863
OXYGEN 16/ENERGY-LEVEL TRANSITIONS
Inner bremsstrahlung in electromagnetic zero--zero transitions in nuclei, 30:31085
OXYGEN 16/HELIUM 3 REACTIONS
Distorted wave Born approximation analysis for the ^{16}O(^{3}He,α)^{15}O reaction (15 MeV; spectroscopic factors), 30:30888
OXYGEN 16/NEUTRON REACTIONS
R-matrix and phase-shift analysis of neutron polarization measurements from n--^{16}O scattering (1 to 4 MeV: multilevel analysis), 30:30889
OXYGEN 16/OXYGEN 16 REACTIONS
Entrance channel effects in the ^{32}S system: comparison of ^{12}C + ^{20}Ne and ^{16}O + ^{16}O elastic scattering (23.3 MeV (c.m.): angular distributions), 30:30880
Microscopic treatment of viscosity in heavy ion reactions, 30:31066
OXYGEN 16/PROTON REACTIONS
Self-consistent wave functions, center-of-mass motion and high-energy particle-nucleus scattering, 30:31098
OXYGEN 16 REACTIONS/COMPOUND-NUCLEUS REACTIONS
γ-ray multiplicity after (HI,xn) reaction (65 to 85 MeV), 30:30983
Investigation of the 3.46 MeV isomeric level of ^{38}K with the ^{24}Mg(^{16}O,pnγ)^{38}K reaction (38 MeV: γ spectra; lifetimes of levels in ^{38}K, ^{38}Ar, ^{35}Cl), 30:30912
Possible resonance anomalies in the ^{16}O + ^{12}C, 30:30887
Search for new isotopes ^{186} ^{187}Tl, 30:30986
States in ^{24}Mg populated by the ^{10}B(^{16}O,d)^{24}Mg and ^{12}C(^{16}O,α)^{24}Mg reactions (40 to 46 MeV: excitation functions), 30:30911
OXYGEN 16 REACTIONS/ELASTIC SCATTERING
Entrance channel effects in the ^{32}S system: comparison of ^{12}C + ^{20}Ne and ^{16}O + ^{16}O elastic scattering (23.3 MeV (c.m.): angular distributions), 30:30880
Microscopic treatment of viscosity in heavy ion reactions, 30:31066
The determination of the differential energy loss of heavy ions backscattered from an infinitely thick solid target (7-35 MeV), 30:30948
OXYGEN 16 REACTIONS/FUSION REACTIONS
Microscopic treatment of viscosity in heavy ion reactions, 30:31066
OXYGEN 16 REACTIONS/INELASTIC SCATTERING
Coulomb nuclear interference in the inelastic scattering of ^{16}O ions from ^{24}Mg (20 to 30 MeV), 30:30905
Polarization in HI inelastic scattering in the Coulomb--nuclear interference region and coupled channel effects (^{56}Fe(^{16}O,^{16}O'), 43 MeV), 30:30920
OXYGEN 17/DEUTERON REACTIONS
1p hole-states in ^{16}O and ^{16}N and the mass dependence of the 1p spin-orbit splitting (Spectroscopic factors), 30:30886
OXYGEN 18/ISOTOPIC EXCHANGE
Investigation of the catalytic properties of compounds of the LnMeO$_3$ type in the homomolecular exchange of oxygen, 30:29028
Investigation of low-temperature homomolecular isotopic oxygen exchange on titanium dioxide, 30:29029
Isotopic study of water gas reaction catalyzed by platinum, 30:29032
OXYGEN EFFECT (RADIOBIOLOGY)
See OXYGEN
OXYGEN IONS/COLLISIONS
Ion beam sputtering. The effect of incident ion energy on atomic mixing in subsurface layers, 30:30483
OXYGEN IONS/ION-ATOM COLLISIONS
The reaction of atomic oxygen with several atmospheric ions (H$^+$, O$^+$, N$^+$, N$^+_2$, O$^-$, O$^-_2$, 1 to 500 eV), 30:30549
OXYGEN IONS/RADIOTHERAPY
Radiobiology with heavy charged particles directed at radiotherapy, 30:31117
OXYMETHYLENE
See FORMALDEHYDE
OXYSULFIDES/OXIDATION
Kinetics of oxidation of uranium oxysulfide, 30:29103
OXYTETRACYCLINE/RADIOSENSITIVITY EFFECTS
Effect of a combination of antibiotics and AET on the survival of irradiated animals (Tetron-pyrrolidinomettryl-oxytetracycline), 30:29746
OZONE/ATOM-MOLECULE COLLISIONS
Infrared laser enhanced reactions: spectral distribution of the NO$_2$ chemiluminescence produced in the reaction of vibrationally excited O$_3$ with NO, 30:30525
OZONE/MONITORING
Quillayute air reference station (Air sampling and monitoring in Washington State), 30:29359 (BNWL-1850(Pt.3))

P

P-N COUNTERS
See JUNCTION DETECTORS
PACEMAKERS
See CARDIAC PACEMAKERS
PADE APPROXIMATION
Convergence of certain Pade approximants, 30:31140
PADUCAH PLANT/NONRADIOACTIVE WASTES
Environmental monitoring report, calendar year 1973, 30:29351 (UCC-ND-279)
PADUCAH PLANT/RADIOACTIVE WASTES
Environmental monitoring report, calendar year 1973, 30:29351 (UCC-ND-279)
PADUCAH PLANT/RADIOACTIVITY
Data. Section IV. Other data (Monitoring), 30:29412
PAIR PRODUCTION/REACTION KINETICS
Is anti p production peripheral or central, 30:30763
PAIRING INTERACTIONS/COUPLING CONSTANTS
Strength of the multipole pairing coupling constant, 30:31000
PALLADIUM 110/ENERGY LEVELS
Static electric quadrupole moment of the first 2$^+$-state in ^{110}Pd, 30:30955 (NP-20122)
PALLADIUM COMPOUNDS/MICROSTRUCTURE
Evaluation of glancing angle x-ray diffraction and MeV ^{4}He backscattering analyses of silicide formation, 30:29939
PALLADIUM HYDRIDES/SUPERCONDUCTIVITY
Isotope effect in the superconducting palladium--hydrogen--deuterium system, 30:30813
Specific heat of superconducting Pd--H alloys, 30:30812
PANCREAS/SCINTISCANNING
Enhancement of pancreatic concentration of ^{75}Se-selenomethionine (Stimulatory effect of urecholine followed by pancreazymin), 30:29855
PAPAIN/RADIOASSAY
Microassay for proteolytic enzymes using a new radioactive anilide substrate (Tritium tracer technique), 30:29834
PARAFFINS
See ALKANES
PARATHYROID GLANDS/SCINTISCANNING
Elimination of intravenously injected ^{125}I-toluidine blue in rabbits (Effectiveness for parathyroid scanning), 30:29812
PARTIAL IONIZATION/MAGNETIC FLUX
Dissipation of magnetic flux and magnetic energy in partially ionized gases, 30:30388
PARTICLE BEAMS/PULSES
Summing of harmonic frequencies by a resonant cable for pulse generation on a capacitive beam deflector, 30:30147
PARTICLE IDENTIFICATION/IONIZATION CHAMBERS
High-resolution ionization measurements in the region of the relativistic rise, 30:29595
PARTICLE INTERACTIONS/ELASTIC SCATTERING
High energy behavior of total and elastic cross sections (Lectures, differential cross sections, small t behavior, dispersion relations, phase, positivity), 30:30641
PARTICLE INTERACTIONS/INELASTIC SCATTERING
Coupled diffusion equations of the hyperspherical formalism, 30:30632
PARTICLE INTERACTIONS/KINETICS
Particle kinematics (Book), 30:30646
PARTICLE INTERACTIONS/MEETINGS
Properties of the fundamental interactions. Volume 9, Part A. 1971 International School of Subnuclear Physics, Erice, Trapani, Sicily, July 8--26, 1971, 30:30638
PARTICLE INTERACTIONS/POMERANCHUK THEOREM
High energy behavior of total and elastic cross sections (Lectures, differential cross sections, small t behavior, dispersion relations, phase, positivity), 30:30641
PARTICLE MODELS
See also COMPOSITE MODELS
DIFFRACTION MODELS
DUAL ABSORPTION MODEL
FIREBALL MODEL
QUARK MODEL
STRING MODELS
VAN HOVE MODEL
VECTOR DOMINANCE MODEL
VENEZIANO MODEL
WEINBERG LEPTON MODEL
PARTICLE MODELS/MESONS
A two-dimensional model for mesons, 30:30725
PARTICLE MODELS/VECTOR MESONS
Note on an infinite-mass limit of the Higgs model, 30:31153
PARTICLE MODELS/Z*RESONANCES
Simple Z$_0$* model, 30:30740
PARTICLE PRODUCTION
See also MULTIPLE PRODUCTION
PHOTOPRODUCTION
PARTICLE PRODUCTION/LORENTZ TRANSFORMATIONS
Bose distribution and the Lorentz contracted geometric model, 30:30751 (IC-73-6)
PARTICLE PRODUCTION/PARTICLE MODELS
Heavy particle production and cluster models of high-energy collisions, 30:30699
PARTICLE SIZE/MEASURING INSTRUMENTS
Improved PETN particle size analyses, 30:31426 (MLM-2098)
PARTICLE-HOLE MODEL/CORRELATIONS
Dynamical implications of correlations, 30:31057

PARTICLE-HOLE MODEL/NUCLEAR SCREENING
  Self-screening of the particle-hole interaction and core polarization of tne effective two-particle interaction (TDA and RPA), 30:31091
PARTICLE-HOLE MODEL/TWO-BODY PROBLEM
  Effective two-body interaction for equivalent particles, 30:31059
PARTON MODEL
  The quark-parton paradox, 30:30715
PARTON MODEL/ELECTRON-NUCLEON INTERACTIONS
  Quark parton model for deep inelastic lepton scattering (Cross sections, lectures), 30:30686
PARTON MODEL/N*RESONANCES
  SU$_6$ quark model, nucleon resonance electroproduction and spin-dependent electroproduction structure functions, 30:30735
PARTON MODEL/NEUTRINO-NUCLEON INTERACTIONS
  Pion distributions in inelastic neutrino interactions (Quark parton model), 30:30689
  Quark parton model for deep inelastic lepton scattering (Cross sections, lectures), 30:30686
PARTON MODEL/REVIEWS
  Partons, 30:30691
PARTON MODEL/SCALE INVARIANCE
  Parton models and asymptotic freedom, 30:30630
PATIENTS/RADIATION DOSES
  Estimation of radiation doses from i. v. administration of selenite Na$_2{}^{75}$SeO$_3$, 30:29793
  Genetic radiation effects (^{147}Pm and ^{238}Pu powered cardiac pacemakers), 30:29700 (AED-CONF-74-030-004)
  In-vivo measurement of the gamma and neutron dose rate on patients with ^{238}Pu pacemakers implanted, 30:29704 (KFK-1851)
  Indirect technique and problems of radiation protection in pediatric X-ray diagnostics, 30:29701 (AED-CONF-74-140-004)
PATIENTS/RADIATION PROTECTION
  Radiation characteristics and controls. I (Radiation protection of dental patients and personnel), 30:29709
PATIENTS/RADIOTHERAPY
  Experimental usage of cysteine in radiation therapy (Radioprotective effects), 30:29722
PATIENTS/SCINTISCANNING
  Affinity of ^{111}In-bleomycin for malignant tumors (In patients and experimental rat tumors), 30:29859
PDP COMPUTERS/PROGRAMMING
  PL/I based multi-tasking operating system, 30:31340 (IS-M-18)
PEA PLANT
    See PISUM
PEBBLE BED REACTORS
  Feasibility problems on UHTR for closed cycle MHD-power plants, 30:31208
PELVIS/BIOLOGICAL RADIATION EFFECTS
  Changes in the number of circulating lymphocytes with chromosomal aberrations following a single exposure of the pelvis to x-irradiation in cancer patients, 30:29706
PENTAERYTHRITOL TETRANITRATE
    See PETN
PEPPERS/BIOLOGICAL RADIATION EFFECTS
  Ascorbic acid content in different stages of ripeness of fruits pepper under the effect of El and irradiation by ^{60}Co, 30:29685
PEPTIDES/RADIOLYSIS
  Reactions of secondary free radicals in the irradiated frozen aqueous solutions of amino acid and peptides, 30:29044
PERMALLOY/MAGNETIC PROPERTIES
  Evaluation of gold-doped permalloy films using ferromagnetic resonance techniques, 30:31454 (UCID-16032)
PEROXIDASES/BIOLOGICAL RADIATION EFFECTS
  Effect of γ irradiation on the charge and size properties of horseradish peroxidase: individual isoenzymes, 30:29651
PERSONNEL
    See also ASTRONAUTS
        MEDICAL PERSONNEL
PERSONNEL/BIOLOGICAL RADIATION EFFECTS
  Human experience (Pu uptake and biological effects in personnel), 30:29772 (LA-UR-74-1300)
PERSONNEL/ERRORS
  Human error quantification, 30:31360 (SCR-610)
PERSONNEL/RADIATION DOSES
  Results of the medical examinations, 30:29829 (AED-CONF-74-221-004)
PERSONNEL/RADIATION PROTECTION
  Code of practice against radiation hazards, 30:29711
PERSONNEL/RADIONUCLIDE KINETICS
  Plutonium. I. Questions of health in a new industry (Accidental exposures), 30:29773
PERSONNEL MONITORING
  Results of the medical examinations, 30:29829 (AED-CONF-74-221-004)
PERTURBATION THEORY
  Degenerate perturbation theory, 30:30566
PERTURBATIONS
    See DISTURBANCES
PETN
    (Pentaerythritol tetranitrate.)
PETN/PARTICLE SIZE
  Improved PETN particle size analyses, 30:31426 (MLM-2098)
PETTEN STEK REACTOR
    See STEK REACTOR
PHAGES
    See BACTERIOPHAGES
PHARMACEUTICALS
    See DRUGS
PHARYNX/BIOLOGICAL RADIATION EFFECTS
  Influence of fractionation on acute and late reactions in vocal cord carcinoma (Radiotheraphy planning), 30:29713
PHENYLACETYLENE
    See TOLAN
PHENYLETHYLENE
    See STYRENE
PHONONS/CLASSICAL MECHANICS
  Classical-particle description of photons and phonons, 30:30659
PHOSPHATASES
    See also ACID PHOSPHATASE
        ALKALINE PHOSPHATASE
PHOSPHATASES/BIOCHEMICAL REACTION KINETICS
  Effect of internally deposited plutonium-239 on the lysosomes of rat liver (Compared with effects from ^{198}Au), 30:29782
PHOSPHATIDES
    See PHOSPHOLIPIDS
PHOSPHIDES/BRAZING ALLOYS
  Nickel brazing below 1025 C of untreated Inconel 718. Use of a getter makes nickel brazing of Inconel 718 and X-750 below 1025 C (1875 F) as easy as nickel brazing of stainless steels in vacuum, 30:29969
PHOSPHIDES/PHOTONS
  Classical-particle description of photons and phonons, 30:30659
PHOSPHOLIPIDS
  Comparative study of the incorporation of ^{32}P into the phospholipids of membranes from Novikoff hepatoma ascites cells and liver cells from normal and tumor bearing animals (Rats), 30:29819
PHOSPHORUS/ADSORPTION
  Effect of irradiation of metal ions on adsorption properties of semiconductor materials. I. Adsorption properties of oxidized surface of silicon (Effect of radioactivity of adsorbed ions), 30:29053
PHOSPHORUS/EMISSION SPECTROSCOPY
  Spectrochemical analysis of uranium oxide by gallium oxide carrier dc arc technique (ASTM Standard E402), 30:28957
PHOSPHORUS 32/BIOLOGICAL RADIATION EFFECTS
  Comparative investigation of mutagenic effects of incorporated isotopes of the most important organogenic elements. VI. Comparison of lethal and mutagenic effects of the decay of ^{32}P and ^{35}S incorporated into cells of Escherichia coli WP-2S Try$^-$, 30:29788
  Pathological changes in mice following the intraperitoneal administration of radionuclides (^{198}Au and ^{32}P), 30:29784
PHOSPHORUS 32/UPTAKE
  Comparative study of the incorporation of ^{32}P into the phospholipids of membranes from Novikoff hepatoma ascites cells and liver cells from normal and tumor bearing animals (Rats), 30:29819
PHOSPHORUS CHLORIDES/PHOTOLYSIS
  ESR spectra of PF$_2$ and SF$_3$ radicals, 30:29067
PHOSPHORUS FLUORIDES/PHOTOLYSIS
  ESR spectra of PF$_2$ and SF$_3$ radicals, 30:29067
PHOSPHORUS FLUORIDES/RADIOLYSIS
  ESR spectra of PF$_2$ and SF$_3$ radicals, 30:29067
PHOSPHORUS OXIDES/X-RAY FLUORESCENCE ANALYSIS
  Compilation of x-ray interaction data for x-ray fluorescence analysis of geological samples, 30:28943 (RISO-297)
PHOSPHORYLASES
    See PHOSPHOTRANSFERASES
PHOSPHOTRANSFERASES
    See also NUCLEASES
        STREPTOKINASE
PHOSPHOTRANSFERASES/BIOLOGICAL RADIATION EFFECTS
  Changes in glycogen localization and content and activity of enzymes metabolizing glycogen in rat brain during maturation under normal conditions and after gamma irradiation, 30:29761
PHOTOCHEMISTRY
  Conversion of complex compounds under the action of light, radiation, and temperature (Book in Russian), 30:29060
PHOTODISINTEGRATION
    See PHOTONUCLEAR REACTIONS
PHOTOGRAPHIC FILMS/DATA PROCESSING
  Application of a computer-simulated Perceptron to a complex photographic scene, 30:31433 (UCID-16373)
PHOTOGRAPHS
    See IMAGES
PHOTOGRAPHY
  New precision, high-contrast photographic resolution target, 30:31457 (UCID-16064)
  Polaroid vectograph process and application as applied to stereo laser and computer-generated 3-dimensional forms, 30:31352 (UCID-15840)

PHOTON-DEUTERON INTERACTIONS
  Relativistic correction in double scattering by deuterons (Glauber formula), 30:30720
PHOTON-ELECTRON INTERACTIONS/COMPTON EFFECT
  Compton scattering subroutine for Monte Carlo calculations, 30:30651 (UCID-15808)
PHOTON-MOLECULE COLLISIONS/EXCITATION
  Raman process in the case of multiphoton excitation of the hydrogen molecule in an intense laser beam, 30:30551
PHOTON-NEUTRON INTERACTIONS/COMPTON EFFECT
  J = 0 fixed pole in the virtual Compton amplitude off proton and neutron, 30:30661
PHOTON-NEUTRON INTERACTIONS/DIFFERENTIAL CROSS SECTIONS
  Photoproduction of π^- from deuterium at laboratory energies 600 to 1250 MeV, 30:30586
PHOTON-NUCLEON INTERACTIONS
  See also PHOTON-NEUTRON INTERACTIONS
    PHOTON-PROTON INTERACTIONS
PHOTON-NUCLEON INTERACTIONS/DIFFERENTIAL CROSS SECTIONS
  Possibility of producing polarized photons by Compton scattering of polarized relativistic electrons, 30:30648 (IC-73-131)
PHOTON-NUCLEON INTERACTIONS/POLARIZATION
  Possibility of producing polarized photons by Compton scattering of polarized relativistic electrons, 30:30648 (IC-73-131)
PHOTON-PHOTON INTERACTIONS/INELASTIC SCATTERING
  Deep inelastic structure functions of the photon, 30:30676
PHOTON-PROTON INTERACTIONS/COMPTON EFFECT
  J = 0 fixed pole in the virtual Compton amplitude off proton and neutron, 30:30661
PHOTON-PROTON INTERACTIONS/ELECTROPRODUCTION
  Absorption corrections in a Mueller Regge analysis of inclusive photo- and electroproduction, 30:30670
PHOTON-PROTON INTERACTIONS/PHOTOPRODUCTION
  Absorption corrections in a Mueller Regge analysis of inclusive photo- and electroproduction, 30:30670
PHOTONS/CLASSICAL MECHANICS
  Classical-particle description of photons and phonons, 30:30659
PHOTONS/POLARIZED BEAMS
  Possibility of producing polarized photons by Compton scattering of polarized relativistic electrons, 30:30648 (IC-73-131)
PHOTONS/STRUCTURE FUNCTIONS
  Deep inelastic structure functions of the photon, 30:30676
PHOTONUCLEAR REACTIONS
  A microscopic description of the negative parity resonances in the mass-4 system by the coupled-channel method, 30:30871
  Isomeric-yield ratio of ^{52}Mn/sup g/ and ^{52}Mn/sup m/ photoproduction from ^{55}Mn at intermediate energies (Lifetimes, 0.3 to 1 GeV), 30:30919
  Particle configurations of giant E1 states in the $^{14}N(\gamma,p_2)$ and $^{14}N(\gamma,p_0)$ processes (Angular distribution, cross sections, spectroscopic factors), 30:30877
  Status report to NCSAC, 30:31011 (UCID-15639)
  Study of nuclear physics using a high-flux reactor (Photonuclear reaction studies using capture γ-rays), 30:31234 (KURRI-TR-110)
  The $^3He(\gamma,\pi^+)^3H$ reaction in the (3,3) resonance region (Cross sections), 30:30869
PHOTONUCLEAR REACTIONS/CROSS SECTIONS
  Experimental photonuclear cross section calculation, 30:31084
PHOTONUCLEAR REACTIONS/PHOTOFISSION
  Photofission in gold at intermediate energy (600 MeV), 30:31002
PHOTONUCLEAR REACTIONS/RESEARCH PROGRAMS
  Selected activities in photonuclear reactions, 1973--1974 (Lawrence Livermore Laboratory), 30:30856 (UCID-16563)
PHOTONUCLEAR REACTIONS/RESONANCE SCATTERING
  Survey for elements to be excited by gamma-rays following thermal neutron capture in vanadium, 30:30959
PHOTOPRODUCTION/INCLUSIVE INTERACTIONS
  Absorption corrections in a Mueller Regge analysis of inclusive photo- and electroproduction, 30:30670
PHOTOPRODUCTION/SU-3 GROUPS
  An SU(3) analysis of vector meson photoproduction and the pomeron, 30:30665
PHOTOSPHERE/CONVECTION
  The solar temperature reversal and convective motions, 30:30339
PHOTOSPHERE/MAGNETIC FIELDS
  Hydraulic concentration of magnetic fields in the solar photosphere. II. Bernoulli effect (Bernoulli effect), 30:30314
  Radio emissions associated with the emergence of new magnetic flux from the solar photosphere, 30:30305
PHOTOTUBES
  New NADS: compatible alpha measuring system, 30:29618 (UCID-15828)
PHYSICAL PROPERTIES/BIBLIOGRAPHIES
  Scientific publications, reports and external lectures in 1973 compiled by Referat Schrifttum, 30:31359 (PTB-L-2)
PHYTOHEMAGGLUTININ/BIOLOGICAL EFFECTS
  Effects of Phytohemaglutinin-P (PHA-P) on bone cells of the tibial and femoral metaphysis of the rats (Uptake of radioisotopes), 30:29800 (COO-119-249)
PIGS
  See SWINE
PINS (FUEL)
  See FUEL PINS
PION BEAMS/RADIOTHERAPY
  Introduction to the discussion on characteristics of installations for radiotherapy with fast neutrons and other types of high-LET radiation, 30:31112
  Negative pions in radiotherapy. A brief review, 30:31116
PION DETECTION/PLASTIC SCINTILLATION DETECTORS
  A high-resolution scintillation counter with particle identification for use with pions, 30:29597
PION DETECTION/TELESCOPE COUNTERS
  Study of a pion-stopping telescope by time-of-flight methods, 30:29590
PION DETECTION/TRANSITION RADIATION DETECTORS
  Transition counters for πK differentiation above 400 GeV, 30:29599
PION DOSIMETRY
  Calculated particle-production spectra from π^- captures in tissue, tissue-equivalent plastic, silicon, and germanium, 30:31120
  Negative pions in radiotherapy. A brief review, 30:31116
PION DOSIMETRY/TISSUE-EQUIVALENT DETECTORS
  Dosimetry of the SIN biomedical pion beam with tissue-equivalent ionization chambers, 30:29555
PION REACTIONS/CAPTURE
  Calculated particle-production spectra from π^- captures in tissue, tissue-equivalent plastic, silicon, and germanium, 30:31120
PION REACTIONS/DIFFRACTION MODELS
  Exact and perturbative solutions of the Van Hove model describing nuclear diffraction dissociation of pions, 30:30722
PION REACTIONS/ELASTIC SCATTERING
  Unitarity corrections to pion-nucleus scattering lengths, 30:30866
PION REACTIONS/INELASTIC SCATTERING
  Momentum-space study of pion-nucleus inelastic scattering (120 to 280 MeV: differential cross sections, form factors DWIA), 30:30897
  Sensitivity of inelastic pion scattering to non-local interactions, 30:31097
PION REACTIONS/MULTIPLE PRODUCTION
  Multiplicity and correlations of secondary particles produced in $\pi^- - ^{12}C$ collisions at 40 GeV/c, 30:30875 (JINR-P1-7523)
PION REACTIONS/SCATTERING
  The πd scattering length from Ksub(α) X-rays, 30:30620
PION REACTIONS/TOTAL CROSS SECTIONS
  Pion-nucleus total cross sections from 88 to 860 MeV, 30:30891
PION-DEUTERON INTERACTIONS/SCATTERING LENGTHS
  The πd scattering length from Ksub(α) X-rays, 30:30620
  Unitarity corrections to pion-nucleus scattering lengths, 30:30866
PION-NEUTRON INTERACTIONS
  Backward production of rho^0 and f^0 mesons in $\pi^+ n$ interactions at 6 GeV/c (Cross sections), 30:30621
PION-NEUTRON INTERACTIONS/INCLUSIVE INTERACTIONS
  Inclusive π^- production in $\pi^+ d$ interactions at 24 GeV/c, 30:30616
PION-NUCLEON INTERACTIONS
  See also PION-NEUTRON INTERACTIONS
    PION-PROTON INTERACTIONS
PION-NUCLEON INTERACTIONS/CROSS SECTIONS
  Finite energy bounds for πN scattering (Related problems in pp and Kp scattering), 30:30748
PION-NUCLEON INTERACTIONS/DIFFRACTION MODELS
  An impact parameter description of single and double diffraction dissociation, 30:30761
PION-NUCLEON INTERACTIONS/PHASE SHIFT
  Parametrization of low energy πN phase shifts, 30:30732
PION-NUCLEON INTERACTIONS/SCATTERING AMPLITUDES
  Asymptotic crossing-even pion--nucleon forward scattering and duality in the complex energy plane (Froissart bound, sum rules, total cross sections), 30:30734
  N and π exchange amplitudes in πN backward scattering, 30:30744
  Off-shell πN amplitudes via a multichannel separable potential, 30:30731
  Practical evaluation of the asymptotic real-part behavior and the search for a possible subtraction constant in the crossing-odd forward pion--nucleon amplitude, 30:30733
  Sensitivity of inelastic pion scattering to non-local interactions, 30:31097
PION-NUCLEON INTERACTIONS/SCATTERING LENGTHS
  Comments on the calculation of the pion-nucleon coupling constant and s-wave scattering lengths, 30:30745
PION-NUCLEON INTERACTIONS/SUM RULES
  Sum rules for forward elastic pion-nucleon scattering, 30:30750
PION-PION INTERACTIONS/ELASTIC SCATTERING
  A new parametrization for the N/D method, 30:30791
  Wide angle scattering in softened field theory (Born diagrams, structure functions, Bethe-Salpeter wave functions), 30:31163

PION-PION INTERACTIONS/PHASE SHIFT
High statistics study of the reaction $\pi^-p \to \pi^-\pi^+n$: apparatus, method of analysis, and general features of results at 17 GeV/c, 30:30617
PION-PION INTERACTIONS/RHO-765 RESONANCES
Possible description of the rho resonance in the simplest model of the $\pi\pi$-interaction (Four-pion interactions,quasipotential), 30:30718 (JINR-P2-7502)
PION-PION INTERACTIONS/SCATTERING LENGTHS
Phenomenological upper and lower bounds on the $\pi\pi$ S-wave scattering lengths, 30:30723
PION-PROTON INTERACTIONS/ANGULAR DISTRIBUTION
High statistics study of the reaction $\pi^-p \to \pi^-\pi^+n$: apparatus, method of analysis, and general features of results at 17 GeV/c, 30:30617
PION-PROTON INTERACTIONS/CROSS SECTIONS
Study of π^+p interactions with strange particle production in five- and six-body final states at 8 GeV/c, 30:30615
PION-PROTON INTERACTIONS/DIFFERENTIAL CROSS SECTIONS
A study of the reactions $\pi^-p \to K^*X$, $K^*\Sigma$ and $K^*Y_1^*(1385)$ at 3.93 GeV/c, 30:30622
PION-PROTON INTERACTIONS/DIFFRACTION MODELS
Elastic-diffraction slopes of π^+p and K^+p scatterings (25.2 and 40.1 GeV/c total cross sections, impact parameters), 30:30736
Experimental results on strong interactions in the NAL hydrogen bubble chamber, 30:30609
Study of double diffraction dissociation in the reaction $\pi^{+-}p \to (3\pi)^{+-}(N\pi)^+$ at 16 GeV/c, 30:30610
PION-PROTON INTERACTIONS/INCLUSIVE INTERACTIONS
Inclusive π^- production in π^+d interactions at 24 GeV/c, 30:30616
PION-PROTON INTERACTIONS/ISOSPIN
Cross channel isospin amplitudes for 3.9 GeV/c $\pi^{+-}p \to \pi(N\pi)$ compared with the predictions of a double exchange model, 30:30623
Isospin analysis of the reaction $\pi^+p \to \pi(N\pi)$ at 11.7 GeV/c (Cross sections, pomeron exchange proton diffractive dissociation), 30:30742
PION-PROTON INTERACTIONS/KAONS NEUTRAL SHORT-LIVED
Analysis of $K_1^0K_1^0$ system in the $\pi^-p \to nK^0$ anti K^0 reaction at 40 GeV/c (Regge trajectories), 30:30730 (ITEF-31)
PION-PROTON INTERACTIONS/MULTIPLICITY
Charged particle multiplicity distributions for 32 GeV/c $K^{+-}p$ and anti pp interactions and for 50 GeV/c $\pi^{+-}p$ interactions (Topological cross sections), 30:30608
PION-PROTON INTERACTIONS/PAIR PRODUCTION
μ-pair production by inelastic πp and anti pp collisions, 30:30738
PION-PROTON INTERACTIONS/PARTIAL WAVES
A partial-wave analysis of three body π^+ proton interactions at low energy, 30:30749
PION-PROTON INTERACTIONS/SCATTERING AMPLITUDES
The real part of the forward scattering amplitude in $\pi^{+-}p$ elastic scattering below 2 GeV/c, 30:30618
PION-PROTON INTERACTIONS/SPECTRA
Study of particle spectra and correlations in the reaction $\pi^+ + p \to n(\text{forward}) + (2\pi,4\pi,6\pi)$ at 8.4 GeV/c (Monte Carlo method, mass spectra), 30:30613 (COO-1428-391(App.A-2))
PION-PROTON INTERACTIONS/TOTAL CROSS SECTIONS
Unitarity, phenomenology and the bare pomeron, 30:30710
PIONIC ATOMS/FINITE-RANGE INTERACTIONS
Finite range effects in pionic atoms, 30:30512
PIONIC ATOMS/X-RAY SPECTRA
The πd scattering length from Kaub(α) X-rays, 30:30620
PIONIZATION
Long range correlations in the pionization component (Multiperipheral cluster model), 30:30754
Semi-inclusive rapidity distributions in a cluster emission model for the pionization component, 30:30756
PIONIZATION/LINEAR MOMENTUM
The effects of momentum conservation on pionization, 30:30712
PIONS
See also PIONS MINUS
PIONS NEUTRAL
PIONS PLUS
PIONS/DECAY
Structure and experimental consequences of chiral SU_3 x SU_3 breaking, 30:30775
PIONS/ELECTROMAGNETIC FORM FACTORS
Pion and kaon form factors and heavy vector mesons, 30:30726
Wide angle scattering in softened field theory (Born diagrams, structure functions, Bethe-Salpeter wave functions), 30:31163
PIONS/ELECTROPRODUCTION
Absorption corrections in a Mueller Regge analysis of inclusive photo- and electroproduction, 30:30670
Pion electroproduction from nuclei near threshold (280 MeV), 30:30671
PIONS/FORM FACTORS
Generalized vector dominance and the pion form factor (Bethe--Salpeter amplitudes and quark form factor), 30:30729
PIONS/MASS
Non-zero masses of π,K, eta and kappa mesons and algebraic realization of SU(3) x SU(3) chiral symmetry, 30:30780
PIONS/MASS DIFFERENCE
Structure and experimental consequences of chiral SU_3 x SU_3 breaking, 30:30775
PIONS/MULTIPLE PRODUCTION
Bound on the average multiplicity of pions in p--p collision at superhigh energy, 30:30757
PIONS/PARTICLE RADII
Pion and kaon form factors and heavy vector mesons, 30:30726
PIONS/PHASE TRANSFORMATIONS
Pion phase transition in chiral symmetry breaking model, 30:30716
PIONS/PHOTOPRODUCTION
Absorption corrections in a Mueller Regge analysis of inclusive photo- and electroproduction, 30:30670
PIONS MINUS/ELECTROPRODUCTION
Measurements of inclusive pion electroproduction (Cross sections, angular distributions), 30:30587
PIONS MINUS/ENERGY LOSSES
Calculations on tissue equivalence for stopping π^- mesons, 30:31119
PIONS MINUS/PARTICLE PRODUCTION
Inclusive π^- production in π^+d interactions at 24 GeV/c, 30:30616
Multiplicity distributions in the reaction $p + p \to p +$ anything (Cross sections, structure function), 30:30759
Negative pion production in proton-proton interactions at 69 GeV/c (Cross sections, structure function), 30:30603
Two body correlations between negative pions in pp interactions at 69 GeV/c, 30:30601
PIONS MINUS/PHOTOPRODUCTION
An experimental investigation of π photoproduction processes on ^3He (Cross sections, angular distributions), 30:30874
Photoproduction of π^- from deuterium at laboratory energies 600 to 1250 MeV, 30:30586
PIONS NEUTRAL/COSMIC RADIATION
Pion inclusive distribution at cosmic-ray energies and comparison with ISR data (15 to 240 TeV, production mechanism), 30:30171
PIONS NEUTRAL/ELECTROPRODUCTION
π^0 electroproduction at the $\Delta(1236)$ resonance at a four-momentum transfer of $q^2=0.3(GeV/c)^2$ (Angular distribution of s- and p-waves, cross sections), 30:30589
π^0-electroproduction on hydrogen near threshold at four-momentum transfers of 0.2, 0.4 and 0.6 GeV^2, 30:30588
PIONS NEUTRAL/MASS DIFFERENCE
Electromagnetic mass differences in a relativistic quark model, 30:30658
PIONS PLUS/ELECTROPRODUCTION
Measurements of inclusive pion electroproduction (Cross sections, angular distributions), 30:30587
Test of the SU_3 breaking in inclusive electroproduction of hadrons (Duality, parton model, quarks, pomeron, scattering amplitudes, structure functions), 30:30772
The pion form factor at a timelike momentum transfer of approximately 1 fm^{-1} from π^+ electroproduction at threshold, 30:30678
PIONS PLUS/FORM FACTORS
The pion form factor at a timelike momentum transfer of approximately 1 fm^{-1} from π^+ electroproduction at threshold, 30:30678
PIONS PLUS/MASS DIFFERENCE
Electromagnetic mass differences in a relativistic quark model, 30:30658
PIONS PLUS/PARTICLE RADII
The pion form factor at a timelike momentum transfer of approximately 1 fm^{-1} from π^+ electroproduction at threshold, 30:30678
PIONS PLUS/PHOTOPRODUCTION
An experimental investigation of π photoproduction processes on ^3He (Cross sections, angular distributions), 30:30874
PISUM/GENETIC RADIATION EFFECTS
Induced mutation in peas. XXVI. Genetically conditioned differences in radiation sensitivity. IV, 30:29694
PITUITARY GLAND/RADIATION DOSES
Carcinogenicity of iodine-131 relative to age at exposure (^{131}I and ^{125}I uptake by thyroid and pituitary glands), 30:29777 (BNWL-SA-5065)
PL-1 LANGUAGE
PL/I based multi-tasking operating system, 30:31340 (IS-M-18)
PLACENTA
Comparative study of placental location by using ^{51}Cr and the Doppler effect, 30:29858
PLACENTA/SCINTISCANNING
Radioisotope placentography with /sup 113m/In. Its value in the diagnosis and treatment of placenta praevia, 30:29865
PLANE-WAVE BORN APPROXIMATION
See BORN APPROXIMATION
PLANETARY ATMOSPHERES/AIRGLOW
Day airglow emissions of 5577-A and 6300 OI lines in Martian atmosphere, 30:30397

PLANETARY ATMOSPHERES/CHEMICAL COMPOSITION
Volatile element influx on Venus from cometary impacts, 30:30402
PLANETARY ATMOSPHERES/RADIATION TRANSPORT
Radiative transfer of partially polarized light (Specific intensity, arbitrary state of motion), 30:30195
PLANETARY NEBULAE/CHEMICAL COMPOSITION
Are stellar surface heavy-element abundances systematically enhanced. (Upper limit, Hayashi-phase convection), 30:30250
PLANETARY NEBULAE/MATHEMATICAL MODELS
Models for nuclei of planetary nebulae and ultraviolet stars, 30:30215
PLANETARY NEBULAE/RADIOWAVE RADIATION
Observations of the H 85α line from planetary nebulae (Total power mode), 30:30240
PLANETARY NEBULAE/WATER VAPOR
First celestial water vapor sources observed at Itapetinga Radio Observatory, Brazil (Reduction in intensity), 30:30287
PLANETS
See also EARTH PLANET
JUPITER PLANET
MARS PLANET
SATURN PLANET
VENUS PLANET
PLANETS/CHEMICAL COMPOSITION
Structure and evolutionary history of the solar system. IV, 30:30332
PLANETS/EMISSION SPECTRA
High-resolution Fourier spectra of stars and planets, 30:30207
PLANKTON/POPULATIONS
Application of sequential estimation methods to counts of phytoplankton, 30:31380 (RT/BIO-(74)7)
PLANKTON/RADIONUCLIDE KINETICS
Plutonium in the Laurentian Great Lakes: food-chain relationships (^{239}Pu; ^{137}Cs), 30:29415 (CONF-740826-3)
PLANT BREEDING
Use of x-rays in sugar beet breeding, 30:29693
PLANT BREEDING/BIOLOGICAL RADIATION EFFECTS
Reciprocal translocation as a new approach to breeding seedless watermelon. I. Some characters of F_1 hybrids with six reciprocal translocations (X radiation), 30:29686
PLANTS
See also BUCKWHEAT
CREPIS
LEGUMINOSAE
MOSSES
TREES
PLANTS/CHEMICAL COMPOSITION
Elemental content of trace elements in vegetation collected at Centralia, Washington (Comparison with Alaskan vegetation), 30:29483 (BNWL-1850(Pt.3))
PLANTS/CONTAMINATION
Dry disposition processes on vegetation canopies (Development of mathematical model), 30:29369 (BNWL-1850(Pt.3))
PLANTS/RADIATION MONITORING
Some ecological attributes and plutonium contents of perennial vegetation in Area 13 (NAEG vegetation studies) (Botany of Nevada Test Site), 30:29445 (NVO-AEIC-74-1)
PLANTS/RADIOCHEMICAL ANALYSIS
Determination of ^{239}Pu and ^{241}Am in large NAEG vegetation samples (Nevada Test Site), 30:28971 (NVO-AEIC-74-1)
PLANTS/RADIOECOLOGY
Radioecology of Pogonatum urnigerum (L.) pal. beauv (Mosses; gamma radiation; Poland), 30:29691
PLANTS/RADIONUCLIDE KINETICS
^{137}Cs, ^{90}Sr, and ^{210}Pb in soils of the Arctic regions, 30:29405
Data. Section IV. Other data, 30:29412
Radiological monitoring program, period covering February 4, 1974--April 30, 1974 (Rio Blanco site), 30:29348 (PNE-RB-51-9)
PLANTS/SAMPLING
General statistical considerations in environmental plutonium studies (Sample selection), 30:29418 (NVO-AEIC-74-1)
REECo field activities and sample logistics in support of the Nevada Applied Ecology Group (Nevada Test Site ecological sample collection and preparation for Pu analysis), 30:29441 (NVO-AEIC-74-1)
PLANTS (POWER)
See POWER PLANTS
PLASMA
See also BEAM-PLASMA SYSTEMS
COLD PLASMA
COLLISIONLESS PLASMA
HIGH-BETA PLASMA
HOMOGENEOUS PLASMA
HOT PLASMA
INHOMOGENEOUS PLASMA
LASER-PRODUCED PLASMA
Thermonuclear fusion power (Research survey), 30:29232
PLASMA/BREMSSTRAHLUNG
Thermally averaged Gaunt factors in non-relativistic electron-ion bremsstrahlung, 30:29185 (UCID-15712)
PLASMA/CONFINEMENT
Arc discharges in a curved magnetic field, 30:29154 (NP-20140)
Summary of containment experiments on the PROTO--CLEO stellarator, 30:29151 (CLM-R-135)
PLASMA/DISTRIBUTION FUNCTIONS
Analytical expression for the E-layer electron velocity distribution, 30:29187 (UCID-16003(Rev.1))
Hypernetted chain solutions for the classical one-component plasma up to GAMMA=7000, 30:29191
PLASMA/ENERGY SPECTRA
On the energy distribution of electrons in a proton-electron plasma with densities higher than the solid-state density, 30:29173 (IPP-3/12)
PLASMA/EQUATIONS OF STATE
New nodal expansion for classical plasmas, 30:30196
PLASMA/HEATING
Effect of intense electromagnetic wave in charged-particle scattering (Born and dipole approximations, Schroedinger equation), 30:30655
PLASMA/INTERSTELLAR SPACE
Introduction to the physics of interstellar plasmas, 30:30183 (CONF-730693-)
PLASMA/KINETIC EQUATIONS
Nuclear correction for Genesis, 30:29180 (UCID-15316)
PLASMA/MICROWAVE RADIATION
Interaction of intense microwave radiation and fully ionized hydrogen plasma. Part 1. High-density system, 30:29233 (UCRL-51631(Pt.1))
PLASMA/PLASMA EXPANSION
Spatial structure of an expanding laser plasma consisting of aluminum ions and nuclei, 30:29177
PLASMA/RELAXATION
Electron-ion relaxation in a dense plasma (Microscopic structure), 30:30259
PLASMA/SYNCHROTRON RADIATION
Calculating electron synchrotron radiation loss from a fusion plasma, 30:29182 (UCID-15513)
Relation between the radiated and received powers due to gyrating electrons in ambient plasma, 30:30275
PLASMA/THERMAL CONDUCTIVITY
The influence of excited states on the reactive thermal conductivity of an L.T.E. hydrogen plasma, 30:29190
PLASMA/THERMODYNAMIC PROPERTIES
Hypernetted chain solutions for the classical one-component plasma up to GAMMA=7000, 30:29191
PLASMA BEAM INJECTION/SCATTERING
Anomalous scattering of the energy of a plasma jet interacting with a gas target, 30:29155
PLASMA DIAGNOSTICS/CAMERAS
LLL compact 10-ps streak camera, 1974 update, 30:29162 (UCRL-75557)
PLASMA DIAGNOSTICS/ELECTRIC PROBES
Collector probe measurements of the parameters of a laser plasma at long distances, 30:29172
PLASMA DIAGNOSTICS/EMISSION SPECTRA
Diagnostics of dense laser plasmas based on the spectra of hydrogen-like and helium-like multiply charged ions, 30:29171
Spectroscopic study in the vacuum ultraviolet of a neon plasma in ELMO, 30:29158 (ORNL-TM-4672)
PLASMA DIAGNOSTICS/EMISSION SPECTROSCOPY
Spectroscopic methods for diagnostics of superdense hot plasma, 30:29163
PLASMA DIAGNOSTICS/FABRY-PEROT INTERFEROMETER
Proposed method of measuring the current distribution in a tokamak plasma, 30:29170
PLASMA DIAGNOSTICS/INTERFEROMETERS
Fast, high sensitivity 10.6 micron interferometer, 30:29161 (UCID-15625)
PLASMA DIAGNOSTICS/LASER RADIATION
Numerical analysis of interferrograms of asymmetric plasma objects, 30:29176
PLASMA DIAGNOSTICS/LASER-RADIATION HEATING
Diagnostics of dense laser plasmas based on the spectra of hydrogen-like and helium-like multiply charged ions, 30:29171
PLASMA DIAGNOSTICS/RAMAN EFFECT
Spectroscopic methods for diagnostics of superdense hot plasma, 30:29163
PLASMA DIAGNOSTICS/RAYLEIGH SCATTERING
Light scattering from Ne, Ar, and Xe arcs (High-pressure nonhomogeneous plasmas), 30:29169
PLASMA DIAGNOSTICS/SPECTRAL SHIFT
Spectroscopic methods for diagnostics of superdense hot plasma, 30:29163
PLASMA DIAGNOSTICS/X RADIATION
Nanosecond time resolved x-ray diagnostics of relativistic electron beam initiated events, 30:29159 (SAND-74-5262)
X-ray measurements on electron distribution in Astron, 30:29160 (UCID-15392)
PLASMA FOCUS/ELECTRON DENSITY
Numerical analysis of interferrograms of asymmetric plasma objects, 30:29176
PLASMA FOCUS DEVICES/ELECTRIC CURRENTS
Break of the current sheath in a noncylindrical Z pinch, 30:29192
PLASMA FOCUS DEVICES/ELECTRON BEAMS
X-ray analysis for electron beam enhancement in the plasma focus device, 30:29174 (UCRL-75910)

PLASMA FOCUS DEVICES/NEUTRON SPECTRA
  Calculation of the neutron spectra from nuclear reactions in Focus type deuterium plasmas. I. General presentation and mathematical analysis, 30:29178 (CEA-N-1711)
  X-ray analysis for electron beam enhancement in the plasma focus device, 30:29174 (UCRL-75910)
PLASMA FOCUS DEVICES/X-RAY SPECTRA
  X-ray analysis for electron beam enhancement in the plasma focus device, 30:29174 (UCRL-75910)
PLASMA GUNS
  Procedure for deuterating titanium, 30:29216 (UCID-15624)
PLASMA INSTABILITY
  See also PLASMA MICROINSTABILITIES
  Some comments on the transverse resistive wall instability (or, ''LNS revisited''), 30:29198 (UCID-15711)
PLASMA INSTABILITY/ELECTRIC DISCHARGES
  Attachment instability in an externally ionized discharge (High-pressure electron beam-sustainer discharge, 74:2 He:H_2O and 1:1 and 9:1 He:CO_2 mixtures), 30:29201
PLASMA INSTABILITY/EXPLOSIVE INSTABILITY
  Explosive and high-frequency instability of electromagnetic waves in a two electron stream system, 30:29202
PLASMA INSTABILITY/HOSE INSTABILITY
  Reduction of hose growth by current tailoring, 30:29199 (UCID-15996)
PLASMA INSTABILITY/RAYLEIGH-TAYLOR INSTABILITY
  Numerical analysis of interferrograms of asymmetric plasma objects, 30:29176
PLASMA INSTABILITY/RESEARCH PROGRAMS
  Investigation of universal plasma instabilities. Annual progress report No. 9, 30:29196 (TID-26639)
PLASMA JETS/ELECTRON DENSITY
  Numerical analysis of interferrograms of asymmetric plasma objects, 30:29176
PLASMA MICROINSTABILITIES/DRIFT INSTABILITY
  Theory of drift-cone modes of collisionless plasma in cylindrical geometry, 30:29195 (LA-5693-MS)
PLASMA MICROINSTABILITIES/NEGATIVE MASS INSTABILITY
  Negative mass instabilities in beam injected plasmas (Baseball devices), 30:29197 (UCID-15540)
PLASMA MICROINSTABILITIES/TWO-STREAM INSTABILITY
  Explosive and high-frequency instability of electromagnetic waves in a two electron stream system, 30:29202
PLASMA PRODUCTION/ELECTRON BEAMS
  Nanosecond time resolved x-ray diagnostics of relativistic electron beam initiated events, 30:29159 (SAND-74-5262)
PLASMA SHEET/ORIGIN
  Origin of the plasma sheet, 30:30465
PLASMA WAVES
  See also ELECTRON PLASMA WAVES
  ION ACOUSTIC WAVES
PLASMA WAVES/INTERACTIONS
  Multimode parametric interactions in a plasma with low-frequency pumping (Initial-value problem, boundary-value problem), 30:29236
PLASMASPHERE/PLASMA DENSITY
  Plasma tail interpretations of pronounced detached plasma regions measured by Ogo 5, 30:30466
PLASTIC SCINTILLATION DETECTORS
  A large plastic scintillator as anticoincidence shield for beta-radiation detectors, 30:29575
  Low-intensity beam monitoring with an image-intensified scintillator detector, 30:30127
PLASTIC SCINTILLATION DETECTORS/PARTICLE IDENTIFICATION
  A high-resolution scintillation counter with particle identification for use with pions, 30:29597
PLASTIC SCINTILLATION DETECTORS/SENSITIVITY
  Luminescence response of thin plastic scintillator detectors to fission fragments from proton-induced fission of ^{232}Th, ^{235}U and ^{238}U, 30:29528
PLASTICS
  See also MYLAR
  NYLON
  ORGANIC POLYMERS
  POLYETHYLENES
  POLYSTYRENE
  POLYURETHANES
  TEFLON
PLASTICS/CHEMICAL PREPARATION
  Studies on the preparation of mortar--plastic composite (Radiation, thermal-catalytic, and radiation-catalytic methods; γ radiation), 30:29045
PLATES (FUEL)
  See FUEL PLATES
PLATINUM/ELECTRODEPOSITION
  Electrodepositing platinum and platinum--iridium alloys from molten cyanides: chemical process studies, 30:31366 (BDX-613-1064(Rev.))
PLATINUM 186/ENERGY LEVELS
  Nuclear Data Sheets for A = 186, 30:30988
PLATINUM 186/NUCLEAR PROPERTIES
  Nuclear Data Sheets for A = 186, 30:30988
PLATINUM ALLOYS/ELECTRODEPOSITION
  Electrodepositing platinum and platinum--iridium alloys from molten cyanides: chemical process studies, 30:31366 (BDX-613-1064(Rev.))
PLATINUM COMPLEXES/CHEMICAL PREPARATION
  Compounds of tetravalent uranium with complex cations of platinum ($[[[Pt(NH_3)_4]_2[U(C_6H_4O_6)_2(C_2O_4)_2]$ and $[Pt(NH_3)t^{4}][U(C_2O_4)_4]\ 3H_2$), 30:29108
PLATINUM COMPLEXES/CRYSTAL LATTICES
  Temperature dependence of the lattice distortion in the one-dimensional conductor $K_2Pt[CN]_4Br_3$ x $3D_2O$ (Neutron spectroscopy), 30:31365 (AED-CONF-74-089-024)
PLATINUM COMPLEXES/RADIOLYSIS
  Radiation-chemical conversions in solutions of Pt(II) and Pt(IV) complexes, 30:29062
PLATINUM ISOTOPES/ALPHA REACTIONS
  Pt (α,xn), 34-50 MeV: γ spectra, 30:31006
PLUMES/DIFFUSION
  Extension of the anaysis of plume washdown to include diffusion, 30:29478 (BNWL-1850(Pt.3))
PLUMES/DROPLETS
  Analytical search for the stochastic-dominating process in the drift-deposition problem, 30:29488 (BNWL-1850(Pt.3))
PLUMES/MOTION
  Simple model for bouyant plumes based on the conservation laws, 30:29460 (BNWL-1850(Pt.3))
PLUTONIUM
  See also PLUTONIUM-ALPHA
  Ventilation design modifications at Los Alamos Scientific Laboratory major plutonium operational areas, 30:29328 (LA-UR-74-1132)
  Ventilation design for new Plutonium Recovery Facility, 30:29329 (RFP-2215)
PLUTONIUM/CASTING
  Plutonium foundry practices at the Lawrence Livermore Laboratory, 30:29958 (UCID-15926)
PLUTONIUM/CHEMICAL ANALYSIS
  Determination of rare earths in plutonium by x-ray emission analysis, 30:28946
PLUTONIUM/CHEMICAL VAPOR DEPOSITION
  Chemical vapor deposition of uranium and plutonium (Patent), 30:29961
PLUTONIUM/DATA COMPILATION
  Information support for the Nevada Applied Ecology Group (Computer file of references on environmental aspects of Pu, U, and Nevada Test Site), 30:29454 (NVO-AEIC-74-1)
PLUTONIUM/DIFFUSION
  Assessment of the long-term exposure due to resuspension, 30:29375 (BNWL-1850(Pt.3))
  Distribution and characterization of plutonium in soils from Nevada Test Site, 30:29443 (NVO-AEIC-74-1)
  Dynamics of plutonium in desert environments. Nevada Applied Ecology Group progress report as of January 1974, 30:29439 (NVO-AEIC-74-1)
  REECo field activities and sample logistics in support of the Nevada Applied Ecology Group (Nevada Test Site ecological sample collection and preparation for Pu analysis), 30:29441 (NVO-AEIC-74-1)
  Resuspension element status report, 30:29450 (NVO-AEIC-74-1)
PLUTONIUM/HEALTH HAZARDS
  Plutonium(II): watching and waiting for adverse effects (Role of US Transuranium Registry), 30:29790
PLUTONIUM/INTESTINAL ABSORPTION
  In vitro plutonium studies using the artificial rumen and simulated abomasal and intestinal fluids (Uptake by ruminants), 30:29809 (NVO-AEIC-74-1)
PLUTONIUM/ION EXCHANGE
  Sorption of tetravalent elements by mordenite. II. Sorption of Pu(IV), 30:28999
PLUTONIUM/ION EXCHANGE CHROMATOGRAPHY
  Ion exchange adsorption of Pu(IV) at extremely low concentrations in a chelating resin, 30:28996
PLUTONIUM/OXIDATION
  Reaction between plutonium(III) and nitrous acid. II. Kinetics of forward reaction, 30:29112
PLUTONIUM/RADIATION MONITORING
  General statistical considerations in environmental plutonium studies (Sample selection), 30:29418 (NVO-AEIC-74-1)
PLUTONIUM/RADIOECOLOGICAL CONCENTRATION
  Grazing studies on selected plutonium-contaminated areas in Nevada (U and Pu uptake by cattle), 30:29448 (NVO-AEIC-74-1)
  Role of soil microorganisms in the movement of plutonium (Nevada Test Site studies), 30:29447 (NVO-AEIC-74-1)
PLUTONIUM/RADIOMETRIC ANALYSIS
  Soils element activities, October 1972--September 1973 (^{241}Am, ^{239}Pu, and ^{240}Pu in soil at Nevada Test Site), 30:29440 (NVO-AEIC-74-1)
PLUTONIUM/REDUCTION
  Kinetics of reduction of plutonium(VI) by oxalate ions, 30:29114
  Reaction between plutonium(III) and nitrous acid. III. Kinetics of reverse reaction, 30:29113
PLUTONIUM/SEPARATION PROCESSES
  Decontaminating uranium by reaction with ClF_3 and HF and volatizing the UF_6 product (Patent), 30:29149

PLUTONIUM/SOLUBILITY
In vitro plutonium studies using the artificial rumen and simulated abomasal and intestinal fluids (Uptake by ruminants), 30:29809 (NVO-AEIC-74-1)
PLUTONIUM/TISSUE DISTRIBUTION
Grazing studies on selected plutonium-contaminated areas in Nevada (U and Pu uptake by cattle), 30:29448 (NVO-AEIC-74-1)
PLUTONIUM/TOXICITY
Plutonium. I. Questions of health in a new industry (Accidental exposures), 30:29773
PLUTONIUM/UPTAKE
Human experience (Pu uptake and biological effects in personnel), 30:29772 (LA-UR-74-1300)
PLUTONIUM 238/RADIATION DOSE DISTRIBUTIONS
In-vivo measurement of the gamma and neutron dose rate on patients with ^{238}Pu pacemakers implanted, 30:29704 (KFK-1851)
PLUTONIUM 238/RADIATION MONITORING
Atmospheric natural aerosols and fallout particulates during 1973 at Richland, Washington and Point Barrow, Alaska, 30:29361 (BNWL-1850(Pt.3))
Data. Section IV. Other data, 30:29412
PLUTONIUM 238/RADIOISOTOPE HEAT SOURCES
10% efficient economic RTG design, 30:29251
Cost effective designing for the economic RTG, 30:29252
Implantable thermal converter as power source for an artificial heart, 30:29258
Light-weight radiosotope thermoelectric generator design, 30:29253
Modular heat source for ^{244}Cm and ^{238}Pu, 30:29245
Nuclear artificial heart bench model (^{238}Pu heat source and Stirling cycle), 30:29259
Nuclear-fueled circulatory support systems. XIII. Augmented performance of the tidal regenerator engine, 30:29262
PLUTONIUM 238/ROOT ABSORPTION
Influence of soil plutonium concentration of plutonium uptake and distribution in shoots and roots of barley (^{239}Pu, ^{240}Pu, ^{238}Pu, ^{241}Am), 30:29825
PLUTONIUM 238/TISSUE DISTRIBUTION
Absorption, distribution, and excretion of plutonium by dairy cattle (^{238}Pu tracer), 30:29810 (NVO-AEIC-74-1)
Distribution of ingested plutonium in chickens and subsequent transport to eggs (^{238}Pu tracer), 30:29811 (NVO-AEIC-74-1)
PLUTONIUM 238/UPTAKE
Human experience (Pu uptake and biological effects in personnel), 30:29772 (LA-UR-74-1300)
PLUTONIUM 239/ALPHA SPECTROSCOPY
Simultaneous determination of alpha-emitting nuclides of radium through californium in soil, 30:28977
PLUTONIUM 239/BIOLOGICAL RADIATION EFFECTS
Effect of internally deposited plutonium-239 on the lysosomes of rat liver (Compared with effects from ^{198}Au), 30:29782
Effect of ^{239}PuO$_2$ particle number and size on the frequency and distribution of chromosome aberrations in the liver of the Chinese hamster, 30:29783
Research in radiobiology. Annual report of work in progress in the internal irradiation program (Pathological effects of bone-seeking radionuclides in beagles), 30:29778 (COO-119-249)
PLUTONIUM 239/DIFFUSION
Resuspension by wind at Rocky Flats (Plutonium monitoring in air and soil), 30:29371 (BNWL-1850(Pt.3))
Resuspension source change at Rocky Flats, 30:29372 (BNWL-1850(Pt.3))
Resuspension of ^{239}Pu, ^{240}Pu, and ^{241}Am particles at Nevada Test Site; prediction of air concentrations of Pu due to resuspension at Eniwetok Atoll, 30:29452 (NVO-AEIC-74-1)
PLUTONIUM 239/INGESTION
NAEG plutonium study modeling program: plutonium transport and dose estimation model (Computer model for evaluation of health hazards to man due to environmental ^{239}Pu, applied to Nevada Test Site), 30:29455 (NVO-AEIC-74-1)
PLUTONIUM 239/INHALATION
NAEG plutonium study modeling program: plutonium transport and dose estimation model (Computer model for evaluation of health hazards to man due to environmental ^{239}Pu, applied to Nevada Test Site), 30:29455 (NVO-AEIC-74-1)
PLUTONIUM 239/NEUTRON REACTIONS
Assessment of known independent yields and the calculation of those unknown in the fission of ^{232}Th, ^{233}U, ^{235}U, ^{238}U, ^{239}Pu, ^{240}Pu, and ^{241}Pu (Odd—even Z effects), 30:31008 (AERE-R-7680)
Contribution to the mutual resonance shielding of ^{238}U and ^{239}Pu, 30:31009 (EURFNR-1162)
PLUTONIUM 239/RADIATION MONITORING
Atmospheric natural aerosols and fallout particulates during 1973 at Richland, Washington and Point Barrow, Alaska, 30:29361 (BNWL-1850(Pt.3))
Data. Section IV. Other data, 30:29412
Distribution and inventory element activities on-NTS and off-NTS (^{239}Pu, ^{240}Pu, and ^{241}Am content of soil samples from Nevada Test Site and environs), 30:29453 (NVO-AEIC-74-1)
Resuspension by wind at Rocky Flats (Plutonium monitoring in air and soil), 30:29371 (BNWL-1850(Pt.3))
Resuspension source change at Rocky Flats, 30:29372 (BNWL-1850(Pt.3))
Soils element activities, October 1972--September 1973 (^{241}Am, ^{239}Pu, and ^{240}Pu in soil at Nevada Test Site), 30:29440 (NVO-AEIC-74-1)
Some ecological attributes and plutonium contents of perennial vegetation in Area 13 (NAEG vegetation studies) (Botany of Nevada Test Site), 30:29445 (NVO-AEIC-74-1)
Statistical analysis of Pu in soil at the Nevada Test Site: some results (Statistical sampling design), 30:29444 (NVO-AEIC-74-1)
PLUTONIUM 239/RADIOCHEMICAL ANALYSIS
Determination of ^{239}Pu and ^{241}Am in large NAEG vegetation samples (Nevada Test Site), 30:28971 (NVO-AEIC-74-1)
PLUTONIUM 239/RADIOECOLOGICAL CONCENTRATION
^{137}Cs, ^{90}Sr, and ^{210}Pb in soils of the Arctic regions, 30:29405
Data. Section IV. Other data, 30:29412
Plutonium in the Laurentian Great Lakes: food-chain relationships (^{239}Pu; ^{137}Cs), 30:29415 (CONF-740826-3)
PLUTONIUM 239/RETENTION
Decorporation of ^{239}Pu and ^{241}Am in the rat and hamster by Zn--DTPA, 30:29813
PLUTONIUM 239/ROOT ABSORPTION
Influence of soil plutonium concentration of plutonium uptake and distribution in shoots and roots of barley (^{239}Pu, ^{240}Pu, ^{238}Pu, ^{241}Am), 30:29825
PLUTONIUM 239/TISSUE DISTRIBUTION
Ecological studies of vertebrates in plutonium-contaminated areas of the Nevada Test Site (^{239}Pu and ^{241}Am content of GI tract, carcass, and pelt of rodents), 30:29449 (NVO-AEIC-74-1)
Effect of delayed lymphadenectomy on ^{239}PuO$_2$ translocation in dogs, 30:29820
Influence of irradiation on the incorporation of radionuclides (^{239}Pu; ^{226}Ra; ^{210}Pb; ^{144}Ce; tritium), 30:29818
Transuranium elements in gonadal tissue (^{239}Pu, ^{241}Am, ^{243}Cm, ^{244}Cm, ^{249}Cf, and ^{252}Cf), 30:29806 (COO-119-249)
PLUTONIUM 239/UPTAKE
Human experience (Pu uptake and biological effects in personnel), 30:29772 (LA-UR-74-1300)
Plutonium, diphosphonates, and bone (Effects of EHDP on ^{239}Pu uptake by bone tissues), 30:29801 (COO-119-249)
PLUTONIUM 240/DIFFUSION
Resuspension of ^{239}Pu, ^{240}Pu, and ^{241}Am particles at Nevada Test Site; prediction of air concentrations of Pu due to resuspension at Eniwetok Atoll, 30:29452 (NVO-AEIC-74-1)
PLUTONIUM 240/NEUTRON REACTIONS
Assessment of known independent yields and the calculation of those unknown in the fission of ^{232}Th, ^{233}U, ^{235}U, ^{238}U, ^{239}Pu, ^{240}Pu, and ^{241}Pu (Odd--even Z effects), 30:31008 (AERE-R-7680)
PLUTONIUM 240/RADIATION MONITORING
Distribution and inventory element activities on-NTS and off-NTS (^{239}Pu, ^{240}Pu, and ^{241}Am content of soil samples from Nevada Test Site and environs), 30:29453 (NVO-AEIC-74-1)
Soils element activities, October 1972--September 1973 (^{241}Am, ^{239}Pu, and ^{240}Pu in soil at Nevada Test Site), 30:29440 (NVO-AEIC-74-1)
Some ecological attributes and plutonium contents of perennial vegetation in Area 13 (NAEG vegetation studies) (Botany of Nevada Test Site), 30:29445 (NVO-AEIC-74-1)
Statistical analysis of Pu in soil at the Nevada Test Site: some results (Statistical sampling design), 30:29444 (NVO-AEIC-74-1)
PLUTONIUM 240/ROOT ABSORPTION
Influence of soil plutonium concentration of plutonium uptake and distribution in shoots and roots of barley (^{239}Pu, ^{240}Pu, ^{238}Pu, ^{241}Am), 30:29825
PLUTONIUM 241/NEUTRON REACTIONS
Assessment of known independent yields and the calculation of those unknown in the fission of ^{232}Th, ^{233}U, ^{235}U, ^{238}U, ^{239}Pu, ^{240}Pu, and ^{241}Pu (Odd--even Z effects), 30:31008 (AERE-R-7680)
PLUTONIUM BASE ALLOYS/CASTING
Plutonium foundry practices at the Lawrence Livermore Laboratory, 30:29958 (UCID-15926)
PLUTONIUM COMPLEXES/CHEMICAL PREPARATION
Preparation of complex perxenates of some actinide elements, 30:29117
PLUTONIUM DIOXIDE/CHEMICAL ANALYSIS
Determination of molybdenum in plutonia cermets by x-ray fluorescence spectrometry, 30:28979
PLUTONIUM DIOXIDE/CRYSTAL STRUCTURE
Lattice defects and atomic radii in UO$_2$ and PuO$_2$, 30:29929
PLUTONIUM DIOXIDE/FABRICATION
Fabrication of (Pu-U) oxide microspheres using an internal gelation method, 30:29926
PLUTONIUM DIOXIDE/FUEL-COOLANT INTERACTIONS
Thermodynamic data program involving plutonia and urania at high temperatures. Quarterly report No. 27, February 1, 1974--April 30, 1974 (LMFBR), 30:31223 (GEAP-12511)

PLUTONIUM DIOXIDE/GELATION
Fabrication of (Pu-U) oxide microspheres using an internal gelation method, 30:29926
PLUTONIUM DIOXIDE/HOT PRESSING
Fabrication of high-density UO$_2$ and (Usub(0.75)Pusub(0.25))O$_2$ by hot pressing, 30:29925
PLUTONIUM DIOXIDE/PHYSICAL RADIATION EFFECTS
Fabrication, irradiation, and postirradiation examination of mixed oxide fuel pin PNL-3-8, 30:31231 (HEDL-TME-74-37)
PLUTONIUM ISOTOPES/RADIATION MONITORING
Environmental monitoring report: United States Atomic Energy Commission, Oak Ridge facilities. Calendar year 1973, 30:29352 (UCC-ND-280)
PLUTONIUM-ALPHA/PHYSICAL RADIATION EFFECTS
Changes in electrical resistance, length, Seebeck coefficient and Hall emf of alpha-plutonium under neutron irradiation in liquid nitrogen and isochronal annealing, 30:30078
POINT BEACH-1 REACTOR/THERMAL EFFLUENTS
Migratory behavior of fish tagged at a nuclear power plant discharge into Lake Michigan, 30:29462 (CONF-740813-2)
POINT BEACH-2 REACTOR/THERMAL EFFLUENTS
Migratory behavior of fish tagged at a nuclear power plant discharge into Lake Michigan, 30:29462 (CONF-740813-2)
POISSON EQUATION/NUMERICAL SOLUTION
Numerical solutions of Poisson's equation by Fourier transform methods, 30:31348 (UCID-15478)
POLAR SUBSTORMS
See MAGNETIC BAYS
POLARIMETERS/PERFORMANCE
A comparison of polarization values for D-D neutrons obtained from Mott-Schwinger and ^{4}He scattering, 30:29511
POLARIZED TARGETS/CALIBRATION
NMR calibration of a polarized nuclear target, part of which is radiation-damaged, 30:30149
POLARIZED TARGETS/PROTONS
Application of microwave techniques to high-energy physics experiments at Argonne National Laboratory, 30:29584
Polarization decay of an ethylene glycol polarized proton target in an intense proton beam, 30:30155
POLIO VIRUS/INACTIVATION
Measurement of the radiation inactivation of attenuated poliovirus by the plaque assay technique (γ radiation), 30:29676 (SLA-74-0065)
POLLEN/FERTILITY
Reciprocal translocation as a new approach to breeding seedless watermelon. I. Some characters of F_1 hybrids with six reciprocal translocations (X radiation), 30:29686
POLONIUM 210/ALPHA DECAY
L shell ionization in the α decay of ^{210}Po, 30:31001
POLONIUM 210/RADIATION MONITORING
Long-lived radon daughters as atmospheric radioactive tracers, 30:29400
POLONIUM 210/RADIOECOLOGICAL CONCENTRATION
^{210}Po radioactivity in organs of selected tunas and other marine fish (Radioecological concentration in Pacific Ocean fishes), 30:29817
POLONIUM 212/ALPHA SPECTRA
Separation of radionuclides using alkyl radicals, 30:29083 (AED-CONF-74-084-002)
POLONIUM 213/RADIATION MONITORING
Scavenging of radioactive material from the atmosphere by surface condensation, 30:29391
POLONIUM 216/ALPHA SPECTRA
Separation of radionuclides using alkyl radicals, 30:29083 (AED-CONF-74-084-002)
POLONIUM COMPLEXES/CHEMICAL PREPARATION
Investigation of complex formation of polonium by an ion exchange method, 30:29120
POLONIUM ISOTOPES/SEPARATION PROCESSES
Separation of radionuclides using alkyl radicals, 30:29083 (AED-CONF-74-084-002)
POLYCARBONATES/STRESSES
Residual stresses and birefringence in polycarbonate plastic, 30:31405 (UCID-15845)
POLYETHYLENES
See also TEFLON
POLYETHYLENES/CHEMICAL RADIATION EFFECTS
Kinetic study of double bonds in polyethylene irradiated by gamma rays, 30:29038
Oxidative degradation products of irradiated polyethylene (Electrons), 30:29054
Radiation effects in polyethylene films studied by pulse radiolysis (Electron beams), 30:29077
POLYETHYLENES/NEUTRON TRANSPORT
Neutron slowing-down in ice and polyethylene at low temperatures (Moderator at 4.2, 77, and 300°K, 0.0018 to 0.090 eV), 30:30843 (IAE-2271)
Shielding benchmark problems, 30:31126 (ORNL-RSIC-25(Suppl.2))
POLYETHYLENES/PROTON REACTIONS
Annual report, 1973, 30:30952 (NP-20122)
POLYNUCLEAR HYDROCARBONS
See CONDENSED AROMATICS
POLYSTYRENE/MECHANICAL PROPERTIES
Tensile and compression test methods for rigid plastic foams, 30:31403 (UCID-15739)
POLYSTYRENE/MOLECULAR STRUCTURE
Measurements of persistence length and temperature dependence of the radius of gyration in bulk atactic polystyrene, 30:31364 (AED-CONF-74-072-002)
POLYTETRAFLUORETHYLENE
See TEFLON
POLYURETHANES/COMPRESSIBILITY
Static compressive testing of rigid polyurethane foam, 30:31384 (BDX-613-1036(Rev.))
POLYURETHANES/MECHANICAL PROPERTIES
Tensile and compression test methods for rigid plastic foams, 30:31403 (UCID-15739)
POLYURETHANES/RADIOSTERILIZATION
Sterilization method and product (Patent), 30:29647
POMERANCHUK PARTICLES/KAON-PROTON INTERACTIONS
Models for the pomeron and low energy K$^+$p scattering (S-channel unitarity model), 30:30746
POMERANCHUK PARTICLES/MEETINGS
Proceedings of the eighth Rencontre de Moriond. Volume II. The pomeron. Conference held at Meribel-les-Allues, France, March 4--16, 1973, 30:30633
POMERANCHUK PARTICLES/PARTICLE PRODUCTION
The pomeron-particle total cross section and diffractive production of showers at very high energies, 30:30760
POMERANCHUK PARTICLES/RENORMALIZATION
Unitarity, phenomenology and the bare pomeron, 30:30710
POMERANCHUK POLES/MEETINGS
Proceedings of the eighth Rencontre de Moriond. Volume II. The pomeron. Conference held at Meribel-les-Allues, France, March 4--16, 1973, 30:30633
POMERANCHUK THEOREM
High energy behavior of total and elastic cross sections (Lectures, differential cross sections, small t behavior, dispersion relations, phase, positivity), 30:30641
POMERONS
See POMERANCHUK PARTICLES
PONDS
See LAKES
POSITRON BEAMS/ACCELERATION
High-power standing-wave triperiodic structure for positron acceleration, 30:30126
POSITRON COLLISIONS
Efficient positronium formation by slow positrons incident on solid targets (Few-eV region), 30:30510
POSITRON COLLISIONS/ANNIHILATION
Positron annihilation in colored KCl, 30:30513
POSITRON DECAY
See BETA-PLUS DECAY
POSITRONIUM/ANNIHILATION
Efficient positronium formation by slow positrons incident on solid targets (Few-eV region), 30:30510
POSITRONS/ANNIHILATION
Automatic corrections for deadtime effects and lineshape changes due to source decay in positron-annihilation experiments, 30:29513
POSITRONS/COLLISIONS
Diffusion of slow positrons from gold (Scattering lengths, Born approximation), 30:30511
POSTULATED PARTICLES
See also GRAVITONS
POMERANCHUK PARTICLES
QUARKS
POSTULATED PARTICLES/SECONDARY COSMIC RADIATION
Search for heavy particles in cosmic rays (6 Proton masses), 30:30579
POTASSIUM/ACTIVATION ANALYSIS
Trace element behavior in soil of some Indonesian sawah's and in sludge of an Indonesian river, 30:28930
Trace elements in precipitation and cloud water in the area of Heidelberg, measured by instrumental neutron activation analysis, 30:28934
POTASSIUM/COSMOCHEMISTRY
Neutral potassium in dusty clouds (Optical depths, gas-to-dust ratio), 30:30358
POTASSIUM/ELECTRIC CONDUCTIVITY
Volume and temperature dependence of the electronic transport properties of fluid alkalis in the semiconducting range (K and Cs), 30:30005
POTASSIUM/ELECTRON-ATOM COLLISIONS
Excitation of resonance lines of K II in electron-atom collisions (20 to 200 eV), 30:30524
POTASSIUM/EMISSION SPECTROSCOPY
Spectrochemical analysis of uranium oxide by gallium oxide carrier dc arc technique (ASTM Standard E402), 30:28957
Spectrographic determination of trace impurities in high purity uranium oxide, 30:28944 (UCID-15952)
POTASSIUM/QUALITATIVE CHEMICAL ANALYSIS
Application of activation analysis to the determination of pollutants in the atmosphere, 30:28914 (IEA-326)
POTASSIUM/TISSUE DISTRIBUTION
Distribution of radioactive and stable cesium in the human body (^{137}Cs; K), 30:29789
POTASSIUM 38/ENERGY LEVELS
Investigation of the 3.46 MeV isomeric level of ^{38}K with the ^{24}Mg(^{16}O,pnγ)^{38}K reaction (38 MeV: γ spectra; lifetimes of levels in ^{38}K, ^{38}Ar, ^{38}Cl), 30:30912

POTASSIUM 40/COSMOCHEMISTRY
  The unique cosmic-ray history of the Malakal chondrite, 30:30170
POTASSIUM BROMIDES/CRYSTAL LATTICES
  Temperature dependence of the lattice distortion in the one-dimensional conductor $K_2Pt[CN]_4Br_3$ x $3D_2O$ (Neutron spectroscopy), 30:31365 (AED-CONF-74-089-024)
POTASSIUM CHLORIDES/POSITRON COLLISIONS
  Positron annihilation in colored KCl, 30:30513
POTASSIUM COMPOUNDS/CHEMICAL RADIATION EFFECTS
  Effects of molecular motion in the ESR spectrum of BrO_3^{2-} ions in $KBrO_3$ single crystals (X radiation), 30:29065
POTASSIUM COMPOUNDS/LATTICE PARAMETERS
  On oxifluorides $A_{12}M(IV)M_3(VI)O_8F_{18}$ with uranium, molybdenum, and tungsten (A = Cs, Rb, K and M(IV) = U, Ce, Mo, W), 30:29006
POTASSIUM COMPOUNDS/MAGNETIC SUSCEPTIBILITY
  On oxifluorides $A_{12}M(IV)M_3(VI)O_8F_{18}$ with uranium, molybdenum, and tungsten (A = Cs, Rb, K and M(IV) = U, Ce, MoW), 30:29006
POTASSIUM IONS/COSMOCHEMISTRY
  Statistical properties of interstellar clouds (Power law), 30:30350
POTASSIUM OXIDES/X-RAY FLUORESCENCE ANALYSIS
  Compilation of x-ray interaction data for x-ray fluorescence analysis of geological samples, 30:28943 (RISO-297)
POTENTIAL SCATTERING
  New description of nuclear scattering at intermediate energies and permissibility of Glauber expression to large-angle elastic scattering, 30:31022
POTENTIAL SCATTERING/FREDHOLM EQUATION
  Connection between Fredholm determinant and Jost function for nonlocal potentials, 30:30788
POTENTIAL SCATTERING/GLAUBER THEORY
  Comments on approximations for the overlap expansion, 30:30786
POTENTIAL SCATTERING/JOST FUNCTION
  Connection between Fredholm determinant and Jost function for nonlocal potentials, 30:30788
  Representations of the Jost solutions and the S matrix for a class of analytic nonlocal potentials (Laplace transform, s waves, spectral function), 30:30785
POTENTIAL SCATTERING/KLEIN-GORDON EQUATION
  Exponential potential and the Klein--Gordon equation (Bound states, phase shifts), 30:30789
POTENTIAL SCATTERING/S MATRIX
  Representations of the Jost solutions and the S matrix for a class of analytic nonlocal potentials (Laplace transform, s waves, spectral function), 30:30785
POTENTIOMETRY/SUPERCONDUCTORS
  Application of Josephson's effect in superconductors for measurements of very small voltages, 30:30842
POWER EXCURSIONS
  See EXCURSIONS
POWER PLANTS
  See also NUCLEAR POWER PLANTS
POWER PLANTS/THERMAL EFFLUENTS
  Mathematical and physical models of heat dissipation, 30:29464
  Physical--chemical effects of cooling systems and thermal discharges on the environment, 30:29465
POWER REACTORS
  See also CALHOUN-1 REACTOR
  CLINCH RIVER BREEDER REACTOR
  COOPER REACTOR
  DESALINATION REACTORS
  DRESDEN-1 REACTOR
  DRESDEN-2 REACTOR
  DRESDEN-3 REACTOR
  DUANE ARNOLD-1 REACTOR
  FUKUSHIMA-1 REACTOR
  HUMBOLDT BAY REACTOR
  JPDR REACTOR
  LUCIE-1 REACTOR
  LUCIE-2 REACTOR
  MAGNOX TYPE REACTORS
  MAINE YANKEE REACTOR
  MIHAMA-1 REACTOR
  MIHAMA-2 REACTOR
  NEWBOLD ISLAND-1 REACTOR
  NEWBOLD ISLAND-2 REACTOR
  NINE MILE POINT-1 REACTOR
  OCONEE-1 REACTOR
  OCONEE-2 REACTOR
  POINT BEACH-1 REACTOR
  POINT BEACH-2 REACTOR
  PROCESS HEAT REACTORS
  SGHWR REACTOR
  SHIMANE-1 REACTOR
  TURKEY POINT-3 REACTOR
  TURKEY POINT-4 REACTOR
POWER REACTORS/MELTDOWN
  Diffusion of radioactive fluid through soil surrounding a large power-reactor station after a core meltdown accident, 30:31254 (UCRL-51494)
POWER REACTORS/PRESSURE REGULATORS
  Fluid pressure regulating and control device (Patent), 30:29622
POWER REACTORS/PRESSURE VESSELS
  Elastic-plastic deformation of cylindrical pressure vessels under cyclic loading, 30:31266
POWER REACTORS/SHIELDING
  Investigations on the shielding of power reactors, 30:31271 (IKE-6-75d)
POWER REACTORS/THERMODYNAMIC CYCLES
  Nuclear energy requirements for hydrogen production from water, 30:31239
POWER TRANSMISSION/SUPERCONDUCTING CABLES
  USAEC-DAT dc superconducting power transmission line project at LASL. Progress report, January 1--March 31, 1974, 30:30820 (LA-5684-PR)
PRASEODYMIUM/ELECTRON COLLISIONS
  Strong 4f resonance effects in rare-earth appearance-potential spectra, 30:30477
PRASEODYMIUM 136/ENERGY LEVELS
  Nuclear Data Sheets for A = 136, 30:30967
PRASEODYMIUM 136/NUCLEAR PROPERTIES
  Nuclear Data Sheets for A = 136, 30:30967
PRASEODYMIUM 143/ENERGY LEVELS
  Nuclear Data Sheets for A = 143, 30:30966
PRASEODYMIUM 143/NUCLEAR PROPERTIES
  Nuclear Data Sheets for A = 143, 30:30966
PRASEODYMIUM 144/BIOLOGICAL RADIATION EFFECTS
  Comparison of external irradiation and consumption of cows' milk as critical pathways for ^{137}Cs, ^{54}Mn and ^{144}Ce--^{144}Pr released to the atmosphere, 30:29423
PRASEODYMIUM 144/RADIOECOLOGICAL CONCENTRATION
  Comparison of external irradiation and consumption of cows' milk as critical pathways for ^{137}Cs, ^{54}Mn and ^{144}Ce--^{144}Pr released to the atmosphere, 30:29423
PRECIPITATION SCAVENGING/TRACER TECHNIQUES
  Entrainment of tracers near the sides of convective clouds (Tantalum, iridium, gold, rhenium, and indium tracer measurements), 30:29481 (BNWL-1850(Pt.3))
  Feasibility study of the use of inert tracers in the national hail research experiment (Inert gold, rhenium, and indium and ^{36}Cl and ^{38}Cl tracer measurements), 30:29427 (BNWL-1850(Pt.3))
  Progress report on in-cloud scavenging in frontal storms, 30:29475 (BNWL-1850(Pt.3))
  Summary of current findings from the analysis of 1972 Quillayute scavenging experiments, 30:29476 (BNWL-1850(Pt.3))
PRECIPITATIONS (ATMOSPHERIC)
  See ATMOSPHERIC PRECIPITATIONS
PRECOMPOUND-NUCLEUS EMISSION
  Intermediate-state transition rates in the exciton model, 30:31093
PRESSURE REGULATORS/DESIGN
  Fluid pressure regulating and control device (Patent), 30:29622
PRESSURE VESSELS/APERTURES
  Pressure vessel penetration techniques (Patent), 30:31286
  Pressure vessel penetration technique (Patent), 30:31287
PRESSURE VESSELS/CLOSURES
  Head closure system (Patent), 30:31197
  Head closure mechanism (Patent), 30:31198
PRESSURE VESSELS/LINING PROCESSES
  Solution of the problem of designing liners for prestressed pressure vessels, 30:29264 (AED-CONF-73-600-001)
PRESSURE VESSELS/NOZZLES
  Nozzle for the cover of a nuclear reactor pressure vessel (Patent), 30:31285
PRESSURE VESSELS/RESEARCH PROGRAMS
  Quarterly progress report on reactor safety programs sponsored by the Division of Reactor Safety Research for April--June 1974 (PWR and BWR), 30:31251 (ORNL-TM-4655(Vol.2))
PRESSURE VESSELS/SPECIFICATIONS
  Trends in structural mechanics. A UK review of the 2nd international conference on structural mechanics in reactor technology. I. Pressure vessels and containments, 30:31192
PRESSURE VESSELS/STRESS ANALYSIS
  Elastic-plastic deformation of cylindrical pressure vessels under cyclic loading, 30:31266
PRESSURE VESSELS/STRESSES
  Solution of the problem of designing liners for prestressed pressure vessels, 30:29264 (AED-CONF-73-600-001)
PRESSURE VESSELS/ULTRASONIC TESTING
  Reactor vessel in-service inspection assembly (Patent), 30:31200
PRESSURIZED WATER REACTORS
  See PWR TYPE REACTORS
PRIMARY COOLANT CIRCUITS/PULSATIONS
  Theory of pump-induced pulsating coolant pressure in pressurized water reactors, 30:31203
PRIMARY COOLANT CIRCUITS/TEMPERATURE MONITORING
  Temperature control and emergency protection against perilous temperatures in nuclear reactor (Patent), 30:31297
PRIMARY COSMIC RADIATION
  Sun and cosmic rays, 30:30327
PRIMARY COSMIC RADIATION/ACCELERATION
  The distribution of cosmic rays in the galaxy and their dynamics as deduced from recent γ-ray observations (Trapping time), 30:30163

PRIMARY COSMIC RADIATION/CHEMICAL COMPOSITION
  Charge composition and energy spectra of cosmic-ray nuclei at energies above 20 GeV per nucleon (Source nuclei, spallation of source nuclei), 30:30164
  Origin of cosmic rays, 30:30169
PRIMARY COSMIC RADIATION/DAILY VARIATIONS
  Variations of cosmic ray intensity in consequence of the semidiurnal anisotropy, 30:30179
PRIMARY COSMIC RADIATION/ENERGY SPECTRA
  Charge composition and energy spectra of cosmic-ray nuclei at energies above 20 GeV per nucleon (Source nuclei, spallation of source nuclei), 30:30164
  Energy spectrum of primary cosmic rays above 10^{12} eV, 30:30176
  Fluctuation studies of large air showers: the composition of primary cosmic ray particles of energy E/sub p/ approximately 10^{18} eV, 30:30175
  Production spectrum of charged cosmic ray pions and the primary cosmic ray nucleon spectrum, 30:30177
PRIMARY COSMIC RADIATION/FLUX DENSITY
  The possible influence of Jupiter on cosmic radiation at the earth, 30:30173
PRIMARY COSMIC RADIATION/ISOTOPE RATIO
  Monte Carlo computation for isotopic analysis of cosmic rays by means of the Earth's magnetic field, 30:30181
PRIMARY COSMIC RADIATION/ORIGIN
  Origin of cosmic rays, 30:30169
PRIMARY COSMIC RADIATION/TEV RANGE
  Fluctuation studies of large air showers: the composition of primary cosmic ray particles of energy E/sub p/ approximately 10^{18} eV, 30:30175
PRINTED CIRCUITS/SURFACE COATING
  Use of EN-7 to encapsulate analyzer assemblies. Final report, 30:31418 (BDX-613-1135(Rev.))
PROBES/PULSE TECHNIQUES
  New method for obtaining probe characteristics (Avoids the difficulties, high particle densities, high energy densities), 30:29167
PROCESS HEAT REACTORS/THERMODYNAMIC CYCLES
  Nuclear energy requirements for hydrogen production from water, 30:31239
PROCESSING (DATA)
  See DATA PROCESSING
PROLACTIN
  See LTH
PROMETHAZINE
  See AMINES
PROMETHIUM 136/NUCLEAR PROPERTIES
  Nuclear Data Sheets for A = 136, 30:30967
PROMETHIUM 143/ENERGY LEVELS
  Nuclear Data Sheets for A = 143, 30:30966
PROMETHIUM 143/NUCLEAR PROPERTIES
  Nuclear Data Sheets for A = 143, 30:30966
PROMETHIUM 147/BETA SPECTROSCOPY
  Determination of promethium-147 in aqueous environmental samples, 30:28969 (DP-MS-73-77)
PROMETHIUM 147/BETAVOLTAIC CELLS
  Advanced betavoltaic power sources, 30:29257
  Optimization of the beta-voltaic cell, 30:29256
PROMETHIUM 147/ENERGY-LEVEL TRANSITIONS
  Gamma--gamma angular correlation in ^{147}Pm (J, π, mixing ratios), 30:30958
PROPAGATION (WAVE)
  See WAVE PROPAGATION
PROPANONE
  See ACETONE
PROPIOLONITRILE/COSMOCHEMISTRY
  Cyanoacetylene: new lines and sources in the galaxy, 30:30374
PROPORTIONAL COUNTERS
  See also BF3 COUNTERS
    HE-3 COUNTERS
  Wavelength shifters for xenon proportional scintillation counters, 30:29523
PROPORTIONAL COUNTERS/PERFORMANCE
  About the use of proportional counters for registration of cosmic ray meson component, 30:29582
  The needle chamber: a new highly versatile detector, 30:29514
PROSTAGLANDIN/CHEMICAL RADIATION EFFECTS
  Method for preparation of biocompatible and biofunctional materials and product thereof (Graft polymerization using high-energy electrons, x or γ radiation, patent), 30:29082
PROTACTINIUM/ACTIVATION ANALYSIS
  Radioactivation analysis in thermal and epithermal neutrons of the IBR-30 reactor of JINR, 30:28929
PROTACTINIUM/SOLVENT EXTRACTION
  Process for separation of protactinium, thorium, and uranium from neutron-irradiated thorium (Using TBP), 30:29150
PROTACTINIUM 231/ALPHA SPECTROSCOPY
  Simultaneous determination of alpha-emitting nuclides of radium through californium in soil, 30:28977
PROTACTINIUM 231/RADIOCHEMICAL ANALYSIS
  Sequential determination of radium-226, radium-228, actinium-227, and thorium isotopes in environmental and process waste samples, 30:28978
PROTACTINIUM 234/GAMMA SPECTROSCOPY
  Gamma-ray assay of low-enriched uranium waste, 30:28986
PROTACTINIUM BROMIDES/VAPOR PRESSURE
  Vapor pressure of protactinium pentabromide, 30:29130
PROTECTION (CORROSION)
  See CORROSION PROTECTION
PROTECTION (RADIATION)
  See RADIATION PROTECTION
PROTECTIVE COATINGS/NUCLEAR POWER PLANTS
  Surface protection in nuclear power plant (Epoxy resin; coating of steel), 30:29946
PROTEINS
  See also ACTIN
    ALBUMINS
    FERRITIN
    GLOBULINS
    HISTONES
    NUCLEOPROTEINS
    PEPTIDES
PROTEINS/BIOSYNTHESIS
  Proteins induced in Bacillus subtilis infected with bacteriophage phi29 (Ultraviolet radiation), 30:29679
PROTEINS/METABOLISM
  Asynchronous turnover of the thin filament proteins, actin, tropomyosin, and troponin by a continuous double isotope method (^{14}C and tritium tracer techniques), 30:29865
PROTO-CLEO STELLARATORS/CONFINEMENT
  Summary of containment experiments on the PROTO--CLEO stellarator, 30:29151 (CLM-R-135)
PROTON BEAMS/RADIOTHERAPY
  Radiobiology with heavy charged particles directed at radiotherapy, 30:31117
PROTON DETECTION/DIELECTRIC TRACK DETECTORS
  Energy spectrometry of protons by means of a dielectric track detector, 30:29569
PROTON DETECTION/PLASTIC SCINTILLATION DETECTORS
  A high-resolution scintillation counter with particle identification for use with pions, 30:29597
PROTON DOSIMETRY/DEPTH DOSE DISTRIBUTIONS
  Radiobiology with heavy charged particles directed at radiotherapy, 30:31117
PROTON DOSIMETRY/DOSE EQUIVALENTS
  Dose fields in convergent irradiation by a narrow beam of protons, 30:31110
PROTON DOSIMETRY/ISODOSE CURVES
  Dose fields in convergent irradiation by a narrow beam of protons, 30:31110
PROTON REACTIONS
  Cross sections of proton--nucleus interactions at high energies (Tables), 30:30854 (AD-777030)
PROTON REACTIONS/BREAKUP REACTIONS
  D(p,2p)n reaction (6 to 11.6 MeV: cross sections, spectra, separable-potential model with Yamaguchi form factors), 30:30855 (NP-20122)
  The deuteron breakup reaction induced by protons of 65, 85 and 100 MeV (Spectra, angular distributions), 30:30872
PROTON REACTIONS/CAPTURE
  A microscopic description of the negative parity resonances in the mass-4 system by the coupled-channel method, 30:30871
  Population of muonic ^{3}He states following the μ-catalysed fusion pμd$\to\mu^{3}$He, 30:30515
PROTON REACTIONS/CHARGE-EXCHANGE REACTIONS
  Gamma angular distributions from ^{107}Ag(rho,n) reaction, 30:30953 (NP-20122)
  Gamma spectra from ^{179}Hf (d,2n), ^{179}Hf (p,n), and ^{181}Ta (α,2n) reactions, 30:30994
  Magnetic rotation of levels of ^{52}Mn and ^{54}Mn following the ^{52} ^{54}Cr(p,n) and ^{51}V(α,n) reactions (2.5- and 3.0-MeV protons, 7.5-MeV alphas; branching ratios, g, lifetimes), 30:30933
  Study of the (p,np) reaction on the isotopes of tin (All stable Sn isotopes, 23.0 and 38.5 MeV), 30:30973
PROTON REACTIONS/COMPOUND-NUCLEUS REACTIONS
  Level densities of ^{62}Cu and ^{64}Cu from the analysis of evaporation spectra (12.5- to 16.0-MeV protons, 16.8- to 21.3-MeV α), 30:30950
PROTON REACTIONS/ELASTIC SCATTERING
  A microscopic description of the negative parity resonances in the mass-4 system by the coupled-channel method, 30:30871
  A three parameter nucleon-nucleus optical model on the energy shell, 30:31104
  Annual report, 1973, 30:30952 (NP-20122)
  Deuteron break-up and proton scattering on ^{58}Ni, 30:30926
  High energy proton scattering by medium and heavy nuclei (1 GeV: differential cross sections, DWIA with Coulomb effects), 30:31087
  On proton-deuteron backward elastic scattering at medium energies (Cross sections), 30:30867
  Self-consistent wave functions, center-of-mass motion and high-energy particle-nucleus scattering, 30:31098
  Variational calculations of reactions involving light nuclei, 30:30861
  ^{70}Zn (p,p) at 3.6 to 6.4 MeV: angular distributions and excitation functions for cross sections and analyzing power, 30:30949

PROTON REACTIONS/EXCITATION FUNCTIONS
Q-values and excitation functions of nuclear reactions. Part C. Estimation of unknown excitation functions and thick target yields for p, d, ^{3}He, and α reactions (Up to 25 or 35 MeV), 30:30960
PROTON REACTIONS/INELASTIC SCATTERING
Blocking with realistic decay functions (Compound-nuclear reaction times), 30:30969
Core polarization in inelastic proton scattering from ^{209}Bi at 61 MeV, 30:31003
High energy proton scattering by medium and heavy nuclei (1 GeV: differential cross sections, DWIA with Coulomb effects), 30:31007
Level densities of ^{63}Cu and ^{65}Cu from the analysis of evaporation spectra (12.5- to 16.0-MeV protons, 16.8- to 21.3-MeV α), 30:30950
Spin-dependent effects in inelastic scattering (^{54}Fe, ^{56}Fe(p,p'), 10 to 49.35 MeV, 19.6 MeV: differential cross sections), 30:30932
PROTON REACTIONS/KNOCK-OUT REACTIONS
The ^{6}Li(p,2p)^{5}He reaction at 100 MeV (Angular correlations and distributions, energy and momentum distributions), 30:30896
PROTON REACTIONS/MULTIPLE PRODUCTION
Multiplicity in proton-nucleus interactions at 200 GeV/c, 30:30604
PROTON REACTIONS/ONE-NUCLEON TRANSFER REACTIONS
One-nucleon transfer reactions in deformed nuclei (Indirect inelastic transitions through intermediate rotational states included), 30:30995
PROTON REACTIONS/PICKUP REACTIONS
Comment on anomalous (p,t) angular distributions due to form factor cancellation, 30:30929
PROTON REACTIONS/QUASI-ELASTIC SCATTERING
The deuteron breakup reaction induced by protons of 65, 85 and 100 MeV (Spectra, angular distributions), 30:30872
PROTON REACTIONS/TOTAL CROSS SECTIONS
Energy dependence of sigma sub(p-air) up to 20TeV, 30:30611
PROTON REACTIONS/TWO-NUCLEON TRANSFER REACTIONS
One- and two-nucleon transfer reactions on deformed nuclei (Generalized optical model; DWBA, coupled-channels and adiabatic theory), 30:31021 (IFA-FT-108-1974)
PROTON SPECTROMETERS
Experimental equipment for spectrometry of electrons and protons between 0.4 and 30keV aboard the AUREOLE satellite, 30:29567
PROTON SPECTROMETERS/SHOWER COUNTERS
A calorimeter for 300GeV neutrons and protons (Layered iron plates and plastic scintillators), 30:29596
PROTON-ANTIPROTON INTERACTIONS/ANNIHILATION
Phase space and multihadron production in annihilation processes at present energies, 30:30669
PROTON-ANTIPROTON INTERACTIONS/DIFFRACTION MODELS
Diffractive processes in anti pp interactions at 5.1 GeV/c, 30:30600
PROTON-ANTIPROTON INTERACTIONS/FIREBALL MODEL
Properties of the nucleon--antinucleon fireball (Statistical bootstrap), 30:30721
PROTON-ANTIPROTON INTERACTIONS/MULTIPLE PRODUCTION
Influence of the kinematical constraints on the transverse momentum correlation features, 30:30602
PROTON-ANTIPROTON INTERACTIONS/MULTIPLICITY
Charged particle multiplicity distributions for 32 GeV/c K^{+-}p and anti pp interactions and for 50 GeV/c π^{+-}p interactions (Topological cross sections), 30:30608
PROTON-ANTIPROTON INTERACTIONS/PAIR PRODUCTION
μ-pair production by inelastic πp and anti pp collisions, 30:30738
PROTON-NEUTRON INTERACTIONS/P INVARIANCE
Parity-nonconserving effects in the reaction $n + p \to d + \gamma$, 30:30752
PROTON-PROTON INTERACTIONS/CORRELATIONS
Two body correlations between negative pions in pp interactions at 69 GeV/c, 30:30601
PROTON-PROTON INTERACTIONS/CROSS SECTIONS
Energy dependence of sigma sub(p-air) up to 20TeV, 30:30611
Finite energy bounds for πN scattering (Related problems in pp and Kp scattering), 30:30748
PROTON-PROTON INTERACTIONS/DIFFRACTION MODELS
Experimental results on strong interactions in the NAL hydrogen bubble chamber, 30:30609
Rapidity-gap separation and study of single-diffraction dissociation in pp collisions at 12 and 24 GeV/c, 30:30612
The pomeron-particle total cross section and diffractive production of showers at very high energies, 30:30760
PROTON-PROTON INTERACTIONS/ELASTIC SCATTERING
A recurrence relation for the polarization in elastic p--p scattering in the framework of a parton model, 30:30765
Wide angle scattering in softened field theory (Born diagrams, structure functions, Bethe-Salpeter wave functions), 30:31163
PROTON-PROTON INTERACTIONS/INCLUSIVE INTERACTIONS
Bose distribution and the Lorentz contracted geometric model, 30:30751 (IC-73-6)
Multiplicity distributions in the reaction $p + p \to p +$ anything (Cross sections, structure function), 30:30759
Negative pion production in proton-proton interactions at 69 GeV/c (Cross sections, structure function), 30:30603
Semi-inclusive rapidity distributions in a cluster emission model for the pionization component, 30:30756
The pomeron-particle total cross section and diffractive production of showers at very high energies, 30:30760
PROTON-PROTON INTERACTIONS/LINEAR MOMENTUM TRANSFER
Large momentum transfer reactions, without partons (Hadronic bremsstrahlung model), 30:30764
PROTON-PROTON INTERACTIONS/MULTIPLE PRODUCTION
Analysis of data on multiparticle production in pp-interactions from 13 up to 300 GeV, 30:30598 (IFVE-SPK-73-69)
Bound on the average multiplicity of pions in p--p collision at superhigh energy, 30:30757
PROTON-PROTON INTERACTIONS/MULTIPLICITY
Measurement of charged particle multiplicities associated with large transverse momentum photons in proton-proton collisions, 30:30605
PROTON-PROTON INTERACTIONS/NEUTRAL CURRENTS
Possible effects of weakly coupled neutral currents in $pp \to l^{+}l^{-} + X$, 30:30762
PROTON-PROTON INTERACTIONS/P INVARIANCE
Measurement of parity violation in proton--proton scattering at 15 MeV (Helicity, total cross sections, errors), 30:30599 (LA-UR-74-1333)
PROTON-PROTON INTERACTIONS/PHASE SHIFT
Possible existence of a diproton resonance. A proposal of p--p scattering experiment at about 500 MeV (Kantor amplitude, differential cross sections, polarization), 30:30607
PROTON-PROTON INTERACTIONS/PIONIZATION
Long range correlations in the pionization component (Multiperipheral cluster model), 30:30754
PROTON-PROTON INTERACTIONS/SCALE INVARIANCE
Scaling of multiplicity distribution in hadron collisions and diffractive-excitation like models, 30:30758
PROTONS/ELECTROMAGNETIC FORM FACTORS
Wide angle scattering in softened field theory (Born diagrams, structure functions, Bethe-Salpeter wave functions), 30:31163
PROTONS/GRAVITATION
F-gravity and the proton--electron mass ratio, 30:31174
PROTONS/MASS
F-gravity and the proton--electron mass ratio, 30:31174
PROTONS/PRIMARY COSMIC RADIATION
Production spectrum of charged cosmic ray pions and the primary cosmic ray nucleon spectrum, 30:30177
PROTONS/RBE
Comment on ''further data on DNA strand breakage by various radiation qualities'' (γ radiation. protons), 30:29660
PROTONS/STRUCTURE FUNCTIONS
Detailed predictions for the p-n structure functions in theories with computable large momenta behaviour, 30:30739
Muon-deuteron deep inelastic scattering, 30:30584
PROTOPLANETS/COLLISIONS
Direct simulation of collision processes. II. The growth of planetesimals, 30:30409
PROTOPLANETS/MASS
Direct simulation of collision processes. II. The growth of planetesimals, 30:30409
PROTOZOA
See also TETRAHYMENA
PROTOZOA/DISTRIBUTION
Recent changes of the foraminiferal assemblages of Jobos Bay and surroundings, Puerto Rico, 30:31376 (CONF-740663-1)
PSEUDOSCALAR MESONS
(Mesons with spin-parity of zero-minus.)
See also ETA MESONS
KAONS
PIONS
PSEUDOSCALAR MESONS/CABIBBO ANGLE
Disturbed non-linear chiral SU(3) x SU(3) dynamics and Cabibbo's angle, 30:30776
PTFE
See TEFLON
PULPS
See SLURRIES
PULSARS/ELECTRONS
Acceleration and radiation of cosmic ray electrons from pulsars, 30:30274
PULSARS/PULSES
On the passage of radiation through inhomogeneous, moving media. VI. Dispersion effects on phase and ray paths in a plane, differentially shearing medium (Basic physical effects, pulse width), 30:30248
PULSARS/STELLAR ATMOSPHERES
On the passage of radiation through inhomogeneous moving media. V. Line absorption and frequency variations of optical depth (Perpendicular incidence), 30:30247
On the passage of radiation through inhomogeneous, moving media. VI. Dispersion effects on phase and ray paths in a plane, differentially shearing medium (Basic physical effects, pulse width), 30:30248

On the passage of radiation through inhomogeneous, moving media. VII. Concerning the validity of the geometrical optics approximation (Basic physical picture, coupled second-order differential equations), 30:30249
PULSE DISCRIMINATORS/ELECTRONIC CIRCUITS
A fast neutron-gamma discriminator, 30:29535
PULSE DISCRIMINATORS/PULSE RISE TIME
Rise-time jitter reduction in timing and amplitude-discrimination circuits, 30:29631
PULSE GENERATORS
Summing of harmonic frequencies by a resonant cable for pulse generation on a capacitive beam deflector, 30:30147
PULSE GENERATORS/CALIBRATION STANDARDS
Reference pulsers for calibration purposes, 30:29628
PULSE INTEGRATORS/OPERATION
Single pulse area measurement system (SPAMS), 30:29496 (UCID-15761)
PULSED NEUTRON TECHNIQUES
Neutron slowing-down in ice and polyethylene at low temperatures, 30:30843 (IAE-2271)
PULSES/MEASURING METHODS
Measurement system for the peak time and amplitude of a pulse, 30:31458 (UCID-16108)
PUMPS/SEALS
Freezing-up shaft seal of machines for the transport of liquids and gases in nuclear power (Patent), 30:29276
PWBA
See BORN APPROXIMATION
PWR TYPE REACTORS
See also CALHOUN-1 REACTOR
LOFT REACTOR
LUCIE-1 REACTOR
LUCIE-2 REACTOR
MAINE YANKEE REACTOR
MIHAMA-1 REACTOR
MIHAMA-2 REACTOR
OCONEE-1 REACTOR
OCONEE-2 REACTOR
OTTO HAHN REACTOR
POINT BEACH-1 REACTOR
POINT BEACH-2 REACTOR
TURKEY POINT-3 REACTOR
TURKEY POINT-4 REACTOR
PWR TYPE REACTORS/AVAILABILITY
Nuclear power availability, 30:31189
PWR TYPE REACTORS/ECCS
Problems of emergency core cooling system, 30:31191
PWR TYPE REACTORS/EXCURSIONS
Comparison of two- and three-dimensional calculations of super prompt critical excursions, 30:31190
PWR TYPE REACTORS/FLUID POISON CONTROL
System for concentrating a moderating solution utilized in a pressurized water nuclear power plant (Patent), 30:31199
PWR TYPE REACTORS/FUEL ASSEMBLIES
Mark C (17 x 17) fuel assembly. Research and development, 30:31195 (BAW-10097)
Transient critical heat flux and spacer grid studies, 30:31201
PWR TYPE REACTORS/FUEL ELEMENTS
Neutronic calculations for experiments with light water reactor fuel in PBF, 30:31187 (BNWL-B-371)
PWR TYPE REACTORS/FUEL MANAGEMENT
Equilibrium approach to optimal in-core fuel management for pressurized water reactors, 30:31310
PWR TYPE REACTORS/IN CORE INSTRUMENTS
Apparatus for in-core instrumentation of pressurized water reactors (Patent), 30:31196
PWR TYPE REACTORS/MAXIMUM CREDIBLE ACCIDENT
Maximum credible accident (MCA) of light water reactor, 30:31260
PWR TYPE REACTORS/PERFORMANCE
Nuclear power availability, 30:31189
PWR TYPE REACTORS/PRESSURE VESSELS
Head closure system (Patent), 30:31197
Head closure mechanism (Patent), 30:31198
Quarterly progress report on reactor safety programs sponsored by the Division of Reactor Safety Research for April--June 1974, 30:31251 (ORNL-TM-4655(Vol.2))
Reactor vessel in-service inspection assembly (Patent), 30:31200
Trends in structural mechanics. A UK review of the 2nd international conference on structural mechanics in reactor technology. I. Pressure vessels and containments, 30:31192
PWR TYPE REACTORS/PRIMARY COOLANT CIRCUITS
Theory of pump-induced pulsating coolant pressure in pressurized water reactors, 30:31203
PWR TYPE REACTORS/QUALITY ASSURANCE
B and W quality assurance program for nuclear equipment, 30:31194 (BAW-10096)
PWR TYPE REACTORS/REACTOR CONTROL SYSTEMS
Block control of a PWR type reactor, 30:31302
PWR TYPE REACTORS/REACTOR SAFETY
Quarterly progress report on reactor safety programs sponsored by the Division of Reactor Safety Research for April--June 1974. I. Light-water-reactor safety, 30:31250 (ORNL-TM-4655(Vol.1))
Quarterly progress report on reactor safety programs sponsored by the Division of Reactor Safety Research for April--June 1974, 30:31251 (ORNL-TM-4655(Vol.2))
PYREX/CRACKS
Acoustic emission monitoring of ring-cracking in glass and alumina, 30:31410 (UCID-16076)
PYROLYTIC GRAPHITE/PHYSICAL RADIATION EFFECTS
Investigation into radiation defects in irradiated pyrographite (Neutrons; 100 to 850°C), 30:30090 (IAE-2266)

Q

QUALITY ASSURANCE
B and W quality assurance program for nuclear equipment (PWR), 30:31194 (BAW-10096)
QUANTUM ELECTRODYNAMICS
Construction of nonlocal quantum electrodynamics of bosons with spin 0 and 1 (Unitarity, macrocausality, relativity, gauge, invariance, finiteness), 30:31144 (JINR-P2-7432)
QUANTUM ELECTRODYNAMICS/INFRARED DIVERGENCES
Infra-red-finite calculations in quantum electrodynamics (S matrix elements, green function, Feynman rules), 30:31149
QUANTUM ELECTRODYNAMICS/QUANTUM OPERATORS
Vacuum polarization tensor and current operator in quantum electrodynamics with compensating current, 30:31156
QUANTUM ELECTRODYNAMICS/VACUUM POLARIZATION
Stieltjes type continued fractions in quantum electrodynamics, 30:31166
Vacuum polarization tensor and current operator in quantum electrodynamics with compensating current, 30:31156
QUANTUM FIELD THEORY
See also LSZ THEORY
QUANTUM ELECTRODYNAMICS
YUKAWA NONLOCAL THEORY
Field theories without Ward-identities (Lagrangian formalism, Poincare group), 30:31145 (KFKI-74-46)
Mathematics of contemporary physics. Proceedings of a conference held at London, England, August 23--September 11, 1971, 30:31154
QUANTUM FIELD THEORY/BOUND STATE
Field quantization on the surface x^2=constant, 30:31159
QUANTUM FIELD THEORY/CAUSALITY
Causality in indefinite metric theories (Shadow states), 30:31164
QUANTUM FIELD THEORY/CONFORMAL GROUPS
D_2-type representation of the conformal group extended by reflections, 30:30628 (KFKI-74-49)
QUANTUM FIELD THEORY/GAUGE INVARIANCE
Anomalous currents in gauge field theories, 30:31161
QUANTUM FIELD THEORY/MASS RENORMALIZATION
The Callan-Symanzik equation and dimensional regularization, 30:31160
QUANTUM FIELD THEORY/PADE APPROXIMATION
Some applications of Pade approximants to quantum field theory models (Reviews, Hamiltonian, eigenvalues), 30:31165
QUANTUM FIELD THEORY/YANG-FELDMAN FORMALISM
Equivalence of Yang--Feldman and action principle quantization, 30:31148
QUANTUM MECHANICS/HEISENBERG PICTURE
Multiplication law in quantum physics. I. The non-relativistic quantum mechanics, 30:31158
QUANTUM MECHANICS/LECTURES
Quantum mechanics. Volume I (Book), 30:31134
Quantum mechanics. Volume II (Book), 30:31135
Quantum physics. Berkeley physics course. Volume 4 (Book), 30:31136
QUARK MODEL
The quark-parton paradox, 30:30715
QUARK MODEL/DUALITY
A dual quark prison, 30:30697
QUARK MODEL/ELECTRON-NUCLEON INTERACTIONS
Quark parton model for deep inelastic lepton scattering (Cross sections, lectures), 30:30686
QUARK MODEL/ELECTROPRODUCTION
Quark model predictions for electroproduction of $3/2^+$ isobars, 30:30662
QUARK MODEL/HADRONS
Quark or bootstrap: triumph or frustration for hadron physics (S matrix), 30:30702
QUARK MODEL/MASS DIFFERENCE
Electromagnetic mass differences in a relativistic quark model, 30:30658
QUARK MODEL/N*RESONANCES
SU_6 quark model, nucleon resonance electroproduction and spin-dependent electroproduction structure functions, 30:30735
QUARK MODEL/NEUTRINO-NUCLEON INTERACTIONS
Quark parton model for deep inelastic lepton scattering (Cross sections, lectures), 30:30686
QUARKS
Kinematical origin of the configuration mixing in the chiral algebra, 30:30719
QUARKS/RADIATION DETECTION
Cloud chamber quark quest one year report (Research summaries), 30:30576 (UCID-15787)

QUARKS/STRING MODELS
  Dual strings in the Amata-Testa quark imprisonment scheme, 30:30647
QUARTZ/DIELECTRIC PROPERTIES
  Dielectric strength of x-cut quartz after thermally induced stress cycling: application to understanding the Sandia Quartz gauge, 30:31396 (SAND-74-0135)
QUASARS/ABSORPTION SPECTRA
  Origin of QSO absorption lines, 30:30289
QUASARS/COORDINATES
  Identification of southern quasi-stellar objects. IV, 30:30276
  Optical identifications from the NRAO 5-GHz radio survey (Quasar-like objects), 30:30282
  Optical identifications and radio spectra of sources found by the Michigan 8-GHz survey (Radio analogue), 30:30283
QUASARS/DOPPLER EFFECT
  On the time evolution of quasar luminosity and redshift distribution, 30:30293
  The interpretation of broad emission lines in high-redshift QSOS (Charge-state distributons), 30:30266
QUASARS/EMISSION SPECTRA
  The interpretation of broad emission lines in high-redshift QSOS (Charge-state distributons), 30:30266
QUASARS/LUMINOSITY
  On the time evolution of quasar luminosity and redshift distribution, 30:30293
QUASARS/POLARIZATION
  Note on linear polarization in the emission frame for radio galaxies and quasars (Wavelength range), 30:30278
  Search for circular polarization in compact radio sources at a wavelength of 2.2 cm (Simultaneous measurements), 30:30284
QUASARS/SPATIAL DISTRIBUTION
  NGC 520 chain of quasars (Peculiar galaxies), 30:30285
QUASARS/SPECTRA
  Identification of some faint radio sources that have flat spectra, 30:30277
QUININE/INTESTINAL ABSORPTION
  Effect of irradiation on gastrointestinal drug absorption in mice and rats (Sulfadiazine;quinime;x radiation), 30:29738
QUINOLINES/TOXICITY
  Study on mechanisms of nervous system disturbance by radioactively labeled chinoform, 30:29879

R

RABBITS/RADIONUCLIDE KINETICS
  Elimination of intravenously injected ^{125}I-toluidine blue in rabbits (Effectiveness for parathyroid scanning), 30:29812
  Influence of irradiation on the incorporation of radionuclides (^{239}Pu; ^{226}Ra; ^{210}Pb; ^{144}Ce; tritium), 30:29818
RADAR
  Instrumenting the LAPQ-1 airborne cloud-mapping radar for shipboard use in Operation Dial Train, 30:31456 (UCID-16051)
  Range-scan radar images and their application to map-matching estimation of location, 30:31429 (SAND-74-0153)
RADAR/ANTENNAS
  Automatic radar-sensitivity measurement. Final report, 30:31417 (BDX-613-1134(Rev.))
RADIATION ACCIDENTS
  Annual report of the Brookhaven DCPA Contract Group (Use of civil defense instrument and manpower resources in response to peacetime radiation accidents), 30:31332 (BNL-19097(Rev.))
RADIATION BELTS/ELECTRON DENSITY
  Behavior of outer radiation belt electrons (> 1.5 MeV) during a geomagnetically disturbed time on 8 March 1970 and its relationship to magnetospheric processes, 30:30471
RADIATION BELTS/PARAMETRIC INSTABILITIES
  Particle saturation of the outer zone: a nonlinear model, 30:30472
RADIATION BURDEN
    See RADIATION DOSES
RADIATION CHEMISTRY
  Conversion of complex compounds under the action of light, radiation, and temperature (Book in Russian), 30:29060
RADIATION CHEMISTRY/RESEARCH PROGRAMS
  Hahn-Meitner-Institut fuer Kernforschung annual report 1973, 30:31334
RADIATION DAMAGE (BIOLOGICAL)
    See RADIATION INJURIES
RADIATION DETECTORS
    See also BEAM MONITORS
      CHERENKOV COUNTERS
      DIELECTRIC TRACK DETECTORS
      GAMMA CAMERAS
      GEIGER-MUELLER COUNTERS
      HODOSCOPES
      IONIZATION CHAMBERS
      LOW LEVEL COUNTERS
      NUCLEAR EMULSIONS
      PROPORTIONAL COUNTERS
      RADIOISOTOPE SCANNERS
      SCINTILLATION COUNTERS
      SEMICONDUCTOR DETECTORS
      SHOWER COUNTERS
      SPECTROMETERS
      TELESCOPE COUNTERS
      TISSUE-EQUIVALENT DETECTORS
      TRANSITION RADIATION DETECTORS
  Solid state radiation sensitive field electron emitter and methods of fabrication thereof (Patent), 30:29504
RADIATION DETECTORS/DEAD TIME
  Dead-time calibrator, 30:29529
RADIATION DETECTORS/PULSE INTEGRATORS
  Single pulse area measurement system (SPAMS), 30:29496 (UCID-16761)
RADIATION DETECTORS/RESPONSE FUNCTIONS
  The performance of single charged-particle detectors under isotropic irradiation, 30:29536
RADIATION DOSES/MATHEMATICAL MODELS
  Comparison of mathematical models for calculation of external gamma doses originating from releases of radioactivity to the atmosphere, 30:29342 (RISO-M-1726)
RADIATION EXPOSURE (DOSES)
    See RADIATION DOSES
RADIATION HYGIENE
    See RADIATION PROTECTION
RADIATION INJURIES/BIOLOGICAL RECOVERY
  Kinetics of recovery in irradiated colonic mucosa of the mouse (Gamma radiation, response of incidentially irradiated intestine), 30:29742
  X-radiation-induced intestinal lesions in protein-deficient rats, 30:29741
RADIATION INJURIES/DIAGNOSIS
  Special laboratory-chemical examination techniques (Diagnosis of radiation injuries), 30:29702 (AED-CONF-74-221-006)
RADIATION MONITORING
    See also PERSONNEL MONITORING
  Annual report of the Brookhaven DCPA Contract Group (Use of civil defense instrument and manpower resources in response to peacetime radiation accidents), 30:31332 (BNL-19097(Rev.))
RADIATION PROTECTION/LEGAL ASPECTS
  Code of practice against radiation hazards, 30:29711
  Radiation characteristics and controls. I (Radiation protection of dental patients and personnel), 30:29709
RADIATION SAFETY
    See RADIATION PROTECTION
RADIATION SOURCES
    (For cosmic sources of radiation see also COSMIC GAMMA SOURCES, COSMIC RADIO SOURCES, and COSMIC X-RAY SOURCES.)
    See also ALPHA SOURCES
      BETA SOURCES
      GAMMA SOURCES
      X-RAY SOURCES
RADIATION SOURCES/REMOTE HANDLING
  Optical coherent radiation (Book), 30:30112
RADIATION SYNDROME/THERAPY
  Effect of a combination of antibiotics and AET on the survival of irradiated animals (Tetron-pyrrolidinomettryl-oxytetracycline), 30:29746
RADICALS
    See also HYDROXYL RADICALS
RADICALS/CHEMICAL REACTIONS
  Reactions of the radiolytically generated hydroxycyclohexadienyl radical in aqueous benzene systems (γ Radiation), 30:29043
RADICALS/ELECTRON SPIN RESONANCE
  Applying statistics to analysis of corrosion data, 30:29056
  Electron spin resonance study on free radicals in the chemical carcinogen, 1,2-dimethylhydrazine induced by x-ray irradiation, 30:29050
  ESR spectra of PF_2 and SF_2 radicals, 30:29067
  Long-lived radiation-induced free radicals in anoxic wet DNA as studied by electron spin resonance spectroscopy, 30:29064
  Radiation-induced radicals in thymine and its derivatives in low temperature glasses, 30:29055
  Unstable intermediates. CXXXVII. α-bromoalkyl radicals in irradiated organic bromides: an electron spin resonance study, 30:29073
  Unstable intermediates. CXLVI. Electron spin resonance spectra for linear $BrCN^-$ and Br_2CN radicals in irradiated cyanogen bromide crystals, 30:29076
RADICALS/ELECTRON-ION COLLISIONS
  Experimental investigation of the effective cross section of excitations of bands of some decay products of water, ammonia, and acetonitrile by slow electrons, 30:30546
RADIO GALAXIES/COORDINATES
  Optical identifications and radio spectra of sources found by the Michigan 8-GHz survey (Radio analogue), 30:30283
RADIO GALAXIES/POLARIZATION
  Note on linear polarization in the emission frame for radio galaxies and quasars (Wavelength range), 30:30278
RADIO GALAXIES/SPECTRA
  Turnover radio spectra of elliptical galaxies (Peak power, frequency at the peak), 30:30345

RADIOACTIVE AEROSOLS
  Formation of secondary aerosols in the atmosphere after ventilated underground nuclear explosions, 30:29390
  Radioactive particle formation after nuclear explosions in the troposphere, 30:29387
RADIOACTIVE AEROSOLS/AERODYNAMICS
  Resuspension element status report (Pu, Nevada Test Site), 30:29450 (NVO-AEIC-74-1)
RADIOACTIVE AEROSOLS/AEROSOL MONITORING
  Method of measuring the mobility, concentration, and isotope composition of radioactive ions, 30:29273
RADIOACTIVE AEROSOLS/CHEMICAL COMPOSITION
  Calculation of fractionation effects following atmospheric nuclear explosions, 30:29386
RADIOACTIVE AEROSOLS/DIFFUSION
  Ground level air concentrations of dust particles downwind from a tailings area during a typical windstorm (Mathematical model), 30:29380 (ORNL-TM-4375)
  Resuspension of ^{239}Pu, ^{240}Pu, and ^{241}Am particles at Nevada Test Site; prediction of air concentrations of Pu due to resuspension at Eniwetok Atoll, 30:29452 (NVO-AEIC-74-1)
RADIOACTIVE AEROSOLS/PARTICLE SIZE
  Particle size distributions of manmade and natural radionuclides, 30:29360 (BNWL-1850(Pt.3))
  Size-distribution relation of high-activity particles in the troposphere in September--December 1967, 30:29392
RADIOACTIVE AEROSOLS/PRECIPITATION SCAVENGING
  Relation between washout of radioactivity and nonradioactive ions in the atmosphere by precipitation, 30:29395
RADIOACTIVE AEROSOLS/RADIATION HAZARDS
  Hot aerosol particles during commercial use of atomic energy (Book in Russian), 30:29344
RADIOACTIVE AEROSOLS/SAMPLING
  Interstage particle losses in a high-volume cascade impactor, 30:29374 (BNWL-1850(Pt.3))
RADIOACTIVE AEROSOLS/WASHOUT
  Relation between washout of radioactivity and nonradioactive ions in the atmosphere by precipitation, 30:29395
  Theories of radioactivity takeup by rain drops, 30:29398
  Use of naturally radioactive substances in studying turbulent exchange and self-scavenging of the atmosphere with surface layer measurements, 30:29396
  Washout of radioactive impurities from the atmosphere in the Central Caucasus mountains, 30:29385
  Washout of hygroscopic and nonhygroscopic aerosols with cloud droplets (^{32}P and ^{89}Sr tracer studies), 30:29393
RADIOACTIVE BIOLOGICAL WASTES
    See RADIOACTIVE WASTES
RADIOACTIVE CLOUDS/RADIATION HAZARDS
  Comparison of mathematical models for calculation of external gamma doses originating from releases of radioactivity to the atmosphere, 30:29342 (RISO-M-1726)
RADIOACTIVE MATERIALS
  Small quantities (Radioactive materials concentrations), 30:29648
RADIOACTIVE WASTE DISPOSAL
    See also STACK DISPOSAL
RADIOACTIVE WASTE DISPOSAL/BIOLOGICAL EFFECTS
  Agricultural impacts of nuclear power generation in New York State (Preliminary survey agricultural data), 30:29438 (COO-3167-102)
RADIOACTIVE WASTE DISPOSAL/GASEOUS WASTES
  Calculations of doses, population doses, and potential health effects due to atmospheric releases of radionuclides from U.S. nuclear power reactors in 1972, 30:29383
  Dry disposition processes on vegetation canopies (Development of mathematical model), 30:29369 (BNWL-1850(Pt.3))
RADIOACTIVE WASTE DISPOSAL/LIQUID WASTES
  Studies on the sorption and fixation of cesium by vermiculite. II, 30:29134
RADIOACTIVE WASTE DISPOSAL/MARINE DISPOSAL
  Advanced waste management studies progress report, April--June 1974, 30:30106 (BNWL-B-223-11)
  Nuclear waste disposal in the oceans (Long-term safety aspects), 30:30110
RADIOACTIVE WASTE DISPOSAL/POLAR REGIONS
  Advanced waste management studies progress report, April--June 1974, 30:30106 (BNWL-B-223-11)
RADIOACTIVE WASTE DISPOSAL/RADIATION HAZARDS
  Atomic energy. V (Norwegin Nature Conservancy Association), 30:29343
  Ecological factors in the siting, design, and operation of a nuclear power station, 30:29354
RADIOACTIVE WASTE DISPOSAL/RADIATION MONITORING
  Health physics and technical considerations concerning the control of gaseous effluents from nuclear power plants, 30:29356 (AED-CONF-74-157-005)
RADIOACTIVE WASTE DISPOSAL/REVIEWS
  The treatment and disposal of radioactive wastes (Review with selected bibliography), 30:29136
RADIOACTIVE WASTE DISPOSAL/SPACE
  Advanced waste management studies progress report, April--June 1974, 30:30106 (BNWL-B-223-11)
RADIOACTIVE WASTE DISPOSAL/STACK DISPOSAL
  Hot aerosol particles during commercial use of atomic energy (Book in Russian), 30:29344
RADIOACTIVE WASTE DISPOSAL/TRANSMUTATION
  Advanced waste management studies progress report, April--June 1974, 30:30106 (BNWL-B-223-11)
RADIOACTIVE WASTE DISPOSAL/UNDERGROUND DISPOSAL
  Advanced waste management studies progress report, April--June 1974, 30:30106 (BNWL-B-223-11)
RADIOACTIVE WASTE MANAGEMENT
    See also RADIOACTIVE WASTE STORAGE
RADIOACTIVE WASTE MANAGEMENT/FORECASTING
  The disposal system in the nuclear fuel cycle (German LFederal Republic), 30:29147
RADIOACTIVE WASTE MANAGEMENT/PLANNING
  Radioactive waste management for nuclear energy center, 30:30107 (BNWL-B-334)
RADIOACTIVE WASTE PROCESSING/REVIEWS
  The treatment and disposal of radioactive wastes (Review with selected bibliography), 30:29136
RADIOACTIVE WASTE PROCESSING/SOLIDIFICATION
  Current storage possibilities of blocks with solidified radioactive wastes at the Institute of Nuclear Research (Bitumens), 30:29137
RADIOACTIVE WASTE STORAGE/CASKS
  Radioactive waste storage (Patent), 30:30109
RADIOACTIVE WASTE STORAGE/SAFETY
  Study of diffusion/leaching phenomena with glasses. Application of risk evaluation to long-term storage, 30:29133 (CEA-R-4550)
RADIOACTIVE WASTES/CHEMICAL ANALYSIS
  Laboratory and hot-cell studies concerning the in-line polarographic determination of uranium in the aqueous waste stream of the KFA-TBP 23/25 process, 30:28941 (JUL-1063-CT)
RADIOACTIVE WASTES/LEACHING
  Study of diffusion/leaching phenomena with glasses. Application of risk evaluation to long-term storage, 30:29133 (CEA-R-4550)
RADIOACTIVE WASTES/RADIATION MONITORING
  Data. Section IV. Other data, 30:29412
  Experience in complying with authorisation conditions for the discharge of liquid and gaseous radioactive effluents from CEGB nuclear stations, 30:31204 (AED-CONF-74-157-007)
  Report of activity, February 1974 (Radioactivity of environmental samples collected throughout France during February 1974), 30:29349 (SCPRI(RM)-2-1974)
RADIOACTIVE WASTES/RADIOMETRIC ANALYSIS
  Gamma-ray assay of low-enriched uranium waste, 30:28986
RADIOACTIVE WASTES/STACK DISPOSAL
  Comparison of mathematical models for calculation of external gamma doses originating from releases of radioactivity to the atmosphere, 30:29342 (RISO-M-1726)
RADIOAPPLICATORS
    See RADIATION SOURCES
RADIOAUTOGRAPHY
    See AUTORADIOGRAPHY
RADIOBIOLOGICAL EFFECTS
    See BIOLOGICAL RADIATION EFFECTS
RADIOCARBON DATING
    See CARBON 14
        ISOTOPE DATING
RADIOCHEMISTRY/RESEARCH PROGRAMS
  Hahn-Meitner-Institut fuer Kernforschung annual report 1973, 30:31334
RADIODIAGNOSIS (RADIONUCLIDES)
    See NUCLEAR MEDICINE
RADIOECOLOGY
  Chemoradioecology of the pelagic zone and the benthos (metals and radionuclides in the hydrobiont and environment) (Book in Russian), 30:29422
RADIOGRAPHS
    See IMAGES
RADIOGRAPHY (AUTO)
    See AUTORADIOGRAPHY
RADIOGRAPHY (BIOMEDICAL)
    See BIOMEDICAL RADIOGRAPHY
RADIOGRAPHY (INDUSTRIAL)
    See INDUSTRIAL RADIOGRAPHY
RADIOINDUCED REACTIONS
    See RADIATION CHEMISTRY
RADIOISOTOPE GENERATORS
  Radionuclide generator production method (Patent), 30:29140
  Radionuclide generator production method (Patent), 30:29144
RADIOISOTOPE HEAT SOURCES
  Unconventional Stirling engines for the artificial heart application, 30:29260
RADIOISOTOPE HEAT SOURCES/COOLING
  Development of a reflux condensing heat pipe for emergency cooling of large cobalt-60 heat source, 30:29255
RADIOISOTOPE HEAT SOURCES/DESIGN
  Modular heat source for ^{244}Cm and ^{238}Pu, 30:29245
RADIOISOTOPE SCANNERS/DESIGN
  Nuclear imaging systems (Patent), 30:29505
  Radiation detection (Patent), 30:29503
RADIOISOTOPES
  Effects of radioactivity on ice nucleation, 30:29367 (BNWL-1850(Pt.3))

RADIOISOTOPES/ISOTOPE PRODUCTION
Radioisotopes from a medium-energy accelerator: the Clinton P. Anderson Meson Physics Facility radioisotope program, 30:30142 (LA-UR-74-1263)
RADIOISOTOPES/RADIOECOLOGICAL CONCENTRATION
Chemoradioecology of the pelagic zone and the benthos (metals and radionuclides in the hydrobiont and environment) (Book in Russian), 30:29422
RADIOMETRIC GAGES/DATA PROCESSING
Contribution of fluctuations in the parameters of the object to the process taking place at the output of a radiometric device, 30:29607
RADIOMETRIC GAGES/DESIGN
General approach to the design of radiation gauges, 30:29608
RADIOMETRIC GAGES/OPTIMIZATION
General approach to the design of radiation gauges, 30:29608
RADIONUCLIDE ADMINISTRATION
Liver studies with various radioactive tracers and methods (Critical evaluation of diagnostic value), 30:29831 (CONF-740708-52)
RADIONUCLIDES
See RADIOISOTOPES
RADIOPHARMACEUTICALS/GAMMA DOSIMETRY
Simplified method for calculating dose-rate distributions from extended volumes containing gamma emitters, 30:31107
RADIOPHARMACEUTICALS/RADIATION HAZARDS
Results of the medical examinations, 30:29829 (AED-CONF-74-221-004)
RADIOPROTECTIVE SUBSTANCES
See also AET
Studies on the radiation protection properties of fenchlorfos and its role in the radioprotection mechanism (Ronnel), 30:29723
RADIOPROTECTIVE SUBSTANCES/CHEMICAL REACTION KINETICS
Competitive radioprotection and radiosensitization in chemical systems (Steady state and pulse radiolysis studies on kinetics of action of various radiosensitizers and radioprotectors), 30:29003
RADIORESISTANCE
See RADIOSENSITIVITY
RADIOSENSITIVITY
Induced mutation in peas. XXVI. Genetically conditioned differences in radiation sensitivity. IV, 30:29694
RADIOSENSITIZERS/BIOCHEMICAL REACTION KINETICS
Metronidazole (Flagyl). A radiosensitizer of hypoxic cells, 30:29674
RADIOSENSITIZERS/CHEMICAL REACTION KINETICS
Competitive radioprotection and radiosensitization in chemical systems (Steady state and pulse radiolysis studies on kinetics of action of various radiosensitizers and radioprotectors), 30:29003
RADIOSENSITIZERS/OXYGEN ENHANCEMENT RATIO
Radiosensitization of hypoxic cells with metronidazole (Flagyl), 30:29699
RADIOSTERILIZATION
Sterilization method and product (Patent), 30:29647
RADIOSURGERY
See RADIOTHERAPY
RADIOTHERAPY
Experimental usage of cysteine in radiation therapy (Radioprotective effects), 30:29722
RADIOTHERAPY/BACKSCATTERING
Back-scattering from metals in superficial therapy with high energy electrons, 30:31108
RADIOTHERAPY/DELAYED RADIATION EFFECTS
Follow-up on the long-term effects of therapeutic irradiation on bone marrow, 30:29715
RADIOTHERAPY/ION BEAMS
Radiobiology with heavy charged particles directed at radiotherapy, 30:31117
RADIOTHERAPY/IRRADIATION PROCEDURES
Dose-limiting tissues in relation to types and location of tumors. Implications for efforts to improve radiation dose distributions (Proton beams), 30:29725
RADIOTHERAPY/NEUTRON SOURCES
Characteristics of ^{252}Cf neutron sources used for radiotherapy, 30:31124
RADIOTHERAPY/PION BEAMS
Negative pions in radiotherapy. A brief review, 30:31116
RADIOTHERAPY/RADIATION QUALITY
Introduction to the discussion on characteristics of installations for radiotherapy with fast neutrons and other types of high-LET radiation, 30:31112
RADIOTHERAPY/RESEARCH PROGRAMS
Cell cycle kinetics and radiation therapy, 30:29662 (UCRL-75441)
RADIOTHERAPY/SIDE EFFECTS
Changes in the cardiovascular system in radiation and medicinal treatment of lung cancer, 30:29729
Changes of the broncho-vascular system of the lung under the influence of local γ irradiation (Following micro- or macro-fractionated therapy), 30:29728
Chromosome aberrations in lymphocytes of peripheral blood after radiation therapy (γ ray; betatron), 30:29731
Condition of the nervous and vascular systems after radiation treatment of lymphogranulomatosis (Hodgkins disease), 30:29730
Influence of fractionation on acute and late reactions in vocal cord carcinoma, 30:29713
Plasma TSH and serum T-4 levels in longer-term follow-up of patients treated with ^{131}I for thyrotoxicosis, 30:29775
Prevention of thrombo-embolism during radiotherapy of carcinoma of the uterine cervix (Radium inserts), 30:29732
Results and complications of the treatment of Bechterew's disease with thorium X (^{224}Ra; arthritis of vertebral column), 30:29774
Systematics of iatrogenic carcinogenesis, 30:29724
Treatment of advanced tumours of head and neck with fast neutrons, 30:29733
RADIOTHORIUM
See THORIUM 228
RADIUM 224/ALPHA DECAY
Perturbed alpha-gamma angular correlation studies of radon recoils into aluminium, 30:31017
RADIUM 224/BIOLOGICAL RADIATION EFFECTS
Morphology and enzyme histochemistry of ^{224}Ra-induced osteosarcomas of the mouse, 30:29785
Results and complications of the treatment of Bechterew's disease with thorium X (^{224}Ra; arthritis of vertebral column), 30:29774
RADIUM 226/ALPHA DECAY
Perturbed alpha-gamma angular correlation studies of radon recoils into aluminium, 30:31017
RADIUM 226/BIOLOGICAL RADIATION EFFECTS
Research in radiobiology. Annual report of work in progress in the internal irradiation program (Pathological effects of bone-seeking radionuclides in beagles), 30:29778 (COO-119-249)
RADIUM 226/RADIATION MONITORING
Feed Materials Production Center environmental monitoring annual report for 1973, 30:29347 (NLCO-1109)
Radioactivity in Brazilian mineral waters, 30:29413
Report of activity, February 1974 (Radioactivity of environmental samples collected throughout France during February 1974), 30:29349 (SCPRI(RM)-2-1974)
RADIUM 226/RADIOCHEMICAL ANALYSIS
Sequential determination of radium-226, radium-228, actinium-227, and thorium isotopes in environmental and process waste samples, 30:28978
RADIUM 226/RADIOMETRIC ANALYSIS
Simultaneous determination of alpha-emitting nuclides of radium through californium in soil, 30:28977
RADIUM 226/TISSUE DISTRIBUTION
Influence of irradiation on the incorporation of radionuclides (^{239}Pu; ^{226}Ra; ^{210}Pb; ^{144}Ce; tritium), 30:29818
RADIUM 228/BIOLOGICAL RADIATION EFFECTS
Research in radiobiology. Annual report of work in progress in the internal irradiation program (Pathological effects of bone-seeking radionuclides in beagles), 30:29778 (COO-119-249)
RADIUM 228/RADIATION MONITORING
Feed Materials Production Center environmental monitoring annual report for 1973, 30:29347 (NLCO-1109)
Radioactivity in Brazilian mineral waters, 30:29413
RADIUM 228/RADIOCHEMICAL ANALYSIS
Sequential determination of radium-226, radium-228, actinium-227, and thorium isotopes in environmental and process waste samples, 30:28978
RADON/RADIATION MONITORING
Vertical distribution of radioactive aerosols in the troposphere above the European part of the USSR in 1964-1967, 30:29389
RADON/SEPARATION PROCESSES
Atmosphere purification of xenon, radon, and radon daughter elements (Patent, fluorination and adsorption), 30:28995
RADON 220/ALPHA SPECTRA
Separation of radionuclides using alkyl radicals, 30:29083 (AED-CONF-74-084-002)
RADON 220/HYPERFINE STRUCTURE
Perturbed alpha-gamma angular correlation studies of radon recoils into aluminium, 30:31017
RADON 220/RADIATION MONITORING
Use of naturally radioactive substances in studying turbulent exchange and self-scavenging of the atmosphere with surface layer measurements, 30:29396
RADON 220/SEPARATION PROCESSES
Separation of radionuclides using alkyl radicals, 30:29083 (AED-CONF-74-084-002)
RADON 222/HYPERFINE STRUCTURE
Perturbed alpha-gamma angular correlation studies of radon recoils into aluminium, 30:31017
RADON FLUORIDES/CHEMICAL PREPARATION
Compounds of rare gases, 30:29089
RAIN/RADIATION MONITORING
Washout of radioactive impurities from the atmosphere in the Central Caucasus mountains, 30:29385
RAIN/RADIOACTIVITY
Specific radioactivity distribution in rain drops, 30:29394
Stochastic approach to studying radioactivity of cloud and rain droplets, 30:29397

RAIN WATER/ACTIVATION ANALYSIS
  Trace elements in precipitation and cloud water in the area of Heidelberg, measured by instrumental neutron activation analysis, 30:28934
RAIN WATER/CHEMICAL ANALYSIS
  Potential application of atomic absorption and anodic stripping voltammetry to the precipitation scavenging program, 30:28937 (BNWL-1850(Pt.3))
RAIN WATER/CONTAMINATION
  Theories of radioactivity takeup by rain drops, 30:29398
RAIN WATER/SAMPLING
  Development an an ideal sampler for below-cloud scavenging studies, 30:29366 (BNWL-1850(Pt.3))
RAINOUT
  See WASHOUT
RAMAN EFFECT/PLASMA DIAGNOSTICS
  Spectroscopic methods for diagnostics of superdense hot plasma, 30:29163
RARE EARTH ALLOYS/ELECTROCHEMISTRY
  Electrochemical investigation of amalgams of rare earth metals. I. Main electrochemical properties of amalgams of rare earth elements, 30:29111
RARE EARTH ALLOYS/MAGNETISM
  Paraprocess near Curie temperature and criteria of appearance of temperature of magnetic compensation in compounds of rare earths with iron, 30:30043
RARE EARTHS
  See also CERIUM
    DYSPROSIUM
    ERBIUM
    EUROPIUM
    GADOLINIUM
    HOLMIUM
    LANTHANUM
    LUTETIUM
    NEODYMIUM
    PRASEODYMIUM
    SAMARIUM
    TERBIUM
    YTTERBIUM
RARE EARTHS/COMPRESSIBILITY
  Compression and anharmonicity of rare-earth metals, 30:30046
RARE EARTHS/ELECTRONIC STRUCTURE
  Widths of 4s and 5s multiplet components in the rare earths, 30:30495
RARE EARTHS/EXTRACTION CHROMATOGRAPHY
  Recent results in the application of column extraction chromatography in inorganic analysis, 30:28989 (ANL-Trans-960)
RARE EARTHS/METALLURGICAL EFFECTS
  Effect of rare earth metals on antimagnetism of chromium, 30:30054
RARE EARTHS/PHOTOEMISSION
  Thermodynamical account of the photoemission spectra of the rare earths, 30:30505
RARE EARTHS/USES
  New uses in technology boost demand for rare earths, 30:29919
RARE GASES
  See also ARGON
    HELIUM
    KRYPTON
    NEON
    RADON
    XENON
RARE GASES/ATOM-MOLECULE COLLISIONS
  Entropy analysis of product energy distributions in nonreactive inelastic collisions, 30:30561
RARE GASES/ENERGY LEVELS
  Grotrian charts for atoms and ions of rare gases, 30:30493
RARE GASES/MEASURING METHODS
  Apparatus for studying the kinetics of the liberation of inert gases from materials during isothermal annealing, 30:30002
RATS/RADIONUCLIDE KINETICS
  Affinity of ^{111}In-bleomycin for malignant tumors (In patients and experimental rat tumors), 30:29859
  Alternate methods for administering chelating agents in decorporation therapy (Removal of actinides from mammals), 30:29798 (COO-119-249)
  Comparison of /sup 115m/Cd retention in rats following different routes of administration, 30:29815
  Decorporation of ^{239}Pu and ^{241}Am in the rat and hamster by Zn--DTPA, 30:29813
  Effect of copper and cadmium on ^{65}Zn absorption in zinc-deficient and zinc-supplemented rats, 30:29814
  Effects of copper, mercury, and zinc on the uptake and distribution of cadmium-115m in the albino rat, 30:29816
  Influence of irradiation on the incorporation of radionuclides (^{239}Pu; ^{226}Ra; ^{210}Pb; ^{144}Ce; tritium), 30:29818
  Metabolism of tritium-labelled sodium acetate, in the rat. A radiation protection approach, 30:29795 (CEA-R-4591)
  Removal by DTPA of internally deposited ^{241}Am. A comparative study on rats and Syrian hamsters, 30:29822
RAYLEIGH-TAYLOR INSTABILITY/NUMERICAL SOLUTION
  Some numerical experiments with low atwood number incompressible Rayleigh--Taylor instabilities, 30:31438 (UCID-15618)
  Two numerical examples of Rayleigh--Taylor instability for a system of five different densities, 30:31437 (UCID-15611)
REACTIVITY/CORRECTIONS
  Calculation of correction factors for pulsed neutron measurements in the ITR critical experiment, 30:31232 (IKE-6-79d)
REACTIVITY/ON-LINE MEASUREMENT SYSTEMS
  Methods for measuring the reactivity and eigenvalue of nuclear reactors (Patent), 30:31301
REACTIVITY METERS/CRITICALITY
  Digital period meter (Critical mass experiments), 30:29491
REACTOR ACCIDENTS
  See also EXCURSIONS
    MAXIMUM CREDIBLE ACCIDENT
    MELTDOWN
    REACTOR CORE DISRUPTION
REACTOR ACCIDENTS/RADIATION HAZARDS
  Atomic energy. V (Norwegin Nature Conservancy Association), 30:29343
REACTOR COMPONENTS
  See also BREEDING BLANKETS
    CORE CATCHERS
    FUEL ELEMENTS
    REACTOR COOLING SYSTEMS
    REACTOR CORES
REACTOR COMPONENTS/RELIABILITY
  Trends in structural mechanics. A UK review of the 2nd international conference on structural mechanics in reactor technology. VII. Reliability analysis, 30:31289
REACTOR COMPONENTS/STABILITY
  SAFR4: a program to evaluate the stability of a rigid blade in parallel fluid flow, 30:31280 (WAPD-TM-1085)
REACTOR COMPONENTS/STRESS ANALYSIS
  Trends in structural mechanics. A UK review of the 2nd international conference on structural mechanics in reactor technology. VI. Inelastic structural analysis, 30:31290
REACTOR CONTROL SYSTEMS
  (The processes and operations ensuring the control and safe running of a nuclear reactor.)
  Block control of a PWR type reactor, 30:31302
REACTOR CONTROL SYSTEMS/DIGITAL COMPUTERS
  A simple time optimal digital control for nuclear reactors, 30:31303
REACTOR CONTROL SYSTEMS/FLUID POISON CONTROL
  System for concentrating a moderating solution utilized in a pressurized water nuclear power plant (Patent), 30:31199
REACTOR CONTROL SYSTEMS/HYDRAULIC CONTROL DEVICES
  Control line disconnect assembly (Patent), 30:31299
  Pressure vessel penetration technique (Patent), 30:31287
  Top actuated reactor control system (Patent), 30:31298
REACTOR CONTROL SYSTEMS/RESEARCH PROGRAMS
  10 years: Laboratory for Reactor Control and Plant Safety, 30:31296 (NP-20130)
REACTOR CONTROL THEORY
  See REACTOR KINETICS
REACTOR COOLING SYSTEMS
  See also PRIMARY COOLANT CIRCUITS
    SECONDARY COOLANT CIRCUITS
  Engineering techniques for nuclear plant cooling, 30:31256
REACTOR CORE DISRUPTION
  Post-accident core retention for LMFBR's. 2. Technical report. Final report for the period 1 July 1972--30 June 1973, 30:31253 (UCLA-ENG-7343)
REACTOR CORE DISRUPTION/TRANSIENTS
  Analysis of the primary containment response using a hydrodynamic-elastic-plastic computer code (Rexco-hep code; LMFBR), 30:31264
REACTOR CORES/DESIGN
  Nuclear data accuracy considerations in reactor design, 30:31276
REACTOR CORES/FUEL ASSEMBLIES
  Fuel assembly for a nuclear reactor (Patent), 30:31292
REACTOR CORES/SEISMIC EFFECTS
  PRELUDE-2: seismic response analysis code for block-type fuel core, 30:31247 (JAERI-M-5560)
REACTOR CORES/TEMPERATURE DISTRIBUTION
  Use of superposition in calculating the temperature of a reactor core cooled by a liquid metal, 30:31277
REACTOR EXPERIMENTAL FACILITIES/FISSION FRAGMENT SPECTROMETERS
  Spectrometer for on-line analysis of radionuclides (SOLAR), 30:29571
REACTOR FUEL ELEMENTS
  See FUEL ELEMENTS
REACTOR KINETICS
  High flux research reactor and research on reactor physics and reactor engineering, 30:31235 (KURRI-TR-110)
  Kinetic experiments in reactor physics, 30:31278
  Nuclear data accuracy considerations in reactor design, 30:31276
REACTOR LATTICES/MATERIAL BUCKLING
  Experiments in pure uranium lattices with unit /sub infinity/. Assemblies SNEAK-8/8Z; UK 1 and UK 5 in ERMINE and HARMONIE, 30:31270 (EURFNR-1189)

REACTOR LATTICES/REACTION KINETICS
Experiments in pure uranium lattices with unit /sub infinity/. Assemblies SNEAK-8/8Z; UK 1 and UK 5 in ERMINE and HARMONIE, 30:31270 (EURFNR-1189)
REACTOR LATTICES/REACTIVITY WORTHS
Experiments in pure uranium lattices with unit /sub infinity/. Assemblies SNEAK-8/8Z; UK 1 and UK 5 in ERMINE and HARMONIE, 30:31270 (EURFNR-1189)
REACTOR MATERIALS
(See also specific materials.)
Adaptation of metallic materials to the conditions of utilization, 30:29986
REACTOR MATERIALS/DEGASSING
Apparatus for studying the kinetics of the liberation of inert gases from materials during isothermal annealing, 30:30002
REACTOR MATERIALS/FRACTURE PROPERTIES
Review of current status of yielding fracture mecnanics, 30:30053
REACTOR MATERIALS/PHYSICAL RADIATION EFFECTS
Radiation damage in reactor structural materials - Formation of pores and its simulation, 30:30062 (AED-CONF-74-044-009)
REACTOR MATERIALS/POROSITY
Radiation damage in reactor structural materials - Formation of pores and its simulation, 30:30062 (AED-CONF-74-044-009)
REACTOR NOISE
Poisson-Algebraic distributions: another family of generalized Poisson profiles in nuclear-reactor noise-analysis, 30:31273 (RT/FI-(74)26)
REACTOR OPERATION/OPTIMIZATION
Optimization of the cyclicity of operation of a research reactor, 30:31237
REACTOR PROTECTION SYSTEMS/TEMPERATURE CONTROL
Temperature control and emergency protection against perilous temperatures in nuclear reactor (Patent), 30:31297
REACTOR SAFETY
(Theoretical and experimental investigations of the behavior of reactor types and designs under various real or hypothetical accidents.)
See also FAULT TREE ANALYSIS
REACTOR SAFETY/BIBLIOGRAPHIES
IRS literature 1965-1973, 30:31246 (IRS-A-4)
REACTOR SAFETY/RESEARCH PROGRAMS
10 years: Laboratory for Reactor Control and Plant Safety, 30:31296 (NP-20130)
Annual colloquium 1973 of the Project Nuclear Safety (Kernforschungszentrum Karlsruhe), 30:31245 (AED-CONF-73-686-000)
Present research of atomic energy safety, 30:31244 (AEC-tr-7569)
Quarterly progress report on reactor safety programs sponsored by the Division of Reactor Safety Research for April--June 1974. I. Light-water-reactor safety (PWR and BWR), 30:31250 (ORNL-TM-4655(Vol.1))
Quarterly progress report on reactor safety programs sponsored by the Division of Reactor Safety Research for April--June 1974 (PWR and BWR), 30:31251 (ORNL-TM-4655(Vol.2))
Second biannual report 1973, 30:31248 (KFK-1908)
REACTORS
See also GAS COOLED REACTORS
GRAPHITE MODERATED REACTORS
LIQUID METAL COOLED REACTORS
POWER REACTORS
TRANSPORTABLE REACTORS
REACTORS/MULTIPLICATION FACTORS
Fluxes and effective multiplication factor evaluation by escape probabilities, 30:31274 (RT/FI-(74)30)
REACTORS/NEUTRON FLUX
Fluxes and effective multiplication factor evaluation by escape probabilities, 30:31274 (RT/FI-(74)30)
RECOMBINATION (GENETIC)
See GENE RECOMBINATION
RECORDING SYSTEMS
MAGREC final report (Magnetic film recorder for fast transients from nuclear events), 30:29619 (UCID-16026)
RECORDING SYSTEMS/PERFORMANCE TESTING
Test methods for high packing density digital magnetic tape recorders, 30:31443 (UCID-15773)
RED DWARF STARS/LUMINOSITY
Influence of binaries on red dwarf density distributions (Galactic plane), 30:30232
RED DWARF STARS/SPATIAL DISTRIBUTION
Influence of binaries on red dwarf density distributions (Galactic plane), 30:30232
RED GIANT STARS/STAR EVOLUTION
Do pulsars make supernovae. II. Calculations of light curves for type II events, 30:30197
RED SHIFT
See DOPPLER EFFECT
REFERENCE THETA-PINCH REACTOR/SPECIFICATIONS
Engineering design study of a Reference Theta-Pinch Reactor (RTPR), 30:29206 (LA-5336)
REGGE CALCULUS/TOTAL CROSS SECTIONS
General features of the reggeon calculus with α>1, 30:31170
REGGE CUTS/REGGE POLES
Possibility that the Pomeron-Reggeon cut contains the Regge pole, 30:30717
REGGE POLES
Strong interaction dynamics (Lectures, Regge exchange), 30:30703
REGGE POLES/BOUNDARY CONDITIONS
Generalization of Regge asymptotic behavior (Lectures), 30:30639
REGGE TRAJECTORIES/HADRONS
Extended hadrons and Regge slope, 30:30695
REGULATORS (VOLTAGE)
See VOLTAGE REGULATORS
REINFORCED MATERIALS/THERMAL FATIGUE
Mechanical properties of metal matrix composites subjected to cyclic temperature changes. Annual report, 1 July 1972--30 June 1973 (6064 Al reinforced with fibers of stainless steel, 34 vol % SiC, 27 vol % B, and 45 vol % B), 30:29973 (AD-774890)
RELATIVITY THEORY
See also GENERAL RELATIVITY THEORY
Special theory of relativity, 30:31137
RELATIVITY THEORY/CONFORMAL GROUPS
Application of a conformal transformation group for relativistic theories, 30:31142 (IAE-2306)
RELATIVITY THEORY/DOPPLER EFFECT
Classical and relativistic Doppler effects, 30:31143 (INIS-mf-1357)
RELATIVITY THEORY/VELOCITY
Velocity of light is direction dependent, 30:31162
REMOTE HANDLING EQUIPMENT/REVIEWS
Optical coherent radiation (Book), 30:30112
RENE 41/WELDED JOINTS
Stress relaxation and strain-age cracking in Rene 41 weldments, 30:29996
RESEARCH REACTORS
See also DEMOCRITUS REACTOR
FRFF REACTOR
ISPRA-1 REACTOR
KUR REACTOR
SUPER KUKLA REACTOR
RESEARCH REACTORS/DESIGN
High flux research reactor and research on reactor physics and reactor engineering, 30:31235 (KURRI-TR-110)
RESEARCH REACTORS/REACTOR KINETICS
Some technical problems on the dynamic studies of the high flux research reactor, 30:31233 (KURRI-TR-110)
RESEARCH REACTORS/REACTOR OPERATION
Optimization of the cyclicity of operation of a research reactor, 30:31237
RESEARCH REACTORS/USES
Study of nuclear physics using a high-flux reactor (Photonuclear reaction studies using capture γ-rays), 30:31234 (KURRI-TR-110)
RESERVOIRS (WATER)
See WATER RESERVOIRS
RESIDUES (RADIOACTIVE)
See RADIOACTIVE WASTES
RESONANCE PARTICLES
See also MESON RESONANCES
RESONANCE PARTICLES/PARTICLE PRODUCTION
Study of π^+p interactions with strange particle production in five- and six-body final states at 8 GeV/c, 30:30615
RESONATING-GROUP METHOD
New analytical derivation of kernels in the resonating group method for composite-particle scattering and molecule-like structures. Derivation from kernels in the generator coordinate method and application to ^{16}O + α, 30:31023
RESPIRATORY SYSTEM DISEASES/DIAGNOSIS
Dual camera studies of pulmonary function with computer processing of data (^{133}Xe tracer), 30:29847
RETICULAR CELLS
See RETICULOENDOTHELIAL SYSTEM
RETICULOENDOTHELIAL SYSTEM/BIOLOGICAL RADIATION EFFECTS
Effects of carbon particles on phagocytic activity of reticuloendothelial system in x-irradiated mice, 30:29753
RETICULOENDOTHELIAL SYSTEM/PHYSIOLOGY
Reticuloendothelial function test in rabbit and man. Experimental and clinical investigation on artificial fat cream and ^{131}IAA, 30:29841
RETINA/BIOLOGICAL RADIATION EFFECTS
Autoradiographic studies of DNA-repair in the retina of rabbits (Gamma radiation), 30:29755
Toxicity to rabbit retina of epithermal neutron beam, 30:29765
RETINA/RADIATION BURNS
Experimental ocular irradiation with accelerated protons (Monkeys), 30:29754
RHENIUM/INTERNAL FRICTION
Internal friction of polycrystalline Re following torsional deformation at liquid nitrogen temperature, 30:29991
RHENIUM/PRODUCTION
High-melting metals and metallic compounds, 30:30021
RHENIUM/USES
High-melting metals and metallic compounds, 30:30021
RHENIUM 183/ENERGY-LEVEL TRANSITIONS
Levels in ^{179}Ta and γ-ray transition probabilities in ^{179}Ta and ^{183}Re, 30:30994

RHENIUM 186/ENERGY LEVELS
  Nuclear Data Sheets for A = 186, 30:30988
RHENIUM 186/NUCLEAR PROPERTIES
  Nuclear Data Sheets for A = 186, 30:30988
RHENIUM ALLOYS/CRYSTAL STRUCTURE
  Effect of lithium vapor on the structure of monocrystals of refractory metals and alloys (W--2 at. percent Rh; W--10 percent Mo; Mo--10 percent Re; Mo--27 percent Re), 30:29955
RHENIUM ALLOYS/ELECTRONIC STRUCTURE
  Nuclear gamma-resonance on nuclei of ^{57}Fe impurity in tungsten--rhenium alloys, 30:30029
RHENIUM ALLOYS/OXIDATION
  Kinetics of molybdenum--rhenium alloy oxidation (MR-47VP), 30:29949
RHEUMATIC DISEASES/THERAPY
  Pharmacodynamics of ^{197}Au and ^{195}Au labeled aurothiomalate in blood. Correlation with course of rheumatoid arthritis, gold toxicity, and gold excretion, 30:29792
RHO-765 RESONANCES
  Possible description of the rho resonance in the simplest model of the $\pi\pi$-interaction (Four-pion interactions,quasipotential), 30:30718 (JINR-P2-7502)
RHO-765 RESONANCES/DECAY
  Upper limit on the rho^0 → etaγ branching ratio, 30:30590
RHO-765 RESONANCES/PARTICLE PRODUCTION
  Backward production of rho^0 and f^0 mesons in π^+n interactions at 6 GeV/c (Cross sections), 30:30621
RHO-765 RESONANCES/PHOTOPRODUCTION
  Relativistic correction in double scattering by deuterons (Glauber formula), 30:30720
RHODIUM 106/RADIATION MONITORING
  Data. Section IV. Other data, 30:29412
  Report of activity, February 1974 (Radioactivity of environmental samples collected throughout France during February 1974), 30:29349 (SCPRI(RM)-2-1974)
RHODIUM 110/ISOMERIC TRANSITIONS
  Isomeric states in ^{97} ^{98} ^{99} ^{100}Rh isotopes, 30:30964
RHODIUM 97/ISOMERIC TRANSITIONS
  Isomeric states in ^{97} ^{98} ^{99} ^{100}Rh isotopes, 30:30964
RHODIUM 98/ISOMERIC TRANSITIONS
  Isomeric states in ^{97} ^{98} ^{99} ^{100}Rh isotopes, 30:30964
RHODIUM ALLOYS/CRYSTAL STRUCTURE
  Effect of lithium vapor on the structure of monocrystals of refractory metals and alloys (W--2 at. percent Rh; W--10 percent Mo; Mo--10 percent Re; Mo--27 percent Re), 30:29955
RIBONUCLEIC ACID
  See RNA
RIBOSE/RADIOLYSIS
  Radiation chemistry of DNA-model compounds. V. Phosphate elimination from ribose-5-phosphate after OH radical attack at C4 (γ radiation), 30:29071
RICHLAND FFTF REACTOR
  See FFTF REACTOR
RIEMANN WAVES
  See SHOCK WAVES
RINGOTRON
  See ELECTRON-RING ACCELERATORS
RINGS (STORAGE)
  See STORAGE RINGS
RIO BLANCO EVENT/HYDROLOGY
  Project Rio Blanco: results from the initial alluvial water quality program, 30:29312 (PNE-RB-59)
  Project Rio Blanco: comparative postdetonation hydrologic testing, 30:29313 (PNE-RB-60)
RIO BLANCO EVENT/RADIATION MONITORING
  Radiological monitoring program, period covering February 4, 1974--April 30, 1974, 30:29348 (PNE-RB-51-9)
RISA
  See ALBUMINS
RNA/LABELLING
  Mechanism of reduction of 1-methyl-4-thiocyanatouracil by bisulfide. A route to in vitro labeling of tRNAs with sulfur-35, 30:29092
ROADS/ENVIRONMENTAL EFFECTS
  Environmental impact handbook for highway systems, 30:31357 (ANL/ES-30)
ROCKS
  See also IGNEOUS ROCKS
ROCKS/ACTIVATION ANALYSIS
  Radioactivation analysis in thermal and epithermal neutrons of the IBR-30 reactor of JINR, 30:28929
ROCKS/AGE ESTIMATION
  ^{40}Ar/^{39}Ar dating of the long range dikes, Newfoundland, 30:29336
ROCKS/CHEMICAL ANALYSIS
  High sensitivity photoneutron detector for 'non-destructive' submicroanalysis of beryllium, 30:29524
  Unknown alpha-emitters in nature, 30:28981
ROCKS/CHEMICAL COMPOSITION
  Mass spectrometric isotope dilution analyses of tin in stony meteorites and standard rocks, 30:30311
ROCKS/NUCLEAR REACTION ANALYSIS
  Simultaneous analysis of uranium and thorium by the delayed fission neutron counting method, 30:28931
ROCKS/X-RAY FLUORESCENCE ANALYSIS
  Compilation of x-ray interaction data for x-ray fluorescence analysis of geological samples, 30:28943 (RISO-297)
ROCKY FLATS PLANT/RADIOACTIVE WASTES
  Resuspension by wind at Rocky Flats (Plutonium monitoring in air and soil), 30:29371 (BNWL-1850(Pt.3))
  Resuspension source change at Rocky Flats, 30:29372 (BNWL-1850(Pt.3))
RODENTS
  See also HAMSTERS
    MICE
    RATS
    SQUIRRELS
RODENTS/RADIONUCLIDE KINETICS
  Ecological studies of vertebrates in plutonium-contaminated areas of the Nevada Test Site (^{239}Pu and ^{241}Am content of GI tract, carcass, and pelt of rodents), 30:29449 (NVO-AEIC-74-1)
RUBIDIUM/EMISSION SPECTROSCOPY
  Spectrochemical analysis of uranium oxide by gallium oxide carrier dc arc technique (ASTM Standard E402), 30:28957
RUBIDIUM COMPOUNDS/LATTICE PARAMETERS
  On oxifluorides $A_{12}M(IV)M_3(VI)O_8F_{18}$ with uranium, molybdenum, and tungsten (A = Cs, Rb, K and M(IV) = U, Ce, MoW), 30:29006
RUBIDIUM COMPOUNDS/MAGNETIC SUSCEPTIBILITY
  On oxifluorides $A_{12}M(IV)M_3(VI)O_8F_{18}$ with uranium, molybdenum, and tungsten (A = Cs, Rb, K and M(IV) = U, Ce, MoW), 30:29006
RUMEN
  See RUMINANTS
RUMINANTS
  See also CATTLE
    SHEEP
RUMINANTS/RADIONUCLIDE KINETICS
  In vitro plutonium studies using the artificial rumen and simulated abomasal and intestinal fluids, 30:29809 (NVO-AEIC-74-1)
RUNAWAY (REACTOR ACCIDENT)
  See EXCURSIONS
RUSSELL-SAUNDERS COUPLING
  See L-S COUPLING
RUTHENIUM/DIFFUSION
  Study of diffusion/leaching phenomena with glasses. Application of risk evaluation to long-term storage, 30:29133 (CEA-R-4550)
RUTHENIUM/SOLVENT EXTRACTION
  3-nitroso-4-hydroxy-5,6-benzocoumarin as a selective reagent for the spectrophotometric determination of ruthenium(III), 30:28966
RUTHENIUM/SPECTROPHOTOMETRY
  3-nitroso-4-hydroxy-5,6-benzocoumarin as a selective reagent for the spectrophotometric determination of ruthenium(III), 30:28966
RUTHENIUM 101/MAGNETIC DIPOLE MOMENTS
  Ratio of the nuclear moments of ^{99}Ru and ^{101}Ru from NMR studies of ferromagnetic alloys, 30:30961
RUTHENIUM 103/RADIATION MONITORING
  Data. Section IV. Other data, 30:29412
  Quillayute air reference station (Air sampling and monitoring in Washington State), 30:29359 (BNWL-1850(Pt.3))
  Report of activity, February 1974 (Radioactivity of environmental samples collected throughout France during February 1974), 30:29349 (SCPRI(RM)-2-1974)
RUTHENIUM 106/DIFFUSION
  Concentration effects of ^{137}Cs, ^{65}Zn, ^{60}Co, and ^{106}Ru sorption by marine sediments with geochemical implications, 30:29409
RUTHENIUM 106/RADIATION MONITORING
  Data. Section IV. Other data, 30:29412
  Determination of fallout radioisotopes from their content in the annual layers of high-mountain glaciers, 30:29408
  Environmental monitoring report: United States Atomic Energy Commission, Oak Ridge facilities. Calendar year 1973, 30:29352 (UCC-ND-280)
  Report of activity, February 1974 (Radioactivity of environmental samples collected throughout France during February 1974), 30:29349 (SCPRI(RM)-2-1974)
RUTHENIUM 106/RADIOCHEMICAL ANALYSIS
  Determination of ruthenium-106 in sea water, 30:28984
RUTHENIUM 106/REMOVAL
  Decontamination of swine, sheep, and cattle surface-contaminated with fission products. II. Removal of radionuclides of zirconium, niobium, ruthenium, and cerium, 30:29823
RUTHENIUM 99/MAGNETIC DIPOLE MOMENTS
  Ratio of the nuclear moments of ^{99}Ru and ^{101}Ru from NMR studies of ferromagnetic alloys, 30:30961
RUTHENIUM OXIDES/PYROLYSIS
  Ruthenium volatility during vitrification of fission products. Part II. Fixation on a steel tube. Peroxide decomposition, 30:29086 (AEC-tr-7575)

S

S CHANNEL/UNITARITY
  Unitarity, phenomenology and the bare pomeron, 30:30716

S MATRIX/FACTORIZATION
Two-body T-matrix factorization and three-nucleon problem, 30:31047
S MATRIX/MATHEMATICAL SPACE
Dipole ghosts and unitarity (Feynman diagrams), 30:30787
S MATRIX/POTENTIAL SCATTERING
Analytic nonlocal potentials. II. Analyticity of the S matrix, for fixed l, its representations, and a dispersion relation for fixed t (Frednolm mthod, lippman-schwinger equation, Jost functions), 30:30784
SACCHAROMYCES CEREVISIAE/METABOLISM
Fractionation of sulfur isotopes by the yeast Saccharomyces cerevisiae, 30:29826
SACCHAROSE/ACTIVATION ANALYSIS
Method for determining sugar/starch contents in aqueous solutions (Using Hg-203-labelled compounds for tracer method or nonradioactive Hg for neutron activation patent), 30:28936
SACCHAROSE/RADIOCHEMICAL ANALYSIS
Method for determining sugar/starch contents in aqueous solutions (Using Hg-203-labelled compounds for tracer method or nonradioactive Hg for neutron activation patent), 30:28936
SACLAY LINAC/CAVITY RESONATORS
High-power standing-wave triperiodic structure for positron acceleration, 30:30126
SAFEGUARDS
See also IAEA SAFEGUARDS
SAFEGUARDS/RECOMMENDATIONS
Report of the advisory panel on safeguarding special nuclear material, 30:30105 (TID-26630)
SAFETY (NUCLEAR)
See RADIATION PROTECTION
SALMON EVENT/RADIATION HAZARDS
Off-site surveillance. Final report. Report on Project Dribble, Salmon Event, Tatum Salt Dome, Mississippi, 22 October 1964, 30:29345 (AD-629357)
SALMONELLA/MUTATIONS
Base-pair deletion at a frameshift hotspot in Salmonella (X rays), 30:29684
SAMARIUM/ACTIVATION ANALYSIS
Determination of rare earths and thorium in apatites by thermal and epithermal neutron-activation analysis, 30:28935
Radioactivation analysis in thermal and epithermal neutrons of the IBR-30 reactor of JINR, 30:28929
Trace elements in precipitation and cloud water in the area of Heidelberg, measured by instrumental neutron activation analysis, 30:28934
SAMARIUM/QUALITATIVE CHEMICAL ANALYSIS
Application of activation analysis to the determination of pollutants in the atmosphere, 30:28914 (IEA-326)
SAMARIUM/QUANTITATIVE CHEMICAL ANALYSIS
Absorption x-ray radiometric analysis using the $K\alpha_2$ lines of the characteristic radiation of targets, 30:28952
SAMARIUM/X-RAY SPECTROSCOPY
Determination of rare earths in plutonium by x-ray emission analysis, 30:28946
SAMARIUM 143/ENERGY LEVELS
Nuclear Data Sheets for A = 143, 30:30966
SAMARIUM 143/NUCLEAR PROPERTIES
Nuclear Data Sheets for A = 143, 30:30966
SAMARIUM 147/NEUTRON REACTIONS
Mass-spectrometric determination of neutron capture cross-sections of the rare earth isotopes (Pile and thermal cross sections), 30:30977 (AEC-tr-7574)
SAMARIUM 148/CARBON 12 REACTIONS
In-beam conversion-electron spectrum for the $^{148}Sm(^{12}C,4n)^{156}Er$ reaction (75 MeV), 30:30965
SAMARIUM 148/NEUTRON REACTIONS
Mass-spectrometric determination of neutron capture cross-sections of the rare earth isotopes (Pile and thermal cross sections), 30:30977 (AEC-tr-7574)
SAMARIUM ALLOYS/CRYSTAL STRUCTURE
Structure of alloys of cobalt with rare earths of the approximate composition RCo_5, 30:30034
SAMARIUM ALLOYS/DOMAIN STRUCTURE
Experimental verification of a model for the magnetization reversal in RCo_5 particles (Sm/sub x/Nd/sub 1+-x/Co_5), 30:30047
SAMARIUM ALLOYS/PHASE STUDIES
Orientation relation between phases in $SmCo_5$--base alloys, 30:30041
SAMARIUM COMPOUNDS/HYPERFINE STRUCTURE
Sign reversal of the 4f contribution to the hyperfine field at Sm in paramagnetic samarium compounds, 30:29997
SAMARIUM COMPOUNDS/MAGNETIC SUSCEPTIBILITY
Synthesis and magnetic properties of samarium and europium titanoniobates ($SmTiNbO_6$; EuTiNbO6), 30:29908
SAMARIUM OXIDES
Effect of complex admixtures of rare-earth oxides on sintering of cerium dioxide, 30:29909
SAND/MOTION
Saltation and creep sampler, 30:29616 (NVO-AEIC-74-1)
SAND/PERMEABILITY
Laminar gas flow through loosely packed Overton sand, 30:29319 (UCID-15818)
SATELLITES
See also MOON
SATELLITES/PHOTOMETRY
Light-variations investigation of variable stars and satellites by means of computer, 30:30209
SATURN PLANET/EQUILIBRIUM
The equilibrium of a rotating body of arbitrary density, 30:30408
SCALE INVARIANCE/REVIEWS
Dilatations, 30:30644
SCALE INVARIANCE/YANG-MILLS THEORY
Scaling and asymptotically free massive Yang--Mills field, 30:31147
SCALING LAWS/GAUGE INVARIANCE
Scaling behaviour in a class of massive non-Abelian gauge theories, 30:30771
SCALING LAWS/STRUCTURE FUNCTIONS
Scaling distribution of large transverse momenta, 30:30634
SCANDIUM/ACTIVATION ANALYSIS
Multielement determination in market-garden soils by instrumental photon activation analysis, 30:28921
Trace element behavior in soil of some Indonesian sawah's and in sludge of an Indonesian river, 30:28930
Trace elements in precipitation and cloud water in the area of Heidelberg, measured by instrumental neutron activation analysis, 30:28934
SCANDIUM/ION EXCHANGE
Selective ion-exchangers containing phosphorus in their functional groups. I. Sorption and separation of some bivalent and trivalent ions, 30:29081
SCANDIUM/QUALITATIVE CHEMICAL ANALYSIS
Application of activation analysis to the determination of pollutants in the atmosphere, 30:28914 (IEA-326)
SCANDIUM/SPECTROPHOTOMETRY
Extraction spectrophotometric determination of scandium with xylenol orange and ethyltridodecylammonium bromide, 30:28953
SCANDIUM 45/ALPHA REACTIONS
Reaction rates of interest in late stages of stellar nycleosynthesis (Estimate of reliability), 30:30255
SCANDIUM 46/COSMOCHEMISTRY
The unique cosmic-ray history of the Malakal chondrite, 30:30170
SCANDIUM 50/ENERGY LEVELS
Nuclear structure calculation of ^{50}Sc and analysis of the $^{48}Ca(^3He,p)^{50}Sc$ reaction (Shell model, Kuo--Brown interaction), 30:30946
SCANNERS (IMAGE)
See IMAGE SCANNERS
SCATTERING
See also ELASTIC SCATTERING
Tests for the purity of the initial ensemble of states in scattering experiments, 30:30783
SCATTERING/CORRELATIONS
Scattering from correlated systems, 30:31056
SCATTERING/EXCHANGE INTERACTIONS
Eigenstate expansions in a soluble model of identical particle scattering, 30:31141
SCATTERING AMPLITUDES
Determination of reaction amplitudes from experimental observables, 30:31028
SCATTERING AMPLITUDES/DISPERSION RELATIONS
Practical evaluation of the asymptotic real-part behavior and the search for a possible subtraction constant in the crossing-odd forward pion--nucleon amplitude, 30:30733
SCAVENGING (ATMOSPHERIC)
See WASHOUT
SCHROEDINGER EQUATION
Quantized friction and the correspondence principle: single particle with friction (Nonlinear time-dependent Schroedinger equation), 30:31075
SCHROEDINGER EQUATION/ANALYTICAL SOLUTION
Eigenstate expansions in a soluble model of identical particle scattering, 30:31141
SCHROEDINGER EQUATION/PADE APPROXIMATION
Solution of the Schroedinger equation using Pade approximants to sum asymptotic series, 30:31139
SCINTIGRAPHY
See SCINTISCANNING
SCINTILLATION COUNTERS
See also GAS SCINTILLATION DETECTORS
LIQUID SCINTILLATION DETECTORS
SOLID SCINTILLATION DETECTORS
SCINTILLATION COUNTERS/PULSE DISCRIMINATORS
A fast neutron-gamma discriminator, 30:29535
SCINTISCANNING
Biologic considerations in anatomic imaging with radionuclides. Progress report, July 1973--June 1974 (Evaluation of diagnostic value of brain, bone, and liver scans), 30:29832 (COO-2427-4)
Liver studies with various radioactive tracers and methods (Critical evaluation of diagnostic value), 30:29831 (CONF-740708-52)
SCINTISCANNING/IODINE 125
Elimination of intravenously injected ^{125}I-toluidine blue in rabbits (Effectiveness for parathyroid scanning), 30:29812
SCRIBA NUCLEAR POWER PLANT
See NINE MILE POINT-1 REACTOR
SEALS/DESIGN
Freezing-up shaft seal of machines for the transport of liquids and gases in nuclear power (Patent), 30:29276

SEAWATER/ACTIVATION ANALYSIS
Use of NH_4-form Chelex 100 chelating resin of low induced activities for neutron activation analysis of manganese in seawater, 30:28927
SEAWATER/CHEMICAL ANALYSIS
Determination of ruthenium-106 in sea water, 30:28984
SEAWATER/CORROSIVE EFFECTS
Corrosion fatigue strength of a titanium alloy at elevated temperature (Ti--Al--Zr; simulated seawater), 30:29945
SEBACEOUS GLANDS
See SKIN
SECOND-CLASS CURRENTS
(Classification of currents according to their properties under G-parity transformations.)
SECOND-CLASS CURRENTS/BETA-PLUS DECAY
K-electron capture to positron emission ratios and the second class currents problem, 30:31076
SECOND-CLASS CURRENTS/K CAPTURE
K-electron capture to positron emission ratios and the second class currents problem, 30:31076
SECONDARY COOLANT CIRCUITS/DESIGN
Process for converting heat produced by a nuclear reactor to electrical energy (Patent), 30:31282
SECONDARY COSMIC RADIATION/COUPLING CONSTANTS
Coupling constants for the cosmic ray muon component, 30:30178
SECONDARY COSMIC RADIATION/PARTICLE PRODUCTION
Search for heavy particles in cosmic rays (6 Proton masses), 30:30579
SECURITY
CAIN system field test (Employee identification system), 30:31446 (UCID-15816)
SEDIMENTS/RADIONUCLIDE MIGRATION
Concentration effects of ^{137}Cs, ^{65}Zn, ^{60}Co, and ^{106}Ru sorption by marine sediments with geochemical implications, 30:29409
Kinetics of the self-purification of a body of water containing strontium-90 as a result of absorption of the radionuclide by the bottom deposits, 30:29414
SEEDS/GENETIC RADIATION EFFECTS
Studies on the use of U-120 cyclotron and fast neutron generator in neutron irradiation of seeds for mutation (Barley; wheat), 30:29692
Use of x-rays in sugar beet breeding, 30:29693
SEEDS/NUCLEAR REACTION ANALYSIS
Nondestructive determination of the nitrogen (protein) content in single kernels of seeds (6-MeV deuterons), 30:28917 (NP-20122)
SEEDS/RADIATION EFFECTS
Effect of chronic and acute gamma irradiation on specific recombination capability of lineage WD maize, 30:29689
SEISMIC EFFECTS/SIMULATION
Dynamic testing of full-scale nuclear power plant structures and equipment, 30:31268
SEISMIC WAVES/ATTENUATION
Regional attenuation of short-period P and S waves in the United States, 30:29303 (AD-776672)
SEISMIC WAVES/DATA PROCESSING
Extended array evaluation program. Special report No. 5. Selection of reference waveforms for matched filter processing of long period signals from seismic events, 30:29304 (AD-776815)
SELECTION RULES/ISOSPIN
Can the $\Delta I = 1/2$ selection rule in the $K \to 2\pi$ decay be satisfied in gauge theories (Free-quark model, Salam-Weinberg model, decay amplitudes), 30:30684
The $\Delta I=1/2$ rule in non-leptonic weak decays, 30:30595
SELENIUM/ACTIVATION ANALYSIS
Application of activation analysis to the determination of pollutants in the atmosphere (Thermal neutrons), 30:28914 (IEA-326)
Multielement determination in market-garden soils by instrumental photon activation analysis, 30:28921
SELENIUM/RAMAN EFFECT
Exciton enhanced Raman scattering of LO phonons in trigonal Se (Longitudinal optical phonons at 1.6K), 30:31425 (LBL-2781)
SELENIUM/STACK DISPOSAL
Trace pollutant emissions in fossil fuel combustion, 30:29469 (BNWL-1850(Pt.3))
SELENIUM/UPTAKE
Elemental content of trace elements in vegetation collected at Centralia, Washington (Comparison with Alaskan vegetation), 30:29483 (BNWL-1850(Pt.3))
SELENIUM 75/RETENTION
Estimation of radiation doses from i. v. administration of selenite $Na_2{}^{75}SeO_3$, 30:29793
SEMICONDUCTOR DETECTORS
See also CDTE SEMICONDUCTOR DETECTORS
JUNCTION DETECTORS
SI SEMICONDUCTOR DETECTORS
SURFACE BARRIER DETECTORS
SEMICONDUCTOR DETECTORS/CALIBRATION
Intensities of γ-rays in the decay of sup(166m)Ho, 30:31125
SEMICONDUCTOR DETECTORS/CHARGE COLLECTION
A perturbation method for calculating the rate of charge collection in a semiconductor detector, 30:29530
SEMICONDUCTOR DETECTORS/PERFORMANCE
Preliminary results on mercuric iodide nuclear radiation detectors, 30:29534
SEMICONDUCTOR MATERIALS
(See also specific semiconductor materials.)
SEMICONDUCTOR MATERIALS/PHYSICAL RADIATION EFFECTS
Study of basic processes in radiation damage. Final report, 1 April 1971--30 November 1973 (Implantation of polarized radioisotopes in metals and semiconductors), 30:30061 (AD-777728)
SEMICONDUCTOR MATERIALS/RESEARCH PROGRAMS
Department of Fundamental Research, Grenoble, semiannual bulletin No. 4, 30:31333 (CEA-N-1688)
SEPARATION PROCESSES
See also DESALINATION
ION EXCHANGE
SEPARATION PROCESSES/SUPERCONDUCTING MAGNETS
High gradient magnetic spearation: an industrial application of magnetism, 30:30832
SERRATIA/BIOLOGICAL RADIATION EFFECTS
Metronidazole (Flagyl). A radiosensitizer of hypoxic cells, 30:29674
SEWAGE
See LIQUID WASTES
SEYFERT GALAXIES/CHEMICAL COMPOSITION
X-ray ionization and the helium abundance in 3C 120 (Time scale, forbidden-line intensities), 30:30347
SEYFERT GALAXIES/RADIOWAVE RADIATION
NGC 1068: possible 3-millimeter radio variability (Standard statistical test), 30:30346
Radio emission from Markarian 6 (Spectral index), 30:30382
SEYFERT GALAXIES/X RADIATION
X-ray ionization and the helium abundance in 3C 120 (Time scale, forbidden-line intensities), 30:30347
SGHWR REACTOR/PERFORMANCE
Not such a bad reactor, 30:31215
SGHWR REACTOR/SPECIFICATIONS
Not such a bad reactor, 30:31215
SHALES/MECHANICAL PROPERTIES
Mechanical properties of a shale from Site U-2, 30:31409 (UCID-16023)
SHEATHS (FUEL)
See FUEL CANS
SHEEP/DECONTAMINATION
Decontamination of swine, sheep, and cattle surface-contaminated with fission products. II. Removal of radionuclides of zirconium, niobium, ruthenium, and cerium (^{95}Zr; ^{95}Nb; ^{106}Ru; ^{144}Ce), 30:29823
SHELL MODELS/NUCLEAR FORCES
Three-body effective interactions in the fsub(7/2) region, 30:30931
SHELL MODELS/NUCLEAR PROPERTIES
Energy density formalism and the shell structure of nuclei, 30:31049
SHELL MODELS/NUCLEON-NUCLEON POTENTIAL
Self-screening of the particle-hole interaction and core polarization of the effective two-particle interaction (TDA and RPA), 30:31091
SHELL MODELS/PERTURBATION THEORY
Degenerate perturbation theory, 30:30566
SHELL MODELS/TWO-BODY PROBLEM
Renormalized effective nuclear interaction by explicit truncation and use of the results of a large configuation space, 30:31060
SHIELDING/NEUTRON TRANSPORT
Investigations on the shielding of power reactors, 30:31271 (IKE-6-75d)
SHIELDING/SAFETY STANDARDS
Shielding benchmark problems, 30:31126 (ORNL-RSIC-25(Suppl.2))
SHIELDING MATERIALS/ELECTRON COLLISIONS
Back-scattering from metals in superficial therapy with high energy electrons, 30:31108
SHIELDING MATERIALS/NEUTRON TRANSPORT
Buildup of scattered radiation behind a shadow shield, 30:31129
SHIELDING MATERIALS/PHOTON TRANSPORT
Buildup of scattered radiation behind a shadow shield, 30:31129
SHIELDING MATERIALS/PRODUCTION
Radiation absorbing shield for personnel and materials and method of making same (Patent), 30:31127
SHIELDING MATERIALS/SPECIFICATIONS
Barites from Boguszow as aggregate for anti-radiation concrete shields, 30:31128
SHIMANE-1 REACTOR/SEISMIC EFFECTS
Comparative forced vibration test of two BWR-type reactor buildings, 30:31265
SHIP PROPULSION REACTORS
See also OTTO HAHN REACTOR
SHIP PROPULSION REACTORS/PLANNING
German marine shipping: changes in structure and future development. General meeting of the Nuclear Energy Research Society, Hamburg, Germany, December 12, 1973, 30:31243
SHIPMENT
See TRANSPORT
SHOAL EVENT
Shoal postshot environment, 30:29317 (UCID-15771)
SHOCK (THERMAL)
See THERMAL SHOCK
SHOCK WAVES/CORRELATIONS
Generalized shock Hugoniots, 30:31400 (UCID-15586)

SHOCK WAVES/REVIEWS
Mathematical review of introductory wave mechanics (Classical mechanics of elastic and shock waves in solids and fluids), 30:31444 (UCID-15603)
SHOWER COUNTERS
(Detects high energy gamma radiation or high energy particles on basis of cascade showers in layered absorbers.)
SHOWER COUNTERS/PERFORMANCE
A calorimeter for 300GeV neutrons and protons (Layered iron plates and plastic scintillators), 30:29596
Study of total-absorption counters for very-high-energy particles (Sandwich of absorber and scintillator plates), 30:29598
SI SEMICONDUCTOR DETECTORS/ELECTRIC CONTACTS
Semiconductor contacts to silicon surface-barrier detectors, 30:29519
SI SEMICONDUCTOR DETECTORS/PERFORMANCE
Semiconductor counters for nuclear radiations produced by ion implantation, 30:29531
SI SEMICONDUCTOR DETECTORS/SENSITIVITY
Some features in the dependence of the pulse-height defect in semiconductor detectors on detected particle energy, 30:29526
SID
See SUDDEN IONOSPHERIC DISTURBANCE
SIGMA MODEL/PHASE TRANSFORMATIONS
Pion phase transition in chiral symmetry breaking model, 30:30716
SILANES/CHEMICAL RADIATION EFFECTS
Reduction of methyl acetate with several hydrosilanes under gamma irradiation, 30:29047
SILICATES/COSMOCHEMISTRY
A quantitative study of silicate extinction (Circumstellar shells, Mie theory), 30:30190
SILICIDES/DEPOSITION
Multicomponent diffusion coatings (Book), 30:29906
SILICIDES/MICROSTRUCTURE
Evaluation of glancing angle x-ray diffraction and MeV ^{4}He backscattering analyses of silicide formation, 30:29939
SILICIDES/PRODUCTION
High-melting metals and metallic compounds, 30:30021
SILICIDES/USES
High-melting metals and metallic compounds, 30:30021
SILICON
Highly resolved electron energy loss spectroscopy of amorphous germanium and silicon layers, 30:31381 (AED-CONF-74-089-025)
SILICON/ABSORPTION SPECTROSCOPY
Atomic absorption spectrometry of impurities in high purity tantalum with heated graphite atomizer, 30:28954
SILICON/CHEMICAL RADIATION EFFECTS
Effect of irradiation of metal ions on adsorption properties of semiconductor materials. I. Adsorption properties of oxidized surface of silicon (Effect of radioactivity of adsorbed ions), 30:29053
SILICON/COSMOCHEMISTRY
High-frequency observations of possible ''heavy-element'' recombination lines (Cosmic value), 30:30267
SILICON/EMISSION SPECTROSCOPY
Spectrochemical analysis of uranium oxide by gallium oxide carrier dc arc technique (ASTM Standard E402), 30:28957
Spectrographic determination of trace impurities in high purity uranium oxide, 30:28944 (UCID-15952)
SILICON/ION CHANNELING
Electronic stopping power of channelled ions in a model incorporating the Pauli principle (Incident ions Z = 1 to 50), 30:31115
SILICON/ION COLLISIONS
Backscattering measurements and surface roughness, 30:30486
SILICON/PHYSICAL RADIATION EFFECTS
Comments on ''Luminescence from electron-irradiated silicon'' (K center, divacancy), 30:30101
Reply to ''Comments on 'Luminescence from electron-irradiated silicon' '', 30:30099
Study of basic processes in radiation damage. Final report, 1 April 1971--30 November 1973 (Implantation of polarized radioisotopes in metals and semiconductors), 30:30061 (AD-777728)
SILICON/PION REACTIONS
Calculated particle-production spectra from π^- captures in tissue, tissue-equivalent plastic, silicon, and germanium, 30:31120
SILICON/VIBRATIONAL STATES
Comments on ''Luminescence from electron-irradiated silicon'' (K center, divacancy), 30:30101
Reply to ''Comments on 'Luminescence from electron-irradiated silicon' '', 30:30099
SILICON 29/HYPERFINE STRUCTURE
Observation and analysis of the primary ^{29}Si hyperfine structure of the E' center in non-crystalline SiO$_2$, 30:30102
SILICON 30/DEUTERON REACTIONS
The coupled-channel Born approximation and J-dependence in ^{30}Si(d,p)^{31}Si (Angular distributions), 30:30907
SILICON 30/SULFUR 32 REACTIONS
Inelastic transfer in the scattering of ^{32}S on ^{30}Si (75 to 80 MeV: angular distributions, DWBA analysis), 30:30906
SILICON 31/EXCITED STATES
The coupled-channel Born approximation and J-dependence in ^{30}Si(d,p)^{31}Si (Angular distributions), 30:30907
SILICON CARBIDES/CHEMICAL REACTIONS
Reactions of boron and silicon carbide with tungsten and titanium, 30:29948
SILICON CARBIDES/FRACTURE PROPERTIES
J-integral as a failure criterion for a Borsic--Al composite, 30:29890 (SAND-74-0193)
SILICON CARBIDES/MECHANICAL PROPERTIES
Mechanical behavior of metal matrix composites. Final report, 1 April 1972--30 April 1973 (B--Al;B/SiC--Ti;tensile, fatigue, and creep behavior;effects of defects), 30:29975 (AD-775359)
SILICON CARBIDES/PHYSICAL RADIATION EFFECTS
Irradiation damage in reaction-bonded silicon carbide, 30:29930
SILICON CARBIDES/THERMAL FATIGUE
Mechanical properties of metal matrix composites subjected to cyclic temperature changes. Annual report, 1 July 1972--30 June 1973 (6064 Al reinforced with fibers of stainless steel, 34 vol % SiC, 27 vol % B, and 45 vol % B), 30:29973 (AD-774890)
SILICON HYDRIDES
See SILANES
SILICON NITRIDES/MECHANICAL PROPERTIES
Some properties of materials of the systems Si$_3$N$_4$--ZrO$_2$, 30:29920
SILICON NITRIDES/THERMODYNAMIC PROPERTIES
Some properties of materials of the systems Si$_3$N$_4$--ZrO$_2$, 30:29920
SILICON OXIDES
See also QUARTZ
SILICON OXIDES/PHYSICAL RADIATION EFFECTS
Observation and analysis of the primary ^{29}Si hyperfine structure of the E' center in non-crystalline SiO$_2$, 30:30102
SILICON OXIDES/SPUTTERING
Sputtering yields and specific energy losses of Ar$^+$ ions with energies from 5 to 30 keV at SiO$_2$, 30:30482
SILICON OXIDES/X-RAY FLUORESCENCE ANALYSIS
Compilation of x-ray interaction data for x-ray fluorescence analysis of geological samples, 30:28943 (RISO-297)
SILICONES/FABRICATION
Process evaluation of new cellular silicone material, 30:31385 (BDX-613-1082(Rev.))
SILICONES/MECHANICAL PROPERTIES
Evaluation of load-deflection tests of 0.060-in.-thick Y-3333 cellular silicone, 30:31407 (UCID-15901)
SILVER/ABSORPTION SPECTROSCOPY
Separation of trace metal impurities from nuclear grade uranium by long-chain amine extraction and direct determination by atomic absorption spectrophotometry, 30:28948
SILVER/ACTIVATION ANALYSIS
Assay of silver in ores by neutron activation, 30:28926
Multielement determination in market-garden soils by instrumental photon activation analysis, 30:28921
Radiochemical separation of fluorine by adsorption on hafnium dioxide: application to the determination of oxygen by activation analysis with charged particles (^{3}He and ^{4}He particles), 30:28923
Trace elements in precipitation and cloud water in the area of Heidelberg, measured by instrumental neutron activation analysis, 30:28934
SILVER/ADSORPTION
Effect of irradiation of metal ions on adsorption properties of semiconductor materials. I. Adsorption properties of oxidized surface of silicon (Effect of radioactivity of adsorbed ions), 30:29053
SILVER/EMISSION SPECTROSCOPY
Spectrochemical analysis of uranium oxide by gallium oxide carrier dc arc technique (ASTM Standard E402), 30:28957
SILVER/FLUORESCENCE SPECTROSCOPY
New discrete atomization cell for atomic fluorescence spectrometry, 30:28947
SILVER/ION CHANNELING
Sputtering experiments with silver single crystals and the channeling phenomena, 30:30481
SILVER/ION COLLISIONS
L- and M-shell ionization of various elements by fast-α-particle bombardment (Cross sections, 1 to 5 MeV), 30:30537
SILVER/SPUTTERING
Sputtering experiments with silver single crystals and the channeling phenomena, 30:30481
SILVER/UPTAKE
Elemental content of trace elements in vegetation collected at Centralia, Washington (Comparison with Alaskan vegetation), 30:29483 (BNWL-1850(Pt.3))
SILVER/X-RAY FLUORESCENCE ANALYSIS
No radioactive silver detectable in silver--uranium ore, 30:28987
SILVER 105/ISOTOPE EFFECTS
The isotope effect for diffusion of silver in gold, 30:29015

SILVER 107/PROTON REACTIONS
Gamma angular distributions from ^{107}Ag(rho,n) reaction, 30:30953 (NP-20122)
SILVER 110/ISOTOPE EFFECTS
The isotope effect for diffusion of silver in gold, 30:29015
SILVER ALLOYS/DIFFUSION
Transport and thermodynamic properties of solids. Progress report, September 1, 1973--August 31, 1974, 30:31390 (COO-1436-41)
SILVER ORES/RADIOACTIVITY
No radioactive silver detectable in silver--uranium ore, 30:28987
SILVER ORES/X-RAY FLUORESCENCE ANALYSIS
No radioactive silver detectable in silver--uranium ore, 30:28987
SIMULATORS/PERFORMANCE
Performance characteristics of Sandia Laboratories 5.8-metre-diameter explosively driven blast simulator, 30:31431 (SLA-74-5239)
SINGLE-PARTICLE MODEL/BINDING ENERGY
Centre of mass motion and single particle separation energies in Hartree-Fock theory, 30:31081
SKELETAL DISEASES
See also OSTEOSARCOMAS
RHEUMATIC DISEASES
SKELETAL DISEASES/DIAGNOSIS
Pitfalls in /sup 99m/Tc polyphosphate skeletal imaging, 30:29849
Value of /sup 99m/Tc-diphosphonate (HEDSPA) as a skeletal scanning agent, 30:29850
SKELETAL DISEASES/RADIOTHERAPY
Results and complications of the treatment of Bechterew's disease with thorium X (^{224}Ra; arthritis of vertebral column), 30:29774
SKELETON/WEIGHT
Weight parameters of adult human skeleton, 30:29885
SKIN
See also HAIR
SKIN/BIOLOGICAL RADIATION EFFECTS
Cortisol metabolism in skin of beagles bearing ^{241}Am: a possible pre-neoplastic change in steroid metabolism, 30:29780 (COO-119-249)
SKIN/FLASH BURNS
Tyrosine aminotransferase induction in rat liver as a response to irradiation or flash burn injuries (Gamma radiation), 30:29757
SKIN/RADIATION INJURIES
Tyrosine aminotransferase induction in rat liver as a response to irradiation or flash burn injuries (Gamma radiation), 30:29757
SKIN/RADIOSENSITIVITY
Radiation and hyperthermal response of normal tissue in situ (Comparison with mammary tumors in mice), 30:29743
SLOW NEUTRONS/SLOWING-DOWN
Neutron slowing-down in ice and polyethylene at low temperatures (Moderator at 4.2, 77, and 300°K, 0.0018 to 0.090 eV), 30:30843 (IAE-2271)
SLUDGES
See SLURRIES
SLUGS (FUEL)
See FUEL RODS
SLURRIES/ACTIVATION ANALYSIS
Betatron activation analysis of cupriferrous flotation pulp (14.9-MeV photons), 30:28920
SMALL INTESTINE/BIOLOGICAL RADIATION EFFECTS
Response of jejunal mucosa to fractionated doses of neutrons or γ-rays, 30:29758
SMALL INTESTINE/RADIATION INJURIES
X-radiation-induced intestinal lesions in protein-deficient rats, 30:29741
SMOKATRON
See ELECTRON-RING ACCELERATORS
SNAP 11 BATTERY/PERFORMANCE TESTING
Performance testing of thermoelectric generators at JPL, 30:29248
SNAP 19 BATTERY/PERFORMANCE TESTING
Performance testing of thermoelectric generators at JPL, 30:29248
SNAP 19 Viking RTG flight configuration and integration testing, 30:29249
SODIUM/ACTIVATION ANALYSIS
Determination of rare earths and thorium in apatites by thermal and epithermal neutron-activation analysis, 30:28935
Multielement determination in market-garden soils by instrumental photon activation analysis, 30:28921
Trace element behavior in soil of some Indonesian sawah's and in sludge of an Indonesian river, 30:28930
SODIUM/BOILING
Study on the test of sodium boiling. I. Loss-of-flow test by a single pin (lmfbr), 30:31258
SODIUM/CHEMICAL ANALYSIS
Comments on oxygen analysis of sodium by equilibration with vanadium: an assessment, 30:28958
SODIUM/CORROSIVE EFFECTS
Study on mass transfer phenomena in the sodium loop of structural materials of the liquid metal fast-breeder reactor, 30:29950
SODIUM/ELECTRON-ATOM COLLISIONS
Polarization of the resonance lines of lithium and sodium atoms by electron impact (Glauber theory), 30:30521 (IC-73-19)
SODIUM/EMISSION SPECTROSCOPY
Spectrochemical analysis of uranium oxide by gallium oxide carrier dc arc technique (ASTM Standard E402), 30:28957
Spectrographic determination of trace impurities in high purity uranium oxide, 30:28944 (UCID-15952)
SODIUM/EXCITATION
Rate coefficients for electron excitation of the first resonance transition in H, Li, Na, Ca, Ca$^+$, and Ba$^+$ calculated from experimental data (Transition probabilities), 30:30246
SODIUM/ION EXCHANGE
Sorption of tetravalent elements by mordenite. II. Sorption of Pu(IV), 30:28999
SODIUM/LEAKS
Alkali metal leak detector method and apparatus (Patent), 30:29621
SODIUM/NEUTRON TRANSPORT
Measurement and calculation of neutron spectra at a sodium--iron interface (14-MeV source), 30:30848 (KFK-1959)
SODIUM/PURIFICATION
Apparatus for refining sodium (Patent), 30:31227
SODIUM/QUALITATIVE CHEMICAL ANALYSIS
Application of activation analysis to the determination of pollutants in the atmosphere, 30:28914 (IEA-326)
SODIUM/RADIOCHEMICAL ANALYSIS
Use of ethyl alcohol and acetic acid to prepare samples of sodium coolant for radiochemical analysis, 30:28983
SODIUM/SOLVENT PROPERTIES
Solubility of tin and germanium in liquid sodium. The sodium--tin partial phase diagram, 30:30049
SODIUM 21/ENERGY LEVELS
Spin and parity of 4.98-MeV level of ^{21}Na nucleus, 30:30909
SODIUM 22/COSMOCHEMISTRY
The unique cosmic-ray history of the Malakal chondrite, 30:30170
SODIUM 23/ISOBARIC ANALOGS
Nuclear structure studies of nuclei around mass number 23, 30:30901 (NP-20122)
SODIUM 24/WASHOUT
Model for cumulus washout of cosmogenic radionuclides, 30:29363 (BNWL-1850(Pt.3))
SODIUM ALLOYS/PHASE DIAGRAMS
Solubility of tin and germanium in liquid sodium. The sodium--tin partial phase diagram, 30:30049
SODIUM CHLORIDES/PHASE TRANSFORMATIONS
Low pressure phase transition in NaCl (29 kbar), 30:31399 (UCID-15454)
SODIUM COMPOUNDS/RADIOSENSITIVITY EFFECTS
Time course of the radioprotective effect and the formation of endogenous colonies of haemopoietic cells in mouse spleen following the administration of sodium fluoroacetate (X Radiation; mice), 30:29747
SODIUM FLUORIDES/ATOM COLLISIONS
The inelastic scattering of He and Ne from a (001) surface of sodium fluoride, 30:30479
SODIUM FLUORIDES/SOLVENT PROPERTIES
Solubility and stability of structural metal difluorides in molten fluoride mixtures, 30:29002 (ORNL-TM-760)
SODIUM OXIDES/X-RAY FLUORESCENCE ANALYSIS
Compilation of x-ray interaction data for x-ray fluorescence analysis of geological samples, 30:28943 (RISO-297)
SOFT X RADIATION/BACKGROUND RADIATION
A search for a cosmological component of the soft X-ray background in the direction of M31 (Alternative interpretations, intergalactic medium), 30:30174
SOILS/ACTIVATION ANALYSIS
Multielement determination in market-garden soils by instrumental photon activation analysis, 30:28921
Trace element behavior in soil of some Indonesian sawah's and in sludge of an Indonesian river, 30:28930
SOILS/CHEMICAL ANALYSIS
Colorimetric determination of molybdenum in oganic-rich soil, 30:28960
Determination of traces of Mo in soils and geological materials by solvent extraction of the molybdenum-thiocyanate complex and atomic absorption, 30:28965
Simultaneous determination of alpha-emitting nuclides of radium through californium in soil, 30:28977
SOILS/CONTAMINATION
Assessment of the long-term exposure due to resuspension, 30:29375 (BNWL-1850(Pt.3))
Resuspension of tracer particles by wind, 30:29370 (BNWL-1850(Pt.3))
Resuspension by wind at Rocky Flats (Plutonium monitoring in air and soil), 30:29371 (BNWL-1850(Pt.3))
Resuspension source change at Rocky Flats, 30:29372 (BNWL-1850(Pt.3))
SOILS/NATURAL RADIOACTIVITY
Radioecology of Pogonatum urnigerum (L.) pal. beauv (Mosses; gamma radiation; Poland), 30:29691
SOILS/PERMEABILITY
Field measurement of permeabilities in NTS Area 9 (Soils in 2- to 12-darcy range), 30:29458 (UCID-15895)

SOILS/RADIATION MONITORING
Airborne release of ^{137}Cs from a contaminated area during a range fire, 30:29376 (BNWL-1850(Pt.3))
Data. Section IV. Other data, 30:29412
Distribution and inventory element activities on-NTS and off-NTS (^{239}Pu, ^{240}Pu, and ^{241}Am content of soil samples from Nevada Test Site and environs), 30:29453 (NVO-AEIC-74-1)
Resuspension by wind at Rocky Flats (Plutonium monitoring in air and soil), 30:29371 (BNWL-1850(Pt.3))
Some ecological attributes and plutonium contents of perennial vegetation in Area 13 (NAEG vegetation studies) (Botany of Nevada Test Site), 30:29445 (NVO-AEIC-74-1)
Statistical analysis of Pu in soil at the Nevada Test Site: some results (Statistical sampling design), 30:29444 (NVO-AEIC-74-1)
SOILS/RADIOACTIVITY
Radioactive contamination of some arable soils in the Lower Silesia in 1972 (^{90}Sr and ^{137}Cs), 30:29402
SOILS/RADIOMETRIC ANALYSIS
Soils element activities, October 1972--September 1973 (^{241}Am, ^{239}Pu, and ^{240}Pu in soil at Nevada Test Site), 30:29440 (NVO-AEIC-74-1)
SOILS/RADIONUCLIDE MIGRATION
Buildup of ^{90}Sr in soils, 30:29406
^{137}Cs, ^{90}Sr, and ^{210}Pb in soils of the Arctic regions, 30:29405
Diffusion of radioactive fluid through soil surrounding a large power-reactor station after a core meltdown accident, 30:31254 (UCRL-51494)
Distribution and characterization of plutonium in soils from Nevada Test Site, 30:29443 (NVO-AEIC-74-1)
Environmental monitoring report, calendar year 1973, 30:29351 (UCC-ND-279)
Environmental monitoring report: United States Atomic Energy Commission, Oak Ridge facilities. Calendar year 1973 (Monitoring), 30:29352 (UCC-ND-280)
Feed Materials Production Center environmental monitoring annual report for 1973, 30:29347 (NLCO-1109)
Horizontal water migration of ^{90}Sr, 30:29407
Portsmouth Gaseous Diffusion Plant environmental monitoring report, 1973, 30:29346 (GAT-781)
Radiological monitoring program, period covering February 4, 1974--April 30, 1974 (Rio Blanco site), 30:29348 (PNE-RB-51-9)
Role of soil microorganisms in the movement of plutonium (Nevada Test Site studies), 30:29447 (NVO-AEIC-74-1)
Soils element activities, October 1972--September 1973 (^{241}Am, ^{239}Pu, and ^{240}Pu in soil at Nevada Test Site), 30:29440 (NVO-AEIC-74-1)
^{90}Sr and ^{137}Cs distribution in different types of soils, 30:29403
^{90}Sr distribution and migration in soils (Measurements of), 30:29404
Study of diffusion/leaching phenomena with glasses. Application of risk evaluation to long-term storage, 30:29133 (CEA-R-4550)
SOILS/SAMPLING
General statistical considerations in environmental plutonium studies (Sample selection), 30:29418 (NVO-AEIC-74-1)
REECo field activities and sample logistics in support of the Nevada Applied Ecology Group (Nevada Test Site ecological sample collection and preparation for Pu analysis), 30:29441 (NVO-AEIC-74-1)
SOLAR ACTIVITY
See also SOLAR FLARES
SOLAR RADIO BURSTS
SOLAR WIND
SOLAR X-RAY BURSTS
SUNSPOTS
Acceleration of thermal particles in collapsing magnetic regions, 30:30317
Sun and cosmic rays, 30:30327
SOLAR ACTIVITY/VARIATIONS
Comparison of activity in solar cycles 18, 19, and 20, 30:30328
SOLAR ATMOSPHERE/MAGNETIC FIELDS
Stokes formulation of non-LTE radiative transfer in a magnetic field, 30:30202
SOLAR ATMOSPHERE/RADIATION TRANSPORT
Stokes formulation of non-LTE radiative transfer in a magnetic field, 30:30202
SOLAR ATMOSPHERE/RESONANCE
Resonance in a semi-infinite isothermal atmosphere, 30:30304
SOLAR CELLS/PHYSICAL RADIATION EFFECTS
Effect of oxygen on unencapsulated cadmium sulfide solar cells, 30:30103
SOLAR CORONA
Coronal inhomogeneities and solar radio emissions, 30:30300
SOLAR CORONA/BRIGHTNESS
Latitudinal distribution of solar wind velocity and its relation to solar EUV corona, 30:30323
SOLAR CORONA/EXPANSION
Coronal expansion and solar wind (Interpretation of solar wind phenomena based on corona processes), 30:30320
SOLAR CORONA/HEATING
New theory of coronal heating, 30:30318
SOLAR FLARES
Comment on ''Propagation anisotropies of solar flare protons and electrons at low energies in interplanetary space'' by R. K. Pyle, 30:30312
Connection of the optical flares with the solar radio bursts, 30:30309
Properties and models of solar flares and cosmic radiation, 30:30297 (CONF-730693-)
SOLAR FLARES/ELECTRONS
Non-relativistic solar electrons, 30:30337
Relativistic electron events in interplanetary space, 30:30338
SOLAR FLARES/EMISSION SPECTRA
Solar-flare and laboratory plasma phenomena, 30:30313
Spectral classifications in the Fe XIX to Fe XXIII isoelectronic sequences, 30:30329
SOLAR FLARES/ENERGETIC SOLAR PARTICLES
Solar flares as sources of energetic particles, 30:30333
SOLAR FLARES/GAMMA RADIATION
Considerations on the neutral component relative to the August 4, 1972 solar event, 30:30296 (CONF-730693-)
SOLAR FLARES/HARD X RADIATION
Rise time in 20 to 32 keV impulsive x-radiation (Two components), 30:30299
SOLAR FLARES/NEUTRONS
Considerations on the neutral component relative to the August 4, 1972 solar event, 30:30296 (CONF-730693-)
SOLAR FLARES/RADIATIONS
Solar-flare and laboratory plasma phenomena, 30:30313
SOLAR FLARES/SHOCK WAVES
Propagation of sudden disturbances through a nonhomogeneous solar wind, 30:30322
SOLAR PARTICLES
See also ENERGETIC SOLAR PARTICLES
Comment on ''Propagation anisotropies of solar flare protons and electrons at low energies in interplanetary space'' by R. K. Pyle, 30:30312
Sun and cosmic rays, 30:30327
SOLAR RADIATION/FLUX DENSITY
Is there a real need for doubling the solar EUV fluxes, 30:30310
Satellite measurements of solar x-ray flux and ground observations of sudden ionospheric disturbances, 30:30413
Solar ultraviolet flux below 50 kilometers, 30:30303
SOLAR RADIO BURSTS
Connection of the optical flares with the solar radio bursts, 30:30309
Coronal inhomogeneities and solar radio emissions, 30:30300
Type I solar radio emission, 30:30302
Type III radio bursts, 30:30301
SOLAR RADIO BURSTS/ELECTRON PLASMA WAVES
Type-III radio bursts and their interpretation, 30:30335
SOLAR RADIO BURSTS/EMISSION
Non-relativistic solar electrons, 30:30337
SOLAR RADIO BURSTS/POLARIZATION
Radio emissions associated with the emergence of new magnetic flux from the solar photosphere, 30:30305
SOLAR RADIO BURSTS/REVIEWS
Type III bursts, 30:30334
SOLAR RADIO BURSTS/SOLAR PARTICLES
Satellite observations of type III solar radio bursts at low frequencies, 30:30336
SOLAR RADIO BURSTS/VARIATIONS
10.5 year period for the slowly varying component of the solar radio flux, 30:30306
SOLAR SPACE HEATING/CONTROL SYSTEMS
Control system design and simulation for solar heated structures, 30:31325 (LA-UR-74-1085)
SOLAR SYSTEM/SOLAR SYSTEM EVOLUTION
Structure and evolutionary history of the solar system. IV, 30:30332
SOLAR WIND
Coronal expansion and solar wind (Interpretation of solar wind phenomena based on corona processes), 30:30320
SOLAR WIND/ELECTRIC CONDUCTIVITY
On electron heat conduction in the solar wind, 30:30324
Sweet's mechanism in the solar wind (Lateral extent of d-sheets), 30:30325
SOLAR WIND/ELECTRON TEMPERATURE
On the nature of the asymptotically adiabatic solution of the two-fluid solar wind (Dimensionless form, electron and proton temperatures), 30:30298
SOLAR WIND/INTERACTIONS
Interaction between an impact-produced neutral gas cloud and the solar wind at the lunar surface, 30:30401
SOLAR WIND/ION TEMPERATURE
On the nature of the asymptotically adiabatic solution of the two-fluid solar wind (Dimensionless form, electron and proton temperatures), 30:30298
SOLAR WIND/MAGNETIC FIELDS
Sweet's mechanism in the solar wind (Lateral extent of d-sheets), 30:30325
SOLAR WIND/SHOCK WAVES
Interplanetary stream interfaces, 30:30321
SOLAR WIND/VELOCITY
Latitudinal distribution of solar wind velocity and its relation to solar EUV corona, 30:30323

  Reliability of the daily quick look solar wind velocities as indicators of interplanetary activity, 30:30400
SOLAR WIND/WAVE PROPAGATION
  Propagation of sudden disturbances through a nonhomogeneous solar wind, 30:30322
SOLAR X-RAY BURSTS/CORRELATIONS
  Some studies on solar x-ray flare-associated optical flares, microwave bursts, and sudden ionospheric disturbances, 30:30307
SOLAR X-RAY BURSTS/ENERGY SPECTRA
  Rise time in 20 to 32 keV impulsive x-radiation (Two components), 30:30299
SOLID SCINTILLATION DETECTORS
  Construction of an adjustable carrying handle for the FIDLER detector, 30:29497 (UCID-15775)
SOLID SCINTILLATION DETECTORS/CONTAMINATION
  Content of radium, uranium, radiothorium, and thorium in some scintillators, 30:29502
SOLID SCINTILLATION DETECTORS/EFFICIENCY
  Efficiencies and response functions of NaI(Tl) crystals for gamma rays from thick disk sources, 30:29517
SOLID SCINTILLATION DETECTORS/OPERATION
  Multi-strip scintillation counters (MSSC), 30:29585
SOLID SCINTILLATION DETECTORS/PERFORMANCE
  Continuous in-line monitor for UF_6 enrichment, 30:29509
SOLID SCINTILLATION DETECTORS/RESPONSE FUNCTIONS
  Efficiencies and response functions of NaI(Tl) crystals for gamma rays from thick disk sources, 30:29517
SOLIDS/EQUATIONS OF STATE
  Consistent vapor equation of state for solids, 30:31406 (UCID-15846)
SOLIDS/MICROANALYSIS
  Extension of quantitative electron beam microanalysis to solids containing light elements, 30:28968 (AED-CONF-74-084-007)
SOLIDS/POSITRON COLLISIONS
  Efficient positronium formation by slow positrons incident on solid targets (Few-eV region), 30:30510
SOLIDS/THERMAL CONDUCTIVITY
  Thermal conductivity of a hard sphere solid, 30:31441 (UCID-15723)
SOLVATED ELECTRONS/ABSORPTION SPECTRA
  Transient spectrum from nanosecond pulse radiolysis of liquid ammonia, 30:29079
SOLVATED ELECTRONS/CHEMICAL REACTION KINETICS
  Reaction of the hydrated electron with benzene studied by pulse radiolysis (5-MeV electron pulses), 30:29081
SOMATIC CELLS
    See also STEM CELLS
        THYMOCYTES
SOMATIC CELLS/MUTATIONS
  Somatic mutation by endogenous radiocarbon, 30:29787
SOMATOTROPIC HORMONE
    See STH
SORGHUM/GENETIC RADIATION EFFECTS
  Studies on inter-relationship of quantitative traits in M_3 and M_4 generations following mutagenic treatments in sorghum (γ Rays; x rays; EMS), 30:29698
SOUTH AMERICA
    See also BRAZIL
SOUTH AMERICA/FALLOUT
  Data. Section III. Air and deposition (Monitoring), 30:29382
  Data. Section I. Milk and food (Monitoring), 30:29421
SOVIET UNION
    See USSR
SPACE FLIGHT/SAFETY
  Problems of space radiobiology and radiation safety in space missions, 30:29712
SPACE PROPULSION REACTORS/FISSIONING PLASMA
  Diagnostics of seeded rf plasmas: an experimental study related to the gaseous core nuclear reactor. Final report, 1 September 1971--31 July 1973 (Argon), 30:31241 (N-74-23299)
SPACECRAFT POWER SUPPLIES/SNAP 19 BATTERY
  SNAP 19 Viking RTG flight configuration and integration testing, 30:29249
SPACECRAFT POWER SUPPLIES/THERMOELECTRIC GENERATORS
  10% efficient economic RTG design, 30:29251
  Cost effective designing for the economic RTG, 30:29252
  Fabrication and testing of a thermoelectric RING converter segment for space applications, 30:29246
  Fault tolerant sequencing (FTS) shunt regulator, 30:29254
  Light-weight radiosotope thermoelectric generator design, 30:29253
  Operational testing of the high performance thermoelectric generator (HPG-02), 30:29250
  Performance testing of thermoelectric generators at JPL, 30:29248
  RTG technology development: where we are/where we are going, 30:29244
  Silicon germanium technology program at JPL, 30:29247
SPECIFIC HEAT/MEASURING METHODS
  Microsecond pulse technique for heat capacity measurement, 30:31424 (LBL-2574)
SPECTROMETERS
    See also BETA SPECTROMETERS
        COSMIC RAY SPECTROMETERS
        ELECTRON SPECTROMETERS
        FISSION FRAGMENT SPECTROMETERS
        GAMMA SPECTROMETERS
        HEAVY ION SPECTROMETERS
        MAGNETIC SPECTROMETERS
        MASS SPECTROMETERS
        NEUTRON SPECTROMETERS
        PROTON SPECTROMETERS
        TIME-OF-FLIGHT SPECTROMETERS
        X-RAY SPECTROMETERS
SPECTROMETERS/RADIAL VELOCITY
  The Palomar radial-velocity spectrometer (Optical basis, very bright stars), 30:30184
SPENT FUEL ELEMENTS/CRUSHING
  Secondary jaw crusher development, 30:29265 (GA-A-12903)
SPENT FUEL ELEMENTS/INSPECTION
  Examination of fuel element cladding including the determination of the mechanical properties, 30:30083
SPENT FUEL ELEMENTS/MECHANICAL DECLADDING
  Nuclear reactor fuel rod splitter (Patent), 30:30111
SPENT FUEL ELEMENTS/REPROCESSING
  Apparatus and method for processing spent nuclear fuel elements (Patent), 30:29146
  Decontaminating uranium by reaction with ClF_3 and HF and volatizing the UF_6 product (Patent), 30:29149
  Method for the suppression of hydrogen during the dissolution of zirconium and zirconium alloys (Patent; Zirflex process), 30:29148
SPENT FUEL ELEMENTS/TRANSPORT
  LMFBR-37-fuel-element shipping cask simulation: test assembly operation and data, 30:30114 (ORNL-TM-3992)
SPENT FUELS/REPROCESSING
  The disposal system in the nuclear fuel cycle (German LFederal Republic), 30:29147
SPERMATOZOA/BIOLOGICAL RADIATION EFFECTS
  Response of spermatogonia of the mouse to hycanthone, and a comparison with the effect of γ rays, 30:29735 (CONF-731222-1)
SPHERES/COLLISIONS
  Comment on the semiclassical scattering of rigid spheres, 30:30530
SPIN ORIENTATION/REVIEWS
  Nuclear orientation: from an exotic to a matured method in nuclear physics, 30:30962
SPIN-ORBIT INTERACTION
    See L-S COUPLING
SPLEEN/BIOLOGICAL RADIATION EFFECTS
  Hydrolysis of 2',3'-cyclic adenosine monophosphate and 3',5'-cyclic adenosine monophosphate in subcellular fractions of normal and neoplastic mouse spleen (X radiation), 30:29739
SPLEEN/RADIONUCLIDE KINETICS
  Effect of delayed lymphadenectomy on $^{239}PuO_2$ translocation in dogs, 30:29820
SPLEEN CELLS/BIOCHEMICAL REACTION KINETICS
  Effect of ionizing radiation on alkaline phosphatase activity in hematopoietic cells of mouse and rat (X rays), 30:29762
SPLEEN COLONY FORMATION
  Time course of the radioprotective effect and the formation of endogenous colonies of haemopoietic cells in mouse spleen following the administration of sodium fluoroacetate (X Radiation; mice), 30:29747
SPLIT DOSE IRRADIATION
    See FRACTIONATED IRRADIATION
SPRAY SYSTEMS (CONTAINMENT)
    See CONTAINMENT SPRAY SYSTEMS
SPRAYED COATINGS/ELASTICITY
  Damping and elastic characteristics of plasma-sprayed coatings of W, nichrome, zirconia, and Cr--Ni spinels, 30:29887
SQUIRRELS/POPULATION DYNAMICS
  Vertebrate behavior and ecology. Progress report, July 1, 1973--June 30, 1974, 30:31377 (COO-1332-103)
STACK DISPOSAL/AEROSOL MONITORING
  Preliminary in-plume measurements near Centralia (Trace gases and particulates, power plant), 30:29472 (BNWL-1850(Pt.3))
STACK DISPOSAL/PLUMES
  Measurement of particulate plume depletion by comparison with inert gas plumes (^{85}Kr tracer studies), 30:29425 (BNWL-1850(Pt.3))
STAINLESS STEEL-304/FATIGUE
  Irradiation effects on reactor structural materials. Semiannual progress report, 1 August 1973--31 January 1974, 30:30060 (AD-777433)
STAINLESS STEEL-304/PHYSICAL RADIATION EFFECTS
  Empirical swelling equations for solution-annealed Type 304 stainless steel (Fast neutrons), 30:30085
  Fabrication, irradiation, and postirradiation examination of mixed oxide fuel pin PNL-3-8, 30:31231 (HEDL-TME-74-37)
  Fast reactor programme. First quarter 1974 progress report, 30:31226 (RCN-212)
STAINLESS STEEL-316/CORROSION
  Thermodynamic data program involving plutonia and urania at high temperatures. Quarterly report No. 27, February 1, 1974--April 30, 1974 (LMFBR), 30:31223 (GEAP-12511)
STAINLESS STEEL-316/MASS TRANSFER
  Study on mass transfer phenomena in the sodium loop of structural materials of the liquid metal fast-breeder reactor, 30:29950

STAINLESS STEEL-316/PHYSICAL RADIATION EFFECTS
A possible mechanism for the formation of a ferromagnetic phase in stainless steel Fe/Cr/Ni/Mo, 17/11/8/2 (type 316L) irradiated in the pile, 30:30077
Irradiation effects on reactor structural materials. Semiannual progress report, 1 August 1973--31 January 1974, 30:30060 (AD-777433)
STAINLESS STEEL-316/SLIP
Grain boundary sliding and structure. Progress report, December 1, 1973--November 30, 1974, 30:29977 (COO-2172-7)
STAINLESS STEELS
See also STAINLESS STEEL-304
STAINLESS STEEL-316
STAINLESS STEELS/MECHANICAL PROPERTIES
Characterizations of fuel element cladding tubes, 30:31279 (RT/MET-(73)1)
STAINLESS STEELS/THERMAL FATIGUE
Mechanical properties of metal matrix composites subjected to cyclic temperature changes. Annual report, 1 July 1972--30 June 1973 (6064 Al reinforced with fibers of stainless steel, 34 vol % SiC, 27 vol % B, and 45 vol % B), 30:29973 (AD-774890)
STANFORD 20-GEV LINAC/ACCELERATOR FACILITIES
A high-quality muon beam in the 10-15 GeV energy range, 30:30150
STAR CLUSTERS/INFRARED RADIATION
Near-infrared magnitudes and (V-K) colors of globular clusters (Weak constants), 30:30219
STAR CLUSTERS/LUMINOSITY
Near-infrared magnitudes and (V-K) colors of globular clusters (Weak constants), 30:30219
STAR CLUSTERS/MASS
Population synthesis applied to eignt young Magellanic Cloud globular clusters (Corresponding age), 30:30216
STAR CLUSTERS/ORBITS
Distribution of orbital eccentricities of the globular clusters, 30:30353
STAR CLUSTERS/PHOTOMETRY
NGC 6193: an emission region with a high ratio of total to selective extinction (Anomalously high value), 30:30239
Population synthesis applied to eignt young Magellanic Cloud globular clusters (Corresponding age), 30:30216
VB 130: A nebulous cluster with an abnormal extinction law (Absorbing material), 30:30363
STAR CLUSTERS/STAR EVOLUTION
Photometry of a Pleiades candidate and composite white dwarfs (Parent star), 30:30234
STAR EVOLUTION
Are stellar surface heavy-element abundances systematically enhanced. (Upper limit, Hayashi-phase convection), 30:30250
Gas density and the rate of star formation in M33 (Initial collapse), 30:30348
Genetic connection between stars O--B0 and diffuse nebulae, 30:30213
STAR EVOLUTION/CHEMICAL COMPOSITION
Island solutions in linear series of static stellar models with core nelium and shell hydrogen burning for M=5,7, and 9 M/subsun/ (Mass loss, secular stability), 30:30198
STAR EVOLUTION/THERMONUCLEAR REACTIONS
URCA processes in convective stellar cores, 30:30200
STARCH/ACTIVATION ANALYSIS
Method for determining sugar/starch contents in aqueous solutions (Using Hg-203-labelled compounds for tracer method or nonradioactive Hg for neutron activation patent), 30:28936
STARCH/RADIOCHEMICAL ANALYSIS
Method for determining sugar/starch contents in aqueous solutions (Using Hg-203-labelled compounds for tracer method or nonradioactive Hg for neutron activation patent), 30:28936
STARCH/RADIOLYSIS
Some physical and chemical properties of fractions separated from gamma-irradiated corn starch, 30:29041
STARS
See also BINARY STARS
CEPHEIDS
DWARF STARS
GIANT STARS
MAGNETIC STARS
MAIN SEQUENCE STARS
NEUTRON STARS
NOVAE
SUN
SUPERNOVAE
T TAURI STARS
STARS/ABSORPTION SPECTRA
Neutral potassium in dusty clouds (Optical deptns, gas-to-dust ratio), 30:30358
Radiative transitions involving the $(2p^2)$ ^3P/sup e/ metastable autodetaching state of H^- (Transition probabilities, Hylleraas bound-state wave function), 30:30245
STARS/ATMOSPHERES
High velocities and cocoon stars, 30:30243
STARS/CONVECTION
URCA processes in convective stellar cores, 30:30200
STARS/EMISSION SPECTRA
High velocities and cocoon stars, 30:30243
High-resolution Fourier spectra of stars and planets, 30:30207
STARS/INFRARED RADIATION
Classification of unidentified sources from a 2-μ southern sky survey (Late types), 30:30220
Infrared observations of Be stars from 2.3 to 19.5 microns (Negative results), 30:30252
STARS/LUMINOSITY
Angular diameter of μ Geminorum (Time scale), 30:30224
STARS/LYMAN LINES
Dust, star, and hydrogen distributions in the Orion association, 30:30242
STARS/MAGELLANIC CLOUDS
Identification of stars in the direction of the Large Magellanic Cloud, 30:30199
STARS/MATHEMATICAL MODELS
Models for nuclei of planetary nebulae and ultraviolet stars, 30:30215
STARS/OPACITY
Radiative transitions involving the $(2p^2)$ ^3P/sup e/ metastable autodetaching state of H^- (Transition probabilities, Hylleraas bound-state wave function), 30:30245
STARS/ORBITS
Parallaxes and proper motions of twelve nearby stars determined with the Sproul 24-in. refractor (Grant machine), 30:30236
STARS/ORIGIN
Genetic connection between stars O--B0 and diffuse nebulae, 30:30213
STARS/PHOTOMETRY
Broad-band 20-μ photometry of 63 stars (Circumstellar shells), 30:30221
Investigation of a Milky Way region in Canis hajor (Obscuring matter), 30:30217
Optical studies of Uhuru sources. VIII. Observations of 92 possible counterparts of x-ray sources, 30:30205
STARS/PROPER MOTION
Parallaxes and proper motions of twelve nearby stars determined with the Sproul 24-in. refractor (Grant machine), 30:30236
Proper motions of faint blue stars near the galactic anticenter. I (Mean error), 30:30237
STARS/ROTATION
Rotational velocities in the Orion association (Early-type stars), 30:30223
STARS/SHOCK WAVES
Ionization shock waves in stars, 30:30212
STARS/SIZE
Angular diameter of μ Geminorum (Time scale), 30:30224
Diameter of μ Geminorum M3 III from lunar occultation (Tnree-channel observation), 30:30225
STARS/SPATIAL DISTRIBUTION
Faint O-B3 stars in the Norma section of the Milky Way (Visual extinction), 30:30233
STARS/SPECTRA
Spectral survey of the southern Milky Way. I. General description and catalog I (l = 306--318°), 30:30352
Spectroscopic observations of interesting Southern stars noted on southern objective-prism plates (R coronae borealis stars), 30:30253
STARS/STABILITY
Pulsational stability of stars in thermal imbalance. III. Analysis in terms of absolute variations (Equivalence proofs, secular motion), 30:30192
Relativistic stellar stability: preferred-frame effects, 30:30206
STARS/STATISTICAL MECHANICS
Equilibrium statistical mechanics of relativistic particles with variable masses. I. Nonquantal theory, 30:30168
STARS/VARIATIONS
Periods of three RR Lyrae type stars, 30:30211
STATISTICAL MECHANICS/RELATIVISTIC RANGE
Equilibrium statistical mechanics of relativistic particles with variable masses. I. Nonquantal theory, 30:30168
STEAM/TWO-PHASE FLOW
Derivation of transfer functions in boiling loops, 30:29292
STEAM GENERATING HEAVY WATER REACTOR
See SGHWR REACTOR
STEAM GENERATORS/DESIGN
Once-through vapor generator (Patent), 30:29278
STEAM GENERATORS/RESEARCH PROGRAMS
LMFBR demonstration plant steam generating system, 30:31217 (CENC-1194(Vol.1)(Suppl.1))
LMFBR demonstration plant steam generating system, 30:31218 (CENC-1194(Vol.2)(Suppl.1))
LMFBR sodium heated steam generator: test model, 30:31219 (CENC-1197(Vol.1))
LMFBR sodium heated steam generator: test model, 30:31220 (CENC-1197(Vol.3))
LMFBR sodium heated steam generator: test model (Structural steel analysis), 30:31221 (CENC-1197(Vol.4))

STEAM TURBINES/CONTROL SYSTEMS
  System and method for operating a steam turbine with independent overspeed protection especially adapted for a nuclear reactor powered steam turbine (Patent), 30:31283
STEAM TURBINES/TEMPERATURE CONTROL
  Electric power plant system and method for operating a steam turbine especially of the nuclear type with electronic reheat control of a cycle steam reheater (Patent), 30:31300
STEEL-1KH18N10T/DUCTILITY
  Effect of electron-beam remelting on the high-temperature ductility of steel 1Kh18N10T irradiated with an integrated flux of $2.7.10^{21}$ neutrons/cm^2, 30:30071
STEEL-1KH18N10T/PHYSICAL RADIATION EFFECTS
  Effect of electron-beam remelting on the high-temperature ductility of steel 1Kh18N10T irradiated with an integrated flux of $2.7.10^{21}$ neutrons/cm^2, 30:30071
STEEL-ASTM-A508/FRACTURE PROPERTIES
  Quarterly progress report on reactor safety programs sponsored by the Division of Reactor Safety Research for April--June 1974, 30:31251 (ORNL-TM-4655(Vol.2))
STEEL-ASTM-A508/PHYSICAL RADIATION EFFECTS
  Quarterly progress report on reactor safety programs sponsored by the Division of Reactor Safety Research for April--June 1974, 30:31251 (ORNL-TM-4655(Vol.2))
STEEL-ASTM-A508/THERMAL STRESSES
  Quarterly progress report on reactor safety programs sponsored by the Division of Reactor Safety Research for April--June 1974, 30:31251 (ORNL-TM-4655(Vol.2))
STEEL-ASTM-A533/FRACTURE PROPERTIES
  Quarterly progress report on reactor safety programs sponsored by the Division of Reactor Safety Research for April--June 1974, 30:31251 (ORNL-TM-4655(Vol.2))
STEEL-ASTM-A533/PHYSICAL RADIATION EFFECTS
  Quarterly progress report on reactor safety programs sponsored by the Division of Reactor Safety Research for April--June 1974, 30:31251 (ORNL-TM-4655(Vol.2))
STEEL-ASTM-A533/THERMAL STRESSES
  Quarterly progress report on reactor safety programs sponsored by the Division of Reactor Safety Research for April--June 1974, 30:31251 (ORNL-TM-4655(Vol.2))
STEEL-ASTM-A543/PHYSICAL RADIATION EFFECTS
  Irradiation effects on reactor structural materials. Semiannual progress report, 1 August 1973--31 January 1974, 30:30060 (AD-777433)
STEELS
  See also CHROMIUM-MOLYBDENUM STEELS
    STAINLESS STEELS
    STEEL-ASTM-A533
STEELS/AGING
  Field-ion microscopic study of aged martensite in an iron--nickel--cobalt--molybdenum alloy (Fe--16 percent Ni--15 percent Co--5 percent Mo; precipitation of Mo), 30:30037
STEELS/CORROSION
  Corrosion and corrosion resistance. IX. Tutzing symposium of the DECHEMA, February 26--March 1, 1973, Tutzing Castle, Starnberger Lake, 30:29943 (CONF-730230-(Absts.))
STEELS/CORROSION RESISTANCE
  Study of the corrosion resistance of titanium alloys and some steels during condensation of alkylphenol with formaldehyde (Steels 3, AT-3, EI-943; Ti alloys VT2-1, VT-14; VT1-0, OT-4, VT5, Ti--5 percent Ta, Ti--33 percent Mo), 30:29947
STEELS/GAMMA RADIOGRAPHY
  Radiography of steel components with a linear electron accelerator, 30:30143
STEELS/INDUSTRIAL RADIOGRAPHY
  Steel castings up to 2 in. in thickness, 30:30044
STEELS/METALLURGY
  Publications from 1970--1972 of the Metallurgical Publishers. Annotated index (Metallurgy; ferrous and nonferrous metals; processing of steels and alloys; corrosion), 30:30042
STEELS/PROTECTIVE COATINGS
  Surface protection in nuclear power plant (Epoxy resin; coating of steel), 30:29946
STEELS/SURFACE COATING
  Multicomponent diffusion coatings (Book), 30:29906
STEELS/WELDING
  Properties of TZM and nuclear behavior of TZM brazements. Various properties of TZM and Zr--5Be and Au--18Ni brazing filler metals are determined for brazing TZM to Zr and to steel, 30:30084
STEK REACTOR/NEUTRON SPECTRA
  Fast reactor programme. First quarter 1974 progress report, 30:31226 (RCN-212)
STELLAR ATMOSPHERES/ABSORPTION SPECTRA
  Dust particles and molecules in the extended atmospheres of carbon stars, 30:30244
STELLAR ATMOSPHERES/CHEMICAL COMPOSITION
  Stellar atmospheres: the sources of interstellar molecules, 30:30241
STELLAR ATMOSPHERES/MAGNETIC FIELDS
  Stokes formulation of non-LTE radiative transfer in a magnetic field, 30:30202
STELLAR ATMOSPHERES/POLARIZATION
  Radiative transfer of partially polarized light (Specific intensity, arbitrary state of motion), 30:30195
STELLAR ATMOSPHERES/RADIATION TRANSPORT
  On the passage of radiation through inhomogeneous moving media. V. Line absorption and frequency variations of optical depth (Perpendicular incidence), 30:30247
  On the passage of radiation through inhomogeneous, moving media. VI. Dispersion effects on phase and ray paths in a plane, differentially shearing medium (Basic physical effects, pulse width), 30:30248
  On the passage of radiation through inhomogeneous, moving media. VII. Concerning the validity of the geometrical optics approximation (Basic physical picture, coupled second-order differential equations), 30:30249
  Radiative transfer of partially polarized light (Specific intensity, arbitrary state of motion), 30:30195
  Stokes formulation of non-LTE radiative transfer in a magnetic field, 30:30202
STELLAR ATMOSPHERES/SPECTRA
  Progress towards an interpretation of stellar spectra (Circumstellar envelopes), 30:30229
STELLAR FLARES
  See also SOLAR FLARES
STELLAR FLARES/COSMIC X-RAY SOURCES
  Simultaneous hard X-ray and optical observations of Sco X-1 and a model of semi-opaque X-ray sources, 30:30294
STEM CELLS/CELL KILLING
  Response of jejunal mucosa to fractionated doses of neutrons or γ-rays, 30:29758
STEREOCHEMISTRY/RESEARCH PROGRAMS
  Department of Fundamental Research, Grenoble, semiannual bulletin No. 4, 30:31333 (CEA-N-1688)
STH
  (Somatotropic hormone; growth hormone.)
STH/RADIOIMMUNOASSAY
  Modification of radioimmunoassay method of human growth hormone estimation, 30:29877
  Radioimmunological determination of proteohormones, 30:29874
STIRLING ENGINES/PERFORMANCE
  Implanted energy conversion system. Annual report, 8 July 1972--8 July 1973, 30:29239 (JUL-73)
STIRLING ENGINES/PERFORMANCE TESTING
  Unconventional Stirling engines for the artificial heart application, 30:29260
STORAGE DEVICES (DATA)
  See MEMORY DEVICES
STORAGE RINGS/BEAM CURRENTS
  Note on the incoherent space charge limit in the High Intensity Storage Ring, 30:30139 (UCID-15686)
STORAGE RINGS/BEAM DYNAMICS
  Resonance excitation by distortion of the β-function coupled with a long range space charge force, 30:30137 (BNL-19192)
STORAGE RINGS/MAGNETIC FIELDS
  Quadrupole fields in a toroidal geometry for the High Intensity Storage Ring, 30:30140 (UCID-15735)
STORAGE RINGS/OPTIMIZATION
  Preliminary orbits and structure of a high intensity storage ring, 30:30138 (UCID-15685)
STORAGE RINGS/PLANNING
  Preliminary orbits and structure of a high intensity storage ring, 30:30138 (UCID-15685)
STORAGE RINGS/SYNCHROTRON RADIATION
  Geometry and optics of synchrotron radiation, 30:30119
STRAINS/MEASURING METHODS
  Dynamic interferometric holography, 30:31440 (UCID-15682)
STRAND BREAKS/BIOLOGICAL REPAIR
  DNA repair in human progeroid cells (Gamma radiation), 30:29673
  Rate of DNA repair in progeric and normal human fibroblasts (Gamma radiation, Hutchinson--Gilford syndrome), 30:29672
  Repair of γ-ray-induced damage in bacteriophage lambda (Escherichia coli), 30:29680
STRAND BREAKS/RADIOINDUCTION
  Chemical nature of the ends of DNA single-strand breaks produced by ionizing γ radiation in vivo and pathways of their reparation (Escherichia coli), 30:29682
  Comment on ''further data on DNA strand breakage by various radiation qualities'' (γ radiation. protons), 30:29660
  Structural study of DNA discontinuities by enzymatic polymerization (γ radiation), 30:29650 (JEN-286)
STRANGE PARTICLES
  See also KAONS
STRANGE PARTICLES/PARTICLE PRODUCTION
  Study of π^+p interactions with strange particle production in five- and six-body final states at 8 GeV/c, 30:30615
STREAMER SPARK CHAMBERS/OPERATION
  Application of microwave techniques to high-energy physics experiments at Argonne National Laboratory, 30:29584
STRENGTH (FRACTURE)
  See FRACTURE PROPERTIES
STREPTOKINASE/CHEMICAL RADIATION EFFECTS
  Method for preparation of biocompatible and biofunctional materials and product thereof (Graft polymerization using high-energy electrons, x or γ radiation, patent), 30:29082

STRESS ANALYSIS/COMPUTER CALCULATIONS
Large user-orientated systems of programs for structural analysis and design, 30:31291
STRESSES
(Mechanics.)
STRESSES/RECORDING SYSTEMS
Photoelastometric recording of stress waves, 30:31434 (UCID-15383)
STRING MODELS
Dual strings in the Amati-Testa quark imprisonment scheme, 30:30647
STRING MODELS/DUALITY
A dual quark prison, 30:30697
STRONG INTERACTIONS
See also CHARGE-EXCHANGE INTERACTIONS
HADRON-HADRON INTERACTIONS
Effective degrees of freedom in strong interaction processes, 30:30705
New description of the initial states, 30:30690
Two-loop diagrams in Yang-Mills theory, 30:31168
STRONG INTERACTIONS/ASYMPTOTIC SOLUTIONS
Asymptotic near freedom, 30:30672
STRONG INTERACTIONS/KINETICS
Strong interaction dynamics (Lectures, Regge exchange), 30:30703
STRONG INTERACTIONS/LINEAR MOMENTUM TRANSFER
Large momentum transfer reactions, without partons (Hadronic bremsstrahlung model), 30:30764
STRONG INTERACTIONS/MULTIPLE PRODUCTION
Experimental results on strong interactions in the NAL hydrogen bubble chamber, 30:30609
STRONG INTERACTIONS/PARTON MODEL
Parton models and asymptotic freedom, 30:30630
STRONG INTERACTIONS/REGGE CUTS
Possibility that the Pomeron-Reggeon cut contains the Regge pole, 30:30717
STRONG INTERACTIONS/RESEARCH PROGRAMS
High Energy Accelerator and Colliding Beam User Group. Progress report (Summaries of research activities at University of Maryland), 30:30575 (TID-26638)
STRONG INTERACTIONS/REVIEWS
Experimental review of strong interactions at high energy, 30:30578
STRONG INTERACTIONS/SYMMETRY BREAKING
SU(3) symmetry breaking and superfluidity of hadronic matter, 30:30781
STRONTIUM/ACTIVATION ANALYSIS
Multielement determination in market-garden soils by instrumental photon activation analysis, 30:28921
STRONTIUM/DIFFUSION
Study of diffusion/leaching phenomena with glasses. Application of risk evaluation to long-term storage, 30:29133 (CEA-R-4550)
STRONTIUM/EMISSION SPECTROSCOPY
Spectrographic determination of trace impurities in high purity uranium oxide, 30:28944 (UCID-15952)
STRONTIUM 86/ISOTOPE RATIO
Determination of ^{87}Sr/^{86}Sr in cenozoic andesites and the related rocks of northwest Sardinia (italy), 30:29340
STRONTIUM 87/ISOTOPE RATIO
Determination of ^{87}Sr/^{86}Sr in cenozoic andesites and the related rocks of northwest Sardinia (Italy), 30:29340
STRONTIUM 89/ABUNDANCE
Calculation of fractionation effects following atmospheric nuclear explosions, 30:29386
STRONTIUM 89/ION EXCHANGE CHROMATOGRAPHY
Chromatography on finely dispersed ionites on inert supports, 30:28997
STRONTIUM 89/RADIATION MONITORING
Data. Section IV. Other data, 30:29412
STRONTIUM 89/RADIOECOLOGICAL CONCENTRATION
Radiological monitoring program, period covering February 4, 1974--April 30, 1974 (Rio Blanco site), 30:29348 (PNE-RB-51-9)
STRONTIUM 90/ABUNDANCE
Calculation of fractionation effects following atmospheric nuclear explosions, 30:29386
STRONTIUM 90/BIOLOGICAL RADIATION EFFECTS
Nuclear testing (^{131}I; ^{90}Sr; ^{137}Cs; ^{14}C; Tritium), 30:29719
Real risks of the nuclear tests (^{131}I; ^{137}Cs; ^{90}Sr), 30:29720
Research in radiobiology. Annual report of work in progress in the internal irradiation program (Pathological effects of bone-seeking radionuclides in beagles), 30:29778 (COO-119-249)
STRONTIUM 90/CHEMICAL STATE
State of ^{90}Sr, ^{137}Cs, and ^{144}Ce in radioactive fallout, 30:29384
STRONTIUM 90/DIFFUSION
Buildup of ^{90}Sr in soils, 30:29406
Horizontal water migration of ^{90}Sr, 30:29407
Kinetics of the self-purification of a body of water containing strontium-90 as a result of absorption of the radionuclide by the bottom deposits, 30:29414
^{90}Sr and ^{137}Cs distribution in different types of soils, 30:29403
^{90}Sr distribution and migration in soils (Measurements of), 30:29404
STRONTIUM 90/ION EXCHANGE
Separation of ^{137}Cs and ^{90}Sr from highly radioactive fission product solutions, 30:28991 (BLG-487)
STRONTIUM 90/RADIATION MONITORING
^{137}Cs, ^{90}Sr, and ^{210}Pb in soils of the Arctic regions, 30:29405
Data. Section III. Air and deposition, 30:29382
Data. Section IV. Other data, 30:29412
Data. Section I. Milk and food, 30:29421
Determination of fallout radioisotopes from their content in the annual layers of high-mountain glaciers, 30:29408
Environmental monitoring report: United States Atomic Energy Commission, Oak Ridge facilities. Calendar year 1973, 30:29352 (UCC-ND-280)
Phase I. Radiation and radioisotope studies with laboratory and domestic animals (Fallout ^{137}Cs, ^{131}I, and ^{90}Sr in food chains), 30:29417 (COO-3167-102)
Radioactive contamination of some arable soils in the Lower Silesia in 1972, 30:29402
Rate of fallout of ^{137}Cs and ^{90}Sr aerosols from the atmosphere, 30:29399
Report of activity, February 1974 (Radioactivity of environmental samples collected throughout France during February 1974), 30:29349 (SCPRI(RM)-2-1974)
STRONTIUM 90/RADIOECOLOGICAL CONCENTRATION
Environmental monitoring report: United States Atomic Energy Commission, Oak Ridge facilities. Calendar year 1973, 30:29352 (UCC-ND-280)
Radiological monitoring program, period covering February 4, 1974--April 30, 1974 (Rio Blanco site), 30:29348 (PNE-RB-51-9)
STRUCTURAL MODELS/TESTING
Methods for the identification of dynamic parameters of mathematical structural models from experimental data, 30:31269
STRUCTURES (MECHANICS)
See MECHANICAL STRUCTURES
STYRENE/CHEMICAL RADIATION EFFECTS
Studies on the preparation of mortar--plastic composite (Radiation, thermal-catalytic, and radiation-catalytic methods; γ radiation), 30:29045
STYRENE POLYMERS
See POLYSTYRENE
SU GROUPS
See also SU-2 GROUPS
SU-3 GROUPS
SU-4 GROUPS
SU-6 GROUPS
SU GROUPS/UNITARY SYMMETRY
Generalized 6j-coefficients and their symmetries, 30:30769
SU-2 GROUPS
Gel'fand-pattern technique applied to the physically important SU(3) x SU(2) is contained in SU(6) decomposition of SU(6), 30:30768
SU-2 GROUPS/CHIRAL SYMMETRY
Is chiral SU$_2$ x SU$_2$ a hidden symmetry, 30:30774
SU-2 GROUPS/SYMMETRY BREAKING
Pion phase transition in chiral symmetry breaking model, 30:30716
Structure and experimental consequences of chiral SU$_3$ x SU$_3$ breaking, 30:30775
SU-2 GROUPS/UNITARY SYMMETRY
Generalized 6j-coefficients and their symmetries, 30:30769
SU-3 GROUPS
Gel'fand-pattern technique applied to the physically important SU(3) x SU(2) is contained in SU(6) decomposition of SU(6), 30:30768
SU-3 GROUPS/CHIRAL SYMMETRY
Consistency conditions in the theory of spontaneous breaking of chiral symmetry, 30:30778
Non-zero masses of π,K, eta and kappa mesons and algebraic realization of SU(3) x SU(3) chiral symmetry, 30:30780
SU-3 GROUPS/SYMMETRY BREAKING
Quark additivity for mass splittings in the psub(z) + infinity frame, 30:30709
Structure and experimental consequences of chiral SU$_3$ x SU$_3$ breaking, 30:30775
SU(3) symmetry breaking and superfluidity of hadronic matter, 30:30781
SU-4 GROUPS
Meson electromagnetic decays from SU(4)/sub w/ and generalized vector dominance (Pion form factor), 30:30650 (NP-20072)
SU-6 GROUPS
Gel'fand-pattern technique applied to the physically important SU(3) x SU(2) is contained in SU(6) decomposition of SU(6), 30:30768
SU-6 GROUPS/N*RESONANCES
SU$_6$ quark model, nucleon resonance electroproduction and spin-dependent electroproduction structure functions, 30:30735
SUCROSE
See SACCHAROSE
SUDDEN IONOSPHERIC DISTURBANCE
Satellite measurements of solar x-ray flux and ground observations of sudden ionospheric disturbances, 30:30413
SUDDEN IONOSPHERIC DISTURBANCE/WAVE PROPAGATION
Propagation of VLF and ELF waves during sudden ionospheric disturbances, 30:30418

SULFADIAZINE/INTESTINAL ABSORPTION
  Effect of irradiation on gastrointestinal drug absorption in mice and rats (Sulfadiazine;quinine;x radiation), 30:29738
SULFATES/WASHOUT
  Relation between washout of radioactivity and nonradioactive ions in the atmosphere by precipitation, 30:29395
SULFHYDRYL COMPOUNDS
  See THIOLS
SULFUR/COSMOCHEMISTRY
  High-frequency observations of possible ''heavy-element'' recombination lines (Cosmic value), 30:30267
SULFUR 32/ISOTOPE SEPARATION
  Fractionation of sulfur isotopes by the yeast Saccharomyces cerevisiae, 30:29826
SULFUR 32 REACTIONS
  Precision lifetime measurement with the coincident high-velocity DSA method, 30:30864
SULFUR 32 REACTIONS/INELASTIC SCATTERING
  Inelastic transfer in the scattering of ^{32}S on ^{30}Si (75 to 80 MeV: angular distributions, DWBA analysis), 30:30906
SULFUR 33/LIFETIME
  Precision lifetime measurement with the coincident high-velocity DSA method, 30:30864
SULFUR 35/BIOLOGICAL RADIATION EFFECTS
  Comparative investigation of mutagenic effects of incorporated isotopes of the most important organogenic elements. VI. Comparison of lethal and mutagenic effects of the decay of ^{32}P and ^{35}S incorporated into cells of Escherichia coli WP-2S Try$^-$, 30:29788
SULFUR 35/RADIOCHEMISTRY
  Mechanism of reduction of 1-methyl-4-thiocyanatouracil by bisulfide. A route to in vitro labeling of tRNAs with sulfur-35, 30:29092
SULFUR CARBIDES
  See CARBON SULFIDES
SULFUR CHLORIDES/ATOM-MOLECULE COLLISIONS
  Angular distributions for the reactive scattering of H and D atoms by polyatomic molecules, 30:30519 (AED-CONF-74-085-004)
SULFUR DIOXIDE/CHEMICAL RADIATION EFFECTS
  Treatment of exhaust gas with electron beam irradiation. I. Treatment of exhaust gas in batch type apparatus, 30:29046
SULFUR DIOXIDE/MONITORING
  Portsmouth Gaseous Diffusion Plant environmental monitoring report, 1973, 30:29346 (GAT-781)
SULFUR HYDRIDES
  See HYDROGEN SULFIDES
SULFUR OXIDES/WASHOUT
  Precipitation scavenging of inorganic pollutants from metropolitan sources: St. Louis, July 1973, 30:29479 (BNWL-1850(Pt.3))
SULFURIC ACID/CHEMICAL RADIATION EFFECTS
  Chemical behavior of intermediates produced in sulfuric acid glass by gamma irradiation. I. Reactivities of mobile electrons with inorganic ions, 30:29048
SUN/ELECTRIC CONDUCTIVITY
  Electrical conductivity of the matter in the subphotospheric layers of the Sun (Kinetic equations), 30:30308
SUN/EMISSION SPECTRA
  Observed departures from LTE in stellar Fe I lines. I. The Sun, 30:30319
SUN/HYDRODYNAMICS
  Acceleration of thermal particles in collapsing magnetic regions, 30:30317
SUN/MAGNETIC FIELDS
  Dynamics of the solar magnetic field. I. Method of examination of force-free magnetic fields, 30:30315
SUN/NEUTRINOS
  Are stellar surface heavy-element abundances systematically enhanced. (Upper limit, Hayashi-phase convection), 30:30250
SUN/TEMPERATURE MEASUREMENT
  Ratio of the temperatures of the quiet sun and the centre of the moon at lambda = 1.3 mm, 30:30330
SUNSPOTS/VARIATIONS
  Long term periodicities in the sunspot cycle (179 year periodicity), 30:30331
SUPER KUKLA REACTOR/REACTOR EXPERIMENTAL FACILITIES
  H.E. firing chambers for use in Super Kukla Reactor, 30:31236 (UCID-15817)
SUPERCONDUCTING CABLES/POWER TRANSMISSION
  Transmission of electrical energy by superconducting cables, 30:30830
SUPERCONDUCTING CABLES/RESEARCH PROGRAMS
  USAEC-DAT dc superconducting power transmission line project at LASL. Progress report, January 1--March 31, 1974, 30:30820 (LA-5684-PR)
SUPERCONDUCTING JUNCTIONS/PROXIMITY EFFECT
  Coherent effects in large arrays of superconducting bridges, 30:30821
SUPERCONDUCTING MAGNETS/ENERGY STORAGE
  Utilization of superconducting devices for the generation and storage of electrical energy, 30:30822
SUPERCONDUCTING MAGNETS/MEETINGS
  Superconducting machines and devices: large systems applications. Conference held at Entreves, Italy, September 5--14, 1973, 30:30823
SUPERCONDUCTING MAGNETS/POWER GENERATION
  Utilization of superconducting devices for the generation and storage of electrical energy, 30:30822
SUPERCONDUCTING MAGNETS/REVIEWS
  Superconducting magnets, 30:30826
SUPERCONDUCTING MAGNETS/USES
  Programs on large scale applications of superconductivity in France, 30:30833
  Programs on large scale applications of superconductivity in the United States, 30:30838
SUPERCONDUCTIVITY/REVIEWS
  Superconductors, 30:30816
SUPERCONDUCTORS
  See also TYPE-II SUPERCONDUCTORS
SUPERCONDUCTORS/BOGOLYUBOV METHOD
  Self-consistent pair potential in superconductors. I. The superconductor--insulator boundary near T/sub c/, 30:30817
SUPERCONDUCTORS/ELECTRICAL PROPERTIES
  Inductance bridge for current-quantum phase measurements in superconductors at zero frequency (Al thin-film meander lines, inductance vs temperature, SQUID magnetometer detector), 30:30839
SUPERCONDUCTORS/MAGNETIC FLUX
  Vortex lattice in magnetic superconductors, 30:30815
SUPERCONDUCTORS/MEETINGS
  Superconducting machines and devices: large systems applications. Conference held at Entreves, Italy, September 5--14, 1973, 30:30823
SUPERCONDUCTORS/PHASE TRANSFORMATIONS
  Superconducting-normal phase boundaries of (La,Th)Ce systems, 30:30814
SUPERCONDUCTORS/REVIEWS
  Superconductors, 30:30816
SUPERCONDUCTORS/SPECIFICATIONS
  Practical superconducting materials, 30:30825
SUPERCONDUCTORS/TRANSITION TEMPERATURE
  Critical temperature of transition-metal alloy superconductors, 30:30811
SUPERCONDUCTORS/USES
  Large scale applications of superconductivity, 30:30824
  Programs on large scale applications of superconductivity in the United Kingdom, 30:30807
  Programs on large scale applications of superconductivity in the Federal Republic of Germany, 30:30834
  Programs on large scale applications of superconductivity in Italy, 30:30835
  Programs on large scale applications of superconductivity in Japan, 30:30836
  Programs on large scale applications of superconductivity in Switzerland, 30:30837
  Programs on large scale applications of superconductivity in the United States, 30:30838
SUPERFLUIDITY/BOGOLYUBOV METHOD
  Condensate density in Bogolyubov hydrodynamics, 30:30796
SUPERFLUIDITY/JOSEPHSON EFFECT
  Fluctuations and superfluid flow, 30:30795
SUPERFLUIDITY/VORTEX FLOW
  Fluctuations and superfluid flow, 30:30795
SUPERGIANT STARS/LUMINOSITY
  Steps toward the Hubble constant. II. The brightest stars in late-type spiral galaxies (Mean correlation line), 30:30393
SUPERGIANT STARS/PHOTOMETRY
  Ultraviolet photometry from the orbiting astronomical observatory. XVI. The stellar Lyman-Alpha absorption line (Upper limits), 30:30251
SUPERHEAVY ELEMENTS
  See TRANS 104 ELEMENTS
SUPERNOVA REMNANTS
  See also CRAB NEBULA
SUPERNOVA REMNANTS/CARBON MONOXIDE
  Observations of galactic carbon monoxide emission at 2.6 millimeters (Visual extinction, excitation temperatures), 30:30265
SUPERNOVAE/LUMINOSITY
  Modulation induced on young supernovae uv and ir luminosity by dust grains, 30:30344 (CONF-730693-)
SUPERNOVAE/NUCLEOSYNTHESIS
  A study of nucleosynthesis during explosive carbon burning (Solar-system material), 30:30257
  Iron production by ^{12}C-detonation supernovae (Severe constraints), 30:30258
SUPERNOVAE/SHOCK WAVES
  Electron-ion relaxation in a dense plasma (Microscopic structure), 30:30259
SUPERNOVAE/STAR EVOLUTION
  Do pulsars make supernovae. II. Calculations of light curves for type II events, 30:30197
SUPERNOVAE/X RADIATION
  Limit on X-ray emission from a supernova during maximum light (Optical rise, observation time), 30:30260
SURFACE AIR
  See also AIR
    EARTH ATMOSPHERE
SURFACE AIR/CHEMICAL ANALYSIS
  Source identification by multi-element analysis of diurnal samples, 30:31371 (UCID-15872)

SURFACE AIR/CONTAMINATION
  Assessment of the long-term exposure due to resuspension, 30:29375 (BNWL-1850(Pt.3))
  Ground level air concentrations of dust particles downwind from a tailings area during a typical windstorm (Mathematical model), 30:29380 (ORNL-TM-4375)
  Resuspension of tracer particles by wind, 30:29370 (BNWL-1850(Pt.3))
  Resuspension by wind at Rocky Flats (Plutonium monitoring in air and soil), 30:29371 (BNWL-1850(Pt.3))
  Resuspension source change at Rocky Flats, 30:29372 (BNWL-1850(Pt.3))
SURFACE AIR/DUSTS
  Fast response light scattering measurements of the characteristics of wind suspended aerosols (Dust suspension by winds), 30:29490 (UCRL-76014(Rev.1))
SURFACE AIR/MONITORING
  Quillayute air reference station (Air sampling and monitoring in Washington State), 30:29359 (BNWL-1850(Pt.3))
SURFACE AIR/NATURAL RADIOACTIVITY
  Natural β-activity of the air in the atmospheric surface layer, 30:29401
SURFACE AIR/RADIATION MONITORING
  Atmospheric natural aerosols and fallout particulates during 1973 at Richland, Washington and Point Barrow, Alaska, 30:29361 (BNWL-1850(Pt.3))
  Behavior and characteristics of radioactive debris from the Chinese nuclear weapons test of June 26, 1973, 30:29362 (BNWL-1850(Pt.3))
  Concentrational distribution of fission products over tropical zone oceans and its relation to atmospheric processes, 30:29368
  Data. Section III. Air and deposition, 30:29382
  Data. Section IV. Other data, 30:29412
  Environmental monitoring report, calendar year 1973, 30:29351 (UCC-ND-279)
  Environmental monitoring report: United States Atomic Energy Commission, Oak Ridge facilities. Calendar year 1973, 30:29352 (UCC-ND-280)
  Feed Materials Production Center environmental monitoring annual report for 1973, 30:29347 (NLCO-1109)
  Operation WHETSTONE: on-site radiological safety report, July 1964--June 1965, 30:29378 (NVO-410-24)
  Operation TOGGLE: on-site radiological safety report, July 1972--June 1973, 30:29379 (NVO-410-25)
  Portsmouth Gaseous Diffusion Plant environmental monitoring report, 1973, 30:29346 (GAT-781)
  Quillayute air reference station (Air sampling and monitoring in Washington State), 30:29359 (BNWL-1850(Pt.3))
  Radiological monitoring program, period covering February 4, 1974--April 30, 1974 (Rio Blanco site), 30:29348 (PNE-RB-51-9)
  Resuspension by wind at Rocky Flats (Plutonium monitoring in air and soil), 30:29371 (BNWL-1850(Pt.3))
  Resuspension source change at Rocky Flats, 30:29372 (BNWL-1850(Pt.3))
  Use of naturally radioactive substances in studying turbulent exchange and self-scavenging of the atmosphere with surface layer measurements, 30:29396
SURFACE AIR/RADIOACTIVITY
  Scavenging of radioactive material from the atmosphere by surface condensation, 30:29391
SURFACE AIR/TURBULENCE
  Use of naturally radioactive substances in studying turbulent exchange and self-scavenging of the atmosphere with surface layer measurements, 30:29396
SURFACE BARRIER DETECTORS/ELECTRIC CONTACTS
  Semiconductor contacts to silicon surface-barrier detectors, 30:29519
SURFACE BARRIER DETECTORS/SENSITIVITY
  Some features in the dependence of the pulse-height defect in semiconductor detectors on detected particle energy, 30:29526
SURFACE WATERS
  See also COASTAL WATERS
    LAKES
    WATER RESERVOIRS
SURFACE WATERS/CONTAMINATION
  Douglas United Nuclear, Inc. reactor and fuel production facilities 1972 environmental release report, 30:29341 (DUN-8133)
SURFACE WATERS/NATURAL RADIOACTIVITY
  Radioactivity in Brazilian mineral waters, 30:29413
SURFACE WATERS/POLLUTION
  Particle deposition rates on a water surface as a function of particle diameter and air velocity, 30:29484 (BNWL-1850(Pt.3))
SURFACE WATERS/RADIATION MONITORING
  Data. Section II. Water, 30:29411
  Data. Section IV. Other data, 30:29412
  Environmental monitoring report, calendar year 1973, 30:29351 (UCC-ND-279)
  Environmental monitoring report: United States Atomic Energy Commission, Oak Ridge facilities. Calendar year 1973, 30:29352 (UCC-ND-280)
  Feed Materials Production Center environmental monitoring annual report for 1973, 30:29347 (NLCO-1109)
  Portsmouth Gaseous Diffusion Plant environmental monitoring report, 1973, 30:29346 (GAT-781)
  Radioactivity in Brazilian mineral waters, 30:29413
  Radiological monitoring program, period covering February 4, 1974--April 30, 1974 (Rio Blanco site), 30:29348 (PNE-RB-51-9)
SURFACE WATERS/RADIONUCLIDE MIGRATION
  Horizontal water migration of ^{90}Sr, 30:29407
SURFACE WATERS/THERMAL POLLUTION
  Physical--chemical effects of cooling systems and thermal discharges on the environment, 30:29465
SURFACE WATERS/WATER POLLUTION
  Douglas United Nuclear, Inc. reactor and fuel production facilities 1972 environmental release report, 30:29341 (DUN-8133)
SURFACES/ATOM COLLISIONS
  Helium scattering from solid surfaces, 30:30480
SURFACES/CHEMICAL ANALYSIS
  Spectroscopy of Auger electrons and its use in metallurgy, 30:31420 (COPPE-TP-6/72)
SURFACES/NUCLEAR REACTION ANALYSIS
  A telescope counter detection system applied to low-energy ion-beam surface analysis, 30:29510
SURVEILLANCE
  See INSPECTION
SURVEY MONITORS
  Construction of an adjustable carrying handle for the FIDLER detector, 30:29497 (UCID-15775)
SWINE/DECONTAMINATION
  Decontamination of swine, sheep, and cattle surface-contaminated with fission products. II. Removal of radionuclides of zirconium, niobium, ruthenium, and cerium (^{95}Zr; ^{95}Nb; ^{106}Ru; ^{144}Ce), 30:29823
SWITCHING CIRCUITS/DESIGN
  State relationships for maximal-length sequence generators, 30:31450 (UCID-15898)
SYMMETRY BREAKING/CP INVARIANCE
  Spontaneous CP-violation and cosmology, 30:30770
SYMMETRY BREAKING/HAMILTONIANS
  Consistency conditions in the theory of spontaneous breaking of chiral symmetry, 30:30778
SYMMETRY BREAKING/REGGE CALCULUS
  Spontaneous symmetry breakdown and Regge intercepts (Higgs mechanism), 30:30707
SYMMETRY GROUPS
  See also CURRENT ALGEBRA
SYMMETRY GROUPS/TOPOLOGY
  Physical significance of the topology of the Bondi--Metzner--Sachs group, 30:30766
SYNCHROTRON RADIATION
  Coherent synchrotron radiation from an intense relativistic electron beam, 30:30580 (AD-773442)
SYNCHROTRON RADIATION/BEAM OPTICS
  Geometry and optics of synchrotron radiation, 30:30119
SYNCHROTRON RADIATION/EMISSIVITY
  Relation between the radiated and received powers due to gyrating electrons in ambient plasma, 30:30275
SYRIAN HAMSTER
  See HAMSTERS

T

T MATRIX
  See S MATRIX
T TAURI STARS/STELLAR ATMOSPHERES
  The T Tauri emission nebula (Circumstellar shells), 30:30185
TANDEM ACCELERATORS
  See VAN DE GRAAFF ACCELERATORS
TANTALUM/ACTIVATION ANALYSIS
  Nondestructive determination of some trace elements in tantalum by proton activation analysis, 30:28922
  Trace element behavior in soil of some Indonesian sawah's and in sludge of an Indonesian river, 30:28930
TANTALUM/ANNEALING
  Reactions occurring during annealing of VIa and Va metals in oxygen, water vapor, and air at low pressures, 30:30022
TANTALUM/ANODIZATION
  Frequency characteristics of anodic oxide films: effects of anodization voltage, 30:29917
TANTALUM/CHEMICAL ANALYSIS
  Atomic absorption spectrometry of impurities in high purity tantalum with heated graphite atomizer, 30:28954
TANTALUM/ELECTRIC CONDUCTIVITY
  Electrical resistance as a function of temperature in pure and doped beta-tantalum films, 30:30059
TANTALUM/ION COLLISIONS
  Energy and charge distribution of backscattered particles during bombardment of metal surfaces with protons (Less than 50 keV), 30:30474 (AED-CONF-74-089-032)
TANTALUM/PRODUCTION
  High-melting metals and metallic compounds, 30:30021
TANTALUM/SOLVENT PROPERTIES
  Solubility of hydrogen in vanadium and niobium at high temperatures (1273 to 2273°K; up to 25 atm; V--H; Nb--H; Ta--H), 30:29918
TANTALUM/STACKING FAULTS
  Stacking faults in refractory metals and alloys, 30:30030
TANTALUM/USES
  High-melting metals and metallic compounds, 30:30021

TANTALUM 179/ENERGY-LEVEL TRANSITIONS
  Levels in ^{179}Ta and γ-ray transition probabilities in ^{179}Ta and ^{183}Re, 30:30994
TANTALUM 179/ROTATIONAL STATES
  Levels in ^{179}Ta and γ-ray transition probabilities in ^{179}Ta and ^{183}Re, 30:30994
TANTALUM 181/ALPHA REACTIONS
  Gamma spectra from ^{179}Hf (d,2n), ^{179}hf (p,n), and ^{181}Ta (α,2n) reactions, 30:30994
TANTALUM 181/NEUTRON REACTIONS
  Coincidence spectra from ^{175}Lu (n,γ) and ^{181}Ta (n,γ) reactions with thermal neutrons, 30:30993
TANTALUM 181/OXYGEN 16 REACTIONS
  Search for new isotopes ^{186} ^{187}Tl, 30:30986
TANTALUM 182/ENERGY-LEVEL TRANSITIONS
  Transition probabilities in the doubly odd nuclei ^{176}Lu and ^{182}Ta, 30:30993
TANTALUM 186/NUCLEAR PROPERTIES
  Nuclear Data Sheets for A = 186, 30:30988
TANTALUM ADDITIONS
  Fatigue-crack growth of Ti--6Al--2Cb-1Ta--0.8Mo alloy in air and natural sea water environments, 30:29972 (AD-765318)
TANTALUM ALLOYS/CORROSION RESISTANCE
  Study of the corrosion resistance of titanium alloys and some steels during condensation of alkylphenol with formaldehyde (Steels 3, AT-3, EI-943; Ti alloys VTZ-1, VT-14; VT1-0, OT-4, VT5, Ti--5 percent Ta, Ti--33 percent Mo), 30:29947
TANTALUM ALLOYS/MECHANICAL PROPERTIES
  Study of some high-temperature strength properties of the niobium alloys 5VMTs, 5VMTsU, and 5VTTs at 1100°C (5VMTs = Nb--5.3W--2.1Mo--0.72Zr; 5VNTsU = Nb--4.9W--2.0Mo--1.15Zr; 5VTTs = 4.5W--2Ta--3.45Zr), 30:30027
TANTALUM ALLOYS/STACKING FAULTS
  Stacking faults in refractory metals and alloys (Mo--16.6, 34.6, and 61.4 at. percent Ta; Mo--49 and 74 at. percent Nb), 30:30030
TANTALUM ALLOYS/SUPERCONDUCTIVITY
  Coherent effects in large arrays of superconducting bridges, 30:30821
TANTALUM BORIDES/OXIDATION
  Oxidation of ZrB_2, TaB_2, NbB_2, and W_2B_5 in atomic oxygen and by anodic polarization, 30:29938
TANTALUM HYDRIDES/PHASE STUDIES
  Solubility of hydrogen in vanadium and niobium at high temperatures (1273 to 2273°K; up to 25 atm; V--H; Nb--H; Ta--H), 30:29918
TANTALUM NITRIDES/ANODIZATION
  Mass anodization of tantalum-nitride resistors, 30:31387 (BDX-613-1155(Rev.))
TANTALUM OXIDES/DIELECTRIC PROPERTIES
  Frequency characteristics of anodic oxide films: effects of anodization voltage, 30:29917
TANTALUM OXIDES/ELECTRICAL PROPERTIES
  Electrical conductivity in metal/oxide/electrolyte systems, 30:29896
TANTALUM OXIDES/SPUTTERING
  Ion beam sputtering. The effect of incident ion energy on atomic mixing in subsurface layers, 30:30483
TAPEWORMS
  See CESTODES
TARGETS
  See also POLARIZED TARGETS
TARGETS/CARBON
  A new technique for the production of carbon foils, 30:30145
TARGETS/CARBON 13
  The preparation of self-supporting ^{13}C-foils using enriched methane gas, 30:30151
TARGETS/COOLING
  A cooling system for thin tritiated titanium targets, 30:30157
TARGETS/SUPPORTS
  Wobble target holder for thin targets in intense light- and heavy-ion beams, 30:30148
TARGETS/TRITIUM
  A cooling system for thin tritiated titanium targets, 30:30157
TECHNETIUM 99/CHEMICAL STATE
  Stabilization of daughter /sup 99m/Tc after β-decay of ^{99}Mo in the hexacarbonyl molybdenum molecule, 30:29109
TECHNETIUM 99/ISOTOPE PRODUCTION
  Process for the production of technetium-99m from neutron irradiated molybdenum trioxide (Patent), 30:29139
  Radionuclide generator production method (Patent), 30:29140
  Radionuclide generator production method (Patent), 30:29144
TECHNETIUM 99/SPIN
  Atomic-beam measurements on refractory elements. . Nuclear spin measurements of ^{99}Mo and sup(99m)Tc, 30:30972
TEFLON/RADIOLYSIS
  Accelerating effect of halogenated methane on the radiation degradation of polytetrafluoroethylene (Gamma radiation), 30:29058
TELESCOPE COUNTERS/COUNTING CIRCUITS
  Input control of counters CU-51 for assembling azimuthal and calibration telescopes T/SKL and ET/SKL, 30:29583
TELESCOPE COUNTERS/DATA PROCESSING
  Spherical harmonic analysis of satellite anisotropy measurements, 30:29533
TELESCOPE COUNTERS/LIQUID SCINTILLATION DETECTORS
  100-channel scintillation telescope, 30:29578
TELESCOPE COUNTERS/PERFORMANCE
  A high-resolution mass-identification system for heavy ions, 30:29564
  A telescope counter detection system applied to low-energy ion-beam surface analysis, 30:29510
TELESCOPE COUNTERS/PROPORTIONAL COUNTERS
  Telescope with proportional gas-discharge counters for analysis of high-energy cosmic ray variations, 30:29581
TELESCOPE COUNTERS/SENSITIVITY
  Diagrams of sensitivity in respect to the zenith angle for scintillation telescopes of arbitrary geometry (Cosmic ray detection), 30:29499
TELESCOPE COUNTERS/TIME-OF-FLIGHT METHOD
  Study of a pion-stopping telescope by time-of-flight methods, 30:29590
TELLURIUM/ACTIVATION ANALYSIS
  Multielement determination in market-garden soils by instrumental photon activation analysis, 30:28921
TELLURIUM/FLUORESCENCE SPECTROSCOPY
  New discrete atomization cell for atomic fluorescence spectrometry, 30:28947
TELLURIUM/SPECTROSCOPY
  Spectrochemical method for determination of tellurium in geological materials, 30:28949
TELLURIUM 130/ENERGY LEVELS
  Nuclear Data Sheets for A = 130, 30:30968
TELLURIUM 130/NUCLEAR PROPERTIES
  Nuclear Data Sheets for A = 130, 30:30968
TELLURIUM 132/ABUNDANCE
  Calculation of fractionation effects following atmospheric nuclear explosions, 30:29386
TELLURIUM 136/NUCLEAR PROPERTIES
  Nuclear Data Sheets for A = 136, 30:30967
TELLURIUM ISOTOPES/ENERGY LEVELS
  Problem of particle-hole symmetry in even--even Cd and Te nuclei, 30:30971
TEMPERATURE (NEUTRON)
  See NEUTRON TEMPERATURE
TEMPERATURE MEASUREMENT
  Monitor for radiation-induced heating (Patent), 30:29624
TENNESSEE/AIR POLLUTION
  Environmental monitoring report: United States Atomic Energy Commission, Oak Ridge facilities. Calendar year 1973 (Monitoring), 30:29352 (UCC-ND-280)
TENNESSEE/RADIOACTIVITY
  Environmental monitoring report: United States Atomic Energy Commission, Oak Ridge facilities. Calendar year 1973 (Monitoring), 30:29352 (UCC-ND-280)
TENNESSEE/WATER POLLUTION
  Environmental monitoring report: United States Atomic Energy Commission, Oak Ridge facilities. Calendar year 1973 (Monitoring), 30:29352 (UCC-ND-280)
TERBIUM/ACTIVATION ANALYSIS
  Determination of rare earths and thorium in apatites by thermal and epithermal neutron-activation analysis, 30:28935
  Trace element behavior in soil of some Indonesian sawah's and in sludge of an Indonesian river, 30:28930
TERBIUM/EXTRACTION CHROMATOGRAPHY
  Contribution to the separation of rare earths by extraction chromatography with di(2-ethylhexyl) phosphoric acid. II. Behavior of the matrix and its influence on the microcomponents, 30:28990 (ANL-Trans-961)
TERBIUM/ION COLLISIONS
  L- and M-shell ionization of various elements by fast-α-particle bombardment (Cross sections, 1 to 5 MeV), 30:30537
TERBIUM 159/ENERGY LEVELS
  Mixing of Nilsson configurations in ^{159}Tb, 30:30992
TERBIUM ALLOYS/MAGNETIC PROPERTIES
  Magnetic properties of alloys of the TbCu--YCu system (77 to 300°K; Curie point; Neel temperature; susceptibility), 30:30031
TERBIUM ALLOYS/SPECIFIC HEAT
  Specific heat in TbZn and HoZn compounds (20 to 300°K; YZn; magnetic properties), 30:29990
TERRAMYCIN
  See OXYTETRACYCLINE
TERRESTRIAL ECOSYSTEMS/RADIONUCLIDE MIGRATION
  Radioactive tracer studies of soil and litter arthropod food chains. Progress report, November 1, 1973--October 31, 1974 (Fallout ^{137}Cs tracer), 30:29419 (SRO-641-13)
TESTES/BIOLOGICAL RADIATION EFFECTS
  Desynchronization of the diurnal rhythm of acid phosphatase activity in male gonads of mice under the influence of uv and x-rays radiation, 30:29751
  Effect of graded doses of ionizing radiation on the human testis, 30:29708
TESTOSTERONE/METABOLISM
  Uptake and metabolism of [4-^{14}C]testosterone in human breast cancer grown in organ culture, 30:29878

TETRAHYMENA
Insensitivity of serially transferred Tetrahymena pyriformis W. to irradiated media, 30:29767
TEXTILES/CONTAMINATION
Unexpected complication in the use of ^{169}Yb--DTPA with respect to hospital health physics, 30:29824
THALLIUM/ACTIVATION ANALYSIS
Multielement determination in market-garden soils by instrumental photon activation analysis, 30:28921
THALLIUM/EMISSION SPECTROSCOPY
Spectrochemical analysis of uranium oxide by gallium oxide carrier dc arc technique (ASTM Standard E402), 30:28957
Spectrographic determination of trace impurities in high purity uranium oxide, 30:28944 (UCID-15952)
THALLIUM/FLUORESCENCE SPECTROSCOPY
New discrete atomization cell for atomic fluorescence spectrometry, 30:28947
THALLIUM/SUBLIMATION
Volatility of microamounts of thallium from PbF$_2$ crystals irradiated with high-energy protons. Fast gas thermochromatographic method of obtaining short-lived thallium isotopes, 30:29142
THALLIUM 186/BETA DECAY
Search for new isotopes ^{186} ^{187}Tl, 30:30986
THALLIUM 186/NUCLEAR PROPERTIES
Nuclear Data Sheets for A = 186, 30:30988
THALLIUM 188/BETA-PLUS DECAY
Half-life and γ rays from decay of ^{188}Tl, 30:30987
THALLIUM 208/SEPARATION PROCESSES
Separation of radionuclides using alkyl radicals, 30:29083 (AED-CONF-74-084-002)
THALLIUM ALLOYS/LATTICE PARAMETERS
Preparation of new β-W phases by film-deposition techniques (Nb$_3$In, Nb$_3$Pb, and Nb$_3$Tl films, unstable phase range), 30:29967
THALLIUM ALLOYS/SUPERCONDUCTIVITY
Preparation of new β-W phases by film-deposition techniques (Nb$_3$In, Nb$_3$Pb, and Nb$_3$Tl films, unstable phase range), 30:29967
THALLIUM CHLORIDES/ENTHALPY
Gaseous halide complexes and their stability, 30:29091
THALLIUM CHLORIDES/FORMATION HEAT
Gaseous halide complexes and their stability, 30:29091
THALLIUM COMPOUNDS/CHEMICAL PREPARATION
Synthesis of high pressure Cd$_2$V$_2$O$_7$ and related compositions, 30:29903
THALLIUM ISOTOPES/GAS CHROMATOGRAPHY
Volatility of microamounts of thallium from PbF$_2$ crystals irradiated with high-energy protons. Fast gas thermochromatographic method of obtaining short-lived thallium isotopes, 30:29142
THALLIUM URANATES/CHEMICAL PREPARATION
Preparation and characterization of a new thallium(I) uranate(VI), Tl$_4$UO$_5$, 30:29090
THERMAL EFFLUENTS
Magnitude of thermal discharges from a developing nuclear economy, 30:31255
Thermal discharges at nuclear power stations. Their management and environmental impacts. A report prepared by a group of experts as the result of a panel meeting held in Vienna, 23--27 October 1972, 30:31252 (STI/DOC-10/155)
Thermal discharges and the siting of nuclear power plants, 30:31257
THERMAL EFFLUENTS/BIOLOGICAL EFFECTS
Aquatic physiology of thermal and chemical discharges (Effects of chlorine), 30:29461 (BNWL-SA-5058)
Biological effects of thermal discharges from nuclear power plants, 30:29466
Migratory behavior of fish tagged at a nuclear power plant discharge into Lake Michigan, 30:29462 (CONF-740813-2)
Possible effects of thermal effluents on fish: a review, 30:29467
Symposium on the effect of hot water of thermoelectric plants on the hydrology and biology of reservoirs (abstracts) March 24--26, 1971, Borok, USSR, 30:29463 (ORNL-tr-2781)
THERMAL EFFLUENTS/DIFFUSION
Mathematical and physical models of heat dissipation, 30:29464
THERMAL EFFLUENTS/STACK DISPOSAL
Simple model for bouyant plumes based on the conservation laws, 30:29460 (BNWL-1850(Pt.3))
THERMAL INSULATION/HEAT TRANSFER
Heat transmission measurements in thermal insulations. Conference held at Philadelphia, Pennsylvania, April 16--17, 1973, 30:29242
THERMAL INSULATION/PERFORMANCE TESTING
High performance thermal insulation for an implantable artificial heart, 30:29241
THERMAL POWER PLANTS/THERMAL EFFLUENTS
Symposium on the effect of hot water of thermoelectric plants on the hydrology and biology of reservoirs (abstracts) March 24--26, 1971, Borok, USSR, 30:29463 (ORNL-tr-2781)
THERMAL SHOCK/MEASURING METHODS
Calorimetric determination of the heat resistance of ring-shaped samples of brittle electric conductors, 30:29960
THERMOCOUPLES/PERFORMANCE TESTING
Silicon germanium technology program at JPL, 30:29247
THERMODYNAMIC CYCLES/EFFICIENCY
Nuclear energy requirements for hydrogen production from water, 30:31239
THERMOELECTRIC GENERATORS/DESIGN
10% efficient economic RTG design, 30:29251
Direct heat rejection path radioisotopic thermoelectric generator (Patent), 30:29240
Light-weight radiosotope thermoelectric generator design, 30:29253
THERMOELECTRIC GENERATORS/ECONOMICS
Cost effective designing for the economic RTG, 30:29252
THERMOELECTRIC GENERATORS/FABRICATION
Fabrication and testing of a thermoelectric RING converter segment for space applications, 30:29246
THERMOELECTRIC GENERATORS/MINIATURIZATION
High voltage miniature radioisotope thermoelectric generators, 30:29263
THERMOELECTRIC GENERATORS/PERFORMANCE TESTING
Fabrication and testing of a thermoelectric RING converter segment for space applications, 30:29246
Operational testing of the high performance thermoelectric generator (HPG-02), 30:29250
Performance testing of thermoelectric generators at JPL, 30:29248
THERMOELECTRIC GENERATORS/RADIOISOTOPE HEAT SOURCES
Modular heat source for ^{244}Cm and ^{238}Pu, 30:29245
THERMOELECTRIC GENERATORS/REVIEWS
RTG technology development: where we are/where we are going, 30:29244
THERMOELECTRIC GENERATORS/THERMOCOUPLES
Silicon germanium technology program at JPL, 30:29247
THERMOELECTRIC GENERATORS/VOLTAGE REGULATORS
Fault tolerant sequencing (FTS) shunt regulator, 30:29254
THERMOLUMINESCENT DOSEMETERS/ANNEALING
Optimal annealing of natural beryl for thermoluminescent dosimetry, 30:29553
THERMOLUMINESCENT DOSEMETERS/READOUT SYSTEMS
Electronics for the LRL automated personnel thermoluminescence dosimetry system, 30:29552 (UCID-15836)
THERMOLUMINESCENT DOSEMETERS/SENSITIVITY
Thermoluminescent response of TLD-100 to 1 to 25 keV electrons. Progress report, July 15, 1973--July 15, 1974, 30:29538 (COO-1105-212)
THERMONUCLEAR REACTIONS/COMPUTER CODES
MEDUSA. A one-dimensional laser fusion code, 30:29227
THERMONUCLEAR REACTIONS/HEAVY ION REACTIONS
Complete nuclear fusion reactions (Angular momentum effects), 30:29205 (GSI-tr-73/20)
THERMONUCLEAR REACTOR WALLS/SHIELDING
Magnetically protected first wall for a laser-induced thermonuclear reaction, 30:29207 (LA-5699-MS)
THERMONUCLEAR REACTORS
See also THERMONUCLEAR REACTOR WALLS
(For use in cases where certain aspects of either hypothetical or real thermonuclear reactors are discussed.)
Adequacy of lithium supplies as a fusion energy source, 30:29222 (UCID-15953)
Thermonuclear fusion power (Research survey), 30:29232
THERMONUCLEAR REACTORS/ECONOMICS
Economic and environmental aspects of a first-generation fusion power plant, 30:29229
THERMONUCLEAR REACTORS/NEUTRON REACTIONS
Recoil energy distributions in CTR-related neutron spectra, 30:29203 (BNL-19043)
THERMONUCLEAR REACTORS/SPECIFICATIONS
Conceptual design of a series of laser-fusion power plants of 100 to 3000 MW(e), 30:29230
THERMONUCLEAR WEAPONS
See NUCLEAR WEAPONS
THERMOSPHERE/HEATING
Heating of the high-latitude thermosphere during magnetically quiet periods, 30:30459
THICKNESS GAGES/ACCURACY
Comparative analysis of the accuracy of absolute and relative methods of thickness measurement using scattered radiation, 30:29606
THICKNESS GAGES/DESIGN
Radioisotope method of measuring the mean fibre diameter of wool samples, 30:29604
THICKNESS GAGES/OPERATION
Beta backscatter measurements of aluminum coatings on mylar substrates, 30:29602 (BDX-613-1028(Rev.))
THIOALCOHOLS
See THIOLS
THIOLS
See also DITHIOLS
THIOLS/OXIDATION
Oxidation of free and coordinated thiols by neptunium(VI) (Thioglycolic acid, methyl thioglycolate, and thiolato ligands in Cr and Co complexes), 30:29132
THORAX
See CHEST
THORIUM/ABUNDANCE
Origin of carbonatitic magma in the light of the Pb-U-Th isotope system, 30:29337

THORIUM/ACTIVATION ANALYSIS
  Determination of rare earths and thorium in apatites by thermal and epithermal neutron-activation analysis, 30:28935
  Trace element behavior in soil of some Indonesian sawah's and in sludge of an Indonesian river, 30:28930
THORIUM/GRAVIMETRIC ANALYSIS
  Preparation, properties, and analytical application of thorium n-phenyl-o-nitrobenzohydroxamate, 30:28962
THORIUM/ION EXCHANGE
  Sorption of tetravalent elements by mordenite. II. Sorption of Pu(IV), 30:28999
THORIUM/NUCLEAR REACTION ANALYSIS
  Simultaneous analysis of uranium and thorium by the delayed fission neutron counting method, 30:28931
THORIUM/RADIATION MONITORING
  Feed Materials Production Center environmental monitoring annual report for 1973, 30:29347 (NLCO-1109)
THORIUM/RADIOMETRIC ANALYSIS
  Radiometric analysis of thorium and uranium, 30:28975
THORIUM/SOLVENT EXTRACTION
  Process for separation of protactinium, thorium, and uranium from neutron-irradiated thorium (Using TBP), 30:29150
THORIUM 227/RADIOCHEMICAL ANALYSIS
  Sequential determination of radium-226, radium-228, actinium-227, and thorium isotopes in environmental and process waste samples, 30:28978
THORIUM 228/ALPHA SPECTRA
  Separation of radionuclides using alkyl radicals, 30:29083 (AED-CONF-74-084-002)
THORIUM 228/BIOLOGICAL RADIATION EFFECTS
  Research in radiobiology. Annual report of work in progress in the internal irradiation program (Pathological effects of bone-seeking radionuclides in beagles), 30:29778 (COO-119-249)
THORIUM 228/RADIATION MONITORING
  Data. Section IV. Other data, 30:29412
THORIUM 230/ALPHA SPECTROSCOPY
  Simultaneous determination of alpha-emitting nuclides of radium through californium in soil, 30:28977
THORIUM 230/RADIATION MONITORING
  Data. Section IV. Other data, 30:29412
THORIUM 230/RADIOCHEMICAL ANALYSIS
  Sequential determination of radium-226, radium-228, actinium-227, and thorium isotopes in environmental and process waste samples, 30:28978
THORIUM 232/NEUTRON REACTIONS
  Assessment of known independent yields and the calculation of those unknown in the fission of ^{232}Th, ^{233}U, ^{235}U, ^{238}U, ^{239}Pu, ^{240}Pu, and ^{241}Pu (Odd--even Z effects), 30:31008 (AERE-R-7680)
THORIUM 232/RADIATION MONITORING
  Data. Section IV. Other data, 30:29412
  Environmental monitoring report: United States Atomic Energy Commission, Oak Ridge facilities. Calendar year 1973, 30:29352 (UCC-ND-280)
THORIUM ALLOYS/MAGNETIC PROPERTIES
  Crystal and magnetic structure of intermetallic compounds of the type Th(Co/sub x/Fe/sub 1-x/)$_5$, 30:29989
THORIUM ALLOYS/SUPERCONDUCTIVITY
  Superconducting-normal phase boundaries of (La,Th)Ce systems, 30:30814
THORIUM CHLORIDES/ENTHALPY
  Gaseous halide complexes and their stability, 30:29091
THORIUM CHLORIDES/FORMATION HEAT
  Gaseous halide complexes and their stability, 30:29091
THORIUM CHLORIDES/MELTING POINTS
  Fusibility diagram of the system LiCl--UCl$_4$--ThCl$_4$, 30:29095
THORIUM COMPLEXES/CHEMICAL PREPARATION
  Preparation, properties, and analytical application of thorium n-phenyl-o-nitrobenzohydroxamate, 30:28962
  Preparation of complex perxenates of some actinide elements, 30:29117
THORIUM COMPLEXES/PYROLYSIS
  Derivatographic investigations on the thermal degradation of pyridine, isoquinoline, α,α-dipyridyl and o-phenantroline, resp. bichromate- or chromate-ion containing metal complexes. II. Zinc(II)-, cadmium(II)-, and manganese(II)-complexes. III. Mercury(I and II)-, uranyl-, thorium-, lanthanum-, and iron-complexes, 30:29122
THORIUM ORES/MINERALIZATION
  Zonality of thorium--niobium mineralization in albitites, 30:29333
THORON
  See RADON 220
THOROTRAST/BIOLOGICAL RADIATION EFFECTS
  Thorotrast-induced neoplasms, 30:29769 (AED-CONF-74-016-002)
THREE-BODY PROBLEM/BREAKUP REACTIONS
  Neutron--neutron effective range parameters from few-nucleon experiments (D(π/sup minus/,2nγ), D(n,2np) reactions), 30:31037
THREE-BODY PROBLEM/CORRELATIONS
  Correlation effects on the ground-state energy and form factor of few-body systems, 30:31045
THREE-BODY PROBLEM/LIPPMANN-SCHWINGER EQUATION
  Use of Lippmann--Schwinger equations in the three-body problem, 30:31044
THREE-BODY PROBLEM/NUCLEONS
  Calculations on few-nucleon systems with correlated wave functions (Binding energy, Coulomb energy), 30:31043
  Ground-state properties of three-nucleon systems: a review (Binding energy, charge form factor, magnetic moment), 30:31039
  Nucleon--nucleon interaction and low-energy properties of three-nucleon systems, 30:31038
  Present status and open problems in few-nucleon systems, 30:31041
  Three-nucleon reactions and off-shell behavior of the nucleon--nucleon interaction, 30:31040
  Two-body T-matrix factorization and three-nucleon problem, 30:31047
THREE-BODY PROBLEM/NUMERICAL SOLUTION
  Application of Trotter's formula to a few-nucleon problem, 30:31046
THREE-BODY PROBLEM/S MATRIX
  Two-body T-matrix factorization and three-nucleon problem, 30:31047
THROAT
  See PHARYNX
THULIUM 169/NEUTRON REACTIONS
  Status report to NCSAC, 30:31011 (UCID-15639)
THULIUM COMPOUNDS/ENERGY LEVELS
  Analysis of the ground configuration of trivalent thulium in single-crystal yttrium vanadate, 30:30487 (AD-776343)
THULIUM ISOTOPES/ROTATIONAL STATES
  Investigations of the level structure and lifetimes of odd Tm isotopes, 30:30979 (NP-20122)
THYMINE/PHOTOCHEMISTRY
  Photochemical addition of amino acids to thymine (UV radiation), 30:29658
THYMINE/RADIOLYSIS
  Radiation-induced radicals in thymine and its derivatives in low temperature glasses (X radiation), 30:29055
THYMOCYTES/BIOLOGICAL RADIATION EFFECTS
  Effect of x rays on the phosphorylation of histon f$_1$ in thymocytes, 30:29653
THYMUS CELLS/RADIOSENSITIVITY
  Sensitivity to radiation and insensitivity to vinblastine of the inducer function of thymus-derived cells (Gamma radiation), 30:29665
THYROID/RADIATION DOSES
  Carcinogenicity of iodine-131 relative to age at exposure (^{131}I and ^{125}I uptake by thyroid and pituitary glands), 30:29777 (BNWL-SA-5065)
THYROID/SCINTISCANNING
  Quantitative thyroid scanning: a reliable thyroid function test (99m-Tc tracer), 30:29853
THYROID STIMULATING HORMONE
  See TSH
THYROTOXICOSIS
  See HYPERTHYROIDISM
TIME-OF-FLIGHT METHOD/CORRELATION FUNCTIONS
  Theory of multi-variable correlation techniques for time-of-flight experiments, 30:29560 (JUL-1050-FF)
TIME-OF-FLIGHT METHOD/PULSED NEUTRON TECHNIQUES
  Neutron slowing-down in ice and polyethylene at low temperatures (Moderator at 4.2, 77, and 300°K, 0.0018 to 0.090 eV), 30:30843 (IAE-2271)
TIME-OF-FLIGHT SPECTROMETERS/ENERGY RESOLUTION
  Resolution function for the rotating-crystal spectrometer, 30:29558 (IFA-FN-44-1974)
TIME-OF-FLIGHT SPECTROMETERS/PERFORMANCE
  Performance of a heavy-ion time-of-flight spectrometer, 30:29573
  The University of Michigan neutron time-of-flight facility, 30:30159
TIME-OF-FLIGHT SPECTROMETERS/RESOLUTION FUNCTIONS
  Resolution of slow neutron spectrometers. I. General method to calculate the resolution function. II. Resolution function for time of flight diffractometry, 30:29559 (IFA-FN-45-1974)
TIMING CIRCUITS/PULSE RISE TIME
  Rise-time jitter reduction in timing and amplitude-discrimination circuits, 30:29631
TIN/ACTIVATION ANALYSIS
  Multielement determination in market-garden soils by instrumental photon activation analysis, 30:28921
TIN/EMISSION SPECTROSCOPY
  Spectrochemical analysis of uranium oxide by gallium oxide carrier dc arc technique (ASTM Standard E402), 30:28957
  Spectrographic determination of trace impurities in high purity uranium oxide, 30:28944 (UCID-15952)
TIN/FLUORESCENCE SPECTROSCOPY
  New discrete atomization cell for atomic fluorescence spectrometry, 30:28947
TIN/ION COLLISIONS
  L- and M-shell ionization of various elements by fast-α-particle bombardment (Cross sections, 1 to 5 MeV), 30:30537
TIN/ISOTOPE DILUTION
  Mass spectrometric isotope dilution analyses of tin in stony meteorites and standard rocks, 30:30311
TIN/SOLUBILITY
  Solubility of tin and germanium in liquid sodium. The sodium--tin partial phase diagram, 30:30049

TIN/SUPERCONDUCTIVITY
  Phase-slip centers and nonequilibrium processes in superconducting tin microbridges, 30:30819
TIN 116/DEUTERON REACTIONS
  Proton-hole states in ^{115}In observed in the ^{116}Sn(d,^{3}He) reaction (50 MeV: angular distributions, DWBA; S), 30:30975
TIN 117/ENERGY LEVELS
  Shell effects on state densities with given number of excited protons and neutrons, 30:31094
TIN 118/HELIUM 3 REACTIONS
  Excitation of the deeply bound gsub(9/2) neutron hole state in ^{117}Sn by a neutron pickup reaction with 81.7 MeV ^{3}He particles (Alpha spectra from reactions with ^{117}Sn and ^{208}Pb), 30:30974
TIN 130/ENERGY LEVELS
  Nuclear Data Sheets for A = 130, 30:30968
TIN 130/NUCLEAR PROPERTIES
  Nuclear Data Sheets for A = 130, 30:30968
TIN ALLOYS/MECHANICAL PROPERTIES
  Mechanical properties of multicomponent alloys based on Ti--Al--Sn (Zr) α-solid solution with β-stabilizing elements (Additions of Mo, V, Cr, Fe, Si, B;properties at up to 950°C), 30:29984
TIN ALLOYS/PHASE DIAGRAMS
  Solubility of tin and germanium in liquid sodium. The sodium--tin partial phase diagram, 30:30049
TIN ALLOYS/PHYSICAL RADIATION EFFECTS
  Influence of neutron irradiation on critical data of type II superconductors (Nb--Sn), 30:30063 (AED-CONF-74-089-006)
TIN ALLOYS/STACKING FAULTS
  Diffraction of x rays on stacking faults in metals with hcp lattices (Ti--Al; Ti--Sn), 30:30024
TIN ALLOYS/SUPERCONDUCTIVITY
  Multifilament Nb_3Sn conductors (Nb_3Sn surface layers on Nb-Cu composite), 30:30809
  The effect of cladding material on ac losses of commercial Nb_3Sn tapes (Pb-Sn and Ag-Sn solders, ferromagnetic nickel flashes, commercial superconducting Cu and Ag clad tapes), 30:30840
TIN CHLORIDES/ENTHALPY
  Gaseous halide complexes and their stability, 30:29091
TIN CHLORIDES/FORMATION HEAT
  Gaseous halide complexes and their stability, 30:29091
TIN COMPOUNDS/CHEMICAL REACTIONS
  Radiation-chemical studies on the generation of lead and tin radicals (By electron scavenging in γ-irradiated 2-MTHF glass at 77°K), 30:29057
TIN ISOTOPES/ISOBARIC ANALOGS
  Study of the (p,np) reaction on the isotopes of tin (All stable Sn isotopes, 23.0 and 38.5 MeV), 30:30973
TIN ISOTOPES/PROTON REACTIONS
  Study of the (p,np) reaction on the isotopes of tin (All stable Sn isotopes, 23.0 and 38.5 MeV), 30:30973
TIN OXIDES/ELECTRONIC STRUCTURE
  ESR spectra and ionic states in the system V_2O_5--SnO_2, 30:29907
TISSUE-EQUIVALENT DETECTORS/CALIBRATION
  Dosimetry of the SIN biomedical pion beam with tissue-equivalent ionization chambers, 30:29555
TISSUE-EQUIVALENT MATERIALS/CHARGED-PARTICLE TRANSPORT
  Calculations on tissue equivalence for stopping π^- mesons, 30:31119
TISSUE-EQUIVALENT MATERIALS/PION REACTIONS
  Calculated particle-production spectra from π^- captures in tissue, tissue-equivalent plastic, silicon, and germanium, 30:31120
TISSUES
  See also RETICULOENDOTHELIAL SYSTEM
    SKIN
TISSUES/BIOLOGICAL RADIATION EFFECTS
  RBE of cyclotron neutrons for effects on normal tissues, 30:29726
  Review of RBE values of 15 MeV neutrons for effects on normal tissues, 30:29764
TISSUES/CHEMICAL ANALYSIS
  Method of ^{3}H-determination in hair, 30:28985
TISSUES/PION REACTIONS
  Calculated particle-production spectra from π^- captures in tissue, tissue-equivalent plastic, silicon, and germanium, 30:31120
TISSUES/RADIONUCLIDE KINETICS
  Influence of irradiation on the incorporation of radionuclides (^{239}Pu; ^{226}Ra; ^{210}Pb; ^{144}Ce; tritium), 30:29818
TISSUES/RADIOSENSITIVITY
  Dose-limiting tissues in relation to types and location of tumors. Implications for efforts to improve radiation dose distributions (Proton beams), 30:29725
TITANATES/MAGNETIC SUSCEPTIBILITY
  Synthesis and magnetic properties of samarium and europium titanoniobates ($SmTiNbO_6$; EuTiNbO6), 30:29906
TITANIUM/ACTIVATION ANALYSIS
  Multielement determination in market-garden soils by instrumental photon activation analysis, 30:28921
  Nondestructive determination of some trace elements in tantalum by proton activation analysis, 30:28922
TITANIUM/BONDING
  Determination of the feasibility of using beta radiation backscatter for the detection of surface contamination of metal panels, 30:29294 (AD-776394)
TITANIUM/CHARGED-PARTICLE TRANSPORT
  Transmission and reflection of electrons by foils, 30:31118
TITANIUM/CHEMICAL ANALYSIS
  Extraction--spectrophotometric methods of determining 0.0--n0.000n% aluminum in materials of metallurgical manufacture (exchange of experience), 30:28956
TITANIUM/CHEMICAL REACTIONS
  Reactions of boron and silicon carbide with tungsten and titanium, 30:29948
TITANIUM/ELECTRON COLLISIONS
  Transmission and reflection of electrons by foils, 30:31118
TITANIUM/EMISSION SPECTROSCOPY
  Spectrographic determination of trace impurities in high purity uranium oxide, 30:28944 (UCID-15952)
TITANIUM/ION-ATOM COLLISIONS
  High-energy calculation of K-shell ejection cross sections as a function of projectile charge (Born approximation), 30:30536
TITANIUM/PHASE TRANSFORMATIONS
  (α + ω) transition in titanium and zirconium in shock waves, 30:30011
TITANIUM/POWDER METALLURGY
  Powder metallurgy of heat-resistant alloys and refractory metals (Book), 30:29963
TITANIUM/SORPTIVE PROPERTIES
  Procedure for deuterating titanium, 30:29216 (UCID-15624)
TITANIUM/STACKING FAULTS
  Diffraction of x rays on stacking faults in metals with hcp lattices, 30:30024
TITANIUM 46/ALPHA REACTIONS
  Reaction rates of interest in late stages of stellar nycleosynthesis (Estimate of reliability), 30:30255
TITANIUM 46/ENERGY LEVELS
  Structure of low-lying 0^+ states in fsub(7/2) shell nuclei from inelastic ^{3}He scattering (29 MeV: differential cross sections, DWBA), 30:30934
TITANIUM 46/HELIUM 3 REACTIONS
  Structure of low-lying 0^+ states in fsub(7/2) shell nuclei from inelastic ^{3}He scattering (29 MeV: differential cross sections, DWBA), 30:30934
TITANIUM 48/ALPHA REACTIONS
  Generalized collective model and α-particle scattering on ^{56}Fe and ^{48}Ti (104 MeV: angular distributions), 30:30945
TITANIUM 48/ENERGY LEVELS
  Structure of low-lying 0^+ states in fsub(7/2) shell nuclei from inelastic ^{3}He scattering (29 MeV: differential cross sections, DWBA), 30:30934
TITANIUM 48/HELIUM 3 REACTIONS
  Structure of low-lying 0^+ states in fsub(7/2) shell nuclei from inelastic ^{3}He scattering (29 MeV: differential cross sections, DWBA), 30:30934
TITANIUM ALLOYS
  See also ALLOY-TZM
    INCONEL X750
    RENE 41
    TITANIUM BASE ALLOYS
TITANIUM ALLOYS/AGING
  Effect of the volume disparity between the precipitation phase and the matrix on the scattering of x rays by aging alloys (EP 199 (Ni--Cr--W--Mo--Al--Ti)), 30:30036
TITANIUM ALLOYS/CORROSION
  Effect of oxygen on the corrosion of vanadium and V--20% Ti by liquid lithium (600 to 1000°C), 30:29954
TITANIUM ALLOYS/CORROSION RESISTANCE
  Electrochemistry of aqueous corrosion: uranium and its alloys (Review), 30:29944 (Y-1949)
TITANIUM ALLOYS/CRYSTAL STRUCTURE
  Structure of alloys of the Nb--Ti--Zr system. Close order of displacement in solid solutions (50 at./percent/Nb; diffusion distribution), 30:30040
TITANIUM ALLOYS/ION EMISSION
  Ionic emission yield for alloys, dependence on the nature of the solute. II. Interpretation, 30:30087
TITANIUM ALLOYS/MECHANICAL PROPERTIES
  Mechanical behavior of metal matrix composites. Final report, 1 April 1972--30 April 1973 (B--Al;B/SiC--Ti;tensile, fatigue, and creep behavior;effects of defects), 30:29975 (AD-775359)
TITANIUM ALLOYS/PHASE TRANSFORMATIONS
  Effect of cold deformation on phase transition in Ti--Nb alloys, 30:30009
TITANIUM ALLOYS/POWDER METALLURGY
  Powder metallurgy of heat-resistant alloys and refractory metals (Book), 30:29963
TITANIUM BASE ALLOYS/CORROSION
  Corrosion fatigue strength of a titanium alloy at elevated temperature (Ti--Al--Zr; simulated seawater), 30:29945
  Thermal and mechanical effects on the corrosion behavior of Ti--6Al--4V. Report for January 1971--January 1972, 30:29942 (AD-777170)
TITANIUM BASE ALLOYS/CORROSION RESISTANCE
  Study of the corrosion resistance of titanium alloys and some steels during condensation of alkylphenol with formaldehyde (Steels 3, AT-3, EI-943; Ti alloys VT2-1, VT-14; VT1-0, OT-4, VT5, Ti--5 percent Ta, Ti--33 percent Mo), 30:29947

TITANIUM BASE ALLOYS/FATIGUE
  Fatigue-crack growth of Ti--6Al--2Cb-1Ta--0.8Mo alloy in air and natural sea water environments, 30:29972 (AD-765318)
TITANIUM BASE ALLOYS/MECHANICAL PROPERTIES
  Mechanical properties of multicomponent alloys based on Ti--Al--Sn (Zr) α-solid solution with β-stabilizing elements (Additions of Mo, V, Cr, Fe, Si, B;properties at up to 950°C), 30:29984
  Precision casting of alloy Ti--6Al--4V (Effects of heat treatments on mechanical properties), 30:29996
TITANIUM BASE ALLOYS/STACKING FAULTS
  Diffraction of x rays on stacking faults in metals with hcp lattices (Ti--Al; Ti--Sn), 30:30024
TITANIUM BORIDES/WEAR RESISTANCE
  Abrasive wear-resistance and failure character of titanium and zirconium borides surface layers (Comparison with steel Kh18N10T), 30:29899
TITANIUM IONS/EMISSION SPECTRA
  Spectral classifications in the Fe XIX to Fe XXIII isoelectronic sequences, 30:30329
TITANIUM OXIDES/X-RAY FLUORESCENCE ANALYSIS
  Compilation of x-ray interaction data for x-ray fluorescence analysis of geological samples, 30:28943 (RISO-297)
TOKAMAK DEVICES/CONFIGURATION
  Equilibrium and stability of elliptical cross section tokamak, 30:29210 (ORNL-TM-4666)
TOKAMAK DEVICES/DIVERTORS
  Bundle divertors and topology, 30:29204 (CLM-R-132)
TOKAMAK DEVICES/EQUILIBRIUM PLASMA
  Computation of MHD equilibria in Tokamak, 30:29179 (CLM-R-133)
TOKAMAK DEVICES/MAGNET COILS
  Method for the calculation of the magnetostatic field from a wide class of current geometries, 30:29211 (RL-74-077)
TOKAMAK DEVICES/PLASMA BEAM INJECTION
  Anomalous scattering of the energy of a plasma jet interacting with a gas target, 30:29155
TOKAMAK DEVICES/PLASMA DIAGNOSTICS
  Proposed method of measuring the current distribution in a tokamak plasma, 30:29170
TOKYO-1 REACTOR
  See FUKUSHIMA-1 REACTOR
TOLAN/HYDROGENATION
  Moessbauer spectroscopic study of the effect of reactor radiation on the iron(III) acetylacetonate-triethylaluminum catalyst, 30:29052
TOLUIDINE BLUE/METABOLISM
  Elimination of intravenously injected ^{125}I-toluidine blue in rabbits (Effectiveness for parathyroid scanning), 30:29812
TONSILS
  See PHARYNX
TOUGHNESS (FRACTURE)
  See FRACTURE PROPERTIES
TRACER TECHNIQUES
  Investigations on material transport and dust formation in revolving furnaces for Clinkering by isotopic tracing, 30:29644
TRACER TECHNIQUES/ERRORS
  Variance in the evaluation of data obtained in radioisotopic tracer investigations, 30:29646
TRACER TECHNIQUES/RESPONSE FUNCTIONS
  Evaluation of response functions which are obtained when radioisotopes are used as a tracer. I. Application of the scaler, 30:29639
  Processing of the response functions obtained by radiotracer measurements. II. Approximation of the measured relations and smoothing of variations by means of Laguerre functions, 30:29638
TRACK DETECTORS (DIELECTRIC)
  See DIELECTRIC TRACK DETECTORS
TRANS 104 ELEMENT COMPOUNDS/SUBLIMATION HEAT
  Prediction of the behaviour of superheavy elements and their chlorides during thermatochromatographic separation (Z = 112 to 117), 30:29138 (GSI-tr-74/15)
TRANS 104 ELEMENTS
  See also ELEMENT 108
  ELEMENT 112
  ELEMENT 117
TRANS 104 ELEMENTS/CHEMICAL PROPERTIES
  Prediction of the behaviour of superheavy elements and their chlorides during thermatochromatographic separation (Z = 112 to 117), 30:29138 (GSI-tr-74/15)
TRANS 104 ELEMENTS/CHROMATOGRAPHY
  Prediction of the behaviour of superheavy elements and their chlorides during thermatochromatographic separation (Z = 112 to 117), 30:29138 (GSI-tr-74/15)
TRANS 104 ELEMENTS/SPONTANEOUS FISSION
  Superheavy elements and the Strutinsky prescription (Single-particle corrections to liquid-drop model), 30:31026
TRANS 104 ELEMENTS/SUBLIMATION HEAT
  Prediction of the behaviour of superheavy elements and their chlorides during thermatochromatographic separation (Z = 112 to 117), 30:29138 (GSI-tr-74/15)
TRANSAMINASES
  See AMINOTRANSFERASES
TRANSDUCERS/CALIBRATION
  Pressure, Force, and Mass Calibration Laboratory, 30:31445 (UCID-15811)
TRANSFER (HEAT)
  See HEAT TRANSFER
TRANSIENTS/RECORDING SYSTEMS
  MAGREC final report (Magnetic film recorder for fast transients from nuclear events), 30:29619 (UCID-16026)
TRANSISTORS
  See also JUNCTION TRANSISTORS
  MOS TRANSISTORS
TRANSISTORS/OSCILLATIONS
  Detection and suppression of transistor oscillation during power burn-in, 30:31419 (BDX-613-1144(Rev.))
TRANSITION ELEMENT COMPOUNDS/PRODUCTION
  High-melting metals and metallic compounds, 30:30021
TRANSITION ELEMENT COMPOUNDS/USES
  High-melting metals and metallic compounds, 30:30021
TRANSITION ELEMENTS/SUPERCONDUCTIVITY
  Critical temperature of transition-metal alloy superconductors, 30:30811
TRANSITION RADIATION DETECTORS/PARTICLE DISCRIMINATION
  Transition counters for πK differentiation above 400 GeV, 30:29599
TRANSPLUTONIUM ELEMENTS
  See also AMERICIUM
  TRANS 104 ELEMENTS
TRANSPLUTONIUM ELEMENTS/EXTRACTION CHROMATOGRAPHY
  Recent results in the application of column extraction chromatography in inorganic analysis, 30:28989 (ANL-Trans-960)
TRANSPORT
  (Limited to the movement of goods and persons.)
TRANSPORT/LEVITATION
  High speed magnetically levitated and propelled mass ground transportation, 30:30829
TRANSPORT/PROPULSION
  High speed magnetically levitated and propelled mass ground transportation, 30:30829
TRANSPORT/SUPERCONDUCTING MAGNETS
  High speed magnetically levitated and propelled mass ground transportation, 30:30829
TRANSPORTABLE REACTORS
  (Capable of being moved when not critical and possibly partly dismantled.)
TRANSPORTABLE REACTORS/DESIGN
  Fuel element for a compact power reactor (Patent), 30:31242
TRANSPORTABLE REACTORS/FUEL ELEMENTS
  Fuel element for a compact power reactor (Patent), 30:31242
TRAPPED ELECTRONS/INFRARED SPECTRA
  Trapped electrons in C_2H_5OD glasses γ-irradiated at 4°K, 30:29068
TREES/DISTRIBUTION
  SAFT: structural analysis of forest trees, 30:31337 (EDFB-IBP-74-4)
1,3,7-TRIMETHYLXANTHINE
  See CAFFEINE
TRIPLET PARTICLES
  See QUARKS
TRITICUM
  See WHEAT
TRITIUM/BETAVOLTAIC CELLS
  Advanced betavoltaic power sources, 30:29257
TRITIUM/BIOLOGICAL HALF-LIFE
  Metabolism of tritium-labelled sodium acetate, in the rat. A radiation protection approach, 30:29795 (CEA-R-4591)
TRITIUM/BIOLOGICAL RADIATION EFFECTS
  Nuclear testing (^{131}I; ^{90}Sr; ^{137}Cs; ^{14}C; Tritium), 30:29719
TRITIUM/BREEDING
  Adequacy of lithium supplies as a fusion energy source, 30:29222 (UCID-15953)
TRITIUM/COSMOCHEMISTRY
  The unique cosmic-ray history of the Malakal chondrite, 30:30176
TRITIUM/DECAY
  Pulse NMR studies of radiation damage in metal tritides (Triton decay in LiT and UT_3), 30:29889 (MLM-2172(OP))
TRITIUM/ELECTROMAGNETIC FORM FACTORS
  Convergence of the hyperspherical expansion treatment of few-nucleon bound states, 30:30859
TRITIUM/HOT ATOM CHEMISTRY
  Identification of high-boiling tritium-labeled compounds formed in reactions of tritium recoil atoms with benzene, 30:29084
  Trajectory studies of hot atom reactions. II. An unrestricted potential for CH_3, 30:29085
TRITIUM/ISOTOPE EFFECTS
  Isotope effects on partition functions and thermodynamic quantities of the stable diatomic hydrides, 30:29020
TRITIUM/ISOTOPE SEPARATION
  Tritium Effluent Control Project. Progress Report: April--June 1974, 30:29026 (MLM-2171(LD))
TRITIUM/ISOTOPIC EXCHANGE
  Tritium Effluent Control Project. Progress Report: April--June 1974, 30:29026 (MLM-2171(LD))

TRITIUM/NEUTRON REACTIONS
  Variational calculations of reactions involving light nuclei, 30:30861
TRITIUM/PROTON REACTIONS
  A microscopic description of the negative parity resonances in the mass-4 system by the coupled-channel method, 30:30871
  Variational calculations of reactions involving light nuclei, 30:30861
TRITIUM/RADIATION MONITORING
  Data. Section II. Water, 30:29411
  Data. Section IV. Other data, 30:29412
  Environmental monitoring report: United States Atomic Energy Commission, Oak Ridge facilities. Calendar year 1973, 30:29352 (UCC-ND-280)
  Radiological monitoring program, period covering February 4, 1974--April 30, 1974 (Rio Blanco site), 30:29348 (PNE-RB-51-9)
  Report of activity, February 1974 (Radioactivity of environmental samples collected throughout France during February 1974), 30:29349 (SCPRI(RM)-2-1974)
TRITIUM/RADIOECOLOGICAL CONCENTRATION
  Radiological monitoring program, period covering February 4, 1974--April 30, 1974 (Rio Blanco site), 30:29348 (PNE-RB-51-9)
TRITIUM/REMOVAL
  Investigation of tritium decontamination. Interim research report (Natural gas decont amination), 30:29326 (UCID-15985)
TRITIUM/SCINTILLATION COUNTING
  Method of ^{3}H-determination in hair, 30:28985
TRITIUM/TARGETS
  A cooling system for thin tritiated titanium targets, 30:30157
TRITIUM/THREE-BODY PROBLEM
  Ground-state properties of three-nucleon systems: a review (Binding energy, charge form factor, magnetic moment), 30:31039
TRITIUM/TISSUE DISTRIBUTION
  Influence of irradiation on the incorporation of radionuclides (^{239}Pu; ^{226}Ra; ^{210}Pb; ^{144}Ce; tritium), 30:29818
  Metabolism of tritium-labelled sodium acetate, in the rat. A radiation protection approach, 30:29795 (CEA-R-4591)
TRITIUM/WAVE FUNCTIONS
  Approximate D-states and meson exchange currents, 30:30870
TRITIUM COMPOUNDS/RADIATION EFFECTS
  Pulse NMR studies of radiation damage in metal tritides (Triton decay in LiT and UT_3), 30:29889 (MLM-2172(OP))
TRITIUM COMPOUNDS/RADIOCHROMATOGRAPHY
  Identification of high-boiling tritium-labeled compounds formed in reactions of tritium recoil atoms with benzene, 30:29084
TRITONS/BINDING ENERGY
  New determination of Mongan's non-local separable potentials for nuclear structure calculations, 30:31036
  Triton binding energy and the deuteron wave function, 30:30862
TROPICAL REGIONS/METEOROLOGY
  Concentrational distribution of fission products over tropical zone oceans and its relation to atmospheric processes, 30:29388
TROPOSPHERE/RADIATION MONITORING
  Vertical distribution of radioactive aerosols in the troposphere above the European part of the USSR in 1964--1967, 30:29389
TROPOSPHERE/RADIOACTIVE AEROSOLS
  Size-distribution relation of high-activity particles in the troposphere in September--December 1967, 30:29392
TROPOSPHERE/WAVE PROPAGATION
  Characteristics of the turbulent atmosphere on the basis of radio source scintillation data, 30:30411
TRYPAFLAVINE
  See ACRIFLAVINE
TRYPSIN/CHEMICAL RADIATION EFFECTS
  Significance of free radicals for the inactivation of trypsin by uv irradiation. Investigations by means of ESR spectroscopy, 30:29657
TRYPSIN/RADIOASSAY
  Microassay for proteolytic enzymes using a new radioactive anilide substrate (Tritium tracer technique), 30:29834
TSH
  (Thyroid stimulating hormone.)
TSH/RADIOIMMUNOASSAY
  Clinical experience with radioimmunological TSH determination (^{131}I tracer techniques), 30:29842
TUFF/BLAST EFFECTS
  Preliminary equation-of-state data for Baneberry altered tuff, 30:29322 (UCID-15874)
TUFF/EQUATIONS OF STATE
  Preliminary equation-of-state data for Baneberry altered tuff, 30:29322 (UCID-15874)
TUMOR CELLS/BIOLOGICAL RADIATION EFFECTS
  Cell cycle kinetics and radiation therapy, 30:29662 (UCRL-75441)
  Cell cycle kinetics and radiation therapy, 30:29662 (UCRL-75441)
  Lack of recovery from radiation damage on colony forming ability and on membrane charge in a Burkitt lymphoma cell line, 30:29668
TUMOR CELLS/CELL PROLIFERATION
  Cell cycle kinetics and radiation therapy, 30:29662 (UCRL-75441)
  Influence of radiation on the layers of tumors in the early formation of tumors, 30:29745
TUMOR CELLS/RADIOSENSITIVITY
  Changes in oxygenation and radiosensitivity of the tumor after irradiation, 30:29763
TUMORS
  See NEOPLASMS
TUNGSTEN/ACTIVATION ANALYSIS
  Nondestructive determination of some trace elements in tantalum by proton activation analysis, 30:28922
TUNGSTEN/ANNEALING
  Reactions occurring during annealing of VIa and Va metals in oxygen, water vapor, and air at low pressures, 30:30022
TUNGSTEN/CHARGED-PARTICLE TRANSPORT
  Helium ion stopping cross sections in bismuth, lead, and tungsten, 30:31114
TUNGSTEN/CHEMICAL ANALYSIS
  Extraction--spectrophotometric methods of determining 0.0--n0.000n% aluminum in materials of metallurgical manufacture (exchange of experience), 30:28956
TUNGSTEN/CHEMICAL REACTIONS
  Reactions of boron and silicon carbide with tungsten and titanium, 30:29948
TUNGSTEN/CRACKS
  Types of cracks in W monocrystals deformed by compression at 77°K, 30:30033
TUNGSTEN/CRYSTAL GROWTH
  Vapor-grown tungsten whiskers induced by vacuum discharges, 30:29968
TUNGSTEN/CRYSTAL STRUCTURE
  Effect of lithium vapor on the structure of monocrystals of refractory metals and alloys, 30:29955
  Formation of a network of spherical micropores and the relation of this with the GK properties of TUNGSRAM-made tungsten metal prepared with oxide additives containing K, Si, and Al, 30:30026
TUNGSTEN/DEBYE-WALLER FACTOR
  Lattice dynamical study of the recoilless fraction of ^{57}Fe in Ni, Mo, W, α-Fe and Cu, 30:30050
TUNGSTEN/DEFORMATION
  Nature of the deformation and flow of metals at and near the interface during abrasion, and its relation to the friction, 30:30051
TUNGSTEN/DEPOSITION
  Nucleation and growth of W films evaporated on NaCl, 30:29959
TUNGSTEN/DISSOLUTION
  Interaction of tungsten with liquid aluminum, 30:30003
TUNGSTEN/EMISSION SPECTROSCOPY
  Spectral assay of components in alloys (exchange of experience), 30:28951
TUNGSTEN/ENERGY TRANSFER
  Energy transfer to a tungsten lattice by ion bombardment, 30:30070
TUNGSTEN/INTERNAL FRICTION
  Effect of temperature and rhenium impurity on the amplitude-dependent, internal friction of tungsten, 30:30056
  Internal friction measurement in high purity tungsten single crystal, 30:29979 (N-74-19370)
TUNGSTEN/ION CHANNELING
  Electronic stopping power of channelled ions in a model incorporating the Pauli principle (Incident ions Z = 1 to 50), 30:31115
TUNGSTEN/MECHANICAL PROPERTIES
  Effect of cyclic deformation on the dislocation structure and mechanical properties of molybdenum, chromium, and tungsten, 30:30028
TUNGSTEN/PLASMA ARC SPRAYING
  Damping and elastic characteristics of plasma-sprayed coatings of W, nichrome, zirconia, and Cr--Ni spinels, 30:29887
TUNGSTEN/POWDER METALLURGY
  Powder metallurgy of heat-resistant alloys and refractory metals (Book), 30:29963
TUNGSTEN/PRODUCTION
  High-melting metals and metallic compounds, 30:30021
TUNGSTEN/QUALITATIVE CHEMICAL ANALYSIS
  Application of activation analysis to the determination of pollutants in the atmosphere, 30:28914 (IEA-326)
TUNGSTEN/SLIDING FRICTION
  Nature of the deformation and flow of metals at and near the interface during abrasion, and its relation to the friction, 30:30051
TUNGSTEN/SLIP
  Pseudoasymmetry of [110] slip in tungsten single crystals, 30:30010
TUNGSTEN/USES
  High-melting metals and metallic compounds, 30:30021
TUNGSTEN 179/ENERGY-LEVEL TRANSITIONS
  Electromagnetic transitions in some odd-neutron deformed nuclei (Lifetimes, transition probabilities in Nilsson model with pairing and band mixing), 30:30990
TUNGSTEN 186/ENERGY LEVELS
  Nuclear Data Sheets for A = 186, 30:30988

TUNGSTEN 186/HEAVY ION REACTIONS
Quasi-fission: a new type of reaction observed in bombarding heavy nuclei by ^{84}Kr and ^{63}Cu ions, 30:30984
TUNGSTEN 186/NUCLEAR PROPERTIES
Nuclear Data Sheets for A = 186, 30:30988
TUNGSTEN 186/PROTON REACTIONS
One-nucleon transfer reactions in deformed nuclei (Indirect inelastic transitions through intermediate rotational states included), 30:30995
TUNGSTEN ALLOYS
See also TUNGSTEN BASE ALLOYS
TUNGSTEN ALLOYS/AGING
Effect of the volume disparity between the precipitation phase and the matrix on the scattering of x rays by aging alloys (EP 199 (Ni--Cr--W--Mo--Al--Ti)), 30:30036
TUNGSTEN ALLOYS/ELECTRONIC STRUCTURE
Nuclear gamma-resonance on nuclei of ^{57}Fe impurity in tungsten--rhenium alloys, 30:30029
TUNGSTEN ALLOYS/MECHANICAL PROPERTIES
Study of some high-temperature strength properties of the niobium alloys 5VMTs, 5VMTsU, and 5VTTs at 1100°C (5VMTs = Nb--5.3W--2.1Mo--0.72Zr; 5VNTsU = Nb--4.9W--2.0Mo--1.15Zr; 5VTTs = 4.5W--2Ta--3.45Zr), 30:30027
TUNGSTEN ALLOYS/POWDER METALLURGY
Powder metallurgy of heat-resistant alloys and refractory metals (Book), 30:29963
TUNGSTEN BASE ALLOYS/CRYSTAL STRUCTURE
Effect of lithium vapor on the structure of monocrystals of refractory metals and alloys (W--2 at. percent Rh; W--10 percent Mo; Mo--10 percent Re; Mo--27 percent Re), 30:29955
TUNGSTEN BASE ALLOYS/GRAIN GROWTH
Recrystallization grain coarsening in the tungsten--nickel system, 30:30004
TUNGSTEN BASE ALLOYS/INTERNAL FRICTION
Effect of temperature and rhenium impurity on the amplitude-dependent, internal friction of tungsten (W--0.1 wt percent Re), 30:30056
TUNGSTEN BORIDES/OXIDATION
Oxidation of ZrB_2, TaB_2, NbB_2, and W_2B_5 in atomic oxygen and by anodic polarization, 30:29938
TUNGSTEN CARBIDES/PRODUCTION
Production of complex zirconium--tungsten carbide on semi-industrial scale, 30:29893
TUNGSTEN COMPOUNDS/LATTICE PARAMETERS
On oxifluorides $A_{12}M(IV)M_3(VI)O_8F_{18}$ with uranium, molybdenum, and tungsten (A = Cs, Rb, K and M(IV) = U, Ce, MoW), 30:29006
TUNGSTEN COMPOUNDS/MAGNETIC SUSCEPTIBILITY
On oxifluorides $A_{12}M(IV)M_3(VI)O_8F_{18}$ with uranium, molybdenum, and tungsten (A = Cs, Rb, K and M(IV) = U, Ce, MoW), 30:29006
TUNGSTEN OXIDES/CRYSTAL STRUCTURE
Electron microscope study of some nonstoichiometric tungsten oxides, 30:29904
TURKEY POINT-3 REACTOR/AERIAL MONITORING
Aerial radiological measuring surveys of the Turkey Point Station, April 1972, 30:29358 (ARMS-72.6.2)
TURKEY POINT-3 REACTOR/REACTOR OPERATION
Semiannual operating report No. 4, January--June 1974, 30:31314 (DOCKET-50250-283)
TURKEY POINT-4 REACTOR/AERIAL MONITORING
Aerial radiological measuring surveys of the Turkey Point Station, April 1972, 30:29358 (ARMS-72.6.2)
TURKEY POINT-4 REACTOR/REACTOR OPERATION
Semiannual operating report No. 4, January--June 1974, 30:31314 (DOCKET-50250-283)
TWO-BODY PROBLEM/VARIATIONAL METHODS
Direct variational calculation of the two-body density matrix, 30:30631
TWO-FIREBALL MODEL
See FIREBALL MODEL
TWO-NUCLEON TRANSFER REACTIONS
One- and two-nucleon transfer reactions on deformed nuclei (Generalized optical model; DWBA, coupled-channels and adiabatic theory), 30:31021 (IFA-FT-108-1974)
TWO-PHASE FLOW/BOUNDARY LAYERS
Two-phase flow and heat transfer at the boundary layer of a thin body of revolution, 30:29291
TWO-PHASE FLOW/INSTABILITY
Derivation of transfer functions in boiling loops, 30:29292
TWO-PHASE FLOW/PRESSURE DROP
New approach to predicting pressure drop in two-phase flows, 30:29293
TYPE-II SUPERCONDUCTORS/ELECTRIC CONDUCTIVITY
Proximity effect on thin NbN-layers, 30:30805 (AED-CONF-74-089-005)
TYPE-II SUPERCONDUCTORS/MAGNETIC FLUX
Kinetics of flux jumps in Type-II superconducting disks, 30:30818
TYPE-II SUPERCONDUCTORS/PHYSICAL RADIATION EFFECTS
Influence of neutron irradiation on critical data of type II superconductors (Nb--Sn), 30:30063 (AED-CONF-74-089-006)
TYPE-III SUPERCONDUCTORS
See TYPE-II SUPERCONDUCTORS
TYROSINE/CHEMICAL RADIATION EFFECTS
Effects of ionizing radiation on tyrosine (X radiation), 30:29040

U

U-3 GROUPS/MATHEMATICAL SPACE
Geometrical interpretation of paraorder 3 of paraquark model, 30:30692
UNICELLULAR ALGAE/LUMINESCENCE
Piezoelectric mechanical-micropipette stimulator. Technical report No. 10, 30:31378 (NYO-3406-18)
UNIFIED GAUGE MODELS/LAGRANGIAN FUNCTION
Derivation of unified gauge theory from a generalized minimal principle, 30:31151
UNITARITY/S CHANNEL
Unitarity, phenomenology and the bare pomeron, 30:30710
UNITED STATES OF AMERICA
See USA
UNIVERSAL BLACKBODY RADIATION
See BLACKBODY RADIATION
UNIVERSE/PARTICLE PRODUCTION
Scalar waves in the mixmaster universe. II. Particle creation (Heisenberg picture, Bogolyubov transformation), 30:30391
UNIVERSE/WAVE PROPAGATION
Scalar waves in the mixmaster universe. II. Particle creation (Heisenberg picture, Bogolyubov transformation), 30:30391
URANATES/FORMATION FREE ENERGY
Heat capacity of α-sodium uranate ($\alpha-Na_2UO_4$) from 5 to 350 K. Standard Gibbs energy of formation at 298.15 K, 30:29128
URANATES/PHASE DIAGRAMS
Fast reactor programme. First quarter 1974 progress report, 30:31226 (RCN-212)
URANATES/SPECIFIC HEAT
Heat capacity of α-sodium uranate ($\alpha-Na_2UO_4$) from 5 to 350 K. Standard Gibbs energy of formation at 298.15 K, 30:29128
URANIUM
See also DEPLETED URANIUM
ENRICHED URANIUM
URANIUM-ALPHA
Uranium in the Great Divide Basin, Wyoming, 30:29336
URANIUM/ABUNDANCE
Origin of carbonatitic magma in the light of the Pb-U-Th isotope system, 30:29337
URANIUM/BURNUP
Utilization of metallic uranium in power channel uranium-graphite reactors, 30:31205
URANIUM/CHEMICAL ANALYSIS
Interlaboratory comparison of chemical analysis of uranium mononitride, 30:28942 (N-74-18812)
Separation of trace metal impurities from nuclear grade uranium by long-chain amine extraction and direct determination by atomic absorption spectrophotometry, 30:28948
URANIUM/CHEMICAL REACTION KINETICS
Interrelationship of thermodynamic and kinetic parameters of redox reactions, 30:29005
URANIUM/CHEMICAL VAPOR DEPOSITION
Chemical vapor deposition of uranium and plutonium (Patent), 30:29961
URANIUM/CORROSION RESISTANCE
Electrochemistry of aqueous corrosion: uranium and its alloys (Review), 30:29944 (Y-1949)
URANIUM/DATA COMPILATION
Information support for the Nevada Applied Ecology Group (Computer file of references on environmental aspects of Pu, U, and Nevada Test Site), 30:29454 (NVO-AEIC-74-1)
URANIUM/DEFORMATION
Nature of the deformation and flow of metals at and near the interface during abrasion, and its relation to the friction, 30:30051
URANIUM/EMISSION SPECTRA
X-ray spectroscopy analysis of the uranium 5f distribution in the metal and in UO_2, 30:30018
URANIUM/EQUATIONS OF STATE
Experimental, very high-temperature, liquid--uranium equation of state, 30:30045
URANIUM/EXTRACTION CHROMATOGRAPHY
Recent results in the application of column extraction chromatography in inorganic analysis, 30:28989 (ANL-Trans-960)
URANIUM/FLUORINATION
Reaction of uranium with a mixture of lithium and calcium fluorides, 30:29110
URANIUM/ION EXCHANGE
Sorption method of isolating uranium and other valuable metals from sea water, 30:28998
URANIUM/IRON 56 REACTIONS
Ternary fission induced by 540 MeV Fe ions on uranium (Branching ratio, potential energy surfaces), 30:31018
URANIUM/NUCLEAR REACTION ANALYSIS
Simultaneous analysis of uranium and thorium by the delayed fission neutron counting method, 30:28931
URANIUM/OXIDATION
Kinetics of uranium(IV)--neptunium(VI) reaction in tributyl phosphate solutions, 30:29102

Oxidation--reduction reactions of actinide elements. XXIV. Kinetics of uranium(IV)--iron(III) reaction in water--isopropanol solutions, 30:29106
URANIUM/POLAROGRAPHY
Laboratory and hot-cell studies concerning the in-line polarographic determination of uranium in the aqueous waste stream of the KFA-TBP 23/25 process, 30:28941 (JUL-1063-CT)
URANIUM/QUALITATIVE CHEMICAL ANALYSIS
Application of activation analysis to the determination of pollutants in the atmosphere, 30:28914 (IEA-326)
URANIUM/RADIATION MONITORING
Data. Section IV. Other data, 30:29412
Environmental monitoring report, calendar year 1973, 30:29351 (UCC-ND-279)
Feed Materials Production Center environmental monitoring annual report for 1973, 30:29347 (NLCO-1109)
Portsmouth Gaseous Diffusion Plant environmental monitoring report, 1973, 30:29346 (GAT-781)
URANIUM/RADIOECOLOGICAL CONCENTRATION
Grazing studies on selected plutonium-contaminated areas in Nevada (U and Pu uptake by cattle), 30:29448 (NVO-AEIC-74-1)
URANIUM/RADIOMETRIC ANALYSIS
Radiometric analysis of thorium and uranium, 30:28975
URANIUM/SEPARATION PROCESSES
Decontaminating uranium by reaction with ClF_3 and HF and volatizing the UF_6 product (Patent), 30:29149
URANIUM/SLIDING FRICTION
Nature of the deformation and flow of metals at and near the interface during abrasion, and its relation to the friction, 30:30051
URANIUM/SOLVENT EXTRACTION
Process for separation of protactinium, thorium, and uranium from neutron-irradiated thorium (Using TBP), 30:29150
URANIUM/TISSUE DISTRIBUTION
Grazing studies on selected plutonium-contaminated areas in Nevada (U and Pu uptake by cattle), 30:29448 (NVO-AEIC-74-1)
URANIUM/X-RAY FLUORESCENCE ANALYSIS
No radioactive silver detectable in silver--uranium ore, 30:28987
URANIUM 233/ALPHA SPECTROSCOPY
Simultaneous determination of alpha-emitting nuclides of radium through californium in soil, 30:28977
URANIUM 233/NEUTRON REACTIONS
Assessment of known independent yields and the calculation of those unknown in the fission of ^{232}Th, ^{233}U, ^{235}U, ^{238}U, ^{239}Pu, ^{240}Pu, and ^{241}Pu (Odd--even Z effects), 30:31008 (AERE-R-7680)
Investigation of the reported mass distribution curves in the fission of ^{233}U with 14.8 MeV neutrons, 30:31010 (ORO-4282-14)
URANIUM 234/RADIOMETRIC ANALYSIS
Continuous in-line monitor for UF_6 enrichment, 30:29509
URANIUM 235/ISOTOPE SEPARATION
Process for separating uranium isotopes (Shock waves; patent), 30:29636
URANIUM 235/NEUTRON REACTIONS
Assessment of known independent yields and the calculation of those unknown in the fission of ^{232}Th, ^{233}U, ^{235}U, ^{238}U, ^{239}Pu, ^{240}Pu, and ^{241}Pu (Odd--even Z effects), 30:31008 (AERE-R-7680)
Energy measurements of delayed neutron groups from ^{235}U, 30:31014
Measurement of internal conversion cascading in ^{235}U fission fragments, 30:31012
Resonance integrals of uranium-235/uranium-238 mixtures, 30:31013
Status report to NCSAC, 30:31011 (UCID-15639)
URANIUM 235/RADIOMETRIC ANALYSIS
Continuous in-line monitor for UF_6 enrichment, 30:29509
URANIUM 237/RADIATION MONITORING
Behavior and characteristics of radioactive debris from the Chinese nuclear weapons test of June 26, 1973, 30:29362 (BNWL-1850(Pt.3))
URANIUM 238/CAPTURE-TO-FISSION RATIO
New methods of measuring ^{238}U capture rate and fast fluxes in a zero energy HTR lattice, 30:31212
URANIUM 238/NEUTRON REACTIONS
Assessment of known independent yields and the calculation of those unknown in the fission of ^{232}Th, ^{233}U, ^{235}U, ^{238}U, ^{239}Pu, ^{240}Pu, and ^{241}Pu (Odd--even Z effects), 30:31008 (AERE-R-7680)
Contribution to the mutual resonance shielding of ^{238}U and ^{239}Pu, 30:31009 (EURFNR-1162)
Resonance integrals of uranium-235/uranium-238 mixtures, 30:31013
Status report to NCSAC, 30:31011 (UCID-15639)
URANIUM 238/RADIOMETRIC ANALYSIS
Gamma-ray assay of low-enriched uranium waste, 30:28986
URANIUM ALLOYS
See also URANIUM BASE ALLOYS
URANIUM ALLOYS/CORROSION RESISTANCE
Electrochemistry of aqueous corrosion: uranium and its alloys (Review), 30:29944 (Y-1949)
URANIUM BASE ALLOYS/METALLURGY
Metallurgical processing and pulsed reactor fuel performance (U--10 Mo alloy), 30:29982 (SLA-73-1121)
URANIUM BROMIDES/MOLECULAR STRUCTURE
Uranium tetrabromide structure. A new MX_4 structure type, 30:29129
URANIUM CARBIDES/PHASE DIAGRAMS
Fast reactor programme. First quarter 1974 progress report, 30:31226 (RCN-212)
URANIUM CARBIDES/THERMODYNAMIC PROPERTIES
Thermodynamic properties and mutual diffusion in the system UC--ZrC, 30:29905
URANIUM CHLORIDES/CHEMICAL REACTION KINETICS
Kinetics of forming ammoniates of uranium tetrachloride, 30:29124
URANIUM CHLORIDES/ENTHALPY
Gaseous halide complexes and their stability, 30:29091
URANIUM CHLORIDES/FORMATION HEAT
Gaseous halide complexes and their stability, 30:29091
URANIUM CHLORIDES/MELTING POINTS
Fusibility diagram of the system LiCl--UCl_4--$ThCl_4$, 30:29095
URANIUM COMPLEXES/CHEMICAL PREPARATION
Compounds of tetravalent uranium with complex cations of platinum ($[[[Pt(NH_3)_4]_2[U(C_4H_4O_6)_2(C_2O_4)_2]$ and $[Pt(NH_3)t^4][U(C_2O_4)_4]\ 3H_2$), 30:29108
Conditions for forming polynuclear hydroxy complexes of hexavalent uranium (Effects of pH of solution and concentration of U on polymerization), 30:29125
Preparation of complex perxenates of some actinide elements, 30:29117
URANIUM COMPLEXES/MAGNETIC SUSCEPTIBILITY
Magnetic susceptibilities of octacoordinated uranium(IV) complexes, 30:29094
URANIUM COMPLEXES/PYROLYSIS
Derivatographic investigations on the thermal degradation of pyridine, isoquinoline, α,α-dipyridyl and o-phenantroline, resp. bichromate- or chromate-ion containing metal complexes. II. Zinc(II)-, cadmium(II)-, and manganese(II)-complexes. III. Mercury(I and II)-, uranyl-, thorium-, lanthanum-, and iron-complexes, 30:29122
URANIUM COMPOUNDS/CHEMICAL PREPARATION
Apparatus for obtaining water-free uranium compounds from suspensions (Patent), 30:29126
Kinetics of forming ammoniates of uranium tetrachloride, 30:29124
URANIUM COMPOUNDS/LATTICE PARAMETERS
On oxifluorides $A_{12}M(IV)M_3(VI)O_8F_{18}$ with uranium, molybdenum, and tungsten (A = Cs, Rb, K and M(IV) = U, Ce, MoW), 30:29006
URANIUM COMPOUNDS/MAGNETIC SUSCEPTIBILITY
On oxifluorides $A_{12}M(IV)M_3(VI)O_8F_{18}$ with uranium, molybdenum, and tungsten (A = Cs, Rb, K and M(IV) = U, Ce, MoW), 30:29006
URANIUM COMPOUNDS/OXIDATION
Kinetics of oxidation of uranium oxysulfide, 30:29103
URANIUM COMPOUNDS/SEPARATION PROCESSES
Decontaminating uranium by reaction with ClF_3 and HF and volatizing the UF_6 product (Patent), 30:29149
URANIUM DEPOSITS
Uranium in the Great Divide Basin, Wyoming, 30:29336
URANIUM DEPOSITS/MINERALIZATION
Hypogenic zonality in hydrothermal uranium deposits, 30:29334
URANIUM DIOXIDE/CHEMICAL PREPARATION
Fueled moderator composition (Patent), 30:29934
URANIUM DIOXIDE/CRYSTAL GROWTH
Epitaxial growth of UO_2 thin films evaporated on NaCl substrates with colloidal centres, 30:29927
URANIUM DIOXIDE/CRYSTAL STRUCTURE
Lattice defects and atomic radii in UO_2 and PuO_2, 30:29929
The structure of vacuum-evaporated UO_2 thin films, 30:29928
URANIUM DIOXIDE/EMISSION SPECTRA
X-ray spectroscopy analysis of the uranium 5f distribution in the metal and in UO_2, 30:30018
URANIUM DIOXIDE/FABRICATION
Fabrication of (Pu-U) oxide microspheres using an internal gelation method, 30:29926
URANIUM DIOXIDE/FUEL-COOLANT INTERACTIONS
Thermodynamic data program involving plutonia and urania at high temperatures. Quarterly report No. 27, February 1, 1974--April 30, 1974 (LMFBR), 30:31223 (GEAP-12511)
URANIUM DIOXIDE/GELATION
Fabrication of (Pu-U) oxide microspheres using an internal gelation method, 30:29926
URANIUM DIOXIDE/GRAIN GROWTH
New aspect of grain growth of sol-gel urania, 30:29921
URANIUM DIOXIDE/HOT PRESSING
Fabrication of high-density UO_2 and (Usub(0.75)Pusub(0.25))O_2 by hot pressing, 30:29925
URANIUM DIOXIDE/PHYSICAL RADIATION EFFECTS
A technique for measuring the density of small fragments of high-density materials both before and after irradiation, 30:29931
Fabrication, irradiation, and postirradiation examination of mixed oxide fuel pin PNL-3-8, 30:31231 (HEDL-TME-74-37)
URANIUM DIOXIDE/SINTERING
Initial-stage sintering of sol-gel urania, 30:29922
URANIUM FLUORIDES
See also URANIUM HEXAFLUORIDE

URANIUM FLUORIDES/SEPARATION PROCESSES
Decontaminating uranium by reaction with ClF_3 and HF and volatizing the UF_6 product (Patent), 30:29149
URANIUM HEXAFLUORIDE/DISTILLATION
Decontaminating uranium by reaction with ClF_3 and HF and volatizing the UF_6 product (Patent), 30:29149
URANIUM HYDRIDES/RADIATION EFFECTS
Pulse NMR studies of radiation damage in metal tritides (Triton decay in LiT and UT_3), 30:29889 (MLM-2172(OP))
URANIUM ISOTOPES/ISOTOPE RATIO
Analysis of ECE data on the basis of isotopic weight fractions, 30:28940 (EUR-4859)
URANIUM ISOTOPES/RADIATION MONITORING
Environmental monitoring report: United States Atomic Energy Commission, Oak Ridge facilities. Calendar year 1973, 30:29352 (UCC-ND-280)
URANIUM NITRIDES/CHEMICAL ANALYSIS
Interlaboratory comparison of chemical analysis of uranium mononitride, 30:28942 (N-74-18812)
URANIUM NITRIDES/PHASE DIAGRAMS
Fast reactor programme. First quarter 1974 progress report, 30:31226 (RCN-212)
URANIUM ORES/MINERALIZATION
Zonality of thorium--niobium mineralization in albitites, 30:29333
URANIUM ORES/ORE PROCESSING
Ground level air concentrations of dust particles downwind from a tailings area during a typical windstorm (Mathematical model), 30:29380 (ORNL-TM-4375)
URANIUM OXIDES
See also URANIUM DIOXIDE
URANIUM OXIDES U308
URANIUM OXIDES/CRYSTAL STRUCTURE
Structure of the double oxide $UMo_{10}O_{32}$, 30:29941
URANIUM OXIDES/MAGNETIC PROPERTIES
Preparation and some magnetic properties of uranium oxide doped YIG crystals ($Y_3Fe_5O_{12}$), 30:29894
URANIUM OXIDES/SEPARATION PROCESSES
Decontaminating uranium by reaction with ClF_3 and HF and volatizing the UF_6 product (Patent), 30:29149
URANIUM OXIDES/THERMODYNAMICS
Effect of altered valent cations on oxygen pressure over urania, 30:29935
URANIUM OXIDES U308/CHEMICAL ANALYSIS
Spectrochemical analysis of uranium oxide by gallium oxide carrier dc arc technique (ASTM Standard E402), 30:28957
Spectrographic determination of trace impurities in high purity uranium oxide, 30:28944 (UCID-15952)
URANIUM OXIDES U308/PHASE TRANSFORMATIONS
New phase transitions in non-stoichiometric U_3O/sub 8-x/ at high temperatures. I. Thermogravimetric study, 30:29924
URANIUM-ALPHA/PEIERLS-NABARRO FORCE
Variation of activation volume and enthalpy during tensile straining of alpha-uranium at room temperature, 30:30035
URANYL COMPLEXES/CHEMICAL PREPARATION
Complex formation of actinides and lanthanides with o-phthalic, 3-nitrophthalic, and 4-nitrophthalic acids. I. Complex formation of uranium (^{233}U tracer), 30:29118
URANYL COMPOUNDS
See also URANYL NITRATES
URANYL COMPOUNDS/CHEMICAL REACTION KINETICS
Reaction of di-2-ethylhexylphosphoric acid and its uranyl salt with diluents. IV. Solutions of $(HR)_2$ and $UO_2(HR_2)_2$ in carbon tetrachloride, 30:29100
Reaction of di-2-ethylhexylphosphoric acid and its uranyl salt with diluents. V. Solutions of $(HR)_2$ and $UO_2(HR_2)_2$ in chloroform, 30:29101
URANYL COMPOUNDS/PHOTOCHEMISTRY
Photochemistry of the uranyl ion, 30:29131
URANYL NITRATES/STABILITY
Stablized uranyl nitrate compositions and uranium impregnation method (Patent), 30:29127
URINE/CHEMICAL ANALYSIS
Chronoamperometric determination of iodine in urine, 30:28939 (CNEA-366)
Direct determination of beryllium in urine by flameless atomic absorption spectrometry, 30:31379 (RFP-2151)
URINE/RADIATION MONITORING
Absorption, distribution, and excretion of plutonium by dairy cattle (^{238}Pu tracer), 30:29810 (NVO-AEIC-74-1)
UROGENITAL SYSTEM DISEASES
Absorption of ^{47}Ca from digestive tract in patients with urolithiasis, 30:29791
US AEC
See also ANL
BETTIS
PADUCAH PLANT
ROCKY FLATS PLANT
US AEC/BUDGETS
Public works for water and power development and Atomic Energy Commission appropriation bill, 1975, Ninety-Third Congress, Second Session, House of Representatives, 30:31331
US AEC/LEGISLATION
AEC omnibus legislation, 1974. Report by the Joint Committee on Atomic Energy, Ninety-Third Congress, Second Session, Senate, 30:31328
AEC omnibus legislation, 1974. Report by the Joint Committee on Atomic Energy, Ninety-Third Congress, Second Session, House of Representatives, 30:31329
USA
See also ALASKA
CALIFORNIA
COLORADO
FLORIDA
KANSAS
KENTUCKY
MAINE
MISSISSIPPI
MISSOURI
NEW YORK
OHIO
OREGON
TENNESSEE
WASHINGTON
WYOMING
USA/FALLOUT
Data. Section III. Air and deposition (Monitoring), 30:29382
Data. Section II. Water (Monitoring), 30:29411
Data. Section I. Milk and food (Monitoring), 30:29421
USSR/FALLOUT
Rate of fallout of ^{137}Cs and ^{90}Sr aerosols from the atmosphere (Monitoring), 30:29399
Washout of radioactive impurities from the atmosphere in the Central Caucasus mountains, 30:29385
USTILAGO
Resistance to Ustilago myadis of WD lineage progeny after chronic gamma irradiation (Maize), 30:29688
UTERINE CERVIX CARCINOMA
See UROGENITAL SYSTEM DISEASES
UTERUS/NEOPLASMS
Histochemical changes in cancer of the corpus uteri after experimental irradiation (X Radiation), 30:29716

V

VACUUM FURNACES/DESIGN
Apparatus for studying the kinetics of the liberation of inert gases from materials during isothermal annealing, 30:30002
VACUUM POLARIZATION
Contribution of hadrons to vacuum polarization, 30:30667
VACUUM SYSTEMS/COLD TRAPS
Protection circuit for a liquid-nitrogen trap filler, 30:31415 (ANL-8111)
VACUUM SYSTEMS/SPECIFICATIONS
Alice vacuum system: Sept. 1969, 30:29218 (UCID-15660)
VALVES/DESIGN
36 inch miter valve design, 30:31435 (UCID-15496)
VALVES/STANDARDS
Class 2 valves for liquid metal service, 30:29267 (RDT-E-1-19T(6-74))
VAN ALLEN BELTS
See RADIATION BELTS
VAN DE GRAAFF ACCELERATORS/BEAM MONITORING
Charge measuring unit of the pulsed electron beam in the Van de Graaff accelerator, 30:30124
VAN DE GRAAFF ACCELERATORS/CONTROL SYSTEMS
An automatic running system for a 500kV Van de Graaff generator, 30:30125
VAN DE GRAAFF ACCELERATORS/ION SOURCES
Beams of Be^+ from an rf ion source, 30:30130
VAN DE GRAAFF ACCELERATORS/OPERATION
Annual report, 1973 (Tandem Accelerator Laboratory, Uppsala, Sweden), 30:30952 (NP-20122)
VAN HOVE MODEL/PION REACTIONS
Exact and perturbative solutions of the Van Hove model describing nuclear diffraction dissociation of pions, 30:30722
VANADATES/CHEMICAL PREPARATION
Synthesis of high pressure $Cd_2V_2O_7$ and related compositions, 30:29903
VANADIUM/ACTIVATION ANALYSIS
Multielement determination in market-garden soils by instrumental photon activation analysis, 30:28921
VANADIUM/ANNEALING
Reactions occurring during annealing of VIa and Va metals in oxygen, water vapor, and air at low pressures, 30:30022
VANADIUM/CORROSION
Effect of oxygen on the corrosion of vanadium and V--20% Ti by liquid lithium (600 to 1000°C), 30:29954
VANADIUM/EMISSION SPECTROSCOPY
Spectrochemical analysis of uranium oxide by gallium oxide carrier dc arc technique (ASTM Standard E402), 30:28957
Spectrographic determination of trace impurities in high purity uranium oxide, 30:28944 (UCID-15952)
VANADIUM/ION EXCHANGE
Sorption method of isolating uranium and other valuable metals from sea water, 30:28998
VANADIUM/REDUCTION
The stability of vanadium and of the alloy V-3Ti-15Nb in liquid lithium at 700°C, 30:29951

VANADIUM/SOLVENT PROPERTIES
Solubility of hydrogen in vanadium and niobium at high temperatures (1273 to 2273°K; up to 25 atm; V--H; Nb--H; Ta--H), 30:29918
VANADIUM/SORPTIVE PROPERTIES
Irradiation effects on reactor structural materials. Semiannual progress report, 1 August 1973--31 January 1974, 30:30060 (AD-777433)
VANADIUM 49/ENERGY-LEVEL TRANSITIONS
Conversion coefficient measurements in ^{49}V (J,r), 30:30928
VANADIUM 51/ALPHA REACTIONS
Magnetic rotation of levels of ^{52}Mn and ^{54}Mn following the ^{52} ^{54}Cr(p,n) and ^{51}V(α,n) reactions (2.5- and 3.0-MeV protons, 7.5-MeV alphas; branching ratios, g, lifetimes), 30:30933
Reaction rates of interest in late stages of stellar nucleosynthesis (Estimate of reliability), 30:30255
Yield functions for ^{51}V(α,rγ) reaction at 7 to 15 MeV, 30:30916 (NP-20122)
VANADIUM ALLOYS
See also VANADIUM BASE ALLOYS
VANADIUM ALLOYS/CORROSION
Thermal and mechanical effects on the corrosion behavior of Ti--6Al--4V. Report for January 1971--January 1972, 30:29942 (AD-777170)
VANADIUM ALLOYS/ION EMISSION
Ionic emission yield for alloys, dependence on the nature of the solute. II. Interpretation, 30:30087
VANADIUM ALLOYS/MECHANICAL PROPERTIES
Mechanical properties of multicomponent alloys based on Ti--Al--Sn (Zr) α-solid solution with β-stabilizing elements (Additions of Mo, V, Cr, Fe, Si, B;properties at up to 950°C), 30:29984
Precision casting of alloy Ti--6Al--4V (Effects of heat treatments on mechanical properties), 30:29995
VANADIUM ALLOYS/REDUCTION
The stability of vanadium and of the alloy V-3Ti-15Nb in liquid lithium at 700°C, 30:29951
VANADIUM BASE ALLOYS/CORROSION
Effect of oxygen on the corrosion of vanadium and V--20% Ti by liquid lithium (600 to 1000°C), 30:29954
VANADIUM CARBIDES/CHEMICAL PREPARATION
Preparation and properties of vanadium monocarbide in the region of homogeneity, 30:29912
VANADIUM CARBIDES/PHYSICAL PROPERTIES
Preparation and properties of vanadium monocarbide in the region of homogeneity, 30:29912
VANADIUM HYDRIDES/PHASE STUDIES
Solubility of hydrogen in vanadium and niobium at high temperatures (1273 to 2273°K; up to 25 atm; V--H; Nb--H; Ta--H), 30:29918
VANADIUM IONS/EMISSION SPECTRA
Spectral classifications in the Fe XIX to Fe XXIII isoelectronic sequences, 30:30329
VANADIUM OXIDES/CRYSTAL DEFECTS
Intrinsic defect conductvity of vanadium pentoxide (Photoconductivity; relaxation time), 30:29915
VANADIUM OXIDES/ELECTRONIC STRUCTURE
ESR spectra and ionic states in the system V_2O_5--SnO_2, 30:29907
VANADIUM OXIDES/MAGNETIC SUSCEPTIBILITY
Magnetic properties of vanadium oxide V_3O_7, 30:29902
VARIABLE STARS/BRIGHTNESS
Study of delta Scuti variables (Possible separation), 30:30226
VARIABLE STARS/LUMINOSITY
Beat phenomenon in Tau Peg (One night), 30:30227
VARIABLE STARS/PHOTOMETRY
Broad-band 20-μ photometry of 63 stars (Circumstellar shells), 30:30221
Light-variations investigation of variable stars and satellites by means of computer, 30:30209
Photometric study of EE Aquarii, 30:30228
VASCULAR DISEASES/DIAGNOSIS
Advantages of theoretical models in interpreting cerebral transit curves (/sup 99m/Tc-pertechnetate tracer), 30:29830 (CONF-740708-20)
VECTOR DOMINANCE MODEL
Meson electromagnetic decays from SU(4)/sub w/ and generalized vector dominance (Pion form factor), 30:30650 (NP-20072)
VECTOR DOMINANCE MODEL/CURRENT COMMUTATORS
Null-plane commutators in the spontaneously broken gauge theory of vector dominance, 30:30637
VECTOR DOMINANCE MODEL/REVIEWS
Dynamical models based on vector-meson dominance and universality (Lectures), 30:30642
VECTOR FIELDS/MASS
Note on an infinite-mass limit of the Higgs model, 30:31153
VECTOR MESONS
(Mesons with spin-one.)
Pion and kaon form factors and heavy vector mesons, 30:30726
VECTOR MESONS/ELECTRODYNAMICS
High-energy scattering of vector particles by external electromagnetic field (Scattering amplitudes, eikonal approximation), 30:30649 (JINR-P2-7511)
VECTOR MESONS/PHOTOPRODUCTION
An SU(3) analysis of vector meson photoproduction and the pomeron, 30:30665
VEGETABLES
(Edible parts of plants only.)
See also BEETS
VEGETABLES/RADIOPRESERVATION
Surface irradiation of spherical vegetables and fruits, 30:29645
Technological foundations for radiation treatment of food products (Gamma radiation; electrons; book in Russian), 30:29681
VEGETATION
See PLANTS
VEHICLES/SAFETY
Tandem towing tests of the MHU-12/M trailer. Final report, October 1972--December 1973 (Nuclear weapon transport), 30:30113 (AD-777254)
VENEZIANO MODEL
See also DUAL RESONANCE MODEL
VENEZIANO MODEL/SCATTERING AMPLITUDES
Off-mass-shell dual amplitudes. III, 30:30714
VENUS PLANET/PLANETARY ATMOSPHERES
Volatile element influx on Venus from cometary impacts, 30:30402
VERMICULITE/SORPTIVE PROPERTIES
Studies on the sorption and fixation of cesium by vermiculite. II, 30:29134
VERTEBRATES
See also FISHES
VERTEBRATES/POPULATION DYNAMICS
Vertebrate behavior and ecology. Progress report, July 1, 1973--June 30, 1974, 30:31377 (COO-1332-103)
VESSELS
See CONTAINERS
VESSELS (PRESSURE)
See PRESSURE VESSELS
VETCH
See VICIA
VICIA/BIOLOGICAL RADIATION EFFECTS
Metronidazole (Flagyl). A radiosensitizer of hypoxic cells, 30:29674
Radiosensitization of hypoxic cells with metronidazole (Flagyl), 30:29699
VINBLASTINE/BIOLOGICAL EFFECTS
Sensitivity to radiation and insensitivity to vinblastine of the inducer function of thymus-derived cells (Gamma radiation), 30:29665
VINYL MONOMERS/CHEMICAL RADIATION EFFECTS
Studies on the preparation of mortar--plastic composite (Radiation, thermal-catalytic, and radiation-catalytic methods; γ radiation), 30:29045
VINYLBENZENE
See STYRENE
VINYLCYANIDE
See ACRYLONITRILE
VIRTUAL PARTICLES/COMPTON EFFECT
$J = 0$ fixed pole in the virtual Compton amplitude off proton and neutron, 30:30661
VIRUSES
See also BACTERIOPHAGES
POLIO VIRUS
VIRUSES/BIOLOGICAL RADIATION EFFECTS
Malignant transformation of hamster embryo fibroblasts following exposure to ultraviolet-irradiated human cytomegalovirus, 30:29677
VIRUSES/RADIOIMMUNOASSAY
Solid phase radioimmunoassay for plant viruses (^{125}I tracer technique), 30:29836
VITAMIN B-12/RADIOIMMUNOASSAY
Practical application of a simplified vitamin B_{12} radioassay (^{57}Co tracer), 30:29856
VITAMIN C
See ASCORBIC ACID
VOLTAGE REGULATORS/DESIGN
Fault tolerant sequencing (FTS) shunt regulator, 30:29254
VOLTAMETRY/COMPARATIVE EVALUATIONS
Comparison of analytical techniques for inorganic pollutants, 30:28924

W

WAGON WHEEL EVENT/ENVIRONMENT
Ecological considerations of Project Wagon Wheel, 30:29459
WALKER CARCINOMA
See EXPERIMENTAL NEOPLASMS
WARD IDENTITY
Broken conformal ward identities in non-abelian gauge theories, 30:31171
WASHINGTON/AIR POLLUTION
Quillayute air reference station (Air sampling and monitoring in Washington State), 30:29359 (BNWL-1850(Pt.3))
Trace pollutant emissions in fossil fuel combustion, 30:29469 (BNWL-1850(Pt.3))
WASHINGTON/CLIMATES
ALE reserve climatology for 1973, 30:29437 (BNWL-1850(Pt.3))
WASHINGTON/FALLOUT
Atmospheric natural aerosols and fallout particulates during 1973 at Richland, Washington and Point Barrow, Alaska, 30:29361 (BNWL-1850(Pt.3))

Behavior and characteristics of radioactive debris from the Chinese nuclear weapons test of June 26, 1973, 30:29362 (BNWL-1850(Pt.3))
Particle size distributions of manmade and natural radionuclides, 30:29360 (BNWL-1850(Pt.3))
Quillayute air reference station (Air sampling and monitoring in Washington State), 30:29359 (BNWL-1850(Pt.3))

WASHINGTON/METEOROLOGY
Comparison of diffusion-deposition model components with experimental results, 30:29434 (BNWL-1850(Pt.3))
Dependence of site evaluation of roughness length and displacement length on value chosen for Von Karman's constant, 30:29432 (BNWL-1850(Pt.3))
Model to compute low-level Montgomery stream functions, 30:29436 (BNWL-1850(Pt.3))
Power spectral analysis of two periods of turbulence data for very stable conditions, 30:29433 (BNWL-1850(Pt.3))
Regional wind resuspension of dust, 30:29373 (BNWL-1850(Pt.3))

WASHINGTON/POLLUTION
Elemental content of trace elements in vegetation collected at Centralia, Washington (Comparison with Alaskan vegetation), 30:29483 (BNWL-1850(Pt.3))

WASHINGTON/WIND
Mesoscale transport and diffusion studies, 30:29435 (BNWL-1850(Pt.3))

WASHOUT/MATHEMATICAL MODELS
Extension of the anaysis of plume washdown to include diffusion, 30:29478 (BNWL-1850(Pt.3))
Model for cumulus washout of cosmogenic radionuclides, 30:29363 (BNWL-1850(Pt.3))

WASTE HEAT/USES
Beneficial uses of waste heat, 30:31308

WASTE SOLUTIONS
See LIQUID WASTES

WATER
See also DRINKING WATER
GROUND WATER
SEAWATER
SURFACE WATERS

WATER/ACTIVATION ANALYSIS
Comparison of analytical techniques for inorganic pollutants, 30:28924
Trace element behavior in soil of some Indonesian sawah's and in sludge of an Indonesian river, 30:28930

WATER/CHEMICAL ANALYSIS
Comparison of analytical techniques for inorganic pollutants, 30:28924
Determination of promethium-147 in aqueous environmental samples, 30:28969 (DP-MS-73-77)

WATER/DECONTAMINATION
Tritium Effluent Control Project. Progress Report: April--June 1974, 30:29026 (MLM-2171(LD))

WATER/NEUTRON TRANSPORT
Measurement of neutron temperature in water by differential and integral methods, 30:30844 (IAE-2274)

WATER/PHOTOIONIZATION
Calculated photoionization cross sections and relative experimental photoionization intensities for a selection of small molecules, 30:30491

WATER/TWO-PHASE FLOW
Derivation of transfer functions in boiling loops, 30:29292

WATER/X-RAY FLUORESCENCE ANALYSIS
Compilation of x-ray interaction data for x-ray fluorescence analysis of geological samples, 30:28943 (RISO-297)

WATER COOLED GRAPHITE MODERATED REACTORS
See LWGR TYPE REACTORS

WATER POLLUTION
Environmental monitoring report: United States Atomic Energy Commission, Oak Ridge facilities. Calendar year 1973 (Monitoring), 30:29352 (UCC-ND-280)

WATER RESERVOIRS/THERMAL POLLUTION
Symposium on the effect of hot water of thermoelectric plants on the hydrology and biology of reservoirs (abstracts) March 24--26, 1971, Borok, USSR, 30:29463 (ORNL-tr-2781)

WATER VAPOR/CONTAMINATION
Scavenging of radioactive material from the atmosphere by surface condensation, 30:29391

WAVE FUNCTIONS/NONLINEAR PROBLEMS
Discrete spectrum of solutions of the wave equation with strong cubic nonlinearity, 30:31131 (AD-776985)

WAVE PROPAGATION/REVIEWS
Mathematical review of introductory wave mechanics (Classical mechanics of elastic and shock waves in solids and fluids), 30:31444 (UCID-15803)

WAVES (SHOCK)
See SHOCK WAVES

WEAK INTERACTIONS/CHIRAL SYMMETRY
Is chiral SU_2 x SU_2 a hidden symmetry, 30:30774

WEAK INTERACTIONS/COUPLING CONSTANTS
Beta asymmetry of ^{35}Ar and the deduced value of the vector coupling constant, 30:30902

WEAK INTERACTIONS/DIMENSIONS
Dimensional regularization for weak interactions, 30:30687

WEAK INTERACTIONS/MEETINGS
Proceedings of the eighth Rencontre de Moriond. Volume I. Electromagnetic and weak interactions. Conference held at Meribel-les-Allues, France, March 4--16, 1973, 30:30663

WEAK INTERACTIONS/NEUTRAL CURRENTS
Experimental study of ^{19}Ne decay and its significance to the study of neutral weak currents, 30:30892

WEAK INTERACTIONS/PARTICLE MODELS
Introduction to renormalizable models of weak interactions, 30:30681

WEAK INTERACTIONS/RESEARCH PROGRAMS
High Energy Accelerator and Colliding Beam User Group. Progress report (Summaries of research activities at University of Maryland), 30:30575 (TID-26638)

WEAK INTERACTIONS/SELECTION RULES
The $\Delta I=1/2$ rule in non-leptonic weak decays, 30:30595

WEINBERG LEPTON MODEL/RADIATIVE CORRECTIONS
Electron decay spectrum in muon decay in the unified theory of weak and electromagnetic interactions, 30:30682

WELDED JOINTS/CRACKS
Stress relaxation and strain-age cracking in Rene 41 weldments, 30:29996

WELDED JOINTS/NONDESTRUCTIVE TESTING
Electro-optic method of tracking an electron-beam weld, 30:31442 (UCID-15769)

WELDED JOINTS/ULTRASONIC TESTING
Reactor vessel in-service inspection assembly (Patent), 30:31200

WELDS
See WELDED JOINTS

WELL LOGGING
Approximation for time relationships in pulsed gamma--gamma logging, 30:29605

WELL LOGGING/PULSED NEUTRON TECHNIQUES
Neutron logging of formation porosity and chlorinity, 30:29429

WEYL FIELD
(Static, cylindrically symmetric gravitational field.)

WEYL FIELD/CONFORMAL INVARIANCE
Conformal invariant spinor theory with third-order derivatives, 30:31155

WHEAT/MUTATIONS
Studies on the use of U-120 cyclotron and fast neutron generator in neutron irradiation of seeds for mutation (Barley; wheat), 30:29692

WHITE DWARF STARS/ABSORPTION SPECTRA
Spectrum of the polarized white dwarf GD 229, 30:30204

WHITE DWARF STARS/CHEMICAL COMPOSITION
Are stellar surface heavy-element abundances systematically enhanced. (Upper limit, Hayashi-phase convection), 30:30250

WHITE DWARF STARS/EMISSION SPECTRA
Wavelength dependence of circular polarization in GD 229, 30:30203

WHITE DWARF STARS/GRAVITATIONAL COLLAPSE
Gravitional radiation from stellar collapse (Point masses, Schwarzschild radius), 30:30231

WHITE DWARF STARS/MAGNETIC FIELDS
A determination by the Zeeman effect of the magnetic field strength in the white dwarf G99-37 (Magnetic stars, stellar profiles), 30:30193

WHITE DWARF STARS/NUCLEOSYNTHESIS
Nucleosynthesis in white-dwarf atmospheres (Infalling material, gamma ray bursts), 30:30256

WHITE DWARF STARS/ORBITS
Analysis of a one-parameter family of triple close approaches occurring in stellar systems (Participating masses), 30:30238

WHITE DWARF STARS/PHOTOMETRY
Photometry of a Pleiades candidate and composite white dwarfs (Parent star), 30:30234

WHITE DWARF STARS/PLASMA
New nodal expansion for classical plasmas, 30:30196

WHITE DWARF STARS/POLARIZATION
A determination by the Zeeman effect of the magnetic field strength in the white dwarf G99-37 (Magnetic stars, stellar profiles), 30:30193
Further observations for circularly polarized radiation from white dwarfs and x-ray sources (Negative results), 30:30218
Wavelength dependence of circular polarization in GD 229, 30:30203

WHITE DWARF STARS/PROPER MOTION
Proper motions of faint blue stars near the galactic anticenter. I (Mean error), 30:30237

WHITE DWARF STARS/STAR ACCRETION
Nucleosynthesis in white-dwarf atmospheres (Infalling material, gamma ray bursts), 30:30256

WILD ANIMALS/POPULATION DYNAMICS
Vertebrate behavior and ecology. Progress report, July 1, 1973--June 30, 1974, 30:31377 (COO-1332-103)

WIND
Fast response light scattering measurements of the characteristics of wind suspended aerosols (Dust suspension by winds), 30:29490 (UCRL-76014(Rev.1))

WIND/DATA PROCESSING
Program descriptions: supplement to mesoscale wind fields and transport estimates determined from a network of wind towers, 30:31343 (NOAA-TM-ERL-ARL-43)

WIND/MATHEMATICAL MODELS
Model to compute low-level Montgomery stream functions (Washington-Oregon area), 30:29436 (BNWL-1850(Pt.3))
WIND/TRACER TECHNIQUES
Peculiarities of the upper cloud layer and suggestions for using radioactive tracer techniques in studying meridional currents, 30:29428
WIRE SPARK CHAMBERS/SPATIAL RESOLUTION
High-resolution cryogenic spark chambers, 30:29594
WOOL/CHEMICAL ANALYSIS
Determination of small amounts of zirconium in wool, 30:28945
WOOL/THICKNESS
Radioisotope method of measuring the mean fibre diameter of wool samples, 30:29604
WORKERS
See PERSONNEL
WORLD-WIDE FALLOUT
See GLOBAL FALLOUT
WOUNDS/CONTAMINATION
Effect of delayed lymphadenectomy on $^{239}PuO_2$ translocation in dogs, 30:29820
WYOMING/URANIUM ORES
Uranium in the Great Divide Basin, Wyoming, 30:29336

X

2X DEVICES/DATA PROCESSING
Proposed 2X data system, 30:29212 (UCID-15434)
2X DEVICES/PLASMA GUNS
Procedure for deuterating titanium, 30:29216 (UCID-15624)
X-RAY DOSIMETRY/DEPTH DOSE DISTRIBUTIONS
Geometric solution of finite x-ray source irradiating two concentric cylinders containing x-ray absorbing material, 30:31123 (UCID-15938)
X-RAY DOSIMETRY/SPATIAL DOSE DISTRIBUTIONS
Geometric solution of finite x-ray source irradiating two concentric cylinders containing x-ray absorbing material, 30:31123 (UCID-15938)
X-RAY FLUORESCENCE ANALYSIS
Sensitivity in trace-element analysis by p,α and ^{16}O induced X-rays, 30:28988
X-RAY FLUORESCENCE ANALYSIS/COMPARATIVE EVALUATIONS
Comparison of analytical techniques for inorganic pollutants, 30:28924
X-RAY FLUORESCENCE ANALYSIS/DATA COMPILATION
Compilation of x-ray interaction data for x-ray fluorescence analysis of geological samples, 30:28943 (RISO-297)
X-RAY RADIOGRAPHY/PERFORMANCE TESTING
Assessment of diagnostic x-ray equipment, 30:31111
X-RAY RADIOGRAPHY/RECOMMENDATIONS
Assessment of diagnostic x-ray equipment, 30:31111
X-RAY RADIOGRAPHY (BIOMEDICAL)
See BIOMEDICAL RADIOGRAPHY
X-RAY SOURCES
See also COSMIC X-RAY SOURCES
X-RAY SOURCES/LASERS
Some necessary conditions on x-ray laser action, 30:29272 (UCRL-74898)
X-ray lasers: necessary conditions and some possible approaches, 30:29271 (UCID-16290)
X-RAY SOURCES/POLARIZATION
Bremsstrahlung polarization from commercial x-ray tubes, 30:31447 (UCID-15829)
X-RAY SPECTROMETERS/RESOLUTION
Spectrometric properties of crystals for x-ray astronomy. I., 30:30272
X-RAY SPECTROSCOPY
Absorption x-ray radiometric analysis using the $K\alpha_2$ lines of the characteristic radiation of targets, 30:28952
X-ZERO RESONANCES
See ETA-958 RESONANCES
XENON/ATOM-ATOM COLLISIONS
Observation of orbiting resonances in the integral cross section of H--Xe (1.0 to 30 MeV (cm)), 30:30532
XENON/ELECTRON-ATOM COLLISIONS
Atomic excitation processes in the discharges of rare gas ion engines, 30:30556
XENON/ION-ATOM COLLISIONS
Differential elastic-scattering measurements of Xe^+ on Xe and Ar^+ on Ar in the 20 to 340-eV range (Oscillations, interference, excitation, potential-curve crossings), 30:30540
XENON/SEPARATION PROCESSES
Atmosphere purification of xenon, radon, and radon daughter elements (Patent, fluorination and adsorption), 30:28995
Recovery of rare gases in air separation and ammonia plants, 30:28993
XENON/THERMAL CONDUCTION
Thermal accommodation coefficients of inert gases on stainless steel and UO_2, 30:30097
XENON 130/ENERGY LEVELS
Nuclear Data Sheets for A = 130, 30:30968
XENON 130/NUCLEAR PROPERTIES
Nuclear Data Sheets for A = 130, 30:30968
XENON 132/CHONDRITES
Xenon isotope anomalies in the carbonaceous chondrite Murray, 30:30162
XENON 132/ENERGY LEVELS
A mechanical beam chopper system for the measurement of half-lives in the millisecond region, 30:30154
XENON 133/CAPILLARY FLOW
Tissue-blood ^{131}I and ^{133}Xe transfer in the presence of raised capillary filtration, 30:29794
XENON 133/RADIATION MONITORING
Environmental monitoring report: United States Atomic Energy Commission, Oak Ridge facilities. Calendar year 1973, 30:29352 (UCC-ND-280)
XENON 136/CHONDRITES
Xenon isotope anomalies in the carbonaceous chondrite Murray, 30:30162
XENON 136/ENERGY LEVELS
Nuclear Data Sheets for A = 136, 30:30967
XENON 136/NUCLEAR PROPERTIES
Nuclear Data Sheets for A = 136, 30:30967
XENON 143/NUCLEAR PROPERTIES
Nuclear Data Sheets for A = 143, 30:30966
XENON COMPLEXES/CHEMICAL PREPARATION
Preparation of complex perxenates of some actinide elements, 30:29117
XENON FLUORIDES/CHEMICAL PREPARATION
Compounds of rare gases, 30:29089
XENON IONS/CHANNELING
Sputtering experiments with silver single crystals and the channeling phenomena, 30:30481
XENON IONS/COLLISIONS
Sputtering experiments with silver single crystals and the channeling phenomena, 30:30481
XENON IONS/ENERGY LOSSES
Charge-state and energy distributions of xenon ions in carbon, 30:31121
XENON IONS/ION-ATOM COLLISIONS
Crossed-molecular-beam study of the kinematics and dynamics of charge-transfer collisions (200 eV), 30:30547
Differential elastic-scattering measurements of Xe^+ on Xe and Ar^+ on Ar in the 20 to 340-eV range (Oscillations, interference, excitation, potential-curve crossings), 30:30540
XENON IONS/ION-MOLECULE COLLISIONS
Crossed-molecular-beam study of the kinematics and dynamics of charge-transfer collisions (200 eV), 30:30547
XENON IONS/STOPPING POWER
Charge-state and energy distributions of xenon ions in carbon, 30:31121
XENON OXIDES/CHEMICAL PREPARATION
Compounds of rare gases, 30:29089

Y

YANG-FELDMAN FORMALISM
Equivalence of Yang--Feldman and action principle quantization, 30:31148
YANG-MILLS THEORY/GREEN FUNCTION
Asymptotic solution of the set of equations for Green's functions in the Yang--Mills field theory, 30:31150
YANG-MILLS THEORY/RENORMALIZATION
Two-loop diagrams in Yang-Mills theory, 30:31168
YANG-MILLS THEORY/SCALE INVARIANCE
Scaling and asymptotically free massive Yang--Mills field, 30:31147
YANKEE MAINE REACTOR
See MAINE YANKEE REACTOR
YEASTS
See also CANDIDA
YEASTS/MUTATIONS
Specificity and frequency of ultraviolet-induced reversion of an iso-1-cytochrome c ochre mutant in radiation-sensitive strains of yeast, 30:29683
YOLK
See EGGS
YOSHIDA SARCOMA
See EXPERIMENTAL NEOPLASMS
YTTERBIUM/ACTIVATION ANALYSIS
Determination of rare earths and thorium in apatites by thermal and epithermal neutron-activation analysis, 30:28935
Trace element behavior in soil of some Indonesian sawah's and in sludge of an Indonesian river, 30:28930
YTTERBIUM 163/ROTATIONAL STATES
Decoupled rotational bands in ^{163} ^{165}Yb, 30:30985
YTTERBIUM 165/ROTATIONAL STATES
Decoupled rotational bands in ^{163} ^{165}Yb, 30:30985
YTTERBIUM 166/ENERGY-LEVEL TRANSITIONS
Decay properties of three ^{166}Lu isomers and the decay of ^{166}Hf (Spectra, log ft, Q, branching ratios, K, J, π, L), 30:30989
YTTERBIUM 166/ROTATIONAL STATES
Decay properties of three ^{166}Lu isomers and the decay of ^{166}Hf (Spectra, log ft, Q, branching ratios, K, J, π, L), 30:30989
YTTERBIUM 166/VIBRATIONAL STATES
Decay properties of three ^{166}Lu isomers and the decay of ^{166}Hf (Spectra, log ft, Q, branching ratios, K, J, π, L), 30:30989

- YTTERBIUM 169/UPTAKE
  - Unexpected complication in the use of ^{169}Yb--DTPA with respect to hospital health physics, 30:29824
- YTTERBIUM 170/NEUTRON REACTIONS
  - Mass-spectrometric determination of neutron capture cross-sections of the rare earth isotopes (Pile and thermal cross sections), 30:30977 (AEC-tr-7574)
- YTTERBIUM 171/DEUTERON REACTIONS
  - One-nucleon transfer reactions in deformed nuclei (Indirect inelastic transitions through intermediate rotational states included), 30:30995
- YTTERBIUM 171/ENERGY LEVELS
  - A mechanical beam chopper system for the measurement of half-lives in the millisecond region, 30:30154
- YTTERBIUM 171/NEUTRON REACTIONS
  - Mass-spectrometric determination of neutron capture cross-sections of the rare earth isotopes (Pile and thermal cross sections), 30:30977 (AEC-tr-7574)
- YTTERBIUM 172/ENERGY LEVELS
  - Shell effects on state densities with given number of excited protons and neutrons, 30:31094
- YTTERBIUM 172/NEUTRON REACTIONS
  - Mass-spectrometric determination of neutron capture cross-sections of the rare earth isotopes (Pile and thermal cross sections), 30:30977 (AEC-tr-7574)
- YTTERBIUM 172/PROTON REACTIONS
  - One-nucleon transfer reactions in deformed nuclei (Indirect inelastic transitions through intermediate rotational states included), 30:30995
- YTTERBIUM 173/NEUTRON REACTIONS
  - Mass-spectrometric determination of neutron capture cross-sections of the rare earth isotopes (Pile and thermal cross sections), 30:30977 (AEC-tr-7574)
- YTTRIUM/EXTRACTION CHROMATOGRAPHY
  - Contribution to the separation of rare earths by extraction chromatography with di(2-ethylhexyl) phosphoric acid. II. Behavior of the matrix and its influence on the microcomponents, 30:28990 (ANL-Trans-961)
- YTTRIUM/ION EXCHANGE
  - Synthesis of reproducible tin(IV) based ion exchangers: separation of lanthanum(III) from yttrium(III), europium(III), and lutetium(III), 30:28994
- YTTRIUM ADDITIONS
  - Oxidation mechanism of Ni_3Al containing yttrium (With and without 0.5 wt percent Y; 900 to 1200°C in air), 30:29953
- YTTRIUM ALLOYS/CRYSTAL STRUCTURE
  - Structure of alloys of cobalt with rare earths of the approximate composition RCo_5, 30:30034
- YTTRIUM ALLOYS/MAGNETIC PROPERTIES
  - Magnetic properties of alloys of the TbCu--YCu system (77 to 300°K; Curie point; Neel temperature; susceptibility), 30:30031
- YTTRIUM ALLOYS/SPECIFIC HEAT
  - Specific heat in TbZn and HoZn compounds (20 to 300°K; YZn; magnetic properties), 30:29990
- YTTRIUM COMPOUNDS/MAGNETIC PROPERTIES
  - Preparation and some magnetic properties of uranium oxide doped YIG crystals ($Y_3Fe_5O_{12}$), 30:29894
- YTTRIUM COMPOUNDS/MAGNETIC SUSCEPTIBILITY
  - Magnetization and Moessbauer spectra of non-crystalline $Y_3Fe_5O_{12}$, 30:29901
- YTTRIUM COMPOUNDS/MOESSBAUER EFFECT
  - Magnetization and Moessbauer spectra of non-crystalline $Y_3Fe_5O_{12}$, 30:29901
- YTTRIUM OXIDES
  - Effect of complex admixtures of rare-earth oxides on sintering of cerium dioxide, 30:29909
- YTTRIUM OXIDES/DISSOCIATION ENERGY
  - Knudsen effusion and mass spectrometric studies of the vaporization of Y_2O_3(s). Dissociation energy of YO(g), 30:29936
- YTTRIUM OXIDES/EVAPORATION
  - Knudsen effusion and mass spectrometric studies of the vaporization of Y_2O_3(s). Dissociation energy of YO(g), 30:29936
- YTTRIUM OXIDES/METALLURGICAL EFFECTS
  - Effect of additivies of yttrium and aluminum oxides on sintering and properties of lanthanum hexaboride, 30:29892
- YUKAWA NONLOCAL THEORY/NUCLEI
  - Meson field theory of nuclei and the N--N interaction, 30:31048

Z

- Z*RESONANCES
  - Simple Z_0* model, 30:30740
- ZEA MAYS
  - See MAIZE
- ZINC/ACTIVATION ANALYSIS
  - Determination of zinc in the presence of scandium by activation analysis combined with thin-layer chromatographic separation (Neutron beams), 30:28928
  - Multielement determination in market-garden soils by instrumental photon activation analysis, 30:28921
  - Trace element behavior in soil of some Indonesian sawah's and in sludge of an Indonesian river, 30:28930
- ZINC/CHEMICAL ANALYSIS
  - Extraction--spectrophotometric methods of determining 0.0--n0.000n% aluminum in materials of metallurgical manufacture (exchange of experience), 30:28956
- ZINC/EMISSION SPECTROSCOPY
  - Spectrochemical analysis of uranium oxide by gallium oxide carrier dc arc technique (ASTM Standard E402), 30:28957
  - Spectrographic determination of trace impurities in high purity uranium oxide, 30:28944 (UCID-15952)
- ZINC/FLUORESCENCE SPECTROSCOPY
  - New discrete atomization cell for atomic fluorescence spectrometry, 30:28947
- ZINC/MONITORING
  - Portsmouth Gaseous Diffusion Plant environmental monitoring report, 1973, 30:29346 (GAT-781)
- ZINC/QUALITATIVE CHEMICAL ANALYSIS
  - Application of activation analysis to the determination of pollutants in the atmosphere, 30:28914 (IEA-326)
- ZINC 65/DIFFUSION
  - Concentration effects of ^{137}Cs, ^{65}Zn, ^{60}Co, and ^{106}Ru sorption by marine sediments with geochemical implications, 30:29409
- ZINC 65/INTESTINAL ABSORPTION
  - Effect of copper and cadmium on ^{65}Zn absorption in zinc-deficient and zinc-supplemented rats, 30:29814
- ZINC 66/ALPHA REACTIONS
  - Spectroscopy of the ^{69}Ga and ^{71}Ga isotopes with the ^{69} ^{71}Ga(α,α'γ)^{69} ^{71}Ga and ^{66} ^{68}Zn(α,pγ)^{69} ^{71}Ga reactions, 30:30941
- ZINC 66/PROTON REACTIONS
  - Level densities of ^{63}Cu and ^{65}Cu from the analysis of evaporation spectra (12.5- to 16.0-MeV protons, 16.8- to 21.3-MeV α), 30:30950
- ZINC 67/NUCLEAR MAGNETIC RESONANCE
  - ^{67}Zn NMR anomalous solvent isotope effect in aqueous solutions (Heavy water or water), 30:29014
- ZINC 68/ALPHA REACTIONS
  - Spectroscopy of the ^{69}Ga and ^{71}Ga isotopes with the ^{69} ^{71}Ga(α,α'γ)^{69} ^{71}Ga and ^{66} ^{68}Zn(α,pγ)^{69} ^{71}Ga reactions, 30:30941
- ZINC 68/ENERGY LEVELS
  - Gamma-ray production due to neutron interactions with ^{68}Zn and the level structure of ^{68}Zn (5.4 MeV: spectra, branching ratios, J, π), 30:30935 (ORNL-4985)
- ZINC 68/NEUTRON REACTIONS
  - Gamma-ray production due to neutron interactions with ^{68}Zn and the level structure of ^{68}Zn (5.4 MeV: spectra, branching ratios, J, π), 30:30935 (ORNL-4985)
- ZINC 68/PROTON REACTIONS
  - Level densities of ^{63}Cu and ^{65}Cu from the analysis of evaporation spectra (12.5- to 16.0-MeV protons, 16.8- to 21.3-MeV α), 30:30950
- ZINC 70/PROTON REACTIONS
  - ^{70}Zn (p,p) at 3.6 to 6.4 MeV: angular distributions and excitation functions for cross sections and analyzing power, 30:30949
- ZINC 71/ENERGY LEVELS
  - A study of isobaric analogue resonances in ^{71}Ga, 30:30949
- ZINC ALLOYS/CORROSION RESISTANCE
  - Corrosion study of the superplastic alloys 70/30 and 80/20 zinc aluminum in a humid atmosphere, 30:31391 (COPPE-TP-8/72)
- ZINC ALLOYS/DIFFUSION
  - Transport and thermodynamic properties of solids. Progress report, September 1, 1973--August 31, 1974, 30:31390 (COO-1436-41)
- ZINC ALLOYS/ELONGATION
  - Method of determining the relative elongation of light alloys close to the solidus on an IMASh-5S-65 unit, 30:30012
- ZINC ALLOYS/PHASE STUDIES
  - Co-solubility of neodymium and zinc in solid magnesium (Mg--Nd--Zn alloys containing up to 3 percent Nd and 8 percent Zn), 30:30007
- ZINC ALLOYS/SPECIFIC HEAT
  - Specific heat in TbZn and HoZn compounds (20 to 300°K; YZn; magnetic properties), 30:29990
- ZINC CHLORIDES/FORMATION HEAT
  - Gaseous halide complexes and their stability, 30:29091
- ZINC COMPLEXES/PYROLYSIS
  - Derivatographic investigations on the thermal degradation of pyridine, isoquinoline, α,α-dipyridyl and o-phenantroline, resp. bichromate- or chromate-ion containing metal complexes. II. Zinc(II)-, cadmium(II)-, and manganese(II)-complexes. III. Mercury(I and II)-, uranyl-, thorium-, lanthanum-, and iron-complexes, 30:29122
- ZINC SULFIDES/X-RAY FLUORESCENCE ANALYSIS
  - Compilation of x-ray interaction data for x-ray fluorescence analysis of geological samples, 30:28943 (RISO-297)
- ZINC TELLURIDES/CHARGED-PARTICLE TRANSPORT
  - Energy loss and projected range of alpha particles in zinc telluride, 30:31113
- ZIRCALOY/SORPTIVE PROPERTIES
  - HYDIZ: a 2-dimensional computer progam for migration of interstitial solutes of finite solubility in a thermal gradient (LWBR Development Program), 30:29983 (WAPD-TM-1157)

ZIRCALOY 2/PHYSICAL RADIATION EFFECTS
Some comments on damage alignment in neutron-irradiated zirconium alloys, 30:30076
ZIRCALOY 4/RUPTURES
Stress-rupture properties of helium-injected Zircaloy-4, 30:30073
ZIRCALOY 4/STRESSES
Stress-rupture properties of helium-injected Zircaloy-4, 30:30073
ZIRCONIUM/ABSORPTION SPECTROSCOPY
Determination of small amounts of zirconium in wool, 30:28945
ZIRCONIUM/ACTIVATION ANALYSIS
Multielement determination in market-garden soils by instrumental photon activation analysis, 30:28921
Nondestructive determination of some trace elements in tantalum by proton activation analysis, 30:28922
ZIRCONIUM/CHEMICAL ANALYSIS
Chemical analysis of zirconium and zirconium-base alloys (Book), 30:28961
ZIRCONIUM/CORROSION RESISTANCE
Aqueous corrosion testing of samples of zirconium and zirconium alloys, 30:29952
ZIRCONIUM/DISSOLUTION
Method for the suppression of hydrogen during the dissolution of zirconium and zirconium alloys (Patent; Zirflex process), 30:29148
ZIRCONIUM/EMISSION SPECTROSCOPY
Spectral assay of components in alloys (exchange of experience), 30:28951
Spectrographic determination of trace impurities in high purity uranium oxide, 30:28944 (UCID-15952)
ZIRCONIUM/GRAVIMETRIC ANALYSIS
Modern methods of determination of zirconium (survey), 30:28911
ZIRCONIUM/PHASE TRANSFORMATIONS
(α + ω) transition in titanium and zirconium in shock waves, 30:30011
ZIRCONIUM/PHOTOMETRY
Modern methods of determination of zirconium (survey), 30:28911
ZIRCONIUM/SOLVENT EXTRACTION
Modern methods of determination of zirconium (survey), 30:28911
ZIRCONIUM/SPECTROSCOPY
Modern methods of determination of zirconium (survey), 30:28911
ZIRCONIUM/STACKING FAULTS
Diffraction of x rays on stacking faults in metals with hcp lattices, 30:30024
ZIRCONIUM/STRESS CORROSION
Stress corrosion cracking of zirconium in methanol—HCl solutions, 30:29957
ZIRCONIUM/TITRATION
Modern methods of determination of zirconium (survey), 30:28911
ZIRCONIUM 89/ELECTRON CAPTURE DECAY
The variation of the life-time of ^{89}Zr in BaTiO$_3$, PbZrO$_3$ and ZrO$_2$, 30:30947
ZIRCONIUM 95/RADIATION MONITORING
Data. Section IV. Other data, 30:29412
Environmental monitoring report: United States Atomic Energy Commission, Oak Ridge facilities. Calendar year 1973, 30:29352 (UCC-ND-280)
Report of activity, February 1974 (Radioactivity of environmental samples collected throughout France during February 1974), 30:29349 (SCPRI(RM)-2-1974)
ZIRCONIUM 95/RADIOCHEMICAL ANALYSIS
Fractional determination of ^{95}Zr and ^{95}Nb in a mixture by reverse phase chromatography, 30:28982
ZIRCONIUM 95/REMOVAL
Decontamination of swine, sheep, and cattle surface-contaminated with fission products. II. Removal of radionuclides of zirconium, niobium, ruthenium, and cerium, 30:29823
ZIRCONIUM ALLOYS
See also ALLOY-TZM
ZIRCONIUM BASE ALLOYS
ZIRCONIUM ALLOYS/CORROSION
Corrosion fatigue strength of a titanium alloy at elevated temperature (Ti--Al--Zr; simulated seawater), 30:29945
ZIRCONIUM ALLOYS/CORROSION RESISTANCE
Aqueous corrosion testing of samples of zirconium and zirconium alloys, 30:29952
Electrochemistry of aqueous corrosion: uranium and its alloys (Review), 30:29944 (Y-1949)
ZIRCONIUM ALLOYS/CRYSTAL STRUCTURE
Structure of alloys of the Nb--Ti--Zr system. Close order of displacement in solid solutions (50 at./percent/Nb; diffusion distribution), 30:30040
ZIRCONIUM ALLOYS/DISSOLUTION
Method for the suppression of hydrogen during the dissolution of zirconium and zirconium alloys (Patent; Zirflex process), 30:29148
ZIRCONIUM ALLOYS/MECHANICAL PROPERTIES
Characterizations of fuel element cladding tubes, 30:31279 (RT/MET-(73)1)
Mechanical properties of multicomponent alloys based on Ti--Al--Sn (Zr) α-solid solution with β-stabilizing elements (Additions of Mo, V, Cr, Fe, Si, B;properties at up to 950°C), 30:29984
Study of some high-temperature strength properties of the niobium alloys 5VMTs, 5VMTsU, and 5VTTs at 1100°C (5VMTs = Nb--5.3W--2.1Mo--0.72Zr; 5VMTsU = Nb--4.9W--2.0Mo--1.15Zr; 5VTTs = 4.5W--2Ta--3.45Zr), 30:30027
ZIRCONIUM ALLOYS/OXIDATION
Quarterly progress report on reactor safety programs sponsored by the Division of Reactor Safety Research for April—June 1974. I. Light-water-reactor safety, 30:31250 (ORNL-TM-4655(Vol.1))
ZIRCONIUM ALLOYS/SUPERCONDUCTIVITY
Superconductivity of Nb--Al--Zr alloys (Phase boundaries;solubility of Zr in Nb$_3$Al), 30:30048
ZIRCONIUM BASE ALLOYS
See also ZIRCALOY
ZIRCONIUM BASE ALLOYS/CHEMICAL ANALYSIS
Chemical analysis of zirconium and zirconium-base alloys (Book), 30:28961
ZIRCONIUM BASE ALLOYS/ELECTRONIC STRUCTURE
Specific heat and superconducting properties of Zr--Mo alloys, 30:30025
ZIRCONIUM BASE ALLOYS/WELDING
Properties of TZM and nuclear behavior of TZM brazements. Various properties of TZM and Zr--5Be and Au--18Ni brazing filler metals are determined for brazing TZM to Zr and to steel, 30:30084
ZIRCONIUM BORIDES/OXIDATION
Oxidation of ZrB$_2$, TaB$_2$, NbB$_2$, and W$_2$B$_5$ in atomic oxygen and by anodic polarization, 30:29938
ZIRCONIUM BORIDES/SOLVENT PROPERTIES
Micro-x-ray spectrum analysis of interphase interaction in the systems ''refractory compound--liquid metal'' (Interaction of liquid Ni with ZrB$_2$), 30:29898
ZIRCONIUM BORIDES/WEAR RESISTANCE
Abrasive wear-resistance and failure character of titanium and zirconium borides surface layers (Comparison with steel Kh18N10T), 30:29899
ZIRCONIUM CARBIDES/CRYSTAL GROWTH
Conditions for three-dimensional correspondence in the heteroepitaxial growth of ZrC (Growth on monocrystalline Mo substrate; intrinsic texture), 30:29914
ZIRCONIUM CARBIDES/ELASTICITY
Temperature dependence of the elastic constants of nonstoichiometric zirconium carbides, 30:29916
ZIRCONIUM CARBIDES/PRODUCTION
Production of complex zirconium--tungsten carbide on semi-industrial scale, 30:29893
ZIRCONIUM CARBIDES/THERMAL SHOCK
Calorimetric determination of the heat resistance of ring-shaped samples of brittle electric conductors (ZrC$_{0.93}$; NbC$_{0.93}$), 30:29900
ZIRCONIUM CARBIDES/THERMODYNAMIC PROPERTIES
Thermodynamic properties and mutual diffusion in the system UC—ZrC, 30:29905
ZIRCONIUM FLUORIDES/SOLVENT PROPERTIES
Solubility and stability of structural metal difluorides in molten fluoride mixtures, 30:29002 (ORNL-TM-760)
ZIRCONIUM OXIDES/CRYSTAL STRUCTURE
Surface stabilization and properties of ZrO$_2$-based solid solutions, 30:29911
ZIRCONIUM OXIDES/MECHANICAL PROPERTIES
Some properties of materials of the systems Si$_3$N$_4$--ZrO$_2$, 30:29920
ZIRCONIUM OXIDES/PLASMA ARC SPRAYING
Damping and elastic characteristics of plasma-sprayed coatings of W, nichrome, zirconia, and Cr--Ni spinels, 30:29887
ZIRCONIUM OXIDES/THERMODYNAMIC PROPERTIES
Some properties of materials of the systems Si$_3$N$_4$--ZrO$_2$, 30:29920
ZIRCONIUM OXIDES/X-RAY FLUORESCENCE ANALYSIS
Compilation of x-ray interaction data for x-ray fluorescence analysis of geological samples, 30:28943 (RISO-297)
ZIRFLEX PROCESS
Method for the suppression of hydrogen during the dissolution of zirconium and zirconium alloys (Patent; Zirflex process), 30:29148
ZOOPLANKTON
See PLANKTON
ZYGOTES
See EMBRYOS

REPORT NUMBER INDEX

Numbers assigned to reports, conference papers and proceedings, translations, and patents are included in this index. Each item is listed by report number; this is followed by the abstract number and a brief notation regarding public availability. The index entries show which reports are on file in the institutions listed on the backs of the covers (Dep.), which reports have been published in open-literature journals (journal citation), and which reports can be purchased (source and price). Whenever a report is identified by more than one number, the availability is given under the primary number, and a cross reference is given under the secondary report number.

The report number codes apply to USAEC reports unless designated otherwise. Non-USAEC reports are identified by parenthetical notes after the report codes; e.g., (non-AEC), (UK), (Canada), (France). The note (Misc.) identifies the codes used for both USAEC and non-USAEC Reports. Patents are listed under the heading "PATENTS"; the country of origin and availability are included in parentheses.

A comprehensive list of both USAEC and non-USAEC report codes is contained in the latest revision of TID-85, *Report Number Series Used by the USAEC Technical Information Center in Cataloging Reports.* This information is also included in the Cumulative Report Number Index (issued annually).

Availability of USAEC Reports

USAEC Reports abstracted in *Nuclear Science Abstracts* are available through one or more of the following sources:

(1) University and public libraries in the United States. A list of these organizations appears on the inside front cover of each issue of *NSA*.

(2) NCR Microcard Editions in Microcard and micronegative form. Orders and inquiries should be sent to: Order Processing Department, 365 South Oak Street, West Salem, Wisconsin 54669.

(3) National Technical Information Service, U. S. Department of Commerce, Springfield, Virginia 22151.

(4) Superintendent of Documents, U. S. Government Printing Office, Washington, D. C. 20402.

(5) Microsurance, Inc., P. O. Box 3522, Oak Ridge, Tenn. 37830, in micronegative form. Purchase details available on request.

(6) Overseas at the organizations listed on the inside of the back cover.

Availability of Non-USAEC Reports

U. S. Reports. Reports of U. S. Government agencies are available to the public from the National Technical Information Service (NTIS). If specific availability is not shown, inquiries may be directed to NTIS.

Non-U. S. Reports. Reports of atomic energy organizations of other countries are available from NTIS for U. S. sale only. Specific availability in the country of origin is shown, when known, at the report number entry. Otherwise, inquiries should be made to the organizations listed below:

AUSTRALIA

Australian Atomic Energy Commission Research Establishment. Available upon request from the Library, Australian Atomic Research Establishment, Private Mail Bag, Sutherland, New South Wales, Australia.

BELGIUM

Centre d'Étude de l'Energie Nucléaire. Available upon request to individuals and organizations from the Centre d'Etude de l'Energie Nucléaire (C.E.N.), Studiecentrum voor Kernenergie (S.C.K.), Technical Information Dept., MOL-DONK (Belgium).

CERN

CERN European Organization for Nuclear Research. Available without charge from CERN European Organization for Nuclear Research, Geneva 23, Switzerland. Copies are deposited in libraries throughout the world.

FRANCE

Commissariat à l'Energie Atomique. Inquiries for reports numbered 1-2199 should be addressed to Service Central de Documentation du C.E.A., Centre d'Etudes Nucléaires de Saclay, Boîte postale n° 2, 91. GIF-sur-YVETTE, FRANCE. Reports numbered 2200 and above are available from La Documentation Française, 31 quai Voltaire, 75, PARIS (7e), FRANCE.

Service Central de Protection contre les Rayonnements Ionisants. Copies are available from Ministère de la Santé Publique, Service Central de Protection contre les Rayonnements Ionisants, B.P. n° 78 Le Vesinet (France) Telex 25667.

GERMANY

Deutsches Elektronen-Synchrotron DESY. Copies are available from Deutsches Elektronen-Synchrotron DESY, Dokumentation, 2000 Hamburg 52, Notkestieg 1, Germany.

Gesellschaft für Kernforschung mbH (KFK). Copies are available from Gesellschaft für Kernforschung mbH, 75 Karlsruhe, Postfach 947, Germany. Copies are also deposited in many national nuclear centers in the world.

Kernforschungsanlage. Copies may be ordered from Zentralbibliothek der Kernforschungsanlage Jülich, Jülich, Bundesrepublik Deutschland.

Hahn-Meitner-Institute für Kernforschung. Available without charge from Hahn-Meitner-Institute für Kernforschung Berlin, Bibliothek, Glienicker Strasse 100, 1 Berlin 39, Germany. Copies are deposited in many national nuclear centers in the world.

Johann-Wolfgang-Goethe Universität, Frankfurt Am Main, Institut für Kernphysik, (IKF). Copies are available from Gmelin Institut, 40-42 Varrentrappstrasse, Frankfurt (Main), West Germany.

ISRAEL

Israel Atomic Energy Commission. Available without charge from Israel Atomic Energy Commission, Soreq Nuclear Research Centre, Yavne, Israel.

ITALY

Centro Informazioni Studi Esperienze (CISE). For sale at CISE Press Office, Casella Postale 3986, Milano, Italy. Copies are deposited in the libraries of various nuclear centers in Italy and abroad.

Comitato Nazionale per l'Energia Nucleare. Copies are available from Comitato Nazionale per l'Energia Nucleare, Divisione Affari Internazionali e Studi Economici, Ufficio Pubblicazioni, Via Belisario, 15, Roma, Italy.

JAPAN

Japan Atomic Energy Research Institute (JAERI). Available from the Staff Supply Cooperative of Japan Atomic Energy Research Institute (JAERI), Tokai-mura, Naka-gun, Ibaraki-ken, Japan. Copies are deposited in depositories in Tokyo, Nagoya, and Osaka.

Nagoya University. Copies are available from Research Information Center, Institute of Plasma Physics, Nagoya University, Nagoya, Japan.

University of Tokyo. Available free of charge from Institute for Nuclear Study, University of Tokyo, Tanashi-Machi, Kitatama-gun, Tokyo, Japan.

NETHERLANDS

Reactor Centrum Nederland. For sale by Reactor Centrum Nederland, 112 Scheveningseweg, 's-Gravenhage, The Netherlands. Copies are deposited in university libraries in Holland and in many national nuclear centers in the world.

NEW ZEALAND

Institute of Nuclear Sciences. Copies are available from Librarian, N. Z. Institute of Nuclear Sciences, D.S.I.R., Private Bag, Lower Hutt, New Zealand. Copies are deposited in other countries.

PAKISTAN

Atomic Energy Center. Copies are available from Atomic Energy Center, P. O. Box 658, Lahore, (West Pakistan).

POLAND

Reports of the Polish nuclear institutes are published by the Nuclear Energy Information Center of the Government Commissioner for Use of Nuclear Energy. Copies are available free of charge from Nuclear Energy Information Center, Palace of Culture and Science, Warsaw, Poland.

SPAIN

Junta de Energia Nuclear. "JEN" reports are available without charge from Servicio de Documentation, Junta de Energia Nuclear, Ciudad Universitaria, Madrid (3), España.

SWITZERLAND

Eidgenössisches Institut für Reaktorforschung. "EIR" reports are available from Eidgenössisches Institut für Reaktorforschung, c/o Bibliothek, 5303 Würenlingen/Switzerland.

TURKEY

Turkish Atomic Energy Commission. Copies are available free of charge from T.A.E.C., Çekmece Nuclear Research Center, P. O. Box 1, Airport, Istanbul, Turkey.

Conferences

Numbers assigned to published conference proceedings as well as individual unpublished papers from conferences are included in this index. A CONF number is assigned to the conference if published proceedings are received and also if only a single paper is received. The base number used is year-month-sequence. Thus, the number CONF-730101 indicates that the conference was held in 1973, in January, and that this was the first January 1973 conference so received. This number would be assigned to complete published proceedings. If individual papers are received, the base number is extended to include a paper number, e.g., CONF-730101-1. As additional papers are received, they are assigned consecutive numbers in the series, CONF-730101-1, CONF-730101-2, etc. This numbering system ensures that all papers received from a conference will be associated with that conference in this index.

Abbreviations Used in Availability Column

AECL	Reports of the Atomic Energy of Canada Limited are for sale by the Scientific Document Distribution Office, Atomic Energy of Canada Limited, Chalk River, Ontario, Canada.
AT	Liquid Metal Fast Breeder Reactor applied technology is available to domestic requesters within the United States from the U. S. Atomic Energy Commission, Technical Information Center, P. O. Box 62, Oak Ridge, TN 37830. Information regarding subscription purchase will be sent on request. Foreign requesters should address inquiries to the above address.
DENM	Reports of the Atomic Energy Commission Research Establishment, Risö, are available on exchange from the Library, Danish Atomic Energy Commission, Risö, Roskilde, Denmark. Also for sale at the price shown from Jul. Gjellerup, Booksellers, 87 Sölvgade, Kobenhavn K., Denmark. Reports of Danatom are available on loan from Research Establishment, Risö, Roskilde, Denmark. Copies are available from Danatom, Aurehojvej 2, Hellerup, Denmark.

Dep.	AEC reports so designated are maintained in the organizations listed on the inside front cover of *NSA*. Prior to July 1, 1965, reports were deposited either in printed copy form or in microform. After that time, all reports have been in the form of micronegatives. Reports from other countries so designated are available in the United States at the organizations listed on the inside front cover of *NSA*.
DRS	Available free from U. S. Atomic Energy Commission, Washington, D. C. 20545. Attn: Director of Regulatory Standards
EM	Inquiries regarding the availability of blueline prints of AEC engineering drawings which were formerly available for sale by NTIS should be addressed to U. S. Atomic Energy Commission, Technical Information Center, P. O. Box 62, Oak Ridge, Tennessee 37830.
EUR	For sale by Centrale de vente des publications des Communautés européennes 37, rue Glesener-Luxembourg.
GPO	For sale by the Superintendent of Documents, Government Printing Office, Washington, D. C. 20402.
IAEA	Available from the International Atomic Energy Agency, Vienna, Austria, and from its sales agencies in various countries throughout the world. A list of these agencies is found in each STI/DOC and STI/PUB publication.
INIS	Available on microfiche at $0.65 per document from INIS Section, International Atomic Energy Agency, P. O. Box 590 A-1011, Vienna, Austria.
LMEC	Available *only to requesters within the United States* from the Liquid Metal Engineering Center, P. O. Box 1449, Canoga Park, CA 91304.
NORW	Reports from Forsvarets Forskningsinstitutt are available from Norwegian Defense Research Establishment, Library, P. O. Box 25, Kjeller, Norway. "KR" reports are available on an exchange basis from the Library, Institutt for Atomenergi, Box 40, Kjeller, Norway. Reports of the Norwegian Reactor School are available from the Library, Institutt for Atomenergi, P. O. Box 40, Kjeller, Norway.
NRC	For sale by the National Research Council of Canada, Ottawa, Ontario, Canada.
NTIS	For sale by the National Technical Information Service (NTIS), U. S. Department of Commerce, Springfield, Virginia 22151. Microfiche copy of each separately bound document can be purchased for $2.25 (domestic) and $3.75 (foreign). Reports issued by organizations outside the United States will be sold by NTIS *only to purchasers within the United States.* Purchasers outside the United States may acquire such reports from the sources described elsewhere in these columns.
OECD	Available from O.E.C.D., Publications 2, rue, André-Pascal, 75 Paris 16^e, France, and from its sales agencies in various countries throughout the world. A list of these agencies is found in each OECD publication.
RSO	Available *only to requesters within the United States* from the Reactor Standards Office, Oak Ridge National Laboratory, P. O. Box X, Oak Ridge, TN 37830.
SWED	"AE" reports (full size or microcopies) are for sale from Aktiebolaget Atomenergi, Studsvik, Library, Fack, S-611 01 NYKÖPING 1, Sweden. Other series are not generally available to the public. Organizations in the Atomic Energy field may obtain copies from Aktiebolaget Atomenergi.
TIC	Available from the U. S. Atomic Energy Commission, Technical Information Center, P. O. Box 62, Oak Ridge, Tennessee 37830.
UK	United Kingdom Atomic Energy Authority reports generally may be purchased from Her Majesty's Stationery Office, P. O. Box 569, London S.E.1. Copies of many UKAEA reports (particularly earlier ones) may be purchased in microcopy form from Micro Methods Ltd., East Ardsley, Wakefield, Yorkshire, England. Copies of UKAEA reports are deposited with the National Lending Library for Science and Technology and 10 public libraries in England; with the USAEC and (through USAEC) with NTIS; and in most national nuclear centers throughout the world. In the USA, UKAEA reports are available on a subscription basis, by subject category, from UNIPUB, Inc., P. O. Box 433, New York, NY 10016, USA; and from Pendragon House, Inc., 1093 Charter Avenue, Redwood City, CA 94063, USA.
UN	Mail orders should be directed to the Sales Section, Room 1059, United Nations Headquarters, New York, New York 10017.
ZAED	Available from ZAED, Kernforschungszentrum, 7501 Leopoldshafen, West Germany.

Report No.	Abstract No.	Availability
AD-	(Misc.)	
629357	30:29345	NTIS, $6.00
765318	30:29972	NTIS
772833	30:30473	NTIS, $3.75
773442	30:30580	NTIS, $3.00
773622	30:30951	NTIS, $3.25
774654	30:30088	NTIS, $4.25
774860	30:29827	NTIS, $13.00
774890	30:29973	NTIS, $4.50
775334	30:29974	NTIS, $3.00
775359	30:29975	NTIS, $4.00
776343	30:30487	NTIS, $4.00
776394	30:29294	NTIS, $3.25
776408	30:31130	NTIS, $5.00
776621	30:29976	NTIS, $3.00
776660	30:30449	NTIS, $4.75
776672	30:29303	NTIS, $3.25
776815	30:29304	NTIS, $4.00
776900	30:29295	NTIS, $3.25
776967	30:29828	NTIS, $11.00
776969	30:30410	NTIS, $3.75
776985	30:31131	NTIS, $5.50
777030	30:30854	NTIS, $3.75
777042	30:30488	NTIS, $3.00
777151	30:29305	NTIS, $4.00
777170	30:29942	NTIS, $3.25
777254	30:30113	NTIS, $3.25
777315	30:29306	NTIS, $3.00
777433	30:30060	NTIS, $4.00
777550	30:29642	NTIS, $3.00
777580	30:29307	NTIS, $7.25
777728	30:30061	NTIS, $3.25
777748	30:29308	NTIS, $3.25
903226	30:29888	NTIS, $9.50
AEC-tr-		
7569	30:31244	Dep. NTIS, $9.75
7574	30:30977	Dep. NTIS, $4.00
7575	30:29086	Dep. NTIS, $4.50
AED-CONF-	(F.R. Germany)	
73-479-009	30:28912	INIS
73-600-001	30:29264	INIS
73-686-000	30:31245	INIS
74-016-002	30:29769	INIS
74-030-003	30:29770	INIS
74-030-004	30:29700	INIS
74-044-009	30:30062	INIS
74-072-002	30:31364	INIS
74-084-002	30:29083	INIS
74-084-004	30:29007	INIS
74-084-007	30:28968	INIS
74-085-001	30:30517	ZAED
74-085-002	30:30518	INIS
74-085-004	30:30519	INIS
74-089-005	30:30805	INIS
74-089-006	30:30063	INIS
74-089-024	30:31365	INIS
74-089-025	30:31381	INIS
74-089-027	30:31382	INIS
74-089-032	30:30474	INIS
74-089-037	30:30064	INIS
74-140-004	30:29701	INIS
74-157-005	30:29356	INIS
74-157-007	30:31204	INIS
74-206-001	30:30089	INIS
74-221-004	30:29829	INIS
74-221-006	30:29702	INIS
74-221-007	30:29703	INIS
74-254-001	30:31383	INIS
AERE-R-	(UK)	
7680	30:31008	Dep. NTIS (US Sales Only), $5.25
7776	30:31414	Dep. NTIS (US Sales Only), $4.00
AFCRL-	(Non-AEC)	
72-0335	30:29888	See AD-903226
AFCRL-TR-	(Misc.)	
73-0348	30:30410	See AD-776969
AFML-TR-	(Non-AEC)	
73-178	30:29975	See AD-775359
AFOSR-TR-	(Misc.)	
74-104	30:30088	See AD-774654
AFSWC-TR-	(Non-AEC)	
73-49	30:30113	See AD-777254
AFWL-TR-	(Misc.)	
73-211	30:29307	See AD-777580
ANL-		
8019	30:29206	See LA-5336
8111	30:31415	Dep. NTIS, $4.00
ANL/ES-		
30	30:31357	Dep. NTIS, $10.00
ANL-Trans-		
960	30:28989	Dep. NTIS, $4.00
961	30:28990	Dep. NTIS, $4.00
ARLV-		
351-28	30:29377	See COM-74-10799
ARMS-		
71.6.5	30:29357	Dep. NTIS, $4.00
72.6.2	30:29358	Dep. NTIS, $4.00
AROD-	(Misc.)	
5378-1S-P	30:30951	See AD-773622
ASTM-B-	(Non-AEC)	
384-74	30:29964	Philadelphia; American Society for Testing and Materials (1974).
ASTM-E-	(Non-AEC)	
146-68	30:28961	Philadelphia; American Society for Testing and Materials (1968).
340-68	30:29965	Philadelphia; American Society for Testing and Materials (1968).
385-73	30:28932	Philadelphia; American Society for Testing and Materials (1973).
402-70	30:28957	Philadelphia; American Society for Testing and Materials (1970).
446-72	30:30044	Philadelphia; American Society for Testing and Materials (1972).
453-72	30:30083	Philadelphia; American Society for Testing and Materials (1972).
ASTM-G-	(Non-AEC)	
2-67	30:29952	Philadelphia; American Society for Testing and Materials (1968).
16-71	30:29056	Philadelphia; American Society for Testing and Materials (1971).
ASTM-STP-	(Non-AEC)	
544	30:29242	Philadelphia; American Society for Testing and Materials (1974). $30.75
AWRE-O-	(UK)	
51/74	30:29309	Dep. NTIS (US Sales Only), $5.50
BAW-	(Misc.)	
10096	30:31194	Dep. NTIS, $7.75
10097	30:31195	
BDX-		
613-1028(Rev.)	30:29602	Dep. NTIS, $4.00
613-1036(Rev.)	30:31384	Dep. NTIS, $4.00
613-1064(Rev.)	30:31366	Dep. NTIS, $4.00
613-1082(Rev.)	30:31385	Dep. NTIS, $4.00
613-1099(Rev.)	30:31367	Dep. NTIS, $4.00
613-1115(Rev.)	30:31416	Dep. NTIS, $7.60
613-1133(Rev.)	30:31386	Dep. NTIS, $4.00
613-1134(Rev.)	30:31417	Dep. NTIS, $4.00
613-1135(Rev.)	30:31418	Dep. NTIS, $4.00
613-1144(Rev.)	30:31419	Dep. NTIS, $4.00
613-1155(Rev.)	30:31387	Dep. NTIS, $4.00
BLG-	(Belgium)	
487	30:28991	Dep. NTIS (US Sales Only), $5.00
BNL-		
19043	30:29203	Dep. NTIS, $4.00
19097(Rev.)	30:31332	Dep. NTIS, $4.25
19153	30:30141	Dep. NTIS, $4.25
19161	30:31388	Dep. NTIS, $4.50
19192	30:30137	Dep. NTIS, $4.00
BNWL-		
1839	30:30065	Dep. NTIS, $4.00
1850(Pt.3)	30:29468	Dep. NTIS, $7.60
BNWL-B-		
223-11	30:30106	Dep. NTIS, $6.50
334	30:30107	Dep. NTIS, $4.50
371	30:31187	Dep. NTIS, $5.00
BNWL-SA-		
4870	30:29776	Dep. NTIS, $4.00
5058	30:29461	Dep. NTIS, $4.75
5065	30:29777	Dep. NTIS, $4.00
CEA-N-	(France)	
1688	30:31333	Dep. NTIS (US Sales Only), $12.00
1711	30:29178	Dep. NTIS (US Sales Only),

Report No.	Abstract No.	Availability
		$14.00
CEA-R-	(France)	
4543	30:29492	Dep. NTIS (US Sales Only), $9.50
4550	30:29133	Dep. NTIS (US Sales Only), $7.50
4552	30:31270	See EURFNR-1169
4591	30:29795	Dep. NTIS (US Sales Only), $4.75
CENC-	(Misc.)	
1194(Vol.1) (Suppl.1)	30:31217	Dep. NTIS, $15.50
1194(Vol.2) (Suppl.1)	30:31218	Dep. NTIS, $13.50
1197(Vol.1)	30:31219	Dep. NTIS, $15.50
1197(Vol.3)	30:31220	Dep. NTIS, $15.00
1197(Vol.4)	30:31221	Dep. NTIS, $10.00
CLM-R-	(UK)	
132	30:29204	Dep. NTIS (US Sales Only), $4.00. UK 50 pence
133	30:29179	Dep. NTIS (US Sales Only), $4.00. UK 50 pence
135	30:29151	Dep. NTIS (US Sales Only), $4.00. UK 50 pence
CNEA-	(Argentina)	
363	30:28938	Dep. NTIS (US Sales Only), $4.00
365	30:31335	Dep. NTIS (US Sales Only), $4.00
366	30:28939	Dep. NTIS (US Sales Only), $4.00
COM-	(Non-AEC)	
74-10799	30:29377	NTIS, $6.25
74-50228	30:30450	GPO, $1.15
74-50233	30:30340	GPO, $0.55
CONF-621106-	(6. annual meeting of the Human Factors Society, New York, New York, USA, 28-30 Nov 1962)	
1	30:31360	See SCR-610
CONF-710360-	(Symposium on the effect of hot water of thermoelectric plants on the hydrology and biology of reservoirs, Borok, USSR, 24-26 Mar 1971)	
(Absts.)	30:29463	See ORNL-tr-2781
CONF-710744-	(Properties of the fundamental interaction NATO-MPI-MRST Advanced Study Institute meeting, Erice, Italy, 8-26 Jul 1971)	
(P9)(PA)	30:30638	Bologna; Editrice Compositori (1973).
CONF-710860-	(Mathematics of contemporary physics conference, London, UK, 23 Aug-11 Sep 1971)	
	30:31154	New York; Academic Press Inc. (1972). $17.50
CONF-720933-	(Symposium on present status and novel developments in the nuclear many-body problem, Rome, Italy, 19-23 Sep 1972)	
P1	30:31031	Bologna; Editrice Compositori (1973).
CONF-730117-	(8. symposium on Mossbauer effect methodology, New York, New York, USA, 28 Jan 1973)	
	30:30092	New York; Plenum Publishing Corporation (1973). $22.50
CONF-730230-	(9. symposium on corrosion and corrosion protection, Tutzing, F.R. Germany, 26 Feb 1973)	
(Absts.)	30:29943	
CONF-730311-	(13. symposium on engineering aspects of magnetohydrodynamics, Stanford, California, USA, 26-28 Mar 1973)	
	30:31207	University, MI; University of Mississippi (1973). $15.00
CONF-730334-	(8. rencontre de moriond conference, Meribel-les-Allues, France, 4-16 Mar 1973)	
P1	30:30663	Orsay, France; Centre National de la Recherche Scientifique (1973).
P2	30:30633	Orsay, France; Centre National de la Recherche Scientifique (1973).
CONF-730479-	(Heat transmission measurements in thermal insulations conference, Philadephia, Pennsylvania, USA, 16-17 Apr 1973)	
	30:29242	Philadelphia; American Society for Testing and Materials (1974). $30.75
CONF-730597-	(USNRL x-ray laser symposium, Washington, District of Columbia, USA, 29 May 1973)	
1	30:29271	See UCID-16290
CONF-730693-	(Proceedings of the summer school on particles and fields in space, Balatonfured, Hungary, 5-15 Jun 1973)	
	30:30160	
CONF-730705-	(6. European conference on controlled fusion and plasma physics, Moscow, USSR, 30 Jul-4 Aug 1973)	
27	30:29272	See UCRL-74898
CONF-730818-	(13. midwestern mechanics conference, Pittsburg, Pennsylvania, USA, 13-15 Aug 1973)	
	30:30570	Pittsburgh; University of Pittsburgh (1973).
CONF-730856-	(5. topical conference in partical physics, Honolulu, Hawaii, USA, 8-21 Aug 1973)	
	30:30577	Honolulu, HI; University Press of Hawaii (1974). $15.00
CONF-7309112-	(Large scale applications of superconductivity and magnetism conference, Entreves, Italy, 5-14 Sep 1973)	
	30:30823	New York; Plenum Publishing Corporation (1974). $39.50
CONF-7309115-	(Symposium and core seminar on the geology and mineral resources of the greater Green River basin, Casper, Wyoming, USA, 17-19 Sep 1973)	
	30:29335	Casper, WY; Wyoming Geological Association (1973).
CONF-731145-	(The production and use of industrial gases symposium, Brighton, UK, 13-15 Nov 1973)	
	30:28992	pounds7.
CONF-731149-	(Conference on bioengineering, Milan, Italy, 20-25 Nov 1973)	
1	30:29705	See RT/FI-(74)16
CONF-731204-	(Digital Equipment Computers Users' Society symposium, San Francisco, California, USA, 27-30 Dec 1973)	
3	30:31340	See IS-M-18
CONF-731220-	(Meeting of the Nuclear Energy Research Society, Hamburg, F.R. Germany, 12 Dec 1973)	
1	30:31243	Munich; Verlag Karl Thiemig AG (1974). $4.50
CONF-731222-	(13. international symposium on physiologic and genetic aspects of reproduction, Salvador, Brazil, 2-7 Dec 1973)	
1	30:29735	Dep. NTIS, $4.25
CONF-731224-	(Project nuclear safety conference, Karlsruhe, F.R. Germany, 11 Dec 1973)	
	30:31245	See AED-CONF-73-686-000
CONF-740115-	(Plutonium information meeting, Los Alamos, New Mexico, USA, 4-5 Jan 1974)	
1	30:29772	See LA-UR-74-1300
CONF-740222-	(Symposium on engineering for the materials/energy challenge, Albuquerque, New Mexico, USA, 28 Feb-1 Mar 1974)	
2	30:31327	See UCRL-75353
CONF-740329-	(Conference on atomic physics, physics of transient phenomena, molecular physics and plasma physics, Stuttgart, F.R. Germany, 4-9 Mar 1974)	
1	30:30519	See AED-CONF-74-085-004
CONF-740340-	(Exhibition and experts meeting on nuclear technology, Frankfurt am Main, F.R. Germany, 18 Mar 1974)	
2	30:30062	See AED-CONF-74-044-009
CONF-740341-	(Electric utility engineering conference, Pittsburgh, Pennsylvania, USA, 3-16 Mar 1974)	
1	30:31222	Dep. NTIS, $4.25
CONF-740342-	(Meeting of lecturers in chemistry, Stuttgart, F.R. Germany, 31 Mar 1974)	
1	30:29083	See AED-CONF-74-084-002
2	30:28968	See AED-CONF-74-084-007
3	30:29007	See AED-CONF-74-084-004
CONF-740343-	(Meeting on deformation and yield in high-	

Report No.	Abstract No.	Availability
	polymer solutions, melts and solids, Wuerzburg, F.R. Germany, 18 Mar 1974)	
1	30:31364	See AED-CONF-74-072-002
CONF-740451-	(Conference on solid state physics, Freudenstadt, F.R. Germany, 1-6 Apr 1974)	
7	30:31365	See AED-CONF-74-089-024
8	30:30063	See AED-CONF-74-089-006
9	30:30064	See AED-CONF-74-089-037
10	30:31382	See AED-CONF-74-089-027
11	30:30805	See AED-CONF-74-089-005
12	30:30474	See AED-CONF-74-089-032
13	30:31381	See AED-CONF-74-089-025
CONF-740465-	(X-ray congress meeting, Baden-Baden, F.R. Germany, 25 Apr 1974)	
2	30:29701	See AED-CONF-74-140-004
CONF-740466-	(Meeting of the working group carbon of the Deutsche Keramische Gesellschaft, Karlsruhe, F.R. Germany, 26 Apr 1974)	
1	30:30089	See AED-CONF-74-206-001
CONF-740509-	(5. international cryogenic engineering conference, Kyoto, Japan, 7-10 May 1974)	
8	30:31324	See LA-UR-74-741
CONF-740554-	(22. annual conference on mass spectrometry and allied topics, Philadelphia, Pennsylvania, USA, 19-24 May 1974)	
1	30:31368	See SLA-73-7063
CONF-740556-	(Seminar on the monitoring of radioactive effluents, Karlsruhe, F.R. Germany, 14 May 1974)	
6	30:31204	See AED-CONF-74-157-007
7	30:29356	See AED-CONF-74-157-005
CONF-740637-	(International conference on reactions between complex nuclei, Nashville, Tennessee, USA, 10-14 Jun 1974)	
(PlandSuppl.)	30:30982	New York; American Elsevier Publishing Company, Inc. (1974).
CONF-740644-	(Takesi Nagata Conference, Pittsburgh, Pennsylvania, USA, 3-4 Jun 1974)	
1	30:31389	Dep. NTIS, $4.00
CONF-740653-	(9. symposium on particle physics, Balatonfured, Hungary, 12-18 Jun 1974)	
2	30:30628	See KFKI-74-49
3	30:31145	See KFKI-74-46
CONF-740662-	(15. annual meeting of the Vereinigung Deutscher Strahlenaerzte e.V. on the authorized physician within the meaning of the radiation protection laws, Karlsruhe, F.R. Germany, 14 Jun 1974)	
2	30:29703	See AED-CONF-74-221-007
3	30:29829	See AED-CONF-74-221-004
4	30:29702	See AED-CONF-74-221-006
CONF-740663-	(7. Caribbean geological conference, Guadeloupe, France, 30 Jun-12 Jul 1974)	
1	30:31376	Dep. NTIS, $4.00
CONF-740664-	(General meeting of the Deutsche Gesellschaft fuer Metallkunde e.V., Bonn, F.R. Germany, 4 Jun 1974)	
2	30:31383	See AED-CONF-74-254-001
CONF-740665-	(Meeting of Mathematical Research Institute, Oberwolfach, F.R. Germany, 9-15 Jun 1974)	
1	30:31345	See SAND-74-5236
CONF-740701-	(2. international conference on nuclear methods in environmental research, Columbia, Missouri, USA, 29-31 Jul 1974)	
2	30:29551	See LA-UR-74-1232
CONF-740702-	(Health Physics Society annual meeting, Houston, Texas, USA, 7-11 Jul 1974)	
7	30:29776	See BNWL-SA-4870
8	30:28969	See DP-MS-73-77
CONF-740708-	(Symposium on dynamic studies with radioisotopes in clinical medicine and research, Knoxville, Tennessee, USA, 15-19 Jul 1974)	
20	30:29830	Dep. NTIS (US Sales Only), $4.00
62	30:29831	Dep. NTIS (US Sales Only), $4.00
CONF-740713-	(17. international conference on high-energy physics, London, UK, 1-10 Jul 1974)	
25	30:30613	See COO-1428-391(App.A-2)
CONF-740715-	(5. international radiation research congress meeting, Seattle, Washington, USA, 14-20 Jul 1974)	
10	30:29777	See BNWL-SA-5065
11	30:29889	See MLM-2172(OP)
13	30:29662	See UCRL-75441
CONF-740722-	(12. international conference on the physics of semiconductors, Stuttgart, F.R. Germany, 15-19 Jul 1974)	
1	30:31425	See LBL-2781
CONF-740805-	(9. Intersociety Energy Conversion Engineering Conference, San Francisco, California, USA, 26-30 Aug 1974)	
	30:29243	New York; American Society of Mechanical Engineers (1974).
CONF-740806-	(Gordon conference, Tilton, New Hampshire, USA, Aug 1974)	
2	30:30856	See UCID-16563
CONF-740807-	(13. air cleaning conference, San Francisco, California, USA, 12-15 Aug 1974)	
17	30:29328	See LA-UR-74-1132
18	30:29329	See RFP-2215
CONF-740809-	(23. annual conference on applications of x-ray analysis, Denver, Colorado, USA, 7-9 Aug 1974)	
1	30:29193	See SLA-74-5242
3	30:29174	See UCRL-75910
7	30:29159	See SAND-74-5262
CONF-740811-	(Meeting of the international Solar Energy Society, Fort Collins, Colorado, USA, 19-23 Aug 1974)	
3	30:31326	See LA-UR-74-1093
4	30:31325	See LA-UR-74-1085
CONF-740813-	(17. conference on Great Lakes research, Hamilton, Ontario, Canada, 12-14 Aug 1974)	
2	30:29462	Dep. NTIS, $4.75
CONF-740820-	(Symposium on the physical and biological effects on the environment of cooling systems and thermal discharges at nuclear power stations, Oslo, Norway, 26-30 Aug 1974)	
2	30:29461	See BNWL-SA-5058
CONF-740822-	(Conference on few body problems in nuclear and particle physics, Quebec, Canada, 27-31 Aug 1974)	
3	30:30599	See LA-UR-74-1333
CONF-740823-	(18. annual meeting of the Society of Photo-Optical Instrumentation Engineers, San Diego, California, USA, 19-23 Aug 1974)	
3	30:31423	See LA-UR-74-1167
4	30:31460	See UCRL-75994
5	30:31356	See UCRL-75662
CONF-740826-	(International Association of Limnology meeting, Winnipeg, Canada, 22-27 Aug 1974)	
3	30:29415	Dep. NTIS, $4.00
CONF-740905-	(International conference on the applications of the Mossbauer effect, Bendor, France, 2-6 Sep 1974)	
2	30:31412	See UCRL-75499(Rev.1)
CONF-740915-	(11. international congress on high speed photography, London, UK, 15-21 Sep 1974)	
2	30:29162	See UCRL-75557
CONF-740921-	(Atmosphere - surface exchange of particulate and gaseous pollutants symposium, Richland, Washington, USA, 4-6 Sep 1974)	
2	30:29489	See UCRL-75902(Rev.1)
3	30:29490	See UCRL-76014(Rev.1)
CONF-740926-	(1. world congress of nuclear medicine and exhibition meeting, Tokyo, Japan, 30 Sep-4 Oct 1974)	
2	30:29781	See COO-3268-5
3	30:30142	See LA-UR-74-1263
CONF-740930-	(14. Hanford biology symposium on radiation and the lymphatic system, Richland, Washington, USA, 30 Sep-2 Oct 1974)	
1	30:29771	Dep. NTIS, $4.00
CONF-740931-	(4. international symposium military applications of blast simulators, Berkshire, UK, 9-12 Sep 1974)	
1	30:31431	See SLA-74-5239
CONF-741017-	(Meeting of the American Nuclear Society, Washington, District of Columbia, USA, 27	

Report No.	Abstract No.	Availability
	Oct-1 Nov 1974)	
9	30:29203	See BNL-19043
COO-		
119-249	30:29778	Dep. NTIS, $20.00
1105-212	30:29536	Dep. NTIS, $4.00
1332-103	30:31377	Dep. NTIS, $7.50
1428-382	30:30597	Dep. NTIS, $5.25
1428-389	30:30626	Dep. NTIS, $4.25
1428-391	30:30574	Dep. NTIS, $4.00
1428-391(App.A-2)	30:30613	Dep. NTIS, $4.50
1436-41	30:31390	Dep. NTIS, $4.00
2172-7	30:29977	Dep. NTIS, $4.00
2277-4	30:29152	Dep. NTIS, $7.00
2427-4	30:29832	Dep. NTIS, $4.00
3077-44	30:31336	Dep. NTIS, $4.00
3167-102	30:29416	Dep. NTIS, $5.50
3237-40	30:30782	Dep. NTIS, $4.00
3268-5	30:29781	Dep. NTIS, $4.00
COPPE-TP-	(Brazil)	
6/72	30:31420	INIS
6/72	30:31391	INIS
DEMO-	(Greece)	
74/5	30:29539	Dep. NTIS (US Sales Only), $7.00
DEU-		
74-2	30:31304	INIS
DNA-	(Non-AEC)	
3248T	30:29308	See AD-777748
DOCKET-50010-	(Dresden Nuclear Power Station, Unit 1, See also DOCKET-50237 and DOCKET-50249, Non-AEC)	
305	30:31311	Dep. NTIS, $17.50
DOCKET-50133-	(Humboldt Bay Power Plant, Unit 3, Non-AEC)	
195	30:31312	Dep. NTIS, $6.75
DOCKET-50220-	(Nine Mile Point Nuclear Station, Unit 1, Non-AEC)	
315	30:31313	Dep. NTIS, $6.75
DOCKET-50237-	(Dresden Nuclear Power Station, Unit 2, See also DOCKET-50010 and DOCKET-50249, Non-AEC)	
598	30:31311	See DOCKET-50010-305
DOCKET-50249-	(Dresden Nuclear Power Station, Unit 3, See also DOCKET-50010 and DOCKET-50237, Non-AEC)	
486	30:31311	See DOCKET-50010-305
DOCKET-50250-	(Turkey Point Plant, Unit 3, See also DOCKET-50251, Non-AEC)	
283	30:31314	Dep. NTIS, $9.50
DOCKET-50251-	(Turkey Point Plant, Unit 4, See also DOCKET-50250, Non-AEC)	
263	30:31314	See DOCKET-50250-283
DOCKET-50269-	(Oconee Nuclear Station, Unit 1, See also DOCKET-50270 and DOCKET-50287, Non-AEC)	
284	30:31315	Dep. NTIS, $21.75
DOCKET-50270-	(Oconee Nuclear Station, Unit 2, See also DOCKET-269 and DOCKET-50287, Non-AEC)	
230	30:31315	See DOCKET-50269-284
DOCKET-50285-	(Fort Calhoun Station, Unit 1, Non-AEC)	
249	30:31316	Dep. NTIS, $13.25
DOCKET-50298-	(Cooper Nuclear Station, Non-AEC)	
233	30:31317	Dep. NTIS, $9.75
DOCKET-50331-	(Duane Arnold Energy Center, Non-AEC)	
277	30:31318	Dep. NTIS, $8.25
DOCKET-50510-	(Blue Hills Station, Unit 1, See also DOCKET-50511, Unit 2, Non-AEC)	
1	30:31319	Dep. NTIS, $12.25
DOCKET-50511-	(Blue Hills Station, Unit 2, See also DOCKET-50510, Unit 1, Non-AEC)	
1	30:31319	See DOCKET-50510-1
DOCKET-STN-50516-	(Jamesport Nuclear Power Station, Unit 1, See also DOCKET-STN-50517, Non-AEC)	
1	30:31320	Dep. NTIS, $7.00
DOCKET-STN-50517-	(Jamesport Nuclear Power Station, Unit 2, See also DOCKET-STN-50516, Non-AEC)	
1	30:31320	See DOCKET-STN-50516-1
DP-MS-		
73-77	30:28969	Dep. NTIS, $4.00
DUN-		
8133	30:29341	Dep. NTIS, $4.00
E-	(Misc.)	
7674	30:28942	See N-74-18812
7724	30:28915	See N-74-20335
7882	30:29979	See N-74-19370
7918	30:29980	See N-74-19371
EDFB-IBP-		
74-4	30:31337	Dep. NTIS, $4.00
EGG-		
1183-1602	30:29358	See ARMS-72.6.2
1183-1605	30:29357	See ARMS-71.6.5
ESD-TR-	(Non-AEC)	
73-346	30:29305	See AD-777151
EUR-	(European Atomic Energy Community)	
4859	30:28940	INIS
4975	30:31225	See KFK-1990
EURFNR-	(European Atomic Energy Community)	
1162	30:31009	Dep. NTIS, $4.00
1163	30:29978	Dep. NTIS, $4.50
1189	30:31270	Dep. NTIS (US Sales Only), $5.45
F-	(Misc.)	
599	30:29808	Dep. NTIS (US Sales Only), $4.00
FIND-		
50335	30:31321	Dep. NTIS, $4.00
50389	30:31322	Dep. NTIS, $4.00
FL-	(Non-AEC)	
180	30:29842	See AD-777550
FRNC-TH-	(France)	
60	30:30104	INIS
GA-A-		
12903	30:29265	Dep. NTIS, $4.00
GAT-		
781	30:29346	Dep. NTIS, $4.00
GEAP-	(Misc.)	
12511	30:31223	Dep. NTIS, $4.00
GKSS-	(F.R. Germany)	
74/E/15	30:31240	INIS
GSI-	(F.R. Germany)	
A1-74	30:30475	INIS
GSI-tr-	(F.R. Germany)	
73/20	30:29205	INIS
74/10	30:30117	INIS
74/15	30:29136	INIS
HASL-		
300(Suppl.2)	30:28970	Dep. NTIS, $7.60
HDL-TR-	(Yugoslavia)	
1653	30:30487	See AD-776343
HEDL-TME-		
74-37	30:31231	AT
HMI-	(F.R. Germany)	
146	30:31334	Berlin, F.R. Germany; HMI (1974).
HMI-B-	(F.R. Germany)	
149	30:31338	Dep. NTIS (US Sales Only), $8.00
IAE-	(USSR)	
2266	30:30090	INIS
2269	30:30520	INIS
2271	30:30643	INIS
2274	30:30844	INIS
2286	30:30627	INIS
2289	30:30978	INIS
2306	30:31142	INIS
2309	30:29008	INIS
IC-	(Italy)	
73-6	30:30751	INIS
73-19	30:30521	INIS
73-131	30:30648	INIS
ICP-		
1045	30:30108	Dep. NTIS, $4.00
IEA-	(Brazil)	
316	30:28913	Dep. NTIS (US Sales Only), $4.00
326	30:28914	Dep. NTIS (US Sales Only), $4.00

Report No.	Abstract No.	Availability
IFA-CRD-	(Romania)	
57-1974	30:29614	Dep. NTIS (US Sales Only), $4.00
IFA-DNBR-	(Romania)	
8-1974	30:30845	Dep. NTIS (US Sales Only), $4.00
9-1974	30:30846	Dep. NTIS (US Sales Only), $4.75
IFA-FN-	(Romania)	
44-1974	30:29558	Dep. NTIS (US Sales Only), $4.25
45-1974	30:29559	Dep. NTIS (US Sales Only), $4.50
IFA-FT-	(Romania)	
107-1974	30:31020	Dep. NTIS (US Sales Only), $4.25
108-1974	30:31021	Dep. NTIS (US Sales Only), $5.20
109-1974	30:31421	Dep. NTIS (US Sales Only), $5.00
IFVE-SPK-	(USSR)	
73-69	30:30598	INIS
IAE-		
5-175	30:31422	INIS
6-75d	30:31271	INIS
6-79d	30:31232	INIS
INIS-mf-	(International Atomic Energy Agency)	
1357	30:31143	INIS
IPP-	(Non-AEC)	
3/12	30:29173	INIS
IRI-	(Netherlands)	
132-73-03	30:30847	INIS
IRS-A-	(F.R. Germany)	
4	30:31246	INIS
IS-		
3444	30:31339	Dep. NTIS, $4.25
IS-M-		
18	30:31340	Dep. NTIS, $4.00
ITEF-	(USSR)	
31	30:30730	INIS
JAERI-M-		
5560	30:31247	NTIS (US Sales Only)
5590	30:31272	NTIS (US Sales Only)
JAPFNR-	(Japan)	
154	30:31224	Dep. NTIS (US Sales Only), $4.00
JEN-	(Spain)	
284	30:29649	Dep. NTIS (US Sales Only), $9.00
286	30:29650	Dep. NTIS (US Sales Only), $16.50
JINR-	(USSR)	
E2-7402	30:30592	INIS
P1-7523	30:30875	INIS
P2-7432	30:31144	INIS
P2-7502	30:30718	INIS
P2-7511	30:30649	INIS
P4-7225	30:31132	INIS
P5-7344	30:31133	INIS
P14-7974	30:31392	Dep. NTIS (US Sales Only), $4.00
JUL-	(F.R. Germany)	
73	30:29239	NTIS, $4.50
1050-FF	30:29560	INIS
1063-CT	30:28941	INIS
1077	30:31305	Dep. NTIS (US Sales Only), $6.50
KFK-	(F.R. Germany)	
1851	30:29704	Dep. NTIS (US Sales Only), $4.75
1865	30:31270	See EURFNR-1169
1908	30:31248	INIS
1935	30:31249	Dep. NTIS (US Sales Only), $5.75
1959	30:30848	,Dep. NTIS (US Sales Only), $7.50
1978	30:31393	Dep. NTIS (US Sales Only), $4.00
1990	30:31225	Dep. NTIS (US Sales Only), $5.00
KFKI-	(Hungary)	
74-46	30:31145	Dep. NTIS (US Sales Only), $4.25
74-49	30:30628	Dep. NTIS (US Sales Only), $4.00
LA-		
5336	30:29206	Dep. NTIS, $7.60
5637-T	30:31395	Dep. NTIS, $10.60
5639-MS	30:29153	Dep. NTIS, $4.00
5683-MS	30:29266	Dep. NTIS, $4.00
5684-PR	30:30820	Dep. NTIS, $4.00
5693-MS	30:29196	Dep. NTIS, $4.00
5694-MS	30:30565	Dep. NTIS, $4.00
5699-MS	30:29207	Dep. NTIS, $4.00
LA-tr-		
74-18	30:29024	Dep. NTIS, $4.25
74-19	30:29025	Dep. NTIS, $4.00
74-30	30:30121	Dep. NTIS, $4.00
LA-UR-		
74-741	30:31324	Dep. NTIS, $4.00
74-1065	30:31325	Dep. NTIS, $4.50
74-1093	30:31326	Dep. NTIS, $4.75
74-1132	30:29328	Dep. NTIS, $4.00
74-1167	30:31423	Dep. NTIS, $4.00
74-1232	30:29551	Dep. NTIS, $4.00
74-1263	30:30142	Dep. NTIS, $4.00
74-1300	30:29772	Dep. NTIS, $5.00
74-1333	30:30599	Dep. NTIS, $4.00
LAMS-		
2610	30:29310	Dep. NTIS, $4.00
LBL-		
2574	30:31424	Dep. NTIS, $7.25
2781	30:31425	Dep. NTIS, $4.00
3072	30:31341	Dep. NTIS, $4.00
LMSC-D-	(Non-AEC)	
401278	30:30061	See AD-777728
LTIRF-	(Non-AEC)	
356/IP	30:30410	See AD-776969
LUIP-CR-	(Sweden)	
74-3	30:29493	Dep. NTIS (US Sales Only), $5.25
MC-	(Romania)	
19-1974	30:31342	Dep. NTIS (US Sales Only), $4.25
MDC-	(Non-AEC)	
G4418	30:29239	See JUL-73
MLM-		
2098	30:31426	Dep. NTIS, $4.00
2171(LD)	30:29026	Dep. NTIS, $4.00
2172(DP)	30:29889	Dep. NTIS, $4.00
N-	(Misc.)	
74-18812	30:28942	NTIS, $3.00
74-19370	30:29979	NTIS, $4.00
74-19371	30:29980	NTIS, $4.00
74-20335	30:28915	NTIS, $4.25
74-20470	30:28916	NTIS, $4.00
74-23299	30:31241	NTIS, $10.00
NASA-CR-	(Misc.)	
137386	30:28916	See N-74-20470
138240	30:31241	See N-74-23299
NASA-TM-X-	(Misc.)	
71506	30:29979	See N-74-19370
71507	30:29980	See N-74-19371
71519	30:28915	See N-74-20335
NASA-TN-D-	(Misc.)	
7536	30:28942	See N-74-18812
NEANDC-	(Switzerland)	
97/U	30:30849	Dep. NTIS (US Sales Only), $4.00
NLCO-		
1109	30:29347	Dep. NTIS, $4.50
NOAA-	(Non-AEC)	
74021906	30:30340	See COM-74-50233
74021907	30:30450	See COM-74-50228
NOAA-TM-ERL-ARL		
37	30:29377	See COM-74-10799
43	30:31343	
NOAA-TR-ERL-	(Non-AEC)	
285	30:30340	See COM-74-50233
286	30:30450	See COM-74-50228
NOLTR-	(Misc.)	
74-4	30:30488	See AD-777042
NP-	(AEC File No. for Non-AEC Reports)	

Report No.	Abstract No.	Availability
20072	30:30650	Dep. NTIS (US Sales Only), $4.00
20106	30:29145	
20122	30:30952	Dep. NTIS (US Sales Only), $7.75
20130	30:31296	Dep. NTIS (US Sales Only), $8.75
20140	30:29154	Dep. NTIS (US Sales Only), $10.75
NRL-	(Misc.)	
7593	30:30854	See AD-777030
NRL-MR-	(Non-AEC)	
2617	30:29972	See AD-765318
2752	30:30060	See AD-777433
NRL-Report-	(Non-AEC)	
7760	30:29981	
NSF/RA/G-	(Non-AEC)	
73-014	30:29311	See PB-231011
NVO-		
142	30:29439	See NVO-AEIC-74-1
410-24	30:29378	Dep. NTIS, $5.75
410-25	30:29379	Dep. NTIS, $4.50
NVO-AEIC-		
74-1	30:29439	Dep. NTIS, $10.60
NYO-		
3406-18	30:31378	Dep. NTIS, $4.00
ORNL-		
4985	30:30935	Dep. NTIS, $5.45
ORNL-NSF-EP-		
73	30:29456	Dep. NTIS, $8.75
ORNL-RSIC-		
25(Suppl.2)	30:31126	Dep. NTIS, $5.45
ORNL-TM-		
760	30:29002	Dep. NTIS, $5.75
3992	30:30114	AT
4375	30:29380	Dep. NTIS, $5.00
4588	30:31344	Dep. NTIS, $4.25
4619	30:29208	Dep. NTIS, $4.75
4655(Vol.1)	30:31250	Dep. NTIS, $5.45
4655(Vol.2)	30:31251	Dep. NTIS, $5.45
4657	30:29209	Dep. NTIS, $4.50
4666	30:29210	Dep. NTIS, $4.50
4672	30:29158	Dep. NTIS, $8.75
4674	30:29381	Dep. NTIS, $5.50
ORNL-tr-		
2781	30:29463	Dep. NTIS, $7.50
2801	30:31358	Dep. NTIS, $7.50
ORO-		
4282-14	30:31010	Dep. NTIS, $4.00
PA-TR-	(Non-AEC)	
4629	30:29295	See AD-776900
PAEC(A)-	(Philippines)	
7332(Suppl.1)	30:28919	Dep. NTIS (US Sales Only), $14.75
PATENTS-	(Canadian: Commissioner of Patents, Ottawa, Canada, KIA OEI; $1.00 per copy)	
941,145	30:29146	
941,155	30:29126	
944,691	30:29647	
PATENTS-	(Czechoslovakian: Dr. Karel Neumann, Advokatni poradna c. 10, Zitna 25, Prague I, Czechoslovakia, Kes. 10 per copy)	
146,221	30:31285	
146,450	30:31297	
146,660	30:29276	
PATENTS-	(German: Deutsches Patentamt, Dienststelle Berlin, Gitschiner Str. 97-103, 1000 Berlin 61, F.R. Germany, DM 3.- per copy, plus postage)	
2136352	30:31188	
2140170	30:31284	
2146346	30:31294	
2335516	30:31301	
PATENTS-	(Netherlands: The Patent Office (Octrooiraad),, Patentslaan 2, Rijswijk 2. H patents, Netherlands, F. 3.00 per copy)	
7,210,084	30:29277	
7,211,133	30:31198	
7,211,400	30:31197	
7,211,772	30:29144	
7,211,781	30:31259	
7,211,897	30:29503	
7,214,024	30:29622	
7,214,381	30:29561	
7,214,774	30:29505	
7,215,142	30:31288	
7,215,216	30:31199	
7,215,811	30:31200	
7,216,867	30:29636	
7,217,247	30:29621	
7,217,555	30:31286	
7,217,556	30:31298	
7,217,568	30:31299	
7,217,571	30:31287	
7,217,655	30:31127	
7,300,178	30:29278	
7,301,065	30:31300	
7,301,442	30:30133	
7,301,833	30:29504	
PATENTS-	(UK: Comptroller-General, The Patent Office (Sale Branch), St. Mary Cray, Orpington, Kent, BR 53rd, UK, 0.25 pounds per copy)	
1,353,556	30:30572	
1,353,733	30:31214	
PATENTS-	(US: Commissioner of Patents, Washington, D.C. 20231, USA, $.50 per copy)	
3,822,146	30:30123	
3,822,185	30:31242	
3,825,499	30:29934	
3,825,500	30:29280	
3,825,649	30:29150	
3,825,650	30:29149	
3,826,091	30:31282	
3,826,094	30:31283	
3,826,617	30:28936	
3,826,678	30:29082	
3,826,753	30:29127	
3,826,754	30:31281	
3,826,921	30:29624	
3,826,996	30:29194	
3,826,997	30:29284	
3,826,998	30:29283	
3,827,935	30:31196	
3,828,197	30:30109	
3,828,276	30:29282	
3,828,277	30:29281	
3,828,518	30:31293	
3,828,868	30:31292	
3,829,313	30:29939	
3,829,551	30:28995	
3,830,292	30:29275	
3,831,248	30:30111	
3,831,912	30:31227	
3,832,222	30:29961	
3,832,439	30:29148	
3,833,428	30:29240	
3,833,469	30:29139	
3,833,509	30:29140	
3,833,809	30:29429	
3,833,815	30:29640	
PB-	(Non-AEC)	
231011	30:29311	NTIS, $4.50
PH-	(Iraq)	
43-67-1408-6	30:29239	See JUL-73
PITHA-	(German Democratic Republic)	
64(1972)	30:30593	INIS
PNC-N-	(Japan)	
251-73-06	30:31224	See JAPFNR-154
PNE-RB-		
51-9	30:29348	
59	30:29312	
60	30:29313	
PTB-L-	(F.R. Germany)	
2	30:31359	INIS
RCN-	(Netherlands)	
212	30:31226	INIS
RDT-E-		
1-19T(6-74)	30:29267	RSO
RFP-		
2151	30:31379	Dep. NTIS, $4.00
2215	30:29329	Dep. NTIS, $4.00
RISO-	(Denmark)	
297	30:28943	Dep. NTIS (US Sales Only), $6.25
RISO-M-	(Denmark)	
1714	30:31427	Dep. NTIS (US Sales Only), $7.75
1726	30:29342	Dep. NTIS (US Sales Only), $12.00
RL-		
74-077	30:29211	Dep. NTIS (US Sales Only),

Report No.	Abstract No.	Availability
		$6.75
74-098	30:30581	Dep. NTIS (US Sales Only), $4.25
RT/BIO-	(Italy)	
(74)7	30:31380	Dep. NTIS (US Sales Only), $6.75
(74)10	30:29736	Dep. NTIS (US Sales Only), $4.50
RT/FI-	(Italy)	
(74)10	30:30850	Dep. NTIS (US Sales Only), $8.00
(74)16	30:29705	Dep. NTIS (US Sales Only), $4.00
(74)17	30:30956	Dep. NTIS (US Sales Only), $4.25
(74)19	30:30851	Dep. NTIS (US Sales Only), $4.25
(74)26	30:31273	Dep. NTIS (US Sales Only), $4.00
(74)30	30:31274	Dep. NTIS (US Sales Only), $4.00
RT/MET-	(Italy)	
(73)1	30:31279	Dep. NTIS (US Sales Only), $5.50
RT/PROT-	(Italy)	
(74)13	30:29457	Dep. NTIS (US Sales Only), $7.00
SAMSO-TR-	(Non-AEC)	
74-73	30:29942	See AD-777170
SAND-		
74-0135	30:31396	Dep. NTIS, $4.00
74-0149	30:31428	Dep. NTIS, $4.00
74-0153	30:31429	Dep. NTIS, $4.00
74-0193	30:29890	Dep. NTIS, $4.75
74-5236	30:31345	Dep. NTIS, $4.00
74-5262	30:29159	Dep. NTIS, $4.00
74-6017	30:29766	Dep. NTIS, $4.00
SCPRI(RM)-	(France)	
2-1974	30:29349	Dep. NTIS (US Sales Only), $4.00
2-1974(Suppl.)	30:29350	Dep. NTIS (US Sales Only), $4.25
SCR-		
610	30:31360	Dep. NTIS, $4.25
SDAC-TR-	(Non-AEC)	
74-1	30:29303	See AD-776672
SEL-	(Misc.)	
26	30:30340	See COM-74-50233
27	30:30450	See COM-74-50228
SLA-		
73-0409	30:31346	Dep. NTIS, $4.75
73-1073	30:31397	Dep. NTIS, $5.25
73-1121	30:29982	Dep. NTIS, $7.50
73-7063	30:31368	Dep. NTIS, $4.00
74-0065	30:29676	Dep. NTIS, $5.50
74-0210	30:29314	Dep. NTIS, $4.00
74-0347	30:31430	Dep. NTIS, $4.00
74-5239	30:31431	Dep. NTIS, $4.00
74-5242	30:29193	Dep. NTIS, $4.00
SM-	(Misc.)	
185/6	30:29831	See CONF-740708-52
185/86	30:29830	See CONF-740708-20
SRO-	(Misc.)	
641-13	30:29419	Dep. NTIS, $5.00
STI/DOC-	(Internatinal Atomic Energy Agency)	
10/155	30:31252	IAEA, $8.00
TID-		
26630	30:30105	Dep. NTIS, $9.25
26631	30:31323	Dep. NTIS, $18.50
26638	30:30575	Dep. NTIS, $4.50
26639	30:29196	Dep. NTIS, $4.00
TRG-Report-	(UK)	
2434	30:29035	Dep. NTIS (US Sales Only), $4.00
TRITA-KKE-	(Sweden)	
7403	30:28972	Dep. NTIS (US Sales Only), $6.00
TRW-ER-	(Misc.)	
7274-9	30:29975	See AD-775359
UCC-ND-		
279	30:29351	Dep. NTIS, $4.50
280	30:29352	Dep. NTIS, $5.50
UCID-		
15203	30:31432	Dep. NTIS, $4.00

Report No.	Abstract No.	Availability
15316	30:29180	Dep. NTIS, $4.75
15369	30:31398	Dep. NTIS, $4.00
15371	30:29268	Dep. NTIS, $4.00
15372	30:29495	Dep. NTIS, $4.25
15373	30:31433	Dep. NTIS, $4.00
15383	30:31434	Dep. NTIS, $4.00
15388	30:31347	Dep. NTIS, $4.00
15392	30:29160	Dep. NTIS, $4.00
15434	30:29212	Dep. NTIS, $4.00
15448	30:29213	Dep. NTIS, $4.00
15454	30:31399	Dep. NTIS, $4.00
15478	30:31348	Dep. NTIS, $4.00
15481	30:29214	Dep. NTIS, $4.00
15487	30:29181	Dep. NTIS, $4.00
15496	30:31435	Dep. NTIS, $4.75
15511	30:29215	Dep. NTIS, $4.00
15513	30:29182	Dep. NTIS, $4.00
15540	30:29197	Dep. NTIS, $4.00
15586	30:31400	Dep. NTIS, $5.00
15597	30:31436	Dep. NTIS, $4.75
15611	30:31437	Dep. NTIS, $4.00
15618	30:31438	Dep. NTIS, $4.50
15623	30:31369	Dep. NTIS, $4.00
15624	30:29216	Dep. NTIS, $4.00
15625	30:29161	Dep. NTIS, $4.00
15628	30:29183	Dep. NTIS, $4.00
15639	30:31011	Dep. NTIS, $4.25
15647	30:29184	Dep. NTIS, $4.50
15649	30:31439	Dep. NTIS, $4.00
15650	30:29217	Dep. NTIS, $9.75
15660	30:29218	Dep. NTIS, $4.00
15662	30:31401	Dep. NTIS, $4.00
15669	30:31402	Dep. NTIS, $4.00
15671	30:31370	Dep. NTIS, $4.00
15682	30:31440	Dep. NTIS, $4.25
15685	30:30138	Dep. NTIS, $4.00
15686	30:30139	Dep. NTIS, $4.00
15695	30:29219	Dep. NTIS, $4.25
15711	30:29198	Dep. NTIS, $4.00
15712	30:29185	Dep. NTIS, $4.75
15722	30:31361	Dep. NTIS, $6.50
15723	30:31441	Dep. NTIS, $4.00
15727	30:29315	Dep. NTIS, $4.00
15735	30:30140	Dep. NTIS, $4.00
15736	30:29316	Dep. NTIS, $4.00
15739	30:31403	Dep. NTIS, $4.00
15743	30:31349	Dep. NTIS, $5.00
15753	30:31350	Dep. NTIS, $4.00
15761	30:29496	Dep. NTIS, $4.00
15765	30:31351	Dep. NTIS, $4.00
15769	30:31442	Dep. NTIS, $4.00
15771	30:29317	Dep. NTIS, $4.00
15773	30:31443	Dep. NTIS, $4.00
15775	30:29497	Dep. NTIS, $4.00
15777	30:29296	Dep. NTIS, $4.00
15784	30:31105	Dep. NTIS, $4.75
15787	30:30576	Dep. NTIS, $5.00
15802(Rev.1)	30:29318	Dep. NTIS, $9.75
15803	30:31444	Dep. NTIS, $9.00
15806	30:29220	Dep. NTIS, $4.00
15808	30:30651	Dep. NTIS, $4.50
15809	30:29087	Dep. NTIS, $4.00
15811	30:31445	Dep. NTIS, $4.00
15815	30:31404	Dep. NTIS, $5.25
15816	30:31446	Dep. NTIS, $5.25
15817	30:31236	Dep. NTIS, $4.00
15818	30:29319	Dep. NTIS, $4.25
15820	30:29186	Dep. NTIS, $4.00
15828	30:29618	Dep. NTIS, $4.00
15829	30:31447	Dep. NTIS, $4.00
15833	30:29269	Dep. NTIS, $4.00
15836	30:29552	Dep. NTIS, $4.25
15840	30:31352	Dep. NTIS, $4.00
15845	30:31405	Dep. NTIS, $4.00
15846	30:31406	Dep. NTIS, $5.25
15855	30:29320	Dep. NTIS, $4.00
15859	30:29891	Dep. NTIS, $4.00
15860	30:29270	Dep. NTIS, $4.00
15865	30:29321	Dep. NTIS, $4.00
15866	30:31448	Dep. NTIS, $4.00
15867	30:29297	Dep. NTIS, $4.00
15872	30:31371	Dep. NTIS, $4.00
15874	30:29322	Dep. NTIS, $4.00
15890	30:31449	Dep. NTIS, $4.75
15895	30:29458	Dep. NTIS, $4.00
15898	30:31450	Dep. NTIS, $4.00
15901	30:31407	Dep. NTIS, $4.75
15907	30:31451	Dep. NTIS, $4.00
15910	30:31372	Dep. NTIS, $4.50
15919	30:29323	Dep. NTIS, $4.00
15926	30:29958	Dep. NTIS, $4.00
15938	30:31123	Dep. NTIS, $4.00
15939	30:29221	Dep. NTIS, $5.00
15941	30:29330	Dep. NTIS, $4.00
15945	30:31353	Dep. NTIS, $4.00
15947	30:31354	Dep. NTIS, $4.00
15952	30:28944	Dep. NTIS, $4.00
15953	30:29222	Dep. NTIS, $4.00
15955	30:31452	Dep. NTIS, $4.00
15956	30:29223	Dep. NTIS, $4.25
15962	30:31408	Dep. NTIS, $4.00

Report No.	Abstract No.	Availability
15972	30:31373	Dep. NTIS, $4.00
15977	30:29224	Dep. NTIS, $4.00
15981	30:29324	Dep. NTIS, $4.00
15983	30:29325	Dep. NTIS, $4.00
15985	30:29326	Dep. NTIS, $4.00
15992	30:31355	Dep. NTIS, $5.00
15996	30:29193	Dep. NTIS, $4.00
15998	30:31453	Dep. NTIS, $4.00
16003(Rev.1)	30:29187	Dep. NTIS, $4.00
16004	30:29188	Dep. NTIS, $4.00
16014	30:31362	Dep. NTIS, $4.75
16023	30:31409	Dep. NTIS, $4.25
16026	30:29619	Dep. NTIS, $4.00
16032	30:31454	Dep. NTIS, $4.00
16034	30:31455	Dep. NTIS, $4.00
16051	30:31456	Dep. NTIS, $4.75
16057	30:29225	Dep. NTIS, $4.00
16064	30:31457	Dep. NTIS, $4.00
16076	30:31410	Dep. NTIS, $4.00
16107	30:29327	Dep. NTIS, $4.25
16108	30:31458	Dep. NTIS, $4.75
16109	30:30066	Dep. NTIS, $4.00
16290	30:29271	Dep. NTIS, $5.00
16563	30:30856	Dep. NTIS, $4.00
16583	30:30131	Dep. NTIS, $4.00
UCLA-		
34P203-18	30:31253	See UCLA-ENG-7343
UCLA-ENG-		
7343	30:31253	Dep. NTIS, $14.50
UCRL-		
13599	30:31459	Dep. NTIS, $4.75
51494	30:31254	Dep. NTIS, $4.00
51537	30:31363	Dep. NTIS, $5.45
51598	30:29189	Dep. NTIS, $5.45
51626	30:31411	Dep. NTIS, $4.00
51629	30:31374	Dep. NTIS, $4.00
51631(Pt.1)	30:29233	Dep. NTIS, $4.00
51636	30:31375	Dep. NTIS, $12.50
74898	30:29272	Dep. NTIS, $4.00
75353	30:31327	Dep. NTIS, $4.00
75441	30:29662	Dep. NTIS, $5.50
75499(Rev.1)	30:31412	Dep. NTIS, $4.00
75557	30:29162	Dep. NTIS, $4.00
75662	30:31356	Dep. NTIS, $4.00
75902(Rev.1)	30:29489	Dep. NTIS, $4.25
75910	30:29174	Dep. NTIS, $4.00
75994	30:31460	Dep. NTIS, $4.00
76014(Rev.1)	30:29490	Dep. NTIS, $4.25
USAAVSCOM-TR-	(Non-AEC)	
73-31	30:29294	See AD-776394
VUF-	(Misc.)	
1021	30:29345	See AD-629357
WAPD-TM-	(Misc.)	
1085	30:31280	Dep. NTIS, $5.00
1157	30:29983	Dep. NTIS, $5.25
WASH-		
1334	30:31306	Dep. NTIS, $5.45
Y-		
1949	30:29944	Dep. NTIS, $5.45
1955	30:31413	Dep. NTIS, $4.00
Y-DD-		
155	30:30115	Dep. NTIS, $4.00
156	30:30116	Dep. NTIS, $4.00
ZAED-BIBL.-	(F.R. Germany)	
02-12	30:29420	Dep. NTIS (US Sales Only), $5.25

☆U. S. GOVERNMENT PRINTING OFFICE: 1974—640-082/11

COMPLETE OR PARTIAL COLLECTIONS OF USAEC REPORTS IN COUNTRIES OTHER THAN THE UNITED STATES

ARGENTINA
Buenos Aires, Comisión Nacional de Energía Atómica

AUSTRALIA
Canberra, National Library of Australia
Sutherland, New South Wales Atomic Energy Research Establishment

AUSTRIA
Vienna, International Atomic Energy Agency (IAEA)
Vienna, Zentralbibliothek der Physikalischen Institute der Universität

BELGIUM
Brussels, European Atomic Energy Community (Euratom)
Mol-Donk, Centre d'Etude de l'Energie Nucléaire

BRAZIL
Rio de Janeiro, Comissão Nacional de Energia Nuclear
São Paulo, Instituto de Energia Atómica

CANADA
Chalk River, Ontario, Atomic Energy of Canada, Ltd.
Hamilton, Ontario, McMaster University
Ottawa, National Research Council

CONGO, REPUBLIC OF
Kinshasa, Trico Nuclear Center

DENMARK
Risö, Danish Atomic Energy Commission

FINLAND
Otaniemi, Teknillinen Korkeakoulu

FRANCE
Saclay, Gif-sur-Yvette, Centre d'Etudes Nucléaires de Saclay

GERMANY, WEST
Karlsruhe, Zentralstelle für Atomkernenergie Dokumentation
Munich, Technische Universität

GREECE
Athens, Nuclear Research Center, Democritus Library

INDIA
Bombay, Trombay, Bhabha Atomic Research Center Library

IRAQ, REPUBLIC OF
Baghdad, Atomic Energy Commission, Nuclear Research Institute

IRELAND
Dublin, University College

ISRAEL
Yavne, Israel Atomic Energy Commission, Soreq Nuclear Research Centre

ITALY
Ispra, Cetis Library
Rome, Centro di Studi Nucleari della Casaccia

JAPAN
Tokyo, National Diet Library
Tokai-Mura, Naka-gun, Ibaraki-ken, Japan Atomic Energy Research Institute

KOREA, REPUBLIC OF
Seoul, Atomic Energy Research Institute

MEXICO
Mexico, D. F., Comisión Nacional de Energía Nuclear

NETHERLANDS, THE
Petten, Reactor Centrum Nederland
The Hague, Bibliothek Octrooiraad

NORWAY
Kjeller, Institutt for Atomenergi

PORTUGAL
Sacavem, Junta de Energia Nuclear

SOUTH AFRICA, REPUBLIC OF
Pretoria, Atomic Energy Board Library

SPAIN
Madrid, Junta de Energia Nuclear, Ciudad Universitaria

SWEDEN
Nyköping, Aktiebolaget Atomenergi Library

SWITZERLAND
Zürich, Swiss Federal Institute of Technology

UNITED KINGDOM
Boston Spa, Wetherby, Yorkshire, British Library Lending Division
Harwell, Didcot, Berkshire, Atomic Energy Research Establishment

IN INTERNATIONAL AGENCIES

EUROPEAN ATOMIC ENERGY COMMUNITY (EURATOM)
Brussels, Belgium
Ispra, Varese, Italy, Cetis Library

OECD NUCLEAR ENERGY AGENCY (NEA)
British Library Lending Division
Boston Spa, Wetherby, Yorkshire, England

INTERNATIONAL ATOMIC ENERGY AGENCY (IAEA)
Vienna, Austria

UNITED STATES
GOVERNMENT PRINTING OFFICE
DIVISION OF
PUBLIC DOCUMENTS
WASHINGTON, D.C. 20402

OFFICIAL BUSINESS

POSTAGE AND FEES PAID
U S GOVERNMENT PRINTING OFFICE

U.S.MAIL

A New USAEC Publication

Nuclear Criticality Safety

R. Douglas O'Dell, Editor

Proceedings of a Short Course
held at the D. H. Lawrence Ranch
near Taos, New Mexico, May 7–11, 1973

Sponsored by the University of New Mexico

Supported by the American Nuclear Society's
Trinity Section and
Nuclear Criticality Safety Division

September 1974
181 pages, $8\frac{1}{2}$ by 11 inches
Library of Congress Catalog Card
Number 74-600168

Available as TID-26286 for
$7.60 (USA) ($10.10 foreign) from

National Technical Information Service
U. S. Department of Commerce
Springfield, Virginia 22161

With the emergence of the nuclear power industry as a large-scale source of energy in the United States, the field of nuclear criticality safety has become increasingly important and has involved an increasing number of persons. *Nuclear Criticality Safety* records the proceedings of a short course designed to give persons from industry, national laboratories, government, and universities—all involved in criticality safety—the opportunity to meet together to exchange ideas and to discuss common problems.

This publication introduces the underlying principles and reviews the state of the art of nuclear criticality safety as well as presents discussions and work sessions on topics of current importance and interest. It contains a reasonably comprehensive coverage of the field of nuclear criticality safety. Not intended to be complete coverage, it is a first step. It will be valuable to anyone directly or indirectly responsible for or interested in the criticality safety of facilities in which radioactive materials are handled.

The topics presented are: The Nature of Fission and the Criticality Process (from protactinium to californium and beyond); Principles of Safety (safety in general, criticality risk in perspective); Consequences of Criticality Accidents; Contingencies and Risk Control (panel discussion); Criticality Experiments and Data; Criticality Computations (an overview); Generic Array Criticality (an analytic representation of reflected arrays of fissile units); Establishing Subcritical Limits; Interpretation of Monte Carlo Results (work–discussion session); Procedures and Practices (work–discussion session); Operator Training (work–discussion session); Process Management (panel discussion); Status of Mixed Oxides and Actinides (work–discussion session); Shielded Facilities (work–discussion session); Fire Protection (work–discussion session); Transportation Problems (work–discussion session); Remarks on Licensing of Nuclear-Fuel-Cycle Facilities; Nuclear Standards; and Regulations and Standards (work–discussion session).